

DPG-Tagung 2022
(DPG Meeting 2022)
of the Condensed Matter Section (SKM)

together with the Division
Quantum Information

and the Working Groups
Equal Opportunities, Young DPG, Young Leaders in Physics



„Regensburg bei Nacht“ / Foto: C. Böll

4 – 9 September 2022
Universität Regensburg

Verhandlungen der Deutschen Physikalischen Gesellschaft (ISSN 2751-0522 [Online])
Reihe VI, Band 57 (2022)
Zitertitel: Verhandl. DPG (VI) 57, 4/2022
Erscheinungsweise: Jährlich 3 - 6 Online-Hefte, je nach Bedarf

Verantwortlich für den Inhalt: Dr. Bernhard Nunner, DPG e. V., Hauptstraße 5, 53604 Bad Honnef
Telefon: +49 (0)2224 9232-0, Telefax: +49 (0)2224 9232-50
© Deutsche Physikalische Gesellschaft e. V., 53604 Bad Honnef

Content

Greeting	5
Organisation	
Organiser	6
Local Organiser	6
Local Secretary	6
Scientific Organisation	
Chair of the Condensed Matter Section	6
Chairs of the Participating Divisions and Working Groups	6
Symposia	7
Organisation of the Exhibition of Scientific Instruments and Literature	7
Sponsors	8
Conference Information	
Conference Venue	9
Parking	9
Transportation	9
Conference Office - Information Desk	9
Lost and found	9
Cloakroom	9
Allocation of the Lecture Halls	10
DPG-App	10
WIFI / LAN	10
Printing Service	10
Presentation / Oral Presentation	10
Poster Presentation.....	11
Notice Board	11
Wilhelm and Else Heraeus Communication Programme	11
Catering	
Coffee	12
Lunch	12
Events	
Tutorials	12
Welcome Evening	12
Opening of the Conference	12
Special Plenary Session with Award Ceremony	12
Public Evening Lecture	13
EinsteinSlam	13
Job Market	13
Exhibition of Scientific Instruments and Literature	14
City Tours	14
Say cheese	14
CO ₂ Compensation	14
Synopsis of the Daily Programme	16
Plenary Talks (PLV).....	45
Prize Talks (PRV)	47
Plenary Special Talks (PSV)	48
Tutorials	49
Symposia	
Entanglement Distribution in Quantum Networks (SYED).....	51
Frontiers of Electronic-Structure Theory: Focus on Artificial Intelligence applied to Real Materials (SYES)	53

From Physics and Big Data to the Design of Novel Materials (SYNM)	55
Frontiers of Orbital Physics: Statics, Dynamics, and Transport of Orbital Angular Momentum (SYOP)	57
High Yield Devices for Photonic Quantum Implementations (SYPQ)	59
Complexity and Topology in Quantum Matter (SYQM)	61
SKM Dissertation Prize (SYSD).....	63
Interplay of Substrate Adaptivity and Wetting Dynamics from Soft Matter to Biology (SYSM)	65
Collective Social Dynamics from Animals to Humans (SYSO)	67
United Kingdom as Guest of Honor (SYUK)	69
Programme of the SKM-Divisions of DPG	
BP Biological Physics	72
CPP Chemical and Polymer Physics	116
DS Thin Films	164
DY Dynamics and Statistical Physics	190
HL Semiconductor Physics	232
KFM Crystalline Solids and their Microstructure	309
MA Magnetism	327
MM Metal and Material Physics	397
O Surface Science	445
SOE Physics of Socio-economic Systems	557
TT Low Temperature Physics	570
VA Vacuum Science and Technology	637
Further Division	
QI Quantum Information	640
Working Groups (DPG)	
AKC Equal Opportunities	665
Index of Authors	667
Index of Exhibitors	701
Exhibition Maps	709
Map of the Main Lecture Hall	713
Campus Map	714
Timetable of the Conference	715

Award Ceremony

Max Planck Medal 2022

Prof. Dr. Annette Zippelius
University of Göttingen

Stern Gerlach Medal 2022

Dr. Frank Eisenhauer
Max Planck Institute for Extraterrestrial Physics (MPE), Garching

Stern Gerlach Medal 2020

Prof. Dr. Joachim Ullrich
Deutsche Physikalische Gesellschaft e.V.

Badge of Honour of the DPG 2019

Prof. Dr. Harald Lesch
Ludwig-Maximilians-University of Munich

Walter Schottky Prize 2022

Dr. Felix Büttner
Helmholtz-Zentrum Berlin

Max Born Prize 2022

Prof. Dr. Claudia Felser
MPI für Chemische Physik, Dresden

SKM Dissertation Prize 2022

(The Laureate will be announced after the SKM-Dissertation Prize Symposium)

Ceremonial Lecture

"Quantum Dots for Green Quantum Technologies"

Prof. Dr. Dieter Bimberg
Technical University of Berlin

Tuesday, 6 September 2022, 14:30 - 17:30

H1 (Audimax)

Dear conference guests,

As President of the German Physical Society, I would like to welcome you to this meeting of the Condensed Matter Section (SKM) with the participating divisions and working groups involved on the campus of the University of Regensburg.

With around 55,000 members, the DPG is the world's largest physics society. It is also one of the most important international communication platforms for research and education in the field of physics and promotes the exchange of knowledge in physics, especially with its conferences.

It is therefore invaluable that this DPG conference once again enables direct encounters. After all, motivation for physics, inspiration and creativity thrive on personal dialogue, on a culture of discourse that must always be cultivated and promoted. This culture is at the same time indispensable for physics with the primacy of basic research, whose findings are not only important for physics, but also for our society.

At the same time, this conference promotes the public visibility of basic research in a special way. In this year, UNESCO's „International Year of Basic Research for Sustainable Development“, the conference is an important contribution by the DPG to draw attention to the importance of basic research, which is often underestimated, at least by the general public - especially as an important component and for the further development of our society, our culture! It is the results of fundamental research that serve as the basis for social decisions and innovations and help to overcome the great challenges facing humanity.

I would like to express my sincere thanks to all those involved for the success of this DPG Conference. First of all, I would like to thank the participating DPG divisions and working groups for organising the scientific programme. My special appreciation also goes to the local organising committee at the University of Regensburg, Prof. Dieter Weiss, Faculty of the Institute of Experimental and Applied Physics. I would like to thank the University of Regensburg for its support and the Wilhelm and Else Heraeus Foundation for once again generously supporting all DPG conferences. I would like to thank the DPG Head Office for its support of all DPG (Spring) Meetings.

A handwritten signature in black ink, appearing to read 'Joachim Ullrich', with a stylized flourish at the end.

Prof. Dr. Joachim Ullrich

President

Deutsche Physikalische Gesellschaft e.V.

Organisation

Organiser

Deutsche Physikalische Gesellschaft e. V.
Hauptstraße 5, 53604 Bad Honnef
Phone +49 (0) 2224 9232-0
Fax +49 (0) 2224 9232-50
Email dpg@dpg-physik.de
Homepage www.dpg-physik.de

Local Organiser

Prof. Dr. Dieter Weiss
Universität Regensburg
Universitätsstr. 31, 93040 Regensburg
Phone +49 (0) 941 943-3197
Email dieter.weiss@physik.uni-regensburg.de

Local Secretary

Cordula Böll M.A.
Universität Regensburg
Universitätsstr. 31, 93040 Regensburg
Email dpg-conference@uni-regensburg.de

Scientific Organisation

Chair of the Condensed Matter Section (SKM)

Prof. Dr. Martin Wolf
Fritz-Haber-Institut der MPG
Abt. Physikalische Chemie
Faradayweg 4-6, 14195 Berlin
Phone +49 (0) 30 84135 111
Email wolf@fhi-berlin.mpg.de

Chairs of the Participating Divisions

- | | |
|---|---|
| (BP) Biological Physics | – Prof. Dr. Joachim Rädler (raedler@lmu.de) |
| (CPP) Chemical and Polymer Physics | – Prof. Dr. Peter Müller-Buschbaum (muellerb@ph.tum.de) |
| (DS) Thin Films | – Priv.-Doz. Dr. Patrick Vogt (patrick.vogt@physik.tu-berlin.de) |
| (DY) Dynamics and Statistical Physics | – Prof. Dr. Markus Bär (markus.baer@ptb.de) |
| (HL) Semiconductor Physics | – Prof. Dr. Axel Lorke (axel.lorke@uni-due.de) |
| (KFM) Crystalline Solids and their
Microstructures | – Prof. Dr. Theo A. Scherer (theo.scherer@kit.de) |
| (MA) Magnetism | – Prof. Dr. Heiko Wende (heiko.wende@uni-due.de) |
| (MM) Metal and Material Physics | – Prof. Dr. Christian Elsässer (christian.elsaesser@iwm.fraunhofer.de) |
| (O) Surface Science | – Prof. Dr. Karsten Reuter (reuter@fhi-berlin.mpg.de) |
| (QI) Quantum Information | – Prof. Dr. Otfried Gühne (otfried.guehne@uni-siegen.de) |
| (SOE) Physics of Socio-economic
Systems | – Priv.-Doz. Dr. Jens C. Claussen (claussen@inb.uni-luebeck.de) |
| (TT) Low Temperature Physics | – Prof. Dr. Elke Scheer (elke.scheer@uni-konstanz.de) |
| (VA) Vacuum Science and Technology | – Dr.-Ing. Stylianos Varoutis (stylianos.varoutis@kit.edu) |

Chairs of the Participating Working Groups

- | | |
|--------------------------------------|--|
| (AKC) Equal Opportunities | – OStR Agnes Sandner (akc@dpg-physik.de) |
| (AKjDPG) Young DPG | – M.Sc. Nils Sommer (sommer@jdpdg.de) |
| (AGyouLeaP) Young Leaders in Physics | – Dr. Tobias Heindel (tobias.heindel@tu-berlin.de)
Dr. Doris Reiter (Doris.Reiter@tu-dortmund.de) |

Symposia

- SYED – Entanglement Distribution in Quantum Networks
- SYES – Frontiers of Electronic-Structure Theory: Focus on Artificial Intelligence applied to Real Materials
- SYNM – From Physics and Big Data to the Design of Novel Materials
- SYOP – Frontiers of Orbital Physics: Statics, Dynamics, and Transport of Orbital Angular Momentum
- SYPQ – High Yield Devices for Photonic Quantum Implementations
- SYQM – Complexity and Topology in Quantum Matter
- SYSO – SKM Dissertation Prize
- SYSM – Interplay of Substrate Adaptivity and Wetting Dynamics from Soft Matter to Biology
- SYSO – Collective Social Dynamics from Animals to Humans
- SYUK – United Kingdom as Guest of Honor

Organisation of the Exhibition of Scientific Instruments and Literature

DPG-Kongress-, Ausstellungs- und Verwaltungsgesellschaft mbH

Hauptstraße 5, 53604 Bad Honnef

Phone +49 (0)2224 9232-0

Fax +49 (0)2224 9232-50

Email dpg@dpg-physik.de

Homepage www.dpg-gmbh.de

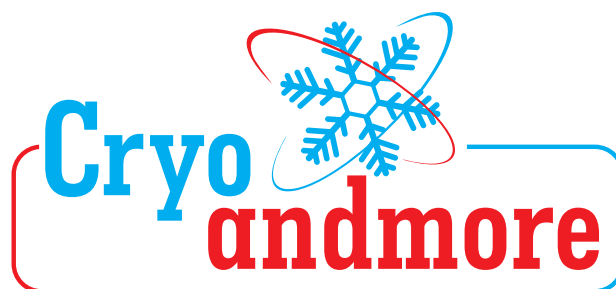
Programme

The scientific programme consists of **3.640** contributions:

11	Plenary talks
1	Evening talk
1	Ceremonial talk
9	Prize talks
4	Lunch talks
49	Topical talks
11	Tutorials
186	Invited talks
2.245	Contributed talks
1.121	Posters
2	Discussions

Sponsors of the DPG Meeting Regensburg 2022

Premium Sponsor:



Main Sponsors:



Sponsors:



Information for Participants

The conference will be held September 4 – 9, 2022.

Conference Information

Conference Venue

University of Regensburg
Universitätsstraße 31
93053 Regensburg

The central activities like registration etc. will take place in the Main Lecture Hall (Audimax) of the University of Regensburg (Universitätsstraße 31). For a detailed map of the campus and the buildings please see the end of this booklet.

Parking at Universität Regensburg

Please note: The underground car parks are closed due to renovation. Please use the new parking garages near BioPark and the parking lots between UR and OTH. There are no parking fees.

Please do not park in areas set aside for special users (“reservierte Stellplätze”) or in handicapped parking areas without a special parking permit. If you do, you may be towed away (with costs). Towed vehicles will be taken to the alternative car park near the building of Chemistry and Pharmacy. It can be reached through the street “Am BioPark”. To reclaim your towed vehicle, please telephone the towing service on +49 (0) 172 8128601. You will be provided with a lock code so you can retrieve your car.

Transportation



Regensburg offers a very good transportation infrastructure. **The conference ticket printed on your conference name tag will authorize you to use all buses of the public transport system (RVV) in Regensburg from September 4 to 9 in the fare zone 1 for free.**

You can reach the **bus stop “Universität”** by the bus lines 2, 4, 6 and 11. Please note: Line 4 takes a different route and does not stop at the main station.

Conference Office – Information Desk

The conference office and the information desk are located in the foyer of the Main Lecture Hall (Audimax H1). The opening hours are:

		Registration	Information Desk
Sunday	September 4	15:00 – 19:00	12:00 – 20:00
Monday	September 5	07:30 – 18:00	07:30 – 22:00
Tuesday	September 6	08:00 – 16:00	08:00 – 22:00
Wednesday	September 7	08:00 – 16:00	08:00 – 22:00
Thursday	September 8	08:00 – 16:00	08:00 – 22:00
Friday	September 9	08:00 – 12:00	08:00 – 15:00

To contact the information desk during the opening hours call +49 (0)941-943 2530.

You will receive the printed short programme and your name tag at the conference office. **The name tag must be worn visibly during the entire conference.** With your name tag you will receive a receipt for your conference fee, the conference ticket for public transport and free coffee at our coffee corners.

The organisers, staff of the conference desk, and the student assistants will be identifiable by coloured name tags and Φ -T-shirts. Please contact them if you have any questions. Do not hesitate to inquire about all necessary information concerning the conference, orientation in Regensburg, accommodation, restaurants, going out, and cultural events at the information desk located in the foyer of the Main Lecture Hall.

Lost and found property

You can bring found items to the information desk in the foyer of the Audimax. There you can also get your lost property back.

Cloakroom

Participants are asked to look carefully after their wardrobe, valuables, laptops, and other belongings. The organisers

decline any liability. You will find a cloakroom in the basement of the Main Lecture Hall (Audimax). The opening hours will be announced. Please note that there is no possibility to store luggage!

Allocation of the Lecture Halls

H1-H10, H22, H23	Main Lecture Hall
H11-H17	Law and Economy Building
H18-H21	Multi-purpose Building
H31, H32	Mathematics Building
H33-H36	Physics Building
H37-H39	Pre-clinical Medicine Building
H43-H48	Chemistry & Pharmacy Building
S051-S054	Ostbayer. Techn. Hochschule (OTH) / University of Applied Sciences (OTH)
Plenary talks, joint Symposia	H1 (Audimax), H2
Lunch Talks	H2
Prize Ceremony, Evening Talks	H1 (Audimax)
Job Market	Kunsthalle (Foyer Audimax, 1 st floor)
Registration Desk	Foyer Audimax (Main Lecture Hall)
Information Desk	Foyer Audimax (Main Lecture Hall)
EinsteinSlam	H1 (Audimax)

With the DPG-App through the DPG Meeting!

The updated DPG-App is ready-to-use and contains additional functions/features: In addition to the option of target groups, the electronic programme booklets for DPG Conferences (E-VERHANDLUNGEN) are accessible and it is possible to compile a „favorite list“ regarding events one wants to attend. Just download the DPG-App for Android or iOS now and utilize the supplemental offerings. You will find more information under <https://www.dpg-physik.de/service/dpg-app.html>.

WIFI

The University of Regensburg is member of the eduroam-network. Users from eduroam institutions, who have registered for eduroam, can use WIFI at the University of Regensburg without local registration in Regensburg. Please ask the computer center/network administration of your home institution for eduroam-registration. Eduroam in Regensburg is possible with WLAN SSID eduroam.

In addition to eduroam WIFI BayernWLAN is offered without prior registration. Furthermore you will have access with StudiWLAN (not at the OTH Regensburg!).

Login required:

“RZ Account”: dpg2022

“RZ Password”: dpg2022

LAN

A few workstations for guests are available in the central library for emergencies. Please sign up directly at the information desk of the central library at th UR! Opening hours: Mo-Fr 10:00 - 14:00.

Printing service „Copy & Paper“

The copyshop at the Forum (Monday to Thursday 08:00-16:00, Friday 08:00-13:00) offers office supplies and printing service up to DIN A0 paper size. You are welcome to print out data from your USB stick or send the copyshop the data in pdf format with the exact details by email: uni@copyandpaper.de. Please note: It is not possible to print posters in DIN A0 format directly at the shop - the printing service needs one day in advance!

Presentation

Scientific presentations will be held either orally or by poster. Presentations with a German abstract will be given in German.

Oral Presentation

Lecturers are requested to provide their presentations electronically. All lecture rooms are equipped with projectors (“beamers”). The projectors mainly display in the 4:3 format. However they are compatible with the 16:9, limited to the display width. Some newer systems also work directly with 16:9. A majority of lecture halls offers radio microphone

amplifiers as well. OHPs are not available.

PCs/laptops will be available in all lecture halls. Therefore, the presentation should be recorded onto a USB stick as back-up in PDF and power point format. Of course, you can also use your own laptop – please consider to bring your own adapter if required.

Contributed talks should take 12 minutes with 3 minutes for discussions; Topical and Invited Talks must not exceed 30 or 45 minutes as specified in the programme. Presentations can be held in German language or in English language (conference language). For further information please contact the division in which you have submitted the lecture or the poster.

All lecture rooms will be opened, at the latest, 30 minutes prior to the lecture. Speakers are requested to be in the lecture room at least 20 minutes prior to the start of the session, to report to the chairperson of the session as well as the technical staff, to receive a brief introduction to the equipment in the lecture room.

Poster Presentation

Sites for poster sessions are named and located as follows:

Poster area 1	Sammelgebäude (Multi-purpose Building)
Poster area 2	Physik (Physics)
Poster area 3	Exhibition tent in front of the Physics Building
Poster area 4	Chemie (Chemistry and Pharmacy)

The poster boards will be marked with the number according to the scientific programme. As there will be several different poster sessions at the poster sites every day, authors are asked to mount their poster max. 2-3 hours before their session. Each poster should display the number according to the scientific programme. Each poster should be no larger than 85 cm x 120 cm (A0 portrait format).

Printing Service: "Copy & Paper". It is not possible to print posters in DIN A0 format directly at the shop – the printing service needs 1 day in advance!

For the mounting of the poster please use the prepared "power strip" at the poster frame. Please make sure to use only power strips for mounting the poster (residue-free removing).

Authors are requested to be available at their poster for at least half of the length of their poster session. Please provide the information when you will be available.

The posters will normally be removed after the session or in the next morning. Any posters remaining on display walls will be removed without requesting your permission before the next poster session. You can get your poster back at the Info Desk. The conference management accepts no liability for the posters.

Notice Board

The programme stated in this document corresponds to the status of the programme publication 12 July 2022 and will not be updated!

All changes to the conference programme (i.e. cancellation of presentations, change of rooms, etc.) will be continuously updated on the notice board of the conference website. The information is identical to the programme updates of the scientific programme and is also available there in other formats (sorted by publication date, filterable by conference parts and as an rss-feed). Please use the form <https://regensburg22.dpg-tagungen.de/programm/notice-board-form> to notify changes or cancellations.

Wilhelm and Else Heraeus Communication Programme

Important notes for participants who apply for a grant of the Wilhelm and Else Heraeus Foundation:

At the beginning of the conference you will receive an identification form at the conference office. The participation in the conference must be certified by the conference desk. You have the possibility to leave this certificate by the staff members of the DPG (recommended!) in the conference office or submit it to the DPG Head Office (DPG-Geschäftsstelle, Hauptstr. 5, 53604 Bad Honnef, Germany) by **September 26, 2022 at the latest**.

For more detailed information refer to <http://regensburg22.dpg-tagungen.de>

The Deutsche Physikalische Gesellschaft thanks the Wilhelm and Else Heraeus Foundation for the generous financial support of young academic talents. We hope that young physicists will continue to seize the offered opportunity for active scientific communication at scientific conferences. A total of about 37,800 young academics were supported by this programme so far.

Catering

Coffee

Free coffee, tea and water will be provided to all registered participants of the conference at DPG-coffee corners located near all exhibition areas and poster areas. All locations are displayed in the map of the campus at the end of this booklet. Please wear your name tag visibly during the entire conference.

In addition you can get refreshments and snacks at the cafeterias in the Multi-purpose Building and in the Buildings of Chemistry, Physics, Philosophy and Law (Monday-Friday). Please pay by your EC- oder credit card. Cash Payment is not possible!

Lunch

Mensa:

Lunch will be supplied in the Mensa of the University (Monday-Friday: 11:00 – 14:00). Prices: about 12.00 € including the meal, one drink and one dessert. Please pay by your EC- oder credit card. Cash Payment is not possible!

Food-Truck:

In addition to the Mensa and the cafeterias a Food truck ("Tommy's Mutzbraten") will offer hearty food in front of the Physics Building (outside).

Uni-Pizzeria:

The Pizzeria UNIKAT offers freshly made Italian food. Reservation recommended!

Campus' Grocery Store

The Campus' Grocery Store "Hechtbauer" at the Forum offers food, beverages and convenience goods (Monday-Friday: 08:00 – 18:00).

Events

Tutorials

On Sunday, September 4, 16:00 – 18:15, there will be tutorial workshops on current scientific topics for interested conference participants, in particular for students and young scientists. All conference participants are welcome.

Topics:

- Careers in science: "To boldly go where no one has gone before"
- Discovering, Creating, and Exploring Novel Atomically-Thin Materials and Heterostructures
- Non-identical moire twins in bilayer graphene
- Introduction to 2D superconducting spintronics

Welcome Evening

Sunday, September 4, 18:30 – 21:30, Mensa

On Sunday evening, a Bavarian Welcome Evening will be held in the Mensa of the University of Regensburg to which all registered participants are kindly invited. Snacks and drinks will be served. "Vieraloe" (Bavarian Brass Music) will entertain you with music.

Do not miss the opportunity to register in the conference office (15:00 – 19:00) before the Welcome Evening as well as the official beginning of the conference. When registering for the conference you will receive your badge and **food and drink vouchers** for the Welcome Evening. Please note that the cloakroom in the lecture hall basement closes on Sunday at 20:00!

Opening of the Conference

The chair of the Condensed Matter Section (SKM) will give a short opening address on Monday, September 5 from 8:25 until 8:30.

Special Plenary Session with Award Ceremony (in German language)

On Tuesday, September 6 at 14:30, the special plenary session with award ceremony and ceremonial lecture will take place in the Audimax (H1).

Am Dienstag, den 6. September um 14:30 Uhr findet im H1 (Audimax) die Festsitzung mit Preisverleihung und anschließendem Festvortrag statt:

Musik

Begrüßung

durch den Örtlichen Tagungsleiter
Prof. Dr. Dieter Weiss, Universität Regensburg

Grußbotschaft (per Video)

des Präsidenten der Universität Regensburg
Prof. Dr. Udo Hebel

Rede

des Präsidenten der Deutschen Physikalischen Gesellschaft
Prof. Dr. Joachim Ullrich

Musik

Preisverleihung

Vergabe der Max-Planck-Medaille 2022

an Prof. Dr. Annette Zippelius, Universität Göttingen

Vergabe der Stern-Gerlach-Medaille 2022

an Dr. Frank Eisenhauer, MPI Garching

Vergabe der Stern-Gerlach-Medaille 2021

an Prof. Dr. Joachim Ullrich, Deutsche Physikalische Gesellschaft e.V.

Vergabe der Ehrennadel 2019

an Prof. Dr. Harald Lesch, LMU München

Vergabe des Walter-Schottky-Preises 2022

an Dr. Felix Büttner, Helmholtz-Zentrum Berlin

Vergabe des Max-Born-Preises 2022

an Prof. Dr. Claudia Felser, MPI für Chemische Physik, Dresden

Vergabe des Dissertationspreises der Sektion Kondensierte Materie (SKM)

(Der Preisträger bzw. die Preisträgerin wird nach dem SKM-Dissertationspreissymposium ernannt)

Musik

Festvortrag (in English Language)

Prof. Dr. Dieter Bimberg, Technische Universität Berlin
„Quantum Dots for Green Quantum Technologies“

Public Evening Lecture (in German language)

Tuesday, September 6, 19:00 to 20:00, Audimax (H1)

Professor Harald Lesch from the Ludwig-Maximilians-Universität München will speak about:

„Grundlagenforschung für Nachhaltigkeit“.

The Evening Lecture is open for all conference participants and interested public. The entrance is free.

EinsteinSlam

Wednesday, September 7, 20:00, Audimax (H1)

Keen to hit the stage and fascinate the audience? The EinsteinSlam is yours! Be smart, take part, let science rock

EinsteinSlam is the competitive art of making complex science accessible to a broad audience. There are just 10 minutes for every attendee to present his/her self-made performance. The event will finish with a public poll in order to evaluate if a particular contribution was either instructive and amusing or rather should have never been performed. All presentations will be given in English. For more information please see www.einstein-slam.de.

Job Market

During the conference various companies and organisations will present their working fields and career opportunities to all interested participants. The presentations will take place from Tuesday, September 6 to Friday, September 9 in the Kunsthalle (Foyer Audimax, 1st floor). The presentations will last for about 30 minutes plus discussion.

Programme:

Tuesday, Sep 6

14:00 – 15:00 Carl Zeiss AG: „ZEISS Semiconductor Manufacturing Technology: Kleinste Strukturen brauchen großartige Köpfe – Wir entwickeln die EUV-Technologien von morgen.“

Wednesday, Sep 7

12:45 – 13:45 Ritzenhoefer GmbH: „Transformation Consulting – Von der Physik zur Sinngebungs-Maschine fürs Topmanagement“

14:00 – 15:00 d-fine: „Auswirkungen von Krisen auf Energieversorger – Einblick in die analytisch-technologische Beratung bei d-fine.“

Thursday, Sep 8

12:45 – 13:45 Basycon Unternehmensberatung GmbH: „Was hat Beratung mit Forschung zu tun?“

14:00 – 15:00 Trumpf GmbH & Co. KG: „Lasersystems for EUV Lithography“

Friday, Sep 9

11:30 – 12:30 Horn & Company: „Horn & Company – Gewinne Einblicke in unsere Projekte zu Data Analytics, Big Data und Künstlicher Intelligenz und lerne unseren Beratungsansatz kennen!“

Exhibition of Scientific Instruments and Literature

From Tuesday to Thursday there will be an exhibition of scientific instruments and literature in the Main Lecture Hall Foyer (Foyer Audimax), Law and Economics Building (“Wirtschaft und Recht”), H6 area and one tent (in front of the Physics Building). Almost 100 companies (see list of exhibitors at the end of this booklet) will present their products. Opening hours are from 09:00 a.m. to 18:00 p.m.. All conference participants are welcome to attend the exhibition. The entrance is free.

City Tours „Regensburg – Experience a Historic City“

Walking Tour in German:

Daily 10:30 & 14:30

Costs: 10,00 EUR/person

Meeting Point: in front of the Tourist Information in the Old Town Hall of Regensburg

Please register online or via e-mail [tourismus\[@\]regensburg.de](mailto:tourismus[@]regensburg.de)

Walking Tour in English:

Tuesday, September 6, 15:30 – 17:00

Costs: 10.00 EUR/person

Meeting point: in front of the Tourist Information in the Old Town Hall of Regensburg

Please register via phone +49 941 507-4410 or via e-mail [tourismus\[@\]regensburg.de](mailto:tourismus[@]regensburg.de)

Bus trip “City Tour”

Information and booking at: <https://www.city-tour.info/en/regensburg/tour>

SAY CHEESE!

The DPG conferences are basically public to the press. Please note: On behalf of DPG, photos and videos will be recorded during the conferences. In the context of public relations, these recordings (as the case may be) will be published on our website, in social media or within prints of the DPG for example.

CO₂ compensation for the DPG conferences

By decision of the Executive Board, the DPG will compensate for fossil CO₂ emissions resulting from mobility for DPG conferences and committee meetings.

Acknowledgement

The Deutsche Physikalische Gesellschaft (DPG) and the Local Organisers want to thank the following institutions for supporting the conference:

- Wilhelm and Else Heraeus Foundation, Hanau
- University of Regensburg
- all industrial sponsors (see page 8 in this booklet)
- and all staff who make this conference possible.

Disclaimer of liability

All participants are asked to take care of their wardrobe and valuables. We assume no liability.

Frühjahrstagung

26. - 31.03.2023 in Dresden

Sektion Kondensierte Materie (SKM)

Biologische Physik
Chemische Physik und Polymerphysik
Dünne Schichten
Dynamik und Statistische Physik
Halbleiterphysik
Kristalline Festkörper und deren Mikrostruktur
Magnetismus
Metall- und Materialphysik
Oberflächenphysik
Physik sozio-ökonomischer Systeme
Tiefe Temperaturen
Vakuumphysik und Vakuumtechnik

Arbeitskreis Chancengleichheit
Arbeitskreis jDPG
Arbeitsgruppe young Leaders in Physics

Tutorien

Industrie- und Buchausstellung

#SKM23

Deadline für Abstract-Einreichung: 01.12.2022



Örtlicher Tagungsleiter:

Prof. Dr. Jochen Geck
Institut für Festkörper- und Materialphysik
Würzburg-Dresden Cluster of Excellence
ct.qmat
Technische Universität Dresden
01062 Dresden

Tagungsort:

Technische Universität Dresden
Hörsaalzentrum
Bergstraße 64
01069 Dresden

skm23.dpg-tagungen.de

Synopsis of the Daily Programme

Sunday, September 4, 2022

TUT

Tutorials

Sessions

16:00	H1	TUT 1	Careers in Science
16:00	H1	TUT 1.1	Careers in science: "To boldly go where no one has gone before" •Manfred Fiebig
16:00	H2	TUT 2	2D Quantum Materials and Heterostructures: From Fabrication to Applications
16:00	H2	TUT 2.1	Discovering, Creating, and Exploring Novel Atomically-Thin Materials and Heterostructures •Joshua Robinson
16:35	H2	TUT 2.2	Non-identical moire twins in bilayer graphene •Rebeca Ribeiro-Palau
17:10	H2	TUT 2.3	Single-photon emitters in 2D materials •Steffen Michaelis de Vasconcellos
17:45	H2	TUT 2.4	Introduction to 2D superconducting spintronics •Elke Scheer
16:00	H3	TUT 3	Functional Ferroics
16:00	H3	TUT 3.1	Domains and domain walls in functional ferroics •Dennis Meier
16:45	H3	TUT 3.2	Theory and simulations of ferroelectrics and related materials •Jorge Iniguez
17:30	H3	TUT 3.3	Atomic scale analysis of ferroic domain walls •Shelly Conroy
16:00	H4	TUT 4	Stochastic Processes from Financial Risk to Genetics
16:00	H4	TUT 4.1	Diffusion approximations for particles in turbulence •Bernhard Mehlig
16:50	H4	TUT 4.2	Probabilities in physics, paradoxes and populations •Tobias Galla
17:40	H4	TUT 4.3	Risk Revealed: Cautionary Tales, Understanding and Communication •Paul Embrechts

18:30	Mensa	Welcome Evening (for registered participants)
-------	-------	--

Monday, September 5, 2022

08:25	H1		Opening
			Plenary Talks
08:30	H1	PLV I	Intrinsic Josephson junctions in $\text{Bi}_2\text{Sr}_2\text{CaCu}_2\text{O}_8$: Generation of Terahertz radiation and beyond •Reinhold Kleiner
14:00	H1	PLV II	Topology and Chirality •Claudia Felser (Laureate of the Max-Born-Prize 2022)
14:00	H2	PLV III	Controlling and exploiting defects in diamond for Quantum Technologies •Mark Newton
			Prize Talk
13:15	H1	PRV I	Ultrafast topological switching of magnetic skyrmions •Felix Büttner (Laureate of the Walter-Schottky-Prize 2022)
			Lunch Talk
13:15	H2	PSV I	Berufsbild: Wissenschaftsmanagement in der deutschen Raumfahrtagentur •Tobias Saltzmann

SYNM

			Invited Talks
15:00	H1	SYNM 1.1	How to tackle the "I" in FAIR? •Claudia Draxl
15:30	H1	SYNM 1.2	Beyond the average error: machine learning for the discovery of novel materials •Mario Boley
16:00	H1	SYNM 1.3	The Phase Diagram of All Inorganic Materials •Chris Wolverton
16:45	H1	SYNM 1.4	Automated data-driven upscaling of transport properties in materials •Danny Perez
17:15	H1	SYNM 1.5	Data-driven understanding of concentrated electrolytes •Alpha Lee
			Session
15:00	H1	SYNM 1	From Physics and Big Data to the Design of Novel Materials

SYOP

			Invited Talks
09:30	H1	SYOP 1.1	Orbital degeneracy in transition metal compounds: Jahn-Teller effect, spin-orbit coupling and quantum effects •Daniel Khomskii
10:00	H1	SYOP 1.2	Orbital magnetism out of equilibrium: driving orbital motion with fluctuations, fields and currents •Yuriy Mokrousov
10:30	H1	SYOP 1.3	Orbitronics: new torques and magnetoresistance effects •Mathias Kläui
11:15	H1	SYOP 1.4	Orbital and total angular momenta dichroism of the THz vortex beams at the antiferromagnetic resonances •Andrei Sirenko
11:45	H1	SYOP 1.5	Observation of the orbital Hall effect in a light metal Ti •Gyung-Min Choi
			Session
09:30	H1	SYOP 1	Frontiers of Orbital Physics: Statics, Dynamics, and Transport of Orbital Angular Momentum

Monday, September 5, 2022

SYSD

			Invited Talks
10:15	H2	SYSD 1.1	Charge localisation in halide perovskites from bulk to nano for efficient opto-electronic applications •Sascha Feldmann
10:45	H2	SYSD 1.2	Nonequilibrium Transport and Dynamics in Conventional and Topological Superconducting Junctions •Raffael L. Klees
11:15	H2	SYSD 1.3	Probing magnetostatic and magnetotransport properties of the antiferromagnetic iron oxide hematite •Andrew Ross
11:45	H2	SYSD 1.4	Quantum dot optomechanics with surface acoustic waves •Matthias Weiss
			Session
10:15	H2	SYSD 1	SKM Dissertation Prize

BP

			Prize Talk, Invited Talks
10:15	H13	BP 2.4	Integrative modeling of dynamic biomolecular structures •Holger Gohlke
09:30	H15	BP 3.1	Basal tension in the wing disc epithelium - what's collagen got to do with it •Elisabeth Fischer-Friedrich (Laureate of the Hertha-Sponer-Prize 2022)
10:30	H16	BP 4.1	Computer simulations of self-motile active droplets and colloid-active gels composites •Davide Davide Marenduzzo
15:00	H15	BP 5.1	The functional nano-architecture of axonal actin •Christophe Leterrier
16:15	H16	BP 6.5	From active bacterial microcolonies to biofilms as model tissues •Vasily Zaburdaev
			Sessions
09:30	H13	BP 2	Computational Biophysics and Neuroscience
09:30	H15	BP 3	Cell Mechanics 1
10:30	H16	BP 4	Active Matter 1
15:00	H15	BP 5	Focus Session: Super Resolution Microscopy and Dynamics of Supramolecular Complexes
15:00	H16	BP 6	Statistical Physics of Biological Systems 1
18:00	P1	BP 7	Poster 1

CPP

			Invited Talks
09:30	H38	CPP 1.1	Ternary blend approach for boosting performance and stability of organic solar cells •Tayebeh Ameri
15:00	H38	CPP 8.1	Stimuli-Responsive Opal Films based on Core-Shell Particle Self-Assembly •Markus Gallei
15:45	H38	CPP 8.3	Self-assembled photonic pigments from bottlebrush block copolymers •Richard Parker
16:45	H38	CPP 8.5	Hierarchically structured mechanochromic deformation-sensing pigments •Jessica Clough
			Sessions
09:30	H38	CPP 1	Organic Electronics and Photovoltaics 1
09:30	H39	CPP 2	Polymer Networks and Elastomers
09:30	H34	CPP 3	Perovskite and Photovoltaics 1
09:30	H36	CPP 4	2D Materials 1
10:00	H19	CPP 5	Wetting, Droplets and Microfluidics

Monday, September 5, 2022

CPP

10:30	H16	CPP 6	Active Matter 1
10:45	H39	CPP 7	Wetting, Fluidics and Liquids at Interfaces and Surfaces
15:00	H38	CPP 8	Focus Session: Photonic Structures from Polymer and Colloidal Self-Assembly
15:00	H39	CPP 9	Modeling and Simulation of Soft Matter
15:00	H36	CPP 10	2D Materials 2
17:15	H38	CPP 11	2D Materials 3
18:00	P1	CPP 12	Poster 1

DS

Invited Talks

09:30	H17	DS 2.1	GaN-based power converters enabling talktive power •Marco Liserre
10:00	H17	DS 2.2	Energy-efficient power electronics based on Gallium Nitride •Oliver Ambacher
10:45	H17	DS 2.4	Potential of Aluminum Nitride for Vertical Power Electronics •Andreas Waag
15:00	H17	DS 6.1	Novel high power device structures: Enabling compact and integrated power ICs •Elison Matioli
15:30	H17	DS 6.2	Ab-initio investigations of V-pits and nanopipes in GaN •Liverios Lymperakis
16:15	H17	DS 6.4	Lateral and Vertical β -Ga ₂ O ₃ Power Transistors for High-Voltage Applications •Kornelius Tetzner

Sessions

09:30	H14	DS 1	Thin Film Properties: Structure, Morphology and Composition (XRD, TEM, XPS, SIMS, RBS, AFM, ...) 1
09:30	H17	DS 2	Focus Session: Innovative GaN-based High-power Devices: Growth, Characterization, Simulation, Application 1
09:30	H36	DS 3	2D Materials 1
11:00	H14	DS 4	Thin Film Properties: Structure, Morphology and Composition (XRD, TEM, XPS, SIMS, RBS, AFM, ...) 2
11:30	H17	DS 5	Organic Thin Films, Organic-Inorganic Interfaces
15:00	H17	DS 6	Focus Session: Innovative GaN-based High-power Devices: Growth, Characterization, Simulation, Application 2
15:00	H36	DS 7	2D Materials 2
17:15	H38	DS 8	2D Materials 3

DY

Invited Talks

09:30	H18	DY 2.1	Roughness growth modes in thin film growth •Martin Oettel
15:00	H19	DY 9.1	Granular matter composed of non-convex grains •Ralf Stannarius
15:30	H20	DY 12.1	A phononic frequency comb from a single resonantly driven nanomechanical mode •Eva Weig
16:30	H20	DY 12.4	From period-doubling bifurcations to time crystals and coherent Ising machines •Oded Zilberberg
17:15	H20	DY 12.6	2D membranes in motion •Herre van der Zant

Sessions

09:30	H18	DY 2	Invited Talk Martin Oettel
10:00	H18	DY 3	Statistical Physics far from Thermal Equilibrium
10:00	H19	DY 4	Wetting, Droplets and Microfluidics
10:00	H20	DY 5	Many-Body Quantum Dynamics 1

Monday, September 5, 2022

DY

10:30	H16	DY 6	Active Matter 1
15:00	H16	DY 7	Statistical Physics of Biological Systems 1
15:00	H18	DY 8	Data Analytics for Complex Systems
15:00	H19	DY 9	Invited Talk Ralf Stannarius
15:00	H39	DY 10	Modeling and Simulation of Soft Matter
15:30	H19	DY 11	Granular Matter and Contact Dynamics
15:30	H20	DY 12	Focus Session: Nonlinear Dynamics of Nanomechanic Oscillators
17:45	H18	DY 13	Big Data and Artificial Intelligence

HL

Invited Talks

09:30	H31	HL 2.1	Observation of quantum Zeno effects for localized spins •Alex Greilich
09:30	H32	HL 3.1	Pushing the limits in real-time measurements of quantum dynamics •Eric Kleinherbers
09:30	H36	HL 6.1	g-factors in van der Waals heterostructures: revealing signatures of interlayer coupling •Paulo E. Faria Junior
15:00	H32	HL 8.1	Crux of Using the Cascaded Emission of a Three-Level Quantum Ladder System to Generate Indistinguishable Photons •Eva Schöll
15:00	H33	HL 9.1	Exceptional points in optics: From bulk materials to one-dimensional confined systems •Chris Sturm
15:30	H33	HL 9.2	Complex Skin Modes in Non-Hermitian Coupled Laser Arrays •Mercedeh Khajavikhan
16:15	H33	HL 9.3	Non-Hermitian effects in exciton polaritons •Eliezer Estrecho
16:45	H33	HL 9.4	Nonlinear dynamics and exceptional points in exciton-polariton condensates •Stefan Schumacher

Sessions

09:30	H31	HL 2	Spin Phenomena in Semiconductors
09:30	H32	HL 3	Quantum Dots and Wires 1: Transport and Electronic Properties
09:30	H33	HL 4	Semiconductor Lasers
09:30	H34	HL 5	Perovskite and Photovoltaics 1
09:30	H36	HL 6	2D Materials 1
15:00	H31	HL 7	(Quantum) Transport Properties
15:00	H32	HL 8	Quantum Dots and Wires 2: Optics 1
15:00	H33	HL 9	Focus Session: Exceptional Points and Non-Hermitian Physics in Semiconductor Systems
15:00	H34	HL 10	Nitrides
15:00	H36	HL 11	2D Materials 2

KFM

Invited Talks

09:30	H5	KFM 2.1	Domain-wall engineering in multiferroic materials •Guillaume Nataf
11:15	H5	KFM 2.5	Charged Higher Order Topologies in Room Temperature Magnetoelectric Multiferroic Thin Films •Shelly Conroy
15:00	H5	KFM 7.1	Multiferroic coupling on the level of domain walls •Mads C. Weber

Sessions

09:30	H5	KFM 2	Focus Session: Defects and Interfaces in Multiferroics 1
09:30	H7	KFM 3	Microscopy and Tomography with X-ray, Photons, Electrons, Ions and Positrons

Monday, September 5, 2022

KFM

09:30	H34	KFM 4	Perovskite and Photovoltaics 1
10:30	S053	KFM 5	New Methods and Developments: Scanning Probe Techniques 1
11:05	H7	KFM 6	Instrumentation and Methods for Micro- and Nanoanalysis
15:00	H5	KFM 7	Focus Session: Defects and Interfaces in Multiferroics 2
15:00	H7	KFM 8	Crystallography in Materials Science, Microstructure and Dielectric Properties
15:00	S053	KFM 9	New Methods and Developments: Scanning Probe Techniques 2

MA

Invited Talk			
15:00	H47	MA 10.1	Magnetic vortices: into the third dimension •Sebastian Gliga
Sessions			
09:30	H37	MA 2	Magnetic Imaging Techniques
09:30	H43	MA 3	Spin-Dependent Phenomena in 2D
09:30	H47	MA 4	Disordered Magnetic Materials
09:30	H48	MA 5	Magnetic Instrumentation and Characterization
11:00	H37	MA 6	Complex Magnetic Oxides
11:00	H43	MA 7	Magnetic Relaxation and Gilbert Damping
15:00	H37	MA 8	Ultrafast Magnetization Effects 1
15:00	H43	MA 9	INNOMAG e.V. Prizes 2022 (Diplom-/Master and Ph.D. Thesis)
15:00	H47	MA 10	Non-Skyrmionic Magnetic Textures
15:00	H48	MA 11	Computational Magnetism 1

MM

Invited Talk, Topical Talks			
09:30	H44	MM 1.1	A novel mechanism to generate metallic single crystals •Carolin Körner
15:00	H44	MM 5.1	Vacancy transport in oxides exposed to high electric fields •Reiner Kirchheim
17:15	H45	MM 9.1	Design of corrosion-free and highly active electrocatalysts and photocatalysts via combinations of ab initio calculations and electrodynamics •Heechae Choi
Sessions			
09:30	H44	MM 1	Invited Talk Carolin Körner
10:15	H44	MM 2	Computational Materials Modelling: Energy Materials
10:15	H45	MM 3	Microstructures and Phase Transformations: Metals & Alloys
10:15	H46	MM 4	Structural Materials
15:00	H44	MM 5	Non-equilibrium Phenomena in Materials Induced by Electrical and Magnetic Fields 1
15:45	H44	MM 6	Computational Materials Modelling: Defects / Alloys
15:45	H45	MM 7	Microstructures and Phase Transformations: Oxides & Perovskites
15:45	H46	MM 8	Materials for Storage and Conversion of Energy
17:15	H45	MM 9	Non-equilibrium Phenomena in Materials Induced by Electrical and Magnetic Fields 2
18:00	P2	MM 10	Poster Session 1

O

Invited Talk, Topical Talks			
09:30	S054	O 1.1	Laser-excited electrons: how hot are they? •Baerbel Rethfeld
10:30	H4	O 3.1	Rational design of single atom electrocatalysts: handle with care •Gianfranco Pacchioni
10:30	S051	O 5.1	Molecular nanostructures on metals vs. graphene •Meike Stöhr

Monday, September 5, 2022

0

10:30	S053	O 7.1	Identification of active electrocatalytic centers using EC- STM under reaction conditions •Aliaksandr Bandarenka
10:30	S054	O 8.1	Dynamic structure changes of bare and modified Cu(111) during CO and water activation •Andrea Auer
15:00	H4	O 10.1	Atomically-precise design of low-nuclearity catalysts •Sharon Mitchell
16:00	H4	O 10.4	Design of Model Single-Atom Catalysts: Metal Adatoms, Monomeric Oxide Units, and Mixed Surface Layers on Oxide Surfaces •Zdenek Dohnalek
17:00	H4	O 10.7	Model catalysis of single atoms on ultrathin solid films •Kai Wu
15:00	S054	O 15.1	Hydration Layer Mapping at Solid-Liquid Interfaces •Angelika Kühnle

Sessions

09:30	S054	O 1	Overview Talk Bärbel Rethfeld
10:30	H3	O 2	Ultrafast Electron Dynamics at Surfaces and Interfaces 1
10:30	H4	O 3	Focus Session: Single Atom Catalysis 1
10:30	H6	O 4	Topology and Symmetry-Protected Materials
10:30	S051	O 5	Organic Molecules at Surfaces 1: Substrate Effects
10:30	S052	O 6	Nanostructures at Surfaces 1
10:30	S053	O 7	New Methods and Developments 1: Scanning Probe Techniques 1
10:30	S054	O 8	Solid-Liquid Interfaces 1: Reactions and Electrochemistry
15:00	H3	O 9	Ultrafast Electron Dynamics at Surfaces and Interfaces 2
15:00	H4	O 10	Focus Session: Single Atom Catalysis 2
15:00	H6	O 11	Electronic Structure Theory
15:00	S051	O 12	Organic Molecules at Surfaces 2: Characterization of Organic Monolayers
15:00	S052	O 13	Nanostructures at Surfaces 2
15:00	S053	O 14	New Methods and Developments 2: Scanning Probe Techniques 2
15:00	S054	O 15	Solid-Liquid Interfaces 2: Structure and Spectroscopy
18:00	P4	O 16	Poster Monday: Ultrafast Processes 1
18:00	P4	O 17	Poster Monday: Organic Molecules at Surfaces 1
18:00	P4	O 18	Poster Monday: 2D Materials 1
18:00	P4	O 19	Poster Monday: Scanning Probe Techniques 1
18:00	P4	O 20	Poster Monday: Solid-Liquid Interfaces
18:00	P4	O 21	Poster Monday: Topology and Symmetry-Protected Materials
18:00	P4	O 22	Poster Monday: Surface Structure, Epitaxy, Growth and Tribology
18:00	P4	O 23	Poster Monday: Nanostructures 1

SOE

Invited Talk

09:30	H11	SOE 2.1	Two-armed bandits versus Carnapian truth seekers and epistemic free riders with bounded confidence •Rainer Hegselmann
-------	-----	---------	--

Sessions

09:30	H11	SOE 2	Invited Talk Rainer Hegselmann: Opinion Formation
10:15	H11	SOE 3	Economic Models
12:00	H11	SOE 4	Financial Risk
12:30	H11	SOE 5	Social Systems, Opinion and Group Dynamics
15:00	H18	SOE 6	Data Analytics for Complex Systems
17:45	H18	SOE 7	Big Data and Artificial Intelligence

Monday, September 5, 2022

TT**Invited Talks**

09:30	H10	TT 1.1	Stability of Floquet Majorana box qubits •Anne Matthies
15:00	H10	TT 5.1	Dynamics of visons and thermal Hall effect in perturbed Kitaev models •Aprem Joy

Sessions

09:30	H10	TT 1	Topology: Majorana Physics
09:30	H22	TT 2	Nanotubes, Nanoribbons and Graphene
09:30	H23	TT 3	Superconductivity: Properties and Electronic Structure
10:00	H20	TT 4	Many-Body Quantum Dynamics 1
15:00	H10	TT 5	Frustrated Magnets – Spin Liquids
15:00	H22	TT 6	Kondo Physics, f-Electron Systems and Heavy Fermions
15:00	H23	TT 7	Fluctuations, Noise, Magnetotransport, and Related Topics
17:15	H10	TT 8	Frustrated Magnets – Strong Spin-Orbit Coupling
18:00	H23	TT 9	Cold Atomic Gases and Superfluids

VA**Sessions**

09:30	H12	VA 1	Rarefied gas dynamics and novel numerical approaches
12:30	H12	VA 2	Vacuum technology: New developments and applications

QI**Invited Talks**

09:30	H8	QI 1.1	Coherence of spin qubits in planar germanium •Nico Willem Hendrickx
09:30	H9	QI 2.1	Measuring the thermodynamic cost of timekeeping •Yelena Guryanova
11:15	H9	QI 2.6	Finite-size effects in quantum thermodynamics •Kamil Korzekwa
15:00	H8	QI 3.1	Generalized randomized benchmarking with short random quantum circuits •Martin Kliesch

Sessions

09:30	H8	QI 1	Implementations: Spin Qubits, Atoms, and Photons
09:30	H9	QI 2	Quantum Thermodynamics and Open Quantum Systems
15:00	H8	QI 3	Certification and Benchmarking of Quantum Systems
18:00	P2	QI 4	Poster: Quantum Information

Tuesday, September 6, 2022

08:30	H1	PLV IV	Plenary Talk Insights from Atomic-Scale Studies on Surfaces •Ulrike Diebold
13:15	H1	PRV II	Prize Talk Water flows in carbon nanochannels: from quantum friction to carbon memories •Lydéric Bocquet (Laureate of the Gentner Kastler Prize 2022)
13:15	H2	PSV II	Lunch Talk, Ceremonial Talk Wissenschaftskommunikation – für wen eigentlich? •Nicolas Wöhrl
16:30	H1	PSV III	Quantum Dots for Green Quantum Technologies •Dieter Bimberg

SYPQ

09:30	H1	SYPQ 1.1	Invited Talks Designing driving protocols for high-fidelity quantum devices using numerically exact predictions •Moritz Cygorek
10:00	H1	SYPQ 1.2	Challenges towards high efficiency quantum dot single photon sources •Arne Ludwig
10:30	H1	SYPQ 1.3	Organic Molecules in photonic quantum technologies •Costanza Toninelli
11:15	H1	SYPQ 1.4	Quantum-dot single-photon sources for quantum photonic networks •Peter Michler
11:45	H1	SYPQ 1.5	Quantum light sources: entanglement generation in semiconductor nanostructures •Ana Predojevic
09:30	H1	SYPQ 1	Session High Yield Devices for Photonic Quantum Implementations

BP

09:30	H15	BP 8.1	Prize Talk, Invited Talk Phase separation in cells: gene localization and noise buffering •Samuel Safran
12:30	H16	BP 9.11	Super-resolution STED and MINFLUX Nanoscopes by Abberior Instruments •Gerald Donnert (Laureate of the DPG-Technologietransferpreis 2022)
09:30	H15	BP 8	Sessions Focus Session: Phase Separation in Biochemical Systems
09:30	H16	BP 9	Bioimaging
10:00	H13	BP 10	Cell Adhesion and Multicellular Systems
10:00	H18	BP 11	Active Matter 2
17:30	P4	BP 12	Poster 2

CPP

09:30	H38	CPP 13.1	Invited Talks Insights into degradation mechanisms in Li-based batteries and advantages of polymer coatings •Neelima Paul
11:30	H38	CPP 18.1	How X-rays can reveal waters mysteries •Katrin Amann-Winkel

Tuesday, September 6, 2022

CPP

Sessions

09:30	H38	CPP 13	Charged Soft Matter, Polyelectrolytes and Ionic Liquid
09:30	H39	CPP 14	Emerging Topics in Chemical and Polymer Physics, New Instruments and Methods
09:30	H36	CPP 15	2D Materials 4
10:00	H18	CPP 16	Active Matter 2
11:00	P2	CPP 17	Poster 2
11:30	H38	CPP 18	Complex Fluids and Colloids, Micelles and Vesicles

DS

Prize Talks

09:40	H17	DS 10.1	Atomic-Scale Optical Spectroscopy at Surfaces •Takashi Kumagai (Laureate of the Gaede-Prize 2020)
10:20	H17	DS 10.2	Slow highly charged ions as a tool for monolayer sensitive nano-engineering •Richard Wilhelm (Laureate of the Gaede-Prize 2021)
11:00	H17	DS 10.3	Quantum Science with Single Atoms and Molecules on Surfaces •Philip Willke (Laureate of the Gaede-Prize 2022)

Sessions

09:30	H14	DS 9	Thin Film Properties: Structure, Morphology and Composition (XRD, TEM, XPS, SIMS, RBS, AFM, ...) 3
09:30	H17	DS 10	Gaede Prize Talks
09:30	H34	DS 11	Focus Session: Quantum Properties at Functional Oxide Interfaces 1
09:30	H36	DS 12	2D Materials 4

DY

Invited Talks

09:30	H18	DY 14.1	Non-Markovian Brownian systems: from single-particle thermodynamics to collective behavior •Sabine Klapp
10:30	H19	DY 17.1	Caustics in turbulent aerosols •Bernhard Mehlig

Sessions

09:30	H18	DY 14	Invited Talk Sabine Klapp
09:30	H19	DY 15	Delay and Feedback Dynamics
10:00	H18	DY 16	Active Matter 2
10:30	H19	DY 17	Invited Talk Bernhard Mehlig
11:15	H19	DY 18	Nonlinear Dynamics 1: Synchronization and Chaos
11:30	H20	DY 19	Many-Body Quantum Dynamics 2
11:30	H38	DY 20	Complex Fluids and Colloids, Micelles and Vesicles

HL

Invited Talks

09:30	H32	HL 12.1	Wafer-Scale Epitaxial Modulation of Quantum Dot Density •Nikolai Bart
09:30	H34	HL 14.1	Materials and Device Engineering for Gallium Oxide-based Electronics •Siddharth Rajan
10:00	H34	HL 14.2	Ferroelectric two-dimensional electron gases for oxide spin-orbitronics •Julien Bréhin
12:15	H34	HL 14.8	Strain-driven dissociation of water on (incipient) ferroelectrics •Chiara Gattinoni
09:30	H36	HL 15.1	Ultrafast all-optical modulation and frequency conversion in 2D materials •Sebastian Klimmer

Tuesday, September 6, 2022

HL

Sessions

09:30	H32	HL 12	Quantum Dots and Wires 3: Growth
09:30	H33	HL 13	Ultra-Fast Phenomena
09:30	H34	HL 14	Focus Session: Quantum Properties at Functional Oxide Interfaces
09:30	H36	HL 15	2D Materials 3

KFM

Prize Talk, Invited Talks, Topical Talk

09:30	H5	KFM 10.1	Einfluss des Sauerstoffgehalts auf das Koerzitivfeld für die Polarisationsumschaltung in HfO_2 aus der Dichtefunktionaltheorie •Luis Azevedo Antunes (Laureate of the Georg-Simon-Ohm-Prize 2022)
10:00	H5	KFM 10.2	Negative capacitance and voltage amplification in ferroelectric heterostructures •Jorge Iniguez
10:30	H5	KFM 10.3	Advanced Phase-field Simulation of Ferroelectrics and Antiferroelectrics •Bai-Xiang Xu
11:15	H5	KFM 10.4	Magnetization processes in SmFeO_3 •Thomas Schrefl

Sessions

09:30	H5	KFM 10	Focus session: Polar Materials Meet Energy demands
09:30	H7	KFM 11	Crystal Structure Defects / Real Structure / Microstructure
09:30	H37	KFM 12	Skyrmions 1
10:15	H46	KFM 13	Materials for Storage and Conversion of Energy

MA

Invited Talks

09:30	H37	MA 12.1	Topological spin structures at surfaces •Stefan Heinze
09:30	H47	MA 14.1	Overriding universality of ferromagnetic phase transitions through nano-scale materials design •Andreas Berger
15:00	H43	MA 17.1	Ultimately fast, small and energy-efficient magnetism: fundamentals and prospects •Johan Mentink
15:30	H43	MA 17.2	From spintronics at limiting temporal and spatial scales in antiferromagnets to an emerging altermagnetic phase •Tomas Jungwirth
16:00	H43	MA 17.3	An electronic structure viewpoint on candidate van der Waals ferromagnets •Phil King
16:30	H43	MA 17.4	Nano-scale skyrmions and atomic-scale spin textures studied with STM •Kirsten von Bergmann

Sessions

09:30	H37	MA 12	Skyrmions 1
09:30	H43	MA 13	Magnonics 1
09:30	H47	MA 14	Cooperative Phenomena: Spin Structures and Magnetic Phase Transitions
09:30	H48	MA 15	Computational Magnetism 2
15:00	H37	MA 16	Frustrated Magnets
15:00	H43	MA 17	PhD Focus Session: The Hitchhiker's Guide to Spin Phenomena at the Space and Time Limit
15:00	H47	MA 18	Spintronics
17:30	P2	MA 19	Poster 1

Invited Talk, Topical Talks			
09:30	H44	MM 11.1	Fast calorimetry: studying phase transitions in slow motion •Jörg F. Löffler
10:15	H45	MM 13.1	Supercompatibility in ceramic micropillars of lanthanum niobate •Olivia A. Graeve
10:45	H45	MM 13.2	X-Ray Spectro(micro)scopy as analytics for field assisted deposition processes •David N. Mueller
12:30	H45	MM 13.7	Field-assisted processing of magnetic materials •Fernando Maccari
Sessions			
09:30	H44	MM 11	Invited Talk Jörg F. Löffler
10:15	H44	MM 12	Computational Materials Modelling: Physics of Ensembles 1
10:15	H45	MM 13	Non-equilibrium Phenomena in Materials Induced by Electrical and Magnetic Fields 3
10:15	H46	MM 14	Materials for Storage and Conversion of Energy
11:45	H46	MM 15	Hydrogen in Materials: Hydrogen Effects
14:00	H44	MM 16	Mechanical Properties
14:00	H46	MM 17	Hydrogen in Materials: Hydrogen Storage
17:30	P2	MM 18	Poster Session 2

Invited Talk, Topical Talks			
09:30	S054	O 24.1	Oxygen Evolution on Rutile Ruthenium and Iridium Dioxides •Yang Shao-Horn
10:30	H2	O 25.1	Designer electronic states in van der Waals heterostructures •Peter Liljeroth
11:00	H2	O 25.2	Magnetic order in a coherent Kondo lattice in the 1T/1H TaSe2 heterostructure •Miguel Ugeda
11:45	H2	O 25.4	Electron-lattice correlations and charge order in two-dimensional materials •Tim Wehling
10:30	S053	O 30.1	Surface Phase Transitions in Atomistic Detail and with Femtosecond Resolution •Wolf Gero Schmidt
10:30	S054	O 31.1	Towards a realistic description of electrified solid-liquid interfaces •Nicolas G. Hörmann
Sessions			
09:30	S054	O 24	Overview Talk Yang Shao-Horn
10:30	H2	O 25	Focus Session: Atomic-Scale Characterization of Correlated Ground States in Epitaxial 2D Materials
10:30	H4	O 26	Surface Magnetism
10:30	H6	O 27	Electron-Driven Processes
10:30	S051	O 28	Organic Molecules at Surfaces 3: Theory
10:30	S052	O 29	Metal substrates 1
10:30	S053	O 30	Semiconductor Surfaces
10:30	S054	O 31	Solid-Liquid Interfaces 3: Reactions and Electrochemistry
11:00	P3	O 32	Poster Tuesday: Adsorption and Catalysis 1
11:00	P3	O 33	Poster Tuesday: Ultrafast Processes 2
11:00	P3	O 34	Poster Tuesday: Scanning Probe Techniques 2
11:00	P3	O 35	Poster Tuesday: Plasmonics and Nanooptics 1

Invited Talk			
09:30	H11	SOE 8.1	Musicians' Synchronization and the Enigma of Swing •Theo Geisel

Tuesday, September 6, 2022

SOE

Sessions

09:30	H11	SOE 8	Invited Talk Theo Geisel: Human Synchronization in Music Performance
10:15	H11	SOE 9	Physics of Contagion Processes
11:15	H19	SOE 10	Nonlinear Dynamics 1: Synchronization and Chaos

TT

Invited Talks

09:30	H3	TT 10.1	Two-fold symmetric superconductivity in few-layer NbSe ₂ •Vlad Pribiag
10:00	H3	TT 10.2	Spin-orbit coupling and triplet pairing in mesoscopic superconductors •marco aprili
10:30	H3	TT 10.3	Supercurrent diode effect in few-layer NbSe ₂ •Nicola Paradiso
11:15	H3	TT 10.4	Superconducting devices in magic-angle twisted bilayer graphene •Folkert de Vries
11:45	H3	TT 10.5	Minigap and Andreev bound states in ballistic graphene •Luca Banszerus

Sessions

09:30	H3	TT 10	Focus Session: Superconductivity in 2d-Materials and their Heterostructures
09:30	H10	TT 11	Topology: Quantum Hall Systems
09:30	H22	TT 12	Correlated Electrons: Materials
09:30	H23	TT 13	Quantum Dots, Quantum Wires, Point Contacts
11:30	H20	TT 14	Many-Body Quantum Dynamics 2
11:15	H23	TT 15	Nano- and Optomechanics

QI

Invited Talks

09:30	H8	QI 5.1	Towards universal quantum computation and simulation with NV centre in diamond •Vadim Vorobyov
09:30	H9	QI 6.1	Towards an Artificial Muse for new Ideas in Quantum Physics •Mario Krenn

Sessions

09:30	H8	QI 5	Implementations: Solid state systems
09:30	H9	QI 6	Quantum Information: Concepts and Methods

Job Market

14:00	Kunsthalle		Carl Zeiss AG: "ZEISS Semiconductor Manufacturing Technology: Kleinste Strukturen brauchen großartige Köpfe – Wir entwickeln die EUV-Technologien von morgen."
-------	------------	--	--

09:00	Foyer Audimax, H6, Economy Bldg, Tent (Physics Building)		Exhibition of Scientific Instruments and Literature (free entrance)
-------	--	--	--

Evening Talk (free entrance)

19:00	H1+H2	PSV IV	Grundlagenforschung für Nachhaltigkeit •Harald Lesch
-------	-------	--------	---

Wednesday, September 7, 2022

			Plenary Talks
08:30	H1	PLV V	Towards useful quantum computing with superconducting qubits •Rami Barends
14:00	H1	PLV VI	Disordered Solids •Annette Zippelius (Laureate of the Max-Planck-Medal 2022)
14:00	H2	PLV VII	Topological insulator lasers •Mordechai Segev
			Prize Talk
13:15	H1	PRV III	Learning the stochastic dynamics of living systems across scales: from single cells to tissues •David Brückner (Laureate of the Gustav-Hertz-Prize 2022)
			Lunch Talk
13:15	H2	PSV V	The German Research Foundation – Funding Opportunities for International Collaborations •Michael Mößle

SYED

			Invited Talks
09:30	H1	SYED 1.1	A multi-node quantum network of remote solid-state qubits •Ronald Hanson
10:00	H1	SYED 1.2	Quantum key distribution with highly entangled photons from GaAs quantum dots •Armando Rastelli
10:30	H1	SYED 1.3	Entanglement distribution with minimal memory requirements using time-bin photonic qudits •Johannes Borregaard
11:15	H1	SYED 1.4	Quantum photonics: interference beyond HOM and quantum networks •Stefanie Barz
11:45	H1	SYED 1.5	Photonic cluster-state generation for memory-free quantum repeaters •Tobias Huber
			Session
09:30	H1	SYED 1	Entanglement Distribution in Quantum Networks

SYSM

			Invited Talks
15:00	H1	SYSM 1.1	Statics and Dynamics of Soft Wetting •Bruno Andreotti
15:30	H1	SYSM 1.2	Droplets on elastic substrates and membranes – Numerical simulation of soft wetting •Sebastian Aland
16:00	H1	SYSM 1.3	Wetting of Polymer Brushes in Air •Sissi de Beer
16:45	H1	SYSM 1.4	Elastocapillary phenomena in cells •Roland L. Knorr
17:15	H1	SYSM 1.5	Active contact line depinning by micro-organisms spreading on hydrogels •Adrian Daerr
			Session
15:00	H1	SYSM 1	Interplay of Substrate Adaptivity and Wetting Dynamics from Soft Matter to Biology

Wednesday, September 7, 2022

SYUK

Invited Talks

09:30	H2	SYUK 1.1	Structure and Dynamics of Interfacial Water •Angelos Michaelides
10:00	H2	SYUK 1.2	A molecular view of the water interface •Mischa Bonn
10:30	H2	SYUK 1.3	Motile cilia waves: creating and responding to flow •Pietro Cicuta
11:00	H2	SYUK 1.4	Cilia and flagella: Building blocks of life and a physicist's playground •Oliver Bäumchen
11:45	H2	SYUK 1.5	Computational modelling of the physics of rare earth – transition metal permanent magnets from SmCo_5 to $\text{Nd}_2\text{Fe}_{14}\text{B}$ •Julie Staunton
15:00	H2	SYUK 2.1	Hysteresis Design of Magnetic Materials for Efficient Energy Conversion •Oliver Gutfleisch
15:30	H2	SYUK 2.2	Non-equilibrium dynamics of many-body quantum systems versus quantum technologies •Irene D'Amico
16:00	H2	SYUK 2.3	Quantum computing with trapped ions •Ferdinand Schmidt-Kaler
16:45	H2	SYUK 2.4	Breaking the millikelvin barrier in cooling nanoelectronic devices •Richard Haley
17:15	H2	SYUK 2.5	Superconducting Quantum Interference Devices for applications at mK temperatures •Sebastian Kempf

Sessions

09:30	H2	SYUK 1	United Kingdom as Guest of Honor I
15:00	H2	SYUK 2	United Kingdom as Guest of Honor II

BP

Invited Talks

09:30	H15	BP 13.1	Cortex mechanics – how subtle modifications matter •Andreas Janshoff
11:00	H13	BP 15.4	The importance of water in membrane receptor function •Anthony Watts
15:00	H15	BP 18.1	Bottom-up molecular control of biomimetic hydrogels •Kerstin G. Blank

Sessions

09:30	H15	BP 13	Cytoskeleton
09:30	H16	BP 14	Active Matter 3
10:00	H13	BP 15	Protein Structure and Single Molecules
10:15	H11	BP 16	Networks: From Topology to Dynamics
15:00	H13	BP 17	Membranes and Vesicles
15:00	H15	BP 18	Biomaterials
15:00	H16	BP 19	Cell Mechanics 2
15:00	H18	BP 20	Active Matter 4
18:00	H15	BP 21	Members' Assembly

CPP

Invited Talk

09:30	H38	CPP 19.1	Elucidating the role of antisolvent polarity on the surface chemistry and optoelectronic properties of lead-halide perovskite nanocrystals •Robert Hoyer
-------	-----	----------	---

Sessions

09:30	H38	CPP 19	Perovskite and Photovoltaics 2
-------	-----	--------	--------------------------------

Wednesday, September 7, 2022

CPP

09:30	H39	CPP 20	General Session to the Symposium: Interplay of Substrate Adaptivity and Wetting Dynamics from Soft Matter to Biology
09:30	H7	CPP 21	Materials for Energy Storage
09:30	H16	CPP 22	Active Matter 3
09:30	H18	CPP 23	Complex Fluids and Soft Matter 1
09:30	H36	CPP 24	2D Materials 5
11:15	H17	CPP 25	2D Materials 6
11:30	H38	CPP 26	Organic Electronics and Photovoltaics 2
11:30	H39	CPP 27	Composites and Functional Polymer Hybrids
15:00	H38	CPP 28	Perovskite and Photovoltaics 3
15:00	H15	CPP 29	Biomaterials
15:00	H17	CPP 30	2D Materials 7
15:00	H18	CPP 31	Active Matter 4
15:00	H34	CPP 32	Perovskite and Photovoltaics 4

DS

Invited Talks			
09:30	H17	DS 14.1	Facet dependence of reconstructions at quantum material interfaces •Eva Benckiser
10:15	H17	DS 14.3	Designing novel electronic phases at oxide interfaces from first principles •Rossitza Pentcheva

Sessions			
09:30	H14	DS 13	Thin Film Applications 2
09:30	H17	DS 14	Focus session: Quantum Properties at Functional Oxide Interfaces 2
09:30	H36	DS 15	2D Materials 5
11:00	H14	DS 16	Thin Film Applications 2
11:15	H17	DS 17	2D Materials 6
15:00	H14	DS 18	Thin Oxides and Oxide Layers 1
15:00	H17	DS 19	2D Materials 7
16:00	P3	DS 20	Poster

DY

Invited Talks			
12:00	H18	DY 29.1	Derivation of a continuum description of sheared jammed soft suspensions from particle dynamics •Eric Bertin
15:00	H19	DY 32.1	Large scale patterns in turbulent Rayleigh-Bénard convection •Stephan Weiss
15:00	H20	DY 33.1	Detecting dynamical quantum phase transitions by string observables •Anatoli Polkovnikov

Sessions			
09:30	H11	DY 21	Invited Talk Dirk Brockmann
09:30	H16	DY 22	Active Matter 3
09:30	H18	DY 23	Complex Fluids and Soft Matter 1
09:30	H19	DY 24	Stochastic Thermodynamics and Information Processing
09:30	H39	DY 25	General Session to the Symposium: Interplay of Substrate Adaptivity and Wetting Dynamics from Soft Matter to Biology
10:00	H20	DY 26	Critical Phenomena and Phase Transitions
10:15	H11	DY 27	Networks: From Topology to Dynamics
11:15	H19	DY 28	Extreme Events, Glasses and Miscellaneous
12:00	H18	DY 29	Invited Talk Eric Bertin
12:45	H11	DY 30	Energy Networks
15:00	H18	DY 31	Active Matter 4
15:00	H19	DY 32	Invited Talk Stephan Weiss
15:00	H20	DY 33	Invited Talk Anatoli Polkovnikov

Wednesday, September 7, 2022

				DY
15:30	H19	DY 34	Fluid Physics: Turbulence and Convection	
15:30	H20	DY 35	Quantum Chaos and Coherent Dynamics	
				HL
				Invited Talk
09:30	H34	HL 19.1	Quantum Interference of Identical Photons from Remote GaAs Quantum Dots •Giang Nam Nguyen	
				Sessions
09:30	H17	HL 16	Focus Session: Quantum Properties at Functional Oxide Interfaces	
09:30	H32	HL 17	Quantum Dots and Wires 4: Devices	
09:30	H33	HL 18	Oxide Semiconductors	
09:30	H34	HL 19	Materials and Devices for Quantum Technology 1	
09:30	H36	HL 20	2D Materials 4	
15:00	H32	HL 21	Optical Properties 1	
15:00	H33	HL 22	Heterostructures, Interfaces and Surfaces	
15:00	H34	HL 23	Perovskite and Photovoltaics 2	
15:00	H36	HL 24	Functional Semiconductors for Renewable Energy Solutions	
18:00	P2	HL 25	Poster 1	
				KFM
				Invited Talk
15:00	H5	KFM 18.1	Deep understanding of advanced optical and dielectric materials for fusion diagnostic applications •Anatoli I. Popov	
				Sessions
09:30	H5	KFM 14	Ferroics – Domains and Domain Walls 1	
09:30	H7	KFM 15	Materials for Energy Storage	
09:30	H33	KFM 16	Oxide Semiconductors	
15:00	H3	KFM 17	Focus Session: Surfaces and Interfaces of (Incipient) Ferroelectrics	
15:00	H5	KFM 18	Focus Session: Diamond and related dielectric materials	
15:00	H7	KFM 19	Ferroics – Domains and Domain Walls 2	
15:00	H34	KFM 20	Perovskite and Photovoltaics 2	
15:00	H36	KFM 21	Functional semiconductors for renewable energy solutions	
17:00	H5	KFM 22	Members' Assembly	
				MA
				Invited Talks
09:30	H37	MA 20.1	Recent developments in X-ray three-dimensional magnetic imaging •Valerio Scagnoli	
10:00	H37	MA 20.2	Magnetic depth profiling with x-ray resonant magnetic reflectivity (XRMR) •Timo Kuschel	
10:30	H37	MA 20.3	Magnetic Bragg Ptychography Studies of Spin Caloritronic •Dina Carbone	
11:15	H37	MA 20.4	Imaging the 3D magnetic texture of skyrmion tubes and approaches towards determining their Hall signature •B. Rellinghaus	
11:45	H37	MA 20.5	Determination of spin chirality and helicity angle by circular dichroism in soft x-ray absorption and resonant elastic scattering •Gerrit van der Laan	
12:15	H37	MA 20.6	Identification of complex spin-textures by novel Hall effects •Juba Bouaziz	
				Sessions
09:30	H37	MA 20	Focus Session: Revealing Multidimensional Spin Textures and their Dynamics via X-rays and Electrons	

Wednesday, September 7, 2022

MA

09:30	H43	MA 21	Terahertz Spintronics
09:30	H47	MA 22	Thin Films: Magnetic Coupling Phenomena / Exchange Bias / Magnetic Anisotropy
09:30	H48	MA 23	Magnetic Domain Walls
15:00	H37	MA 24	Spin Transport and Orbitronics, Spin-Hall Effects
15:00	H43	MA 25	Ultrafast Magnetization Effects 2
15:00	H48	MA 26	Molecular Magnetism

MM

Invited Talk, Topical Talks			
09:30	H44	MM 19.1	High-Entropy Alloys: Materials design in high dimensional chemical space from ab initio thermodynamics •Fritz Körmann
10:15	H46	MM 22.1	Ingredients for effective computer-augmented experimental materials science •Christoph T. Koch
11:45	H46	MM 22.5	Physics guided machine learning tools in analytical transmission electron microscopy •Cecile Hebert
15:45	H45	MM 24.1	Electromigration effects on the atomic ordering process in hard magnetic L1 ₀ intermetallic phases •Daniel Urban
17:30	H45	MM 24.6	From Uncovering the Mechanisms of Flash Sintering to Realizing Ultrafast Sintering without Electric Fields and Discovering Electrochemically Driven Microstructural Evolution •Jian Luo
18:00	H45	MM 24.7	Electric fields effects in ionic conductors during flash sintering and ion exchange •Mattia Biesuz
15:45	H46	MM 25.1	Automated atomistic calculation of thermodynamic and thermophysical data •Jan Janssen
17:15	H46	MM 25.5	Understanding Dislocation Flow and Avalanches in High Entropy Alloys by Machine Learning-based Data Mining of In-Situ TEM Experiments •Stefan Sandfeld
Sessions			
09:30	H44	MM 19	Invited Talk Fritz Körmann
10:15	H44	MM 20	Computational Materials Modelling: HEA, Alloys & Nanostructures
10:15	H45	MM 21	Transport in Materials: Thermal transport
10:15	H46	MM 22	Data Driven Materials Science: Experimental Data Treatment and Machine Learning
15:45	H44	MM 23	Computational Materials Modelling: Magnetic & Electrical Properties
15:45	H45	MM 24	Non-equilibrium Phenomena in Materials Induced by Electrical and Magnetic Fields 4
15:45	H46	MM 25	Data Driven Materials Science: Computational Frameworks / Chemical Complexity
18:45	H44	MM 26	Members' Assembly

O

Invited Talk, Topical Talks			
09:30	S054	O 36.1	Heterogeneous chemistry of liquid-vapor interfaces investigated with X-ray photoelectron spectroscopy •Hendrik Bluhm
10:30	H3	O 37.1	Merging integrated photonics with free-electron beams •Armin Feist
10:30	H4	O 38.1	Electrochemical Microcalorimetry •Rolf Schuster
15:00	H3	O 44.1	In search of electrostatic happiness at surfaces •Nicola Spaldin

Wednesday, September 7, 2022

0

15:30	H3	O 44.2	Synthesis and Characterisation of Ultra-thin Aurivillius Phase Multiferroics •Lynette Keeney
16:45	H3	O 44.6	Water-oxidation catalysis on surfaces of ferroelectrics •Ulrich Aschauer
18:00	H3	O 44.10	Spin-orbitronics and superconductivity in KTaO ₃ twodimensional electron gases •Srijani Mallik
15:00	H4	O 45.1	Addressing Electronic Effects in Catalysis by Intermetallic Compounds •Marc Armbrüster
16:15	H4	O 45.5	Understanding liquid metal catalysts for graphene synthesis using machine learning interatomic potentials •Hendrik H. Heenen
16:45	H4	O 45.6	Ionic liquids and deep eutectic solvents - sustainable media for selective molecular recognition and adsorption •Jan Blasius
15:00	S051	O 47.1	Quantum control of multi-spin architectures on a surface •Yujeong Bae
16:30	S051	O 47.6	Free coherent evolution of a coupled atomic spin system initialized by electron scattering •Sander Otte

Sessions

09:30	S054	O 36	Overview Talk Hendrik Bluhm
10:30	H3	O 37	Plasmonics and Nanooptics 1
10:30	H4	O 38	Solid-Liquid Interfaces 4: Reactions and Electrochemistry
10:30	H6	O 39	Tribology
10:30	S051	O 40	Organic Molecules at Surfaces 4: Chemistry on Surfaces
10:30	S052	O 41	Graphene: Growth, Substrate Interaction, Intercalation, and Doping
10:30	S053	O 42	Metal substrates 2
10:30	S054	O 43	Frontiers of Electronic Structure Theory: Focus on Artificial Intelligence Applied to Real Materials 1
15:00	H3	O 44	Focus Session: Surfaces and Interfaces of (Incipient) Ferroelectrics
15:00	H4	O 45	Focus Session: Catalysis at Liquid Interfaces
15:00	H6	O 46	New Methods and Developments 3: Theory
15:00	S051	O 47	Focus Session: Atomic-Scale Studies of Spins on Surfaces with Scanning Tunneling Microscopy 1
15:00	S052	O 48	2D Materials 1: Electronic Structure of Transition Metal Dichalcogenides
15:00	S053	O 49	Oxide Surfaces 1
15:00	S054	O 50	Frontiers of Electronic Structure Theory: Focus on Artificial Intelligence Applied to Real Materials 2
18:00	P4	O 51	Poster Wednesday: Atomic-Scale Studies of Spins on Surfaces with Scanning Tunneling Microscopy
18:00	P4	O 52	Poster Wednesday: Adsorption and Catalysis 2
18:00	P4	O 53	Poster Wednesday: Spins and Magnetism
18:00	P4	O 54	Poster Wednesday: 2D Materials 2
18:00	P4	O 55	Poster Wednesday: Organic Molecules at Surfaces 2
18:00	P4	O 56	Poster Wednesday: Nanostructures 2
18:00	P4	O 57	Poster Wednesday: Electronic Structure
18:00	P4	O 58	Poster Wednesday: New Methods and Developments, Frontiers of Electronic Structure Theory
18:00	P4	O 59	Poster Wednesday: Plasmonics and Nanooptics 2

SOE

Invited Talk

09:30	H11	SOE 11.1	The Corona Data Donation Project - When Citizens Collaborate to Fight a Pandemic •Dirk Brockmann
-------	-----	----------	---

Wednesday, September 7, 2022

SOE

Sessions

09:30	H11	SOE 11	Invited Talk Dirk Brockmann: Big Data in Epidemic Dynamics
10:15	H11	SOE 12	Networks: From Topology to Dynamics
12:45	H11	SOE 13	Energy Networks
15:00	H11	SOE 14	Computational Social Science
17:00	H11	SOE 15	Traffic Dynamics, Urban and Regional Systems
18:15	H11	SOE 16	Members' Assembly

TT

Invited Talks

09:30	H10	TT 16.1	Multimethod, multimessenger approaches to models of strong correlations •Thomas Schäfer
15:00	H10	TT 22.1	Evidence for orbital loop current magnetism in Sr_2RuO_4 •A. Di Bernardo
17:15	H10	TT 22.8	Role of the film geometry in the electronic reconstruction of infinite-layer nickelates on $\text{SrTiO}_3(001)$ •Benjamin Geisler

Sessions

09:30	H10	TT 16	Correlated Electrons: Method Development
09:30	H22	TT 17	Cryogenic Detectors and Cryotechnique
09:30	H23	TT 18	Topological Insulators
11:45	H23	TT 19	Topological Superconductors
15:00	P1	TT 20	Topology: Poster Session
15:00	P1	TT 21	Correlated Electrons: Poster Session
15:00	H10	TT 22	Unconventional Superconductors
15:00	H22	TT 23	Frustrated Magnets – General
15:00	H23	TT 24	Quantum-Critical Phenomena

QI

Invited Talk

15:00	H9	QI 8.1	Exploring Quantum Materials with Quantum Sensors •Uri Vool
-------	----	--------	---

Sessions

15:00	H8	QI 7	Quantum Communication and Networks
15:00	H9	QI 8	Quantum Sensors and Metrology

Job Market

12:45	Kunsthalle		Ritzenhoefer GmbH: „Transformation Consulting – Von der Physik zur Sinngebungs-Maschine fürs Topmanagement“
14:00	Kunsthalle		d-fine: "Auswirkungen von Krisen auf Energieversorger – Einblick in die analytisch-technologische Beratung bei d-fine"

09:00	Foyer Audimax, H6, Economy Bldg, Tent (Physics Building)		Exhibition of Scientific Instruments and Literature (free entrance)
-------	--	--	--

20:00	H1		EinsteinSlam
-------	----	--	---------------------

Thursday, September 8, 2022

Plenary Talks			
08:30	H1	PLV VIII	Physics of Structure Formation in Living Systems •Stephan Grill
14:00	H1	PLV IX	Evolutionary transitions: universality, complexity and predictability •Ricard Sole
14:00	H2	PLV X	Semiconductor quantum optics: from artificial atoms to atomically thin materials •Jonathan Finley
Lunch Talk			
13:15	H2	PSV VII	Berufsbild: Wissenschaftskommunikation und Museumsdidaktik •Kim Ludwig-Petsch

SYES

Invited Talks			
15:00	H1	SYES 1.1	Machine-learning-driven advances in modelling inorganic materials •Volker L. Deringer
15:30	H1	SYES 1.2	Machine-Learning Discovery of Descriptors for Square-Net Topological Semimetals •Eun-Ah Kim
16:00	H1	SYES 1.3	Four Generations of Neural Network Potentials •Jörg Behler
16:30	H1	SYES 1.4	Using machine learning to find density functionals •Kieron Burke
17:00	H1	SYES 1.5	Coarse graining for classical and quantum systems •Cecilia Clementi
Session			
15:00	H1	SYES 1	Frontiers of Electronic-Structure Theory: Focus on Artificial Intelligence Applied to Real Materials

SYSO

Invited Talks			
09:30	H1	SYSO 1.1	Capturing group interactions: The next frontier of modeling social and biological systems •Frank Schweitzer
10:00	H1	SYSO 1.2	Modelling Individual Mobility Behavior •Laura Maria Alessandretti
10:30	H1	SYSO 1.3	Validating argument-based opinion dynamics with survey experiments •Sven Banisch
11:15	H1	SYSO 1.4	Self-organization, Criticality and Collective Information Processing in Animal Groups •Pawel Romanczuk
11:45	H1	SYSO 1.5	Collective dynamics and physiological interactions in bird colonies •Hanja Brandl
Session			
09:30	H1	SYSO 1	Collective social dynamics from animals to humans

BP

Invited Talks			
09:30	H15	BP 22.1	Cell and tissue mechano-plasticity in development •Verena Ruprecht
10:30	H16	BP 24.1	Actin waves as building blocks of cellular function •Carsten Beta
15:00	H15	BP 26.1	Molecular robots working cooperatively in swarm •Akira Kakugo

Thursday, September 8, 2022

BP**Sessions**

09:30	H15	BP 22	Migration and Multicellular Systems
10:00	H13	BP 23	Evolution
10:30	H16	BP 24	Systems Biology, Gene Expression, Signalling
11:00	H13	BP 25	Bioinspired Systems
15:00	H15	BP 26	Focus Session: Bioinspired Systems
15:00	H16	BP 27	Statistical Physics of Biological Systems 2

CPP**Invited Talks**

09:30	H38	CPP 33.1	Cooperative and non-Gaussian dynamics of entanglement strands in polymer melts •Margarita Kruteva
10:30	H39	CPP 37.1	Non-equilibrium Properties of Thin Polymer Films •Günter Reiter
15:00	H38	CPP 40.1	Computational Design of Organic Semiconductors •Harald Oberhofer
15:00	H39	CPP 41.1	Interface-induced crystallization in polymers: From model systems to applications for semiconducting polymers •Oleksandr Dolynchuk

Sessions

09:30	H38	CPP 33	Focus Session: Soft Matter and Nanocomposites: New Opportunities with Advanced Neutron Sources 1
09:30	H39	CPP 34	Hydrogels and Microgels
09:30	H17	CPP 35	2D Materials 8
10:00	H18	CPP 36	Complex Fluids and Soft Matter 2
10:30	H39	CPP 37	Interfaces and Thin Films and Responsive and Adaptive Systems
11:15	H36	CPP 38	2D Materials 9
11:30	H38	CPP 39	Molecular Electronics and Excited State Properties
15:00	H38	CPP 40	Organic Electronics and Photovoltaics 3
15:00	H39	CPP 41	Crystallization, Nucleation and Self-Assembly
15:00	H31	CPP 42	Perovskite and Photovoltaics 5
18:00	H39	CPP 43	Members' Assembly

DS**Sessions**

09:30	H14	DS 21	Layer Deposition (ALD, MBE, Sputtering, ...)
09:30	H17	DS 22	2D Materials 8
10:45	H14	DS 23	Optical Analysis of Thin Films (Reflection, Ellipsometry, Raman, IR-DUV Spectroscopy, ...)
11:15	H36	DS 24	2D Materials 9
15:00	H14	DS 25	Transport Properties
16:15	H14	DS 26	Thin Oxides and Oxide Layers 2

DY**Invited Talk**

09:30	H20	DY 37.1	Controlled and robust phase separation in cells •David Zwicker
-------	-----	---------	---

Sessions

09:30	H22	DY 36	Quantum Coherence and Quantum Information Systems
09:30	H20	DY 37	Invited Talk David Zwicker
10:00	H18	DY 38	Complex Fluids and Soft Matter 2
10:00	H19	DY 39	Pattern Formation and Reaction-Diffusion Systems
10:00	H20	DY 40	Brownian Motion and Anomalous Diffusion

Thursday, September 8, 2022

DY

15:00	H22	DY 41	Nonequilibrium Quantum Many-Body Systems
15:00	H16	DY 42	Statistical Physics of Biological Systems 2
15:00	P2	DY 43	Poster Session: Quantum Chaos and Many-Body Dynamics
15:00	P2	DY 44	Poster Session: Statistical Physics and Critical Phenomena
15:00	P2	DY 45	Poster Session: Nonlinear Dynamics, Pattern Formation, Data Analytics and Machine Learning
15:00	P2	DY 46	Poster Session: Complex Fluids, Soft Matter, Active Matter, Glasses and Granular Materials
18:30	H19	DY 47	Members' Assembly

HL**Invited Talks**

09:30	H33	HL 27.1	What limits state-of-the-art chalcopyrite solar cells? •Susanne Siebentritt
10:00	H33	HL 27.2	Approaches to improve CIGS absorber quality and the CIGS/buffer interface to reach 24% efficiency and beyond •Wolfram Witte
16:30	H32	HL 33.6	Ultrastrong light-matter coupling in materials •Niclas S. Mueller
15:00	H33	HL 34.1	Super-high efficiency CIGS devices: current status and pathways forward •Romain Carron
15:30	H33	HL 34.2	Highlights from the development of the world record Cd-free CIGSSe 30x30cm ² solar module •Anastasia Zelenina
17:00	H33	HL 34.5	Digital Twins - a simulation model for Cu(In,Ga)Se ₂ solar cells of high and moderate efficiency •Matthias Maiberg

Sessions

09:30	H32	HL 26	Quantum Dots and Wires 5: Optics 2
09:30	H33	HL 27	Focus Session: Perspectives in Cu(In,Ga)Se 1
09:30	H34	HL 28	Organic Semiconductors 1
09:30	H36	HL 29	2D Materials: Graphene
11:00	P3	HL 30	Poster 2
11:15	H36	HL 31	2D Materials 5
15:00	H31	HL 32	Perovskite and Photovoltaics 3
15:00	H32	HL 33	Optical Properties 2
15:00	H33	HL 34	Focus Session: Perspectives in Cu(In,Ga)Se 2
15:00	H34	HL 35	Acoustic Waves and Nanomechanics
15:00	H36	HL 36	Materials and Devices for Quantum Technology 2
16:30	H34	HL 37	Thermal Properties
18:00	H34	HL 38	Members' Assembly

KFM**Sessions**

09:30	H37	KFM 23	Skyrmions 2
10:30	H6	KFM 24	New Methods and Developments: Spectroscopies, Diffraction and Others
15:00	P2	KFM 25	Poster
15:00	H10	KFM 26	Focus Session: Topological Devices
15:00	H31	KFM 27	Perovskite and Photovoltaics 3
15:00	H37	KFM 28	Topological Insulators
15:00	H47	KFM 29	Multiferroics and Magnetoelectric Coupling

Thursday, September 8, 2022

MA

15:00	H37	MA 31.1	Invited Talk Neutron scattering on magnetic topological materials: From topological magnon insulators to emergent many-body effects •Yixi Su
09:30	H37	MA 27	Sessions Skyrmions 2
09:30	H43	MA 28	Magnonics 2
09:30	H47	MA 29	Caloric Effects in Magnetic Materials
09:30	H48	MA 30	Surface Magnetism
15:00	H37	MA 31	Topological Insulators
15:00	H43	MA 32	Bulk Materials: Soft and Hard Permanent Magnets
15:00	H47	MA 33	Multiferroics and Magnetoelectric Coupling
15:00	H48	MA 34	Functional Antiferromagnetism
16:00	P4	MA 35	Poster 2
18:00	H37	MA 36	Members' Assembly

MM

09:30	H44	MM 27.1	Invited Talk Crystal rotation kinematics during the tribological loading of high-purity copper •Christian Greiner
09:30	H44	MM 27	Sessions Invited Talk Christian Greiner
10:15	H44	MM 28	Transport in Materials: Diffusion / Electrical Transport & Magnetism
10:15	H45	MM 29	Data Driven Materials Science: Design of Functional Materials
10:15	H46	MM 30	Liquid and Amorphous Metals
11:45	H44	MM 31	Computational Materials Modelling: Physics of Ensembles 2
11:45	H45	MM 32	Nanomaterials: Surface Effects
15:45	H44	MM 33	Computational Materials Modelling: Process Schemes / Oxides
15:45	H45	MM 34	Data Driven Materials Science: Interatomic Potentials / Reduced Dimensions
15:45	H46	MM 35	Nanomaterials: Structure & Properties

O

09:30	S054	O 60.1	Invited Talk, Topical Talks Exciting states in atomically thin layers •Thorsten Deilmann
10:30	H2	O 61.1	Single Molecule Nonlinearity in a Plasmonic Waveguide •Markus Lippitz
10:30	H6	O 63.1	Element and Structure Analysis of Surfaces Using Positrons •Christoph Hugenschmidt
10:30	S053	O 66.1	Charge-ordered states on incipient ferroelectric polar surfaces •Cesare Franchini
15:00	H3	O 68.1	Exploring Excitonic Excitations in Momentum Space •Keshav Dani
15:30	H3	O 68.2	Moiré interlayer and charge-transfer excitons in space and time: new experiments enabled by time-resolved momentum microscopy •Stefan Mathias
16:30	H3	O 68.5	Momentum and energy dissipation of hot electrons in metals and metal-molecular heterostructures •Benjamin Stadtmueller
17:30	H3	O 68.8	Is there a perfect electron analyzer for time-resolved ARPES? •Laurenz Rettig
15:00	H4	O 69.1	Theoretical Investigations of Size and Support Effects in Heterogeneous Catalysis •Felix Studt
15:00	H6	O 70.1	Stability and dynamics of cluster catalysts and their supports •Barbara A. J. Lechner

Thursday, September 8, 2022

O

15:00	S051	O 71.1	Theory for Electron Spin Resonance based on electron transport •Nicolas Lorente
16:45	S051	O 71.7	Stochastic resonance as a new tool to investigate spin dynamics •Susanne Baumann
Sessions			
09:30	S054	O 60	Overview Talk Thorsten Deilmann
10:30	H2	O 61	Plasmonics and Nanooptics 2
10:30	H4	O 62	Surface Reactions and Heterogeneous Catalysis 1
10:30	H6	O 63	New Methods and Developments 4: Spectroscopies, Diffraction and Others
10:30	S051	O 64	Gerhard Ertl Young Investigator Award
10:30	S052	O 65	2D Materials 2: Growth, Structure and Substrate Interaction
10:30	S053	O 66	Oxide Surfaces 2
10:30	S054	O 67	Frontiers of Electronic Structure Theory: Focus on Artificial Intelligence Applied to Real Materials 3
15:00	H3	O 68	Focus Session: Time-Resolved Momentum Microscopy
15:00	H4	O 69	Surface Reactions and Heterogeneous Catalysis 2
15:00	H6	O 70	Supported nanoclusters: Structure, Reactions, Catalysis
15:00	S051	O 71	Focus Session: Atomic-Scale Studies of Spins on Surfaces with Scanning Tunneling Microscopy 2
15:00	S052	O 72	2D Materials 3: hBN and Electronic Structure
15:00	S053	O 73	Electronic Structure of Surfaces 1
15:00	S054	O 74	Organic Molecules at Surfaces 5: Molecular Switches
19:00	H1	O 75	Members' Assembly
19:30	H1	O 76	Post-Deadline Session

SOE

Session			
15:00	P2	SOE 17	Poster

TT

Invited Talks			
09:30	H3	TT 25.1	Topology: Open and with diverse backgrounds •Tobias Meng
10:30	H23	TT 28.5	Towards an ab-initio theory of Anderson localization for correlated electrons •Liviu Chioncel
15:00	H10	TT 32.1	Supercurrents in HgTe-based topological nanowires •Dieter Weiss
15:30	H10	TT 32.2	Majorana bound states and non-reciprocal transport in topological insulator nanowire devices •Henry Legg
16:00	H10	TT 32.3	Integration of topological insulator Josephson junctions in superconducting qubit circuits •Tobias W. Schmitt
16:45	H10	TT 32.4	Universal fluctuations of the induced superconducting gap in an elemental nanowire •Matthieu Delbecq
17:15	H10	TT 32.5	Exploring the full potential of edge channel transport in HgTe based two-dimensional topological insulators •Saqib Shamim
Sessions			
09:30	H3	TT 25	Topological Semimetals
09:30	H10	TT 26	Superconductivity: Tunnelling and Josephson Junctions
09:30	H22	TT 27	Quantum Coherence and Quantum Information Systems
09:30	H23	TT 28	Correlated Electrons: Theory 1
15:00	P1	TT 29	Transport: Poster Session

Thursday, September 8, 2022

TT

15:00	P1	TT 30	Superconductivity: Poster Session
15:00	P1	TT 31	Superconducting Electronics and Cryogenics: Poster Session
15:00	H10	TT 32	Focus Session: Topological Devices
15:00	H22	TT 33	Nonequilibrium Quantum Many-Body Systems
15:00	H23	TT 34	Correlated Electrons: Theory 2
19:00	H22	TT 35	Members' Assembly

QI

09:30	H9	QI 10.1	Invited Talk Entanglement Transition in the Projective Transverse Field Ising Model •Hans Peter Büchler
-------	----	---------	--

09:30	H8	QI 9	Sessions Quantum Correlations
09:30	H9	QI 10	Quantum Simulation and Many-Body Systems
14:00	H8	QI 11	Members' Assembly
15:00	H8	QI 12	Quantum Computing and Algorithms

12:45	Kunsthalle	Job Market Basycon Unternehmensberatung GmbH: "Was hat Beratung mit Forschung zu tun?"
14:00	Kunsthalle	Trumpf GmbH & Co. KG: "Lasersystems for EUV Lithography"

09:00	Foyer Audimax, H6, Economy Bldg, Tent (Physics Building)	Exhibition of Scientific Instruments and Literature (free entrance)
-------	--	--

Friday, September 9, 2022

08:30	H1	PLV XI	Plenary Talk Spinwaves as experimental probes •Christian Back
-------	----	--------	--

SYQM

09:30	H1	SYQM 1.1	Invited Talks The role of crystalline symmetries in topological materials: the topological materials database •Maia Vergniory
10:00	H1	SYQM 1.2	Microwave Bulk and Edge Transport in HgTe-Based 2D Topological Insulators •Erwann Bocquillon
10:30	H1	SYQM 1.3	Spectral Sensitivity of Non-Hermitian Topological Systems •Jan Carl Budich
11:15	H1	SYQM 1.4	Topological photonics and topological lasers with coupled vertical resonators •Sebastian Klembt
11:45	H1	SYQM 1.5	Spectroscopic Studies of the Topological Magnon Band Structure in a Skyrmion Lattice •Markus Garst
09:30	H1	SYQM 1	Session Complexity and Topology in Quantum Matter

BP

09:30	H39	BP 28	Sessions Biopolymers, Biomaterials and Bioinspired Functional Materials Active Matter 5
10:00	H18	BP 29	

CPP

09:30	H38	CPP 44.1	Invited Talks Connecting dynamics and phase behavior of proteins: The neutron perspective •Frank Schreiber
10:45	H38	CPP 44.5	Magnetic particle self-assembly at functionalized interfaces •Max Wolff
09:30	H39	CPP 45.1	New biobased material concepts using scattering techniques to elucidate and control nanoscale assembly •Daniel Söderberg
09:30	H38	CPP 44	Sessions Focus Session: Soft Matter and Nanocomposites: New Opportunities with Advanced Neutron Sources 2
09:30	H39	CPP 45	Biopolymers, Biomaterials and Bioinspired Functional Materials
09:30	H36	CPP 46	2D Materials 10
10:00	H18	CPP 47	Active Matter 5
11:30	H38	CPP 48	Electrical, Dielectrical and Optical Properties of Thin Films
11:30	H39	CPP 49	Polymer and Molecular Dynamics, Friction and Rheology
12:30	H38	CPP 50	Nanostructures, Nanostructuring and Nanosized Soft Matter
13:15	S054	CPP 51	Overview Talk Claus M. Schneider

DS

09:30	H36	DS 27	Session 2D Materials 10
-------	-----	-------	-----------------------------------

Friday, September 9, 2022

DY

09:30	H19	DY 48.1	Invited Talk Photonic Reservoir Computing: Analytic insights and possibilities for optimization •Kathy Lüdge
			Sessions
09:30	H19	DY 48	Invited Talk Kathy Lüdge
09:30	H20	DY 49	Statistical Physics: General
10:00	H18	DY 50	Active Matter 5
10:00	H19	DY 51	Machine Learning in Dynamics and Statistical Physics
11:30	H19	DY 52	Nonlinear Dynamics 2: Stochastic and Complex Systems, Networks

HL

10:45	H33	HL 40.5	Invited Talk Ultrafast subcycle dynamics of deep-strong light-matter coupling •Joshua Mornhinweg
			Sessions
09:30	H32	HL 39	Quantum Dots and Wires 6: II-VI and related
09:30	H33	HL 40	THz and MIR Physics in Semiconductors
09:30	H34	HL 41	Organic Semiconductors 2
09:30	H36	HL 42	2D Materials 6

KFM

			Sessions
09:30	H37	KFM 30	Skymions 3
11:30	H38	KFM 31	Electrical, Dielectrical and Optical Properties of Thin Films

MA

			Sessions
09:30	H37	MA 37	Skymions 3
09:30	H43	MA 38	Electron Theory of Magnetism and Correlations
09:30	H47	MA 39	Magnetic Particles / Clusters
09:30	H48	MA 40	Weyl Semimetals
11:30	H47	MA 41	Micro- and Nanostructured Magnetic Materials
11:30	H48	MA 42	Magnetic Heuslers

O

			Invited Talks, Topical Talk
09:30	S054	O 77.1	Sub-molecular fluorescence microscopy with STM •Guillaume Schull
10:30	H4	O 79.1	Exploitation of Heterocycles for N-doped Graphene Nanomaterials •Shi-Xia Liu
13:15	S054	O 84.1	Exploring the Mysteries of Topology in Quantum Materials •Claus M. Schneider
			Sessions
09:30	S054	O 77	Overview Talk Guillaume Schull
10:30	H3	O 78	Plasmonics and Nanooptics 3
10:30	H4	O 79	Surface Reactions and Heterogeneous Catalysis 3
10:30	S051	O 80	Focus Session: Atomic-Scale Studies of Spins on Surfaces with Scanning Tunneling Microscopy 3
10:30	S052	O 81	2D Materials 4: Heterostructures
10:30	S053	O 82	Electronic Structure of Surfaces 2
10:30	S054	O 83	Frontiers of Electronic Structure Theory: Focus on Artificial Intelligence Applied to Real Materials 4
13:15	S054	O 84	Overview Talk Claus M. Schneider

Friday, September 9, 2022

SOE

Sessions

09:30	H19	SOE 18	Invited Talk Kathy Lüdge
10:00	H19	SOE 19	Machine Learning in Dynamics and Statistical Physics
11:30	H19	SOE 20	Nonlinear Dynamics 2: Stochastic and Complex Systems, Networks

TT

Invited Talks

09:30	H10	TT 36.1	Coherent control of lattice and electronic states •Steven Johnson
10:00	H10	TT 36.2	New opportunities for light-matter control of quantum materials •Michael Sentef
10:30	H10	TT 36.3	Coherent electronic control of an insulator-to-metal transition •Claudio Giannetti
11:15	H10	TT 36.4	Nanoscale transient magnetization dynamics: A comprehensive EUV TG study •Laura Foglia
11:45	H10	TT 36.5	Ultrafast magnetism of antiferromagnets •Alexey Kimel

Sessions

09:30	H10	TT 36	Focus Session: Ultrafast Spin, Lattice and Charge Dynamics of Solids
09:30	H22	TT 37	Superconducting Electronics: SQUIDs, Qubits, Circuit QED
09:30	H23	TT 38	Superconductivity: Theory
11:15	H23	TT 39	Correlated Electrons: Charge Order

QI

Invited Talks

09:30	H8	QI 13.1	Scalable control of superconducting qubits •Stefan Filipp
09:30	H9	QI 14.1	Testing quantum theory with generalized noncontextuality •Markus P. Müller

Sessions

09:30	H8	QI 13	Implementations: Superconducting Qubits
09:30	H9	QI 14	Quantum Foundations

AKC

Invited Talk

09:30	H2	AKC 1.1	Closing the gender gap: avoid dropout in the postdoc and junior professor phase •Petra Rudolf
-------	----	---------	--

Session

09:30	H2	AKC 1	Career in Academia
-------	----	-------	--------------------

Job Market

11:30	Kunsthalle		Horn & Company: "Gewinne Einblicke in unsere Projekte zu Data Analytics, Big Data und Künstlicher Intelligenz und lerne unseren Beratungsansatz kennen!"
-------	------------	--	--

Sessions

– Plenary Talks –

Plenary Talk PLV I Mon 8:30 H1

Intrinsic Josephson junctions in $\text{Bi}_2\text{Sr}_2\text{CaCu}_2\text{O}_8$: Generation of Terahertz radiation and beyond — •REINHOLD KLEINER — Physikalisches Institut, Center for Quantum Science (CQ) and LISA⁺, Universität Tübingen

The layered superconductor $\text{Bi}_2\text{Sr}_2\text{CaCu}_2\text{O}_8$ (BSCCO) is known to intrinsically form a stack of Josephson tunnel junctions (IJJs). Each junction is formed by adjacent superconducting CuO_2 layers and the insulating BiO and SrO layers in between. Due to the fact that the BiO layers are coupled by van der Waals forces, stacks of consisting of only a few IJJs up to several thousands of IJJs can be created by using exfoliation methods combined with lithography. After an initial phase of investigations on small-sized stacks, in recent years the focus was on the generation of terahertz (THz) radiation, making use of stacks consisting of a large number of IJJs. The stacks mainly radiate in the frequency range between 0.5 THz and 2 THz, which inside the so-called THz gap. Beyond THz generation BSCCO received attention in the context of 2D materials and it was also shown recently that IJJ stacks can host electromagnetic modes acting as a discrete classical space-time crystal, developing periodic order both in space and time. In the talk, after some introduction, I will present the recent status on the field of THz generation. I will then turn to the possible realization of a discrete space-time crystal based on BSCCO IJJ stacks.

Plenary Talk PLV II Mon 14:00 H1

Topology and Chirality — •CLAUDIA FELSER — Max Planck Institute for Chemical Physics of Solids, Dresden, Germany — Laureate of the Max-Born-Prize 2022

Topology, a well-established concept in mathematics, has nowadays become essential to describe condensed matter. At its core are chiral electron states on the bulk, surfaces and edges of the condensed matter systems, in which spin and momentum of the electrons are locked parallel or anti-parallel to each other. Magnetic and non-magnetic Weyl semimetals, for example, exhibit chiral bulk states that have enabled the realization of predictions from high energy and astrophysics involving the chiral quantum number, such as the chiral anomaly, the mixed axial-gravitational anomaly and axions. The potential for connecting chirality as a quantum number to other chiral phenomena across different areas of science, including the asymmetry of matter and antimatter and the homochirality of life, brings topological materials to the fore.

Plenary Talk PLV III Mon 14:00 H2

Controlling and exploiting defects in diamond for Quantum Technologies — •MARK NEWTON, BEN GREEN, CHLOE NEWSOM, IMOGEN GULLICK, and GLORIA ZHAO — Department of Physics, University of Warwick, Coventry UK

Point defects in diamond have great potential for use in a range of quantum technologies. For example as single photon sources and quantum bits that can be exploited in quantum information processing and as the heart of sensors that will transform the way we do analytical science and medical imaging. The negatively charged nitrogen-vacancy centre is an amazing defect in diamond that possesses properties highly suited to many of these applications. However, it does have some challenging weaknesses and full exploitation of the optical and spin properties of this and other defects necessitates that we control their position, orientation and environment to optimise all of the desirable properties simultaneously, especially near the surface of the diamond. I will review our understanding of the production of intrinsic defects and present new data on the creation of defect complexes by doping, electron irradiation, short pulse laser irradiation, ion implantation and annealing. The success and failure of different combinations of processing steps to control and optimise the local defect environment will be discussed and the ongoing search for alternate colour centres with comparable spin properties and superior optical properties will be reviewed.

Plenary Talk PLV IV Tue 8:30 H1

Insights from Atomic-Scale Studies on Surfaces — •ULRIKE DIEBOLD — Institute of Applied Physics, TU Wien, Vienna, Austria

The arrangement of the top layer of atoms on a solid and the resulting electronic and chemical properties affect and sometimes even dominate its functionality. In the talk, I will showcase how we can use basic physical phenomena – tunneling, diffraction, and change in resonance frequencies – to measure surface properties in an atom-by-atom fashion. Such experiments can be interlinked tightly with theoretical computations by investigating well-defined samples in a controlled environment. Examples include assessing the acidity of individual surface atoms, pushing the size of catalytically-active nanoclusters to their physical limit, and extending ultrahigh-vacuum experiments to the liquid phase.

Plenary Talk PLV V Wed 8:30 H1

Towards useful quantum computing with superconducting qubits — •RAMI BARENS — Institute for Functional Quantum Systems (PGI-13), Forschungszentrum Jülich

One of the outstanding scientific challenges of this decade is the construction of an architecture and development of a methodology that can enable useful quantum computing. Superconducting quantum circuits have demonstrated unparalleled performance, by outperforming the world's most powerful supercomputers on a specific sampling task. Yet, applying quantum computing to real-world problems has remained elusive. The performance of current systems is limited, and the development of algorithms that make efficient use of present-day hardware is only starting. I will discuss the challenges in going from the current exploratory phase towards one where addressing real-world problems could be accomplished.

Plenary Talk PLV VI Wed 14:00 H1

Disordered Solids — •ANNETTE ZIPPELIUS — Institut für Theoretische Physik, Universität Göttingen, 37077, Germany — Laureate of the Max-Planck-Medal 2022

We discuss a phase of matter which is characterized by 1) random localization of the atoms or molecules and 2) a finite restoring force for static shear deformations. The following questions will be addressed: What is an appropriate order parameter for the amorphous solid state? How can we characterize its random structure? How do long range elastic correlations develop at the glass transition? These questions will be discussed by means of a statistical mechanical theory of disordered system as well as generalized hydrodynamics.

Plenary Talk PLV VII Wed 14:00 H2

Topological insulator lasers — •MORDECHAI SEGEV — Technion - Israel Institute of Technology

Topological Insulator Lasers are arrays of semiconductor lasers arranged on a photonic chip in a way that endows them with topological features. We utilize the topological features of robustness and nonzero group velocity, both associated with the topological edge states, to force injection locking of tens of semiconductor lasers, eventually giving rise to many lasers working together as a single high order radiation source. The concepts of topological insulator lasers will be reviewed, while current challenges and recent progress will be described.

Plenary Talk PLV VIII Thu 8:30 H1

Physics of Structure Formation in Living Systems — •STEPHAN GRILL — MPI-CBG, Dresden

One of the most remarkable examples of self-organized structure formation is the development of a complex organism from a single fertilized egg. With the identification of many molecules that participate in this process of morphogenesis, attention has now turned to capturing the physical principles that govern the emergence of biological form. What are the physical laws that govern the dynamics and the formation of structure in living matter? Much of the force generation that drives morphogenesis stems from the actomyosin cortical layer inside cells, which endows the surface of the cell with the ability to generate active forces and stresses that can drive reshaping. We combine theory and experiment and investigate how the actomyosin cell cortex self contracts, reshapes and deforms, and how these physical activities couple to regulatory biochemical pathways to give rise to the emergence of shape in living systems.

Plenary Talk PLV IX Thu 14:00 H1

Evolutionary transitions: universality, complexity and predictability — •RICARD SOLE — Universitat Pompeu Fabra, Barcelona, Spain — Santa Fe Institute, Santa Fe, USA

The evolution of life in our biosphere has been marked by several major innovations. Such major complexity shifts include the origin of cells, genetic codes or multicellularity to the emergence of language, cognition or even consciousness. Understanding the nature and conditions for evolutionary innovation is a major challenge for evolutionary biology. Along with data analysis, phylogenetic studies and dedicated experimental work, theoretical and computational studies are an essential part of this exploration. With the rise of synthetic biology, evolutionary robotics, artificial life and advanced simulations, novel perspectives to these problems have led to an emerging new synthesis, where evolutionary innovations can be understood in terms of phase transitions, as defined in physics. Such mapping (if correct) would help in defining a general framework to establish a theory of evolutionary change and the role played by chance and constraints in shaping living complexity.

Plenary Talk

PLV X Thu 14:00 H2

Semiconductor quantum optics: from artificial atoms to atomically thin materials — •JONATHAN FINLEY — Walter Schottky Institut, Am Coulombwall 4, 85748 Garching, Germany

Optically active confined spins in solids such as III-V semiconductor quantum dots (QDs), colour centres in diamond and atomic-scale defects in 2D-semiconductors are of interest for a wide range of applications in quantum science and technology. For example, in the context of photon-based quantum communication and computation electron and hole spins localized in single QDs can be used for the high rate ($\sim GHz$) on-demand generation of single photons with excellent Hong-Ou-Mandel (HOM) quantum indistinguishability, as well as entangled multi-photon cluster states. We will explore the factors currently limiting the performance of QD based non-classical light sources and discuss how methods derived from the quantum optical toolbox, such as incoherent spin pumping and coherent quantum state preparation can be used to both suppress unwanted re-excitation processes, that lead to multi-photon errors, while precisely timed stimulation pulses reduce the timing jitter of emit-

ted photons, leading to much improved HOM indistinguishability. For few-spin systems hosted by electrically tunable QD-molecules, we will show how selective optical-charge generation can be used to suppress coupling of S-T spin states to electric and magnetic field fluctuations. Finally, we will explore how spin states in 2D-semiconductors are highly sensitive to lattice and macroscopic vibrational modes, providing interesting perspectives in quantum sensing and metrology.

Plenary Talk

PLV XI Fri 8:30 H1

Spinwaves as experimental probes — •CHRISTIAN BACK — Physik-Department, TU München, Garching, Germany

Spin waves - the dynamic eigenmodes of magnetically ordered systems - are suitable as potential information carriers in future nanoscale microwave devices with frequencies ranging from a few GHz to several THz. It has been shown that their frequency, amplitude and phase can be relatively easily controlled. In this talk, I will revisit some of the fundamental properties of spin waves in thin magnetic films, show how we can image them with high resolution, and give examples of how they can also be used to detect fundamental properties such as spin-orbit fields.

Sessions

– Prize Talks –

Prize Talk

PRV I Mon 13:15 H1

Ultrafast topological switching of magnetic skyrmions — •FELIX BÜTTNER — Helmholtz-Zentrum Berlin, Berlin, Germany — Laureate of the Walter-Schottky-Prize 2022

Magnetic skyrmions are non-collinear arrangements of spins, characterized by a defining non-trivial topology and a quasi-particle character. Skyrmions can be of nanometer-scale size, even at room temperature and - upon suitable stimulation - they can move coherently within their hosting material. Both, the stability and the emergent quasi-particle dynamics of skyrmions, can be linked to their topology, and these exotic properties have widely inspired research in fundamental and applied physics alike. In this talk, I will first give an overview of the field of skyrmionics before discussing one particularly fascinating aspect in greater depth: the possibility to switch, i.e., nucleate or annihilate, magnetic skyrmions despite their topological protection. I will show that the topological nucleation energy barrier of skyrmions, which can be understood from a simple product of magnetic exchange energy and film thickness, can surprisingly be lifted by heating the system into a newly discovered fluctuation state. This allows the simultaneous nucleation of an extended array of skyrmions, even on a picosecond time scale, as we could evidence by direct experimental observation. I will discuss this mechanism in the context of topological phase transitions and conclude with a perspective on technological applications.

Prize Talk

PRV II Tue 13:15 H1

Water flows in carbon nanochannels: from quantum friction to carbon memories — •LYDÉRIC BOCQUET — Laboratoire de Physique, Ecole Normale Supérieure and CNRS, Paris — Laureate of the Gentner-Kastler-Prize 2022

In this talk, I will discuss various experimental and theoretical results that we obtained recently on the transport of water and ions in ultra-confinement. I will in particular focus on the odd properties of the water-carbon couple, which highlights a variety of strange transport properties. I will first discuss the ultra-fast, and radius dependent, flows of water in carbon nano-structures [1]. We demonstrate that this phenomenon is a consequence of an unconventional quantum friction at the water-carbon interface, taking its root in the coupling between

water collective modes with electronic excitations [2]. I will then explore far from equilibrium transport of ions across quasi two-dimensional slits. We predict that under an electric field, ions assemble into elongated clusters - as a consequence of a 2D Wien effect -, whose slow dynamics results in the emergence of long-term memory [3]. This phenomenon, known as the memristor effect, can be harnessed to build an elementary neuron. Experimental demonstrations of this effect in the 2D nanochannels allow for the development of elementary ion-based computing, with basic forms of Hebbian learning [4].

References [1] E. Secchi, et al., Nature 537 210 (2016) [2] N. Kavokine, M.-L. Bocquet and L. Bocquet, Nature, 602, 84-90 (2022) [3] P. Robin, N. Kavokine, and L. Bocquet, Science, 373, 687-691 (2021) [4] P. Robin, et al., submitted (2022).

Prize Talk

PRV III Wed 13:15 H1

Learning the stochastic dynamics of living systems across scales: from single cells to tissues — •DAVID BRÜCKNER — Institute of Science and Technology, Am Campus 1, 3400 Klosterneuburg, Austria — Laureate of the Gustav-Hertz-Prize 2022

Many biological phenomena, including embryo development, immune response, and cancer, rely on the coordinated movement of cells in complex environments. In all these processes, cells face a dual physical challenge: they navigate confining extra-cellular environments, in which they squeeze through thin constrictions; and they communicate with close-by cells to organize their collective behaviour. The motion of cells is powered by a complex machinery whose molecular basis is increasingly well understood. However, a quantitative understanding of the functional cell behaviours that emerge at the cellular scale remains elusive. This raises a central question: are there simple dynamical 'laws' that describe the dynamics of confined cell migration and cell-cell interactions? In this talk, I will discuss how we can use stochastic inference methods to learn the dynamics of migrating cells directly from observed experimental trajectories. I will show how these approaches give insight into the non-linear dynamics governing confined single cell migration, the pair-wise collisions of cancerous and healthy cell types, as well as collective cell migration at the tissue level.

Sessions

– Plenary, Ceremonial, Evening Talks and Discussions –

Lunch Talk

PSV I Mon 13:15 H2

Berufsbild: Wissenschaftsmanagement in der deutschen Raumfahrtagentur — •TOBIAS SALTZMANN — Deutsches Zentrum für Luft- und Raumfahrt (DLR), Bonn

It's no rocket science – Forschungsförderung im Spannungsfeld zwischen Industrie, Wissenschaft und Politik.

Lunch Talk

PSV II Tue 13:15 H2

Wissenschaftskommunikation - für wen eigentlich? — •NICOLAS WÖHRL, PETER KOHL und AXEL LORKE — Fakultät für Physik und SFB 1242, Universität Duisburg-Essen, 47048 Duisburg

Auch Physiker:innen sind gefragt, wenn es um Wissenschaftskommunikation geht, z.B. bei Themen wie Quantenkryptographie, alten und neuen Energietechniken oder dem Klimawandel. Wie notwendig (und manchmal schwierig) gelungene Kommunikation ist, wurde uns während der Corona-Krise eindrück-

lich vor Augen geführt. Forschende übernahmen eine wichtige Rolle als Mittler zwischen Fachliteratur und populärer Darstellung. So wurde Fehlinformationen und Verschwörungs"theorien" überzeugend entgegengetreten. Und zwar erfolgreich: Das "Wissenschaftsbarometer 2021" zeigt, dass während der Pandemie das Vertrauen in die Wissenschaft stieg. Systeme und Probleme werden komplexer, und wir brauchen eine informierte Öffentlichkeit, um wissenschaftsbasierte Entscheidungen zu treffen und umzusetzen. Dabei geht es nicht nur um Forschungsergebnisse, sondern auch darum, Prozesse und Methoden von wissenschaftlicher Arbeit transparent abzubilden - eine Aufgabe, die prinzipiell alle Forschenden übernehmen können. Im Vortrag diskutieren wir u. a.: Wie kann Öffentlichkeitsarbeit neben allen anderen Aufgaben in Forschung und Lehre gelingen? Welchen Stellenwert hat sie in der Ausbildung? Warum brauchen wir neben Pressestellen und Journalismus auch kommunikative Wissenschaftler:innen? Wie sollte Unterstützung für Forschende in Zukunft aussehen? Und welchen Nutzen hat die Kommunikation mit der Öffentlichkeit für die Wissenschaftler:innen selbst?

PSV III: Award Ceremony and Ceremonial Lecture

Time: Tuesday 14:30–17:15

Location: H1

Ceremonial Talk

PSV III H1

Quantum Dots for Green Quantum Technologies — •DIETER BIMBERG — TU Berlin and CIOMP of CAS Changchun — Laureate of the Stern-Gerlach-Medal 2020

Universal self-organization at surfaces of semiconductors leads to the formation of self-similar quantum dots (QDs). Their electronic and optical properties are close to those of atoms in a dielectric cage. All their energy levels are however only twofold degenerate [1]. The few particle states like excitons are strongly Coulomb-correlated due to the carrier localisation. Their energies depend on shape and size of the dots, such that positive, zero or negative biexciton binding energies and fine-structure splitting appear [2].

Applications of single, few and millions of QDs for novel Quantum Technologies will be elucidated.

a. Single QDs can be emitters of Q-bits on demand or entangled photons for future quantum cryptography systems. In electrically pumped RCLED structures, emission of q-bits at rates beyond 1 Gbit/s were shown [3, 4].

b. Hybridization of Flash and DRAMs, bringing together the advantages of both types of memories, is the "Holy Grail" of memories and ensures future memory development after the end of Moore's law. The goal of non-volatility (i.e. storage time > 10 years) can be achieved for the storage of holes in type I I (InGa)Sb QDs embedded in a (AlGa)P matrix [5].

c. The demand for higher data rates in optical networks, requires novel ultra-high bit rate, energy efficient sources. QD Lasers based on GaAs emit up to the

O-band at 1.3 μm , showing record low jitter and complete temperature stability up to 80°C. Passive mode-locking generates pulses in the sub-ps range at repetition rates up to 90 GHz. The hat spectrum of one single laser of several tens of closely spaced narrow lines is thus a potential pulse source for bit rates up to ≈ 6 Tbit/s using higher order modulation formats like DQPSK [6]

[1] M. Grundmann, O. Stier, D. Bimberg, *Pyramidal Quantum Dots – Strain Distribution, Optical Phonons, and Electronic Structure*, Phys. Rev. B **52**, 11969 (1995); O. Stier, M. Grundmann, D. Bimberg, *Electronic and optical properties of strained quantum dots modelled by 8-band k.p theory*, Phys. Rev. B **59**, 5688 (1999)

[2] S. Rodt, A. Schliwa, K. Pötschke, F. Guffarth, D. Bimberg, *Correlation of structural and few particle properties of self-organized InAs/GaAs quantum dots*, Phys. Rev. B **71**, 155325 (2005)

[3] A. Schliwa, M. Winkelkemper, A. Lochmann, E. Stock, D. Bimberg, *(InGa)As/GaAs quantum dots grown on a (111) surface as ideal sources of entangled photon pairs*, Phys. Rev. B **80**, 601307(R) (2009)

[4] W. Unrau, D. Bimberg, *Flying q-bits and entangled photons*, Laser Photonics Review **8**, 276 (Wiley, 2014)

[5] L. Bonato, F. I. Arikian, L. Desplanque, C. Coignon, X. Wallart, Yi Wang, P. Ruterana, D. Bimberg, *Hole Localization Energy of 1.18 eV in GaSb quantum dots embedded in GaP*, Phys. Stat. Sol (b) **10**, 1877 (2016)

[6] G. Eisenstein, D. Bimberg (eds.), *Green Photonics and Electronics* (Springer, 2017)

Evening Talk

PSV IV Tue 19:00 H1+H2

Grundlagenforschung für Nachhaltigkeit — •HARALD LESCH — LMU Physik, München Deutschland

Grundlagen der Physik sind meist weit weg von den direkten Anwendungen. Aber bei dem Thema Nachhaltigkeit haben wir keine Zeit mehr. Hier gilt es schnell und mutig darüber zu sprechen und auch zu handeln. Klimawandel und Energiewende sind beides Themen, deren Lösung unter Zeitdruck entwickelt werden muss. So zeigt sich die Thermodynamik als Mutter aller Theorien als wichtige Begrenzung unserer Möglichkeiten auch bei den erneuerbaren Energien. Die Forschung an komplexen Systemen liefert uns wichtige Hinweise über deren resiliente Eigenschaften. Und währenddessen müssen wir ständig versuchen im Land der physikalischen Optionen neue Möglichkeiten zu entdecken. Mit anderen Worten, es geht um Physik unter Druck, unter Zeitdruck.

Lunch Talk

PSV V Wed 13:15 H2

The German Research Foundation - Funding Opportunities for International Collaborations — •MICHAEL MÖSSLE, MARIO BOMERS, and JOANNA KOWALSKA — Deutsche Forschungsgemeinschaft, Bonn

The German Research Foundation (DFG) is the central funding organization for basic research in Germany. As a self-governing organization for science and research it offers a broad spectrum of funding opportunities from individual grants to larger coordinated programs. The talk will be focused on the DFG funding opportunities for international collaborations. In particular, we will cover the possibilities to include international partners in regular DFG funding schemes,

funding opportunities for bi- and multilateral projects and funding possibilities for early-career researchers like the Walter-Benjamin-Programme. This programme offers postdoctoral fellowships for a stay abroad as well as postdoctoral positions within Germany.

Discussion

PSV VI Thu 13:15 H1

Publizieren offen für den Umbruch? — •MARTIN WOLF — Fritz-Haber-Institut der MPG

Das wissenschaftliche Publikationswesen befindet sich zurzeit in einem Umbruch, der die traditionelle Rolle der Verlage in Frage stellt. Wunsch der Forschungsgemeinschaft sind allgemeine Zugänglichkeit zu wissenschaftlichen Ergebnissen („Open Access“), bei gleichzeitiger Kosten- und Datentransparenz und niedrigschwelligem Marktzugang für neue Akteure und Modelle. Dem steht ein sehr erfolgreiches, etabliertes Publikationswesen gegenüber, das den Autoren Kontinuität und Reputation verspricht und durch die Summe der Publikationsentscheidungen sowie Qualitäts- und Reputationskriterien der wissenschaftlichen Gemeinschaft gestützt wird. Ein Reformschritt ist die DEAL Vereinbarung, die „Publish & Read“ zu pauschalieren Kosten ermöglicht. Diese Themen sollen bei der Diskussionsveranstaltung von eingeladenen Sprechern adressiert werden, gefolgt von Beiträgen aus dem Publikum.

Lunch Talk

PSV VII Thu 13:15 H2

Berufsbild: Wissenschaftskommunikation und Museumsdidaktik — •KIM LUDWIG-PETSCH — Deutsches Museum München

Tutorials

TUT 1: Careers in Science (joint session MA/TUT)

Time: Sunday 16:00–17:30

Location: H1

Tutorial

TUT 1.1 Sun 16:00 H1

Careers in science: "To boldly go where no one has gone before" — •MANFRED FIEBIG — Department of Materials, ETH Zurich

What does it take to do a career in science and become a university professor? An obvious answer is: you have to do outstanding research. But just doing great science plays a surprisingly small part — and what defines scientific work as outstanding anyway? Then, you also need to communicate your findings well. The best result is worth little if you present it in an awful talk or manuscript. You also need to be "good with people", may these be your students or your colleagues.

Even luck can play an important role in a successful scientific career, but is very important to distinguish luck from "luck". I will refer to all these points and analyze what "being lucky" has actually to do with luck. I will present a list of points that I consider essential for a prosperous start into a scientific career. Some of these points are surprisingly unnoticed, so following them may put you ahead of the crowd.

Questions and discussion

TUT 2: 2D Quantum Materials and Heterostructures: From Fabrication to Applications (joint session HL/TUT)

Time: Sunday 16:00–18:20

Location: H2

Tutorial

TUT 2.1 Sun 16:00 H2

Discovering, Creating, and Exploring Novel Atomically-Thin Materials and Heterostructures — •JOSHUA ROBINSON — The Pennsylvania State University, University Park, PA, USA

The last decade has seen an exponential growth in the science and technology of two-dimensional materials. Beyond graphene, there is a huge variety of layered materials that range in properties from insulating to superconducting. Furthermore, heterogeneous stacking of 2D materials also allows for additional dimensionality for band structure engineering. In this talk, I will discuss recent breakthroughs in two-dimensional atomic layer synthesis and properties, including novel 2D heterostructures and realization of unique 2D allotropes of 3D materials (e.g. 2D metals and oxides). Our recent works demonstrate that the properties and doping of 2D materials, especially synthetic 2D materials, are extremely sensitive to the substrate choice. I will discuss substrate impact on 2D layer growth and properties, doping of 2D materials, selective area synthesis of 2D materials, and creating 2D allotropes from traditionally 3D materials for photonic and quantum applications. Our work and the work of our collaborators has led to a better understanding of how substrate not only impacts 2D crystal quality, but also doping efficiency in 2D materials, and stabilization of 3D materials at their quantum limit.

Tutorial

TUT 2.2 Sun 16:35 H2

Non-identical moire twins in bilayer graphene — •REBECA RIBEIRO-PALAU¹, EVERTON ARRIGHI¹, VIET-HUNG NGUYEN², MARIO DI LUCA¹, GAIA MAFFIONE¹, KENJI WATANABE³, TAKASHI TANIGUCHI³, DOMINIQUE MAILLY¹, and JEAN-CHRISTOPHE CHARLIER² — ¹Universite Paris-Saclay, CNRS, Centre de Nanosciences et de Nanotechnologies (C2N), 91120 Palaiseau, France — ²Institute of Condensed Matter and Nanosciences, Universite catholique de Louvain (UCLouvain), 1348 Louvain-la-Neuve, Belgium — ³National Institute for Materials Science, 1-1 Namiki, Tsukuba, Japan

I will present recent results which demonstrate that the moire superlattice formed by a bilayer graphene aligned with BN, is present every 60 deg, but the symmetry is broken between the 0 deg and 60 deg alignments, creating non-identical "moire twins" with different electronic properties. In particular, electron transport measurements display a fully developed valley Hall effect at 0 deg while on the contrary, it is completely absent at 60 deg. We explain this effect by performing numerical simulations, which highlight the central role of the atomic-scale structural relaxation of the second graphene layer. This in-plane atomic relaxation, different for the two alignments, impacts on the electronic band structure of our system. Our results demonstrate that in situ control of the rotational order provides a unique insight on the interplay between mechanical and electronic properties, and increases the possibilities for band-structure engineering on van der Waals heterostructures.

Tutorial

TUT 2.3 Sun 17:10 H2

Single-photon emitters in 2D materials — •STEFFEN MICHAELIS DE VASCONCELLOS — University of Münster, Institute of Physics and Center for Nanotechnology, Wilhelm-Klemm-Str. 10, 48149 Münster, Germany

Single-photon sources are key components for quantum technologies, such as communications, cryptography, computation, and metrology. Recently, the family of solid-state quantum light emitters was joined by single-photon sources in atomically thin materials [1]. Compared to 3D bulk materials, the 2D host crystals with their high structural flexibility allow for a high photon extraction efficiency, new methods for the deterministic creation, and convenient integration with photonic circuits.

In this tutorial, I will introduce the basic properties of single-photon emitters in different 2D van der Waals material systems and discuss present experimental methods for their creation, control, and coupling to photonic nanostructures.

[1] S. Michaelis de Vasconcellos et al., "Single-Photon Emitters in Layered Van der Waals Materials," Phys. Status Solidi B **2022**, 259, 2100566

Tutorial

TUT 2.4 Sun 17:45 H2

Introduction to 2D superconducting spintronics — •ELKE SCHEER — Department of Physics, University of Konstanz, Konstanz

The proximity effect between a conventional (s-wave) 3D superconductor (S) and a ferromagnet (F) can lead to the formation of Cooper pairs with parallel-spin (spin-triplet) alignment instead of the conventional antiparallel-spin (spin-singlet) state. The demonstration of spin-triplet generation in S/F systems [1,2] has inaugurated the field of superconducting spintronics aiming at developing energy-efficient spintronic devices [3]. Both superconductivity and ferromagnetism depend on the dimensionality of the system, but have been shown to exist in 2D or quasi-2D systems [4,5]. The possibility to exfoliate layered van der Waals (vdW) materials down to the few-layer limit [6] in combination with the existence of S and of F vdW materials makes this material basis in particular promising to explore triplet S in 2DS/2DF heterostructures. In this tutorial talk I will briefly recall the physics of SF spintronics in 3D, before I will describe the particular properties and challenges in the investigation of 2D-SF hybrid systems and give an overview over the so far best-studied material combinations and target devices.

[1] R. Keizer et al., Nature **95**, 825 (2006)

[2] A. Buzdin, Rev. Mod. Phys. **77**, 935 (2005)

[3] J. Linder & J. Robinson, Nature Phys. **11**, 307 (2015)

[4] B. Huang et al., Nature **546**, 270 (2017)

[5] M. Smidman et al., Rep. Prog. Phys. **80**, 036501 (2017)

[6] A. K. Geim & I. V. Grigorieva, Nature **499**, 419 (2013).

TUT 3: Functional Ferroics (joint session KFM/TUT)

Chair: Dr. Jan Schultheiß (Augsburg University / NTNU Trondheim)

Time: Sunday 16:00–18:15

Location: H3

Tutorial TUT 3.1 Sun 16:00 H3

Domains and domain walls in functional ferroics — •DENNIS MEIER — Department of Materials Science and Engineering, Norwegian University of Science and Technology — Center for Quantum Spintronics, Department of Physics, Norwegian University of Science and Technology, Trondheim, Norway

Ferroic materials with spontaneous magnetic or electric long-range order are a rich source for functional phenomena. Ferromagnets, for example, are used in hard discs and read heads, whereas ferroelectrics find application as capacitors, energy harvesters, and in tunnel junctions. The rich functionality of ferroic materials is closely linked to their domain structures and the responses of the domains to external stimuli.

In this tutorial, I will give an introduction to the fundamentals that underpin the domain formation in ferroics and discuss different microscopy techniques that allow for imaging electric and magnetic domains. Furthermore, we will talk about more exotic systems, such as improper ferroelectrics and multiferroics, where the interplay of coexisting order parameters gives rise to completely new domain and domain wall properties at the nanoscale. Open experimental challenges will be addressed, as well as future application and research opportunities.

Tutorial TUT 3.2 Sun 16:45 H3

Theory and simulations of ferroelectrics and related materials — •JORGE INIGUEZ — Luxembourg Institute of Science and Technology — University of Luxembourg

In this tutorial I will introduce the theoretical and simulation methods most frequently employed to investigate ferroelectrics and related materials (antiferroelectrics, multiferroics). I will start from the general electronic-structure methods that permit predictive calculations at the atomic scale, and introduce successive simplifications to eventually reach continuum field schemes that give us access to the mesoscale. I will illustrate the specificity and usefulness of the different approaches by presenting, for each of them, one or two classic examples

of application. In passing, this will allow me to emphasize the key role that simulation has played in our field, and to touch upon interesting possibilities for application in energy-related problems.

Jorge Íñiguez's work on ferroelectrics and related materials is mainly funded by the Luxembourg National Research Fund, currently through projects FNR/C18/MS/12705883/REFOX/Gonzalez, INTER/NWO/20/15079143, and C21/MS/15799044.

Tutorial TUT 3.3 Sun 17:30 H3

Atomic scale analysis of ferroic domain walls — •SHELLY CONROY — Department of Materials, London Centre of Nanotechnology, Imperial College London, United Kingdom

The dynamic interfaces of ferroic materials known as domain walls by-pass the static limitations of traditional nano-device designs. In contrast to hetero-interfaces between different materials, domain walls can be created, moved and removed via an applied stimulus. By combining multiple ferroic properties such as electricity and magnetism, new multi-functional interactive device applications are possible. As these mobile walls can be atomically sharp, it is essential to have physical characterisation at this scale spatially and time-resolved. In this tutorial, I will give an introduction to electron microscopy techniques starting with how to identify domain patterns in the bulk samples, and the most appropriate electron microscopy techniques to use with increasing magnification, leading to pico-meter characterisation. We will discuss some of the most recent advances in electron microscopy characterisation methods for ferroelectrics such as visualising electric charge density at sub-angstrom resolution, and the benefits of coupling polarisation characterisation with electron energy loss spectroscopy band structure analysis. We will then talk about how one can probe multiferroic properties such as magnetic field, strain and phonon modes. As one of the most exciting aspects of ferroic domain walls is their mobility, the various in situ options to investigate their dynamics will be detailed.

TUT 4: Stochastic Processes from Financial Risk to Genetics (joint session SOE/TUT/BP/DY)

Macroscopic and microscopic models from Economy to Biology must account for stochasticity on various levels. While classical physics strives for deterministic descriptions through differential equations from fundamental level to thermodynamics, many physics-based models on higher level explicitly include stochasticity from various sources. Discrete and continuous stochastic processes then become the mathematical foundation of these models. This tutorial highlights classical as well as current methods and approaches of probabilistic models and stochastic processes in physics, biology as well as socio-economic systems, thereby bridging the risk to extinction in genetics with its economic counterpart. (Session organized by Jens Christian Clausen.)

Time: Sunday 16:00–18:30

Location: H4

Tutorial TUT 4.1 Sun 16:00 H4

Diffusion approximations for particles in turbulence — •BERNHARD MEHLIG — University of Gothenburg, Gothenburg, Sweden

The subject of this tutorial is the dynamics of particles in turbulence, such as micron-sized water droplets in the turbulent air of a cumulus cloud. The particles respond in intricate ways to the turbulent fluctuations. Non-interacting particles may cluster together to form spatial patterns – even though the turbulent fluid is incompressible [1]. In this tutorial I explain how to understand spatial clustering using diffusion approximations, highlighting an analogy with Kramers' escape problem [2]. I introduce/review the necessary elements of diffusion theory. My goal is to give a pedagogical introduction to diffusion approximations in non-equilibrium statistical physics, using particles in turbulence as an example.

[1] K. Gustavsson and B. Mehlig, Statistical models for spatial patterns of heavy particles in turbulence, *Adv. Phys.* 65 (2016) 57 (read Sections 1, 3.1, and 6.1).

[2] H. A. Kramers, Brownian motion in a field of force and the diffusion model of chemical reactions, *Physica* 7 (1940) 284 (read up to eq. (17)).

Tutorial TUT 4.2 Sun 16:50 H4

Probabilities in physics, paradoxes and populations — •TOBIAS GALLA — Instituto de Física Interdisciplinaria Sistemas Complejos, IFISC (CSIC-UIB), Campus Universitat Illes Balears, E-07122 Palma de Mallorca, Spain

It is notoriously hard for humans to develop a good intuition for probabilities and stochastic processes. Our brains are not able to do this naturally, and there

are numerous mistakes which are easy to make. These mistakes are in fact made regularly in the press (sometimes perhaps deliberately). More worrisome, decision makers such as judges, doctors or politicians are also prone to mishandling probabilities. In this tutorial I will outline a few of these traps, and how to avoid them. I will also discuss the nature of probabilistic models of physical processes – is there genuine randomness in the world around us? I will then present a number of instances in which physics approaches combined with stochastic modelling can make a difference. As one example, I will outline experimental and theoretical results which highlight the importance of stochastic processes in population dynamics. Other examples will include stochastic processes in genetics, the evolution of cancer and in game theory.

Tutorial TUT 4.3 Sun 17:40 H4

Risk Revealed: Cautionary Tales, Understanding and Communication — •PAUL EMBRECHTS — Department of Mathematics, ETH Zürich

The title of the tutorial refers to a forthcoming book, to be published by Cambridge University Press, co-authored with Valérie Chavez-Demoulin (Lausanne) and Marius Hofert (Waterloo). Extreme Value Theory (EVT) offers a mathematical tool for the modeling of so-called What-If events, or stress scenarios. I will present several examples of risk-based decision-making and show how EVT can be used as part of the solution. The current pandemic has clearly shown that the communication of scientific evidence has a difficult stand in the ubiquitous environment of social media. I will discuss some examples of this struggle.

Entanglement Distribution in Quantum Networks (SYED)

jointly organised by
the Quantum Information Division (QI) and
the Semiconductor Physics Division (HL)

Christoph Becher,
Universität des Saarlandes
66123 Saarbrücken
christoph.becher@physik.uni-
saarland.de

Sven Höfling,
Julius-Maximilians-Universität,
97074 Würzburg
sven.hoefling@physik.uni-
wuerzburg.de

Peter van Loock,
Johannes Gutenberg-Universität,
55128 Mainz,
loock@uni-mainz.de

Scalable quantum networks, i.e., links between quantum nodes that are capable of storing and processing quantum information, promise advantages in many applications such as secure quantum communication, networks of distributed quantum sensors and connecting quantum computers. A common prerequisite is the ability to create and distribute entangled states as resource for establishing such a network. This symposium reviews some recent developments in the field of entanglement generation and distribution in quantum networks with solid state and photonic qubit systems, both from an experimental and conceptual perspective.

Overview of Invited Talks and Sessions

(Lecture hall H1)

Invited Talks

SYED 1.1	Wed	9:30–10:00	H1	A multi-node quantum network of remote solid-state qubits — •RONALD HANSON
SYED 1.2	Wed	10:00–10:30	H1	Quantum key distribution with highly entangled photons from GaAs quantum dots — •ARMANDO RASTELLI, SANTANU MANNA, SAIMON COVRE DA SILVA, GABRIEL UNDEUTSCH, CHRISTIAN SCHIMPF
SYED 1.3	Wed	10:30–11:00	H1	Entanglement distribution with minimal memory requirements using time-bin photonic qubits — •JOHANNES BORREGAARD
SYED 1.4	Wed	11:15–11:45	H1	Quantum photonics: interference beyond HOM and quantum networks — •STEFANIE BARZ
SYED 1.5	Wed	11:45–12:15	H1	Photonic cluster-state generation for memory-free quantum repeaters — •TOBIAS HUBER

Sessions

SYED 1.1–1.5	Wed	9:30–12:15	H1	Entanglement Distribution in Quantum Networks
--------------	-----	------------	----	--

Sessions

– Invited Talks –

SYED 1: Entanglement Distribution in Quantum Networks

Time: Wednesday 9:30–12:15

Location: H1

Invited Talk SYED 1.1 Wed 9:30 H1**A multi-node quantum network of remote solid-state qubits** — •RONALD HANSON — QuTech and Kavli Institute of Nanoscience Delft, Delft University of Technology, The Netherlands

Future quantum networks may harness the unique features of entanglement in a range of exciting applications, such as quantum computation and simulation, secure communication, enhanced metrology for astronomy and time-keeping as well as fundamental investigations. To fulfill these promises, a strong worldwide effort is ongoing to gain precise control over the full quantum dynamics of multi-particle nodes and to wire them up using quantum-photon channels.

We report on the realization of a three-node entanglement-based quantum network based on diamond NV centers and demonstrate several quantum network protocols without post-selection: the distribution of genuine multipartite entangled states across the three nodes, entanglement swapping through an intermediary node [1], and qubit teleportation between non-neighbouring nodes [2]. Moreover, we will discuss future challenges and prospects for quantum networks, including increasing the distance between nodes to metropolitan scales [3] and the role of next-generation integrated devices.

[1] M. Pompili, S.L.N. Hermans, S. Baier et al., *Science* 372, 259 (2021).[2] S.L.N. Hermans, M. Pompili et al., *Nature* 605, 663 (2022).

[3] Arian Stolk, Kian L. van der Enden et al., arXiv: 2202.00036 (2021).

Invited Talk SYED 1.2 Wed 10:00 H1**Quantum key distribution with highly entangled photons from GaAs quantum dots** — •ARMANDO RASTELLI, SANTANU MANNA, SAIMON COVRE DA SILVA, GABRIEL UNDEUTSCH, and CHRISTIAN SCHIMPF — Institute of Semiconductor and Solid State Physics, Johannes Kepler Universität Linz, Linz, Austria

Entanglement is one of the most peculiar phenomena in quantum science and a key resource for quantum technologies. More than two decades after the initial proposal [1], semiconductor quantum dots (QDs) are now beginning to outperform other sources for the generation of entangled photon pairs. Among different material systems, QDs in the (Al)GaAs platform have demonstrated the highest degree of polarization entanglement to date together with other appealing features for quantum science and technology [2]. In this talk, we will discuss the properties of GaAs QDs obtained by the droplet etching method and present recent results relevant to their application in quantum communication, i.e. entanglement-based quantum key distribution [3,4], quantum teleportation and entanglement swapping.

References [1] O. Benson et al., *Phys. Rev. Lett.* 84, 2513*2516 (2000). [2] S. F. C. da Silva et al., *Appl. Phys. Lett.* 119, 120502 (2021). [3] C. Schimpf et al., *Adv. Photonics* 3, (2021). [4] C. Schimpf et al., *Sci. Adv.* 7, eabe8905 (2021).

Invited Talk SYED 1.3 Wed 10:30 H1**Entanglement distribution with minimal memory requirements using time-bin photonic qudits** — •JOHANNES BORREGAARD — QuTech and Kavli Institute of Nanoscience, Delft University of Technology, 2628 CJ, Delft, The Netherlands

Generating multiple entangled qubit pairs between distributed nodes is a prerequisite for a future quantum internet. To achieve a practicable generation rate, standard protocols based on photonic qubits require multi-qubit quantum memories with long coherence times, which remains a significant experimental chal-

lenge. In this talk, I will discuss a novel protocol based on time-bin photonic qudits that allow for the simultaneous generation of multiple entangled pairs between two distributed qubit registers. By adopting the qudit protocol, the required memory time is independent of the transmission loss between the nodes in contrast to standard qubit approaches. Consequently, a significant boost of the capabilities of near-term quantum communication hardware can be achieved paving the way for a practical quantum internet.

15 min. break**Invited Talk** SYED 1.4 Wed 11:15 H1**Quantum photonics: interference beyond HOM and quantum networks** — •STEFANIE BARZ — Institute for Functional Matter and Quantum Technologies, University of Stuttgart, Germany — Center for Integrated Quantum Science and Technology (IQST), University of Stuttgart, Germany

In the first part of my talk, I will talk about recent experiments on quantum interference. I will show the impact of distinguishability and mixedness - two fundamental properties of quantum states - on quantum interference. I will demonstrate that these two properties can influence the interference of multiple particles in very different ways, leading to effects that cannot be observed in the interference of two particles alone. In the second part of my talk, I will report on our recent work in quantum networks. I will talk about a crucial component of a photonic quantum network: Bell-state measurements and report on an experimental demonstration of a scheme that allows obtaining a success probability of more than 50%. Finally, I will show the implementation of a novel protocol for networked key exchange using cluster states as a resource.

Invited Talk SYED 1.5 Wed 11:45 H1**Photonic cluster-state generation for memory-free quantum repeaters** — •TOBIAS HUBER — Lehrstuhl für Technische Physik, University of Würzburg, Würzburg, Germany

Many different hardware implementations show very promising results towards implementing quantum repeater nodes based on local memories [1]. While defects in diamond are currently the frontrunners, due to already demonstrated 3-node networks [2] and the possibility to enter the quantum repeater advantage regime (when comparing to direct links, considering losses at the given wavelength) [3], semiconductor quantum dots offer an intriguing alternative. Semiconductor quantum dots have the advantages of easy fabrication which leads to high device efficiencies. Furthermore, protocols for deterministic generation of linear photonic-cluster states do exist and have been already demonstrated experimentally [4]. With only moderate resource overhead a quantum repeater graph state can be fused from linear cluster states, opening the pathway towards memory-less 3rd generation quantum repeaters.

In this talk I will present our recent advances in device design and cluster-state generation with semiconductor quantum dots.

[1] van Loock et al. *Adv. Quantum Technol.* 3, 1900141 (2020)[2] Pompili et al. *Science* 372, 259-264 (2021)[3] Bhaskar et al. *Nature* 580, 60-64 (2020)[4] Schwartz et al. *Science* 354, 434 (2016)

Frontiers of Electronic-Structure Theory: Focus on Artificial Intelligence Applied to Real Materials (SYES)

jointly organised by
the Surface Science Division (O),
the Metal and Material Physics Division (MM),
the Thin Films Division (DS) and
the Semiconductor Physics Division (HL)

Michele Ceriotti
EPFL COSMO
MXG 337 - Station 12
CH-1015 Lausanne
michele.ceriotti@epfl.ch

Georg Kresse
University of Vienna
Sensengasse 8/12
A-1090 Wien
georg.kresse@univie.ac.at

Mariana Rossi
MPI for the Structure and Dynamics of Matter
Luruper Chaussee 149, Geb. 99
22761 Hamburg
mariana.rossi@mpsd.mpg.de

Machine learning methods have gained a prominent spot in the research of materials and molecules, especially in the context of the atomic-scale modeling of their properties. The growing understanding of how machine-learning methods should be adapted to the specific requirements of the field is making them progressively more effective and easy to use. Machine-learning techniques use the predictions of electronic-structure theory to train surrogate models that can compute the same properties with similar accuracy at much reduced cost. The combination of physics-based and data-driven paradigms is extending dramatically the reach of electronic-structure theory, as its predictive accuracy can now be applied to more complex, larger-scale problems and longer timescales. The field has been evolving so fast that in the past years we have witnessed considerable breakthroughs enabled by this combination: first-principles accuracy assessment of finite-temperature thermodynamics, including also subtle effects such as quantum nuclear fluctuations, has become commonplace; predictions of microscopic quantities beyond the interatomic potential energy are making it possible to incorporate functional properties into a fully-predictive machine-learning framework; inverse design and generative models are simplifying the search of configurational and composition spaces for compounds with optimal performance; including information and training data calculated from methods that go beyond density functional theory allows to make predictions systematically improvable.

Overview of Invited Talks and Sessions

(Lecture hall H1)

Invited Talks

SYES 1.1	Thu	15:00–15:30	H1	Machine-learning-driven advances in modelling inorganic materials — •VOLKER L. DERINGER
SYES 1.2	Thu	15:30–16:00	H1	Machine-Learning Discovery of Descriptors for Square-Net Topological Semimetals — •EUN-AH KIM
SYES 1.3	Thu	16:00–16:30	H1	Four Generations of Neural Network Potentials — •JÖRG BEHLER
SYES 1.4	Thu	16:30–17:00	H1	Using machine learning to find density functionals — •KIERON BURKE
SYES 1.5	Thu	17:00–17:30	H1	Coarse graining for classical and quantum systems — •CECILIA CLEMENTI

Sessions

SYES 1.1–1.5	Thu	15:00–17:30	H1	Frontiers of Electronic-Structure Theory: Focus on Artificial Intelligence Applied to Real Materials
--------------	-----	-------------	----	---

Continuation as topical sessions in O

O 43.1–43.10	Wed	10:30–13:00	S054	Frontiers of Electronic Structure Theory: Focus on Artificial Intelligence Applied to Real Materials 1
O 50.1–50.12	Wed	15:00–18:00	S054	Frontiers of Electronic Structure Theory: Focus on Artificial Intelligence Applied to Real Materials 2
O 67.1–67.9	Thu	10:30–12:45	S054	Frontiers of Electronic Structure Theory: Focus on Artificial Intelligence Applied to Real Materials 3
O 83.1–83.10	Fri	10:30–13:00	S054	Frontiers of Electronic Structure Theory: Focus on Artificial Intelligence Applied to Real Materials 4

Sessions

– Invited Talks –

SYES 1: Frontiers of Electronic-Structure Theory: Focus on Artificial Intelligence Applied to Real Materials

Time: Thursday 15:00–17:30

Location: H1

Invited Talk

SYES 1.1 Thu 15:00 H1

Machine-learning-driven advances in modelling inorganic materials — •VOLKER L. DERINGER — University of Oxford, Oxford, UK

Understanding the links between structures and properties of materials is an important research challenge. Computer simulations based on quantum-mechanical methods give access to small-scale models, but quickly reach their limits when structurally complex systems are to be studied. Here, I will showcase recent advances in modelling inorganic functional materials that have been enabled by machine learning (ML) based interatomic potentials. Specifically, I will demonstrate the power of ML-driven simulations in exploring the structures of amorphous elemental systems, at ambient and high pressure, and I will discuss future perspectives for modelling compositionally more complex materials.

Invited Talk

SYES 1.2 Thu 15:30 H1

Machine-Learning Discovery of Descriptors for Square-Net Topological Semimetals — •EUN-AH KIM — Cornell University, Ithaca, NY, USA

The accumulation of massive amounts of materials data motivates data-based machine learning (ML) approaches. However, an extensive database of materials relying on high-throughput density functional theory (DFT) can be unreliable for emergent properties. Much needed is an approach that can articulate and build on expert human researchers' insights. The tolerance factor introduced in Refs [1-2] articulates a chemical insight for identifying topological semimetals among square-net materials and presents an opportunity to develop such a human-machine synergy. Hence, we developed a supervised-unsupervised hybrid approach combining non-linear Gaussian Process (GP) regression [3] with supervised metric learning to discover descriptors for topological semimetals. Simultaneously, we curated a database containing 1279 square-net materials featuring different physical and chemical attributes and the binary label for the topological property associated with each material. Application of the GP model to the database rediscovers the tolerance factor and offers new theoretical insight.

[1] Klemenz, et al, *J. Am. Chem. Soc.* 2020, 142, 13, 6350-6359

[2] Klemenz, et al, *Annual Review of Materials Research* 2019 49:1, 185-206

[3] D. Milios, et al, *Advance in Neural Information Processing Systems*, page 11, 2018

Invited Talk

SYES 1.3 Thu 16:00 H1

Four Generations of Neural Network Potentials — •JÖRG BEHLER — Universität Göttingen, Germany

A lot of progress has been made in recent years in the development of machine learning potentials for atomistic simulations, with neural network potentials (NNPs) being an important example. While the first generation of NNPs has been restricted to small systems, the second generation extended the applicability of ML potentials to high-dimensional systems containing thousands of atoms by constructing the total energy as a sum of environment-dependent atomic energies. Long-range electrostatic interactions can be included in third-generation

NNPs employing environment-dependent charges, but only recently limitations of this locality approximation could be overcome by the introduction of fourth-generation NNPs, which are able to describe non-local charge transfer using a global charge equilibration step. In this talk an overview about the historical evolution of high-dimensional neural network potentials will be given along with an overview of typical applications in large-scale atomistic simulations.

Invited Talk

SYES 1.4 Thu 16:30 H1

Using machine learning to find density functionals — •KIERON BURKE — University of California, Irvine, USA

Over the past decade, advances in machine learning have led to the creation of new approximate density functionals. I will review this area, with an emphasis on very recent developments. How do such functionals compare to those of human design? What are their advantages and their limitations? For example, can they work for strongly correlated systems? I will consider both the exchange-correlation energy used in Kohn-Sham DFT and the non-interacting kinetic energy functional, needed to bypass the KS equations.

• How Well Does Kohn-Sham Regularizer Work for Weakly Correlated Systems? B. Kalita, R. Pederson, J. Chen, L. Li, and K. Burke, *J. Phys. Chem. Lett.* (2022).

• Machine learning and density functional theory R. Pederson, B. Kalita, and K. Burke, *Nat. Rev. Phys.* (2022).

• Kohn-Sham Equations as Regularizer: Building Prior Knowledge into Machine-Learned Physics L. Li, S. Hoyer, R. Pederson, R. Sun, E. Cubuk, P. Riley, and K. Burke, *Phys. Rev. Lett.* 126, 036401 (2021).

• Using Machine Learning to Find New Density Functionals B. Kalita and K. Burke, Article in Roadmap on Machine Learning in Electronic Structure (2022).

Invited Talk

SYES 1.5 Thu 17:00 H1

Coarse graining for classical and quantum systems — •CECILIA CLEMENTI — Freie Universität Berlin, Germany

The last years have seen an immense increase in high-throughput and high-resolution technologies for experimental observation as well as high-performance techniques to simulate molecular systems at a microscopic level, resulting in vast and ever-increasing amounts of high-dimensional data. However, experiments provide only a partial view of the molecular processes and are limited in their temporal and spatial resolution. On the other hand, simulations are still not able to completely characterize large and/or complex molecular processes over long timescales, thus leaving significant gaps in our ability to study these processes at a physically relevant scale. We present our efforts to bridge these gaps, by combining statistical physics with state-of-the-art machine-learning methods to design optimal coarse models for complex macromolecular systems. We derive simplified molecular models to reproduce the essential information contained both in microscopic simulation and experimental measurements.

From Physics and Big Data to the Design of Novel Materials (SYNM)

jointly organised by
the Metal and Material Physics Division (MM),
the Chemical and Polymer Physics Division (CPP),
the Semiconductor Physics Division (HL), and
the Thin Films Division (DS)

Jörg Neugebauer
Max-Planck-Institut für
Eisenforschung
Düsseldorf
neugebauer@mpie.de

Matthias Scheffler
Fritz-Haber-Institut der
Max-Planck-Gesellschaft
Berlin
scheffler@fhi-berlin.mpg.de

Kurt Kremer
Max-Planck-Institut für
Polymerforschung
Mainz
kremer@mpip-mainz.mpg.de

Combining concepts from big data analytics with experimental and theoretical techniques in solid state physics has opened exciting new routes to designing materials with superior mechanical, electronic or optical properties as well as to enhance resolution and performance of established experimental techniques as e.g. electron microscopy, x-ray diffraction, or atom probe tomography. The symposium will bring together leading experts who pioneer the application of these techniques for their respective fields. The intention is to show success stories but also to critically discuss present limitations as well as emerging areas. A critical aspect that will be in the focus of the symposium is that big data analytics alone, i.e. without a deep understanding of the underlying physics, turns out to be insufficient in successfully addressing experiment or materials related challenges.

Overview of Invited Talks and Sessions

(Lecture hall H1)

Invited Talks

SYNM 1.1	Mon	15:00–15:30	H1	How to tackle the "I" in FAIR? — •CLAUDIA DRAXL
SYNM 1.2	Mon	15:30–16:00	H1	Beyond the average error: machine learning for the discovery of novel materials — •MARIO BOLEY, SIMON TESHUVA, FELIX LUONG, LUCAS FOPPA, MATTHIAS SCHEFFLER
SYNM 1.3	Mon	16:00–16:30	H1	The Phase Diagram of All Inorganic Materials — •CHRIS WOLVERTON
SYNM 1.4	Mon	16:45–17:15	H1	Automated data-driven upscaling of transport properties in materials — •DANNY PEREZ, THOMAS SWINBURNE
SYNM 1.5	Mon	17:15–17:45	H1	Data-driven understanding of concentrated electrolytes — •ALPHA LEE

Sessions

SYNM 1.1–1.5	Mon	15:00–17:45	H1	From Physics and Big Data to the Design of Novel Materials
--------------	-----	-------------	----	---

Sessions

– Invited Talks –

SYNM 1: From Physics and Big Data to the Design of Novel Materials

Time: Monday 15:00–17:45

Location: H1

Invited Talk

SYNM 1.1 Mon 15:00 H1

How to tackle the "I" in FAIR? — •CLAUDIA DRAXL — Physics Department, Humboldt-Universität Berlin, Germany

Veracity, one of the 4V challenges of Big Data, is an issue for the FAIRness of materials-science results. This concerns in particular, the interoperability. On the computational side, the precision of different DFT codes was thoroughly investigated [1]. Later, it was demonstrated how ultimate precision for molecules and solids can be reached [2] and how different methodology impacts the results [3]. Also code-specific uncertainties coming from numerical settings were assessed [4]. More recently, we demonstrated [5] how a spectral fingerprint, combined with a similarity metric, can be used for establishing quantitative relationships between materials data. Besides the identification of electronically similar materials, this approach can be used for assessing uncertainty in data that potentially come from different sources. Various examples highlight how to quantify differences between measured optical spectra or the impact of methodology and computational parameters on calculated spectral properties. Moreover, combining our fingerprint with a clustering approach allows us to explore materials spaces in view of finding (un)expected trends or patterns [6].

[1] K. Lejaeghere et al., *Science* 351, aad3000 (2016). [2] A. Gulans et al., *PRB* 97, 161105(R) (2018). [3] A. Gulans and C. Draxl, <https://arxiv.org/abs/2204.02751> [4] C. Carbogno, et al., *npj Comput. Mater.* 8, 69 (2022). [5] M. Kuban, et al., *MRS Bulletin Impact* (2022); <https://arxiv.org/abs/2204.04056> [6] M. Kuban et al., <https://arxiv.org/abs/2201.02187>

Invited Talk

SYNM 1.2 Mon 15:30 H1

Beyond the average error: machine learning for the discovery of novel materials — •MARIO BOLEY¹, SIMON TESHUVA¹, FELIX LUONG¹, LUCAS FOPPA², and MATTHIAS SCHEFFLER² — ¹Monash University — ²Fritz Haber Institute of the Max Planck Society

Machine learning models promise to radically accelerate the discovery of novel functional materials by rapidly screening huge candidate spaces for materials with rare combinations of properties. While current models allow for accurate property prediction on average, e.g., indicated by the root mean squared error, such measures are only loosely connected to materials discovery. They do not capture that discovery is a process, where models are repeatedly retrained with new data. Moreover, they depend on some fixed sampling distribution, which is irrelevant when actively exploring candidates and distorted by the overwhelming mass of mediocre materials. Finally, they do not reflect model uncertainty, which is a crucial parameter for effective active learning strategies. Here, based on the example of searching for stable and stress resistant double perovskites under a bandgap constraint, we evaluate models in terms of their optimisation regret—a function of consecutive improvements of the target property by newly discovered materials. In particular, we employ non-parametric regression models (Gaussian processes and random forests) within the “expected improvement” search strategy. Starting from an initial dataset of 815 computed double perovskite properties, we are able to discover materials with improved target values already within the first 20 newly acquired data points.

Invited Talk

SYNM 1.3 Mon 16:00 H1

The Phase Diagram of All Inorganic Materials — •CHRIS WOLVERTON — Northwestern University, Evanston, IL USA

One of the holy grails of materials science, unlocking structure-property relationships, has largely been pursued via bottom-up investigations of how the arrangement of atoms and interatomic bonding in a material determine its macro-

scopic behavior. Here we consider a complementary approach, a top-down study of the organizational structure of networks of materials, based on the interaction between materials themselves. We demonstrate the utility of applying network theory to materials science in two applications: First, we unravel the complete *phase stability network of all inorganic materials* as a densely-connected complex network of 21,000 thermodynamically stable compounds (nodes) interlinked by 41 million tie-lines (edges) defining their two-phase equilibria, as computed by high-throughput density functional theory. Using the connectivity of nodes in this phase stability network, we derive a rational, data-driven metric for material reactivity, the *nobility index*, and quantitatively identify the noblest materials in nature. Second, we apply network theory to the problem of synthesizability of inorganic materials, a grand challenge for accelerating their discovery using computations. We use machine-learning of our network to predict the likelihood that hypothetical, computer generated materials will be amenable to successful experimental synthesis.

15 min. break

Invited Talk

SYNM 1.4 Mon 16:45 H1

Automated data-driven upscaling of transport properties in materials — •DANNY PEREZ¹ and THOMAS SWINBURNE² — ¹Los Alamos National Laboratory, Los Alamos, USA — ²CRNS/CINaM, Marseille, France

Transport properties of complex defects are crucial factors that control the performance of many material systems, e.g., the radiation tolerance of materials for nuclear fusion or fission applications. Characterizing the transport of complex defects is however notoriously tedious and time-consuming, especially as the defects grow, leading to a combinatorial explosion in the number of possible conformations and local transition pathways. I will present a large-scale data-driven approach to automatically obtain reduced-order models of defect evolution, transport coefficients, as well as effective continuum transport equations, from large number of short molecular dynamics (MD) simulations. The optimal MD simulations to carry out are identified on-the-fly using a Bayesian uncertainty quantification framework and automatically executed on a massively-parallel task-execution infrastructure. We show how this microscopic information can be systematically and efficiently upscaled into meso and macro-scale representations that can inform microstructure evolution models.

Invited Talk

SYNM 1.5 Mon 17:15 H1

Data-driven understanding of concentrated electrolytes — •ALPHA LEE — Department of Physics, University of Cambridge, Cambridge, UK

Electrolytes play an important role in a plethora of applications ranging from energy storage to biomaterials. Notwithstanding this, the structure and dynamics of concentrated electrolytes remain enigmatic. In this talk, I will show how machine learning can unravel hidden patterns in simulations of electrolytes, helping us understand the structure of concentrated electrolytes and mechanisms of ion transport. In the first part of my talk, I will illustrate how debates such as extent of “ion pairing” in concentrated electrolytes can be addressed using methods in unsupervised machine learning and Bayesian hypothesis testing. In the second part of my talk, I will discuss how machine learning help relate local ionic structure to molar ionic conductivity. This furnishes microscopic insights on what are the drivers of conductivity as a function of ion concentrations. More broadly, I will discuss the role that machine learning can play in not only delivering predictive models, but also serving as an “intuition pump” to understand complex soft matter systems.

Frontiers of Orbital Physics: Statics, Dynamics, and Transport of Orbital Angular Momentum (SYOP)

jointly organised by
the Magnetism Division (MA),
the Surface Science Division (O),
the Crystalline Solids and their Microstructure Division (KFM),
the Thin Films Division (DS),
the Semiconductor Physics Division (HL) and
the Low Temperature Physics Division (TT)

Ingrid Mertig
Martin-Luther-Universität Halle-Wittenberg
06099 Halle
ingrid.mertig@physik.uni-halle.de

The interplay of orbital, spin, and lattice leads to not only exotic phases of matter such as orbital ordering in multiferroic materials and orbital Chern insulator states in twisted bilayer graphene but also dynamic phenomena including orbital Hall effect, orbital torque, and topological orbital magnetoelectric response. While so far the focus has been on spin currents, orbital currents, the flow of the electrons with finite orbital angular momentum, is found to be extremely efficient in many materials and can outperform conventional spin current effects. As recently demonstrated, orbital currents can additionally play a pivotal role in generating spin currents thus leading to torques with unprecedented amplitude to manipulate magnetization. On the other hand, optical means including vortex beams provide a potentially outstanding means of generating and manipulating orbital order and orbital transport. So far these effects have been observed in metallic heterostructures where light metals and their oxides generate strong orbital currents as well as oxidic 2DEG heterostructures that show efficient orbital to charge conversion thus showing that orbital currents can play a role in many systems. Developing methods and materials for harnessing orbital currents can thus potentially have significant impact and open a new direction in spintronics research. This session brings experts on the orbital physics from different areas of condensed matter physics in one place to promote collaborations beyond the boundaries of each community, share knowledge on cutting edge theoretical and experimental methods, and discuss challenges and future directions of the orbital physics. The invited speakers include not only experts on oxide multiferroic materials and spintronic devices but also on new experimental techniques that can unambiguously detect the orbital ordering and dynamics in solids and optical methods.

Overview of Invited Talks and Sessions

(Lecture hall H1)

Invited Talks

SYOP 1.1	Mon	9:30–10:00	H1	Orbital degeneracy in transition metal compounds: Jahn-Teller effect, spin-orbit coupling and quantum effects — •DANIEL KHOMSKII
SYOP 1.2	Mon	10:00–10:30	H1	Orbital magnetism out of equilibrium: driving orbital motion with fluctuations, fields and currents — •YURIY MOKROUSOV
SYOP 1.3	Mon	10:30–11:00	H1	Orbitronics: new torques and magnetoresistance effects — •MATHIAS KLÄUI
SYOP 1.4	Mon	11:15–11:45	H1	Orbital and total angular momenta dichroism of the THz vortex beams at the antiferromagnetic resonances — •ANDREI SIRENKO
SYOP 1.5	Mon	11:45–12:15	H1	Observation of the orbital Hall effect in a light metal Ti — •GYUNG-MIN CHOI

Sessions

SYOP 1.1–1.5	Mon	9:30–12:15	H1	Frontiers of Orbital Physics: Statics, Dynamics, and Transport of Orbital Angular Momentum
--------------	-----	------------	----	---

Sessions

– Invited Talks –

SYOP 1: Frontiers of Orbital Physics: Statics, Dynamics, and Transport of Orbital Angular Momentum

Time: Monday 9:30–12:15

Location: H1

Invited Talk

SYOP 1.1 Mon 9:30 H1

Orbital degeneracy in transition metal compounds: Jahn-Teller effect, spin-orbit coupling and quantum effects — •DANIEL KHOMSKII — II Physikalisches Institut Universitaet zu Koeln Zulpicher Str. 77 50937 Koeln, Germany

Transition metal compounds with orbital degeneracy display a number of specific interesting properties [1, 2]. Among them there are first of all the cooperative Jahn-Teller (JT) effect and corresponding orbital ordering. For t_{2g} electrons also spin-orbit coupling (SOC) may play crucial role: for these states orbital moment is not quenched by crystal field. There may be a very nontrivial effects connected with the mutual influence of Jahn-Teller effect and SOC. In most cases SOC suppresses JT effect, but there are situation in which it can instead promote, activate it. Also very nontrivial quantum effects can occur in this case. In my talk, after a short general introduction, I will discuss in particular this mutual interplay of JT effect and SOC for different situations [3, 4]. [1] Daniel I. Khomskii and Sergey V. Streltsov, “Orbital Effects in Solids: Basics, Recent Progress, and Opportunities”, *Chem. Rev.* 121, 2992-3030 (2021) [2] D.I. Khomskii, “Orbital physics: glorious past, bright future”, *ECS J. Solid State Sci. Technol.* 11, 054004 (2022) (special issue in honour of 100 birthday of J.B. Goodenough) [3] S. V. Streltsov, D. I. Khomskii, “Jahn-Teller effect and spin-orbit coupling: friends or foes?”, *Phys. Rev. X* 10, 031043 (2020) [4] Sergey V. Streltsov, Fedor V. Temnikov, Kliment I. Kugel, and Daniel I. Khomskii, “Interplay of the Jahn-Teller Effect and Spin-Orbit Coupling: The Case of Trigonal Vibrations”, *Phys. Rev. B* 105, 205142 (2022)

Invited Talk

SYOP 1.2 Mon 10:00 H1

Orbital magnetism out of equilibrium: driving orbital motion with fluctuations, fields and currents — •YURIY MOKROUSOV — Forschungszentrum Jülich GmbH, Jülich, Germany — Johannes Gutenberg-University Mainz, Mainz, Germany

In modern spintronics properties of non-equilibrium orbital polarization and orbital currents start to attract significant attention. In this talk we will review the theory of orbital magnetism in low-symmetric crystals and corresponding current-induced orbital magnetization. We will in particular show that applied electrical currents and optical pulses can drive non-equilibrium orbital magnetism and currents of orbital angular momentum. These orbital currents can be used to transmit angular momentum over large distances in solids, and can be utilized to exert sizeable orbital torques on magnetization thus enabling magnetic switching even in light materials with weak spin-orbit interaction. Moreover, we will underline that in fluctuating magnets spin excitations can mediate a significant orbital response which can be coupled to temperature gradients so as to ignite thermal orbital currents. We will thus attempt to promote a paradigm that unleashing non-equilibrium orbital physics and entanglement of spin and orbital degrees of freedom in diverse classes of materials can lead to much richer physics than previously expected, and might provide a key to realization of novel properties of matter out of equilibrium as well as energy-efficient applications.

Invited Talk

SYOP 1.3 Mon 10:30 H1

Orbitronics: new torques and magnetoresistance effects — •MATHIAS KLÄUI — Institute of Physics, Johannes Gutenberg University Mainz, 55099 Mainz, Germany

Experimentally, orbital currents for efficient manipulation of magnetization have only recently started to be explored. We studied spin orbit torques generated in TmIG/Pt/(Cu(O)_x) heterostructures. Varying the CuO_x and Pt layer thicknesses, we realized a 16x increase of the spin orbit torques exerted on the TmIG

compared to conventional TmIG/Pt [1]. Such an enhancement is extremely surprising if one considers only conventional spin-charge interconversion based on spin orbit coupling effects and given the low spin-orbitcoupling of Cu and Cu(O)_x one does not expect large torques. However, the results can be naturally explained as Cu(O)_x can generate large orbital currents that are then converted to spin currents in the Pt layer, which then manipulate the TmIG extremely efficiently. In addition, we found in Py/Cu(O)_x a Orbital Rashba-Edelstein Magnetoresistance effect related to the conventional spin Hall magnetoresistance [2]. In particular in this work, the length scale of the orbital to spin current conversion in Py could be identified as a key step to harnessing orbital currents efficiently even without a heavy metal-based orbital to spin conversion layer [3]. [1] S. Ding, MK et al., *Phys. Rev. Lett.* 125, 177201 (2020) [2] S. Ding, MK et al., *Phys. Rev. Lett.* 128, 067201 (2022) [3] D. Go, MK et al., *Perspectives Review in EPL* 135, 37001 (2021)

15 min. break**Invited Talk**

SYOP 1.4 Mon 11:15 H1

Orbital and total angular momenta dichroism of the THz vortex beams at the antiferromagnetic resonances — •ANDREI SIRENKO — Department of Physics, New Jersey Institute of Technology, Newark, New Jersey 07102, USA

Light beams with orbital angular momentum (OAM), or vortex beams, can couple to magnetism exhibiting dichroisms in a magnetized medium. Terahertz (THz) vortex beams with various combinations of the orbital angular momentum $L = +/-1, +/-2, +/-3$, and $+/-4$ and spin angular momentum $S = +/-1$, or conventional circular polarization, were used for studies of the magnon spectra at the antiferromagnetic resonance conditions in TbFe₃(BO₃)₄ and Ni₃TeO₆ single crystals. In both materials we observed strong vortex beam dichroism for the magnon doublet, which is split in an external magnetic field applied along the spin ordering direction. The absorption conditions at the magnon frequencies depend on the total angular momentum of light J that is determined by the combination of the spin and orbital angular momenta: $J = S + L$. For the higher orders of l , the selection rules for AFM resonances dictated by l completely dominate over that for conventional circular polarization. Our results demonstrate the high potential of the vortex beams with OAM as a new spectroscopic probe of magnetism in matter. This work was performed in collaboration with T. N. Stanislavchuk, P. Marsik, L. Bugnon, M. Soulier, C. Bernhard, V. Kiryukhin, and S.-W. Cheong.

Invited Talk

SYOP 1.5 Mon 11:45 H1

Observation of the orbital Hall effect in a light metal Ti — •GYUNG-MIN CHOI — Sungkyunkwan University, Suwon, Korea

The orbital angular momentum is a core ingredient of orbital magnetism, spin Hall effect, giant Rashba spin splitting, orbital Edelstein effect, and spin-orbit torque. However, its experimental detection is tricky. In particular, direct detection of the orbital Hall effect remains elusive despite its importance for the electrical control of magnetic nanodevices. Here we report the direct observation of the orbital Hall effect in a light metal Ti1. The Kerr rotation by the accumulated orbital magnetic moment is measured at Ti surfaces, whose result agrees with theoretical calculations semi-quantitatively. As another evidence, we measured the orbital torque in the Ti/ferromagnet heterostructures, from which we determine the orbital Hall angle >0.21 . Our experimental results confirm the orbital Hall effect in a light metal Ti and hint at opportunities in the emerging field of orbitronics.

High Yield Devices for Photonic Quantum Implementations (SYPQ)

jointly organised by
the Semiconductor Physics Division (HL) and
the Working Group young Leaders in Physics (AGyouLeaP)

Simone Portalupi
University of Stuttgart
s.portalupi@ihfg.uni-stuttgart.de

Doris Reiter
TU Dortmund
doris.reiter@tu-dortmund.de

Stephan Götzinger
MPI Erlangen
stephan.goetzinger@mpl.mpg.de

The symposium aims at discussing the challenges and achievements in realizing photonic devices for quantum applications. This will cover growth, fabrication, quantum optical measurements, and theoretical modelling. Platforms like semiconductors, organic molecules, and transparent materials will be examples of the discussed topics. Particular attention will be posed in discussing and selecting results which have a clear impact in transferring quantum technologies to real world implementations. Focus will be given as well to all techniques that allows boosting not only the device performances but also the fabrication yield (ideally to mass production), like deterministic technologies, lithography and 3D printed approaches.

Overview of Invited Talks and Sessions

(Lecture hall H1)

Invited Talks

SYPQ 1.1	Tue	9:30–10:00	H1	Designing driving protocols for high-fidelity quantum devices using numerically exact predictions — •MORITZ CYGOREK, ERIK M. GAUGER
SYPQ 1.2	Tue	10:00–10:30	H1	Challenges towards high efficiency quantum dot single photon sources — •ARNE LUDWIG
SYPQ 1.3	Tue	10:30–11:00	H1	Organic Molecules in photonic quantum technologies — •COSTANZA TONINELLI
SYPQ 1.4	Tue	11:15–11:45	H1	Quantum-dot single-photon sources for quantum photonic networks — •PETER MICHLER
SYPQ 1.5	Tue	11:45–12:15	H1	Quantum light sources: entanglement generation in semiconductor nanostructures — •ANA PREDOJEVIC

Sessions

SYPQ 1.1–1.5	Tue	9:30–12:15	H1	High Yield Devices for Photonic Quantum Implementations
--------------	-----	------------	----	--

Sessions

– Invited Talks –

SYPQ 1: High Yield Devices for Photonic Quantum Implementations

Time: Tuesday 9:30–12:15

Location: H1

Invited Talk

SYPQ 1.1 Tue 9:30 H1

Designing driving protocols for high-fidelity quantum devices using numerically exact predictions — •MORITZ CYGOREK and ERIK M. GAUGER — Heriot-Watt University, Edinburgh, UK

Improving the quality of quantum devices, such as solid state quantum dots as emitters of non-classical light, is not only a matter of device fabrication. Engineering operation protocols by combining coherent driving, adiabatic rapid passage, Stark tuning, and phonon-assisted state preparation is key to enhancing devices robustness and fidelity. This turns a hardware problem into the software problem of predicting the dynamics of quantum devices. The challenge for solid state devices is the simultaneously strong coupling to phonon environments, strong time-dependent driving, and possibly strong interactions with structured photonic environments. After a series of conceptual developments in less than a decade, it has become possible to describe the dynamics of such devices numerically exactly, i.e., to fully account for all effects described by the microscopic Hamiltonians to arbitrary precision. While prior numerically exact methods had been practicable only for very small idealised quantum systems, now, easy-to-use computational tools are publicly available that provide numerically exact results even for the multi-scale dynamics of small quantum networks strongly coupled to multiple environments with long memory times. Here, I summarise these developments and discuss their impact for the design of driving protocols for real-world quantum device. Furthermore, I discuss the prospects and challenges for a universal solver of arbitrary open quantum systems.

Invited Talk

SYPQ 1.2 Tue 10:00 H1

Challenges towards high efficiency quantum dot single photon sources — •ARNE LUDWIG — Ruhr-Universität Bochum, Germany

A key component for photonic quantum devices is a source of high-fidelity photonic qubits, a single photon source (SPS) [1]. A promising route to create such a device employs semiconductor quantum dots (QDs) in photonic cavities. These approaches exploit the exquisite toolbox of semiconductors, in particular scalable manufacturing.

However, noise processes hampering these [2]. A main contributor to decoherence and low efficiency is random charge rearrangements in the semiconductor environment or the QD itself. A random change of the QD charge state from e.g. Auger processes [3] or photoionization [4] can switch the emitter temporarily off [3,5].

Noise from a fluctuating electrostatic environment is called charge noise. One way to efficiently suppress this, is to embed the QDs in the high purity material undoped region of a p-i-n-diode [6,7]. This approach combined with a tuneable cavity has been pursued to realize a highly efficient fiber-coupled SPS with an end-to-end efficiency of 57% [8].

[1] P. Senellart et al., *Nat Nano* **12**, 1026 (2017). [2] A.V. Kuhlmann et al., *Nat Phys* **9**, 570 (2013). [3] A. Kurzmann et al., *Nano Lett* **16**, 3367 (2016). [4] P. Lochner et al., *Phys. Rev. B* **103**, 075426 (2021). [5] G. Gillard et al., *npj Q Inf* **7**, 43 (2021). [6] D. Najer et al., *Nature* **575**, 622 (2019). [7] L. Zhai et al., *Nat Commun* **11**, 4745 (2020). [8] N. Tomm et al., *Nat Nano* **16**, 399 (2021).

Invited Talk

SYPQ 1.3 Tue 10:30 H1

Organic Molecules in photonic quantum technologies — •COSTANZA TONINELLI — CNR-INO, LENS Via Nello Carrara 1, 50019 Sesto Fiorentino (FI), Italy

In this contribution I will discuss the prospects of using polyaromatic hydrocarbons as quantum emitters for photonic quantum technologies. I will revise our

recent advances in the development of molecule-based single photon sources and related applications. The possibility of scaling up the number of sources on chip will be discussed, in terms of integration strategies and novel tuning methods. Finally I will show recent results on the use of molecules as low-invasivity thermal sensors.

[1] S. Pazzagli, et al., *ACS Nano* **12**, 4295, 4303 (2018)

[2] M. Colautti, et al., *Adv. Q. Tech.* **3**, 7 cover (2020)

[3] C. Ciancio, et al., *ACS Photonics* **6**, 12, 3120 3125 (2019)

[4] M. Colautti, et al., *ACS Nano* (2020) 10.1021/acsnano.0c05620

[5] P.Lombardi et al., *Appl. Phys. Lett.* **118**, 204002 (2021)

[6] R. Duquennoy et al., arXiv:2201.07140v1, accepted in *Optica*

[7] M. Ghulam et al., arXiv:2202.12635

15 min. break

Invited Talk

SYPQ 1.4 Tue 11:15 H1

Quantum-dot single-photon sources for quantum photonic networks — •PETER MICHLER — University of Stuttgart, Institute for semiconductor optics and functional interfaces, Stuttgart, Germany

In many foreseen implementations of quantum photonic networks, photons must be able to propagate over long distances in silica fibers with limited absorption and wave packet dispersion. When propagating into silica fibers, photons in the so-called telecom C-band (1530-1565 nm) will experience the absolute minimum of absorption whereas in the O-band (1260-1360 nm) they can travel with vanishing dispersion together with limited absorption.

In this talk, we report about recent highlights achieved with quantum dots emitting in the telecom O- and C-band [1,2]. This includes bright Purcell enhanced single-photon sources based on quantum dots in circular Bragg gratings [2] and the study of resonance fluorescence of single In(Ga)As QDs emitting in the telecom C-band [3]. Moreover, we present an efficient and stable fiber-to-chip coupling, which enables the injection of single photons from telecom quantum dots into a silicon-on-insulator chip [4].

[1] S. L. Portalupi, M. Jetter and P. Michler, *Semicond. Sci. Technol.* **34**, 053001 (2019) [2] S. Kolatschek et al., *Nano Lett.* **21**, 7740 (2021) [3] C. Nawrath et al., *Appl. Phys. Lett.* **118**, 244002 (2021) [4] S. Bauer et al., *Appl. Phys. Lett.* **119**, 211101 (2021)

Invited Talk

SYPQ 1.5 Tue 11:45 H1

Quantum light sources: entanglement generation in semiconductor nanostructures — •ANA PREDOJEVIC — Stockholm University, Stockholm, Sweden

Single quantum dots are established emitters of single photons and entangled photon pairs. By means of resonant excitation they generate photon pairs with high efficiency, low multi-photon contribution, and suitable for entangling schemes such as time-bin entanglement. The entanglement of photons generated by quantum dots can be employed in free-space and fibre-based quantum communication. In addition to this, some applications of entanglement are more versatile if the photons are entangled simultaneously in more than one degree of freedom - hyperentangled, which we also demonstrated using quantum dots. However, the achievable degree of entanglement and the source readiness to be deployed in quantum communication protocols depend on additional functionalities, including high photon collection efficiency. I will present engineered photonic systems that allow for entangled photon pair sources to be more efficient. Also, I will introduce novel methods to characterize sources of entangled photons.

Complexity and Topology in Quantum Matter (SYQM)

jointly organised by
 the Semiconductor Physics Division (HL),
 the Low Temperature Physics Division (TT),
 the Dynamics and Statistical Physics Division (DY), and
 the Thin Films Division (DS)

Matthias Vojta
 Technische Universität Dresden
 matthias.vojta@tu-dresden.de

Ralph Claessen
 Julius-Maximilians-Universität Würzburg
 claessen@physik.uni-wuerzburg.de

Over the past two decades the mathematical concept of topology has emerged into a powerful tool for understanding and classifying quantum matter. The existence of global invariants in a physical system not only gives rise to novel types of quantum phases beyond Landau's concept of broken symmetries and local order parameters, but may also lead to "topological protection" of otherwise rather delicate quantum states with respect to external perturbations, with obvious application potential for future quantum technologies. Topological physics is, in fact, ubiquitous. This symposium is dedicated to giving an overview of its unifying relevance in widely differing areas of condensed matter physics, ranging from electronic band structures to quantum magnetism to photonics devices. The talks will also cover the impact of topology in out-of-equilibrium systems.

Overview of Invited Talks and Sessions

(Lecture hall H1)

Invited Talks

SYQM 1.1	Fri	9:30–10:00	H1	The role of crystalline symmetries in topological materials: the topological materials database — •MAIA VERGNIORY
SYQM 1.2	Fri	10:00–10:30	H1	Microwave Bulk and Edge Transport in HgTe-Based 2D Topological Insulators — •ERWANN BOCQUILLON, MATTHIEU C. DARTAILH, ALEXANDRE GOURMELON, HIROSHI KAMATA, KALLE BENDIAS, SIMON HARTINGER, JEAN-MARC BERROIR, GWENDAL FÈVE, BERNARD PLAÇAIS, LUKAS LUNCZER, RAIMUND SCHLERETH, HARTMUT BUHMANN, LAURENS MOLENKAMP
SYQM 1.3	Fri	10:30–11:00	H1	Spectral Sensitivity of Non-Hermitian Topological Systems — •JAN CARL BUDICH
SYQM 1.4	Fri	11:15–11:45	H1	Topological photonics and topological lasers with coupled vertical resonators — •SEBASTIAN KLEMBT
SYQM 1.5	Fri	11:45–12:15	H1	Spectroscopic Studies of the Topological Magnon Band Structure in a Skyrmion Lattice — •MARKUS GARST

Sessions

SYQM 1.1–1.5	Fri	9:30–12:15	H1	Complexity and Topology in Quantum Matter
--------------	-----	------------	----	--

Sessions

– Invited Talks –

SYQM 1: Complexity and Topology in Quantum Matter

Time: Friday 9:30–12:15

Location: H1

Invited Talk SYQM 1.1 Fri 9:30 H1
The role of crystalline symmetries in topological materials: the topological materials database — •MAIA VERGNIORY — Max Planck for Chemical Physics of Solids, Nöthnitzer Str. 40, 01187 Dresden, Germany

Quantum materials are a collection of atoms with interacting electrons and nuclei displaying emergent behaviour and topological properties. The past two decades has witnessed an explosion in the field of topological materials: from weak interacting electrons to strongly correlated ones, topological materials represent one of the most exciting application for future technologies. High performance electronics, quantum information or ultrafast spintronics are just a few of the possible technologies that can be developed based on these materials. In this talk I will discuss the route to go from pure mathematical prediction of topological properties, through high through-put materials search to device fabrication. I will discuss both topological insulators, in non magnetic and magnetic phases as well as topological (chiral) semimetals using the the modern theory of topological band structure. Topological Quantum Chemistry built upon symmetry-based considerations and complemented with chemical theories of bonding, ionization, and covalence. Consequently, it describes the universal global properties of all possible band structures and materials. Beyond the single particle picture, I will present our formalism based on Green's functions aiming to discover topological correlated phases in materials displaying electronic entanglement.

Invited Talk SYQM 1.2 Fri 10:00 H1
Microwave Bulk and Edge Transport in HgTe-Based 2D Topological Insulators — •ERWANN BOCQUILLON^{1,2}, MATTHIEU C. DARTIAILH¹, ALEXANDRE GOURMELON¹, HIROSHI KAMATA¹, KALLE BENDIAS^{3,4}, SIMON HARTINGER^{3,4}, JEAN-MARC BERROIR¹, GWENDAL FÈVE¹, BERNARD PLAÇAIS¹, LUKAS LUNCZER^{3,4}, RAIMUND SCHLERETH^{3,4}, HARTMUT BUHMANN^{3,4}, and LAURENS MOLENKAMP^{3,4} — ¹Laboratoire de Physique de l'École Normale Supérieure, ENS, PSL Research University, CNRS, Sorbonne Université, Université Paris-Cité, 24 rue Lhomond, 75005 Paris — ²Physikalisches Institut 2, Universität zu Köln, D-50937 Köln — ³Physikalisches Institut (EP3), Universität Würzburg, D-97074 Würzburg — ⁴Institute for Topological Insulators, Universität Würzburg, D-97074 Würzburg

Research on the helical edge states of 2D topological insulators is motivated by exotic fundamental physics, robust topological quantum computation and novel spinorbitronics. In this talk, we report on the use of microwave methods to investigate dynamical transport in HgTe-based 2D topological insulators. More specifically, capacitance spectroscopy highlights the response of the edges which host very mobile carriers, while bulk carriers are drastically slowed down in the gap. Charge relaxation timescales are shorter on the edges, which suggests that edge states can be selectively addressed on timescales over which bulk carriers are frozen. Additionally, we also propose edge resonator geometries to characterize Coulomb interaction by via high-frequency measurements.

Invited Talk SYQM 1.3 Fri 10:30 H1
Spectral Sensitivity of Non-Hermitian Topological Systems — •JAN CARL BUDICH — Institute of Theoretical Physics, Technische Universität Dresden and Würzburg-Dresden Cluster of Excellence ct.qmat, 01062 Dresden, Germany
 In a wide variety of physical scenarios ranging from classical meta-materials to correlated quantum many-body systems, non-Hermitian (NH) Hamiltonians have proven to be a powerful and conceptually simple tool for effectively describing dissipation. Motivated by recent experimental discoveries, investigating the topological properties of such NH systems has become a broad frontier of cur-

rent research. In this talk, I will focus on a remarkable spectral sensitivity unique to NH topological systems. After an introductory discussion of the general theoretical background of this algebraic phenomenon, I will present several of its salient physical manifestations, including its impact on quasi-particles in correlated solids, and its potential for devising novel high-precision sensors.

15 min. break

Invited Talk SYQM 1.4 Fri 11:15 H1
Topological photonics and topological lasers with coupled vertical resonators — •SEBASTIAN KLEMBT — Chair for Applied Physics and Würzburg-Dresden Cluster of Excellence ct.qmat, Universität Würzburg, Am Hubland, D-97074 Würzburg, Germany.

Topological Photonics is an emerging and novel field of research, adapting concepts from condensed matter physics to photonic systems adding new degrees of freedom. After the first demonstrations of topological photonic insulators, the field has moved on to study and exploit the inherent non-hermiticity of photonic systems and the interplay with their topological nature. In my talk I will discuss novel photonic lattice devices resulting from the coupling of individual vertical III-V semiconductor microresonators. So-called exciton-polaritons (hybrid states of light and matter) can emerge in the strong coupling regime. By choosing precise lattice geometries we are able to tailor optical band structures realizing novel photonic lattice. Here, the specific geometry as well as the hybrid light-matter nature allow for ways to break time-reversal symmetry and implement topologically non-trivial systems. Thus we were able to experimentally demonstrate the first exciton-polariton topological insulator, manifesting in chiral, topologically protected edge modes. In order to study topological effects in combination with optical non-linearities, topological lasers have been envisaged and realized. They exploit topological effects to efficiently couple and phase-lock extended arrays of lasers to behave as one single coherent laser. Here, I report on the first experimental demonstration of a topological insulator vertical cavity laser array.

Invited Talk SYQM 1.5 Fri 11:45 H1
Spectroscopic Studies of the Topological Magnon Band Structure in a Skyrmion Lattice — •MARKUS GARST — Karlsruhe Institute of Technology
 When magnons propagate across a non-collinear magnetic texture, they collect a Berry phase that can be interpreted as the flux of a synthetic orbital magnetic field. The magnon thus experiences a synthetic Lorentz force that bends the quasi-classical trajectories of the magnons. For a magnetic skyrmion lattice, the average synthetic field is finite such that the magnons are confined to cyclotron orbits of the corresponding magnon Landau levels. This is reflected in a magnon band structure with finite Chern numbers. Here, we report on a series of spectroscopic studies of this band structure using various techniques that allow to probe different regimes in energy-momentum space: magnetic resonance spectroscopy [1], spin-wave spectroscopy [2], inelastic neutron scattering [3] and Brillouin light scattering [4,5]. These techniques have been applied to various cubic chiral magnets like MnSi, FeCoSi and Cu₂OSeO₃, that are well described by a universal effective continuum theory parametrized by a few parameters only. The combined data from all techniques are found to be in quantitative agreement with theory.

[1] R. Takagi et al. Phys. Rev. B 104, 144410 (2021). [2] S. Seki et al. Nat. Commun. 11, 256 (2020). [3] T. Weber et al. Science 375, 1025 (2022). [4] N. Ogawa et al. PNAS 118, e2022927118 (2021). [5] P. Che et al. unpublished.

SKM Dissertation Prize 2022 (SYSD)

jointly organised by
the divisions of the Condensed Matter Section (SKM)

Sarah Köster
Georg-August-Universität Göttingen
Institut für Röntgenphysik
Friedrich-Hund-Platz 1
37077 Göttingen
sarah.koester@phys.uni-goettingen.de

The divisions belonging to the Condensed Matter Section (SKM) of the DPG award annually the SKM Dissertation Prize. The prize acknowledges outstanding research during the PhD work in the research areas of SKM completed in 2020 or 2021, and its excellent oral presentation. Based on nominations a jury formed by the chairpersons of all SKM divisions has selected four finalists for the award to present their work in this symposium. The winner will be selected after the symposium and publicly announced Tuesday, September 6th, in the afternoon during the ceremonial session.

Overview of Invited Talks and Sessions

(Lecture hall H2)

Invited Talks

SYSD 1.1	Mon	10:15–10:45	H2	Charge localisation in halide perovskites from bulk to nano for efficient optoelectronic applications — •SASCHA FELDMANN
SYSD 1.2	Mon	10:45–11:15	H2	Nonequilibrium Transport and Dynamics in Conventional and Topological Superconducting Junctions — •RAFFAEL L. KLEES
SYSD 1.3	Mon	11:15–11:45	H2	Probing magnetostatic and magnetotransport properties of the antiferromagnetic iron oxide hematite — •ANDREW ROSS
SYSD 1.4	Mon	11:45–12:15	H2	Quantum dot optomechanics with surface acoustic waves — •MATTHIAS WEISS

Sessions

SYSD 1.1–1.4	Mon	10:15–12:15	H2	SKM Dissertation Prize
--------------	-----	-------------	----	-------------------------------

Sessions

– Invited Talks –

SYSD 1: SKM Dissertation Prize

Time: Monday 10:15–12:15

Location: H2

Invited Talk SYSD 1.1 Mon 10:15 H2

Charge localisation in halide perovskites from bulk to nano for efficient optoelectronic applications — •SASCHA FELDMANN — Cavendish Laboratory, University of Cambridge, Cambridge, UK — Rowland Institute, Harvard University, Cambridge, USA

Halide perovskites have emerged as high-performance semiconductors for efficient optoelectronic devices like solar cells or LEDs. Yet, we still do not fully understand why these materials work so efficiently, given that we can process them crudely from solution, likely introducing many defects detrimental to devices based on conventional crystalline semiconductors like silicon. In this talk, I will give an overview of our recent work on understanding the high luminescence yields observed in i) bulk mixed-halide thin films and ii) atomically doped nanocrystals. We show that spatially varying energetic disorder in the electronic states of mixed-halide films causes local charge accumulation, which unearths a strategy for efficient charge extraction at low-light conditions for solar cells and for efficient light emission in LEDs operating at low currents. In doped perovskite nanocrystals, we find that the dopant-induced lattice periodicity breaking results in the transient localisation of charges with an increased overlap of electron and hole wavefunctions. This leads to increased radiative rates - a property that is typically intrinsic to a semiconductor and hard to change - together with reduced non-radiative losses, paving the way to highly efficient LEDs and quantum applications. Overall, these findings hint at energetic disorder in these materials not only being tolerated but potentially helpful in explaining their high performance.

Invited Talk SYSD 1.2 Mon 10:45 H2

Nonequilibrium Transport and Dynamics in Conventional and Topological Superconducting Junctions — •RAFFAEL L. KLEES — University of Konstanz, D-78457 Konstanz, Germany

In this talk, I will give a brief overview about the main content of my dissertation. Recently, it has been shown that multiterminal superconducting junctions (MSJs) provide an ideal platform to mimic topological systems in a controlled manner [1]. In the first part, we will construct deterministic model systems of MSJs based on quantum dots that show nontrivial Andreev bound states in terms of a nonzero first and second Chern number. We will also see how the underlying object of quantum geometry and topology, the quantum geometric tensor [2], can be accessed with the help of polarized microwave spectroscopy [3]. In the second part, I will report on the theory behind recent scanning tunneling microscope (STM) experiments between single superconducting Yu-Shiba-Rusinov (YSR) bound states that form in localized magnetic impurities on superconducting substrates [4]. Motivated by these experiments, we study YSR-functionalized STM tips and present a detailed analysis of multiple Andreev reflection processes mediated by YSR states giving rise to a very complex subgap structure in the current-voltage characteristics [5]. [1] R.-P. Riwar *et al.*, *Nat. Commun.* **7**, 11167 (2016). [2] M. Kolodrubetz *et al.*, *Phys. Rep.* **697**, 1 (2017). [3] R. L. Klees *et al.*, *Phys. Rev. Lett.* **124**, 197002 (2020); *Phys. Rev. B* **103**, 014516 (2021); H.

Weisbrich *et al.*, *PRX Quantum* **2**, 010310 (2021). [4] H. Huang *et al.*, *Nat. Phys.* **16**, 1227 (2020). [5] A. Villas *et al.*, *Phys. Rev. B* **103**, 155407 (2021).

Invited Talk SYSD 1.3 Mon 11:15 H2

Probing magnetostatic and magnetotransport properties of the antiferromagnetic iron oxide hematite — •ANDREW ROSS — Johannes Gutenberg Universität-Mainz, Mainz, Germany

With spin dynamics in the THz regime, a lack of stray fields and a high stability in external magnetic fields, antiferromagnets have several benefits over ferromagnets for spintronics applications. In this talk I will discuss two key steps towards functionalising antiferromagnetic insulators, focussing on the antiferromagnetic iron oxide, hematite, the main component of rust.

First, I will demonstrate how spin Hall magnetoresistance measurements can be used to extract the strengths of key antiferromagnetic anisotropies for both bulk and thin film samples responsible for the equilibrium orientation of the magnetic ordering.

Then, I will show how we can use antiferromagnetic insulators for information transport via quantised magnetic excitations, magnons. Polarised magnons are electrically excited by an interfacial spin-bias and carried over micrometres by the antiferromagnetic Neel order, facilitated by the relative orientation of the antiferromagnetic Neel vector and the low damping of hematite. By performing direct magnetic imaging of the domain structure, the strong attenuation of the magnon transport by a multi-domain structure is elucidated. Overall, the results I will present demonstrate the feasibility and promise of the prototypical antiferromagnet hematite for antiferromagnetic spintronic devices.

Invited Talk SYSD 1.4 Mon 11:45 H2

Quantum dot optomechanics with surface acoustic waves — •MATTHIAS WEISS — Institut für Physik, Universität Augsburg — Physikalisches Institut, WWU Münster

Phonons, the quanta of mechanical vibrations, represent fundamental excitation in solid state materials and interact strongly with literally any other system. This universal coupling and their low susceptibility to dissipation makes phonons ideally suited to manipulate dissimilar systems and interface them in hybrid technologies.

In this talk, I show experiments of the interaction between the coherent phonon field of a surface acoustic wave and a single quantum emitter, a semiconductor quantum dot, employing resonant light scattering. This approach provides an ideal testbed to study electron-phonon interactions and to implement optomechanical control schemes. I show that the dynamic strain field of the acoustic wave modulates the dot's sharp optical transition at gigahertz frequencies enabling precisely triggered single photon emission and the generation of phononic sidebands in the optical spectrum. When combining two acoustic waves of different frequencies, spectral components are programmed by coherent wave mixing of photons and phonons by the quantum dot. I will discuss the experimental observations using a simple model of coupled phonon emission and absorption processes obeying well-defined phase matching conditions.

Interplay of Substrate Adaptivity and Wetting Dynamics from Soft Matter to Biology (SYSM)

jointly organised by
the Chemical and Polymer Physics Division (CPP),
the Biological Physics Division (BP), and
the Dynamics and Statistical Physics Division (DY)

Uwe Thiele
Institut für Theoretische Physik
Westfälische Wilhelms-Universität Münster
u.thiele@uni-muenster.de

Karin John
Laboratoire Interdisciplinaire de Physique
Université Grenoble Alpes, CNRS
karin.john@univ-grenoble-alpes.fr

Stefan Karpitschka
AG Grenzflächen komplexer Flüssigkeiten
Max-Planck-Institut für Dynamik &
Selbstorganisation
Göttingen
stefan.karpitschka@ds.mpg.de

Ralf Seemann
AG Geometrie fluider Grenzflächen,
Experimentalphysik
Universität des Saarlandes
Saarbrücken
ralf.seemann@ds.mpg.de

The basic understanding and practical application of the coupled dynamics of a (de)wetting liquid and adaptive soft substrates is attracting increasing interest in fields spanning chemical and biological physics, material science, and hydrodynamics. Examples of substrates include flexible elastomers or hydrogels that form dissipation-rich wetting ridges, polymer brushes that adapt their wettability and mechanical properties by absorbing liquid, or membraneless organelles in a biological cell whose creation and manipulation involves their adhesion to flexible membranes. Wetting interactions may also be manipulated by spatio-temporally structured external fields allowing, for example, wettability-switching triggered by electric fields or light irradiation. In all these systems, capillary and wetting energies interact with elastic properties, possible decomposition and mixing processes as well as absorption, adsorption and desorption processes resulting in feedback mechanism that influence the static and dynamic behaviour of the liquid-substrate system.

In general, one can say that intricate multiscale dynamics results from the coupling of different non-equilibrium processes, that is various mechanisms of energy dissipation may dominate on different time- and length scales, ultimately determining the dynamic behaviour. Furthermore, the interplay of several degrees of freedom offers new possibilities for a targeted control of dynamic wetting processes, but also poses new challenges for experimental investigation and theoretical description: Recent developments in length-scale-bridging experimental techniques allow for in situ (and in vivo) visualisation enabling quantitative analysis while methods from statistical physics to computational fluid and solid dynamics give unprecedented multiscale insight.

Overview of Invited Talks and Sessions

(Lecture hall H1)

Invited Talks

SYSM 1.1	Wed	15:00–15:30	H1	Statics and Dynamics of Soft Wetting — •BRUNO ANDREOTTI
SYSM 1.2	Wed	15:30–16:00	H1	Droplets on elastic substrates and membranes - Numerical simulation of soft wetting — •SEBASTIAN ALAND
SYSM 1.3	Wed	16:00–16:30	H1	Wetting of Polymer Brushes in Air — LARS VELDSCHOLTE, GUIDO RITSEMA VAN ECK, LIZ MENSINK, JACCO SNOEIJER, •SISSI DE BEER
SYSM 1.4	Wed	16:45–17:15	H1	Elastocapillary phenomena in cells — •ROLAND L. KNORR
SYSM 1.5	Wed	17:15–17:45	H1	Active contact line depinning by micro-organisms spreading on hydrogels — MARC HENNES, JULIEN TAILLEUR, GAËLLE CHARRON, •ADRIAN DAERR

Sessions

SYSM 1.1–1.5	Wed	15:00–17:45	H1	Interplay of Substrate Adaptivity and Wetting Dynamics from Soft Matter to Biology
--------------	-----	-------------	----	---

Sessions

– Invited Talks –

SYSM 1: Interplay of Substrate Adaptivity and Wetting Dynamics from Soft Matter to Biology

Time: Wednesday 15:00–17:45

Location: H1

Invited Talk SYSM 1.1 Wed 15:00 H1**Statics and Dynamics of Soft Wetting** — •BRUNO ANDREOTTI — LPENS, 24 rue Lhomond, 75005 Paris

The laws of wetting are well-known for drops on rigid surfaces, but these change dramatically when the substrate is soft and deformable. The combination of wetting and the intricacies of soft polymeric interfaces has provided many rich examples of fluid-structure interaction, both in terms of phenomenology as well as from the fundamental perspective. In this colloquium, I will discuss experimental and theoretical progress on the statics and dynamics of soft wetting. In this context, I will critically revisit the foundations of capillarity, such as the nature of solid surface tension, the microscopic mechanics near the contact line, and the dissipative mechanisms that lead to unexpected spreading dynamics.

Invited Talk SYSM 1.2 Wed 15:30 H1**Droplets on elastic substrates and membranes - Numerical simulation of soft wetting** — •SEBASTIAN ALAND — TU Freiberg, Germany

Wetting of flexible substrates plays a major role in a broad variety of phenomena. The interaction between droplets and their surrounding is at small length scales dominated by surface tension forces. These forces may lead to significant deformation of the surrounding structure if either very soft or very thin (e.g. a biological membrane). The interplay between wetting dynamics and structure mechanics leads to a range of fascinating phenomena from stick-slip motion to droplet-mediated remodeling of membranes.

In this talk, we present a computational model which is capable to shed some light on such elastocapillary phenomena. The model captures the interaction between two immiscible fluids and a soft structure or membrane. The discretization is based on a combination of a phase-field model with a moving finite-element grid. In numerical tests we demonstrate that this novel method is robust, flexible and accurate. We confirm analytical theory of droplet surfing on Kelvin-Voigt substrates and find an explanation for the experimentally observed stick-slip phenomenon. Finally, we present first simulations of droplet-mediated membrane remodeling.

Invited Talk SYSM 1.3 Wed 16:00 H1**Wetting of Polymer Brushes in Air** — LARS VELDSCHOLTE, GUIDO RITSEMA VAN ECK, LIZ MENSINK, JACCO SNOEIJER, and •SISSI DE BEER — Sustainable Polymer Chemistry Group, Department of Molecules & Materials, MESA+ Institute for Nanotechnology, University of Twente, P.O. Box 217, 7500 AE Enschede, The Netherlands

For the development of brush-based functional surface-coatings, it is critical to understand their properties, because they will determine their performance and user-experience. Polymer brush wetting is a key parameter in this. In this presentation we will show that brushes can display counter-intuitive wetting properties. We aim to unravel those by combining molecular dynamics simulations, contact angle goniometry and ellipsometry laboratory experiments.

15 min. break

Invited Talk SYSM 1.4 Wed 16:45 H1**Elastocapillary phenomena in cells** — •ROLAND L. KNORR — Interfacial Cell Biology Lab, Integrative Research Institute for the Life Sciences, Humboldt-Universität zu Berlin, Germany — Graduate School and Faculty of Medicine, The University of Tokyo, Japan

Compartmentalisation is essential for eukaryotic cell function, allowing the division of processes into membrane-bound, specialised compartments, such as organelles. In recent years, intracellular phase separation has garnered much attention as a non-membrane means of organising components through the formation of droplet-like compartments, which are functionally implicated in both health and disease. Evidence suggests that droplet clearance involves autophagy, a highly-conserved cellular recycling system in which membrane sheets expand and bend to isolate and degrade portions of the cell interior.

Here, we investigate the mechanisms of droplet sequestration by membrane sheets in both living and synthetic cells. A minimal theoretical model shows that the surface tension of wetting droplets determines whether membrane sheets isolate the droplet phase in a whole or piecemeal fashion. We also find that wetting droplet induce local membrane spontaneous curvature changes, resulting in the reversal of the bending direction of membrane sheets and, thus, in cytosol sequestration [Nature 2020, 2021]. Further, we demonstrate that the morphogenesis of protein storage vacuoles in plants underlies similar physical principles [PNAS, JCB 2021]. I propose that droplet-mediated autophagy and vacuole remodelling represent a novel class of cellular processes driven by elastocapillary.

Invited Talk SYSM 1.5 Wed 17:15 H1**Active contact line depinning by micro-organisms spreading on hydrogels** — MARC HENNES^{1,2}, JULIEN TAILLEUR^{1,3}, GAËLLE CHARRON¹, and •ADRIAN DAERR¹ — ¹Université Paris Cité, UMR 7057 Matière et Systèmes Complexes, France — ²Universität zu Köln, Institut für Biologische Physik — ³CNRS, France

Capillary forces, capable of pinning millimetre-sized water droplets on inclined surfaces, become enormous at the bacterial scale, exceeding typical propulsion forces of microbes by several orders of magnitude. It is thus fascinating to explore the tricks that micro-organisms have evolved to overcome contact line pinning and spread across substrates. I will discuss specifically the spreading of bacteria (*Bacillus subtilis*) across agar hydrogels.

Recently we discovered a mode of collective bacterial motility in humid environment through the depinning of bacterial droplets[1]. Bacteria harness a variety of phenomena, drawing both on the porosity and the softness of the substrate, that result in unpinning the contact line, hence inducing a collective slipping of the colony across surfaces at slopes that can be as small as 0.5°. The exploited microscopic mechanisms could play a role in other contexts, including biofilm formation and flagella dependent migration modes like swarming, and highlight the possibilities of tuning the wetting dynamics on soft porous substrates.

[1] M. Hennes, J. Tailleur, G. Charron, A. Daerr, Proc. Nat. Acad. Sc. USA **114**, 5958–5963, (2017), doi: 10.1073/pnas.1703997114

Collective Social Dynamics from Animals to Humans (SYSO)

jointly organised by
the Physics of Socio-economic Systems Division (SOE),
the Dynamics and Statistical Physics Division (DY), and
the Biological Physics Division (BP)

Fakhteh Ghanbarnejad
Departments of Physics
Sharif University of Technology
Tehran, Iran
fakhteh.gh@sharif.edu

Philipp Hövel
School of Mathematical Sciences
University College Cork
Cork, Irland
philipp.hoevel@ucc.ie

Eckehard Olbrich
Max Planck Institute for Mathematics in
the Sciences
Leipzig, Germany
eckehard.olbrich@mis.mpg.de

Collective opinion formation, emergence of hierarchies and collective dynamics on markets are typical phenomena both of bacterial and animal as well as of socio-economic communities. Statistical physics concepts widely contributed to the understanding of such nonlinear collective phenomena. Collective movement of humans in public space have been an early studied dynamics of active Brownian motion. This symposium integrates individual modeling of human and animal behaviour, movement and mobility, opinion formation, information processing and group interactions towards an understanding of the self-organizing dynamics in societies.

Overview of Invited Talks and Sessions

(Lecture hall H1)

Invited Talks

SYSO 1.1	Thu	9:30–10:00	H1	Capturing group interactions: The next frontier of modeling social and biological systems — •FRANK SCHWEITZER
SYSO 1.2	Thu	10:00–10:30	H1	Modelling Individual Mobility Behavior — •LAURA MARIA ALESSANDRETTI
SYSO 1.3	Thu	10:30–11:00	H1	Validating argument-based opinion dynamics with survey experiments — •SVEN BANISCH
SYSO 1.4	Thu	11:15–11:45	H1	Self-organization, Criticality and Collective Information Processing in Animal Groups — •PAWEL ROMANCZUK
SYSO 1.5	Thu	11:45–12:15	H1	Collective dynamics and physiological interactions in bird colonies — •HANJA BRANDL

Sessions

SYSO 1.1–1.5	Thu	9:30–12:15	H1	Collective social dynamics from animals to humans
--------------	-----	------------	----	--

Sessions

– Invited Talks –

YSO 1: Collective social dynamics from animals to humans

Time: Thursday 9:30–12:15

Location: H1

Invited Talk

SYSO 1.1 Thu 9:30 H1

Capturing group interactions: The next frontier of modeling social and biological systems — •FRANK SCHWEITZER — Chair of Systems Design, ETH Zürich, Switzerland

Complex social and biological systems comprised of many interacting agents are often represented as networks. This implies to decompose interactions between many agents into concurrent dyadic interactions of pairs of agents. Such a reduction is recently challenged with different approaches, which are addressed in this talk: (i) temporal network models reflect the causal relation between interactions occurring at different time steps, (ii) hyperedge network models capture group interactions by constructing higher-order networks, (iii) inference network models reveal information hidden behind observed interaction patterns. Combined, we obtain a very rich picture of social structures that emerge and adapt at different time scales and at different size levels (dyads, groups, communities, networks). Two examples of real-world social organizations (Bechstein bats, software developers) are used to illustrate our insights.

Invited Talk

SYSO 1.2 Thu 10:00 H1

Modelling Individual Mobility Behavior — •LAURA MARIA ALESSANDRETTI — Technical University of Denmark, Copenhagen, Denmark

From choosing a restaurant for dinner, to deciding whether to cycle or drive, spatial decisions are ubiquitous in human day-to-day lives. Taken together, these choices underlie critical societal phenomena, including the spread of epidemics, traffic congestion, and the emergence of urban segregation. In this talk, I will present recent empirical findings on the mechanisms underlying individual mobility behaviour, made possible by the study of comprehensive, high-resolution mobility data, and modelling approaches. The talk will touch upon key aspects in mobility, such as the interplay between exploration and exploitation, the effect of cognitive constraints, the relation between social and spatial behavior, and the effect of spatial scales. I will conclude with a perspective on open questions and future directions.

Invited Talk

SYSO 1.3 Thu 10:30 H1

Validating argument-based opinion dynamics with survey experiments — •SVEN BANISCH — Karlsruhe Institute of Technology, Institute of Technology Futures, Germany

We combine experimental research on the biased processing of arguments with a computational theory of collective opinion dynamics. While the biased processing of arguments has been frequently reported in social-psychological literature, its integration into argument-based models of opinion dynamics has been missing. In this paper we operationalize the argument communication process employed in these models in conjunction with an experimental design developed to measure biased processing and the resulting attitude changes in the context of energy production technologies. This allows us to analytically compute the expected attitude change through exposure to an unbiased set of arguments for different strengths of biased processing. Calibrating the microlevel assumptions with the experimental data shows a clear signature of moderate biased processing. We further extend the model by incorporating an unbiased external information source providing random arguments at a certain rate (as opposed to receiving arguments from others). The macroscopic opinion distributions emerging from this at the collective level are one-sided clearly in favor

(green) or against (coal) a technology and match the surveyed attitudes if we control for the impact of social influence. Sociological model-building reveals that the relationship between biased processing and attitude polarization is not as direct as typical assumed in the psychological literature.

15 min. break

Invited Talk

SYSO 1.4 Thu 11:15 H1

Self-organization, Criticality and Collective Information Processing in Animal Groups — •PAWEL ROMANCZUK — Institute for Theoretical Biology, Department of Biology, Humboldt Universität zu Berlin, Germany — Bernstein Center for Computational Neuroscience, Berlin — Research Cluster of Excellence “Science of Intelligence”, Berlin

Collective behavior of animals is a fascinating example of self-organization in biology. In contrast to non-living physical systems, collective animal behavior and the underlying social interactions are the result of evolutionary adaptations. Being and acting in a group is believed to confer fitness benefits to individuals, for example by promoting exchange of social information, accurate collective decisions, or protection from predators. In this context, it has been argued that animal collectives should operate in a special parameter region close to critical points, i.e. close to phase transitions between different collective states, where various aspects of collective information processing become optimal. Here, we will investigate the *criticality hypothesis* for animal collective behavior from different angles by combining model simulations together with laboratory and field experiments on collective predator response in fish.

Invited Talk

SYSO 1.5 Thu 11:45 H1

Collective dynamics and physiological interactions in bird colonies — •HANJA BRANDL — University of Konstanz, Konstanz, Germany — Max Planck Institute of Animal Behavior, Konstanz, Germany — University of Zurich, Zurich, Switzerland

Social behaviours can help animals survive in harsh and unpredictable environments by giving them access to information about where resources are or the presence of predators. To reap these benefits requires individuals to form and maintain social bonds with others, then enabling them to coordinate key activities such as foraging together or to synchronise reproduction. However, the social networks that form among individuals promote not only benefits. Social connectivity can also have negative consequences, such as the transmission of physiological stress from one individual to another. As humans, we have all experienced situations where interacting with stressed friends or family members has made us feel stressed ourselves. As the stress response is highly conserved across vertebrates, it is highly likely that stress transmission is common in other animal societies and could amplify the effects of stress exposure in animal collectives; yet, its consequences remain almost completely unexplored.

In this talk, I present findings from my research on avian societies in the wild and the laboratory, using behavioural experiments and fine-scale tracking to unravel the mechanisms, functions, and consequences of birds’ social bonds. I discuss methods, frameworks, and limitations in studying animal social networks using examples from my work on zebra finches, but will also give an outlook into other study systems.

Symposium United Kingdom as a Guest of Honor (SYUK)

organised by the DPG Condensed Matter Section (SKM)

Martin Wolf

Fritz Haber Institute of the Max Planck Society

Faradayweg 4-6

14195 Berlin

wolf@fhi-berlin.mpg.de

The “Guest of Honor” symposia celebrates the European physics community in general and the links in science across Europe. Thereby, the German Physical Society aims to foster collaborations between individual scientists, research groups and institutions.

This year’s “Guest of Honor” symposium honors the numerous ties between United Kingdom and Germany (beyond Brexit) by highlighting five fields of common interest. Each is represented by a pair of Invited Talks from distinguished scientist from UK and Germany.

Overview of Invited Talks and Sessions

(Lecture hall H2)

Invited Talks

SYUK 1.1	Wed	9:30–10:00	H2	Structure and Dynamics of Interfacial Water — •ANGELOS MICHAELIDES
SYUK 1.2	Wed	10:00–10:30	H2	A molecular view of the water interface — •MISCHA BONN
SYUK 1.3	Wed	10:30–11:00	H2	Motile cilia waves: creating and responding to flow — •PIETRO CICUTA
SYUK 1.4	Wed	11:00–11:30	H2	Cilia and flagella: Building blocks of life and a physicist’s playground — •OLIVER BÄUMCHEN
SYUK 1.5	Wed	11:45–12:15	H2	Computational modelling of the physics of rare earth - transition metal permanent magnets from SmCo₅ to Nd₂Fe₁₄B — •JULIE STAUNTON
SYUK 2.1	Wed	15:00–15:30	H2	Hysteresis Design of Magnetic Materials for Efficient Energy Conversion — •OLIVER GUTFLEISCH
SYUK 2.2	Wed	15:30–16:00	H2	Non-equilibrium dynamics of many-body quantum systems versus quantum technologies — •IRENE D’AMICO
SYUK 2.3	Wed	16:00–16:30	H2	Quantum computing with trapped ions — •FERDINAND SCHMIDT-KALER
SYUK 2.4	Wed	16:45–17:15	H2	Breaking the millikelvin barrier in cooling nanoelectronic devices — •RICHARD HALEY
SYUK 2.5	Wed	17:15–17:45	H2	Superconducting Quantum Interference Devices for applications at mK temperatures — •SEBASTIAN KEMPF

Sessions

SYUK 1.1–1.5	Wed	9:30–12:15	H2	United Kingdom as Guest of Honor I
SYUK 2.1–2.5	Wed	15:00–17:45	H2	United Kingdom as Guest of Honor II

Sessions

– Invited Talks –

SYUK 1: United Kingdom as Guest of Honor I

Time: Wednesday 9:30–12:15

Location: H2

Invited Talk SYUK 1.1 Wed 9:30 H2**Structure and Dynamics of Interfacial Water** — •ANGELOS MICHAELIDES — University of Cambridge, Cambridge, UK

There are few molecules, if any, more important than water. However, remarkably little is known about how it interacts with surfaces, particularly at the molecular level. In this talk I will discuss some of our recent work on the application and development of a variety of state of the art computer simulation methods to better understand the structure and dynamics of water at surfaces and under confinement. Specific topics discussed will include work carried out in collaboration with experimentalists to understand the growth and diffusion of ice clusters at metal surfaces, heterogeneous ice nucleation, and water confined within 1- and 2-dimensional membranes. Methodological developments aimed at providing more accurate treatments of adsorption on and bonding within solids will also be covered, as well as an efficient machine learning strategy for simulating complex aqueous interfaces.

Invited Talk SYUK 1.2 Wed 10:00 H2**A molecular view of the water interface** — •MISCHA BONN — Max Planck, Mainz, Germany

Water surfaces and interfaces are ubiquitous, not just in nature, but also in many technological applications. Water is a rather unique liquid, owing to its strong intermolecular interactions: strong hydrogen bonds hold water molecules together. At the surface of water, the water hydrogen-bonded network is abruptly interrupted, conferring distinct properties on the interface, compared to bulk. I will present some challenges and progress in the study of interfacial water. Specifically, I will address how to study the ~ 1 monolayer of water molecules that is in direct contact with the other phase, and distinguish this \sim Angstrom-thin layer from the bulk. The question rises how large the interface is. And can we describe the interfacial region as a modified dielectric continuum, or do we need to consider molecular structure?

Invited Talk SYUK 1.3 Wed 10:30 H2**Motile cilia waves: creating and responding to flow** — •PIETRO CICUTA — University of Cambridge, Cambridge, UK

Motile cilia are active filaments present on the surface of various human organs, where they perform crucial functions by driving surface flows. Structurally, they are conserved across the eukaryotes. Cilia can affect each other, for example leading to phase locking of their beating, by the forces they exert on each other through the fluid and in some cases through the cell cytoskeleton.

Some beautiful physics has been developed by various teams in the last decade to understand how the details of beating on each cilium can lead to specific phase locking, and to the emergence of collective waves. In recent work we have explored the role of external flows, both oscillatory and constant. Analogies can be drawn between these flows and the effect of external magnetic fields in magnetic systems.

We present both experimental results, and numerical explorations of a simple class of "rower" models of motile cilia.

Invited Talk SYUK 1.4 Wed 11:00 H2**Cilia and flagella: Building blocks of life and a physicist's playground** — •OLIVER BÄUMCHEN — Chair of Experimental Physics V, University of Bayreuth, Bayreuth, Germany

Flagella and cilia are actively beating, hair-like cellular appendages that represent universal building blocks of life. They inherit various essential functions that range from driving fluid flows in the mammalian brain and transporting mucus in the respiratory tract to realizing microbial motility and navigation through complex environments. While large-scale flows are achieved through the coordination of dense ciliary carpets, only a few isolated flagella are needed in order to propel a single-celled microorganism. These flagella displace the surrounding fluid by means of periodic motions, while precisely timed modulations of their beating enable the cell to steer towards or away from specific locations. In this presentation I will focus on the interactions of flagella with interfaces and elucidate how physical principles advance our understanding of microbial motility and emergent phenomena in microbial suspensions. Microorganisms that are equipped with photoreceptors may adapt their flagella beating and also actively switch their flagella-surface interactions in response to light cues. These skills allow photoactive microorganisms to effectively adapt to variable light conditions in their natural habitats and make flagellated microbes a fascinating playground for physicists.

15 min. break

Invited Talk SYUK 1.5 Wed 11:45 H2**Computational modelling of the physics of rare earth - transition metal permanent magnets from SmCo_5 to $\text{Nd}_2\text{Fe}_{14}\text{B}$** — •JULIE STAUNTON — University of Warwick, Coventry CV4 7AL, U.K.

Magnetic materials are ubiquitous, technologically indispensable and a deeper understanding of the physics is needed for the design of new permanent magnets. Most strong magnets contain both rare earths (RE) and transition metals (TM) and this talk will describe recently developed *ab initio* modelling of intrinsic properties. Each RE atom has a magnetic moment, set up by its nearly localised f-electrons, immersed in a glue of septillions of valence electrons coming from all the RE and TM atoms. Local magnetic moments associated with the TM atoms also emerge from this complex electron fluid. The magnetic properties stem from the behaviour of the RE and TM local moments, the atomic arrangements and on the overall response to applied fields. *Ab initio* Density Functional Theory-based Disordered Local Moment (DLM-DFT) theory provides a parameter-free, accurate account of the electrons and incorporates the effects of the fluctuating local moments by averaging over them to describe temperature dependent effects. After demonstrating the computational modelling with calculations of the light RE- Co_5 permanent magnet class, the rich and complex behaviour associated with the Fe atoms in $\text{Nd}_2\text{Fe}_{14}\text{B}$ will be described together with its role in determining the hard magnetic properties of this champion magnet.

SYUK 2: United Kingdom as Guest of Honor II

Time: Wednesday 15:00–17:45

Location: H2

Invited Talk SYUK 2.1 Wed 15:00 H2**Hysteresis Design of Magnetic Materials for Efficient Energy Conversion** — •OLIVER GUTFLEISCH — TU Darmstadt, Material Science

High performance permanent magnets are key components of energy-related technologies, such as direct drive wind turbines and e-mobility. They are also important in robotics and automatization, sensors, actuators, and information technology. The magnetocaloric effect is the key for new and disruptive solid state-based refrigeration. Magnetic hysteresis and its inherent energy product - characterises the performance of all magnetic materials. Despite considerable progress in the modelling, characterisation and synthesis of magnetic materials, hysteresis is a long-studied phenomenon that is still far from being completely understood. Discrepancies between intrinsic and extrinsic magnetic properties remain an open challenge and magnets do not operate yet at their physical limits. Basic material requirements, figure of merits, demand and supply, criticality of strategic elements are explained for both permanent magnets and magne-

tocalorics referring to the benchmark materials NdFeB and LaFeSi . The search for perfect defects is driving the material design strategy.

This work was supported by the Deutsche Forschungsgemeinschaft (DFG, German Research Foundation) Project-ID 405553726 CRC - TRR 270 - Cooperative Research Center HoMMage.

Invited Talk SYUK 2.2 Wed 15:30 H2**Non-equilibrium dynamics of many-body quantum systems versus quantum technologies** — •IRENE D'AMICO — University of York, York, UK

Quantum technologies take advantage of properties developed by quantum systems when driven out of equilibrium. For example, quantum computation is based on an accurate, controlled driving of these systems to perform specific dynamics which produce entanglement, compute basic gates, and eventually leads to the completion of a numerical algorithm. Thermal fluctuations are often an enemy which spoils the controlled out-of-equilibrium dynamics. On the other

side, quantum thermodynamics takes advantage of thermal - and quantum - fluctuations to create engines and refrigerators of sizes well below the thermodynamic limit and properties still under discussion. In this talk we will first focus on engineering robust properties for distributed quantum computing using spin-networks [1]: here the twist is *not* to drive the out-of-equilibrium dynamics, but let the system Hamiltonian do the job. We will then turn up the temperature, and consider a less-explored aspect of quantum thermodynamics, that is the effects and signatures of many-body interactions on few-electrons' quantum machines [2].

[1] L. Mortimer et al., *Adv. Quantum Technologies* 4, 2100013 (2021); A. H. Alsulami et al., arXiv:2202.02632

[2] K. Zawadzki et al., *Phys. Rev. Research* 2,033167 (2020); M. Herrera et al. *Phys. Rev. Lett.* 127, 030602 (2021); G. A. Canella et al., preprint (2022)

Invited Talk SYUK 2.3 Wed 16:00 H2
Quantum computing with trapped ions — •FERDINAND SCHMIDT-KALER — QUANTUM, Uni Mainz

Quantum technologies allow for fully novel schemes of hybrid computing. We employ modern segmented ion traps. I will sketch architectures, the required trap technologies and fabrication methods, control electronics for quantum register reconfigurations, and recent improvements of qubit coherence and gate performance. Currently gate fidelities of 99.995% (single bit) and 99.8% (two bit) are reached. We are implementing a reconfigurable qubit register and have realized multi-qubit entanglement [1] and fault-tolerant syndrome readout [2] in view for topological quantum error correction [3], since current aim is to leave the noisy area of quantum computing. Complementary to gate tomography, we employ thermodynamically-inspired methods within the frameworks of global passivity and passivity deformation where system qubits undergoing unitary evolution but may optionally be coupled also to an unobserved environment qubit, resulting in a heat leak [4].

[1] Kaufmann et al, *Phys. Rev. Lett.* 119, 150503 (2017) [2] J. Hilder, et al, *Phys. Rev. X* 12.011032 (2022) [3] Bermudez, et al, *Phys. Rev. X* 7, 041061 (2017) [4] D. Pijn, et al., *Phys. Rev. Lett.* 128 110601 (2022)

15 min. break

Invited Talk SYUK 2.4 Wed 16:45 H2
Breaking the millikelvin barrier in cooling nanoelectronic devices — •RICHARD HALEY — Physics Department, University of Lancaster, Lancaster LA1 4YB, UK

Over the last several years a number of groups across Europe have been developing techniques to cool the electrons in nano-fabricated devices to sub-

mK temperatures. Cooling device electrons into the microkelvin regime, below the canonical limit of around 10 millikelvin, enhances sensitivity for observing known and new physical phenomena, and improves the performance of quantum technologies, sensors and metrological standards.

There are two main challenges. First, one must provide a technique which will deliver electron temperatures colder than a dilution refrigerator and which is relatively easy to implement. Currently the microkelvin regime is really only accessible in specially dedicated labs. Second, one must understand the thermal links between the microkelvin cooling platform and the electrons in the device of interest, bearing in mind that nanoscale systems are typically also more susceptible to nuisance heating than bulk materials. Progress has been made with three methods and combinations thereof: immersion cooling in liquid helium; demagnetisation cooling of electrical leads and contacts; and the demagnetisation of material deposited directly onto device chips.

Here we review the current state-of-the-art in cooling nanoelectronic devices, and ways to make the techniques easier to adapt and adopt.

Invited Talk SYUK 2.5 Wed 17:15 H2
Superconducting Quantum Interference Devices for applications at mK temperatures — •SEBASTIAN KEMPF — Institute of Micro- and Nanoelectronic Systems, Karlsruhe Institute of Technology, Hertzstraße 16, 76187 Karlsruhe, Germany.

Superconducting quantum interference devices (SQUIDs) are among the most sensitive wideband devices for measuring any quantity that can be naturally converted into magnetic flux. They are intrinsically compatible with Kelvin and sub-Kelvin operation temperatures, offer great sensitivity to even tiniest signals and often show a noise level close to the quantum limit. For this reason, SQUIDs are routinely used for various applications such as investigating magnetic nanoparticles, diagnostics in health care, "non-invasive" mineral deposit exploration, low-field magnetic resonance imaging, quantum information processing or the readout of low-impedance cryogenic particle detectors. However, SQUID based measurements are susceptible to suffer from parasitic Joule heating, often preventing to reach very low sub-K temperatures.

Using the example of cryogenic low-impedance detectors, we discuss strategies to minimize parasitic SQUID Joule heating to ultimately operate single-channel detectors as well as mid- and large-scale detector arrays at lowest mK temperatures. We particularly show that on-chip thermal decoupling of shunt resistors and sample environment or dispersive SQUID readout allow for performing SQUID based measurements down to very low temperatures. Moreover, we discuss a SQUID based multiplexer allowing for simultaneous readout of hundreds and thousands of signal sources with only several nW of power.

Biological Physics Division Fachverband Biologische Physik (BP)

Joachim Rädler
Lehrstuhl Physik weicher Materie
Fakultät für Physik
Ludwig-Maximilians-Universität München
Geschwister-Scholl-Platz 1
80539 München
raedler@lmu.de

Overview of Invited Talks and Sessions

(Lecture halls H13, H15, and H16; Poster P1 and P4)

Invited Talks

BP 2.4	Mon	10:15–10:45	H13	Integrative modeling of dynamic biomolecular structures — •HOLGER GOHLKE
BP 4.1	Mon	10:30–11:00	H16	Computer simulations of self-motile active droplets and colloid-active gels composites — •DAVIDE DAVIDE MARENDUZZO
BP 5.1	Mon	15:00–15:30	H15	The functional nano-architecture of axonal actin — •CHRISTOPHE LETERRIER
BP 6.5	Mon	16:15–16:45	H16	From active bacterial microcolonies to biofilms as model tissues — •VASILY ZABURDAEV
BP 8.1	Tue	9:30–10:00	H15	Phase separation in cells: gene localization and noise buffering — •SAMUEL SAFRAN
BP 13.1	Wed	9:30–10:00	H15	Cortex mechanics - how subtle modifications matter — •ANDREAS JANSHOFF
BP 15.4	Wed	11:00–11:30	H13	The importance of water in membrane receptor function — •ANTHONY WATTS
BP 18.1	Wed	15:00–15:30	H15	Bottom-up molecular control of biomimetic hydrogels — •KERSTIN G. BLANK
BP 22.1	Thu	9:30–10:00	H15	Cell and tissue mechano-plasticity in development — •VERENA RUPRECHT
BP 24.1	Thu	10:30–11:00	H16	Actin waves as building blocks of cellular function — •CARSTEN BETA
BP 26.1	Thu	15:00–15:30	H15	Molecular robots working cooperatively in swarm — •AKIRA KAKUGO

Invited Talks of the joint Symposium SKM Dissertation Prize 2022 (SYSD)

See SYSD for the full program of the symposium.

SYSD 1.1	Mon	10:15–10:45	H2	Charge localisation in halide perovskites from bulk to nano for efficient optoelectronic applications — •SASCHA FELDMANN
SYSD 1.2	Mon	10:45–11:15	H2	Nonequilibrium Transport and Dynamics in Conventional and Topological Superconducting Junctions — •RAFFAEL L. KLEES
SYSD 1.3	Mon	11:15–11:45	H2	Probing magnetostatic and magnetotransport properties of the antiferromagnetic iron oxide hematite — •ANDREW ROSS
SYSD 1.4	Mon	11:45–12:15	H2	Quantum dot optomechanics with surface acoustic waves — •MATTHIAS WEISS

Invited Talks of the joint Symposium United Kingdom as Guest of Honor (SYUK)

See SYUK for the full program of the symposium.

SYUK 1.1	Wed	9:30–10:00	H2	Structure and Dynamics of Interfacial Water — •ANGELOS MICHAELIDES
SYUK 1.2	Wed	10:00–10:30	H2	A molecular view of the water interface — •MISCHA BONN
SYUK 1.3	Wed	10:30–11:00	H2	Motile cilia waves: creating and responding to flow — •PIETRO CICUTA
SYUK 1.4	Wed	11:00–11:30	H2	Cilia and flagella: Building blocks of life and a physicist's playground — •OLIVER BÄUMCHEN
SYUK 1.5	Wed	11:45–12:15	H2	Computational modelling of the physics of rare earth - transition metal permanent magnets from SmCo_5 to $\text{Nd}_2\text{Fe}_{14}\text{B}$ — •JULIE STAUNTON
SYUK 2.1	Wed	15:00–15:30	H2	Hysteresis Design of Magnetic Materials for Efficient Energy Conversion — •OLIVER GUTFLEISCH
SYUK 2.2	Wed	15:30–16:00	H2	Non-equilibrium dynamics of many-body quantum systems versus quantum technologies — •IRENE D'AMICO

SYUK 2.3	Wed	16:00–16:30	H2	Quantum computing with trapped ions — •FERDINAND SCHMIDT-KALER
SYUK 2.4	Wed	16:45–17:15	H2	Breaking the millikelvin barrier in cooling nanoelectronic devices — •RICHARD HALEY
SYUK 2.5	Wed	17:15–17:45	H2	Superconducting Quantum Interference Devices for applications at mK temperatures — •SEBASTIAN KEMPF

Invited Talks of the joint Symposium Interplay of Substrate Adaptivity and Wetting Dynamics from Soft Matter to Biology (SYSM)

See SYSM for the full program of the symposium.

SYSM 1.1	Wed	15:00–15:30	H1	Statics and Dynamics of Soft Wetting — •BRUNO ANDREOTTI
SYSM 1.2	Wed	15:30–16:00	H1	Droplets on elastic substrates and membranes - Numerical simulation of soft wetting — •SEBASTIAN ALAND
SYSM 1.3	Wed	16:00–16:30	H1	Wetting of Polymer Brushes in Air — LARS VELDSCHOLTE, GUIDO RITSEMA VAN ECK, LIZ MENSINK, JACCO SNOEIJER, •SISSI DE BEER
SYSM 1.4	Wed	16:45–17:15	H1	Elastocapillary phenomena in cells — •ROLAND L. KNORR
SYSM 1.5	Wed	17:15–17:45	H1	Active contact line depinning by micro-organisms spreading on hydrogels — MARC HENNES, JULIEN TAILLEUR, GAËLLE CHARRON, •ADRIAN DAERR

Invited Talks of the joint Symposium Collective Social Dynamics from Animals to Humans (SYSO)

See SYSO for the full program of the symposium.

SYSO 1.1	Thu	9:30–10:00	H1	Capturing group interactions: The next frontier of modeling social and biological systems — •FRANK SCHWEITZER
SYSO 1.2	Thu	10:00–10:30	H1	Modelling Individual Mobility Behavior — •LAURA MARIA ALESSANDRETTI
SYSO 1.3	Thu	10:30–11:00	H1	Validating argument-based opinion dynamics with survey experiments — •SVEN BANISCH
SYSO 1.4	Thu	11:15–11:45	H1	Self-organization, Criticality and Collective Information Processing in Animal Groups — •PAWEŁ ROMANCZUK
SYSO 1.5	Thu	11:45–12:15	H1	Collective dynamics and physiological interactions in bird colonies — •HANJA BRANDL

Sessions

BP 1.1–1.3	Sun	16:00–18:30	H4	Tutorial: Stochastic Processes from Financial Risk to Genetics (joint session SOE/TUT/BP/DY)
BP 2.1–2.9	Mon	9:30–12:15	H13	Computational Biophysics and Neuroscience
BP 3.1–3.10	Mon	9:30–12:30	H15	Cell Mechanics 1
BP 4.1–4.7	Mon	10:30–12:45	H16	Active Matter 1 (joint session BP/PPP/DY)
BP 5.1–5.7	Mon	15:00–17:30	H15	Focus Session: Super Resolution Microscopy and Dynamics of Supramolecular Complexes
BP 6.1–6.7	Mon	15:00–17:15	H16	Statistical Physics of Biological Systems 1 (joint session BP/DY)
BP 7.1–7.46	Mon	18:00–20:00	P1	Poster 1
BP 8.1–8.12	Tue	9:30–13:00	H15	Focus Session: Phase Separation in Biochemical Systems
BP 9.1–9.11	Tue	9:30–13:00	H16	Bioimaging
BP 10.1–10.9	Tue	10:00–12:30	H13	Cell Adhesion and Multicellular Systems
BP 11.1–11.11	Tue	10:00–13:00	H18	Active Matter 2 (joint session DY/BP/PPP)
BP 12.1–12.66	Tue	17:30–19:30	P4	Poster 2
BP 13.1–13.11	Wed	9:30–12:45	H15	Cytoskeleton
BP 14.1–14.10	Wed	9:30–12:30	H16	Active Matter 3 (joint session BP/PPP/DY)
BP 15.1–15.7	Wed	10:00–12:15	H13	Protein Structure and Single Molecules
BP 16.1–16.6	Wed	10:15–12:45	H11	Networks: From Topology to Dynamics (joint session SOE/BP/DY)
BP 17.1–17.7	Wed	15:00–17:00	H13	Membranes and Vesicles
BP 18.1–18.8	Wed	15:00–17:30	H15	Biomaterials (joint session BP/PPP)
BP 19.1–19.8	Wed	15:00–17:15	H16	Cell Mechanics 2
BP 20.1–20.9	Wed	15:00–17:30	H18	Active Matter 4 (joint session DY/BP/PPP)
BP 21	Wed	18:00–19:00	H15	Members' Assembly
BP 22.1–22.9	Thu	9:30–12:15	H15	Migration and Multicellular Systems
BP 23.1–23.3	Thu	10:00–10:45	H13	Evolution
BP 24.1–24.6	Thu	10:30–12:30	H16	Systems Biology, Gene Expression, Signalling
BP 25.1–25.4	Thu	11:00–12:00	H13	Bioinspired Systems
BP 26.1–26.8	Thu	15:00–17:30	H15	Focus Session: Bioinspired Systems

BP 27.1–27.6	Thu	15:00–16:30	H16	Statistical Physics of Biological Systems 2 (joint session BP/DY)
BP 28.1–28.6	Fri	9:30–11:15	H39	Biopolymers, Biomaterials and Bioinspired Functional Materials (joint session CPP/BP)
BP 29.1–29.11	Fri	10:00–12:45	H18	Active Matter 5 (joint session DY/BP/ CPP)

Members' Assembly of the Biological Physics Division

Wednesday 18:00–19:00 H15

- Report
- Election
- Miscellaneous

Sessions

– Invited Talks, Prize Talks, Tutorials, Contributed Talks, and Posters –

BP 1: Tutorial: Stochastic Processes from Financial Risk to Genetics (joint session SOE/TUT/BP/DY)

Macroscopic and microscopic models from Economy to Biology must account for stochasticity on various levels. While classical physics strives for deterministic descriptions through differential equations from fundamental level to thermodynamics, many physics-based models on higher level explicitly include stochasticity from various sources. Discrete and continuous stochastic processes then become the mathematical foundation of these models. This tutorial highlights classical as well as current methods and approaches of probabilistic models and stochastic processes in physics, biology as well as socio-economic systems, thereby bridging the risk to extinction in genetics with its economic counterpart. (Session organized by Jens Christian Clausen.)

Time: Sunday 16:00–18:30

Location: H4

See SOE 1 for details of this session.

BP 2: Computational Biophysics and Neuroscience

Time: Monday 9:30–12:15

Location: H13

BP 2.1 Mon 9:30 H13

Non-ideality in lipid mixtures, a molecular dynamics study — •LISA BEREZOVSKA¹, FABRICE THALMANN¹, and RAISA KOCIURZYNSKI² — ¹Institut Charles Sadron, CNRS and University of Strasbourg, 23 rue du Loess, F-67034 Strasbourg, France — ²Faculty of Biology, Albert-Ludwigs-University Freiburg, Schänzlestraße 1, 79104 Freiburg, Germany

Biological membranes are complex environments characterized by multicomponent lipid mixtures [1]. We investigate in this work binary lipid bilayers using the SPICA coarse-grained molecular dynamics model.

Adapting the Kirkwood-Buff theory of liquid mixtures [2] to finite wavelength density fluctuations statistics, we compare various practical approaches for determining the interaction parameters in a theory of regular solution description of these numerical lipid mixtures.

[1] Ole G. Mouritsen, L. A. Bagatolli. *Life as a matter of fat*, Springer-Verlag GmbH, 2015

[2] A. Ben-Naim, *Water and Aqueous Solutions: Introduction to a Molecular Theory*, Plenum Press, 1974

[3] Lisa Berezovska, Raisa Kociurzynski, Fabrice Thalmann, in preparation

BP 2.2 Mon 9:45 H13

Membrane-mediated interactions between non-spherical elastic particles — •JIARUL MIDYA, THORSTEN AUTH, and GERHARD GOMPPER — Theoretical Physics of Living Matter (IBI-5/IAS-2), Forschungszentrum Jülich, D-52425 Jülich, Germany

Transport of particles across lipid-bilayer membranes is important for biological cells to exchange information and material with the environment. Large particles often get wrapped by membranes [1]. However, many particles in vivo and in vitro are deformable, e.g., vesicles, filamentous viruses, macromolecular condensates, polymer-grafted nanoparticles, and microgels. Vesicles may serve as a generic model system for deformable particles [2]. Using the Helfrich Hamiltonian, triangulated membranes, and energy minimization, we predict the interplay of vesicle shapes and wrapping states. Increasing particle softness enhances the stability of shallow-wrapped and deep-wrapped states over non-wrapped and complete-wrapped states. The free membrane mediates an interaction between partial-wrapped vesicles. For the deep-wrapped vesicles, we predict a purely repulsive interaction. For shallow-wrapped states, interaction potential depends on the mutual orientation of the vesicles. Our predictions may guide the design and fabrication of deformable particles for efficient use in medical applications, such as targeted drug delivery.

[1] S. Dasgupta et al., *J. Phys.: Condens. Matter* **29**, 373003 (2017); [2] X. Yi et al., *Phys. Rev. Lett.* **107**, 098101 (2011).

BP 2.3 Mon 10:00 H13

RNA structure prediction via Machine Learning — •ALEXANDER SCHUG^{1,2}, OSKAR TAUBERT⁴, CHRISTIAN FABER¹, MEHARI ZERIHUN¹, FABRIZIO PUCCI¹, FABRICE VON DER LEHR³, PHILIPP KNECHTGES³, MARIE WEI^{4,5}, CHARLOTTE DEBUS^{4,5}, DANIEL COQUELIN^{4,5}, STEFAN KESSELHEIM^{1,5}, ACHIM BASERMANN³, ACHIM STREIT⁴, and MARKUS GÖTZ^{4,5} — ¹Jülich Supercomputing Centre, FZ Jülich, Jülich — ²Faculty of Biology, University of Duisburg/Essen — ³Institute

for Software Technology, German Aerospace Centre (DLR) — ⁴Steinbuch Centre for Computing, Karlsruhe Institute of Technology — ⁵Helmholtz AI

Knowledge of biomolecular structure is necessary to gain any detailed understanding of their function. For proteins, tools rooted in statistical physics such as Direct Coupling Analysis (DCA) or Machine Learning driven approaches (ML) such as Alpha Fold 2 exploit massive sequence databases to trace evolutionary patterns for structure predictions. We demonstrate how additional information, such as low-resolution experimental information (e.g. SAXS or FRET) can be integrated. For RNA there are significantly less data available than for proteins, which makes ML more challenging. Still, we demonstrate how contact prediction for RNA can be vastly improved both via simple convolutional neural networks but also by unsupervised deep-learning approaches by combining multiple self-supervised learning tasks. In an empirical evaluation for RNA, we find a strong increase of prediction quality.

Invited Talk

BP 2.4 Mon 10:15 H13

Integrative modeling of dynamic biomolecular structures — •HOLGER GOHLKE — Institute for Pharmaceutical and Medicinal Chemistry, Heinrich Heine University Düsseldorf, 40225 Düsseldorf, Germany — John von Neumann Institute for Computing (NIC), Jülich Supercomputing Centre (JSC), Institute of Biological Information Processing (IBI-7: Structural Biochemistry), and Institute of Bio- and Geosciences (IBG-4: Bioinformatics), Forschungszentrum Jülich GmbH, 52425 Jülich, Germany

Structures of biomacromolecules and their complexes are essential to understand the underlying molecular mechanisms of the biological processes. If biomolecular systems are complex, information from multiple experimental and computational methods is combined by integrative modeling (IM) for generating integrative structure models. We will describe how molecular modeling and simulations contributed to a high-resolution NMR characterization of all apparent states of the prototypic 10*23 DNase and to rationally selecting a single-atom replacement, with which the performance of the DNase could be considerably enhanced. Furthermore, we will address how to overcome the sparsity of FRET experiments to provide state-specific structural information of complex dynamic biomolecular assemblies and probe the robustness of Maximum Entropy Method reconstructions for a flexible system with ordered parts using FRET data as experimental information.

15 min. break

BP 2.5 Mon 11:00 H13

Mechanical stimulation in stem cell-derived 3D neuronal networks — •ELIJAH SHELTON¹, KATJA SALBAUM^{1,2}, FILIPPO KIESSLER¹, PAULINA WYSMOLEK³, SELINA SONNTAG¹, and FRIEDHELM SERWANE^{1,2,4} — ¹Faculty of Physics and Center for NanoScience, Ludwig-Maximilians-Universität, Munich, Germany — ²Graduate School of Systemic Neuroscience (GSN), Munich, Germany — ³Max Planck Institute for Medical Research, Heidelberg, Germany — ⁴Munich Cluster for Systems Neurology (SyNergy), Germany

Neurons sense and respond to mechanical factors in their local microenvironment. For example, firing activity is modulated in response to amplitude and location of a mechanical stimulation as single cell in vitro experiments have shown.

However, it is unclear (i) how these observations translate to the scale of neuronal tissues and (ii) how mechanical stimulation informs the formation and function of neurons in 3D networks. To tackle this problem, we combine stem cell-derived neuronal organoids, magnetic droplets as mechanical actuators, and calcium imaging as tool for neuronal characterization. Using 30-50 micron diameter magnetic droplets, we produce controlled and precise mechanical stimulations inside these 3D tissues. We visualize electrophysiological activity within these networks using genetically encoded calcium sensors and confocal fluorescence microscopy. Here, I present recent mechanical and electrophysiological measurements within these neuronal organoids. Such kinds of recordings might provide insights into how mechanical forces can influence both form and function of neuronal networks.

BP 2.6 Mon 11:15 H13

Characterizing spreading dynamics of subsampled systems with nonstationary external input — JORGE DE HEUVEL¹, JENS WILTING², MORITZ BECKER³, VIOLA PRIESEMANN², and •JOHANNES ZIERENBERG² — ¹University of Bonn, Bonn, Germany — ²Max Planck Institute for Dynamics and Self-Organization, Göttingen Germany — ³University Medical Center Göttingen, Göttingen Germany

Many systems with propagation dynamics, such as spike propagation in neural networks and spreading of infectious diseases, can be approximated by autoregressive models. The estimation of model parameters can be complicated by the experimental limitation that one observes only a fraction of the system (subsampling) and potentially time-dependent parameters, leading to incorrect estimates. We show analytically how to overcome the subsampling bias when estimating the propagation rate for systems with certain nonstationary external input. This approach is readily applicable to trial-based experimental setups and seasonal fluctuations as demonstrated on spike recordings from monkey prefrontal cortex and spreading of norovirus and measles.

BP 2.7 Mon 11:30 H13

Mesoscopic description of metastability and hippocampal replay in neural networks with short-term plasticity — BASTIAN PIETRAS¹, VALENTIN SCHMUTZ², and •TILO SCHWALGER³ — ¹Universitat Pompeu Fabra, Barcelona, Spain — ²Brain Mind Institute, School of École Polytechnique Fédérale de Lausanne (EPFL), Lausanne, Switzerland — ³Technische Universität Berlin

Sequences of metastable states in neuronal population activities have been linked to various sensory and cognitive functions. Two prominent mechanisms of metastable dynamics are noise-induced transitions among attractors and deterministic transitions induced by slow fatigue processes. The dependence of these mechanisms on neural circuit parameters at the microscopic scale are largely unclear. Starting with a network of linear-nonlinear Poisson spiking neurons with synaptic short-term plasticity, we use a bottom-up approach and derive a stochastic neural-mass model at the mesoscopic scale that links to the microscopic circuit parameters. We apply the mesoscopic model to investigate hippocampal "replay" events, i.e. spontaneous sequences of metastable activa-

tions of place cells. We study a spiking-neural-network for depression-induced metastability of place-cell activity. The corresponding mesoscopic model precisely reproduces the statistics of metastable events in the microscopic network model. This enables us to efficiently explore the full range of neuron numbers including the thermodynamic limit. We find a novel dynamical regime in finite-size networks where metastable replay events are fluctuation-driven and exhibit biologically plausible irregularity.

BP 2.8 Mon 11:45 H13

Decision-making and dynamics in a small neural network — •MONIKA SCHOLZ — Max Planck Institute for Neurobiology of Behavior - caesar

The nematode *C. elegans* feeds on small microbes which it ingests using a pumping action of the pharynx. Its pharyngeal nervous system, which controls feeding, comprises only 20 neurons. We aim to understand how the animal adapts its feeding rate to environmental conditions and metabolic needs, using a combination of theoretical modelling, voltage imaging and behavioral observations. When imaging the animals feeding behavior we identify two modes of regulating food intake: First, we find burst-pause dynamics which we link to a decision-making process where the animal attempts to measure the external food concentration. We also find a second mode of action, in which the pumping frequency is smoothly adapted to reflect the quality of the available food. Using a conductance model of the pharyngeal muscle and its key regulatory circuit, we ask which of these modes of regulation are in the muscular excitability and which are driven by phasic inputs by the nervous system. We will discuss the utility of this small nervous system in understanding computational principles connecting neural activity to behavior.

BP 2.9 Mon 12:00 H13

Available processing time regulates optimal balance between sensitivity and precision — SAHEL AZIZPOUR¹, •JOHANNES ZIERENBERG², VIOLA PRIESEMANN², and ANNA LEVINA³ — ¹Donders Institute for Brain, Cognition and Behavior, Nijmegen, Netherlands — ²Max Planck Institute for Dynamics and Self-Organization, Göttingen Germany — ³Eberhard Karls University of Tübingen, Tübingen, Germany

Solving everyday tasks naturally leads to a trade-off between the time spent on processing some input and the accuracy of the outcome. In particular, fast decisions have to rely on uncertain information about inputs. However, standard estimates of information processing capabilities, such as the dynamic range, are defined based on infinite-time averages that do not incorporate noise effects from finite processing times. Here, we develop estimates of processing capability that explicitly account for noisy outputs. We use these measures to show that limiting the processing time in recurrent neural networks can drastically affect the sensitivity and precision of outcomes. This way, optimal dynamical states shift away from the conventionally expected critical point toward subcritical states for finite processing times. Our results thus highlight the necessity to explicitly account for processing times in future estimates of information processing capabilities.

BP 3: Cell Mechanics 1

Time: Monday 9:30–12:30

Location: H15

Prize Talk

BP 3.1 Mon 9:30 H15

Basal tension in the wing disc epithelium - what's collagen got to do with it — KARLA YANIN GUERRA SANTIALLAN^{1,3}, CHRISTIAN DAHMANN², and •ELISABETH FISCHER-FRIEDRICH^{1,3,4,5} — ¹Cluster of Excellence Physics of Life, Technische Universität Dresden, Dresden, Germany — ²Institute of Genetics, Technische Universität Dresden, Dresden, Germany — ³Biotechnology Center, Technische Universität Dresden, Dresden, Germany — ⁴Faculty of Physics, Technische Universität Dresden, Dresden, Germany — ⁵Laureate of the Hertha-Sponer-Prize 2022

Healthy tissue morphogenesis is an important prerequisite for organ function. During development, epithelial folding is a major element of tissue morphogenesis. It has been shown that epithelial folding can be driven through a reduction of basal cell tension. However, a comprehensive analysis of the regulating factors of basal tension is still lacking. In this study, we use indentation with the cantilever of an atomic force microscope to estimate mechanical tension at the basal cell boundary in the wing disc epithelium of the 3rd instar larva of *Drosophila melanogaster*. We find that basal tension is not only affected by contractility of the actin cytoskeleton but is strongly influenced by the presence of the basement membrane as well as osmotic pressure. Our data suggest that elastic stresses in the basement membrane induced by basement membrane stretch, e.g. via osmotic swelling, may be a key factor in the adjustment of basal tension.

BP 3.2 Mon 10:00 H15

Viscoelasticity of spherical cellular aggregates — •ANTOINE GIROT^{1,2}, MARCIN MAKOWSKI¹, MARCO RIVETTI¹, CHRISTIAN KREIS^{1,3}, ALEXANDROS FRAGKOPOULOS^{1,2}, and OLIVER BÄUMCHEN^{1,2} — ¹Max Planck Institute for Dynamics and Self-Organization (MPIDS), 37077 Göttingen, Germany — ²University of Bayreuth, Experimental Physics V, 95447 Bayreuth, Germany — ³Department of Physical and Environmental Sciences, University of Toronto, ON Toronto, Canada

Understanding the complexity of many biophysical processes such as the dynamics of biological tissues requires a proper mechanical characterization of multicellular aggregates. Current experimental techniques, however, are typically limited to systems that are not larger than an individual cell. We employ *in vivo* micropipette force measurements combined with optical detection to precisely measure the force response and the deformation of living organisms simultaneously. In this presentation, we use this approach to investigate the mechanical behaviour of *Volvox globator*, a multicellular aggregate composed of thousands of bi-flagellated cells forming a spherical monolayer filled with mucilage. *Volvox* is considered a model system, e.g. to study the evolution from single cells to multicellular life. We show that a model that couples elastic and viscous components is in excellent agreement with the mechanical response of *Volvox* and therefore can be used to extract the viscoelastic properties. We find that the viscous component is rate-dependent and exhibits a shear-thinning behaviour, while the elasticity of the cellular monolayer depends on the size of the colony.

BP 3.3 Mon 10:15 H15

Phase field model for the mechanics and migration of nucleated cells — •ROBERT CHOJOWSKI, ULRICH S. SCHWARZ, and FALCO ZIEBERT — Institute for Theoretical Physics and BioQuant, Heidelberg University, Germany

Eukaryotic cells are built from many different constituents of varying sizes and properties. Of these organelles, the nucleus is by far the largest one. During recent years, it has become clear that many cellular functions are modulated by the nucleus, including mechanosensing of the environment and cell migration in complex environments. Its stiffness has been determined by AFM and micropipette experiments to be up to 10-fold higher than the stiffness of the surrounding cytoplasm. Despite its physical and biological importance, the nucleus is often neglected in models for cell mechanics and migration. Here we extend our reversible elastic phase field method [1] by a compartment with nuclear elasticity. We validate our numerical implementation by comparing to the analytical solution of a homogeneously adhered disk-like cell. We then simulate the effect of the nucleus for several interesting experimental setups, in particular for cell migration through a narrow channel.

[1] R. Chojowski, U.S. Schwarz, F. Ziebert, Reversible elastic phase field approach and application to cell monolayers, *Eur. Phys. J. E* 43, 63 (2020)

BP 3.4 Mon 10:30 H15

Mechanical Properties of the Premature Lung — •JONAS NAUMANN¹, NICKLAS KOPPE¹, ULRICH HERBERT THOME², MANDY LAUBE², and MAREIKE ZINK¹ — ¹Research Group Biotechnology and Biomedicine, Peter-Debye-Institute for Soft Matter Physics, Leipzig University, 04103 Leipzig, Germany — ²Center for Pediatric Research Leipzig, Department of Pediatrics, Division of Neonatology, Leipzig University, 04103 Leipzig, Germany

Even though mechanical ventilation is a life-saving therapy for premature infants suffering from respiratory distress syndrome, prolonged ventilation and related mechanical load may cause subsequent pulmonary diseases such as bronchopulmonary dysplasia. To study the effect of mechanical stress on the immature lung, premature rat lungs were subjected to rheology experiments in compression and tension at different velocities. Here, fetal lungs behaved significantly stiffer with increasing deformation velocities as also used during high-frequency ventilation. A higher Young's modulus of fetal rat lungs compared to adult controls clearly pointed towards altered tissue characteristics. Furthermore, influences of hydrostatic pressure differences on the electrophysiology of lung epithelial cells were studied with a pressure-adjustable Ussing chamber. We observed a strong impact of hydrostatic pressure on vectorial sodium transport, important for alveolar fluid clearance. These pressure-dependent cellular alterations might explain clinical observations of ventilation-induced side effects.

15 min. break

BP 3.5 Mon 11:00 H15

Novel Optofluidic Particle Trap Enables FemtoNewton Force Sensing — •ILIYA STOEVI^{1,2}, BENJAMIN SEELBINDER^{1,2}, ELENA ERBEN^{1,2}, NICOLA MAGHELLI^{1,2}, and MORITZ KREYSING^{1,2,3} — ¹Max Planck Institute of Molecular Cell Biology and Genetics, Pfotenhauerstraße 108, 01307, Dresden, Germany — ²Centre for Systems Biology, Pfotenhauerstraße 108, 01307, Dresden, Germany — ³Cluster of Excellence Physics of Life, TU Dresden, Arnoldstraße 18, 01307, Dresden, Germany

Here we show how thermoviscous expansion phenomena can be used to generate a new contactless particle trap that is characterised by a linear force-extension relationship and can therefore be employed in non-invasively measuring femtoNewton forces with thermally limited sensitivity. Our new method combines optics with microfluidics, lifting prerequisites related to the probe material and resulting in only moderate heating at the position of the micromanipulated object. This offers an appealing alternative to the use of optical tweezers in highly delicate samples and living systems. As a follow-up work, we aim to explore the opportunity of using these thermoviscous flows in a novel phase-sensitive microrheology approach by building on the formalism established in classic bulk rheology. We anticipate that our new method would be of interest to material scientists and mechanobiologists alike as it provides a route towards measuring the mechanics of highly viscous media, tenuous gels and likely even cellular cytoplasm or embryonic ooplasm. Further refinements of the method aim at removing the need for using fluorescent tags and/or external probes.

BP 3.6 Mon 11:15 H15

Theoretical model reveals significance of microtubules poleward flux in chromosome congression — •IVAN SIGMUND, DOMAGOJ BOŽAN, and NENAD PAVIN — University of Zagreb, Faculty of Science

At the onset of mitosis, a living cell forms mitotic spindle to ensure proper division of duplicated chromosomes between two daughter cells, whereas malfunctioning spindles can lead to chromosome missegregation. During prometaphase chromosomes are initially randomly distributed and in interaction with microtubules experience forces that congress them in spindle equator. Here we investigate what are the dominant forces that drive chromosome congression. By introducing a theoretical model, we show that length dependent poleward flux

generates a net force towards the spindle equator. This poleward flux is generated by motor proteins which accumulate along the region of antiparallel microtubule overlaps. On the other hand, forces exerted by passive crosslinkers, that accumulate within the region of parallel microtubule overlaps, are off-centering, and can impair chromosome congression. Thus, our model reveals the significance of microtubule poleward flux in chromosome congression.

BP 3.7 Mon 11:30 H15

Red blood cell shape transitions and dynamics in time-dependent capillary flow — •KATHARINA GRAESEL¹, STEFFEN M. RECKTENWALD², FELIX M. MAURER², THOMAS JOHN², CHRISTIAN WAGNER^{2,3}, and STEPHAN GEKLE¹ — ¹Biofluid Simulation and Modeling, Theoretische Physik VI, University of Bayreuth — ²Dynamics of Fluids, Experimental Physics, Saarland University — ³Physics and Materials Science Research Unit, University of Luxembourg

Red blood cells in small microchannels flow in characteristic shapes, mainly symmetric croissants at the channel center and non-symmetric off-centered slippers. While these shapes have been studied for some time, not much is known about the transition dynamics between different states. Here, we use boundary-integral simulations together with microfluidic experiments in time-dependent flows to observe and understand red blood cell shape transitions. The transition from the croissant to the slipper shape happens much faster than the opposite transition. We find that the center of mass of slipper cells shows lateral oscillations due to the tank-treading movement of the RBC membrane. The oscillation frequency increases with the cell velocity and the viscosity of the surrounding fluid.

BP 3.8 Mon 11:45 H15

Elastic modulus of lipid-loaded platelets investigated with scanning ion conductance microscopy (SICM) — •HENDRIK VON EYSMONDT¹, JOHANNES RHEINLAENDER¹, MADHUMITA CHATTERJEE², and TILMAN E. SCHÄFFER¹ — ¹Institute of Applied Physics, Eberhard-Karls-University Tübingen, Germany — ²Department of Cardiology and Angiology, University Hospital Tübingen, Germany

Platelets are small, nucleate blood cells involved in blood hemostasis, wound healing, and immune response as well as in diseases like atherosclerosis and coronary artery disease. Both low-density lipoprotein (LDL) and its oxidized form (OxLDL) increase the prothrombotic potential of platelets. Recently, it was shown that a chemokine receptor ACKR3/CXCR7 agonist inhibits platelet activation and thrombus formation, offering a new therapeutic choice for hyperlipidemic patients. However, the impacts of LDL, OxLDL, and CXCR7-agonist on platelet morphology and mechanics have not yet been identified.

We therefore investigated the influence of LDL, OxLDL, and CXCR7-agonist on platelet morphology and mechanics using SICM. We showed that CXCR7-agonist pre-treatment reduced the initial spreading rate on collagen, the final spreading area on both collagen and fibrinogen, and the elastic modulus on fibrinogen. We also showed that OxLDL, but not LDL, significantly alters the morphology and elastic modulus of lipid-loaded platelets and that CXCR7-agonist pretreatment can reverse some of the effects of OxLDL.

BP 3.9 Mon 12:00 H15

Measuring the Tension of Droplets and Living Cells with the Scanning Ion Conductance Microscope — •JOHANNES RHEINLAENDER and TILMAN E. SCHÄFFER — Institute of Applied Physics, University Tübingen, Germany

It is well known that surface tension can dominate the mechanics of micro- and nanoscale systems. However, probing the mechanics of elastic interfaces at the micrometer scale can be difficult because of the complex probe-sample interactions or the unknown underlying geometry. Here, we introduce a method to measure the surface tension of interfaces at the micrometer scale in a contact-free manner using the scanning ion conductance microscope (SICM). The SICM is based on recording the ion current through a nanopipette and was recently extended to also measure the mechanical stiffness of soft samples utilizing a microfluidic flow through the nanopipette opening. By measuring the three-dimensional shape and mechanical stiffness of oil droplets on various surfaces, we show that we can quantitatively measure their surface tension independently of their shape over more than three orders of magnitude. Applying this concept to living cells, we show that we can quantitatively measure their local stiffness and average (cortical) tension in a contact-free way. Living cells exhibit cortical tensions on the order of few mN/m, which we found to strongly vary with cell type and external conditions. For example, we show that normal and cancer cells strongly differ in their cortical tension, which demonstrates that the SICM is a versatile tool to measure the mechanical properties of living cells.

BP 3.10 Mon 12:15 H15

The secret life of sarcomeres: stochastic heterogeneity of sarcomeres in beating stem-cell-derived cardiomyocytes — •DANIEL HÄRTTER^{1,2}, LARA HAUKE¹, WOLFRAM-HUBERTUS ZIMMERMANN¹, and CHRISTOPH F. SCHMIDT² — ¹Institute of Pharmacology and Toxicology, Göttingen University Medical Center, Germany — ²Department of Physics and Soft Matter Center, Duke University, Durham, NC, USA

Sarcomeres are the basic contractile units of cardiac muscles. We tracked single sarcomere motion in individual hiPSC-derived cardiomyocytes at high resolution, using a novel set of experimental and computational tools. While the emergent cell-level motion is smooth, individual sarcomeres are highly motile and behave heterogeneously during beating cycles. In response to rigid mechanical constraints, sarcomeres are forced into a tug-of-war-like competition. Automated, machine-learning-supported analysis of a large data set (>1200 cells) indicates that sarcomere heterogeneity is not caused by static non-uniformity

between sarcomeres (e.g., strong/weak), but can be primarily attributed to the stochastic and non-linear nature of sarcomere dynamics and thus occurs intrinsically during cardiomyocyte beating. We show that a simple dynamic model reproduces crucial experimental findings by assuming a non-monotonic force-velocity relation for single sarcomeres, as previously predicted for ensembles of motor proteins. This led us to a novel, active matter perspective on sarcomere motion, with sarcomeres as interacting, non-linear and stochastic agents, in contrast to the prevailing mechanistic view on muscle contraction.

BP 4: Active Matter 1 (joint session BP/CPP/DY)

Time: Monday 10:30–12:45

Location: H16

Invited Talk

BP 4.1 Mon 10:30 H16

Computer simulations of self-motile active droplets and colloid-active gels composites — •DAVIDE DAVIDE MARENDUZZO — School of Physics and Astronomy, University of Edinburgh, Edinburgh, UK

In this talk we will show results from computer simulations probing the behaviour of composite materials based on active gels.

In the first part of the talk we will investigate the behavior of active nematic or cholesteric droplets inside an isotropic fluid. In different regions of parameter space, we find regular motility and chaotic behaviour, and discuss the relevance of these results to biophysical systems such as microbial motility.

In the second part of the talk, we will study the dynamics of a dispersion of passive colloidal particles in an active nematic host. We find that activity induces a dynamic clustering of colloids even in the absence of any preferential anchoring of the active nematic director at the particle surface. When such an anchoring is present, active stresses instead compete with elastic forces and re-disperse the aggregates observed in passive colloid-liquid crystal composites.

BP 4.2 Mon 11:00 H16

Chloroplasts in dark-adapted plants show active glassy behavior — •NICO SCHRAMMA, CINTIA PERUGACHI ISRAËLS, and MAZI JALAL — University of Amsterdam, Amsterdam, Netherlands

Photosynthesis in plants is one of the main drivers for the survival of whole ecosystems on earth. To guarantee the efficiency of this process, plants have to actively adapt to ever-changing light conditions. On large time scales plants can grow towards the light. However, this process is too slow to adapt towards transient stimuli. To do this plants can re-arrange the intracellular structure by the active motion of chloroplasts on short timescales. These organelles are confined between the cell membrane and vacuole and can move inside the cytoplasm via actin polymerization forces. Remarkably, the simple - yet elegant - interplay of light-sensing and active forces leads to various modes of collective motion. Here, we show that the chloroplasts under dark conditions are densely packed systems, driven by a-thermal noise and can exhibit active glassy motion. Furthermore, we aim to establish chloroplast motion as a new framework to study the dynamics of light-controlled dense biological systems featuring intriguing dynamic phase transitions.

BP 4.3 Mon 11:15 H16

Activity-induced polar patterns of filaments gliding on a sphere — •CHIAO-PENG HSU, ALFREDO SCIORTINO, YU ALICE DE LA TROBE, and ANDREAS BAUSCH — Center for Protein Assemblies and Lehrstuhl für Zellbiophysik E27, Physics Department, Technische Universität München, Garching, Germany

Active matter systems feature the ability to form collective patterns as observed in a plethora of living systems, from schools of fish to swimming bacteria. While many of these systems move in a wide, three-dimensional environment, several biological systems are confined by a curved topology. The role played by a non-Euclidean geometry on the self-organization of active systems is not yet fully understood, and few experimental systems are available to study it. Here, we introduce an experimental setup in which actin filaments glide on the inner surface of a spherical lipid vesicle, thus embedding them in a curved geometry. We show that filaments self-assemble into polar, elongated structures and that, when these match the size of the spherical geometry, both confinement and topological constraints become relevant for the emergent patterns, leading to the formation of polar vortices and jammed states. These results experimentally demonstrate that activity-induced complex patterns can be shaped by spherical confinement and topology.

15 min. break

BP 4.4 Mon 11:45 H16

The effect of chiral flows on pattern formation on active cell surfaces — LUCAS WITWER², ELOY DE KINKELDER¹, and •SEBASTIAN ALAND^{1,2} — ¹TU Freiberg — ²HTW Dresden

Mechanochemical processes play a crucial role during morphogenesis, the formation of complex shapes and tissues out of a single cell. On the cellular level,

the actomyosin cortex governs shape and shape changes. This thin layer of active material underneath the cell surface exerts an active contractile tension, the strength of which being controlled by the concentration of force-generating molecules. Advective transport of such molecules leads to a complex interplay of hydrodynamics and molecule concentration which gives rise to pattern formation and self-organized shape dynamics. In this talk, we present a novel numerical model to simulate an active viscoelastic surface immersed in viscous fluids. The resulting patterning, flows and cell shape dynamics are shown for different parameter configurations. It is further demonstrated that adding a chiral (i.e. counter-rotating) force at the cell surface can promote a ring of high molecule concentration and facilitate cell division.

BP 4.5 Mon 12:00 H16

Premelting controlled active matter in ice — •JEREMY VACHIER¹ and JOHN S. WETTLAUFER^{1,2} — ¹Nordita, KTH Royal Institute of Technology and Stockholm University, Hannes Alfvéns väg 12, SE-106 91 Stockholm, Sweden — ²Yale University, New Haven, Connecticut 06520-8109, USA

Self-propelled particles can undergo complex dynamics due to a range of bulk and surface interactions. In the case of a foreign particle inside a subfreezing solid, such as a particle in ice, a premelted film can form around it allowing the particle to migrate under the influence of an external temperature gradient, which is a phenomenon called thermal regelation. It has recently been shown that the migration of particles of a biological origin can accelerate melting in a column of ice and thereby migrate faster. We have previously shown that the effect of regelation plays a major role in the migration of inert particles and impurities inside ice, with important environmental implications. In particular, the question of how the activity affects a particle's position over time is essential for paleoclimate dating methods in ice cores. We re-cast this class of regelation phenomena in the stochastic framework of active Ornstein-Uhlenbeck dynamics and make predictions relevant to this and related problems of interest in geophysical and biological problems.

BP 4.6 Mon 12:15 H16

Emergent collective behavior of active Brownian particles with visual perception — •RAJENDRA SINGH NEGI, ROLAND G. WINKER, and GERHARD GOMPPER — Theoretical Physics of Living Matter, Institute of Biological Information Processing (IBI-5), Forschungszentrum Jülich, 52425 Jülich, Germany

Collective behavior of self-propelled agents emerges from the dynamic response of individuals to various input signals [1,2]. One such input signal is visual perception. We explore the behavior of a model of self-steering active Brownian particles with visual perception in two dimensions [3]. Several non-equilibrium structures like motile worms, worm-aggregate coexistence, aggregates, and a dilute-gas phase are obtained, depending on the system parameters. The strength of the response to the visual signal, vision angle, packing fraction, rotational diffusion, and activity (velocity v_0) determine the location and extent of these phases in the phase diagram. The radius-of-gyration tensor is used to distinguish between the worm and the aggregate phase. Our results help to understand the collective behavior of cognitive self-propelled particles, like animal herds and micro-robotic swarms.

[1]. J. Elgeti, R. G. Winkler, and G. Gompper, Rep. Prog. Phys. **78**, 056601 (2015).

[2]. M. R. Shaebani, A. Wysocki, R. G. Winkler, G. Gompper, and H. Rieger, Nat. Rev. Phys. **2**, 181 (2020).

[3]. L. Barberis and F. Peruani, Phys. Rev. Lett. **117**, 248001 (2016).

BP 4.7 Mon 12:30 H16

Diffusiophoretic propulsion of an isotropic active particle near a finite-sized disk — •ABDALLAH DADDI-MOUSSA-IDER¹, ANDREJ VILFAN^{1,2}, and RAMIN GOLESTANIAN^{1,3} — ¹Max Planck Institute for Dynamics and Self-Organization (MPIDS), 37077 Göttingen, Germany — ²Jozef Stefan Institute, 1000 Ljubljana, Slovenia — ³Rudolf Peierls Centre for Theoretical Physics, University of Oxford, Oxford OX1 3PU, United Kingdom

We employ a far-field analytical model to quantify the leading-order contribution to the induced phoretic velocity of an isotropic active colloid near a finite-

sized disk of circular shape resting on an interface separating two immiscible viscous incompressible Newtonian fluids. To this aim, we formulate the solution of the phoretic problem as a mixed-boundary-value problem which we then transform into a system of dual integral equations on the inner and outer domains. Depending on the ratio of different involved viscosities and solute solubilities, the sign of phoretic mobility and chemical activity, as well as the ratio of particle-

interface distance to the radius of the disk, we find the isotropic active particle to be repelled from the interface, be attracted to it, or reach a stable hovering state and remain immobile near the interface. Our results may prove useful in controlling and guiding the motion of self-propelled phoretic active particles near aqueous interfaces.

A. Daddi-Moussa-Ider, A. Vilfan, R. Golestanian, *J. Fluid Mech.* **940** A12 (2022)

BP 5: Focus Session: Super Resolution Microscopy and Dynamics of Supramolecular Complexes

organized by Jonas Ries (EMBL Heidelberg) and Ulrich Schwarz (Heidelberg University)

Time: Monday 15:00–17:30

Location: H15

Invited Talk

BP 5.1 Mon 15:00 H15

The functional nano-architecture of axonal actin — •CHRISTOPHE LETERRIER — Aix Marseille Université, CNRS, INP UMR7051, NeuroCyto, Marseille, France

The intricate arborization and molecular identity of axons is maintained for decades, but must also continuously adapt to changes in the environment and modulate the activity of neurons. Axons fulfill these paradoxical demands thanks to a unique cytoskeletal organization that ensures the coordinated transport, anchoring and assembly of axonal components. In our lab, we use super-resolution microscopy to delineate and map the nanoscale architecture of actin-based structures within the axon: the periodic actin/spectrin submembrane scaffold, intra-axonal hotspots and trails, and presynaptic actin assemblies. We are exploring their molecular organization and functions by combining versatile labeling approaches, correlative live-cell/super-resolution/electron microscopy and quantitative analysis that allow for high-content, nanoscale interrogation of the axonal architecture.

BP 5.2 Mon 15:30 H15

Photon-stream-based aberration correction for STED microscopy — •DEBADRITA GHOSH, CLAUDIA GEISLER, and ALEXANDER EGNER — Institute for Nanophotonics, Goettingen, Germany

Stimulated emission depletion (STED) microscopy is the most prominent super-resolution fluorescence microscopy method and achieves a resolution far beyond the diffraction limit. However, like all these methods, it is adversely affected by sample-induced aberrations, which can degrade the achievable resolution and image quality significantly. These aberrations are caused by wavefront distortions due to refractive index variations, for example within thick biological specimens. This challenge can be addressed by using adaptive optics (AO) in a feedback-controlled manner such that the wavefront distortions are compensated and the image quality is restored. Typically, the feed-back loop uses image features which necessitates repeated acquisitions of the same field-of-view. This approach, therefore, is slow and prone to unwanted photo-bleaching. Here, we present an AO correction scheme that does not rely on image features, but exploits the dependence of the fluorescence lifetime on the local STED intensity. In principle, our photon-stream-based metric can be evaluated on a single image pixel, which makes it photon-budget-friendly and allows to correct aberrations rapidly in parallel with image acquisition. We successfully utilized this new metric for automated and continuous aberration correction in biological samples, making imaging fast and easy even for users without expert knowledge.

BP 5.3 Mon 15:45 H15

Cytoskeletal organization of red blood cells during malaria infections investigated with super-resolution microscopy and pair cross-correlation analysis — •PINTU PATRA¹, CECILIA P. SANCHEZ², MICHAEL LANZER², and ULRICH S. SCHWARZ¹ — ¹Institute for Theoretical Physics & BioQuant, Heidelberg University, Germany — ²Center of Infectious Diseases, Parasitology, University Hospital Heidelberg, Germany

Measuring the distance between molecules is key to understanding the molecular organization of biological systems. The pair cross-correlation (PCC) function computed from two-color super-resolution microscopy images provides a measure of co-localization between differently labeled molecules. Here, we theoretically compute the PCC-function between two molecules by using 2D Gaussian distribution as the effective point spread function for single molecules. By fitting this function to simulated data based on experimentally measured images, one can estimate both small and large separation distances. We apply this method to malaria-infected red blood cells and demonstrate that the knob-associated histidine-rich protein (KAHRP), which is used by the parasite to remodel the spectrin-actin network from a distance, relocalizes from the ankyrin bridges to the actin-based junctional complexes during the 48 hours course of the infection.

15 min. break

BP 5.4 Mon 16:15 H15

Superresolution microscopy for structural cell biology — •JONAS RIES — EMBL Heidelberg

Superresolution microscopy, such as single-molecule localization microscopy (SMLM), is becoming a key technique for structural cell biology, ideally complementing electron microscopy. I will discuss projects in my group in which we push SMLM towards nanometer resolution in 3D and multicolor with the aim to investigate the structure and dynamics of molecular machines in cells. I will show how these technologies allowed us to gain mechanistic insights into the machinery that drives endocytosis. Endocytosis is an essential cellular function by which cells take up molecules from the environment. We were able to reconstruct the dynamics of this process from thousands of snapshots taken in fixed cells. I will conclude with first results illustrating the potential of MINFLUX to image dynamic structural changes of protein machines in the living cell with nanometer resolution. Specifically, I will show how we resolved the precise stepping motion of the motor protein kinesin in living cells.

BP 5.5 Mon 16:45 H15

Spatiotemporal SARS-CoV-2 binding dynamics investigated with 100 Hz ROCS microscopy and thermal fluctuation analysis — •DOMINIK HUBER and ALEXANDER ROHRBACH — Laboratory for Bio- and Nanophotonics, Department of Microsystems Engineering - IMTEK, University of Freiburg, 79110 Freiburg, Germany

The emergence of the new severe acute respiratory syndrome corona virus 2 (SARS-CoV-2) in recent years has caused tremendous interest in investigating the interactions between viruses and cells. Especially the imaging and tracking of viruses are of great importance to see and understand the binding and uptake of viruses into cells and to be able to intervene in these processes. Due to their small size and fast movement imaging virus dynamics is a very challenging task, which has so far been achieved with different fluorescence methods, being limited by photo bleaching and imaging speed.

In our research we apply Rotating Coherent Scattering (ROCS) microscopy in order to visualize the diffusion of SARS-CoV-2 virus like particles (VLPs) close to A549 lung epithelial cells. ROCS microscopy allows for label-free imaging with more than 100 Hz temporal at 150 nm spatial resolution. The high contrast image stacks enable single particle tracking and characterization of the binding process and strength of VLPs with SARS-CoV-2 spike proteins to A549 cells using thermal fluctuation analysis.

BP 5.6 Mon 17:00 H15

Transient Optoplasmonic Detection of Single Proteins on the Nanosecond Time Scale — •MARTIN D. BAASKE^{1,2}, NASRIN ASGARI¹, DEEP PUNJ¹, and MICHEL ORRIT¹ — ¹Leiden University, Leiden, Netherlands — ²Johannes Gutenberg-University, Mainz, Germany

Label-free optical detection schemes commonly rely on specific chemical interactions between receptor and target molecule in order to facilitate analyte recognition. Here I present our first steps on a novel pathway to fingerprint proteins via analysis of their motion, i.e., physical properties such as Stokes radius and polarizability rather than chemical interactions. We show that via a polarization selective technique and careful optimization of a confocal microscope single gold nanorods, which are commonly used as labels, can be transformed into high-speed nanoscale sensors. We perform photothermal spectroscopy on single gold nanorods and use it as a means to probe their sensitivity to refractive index changes with respect to the experimental parameters * in turn allowing us to optimize the later on a rod-to-rod basis. This enables the detection single protein molecules traversing plasmonic near fields with previously time resolutions on the nanosecond scale.

BP 5.7 Mon 17:15 H15

Modeling the assembly and invagination of clathrin lattices at the cell membrane — •FELIX FREY^{1,2} and ULRICH S. SCHWARZ³ — ¹Department of Bioscience, Delft University of Technology, Delft, the Netherlands — ²Institute of Science and Technology Austria, Klosterneuburg, Austria — ³Institute for Theoretical Physics and BioQuant-Center, Heidelberg University, Heidelberg, Germany

Biological cells constantly relay material and information across their plasma membranes. For particles with sizes between 50 and 200 nm, clathrin-mediated endocytosis (CME) is the main uptake route. In CME clathrin triskelia assemble at the cell membrane and form a clathrin lattice. After initially growing flat the lattice starts to curve before it reaches its final size [1]. However, how this flat-to-curved transition proceeds in detail is still elusive, because theoretically several pathways can be envisioned [2]. When confronted with conventional imaging data, a microscopic model for the growth of clathrin lattices indeed suggests

some level of plasticity as required for bending [3]. Recently we have combined mathematical modeling with 3D superresolution microscopy to determine the dynamics of membrane invagination. We find that membrane curvature is generated cooperatively between the triskelia of the clathrin lattice [4].

[1] D. Bucher, F. Frey et al., Nat. Commun. 9, 1109 (2018). [2] F. Frey and U.S. Schwarz, Soft Matter 16, 10723 (2020). [3] F. Frey et al., New J. of Phys. 22, 073043 (2020). [4] M. Mund et al., bioRxiv, doi:10.1101/2021.10.12.463947 (2022).

BP 6: Statistical Physics of Biological Systems 1 (joint session BP/DY)

Time: Monday 15:00–17:15

Location: H16

BP 6.1 Mon 15:00 H16

Dynamics and Fair Risk Sharing in Groups of Intelligent, Egoistic Individuals — SAMUEL MONTER¹, VEIT-LORENZ HEUTHE¹, EMANUELE PANIZON², and CLEMENS BECHINGER¹ — ¹FB Physik, Universität Konstanz, Konstanz, Germany — ²Department of Quantitative Life Science, ICTP, Trieste, Italy

Many animal species organize in social groups of fascinating complexity. The evolutionary biologist W.D. Hamilton hypothesized that the gregariousness of some animals can be explained solely from the egoistic motivation to decrease the risk of predation [1]. As a quantitative measure of this risk, he considered the Voronoi area around each animal. Many collective behavior studies try to capture this motivation by imposing interaction rules or neglect the driving motive altogether when modeling the dynamics of animals. In this study we train a swarm of individuals in a Multi Agent Reinforcement Learning (MARL) framework according to Hamilton's hypothesis, i.e. to decrease their predation risk. Thus, we gain insights into the dynamics of an ensemble of selfishly motivated individuals unbiased by any a priori assumption about interactions. We find that the individuals learn to cluster into groups which exhibit dynamic steady states resembling the behavior of natural swarms. Additionally, the predation risk is shared evenly within the groups, counterintuitive to the selfish motivation of each individual. Our findings suggest that gregariousness could indeed be driven by selfish motives in accordance with Hamilton's hypothesis.

[1] W. D. Hamilton, Journal of theoretical Biology 1971, 31, 295-311.

BP 6.2 Mon 15:15 H16

Boundary-driven epithelial ordering: from the mouse embryo to topological defects — PAMELA GURUCIAGA¹, TAKAFUMI ICHIKAWA², TAKASHI HIIRAGI³, and ANNA ERZBERGER¹ — ¹European Molecular Biology Laboratory, Heidelberg, Germany — ²Kyoto University, Kyoto, Japan — ³Hubrecht Institute, Utrecht, The Netherlands

In physical problems boundaries are typically considered to be simple, static and externally fixed. Biological systems however not only interact with their surroundings, but also alter them in ways that feed back on their own dynamics. We address this complex interaction in the context of epithelial development. Motivated by observations of an interplay between apico-basal polarity and boundary geometry in mouse epiblast morphogenesis, we develop a theory for epithelial ordering based on the Landau-de Gennes approach to surface-induced order in liquid crystals. We introduce a vector order parameter to represent the polarity, and model its interaction with the boundaries by a weak anchoring energy. We calculate the alignment fields arising from different boundary curvatures, and compare our predictions with imaging data of the morphogenetic process. Our work highlights the role of extraembryonic tissue in embryogenesis, while identifying interesting physical phenomena, such as boundary-dependent transitions in the structure of topological defects.

BP 6.3 Mon 15:30 H16

A competitive advantage through fast dead matter elimination in confined cellular aggregates — YOAV G. POLLACK^{1,2}, PHILIP BITTICH¹, and RAMIN GOLESTANIAN^{1,3} — ¹Max Planck Institute for Dynamics and Self-Organization (MPI-DS), Göttingen, 37077, Germany. — ²Max Planck Institute for Multidisciplinary Sciences (MPI-NAT), Göttingen, 37077, Germany. — ³Rudolf Peierls Centre for Theoretical Physics, University of Oxford, Oxford, OX1 3PU, UK.

Competition of different cell types for limited space is relevant in biological processes such as tissue morphogenesis and tumor growth. Predicting the outcome for non-adversarial competition of such growing active matter is non-trivial, as it depends on how processes like growth, proliferation and the degradation of cellular matter are regulated in confinement; regulation that happens even in the absence of competition to achieve homeostasis. We show that passive by-products of the processes maintaining homeostasis can significantly alter fitness, enabling cell types with lower homeostatic pressure to outcompete those with higher homeostatic pressure. We reveal that interfaces play a critical role for this specific kind of competition: There, growing matter with a higher proportion of active cells can better exploit local growth opportunities that continuously arise as the active processes keep the system out of mechanical equilibrium. Our results show that optimizing the ratio of growing (active) to dead (passive) cells

can be as important to survival as growth rates and their sensitivity to mechanical cues.

BP 6.4 Mon 15:45 H16

A biophysical model of DNA methylation ageing — AIDA HASHTROUD and STEFFEN RULANDS — Max Planck Institute for the Physics of Complex Systems, Dresden, Germany

Machine learning models can accurately predict biological age and time of death based on sequencing measurements of DNA methylation marks. The mechanistic basis underlying these methylation clocks is poorly understood. Here, using a combination of tools from statistical physics and sequencing experiments we show that biological age can be predicted as a result of collective processes in the boundaries between genomic regions of different densities of cytosine-guanine pairs (CpGs). Specifically, we define a biophysical model predicting the time evolution of DNA methylation patterns during ageing based on a wave localization mechanism of tilted competition between antagonistic chromatin modifiers. Our work shows that biological age can be predicted from DNA methylation patterns using models with few parameters inspired by statistical physics.

15 min. break

Invited Talk

BP 6.5 Mon 16:15 H16

From active bacterial microcolonies to biofilms as model tissues — VASILY ZABURDAEV — Friedrich-Alexander-Universität Erlangen-Nürnberg, Erlangen, Germany — Max-Planck-Zentrum für Physik und Medizin, Erlangen, Germany
Bacterial intrinsic activity is evident on all stages of their life cycle. We will start by following how individual cells deploy forces to attach and move on surfaces. We suggest how these active movements may be harnessed to generate work and, for example, cells can power the rotation of micro-turbines. When let to move and interact, however, bacteria will find each other and form microcolonies that consist of several thousands of cells. Microcolonies are often the functional units of the bacterial existence in natural settings and in the context of disease. We will provide theoretical framework describing the bacterial microcolonies as active viscoelastic materials and discuss how this theory might be useful in eukaryotic systems such as organoids, tumour spheroids or clustering immune cells. Microcolonies may further develop into even more complex bacterial communities known as biofilms - there, bacteria embed themselves in the self-secreted extracellular matrix creating an analogue of multicellular tissues. We will outline some future research avenues deepening this analogy and illustrate it with an intriguing example of wound healing in bacterial biofilms.

BP 6.6 Mon 16:45 H16

Playing it safe: information constrains collective betting strategies — PHILIPP FLEIG^{1,2} and VIJAY BALASUBRAMANIAN² — ¹Max Planck Institute for Medical Research, 69120 Heidelberg, Germany — ²Department of Physics & Astronomy, University of Pennsylvania, Philadelphia, PA 19104, USA

Risk is an inherent part of life and biological functions are partly shaped by the need to reduce risk. Broadly, risk arises from stochastic interactions of an organism with its environment. Every time an organism displays a particular response or behaviour (e.g. expresses a phenotype or exhibits a certain immune response), it is placing a bet with potential impact on its biological fitness. The more precisely the statistics of the environment are known to the organism, the more successfully bets can be placed. However, an organism typically has limited information about the statistics of the environment. This limitation should be accounted for in the adaptation of biological functions to the environment. We develop a theoretical principle where information geometric model complexity guides stochastic biological functions towards less risky betting strategies. In the framework of Bayesian inference, we show that given finite information about the environment, there is an optimally safe adaptation strategy set by the Bayesian prior. Furthermore, in a toy model of stochastic phenotypic switching by bacteria, we demonstrate how the implementation of our principle of "playing it safe" increases the fitness (population growth rate) of the bacterial collective. We suggest that the principle applies broadly to problems of adaptation, learning and evolution.

BP 6.7 Mon 17:00 H16

Quantification of intracellular information flow — •MIRNA KRAMAR¹, MATHIEU COPPEY¹, THIERRY MORA², and ALEKSANDRA WALCZAK² — ¹UMR 168, Institut Curie, Paris — ²Laboratoire de Physique, Ecole Normale Supérieure, Paris

Signalling pathways are cascades of biochemical reactions which transduce signals from the exterior to the interior of the cell. By essence, these pathways convey information about the outside world which cells collect and process to adapt and guide decisions. The cell's ability to govern its functions correctly and precisely while relying on these intricate biochemical networks is surprising given the crowded and noisy cell interior, which indicates that the mechanisms cells use to process information are highly sophisticated. While our understanding

of the constituents of the cellular machinery and the processes taking place in the cell is steadily increasing, little is known about the information flow within the cell. Are pathways conveying only on/off signals, or is there more graded information being transduced?

Here, we measure and quantify the information relayed through the MAPK signalling pathway, one of the key signalling pathways in eukaryotic systems. Using a synergy of an optogenetic experimental setup and a data analysis pipeline based on information theory, we quantify the input-output relationships within the MAPK signalling pathway. We show that the capacity of the pathway far exceeds the 1-bit value (on/off), and that collective systems of cell seem to exploit this capacity.

BP 7: Poster 1

Time: Monday 18:00–20:00

Location: P1

BP 7.1 Mon 18:00 P1

Assessing biomolecular interactions across scales using optical tweezers — •ROMAN RENGER, NICHOLAS LUZZIETTI LUZZIETTI, and PHILIPP RAUCH — LUMICKS, Amsterdam, Netherlands

Biological processes involving proteins interacting with nucleic acids, cell membranes or cytoskeletal filaments are key to cell metabolism and hence to life in general. Detailed insights into these processes provide essential information for understanding the molecular basis of physiology and the pathological conditions that develop when such processes go awry. The next scientific breakthrough consists in the direct, real-time observations and measurements of the most fundamental mechanisms involved in biology. Single-molecule technologies offer a powerful opportunity to meet these challenges and to study dynamic protein function and activity in real-time and at the single-particle level. Here, we present our efforts for further enabling discoveries in the field of biology and biophysics using the combination of optical tweezers with correlative fluorescence microscopy (widefield, TIRF, confocal and STED) and label-free Interference Reflection Microscopy (IRM). We present several examples in which our technology has enhanced the understanding of basic biological phenomena, ranging from protein structure to intracellular organization. Furthermore, we show that advances in hybrid single-molecule methods can be turned into an easy-to-use and stable instrument that has the ability to open up new avenues in many research areas.

BP 7.2 Mon 18:00 P1

Transport in complex intracellular environments — •MOHAMMAD AMIN ESKANDARI, BART VOS, MATTIAS LUBER, and TIMO BETZ — Third Institute of Physics - Biophysics Georg August University Göttingen

Active transport is vital for targeted delivery of organelles, proteins and signalling molecules in eukaryotic cells and defects in active transport are linked to different diseases such as Alzheimer's disease. Kinesin and dynein are two motor proteins which are responsible to carry the cargoes along the microtubule filaments. Since the cytoplasm is a highly crowded environment, the motion of cargoes can be hindered by some sorts of obstacles and this brings us to the question how these motors can generate a processive motion in such an environment to bypass the roadblocks. In this project, we aim to investigate the possible mechanisms that kinesin and dynein can use to overcome the obstacles.

BP 7.3 Mon 18:00 P1

Single Particle Tracking of Molecular Motors under Different Physiological Conditions — •ADRIAN LENTZ, PAULINA BLAIR, DANIEL KUCKLA, PHILIPP HAGEMANN, and CORNELIA MONZEL — Experimental Medical Physics, Heinrich-Heine University, Düsseldorf, Germany

Single particle tracking (SPT) is a powerful tool to gain insights into the dynamics of molecular motors. These proteins convert the chemical energy of adenosine triphosphate (ATP) into a forward motion to transport vesicles along the microtubule network. In our study we investigate the linear motion of the kinesin variant Kif5C, which is normally found in neuronal cells. A genetically modified Kif5C with fused green fluorescent protein was monitored with millisecond resolution and analysed with an algorithm that links precisely detected particle positions to trajectories. We establish a point density based classification of trajectories into different molecular gaits and determine diffusion, velocity and processivity of the Kif5C motor. We show a systematic analysis of the influence of different acquisition times on the motor motion determination and compare Kif5C transport in the human cell lines HeLa, MCF-7, HEK, NIH/3T3 and COS-7. Of central interest was then to measure the effect of different physiological conditions, e.g. absence or high concentration of glucose and high amount of ATP, on the Kif5C dynamics.

BP 7.4 Mon 18:00 P1

Towards Advanced Single Particle Tracking of Molecular Motors by Quantum Dot Labeling and Monitoring of the Cytoskeletal Environment — •PAULINA BLAIR, ADRIAN LENTZ, XIAOYUE SHANG, DANIEL KUCKLA, PHILIPP HAGEMANN, and CORNELIA MONZEL — Experimental Medical Physics, Heinrich-Heine Universität, Düsseldorf, Germany

The molecular motor Kif5C plays a central role in the intracellular transport and synaptic transmission of neuronal cells. To understand how Kif5C mediated transport depends on its environment, it is essential to track the motor in the cytoplasmic context. We aim to advance the single molecule tracking of Kif5C by Quantum Dot labeling as well as by characterising the cytoskeletal environment. Quantum Dots are nanoscale semiconductors, which in contrast to genetically encoded fluorophores, offer tracking at enhanced spatio-temporal resolution and over long time scales. In this project we express Kif5C genetically fused to a streptavidin molecule in live cells. Quantum Dots functionalised with biotin are added to the cell sample to bind via streptavidin-biotin interaction to Kif5C. Molecular motors are recorded with millisecond resolution and are analysed using a global Linear Assignment Approach. The microtubule is stained using a silicon rhodamine-based fluorophore. We then derive parameters such as network density or intersections to correlate it with the motor protein dynamics.

Our data will provide insights on the benefit of Quantum Dot labeling, on molecular motor gaits such directed, superdiffusive and subdiffusive motion as well as on effects of the cytoskeletal environment.

BP 7.5 Mon 18:00 P1

Quantification of molecule-spanning protein dynamics with fluorescence correlation spectroscopy — •VERONIKA FRANK¹, JEAN-BENOÎT CLAUDE², JÉRÔME WENGER², and THORSTEN HUGEL^{1,3} — ¹Institute of Physical Chemistry, University of Freiburg, Germany — ²Fresnel Institute, CNRS, Aix Marseille University, France — ³Signaling research centers BIOSO and CIBSS, University of Freiburg, Germany

Protein conformational kinetics and their regulation occur on many time and length scales. Fluorescence methods have mainly focused on the hundreds of microseconds to minutes time scale and NMR on the picosecond time scale. Here we explore the several nanoseconds to microseconds time scale for the multidomain molecular chaperone heat shock protein Hsp90, a homodimer with a molecular weight of 90 kDa per monomer. Hsp90 is a therapeutic target for cancer therapy, but its dynamics and its dynamic interactions with other proteins are not yet fully understood.

Here we use fluorescence correlation spectroscopy and zero-mode waveguide nanoapertures to measure and understand fast molecule-spanning dynamics and how they are affected by interactors.

BP 7.6 Mon 18:00 P1

AniMol: A quick interactive web-based molecular trajectory visualiser — JAMES PANAYIS, JAMES PARTINGTON, and •RUDOLF A. RÖMER — Department of Physics, University of Warwick, Coventry, CV4 7AL, UK

We present software developed to interactively visualise dynamic molecular trajectories in web browsers. This tool allows for quick and efficient interaction with large flexing/moving molecular structures and helps to more easily understand results of in-silico modeling processes, for example protein dynamics simulations. The browser-based software simplifies workflows as no installation is required, and there are very few limitations due to hardware or software compatibilities. We achieve this using a lightweight state-of-the-art graphics engine, and compiling our code to WebAssembly (WASM), a portable compilation target for programming languages supported by all major browsers since 2017. We also present a webserver (animol.warwick.ac.uk) utilising this software offering cloud storage and retrieval of molecular trajectories, to aid collaboration and communication of results.

BP 7.7 Mon 18:00 P1

Correlation-based feature selection to identify functional dynamics in proteins — •GEORG DIEZ, DANIEL NAGEL, and GERHARD STOCK — Physikalisches Institut, Albert-Ludwigs-Universität Freiburg

Molecular dynamic simulations provide an effective tool for a deeper understanding of proteins and their functioning. In order to shed light on the underlying mechanisms of processes, one typically models the dynamics using some key internal coordinates (or features) which capture the most important conformational changes of the protein. However, one often ends up in a high-dimensional feature space which hampers a straightforward interpretation of the typically very complex dynamics. Adopting the Leiden community detection algorithm [1], we present an effective and scalable approach to divide the feature space into subsets which describe collective motion. By applying this approach to the functional dynamics of different protein systems with varying size, we show that it allows to identify and discard uncorrelated motion and noise. Moreover, it provides an effective dimensionality reduction scheme by extracting the key features, and leads to a detailed understanding of the underlying mechanisms.

[1] Traag et al., "From Louvain to Leiden: guaranteeing well-connected communities", *Sci. Rep.*, 2019

BP 7.8 Mon 18:00 P1

Reversible protein immobilization and biosensing on liquid-gated GFETs — •MYKOLA FOMIN¹, LARA JORDE², CHANGJIANG YOU², JACOB PIEHLER², and CAROLA MEYER¹ — ¹Department of Physics, Osnabrück University, Germany — ²Department of Biology/Chemistry and CellNanOs Center, Osnabrück University, Germany

Apart from the standard requirements such as selectivity, sensitivity, and biological compatibility, effective electronic biosensors are facing the demand for the fabrication of cost-efficient devices. Cost and resource efficiency would benefit from re-use of the biosensor after detection, which can be achieved by reversible immobilization of the molecules in question. While multiple biosensors have already been demonstrated to generate a response to a specific analyte molecule and its various concentrations, reversible protein monitoring remains a challenging task. Besides, during such measurements on graphene exists a risk of unspecific attachment to the channel with following protein denaturation. This work aims to demonstrate reversible protein immobilization detected by current changes of a liquid-gated GFET. PEG-tris-NTA on a lipid monolayer is used for site-specific immobilization of histidine-tagged proteins. The lipid layer forms a 2,5 nm hydrophilic cover over the channel that prevents unspecific protein attachment and its denaturation, resulting in enhanced biocompatibility [1]. We track the current changes upon attachment of histidine-tagged GFP to the device and their removal upon imidazole wash.

[1] L. Jorde. et al.(2021), doi: 10.1063/5.0035871.

BP 7.9 Mon 18:00 P1

Hierarchical dynamics as result of log-periodic oscillations in proteins — •EMANUEL DORBATH, GERHARD STOCK, and STEFFEN WOLF — Albert-Ludwigs-Universität, Freiburg, Germany

Logarithmic oscillations were observed in earthquakes, financial crashes and several biomolecular systems such as proteins. In many protein systems it is generally assumed, that the time scales, ranging from femtoseconds up to microseconds and longer, are in fact not independent but structured hierarchical in the sense that the fast time scales are a prerequisite for the slower ones.

This hierarchy can be well described via the free energy landscape which then gives rise to the logarithmic oscillations and a power-law. From the logarithmic oscillations, multiple relaxation times can be derived extending over several orders of magnitude [Metzler 1999].

Here, an analysis is presented to derive the respective time scales using logarithmic oscillations in non-equilibrium simulations. For this three systems are studied: A 1-dimensional model with an inherent hierarchical energy landscape is used as proof of principle and demonstration of the method. The second one is the simple hierarchical peptide Aib9 with two helical states which has been researched already in the past [Buchenberg 2015]. Finally, the widely studied PDZ2 domain is studied which shows complex conformational folding and re-structure mechanisms.

BP 7.10 Mon 18:00 P1

The effect of D₂O on the pressure dependent protein-protein interaction in aqueous lysozyme solutions — •MICHELLE DARGASZ, JAQUELINE SVELKOUKS, and MICHAEL PAULUS — Fakultät Physik/DELTA, TU Dortmund, 44221 Dortmund, Germany

In some experimental techniques such as neutron scattering, the substitution of H₂O with D₂O is used to obtain a useful signal. It was assumed that the exchange of the solvent does not have a major influence on the protein structure and interactions. However, measurements with lysozyme in D₂O revealed a larger attractive component of the protein-protein interaction potential [1]. In this study, the pressure-dependent behavior of high concentrated lysozyme solutions with H₂O and D₂O was considered using SAXS at the beamline BL2 of the synchrotron radiation source DELTA (Dortmund Germany). In previous mea-

surements a non-linear relationship between the interaction potential and the exerted pressure was observed [2]. This was also visible in this study, as a shift in the correlation peak of the scattering curve occurs as a function of pressure. Up to approx. 2 kbar, a shift to larger q-values occurs, which is reversed with further increasing pressure up to 4 kbar. Since this effect occurs equally in H₂O as well as D₂O, it can be assumed that the water structure plays a rather minor role for the nonlinear correlation.

[1] C. Gripon, *Journal of Crystal Growth* 178, 575-584 (1997)

[2] Martin A. Schroer, *Phys. Rev. Lett.* 106, 178102 (2011)

BP 7.11 Mon 18:00 P1

Coarsening of biomolecular condensates regulate crossover placement in Meiosis I — •MARCEL ERNST and DAVID ZWICKER — Max Planck Institute for Dynamics and Self-Organization, Göttingen, Germany

During meiosis, genetic information from female and male chromosomes is exchanged in a process called crossover. The dynamics that determine the positioning of these crossovers is largely not understood. Experimental observations consistently reveal two key findings: First, the number of crossovers per chromosome is at least one and is usually small, between one and three. Second, there is crossover interference, which prevents nearby crossovers on a single chromosome. We hypothesize that crossovers are determined by biomolecular condensates, which coarsen by exchanging material along chromosomes. We present theoretical and numerical results suggesting scaling laws analogous to Lifshitz-Slyozov-Wagner theory that predict the final number of crossovers, and their spatial structure as a function of coarsening time, chromosome length, and the initial amount of material. These results are consistent with current experimental findings in *Arabidopsis thaliana* and suggest how cells use a fundamental coarsening process to regulate spatial patterns.

BP 7.12 Mon 18:00 P1

Controlling size, phase transitions, and reactions in microfluidic double-emulsion droplets — •PAULA GIRONES PAYA, SEBASTIAN W. KRAUSS, and MATTHIAS WEISS — Experimental Physics I, University of Bayreuth

Double-emulsion based assays have been widely used in a large number of experiments such as in bio-inspired microreactors or in direct evolution assays. Despite the advanced techniques that have been developed to produce picoliter-sized droplets, a better manipulation of the droplet interior remains a challenge. Here, we demonstrate how hundreds of double emulsion droplets, trapped in a microfluidic sieve, can be grown and shrunk by controlling the salt concentration in the carrier liquid. Alternating the osmotic pressure leads to a rapid and reversible volume change of the aqueous droplet interior, resulting in a reversible phase separation of an enclosed binary fluid. The phase separation is shown to be a versatile tool to control, for example, the dissociation and re-association of double-stranded DNA or to monitor an enzymatic reaction via a pH sensitive fluorescence reporter.

BP 7.13 Mon 18:00 P1

Nucleation of chemically active droplets — •NOAH ZIETHEN and DAVID ZWICKER — Max Planck Institute for Dynamics and Self-Organization, Göttingen, Germany

Liquid-liquid phase separation emerged as a crucial organizing principle inside biological cells giving rise to a plethora of intracellular compartments. Unique to the cellular context, these condensates can consist of only a few hundred molecules and are affected by non-equilibrium processes. In particular, active chemical conversion between condensate material and proteins in the surrounding cytoplasm can control their size. Moreover, the significant concentration fluctuations due to the small molecule numbers imply that spontaneous nucleation and dissolution are likely. Yet, it is unclear how the driven reactions affect these stochastic processes. Here, we investigate the influence of chemical reactions on the nucleation behavior of active droplets using a stochastic field theory. We find a decrease in the nucleation rate with the increased strength of the chemical reactions. Using classical nucleation theory, we can reduce the full dynamics to an analytical expression for the free energy, which only depends on the droplet radius and the strength of the chemical reactions. The chemical reactions increase the energy barrier, which the system needs to overcome to form a droplet. Additionally, the binodal and the spinodal line are moved towards the center of the phase diagram. Cells might use these effects to control the nucleation behavior of intracellular droplets or even suppress their formation completely.

BP 7.14 Mon 18:00 P1

Liquid-liquid phase separation of promoter and gene-body condensates in multi-scale simulations — •ARYA CHANGIARATH SIVADASAN^{1,2} and LUKAS STELZL^{1,2} — ¹Institute of Physics, JGU Mainz — ²Faculty of Biology JGU Mainz and institute of Molecular Biology (IMB), Mainz

Liquid-Liquid phase separation plays an important role in the formation of localized nuclear hubs of RNAPII during the transcription process. Our research is focused on understanding the molecular basis of phase separation of CTD, the largest subunit of RNAPII, using molecular dynamics (MD) simulation methods.

We investigated how the CTD phase separation is affected by differences in CTD sequences using coarse-grained MD simulations and the results indicate that deviation from the ideal heptapeptide sequence has less tendency to phase separate, which suggests that these deviations from the ideal heptapeptide repeats are important for responsive regulation of transcription. Moreover, we are looking at how phosphorylation of CTD and the presence of other biomolecules that can influence CTD phase behavior. Hyper-phosphorylation prevents phase separation as the negatively charged phosphate groups repel each other. We show how hyperphosphorylated CTD might co-phase separate in elongation with HRD of Cylin-T1 in accordance with the experiment. To explore more on this, we studied the phase behavior of CTD and phosphorylated CTD in the presence of HRD and the results show that they co phase separate into a large cluster, but do not mix, which may help to physically distinguish between the initiation and elongation stages of transcription.

BP 7.15 Mon 18:00 P1

Mechanical growth and auxin patterning in plant tissues — •MATHIAS HÖFLER¹ and KAREN ALIM^{1,2} — ¹Physics Department and CPA, Technische Universität München — ²Max-Planck-Institut für Dynamik und Selbstorganisation, Göttingen

Individual cell shape and growth underlies a high variance in living organisms. It is puzzling how on a larger scale, the morphogenesis of a tissue can be a reliably stable and efficient process. Theory and experiment show that there is a mechanical and biochemical feedback loop for tissue development and morphogenesis. Mechanical forces in plants have a pronounced effect on the microtubule orientation in cells, thereby changing the cell's mechanical properties, causing an impact on the magnitude and direction, hence anisotropy, of cell growth. Here we study the effect of cell mechanics on the bidirectional, radial growth of tissue in the plant stem. We investigate feedback mechanisms, stress patterns and how these affect tissue and early organ shape and development. For the latter, we furthermore study the role of the growth hormone auxin in the shoot apical meristem (SAM). Here, auxin induces cell wall loosening thus enhancing mechanical growth via biochemical feedback.

BP 7.16 Mon 18:00 P1

Characterizing flexibility and mobility in the natural mutations of the SARS-CoV-2 spikes — JAMES PANAYIS¹, DOM BELLINI², and •RUDOLF A. RÖMER¹ — ¹Department of Physics, University of Warwick, Coventry, CV4 7AL, UK — ²MRC Laboratory of Molecular Biology, Cambridge CB2 0QH, UK

We perform in-silico modelling of the SARS-CoV-2 spike protein and its mutations, using structures from the Protein Data Bank (PDB), to ascertain their dynamics, flexibility and rigidity. Identifying the precise nature of the dynamics for the spike proteins enables, in principle, the use of further in-silico design methods to quickly screen both existing and novel drugs that may hinder these natural dynamics. We use a recent protein flexibility modelling approach, combining methods for deconstructing a protein structure into a network of rigid and flexible units with a method that explores the elastic modes of motion of this network, and a geometric modelling of flexible motion. We also conduct this analysis on synthetic structures of some newer variants (α , β , γ , δ , λ , ρ) for some of which structure files are not yet available from the PDB. All proteins are thermalised for at least 1ns with NAMD to human body temperature before the flexibility analysis.

BP 7.17 Mon 18:00 P1

Effects of CTCF and Cohesin complexes and nucleosome positions on chromatin loops. — •AYMEN ATTOU, TILO ZÜLSKE, and GERO WEDEMANN — University of Applied Sciences Stralsund, Institute for Applied Computer Science, 18435 Stralsund, Germany

The spatial organization of the eukaryotic genome plays an important role in regulating transcriptional activity. In the nucleus, chromatin forms loops that assemble into fundamental units called topologically associating domains, which facilitate or inhibit long range contacts. These loops are formed and held together by a ring-shaped protein complex involving cohesin and CTCF. To analyse the effects of cohesin and CTCF, an established coarse-grained computer model of chromatin with a resolution of single nucleosomes was extended by integrating potentials describing CTCF and cohesin. We performed Monte Carlo simulations combined with replica exchange procedure with regular spaced nucleosomes and experimentally determined nucleosome positions in presence of cohesin-CTCF as well as depleted systems as control. The simulations generated a statistical representative ensemble of configurations in thermal equilibrium. We studied differences in the spatial structure and of contacts probabilities of different domains. That allowed us to understand the impact of cohesin and CTCF on the 3D structure of chromatin and how nucleosome positions can impact the conformations of the chromatin loops during the residence time of the loop anchor, with presumed consequences for transcriptional activity.

BP 7.18 Mon 18:00 P1

In Silico Tumor Invasion — •ERIC BEHLE¹, JULIAN HEROLD², and ALEXANDER SCHUG¹ — ¹JSC, Jülich Research Centre, Wilhelm-Johnen-Straße, 52428 Jülich, Germany — ²Karlsruhe Institute of Technology, Kaiserstraße 12, 76131 Karlsruhe, Germany

To this day, cancer remains an insufficiently understood disease plaguing humanity. In particular, the mechanisms driving tumor invasion still require extensive study. Current investigations address collective cellular behavior within tumors, which leads to solid or fluid tissue dynamics. Furthermore, the extracellular matrix (ECM) has come into focus as a driving force facilitating invasion. To complement the experimental studies, computational models are employed, and advances in computational power within HPC systems have enabled the simulation of macroscopic tissue arrangements. In line with this, we hereby present our work using Cells in Silico (CiS), a high performance framework for large-scale tissue simulation developed by us. Combining a cellular potts model and an agent-based layer, CiS is capable of simulating tissues composed of millions of cells, while accurately representing many physical and biological properties. We aim to parameterize CiS via a bottom-up approach, starting with experimental data from small systems. We focused our studies on tumor spheroids, spherical aggregates composed of thousands of individual cells, which are one of the main workhorses of tumor analysis. We investigated the invasion dynamics and their dependence on the ECM density, and further aim to apply our model to the realistic simulation of larger systems.

BP 7.19 Mon 18:00 P1

Time resolved signal propagation in a photoswitched PDZ3 domain — •AHMED ALI, ADNAN GULZAR, STEFFEN WOLF, and GERHARD STOCK — Institute of Physics, University of Freiburg, Germany

Allostery is one of the most important mechanisms for biomolecular regulation. Generally, it involves a perturbation such as a binding event at one side of a macromolecule to affect another distant functional site. However, how such a perturbation propagates through the protein in detail is still not well understood. To establish a minimal allosteric model system, the third PDZ domain (PDZ3) of the postsynaptic density-95 (PSD-95) protein has been considered. The PDZ3 domain binds to the C-terminus of target proteins and regulates the signal propagation in PSD-95. In addition to the common and conserved central β -sheets and two α -helices present in all PDZ variants, PDZ3 contains a third C-terminal α -helix (α_3 -helix) that packs against the β -sheet at a considerable distance to the ligand binding pocket.

In this work, we aim for a detailed understanding of the microscopic dynamics of allosteric communication between α_3 and the ligand binding pocket. In addition, we explicitly aim at finding intraprotein changes appearing on the same time scales as found in recent time-resolved IR spectroscopic experiments. Consequently, we perform direct nonequilibrium molecular dynamics (MD) simulations of PDZ3. We characterize the α_3 -switched response by a combination of principal component analysis, clustering methods, and machine learning and characterize the microscopic mechanism behind the allosteric communication between α_3 and the ligand binding site.

BP 7.20 Mon 18:00 P1

Enabling computer simulations of chromatin at physiological density with a resolution of individual nucleosomes — •TILO ZÜLSKE, AYMEN ATTOU, and GERO WEDEMANN — University of Applied Sciences Stralsund, System Engineering and Information Management, 18435 Stralsund, Germany

The spatial structure of chromatin in the nucleus is important for processes such as the regulation of transcription by facilitating contacts over long distances or by hindering spatial accessibility. Despite extensive research, the spatial structure of chromatin remains enigmatic. Coarse-grained computer simulation models of chromatin help to understand the existing variation of experimental data. Nucleosomes were modelled as spherocylinders connected by elastic segments describing linker DNA. Interactions include stretching, bending, torsion, electrostatic and internucleosomal interactions. Nucleosomes were spaced equidistantly and randomly. Configurations were sampled utilizing Metropolis Monte Carlo and replica exchange algorithms. We studied synthetic fibers of 1.1 Mbp utilizing with periodic boundary conditions that mimic density behavior at different concentrations. The systems comprised 6000 nucleosomes which was more than an order of magnitude larger than the systems computed by us so far. Comparison with experimental results deliver crucial insights how nucleosome positions and density affect the spatial structure and contacts.

BP 7.21 Mon 18:00 P1

Numerical study of the driving forces behind the slipper formation for RBC cells in rectangular microchannels. — •BERIN BECIC — Biofluid Simulation and Modeling, Theoretische Physik VI, Universität Bayreuth

Red blood cells in rectangular microchannel flows exhibit two types of motions. At low velocities they tend to migrate towards the center and take symmetric croissant like shapes whereas for high velocities they migrate along the axis with the larger dimension and take an asymmetric slipper shape. Based on these results the behavior of the asymmetric off-centered slipper-movement was studied

further via the boundary integral method. There it was observed that surprisingly this motion is only weakly dependent on the cell's elastic properties. Additionally it was found that the flow profile perpendicular to the direction of the displacement of the centered position plays a crucial role in stabilizing the slipper state and suppressing the tumbling motion expected from considering the behavior in a pure shear flow.

BP 7.22 Mon 18:00 P1

Brownian dynamics simulations of deformable cells in ordered polymer networks — •JAN TIMO BACHMANN^{1,2} and ANDREAS ZÖTTL² — ¹TU Darmstadt, Germany — ²University of Vienna, Austria

Various Cells migrate in different environments and in response to different stimuli. Cell migration may include the navigation and locomotion through complex environments, as in the case of Leukocyte migration where cells have to translocate through small pores in the extracellular matrix (ECM) by squeezing their cell body considerably. To investigate the influence of pores in the ECM on cell velocity and deformation we study a simplified model of an externally driven deformable cell moving through ordered polymer networks by means of Brownian dynamics simulations.

The cell velocity shows oscillatory behaviour with minima before and maxima after each network pore. The speed maxima can exceed the terminal velocity of the respective cell in a network-free fluid, indicating that in the squeezing process elastic interaction energy with the network is utilized to locally enhance the cell speed. The mean velocity through the network as a function of the bending modulus of the cell surface bending potential shows a non-linear unimodal curve. We further show how the interplay of pore size and cell elasticity determines the cell velocity.

BP 7.23 Mon 18:00 P1

Modelling of cell proliferation in epithelial tissue — •KEVIN HÖLLRING¹, SARA KALIMAN¹, LOVRO NUIC², LUCA ROGIC², SIMONE GEHRER¹, MAXIME HUBERT¹, and ANA-SUNČANA SMITH^{1,2} — ¹PULS Group, FAU Erlangen-Nürnberg, Germany — ²Group for Computational Life Sciences, Ruđer Bošković Institute, Zagreb, Croatia

The extracellular microenvironment (ECM) of epithelial cells is known to mechanically govern the properties and behavior of cells and tissues like cell differentiation, size and motility. Yet its effect on the division rate of cells in tissues has not been analyzed in detail to our knowledge. In this work, we use MDCK-II cells grown on glass and 11 kPa PDMS substrates to provide evidence for a local cell density dependent division rate in an ECM stiffness dependent manner but independent of the age of the model- tissue, its internal structure or state.

We provide a theoretical model for microscopic tissue growth in a local microenvironment with well-defined average cell-density in agreement with experimental data and Dissipative Particle Dynamics (DPD) tissue simulations. We also propose an extension to the macroscopic tissue description via the Fisher-Kolmogorov equation (FK) accounting for our new findings that is able to reproduce characteristic edge behavior of tissues that has not been able to be reproduced by the FK formalism alone.

This work therefore sheds a new light on the influence of the ECM stiffness on the maturation of epithelial tissues and the important influences of different time scales for tissue growth and cell division.

BP 7.24 Mon 18:00 P1

Finding protein-ligand unbinding pathways in dcTMD simulations using distance-based clustering — •VICTOR TÄNZEL — Institute of Physics, Albert Ludwigs University, Freiburg, Germany

The exploration of protein-ligand dynamics by fully atomic simulations is of immense interest, for example in drug design, yet remains unfeasible in unbiased molecular dynamics (MD). To trigger rare events, we employ dissipation-corrected targeted MD (dcTMD) simulations, in which a moving distance constraint biases a prechosen reaction coordinate x , here the protein-ligand distance. The method combines a Markovian Langevin equation with a second-order cumulant expansion of the Jarzynski equality. From the required constraint forces, a free energy profile $\Delta G(x)$ as well as a friction coefficient $\Gamma(x)$ are extracted.

Transitions often occur along multiple pathways. In order to find these pathways, we study distance-based clustering approaches combining a pairwise ligand RMSD with the Leiden community detection algorithm. Here, we demonstrate the capabilities of this approach with the example of the A2A-ZMA complex and estimate (un-)binding rates.

BP 7.25 Mon 18:00 P1

Protein folding as described by different internal coordinates — •SOFIA SARTORE — Albert-Ludwigs-Universität Freiburg

Proteins reach their final structure (native state) through a process named folding. A powerful tool to investigate such process are molecular dynamics simulations, that can simulate the folding of a protein, giving as output a folding trajectory up to hundreds of microseconds long. This trajectory however needs to be further interpreted and analyzed in order to obtain an understandable model of

the process, consisting of states that correspond to metastable conformation of the protein during the folding. To build such states, identifying the main features that are responsible for the folding of the protein is of utmost importance, as well as choosing appropriate coordinates to describe the dynamics under study. Using internal coordinates such as dihedral angles or interatomic distances proves to be convenient, since they disregard the overall motion of the system. In this poster we analyse what influence the choice of different input coordinates has on the resulting picture of the process: we compare an analysis of the fast folding protein HP35 based on dihedral angles as internal coordinates with one based on contacts, a particular set of interatomic distances that satisfy specific requirements. We find that using different input coordinates highlights different dynamics of the system, resulting in different descriptions of the same physical process.

BP 7.26 Mon 18:00 P1

Machine Learning based parametrization of tumor simulation — •JULIAN HEROLD¹, ERIC BEHLE², and ALEXANDER SCHUG² — ¹Karlsruhe Institute of Technology (KIT), Kaiserstraße 12, 76131 Karlsruhe, Germany — ²JSC, Jülich Research Centre, Wilhelm-Johnen-Straße, 52428 Jülich, Germany

Despite decades of substantial research, cancer remains a ubiquitous scourge in the industrialized world. Effective treatments require a thorough understanding of macroscopic cancerous tumor growth out of individual cells in the tissue and microenvironment context.

Here, we aim to introduce the critical scale-bridging link between clinical imaging and quantitative experiments focusing on small clusters of cancerous cells by applying machine learning to drive model building between them. We deploy Cells in Silico (CiS), a high performance framework for large-scale tissue modeling developed by us. Based on both a cellular potts model and an agent-based layer, CiS is capable of accurately representing many physical and biological properties, such as individual cell shapes, cell division, cell motility etc.

The strong representational capacity of our model comes with the need to adjust a large number of parameters according to experimental findings. We present a generalized approach to optimize these parameters which allows the use of different sources of experimental data.

One major hurdle to achieve this goal is finding appropriate objective functions. To overcome this we implemented a variation of the Particle Swarm Optimization algorithm which learns the objective function during the optimization process.

BP 7.27 Mon 18:00 P1

Coarse-Grained Force Fields for Intrinsically Disordered Proteins — •YANNICK WITZKY, D. JANKA BAUER, ARASH NIKOUBASHMAN, and FRIEDERIKE SCHMID — Inst. für Physik, Universität Mainz, Germany

Simulations of systems containing many long proteins that perform liquid-liquid phase separation (LLPS) are usually computed with coarse-grained united residue force fields that allow for feasible runtime. One of these commonly used force fields was developed by Dignon et al.[1], where the proteins are modeled as bead-spring chains in an implicit solvent. As a reference we also used the bottom up coarse-grained UNRES force field [2] that resolves many more protein characteristics and is originally used for folding predictions. The results of simulations of four variants of an intrinsically disordered protein from both force fields are discussed in prospect of their polymer characteristics and the implications for simulations of LLPS-systems.

[1] Dignon et al.(2018) PLoS Comput Biol 14(1): e1005941

[2] Sieradzan et al.(2019) J. Phys. Chem. B, 123, 27, 5721-572

BP 7.28 Mon 18:00 P1

Nano-tribological investigation of the influence of specific synovial fluid components on lubrication of artificial joint materials — •ALEX KREIS¹, LUKAS BÖTTCHER¹, REGINA LANGE¹, PAUL HENKE², RAINER BADER², INGO BARKE¹, and SYLVIA SPELLER¹ — ¹Institute of Physics, University of Rostock — ²Biomechanics and Implant Technology Research Laboratory, University Medical Center Rostock

The human synovial fluid in native and endoprosthetic joints enables outstanding lubrication and low wear. The question is how this fluid or its specific components, such as hyaluronic acid and albumin, participate in this performance on a nanoscopic scale. In this work we aim to determine the frictional forces between the force microscope (AFM) tip (Si3N4) and typical materials for articulating components of endoprosthetic implants, such as ceramics, ultra-high molecular weight polyethylene (UHMWPE) and cobalt-chromium (CoCr) based alloy by means of lateral force microscopy (LFM). As reference we use force loops acquired on borosilicate glass surfaces in water. Further we plan to investigate and discuss the influence of the chain length of hyaluronic acid on tribological properties of each of these materials.

BP 7.29 Mon 18:00 P1

Microscale resonators for microfluidic based Nuclear Magnetic Resonance spectroscopy — •ALALEH MIRHAJVARZANEH¹, PIOTR LEPUCKI¹, ADAM P. DIOGUARDI¹, ALEKSANDR I. EGUNOV¹, MARCO ROSENKRANZ¹, RENATO

HUBER¹, DANIIL KARNAUSHENKO¹, DMITRY D. KARNAUSHENKO¹, OLIVER G. SCHMIDT^{3,4}, BERND BÜCHNER^{1,2}, and HANS-JOACHIM GRAFE¹ — ¹Leibniz Institute for Solid State and Materials Research (IFW) Dresden — ²Dresden University of Technology, Faculty of Physics — ³Research Center for Materials, Architectures and Integration of Nanomembranes (MAIN), Chemnitz — ⁴Chemnitz University of Technology, Material Systems for Nanoelectronics

Over the past few decades efforts to miniaturize Nuclear Magnetic Resonance (NMR) spectroscopy have resulted in the down-scaling of the core of an NMR system to microscale detectors. This achievement has unfolded a new era of NMR spectroscopy, with applications particularly in biological studies, where the sample size can scale down to micro- or nanoliters (nL), typical of microorganism and cell cultures. Our novel microcoil is a 3D microscale resonator with an integrated microfluidic system that offers high sensitivity and resolution (8ppb) for analyte volumes as small as 1.5nL, one of the smallest reported detection volumes in the field of NMR spectroscopy. Additionally, the integrated microfluidic system optimizes the filling factor of the device to reach almost 100%. The rolled-up microcoil can potentially be employed for high-resolution micro-NMR analysis of biological samples.

BP 7.30 Mon 18:00 P1

Altered local chromatin dynamics in stressed cells — •REBECCA BENELLI and MATTHIAS WEISS — Experimental Physics I, University of Bayreuth, Germany
The dynamic re-organization of chromatin is of crucial importance for cell viability and replication. During interphase, chromatin is mostly decondensed to allow for the transcription of genes, i.e. individual chromatin elements can be supposed to move like monomers of a polymer. Yet, recent reports have suggested chromatin to behave like a solid body on mesoscopic scales, questioning any free motion of chromatin elements. To explore the motion of integral chromatin markers, we have performed extensive single-particle tracking on telomeres under varying conditions. In agreement with previous findings, we observed a strongly subdiffusive and anti-persistent motion of telomeres in untreated culture cells, akin to the motion of monomers in a Rouse polymer. Reducing the ambient temperature or challenging cells by hyper- or hypo-osmotic stress resulted in a significant reduction of telomere mobility. In addition, significant jumps of telomeres between dynamically caged loci, observed in untreated cells, subsided or even vanished in response to these challenges. Altogether, our data indicate that local chromatin dynamics with long-range jumps between different loci are possible in untreated cells whereas a more compact/solid configuration of chromatin might explain the strongly reduced mobility of telomeres in stressed cells.

BP 7.31 Mon 18:00 P1

Image segmentation of irradiated tumour spheroids by Fully Convolutional Networks — •MATTHIAS STRELLER¹, SONA MICHLIKOVÁ², LEONI A. KUNZ-SCHUGHART², STEFFEN LANGE¹, and ANJA VOSS-BOEHME¹ — ¹University of Applied Sciences Dresden — ²OncoRay, National Center for Radiation Research in Oncology

Multicellular tumour spheroids are an established in-vitro model to quantify the effectiveness of cancer therapies. Spheroids are treated with radiotherapy and their therapeutic response over time is most frequently monitored via microscopic imaging. For analysis, it is necessary to segment the spheroids in these images, to extract their characteristics like the average diameter or circularity. While several image analysis algorithms have been developed for the automatic segmentation of spheroid images, they focus on more or less compact and circular spheroids with clearly distinguishable outer rim throughout growth. In contrast, treated spheroids are usually obscured by debris of dead cells and might be partly detached and destroyed. We train and optimize two Fully Convolutional Networks, in particular UNet and HRNet, to create an automatic segmentation which covers both cases, spheroids with and without therapy. While we successfully demonstrate the automatic segmentation for one spheroid type, we plan to extend the segmentation to other spheroid models.

BP 7.32 Mon 18:00 P1

Investigating Nanoparticle Dynamics in a High-Finesse Optical Microcavity — LARISSA KOHLER, •SHALOM PALKHIVALA, and DAVID HUNGER — Karlsruhe Institute of Technology – Institute of Physics, Karlsruhe, Germany

We explore the dynamics of nanoparticles using a novel fibre-based high-finesse Fabry-Perot microcavity with integrated microfluidic channels. Silica nanospheres with radii down to 25 nm and gold nanorods with lengths of 20 nm have thus been investigated.

The three-dimensional Brownian motion of a single nanosphere in the cavity has been tracked by the simultaneous measurement of the fundamental and higher-order transverse modes. The particle's position was derived with spatial and temporal resolutions of down to 8 nm and 0.3 ms respectively.

To resolve the faster motion of even smaller nanoparticles, a cavity-locking system has been implemented. This achieved an rms stability of 4% of the resonance linewidth in a water-filled cavity having a finesse of 5×10^4 . Hence, the dynamics of 20 nm gold nanorods could be detected with high measurement bandwidth. We shall report progress towards a quantitative evaluation of

nanorod diffusion, and the measurement of nanoparticle rotation using a cavity-locked polarisation-splitting scheme.

Based on this, we aim to explore the dynamic and optical behaviour of single biomolecules, such as DNA.

BP 7.33 Mon 18:00 P1

Fixed 4-channel detection in 2D polarization fluorescence imaging (2DPOLIM) and compensation of depolarization caused by dichroic mirrors — •YÜTONG WANG^{1,2}, ASAD HAFEEZ^{1,2}, DIJO MOONNUKANDATHIL JOSEPH^{1,2}, MOHAMMAD SOLTANINEZHAD^{1,2}, RAINER HEINTZMANN^{1,2}, and DANIELA TÄUBER^{1,2} — ¹Leibniz Institute of Photonic Technology — ²Friedrich-Schiller-University Jena, Germany

Polarization resolved fluorescence imaging (POLIM) can reveal macromolecular structure in the range of 2-10 nm via Förster resonance energy transfer between similar fluorophores (homo-FRET, emFRET). 2D POLIM is superior to conventional fluorescence anisotropy methods for studies of anisotropic samples[1,2]. Implementing a variable electrooptic polarization control in the excitation together with a fixed 4-channel detection[3] speeds up the acquisition giving access to polarization resolved snapshots of dynamic samples. A major issue in POLIM setups is depolarization caused by the multilayer coating of dichroic mirrors, which introduces phase shifts between s- and p-polarized components. We implemented two pairs of dichroics with orientations crossed to each other. By this, incident s- and p-polarization is exchanged within each pair. The design proved to be an effective and reliable approach to significantly improve the quality of polarization by compensating the depolarization introduced by a single dichroic. – Funding: DFG-Ta1049/2 – [1] R. Camacho et al. Adv. Mater. 2019, 1805671. [2] R. Camacho et al. Commun. Biol. 2018, 1, 157. [3] F. Zimmermann et al. in Optically Induced Nanostructures, 2015.

BP 7.34 Mon 18:00 P1

Scanning small angle x-ray scattering of hydrated, keratin-rich cells — •BORAM YU¹, CHIARA CASSINI¹, SOPHIE-CHARLOTTE AUGUST¹, MANFRED BURGHAMMER², and SARAH KÖSTER¹ — ¹Institute for X-Ray Physics, Universität Göttingen, Germany — ²ESRF, Grenoble, France

Intermediate filaments (IFs), one of the three main components of the cytoskeleton, form a network that contributes to cell mechanic. Thus, collecting structural information about IFs in their physiological setting, i.e., in whole cells, is crucial. We use scanning small angle x-ray scattering(SAXS) to obtain this information, as it offers both real space overview images with moderate resolution and reciprocal space information with high resolution. X-ray imaging of cells in aqueous state is challenging as their electron density contrast is low. Additionally, the aqueous environment contributes to extremely rapidly spreading radiation damage. For this reason, a fast-scanning mode is employed by moving the sample continuously through the beam rather than step by step, resulting in a significant reduction in exposure time, thus diminishing the radiation damage. As a benchmark for ordered intracellular structures, we investigate mammalian cells expressing the IF protein keratin. A purpose-built chamber maintains the cells hydrated while minimizing the volume of the liquid in the optical path. Despite weak contrast and short exposure times, we are able to retrieve the local main orientation of subcellular structures, thus demonstrating how scanning SAXS offers valuable information from hydrated cells.

BP 7.35 Mon 18:00 P1

Microfluidics-based analysis of the mobility and migration pattern of Trypanosoma brucei — •HANNES WUNDERLICH¹, LUCAS BREHM², JANA JENTZSCH², SEBASTIAN KRAUSS¹, KLAUS ERSFELD², and MATTHIAS WEISS¹ — ¹Experimental Physics I, University of Bayreuth, Germany — ²Molecular Parasitology, University of Bayreuth, Germany

Trypanosoma brucei is a unicellular parasite that causes the African sleeping sickness after entering the human bloodstream. An active movement of trypanosomes, mediated by the beating of a microtubule-powered flagellum that spirals along the elastic cell body, is crucial for escaping the host's immune response. A highly ordered, subpellicular array of aligned microtubules beneath the cell membrane determines the effective elasticity of parasite and hence its propulsion during flagellar beating. Using soft lithography to create well-defined two-dimensional chambers, we have studied the mobility and migration pattern of trypanosomes without and with genetically induced changes of posttranslational microtubule modifications. Using a set of informative measures that have been developed for (persistent) random walks, we have analyzed trypanosome trajectories that exhibit clear run-and-tumble patterns. Our data reveal that posttranslational modifications of microtubules significantly alter trypanosome mobility and migration.

BP 7.36 Mon 18:00 P1

Topological artifacts in mid-IR photo-induced force microscopy (PiF-IR) — •SAJIB BARUA^{1,2}, HARDIK GADHER^{1,3}, UWE HÜBNER¹, and DANIELA TÄUBER^{1,2} — ¹Leibniz Institute of Photonic Technology, Jena — ²Institute of Physical Chemistry & Abbe Center of Photonics, Friedrich-Schiller-University Jena, Germany — ³Leibniz University Hannover, Germany

The use of tapping mode atomic force microscopy (AFM) for detecting mid IR absorption can provide nanoscale chemical information. Several studies report on successful applications for qualitative characterization of biomaterials [1]. Implementing such methods for quantitative evaluation of chemical sample compositions requires further understanding of underlying physical processes [2]. In general, the surface of biological cells and tissue is rough on a sub-micron scale. This may cause artifacts in signal detection due to non-planar interactions with the AFM tip. We use structured polymer layers to investigate implications of sample topography on the signal intensity in mid-IR photo-induced force microscopy (PiF-IR). – [1] Wang et al. Super-Resolution Mid-Infrared Spectro-Microscopy of Biological Applications through Tapping Mode and Peak Force Tapping Mode Atomic Force Microscope. *Adv. Drug Deliv. Rev.* 2022, 180. [2] Täuber et al. Interference Effects in Nanoscale Infrared Spectroscopy Methods, submitted.

BP 7.37 Mon 18:00 P1

Investigation of biofilm formation on metal surfaces — •BERNHARD KALTSCHMIDT¹, ANNIKA KIEL², EHSAN ASGHARI², JULIAN CREMER³, DARIO ANSELMETTI³, BARBARA KALTSCHMIDT², CHRISTIAN KALTSCHMIDT², and ANDREAS HÜTTEN¹ — ¹Thin Films & Physics of Nanostructures, University of Bielefeld — ²Department of Cell Biology, University of Bielefeld — ³Biophysics & Nanosciences - "Physics of Life", University of Bielefeld

Biofilms can cause major problems in many different areas, such as corrosion and contamination of medical products. The aim of this work was to investigate biofilm formation on stainless steels and on sputtered transition metals. Steel disks of the chromium steels 1.4016, 1.4301 and 1.4510 were inoculated with bacteria in LB medium for 7 and 14 days. As bacteria we used *Pseudomonas aeruginosa*, which we use as our in vitro model for strong biofilm formation. After 14 days the first signs of bio-corrosion were detected by scanning electron microscopy (SEM) and atomic force microscopy. In another series of investigations, glass slides were coated with the transition metals Gold, Ruthenium and Tantal by magnetron sputtering and incubated with *Pseudomonas aeruginosa* for 24 hours. An uncoated glass surface served as a reference. Comparative studies of biofilm growth on the reference and on the different transition metals were carried out using SEM, confocal laser scanning microscopy and the colony forming unit assay. The analysis revealed that biofilm growth on transition metals is severely hindered compared to our non coated glass slide reference.

BP 7.38 Mon 18:00 P1

Observation of two-step aggregation kinetics of amyloid- β 42 peptide from fractal analysis — •SOHAM MUKHOPADHYAY — Chair of Mathematics in Life Sciences, Friedrich-Alexander Universität Erlangen-Nürnberg, Cauerstr. 11, 91058 Erlangen, Germany — Max-Planck-Zentrum für Physik und Medizin, Erlangen, Germany

Proteins are responsible for controlling and catalyzing the reactions and processes that make life possible. Proper folding of protein molecules into their native states is critical for them to function correctly; conversely, misfolded proteins often cause damaging effects on the biological processes they are involved in. Misfolded proteins often undergo self-aggregation, a process that has been the subject of intense research due to its importance in biological contexts. Of particular interest is the formation of stable filamentous aggregates termed amyloids — implicated in the pathology of several diseases such as Alzheimer's, Parkinson's, type-II diabetes, etc. Several models propose a two-step aggregation mechanism, with linearly growing fibrils and branch formation through secondary growth.

In this work, we employ tools from fractal geometry to develop an analysis technique for images of protein aggregation obtained from TIRF microscopy. Fractal geometry provides an instinctive framework for analyzing 1- and 2-dimensional growth. We use this framework to study the aggregation of the amyloid- β 42 peptide and find the initial aggregation to proceed in a one-dimensional fashion, with later branching events leading to two-dimensional growth. This provides direct evidence for the two-step aggregation model.

BP 7.39 Mon 18:00 P1

Influence of varying pH on individual and collective behavior of filamentous cyanobacteria — •FRANZISKA PAPANFUSS, MAXIMILIAN KURJAHN, ANTARAN DEKA, and STEFAN KARPITSCHKA — MPI for Dynamics and Self-Organization, Göttingen, Germany

Photoautotrophic cyanobacteria are responsible for about 10 % of global primary production of reduced carbon and represent a sustainable source of carbon dioxide neutral bio-fuel. Adaptation to environmental changes is a key factor of their evolutionary success, but the emergent phenomena that couple the individual to their collective behavior remain elusive. Here, we investigate three species of filamentous cyanobacteria cultivated in pH-buffered and non-buffered medium over three weeks of cultivation. During cultivation, colony-scale properties like external pH and aggregate morphology were measured as well as properties of individual filaments like gliding velocity and absorption spectra. In the non-buffered cultures, pH varies in dependence on light-driven photosynthesis. Different species seem to adapt colony morphology from compact aggregates to

reticulate layers at different pH values in the low alkaline range. Yet, the external pH has no influence on the gliding velocities, but influences the abundance of the dominant photo-pigments Chlorophyll-a, beta-carotene and phycocyanin in some species. Our investigations show that the pH is not only governed by the photosynthetic activity, but also influences the fate of the cyanobacterial colony in a regulating feedback mechanism.

BP 7.40 Mon 18:00 P1

Identifying malignant tissue using Laser Induced Breakdown Spectroscopy (LIBS) and Neural Networks — •ELENA RAMELA CIOBOTEA¹, CHRISTOPH BURGHARD MORSCHER¹, CRISTIAN SARPE¹, BASTIAN ZIELINSKI¹, HENDRIKE BRAUN¹, ARNE SENFTLEBEN¹, JOSEF RÜSCHOFF², and THOMAS BAUMERT¹ — ¹Kassel Universität, Kassel, Germany — ²Institut für Pathologie Nordhessen, Kassel, Germany

The problem of differentiating cancerous tissue from a healthy one is currently solved in the diagnostic process through microscopic imaging of stained biopsy sections by pathologists. During surgical removal of cancerous tissue, oncological safety margins must be established to ensure the complete removal of the tumor without affecting much of the neighboring healthy tissue. For this purpose, on-site pathological analysis is done on freshly frozen, stained cuts, which is time consuming. We investigate a new approach to minimize the time of discrimination between malign and benign tissue by an in situ, non-contact spectroscopic analysis. In a proof of principle experiment, a plasma is generated by focusing an 800 nm femtosecond laser on the pathologic postoperative sample. The spectrum of plasma radiation contains information on the element composition of the ablated tissue. Since the recorded spectra are complex and full of information, neural networks are employed to find differences between malign and benign tissue with a high speed and accuracy. This contribution presents the experimental parameters that allow for the best possible differentiation of some biological tissues through fs-LIBS by minimizing deviations between the measurements.

BP 7.41 Mon 18:00 P1

Deep learning for single particle tracking in noisy data — •MATTIAS LUBER, MOHAMMAD AMIN ESKANDARI, and TIMO BETZ — University of Goettingen, Goettingen, Germany

The quantitative analysis of particle motion critically depends on the quality of particle trajectory detection. Especially the position detection of particles in fluorescence microscopy images is an important task faced in biophysics. Trajectories are used to study processes like intra-cellular transport protein diffusion within and through membranes and the reconstruction of force fields driving the particle motion. In such settings, high spatial and temporal resolution are desired. However, in practice those factors have contradictory measurement requirements. High temporal resolution requires short exposure times, which limit the photon budget and thus lead to low signal to noise ratios. We developed an approach to reconstruct the particle position from noisy images, by applying U-NET based deep learning models to fluorescence microscopy images. Using this we can successfully track particles with shorter exposure times, compared to traditional denoising techniques.

BP 7.42 Mon 18:00 P1

Analyses of the outer membrane of vital mitochondria — •ERIC LIEBERWIRTH¹, CHRISTIAN VÖLKNER¹, REGINA LANGE¹, ANJA SCHAEFER², MAGDALENA OTTE², ARMIN SPRINGER³, MARKUS FRANK³, INGO BARKE¹, SIMONE BALTRUSCH², and SYLVIA SPELLER¹ — ¹University of Rostock, Institute of Physics, 18059 Rostock, Germany — ²Rostock University Medical Center, Institute for Medical Biochemistry and Molecular Biology, 18057 Rostock, Germany — ³Rostock University Medical Center, Medical Biology and Electron Microscopy Center, 18057 Rostock, Germany

A network of mitochondria enables a cell to perform oxidative metabolism. These organelles have a double membrane that is subject to constant remodeling during the regular fusion and fission processes. This study aims to gain more knowledge about the outer membrane containing translocase, porin and ion channels. Via Scanning Ion Conductance Microscopy (SICM) it is possible to measure the outer membrane of vital mitochondria at lateral spatial resolution of approx. 50 nm and at height resolution of a few nanometer. We immobilize the organelle in phosphate buffered saline (PBS) on collagen-coated substrates and scan the outer membrane with nanopipettes. Though the nanoprobe was, on each pixel, approached from top, the observed shapes exhibit forward-backward hysteresis and flat plateaus. The corrugation amplitude amounts to a few 10 nm and soft steps are present. Labeling translocase of the outer membrane (TOM) with nanoscopic gold particles may help learning about their spatial distribution and help to identify signatures in SICM and SEM.

BP 7.43 Mon 18:00 P1

Multiple thermophoretic particle trapping at single molecule resolution — •BENJAMIN FANSELOW, TOBIAS THALHEIM, and FRANK CICHOS — Peter-Debye Institute for Soft Matter Physics, Leipzig University, Germany

Achieving single molecule resolution for microscopy enabled to gain valuable insight into processes, that otherwise would be hidden in the ensemble, such as

amyloid fibril fragmentation, volume exclusion of DNA molecules, or localization of proteins within a cell. One technique is the combination of fluorescence microscopy with thermophoretic trapping. It utilizes thermophoresis for confining freely diffusing single molecules within a liquid into a region of interest and allows observing these molecules without surface immobilization, over a time period of several minutes. The required temperature fields are generated via optical heating using a focused laser beam steered on a thin chromium layer. So far, only one trap at a time could be used, entailing multiple time-consuming measurements to achieve a reasonable statistics. We present the realization and characterization of up to four thermophoretic traps, which can be controlled simultaneously while preserving the single molecule resolution. This mode is characterized by a model system of 200-nm polystyrene particles in water, trapped with a feedback assisted mode. Analyzing the molecule displacement framewise, the trap stiffness and temperature induced velocities can be calculated. While it could be shown, that the stiffness is scalable with the laser power and the number of used traps, it also revealed an upper limit caused by the feedback loop frequency.

BP 7.44 Mon 18:00 P1

adaptive interferometric light-sheets for resolution enhanced imaging — •MEELAD LALENEJAD and ALEXANDER ROHRBACH — Laboratory for Bio- and Nano-Photonics, Department of Microsystems Engineering (IMTEK), University of Freiburg, Georges-Koehler-Allee 102, 79110 Freiburg, Germany

The success of light-sheet microscopy bases on the idea that only the parts of the object being are illuminated with laser beams from the side, which are in focus of the objective lens. This concept leads to increased image contrast and reduces photo-bleaching / -toxicity. In addition, larger volumes are scanned plane-wise or line-wise, such that LSM is significantly faster than point-wise scanning methods. However, compromises in spatial resolution have had to be made because of objective lenses with limited numerical aperture and aberrations from light scattering. On the detection side, such phase aberrations could often be corrected with adaptive optics. However, spatial light modulation and phase adaptation of the illumination side still leave plenty of room for improvements. In our research we want to combine the principles of holographically shaped illumination beams with interferometric arrangements of the illumination beams. Since the modulation contrast can be deteriorated by refractive index inhomogeneities of the sample, future phase adaptation for each of the counter propagating beams shall be used as an effective aberration compensation. Using the principles of structured illumination microscopy, we show 3D images in scattering media such as cancer cell clusters obtained from two laterally scanned, counter-propagating Bessel beams.

BP 7.45 Mon 18:00 P1

Absorption-based specificity in ROCS microscopy — •VICTOR CHUMAN and ALEXANDER ROHRBACH — University of Freiburg, Department of Microsystems Engineering - IMTEK, Laboratory for Bio- and Nano-Photonics, Georges-Köhler-Allee 102, 79110 Freiburg, Germany

Fluorescence techniques dominate the field of live-cell microscopy, but bleaching and motion blur from too long integration times limit dynamic investigations of small objects. High contrast, label-free life-cell imaging of thousands of acquisitions at 150nm and 200 Hz is possible by Rotating Coherent Scattering (ROCS) microscopy, where intensity speckle patterns from all azimuthal illumination directions are added up within a few milliseconds. However, ROCS lacks the important imaging feature of specificity. We address this deficiency by using different absorption markers, characterized by their different complex valued refractive indices to achieve a difference in image contrast in the observed structures. We demonstrate how different gray values in the image are obtained from interferences between scattered and unscattered light, resulting from material dependent phase shifts of the scattered light. Absorption-based specificity in ROCS imaging may open new fields of applications, adding on top of its high spatio-temporal resolution.

BP 7.46 Mon 18:00 P1

Novel concepts in scanned light-sheet microscopy to improve speed, contrast and resolution — •YATISH YATISH^{1,2,3} and ALEXANDER ROHRBACH^{1,2} — ¹Laboratory for Bio- and Nano-Photonics, Department of Microsystems Engineering-IMTEK, University of Freiburg, 79110 Freiburg, Germany — ²CIBSS - Centre for Integrative Biological Signalling Studies, Freiburg, Germany — ³Spemann Graduate School of Biology and Medicine (SGBM), University of Freiburg, Freiburg, Germany

Light-sheet microscopy (LSM) enables fast 3D, high contrast imaging offering effective sectioning and low photo-toxicity. LSM allows to investigate the issue of light scattering in both the illumination and detections, and to better understand the complex image formation. Switchable computer holograms can generate special Bessel beams that are scanned through the object offering increased penetration depths due to their self-reconstruction capability. These beams generate images with better contrast and resolution, when combined with confocal line detection. A future challenge will be to automatically adapt the illumination beam dimensions to the specific structure of object to enhance the 3D image quality. We have investigated the propagation of different beams through classes of spheres. All experiments were performed in combination with advanced computer simulations to better understand the effects of scattering. This includes the loss in quality of bead images along the optical illumination and detection axes through bead clusters, but also the position dependent scattering and absorbing of illumination and fluorescence light in cancer cell clusters.

BP 8: Focus Session: Phase Separation in Biochemical Systems

organized by Christoph Weber (University of Augsburg) and David Zwicker (MPIDS Göttingen)

Time: Tuesday 9:30–13:00

Location: H15

Invited Talk

BP 8.1 Tue 9:30 H15

Phase separation in cells: gene localization and noise buffering — •SAMUEL SAFRAN — Weizmann Institute of Science, Rehovot, Israel

Biomolecular condensates formed by phase separation allow the cell to organize itself in space and can promote or inhibit biochemical reactions. I will focus upon recent observations of phase separation of chromatin (chains of DNA and proteins) in the nucleus that suggests a new paradigm in which the genetic material is separated into domains, which in some cases, have a complex, marshland, mesoscale structure. How this mesoscale structure affects gene expression noise is a topic of current research. While many of the equilibrium properties of biomolecular condensates can be understood by extensions of statistical physics, biological molecules often do not maintain constant overall compositions, in contrast to equilibrium phase separation; over time, the cell stochastically produces and degrades many proteins, resulting in a noise-induced concentration distribution. Our theory shows how in the limit of slow production/degradation relative to molecular diffusion, one can incorporate the effects of such noise into the equilibrium phase diagram to predict the extent of noise reduction (buffering) by the phase separation in multicomponent systems.

BP 8.2 Tue 10:00 H15

RNA polymerase II clusters form in line with surface condensation on regulatory chromatin — •TIM KLINGBERG^{1,2}, AGNIESZKA PANCHOLI³, WEICHUN ZHANG³, ROSHAN PRIZAK³, IRINA MAMONTOVA³, MARCEL SOBUECKI³, ANDREI YU KOBITSKI³, GERD ULRICH NIENHAUS³, VASILY ZABURDAEV^{1,2}, and LENNART HILBERT³ — ¹Friedrich-Alexander-Universität Erlangen-Nürnberg — ²Max-Planck-Zentrum für Physik und Medizin — ³Karlsruhe Institute of Technology
Transcription of eukaryotic genes by the RNA polymerase II (Pol II) has two

major control points: recruitment to the regulatory region of a specific gene, and subsequent release into the elongation of RNA transcripts. We find that recruited Pol II forms macromolecular clusters with a large variety of shapes in the embryos of zebrafish, which we investigated by live and super-resolution microscopy. To delineate the essential physical mechanisms underlying Pol II cluster formation, we use coarse-grained lattice kinetic Monte Carlo simulations containing monomeric particles (recruited Pol II) that can interact with polymer chains (regulatory regions). We propose that the regulatory chromatin regions act as surfaces for the condensation of recruited Pol II into a liquid-phase. The numerical simulations of our model qualitatively reproduce the different forms of RNA Pol II clusters that we detected with microscopy. Taken together, our results suggest that recruited Pol II contributes to the surface-associated condensates, whereas elongating Pol II is excluded from these condensates and thereby drives unfolding of the condensates.

BP 8.3 Tue 10:15 H15

Lattice based model and continuum theory of active microemulsion — •RAKESH CHATTERJEE^{1,2}, HUI-SHUN KUAN^{1,2}, and VASILY ZABURDAEV^{1,2} — ¹Friedrich-Alexander University, Erlangen-Nuremberg, Erlangen, Germany — ²Max-Planck-Zentrum für Physik und Medizin, Erlangen, Germany

During transcription, RNA polymerase II (Pol II) attaches and moves along the DNA strand to produce messenger-RNA (mRNA) transcript. It has been recently shown that in the nucleus, DNA and RNA are spatially organised in agreement with a microphase separation process [1], where the full phase separation of the RNA-rich phase from DNA is prevented by the transcribing Pol II playing the role of an amphiphile. To gain the comprehensive understanding of physical mechanisms behind this process we propose a phenomenological lattice model

where DNA, mRNA and Pol II serve as the three basic components similar to the equilibrium oil-water-amphiphile system, which exhibits two and three phase coexistence. Here however, Pol II undergoes chemical transitions reflecting different stages of the transcription process. In the model, it is realised by assuming transient dynamics of the amphiphiles which switches between active and inactive states. Numerical simulations of the lattice model show that amphiphile activity significantly modifies phase behaviour of the system compared to the equilibrium scenario. Furthermore, by rigorous coarse-graining of the lattice model we could derive the continuum theory and predict the relaxation dynamics of the dynamic structure factor of active microemulsion.

[1] Hilbert et.al, Nature Comm. 12, (1) 2021.

BP 8.4 Tue 10:30 H15

Molecular assembly lines regulate the size of active droplets — •TYLER HARMON — Leibniz Institute for Polymer Research, Dresden, Germany

Large protein complexes are assembled from protein subunits to form a specific structure. In our previous work, we used theory to propose that assembly into the correct structure could be reliably achieved through an assembly line with a specific sequence of assembly steps. We illustrated that the assembly line can be self-organized through utilizing existing membraneless organelles. In this way, the droplet directly regulates the formation of the assembly line.

In this work we explore how the assembly line can directly regulate the droplet. It has been observed that the core element can act as an important structural factor for the droplet formation. By introducing this feature into the model, we see that the assembly line also regulates the size of the droplet in a productive way.

BP 8.5 Tue 10:45 H15

Droplet differentiation induced by chemical reactions — •XI CHEN¹, FRANK JÜLICHER², JENS-UWE SOMMER¹, and TYLER HARMON¹ — ¹Leibniz-Institut für Polymerforschung Dresden, Institut Theory der Polymere, 01069 Dresden — ²Max Planck Institute for the Physics of Complex Systems, 01187 Dresden

Membraneless compartments are formed in cells by liquid-liquid phase separation. The compartments enrich many components including enzymes which resemble chemically active droplets. A major paradigm for studying these droplets is to consider two types of species, scaffolds, which thermodynamically hold the droplets together, and clients, such as enzymes which utilize the droplets that are formed. We investigate through theory a model system where two competing enzymes which can modify the scaffold, for example a kinase and a phosphatase, are clients to the droplets. Interestingly, by introducing a preferential affinity between enzymes and their product scaffold, the system becomes unstable and differentiates into two types of droplets concentrated in either modified scaffold. Additionally, these features can lead to unexpected behaviors such as droplets which repel each other. This may correspond to an unexplored mechanism of the spatial control of biochemical reactions in biological cells.

15 min. break

BP 8.6 Tue 11:15 H15

Non-specific adhesive forces reorganize the cytoskeleton around membraneless organelles — •THOMAS J. BÖDDEKER, KATHRYN A. ROSOWSKI, ROBERT W. STYLE, and ERIC R. DUFRESNE — Department of Materials, ETH Zurich, Switzerland

Phase-separation of biomolecules in cells takes place in a complex environment crossed by multiple filaments of the cytoskeleton or chromatin. To understand the potential coupling between emerging droplets and the surrounding network, we study the interactions of stress granules, a phase-separated protein-RNA droplet in the cytosol, with the microtubule network. Statistical tools similar to the radial distribution function enable us to quantify long-ranged enhancement in microtubule density in the vicinity of stress granules. When microtubules are depolymerized, the molecular subunits partition to the surface of the droplet. We interpret the data using a thermodynamic model, revealing a weak non-specific affinity of the subunits to the surface of about $0.1 k_b T$. As filaments polymerize, the affinity is amplified leading to significant adhesion of filaments to the granule surface. This adhesion leads to reorganization of filaments around the granule and makes microtubule rich regions of the cell energetically favorable for stress granules. We find that the liquid nature of membraneless organelles leads to non-specific adhesion of larger particles to their surface due to the surface tension of these protein droplets, reminiscent of Pickering emulsions.

T.J. Böddeker, et. al. Nature Physics 18, 571 2022

BP 8.7 Tue 11:30 H15

Catalysis-Induced Phase Separation and Autoregulation of Enzymatic Activity — MATTHEW W. COTTON^{1,2}, RAMIN GOLESTANIAN^{2,3}, and JAIME AGUDO-CANALEJO^{2,4} — ¹Mathematical Institute, University of Oxford, Oxford, United Kingdom — ²Department of Living Matter Physics, Max Planck Institute for Dynamics and Self-Organization, Göttingen, Germany — ³Rudolf Peierls Centre for Theoretical Physics, University of Oxford, Oxford, United Kingdom — ⁴Institute for Theoretical Physics, University of Heidelberg, Heidelberg, Germany

Studying the effect of non-equilibrium activity on intracellular phase separation is a very active research area, but all previous studies have still relied on equilibrium interactions as the driver for phase separation. Here, we present a thermodynamically consistent model describing the dynamics of a multi-component mixture where one enzyme component catalyzes a reaction between other components. We find that the catalytic activity alone can induce phase separation for sufficiently active systems and large enzymes, without any equilibrium interactions between components [1]. In the limit of fast reaction rates, binodal lines can be calculated using a mapping to an effective free energy. We also explain how this catalysis-induced phase separation (CIPS) can act to autoregulate the enzymatic activity, which points at the biological relevance of this phenomenon.

[1] M. W. Cotton, R. Golestanian, and J. Agudo-Canalejo, arXiv:2205.12306 (2022).

BP 8.8 Tue 11:45 H15

Structure and dynamics of water molecules in FUS protein molecular condensates — •DANIEL CHAVEZ ROJAS, MARTIN GIRARD, and JOSEPH RUDZINSKI — Max Planck Institute for Polymer Research, Mainz, Germany

There is evidence that molecular condensates of the FUS protein play a role in the development of some neurodegenerative diseases like ALS. For this reason, understanding the molecular mechanism by which these condensates form at an atomistic level is of therapeutic interest. The molecular structure and water-protein interactions of these condensates is poorly understood. In order to study these interactions, we make use of multi-scale molecular dynamics simulations. Through the analysis of these simulations we report on the water-protein hydrogen bonding interactions of the individual amino acids of FUS proteins in the condensate versus in solution.

BP 8.9 Tue 12:00 H15

Regulation of chromatin microphase separation by adsorbed protein complexes — •OMAR ADAME-ARANA, GAURAV BAJPAI, DANA LORBER, TALILA VOLK, and SAMUEL A. SAFRAN — Weizmann Institute of Science, Rehovot, Israel
The spatial arrangement of chromatin in the nucleus serves as a template for DNA transcription. Regions of chromatin that are loosely packed (active regions) are accessible to the transcription machinery and can be readily transcribed; in contrast, regions that are tightly packed are usually not transcribed (inactive regions). These two types of chromatin regions separate from the nucleoplasm and further form distinct compartments reminiscent of microphase separation. Chromatin phase separation due to self-attraction has been experimentally described in the past. But what controls the further, observed microphase separation into active and inactive chromatin regions? Here, we present a minimal theory in which the inactive regions experience poor solvent conditions (due to self-attraction,) but where the solvent quality for the active chromatin regions can be regulated by the adsorption of protein complexes. Using the theory of polymer brushes as well as Brownian dynamics simulations, we find that such adsorption leads to swelling of the active regions which in turn, decreases the thickness (in a flat geometry) or radius of curvature (in a spherical geometry) of the inactive chromatin microphase. We compare the theory with experiments to suggest that the solvent quality modulated by adsorption of protein complexes may be a key contributing factor in establishing and regulating the physical organization of the genome.

BP 8.10 Tue 12:15 H15

(De)hydration far away from equilibrium can speed up chemical processes — •IVAR SVALHEIM HAUGERUD, PRANAY JAISWAL, and CHRISTOPH WEBER — Institute of Physics, Universität Augsburg, Augsburg, Germany

Under early earth conditions, wet-dry cycles and phase-separated droplets are believed to facilitate chemical processes. Recent experimental studies suggest that chemical reactions can accelerate when subject to non-equilibrium conditions of hydration or dehydration. We develop a theoretical model studying the interplay between wet-dry cycles, phase separation, and chemical processes. We find that both hydration and dehydration can significantly increase chemical reaction rates. Interestingly, we show that the conditions that enhance reaction rates coincide with the conditions necessary for the mixture to phase separate. The findings show under what conditions the physics of wet-dry cycles can play a role similar to enzymes in living cells, speeding up slow reactions in prebiotic soups.

BP 8.11 Tue 12:30 H15

Chemically Active Wetting — •SUSANNE LIESE¹, XUEPING ZHAO², FRANK JÜLICHER², and CHRISTOPH WEBER¹ — ¹University of Augsburg, Germany — ²MPI Physics of Complex Systems, Dresden, Germany

In living cells, the wetting of condensed phases at membrane surfaces provides a mechanism for positioning biomolecules. Biomolecules can also bind to such membrane surfaces. In living cells, this binding is often chemically active since it is maintained away from equilibrium by supplying energy and matter. Here, we investigate how active binding on membranes affects the wetting of condensates. To this, we derive the non-equilibrium thermodynamic theory of active wetting. We find that active binding significantly alters the wetting behavior leading to non-equilibrium steady states with condensate shapes reminiscent of a fried egg

or a mushroom. We further show that such condensate shapes are determined by the strength of active binding in the dense and dilute phases, respectively. Strikingly, such condensate shapes can be explained by an electrostatic analogy where binding sinks and sources correspond to electrostatic dipoles along the triple line. Through this analogy, we can understand how fluxes at the triple line control the three-dimensional shape of condensates.

BP 8.12 Tue 12:45 H15

Interface resistance can govern transport of molecules across phase boundaries — •LARS HUBATSCH^{1,2}, ANATOL FRITSCH^{1,2}, TYLER HARMON³, FRANK JÜLICHER^{2,4}, CHRISTOPH WEBER⁵, and ANTHONY HYMAN^{1,2} — ¹Max Planck Institute of Molecular Cell Biology and Genetics — ²Center for Systems Biology Dresden — ³Leibniz Institute for Polymer Research — ⁴Max Planck Institute for the Physics of Complex Systems — ⁵University of Augsburg

Cells can achieve compartmentalization of biochemical processes via organelles

by the selective admission of biomolecules. Organelles are enclosed by a membrane or, in the case of biomolecular condensates, by the condensate-bulk interface. While transport across membranes has been studied for decades, it is less clear how biomolecular condensates regulate transport across their interface. Using a combination of live-imaging and theory, we show that the flux of molecules across the condensate-bulk interface exhibits transients that cannot be explained by local equilibrium between the coexisting phases, a phenomenon also referred to as interface resistance. It is unclear whether this interface resistance stems from molecules adsorbing to the interface or from a kinetic barrier reflecting molecules at the interface. Using single-particle imaging of PGL-3 droplets, we observe no accumulation of molecules at the interface. This observation suggests that molecules are reflected rather than adsorbed at the interface. We quantify the strength of interface resistance by accounting for molecule dynamics outside, inside, and at the droplet interface and thus provide a framework to characterize molecular fluxes across condensate-bulk interfaces.

BP 9: Bioimaging

Time: Tuesday 9:30–13:00

Location: H16

BP 9.1 Tue 9:30 H16

Nano-infrared spectroscopic imaging (NanIRim): Promises and Challenges for Application in Biophotonics — •DANIELA TÄUBER — Leibniz Institute of Photonic Technology, Jena, Germany — Friedrich-Schiller University Jena, Germany

A number of nano IR spectroscopic methods have been developed, which provide chemical information at subcellular and single molecule level. High spatial resolution leads to a reduction of the number of chemical bonds contributing to the signal. Thus, variations have to be identified above a heterogeneous background. Since 2019, I have investigated advantages and limitations of mid IR photo-induced force microscopy (PIF-IR) together with my team and collaborators. We applied PIF-IR to materials ranging from organic monolayers on various substrates, and biopolymer compositions to single bacteria and human retina. Recently, we studied interference effects in layered systems comparing experimental and calculated FTIR spectra of polymer films on different substrates to PIF-IR spectra. PIF-IR enables hyperspectral imaging at a fascinating spatial resolution of ~5 nm. A drawback are the small data sets. We applied PIF-IR to well-known interactions of antibiotics with *Bacillus subtilis*. To meet the challenge of finding the local interactions in hyperspectral images of single bacteria, we developed an advanced cluster analysis together with colleagues in the Heintzmann Lab. Our findings are very promising for successful applications of PIF-IR to the investigation of local variations in the surface areas of cells and tissues. Such visualization at the single cell level will boost our understanding of interactions in the Life Sciences

BP 9.2 Tue 9:45 H16

Phase reconstruction of low-energy electron holograms of individual proteins — •HANNAH OCHNER¹, SVEN SZILAGYI¹, MORITZ EDTE¹, STEPHAN RAUSCHENBACH^{1,2}, LUIGI MALAVOLTI¹, and KLAUS KERN^{1,3} — ¹Max Planck Institute for Solid State Research, Stuttgart — ²Department of Chemistry, University of Oxford — ³Institut de Physique, École Polytechnique Fédérale de Lausanne

Low-energy electron holography (LEEH) can image proteins and their conformational variability on the single-molecule level [1,2]. However, the technique does not yield a real-space image, but rather a hologram from which the information about the molecule needs to be recovered via a reconstruction process. While a one-step reconstruction process can reproduce molecular size and shape via amplitude imaging, it cannot directly recover the phase information encoded in the hologram. Here, we apply an iterative phase retrieval algorithm to experimentally acquired low-energy electron holograms of proteins. This allows us to reconstruct the phase shift induced by the protein along with its amplitude distribution. We provide evidence that phase imaging is sensitive to changes in local potential, as indicated by the strong correlation between reconstructed phase shift and the number of scatterers in the electron path, and the strong phase signatures induced by localised charges. LEEH phase imaging thus yields insights into structural features beyond size and shape and could, at high spatial resolution, open up the possibility of chemically sensitive single-molecule imaging.

[1] PNAS,2017;114(7) [2] PNAS,2021;118(51) e2112651118

BP 9.3 Tue 10:00 H16

Investigation of human platelet volume changes with scanning ion conductance microscopy (SICM) — •KONSTANTIN KRUTZKE, JAN SEIFERT, JOHANNES RHEINLAENDER, and TILMAN E. SCHÄFFER — Institute of Applied Physics, Eberhard-Karls-Universität Tübingen, Germany

Human blood platelets (thrombocytes) are anucleate cells that play an important role in wound closure in the case of vessel injury. Changes in morphology

and activation of platelets are linked to blood vessel diseases such as atherosclerosis or can cause thrombosis. Water-induced swelling promotes procoagulant activity and possibly initiates thrombosis. Volume changes of platelets can be measured by light transmittance or light scattering techniques. However, these studies have only qualitatively shown that platelets regulate their volume as a response to different osmotic conditions and usually have not been performed on a single-cell level. To elucidate the volume regulatory mechanisms of platelets, we used scanning ion conductance microscopy (SICM) to quantitatively measure dynamic volume changes of single adhered platelets under different osmotic conditions with down to sub-minute time-resolution. SICM is a nanopipette-based, contact-free imaging technique ideally suited for sensitive live cells such as platelets. Our data show that rapid volume regulation of non-activated adherent platelets occurs in direct response to different osmotic conditions. Activated platelets, however, seem not to be able to regulate their volume when the osmolarity changes. We thereby highlight the usability of SICM for high-speed volume measurements.

BP 9.4 Tue 10:15 H16

Pool formation of synaptic vesicles by synapsin investigated by X-ray diffraction and cryo-EM — •JETTE ALFKEN¹, CHARLOTTE NEUHAUS¹, MORITZ STAMMER¹, MARCELO GANZELLA³, ARSEN PETROVIC⁴, RUBÉN FERNÁNDEZ-BUSNADIEGO⁴, REINHARD JAHN³, DRAGOMIR MILOVANOVIC², and TIM SALDITT¹ — ¹Georg-August-Universität, Institute for X-ray Physics, 37077 Göttingen — ²Laboratory of Molecular Neuroscience, German Center for Neurodegenerative Diseases (DZNE), 10117 Berlin — ³Laboratory of Neurobiology, Max Planck Institute for Multidisciplinary Sciences, 37077 Göttingen, Germany — ⁴Institute of Neuropathology, University Medical Center Göttingen, 37099 Göttingen

Synaptic vesicles (SVs) are organized in dense pools close to the synaptic membrane. A key protein for this structural arrangement within the synapse is synapsin, which forms droplets containing SVs, due to liquid-liquid phase separation. To study the structure and interactions underlying pool formation in a controlled in vitro model, we have investigated phases made of SVs purified from rat brain and varied synapsin concentration. We have studied the pools by two complementary techniques: cryo-EM yielding the 3D structural arrangement of the adhering vesicles in pools at resolution of a few nanometers in the vitrified state, and solution SAXS under varied buffer conditions and concentrations. In addition, the pools were studied for comparison in a controlled system consisting of artificially prepared lipid vesicles and synapsin. We report these experiments and preliminary results (data analysis still ongoing).

15 min. break

BP 9.5 Tue 10:45 H16

Understanding calcareous biomineralization on the nanoscale through in-vivo growth imaging by x-ray nanodiffraction — •TILMAN GRÜNEWALD¹, JEREMIE VIDAL-DUPIOLE², JULIEN DUBOISSET¹, BRUNO PETTON³, JACQUELINE LEGRAND³, MICHAEL SZTUCKI⁴, MANFRED BURGHAMMER⁴, and VIRGINIE CHAMARD¹ — ¹Institut Fresnel, Marseille, France — ²Ifremer, Montpellier, France — ³Ifremer, Plouzané, France — ⁴ESRF, Grenoble, France

Biomineralized tissues combine properties such as low weight with high-strength and are formed from abundant atoms via low-energy processes. However, the nanostructural formation process of biominerals is not well understood, relying on post-mortem investigations of the bivalve growth edge [1]. Insights by in-vivo experiments requires studying a live organism in its environment at the crystalline level with sub-um spatial resolution. The associated problems have been overcome by 4th generation synchrotrons, enabling faster measurements.

Here, an experimental approach we developed and validated is outlined, enabling us to observe the first nanoscale-resolved, temporal follow-up of the shell growth in a living, mineralizing *Crassostrea gigas* oyster shell by nanofocus x-ray Bragg diffraction.

We show that crystallization occurs without the presence of the animal mantle, over several hours and follows a layer-by-layer deposition scheme with slightly misaligned grains. These results imply a cyclic crystallization, driven by a physico-chemical mechanism. This provides the animal with an efficient way of building its shell.

[1] Duboisset et al. 10.1016/j.actbio.2022.01.024

BP 9.6 Tue 11:00 H16

An open-top scanned oblique lightsheet microscope for neuronal network imaging — •ACHIM THEO BRINKOP¹, STEFAN STÖBERL¹, FLORIAN SCHORRE¹, and FRIEDHELM SERWANE^{1,2,3} — ¹Faculty of Physics, LMU Munich, Germany — ²Munich Cluster for Systems Neurology (SyNergy), Germany — ³Graduate School of Systemic Neuroscience (GSN), Munich, Germany

Understanding signal processing in neuronal networks such as brain organoids on a single-neuron level has remained a challenge. Imaging network activity requires a millisecond temporal resolution with single-neuron spatial resolution, all in an observation volume containing the 3D network. Advances in lightsheet microscopy have brought this goal closer to experimental reach, but at the cost of complex optical set-ups which (i) impose geometrical constraints to sample mounting or (ii) require multiple imaging objectives with custom optical components.

We report on the development of an open-top single-objective oblique lightsheet microscope which reduces the complexity compared to existing set-ups. We implement the open-top geometry by using only two primary objectives. The lightsheet is digital scanned by a fast galvo mirror to maintain high image quality. Our first prototype with excitation wavelengths of 561 (488, 638) nm is expected to allow for a $1/e^2$ -resolution of 1.84 (1.47, 1.95) μm axially and 0.27 (0.23, 0.30) μm laterally. It offers a volumetric temporal resolution of 8 (2) Hz for a volume of 400 x 90 (360) x 100 μm^3 .

With this set-up, we aim to gain insights into large neuronal networks of retina organoids, both in wildtype and disease condition.

BP 9.7 Tue 11:15 H16

Extraction of Calcium Traces from Volumetric Lightsheet Images of 3D Neuron Ensembles — •FILIPPO KIESSLER¹, PAULINA WYSMOLEK⁴, KATJA SALBAUM^{1,2}, ELIJAH SHELTON¹, SELINA SONNTAG¹, and FRIEDHELM SERWANE^{1,2,3} — ¹Faculty of Physics and Center for NanoScience, Ludwig-Maximilians-Universität München, Munich — ²Graduate School of Systemic Neuroscience (GSN), Munich, Germany — ³Munich Cluster for Systems Neurology (SyNergy), Germany — ⁴Max Planck Institute for Medical Research, Heidelberg, Germany

In vitro systems resembling brain regions, such as brain organoids, are slowly changing the field of neuroscience. However, characterization of their electrical activity has remained a challenge as this requires electrophysiological readout in 3D at single-neuron resolution. We use a custom-built single-photon light-sheet microscope to record calcium activity in 3D neuron ensembles which we grow from mouse embryonic stem cells. To extract calcium intensities from the volumetric light-sheet data, we developed a custom software pipeline that augments the CaImAn software. Our pipeline includes a median filter to remove sample bleaching effects. In addition, typical artifacts arising from the illumination of our light-sheet microscope are removed with a custom Fourier filter. With this setup we obtained connectivity graphs based on correlation of the extracted calcium traces. We envision this platform as a non-invasive toy-model to understand neuronal information generation and processing.

BP 9.8 Tue 11:30 H16

Thermal fluctuations of the trapped bead as the complementary tool to the microscopy for investigation of a phagocytosis. — •TETIANA UDOD and ALEXANDER ROHRBACH — Lab for Bio- and Nano-Photonics, Department of Microsystems Engineering (IMTEK), University of Freiburg, Georges-Koehler-Allee 102, 79110 Freiburg, Germany

Phagocytosis, the uptake of particle by cells, is typically investigated in vivo by different microscopy techniques, such as Brightfield, DIC, or Fluorescence microscopy. But even with highest possible resolution we can't observe receptor binding or derive binding strengths to the cell membrane during binding and uptake. In addition to continuously recording 3D stacks of J774 macrophages cells by DIC microscopy, we record the thermal fluctuations of beads during the engulfment process. We measure the bead's position in 3D with nanometer precision at MHz rates with back focal plane interferometry. Running both methods in parallel we can correlate the bead position relative to the cell to record changes in binding parameters like stiffnesses or, viscous drags derived from position fluctuations. Furthermore, remaining measurement ambiguities are resolved by Brownian Dynamic simulations.

To better understand such processes we use a combination of experiments with Photonic Force Microscopy, Brownian Dynamic simulation and analytical theory.

BP 9.9 Tue 11:45 H16

Assessing the cochlear morphology from the whole organ down to cellular resolution with multi-scale phase-contrast x-ray tomography — •JANNIS JUSTUS SCHAEFER¹, CHRISTOPH KAMPSHOFF², BETTINA WOLF², DANIEL KEPPELER², TOBIAS MOSER², and TIM SALDIT¹ — ¹Institut für Röntgenphysik, Georg-August-Universität Göttingen — ²InnerEarLab, Universitätsmedizin Göttingen

The cochlea is the receptor organ of the inner ear which transduces sound into neuronal activity. Both fundamental aspects of signal transduction and neurophysiology as well as biomedical research (implant technology, hearing loss and disorders) require 3D imaging techniques capable to quantify the micro-anatomy (1).

We present multi-scale 3D imaging of small-animal cochleae by phase-contrast x-ray tomography (PC-CT) using both synchrotron radiation (SR) and lab μ -CT to assess the morphology of the cochlea, orientation of cochlear implants (CIs), and the number and density of spiral ganglion neurons (SGNs). Due to optimization in sample preparation, image acquisition and phase retrieval we achieve high contrast for unstained soft tissue. Without extensive sample preparation, shape and volume of every SGN in the entire organ can be identified. In the high-resolution PC-CT, and in the parallel beam, we reach cellular resolution in the organ of Corti. Lab μ -CT is suitable to analyze cochlear morphology and to assess the correct positioning of CIs and resulting (non-)optimal signal transduction.

(1) Keppeler et al. (2021), PNAS 118(18), e2014472118

15 min. break

BP 9.10 Tue 12:15 H16

Studying biomolecular dynamics and structure with high-speed atomic force microscopy — •DIMITAR STAMOV, ANDREAS KRAUS, ANDRÉ KÖRNIG, and HEIKO HASCHKE — JPK BioAFM, Bruker Nano GmbH, Am Studio 2D, 12489 Berlin, Germany

Studying the molecular dynamics and structural conformations is important for understanding the function and biological significance of samples ranging from single membrane proteins to complex macromolecular systems. Recent atomic force microscopy (AFM) developments have led to unprecedented imaging rates in fluid, enabling temporal resolution on the sub-20-millisecond scale.

Annexin V (A5) serves as an important regulator of membrane repair in eukaryotic cells, where it shows a strong Ca^{2+} binding affinity to phosphatidylserine. We have used high-speed AFM to study the 2D crystal formation in a model system containing supported lipid bilayers and A5 molecules. We demonstrate the lateral dynamics and preferred structural orientations of the mobile A5 trimers.

We previously demonstrated that pUC19 plasmids bind to poly-L-ornithine substrate in supercoiled states that are very high in torsional energy, thereby driving dehybridization of the double-helical DNA strands. Here we have quantified the process kinetics with a temporal resolution of 25 ms per frame and identified stages that include formation of metastable dehybridization bubbles, thermodynamic single strand fluctuations, and ultimately rehybridization to an intact double-stranded state.

Prize Talk

BP 9.11 Tue 12:30 H16

Super-resolution STED and MINFLUX Nanoscopes by Abberior Instruments — •GERALD DONNERT — Abberior Instruments GmbH, Göttingen, Germany — Laureate of the Technology-Transfer-Prize 2022

Abberior Instruments GmbH was founded 10 years ago from the laboratory of Nobel Laureate Stefan Hell at the Max Planck Institute in Göttingen. In 2022, Abberior Instruments was awarded the Technology Transfer Prize of the German Physical Society (DPG).

Abberior Instruments develops and markets super-resolution light microscopes, namely confocal plus STED microscopes and MINFLUX microscopes. The latter are the latest generation of super-resolution instruments with resolutions down to the molecular level, i.e. 1 nm resolution; unrivaled in resolution today. Understanding life at the molecular level - both in terms of structure and dynamics - is a human dream and is becoming feasible with the latest generation of super-resolution instruments with multicolor capabilities. We expect to soon gain new insights into the dynamic structural changes of e.g. protein machines in living cells.

In this talk, I will present the latest imaging and tracking results with our super-resolution STED and MINFLUX nanoscopes, such as single-particle tracking of lipids in lipid membranes, the structure of nuclear pore complex (NPC) subunits, and the nanoscale assembly of proteins in neuronal synapses.

BP 10: Cell Adhesion and Multicellular Systems

Time: Tuesday 10:00–12:30

Location: H13

BP 10.1 Tue 10:00 H13

Physics of gut motility governs digestion and bacterial growth — •AGNESE CODUTTI^{1,2}, JONAS CREMER³, and KAREN ALIM^{1,2} — ¹Physics Department and CPA, Technische Universität München — ²Max-Planck-Institut für Dynamik und Selbstorganisation, Göttingen — ³Stanford University

Malfunctioning of the small intestine contractility and the ensuing bacterial population therein are linked to a plethora of diseases. We, here, study how the small intestine's variety of contractility patterns impacts nutrient uptake and bacterial population. Our analytical derivations in agreement with simulations identify flow velocity as the key control parameter of the nutrients uptake efficiency and bacterial growth, independently of the specifics of contractility patterns. Self-regulating flow velocity in response to the number of nutrients and bacteria in the gut allows achieving 100% efficiency in nutrient uptake. Instead of the specifics of intestine contractility, our work points to the flow velocity and its variation in time within the intestine to prevent malfunctioning.

BP 10.2 Tue 10:15 H13

Blue-light photoreceptors regulating light-switchable adhesion in *Chlamydomonas reinhardtii* — •RODRIGO CATALAN^{1,2}, ANTOINE GIROT^{1,2}, ALEXANDROS FRAGKOPOULOS^{1,2}, SIMON KELTERBORN³, DARIUS RAUCH³, PETER HEGEMANN³, and OLIVER BÄUMCHEN^{1,2} — ¹Max Planck Institute for Dynamics and Self-Organization (MPIDS), 37077 Göttingen, Germany — ²University of Bayreuth, Experimental Physics V, 95447 Bayreuth, Germany — ³Humboldt University Berlin, Institute of Biology, 10115 Berlin, Germany

Photoactive organisms have evolved a variety of light-sensitive molecules, called photoreceptors, which regulate phenotypes such as phototaxis, circadian life cycle and sexual reproduction. Recently it was discovered that the unicellular, eukaryotic microalga *Chlamydomonas reinhardtii* exhibits light-switchable flagellar adhesion to surfaces [Kreis *et al.*, Nature Physics, 2018]; a phenotype triggered by a blue-light photoreceptor. Using single-cell micropipette force measurements, we show that the action spectrum of flagellar adhesion forces in wild-type (WT) cells resembles the adsorption spectrum of photoreceptors called cryptochromes. Furthermore, adsorption experiments show that the number of WT cells adsorbing to surfaces under blue light increases after the start of the cells' day-phase, which coincides with the light degradation of plant cryptochrome (pCRY). Adhesion force and adsorption experiments of WT and photoreceptor deletion mutants illuminate the role of photoreceptors in this adhesion phenotype.

BP 10.3 Tue 10:30 H13

Motility and collective behavior of gliding *Chlamydomonas* populations — •ALEXANDROS FRAGKOPOULOS^{1,2}, SEBASTIAN TILL¹, FLORIAN EBMEIER¹, MARCO G. MAZZA^{1,3}, and OLIVER BÄUMCHEN^{1,2} — ¹Max Planck Institute for Dynamics and Self-Organization (MPIDS), 37077 Göttingen, Germany — ²University of Bayreuth, Experimental Physics V, 95447 Bayreuth, Germany — ³Department of Mathematical Sciences, Loughborough University, Loughborough, Leicestershire LE11 3TU, UK

The model microbe *Chlamydomonas reinhardtii*, a unicellular biflagellated microalga, can adhere and colonize almost any surface under particular light conditions. Once the cells attach to a surface, an intraflagellar transport machinery translocates the cell body along the flagella, which are oriented in a 180° configuration. This motion is known as gliding motility. We find that gliding enables surface-associated *Chlamydomonas* cells to cluster and form compact, interconnected microbial communities [1]. We detect and analyze the movement of single cells and characterize the spatio-temporal evolution of the morphology of the colony. The motion of single cells exhibits rapid movements, followed by prolonged immobility. By analyzing the cell clustering, we observe the colony transitioning from local clusters to a single global network with increasing cell density. Simulations based on a purely mechanistic approach cannot capture the non-random cell positions. However, by including flagellar mechanosensing through a cognitive model, we quantitatively reproduce the experimental observations.

[1] Till *et al.*, arXiv:2108.03902v1

BP 10.4 Tue 10:45 H13

Spatiotemporally resolved single-cell growth in bacterial biofilms — •ERIC JELLI^{1,2,3}, TAKUYA OHMURA^{2,4}, NIKLAS NETTER^{2,3,4}, MARTIN ABT^{2,3}, EVA JIMÉNEZ-SIEBERT^{2,3,4}, KONSTANTIN NEUHAUS^{2,3,4}, DANIEL KARL-HEINZ RODE^{2,3,4}, and KNUT DRESCHER^{2,3,4} — ¹Max Planck Institute for Neurobiology of Behavior - caesar, Bonn, Germany — ²Max Planck Institute for Terrestrial Microbiology, Marburg, Germany — ³Department of Physics, Philipps-Universität Marburg, Marburg, Germany — ⁴Biozentrum - University of Basel, Basel, Switzerland

Bacterial biofilms are dense multicellular communities that are embedded in a self-produced matrix. The high density of cells gives rise to nutrient, oxy-

gen, and metabolite gradients in space and time. To understand the underlying spatio-temporal growth principles in biofilms, single-cell segmentation algorithms are required. Current Deep Learning algorithms provide the required accuracy for tracking-dependent investigations, yet depend on suitable large training datasets.

We used an iterative training pipeline to densely annotate complete biofilms with thousands of cells in 3D. The pipeline reduced the required manual labeling steps which would otherwise be prohibitive for a dataset of a similar size. The collected data enabled us to compare the single-cell segmentation accuracy of recent Deep Learning algorithms with the results of classical biofilm segmentation approaches. We used the trained algorithms for single-cell tracking in 3D time-lapse confocal microscopy data and identified regions with different division rates inside the microbial communities.

15 min. break

BP 10.5 Tue 11:15 H13

The advantage of network topology in avoidance reaction — •SIYU CHEN¹, JEAN-DANIEL JULIEN¹, and KAREN ALIM^{1,2} — ¹Max-Planck-Institut für Dynamik und Selbstorganisation, Göttingen — ²Physics Department and CPA, Technische Universität München, München

The unicellular slime mould *Physarum polycephalum* stands out among other unicellular organisms for having a network-shaped body. Which advantage does a network structure provide when facing a challenging environment with adverse conditions? We, here, follow how network topology impacts *P. polycephalum*'s avoidance response to adverse blue light. We stimulate either an elongated amoeboid or a simple Y-shaped networked specimen and quantify the retraction velocity of the light-exposed body part. The result shows that Y-shaped specimen can complete the avoidance retraction without increasing the migration velocity, while an elongated amoeboid requires bursts of higher velocities - an energetically costly expense. Our theoretical predictions suggest that a light-triggered change in cytoplasm viscosity may account for the difference in response, as the more complex topology of a network allows *P. polycephalum* to maintain large flows that enable quick retraction out of the blue light. The difference in the retraction behaviour suggest the complexity of network topology provides a key advantage in dealing with adverse environments. Our findings could lead to the better understanding of the evolutionary transition from unicellular to multicellularity.

BP 10.6 Tue 11:30 H13

Model-Based Prediction of an Effective Adhesion Parameter Guiding Multi-Type Cell Segregation — •PHILIPP ROSSBACH, HANS-JOACHIM BÖHME, STEFFEN LANGE, and ANJA VOSS-BÖHME — DataMedAssist, HTW - University of Applied Sciences, 01062 Dresden, Germany

The process of cell-sorting is essential for development and maintenance of tissues. With the Differential Adhesion Hypothesis, Steinberg proposed that cell-sorting is determined by quantitative differences in cell-type-specific intercellular adhesion strengths. An implementation of the Differential Adhesion Hypothesis is the Differential Migration Model by Voss-Böhme and Deutsch. There, an effective adhesion parameter was derived analytically for systems with two cell types, which predicts the asymptotic sorting pattern. However, the existence and form of such a parameter for more than two cell types is unclear. Here, we generalize analytically the concept of an effective adhesion parameter to three and more cell types and demonstrate its existence numerically for three cell types based on in silico time-series data that is produced by a cellular-automaton implementation of the Differential Migration Model. Additionally, we classify the segregation behavior using statistical learning methods and show that the estimated effective adhesion parameter for three cell types matches our analytical prediction. Finally, we demonstrate that the effective adhesion parameter can resolve a recent dispute about the impact of interfacial adhesion, cortical tension and heterotypic repulsion on cell segregation.

BP 10.7 Tue 11:45 H13

Is cell segregation like oil and water: asymptotic versus transitory regime — •FLORIAN FRANKE^{1,2}, SEBASTIAN ALAND^{2,3}, HANS-JOACHIM BOEHME^{1,2}, ANJA VOSS-BOEHME^{1,2}, and STEFFEN LANGE^{1,2} — ¹DataMedAssist, HTW Dresden — ²Faculty of Informatics/Mathematics, HTW Dresden - University of Applied Sciences — ³Faculty of Mathematics and Computer Science, TU Freiberg

Segregation of different cell types is a crucial process for the pattern formation in tissues. Since the involved cell interactions are complex and difficult to measure individually in experiments, mathematical modelling plays an increasingly important role to unravel the mechanisms governing segregation. The analysis of these theoretical models focuses mainly on the asymptotic behavior at large times, in a steady regime and for large numbers of cells. Most famously, cell-segregation models based on the minimization of the total surface energy,

a mechanism also driving the demixing of immiscible fluids, are known to exhibit asymptotically a particular algebraic scaling behavior. However, it is not clear, whether the asymptotic regime of the numerical models is relevant at the spatio-temporal scales of actual biological processes and in-vitro experiments. By developing a mapping between cell-based models and experimental settings, we are able to directly compare previous experimental data to numerical simulations of cell segregation quantitatively. We demonstrate that the experiments are reproduced by the transitory regime of the models rather than the asymptotic one. Our work puts a new perspective on previous model-driven conclusions on cell segregation mechanisms.

BP 10.8 Tue 12:00 H13

Self-Buckling of filamentous cyanobacteria reveals gliding forces — •MAXIMILIAN KURJAHN¹, ANTARAN DEKA¹, ANTOINE GIROT^{1,2}, LEILA ABBASPOUR^{3,4}, STEFAN KLUMPP^{3,4}, MAIKE LORENZ⁵, OLIVER BÄUMCHEN^{1,2}, and STEFAN KARPITSCHKA¹ — ¹Max Planck Institute for Dynamics and Self-Organization (MPI-DS), Göttingen — ²Experimental Physics V, University of Bayreuth — ³Max Planck School Matter to Life, University of Göttingen — ⁴Institute for Dynamics of Complex Systems, University of Göttingen — ⁵Department of Experimental Phycology and SAG Culture Collection of Algae, University of Göttingen

Filamentous cyanobacteria are one of the oldest and today still most abundant lifeforms on earth, with manifold implications in ecology and economics. These phototrophic organisms form long and flexible filaments that do not actively swim in bulk liquid but exhibit gliding motility in contact with solid surfaces. The underlying force generating mechanism of their gliding apparatus is not yet understood. We measure their bending modulus with micropipette force sen-

sors, and investigate how filaments buckle after gliding onto an obstacle. Comparing Kirchhoff theory to the experiments, we derive the active forces and the friction coefficients associated with gliding from the observed critical filament length for buckling. Remarkably, we find that these two quantities are strongly coupled, while dependencies on other observables are largely absent. The critical length also aligns with the peak of their natural length distribution, indicating the importance of buckling for their collective.

BP 10.9 Tue 12:15 H13

Structural and mechanical properties of filamentous cyanobacteria — •MIXON FALUWEKI^{1,2} and LUCAS GOEHRING¹ — ¹Nottingham Trent University, Nottingham, UK. — ²Malawi University of Science and Technology, Limbe, Malawi.

Filamentous cyanobacteria, long strands of connected cells, are one of Earth's earliest forms of life. They are found in multiple environments playing different roles and forming large-scale patterns in structures like biomats and stromatolites. The mechanical properties of these structures contribute to cyanobacteria's success in inhabiting their environments and are useful in applications such as algae-based biofuel production. One of the most important mechanical properties of these active polymers is the bending modulus or flexural rigidity. Here, we quantify the flexural rigidity of three cyanobacteria species, of order *Oscillatoriales*, via bending tests in a microfluidic flow device, where single cyanobacteria filaments are introduced into the microfluidic channel and deflected by fluid flow. Our measurements are confirmed separately by measuring the Young's modulus and cell wall thickness using atomic force microscopy and transmission electron microscopy, respectively. These measurements can be used to model interactions between cyanobacteria, or with their environment, and how their collective behaviour emerges from such interactions.

BP 11: Active Matter 2 (joint session DY/BP/ CPP)

Time: Tuesday 10:00–13:00

Location: H18

See DY 16 for details of this session.

BP 12: Poster 2

Time: Tuesday 17:30–19:30

Location: P4

BP 12.1 Tue 17:30 P4

Holographic vibration spectroscopy: Probe- and contact-free viscoelastic analysis of adherent cells — •BOB FREGIN^{1,2}, STEFANIE SPIEGLER^{1,2}, and OLIVER OTTO^{1,2} — ¹ZIK HIKE, University of Greifswald, Greifswald, Germany — ²DZHK, University Medicine Greifswald, Greifswald, Germany

Cell mechanical properties can be used as an inherent biomarker for cell state, fate and function. Several high-throughput methods are available to characterize suspension cells, e.g., peripheral blood cells, without any labeling. However, fast and robust methods are lacking for adherent cells, although the majority of cells, e.g., in our human body, is aggregated into tissues.

Here, we introduce a new probe- and contact-free method for label-free mechanical phenotyping of adherent cells at high spatiotemporal resolution. While cells are excited mechanically by a vibration in the range of 100 kHz, their response is determined optically from cell height oscillations utilizing holographic laser Doppler interferometry. In proof-of-concept experiments on a monolayer of induced pluripotent stem cells (iPSCs), we present a cell amplitude response as a function of varying excitation amplitudes. This amplitude response is proportional to the elastic properties of a cell.

In future work, we plan to perform a spectroscopic evaluation, where experiments are carried out at multiple frequencies. Further, we aim to extend our analysis to a complete viscoelastic description.

BP 12.2 Tue 17:30 P4

Heterogenous cell structures in AFM and shear flow simulations — •SEBASTIAN WOHLRAB, SEBASTIAN MÜLLER, and STEPHAN GEKLE — Theoretical Physics VI, University of Bayreuth

In biophysical cell mechanics simulations, the complex inner structure of cells is often simplified as homogeneous material. However, this approach neglects individual properties of the cell's components, e.g., the significantly stiffer nucleus.

By introducing a stiff inhomogeneity inside our hyperelastic cell, we investigate it during AFM compression and inside shear flow in finite-element and Lattice Boltzmann calculations.

We show that a heterogenous cell exhibits almost identical deformation behavior under load and in flow as compared to a homogeneous cell with equal averaged stiffness, supporting the validity of the homogeneity assumed in both mechanical characterization as well as numerical computations.

BP 12.3 Tue 17:30 P4

Cell migration dynamics and nuclear deformation in three-dimensional micro-dumbbells — •STEFAN STÖBERL¹, JOHANNES FLOMMERSFELD², MAXIMILIAN M. KREFT¹, CHASE P. BROEDERS², and JOACHIM O. RÄDLER¹ — ¹Faculty of Physics and Center for NanoScience, Ludwig-Maximilians-University, Munich, Germany — ²Department of Physics and Astronomy, Vrije Universiteit Amsterdam, 1081 HV Amsterdam, The Netherlands

Cell migration plays a key role in physiological processes such as wound healing, cancer metastasis and immune response. In previous work we have studied the non-linear dynamics of single cells migrating between two surface-patterned adhesion sites guided by a bridging line.

Here we study the dynamics of MDA-MB-231 cells captured in three-dimensional (3D)-dumbbell-like microcavities. The structures formed by photolithography of PEG-norbornene hydrogels provide a soft and hence deformable frame, while cells attach and migrate on a fibronectin coated bottom. In our experiments we find that the dwell-time of cells before transitioning is retarded when the width of the dumbbell-constriction is narrowed below 8 μm. We are hypothesizing that the observed deformation of the nucleus, which is the biggest organelle in the cell, determines the time course of the repeated stochastic transitions. To study the external and internal forces involved we measure the displacement field of beads embedded in the vicinity of the 3D constriction.

BP 12.4 Tue 17:30 P4

The Weakness of Senescent Dermal Fibroblasts — •LYDIA REBEHN¹, SAMIRA KHALAJI¹, FENNEKE KLEINJAN¹, ANJA KLEEMANN¹, PATRICK PAUL¹, CONSTANTIN HUSTER³, ULLA NOLTE¹, KARMVEER SINGH², TANER PULA⁴, PAMELA FISCHER-POSOVSZKY⁴, KARIN SCHARFFETTER-KOCKANEK², and KAYE GOTTSCHALK¹ — ¹Institute for Experimental Physics, Ulm University, Ulm, Germany — ²Department of Dermatology and Allergology, Ulm University, Ulm, Germany — ³Institut für Theoretische Physik, Universität Leipzig, Leipzig, Germany — ⁴Department of Pediatrics and Adolescent Medicine, Ulm University, Ulm, Germany

As human tissues age, there is chronological accumulation of biophysical changes from internal and environmental factors. Skin aging leads to loss of dermal matrix integrity via degradation and decreased elasticity. The mechanical properties of the dermal matrix are maintained by fibroblasts, whose properties change during replicative aging. Here, we compare biophysical proper-

ties of young versus proliferatively aged primary fibroblasts via fluorescence and traction force microscopy, single-cell AFM, and microrheology of the cytoskeleton. Results show senescent fibroblasts have decreased cytoskeletal tension and myosin II regulatory light chain phosphorylation, in addition to significant loss of traction force. The alteration of cellular forces is harmful to the process of building and maintaining extracellular matrix, while decreased cytoskeletal tension can amplify epigenetic changes involved in senescence. Exploration of these mechanical phenomena provide possibilities for unexplored pharmaceutical targets against aging.

BP 12.5 Tue 17:30 P4

Unravelling the collective behaviour of protrusions for directed migration — •LUCAS TRÖGER¹ and KAREN ALIM^{1,2} — ¹Physics Department and CPA, Technische Universität München — ²Max Planck Institute for Dynamics and Self-Organization, Göttingen

Living systems are often challenged to coordinate collective behaviour of individual entities across large spatial scales. The morphology of amoeboid cells, for example, arises due to the coordination of randomly forming protrusions that facilitates the cell's directed migration. The slime mold *Physarum polycephalum* grows as a single giant cell of network-like shape, spanning orders of magnitude in size ranging from 500 micrometers to tens of centimeters. Due to the large extent, chemotaxis and morphogenesis of the entire cell require a mechanism for coordination among competing protrusions. *P. polycephalum* is renowned for its organism-wide cytoplasmic fluid flows spanning the fluid-filled tubular network in a peristaltic wave. These strong and large-scale flows make this organism an ideal model to investigate the role of fluid flows in coordinating the collective behaviour of competing protrusions during the morphological changes in chemotaxis. We perform experiments of chemotaxing *P. polycephalum* specimen of varying sizes and quantify the dynamics of individual protrusions in addition to the chemotactic performance of the entire specimen. We correlate growing and retracting protrusions over time to identify the mechanism of communication. The project will teach us how fluid flows control the collective behaviour of protrusions during directed migration.

BP 12.6 Tue 17:30 P4

Neutrophil mechanotransduction during durotaxis — •FATEMEH ABBASI¹, MATTHIAS BRANDT², and TIMO BETZ¹ — ¹Third Institute of Physics-Biophysics, Georg August University Göttingen — ²Institute of Cell Biology, ZMBE, University of Münster

In Vivo, cells experience complex tissue environments with various chemical and physical features. 3D confinement is one of the major physical obstacles for cells in their natural environment. Neutrophils are among the most abundant immune cells in our body, which have to cope with various physical constrictions on their way from production to the infection site. In addition to confinement, the stiffness of the microenvironment is another mechanical feature these rapidly moving cells are exposed to. Neutrophils experience various tissue stiffness, from 1 kPa (bone marrow) to 20 MPa (bone). Previous studies have demonstrated that these cells are responsive to their microenvironment stiffness by adjusting their adhesion and spreading. Based on this knowledge we decided to combine confinement and stiffness change and investigate the impact of 3D stiffness gradient on cell behaviour and migration, a fact called durotaxis. We hypothesized that stiffness gradient might be a triggering factor of neutrophil migration toward the infection site. We confine neutrophils in between 2 layers of polyacrylamide hydrogels with 2 different stiffness and keep this distance stable for the desired period of time to investigate cell mechanotransduction during durotaxis from different points of view. Our preliminary results regarding the neutrophil durotaxis show a surprising and transient force peak on the soft substrate during cell shifting.

BP 12.7 Tue 17:30 P4

Cytoskeletal Networks in Cells Under Strain — •RUTH MEYER, ANNA V. SCHEPERS, PETER LULEY, and SARAH KÖSTER — Institute for X-Ray Physics, University of Göttingen

The cytoskeleton of eukaryotic cells mainly consists of three types of filamentous proteins: F-actin, microtubules and intermediate filaments (IFs). In contrast to microtubules and actin filaments, IFs are expressed in a cell-type specific manner, and keratins are found in epithelial cells. In certain cell types, the IF keratin forms a layer close to the membrane, referred to as an "IF-cortex". It has been observed that this IF-cortex arranges in a "rim-and-spokes" structure in epithelia. Based on this hypothesis, IFs and actin filaments might add complementary mechanical properties to the cellular cortex. When stretching single IFs, it was previously shown that IFs remain undamaged even at high forces. We now ask the question of whether this unique force-extension behavior of single IFs is also relevant in the filament network within a cell. The experiment is conducted by seeding cells on an elastic substrate and then stretching the substrate uniaxially or equibiaxially to high strains. In combination with fluorescence and atomic force microscopy, this setup allows us to study the structure and the mechanical properties of actin and IF networks close to the cell membrane.

BP 12.8 Tue 17:30 P4

Cell mechanics and cytoskeletal structures under uniaxial, equibiaxial strain — •ANNA V. SCHEPERS, RUTH MEYER, PETER LULEY, and SARAH KÖSTER — Universität Göttingen

The cytoskeleton, which largely determines the mechanical properties of cells, has to withstand various mechanical stresses throughout the lifetime of a cell. In mechanically stressed cells, structural and mechanical changes often go hand-in-hand. Understanding how cytoskeletal remodelling accompanies the mechanical changes will give insight into the mechanism by which cells adjust to mechanical load and how this reaction might be altered in diseases. Remodelling of the cytoskeleton has been observed under uniaxial and equibiaxial stretching. However, combined structural and force measurements under well-defined mechanical conditions are sparse. We therefore present a uniform, equibiaxial cell stretching device that is compatible with fluorescence microscopy as well as single cell force spectroscopy. The device allows for the study of living single cells or cell monolayers throughout equibiaxial stretching. Changes in the mechanical properties of cells can thus be linked to the remodelling of the cytoskeleton.

BP 12.9 Tue 17:30 P4

Force generation in human blood platelets mediated by actin structures — •ANNA ZELENÁ¹, JOHANNES BLUMBERG², ULRICH S. SCHWARZ², and SARAH KÖSTER¹ — ¹Institute for X-Ray Physics, University of Göttingen, Germany — ²Institute for Theoretical Physics, University Heidelberg, Germany

Blood platelets are known for their importance in blood clotting: Their correct function significantly affects the early steps of wound closing and thus restoration of blood circulation. The hemostatic function of platelets is directly connected to their mechanics and cytoskeletal morphology, however, the exact mechanism and connection between them remain elusive. As was previously investigated, the reorganization of the platelet cytoskeleton upon spreading is a very fast process, which occurs within minutes, and it leads to pronounced stress fiber morphologies. In this study, we investigate single platelets by combining traction force measurements with fluorescence imaging of the actin structures in a time-resolved manner. Thus, we can spatially and temporally correlate the force generation with the emerging actin structures. Interestingly, the spots of highest force remain very stable in time and spatially align very closely with the visualized end points of fibrous actin structures. Additionally, our data show that the force generation is a very robust mechanism independent of changes in the amount of added thrombin in solution or fibrinogen coverage on the substrate, which may be physiologically important so as to ensure reliable blood clotting independent of environmental parameters.

BP 12.10 Tue 17:30 P4

Mechanical fingerprint of the intra-cellular space — •TILL M MÜNKER and TIMO BETZ — University of Göttingen, Göttingen, Germany

Many important cellular functions such as organelle positioning and internal cargo transport are dependent on the viscoelastic intracellular mechanical properties of cells. A range of different mechanical models has been proposed to describe these properties. Whilst simple models such as Maxwell or Kelvin-Voigt models don't seem sufficient to capture the full complexity of cells, more elaborate models like generalized Kelvin-Voigt models require a huge number of parameters. This hinders the comparison and interpretation of experimental findings. Further, from a physics perspective, cells are systems out of thermodynamic equilibrium, permanently consuming metabolic energy to carry out mechanical work. The level of "non-equilibrium" can be proposed as an indicator for cell type, cell state or even diseases. To determine both, the viscoelastic properties and the cellular activity, we use optical tweezers based active and passive microrheology in a diverse group of 9 different cell-types. Surprisingly, despite differences in origin and function, the complex moduli of all cell types can be described using a 4 parameter based fractional Kelvin-Voigt model. Additionally, the frequency dependent activity can be described with a simple power law. This approach allows to reduce those complex and frequency dependent properties down to a fingerprint of 6 parameter. Further principal component analysis shows that only 2 of them may be sufficient to characterize the mechanical intracellular state.

BP 12.11 Tue 17:30 P4

Measuring the stiffness of neuronal growth cones with scanning ion conductance microscopy — •AYLIN BALMES¹, HANNES SCHMIDT², and TILMAN E. SCHÄFFER¹ — ¹Institute of Applied Physics, University Tübingen, Germany — ²Interfaculty Institute of Biochemistry (IFIB), University Tübingen, Germany

It was recently demonstrated that nanoscale dynamic structural changes in live neurons can be visualized using scanning ion conductance microscopy (SICM). In SICM imaging the sample is scanned with an electrolyte-filled nanopipette to which a voltage and a pressure are applied and the ion current through the nanopipette is measured. The sample topography and stiffness (Young's modulus) can thereby be derived with high spatial and temporal resolution. There is no direct mechanical contact between the probe and the sample during SICM imaging, making it a very suitable technique to study fragile samples such as neurons. In this study we use SICM to investigate the stiffness of growth cones of dorsal

root ganglion (DRG) neurons, which have previously been used to study axonal branching, an important process in neuronal development. Studies showed that a signaling cascade involving the second messenger cyclic guanosine monophosphate (cGMP) which is generated upon binding of C-type natriuretic peptide (CNP) to the receptor guanylyl cyclase B regulates the bifurcation of DRG axons. Our measurements show that the presence of cGMP and CNP reduces growth cone stiffness. This alteration in stiffness could be linked to changes in the actin cytoskeleton and might play a role in the regulation of axon bifurcation.

BP 12.12 Tue 17:30 P4

Optimization of patterned polyacrylamide gels for traction force microscopy — •INA BRAUN, MOHAMMAD ARMIN ESKANDARI, FATEMEH ABASSI, and TIMO BETZ — Third Institute, Biophysics, Georg August Universität, Göttingen, Germany

Combining micropatterned adhesion with soft polyacrylamide gels is widely described in literature, however the practical experience shows a series of possible artifacts. The problems are typically a variation of fluorescent bead localization in response to the ECM proteins applied. In detail we find changes in the bead distribution that we aim to understand and avoid. Micropatterns of various ECM proteins are initially created on glass coverslips using a photomask. Subsequently, they are transferred on the polyacrylamide gels containing fluorescent beads during the polymerization process. In an additional step we compare the classical protocol of pattern transfer during polymerization with a more specific approach by including NHS-acrylamide in the hydrogel premix. After pattern transfer we quantify the bead localization, homogeneity and potential clustering at the pattern sites with the non-patterned regions. We optimize the bead distribution by systematic variation of pH value and ion composition of the premix. The potential of cell adhesion and traction force microscopy is assessed in the final step.

BP 12.13 Tue 17:30 P4

Dystrophin as a tension regulator in human skeletal muscles — •MARIAM RISTAU¹, ARNE HOFEMEIER^{1,2}, and TIMO BETZ¹ — ¹Third Institute of Physics - Biophysics, Georg-August-University Göttingen, Germany — ²ZMBE - Institute of Cell Biology, University of Münster, Germany

Skeletal muscles are associated with contraction, movement and force generation. They are important for maintaining posture and maintaining bone and joint stability. Muscular dystrophies such as Duchenne muscular dystrophy (DMD) result in progressive weakening of skeletal muscles. DMD is caused by the loss of the protein dystrophin which is thought to stabilize and protect muscle fibers from injury. In the progression of the disease, damaged muscle fibers degrade, muscle mass is lost and greater functional impairments develop. We have studied the contractile potential of myoblasts and reconstituted tissue derived from healthy and DMD patients, and found that they were mechanically different in muscle tension and contractility. DMD derived myoblast exhibited an overall weaker contractility compared to healthy derived myoblast. In contrast, DMD derived myoblast showed an overall higher muscle tension, suggesting that dystrophin may function as a tension regulator in skeletal muscles. In order to rule out the possibility that these findings are due to patient variability we intend to establish a genetic model in which we knockout dystrophin with the CRISPR/Cas9 system in healthy myoblasts and rescue dystrophin in DMD myoblasts by integrating micro-dystrophins (μ Dys).

BP 12.14 Tue 17:30 P4

Modelling internal cell structure for bioprinting processes — •RICHARD KELLNBERGER, FABIAN HÄUSL, MORITZ LEHMANN, and STEPHAN GEKLE — Universität Bayreuth, Bayreuth, Deutschland

The deformation cells experience during bioprinting processes depends on the structure of the cell and the stresses exerted by the surrounding fluid. We extended a Lattice-Boltzmann solver with a cell model using the immersed boundary method to model the cell membrane as well as discretizing the cell as elastic tetrahedrons in order to model the cytoskeleton. Furthermore, we extended the fluid model to take viscoelastic effects into account. With these extended models we improve our qualitative investigations of the deformation of cells during the printing process.

BP 12.15 Tue 17:30 P4

Neutrophil cell behavior as a response to mechanical confinement and substrate stiffness — •KATHARINA RIECK^{1,2,3}, FATEMEH ABBASI^{2,3}, MATTHIAS BRANDT², and TIMO BETZ^{2,3} — ¹Department of Physics, University of Münster, Germany — ²Institute of Cell Biology, ZMBE, University of Münster, Germany — ³Third Institute of Physics, Biophysics, University of Göttingen, Germany

Neutrophils are among the first immune cells attacking invading microorganisms in our body. To reach the site of infection they must undergo extreme cellular deformations while experiencing high shear stress during their migration through highly confined microenvironments. In order to investigate the mechanisms driving their confined migration and cell shape adjustment, we probe cell behavior and traction force generation in different levels of confinement with variable stiffnesses of the confining boundaries. We seed Neutrophils between two polyacrylamide (PAA) gels of the same stiffness and vary substrate Young's

modulus (3kPa, 15kPa, 30kPa) as well as the distance between the gels. This allows to examine the impact of microenvironment stiffness and confinement level on cell migration and forces. Using the substrate elastic modulus and cell induced gel deformation we are able to measure their traction stress. Our preliminary results demonstrate that cells exert higher traction forces on stiffer substrates. In confinement cells show higher traction forces than on 2D substrates. Furthermore, cells are more motile in confinement and show more motility on gels of higher stiffnesses. However, no significant difference of traction forces in different levels of confinement was observed.

BP 12.16 Tue 17:30 P4

Development of a platform for accessing the membrane tension of cells in microchannels — •ERIC SÜNDERMANN, BOB FREGIN, DOREEN BIEDENWEG, STEFANIE SPIEGLER, and OLIVER OTTO — ZIK HIKE, University of Greifswald, Greifswald, Germany

Real-time deformability cytometry (RT-DC) is a biomechanical method which is able to characterise the physical properties of cells. To do so, the cells travel through a microfluidic chip assembled on an inverted microscope. Every cell is imaged by a high-speed camera, and its shape is fitted to calculate the deformation. While the acting stress and cell tension can be derived from hydrodynamic simulations we can not disentangle different tension contributors.

Here, we introduce a new method of directly accessing the membrane tension of a cell, passing a microfluidic constriction. Measurements are carried out in a microfluidic channel, and the cells are illuminated with a pulsed laser. The cells were stained with the Flipper-TR probe, which has a fluorescent lifetime depending on the membrane tension. The signal is acquired with a fluorescence lifetime imaging (FLIM) point detector.

In preliminary experiments, we measure the membrane tension and simultaneously image the cells to perform RT-DC leading to the cell mechanical properties. Having access to the ensemble mechanical properties of a cell as well as its membrane tension, the method allows for studying the interaction between the latter and the derived cortex tension. In future studies, we also want to investigate the tension distribution on the cell membrane.

BP 12.17 Tue 17:30 P4

Nuclear mechanics probed by optical tweezers-based active microrheology — •BART VOS¹, IVAN AVILOV², TYLL MÜNCKER¹, PETER LENART², and TIMO BETZ¹ — ¹Third Institute of Physics, University of Göttingen, Göttingen, Germany — ²Max Planck Institute for Biophysical Chemistry, Göttingen, Germany

Mechanics play a crucial role in a wide range of cellular processes, from differentiation to division and metastatic invasion. Consequently, the mechanical properties of the cytoskeleton, providing shape, motility and mechanical stability to the cell, have been extensively studied. However, remarkably little is known about the mechanical environment within the nucleus of a cell, and fundamental questions remain unanswered, such as the role of nuclear actin or the sudden "freezing" of the cell during cellular division that prevents diffusion or active mixing of the nucleus and the cytoplasm.

To address these questions, we perform optical tweezers-based microrheology in the nucleus. Microrheology has proven to be a suitable tool for intracellular mechanical measurements, as it enables local, non-invasive measurements. However, although the cytoskeleton has been extensively studied this way, the cell nucleus has not been investigated, mainly due to difficulties with inserting appropriate probe particles. By using starfish oocytes that have larger dimensions than most other cell types, we are able to perform microinjection of micrometer-sized particles. We observe, similar to the cytoskeleton, viscoelastic behavior of the nucleoplasm. In addition, we mechanically follow the oocyte during its development after fertilization.

BP 12.18 Tue 17:30 P4

Predicting the distribution of mechanical stresses in the *S. aureus* cell wall during the cell cycle — •SHEILA HOSHYARIPOUR¹, MARCO MAURI¹, JAMIE K. HOBBS², SIMON J. FOSTER², and ROSALIND J. ALLEN¹ — ¹Friedrich-Schiller-Universität Jena, Jena, Germany — ²University of Sheffield, Sheffield, United Kingdom

Staphylococcus aureus is a Gram-positive bacterium which is clinically important due to its ability to act as an opportunistic pathogen and to generate antibiotic-resistant strains. During the cell cycle, the cell synthesizes a flat septum that divides the spherical cell into two hemispheres. Division then happens in few milliseconds, suggesting an important role for mechanics in the separation process. In this work, we used concepts from mechanical engineering to create an elastic model of the cell wall, in order to predict the spatial distribution of stress in the cell wall, and the induced deformations, during the cell cycle. Our modelling shows that the presence of the growing septum decreases the cell wall stress in its vicinity and leads to an invagination. The amount of this invagination and reduction in stress depends on the mechanical and geometrical properties of the cell wall and the septum. For a smaller cell with thicker wall, the stress is less during the whole cell cycle, and a stiffer septum leads to more invagination. Comparing these predictions with experimental data for various mutants in the presence and absence of cell-wall targeting antibiotics should provide a useful tool for understanding the role of mechanical stress in the *S. aureus* cell cycle.

BP 12.19 Tue 17:30 P4

Optical Stretcher for Adherent Cells — •ALEXANDER JANIK, TOBIAS NECKER-NUSS, and OTHMAR MARTI — Institute of Experimental Physics, Ulm University
We have demonstrated a method to stretch adherent cells with a parallel laser beam, that is capable of distinguishing between stiff and softened cells. Recently, a new method for the detection of the membrane displacement was developed. It relies on off-axis interferometry, which allows for high precision as well as arbitrary positioning of the probed spot and makes the method completely contact-free.

BP 12.20 Tue 17:30 P4

Cell volume changes in confined environments on short timescales — •FELIX GRAF, BOB FREGIN, DOREEN BIEDENWEG, YESASWINI KOMARAGIRI, STEFANIE SPIEGLER, and OLIVER OTTO — ZIK HIKE, University of Greifswald, Greifswald, Germany

Dynamic real-time deformability cytometry (dRT-DC) is a high-throughput method for extracting the viscoelastic material properties of cells. Cells are dynamically tracked while they translocate through a microfluidic channel and deform in response to the hydrodynamic stress. We extend the time-dependent analysis of dRT-DC towards cellular volume and perform experiments on vesicles and different cell lines in a channel of $30 \times 30 \mu\text{m}^2$ cross-section with buffers as well as cell velocities resembling physiological conditions. Our measurements reveal a volume change of $\approx 5 - 10\%$ on a millisecond timescale over the entire length of the microchannel, which is $300 \mu\text{m}$. We propose an explanation of our observation by water transport through transmembrane channel proteins. In preliminary experiments, we examined the relationship between the presence and amount of channel proteins, as well as the applied stress and the volume change observed in vesicles and cells. We expect our results to provide insights into the processes involved in physiological volume changes of cells in flow.

BP 12.21 Tue 17:30 P4

New directions in traction force microscopy — •JOHANNES W. BLUMBERG^{1,2}, TIMOTHY J. HERBST³, ULLRICH KOETHE⁴, and ULRICH SCHWARZ^{1,2} — ¹Institute for Theoretical Physics, Heidelberg University, Germany — ²BioQuant, Heidelberg University, Germany — ³German Cancer Research Center (DKFZ), Heidelberg, Germany — ⁴Visual Learning Lab, IWR, Heidelberg University, Germany
In traction force microscopy (TFM), the mechanical forces of cells adhering to an elastic substrate are estimated from the substrate displacements as measured by the movement of embedded marker beads. While it is straightforward to calculate the deformation field resulting from a given traction pattern (direct problem), it is challenging to estimate the traction pattern from the deformation field (ill-posed inverse problem). Usually, an estimate is obtained by minimizing the mean squared distance between experimentally observed and predicted displacements (inverse TFM). Here we explore two alternative approaches in TFM. First, we compare inverse TFM to the direct method, in which the stress tensor is calculated directly from the displacement data, thus avoiding the use of a loss function. Second, we explore the potential of machine learning and convolutional neuronal networks. By applying recently developed conditional invertible neuronal networks (cINN), we can address questions regarding the stability and uniqueness of the obtained traction field estimates.

BP 12.22 Tue 17:30 P4

Quantifying the relation between cell membrane and nucleus through Shape-based Voronoi tessellation — •MADHURA RAMANI¹, MAXIME HUBERT¹, SARA KALIMAN¹, SIMONE GEHRER¹, FLORIAN REHFELDT², and ANA-SUNČANA SMITH^{1,3} — ¹PULS group, FAU Erlangen-Nürnberg, Erlangen, Germany — ²Experimental Physics 1, Universität Bayreuth, Bayreuth, Germany — ³Group for Computational Life Sciences, Ruđer Bošković Institute, Zagreb, Croatia
Numerous disorders caused by genetic alterations emphasize the importance of nuclear shape and position within the cell. It is crucial to understand how the cell and nuclei relate mechanically to each other in various conditions. We investigate this relation using confluent MDCK-II monolayers grown unconstrained on substrates of various elasticities. The synergy between the cell membrane and nucleus is measured through the quality of the Shape-based Voronoi Tessellation (SVT), which is then compared to the tessellation of space provided by the cell membranes in the tissue. To address the precision, we compare SVT-extracted morphological information to the corresponding membrane-segmented ones and show that the method outclasses classical Voronoi Tessellation. As the SVT relies on the nuclei position to approximate the cell membrane, we present a systematic measure of the distance between the cell and nucleus center of mass. Our method offers insights regarding the mechanical feedback between the cell membrane shape and nuclei positioning, and is central in the creation of theoretical and numerical models of tissues.

BP 12.23 Tue 17:30 P4

Reactive oxygen species induce cell stiffening through lysosomal disruption and subsequent intracellular acidosis in HL60 cells — •YESASWINI KOMARAGIRI^{1,2}, RICARDO HUGO PIRES^{1,2}, STEFANIE SPIEGLER^{1,2}, HUY TUNG DAU¹, DOREEN BIEDENWEG¹, CLARA ORTEGON SALAS³, MD FARUQ HOSSAIN¹,

BOB FREGIN^{1,2}, STEFAN GROSS^{2,3}, MANUELA GELLERT³, UWE LENDECKEL³, CHRISTOPHER LILLIG³, and OLIVER OTTO^{1,2} — ¹ZIK HIKE, University of Greifswald, Greifswald, Germany — ²DZHK, University Medicine Greifswald, Greifswald, Germany — ³University Medicine Greifswald, Greifswald, Germany

Reactive oxygen species (ROS) are important players of redox homeostasis and associated with cellular alterations in both, physiological and pathological conditions. Effects of different ROS on the cytoskeleton have been reported earlier; however, the exact mechanism by which they alter cell mechanics remains to be understood. Here, we used varying concentrations of hydrogen peroxide to induce intracellular ROS in human myeloid precursor cells (HL60). Using real-time fluorescence and deformability cytometry, we combined the mechanical characterization of cells with simultaneous fluorometric assessment of intracellular superoxide levels. Our work reveals a direct correlation of cell stiffening with increasing levels of superoxide. While no global changes of F-actin or microtubule networks could be observed, we show increased elastic properties as a consequence of lysosomal damage followed by intracellular acidification.

BP 12.24 Tue 17:30 P4

Nuclear Volume, Density and Dry Mass are Controlled by Chromatin and Nucleocytoplasmic Transport — •OMAR MUÑOZ^{1,2}, ABIN BISWAS^{1,3,4}, KYOOHYUN KIM^{1,3}, SIMONE REBER⁴, VASILY ZABURDAEV^{1,2}, and JOCHEN GUCK^{1,3} — ¹Max Planck Zentrum für Physik und Medizin — ²Department of Biology, Friedrich-Alexander-Universität Erlangen-Nürnberg — ³Max Planck Institute for the Science of Light — ⁴IRI Life Sciences, Humboldt-Universität zu Berlin

The cell nucleus is an organelle responsible for hosting essential processes such as DNA replication and transcription. Many important biophysical properties of the nucleus are not well understood, for example, its density is lower than the density of the cytoplasm despite the nucleus hosting the highly compressed genome. Motivated by this observation, we combined optical diffraction tomography and confocal fluorescence microscopy and measured, in real time, the material properties of nuclei reconstituted in *Xenopus* egg extract. We found that nuclear growth has two phases: the first one driven by chromatin decondensation and the second one, by nucleocytoplasmic transport and replication. We also developed a simple theoretical model, where nuclear volume is determined by an entropic polymer pressure exerted by chromatin and an osmotic pressure caused by the protein concentration gradient across the nuclear envelope. The good agreement between the model predictions and experimental results supports a view, where chromatin and nucleocytoplasmic transport are essential contributors to the biophysical properties of the nucleus.

BP 12.25 Tue 17:30 P4

Mechanical Characterization of Pharmaceutical Nanoparticles — •HENRIK SIBONI^{1,2}, LEONHARD GRILL¹, and ANDREAS ZIMMER² — ¹Single Molecule Chemistry, Institute of Chemistry, University of Graz — ²Pharmaceutical Technology & Biopharmacy, Institute of Pharmaceutical Sciences, University of Graz
Nanoscale Drug Delivery Systems are becoming an essential part of modern medicine, but lack of understanding of the underlying physical mechanisms hinders its progress. Focusing on self-assembled nanoparticles called proticles, we employ Atomic Force Microscopy to gain new insights. We find that we are able to characterize particle shape and its dependence on formulation. We further show that proticles can be imaged on biological cells and that the mechanical changes in cells can be measured using nanoindentation experiments. Our methods can be used in the future to accelerate early-stage development of pharmaceutical nanoparticles.

BP 12.26 Tue 17:30 P4

The role of vimentin phosphorylation in mechanotransduction — •JULIA KRAXNER^{1,2} and HOLGER GERHARDT^{1,2} — ¹Max Delbrück Center for Molecular Medicine in the Helmholtz Association (MDC), Berlin — ²German Centre for Cardiovascular Research (DZHK)

Vascular endothelial cells (VECs) need to be able to constantly sense, withstand and adapt to varying mechanical stresses. One way cells adapt their mechanics to these varying requirements is through differential expression of cytoskeletal proteins. Here, we focus on the intermediate filament vimentin and introduce post-translational modifications (PTMs). Interestingly, PTMs provide a mechanism for mechanical modulation on short time scales. We study the impact of one such PTM, phosphorylation and one effect of phosphorylation is, for example, the disassembly of intermediate filaments. Experiments on VECs under flow reveal an increase of specific phosphorylation sites in vimentin. We investigate the role of these phosphorylation sites on the mechanotransduction. Therefore, we want to combine traction force microscopy under flow with mutations in vimentin which inhibit phosphorylation of specific sites. Additionally, we plan on tuning the substrate stiffness to study the effect of tissue mechanics observed in aging of the vascular system and possible effects on mechanotransduction. These insights have the potential to improve our understanding of the complex mechanism of mechanotransduction in vascular endothelial cells.

BP 12.27 Tue 17:30 P4

Towards observing entry of Particulate Matter into lung cells using Photonic Force Microscopy — •JEREMIAS GUTEKUNST and ALEXANDER ROHRBACH — Lab for Bio- and Nano-Photonics, Department of Microsystems Engineering (IMTEK), University of Freiburg, Georges-Koehler-Allee 102, 79110 Freiburg, Germany,

The uptake of Particulate Matter (PM) into lung cells increases the risk of stroke and coronary heart disease. Following an in vitro approach, we expose single particulates to lung epithelial cells on a coverslip and examine their fluctuation based binding and entry paths with a photonic force microscope (PFM). The PFM consists of a highly focused laser beam, which is used to optically trap and interferometrically track a PM particle at 1 MHz frequency and with nm precision.

The central part of this work is to investigate the influence of additional scatterers below and above the nano particle of a PFM. The understanding of their optical influence is crucial, as in particle entry experiments the cell scatters light and alters the interference signal used to track the probe. We address the problem by simplifying and controlling the situation: In addition to the particle used as a probe, we introduce a further particles positioned in the same beam path, but trapped with a second laser. By decorrelating the combined scattering signals on different frequencies, we want to recover the precise position of the trapped PM probe on a broad temporal bandwidth to reliably study cell particle interactions.

BP 12.28 Tue 17:30 P4

Motion-correlated particle transport along filopodia and lamellipodia — •MARIO BREHM and ALEXANDER ROHRBACH — Laboratory for Bio- and Nanophotonics, Department of Microsystems Engineering - IMTEK, Georges-Köhler-Allee 102, 79110 Freiburg, Germany

Macrophages play an important role in cleaning up the body from cell debris, bacteria and viruses. As a prior step to phagocytosis, extracellular particles can attach to cell protrusions like filopodia and be pulled towards the cell body. Our data points to the idea that particles such as bacteria or viruses get mechanically coupled to the actin fibers within the cell, similarly to focal adhesions. The aim of this study is to improve mechanistic models that describe the mechanical coupling of extracellular particles to proteins connected to the retrograde flow of actin fibers. In addition, we investigate whether and how the transport along filopodia and lamellipodia differ from each other.

The high image contrast combined with the high temporal and spatial resolution of ROCS microscopy enables us to observe directed motion and fluctuations along filopodia at 100 Hz and without fluorescence. By recording, tracking and analyzing the nanoparticle's fluctuations it is possible to derive changes of the particle's viscoelastic properties and their relation to molecular bonds during their transport along the cell's protrusions.

BP 12.29 Tue 17:30 P4

Local organization of F-actin studied via Förster resonance energy transfer using 2D polarization fluorescence imaging (2DPOLIM) — •MOHAMMAD SOLTANINEZHAD^{1,2}, RAINER HEINTZMANN^{1,2}, ADRIAN T. PRESS^{3,4}, and DANIELA TÄUBER^{1,2} — ¹Leibniz Institute of Photonic Technology, Jena — ²Institute of Physical Chemistry & Abbe Center of Photonics, Friedrich-Schiller-University Jena, Germany — ³Department of Anesthesiology and Intensive Care Medicine, Jena University Hospital — ⁴Faculty of Medicine, Friedrich Schiller University Jena, Germany

2D polarization fluorescence imaging (2DPOLIM) provides complete in-plane evaluation of the polarization state of the sample[1,2], giving access to macromolecular arrangement in the range of 2-10 nm via Förster resonance energy transfer between similar fluorophores (homo-FRET, emFRET). Phalloidin-dye complexes map the structure of F-Actin, by binding specifically. We applied 2DPOLIM to phalloidin-DY490 stained liver tissue of mice from different treatment groups in the context of polymicrobial sepsis[1,3]. Qualitative analysis showed significant differences in the molecular arrangement of F-actin in agreement with the survival of the animals. Further information will be obtained from comparing the experimental data to a series of simulations[2]. — Funding by DAAD-GSSP, DFG-Ta1049/2, Interdisziplinäre Zentrum für Klinische Forschung Jena (AMSP-05). — [1] D. Täuber et al. ELMI 2021, <https://doi.org/10.22443/RMS.ELMI2021.6>. [2] R. Camacho et al. Commun. Biol. 2018, 1, 157. [3] A.T. Press et al. EMBO Mol. Med. 2021, 13 (10), e14436.

BP 12.30 Tue 17:30 P4

Interactions between cytoskeletal filaments — •MAGDALENA HAAF, ANNA SCHEPERS, and SARAH KÖSTER — Institute of X-Ray Physics, Göttingen, Germany

The cytoskeletal filaments –F-actin, microtubules and intermediate filaments (IFs)– constitute an interpenetrating network that performs essential cellular functions. Next to the mechanical properties of the single filaments, the interactions between the filamentous proteins play an important role in cytoskeletal network mechanics. To gain a deeper understanding of the composite network it is useful to quantify such interactions in a controlled setting. Cell experiments have revealed a functional and structural interplay between F-actin and vimentin

IFs. However, in reconstituted systems studies of mixed networks come to conflicting conclusions. To clearly solve this conflict, it is crucial to simplify the system even further to the single filament level. We use a quadruple optical trap in combination with microfluidics and confocal microscopy to directly quantify the interaction strength and dynamics between F-actin and vimentin IFs. Our approach allows us to characterize the interactions independent of the network morphology. This setup further enables us to probe the influence of electrostatic and hydrophobic effects on the interactions between single filaments.

BP 12.31 Tue 17:30 P4

Comparative investigation of F-actin using Nano IR spectroscopic and polarization resolved fluorescence microscopy imaging — •DIJO MOON-NUKANDATHIL JOSEPH^{1,2}, LUKAS SPANTZEL^{2,3}, KATHARINA REGLINSKI^{1,2}, ASAD HAFEZ^{1,2}, YUTONG WANG^{1,2}, MOHAMMAD SOLTANINEZHAD^{1,2}, CHRISTIAN EGELING^{1,2}, RAINER HEINTZMANN^{1,2}, MICHAEL BÖRSCH^{2,3}, and DANIELA TÄUBER^{1,2} — ¹Leibniz Institute of Photonic Technology, Jena — ²Friedrich-Schiller University Jena — ³University Hospital Jena, Germany

Fibrillar actin is one of the major structural components in cells. Thus, its organization has been studied extensively. Nevertheless there are still open questions, in particular, related to pathogenic infections. We examine the potential contributions of two complementary recently developed imaging methods for increasing our understanding on local F-actin: IR spectroscopic photo-induced force microscopy (PiF-IR) and 2D polarization resolved fluorescence microscopy imaging (2DPOLIM). PiF-IR provides local chemical information at high spatial resolution below 10 nm. 2DPOLIM allows to study the local aggregation of fluorescence labeled F-actin via Förster resonance energy transfer (FRET) in the range of 2-10 nm [1]. — Funding by DAAD-GSSP, DFG-Ta1049/2 – [1] R. Camacho et al. Commun. Biol. 2018, 1, 157.

BP 12.32 Tue 17:30 P4

How do muscles self-assemble? — •FRANCINE KOLLEY¹, IAN D. ESTABROOK¹, CLEMENT RODIER², FRANK SCHNORRER², and BENJAMIN M. FRIEDRICH^{1,3} — ¹cfaed, TU Dresden — ²IBDM, Aix Marseille University — ³Physics of Life, TU Dresden.

For voluntary movements, all animal life relies myofibrils in striated muscle, which are highly organised crystal-like cytoskeletal structures comprising chains of micrometer-sized sarcomeres. The size of sarcomeres is supposedly set by giant proteins such as titin. Titin elastically links myosin molecular motors in the middle of a sarcomere to a structure called Z-disc rich in actin crosslinkers at the sarcomere boundary. To investigate putative mechanisms for the self-assembly of myofibrils, we develop minimal mathematical models. We show that minimal models accounting for non-local interactions between three key proteins is sufficient to account for the spontaneous emergence of periodic sarcomeric patterns. We employ mean-field models, as well as agent-based simulations, which reveal the influence of small-number fluctuations on emergent patterns. Additionally, analysing images of the *Drosophila* flight muscle during early development provided by the Schnorrer lab (IBDM, Marseilles), we were able to identify titin as the first protein forming periodic patterns, with myosin and later actin following subsequently, which constrains possible models.

BP 12.33 Tue 17:30 P4

Simulation and machine-learning-based analysis of active Brownian magnetic microswimmers — •ANAS HUSSIN, SASCHA LAMBERT, and STEFAN KLUMPP — Institute for the Dynamics of Complex Systems, University of Göttingen, Göttingen

Magnetic microswimmers, whether these are biological organisms or designed nanomachines, show promise in biomedical microrobotics, as they can be steered remotely with a magnetic field. Often, these swimmers encounter complex environments characterized by obstacles and confinement. To understand their navigation in such complex environment, we simulate their swimming as active Brownian particles with an intrinsic magnetic moment and interactions with obstacles and walls that can be of hydrodynamic and/or steric nature. In addition, we use the resulting trajectories to train a neural network with an optimized architecture in order to explore the ability of machine learning algorithms to infer parameters of the motion from trajectories.

BP 12.34 Tue 17:30 P4

Function of Morphodynamics in Foraging *Physarum polycephalum* — •LISA SCHICK^{1,2} and KAREN ALIM^{1,2} — ¹Physics Department and CPA, Technische Universität München — ²Max-Planck-Institut für Dynamik und Selbstorganisation, Göttingen

Foraging for nutrients and shelter in a heterogeneous environment is key for the survival of living organisms. Foraging behaviour of animals is generally viewed as optimised for maximal energy uptake per search time by balancing time spent for environmental exploration and food exploitation. Yet, it is unclear which foraging behaviour can be adopted by spatially extended organisms like the unicellular slime mould *Physarum polycephalum*. What foraging strategy does the large and adaptive network-like morphology allow for? Here, we follow the plasmodial network of *P. polycephalum* as it adapts its morphology, gradually moving its body mass as it is foraging for food. We evaluate the morphodynamics of the foraging plasmodia by calculating morphology and velocity of the specimen. We

identify three different morphological states by network compactness and the density of moving fronts. In order to understand the purpose of the continuous morphological changes, we investigate the energy distribution within the different morphologies. In particular we discuss how the morphological variability allows the organism to adjust its energetic costs during foraging.

BP 12.35 Tue 17:30 P4

Lattice based model to study wound healing in biofilms — •YUSONG YE¹, MNAR GHAYEB², LIRAZ CHAI², and VASILY ZABURDAEV¹ — ¹Friedrich-Alexander-Universität Erlangen-Nürnberg (FAU) & Max-Planck-Zentrum für Physik und Medizin, Erlangen, Germany — ²Institute of Chemistry, The Hebrew University of Jerusalem, Jerusalem, Israel

Biofilms are multicellular heterogeneous bacterial communities excelling in social-like cooperation, division of labor, and resource capture. Bacteria in biofilms are embedded in the self-produced extracellular matrix (ECM). Increasingly more often an analogy between biofilms and higher multicellular organisms is drawn. One illustrative example is the process of wound healing. While it is extensively studied in eukaryotic tissues, the mechanisms of wound healing in biofilms are barely understood. The wound healing in biofilm is a regulated growth by which bacteria alter their physiological state in response to a damage. Motivated by experiments in a model biofilm forming bacteria *Bacillus subtilis*, we developed a lattice based model of a biofilm growth. It explicitly considers cells and ECM produced by cells, as well as nutrient fluxes and helps to elucidate the role of biofilm components (matrix, cells), aging, and nutrient availability in damage repair. Division of labor (growth vs. ECM production) and nutrient consumption play key roles in heterogeneous wound closure. Even under most general assumptions, the model qualitatively reproduces the wound healing phenotypes observed in our experiments and can be further generalised to include signalling and regulatory mechanisms.

BP 12.36 Tue 17:30 P4

Fluid Flow and Microvascular Remodeling — •FATEMEH MIRZAPOUR-SHAFIYI¹ and KAREN ALIM^{1,2} — ¹Physics Department and CPA, Technische Universität München — ²Max Planck Institute for Dynamics and Self-Organization, Göttingen

As a transport network optimised through evolution, vessel morphology is adapted to minimise energetic costs of dissipation and homogenize flow transport in the network. Resource-deprived tissues produce chemotactic agents to induce vessel formation during development and in tissue homeostasis. The primitive, mesh-like vascular network formed through neovascularisation is highly ramified. Later, vascular network is normalised into a hemodynamically preferred tree-like structure. The normalisation process, termed vessel remodeling, leads to an organ-specific network architecture which better meets the metabolic needs of its surrounding tissue. As vessel growth and remodeling is found impaired in various disease states, several factors regulating vessel formation and branching morphology were identified over the past decades. However, while some of these factors have been undergoing clinical trials, their effects on transport properties of the altered vessel morphology are not fully elucidated yet. Establishing a perfusable human capillary-on-a-chip (hCOC) model system, here we aim to investigate how vascular morphology correlates with fluid flows. Our hCOC model allows extensive quantitative analyses of network morphology and adaptive remodeling under fluid flow applied by a low-pressure syringe pump. Results of our analyses will contribute to the next generation therapeutics targeting vessel development.

BP 12.37 Tue 17:30 P4

Cancer tissue dynamics as active liquids — •MAHBOUBEH FARAJIAN¹, SWETHA RAGHURAMAN², ALEJANDRO JURADO JIMENEZ¹, FATEMEH ABBASI¹, and TIMO BETZ¹ — ¹Third Institute of Physics - Biophysics Georg August University Göttingen — ²Institute for Cell biology ZMBE - University of Münster

Collective cell migration can be found in some key biological processes such as Metastasis, wound healing and tissue rearrangement. While the molecular mechanisms of collective migration already represent a strong research focus, the mechanical processes driving it are currently less studied. Here we propose to answer this question: "Can statistical mechanics explain the local and global characteristics of cell migration in the tumors?" Someone can imagine 3 kinds of phenotypes regarding the collective cell migration: "Sub-diffusive", "Diffusive" and "Super-diffusive" motion. We aim to change the physical parameters of the environment such as Volume (by letting the tumor models grow) and Pressure (by addition of Dextran to the environment), and then look at the statistical mechanics of the cells' collective motion, different phenotypes and the transition between different phenotypes. and we use 3D individual cell tracks for this aim.

BP 12.38 Tue 17:30 P4

Assessing statistical properties of resident tissue macrophages — •MIRIAM SCHNITZERLEIN^{1,2}, ANJA WEGNER³, STEFAN UDERHARDT³, and VASILY ZABURDAEV^{1,2} — ¹Department of Biology, Friedrich-Alexander-Universität Erlangen-Nürnberg, Germany — ²Max-Planck-Zentrum für Physik und Medizin, Erlangen, Germany — ³Department of Internal Medicine 3 - Rheumatol-

ogy and Immunology, Friedrich-Alexander-Universität Erlangen-Nürnberg und Universitätsklinikum Erlangen, Germany

Resident tissue macrophages (RTMs) are present in essentially all tissues in the human body. While macrophages in general are mostly known as part of the immune response, RTMs are additionally crucial for ensuring tissue homeostasis. This includes removing dead cells, providing growth factors and protecting the tissue from inflammatory damage. To monitor their surroundings, RTMs show continuous sampling behaviour by extensions and retractions of protrusions as well as endocytosis behaviour. Quantifying the growth and shrinkage of protrusions under different conditions is thereby essential to understand the overall dynamics of RTMs together with their approach of ensuring tissue homeostasis. In this project, we have employed a high-resolution intravital imaging protocol to generate movies of RTMs *in vivo*. Subsequently we have built an image processing pipeline to assess cell properties - such as area and perimeter of whole RTMs or the diffusion coefficient and thereby the dynamics of their protrusions. Such measurements will help to build a mathematical model for protrusion dynamics as well as to establish a biophysical model of RTMs.

BP 12.39 Tue 17:30 P4

3D Force Model of early zebrafish development via NeuralODEs — •LEON LETTERMANN, SEBASTIAN HERZOG, ALEJANDRO JURADO, FLORENTIN WÖRGÖTTER, and TIMO BETZ — 3rd Institute of Physics - Biophysics, University of Göttingen, Friedrich-Hund-Platz 1, 37077 Göttingen

The astonishing process of embryo development still poses a great variety of unanswered questions today. Motivated by the importance of understanding cell migration and organization patterns, we want to study the movements in the early development of zebrafish embryos on a mesoscopic scale. A coarse-grained tissue flow obtained from light sheet microscopy data is analyzed based on a hydrodynamic model. This model is enhanced by active stresses and forces, redirecting the flow away from a dead liquid's description. Using a Neural Ordinary Differential Equation, the active contributions can be reconstructed from observations, shedding light on the distribution of active forces and stresses in the embryo. This allows for quantifying symmetry breaking due to active effects and early recognition of the forming body axes.

BP 12.40 Tue 17:30 P4

Tissue tension during zebrafish development — •MING HONG LUI^{1,2}, ALEJANDRO JURADO¹, LEON LETTERMANN¹, and TIMO BETZ^{1,2} — ¹3rd Institute of Physics - Biophysics, University of Göttingen, Friedrich-Hund-Platz 1, 37077 Göttingen — ²Max Planck School Matter to Life

Understanding the morphogenesis during development is one of the emerging fields where the interaction between developmental and tissue biology with biophysics has provided a series of deep new insights into nature's physical working principles. In particular, during embryonic development of zebrafish, cells in the blastoderm exhibit collective migration towards the yolk in a process known as epiboly, as well as the subsequent gastrulation that involves symmetry breaking. These elegantly robust processes are facilitated by both biochemical and mechanical interactions. To determine how tissue stresses contribute mechanically we use photoablation to create mechanical defects in the tissue and record the subsequent tension relaxation using light sheet microscopy of the whole embryonic volume. We analyze and contrast the nuclei trajectories, density, velocity and force maps with and without the ablative perturbation. From the changes in these quantities, we can infer the adaptive response of the embryo, the source of force generation, and the role played by tissue tension in guiding the coordinated movement.

BP 12.41 Tue 17:30 P4

Single Cell Force Spectroscopy: The Impact of Cell Contact Area — •SOPHIE GEIGER¹, MARIA VILLIOU^{1,2,3}, and CHRISTINE SELHUBER-UNKEL^{1,2,3} — ¹Institute for Molecular Systems Engineering, University of Heidelberg, DE — ²Max Planck Schools: Matter to Life, University of Heidelberg, DE — ³Cluster of Excellence 3DMM2O KIT & Heidelberg University, DE

Single cell force spectroscopy is a versatile method for characterising cell-substrate interactions. It has already been applied in several studies to investigate the effect of photomechanical stimulation and the influence of structuring molecules on cell detachment forces.

A critical aspect is the contact area between cell and substrate, as a larger contact area usually leads to higher cell detachment forces. However, the contact area between cell and substrate varies with cell size and with the deformation of the cell pressed onto the surface.

We aim to avoid the distortion that these variations exert on the cell detachment forces by limiting the adhesion area. This is achieved using micropatterned substrates. We use light-induced molecular adsorption of proteins (LIMAP) to generate circular fibronectin micropatterns on an inert background. In a systematic study, we investigate the dependence of cell detachment forces on the cell-substrate interaction surface.

BP 12.42 Tue 17:30 P4

Investigation of the binding behaviour of proteins in various patterns — •JONAS WALTHER¹ and ANA-SUNČANA SMITH^{1,2} — ¹PULS Group, Department of Physics, Interdisciplinary Center for Nanostructured Films, Friedrich-Alexander-Universität Erlangen-Nürnberg, Cauerstraße 3, 91058 Erlangen, Germany — ²Group for Computational Life Sciences, Ruđer Bošković Institute, Zagreb, Croatia

The coupling of two or more cellular membranes is an important part of cell interactions and therefore affects many biological mechanisms. Cells may restrict the movement of proteins in certain areas of their membrane creating functionally specialized regions, or membrane domains. Here we analyse whether the arrangement of proteins in different patterns changes the binding kinetics of the proteins. In our investigation we combine kinetic Monte Carlo simulations and explicit calculations of the binding rates of the patterns. Results show that there is indeed a difference in binding of the different patterns. An important factor seems to be the amount of proteins within a pattern due to the correlations between the proteins. The exact difference of the binding rates depends on the mechanical properties of the membrane and the proteins. We furthermore analyse the dynamics of bond formation and compare the results to experimental data on the activation of natural-killer cells binding to analogous patterns (experiment by the group of Mark Schwartzman at the Ben-Gurion University of the Negev).

BP 12.43 Tue 17:30 P4

Electrostimulation of osteoblasts on coated planar resistive electrodes — •FRANZIŠKA DORN¹, CHRISTIAN VÖLKNER¹, MEIKE GENZOW², MARTINA GRÜNING², SVEN NEUBER³, REGINA LANGE¹, INGO BARKE¹, CHRISTIANE A. HELM³, BARBARA NEBE², and SYLVIA SPELLER¹ — ¹Institute of Physics, University of Rostock — ²University Medical Center Rostock, University of Rostock — ³Institute of Physics, University of Greifswald

The development of electrically active implants may profit from knowledge and understanding of how osteoblasts respond to electrostimulation. Besides the aim to find routes to accelerate adhesion of osteoblasts, the cellular response in terms of migration and deformation is interesting. For our experiments we use a planar resistive electrode configuration with DC electrostimulation. The glass substrate is covered with a few bilayers of polyelectrolyte (PDADMA/PEI) with carbon nanotubes incorporated to enhance electrical conductivity. In physiologic medium the sheet resistance increases from few kΩ to more than 10 kΩ. Human osteoblast-like cells (MG-63) were seeded on the electrode and, after 24 h cell growth, stimulated by a couple of cycles at voltages between 1V and 2V. The observed cellular shape changes and mobility are only subtle and the dependence on the orientation of the electric field axes is not obvious. Experiments at an earlier phase in the adhesion process i.e., in a shorter time frame of cell adhesion, are considered. [1] C. Voelkner, et al, Beilstein J. Nanotechnol. 12, 242 (2021) [2] M. Gruening, et al, Front. Biotechnol. 8,1016 (2020) [3] H. Rebl, et al, Adv. Engin. Mater. 12, B356 (2010)

BP 12.44 Tue 17:30 P4

The zeta potential as parameter in electric field landscapes for guiding cell adhesion — •WANDA WITTE¹, CHRISTIAN VÖLKNER¹, REGINA LANGE¹, SUSANNE SEEMANN², BARBARA NEBE², INGO BARKE¹, and SYLVIA SPELLER¹ — ¹Institute of Physics, University of Rostock, Rostock, Germany — ²Department of Cell Biology, Rostock University Medical Center, Rostock, Germany

In osseointegration of implants, chemical and physical material properties influence initial cell adhesion. The relevant surface potential for cells is the zeta potential at the shear plane or hydrodynamic distance. We investigate how the zeta potential of glass can be modified by an aggregated molecular monolayer, with the aim of using the zeta potential to create electric field landscapes. To achieve the aggregation of a molecule monolayer, amine-terminated dendrimers and albumin were deposited on the glass by micro-contact printing or immersion. An electrokinetic analyzer was used to determine the zeta potential of the coated and uncoated samples. The successful physisorption of molecules was verified by fluorescence microscopy and force microscopy (AFM). It could be shown that the application of albumin or amine-terminated dendrimers increases the zeta potential by approx. 25 eV and 40 eV. The choices and shape responses of osteoblasts (MG-63) in molecule stripe landscapes are discussed.

BP 12.45 Tue 17:30 P4

Quantification of the dynamics of confluent endothelial cells — •ANSELM HOHLSTAMM, ANDREAS DRUSSEN, and PETER DIETERICH — Institut für Physiologie, Medizinische Fakultät, TU Dresden

Cooperative cell dynamics resulting from a complex interplay of single cell migration and cell-to-cell interactions plays a fundamental role in maintaining a confluent cell layer despite continuous changes in cell numbers and environmental conditions. It is the aim of this work to extract the essential components of this dynamics. Therefore, we seeded human umbilical vein endothelial cells and stained their nuclei with a fluorescent dye. Cells were observed within 48 hours (dt = 10 minutes). We obtained up to 50.000 cell trajectories within an area of 6 x 7 millimeters for 10 different experiments. All analyses were performed under

nearly confluent conditions. Cells continued to show lively proliferations and a non-stationary behavior indicated by a two-phase decay of the mean squared velocity. This behavior is accompanied by a decay of the velocity correlation. In addition, we found an exponential repulsion between cells that could transiently rise cell velocities due to cell proliferations. We put these observations into a mathematical model coupling cell proliferation and mean squared velocities over time. Bayesian analysis was applied to determine the best model and its parameters. In summary, we are able to perform a characterization of the complex cell dynamics. This approach can be used for simulations and application to different experimental conditions.

BP 12.46 Tue 17:30 P4

Adaptive microfluidics using hydrogels with irreversible response — •ONURCAN BEKTAS^{1,2,3,4}, CHARLOTT LEU³, JOACHIM RÄDLER^{1,3}, and KAREN ALIM^{1,2,5} — ¹Max Planck School Matter to Life, Germany — ²Physics Department and CPA, Technische Universität München — ³Faculty of Physics and and Center for NanoScience (CeNS), Ludwig-Maximilians-Universität München, München, Germany — ⁴Physics Department, University of Göttingen, Göttingen — ⁵Max Planck Institute for Dynamics and Self-Organization, Göttingen

Microfluidic devices have triggered technological revolutions in biology and separation technology. Their increased surface-to-volume ratio shortens reaction times, and make reactions more accurate and effective in an automated fashion, thus reducing error rates and allowing for highthroughput assays. However, fabricating multifunctional devices with integrated modules requires complicated control systems and is by far from being trivial. Here we present a novel bio-inspired approach to design adaptable microfluidic devices that can adapt the sizes of its channels using local feedback mechanisms for uniform flow. We fabricate a random porous media using an hydrogel made of Poly(ethylene glycol)-norbornene backbone and MMP-degradable cross-linker. When perfused with MMP-1 enzyme, the boundaries of the channels are cleaved such that the size of the channels and the flow are coupled. We investigate how the feedback mechanism between the flow and the channel size allows the network to optimise the flow rate distribution. Our methodology will lay the foundation for designing microfluidic devices that are adaptive to biological activity.

BP 12.47 Tue 17:30 P4

Adaptive microfluidics using irreversibly responsive hydrogels — •ONURCAN BEKTAS^{1,2,3,4}, CHARLOTT LEU³, JOACHIM RÄDLER^{1,3}, and KAREN ALIM^{1,2,5} — ¹Max Planck School Matter to Life, Germany — ²Physics Department and CPA, Technische Universität München — ³Faculty of Physics and and Center for NanoScience (CeNS), Ludwig-Maximilians-Universität München, Germany — ⁴Physics Department, University of Göttingen, Göttingen — ⁵Max Planck Institute for Dynamics and Self-Organization, Göttingen

Microfluidic devices have triggered a technological revolution in the pharmaceutical industry and biotechnology. Integrated modular microfluidic devices allow for high throughput assays while making them more precise by eliminating human-induced errors. The fabrication process, however, introduces inhomogeneities which limit the efficiency and the precision of the produced devices. Here, we present a novel bio-inspired approach to designing adaptable microfluidic devices that can adapt the sizes of their channels using local feedback mechanisms for uniform flow. We test our approach by fabricating a random porous media using Matrix-Metalloproteinase(MMP)-degradable poly(ethylene glycol)-norbornene hydrogel and measure how the flow rate distribution changes by using Particle Image Velocimetry technique. As the device is perfused with an MMP-enzyme, the degradation of the hydrogel is coupled to the flow. We investigate how this coupling could result in a uniform flow. Our method could be used to eliminate inhomogeneities introduced during the fabricating processes to produce spatially homogeneous microfluidic devices.

BP 12.48 Tue 17:30 P4

Self-organization of microtubule filaments in energy dissipative evaporating droplet — •VAHID NASIRIMAREKANI, OLINKA RAMIREZ-SOTO, STEFAN KARPITSCHKA, and ISABELLA GUIDO — Max Planck Institute for Dynamics and Self-Organization, 37077 Göttingen, Germany

Cytoskeletal assemblies such as microtubule networks and motor proteins of the kinesin family drive vital cellular processes that, together with cargo delivery and cell division, also include providing mechanical stability when cells are exposed to external stresses. How these self-organising structures can orchestrate such response is not yet well understood. In this study, we develop a bioinspired system resembling intracellular cytoskeletal networks and characterise its activity under the influence of external stress. For this purpose, we confine an active network of microtubules and kinesin motors in an evaporating aqueous droplet. This setup serves as a bioreactor that enables to apply forces to the active system. Namely, the flow field generated by the Marangoni and capillary flow couples with the active stress of the microtubule-motor protein network. We observe that this coupling influences the spatio-temporal distribution of the driving forces and the emergent behaviour of the system, which shows contracting and relaxing behaviour. By analysing such non-equilibrium systems, our study can contribute to understand the response of biological structures to cues from the external environment.

BP 12.49 Tue 17:30 P4

Establishment of a microfluidic UV-Vis analysis of single cell *E. coli* — •TIM R. BAUMANN¹, ALEXANDER GRÜNBERGER², DARIO ANSELMETTI¹, HARALD GRÖGER³, and MARTINA VIEFHUES¹ — ¹Experimental Biophysics & Applied Nanosciences, Department of Physics, Bielefeld University — ²Multiscale Bioengineering, Department of Technology, Bielefeld University — ³Industrial organic chemistry and biotechnology, Department of Chemistry, Bielefeld University

Whole-cell biocatalysts like, *E. coli* DH5- α are widely used in industrial organic chemistry and biotechnology. For efficient production an appropriate cultivation media composition is of high importance. Harmful organic solvents, like ethanol are needed to solve insoluble substrates, those often lead to a permeabilisation of the bacterial membranes. In this study, we established a microfluidic method to analyse the impact of ethanol on leaching of certain intracellular cofactors e.g., NAD(P)H and exploited the contribution of NAD(P)H to the cells autofluorescence. In order to detect the losses in intensity due to leaching, a UV-LiF analysis of single cells was conducted, using a Nd:YAG Laser ($\lambda = 266$ nm). We evaluated the impact of incubation in 5% ethanol for either 5 or 10 minutes on single cells in a PDMS microfluidic chip with a UV transparent fused silica base layer, including a carbon black PDMS spot at the detection point to reduce the PDMS's autofluorescence. The intensity data was assessed and plotted in histograms. Those exhibited a reduction of the FWHM and a displacement of the distribution maxima to smaller intensities depending on the incubation time and proved the cofactor leaching due to ethanol exposition.

BP 12.50 Tue 17:30 P4

Study of the temporal stability of evaporated SLBs for technological applications — •NANCY GOMEZ-VIERLING¹, MARCELO A. CISTERNAS², MARÍA JOSÉ RETAMAL¹, NICOLÁS MORAGA¹, MARCO A. SOTO-ARRIAZA³, TOMÁS P. CORRALES⁴, FELIX KLEEMANN⁵, and ULRICH G. VOLKMANN¹ — ¹Instituto de Física and CIEN-UC, P. Univ. Católica de Chile — ²Escuela de Ingeniería Industrial, Univ. de Valparaíso, Chile — ³Facultad de Química y Farmacia and CIEN-UC, P. Univ. Católica de Chile — ⁴Departamento de Física, UTFSM, Valparaíso, Chile — ⁵Departamento de Física, Technische Universität Clausthal, Germany. Artificial membranes are models for biological systems. We introduce a dry two-step self-assembly method, first performing a high-vacuum evaporation of phospholipid molecules over silicon, followed by an annealing step in air. Our evaporated membranes show long-term stability and no restructuring after storage in air during at least fifteen months. This extreme stability of the Supported Lipid Bilayer (SLB) structures make this system interesting for technical applications in the field of functional biointerfaces, e.g., for fabrication of biosensors and membrane protein platforms, including cleanroom-compatible fabrication technology. It is expected that SLBs can help to gain insight into the lifetime of viral structures protected by a surrounding phospholipid bilayer adsorbed on static solid surfaces or on inhalable particulate material (PM), which contributes to the spread of the SARS-CoV-2 virus. Acknowledgment: FONDECYT grant numbers 1180939 (UGV), 1171047 (MS-A) and 1211901 (TPC).

BP 12.51 Tue 17:30 P4

Measurements of topologies and Young moduli of DPPC films deposited from the gas phase onto silicon substrates at different temperatures — •NICOLÁS MORAGA¹, GABRIEL ALFARO¹, NANCY GOMEZ-VIERLING¹, DANIEL SAAVEDRA¹, MARCELO A. CISTERNAS², MARÍA JOSÉ RETAMAL¹, MARCO A. SOTO-ARRIAZA³, TOMÁS P. CORRALES⁴, FELIX KLEEMANN⁵, and ULRICH G. VOLKMANN¹ — ¹Instituto de Física and CIEN-UC, P. Univ. Católica de Chile — ²Escuela de Ingeniería Industrial, Univ. de Valparaíso, Chile — ³Facultad de Química y de Farmacia and CIEN-UC, P. Univ. Católica de Chile — ⁴Departamento de Física, UTFSM, Valparaíso, Chile — ⁵Departamento de Física, Technische Universität Clausthal, Clausthal, Germany. Supported lipid bilayers (SLBs) are suited to gain insight into the physical behavior of cell membranes. In this work, DPPC deposition by Physical Vapor Deposition (PVD) is performed on silicon (100) substrates at different substrate temperatures and deposition rates. Our goal is finding growth parameters, to optimize coverage and homogeneity of the DPPC SLBs. We observe a modification of topologies and Young moduli and an optimization of the homogeneity for substrate temperatures between 310 and 315 K and deposition rates in the range of 0,78 to 0,93 Å/min. Homogeneous, planar biomimic phospholipid membranes avail protein insertion and an easier detection of ionic channels which will form in case of Gramicidin [Kelkar et. al, BBA 1768 (2007) 2011-25]. Acknowledgment: FONDECYT grant numbers 1180939 (UGV), 1171047 (MS-A) and 1211901 (TPC).

BP 12.52 Tue 17:30 P4

The effect of additives on the lamellar-to-cubic transition dynamics of monoolein at excess water conditions — •JAQUELINE SAVELKOULS, MICHELLE DARGASZ, GÖRAN SURMEIER, and MICHAEL PAULUS — Fakultät Physik/DELTA, Technische Universität Dortmund, 44221 Dortmund, Germany. Monoolein is an amphiphilic lipid, which is of particular interest in the pharmaceutical industry. Monoolein swells in excess water and forms several lyotropic

liquid crystalline structures. In the cubic Pn3m phase, monoolein can release a previously added drug by slow diffusion in the human body [1]. Measurements are performed at the beamline BL2 of the synchrotron radiation source DELTA (Dortmund, Germany) using the small angle X-ray scattering (SAXS) set-up to study the pressure-induced transition from the lamellar crystalline phase to the cubic Pn3m phase. 20 wt% monoolein was mixed in water with salts or drugs. Diffraction patterns are recorded, from which the lattice constants for each phase can be determined. The results show that a much larger lattice constant of the Pn3m phase is formed after the pressure jump compared to the equilibrium state before the pressure increase. Given some time, the system relaxes, causing the lattice constant to approach the equilibrium lattice constant. The rate of relaxation depends on the added additives. In summary, the formation of the liquid crystalline phases of monoolein allows drugs to be released over a long period of time. The speed of diffusion can be optimized by the addition of salts.

[1] Adriana Ganem-Quintanar, "Monoolein: A Review of the Pharmaceutical Applications", p.813 (2000)

BP 12.53 Tue 17:30 P4

Simulation of Double-Walled Vesicles Surrounded by Mixed Membranes — •PAUL LOUIS SONEK and FRIEDERIKE SCHMID — Johannes Gutenberg-Universität, Mainz, Germany

The simulation of membranes from cells and organelles has been a subject of research for quite some time. Some organelles, like the mitochondria, are surrounded by two membranes, where the area of the inner one is much larger than that of the outer one. Such organelles are characterized by numerous invaginations in the inner membrane. The goal of our work is to investigate to which extent simple membrane models can reproduce such structures.

We use the triangulated surface model of Noguchi and Gompper [1] to model double-walled vesicles and combine it with a field model on the model's surface to simulate a membrane with different lipid compositions on different parts of the membrane. Depending on the volume and surface of the inner membrane, we obtain different stable and metastable shapes for the resulting invagination, including flat invaginations, which have a shape similar to the ones observed in mitochondria. Furthermore, configurations with more than one of such folds are found to be metastable.

Our results may shed light on the mechanisms responsible for the peculiar membrane shapes observed in organelles.

[1] H. Noguchi, G. Gompper, Phys. Rev. E 72, 011901 (2005).

BP 12.54 Tue 17:30 P4

Single-particle Diffractive Imaging at the European XFEL: Instrumentation, Data Acquisition and Hit-finding — •MORITZ STAMMER¹, CHARLOTTE NEUHAUS¹, JETTE ALFKEN¹, MARKUS OSTERHOFF¹, RICHARD BEAN², JOHAN BIELECKI², JUNCHENG E², SAFI RAFIE-ZINEDINE², RAPHAEL DE WIJN², ROMAIN LETRUN², ADRIAN MANCUSO², REINHART JAHN³, and TIM SALDITT¹ — ¹Georg-August-Universität, Institute for X-ray Physics, 37077 Göttingen — ²Scientific Instrument SPB/SFX, European XFEL GmbH, Holzkoppel 4, 22869 Schenefeld Germany — ³Laboratory of Neurobiology, Max Planck Institute for Multidisciplinary Sciences, 37077 Göttingen, Germany

The European XFEL provides state-of-the-art instrumentation for absorbing single-pulse, single-particle coherent diffractive imaging, which we have used to investigate synaptic vesicles, harvested from rat brain, with high spatial resolution. The method involves serial bio-sample delivery by aerosol jet such that droplets incorporating single particles are probed by femto-second pulses. In this way two prevalent challenges of SAXS (polydispersity and radiation damage for high brilliance beams) can be met. Stochastic distribution of sample and a nano-focused beam means only a fraction of the recorded data was of interest (1.2 PB in total, roughly $3 \cdot 10^8$ images). We present technical details behind the data acquisition used for this proof-of-concept experiment at the SPB instrument of the European FEL as well as our strategy in "hit-finding". Further, first steps towards electron density reconstruction will be presented as well as comparison to preceding SAXS work.

BP 12.55 Tue 17:30 P4

Live imaging on single cell arrays (LISCA) as platform to study mRNA codon optimization based on ribosome modelling — •JUDITH MÜLLER¹, GERLINDE SCHWAKE¹, ANITA REISER¹, DANIEL WOSCHÉE¹, ZAHARA ALIREZAEIJANJANI³, JOACHIM RÄDLER¹, and SOPHIA RUDORF² — ¹Ludwig-Maximilians-Universität, München — ²Leibniz Universität, Hannover — ³Max Planck Institute of Colloids and Interfaces, Potsdam

mRNA based therapies have the potential to evolve as one of the most powerful therapeutic technologies of our future. Massive efforts have been made to deeply study the underlying mechanisms of mRNA delivery and translation. Synonymous re-coding of the mRNA's open reading frame is one approach to investigate and optimize the physics of mRNA translation. In this project, we evaluate the potential of bias in codon usage on influencing the mRNA's translation and degradation kinetics. Live imaging on single cell arrays (LISCA) enables the quantification of translation of hundreds of single cells in parallel on microstructured surfaces. By describing the translation in biochemical rate equations, we analyse mRNA expression and degradation rates with high accuracy. Ribosome

movement on the open reading frame (ORF) is simulated to generate mRNA constructs coding for reporter genes with varying ribosome speeds and densities. We observe distinct differences in expression and degradation rates for GFP mRNAs with various optimized ORFs in agreement with simulation. Secondly, we study how specifically provoked ribosome jams on the ORF influence mRNA stability.

BP 12.56 Tue 17:30 P4

The pH dependent phase transition in lipid nanoparticle cores leads to changes of protein expression in single cells — •JULIAN PHILIPP¹, LENNART LINDFORS², and JOACHIM RÄDLER¹ — ¹LMU, Munich, Germany — ²AstraZeneca, Mölndal, Sweden

Lipid nanoparticles developed into the most powerful delivery platform for mRNA based vaccination and therapies. In general LNPs are core/shell particles exhibiting PEG-lipid and DSPC at the surface and ionizable lipid, cholesterol and mRNA in the core. However, the pH dependent changes induced by ionizable lipids in the context of endosomal release are little understood. Here we study the ionizable lipids MC3, KC2, DLin-DMA as model systems as they exhibit different efficacy despite similar pK values. Using synchrotron X-ray scattering we study the structure of bulk phases containing ionizable lipid/cholesterol with and without polyA as mRNA surrogate. The bulk phases exhibit ordered mesophases at low pH and a transition into isotropic swollen phases at higher pH. We find inverse hexagonal H_{II} lipid phases in case of MC3 and KC2 and cubic Pn3m and H_{II} phases in case of DLin. Bulk phases with polyA show coexistence of pure lipid phases and condensed nucleic acid lipid phases. We show that the observed bulk structures are consistent with the SAXS scattering profile of mRNA containing LNPs. The difference in structural features is also consistent with the delayed onset and reduced level of GFP expression observed in single cell time courses after transfection with DLin LNPs compared to MC3 and KC2. We conclude that pH dependent bulk phase transitions trigger endosomal release.

BP 12.57 Tue 17:30 P4

Spatial-Stochastic Model of Cell Fate Decisions in Early Mouse Development — •MICHAEL ALEXANDER RAMIREZ SIERRA¹, TIM LIEBISCH^{1,2}, SABINE C. FISCHER³, FRANZISKA MATTHÄUS^{1,2}, and THOMAS R. SOKOLOWSKI¹ — ¹Frankfurt Institute for Advanced Studies (FIAS), Frankfurt am Main, Germany — ²Goethe Universität Frankfurt am Main, Germany — ³Julius-Maximilians-Universität Würzburg, Germany

The delicate balance necessary for ensuring reliable specification of cell lineages is an intriguing problem in developmental biology. As an important paradigm in tissue development, the early mouse embryo cell fate decisions have been extensively researched, but the underlying mechanisms remain poorly understood. Current approaches to this problem still primarily rely on deterministic modeling techniques, although stochasticity is an inherent feature of this biological process. We are developing a multi-scale event-driven spatial-stochastic simulator for emerging-tissue development. We build up new simulation schemes for incorporating suitable tissue-scale phenomena, and we fix important parameters by using experimental values or numerical optimization to infer biophysically-feasible regimes. We first explore the characteristics of this system in a single-cell setting. We then extend the study to a multi-cellular setting in order to understand how positional information is robustly achieved and preserved. Our latest results indicate a potential signaling mechanism for reliable patterning emergence, despite strong constraints imposed by cell cycles. We are closely exploring how these signals redefine cell fates.

BP 12.58 Tue 17:30 P4

Protein Dynamics in the Complex Physical Environment of the Synapse — •SIMON DANNENBERG, SARAH MOHAMMADINEJAD, and STEFAN KLUMPP — Institut für Dynamik komplexer Systeme Georg-August-Universität Göttingen, Göttingen, Germany

The synapse is a complex environment that is densely packed with proteins and has an internal geometry structured by membranes. This affects the mobility of proteins involved in signal transmission and hence, their availability at corresponding reaction sides.

In our work we use dynamic Monte Carlo simulations to investigate the individual influences of different physical features of the synapse on protein mobility. The simulations are parameterized by mobility measurements via FRAP experiments. By simulating protein mobility in synapses with different geometric features such as synapse volume and vesicle number, we study the influence of these features on concentration profiles in the synapse and other key aspects of signal transmission.

BP 12.59 Tue 17:30 P4

Single Cell Prime Editing Kinetics — •NATHALIE SCHÄFFLER¹, JULIAN GEILENKEUSER², DONG-JIUNN JEFFERY TRUONG², GIL WESTMEYER², and JOACHIM RÄDLER¹ — ¹LMU München, Deutschland — ²Institute for Synthetic Biomedicine, Helmholtz-Zentrum München, Deutschland
CRISPR-Cas technology opens up new ways of approaching biological computing, taking advantage of the native language of biology and the inherent possibilities of DNA which could enable easier parallelism and higher storage capacities.

However, to effectively leverage this technology a solid understanding of the kinetics and efficiency of gene editing is essential.

A key advancement in CRISPR-Cas is Prime Editing (PE), which enables precise "search-and-replace" of specific DNA sections without templates. However, PE requires delivery of both the PE specific Cas-9 protein and a guide RNA (pegRNA) into living cells. Two common strategies of non-viral in vivo delivery are via mRNA or pDNA constructs encoding both PE components. We compare these two methods and study their efficiency and timing using Live Imaging on Single Cell Arrays (LISCA).

Our experiments use a HEK293T cell line with stable expressing blue shifted mGreenLantern (mGL) as reporter system, taking advantage of the fact that only a short DNA sequence edit is needed to reverse the blue shift back to the green mGL. By recording the single cell kinetics and statistics of PE converting bs-mGL into mGL starting from the time point of transfection, we can assess editing times and efficiencies.

BP 12.60 Tue 17:30 P4

Self-generated oxygen gradients control the collective aggregation of photosynthetic microbes — •ALEXANDROS FRAGKOPOULOS^{1,2}, JEREMY VACHIER¹, JOHANNES FREY¹, FLORA MAUD LE MENN¹, MARCO G. MAZZA^{1,3}, MICHAEL WILCZEK^{1,4}, DAVID ZWICKER¹, and OLIVER BÄUMCHEN^{1,2} — ¹Max Planck Institute for Dynamics and Self-Organization, 37077 Göttingen, Germany — ²University of Bayreuth, Experimental Physics V, 95447 Bayreuth, Germany — ³Interdisciplinary Centre for Mathematical Modelling and Department of Mathematical Sciences, Loughborough University, Loughborough, Leicestershire LE11 3TU, UK — ⁴University of Bayreuth, Theoretical Physics I, 95447 Bayreuth, Germany

In the absence of light, photosynthetic microbes can still sustain essential metabolic functionalities and motility by switching their energy production from photosynthesis to oxygen respiration. For suspensions of motile *C. reinhardtii* cells above a critical density, we demonstrate that this switch reversibly controls collective microbial aggregation [1]. Aerobic respiration dominates over photosynthesis in conditions of low light, which causes the microbial motility to sensitively depend on the local availability of oxygen. For dense microbial populations in self-generated oxygen gradients, microfluidic experiments and continuum theory based on a reaction-diffusion mechanism show that oxygen-regulated motility enables the collective emergence of highly localized regions of high and low cell densities.

[1] Fragkopoulou et al., J.R. Soc. Interface 18, 20210553 (2021).

BP 12.61 Tue 17:30 P4

Physical heterogeneities in bacterial mixtures under flow — •GIACOMO DI DIO, VICTOR SOURJIK, and REMY COLIN — Max Planck Institute for Terrestrial Microbiology, Marburg, Germany

Bacteria are often found in heterogeneous communities organized through physical interaction with their surrounding environment. Although external physical constraints like shear flow are frequent in natural situations, little is still known about their effect on the distribution of bacteria within complex communities. Under no flow condition, previous experiments have shown the emergence of large density fluctuations of passive bacterial cells driven by the activity of motile bacteria with which they are mixed. Through microfluidic experiments, we investigate how the spatiotemporal organization and the density distribution of a binary mixture of active and passive *E. coli* bacteria react under different configurations of shear flow. Our initial focus is on the effect of Poiseuille flow (linear shear profile) on the mixture, but we also plan to study the behavior under Couette flow. We notably focus on possible transport effects emerging from the combined action of external shear and active swimming on the non-motile species of the mixture. Our experiments aim at understanding the physical roles of flow and shear in the spatiotemporal organization of multispecies bacterial communities

BP 12.62 Tue 17:30 P4

Fast sorting of microfluidic droplets by content type with combined bright field and fluorescence detection — •JONAS PFEIL, PATRICIA SCHWILLING, and OTHMAR MARTI — Universität Ulm, Ulm, Germany

Droplet-based microfluidics in context of fluorescent imaging can be used for a multitude of applications in biophysics, medicine, and lab-on-a-chip. One remaining issue in the encapsulation process of particle-like objects is that the number of encapsulated objects is Poisson or Poisson-like distributed. A sorting step immediately after the encapsulation reduces the number of falsely-laden droplets.

Here we present results of sorting of beads with similar diameters and different fluorescent signals. Therefore, we encapsulate similar sized beads with different fluorescent signature and sort them using a time multiplexed imaging approach to simultaneously detect the population for each bead type. Thereby, we show that it is possible to achieve a user-defined, homogeneous configuration of fluorescent and non fluorescent particles in droplets.

BP 12.63 Tue 17:30 P4

Physics of optimal odor detection — •SWATI SEN and DAVID ZWICKER — Max Planck Institute for Dynamics and Self-organization, Göttingen, Germany

Animals need to detect and discriminate odors for survival. In contrast to other senses, olfaction is shaped by physical processes, including odorant transport by the airflow and adsorption in the nasal mucus layer. These processes crucially affect what the brain can learn about the chemical composition of the environment. We study how the olfactory system relays information by using a simplified theoretical description of the airflow and the adsorption in the mucus. We predict the length scales over which odorants absorb along the olfactory epithelium. This length scale depends significantly on the odorant's solubility but is only weakly affected by odorant diffusivity and adsorption strength of mucus wall. We use these predictions to obtain the optimal arrangement of odorant receptor neurons that maximizes the information relay to the brain. We notice that the receptors sensitive to odorants with shorter adsorption length scale always reside closer to the cavity inlet side and cover the cavity in an increasing fraction of total cavity length with adsorption length scale. Taken together, we study design principles of optimal odor information encoding using a simple fluid dynamical model and information theory. Our approach could help to understand the natural olfaction process and develop artificial noses.

BP 12.64 Tue 17:30 P4

Assembly of plant-pollinator networks with rare and common plants — •LUCA SCHÄFER, LARA BECKER, and BARBARA DROSSEL — TU Darmstadt, Darmstadt, Germany

Species interaction networks are subject to natural and anthropogenic disturbances that lead to their disassembly, while natural regeneration or restoration efforts facilitate their reassembly. Since over 90% of all angiosperms are pollinated by animals, understanding the stability and assembly of plant-pollinator networks is crucial for ecosystem conservation.

We introduce and investigate a model for the assembly of plant-pollinator networks from an infinite species pool, based on trait-matching between plants and animals. Population dynamics equations include different intraspecific competition strengths and niche width, to allow for the occurrence of rare (high intraspecific competition and small niche width) and common plants. We show that computer simulations of the model lead to the emergence of plant-pollinator networks where rare plants can persist despite the effect of pollen dilution. Over time, pollinators become more specialized, but this trend is stopped if stochasticity in the form of demographic noise is taken into account.

BP 12.65 Tue 17:30 P4

Statistical modelling of cerebral blood flow and transport in microvascular networks — •FLORIAN GOIRAND¹, TANGUY LE BORGNE², and LORTHOIS SYLVIE³ — ¹Center for Protein Assemblies, Physics Department, Technische Universität München, Garching bei München, Germany — ²University of Rennes, CNRS, Géosciences Rennes, UMR 6118, Rennes, France — ³Institut de Mécanique des Fluides de Toulouse, UMR 5502, CNRS, University of Toulouse, Toulouse, France

Despite of the high dependency of brain cells function on the efficiency of blood transport throughout the micro-vasculature, only little is known about the physical processes that drive neural cell supply. Here, based on the statistical analysis of realistic blood flow computations in mouse brain micro-vascular networks, we develop a statistical framework relating the structure of micro-vascular networks to the observed blood flow and transport heterogeneities. In particular, this framework enables to investigate the detrimental consequences of the cerebral blood flow decrease, a key phenomenon at early stage of Alzheimer's disease. We notably predict, in agreement with simulations, that the anomalous nature of the transport induces a non-linear evolution of the size of the regions exhibiting a critical concentration in oxygen or in neuro-toxic metabolic wastes with the decrease of the cerebral blood flow, unraveling an additional mechanism contributing to Alzheimer's disease progress.

BP 12.66 Tue 17:30 P4

Investigation of nonlinear effects on polarizable μ beads in AC/DC-Dielectrophoresis — •TIM R. BAUMANN, DARIO ANSELMETTI, and MARTINA VIEFHUES — Experimental Biophysics & Applied Nanosciences, Department of Physics, Bielefeld University

Dielectrophoresis (DEP) is a common selective force used for separation applications in microfluidics. Due to a non-uniform electric field, polarizable particles migrate through a fluid. Depending on the applied electric field, intrinsic parameters like surface charge, polarizability or ion mobility and extrinsic parameters like pH-value objects lead to acceleration, deceleration or trapping in dielectrophoretic potentials. Thus, analysis of the migration in electric fields yields access to characteristic electric parameter of particles. The direction of movement is given by the value of charge and the direction of the electric field. Here a constant direct current (DC) is set in range 0 – 40 V and incrementally raised by 5 V to drive the beads through a microfluidic device. An alternating current (AC) ($f = 1\text{ kHz}$) ranging from 100 – 450 V in amplitude (increment size: 50 V) was superimposed to generate dielectrophoretic trapping forces that should decelerate the beads. An increase of migration velocity was observed though, which is assumed to be due to higher order terms of the electric field as recently presented by the group of Perez-Gonzales for DC electric fields [1]. In this work, we investigate if this effect also applies in AC electric fields. [1]Anal. Chem. 2020, 92, 12871-12879

BP 13: Cytoskeleton

Time: Wednesday 9:30–12:45

Location: H15

Invited Talk

BP 13.1 Wed 9:30 H15

Cortex mechanics - how subtle modifications matter — •ANDREAS JANSHOFF — Institute of Physical Chemistry, Tammannstr. 6, University of Goettingen, 37077 Goettingen

Cell cortices are responsible for the resilience and morphological dynamics of cells. Measuring their mechanical properties is impeded by contributions from other filament types, organelles, and the crowded cytoplasm. Therefore, we established two routes to examine its essential features using i) a bottom-up approach to create artificial minimal actin cortices (MACs) and b) by extracting cortices from living cells. Apical cell membranes of confluent MDCK II cells as well as MACs were deposited or formed on porous substrates and either locally deformed using an atomic force microscope setup or explored by microrheology techniques. Force cycles could be described with a time-dependent area compressibility modulus obeying the same power law as employed for whole cells. We found that subtle modifications such as the composition of the plasma membrane and origin of actin, i.e., the chosen isoform or its posttranslational modification are important for the dynamics and mechanics of the cortex. We found that the presence of phosphatidylserine in the inner leaflet of the plasma membranes is crucial for cortex contractility and efficient binding of F-actin to the membrane.

BP 13.2 Wed 10:00 H15

Dynamic bridging explains sub-diffusive movement of chromosomal loci — •SRIKANTH SUBRAMANIAN and SEÁN MURRAY — Max Planck Institute for Terrestrial Microbiology, Marburg, Germany

Chromosomal loci in bacterial cells show a robust sub-diffusive scaling of the mean square displacement (MSD) $\sim \tau^\alpha$, with $\alpha < 0.5$ under various growth conditions and antibiotic treatments. Recent experiments have also shown that

DNA-bridging Nucleoid Associated Proteins (NAPs) play an important role in chromosome organisation and compaction. Here, using polymer simulations we investigate the role of DNA bridging in determining the dynamics of chromosomal loci. We find that bridging compacts the polymer and reproduces the sub-diffusive dynamics of monomers at timescales shorter than the bridge lifetime. Furthermore, the measured scaling exponent defines a relationship between chromosome compaction and bridge lifetime. Importantly, measuring the MSD of tagged chromosomal loci in WT and NAP mutant ($\Delta\text{H-NS}$) we find that the decompact mutant has a higher scaling exponent as expected. Based on the observed mobility of chromosomal loci and our simulations, we predict a lower bound on the average bridge lifetime of NAPs to be around 5 seconds.

BP 13.3 Wed 10:15 H15

Image analysis and modelling of nascent sarcomeres during myofibrillogenesis — •IAN D. ESTABROOK¹, FRANCINE KOLLEY¹, CLÉMENT RODIER², FRANK SCHNORRER², and BENJAMIN M. FRIEDRICH^{1,3} — ¹cfaed, TU Dresden — ²IBDM, Aix Marseille University — ³Physics of Life, TU Dresden.

All animals possess striated muscle, which enable their voluntary movements. Inside muscle cells, actin and myosin molecular motors together with actin crosslinkers and the giant protein titin are arranged in long chains of sarcomeres in so-called myofibrils of almost crystalline regularity. Despite their physiological importance, it remains poorly understood how myofibrils spontaneously self-assemble during myofibrillogenesis. To investigate this molecular pattern formation process, our group combines image analysis and mathematical modelling, in close collaboration with the experimental Schnorrer lab.

We automatically analysed thousands of sarcomeres using a custom Matlab-based feature detection algorithm to analyse three-dimensional multi-channel fluorescence images of the *Drosophila* flight muscle. This allows us to compute

averaged spatial intensity profiles of key proteins at different stages of myofibrillogenesis, providing a pseudo-time course of sarcomere assembly. Additionally, we observe rare abnormal sarcomeres, which reveals a new mechanism by which a 'mother sarcomere' splits into two 'daughter sarcomeres'. This data drives mathematical modelling: minimal models demonstrate that non-local interactions between spatially extended myosin and titin molecules, as well as actin crosslinkers are sufficient to replicate sarcomeric pattern formation.

BP 13.4 Wed 10:30 H15

Torques within microtubule bundles generate the curved shape of the mitotic spindle — •ARIAN IVEC¹, MAJA NOVAK¹, MONIKA TRUPINIĆ², IVANA PONJAVIĆ², IVA TOLIĆ², and NENAD PAVIN¹ — ¹Department of Physics, Faculty of Science, University of Zagreb, Bijenička cesta 32, 10000 Zagreb, Croatia — ²Division of Molecular Biology, Ruder Bošković Institute, Bijenička cesta 54, 10000 Zagreb, Croatia

The mitotic spindle is a complex micro-machine made up of microtubules and associated proteins, which are highly ordered in space and time to ensure its proper biological functioning. A functional spindle has a characteristic shape, which includes curved bundles of microtubules that are twisted around the pole-to-pole axis. An understanding of both how the linear and rotational forces define the overall shape of the mitotic spindle and how the twisted shapes arise as a result of interactions between microtubules and motor proteins is still missing. To answer this, we model the entire spindle by using a mean-field approach, in which we describe the forces and torques along microtubule bundles throughout the spindle. We compare our theoretical modeling with experimentally observed shapes of bundles in the mitotic spindle, including both unperturbed spindles and those compressed by an external force. We conclude that the observed shape of the spindle is predominately determined by rotational forces. Additionally, we find that a difference in bending forces explains the disparity in the shapes of inner and outer bundles, and that the chirality of the spindle is the result of a constant twisting moment.

BP 13.5 Wed 10:45 H15

Length-dependent poleward flux of sister kinetochore fibres promotes chromosome alignment — •DOMAGOJ BOŽAN — Department of Physics, Faculty of Science, University of Zagreb, Bijenička cesta 32, 10000 Zagreb, Croatia

Chromosome alignment at the spindle equator promotes proper chromosome segregation and depends on pulling forces exerted at kinetochore fiber tips together with polar ejection forces. However, kinetochore fibers are also subjected to forces exerted by motor proteins that drive their poleward flux. Here we introduce a flux-driven centering model that relies on flux generated by forces within the overlaps of bridging and kinetochore fibers. This centering mechanism works so that the longer kinetochore fiber fluxes faster than the shorter one, moving the kinetochores towards the center. Our collaborators developed speckle microscopy in human spindles and confirmed the key prediction that kinetochore fiber flux is length-dependent. The experiments also confirmed that kinetochores are better centered when overlaps are shorter and the kinetochore fiber flux markedly slower than the bridging fiber flux. Furthermore, we extend the model to describe congression of chromosomes by considering dynamics of microtubule-kinetochore attachments and motor proteins at kinetochores and find that the length-dependent forces exerted by microtubules from farther pole can overcome the forces exerted by the greater number of microtubules from nearer pole. Thus, length-dependent sliding forces exerted by the bridging fiber onto kinetochore fibers promote chromosome congression and alignment.

15 min. break

BP 13.6 Wed 11:15 H15

Mechanical properties of keratin and vimentin intermediate filaments — •CHARLOTTA LORENZ¹, JOHANNA FORSTING¹, STEFAN KLUMPP², and SARAH KÖSTER¹ — ¹Institute for X-Ray Physics, University of Göttingen, Göttingen, Germany — ²Institute for the Dynamics of Complex Systems, University of Göttingen, Göttingen, Germany

Different cell types require different mechanical properties. Prominent examples include cell contracting muscle cells, or migrating versus non-migrating cells. Cells change from a migrating to a non-migrating phenotype during cancer metastasis, wound-healing and embryogenesis (epithelial-to-mesenchymal transition). Interestingly, the expression of different intermediate filament (IF) proteins correlates with this transition: epithelial-like cells express mostly keratin, whereas mesenchymal cells primarily express vimentin. We compare the mechanical response of keratin and vimentin on the single filament level using optical tweezers. We find that both filament types dissipate a large amount of mechanical input energy, which predestines them to act as a cellular shock absorbers, yet by very different mechanisms, internal friction of sliding filament subunits, or nonequilibrium unfolding of alpha helices for keratin and vimentin filaments, respectively. We conclude that cells can tune their mechanics by differential expression of keratin versus vimentin.

BP 13.7 Wed 11:30 H15

Influence of vimentin intermediate filaments on microtubules in cells — •ANNA BLOB¹, ROMAN DAVID VENTZKE^{1,2}, CAROLIN SCHLEIN¹, LAURA SCHAEDEL³, AXEL MUNK², and SARAH KÖSTER¹ — ¹Institute for X-Ray Physics, University of Göttingen — ²Institute for Mathematical Stochastics, University of Göttingen — ³Center for Biophysics, Saarland University

The cytoskeleton in eucaryotic cells is an intricate network of three different filamentous proteins: microtubules, actin filaments and intermediate filaments. Together, they are essential for the mechanical properties as well as important functions of the cell, such as intracellular transport and division. Each protein has its own unique properties and there is evidence for important interactions between them. It has been shown that vimentin intermediate filaments stabilize microtubules in vitro and can template the microtubule network in migrating cells. Following up on this idea, we are interested in the influence of vimentin networks on microtubule mechanics. Cellular microtubules show characteristic buckling and bending behavior that is still not fully understood. Investigating the role of vimentin for the bending of microtubules will improve our understanding of the mechanical consequences and importance of the interactions between these filament systems. We compare microtubule networks in vimentin-knockout and wildtype mouse fibroblasts on micropatterns. Microscopy images are processed and analyzed with respect to the curvature of microtubules. We find that the local curvature of microtubules depends on the cellular region and increases with increasing vimentin density.

BP 13.8 Wed 11:45 H15

Microscopic modelling of forces and torques in the mitotic spindles — •MAJA NOVAK¹, ARIAN IVEC¹, IVA M. TOLIĆ², and NENAD PAVIN¹ — ¹University of Zagreb, Faculty of Science, Bijenička c. 32, 10 000 Zagreb — ²Rudjer Bosković Institute, Biophysics of Cell Division, Bijenička c. 54, 10000 Zagreb

The mitotic spindle is a complex micro-machine built from microtubules and associated proteins, with a purpose to properly separate genetic material into two nascent cells. In our previous work we found that microtubule bundles in human spindles follow a left-handed helical path [1], from which we concluded that torques, in addition to forces, exist in the mitotic spindle. However, theoretical description of molecular origin of forces and torques in the mitotic spindle is still missing. Here we show that single-molecule rotational forces regulate the volume of mitotic spindle, where larger twisting moment increases the spindle width. Our model describes microtubules as flexible rods, which are cross-linked by the motor proteins and passive linkers. The model predicts angular distribution of microtubules at the pole, based on experimentally observed shapes of microtubule bundles in the spindle midzone. Finally we found that the bending and twisting moment at the pole change between the inner and outer bundles in a manner qualitatively similar to curvature and twist obtained from the experimental data. In conclusion, our microscopic description opens up the possibility to quantify and understand both function and details of the twisting moment in the mitotic spindle. [1] Novak et al., Nat. Commun.(2018)9:3571

BP 13.9 Wed 12:00 H15

Correlative Super-Resolution Microscopy and Structural Analysis of Cells and Tissues — •DIMITAR STAMOV, TANJA NEUMANN, ANDRÉ KÖRNIG, TORSTEN MÜLLER, and HEIKO HASCHKE — JPK BioAFM, Bruker Nano GmbH, Am Studio 2D, 12489 Berlin, Germany

Active forces in biological systems define the interactions between single molecules, growing cells and developing tissues. Cells adapt their shape and react to the surrounding environment by a dynamic reorganization of the F-actin cytoskeleton. We will demonstrate how cell spreading and migration in living KPG-7 fibroblasts and CHO cells, can be studied with high-speed AFM and associated with spatially resolved cytoskeletal reorganization events. We will further extend this with high-speed mechanical mapping of confluent cell layers, which in combination with optical tiling can be applied to automated analysis of large sample areas. We will show how AFM imaging and super-resolution 2color easy3D STED measurements can be combined and will show results of colocalized imaging and sample manipulation with a precision below the diffraction limit. We will discuss how to calculate the viscoelastic properties, characterized by the dynamic storage and loss modulus distribution in such samples.

BP 13.10 Wed 12:15 H15

Processive molecular motors stimulate microtubule turnover — WILLIAM LECOMPTÉ¹, SARAH TRICLIN², LAURENT BLANCHOIN^{2,3}, MANUEL THÉRY^{2,3}, and •KARIN JOHN¹ — ¹Univ. Grenoble-Alpes, CNRS, Laboratoire Interdisciplinaire de Physique, 38000 Grenoble, France. — ²Univ. Grenoble-Alpes, CEA, CNRS, INRA, Institute de Recherche Interdisciplinaire de Grenoble, Laboratoire de Physiologie Cellulaire & Végétale, CytoMorpho Lab, 38054 Grenoble, France — ³Univ. Paris Diderot, INSERM, CEA, Hôpital Saint Louis, Institut Universitaire d'Hématologie, UMRS1160, CytoMorpho Lab, 75010 Paris, France

Microtubules (MTs) and molecular motors are ubiquitous in eukaryotic cells and are vital for many key cellular functions (eg. chromosome segregation, intracellular protein transport). Recent experiments have shown that processive molecular motors may damage the underlying microtubule lattice yet a mechanistic

model has remained elusive. Here we investigate theoretically how molecular motors collectively remodel the shaft lattice, as opposed to a vision, where a single motor damages the microtubule as a rare event. Our leading concept is, that the walk of molecular motors locally and transiently destabilizes the lattice and may facilitate the removal of tubulin dimers. This mechanism (i) accelerates fracture of MTs in the absence of free tubulin and (ii) stimulates localized free tubulin dimer incorporation. The model reveals that a small transient perturbation (a few kT with a lifetime of 0.1 s) induced by the motor's walk is sufficient to modify significantly the lattice dynamics.

BP 13.11 Wed 12:30 H15

investigating cardio-myocyte scar formation on a single cell level using ROCS microscopy — •ARASH FELEKARY¹, ALEXANDER ROHRBACH¹, STEPHANIE SCHMID², and EVA ROG-ZIELINSKA² — ¹IMTEK, Lab for Bio- and Nano-Photonics, Freiburg, Germany — ²Institute for Experimental Cardiovascular Medicine, Freiburg, Germany

Rotating coherent scattering (ROCS) microscopy is a label-free super-resolution microscopy technique enabling 150 nm spatial and 10 ms temporal resolution, which is highly beneficial for live-cell imaging. We have applied ROCS in total internal reflection (TIR) mode to acquire high-quality images from tunneling nanotubes (TNTs). TNTs or membrane nanotubes, are more than 10 micrometers in length and about 100 nm thin and directly connect distant cells. It seems that after heart injuries, such as myocardial infarction, mechanical and biochemical communication between heart fibroblasts (FB) and cardio myocytes (CM) is established by TNTs, which helped to generate an extracellular matrix (ECM). TNTs could be involved in the exchange of small molecules and ions between neighbor cells, injury-signal recognition, and directed collagen deposition. We measured the interaction between CMs and FBs, i.e. the dynamics of TNT fluctuations by 100 Hz ROCS movies. With a post-processing activity analysis with frequency decomposition, we detected TNT stiffening over minutes. Computer simulations of stimulated TNT motions or thermal particle motions help to confirm or reject the underlying assumptions forming a mechanistic picture.

BP 14: Active Matter 3 (joint session BP/PP/DY)

Time: Wednesday 9:30–12:30

Location: H16

BP 14.1 Wed 9:30 H16

Collective foraging of microrobots trained by reinforcement learning — •ROBERT C. LÖFFLER¹, EMANUELE PANIZON², and CLEMENS BECHINGER¹ — ¹Fachbereich Physik, Universität Konstanz, Konstanz, Germany — ²Department of Quantitative Life Science, International Centre for Theoretical Physics, Trieste, Italy

From bacteria to mammals, collective behavior can be observed on all scales in nature. It is generally driven by the benefit to individuals when cooperating with others. However, the exact motivation of individuals to participate is challenging to investigate, as biological creatures are complex systems themselves. At the same time engineers seek to create collective groups of autonomous systems to perform dedicated tasks by cooperation.

Here we present an experimental model system of feedback-controlled microswimmers which are trained with multi agent reinforcement learning in an actor-critic scheme. A group of active particles is situated in a 2D environment containing a virtual food source which is changing position over time. Despite being rewarded individually for being inside the food source, particles show cohesive collective motion forming flocks and swirls. This is driven by the benefit of social information and collision avoidance, resulting in faster migration to a relocated food source. Understanding those mechanisms behind the emergence of collective behavior is of biological interest as well as to understand human crowd behavior and to design future robotic systems.

BP 14.2 Wed 9:45 H16

Collective response of microrobotic swarms to external threats — •CHUN-JEN CHEN¹ and CLEMENS BECHINGER^{1,2} — ¹Fachbereich Physik, Universität Konstanz, 78464 Konstanz, Germany — ²Centre for the Advanced Study of Collective Behaviour, Universität Konstanz, 78464 Konstanz, Germany

Many animal species organize within groups to achieve advantages compared to being isolated. Such advantages can be found e.g. in collective responses which are less prone to individual failures or noise and thus provide better group performance. Inspired by social animals, here we demonstrate with a swarm of microrobots made from programmable active colloidal particles (APs) that their escape from a hazardous area can originate from a cooperative group formation. As a consequence, the escape efficiency remains almost unchanged even when half of the APs are not responding to the threat. Our results not only confirm that incomplete or missing individual information in robotic swarms can be compensated by other group members but also suggest strategies to increase the responsiveness and fault-tolerance of robotic swarms when performing tasks in complex environments.

BP 14.3 Wed 10:00 H16

Soft robots powered by magnetically driven active particles — •HONGRI GU and CLEMENS BECHINGER — Fachbereich Physik, University of Konstanz, Germany

Active matter describes systems of a large number of self-driving particles that convert surrounding energy into active motion. Many of the emergent behaviors resemble life-like behaviors in nature. However, it is still unclear how one can utilize such active collective motions for engineering and robotic applications. In this talk, we would like to bridge the research fields of active matter and soft robots by designing soft machines powered by active matter. The main objective is to investigate the general interactions between swarm active particles and soft structures and use this knowledge to design a new type of soft robots that are driven by swarm active particles. To facilitate the investigation, we built a highly customizable fabrication process for magnetic composite soft structures at mesoscales based on two-step micromolding. We also built a modular mag-

netic actuation system based on rotating permanent magnets. This new experimental platform has an enormous design space for magnetic soft matters with the capability to tune individual system parameters. By carefully designing these parameters, it is possible to precisely tune the local magnetic, elastic, and hydrodynamic interactions between active particles and soft structures. This new type of soft machine can potentially take advantage of the robust dynamic states of the active matter, which can recover their functions from extreme mechanical deformations.

BP 14.4 Wed 10:15 H16

Microswimmers in viscosity gradients — •SEBASTIAN ZIEGLER¹, MAXIME HUBERT¹, and ANA-SUNČANA SMITH^{1,2} — ¹PULS Group, Friedrich-Alexander-Universität Erlangen-Nürnberg, Germany — ²Division of Physical Chemistry, Ruder Bošković Institute Zagreb, Croatia

Regions of variant viscosity are ubiquitous in both inanimate systems as well as in living systems. It is therefore of great interest to understand the effect of viscosity gradients on the mobility of both passive particles as well as on active systems. We firstly study a system of passive spheres and provide a general expression for the asymptotic mobility matrix in small viscosity gradients. We apply this result to linear viscosity gradients, where we unveil the existence of radially constant flows and elaborate on the effect of asymmetry of the particle position within the finite-size gradient, which hitherto has not been considered.

These results are subsequently applied to bead-spring microswimmers as model systems for self-propelling active matter. In contrast to the common approach of prescribing the stroke of the swimmer, we here employ a force-based swimmer model, allowing for an adaption of the swimming stroke to the environment, and reveal the rich viscotactic properties of such a microswimmer. We also construct a simple swimmer inspired by the *Chlamydomonas* algae and compare the viscotactic behavior of the biological swimmer to ours.

15 min. break

BP 14.5 Wed 10:45 H16

Noisy pursuit of active Brownian particles — •SEGUN GOH, ROLAND G. WINKER, and GERHARD GOMPPER — IBI-5, Forschungszentrum Jülich, 52425 Jülich, Germany

Many biological and artificial agents are not only motile, but also capable of adjusting their motion based upon information gathered from their environment. This study considers sensing of a target and as a consequence reorientation of the direction of self-propulsion, which enables active pursuit. Specifically, an active Brownian particle is employed as a model agent to investigate pursuit dynamics in two dimensions, for both stationary as well as moving targets. We discuss how the interplay between intrinsic persistent self-propulsion and active reorientation by sensing gives rise to unexpected complex behaviors. In particular, the noise plays a pivotal role with both positive and negative influences on the success of pursuit. Numerical simulations and analytical calculations reveal that strong motility results in overshooting of the target, while pursuers cannot approach the target effectively at low Péclet numbers. Moreover, we propose a strategy to sort active pursuers according to their motility and reorientation capability by employing particular target trajectories.

BP 14.6 Wed 11:00 H16

Rheotaxis of the ciliate — •TAKUYA OHMURA¹, YUKINORI NISHIGAMI², and MASATOSHI ICHIKAWA³ — ¹Biozentrum, University of Basel, Switzerland — ²Research Institute for Electronic Science, Hokkaido University, Japan — ³Department of Physics, Kyoto University, Japan

Rheotaxis, a property of organisms to move against an external flow, has a crucial role to stay in living environment. For instance, freshwater fishes in rivers swim upstream to avoid being swept away to the sea. Interestingly, recent studies reported that not only fish but also swimming cells show rheotaxis. We elucidated the rheotaxis of the ciliate, *Tetrahymena*, a well-known single-celled freshwater microorganism swimming by cilia [1]. While that microorganism doesn't have a sensor to detect flow direction and micrometer-sized particles are swept away downstream in a viscous flow, what dynamics underlie the rheotaxis of the ciliate? Our experiments revealed that the ciliate slid upstream along a wall, which indicates that the cells receive rotational torque from shear flow to align swimming orientation. To evaluate the shear torque, we performed a numerical simulation with a hydrodynamic model swimmer adopting cilia dynamics in a shear flow. The result suggests that the ciliate automatically slides upstream by using cilia-stalling mechanics.

[1] T. Ohmura, et al., *Science Advances*, 7(43), eabi5878 (2021).

BP 14.7 Wed 11:15 H16

Analytical study of active semiflexible ring polymer — •CHRISTIAN A. PHILIPPS, GERHARD GOMPPER, and ROLAND G. WINKLER — Forschungszentrum Jülich, Jülich, Germany

Nature provides a variety of active matter systems, with self-propelled agents consuming internal energy or extracting it from their vicinity for locomotion [1]. Examples on the cellular level are self-propelled semiflexible actomyosin ring-like filaments driven by myosin motors in the cytoskeleton. We present a theoretical study of an active ring polymer [2] with tangential propulsion applying the continuous Gaussian semiflexible polymer model [3]. By a normal-mode expansion, the ring polymer conformational and dynamical properties, emerging by the homogeneous active force, and its interplay with rigidity are determined. Remarkably, the ring conformations are unaffected by activity for any rigidity. In contrast to linear filaments, the center-of-mass motion is independent of propulsion. However, activity strongly influences the internal dynamics with an activity enhanced diffusive for the flexible and a ballistic regime for the semiflexible ring polymer. Furthermore, a dominant rotational mode over several orders of magnitude in time emerges for high activities, which implies a rotational motion of the entire ring polymer. [1] R. G. Winkler, G. Gompper, *J. Chem. Phys.* 153, 040901 (2020); [2] M. Mousavi, R. G. Winkler, G. Gompper, *J. Chem. Phys.* 150, 064913 (2019); [3] T. Eisenstecken, G. Gompper, R. G. Winkler, *Polymers* 8, 304 (2016).

BP 14.8 Wed 11:30 H16

Dynamical Renormalization Group approach to the collective behavior of natural swarms — ANDREA CAVAGNA¹, LUCA DI CARLO¹, IRENE GIARDINA¹, TOMAS GRIGERA^{1,3}, GIULIA PISEGNA^{1,2}, and MATTIA SCANDOLO¹ — ¹Sapienza Università di Roma, Roma IT — ²Max Planck Institute for Dynamics and Self-Organization, Goettingen DE — ³IFLYSIB, La Plata, Argentina

Recent data on strongly correlated biological systems showed the validity of scaling laws as one of the fundamental traits of collective behaviour. Experiments on natural swarms of insects unveiled traces of critical dynamics, with inertial features and a dynamical critical exponent $z=1.2$. To rationalize this evidence, we develop an inertial active field theory in which the velocity is coupled to its generator of internal rotations, namely the spin, through a mode-coupling interaction. We study its near-critical regime with a one-loop Renormalization Group

approach under the assumption of incompressibility. The presence of friction in the dynamics of the spin rules a paramount crossover between two fixed points: the unstable underdamped fixed point with $z=1.3$ and the stable overdamped fixed point with $z=1.7$, where dissipation takes over. We show how finite-size systems with weak dissipation, such as swarms, can actually exhibit the critical dynamics of the unstable fixed point thus providing a theoretical result which is in fair agreement with experimental data.

15 min. break

BP 14.9 Wed 12:00 H16

Dynamics and rheology of active suspensions in viscoelastic media — •AKASH CHOUDHARY¹, SANKALP NAMBIAR², and HOLGER STARK¹ — ¹Institute of Theoretical Physics, Technische Universität Berlin, 10623 Berlin, Germany — ²Nordita, KTH Royal Institute of Technology and Stockholm University, Stockholm 10691, Sweden

Active suspensions are systems of motile organisms or active motors that are driven out of equilibrium through self-propulsion. This localized energy-work conversion imparts rich phenomenology and anomalous macroscale properties that are in stark contrast to passive suspensions and polymeric fluids. Motivated by the ubiquitous microbial systems in biological fluids, we analyse the impact of non-Newtonian fluids on the rheological response of active suspensions to steady shear flows.

We first study the suspension at an individual scale and show that elongated pushers (representative of *E. coli*) and pullers (*C. reinhardtii*) exhibit diverse orbital dynamics in a viscoelastic fluid. We find that the active stresses not only modify the Jeffery orbits, well-known for viscous fluids, but microswimmers can even resist flow-induced rotation and align themselves at an angle with the flow. To analyze the impact of such behavior on the bulk rheological response, we study an ensemble of a dilute suspension of such swimmers in the presence of stochastic noise from bacterial tumbling and rotary diffusion. In comparison to Newtonian media, the polymeric elastic stresses substantially and non-monotonically amplify the swimmer-induced viscosity, in particular, the superfluid transition of pusher solutions.

BP 14.10 Wed 12:15 H16

Intercellular transport in *Chara corallina* — •FLORIAN VON RÜLING¹, ANNA ALOVA², ALEXANDER BULYCHEV², and ALEXEY EREMIN¹ — ¹Otto von Guericke University Magdeburg, Germany — ²Moscow, Russia

We explore the kinetics of the intercellular transport between the giant cells of characean algae. The transport involves advection via cytoplasmic streaming and diffusion through the plasmodesmata, pores that penetrate the cell walls. Using fluorescent dye as a tracer, we measure the permeation through the node of tandem cells. The permeability is extracted from the experimental data using an advection-diffusion model. The current work is focused on the roles of cytoplasmic streaming and the nodal cells in the transport mechanism. To separate the diffusive permeation from the advective contribution, cyclosis was temporarily inhibited using action potentials. Streaming cessation results in dye accumulation in the vicinity of the node. The shape of regions with high dye concentration indicates that action potentials may induce closure of the plasmodesmata in central nodal cells.

BP 15: Protein Structure and Single Molecules

Time: Wednesday 10:00–12:15

Location: H13

BP 15.1 Wed 10:00 H13

Using physics to understand and fight viruses — •JAN LIPPERT¹, WILLEM VANDERLINDEN¹, PAULINE KOLBECK¹, SOPHIA GRUBER², MAGNUS BAUER³, and HERMANN GAUB² — ¹Utrecht University — ²LMU Munich — ³Stanford University

Viruses can cause human disease, with dramatic and global consequences. Here, I will present how we use single-molecule approaches to investigate aspects of the life cycles of SARS-CoV-2 and HIV. First, we have developed a tethered ligand assay to investigate how SARS-CoV-2 attaches to human cells. Using magnetic tweezers and AFM force spectroscopy, we obtain a comprehensive view of the force stability of the critical first interaction of the virus with our cells (Bauer, Gruber, et al. *PNAS* 2022) and investigate the current variants of concern. We find differences in force stability that help rationalize the epidemiology of the different variants (Gruber et al., unpublished). Second, we use magnetic tweezers and AFM imaging to investigate the interactions of retroviral integrases with DNA. We obtain a comprehensive view of the free energy landscape of retroviral integration for prototype foamy virus (Vanderlinden et al. *Nature Comm.* 2019) and find that, in addition to its well known catalytic role, HIV integrase can efficiently condense DNA into biomolecular condensates (Kolbeck et al., unpublished).

BP 15.2 Wed 10:15 H13

Angle-dependent strength of a single chemical bond by stereographic force spectroscopy — WANHAO CAI¹, •JAKOB TÓMAS BULLERJAHN², MAX LALLEMANG^{1,3}, KLAUS KROY⁴, BIZAN BALZER^{1,3,5}, and THORSTEN HUGEL^{1,3} — ¹Institute of Physical Chemistry, University of Freiburg, Germany — ²Department of Theoretical Biophysics, Max Planck Institute of Biophysics, Frankfurt am Main, Germany — ³Cluster of Excellence livMatS@FIT - Freiburg Center for Interactive Materials and Bioinspired Technologies, University of Freiburg, Germany — ⁴Institute for Theoretical Physics, Leipzig University, Germany — ⁵Freiburg Materials Research Center, University of Freiburg, Germany

A wealth of chemical bonds and polymers have been studied with single-molecule force spectroscopy, usually by applying a force perpendicular to the anchoring surface. However, the direction-dependence of the bond strength lacks fundamental understanding. Here we establish stereographic force spectroscopy to study the single-bond strength for various pulling angles. Surprisingly, we find that the apparent bond strength increases with increasing pulling angle relative to the anchoring surface normal, indicating a sturdy mechanical anisotropy of a chemical bond. This finding can be rationalized by a fixed pathway for the rupture of the bond, resulting in an effective projection of the applied pulling force

onto a nearly fixed rupture direction. Our study is fundamental for the molecular understanding of the role of the direction of force application in molecular adhesion and friction.

BP 15.3 Wed 10:30 H13

Rebinding kinetics from single-molecule force spectroscopy experiments close to equilibrium — •JAKOB TÓMAS BULLERJAHN¹ and GERHARD HUMMER^{1,2} — ¹Department of Theoretical Biophysics, Max Planck Institute of Biophysics, 60438 Frankfurt am Main, Germany — ²Institute of Biophysics, Goethe University Frankfurt, 60438 Frankfurt am Main, Germany

Analysis of bond rupture data from single-molecule force spectroscopy experiments commonly relies on the strong assumption that the bond dissociation process is irreversible. However, with increased spatiotemporal resolution of instruments it is now possible to observe multiple unbinding-rebinding events in a single pulling experiment. Here, we augment the theory of force-induced unbinding by explicitly taking into account rebinding kinetics, and provide approximate analytic solutions of the resulting rate equations. Furthermore, we use a short-time expansion of the exact kinetics to construct numerically efficient maximum likelihood estimators for the parameters of the force-dependent unbinding and rebinding rates, which pair well with and complement established methods, such as the analysis of rate maps. We provide an open-source implementation of the theory, evaluated for Bell-like rates, which we apply to synthetic data generated by a Gillespie stochastic simulation algorithm for time-dependent rates.

15 min. break

Invited Talk

BP 15.4 Wed 11:00 H13

The importance of water in membrane receptor function — •ANTHONY WATTS — Biochemistry Department, South Parks Road, Oxford, OX1 3QU, UK

Resolving conformational changes in membrane receptors in response to a stimulus, and capturing their functionally relevant dynamics, is very challenging. Over the years we have addressed this challenge using a range of spectroscopic approaches^{1,2,3} on functionally competent photoreceptors, often in their natural membranes⁴ or Lipodisks⁵. We have complemented this work with functional studies, mass spec characterization⁶ and very high resolution (1.07Å) crystallography^{7,8}, as well as photo-induced x-ray, free electron laser studies (XFELS), without the use of detergents and including natural lipids. This high-resolution information reveals waters and their importance in both receptor activation-desensitization and QM(SCC-DFTB)/MM MD trajectories give information about the activation process. The system studied is achearhodopsin-3 (AR3), a photoreceptor utilized widely in optogenetics despite the lack of structures. The arrangement of internal water networks is responsible for the faster photocycle compared to homologs. These insights have generic implications for other receptors. (1). Higman et al., (2011) *Angew. Chemie* 50(36):8432 (2). Dijkman et al., (2018) *Nature Comms.* 9:1710 (3). Dijkman et al., (2020) *Science Advances*, 6:33 (4). Lavington & Watts (2020) *Biophys. Rev.* 12:1287 (5). Juarez et al., (2019) *Chem. Phys. Lipids* 221:167 (6). Hoi et al., (2021) *Nano Letters*, 21(7):2824 (7). Axford et al., (2022) *Acta Cryst D*78:52 (8). Juarez et al (2021) *Nature Comms.* 12:629

BP 15.5 Wed 11:30 H13

Exploring the molecular details of the role of methylation and ATP in chemotaxis signaling — •HIMANSHU JOSHI¹ and MEHER PRAKASH² — ¹Jawaharlal Nehru Centre for Advanced Scientific Research (JNCASR), Bengaluru, 560064 — ²EPFL EssentialTech Center, Switzerland

Chemotaxis is the movement of bacteria in response to the surrounding chemical concentration gradients. Bacteria perform runs and tumbles due to the anti-clockwise and clockwise rotation of their flagella depending on the type and gradient of chemical concentration. The molecular concentration sensed by the binding of nutrients is transmitted across the membrane and over 200 Angstroms for a kinase domain actuation. The question then arises as to what is the molecular basis of this signal propagation? Performing long all atom molecular dynamics (MD) simulations on the CryoEM structures that have become recently available, we study the plausible interactions between the methylation and the ATP hydrolysis. Our study, the MD first one which includes methylation and ATP, finds several correlations with the experimental data such as the matching contacts among the dynamic domains, the intermediate state, higher gamma-phosphate coordination by the methylated protein. The results on this very important signaling mechanism are encouraging, a validation which is non-trivial when performing MD on an extended spatial or time scale or with a new class of proteins (fibrillar in this case), to perform further MD studies on this large protein complex.

BP 15.6 Wed 11:45 H13

Identifying the Functional Dynamics in Proteins - Divide and Conquer the Feature Space — •DANIEL NAGEL, GEORG DIEZ, and GERHARD STOCK — Biomolecular Dynamics, Institute of Physics, Albert-Ludwigs-Universität, 79104 Freiburg, Germany

The function of proteins is closely linked to their conformational changes. To support experiments, molecular dynamics simulations allow high spatiotemporal resolution while generating large amounts of data. To model and interpret them, it is essential to identify suitable features, such as backbone dihedral angles or interresidual distances. However, in this high-dimensional feature space—in addition to the motion of interest—one finds uncorrelated motions described by small subsets of features, which poses a difficult challenge for the subsequent dimensionality reduction and understanding of the underlying biological process.

In the following we present an effective and scalable correlation-based feature selection method (MoSAIC) that identifies functional dynamics in the feature space and separates it from noise in order to facilitate the further analysis. To demonstrate the different application purposes, we adopt the unsupervised method to systems of various complexity.

G. Diez, D. Nagel, and G. Stock, Correlation-based feature selection to identify functional dynamics in proteins, arxiv:2204.02770, 2022

BP 15.7 Wed 12:00 H13

Understanding friction in ligand protein systems — •MIRIAM JÄGER¹, WANHAO CAI², JAKOB T. BULLERJAHN³, THORSTEN HUGEL², STEFFEN WOLF¹, and BIZAN N. BALZER² — ¹Biomolecular Dynamics, Institute of Physics, University of Freiburg, Hermann-Herder-Str. 3, 79104 Freiburg, Germany — ²Institute of Physical Chemistry, University of Freiburg, Albertstr. 21, 79104 Freiburg, Germany — ³Department of Theoretical Biophysics, Max Planck Institute of Biophysics, 60438 Frankfurt am Main, Germany

Both experiments and simulations have shown the importance of friction in biomolecular system dynamics. To gain a deeper understanding of the connection between directional forces and friction, we study the streptavidin-biotin complex in a combination of stereographic force spectroscopy experiments and biased molecular dynamics simulations. While experiments show an increasing mean rupture force and rupture force variance with steeper pulling angles, the simulations display similar internal friction, but an anisotropy in the free energy barriers. Based on the simulation results, we propose that this anisotropy in barriers manifests itself in experiments as the increase in friction. This effect can be viewed as anisotropic friction.

BP 16: Networks: From Topology to Dynamics (joint session SOE/BP/DY)

Time: Wednesday 10:15–12:45

Location: H11

See SOE 12 for details of this session.

BP 17: Membranes and Vesicles

Time: Wednesday 15:00–17:00

Location: H13

BP 17.1 Wed 15:00 H13

Lipid domain diffusion in confined geometry — •CLAUDIA STEINEM, NIKOLAS K. TEIWES, and OLE M. SCHÜTTE — Georg-August Universität, Göttingen, Germany

Pore-spanning membranes (PSMs) are well-suited to investigate lipid domain diffusion. Recent findings have highlighted the dynamic nature of such lipid domains in the plasma membrane of mammalian cells and the key role of the underlying cytoskeleton network in confining their diffusion. We established PSMs

composed of DOPC, sphingomyelin, and cholesterol with co-existing liquid ordered (lo)/liquid disordered (ld) domains on silicon substrates with micrometer-sized pores to investigate the diffusion of lo-domains confined in the freestanding parts of the PSMs. We compared the lo-domains in the artificial PSMs with PSMs derived from spreading giant plasma membrane vesicles (GPMVs) obtained from HEK-293 cells. In both cases, mobile ordered domains are visualized by fluorescence microscopy. From the trajectories of the individual mobile domains, the MSD is determined, which provides the diffusion constants as a

function of domain size. The analysis reveals that the domains' diffusion constants are slowed down by orders of magnitude due to the confinement in the PSM, where the drag force is governed by both the friction in the bilayer and the coupling to the aqueous phase compared to the unrestricted case. From the analysis, the membrane surface viscosity can be extracted, which is by a factor of four smaller in case of the naturally derived membranes compared to the artificial ones, which can be explained in terms of the large protein content in the GPMV-derived membranes.

BP 17.2 Wed 15:15 H13

SAXS measurements of photoswitching in azobenzene lipid vesicles — MARTINA OBER¹, ADRIAN MÜLLER-DEKU², OLIVER THORN-SESHOLD², and •BERT NICKEL¹ — ¹Faculty of Physics and CeNS, Ludwig-Maximilians-Universität München, Geschwister-Scholl-Platz 1, Munich 80539, Germany — ²Department of Pharmacy, Ludwig-Maximilians-Universität München, Butenandtstraße 5-13, Munich 81377, Germany,

We study the switching of photoresponsive lipids that allow for precise and reversible manipulation of membrane shape, permeability, and fluidity. Though these macroscopic responses are clear, it is unclear how large the changes of trans/cis ratio are, and whether they can be improved. Here, we use small-angle X-ray scattering to measure the thickness of photoswitchable lipid membranes, and we correlate lipid bilayer thickness to trans/cis ratios [1]. This reveals an unexpected dependency of photoswitching ratio upon aqueous phase composition. In buffer with ionic strength, we observe thickness variations twice as large as previously observed. Furthermore, soft X-rays can quantitatively isomerise photolipid membranes to the all-trans state; enabling X-ray-based membrane control. High energy X-rays do not influence the state of the photoswitches, presumably because they deposit less dose in the sample.

[1] M. Ober et al, *Nanophotonics* 2022; 11(10): 2361, DOI <https://doi.org/10.1515/nanoph-2022-0053>

BP 17.3 Wed 15:30 H13

Buoyant adhered vesicles in finite-range membrane-substrate interactions — •LUCIA WESENER and MARCUS MÜLLER — Georg-August University, Göttingen, Germany

Constructing switchable interlayers between soft, biological objects and hard solids is a major challenge to dynamically regulate interface interactions. Here, we focus on the adhesion of lipid vesicles on bio-inspired polymer substrates. Experiments on the adhesion of liquid droplets or vesicles on switchable surfaces often facilitate contact with the substrate by a density difference. But when compared to theoretical expectations, this key experimental characteristic as well as the finite range of the membrane-substrate interaction have mostly been neglected. Thus, we systematically studied the adhesion of axially symmetric vesicles for finite-range membrane-substrate interaction and buoyancy through simulations. We investigated the adhesion transition of vesicles in the absence of thermal fluctuations. For downward buoyancy, vesicles sediment onto the substrate and there is no mean-field adhesion transition. Whereas for upward buoyancy, adhered vesicles are metastable at best. A proper adhesion transition can only occur at zero buoyancy. Moreover, length scales such as the capillary length, extrapolation length, and curvature-decay scale exhibit a pronounced dependence on interaction range and buoyancy and should not be used uninformed. Whereas these characteristics significantly modified the adhesion diagram, the local transversality condition - relating contact curvature to adhesion strength and vesicle's bending rigidity - remains accurate in the presence of moderate buoyancy.

BP 17.4 Wed 15:45 H13

Seaweed and dendritic domains of erucic acid monolayers — •FLORIAN GELLERT, HEIKO AHRENS, HARM WULFF, and CHRISTIANE A. HELM — Institute of Physics, University of Greifswald, Germany

Nucleation and growth of domains in the liquid expanded/liquid condensed phase transition in monolayers of erucic acid at the air/water interface is studied with a Brewster Angle Microscope. With increase of the compression speed of the monolayer, the growth mode of the domains changes from seaweed to dendritic. Seaweed domains have broad tips, and wide, variable side branch spacing. Dendritic domains have narrower tips, and small, well-defined side branch spacing and a larger fractal dimension. The domains have different growth mechanisms: seaweed domains grow by surface diffusion while dendrite domains grow

by diffusion in the subphase (Marangoni effect). The hydrodynamic models of domain growth will be discussed.

15 min. break

BP 17.5 Wed 16:15 H13

Asymmetric membranes, chemical potentials and homeostasis — •MARTIN GIRARD — Max-Planck-Institut für Polymerforschung

The properties of membranes in cells are tightly regulated. For instance, Sineski clearly established that E. Coli cells maintain a viscosity of around 2 poise, which is achieved by modulating the chemical composition of the membrane. How cells choose to alter this composition is not obvious, and has been associated with various controversies over the years.

I have recently introduced usage of chemical potential in computer simulations as a proxy for membrane homeostasis in cells. In coarse-grained simulations, this results in surprisingly good agreement between trends measured in cells and simulation results. I have also shown that this model can be used as a proxy for flippase proteins, and thus enables simulations of asymmetric membranes. Using this model, I will show that imposing asymmetries in membranes can result in surprising behavior. For example, that cholesterol concentration can become correlated with the presence of unsaturated lipids, in accord with experimental measurements. I will discuss the biological implications of these results.

BP 17.6 Wed 16:30 H13

Coherent Diffractive Imaging of Synaptic Vesicles by Femtosecond FEL pulses — •CHARLOTTE NEUHAUS¹, JETTE ALFKEN¹, MORITZ STAMMER¹, SPB TEAM², MARCELO GANZELLA³, REINHARD JAHN³, and TIM SALDITT¹ — ¹Georg-August-Universität, Institute for X-ray Physics, Friedrich-Hund-Platz 1, 37077 Göttingen — ²European XFEL, Holzkoppel 4, 22869, Schenefeld, Germany — ³Department of Neurobiology, Max-Planck-Institut für Multidisziplinäre Sciences, Am Faßberg 11, 37077, Göttingen, Germany

Synaptic Vesicles (SVs) are secretory organelles which store neurotransmitters in presynaptic nerve endings. Due to the small size of vesicles ($R \approx 20$ nm), a high spatial resolution is needed to gain more insights into the structure and structural dynamics of SVs, including functional lipid and protein components. To this end, solution SAXS experiments were previously used, yielding information about the average electron density of SVs. However, many of the relevant structural properties and parameters are screened by ensemble averaging, given the substantial polydispersity of SVs and unavoidable contaminations in the preparations. To overcome these limitations, we have carried out serial diffraction experiments on single vesicles (including lipid vesicles, proteoliposomes and SVs) delivered by an aerosol jet into a nano-focused X-ray Free Electron Laser (XFEL) beam. By the 'diffraction before destroy' principle, the individual vesicles can be probed without radiation damage. Thousands of diffraction patterns can now be analyzed and reconstructed. We report these experiments and preliminary results (data analysis still ongoing).

BP 17.7 Wed 16:45 H13

Dynamics of active vesicles — PRIYANKA IYER, MASOUD HOORE, THORSTEN AUTH, GERHARD GOMPPER, and •DMITRY FEDOSOV — Institute of Biological Information Processing and Institute for Advanced Simulation, Forschungszentrum Juelich, Juelich 52425, Germany

Biological cells are able to generate intricate structures and respond to external stimuli, sculpting their membrane from inside. Simplified biomimetic systems can aid in understanding the principles which govern these shape changes and elucidate the response of the cell membrane under strong deformations. We employ simulations of vesicles enclosing active self-propelled particles to investigate different non-equilibrium shapes with tether-like protrusions and highly branched, dendritic structures. Furthermore, adhesive interactions between active particles and the membrane result in highly branched tethers at low particle activity, where the system exhibits 'pseudo-equilibrium' shapes. The resulting membrane fluctuations present anomalous behaviour at high adhesive strengths, as they show an initial decrease with increasing activity. The active particles show ordering at the membrane surface which initially increases with activity and then decreases. The obtained state diagram characterizes shapes of active vesicles for various conditions applied.

BP 18: Biomaterials (joint session BP/PPP)

Time: Wednesday 15:00–17:30

Location: H15

Invited Talk

BP 18.1 Wed 15:00 H15

Bottom-up molecular control of biomimetic hydrogels — •KERSTIN G. BLANK — Johannes Kepler University, Institute of Experimental Physics, Altenberger Str. 69, 4040 Linz, Austria

The development of biomimetic hydrogels has greatly facilitated fundamental studies aimed at understanding cellular mechanosensing and mechanotransduction processes. It is now widely accepted that cells sense the elastic and viscoelastic properties of their surroundings and respond to these properties via a

range of different mechanisms. It is still unknown, however, how cells determine these material properties. Hydrogels are usually characterized as bulk samples while cells interact with these materials in a highly localized manner via specific receptor-ligand interactions. It is thus essential to adopt the cellular point of view and establish a link between microscopic and macroscopic material properties. Towards this goal, we utilize biomimetic hydrogels consisting of mechanically characterized synthetic polymers and extracellular matrix-inspired peptides that serve as physical crosslinks. Using selected examples, we show how crosslink thermodynamics, kinetics and mechanics as well as network topology affect the linear and non-linear viscoelastic properties of molecularly programmed hydrogels. In particular, we highlight that both individual crosslink properties and network topology affect network stress relaxation and show how molecular bond rupture correlates with bulk material failure. Our modular hydrogel system allows for tuning different parameters independently and thus serves as an excellent platform for disentangling the roles of different material properties on cellular responses.

BP 18.2 Wed 15:30 H15

The role of protein constriction in the fission of membrane tubes — •RUSSELL SPENCER and MARCUS MÜLLER — Georg-August Universität Göttingen, Institute for Theoretical Physics, 37077 Göttingen, Germany

Membrane remodelling, such as fusion and fission, is involved in a variety of basic, cellular processes. When unaided, the free energy barriers for such remodelling can be prohibitively high, so biological systems employ proteins as catalysts. This work investigates the influence of proteins, such as dynamin, which constrict membrane tubes in order to lower the barrier to fission. We are particularly interested in their role in double-membrane fission as it occurs in mitochondrial division. This work employs self-consistent field theory and utilizes the string method to find the Minimum Free Energy Path (MFEP) in order to determine the most likely pathway for the transition. In addition to lowering the free energy barrier, constriction of the tubes also affects the dominant transition pathway. This work explores the interplay between membrane tension and constriction and the effects that these influences have on fission mechanisms of single and double membrane tubes.

BP 18.3 Wed 15:45 H15

Rate-Independent Hysteretic Energy Dissipation in Collagen Fibrils — ROBERT MAGERLE, •PAUL ZECH, MARTIN DEHNERT, ALEXANDRA BENDIXEN, and ANDREAS OTTO — Fakultät für Naturwissenschaften, Technische Universität Chemnitz, 09107 Chemnitz, Germany

Nanoindentation data measured with an atomic force microscope on hydrated collagen fibrils above the glass transition, display a rate-independent hysteresis with return point memory. It is caused by the interplay of elastoplastic deformation during tip indentation followed by elastocapillary recovery of the indent during tip retraction. This previously unknown energy dissipation mechanism dominates at slow indentation rates, where viscous friction is negligible. A generic hysteresis model, based on force-distance data measured during one approach-retract cycle, predicts the force (output) for arbitrary indentation trajectories (input). This model describes collagen fibrils' elastic as well as their dissipative nanomechanical properties with high fidelity for a large range of tip velocities and indentation amplitudes.

15 min. break

BP 18.4 Wed 16:15 H15

Partition complex structure arises from sliding and bridging — •LARA CONNOLLEY and SEAN MURRAY — Max Planck Institute for Terrestrial Microbiology, Marburg, Germany

Chromosome segregation is vital for cell replication and in many bacteria is controlled by the ParABS system. A key part of this machinery is the association of ParB proteins to the parS-containing centromeric region to form the partition complex. Despite much work, the formation and structure of this nucleoprotein complex has remained unclear. However, it was recently discovered that CTP binding allows ParB dimers to entrap and slide along the DNA, as well as leading to more efficient condensation through ParB-ParB-mediated DNA bridging. Here, we use stiff polymer simulations to show how these properties of sliding and bridging can explain partition complex formation. We find that dynamic ParB bridges condense the DNA through the formation of two structures, hairpins and helices. In separate stochastic simulations, we show that ParB sliding accurately predicts the experimentally measured multi-peaked binding profile of *Caulobacter crescentus*, indicating that bridging and other potential roadblocks are sufficiently short-lived that they do not hinder ParB spreading. Indeed, upon coupling the two simulation frameworks into a unified sliding and bridging polymer model, we find that short lived ParB bridges do not hinder ParB sliding from the parS sites, and can reproduce the binding profile of ParB as well as the overall condensation of the nucleoprotein complex. Overall, our model clarifies the mechanism of partition complex formation and predicts its fine structure.

BP 18.5 Wed 16:30 H15

Single-chain and condensed-state behavior of hnRNPA1 from molecular simulations — •D. JANKA BAUER¹, LUKAS STELZL^{1,2}, and ARASH NIKOUBASHMAN¹ — ¹Institute of Physics, Johannes Gutenberg University Mainz, Germany — ²Biocenter, Institute of Molecular Physiology, Johannes Gutenberg University Mainz, Germany

Intrinsically disordered proteins (IDPs) are essential components for the formation of membraneless organelles, which play key functional and regulatory roles within biological systems. These complex assemblies form and dissolve spontaneously over time via liquid-liquid phase separation of IDPs. Mutations in their amino acid sequence can alter their phase behavior, which has been linked to the emergence of cancer and neurodegenerative diseases. In this work, we study the conformations and phase behavior of a low-complexity domain of heterogeneous nuclear ribonucleoprotein A1 (hnRNPA1), using coarse-grained molecular simulations. We systematically analyze how the single-chain and condensed-state behavior are affected by the number of aromatic residues within the examined sequences. We find a significant compaction of the chains and an increase in the critical temperature with increasing number of aromatic residues within the IDPs. Both observations strongly support the hypothesis that aromatic residues play a dominant role for driving condensation, which is further corroborated by a detailed analysis of the intermolecular contacts. By establishing quantitative comparisons to the experimental phase behavior, we start to critically assess the reliability of coarse-grained IDP models.

BP 18.6 Wed 16:45 H15

Water flow elastography for minimal invasive surgery — •PAUL KALWA and TILMAN SCHÄFFER — University of Tübingen, Germany

Mechanical properties of tissue are of great interest for physicians to differentiate healthy from malign tissue, to determine the status or extent of a disease, and to investigate tissue ageing. The measurement of these properties is therefore a helpful tool for diagnosis. Many elastography techniques have been established and are used in medicine today. However, most of these techniques are not applicable in minimal invasive surgery (MIS), because there the size of probes is limited to a few millimeters and the handling is restricted. We introduce water flow elastography, a novel technique that benefits from a small and inexpensive probe. This technique uses a specialized probe to flow pressurized water against the sample surface, thereby inducing a local indentation. The volume of the indentation, which is measured with a flow meter, is used to quantify the Young's modulus with the help of finite element simulations. We measure the Young's modulus of silicone samples and porcine organs and validate the results with a commercial testing machine, finding agreement within 15%. We also discuss the suitability of this technique for the determination of viscoelastic tissue properties and for the application in endoscopes for MIS in the future.

BP 18.7 Wed 17:00 H15

Turning the Corner on the Image Method in Linear Elasticity and Low-Reynolds-Number Hydrodynamics — •TYLER LUTZ, LUKAS FISCHER, SONJA RICHTER, and ANDREAS MENZEL — Institut für Physik, Otto-von-Guericke-Universität Magdeburg, Universitätsplatz 2, 39106 Magdeburg

In both linear elasticity and low-Reynolds-number hydrodynamics, extensions of the image method—familiar from elementary electrostatics—have been developed to deduce the displacement (resp. velocity) fields arising from point forces applied in the vicinity of a single, flat, infinitely extended boundary. In this work, we assess the applicability of these methods to domains described by multiple, mutually orthogonal boundaries in 2 and 3 dimensions. Already in the case of a single flat boundary, the necessary image forces depend on the specific boundary conditions considered; the images become progressively more complex as one goes from free-slip to no-slip and stress-free surfaces. By iterating the image method for forces near corners or edges, we explicitly show that this method fails to generate a self-consistent image if any more than one boundary is anything other than a free-slip surface. For the situations in which the image method may be successfully applied, we explicitly construct and survey the qualitative features of the point-force Green's function near corners.

BP 18.8 Wed 17:15 H15

Adsorption of laminin and cellular response of neurons and glial cells on ion implanted titania nanotube scaffolds — •JAN FRENZEL^{1,2,3}, ASTRID KUPFERER^{1,2}, MAREIKE ZINK³, and STEFAN G. MAYR^{1,2} — ¹Leibniz Institute of Surface Engineering (IOM), Permoserstraße 15, 04318 Leipzig, Germany — ²Division of Surface Physics, Department of Physics and Earth Sciences, Linnéstraße 5, 04103 Leipzig, Germany — ³Research Group Biotechnology and Biomedicine, Department of Physics and Earth Sciences, Linnéstraße 5, 04103 Leipzig, Germany

Brain-machine interfaces are used in a wide spectrum of neuroscience, as for time-resolved sensing of neural activities and for tackling neurodegenerative diseases. Currently established cultivation platforms, including cellulose filters, often result in loss of long-term adhesion, rejection reaction and glial scarring or do not allow for electrical contact due to their insulating properties. As we demonstrate, ion implanted titania nanotube scaffolds (TNS) are a promising

candidate to overcome these issues, since they combine a high biocompatibility with a sufficient large electrical conductivity. In our experiments, we explain how ion implantation induced changes of surface characteristics affect the adsorption of laminin and the viability and adhesion of neurons and glial cells. We link the

hindered laminin adsorption due to implantation to the shrinkage of tube diameter and rise of zeta potential. The stable and high neuron viability on all TNS but suppressed glial cell formation of implanted TNS gives rise for a potential interface material. Funding by SMWK (100331694) is gratefully acknowledged.

BP 19: Cell Mechanics 2

Time: Wednesday 15:00–17:15

Location: H16

BP 19.1 Wed 15:00 H16

Light, proteins, and shape: exploiting protein pattern formation for light-controlled oocyte deformations — JINGHUI LIU², •TOM BURKART¹, ALEXANDER ZIEPKE¹, ERWIN FREY¹, and NIKTA FAKHRI² — ¹Arnold Sommerfeld Center for Theoretical Physics (ASC) and Center for NanoScience (CeNS), Department of Physics, Ludwig-Maximilians-Universität München, Munich, Germany — ²Department of Physics, Massachusetts Institute of Technology, Cambridge, MA 02139

To coordinate shape deformations, in particular cell division, cells rely on chemical reaction networks that process spatial and temporal cues, such as cell cycle signals, and control the mechanical activity that generates the required deformation. In starfish oocytes, a Rho-GTP protein pattern on the cell membrane regulates actomyosin contractility which induces large-scale cell deformations during meiotic anaphase. By engineering optogenetic activators of Rho-GTP, the native control mechanism can be hijacked to manually trigger the actomyosin contractility and thereby deform the oocyte even before entering meiotic anaphase. We study how such an artificial guiding cue is processed by the mechanochemical machinery in starfish oocytes. We combine simulations of the protein reaction-diffusion dynamics with the dynamic shape deformation of the oocyte to predict spatio-temporal light activation patterns that produce custom cell deformations. Our results contribute to the development of an overarching theoretical framework that allows to study and design minimal artificial cells capable of self-regulated and externally controlled shape changes.

BP 19.2 Wed 15:15 H16

Modeling Cell Shape and Forces on Structured Environments in Three Dimensions — •RABEA LINK and ULRICH SEBASTIAN SCHWARZ — Institute for Theoretical Physics, University Heidelberg, Germany

Micropatterns are a widely used tool to standardize the mechanical environment single cells or cell collectives experience in experiments. In recent years, microstructures manufactured with direct laser writing have tremendously increased the design possibilities of structured environments for cells. We model the shape, spreading dynamics and forces of a single cell with external adhesive cues using a three-dimensional compartmentalized Cellular Potts Model on 2D micropatterns and in 3D structured environments. This allows us to investigate the influence of the nucleus on the cell shape and spreading dynamics. In addition, we compare the cell shapes obtained by the Cellular Potts Model with the minimal energy shape of a surface under tension in the same mechanical environment and with experimental results.

BP 19.3 Wed 15:30 H16

Exploiting nonlinear elasticity for robust mechanosensation in disordered fiber networks — ESTELLE BERTHIER¹, •PIERRE RONCERAY², and CHASE BROEDERSZ^{1,3} — ¹Arnold-Sommerfeld-Center for Theoretical Physics and Center for NanoScience, Ludwig-Maximilians-Universität München, Germany — ²Centre Turing and Centre de Physique Théorique, Université Aix-Marseille, France — ³Department of Physics and Astronomy, Vrije Universiteit Amsterdam, Netherlands

Cell behavior is steered by guiding cues from their surrounding extracellular environment. Cells anchor to the extracellular matrix (ECM) and perform mechanosensation: they probe their surrounding's mechanical response and regulate their behavior according to the stiffness they sense. Yet, the robustness of cellular mechanosensing is physically limited by the ECM intrinsic disorder and complex mechanical response of both the network and its constituents. Thus, it remains what strategies cells employ to accurately interpret mechanical guiding cues of such a heterogeneous environment.

Using a theoretical framework for disordered fiber networks, we evaluate the mechanical information cell can obtain by performing local measurements. We show that the signal-to-noise ratio of stiffness measurements increases dramatically in the nonlinear regime: the measurements become insensitive to local structural fluctuations of the network. We provide a scaling argument supporting that the local measurement effectively behaves as a sensory device of larger size.

BP 19.4 Wed 15:45 H16

Competition between cell deformation and depletion force: Quantified by 3D image analysis of red blood cell doublets — •MEHRNAZ BABAKI^{1,2}, MINNE PAUL LETTINGA^{1,2}, and DMITRY FEDOSOV³ — ¹Biomacromolecular Systems and Processes (IBI-4), Forschungszentrum Jülich GmbH, Jülich, Germany —

²Laboratory for Soft Matter and Biophysics, KU Leuven, Leuven, Belgium —

³Theoretical Physics of Living Matter (IBI-5/IAS-2), Forschungszentrum Jülich GmbH, Jülich, Germany

Understanding cell deformation associated with an external force is the key to a full comprehension of the behaviour of cells under mechanical loading. Red Blood Cells (RBCs) are an extreme example of deformable cells. The high deformability of RBCs influences the blood flow and blood circulation in both physiological and pathophysiological conditions as well as RBC aggregation

We investigated the deformation of RBCs using analysis of the 3D reconstructed confocal images of the RBCs in aggregated doublets. Here we use non-absorbing rod-like particles, causing depletion attraction. Our analysis yields the change in the bending energy of RBCs in a doublet, as well as the change in the depletion energy.

We identified a sequence of configurational transitions of RBC doublets upon increasing rod-like particles concentration, thus maximizing the free volume available for the depletants at the cost of deformation energy. We compared the experimental results with simulations, where we explored the different energy contributions to deformation, as well as the stability of RBC doublets at low depletion force.

15 min. break

BP 19.5 Wed 16:15 H16

Butterfly scale morphogenesis: Wrinkling on the micron scale — •JAN TOTZ¹, ANTHONY McDOUGAL², and MATHIAS KOLLE² — ¹Departments of Mathematics and Mechanical Engineering, Massachusetts Institute of Technology, Cambridge MA 02139, USA — ²Department of Mechanical Engineering, Massachusetts Institute of Technology, Cambridge MA 02139, USA

Micron-scale surface modulations such as wrinkles or folds underly a number of modern engineering applications, such as photonic structures in photovoltaics and flexible metasurfaces. Controlled and precise fabrication of these modulations is a challenge for human manufacturing techniques. In stark contrast, biological systems robustly utilize morphological changes in their developmental program to create multi-germ bodies, hairs and scales on spatial scales which would be costly to replicate with human manufacturing. In this talk I will present recent measurements of in-vivo butterfly scale development exhibiting wrinkling. The observations are rationalized with a numerical finite element simulation and a parsimonious continuum mechanics model.

BP 19.6 Wed 16:30 H16

Active morphogenesis of patterned epithelial shells — •DIANA KHOROMSKAIA¹ and GUILLAUME SALBREUX^{1,2} — ¹The Francis Crick Institute, 1 Midland Road, NW1 1AT, United Kingdom — ²University of Geneva, Quai Ernest Ansermet 30, 1205 Genève, Switzerland

Shape transformations of epithelial tissues in three dimensions, which are crucial for embryonic development or in vitro organoid growth, can result from active forces generated within the cytoskeleton of the epithelial cells. How the interplay of local differential tensions with tissue geometry and with external forces results in tissue-scale morphogenesis remains an open question. Here, we describe epithelial sheets as active viscoelastic surfaces and study their deformation under patterned internal tensions and bending moments. In addition to isotropic effects, we take into account nematic alignment in the plane of the tissue, which gives rise to shape-dependent, anisotropic active tensions and bending moments. We present phase diagrams of the mechanical equilibrium shapes of pre-patterned closed shells and explore their dynamical deformations. Our results show that a combination of nematic alignment and gradients in internal tensions and bending moments is sufficient to reproduce basic building blocks of epithelial morphogenesis, including fold formation, budding, neck formation, flattening, and tubulation.

BP 19.7 Wed 16:45 H16

Condensed topological defects in compressible active nematics — •IVAN MARYSHEV¹, TIMO KRÜGER¹, and ERWIN FREY^{1,2} — ¹LMU, München, Germany — ²Max Planck School Matter to Life, München, Germany

So far, topological defects with plus/minus 1/2 charges have been considered to be characteristic features of homogeneous active nematics. Phase-separated systems, in turn, have been known for the formation of dense nematic bands. Here, we use the agent-based model for weakly-aligning self-propelled filaments and, for the first time, demonstrate that phase-separated active nematics form -1/2

defects of a new kind. In contrast to the homogeneous case, these new defects correspond to high-density regions and coexist with bending bands. We also observe filamentous arc ejections - formations of lateral arcuate structures that separate from the band's bulk and move in a transverse direction. We show that the key control parameters defining the transition from the topologically charged structures to stable bands are the initial density of particles and their path persistence length. Finally, we develop hydrodynamic theory recapitulating observed phenomena.

BP 19.8 Wed 17:00 H16

Spherical harmonics analysis of in vivo force probes for tissue stress quantification — •ALEJANDRO JURADO¹, BERNHARD WALLMEYER², CHRISTOPH ENGWER², and TIMO BETZ¹ — ¹Third Institute of Physics - Biophysics, Friedrich-Hund-Platz 1, University of Göttingen — ²Institute of Cell Biology, ZMBE, Von-Esmarch-Str. 56, University of Münster

The mechanical analysis of tissue motion offers a new insight in key biological processes such as embryogenesis, cancer cell invasion and wound healing.

Force quantification at this scale has been drastically improved with the emergence of *in vivo* sensors such as oil droplets or hydrogel beads which open up the possibility of non-invasive studies. Many approaches in recent literature rely on numerical processes to iteratively reconstruct the surface of measured beads, which can be computationally expensive and rendering results that are difficult to interpret. In this work we present the analysis of arbitrarily deformed beads based on the expansion in Spherical Harmonics in a Python custom software. We exploit the fast converging algorithms offered by SHTools [1] to reduce the great complexity of three-dimensional radial deformations to an affordable harmonic coefficient table which is directly fed into an analytical solution of the Navier-Cauchy equation. As a first proof-of-concept we show the performance of the software with polyacrylamide beads injected into zebrafish embryo at early developmental stages, in which the stress field could help understanding the processes of epiboly and shield formation.

[1] Wiczczonek M.A., Meschede M., 2018. *Geochem. Geophys. Geosyst.* 19(8), 2574-2592

BP 20: Active Matter 4 (joint session DY/BP/PPP)

Time: Wednesday 15:00–17:30

Location: H18

See DY 31 for details of this session.

BP 21: Members' Assembly

Time: Wednesday 18:00–19:00

Location: H15

All members of the Biological Physics Division are invited to participate.

BP 22: Migration and Multicellular Systems

Time: Thursday 9:30–12:15

Location: H15

Invited Talk

BP 22.1 Thu 9:30 H15

Cell and tissue mechano-plasticity in development — •VERENA RUPRECHT — Centre for Genomic Regulation (CRG), Barcelona, Spain

The development of a single fertilised cell into an embryo is a highly dynamic process that establishes the structural and functional architecture of the organism. The building of complex multicellular structures fundamentally emerges from the spatio-temporal coordination of dynamic behaviours at the single cell level. How this multi-scale process occurs with high fidelity and robustness is still a major open question. Here I will discuss how embryonic stem cells are able to sense and adapt to mechanical shape deformations in their 3D tissue environment. I will explore the function of the cell nucleus as an intracellular mechano-sensor and how it can act as a non-genetic controller of cell mechanics and migration plasticity. I will further discuss how cellular error correction is established in the earliest stages of embryo development by mechanical cell co-operation that promotes the efficient phagocytic clearance of aberrant apoptotic cells. Theoretical modelling of mechanical force fluctuations at the cell cortex and protrusive force generation in cell collectives will be presented to mechanistically describe the emergence of mechano-plasticity at the single cell and tissue level mediating robust embryo development.

BP 22.2 Thu 10:00 H15

Active T1 transitions in cellular networks — •CHARLIE DUCLUT^{1,2}, JORIS PAIJMANS¹, MANDAR M. INAMDAR³, CARL D. MODES^{4,5,6}, and FRANK JÜLICHER^{1,5,6} — ¹Max Planck Institute for the Physics of Complex Systems, Nöthnitzer Str. 8, 01187 Dresden, Germany — ²Université Paris Cité, Laboratoire Matière et Systèmes Complexes, Paris, France — ³Department of Civil Engineering, Indian Institute of Technology Bombay, Powai, Mumbai 400076, India — ⁴Max Planck Institute for Molecular Cell Biology and Genetics (MPI-CBG), Dresden 01307, Germany — ⁵enter for Systems Biology Dresden, Pfothenhauerstrasse 108, 01307 Dresden, Germany — ⁶Cluster of Excellence, Physics of Life, TU Dresden, Dresden 01307, Germany

In amorphous solids as in tissues, neighbour exchanges can relax local stresses and allow the material to flow. In this talk, I will use an anisotropic vertex model to study T1 rearrangements in polygonal cellular networks. We consider two different physical realization of the active anisotropic stresses: (i) anisotropic bond tension and (ii) anisotropic cell stress. Interestingly, the two types of active stress lead to patterns of oriented T1 transitions that are different. I will describe and explain these observations through the lens of a continuum description of the tissue as an anisotropic active material. I will furthermore discuss the energetics of the tissue and express the energy balance in terms of internal elastic energy,

mechanical work, chemical work and heat. This allows us to define active T1 transitions that can perform mechanical work while consuming chemical energy.

BP 22.3 Thu 10:15 H15

Bistability between sessile and motile solutions in a nonlinear active gel model for cell migration — •OLIVER M. DROZDOWSKI, FALCO ZIEBERT, and ULRICH S. SCHWARZ — Institute for Theoretical Physics and BioQuant, Heidelberg University, 69120 Heidelberg, Germany

Cell motility is one of the hallmarks of life and often is based on flow in the actin cytoskeleton that is driven by myosin II motors. The standard model to describe such flows is active gel theory, in which myosin II contractility enters as active stress. Recently, we have shown how to include optogenetic control in a minimal active gel model [1]. Here we ask how active gel descriptions of motility need to be modified to explain the experimental observation that a cell's state can be switched between sessile and motile. We show that such bistability emerges in active gel theory if the myosin II motors are modeled as a supercritical van der Waals fluid, including volume exclusion and short-range attraction. We present phase diagrams in cell adhesion and contractility that include sessile, bistable and motile regimes in experimentally relevant parameter ranges. Including optogenetic perturbations of contraction, as done before for a simpler model [1], we find that such external activation can be used to control cell locomotion, in agreement with recent experiments [2].

[1] O. M. Drozdowski, F. Ziebert, and U. S. Schwarz, *Phys. Rev. E* 104, 024406 (2021),

[2] A. Hadjitheodorou, et al., *Nat. Commun.* 12, 6619 (2021).

BP 22.4 Thu 10:30 H15

Rotation of an aspherical organoid within its matrix - a continuum model — •ANNE MATERNE¹, CHARLIE DUCLUT^{1,2}, and FRANK JÜLICHER^{1,3,4} — ¹Max Planck Institute for the Physics of Complex Systems, Dresden, Germany — ²Université Paris Cité, Laboratoire Matière et Systèmes Complexes, Paris, France — ³Center for Systems Biology Dresden, Dresden, Germany — ⁴Cluster of Excellence Physics of Life, TU Dresden, Germany

Organoids and other 3D *in vitro* multicellular systems have frequently been observed to display rotational motion within their matrix. Collective rotational motion can also be witnessed *in vivo*, for example in the *Drosophila* egg chamber. We propose that this motion results from cell-matrix interactions. Cells are thought to move similarly to 2D migration - however, a (near-)spherical geometry of cell clusters can lead to the observed rotation in 3D. Here, we present a

continuum mechanics description of an organoid rotating within its embedding matrix. We discuss the extreme cases of the matrix being either purely elastic or purely viscous. The organoid is considered to be a non-deformable solid with a surface polarity field, exerting traction forces on the matrix. Importantly, our study is not limited to perfectly spherical organoids but takes small shape deformations into account. This permits to distinguish between purely rotational and deformation-induced cell-matrix interactions. Our work clarifies how matrix material properties and cellular traction forces enable collective organoid rotation. Reciprocally, the rotating organoid can serve as an active rheology probe, revealing key information about the matrix properties.

15 min. break

BP 22.5 Thu 11:00 H15

Exploiting Onsager regression in passive measurements to reveal active mechanics of living systems — TILL MÜNCKER, GABRIEL KNOTZ, MATTHIAS KRÜGER, and •TIMO BETZ — Faculty of Physics, Georg-August-University Göttingen

Understanding life is arguably among the most complex scientific problems faced in modern research. From a physics perspective, living systems are complex dynamic entities that operate far from thermodynamic equilibrium. This active, non-equilibrium behaviour, with its constant hunger for energy, allows life to overcome the dispersing forces of entropy, and hence drives cellular organisation and dynamics at the micrometer scale. Unfortunately, most analysis methods provided by the powerful toolbox of statistical mechanics cannot be used in such non-equilibrium situations, forcing researchers to use sophisticated and often invasive approaches to study the mechanistic processes inside living organisms. Inspired by Onsager's regression hypothesis, we introduce here a Mean Back Relaxation (MBR) observable, which detects active motion in purely passive measurements of particle fluctuations. The MBR, which is based on three point probabilities, is theoretically and experimentally shown to exhibit markers of non-equilibrium, i.e., of detailed balance breaking dynamics. We furthermore observe an astonishing relation between the MBR and the effective non-equilibrium energy in living cellular systems. This is used to successfully predict the viscoelastic response function and the complex shear modulus from a purely passive approach, hence opening the door for rapid and simple passive mechanics measurements even in active systems.

BP 22.6 Thu 11:15 H15

Redirecting early embryogenesis of the model organism *Caenorhabditis elegans* via altered mechanical cues — •VINCENT BORNE and MATTHIAS WEISS — Experimental Physics I, University of Bayreuth, Universitätsstr. 30, D-95447 Bayreuth, Germany

During early development, somatic and germline precursor cells of the model organism *Caenorhabditis elegans* undergo an apparently predetermined and robust division scheme, suggesting early embryogenesis to run on autopilot. While the role of biochemical signaling in this process has long been recognized, the influence of mechanical forces for proper cell arrangement until gastrulation has only recently been revealed. Aiming to further explore, how mechanical cues contribute to proper embryogenesis, we have challenged the natural development at early stages via laser microsurgery and physical compression. As a result, we were able to significantly perturb the embryonic division scheme with both approaches, leading to catastrophic failures of cell divisions. While defects introduced by laser ablation remained mostly restricted to cells that had been challenged, compression frequently resulted in a global perturbation: Cytokinesis was compromised, leading to multinucleated cells or even a syncytium state in which nuclei kept on dividing up to stages of 60 nuclei or more with similar timing characteristics as observed in unperturbed embryos. Our data therefore underline the crucial role of properly adjusted mechanical cues during the early embryogenesis of *C. elegans*.

BP 22.7 Thu 11:30 H15

Active cell mechanisms reveal rich tissue-wide structures and dynamics in simulations — •MAXIME HUBERT¹, LOVRO NUIC², KEVIN HÖLLRING¹, and ANA-SUNČANA SMITH^{1,2} — ¹PULS group, FAU Erlangen-Nürnberg, Erlangen, Germany — ²Group for Computational Life Sciences, Ruder Bošković Institute, Zagreb, Croatia

Dissipative Particle Dynamics simulations provide a robust numerical platform of investigation to understand the dynamics of epithelial tissues. The technique allows to implement various properties at the cell level that can be related to tissue-wide structures and dynamics on various time scales, from hours to days in experiments. In this talk, we present our recent progresses in the field of epithelium numerical simulations by implementing different active ingredients that relate to the immediate neighbourhood of the cell within a tissue monolayer. We show, through comparisons with experiments performed with MDCK-II cells, that we are able to capture the formation of macroscopic compartments of the tissue, the complex relation between average cell velocity and cell density, and the rate of expansion of the tissue. These results highlight the importance of "nuclei"-based approaches along with "membrane"-based approaches in order to provide a complete numerical and mechanical perspective of epithelial tissues across various time- and length-scales.

BP 22.8 Thu 11:45 H15

'Forcing' changes in health and disease: New access into bioengineered skeletal muscle mechanics — •ARNE HOFMEIER^{1,2}, TILL MÜNCKER², FABIAN HERKENRATH¹, and TIMO BETZ^{1,2} — ¹University of Muenster, Muenster, Germany — ²University of Goettingen, Goettingen, Germany

Mechanical properties of skeletal muscles are tightly related to proper functionality, which makes experimental access to the biomechanics of skeletal muscle tissue a key requirement to advance our understanding of muscle function, development and disease. Recently devised in vitro culture chambers allow for raising 3D skeletal muscle tissues under controlled conditions and to measure global tissue force generation. However, these PDMS-based systems are inherently incompatible with high resolution microscopy. Here, we present a new chamber design that allows real-time high resolution 3D microscopy and simultaneous non-invasive quantification of global contractile forces and local tension during muscle formation for the first time. With this in hand, we observed an early mechanical homeostasis within mouse myoblast derived skeletal muscle tissues after one week of development, despite progressing myotube maturation. Additionally, we raised human in vitro skeletal muscles derived from patients suffering from Duchenne muscular dystrophy caused by loss of a functional membrane linker protein, called dystrophin. Interestingly, bioengineered Duchenne skeletal muscles displayed a disturbed mechanical homeostasis that correlates with functional impairment, suggesting a novel function of dystrophin being a molecular tension sensor and regulator.

BP 22.9 Thu 12:00 H15

On multistability and constitutive relations of cell motion on Fibronectin lanes — BEHNAM AMIRI¹, •JOHANNES CLEMENS JULIUS HEYN², JOACHIM OSKAR RÄDLER², and MARTIN FALCKE^{1,3} — ¹Max Delbrück Center for Molecular Medicine in the Helmholtz Association, Robert Rössle Str. 10, 13125 Berlin, Germany — ²Ludwig-Maximilians-Universität München (LMU), Fakultät für Physik, Geschwister-Scholl-Platz 1, 80539 München, Germany — ³Dept. of Physics, Humboldt University, Newtonstr. 15, 12489 Berlin, Germany

Migration of eukaryotic cells is a fundamental process for embryonic development, wound healing, immune responses, and tumour metastasis. Many cell types exhibit coexisting steady and oscillatory morphodynamics on flat substrates. There is, however, little quantitative understanding of how adhesion controls these dynamic states.

We study the motion of MDA-MB-231 cells on microlanes of a broad range of Fibronectin densities to address this topic and derive a biophysical model.

The experiments exhibit cells with steady or oscillatory morphodynamics and either spread or moving with spontaneous transitions between the dynamic states. Our biophysical model is based on the force balance at the protrusion edge, the noisy clutch of retrograde flow and a response function of friction and membrane drag to integrin signaling. The theory reproduces the experimentally observed cell states, characteristics of oscillations and state probabilities.

BP 23: Evolution

Time: Thursday 10:00–10:45

Location: H13

BP 23.1 Thu 10:00 H13

New phenotypes appear in an evolving population in non-Poissonian bursts — •NORA S. MARTIN¹, STEFFEN SCHAPER¹, CHICO Q. CAMARGO^{1,2}, and ARD A. LOUIS¹ — ¹Department of Physics, University of Oxford, Oxford, UK — ²Department of Computer Science, University of Exeter, Exeter, UK

For adaptive evolution, a central question is when and how frequently random mutations produce the specific rare adaptive phenotypes that have a selective advantage. A widely studied scenario is the following: a population starts with a given initial phenotype and accumulates neutral mutations, and new phenotypes are also introduced at a certain rate. Many theories implicitly assume that

new phenotypes appear through simple stochastic processes which lead to Poissonian statistics. In this contribution, we use simulations on the biophysically motivated computational genotype-phenotype map from RNA sequences to secondary structures and show that new structures appear in highly non-Poissonian “bursts”. In other words, if a new structure appears once, it is highly likely to appear multiple times in a relatively small number of generations. We show that there are several sources for this non-Poissonian behaviour, for example correlations in the mappings from genotypes to phenotypes, which may be a generic property of realistic genotype to phenotype maps. We find that these bursts can affect probabilities of fixation, especially when there are multiple competing adaptive phenotypes.

BP 23.2 Thu 10:15 H13

Proliferative advantage of specific aneuploid cells drives evolution of tumor karyotypes — •LUCIJA TOMAŠIĆ¹, IVANA BAN¹, MARIANNA TRAKALA², IVA TOLIĆ³, and NENAD PAVIN¹ — ¹Department of Physics, Faculty of Science, University of Zagreb, Croatia — ²David H. Koch Institute for Integrative Cancer Research, Howard Hughes Medical Institute, Massachusetts Institute of Technology, Cambridge, Massachusetts 02142, USA — ³Division of Molecular Biology, Ruder Bošković Institute, Croatia

Most tumors have abnormal karyotypes, which arise from mistakes during mitotic division of healthy euploid cells and evolve through numerous complex mechanisms. In a recent mouse model with high levels of chromosome mis-segregation, chromosome gains dominate over losses both in pretumor and tumor tissues, whereas tumors are characterized by gains of chromosomes 14 and 15. However, the mechanisms driving clonal selection leading to tumor karyotype evolution remain unclear. Here we show, by introducing a mathematical model based on a concept of a macro-karyotype, that tumor karyotypes can be explained by proliferation-driven evolution of aneuploid cells. In pretumor cells,

increased apoptosis and slower proliferation of cells with monosomies lead to predominant chromosome gains over losses. Tumor karyotypes with gain of one chromosome can be explained by karyotype-dependent proliferation, while for those with two chromosomes an interplay with karyotype-dependent apoptosis is an additional possible pathway. Thus, evolution of tumor-specific karyotypes requires proliferative advantage of specific aneuploid karyotypes.

BP 23.3 Thu 10:30 H13

Data-driven modeling of social interactions in bats across time scales — •FRANK SCHWEITZER¹, PAVLIN MAVRODIEV¹, and GERALD KERTH² — ¹Chair of Systems Design, ETH Zürich, Switzerland — ²Applied Zoology and Nature Conservation, University of Greifswald, Germany

The study of bat's social and foraging behavior is of great relevance to forecast the outbreak and distribution of virus induced diseases. To analyze this behavior we use a large-scale data set from two colonies of Bechstein's bats over five years. From this data, we reconstruct the social interactions of bats at three different time scales: (a) At the scale of minutes: social influence and information transfer. This leads to the formation of leader-follower pairs, where an informed individual leads an uninformed one to a roost box. (b) At the time scale of days: fission-fusion dynamics. This leads to the formation and dissolution of roosting groups of different size, composed of different individuals. (c) At the time scale of months: Emergence of social structures. This leads to the formation of communities within a colony. While the analysis of (a) requires statistical data analysis and hypothesis testing, for (b) we employ agent-based models, and for (c) social network analysis. The combination of these approaches allows us to bridge time scales in social behavior, which cannot be observed together. With our models we are able to develop the bigger picture of how social interactions feed back to long-term social structures.

BP 24: Systems Biology, Gene Expression, Signalling

Time: Thursday 10:30–12:30

Location: H16

Invited Talk

BP 24.1 Thu 10:30 H16

Actin waves as building blocks of cellular function — •CARSTEN BETA — Institute of Physics and Astronomy, University of Potsdam, Potsdam, Germany
Many cellular functions, such as motility, phagocytosis, and cell division, are driven by coherent patterns of activity in the actin cytoskeleton. Among them, actin waves are a recurrent motive that is commonly observed across different cell types. Here, we present experimental results demonstrating the rich variety of wave patterns in the actin cortex of motile amoeboid cells. We show that ring-shaped actin waves, commonly acting as precursors of macropinocytic cups, can mediate switches between different modes of motility, a pseudopod-based amoeboid mode, and a more persistent, wave-driven migratory mode, reminiscent of keratocyte motility. In multinucleate, oversized amoeboid cells, the same waves may also trigger spontaneous, cell cycle-independent cytofission events, resulting in mononucleated daughter cells of a well-defined size. We also demonstrate that a second wave pattern can coexist with the ring-shaped macropinocytic waves. It emerges in a cell-size dependent manner and consists of rapidly moving planar pulses that show typical signatures of an excitable system. Our experimental findings demonstrate the functional versatility of cortical waves patterns. They can be rationalized based on minimal reaction-diffusion models that mimic the evolution of cortical wave patterns and are coupled to a dynamic phase field to take the cell shape evolution into account. In addition, bifurcation analysis provides a more detailed understanding of how regimes of pattern coexistence may emerge.

BP 24.2 Thu 11:00 H16

Quantifying Dynamic Information Transfer in Stochastic Biochemical Networks — •ANNE-LENA MOOR^{1,2} and CHRISTOPH ZECHNER^{1,2} — ¹Max-Planck Institute of Molecular Cell Biology and Genetics, Dresden Germany — ²Center for Systems Biology, Dresden, Germany

Transmission and encoding of information are fundamental processes for the functioning of biochemical systems. Information theoretical concepts, such as the mutual information, provide a rigorous mathematical framework to study intracellular signal transmission. In many biological systems, information is encoded in the time-trajectory of signalling components as opposed to instantaneous levels. However, performing information theoretical analysis on the trajectory-level is computationally demanding. In this work, we present an effective approach to calculate mutual information between complete trajectories of biochemical components. The resulting measure provides useful insights into the dynamic information transfer through networks of chemical reactions.

BP 24.3 Thu 11:15 H16

Optimal ligand discrimination by asymmetric dimerization of interferon receptors — •PATRICK BINDER^{1,2,3}, NIKOLAS D. SCHNELLBÄCHER^{1,2}, THOMAS HÖFER^{2,3}, NILS B. BECKER^{2,3}, and ULRICH S. SCHWARZ^{1,2} — ¹Institute for Theoretical Physics, Heidelberg University, 69120 Heidelberg, Germany — ²BioQuant Center for Quantitative Biology, Heidelberg University, 69120 Heidelberg, Germany — ³Theoretical Systems Biology, German Cancer Research Center, 69120 Heidelberg, Germany

In multicellular organisms, antiviral defense is mediated by ligands. These signaling molecules are usually characterized by highly inhomogeneous distributions due to scarcity of producer cells, diffusion and localized degradation. And yet, a molecular hub of the antiviral response, the interferon I receptor (IFNAR), discriminates between ligand types by their affinity regardless of concentration. In my talk, I address the long-standing question of how a single receptor can decode robustly ligand type. I frame ligand discrimination as an information-theoretic problem and systematically compare the major classes of receptor architectures: allosteric, homodimerizing, and heterodimerizing. As a result, asymmetric heterodimers achieve the best discrimination power over the entire physiological range of local ligand concentrations, enabling sensing of ligand presence and type. IFNAR exhibits this optimal architecture, suggesting that it has evolved the optimal design to detect and separate the presence of different ligand types in a noisy environment.

15 min. break

BP 24.4 Thu 11:45 H16

Rationalizing the optimality of the Drosophila gap gene system by ab-initio derivation of optimal solutions for morphogenetic patterns — •THOMAS R. SOKOLOWSKI^{1,2}, THOMAS GREGOR^{3,4}, WILLIAM BIALEK³, and GAŠPER TKAČIK¹ — ¹IST Austria, Am Campus 1, A-4300 Klosterneuburg, Austria — ²Present Address: Frankfurt Institute for Advanced Studies, Ruth-Moufang-Str. 1, D-60438 Frankfurt, Germany — ³Department of Physics, Princeton University, Princeton, NJ 08540, U.S.A. — ⁴Institut Pasteur, Department of Developmental and Stem Cell Biology, 25 Rue du Dr. Roux, F-75015, Paris, France

Early fruit fly development is outstandingly precise in spite of the high level of stochasticity in the underlying biochemical processes. While the gap gene system driving fly embryo patterning has been shown to encode positional information optimally, the precise mechanisms that enable this remain elusive. We show that optimal solutions for the gap gene regulatory network can be obtained by optimizing a biophysically realistic spatial-stochastic embryo model, without inferring from data. Firstly, our predictions mechanistically explain how the observed developmental precision can be attained. Secondly, by exploring rich sets of optimal solutions, we elucidate the role of key components controlling early

fly patterning. To our knowledge our work provides the first successful ab-initio derivation of a nontrivial biological network in a biophysically realistic setting. Our results suggest that even though real biological networks are hard to intuit, they may represent optimal solutions to optimization problems which evolution can find.

BP 24.5 Thu 12:00 H16

Stability of gene expression patterns in developmental systems with dynamic morphogen sources — •MACIEJ MAJKA — Jagiellonian University, Krakow, Poland

In developmental systems cells determine their fate by decoding chemical signals, called morphogens. In this presentation I will address the problem of gene expression patterns stability in the systems where two diffusible morphogens affect each other production and control the growth of their own source regions. Such systems are encountered in e.g. spinal cord development, limb formation and many others. The reaction-diffusion equation with bi-stable production term is employed as a generic model for this problem. The phase transition is found, between the phase of indeterminate patterning, where region of mixed gene expression is ever growing, and the phase of travelling gene expression patterns, where two expression domains form and preserve a well-defined contact zone. A sub-class of genuinely stationary patterns is then identified, alongside the exact conditions ensuring this stability. This allows me to classify the pattern stability for all possible two-gene regulatory motifs.

BP 24.6 Thu 12:15 H16

Conditions and trade-offs to enhance protein production in synthetic bacterial communities — •MARCO MAURI^{1,3}, JEAN-LUC GOUZÉ², HIDDE DE JONG³, and EUGENIO CINQUEMANI³ — ¹Friedrich Schiller University, Jena, Germany — ²University Côte d'Azur, Sophia-Antipolis, France — ³Univ. Grenoble Alpes Inria, Grenoble, France

In nature, microorganisms occur in communities comprising a variety of mutually interacting species. To overcome the complexity of natural communities, a rapidly growing research field concerns the rational design and engineering of synthetic microbial consortia.

Here, based on a quantitative model of a prototypical synthetic microbial consortium, we discuss the precise conditions under which a consortium outperforms individual species in the production of a recombinant protein. Moreover, we identify the inherent trade-offs between productivity and efficiency of substrate utilization [1].

[1] Mauri M, Gouze' JL, de Jong H, Cinquemani E (2020) Enhanced production of heterologous proteins by a synthetic microbial community: Conditions and trade-offs. PLOS Computational Biology 16(4): e1007795. <https://doi.org/10.1371/journal.pcbi.1007795>

BP 25: Bioinspired Systems

Time: Thursday 11:00–12:00

Location: H13

BP 25.1 Thu 11:00 H13

Bottom-up assembly of synthetic cell-based tumor immune microenvironments in pancreatic cancer organoids — •OSKAR STAUFER — University of Oxford, Kennedy Institute of Rheumatology, Oxford, United Kingdom

Understanding the communication and interactions between tumour and immune cells is pivotal for holistic understanding of tumour biology and therapy. I present strategies to recreate immune cells, the defining elements of the tumor immune microenvironment (TIME), as synthetic cells by bottom-up assembly from their single molecular building blocks. The programmable synthetic cells are introduced into tumor organoids to function as lifelike leukocyte mimics presenting immune effector functions. By this, a molecularly defined artificial TIME (ART-TIME) is created inside tumor models. The central objective of this approach is to reduce the complexity of the intricate TIME composition to a comprehensible and systematic level by applying a novel bioinspired systems approach. This strategy links TIME architectures to cancer adaptation and immune evasion for quantitative description of therapy resistance. ART-TIME strive to de-convolute the dynamic complexity of the tumor immune microenvironment towards a rational dissection. Strategies for stable incorporation of synthetic cells into organoids, chemical, biophysical and ultrastructural characterizations of the synthetic immune cells as well as their molecular interactions with cancer cells inside the organoids are presented.

BP 25.2 Thu 11:15 H13

Frustrated frustules: geometrical frustration in *Coscinodiscus* diatom frustules — •MARIA FEOFILOVA and ERIC DUFRESNE — Vladimir-Prelog-Weg 5, 8093 Zürich, Switzerland

Diatoms are single-celled organisms with a cell wall made of silica, called the frustule. Their elaborate patterns have fascinated scientists for years, however little is known about the biological and physical mechanisms involved in their organizations.

In this work, we take a top-down approach and examine the micron-scale organization of diatoms from the *Coscinodiscus* family. We find two competing tendencies of organization, which appear to be controlled by distinct biological pathways. On one hand, micron-scale pores organize locally on a triangular lattice. On the other, lattice vectors tend to point globally toward a center of symmetry. This competition results in a frustrated triangular lattice, populated with geometrically necessary defects whose density increases near the center.

BP 25.3 Thu 11:30 H13

Structured keratin films as artificial nail plate model — •KIM THOMANN, ANDREAS SPÄTH, and RAINER H. FINK — Lehrstuhl für Physikalische Chemie II, Friedrich-Alexander Universität Erlangen-Nürnberg, Egerlandstr. 3, D-91058, Erlangen, Germany

Human fingernails can be studied ex vivo only in form of clippings which offer limited insight as they do not necessarily reflect the behavior of the whole nail. Keratin films (KFs) may potentially serve as human fingernail substitute, which is especially relevant for the medical and cosmetics sector. In order to model the nail's adhesive characteristics, structured and unstructured films from keratin extracted from human hair and nails were produced. The fingernail being the reference, the KFs were characterized with a number of complementary techniques, including SEM, confocal microscopy, contact angle (CA) measurements, XPS, ATR-FTIR and SAXS. In terms of composition, the prepared films show good resemblance, regardless of keratin origin. The nail's microstructured topography is well matched by the structured KFs. CA measurements revealed that the surface free energy is in the same range for both KF types. However, the structured KFs fit the nail's component composition better. Thus, the structured KFs represent a good approach to achieve a satisfying model in terms of wetting while combining both composition and topography aspects. The research is funded by the BMBF within project 05K19WE2.

BP 25.4 Thu 11:45 H13

Memory effect of red blood cells in a 3D microfluidic chip — •AMIRREZA GHOLIVAND^{1,2} and MINNE PAUL LETTINGA^{1,2} — ¹Forschungszentrum Jülich, IBI-4, Jülich, Germany — ²KU Leuven, Laboratory of Soft Matter and Biophysics, Leuven, Belgium

The significance of healthy blood vessels and blood flow for proper brain functioning is becoming more recognized, for example due to its involvement in the development of human neurodegenerative disorders, notably Alzheimer's disease. Therefore, it is of interest to develop a platform to investigate blood flow and blood cell behavior through the brain vasculature.

Here we present model 3-D microfluidic channels to study the RBCs flow through different vessels geometry and their flow dynamics. RBCs in microcirculation and at bifurcation may attain different memory effect, which we studied systematically varying the interaction strength between the red blood cells and the complexity of flow geometries. To this end, we make use of a novel technique, Selective Laser-induced Etching (SLE), which can produce 3D structures in glass with any desirable shape. To study the shape memory of the vessels the second generation of the bifurcation has been implemented with a parallel and perpendicular orientation relative to the first bifurcation. Using ultra-fast microscopy in combination with velocimetric analysis, we identify a new memory effect, where there is a shift in the maximum velocity, depending on the orientation of the downstream bifurcation.

BP 26: Focus Session: Bioinspired Systems

organized by Isabella Guido (MPI for Dynamics and Self-Organization, Göttingen) and Kerstin Göpfrich (MPI for Medical Research, Heidelberg)

Time: Thursday 15:00–17:30

Location: H15

Invited Talk

BP 26.1 Thu 15:00 H15

Molecular robots working cooperatively in swarm — •AKIRA KAKUGO — Hokkaido University, Sapporo, Japan

Cooperation is a strategy that has been adopted by groups of organisms to execute complex tasks more efficiently than single entities. Cooperation increases the robustness and flexibility of the working groups and permits sharing of the workload among individuals. Here, we demonstrate molecular transportation through the cooperative action of a large number of artificial molecular machines, photoresponsive DNA-conjugated microtubules driven by kinesin motor proteins. Mechanical communication via conjugated photoresponsive DNA enables these microtubules to organize into groups upon photoirradiation. The groups of transporters load and transport cargo, and cargo unloading is achieved by dissociating the groups into single microtubules. The group formation permits the loading and transport of cargoes with larger sizes and in larger numbers over long distances compared with single transporters. We also demonstrate that cargo can be collected at user-determined locations defined by ultraviolet light exposure.

BP 26.2 Thu 15:30 H15

Self-organization of microtubule filaments in energy dissipative evaporating droplet — •VAHID NASIRIMAREKANI, OLINKA RAMIREZ-SOTO, STEFAN KARPITSCHKA, and ISABELLA GUIDO — Max Planck Institute for Dynamics and Self-Organization, 37077 Göttingen, Germany

Cytoskeletal assemblies such as microtubule networks and motor proteins of the kinesin family drive vital cellular processes that, together with cargo delivery and cell division, also include providing mechanical stability when cells are exposed to external stresses. How these self-organising structures can orchestrate such response is not yet well understood. In this study, we develop a bioinspired system resembling intracellular cytoskeletal networks and characterise its activity under the influence of external stress. For this purpose, we confine an active network of microtubules and kinesin motors in an evaporating aqueous droplet. This setup serves as a bioreactor that enables to apply forces to the active system. Namely, the flow field generated by the Marangoni and capillary flow couples with the active stress of the microtubule-motor protein network. We observe that this coupling influences the spatio-temporal distribution of the driving forces and the emergent behaviour of the system, which shows contracting and relaxing behaviour. By analysing such non-equilibrium systems, our study can contribute to understand the response of biological structures to cues from the external environment.

BP 26.3 Thu 15:45 H15

Amphiphile-stabilized microemulsions formed from synthetic DNA-nanomotifs — XENIA TSCHURIKOW¹, MAI TRAN², RAKESH CHATTERJEE^{3,4}, VASILY ZABURDAEV^{3,4}, KERSTIN GÖPFRICH², and •LENNART HILBERT¹ — ¹Karlsruhe Institute of Technology — ²Max Planck Institute for Medical Research — ³Friedrich-Alexander-Universität Erlangen — ⁴Max-Planck-Zentrum für Physik und Medizin

DNA in the nuclei of pluripotent cells exhibits a unique, finely dispersed microdomain pattern. This pattern is formed from DNA and RNA, which behave as two separating phases, and is stabilized in a microemulsified configuration by amphiphiles forming at sites where DNA is transcribed into RNA. Here, we synthetically reproduce such an amphiphile-stabilised microemulsion using DNA oligo-based nanomotifs. Specifically, we implemented a droplet phase in the form of DNA-nanomotifs with three self-affine "sticky ends", to which we add amphiphile particles that additionally harbour negative charges that are repelled from DNA-dense droplets. We confirmed behaviors expected upon amphiphile addition in titration experiments, time-lapse microscopy, and by mapping the amphiphile distribution within droplets. We are currently carrying out lattice simulations with multi-ended particles, which explicitly capture the interaction rules that are encoded via the different DNA-nanomotif ends. Our work provides an avenue towards the model-guided design of more complex multi-phase systems, to reproduce, for instance, the multitude of nuclear bodies observed in biological cells.

15 min. break

BP 26.4 Thu 16:15 H15

Bottom-up assembly of synthetic cells with bio-inspired DNA-based cytoskeletons — •KEVIN JAHNKE¹, PENGFEI ZHAN², MAJA ILLIG¹, NA LIU², and KERSTIN GÖPFRICH¹ — ¹Max Planck Institute for Medical Research — ²Stuttgart University

The bottom-up assembly of synthetic cells with a functional cytoskeleton sets a major milestone to understand cell mechanics and to develop man-made cellular machines. However, the combination of multiple elements and functions remained elusive, which stimulates endeavors to explore entirely synthetic bio-inspired and rationally designed solutions towards engineering life. To this end, DNA nanotechnology represents one of the most promising routes. Here, we demonstrate functional DNA-based cytoskeletons operating in microfluidic cell-sized compartments and lipid vesicles. The synthetic cytoskeletons consist of DNA tiles self-assembled into filament networks (Zhan*, Jahnke* et al., in press at Nat. Chem. 2022; Jahnke et al., ACS Nano 2022). These synthetic cytoskeletons can be rationally designed and controlled to imitate features of natural cytoskeletons, including ATP-triggered polymerization, morphology control and vesicle transport in cell-sized confinement. Also, they possess engineerable characteristics, including assembly and disassembly powered by DNA hybridization, light or aptamer-target interactions. Moreover, we incorporate membrane-spanning DNA origami signalling units to allow for mechanochemical signal transduction across the GUV membrane (Jahnke, Illig et al., biorxiv 2022). This work underpins DNA nanotechnology as a key player in building synthetic cells from the bottom up.

BP 26.5 Thu 16:30 H15

Synchronization, enhanced catalysis of mechanically coupled enzymes and how to design them — •MICHALIS CHATZITTOFI¹, JAIME AGUDO-CANALEJO¹, TUNRAYO ADELEKE-LARODO², PIERRE ILLIEN³, and RAMIN GOLESTANIAN^{1,2} — ¹Department of Living Matter Physics, MPI -DS, D-37077 Göttingen, Germany — ²Rudolf Peierls Centre for Theoretical Physics, University of Oxford, OX1 3PU, UK — ³Sorbonne Université, CNRS, Laboratoire Physicochimie des Electrolytes et Nanosystemes Interfaciaux, 75005, France

Enzymes are the catalysts of the chemical processes that take place in living organisms. These processes, during which chemical energy is converted to mechanical energy and heat, occur stochastically as a result of a noise-activated barrier-crossing event. Despite this stochasticity, it has been shown recently that two mechanically coupled enzymes can synchronize their catalytic reaction [1]. Even more interestingly, the coupling enhances the catalysis of the two enzymes. This effect can be understood as arising from a bifurcation in the deterministic dynamics of the system. In this work, we use a similar approach to describe the dynamics of an enzyme by assuming that the enzyme is attached to a passive molecule. The goal is to design the properties of the enzyme so that its motion favours a chemical reaction, for example dissociation or a shape switch of the molecule. A bifurcation in the deterministic dynamics can cause a change in the molecules state after one enzymatic reaction. The stochastic simulations, also show that the enzyme's activity affects the state of the molecule.

[1] J. Agudo-Canalejo, et al., Phys. Rev. Lett. 127, 208103 (2021).

BP 26.6 Thu 16:45 H15

Dynamic formation and size control of cell-like compartments — •SEBASTIAN W. KRAUSS, PIERRE-YVES GIRES, MITHUN THAMPI, and MATTHIAS WEISS — Experimental Physics I, University of Bayreuth, Germany

A fundamental feature of living matter is its spatial organization into individual units, with the replication of template-like entities during cell division supposedly being the most familiar process linked to this feature. Yet, spatially ordered arrays of cell-like compartments ("protocells") also emerge spontaneously in homogeneous, isotropic *Xenopus* egg extracts in the absence of template structures and genetic material. We show that the geometry of these patterns has properties of a random-packing problem, i.e. randomly placed seeds grow at a uniform rate until competition for material becomes limiting. We also show that the pattern undergoes a coarse-graining over time while maintaining its overall organization. Moreover, fluorescence imaging reveals the cytoskeleton to be the driving force behind the compartmentalization. In line with this notion, a perturbed dynamics of microtubules is observed to result in strongly reduced protocell areas. Altogether, our experimental observations suggest that space compartmentalization in living matter relies on few but robust generic physico-chemical principles.

BP 26.7 Thu 17:00 H15

New insights into the DNA origami silicification reaction mechanism by in situ small angle X-ray scattering — •AMELIE HEUER-JUNGEMANN^{1,3}, MARTINA OBER², LEA WASSERMANN¹, ANNA BAPTIST¹, and BERT NICKEL^{2,3} — ¹Max Planck Institut für Biochemie, Am Klopferspitz 18, 82152 Martinsried — ²Ludwig-Maximilians-Universität, Geschwister-Scholl-Platz 1, 80539 München — ³Center for Nanoscience, LMU München, Geschwister-Scholl-Platz 1, 80539 München

DNA origami allows for the formation of arbitrarily shaped nanostructures with nm precision control. Yet, many potential real-life applications have been hampered due to the biological instability of DNA origami: Silicification provides an excellent way of increasing DNA origami stability. However, so far, it remains unclear how silicification affects the internal structure of the DNA origami and whether the whole DNA framework is embedded or if silica just forms an outer shell. By using in situ small angle x-ray scattering (SAXS), we were able to show that silica growth is not restricted to the outer origami surface, but also occurs on the inner surface, penetrating the whole structure and induces substantial condensation of the structure at early reaction times. Remarkably, we found that thermal stabilization of the origami up to 60°C as well as resistance towards degradation by nucleases could already be observed for sub-nm silica deposition in the highly condensed state. In this state DNA origami addressability could also be retained, resulting in the first fully site-specifically addressable silica nanostructure.

BP 26.8 Thu 17:15 H15

Energy transfer between coupled colloidal clusters — •ANDREAS EHRMANN and CARL GODDRICH — Institute of Science and Technology Austria, Am Campus 1, 3400 Klosterneuburg, Austria

Can biology-inspired complexity be obtained without biochemical components? Can we replicate ubiquitous biological processes using only model physical building blocks like DNA-coated colloids that have simple but programmable interactions? The last decades have seen tremendous progress in understanding the self-assembly mechanisms that enable the formation of complex, sub-micron scale structures, but embedding these structures with bio-inspired functional behaviors remains a considerable challenge. Here, we demonstrate a scheme for transferring energy between two colloidal clusters, in analogy to ATP hydrolysis. By coupling the two clusters, we show how the one acting as a receiver catalyzes a structural transition in the one acting as a fuel source, releasing energy that drives the receiver into a higher energy structural state. The coupled system shows a significantly reduced mean-first passage time. This work demonstrates that a fundamental and enabling biological process can be replicated without complex biochemical reactions. In contrast, theories of active matter often focus on the effect of energy consumption, not on the mechanism itself. However, the mechanism is intimately connected to the type of physical phenomena that can result. In a next step, we extend the scheme to convert energy into work by driving a net flux in the receiver, which is not possible in equilibrium and requires a fuel source.

BP 27: Statistical Physics of Biological Systems 2 (joint session BP/DY)

Time: Thursday 15:00–16:30

Location: H16

BP 27.1 Thu 15:00 H16

Sensing and making sense of fluctuating cellular states — •FELIX J. MEIGEL¹, LINA HELLMIG², PHILIPP MERGENTHALER², and STEFFEN RULANDS^{1,3} — ¹Max Planck Institute for Physics of Complex Systems, Dresden — ²Neurology Department, Charité University Medicine Berlin — ³Center for Systems Biology Dresden

The self-organisation of cells into complex tissue relies on the tight regulation of cellular responses to fluctuating cues. Typically, the regulation of cell decisions is attributed to pathways controlling the concentration of molecular species in response to intrinsic or extrinsic signal. Here, by contrast, we show in the paradigmatic example of cell death that cells manipulate how fluctuations propagate across spatial scales to regulate cellular behavior. Specifically, we find that the feedback between molecular and mesoscopic organelle fluctuations gives rise to a quasi-particle degree of freedom whose intriguing kinetic properties construct a kinetic low-pass filter of time-dependent concentrations of signaling molecules. We show that the collective dynamics of the quasi-particle degree of freedom exhibits different kinetics on different temporal scales. This allows cells to distinguish between fast fluctuations and slow, biologically relevant changes in environmental signals. We demonstrate an order of magnitude effect of this phenomenon on the quality of the cell death decision and validate our predictions experimentally by dynamically perturbing the intrinsic apoptosis pathway. Our work reveals a new mechanism of cell fate decision making.

BP 27.2 Thu 15:15 H16

Guidance and optimization in branching morphogenesis — •MEHMET CAN UCAR and EDOUARD HANNEZO — Institute of Science and Technology Austria, Am Campus 1, 3400 Klosterneuburg, Austria

The development of branched, tree-like biological structures such as lung, kidney, or the neurovascular system has been a pivotal question in biology, physics and mathematics. Recently, many studies based on combinatorial, mechanical, or stochastic models explored local, selforganizing rules leading to branched morphologies in specific systems. However, in addition to local interactions, the growth of branched structures is also regulated globally by external chemical or mechanical guidance cues. In this talk, we present our recent theoretical framework that integrates local and global regulatory mechanisms of branching morphogenesis. Combining analytical theory and numerical simulations, we show that branch orientations follow a generic scaling law that depends on the strength of global guidance. Local interactions such as self-avoidance of branches, on the other hand, lead to denser, efficiently space-filling networks, with a minimal influence on the overall shape and territory. These quantitative predictions of the model are corroborated by experimental data on sensory neurons in the zebrafish caudal fin. Finally, we discuss effects of local interactions on optimal tiling of space in branched distribution networks such as in lymphatic vasculature.

BP 27.3 Thu 15:30 H16

Random force yielding transition in spherical epithelia — ABOUTALEB AMIRI¹, CHARLIE DUCLUT², FRANK JÜLICHER¹, and •MARKO POPOVIĆ¹ — ¹Max Planck Institute for Physics of Complex Systems, Dresden — ²Université Paris Diderot, Paris

Developing biological tissues are often described as active viscoelastic fluids on long time-scales, due to fluidization by cell division and apoptosis. However, on shorter time-scales they can behave as amorphous solids with a finite yield stress

[Mongera et al., Nature, 2018]. Under shear stress beyond the yield stress value amorphous solids begin to flow. This yielding transition is a dynamical phase transition characterized by a diverging correlation length and a set of critical exponents. Developing tissues are active matter systems whose constitutive cells can propel themselves by exerting traction forces. Recently, a remarkable correspondence has been proposed between uniformly sheared amorphous solids and dense self-propelled particle systems [Morse et al., PNAS, 2021] based on the identical scaling of non-linear properties of their energy landscapes. Here, we use a vertex model of epithelial tissues to study how randomly oriented traction forces fluidize a spherical epithelial tissue. In particular, we identify a sharp transition between quiescent and randomly flowing states separated by the critical value of the traction force magnitude, analogous to the yield stress. Moreover, we show that this transition is characterized by the same set of exponents as the classical yielding transition, and the corresponding scaling relations provide a non-trivial relation between cell geometry, cell rearrangement dynamics and tissue flow.

BP 27.4 Thu 15:45 H16

Biological tissues as living amorphous solids — •ALI TAHA EI and MARKO POPOVIĆ — Max Planck Institute for Physics of Complex Systems, Dresden

Biological tissues are often described as viscoelastic fluids on long time-scales. However, on shorter times-scales, tissues can behave as amorphous solids, such as clay, changing shape only when exposed to a shear stress above the material yield stress Σ_c . Amorphous solids near Σ_c display critical behaviour with a diverging correlation length-scale characterising dynamics of plastic activity. Here, we ask how would this critical behaviour be affected by active processes present in biological tissues, such as cell divisions.

In order to model yielding of biological tissues we employ the mesoscopic elasto-plastic model, commonly used to describe yielding of amorphous solids. Here, we extend the classical elasto-plastic model by introducing cell divisions as an additional source of plastic activity. We find that cell divisions strongly fluidise the solid phase of the system at stresses lower than Σ_c , consistent with literature. Furthermore, we find that critical behaviour is strongly suppressed, leading to localised dynamics of plastic activity nucleated by cell divisions. Finally, in our model we can describe how well is the cell division orientation aligned with local shear stress. We find that low alignment strength leads to less mechanically stable tissues where, consequently, most of the plastic flow arises from cell rearrangements, and vice versa.

BP 27.5 Thu 16:00 H16

Order-disorder transition in epithelial tissues — •KARTIK CHHAJED, MARKO POPOVIĆ, and FRANK JÜLICHER — Max Planck Institute for Physics of Complex Systems, Dresden

Two dimensional packings of cells in developing epithelial tissues are commonly found to be disordered. However, highly organised packings can emerge during development, such as hexagonal pattern of ommatidia in the eye epithelium of the fruit fly. Here, we observe a disorder to order transition in the packing of the fruit fly pupal wing epithelium. In particular, we find a sudden increase in the hexatic order parameter ψ_6 , which suggests a presence of hexatic and crystalline phases in two dimensional systems, as described by the classical KTHNY theory. The melting transition scenario with the intermediate hexatic phase has been reproduced in a model of epithelial tissues [Pashupalak et al. Soft Mat-

ter, 2020] where the stochastic active forces generated by the cells play the role of an effective temperature. However, both KTHNY theory and recent literature on packings of epithelial tissues assume uniform properties of particles and cells, respectively. In a proliferating tissue cells grow and divide, which inevitably leads to a heterogeneity of cell sizes. Here, we use the vertex model of epithelial tissues to study how the disorder to order transition is affected by the heterogeneity of cell sizes. We find that reducing cell heterogeneity as a control parameter drives the system through an ordering transition. We compare our results with the experimental data of the fruit fly wing to identify the role of cell size heterogeneity in the observed disorder to order transition.

BP 27.6 Thu 16:15 H16

The Influence of Contact Maps on RNA Structure Prediction — •CHRISTIAN FABER¹ and ALEXANDER SCHUG^{1,2} — ¹Jülich Supercomputing Centre, FZ Jülich — ²Steinbuch Centre for Computing, KIT

The 3d structure of Proteins and non coding RNA are essential for their function, but hard to determine via NMR or x-ray crystallography. Therefore an effective

way of simulation with the knowledge of the sequence only would be a huge improvement. Impressive progress has been made in recent years, most notably AlphaFold2 for protein structure prediction using Machine Learning techniques. Such a break through is still missing for RNA.

For RNA, there are folding programs such as SimRNA, that simulate the structure with a physical force field [1]. The outcome can be improved by incorporating evolutionary data from homologous sequences. From the evolutionary data, we can make predictions about possible contacts in the form of contact maps [2].

We investigate how contact maps can influence prediction quality and what are particularly valuable contacts. From these insights we develop new measures for machine learning algorithms.

[1] Boniecki, M. J. et al. *SimRNA: a coarse-grained method for RNA folding simulations and 3D structure prediction*. Nucleic Acids Research 44, e63 (2016).

[2] Weigt, M., White, R. A., Szurmant, H., Hoch, J. A., Hwa, T. *Identification of direct residue contacts in protein-protein interaction by message passing*. PNAS 106, 67-72 (2009).

BP 28: Biopolymers, Biomaterials and Bioinspired Functional Materials (joint session CPP/BP)

Time: Friday 9:30–11:15

Location: H39

See CPP 45 for details of this session.

BP 29: Active Matter 5 (joint session DY/BP/PP)

Time: Friday 10:00–12:45

Location: H18

See DY 50 for details of this session.

Chemical and Polymer Physics Division Fachverband Chemische Physik und Polymerphysik (CPP)

Peter Müller-Buschbaum
Technische Universität München
Lehrstuhl für Funktionelle Materialien
James-Franck-Straße 1
85748 Garching
muellerb@ph.tum.de

Hans-Jürgen Butt
Max-Planck-Institut für
Polymerforschung
Ackermannweg 10
55128 Mainz
butt@mpip-mainz.mpg.de

Jens-Uwe Sommer
Leibniz-Institut für Polymerforschung
Dresden e.V.
Hohe Strasse 6
01069 Dresden
sommer@ipfdd.de

Overview of Invited Talks and Sessions

(Lecture halls H38 and H39; Poster P1 and P2)

Invited Talks

CPP 1.1	Mon	9:30–10:00	H38	Ternary blend approach for boosting performance and stability of organic solar cells — •TAYEBEH AMERI
CPP 8.1	Mon	15:00–15:30	H38	Stimuli-Responsive Opal Films based on Core-Shell Particle Self-Assembly — •MARKUS GALLEI
CPP 8.3	Mon	15:45–16:15	H38	Self-assembled photonic pigments from bottlebrush block copolymers — •RICHARD PARKER, TIANHENG ZHAO, ZHEN WANG, CLEMENT CHAN, SILVIA VIGNOLINI
CPP 8.5	Mon	16:45–17:15	H38	Hierarchically structured mechanochromic deformation-sensing pigments — •JESSICA CLOUGH, CÉDRIC KILCHOER, BODO WILTS, CHRIS WEDER
CPP 13.1	Tue	9:30–10:00	H38	Insights into degradation mechanisms in Li-based batteries and advantages of polymer coatings — •NEELIMA PAUL
CPP 18.1	Tue	11:30–12:00	H38	How X-rays can reveal waters mysteries — •KATRIN AMANN-WINKEL
CPP 19.1	Wed	9:30–10:00	H38	Elucidating the role of antisolvent polarity on the surface chemistry and optoelectronic properties of lead-halide perovskite nanocrystals — •ROBERT HOYE
CPP 33.1	Thu	9:30–10:00	H38	Cooperative and non-Gaussian dynamics of entanglement strands in polymer melts — •MARGARITA KRUTEVA, MICHAELA ZAMONI, INGO HOFFMANN, JÜRGEN ALLGAIER, LUTZ WILLNER, ANDREAS WISCHNEWSKI, MICHAEL MONKENBUSCH, DIETER RICHTER
CPP 37.1	Thu	10:30–11:00	H39	Non-equilibrium Properties of Thin Polymer Films — •GÜNTER REITER, SIVASURENDER CHANDRAN
CPP 40.1	Thu	15:00–15:30	H38	Computational Design of Organic Semiconductors — •HARALD OBERHOFFER
CPP 41.1	Thu	15:00–15:30	H39	Interface-induced crystallization in polymers: From model systems to applications for semiconducting polymers — MUHAMMAD TARIQ, ROBERT KAHL, MUKUNDAN THELAKKAT, THOMAS THURN-ALBRECHT, •OLEKSANDR DOLYNCHUK
CPP 44.1	Fri	9:30–10:00	H38	Connecting dynamics and phase behavior of proteins: The neutron perspective — •FRANK SCHREIBER
CPP 44.5	Fri	10:45–11:15	H38	Magnetic particle self-assembly at functionalized interfaces — •MAX WOLFF
CPP 45.1	Fri	9:30–10:00	H39	New biobased material concepts using scattering techniques to elucidate and control nanoscale assembly — •DANIEL SÖDERBERG

Invited Talks of the joint Symposium SKM Dissertation Prize 2022 (SYSD)

See SYSD for the full program of the symposium.

SYSD 1.1	Mon	10:15–10:45	H2	Charge localisation in halide perovskites from bulk to nano for efficient optoelectronic applications — •SASCHA FELDMANN
SYSD 1.2	Mon	10:45–11:15	H2	Nonequilibrium Transport and Dynamics in Conventional and Topological Superconducting Junctions — •RAFFAEL L. KLEES
SYSD 1.3	Mon	11:15–11:45	H2	Probing magnetostatic and magnetotransport properties of the antiferromagnetic iron oxide hematite — •ANDREW ROSS
SYSD 1.4	Mon	11:45–12:15	H2	Quantum dot optomechanics with surface acoustic waves — •MATTHIAS WEISS

Invited Talks of the joint Symposium From Physics and Big Data to the Design of Novel Materials (SYNM)

See SYNM for the full program of the symposium.

SYNM 1.1	Mon	15:00–15:30	H1	How to tackle the "I" in FAIR? — •CLAUDIA DRAXL
SYNM 1.2	Mon	15:30–16:00	H1	Beyond the average error: machine learning for the discovery of novel materials — •MARIO BOLEY, SIMON TESHUVA, FELIX LUONG, LUCAS FOPPA, MATTHIAS SCHEFFLER
SYNM 1.3	Mon	16:00–16:30	H1	The Phase Diagram of All Inorganic Materials — •CHRIS WOLVERTON
SYNM 1.4	Mon	16:45–17:15	H1	Automated data-driven upscaling of transport properties in materials — •DANNY PEREZ, THOMAS SWINBURNE
SYNM 1.5	Mon	17:15–17:45	H1	Data-driven understanding of concentrated electrolytes — •ALPHA LEE

Invited Talks of the joint Symposium United Kingdom as Guest of Honor (SYUK)

See SYUK for the full program of the symposium.

SYUK 1.1	Wed	9:30–10:00	H2	Structure and Dynamics of Interfacial Water — •ANGELOS MICHAELIDES
SYUK 1.2	Wed	10:00–10:30	H2	A molecular view of the water interface — •MISCHA BONN
SYUK 1.3	Wed	10:30–11:00	H2	Motile cilia waves: creating and responding to flow — •PIETRO CICUTA
SYUK 1.4	Wed	11:00–11:30	H2	Cilia and flagella: Building blocks of life and a physicist's playground — •OLIVER BÄUMCHEN
SYUK 1.5	Wed	11:45–12:15	H2	Computational modelling of the physics of rare earth - transition metal permanent magnets from SmCo₅ to Nd₂Fe₁₄B — •JULIE STAUNTON
SYUK 2.1	Wed	15:00–15:30	H2	Hysteresis Design of Magnetic Materials for Efficient Energy Conversion — •OLIVER GUTFLEISCH
SYUK 2.2	Wed	15:30–16:00	H2	Non-equilibrium dynamics of many-body quantum systems versus quantum technologies — •IRENE D'AMICO
SYUK 2.3	Wed	16:00–16:30	H2	Quantum computing with trapped ions — •FERDINAND SCHMIDT-KALER
SYUK 2.4	Wed	16:45–17:15	H2	Breaking the millikelvin barrier in cooling nanoelectronic devices — •RICHARD HALEY
SYUK 2.5	Wed	17:15–17:45	H2	Superconducting Quantum Interference Devices for applications at mK temperatures — •SEBASTIAN KEMPF

Invited Talks of the joint Symposium Interplay of Substrate Adaptivity and Wetting Dynamics from Soft Matter to Biology (SYSM)

See SYSM for the full program of the symposium.

SYSM 1.1	Wed	15:00–15:30	H1	Statics and Dynamics of Soft Wetting — •BRUNO ANDREOTTI
SYSM 1.2	Wed	15:30–16:00	H1	Droplets on elastic substrates and membranes - Numerical simulation of soft wetting — •SEBASTIAN ALAND
SYSM 1.3	Wed	16:00–16:30	H1	Wetting of Polymer Brushes in Air — LARS VELDSCHOLTE, GUIDO RITSEMA VAN ECK, LIZ MENSINK, JACCO SNOEIJER, •SISSI DE BEER
SYSM 1.4	Wed	16:45–17:15	H1	Elastocapillary phenomena in cells — •ROLAND L. KNORR
SYSM 1.5	Wed	17:15–17:45	H1	Active contact line depinning by micro-organisms spreading on hydrogels — MARC HENNES, JULIEN TAILLEUR, GAËLLE CHARRON, •ADRIAN DAERR

Sessions

CPP 1.1–1.12	Mon	9:30–13:00	H38	Organic Electronics and Photovoltaics 1
CPP 2.1–2.4	Mon	9:30–10:30	H39	Polymer Networks and Elastomers
CPP 3.1–3.11	Mon	9:30–12:45	H34	Perovskite and Photovoltaics 1 (joint session HL/CPP/KFM)
CPP 4.1–4.10	Mon	9:30–12:45	H36	2D Materials 1 (joint session HL/CPP/DS)
CPP 5.1–5.8	Mon	10:00–12:15	H19	Wetting, Droplets and Microfluidics (joint session DY/CPP)
CPP 6.1–6.7	Mon	10:30–12:45	H16	Active Matter 1 (joint session BP/CPP/DY)
CPP 7.1–7.8	Mon	10:45–13:00	H39	Wetting, Fluidics and Liquids at Interfaces and Surfaces
CPP 8.1–8.5	Mon	15:00–17:15	H38	Focus Session: Photonic Structures from Polymer and Colloidal Self-Assembly
CPP 9.1–9.10	Mon	15:00–17:45	H39	Modeling and Simulation of Soft Matter (joint session CPP/DY)
CPP 10.1–10.12	Mon	15:00–18:30	H36	2D Materials 2 (joint session HL/CPP/DS)
CPP 11.1–11.2	Mon	17:15–17:45	H38	2D Materials 3 (joint session CPP/DS)
CPP 12.1–12.80	Mon	18:00–20:00	P1	Poster 1
CPP 13.1–13.6	Tue	9:30–11:15	H38	Charged Soft Matter, Polyelectrolytes and Ionic Liquid

CPP 14.1–14.7	Tue	9:30–11:15	H39	Emerging Topics in Chemical and Polymer Physics, New Instruments and Methods
CPP 15.1–15.8	Tue	9:30–12:00	H36	2D Materials 4 (joint session HL/CPP/DS)
CPP 16.1–16.11	Tue	10:00–13:00	H18	Active Matter 2 (joint session DY/BP/CPP)
CPP 17.1–17.41	Tue	11:00–13:00	P2	Poster 2
CPP 18.1–18.5	Tue	11:30–13:00	H38	Complex Fluids and Colloids, Micelles and Vesicles (joint session CPP/DY)
CPP 19.1–19.5	Wed	9:30–11:00	H38	Perovskite and Photovoltaics 2
CPP 20.1–20.7	Wed	9:30–11:15	H39	General Session to the Symposium: Interplay of Substrate Adaptivity and Wetting Dynamics from Soft Matter to Biology (joint session CPP/DY)
CPP 21.1–21.7	Wed	9:30–12:05	H7	Materials for Energy Storage (joint session KFM/CPP)
CPP 22.1–22.10	Wed	9:30–12:30	H16	Active Matter 3 (joint session BP/CPP/DY)
CPP 23.1–23.9	Wed	9:30–12:00	H18	Complex Fluids and Soft Matter 1 (joint session DY/CPP)
CPP 24.1–24.9	Wed	9:30–12:00	H36	2D Materials 5 (joint session HL/CPP/DS)
CPP 25.1–25.7	Wed	11:15–13:00	H17	2D Materials 6 (joint session DS/CPP)
CPP 26.1–26.6	Wed	11:30–13:00	H38	Organic Electronics and Photovoltaics 2
CPP 27.1–27.6	Wed	11:30–13:00	H39	Composites and Functional Polymer Hybrids
CPP 28.1–28.8	Wed	15:00–17:15	H38	Perovskite and Photovoltaics 3
CPP 29.1–29.8	Wed	15:00–17:30	H15	Biomaterials (joint session BP/CPP)
CPP 30.1–30.4	Wed	15:00–16:00	H17	2D Materials 7 (joint session DS/CPP)
CPP 31.1–31.9	Wed	15:00–17:30	H18	Active Matter 4 (joint session DY/BP/CPP)
CPP 32.1–32.11	Wed	15:00–18:15	H34	Perovskite and Photovoltaics 4 (joint session HL/CPP/KFM)
CPP 33.1–33.6	Thu	9:30–11:15	H38	Focus Session: Soft Matter and Nanocomposites: New Opportunities with Advanced Neutron Sources 1
CPP 34.1–34.3	Thu	9:30–10:15	H39	Hydrogels and Microgels
CPP 35.1–35.8	Thu	9:30–11:30	H17	2D Materials 8 (joint session DS/CPP)
CPP 36.1–36.6	Thu	10:00–11:30	H18	Complex Fluids and Soft Matter 2 (joint session DY/CPP)
CPP 37.1–37.8	Thu	10:30–13:00	H39	Interfaces and Thin Films and Responsive and Adaptive Systems
CPP 38.1–38.4	Thu	11:15–12:15	H36	2D Materials 9 (joint session HL/CPP/DS)
CPP 39.1–39.6	Thu	11:30–13:00	H38	Molecular Electronics and Excited State Properties
CPP 40.1–40.9	Thu	15:00–17:45	H38	Organic Electronics and Photovoltaics 3
CPP 41.1–41.8	Thu	15:00–17:30	H39	Crystallization, Nucleation and Self-Assembly
CPP 42.1–42.6	Thu	15:00–16:30	H31	Perovskite and Photovoltaics 5 (joint session HL/CPP/KFM)
CPP 43	Thu	18:00–19:00	H39	Members' Assembly
CPP 44.1–44.5	Fri	9:30–11:15	H38	Focus Session: Soft Matter and Nanocomposites: New Opportunities with Advanced Neutron Sources 2
CPP 45.1–45.6	Fri	9:30–11:15	H39	Biopolymers, Biomaterials and Bioinspired Functional Materials (joint session CPP/BP)
CPP 46.1–46.9	Fri	9:30–12:00	H36	2D Materials 10 (joint session HL/CPP/DS)
CPP 47.1–47.11	Fri	10:00–12:45	H18	Active Matter 5 (joint session DY/BP/CPP)
CPP 48.1–48.4	Fri	11:30–12:30	H38	Electrical, Dielectrical and Optical Properties of Thin Films (joint session CPP/KFM)
CPP 49.1–49.6	Fri	11:30–13:00	H39	Polymer and Molecular Dynamics, Friction and Rheology
CPP 50.1–50.2	Fri	12:30–13:00	H38	Nanostructures, Nanostructuring and Nanosized Soft Matter
CPP 51.1–51.1	Fri	13:15–14:00	S054	Overview Talk Claus M. Schneider (joint session O/CPP)

Members' Assembly of the Chemical and Polymer Physics Division

Thursday 18:00–19:00 H39

- Report of the current speaker team
- Election of the second deputy speaker
- Miscellaneous

From	To	Sunday 04.09.2022	Monday 05.09.2022	Tuesday 06.09.2022	Wednesday 07.09.2022	Thursday 08.09.2022	Friday 09.09.2022
8:30	8:45						
8:45	9:00						
9:00	9:15						
9:30	9:45						
9:45	10:00						
10:00	10:15						
10:15	10:30						
10:30	10:45						
10:45	11:00						
11:00	11:15						
11:15	11:30						
11:30	11:45						
11:45	12:00						
12:00	12:15						
12:15	12:30						
12:30	12:45						
12:45	13:00						
13:00	13:15						
13:15	13:30						
13:30	13:45						
13:45	14:00						
14:00	14:15						
14:15	14:30						
14:30	14:45						
15:00	15:15						
15:15	15:30						
15:30	15:45						
15:45	16:00						
16:00	16:15						
16:15	16:30						
16:30	16:45						
16:45	17:00						
17:00	17:15						
17:15	17:30						
17:30	17:45						
17:45	18:00						
18:00	18:15						
18:15	18:30						
18:30	18:45						
18:45	19:00						
19:00	19:15						
19:15	19:30						
19:30	19:45						
19:45	20:00						
20:00	20:30						
20:30	21:00						
21:00	21:30						
21:30	22:00						

Sessions

– Invited Talks, Contributed Talks, and Posters –

CPP 1: Organic Electronics and Photovoltaics 1

Time: Monday 9:30–13:00

Location: H38

Invited Talk

CPP 1.1 Mon 9:30 H38

Ternary blend approach for boosting performance and stability of organic solar cells — •TAYEBEH AMERI — University of Edinburgh, School of Engineering, Edinburgh, UK

Organic solar cells (OSCs) have now reached power conversion efficiencies over 18% on laboratory-scale devices, an important milestone towards their commercialization. The evolution in organic photovoltaic technology along with introducing non-fullerene acceptor materials and ternary blend approach caused this significant boost in the performance of solar cells.

However, for longer than a decade, when researchers were focused on boosting the power conversion efficiency of solar cells, the importance of lifetime and stability issues was overlooked by the organic photovoltaic community. Recently, more studies have been conducted and reported on the lifetime and stability of OSCs, employing different strategies to either understand the degradation mechanisms or enhance the lifetime of solar cells.

In this presentation, we overview how the ternary blend approach was developed to boost the power conversion efficiency. Moreover, we discuss how this approach can also address the stability issues related to the mostly used electron transport layer of zinc oxide and significantly increase the photostability of organic solar cells. And finally, we explain how zinc oxide must be manufactured and pretreated to avoid UV light activation, and in parallel, increase the thermal stability of the devices.

CPP 1.2 Mon 10:00 H38

Structure control during in situ printing of donor-acceptor blend films — KERSTIN S. WIENHOLD¹, MANUEL A. REUS¹, DAN YANG¹, BAOJUN LIN², HENG ZHAO², WEI MA², and •PETER MÜLLER-BUSCHBAUM^{1,3} — ¹TU München, Physik-Department, LS Funktionelle Materialien, 85748 Garching — ²State Key Laboratory for Mechanical Behavior of Materials, Xi'an Jiaotong University, Xi'an, 710049 China — ³Heinz Maier-Leibnitz Zentrum (MLZ), TU München, 85748 Garching, Germany

Among the next generation solar cells, in particular organic photovoltaics are gaining impact as a promising alternative to conventional silicon-based solar cells. However, despite big achievements in the last years, it remains an unresolved challenge to fabricate large-area organic solar cells without sacrificing efficiencies. The reason behind is that basic understanding is still very limited due to the complexity of the systems. Moreover, presently a substantial number of researchers use spin-coating for film fabrication, which is not compatible with the needs of a large scale production. Thus, using up-scalable fabrication methods such as printing are of immanent interest. In the present work, we use GISAXS and GIWAXS in situ during printing of donor:acceptor blends to gain fundamental understanding about the underlying film formation processes. Different examples of polymer donors and small molecule acceptors are presented and the resulting morphologies are correlated with solar cell device performance.

CPP 1.3 Mon 10:15 H38

Revealing the Thermally Induced Degradation of PM6:Y6 based Bulk Heterojunction Organic Solar Cell — •SHAHIDUL ALAM, HUA TANG, MARYAM ALQURASHI, WEJDAN ALTHOBAITI, SI CHEN, HAYA ALDOSARI, JAFAR I. KHAN, and FRÉDÉRIC LAQUAI — King Abdullah University of Science and Technology (KAUST), KAUST Solar Center (KSC), Physical Sciences and Engineering Division (PSE), Material Science and Engineering Program (MSE), Thuwal 23955-6900, Kingdom of Saudi Arabia

Thermally-induced degradation in bulk-heterojunction OSCs is an obvious barrier to the fabrication of stable devices. Thus, practical approaches and strategies need to be identified their inherent thermal instability. In this work, the thermally induced degradation of the most commonly used system PM6:Y6 is investigated by varying temperatures and different exposure conditions. The degradation pathways have been identified by applying several opto-electrical and spectroscopic characterizations methods. Due to the reduced charge carrier mobility and extraction probability, the thermally degraded device exhibits significant losses in the VOC and FF. Furthermore, the field dependence of charge generation, charge extraction, photo-generated charge density, and charge recombination dynamics in solar cells were studied by the TDCF optical-pump electronic-probe technique. By using all the analyses, we can explain the significant recombination process that dominates device performance and thermal stability. Finally, device simulation by SETFOS of the JV characteristics was used to confirm experimentally determined thermally induced degradation.

CPP 1.4 Mon 10:30 H38

Developing the next generation of photovoltaics with high efficiencies — •ELISABETH ERBES^{1,2}, MATTHIAS SCHWARTZKOPF¹, CONSTANTIN HARDER^{1,3}, SUSANN FRENZKE¹, BENEDIKT SOCHOR¹, NAIREETA BISWAS^{1,2}, STEPHAN V. ROTH^{1,4}, and SIMONE TECHERT^{1,2} — ¹Deutsches Elektronen-Synchrotron (DESY), Hamburg, Germany — ²Institute for X-ray Physics, Goettingen University, Goettingen, Germany — ³Technical University of Munich, Munich, Germany — ⁴Department of Fibre and Polymer Technology, KTH Royal Institute of Technology, Stockholm, Sweden

A crucial challenge in bio-inspired energy research is to develop a rationale for the synthesis and use of sustainable, bio-based materials. Cellulose fibers have excellent mechanical strength, are thermally stable, are very lightweight and have a very low surface roughness in thin films. On the other hand, the use of small molecules in OSC is well known to increase the power conversion efficiency. The idea is to combine the use of cellulose and small molecules to create a sustainable organic solar cell with high efficiencies. The current study aims to investigate systematically the OSC matrix PM6:Y6 doped with optical-light absorbing, electron transfer (ET) dyes. The structural and morphological integrity of the dyes were studied with grazing incidence small angle and wide angle X-ray scattering techniques (in situ GISAXS and static GIWAXS) and photo-sensitization experiments. This analysis showed us the intercalation dynamics, distribution and function of pyrene-based photo-dopants within the PM6:Y6 matrix and whether these dopants alter the overall polymer structures.

CPP 1.5 Mon 10:45 H38

Ultrafast charge carriers separation at organic donor-acceptor interfaces - Influence of molecular vibrations — •MAXIMILIAN F. X. DORFNER¹, SEBASTIAN HUTSCH¹, RAFFAELE BORRELLI², MAXIM F. GELIN³, and FRANK ORTMANN¹ — ¹Department of Chemistry, Technische Universität München, 85748 Garching b. München (Germany) — ²DISAFA, University of Torino, Largo Paolo Braccini 2, I-10095 Grugliasco (TO), Italy — ³School of Sciences, Hangzhou Dianzi University, Hangzhou 310018, China

In this work the charge transfer dynamics of photogenerated excitons at a donor-acceptor interface of an organic solar cell blend is examined. This is done by means of a fully quantum mechanical treatment of an effective Holstein model including the relevant electronic orbitals coupled to over one hundred vibrational modes, parametrized by density functional theory calculations. To solve this coupled electron-phonon system we make use of the numerically quasi-exact matrix-product-state ansatz. We find that, depending on the driving energy, different mechanisms are predominantly responsible for the charge separation at the interface. For near zero driving the ultrafast electron transfer is prevalently due to kinetic processes, while at larger driving the separation of carriers can be traced back to dissipative phonon emission connected with the dominant molecular vibrations. This charge transfer picture is consistent with a novel semi-classical hopping approach, with which we compare. These results show that dissipation of energy to the phonon is essential for charge separation for systems with a moderate driving force.

CPP 1.6 Mon 11:00 H38

Revealing the formation kinetics of the active layer for non-fullerene organic solar cells — •XINYU JIANG¹, SUO TU¹, MANUEL A. REUS¹, JULIJA REITENBACH¹, CHRISTIAN L. WEINDL¹, MATTHIAS SCHWARTZKOPF², STEPHAN V. ROTH², and PETER MÜLLER-BUSCHBAUM¹ — ¹Lehrstuhl für Funktionelle Materialien, Physik Department, Technische Universität München, James-Frank-Str. 1, 85748 Garching, Germany — ²DESY, Notkestraße 85, 22607 Hamburg

Bulk heterojunction (BHJ) organic solar cells have gained significant improvements in the past few years, however, traditional laboratory deposition methods like spin coating are limited to small-scale production. In addition, it is difficult to observe the structure formation process of the active layer during deposition, which is crucial for gaining a fundamental understanding. Encouragingly, the emergence of printing techniques and the development of in-situ observation technology open new windows for larger-area device manufacturing and inspection of the formation process of the printed active layer, respectively. In this work, we fabricate an active layer, which contains a donor polymer (PDTBT2T-FTBDT) and a non-fullerene acceptor (BTP-4F) with a slot-die coating. The structure formation of the polymer domains kinetics is followed in-situ during the printing process with GIWAXS and UV-Vis spectroscopy measurements, respectively. Thus, structure evolution is coupled with optical properties during

the printing process, thereby providing an understanding of the drying of non-fullerene organic BHJ thin films.

15 min. break

CPP 1.7 Mon 11:30 H38

Re-evaluation of Published Figures of Merit and Introduction of Novel figure of merit for Transparent Conducting Electrodes used in Photovoltaics — •AMAN ANAND^{1,2}, MD MOIDUL ISLAM^{1,2}, RICO MEITZNER^{1,2}, ULRICH S. SCHUBERT^{1,2}, and HARALD HOPPE^{1,2} — ¹Laboratory of Organic and Macromolecular Chemistry (IOMC), Friedrich Schiller University Jena, Humboldtstraße 10, 07743 Jena, Germany — ²Center for Energy and Environmental Chemistry Jena (CEEC Jena), Friedrich Schiller University Jena, Philosophenweg 7a, 07743 Jena, Germany

Transparent conductive electrodes (TCEs) are one of the important components of photovoltaic technologies. Since they are transparent and conductive, they allow light to enter the device and the photocurrent generated to be drawn into the outer electric circuit. In theory, TCEs should have the highest light transmission and conductivity. Both traits, however, must be balanced. The selection of the best TCE depends on the photovoltaic material system and is evaluated using so-called figures-of-merit (FOM). A novel and exact FOM is presented here that explicitly analyzes the impact on photovoltaic performance. This novel and exact FOM has several important properties, including i) proportionality to the solar device's potential power output, ii) normalization to the theoretically ultimately attainable photovoltaic performance, and, thus, iii) significant direction for the development of advanced TCEs. This work reassesses and compares a variety of realized state-of-the-art semitransparent electrodes.

CPP 1.8 Mon 11:45 H38

Cycling stability of cellulose-based electronics — •STEPHAN V. ROTH^{1,2}, CALVIN J. BRETT^{1,2}, OLA K. FORSLUND¹, ELISABETTA NOCERINO¹, LUCAS P. KREUZER³, LIONEL PORCAR⁴, NORIFUMI L. YAMADA⁵, MARTIN MANSSON¹, PETER MÜLLER-BUSCHBAUM³, and L. DANIEL SÖDERBERG¹ — ¹KTH Royal Institute of Technology, SE-10044 Stockholm — ²DESY, D-22607 Hamburg — ³TU München, Physik-Department, Lehrst. f. Funktionelle Materialien, D-85748 Garching — ⁴ILL, F-38042 Grenoble — ⁵KEK, Tokai (JPN)

In organic electronics, hybrid materials combining high-strength biomaterials and conducting organic polymers allow for disentangling mechanical flexibility and functionality. Yet, degradation in such complex organic electronics applications is still less addressed. We thus combine sprayed cellulose nanofibrils (CNF) templates due to their hierarchical, nanoporous morphology and a conductive polymer blend poly(3,4-ethylenedioxythiophene):poly(styrenesulfonate) (PEDOT:PSS) to correlate the impact of cyclic relative humidity changes with device performance and nanostructure evolution. The conductivity of the CNF/PEDOT:PSS hybrid shows reversible changes: The PEDOT:PSS blend undergoes cyclic wetting/dewetting on the CNF backbone accompanied by swelling and deswelling of PEDOT:PSS moieties in the pores. The cycling stability of the device performance is ensured by reversible rearrangement of the CNF backbone. With CNF acting as structural reinforcing template, interestingly, no macroscopic swelling is observed, proving the applicability in e.g. supercapacitors.

CPP 1.9 Mon 12:00 H38

Dual-Gate Organic Electrochemical Transistors and Circuits — •HSIN TSENG, ANTON WEISSBACH, KARL LEO, and HANS KLEEMANN — Dresden Integrated Center for Applied Physics and Photonic Materials, TU Dresden, Dresden, Germany

Organic mixed ionic-electronic conductors (OMIECs) are currently in the spotlight of research for diverse applications. Among all, organic electrochemical transistors (OECTs) stand out as organic synaptic devices for integrated bioelectronics leading to neuromorphic computing applications, thanks to their low operating voltage, biocompatibility, and the ionic and electronic interactions in OMIECs. Modifying OMIECs by molecular design enables accumulation-mode OECTs, resulting in broad IC applications. However, the side chain molecular design of the polymer is unfavorable for IC design and manufacturing processes. Here, we show an OECT with photo-patternable solid electrolyte advancing towards integrated circuits. We discuss how alterable device parameters can be employed to adjust the OECT performance. In particular, we demonstrate how the biasing conditions govern the time constant of OECTs. In addition, we discuss how a dual-gate OECT architecture can be employed to tune the threshold voltage of OECTs and control the ionic and electronic charge transport in the electrolyte and OMIECs without any complicated molecular design. The elec-

trical analysis of solid-state electrolyte OECTs provides new insights stimulating higher investigations on ionic and electronic interactions and coupled transport properties in OMIECs and paves the foundation for the integration of OECTs for advanced applications.

CPP 1.10 Mon 12:15 H38

Design of Monolithic All-Organic Oxygen Sensors — •TONI BÄRSCHNEIDER and SEBASTIAN REINEKE — Dresden Integrated Center for Applied Physics and Photonic Materials (IAPP), Technische Universität Dresden

Organic electronic devices, such as light-emitting diodes (OLEDs) and photodetectors (OPDs), are ideal for sensor application because of their versatility and flexibility. Additionally, they can be easily fabricated on any substrate, making monolithic sensor application possible. This allows for an easy miniaturization and a cheap fabrication. Organic room temperature phosphorescence (RTP) materials are well suited for optical oxygen sensors because of their strong oxygen dependency.

In this work, we developed a monolithic all-organic oxygen sensor which is composed a RTP sensing layer, an ultraviolet OLED as excitation source, and a novel narrow bandwidth OPD for detection. The RTP sensing layer shows fluorescence and phosphorescence at room temperature at the same time which enables self-referencing to avoid photodegradation-caused distortion. Due to the long phosphorescence lifetime, sensing within the ultra-trace range is possible.

The presented sensors overcome drawbacks of common optical oxygen sensors such as complexity, expensive read-out electronics, and a lack of possible miniaturization.

CPP 1.11 Mon 12:30 H38

Towards all solution-processed OFETs using microcontact printed electrodes

— •KIRILL GUBANOV¹, MANUEL JOHNSON¹, MELDA AKAY¹, KIM THOMANN¹, DAN SHEN^{1,2}, XING CHENG², and RAINER H. FINK¹ — ¹Physikalische Chemie II, Friedrich-Alexander Universität Erlangen-Nürnberg, Germany — ²South University of Science and Technology, Shenzhen, China

Printed electronics is expected to facilitate low-cost solvent prepared devices for potential applications in RFID, flexible displays, OLEDs and transistors. Furthermore, microcontact printing may be used in a large-scale production using roll-to-roll printing with direct access to structures on the micrometer level. The preparation of the microstructured conductive electrodes using PEDOT:PSS ink for applications in OFETs was successful in various aspects: the electrodes were fabricated with very good structural definition and high reproducibility on solvent-prepared 2D-extended single-crystalline C8-BTBT films. A defined mechanical load of the PDMS stamps pre-treated with O₂ plasma yielded good structural quality and competitive electrical performance. In particular, the implementation of the MWCNTs in the PEDOT:PSS ink has a direct impact on the charge carriers transport efficiency, leading to the contact resistance decrease. In addition to electrical characterization made with KPFM and IV-curves, the morphology and structure analysis was performed using VLM, AFM and 3D Microscopy, providing with an insight into the structural quality of the contacts and relate their structures to the overall device performances. The research is funded by the BMBF (contract 05K19WE2).

CPP 1.12 Mon 12:45 H38

Effect of trap states on the performance of organic photodetectors — •JAKOB WOLANSKY¹, SEBASTIAN HUTSCH², FELIX TALNACK¹, MICHEL PANHANS², JONAS KUBLITSKI¹, STEFAN MANNFELD¹, FRANK ORTMANN², JOHANNES BENDUHN¹, and KARL LEO¹ — ¹Technische Universität Dresden, Dresden, Germany — ²Technische Universität München, Garching b. München, Germany

Due to the broad range of modern applications, the demand for photodetectors is drastically increasing, and in particular, organic photodetectors (OPDs) can meet the diverse requirements. However, the specific detectivity of OPDs is significantly below the thermal limit and is currently restricted by the high noise spectral density. Kublitski *et al.* [1] recently showed that the shot noise and hence the dark current (J_D) dominates the noise spectral density at negative bias. Further, the authors suspect that mid-gap trap states cause the high J_D .

Here, we study devices with a well-performing absorber layer without an electron acceptor and, therefore, we do not expect any charge-transfer states to form. Nevertheless, we can observe sub-bandgap absorption in ultra-sensitive external quantum efficiency measurements. By utilizing different device processing parameters and employing different interface layers, we identify the origin of these sub-bandgap excitations. Interestingly, we observe a clear correlation between the device performance and the presence and quantity of trap states. The relation between molecular structure and device performance gives a new direction for reducing J_D further in OPDs and improving their specific detectivity. [1] Kublitski, J. *et al.* Nat Commun 12, 551 (2021)

CPP 2: Polymer Networks and Elastomers

Time: Monday 9:30–10:30

Location: H39

CPP 2.1 Mon 9:30 H39

The non-ideal preparation state of polymer (model) networks — •MICHAEL LANG¹ and TONI MÜLLER^{1,2} — ¹Institut Theorie der Polymere, Leibniz Institut für Polymerforschung Dresden, Hohe Straße 6, 01069 Dresden, Germany — ²Institut für Theoretische Physik, Technische Universität Dresden, Zellescher Weg 17, 01069 Dresden, Germany

We demonstrate that the phantom modulus can be split into two major contributions: the cycle rank of the active network structure and a correction resulting predominantly from non-ideal chain conformations at the instance of cross-linking. The correction contains several contributions related to loop formation, an effective repulsion between network junctions, and an excess strain of chains that develops towards the end of the reactions, if reaction partners become sparse. This challenges the text-book assumption that network strands are incorporated into the network with the same conformations as a free chain inside the reaction container. Our results are relevant for developing a better understanding of rubber elasticity and its dependence on the network formation process.

CPP 2.2 Mon 9:45 H39

Nonlinear elasticity under constraints and predeformations: a group theoretical approach — •SEGUN GOH^{1,2}, HARTMUT LÖWEN², and ANDREAS M. MENZEL³ — ¹Forschungszentrum Jülich, 52425 Jülich, Germany — ²Heinrich-Heine Universität Düsseldorf, 40225 Düsseldorf, Germany — ³Otto-von-Guericke-Universität Magdeburg, 39106 Magdeburg, Germany

The mechanical response of elastic materials frequently involves predeformations. Moreover, if an active or driven material is exposed to an external condition, a mismatch between the activity/driving and external condition may lead to a hidden predeformation in the system in its mechanical equilibrium state. Then the assumption of linear response breaks down, making descriptions of nonlinear elasticity compulsory even if the applied deformation is infinitesimally small. In this talk, we discuss how to develop a theoretical framework to meet this challenge and thereby, to address elasticity consistently for both small and large deformations. Specifically, employing concepts from group theory and Lie algebra, we suggest an idea to construct finite deformation gradients from infinitesimal group generators. Generalized nonlinear shear deformations and elastic moduli are defined subsequently. Possible applications will also be discussed.

CPP 2.3 Mon 10:00 H39

Surface structure and rheology of amphiphilic co-polymer networks on different length scales — •KEVIN HAGMANN¹, NORA FRIBICZER², SEBASTIAN SEIFFERT², CAROLIN BUNK³, FRANK BÖHME³, and REGINE VON KLITZING¹ — ¹Institute for Condensed Matter Physics, Technische Universität Darmstadt, D-64289 Darmstadt — ²Department of Chemistry, Johannes Gutenberg University Mainz, D-55128 Mainz — ³Leibniz-Institut für Polymerforschung Dresden e.V., D-01069 Dresden

This study focuses on the relation between structure, swelling abilities and mechanical/rheological properties of films of amphiphilic co-polymer networks (ACNs). First, the correlation between different synthesis strategies for gel films and their resulting properties will be described. Secondly, the effect of solvents of different polarity on the swelling ability will be presented on different length scales. For this purpose, topology and near surface structure are studied with atomic force microscopy (AFM) and grazing incidence small angle x-ray scattering (GISAXS), respectively. We also put special emphasis on the determination of mechanical and rheological properties laterally and orthogonally to the gel surface by carrying out dynamic AFM indentation experiments. In order to evaluate heterogeneities the mechanical and rheological behaviour at the interface of the ACNs will be presented on various length scales (nm - μ m). The study shows that the synthesis strategy has a strong effect on the gel structure and on nano/microrheological properties. The structure and rheology of gel films will be compared with results obtained of the respective bulk gel.

CPP 2.4 Mon 10:15 H39

Correlations of infrared spectroscopy and DSC measurements to determine the yield of scission under irradiation in biopolyesters — •DAVID KRIEG, MIRKO RENNERT, and MICHAEL NASE — Institut für Biopolymerforschung der Hochschule für Angewandte Wissenschaften Hof

Under the influence of ionizing irradiation, biopolyesters can either undergo crosslinking or scissioning. It was shown that the yield of crosslinking for polyesters such as polybutylenadipat-terephthalat (PBAT) can be correlated to changes in peaks in the IR spectrum and the onset time of the melting peak while heating during DSC measurements using the Avrami equation [Kijchavengkul 2008]. For biopolyesters such as polyhydroxybutyrate (PHB) and polylactic acid (PLA) scissioning is the dominant process under irradiation. This talk will go into detail, whether similar correlations as seen in crosslinking PBAT can be found in PLA and PH3B, when scission is the dominant reaction and what structural changes in the polymer make this correlation possible.

CPP 3: Perovskite and Photovoltaics 1 (joint session HL/CPP/KFM)

Time: Monday 9:30–12:45

Location: H34

See HL 5 for details of this session.

CPP 4: 2D Materials 1 (joint session HL/CPP/DS)

Time: Monday 9:30–12:45

Location: H36

See HL 6 for details of this session.

CPP 5: Wetting, Droplets and Microfluidics (joint session DY/CPP)

Time: Monday 10:00–12:15

Location: H19

See DY 4 for details of this session.

CPP 6: Active Matter 1 (joint session BP/CPP/DY)

Time: Monday 10:30–12:45

Location: H16

See BP 4 for details of this session.

CPP 7: Wetting, Fluidics and Liquids at Interfaces and Surfaces

Time: Monday 10:45–13:00

Location: H39

CPP 7.1 Mon 10:45 H39

Coupling of liquid-liquid phase separation and wetting dynamics — •YUCHUANG CHAO, OLINCA RAMÍREZ-SOTO, CHRISTIAN BAHR, and STEFAN KARPITSCHKA — Max Planck Institute for Dynamics and Self-Organization, 37077 Göttingen, Germany

The interplay of phase separation and surface wetting is of great interest for various fields, ranging from industrial applications of oil recovery to the formation of membraneless organelles in living cells. Most of previous studies focus on understanding the interaction of phase separation with static wetting, i.e., pinned contact line conditions; nevertheless, how phase separation interacts with dynamical wetting, for instance, advancing contact lines is still unclear. Here, using highly mobile, Marangoni-contracted droplets of evaporating, binary liquid mixtures with a well-defined miscibility gap on fully wetting substrates, we explore the interplay of phase separation and wetting dynamics. Interestingly, we observe an abrupt wetting transition: from a contracted droplet state in the one-phase region to an actively driven spreading motion in the two-phase region; This is caused by the strong coupling of liquid-liquid phase separation and advancing contact lines, together with effects of evaporative enrichment and surface forces. Our finding may enable the development of novel surface processing strategies.

CPP 7.2 Mon 11:00 H39

Liquid phase separation during soft dynamic wetting — •LUKAS HAUER¹, ZHUOYUN CAI², JONATHAN T. PHAM², and DORIS VOLLMER¹ — ¹Max Planck Institute for Polymer Research, Ackermannweg 10, 55128 Mainz, Germany — ²Department of Chemical and Materials Engineering, University of Kentucky, Lexington, Kentucky, USA

Droplets sitting on soft substrates deform the material around the three-phase contact line, i.e., the formation of the wetting ridge. While on liquid films the ridge geometry is solely governed by capillarity, on (visco)elastic films elastic contributions add to the ridge geometry. Recently, on (visco)elastic materials a capillary induced phase-separated region of pure liquid was observed. Here, we investigate this phase separation on crosslinked PDMS films with differing amounts of free oligomer chains during dynamic wetting. We let droplets forcefully slide over PDMS films while monitoring the ridge zone with laser scanning confocal microscopy. Different dyes in the crosslinked network and in the free oligomers enable discrimination between the two phases. We find that phase-separation competes with the motion of the droplet: by tuning the droplets' speed, the phase-separated ridge height ranges from $> 30 \mu\text{m}$ (at $5 \mu\text{m/s}$) to no phase separation at all for fast speeds.

15 min. break

CPP 7.3 Mon 11:30 H39

Deep learning to analyze sliding drops — •SAJJAD SHUMALY, FAHMEH DARVISH, XIAOMEI LI, ALEXANDER SAAL, CHIRAG HINDUJA, WERNER STEFFEN, OLEKSANDRA KUKHARENKO, RÜDIGER BERGER, and HANS-JÜRGEN BUTT — Max Planck Institute for Polymer Research, Ackermannweg 10, D-55128, Mainz, Germany

Investigation of drop sliding forces requires knowledge of the shape of the drop close to the three-phase contact line. State-of-the-art contact angle measurement methods are designed for analyzing symmetric and high-resolution images of the drop. The analysis of videos of drops sliding down a tilted plane is hampered due to the low-resolution of the cutout area where the drop is visible. The drop is just a part of the whole image. In addition, drops sliding down a tilted plate are unsymmetrical in shape and the three-phase contact line may deform due to the sticky points.

In order to increase the accuracy of the measured contact angle, we trained a deep learning-based super-resolution model with an up-scale ratio of 3, i.e. the trained model is able to enlarge droplet images 9 times. In the second step, we performed an optimized polynomial fitting approach to measure the contact angle even for symmetric, asymmetric, or deformed droplets without the need for liquid parameters. To find the best parameters for polynomial fitting in our special problem, we conducted a systematic experiment using synthetic images.

CPP 7.4 Mon 11:45 H39

How often a Drops Sticks and Slips at a Wetting Transition — CHIRAG HINDUJA¹, ALEXANDRE LAROCHE^{1,2}, SAJJAD SHUMALY¹, YUJIAO WANG^{3,4}, DORIS VOLLMER¹, HANS-JÜRGEN BUTT¹, and •RÜDIGER BERGER¹ — ¹Max Planck Institute for Polymer Research, 55128 Mainz, Germany — ²University of Zurich, 8057 Zurich, Switzerland — ³Key Laboratory of Interfacial Physics and Technology, Shanghai Institute of Applied Physics, Chinese Academy of Sciences, Shanghai 201800, China — ⁴University of Chinese Academy of Sciences, Beijing 100049, China

We will discuss forces of sliding drops at a sharp wetting transitions featuring no topographic variation. Such surfaces with different wetting properties were

made from chemical vapor deposition of trichlorooctylsilane (OTS) and trichloro(perfluoro) octylsilane (PFOCTS). We observed that drops sliding from an area of low to high contact angle hysteresis exhibit two force maxima. The drop motion is characterized by pinning of the advancing and receding contact lines, respectively. Accordingly, the motion of the drop follows two stick-slip processes. Drops sliding from an area of high to low contact angle hysteresis exhibit a single local force maximum, a single stick process, but two slip processes.

Sliding forces of drops were measured by a novel tool named scanning Drop Adhesion Force Instrument (sDAFI) which we use to image, locate and characterize wetting properties of cm-large areas with a resolution down to the micrometer-scale.

CPP 7.5 Mon 12:00 H39

Tunable lamellar topography driven by wetting dynamics — •GISSELA CONSTANTE¹, INDRA APSITE¹, PAUL AUERBACH², SEBASTIAN ALAND², DENNIS SCHÖNFELD³, THORSTEN PRETSCH³, PAVEL MILKIN¹, and LEONID IONOV^{1,4} — ¹University of Bayreuth, Bayreuth, Germany — ²Hochschule für Technik und Wirtschaft Dresden, Dresden, Germany — ³Fraunhofer Institute for Applied Polymer Research IAP, Postdam, Germany — ⁴Bavarian Polymer Institute, Bayreuth, Germany

The fabrication of switchable surfaces has been of interest in several fields such as biotechnology, industry, and others. The selection of materials and methods is crucial to provide proper control on the tunable surface. In this research, an exceptional high aspect ratio lamellar surface topography was fabricated by melt-electrowriting of microfibers of a shape-memory thermo-responsive polyurethane. Two different types of stimuli: temperature and light exposition were applied to modify the mechanical properties of shape memory polymer and thus program deformation and recovery of the surface. Wetting studies showed that the deformation of the high aspect ratio lamellar surface can be tuned not only manually, but as well by a liquid droplet. This behavior is controlled by temperature changes during direct heating/cooling or by exposure to light. The liquid in combination with thermo-responsive topography presents a new type of wetting behavior. This feature opens the possibility to apply such topographies for the design of smart elements for microfluidic devices, for example, smart valves.

CPP 7.6 Mon 12:15 H39

Gradient dynamics model for sessile drop evaporation in a gap: from simple to applied scenarios — •SIMON HARTMANN¹, UWE THIELE¹, CHRISTIAN DIDDENS², and MAZIYAR JALAL³ — ¹Institut für Theoretische Physik and Center for Nonlinear Science, Universität Münster — ²Physics of Fluids group, Max Planck Center Twente for Complex Fluid Dynamics, and J. M. Burgers Center for Fluid Dynamics, University of Twente — ³Van der Waals-Zeeman Institute, Institute of Physics, University of Amsterdam

We consider an evaporating drop of volatile partially wetting liquid on a rigid solid substrate. In addition, the setup is covered with a plate, forming a narrow gap with the substrate. First, we develop an efficient mesoscopic description of the liquid and vapor dynamics in a gradient dynamics form. It couples the diffusive dynamics of the vertically averaged vapour density in the narrow gap to an evolution equation for the drop profile. The dynamics is purely driven by a free energy functional that incorporates wetting, bulk and interface energies of the liquid as well as vapour entropy.

Subsequently, we employ numerical simulations to validate the model against both experiments and simulations based on Stokes equation. Finally, we show that the gradient dynamics approach allows for extensions of our model to cover more intricate scenarios, e.g., spreading drops of volatile liquid on polymer brushes or on porous media.

CPP 7.7 Mon 12:30 H39

Dewetting of thin lubricating films under aqueous drops on high and low surface energy surfaces — •BIDISHA BHATT, SHIVAM GUPTA, VASUDEVAN SUMATHI, SIVASURENDER CHANDRAN, and KRISHNACHARYA KHARE — Indian Institute of Technology Kanpur, Kanpur, India

Understanding the stability of thin liquid films under different environments is important due to their potential applications, such as coatings, paints, and printing, to name a few. In this work, we investigate the stability of thin liquid films of a lubricating fluid under aqueous drops on slippery surfaces. Lubricating films under aqueous drops are found stable when the total excess free energy of the system is positive, which otherwise would dewet into droplets on hydrophilic surfaces. The dewetting dynamics and the apparent contact angle of the aqueous drop depend on the thickness of the lubricating film and the final morphology depends on interfacial boundary conditions between film and the substrate. However, the lubricating films on hydrophobic surfaces are stable under the aqueous drops, yet they can be destabilized using external perturbations like an electric field. Due to the electric field, surface capillary waves are

generated at the film-drop interface, and the amplitude of the waves grows exponentially with time, similar to spinodal dewetting. Experimentally observed wavelength and growth rate of the surface capillary waves show good agreement with the theoretically predicted value using linear stability analysis. The dewetted droplets coalesce and form a uniform film again upon removing the applied voltage, making the dewetting process fully reversible.

CPP 7.8 Mon 12:45 H39

Cloaking Transition of Droplets on Lubricated Brushes — •RODRIQUE BADR¹, FRIEDERIKE SCHMID¹, DORIS VOLLMER², and LUKAS HAUER² — ¹Johannes Gutenberg University, Mainz, Germany — ²Max Plank Institute for Polymer Physics, Mainz, Germany

We study the equilibrium properties and wetting behavior of a simple liquid on a polymer brush, with and without the presence of lubricant. We investigate the behavior of the brush in terms of grafting density and the amount of lubricant present. As for the wetting behavior, we study a sessile droplet on top of the brush. Our model and choice of parameters results in the formation of a wetting ridge and in the cloaking of the droplet by the lubricant, a phenomenon that is observed experimentally and is of integral importance to the dynamics of sliding droplets. We quantify the cloaking in terms of its thickness, which increases with the amount of lubricant present, and provide thermodynamic theory to explain the behavior. In addition, we investigate the dependence of contact angles on the size of the droplet and the possible effect of line tension, as well as the dependence on the cloaking/lubrication of the brush.

CPP 8: Focus Session: Photonic Structures from Polymer and Colloidal Self-Assembly

organized by Ilja Gunkel (University of Fribourg) and Bodo Wilts (University of Salzburg)

Time: Monday 15:00–17:15

Location: H38

Invited Talk

CPP 8.1 Mon 15:00 H38

Stimuli-Responsive Opal Films based on Core-Shell Particle Self-Assembly — •MARKUS GALLEI — Lehrstuhl für Polymerchemie, Universität des Saarlandes, Campus C4 2, Saarbrücken

In the last decade stimuli-responsive polymers have proven their feasibility for a wide range of important applications. These polymers are capable of changing their conformation, solubility, or they can even break or form covalent bonds upon a change of temperature or pH, light irradiation or by electrochemical stimuli, or combinations thereof. The presentation will focus on materials, which contain at least one selectively addressable segment, either chemically or physically. Functional porous nanostructures based on inverse opal films obtained after shear-induced particle self-assembly will be highlighted and discussed in more detail. In the case of soft colloidal crystal and their inverted structures, external triggers additionally lead to a remarkably fast and reversible change of their intriguing optical properties. Moreover, such opal structures can be used for the design of smart catch and release systems based on responsive moieties, but also as soft templates for ceramic materials. The talk will give some recent examples for the rational design of functional organic as well as hybrid porous materials with hierarchical architectures. Some of the highlighted polymer or polymer-templated structures can be advantageously used for direct conversion into ordered ceramic or carbonaceous materials. Herein presented preparation strategies will pave the way for a manifold of applications in the field of sensing and robust membrane technologies.

CPP 8.2 Mon 15:30 H38

Strategies for increased colour saturation in colloidal photonic crystals — •GUDRUN BLEYER¹, CARINA BITTNER¹, LUKAS ROEMLING¹, NICO NEES², ERIC GOERLITZER¹, and NICOLAS VOGEL¹ — ¹Institute of Particle Technology (LFG), FAU, Erlangen, Germany — ²Chair of Applied Mathematics, FAU, Erlangen, Germany

Monodisperse polystyrene nanoparticles are easily synthesized using surfactant free emulsion polymerization, making them ideal accessible building block for photonic crystals via self-assembly.

However, structures made only with polystyrene display a whitish hue of colour as incoherent scattering at defects in the crystal structure overlaps with the photonic stop band from constructive interference. We investigate how the colour saturation in colloidal photonic crystals depends on the local and global ordering of the particles and the absorptive properties of additive materials.

First, we assemble photonic crystals using two methods resulting in structures displaying different defect characteristics. We then correlate the photonic properties as a function of these defects using correlative microscopy connecting optical imaging, reflectance spectra and SEM measurements to establish the structure-property relationship.

Secondly, we introduce absorbing material at defined positions within the colloidal photonic crystal with the goal to optimize not only the amount but the absorber position as well, allowing for an optimized colour saturation.

Invited Talk

CPP 8.3 Mon 15:45 H38

Self-assembled photonic pigments from bottlebrush block copolymers — •RICHARD PARKER, TIANHENG ZHAO, ZHEN WANG, CLEMENT CHAN, and SILVIA VIGNOLINI — Yusuf Hamied Department of Chemistry, University of Cambridge, United Kingdom

The self-assembly of bottlebrush block copolymers (BBCPs) into photonic materials has drawn significant attention due to the flexibility and diversity of the building blocks that can be synthesised. In this talk we will introduce a robust strategy for the fabrication of hierarchical photonic pigments via the confined self-assembly of BBCPs within emulsified microdroplets. By utilising an amphiphilic BBCP and optimising the emulsification conditions, we will demon-

strate the formation of structurally coloured particles with a correlated disordered structure (i.e. a photonic glass) and compare them to particles with a highly-ordered concentric lamellar structure (i.e. a 1D photonic crystal). The mechanisms behind these two different architectures will be proposed and methods to tune the reflected colour of the respective systems considered. Finally, the strengths and weaknesses of the two approaches will be summarised in terms of the optical properties of the particles, the scalability of the approach and their viability as real-world colorants.

CPP 8.4 Mon 16:15 H38

Elucidating the chiral self-assembly of cellulose nanocrystals for photonic films — •THOMAS PARTON, RICHARD PARKER, GEA VAN DE KERKHOFF, AURIMAS NARKEVICIUS, JOHANNES HAATAJA, BRUNO FRKA-PETESIC, and SILVIA VIGNOLINI — Department of Chemistry, University of Cambridge, United Kingdom

Cellulose nanocrystals (CNCs) are naturally-sourced elongated nanoparticles that form a cholesteric colloidal liquid crystal phase in suspension. Interestingly, this helicoidal arrangement can be preserved upon drying to create films with vibrant structural colour. However, while CNCs have drawn significant attention as a way to produce sustainable photonic materials, the underlying mechanism by which chirality arises in the mesophase remains unclear. Although the morphology of individual CNCs is believed to play an important role, most particles are not strongly twisted, and the suspensions exhibit considerable polydispersity in both particle size and shape.

In this study, we performed an in-depth morphological analysis of CNCs observed using transmission electron microscopy (TEM) and atomic force microscopy (AFM). We sequentially tuned the size and shape of the CNCs using ultrasonication and correlated the morphology of individual nanoparticles with their ensemble liquid crystalline behaviour and photonic response. This analysis revealed that a sub-population of CNC “bundles” (i.e. clusters of laterally-bound elementary crystallites) act as chiral dopants, analogous to those used for molecular liquid crystals, and are therefore essential for the formation of the cholesteric phase.

15 min. break

Invited Talk

CPP 8.5 Mon 16:45 H38

Hierarchically structured mechanochromic deformation-sensing pigments — •JESSICA CLOUGH¹, CÉDRIC KILCHOER¹, BODO WILTS^{1,2}, and CHRIS WEDER¹ — ¹Adolphe Merkle Institute, University of Fribourg, Chemin des Verdiers 4, Fribourg 1700, Switzerland — ²Chemistry and Physics of Materials, University of Salzburg, Jakob-Haringer-Str. 2a, 5020 Salzburg, Austria.

Mechanochromic materials can change their colour in response to mechanical force and are useful for fundamental studies as well as practical applications. A versatile platform with extended sensing capabilities would be valuable for monitoring complex mechanical behaviours and failure events. Here, we report that this is possible by combining photonic structures, which alter their reflection upon deformation, and covalent mechanophores, whose absorption changes upon mechanically induced bond scission, in hierarchically structured assemblies. This was achieved by synthesising microspheres of an elastic polymer with spiropyran-based cross-links and incorporating non-close-packed silica nanoparticles into this matrix. The shift of the reflection band produced by the silica is noticeable at less than 1% strain, while the conversion of the spiropyran can require strains exceeding 50%. The two responses can be tailored via the silica content and the cross-link density. The mechano-sensing pigments can readily be incorporated into different materials of interest and probe local deformations from within. This was demonstrated by monitoring high-strain deformation of poly(dimethyl siloxane) in compression and local strain field variations caused by the necking of semicrystalline polyethylene.

CPP 9: Modeling and Simulation of Soft Matter (joint session CPP/DY)

Time: Monday 15:00–17:45

Location: H39

CPP 9.1 Mon 15:00 H39

Machine Learning of consistent thermodynamic models using automatic differentiation — •DAVID ROSENBERGER¹, KIPTON BARROS², TIMOTHY GERMAN², and NICHOLAS LUBBERS² — ¹Freie Universität Berlin, Berlin, Germany — ²Los Alamos National Laboratory, Los Alamos, NM, USA

Instead of fitting suitable analytical expressions to thermophysical data, we propose to combine automatic differentiation and artificial neural networks (ANNs) to obtain complex equations of state (EOS) for arbitrary systems. Rather than training directly on the properties of interest, we train an ANN on a model free energy whose partial derivatives match the thermophysical properties measured in experiment. We show that this method is advantageous over direct learning of thermodynamic properties, in terms of both accuracy and the exact preservation of the Maxwell relations. Furthermore, the method can implicitly solve the integration problem of computing the free energy of a system without explicit integration given appropriate data to learn from.

CPP 9.2 Mon 15:15 H39

Atomistic Machine Learning for Aqueous Ionic Solutions — •PHILIP LOCHE, KEVIN K. HUGUENIN-DUMITTAN, and MICHELE CERIOTTI — Laboratory of Computational Science and Modeling, IMX, École Polytechnique Fédérale de Lausanne, 1015 Lausanne, Switzerland

Accurate modeling of matter at the atomic scale requires to simultaneously account for the quantum nature of the chemical bond - that usually manifests itself on short time and length scales - and long-range interactions, such as electrostatics and dispersion, that occur on a large scale and often result in phenomena with a long characteristic time. Electronic structure calculations provide an accurate description of both quantum and long-range effects, but are computationally demanding, and scale poorly with system size. Machine learning (ML) approaches have emerged as a very effective strategy to build surrogate models that provide comparable accuracy at a fraction of the cost, but the most widespread techniques base their efficiency and transferability on a local description of atomic structure, which makes them ill-equipped to deal with long-range effects.

Here, we are going to connect local and long range physics in a data driven ML approach by applying the current ML techniques to, condensed-phase systems, involving the characterization of aqueous ionic solutions. We show that only a combination of a long and a short range approach is able to predict short distanced molecular vibrations as well as a long ranged ionic screening lengths.

CPP 9.3 Mon 15:30 H39

Identification of glass transition temperature for polymer melts using data-driven methods — •ATREYEE BANERJEE, HSIAO-PING HSU, OLEKSANDRA KUKHARENKO, and KURT KREMER — Max Planck Institute for Polymer Research, Ackermannweg 10, 55128 Mainz, Germany

On fast cooling, the dynamics of polymer melts slow down exponentially, leading to solid glassy states without any drastic change in the structural structure. We employ data-driven methods based on purely conformational fluctuations to identify the glass transition temperature for a coarse-grained weakly semi-flexible polymer model. More precisely, we used principal component analysis (PCA) to quantify the conformational fluctuations and identify a sharp change in fluctuation around the glass transition temperature. The first eigen value of PCA shows a clear difference below and above glass transition temperatures. The new method of glass transition temperature predicted from PCA considers local structural fluctuations and does not depend on any fitting parameters like the existing methods.

CPP 9.4 Mon 15:45 H39

Systematic parametrization of non-Markovian dissipative thermostats for coarse-grained molecular simulations with accurate dynamics — •VIKTOR KLIPPENSTEIN and NICO F. A. VAN DER VEGT — Eduard-Zintl-Institut für Anorganische und Physikalische Chemie, Technische Universität Darmstadt, 64287 Darmstadt, Germany

The Mori-Zwanzig theory, in principle, allows to derive an exact equation of motion for coarse-grained degrees of freedom based on the dynamics of an underlying fine-grained reference system.[1] Still, in practice the simultaneous representation of structural and dynamic properties in particle-based models poses a complicated problem, e.g. due to the non-linearity of the exact coarse-grained equation of motion.

A viable approximate approach is to start from a conservative coarse-grained force-field and to extend the standard Newtonian equation of motion used in molecular simulation with a linear generalized Langevin thermostat. We demonstrate how such a thermostat can be parametrized to correctly represent dynamic properties, both in a purely bottom-up approach[2,3] or by applying iterative optimization.[3] We consider the Asakura-Oosawa model as a simple test case.[3] [1] V. Klippenstein, M. Tripathy, G. Jung, F. Schmid, and N. F. A. van der Vegt, *The Journal of Physical Chemistry B* 125, 4931 (2021).

[2] V. Klippenstein and N. F. A. van der Vegt, *The Journal of Chemical Physics* 154, 191102 (2021).

[3] V. Klippenstein and N. F. A. Van Der Vegt, *The Journal of Chemical Physics* under review (2022).

CPP 9.5 Mon 16:00 H39

Stretching biopolymers with fluctuating bending stiffness — •PANAYOTIS BENETATOS — Kyungpook National University, Daegu, South Korea

In many biopolymers, the local bending stiffness fluctuates. For example, DNA-binding proteins attach to and detach from DNA to regulate cellular functions, thus causing a change in the local bending stiffness of the polymer backbone. This could also happen due to internal conformational transitions, such as the DNA denaturation or the helix-coil transition in polypeptides. What all these cases have in common is that the change in the local flexibility is transient and reversible. In order to analyse the conformational and elastic behaviour of such biopolymers, we propose a minimal but encompassing model of a freely jointed chain with reversible hinges (rFJC). We show that the tensile response of a rFJC is remarkably different from that of the usual freely jointed chain (uFJC). At small stretching forces, the rFJC is more compliant than the uFJC and the size (mean square end-to-end distance) of the former is greater than that of the latter. At strong stretching forces, in contrast, the rFJC is much stiffer than the uFJC. In this talk, we also discuss a strongly stretched wormlike chain with fluctuating local bending stiffness. We show that, under certain conditions, we get significant ensemble inequivalence (Gibbs vs Helmholtz).

CPP 9.6 Mon 16:15 H39

Modulating internal transition kinetics of responsive macromolecules by collective crowding — •NILS GÖTH, UPAYAN BAUL, MICHAEL BLEY, and JOACHIM DZUBIELLA — Applied Theoretical Physics—Computational Physics, Physikalisches Institut, Albert-Ludwigs-Universität Freiburg, 79104 Freiburg, Germany

Packing and crowding are used in biology as mechanisms to (self-) regulate internal molecular or cellular processes based on collective signaling. Here, we study how the transition kinetics of an internal “switch” of responsive macromolecules is modified collectively by their spatial packing. We employ Brownian dynamics simulations of a model of Responsive Colloids, in which an explicit internal degree of freedom—here, the particle size—moving in a bimodal energy landscape self-consistently responds to the density fluctuations of the crowded environment. The bimodal energy landscape is motivated by existing two-state behavior like in protein folding or hydrogels with bimodal volume transitions. We demonstrate that populations and transition times for the two-state switching kinetics can be tuned over one order of magnitude by “self-crowding”. An exponential scaling law derived from a combination of Kramers’ and liquid state perturbation theory is in very good agreement with the simulations.

[1] Upayan Baul, NG, MB, and JD, *J. Chem. Phys.* 155, 244902 (2021).

15 min. break

CPP 9.7 Mon 16:45 H39

Modelling process-structure-properties of polymer nanocomposites — •JANETT PREHL, CONSTANTIN HUSTER, and KARL HEINZ HOFFMANN — TU Chemnitz, Chemnitz, Germany

Twin polymerization is a complex chemical reaction process leading to a broad range of organic-inorganic nano composite materials.

Within this presentation we will show our latest results [1] on the theoretical analysis of the structure formation process of twin polymerization via a previously introduced lattice-based Monte Carlo method, the reactive bond fluctuation model [2]. We analyze the effects of various model parameters, such as movability, attraction, or reaction probabilities on structural properties, like the specific surface area, the radial distribution function, the local porosity distribution, or the total fraction of percolating elements.

From these examinations, we may identify structural key factors and thus chemical properties of the underlying components that need to be adapted to fulfill desired requirements for possible applications.

[1] Prehl, J. and Huster, C., *polymers* 11 (2019) 878

[2] Hoffmann, K.H. and Prehl, J., *Reac. Kinet. Mech. Cat.* 123 (2018) 367-383; Huster, C., Nagel, K., Spange, S., and Prehl, J., *Chem. Phys. Lett.* 713 (2018) 145-148

CPP 9.8 Mon 17:00 H39

A cosolvent surfactant mechanism affects polymer collapse in miscible good solvents — •SWAMINATH BHARADWAJ¹, DIVYA NAYAR^{1,2}, CAHIT DALGICDIR¹, and NICO VAN DER VEGT¹ — ¹Technische Universität Darmstadt, Germany — ²IIT Delhi, India

The coil-globule transitions of aqueous polymers are of profound significance in understanding the structure and function of responsive soft matter. In particu-

lar, the remarkable effect of amphiphilic cosolvents (which preferentially adsorb on the polymer surface) that leads to both swelling and collapse of stimuli responsive polymers is still hotly debated in the literature [1]. The predominant focus has been on the attractive polymer-(co)solvent interactions and the role of solvent-excluded volume interactions has been largely neglected. The solvent-excluded volume contribution to the solvation free energy corresponds to the formation of a repulsive polymer-solvent interface.

Using MD simulations, we herein demonstrate that alcohols reduce the free energy cost of creating a repulsive polymer-solvent interface via a surfactant-like mechanism which surprisingly drives polymer collapse at low alcohol concentrations. This hitherto neglected role of interfacial solvation thermodynamics is common to all coil-globule transitions [2], and rationalizes the experimentally observed effects of higher alcohols and polymer molecular weight on the coil-to-globule transition of thermoresponsive polymers [2]. This mechanism is generic and applicable to other solutions containing amphiphilic cosolvents or cosolutes.

References: [1] S. Bharadwaj et al., *Soft Matter*, 2022, 18, 2884. [2] S. Bharadwaj et al., *Commun. Chem.*, 2020, 3, 165.

CPP 9.9 Mon 17:15 H39

Water transport in soft nanoporous materials: Impact of mechanical response on dynamics, slippage and permeance — •ALEXANDER SCHLAICH^{1,2}, MATTHIEU VANDAMME³, MARIE PLAZANET², and BENOIT COASNE² — ¹Stuttgart Center for Simulation Science (SC SimTech), University of Stuttgart, Germany — ²Univ. Grenoble Alpes, CNRS, LIPhy, 38000 Grenoble, France — ³Navier, Ecole des Ponts, Univ. Gustave Eiffel, CNRS, Marne-la-Vallée, France
Transport of water in soft porous materials is relevant to applications such as ultrafiltration and reverse osmosis processes, where polymeric membranes are employed in filtration/separation, or energy related processes. While water transport in hard porous materials such as porous silica glasses is well studied, the situation in soft matter is much more puzzling and remains unclear due to the combination of surface heterogeneity, the diffuse boundary location and pore deformations due to mechanical stresses.

In this work we study water in chemically realistic hydrophobic pores at different thermodynamic and mechanical conditions using atomistic molecular dynamics simulations. In detail, we analyze pore swelling, adsorption and confinement effects as well as microscopic diffusion mechanisms and transport effects due to pore size fluctuations. Strikingly, we find that hydrodynamic continuum models remain valid for planar flow of water even in monolayer confinement in soft pores.

CPP 9.10 Mon 17:30 H39

Solvation structure of polymer cathodes for Li/S batteries — •DIPTESH GAYEN¹, YANNIK SCHUETZE², SEBASTIEN GROH¹, and JOACHIM DZUBIELLA¹ — ¹Institute of Physik, University of Freiburg, Freiburg, Germany — ²Helmholtz Zentrum Berlin, Berlin

Lithium-sulfur (Li/S) batteries are regarded as one of the most promising next-generation energy storage devices. Meanwhile, some challenges inherent to Li/S batteries remain to be solved, for instance, the polysulfide shuttle effect and the volume expansion of the cathode during discharge. To suppress the above-mentioned drawbacks, polymeric cathodes, e.g., based on poly(4-(thiophen-3-yl) benzenethiol) (PTBT) are considered sulfur host material (S/PTBT). Here, we use molecular dynamics (MD) computer simulations to study the structure and dynamics of a single PTBT chain at 300 K in different concentrations and compositions of dimethoxyethane (DME) and dioxolane (DOL) solvents. The force-field parameters for this polymer were constructed based on the OPLS database, with missing parameters newly developed by us by benchmarking to density-functional theory calculations. We report results on polymer conformational behavior, solvent-specific adsorption, and thermodynamic properties such as the partial molar volume. Our results show that DOL is more absorbed at the PTBT compare to DME. We find no significant effect of the solvent on the structure factor of the polymer. Our simulation model enables future systematic studies of PTBT in various solvent mixtures, in particular electrolytes, for the optimizations of modern Li/S batteries.

CPP 10: 2D Materials 2 (joint session HL/CPP/DS)

Time: Monday 15:00–18:30

Location: H36

See HL 11 for details of this session.

CPP 11: 2D Materials 3 (joint session CPP/DS)

Time: Monday 17:15–17:45

Location: H38

CPP 11.1 Mon 17:15 H38

On the electronic pi-system of 2D covalent organic frameworks — •KONRAD MERKEL, JOHANNES GREINER, and FRANK ORTMANN — TU München
We investigate a family of 2D hexagonal covalent organic frameworks (COFs) with different linker monomers regarding their electronic structure and pi-conjugation. Molecular orbitals can be obtained from maximally localized Wannier functions and turn out to be sigma- and pi-like orbitals forming distinct sigma- and pi-bands, respectively. The Wannier description enables a detailed analysis of the topology, effective coupling and delocalization of the entire pi-system. We identify conjugated states that are delocalized across multiple building blocks of the COF and show their robustness against perturbations like out-of-plane rotations of molecular fragments and different strength of Anderson disorder. Furthermore, we apply the nucleus-independent chemical shift (NICS), which is an established measure of aromaticity. All results are compared for different types of linker units with different degrees of pi-conjugation.

CPP 11.2 Mon 17:30 H38

Permeation of gases through molecularly thin carbon nanomembranes — •VLADISLAV STROGANOV¹, DANIEL HÜGER¹, TABATA NÖTHEL¹, CHRISTOF NEUMANN¹, UWE HÜBNER², MICHAEL STEINERT¹, MONIKA KRUK³, PIOTR CYGANIK³, and ANDREY TURCHANIN¹ — ¹Friedrich-Schiller University Jena, Jena, Germany — ²Leibniz Institute of Photonic Technology, Jena, Germany — ³Jagiellonian University, Kraków, Poland

Atomically thin carbon nanomembranes (CNMs) are promising candidates for next generation filtration and gas separation technologies. However, the gas permeation mechanism through CNMs is not fully understood yet. To improve this knowledge, we investigated permeation of helium, deuterium, water vapor and other gases through a series of CNMs under different conditions. The CNMs were synthesized from biphenyl substituted carboxylic acids on silver substrate $C_6H_5-C_6H_4-(CH_2)_n-COOAg$, with different lengths of aliphatic linker $n = 2 - 6$. A CNM based on terphenyl thiol (TPT) was used as a well-known reference system. We demonstrated that even the smallest variation in the structure of the molecular precursor lead to significant change of the permeation properties.

CPP 12: Poster 1

Active Matter (12.1-12.2), Biopolymers, Biomaterials and Bioinspired Functional Materials (12.3-12.9), Charged Soft Matter, Polyelectrolytes and Ionic Liquids (12.10-12.15), Complex Fluids and Colloids, Micelles and Vesicles (12.16-12.19), Emerging Topics in Chemical and Polymer Physics, New Instruments and Methods (12.20-12.22), Modeling and Simulation of Soft Matter (12.23-12.28), Responsive and Adaptive Systems (12.29-12.35), Wetting, Fluidics and Liquids at Interfaces and Surfaces (12.36-12.39), Electrical, Dielectrical and Optical Properties of Thin Films (12.40-12.41), Hybrid and Perovskite Photovoltaics (12.42-12.54), Molecular Electronics and Excited State Properties (12.55-12.58), Organic Electronics and Photovoltaics (12.59-12.80)

Time: Monday 18:00–20:00

Location: P1

CPP 12.1 Mon 18:00 P1

Janus particles: Challenges in the preparation process and analysis of their thermophoretic self-propulsion — •FRANZISKA JAKOB and REGINE VON KLITZING — Institute for Condensed Matter Physics, Technische Universität Darmstadt, D-64289 Darmstadt

Active colloidal particles with different functionalities at their opposite sides are named Janus particles - motivated by the Roman mythological god. One possible propulsion mechanism is thermophoretic self-propulsion. When laser light ($\lambda = 532$ nm) illuminates a gold-capped particle, a local temperature gradient is generated along the particle surface due to surface plasmon excitation of the gold cap. This gradient perturbs the equilibrium conditions of the surrounding medium and finally leads to particle self-propulsion.

This contribution focuses on various preparation processes of self-thermophoretic gold-polystyrene (Au-PS) microswimmers. The influence of the preparation technique on the gold cap size and the resulting self-thermophoretic behavior of the Janus particle will be presented. For this purpose, Janus particles are prepared either by metal sputtering, thermal evaporation, or by a combination of gel trapping technique and metal sputtering. With scanning electron microscopy (SEM) and energy-dispersive X-ray spectroscopy (EDX), the dimension of the gold cap was investigated. Dark-field microscopy (DFM) combined with a LabView program enables real-time tracking of the Janus particles. The study shows that the preparation method strongly affects the gold cap size of the Janus particles and thus influences their self-thermophoretic velocity.

CPP 12.2 Mon 18:00 P1

Modeling Chemotaxis and Cross-Diffusion using MD and cDFT — •PHILIPP STÄRK — SC Simtech, Uni Stuttgart, Germany

Multiple experimental studies have observed diffusion of certain particle types—such as catalysts—along concentration gradients of other species. Using stochastic, coarse grained reaction dynamics in MD simulations, we present simplified models for this behavior. Furthermore, we present a classical Density Functional Theory which provides a simple model for cross-diffusion on a broader class of particle types.

CPP 12.3 Mon 18:00 P1

Cellulose-based programmable, robust, and healable actuators for smart packaging devices — •QING CHEN¹, BENEDIKT SOCHOR¹, ANDREI CHUMOKOV¹, MARIE BETKER^{1,2}, NILS ULRICH^{3,4}, MARIA E. TOIMIL-MOLARES⁴, KORNELIYA GORDEYEVA², DANIEL SÖDERBERG², VOLKER KÖRSTGENS⁵, MATTHIAS SCHWARTZKOPF¹, PETER MÜLLER-BUSCHBAUM⁵, and STEPHAN ROTH^{1,2} — ¹DESY, 22607 Hamburg, Germany — ²KTH, 10044 Stockholm, Sweden — ³GSI Helmholtz Center, 64291, Darmstadt, Germany — ⁴TU Darmstadt, 64287 Darmstadt, Germany — ⁵TU Munich, 85748 Garching, Germany

Programmable actuators are promising candidates for smart devices. Herein, we fabricated a cellulose-based actuator with polyvinyl alcohol (PVA) and polystyrene sulfonate (PSS) as reinforcement. Driven by moisture, the actuators bend in programmable directions when we cut the films at different oblique angle with respect to its radial axis. Furthermore, the actuator shows an exceptional elongation-at-break of 77%. Ultra-Small-Angle X-ray Scattering and scanning electron microscopy examination at the necking region of the film yields the formation of cavities with an average width of 75 nm. They decrease to 16.5 nm with an elevating relative humidity (RH) from 0 to 100% and remains constant when the RH decreases from 100% to 0%. The programmable, robust, and healing ability of the actuator suggests its potential as smart packaging devices.

CPP 12.4 Mon 18:00 P1

A Raman spectroscopic study of the pyrolysis of lactose and tannins — •SIMON BREHM, CAMELIU HIMCINSCHI, JAKOB KRAUS, and JENS KORTUS — TU Bergakademie Freiberg, Germany

Lactose and tannin are naturally occurring and eco-friendly alternatives to commonly used binders for carbon-bonded alumina filters that are applied in steel melt filtration. A contribution to understand the production process of these filters is the investigation of the pyrolysis process of the binders. In this work, lactose and different tannins were investigated by *in situ* and *ex situ* Raman spectroscopy. The transformation of the tannin and lactose molecules to a system of

amorphous carbon and at even higher temperatures to nanocrystalline graphite could be observed in the Raman spectra. In addition, intermediate pyrolysis products of the investigated tannins as well as their pyrolysis temperatures could be determined.

CPP 12.5 Mon 18:00 P1

F-Actin photocleavage as an artificial secondary nucleation model — •STEPHAN SYDOW, TOBIAS THALHEIM, JÖRG SCHNAUSS, and FRANK CICHOS — Peter Debye Institute for Soft Matter Physics, Universität Leipzig, Leipzig, Germany.

The aggregation of soluble proteins into highly ordered, insoluble amyloid fibrils is characteristic for a range of neurodegenerative disorders, like Alzheimer's or Parkinson's disease. The kinetics in the formation of amyloid fibrils are governed by multiple aggregation mechanisms, which are present simultaneously. One of these being the unspecific spontaneous breaking of Amyloid fibrils, whose cause, rate and break size distribution are still unknown, due to them being hidden in ensemble measurements.

We employ an artificial model system with a controllable fragmentation rate to compare it with current amyloid kinetic models, all assuming a homogeneous break size distribution. Fluorescence labelled Actin filaments exhibit photocleavage. By laser illumination of single, homogeneously labelled filaments in solution, we are able to control the breakage rate. The length and position of filaments and fragments are imaged over time by fluorescence microscopy.

We show, that Actin filaments exhibit a homogeneous break size distribution, verifying our artificial model system. Additionally, the fragment size distribution is independent of the intensity dependent, induced cleavage rate, thus it enables the direct comparison to current amyloid models.

CPP 12.6 Mon 18:00 P1

Mapping nanomechanics and energy dissipation of collagen fibrils in tendon — •MARTIN DEHNERT, PAUL ZECH, MARIO ZERSON, and ROBERT MAGERLE — Fakultät für Naturwissenschaften, Technische Universität Chemnitz, Germany

We study the nanomechanical properties of hydrated collagen fibrils with AFM-based nanoindentation measurements. Force-distance (FD) data measured with tip velocities $< 1 \mu\text{m/s}$ display a rate-independent hysteresis with return point memory depending on only one return point. With different indentation protocols, we show that stress relaxation and creep do not influence the time evolution of the FD data. The main cause of hysteresis is the elastoplastic deformation of collagen fibrils above the glass transition. We explore the variations of these nanomechanical properties in sets of unfixed hydrated collagen fibrils isolated from native chicken Achilles tendon and compare them with collagen fibrils embedded in the natural tendon. AFM imaging in the air with controlled humidity preserves the tissue's native water content and allows for high-resolution imaging and nanoindentation measurements. This sheds new light on the role of interfibrillar bonds, the mechanical properties of the interfibrillar matrix, and the biomechanics of native tendon.

CPP 12.7 Mon 18:00 P1

Hydrogel-based electrodes for brain wave detection — •GÖKAY ERBİL¹, HSIN-YIN CHIANG², VOLKER KÖRSTGENS¹, and PETER MÜLLER-BUSCHBAUM¹ — ¹TU München, Physik-Department, LS Funktionelle Materialien, 85748 Garching — ²Cephalgo, 75014 Strasbourg, France

Electroencephalography (EEG) as method for detecting brain waves is gaining importance for medical applications, since it can non-invasively provide information. Currently, both wet electrodes and dry electrodes are in use for clinical and commercial applications. With both concepts, one has to deal with certain challenges. Dry electrodes often show motion artifacts due to changes in contact and pressure applied between skin and electrode altering the signal quality. For wet electrodes on the other hand, a decrease in signal quality is usually observed with long term signal acquisitions. In this work, mussel inspired hydrogels are presented to address these challenges. The hydrogel electrodes containing tannic acid and silver nanoparticles are optimized in terms of high conductivity and adhesive properties. The elevation of brain waves collected with a headset comprised of hydrogel electrodes is demonstrated in an EEG setup for long term analysis.

CPP 12.8 Mon 18:00 P1

Spin-Based Quantum Sensing with Endohedral Fullerenes — •MARCO SOMMER¹, DON-SHENG GUO¹, ANDREAS HENNIG¹, JOHANN P. KLARE¹, and WOLFGANG HARNEIT² — ¹Universität Osnabrück, Osnabrück, Deutschland — ²Nankai University, Tianjin, China

The endohedral fullerene N@C₆₀ in an inhomogeneous environment is investigated with the goal to establish the N@C₆₀ with its outstanding spin properties as a spin label for coupling experiments in biological systems at room temperature. To reveal the preservation of these spin features, the N@C₆₀ is transferred into Triton X-100 micelles, a deep cavitated calixarene (SAC4A) as well as the cavity formed by two γ -cyclodextrins building a non-covalently bonded guest-host complex. The spectroscopic tools are based primarily on continuous wave (cw) and pulsed electron paramagnetic resonance (EPR) techniques, in addition to absorption measurements in the ultraviolet-visible light (UV/vis) range and molecular modelling with molecular dynamic (MD) simulation of the complexes. The resulting spin properties are examined with cw and pulsed EPR spectroscopy. The computational modelling and MD simulations of the complexes in combination with UV/vis spectroscopy serves for the unravelling of the arrangement. Initial experiments show a successful transfer of the highly hydrophobic N@C₆₀ into the aqueous phase. The resulting spin-spin relaxation time T₂ strongly depends on the the N@C₆₀'s encapsulation system. Inhomogeneous environments (Triton X-100) decrease the transverse relaxation time whereas a symmetric system (γ -cyclodextrin) provides an increase in T₂.

CPP 12.9 Mon 18:00 P1

Studying the nanomechanical properties of functional organic and biologic macromolecules — ILKA M. HERMES¹, ANDREA CERRATA², VLADIMIR KOROLKOV², and •ALEXANDER KLASSEN² — ¹Leibniz-Institut für Polymerforschung Dresden e.V., Dresden, Germany — ²Park Systems Europe GmbH, Mannheim, Germany

As the functionality of organic and biologic macromolecules is often determined by their nanomechanical properties, visualizing the distribution of mechanical properties on the nanoscale provides crucial insights for soft matter research. [1,2] Here, we present a study on structural and nanomechanical properties of functional organic and biologic macromolecules in different environments as well as under external stimuli, such as temperature, ion concentration and pH. Force-distance measurements with atomic force microscopy (AFM) resolve adhesion and elasticity by pressing a nanometer-sized tip on the end of a cantilever onto the surface. However, the correlation of mechanical data from force-distance measurements to the local sample morphology additionally requires topographic sample information. PinPoint™ nanomechanical imaging simultaneously acquires topographic and force-distance data within short amounts of time and is therefore ideally suited to investigate organic and biologic macromolecules.

1. S. Perni et al., *Langmuir* 32, 7965-7974 (2016).

2. E. E. Bastounis et al., *Mol. Biol. Cell* 29, 1571-1589 (2018).

CPP 12.10 Mon 18:00 P1

Huge pKa-Shifts in Weak Polyelectrolyte Brushes Explained by Coarse-Grained Simulations — •DAVID BEYER¹, CHRISTIAN HOLM¹, and PETER KOŠOVAN² — ¹Institute for Computational Physics, University of Stuttgart, D-70569 Stuttgart, Germany — ²Department of Physical and Macromolecular Chemistry, Charles University, Prague, Czechia

Following recent experiments, we study the titration behaviour of weak (pH-responsive) polyelectrolyte brushes at different salt concentrations using coarse-grained computer simulations. To account for charge regulation and the exchange of small ions with the bulk solution, we make use of the Grand-Reaction Monte-Carlo method (G-RxMC). Our simulations yield ionization curves which strongly deviate from the ideal result. Furthermore, we observe a strong dependence of the deviation on the bulk salt concentration, amounting to a shift of approximately one unit of pH as the salt concentration decreases by one order of magnitude. We theoretically explain the observed titration behaviour as a consequence of the Donnan partitioning between the brush and the bulk solution. To confirm our theoretical explanation we measure the pH inside the brush, which eliminates the Donnan contribution. Our results show that the Donnan effect can account for a shift in pH between the bulk and the brush of more than 4 units in extreme cases. We finally plot the degree of ionization as a function of the pH inside the brush, thus eliminating the Donnan contribution. Up to a small shift due to the electrostatic interactions, the resulting curves almost coincide with the ideal result, thus confirming our hypothesis.

CPP 12.11 Mon 18:00 P1

Narrow Gap Flow Electrolysis Cells: Atomistic Computer Simulation of Electric Field Effects on Water/Organic Mixtures — •ANASTASIOS SOURPIS and FRIEDERIKE SCHMID — Johannes Gutenberg University, Mainz, Germany

Electrolyte-free electrolysis fuel cells are central to a sustainable future with clean water. With growing industrial development, for example, toxic heavy metals, radioactive ions, and inorganic compounds are increasingly discharged into the environment and our sources of drinking water. In novel cutting-edge developed

electrolysis fuel cells [1] the case of electrolyte-free electrolysis has been observed for mixtures of water and acetonitrile. These high modular flow cells of electro organic synthesis are very promising for the production of fine chemicals and pharmaceutically active agents. The purpose of this study is to qualitatively and quantitatively evaluate the effect of electric fields on electrolysis cells. Especially in the case of acetonitrile and water mixtures, we have focused on understanding by atomistic simulations the existence of the electrical conductance and how this can be described on larger scales.

CPP 12.12 Mon 18:00 P1

Controlling the phase transitions in surfactant-dna complexes — A.V. RADHAKRISHNAN^{1,2}, S. MADHUKAR¹, A. CHOUDHARI¹, and •V.A. RAGHUNATHAN¹ — ¹Raman Research Institute Bangalore 560080 India — ²Experimental Physics I, University of Bayreuth, Bayreuth 95447 Germany

Surfactant-DNA complexes are a special class of polyelectrolyte complexes where one of the macroions is formed by self assembly. They have been studied for their interesting electrostatics and potential applications for gene delivery and photonic applications. The gain in counter ion entropy is driving the complex formation and there is an interesting interplay of electrostatics and entropy leading to a rich phase behavior. The self assembled macroion can be formed either by a bilayer forming lipid or a micelle forming surfactant. We have studied the structural transitions in complexes formed by cationic surfactants such as CTAB, CTAT, DTAB with ds-DNA and constructed phase diagrams. Using small angle xray scattering and polarizing optical microscopy and elemental analysis the presence of a various phases, including a square phase(S), hexagonal phase (H) and a hexagonal super lattice phase (Hs) are identified. Detailed modeling of these structures have been carried out based on the electron density maps to propose the packaging of the macroions in the lattices. Striking differences in the phase diagrams and various ways of controlling the structural transitions will be discussed.

CPP 12.13 Mon 18:00 P1

Poly((trifluoromethane)sulfonimide lithium styrene) as single-ion conducting binder for lithium iron phosphate electrodes in lithium-ion batteries — •FABIAN A.C. APFELBECK¹, JULIAN E. HEGER¹, TIANFU GUAN¹, MATTHIAS SCHWARTZKOPF², STEPHAN V. ROTH^{2,3}, and PETER MÜLLER-BUSCHBAUM^{1,4} — ¹TU München, Physik- Department, LS Funktionelle Materialien, 85748 Garching — ²DESY, 22607 Hamburg — ³Royal Institute of Technology KTH, 100 44 Stockholm — ⁴MLZ, TU München, 85748 Garching

Lithium-ion batteries turned out as an indispensable energy supplier in modern society which however suffers from safety concerns due to the flammability of the liquid electrolyte. Solid polymer electrolytes (SPEs) represent a safe alternative to conventional electrolytes. Especially single-ion conducting polymers (SICPs), which have the anion covalently bonded to the backbone of the polymer and thus a theoretical transference number of unity, attracted strong interest in battery research. For full-cell performance investigation of these battery cells, the ion-conducting polymer electrolyte is often used as binder instead of the neutral polyvinylidenfluorid (PVDF) in order to enhance ion conduction in the electrode and decrease the interfacial contact. Here, lithium iron phosphate (LFP) cathodes with different weight ratios of PVDF and the SICP poly((trifluoromethane)sulfonimide lithium styrene) (PSTFSLi) as binders are prepared and analysed with real (scanning electron microscopy) and reciprocal (grazing-incidence small/wide angle x-ray scattering) space techniques.

CPP 12.14 Mon 18:00 P1

Influence of Li Salt concentration in poly(propylene carbonate) based solid polymer electrolytes — •THIEN AN PHAM^{1,2}, RALPH GILLES¹, and PETER MÜLLER-BUSCHBAUM^{1,2} — ¹MLZ, TU München, 85748 Garching — ²TU München, Physik-Department, LS Funktionelle Materialien, 85748 Garching

Li metal exhibits a high specific capacity as well as a low discharge potential that makes it interesting as an anode material for Li ion batteries. But Li dendrite growth remains a major safety in cells with liquid electrolyte. Solid polymer electrolytes (SPE) show a higher mechanical stability in comparison to their liquid counterparts and thus, can inhibit dendrite growth. In order to achieve even higher energy densities, high-energy cathode materials such as Ni rich layered transition metal oxides should be combined with Li metal anodes. However, the high operation potentials of those cathodes are a challenge for SPE. Poly(propylene carbonate) (PPC) has an intrinsically high oxidation voltage exceeding 4.5 V making it suitable for high voltage operation. Here, SPE with PPC as polymer host and Lithium bis(trifluoromethanesulfonyl)imide (LiTFSI) as Li salt are prepared and the influence of the salt concentration on the SPE properties are studied with electrochemical impedance spectroscopy and differential scanning calorimetry. Results have shown that the ionic conductivity increasing and the glass transition temperature is decreasing with higher amount of LiTFSI.

CPP 12.15 Mon 18:00 P1

Influence of Solvent and Lithium Salt on the Structure and Performance of NCM111 Cathode for Lithium Ion Batteries — •YUXIN LIANG¹, ZHUIJUN XU¹, KUN SUN¹, TIANFU GUAN¹, FABIAN APFELBECK¹, PAN DING², and PETER MÜLLER-BUSCHBAUM^{1,3} — ¹TU München, Physik-Department, LS Funktionelle Materialien, 85748 Garching — ²TU München, Walter Schottky Institute, Experimental Semiconductor Physics, 85748 Garching — ³MLZ, TU München, 85748 Garching

Lithium ion batteries (LIBs) with a wide range of applications have emerged as the most promising candidate for electrochemical energy storage due to its higher specific energies, volumetric energy densities and power densities. However, lithium dendrite will grow and the Coulombic efficiency (CE) will decrease with Li plating and stripping. During past decades, more and more state-of-art materials has been developed to alleviate the abovementioned problems. Nevertheless, fundamental research on the component composition and the effect of additive and solvent on LIBs is still lacking. It is of great value to get a deep understanding and therefore optimize the fabrication process for future studies on the electrode/electrolyte interface of LIBs. In this project, we select the LiNi_{0.33}Mn_{0.33}Co_{0.33}O₂ as cathode material to find out the effect of different solvents and extra lithium salt (LiTFSI) on the performance of LIBs. The Li/cathode cells were assembled to observe the battery performance and grazing incidence wide-angle X-ray scattering (GIWAXS) technique is used to detect structure change within the cathode before and after cycling.

CPP 12.16 Mon 18:00 P1

Scaling mechanical instabilities in drying micellar droplets — •JAYANT KUMAR DEWANGAN¹, NANDITA BASU², and MITHUN CHOWDHURY¹ — ¹Lab of Soft Interfaces, Metallurgical Engineering and Materials science, IIT Bombay, Mumbai 400076, India — ²Department of Chemistry, IIT Bombay, Mumbai 400076, India

We present unique wrinkling patterns produced by evaporating sessile micellar aqueous droplets on rigid and soft substrates kept at temperatures far above ambient. The wrinkling patterns vary dramatically depending on the material's elastic modulus and substrate, the concentration of the micellar solution, and the temperature of the substrate. Coffee-ring-like morphologies are observed at very low concentration regimes (CTAB concentration < 0.0364 wt%), devoid of any wrinkling morphology, regardless of substrate temperature. Droplets deposited at a temperature above 85°C wrinkle formation begins at the droplet peripheral zone, radial on the stiff glass annular on soft cross-linked PDMS substrate, at the high initial concentration regime (CTAB concentration > 0.0364 wt%). Radial wrinkles on the glass substrate and annular wrinkles on the cross-linked PDMS substrate nucleate from the edges connecting to the deposit's central region at CTAB concentration > 2.73 wt%. The ratio of the width of the gel-like deposit to the radius of the droplet scales with surfactant concentration is dependent on the initial equilibrium contact angle of micellar droplets. Our findings support previous literature on mechanical instabilities of dried deposits by interdependent scaling relationships between deposit radius, wavelength of wrinkle, thickness, and elastic modulus.

CPP 12.17 Mon 18:00 P1

A scaled-down double-pass optical beam deflection setup for the measurement of diffusion and thermodiffusion in liquid mixtures — MAREIKE HAGER, •ROMAN REH, and WERNER KÖHLER — Physikalisches Institut, Universität Bayreuth, Germany

We report about a compact double-pass optical beam deflection (OBD) setup for measurements on diffusion and thermodiffusion in liquid mixtures. A laser beam transmitted through the sample gets back-reflected behind the OBD-cell and, thus, traverses the sample volume a second time. Applying a vertical temperature gradient to the sample leads to thermodiffusion and the beam gets deflected by the resulting gradient in refractive index due to the gradients in temperature and concentration. A beamsplitter guides the beam towards a camera, where the time dependent laserposition is recorded. The signal then gives information about the diffusion processes. Since the laser beam propagates on the same path between the beamsplitter and the cell before and after getting deflected in the sample and since the double-transmission geometry allows little distance between cell and camera, the whole setup could be built very compact. Measurements with different binary mixtures are in good agreement with measurements with a single-transmission-OBD. We present a matrix formalism to describe the optical transfer function of the instrument.

CPP 12.18 Mon 18:00 P1

Particle sorting by Marangoni convection in microfluidic channels — •ROMAN REH, LORENZ KIEL, DANIEL ZAPF, and WERNER KÖHLER — Physikalisches Institut, Universität Bayreuth, Germany

Thermosolutal and thermocapillary Marangoni convection at a liquid-gas interface in a T-shaped microchannel structure of approximately 100 × 20 μm² cross section creates localized vortices that can be used for particle trapping, steering, and sorting. Experiments have been performed with water-ethanol mixtures as carrier liquid and dispersed micrometer-sized polystyrene beads. Due to colli-

sions with the meniscus, particles are displaced from streamlines that approach the interface closer than one particle radius. These streamlines feed liquid volumes that are entirely cleared of particles. Particle accumulations structures form inside the vortex, from where only small particles can escape by diffusion. Since the critical streamline, which separates the depletion from the accumulation region, depends on the particle radius, the mechanism can be used for particle sorting by superposition of a Poiseuille flow and splitting of the flow downstream from the meniscus. In the simplest case, the initially homogeneous flow is split into two arms, one where the particles are enriched and one where all particles are removed from the liquid. The microchannel structures consist of crosslinked PDMS and the dispersed particles are observed by video microscopy. Numerical simulations are performed that almost perfectly match the experimental observations.

CPP 12.19 Mon 18:00 P1

Dynamic Ellipsometric Light Scattering: A Feasibility Study — •REINHARD SIGEL — Markdorf, Germany

For colloidal particles dispersed in water, ellipsometric light scattering (ELS) has been established as a means for the characterization of the particles' interface layers [1,2]. These layers are important for the colloidal stabilization. We explore theoretically a combination of ELS with photon correlation measurements to access the fluctuation amplitude and dynamics of soft colloidal layers (e.g. in steric stabilization). They are connected to mechanical properties of the layers and are complementary to the structure information of conventional ELS. The investigation builds on preceding work on Mie scattering by soft core-shell particles [3], correlation ellipsometry [4], extraction of the coherent scattering properties in ELS for polydisperse samples [5,6], and the detection of incoherent dynamics in the ellipsometry minimum [7].

- [1] A. Erbe, K. Tauer, R. Sigel, Phys. Rev. E 73, 031406 (2006)
- [2] R. Sigel, Curr. Opin. Colloid Interface Sci. 14, 426-437 (2009).
- [3] D. J. Ross, R. Sigel, Phys. Rev. E 85, 056710 (2012)
- [4] R. Sigel, Soft Matter 13, 1132-1141 (2017)
- [5] R. Sigel, A. Erbe, Appl. Opt. 47, 2161-2170 (2008)
- [6] A. Erbe, K. Tauer, R. Sigel, Langmuir 25, 2703-2710 (2009).
- [7] A. Erbe, R. Sigel, Phys. Chem. Chem. Phys. 15, 19143-19146 (2013)

CPP 12.20 Mon 18:00 P1

Improved virtual orbitals for charge transfer excitations in time dependent DFT — •ROLF WÜRDEMANN¹ and MICHAEL WALTER^{2,3} — ¹Freiburger Materialforschungszentrum, Freiburg, Germany — ²Freiburger Zentrum für interaktive Werkstoffe und bioinspirierte Technologien, Freiburg, Germany — ³Fraunhofer-Institut für Werkstoffmechanik, Freiburg, Germany

Charge transfer excitations (CTE) are of high importance in photovoltaics, organic electronics and molecular and organic magnetism. Range separated functionals (RSF) can be used to correctly determine the energetics of CTEs within linear response time dependent density functional theory (TDDFT).

TDDFT becomes numerically very demanding on grids if hybrid or RSF are used due to the inclusion of exact exchange derived from Hartree-Fock theory.

We present an implementation of RSF on real space grids and discuss a way to circumvent the problem mentioned above by utilizing Huzinagas improved virtual orbitals (IVOs) that form an improved basis for this type of calculations. The CTE energetics can be obtained by means of DFT ground-state calculations using IVOs[1].

- [1] R. Würdemann, M. Walter, J. Chem. Theory Comput. 2018, 14, 7, 3667-3676

CPP 12.21 Mon 18:00 P1

Unravelling Superpositions in GI-XPCS by simultaneous GT-GI-XPCS on Spincoated Thin Films — •CHRISTOPHER R. GREVE¹, MEIKE KUHN¹, FABIAN ELLER¹, GUILLAUME FREYCHET³, ALEXANDER HEXEMER², LUTZ WIEGART³, and EVA M. HERZIG¹ — ¹Dynamik und Strukturbiologie - Herzig Group, Universität Bayreuth, Universitätsstr. 30, 95447 Bayreuth, Germany — ²CAMERA, Lawrence Berkeley National Lab Berkeley CA, USA — ³NSLSII, Brookhaven National Lab, Upton NY, USA

X-Ray Photon Correlation Spectroscopy (XPCS) is a flexible tool to quantify dynamics on the nanometer scale in bulk samples and is used in grazing incidence (GI) geometry for application to thin films. By measurements in GI geometry distortions to the scattering signal are introduced, related to refraction and reflection events, known from the Distorted Wave Born Approximation (DWBA). These reflection and refraction events lead to superpositions of signal on the detector, resulting in alterations of analyzed quantities. We applied an approach to quantify the influence of events within the DWBA on decorrelation analysis by measuring grazing incidence transmission (GT) XPCS and GI-XPCS simultaneously for various thin films. Combining GI-GT-XPCS results with calculations of Fresnel coefficients within the simplified DWBA the origin of scattering contributions is determined. Calculations of the non-linear effect of refractions are added to identify comparable regions within GI and GT. Thus, elucidating differences for phenomena like altered decorrelation times, allowing a valid analysis of GI-XPCS experiments for certain experimental conditions.

CPP 12.22 Mon 18:00 P1

Propagation of learned sequence patterns to larger chain length using TransEncoder neural networks — •HUZAIFA SHABBI, MARCO WERNER, and JENS UWE SOMMER — Leibniz Institute for Polymer Research Dresden

In this work, we investigate artificial neural networks that are capable of learning and transferring hidden variables in chemical sequences from a small sequence length to a larger one. Patterns in the relation between the hydrophilic/hydrophobic sequence of a copolymer and its free energy of interaction with a lipid membrane have been learned with the aid of AutoEncoder neural networks, which were employed to translate between these two properties (TransEncoder)[1]. We demonstrate that the latent space parameters learned by the TransEncoder allow for a physical interpretation of the contributions to the free energy. Furthermore, the learned patterns for a smaller sequence length can be transferred towards a higher sequence length of our interest, which not only significantly reduces the number of training examples required but also increases the accuracy in comparison to the training for individual polymer sequence length. We investigate the computational efficiency and the convergence of learned patterns when multiple chain lengths are addressed at once.

[1] M. Werner, ACS Macro Letters 10, 1333 (2021).

CPP 12.23 Mon 18:00 P1

Crystallization of short polymer chains at hard walls: stochastic approximation Monte Carlo simulation (SAMC) — •EVGENIIA FILIMONOVA, TIMUR SHAKIROV, and VIKTOR IVANOV — Martin-Luther-University Halle-Wittenberg, Institute of Physics, 06099, Halle, Germany

Our research is devoted to crystallization in polymer melts in the presence of hard walls. An interface to a solid material can initiate crystallization in polymer liquids by either heterogeneous nucleation or prefreezing. Our goal is to reveal physical factors which are responsible for one of these two scenarios of surface-induced polymer crystallization. We use coarse-grained model and perform stochastic approximation Monte Carlo (SAMC) simulation. We have developed an approach that allows us to identify the translational and orientational local ordering by means of comparing our system configurations with reference crystalline structures of different symmetries. In addition to calculating the usual order parameters (Steinhardt parameters, common neighbours analysis, nematic order parameter, etc.), we suggested new order parameters based on scalar products of bonds between nearest neighbours. We observe a coexistence of an isotropic structure in the center of the film with ordered structures at the walls at intermediate values of energies (in microcanonical analysis). A change in the crystal structure accompanying a change in density at different energies is also shown. Financial support of the International Graduate School AGRIPOLY supported by the European Social Fund (ESF) and the Federal State Saxony-Anhalt is acknowledged.

CPP 12.24 Mon 18:00 P1

Simulation of reversible chain association using the reaction ensemble Monte Carlo — •PABLO M. BLANCO and PETER KOŠOVAN — Department of Physical and Macromolecular Chemistry, Faculty of Science, Charles University, Hlavova 8, 128 00 Prague 2, Czech Republic.

Reversible association reactions are the key feature of many self-healing polymeric materials and controlled release systems. Simulations and theory are lagging behind the experimental progress in investigating such systems, partly due to the lack of a suitable implementation of an algorithm that would allow for such reversible reactions. In this work, we present an implementation of such reversible reactions within the Reaction-ensemble Monte Carlo framework (RxMC). To validate the algorithm, we simulated the polycondensation reactions, illustrated in Fig.1 (top). These reactions are common in polymer chemistry, and analytical predictions of the distribution of chain lengths at equilibrium are available, serving as an ideal test case for numerical simulations. Starting from the free monomers, we let the system evolve towards equilibrium, resulting in an ensemble of chains of various chain lengths, depending on the value of the equilibrium constant of the reaction. By comparing our simulation results with the theoretical predictions, we investigate the limitations of the algorithm, possible finite-size effect, and efficiency of its implementation. After initial validation, this reaction algorithm will be implemented in the ESPResSo simulation software (www.espressomd.org) that will enable its application to a broad class of problems involving reversible association reactions.

CPP 12.25 Mon 18:00 P1

Modelling electrode interfaces via multi-scale simulations — •HENRIK KONSTANTIN JÄGER, PHILIPP STÄRK, and ALEXANDER SCHLAICH — Stuttgart Center for Simulation Science (SC SimTech), University of Stuttgart, Germany

We investigate the interactions of ions at a graphene interface via first-principle simulations using ab initio molecular dynamics. In a multi-scale approach we employ first principle calculations to parametrize semi-classical electrode models based on the Tomas-Fermi screening approach, allowing to access dynamics and adsorption at common electrode-electrolyte interfaces.

CPP 12.26 Mon 18:00 P1

Combined first-principles statistical mechanics approach to sulfur structure in organic cathode hosts for polymer based lithium-sulfur (Li-S) batteries — •YANNIK SCHÜTZE^{1,2}, RANIELLE OLIVEIRA DE SILVA^{1,3}, JIAOYI NING¹, JÖRG RAPPICH¹, YAN LU^{1,3}, VICTOR G. RUIZ¹, ANNIKA BANDE³, and JOACHIM DZUBIELLA^{1,4} — ¹Helmholtz-Zentrum Berlin für Energie und Materialien GmbH, Germany — ²Freie Universität Berlin, Germany — ³Universität Potsdam, Germany — ⁴Albert-Ludwigs-Universität Freiburg, Germany

Polymer-based batteries that utilize organic electrode materials are considered viable candidates to overcome the common drawbacks of lithium-sulfur (Li-S) batteries. A promising cathode can be developed using a conductive, flexible, and free-standing polymer, poly(4-thiophen-3-yl)benzenethiol (PTBT), as the sulfur host material. Here, we present a combination of electronic structure theory and statistical mechanics to characterize the structure of the initial state of the charged cathode on an atomic level. We perform a stability analysis of differently sulfurized TBT dimers as the basic polymer unit calculated within density-functional theory (DFT) and combine this with a statistical binding model for the binding probability distributions of the vulcanization process. This multi-scale approach allows us to bridge the gap between the local description of the covalent bonding process and the derivation of the macroscopic properties of the cathode.

CPP 12.27 Mon 18:00 P1

Correcting Coarse-Grained Dynamics of Molecular Liquids and Their Mixtures Using an Efficient Iterative Memory Reconstruction Method — •MADHUSMITA TRIPATHY, VIKTOR KLIPPENSTEIN, and NICO FA VAN DER VEGT — Eduard-Zintl-Institut für Anorganische und Physikalische Chemie, Technische Universität Darmstadt, 64287 Darmstadt, Germany

Generalized Langevin equation (GLE) based coarse-grained (CG) models are considered to be the most reliable models for dynamically consistent coarse-graining [1]. However, their implementation in molecular simulation is not straight-forward owing to their inherent complexity [2]. With an aim to employ computationally tractable GLE based CG models for dynamic coarse graining of complex molecular systems, we coarse-grain two molecular liquids and their mixtures at various compositions following a novel iterative optimization scheme. Using the memory kernel from an isotropic GLE model as a starting point, we use an efficient iterative memory reconstruction method, which can closely reproduce the underlying fine-grained (FG) dynamics, assessed in terms of the velocity auto-correlation function, within a few iterations. We use this iterative method to correct the artificial dynamic speed-up in CG molecular dynamics (MD) simulations of pure molecular liquids and the relative dynamic speed-up in their mixtures. Furthermore, we investigate the transferability of the resulting memory kernels to molecular mixtures with varying composition.

[1] Klippenstein et al. J. Phys. Chem. B 125 (19), 4931-4954 [2] Glatzel and Schilling, Europhys Lett. 136 36001 (2021)

CPP 12.28 Mon 18:00 P1

Aggregation of flexible-semiflexible multiblock-copolymers in a dilute solution: MD simulation — •VIKTOR IVANOV^{1,2}, ELIZAVETA SIDLER², JULIA MARTEMYANOVA², TIMUR SHAKIROV¹, and WOLFGANG PAUL¹ — ¹Martin-Luther-University Halle-Wittenberg, Institute of Physics, 06099, Halle, Germany — ²Moscow, Russia

We study aggregation of several regular multi-block copolymer chains in a dilute solution. Chains consist of flexible (F) and semi-flexible (S) blocks with equal composition of F- and S-units having different affinity to a solvent, which is poor for both components. We use coarse-grained MD simulation. Our main goal is to find conditions (values of model parameters) for a shape-persistent aggregation of globules with different non-trivial globular morphologies which are formed in poor solvent, including structures with high orientational ordering of S-blocks and with micro-segregation of S- and F-blocks. Stable aggregates of the following highly anisotropic morphologies have been obtained: "core-shell", "bundle", "dumbbell", "disk", worm-like micelles ("tubes"). The driving forces for formation of structured globules and their anisotropic aggregates are usual van-der-Waals interactions, block length and intramolecular stiffness (there are no specific interactions in our model). We acknowledge the financial support from RFBR (grant 19-53-12006-NNIO-a) and DFG (project PA 473/18-1) and thank Moscow State University Supercomputer Center for providing computational resources.

CPP 12.29 Mon 18:00 P1

A combined experimental-theoretical study of azo-SAM restructuring under light stimulus: New insights — ALEXEY KOPYSHEV^{1,2}, AMRITA PAL¹, SVETLANA SANTER², and •OLGA GUSKOVA¹ — ¹IPF Dresden, 01069 Dresden, Germany — ²University of Potsdam, 14469 Potsdam, Germany

The topography transformation of the self-assembled (SAM) layers of azobenzene (azo) surfactant [1] on mica is studied using AFM and modeled in all-atom MD simulations. Under blue light, when azo adopts the trans-state, the smooth SAMs are formed. Under UV stimulus due to a shift in equilibrium between trans and cis isomers, a rapid change in the topography of SAMs occurs. Sub-

sequent blue light irradiation leads to the stabilization of SAMs and smoothing of the upper layers. The explanation of the layer restructuring/mass transport is proposed in simulations. First, we observe that the cis isomers diffuse slower within the adsorbed layers. Second, the expulsion of the cis isomers from SAM is detected independently of the layer compositions. Third, the vertical diffusion for trans isomers is negligible, whereas for cis-state it is comparable to diffusion within the layer. Thus, the change in the topography of SAMs under UV light seen in AFM is related to the vertical diffusion of cis azo. The work is supported by DFG (project GU1510/5-1). [1] Titov E. et al. *ChemPhotoChem* 5 (2021) 926.

CPP 12.30 Mon 18:00 P1

Molecular switch based on bithiophene-azobenzene: How to control conductance through the monolayer using light — •VLADYSLAV SAVCHENKO and OLGA GUSKOVA — IPF Dresden, 01069 Dresden, Germany

Molecular switches based on azobenzene (azo) are defined as light-responsive molecules which can change between two configurational states. Responsive azo monolayers can be used to modulate the work function of the electrodes. In this study, we investigate using DFT what happens to the structures, electronic properties, and the charge redistribution within azo-bithiophene (azo-bt) monolayers depending on the light stimulus. Two types of switches differing in the order of azo and bt counting from the anchor group are modeled: azo-bt and bt-azo. Bt-azo switch is known from the literature [1], while the azo-bt is a product of rational design [2]. We study trans- and cis-isomers for each switch being in a contact with a gold cluster (C-AFM tip). A giant ON/OFF conductance ratio upon UV light observed in the experiment [1] results from an improved electronic coupling between the cis-isomers and the gold tip (ON-state) [1]. The trans-isomers of the simulated switches play the role of the insulators (OFF-state). Moreover, we show which molecular properties are enhanced by molecular design. This study opens up new avenues for the development of the rational design of electrode surface modifications. The work is supported by DFG, project GU1510/5-1. [1] Smaali K. et al. *ACS Nano* 4 (2021) 2411. [2] Savchenko V.A. et al. *Herald of TvSU. Ser. Chemistry* 3 (2021) 7.

CPP 12.31 Mon 18:00 P1

Non-invasively induced amphiphilic self-assemblies from orthogonally switchable block copolymers — •PEIRAN ZHANG¹, RENÉ STEINBRECHER², ANDRE LASCHESKY^{2,3}, PETER MÜLLER-BUSCHBAUM⁴, and CHRISTINE M. PAPADAKIS¹ — ¹Fachgebiet Physik weicher Materie, Physik-Department, TU München, Garching — ²Institut für Chemie, Universität Potsdam — ³Fraunhofer IAP, Potsdam-Golm — ⁴Lehrstuhl für Funktionelle Materialien, Physik-Department, TU München, Garching

Amphiphilic self-assemblies arising from orthogonally switchable block copolymers are promising candidate in drug delivery, due to their structure and transformation diversity, which is superior to the presently most studied singly responsive copolymers [1]. To induce this process completely non-invasively, light in combination with temperature is utilized as the stimulus. Introduction of suitable photoactive functional groups could modulate the LCST of the copolymer, thereby achieving the stage that all aggregate scenarios could be concluded in a certain temperature range. For characterization of the copolymer structure, measurements are implemented by dynamic light scattering (DLS), small angle X-ray scattering (SAXS) and -neutron scattering (SANS), while the phase behavior as well as phase transition kinetics are investigated by the time-resolved scattering methods.

[1] C. M. Papadakis, et al., *Langmuir* 2019, 35, 9660-9676.

CPP 12.32 Mon 18:00 P1

Effect of architecture in thermoresponsive methacrylate terpolymers based on PEG analogues — •FEIFEI ZHENG¹, EIRINI MELAMPANAKI¹, WENQI XU¹, ANNA P. CONSTANTINOU², THEONI K. GEORGIU², and CHRISTINE M. PAPADAKIS¹ — ¹Physics Department, Technical University of Munich, Garching, Germany — ²Department of Materials, Imperial College, London, England

The LCST polymers have attracted great interest for the biomedical sectors, as they have the advantage of being water-soluble at room temperature, while they can form a gel at body temperature [1]. Here, we address the effect of polymer architecture of poly(ethylene glycol) based thermoresponsive terpolymers featuring A, B and C blocks. These consist of the hydrophilic oligo(ethylene glycol) methyl ether methacrylate (OEGMA300, A), hydrophobic n-butyl methacrylate (B), and thermoresponsive di(ethylene glycol) methyl ether methacrylate (C). Several architectures have been synthesised via group transfer polymerisation, varying from statistical, to gradient to block structures. The results from dynamic light scattering indicate that the BABC tetrablock terpolymer and ABC gradient polymer form smaller micelles than ABC triblock terpolymer. This difference points to the importance of the exposed OEGMA300 block for micelle stabilization: bending it back in the BABC architecture enhances the effect of the thermoresponsive block on the thermal behavior.

[1] A. P. Constantinou, B. Zhan et al., *Macromolecules*, 2021, 54, 1943.

CPP 12.33 Mon 18:00 P1

Unique colorimetric response of polydiacetylene-Na⁺ microcrystals for detection of hydrochloric acid by naked eye — •RUNGARUNE SAYMUNG¹, CHRISTINE M. PAPADAKIS², NISANART TRAIIPHOL³, and RAKCHART TRAIIPHOL¹ — ¹School of Materials Science and Innovation, Faculty of Science, Mahidol University, Nakhon Pathom, Thailand — ²Physics Department, Technical University of Munich, Garching, Germany — ³Materials Science Department, Faculty of Science, Chulalongkorn University, Bangkok, Thailand

Polydiacetylenes (PDA), a class of conjugated polymers, are very promising as colorimetric sensors because the change of the color can be easily observed. The commercially available PDA with carboxylic head groups changes color from blue at acidic to red in basic condition. To develop this class of materials for pH sensing applications, many research groups synthesize PDA-based materials by structural modification or addition of foreign materials. Studies by our research group illustrate that incorporating ZnO nanoparticles with PDAs lead to colorimetric response to both acids and bases. Herein, we explore a new route by introducing Na⁺ ions into the PDA system. Upon exposure to hydrochloric acid (HCl) solution, the PDA-Na microcrystals exhibit a unique red to blue color-transition, which has never been observed before. To understand the origins of this behavior, various techniques are employed including Fourier-transformed infrared spectroscopy (FT-IR), scanning electron microscope (SEM), and X-ray diffraction (XRD).

CPP 12.34 Mon 18:00 P1

Anionic surfactant detection using polydiacetylene-based nanocomposites — •WATSAPON YIMKAEW¹, CHRISTINE M. PAPADAKIS², RAKCHART TRAIIPHOL³, and NISANART TRAIIPHOL¹ — ¹Laboratory of Advanced Chromic Materials, Department of Materials Science, Faculty of Science, Chulalongkorn University, Bangkok, Thailand — ²Physics Department, Technical University of Munich, Garching, Germany — ³Laboratory of Advanced Polymer and Nanomaterials, School of Materials Science and Innovation, Faculty of Science, Mahidol University, Nakhon Pathom, Thailand

Polydiacetylenes (PDAs) are color-responsive polymers to various stimuli. The development of PDAs as anionic surfactant sensors by structural modification involved complicated and costly processes. In this study, we introduce a facile approach for preparing polydiacetylene/zinc (II) ion/zinc oxide (PDA/Zn²⁺/ZnO) nanocomposites utilized for anionic surfactant detection. Cationic surfactant, cetyltrimethylammonium bromide (CTAB) is incorporated into the nanocomposites via a simple mixing process to adjust their color transition behaviors. Addition of CTAB at 1 mM induces the blue-to-yellow color transition of the nanocomposites. Interestingly, the nanocomposites exhibit yellow-to-red color transition in response to sodium dodecyl sulfate (SDS). This demonstrates the ability of the nanocomposites as anionic surfactant sensors. A key mechanism of the color transition is the interaction between CTAB and SDS, which induces perturbation in the outer layers of the nanocomposites.

CPP 12.35 Mon 18:00 P1

Tunable morphologies in charged multiblock terpolymers in thin film geometry: effect of solvent vapor annealing — •BAHAR YAZDANSHENAS¹, FLORIAN A. JUNG¹, MAXIMILIAN SCHART¹, CONSTANTINOS TSIPTILIANIS², and CHRISTINE M. PAPADAKIS¹ — ¹Technische Universität München, Physik-Department, Fachgebiet Physik weicher Materie, Garching, Germany — ²University of Patras, Department of Chemical Engineering, Patras, Greece

Thin films of a pentablock terpolymer with a symmetric architecture of two types of pH-responsive midblocks and short hydrophobic end blocks are investigated. As-prepared spin-coated films from different pH-values have previously shown highly tunable and non-monotonous behavior of the lateral structure sizes, based on the charge [1]. However, with the high glass transition temperatures of the middle pH-responsive block and the hydrophobic end blocks, the films were not necessarily in equilibrium. Here, we investigate further accessible morphologies by swelling the films in the vapors of solvents having different selectivity. Results from spectral reflectance and atomic force microscopy suggest that water (exclusively swelling the pH-responsive blocks) leaves the nanostructures intact, while methanol (swelling all blocks) results in a reorganization. Mixtures of these vapors allow to tune the solubilities of the blocks and thus to find the minimum amount of methanol needed for equilibration.

[1] F. A. Jung, C. M. Papadakis et al., *Adv. Funct. Mater.* 2021, 31, 2102905.

CPP 12.36 Mon 18:00 P1

Transport of thin water films: from thermally activated random walks to hydrodynamics — SIMON GRAVELLE¹, CHRISTIAN HOLM¹, and •ALEXANDER SCHLAICH² — ¹Institute for Computational Physics, University of Stuttgart, Germany — ²Stuttgart Center for Simulation Science (SC SimTech), University of Stuttgart, Germany

Under ambient atmospheric conditions, a thin film of water wets many solid surfaces, including insulators, ice, and salt. The film thickness as well as its transport behavior sensitively depend on the surrounding humidity. Understanding this intricate interplay is of highest relevance for water transport through porous media, particularly in the context of soil salinization induced by evaporation. Here,

we use molecular simulations to evaluate the transport properties of thin water films on prototypical salt and soil interfaces.

Our results show two distinct regimes for water transport: at low water coverage, the film permeance scales linearly with the adsorbed amount, in agreement with the activated random walk model. Finally, in the context of water transport through porous material, we determine the humidity-dependent crossover between a vapor dominated and a thin film dominated transport regimes depending on the pore size.

CPP 12.37 Mon 18:00 P1

Predicting static wetting morphology of aqueous drops on lubricated surface — •SHIVAM GUPTA, BIDISHA BHATT, MEENAXI SHARMA, and KRISHNACHARYA KHARE — Indian Institute of Technology Kanpur, Kanpur, India

Static wetting behavior of liquid drops on thin liquid-coated solid surfaces is very different compared to dry solid surfaces. Conventionally, the equilibrium wetting behavior on deformable (soft or thin liquid coated) surfaces is characterized by the Neumann's contact angle, which solely depends on the various interfacial energies of the participating phases. However, due to the difficulty in identifying the Neumann's point, it is often convenient to define apparent contact angles on such surfaces. By controlling the various interfacial energies, drops can be either made to directly contact the substrate or float on the thin liquid layer supported by the substrate resulting in different apparent angles and thus different wetting morphology. Although such systems are highly prevalent, however, to our knowledge, there is no study reported to date that can beforehand predict the static wetting behavior and the quasi-static interfacial profiles as a function of various system parameters, e.g., substrate wettability, thickness of the liquid film, and drop volume. We propose a method to beforehand predict the interfacial profiles using numerical computation with Surface Evolver software. Experimental studies are also performed to validate the simulations. A good quantitative agreement is found for the variation of the drop contact angle as a function of various systems parameters.

CPP 12.38 Mon 18:00 P1

In-situ white light, near infrared spectroscopy on thin films and photonic crystals of nanoporous silicon during liquid imbibition — •GUIDO DITTRICH^{1,2}, RAUL URTEAGA³, and PATRICK HUBER^{1,2} — ¹Hamburg University of Technology, Institute of Materials and X-Ray Physics, 21073 Hamburg, Germany — ²Deutsches Elektronen-Synchrotron DESY, Centre for X-Ray and Nano Science CXNS, Hamburg, Germany — ³IFIS-Litoral (Universidad Nacional del Litoral-CONICET), Guemes 3450, 3000 Santa Fe, Argentina

Nanoporous materials offer a high specific surface area and spatial confinement. Scientists are aiming to abuse these properties for functional materials in a variety of fields, e.g. thermoelectrics, catalysis, Lab-on-a-Chip as well as energy storage and harvesting applications. Understanding the fundamental transport mechanisms on the nanoscale is required and drives the progress. We present a method to measure liquid imbibition in nanoporous silicon (np-Si) with a resolution even resolving spreading of ultra-thin precursor films in nanopore space with a time resolution of microseconds. Therefore, a photonic crystal (PC) is etched in at a chosen height during the fabrication. The PC has a specific resonance wavelength, which can be monitored with white light spectroscopy. Imbibition by fluids, in our case oligostyrenes, into the central defect of the PC changes the effective refractive index and causes a proportional shift of the resonance wavelength. This offers very localized information on the nanopore filling at the position of the PC. Producing only thin np-Si films, one can measure the shift of the thin film interference with a NIR-spectrometer simultaneously.

CPP 12.39 Mon 18:00 P1

Single-nanochannel X-ray diffraction on the liquid crystal C8BTBT confined in anodic aluminium oxide membranes — •MARK BUSCH^{1,2}, ZHUOQING LI^{1,2}, MILENA LIPPMANN², ANDREAS SCHROPP², JOHANNES HAGEMANN², CHRISTIAN SCHROER^{2,3}, and PATRICK HUBER^{1,2} — ¹TU Hamburg, Institut für Material- und Röntgenphysik — ²Deutsches Elektronen-Synchrotron DESY — ³Universität Hamburg

We investigate the self-assembly of the liquid crystal C8BTBT within anodic aluminium oxide (AAO) nanochannels in dependence of channel wall chemistry and the diameter of the channels from 60 to 180 nm. Conventional X-ray diffraction experiments use a comparatively large beam and therefore deliver a structural information which is averaged over a large number of nanochannels. In contrast here we investigate the structure of liquid crystals within individual nanochannels by employing an X-ray beam with a diameter in the nanometre range.

CPP 12.40 Mon 18:00 P1

Investigation of the charge transport of ionic liquid post-treated PEDOT:PSS thin films with in-situ surface plane impedance spectroscopy, under the influence of varying temperature and humidity — •TOBIAS SCHÖNER¹, ANNA LENA OECHSLE¹, and PETER MÜLLER-BUSCHBAUM^{1,2} — ¹Lehrstuhl für Funktionelle Materialien, Physik- Department, Technische Universität München, James-Frank-Strasse 1, 85748 Garching, Germany — ²Heinz Maier-Leibnitz-

Zentrum (MLZ), Technische Universität München, Lichtenbergstr. 1, 85748 Garching, Germany

Thermoelectric materials based on polymers are attractive due to their large-scale and low cost processability, high mechanical flexibility, low or no toxicity, lightness and intrinsically low thermal conductivity. One highly investigated polymer with promising thermoelectric properties is poly(3,4-ethylene dioxithiophene):poly(styrene sulfonate) (PEDOT:PSS). The post-treatment of PEDOT:PSS thin films with ionic liquids (ILs) enhances the thermoelectric properties for the practical application by simultaneously improving the inter-domain conductivity and optimizing the charge carrier concentration. Our recent investigation focuses on the influence of the environmental parameters temperature and humidity on the electronic and ionic charge transport properties in the thin films. For this, the thermoelectric films are contacted with a self-built setup in a planar way and inserted into a humidity chamber. By using a potentiostat surface-plane Galvanostatic Electrochemical Impedance Spectroscopy (GEIS) measurements under alternating humidity and temperature can be performed.

CPP 12.41 Mon 18:00 P1

Optimization Strategies for Purely Organic Room-Temperature Phosphorescence — •HEIDI THOMAS and SEBASTIAN REINEKE — Dresden Integrated Center for Applied Physics and Photonic Materials (IAPP) and Institute for Applied Physics, TU Dresden

The development of organic materials displaying room-temperature phosphorescence (RTP) with lifetimes in the range of several hundred milliseconds is a research field that has attracted more and more attention in the last years. By using amorphous purely organic systems, we have been able, for example, to develop programmable luminescent tags. Still, the potential of such emitter systems is far from being exploited. We present a new family of organic luminescent derivatives embedded in amorphous matrices with phosphorescence lifetimes up to 2.6 s, extending their applicability. Hydrogen bonds between the emitters and the matrix presumably suppress vibrational dissipation, thus enabling bright long-lived phosphorescence. Further optimization of the host:emitter system is related to the film preparation technique. By varying host polymer, post-annealing temperature, and fabrication procedure, we analyze the phosphorescence lifetime, the photoluminescent quantum yield, and the phosphorescence-to-luminescence ratio. The film thickness turns out to affect the performance the most: Going from thin to thick spin-coated films, the phosphorescence lifetime could be increased by a factor of up to 2.5.

CPP 12.42 Mon 18:00 P1

Investigating the Impact of Surfactants on Perovskite Crystallization during Thin Film Solution Processing Using In Situ Optical Spectroscopy — •TOBIAS SIEGERT, SIMON BIBERGER, KONSTANTIN SCHÖTZ, and FABIAN PANZER — University, Bayreuth, Germany

Recent reports have shown that adding surfactants in the solution processing of halide perovskites, e.g. by blade-coating, can improve their morphology and optoelectronic properties[1]. In general the crystallization processes of halide perovskites that occur during thin film formation largely determine the final film morphology. Thus, here we investigate the change in crystallization dynamics upon addition of surfactants to the solution processing of halide perovskites. We monitor the film formation processes by multimodal optical in situ spectroscopy[2], so that detailed insights about the film formation process of halide perovskites can be gained[3,4]. This finally allows us to elucidate the exact role and the impact of the presence of surfactants during solution processing on the crystallization behavior of the perovskite.

[1] Deng et al. Nat Energy 2018

[2] Buchhorn, Wedler, Panzer. J. Phys. Chem. A 2018

[3] Chauhan, Zhong et al. J. Mater. Chem. A. 2020

[4] Schötz et al. Adv. Optical Mater. 2021

CPP 12.43 Mon 18:00 P1

Fabrication and Characterisation of Two-Step Slot-Die Coated Methylammonium-Formamidinium Lead Iodide Perovskite Solar Cells — •THOMAS BAIER, MANUEL A. REUS, LENNART K. REB, and PETER MÜLLER-BUSCHBAUM — TU München, Physik-Department, LS Funktionelle Materialien, 85748 Garching

Perovskite solar cells (PSCs) are very promising in contributing in the renewable energy mix of the future. They have high power conversion efficiencies and are made of low-cost materials. Especially in combination with slot-die coating as promising thin-film deposition technique for organic-inorganic hybrid perovskite materials, they offer the chance for fast and cheap roll-to-roll solar cell production.

In this work two-step slot-die coated lead iodide layers and slot-die coated methylammonium-formamidinium iodide perovskite solar cells have been prepared. Depending on slot-die coating parameters and additives used in the ink that enhance thin-film formation and optoelectronic properties of the final perovskite semiconductor absorber, morphology changes are observed in the final film. The morphology is investigated by reciprocal (X-ray diffraction) and real-

space methods (SEM). Furthermore, the two-step slot-die coated solar cells are produced and characterized via their respective performance parameters.

CPP 12.44 Mon 18:00 P1

First-principles study of the electronic and optical properties of perovskite solution precursors — •FREERK SCHÜTT¹, ANA M. VALENCIA^{1,2}, and CATERINA COCCHI^{1,2} — ¹Institut für Physik, Carl von Ossietzky Universität Oldenburg — ²Humboldt-Universität zu Berlin und IRIS Adlershof, Berlin

Metal halide perovskites have shown great promise for next-generation optoelectronic applications but the predominant employment of Pb poses a problem in terms of environmental sustainability of these compounds. Replacing Pb with Sn represents a viable solution, however, despite recent efforts in this direction [1], knowledge of Sn-based perovskites and precursors is to date still insufficient. In a first-principles work based on time-dependent density-functional theory coupled to the polarizable continuum model, we systematically investigate electronic and optical properties of SnI_2M_4 complexes, with M being common solvent molecules. We find that the structural, electronic, and optical properties are strongly affected by the choice of the solvent. By rationalising the behavior of 15 of such compounds even in comparison with lead-halide counterparts [2,3], we provide useful indications to complement experiments in the choice of the solvent molecules for SnI_2 -based solution complexes and in their characterization towards the production of thin films. [1] Di Girolamo et al., ACS Energy Lett. 6, 959 (2021). [2] Schier et al., Phys. Status Sol. B 258, 2100359 (2021). [3] Procidia et al., PCCP 23, 21087 (2021).

CPP 12.45 Mon 18:00 P1

Ionic liquids tailoring crystal orientation for stable and high fill factor perovskite solar cells — •YUQIN ZOU¹, LUKAS V SPANIER¹, JULIAN E HEGER¹, SHANSHAN YIN¹, CHRISTOPHER R EVERETT¹, and PETER MÜLLER-BUSCHBAUM MÜLLER-BUSCHBAUM^{1,2} — ¹TU München, Physik-Department, LS Funktionelle Materialien, 85748 Garching — ²MLZ, TU München, 85748 Garching

Ionic liquids with superior electrical conductivity and thermal stability are used as effective and practical dopants to improve the long-term operation stability and the photovoltaic performance of perovskite solar cells (PSCs). We study different ionic liquids in the perovskite component. Using grazing-incidence wide-angle X-ray scattering (GIWAXS), we discover that the incorporation of ionic liquids is beneficial for obtaining homogeneous spherical nano-particle films and tuning the film crystal orientation. We select 1-butyl-1-methylpyrrolidinium tetrafluoroborate (Pyr13BF4) as the main additive to investigate the charge carrier dynamic behavior of PSCs underdoped with Pyr13BF4 using TRPL, TPC, TPV and OCVD methods. In addition to enhancing the fill factor and optimizing energy level alignment, this additive promotes charge transfer and extraction, reduces the charge carrier accumulation in the bulk, and retards recombination. Under ambient atmosphere, the un-encapsulated PSCs retain 97% of their initial efficiencies for 4368 h.

CPP 12.46 Mon 18:00 P1

Improving morphology and efficiency of slot-die coated perovskite solar cells — •CHRISTOPH G. LINDENMEIR¹, ANDREA VITALONI¹, LENNART K. REB¹, MANUEL A. REUS¹, and PETER MÜLLER-BUSCHBAUM^{1,2} — ¹TU München, Physik-Department, LS Funktionelle Materialien, 85748 Garching — ²MLZ, TU München, 85748 Garching

During the last years perovskite solar cells (PSCs) received high attention in industry and research for sustainable power production. Especially due to their low material costs, low weight, high power conversion efficiencies, and the possibility to fabricate them via simple solution-based deposition techniques like slot-die coating or spray coating. Because of the possibility of up-scaling and using minimal material, slot-die coating is one of the most promising techniques to produce high efficiency PSCs. In this work, we compare the properties of slot-die coated PSCs with different perovskite compositions. The perovskite layer is printed out of a solution, containing different ratios of lead iodide (PbI_2), methylammonium iodide (MAI), formamidinium iodide (FAI), and methylammonium chloride (MACl) in a solvent mixture of 2-methoxyethanol (2-ME) and dimethyl sulfoxide (DMSO). To improve the film quality of the printed perovskite layer, the influence of nitrogen gas quenching is extensively studied and the print process optimized. The resulting high-quality thin films are analyzed with optical and structure characterization methods like spectroscopy and X-ray scattering methods. For further information, current-voltage and external quantum efficiency measurements are carried out.

CPP 12.47 Mon 18:00 P1

Slot-die coated perovskite quantum dot layers for solar cell application — •AHMED KRIFA¹, MANUEL A. REUS¹, LENNART K. REB¹, and PETER MÜLLER-BUSCHBAUM^{1,2} — ¹TU München, Physik-Department, LS Funktionelle Materialien, 85748 Garching — ²MLZ, TU München, 85748 Garching

Perovskite quantum dots (PQDs) are semiconductor nanocrystals that have received tremendous attention in photovoltaic devices due to their exceptional optical and electronic properties. PQD solar cells (PQDSCs) have shown great potential to overcome many drawbacks of their large-grain perovskite thin-film

(often called bulk) counterparts, such as high defect tolerance and better stability due to the controlled surface properties of the quantum dots. Over the past few years, PQDSCs have shown a quick increase in efficiency, already exceeding 16%, and high stability. However, the fabrication of these solar cells is based on the spin-coating technique, which leads to significant waste. In this work, we develop and optimize a printing process for PQDs layers and study them with various techniques such as UV-Vis, scanning electron microscopy and X-ray diffraction to achieve an up scalable fabrication of PQDSCs.

CPP 12.48 Mon 18:00 P1

In situ study of superlattice self-assembly during printing of perovskite quantum dot films for solar cell applications — •DAVID P. KOSBAHN¹, MANUEL A. REUS¹, and PETER MÜLLER-BUSCHBAUM^{1,2} — ¹TU München, Physik-Department, LS Funktionelle Materialien, 85748 Garching — ²MLZ, TU München, 85748 Garching

Research into quantum dots (QDs) of lead halide perovskites (LHPs) has become increasingly popular due to their stability and tunable optoelectronic properties. Their controllable surface chemistry and simple preparation make them a promising alternative to bulk perovskite solar cells. The power conversion efficiency (PCE) of $\text{Cs}_x\text{FA}_{1-x}\text{PbI}_3$ QD solar cells (QDSCs) has been steadily rising, up to a recent record efficiency surpassing 16%. However, the orientation and self-assembly of the colloidal precursor into a superstructure is not yet well-understood. In this work, we study the formation of perovskite QD films using in situ grazing-incidence wide-angle X-ray scattering (GIWAXS) in real time, to achieve a better understanding of the kinetics involved in their fabrication.

CPP 12.49 Mon 18:00 P1

Operando study of light and moisture induced degradation of perovskite solar cell — •KUN SUN¹, JULIAN E. HEGER¹, MANUEL A. REUS¹, XINYU JIANG¹, LUKAS V. SPANIER¹, SIGRID BERNSTORFF², and PETER MÜLLER-BUSCHBAUM^{1,3} — ¹TU München, Physik-Department, LS Funktionelle Materialien, 85748 Garching — ²Eletra-Sincrotrone Trieste, 34149 Basovizza — ³MLZ, TU München, 85748 Garching

Perovskite solar cells (PSCs) are among the most promising photovoltaic technologies and reached a certified 25.5% efficiency owing to their tuneable bandgap, high charge carrier mobility, long diffusion length and so on. The long-term operational stability of PSCs, however, has been not investigated. Herein, we probe the structure change with grazing-incidence small-angle scattering and solar cell performance under 1-sun illumination and high humidity. We find that PSCs fabricated with and without caesium iodide (CsI) show differences in the device degradation and morphology change. The decrease of open-circuit voltage (VOC) can be attributed to the morphology changes and the evolution of crystalline grain size. With the additive of CsI, solar cells show slow decay of VOC, correlated to improved morphology of active layer and passivation of trap states. Our work presents a crucial step towards a fundamental understanding of morphology change combined with solar cell parameters during the device operation.

CPP 12.50 Mon 18:00 P1

Non-invasive characterization of degradation in inverted planar perovskite solar cells via reflectance and optical modelling. — •CHIKEZIE WILLIAMS UGOKWE^{1,2}, KEHINDE OGUNMOYE^{1,2}, ULRICH S. SCHUBERT^{1,2}, and HARALD HOPPE^{1,2} — ¹Center for Energy and Environmental Chemistry Jena (CEEC Jena), Friedrich Schiller University Jena, Philosophenweg 7a, 07743 Jena, Germany — ²Institute for Organic and Macromolecular Chemistry (IOMC), Friedrich Schiller University Jena, Humboldtstrasse 10, 07743 Jena, Germany

Despite gains in efficiency since their discovery a little more than a decade ago, hybrid perovskite solar cells (PSCs) are still plagued by poor stability. This poor stability also interferes with their characterization to the point where widely used and easily applicable methods of studying in situ degradation, such as scanning electron microscopy, X-ray diffraction, impact the result because they are invasive and introduce some forms of degradation themselves.

We pursued a non-invasive approach for characterizing the evolution of degradation in PSCs using a combination of optical characterization, modelling, and simulation. Using a software package for coherent light propagation in thin film layer stacks, reflectance and transmittance spectra were used to model the complex refractive index of each functional layer. The evolution of degradation was then studied for ageing methylammonium PSC using periodically measured reflectance data. We will discuss if the evolution of lead iodide, the undoubtable by-product of degradation can be detected using optical simulation.

CPP 12.51 Mon 18:00 P1

Charge Carrier Properties of $\text{Cs}_2\text{AgBiBr}_6$ in Thin Films for Perovskite Solar Cells — •TIM P. SCHNEIDER, JONAS HORN, and DERCK SCHLETTWEIN — Justus-Liebig-Universität Gießen, Institut für Angewandte Physik

The double perovskite $\text{Cs}_2\text{AgBiBr}_6$ is regarded as a potential candidate to replace the toxic lead perovskites currently used in perovskite solar cells and can potentially be used for photo- and x-ray detection. For any such technical application the electrical properties of the double perovskite play an important role. There-

fore, the charge transport in $\text{Cs}_2\text{AgBiBr}_6$ was systematically studied in different sample geometries. Thin films were prepared onto micro-structured interdigitated metal electrode arrays as well as sandwiched between different electron-conducting or hole-conducting layers that are often used in perovskite solar cells, to achieve single-carrier-devices. Aside from estimates of the conductivity and a discussion of possible trapping of charge carriers, the obtained current-voltage characteristics yielded insights into contact formation, hysteresis and intrinsic ion migration. Further, atomic force microscopy showed a strong influence of the underlying substrate on the morphology of the $\text{Cs}_2\text{AgBiBr}_6$ thin films.

CPP 12.52 Mon 18:00 P1

Decoding the Self-assembled Plasmonic Nano-structure in Colloidal Quantum Dots for Photodetectors — •TIANFU GUAN, WEI CHEN, CHRISTIAN L. WEINDL, SUZHE LIANG, and PETER MÜLLER-BUSCHBAUM — Technische Universität München, Physik-Department, Lehrstuhl für Funktionelle Materialien, James-Frankk-Straße 1, 85748 Garching, Germany

Hybrid plasmonic nanostructures have raised great interest for being used in a variety of optoelectronic devices, due to the surface plasmon resonance (SPR). Charge carriers trapped in colloidal quantum dots (QDs) at localized surface defects is a key issue in photodetectors. Self-assembled hybrid metal/quantum dots can couple plasmonics and quantum properties to photodetectors and modify their functionality. Arranged and localized hybrid nanostructures impact on excitons traps and light harvesting. Here, we demonstrate a coupling hybrid structure using self-assembled gold nanoparticles (Au NPs) doped in PbS QDs solid for mapping the interface structures and the motion of excitons. Grazing incidence small angle X-ray scattering (GISAXS) was used to characterize the order of the Au NPs in the hybrid structure. Furthermore, by correlating the sizes of the Au NPs in the hybrid structure with corresponding differences in photodetector performance, we could obtain the interface carriers trapping influences in the coupling structure.

CPP 12.53 Mon 18:00 P1

Einfluss von CO₂ auf die Zusammensetzung von Produkten bei der Hydrierung von Kohlenstoffoxiden an einem Katalysator mit GdFeO₃-Perowskitstruktur — •POLINA AKHMINA — Moscow, Russia

Heute stehen viele Menschen in der Welt vor der Notwendigkeit, den ständig wachsenden Energiebedarf zu decken. Einen wichtigen Platz nimmt die Energie von Kohlenwasserstoffen ein, eine der vielversprechenden Methoden zu deren Synthese ist die Fischer-Tropsch-Synthese. Bekannte Katalysatoren für die Fischer-Tropsch-Synthese sind Verbindungen auf Eisen- und Kobaltbasis, auch komplexe Oxide mit der ABO₃-Perowskitstruktur (A-Kation eines Alkali- oder Seltenerdmetalls, B - Übergangsmetallkation) finden ihre Anwendung. Es wurde ein Experiment mit der Feststellung der Wirkung der Einführung von Kohlendioxid in die Zusammensetzung des Synthesegases CO:H₂ durchgeführt. Das Reaktionsgemisch wurde auf einem Gaschromatographen mit einer Edelstahlsäule analysiert, die Menge der Produkte wurde aus der Fläche der chromatographischen Peaks bestimmt. Als Ergebnis wurde erfahren, dass, im Fall wenn der Gehalt von CO₂ in der Reaktionsmischung 17 % ist (Verhältnis der Reagenzien (CO:CO₂): H₂ = (1:1:2)), im Vergleich zu der Reaktionsmischung ohne Kohlendioxid, ist eine Erhöhung der Menge der gebildeten leichten Olefinen und eine Erhöhung der Olefin/Paraffin-Verhältnisse bemerkt. Außerdem gab es eine Verringerung der Umwandlung von CO. Einer der möglichen Gründe für die Verringerung der Umwandlung ist das Auftreten eines Boudouard Nebenreaktion: $2\text{CO} = \text{C} + \text{CO}_2$

CPP 12.54 Mon 18:00 P1

Semiconducting Carbon Nitride Thin Films — •HSU THAZIN MYINT¹, LENNART K. REB¹, MANUEL A. REUS¹, NARENDRA CHAULAGAIN², KARTHIK SHANKAR², and PETER MÜLLER-BUSCHBAUM^{1,3} — ¹TU München, Physik-Department, LS Funktionelle Materialien, 85748 Garching — ²University of Alberta, Department of Electrical and Computer Engineering, Edmonton, AB T6G 1H9, Canada — ³MLZ, TU München, 85748 Garching

Researchers endeavoring for a clean energy resource have focused on a semiconducting material called graphitic carbon nitride ($g\text{-C}_3\text{N}_4$). The unique property of this material is being environmentally benign due to its metal-free nature, and high solubility in water. Moreover, the earth-abundance of carbon and nitrogen enables easy synthesis at low costs. The astonishing optoelectronic properties, high stability, and absorption in UV-visible region with band-gap energy of 2.7eV render $g\text{-C}_3\text{N}_4$ a prime center for the extensive applications such as solar energy utilization. Fabrication of homogeneous $g\text{-C}_3\text{N}_4$ thin films with tailored thickness and morphology is important to develop novel applications. However, the material deposition to achieve homogeneous thin films is still challenging, rendering information about the bulk material properties essential for device application largely unknown to date. In this work, the low waste and scalable slot-die coating method is fine-tuned to get uniform and high-quality films with good adhesion onto the substrates. The final optimized thin-film properties are studied in terms of spectroscopic, morphological and structural characterization methods.

CPP 12.55 Mon 18:00 P1

Comparison of exciton diffusion in organic and inorganic semiconductors — •DOMINIK MUTH, MARINA GERHARD, GREGOR WITTE, DANIEL BISCHOF, and SEBASTIAN ANHÄUSER — Philipps Universität, Marburg, Deutschland

The mechanisms of exciton and charge carrier transport in organic and inorganic semiconductors differs greatly. To characterize transport processes on the picosecond time scale, a streak camera coupled with a megahertz laser system is employed. The spatio-temporal evolution of the excitation profile is studied at temperatures between 77 K and 295 K. Detailed analysis of the spatial broadening allows us to estimate the underlying exciton diffusion coefficients as a function of time and temperature. In single crystalline tetracene we find evidence for highly dispersive exciton transport, which indicates that excitons populate more localized states on a time scale of a few hundred picoseconds. Moreover, the diffusion coefficients show clear temperature dependence, which will be discussed in this contribution.

CPP 12.56 Mon 18:00 P1

Matrix Influence on the Photodynamics of a TADF-Emitting Molecule — •BJÖRN EWALD¹, ULRICH MUELLER¹, JONAS GEHRIG¹, JONAS BELLMANN¹, and JENS PFLAUM^{1,2} — ¹Experimental Physics VI, University of Würzburg, 97074 Würzburg — ²ZAE Bayern, 97074 Würzburg

The singlet-triplet dynamics of thermally activated delayed fluorescence (TADF) emitters is of high technological relevance for their application in 3rd generation Organic Light Emitting Diodes. In this respect, the molecular and solid-state properties of the matrix material hosting the molecular TADF-dopant, may drastically influence its confirmation, the related energetics and thus, its rate dynamics and the overall OLED efficiency. By virtue of their dark and long-living nature, spectroscopic access to the population dynamics of involved triplet states in such host-guest systems is not trivial. Here we applied a spectroscopic method, based on transient intensity-modulated photoluminescence (TIM-PL). Resting on a generic three level scheme, this technique yields access to the singlet-triplet population dynamics and the corresponding rates in TADF host-guest blends. We studied the photophysics of the TADF-emitter TXO-TPA doped into matrices with different crystalline order (PMMA and mCP). We can confirm that local matrix effects impose a significant impact on the rate dynamics and the singlet-triplet conversion. Particularly the intersystemcrossing rate can be drastically influenced by the local matrix environment. Hence the data obtained by the TIM-PL method, allow for a more rational selection of suited TADF guest-matrix combinations.

CPP 12.57 Mon 18:00 P1

Optically Detected Magnetic Resonance (ODMR) studies on Pentacene doped p-Terphenyl microcrystals — •DOMINIK WINTER¹, BJÖRN EWALD¹, and JENS PFLAUM^{1,2} — ¹Experimental Physics VI, University of Würzburg, 97074 Würzburg — ²ZAE Bayern, 97074 Würzburg

The characteristic wavefunctions of the pentacene triplet states offer the possibility to maintain an asymmetric occupation of the various sublevels even at room temperature. Exposing pentacene single molecules embedded in a crystalline environment to microwaves of suited frequency, a controlled variation in population of the resonant triplet states can be achieved and optically detected - a technique termed optically detected magnetic resonance (ODMR). Here we report on our first results on the triplet polarization of pentacene doped p-terphenyl microcrystals prepared by microspacing in-air sublimation (MAS). By means of zero-field ODMR we analyze the microwave-induced transitions between the contributing triplet states. We will demonstrate and evaluate how the fast and easy method of MAS provides microcrystals that show an enhanced nuclear spin polarization. This process of triplet-induced dynamic nuclear polarization (DNP), is considered a potential approach to enhance the nuclear spin polarization of water and, thus, to significantly improve the image contrast of magnetic resonance imaging (MRI) as well as the sensitivity of non-invasive methods for structural characterization [1].

[1] K. Nishimura et al., Phys. Chem. Chem. Phys., 2019,21, 16408-16412

CPP 12.58 Mon 18:00 P1

Dye-induced Fluorescence Quenching of Quantum Dots having Different Excited State Lifetimes and Confinement Potentials — •SALEEM AL-MASKARI¹, ABEY ISSAC¹, EKLAS AL-GHATTAMI¹, SR VARANASI¹, R.G. SUMESH SOFIN¹, and OSAMA K. ABOU-ZIED² — ¹Department of Physics, College of Science, Sultan Qaboos University, Muscat, 123, Oman — ²Department of Chemistry, College of Science, Sultan Qaboos University, Muscat, 123, Oman

We study the role of quantum confinement and the excited-state lifetime on the fluorescence quenching of heavy metal free quantum dots (QDs). Two different types of QDs are selected, namely CuInS₂/ZnS (CIS) and InP/ZnS (InP). Quantum confinement in CIS QDs is weak (exciton Bohr radius $a_B = 4.3$ nm versus particle size = 3.5 nm) whereas that in InP QDs is strong ($a_B = 15$ nm versus particle size = 3.9 nm). Moreover, the excited-state lifetime of CIS QDs is ca. 298 ns whereas that of InP QDs is ca. 37 ns. Rhodamine 575 (Rh575) dye molecules adsorbed on the surface of QDs are used as the quencher. Stern-Volmer analysis of steady-state and time-resolved optical spectroscopy data reveal that in CIS-

Rh575 and InP-Rh575 assemblies, although static and dynamic quenching are present, dynamic quenching is dominating. Further, quenching is more efficient in CIS-Rh575 assembly. We propose a model based on the quantum mechanical tunneling of the excited QD electron onto the dye induced surface states and subsequent non-radiative relaxation as the quenching mechanism. In addition, the long-lived excited state of CIS QDs support the tunneling mediated quenching in CIS-Rh575 assembly.

CPP 12.59 Mon 18:00 P1

sustainable materials for building-integrated photovoltaics — •ZIMEI CHEN¹, MARIE BETKER^{1,2}, CONSTANTIN HARDER^{1,3}, BENEDIKT SOHOR¹, MATTHIAS SCHWARZKOPF¹, DANIEL SÖDERBERG², NADJA KÖLPIN¹, ARIK WILLNER¹, and STEPHAN V. ROTH^{1,2} — ¹Deutsches Elektronen-Synchrotron (DESY), 22607 Hamburg, Germany — ²KTH Royal Institute of Technology, SE-100 44 Stockholm, Sweden — ³Technische Universität München, 85748 Garching, Germany Cellulose nanofibrils (CNF) as a bio-based material are very attractive due to their resource-saving and renewable property. They are biocompatible, flexible, lightweight, transparent and show excellent mechanical strength. With functionalized properties, they can be used as substrate for incorporating photovoltaic or electronic devices. In this project, we are going for building-integrated photovoltaics. Solar cells with PEDOT:PSS as electron blocking layer, P3HT:PCBM as photoactive layer and ZnO as hole blocking layer will be designed both in standard and inverted devices directly deposited on a CNF composite. A CNF / Ag nanowires mixture can be used as electrode material to improve the conductivity of Ag metal as electrode. Spray deposition will be used as a suitable technique to fabricate such functional layers in a large scale with homogeneous surface and a low roughness. in-situ grazing incidence small- and wide-angle X ray scattering (GISAXS/GIWAXS) will be used to observe the nanostructuring of each layer on the CNF composite base material and to optimize the fabrication process.

CPP 12.60 Mon 18:00 P1

P3HT:PCBM Polymer Solar Cells from a Didactic Perspective — •SHAHIDUL ALAM¹, AMAN ANAND², MD MOIDUL ISLAM², RICO MEITZNER², AURELIEN SOKENG DJOUMESSI², JOSEF SLOWIK², ZEKARIAS TEKLU², PETER FISCHER³, CHRISTIAN KÄSTNER³, JAFAR I. KHAN¹, ULRICH S. SCHUBERT², FRÉDÉRIC LAQUAI¹, and HARALD HOPPE¹ — ¹King Abdullah University of Science and Technology (KAUST), KAUST Solar Center (KSC), Physical Sciences and Engineering Division (PSE), Kingdom of Saudi Arabia — ²Friedrich Schiller University Jena, Germany — ³Ilmenau University of Technology, Germany

In this work, we studied the influence annealing process on the performance of the common polymer:fullerene bulk heterojunction solar cells with conventional architecture, comprising P3HT:PC60BM blend as a photoactive layer. The non-annealed active layer device exhibited a power conversion efficiency of less than 1%, which was significantly lower than the pre and post-annealed device. In order to investigate the impact of pre and post thermal annealing on the natural morphological state of the polymer, regiorandom and regioregular type P3HT were used in photoactive layers. Changes in solar cell performance were associated with different extraction probabilities due to changed annealing conditions. Several spectroscopic techniques like EL, SS-PL, and TR-PL were employed to comprehend the phenomenon of charge photogeneration processes. Finally, to explore the morphological changes upon annealing, AFM and ELI measurements were performed on films and solar cells, respectively.

CPP 12.61 Mon 18:00 P1

Simultaneously enhanced performance and stability of NFA solar cells with PETMP interfacial process — •ZERUI LI^{1,2}, CHANGQI MA², and PETER MÜLLER-BUSCHBAUM¹ — ¹TU München, Physik-Department, LS Funktionelle Materialien, 85748 Garching — ²i-Lab &Printed Electronics Research Center, Suzhou Institute of Nano-Tech and Nano-Bionics, Chinese Academy of Sciences (CAS), Suzhou 215123, P. R. China

With the rapid development of novel non-fullerene acceptors (NFA), the PCE of NFA solar cells has reached over 18.6%, while the poor stability is still the limitation for application. For NFA solar cells, the hydroxyl radicals of ZnO forming under illumination would cause the degradation of the acceptor material, which is one key source for performance decrease. They could be effectively suppressed through modifying ZnO with radical trapping agents, such as 2-phenylethylmercaptan (PET). Unfortunately, PET is highly toxic with a bad smell. Here, PETMP with similar end group as PET is used as the alternative and it's found to be able to suppress the formation of hydroxyl radicals as well as to improve the device stability. Moreover, PETMP can improve the Jsc of devices through promoting the vertical phase separation of the active layer. Lastly, other similar derivatives is also tried and the amount of sulfhydryl is found to be highly important to the enhanced performance and stability, since only molecules with more sulfhydryl groups could work well. The interaction between PETMP and ZnO is the key factor promoting such a benefit. This work provides a perfect interfacial modification agent for more stable NFA solar cells.

CPP 12.62 Mon 18:00 P1

Improved hole extraction selectivity of polymer solar cells by combining PEDOT:PSS with WO₃ — •AURELIEN SOKENG DJOUMESSI^{1,2}, SHAHIDUL ALAM^{1,2}, JOSE PRINCE MADALAIMUTHU^{1,2}, AMAN ANAND^{1,2}, JOSEF SLOWIK^{1,2}, THEO PFLUG^{3,4}, RICO MEITZNER^{1,2}, ROLAND ROESCH^{1,2}, ENRICO GNECCO⁵, ALEXANDER HORN³, ULRICH S. SCHUBERT^{1,2}, and HARALD HOPPE^{1,2} — ¹Center for Energy and Environmental Chemistry Jena (CEEC Jena), Friedrich Schiller University Jena, Philosophenweg 7a, 07743 Jena, Germany — ²Laboratory of Organic and Macromolecular Chemistry (IOMC), Friedrich Schiller University Jena, Humboldtstrasse 10, 07743 Jena, Germany — ³Laserinstitut Hochschule Mittweida, Hochschule Mittweida, Schillerstraße 10, 09648 Mittweida, Germany — ⁴Institut für Physik, Technische Universität Chemnitz, Reichenhainer Straße 70, 09126 Chemnitz, Germany — ⁵Otto Schott Institute of Materials Research, Friedrich Schiller University Jena, Löbdergraben 32, 07743 Jena, Germany

Since the device performance and stability of polymer solar cells strongly depend on the interfacial charge extraction layers, we investigated the impact of hole transport layer (HTL) in the devices by varying the HTL material and layer stack systematically between PEDOT:PSS and a sol-gel derived tungsten oxide (WO₃). Interestingly there was an increase of the work function upon stacking both materials and the triple layer WO₃/PEDOT:PSS/WO₃ configuration resulted in the best device performance and an increased reproducibility in the lifetime compared to the use of pristine WO₃ and PEDOT:PSS

CPP 12.63 Mon 18:00 P1

Compatible solution-processed interface materials for improving efficiency and prolonging the lifetime of polymer solar cells — •ZHUO XU^{1,2}, JOSE PRINCE MADALAIMUTHU^{1,2}, JOSEF BERND SLOWIK^{1,2}, RICO MEITZNER^{1,2}, SHAHIDUL ALAM^{1,2,3}, ULRICH S. SCHUBERT^{1,2}, and HARALD HOPPE^{1,2} — ¹Laboratory of Organic and Macromolecular Chemistry (IOMC), Friedrich Schiller University Jena, Humboldtstraße 10, 07743 Jena, Germany. — ²Center for Energy and Environmental Chemistry Jena (CEEC Jena), Friedrich Schiller University Jena, Philosophenweg 7a, 07743 Jena, Germany. — ³King Abdullah University of Science and Technology (KAUST), KAUST Solar Center (KSC), Physical Sciences and Engineering Division (PSE), Material Science and Engineering Program (MSE), Thuwal 23955-6900, Kingdom of Saudi Arabia

The electron transport layer in a solar cell is one of the main components which plays a crucial role in the separation of charges and improving the efficiency of the solar cells. Herein, solution-processed organic solar cells (PBDTTT-CT:PC70BM) were fabricated with PDINO, Titanium Oxide, and PDINO:TiOx as an ETL. The effect of different ETLs on the performance of solar cells was observed. An efficiency of 7.94% was achieved when PDINO:TiOx was used as an ETL which is one of the highest reported efficiencies for halogen-free solvent processed PBDTTT-CT:PC70BM polymer solar cells. Meanwhile, lower recombination and higher exciton dissociation probability were observed in PDINO:TiOx based PSCs, as well as the superior stability at 45 °C in air.

CPP 12.64 Mon 18:00 P1

Investigation of solvent dependent morphology degradation of PTQ-2F:BTP-4F bulk heterojunctions — •LUKAS V. SPANIER¹, RENJUN GUO¹, JULIAN E. HEGER¹, YUQIN ZOU¹, MATTHIAS NUBER², MATTHIAS SCHWARTZKOPF³, HRISTO IGLEV², REINHARD KIENBERGER², STEPHAN V. ROTH³, and PETER MÜLLER-BUSCHBAUM^{1,4} — ¹TU München, Physik-Department, LS Funktionelle Materialien, 85748 Garching — ²TU München, Physik-Department, LS Laser- und Röntgenphysik, 85748 Garching — ³DESY, 22607 Hamburg — ⁴MLZ, TU München, 85748 Garching

Lately, organic solar cells (OSCs) have gained increasing attention due to their rapidly increasing efficiencies as well as the relatively easy scalability in their manufacture. To make the manufacturing process of the bulk-heterojunction (BHJ) more environmentally friendly, increased efforts have recently been made to use halogen-free solvents, which, however, can lead to reduced efficiencies.

We investigate and compare the changes in morphology and performance stability of PTQ10:BTP-4F OSCs processed from various solvents, utilising operando grazing-incidence small and wide angle X-ray scattering during illumination and solar cell operation. We further show the impact of solvent composition on the charge carrier generation in the respective BHJs using time-resolved transient absorption spectroscopy, analysing the connection between thin-film morphology and device performance in polymer:non-fullerene acceptor OSCs.

CPP 12.65 Mon 18:00 P1

Polysulfobetaines as electron transport layers in organic solar cells employing a PBDBTCl-DTBT:BTP-4F active layer — •SEBASTIAN COEN¹, APOSTOLOS VAGIAS², JOHANNA EICHHORN³, LUKAS SPANIER¹, ZERUI LI¹, XINYU JIANG¹, ANDRÉ LASCHEWSKY^{4,5}, and PETER MÜLLER-BUSCHBAUM^{1,2} — ¹TU München, Physik-Department, LS Funktionelle Materialien, 85748 Garching — ²MLZ, TU München, 85748 Garching — ³WSI, TU München, AG Experimentelle Halbleitersphysik, 85748 Garching — ⁴Universität Potsdam, Institut für Chemie, 14476 Potsdam-Golm — ⁵Fraunhofer IAP, 14476 Potsdam-Golm

Zwitterionic polymers (e.g. polysulfobetaines) have so far been systematically explored as antifouling agents due to their total electroneutrality and superhy-

drophilicity. These macromolecules carry a permanent dipole moment because of the simultaneous presence of positive and negative charges on the backbone. However, this dipole moment can affect the optoelectronic properties and charge transport when such polymers are considered as interlayers for organic solar cells. So far, the role of polyzwitterions as interlayers of organic photovoltaics remains unexplored. We investigate the use of one specific polysulfobetaine (PSPE) in this work. We study its optoelectronic and morphological properties under the aspect of usage in an organic solar cell. For this solar cell, we use an active layer of a PBDBTCl-DTBT:BTP-4F blend with an architecture of ITO/PEDOT:PSS/Active Layer/PSPE or PDIN/Ag. PDIN is a reference electron transport layer material showing similar band positions as PSPE.

CPP 12.66 Mon 18:00 P1

Possibilities and limitations for the alignment of polymer chains in photo-voltaic materials — •ROBIN TEICHGREBER, FABIAN ELLER, and EVA M. HERZIG — Dynamik und Strukturbildung - Herzig Group, Universität Bayreuth, Universitätsstr. 30, 95447 Bayreuth, Germany

The arrangement of the polymer chains on the nanoscale in thin films influences the optical and electrical properties of the material in a decisive way. For efficient charge transport, a sufficient alignment of the polymers is necessary. Due to the sensitive nature of the microstructure to various influencing variables such as concentration, solubility, and temperature, this goal presents an experimental challenge. However, a deliberate alignment will allow to probe optical and electric photovoltaic properties more systematically. Li et al. [1] have shown that thin films with a high degree of alignment can be produced via dip-coating by varying the coating speed and concentration using the polymer PII-2T. The simple nature of the dip-coating process makes it attractive, also for other polymers, should similar results be obtainable. Here, it will be shown which results can be obtained in a dip-coating based process with P3HT and high performance polymers like PM6. For this purpose, different influencing variables such as coating speed, concentration, solvent quality and temperature are evaluated. In addition, the process is extended to include pre-processing and post-processing steps.

[1] Li, Qi-Yi; Yao, Ze-Fan; Lu, Yang; Zhang, Song; Ahmad, Zachary; Wang, Jie-Yu; et al. *Adv. Electron. Mater.*, 6 (6), 2000080, 2020

CPP 12.67 Mon 18:00 P1

PbS quantum dot solar cells with a IZO buffer layer at quantum dot/ZnO interface — •HUAYING ZHONG¹, WEI CHEN^{1,2}, LUKAS V. SPANIER¹, CHRISTOPHER R. EVERETT¹, MANUEL A. REUS¹, XINYU JIANG¹, SHANSHAN YIN¹, MARLENE SOPHIE HÄRTEL³, JIAHUAN ZHANG³, BERTWIN BILGRIM OTTO SEIBERTZ⁴, MATTHIAS SCHWARTZKOPF⁵, STEPHAN V. ROTH⁵, and PETER MÜLLER-BUSCHBAUM^{1,6} — ¹TU München, Physik-Department, 85748 Garching, Germany — ²James-Frank-Strasse 1 — ³HZB, Solar Energy, 14109 Berlin — ⁴TU Berlin, Department of Technology for Thin-film Components, 10623 Berlin — ⁵DESY, 22607 Hamburg — ⁶MLZ, TU München, 85748 Garching

Colloidal quantum dots (CQDs) have generated great interests in various optoelectronic devices due to their size-tunable bandgap, low-temperature solution processability. Lead sulfide (PbS) CQDs with large Bohr radius enable solar cells to harvest infrared photons of the solar spectrum beyond the absorption edge of crystalline silicon and perovskites. Interface engineering, as one of strategies to improve device performance, is designed to form an energy cascade to enable an efficient charge transfer and promote exciton dissociation. Moreover, it can also offer good interfacial contact and improve device air stability by selecting appropriate materials. Here, we sputter the indium zinc oxide (IZO) as the interlayer between PbS QDs absorption layer and ZnO nanoparticle (NP) electron transport layer (ETL), to fabricate PbS QD solar cells and study the trap densities and charge transport process at QDs interfaces.

CPP 12.68 Mon 18:00 P1

Preparation of Highly Crystalline ZnO Thin Films at Low Temperatures using ZnO Nanoparticles to Enable High-Quality Organic Solar Cells On Flexible Substrates — •EMANUEL ANWANDER, LUKAS V. SPANIER, and PETER MÜLLER-BUSCHBAUM — TU München, Physik-Department, Lehrstuhl für Funktionelle Materialien James-Frank-Straße 1, 85748 Garching

The possibility to build flexible light weight OSCs makes them very promising for aviation and aerospace applications. Therefore, inexpensive and scalable materials such as PET or PEN are desirable substrates. Conventional sol-gel preparation of ZnO thin films, which have proven to be the best choice for electron transport layers (ETLs) in inverted OSCs, requires annealing at temperatures up to 200°C. Since PET and PEN have glass transition temperatures of 69°C and 113°C, respectively, and are long term heat resistant at a maximum of 120°C and 155°C, respectively, a way to produce high-quality ZnO thin films at low temperatures is required. One approach to achieve this goal is to use a solution of pre-synthesized ZnO nanoparticles. These nanoparticles exhibit high crystallinity and thus good ZnO thin films that have higher charge carrier mobility and lower recombination rates than the sol-gel ZnO films can be formed at room temperature without annealing. This approach allows the realization of lightweight OSCs on flexible substrates that have the same or even higher efficiencies than conventional OSCs on rigid substrates with ETLs prepared using the sol-gel method.

CPP 12.69 Mon 18:00 P1

Calculation of vibronic progressions for PPE-PPV polymers — MONTASSAR CHAABANI¹, SAMIR ROMDHANE¹, and •WICHARD BEENKEN² — ¹Laboratoire Matériaux Avancés et Phénomènes Quantiques, Faculté des Sciences de Tunis, Université Tunis El Manar, Campus Universitaire Tunis, 2092, Tunisia — ²Institut für Physik, Technische Universität Ilmenau, Weimarer Str. 32, 98693 Ilmenau, Germany

We have calculated the vibronic progressions for absorption and photoluminescence spectra of conjugated copolymers with alternating PPE and PPV units and various side-chains.

CPP 12.70 Mon 18:00 P1

Investigation of Crystal Structure of Polydiketopyrrolopyrrole Copolymers — •ROBERT KAHL¹, GERT KRAUSS², ANDREAS ERHARDT², OLEKSANDR DOLYNCHUK¹, MUKUNDAN THELAKKAT², and THOMAS THURN-ALBRECHT¹ — ¹Experimental Polymer Physics, Martin Luther University Halle-Wittenberg — ²Applied Functional Polymers, University of Bayreuth

Polydiketopyrrolopyrrole (PDPP) copolymers are promising materials for applications in organic solar cells and transistors. Their chemical structure offers many possibilities for modifications, allowing to adjust their optoelectronic properties according to the desired application. Here, we investigated the molecular ordering and thermal properties in bulk (WAXS, DSC, TGA) and in thin films (GIWAXS, AFM) of three exemplary PDPPs, two donor polymers: PDPP[T]₂{2-HD}₂-T (PDPP_T) with thiophene flanking units and PDPP[T]₂{2-HD}₂-T{DEG} (PDPP_{T-OEG}) with thiophene flanking units and an additional OEG side chain, and one acceptor polymer: PDPP[Py]₂{2-HD}₂-T (PDPP_{Py}) with pyridine flanking units. In the ordered state, all three PDPPs show regular π - π -stacked backbones ($d_{020} = 3.7 - 3.9 \text{ \AA}$) and a regular layered structure of demixed backbones and side chains ($d_{100} = 18.7 - 19.1 \text{ \AA}$). While PDPP_T and PDPP_{T-OEG} only have sanidic liquid crystalline order, PDPP_{Py} has a complex triclinic structure. PDPP_{T-OEG} has the lowest melting temperature and PDPP_{Py} the poorest thermal stability of the three. These results demonstrate the significant influence of seemingly small chemical modifications on crystal structure and thermal properties of PDPPs.

CPP 12.71 Mon 18:00 P1

Fluorinated thieno-quinoxalines - a systematic study on conformational locking and accompanied electronic characteristics — •M.M. ISLAM^{1,2}, A.M. ANTON^{1,2}, R. MEITZNER^{1,2}, C.L. CHOCHOS^{3,4}, U.S. SCHUBERT^{1,2}, and H. HOPPE^{1,2} — ¹Laboratory of Organic and Macromolecular Chemistry (IOMC), Friedrich Schiller University Jena, Humboldtstrasse 10, 07743 Jena, Germany — ²Center for Energy and Environmental Chemistry Jena (CEEC Jena), Friedrich Schiller University Jena, Philosophenweg 7a, 07743 Jena, Germany — ³Institute of Chemical Biology, National Hellenic Research Foundation, 48 Vassileos Constantinou Avenue, Athens 11635, Greece. — ⁴Advent Technologies SA, Patras Science Park, Stadiou Street, Platani-Rio, 26504, Patra, Greece

Low band-gap thieno-quinoxaline derivatives are promising donor materials in organic solar cells. Fluorination, on the one hand, can lower both the HOMO as well as LUMO energy levels and thus enhance stability. On the other hand, electron exchange between hydrogen or sulfur and fluorine atoms might cause non-covalent interactions and steric hindrance. Six thieno-quinoxaline derivatives with systematically fluorinated sites have been investigated in solution, pristine films, and blends with ITIC as acceptor. UV-Vis absorption spectra reveal the sensitivity of stacking depending on the particular fashion of fluorination, which affects the size of photochromic units. The stacking propensity is corroborated by DFT simulations. Fluorescence spectroscopic indicates different photoluminescence pathways indicated by excitation-independent and excitation-selective PL signals.

CPP 12.72 Mon 18:00 P1

Optically detected magnetic resonance of OLED materials using a confocal microscope — •PASCAL SCHADY, FABIAN BINDER, MONA LÖTHER, VLADIMIR DYAKONOV, and ANDREAS SPERLICH — Experimental Physics VI, Julius Maximilian University of Würzburg, 97074 Würzburg

Optically detected magnetic resonance (ODMR) is a specialized technique to investigate spin-dependent optical transitions in solids. This method is also applicable for examining photoluminescence characteristics of semiconducting organic materials which are becoming increasingly popular for, e.g. display applications. In typical ODMR setups a laser beam is guided into a microwave-cavity from one side while the emission spectrum of the sample is detected from the other. To improve upon that, we build a confocal microscope around the cavity, such that white light as well as a laser beam are guided through the cavity opening onto the sample, allowing us to locally excite sample spots while monitoring the laser spot and photoluminescence through a camera and photodetector. By implementing these upgrades we aim to enhance sensitivity while also enabling improved control over the investigated sample spot in order to highlight excited state spin physics processes of potential organic light emitting diode materials.

CPP 12.73 Mon 18:00 P1

Conception and realization of a highly automated physical vapor deposition system for the fabrication of organic light-emitting diodes — •FABIAN BINDER, MONA LÖTHER, VLADIMIR DYAKONOV, and ANDREAS SPERLICH — Experimental Physics VI, Julius Maximilian University of Würzburg, 97074 Würzburg

Organic light emitting diodes (OLEDs) are most commonly produced in ultra-high vacuum by physical vapor deposition of different organic and metallic layers on a carrier substrate. We designed a production system that should enable an almost completely automated production of the OLED-devices by the use of many sensor solutions and electric stepper motors. The different stepper motors allow a smooth and precise positioning of the OLED-sample above the evaporation crucibles in the vacuum chamber. Being positioned over an evaporation crucible, the sample needs to rotate with a defined speed to achieve an even deposition of the material. In order to vapor-deposit material, a certain, material-specific temperature range is required. This is realized by a software-based temperature controller which manages the evaporation rate according to the specifications of the user. A user interface makes it possible to design the desired OLED layer stack and provides information about the production progress. Finally, the first OLED devices will be produced and an electrical characterization of these devices, such as an investigation on the quantum efficiency will be done.

CPP 12.74 Mon 18:00 P1

Nanoscale alignment and chemical characterization of self-assembled all polymer donor-acceptor blends — •DIJO MOONNUKANDATHIL JOSEPH^{1,2}, JUANZI SHI³, WANZHU CAI⁴, HARDIK GADHER¹, MOHAMMAD SOLTANINZEHAD^{1,2}, IVAN G. SCHEBLYKIN³, and DANIELA TÄUBER^{1,2} — ¹Leibniz Institute of Photonic Technology, Jena — ²Friedrich-Schiller University Jena, Germany — ³Lund University, Lund, Sweden — ⁴Jinan University, Guangzhou, China

Control of light polarization properties in self-assembled all-polymer donor-acceptor blends enables intrinsic polarization-sensitive applications in organic optoelectronics. In general, the polarization properties of thin conjugated polymer films are related to the polymer chain alignment in the film. Macroscopic domains of polymer alignment were demonstrated in thin films of a quinoxaline-thiophene copolymer (TQ1), which had been self-assembled via floating film transfer [1]. The nano-chemical characterization of thin polymer films can be achieved by nano-infrared spectroscopy (NanIR) methods [2]. We use 2D polarization imaging for characterizing the polarization properties of several thin polymer blend films fabricated via floating film transfer. In addition we investigate the chemical nanostructure of these films using mid-infrared photoinduced force microscopy. — [1] Täuber et al. ACS Omega 2017, 2, 32-40. [2] L. Xiao, Z.D. Schultz, Anal. Chem. 2018, 90 (1), 440-458.

CPP 12.75 Mon 18:00 P1

Ground-state charge transfer and influence on charge carrier transport in organic donor-acceptor mixtures — •HONGWON KIM¹, FLORIAN FENZEL¹, DOMENIK VÖGEL¹, ANDREAS OPITZ², and WOLFGANG BRÜTTING¹ — ¹Experimental Physics IV, Institute of Physics, University of Augsburg, 86135 Augsburg — ²Supramolekulare Systeme, Institut für Physik, Humboldt-Universität zu Berlin, 12489 Berlin

In organic semiconductors, charge transfer (CT) states form at interfaces or in mixtures of electron accepting and donating molecules. Their mutual electronic interaction is accompanied by a partial or full transfer of electric charges. This charge transfer is crucial to generate excess charges in (opto-)electronic devices, i.e. to facilitate electrical doping.

We have investigated donor-acceptor thin films consisting of electron donating molecules (DIP, 6T, DBTTF, and DBP) mixed with strong acceptors (F6TCNNQ and HATCN). It is investigated that the thermal activation energy (E_a) decreases and the electrical conductivity (σ) increases through doping by strong acceptors. Furthermore, the formation of CT states accelerates this doping effect and a highly improved conductivity can be obtained on DBTTF/F6TCNNQ as well as DIP/F6TCNNQ mixed thin films. This high conductivity is a result of increased concentration of charge carriers by doping effect as well as its improved mobility by CT states formation. However, the formation of CT states also has characteristic spectroscopic signatures and affects the growth behavior of molecular donor-acceptor blends.

CPP 12.76 Mon 18:00 P1

Morphology and stability study of organic thin films — •MEIKE KUHN¹, CHRIS MCNEILL², and EVA M. HERZIG¹ — ¹Dynamik und Strukturbildung - Herzig Group, Universität Bayreuth, Universitätsstr. 30, 95447 Bayreuth, Germany — ²Material Science and Engineering, Monash University, 20 Research Way, Clayton

New, promising materials with high efficiency are constantly being discovered for organic solar cells. Often, these materials are chosen to mainly maximize efficiency. However, stability also plays an important role when selecting promising materials. The stability of organic materials depends on many variables, such as photochemical stability, photostability and morphological stability. In this anal-

ysis, we will attempt to gain a better understanding of nanostructural changes and hence morphological stability. [1] Using GIWAXS and absorption measurements, we systematically investigate how the ageing process affects the structure. In particular, we investigate the behaviour of the morphological ageing mechanisms, such as the orientation and aggregation of the material, as a function of temperature and substrate properties. These experiments are carried out on organic polymers such as PM6.

[1] C. Wöpke; C. Göhler; M. Saladina; X. Du; L. Nian; C. Greve; C. Zhu; K. M. Yallum; Y. J. Hofstetter; D. Becker-Koch; N. Li; T. Heumüller; I. Milekhin; D. R. T. Zahn; C. J. Brabec; N. Banerji; Y. Vaynzof; E. M. Herzig; R. C. I. MacKenzie; C. Deibel, Nat. Comm., accepted

CPP 12.77 Mon 18:00 P1

Photoluminescence and Quantum Yield of a deep blue TADF emitter — •MONA LÖTHER, FABIAN BINDER, PASCAL SCHADY, JEANNINE GRÜNE, VLADIMIR DYAKONOV, and ANDREAS SPERLICH — Experimental Physics VI, Julius Maximilian University of Würzburg, 97074 Würzburg

Organic light-emitting diodes (OLEDs) based on thermally activated delayed fluorescence (TADF) are becoming increasingly important due to their advantages over OLEDs of earlier generations as they enable access to triplet excitons via reverse intersystem crossing (rISC) without the need of resources-limited rare metal complexes. However, TADF OLEDs have yet to reach commercial viability, as an efficient and durable blue OLED remains to be found. A promising design for a blue host-dopant system is N7,N7,N13,N13,5,9,11,15-octaphenyl-5,9,11,15-tetrahydro-5, 9,11,15-tetraaza-19b, 20b diboradiazaphtho[3,2,1-de:10, 20, 30-jk]pent-acene-7,13-diamine (ν -DABNA). This system belongs to the multiresonant TADF compounds, represented typically by narrow band emission, high photoluminescence quantum yield (PLQY) and a small singlet-triplet gap ΔE_{ST} . In order to characterize its optical properties we examined the steady state photoluminescence (PL), transient photoluminescence (trPL) and PLQY. Furthermore, we used different host systems to survey the behavior of ν -DABNA in a host-emitter system. With these optical characterization methods we are able to better understand the promising candidate of TADF OLEDs with high efficiencies and color purity.

CPP 12.78 Mon 18:00 P1

Towards efficient blue perovskite lead-halide nanocrystal light emitting diodes — •TASSILO NAUJOKS¹, ADRIAN HOCHGESANG², CHRISTOPHER KIRSCH³, MARCUS SCHEELE³, MUKUNDAN THELAKKAT², and WOLFGANG BRÜTTING¹ — ¹Institut für Physik, Universität Augsburg, Germany — ²Universität Bayreuth, Germany — ³Institut für Physikalische und Theoretische Chemie, Universität Tübingen, Germany

The research focus for affordable solution-processed light-emitters has been shifted towards quantum-dot materials in recent years. High quantum yields (QY) even with inorganic nanocrystals (NC) capped by organic ligands have been achieved. One prominent, particularly highly luminescent type of NC is lead-halide perovskite with tunable colour by halide composition achieving near-unity QY.

While for red and green emitting NCs the quantum efficiency in the resulting LEDs is engineered to a satisfactory level, blue perovskite NCs are still underperforming. One issue with blue and therefore wider bandgap NCs lies in the very deep valence level. With that, hole injection into the NCs is significantly impaired. Here we present two approaches to enhance hole-injection into blue LHP NCs. The use of carbazole moieties either within the ligand on the NC surface or as a TCTA-doped polyvinyl-carbazole (PVK) polymeric hole transport layer increases the efficiency in perovskite NC LEDs. We propose that the carbazole group effectively blocks electrons, while its deep HOMO facilitates the injection into the similarly deep valence level of the blue perovskites.

CPP 12.79 Mon 18:00 P1

Photoinduced metastable and trapped charge-carrier pairs in neat amorphous films of OLED host materials — SEBASTIAN LULEI¹, JEANNINE GRÜNE¹, ANDREAS SPERLICH¹, •VLADIMIR DYAKONOV¹, ANDREI STANKEVYCH², ANDREY KADASSHCHUK², and ANNA KÖHLER² — ¹Experimental Physics 6, Julius Maximilian University of Würzburg, 97074 Würzburg — ²Soft Matter Optoelectronics and Bavarian Polymer Institute (BPS), 95448 Bayreuth

We discuss light-induced ESR (LESR) transients, PL-detected magnetic resonance (PLDMR), and thermally-stimulated luminescence (TSL) in neat amorphous thin films of 3',5'-di(9H-carbazol-9-yl)-[1,1'-biphenyl]-3-carbonitrile (mCBP-CN), which is commonly used as a host material for blue emitters based on thermally activated delayed fluorescence (TADF) in OLED devices. While the half-field LESR signal associated with triplet excitations shows fast saturation being comparable with the triplet lifetime, the full-field LESR featured extremely slow kinetics of both growth and decay at T=10K. The latter implies very slow accumulation and subsequent recombination of the photogenerated charge carriers due to shallow charge trapping at such low temperatures. These results are in good agreement with the observation of a long isothermal afterglow lasting up to thousands of seconds at 5K. Further, the persistent LESR signal is detected in

the same temperature range as the TSL emission, implying that both are caused by the same trapped carriers. Finally, PLDMR showed signals from closed-by triplet states, emitting through fluorescence.

CPP 12.80 Mon 18:00 P1

Graphene nanoribbons synthesized on Au(111) and Au(788) in ultra-high vacuum conditions and by atmospheric pressure chemical vapor deposition method — •VASILII OSIPOV, YI HAN, PHILIPP WEITKAMP, MAX REIMER, DIRK HERTEL, and KLAUS MEERHOLZ — Chemistry department, University of Cologne, Germany

Graphene nanoribbons (GNRs) are an interesting class of materials due to their tunable width- and edge-type-dependent electronic structure. The state-of-the-art methods of GNRs synthesis are bottom-up processes involving polymerization of precursor molecules at catalytic surfaces, and are typically performed ei-

ther in ultra-high vacuum (UHV) conditions or by atmospheric pressure chemical vapor deposition (AP-CVD) technique. Despite leading to GNR layers of reduced quality, the AP-CVD method possesses advantages of simplicity and better scalability compared to the UHV one, which make it a promising option for developing routes for synthesis of new types of GNRs. We present results of AP-CVD synthesis of GNRs from different precursors and their comparison to GNRs of corresponding types obtained by UHV method, using Raman spectroscopy. Particularly, degree of GNRs growth geometrical anisotropy, induced by using Au(788) growth substrate instead of Au(111), is investigated by observing the polarization-angle-dependent Raman intensity. This should eventually contribute to better understanding of the processes of GNRs synthesis and to development of technologies for functional (templating) materials for organic electronics.

CPP 13: Charged Soft Matter, Polyelectrolytes and Ionic Liquid

Time: Tuesday 9:30–11:15

Location: H38

Invited Talk

CPP 13.1 Tue 9:30 H38

Insights into degradation mechanisms in Li-based batteries and advantages of polymer coatings — •NEELIMA PAUL — Heinz Maier-Leibnitz Zentrum (MLZ), TU München, Lichtenbergstr. 1, 85748 Garching, Germany

Lithium-ion batteries are present in portable electronics, electric vehicles and grid-scale energy storage and are an inherent part of our daily life. They offer high energy density, high power density, stable temperature performance, and are safe. However, they eventually suffer from capacity fade due to some intrinsic degradation mechanisms, and thus have a limited cycle life. To increase their lifetime, knowledge of the responsible degradation/aging mechanism is crucial and most beneficial if determined without destructive disassembly of the battery. I will demonstrate how parameters responsible for aging such loss of mobile Li inventory, active material degradation, metallic Li plating, can be monitored and quantified using both operando and post-mortem neutron techniques. Thereafter, I will describe the main degradation mechanism in Li-metal batteries and show how this can be overcome by applying viscoelastic polymer coatings with a specific mechanical strength to the anode surface.

CPP 13.2 Tue 10:00 H38

Electrostatically Cross-Linked Reversible Gels - Effects of pH and Ionic Strength — ROMAN STAÑO^{1,4}, •PETER KOŠOVAN¹, ANDREA TAGLIABUE², and CHRISTIAN HOLM³ — ¹Faculty of Science, Charles University, Prague, Czechia — ²Università degli Studi dell'Insubria, Como, Italy — ³Institute for Computational Physics, University of Stuttgart, Germany — ⁴University of Vienna, Austria

Mixing of oppositely charged macromolecules can lead to the formation of electrostatically cross-linked coacervate gels. In this simulation study, we determine the conditions under which four-armed star copolymers with charged end-blocks are able to form such coacervate gels. The cationic charged blocks consist of quenched charges, whereas the anionic blocks contain pH-responsive weak acid groups. We used the Grand-reaction method to determine the phase stability, equilibrium composition, and structural properties of these systems in equilibrium with a supernatant solution at various pH levels and salt concentrations. Depending on the pH and hence on the charge state of the polyanion blocks, we observed the emergence of three regimes: a solution, a sol of isolated star clusters, and a gel*percolating network of stars. Moreover, we demonstrate that the charge state of the stars in the gel phase can be well described by the ideal Henderson-Hasselbalch (HH) equation, despite the presence of strong interactions violating ideality. We can explain this surprising result by cancellation of two stongly non-ideal effects. This observation explains why various experiments on coacervate gels can be well described by the HH equation, although its assumption of ideality is violated.

CPP 13.3 Tue 10:15 H38

Temperature Dependence of PSS diffusion in multilayers of entangled PDADMA: more than one diffusion constant — •ANNEKATRIN SILL¹, PETER NESTLER², PETER THRAN¹, and CHRISTIANE A. HELM¹ — ¹University of Greifswald, Institute of Physics, D-17489 Greifswald, Germany — ²ZIK HIKE-Biomechanics, University of Greifswald, D-17489 Greifswald, Germany

Layer-by-layer assembly is a widely used tool for engineering materials and coatings, but the dynamics of the constituent polymer chains remain poorly understood. Using neutron reflectivity, the vertical diffusion of polyanion PSS (Mw(PSS) = 75.6 kDa) within PSS/PDADMA (Mw(PDADMA) = 72.1 kDa) multilayers is probed while annealing in 1 M NaCl solution at different temperatures. The observed diffusion could not be described by a simple diffusion model. Instead, two different PSS fractions (one mobile and one almost immobile, i.e. different diffusion constants) are the simplest model to describe the time dependence of the scattering length density profiles. Increasing the annealing temperatures (20 - 50 °C) increases the diffusion constant of both the fast and slow PSS

fraction. Additionally, the fraction of fast PSS molecules is increased. We suggest that an immobile or nearly immobile fraction of polyelectrolytes is always present when the polymer length is beyond the entanglement limit and the sticky reptation model fails.

CPP 13.4 Tue 10:30 H38

Ratcheting charged polymers through symmetric nanopores using pulsed fields: Designing a low pass filter for concentrating DNA — •LE QIAO and GARY W. SLATER — Department of Physics, University of Ottawa, Ottawa, Ontario K1N 6N5, Canada

Size-based separation of DNA molecules is crucial for molecular analyses such as genome sequencing. To date, gel electrophoresis is the most commonly used separation method in the laboratory. However, due to poor resolution for larger molecules and difficult sample recovery, it cannot meet the goal of bulk separation. Alternatively, micro/nanofluidics offers a relatively inexpensive, label-free, and continuous separation with high throughput. In this talk, I will present a new proof-of-concept idea for the separation of DNA by contour length using a nanofluidic ratchet by combining nanopore translocation and pulsed fields. Using Langevin dynamics simulations, we show that it is possible to design pulsed fields to ratchet semiflexible molecules such that only short chains are successfully translocated, effectively turning the nanopore process into a molecular low-pass filter. The process itself can be performed with many pores in parallel, and it is possible to integrate it directly into nanopore sequencing devices, increasing its potential utility.

CPP 13.5 Tue 10:45 H38

Tuning water-in-salt electrolytes: impact of concentration and anion structure on local and long-ranged dynamics probed by NMR — •DOMINIK GAPPA, ELISA STEINRÜCKEN, MANUEL BECHER, and MICHAEL VOGEL — TU Darmstadt, Institut für Physik kondensierter Materie, Darmstadt, Germany

Water-in-salt electrolytes (WiSE) are highly concentrated aqueous solutions of (Li-)salts. Newly developed WiSE, as they are nonflammable, nontoxic, have a high lithium-ion density and a wide electrochemical stability window (ESW), are promising materials for applications as lithium-ion electrolytes. Due to the high amount of the solute and, thus, strong electrostatic interactions between the components they show complex molecular dynamics. A full understanding of interaction mechanism, e.g. the impact of the concentration and anion structure on the dynamics is still elusive. We investigate LiTFSI, which has a wide ESW for different salt concentrations in water. In particular, we exploit the isotope selectivity of Nuclear Magnetic Resonance (NMR) to observe the behavior of the constituents of LiTFSI-H₂O mixtures with various concentrations separately via ¹H, ⁷Li and ¹⁹F NMR. The anion structure is modified by extending one side group of the originally symmetric TFSI anion, leading to increasingly heterogeneous dynamics. Local dynamics are investigated by spin-lattice relaxation, including field-cycling NMR, and long-ranged transport by diffusion experiments. Rotational correlation times and diffusion coefficients are extracted to scrutinize the validity of the Stokes-Einstein relation.

CPP 13.6 Tue 11:00 H38

Tuning the Electronic and Ionic Thermoelectric Transport Properties in Polymer Electrolytes by Carbon Based Additives — •MAXIMILIAN FRANK¹ and JENS PFLAUM^{1,2} — ¹Experimental Physics VI, University of Würzburg, 97074 Würzburg — ²ZAE Bayern, 97074 Würzburg

Ionic transport constitutes a key process in organic-based electrochemical energy storage media. As such, it also offers intriguing possibilities for the utilization of these materials in thermoelectrics (TE) to recuperate waste heat into electrical power. In this work we present our results on the electrical and thermoelectrical characterization of a methacrylate based solution processable solid polymer electrolyte. By means of impedance spectroscopy over a broad frequency

regime from 100 mHz up to 500 kHz and in a technologically relevant temperature range between 263 K and 363 K we investigate the dynamics of charge carriers in the solidified electrolyte. Furthermore, we demonstrate that the electronic and ionic transport properties can be efficiently varied by the ratio between Lithium-salt and carbon-based additives, in this case, carbon nanotubes.

Even more, we can reverse the sign of the occurring thermovoltage, which allows for different TE operational modes depending on ambient temperature. A proof-of-concept all organic TEG verifies the functionality of our approach and, thereby, substantiates the potential of mixed ionic and electronic materials for future TE applications.

CPP 14: Emerging Topics in Chemical and Polymer Physics, New Instruments and Methods

Time: Tuesday 9:30–11:15

Location: H39

CPP 14.1 Tue 9:30 H39

Where is the Water? — •MAXIMILIAN FUCHS^{1,2}, EDUARDO MACHADO CHARRY^{1,2}, GREGOR BÖHM^{1,2}, ROLAND RESEL¹, and KARIN ZOJER^{1,2} — ¹Institute of Solid State Physics, NAWI Graz, Graz University of Technology, Austria — ²Christian Doppler Laboratory for Mass Transport through Paper, Graz University of Technology, Austria

The take up of liquid water by paper is a complex interplay between capillary transport and swelling of cellulose-lignin-based fibers. Though paper is a convenience product used every day, little is known how swelling affects the pore space between fibers and the subsequent transport within it. We used X-ray microcomputed tomography to monitor the spread of water in-situ. The sequence of 3D-images, segmented by a neural network, traces the time-dependent progression of swelling and liquid transport up to one hour after the application of water. We find that water not only swells the fiber walls, but also expands the pore space between the fibers. Even more remarkable is that there is no liquid water in the pores between the fibers of the examined paper. Rather, liquid water was found exclusively in the fiber lumen.

CPP 14.2 Tue 9:45 H39

Rational Design of Novel Photoswitches with Generative Models — •ROBERT STROTHMANN, CHRISTIAN KUNKEL, JOHANNES T. MARGRAF, and KARSTEN REUTER — Fritz-Haber-Institut der MPG, Berlin, Germany

The sheer vastness of chemical spaces poses a daunting challenge to molecular discovery through high-throughput screening based on exhaustive sampling. Generative models (GMs) are an emerging machine learning (ML) approach that enables a more guided discovery. Implicitly learning chemical design rules from large reference data sets and suitable descriptors of a targeted functionality, GMs directly propose promising, yet diverse candidates.

Here we explore the use of GMs for the design of novel molecular photoswitches. In order to guarantee the desired functionality in the generated molecules, we specifically employ scaffold decoration methods that append chemically meaningful side-groups to a predefined photochromic core. In a second step, the creation process needs to be conditioned towards performant switching capabilities. In the absence of sufficient corresponding experimental reference data, this conditioning is based on synthetic first-principles data. To this end, we discuss computationally efficient descriptors assessing addressability and robustness.

CPP 14.3 Tue 10:00 H39

Transferable hidden variables in sequence space learned by transcoder neural networks — •MARCO WERNER — Institut Theorie der Polymere, Leibniz-Institut für Polymerforschung Dresden, Germany

The relation between chemical sequences and the properties of polymers is investigated using artificial neural networks with a bottleneck layer of neurons. By training such AutoEncoder networks to translate between sequence and property (TransEncoder¹), one may identify variables that control the physical relationship behind. Here, networks were trained to predict the effective free energy landscape of a copolymer interacting with a lipid membrane depending on its sequence of hydrophilic and hydrophobic monomers. TransEncoders that were split into separate encoder-decoder channels have learned to decompose the free energy into independent components that were physically meaningful. For instance, they reflect theoretical concepts such as solutions of the Edwards equation. Sequence-complete data sets for training were obtained via Rosenbluth sampling of single chains in a given density field. It is demonstrated that once the sequence patterns were learned based on the large data set for chain length $N = 14$, a small number of ~ 20 examples was sufficient to transfer-learn the prediction to a more detailed simulation model with explicit lipids and solvent (accuracy $0.5k_B T$). The results open a perspective to physics-informed inverse searches, for instance, for copolymer sequences leading to the smallest translocation time through a membrane. [1] M. Werner, ACS Macro Lett. 10, 1333 (2021).

CPP 14.4 Tue 10:15 H39

Improved virtual orbitals for the calculation of X-ray absorption spectra for organic molecules — •ROLF WÜRDEMANN¹ and MICHAEL WALTER^{2,3} — ¹Freiburger Materialforschungszentrum, Freiburg, Germany — ²Freiburger Zentrum für interaktive Werkstoffe und bioinspirierte Technologien, Freiburg, Germany — ³Fraunhofer-Institut für Werkstoffmechanik, Freiburg, Germany

X-ray absorption spectroscopy (XAS) is an element specific local probe used for the analysis of materials. One way to compare and interpret experimentally measured spectra is to perform ab initio calculations of XAS spectra for molecules in given geometries. This opens a way to distinguish between different isomers and gain a deeper understanding of the bonding situation.

Common ways to calculate XAS spectra by density functional theory (DFT) either utilize fractional charges in the frozen cores or restrict the state-space of linear time-dependent DFT. In our contribution we examine the possibility to utilize the combination of range-separated functionals (RSF) with Huzingas improved virtual orbitals to calculate XAS spectra. This combination has been successful in the calculation of charge transfer excitations[1].

[1] R. Würdemann, M. Walter, J. Chem. Theory Comput. 2018, 14, 7, 366

CPP 14.5 Tue 10:30 H39

Transport of organic volatiles through paper: physics-informed neural networks for solving inverse and forward problems — •ALEXANDRA SEREBRENNIKOVA^{1,4}, RAIMUND TEUBLER^{2,4}, LISA HOFFELLNER^{2,4}, ERICH LEITNER^{2,4}, ULRICH HIRN^{3,4}, and KARIN ZOJER^{1,4} — ¹Institute of Solid State Physics, TU Graz, Petersgasse 16, Graz, 8010, Austria — ²Institute of Analytical Chemistry and Food Chemistry, TU Graz, Stremayrgasse 9/II, Graz, 8010, Austria — ³Institute of Bioproducts and Paper Technology, TU Graz, Inffeldgasse 23, Graz, 8010, Austria — ⁴Christian Doppler Laboratory for mass transport through paper, Petersgasse 16, Graz, 8010, Austria

Transport of volatile organic compounds (VOCs) through porous media with active surfaces takes place in many applications, e.g., in cellulose-based materials for packaging. To date, mathematical models proposed in literature for this complex process are scarce and have not been systematically compiled together with experimental data.

Based on a model for water-vapor transport through paper (Ramarao et al. (2003)), we propose to describe transport of VOCs via diffusion in pores and sorption to fibers. It is key to determine the necessary material parameters for the model. Using experiments for that is challenging, as the related system of non-linear PDEs does not offer analytical solutions.

We demonstrate for dimethyl sulfoxide and n-tetradecane, how combining experimental concentration data with physics-informed neural networks yields these parameters as solution of an inverse problem.

CPP 14.6 Tue 10:45 H39

STED-Inspired Sub Diffractive Cationic Lithography — •SOURAV ISLAM¹, MARCO SANGERMANO², and THOMAS KLAR¹ — ¹Institute of Applied Physics, Johannes Kepler University Linz, 4040 Linz, Austria — ²Department of Applied Science and Technology, Politecnico Di Torino, Torino, Italy

Cationic polymerization has come out as a low cost, efficient, bio-compatible alternative to radical polymerization because of lower toxicity of the monomers, lower shrinkage stress, no oxygen inhibition. Although the mechanism of cationic polymerization is well understood(1), the knowledge about two-photon induced cationic polymerization is still insufficient. In our work, we try to fill the void in the knowledge of two photon induced cationic polymerization and the scope of STED-inspired (2) sub diffractive lithography. 3,4-Epoxy cyclohexylmethyl 3,4 epoxy cyclohexanecarboxylate (CE) was used as monomer and Triarylsulfonium hexafluoroantimonate salts and 2-Isopropylthioxanthone (ITX) were used as onium salt and photo-sensitizer, respectively. 110fs laser pulses of 780nm wavelength were used to write two-photon polymer lines with a feature size of 315nm. Furthermore, 60% suppression of polymerization was achieved using an additional 660nm continuous beam overlapped with 780nm beam. To obtain further reduction of the feature size, a donut shaped beam profile was produced by installing a 2-pi phase plate in the 660 nm beam path. This way, lines of 195 nm feature size were achieved. 1.M. Sangermano Pure and Applied Chemistry, 84, 2089 (2012). 2.Fischer, Wegener, Opt. Mat. Exp. 1, 614 (2022)

CPP 14.7 Tue 11:00 H39

Photoluminescence spectroscopy for the detection of microplastics - the Nile Red approach — •SRUMIKA KONDE, STEFAN BRACKMANN, MARINA GERHARD, and MARTIN KOCH — Department of Physics and Material Sciences Center, Philipps-University of Marburg, Germany

For the detection and classification of microplastics, most researchers commonly use FTIR or Raman spectroscopy. These state-of-the-art methods are, how-

ever, laborious, cost-intensive, and time-consuming. To establish a less arduous and inexpensive approach, we propose photoluminescence-based multispectral imaging. Based on the parallel research in our workgroup, we have found that the autofluorescence of plastics lies predominantly in the UV region. To accommodate the identification in the visible region we use a solvatochromic dye called Nile Red. PLE/PL spectra of stained plastics and stained natural materials have

been analyzed to determine the right excitation and emission windows for building an imaging system. This analysis has been performed using LDA (linear discriminant analysis). Based on our analysis we propose a system consisting of a blue excitation LED, an RGB camera, and two bandpass filters which would yield about 98% accuracy in isolating plastics from natural materials.

CPP 15: 2D Materials 4 (joint session HL/CPP/DS)

Time: Tuesday 9:30–12:00

Location: H36

See HL 15 for details of this session.

CPP 16: Active Matter 2 (joint session DY/BP/CPP)

Time: Tuesday 10:00–13:00

Location: H18

See DY 16 for details of this session.

CPP 17: Poster 2

Topics: 2D Materials (17.1-17.3), Composites and Functional Polymer Hybrids (17.4-17.6), Crystallization, Nucleation and Self-Assembly (17.7-17.12), General Session to the Symposium: Interplay of Substrate Adaptivity and Wetting Dynamics from Soft Matter to Biology (17.13-17.15), Hydrogels and Microgels (17.16-17.21), Interfaces and Thin Films (17.22-17.31), Nanostructures, Nanostructuring and Nanosized Soft Matter (17.32-17.35), Polymer and Molecular Dynamics, Friction and Rheology (17.36-17.38), Polymer Networks and Elastomers (17.39-17.41).

Time: Tuesday 11:00–13:00

Location: P2

CPP 17.1 Tue 11:00 P2

Simulation of vapour flow through aperture arrays for quantifying gravimetric mass loss measurements — •RIKO KORZETZ, LENNART SCHULTE, and ANDRÉ BEYER — Bielefeld University

Gravimetric mass loss measurements are frequently employed to investigate the permeative behaviour of 2D membranes with respect to vapours of different solvents. Due to constraints in these measurements, insufficient circulation causes the build-up of concentration gradients in the vapour phase, which is known as concentration polarization. This leads to a seemingly non-intuitive permeation behaviour, which complicates the evaluation of the measured data.

Here, we present finite-element simulations that were employed to investigate this effect with respect to different types of membrane supporting apertures and aperture arrays. Both open orifices as well as membranes with different permeance values have been modelled to achieve a quantitative understanding of the relevant effects in mass loss measurements.

We found that for open orifices and apertures with highly permeable membranes, the diffusion from the bulk towards the membrane is the rate-limiting step. This results, for example, in a linear dependence between the permeation rate and the edge length of single open orifices. On the other hand, a dependence on the free-standing area occurs in the case of membranes with a sufficiently low permeance. We devised a phenomenological model to describe the permeation rate in dependence of the membrane permeance as well as support geometry, which allows correction of these effects when evaluating such measured data.

CPP 17.2 Tue 11:00 P2

Preparation and characterization of photosensitive nanomembranes — •VERENA MÜLLER¹, MARIA KÜLLMER¹, FLORIAN KÜLLMER^{1,2}, HANS-DIETER ARNDT², and ANDREY TURCHANIN¹ — ¹Friedrich Schiller University Jena, Institute of Physical Chemistry, Lessingstraße 10, 07743 Jena, Germany — ²Friedrich Schiller University Jena, Institute of Organic Chemistry and Macromolecular Chemistry, Humboldtstraße 10, 07743 Jena

Carbon nanomembranes (CNMs) are two-dimensional (2D) organic materials with a molecular thickness that are synthesized by low-energy electron irradiation of aromatic self-assembled monolayers (SAMs). Using the molecular design, CNMs can be prepared with tunable physical and chemical properties and employed on their own, e.g. as separation membranes or in combination with other 2D materials in hierarchically assembled van-der-Waals heterostructures. Here we present the engineering of photosensitive nanomembranes *via* post-functionalization of ~ 1 nm thick amino-terminated CNMs with azobenzene molecules. We characterize their properties using surface science techniques including X-ray photoelectron spectroscopy (XPS) and compare the obtained characteristics with the azobenzene-based SAMs.

CPP 17.3 Tue 11:00 P2

Selective Diffusion of CO₂ and H₂O through Carbon Nanomembranes in Aqueous Solution as Studied with Radioactive Tracers — RAPHAEL DALPKE¹, ANNA DREYER², RIKO KORZETZ¹, •LENNART SCHULTE¹, ANDRÉ BEYER¹, and KARL JOSEF DIEZ² — ¹Faculty of Physics, Bielefeld University — ²Faculty of Biology, Bielefeld University

A well-known approach of improving membrane separation processes is the attempt to utilize 2D materials. In particular, carbon nanomembranes (CNMs) are promising candidates due to their extremely high areal pore density. Specifically, CNMs made from terphenylthiol (TPT) exhibit a very high water permeance while blocking ions as well as many gases and vapours. Here, we present permeation measurements of TPT-CNMs utilizing radioactive tracer molecules to characterize diffusion of [³H]H₂O, [¹⁴C]NaHCO₃, and [³²P]H₃PO₄ in aqueous solution. For full consideration of concentration polarization and outgassing effects a mathematical model was developed and verified using finite-element simulations. The experiment shows that water and carbonate can pass through the CNM while phosphate ions are completely blocked. Considering ion conductivity measurements, the obtained diffusion coefficients indicate that the permeation across the membrane primarily occurs by transport of neutral species.

CPP 17.4 Tue 11:00 P2

Dipolar Molecular Rotors in Surface-Anchored Metal Organic Frameworks — •XIANGHUI ZHANG¹, SEBASTIAN HAMER², RITESH HALDAR³, DANIEL REUTER⁴, FLORIAN PANEFF¹, DIRK VOLKMER⁴, PETER LUNKENHEIMER⁴, ANDRÉ BEYER¹, IAN HOWARD³, and RAINER HERGES² — ¹Faculty of Physics, Bielefeld University, 33615 Bielefeld — ²Otto-Diels-Institute for Organic Chemistry, Christian-Albrechts-University of Kiel, 24098 Kiel — ³Karlsruhe Institute of Technology (KIT), 76344 Karlsruhe — ⁴Institute of Physics, Augsburg University, 86135 Augsburg, Germany

Molecular rotors arranged in the surface-anchored metal-organic frameworks (SURMOF) were investigated. The rotating part of each linker molecule consists of a fluorine-substituted phenyl group connected with acetylene linkages to the Cu clusters. Dielectric spectroscopy was used to investigate the rotation dynamics of molecular rotors in a parallel capacitor assembly. We determined an activation energy of 10 kJ/mol for one SURMOF type consisting of 3-[4-(2-carboxyethyl)-2,3-difluoro-phenyl]prop-2-ynoic acid (C₁₂H₄F₂O₄) as dipolar linkers and 1,4-diazabicyclo(2.2.2)octane (DABCO) as pillars, at temperatures above 170 K. A smaller barrier of about 2 kJ/mol was found for the corresponding SURMOFs without any pillars. The analog made from the non-polar linker was used as a control system and showed no dielectric relaxation processes down to 20 K. The observed activation energy barriers are consistent with *ab initio* DFT modelling and classical dipole-dipole interaction calculations.

CPP 17.5 Tue 11:00 P2

Design, fabrication and nano-scale characterization of novel SEI layers — •ZHUIJUN XU¹, YANJUN CHENG², YONGGAO XIA², and PETER MÜLLER-BUSCHBAUM^{1,3} — ¹TU München, Physik-Department, LS Funktionelle Materialien, 85748 Garching, Germany — ²Ningbo Institute of Materials Technology and Engineering, Chinese Academy of Sciences, 315201, Ningbo, China — ³MLZ, TU München, 85748 Garching, Germany

Rechargeable lithium metal batteries have been recognized as one of the most promising energy storage devices due to their superior energy density. However, serious safety concerns and poor cyclability are challenges originating from an uncontrolled lithium dendrite growth and an unstable solid electrolyte interface (SEI) layer. One strategy to suppress dendrite growth is a surface modification with amphiphilic block copolymers, such as PDMS-b-PAA, which bear some clear advantages including absorbing mechanical stress, conducting lithium ion and controlling the lithium dendrite growth process. With ex-situ scattering techniques or in-situ scattering studies, the structures of the surface modified lithium metal anodes and structure formation processes are studied. In particular, by applying GISAXS, the horizontal structures and vertical structures of the polymer films on the lithium metal surfaces are investigated.

CPP 17.6 Tue 11:00 P2

In situ GISAXS printing of inorganic-organic hybrid nanostructures based on biopolymer templating — •LINUS F. HUBER¹, STEPHAN V. ROTH³, KUN SUN¹, MANUEL A. REUS¹, and PETER MÜLLER-BUSCHBAUM^{1,2} — ¹TU München, Physik-Department, LS Funktionelle Materialien, 85748 Garching — ²MLZ, TU München, 85748 Garching — ³Deutsches Elektronen-Synchrotron (DESY), Notkestr. 85, 22607 Hamburg, Germany

Inorganic-organic hybrid nanostructures are interesting for the energy conversion through the thermoelectric effect. Thermoelectric generators based on abundant, environmentally friendly and affordable materials have historically had low efficiencies. The electrical conductivity, the Seebeck coefficient and the thermal conductivity need to be individually improved, to significantly enhance the thermoelectric figure of merit. Nanostructuring can improve these parameters and maximize the performance of thermoelectric materials. Beta-lactoglobulin is a bovine whey protein that is used as a template during sol-gel synthesis. Different titania thin film morphologies can be achieved by changing the pH-value and the beta-lactoglobuline concentration. To investigate the different titania morphologies, in situ GISAXS, GIWAXS and SEM are used. In situ GISAXS printing enables a time resolved investigation of the structure formation, domain sizes and domain distances. UV-Vis and PL are used to analyze differences in the optical properties of the thin films. These structural and optical changes are then correlated with measurements of the Seebeck coefficient and the electrical conductivity.

CPP 17.7 Tue 11:00 P2

Two-step nucleation in confined geometry on a lattice gas model — •JACOB HOLDER, RALF SCHMID, and PETER NIELABA — Physics Department University of Konstanz, Konstanz, Germany

We deploy a degenerated Ising model to describe nucleation and crystallization from solution in a confined two-component system. The free energy is calculated using Metadynamics simulation. With nudged elastic band simulation we calculate the minimum energy path and give properties of the crystallization path. From the parameters and setup we find necessary conditions for the occurrence of two-step nucleation in our system.

CPP 17.8 Tue 11:00 P2

Nucleation patterns in polymer crystallization analyzed by machine learning — •ATMIKA BHARDWAJ^{1,2}, MARCO WERNER¹, and JENS-UWE SOMMER^{1,2} — ¹Leibniz-Institut für Polymerforschung Dresden e. V., Hohe Str. 6, Germany 01069 — ²Technische Universität Dresden (TUD)

Today, many efforts seek to link machine learning (ML) algorithms to the concepts of theoretical physics. Our work focuses on developing ML tools to derive meaningful interpretations from the data generated through molecular dynamics simulations. We aim to find and quantify the nucleation patterns in polymer crystallization. The transition dynamics occurring under-cooled polymer melt is a local environmental phenomenon rather than a property of individual particles (or monomers), and depends on subtle conformation patterns such as entanglements between the chains. Our first objective is to define a set of fingerprint parameters to capture the crucial information in the local conformation and a monomer's environment and to quantify the degree of crystallinity. We use self-supervised auto-encoders to contain those local fingerprints. The second objective is to recognize the precursors or nucleation sites that stimulate crystal growth before the occurrence of such growth. We are currently working on both convolutional neural networks and recurrent neural networks to investigate the spatial and temporal patterns of the precursors.

CPP 17.9 Tue 11:00 P2

Laser control over crystallization and morphology of tetracene thin films — •STEFAN KOWARIK¹, ANDIKA ASYUDA², LINUS PITHAN³, and ANDREAS OPITZ⁴ — ¹Physical Chemistry, University of Graz, Austria — ²Institute for Physical Chemistry, Universität Heidelberg, Germany — ³Institut für Angewandte Physik, Universität Tübingen, Germany — ⁴Institut für Physik, Humboldt-Universität zu Berlin, Germany

Nucleation and crystallization in thin-film growth are notoriously difficult to steer, but optical control offers exciting new possibilities for selecting specific polymorphic forms [1] or aligning the crystallite orientation in thin films [2]. Here we report an increase in crystallite size in vacuum-deposited tetracene thin films under illumination with a wavelength tuned to a specific absorption band of tetracene crystals. The morphological changes are induced with linearly and circularly polarized light and the larger crystallite size is accompanied by higher photoluminescence of tetracene. We propose a mechanism based on optical heating of specifically oriented crystals during growth, which leads to enhanced surface migration processes in these crystals and consequently larger crystals via Oswald ripening effects. The light-induced temperature effects are distinct from substrate heating both for linearly and circularly polarized light. Laser illumination, therefore, is a novel control parameter of growth and enables high crystallinity even for low substrate temperature deposition.

[1] L. Pithan, et al., *Crystal Growth & Design* 15.3 (2015): 1319-1324. [2] L. Pithan, et al., *Advanced Materials* 29.6 (2017): 1604382.

CPP 17.10 Tue 11:00 P2

Synthesis of Hard-Carbon Microspheres with Binary Size Distribution via Hydrothermal Carbonization of Trehalose — •MARTIN WORTMANN¹, WALDEMAR KEIL², MICHAEL WESTPHAL¹, ELISE DIESTELHORST³, JAN BIEDINGER¹, BENNET BROCKHAGEN³, GÜNTER REISS¹, CLAUDIA SCHMIDT², KLAUS SÄTTLER⁴, and NATALIE FRESE¹ — ¹Bielefeld University, Bielefeld, Germany — ²Paderborn University, Paderborn, Germany — ³Bielefeld University of Applied Sciences, Bielefeld, Germany — ⁴University of Hawaii, Honolulu, USA

Hard Carbon microspheres (HCS) were synthesized via hydrothermal carbonization (HTC) of trehalose and subsequent pyrolytic post-carbonization at 1000°C. It was found that HTC of trehalose, in contrast to other saccharides, results in a distinctly binary sphere diameter distribution with monodisperse small spheres and polydisperse large spheres. Pore formation, as visualized by charge-compensated helium ion microscopy, results in a strong increase in BET surface area. The chemical composition and crystallinity were examined before and after pyrolysis using a variety of spectroscopic methods. Strong compositional similarities were found to other saccharide-derived hydrochars, with a cross-linked furan-based polymer-structure before, and nano-crystalline carbon structure after pyrolysis. The binary size-distribution and large BET surface area make trehalose-derived HCS a highly promising material for applications in energy storage or catalysis.

CPP 17.11 Tue 11:00 P2

Physics of supersaturated, agitated sucrose solutions: Crystal nucleation and growth — •HANNAH M. HARTGE and THOMAS A. VILGIS — Max Planck Institute for Polymer Research, Mainz, Germany

Supersaturated sucrose solutions that have been sufficiently cooled without nucleation constitute a meta-stable system in which agitation promotes fast crystallization. Applications of this physically interesting process can be found for example in the production of fondant in confectionery. While just water and sucrose are present, the system goes through complex thermodynamic processes during crystallization, which are highly dependent on composition, temperature, and agitation.

In this work, we investigate how temperature and concentration affect nucleation, crystal growth and final particle size distribution of highly supersaturated sucrose solutions under agitation. To do so, the torque was measured during kneading of the samples at controlled temperature, followed by light microscopy and corresponding image analysis. When crystallization times were compared to classical nucleation theory, variations were found to be related to temperature and supersaturation in the same way as indicated by induction time models of statistical physics. Additionally, size distributions of the resulting crystal phases showed a strong dependence on temperature during agitation, sucrose content and according initial supersaturation.

CPP 17.12 Tue 11:00 P2

Following the directed self-assembly of crystallizable block co oligomers via in situ AFM — •ALEXANDER MEINHARDT and THOMAS F. KELLER — Centre for X-ray and Nano Science (CXNS), Deutsches Elektronen-Synchrotron DESY, Hamburg, Germany

Bottom up nanofabrication utilizing the molecular self-assembly of block co-oligomers with sub-10 nm domain sizes are widely discussed as a promising route for next generation photolithography. Double crystalline co-oligomers can be used to create well defined, high-fidelity nanostructures by controlling the competing driving forces microphase separation and crystallization. We re-

port on the surface nanostructure formation and its temporal evolution during annealing of thin films of an amphiphilic double crystalline polyethylene-block-poly(ethylene oxide) co-oligomer (PE-b-PEO) on planar and patterned surfaces. Directing the self-assembly of such systems with physical or chemical guiding patterns can enable the formation of defined, large scale amphiphilic nanostructures, which could be of interest for various applications, e.g., biomaterials, photonics, and nanotechnology. However, there still remain several challenges regarding the characterization, defect density, pattern fidelity, and post processing of such block copolymer nanopatterns. By investigating the directed self-assembly (DSA) of the PE-b-PEO using AFM in situ, we aim to tune the balance of the involved driving forces and in turn create optimized nano-templates.

CPP 17.13 Tue 11:00 P2

Influence of the surface roughness and surface chemistry to understand slide electrification — •BENJAMIN LEIBAUER, WERNER STEFFEN, and HANS-JÜRGEN BUTT — Ackermannweg 10 55128 Mainz

In the last few years a lot of studies have shown that by contact electrification between water droplets and hydrophobic surfaces, it is possible to generate electricity in an environmentally friendly way.[1] The physical processes are still being discussed today and to extend the understanding Stetten et al.[2] have established an experimental setup that allows the drop charge of individual drops. In the work presented here we have studied with this setup the influence of the surface roughness and the chemistry of the substrates on hydrophobic to superhydrophobic substrates. We found that for the drop charge both parameters have an influence on at least the same order of magnitude.

[1] C. Wu, A. C. Wang, W. Ding, H. Guo, Z. L. Wang, *Advanced Energy Materials* 2019, 9, 1802906. [2] A. Z. Stetten, D. S. Golovko, S. A. Weber, H.-J. Butt, *Soft Matter* 2019, 15, 8667-8679.

CPP 17.14 Tue 11:00 P2

Dewetting dynamics and equilibrium droplet shapes for of visco-elastic substrates — •KHALIL REMINI¹, LEONIE SCHMELLER², DIRK PESCHKA², BARBARA WAGNER², and RALF SEEMANN¹ — ¹Experimental Physics, Saarland University, Saarbrücken, Germany — ²Weierstrass-Institute, Berlin University, Berlin, Germany

In our study we are interested in the dewetting of liquid polymer layers (Polystyrene 18 kg/mol) with about 100 nm thickness from visco-elastic polydimethylsiloxane surfaces with elasticity ranging $E = 1.2$ MPa for Sylgard 184 to $E = 3$ kPa for Cy52-276. When heating the samples to temperatures where PS is liquid, holes nucleate in the initially uniform PS film. These holes grow during dewetting, coalesce and eventually form sessile droplets of a few micrometers in diameter sitting on the PDMS surface. Due to the particular situation of the adaptive PDMS substrate, we observe characteristic qualitative and quantitative differences in rim shapes, (dynamic) contact angles and dewetting velocities which are indicating differences in the underlying energy dissipation but might result also from potential phase separation of liquid and cross linked PDMS close to the three-phase contact line. To shed light on the impact of viscous and elastic properties and potential phase separation at the three phase contact line, we aim at a quantitative comparison of sessile (equilibrium) droplets on substrates having different elasticities and thus elastocapillary lengths.

CPP 17.15 Tue 11:00 P2

Messung von Kräften zwischen Tropfen und bewegten Oberflächen — •MARISA FISCHER, SIMON SCHUBOTZ, JENS-UWE SOMMER, ANDREAS FERY und GÜNTER AUERNHAMMER — Leibniz-Institut für Polymerforschung Dresden e.V., 01069 Dresden, Germany

Um einen Tropfen über eine Oberfläche zu bewegen, wird eine Kraft benötigt, die von deren Eigenschaften abhängt. Das zur Messung dieser Kraft entwickelte Drop Adhesion Force Instrument (DAFI) erlaubt die freie Wahl der Geschwindigkeit der Drei-Phasen Kontaktlinie und der Größe des Tropfens [1]. Die Kraftmessung erfolgt mittels des Hookschen Gesetzes, indem die Auslenkung einer im Tropfen befindlichen Glaskapillare gemessen wird.

Ein von der Bewegung des Tropfens aufgenommenes Video wird mit einem von uns entwickelten Analyseprogramm ausgewertet. Für die Übertragung größerer Kräfte wird ein Glasplättchen am Kapillarende befestigt, welches die Adhäsion zwischen Tropfen und Kapillare erhöht.

Mit dem entwickelten Aufbau wurden die Kräfte zwischen Wassertropfen und Polydimethylsiloxan (PDMS) sowie Poly(N-isopropylacrylamide) (PNiPAAm) Polymerbürsten untersucht. Dabei zeigte sich ein Zusammenhang zwischen dem Zustand der Oberfläche und der Kraft.

[1] D. W. Pilat u. a., *Langmuir* 2012, 28, 49, 16812-16820

CPP 17.16 Tue 11:00 P2

In-situ Monitoring of Hard-Core Soft-Shell Microgels During Monolayer Drying — •JULIAN RINGLING, KEUMKYUNG KUK, and MATTHIAS KARG — Heinrich-Heine-Universität, Düsseldorf, Germany

Hard-core soft-shell (HCSS) microgels are interesting colloids with the potential to be used as model systems to understand crystallization and melting processes [1]. They spread at the air/water interface and self-assemble into 2D monolayers

in which the cores do not touch directly due to shell-shell repulsion. Compression of such a monolayer allows control over the inter-particle distance by compressing the soft and deformable shell [2]. After transferring a compressed monolayer to a substrate, various structures can be observed [3]. Understanding and controlling the formation of those structures is essential for the use of the system as a model for crystallization.

Previously our group discovered a difference in monolayer structure at the air/water interface in comparison to the dried monolayer after transfer onto a substrate when using micron-sized silica-poly(N-isopropylacrylamide) HCSS microgels. To understand the phase transition/structural change occurring, we have monitored this phase transition/structural change using fluorescence and light microscopy. Here we present results from in-situ observations of drying 2D colloidal monolayers focussing on the effect of different parameters on drying and assembly behaviour.

[1] G. Wie et al., *Soft Matter*, 2013, 9, 9924-9930

[2] J. Tang et al., *ACS Omega*, 2018, 3, 12089-12098

[3] S. Ciarella et al., *Langmuir*, 2021, 37, 5364-5375

CPP 17.17 Tue 11:00 P2

Investigation of Cononsolvency Phase Transition of Poly(sulfobetaine)-based Diblock Copolymer Thin Films — •PEIXI WANG¹ and PETER MÜLLER-BUSCHBAUM^{1,2} — ¹Technische Universität München, James-Frank-Straße 1, 85748 Garching, Germany — ²Heinz Maier-Leibnitz Zentrum (MLZ), Lichtenbergstr. 1, 85748 Garching, Germany

Co-nonsolvency occurs if a mixture of two good solvents causes the collapse or demixing of polymers into a polymer-rich and solvent-rich phase in a certain range of compositions of these two solvents. The nonionic thermo-responsive polymer, poly(N-isopropylmethacrylamide) (PNIPMAM), which features a lower critical solution temperature (LCST) in aqueous solution, has been widely used to investigate its collapse transition behavior in a mixture of two competing good solvents. However, co-nonsolvency response of its block copolymer containing the zwitterionic poly(sulfobetaine)s, especially poly(4-(3-methacrylamidopropyl)dimethylammonio)butane-1-sulfonate) (PSBP)*which exhibits a lower upper critical solution temperature (UCST) and shows a strong swelling transition in aqueous media, is newly studied. We focus on the co-nonsolvency behavior of PSBP-b-PNIPMAM thin films in water/acetone mixtures by in situ time-of-flight neutron reflectometry (TOF-NR) and spectral reflectance (SR). Furthermore, Fourier transform infra-red (FTIR) spectroscopy is applied to investigate the interactions between the polymer thin film and water/co-solvent, which is closely related to their deuteration level.

CPP 17.18 Tue 11:00 P2

Core-shell microgels synthesized in continuous flow: Deep insight into shell growth by temperature-dependent FTIR spectroscopy — •PASCAL FANDRICH¹, MARCO ANNEGARN¹, LARS WIEHEMEIER¹, INA EHRING¹, TILMAN KOTTKE², and THOMAS HELLEWEG¹ — ¹Physical and Biophysical Chemistry, Bielefeld University, 33615 Bielefeld, Germany — ²Biophysical Chemistry and Diagnostics, Bielefeld University, 33615 Bielefeld, Germany

While core-shell microgels have been intensively studied in their fully synthesized state, the formation mechanism of the shell growth has not been completely understood. Such insight is decisive for a customization of microgel properties for applications. In a novel approach, we synthesized microgels based on a N-isopropylmethacrylamide (NiPMAM) core and a N-n-propylacrylamide (NnPAM) shell in a continuous flow reactor. The shell growth is studied depending on the solution's time of residence inside the reactor. PCS experiments reveal a significant decrease of the volume phase transition temperatures of the core and the shell respectively, with increasing residence time. At early stages, a decreased swelling capacity is found before a discrete NnPAM shell is formed. Temperature-dependent FTIR spectroscopy shows that the decreased swelling capacity originates from a pronounced interpenetrated network between NnPAM and NiPMAM. AFM images resolve a raspberry-like structure after 3 min, pointing to an aggregation of NnPAM domains before the distinct shell forms.

CPP 17.19 Tue 11:00 P2

How ultrasound accelerates microgel adsorption kinetics — •LUCA MIRAU¹, SEBASTIAN STOCK¹, AMIN RAHIMZADEH¹, SONJA WISMATH², MATTHIAS RUTSCH², MARIO KUPNIK², and REGINE VON KLITZING¹ — ¹Department of Physics, TU Darmstadt, Hochschulstr. 8, 64289 Darmstadt — ²Measurement and Sensor Technology, TU Darmstadt, Merckstraße 25, 64283 Darmstadt

Poly-N-isopropylacrylamide (PNIPAM) based microgels (MGs) are surface-active and offer great opportunities as stabilizers of emulsions and foams. Due to their thermosensitive response, the MGs enable also destabilization on demand. However, emulsion formation implies energy input by stirring or ultrasonication. To understand this formation process, it is important to understand the interfacial adsorption of the MGs. A fast trigger to affect the adsorption process is given by ultrasonication. The present study shows the effect of ultrasound on the adsorption kinetics of PNIPAM MGs at the water-oil interface monitored by drop shape tensiometry. The adsorption kinetics of MGs accelerates with in-

creasing ultrasonication intensity. The variation of different parameters, such as ultrasonic frequency, MG crosslinker density, concentration and phase composition, indicates that both acoustic streaming as well as ultrasound induced deswelling of MGs due to breakage of hydrogen bonding cause this acceleration.

CPP 17.20 Tue 11:00 P2

Interaction of soft microgel with solid silica particles at the air-water interface — •CARINA SCHNEIDER, SEBASTIAN STOCK, KEVIN GRÄFF, FRANZISKA JAKOB, and REGINE VON KLITZING — Department of Physics, TU Darmstadt, Hochschulstraße 8, 64289, Darmstadt

Emulsions stabilized by multiple particle systems are interesting in various research fields, e. g., in the food industry or interfacial catalysis. The interaction of two or more nano-particle systems of different properties at liquid interfaces is important for the coalescence behavior of emulsion droplets stabilized by these particle mixtures. For instance, a mixture of hydrophilic microgel particles (MGs) and hydrophobic silica nano-particles (SiNP) is able to stabilize water in oil emulsions, which is not possible with MGs alone. Therefore, it is of special interest to understand the interaction of those particles at the interface. In this context, their lateral compression may simulate the droplet interfaces under coalescence conditions. For this purpose, we spread mixtures of poly-NIPAM MGs and spherical SiNPs at the air-water interface of a Langmuir trough and determined the compression isotherms. For deeper insights into the lateral structure formation, the particle layers were transferred onto Silicon wafers and scanned by atomic force microscopy. For low compressions, the elastic MG network dominates the isotherm while SiNP are situated between the MGs with low impact. For higher compressions, the inelastic SiNP structures are pushed onto the MGs and take over the resistance to the outer pressure.

CPP 17.21 Tue 11:00 P2

Adsorption kinetics of microgel particles at the air/water interface — •KAI LUCA SPANHEIMER, DANIEL JÄGER, SEBASTIAN STOCK, and REGINE VON KLITZING — Department of Physics, TU Darmstadt, Hochschulstraße 8, 64289 Darmstadt

Interest in microgel particles (MGs) based on poly-N-isopropyl acrylamide (PNIPAM) as surface-active material remains high. The nano- to micrometer sized, cross-linked polymer particles are able to adsorb to water/air or water/oil interfaces spontaneously. Combined with their ability to act as carriers for drugs, recent studies showed, that they may act as transport vehicles for amphiphilic catalysts to the interface, resulting in improved interfacial catalysis, e. g., in Pickering emulsions. Despite much research on the interaction of MGs with various low and higher molecular weight material, the adsorption of MG/catalyst complexes at the interface is not yet well understood. In the presented work, the adsorption kinetics at the air/water interface is measured via change in surface tension over time by drop shape analysis. In order to disentangle different effects in case of MG/catalyst complexes the adsorption kinetics of pure MGs and mixtures of MGs with simple anionic and cationic surfactants as model systems for the catalysts is studied and compared with the adsorption of MG/catalyst complexes.

CPP 17.22 Tue 11:00 P2

A molecular dynamics approach to understand and control the catalyst enrichment at the IL/vacuum interface in SILP systems — MATTIA LIVRAGHI¹, CHRISTIAN WICK^{1,2}, •DAVID MATTHEW SMITH^{1,3}, and ANA-SUNČANA SMITH³ — ¹PULS Group, Institute for Theoretical Physics and Interdisciplinary Center for Nanostructured Films (IZNF), Friedrich-Alexander Universität Erlangen-Nürnberg (FAU), 91058 Erlangen, Germany — ²Competence Unit for Scientific Computing (CSC), FAU, 91058 Erlangen, Germany — ³Group of Computational Life Sciences, Division of Physical Chemistry, Ruder Bošković Institute, 10000 Zagreb, Croatia

Supported Ionic Liquid Phase Catalysis (SILP) improves the catalytic turnover by smearing a thin IL layer onto a support material, reducing the need for slow reactant transport inside viscous ILs. Next generation SILP technology will rely on confining the catalyst to the vacuum interface, spatially localising the chemical reaction. This will require a deep understanding of the interface enrichment and structuring of the individual chemical components. We investigated ionic liquids made of iodide and polyethylene glycol imidazolium cations. Therefore, we parameterized atomic charges for the new ILs using multiple conformations during the RESP fitting procedure, compatible with the GAFF force field, and validated our simulations against experimental data. The (also newly parameterized) catalysts are Nickel(II) coordination compounds with task-specific carbene ligands. We investigate the influence of the structures of the ligands and the ILs chain on controlling the catalyst's distribution in and affinity for the IL-vacuum interface.

CPP 17.23 Tue 11:00 P2

Morphology control of titania thin films in a low temperature process — •GUANGJIU PAN¹, SHANSHAN YIN¹, NIAN LI¹, TIANFU GUAN¹, RENJUN GUO¹, SUZHE LIANG¹, YUQIN ZOU¹, CAROLINE EHGARTNER², NICOLA HÜSING², and PETER MÜLLER-BUSCHBAUM^{1,3} — ¹TU München, Physik-Department, LS Funktionelle Materialien, 85748 Garching, Germany — ²Materialchemie,

Chemie und Physik der Materialien, Universität Salzburg, 5020 Salzburg, Austria — ³MLZ, TU München, 85748 Garching, Germany

A low-temperature routine to realize inorganic electron-transport layers (ETLs) is important for the commercialization of perovskite solar cells. Fabricating ETLs at low temperature is energy saving and compatible with flexible substrates. In this work, titania thin films are synthesized at low temperature (below 100 Celsius degree) with a polymer template sol-gel method based on the amphiphilic diblock copolymer polystyrene-b-polyethylene oxide (PS-b-PEO), in combination with selective incorporation of the titanium precursor ethylene glycol-modified titanate (EGMT). Tailoring titania film morphology in the low-temperature process is achieved by managing phase separation of the polymer template. The ratio of polymer, precursor, solvent, and catalyst for the sol-gel solution is varied to tune the thin film morphologies. The surface morphologies of titania films are probed via scanning electron microscopy and GISAXS. The optical properties of the films are examined with ultraviolet-visible spectroscopy.

CPP 17.24 Tue 11:00 P2

Soft Matter Food Physics: Oat Drink Foams — •JUDITH HEGE, ANTONIA-LOUISA SCHLICHTING, JANA REEH, and THOMAS A. VILGIS — Max Planck Institute for Polymer Research, Mainz, Germany

For various applications, oat drink needs to provide a capacity to form stable, creamy, homogeneous foams. Such macroscopic foam properties are based on molecular interactions at the air-water interfaces and protein kinetics within the lamellae. However, the underlying structure-function relationships between molecular interactions and macroscopic foam properties are not yet fully understood, especially for multicomponent systems like plant-based drinks. Therefore, this study probed foams formed by an oat drink containing only water, oats, canola oil and salt.

Investigations focused on the influence of enzyme treatment, canola oil addition, heat treatment and homogenization parameters on foam properties. Accordingly, time-dependent foam height measurements were performed and supported by light microscopy, photography, and particle size measurements to compare the findings on the macroscopic scale with bubble size evolution and oil droplet distribution.

This study showed that protease treatment resulted in a higher foaming capacity, but lower foam stability and that heat treatment lessened the foam stability. Furthermore, addition of small contents of canola oil increased the foaming capacity, however, higher canola oil contents reduced foam stability. Furthermore, a longer duration and higher speed of homogenization treatment caused a more homogeneous emulsion and increased foaming capacity as well as foam stability.

CPP 17.25 Tue 11:00 P2

Spatial resolution of particle transport at interfaces — •KEVIN HÖLLRINGER¹, ANDREAS BAER¹, DAVID M. SMITH², and ANA-SUNČANA SMITH^{1,2} — ¹PULS Group, FAU Erlangen-Nürnberg, Germany — ²Group for Computational Life Sciences, Ruder Bošković Institute, Zagreb, Croatia

Confined geometries play an important role in various applications, where it is generally important to be able to predict particle transport and mobility. Commonly used techniques like the Einstein-approach using the Mean Square Displacement (MSD) as well as Auto-correlation-function (ACF) related techniques rely on strong assumptions about spatial isotropy and homogeneity tied to conditions on local symmetry, that are not satisfied in these confined geometries, making it especially hard to resolve interface-orthogonal particle dynamics. Still other techniques like jump-diffusion are only able to approximate relative mobility and require calibration for each system.

We propose a theoretical model for resolving absolute interface-perpendicular diffusion based on the time particles spend within subspaces of confined systems that accurately predicts diffusion for simple point-like particles like water. In addition, we also present an extension to that model taking into account internal deformational degrees of freedom that can affect the observed particle lifetime.

By application of the proposed models to water as well as Imidazolium-based ionic liquids, we confirm their accuracy and versatility in the analysis of complex particle dynamics thus also proving their applicability to confined geometries.

CPP 17.26 Tue 11:00 P2

In-situ investigation during gold HiPIMS deposition onto polymers — •YUSUF BULUT^{1,2}, KRISTIAN RECK³, MATTHIAS SCHWARTZKOPF¹, JONAS DREWES³, SUZHE LIANG², TIANFU GUAN², THOMAS STRUNKUS³, FRANZ FRAUPEL³, PETER MÜLLER-BUSCHBAUM^{2,4}, and STEPHAN V. ROTH^{1,5} — ¹DESY, 22607 Hamburg — ²TU München, Physik Department, Lehrstuhl für Funktionelle Materialien, 85748 Garching — ³CAU, Chair for Multicomponent Materials, Faculty of Engineering, 24143 Kiel — ⁴MLZ, TU München, 85748 Garching — ⁵KTH Royal Institute of Technology, Department of Fibre and Polymer Technology, SE-100 44 Stockholm

Gold deposition via high power impulse magnetron sputtering (HiPIMS) allows to coat thin metal layers on heat sensitive materials such as polymers allowing for increased adhesion and density. HiPIMS allows deposition at a lower total deposited thermal energy in comparison to conventional magnetron sputtering, but this energy is delivered in a very short pulse exhibiting very high power and

ionization. The consequences for the nucleation and growth processes during HiPIMS deposition are not sufficiently known. Therefore, we investigate the morphology evolution of thin gold layers on four polymer templates, namely polystyrene (PS), polyvinylalcohol (PVA), polystyrene sulfonic acid (PSS) and poly-4-vinylpyridin (P4VP). These polymers show different functional moieties and thus are expected to influence the growth of the gold layer. We present first results of our in situ investigations combining grazing-incidence small angle X-ray scattering (GISAXS), grazing incidence wide angle X ray scattering (GIWAXS).

CPP 17.27 Tue 11:00 P2

High-concentration Lithium-ion Electrolyte Overcomes the Challenges of High-temperature Lithium Batteries — •TIANLE ZHENG¹, YAJUN CHENG², and PETER MÜLLER-BUSCHBAUM¹ — ¹TU München, Physik-Department, LS Funktionelle Materialien, 85748 Garching — ²Ningbo Institute of Materials Technology & Engineering, Chinese Academy of Sciences, Ningbo, 315201, Zhejiang Province, P. R. China

Traditional Li-ion batteries, on the other hand, are severely constrained in high-temperature applications due to the low thermal stability of the electrolyte/electrode interface and electrolyte decompositions in the cell. Herein, we demonstrate a new electrolyte that achieves an excellent stable long-term cycling at 100 °C, well beyond the typical 60 °C limits of normal conventional Li-ion batteries. The high concentrated lithium oxalylidifluoroborate (LiODFB) is selected as the only lithium salt with a carefully designed high thermal stability solvent group. As a result, this unique high-concentration electrolyte can promote to form a stable and inorganic solid electrolyte interface (SEI) layer on the electrode at elevated temperature, leading to improved performance in MCMB/Li and lithium iron phosphate (LFP)/Li half-cells, and achieve reversible capacities of 160 and 350 mA h/g, respectively, with Coulombic efficiencies (CEs) > 99.3%. Subsequently, we further investigate the mechanism of high concentration LiODFB electrolytes by molecular dynamics (MD) simulations and XPS characterization techniques, exploring a new way for future high-temperature electrolytes for Li-ion batteries.

CPP 17.28 Tue 11:00 P2

Sol-gel based tailored lithium-ion battery electrodes — •IVANA PIVARNÍKOVÁ^{1,2}, RALPH GILLES¹, and PETER MÜLLER-BUSCHBAUM^{1,2} — ¹MLZ, TU München, 85748 Garching — ²TU München, Physik-Department, LS Funktionelle Materialien, 85748 Garching

Silicon based materials have been considered as one of the most promising candidates for the next-generation lithium-ion battery anodes, thanks to its low cost, non-toxicity and high theoretical gravimetric capacity (4200 mAh/g). One of the concepts for a suitable application is to design the mesoporous Si-based material via copolymer assisted sol-gel synthesis. This wet chemical method consists of the formation of the organic-inorganic composites by a self-assembly mechanism, where the organic phase (PEO-b-PPO-b-PEO non-ionic triblock copolymer) serves as a template for the inorganic structure (SiO_x). The tetraethoxysilane (TEOS) is used as a Si precursor. The solution mix is spin-coated onto the cleaned Si substrates and the removal of the template is done by calcination at high temperature (400 °C). The properties of the thin films can be tuned by adjusting the synthesis conditions such as concentration of the reaction compounds, choice of the deposition technique, choice of the final calcination step or choice of additives. The aim is to reach the desired thickness, porosity, conductivity and mechanical stability for a successful Li-ion battery anode application. The produced thin films are characterized by scanning electron microscopy (SEM), grazing incidence small-angle X-ray scattering (GISAXS), profilometry and ellipsometry measurements.

CPP 17.29 Tue 11:00 P2

Silicon-germanium based coating of anodes for Lithium-ion batteries — •KEXIN WU¹, CHRISTIAN L. WEINDL¹, and PETER MÜLLER-BUSCHBAUM^{1,2} — ¹TU München, Physik-Department, LS Funktionelle Materialien, 85748 Garching — ²MLZ, TU München, 85748 Garching

Lithium-ion batteries (LIBs) have received increasing attention over several decades as an indispensable role in energy storage. The application of silicon anodes is hindered by their volumetric expansion after full lithiation, which causes collapse with three failure mechanisms including electrode pulverization, disconnection between the electrode and current collector, and continuous breaking and re-growth of the solid electrolyte interface (SEI) layer. To tackle this critical issue, the construction of hierarchical structures is a promising way to increase the stability of active materials. In our studies, Si/Ge hierarchical structures are built by chemical templating of pre-nanostructure self-assembled polystyrene nanoparticles, using an amphiphilic polystyrene-block-polyethylene oxide (PS-b-PEO) diblock copolymer as structure-directing agent. The diblock copolymers undergo microphase separation, which is further modified by solvent vapor annealing with dichloromethane (DCM) and SiCl₄. By pyrolysis, mesoporous thin films are achieved. The desirable morphological and crystallographic studies are accomplished by GISAXS SEM, AFM, and GIWAXS. The study is completed by galvanostatic cycling tests and impedance spectroscopy.

CPP 17.30 Tue 11:00 P2

Modeling of Nano-Porous Electrode Systems via Molecular Dynamics — •PHILIPP STÄRK — SC Simtech, Uni Stuttgart, Germany

We use grand canonical Monte Carlo combined with atomistic-level MD to simulate open electrode systems at a constant potential. Using a multi-scale approach, our aim is to aid in the design of energy storage devices/electrocatalysis applications. In order to achieve this goal, we use different constant potential approaches to characterise the atomistic mechanisms behind charging and electrocatalytic product transport.

CPP 17.31 Tue 11:00 P2

Charging of dielectric surfaces in contact with aqueous electrolyte – the influence of CO₂ — •PETER VOGEL¹, NADIR MÖLLER¹, PRAVASH BISTA², STEFAN WEBER², HANS-JÜRGEN BUTT², BENNO LIEBCHEN³, and THOMAS PALBERG¹ — ¹Institut für Physik, Johannes Gutenberg Universität, 55128 Mainz (Germany) — ²Max Planck Institut für Polymerforschung, 55128 Mainz (Germany) — ³Institut für Physik kondensierter Materie, Technische Universität Darmstadt, 3 64289 Darmstadt (Germany)

The charge state of dielectric surfaces in aqueous environments is of fundamental and technological importance. We use super-heterodyne light scattering in a custom-made cell to study the influence of dissolved CO₂ on the charging of three, chemically different surfaces. We compare an ideal, CO₂-free reference state to ambient CO₂ conditions. Systems are conditioned under conductometric control at different low concentrations of NaCl. As expected for constant charge densities, ζ-potentials drop upon increasing the salt concentration in the reference state. Presence of CO₂ leads to an overall lowering of ζ-potentials. Moreover, for the inorganic dielectric, the salt dependent drop is significantly weakened, and it is inverted for the organic dielectrics. We suggest that at ambient conditions, the charge state of dielectric surfaces is related to dielectric charge regulation caused by the salt concentration dependent adsorption/desorption of CO₂.

CPP 17.32 Tue 11:00 P2

Characterization of Nd complexes and processing of photonic crystal structures — •MIRIAM GERSTEL¹, MUHAMMAD SHAHARUKH¹, INGO KÖHNE², PAUL MERTIN³, RUDOLF PIETSCHNIG², BERND WITZIGMANN³, JOHANN PETER REITHMAIER¹, and MOHAMED BENYOUCHEF¹ — ¹Institute of Nanostructure Technologies and Analytics (INA) — ²Institute of Chemistry — ³Institute of Computational Electronics and Photonics, CINSaT, University of Kassel, Germany

Lanthanide (Ln) ions are unique for applications in lighting, sensing, and display technologies. In our approach, we investigate the potential of using Ln(III) complexes as attractive luminescent materials due to its characteristics of narrow emission bands and wide emission spectrum. Two different types of Nd(III) complexes are investigated: Nd complexes with phosphonate ligands with varying aromatic residues and complexes where the Nd ion is incorporated in a polyoctahedral silsesquioxane cage. Optical properties of Nd complexes are determined by photoluminescence (PL) spectroscopy, which reveals three emission bands of Nd(III) ions in the NIR region. To achieve a low-density molecular distribution on the sample surface, the complexes are dissolved in dichloromethane and drop-casted on a flat surface. For light enhancement, molecules will be immobilized on photonic crystal cavities (PhCs). The fabrication of PhCs by electron-beam lithography, inductively coupled plasma reactive ion etching and selective wet etching techniques is discussed. This work is supported by the state of Hesse in the frame of LOEWE priority project SMolBits.

CPP 17.33 Tue 11:00 P2

Fabrication of photonic crystals for integration of molecules — •ÖZLEM URCAN¹, RANBIR KAUR¹, MUHAMMAD SHAHARUKH¹, INGO KÖHNE², RUDOLF PIETSCHNIG², JOHANN PETER REITHMAIER¹, and MOHAMED BENYOUCHEF¹ — ¹Institute of Nanostructure Technologies and Analytics (INA), Kassel, Germany — ²Institute of Chemistry, Kassel, Germany

The control of light-matter interaction is an enabling technique for many emerging quantum technology applications. Photonic crystals (PhCs) are of particular interest since they can confine light in small mode volumes producing a strong interaction between light and emitters located in or near the cavity. Emitters such as lanthanide (Ln) molecules offer the potential of scalable quantum systems due to their characteristic narrow linewidth and wide emission spectrum.

This work focuses on the fabrication of PhCs by electron-beam lithography, inductively coupled plasma reactive ion etching and selective wet etching techniques and investigating different process parameters influencing the quality of PhCs. The morphological and optical properties of PhCs are characterized by scanning electron microscopy and micro-photoluminescence spectroscopy. In order to enhance the light emission, Ln molecules will be immobilized on the processed PhC cavities.

This work is supported by the state of Hesse in the frame of LOEWE priority project SMolBits

CPP 17.34 Tue 11:00 P2

Propandehydrirkungskatalysatoren mit den Eisen(III)oxid-Nanopartikeln — •IRINA BELOVA — Moscow, Russia

Propylen ist ein sehr wichtiger Industrierohstoff, aber das Wachstum seiner Produktion hat mit dem Wachstum des Verbrauchs nicht Schritt gehalten. Das größte Potenzial im Bereich der Propylenherstellung haben die Reaktionen der direkten und oxidativen Dehydrierung von Propan. Wir haben versucht, einen Propan-Dehydrierungskatalysator als Eisen-Nanopartikeln auf Aluminiumoxid zu erhalten. Um Nanopartikel zu bilden, griffen wir auf die Bildung von Eisenkomplexen mit Phenanthrolin zurück. Bei der Reaktion der direkten Propandehydrierung gibt es bei diesen Katalysatoren eine geringe Selektivität. Dabei schreitet Cracken schreitet aktiv voran. Es gibt jedoch immer noch eine Propandehydrierung. Wir planen, mit Sauerstoff gemischtes Propan benutzen. Wir erwarten, dass die *milde* Oxidation von Propan mit Sauerstoff besser verläuft.

CPP 17.35 Tue 11:00 P2

Polydisperse curved polymer brushes — •MARIOS GIANNAKOU and FRIEDERIKE SCHMID — University of Mainz

In the past, polymer brushes have been investigated in the monodisperse limit or in flat geometries. These circumstances however aren't as experimentally relevant, as monodisperse brushes are difficult to construct and brushes are found in curved geometries most of the times. Here, we attempt to resolve this issue by extending the already established mean-field theory describing polymer brushes developed by Cates et al.. We develop a numerical method that allows us to investigate cylindrical and spherical geometries for arbitrary polydispersities. We then explore the uniform, Schulz-Zimm and monodisperse polymer distributions, and comment on the results.

CPP 17.36 Tue 11:00 P2

Temperature-dependent conformation behavior of isolated Poly(3-hexylthiophene) chains — •SANWARDHINI PANTAWANE and STEPHAN GEKLE — Biofluid Simulation and Modeling Theoretische Physik VI Universität Bayreuth 95440 Bayreuth Germany

We use atomistic as well as coarse-grained molecular dynamics simulations to study the conformation of a single Poly(3-hexylthiophene) chain as function of temperature. We find that mainly bundle and toroid structures appear with bundles becoming more abundant for decreasing temperatures and even more after adding solvent (THF), leading to a prominent swelling of the molecular size at a temperature of about 220K. This swelling is in close agreement with the interpretation of recent spectroscopic experiments (Panzer et al. J Phys Chem Lett 8, 114 (2017)). We further relate the temperature dependence of P3HT to that of simple Lennard-Jones model polymers in vacuum.

CPP 17.37 Tue 11:00 P2

Dynamic Origin of the Entropic Force on a Semi-Confined Chain — •RODRIQUE BADR¹, LAMA TANNOURY², and LEONID KLUSHIN³ — ¹Johannes Gutenberg University, Mainz, Germany — ²Martin Luther University, Halle-Wittenberg, Germany — ³American University of Beirut, Beirut, Lebanon

Thermodynamics predicts that the free energy of confinement

$$F = B \frac{L}{D}$$

for a chain confined in a tube with thin and thick walls is the same in both cases. This equivalence implies that the force acting to eject the chain from semi-confinement is also the same. Thermodynamics, however, does not explain the dynamical origin of the force, but one can understand the force as originating from contacts with the surface of the boundary. Intuition suggests that the thin boundary should amount to fewer contacts and thus lead to a smaller ejection force when compared to the case of a thick boundary. Using coarse-grained molecular dynamics (MD) simulations, we support and validate the thermodynamic prediction that the magnitude of the ejection force is the same for different thicknesses of the boundary.

The forces are also found to be in good agreement with the scaling laws predicted by the thermodynamic approach. Finally, the results from our MD simulations provide an explanation of the origin of this equivalence of entropic forces, through the analysis of the radial distribution of contributions from the boundary to the ejection force.

CPP 17.38 Tue 11:00 P2

Computational study of the rheology of nanoparticle-polymer composites — •LEON HILLMANN, NIKLAS BLAGOJEVIC, and MARCUS MÜLLER — Institute for Theoretical Physics, Georg-August-Universität Göttingen, Germany

Matrix-filler interactions in nanoparticle-polymer composites play a crucial role in the manufacturing process as well as the properties of the final material. Therefore, understanding the interplay between the parameters, such as shape, concentration, and size, is paramount for the design process of new compos-

ites. Computer simulations of these materials, however, pose several challenges due to the vast differences in the length scales involved, ranging from atomistic forces up to large-scale self-assembling structures. Here, a single nanoparticle embedded in polymer melt, represented by a highly coarse-grained, Gaussian, bead-spring model, is studied by dissipative particle dynamics (DPD) simulations. The nanoparticle-polymer interaction is adjusted with iterative Boltzmann inversion to match predictions of the density profile from atomistic simulations. Measurements of the nanoparticle's velocity autocorrelation function are then used to determine the memory kernel in a generalized Langevin equation. To what extent does the motion of the nanoparticle provide information about the viscoelastic properties of the surrounding melt? To this end, a numerical solution of the corresponding inverse problem is presented, which arises from a reformulation of the problem as the inversion of a triangular Toeplitz matrix. The results are finally compared with the predictions made by the Rouse model for unentangled polymer melts.

CPP 17.39 Tue 11:00 P2

Anomalous Diffusion of Diisocyanate in Cross-linked Silicone — •MARTIN WORTMANN¹, KLAUS VIERTTEL², NATALIE FRESE¹, WALDEMAR KEIL³, CLAUDIA SCHMIDT³, and BRUNO HÜSGEN² — ¹Bielefeld University, Bielefeld, Germany — ²Bielefeld University of Applied Sciences, Bielefeld, Germany — ³Paderborn University, Paderborn, Germany

In industrial applications of polyurethane vacuum casting, silicone casting molds are used to replicate complex three-dimensional master patterns for prototypes and small series production. The undesired diffusion of isocyanate from the casting resin into the silicone causes gradual degradation of the casting molds. In this contribution, we present mathematical models for the anomalous diffusion process and a comprehensive description of the underlying chemical and physical mechanisms. The polymerization of the isocyanate with residual moisture to polyurea within the silicone matrix leads to a time dependence of both the surface concentration and the diffusion coefficient. The resulting concentration distribution over time and cross-section is modelled by analytical solutions to the diffusion equation.

CPP 17.40 Tue 11:00 P2

Molecular Dynamics Simulation of Free chain Diffusion into a Regular Network — •JUDE ANN VISHNU¹ and FRIEDERIKE SCHMID² — ¹Johannes Gutenberg University, Mainz, Germany — ²Johannes Gutenberg University, Mainz, Germany

Thermo-sensitive hydrogels have attracted considerable attention in the field of bio chemistry and bio-medicine. Earlier works show that microfluidics can be used to create core-shell particle with decoupled elasticity and surface adhesiveness. However these experiments could not achieve proper control over the core-shell interconnectivity. We use MD simulations to understand and quantify the diffusive interpenetration of these shell polymers into a core gel. The simulation uses a Regular network to model the gel which is diffusively invaded via a polymer solution. We look into the interfacial profile and the ways to control this core-shell connectivity. The density profiles show a clear dependence of penetration on shell polymer concentrations. This is also seen in the degree of interfacial integration and diffusion depths. Finally the analysis of diffused free chain within the gel shows the emergence of large clusters leading to percolation. These results give us insight into how the factors like the core-shell polymer contact time, shell polymer concentration, etc can help us fine tune the core-shell connectivity in experiments.

CPP 17.41 Tue 11:00 P2

Nucleation of separating liquid phases in elastic polymer networks — •CHARLOTTA LORENZ, CARLA FERNÁNDEZ-RICO, and ERIC DUFRESNE — Soft and Living Materials, ETH Zurich, Zurich, Switzerland

Arrested phase separation is a key mechanism used by living systems to create well-controlled nanostructures. One of the most salient examples is structural color as present in some bird and insect species. Besides fascinating optical properties, phase-separating composite systems can have astonishing mechanical properties: For example, liquid inclusions can stiffen polymer networks. These mechanical properties have been less studied compared to the optical properties. To study the mechanical properties we use a sample system of a polymer network made of PDMS and fluorinated oil. We aim to control mechanical properties by tuning the structure of the phase-separated domains. Structure of the phase separating domains can be influenced by their nucleation. We vary typical parameters which could determine the nucleation such as the mesh size of the polymer network and total liquid fraction. We employ small-angle X-ray scattering, tensile tests and indentation experiments to study nucleation and mechanical properties of phase-separating samples. Our studies can result in mechanically highly flexible, self-assembled materials, which are comparatively fast and easy to produce.

CPP 18: Complex Fluids and Colloids, Micelles and Vesicles (joint session CPP/DY)

Time: Tuesday 11:30–13:00

Location: H38

Invited Talk

CPP 18.1 Tue 11:30 H38

How X-rays can reveal waters mysteries — •KATRIN AMANN-WINKEL — Max-Planck-Institut für Polymerforschung, Mainz, Germany — Johannes Gutenberg Universität Mainz, Institut für Physik, Mainz, Germany — Stockholm University, Department of Physics, Stockholm, Sweden

Water is ubiquitous and the most important liquid for life on earth. Although the water molecule is seemingly simple, various macroscopic properties of water are most anomalous, such as the density maximum at 4 °C or the divergence of the heat capacity upon cooling. Computer-simulations suggest that the anomalous behaviour of ambient and supercooled water could be explained by a two state model of water. An important role in this ongoing discussion plays the amorphous forms of water [1]. Since the discovery of two distinct amorphous states of ice with different density (high- and low density amorphous ice, HDA and LDA) it has been discussed whether and how this phenomenon of polymorphism at high pressures is connected to the occurrence of two distinct liquid phases (HDL and LDL). X-ray scattering experiments on both supercooled water [2] and amorphous ice [3] are of major importance for our understanding of water. In my talk I will give an overview on our recent experiments on supercooled water and amorphous ices. [1] K. Amann-Winkel et al., *Waters controversial glass transition*, *Rev. Mod. Phys.* 88, (2016) [2] K.H. Kim, et al., *SCIENCE* 358, 1589 (2017) [3] K.H. Kim, et al., *SCIENCE* 370, 6519, 978 (2020)

CPP 18.2 Tue 12:00 H38

Electrostatic Shielding Behavior of Keggin Anions in Aqueous Solution — •THOMAS TILGER and REGINE VON KLITZING — Department of Physics, Technische Universität Darmstadt, Darmstadt, 64289, Germany

Natural colloidal dispersions have accompanied mankind in the form of blood or milk ever since. Besides this, artificial systems have gained a significant importance for our daily life during the last decades.

Therefore, it is of special interest to gain an understanding of which interparticle forces govern the stability of colloidal dispersions and how this stability can be tailored. In electrolyte solutions, the classical DLVO theory describes these interactions. Whilst this description provides a good agreement with experimental data for 1:1 electrolytes, larger deviations appear for systems of higher valency. For a detailed examination of the van der Waals and electrostatically dominated regimes, we directly measure the forces between colloidal silica particles in aqueous solutions by the colloidal probe AFM (atomic force microscopy) technique.

Varying the concentration of monovalent salts and acids allows us to demonstrate the transition from the double layer to the van der Waals dominated regime and to determine the pH dependence of the colloidal probes double layer potential. Similar measurements for phosphotungstic (PTA, a 1:3 system) and silicotungstic acid (STA, a 1:4 system) - both nanometer-sized anions of the Keggin type - can still be described with the DLVO theory, but reveal significant deviations between the calculated and measured ionic strengths.

CPP 18.3 Tue 12:15 H38

Influence of the imbibition of colloids through the morphology of porous CNF layers — •CONSTANTIN HARDER^{1,2}, MARIE BETKER^{1,3}, ALEXAKIS E. ALEXAKIS³, ANDREI CHUMAKOV¹, BENEDIKT SOCHOR¹, ELISABETH ERBES^{1,4}, MARC GENSCH^{1,2}, QING CHEN¹, CALVIN BRETT^{1,3}, JAN RUBECK¹, MATTHIAS SCHWARTZKOPF¹, EVA MALMSTRÖM³, DANIEL SÖDERBERG³, PETER MÜLLER-BUSCHBAUM^{2,5}, and STEPHAN V. ROTH^{1,3} — ¹DESY, 22607 Hamburg, Germany — ²TU München, Physik-Department, LS Funktionelle Materialien, 85748 Garching, Germany — ³KTH Royal Institute of Technology, 10044 Stockholm, Sweden — ⁴Institute for X-ray Physics, Goettingen University, 37077 Goettingen, Germany — ⁵MLZ, TU München, 85748 Garching, Germany

Functionalization of porous materials in terms of optical, chemical, and mechanical properties is readily achieved by applying colloidal layers. Our goal is to functionalize porous cellulose nanofibril (CNF) templates by applying tailored core-shell colloids with specific surface properties. The colloidal layer formation influencing the surface properties can be tuned by the deposition conditions and subsequent annealing. Therefore, we applied colloidal inks (poly(butyl methacrylate) and poly(sobrerol methacrylate) in aqueous dispersion) with different glass transition temperatures T_g as the colloidal layers on the CNF templates. During the deposition, the colloids partially enter the CNF layer to fill the CNF voids and remain on the CNF surface, leading to complex drying processes. The morphology of the mixed CNF / colloidal thin film changes when T_g of the colloids is exceeded.

CPP 18.4 Tue 12:30 H38

Elastic core-shell materials and their deformational behavior — JANNIS KOLKER¹, •LUKAS FISCHER², ANDREAS M. MENZEL², and HARTMUT LÖWEN¹ — ¹Institut für Theoretische Physik II, Heinrich-Heine-Universität Düsseldorf, Düsseldorf, Germany — ²Institut für Physik, Otto-von-Guericke-Universität Magdeburg, Magdeburg, Germany

Elastic materials consisting of an inner part, a core, and an outer part, a shell, of possibly different material properties can be found from planetary scales down to the colloidal microscale. We here describe a situation amenable to analytical theory, namely the linear elastic deformation of a spherical core-shell system in response to an equatorial load in form of a force line density [1]. The relevance of this setup lies in, e.g., functionalized microgel particles absorbed to fluid-fluid interfaces or macroscopic illustrative show-and-tell objects.

Situations of different elastic properties and sizes of core and shell are analyzed to study their influence on the deformational response of the whole system. For example, tuning the two Poisson ratios allows to adjust the relative degree of oblate or prolate deformations and change in volume between core and shell. Due to the overall spherical shape and the two-component structure, the stress and strain distributions become rather inhomogeneous. Using different core and shell materials in colloidal microgel particles allows for inner functionalization while simultaneously adjusting the outer wetting properties.

[1] J. Kolker, L. Fischer, A. M. Menzel, H. Löwen, *J. Elasticity*, in press.

CPP 18.5 Tue 12:45 H38

Effective Thomas-Fermi screening approach and wetting transition at charge/metal interfaces — •ALEXANDER SCHLAICH^{1,2}, DONGLIANG JIN^{1,3}, LYDERIC BOCQUET⁴, and BENOIT COASNE¹ — ¹Univ. Grenoble Alpes, CNRS, LIPhy, Grenoble, France — ²Stuttgart Center for Simulation Science, Universität Stuttgart, Germany — ³Institut für Theoretische Physik, Technische Universität Wien, Austria — ⁴Laboratoire de Physique de l'École Normale Supérieure, CNRS, Université PSL, Sorbonne Université, Sorbonne Paris Cité, Paris, France

At the nanometer scale the commonly employed image charge approach to obtain the electrostatic interactions close to a metallic interface breaks down due to the finite screening in any real metal. We develop an effective approach that allows dealing with any real metal using the Thomas-Fermi formalism. [1]

We find a microscopic picture based on the Gibbs-Thomson equation for capillary freezing of an ionic liquid. An unprecedented wetting transition is found upon switching the confining medium from insulating to metallic. The wetting behavior at imperfect metals raises new challenging questions on the complex behavior of charged systems in the vicinity or confined within surfaces.

[1] A. Schlaich, D. Jin, L. Bocquet & B. Coasne, *Nat. Mater.* 1 (2021).

CPP 19: Perovskite and Photovoltaics 2

Time: Wednesday 9:30–11:00

Location: H38

Invited Talk

CPP 19.1 Wed 9:30 H38

Elucidating the role of antisolvent polarity on the surface chemistry and optoelectronic properties of lead-halide perovskite nanocrystals — •ROBERT HOYE — Department of Materials, Imperial College London, Exhibition Road, London SW7 2AZ, United Kingdom

Lead-halide perovskites (LHPs) have emerged as highly-promising contenders for light-emission applications, particularly in the form of nanocrystals (NCs), owing to their advantages of high photoluminescence quantum yield (PLQY), along with tunable, sharp emission peaks. Achieving high-quality NCs critically depends on the purification process, which often makes use of an antisolvent. Despite its important role, the mechanism by which the antisolvent influences the surface properties of the NCs is not well understood. In this talk, we examine

the influence of the polarity of the antisolvent on the properties of the model NC system CsPbBr₃I_{3-x}. The antisolvents we compare are (in order of increasing polarity): methyl acetate, acetone and butanol. We find that as the polarity of the antisolvent increases, there is a greater blue-shift in the photoluminescence peak, owing to the removal of iodide. Through detailed nuclear magnetic resonance measurements, we find that this occurs due to more polar antisolvents having a higher propensity to induce a condensation reaction between the oleic acid and oleylamine ligands on the NCs, leading to their removal in the form of amides, which leads to the removal of surface iodides. This work shows that minimising surface damage to LHP NCs requires the selection of low polarity antisolvents.

CPP 19.2 Wed 10:00 H38

Simulation of the impact of processing conditions on the perovskite film morphology — •MARTIN MAJEWSKI, OLIVIER RONSIN, and JENS HARTING — Forschungszentrum Jülich GmbH, Helmholtz Institute Erlangen- Nürnberg (IEK-11), Dynamics of Complex Fluids and Interfaces, Cauerstraße 1, 91058 Erlangen, Germany

The solution-processed perovskite layer forms complex structures during drying. This morphology of the dry film heavily influences the efficiency of the final solar cell. The impact of the physical mechanisms on the morphology, like for example nucleation and evaporation rate, in a drying, crystallizing wet film is not really understood yet. Therefore a better understanding of the interplay of these phenomena is needed.

We will present phase field simulations which are capable to describe the main physical processes like: evaporation, diffusion, spontaneous nucleation, crystal growth and advection, to investigate the impact of processing conditions on the final morphology of the perovskite film. Comparisons of the simulation to the theory will be presented. First simulations of drying solutions, including all physical phenomena, will be shown and compared to experiments.

CPP 19.3 Wed 10:15 H38

Influence of crystallization on the structural and optical properties of lead-free Cs₂AgBiBr₆ perovskite crystals — •MELINA ARMER¹, JULIAN HÖCKER², CARSTEN BÜCHNER¹, SOPHIE HÄFELE¹, PATRICK DÖRFLINGER¹, MAXIMILIAN T. SIRTIL³, KRISTOFER TVINGSTEDT¹, THOMAS BEIN³, and VLADIMIR DYAKONOV¹ — ¹Experimental Physics VI, Julius Maximilian University of Würzburg, 97074 Würzburg — ²Ludwigs Maximilian University München, 80539 München — ³Ludwigs Maximilian University München, 81377 München

As conventional perovskite solar cells contain lead and therefore suffer from toxicity issues, finding stable lead-free materials for the application in perovskite photovoltaics has become an essential problem to be solved. In this work, lead-free Cs₂AgBiBr₆ single crystals have been synthesized by slowly evaporating organic solvents and by using the well-known controlled cooling technique. The evaluation of solubility curves showed that slow evaporation enables crystal growth in a wide range of temperatures. We further used the controlled cooling technique as a reference to the slow evaporation method to grow crystals at different temperatures. The quality of the synthesized crystals was characterized by X-ray diffraction (XRD) and energy dispersive X-ray (EDX) measurements. Furthermore, photoluminescence excitation (PLE) and absorption measurements were conducted to investigate the relationship between Urbach energy and the growth method and temperature. As a result, we found that growth temperatures significantly impact the amount of tail-states present in the perovskite crystals.

CPP 19.4 Wed 10:30 H38

Real-time texture and phase evolution tracking of the annealing process of slot-die coated perovskite by in situ GIWAXS — •MANUEL A. REUS¹, LENNART K. REB¹, ALEXANDER F. WEINZIERL¹, CHRISTIAN L. WEINDL¹, RENJUN GUO¹, TIANXIAO XIAO¹, MATTHIAS SCHWARTZKOPF², ANDREI CHUMAKOV², STEPHAN V. ROTH², and PETER MÜLLER-BUSCHBAUM^{1,3} — ¹TU München, Physik-Department, LS Funktionelle Materialien, 85748 Garching — ²DESY, 22607 Hamburg — ³MLZ, TU München, 85748 Garching

In perovskite solar cell material research the thin-film morphology determines the quality of the absorber material and consequently device performance. To scale up material deposition towards, e.g., roll-to-roll compatible techniques, the influence of the deposition method on morphology needs to be known to control the process. Here, we apply in situ grazing-incidence wide-angle x-ray scattering (GIWAXS) on the annealing process of slot-die coated lead iodide and slot-die coated methylammonium iodide, that react to perovskite under heat. We track the conversion in real-time and extract relevant parameters concerning texture and phase evolution. As a reference, we show GIWAXS data of spin-cast equivalent systems and show the resulting morphology and kinetics differences traced back to the deposition method.

CPP 19.5 Wed 10:45 H38

Temperature-reduced and rapid growth of hybrid perovskite single crystals — •JULIAN HÖCKER^{1,2}, FELIX BRUST¹, MELINA ARMER¹, and VLADIMIR DYAKONOV¹ — ¹Experimental Physics VI, Julius Maximilian University of Würzburg, 97074 Würzburg, Germany — ²Experimental Physics - Soft Condensed Matter, Ludwig Maximilian University of Munich, 80539 Munich, Germany

Organolead trihalide perovskite single crystals are gaining more and more interest in the field of semiconductor research since they can be used for a variety of technical applications, like photodetectors or solar cells. To date, exclusively solution-processed perovskite crystals have been used for the fabrication of such device prototypes. A supersaturated perovskite solution is caused either by a temperature change, solvent evaporation, chemical reaction, or a combination of the methods. The aim of the various processes is to achieve rapid growth of crystals with controlled structure, size, shape, and yield. In addition, the crystalline components must exhibit high physical and chemical qualities to be applied as semiconducting components. However, these high requirements and numerous criteria cannot always be fully met by standard techniques like inverse temperature crystallisation. In order to grow large-sized OLTP single crystals in a controlled and simple manner from solution in the shortest possible time, we developed a crystallisation process based on primary alcohols. As a result, the blends based on perovskite precursor solution and alcohols lead to a significant reduction in their retrograde solubility and enable a temperature-reduced crystallisation pathway to grow single crystals.

CPP 20: General Session to the Symposium: Interplay of Substrate Adaptivity and Wetting Dynamics from Soft Matter to Biology (joint session CPP/DY)

Time: Wednesday 9:30–11:15

Location: H39

CPP 20.1 Wed 9:30 H39

Adaptive two capacitor model to describe slide electrification in moving water drops — •PRAVASH BISTA¹, AMY Z. STETTEN¹, WILLIAM S.Y. WONG¹, HANS-JÜRGEN BUTT¹, and STEFAN A.L. WEBER^{1,2} — ¹Max Planck Institute for Polymer Research, Ackermannweg 10, 55128 Mainz, Germany — ²Johannes Gutenberg University, Department of Physics, Staudingerweg 10, 55128 Mainz, Germany

Slide electrification is a contact-charge separation where neutral water drops slide over a neutral hydrophobic surface, accumulating and leaving behind a net charge. The accumulated drop charge for successive sliding drops decreases and eventually reaches a steady state. On hydrophobic and hydrophilic mixed surfaces, even a polarity flipping of drop charge depending on a drop rate was observed. Here, we describe this effect in terms of a voltage generated at the three-phase contact line. This voltage moves charges between capacitors, one formed by the drop combined with the solid surface and one on the solid-surface. By introducing an adaptation of the voltage upon water contact, we can model drop charge experiments on different surfaces, including more exotic ones with drop-rate-dependent charge polarity. Thus, the adaptive two capacitor model enables new insights into the molecular details of the charge separation mechanism.

CPP 20.2 Wed 9:45 H39

Memory effects of PNIPAAm brushes in different atmospheres — •SIMON SCHUBOTZ, MARISA FISCHER, JENS-UWE SOMMER, PETRA UHLMANN, ANDREAS FERY, and GÜNTER AUERNHAMMER — Leibniz-Institut für Polymerforschung Dresden e.V., 01069 Dresden, Germany

Some polymer brushes show a co-nonsolvency effect: They collapse in a mixture of two good solvents at some specific mixing ratio. In contrast to previous studies we concentrate on partial wetting of co-nonsolvent polymer brushes, i.e., on

the dynamics of a three-phase contact line moving over such brushes.

We found that Poly(N-isopropylacrylamide) (PNIPAAm) brushes experiences a memory effect when consecutively depositing drops at the same position. Previously deposited drops adapt the brush and changes the wetting behavior (advancing contact angle) of subsequent drops.

We measure water drops in an ethanol-saturated atmosphere on PNIPAAm brushes. The measurements show that the memory effect is strongly effected by an ethanol-enriched atmosphere. At the three-phase contact line, due to evaporation from the drop, the composition of the atmosphere and probably also the brush will transition from an ethanol-rich state to a water-enriched state. Thus, the brush might pass through the co-nonsolvency regime. On large time scales the ethanol enriched gas phase and the water drop will become mixtures of ethanol and water. We present strategies to counter this mixing effect.

CPP 20.3 Wed 10:00 H39

Fast contact lines on soft solids — •HANSOL JEON^{1,2} and STEFAN KARPITSCHKA¹ — ¹Max Planck Institute for Dynamics and Self-Organization, Göttingen, Germany — ²Georg-August-Universität Göttingen, Göttingen, Germany

When a droplet is resting on a soft surface, the capillary forces deform the surface into a sharp wetting ridge. The amplitude of the wetting ridge is determined by elasto-capillary length, but the angles by which the interfaces meet at the ridge tip only depend on the balance of surface tensions, the so-called Neumann balance. For moving contact lines, dissipation in the wetting ridge leads to viscoelastic braking. In recent literature, various effects that could alter Neumann balance and viscoelastic braking have been suggested, ranging from free, extractable oligomers to point forces emerging from bulk viscoelasticity.

We visualize moving wetting ridges at high spatio-temporal resolution and determine the tip geometry for various liquids and PDMS substrates. We observe an increase of the ridge opening angle at large speeds, even for very mild deformations caused by the low surface tension of a fluorinated oil. We also find no significant change in ridge rotation and opening angle for gels with different fractions of cross-linked and free chains, nor for different bulk rheological properties. These findings highlight the need for a non-trivial surface constitutional relation that is different from the bulk.

CPP 20.4 Wed 10:15 H39

Mixed grafted homopolymer and diblock copolymer functional brush layers upon humidity alterations: nanoscale morphology and transformations —

•APOSTOLOS VAGIAS¹, THEODORE MANOURAS², ELEFTHERIOS KOUFAKIS^{2,3}, PEIXI WANG⁴, MARCELL WOLF¹, FABIAN A. C. APFELBECK⁴, SIGRID BERNSTORFF⁵, MARIA VAMVAKAKI^{2,3}, and PETER MÜLLER-BUSCHBAUM^{1,4} — ¹Heinz Maier-Leibnitz Zentrum (MLZ), Technische Universität München, 85748 Garching, Germany — ²Foundation for Research and Technology (F.O.R.T.H.) Hellas, Institute of Electronic Structure and Laser, 700 13 Heraklion, Crete, Greece — ³Department of Materials Science and Technology, University of Crete, 700 13 Heraklion, Crete, Greece — ⁴Physik-Department, Lehrstuhl für Funktionelle Materialien, Technische Universität München, 85748 Garching, Germany — ⁵Elettra Sincrotrone Trieste S.C.p.A., Basovizza, 34149 Trieste, Italy Using in situ grazing-incident small-angle X-ray scattering (GISAXS) measurements during water vapor uptake, we study the nanostructure morphology in the dry state, during vapor swelling and in the fully swollen state, for thin (<100nm) films of poly(2-(dimethylamino)ethyl methacrylate) (PDMAEMA) and poly(fluoroalkyl methacrylate) (POFPMA) homopolymer and PDMAEMA-b-POFPMA block copolymer dual functional, bactericidal and antifouling brushes. Our surface energy and swelling studies, stress on the role alkyl chain length, charged groups and brush topology in morphology, for the brush functionality.

CPP 20.5 Wed 10:30 H39

Steering droplets on substrates with periodic wettability patterns and deformations —

•JOSUA GRAWITTER and HOLGER STARK — Technische Universität Berlin, Institut für Theoretische Physik, Straße des 17. Juni 135, 10623 Berlin Droplets are set in motion on substrates with a spatio-temporal wettability pattern as generated, for example, on light-switchable surfaces. To study such cases, we implement the boundary-element method to solve the governing Stokes equations for the fluid flow field inside and on the surface of a droplet and supplement it by the Cox-Voinov law for the dynamics of the contact line. Our approach reproduces the relaxation of an axisymmetric droplet in experiments, which we initiate by instantaneously switching the uniform wettability of a substrate quantified by the equilibrium contact angle.

First, we investigate a droplet on substrates with planar-wave-like wettability profile by varying the speed and wave length of the pattern. When the profile moves slowly, it moves the droplet moves steadily forward. Above a critical pattern speed the droplet performs steady oscillations, the effective (time-averaged) velocity of which decreases with the square of the pattern speed.

Second, we investigate a droplet on substrates which deform periodically according to a planar-wave profile. We analyze the effective velocity again as a function of wave speed and length and investigate specifically the influence of curvature changes on droplet motion.

CPP 20.6 Wed 10:45 H39

Spontaneous charging affects the motion of sliding drops — XIAOMEI LI¹, PRAVASH BISTA¹, RÜDIGER BERGER¹, STEFFEN HARDT², HOLGER MARSCHALL³, HANS-JÜRGEN BUTT¹, and •STEFAN A.L. WEBER^{1,4} — ¹MPI for Polymer Research, Ackermannweg 10, Mainz, Germany — ²Institute for Nano- and Microfluidics, Technische Universität Darmstadt, Darmstadt, Germany — ³Computational Multiphase Flows, Technische Universität Darmstadt, Darmstadt, Germany — ⁴Institute of Physics, Johannes Gutenberg University Mainz, Mainz, Germany

The motion of water drops on surfaces is still far from being fully understood. Previous understanding is that drop motion is dictated by viscous dissipation and activated dynamics at the contact line. To accurately measure the forces experienced by moving drops, we imaged their trajectory when sliding down a tilted surface, and applied the relevant equations of motion [1]. We found that drop motion on low-permittivity substrates is substantially influenced by electrostatic forces. Our findings confirm that electrostatics must be taken into consideration for the description of the motion of water, aqueous electrolytes and ethylene glycol on hydrophobic surfaces. Our results are relevant for improving the control of drop motion in many applications, including printing, microfluidics, water management and triboelectric nanogenerators. [1] Li, X. et al. Spontaneous charging affects the motion of sliding drops. *Nat. Phys.* (2022).

CPP 20.7 Wed 11:00 H39

Dynamic mesoscopic model for two-component compound drops — •JAN DIEKMANN and UWE THIELE — Westfälische Wilhelms-Universität, Münster, Deutschland

We consider a mesoscopic model for two immiscible fluids forming two-layer liquid films or compound drops on a rigid solid substrate. The earlier macroscale description [1,2] is connected to our mesoscopic approach (building on [3]) via consistency conditions. Thereby we relate macroscale and mesoscale versions of the Young and Neumann relations at the liquid 1/solid/gas and liquid 1/liquid 2/gas contact lines, respectively. Furthermore, we employ the mesoscale model to investigate selected dewetting and coarsening processes for physically realistic parameters. The steady compound drops emerging from the time simulations are related to bifurcation scenarios determined via macroscale and mesoscale descriptions.

[1] L. Mahadevan, M. Adda-Bedia, and Y. Pomeau. "Four-phase merging in sessile compound drops". In: *J. Fluid Mech.* 451 (2002), pp. 411-420. [2] M. J. Neeson et al. "Compound sessile drops". In: *Soft Matter* 8 (2012), pp. 11042-11050. doi: 10.1039/c2sm26637g. [3] A. Pototsky et al. "Morphology changes in the evolution of liquid two-layer films". In: *J. Chem. Phys.* 122 (2005), p. 224711. doi: 10.1063/1.1927512. [4] Uwe Thiele et al. "Equilibrium contact angle and adsorption layer properties with surfactants". In: *Langmuir* 34.24 (2018), pp. 7210-7221.

CPP 21: Materials for Energy Storage (joint session KFM/CPP)

Chair: Prof. Dr. Theo Scherer (KIT, Karlsruhe)

Time: Wednesday 9:30–12:05

Location: H7

See KFM 15 for details of this session.

CPP 22: Active Matter 3 (joint session BP/CPP/DY)

Time: Wednesday 9:30–12:30

Location: H16

See BP 14 for details of this session.

CPP 23: Complex Fluids and Soft Matter 1 (joint session DY/CPP)

Time: Wednesday 9:30–12:00

Location: H18

See DY 23 for details of this session.

CPP 24: 2D Materials 5 (joint session HL/CPP/DS)

Time: Wednesday 9:30–12:00

Location: H36

See HL 20 for details of this session.

CPP 25: 2D Materials 6 (joint session DS/CPP)

Time: Wednesday 11:15–13:00

Location: H17

See DS 17 for details of this session.

CPP 26: Organic Electronics and Photovoltaics 2

Time: Wednesday 11:30–13:00

Location: H38

CPP 26.1 Wed 11:30 H38

Large Area Semitransparent Near-Infrared Organic Photodetectors — YAZHONG WANG¹, •TIANYI ZHANG¹, LOUIS CONRAD WINKLER¹, DONATO SPOLTORE², JOHANNES BENDUHN¹, and KARL LEO¹ — ¹Dresden Integrated Center for Applied Physics and Photonic Materials, Technische Universität Dresden, Dresden, Germany — ²Department of Mathematical, Physical and Computer Sciences, University of Parma, V.le delle Scienze 7/A, 43124 Parma, Italy

Organic photodetector (OPD) is a promising technology for several sensing applications. With advances in material synthesis and device engineering, OPDs can rival their inorganic counterparts due to their tunable absorption, lightweight, facile fabrication, low cost, and comparable performance. Here, we demonstrate a semi-transparent large area (256 mm²) near-infrared OPD. Through vacuum deposition and optimization of the thickness of the back metal contact layer, a promising average visible transmittance up to 34.6% is achieved while maintaining 36.0% of external quantum efficiency at 790 nm. Judicious design for combining wide-optical gap buffer layers with semi-transparent electrodes results in the remarkable specific detectivity of 1.4×10^{13} (6.44 mm²) and 1.1×10^{12} (large area) Jones, respectively. Those performances are comparable with commercial silicon photodiodes. To the best of our knowledge, our device is the best see-through, large-area, near-infrared OPD, which enables a higher level of photon detection and integration into image sensors. The transparency and good stability of these OPDs make them excellent candidates for various biomedical sensing applications and the internet of things.

CPP 26.2 Wed 11:45 H38

Exploring Highly Ordered Rubrene:C₆₀ Heterojunctions for Organic Photodetectors — •ANNA-LENA HOFMANN¹, LUCY WINKLER¹, MAX HERZOG¹, EVA BITTRICH², JAKOB WOLANSKY¹, MARTIN KROLL¹, JOHANNES BENDUHN¹, and KARL LEO¹ — ¹Institute of Applied Physics, Technische Universität Dresden, Nöthnitzer Str. 61, 01187 Dresden, Germany — ²Leibniz-Institut für Polymerforschung Dresden e.V., Dresden, Germany

Rubrene can form highly ordered phases, demonstrating an unusually high charge carrier mobility for holes ($> 10 \text{ cm}^2 \text{V}^{-1} \text{s}^{-1}$) even in thin films. Therefore it is a promising material for high-performance organic photodetectors (OPDs). To study the impact on OPDs, crystalline triclinic rubrene is compared to amorphous rubrene. Planar heterojunctions (PHJs) and bulk heterojunctions (BHJs) are fabricated for both material systems. For the latter, rubrene is doped with 2, 5, and 10 wt% of C₆₀. Linearly polarized microscopy is used to get the first insight into the morphology, which is then completed by ellipsometry, atomic force microscopy (AFM), and x-ray diffraction (XRD). For the electrical characterization, the external quantum efficiency (EQE) and IV characteristics are obtained, where an additional crystalline sample with a neat C₆₀ layer is investigated. The neat layer of C₆₀ achieves an enormous improvement of the EQE. This makes the PHJ a more favourable device architecture. Even though triclinic rubrene reaches a higher EQE and has a broader spectral response, it does underperform in optimized OPDs concerning the specific detectivity since the dark current is three magnitudes higher than the amorphous counterpart.

CPP 26.3 Wed 12:00 H38

Hybrid Energy Harvester based on Triboelectric Nanogenerator and PbS Quantum Dot Solar Cell — •TIANXIAO XIAO¹, WEI CHEN¹, WEI CAO¹, and PETER MÜLLER-BUSCHBAUM^{1,2} — ¹Physik-Department, LS Funktionelle Materialien, 85748 Garching — ²MLZ, TU München, 85748 Garching

Developing clean energy lies in the heart of the sustainable development of human society. Triboelectric nanogenerators (TENGs) originating from Maxwell's displacement current is a new type of energy harvester for harnessing ambient mechanical energy based on the coupling of triboelectrification and electrostatic induction effect. Compared with other counterparts, owing to the light-weight, low-cost, and easy fabrication TENGs become one of the most promising candidates in the replacement of conventional fossil fuels and attract worldwide attention in the past years. However, to further increase the energy harvesting efficiency and broaden application fields, integrating the TENG with other kinds of energy harvesters in one device is a possible way to meet these needs. In the present work, a TENG based hybrid energy harvester is designed and fabricated on the flexible polyethylene terephthalate (PET) substrate. This hybrid device consists of a single-electrode mode TENG component and a PbS quantum dot (QD) based solar cell component, which can harness both mechanical and solar energy from ambient environment to directly generate electricity.

CPP 26.4 Wed 12:15 H38

In Situ and In Operando KPFM Studies on OFET Based on Hexadecafluoro-Copper-Phthalocyanine (F₁₆PcCu) to Access Energy Level Alignment and Electrical Contact Resistance — •PASCAL SCHWEITZER, CLEMENS GEIS, and DERCK SCHLETTWEIN — Justus-Liebig-Universität Gießen, Institut für Angewandte Physik

Contact resistances are considered a show-stopper for organic field effect transistors (OFET). Perfluorinated copper-phthalocyanine (F₁₆PcCu) is a promising chemically stable n-conductor to build complementary logical circuits with established p-conductors. A reasonably high charge carrier mobility $\mu_{ext} \approx 2 \times 10^{-3} \text{ cm}^2/\text{Vs}$ was estimated from device performance affected, however, by neglected contact resistances. In this work, we used *in operando* Kelvin probe force microscopy under high vacuum to study the influence of contact resistances at the source and drain electrodes on the OFET performance. Non-contact potentiometry at different applied external voltages revealed relevant voltage drops at the electrode interface and in the adjacent contact region. Based on these voltage drops and measured device currents significant contact resistances were calculated. Correcting for such parasitic voltage drops, contact-free μ_{ch} was obtained, substantially higher than μ_{ext} . The growth mode of F₁₆PcCu on application-relevant polycrystalline gold substrates and shifts of the energy levels were studied by *in situ* KPFM and an injection barrier was confirmed. From these results, we conclude that the model of thermionic emission, often used for contact resistances, is not completely sufficient to describe the present case.

CPP 26.5 Wed 12:30 H38

Thin films of electron donor-acceptor complexes: characterisation of mixed-crystalline phases and implications for electrical doping — •ANDREAS OPITZ¹, GIULIANO DUVA², MARIUS GEBHARDT³, HONGWON KIM³, EDUARD MEISTER³, TINO MEISEL¹, PAUL BEYER¹, VALENTINA BELOVA², CHRISTIAN KASPER⁴, JENS PFLAUM⁴, LINUS PITHAN^{4,5}, ALEXANDER HINDERHOFER², FRANK SCHREIBER², and WOLFGANG BRÜTTING³ — ¹Institut für Physik, Humboldt-Universität zu Berlin, Germany — ²Institut für Angewandte Physik, Universität Tübingen, Germany — ³Institut für Physik, Universität Augsburg, Germany — ⁴Experimentelle Physik VI, Julius-Maximilians-Universität Würzburg, Germany — ⁵European Synchrotron Radiation Facility, Grenoble Cedex 9, France

Electron donor-acceptor (EDA) complexes are of interest as low-band gap molecular semiconductors and as dopants for molecular semiconducting matrices. Our recent work establishes a link between optical, structural and vibrational properties of EDA complexes as well as the electrical doping by them. [1] Here, we report on optical and electrical properties of EDA complexes. All studied donor:acceptor systems form mixed crystalline structures and the EDA complex is characterised by the complex-related absorption, which cross the neutral-to-ionic boundary. Our measurements reveal an exponential relation between electrical conductivity and activation energy of transport for all complex-doped systems related to the separation of Coulombically bound charges.

[1] A. Opitz *et al.*, *Mater. Adv.* **3** (2022). DOI: 10.1039/D1MA00578B

CPP 26.6 Wed 12:45 H38

Effect of phenylation vs. functionalization for tetracene-based electron transport materials — •MARYKE KOUYATE, SEBASTIAN HUTSCH, and FRANK ORTMANN — Technical University of Munich, Munich, Germany

In analogy to the tetracene/rubrene system, new electron transport materials (ETMs) are designed by modifying the outer benzene rings of tetracene with electron-withdrawing groups and attaching four phenyl groups to the modified backbone. Subsequent crystal structure prediction and charge transport calculations provided further insights in the structural effect of tetra-phenylation on tetracene based systems and the impact on charge transport properties. A strong effect of core-end modification on the molecular packing and charge transport properties for molecules without phenylation is revealed. These structures differ significantly from the known crystal structure of tetracene. Tetra-phenylation, on the other hand, reduces the impact of core-end modification and crystal structures close to the high-mobility orthorhombic rubrene structure are obtained, suggesting a considerable steric effect of the bulky phenyl-groups. We finally compare the charge-transport properties between the tetracene/rubrene reference systems and ETMs with and without phenyl functionalization.

CPP 27: Composites and Functional Polymer Hybrids

Time: Wednesday 11:30–13:00

Location: H39

CPP 27.1 Wed 11:30 H39

Polymer - Organic Metal Composites for Waste Heat Recovery — •MARIE SIEGERT¹ and JENS PFLAUM^{1,2} — ¹Experimental Physics VI, University of Würzburg, 97074 Würzburg — ²ZAE Bayern, 97074 Würzburg

The interest in organic thermoelectrics has greatly gained traction over the last decade due to its great potential in waste heat recovery based on sustainable, low-cost materials. For instance, polymers can be solution processed on industrial scale and display aptly low thermal conductivity, but lack high electrical conductivity due to their inherent disorder. Organic molecular metals, on the other hand, exhibit superior electrical conductivity over a wide temperature range, but the complexity of preparation currently limits scalable applications [1]. Here, we report on an approach utilizing suitable polymers in combination with the p-type organic metal TTT₂I₃ and the n-type Cu(DCNQI)₂, thus exploiting the benefits of both material classes. As demonstrated by our preliminary experimental data, these composite materials do not only allow for a controlled variation of the thermoelectric properties via the respective amount of organic metal additive but also show significant improvements with respect to their mechanical integrity upon thermal treatment. The related thermoelectric properties of the composites will be evaluated with regard to their application in thin film based organic thermoelectric generators for waste heat recovery. The Deutsche Bundesstiftung Umwelt (DBU) is acknowledged for financial support.

[1] F. Huewe, A. Steeger, et al. Adv. Mat. 29 (2017) 1605682

CPP 27.2 Wed 11:45 H39

From spinning to spraying functional materials: structural and thermoelectric properties of gold doped spin-casted and spray-deposited P3HT-based thin films — •BENEDIKT SOHOR¹, ANNA-LENA OECHSLE², CONSTANTIN HARDER^{1,2}, ALEXEI VOROBIEV^{3,4}, PETER MÜLLER-BUSCHBAUM^{2,5}, and STEPHAN V. ROTH^{1,6} — ¹Deutsches Elektronen-Synchrotron DESY, Notkestr. 85, 22607 Hamburg, Germany — ²Technical University Munich, Physics Department, James-Frank-Str. 1, 85748 Garching, Germany — ³Institute Laue-Langevin, 71 Avenue des Martyrs, 38042 Grenoble Cedex 9, France — ⁴Uppsala University, Department of Physics and Astronomy, Lägerhyddsvägen 1, 752 37 Uppsala, Sweden — ⁵Research Neutron Source Heinz Maier-Leibnitz, FRM II, Lichtenbergstr. 1, 85748 Garching, Germany — ⁶KTH Royal Institute of Technology, Teknikringen 56-58, 100 44 Stockholm, Sweden

Poly(3-hexylthiophen-2,5-diyl) (P3HT) is one of the most prominent semiconducting, conjugated polymers in the fields of organic electronics and photovoltaics. Upon addition of a suitable metal dopant, e.g. chloroauric acid (HAuCl₄), thin P3HT films exhibit thermoelectric properties with large values for the power factor and figure of merit. To investigate the possibility and efficiency of future scalable industrial manufacturing, spin-casted and spray-deposited P3HT films were compared correlating their structural differences with their thermoelectric performance upon doping using AFM, GISAXS/GIWAXS, XRR and NR measurements.

CPP 27.3 Wed 12:00 H39

In-situ GISAXS Observation and Large Area Homogeneity Study of Slot-Die Printed PS-b-P4VP and PS-b-P4VP/FeCl₃ Thin Films — •SHANSHAN YIN¹, TING TIAN¹, CHRISTIAN L. WEINDL¹, KERSTIN S. WIENHOLD¹, QING JI², YAJUN CHENG², YANAN LI³, CHRISTINE M. PAPADAKIS³, MATTHIAS SCHWARTZKOPF⁴, STEPHAN V. ROTH^{4,5}, and PETER MÜLLER-BUSCHBAUM^{1,6} — ¹TU München, Physik-Department, LS Funktionelle Materialien, 85748 Garching — ²NIMTE, Chinese Academy of Sciences, 315201, P. R. China — ³TU München, Physik-Department, Fachgebiet Physik weicher Materie, 85748 Garching — ⁴DESY, 22607 Hamburg — ⁵Royal Institute of Technology KTH, 100 44 Stockholm — ⁶MLZ, TU München, 85748 Garching

Mesoporous hematite (Fe₂O₃) thin films with high surface-to-volume ratios show great potential as photoelectrodes or electrochemical electrodes in energy conversion and storage. In the present work, with the assistance of an up-scalable slot-die coating technique, highly ordered Fe₂O₃ thin films are successfully printed based on the amphiphilic diblock copolymer poly(styrene-*b*-4-vinyl pyridine) (PS-*b*-P4VP) as a structure-directing agent. Pure PS-*b*-P4VP films are printed under the same conditions for comparison. The micellization of the diblock copolymer in the solution, the film formation process of the printed thin films, the homogeneity of the dry films in the lateral and vertical direction as well as the morphological and compositional information of the calcined hybrid PS-*b*-P4VP/FeCl₃ thin film are investigated.

CPP 27.4 Wed 12:15 H39

Morphology transformation pathway of block copolymer- directed cooperative self-assembly of ZnO hybrid films monitored in situ during slot-die coating — •TING TIAN¹, SHANSHAN YIN¹, SUO TU¹, CHRISTIAN L. WEINDL¹, KERSTIN S. WIENHOLD¹, SUZHE LIANG¹, MATTHIAS SCHWARTZKOPF², STEPHAN V. ROTH^{2,3}, and PETER MÜLLER-BUSCHBAUM^{1,4} — ¹TU München, Physik-Department, LS Funktionelle Materialien, 85748 Garching — ²DESY, 22607 Hamburg — ³KTH, Department of Fibre and Polymer Technology, 10044 Stockholm, Sweden — ⁴MLZ, TU München, 85748 Garching

Co-assembly of diblock copolymers (DBC) and inorganic precursors that takes inspiration from the rich phase separation behavior of DBCs can enable the realization of a broad spectrum of functional nanostructures with the desired sizes. In a DBC assisted sol*gel chemistry approach with polystyrene-block-poly(ethylene oxide) and ZnO, hybrid films are formed with slot-die coating. In situ GISAXS measurements are performed to investigate the self-assembly and co-assembly process during the film formation. Combining complementary ex situ characterizations, several distinct regimes are differentiated to describe the morphological transformations from the solvent-dispersed to solidified films. The comparison of the assembly pathway evidences that the key step in the establishment of the pure DBC film is the coalescence of spherical micelles toward cylindrical domains. Due to the presence of the precursor, the formation of cylindrical aggregates in the solution is crucial for the structural development of the hybrid film.

CPP 27.5 Wed 12:30 H39

Programmable Luminescent Tags: Utilizing the interplay of room temperature phosphorescence and oxygen as an information storage device — •TIM ACHENBACH, MAX GMELCH, HEIDI THOMAS, and SEBASTIAN REINEKE — Technische Universität Dresden, Germany

By utilizing the interaction between molecular oxygen and the room temperature phosphorescence of organic materials, continuous-wave-readable and sub-second programmable luminescent tags (PLT) can be realized. They are transparent, flexible and provide a resolution of up to 700 dpi. Information is imprinted by illuminating the PLT with UV light through a shadow mask. By heating the PLT, the information can be erased and a new writing cycle can be started again.

The device consists of two layers on a substrate. The functional layer comprises an organic biluminescent emitter doped into a polymer. The second layer is an oxygen barrier layer. After wet processing in air, molecular oxygen is present in the functional layer of the device, quenching the phosphorescence of the emitter. As energy is transferred to the oxygen during this interaction, it is excited to its highly reactive singlet state and binds to its environment. Over time, all molecular oxygen in the illuminated areas undergoes this photoconsumption process, and a phosphorescent pattern in shape of the mask becomes visible. The oxygen barrier becomes more permeable at elevated temperatures, allowing an oxygen refill of the functional layer by heating the device. This resets the device and it can be rewritten after a short cooling phase.

CPP 27.6 Wed 12:45 H39

Spatio-temporal Imaging of Programmable Luminescent Tags reveals Planar Oxygen Diffusion Properties in Polymer Films — •RICHARD KANTELBERG, TIM ACHENBACH, ANTON KIRCH, and SEBASTIAN REINEKE — Dresden Integrated Center for Applied Physics and Photonic Materials (IAPP) and Institute for Applied Physics, Technische Universität Dresden, Germany

Programmable Luminescent Tags based on oxygen quenched organic room temperature phosphorescence show application potential in UV sensing and rewritable labelling. This work demonstrates, that the concept can also be exploited to resolve oxygen diffusion properties in thin polymer films, which are essential in everyday applications from medical encapsulation to industrial packaging. In contrast to many established methods, the investigated principle comes without the need of complex pressure sensitive setups or vacuum technology and potentially allows high spatial accuracy. The time-resolved tracking of a two-dimensional phosphorescent pattern reveals the in-plane oxygen diffusion coefficient and considers the photoconsumption of oxygen during the measurement. The diffusion coefficients are determined at the representative case of polystyrene glasses with molecular weights between 13 000 and 350 000 g/mol.

CPP 28: Perovskite and Photovoltaics 3

Time: Wednesday 15:00–17:15

Location: H38

CPP 28.1 Wed 15:00 H38

Optically-Induced Long-lived Chirality Memory in the Color Tunable Chiral Lead-Free Semiconductor (R)/(S)-CHEA4Bi2BrxI10-x (x = 0 - 10) — •SHANGPU LIU¹, MARKUS HEINDL¹, NATALIE FEHN², SEBASTIAN CAICEDO-DÁVILA¹, SILVA KRONAWITTER², GREGOR KIESLICH², DAVID EGGER¹, ARAS KARTOUZIAN², and FELIX DESCHLER¹ — ¹Walter Schottky Institute and Department of Physics, TUM, Garching, Germany — ²Catalysis Research Center, TUM, Garching, Germany

Hybrid organic-Inorganic networks that incorporate chiral molecules have attracted great attention due to their potential in semiconductor lighting applications and optical communication. Here we introduce the chiral organic molecules (R/S)-CHEA into bismuth-based structures with an edge-sharing octahedral motif, to synthesize chiral (R/S)-CHEA4Bi2BrxI10-x crystals and thin films. Using single-crystal X-ray diffraction measurements and density-functional theory calculations, we identify crystal and electronic band structures. We investigate the material optical properties and find circular dichroism, which we tune by the bromide-iodide ratio over a wide wavelength range from 300-500 nm. Further, we employ transient absorption spectra and time-correlated single photon counting to investigate charge carrier dynamics, which show long-lived excitations with unexpected optically-induced chirality memory up to 10s of nanosecond timescales. Our demonstration of chirality memory in a color-tunable and chiral lead-free semiconductor opens a new avenue for the discovery of high-performance spintronic materials with optical functionalities.

CPP 28.2 Wed 15:15 H38

Time-Resolved Microwave Conductivity on ionic liquid doped Lead Halide Perovskites — •PATRICK DÖRFLINGER¹, VALENTIN SCHMID¹, YONG DING², MOHAMMAD KHAJA NAZEERUDDIN², and VLADIMIR DYAKONOV¹ — ¹Experimental Physics VI, Julius Maximilian University of Würzburg, 97074 Würzburg — ²Group for Molecular Engineering of Functional Materials, Institute of Chemical Sciences and Engineering, EPFL Valais, Sion 1950, Switzerland

In the past decade, perovskite solar cells evolved to one of the most promising photovoltaic materials with steadily rising power conversion efficiencies, now exceeding 25%. Nonetheless, Organolead Halide Perovskites suffer from insufficient long-term stability. Especially the stability under thermal stress is crucial towards commercialization. Ionic liquids as an additive into the precursor solution are candidates to overcome this issue. Besides the increased resistivity against higher temperatures, alterations of important material properties like mobility and lifetime are expected. Therefore, we used Time-Resolved Microwave Conductivity (TRMC) to determine the mobility and lifetime of photo-generated charge carriers in the perovskite layer. In addition, with Steady-State Microwave Conductivity (SSMC) we can provide insights into the predominant recombination pathways. Combined, we investigated the influence of the ionic liquids on the perovskite material properties and gain deeper understanding of the charge carrier dynamics.

CPP 28.3 Wed 15:30 H38

Hidden interfaces: How ferroelastic domain walls affect the charge diffusion in perovskite solar cells — •ILKA M. HERMES^{1,2}, ANDREAS BEST², KALOIAN KOYNOV², HANS-JÜRGEN BUTT², and STEFAN A. L. WEBER² — ¹Leibniz Institute for Polymer Research Dresden e.V., Dresden, Germany — ²Max Planck Institute for Polymer Research, Mainz, Germany

Ferroelastic domains form during phase transitions that change the crystal system. By arranging in domains with alternating unit cell orientation, the material lowers its overall strain. The walls that separate ferroelastic domains typically feature some structural anomalies, which can affect the electronic properties of the crystal by increasing the defect concentration, introducing dopants or forming a local electric polarization via the flexoelectric effect. Here, we explored the implications of ferroelastic domain walls for the photo-carrier transport in methylammonium lead iodide, a solar cell light absorber used in perovskite solar cells. Via correlative spatial and time-resolved photoluminescence microscopy and electromechanical atomic force microscopy, we could link the presence of domain walls to the occurrence of an anisotropic charge diffusion, where charges move faster parallel to domain walls than perpendicular. Moreover, the ferroelastic nature of the domains promises a targeted engineering of the domain wall arrangement using the application of external stress or heat treatments across the material's cubic-tetragonal phase transition: a perpendicular alignment of the domain walls with respect to the extraction layer interfaces should facilitate faster and more efficient charge extraction.

CPP 28.4 Wed 15:45 H38

Degradation mechanisms of perovskite solar cells under vacuum and one atmosphere of nitrogen — •RENJUN GUO¹, WEI CHEN¹, LENNART K. REB¹, MANUEL A. SCHEEL¹, MATTHIAS SCHWARTZKOPF², STEPHAN V. ROTH², and PETER MÜLLER-BUSCHBAUM¹ — ¹Technische Universität München, Garching, Germany — ²Deutsches Elektronen-Synchrotron, Hamburg, Germany

Extensive studies have focused on improving the operational stability of perovskite solar cells. Only a few studies survey the fundamental degradation mechanisms related to the device performance, and these studies were executed under various experimental conditions. Thus, we investigate the degradation mechanisms of high-efficiency perovskite solar cells under vacuum and a nitrogen atmosphere, as based on the International Summit on Organic Photovoltaic Stability protocols. We use synchrotron radiation-based operando grazing-incidence X-ray scattering methods. Unlike what was seen in previous reports, we find that the perovskite lattice can also experience a lattice shrinkage under operation. Moreover, we reveal that the atmosphere has a paramount influence on phase segregation, lattice distortion, and morphology deformation during operation of mixed cation lead mixed halide perovskite solar cells. This, in turn, degrades the performance of the respective perovskite solar cells. Our discoveries emphasize the importance of different types of inert atmospheres as critical parameters, which must be considered in future scientific studies and the industrial screening of longevity for photovoltaic modules.

CPP 28.5 Wed 16:00 H38

Determination of the Optimum Dead Area Width of Laser-Patterned, Series-Interconnected Perovskite Solar Cells — •NICOLAS OTTO¹, CHRISTOF SCHULTZ¹, GUILLERMO FARIAS BASULTO², JANARDAN DAGAR³, MARKUS FENSKE¹, RUTGER SCHLATMANN^{1,2}, EVA UNGER³, and BERT STEGEMANN¹ — ¹HTW Berlin - University of Applied Sciences, Wilhelminenhofstr. 75A, D-12459 Berlin — ²HZB für Materialien und Energie, PVcomB, Schwarzschildstr. 3, D-12489 Berlin — ³HZB für Materialien und Energie, Young Investigator Group Hybrid Materials Formation and Scaling, Kekuléstraße 5, D-12489 Berlin, Germany

Based on recent work on minimizing the interconnection width of laser patterned perovskite solar cells the optimum dead area width was determined. In order to use the largest possible aperture area, the dead area width should be as small as possible while still providing full electrical functionality. For this purpose the width between the P2 and the P3 scribes was varied ranging from overlapping to patterning with safety area. By also reducing the P1/P2 spacing an optimum dead area width can be achieved. The detailed scribe line characterization was done by optical microscopy imaging, electrical j-V measurements and compositional analyses. Minimodules with three in series connected cells were then produced. The results show that overlapping scribe lines as well as included safety areas cause avoidable electrical losses. Consequently, an optimum is achieved for arranging the scribe lines as closely as possible. In our study an optimal scribe line width of about 230 micrometres was realized.

CPP 28.6 Wed 16:15 H38

Performance of Perovskite and Organic Solar Cells in Space — •LENNART REB¹, MICHAEL BÖHMER², BENJAMIN PREDSCHLY¹, SEBASTIAN GROTT¹, LUKAS SPANIER¹, CHRISTIAN WEINDL¹, GORAN IVANDEKIC¹, RENJUN GUO¹, CHRISTOPH DREISSIGACKER³, JÖRG DRESCHER³, ROMAN GERNHÄUSER², ANDREAS MEYER³, and PETER MÜLLER-BUSCHBAUM^{1,4} — ¹TU München, Physik-Department, Lehrstuhl für Funktionelle Materialien, Garching, Germany — ²TU München, Physik-Department, Zentrales Technologielabor, Garching, Germany — ³Deutsches Zentrum für Luft- und Raumfahrt (DLR), Institut für Materialphysik im Weltraum, Köln, Germany — ⁴Heinz Maier-Leibnitz-Zentrum, Garching, Germany

Perovskite and organic solar cells have become a hot research topic in the last few years. The lightweight thin-film solar cells exhibit an exceptional power per mass that exceeds their inorganic counterparts by magnitudes, particularly interesting for space applications. Recently, we launched perovskite and organic solar cells to space on a suborbital rocket flight for the first time [1, 2]. The perovskite and organic solar cells operate in space conditions and produce reasonable power per area of up to 14 and 7 mW cm⁻², respectively. Here we derive, with a detailed solar irradiation reconstruction, the irradiation-dependent solar cell performance parameter evolutions, and conclude the solar cell efficiency under strong AMO irradiation. [1] L. Reb et al., *Joule* 4, 1880-1892 (2020), doi.org/10.1016/j.joule.2020.07.004. [2] L. Reb et al., *Rev. Sci. Instrum.* 92 (2021), doi.org/10.1063/5.0047346.

15 min. break

CPP 28.7 Wed 16:45 H38

Quantum Efficiency Enhancement of Lead-Halide Perovskite Nanocrystal LEDs by Organic Lithium Salt Treatment — •ROSHINI JAYABALAN¹, TASSILO NAUJOKS¹, CHRISTOPHER KIRSCH², FENGSHUO ZU³, MUKUNDHA MANDAL⁴, JAN WAHL², MARTIN WAIBEL¹, ANDREAS OPITZ³, NORBERT KOCH^{3,5}, DENIS ANDRIENKO⁴, MARCUS SCHEELE², and WOLFGANG BRÜTTING¹ — ¹Universität Augsburg, 86135 Augsburg, Germany — ²Universität Tübingen, 72076 Tübingen, Germany — ³Institut für Physik & IRIS Adlershof, Humboldt-Universität zu Berlin, Germany — ⁴Max Planck Institut für Polymerforschung, 55128 Mainz, Germany — ⁵Helmholtz-Zentrum Berlin für Materialien und Energie GmbH, 12489 Berlin, Germany

Owing to large specific surface area in lead halide perovskite nanocrystals, surface passivation using ligands is crucial to attain high photoluminescent quantum yield (PLQY). With respect to device fabrication, such passivation methods must also enable balanced charge injection to achieve high efficiency and operational stability. In this regard, this talk will discuss on the results of post-passivation treatment of CsPbBr₃ nanocrystals with LiTFSI, an organic lithium salt. The results from such treatment have proven to be propitious for the nanocrystals - yielding higher PLQY, longer exciton lifetime and improved light outcoupling. Consequently, a significant improvement is observed in the devices fabricated using such post post-treated nanoparticles. Lastly, photoelectron spectroscopy and density functional theory modelling is employed to understand the impact of LiTFSI post-treatment on the performance of a perovskite based LED.

CPP 28.8 Wed 17:00 H38

Tunable mesoporous and optoelectronics properties of zinc titanate films using sol-gel technique — •YANAN LI¹, NIAN LI¹, APOSTOLOS VAGIAS², and PETER MÜLLER-BUSCHBAUM¹ — ¹Physics Department, Technical University of Munich, 85748 Garching, Germany — ²Heinz Maier-Leibnitz Zentrum (MLZ), Technische Universität München, 85748 Garching, Germany

Mesoporous films consisting of zinc titanate have high potential applications in photocatalysis, solar cells, and sensors due to tailoring their semiconductive properties. In the present work, we investigate the morphologies of mesoporous zinc titanate films obtained by changing the ratio of two inorganic precursors after calcining hybrid films consisting of organic-inorganic materials. The amphiphilic diblock copolymer poly(styrene)-*b*-poly(ethyleneoxide) PS-*b*-PEO self-assembles into core-shell micelles in a mixture of N,N-dimethylformamid/hydrogen chloride playing the role as structure directing template. The inorganic precursors, zinc acetate dehydrate and titanium tetraisopropoxide, are loaded in the micellar shell due to hydrogen bonds between PEO and precursors. We use slot-die and spin-coating methods to prepare hybrid films, and investigate the influence of the different deposition methods on the film morphologies. Moreover, we investigate how mesoporous structures and crystal phases depend on calcination temperatures. The morphologies of the hybrid films are characterized using grazing incidence small-angle X-ray scattering (GISAXS) and scanning electronic microscopy (SEM).

CPP 29: Biomaterials (joint session BP/CPP)

Time: Wednesday 15:00–17:30

Location: H15

See BP 18 for details of this session.

CPP 30: 2D Materials 7 (joint session DS/CPP)

Time: Wednesday 15:00–16:00

Location: H17

See DS 19 for details of this session.

CPP 31: Active Matter 4 (joint session DY/BP/CPP)

Time: Wednesday 15:00–17:30

Location: H18

See DY 31 for details of this session.

CPP 32: Perovskite and Photovoltaics 4 (joint session HL/CPP/KFM)

Time: Wednesday 15:00–18:15

Location: H34

See HL 23 for details of this session.

CPP 33: Focus Session: Soft Matter and Nanocomposites: New Opportunities with Advanced Neutron Sources 1

organized by Stephan Förster (FZ Jülich), Thomas Gutberlet (FZ Jülich), Peter Müller-Buschbaum (TUM) and Walter Richtering (RWTH Aachen)

Time: Thursday 9:30–11:15

Location: H38

Invited Talk

CPP 33.1 Thu 9:30 H38

Cooperative and non-Gaussian dynamics of entanglement strands in polymer melts — •MARGARITA KRUTEVA¹, MICHAELA ZAMPONI², INGO HOFFMANN³, JÜRGEN ALLGAIER¹, LUTZ WILLNER¹, ANDREAS WISCHNEWSKI¹, MICHAEL MONKENBUSCH¹, and DIETER RICHTER¹ — ¹Forschungszentrum Jülich GmbH, Jülich Centre for Neutron Science (JCNS-1: Neutron Scattering and Biological Matter), 52425 Jülich, Germany — ²Forschungszentrum Jülich GmbH, Jülich Centre for Neutron Science at MLZ, Lichtenbergstraße 1, 85748 Garching, Germany — ³Institut Laue-Langevin (ILL), B.P. 156, F-38042 Grenoble Cedex 9, France

We report neutron spin echo investigations on the motion of short tracer chains in highly entangled melts [1,2]. The tracers were found to undergo sub-diffusion behavior. Unexpectedly the sub-diffusion is limited by a distance very close to the tube diameter of the respective highly entangled host. The cross-over distance to Fickian diffusion, thereby, is independent of the tracer's length. The Fickian

diffusivity agreed with the macroscopic results. We found that the Rouse dynamics of the tracers is strongly non-Gaussian with a related segment displacement distribution narrower than the Gaussian counterpart. These results were understood as a consequence of highly cooperative motion of the tracers with the host that mirrors the host dynamics within the tube. The phenomena were found both in a polyolefin (polyethylene) as well as in a polyether (polyethylene-oxide) indicating their generality. (1) Zamponi, M. et al. Phys. Rev. Lett. 2021, 126 (18), 187801. (2) Kruteva, M. et al. Macromolecules 2021, accepted.

CPP 33.2 Thu 10:00 H38

Molecular weight dependent dynamics of polymers grafted on nanoparticles. — •AAKASH SHARMA¹, MARGARITA KRUTEVA¹, MICHAELA ZAMPONI², SASCHA EHLERT¹, DIETER RICHTER¹, and STEPHAN FÖRSTER¹ — ¹Forschungszentrum Jülich GmbH, Jülich Centre for Neutron Science (JCNS-1: Neutron Scattering and Biological Matter), 52425 Jülich, Germany — ²Forschungszentrum Jülich

GmbH, Jülich Centre for Neutron Science at MLZ, Lichtenbergstraße 1, 85748 Garching, Germany

Grafting polymer chains on nanoparticles prevents their undesired aggregation leading to improved properties. Whereas, grafting induces inevitable alteration in the dynamics of polymer chains, which affects macroscopic properties e.g. viscoelasticity. It has been established that the polymer chain dynamics is retarded in grafted chains. However, literature lacks consensus on whether the segmental dynamics of grafted chains is accelerated or retarded. We study the segmental dynamics of polyisoprene grafted on spherical nanoparticles using neutron backscattering. The analysis of relaxation times led to the conclusions: (i) Low molecular weight (MW) grafted polymer display reduced local relaxation (ii) At high MW and equal grafting density faster segmental dynamics than the free polymer is observed. We prove that these conflicting results are seemingly artifacts of the traditional analysis method. We invoke an elegant methodology and show that the underlying physics of grafted polymer is unchanged. However, spatial variation of the relaxation times across the grafted chain causes the average dynamics to transition with molecular weight.

CPP 33.3 Thu 10:15 H38

Structure and Dynamics of Polymer Brushes and Microgels at Interfaces measured with Neutron Scattering — •OLAF HOLDERER¹ and STEFAN WELLERT² — ¹Jülich Centre for Neutron Science at MLZ, Forschungszentrum Jülich GmbH, 85748 Garching, Germany — ²Department of Chemistry, Technische Universität Berlin, 10623 Berlin, Germany

It is an experimental challenge to access structural and dynamic properties of brushes and microgels at the solid liquid interface [1]. Neutron scattering techniques such as Grazing Incidence Small Angle Neutron Scattering (GISANS) for structural investigations and Grazing Incidence Neutron Spin Echo Spectroscopy (GINSES) provide a means of studying structural and dynamic properties on molecular length scales at the interface. Simulations of the experimental conditions in the framework of the Distorted Wave Born Approximation help interpreting the static and dynamic scattering signals [2]. Examples of thermoresponsive microgels with different architecture and brushes at the interface are presented to illustrate the possibilities and challenges of this type of interface studies.

[1] J. Witte, T. Kyrey, J. Lurtzki, A.M. Dahl, M. Kühnhammer, R. von Klitzing, O. Holderer, S. Wellert, ACS Appl. Polym. Mater. 2021, 3, 2, 976-985

[2] T. Kyrey, M. Ganeva, J. Witte, R. von Klitzing, S. Wellert, O. Holderer, J. Appl. Cryst. (2021) 54, 72-79

CPP 33.4 Thu 10:30 H38

In-situ neutron reflectometry measurements of polyelectrolyte diffusion in Layer-by-Layer films in aqueous solution at ILL — •ANNEKATRIN SILL¹, HEIKO AHRENS¹, OLAF SOLTWEDEL², PHILIPP GUTFREUND³, and CHRISTIANE A. HELM¹ — ¹University of Greifswald, Institute of Physics, D-17489 Greifswald, Germany — ²Technische Universität Darmstadt, Institute for Condensed Matter Physics, D-64289 Darmstadt, Germany — ³Institut Laue-Langevin, F-38042 Grenoble, France

Up to now, we measured vertical polyelectrolyte diffusion in Layer-by-Layer films by immersing the film for a defined amount of time in the annealing solution. Then the film was dried, and a snapshot was taken. With the snapshot method, one can get good results, but we wanted to develop an improved method. For the first time, the dynamics of our films were studied in-situ at the

Institut Laue-Langevin (ILL) on instrument D17. This neutron reflectometer with horizontal scattering geometry is suitable for in-situ measurements, using wavelengths from 2 to 27 Å with great flexibility in resolution. We used the slab architecture with selective polyanion deuteration to study vertical polyanion diffusion. As polycation linear PDADMA was used, PSS/PSSd was the polyanion. Each film consisted of a protonated and a deuterated slab. Varied were the salt concentration and the temperature of the annealing solution. The diffusion constant was determined and compared to the snapshot measurements in air.

CPP 33.5 Thu 10:45 H38

Kinetics of mesoglobule formation and dissolution in solutions of thermoresponsive polymers after fast pressure jumps — BART-JAN NIEBUUR¹, LEONARDO CHIAPPISI², ALFONS SCHULTE³, and •CHRISTINE M. PAPADAKIS¹ — ¹Technical University of Munich, Physics Department, Garching, Germany — ²Institut Laue-Langevin, Grenoble, France — ³University of Central Florida, Department of Physics and College of Optics and Photonics, Orlando FL, U.S.A.

The thermoresponsive polymer poly(*N*-isopropylacrylamide) (PNIPAM) features lower critical solution temperature behavior in aqueous solution with the cloud point depending on pressure [1]. Fast pressure jumps across the coexistence line in combination with time-resolved small-angle neutron scattering elucidate the pathways of mesoglobule formation and disintegration over a wide range of length scales with a time resolution of 50 milliseconds. Varying the start and target pressures gives insight into the role of thermodynamic and kinetic factors governing mesoglobule formation [2,3]. For disintegration, the osmotic pressure of the solvent within the mesoglobules is the decisive factor for the mechanism and the time scales [4]. These results are of importance for applications of thermoresponsive polymers as switches. 1. B.-J. Niebuur et al., ACS Macro Lett. 6, 1180 (2017). 2. B.-J. Niebuur et al., ACS Macro Lett. 7, 1155 (2018). 3. B.-J. Niebuur et al., Macromolecules 52, 6416 (2019). 4. B.-J. Niebuur et al., RSC Nanoscale 13, 13421 (2021).

CPP 33.6 Thu 11:00 H38

Simultaneous SAXS/SANS method: A novel nanoanalytical tool — •EZZELDIN METWALLI¹, KLAUS GÖTZ¹, TOBIAS ZECH¹, CHRISTIAN BÄR¹, ANNE MARTEL², LIONEL PORCAR², and TOBIAS UNRUH¹ — ¹Institute for Crystallography and Structural Physics (ICSP), Friedrich-Alexander-Universität Erlangen-Nürnberg, Staudtstr. 3, 91058 Erlangen, Germany — ²Institut Laue-Langevin, 71, Avenue des Martyrs, Grenoble, 38042, France

Exploiting X-ray and neutron beams at the same sample volume enables unprecedented investigations of nanomaterials using small angle scattering (SAS) technique. A portable small angle X-ray scattering (SAXS) instrument with a proper geometrical dimension was successfully designed, constructed and implemented at D22 zone of Institut Laue Langevin (ILL) in France for simultaneous SAXS/SANS experiments. Compared with an independent experimental approach, the simultaneous SAXS/SANS experimental approach ensures the exactness of the probed samples, especially for time-resolved studies. The SAXS/SANS experimental setup will indispensably permit to instantaneously analyse and understand the complicated correlated nanostructures of two different types of nanoscale components in the same sample volume. For instance, a temporal structural cross-correlation between organic stabilizing agent (cetyltrimethylammonium bromide; CTAB micelles) and gold seeds, which cooperate in the formation of different size/shape of large stabilized gold nanorods during the synthesis process [1] was successfully probed. [1] T. Zech, et al., Part Part Syst Charact, 39, 2100172, 2022.

CPP 34: Hydrogels and Microgels

Time: Thursday 9:30–10:15

Location: H39

CPP 34.1 Thu 9:30 H39

Simulations explain the Swelling Behavior of Hydrogels with Alternating Neutral and Weakly Acidic Blocks — •DAVID BEYER¹, PETER KOŠOVAN², and CHRISTIAN HOLM¹ — ¹Institute for Computational Physics, University of Stuttgart, D-70569 Stuttgart, Germany — ²Department of Physical and Macromolecular Chemistry, Charles University, Prague, Czechia

We use computer simulations to study a coarse-grained model of a weak (pH-responsive) polyelectrolyte hydrogel which consists of a covalent, regular tetrafunctional network of four-armed neutral and acidic stars, coupled to a reservoir of small ions. A similar system consisting of tetrapoly-(acrylic acid) and tetrapoly(ethylene glycol) was recently investigated experimentally by the Sakai group. To model the ionization equilibrium of the weak groups and the exchange of small ions with the reservoir, we make use of the recently developed Grand-Reaction Monte-Carlo method (G-RxMC). We determine the free swelling equilibrium for different salt concentrations and pH values of the reservoir. The results for the swelling ratio are in good agreement with the experimental data for high and intermediate pH values. We obtain titration curves which display a sig-

nificant deviation from the ideal Henderson-Hasselbalch equation due to charge correlations and Donnan partitioning. Contrary to a previous conjecture, our results show that counterion condensation does not explain the observed swelling behavior. Finally, we investigate the gel structure and observe that the swelling is dominated by the stretching of the acidic blocks.

CPP 34.2 Thu 9:45 H39

Importance of pH in Synthesis of pH-Responsive Cationic Nano- and Microgels — •MARCO ANNEGARN, MAXIM DIRKSEN, and THOMAS HELLWEG — Department of Physical and Biophysical Chemistry, Bielefeld University, Universitätsstraße 25, 33615 Bielefeld, Germany

While cationic nano- and microgels are potentially useful for transfection of cells or the immobilization of biomacromolecules, their synthesis often has certain drawbacks regarding size, polydispersity, yield and incorporation of the cationic comonomer. Since many cationic comonomers like primary or secondary amines are pH-responsive, their charge relies on the surrounding pH. Therefore, a range of poly(*N*-isopropylacrylamide) (PNIPAM) microgels with

the primary amine *N*-(3-aminopropyl)methacrylamide hydrochloride (APMH) as the cationic comonomer were synthesized at different reaction pH. The microgels were analyzed with respect to their size, thermoresponsive swelling behavior, synthesis yield, polydispersity and APMH-incorporation.

The results show that the reaction pH has a strong influence on all the mentioned parameters and can be utilized to tailor the microgels properties. While the influence of the pH on such microgels has been examined repeatedly after synthesis, the influence of the reaction pH during synthesis is mostly ignored. Hence, a precise pH-control during the synthesis of microgels with pH-responsive moieties is crucial to gain reproducible and comparable results.

CPP 34.3 Thu 10:00 H39

Behaviour of a magnetic nanogel in a shear flow — •IVAN NOVIKAU¹, EKATERINA NOVAK², ELENA PYANZINA², and SOFIA KANTOROVICH^{1,2} — ¹University of Vienna, Austria — ²Russia

Magnetic nanogels (MNG) are promising magneto-controllable drug carriers. In order to develop this potential, one needs to study MNG's behavior in various

microfluidic systems, one of which can be modelled as a channel with a given flow.

Considering the size of the MNG and typical time and velocity scales involved in their nanofluidics, experimental characterisation of the system is challenging. In this work, we perform molecular dynamics (MD) simulations combined with the Lattice-Boltzmann (LB) scheme aiming at describing the impact of the shear rate on the shape, magnetic structure and motion of an MNG.

We find that in a shear flow, the centre of mass of an MNG tends to be in the centre of a channel and to move, preserving the distance to both walls. The MNG monomers along with translation are involved in two more types of motion, they rotate around the centre of mass and oscillate with respect to the latter. It results in synchronised tumbling and wobbling of the whole MNG accompanied by its volume oscillates. We show that the volume oscillations and rotations are two faces of the same periodic process whose frequency is a growing function of the shear rate and depends on strength of magnetic interaction between magnetic nanoparticles. We demonstrate that the oscillations of the volume lead to the periodic changes in MNG magnetic energy.

CPP 35: 2D Materials 8 (joint session DS/CPP)

Time: Thursday 9:30–11:30

Location: H17

See DS 22 for details of this session.

CPP 36: Complex Fluids and Soft Matter 2 (joint session DY/CPP)

Time: Thursday 10:00–11:30

Location: H18

See DY 38 for details of this session.

CPP 37: Interfaces and Thin Films and Responsive and Adaptive Systems

Time: Thursday 10:30–13:00

Location: H39

Invited Talk

CPP 37.1 Thu 10:30 H39

Non-equilibrium Properties of Thin Polymer Films — •GÜNTER REITER¹ and SIVASURENDER CHANDRAN² — ¹Physikalisches Institut, Albert-Ludwigs Universität Freiburg — ²Department of Physics, Indian Institute of Technology Kanpur, Uttar Pradesh 208016, India

Rapid industrial processes often freeze polymers in non-equilibrium conformations, which, in turn, cause material properties that are significantly different from the predictions of equilibrium theories. Thus, by choosing appropriate processing pathways, we potentially can control macroscopic properties and performance of polymers. However, due to our current lack of fundamental understanding of the behavior of non-equilibrated polymers, we have to rely on empirical knowledge, imposing trial-and-error approaches for achieving desired properties. Considering these aspects, we discuss recent studies on polymer films revealing that quantitative relations exist between properties and processing pathways, suggesting possible relations for processing-induced deviations in chain conformations. These relations propose that long-living and long-ranged correlations between polymers have been induced by processing, as indicated by the observation of relaxation times much longer than known for equilibrated polymers. We present an example where control of processing conditions for thin films allowed to translate the molecular relaxations during equilibration into a predictable lifting of macroscopic loads.

CPP 37.2 Thu 11:00 H39

Water Induced Polymer Reorientation at a Polystyrene/ Polyacrylic Acid Surface — XIAOMEI LI¹, MIRELA ENCHEVA², KALOIAN KOYNOV¹, HANS-JÜRGEN BUTT¹, ELLEN BACKUS², and •RÜDIGER BERGER¹ — ¹Max Planck Institute for Polymer Research, 55128 Mainz, Germany — ²University of Vienna, Währinger Straße 42, 1090 Vienna, Austria

Polymers are capable of undergoing adaptation phenomena triggered by exposure to liquids. Here we study the adaptation of copolymer films formed by polystyrene and polyacrylic acid (PS/PAA) after water exposure. We measured the dynamic advancing and receding contact angles (CA) of water drops sliding down a PS/PAA film. We associate the gradual increase in advancing CA with drop velocity to the adaptation process to water. By applying adaptation theory, we estimated the time constant of this adaptation process to be much smaller than 1 s. The changes in contact angles may be caused by swelling of the copolymer and/or by a reorientation of the hydrophilic segments (PAA) towards the surface. Therefore, we performed vibrational sum frequency generation (SFG) spectroscopy which is surface sensitive. SFG experiments before and after exposing the copolymer to water reveal a decrease in intensity of the vibrational band representing the PS segments, suggesting a reorientation of the polymer groups at the surface upon contact with water.

15 min. break

CPP 37.3 Thu 11:30 H39

Tailoring the Optical Properties of Sputter-Deposited Gold Nanostructures on Nanostructured TiO₂ Templates based on in situ GISAXS Determined Growth Laws — •SUZHE LIANG¹, WEI CHEN¹, SHANSHAN YIN¹, SIMON J. SCHAPER¹, JONAS DREWES², NIKO CARSTENS², THOMAS STRUNSKUS², FRANZ FAUPEL², MARC GENSCH^{1,3}, MATTHIAS SCHWARTZKOPF³, STENPHAN V. ROTH^{3,4}, YA-JUN CHENG⁵, and PETER MÜLLER-BUSCHBAUM^{1,6} — ¹TU München, Physik-Department, LS Funktionelle Materialien, 85748 Garching — ²LS Materialverbunde, Institut für Materialwissenschaft, CAU, 24143 Kiel — ³DESY, 22607 Hamburg — ⁴Department of Fibre and Polymer Technology, KTH, SE-100 44 Stockholm, Sweden — ⁵NIMTE, CAS, 315201 Ningbo, China — ⁶MLZ, TU München, 85748 Garching

Au/TiO₂ nanohybrid materials have attracted significant attention due to the outstanding optical, photocatalytic and photovoltaic performance. We use customized polymer templating to achieve TiO₂ nanostructures with different morphologies. Au/TiO₂ hybrid thin films are fabricated by sputter deposition, meanwhile in situ GISAXS during the deposition process is applied to in-depth understand the Au morphology on the TiO₂ templates. The resulting Au nanostructure is largely influenced by the TiO₂ template morphology. Based on the detailed understanding of the Au growth process, characteristic distances can be selected to achieve tailored Au nanostructures at different Au loadings. For selected sputter-deposited Au/TiO₂ hybrid thin films, the optical response with a tailored localized surface plasmon resonance is demonstrated.

CPP 37.4 Thu 11:45 H39

Investigations of ultra-thin film behavior of polycarbonate on inorganic surfaces — •HASSAN OMAR, PAULINA SZYMONIAK, and ANDREAS SCHÖNHALS — Bundesanstalt für Materialforschung und -prüfung (BAM), Berlin, Germany

Thin polymer films are of vital importance due to their low production costs and wide range of applications in sensors, electronics, and coatings. Their geometry is ideal for the study of confinement effects on the thermodynamic properties and segmental dynamics of polymers. However, there is little research into these effects for main chain polymers such as polycarbonate (PC). PC has important applications due to its improved mechanical, optical, and thermal stability compared to other polymers. For this investigation, films of PC ranging from 200 nm to 7 nm were prepared on both glass and silica substrates to measure the dielectric and calorimetric behavior. The methodology consisted of broadband dielectric spectroscopy (BDS), ellipsometry, atomic force microscopy (AFM), and sum frequency generation (SFG). Using ellipsometry, the glass transition was shown to increase with decreasing film thickness. This was further proved by BDS for

glassy dynamics for thin films employing different sample geometries (crossed electrode and nanostructured capacitors). The properties and influence of the adsorbed layer on the molecular mobility was also addressed by a combination of AFM, SFG and BDS.

CPP 37.5 Thu 12:00 H39

Fabrication and Characterization of Hydrophobic Porous Metallic Membranes for High-Temperature Applications — SARA CLARAMUNT¹, MUHAMMAD KHURRAM², WALTHER BENZINGER¹, MANFRED KRAUT¹, and ROLAND DITTMAYER¹ — ¹Institute for Micro Process Engineering, Karlsruhe Institute of Technology, 76131 Karlsruhe, Germany — ²Institute for Physics, University of Greifswald, 17489 Greifswald, Germany

Hydrophobic porous metallic membranes can be integrated into a microreactor for in-situ separation of steam at high temperatures. This study investigates the fabrication and characterization of hydrophobic coatings on metallic substrates. Two different coating methods were explored: (1) plasma enhanced-chemical vapor deposition to form amorphous carbon silicon-doped a-C:H:Si:O thin films and (2) direct immersion in fluoroalkyl silane (FAS-13) solution using dip coating to form self-assembled monolayers. The results on wettability as well as SEM images and Energy Dispersive Spectroscopy/Wavelength Depressive Spectroscopy analyses indicate that the coated sintered stainless-steel membranes are adequate as hydrophobic surfaces, maintaining the porosity of the substrate and withstanding high temperatures. Especially the FAS-13 coating shows very good resistance to temperatures higher than 250°C. These findings are of special significance for the fabrication of porous metal membranes for the separation of steam in high-temperature applications.

CPP 37.6 Thu 12:15 H39

Superlattice deformation via uniaxial strain and its impact on photoluminescence in PbS quantum dot thin films — JULIAN E. HEGER¹, WEI CHEN¹, HUAYING ZHONG¹, TIANXIAO XIAO¹, CONSTANTIN HARDER^{1,2}, FABIAN A. C. APFELBECK¹, ALEXANDER WEINZIERL¹, REGINE BOLDT³, LUCAS SCHRAA³, ERIC EUCHLER³, ANNA K. SAMBALE³, KONRAD SCHNEIDER³, MATTHIAS SCHWARTZKOPF², STEPHAN V. ROTH^{2,4}, and PETER MÜLLER-BUSCHBAUM^{1,5} — ¹TU München, Physik-Department, LS Funktionelle Materialien, 85748 Garching — ²DESY, 22607 Hamburg — ³Leibniz-Institut für Polymerforschung IPFDD, 01069 Dresden — ⁴Royal Institute of Technology KTH, 100 44 Stockholm — ⁵MLZ, TU München, 85748 Garching

Colloidal lead sulfide quantum dots (PbS CQDs) show high potential for the application in flexible electronics, as they are solution processible with tunable optoelectronic properties. In thin films, PbS CQDs form a superlattice morphology that tailors these optoelectronic properties. For instance, electronic coupling between adjacent PbS CQDs is dependent on the inter-dot distance in the superlattice. In this work, we investigate the superlattice deformation during applied

external strain. For this, PbS CQDs thin films are prepared on flexible PDMS substrates. The samples are investigated with in situ GISAXS and photoluminescence measurements at different levels of strain to correlate the deformation-induced morphological changes to the optoelectronic performance.

CPP 37.7 Thu 12:30 H39

The surface of electrolyte solutions is stratified — YAIR LITMAN, KUO-YANG CHIANG, TAKAKAZU SEKI, YUKI NAGATA, and MISCHA BONN — MPI for Polymer Research, Mainz, Germany.

The electrical-double layer (EDL) model has been used during the last two decades to describe the behaviour of ions at the water/air interface, and also as a framework to analyze and interpret several types of surface-selective experimental measurements. In this work, we present a combination of surface-sensitive heterodyne-detected vibrational sum frequency generation (VSFG) and *ab initio* based molecular dynamics simulations to study the liquid/air interface of different aqueous electrolyte solutions. Our VSFG measurements clearly demonstrate that the EDL model is an incomplete microscopic picture to understand the interface of NaCl, NaBr and NaCl aqueous solutions and it is completely inappropriate for the NaOH and CsF cases. Based on our simulations, we propose that the surface of electrolyte solutions is stratified into two water layers, one depleted and the other enriched with ions, creating an effective liquid-liquid interface buried a few Å inside the solution.

CPP 37.8 Thu 12:45 H39

A purely ionic voltage effect soft triode — ELALYAA MOHAMED, SABINE JOSTEN, and FRANK MARLOW — Kaiser-Wilhelm-Platz 1, 45470 Mülheim an der Ruhr
Iontronics is a concept of connecting ionic transport, storage and reactions with electronics. As ions are the language of nature and electrons are the language of man-made information processing, connecting both may lead to more understanding of nature as well as to new computational systems which might be called neuromorphic. In the last decade, many iontronic devices were invented and studied. However, developing of iontronics requires the invention of more flexible devices. In our lab we developed a purely ionic voltage effect soft triode (IVEST) based on interfacial ion adsorption and redox oxidizer depletion. The IVEST was built with no need of sophisticated or expensive materials. This device is an electrochemical micro-cell, which consists of a top electrode and two bottom electrodes. The basic idea of this device is to control the concentration and diffusion of ions by the voltage applied on the top electrode. In different electrical circuit configurations, it can show amplification or memory effects. The device had an electrical current amplification reaching 52 and memory effects in the electrical resistance lasting for up to 6 h. These values were achieved by tuning an electrode interface, the electrolyte and diffusion properties. They might be promising for neuromorphic applications.

CPP 38: 2D Materials 9 (joint session HL/CPP/DS)

Time: Thursday 11:15–12:15

Location: H36

See HL 31 for details of this session.

CPP 39: Molecular Electronics and Excited State Properties

Time: Thursday 11:30–13:00

Location: H38

CPP 39.1 Thu 11:30 H38

Fluorinated Acenes: Controlling Molecular Electronic Levels, Crystalline Phases and Optoelectronic Properties — DANIEL BISCHOF¹, PHILIPP E. HOFMANN², MATTHIAS W. TRIPP², MARC ZEPLICHAL³, SEBASTIAN ANHÄUSER¹, TOBIAS BREUER¹, SERGEI I. IVLEV², MARINA GERHARD¹, ANDREAS TERFORT³, ULRICH KOERT², and GREGOR WITTE¹ — ¹Fachbereich Physik, Philipps-Universität Marburg — ²Fachbereich Chemie, Philipps-Universität Marburg — ³Goethe Universität Frankfurt

Acenes serve as prototypical molecular materials to study structure-property relationships. Here, we systematically analyze the influence of the acene length and the degree of fluorination on their structure and optoelectronic properties [1-3]. Our results show that the optical gap decreases with increasing acene length, while the degree of fluorination determines the precise energy levels of the frontier orbitals HOMO and LUMO, whereas the optical gap is barely affected upon fluorination. Partial fluorination also influences the molecular electrostatic potential (MEP) and leads to a change in the molecular packing from herringbone packing for pristine and perfluorinated acenes to a planar stacking motif. These structural changes also affect the photoluminescence properties and induce a red-shifted PL for the stacked molecules due to excimer formation. The presented insights are not limited to acenes, but can be extended to other π -conjugated systems.

[1] P. E. Hofmann, et al. *Angew. Chem. Int. Ed.* 59, 16501 (2020).

[2] D. Bischof et al. *J. Phys. Chem. C* 125, 19000 (2021).

[3] D. Bischof et al. *Chem. Eur. J.* 28, e202103653 (2022).

CPP 39.2 Thu 11:45 H38

Time-resolved spectroscopy study of the dynamics of charge transfer processes in strongly interacting organic donor/acceptor compounds — NICO HOFEDITZ¹, CHRISTOPH P. THEURER², JULIAN HAUSCH², KATHARINA BROCH², WOLFRAM HEIMBRODT¹, and MARINA GERHARD¹ — ¹Department of Physics, Philipps-Universität Marburg, Germany — ²Institut für Angewandte Physik, Universität Tübingen, Germany

Doping of organic semiconductors with strong acceptor molecules is an effective way to tailor their electronic properties. Here, we investigate the photoexcitation dynamics of blends of tetracene and the strong acceptor F4-TCNQ to better understand how acceptors alter the transport of charge carriers and excitons. The mixtures feature a phase of relatively pure tetracene as well as an intimately mixed phase. In the mixed phase donor and acceptor molecules for charge transfer complexes that efficiently quench excitons from the pure phases. That leads to faster photoluminescence dynamics in the blends with respect to neat tetracene. We investigate the low temperature photoluminescence through global analysis and find constrained dynamics in the blends which we attribute to localization effects and energetic disorder in the tetracene domains.

CPP 39.3 Thu 12:00 H38

Ultrafast excited states dynamics of two orthogonal molecular photoswitches — •TANJA SCHMITT¹, LI-YUN HSU², EVA BLASCO², and PETRA TEGEDER¹ — ¹Physical Chemistry, Ruprecht-Karls-Universität Heidelberg — ²Organic Chemistry, Ruprecht-Karls-Universität Heidelberg

Molecular photoswitches are widely used in physics, chemistry, biology and material sciences. The use of multiple photoswitches at one time opens diverse opportunities for further improved and more complicated systems. This requires orthogonal addressability of the photoswitches and ideally reversible processes. Herein, we report a mixture of two reversible and orthogonal photoswitches which could potentially be used in four-dimensional printing. We report the first study of their ultrafast excited state dynamics when they are addressed orthogonally as well as simultaneously to gain insight in their interaction. In addition, the environmental influence of the excited state dynamics of the orthogonal photoswitches is examined using different solvents as well as films.

CPP 39.4 Thu 12:15 H38

Charge Transfer and Singlet Fission in Pentacene/Acceptor thin films — •MARTIN RICHTER¹, CHRISTOPH THEURER², DEBKUMAR RANA^{1,3}, KATHARINA BROCH², and PETRA TEGEDER^{1,3} — ¹Physikalisch-Chemisches Institut, Universität Heidelberg, Im Neuenheimer Feld 253/229, 69120 Heidelberg, Germany — ²Institut für Angewandte Physik, Universität Tübingen, Auf der Morgenstelle 10, 72076 Tübingen, Germany — ³Centre for Advanced Materials, Universität Heidelberg, Im Neuenheimer Feld 225, 69120 Heidelberg, Germany

Singlet fission (SF) is a process where a singlet excited state is converted into two triplet excited states. Since SF is exothermic in pentacene (PEN), it is an excellent material to investigate charge transfer (CT) interactions with electron acceptors. Here, stacked bi-layers of PEN either with 2,3,5,6-tetrafluoro-7,7,8,8-tetracyanoquinodimethane (F4-TCNQ) or 2,2'-(perfluoronaphthalene-2,6-diylidene)dimalononitrile (F6-TCNNQ) were investigated with transient absorption spectroscopy. The experiments show formation of triplet pairs, due to the SF process with a slightly slower time constant compared to the pure PEN. Subsequently a separation of the correlated triplet pair can be observed, a process that has been identified also in PEN thin films. A drastic reduction of the triplet lifetime is extracted with both acceptors. Further, evidence for diffusion of excitons to the interface followed by charge formation is found for layers with F4-TCNQ, supported by the shifting of an absorption band, caused by electric fields.

CPP 39.5 Thu 12:30 H38

Understanding charge transfer excitations in Bacteriochlorophyll dimers from first principles — •ZOHREH HASHEMI¹, MATTHIAS KNODT¹, and LINN LEPPERT^{1,2} — ¹Institute of Physics, University of Bayreuth, Germany — ²MESA+ Institute for Nanotechnology, University of Twente, Netherlands

Bacteriochlorophyll (BCL) molecules are the main pigments driving the primary excitation and charge transfer processes in photosynthetic bacteria. They are organized in highly coordinated multichromophoric complexes, embedded in protein, guaranteeing an efficient transfer of excitation energy from the light harvesting antennae to the reaction center where a charge transfer excitation triggers. In this contribution we focus on the electronic and excited state structure of BCL monomers and dimers found in the reaction center and light harvesting apparatus of the purple bacterium *Rhodobacter sphaeroides*. We assess the accuracy of ab initio GW+Bethe-Salpeter equation approach for BCL monomers considering a wide range of excitation energies, and find excellent agreement with experimental data and correlated wavefunction-based approaches. We also discuss notable differences to results from state-of-the-art time-dependent density functional theory, which can be traced back to the treatment of electron-hole interactions in both methods [1]. For dimeric systems we show that the energy and character of charge transfer excitations is strongly affected by distance and orientation of the BCL molecules, providing an intuitive understanding for the role of these excitations in different parts of the photosynthetic apparatus.

CPP 39.6 Thu 12:45 H38

Temperature Dependent Optical Transition in Zinc Phthalocyanine Single Crystals — •LISA SCHRAUT-MAY¹, SEBASTIAN HAMMER¹, KILIAN FRANK², BERT NICKEL², and JENS PFLAUM^{1,3} — ¹Experimental Physics VI, Julius Maximilian University, 97074 Würzburg — ²Department of Physics and Center for Nano Science, Ludwig Maximilian University, 80539 Munich — ³Bavarian Center for Applied Energy Research, 97074 Würzburg

By its various polymorphs, Zinc Phthalocyanine (ZnPc) serves as an excellent model system to study the interplay between molecular packing on microscopic length scales and the resulting photophysical properties [1]. Here, we address the dependence of the excitonic coupling on the underlying crystal structure of the thermodynamically stable ZnPc β -phase. For this purpose, we conducted complementary temperature dependent X-ray diffraction as well as polarisation dependent photoluminescence (PL) studies on ZnPc single crystals. By means of the PL signals spectral characteristics we observed a continuous transition from a J- into an H-aggregated state between 300 K and 100 K. Remarkably, below 100 K an exceptionally sharp PL peak evolves being indicative for the formation of a superradiant J-aggregate. As there is no indication for a discrete structural phase transition, we interpret the resulting PL signal in this temperature range by a model of vibronically coupled excitons steered by the gradual anisotropic thermal contraction of the crystal lattice [2]. We thank the Bavarian research network SolTech for financial support. [1] Hammer et al., Appl. Phys. Lett. (2019) [2] Hestand et al., Chem. Rev. (2018)

CPP 40: Organic Electronics and Photovoltaics 3

Time: Thursday 15:00–17:45

Location: H38

Invited Talk

CPP 40.1 Thu 15:00 H38

Computational Design of Organic Semiconductors — •HARALD OBERHOFER — Chair for Theoretical Physics VII, Universität Bayreuth — Chair for Theoretical Chemistry, Technische Universität München

Organic electronics—in the form of field effect transistors, light emitting diodes, or solar cells—are slowly finding their use in everyday consumer devices. To date, most of the employed materials have been discovered by structural tuning of a promising compound family, thereby relying on intuition, experience, or simply trial and error. While sometimes quite successful, such incremental changes only lead to a local exploration of the vast chemical space of possible molecules, potentially overlooking many interesting materials.

In contrast, modern data-driven strategies allow the extraction of general design rules through the systematic of the available design space. Often, these take the form of a computational funnel, where large databases are searched by computing relevant properties, so-called descriptors, for each element of the database. While this can point towards promising yet so-far overlooked theoretical and experimental design routes for organic electronics materials such an approach is limited by the employed database, not really allowing any insight beyond. Therefore, we trained machine-learned surrogate models for the most important organic semiconductor properties. These form the basis for an active machine learning scheme that allows us to sample the, in principle, unlimited space of organic molecules searching for materials not considered so far.

CPP 40.2 Thu 15:30 H38

Reorganization energies of flexible organic molecules as a challenging target for machine learning enhanced virtual screening — •KE CHEN^{1,2}, CHRISTIAN KUNKEL^{1,2}, KARSTEN REUTER^{1,2}, and JOHANNES T. MARGRAF^{1,2} — ¹Technische Universität München, Garching, Germany — ²Fritz-Haber-Institut der Max-Planck-Gesellschaft, Berlin, Germany

The molecular reorganization energy λ strongly influences the charge carrier mobility of organic semiconductors and is therefore an important target for molecular design. Machine learning (ML) has the potential to accelerate this process by providing accurate surrogate models in design space. Unfortunately, λ poses a significant challenge for ML-models as it simultaneously depends on the neutral and ionized potential energy surfaces of the molecule.

In this contribution, we address the questions of how ML models for λ can be improved and what their benefit is in high-throughput virtual screening (HTVS). We find that, while improved predictive accuracy with respect to a semi-empirical baseline model is achieved, the benefits for molecular discovery are actually somewhat marginal. In particular, ML-enhanced HTVS is more effective in identifying promising candidates but leads to a less diverse sample set.

CPP 40.3 Thu 15:45 H38

Protonation-Induced Charge Transfer and Polaron Formation in Organic Semiconductors Doped by Lewis Acids — •FABIAN BAUCH, CHUAN-DING DONG, and STEFAN SCHUMACHER — Physics Department and CeOPP, Paderborn University, Germany

Organic electronics rely crucially on doping to enhance the conductivity of organic semiconductors (OSC). Lewis acid doping of OSC is currently of great interest as an alternative to typical molecular p-type doping. Recently, the underlying process was understood to be based on the electron transfer (ET) from a neutral polymer to the protonated polymer [Nat. Mater. 18, 1327 (2019)]. In this work, we provide insight into the microscopic process by investigating the influence of protons on the electronic properties of the copolymer PCPDT-BT using DFT calculations. [1] We find that a single proton on the backbone can give rise to a polaron coupled to the proton position. Two protons on the same polymer backbone can induce a long range intrachain ET, resulting in a polaron

decoupled from the proton positions, more fit to act as charge carrier. We also demonstrate the possibility of ET between a neutral polymer and a doubly protonated polymer. The experimental data on the doping of PCPDT-BT via Lewis acid BCF agree well with our simulated vertical excitation spectra for an ensemble of protonated species with increasing amounts of protons. Our results highlight the important role of multiple protonation of the OSC backbone in completing the mechanistic picture of Lewis acid doping. [1] F. Bauch, C. Dong, and S. Schumacher, RSC Advances 12, 13999 (2022).

CPP 40.4 Thu 16:00 H38

Adsorption layers of diketopyrrolopyrrole acceptor blocks on graphite: Self-assembly and structure in all-atom modelling — MOUFDI HADJAB¹ and •OLGA GUSKOVA² — ¹Boudiaf University of M'Sila, 28000 M'Sila, Algeria — ²IPF Dresden, 01069 Dresden, Germany

In this computational work, we investigate the adsorption layers of electron-deficient N-unsubstituted difuran-diketopyrrolopyrroles (DPP). Three conformational states differing in the mutual orientation of the central DPP unit and furan flanks are distinguished: cis-cis, trans-trans, and cis-trans. The adsorption layers are obtained during in-silico self-assembly on graphite surface through intermolecular hydrogen bonding in all-atom MD simulations. The experimental process for the construction of the adsorption layers, called the droplet deposition technique, is reproduced in the modeling. In all simulated systems, the formation of stable supramolecular polymers is observed which build the ordered carpets on the surface. However, the binding energetics and strength and the type of hydrogen bonding are highly sensitive to the molecular conformation. We quantify each of these characteristics and provide a molecular picture of difuran-DPP layers relevant for organic field-effect transistor applications. OG thanks DFG (project GU1510/5-1) for financial support.

CPP 40.5 Thu 16:15 H38

Understanding Phonon Properties and the Thermal Conductivity of Crystalline Polymers — •LUKAS REICHT, LUKAS LEGENSTEIN, TOMAS KAMENCEK, SANDRO WIESER, and EGBERT ZOJER — Graz University of Technology, Austria
Disordered polymers are characterized by a very low thermal conductivity on the order of 0.1 W/mK. In contrast, recent studies have shown that aligned (crystalline) polymers can have thermal conductivities comparable to those of metals. Given these prospects, it is interesting to understand, how the thermal conductivity of a polymer depends on its chemical structure. A crucial step in that context is to investigate phonons and their influence on thermal transport. For simulating the phonons, we relied on density-functional theory (DFT) calculations combining phonopy and the Vienna Ab initio Simulation Package (VASP). In a second step, anharmonic force constants and thermal conductivities were calculated with phono3py and hiPhive. Additionally, we explored the capabilities of on-the-fly machine learned force fields (ML-FF), trained on DFT data, as implemented in VASP. These approaches were tested and benchmarked for polyethylene as a comparably simple model system. The final goal of our work is to then apply the above methodology to other polymers, systematically varying the structure of the backbone, thereby finding structure-to-property relations. These polymers include poly(p-phenylene), polythiophene, polyfuran, polysephenophene, poly(3-hexylthiophen-2,5-diyl) (P3HT) and Poly(p-phenylene vinylene) (PPV).

15 min. break

CPP 40.6 Thu 16:45 H38

Assessing Crystal Structure Prediction Based on Density Functional Tight Binding and Evolutionary Algorithms — •SEBASTIAN HUTSCH and FRANK ORTMANN — Department of Chemistry, Technical University of Munich

The prediction of crystal structures for organic molecules is a computationally expensive task due to the large number of atoms in the unit cell and the associated number of possible configurations. The computational load can be compensated by the use of classical force fields, which however lack transferability to new molecules and necessitate an extensive training for complex molecules. Here, we study an approach to crystal structure prediction based on evolutionary algorithms and a combination of Density Functional Tight Binding (DFTB) and Density Functional Theory (DFT). This combination allows us to efficiently compute crystal structures for new materials on a high level of accuracy. A compar-

ison of the calculated crystal structures with experimentally known structures will be made.

CPP 40.7 Thu 17:00 H38

Singlet Fission search in polyacene molecules in gas-phase and on rare-gas clusters using ab initio methods — •SELMANE FERCHANE¹, ALEXANDER EISEL², and MICHAEL WALTER^{1,3,4} — ¹Institute of Physics, University of Freiburg, Germany — ²Max Planck Institute for the Physics of Complex Systems, Dresden, Germany — ³FIT Freiburg Center for Interactive Materials and Bioinspired Technologies, University of Freiburg, Germany — ⁴Fraunhofer IWM, Freiburg, Germany

Singlet fission (SF), is a spontaneous photo-excited splitting phenomenon. Where an organic chromophore dimer, converts its singlet exciton into a pair of triplet excitons. A great promise for future photon-to-current conversion of solar energy using organic materials with high efficiency. To get more insight into these processes of SF, we employed different ab initio theories and approaches in our investigation, namely, density functional theory (DFT), TD-DFT, MCTDH, and CASPT2/CASSCF. Since the spatial orientation is crucial to whether the molecule will go SF and the rate of it due to the orbital coupling of both molecules, based on recent studies. We calculate the most favorable orientation of the chromophores with the binding energies in the gas phase and adsorbed on Argon and Neon surfaces. Then we calculate the lowest-lying excited states that contribute to the singlet and triple transition plus the search for the possible conical intersection that crosses the surface potential energies.

CPP 40.8 Thu 17:15 H38

Materials design based on theoretical characterization: Improving open-shell organic molecules for electronic applications — •SEBASTIAN SCHELLHAMMER¹ and FRANK ORTMANN² — ¹Dresden Integrated Center for Applied Physics and Photonic Materials (IAPP) and Institute for Applied Physics, Technische Universität Dresden, Dresden, 01187 Germany — ²Department of Chemistry, Technische Universität München, Lichtenbergstr. 4, 85748 Garching b. München

In recent years, organic molecules with stable open-shell ground states have attracted growing interest due to their outstanding properties, i.e. responsive spin structures, high-spin ground states, two-photon absorption, or small band gap. Although a growing number of interesting materials has appeared, molecules often lack thermal stability impeding their application in electronic devices. In this presentation, we will highlight routes but also dead ends in the quest for high-spin configurations in hydrocarbons. We benchmark a computational approach for the characterization of open-shell organic structures, which combines predictability with appropriate simulation resources. For polycyclic heteroaromatic hydrocarbons containing a benzoisindole core, we explain why a supposedly open-shell material does not provide the desired characteristics. On the contrary, we discuss the promising characteristics of stable polycyclic hydrocarbon diradicaloids as well as related tetradicaloids. Based on these analyses, design rules for optimized material properties are extracted, which helps to exploit the full potential of promising material groups.

CPP 40.9 Thu 17:30 H38

Simulation organic semiconductors with tensor network techniques — •SAM MARDAZAD¹, YIHE XU², XUEXIAO XANG², MARTIN GRUNDNER³, ULRICH SCHOLLWÖCK³, HAIBO MA², and SEBASTIAN PAECKEL³ — ¹Heriot-Watt University, Edinburgh — ²School of Chemistry and Chemical Engineering, Nanjing University — ³Department of Physics, Arnold Sommerfeld Center of Theoretical Physics, University of Munich

Organic solar cells provide the possibility to enhance the efficiency and to overcome the Shockley-Queisser limit. In this talk we present results for the simulation of quantum transport effects in a tetracene para dimers, a large organic molecule modelled by a Frenkel-exciton Hamiltonian. We account for the full quantum dynamics going beyond the Born-Oppenheimer approximation. For that purpose we use a new numerically unbiased representation of the molecule's wave function enabling us to compare with experiments, exhibiting good agreement. With this powerful approach we map out a phase diagram aiming and determining the experimental sweet spot yielding the highest charge carrier production rate. Furthermore, we develop a physical picture indicating that the coherent time scale in which most of the yield is generated is driven by a renormalization of the bare modes and make suggestions on how to manipulate this for the development of more efficient organic solar cells.

CPP 41: Crystallization, Nucleation and Self-Assembly

Time: Thursday 15:00–17:30

Location: H39

Invited Talk

CPP 41.1 Thu 15:00 H39

Interface-induced crystallization in polymers: From model systems to applications for semiconducting polymers — MUHAMMAD TARIQ¹, ROBERT KAHL¹, MUKUNDAN THELAKKAT², THOMAS THURN-ALBRECHT¹, and •OLEKSANDR

DOLYNCHUK¹ — ¹Experimental Polymer Physics, Martin Luther University Halle-Wittenberg — ²Applied Functional Polymers, University of Bayreuth

Crystallization is usually initiated at interfaces. Understanding the physical process underlying interface-induced crystallization (IIC) is of fundamental inter-

est and is relevant for material applications. IIC of liquids can occur either by heterogeneous nucleation (HN) or by the equilibrium phenomenon of prefreezing. First, we present a combined theoretical and experimental study of the effect of the substrate-material interactions on the thermodynamics of prefreezing and on the kinetics of HN in model polymers on various substrates. Second, the acquired knowledge about IIC elucidates the role of interfaces for crystal orientation in films of conjugated polymers, which is important for device performance. Using polythiophenes as model conjugated polymers, we show that different crystal orientations can be formed at the interfaces to a substrate and vacuum as a result of two competing interfacial interactions. Our results demonstrate that increasing the polarity of polythiophene side chains influences the interactions at the interfaces, resulting in a change of crystal orientations. Thus, we disclose the crucial role of the interfacial interactions for crystallization kinetics, thin film morphology, and control of molecular orientation in films of model and semiconducting polymers.

CPP 41.2 Thu 15:30 H39

Determination of Morphologically Tailored Chirality in Supramolecular Nanostructures by X-ray Scattering — •ASENA CERHAN HAINK¹, FELIX WENZEL², KLAUS KREGER², HANS-WERNER SCHMIDT², RICHARD HILDNER³, and EVA M. HERZIG¹ — ¹Dynamik und Strukturbiologie-Herzig Group, Universität Bayreuth, Universitätsstr.30, 95447 Bayreuth, Germany — ²Makromolekulare Chemie I, Universität Bayreuth, Universitätsstr.30, 95447 Bayreuth, Germany — ³Zernike Institute for Advanced Materials, University of Groningen, Nijenborgh 4, 9747 AG Groningen, Netherlands

Designed supramolecular nanostructures allow control over their optical and electronic properties which make them promising candidates for light-harvesting applications. Recently, we presented long-range (μm) transport of excitation energy in supramolecular nanofibres based on a carbonyl-bridged triarylamine (CBT). Here, we study supramolecular CBT building blocks with chiral side groups, which result in a distinct circular dichroism (CD) signal from self-assembled nanofibres. For bundles of supramolecular nanofibres, we observe an inversion in the CD signal as a function of temperature. To understand the origin of this effect, we performed morphological characterisation using temperature-dependent Wide Angle X-ray Scattering on the CBT-based bundles. We demonstrate systematic temperature-dependent variations in the π - π stacking and the column-column distances, which indicates that the CBT-based bundles have thermoelastic behaviour and change chirality at the critical temperature.

CPP 41.3 Thu 15:45 H39

Learning the Crystallisation Behaviour of Bidisperse Branched Model Polymers using Coarse-Grained Molecular Dynamics Simulations — •WILLIAM FALL¹, JOERG BASCHNAGEL¹, OLIVIER LHOST², and HENDRIK MEYER¹ — ¹Institut Charles Sadron, 23 rue du Loess, 67034 Strasbourg Cedex, France. — ²TotalEnergies One Tech Belgium, Zone Industrielle C, 7181 Feluy, Belgium

Model polymer systems allow fundamental questions about polymer crystallisation to be tackled precisely. Molecular dynamics (MD) simulations can provide insights but studying large lamellar structures is challenging. Meyer and Muller-Plathe set the stage for molecular dynamics (MD) simulations of large lamella structures, by demonstrating that reproducing local crystalline structures is unimportant when large crystalline and amorphous regions dominate properties. Here, the role of short chain branches (SCBs) (C4) on the melt and crystalline properties of monodisperse polyethylene systems (C400) is investigated, using CGMD simulations. SCBs are grown into the melt to minimise computational expense, providing access to large systems. Cooling and heating cycles reveal the crystalline morphology depends strongly on both cooling rate and number of branches. Bidisperse mixtures of ultra-long C4000 and C400 are also studied, with different branch distributions, which mimic industrial PE morphologies. Via self-seeding, well aligned lamella are grown and morphological features, i.e. tie chains analysed. We begin to address how these features influence crystalline structure and material properties. We thank TotalEnergies for funding and GENCI/IDRIS (Orsay) and CAIUS/HPC centre.

CPP 41.4 Thu 16:00 H39

Aggregation and ordering in small alkane systems — •TIMUR SHAKIROV and WOLFGANG PAUL — University of Halle, Halle, Germany

Ordering of small alkanes differs drastically from the bulk one. The difference is not only quantitative but also qualitative: short-chain single alkanes fold at low temperatures into non-trivial structures [1] in contrast to fully-stretched-chain lamellae in bulk. For the few chain systems we demonstrate the leading role of torsional stiffness in the ordered structure formation and investigate the corresponding conformations, which vary from spirals to tilted lamellae. For the fully stretched chain lamellae we find a two-step ordering, the indications of which remain at least up to 16 chain aggregates. In contrast to the low-temperature ordering, the aggregation or liquid-vapor transition leads to similarly disordered structures for all system sizes, which allows correction of size effects and extrapolation of the estimated aggregation temperatures to the thermodynamic limit. Our calculations of aggregation/boiling temperatures at normal pressure are in

good agreement with experimental data. The presented equilibrium results are based on Wang-Landau-type Monte Carlo simulations [2,3] of a chemically realistic united atom model [4].

[1] T. Shakirov, and W. Paul, J. Chem. Phys. 2019, 150, 084903.

[2] F. Liang et al, J. Am. Stat. Assoc. 2007, 102, 305-320.

[3] T. Shakirov, Comp. Phys. Commun. 228 (2018), 38-43.

[4] W. Paul, D. Y. Yoon, and G. D. Smith, J. Chem. Phys. 103 (1995) 1702-1709.

CPP 41.5 Thu 16:15 H39

How the competition between crystal growth and intracrystalline chain diffusion determines the lamellar thickness in semicrystalline polymers — MARTHA SCHULZ, MAREEN SCHÄFER, KAY SAALWÄCHTER, and •THOMAS THURN-ALBRECHT — Institut für Physik, Martin-Luther-Universität Halle-Wittenberg, 06099 Halle

The non-equilibrium thickness of lamellar crystals in semicrystalline polymers varies significantly between different polymer systems and depends on the crystallization temperature T_c . There is currently no consensus on the mechanism of thickness selection. Previous work has highlighted the decisive role of intracrystalline chain diffusion (ICD) in special cases, but a systematic dependence of lamellar thickness on relevant timescales such as that of ICD and stem attachment has not yet been established. Studying the morphology by small-angle X-ray scattering and the two timescales by NMR methods and polarization microscopy, we present data on poly(oxymethylene), a case with relatively slow ICD. It fills the gap between previously studied cases of absent and fast ICD, enabling us to establish a quantitative dependence of lamellar thickness on the competition between the noted timescales.

Ref. Nature Communications, 13.1 (2022): 1-10.

15 min. break

CPP 41.6 Thu 16:45 H39

The Crucial Role of Solvation Forces in Inter-Nanoplatelet Interactions and Stack Formation — •NANNING PETERSEN, MARTIN GIRARD, ANDREAS RIEDINGER, and OMAR VALSSON — Max Planck Institute for Polymer Research, Ackermannweg 10, D-55128 Mainz

Cadmium selenide nanoplatelets show the tendency to form stacks in apolar alkane solvents. This effect is very similar to the stack formation of micron-sized discs, which can be induced by depletion forces. However, the interplay of the various forces leading to stack formation of nanoplatelets remains unclear. Solvation forces are in their origin and behaviour very similar to depletion forces.

Here, we use coarse-grained molecular dynamics simulations of nanoplatelets in octane solvent to investigate the role of solvation forces in nanoplatelet interactions. We demonstrate that solvation forces resulting from solvent layering are sufficiently strong to stabilize nanoplatelet stacks. We examine the dependence of solvation forces on the nanoplatelets' ligand shell, size, and other parameters. In particular, we demonstrate that for sufficiently large nanoplatelets, solvation forces are proportional to the interacting facet area, and their strength is intrinsically tied to the softness of the ligand shell. The solvation forces exhibit an oscillatory nature; increases in their strength leads to a stronger attraction between close nanoplatelet facets and in addition to an increase in the kinetic barriers.

[1] N. Petersen, M. Girard, A. Riedinger, and O. Valsson, ChemRxiv, doi:10.26434/chemrxiv-2022-mw1cs (2022)

CPP 41.7 Thu 17:00 H39

In situ small-angle X-ray scattering and total scattering to study CuPd nanoparticle growth and self-assembly — •KILIAN FRANK¹, DAVIDE DERELLI², DOROTA KOZIEJ², and BERT NICKEL¹ — ¹Faculty of Physics and Center for Nanoscience (CeNS), Ludwig-Maximilians-Universität, Geschwister-Scholl-Platz 1, 80539 München, Germany — ²University of Hamburg, Institute for Nanostructure and Solid-State Physics, Center for Hybrid Nanostructures, 22761, Hamburg, Germany

Combining noble metals with abundant materials is a promising design strategy for new catalytic nanomaterials, e.g. for CO₂ reduction. Reliable synthesis routes of nanoparticles with a low size dispersity are required, but often an understanding of the formation pathway is lacking. Therefore, we investigated the entire synthesis of CuPd alloy nanoparticles using simultaneous small-angle X-ray scattering (SAXS) and the atomic pair distribution function obtained from total scattering (TS) to establish the sequence of structures from the atomic level to the nanoscale. We use a dedicated reaction cell for heating and stirring at the high-energy beamline P07 (PETRA III, DESY), extending our previous studies on cobalt oxide nanoparticle formation (<https://doi.org/10.1038/s41467-021-24557-z>). We characterize the transformation of precursors and early nucleation by TS, and the subsequent particle growth and assembly by SAXS in a model-based analysis. Upon cooling, we observe a rich temperature-dependent phase behavior of particle assemblies. These can serve as a potential templating strategy for efficient particle-based catalysts.

CPP 41.8 Thu 17:15 H39

Ligand-stabilized gold nanorods as an ideal model system for anisotropic colloids — •MARCEL KRÜSMANN and MATTHIAS KARG — Physikalische Chemie I: Kolloide und Nanooptik, Heinrich-Heine-Universität Düsseldorf, Düsseldorf, 40225, Germany

Anisotropic colloidal particles have interesting optical, electronic and self-assembly properties. Yet the investigation of their phase behavior is often difficult due to limitations in quantity, monodispersity and colloidal stability for many particles. An additional challenge is the precise determination of particle number concentrations.

The easily scalable synthesis of gold nanorods gives access to monodisperse anisotropic colloids with a broad range of aspect ratios. The functionalization of gold nanorods with a polymer ligand increases the colloidal stability and removes the large excess of surfactant that is most often used in particle synthesis.

These anisotropic particles can now be studied with various methods. One of these methods is small-angle X-ray scattering for which gold has an excellent contrast. In combination with the good colloidal stability it is now possible to not only study the form factor but also the structure factor at high concentrations and/or during induced aggregation. The addition of absolute intensity measurements gives access to the particle number concentration, that can be related to measured extinction from spectroscopy.

CPP 42: Perovskite and Photovoltaics 5 (joint session HL/CPP/KFM)

Time: Thursday 15:00–16:30

Location: H31

See HL 32 for details of this session.

CPP 43: Members' Assembly

Time: Thursday 18:00–19:00

Location: H39

All members of the Chemical and Polymer Physics Division are invited to participate.

CPP 44: Focus Session: Soft Matter and Nanocomposites: New Opportunities with Advanced Neutron Sources 2

organized by Stephan Förster (FZ Jülich), Thomas Gutberlet (FZ Jülich), Peter Müller-Buschbaum (TUM) and Walter Richtering (RWTH Aachen)

Time: Friday 9:30–11:15

Location: H38

Invited Talk

CPP 44.1 Fri 9:30 H38

Connecting dynamics and phase behavior of proteins: The neutron perspective — •FRANK SCHREIBER — Universität Tübingen, Germany

We discuss the combination of various neutron scattering techniques to shed light on the dynamics of proteins in aqueous solution. This includes several processes, such as backbone and side-chain fluctuations, interdomain motions, as well as global rotational and translational (i.e. center of mass) diffusion. Since protein dynamics is related to protein function and essential transport processes, a detailed mechanistic understanding and monitoring of protein dynamics in solution is highly desirable. In particular, we connect it to the overall phase behavior in terms of clustering, crowding, crystallization, and phase separation [1], employing a combination of elastic, quasi-elastic, and inelastic scattering [2] as well as complementary techniques, such as X-ray photon correlation spectroscopy (XPCS) and simulations [3]. Finally, we comment on future perspectives with advanced neutron sources. Invaluable contributions by numerous collaborators are gratefully acknowledged.

[1] M. Grimaldo et al., *JPCL*, 10, 1709 (2019) [2] M. Grimaldo et al., *Quarterly Reviews of Biophysics*, 52, e7 (2019) [3] A. Girelli et al., *Phys. Rev. Lett.* 126 (2021) 138004

CPP 44.2 Fri 10:00 H38

Self-assembly of supramolecular magnetic polymers with monomers of different sizes — EKATERINA NOVAK¹, ELENA PYANZINA¹, •MARINA GUPALO¹, and SOFIA KANTOROVICH^{1,2} — ¹Ekaterinburg, Russia — ²University of Vienna, Vienna, Austria

In this paper we studying the effect of polydispersity of magnetic particles on the self-assembly of supramolecular magnetic polymers. Magnetic polymers are widely used to create new magnetically controlled materials and represent an analogue of polymer chains, where polymer molecules serve as crosslinks, and magnetic particles replace monomers. We propose to consider the bidisperse model, which takes into account only two fractions of particles in size, which is enough to track the main influence of polydispersity on the self-organization of a magnetic polymer. Using the method of computer simulation of Langevin's dynamics, we study various structural parameters of an individual magnetic polymer of different configurations: a chain, a closed ring, an X-shaped and Y-shaped magnetic filament. For analysis of the qualitative changes in equilibrium properties with temperature were used radius of gyration and magnetic moment, the general microstates are also defined. It turned out that the considered new types of polymer configuration compared with the monodisperse model significantly affect the equilibrium properties. This work was supported by RSF grant 19-72-10033.

CPP 44.3 Fri 10:15 H38

Pathways of micellar collapse and swelling of PMMA-*b*-PNIPAM in aqueous solution after a rapid change of pressure — •PABLO A. ALVAREZ HERRERA¹, JOHANNES ALLWANG¹, FEIFEI ZHENG¹, CRISTIANE HENSCHEL², LEONARDO CHIAPPISI³, ALFONS SCHULTE⁴, ANDRÉ LASCHEWSKY², and CHRISTINE M. PAPADAKIS¹ — ¹TU München, Physik-Department, Garching, Germany — ²Institut für Chemie, Potsdam-Golm, Germany — ³Institut Laue-Langevin, Grenoble, France — ⁴University of Central Florida, Orlando, USA

In aqueous solution, diblock copolymers consisting of a permanently hydrophobic and a thermo-responsive block can self-assemble into different morphologies. In particular, poly (methyl methacrylate)-*b*-poly(*N*-isopropylacrylamide) (PMMA-*b*-PNIPAM) forms spherical micelles featuring a PMMA core and a thermo-responsive PNIPAM shell. At atmospheric pressure, the micellar shell dehydrates, and the collapsed micelles form aggregates when heating above the cloud point of PNIPAM [1]. This phase transition can be also induced by changing the pressure. In this contribution, we study the micellar collapse and their posterior aggregation by kinetic small-angle neutron scattering (SANS) in combination with rapid pressure jumps across the co-existence line. The disintegration of the aggregates and the micellar swelling are also investigated by performing the pressure jump in the opposite direction.

[1] C.-H. Ko, C. M. Papadakis et al., *Macromolecules* 54, 384 (2021).

CPP 44.4 Fri 10:30 H38

Investigation of the Effect of Magnesium Salts with Chaotropic Anions on the Swelling Behavior of PNIPAM Thin Films — •JULIJA REITENBACH¹, CHRISTINA GEIGER¹, PEIXI WANG¹, ROBERT CUBITT², DIRK SCHANZENBACH³, ANDRÉ LASCHEWSKY³, CHRISTINE M. PAPADAKIS⁴, and PETER MÜLLER-BUSCHBAUM¹ — ¹TU München, Physik-Department, Lehrstuhl für Funktionelle Materialien, James-Frank-Str. 1, 85748 Garching — ²Institut Laue-Langevin, 71 Avenue des Martyrs, CS 20156, 38042 Grenoble Cedex 9, France — ³Universität Potsdam, Institut für Chemie, Karl-Liebknecht-Str. 24-25, 14476 Potsdam-Golm — ⁴TU München, Physik-Department, Physik weicher Materie, 85748 Garching

Thermoresponsive polymer thin films have gained a lot of attention in the past decades due to their attractiveness for a wide range of applications. A variety of polymer showing LCST- or UCST-type behavior are known, and their transition temperatures can be influenced by various factors such as molar mass, end groups, copolymerization, or by the addition of salts. For polymers in aqueous solution, it was found that the folding of the polymer chains can be strongly influenced by the type of salt and this ability follows a trend called the Hofmeister series. While this effect is well known in solution, the influence on the swelling behavior of PNIPAM thin films has yet to be investigated thoroughly. We aim

to elucidate the underlying mechanism by spectral reflectance and time-of-flight neutron reflectometry on a macroscopic scale and by in situ Fourier-transform infrared spectroscopy on a molecular level.

Invited Talk CPP 44.5 Fri 10:45 H38
Magnetic particle self-assembly at functionalized interfaces — •MAX WOLFF — Department for Physics and Astronomy, Uppsala University, Uppsala, Sweden
 Neutrons allow the study of buried interfaces and are directly sensitive to magnetic induction. This makes grazing incidence neutron scattering an ideal tool for the study of self-assembled magnetic particles.

In this talk I will discuss the self-assembly of monodisperse colloidal magnetite nanoparticles from a dilute water-based ferrofluid onto functionalized silicon

surfaces. The density of the layer adjacent to the substrate is determined by the interaction between the particles and the substrate. Dense layers form for chemical binding and magnetic substrates, while less dense and no layering is found for physisorption and repulsive interactions. Once adsorbed subsequent layers assemble due to magnetic dipolar forces. The layering gets more pronounced for larger dipole moments of the particles. Once formed the density and structure of the layers may be tuned by magnetic and/or shear fields.

Magnetic particles may also be used to self-assemble polymer micelles. Applied magnetic fields may result in a micro shear effect aligning the domains of micellar crystals. By stroboscopic reintegration this reorientation process may be followed on time scales down to ms and resonant enhancement may aid the identification of off-specular and grazing incidence small angle scattering.

CPP 45: Biopolymers, Biomaterials and Bioinspired Functional Materials (joint session CPP/BP)

Time: Friday 9:30–11:15

Location: H39

Invited Talk CPP 45.1 Fri 9:30 H39
New biobased material concepts using scattering techniques to elucidate and control nanoscale assembly — •DANIEL SÖDERBERG — KTH Royal Institute of Technology, Department of Fibre and Polymer technology, Stockholm, Sweden
 Cellulose, the most abundant biopolymer on earth, can be crucial in mitigating fossil-based resources to more sustainable solutions. It is used as an engineering material, e.g. sawn timber, pulp for papermaking or as a polymer as a basis for plastic materials.

Cellulose nanofibres (CNF) constitute the structural component of plants, it is a semi-crystalline, semi-flexible rod-like nanoparticle having cross-sections in the order of 4-5 nm and lengths around one micrometre. Based on technical developments during the last decades, it is today possible to extract the CNF in large quantities, which has promoted significant research efforts aiming at new material concepts and devices based on cellulose.

Small and wide-angle x-ray scattering have been used to understand nanoscale assembly during fibre spinning from a CNF dope using microfluidics, allowing the tuning of the hierarchical structure, resulting in 100% bio-based filaments with exceptional properties. Furthermore, to develop scalable engineering processes, an in-depth understanding of nanoscale diffusion and the effects of nanoparticle interaction in low-concentration crowded systems has been pursued by combining light-scattering, X-ray Photon Correlation Scattering and coarse-grain modelling.

CPP 45.2 Fri 10:00 H39
A Semisynthetic Superparamagnetic Nanoprobe for Protein Targeting and Manipulation — •ANDREAS NEUSCH¹, IULIA NOVOSELOVA¹, NIKOLAOS TETOS², MICHAEL FARLE², ULF WIEDLAND², and CORNELIA MONZEL¹ — ¹Heinrich-Heine University Düsseldorf, Germany — ²University of Duisburg-Essen, Germany

Probing and manipulating biological functions requires tools to target and modify the proteins involved in the respective process. In recent years Magnetogenetics emerged as an approach where magnetic nanoparticles (MNPs) and external magnetic fields are used to realize such manipulation (Lisse et al., *Adv. Mater.*, 29, 1700189 (2017)). The advantages of this combination lies within the deep tissue penetration of magnetic fields and the possibility to apply stimuli on nanoscales leading to spatial redistribution, force application, or heat generation of proteins. However, a precise active perturbation requires MNPs to be monodisperse, biocompatible, tunable with regard to their magnetic properties, as well as exhibiting a modifiable molecular shell (Monzel et al., *Chem. Sci.* 8, 7330-7338 (2017)). Here, we synthesize a bioinspired semisynthetic MNP - Magnetoferritin (MFT) -, which fulfils these demands. MFT is based on the globular iron storage protein complex ferritin that converts iron ions to a ferrihydrite core but can be synthetically loaded with a magnetic iron oxide core (Novoselova et al., *Nanomaterials*, 11, 2267 (2021)). MFT was chemically, physically and magnetically characterized both in vitro and in vivo. We demonstrate how MFT can be used to target proteins on living cells as well as to spatially manipulate MFTs in a single cell environment.

CPP 45.3 Fri 10:15 H39
Bioinspired electrodes for brain wave detection — •VOLKER KÖRSTGENS¹, GÖKAY ERBİL¹, ANDREAS ZHENG¹, HSIN-YIN CHIANG², and PETER MÜLLER-BUSCHBAUM¹ — ¹TU München, Physik-Department, LS Funktionelle Materialien, 85748 Garching — ²Cephalgo, 67000 Strasbourg, France

With increasing demands in brain computer interfaces (BCI) measuring biosignals non-invasively becomes more important. Applications like measuring brain waves via electroencephalography (EEG) with dry electrodes remains challenging as for a steady biosignal acquisition adhesion to the skin has to be maintained all the time. We present two different approaches inspired by nature for such electrodes. In our first approach we developed micro-structured dry adhesive electrodes based on polydimethylsiloxane (PDMS) with conductive fillers.

The EEG-performance and adhesive properties of these electrodes will be discussed and compared to the concept of mussel-inspired hydrogels we follow in our second approach.

CPP 45.4 Fri 10:30 H39
Anionically functionalized glycogens efficiently encapsulate cationic peptides — HANNA ZHUKOUSKAYA¹, PABLO M. BLANCO², ZULFIYA ČERNOCHOVÁ¹, LUCIE ČTVERÁČKOVÁ¹, ROMAN STAÑO³, EWA PAVLOVA¹, MIROSLAV VETRÍK¹, PETER ČERNOCH¹, MIROSLAV ŠLOUF¹, MARCELA FILIPOVÁ¹, MIROSLAV ŠTĚPÁNEK², MARTIN HRUBÝ¹, PETER KOŠOVAN², and JIŘÍ PÁNEK¹ — ¹Institute of Macromolecular Chemistry, Czech Academy of Sciences, Heyrovského nám. 2, 162 06 Prague 6, Czech Republic — ²Department of Physical and Macromolecular Chemistry, Faculty of Science, Charles University, Hlavova 8, 128 40 Prague 2, Czech Republic — ³Faculty of Physics, University of Vienna, Kolingasse 14-16, 1090 Vienna, Austria

We developed and tested novel acid-functionalized glycogen conjugates as supramolecular carriers for efficient encapsulation and inhibition of a model cationic peptide melittin, which is the main component of honeybee venom. Systematic investigation of this model system allowed us not only to test its potential application as honeybee venom antidote but also to assess the role of the degree of substitution and solution pH in the interactions of these anionic carriers with multivalent cationic cargos. Our results demonstrate that the concept of electrostatically driven encapsulation by acid-functionalized glycogens should be applicable not only to the model case of melittin but also to other multivalent cationic biomolecules.

CPP 45.5 Fri 10:45 H39
Dissipative Assembly: Controlling Changes of Membrane Topology by Reaction Cycles — •GREGOR IBBEKEN and MARCUS MÜLLER — Institut für Theoretische Physik, Georg-August Universität, Friedrich-Hund-Platz 1, 37075 Göttingen

Coupling a self-assembling system to a reaction cycle, we go beyond equilibrium self-assembly toward systems that dissipate energy and thus exhibit new, unique features of dynamic self-organization. We consider polymers which can switch between a hydrophilic and an amphiphilic state and in the latter self-assemble to form vesicles in aqueous solution. This can occur either by macromolecular or monomeric reactions. In both cases a precursor reacts with a fuel to a product, which itself can decay back to the precursor. We perform particle-based simulations using a soft, coarse grained model for polymers. For the macromolecular reactions we find two drastically different scenarios depending on the fuel volatility: (i) For high fuel volatility, the coupling of inactivated to activated polymers introduces a length scale which dictates the maximal vesicle size and prevents fusion beyond this. This results in an interplay between the architecture and the reaction-rate-determined length and time scales. (ii) For less volatile fuel, a fuel gradient arises in the system. This results in the compartments moving within the fuel gradient to approach the source. In doing so the moieties gain material over long times which drastically changes the formation mechanism of the vesicles. Finally, we show that the above reaction mechanism can be mimicked by monomeric reactions by the use of multiple, inhomogeneously distributed fuels.

CPP 45.6 Fri 11:00 H39
Influence of molecular weight of polycation polydimethyldiallylammonium and carbon nanotube content on the electric conductivity of layer-by-layer films — •SVEN NEUBER¹, ANNEKATRIN SILL¹, PETER NESTLER², HEIKO AHRENS¹, and CHRISTIANE A. HELM¹ — ¹University of Greifswald, Institut of Physics, Greifswald, Germany — ²TÜV NORD EnSys GmbH & Co. KG, Greifswald, Germany

For biological and engineering applications, nm-thin films with high electrical conductivity and tunable sheet resistance are desirable. Multilayers of poly-

dimethyldiallylammonium chloride (PDADMA) with two different molecular weights (322 and 44.3 kDa) and oxidized carbon nanotubes (CNTs) were constructed using the layer-by-layer technique. Both the film thickness and the surface coverage of the CNTs increased linearly with the number of CNT/PDADMA bilayers deposited (dfilm up to 80 nm). Atomic force microscopy images showed a predominantly surface-parallel orientation of CNTs. Ohmic behavior with constant electrical conductivity of each CNT/PDADMA film and conductivity

up to 4×10^3 S/m was found. A change in PDADMA molecular weight by almost a factor of ten does not affect the film thickness and electrical conductivity, only the film/air roughness is reduced. However, increasing CNT concentration in the deposition dispersion from 0.15 up to 0.25 mg/ml results in an increased thickness of a CNT/PDADMA bilayer (by a factor of three). The increased bilayer thickness is accompanied by a decreased CNT coverage and a decreased electrical conductivity (by a factor of four).

CPP 46: 2D Materials 10 (joint session HL/CPP/DS)

Time: Friday 9:30–12:00

Location: H36

See HL 42 for details of this session.

CPP 47: Active Matter 5 (joint session DY/BP/CPP)

Time: Friday 10:00–12:45

Location: H18

See DY 50 for details of this session.

CPP 48: Electrical, Dielectrical and Optical Properties of Thin Films (joint session CPP/KFM)

Time: Friday 11:30–12:30

Location: H38

CPP 48.1 Fri 11:30 H38

Mechanical nanoscale polarization switching in ferroelectric polymer films — •KATHRIN DÖRR, MARTIN KOCH, DIANA RATA, and ROBERT ROTH — MLU Halle-Wittenberg

Ferroelectric polymer films offer strong advantages like mechanical flexibility, biocompatibility, optical transparency and low-cost processing. However, their dielectric or piezoelectric performance is often inferior to that of oxide ferroelectric materials. Key to that is the electric dipolar order which is naturally lower in semicrystalline polymers than in crystalline ferroelectrics. We introduce the reorientation and alignment of the electric polarization in thin films utilizing the mechanical effect of an unbiased scanning force microscopy tip, providing a versatile tool for nanoscale domain writing [1]. Thin films (50 - 150 nm) of P(VDF-TrFE) (78:22) on graphite were prepared with dense (110)-oriented beta-phase lamellae randomly oriented in the film plane. Domain patterns with resolution down to 50 nm have been written with four (out of six possible) local polarization orientations. Written domains show excellent long-time stability. We discuss a ferroelastic origin of the mechanical polarization switching and make suggestions for how to utilize the domain patterns in thin film devices. [1] Adv. Electron. Mater. 2022, 2101416

CPP 48.2 Fri 11:45 H38

In-situ investigations of morphology degradation and oxidation level changes in EMIM DCA post-treated PEDOT:PSS thin films upon external influence — •ANNA LENA OECHSLE¹, JULIAN E. HEGER¹, NIAN LI¹, SHANSHAN YIN¹, SIGRID BERNSTORFF², and PETER MÜLLER-BUSCHBAUM^{1,3} — ¹TU München, Physik-Department, LS Funktionelle Materialien, 85748 Garching — ²ELETTRA, 34149 Basovizza TS, Italy — ³MLZ, TU München, 85748 Garching

Nowadays thermoelectric generators are considered a promising technique for heat waste recovery as they enable a direct conversion of a temperature gradient into electrical power. Especially, organic thermoelectric polymers are attractive, owning some advantages like low cost, lightness and high mechanical flexibility, low or no toxicity, as well as a usually low thermal conductivity. In our work we show the positive effect of ionic liquid (IL) treatment on the thermoelectric properties, Seebeck coefficient and electrical conductivity, of semi-conducting PEDOT:PSS thin films. Furthermore with different in-situ experiments like GISAXS (grazing incidence small angle x-ray scattering), UV-Vis, and conductivity measurements we examine the inner film morphology and oxidation level changes upon operation at different ambient conditions.

CPP 48.3 Fri 12:00 H38

Improvement of TE properties of PEDOT:PSS films via DMSO addition and DMSO/salt post-treatment resolved from a fundamental view — •SUO TU¹, TING TIAN¹, ANNA-LENA OECHSLE¹, SHANSHAN YIN¹, XINYU JIANG¹, WEI CAO¹, NIAN LI¹, MANUEL A. REUS¹, LENNART K. REB¹, SHUJIN HOU², ALI-AKSANDR S. BANDARENKA², MATTHIAS SCHWARTZKOPF³, STEPHAN V. ROTH³, and PETER MÜLLER-BUSCHBAUM^{1,4} — ¹TU München, Physik-Department, LS Funktionelle Materialien, 85748 Garching — ²TU München, Physik-Department, Physik der Energiewandlung und -speicherung, 85748 Garching — ³DESY, 22607 Hamburg — ⁴MLZ, TU München, 85748 Garching

The combination of DMSO-solvent doping and physical-chemical DMSO/salt de-doping in a sequence has been used to improve the thermoelectric PEDOT:PSS films. The initial DMSO-doping treatment induces a distinct phase separation by facilitating the aggregation of the PEDOT molecules. At the same time, the subsequent DMSO/salt de-doping post-treatment strengthens the selective removal of the surplus non-conductive PSS chains. Substantial alterations in the oxidation level, chain conformations, PEDOT crystallites and their preferential orientation are observed upon treatment on the molecular level. At the mesoscale level, the purification and densification of PEDOT-rich domains enable the realization of inter-grain coupling by the formation of the electronically well-percolated network. Thereby, both electrical conductivity and Seebeck coefficient are optimized.

CPP 48.4 Fri 12:15 H38

Exciton dynamics in surface-mounted metal-organic frameworks: A femtosecond transient absorption study — •VIPILAN SIVANESAN¹, MARTIN RICHTER¹, DEBKUMAR RANA¹, RITESH HALDAR², CHRISTOPH WÖLL², and PETRA TEGEDER¹ — ¹Physikalisch-Chemisches Institut, Universität Heidelberg, Germany — ²Institute of Functional Interfaces, Karlsruhe Institute of Technology, Germany

For the optimization of organic optoelectronic devices, it is important to understand the ultrafast electronically excited state dynamics in organic semiconductors after optical excitation. For instance, different molecular packing and relative orientations of the optically active chromophores can affect the excitonic coupling strength. This can be studied in crystalline molecular assemblies by integrating these chromophores into surface-mounted metal-organic frameworks (SURMOFs) as organic linkers. Varying the side-groups of the molecules enables to engineer the crystal structure to tune the excitonic coupling. To analyse the influence of this crystal engineering on the ultrafast dynamics we investigated thin films of chromophore functionalized Zn-SURMOF by means of femtosecond transient absorption.

CPP 49: Polymer and Molecular Dynamics, Friction and Rheology

Time: Friday 11:30–13:00

Location: H39

CPP 49.1 Fri 11:30 H39

Molecular Mobility and Physical Aging in Polymers of Intrinsic Microporosity (PIM-1) Revisited: A Big Glassy World — •FARNAZ EMAMVERDI, MARTIN BÖHNING, and ANDREAS SCHÖNHALS — Bundesanstalt für Materialforschung und -prüfung (BAM), Berlin, Germany

Polymers of Intrinsic Microporosity (PIMs) are promising candidates for the active layer in gas separation membranes because of their high permeability and reasonable permselectivity. However, PIMs suffer from a decrease in performance with time due to physical aging. The initial microporous structures approach a denser state via local rearrangements, leading to a reduction of the permeability. Hence a characterization of the molecular mobility in these materials can provide valuable information about physical aging. In this work, the dielectric behavior of PIM-1 films and their behavior upon heating (aging) were revisited during different heating/cooling cycles in a broad temperature range between 133 K and 523 K. In addition, the obtained results were compared with data of samples that were annealed at ambient temperatures for different time. Multiple dielectric processes were observed like different relaxations due to local fluctuations and a Maxwell-Wagner-Sillars polarization effects due to the microporosity. The temperature dependence of the rates of all the processes follows the Arrhenius law where the estimated activation energy depends on the process. The influence of the thermal history on the processes is discussed in detail.

CPP 49.2 Fri 11:45 H39

Orientation approach to the light-induced surface relief gratings formation in azopolymer materials — •NINA TVERDOKHLEB, BHARTI YADAV, and MARINA SAPHIANNIKOVA — Leibniz-Institut für Polymerforschung Dresden e. V., PF 120411, 01005 Dresden

The phenomenon of azopolymer deformation giving rise to surface relief gratings (SRG) under the influence of polarized light was discovered two and a half decades ago. Despite the numerous different theoretical approaches to this effect, an accurate representation that would interpret all peculiarities of this phenomenon is absent. At present, the light-induced orientation of polymer backbones looks like the most promising explanation [1]. With help of this orientation approach and the finite element modeling software ANSYS, we simulate the viscoplastic formation of sinusoidal protrusions produced by the applied light-induced stress on the thin azopolymer films. We explain the difference in SRG height for irradiation with various interference patterns. It is found that the mechanical boundary conditions have a crucial impact on the output. The results of our viscoplastic modeling are in good agreement with recent experiments [2]. [1] B. Yadav et al. J. Phys. Chem. B 122 (2019) 2001-2009. [2] B. Yadav, N. Tverdokhlebe et al. Macromol. Mater. Eng. (2022) 2100990.

CPP 49.3 Fri 12:00 H39

Measuring Volume Exclusion on Single Polymer Chains Diffusing in Solution — •TOBIAS THALHEIM and FRANK CICHOS — Peter Debye Institute for Soft Matter Physics, Leipzig University, Germany

Excluded volume effects in single polymer chains occur due to long-range interactions of distant segments in the chain which cannot pass through each other entailing a strong influence of the static as well as the dynamic behavior of the polymer. Various theoretical descriptions were thus devised to incorporate these effects in the interpretation of experimental outcomes. A theory by Schäfer and Krüger incorporating this real-polymer phenomenon predicts a distribution function which describes the total segment density about an individual polymer's center of mass. This distribution function augments the picture of an ideal Gaussian chain by correction functions that account for volume exclusion and which were derived in the framework of renormalization groups. Although this permits the assessment of the role of volume exclusion for single chains in contrast to usual accesses via scaling theories or ensemble measurements, this theory has never been tested before. We report on experiments including two types of freely-diffusing double-stranded DNA molecules that utilize Schäfer's and Krüger's theory to investigate these effects. We show that for short λ -DNA molecules volume exclusion is of minor importance, whereas long T4-DNA molecules exhibit prominent volume exclusion. Furthermore, we employ a thermophoretic trapping method to test this theory on single compressed polymers subjected to a virtual harmonic potential.

CPP 49.4 Fri 12:15 H39

Dynamics in polymer-fullerene blends for photovoltaic applications studied with quasielastic neutron scattering — •DOMINIK M. SCHWAIGER¹, WIEBKE LOHSTROH², and PETER MÜLLER-BUSCHBAUM^{1,2} — ¹TU München, Physik-Department, LS Funktionelle Materialien, 85748 Garching — ²MLZ, TU München, 85748 Garching

In organic photovoltaics, donor - acceptor bulk heterojunctions are often used as active layer due to their superior performance compared to e.g. planar structured devices. In this optically active polymer layer, photons are absorbed, excitons are created, subsequently dissipated at a material interface and hence free charges are provided. A promising low-bandgap electron donor material is the conjugated polymer PTB7 that is often used in combination with the fullerene derivative PCBM. Besides a large number of studies on structure and electrical properties, the level of knowledge about dynamics in this system is very limited. We investigated films of PTB7, PCBM and different blends of these two, prepared out of chlorobenzene solutions. Quasielastic neutron scattering experiments were performed to determine hydro- gen dynamics on a pico- to nanosecond timescale. In addition, two well established techniques for performance enhancement in organic photovoltaics, namely the addition of DIO to the casting solution and a methanol posttreatment of the active layer, are applied and their influence on the polymer dynamics is investigated.

CPP 49.5 Fri 12:30 H39

Equilibration of free-standing films of highly entangled polymer melts — •HSIAO-PING HSU and KURT KREMER — Max-Planck-Institut für Polymerforschung, Ackermannweg 10, 55128, Mainz, Germany

Equilibrating confined and free-standing films of highly entangled polymer melts is a challenge for computer simulations. We approach this problem by first studying polymer melts based on a soft-sphere coarse-grained model confined between two walls. The distance of the walls is compatible with the simulation box of bulk melts in equilibrium, while periodic boundary conditions in the directions parallel to the walls are kept. Then we successively insert more fine grained polymer representations until the underlying microscopic details of the bead-spring model are reached. Tuning the wall potential, the monomer density of confined polymer melts in equilibrium is kept at bulk melt density even near the walls. Switching to another recently developed variant of the bead-spring model we can study melts at zero pressure [1] and study free-standing polymer films [2]. Furthermore, this also allows us to study free-standing films under strain and analyze the influence of entanglements on the local film morphology.

[1] H.-P. Hsu, K. Kremer, J. Chem. Phys. 150, 091101 (2019); 150, 159902 (2019).

[2] H.-P. Hsu, K. Kremer, J. Chem. Phys. 153, 144902 (2020); 156, 019901 (2022).

CPP 49.6 Fri 12:45 H39

Liquid flow through nanoporous media: non-linear response and blocking — •ROYA EBRAHIMI VIAND¹ and FELIX HÖFLING^{1,2} — ¹Department of Mathematics and Computer Science, Freie Universität Berlin, Germany — ²Zuse Institute Berlin, Germany

Directed fluid flow is a major transport mechanism in porous media that can either be generated by pumps or emerge in response to a pressure gradient. The pressure-flow relation and how it depends on the structure and geometry of the medium is investigated by non-equilibrium molecular dynamics (NEMD) simulations of a flow of dense liquids through regular bead packings as a model for nanoporous medium. Upon decreasing the porosity, we find a significant non-linear response. The linear permeability varies over two orders of magnitude and vanishes beyond a critical porosity. Our simulations further exhibit a substantial increase in temperature inside the porous medium, which we attribute to the local balance of energy fluxes using fluid mechanical conservation laws. Finally, we show that a recent NEMD approach based on the adaptive resolution simulation (AdResS) technique can help to decrease the required simulation volume considerably [1,2]. This simulation approach is expected to be highly applicable for research on flow in porous as well as biological media.

[1] R. Ebrahimi Viand et al., J. Chem. Phys. 153, 101102 (2020)

[2] R. Klein, R. Ebrahimi Viand et al., Adv. Theory Simul. 4, 2100071 (2021)

CPP 50: Nanostructures, Nanostructuring and Nanosized Soft Matter

Time: Friday 12:30–13:00

Location: H38

CPP 50.1 Fri 12:30 H38

The effect of solvent vapor annealing on diblock copolymer templated mesoporous Si/Ge/C thin films — •CHRISTIAN L. WEINDL¹, CHRISTIAN E. FAJMAN², MICHAEL A. GIEBEL², KERSTIN S. WIENHOLD¹, SHANSHAN YIN¹, TING TIAN¹, CHRISTINA GEIGER¹, LUCAS P. KREUZER⁵, MATTHIAS SCHWARTZKOPF³, STEPHAN V. ROTH^{3,4}, THOMAS F. FÄSSLER², and PETER MÜLLER-BUSCHBAUM^{1,5} — ¹TU München, Physik-Department, LS Funktionelle Materialien, 85748 Garching — ²TU München, LS Anorganische Chemie mit Schwerpunkt Neue Materialien, Chemie-Department, 85748 Garching — ³DESY, 22607 Hamburg — ⁴Royal Institute of Technology KTH, 100 44 Stockholm — ⁵MLZ, TU München, 85748 Garching

The latest research has revealed promising results for silicon (Si) and germanium (Ge) as anode materials for lithium-ion batteries. These two group 14 semiconductors are considered auspicious additives in graphite anodes due to their high specific capacity (Si) and electron mobility (Ge). This study aims to synthesize a mesoporous Si/Ge/C structure by using a wet chemical sol-gel approach with the structure-directing amphiphilic diblock copolymer PS-*b*-PEO and the Zintl cluster $K_{12}Si_xGe_{17-x}$. Furthermore, we investigate the structural changes on the spin-coated thin films upon exposure to a saturated toluene/butanol atmosphere. For morphological analysis, scanning electron microscopy will be combined with grazing-incidence small-angle x-ray scattering (GISAXS). Moreover, energy-dispersive X-ray spectroscopy, Raman spectroscopy and powder X-ray diffraction are used for further elemental and crystalline phase analysis.

CPP 50.2 Fri 12:45 H38

The kinetics and free-energy landscape of grain-boundary motion in cylinder-forming copolymers — •NIKLAS BLAGOJEVIC and MARCUS MÜLLER — Universität Göttingen, Institut für Theoretische Physik

Block copolymers which self-assemble into a dense array of hexagonally-packed cylinders are promising candidates for filtering membranes with pore sizes in the nanometer range used to extract or to purify a substance. The cylinders act as selective transport channels and it is important to align the cylinders along the desired flux direction. A fundamental understanding on how to control the cylinder orientation in the processing of the membrane, however, is incomplete and successful applications have often relied on trial-and-error searches in the high-dimensional space of process parameters.

To gain fundamental understanding about orientation mechanisms of cylindrical copolymer phases, we employ large-scale computer simulations of a particle based model in a highly efficient GPU-parallel implementation with sophisticated free-energy techniques. With this, we study the kinetics of grain-boundary motion of cylindrical copolymer domains – resembling the (re-)orientation mechanisms – and the Minimum Free-Energy Path of the associated changes of the domain topology. The simulation study has provided direct insights into the kinetics and the free-energy landscapes of orientation mechanisms and ordering in the early and late stages.

CPP 51: Overview Talk Claus M. Schneider (joint session O/CPP)

Time: Friday 13:15–14:00

Location: S054

See O 84 for details of this session.

Thin Films Division Fachverband Dünne Schichten (DS)

Patrick Vogt
Institut für Festkörperphysik
Technische Universität Berlin
Hardenbergstr. 36
10623 Berlin
patrick.vogt@physik.tu-berlin.de

Overview of Invited Talks and Sessions

(Lecture halls H14 and H17; Poster P3)

Invited Talks

DS 2.1	Mon	9:30–10:00	H17	GaN-based power converters enabling talktive power — •MARCO LISERRE
DS 2.2	Mon	10:00–10:30	H17	Energy-efficient power electronics based on Gallium Nitride — •OLIVER AMBACHER
DS 2.4	Mon	10:45–11:15	H17	Potential of Aluminum Nitride for Vertical Power Electronics — •ANDREAS WAAG, KLAAS STREMPER, LUKAS PETERS, CHRISTOPH MARGENFELD, SAMUEL FABER, FRIEDHARD RÖMER, BERND WITZIGMANN
DS 6.1	Mon	15:00–15:30	H17	Novel high power device structures: Enabling compact and integrated power ICs — •ELISON MATIOLI
DS 6.2	Mon	15:30–16:00	H17	Ab-initio investigations of V-pits and nanopipes in GaN — •LIVERIOS LYMPERAKIS, SU-HYUN YOO, JÖRG NEUGEBAUER
DS 6.4	Mon	16:15–16:45	H17	Lateral and Vertical β-Ga₂O₃ Power Transistors for High-Voltage Applications — •KORNELIUS TETZNER, MICHAEL KLUPSCH, KARINA ICKERT, RALPH-STEPHAN UNGER, ZBIGNIEW GALAZKA, TA-SHUN CHOU, SAUD BIN ANOOZ, ANDREAS POPP, JOACHIM WÜRFL, OLIVER HILT
DS 14.1	Wed	9:30–10:00	H17	Facet dependence of reconstructions at quantum material interfaces — •EVA BENCKISER
DS 14.3	Wed	10:15–10:45	H17	Designing novel electronic phases at oxide interfaces from first principles — •ROSSITZA PENTCHEVA

Invited Talks of the joint Symposium **Frontiers of Orbital Physics: Statics, Dynamics, and Transport of Orbital Angular Momentum (SYOP)**

See SYOP for the full program of the symposium.

SYOP 1.1	Mon	9:30–10:00	H1	Orbital degeneracy in transition metal compounds: Jahn-Teller effect, spin-orbit coupling and quantum effects — •DANIEL KHOMSKII
SYOP 1.2	Mon	10:00–10:30	H1	Orbital magnetism out of equilibrium: driving orbital motion with fluctuations, fields and currents — •YURIY MOKROUSOV
SYOP 1.3	Mon	10:30–11:00	H1	Orbitronics: new torques and magnetoresistance effects — •MATHIAS KLÄUI
SYOP 1.4	Mon	11:15–11:45	H1	Orbital and total angular momenta dichroism of the THz vortex beams at the antiferromagnetic resonances — •ANDREI SIRENKO
SYOP 1.5	Mon	11:45–12:15	H1	Observation of the orbital Hall effect in a light metal Ti — •GYUNG-MIN CHOI

Invited Talks of the joint Symposium **SKM Dissertation Prize 2022 (SYSD)**

See SYSD for the full program of the symposium.

SYSD 1.1	Mon	10:15–10:45	H2	Charge localisation in halide perovskites from bulk to nano for efficient optoelectronic applications — •SASCHA FELDMANN
SYSD 1.2	Mon	10:45–11:15	H2	Nonequilibrium Transport and Dynamics in Conventional and Topological Superconducting Junctions — •RAFFAEL L. KLEES
SYSD 1.3	Mon	11:15–11:45	H2	Probing magnetostatic and magnetotransport properties of the antiferromagnetic iron oxide hematite — •ANDREW ROSS
SYSD 1.4	Mon	11:45–12:15	H2	Quantum dot optomechanics with surface acoustic waves — •MATTHIAS WEISS

Invited Talks of the joint Symposium From Physics and Big Data to the Design of Novel Materials (SYNM)

See SYNM for the full program of the symposium.

SYNM 1.1	Mon	15:00–15:30	H1	How to tackle the "I" in FAIR? — •CLAUDIA DRAXL
SYNM 1.2	Mon	15:30–16:00	H1	Beyond the average error: machine learning for the discovery of novel materials — •MARIO BOLEY, SIMON TESHUVA, FELIX LUONG, LUCAS FOPPA, MATTHIAS SCHEFFLER
SYNM 1.3	Mon	16:00–16:30	H1	The Phase Diagram of All Inorganic Materials — •CHRIS WOLVERTON
SYNM 1.4	Mon	16:45–17:15	H1	Automated data-driven upscaling of transport properties in materials — •DANNY PEREZ, THOMAS SWINBURNE
SYNM 1.5	Mon	17:15–17:45	H1	Data-driven understanding of concentrated electrolytes — •ALPHA LEE

Invited Talks of the joint Symposium United Kingdom as Guest of Honor (SYUK)

See SYUK for the full program of the symposium.

SYUK 1.1	Wed	9:30–10:00	H2	Structure and Dynamics of Interfacial Water — •ANGELOS MICHAELIDES
SYUK 1.2	Wed	10:00–10:30	H2	A molecular view of the water interface — •MISCHA BONN
SYUK 1.3	Wed	10:30–11:00	H2	Motile cilia waves: creating and responding to flow — •PIETRO CICUTA
SYUK 1.4	Wed	11:00–11:30	H2	Cilia and flagella: Building blocks of life and a physicist's playground — •OLIVER BÄUMCHEN
SYUK 1.5	Wed	11:45–12:15	H2	Computational modelling of the physics of rare earth - transition metal permanent magnets from SmCo₅ to Nd₂Fe₁₄B — •JULIE STAUNTON
SYUK 2.1	Wed	15:00–15:30	H2	Hysteresis Design of Magnetic Materials for Efficient Energy Conversion — •OLIVER GUTFLEISCH
SYUK 2.2	Wed	15:30–16:00	H2	Non-equilibrium dynamics of many-body quantum systems versus quantum technologies — •IRENE D'AMICO
SYUK 2.3	Wed	16:00–16:30	H2	Quantum computing with trapped ions — •FERDINAND SCHMIDT-KALER
SYUK 2.4	Wed	16:45–17:15	H2	Breaking the millikelvin barrier in cooling nanoelectronic devices — •RICHARD HALEY
SYUK 2.5	Wed	17:15–17:45	H2	Superconducting Quantum Interference Devices for applications at mK temperatures — •SEBASTIAN KEMPF

Invited Talks of the joint Symposium Frontiers of Electronic-Structure Theory: Focus on Artificial Intelligence Applied to Real Materials (SYES)

See SYES for the full program of the symposium.

SYES 1.1	Thu	15:00–15:30	H1	Machine-learning-driven advances in modelling inorganic materials — •VOLKER L. DERINGER
SYES 1.2	Thu	15:30–16:00	H1	Machine-Learning Discovery of Descriptors for Square-Net Topological Semimetals — •EUN-AH KIM
SYES 1.3	Thu	16:00–16:30	H1	Four Generations of Neural Network Potentials — •JÖRG BEHLER
SYES 1.4	Thu	16:30–17:00	H1	Using machine learning to find density functionals — •KIERON BURKE
SYES 1.5	Thu	17:00–17:30	H1	Coarse graining for classical and quantum systems — •CECILIA CLEMENTI

Invited Talks of the joint Symposium Complexity and Topology in Quantum Matter (SYQM)

See SYQM for the full program of the symposium.

SYQM 1.1	Fri	9:30–10:00	H1	The role of crystalline symmetries in topological materials: the topological materials database — •MAIA VERGNIORY
SYQM 1.2	Fri	10:00–10:30	H1	Microwave Bulk and Edge Transport in HgTe-Based 2D Topological Insulators — •ERWANN BOCQUILLON, MATTHIEU C. DARTIAILH, ALEXANDRE GOURMELON, HIROSHI KAMATA, KALLE BENDIAS, SIMON HARTINGER, JEAN-MARC BERROIR, GWENDAL FÈVE, BERNARD PLAÇAIS, LUKAS LUNCZER, RAIMUND SCHLERETH, HARTMUT BUHMANN, LAURENS MOLENKAMP
SYQM 1.3	Fri	10:30–11:00	H1	Spectral Sensitivity of Non-Hermitian Topological Systems — •JAN CARL BUDICH
SYQM 1.4	Fri	11:15–11:45	H1	Topological photonics and topological lasers with coupled vertical resonators — •SEBASTIAN KLEMBT
SYQM 1.5	Fri	11:45–12:15	H1	Spectroscopic Studies of the Topological Magnon Band Structure in a Skyrmion Lattice — •MARKUS GARST

Sessions

DS 1.1–1.5	Mon	9:30–10:45	H14	Thin Film Properties: Structure, Morphology and Composition (XRD, TEM, XPS, SIMS, RBS, AFM, ...) 1
DS 2.1–2.4	Mon	9:30–11:15	H17	Focus Session: Innovative GaN-based High-power Devices: Growth, Characterization, Simulation, Application 1
DS 3.1–3.10	Mon	9:30–12:45	H36	2D Materials 1 (joint session HL/CPP/DS)
DS 4.1–4.3	Mon	11:00–11:45	H14	Thin Film Properties: Structure, Morphology and Composition (XRD, TEM, XPS, SIMS, RBS, AFM, ...) 2
DS 5.1–5.6	Mon	11:30–13:00	H17	Organic Thin Films, Organic-Inorganic Interfaces
DS 6.1–6.4	Mon	15:00–16:45	H17	Focus Session: Innovative GaN-based High-power Devices: Growth, Characterization, Simulation, Application 2
DS 7.1–7.12	Mon	15:00–18:30	H36	2D Materials 2 (joint session HL/CPP/DS)
DS 8.1–8.2	Mon	17:15–17:45	H38	2D Materials 3 (joint session CPP/DS)
DS 9.1–9.6	Tue	9:30–11:00	H14	Thin Film Properties: Structure, Morphology and Composition (XRD, TEM, XPS, SIMS, RBS, AFM, ...) 3
DS 10.1–10.3	Tue	9:30–11:30	H17	Gaede Prize Talks
DS 11.1–11.8	Tue	9:30–12:45	H34	Focus Session: Quantum Properties at Functional Oxide Interfaces 1 (joint session HL/DS)
DS 12.1–12.8	Tue	9:30–12:00	H36	2D Materials 4 (joint session HL/CPP/DS)
DS 13.1–13.5	Wed	9:30–10:45	H14	Thin Film Applications 2
DS 14.1–14.4	Wed	9:30–11:00	H17	Focus session: Quantum Properties at Functional Oxide Interfaces 2 (joint session DS/HL)
DS 15.1–15.9	Wed	9:30–12:00	H36	2D Materials 5 (joint session HL/CPP/DS)
DS 16.1–16.4	Wed	11:00–12:00	H14	Thin Film Applications 2
DS 17.1–17.7	Wed	11:15–13:00	H17	2D Materials 6 (joint session DS/CPP)
DS 18.1–18.4	Wed	15:00–16:00	H14	Thin Oxides and Oxide Layers 1
DS 19.1–19.4	Wed	15:00–16:00	H17	2D Materials 7 (joint session DS/CPP)
DS 20.1–20.52	Wed	16:00–18:00	P3	Poster
DS 21.1–21.4	Thu	9:30–10:30	H14	Layer Deposition (ALD, MBE, Sputtering, ...)
DS 22.1–22.8	Thu	9:30–11:30	H17	2D Materials 8 (joint session DS/CPP)
DS 23.1–23.6	Thu	10:45–12:15	H14	Optical Analysis of Thin Films (Reflection, Ellipsometry, Raman, IR-DUV Spectroscopy, ...)
DS 24.1–24.4	Thu	11:15–12:15	H36	2D Materials 9 (joint session HL/CPP/DS)
DS 25.1–25.4	Thu	15:00–16:00	H14	Transport Properties
DS 26.1–26.4	Thu	16:15–17:15	H14	Thin Oxides and Oxide Layers 2
DS 27.1–27.9	Fri	9:30–12:00	H36	2D Materials 10 (joint session HL/CPP/DS)

Sessions

– Invited Talks, Prize Talks, Contributed Talks, and Posters –

DS 1: Thin Film Properties: Structure, Morphology and Composition (XRD, TEM, XPS, SIMS, RBS, AFM, ...) 1

Time: Monday 9:30–10:45

Location: H14

DS 1.1 Mon 9:30 H14

Low-energy ion channeling in nanocubes — •SHIVA CHOUPANIAN¹, WOLFHARD MÖLLER², MARTIN SEYRING¹, and CARSTEN RONNING¹ — ¹Institute of Solid State Physics, Friedrich Schiller University Jena — ²Helmholtz-Zentrum Dresden-Rossendorf

Focused ion beam (FIB) processing with low-energy ions has become a standard technique for the manipulation of nanostructures. Many underlying ion beam effects that deviate from conventional high-energy ion irradiation of bulk systems are considered today; however, ion channeling with its consequence of significant deeper penetration depth has been only theoretically investigated in this regime. We present here an experimental approach to determine the channeling of low-energy ions in crystalline nanoparticles by measuring the sputter yield derived from SEM images taken after irradiation under various incident ion angles. Channeling maps of 30 and 20 keV Ga⁺ ions in Ag nanocubes have been identified and fit well with the theory. Indeed, channeling has a significant impact on the transport of energetic ions in crystals due to the large critical angle at low ion energies, thus being relevant for any FIB-application. Consequently, the obtained sputter yield clearly differs from amorphous materials; therefore, it is recommended not to rely only on, e.g., ion distribution depths predicted by standard Monte-Carlo (MC) algorithms for amorphous materials.

DS 1.2 Mon 9:45 H14

Tuning the properties of thin films via disorder — •ALESSANDRO TROGLIA¹, JORIK VAN DE GROEP², ANNE DE VISSER², and ROLAND BLIEM^{1,2} — ¹Advanced Research Center for Nanolithography (ARCNL), Science Park 106, 1098 XG Amsterdam, The Netherlands (NL) — ²Van der Waals-Zeeman Institute, University of Amsterdam, Science Park 904, 1098 XH Amsterdam, The Netherlands (NL)

Structural disorder in thin films is often considered detrimental compared to the well-defined nature of epitaxial layers. However, some examples of amorphous thin films show superior properties such as better corrosion resistance, mechanical strength and catalytic performance. Here we investigate amorphous and crystalline CuZr thin films of identical composition. Grazing-incidence x-ray diffraction (GI-XRD) demonstrate that amorphous and crystalline CuZr thin films were achieved by varying the substrate temperature during deposition with pulsed laser deposition (PLD). The effect of disorder is clearly visible in the optical, transport and corrosion properties. The amorphous films are optically transparent in the visible, while polycrystalline films are dark and reflective. The temperature-dependent electronic transport changes its mode from a bad metal to a charge-hopping conductor with an increase in structural disorder. Moreover, we observe a higher oxidation resistance of amorphous CuZr thin films due to the absence of grain boundaries. These results pave the way to the synthesis of metallic thin films with superior and tunable properties via disorder for customizing materials properties to their technological applications.

DS 1.3 Mon 10:00 H14

Faster and lower dose X-ray reflectivity measurements enabled by physics-informed modelling and artificial intelligence co-refinement — •DAVID MARECEK¹, JULIAN OBERREITER¹, ANDREW NELSON², and STEFAN KOWARIK¹ — ¹Physikalische und Theoretische Chemie, Universität Graz, Graz, 8010, Austria — ²ANSTO, Locked Bag 2001, Kirrawee DC, NSW, 2232, Australia

We present an approach for analysis of real-time X-ray reflectivity (XRR) process data not just as a function of the reciprocal space vector q as is commonly done, but as a function of both q and time. We restrict the real-space structures extracted from the XRR curves to be solutions of a physics-informed growth model, and use state-of-the-art convolutional neural networks (CNNs) and differential evolution fitting to co-refine multiple time-dependent XRR curves $R(q,t)$ of a

thin film growth experiment. Thereby it becomes possible to correctly analyze XRR data with a fidelity corresponding to standard fits of individual XRR curves even if they are sparsely sampled with a 7-fold reduction of XRR datapoints, or if the data is noisy due to a 200-fold reduction in counting times. Our approach of using a CNN analysis and of including prior information through a kinetic model is not limited to growth studies, but can be easily extended to other kinetic X-ray or neutron reflectivity data to enable faster measurements with lower beam damage.

DS 1.4 Mon 10:15 H14

Scattergram analysis and filtering of differential phase contrast STEM images — •JULIUS BÜRGER^{1,2}, MAJA GROLL^{1,2}, THOMAS RIEDL^{1,2}, and JÖRG K. N. LINDNER^{1,2} — ¹Nanostructuring, Nanoanalysis and Photonic Materials Group, Dept. of Physics, Paderborn University, Paderborn, Germany — ²Center for Optoelectronics and Photonics Paderborn (CeOPP), Paderborn, Germany

Differential phase contrast (DPC) in scanning transmission electron microscopy allows the imaging and quantification of electric fields in solid specimen by measuring the transferred (first) momentum perpendicular to the optical axis imposed on the beam by the specimen's electrostatic potentials. Owing to the high-resolution capability of modern Cs-corrected transmission electron microscopes, electric fields and charge densities can be revealed with sub-atomic resolution. However, the requirements are very high, since the field distributions being measured by a position sensitive detector are drastically influenced by numerous factors, such as the lens aberrations, dynamic diffraction effects, noises, and the detector response function. We demonstrate how these influences can be readily detected in a DPC image using the so-called scattergram, which is a two-dimensional histogram of all transferred momenta, and particularly focus on the effect of noise and detector rotation by comparing DPC measurements and simulations for Si [110] performed with a segmented annular quadrant detector. In this regard, we introduce a novel method, the scattergram filtering, revealing the position of characteristic features in DPC images.

DS 1.5 Mon 10:30 H14

Contrast modes in transmission experiments using broad and focussed keV ion beams — •SVENJA LOHMANN^{1,2}, GREGOR HLAWACEK¹, RADEK HOLEŇÁK², NICO KLINGNER¹, DANIEL PRIMETZHOFFER², and EDUARDO SERRALTA^{1,3} — ¹Institute of Ion Beam Physics and Materials Research, Helmholtz-Zentrum Dresden-Rossendorf, Dresden, Germany — ²Department of Physics and Astronomy, Uppsala University, Uppsala, Sweden — ³Technische Universität Dresden, Germany

The helium ion microscope (HIM) is an instrument for high-resolution imaging, composition analysis, and materials modification at the nanoscale. Ion transmission experiments could further improve the analytical capabilities of this technique, and multiple contrast modes are possible. We explore the latter at keV ion energies using a HIM in a scanning transmission approach as well as a broad beam in combination with a time-of-flight (ToF) set-up. Both systems employ position-sensitive detectors allowing for analysis of angular distributions.

In the ToF-system, we find a strong trajectory-dependence of the measured specific energy loss attributed to charge-exchange events in close collisions [Phys. Rev. Lett. 124 (2020), 096601]. Channelling and blocking of transmitted ions allows for mapping of intensity as well as different energy loss moments [Ultramicroscopy 217 (2020), 113051]. In the HIM we demonstrate different contrasts, e.g., due to orientation of nanocrystals, channelling in single-crystalline membranes and material contrast for layered films [Beilstein J. Nanotechnol. 11 (2020), 1854].

DS 2: Focus Session: Innovative GaN-based High-power Devices: Growth, Characterization, Simulation, Application 1

Organizers:

Bernd Witzigmann, University Erlangen-Nürnberg

Frank Bertram, Magdeburg University

The transition to globally sustainable energy generation requires a further significant rise of sharing electrical energy. Power electronics is a key technology enabling efficient distribution, conversion, and use of these large amounts of electrical energy. Thanks to the advances in semiconductor materials with solid-state properties, power electronics research remains a focal point. The remarkable progress in wide-bandgap semiconductor materials such as Gallium Nitride (GaN) allows for power devices reaching switching speeds an order of magnitude above the state of the art, with significantly reduced ohmic and dynamic losses, and improved thermal properties. GaN-based devices and circuits therefore enable the design of highly compact power-electronic systems with highest efficiencies. Considerable energy savings are possible, e.g. with energy and vehicle technology alone, a previously unused potential of up to 35% can be exploited. This not only offers economic advantages, but also significantly reduces the CO₂ equivalents associated with the applications.

Time: Monday 9:30–11:15

Location: H17

Invited Talk DS.2.1 Mon 9:30 H17

GaN-based power converters enabling talktive power — •MARCO LISERRE — Kiel University, Kiel, Germany

GaN power semiconductors with their extremely fast switching characteristics enable not only electrical energy conversion which is almost free from switching losses but also to bridge for the first time two fields which have been developing separately for more than 70 years: energy and information transfer. This contribution will start from the physical characteristics of GaN power semiconductors to show what they allow in power conversion and how they can lead to realize power exchange which carries also information.

Invited Talk DS.2.2 Mon 10:00 H17

Energy-efficient power electronics based on Gallium Nitride — •OLIVER AMBACHER — Sustainable Systems Engineering (INATECH), Albert-Ludwigs-Universität, Freiburg

Around 40% of the energy converted worldwide by technical systems is already provided in the form of electricity. This share is expected to increase to around 60% in 2040. These enormous amounts of energy not only have to be generated in a way that conserves resources and the environment, but also distributed and used efficiently. The power electronics required for this is an "emerging field" of electrical engineering, which makes it possible to provide electrical energy optimally adapted for a wide variety of applications. These applications include the integration of renewable energy sources into the electrical supply network, drive technology for electromobility, the power supply for data centers or the high-frequency network for mobile communications. Using the example of the development and use of particularly energy-efficient gallium nitride-based power electronic circuits, the presentation will illustrate the high potential for saving energy that further optimization of semiconductor materials and micro-electronic components offers and how sustainable electronic systems can be realized from them. Based on a basic understanding of the "atomic building blocks", functional material properties are derived and presented for the design of novel power electronic devices and components. These GaN-based components are demonstrated for high performance amplifiers and voltage converters that are characterized by particularly energy-efficient operation.

DS.2.3 Mon 10:30 H17

Influence of space-charge region on luminescence in a lateral GaN superjunction — •GORDON SCHMIDT¹, PETER VEIT¹, FRANK BERTRAM¹, JÜRGEN CHRISTEN¹, ARNE DEBALD², MICHAEL HEUKEN^{2,3}, THORSTEN ZWEIFENNIG², HOLGER KALISCH², and ANDREI VESCAN² — ¹Otto-von-Guericke-University Magdeburg, Magdeburg, Germany — ²RWTH Aachen University, Aachen, Germany — ³AIXTRON SE, Herzogenrath, Germany

The superjunction concept, based on charge compensation in the drift region by fully balanced n- and p-regions, is intended to break the tradeoff between breakdown voltage and on-resistance in GaN-based power devices.

In this study, a lateral GaN p-n⁺ superjunction was investigated by scanning transmission electron microscope cathodoluminescence microscopy. The structure was grown on top of a GaN/sapphire template. After the growth of an AlGaIn marker layer, the superjunction was epitaxially deposited composed of alternating 91 nm thick p-GaN with $5 \cdot 10^{18} \text{ cm}^{-3}$ Mg doping and 23 nm thick n⁺GaN with $1 \cdot 10^{19}$ Si doping. Finally, the structure was capped by a n⁺GaN layer. To probe the space charge region of the superjunction, the luminescence evolution across the pn⁺p junctions was investigated at T = 16 K. Donor-acceptor-pair recombination (DAP) is dominating the spectrum in the n-doped layers. In the near-band-edge region, bound exciton luminescence is observed in GaN:Mg. Both, excitons bound to an acceptor as well as to a donor exhibit reduced intensity in the space-charge region indicating exciton dissociation by the built-in electric field.

Invited Talk DS.2.4 Mon 10:45 H17

Potential of Aluminum Nitride for Vertical Power Electronics — •ANDREAS WAAG^{1,2}, KLAAS STREMPPEL^{1,2}, LUKAS PETERS^{1,2}, CHRISTOPH MARGENFELD^{1,2}, SAMUEL FABER³, FRIEDHARD RÖMER³, and BERND WITZIGMANN³ — ¹Institute of Semiconductor Technology, Technische Universität Braunschweig, Hans-Sommer-Straße 66, 38106 Braunschweig, Germany — ²Laboratory for Emerging Nanometrology (LENA), Technische Universität Braunschweig, Langer Kamp 6, 38106 Braunschweig, Germany — ³Institute for Optoelectronics, Friedrich-Alexander Universität Erlangen-Nürnberg, Konrad-Zuse Str. 3/5, 91052 Erlangen, Germany

Owing to its excellent material properties, AlN is considered to be highly promising for power electronics. One of the main obstacles for AlN, however, is the poor availability of single crystal substrates. A particularly promising technique is the high temperature annealing (HTA) of sputtered AlN thin films on sapphire. AlN is one of the few compound semiconductors, which is curing its crystal lattice during HTA without thermal decomposition or evaporation if processed in a face-to-face configuration.

In addition to the material aspects, we discuss the design of AlN devices, supported by TCAD simulations, combining microscopic drift-diffusion currents with electron/hole continuity equations and the Poisson equation.

DS 3: 2D Materials 1 (joint session HL/CPP/DS)

Time: Monday 9:30–12:45

Location: H36

See HL 6 for details of this session.

DS 4: Thin Film Properties: Structure, Morphology and Composition (XRD, TEM, XPS, SIMS, RBS, AFM, ...) 2

Time: Monday 11:00–11:45

Location: H14

DS 4.1 Mon 11:00 H14

Scaling and confinement in ultrathin chalcogenide films as exemplified by GeTe — •PETER KERRES — 1st Institute of Physics "new Materials", RWTH Aachen University, 52066 Aachen, Germany

Chalcogenides such as GeTe, PbTe, Sb₂Te₃, and Bi₂Se₃ are characterized by an unconventional combination of properties enabling a plethora of applications ranging from thermo-electrics to phase change materials, topological insulators and photonic switches. Chalcogenides possess pronounced optical absorption, relatively low effective masses, reasonably high electron mobilities, soft bonds, large bond polarizabilities and low thermal conductivities. These remarkable characteristics are linked to an unconventional bonding mechanism characterized by a competition between electron delocalization and electron localization. Confinement, i.e. the reduction of the sample dimension as realized in thin films should alter this competition and modify chemical bonds and the resulting properties. Here, we demonstrate for crystalline films of GeTe pronounced changes of optical and vibrational properties, while amorphous films of GeTe show no similar thickness dependence. For crystalline films, this thickness dependence persists up to remarkably large thicknesses of 40 nm. x-ray diffraction and accompanying simulations employing density functional theory relate these changes to thickness dependent structural (Peierls) distortions, due to an increased electron localization between adjacent atoms upon reducing the film thickness. We expect a thickness dependence and hence potential to modify film properties for all chalcogenide films with a similar bonding mechanism.

DS 4.2 Mon 11:15 H14

Solid-state microstructural evolution and dewetting of Co_xCu_{100-x} thin films — •FARNAZ FARZAM¹, BÁRBARA BELLÓN¹, MATTEO GHIDELLI^{1,2}, MARÍA JAZMIN DUARTE CORREA¹, DOMINIQUE CHATAIN³, and GERHARD DEHM¹ — ¹Max-Planck-Institut für Eisenforschung GmbH, Düsseldorf, Germany — ²LSPM, CNRS, Université Sorbonne Paris Nord, Villetaneuse, France — ³Aix-Marseille Univ, CNRS, CINaM, Marseille, France

Metallic thin films can undergo severe microstructural and morphological evolution, while maintaining their solid state at high temperatures below their melt-

ing point (T_M). These structural changes such as hillock formation and texture evolution can be followed by solid-state dewetting (SSD) in which capillary forces finally break up the film into isolated particles. Here, we investigate the microstructural evolution of Co_xCu_{100-x} thin films with x equal to 15, 38 and 75 at.%. Films were deposited on (0001) sapphire and annealed below their T_M . Subsequently, characterization has been carried out using scanning and transmission electron microscopy (SEM, TEM), and X-ray diffraction (XRD). Upon annealing, Cu-rich hillocks form in all three compositions prior to voids at which dewetting initiates. The onset temperature of the formation of these hillocks depends on the composition of the film. Moreover, a phase separation of FCC Co and FCC Cu is observed. Finally, we show an orientation relationship of Cu (FCC) and Co (FCC)-rich isolated particles with sapphire: $Cu/Co(111) \pm [1\bar{1}0] \parallel Al_2O_3(0001)[10\bar{1}0]$.

DS 4.3 Mon 11:30 H14

Analysis of 3D check board pattern formation in NiCoMnAl shape memory alloys with alternating austenitic and martensitic layers — •DARIO STIERL, ANDREAS BECKER, LAILA BONDZIO, TAPAS SAMANTA, INGA ENNEN, and ANDREAS HÜTTEN — Center for Thin Films and Physics of Nanostructures, Physics Department, Bielefeld University, 33615 Bielefeld, Germany

NiMnX (X=Al, Ga, Sn, In) magnetic shape memory Heusler alloys are considered as promising materials for magnetocaloric cooling applications due to their magnetoelastic coupling near room temperature. The thermal hysteresis could be reduced in NiCoMnAl thin films with alternating active transforming austenitic layers and martensitic intercalations. The stoichiometry of these two layers is chosen in such a way that their thermal hysteresis does not overlap. In addition, a 3D check board pattern becomes visible in HRTEM cross section images if the austenite active layers and martensite intercalations possess similar thicknesses.

In this contribution we aim for an improved understanding of the 3D check board pattern formation. Therefore, we varied the number of the alternating layers in one series and changed the ratio between the thicknesses of the two different layers in a different series. Furthermore, we analyzed the samples with XRD and temperature dependent magnetization measurements.

DS 5: Organic Thin Films, Organic-Inorganic Interfaces

Time: Monday 11:30–13:00

Location: H17

DS 5.1 Mon 11:30 H17

RuTPP thin films: morphology, dimerization and CO adsorption — •JAKOB HAUNS¹, JOHANNES SEIBEL¹, ARTUR BÖTTCHER¹, LUKAS GERHARD², WULF WULFHEKEL², and MANFRED KAPPES¹ — ¹Institute of Physical Chemistry, KIT, 76131 Karlsruhe, Germany — ²Institute of Nanotechnology, KIT, 76344, Eggenstein-Leopoldshafen, Germany

Thin RuTPP-2H films were grown on HOPG under UHV conditions by applying the Low Energy Cluster Beam Deposition method, LECBD [1]. We used the mass-selected (RuTPP-2H)⁺ beam resulting from electron impact induced ionization and fragmentation of the effusive flux of RuTPP molecules. The morphology of the films grown here were systematically studied by means of STM, UPS, XPS and desorption spectroscopy. The temperature programmed desorption (TPD) spectra, taken for sub- and multilayers enable to determine the binding energies explaining the unique stability of the films. In particular this analysis revealed the thermally activated formation of stable desorbable dimers for layers thicker than one monolayer. By combining STM and UPS we found spectral markers for the monomers and dimers deposited on HOPG. XPS/UPS based study of the CO adsorption on RuTPP-2H submonolayers revealed pronounced modifications of the valence band. These findings are supported by extensive DFT calculations which enable to identify the major CO-(RuTPP-2H) binding sites.

[1] J. Weippert, et al., J. Phys. Chem. C 2018, 122, 28588*28600

DS 5.2 Mon 11:45 H17

Low-Temperature Atomic Layer Deposition of Al₂O₃ Thin Films on Spin-Coated Carbon Nanomembranes — •JAN BIEDINGER, NATALIE FRESE, RAPHAEL DALPKE, BERNHARD KALTSCHMIDT, MARTIN WORTMANN, ANDREAS HÜTTEN, ARMIN GÖLZHÄUSER, and GÜNTER REISS — Bielefeld University, Germany

Carbon nanomembranes are stable, carbon-based 2D sheets that have been investigated in recent years due to their wide range of potential applications, in nanofiltration, nanoelectromechanical systems, microelectronics or energy storage [1]. Atomic layer deposition relies on alternating self-limiting gas-surface

reactions, resulting in smooth, conformal and defect-free coatings with precise thickness control [2]. In the presented work, carbon nanomembranes were coated with aluminum oxide (Al₂O₃) via a thermal atomic layer deposition process at a substrate temperature of 60°C including the reactants trimethylaluminum and water. Structural and compositional investigations of these bilayer systems by atomic force, helium ion and transmission electron microscopy as well as depth profile X-ray photoelectron spectroscopy and energy dispersive X-ray analysis, respectively, reveal a homogeneous and conformal coating of the entire sample, resulting in effective surface modification. In addition, gas permeation measurements were carried out to explore potential applications of such hybrid membranes, demonstrating atomic layer deposition offers a simple way of tuning carbon nanomembranes.

[1] A. Turchanin and A. Gözlhäuser, Adv. Mater. 28, 6075 (2016)

[2] S. M. George, Chem. Rev. 110, 111 (2010)

DS 5.3 Mon 12:00 H17

Contact Primers: A new Approach to Reducing Contact Resistance in Organic Field-Effect Transistors — •YURI RADIEV and GREGOR WITTE — Molekulare Festkörperphysik, Philipps-Universität Marburg, Renthof 7, 35037 Marburg, Germany

Methods to reduce contact resistance have long been of interest to researchers that aim to improve performance of organic electronic devices. Caused by the injection barrier at the metal-organic semiconductor interface, contact resistance was shown to be one of the main obstacles on the way to producing high-frequency organic field-effect transistors (OFETs), limiting the switching frequency of such transistors to well below gigahertz range [1]. In this work we report on the contact primer method [2] – a method that allows selective modification of the work function of the electrodes in a bottom gate-bottom contact OFET structure. The modified work function reduces the charge carrier injection barrier and improves the morphology of the subsequently deposited thin film on top. We demonstrate this effect for both p- and n-type OFETs by employing various organic contact primer materials to increase and reduce the work function of gold electrodes, respectively. Combining this device-oriented ap-

proach with a rigorous investigation of the employed material systems on model substrates, we are able to achieve deeper understanding of the phenomena that lead to a reduced contact resistance [3].

[1] U. Zschieschang, et al., *Adv. Func. Mater.* 30, 1903812 (2020).

[2] F. Widdascheck, et al., *Adv. Funct. Mater.* 29, 1808385 (2019).

[3] Y. Radiev, et al., *Org. Electron.* 89, 106030 (2021).

DS 5.4 Mon 12:15 H17

Patterned Growth of Organic Semiconductor Films by Electron Irradiation Induced F-Centers on Alkali Halide Substrates — •DARIUS GÜNDER¹, VALENTIN DIEZ-CABANES², ANDREA HUTTNER¹, TOBIAS BREUER¹, VINCENT LEMAU², JEROME CORNIL², and GREGOR WITTE¹ — ¹Molekulare Festkörperphysik, Philipps-Universität Marburg — ²Laboratory for Chemistry of Novel Materials, University of Mons

In this study, a new approach is introduced to control structural properties of organic films. Combining AFM, SEM and XRD we demonstrate that electron irradiation induced F-centers (halide vacancies) on KCl(100) surfaces strongly influence the molecular orientation and epitaxial alignment of dinaphthothienothiophene (DNNT) thin films. Due to electrostatic interactions between F-centers and interfacial DNNT molecules, as validated by DFT calculations, DNNT molecules adopt a recumbent molecular orientation and form elongated fibers instead of hexagonally shaped island with upright molecular orientation present on pristine KCl. Interestingly, both morphologies exhibit epitaxial alignments that are understood by higher-order commensurabilities. By inducing F-centers only at defined surface regions, this F-center controlled growth is utilized to achieve laterally patterned DNNT films that are even transferable to other substrates by a wet transfer process.

DS 5.5 Mon 12:30 H17

The Role of Molecular Packing in Strongly Coupled Metal-Organic Hybrid Structures — •MAXIMILIAN RÖDEL¹, POLINA LISINETSAYA², MAXIMILIAN RUDLOFF¹, THOMAS STARK³, JOCHEN MANARA³, ROLAND MITRIC², and JENS PFLAUM^{1,3} — ¹Experimental Physics VI, University of Würzburg, 97074 Würzburg — ²Institut für Physikalische und Theoretische Chemie, University of Würzburg, 97074 Würzburg — ³ZAE Bayern, 97074 Würzburg

DS 6: Focus Session: Innovative GaN-based High-power Devices: Growth, Characterization, Simulation, Application 2

Organizers:

Bernd Witzigmann, University Erlangen-Nürnberg

Frank Bertram, Magdeburg University

Synopsis (see part I)

Time: Monday 15:00–16:45

Location: H17

Invited Talk

DS 6.1 Mon 15:00 H17

Novel high power device structures: Enabling compact and integrated power ICs — •ELISON MATIOLI — EPFL, Lausanne, Switzerland

This talk will discuss new technologies to drastically reduce the sheet resistance in these semiconductors. Combined with a judicious design of the electric field distribution, based on nanostructures, this approach enables to concurrently reduce the on-resistance and increase the breakdown voltage of power devices, leading to figures of merit far beyond the state-of-the-art. To manage the large heat fluxes in power devices, I will present new technologies based on integrated microfluidic cooling inside the device. By co-designing microfluidics and electronics within the same semiconductor substrate, a monolithically integrated manifold microchannel cooling structure was produced with efficiency beyond what is currently available. Our results show that heat fluxes exceeding 1.7 kW/cm² could be extracted using only 0.57 W/cm² of pumping power. The proposed cooling technology should enable further miniaturization of electronics, and greatly reduce the energy consumption in cooling of electronics. Furthermore, by removing the need for large external heat sinks, this approach enables the realization of very compact power converters integrated on a single chip.

Invited Talk

DS 6.2 Mon 15:30 H17

Ab-initio investigations of V-pits and nanopipes in GaN — •LIVERIOS LYMPERAKIS^{1,2}, SU-HYUN YOO², and JÖRG NEUGEBAUER² — ¹Department of Physics, University of Crete, Heraklion, Greece — ²Computational Materials Design Department, Max-Planck-Institut für Eisenforschung GmbH, Düsseldorf, Germany

Dislocations in nitrides constitute a long-standing and controversial topic. Nevertheless, screw dislocations in GaN have recently attracted considerable inter-

The coupling between excited states in fluorinated zinc-phthalocyanine thin films (F_nZnPc, with n = 0,4,8,16) and surface plasmons in gold layers underneath enables unique insights in the resulting exciton-plasmon polariton coupling phenomena and their energetics. In particular, the increase of the molecular van der Waals radii by the degree of fluorination offers an additional degree of freedom to analyze the role of molecular orientation and aggregation on the resulting dispersion curves. As such, we were able to identify up to four anticrossings in the layered Au/F_nZnPc samples which can be attributed to: 1) a coexisting F₁₆ZnPc β-polymorph, 2) monomers, preferentially located at the metal interface, and 3) aggregated α-phase regions located within the F_nZnPc films. While energy and splitting of the monomer-related anticrossing are determined by the average tilting and the close proximity to the metal surface, the coupling associated with the aggregate can be consistently described by a change in F_nZnPc dipole density. Supported by structural data and TDDFT calculations in combinations with a Jaynes-Cummings model, Au/F_nZnPc bilayers prove to be a versatile platform to study the primary light-matter interactions.

DS 5.6 Mon 12:45 H17

Strong Quenching of Dye Fluorescence in Perylene Orange/TMDC Hybrid Structures — •TIM VÖLZER, ALINA SCHUBERT, ERIK VON DER OELSCHNITZ, INGO BARKE, SYLVIA SPELLER, TOBIAS KORN, and STEFAN LOCHBRUNNER — Institut für Physik, Universität Rostock, Albert-Einstein-Str. 23, 18059 Rostock

While monolayer transition metal dichalcogenides (1L-TMDCs) have emerged as 2D semiconductors with multiple applications in optoelectronics, their combination with dye molecules to form promising hybrid structures, since they should allow charge transfer after optical excitation as required for photodetectors or solar cells. Here, we discuss the preparation of such systems, i.e. the deposition of perylene orange (PO) onto substrates by means of spin coating, stamping, and thermal vapor deposition (TVD) and compare these methods regarding the quality of the dye layer and practicability of the process. For TVD-fabricated 1L-TMDC/PO hybrid structures, we observe a drastic quenching of the dye fluorescence in terms of both intensity and lifetime reduction for all used TMDCs compared to hBN/PO references. This quenching is attributed to electron or hole transfer depending on the energy levels of the molecule and the specific TMDC, respectively.

est due to their potential effect on power electronic devices' performance. An intriguing feature of these dislocations is that they trigger the formation of V-pits and nanopipes in GaN. However, a full understanding of their origin, size, and shape is still lacking. The nucleation and properties of these defects are governed by the complex interplay between dislocation's strain and core energies, surface energies, and oversaturation. In the present work, we combine density functional theory calculations with elasticity theory and we shed light on the aforementioned interplay. Based on these calculations we derive phase diagrams that describe the equilibrium size and shape of V-pits and nanopipes as a function of the ambient growth conditions, i.e., the Ga and H chemical potentials as well as the oversaturation. Our calculations indicate that under H-rich conditions, V-pits and nanopipes can spontaneously form due to the preferential decoration of the bounding surfaces by hydrogen. Based on these results we will further discuss their electronic properties as well as their potential to preferentially accommodate impurities/dopants.

DS 6.3 Mon 16:00 H17

Metal micro-contacts deposited by focused electron and ion beam: impact on electrical properties — •KONSTANTIN WEIN, GORDON SCHMIDT, FRANK BERTRAM, SILKE PETZOLD, PETER VEIT, CHRISTOPH BERGER, ANDRÉ STRITTMATTER, and JÜRGEN CHRISTEN — Otto-von-Guericke-University Magdeburg, Magdeburg, Germany

In this study, we want to concentrate on the local deposition of platinum and tungsten as metal micro-contacts by electron- as well as ion-beam in a focused ion beam microscope (FIB). We are using a Thermo Fisher Scientific Scios 2 HighVac dual-beam with liquid gallium ion source. Either the focused electron beam or the ion beam are used to crack the precursor molecule bonds and induce the complex metal deposition process.

For the investigation of the electrical properties Pt/W stripes were deposited between macroscopic lithographic Au pads on top of insulating SiO₂/Si template. Parameters like Ga- and e-beam current, acceleration voltage, dwell time and pixel overlap were systematically investigated and optimized with regard to best electrical properties. The trade-off between efficient incorporation of conductive material and sputtering has to be determined. We observe almost insulating properties for layers deposited by electron beam radiation. On the other hand, the ion beam induced deposition layers behave ohmic and exhibit electrical conductivity up to $4.6 \frac{10^5}{\Omega \cdot \text{cm}}$ for tungsten.

Invited Talk

DS 6.4 Mon 16:15 H17

Lateral and Vertical β -Ga₂O₃ Power Transistors for High-Voltage Applications — •KORNELIUS TETZNER¹, MICHAEL KLUPSCH¹, KARINA ICKERT¹, RALPH-STEPHAN UNGER¹, ZBIGNIEW GALAZKA², TA-SHUN CHOU², SAUD BIN ANOOZ², ANDREAS POPP², JOACHIM WÜRFEL¹, and OLIVER HILT¹ — ¹Ferdinand-Braun-Institut, Leibniz-Institut für Höchstfrequenztechnik (FBH), Gustav-

Kirchhoff-Straße 4, 12489 Berlin, Germany — ²Leibniz-Institut für Kristallzüchtung (IKZ), Max-Born-Straße 2, 12489 Berlin, Germany

Beta gallium oxide (β -Ga₂O₃) with its ultra-wide bandgap of 4.8 eV has emerged as a promising semiconducting material for the fabrication of next-generation power electronic devices. The estimated dielectric strength of 8 MV/cm in combination with the expected Baliga's figure of merit are promising indicators to pave the way for the realization of power devices with even higher breakdown voltages and efficiencies than their SiC and GaN counterparts. This presentation will give an overview on the current status of lateral and vertical β -Ga₂O₃ power transistor devices with a special emphasis on results obtained at FBH and IKZ. For both cases different concepts for bulk crystal growth, epitaxial layer structures and device designs suitable for reaching the targeted performance will be discussed especially in terms of breakdown voltage and channel current density. In this regard, certain material and device related challenges are identified which need to be addressed perspectively in order to overcome current breakdown limitations.

DS 7: 2D Materials 2 (joint session HL/CPP/DS)

Time: Monday 15:00–18:30

Location: H36

See HL 11 for details of this session.

DS 8: 2D Materials 3 (joint session CPP/DS)

Time: Monday 17:15–17:45

Location: H38

See CPP 11 for details of this session.

DS 9: Thin Film Properties: Structure, Morphology and Composition (XRD, TEM, XPS, SIMS, RBS, AFM, ...) 3

Time: Tuesday 9:30–11:00

Location: H14

DS 9.1 Tue 9:30 H14

Structural properties of iron dichalcogenide thin films deposited by selenization process — •LUQMAN MUSTAFA¹, ANDREAS KREYSSIG¹, JILL FORTMANN², AURELIJA MOCKUTE², ALFRED LUDWIG², and ANNA E. BÖHMER¹ — ¹Institute for Experimental Physics IV, Ruhr-Universität Bochum, Germany — ²Materials Discovery and Interfaces, Institute for Materials, Ruhr University Bochum, Germany

Transition-metal dichalcogenides with marcasite structure have been extensively studied for their applications in light energy conversion and photoelectrochemical devices. Lately this structure type has also gained interest for its magnetic properties as a candidate for the newly-predicted altermagnetic order.

We report on the formation of (Fe,X)Se₂, (X= Co, Mn, Cr...) thin films by ex-situ selenization of amorphous transition metal thin films. Using combinatorial deposition allowed to efficiently explore a wide range of substitution at the iron site with different transition metals (for example Co, Mn, Cr). The dependence of structural properties and phase stability on the selenization temperature and substitution level has been investigated. The process may be adapted for other transition metal dichalcogenides thin films, such as FeSb₂, and is therefore a unique tool to study a broad material family and its possible substitution ranges.

DS 9.2 Tue 9:45 H14

Structural and elastic properties of Sc_xAl_{1-x}N — •SASKIA MIHALIC¹, ARMIN DADGAR², NICLAS M. FEIL¹, CHRISTOPHER LÜTTICH², ANDRÉ STRITTMATTER², and OLIVER AMBACHER¹ — ¹Department of Sustainable Systems Engineering, University of Freiburg, Germany — ²Department of Semiconductor Epitaxy, Otto von Guericke University Magdeburg, Germany

The hexagonal compound alloy scandium aluminum nitride (Sc_xAl_{1-x}N) shows an enhancement of the piezoelectric module $d_{33}(x)$ by more than 300 % compared to aluminum nitride (AlN). Therefore, Sc_xAl_{1-x}N is a highly promising material for the implementation of acoustic resonators for mobile communication systems, although usually a larger stiffness of the material is required. The direction-dependent elastic behavior of hexagonal Sc_xAl_{1-x}N crystals is represented by the reciprocal Young's modulus $S_{11}^*(x)$ and aids in identifying the best trade-off between piezoelectric and elastic properties of anisotropic Sc_xAl_{1-x}N for microacoustic applications. To confirm the calculations with experimental results, thin films of Sc_xAl_{1-x}N(0001) and ScN(111) on Si-substrates were grown by reactive magnetron sputter epitaxy. The structural properties of thin films have been investigated by high-resolution X-Ray diffractometry (HRXRD) and high-resolution transmission electron microscopy (HRTEM). Furthermore, we will present a detailed comparison of theoretical and experimental results of

the piezoelectric and stiffness coefficients achieved by the analysis of Sc_xAl_{1-x}N-based SAW resonators.

DS 9.3 Tue 10:00 H14

Structural analysis of Sc_xAl_{1-x}N thin films — •REBECCA PETRICH¹, YOUNES SLIMI¹, HAUKE HONIG², LORENZ STEINACKER², KATJA TONISCH¹, RAPHAEL KUHNEN³, DIETMAR FRÜHAUF³, and STEFAN KRISCHOK¹ — ¹TU Ilmenau, FG Technische Physik I, IMN MacroNano, 98693 Ilmenau — ²TU Ilmenau, FG Werkstoffe der Elektrotechnik, IMN MacroNano, 98693 Ilmenau — ³Endress+Hauser SE+Co. KG, TTD Technologieentwicklung, 79689 Maulburg

The further and new development of functional materials is an important and constant research approach for the optimization of microelectromechanical systems. In the field of piezoelectric materials, AlN stands out due to its good piezoelectric properties and its CMOS compatibility, its very good thermal stability and high sound velocity. While the basic research for this material is considered to be largely completed, research for the scandium-based alloy Sc_xAl_{1-x}N is still in its infancy. The need for investigation is particularly high for alloys with scandium concentrations of more than x = 15%. For this purpose, Sc_xAl_{1-x}N thin films were deposited and analyzed using pulsed magnetron sputtering in a concentration range between x = 15% and 35%. Starting with the crystal orientation (X-ray diffractometry) and the layer composition (energy-dispersive X-ray spectroscopy) through to the surface roughness (atomic force microscopy), optical parameters for determining the layer thickness and dielectric function (spectroscopic UV-Vis ellipsometry) were also examined and compared to pure AlN. In addition, the homogeneity of the layer properties was examined over different radii on 4" Si wafers.

DS 9.4 Tue 10:15 H14

Phase behavior of dumbbell monolayers obtained via Langmuir-Blodgett-like Brownian dynamics simulations — •ANTON LÜDERS, ROUVEN STUCKERT, ELLEN ZANDER, ALEXANDER WITTEMANN, and PETER NIELABA — Universität Konstanz, Konstanz, Deutschland

We explore the structure formation and the phase behavior of thin films of dumbbell colloids. For this, we first determine empiric formulas for the microscopic diffusion coefficients of dumbbells using a bead-shell approach. These diffusion coefficients are used to perform two-dimensional Brownian dynamics (BD) simulations where the area fraction of the system is adjusted via movable barriers at the boundaries of the simulation box. The results of the simulations are compared to Langmuir-Blodgett experiments with dumbbell monolayers at the air/water interface. Using Voronoi diagrams and the Voronoi cell shape factor,

the influence of the area fraction on the structure of the monolayers is investigated. The simulations and the experiments show - in excellent agreement with each other - that an increase of the area fraction leads to a higher percentage of domains containing particles with six nearest neighbors. Especially in dense systems, these domains can consist of aligned particles with uniform Voronoi cells. Thus, the increase of the area fraction enhances the order of the monolayers. The remarkable qualitative agreement of the simulations and the experiments indicates a versatile way of characterizing colloidal monolayers by BD simulations which opens up perspectives for application to a broad range of nanoparticle-based thin film coatings.

DS 9.5 Tue 10:30 H14

Thermal Laser Epitaxy of Refractory Metals — •LENA NADINE MAJER, HONGGUANG WANG, WOLFGANG BRAUN, PETER A. VAN AKEN, JOCHEN MANNHART, and SANDER SMINK — Max Planck Institute for Solid State Research, Heisenbergstraße 1, 70569 Stuttgart, Germany

In thermal laser epitaxy, both the substrate and the individual evaporation sources are heated by high-power continuous-wave lasers. This method combines the advantages of MBE and PLD, allowing the efficient thermal evaporation and epitaxial deposition of practically any combination of elements from the periodic table. We demonstrate and discuss the epitaxial growth of refractory metals on c-cut sapphire. As examples we present Ru and Ta growth, because they are of particular interest for many technological applications. We have optimized the growth parameters to obtain epitaxial films of superior quality, which are apparently devoid of defects over large areas. The films have been characterized by AFM, RHEED, STEM, and X-ray analysis, revealing that the layers grow

single phase, with a low surface roughness and that the interface between the layer and the substrate is atomically sharp.

DS 9.6 Tue 10:45 H14

Temperature-dependent C-AFM measurements on rhodium paddle-wheel coordination polymers — DANIEL STEINBACH, SOPHIE GERSDORF, and •FLORIAN MERTENS — Institute of Physical Chemistry, TU Bergakademie Freiberg, Germany

To overcome one of the disadvantages of most coordination polymers and metal-organic frameworks being insulators, conjugated coordination polymers are investigated regarding their electrical conductivity. To obtain a potentially conductive system paddle-wheel structures with a documented metal-metal bond, here rhodium derivatives, were linked via conjugated organic molecules like pyrazine. Coordination polymers of this type were first synthesized as bulk materials, characterized using XRD, TG-DSC and XPS and then deposited as coatings on gold surfaces. Subsequently, the topography of the deposited layers was determined. The morphological properties of the coatings were correlated with the properties of the basic coordination polymer components.

The conductivity was investigated via temperature-dependent C-AFM measurements. As expected no conductivity is measurable for coordination polymers containing acetates based paddle-wheels even if they are linked with a tridentate conjugated ligand. For the $[\text{Rh}_2(\text{acam})_4(\text{pyz})]_n$ (Hacam = acetamide) coordination polymer a strong temperature and field dependency of the conductivity was observed. From the corresponding measurements an Arrhenius type activation energy of app. 0.3-0.4 eV was derived. In addition, various conduction mechanisms were discussed.

DS 10: Gaede Prize Talks

Time: Tuesday 9:30–11:30

Location: H17

Laudatio

Prize Talk

DS 10.1 Tue 9:40 H17

Atomic-Scale Optical Spectroscopy at Surfaces — •TAKASHI KUMAGAI — Fritz Haber Institute, Berlin, German — Institute for Molecular Science, Okazaki, Aichi, Japan — Laureate of the Gaede-Prize 2020

Light-matter interactions can be largely enhanced in the presence of optical near fields. Atomic-scale light-matter interactions in plasmonic “picocavities” has emerged as a new frontier of fundamental light science and technology [1]. However, the investigation of such light-matter interactions still involves significant challenges in both experiment and theory. A combination of plasmon-enhanced spectroscopy with low-temperature STM can provide a unique way to investigate intriguing physics resulting from the strong interaction between cavity-mode plasmon and matter even at atomic scales [2]. I will discuss our recent development toward atomic-scale optical spectroscopy in plasmonic STM junctions [3].

References: [1] Nat. Mater. 18, 668 (2019). [2] Nat. Rev. Phys. 3, 411 (2021). [3] Phys. Rev. Lett. 128, 206803 (2022); Nano Lett. 22, 2170 (2022); ACS Photonics 8, 2610 (2021); Nano Lett. 21, 4057 (2021); Nano Lett. 20, 5879 (2020); Nano Lett. 19, 5725 (2019); Nano Lett. 19, 3597 (2019).

Laudatio

Prize Talk

DS 10.2 Tue 10:20 H17

Slow highly charged ions as a tool for monolayer sensitive nano-engineering — •RICHARD WILHELM — TU Wien, Institute of Applied Physics, Vienna, Austria — Laureate of the Gaede-Prize 2021

Heavy ions in high charge states can be prepared with kinetic energies in the keV energy range. These slow ions interact with surface electrons upon impact of a material which leads to their neutralisation and consequently to the deposition of several ten keV of potential energy. Over the past 20 years it has been a puzzle how fast and consequently how surface sensitive this energy deposition is. With the use of freestanding two-dimensional materials we can now limit the interac-

tion time of the ions with a solid to the femtosecond regime. We find that most of the neutralisation of the ions takes place in a single atomic monolayer of material. In this contribution I will discuss recent advancements in the study of ion neutralisation dynamics inside of solids as well as the efficiency of potential energy driven sputtering of atoms. The latter depends on the type of material and can be confined to a single monolayer only, despite the high amount of deposited energy.

Laudatio

Prize Talk

DS 10.3 Tue 11:00 H17

Quantum Science with Single Atoms and Molecules on Surfaces — •PHILIP WILLKE — Karlsruhe Institute of Technology, Physikalisches Institut, Karlsruhe, Germany — Laureate of the Gaede-Prize 2022

The quantum nature of a physical system often emerges from its fundamental building blocks and demands a profound understanding to harvest its advantages for quantum devices. In this talk, I will introduce a new architecture for coherent control of spins on surfaces, by combining electron spin resonance (ESR) and scanning tunneling microscopy (STM) [1]. This technique allows to address single atoms and molecules on surfaces with unprecedented energy resolution. Thus, it can be used to sense the magnetic coupling between spin centers on the nanoscale [2]. In addition, when scanning the STM tip across the surface it permits to perform magnetic resonance imaging on the atomic scale [3]. The high energy resolution also grants access to the hyperfine interaction between the electron and nuclear spin of different atomic species [4]. Recently, we could extend this technique also to spin resonance on individual molecules [5]. Lastly, by employing pulsed ESR schemes, a coherent manipulation of the surface spin becomes possible, for instance in Rabi and Hahn echo schemes [6]. This opens up a path towards quantum information processing and quantum sensing using atomic building blocks, including atoms and molecules. [1] S. Baumann et al., Science 350 (2015) [2] T. Choi et al. Nat. Nano 12 (2017) [3] P. Willke et al., Nat. Phys. 15 (2019) [4] P. Willke et al., Science 362 (2018) [5] X. Zhang et al., Nat. Chem. 14 (2022) [6] K. Yang et al., Science 366 (2019)

DS 11: Focus Session: Quantum Properties at Functional Oxide Interfaces 1 (joint session HL/DS)

Modern oxide materials exhibit a rich variety of physical properties that lead to potential applications such as sensors and detectors, solar energy harvesting, transparent and power electronics. Understanding their quantum properties at surfaces and interfaces may play a decisive role for functionalities in high-electron-mobility transistors, quantum electronics or topological quantum computation. These typically require homo- or heteroepitaxial layers of high crystallinity and investigation methods designed to reveal the fascinating physics at (complex) oxide interfaces. This session sets a focus on growth of oxide interfaces, the experimental and theoretical investigation of their novel physical, in particular quantum properties as well as fabrication and characterization of demonstrator devices.

Organized by Martin Albrecht, Oliver Bierwagen, and Saskia F. Fischer

Time: Tuesday 9:30–12:45

Location: H34

See HL 14 for details of this session.

DS 12: 2D Materials 4 (joint session HL/ CPP/DS)

Time: Tuesday 9:30–12:00

Location: H36

See HL 15 for details of this session.

DS 13: Thin Film Applications 2

Time: Wednesday 9:30–10:45

Location: H14

DS 13.1 Wed 9:30 H14

Investigation of Production Techniques for Sputtered Tungsten Thin Films — •TOBIAS ORTMANN¹, ANDREAS ERHART¹, MARGARITA KAZNACHEEVA¹, ANGELINA KINAST¹, ALEXANDER LANGENKÄMPER¹, LUCA PATTAVINA¹, WALTER POTZEL¹, JOHANN RIESCH², JOHANNES ROTHE¹, NICOLE SCHERMER¹, STEFAN SCHÖNERT¹, RAIMUND STRAUSS¹, VICTORIA WAGNER¹, and ALEXANDER WEX¹ — ¹Technische Universität München, Physik Department Lehrstuhl E15, James-Frank-Straße 1, D-85748 Garching — ²Max-Planck-Institut für Plasmaphysik, Boltzmannstraße 2, D-85748 Garching bei München

Cryogenic rare event searches like the CRESST and the NUCLEUS experiments use TES (Transition Edge Sensors) as phonon sensors to read out their target crystals. This type of sensors utilizes the superconducting phase transition of tungsten to measure the energy deposited in the absorbers. The most established method of production for these films is electron beam physical vapor deposition. For future large scale production the application of argon DC-magnetron sputtering is investigated in terms of film quality and reproducibility. The most recent results of these investigations are presented. The research was supported by the DFG through the Excellence Cluster ORIGINS and the SFB1258, and the BMBF: 05A17WO4 and 05A17VTA.

DS 13.2 Wed 9:45 H14

Preparation of RuVO₂ alloy thin films and their uncooled infrared detection performance — •HAO LU^{1,2,3}, YUNBIN HE³, and PETER J. KLAR^{1,2} — ¹Institute of Experimental Physics I, Justus-Liebig-University, Giessen, Germany — ²Center for Materials Research (ZfM), Justus-Liebig-University, Giessen, Germany — ³School of Materials Science and Engineering, Hubei University, Wuhan 430062, China

Vanadium dioxide (VO₂) films are the most popular materials for sensing layers in uncooled IR detectors because of their high TCR of -2.0%/K, low noise, low thermal conductivity. The monoclinic phase (M1) of VO₂ undergoes an insulator-to-metal transition at 341K which is accompanied by the crystal structure changing from tetragonal to rutile. The structural phase transition exhibits a thermal hysteresis, which reduces the sensitivity of the minimum temperature change detectable indicative for the IR intensify. So we focused on decreasing the thermal hysteresis width whilst increasing TCR, and carried out the following study: (022) oriented RuVO₂ alloy thin films were prepared on TiO₂ (110) substrates by pulsed laser deposition. It was found that the thermal hysteresis width of RuVO₂ (M1) for Ru content contents above 7% is smaller than for corresponding binary VO₂. The TCR of such RuVO₂ alloy films was -5.2%/K, and the thermal hysteresis was no longer observable from electrical properties. This work demonstrates the potential of VO₂ (M1) for the development of the IR detector.

DS 13.3 Wed 10:00 H14

Tracking the evolution of polarization in BiFeO₃-based devices — •MARVIN MÜLLER¹, YEN-LIN HUANG², SAÜL VÉLEZ³, RAMAMOORTHY RAMESH², MANFRED FIEBIG¹, and MORGAN TRASSIN¹ — ¹Department of Materials, ETH Zurich, Switzerland — ²Department of Material Science and Engineering, University of California, Berkeley, USA — ³Department of Physics, Universidad Autónoma de Madrid, Spain

The integration of magnetoelectric multiferroics, hosting coexisting and coupled ferromagnetic and ferroelectric orders, into magnetoelectric spin-orbit logic devices holds promises for unprecedented performance and reduction of energy consumption by several orders of magnitude. While static properties such as the coercive electric field have been thoroughly studied and optimized, investigations on the evolution of the ferroic orders during electric-field switching cycles are sparse.

Here, we study the three-dimensional evolution of the net polarization in the technologically highly relevant magnetoelectric material La_{0.15}Bi_{0.85}FeO₃. Using optical second-harmonic generation microscopy, we access the polarization of the films integrated in capacitor heterostructures operando. We demonstrate that electric-field training results in a spontaneous domain ordering and a giant enhancement of the net in-plane polarization in La_{0.15}Bi_{0.85}FeO₃. Finally, we distinguish between the behavior of the in-plane and out-of-plane polarization during the electric poling. Our investigations thus give unprecedented insights into the polarization dynamics in integrated BiFeO₃-based devices.

DS 13.4 Wed 10:15 H14

Photoelectrochemical properties of CuBi₂O₄-based electrodes prepared via spin-coating for solar water splitting. — •FRANCESCO CADDEO, MARCO KRUEGER, SOPHIE MEDICUS, CARINA HEDRICH, ROBERT ZIEROLD, and DOROTA KOZIEJ — University of Hamburg, Institute of Nanostructure and Solid State Physics Luruper Chaussee 149, D-22761 Hamburg, Germany

Photoelectrochemical (PEC) water splitting is one of the most promising technologies for the conversion of solar energy into hydrogen gas, which can be stored and used on demand as a fuel with net-zero CO₂ emissions. Copper bismuth oxide (CuBi₂O₄) is recently emerging as a promising metal-oxide to be used as a light harvesting material in the photocathode of a PEC cell and is attracting increasing attention due to its well-suited bandgap of ca. 1.8 eV, its conduction band position of -0.7 V vs RHE (Reversible Hydrogen Electrode) and its highly anodic onset potential of ca. 0.8 V vs RHE, which makes it an ideal material to be implemented in a tandem device for unassisted solar water splitting. In our labs, we have developed a spin-coating procedure that allows us to fabricate highly uniform CuBi₂O₄ films with pure crystalline phase and various thicknesses on top of fluorine-doped tin oxide coated glass (FTO) used as a support. During my presentation, I will talk about recent results on the synthesis, characterization and photoelectrochemical properties of CuBi₂O₄ based photo-electrodes protected with a uniform coating of TiO₂ overlayer deposited using Atomic Layer Deposition (ALD).

DS 13.5 Wed 10:30 H14

Growth and electrical properties of sputtered gallium oxide device — •AMAN BAUNTHIYAL, MARCO SCHOWALTER, THORSTEN MEHRTENS, ANDREAS ROSENAUER, SEYED MAJID MAHDIAN, JON-OLAF KRISPONEIT, and JENS FALTA — Institute of Solid State Physics, University of Bremen, Germany

Due to the scalability limitations of conventional semiconductor based devices, there is a high demand for powerful memory devices. Resistive switching (RS) is a promising phenomenon especially for future resistance random access memories. In the last few years, gallium oxide has attracted the interest of researchers toward RS applications due to its very large breakdown voltage and concentration

sensitive to oxygen content. In this work, we present devices with RF sputtered gallium oxide on ultra smooth Ru/Al₂O₃ for non-volatile RAMs.

Sputter deposition of gallium oxide on Ru(0001)/Al₂O₃ at 400°C results in the good crystallinity with diffraction spots matching the β -Ga₂O₃ structure as confirmed by transmission electron diffraction (TED). For device completion, top electrodes (TE) were fabricated by depositing Al/Ag using the e-beam evaporation. X-ray photoelectron spectroscopy (XPS) confirmed a very large amount of

oxygen vacancies in gallium oxide film. A RS behaviour in Al TE devices with an ON/OFF ratio of more than 10⁴ is suggested to be related to formation/rupture of oxygen vacancies filaments. In the case of Ag TE devices, RS is assigned to electro-metallization of Ag electrode. The stable endurance cycle and long retention time of > 10⁴ seconds qualify these devices as a future prototype for non volatile ReRAMs.

DS 14: Focus session: Quantum Properties at Functional Oxide Interfaces 2 (joint session DS/HL)

Time: Wednesday 9:30–11:00

Location: H17

Invited Talk

DS 14.1 Wed 9:30 H17

Facet dependence of reconstructions at quantum material interfaces — •EVA BENCKISER — Max Planck Institute for Solid State Research, Stuttgart, Germany
Oxide heterostructures promise a rational design of quantum materials with specific, functional properties such as magnetism and superconductivity. Our research aims to gain a fundamental understanding of spin, orbital, charge and lattice reconstructions at complex transition-metal oxide interfaces, mainly using x-ray spectroscopy.

In my talk, I will focus on implications of the choice of the crystallographic facet of the interface by showing examples of two prototypical correlated-electrons materials. In NdNiO₃ epitaxial thin films we observe modifications of the metal-insulator transition, which we explain by the facet dependence of the bond-order instability in the system [1]. The choice of a specific interface facet, in turn, allows to manipulate the complex spin order in ultrathin NdNiO₃ slabs [2]. In YVO₃ heterostructures, an artificial, layered orbital occupation pattern can be realized by the choice of the interface facet [3]. I have conducted the above-mentioned studies in collaboration with many scientists who are co-authors of the publications listed below.

[1] Y. E. Suyolcu, K. Fürsich *et al.*, Phys. Rev. Materials **5**, 045001 (2021). [2] M. Hepting *et al.*, Nature Physics **14**, 1097 (2018). [3] P. Radhakrishnan *et al.*, Phys. Rev. B **104**, L121102 (2021); Phys. Rev. B **105**, 165117 (2022).

DS 14.2 Wed 10:00 H17

A detailed interface and surface analysis of BaSnO₃ in LaInO₃/BaSnO₃ heterostructures — •MARTINA ZUPANCIC¹, WAHIB AGGOUNE², DANIEL PFÜTZENREUTER¹, ZBIGNIEW GALAZKA¹, HOUARI AMARI¹, CLAUDIA DRAXL², JUTTA SCHWARZKOPF¹, and MARTIN ALBRECHT¹ — ¹Leibniz-Institut für Kristallzüchtung, Berlin, Germany — ²Institut für Physik and IRIS Adlershof, Humboldt-Universität zu Berlin, Berlin, Germany

LaInO₃/BaSnO₃ heterostructures have lately attracted a lot of interest due to the high electron mobility of ~300cm²/Vs in BaSnO₃ and the formation of a 2DEG at the interface. In LaAlO₃/SrTiO₃ system, the origin of the 2DEG is attributed to the polar discontinuity and an electronic reconstruction at the n-type LaO-TiO₂ interface. Controlling the interface termination is therefore crucial to accomplish heterostructures with desired properties. Here, we combine density-functional theory, atomic resolution transmission electron microscopy, energy dispersive X-ray spectroscopy, and electron energy loss spectroscopy (EELS) to study the LaInO₃/BaSnO₃ interface. Experiment and theory are in excellent agreement and show that free BaSnO₃ (100) surfaces are BaO terminated, while the interface between BaSnO₃ and LaInO₃ is SnO₂ terminated. This finding indicates that during the growth of LaInO₃ layer on BaSnO₃ Ba atoms exchange from the subsurface to the surface. Preliminary EELS analysis of a few monolayer thick LaInO₃ grown on BaSnO₃ shows indications of Ba atoms on the LaInO₃ surface, confirming that atomic exchange in this system promotes the energetically favorable SnO₂-LaO interface.

Invited Talk

DS 14.3 Wed 10:15 H17

Designing novel electronic phases at oxide interfaces from first principles — •ROSSITZA PENTCHEVA — Department of Physics and Center for Nanointegration (CENIDE), University of Duisburg-Essen, Germany

Transition metal oxide interfaces exhibit a rich plethora of functional properties that are not available in the respective bulk compounds and open possibilities for electronics, spintronics and energy conversion applications. Over the past years several control parameters of novel behavior have been identified and systematically explored such as the symmetry breaking at the interface, the effect of strain, confinement and crystallographic orientation, the electrostatic doping at polar interfaces [1]. Based on the insight from density functional theory calculations including an on-site Hubbard term, I will address the formation of unanticipated charge, spin and orbital reconstructions in perovskite-derived superlattices and thin films with (001) and (111) orientation that can lead to e.g. metal-to-insulator transitions and/or topologically nontrivial states which are fascinating not only from a fundamental point of view but also potentially interesting for thermoelectric applications [2].

Research supported by the German Research Foundation DFG within CRC/TRR80. [1] M. Lorenz *et al.*, J. Phys. D: Appl. Phys. **49**, 433001 (2016). [2] B. Geisler, P. Yordanov, M. E. Gruner, B. Keimer, R. Pentcheva, Phys. Status Solidi B **259**, 2100270 (2022)

DS 14.4 Wed 10:45 H17

Orbital engineering in vanadate heterostructures — •PADMA RADHAKRISHNAN¹, BENJAMIN GEISLER², KATRIN FÜRSTICH¹, DANIEL PUTZKY¹, YI WANG¹, SVEN ILSE³, GEORG CHRISTIANI¹, GENNADY LOGVENOV¹, PETER WOCHNER¹, PETER VAN AKEN¹, EBERHARD GOERING³, ROSSITZA PENTCHEVA², and EVA BENCKISER¹ — ¹Max Planck Institute for Solid State Research, Heisenbergstrasse 1, 70569 Stuttgart, Germany — ²Department of Physics and Center for Nanointegration (CENIDE), Universität Duisburg-Essen, Lothastrasse 1, 47057 Duisburg, Germany — ³Max Planck Institute for Intelligent Systems, Heisenbergstrasse 3, 70569 Stuttgart, Germany

A promising approach for the manipulation of quantum states involves the epitaxial stabilization of certain orbital occupations, i.e. orbital engineering. Here we use resonant x-ray reflectometry to extract quantitative depth-dependent x-ray linear dichroism profiles of thin slabs of YVO₃ embedded in a superlattice with LaAlO₃. Our data reveal an artificial, layered orbital polarization, where the average occupation of *xz* and *yz* orbitals at the interface is inverted compared to the central layers of YVO₃. We attribute this effect to a combination of epitaxial strain and spatial confinement by LaAlO₃. Further, insights from *ab initio* calculations and scanning transmission electron microscopy indicate that the selection of a suitable spacer layer material, layer thickness of the transition metal oxide, facet of substrate, and sign of strain can together implement a desired orbital polarization pattern. Our study demonstrates the use of orbital engineering as a promising approach for the theory-guided rational design of quantum materials.

DS 15: 2D Materials 5 (joint session HL/ CPP/DS)

Time: Wednesday 9:30–12:00

Location: H36

See HL 20 for details of this session.

DS 16: Thin Film Applications 2

Time: Wednesday 11:00–12:00

Location: H14

DS 16.1 Wed 11:00 H14

High Open-Circuit Voltage Cs₂AgBiBr₆ Carbon-Based Perovskite Solar Cells Via Green Processing of Ultrasonic Spray-Coated Carbon Electrodes from Waste Tire Sources — •FABIAN SCHMITZ and TERESA GATTI — Center for Materials Research, Justus Liebig University, Giessen, Germany

Although top-notch lead-based perovskite solar cells (PSCs) achieve power conversion efficiencies >25%, they are still hindered from commercial implementation by their low environmental stability, high toxicity and optimizable costs. The latter could be reduced by eliminating the metal back electrode as well as the hole-transport material by substituting both with a conductive carbon material.

terial to create carbon-based PSCs (C-PSCs). Furthermore, the utilization of perovskite materials based on other metallic compounds could tackle the other two issues of stability and toxicity. A promising example that combines both high environmental stability and low toxicity is the double perovskite $\text{Cs}_2\text{AgBiBr}_6$.

In our work, we present the deposition of "green" carbon electrodes onto $\text{Cs}_2\text{AgBiBr}_6$ thin films via high-throughput ultrasonic spray coating to prepare lead-free C-PSCs. For our sustainable approach, we started from a carbon material obtained from the hydrothermal recycling of waste tires and dispersed it in isopropanol. This additive-free ink worked as a precursor for the upscalable ultrasonic spray deposition method to fabricate carbon electrodes under ambient atmosphere and at a low substrate temperature. Through this procedure we obtained C-PSCs with record open-circuit voltages of >1.2 V.

DS 16.2 Wed 11:15 H14

Indirect band gap semiconductors for thin-film photovoltaics: High-throughput calculation of phonon-assisted absorption — •JIBAN KANGSABANIK, MARK KAMPER SVENDSEN, ALIREZA TAGHIZADEH, and KRISTIAN S. THYGESEN — Technical University of Denmark, Denmark

Photovoltaics is one of the most promising ways towards meeting the ever-increasing global energy demand in a sustainable and eco-friendly way. Thin-film materials (GaAs, CdTe, InP, CIGS, MAPb₃, etc) are rapidly growing in terms of market share in recent times, showing comparable efficiencies to the current Si-based technology. Currently, these well-known thin-film materials possess some major drawbacks associated with low material abundance (In, Ga), toxicity (Cd, As, Pb), and long-term device stability (perovskites). As such, finding new materials with desirable physical attributes remains one of the key aspects in this area. Indirect bandgap semiconductors, which occupy a major portion of the semiconductor space are mostly ignored in recent material screening studies. Here, we propose a recipe to evaluate PV efficiency for indirect gap materials via calculating phonon-assisted absorption, which is high-throughput friendly. Using this recipe, we evaluate chemically stable unary and binary materials from the Open Quantum Materials Database for PV application. From our final screening, we identify well-known binary thin film materials (GaAs, CdTe, and InP) as well as a number of the emerging PV materials (PbS, SnS, Se, GeSe, etc). Additionally, we find a number of indirect gap materials with potential for thin-film PV device application.

DS 16.3 Wed 11:30 H14

Physical unclonable function based on unsorted carbon nanotube random networks in multi-contact field-effect transistors — JONAS SCHROEDER¹, •JAMES W. BORCHERT¹, PATRICK SCHUSTER², PETER EDER², STEFAN HEISERER³, JOSEF BIBA³, GEORG S. DUESBERG³, ULRICH RÜHRMAIR^{2,4}, and R. THOMAS

WEITZ¹ — ¹Georg-August Universität Göttingen, Göttingen, Germany — ²Ludwig-Maximilians-Universität München, München, Germany — ³Universität der Bundeswehr München, Neubiberg, Germany — ⁴University of Connecticut, Storrs CT 06269, USA

The standard practice in cryptography of using digital binary keys that are permanently stored on devices is prohibitively inefficient for some applications and open to both physical and software-based attacks. A promising alternative approach known as 'physical unclonable function' (PUF) instead uses the inherent random variation in fabrication to create physical 'keys' that produce unique randomized responses to defined challenges. Electrical PUF devices based on random networks of unsorted carbon nanotubes (CNTs) have shown promise, but so far have been limited in terms of scaling up the number of challenge-response pairs (CRPs) that can be extracted. Here, we demonstrate how gating the CNT networks might be a useful method for expanding the number of CRPs, thus strengthening the scalability of the PUF. We show CNT networks implemented in modified field-effect transistors with up to 12 contacts. The output randomness and stability of the devices are investigated, and further routes for improvement are discussed.

DS 16.4 Wed 11:45 H14

Redox-based Memristive Devices for Neuromorphic Systems — •BENJAMIN SPETZLER, SEONGAE PARK, ANNA LINKENHEIL, TZVETAN IVANOV, and MARTIN ZIEGLER — Technical University Ilmenau, Ilmenau, Germany

Redox-based memristive devices have demonstrated promising properties for their application as synaptic elements in neuromorphic computing systems. The device characteristics are the product of a variety of complex mechanisms, and electronic and ionic processes need to be precisely tuned, which requires a deep understanding of the underlying physical mechanisms and control of the fabrication parameters. We present redox-based memristive elements and show how their properties can be tailored by systematic design variations for applications in neuromorphic computing architectures. In this context, the influence of different oxide layer systems and electrode materials on the device characteristics is analyzed to assess their properties for neuromorphic computing. The experimental findings are supported by a numerical device model, which connects the physical processes with technology parameters, and permits a deeper understanding of the origin of the current-voltage hysteresis. Furthermore, we discuss the system integration of memristive devices and present memristive device arrays.

This work was partially funded by the Carl-Zeiss Foundation via the Project MemWerk and the German Research Foundation (DFG) through the Collaborative Research Centre CRC 1461 "Neurotronics- Bio-Inspired Information Pathway".

DS 17: 2D Materials 6 (joint session DS/PPP)

Time: Wednesday 11:15–13:00

Location: H17

DS 17.1 Wed 11:15 H17

Curvature-induced spin-orbit splitting in transition metal dichalcogenide nanotubes and wrinkles — MOHAMMADREZA DAQQSHIRAZI and •THOMAS BRUMME — Theoretical Chemistry, TU Dresden

Strain engineering provides a powerful means to tune the properties of 2D materials. Homogeneous strain fields have been studied extensively, and there are standard techniques for altering properties of 2D materials even in industry. On the other hand, much less is known about how inhomogeneous strain affects the electronic properties of 2D materials. We employed DFT to understand the correlation between the atomic and the electronic structure in nanoscale wrinkles and nanotubes of the prototypical transition metal dichalcogenide WSe_2 . Our research shows that the symmetry breaking in these structures lead to strong Rashba-like spin-orbit splitting of the bands at the Γ point and that they thus may be utilized in future tunable spintronics devices.

DS 17.2 Wed 11:30 H17

Moiré-Bose-Hubbard model for interlayer excitons in twisted transition metal dichalcogenide heterostructures — •NICLAS GÖTTING, FREDERIK LOHOF, and CHRISTOPHER GIES — Institute for Theoretical Physics, University of Bremen, Bremen

Introducing a twist between two superimposed TMD monolayers results in a new superlattice whose properties heavily depend on the twist angle. These so-called moiré structures of TMD materials like MoS_2/WS_2 can host interlayer excitons (IXs) which perceive the varying atomic registry over the moiré unit cell as an effective moiré potential. In such structures, correlated states can emerge, in which the IXs are strongly localized to the potential minima due to exciton-exciton interactions.

We investigate the phases of these trapped moiré IXs by approximating them as bosonic particles and mapping the system onto a Bose-Hubbard model [1].

Our methods allow us to calculate the hopping and two-particle interaction terms of the Bose-Hubbard model for n -th nearest neighbors. To examine the strong impact of dielectrics surrounding the heterobilayer, we introduce a Keldysh potential to the calculation and thereby obtain first results of the twist-angle dependent phases of moiré IXs in twisted TMD heterobilayers.

[1] Götting et al., Phys. Rev. B 105, 165419 (2022)

DS 17.3 Wed 11:45 H17

Enhanced Potassium Storage Capability of Two-Dimensional Transition-Metal Chalcogenides — •VINCENT HARTMANN and YONG LEI — Fachgebiet Angewandte Nanophysik, Institut für Physik & IMN MacroNano, Technische Universität Ilmenau, 98693 Ilmenau, Germany

Potassium-ion batteries (PIBs) have been considered a promising alternative to lithium-ion batteries due to their merits of high safety and low cost. Two-dimensional transition metal chalcogenides (2D TMCs) with high theoretical specific capacities and unique layered structures have been proven to be amenable materials for PIB anodes. However, some intrinsic properties including severe stacking and unsatisfactory conductivity restrict their electrochemical performance, especially rate capability. Herein, a heterostructure of high-crystallized ultrathin MoSe_2 nanosheet-coated multiwall carbon nanotubes was prepared and its electrochemical properties were investigated. In such a heterostructure, the constructive contribution of CNTs not only suppresses the restacking of MoSe_2 nanosheets but also accelerates electron transport. Meanwhile, the MoSe_2 nanosheets loaded on CNTs exhibit an ultrathin feature, which can expose abundant active sites for the electrochemical reaction and shorten the K^+ diffusion length. Therefore, the synergistic effect between ultrathin MoSe_2 and CNTs endows the resulting nanocomposite with superior structural and electrochemical properties. Additionally, the high crystallinity of the MoSe_2 nanosheets further leads to the improvement of electrochemical performance.

DS 17.4 Wed 12:00 H17

Single photon emission of quantum emitters in WSe2 monolayers and their temperature-dependent coherence properties — •MARTIN VON HELVERSEN¹, PAUL SCHLAUGAT¹, CHIRAG PALEKAR¹, CARLOS ANTÓN-SOLANAS², BÁRBARA ROSA¹, CHRISTIAN SCHNEIDER², and STEPHAN REITZENSTEIN¹ — ¹Institute for solid state physics, Technische Universität Berlin, 10623 Berlin, Germany — ²Institute for Physics, Carl von Ossietzky Universität Oldenburg, 26111 Oldenburg, Germany

Two-dimensional van der Waals monolayers have appeared as novel type of semiconducting materials, which provide a platform for the exploration of their highly interesting optical, electronic and structural properties. Within the transition-metal dichalcogenides, WSe2 has turned out to be the most promising platform for two-level single-photon emitters, generated either by applied strain to the monolayer-flake [1,2], or by defects in the material [2]. However, the quality of the generated photons still lacks behind other systems as for example semiconductor quantum dots. In this work, we study single emitters of a strained WSe2-monolayer showing linewidths around 100 μeV at 4 K. In quasi-resonant pulsed optical excitation a second-order autocorrelation value down to $g^{(2)}(0)=0.037(5)$ is measured. We further study their temperature dependent first-order coherence properties via a scanning Michelson interferometer, which yields coherence times up to 48 ps.

[1] L. N. Tripathi et al., ACS Photonics 5, 1919 (2018)

[2] K. Parto et al., Nat. Commun. 12, 3585 (2021)

DS 17.5 Wed 12:15 H17

Spin-defect characteristics of single sulfur vacancies in monolayer MoS₂ — •ALEXANDER HÖTGER¹, TOMER AMIT², JULIAN KLEIN³, KATJA BARTHELMI¹, THOMAS PELINI⁴, ALEX DELHOMME⁴, SERGIO REY⁵, MAREK POTEMSKI^{4,6}, CLÉMENT FAUGERAS⁴, GALIT COHEN², DANIEL HERNANGÓMEZ-PÉREZ², TAKASHI TANIGUCHI⁷, KENJI WATANABE⁷, CHRISTOPH KASTL¹, JONATHAN FINLEY¹, SIVAN REFAELY-ABRAMSON², ALEXANDER HOLLEITNER¹, and ANDREAS STIER¹ — ¹Walter Schottky Institute, Garching, Germany — ²Weizmann Institute of Science, Rehovot, Israel — ³Massachusetts Institute of Technology, Cambridge, USA — ⁴Laboratoire National des Champs Magnétiques Intenses, Grenoble, France — ⁵Technical University of Denmark, Lyngby, Denmark — ⁶University of Warsaw, Warszawa, Poland — ⁷National Institute for Materials Science, Tsukuba, Japan

Single spin defects in 2D transition-metal dichalcogenides are natural spin-photon interfaces for quantum applications. Here we report high-field magneto-spectroscopy from three emission lines of He-ion induced sulfur vacancies in monolayer MoS₂. The distinct valley-Zeeman splitting and the brightening of dark states necessitates spin-valley selectivity of the defect states and lifted spin-degeneracy at zero field. Comparing our results to ab-initio calculations identifies the nature of the defect luminescence. Analysis of the optical degree of circular polarization reveals that the Fermi level is a parameter that enables the tunability of the emitter. These results show that defects in 2D semiconductors may be utilized for quantum technologies.

DS 17.6 Wed 12:30 H17

Probing excitonic population dynamics by nonlinear optical wave mixing in monolayer WSe2 — •JONAS M. BAUER, LIJUE CHEN, PHILIPP WILHELM, SEBASTIAN BANGE, JOHN M. LUPTON, and KAI-QIANG LIN — Department of Physics, University of Regensburg, 93053 Regensburg, Germany

Monolayer semiconductors are emerging platforms for strong nonlinear light-matter interaction, due to their giant oscillator strength of tightly bound excitons. Recently, we reported the existence of a new excitonic species, the high-lying exciton (HX), in monolayer WSe2. The HX appears at around twice the energy of the band-edge A-exciton, forming a ladder-type excitonic three-level system. We demonstrate excitonic quantum interference in monolayers [1] and twisted bilayers [2]. Here, we apply time-resolved nonlinear spectroscopy to probe the excitonic dynamics. We find that a significant time difference between two light pulses is necessary for optimal sum-frequency generation (SFG) and four-wave mixing (FWM) if one of the pulses is in resonance with an excitonic transition. The experimental results are rationalized by numerical calculations based on a density-matrix approach and provide insights into coherent exciton dynamics on a femtosecond scale.

[1] K.-Q. Lin, S. Bange, & J. M. Lupton, Nat. Phys. 15, 242-246 (2019).

[2] K.-Q. Lin, J.M. Bauer et al., Nat. Commun. 12, 1553 (2021).

DS 17.7 Wed 12:45 H17

Characterization of 2D WSe2 by high-resolution STEM and Differential Phase Contrast STEM — •MAJA GROLL¹, JULIUS BÜRGER¹, IOANNIS CALTZIDIS², MARC SARTISON², KLAUS JÖNS², and JÖRG LINDNER¹ — ¹Nanostructuring, Nanoanalysis and Photonic Materials Group, Department of Physics, Paderborn University, Germany — ²Hybrid Quantum Photonic Devices, Department of Physics, Paderborn University, Germany

2D transition metal dichalcogenides (TMDs) are gaining attention as their optical and electronic properties differ from those of their bulk counterparts. In particular, layer thickness-dependent properties, such as the transition from an indirect to a direct band gap in monolayers, make these materials interesting for photonic and optoelectronic applications. At the same time 2D-TMDs are ideal materials for the advancement of new techniques in scanning transmission electron microscopy (STEM) like differential phase contrast (DPC)-STEM. Using a spherical aberration corrected STEM, this technique enables the quantification of atomic electric fields with sub-atomic resolution if the specimen is sufficiently thin. In order to examine the atomic electric fields of TMDs, we transferred mechanically exfoliated mono- and multilayers of tungsten diselenide (WSe2) to TEM grids. The atomic structure of WSe2 flakes and their thickness are studied using TEM, energy filtered TEM and STEM. STEM-DPC measurements are performed using an eight-fold segmented bright-field STEM detector measuring the beam deflection due to the internal fields. Results are presented for WSe2 flakes of different thickness and compared with simulations.

DS 18: Thin Oxides and Oxide Layers 1

Time: Wednesday 15:00–16:00

Location: H14

DS 18.1 Wed 15:00 H14

Simulation analysis of sneak paths effect in the memristor-based crossbar topology — •ZIANG CHEN^{1,2,3}, HAO CAI^{1,2,3}, CHRISTOPHER BENDEL⁴, FENG LIU⁵, XIANYUE ZHAO^{1,2,3}, HEIDEMARIE SCHMIDT^{1,2}, STEPHAN MENZEL⁵, and NAN DU^{1,2,3} — ¹*FSU Jena, Jena, Germany — ²*IPHT, Jena, Germany — ³*TU Chemnitz, Chemnitz, Germany — ⁴*RWTH Aachen, Aachen, Germany — ⁵*FZJ, Juelich, Germany

The high demand for performance and energy efficiency poses challenges for computing systems. The memristor-based crossbar architecture is enthusiastically regarded as a potential competitor to traditional solutions. Nonetheless, due to the lack of a switching control per cell, the memristor-based crossbar architecture suffers from the sneak paths that limit the range of accurate operation of the crossbar array. In this talk, the memristor-based passive crossbar geometry is studied and different topological patterns—one word line pull-up (OneWLPU) and all word line pull-up (AllWLPU)—is presented. In the worst-case scenario of two crossbar topological patterns, the read margin is defined as an accurate estimation for the sneak paths effects. For suppressing the sneak paths effects, in the Cadence simulation of two crossbar topological patterns based on the mathematical memristor model, the relevance between the read margin and other functional elements in the crossbar topology, i.e. pull-up resistance, line resistance, On/Off ratio, is revealed and analyzed. This work offers a beneficial reference and feasible solutions for the future optimization of crossbar topology with the intention of diminishing sneak paths effects.

DS 18.2 Wed 15:15 H14

Mapping the local strain distribution of oxide membranes using polarization-dependent micro-Raman spectroscopy — •MATTHIAS T. ELM, ALEXANDER KONETSCHNY, MARCEL WEINHOLD, CHRISTIAN HEILIGER, and PETER J. KLAR — Justus-Liebig University, Gießen, Germany

Free-standing ceramic membranes are of great interest for miniaturized electrochemical devices, such as micro-solid oxide fuel cells, sensors or memory devices. Free-standing membranes exhibit residual strain, which alters the electrical conductivity and, thus, the performance of the device. Detailed knowledge of the local strain distribution in the membrane is therefore of paramount importance. Here, we show that the local strain state of the membrane can be monitored using polarization dependent micro-Raman mapping. Due to the residual strain the triply degenerate F_{2g} mode splits and the contribution of their Raman intensity to the overall Raman signal depends on the measurement geometry and the polarization of the incoming and scattered light. Varying the polarization of the incoming excitation light results in different averaging of the Raman-active modes. These results clearly demonstrate that polarization-dependent Raman measurements have the potential to yield additional insight into the local strain distribution in free-standing oxide membranes.

DS 18.3 Wed 15:30 H14

Soft RIXS study of alumina-titania thin films heterostructure to reveal the nature of 2-dimensional electron system — •DEOK-YONG CHO — Department of Physics, Jeonbuk National University, South Korea

Al₂O₃/TiO₂ binary oxide heterostructure is a novel 2-dimensional electron system (2DES) compatible with mass production. The electronic structure of the 2DES was examined using resonant inelastic soft X-ray scattering. The TiO₂ thickness-dependent evolution in the Ti L₃-edge energy loss features unequivocally evidenced the presence of Ti³⁺ state at the interface and a substantial electron-phonon coupling effects. This suggests that the 2DES properties can be controlled via well-established TiO₂ engineering so that the binary oxide heterostructure would be a promising candidate for 2DES-based device application.

This work was done in collaboration with Yu-Cheng Shao, Cheng-Tai Kuo, Xuefei Feng and Yi-De Chuang (Advanced Light Source, USA), and Tae Jun Seok, Ji Hyeon Choi and Tae Joo Park (Hanyang University, South Korea). DOI: 10.1002/adfm.202104430

DS 18.4 Wed 15:45 H14

Tuning the electrochemical properties of multifunctional CoO_x catalyst layers by plasma-enhanced atomic layer deposition — •MATTHIAS KUHLE, GABRIEL GRÖTZNER, LAURA WAGNER, ALEX HENNING, IAN SHARP, and JOHANNA EICHHORN — Walter Schottky Institute, Technical University of Munich, Munich, Germany

Artificial photosynthetic systems are often limited by the poor efficiency and material instability of photoelectrodes under harsh PEC conditions. One strategy towards stable and efficient systems is to interface the semiconductor light absorber with conformal and ultra-thin catalytic layers, which still permit interfacial charge transport and minimize losses due to parasitic light absorption. In this context, conformal, biphasic Co₃O₄/Co(OH)₂ catalyst layers were fabricated by means of plasma-enhanced atomic layer deposition (PE-ALD), which are simultaneously robust and electrochemically active. The nanocrystalline Co₃O₄ layer forms a durable interface to the substrate and the disordered Co(OH)₂ surface layer significantly improves the electrocatalytic oxygen evolution reaction activity. Here, we show that non-saturated oxidation reactions can be applied to tune catalytic activity, chemical stability, and physical properties of the PE-ALD layer by leveraging low plasma exposure time and low plasma power. Based on these insights, the CoO_x films are interfaced with polycrystalline semiconductor thin films to generate highly stable and efficient multilayer photoelectrode assemblies. Overall, this work highlights the use of PE-ALD as a promising approach for engineering catalyst/semiconductor interfaces to create efficient and stable photoelectrodes.

DS 19: 2D Materials 7 (joint session DS/PPP)

Time: Wednesday 15:00–16:00

Location: H17

DS 19.1 Wed 15:00 H17

Gate-Tunable Helical Currents in Commensurate Topological Insulator/Graphene Heterostructures — •JONAS KIEMLE^{1,2}, LUKAS POWALLA^{3,4}, KATHARINA POLYUDOV^{3,4}, LOVISH GULATI³, MAANWINDER SINGH^{1,2}, ALEXANDER HOLLEITNER^{1,2}, MARKO BURGHARD^{3,4}, and CHRISTOPH KASTL^{1,2} — ¹Walter Schottky Institut and Physics Department, Technical University of Munich, Garching, Germany — ²MCQST, München, Germany — ³Max-Planck-Institut für Festkörperforschung, Stuttgart, Germany — ⁴Institut de Physique, Ecole Polytechnique Fédérale de Lausanne, Lausanne, Switzerland

Van der Waals heterostructures made from graphene and three-dimensional topological insulators promise very high electron mobilities, a non-trivial spin texture and a gate-tunability of electronic properties. Here, we explore epitaxially grown interfaces between graphene and the lattice-matched topological insulator Bi₂Te₂Se. For this heterostructure, spin-orbit coupling proximity has been predicted to impart an anisotropic and electronically tunable spin texture. Polarization-resolved second-harmonic generation, Raman spectroscopy, and time-resolved magneto-optic Kerr microscopies are combined to demonstrate that the atomic interfaces align in a commensurate symmetry with characteristic interlayer vibrations. By polarization-resolved photocurrent measurements, we find a circular photogalvanic effect which is drastically enhanced at the Dirac point of the proximitized graphene. We attribute the peculiar gate-tunability to the proximity-induced interfacial spin structure.

DS 19.2 Wed 15:15 H17

Topological Invariant of Acoustic Phonons in 2D materials — •GUNNAR LANGE¹, ADRIEN BOUHON¹, BARTOMEU MONSERRAT^{1,2}, and ROBERT-JAN SLAGER¹ — ¹Cavendish Laboratory, University of Cambridge, UK — ²Department of Materials Science and Metallurgy, University of Cambridge, UK
2D materials that live in a 3D space display an unusual acoustic phonon mode: the flexural mode. This mode disperses quadratically away from the center of the acoustic Brillouin zone, and corresponds to a flexing of the material out-of-plane. This differs markedly from the linear dispersion displayed by the in-plane modes, and leads to an unusual triple degeneracy at the zone center. This triple degeneracy is enforced by the Nambu-Goldstone theorem, rather than symmetry, as will be discussed. Such band degeneracies frequently have associated topological invariants. For this triple degeneracy, the topological invariant turns out to generically be of quaternionic type (Euler topology), but reduces to a \mathbb{Z}_2 invariant under fairly general assumptions. The invariant has important implications for 2D materials grown on a substrate, as it dictates how the bands are split due to the presence of the substrate. This will be discussed in the context of graphene, where the \mathbb{Z}_2 invariant turns out to be non-trivial.

This talk is based on: Lange, G. F., Bouhon, A., Monserrat, B., and Slager, R.-J., "Topological continuum charges of acoustic phonons in two dimensions and the Nambu-Goldstone theorem" Phys. Rev. B **105**, 064301 (2022)

DS 19.3 Wed 15:30 H17

Coupled Bilayer Graphene Quantum Dots — •ANGELIKA KNOTHE^{1,2} and VLADIMIR FAL'KO^{2,3} — ¹Institute of Physics, Technische Universität Chemnitz, D-09107 Chemnitz, Germany — ²National Graphene Institute, University of Manchester, Manchester, UK — ³Henry Royce Institute for Advanced Materials, University of Manchester, Manchester, UK

Bilayer graphene quantum dots are promising for spin and valley qubits [1,2,3]. A functional quantum information architecture requires scalable multi-qubit systems. We theoretically study electrostatically confined double-dots and few-dot arrays in bilayer graphene. We quantify the inter-dot couplings for different dot parameters such as the field-induced gap, the confinement shape, and the inter-dot distance. This dependence on external parameters allows tuning the dot arrays into different regimes for which we study the extended Hubbard Hamiltonians and identify the spin and valley level structure. Our results will help to advance the use of bilayer graphene quantum dots for quantum technologies.

[1] A. Knothe, L. I. Glazman, V. Fal'ko, New Journal of Physics **24** (4), 043003 (2022)

[2] S. Möller, L. Banszerus, A. Knothe, C. Steiner, E. Icking, S. Trellenkamp, F. Lentz, K. Watanabe, T. Taniguchi, L. Glazman, V. Fal'ko, C. Volk, C. Stampfer, Phys. Rev. Lett. **127**, 256802 (2021)

[3] A. Knothe, V. Fal'ko, Phys. Rev. B **101**, 235423 (2020)

DS 19.4 Wed 15:45 H17

Electron cavity optics in bilayer graphene — LUKAS SEEMANN¹, •ANGELIKA KNOTHE¹, KLAUS RICHTER², and MARTINA HENTSCHEL¹ — ¹Institute of Physics, Technische Universität Chemnitz, D-09107 Chemnitz, Germany — ²Institut für Theoretische Physik, Universität Regensburg, 93040 Regensburg, Germany

Rapid developments in the field of 2D materials and their nanostructures make it possible to trap charge carriers with different dispersions in various confinement geometries with a high degree of control. This progress now allows studying 2D electron optics phenomena enriched by the charge carriers' different electronic and topological properties compared to the photonic case. Here, we theoretically investigate cavities in gapped bilayer graphene employing an approach based on ray-wave correspondence [1]. We identify the influence of the materials' trigonally warped band structure [2] on the fermion optics characteristics that we show to be conveniently tuneable by gate voltages. Similar considerations can be applied to electron optics in other 2D materials.

[1] J.-K. Schrepfer, S. Chen, M.-H. Liu, K. Richter, and M. Hentschel, Phys. Rev. B **104**, 155436 (2021)

[2] C. Gold, A. Knothe, A. Kurzman, A. Garcia-Ruiz, K. Watanabe, T. Taniguchi, V. Fal'ko, K. Ensslin, T. Ihn, Phys. Rev. Lett. **127**, 046801 (2021)

DS 20: Poster

Time: Wednesday 16:00–18:00

Location: P3

DS 20.1 Wed 16:00 P3

Thickness effect on ferroelectric domain formation in compressively strained K_{0.65}Na_{0.35}NbO₃ epitaxial films — •YANKUN WANG^{1,2}, SAUD BIN ANOOZ¹, GANG NIU², MARTIN SCHMIDBAUER¹, LINGYAN WANG², WEI REN², and JUTTA SCHWARZKOPF¹ — ¹Leibniz-Institut für Kristallzüchtung, Max-Born-Str. 2, 12489 Berlin, Germany — ²Electronic Materials Research Laboratory, Xi'an Jiaotong University, Xi'an, China

Ferroelectrics are of increasing interest for a broad range of applications such as nonvolatile memory devices, transducers and MEMS sensors. Herein, the influence of thickness in epitaxial K_{0.65}Na_{0.35}NbO₃ ferroelectric thin films grown on (110) TbScO₃ substrate is systematically studied. By combining piezoresponse force microscopy and high-resolution x-ray diffraction, the occurrence of 90° stripe domains was demonstrated for the films with a thickness above 11 nm, while the domain periodicity is in good agreement with Kittel's law. Furthermore, up to a thickness of 93 nm, elastic strain relaxation induced by the formation of ferroelectric domains is observed, whereas plastic strain relaxation plays only a minor role. With increasing film thickness three successive phases of ferroelectric domains were observed: i) Irregularly arranged orthorhombic c domains in the thinnest film, ii) periodically arranged 90° monoclinic MC domains up to a thickness of 25 nm and iii) flux closure vortex-like structure in thicker films to achieve the lowest equilibrium energy. These results demonstrate the importance of understanding the lattice relaxation mechanisms for intentional tuning of ferroelectric thin film properties.

DS 20.2 Wed 16:00 P3

X-ray characterization of an above-RT bi-stable sublimable molecular spin-crossover Fe(II)-complex — •YAHYA SHUBBAK¹, MIGUEL GAVARA EDO², ARNO EHRESMANN¹, and EUGENIO CORONADO MIRALLES² — ¹Institute of Physics & Center for Interdisciplinary Nanostructure Science and Technology (CINSaT), University of Kassel, D-34132 Kassel — ²Institute of Molecular Science (ICMol), University of València, S-46980 Paterna

Spin crossover (SCO) molecules are a promising type of material that can undergo reversible switching between low-spin (LS)- and high-spin (HS)-states upon external stimuli (heat, light, pressure, etc.)[1], making them useful for information technology, data storage and optoelectronics[2]. However, most SCO molecules need to be cooled significantly for this transition to be observable. We have investigated the hitherto unknown electronic structure of the complex molecule bis[hydrotris(1,2,4-triazol-1-yl)borate]iron(II) ([Fe(HB(tz)3)2])[3] capable of above-RT transition by XPS and XAS measurements, since the distinct electronic structure in both spin-states unmistakably prove the transition between them.

[1]P. Gütllich and H. A. Goodwin. "Spin Crossover in Transition Metal Compounds I." Springer Berlin Heidelberg, May 2004. 356 pp. [2]E. P. Geest et al., "Contactless Spin Switch Sensing by Chemo*Electric Gating of graphene". In: *Advanced Materials* (2020), p. 1903575. [3]S. Rat et al., "Solvatomorphism and structural-spin crossover property relationship in bis[hydrotris(1,2,4-triazol-1-yl)borate]iron(ii)". In: *CrystrEngComm* 19.24 (2017).

DS 20.3 Wed 16:00 P3

Insights into the evaporation behaviour of FAI: material degradation and consequences for perovskite solar cells — MARTIN KROLL¹, SEREN DILARA ÖZ³, ZONGBAO ZHANG¹, RAN JI¹, •TIM SCHRAMM^{1,2}, TOBIAS ANTRACK¹, YANA VAYNZOF^{1,2}, SELINA OLTHOFF³, and KARL LEO¹ — ¹Dresden Integrated Center for Applied Physics and Photonic Materials, IAPP — ²Center for Advancing Electronics Dresden, CFAED — ³Department of Chemistry, University of Cologne

Thermal co-evaporation is a promising method for large-scale uniform perovskite deposition. In this work, we look at the decomposition of formamidinium iodide (FAI) upon evaporation in high vacuum by tracking the composition of the residual gas with a mass spectrometer. We find that the precursor material degrades during the evaporation process into hydrogen cyanide (HCN) and sym-triazine (C₃H₃N₃), leading to an increase in pressure, which is commonly observed during the deposition of FAI. Using optical characterization as well as x-ray photoelectron spectroscopy on co-deposited perovskite films, we demonstrate that this background pressure strongly affects the resulting film's stoichiometry. Using two different vacuum setups, we are able to show that significant changes are imposed, e.g. on the optimized co-evaporation rates, by the specific vacuum chamber setup. Our results have important implications for the optimized evaporation of FA-based perovskites as they identify key issues related to the deposition of the FAI precursor.

DS 20.4 Wed 16:00 P3

In situ surface X-ray diffraction studies at high temperatures of Co oxide model catalysts for electrochemical water splitting — •CARL HENDRIC SCHARF¹, CANRONG QIU¹, JOCHIM STETNER¹, OLVIDO IRRAZÁBAL-MOREDA², MATHILDE BOUVIER³, FOUAD MAROUN³, and OLAF MAGNUSSEN¹ — ¹Institute of Experimental and Applied Physics, Kiel, Germany — ²European Synchrotron Radiation Facility (ESRF), Grenoble, France — ³Physique de la Matière Condensée, Ecole Polytechnique, Palaiseau, France

The development of low-cost electrocatalysts for electrochemical water splitting is of great interest for hydrogen technology. Among the best precious-metal-free electrode materials for the anodic oxygen evolution reaction (OER) in alkaline electrolysis are Co oxides such as Co₃O₄ and CoOOH. It was shown previously that a sub-nm thick CoO_x(OH)_y skin layer is formed in the pre-OER potential range, which forms the active phase during OER. Furthermore, reversible and irreversible structural changes in the oxide bulk were detected in the pre-OER regime. So far the vast majority of publications on Co oxide OER electrolysis have been performed at room temperature. We present first results up to 60°C (typ. operating temperatures of commercial electrolyzers). Using operando surface X-ray diffraction Co₃O₄ and CoOOH epitaxial films electrodeposited on Au(111) were studied in 0.1M NaOH at Petra III, Desy. These data are correlated with the electrochemical properties, determined by Cyclic Voltammetry and Optical Reflectivity, in order to provide insights into the temperature-dependence of skin layer thickness, bulk lattice changes and the stability of the oxides.

DS 20.5 Wed 16:00 P3

Growth of CoO Thin Films for Application in Superconductor - Magnet Heterostructures — •AMY MCGLINCHY — Trinity College Dublin, Ireland

Cobalt monoxide, CoO, is an antiferromagnet (AF) with a Néel temperature of 293K. It is utilised to pin the magnetisation of Co layers via exchange bias and is employed in magnetic heterostructures. The interaction between ferromagnet (F) and AF layers is predicted to generate long-range spin-triplet superconductivity in F-S-AF heterostructures [1]. CoO is a good candidate for the AF due to its strong magnetism, stability and low Neel temperature, which facilitates in-field cooling through the transition, improving magnetic uniformity. For the most part, CoO is synthesized by the oxidation of Co thin films. A fundamental understanding of how the Co phase (fcc or hcp) and oxidation environment influence the crystalline quality and surface morphology of the resultant CoO is lacking. In this work, we investigate the crystalline quality of the CoO as a function of Co phase and oxidation environment. As a second step towards a F-S-AF heterostructure, we also investigate the superconducting properties of superconducting Nb grown on the different CoO films. The properties of the niobium - especially at low thickness relevant to heterostructures - will, in theory, be influenced by the CoO magnetic and surface structure. I. L. G. Johnsen et al., *Phys. Rev. B*, 103, L060505 (2021).

DS 20.6 Wed 16:00 P3

Pseudo-2-dimensional Ga₂O₃ structures grown on Al₂O₃ using metal-oxide catalyzed epitaxy (MOCATAXY) — •JUSTIN ANDREAS BICH¹, MARCO SCHOWALTER¹, TJARK LIESTMANN¹, SUSHMA RAGHUVANSY¹, JONATHAN MCCANDLESS², MANUEL ALONSO-ORTS¹, ANDREAS ROSENAUER¹, MARTIN EICKHOFF¹, and PATRICK VOGT¹ — ¹Institute of Solid-State Physics, Bremen University, Otto-Hahn-Allee 1, 28359 Bremen, Germany — ²School of Electrical and Computer Engineering, Cornell University, Ithaca, New York 14853, USA

Ga₂O₃ has attracted attention as a new wide-bandgap semiconductor—which can be alloyed with Al₂O₃—for high-power applications. However, the growth of group-III sesquioxides by molecular-beam epitaxy differs substantially from other material systems, e.g., III-V materials.

In this work, we present the growth of ultra-thin α-Ga₂O₃ (0001) on α-Al₂O₃ (0001) in a controlled self-passivating manner. Using MOCATAXY, we observe the formation of this 'pseudo' 2-dimensional (2D) α-Ga₂O₃ thin film and its growth passivation after reaching 2 nm thickness. This α-Ga₂O₃ 2D thin film serves as a template for growing α-Ga₂O₃/α-Al₂O₃ quantum wells.

We present reflection-high energy electron diffraction, x-ray photoelectron spectroscopy, atomic force microscopy, x-ray diffraction, x-ray reflectivity, and transmission electron microscopy data, showing the existence and characteristics of this 'pseudo' 2D α-Ga₂O₃ thin film grown by MOCATAXY, and explain our results using a kinetic and thermodynamic framework.

DS 20.7 Wed 16:00 P3

An unconventional octahedral metal: AgSnTe₂ — •SOPHIA WAHL, CHRISTIAN TEICHRIB, CARL-FRIEDRICH SCHÖN, MARIA HÄSER, YUAN YU, and MATTHIAS WUTTIG — 1. Institute of Physics (Ia), RWTH Aachen University, Aachen, Germany

Phase-change materials (PCMs) provide a unique combination of properties. Switching from the amorphous to crystalline structural phase, their optical and

electrical properties change significantly. While conventional PCMs undergo a change from covalent to metavalent bonding upon crystallization accompanied by a dielectric behavior in both phases [1], we observe a change from dielectric to metallic in the optical and electrical properties for the unconventional metal AgSnTe₂ (AST).

We analyze the dielectric properties of amorphous and crystalline AST samples by employing optical spectroscopy from the infrared to UV/Vis range. Through a Kramers-Kronig analysis of the data, we can separate the contributions of the optical functions accordingly and yield insight into the nature of bonding. Transport measurements and the investigation of bond rupture in atom probe tomography support the findings and all imply a non-conventional bonding mechanism in crystalline AST.

This work is aiming to define a whole set of new plasmonic PCMs which are all located in one region of the materials bonding map[2].

[1] Wuttig et al., Nat. Photonics, 11, 2017

[2] Raty et al., Adv. Mater., 31, 2019

DS 20.8 Wed 16:00 P3

Structural and electronic investigations of Bismuth multilayers with DFT — •FABIAN TEICHERT¹, CHITRAN GHOSAL¹, UWE GERSTMANN², CHRISTOPH TEGENKAMP¹, and ANGELA THRÄNHARDT¹ — ¹Institute of Physics, Chemnitz University of Technology, Chemnitz, Germany — ²Department of Physics, Paderborn University, Paderborn, Germany

Bismuth shows a variety of interesting properties as bulk material but also as thin film, e.g. it is a topological insulator, shows strong spin-orbit coupling effects and has a semimetal-semiconductor transition concerning film thickness. The focus of this presentation will be on density functional theory (DFT) calculations, which have been done for Bi(110) multilayers to get insights into the concrete structure and electronic states. We compare the results with Bi multilayers, which have been grown epitaxially on graphene substrate and where (110) slabs have been figured out. They are treated with scanning tunneling microscopy (STM) measurements for various slab thicknesses. We found an even/odd scheme concerning the number of monolayers as well as concerning the number of bilayers indicating a structural relaxation like the black phosphorus allotrope. Further calculations with graphene and highly oriented pyrolytic graphite (HOPG) substrate have been performed to figure out if structurally separated and electronically decoupled layers are present at the substrate interface. Concerning the electronic properties, we present the calculated bandstructures and density of states and comparisons with the measured differential conductance, which are in good agreement.

DS 20.9 Wed 16:00 P3

Twisted bilayer antimonene — •STEFAN WOLFF, ROLAND GILLEN, and JANINA MAULTZSCH — Department of Physics, Chair of Experimental Physics, Friedrich-Alexander-Universität Erlangen-Nürnberg, Staudtstr. 7, 91058 Erlangen, Germany

Antimony has proven to be a promising candidate for two-dimensional (2D) mono-elemental materials. In bulk form, it is a layered crystal comprising sheets of antimony atoms arranged in a hexagonal buckled honeycomb lattice called antimonene. The natural stacking order follows an ABC-pattern, in which each subsequent layer is shifted by one third. Other than many other 2D materials, the interlayer bonds in few-layer antimonene show partially covalent character. Due to this covalent character, changes of the local stacking order via rotation and translation may lead to new interesting features and properties of the material. Density functional theory (DFT) is used to simulate twisted bilayer antimonene structures with different rotation angles and to investigate their physical properties. Moiré patterns and local stacking orders can be found, which lead to a non-uniform bond length distribution. Additionally, our investigation of the charge density shows how the overlap of atomic orbitals in certain areas changes, depending on the proximity of atoms from neighboring layers. A comprehensive understanding of how the properties of twisted bilayer antimonene are modified compared to naturally stacked bilayer antimonene may lead to future applications making use of well-constructed, favorable stacking orders in layered materials.

DS 20.10 Wed 16:00 P3

Determination of circularly polarized light-triggered chiral excitons in organic light harvesting devices — •OTGONBAYAR ERDENE-OCHIR, DIRK HERTEL, and KLAUS MEERHOLZ — Chemistry Department, University of Cologne, Cologne, Germany

Organic-chiroptics have not been a focus of the research area due to the trace amount of circular dichroism (CD) nature has provided in most chiral molecules. However, aggregation of chiral prolinol functionalized squaraine offers giant intrinsic CD behavior. The CD effect is related not only to the difference of left- and right-handed circularly polarized (CP) light absorption for the organic chiral molecule, but also associated with their excitonic nature based on the formation of molecular aggregates. This work discusses the determination of the selective chiral excitons via direct right- and left-handed CP laser radiation. The enantiomer of squaraine derivative (S,S)-ProSQ-C16 is a strongly CD-active material

featuring maximum absorbance at ca. 780 nm after thermal annealing of a thin film. We introduced (S,S)-ProSQ-C16 as a p-type active material in a planar heterojunction (PHJ) and bulk heterojunction (BHJ) blend for the photovoltaic devices, together with the fullerenes C60 and PCBM as acceptors, respectively. We used normal-incident transmission Mueller Matrix method to determine the intrinsic CD effects of the thin film. An electronic characterization of the chiral exciton within the PHJ and BHJ systems are quantified. The efficiency of the chiroptical response is estimated by the dissymmetry factor. A systematic correlation between optical and electronic dissymmetry factors will be discussed.

DS 20.11 Wed 16:00 P3

Molecular dynamics simulations of carbon nanomembranes (CNMs): Formation and mechanical properties — •LEVIN MIHLAN, JULIAN EHRENS, and JÜRGEN SCHNACK — Universität Bielefeld, Universitätsstrasse 25, D-33615 Bielefeld

CNMs are made by electron-induced crosslinking of aromatic self-assembled monolayers (SAMs) [1,2]. Their supposedly irregular internal structure cannot be adequately investigated by standard spectroscopic techniques, however, a determination of, e.g. Young's moduli is possible. In order to propose possible internal structures obtained from various initial configurations of the SAM and irradiation processes, we investigate the monolayers with respect to the Young's modulus in terms of classical molecular dynamics calculations using LAMMPS and compare to experimental values. We present three distinct methods to calculate the Young's modulus: Global scaling of all coordinates, stress-strain response from clamped straining and barostated dynamics. Discrepancies among the methods with regard to vastly different outcomes will be discussed considering finite size effects. CNMs can be used for water filtration, a property that is closely related to the distribution of holes in the membrane [3]. With a hole-detection algorithm for our simulated CNMs we can investigate the hole distributions too and use this as a second observable for comparison with experimental data.

[1] Dementyev, Petr, et al. ChemPhysChem 21.10 1006, 2020

[2] Ehrens, Julian, et al. Phys. Rev. B 103 115416, 2021

[3] Y. Yang, et al. ACS Nano vol. 12 no. 12 pp. 4695-4701, 2018

DS 20.12 Wed 16:00 P3

Microscopic theory of X-ray absorption spectroscopy — •JORIS STURM, DOMINIK CHRISTIANSEN, MALTE SELIG, and ANDREAS KNORR — Institut für Theoretische Physik, Nichtlineare Optik und Quantenelektronik, Technische Universität Berlin, Hardenbergstr. 36, 10623 Berlin, Germany

X-ray absorption near-edge spectroscopy (XANES) and extended X-ray absorption fine structure (EXAFS) are two widely used methods to investigate the structure of solid states. Unfortunately, for both techniques, mostly heuristic models are available [1,2,3].

In this contribution, we present the first self-consistent Maxwell-Bloch approach based on Heisenberg equation of motion formalism for the unified description of XANES and EXAFS for 2D solid-state materials and apply it to the exemplary material graphene. For XANES we reproduce the experimentally observed absorption peaks and polarization-dependent selection rules of the included orbitals. Furthermore, the rigorous treatment of the Bloch theorem allows us to calculate the Fourier transformed EXAFS spectrum [2] predicting so far uninterpreted features which have not been assigned within scattering theory [1].

[1] Sayers, Dale E., et al., PRL 27 (1971): 1204

[2] Buades, Bárbara, et al., Optica 5 (2018): 502

[3] Chowdhury, M. T., R. Saito, and M. S. Dresselhaus, PRB 85 (2012): 115410.

DS 20.13 Wed 16:00 P3

Confinement induced coherent phonon softening in Sb₂Te₃ thin films — •JONATHAN FRANK¹, JULIAN MERTENS¹, FELIX HOFF¹, MOHIT RAGHUWANSHI², and MATTHIAS WUTTIG¹ — ¹Institute of Physics (IA), RWTH Aachen University, Aachen, Germany — ²Forschungszentrum Jülich, Jülich, Germany

Femtosecond reflection-type optical pump-probe experiments on a thickness-series of MBE-grown Sb₂Te₃ thin films were carried out to study confinement effects of coherent optical phonons. Therefore, an isotropic detection scheme was applied to investigate the ultrafast dynamics of the LO-phonon mode of A1g-symmetry in Sb₂Te₃ thin films ranging from 1.3 to 55 nm. The ultrafast response of each thin film contains a distinct coherent feature uncovered by damped harmonic oscillations in the transient reflectivity traces. It is shown that coherent optical phonons are efficiently photoexcited in thin films of only a few quintuple layers. This finding supports the hypothesis that electron-phonon coupling in ultrathin sesqui-chalcogenide films does not fundamentally differ from bulk which is essential for the performance in strongly scaled applications as for example in topological insulators. Furthermore, a slight decrease in phonon-frequency accompanied by a more pronounced decrease in phonon-lifetime is observed in films smaller than ten nanometers; both quantities nearly monotonously decrease with film thickness. We ascribe this phonon softening to a decreased interlayer coupling in films of a few quintuple layers compared to a more bulk-like behavior observed in the thicker films.

DS 20.14 Wed 16:00 P3

Characterization of layer systems by combination of X-ray reflectivity and hyperspectral imaging — •STEFFEN BIEDER¹, FLORIAN GRUBER², PATRICK SCHLENZ³, PHILIPP WOLLMANN², CHRISTIAN ALBERS¹, SUSANNE DOGAN¹, MICHAEL PAULUS¹, NICOLA THIERING¹, CHRISTIAN STERNEMANN¹, and STEFFEN CORNELIUS³ — ¹TU Dortmund, 44227 Dortmund, Germany — ²Fraunhofer IWS, Winterbergstrasse 28, 01277 Dresden, Germany — ³Fraunhofer FEP, Winterbergstrasse 28, 01277 Dresden, Germany

Different thin film multilayers consisting of indium tin oxide, zinc tin oxide and silver deposited on flexible PET foils were studied using X-ray reflectivity and hyperspectral imaging aiming for an online quality control of the coatings' manufacturing process. The X-ray reflectivity data measured at beamline BL9 of the DELTA synchrotron radiation source provide detailed information on layer thickness with Angström resolution, roughness and electron density. These results are used to establish statistical models in order to analyze and interpret the data obtained from hyperspectral imaging. Latter is foreseen to be implemented into the foils' production line for in-situ detection of thickness changes during the production process.

The authors acknowledge funding from the European Union's Horizon 2020 research and innovation programme under grant agreement No 862055. We thank DELTA for providing synchrotron radiation.

DS 20.15 Wed 16:00 P3

Surface second harmonic generation in dielectric nanofilms — •FATEMEH ALSADAT ABTAHI¹, PALLABI PAUL^{1,2}, SEBASTIAN BEER¹, ADRIANA SZEGHALIMI^{1,2}, STEFAN NOLTE^{1,2}, and FALK EILENBERGER^{1,2,3} — ¹Institute of Applied Physics, Friedrich-Schiller-University, Jena, Germany — ²Fraunhofer-Institute for Applied Optics and Precision Engineering IOF, Jena, Germany — ³Max Planck School of Photonics, Jena, Germany

Second-harmonic generation (SHG) is a second-order nonlinear optical process that is not allowed in media with inversion symmetry. However, due to the broken symmetry at the surface, surface SHG can still occur in such materials. We experimentally investigate the surface SHG in the periodic stacks of ultrathin dielectric layers. Uniform, dense and optically homogeneous multilayer stacks of SiO₂/TiO₂ were grown by Plasma Enhanced Atomic Layer Deposition (PEALD) on fused silica substrates. With this technique individual layers of a thickness of less than 2 nm can be fabricated, increasing the number of SHG-active surfaces substantially. Because of the material discontinuity, in each surface of this structure, the symmetry is broken and surface SHG will occur. By changing the Angle of Incidence (AOI) and having constructive interference between all fundamental/SHG signals from different surfaces, we are able to enhance the surface SHG. We experimentally show that under large angles of incidence > 20 degrees there is substantial SHG, well beyond the level, which can be expected for simple surfaces.

DS 20.16 Wed 16:00 P3

Surface-Enhanced Raman Spectroscopy and Transient Reflectivity of Strained LSMO Thin Films — •LEONARD SCHÜLER, TIM TITZE, STEFAN MATHIAS, DANIEL STEIL, and VASILY MOSHNYAGA — I. Physikalisches Institut, Georg-August-Universität Göttingen

The effect of lattice strain on the structural and electronic surface reconstruction of epitaxial La_{0.7}Sr_{0.3}MnO₃/LaAlO₃ (LSMO/LAO) thin films has been studied by surface-enhanced optical measurements. Surface sensitivity is achieved by deposition of gold nanoparticles, in which the localized surface plasmon resonance enhances laser electric fields at the surface, enabling surface-enhanced Raman spectroscopy (SERS) and pump-probe reflectivity (SE-PPR) studies of the LSMO films. For this system, SERS reveals a structural surface reconstruction and signals an insulating surface state characterized by strong Jahn-Teller modes which are not present in the conventional Raman spectra of the ferromagnetic metallic LSMO/LAO films. Furthermore, a structural transition of the insulating surface is shown at T* = 200-220 K possibly related to charge ordering (CO). SE-PPR indicates that it is possible to photoinduce a ferromagnetic metallic phase at the surface above the assumed CO transition temperature.

DS 20.17 Wed 16:00 P3

In-situ spectroscopic ellipsometry analysis of SiO₂ on Si under different atmosphere and temperature — •XINYU ZHOU, YOUNES SLIMI, STEFAN KRISCHOK, and RÜDIGER SCHMIDT-GRUND — Technische Universität Ilmenau, Fachgebiet Technische Physik I, Weimarer Straße 32, 98693 Ilmenau, Germany In-situ Spectroscopic ellipsometry has been applied to obtain optical constants and thin film thicknesses of SiO₂ on Si under different atmospheres (nitrogen, dry air) and temperatures. We found changes in refractive index and thickness of the SiO₂ layer under different conditions due to oxidation and material ablation. We further present our recent developments in building up an in-situ ellipsometry system for photo-electrochemical applications.

DS 20.18 Wed 16:00 P3

Spectroscopic Ellipsometry of transition metal oxide thin films — •NAHID AHMADIAN^{1,2}, TERESA I. MADEIRA^{1,2}, and DIETRICH R.T. ZAHN^{1,2} — ¹Chemnitz University of Technology, Chemnitz, Germany — ²Center for Materials, Architectures and Integration of Nanomembranes (MAIN), D-09107, Chemnitz, Germany

Transition metal oxides such as HfO₂ or TiO₂ with bandgaps of 5.3-5.9 eV and 3.0-3.4 eV, are transparent in the visible range of the spectrum, i.e. their extinction coefficient in this range is very low close to zero while the refractive index varies as a function of photon energy. In this work, we tested four dispersion models: Sellmeier, Cauchy, extended Cauchy, and Tauc-Lorentz aiming at understanding the mathematical and physical differences of these approximations, their robustness and limitations in addressing amorphous and crystalline phases of thin films of HfO₂ deposited by atomic layer deposition (ALD) on Si(100) and TiO₂ thin films prepared on Si(100) by magnetron sputtering and spin coating. The spectroscopic ellipsometry measurements were performed using a M-2000 T-Solar from J.A. Woollam. Spectra covering a range of energies 0.7 (IR) – 5 eV (UV) were taken in air at room temperature and analyzed using CompleteEASE. We conclude that multiple oscillators are required to treat the crystalline phases in comparison to the amorphous, and when very good solutions are obtained from all oscillators, the choice to use one or the other is based on complexity: the less the fit parameters the best.

DS 20.19 Wed 16:00 P3

Reaction of Tetrapyrrole Thin Films with Alkali Metals — •LEONARD NEUHAUS¹, STEFAN RENATO KACHEL¹, PETER SCHWEYEN², MARK HUTTER¹, MAIK SCHÖNIGER¹, FLORIAN MÜNSTER¹, LUKAS RUPPENTHAL¹, JAN HERRITSCH¹, MARIE-IRENE ALBUS¹, MARTIN BRÖRING², and J. MICHAEL GOTTFRIED¹ — ¹Fachbereich Chemie, Philipps-Universität Marburg, Germany — ²Institut für Anorganische und Analytische Chemie, Technische Universität Braunschweig, Germany

Tetrapyrroles such as porphyrins play an import role in living organism and for various modern technologies. While most previous publications related to tetrapyrrole thin films focus on transition metal complexes, we want to expand the field by exploring the reaction of various tetrapyrrole films with alkali metals. For this purpose, we prepared multilayer films of tetraphenylporphyrin and an octaalkylcorrol on a Au(111) surface and studied their reactions with Li and Cs, thus covering the extremes of the lightest and heaviest stable alkali metal. For all studied systems, X-ray photoelectron spectroscopy (XPS) showed, changes in the N 1s region that indicate formation of the corresponding tetrapyrrole metal complexes. Complementary studies with temperature programmed reaction (TPR) provided unambiguous mass spectrometric evidence for the formation of the metal complexes. TPR also showed that the number of alkali metal atoms attached to a tetrapyrrole ligand can exceed the number of pyrrolic hydrogen atoms in the free-base tetrapyrrole.

DS 20.20 Wed 16:00 P3

Thermoelectric Characterization of Polymer Thin Films with Ag-nanowire Additives — •SOHRAAB SCHERZAD¹, MARIE SIEGERT¹, and JENS PFLAUM^{1,2} — ¹Experimental Physics VI, University of Würzburg, 97074 Würzburg — ²ZAE Bayern, 97074 Würzburg

Along the process of power conversion from primary energy carriers vast amounts of waste heat in the low and mid temperature range occur. A possible solution to recover this waste heat is offered by thermoelectric generators which rely on the Seebeck effect and are able to directly convert thermal into electrical energy. Polymeric semiconductors, operating in this temperature regime, offer a sustainable and low-cost alternative to inorganic thermoelectrics. Their characteristics include a sufficiently low thermal conductivity κ , but also a low electrical conductivity σ , due to the low charge carrier concentration and generic disorder. Here we report on composite thin films made of Ag-nanowires embedded in PEDOT:PSS polymer matrices, which lead to changes in the electrical conductivity compared to pure PEDOT:PSS. Ag-nanowires are considered to be a suitable additive for increasing σ of the resulting composite and its impact on κ will also be studied. First results on the thermoelectric properties of this material combination will be presented together with structural information obtained by X-ray diffraction and atomic force microscopy. Based on this complementary information we will critically discuss the potential of the presented approach for application in TEGs.

DS 20.21 Wed 16:00 P3

Plasmonic-induced Thermoelectric Effects in Metal-organic Hybridstructures — •LUCCA MACHER¹, PAUL HOPPSTOCK¹, MAXIMILIAN FRANK¹, MAXIMILIAN RÖDEL¹, and JENS PFLAUM^{1,2} — ¹Experimental Physics VI, University of Würzburg, 97074 Würzburg — ²Bavarian Center for Applied Energy Research (ZAE Bayern), 97074 Würzburg

Local heat generation by plasmonic excitations in noble metal nanoparticles is of high technological interest for numerous applications such as photo-thermal chemistry or cancer therapy. In this work we utilize this approach to create a thermal gradient by the absorption of light in metal-organic hybrid structures.

The latter are based on arrays of nanostructured gold and silver triangles in combination with solution processed p-type PEDOT:PSS films. As we can demonstrate, a defined temperature enhancement and thus, gradient evolves upon resonantly exciting local plasmons in the Au or Ag nanoparticle arrays. The amplitude of this enhancement amounts to $\Delta T = 0.5$ K for an incident light power of 1.4 mW/mm². Accordingly, this plasmon-induced temperature gradient which is aligned along the PEDOT:PSS polymer layers results in a significant enhancement of the thermovoltage to $V_T = 24$ μ V/K as compared to neat PEDOT:PSS ($V_T = 12$ μ V/K). An application-oriented approach was carried out as well, using arrays of nanostructured gold triangles covered by a transparent polymer-gel electrolyte PEGMA/BEMA in a window-like device architecture. A temperature gradient of $\Delta T = 0.1$ K for an incident light power of 1.8 mW/mm² was determined along the PEGMA/BEMA layer.

DS 20.22 Wed 16:00 P3

Self-assembled monolayers of molecular spin-crossover (SCO) switches — •FABIAN STRELLER¹, STEPHEN GOODNER², MARAT KHUSNIYAROV², and RAINER FINK¹ — ¹Lehrstuhl für Physikalische Chemie II, Friedrich Alexander Universität Erlangen Nürnberg, Germany — ²Lehrstuhl für Anorganische und Allgemeine Chemie, Friedrich Alexander Universität Erlangen Nürnberg, Germany Spin-crossover (SCO) complexes are regarded as promising materials in applications such as spintronics, molecular electronics and ultra-high-density memory systems. They can be switched by external stimuli, e.g., change of temperature, pressure, or illumination with light. In the investigated complexes switching occurs between diamagnetic low-spin (LS) and paramagnetic high-spin (HS) species by either a simple SCO, or a valence tautomeric (VT) transition accompanied by a SCO. While the mentioned applications seem promising, one big challenge that needs to be overcome is the transfer of the systems from solution or bulk towards thin films or even monolayers on well-defined surfaces. Six-coordinate iron(II) complexes have been used as SCO materials, whereas six-coordinate Co complexes with redox active dioxolene ligands were chosen as VT materials. Both materials can be attached to the surface via a bidentate phenanthroline ligand containing moieties suitable for bonding to the substrate. Here we report a step by step formation of single-layer films on Au(111) surfaces. The thus created specimens were characterized by atomic force microscopy (AFM), x-ray photoelectron spectroscopy (XPS) and near edge x-ray absorption fine structure (NEXAFS).

DS 20.23 Wed 16:00 P3

Chern number control in quantum anomalous Hall insulators by external fields — •YURIKO BABA^{1,2}, FRANCISCO DOMÍNGUEZ-ADAME¹, and RAFAEL A. MOLINA-FERÁNDEZ² — ¹GISC, Departamento de Física de Materiales, Universidad Complutense, E-28040 Madrid, Spain — ²Instituto de Estructura de la Materia, IEM-CSIC, E-28006 Madrid, Spain

Topological magnetic insulators have been discovered as a new platform for observing Quantum Anomalous Hall states with high Chern number C . In three-dimensional structures of stacking layers of magnetically doped and undoped topological insulators of Bi₂(Se,Te)₃, the number of chiral edge channels can be controlled by the width and number of layers and by the doping concentration. This has been recently measured by Zhao et al. [1] in Cr doped samples, showing this feature up to $C = 5$.

In this theoretical work, we explore the possibilities of tuning the chiral channels of the aforementioned materials in the presence of electric fields in multilayered structures. The external field tunes the Chern number and changes the number of topological channels dynamically without the need of replacing the sample to modify the Chern number. The tuneability has a remarkable impact on the transport properties of pristine and disordered samples.

[1] Zhao, Y. F. et al., Nature, 588 (2020) 419

DS 20.24 Wed 16:00 P3

topological magnons and thermal hall conductivity in 2D magnets — •HAMID NOURI and HONGBIN ZHANG — Technical University of Darmstadt, 64287 Darmstadt, Germany

Two-dimensional (2D) materials provide a fascinating playground for emergent phenomena driven by enhanced thermal and quantum fluctuations, in particular the nontrivial topological phases with the associated dissipationless transport properties. For 2D magnetic insulators, magnons can also host Dirac and Weyl points with nonzero Berry curvature, leading to finite thermal Hall conductivities. In this work, based on the linear response spin-wave theory, we investigated a Hamiltonian formulated on 2D lattices comprising the Heisenberg exchange, Dzyaloshinskii-Moriya interaction (DMI) interactions, single-ion anisotropy, external magnetic fields, and found that the gapped magnon bands exhibit nonzero Chern numbers of ± 1 due to finite DMI which acts like effective spin-orbit coupling. The thermal Hall conductivity is evaluated based on the Boltzmann transport theory, suggesting a novel approach to designing 2D thermal management materials. The realization of such Hamiltonians in experimentally available 2D materials will be discussed as well.

DS 20.25 Wed 16:00 P3

Bottom-up preparation of large area van-der-Waals heterostructures by the subsequent growth of 2D transition metal dichalcogenides layers — •DEVENDRA PAREEK¹, MARCO A. GONZALEZ¹, NEDAL GREWO¹, MARTEN L. JANSSEN¹, LEON A. GRÄPER¹, KUMARAHGIRI ARUNAKIRI¹, KAYODE. L. ALIM¹, MARTIN SILIES^{1,2}, JÜRGEN PARISI¹, LEVENT GÜTAY¹, and SASCHA SCHÄFER¹ — ¹Ultrafast Nanoscale Dynamics, Institute of Physics, Carl von Ossietzky University of Oldenburg, Oldenburg, Germany — ²Institute for Lasers and Optics, University of Applied Sciences Emden/Leer, Emden, Germany

We report the preparation of as-grown two-dimensional transition metal dichalcogenides (2D-TMDC) heterostructures from a processing route employing a combination of atomic layer deposition of monolayer MoS₂ and solution-based processing of ultrathin Mo(S/Se)₂ and W(S/Se)₂ films. Grown on centimeter-scale sapphire substrates, spatially uniform optoelectronic characteristics of the individual TMDC layers and heterostructures are demonstrated down to micrometer length scales using photoluminescence, Raman spectroscopy, and light-beam-induced current measurements. Preliminary observations on enhanced photogenerated currents in MoS₂-MoS₂/WS₂ lateral heterostructures demonstrate the suitability of this approach for the preparation of functional devices on macroscopic length scales. Finally, we also discuss the possibilities to synthesize these compounds at temperatures below 400 °C, making them suitable for a broad range of substrate materials.

DS 20.26 Wed 16:00 P3

Twist-angle dependent proximity induced spin-orbit coupling in graphene/transition-metal dichalcogenide and graphene/topological insulator heterostructures — •THOMAS NAIMER¹, KLAUS ZOLLNER¹, MARTIN GMITRA², and JAROSLAV FABIAN¹ — ¹Uni Regensburg, Regensburg, Germany — ²Pavol Jozef Šafárik University, Košice, Slovakia

We investigate the proximity-induced spin-orbit coupling in twisted heterostructures of graphene/transition-metal dichalcogenides (MoS₂, WS₂, MoSe₂, and WSe₂) as well as graphene/topological insulators (Bi₂Se₃ and Bi₂Te₃) from first principles. To correct for strain induced band offsets, we apply a perpendicular electric field. The resulting corrected band structure is then fitted around the Dirac point to an established spin-orbit Hamiltonian, yielding the twist angle dependencies of the (Rashba and valley-Zeeman) spin-orbit coupling. This work was funded by the Elite Network of Bavaria, the Deutsche Forschungsgemeinschaft (DFG, German Research Foundation), SFB 1277, SPP 2244 and by the European Union Horizon 2020 Research and Innovation Program under contract number 881603 (Graphene Flagship). M.G. acknowledges VEGA 1/0105/20.

DS 20.27 Wed 16:00 P3

Valley depolarization of excitons in encapsulated MoSe₂-WSe₂ heterostructures with controlled moiré potentials — •ANDREAS BEER¹, ANNA WEINDL¹, NICLAS MAIER¹, ANTONY GEORGE², ANDREY TURCHANIN², and CHRISTIAN SCHÜLLER¹ — ¹Universität Regensburg — ²Friedrich-Schiller-Universität Jena

Our focus is the investigation of the temporal and spatial dynamics of interlayer excitons in MoSe₂-WSe₂ heterostructures with well-defined moiré potentials, based on CVD grown samples. The so called hot pickup method enables us to fabricate such heterostructures out of CVD grown triangulars in a controlled, dry, PDMS-free and easy way.

To understand the valley depolarization mechanism in TMDC monolayers and heterostructures we perform time resolved pump probe measurement. First measurements on twisted TMDC exfoliated heterostructures reveal twist-angle-dependent decay times of the interlayer exciton.

DS 20.28 Wed 16:00 P3

Protection of QSHI indenene from air via intercalation — •CEDRIC SCHMITT^{1,2}, JONAS ERHARDT^{1,2}, SIMON MOSER^{1,2}, and RALPH CLAESSEN^{1,2} — ¹Physikalisches Institut, Universität Würzburg, D-97074 Würzburg, Germany — ²Würzburg-Dresden Cluster of Excellence ct.qmat, Universität Würzburg, D-97074 Würzburg, Germany

In the search for new quantum materials, ultrathin metals are interesting as they push bulk properties to the 2D limit and foster novel quantum effects. Unfortunately, these systems are prone to oxidation in air, making them useless for quantum transport devices. Metal intercalation is a relatively new capping method, that utilizes graphene, an inert quantum material that can be easily produced by heating of a SiC substrate [1,2]. Hereby, the metal is intercalated between the SiC/graphene layer, thus forming freestanding graphene, which is believed to protect the intercalated layers against oxidation [3]. Hitherto studies focused mainly on identifying stable allotropes but lacking a detailed investigation of metal coverage and oxidation [3]. Here, we study the intercalation of indenene, a recently discovered QSHI on a triangular lattice [4]. First experiments indicate the indium layer to remain intact upon air exposure, indeed pointing to an effective protective function of the overlayer graphene.

[1] K. S. Novoselov et al. Science 306, 666 (2004)

[2] C. Berger et al. J. Phys. Chem. B 108, 19912 (2004)

[3] N. Briggs et al. Nat. Mater. 19, 637-643 (2020)

[4] M. Bauernfeind et al. Nat. Commun. 12, 5396 (2021)

DS 20.29 Wed 16:00 P3

Electronic Structure of $[(\text{SnSe})_{1+\delta}]_m(\text{TiSe}_2)_n$ investigated by Photoelectron Spectroscopy — •NIELS RÖSCH¹, FABIAN GÖHLER¹, DANIELLE M. HAMANN², DAVID C. JOHNSON², and THOMAS SEYLLER¹ — ¹Technische Universität Chemnitz, Institut für Physik, 09126 Chemnitz — ²University of Oregon, Department of Chemistry, Eugene OR 97401

The Modulated Elemental Reactants (MER) synthesis is a new method for producing multilayer heterostructures. A precursor is created in MER by using consecutive physical vapour deposition. The precursor's structure and composition can be deliberately changed to mimic the desired heterostructure. After that, the precursor is crystallized by annealing it at low temperatures in an inert environment. Low temperatures allow thermodynamically metastable films to form, albeit at the cost of turbostratic rotational disorder between layers. By systematically modifying the stacking sequence of individual layers, this approach can be used to create a succession of layered heterostructures.

X-ray photoelectron spectroscopy was used to investigate the electrical structure of a sequence of $[(\text{SnSe})_{1+\delta}]_m(\text{TiSe}_2)_n$ heterostructures [1]. It is demonstrated that electrons are transferred from the SnSe layers to the TiSe_2 layers. Understanding charge transfer in heterostructures is important for future applications, as controlled stacking of the heterostructure may allow for targeted doping.

[1] Göhler, F., Hamann, D. M., Rösch, N., et al., *J. Mater. Res.* 34 (12): (2019)

DS 20.30 Wed 16:00 P3

Atomistic Simulations of Defects Production Under Ion Irradiation in Epitaxial Graphene on SiC — •MITISHA JAIN¹, SILVAN KRETSCHMER¹, KATJA HÖFLICH^{2,3}, JOAO MARCELO J. LOPES⁴, and ARKADY KRASHENINNIKOV¹ — ¹Institute of Ion Beam Physics and Materials Research, Helmholtz-Zentrum Dresden-Rossendorf, Bautzner Landstraße 400, 01328 Dresden, Germany — ²Ferdinand-Braun Institut gGmbH, Leibniz-Institut für Höchstfrequenztechnik, Berlin, Germany — ³Helmholtz-Zentrum Berlin für Materialien und Energie GmbH, Berlin, Germany — ⁴Paul-Drude-Institut für Festkörperelektronik, Leibniz-Institut im Forschungsverbund Berlin e.V., Berlin, Germany

In this work, using atomistic simulations at the analytical potential and density-functional theory (DFT) levels, we theoretically study defect production in EG on SiC by ion beams (He and Ne ions). We explicitly consider the effects of the substrate (bulk SiC) on the response of graphene to irradiation. Since the substrate affects the number of displaced carbon atoms and vacancy types in EG, we present information about the number, types and location of defects produced in each layer of EG to guide the experiment in tailoring the defect production. Motivated by the He FIB experiments (aiming at nucleation sites of h-BN growth, operating at 30 keV), our considerations apply to the typical ion energies used in HIM, that is 10-30 keV.

DS 20.31 Wed 16:00 P3

Low energy ion induced effects on core-shell nano particles — •JULIAN LISSON, SHIVA CHOUPANIAN, and CARSTEN RONNING — Institute of Solid State Physics, Friedrich Schiller University Jena, Max-Wien-Platz 1, 07743 Jena, Germany
Ion irradiation can be used for manipulating the shape and properties of nano-materials. However, the compartment of nano materials irradiated with energetic ions differs from bulk and thin films due to the mesoscopic properties of nanoparticles. The succeeding effects such as sputtering and ion beam mixing are strongly coupled and are dependent on the properties of the irradiated target. In this study, the effect of Ga⁺ ions with an energy range of 10-30 keV on different nanomaterials of Au, Ag, Au-Ag mix, and core-shell nanoparticles dispersed on Si substrates has been investigated. The sputter yield for each nanomaterial has been measured. Comparing the sputter yield and morphology changes of the nanoparticles, we observe that the ion beam mixing at the interface of the Au-Ag core-shell nano particles is prominent. The sputter yield dependence is changing when ion beam mixing is occurring and leads to dissimilar morphology changes of the core-shell nanoparticles due to preferential sputtering.

DS 20.32 Wed 16:00 P3

Lattice dynamics in tuneable thin films with Ruddlesden-Popper structure — •VERONICA GOIAN¹, NATALIE DAWLEY², JINGSHU ZHANG², CHRISTELLE KADLEC¹, NATHAN D. ORLOFF³, REINHARD UECKER⁴, STEFFEN GANSCHOW⁴, DARRELL G. SCHLOM^{2,5}, and STANISLAV KAMBA¹ — ¹Institute of Physics ASCR, Prague, Czech Republic — ²Department of Materials Science and Engineering, Cornell University, Ithaca, NY, USA — ³National Institute of Standards and Technology, Boulder, CO, USA — ⁴Leibniz-Institut für Kristallzüchtung, Berlin, Germany — ⁵Kavli Institute at Cornell for Nanoscale Science, Ithaca, NY, USA
In this work, we will compare the phonon dynamics of $(\text{SrTiO}_3)_6\text{SrO}$ (SrRP6) thin film with $(\text{SrTiO}_3)_5(\text{BaTiO}_3)_1\text{SrO}$ (BaRP6) and $\text{Sr}_{5/6}\text{Ba}_{1/6}\text{TiO}_3$ (SBT) thin films, all deposited on (110) DyScO_3 substrates. The XRD measurements and the rocking curves prove the thin films are single phase and epitaxially grown on the substrates. The lattice dynamics of the thin films were determined using THz and IR spectroscopies down to 10 K. Many phonons exhibit anomalies near temperatures of the ferroelectric phase transitions. We found out that the 100 nm BaRP6 and SBT thin films have T_C about 40-50 K higher than previously

studied 50 nm thin films, which is due to slightly relaxed strain in the thin films. We will also compare the temperature behavior of the complex permittivity of BaRP6 and SBT thin films with behavior of $\text{Ba}_x\text{Sr}_{1-x}\text{TiO}_3$ ($x=0.1..0.6$) ceramics and will discuss the reason for high tuneability of permittivity and low dielectric loss in strained thin films.

DS 20.33 Wed 16:00 P3

Stabilized ferromagnetism in LPCMO thin films by using buffer layers — •PIA HENNING¹, KAREN STROH¹, VITALY BRUCHMANN-BAMBERG¹, OLEG SHAPOVAL², and VASILY MOSHNYAGA¹ — ¹Erstes Physikalisches Institut, Georg-August-Universität-Göttingen, Göttingen, Germany — ²IIES, Academy of Sciences of Republic Moldova, Chisinau, Republic of Moldova

$(\text{La}_{0.6}\text{Pr}_{0.4})_{0.7}\text{Ca}_{0.3}\text{MnO}_3$ (LPCMO) is an A-site substituted perovskite manganite and is mostly known for the colossal magnetoresistance (CMR) effect. Relatively thick LPCMO films ($d \approx 50-100$ nm) with a coupled ferro-to-paramagnet and a metal-to-insulator transition (MIT) and CMR can be heteroepitaxially grown on $\text{MgO}(200)$ substrates, where a relaxed growth due to misfit dislocations is achieved. However, very thin LPCMO films with $d \leq 20$ nm on $\text{MgO}(200)$ do not show a MIT and CMR. On the alternative substrate $\text{SrTiO}_3(100)$, LPCMO grows coherently strained and with good surface morphology, but lacks an MIT and CMR even for $d \leq 50$ nm.

To enable high-quality LPCMO thin film growth on SrTiO_3 substrates, the introduction of a buffer layer to bridge the lattice mismatch of film and substrate is inevitable. Based on this, we investigate the growth of LaAlO_3 (LAO) buffer layers on SrTiO_3 and the influence of LAO buffer layers on the growth of LPCMO in order to improve the magnetic and electric properties. Specifically, the interplay of buffer and film thickness is studied. It is demonstrated the possibility of high quality thin film growth of LPCMO on buffered STO and a stabilization of the ferromagnetic-metallic phase.

DS 20.34 Wed 16:00 P3

Electronic Reconstruction and Anomalous Hall Effect at the $\text{LaAlO}_3/\text{SrRuO}_3$ Interface — •MERIT SPRING¹, JI SOO LIM¹, MARTIN KAMP¹, LOUIS VEYRAT², PAVEL POTAPOV², AXEL LUBK², BERND BÜCHNER², MICHAEL SING¹, and RALPH CLAESSEN¹ — ¹Physikalisches Institut und Würzburg-Dresden Cluster of Excellence ct.qmat, 97074 Würzburg, Germany — ²Leibniz Institute for Solid State and Materials Research and Würzburg-Dresden Cluster of Excellence ct.qmat, 01069 Dresden, Germany

4d and 5d transition metal oxides are a promising class of materials for topological phases in the context of electron correlations. Recently, the ferromagnetic metal SrRuO_3 (SRO) grown on a SrTiO_3 (STO) (001) substrate has been reported to exhibit electronic-reconstruction induced interfacial charge pinning accompanied by a topological transition of its electronic bands when capped with a LaAlO_3 (LAO) layer [1]. LAO is a polar oxide and the electronic reconstruction in a heterosystem of LAO/STO caused by the polar discontinuity at the interface is well known. For the LAO/SRO system a similar behaviour is expected and charge is thought to be accumulated at the very interface giving rise to strong inversion-symmetry breaking and hence change in the momentum-space topology [1]. Here we show the observation of signatures of an anomalous Hall effect in 4uc SRO films capped with LAO but also with non-polar STO. We correlate these findings with angle-dependent XPS data that allow for depth-profiling the oxidation state of ruthenium in both systems.

[1] Thiel, T. C. et al., *Phys. Rev. Lett.* 127, 127202 (2021)

DS 20.35 Wed 16:00 P3

Epitaxial growth of $\text{IrO}_2(110)$ thin films on $\text{TiO}_2(110)$ substrates by pulsed-laser-deposition — •TIM WALDSAUER¹, PHILIPP KESSLER¹, THEODORE PELLEGRIN¹, CHRISTOPHER REISER¹, RALPH CLAESSEN¹, VEDRAN JOVIC², and SIMON MOSER¹ — ¹JMU Physikalisches Institut, am Hubland, Würzburg, Germany — ²GNS National Isotope Center, Gracefield Rdd, Gracefield, New Zealand

Iridium dioxide (IrO_2), a state-of-the-art catalyst for the electrocatalytic oxygen evolution reaction in water splitting, has recently been shown to exhibit exotic physical phenomena such as the inverse spin Hall effect. The latter is supposed to promote easy switching of its majority charge carriers. For both fundamental spectroscopic studies as well as device applications, IrO_2 samples of high bulk and surface crystalline order are required. Here, we present a growth study of rutile $\text{IrO}_2(110)$ thin films on $\text{TiO}_2(110)$ substrates by pulsed-laser-deposition (PLD). Film characterization by AFM, RHEED and XPS shows stoichiometric growth of thin films with high bulk crystallinity but a granular surface at higher thicknesses. Strategies to enhance the surface quality, e.g., through utilization of an oxygen plasma are outlined and first results are presented.

DS 20.36 Wed 16:00 P3

2D electronic states at $\text{Fe}_x\text{O}_y/\text{STO}$ interfaces — •PIA M. DÜRING¹, PAUL ROSENBERGER^{1,2}, LUTZ BAUMGARTEN³, FATIMA ALARAB⁴, FRANK LECHERMANN⁵, VLADIMIR N. STROCOV⁴, and MARTINA MÜLLER¹ — ¹Fachbereich Physik, Universität Konstanz, 78457 Konstanz, Germany — ²Fakultät Physik, Technische Universität Dortmund, 44221 Dortmund, Ger-

many — ³FZ Jülich GmbH, PGI-6, 52425 Jülich, Germany — ⁴PSI, Swiss Light Source, CH-5232 Villigen PSI, Switzerland — ⁵Institut für Theoretische Physik III, Ruhr-Universität Bochum, 44780 Bochum, Germany

Oxide interfaces play an important role in investigating phenomena like 2D electronic states which can feature properties like magnetism, superconductivity or the spin Hall effect. While 2DEGs have been reported for various oxide systems like LAO/STO or EuO/STO, the direct experimental evidence for the counterpart, the 2DHG, is still lacking. Using our UHV-MBE system, we grow high-quality oxide heterostructures to investigate these properties using synchrotron radiation. Here presented are the results of resonant photoelectron spectroscopy measurements that reveal the emergence of different 2DESs at $\text{Fe}_x\text{O}_y/\text{STO}$ interfaces which suggests a dependence of the 2D interface properties on the oxidation state of Fe.

DS 20.37 Wed 16:00 P3

Stabilization of ferromagnetic metallic ground state in epitaxial $(\text{La}_{1-y}\text{Pr}_y)_{0.7}\text{Ca}_{0.3}\text{MnO}_3/\text{SrTiO}_3$ thin films by using buffer layers — •PIA HENNING¹, KAREN STROH¹, VITALY BRUCHMANN-BAMBERG¹, OLEG SHAPOVAL², and VASILY MOSHNYAGA¹ — ¹Erstes Physikalisches Institut, Georg-August-Universität-Göttingen, Göttingen, Germany — ²IEN, Academy of Sciences of Republic Moldova, Chisinau, Republic of Moldova

$(\text{La}_{1-y}\text{Pr}_y)_{0.7}\text{Ca}_{0.3}\text{MnO}_3$ (LPCMO) is an A-site substituted perovskite manganite, mostly known for the colossal magnetoresistance (CMR) effect. Relatively thick, $d=50-100$ nm, and stress-free LPCMO films with coupled ferro/paramagnetic and metal/insulator transition (MIT) and CMR $\sim 10^4\%$ can be heteroepitaxially grown by the metalorganic aerosol deposition technique on MgO(200) substrates, where strain relief occurs due to misfit dislocations. However, thin LPCMO films $d<20$ nm on MgO(200) do not show MIT and CMR. Alternatively, LPCMO/SrTiO₃ (LPCMO/STO) films grow coherently strained and with smooth surface morphology, however lacking the MIT and CMR even for $d>50$ nm. To obtain epitaxial LPCMO films with optimal metal-insulator transition sharpness and temperature we have employed a strain-engineered LaAlO₃ buffer layer to bridge the lattice mismatch of the LPCMO film and SrTiO₃(100) substrate. The influence of LaAlO₃ buffers on the magnetic and electric properties of epitaxial LPCMO films was studied. A high-quality growth of LPCMO/LAO/STO films and stabilization of the ferromagnetic-metallic phase for 10 nm thick LPCMO films were demonstrated.

DS 20.38 Wed 16:00 P3

Metal-insulator transition in $\text{AgSb}_{1-x}\text{Sn}_x\text{Te}_2$ alloys — •CHRISTIAN TEICHRIB and MATTHIAS WUTTIG — I. Physikalisches Institut (IA)

Metal-insulator transitions describe the localisation of charge carriers upon the change of a physical parameter. They can occur as a result of electron correlations (Mott transition) or disorder (Anderson transition) but a distinction between these two mechanisms is generally difficult and often both effects play a role in the transition. Phase change materials show a multitude of remarkable properties that make them suitable for the investigation of localisation phenomena. Their density of states at the Fermi level can be varied through chemical composition and disorder can be tuned through thermal annealing. This allows for the electrical resistivity to be modified over several orders of magnitude and a transition from a metallic to an insulating state to occur.

We present electrical transport and structural data for $\text{AgSb}_{1-x}\text{Sn}_x\text{Te}_2$ alloys where a metal-insulator transition is observed upon variation of the stoichiometry. The nature of the transition is investigated using the temperature dependence of the resistivity, magnetoresistance data, and the Hall effect.

DS 20.39 Wed 16:00 P3

Cryogenic Transport And Dielectric Properties Of Atomically Thin 2D-Polar Metals — •SVEN BÖKEMEIER¹, PIERRE-MAURICE PIEL¹, JAKOB HENZ¹, MARGAUX LASSUNIÈRE¹, JOSHUA ROBINSON², SIYAVASH RAJABPOUR², ALEXANDER VERA² und URSULA WURSTBAUER¹ — ¹Physikalisches Institut, Westfälische Wilhelms-Universität, Münster, — ²MatSE; Center for 2DLM; Atomic, 2D Crystal Consort, PennState University, USA

2D layered materials are of great interest due to their electronic and optical properties that can be manipulated to a high degree. A novel class of atomically thin materials are 2D polar metals such as 2D Ga or 2D In and their ternary alloys that exhibit fascinating properties like strong nonlinear optical properties emerging by giant second harmonic generation [1], epsilon near zero behavior in the visible and NIR range [2] and alloy dependent superconductivity [3]. Intriguingly, 2D Ga exhibits a superconducting phase transition around 4K, while 2D In remains a metal down to $< 800\text{mK}$ [3]. The 2D polar metals are prepared via confinement hetero-epitaxy (CHet) by intercalating metals between epitaxial graphene and the hosting SiC crystal resulting in atomically thin half-van der Waals materials [1]. We report on combined temperature dependent transport and spectroscopic ellipsometry experiments in order to develop a better understanding of the alloy dependent emerging superconductivity of thin 2D Ga and 2D GaIn films. [1] M. A. Steves et al. Nano Lett. 2020, 20, 11, 8312*8318. [2] K. Nisi et al. Adv. Mater. 2021, 2104265 [3] S. Rajabpour et al. Adv. Funct. Mater. 2020, 2005977

DS 20.40 Wed 16:00 P3

Magnetic Field-Dependent Thermal Conductivity in Manganite Thin Films — •VITALY BRUCHMANN-BAMBERG, KAREN STROH, PIA HENNING, and VASILY MOSHNYAGA — I. Physik. Inst. Universität Göttingen, Friedrich-Hund-Platz 1, 37077 Göttingen

In perovskite manganites strong electron-phonon and spin-phonon coupling give rise to intriguing magneto-electric phenomena like colossal magnetoresistance (CMR), i.e. reduction of electrical resistivity by several orders of magnitude in an applied magnetic field of few Tesla. Since thermal conductivity of a solid contains both lattice and electronic contributions, a question of its manipulation by an external magnetic field can be addressed in CMR manganites.

Here we present temperature- and magnetic-field-dependent measurements of thermal conductivity by means of 3ω -technique in $(\text{La}_{0.6}\text{Pr}_{0.4})_{0.7}\text{Ca}_{0.3}\text{MnO}_3/\text{MgO}(100)$ thin films with a CMR ratio of $[\text{R}(0\text{T})-\text{R}(5\text{T})]/\text{R}(5\text{T})\approx 10^4\%$. The observed significant change of the thermal conductivity, κ , in magnetic field $[\kappa(5\text{T})-\kappa(0\text{T})]/\kappa(0\text{T}) = 16\%$ close to $T_C \approx 200\text{K}$ is caused by the electronic contribution in agreement with the Wiedemann-Franz law.

DS 20.41 Wed 16:00 P3

Phonon-dominated energy transport in purely metallic thin films — •MARC HERZOG¹, ALEXANDER VON REPPERT¹, JAN-ETIENNE PUDELL^{1,2}, CARSTEN HENKEL¹, MATTHIAS KRONSEDER³, CHRISTIAN BACK^{3,4}, ALEXEI MAZNEV⁵, and MATIAS BARGHEER^{1,6} — ¹Inst. f. Physik & Astronomie, Universität Potsdam, Germany — ²European XFEL, Schenefeld, Hamburg, Germany — ³Inst. f. Experimentelle & Angewandte Physik, Universität Regensburg, Germany — ⁴Fakultät f. Physik, Technische Universität München, Germany — ⁵Department of Chemistry, MIT, Cambridge, USA — ⁶Helmholtz-Zentrum Berlin, Germany

In various branches of physical sciences it is assumed that electrons are the main carriers of thermal energy in metals. We use ultrafast x-ray diffraction to quantify the energy exchange among the metallic constituents in nanoscale thin films after laser excitation. Modeling the data with two-temperature models describing the energy exchange between non-equilibrium electrons and phonons provides clear evidence that phonons dominate the heat transport within gold films thinner than approx. 10 nm. Our fundamental experimental findings shift the paradigm of energy being solely transported by electron in noble metals. These results may be relevant for the description of non-equilibrium thermal transport in diverse fields ranging from thermal management in nanoelectronics, spin-caloritronics and ultrafast spin dynamics to photothermal processes and plasmonic chemistry.

DS 20.42 Wed 16:00 P3

Combinatorial Synthesis of $\text{Pb}_{1-x}\text{Sn}_x\text{Se}$ Films with Sputter Deposition — •THOMAS SCHMIDT, PETER KERRES, and MATTHIAS WUTTIG — RWTH Aachen University, Aachen, Germany

PbSe and SnSe are two chalcogenides with a wide range of applications of their properties, in particular as thermoelectrics. Interestingly, these two iso-electronic materials employ different bonding mechanisms. While at room temperature SnSe utilizes covalent bonds, PbSe is characterized by a more unconventional bonding mechanism, coined metavalent bonding. Therefore, we expect significant property changes upon crossing the border between those two bonding mechanisms. Such a change opens up the possibility to tailor material properties with sample stoichiometry. We have thus studied optical and electrical properties of $\text{Pb}_{1-x}\text{Sn}_x\text{Se}$ films as a function of stoichiometry. Effective sample-production has been employed to facilitate this analysis. In this study the compositions around $x=0.5$, at which a structural transition is expected, are confocally sputtered and subsequently analyzed. The two targets PbSe (cubic structure) and SnSe (orthorhombic structure) were focused on the different ends of the 7.5 cm long Si-substrate. The resulting stoichiometry gradient in the sample was determined by energy dispersive X-ray spectroscopy and linked to the evolution of structure (X-ray diffraction) and optical properties (spectroscopic ellipsometry and reflectometry).

DS 20.43 Wed 16:00 P3

Growth of Crystalline High-Entropy Alloy thin Films by Magnetron Sputtering — •HOLGER SCHWARZ¹, THOMAS UHLIG², ERIC WONG¹, PETER HENNING¹, GUNTRAM WAGNER², and THOMAS SEYLLER¹ — ¹Institute of Physics, Faculty of Natural Sciences, TU Chemnitz, 09126 Chemnitz, Germany — ²Institute of Materials Science and Engineering, Faculty of Mechanical Engineering, TU Chemnitz, 09126 Chemnitz, Germany

Multicomponent alloys of at least four elements with near equimolar percentage were first reported and investigated by Cantor et al. in 2004 [1] and are nowadays often referred to as High-Entropy Alloys (HEAs) [2]. This group of materials has raised high attention in the field of material research due to its almost infinite possibilities of element combination and resulting physical properties. We demonstrate the fabrication of crystalline HEA thin films on MgO(100) and Al₂O₃(0001) single crystal substrates from homemade targets via magnetron sputtering. Low electron energy diffraction and X-ray diffraction experiments confirmed the formation of single phase crystalline HEA films. The surface elemental composition is investigated by X-ray photoelectron spec-

troscopy whereas the bulk stoichiometry is measured by energy dispersive X-ray spectroscopy. Angle resolved photoemission spectroscopy was used to investigate the band structure of the thin films.

[1] B. Cantor, I. Chang, P. Knight, A. Vincent, *Mat. Sci. Eng. A*, 213-218, 375-377 (2004)

[2] D.B. Miracle, *JOM*, 2130-2136, 69 (2017)

DS 20.44 Wed 16:00 P3

Different approaches to deposit tungsten-doped vanadium dioxide by ion-beam sputter-deposition — •JILL KESSLER, SEBASTIAN LEONARD BENZ, ISABEL MÜLLER, MARTIN BECKER, and SANGAM CHATTERJEE — Institute for Exp. Physics I and Center for Materials Research (LaMa), Justus Liebig University Giessen, Germany

The complexity of the phase diagram of vanadium oxides makes the reproducible growth of thin films of defined phases by nonequilibrium techniques challenging. Here, we discuss thermochromic VO₂, which exhibits a significant change in optical transparency and reflectivity and, thus, is an ideal candidate for the use in smart windows. However, the bulk phase transition temperature of 68 °C is too high for useful applications. Doping VO₂ with tungsten drives the thermochromic key measures close to the desired range.

We present different approaches for tungsten doping of VO₂ based on ion-beam sputter-deposition. We employ tungsten screws that are inserted into the vanadium target. Furthermore, a pre-doped vanadium target is used. In another approach we employ two targets of vanadium and tungsten, respectively, to be sputtered simultaneously. Here, a compositional gradient allows for identification of the optimum doping concentration. The different approaches are compared regarding thin film properties and overall reproducibility of the growth process.

Raman spectroscopy and X-ray photoelectron spectroscopy provide structural and compositional analysis. UV/Vis/NIR spectroscopy yields the thermochromic performance.

DS 20.45 Wed 16:00 P3

Enhanced amorphization of Cu-Sn-I alloy thin films fabricated by reactive magnetron sputtering — •CHRISTIANE DETHLOFF, SOFIE VOGT, TILLMANN STRALKA, DANIEL SPLITH, HOLGER VON WENCKSTERN, and MARIUS GRUNDMANN — Universität Leipzig, Leipzig, Deutschland

CuI is a promising p-type semiconductor for optoelectronic applications due to various advantageous material properties such as transparency in the visible spectrum [1] and its earth abundant, cheap and non-toxic constituents. Growth of amorphous layers of CuI by solution processing has already been reported [2, 3]. The feasibility of deposition of the amorphous Cu-Sn-I alloy has not yet been demonstrated for a physical, scalable process, such as sputtering.

We present our investigations of the influence of the process parameters during the deposition of a Cu-Sn-I-alloy using reactive co-sputtering of Cu and Sn in a reactive iodine ambient. A dependence of the growth rate, the thin films morphology and the electrical properties on the process parameters i.e. the magnitude of the electrical power applied at the sputtering sources, the iodine partial pressure and the chamber pressure. A decrease of crystallinity was observed by XRD measurements for increasing sputtering power applied on the tin target as well as with increasing chamber pressure. LSM and AFM measurements yielded root-mean-square surface roughnesses below 10 nm.

[1] M. Grundmann *et al.* *Phys. Status Solidi A* 210, 1671 (2013);

[2] H. Wu *et al.* *Appl. Phys. Lett.* 118, 222107 (2021);

[3] T. Jun *et al.* *Advanced materials* 30, e1706573 (2018).

DS 20.46 Wed 16:00 P3

Overcoming the integration issues between 2D materials and waveguides — •OSCAR CAMACHO IBARRA¹, IOANNIS CALTZIDIS¹, SELIM SCHARMER², SAMUEL GYGER², MARC SARTISON¹, and KLAUS D. JÖNS¹ — ¹HQPD lab, Department of Physics, Paderborn University, Germany — ²Quantum Nanophotonics, KTH Royal Institute of Technology, Sweden

To achieve fully operational quantum photonic integrated circuits, developing a scalable platform capable of supplying an efficient coupling between single-photon emitters and photonic circuitry is essential. A hybrid approach is the most favorable to integrate single-photon emitters with other on-chip components since the advantages of each material platform are exploited. Single-photon emitters hosted in 2D materials are emerging technologies and promising candidates for future scalable photonic circuits. However, the coupling of light from these emitters into waveguides remains challenging: In particular, higher coupling efficiency and reduction of spectral jitter are needed. Both issues can be simultaneously overcome by implementing a cavity in the photonic circuit. In this work, 1D photonic crystal cavities were designed and simulated for later integration of 2D emitters. These photonic crystal cavities are designed to be efficiently coupled to waveguide modes, and they possess high-quality factors and small mode volumes, resulting in prominent Purcell factors. Furthermore, the cavity geometrical structure can act as nucleation sites for strain-driven single-photon emitters, allowing a self-alignment process between emitter and cavity.

DS 20.47 Wed 16:00 P3

Propagation and manipulation of Bloch Surface Waves and Bloch Surface Wave Polaritons in ZnO — •SEBASTIAN HENN, SIMON BRIESENICK, CHRIS STURM, and MARIUS GRUNDMANN — 1Universität Leipzig, Faculty of Physics and Earth Sciences, Felix Bloch Institute for Solid State Physics, Linnéstr. 5, 04103 Leipzig, Germany

In this contribution we demonstrate experimentally the control of the propagation of Bloch Surface Waves (BSW) in the transparent spectral range and Bloch Surface Wave Polaritons (BSWP) in the vicinity of excitonic transitions in ZnO. BSWP are bosonic quasi-particles originating from the strong coupling between BSW and excitons and exist along the ambient interface of a distributed Bragg reflector (DBR) with a thin ZnO top layer [1]. Using shallow optical diffraction gratings with sub-micron sized lattice constant, incident light is coupled into and out of the Bloch modes, which propagate along the surface interface between the gratings. Depending on the geometry of the sample and roughness of the surface layer the low-loss nature of evanescent BSW allows long-range lateral propagation of BSWP, on the order of micrometers, making this an interesting candidate for on-chip polaritonic devices. We determine the propagation lengths and test the coupling efficiency of the gratings, which are modelled using RCWA computations.

[1] S. Henn *et al.*, *New J. Phys.* 23, 093031 (2021)

DS 20.48 Wed 16:00 P3

Improvement of the Architecture of Water-Based Dye-Sensitized Solar Cells — •SARA DOMENICI, ANDREAS RINGLEB, and DERCK SCHLETTWEIN — Justus-Liebig-Universität Gießen, Institut für Angewandte Physik

Dye-sensitized solar cells (DSSCs) have emerged as a possible alternative technology for the conversion of sunlight into electrical energy. Aqueous electrolytes would considerably increase their sustainability. Aside from chemical instabilities, the power conversion efficiencies of aqueous DSSCs remain significantly lower compared to other DSSCs. One main problem which is dealt with in the present work, consist in low diffusion coefficients of appropriate redox couples. Aqueous DSSCs were assembled using screen-printed TiO₂ semi-conducting layers sensitized with an organic dye, XY1b. The redox couple was TEMPO/TEMPO⁺ dissolved in aqueous LiClO₄ with MBI added as organic corrosion inhibitor. To improve the accessibility of the photoanodes for the redox couple, the size of TiO₂ nanoparticles was varied. Further, this helps to add a scattering layer. In a second approach, the sealing method for the cells was adjusted. For instance, the distance between the working electrode and the counter electrode was tuned by using different sealant materials, such as hotmelt foils or UV glue, in order to allow short pathways for ion conduction. In this context, interactions of different sealant materials and the organic redox mediators have to be considered. The influence of the different approaches on cell efficiency will be discussed.

DS 20.49 Wed 16:00 P3

Development of a Transport Layer for the Integration of a TiO₂-based Photoanode on a Silicon Wafer for Solar Water Splitting — •LUIA BUSCH, DENNIS BERENDS, and KAI GEHRKE — DLR Institut für Vernetzte Energiesysteme, Oldenburg, Germany

Recently, Segev *et al.* [1] proposed a three-terminal hybrid photoelectrochemical (PEC) / photovoltaic (PV) device for improved solar spectrum utilization. The concept integrates a TiO₂ photoanode on an IBC silicon wafer in tandem configuration. To overcome the rather large bandgap of TiO₂, which still limits the absorption of the solar spectrum and therefore the efficiency of the PEC, a sub-stoichiometric TiO₂ layer is advantageous. However, contacting the two semiconductors directly would result in a high recombination of the free charge carriers and thus low currents in the cell, due to band mismatch. By adding a transport layer between the two materials, for example a tunnel recombination junction, an improved current flow can be achieved. Within this work, the development of such a transport layer is presented in order to integrate a sub-stoichiometric TiO₂ photoanode on a Si wafer. For this purpose, the optoelectronic properties of the two semiconductor materials are characterized to select a suitable transport layer material by simulating the band alignment with AFORS-HET. Based on these results, a possible transport layer is developed and integrated into the tandem structure for electrochemical characterization.

[1] G. Segev *et al.*, In: *Nature materials*, 17(12):1115-1121, 2018. doi: 10.1038/s41563-018-0198-y

DS 20.50 Wed 16:00 P3

Hybrid thin film for H₂ evolution applications — •MORGAN LE DÛ¹, MANUEL ANDREE REUS¹, KUN SUN¹, ZERUI LI¹, CRISTIANE HENSCHL², ANDRE LASCHEWSKY^{2,3}, SIGIRD BERNSTORFF⁴, and PETER MÜLLER-BUSCHBAUM^{1,5} — ¹TU München, Physik-Department, LS Funktionelle Materialien, 85748 Garching — ²Universität Potsdam, Institut für Chemie, 14476 Potsdam-Golm — ³Fraunhofer Institut für Angewandte Polymerforschung, 14476 Postdam-Golm — ⁴Elettra-Sincrotrone Trieste, Basovizza, 34149 Trieste, Italy — ⁵MLZ, TU München, 85748 Garching

Photocatalysis via water splitting reaction is a way to implement the sun to produce hydrogen-based energy. Recently, Pt loaded graphitic carbon nitride (g-

CN) has been found as a promising photocatalyst for H₂ evolution under visible light. The aim of this work is to bring this material in a polymer thin film configuration to make it suitable for industrial purposes. Poly(N-isopropylacrylamide) exhibits good swelling capacity of water vapor and seems to be suitable for such a hybrid thin film system. A new isomer of PNIPAM, poly(N-vinylisobutyramide) (PNVIBAM) raised our attention due to its higher lower critical solution temperature (LCST) in aqueous solution ($\approx 39^\circ\text{C}$) which makes it more stable in ambient environment. Spray coating has been chosen to be the deposition technique of PNVIBAM/g-CN/Pt hybrid films. A comparative study of the photocatalyst concentrations is presented. Grazing incident small angle x-ray scattering is the main tool of this work. G-CN/Pt blended polymer films structure is analysed under light irradiation condition.

DS 20.51 Wed 16:00 P3

Fabrication and electrochemical characterization of 2D membranes — •YOSSARIAN LIEBSCH — Universität Duisburg-Essen, AG Schleberger, Germany
Membranes are critical components in widely used industrial and technical processes, e.g., water filtration, desalination and energy storage and conversion. With their extreme thinness of only a few angstrom, two-dimensional (2D) materials have the potential to be used as highly efficient membranes, possibly outperforming conventional membranes by orders of magnitude. We fabricated two different types of 2D membranes: Membranes made of commercially available CVD-grown graphene and membranes made of self grown CVD MoS₂. The membranes were made by transferring the 2D material onto a 3 μm micropore. Subsequently the membranes were plasma etched (graphene) or irradiated

by highly charged ions (MoS₂) in order to create nanopores. Raman and photoluminescence spectroscopy was used to analyse the membranes in terms of doping, stress and defects density. Additionally an electrochemical characterization of the membranes was done in a custom build membrane potential measurement stand. In case of the graphene membranes the measured membrane potentials were in good agreement to the well-known Theorell-Meyer-Sievers Theory. However for the MoS₂ membranes no potential could yet be measured. In upcoming experiments with this electrochemical cell we aim to investigate the correlations between the pore creation mechanisms and intrinsic membrane properties like pore size, pore chemistry and surface charge density.

DS 20.52 Wed 16:00 P3

Laser-assisted polarization switching dynamics in ferroelectric thin films — •REKIKUA ALEMAYEHU¹, MATTHIAS RÖSSELE², and MATIAS BARGHEER^{1,2} — ¹Institute of Physics and Astronomy, University of Potsdam, Karl-Liebknecht-Str. 24-25, 14476 Potsdam, Germany — ²Helmholtz Zentrum Berlin, Albert-Einstein-Str. 15, 12489 Berlin, Germany

Nucleation and growth of domains with opposite polarization moderates the electric field-induced polarization reversal process in ferroelectric materials. Accordingly, the domain wall velocity governs the timescale of polarization switching. Achieving the ultimate switching time in ferroelectrics is a fundamental quest to improve the device response time. Here we show laser-assisted polarization switching dynamics in metal-ferroelectric-metal heterostructure via heat and strain waves induced by a femtosecond laser pulse.

DS 21: Layer Deposition (ALD, MBE, Sputtering, ...)

Time: Thursday 9:30–10:30

Location: H14

DS 21.1 Thu 9:30 H14

Surface-Diffusion Control Enables Tailored-Aspect-Ratio Nanostructures in Area-Selective Atomic Layer Deposition — •PHILIP KLEMENT¹, DANIEL ANDERS¹, LUKAS GÜMBEL¹, MICHELE BASTIANELLO¹, FABIAN MICHEL¹, JÖRG SCHÖRMANN¹, MATTHIAS T. ELM^{1,2}, CHRISTIAN HEILIGER³, and SANGAM CHATTERJEE¹ — ¹Institute of Experimental Physics I & Center for Materials Research (ZfM), Justus Liebig University Giessen, Giessen, Germany — ²Institute of Physical Chemistry, Justus Liebig University Giessen, Giessen, Germany — ³Institute of Theoretical Physics & Center for Materials Research (ZfM), Justus Liebig University Giessen, Giessen, Germany

Area-selective atomic layer deposition is a key technology for modern microelectronics as it enables material deposition only in specific areas. Typically, the selectivity originates from surface modifications of the substrate that allow or block precursor adsorption. The control of the deposition process currently remains a major challenge as the selectivity of the no-growth areas is lost quickly. Here, we show that surface modifications of the substrate strongly manipulate the surface diffusion. The selective deposition of TiO₂ on poly (methyl methacrylate) and SiO₂ yields localized nanostructures with tailored aspect ratios. Controlling the surface diffusion allows to tune such nanostructures as it boosts the growth rate at the interface of the growth and no-growth areas. Kinetic Monte-Carlo calculations reveal that species move from high to low diffusion areas.

DS 21.2 Thu 9:45 H14

Molecular-beam epitaxy of Cd- and Nb-containing Bi_xSe_y-based compounds for novel topological materials — •CHRISTOPH RINGKAMP¹, ABDUR REHMAN JALIL², ERIK ZIMMERMANN¹, PETER SCHÜFFELGEN¹, THOMAS SCHÄPERS¹, GREGOR MUSSLER¹, and DETLEV GRÜTZMACHER¹ — ¹PGI-9, Forschungszentrum Jülich — ²PGI-10, Forschungszentrum Jülich

Topological insulators (TIs) have gained a lot of interest in recent years because of their unique topologically protected surface states. Prominent examples of 3-dimensional topological insulators are Bi₂Te₃, Sb₂Te₃, and Bi₂Se₃ and alloys thereof. The combination of TI with superconductors and using the proximity effect to induce superconductivity in the TI is of fundamental interest in physics and may direct a possible avenue towards novel applications in the field of quantum computation. Here the successful deposition of Cd- and Nb-containing Bi_xSe_y films by molecular beam epitaxy is reported. Carefully adjusting the growth parameter, single-crystal CdBi₂Se₄ and (BiSe)_{1,10}NbSe₂ thin films have been grown on sapphire substrates. For both materials, transmission electron microscopy images reveal the expected stacking sequences of atomic layers within the deposited films, indicating the presence of the anticipated stoichiometry. First data of the electrical transport of (BiSe)_{1,10}NbSe₂ films show superconducting behavior with a transition temperature of 0.4 K.

DS 21.3 Thu 10:00 H14

Growth and Characterization of Epitaxial (Cr_{1-x}Mnx)₂GaC MAX Phase Thin Films by Pulsed Laser Deposition — •IVAN TARASOV, HANNA PAZNIAK, MICHAEL FARLE, and ULF WIEDWALD — Faculty of Physics and Center for

Nanointegration (CENIDE), University of Duisburg-Essen, 47057 Duisburg, Germany

Due to their nanolaminated structure, tunable chemistry, and high oxidation resistance, MAX phases (where M is an early transition metal, A is a main group element, and X is carbon or nitrogen) are interesting materials for a wide variety of applications. The partial substitution of M atoms is one of the ways to tailor their properties to specific applications. In this study, we grow (Cr_{1-x}Mnx)₂GaC MAX phase films to fine-tune their magnetic response by stoichiometry variations for x = 0-1. High-quality epitaxial (Cr_{1-x}Mnx)₂GaC MAX phase films (thickness 30 * 100 nm) are synthesized by pulsed laser deposition on MgO (111) substrates using (Mn₅₀Cr₅₀)₆₆Ga₃₄, Mn_{0.66}Ga_{0.34}, Cr₆₆Ga₃₄ and C targets. The combination of structural and morphological characterization reveals a strong competition between the (Cr_{1-x}Mnx)₂GaC MAX phase and (Cr_{1-x}Mnx)₃GaC, (Cr_{1-x}Mnx)₃Ga phases. We suppress the formation of side phases by variation of the growth temperature and the formation of seed layers. Vibrating sample magnetometry of the MAX phase reveals increasing magnetization and ordering temperature with increasing Mn content. Funding by the Deutsche Forschungs*gemeinschaft (DFG) within CRC/TRR 270, project B02 (Project-ID 40553726) is gratefully acknowledged.

DS 21.4 Thu 10:15 H14

Optical Quantizing Structures in Al₂O₃/TiO₂ Heterostructures by Plasma Enhanced Atomic Layer Deposition (PEALD) — •PALLABI PAUL^{1,2} and ADRIANA SZEGHALMI^{1,2} — ¹Friedrich Schiller University Jena, Germany — ²Fraunhofer Institute for Applied Optics and Precision Engineering, Jena, Germany

Atomically thin heterostructures are promising candidates for various optoelectronic and photonic applications. Here we present on the properties of Al₂O₃/TiO₂ nano-composites grown by PEALD. The growth, dispersion relation, optical bandgap and composition of such structures are systematically studied by means of UV/VIS spectrophotometry, ellipsometry, XRR, STEM, and XPS techniques. The refractive index and the indirect bandgap of the heterostructures depend on the ratio of the two oxides, while the bandgap is very sensitive to the thicknesses of the barrier and quantum well layers. A large blue shift of the absorption edge from 400 nm to 320 nm is obtained by changing the TiO₂ (quantum well) thickness from 2 nm to 0.1 nm. PEALD unfolds the possibility of achieving optical quantizing effects within complex heterostructures enabling control of their structures down to atomic scale. Selected compositions are identified for applications in antireflection coatings at 355 nm wavelength. Interference multilayers of TiO₂/Al₂O₃ composites as high refractive index material and SiO₂ as the low refractive index show very low reflectance and optical losses at 355 nm wavelength with transmittance values of approximately 99%. Such heterostructures overcome the limitations of the low bandgap dielectric TiO₂ for optical applications in the UV spectral range.

DS 22: 2D Materials 8 (joint session DS/ CPP)

Time: Thursday 9:30–11:30

Location: H17

DS 22.1 Thu 9:30 H17

Calculation of Elastic Properties in Monolayer Covalent-Organic Frameworks — •DAVID BODESHEIM¹, ANTONIOS RAPTAKIS¹, JONATHAN HEINZE¹, AREZOO DIANAT¹, ROBERT BIELE¹, ALEXANDER CROY², and GIANAURELIO CUNIBERTI¹ — ¹TU Dresden, Dresden, Germany — ²FSU Jena, Jena, Germany

Covalent-Organic Frameworks (COFs) are crystalline porous materials that are based on organic monomeric units, so called building blocks. Through recent experimental progress, mono- and few-layer COF materials have been synthesized, providing a new class of 2D materials.[1,2] From a computational point of view, however, accurately calculating properties of these materials is demanding as their unit cells are usually very big. In this work, we calculate elastic properties for a multitude of 2D COFs in a high-throughput manner. The calculations are based on classical force-fields and are compared with higher level of theory like density functional based tight binding (DFTB). We show how force-fields can be very useful for mechanical property calculation, how their accuracy can be improved, and typical fallacies for 2D COFs. Furthermore, we introduce models to predict mechanical properties from the properties of their monomeric building blocks.[3] This paves the way for accurate multiscale modeling, high-throughput calculations, and materials design with properties on demand.

[1] A. Ortega-Guerrero, et al. ACS Appl. Mater. Interfaces, 13, 22, 26411-26420 (2021).

[2] Z. Wang, et al., Nat. Synth., 1, 69-76 (2022).

[3] A. Raptakis, et al. Nanoscale, 13, 1077 (2021).

DS 22.2 Thu 9:45 H17

Light-Matter Interaction in 2D Polar Metals — •MARGAUX LASSAUNIÈRE¹, WEN HE², KATHARINA NISI¹, SHRUTI SUBRAMANIAN³, SIAVASH RAJABPOUR³, ALEXANDER VERA³, NATHALIE BRIGGS³, SU YING QUEK², JOSHUA ROBINSON³, and URSULA WURSTBAUER¹ — ¹Institut of Physics, Münster University, Germany — ²Department of Physics, National University of Singapore, Singapore — ³MatSE; Center for 2DLM; ATOMIC; 2D Crystal Consort.; Penn State University, USA

Understanding and controlling the light-matter interaction in thin metal films is of high technological relevance. Here, we study the linear optical response of atomically thin 2D gallium, 2D indium as well as their alloys embedded in half-van der Waals heterostructures by spectroscopic imaging ellipsometry. The thin films are prepared via confinement heteroepitaxy (Chet). In a systematic study of the dielectric functions, we separate free and bound electron contributions to the optical response, with the latter pointing towards the existence of thickness-dependent quantum confinement phenomena and epsilon near zero (ENZ) behaviour [1]. The resonance energies of the observed ENZ behaviour are dependent on the number of atomic metal layers, materials, and alloying [2]. Their tunability makes 2D polar metals attractive for quantum engineered metal films, tunable (quantum-)plasmonics and nano-photonics.

[1] K. Nisi et al. Adv. Mater. 2021, 2104265

[2] S. Rajabpour et al. Adv. Funct. Mater. 2020, 2005977

DS 22.3 Thu 10:00 H17

Layer dependent anisotropic dielectric function of the magnetic semiconductor CrSBr — •PIERRE-AURICE PIEL¹, MARGAUX LASSAUNIÈRE¹, JULIAN KLEIN², and URSULA WURSTBAUER¹ — ¹Institute of Physics, Muenster University, Germany — ²Department of Materials Science and Engineering, Massachusetts Institute of Technology, USA

The van der Waals (vdW) material CrSBr is a 2D magnetic semiconductor with ferromagnetic ordering within each layer. Adjacent layers, however, are coupled antiferromagnetically. As a vdW semiconductor with a direct band gap, the light matter interaction is determined by strong excitonic resonances that are highly anisotropic in the crystal plane. We experimentally determine the complex dielectric function in the near infrared to visible regime along the two main crystal directions by spectroscopic imaging ellipsometry (SIE) measurements and regression analysis to a multilayer model. Unlike other vdW semiconductors such as MoS2 or WSe2 [1], the rich excitonic signatures in the dielectric function are highly anisotropic and show only minor distinct dependence on the number of layers. Even more striking, we find that the excitonic resonance are better pronounced for multilayer compared to monolayer CrSBr with significantly reduced line-width even at room temperature. [1] Wurstbauer et al. J. Phys. D: Appl. Phys. 50, 173001 (2017).

DS 22.4 Thu 10:15 H17

Tracing the Superconducting Phase Transition in Atomically Thin 2D Polar Gallium by Transport and Spectroscopic Ellipsometry — •JAKOB HENZ¹, MARGAUX LASSAUNIÈRE¹, PIERRE-AURICE PIEL¹, SIAVASH RAJABPOUR², ALEXANDER VERA², JOSHUA ROBINSON², and URSULA WURSTBAUER¹ — ¹Institute of Physics, Muenster University, Germany — ²MatSE; Center for 2DLM; Atomic; 2D Crystal Consort, PennState University, USA

Half van der Waals 2D polar metals are a novel class of 2D materials, realized by confinement heteroepitaxial growth (CHet). Hereby, metal atoms such as gallium or indium are intercalated between graphene and a silicon carbide substrate. This results in large area, environmentally stable, 2D metals with a bonding gradient in z-direction ranging from covalent over metallic to vdW within only two to three atomic layers. The materials feature interesting properties such as superconductivity¹ and a large plasmonic response in the visible range². 2D gallium is studied by temperature dependent spectroscopic ellipsometry and transport measurements down to below 1K. We extract the dielectric function in the visible to near infrared range with a special focus on signatures across the phase transition from metallic to superconducting behavior unambiguously identified from the abrupt drop in the temperature dependent sheet resistance at the transition temperature T_C of about 3.5 K.

1 S. Rajabpour et al., Adv. Mater. 2104265 (2021)

2 Nisi et al., Adv. Funct. Mater. 2005977, 1-11 (2020)

DS 22.5 Thu 10:30 H17

Epitaxial growth of Fe_{5-x}GeTe₂ films with a Curie temperature above 300 K on graphene — HUA LV¹, JENS HERFORT¹, JÜRGEN SCHUBERT², MICHAEL HANKE¹, MANFRED RAMSTEINER¹, and •JOAO MARCELO J. LOPES¹ — ¹Paul-Drude-Institut für Festkörperelektronik, Leibniz-Institut im Forschungsverbund Berlin e.V., Germany — ²Peter Grünberg Institut (PGI-9), Forschungszentrum Jülich, Germany

Synthesis of magnetic 2D materials exhibiting transition temperatures at or above 300 K is a crucial step towards the development of ultra-compact spintronic devices. Here, we report our recent progress on epitaxial growth of the 2D ferromagnet Fe_{5-x}GeTe₂ via MBE on graphene on SiC(0001). Thin films with a thickness of about 10 nm and different Fe concentrations were studied. Characterization performed with methods such as in-situ RHEED and grazing incidence X-ray diffraction confirmed the formation of epitaxial layers with good crystalline quality. Magneto-transport measurements and SQUID magnetometry were employed to assess the electrical and magnetic properties. They reveal that the MBE-grown Fe_{5-x}GeTe₂ exhibits a metallic behavior for all investigated Fe concentrations. In addition, composition-dependent magnetic anisotropies and Curie temperatures (T_C) were deduced. For the Fe content close to 5, a predominant easy out-of-plane orientation and T_C well above 300 K were measured. These results are relevant for the further development of wafer-scale fabrication of magnetic 2D materials aiming at the realization of multifunctional, atomically thin devices.

DS 22.6 Thu 10:45 H17

Antisymmetric magnetoresistance in a Fe₃GeTe₂-Fe₂GeTe₂ van der Waals ferromagnetic homojunction — •JAN BÄRENFÄNGER¹, KENJI WATANABE², TAKASHI TANIGUCHI², JONATHAN EROMS¹, DIETER WEISS¹, and MARIUSZ CIORGA¹ — ¹Institut für Experimentelle und Angewandte Physik, Universität Regensburg, 93040 Regensburg, Germany — ²NIMS, 1-1 Namiki, Tsukuba, Ibaraki 305-0044, Japan

The emergence of novel two-dimensional (2D) magnetic van der Waals (vdW) materials have breathed new life into the field of spintronics. The weak vdW interaction between layers of strong covalent bonds enables the exfoliation of these materials down to monolayers. Furthermore, vdW heterostructures can easily be fabricated by stacking them on top of each other like LEGO blocks, bringing a platform for novel spintronic devices. Here, we report an antisymmetric magnetoresistance (MR) in an Fe₃GeTe₂-Fe₂GeTe₂ (FGT) vdW homojunction. We attribute it to eddy currents emerging at the interface of the antiparallel, perpendicular-to-plane magnetized FGT flakes, due to the different sign of the anomalous Hall effect in both flakes. These eddy currents perturb the measured longitudinal resistance, resulting in the observed antisymmetry. Such an interpretation is supported by the observation of a sign change of the MR when measuring the voltage drop along the opposite edges of the transport channel. This work highlights the potential for new spintronic applications using vdW ferromagnets.

DS 22.7 Thu 11:00 H17

Charge-transfer stabilization, modulation doping, and CDW phase in layered ferecystal heterostructures — •FABIAN GÖHLER¹, SHRINIDHI RAMASUBRAMANIAN¹, SANAM K. RAJAK¹, NIELS RÖSCH¹, ADRIAN SCHÜTZE¹, SUSANNE WOLFF¹, MARISA CHOFFEL², DMITRI L. M. CORDOVA², DAVID C. JOHNSON², and THOMAS SEYLLER¹ — ¹Chemnitz University of Technology, 09126 Chemnitz, Germany — ²University of Oregon, Eugene 97403, USA

A virtually unlimited number of metastable, layered heterostructures - called *ferrecrystals* due to the non-epitaxial alignment between layers - can be grown via the self-assembly of layered amorphous precursors. [1] In this contribution, we want to highlight recent investigations on the electronic structure and interlayer interactions in several series of compounds using photoemission spectroscopy (PES).

In the Bi-Mo-Se system, the formation of the metallic 1T-polytype of MoSe₂ is aided by charge transfer from rock-salt structured BiSe. By systematically stacking BiSe, Bi₂Se₃, and MoSe₂, the mechanisms which stabilize these structures can be understood. [2]

Compounds prepared from PbSe and VSe₂ layers show charge transfer between layers as well, allowing to tune transport properties via modulation doping. Additionally, the emergence of a charge density wave in the VSe₂ layers has been reported below 100 K [3], and was investigated by angle-resolved PES.

[1] Esters et al., *Angew. Chem. Int. Ed.* **54**, 1130 (2015).

[2] Göhler et al., *J. Phys. Chem. C* **125**, 9469 (2021).

[3] Cordova et al., *Chem. Mater.* **31**, 8473 (2019).

DS 22.8 Thu 11:15 H17

Impact of opto-electronic measurements on the properties of hexagonal boron nitride as a dielectric — •JO BERTRAM¹, LUCA KOTEWITZ¹, MANFRED ERSFELD¹, FRANK VOLMER¹, KENJI WATANABE², TAKASHI TANIGUCHI³, CHRISTOPH STAMPFER¹, and BERND BESCHOTEN¹ — ¹2nd Institute of Physics

and JARA-FIT, RWTH Aachen University, 52074 Aachen, Germany — ²Research Center for Functional Materials, National Institute for Materials Science, Tsukuba, Japan — ³International Center for Materials Nanoarchitectonics, National Institute for Materials Science, Tsukuba, Japan

Hexagonal boron nitride (hBN) serves as an atomically flat, insulating substrate for a large variety of 2D heterostructures. However, recent opto-electronic experiments showed that optically triggered leakage currents passing through hBN pose a serious bottleneck for reliable gating of 2D semiconductors [1]. Motivated by these observations, we report on photo-induced charge transport through hBN in graphite-hBN-graphite devices. Furthermore, we examine the impact of illuminating hBN employed as a gate dielectric on the charge carrier density of graphene Hall bar devices. Our results indicate that hBN exhibits optically active electronic states, which partially screen the gate electric field under light illumination. Interestingly, we observe a strong asymmetry of this effect for positive and negative electric fields showing that hBN does not behave as an ideal dielectric within the plate capacitor model especially in opto-electronic experiments.

[1] F. Volmer et al., *Phys. Status Solidi RRL* **14**, 2000298 (2020)

DS 23: Optical Analysis of Thin Films (Reflection, Ellipsometry, Raman, IR-DUV Spectroscopy, ...)

Time: Thursday 10:45–12:15

Location: H14

DS 23.1 Thu 10:45 H14

Raman characterisation of composite thin films of PEDOT:PSS and Cu₂ZnSnS₄ nanocrystals — •YEVHENII HAVRYLIUK^{1,2,3}, VOLODYMYR DZHAGAN³, OLEKSANDR SELYSHCHEV^{1,2}, and DIETRICH R.T. ZAHN^{1,2} — ¹Semiconductor Physics, Chemnitz University of Technology, Chemnitz, Germany — ²Center for Materials, Architectures, and Integration of Nanomembranes (MAIN), Chemnitz, Germany — ³V.E. Lashkaryov Institute of Semiconductor Physics NAS of Ukraine, Kyiv, Ukraine

The increasing demand for renewable energy sources powers the high research interest in the fields of photovoltaics and thermoelectrics. One of the materials promising in these fields are Cu₂ZnSnS₄ (CZTS) family compounds. CZTS nanocrystals (NCs) for third generation photovoltaics can be obtained by low-temperature "green" colloidal synthesis. Another material widely studied especially for thermoelectric applications is PEDOT:PSS. Usually these two materials are used as separate layers in devices. However, using them in a composite layer probably can reveal even more interesting properties. Therefore, we investigated such composite films with different polymer/NC ratios. Raman spectroscopy was used as a main characterization method. We detected the modification of the structure of PEDOT:PSS films upon incorporation of NCs and found that the formation of the CZTS NCs films using a drop-casting method occurs differently in the presence of even a small amount of PEDOT:PSS. The change in the stability of the PEDOT:PSS/CZTS composite under intense laser irradiation, in comparison with the pure components, was also investigated.

DS 23.2 Thu 11:00 H14

dielectric function of Al(1-x)ScxN obtained by spectroscopic ellipsometry. — •YOUNES SLIMI¹, REBECCA PETRICH¹, RÜDIGER SCHMIDT-GRÜND¹, HAUKE-LARS HONIG², CHRISTINA HELM³, HEIKE BARTSCH³, JENS MÜLLER³, PETER SCHAAF², and STEFAN KRISCHOK¹ — ¹Fachgebiet Technische Physik I, IMN Macro Nano, Technische Universität Ilmenau, 98693 Ilmenau — ²Fachgebiet Werkstoffe der Elektrotechnik, Institut für Werkstofftechnik und Institut für Mikro- und Nanotechnologien MacroNano, Technische Universität Ilmenau, 98693 Ilmenau — ³Fachgebiet Elektroniktechnologie, Technische Universität Ilmenau, IMN Macro Nano, 98693 Ilmenau

Scandium Aluminum Nitride alloy (ScxAl1-xN) thin films were prepared via the sputtering technique. The samples then were measured by spectroscopic ellipsometry (SE) and analysed to determine the sample's dielectric function (DE) by means of numeric b-spline and line shape model dielectric functions. We found a redshift of the bandgap (E_g) and an increasing refractive index with increasing Sc content. As AlN is hexagonal and ScN cubic, the birefringence also reduces when Sc is incorporated into the alloy. Therefore, the samples were measured with XRD and EDX to determine the crystal structure and lattice constant as a function of Sc percentage.

DS 23.3 Thu 11:15 H14

Analysis of CVD coatings with Raman spectroscopy — •MAXIMILIAN VON ROEDER, PETER J. KLAR, and SANGAM CHATTERJEE — Institute of Experimental Physics I, Giessen, Germany

The interphase between fibre and matrix is an important component in the preparation of ceramic matrix composites. The understanding of the nature of the coating is crucial for the optimization of CMC materials. Chemical vapour infiltration is the most frequent method of fibre coating. Homogeneity, low error density and controlled thickness are the key properties that the coating has to satisfy. Most characterization methods for the coating are very local probes. We ap-

plied rough Raman mapping measurements together with principal component analysis to get a broader picture for a larger sample. We studied SiC Hi-Nicalon S fibres with BN/SiC and C coating prepared by chemical vapour infiltration. With a data filtering algorithm to erase the raman spectra of the background we were able to obtain a colour coded maps of the samples. We tested this method with different samples where we introduced errors of different magnitude to determine the sensitivity of the approach. This method provides a quick and easy way to examine a sample with the extensions up to a few centimeters. In this fashion it is possible to study a larger fraction of a prepared material which leads to a higher reliability in quality control.

DS 23.4 Thu 11:30 H14

Time-resolved femtosecond ellipsometry — •SHIRLY ESPINOZA — ELI Beamlines, Institute of Physics, Czech Academy of Science, Prague, Czech Republic

The ellipsometry technique is well extend for the study of thin film material. Thanks to femtosecond pulse lasers, we developed a time-resolved femtosecond ellipsometry technique, where a pump beam from any wavelength between 200 nm and 2000 nm excite the material and second pulse, the probe beam, with a continuous spectrum from 350 nm * 750 nm measure the dielectric function of the material. The pump and the probe beam can be separated in time from femtoseconds until nanoseconds generating a time-scan of the relaxation of the material. The time-resolved ellipsometry technique is available to the scientific community at the user-oriented infrastructure ELI Beamlines located few kilometers from Prague, Czech Republic. Examples of successful experiments will be presented and the details of how to apply for beamtime will be shared.

DS 23.5 Thu 11:45 H14

Chalcogenides for Photonic Applications in the Visible — •FELIX HOFF¹, CARL-FRIEDRICH SCHOEN¹, MAXIMILIAN MUELLER¹, YIMING ZHOU¹, PETER KERRES¹, HÄSER MARIA¹, and MATTHIAS WUTTIG^{1,2,3} — ¹I. Institute of Physics (IA), RWTH Aachen University — ²Juelich-Aachen Research Alliance (JARA FIT and JARA HPC) — ³PGI 10 (Green IT), Forschungszentrum Juelich GmbH

Due to its large bandgap, the chalcogenide phase-change material (PCM) Sb₂S₃ is interesting for photonic applications, such as photonic switches in the visible range. Recent publications report contradictory findings concerning the switching speed. Since this property is decisive for many applications, it is important to better understand the crystallization process. To understand glass dynamics and crystallization kinetics, calorimetric measurements were performed. In addition, the optical properties were measured by optical spectroscopy and Ellipsometry. Supporting density functional theory (DFT) calculations are used and a comparison with typical PCMs is made. Sb₂S₃ has significant optical contrast in the visible spectral range, but lower maximum contrast than typical PCMs. It has been shown that crystallization takes significantly longer and has a broader stochastic distribution than for typical PCMs. Furthermore, crystallization occurs in the undercooled liquid phase for a range of heating rates which span over six orders of magnitude, so the glass transition could be studied. Our observations can be explained by the covalent bonding of Sb₂S₃. They can be understood in the context of a quantum mechanical map, which can be utilized to design materials for photonic applications.

DS 23.6 Thu 12:00 H14

IR dual-comb polarimetry of a nanofiber scaffold — •KARSTEN HINRICH¹, BRIANNA BLEVINS^{2,3}, ANDREAS FURCHNER⁴, NATARAJA SEKSHAR YADAVALLI^{2,3}, SERGIY MINKO^{2,3,5}, RAPHAEL HORVATH⁶, and MARKUS MANGOLD⁶ — ¹Leibniz-Institut für Analytische Wissenschaften - ISAS e.V., Schwarzschildstraße 8, 12489 Berlin, Germany — ²Nanostructured Materials Laboratory, The University of Georgia — ³Department of Chemistry, The University of Georgia — ⁴Helmholtz-Zentrum Berlin für Materialien und Energie GmbH, Division Energy and Information, Schwarzschildstraße 8, 12489 Berlin, Germany — ⁵Department of Textile, Fiber, and Polymer Sciences, The University of Georgia, Athens, Georgia 30602, United States — ⁶IRsweep AG, Laubisruetistrasse 44, 8712 Staefa, Switzerland

In this study the transmission properties of an anisotropic nanofiber scaffold are investigated non-invasively under ambient conditions by IR dual-comb polarimetry (DCP). Good agreement between DCP and classical FTIR polarimetry is found for amplitude and phase measurements at various azimuthal sample rotations, proving DCP as a new method for the study of such anisotropic samples in very short measurement times. A spectral information in the range of 1200 cm⁻¹ to 1300 cm⁻¹ can be achieved in 0.065 ms at 1.4 cm⁻¹ spectral resolution showing the potential for imaging applications, time resolved studies and hyperspectral spectroscopy of anisotropic samples. We acknowledge financial support by the EU through EFRE 1.8/13 and the Horizon 2020 grant 820419 and by the BMBF through CatLab (03EW0015A).

DS 24: 2D Materials 9 (joint session HL/ CPP/DS)

Time: Thursday 11:15–12:15

Location: H36

See HL 31 for details of this session.

DS 25: Transport Properties

Time: Thursday 15:00–16:00

Location: H14

DS 25.1 Thu 15:00 H14

Visualization of metallic filament formation in rare-earth nickelates via optical microscopy — •THEODOR LUIBRAND¹, STEFAN GUÉNON¹, FARNAZ TAHOUNI-BONAB¹, JAVIER DEL VALLE², CLARIBEL DOMÍNGUEZ², WILLEM RISCCHAU², LUCIA VARBARO², STEFANO GARIGLIO², RODOLFO ROCCO³, SOUMEN BAG³, MARCELO ROZENBERG³, JEAN-MARC TRISCONÉ², REINHOLD KLEINER¹, and DIETER KOELLE¹ — ¹Physikalisches Institut, Center for Quantum Science (CQ) an LISA⁺, Universität Tübingen, 72076 Tübingen, Germany — ²Department of Quantum Matter Physics, Université de Genève, 1211 Geneva, Switzerland — ³Université Paris-Saclay, CNRS, Laboratoire de Physique des Solides, 91405 Orsay, France

In recent years, there has been growing interest in resistive switching in strongly correlated materials. Resistive switching is at the core of memristive devices, which are considered as crucial elements in the emerging field of neuromorphic computing. However, in many systems, the details of the resistive switching mechanisms are elusive. We investigated the resistive switching of two types of rare-earth nickelate (NdNiO₃ and SmNiO₃) thin film devices. Both materials undergo insulator-to-metal transitions (IMT) from low-temperature antiferromagnetic or paramagnetic insulating to high-temperature paramagnetic metallic phases. Current-voltage characteristics acquired at device temperatures near the IMT show jumps towards lower voltages indicating resistive switching. We find that these events are accompanied by the formation of spatially confined conducting filaments, which is revealed by a change in reflectivity in optical images.

DS 25.2 Thu 15:15 H14

Towards ultraclean correlated metal CaVO₃ - Electric Transport Measurements — •MAHNI MÜLLER¹, TATIANA KUZNETSOVA², ROMAN ENGEL-HERBERT^{2,3}, and SASKIA F. FISCHER¹ — ¹Novel Materials Group, HU Berlin, 10099 Berlin, Germany — ²Department of Materials Science and Engineering, The Pennsylvania State University, University Park, PA 16802, USA. — ³Paul-Drude-Institut für Festkörperelektronik, 10117 Berlin, Germany

High-performance and cost-effective transparent materials are in great demand in the optoelectronic industry. The enhancement of the carrier effective mass through strong electron-electron interactions in correlated metals is a promising approach to achieve both high-optical transparency and high-electrical conductivity [1].

In this work we study the electric transport characteristics of CaVO₃ films with a thickness of 55 nm grown on LAO substrates. The films were deposited by hybrid molecular beam epitaxy with different partial pressures of the metalorganic vanadium oxytriisopropoxide precursor. Calcium was supplied through a solid state effusion cell. The optimal growth window estimated by X-ray diffraction was narrowed down by residual-resistance ratio (RRR) measurements. Temperature dependent resistivity and hall measurements were performed between 4.2 K and 300 K. The RRR was tripled compared to previous substrate [2]. Furthermore, the films with highest RRR ≈ 98 showed an increase of mobility with decreasing temperature with over 2000 $\frac{\text{cm}^2}{\text{Vs}}$ at 4.2 K.

[1] Zhang, Lei, *et al.*; Nature materials **15.2**, 204-210 (2016).[2] Eaton, Craig, *et al.*; J. Vac. Sci. Technol. **35.6**, 061510, (2017).

DS 25.3 Thu 15:30 H14

Electro-Thermal Resistive Switching at the Insulator to Metal Transition in Strongly Correlated Materials — •STEFAN GUÉNON¹, MATTHIAS LANGE¹, YOAV KALCHEIM^{2,3}, THEODOR LUIBRAND¹, FARNAZ TAHOUNI¹, REINHOLD KLEINER¹, IVAN K SCHULLER², and DIETER KOELLE¹ — ¹Physikalisches Institut, Center for Quantum Science (CQ) and LISA⁺, Universität Tübingen, 72076 Tübingen, Germany — ²Department of Physics and Center for Advanced Nanoscience, University of California - San Diego La Jolla, CA 92093, USA — ³Department of Materials Science and Engineering, Technion - Israel Institute of Technology, Technion City, 32000 Haifa, Israel

Electro-thermal (Joule-heating driven) resistive switching devices are investigated in the emerging field of neuromorphic computing. In a bio-mimetic approach, the memristive properties of such devices are used to emulate neurons and synapses. This talk explains how the considerable resistance change at the insulator-to-metal transition leads to electro-thermal instability. A metallic filament forms above a certain threshold current due to current and temperature redistribution if a device is electrically biased in this unstable temperature regime. We will complement the explanation with experimental results from microscopic studies on V₂O₃-devices, in which photomicrographs were acquired during filament formation. Further, we will discuss how additional device properties like thermal hysteresis or structural phase separation affect electro-thermal resistive switching. The U.S. Department of Energy supported this work under Award # DE-SC0019273.

DS 25.4 Thu 15:45 H14

Parallel field magnetoconductance in epitaxial bismuth quantum films — •JULIAN KOCH¹, DOAA ABDELBARAY², PHILIPP KRÖGER², PRIYANKA YOGI², CHRISTOPH TEGENKAMP¹, and HERBERT PENÜR² — ¹Institut für Physik, TU Chemnitz, Reichenhainerstr. 70, 09126 Chemnitz — ²Institut für Festkörperphysik, Leibniz Universität Hannover, Appelstraße 2, 30167 Hannover

The magnetoconductance (MC) of epitaxial Bi films on Si(111) (thickness 20-100 bilayers) was measured at $T = 9$ K in magnetic fields oriented in-plane parallel and perpendicular to the electric dc current I . Contributions to MC by weak antilocalization (WAL), by weak localization (WL) as well as by diffuse scattering were identified, which all turned out to be independent of the angle between B and I . In addition, only for $B \perp I$ a contribution to MC was found that increases with increasing B and is, to first approximation, $\propto B^2$. It is ascribed to ballistic scattering between the Rashba-split interfaces that allow Umklapp scattering without spin flip.

At small thicknesses the MC curves are dominated by WAL originating from the surface/interface states. However, the coupling between the interfaces, necessary for the observation of WAL in an in-plane B-field, happens through quantized bulk states instead of tunneling. Moreover, the admixing of the quantized bulk states with increasing film thickness not only increases diffuse scattering, but also modifies the WAL component, effectively introducing a WL-like component, above 50 BL. Thus, our findings suggest an intriguing interplay in magnetotransport between 2D and quantized 3D states.

DS 26: Thin Oxides and Oxide Layers 2

Time: Thursday 16:15–17:15

Location: H14

DS 26.1 Thu 16:15 H14

Studying the differences of Ga₂O₃ grown by conventional molecular-beam epitaxy (MBE) and suboxide MBE (S-MBE) — •SUSHMA RAGHUVANSY¹, JUSTIN A. BICH¹, TJARK LIESTMANN¹, JONATHAN McCANDLESS², MANUEL ALONSO-ORTS¹, DARRELL G. SCHLOM³, MARTIN EICKHOFF¹, and PATRICK VOGT^{1,3} — ¹Institute of Solid-State Physics, Bremen University, Otto-Hahn-Allee 1, 28359 Bremen, Germany — ²School of Electrical and Computer Engineering, Cornell University, Ithaca, New York 14853, USA — ³Department of Materials Science and Engineering, Cornell University, Ithaca, New York 14853, USA

The growth of Ga₂O₃ by conventional MBE, i.e., when supplying elemental Ga and active O, is limited by the formation and subsequent desorption of its volatile suboxide, Ga₂O. During suboxide MBE (S-MBE), a recently developed new MBE variant, suboxides (here: Ga₂O) are supplied during growth, bypassing the reaction limiting steps experienced during conventional Ga₂O₃ MBE growth by conventional MBE, and extending its kinetic and thermodynamic limits. S-MBE enables the synthesis of Ga₂O₃ at much higher growth rates (> 1 μm h⁻¹) and displays improved crystallinity and surface morphology compared with Ga₂O₃ thin films grown by conventional MBE.

This talk presents a direct comparison of Ga₂O₃ thin films grown by conventional MBE versus Ga₂O₃ thin films grown by S-MBE. We will show the impact of both MBE variants on the crystallinity and surface morphology of Ga₂O₃/Al₂O₃ heterostructures.

DS 26.2 Thu 16:30 H14

Comparative Study of a Ga₂O₃ nucleation layer and its impact on Ga₂O₃ growth on Al₂O₃ by molecular beam epitaxy — •ALEXANDER KARG, ADRIAN MESSOW, MANUEL ALONSO-ORTS, STEPHAN FIGGE, PATRICK VOGT, and MARTIN EICKHOFF — Institute of Solid-State Physics, University Bremen, Bremen, Germany

Ga₂O₃ is a wide bandgap semiconductor and is seen as a promising candidate for e.g. future high-power electronics, and UV-detectors. The availability of single crystalline substrates makes the material attractive for device fabrication. Because of easier access, the majority of experiments were carried out by heteroepitaxy on e.g. Al₂O₃ substrates. In this study, the influence of the Al₂O₃ substrate on the nucleation and layer growth is investigated and compared with the use of a beta-Ga₂O₃ buffer layer to mimic homoepitaxial conditions. It was found that the effective Me to O ratio on the surface differs substantially and the amount of the available species (especially active oxygen) for growth could be estimated with respect to the different growth surfaces (0001) Al₂O₃ and (-201) beta-Ga₂O₃. This study was transferred to In₂O₃ growth to determine the different oxidation efficacies of the cations Indium and Gallium. Furthermore, the influence of the plasma power on the nucleation behavior of Ga₂O₃ and In₂O₃ as well as its influence on the growth kinetics itself and the layer properties will be discussed.

DS 26.3 Thu 16:45 H14

The effect of post-growth annealing of titanium dioxide thin films prepared by a sol-gel process on the photocatalytic activity — •LU HE¹, SHUO NIU¹, DIETRICH.R.T. ZAHN^{1,2}, and TERESA I. MADEIRA^{1,2} — ¹Technische Universität Chemnitz, Semiconductor Physics, D-09107 Chemnitz, Germany — ²Center for Materials, Architectures and Integration of Nanomembranes (MAIN), Chemnitz University of Technology, 09107 Chemnitz, Germany

TiO₂ thin films revealed competitive performance for photocatalytic applications[1,2]. Here, a set of TiO₂ thin films are synthesized using a sol-gel process and spin coated on p-type Si(100) substrates with a native oxide layer. The as-deposited thin films are annealed at various temperatures from 400 to 800 °C for 3 hours in ambient conditions.

Characterization is performed using various methods[3] on phases (UV-Raman & X-Ray diffractometry), film thickness and optical constants (Spectroscopic ellipsometry), morphology(Atomic Force Microscopy). Photocatalytic results on photodegradation of acetone to CO₂ are obtained in a self-designed gas (reactant)-solid (photocatalyst) reaction chamber. The decrease/increase of acetone/CO₂ is monitored via in-situ Fourier Transform Infrared Spectroscopy.

Quantitative data analysis is performed and correlated to indicate the effect of post annealing on the optical and structural properties of the titanium dioxide thin films and their photocatalytic activities.

1. Song,H et al, Conf. Lasers Electro-Optics,CLEO 2019
2. Nalajala et al, C.S.RSC Adv. 9 2019.
3. Gartner,M et al, Sol-Gel Sci. Technol. 2021

DS 26.4 Thu 17:00 H14

Oxidation behavior of SMART alloys and MAX phases materials and applicability in solar receivers. — •LEONARDO GUIMARÃES LEAL LEALDINI¹, ANDREY LITNOVSKY^{1,2}, and JESUS GONZALEZ-JULIAN^{1,3} — ¹Forschungszentrum, Jülich GmbH, 52425 Jülich, Germany — ²115409 Moscow, Russia — ³Institute of Mineral Engineering, RWTH Aachen University, 52064 Aachen, Germany

In the concept of materials for high-temperature application, two types of are being investigated: SMART alloys and MAX phase materials. W-Cr-Y SMART alloys were first designed for future fusion power plants. Studies suggests that SMART alloy containing Cr and Y is capable of forming a Cr₂O₃ layer and maintaining it at 1273K which avoids the generation of tungsten oxide. MAX Phase materials are able to provide great properties like oxidation resistance at high temperatures. Cr₂AlC and Ti₂AlC are two MAX phases that, in initial studies, provided a good oxidation response. Studies showed that Cr₂AlC MAX phase and W-Cr-Y SMART alloy when exposed to 1273K and in humid atmosphere present good resistance to oxidation. Both were capable of withstand more than 20 hours in these conditions with a gain of mass lower than 0.3g/cm². The main objective of this research is to evaluate the feasibility of both MAX phase materials and propose a new W-Al-Y SMART alloy, using them as solar receivers in concentrated solar power plants.

DS 27: 2D Materials 10 (joint session HL/ CPP/DS)

Time: Friday 9:30–12:00

Location: H36

See HL 42 for details of this session.

Dynamics and Statistical Physics Division Fachverband Dynamik und Statistische Physik (DY)

Markus Bär
Physikalisch-Technische Bundesanstalt
FB 8.4 - Modellierung und Datenanalyse
Abbestraße 2 - 12
10587 Berlin
markus.baer@ptb.de

Overview of Invited Talks and Sessions

(Lecture halls H18, H19, and H20; Poster P2)

Invited Talks

DY 2.1	Mon	9:30–10:00	H18	Roughness growth modes in thin film growth — •MARTIN OETTEL
DY 9.1	Mon	15:00–15:30	H19	Granular matter composed of non-convex grains — •RALF STANNARIUS
DY 12.1	Mon	15:30–16:00	H20	A phononic frequency comb from a single resonantly driven nanomechanical mode — •EVA WEIG
DY 12.4	Mon	16:30–17:00	H20	From period-doubling bifurcations to time crystals and coherent Ising machines — •ODED ZILBERBERG, TONI L. HEUGEL, JAN KOŠATA, JAVIER DEL PINO, R. CHITRA, ALEXANDER EICHLER
DY 12.6	Mon	17:15–17:45	H20	2D membranes in motion — •HERRE VAN DER ZANT
DY 14.1	Tue	9:30–10:00	H18	Non-Markovian Brownian systems: from single-particle thermodynamics to collective behavior — •SABINE KLAPP
DY 17.1	Tue	10:30–11:00	H19	Caustics in turbulent aerosols — •BERNHARD MEHLIG
DY 29.1	Wed	12:00–12:30	H18	Derivation of a continuum description of sheared jammed soft suspensions from particle dynamics — •ERIC BERTIN, NICOLAS CUNY, ROMAIN MARI
DY 32.1	Wed	15:00–15:30	H19	Large scale patterns in turbulent Rayleigh-Bénard convection — •STEPHAN WEISS
DY 33.1	Wed	15:00–15:30	H20	Detecting dynamical quantum phase transitions by string observables — •ANATOLI POLKOVNIKOV, AMIT DUTTA, SOUVIK BANDYOPADHYAY
DY 37.1	Thu	9:30–10:00	H20	Controlled and robust phase separation in cells — •DAVID ZWICKER
DY 48.1	Fri	9:30–10:00	H19	Photonic Reservoir Computing: Analytic insights and possibilities for optimization — LINA JAURIGUE, FELIX KÖSTER, •KATHY LÜDGE

Invited Talks of the joint Symposium SKM Dissertation Prize 2022 (SYSD)

See SYSD for the full program of the symposium.

SYSD 1.1	Mon	10:15–10:45	H2	Charge localisation in halide perovskites from bulk to nano for efficient optoelectronic applications — •SASCHA FELDMANN
SYSD 1.2	Mon	10:45–11:15	H2	Nonequilibrium Transport and Dynamics in Conventional and Topological Superconducting Junctions — •RAFFAEL L. KLEES
SYSD 1.3	Mon	11:15–11:45	H2	Probing magnetostatic and magnetotransport properties of the antiferromagnetic iron oxide hematite — •ANDREW ROSS
SYSD 1.4	Mon	11:45–12:15	H2	Quantum dot optomechanics with surface acoustic waves — •MATTHIAS WEISS

Invited Talks of the joint Symposium United Kingdom as Guest of Honor (SYUK)

See SYUK for the full program of the symposium.

SYUK 1.1	Wed	9:30–10:00	H2	Structure and Dynamics of Interfacial Water — •ANGELOS MICHAELIDES
SYUK 1.2	Wed	10:00–10:30	H2	A molecular view of the water interface — •MISCHA BONN
SYUK 1.3	Wed	10:30–11:00	H2	Motile cilia waves: creating and responding to flow — •PIETRO CICUTA
SYUK 1.4	Wed	11:00–11:30	H2	Cilia and flagella: Building blocks of life and a physicist's playground — •OLIVER BÄUMCHEN

SYUK 1.5	Wed	11:45–12:15	H2	Computational modelling of the physics of rare earth - transition metal permanent magnets from SmCo_5 to $\text{Nd}_2\text{Fe}_{14}\text{B}$ — •JULIE STAUNTON
SYUK 2.1	Wed	15:00–15:30	H2	Hysteresis Design of Magnetic Materials for Efficient Energy Conversion — •OLIVER GUTFLEISCH
SYUK 2.2	Wed	15:30–16:00	H2	Non-equilibrium dynamics of many-body quantum systems versus quantum technologies — •IRENE D'AMICO
SYUK 2.3	Wed	16:00–16:30	H2	Quantum computing with trapped ions — •FERDINAND SCHMIDT-KALER
SYUK 2.4	Wed	16:45–17:15	H2	Breaking the millikelvin barrier in cooling nanoelectronic devices — •RICHARD HALEY
SYUK 2.5	Wed	17:15–17:45	H2	Superconducting Quantum Interference Devices for applications at mK temperatures — •SEBASTIAN KEMPF

Invited Talks of the joint Symposium Interplay of Substrate Adaptivity and Wetting Dynamics from Soft Matter to Biology (SYSM)

See SYSM for the full program of the symposium.

SYSM 1.1	Wed	15:00–15:30	H1	Statics and Dynamics of Soft Wetting — •BRUNO ANDREOTTI
SYSM 1.2	Wed	15:30–16:00	H1	Droplets on elastic substrates and membranes - Numerical simulation of soft wetting — •SEBASTIAN ALAND
SYSM 1.3	Wed	16:00–16:30	H1	Wetting of Polymer Brushes in Air — LARS VELDSCHOLTE, GUIDO RITSEMA VAN ECK, LIZ MENSINK, JACCO SNOEIJER, •SISSI DE BEER
SYSM 1.4	Wed	16:45–17:15	H1	Elastocapillary phenomena in cells — •ROLAND L. KNORR
SYSM 1.5	Wed	17:15–17:45	H1	Active contact line depinning by micro-organisms spreading on hydrogels — MARC HENNES, JULIEN TAILLEUR, GAËLLE CHARRON, •ADRIAN DAERR

Invited Talks of the joint Symposium Collective Social Dynamics from Animals to Humans (SYSO)

See SYSO for the full program of the symposium.

SYSO 1.1	Thu	9:30–10:00	H1	Capturing group interactions: The next frontier of modeling social and biological systems — •FRANK SCHWEITZER
SYSO 1.2	Thu	10:00–10:30	H1	Modelling Individual Mobility Behavior — •LAURA MARIA ALESSANDRETTI
SYSO 1.3	Thu	10:30–11:00	H1	Validating argument-based opinion dynamics with survey experiments — •SVEN BANISCH
SYSO 1.4	Thu	11:15–11:45	H1	Self-organization, Criticality and Collective Information Processing in Animal Groups — •PAWEŁ ROMANCZUK
SYSO 1.5	Thu	11:45–12:15	H1	Collective dynamics and physiological interactions in bird colonies — •HANJA BRANDL

Invited Talks of the joint Symposium Complexity and Topology in Quantum Matter (SYQM)

See SYQM for the full program of the symposium.

SYQM 1.1	Fri	9:30–10:00	H1	The role of crystalline symmetries in topological materials: the topological materials database — •MAIA VERGNIORY
SYQM 1.2	Fri	10:00–10:30	H1	Microwave Bulk and Edge Transport in HgTe-Based 2D Topological Insulators — •ERWANN BOCQUILLON, MATTHIEU C. DARTIALH, ALEXANDRE GOURMELON, HIROSHI KAMATA, KALLE BENDIAS, SIMON HARTINGER, JEAN-MARC BERROIR, GWENDAL FÈVE, BERNARD PLAÇAIS, LUKAS LUNCZER, RAIMUND SCHLERETH, HARTMUT BUHMANN, LAURENS MOLENKAMP
SYQM 1.3	Fri	10:30–11:00	H1	Spectral Sensitivity of Non-Hermitian Topological Systems — •JAN CARL BUDICH
SYQM 1.4	Fri	11:15–11:45	H1	Topological photonics and topological lasers with coupled vertical resonators — •SEBASTIAN KLEMBT
SYQM 1.5	Fri	11:45–12:15	H1	Spectroscopic Studies of the Topological Magnon Band Structure in a Skyrmion Lattice — •MARKUS GARST

Sessions

DY 1.1–1.3	Sun	16:00–18:30	H4	Tutorial: Stochastic Processes from Financial Risk to Genetics (joint session SOE/TUT/BP/DY)
DY 2.1–2.1	Mon	9:30–10:00	H18	Invited Talk Martin Oettel
DY 3.1–3.9	Mon	10:00–12:30	H18	Statistical Physics far from Thermal Equilibrium
DY 4.1–4.8	Mon	10:00–12:15	H19	Wetting, Droplets and Microfluidics (joint session DY/PPP)

DY 5.1–5.10	Mon	10:00–12:45	H20	Many-Body Quantum Dynamics 1 (joint session DY/TT)
DY 6.1–6.7	Mon	10:30–12:45	H16	Active Matter 1 (joint session BP/CPP/DY)
DY 7.1–7.7	Mon	15:00–17:15	H16	Statistical Physics of Biological Systems 1 (joint session BP/DY)
DY 8.1–8.10	Mon	15:00–17:45	H18	Data Analytics for Complex Systems (joint session DY/SOE)
DY 9.1–9.1	Mon	15:00–15:30	H19	Invited Talk Ralf Stannarius
DY 10.1–10.10	Mon	15:00–17:45	H39	Modeling and Simulation of Soft Matter (joint session CPP/DY)
DY 11.1–11.9	Mon	15:30–18:00	H19	Granular Matter and Contact Dynamics
DY 12.1–12.6	Mon	15:30–17:45	H20	Focus Session: Nonlinear Dynamics of Nanomechanic Oscillators
DY 13.1–13.2	Mon	17:45–18:15	H18	Big Data and Artificial Intelligence (joint session SOE/DY)
DY 14.1–14.1	Tue	9:30–10:00	H18	Invited Talk Sabine Klapp
DY 15.1–15.4	Tue	9:30–10:30	H19	Delay and Feedback Dynamics
DY 16.1–16.11	Tue	10:00–13:00	H18	Active Matter 2 (joint session DY/BP/CPP)
DY 17.1–17.1	Tue	10:30–11:00	H19	Invited Talk Bernhard Mehlig
DY 18.1–18.7	Tue	11:15–13:00	H19	Nonlinear Dynamics 1: Synchronization and Chaos (joint session DY/SOE)
DY 19.1–19.6	Tue	11:30–13:00	H20	Many-Body Quantum Dynamics 2 (joint session DY/TT)
DY 20.1–20.5	Tue	11:30–13:00	H38	Complex Fluids and Colloids, Micelles and Vesicles (joint session CPP/DY)
DY 21.1–21.1	Wed	9:30–10:15	H11	Invited Talk Dirk Brockmann (joint session SOE/DY)
DY 22.1–22.10	Wed	9:30–12:30	H16	Active Matter 3 (joint session BP/CPP/DY)
DY 23.1–23.9	Wed	9:30–12:00	H18	Complex Fluids and Soft Matter 1 (joint session DY/CPP)
DY 24.1–24.6	Wed	9:30–11:15	H19	Stochastic Thermodynamics and Information Processing
DY 25.1–25.7	Wed	9:30–11:15	H39	General Session to the Symposium: Interplay of Substrate Adaptivity and Wetting Dynamics from Soft Matter to Biology (joint session CPP/DY)
DY 26.1–26.6	Wed	10:00–11:30	H20	Critical Phenomena and Phase Transitions
DY 27.1–27.6	Wed	10:15–12:45	H11	Networks: From Topology to Dynamics (joint session SOE/BP/DY)
DY 28.1–28.7	Wed	11:15–13:00	H19	Extreme Events, Glasses and Miscellaneous
DY 29.1–29.1	Wed	12:00–12:30	H18	Invited Talk Eric Bertin
DY 30.1–30.2	Wed	12:45–13:15	H11	Energy Networks (joint session SOE/DY)
DY 31.1–31.9	Wed	15:00–17:30	H18	Active Matter 4 (joint session DY/BP/CPP)
DY 32.1–32.1	Wed	15:00–15:30	H19	Invited Talk Stephan Weiss
DY 33.1–33.1	Wed	15:00–15:30	H20	Invited Talk Anatoli Polkovnikov
DY 34.1–34.6	Wed	15:30–17:15	H19	Fluid Physics: Turbulence and Convection
DY 35.1–35.9	Wed	15:30–18:00	H20	Quantum Chaos and Coherent Dynamics
DY 36.1–36.11	Thu	9:30–12:30	H22	Quantum Coherence and Quantum Information Systems (joint session TT/DY)
DY 37.1–37.1	Thu	9:30–10:00	H20	Invited Talk David Zwicker
DY 38.1–38.6	Thu	10:00–11:30	H18	Complex Fluids and Soft Matter 2 (joint session DY/CPP)
DY 39.1–39.8	Thu	10:00–12:15	H19	Pattern Formation and Reaction-Diffusion Systems
DY 40.1–40.7	Thu	10:00–12:00	H20	Brownian Motion and Anomalous Diffusion
DY 41.1–41.12	Thu	15:00–18:15	H22	Nonequilibrium Quantum Many-Body Systems (joint session TT/DY)
DY 42.1–42.6	Thu	15:00–16:30	H16	Statistical Physics of Biological Systems 2 (joint session BP/DY)
DY 43.1–43.8	Thu	15:00–18:00	P2	Poster Session: Quantum Chaos and Many-Body Dynamics
DY 44.1–44.20	Thu	15:00–18:00	P2	Poster Session: Statistical Physics and Critical Phenomena
DY 45.1–45.13	Thu	15:00–18:00	P2	Poster Session: Nonlinear Dynamics, Pattern Formation, Data Analytics and Machine Learning
DY 46.1–46.22	Thu	15:00–18:00	P2	Poster Session: Complex Fluids, Soft Matter, Active Matter, Glasses and Granular Materials
DY 47	Thu	18:30–19:15	H19	Members' Assembly
DY 48.1–48.1	Fri	9:30–10:00	H19	Invited Talk Kathy Lüdge (joint session DY/SOE)
DY 49.1–49.10	Fri	9:30–12:15	H20	Statistical Physics: General
DY 50.1–50.11	Fri	10:00–12:45	H18	Active Matter 5 (joint session DY/BP/CPP)
DY 51.1–51.5	Fri	10:00–11:15	H19	Machine Learning in Dynamics and Statistical Physics (joint session DY/SOE)
DY 52.1–52.5	Fri	11:30–12:45	H19	Nonlinear Dynamics 2: Stochastic and Complex Systems, Networks (joint session DY/SOE)

Members' Assembly of the Dynamics and Statistical Physics Division

Thursday 18:30–19:15 H19

Sessions

– Invited Talks, Tutorials, Contributed Talks, and Posters –

DY 1: Tutorial: Stochastic Processes from Financial Risk to Genetics (joint session SOE/TUT/BP/DY)

Macroscopic and microscopic models from Economy to Biology must account for stochasticity on various levels. While classical physics strives for deterministic descriptions through differential equations from fundamental level to thermodynamics, many physics-based models on higher level explicitly include stochasticity from various sources. Discrete and continuous stochastic processes then become the mathematical foundation of these models. This tutorial highlights classical as well as current methods and approaches of probabilistic models and stochastic processes in physics, biology as well as socio-economic systems, thereby bridging the risk to extinction in genetics with its economic counterpart. (Session organized by Jens Christian Clausen.)

Time: Sunday 16:00–18:30

Location: H4

See SOE 1 for details of this session.

DY 2: Invited Talk Martin Oettel

Time: Monday 9:30–10:00

Location: H18

Invited Talk DY 2.1 Mon 9:30 H18
Roughness growth modes in thin film growth — •MARTIN OETTEL — Uni Tübingen, Institut für Angewandte Physik

Thin film growth is one of the fundamental nonequilibrium processes in statistical physics and it is also very relevant for applications. In the past years, experimental attention has shifted from the growth of metallic films (with fairly isotropic particles) to growth of organic films with possibly very anisotropic particles. In view of applications, the film morphology (notably the film roughness) is a central object of interest. To study that, we employ simple lattice models for isotropic and anisotropic particles to elucidate principal film growth modes with a focus on the intermediate thickness regime. For isotropic particles we find 4

principal growth modes with fairly sharp transitions between them [1]. E.g., a dynamic layering transition separates layer-by-layer and island growth and can be viewed as a nonequilibrium counterpart of wetting/layering transitions. Anisotropy in the interactions between the lattice particles does not change the roughness growth modes but adds further orientational transitions [2]. Further, we have studied monolayer growth for lattice particles which are also anisotropic in their hard-core shape. There, the deposition process corresponds to trajectories in the space of macroscopic order parameters (density, orientation) which connect rather small equilibrium domains and which describe generalized nucleation and arrest processes.

[1] E. Empting et al., Phys. Rev. E 103, 023302 (2021). [2] E. Empting, N. Bader, and M. Oettel, Phys. Rev. E 105, 045306 (2022).

DY 3: Statistical Physics far from Thermal Equilibrium

Time: Monday 10:00–12:30

Location: H18

DY 3.1 Mon 10:00 H18
Relaxation to a parity-time symmetric generalized Gibbs ensemble after a quantum quench in a driven-dissipative Kitaev chain — •ELIAS STARCHL and LUKAS SIEBERER — Institute for Theoretical Physics, University of Innsbruck, Austria

After a quench, isolated thermalizing quantum many-body systems relax locally to an equilibrium state that is universally determined by conservation laws and the principle of maximum entropy. In contrast, open quantum systems, subjected to Markovian drive and dissipation, typically evolve toward nonequilibrium steady states that are highly model-dependent. However, focusing on a driven-dissipative Kitaev chain, we show that relaxation after a quantum quench can be described by a maximum entropy ensemble, if the Liouvillian governing the dynamics has parity-time (PT) symmetry. We dub this ensemble, which is determined by the biorthogonal eigenmodes of the adjoint Liouvillian, the PT-symmetric generalized Gibbs ensemble (PTGGE). Resembling isolated systems, thermalization becomes manifest in the growth and saturation of entanglement, and the relaxation of local observables. In contrast, the directional pumping of fermion parity represents a phenomenon that is unique to relaxation dynamics in driven-dissipative systems. We expect that our results apply rather generally to integrable, driven-dissipative bosonic and fermionic quantum many-body systems with PT symmetry.

DY 3.2 Mon 10:15 H18
Finite-time dynamical phase transition in non-equilibrium relaxation — •JAN MEIBOHM^{1,2} and MASSIMILIANO ESPOSITO¹ — ¹Complex Systems and Statistical Mechanics, Department of Physics and Materials Science, University of Luxembourg, L-1511 Luxembourg, Luxembourg — ²Department of Mathematics, King's College London, London WC2R 2LS, United Kingdom

We uncover a finite-time dynamical phase transition in the thermal relaxation of a mean-field magnetic model. The phase transition manifests itself as a cusp singularity in the probability distribution of the magnetization that forms at a critical time. The transition is due to a sudden switch in the dynamics, charac-

terized by a dynamical order parameter. We derive a dynamical Landau theory for the transition that applies to a range of systems with scalar, parity-invariant order parameters. Close to criticality, our theory reveals an exact mapping between the dynamical and equilibrium phase transitions of the magnetic model, and implies critical exponents of mean-field type. We argue that interactions between nearby saddle points, neglected at the mean-field level, may lead to critical, spatiotemporal fluctuations of the order parameter, and thus give rise to novel, dynamical critical phenomena.

DY 3.3 Mon 10:30 H18
Mori-Zwanzig formalism for general relativity: a new approach to the averaging problem* — •MICHAEL TE VRUGT¹, SABINE HOSSENFELDER², and RAPHAEL WITTKOWSKI¹ — ¹Institut für Theoretische Physik, Center for Soft Nanoscience, Westfälische Wilhelms-Universität Münster, D-48149 Münster, Germany — ²Frankfurt Institute for Advanced Studies, D-60438 Frankfurt am Main, Germany

Cosmology provides a coarse-grained description of the universe that is valid on very large length scales. However, the Einstein field equations are not valid for coarse-grained quantities since, due to their nonlinearity, they do not commute with an averaging procedure. Thus, it is unclear in which way small-scale inhomogeneities affect large-scale cosmology (backreaction). In this work [1], we address this problem by extending the Mori-Zwanzig projection operator formalism, a highly successful coarse-graining method from statistical mechanics, towards general relativity. This allows to derive a dynamic equation for the Hubble parameter in which backreaction is taken into account through memory and noise terms. Our results are linked to cosmological observations.

[1] M. te Vrugt, S. Hossensfelder, R. Wittkowski, Physical Review Letters 127, 231101 (2021)

*Funded by the Deutsche Forschungsgemeinschaft (DFG) – WI 4170/3-1

DY 3.4 Mon 10:45 H18

Synthetic horizons in 1D tight-binding model and thermalisation of the many-body groundstate — •LOTTE MERTENS^{1,2}, ALI G. MOGHADDAM^{2,3}, DMITRY CHERNYAVSKY², CORENTIN MORICE¹, JEROEN VAN DEN BRINK^{2,4}, and JASPER VAN WEZEL¹ — ¹Institute for Theoretical Physics and Delta Institute for Theoretical Physics, University of Amsterdam, 1090 GL Amsterdam, The Netherlands — ²Institute for Theoretical Solid State Physics, IFW Dresden, Helmholtzstr. 20, 01069 Dresden, Germany — ³Department of Physics, Institute for Advanced Studies in Basic Sciences (IASBS), Zanjan 45137-66731, Iran — ⁴Institute for Theoretical Physics and Würzburg-Dresden Cluster of Excellence ct.qmat, Technische Universität Dresden, 01069 Dresden, Germany

Open problems in general relativity have motivated the search for analogue gravitational systems in condensed matter implementations. In one such system, a 1D tight-binding model with position-dependent hopping, the possibility of realizing an analogue gravitational horizon has recently been demonstrated. Here, we introduce the concept of emergent temperature, inspired by Unruh radiation, and show that it arises naturally in tight-binding lattice models featuring a horizon. Despite finding many similarities between the emergent lattice temperature and the gravitational Unruh temperature, we show that the nature of the thermal spectrum in the lattice theory is radically different from that in the continuum limit. Additionally, we provide a detailed analysis of outgoing radiation showing the conditions under which the horizon behaves purely as a thermal source.

DY 3.5 Mon 11:00 H18

Renormalized Fluctuation Expansion for Non-Equilibrium Disordered Networks — •MICHAEL DICK^{1,2,3}, ALEX VAN MEEGEN^{1,4}, and MORITZ HELIAS^{1,5} — ¹Institute of Neuroscience and Medicine (INM-6) and Institute for Advanced Simulation (IAS-6) and JARA-BRAIN Institute I, Jülich Research Centre, 52425 Jülich, Germany — ²Department of Computer Science 3 - Software Engineering, RWTH Aachen University, Aachen, Germany — ³Peter Grünberg Institut (PGI-1) and Institute for Advanced Simulation (IAS-1), Jülich Research Centre, 52425 Jülich, Germany — ⁴Institute of Zoology, University of Cologne, 50674 Cologne, Germany — ⁵Department of Physics, Faculty 1, RWTH Aachen University, Aachen, Germany

It is frequently hypothesized that cortical networks display hallmarks of critical dynamics. Such critical dynamics are beyond the validity of a mean-field approximation because it inherently neglects fluctuations. Thus, a renormalized theory is necessary. We consider an archetypal neural network model which displays a magnetic as well as a chaotic transition. Based on the analogue of a quantum effective action, we derive self-consistency equations for the first two renormalized Greens functions. Their self-consistent solution reveals critical slowing down near the transition to the ferromagnetic state and an optimal level of disorder which favors collective behavior. The quantitative theory explains the shape of the single-unit autocorrelation function, featuring multiple temporal scales, and the population autocorrelation function.

15 min. break

DY 3.6 Mon 11:30 H18

Modeling flash sintering conditions with Boltzmann equations — •MAGDULIN DWEDARI, LOTHAR BRENDEL, and DIETRICH WOLF — University of Duisburg-Essen, Lotharstraße 1, 47057 Duisburg

In a flash sintering experiment, a suitable combination of electric field and furnace heating is applied to the sample, which makes it possible to sinter it in a matter of seconds and at significantly lower temperatures compared to conventional sintering. An established hypothesis that explains the key signatures of a flash sintering event, such as a surge in conductivity, is that the electric field causes a rapid generation of Frenkel defects in the sample. With molecular dynamic simulations it has been confirmed that a phonon proliferation at the Brillouin-Zone edge can cause a Frenkel defect concentration 10^{15} times higher than the thermal concentration.

To study the effects of an electric field on the phonon distribution, we model the electron system governed by an electric field and the phonon system coupled to an external heat bath with two coupled Boltzmann equations. The key difference to previous work exciting the electron system via a laser pulse is that our excita-

tion term models the effects of the electric field and is therefore continuous and imposes a cylindrical symmetry.

DY 3.7 Mon 11:45 H18

Barrier crossing in a viscoelastic bath — •FÉLIX GINOT¹, JULIANA CASPERS², MATTHIAS KRÜGER², and CLEMENS BECHINGER¹ — ¹Fachbereich Physik Universität Konstanz, 78457 Konstanz, Germany — ²Georg-August Universität Göttingen, 37073 Göttingen, Germany

The activated, i.e., fluctuation-assisted hopping of a Brownian particle across an energy barrier ΔU is a fundamental process with important applications across science, such as in chemical reactions, protein folding, or drug absorption. Such processes can be rationalized using Kramers theory, which predicts the hopping rate $\nu \propto \exp(-\Delta U/k_B T)$ with $k_B T$ the thermal energy, in agreement with experimental observations. Many systems, however, cannot be described in terms of a single degree of freedom, notably when memory effects need to be taken into account. In this work we experimentally investigate barrier crossing of a Brownian particle in a double-well potential suspended in a viscoelastic solvent which exhibits non-Markovian behavior, i.e., memory. For potential barriers up to several $k_B T$ we find the hopping dynamics to be characterized not by a single but by *two* time scales which can differ by more than two orders of magnitude. While the long time scale increases exponentially with ΔU (as in Kramers theory), the short one is almost unaffected by the barrier height. The latter results from elastic energy fluctuations of the viscoelastic bath due to excitations arising from the particle's hopping motion. Our results, which are in agreement with a simple model where the fluid is described as a Maxwell medium, have immediate consequences for the above examples, e.g., altering the interpretation and prediction of lifetimes.

DY 3.8 Mon 12:00 H18

Scalar Active Mixtures: The Nonreciprocal Cahn-Hilliard Model — •SUROPRIYA SAHA¹, JAIME AGUDO-CANALEJO¹, and RAMIN GOLESTANIAN^{1,2} — ¹Department of Living Matter Physics, Max Planck Institute for Dynamics and Self-Organization — ²Rudolf Peierls Centre for Theoretical Physics, University of Oxford

Pair interactions between active particles need not follow Newton's third law. In this work, we propose a continuum model of pattern formation due to nonreciprocal interaction between multiple species of scalar active matter. The classical Cahn-Hilliard model is minimally modified by supplementing the equilibrium Ginzburg-Landau dynamics with particle-number-conserving currents, which cannot be derived from a free energy, reflecting the microscopic departure from action-reaction symmetry. The strength of the asymmetry in the interaction determines whether the steady state exhibits a macroscopic phase separation or a traveling density wave displaying global polar order. The latter structure, which is equivalent to an active self-propelled smectic phase, coarsens via annihilation of defects, whereas the former structure undergoes Ostwald ripening. The emergence of traveling density waves, which is a clear signature of broken time-reversal symmetry in this active system, is a generic feature of any multicomponent mixture with microscopic nonreciprocal interactions.

DY 3.9 Mon 12:15 H18

Quantum thermodynamics of nonadiabatically driven systems: The effect of electron-phonon interaction — •JAKOB BÄTGE¹, AMIKAM LEVY³, WENJIE DOU², and MICHAEL THOSS¹ — ¹Institute of Physics, University of Freiburg, Freiburg, Germany — ²Department of Physics, School of Science, Westlake University, Hangzhou, China — ³Department of Chemistry, Bar-Ilan University, Ramat-Gan, Israel

The development and optimization of quantum devices have increased the interest in dynamics and thermodynamics of systems on the scale of single atoms and molecules. In this contribution, we investigate the nonequilibrium quantum dynamics of a driven nanosystem with two different approaches. By comparing results from the numerically exact hierarchical equations of motion method [1] and a Markovian quantum master equation [2], we analyze non-Markovian effects in the system dynamics. Furthermore, we discuss nonadiabatic effects in thermodynamic quantities induced by electronic-vibrational coupling.

[1] J. Bätge *et al.*, Phys. Rev. B **103**, 235413 (2021)[2] R. Dann *et al.*, Phys. Rev. A **98**, 052129 (2018)

DY 4: Wetting, Droplets and Microfluidics (joint session DY/CPP)

Time: Monday 10:00–12:15

Location: H19

DY 4.1 Mon 10:00 H19

Lattice Boltzmann simulations of dense suspensions of soft particles with interface viscosity — •FABIO GUGLIETTA¹, OTHMANE AOUANE¹, FRANCESCA PELUSI¹, MARCELLO SEGA¹, and JENS HARTING^{1,2} — ¹Helmholtz Institute Erlangen-Nürnberg, Germany — ²Department of Chemical and Biological Engineering and Department of Physics, FAU Erlangen-Nürnberg, Germany

Interface viscosity (IV) plays a major role in the dynamics of single droplets and viscoelastic capsules by influencing their transient dynamics and steady-state deformation. For example, it has recently become clear that numerical models for red blood cells must include IV to account for their realistic description. Therefore, IV can be expected to play a significant role in determining also the dynamics and rheology of their dense suspensions. However, as no detailed inves-

tigation exists on the effects of IV in the dense suspensions of soft capsules, we aim to fill this gap by including it in computational fluid dynamics models. Here, we address this problem for the first time by performing numerical simulations in the framework of the immersed boundary - lattice Boltzmann method. This approach proved to be a valid numerical tool to provide a realistic description of soft particles immersed in Newtonian fluids. We employ a recent numerical model to account for IV by relying on the discretised Boussinesq-Scriven tensor, which provides a continuum description of a 2D viscous fluid. We show that the IV influences (a) the time it takes for particles to deform during the transient phase and (b) the final shape of the particles in the steady-state at different volume fraction values.

DY 4.2 Mon 10:15 H19

Wetting dynamics of droplets: an immersed boundary lattice Boltzmann approach — •FRANCESCA PELUSI¹, OTHMANE AOUANE¹, FABIO GUGLIETTA¹, MARCELLO SEGA¹, and JENS HARTING^{1,2} — ¹Helmholtz Institute Erlangen-Nürnberg, Germany — ²Department of Chemical and Biological Engineering and Department of Physics, FAU, Germany

Many applications in computational fluid dynamics require the immersed boundary (IB) method to couple the dynamics of well-defined structures with that of a surrounding fluid. If the latter is simulated with a lattice Boltzmann (LB) method, the resulting IBLB approach is known to be a very versatile tool, for example, in studying dense suspensions of red blood cells. However, little attention has been devoted so far to applying this approach to substrate wetting problems. Here, we report on an IBLB-based investigation of the wetting of droplets interacting with a solid surface. In our model, the droplet surface tension contributes to the force the droplet (structure) communicates to the surrounding fluid. We characterize Newtonian droplets' static and dynamic contact angles and show how surface/IB-nodes interaction tuning allows obtaining the desired wetting properties. Furthermore, the flexibility of the IBLB approach will enable us to model non-Newtonian surface rheology, opening the possibility of simulating the unusual wetting behavior of gallium droplets. Indeed, liquid gallium develops an oxide layer at the liquid surface when in contact with the oxygen, which affects its adhesive properties with significant consequences for its high-tech applications, such as catalysis.

DY 4.3 Mon 10:30 H19

Viscosity-induced Destabilization of a Liquid Sheet in Inertial Microfluidics — •KUNTAL PATEL and HOLGER STARK — Institut für Theoretische Physik, Technische Universität Berlin, Berlin, Germany

Lab-on-a-chip devices based on inertial microfluidics function between Stokes and turbulent regimes, which enables to achieve high throughput. In the present work, we study the motion of a liquid sheet of thickness t_s and viscosity μ_1 in a two-dimensional microchannel of width w , filled with a viscous fluid (viscosity μ_2 , $m = \mu_2/\mu_1 > 1$). At finite Reynolds number Re , a small perturbation at the interfaces separating the sheet from the surrounding fluid can result in a rapid destabilization of interfaces and may lead to a break-up. The present work gives a proof-of-concept of how viscosity-driven interfacial instability can be exploited for a controlled droplet production in inertial microfluidics. Such microfluidic droplets are utilized in food and pharmaceutical related applications and as chemical reactors in Lab-on-a-chip devices.

In our computational linear stability analysis based on the Orr-Sommerfeld equation, we observe that the growth rate of the fastest growing mode ξ^* increases with Re . Furthermore, the dependence of ξ^* on m and t_s is quantified by the scaling law $\xi^* \propto mt_s^{2.5}$, which is valid for thin sheets in moderate Re flows with relatively weak interfacial tension Γ . In the second part, our lattice Boltzmann simulations starting from a single-mode perturbation of wavelength λ reveal that the interfacial instability causes the liquid sheet to break up and ultimately to form droplets when $\lambda \geq 0.5w$. We also identify different interface breakup mechanisms leading to droplet formation.

DY 4.4 Mon 10:45 H19

Imaging, Analysis and Sorting in Microfluidic Systems: Correlative Multi-Contrast, Multi-Parameter Applications — •TOBIAS NECKERNUSS¹, PATRICIA SCHWILLING², JONAS PFEIL^{1,2}, DANIEL GEIGER¹, and OTHMAR MARTI² — ¹Sensific GmbH — ²Institute for Experimental Physics, Ulm University

Droplet-based microfluidics is a promising approach in biology, pharmacy, medicine, and lab-on-a-chip applications. One remaining problem is the lack of a suitable fast image-based detection method that enables droplet- and content-based analysis and sorting with rates fast enough to be sufficient for high-throughput measurements and to enable surveilled lab scale production. We demonstrate recent advances for high-speed, real-time, image-based analysis and manipulation of microfluidic systems. With rates of up to 3000 particles or droplets per second we show applications of our system in the field of droplet-based microfluidics. Here, we concentrate on droplet-content analysis and have a sneak look at further potential applications in biology and image-based cell analysis. We introduce new contrast types for image-based analysis like brightfield, darkfield, phase contrast, fluorescence and combinations thereof. Combining new cutting edge hardware technology with specifically tailored software

and integration of external lab infrastructure enables us reach new dimensions in image based particle analysis and sorting.

15 min. break

DY 4.5 Mon 11:15 H19

the obstacle effect on soft sphere discharging in quasi-2D silo — •JING WANG¹, KIRSTEN HARTH^{1,2}, DMITRY PUZYREV¹, and RALF STANNARIUS¹ — ¹Institute of Physics, Otto von Guericke University Magdeburg, Universitätsplatz 2, D-39106 Magdeburg, Germany — ²Department of Engineering, Brandenburg University of Applied Sciences, Magdeburger Straße 50, D-14770 Brandenburg an der Havel, Germany

Soft smooth particles in silo discharge show their own characteristics, for example, non-permanent clogging and intermittent flow. We conduct experiment on soft, low-frictional hydrogel spheres compared with hard, frictional spheres in a quasi-2D silo. We introduce a competitive behavior of these spheres during their discharge by placing an obstacle in front of the outlet of the silo. High-speed optical imaging is applied to capture the process of discharge. By the method of particle tracking velocimetry (PTV), the fields of velocity, egress time, packing fraction, and kinetic stress are analysed in the study.

DY 4.6 Mon 11:30 H19

Coalescence of isotropic and nematic droplets in quasi 2D liquid crystal films — •CHRISTOPH KLOPP, ALEXEY EREMIN, and RALF STANNARIUS — Institute for Physics, Otto von Guericke University Magdeburg, Germany

Coalescence of droplets is ubiquitous in nature and modern technology. Various experimental and theoretical studies explored droplet dynamics in three dimensions (3D) and on two-dimensional (2D) solid or liquid substrates, e.g. [1-3]. Here, we demonstrate coalescence of isotropic and nematic droplets in quasi-2D liquids, viz. overheated smectic A freely suspended films. We investigated their dynamics experimentally and measured the shape deformation during the entire merging process using high-speed imaging and interferometry. This system is a unique example where the lubrication approximation can be directly applied, and the smectic membrane plays the role of a precursor film. Our studies reveal the scaling laws of the coalescence time depending on the droplet size and the material parameters. We also compared the dynamics of isotropic and nematic droplets and additionally analyzed the results based on an existing model for liquid lens coalescence on liquid and solid surfaces [4].

This study was supported by DLR and DFG within the OASIS and OASIS-Co projects WM2054 and STA 425/40.

[1] J. D. Paulsen et al., Nat. Commun., 5, 3182 (2014)

[2] D. G. A. L. Aarts et al., Phys. Rev. Lett., 95, 164503 (2005)

[3] N. S. Shuravin et al., Phys. Rev. E, 99, 062702 (2019)

[4] C. Klopp et al., Langmuir, 36, 10615 (2020)

DY 4.7 Mon 11:45 H19

Using feedback-controlled thermoviscous flows to precisely position microparticles — •ELENA ERBEN, ANTONIO MINOPOLI, NICOLA MAGHELLI, BENJAMIN SEELBINDER, ILIYA D. STOEVEV, SERGEI KLYKOV, and MORITZ KREYSING — Max Planck Institute of Molecular Cell Biology and Genetics, Dresden, Germany

Optical positioning of microscale objects has proven key for advancing fundamental biological research and holds great potential for other disciplines as well. The most widely used among these methods are optical tweezers which enable the precise control and manipulation of multiple particles. However, they require probes of high refractive index contrast and low absorption and exclude the use of photosensitive samples. Here we present a novel optofluidic technique that leverages optical-control capabilities and the gentle nature of hydrodynamic flows, thus lifting the aforementioned constraints. Our approach is based on optically-induced thermoviscous flows generated by the repeated scanning of a moderately heating infrared laser beam [1]. We have combined thermoviscous flows with feedback control to confine micron-sized particles with a precision of up to 24 nm without exposing them directly to laser light [2]. Recently, we extended this approach beyond single-object manipulation to further enable simultaneous control of multiple particles. With this contribution, we furthermore discuss combinations with implicit force sensing [3] and the potential for future application in and beyond the life science sector.

[1] Weinert et al., Phys. Rev. Lett., 2008; [2] Erben et al., Opt. Express, 2021;

[3] Stoevev et al., eLight, 2021.

DY 4.8 Mon 12:00 H19

Active thin films — •TILMAN RICHTER¹, PAOLO MALGARETTI¹, STEFAN ZITZ², and JENS HARTING¹ — ¹Forschungszentrum Jülich GmbH, Helmholtz Institute Erlangen-Nürnberg (IEK-11), Dynamics of Complex Fluids and Interfaces, Cauerstraße 1, 91058 Erlangen, Germany — ²Roskilde University, Department of Science and Environment, Roskilde, Denmark

Thin liquid films are important for many microfluidic applications such as printing or coating of e.g. printable electronics or photovoltaic cells where a evenly spread thin film of certain properties is of utmost importance. It is well known that a thin film on a solid substrate can be unstable and droplet formation may

rise, especially for very thin films. The dynamics of thin liquid films and their instability has been the subject of intensive experimental, analytical, and numerical studies, the latter often based on the thin film equation. We propose a set of newly developed equations for the influence of chemical active colloids suspended in a thin liquid film based on the lubrication approximation, advection-diffusion and, the Fick-Jackobs approximation. For this novel set of equations

we perform a linear stability analysis (LSA) that reveals surprisingly interesting dynamics. We identify the subset of parameters for which the thin film becomes stable, as well as a variety of different dominating wave-modes. This allows us to control not only the stability but also the droplet size distribution after film rupture. In order to assess the asymptotic state of the thin film, the LSA results are compared against numerical simulations using the Lattice Boltzmann method.

DY 5: Many-Body Quantum Dynamics 1 (joint session DY/TT)

Time: Monday 10:00–12:45

Location: H20

DY 5.1 Mon 10:00 H20

Squeezed-field path integral method for fermionic superfluid systems — •DAPENG LI — Luruper Chaussee 149, Gebäude 69 22761 Hamburg

We develop a squeezed field path integral method for fermionic superfluid systems including BCS superconductors and unconventional superfluid systems. In this method, the squeezing parameters of the Bogoliubov transformation for fermions become dynamical variables representing bosonic collective excitations on superfluid systems. Using this method, we analyze the spectral function of the single particle excitations for BCS superconductors. We demonstrate that, as a main consequence of the method, a bosonic branch corresponding to the Higgs mode appears as a sideband branch, in addition to the single particle excitation branches obtained from the BCS mean-field approximation. Moreover, we show that our framework can also be applied to low-energy excitations of systems with unconventional orders.

DY 5.2 Mon 10:15 H20

Suppression of inter-band heating for random driving — •HONGZHENG ZHAO^{1,2}, JOHANNES KNOLLE^{2,3,4}, RODERICH MOESSNER¹, and FLORIAN MINTERT² — ¹Max Planck Institute for the Physics of Complex Systems, Dresden, Germany — ²Imperial College London, London, United Kingdom — ³Technical University of Munich, Munich, Germany — ⁴Munich Center for Quantum Science and Technology, Munich, Germany

Heating to high-lying states strongly limits the experimental observation of driving induced non-equilibrium phenomena, particularly when the drive has a broad spectrum. Here we show that, for entire families of structured random drives known as random multipolar drives, particle excitation to higher bands can be well controlled even away from a high-frequency driving regime. This opens a window for observing drive-induced phenomena in a long-lived prethermal regime in the lowest band. Reference: arXiv:2201.08130

DY 5.3 Mon 10:30 H20

Anomalous hydrodynamics and exact quantum scars in frustration-free Hamiltonians — •JONAS RICHTER and ARIJEET PAL — University College London, UK

We study the interplay between quantum scarring and weak Hilbert-space fragmentation in a class of one-dimensional spin-1 frustration-free projector Hamiltonians, known as deformed Motzkin chain. We show that the particular form of the projectors causes the emergence of disjoint Krylov subspaces, with an exact quantum scar being embedded in each subspace, leading to slow growth of entanglement and localized dynamics for specific out-of-equilibrium initial states. Focusing on infinite temperature, we unveil that spin transport is subdiffusive, which we corroborate by simulations of constrained stochastic cellular automaton circuits. Compared to dipole moment conserving systems, the deformed Motzkin chain belongs to a different universality class with distinct dynamical transport exponent and only polynomially many Krylov subspaces. Based on J. Richter and A. Pal, Phys. Rev. Research 4, L012003 (2022).

DY 5.4 Mon 10:45 H20

Influence functional of quantum many-body systems — •ALESSIO LEROSE, MICHAEL SONNER, JULIAN THOENISS, and DMITRY ABANIN — University of Geneva, Switzerland

Feynman-Vernon influence functional (IF) was originally introduced to describe the effect of a quantum environment on the dynamics of an open quantum system. We apply the IF approach to describe quantum many-body dynamics in isolated spin systems, viewing the system as an environment for its local subsystems. While the IF can be computed exactly only in certain many-body models, it generally satisfies a self-consistency equation, provided the system, or an ensemble of systems, are translationally invariant. We view the IF as a fictitious wavefunction in the temporal domain, and approximate it using matrix-product states (MPS). This approach is efficient provided the temporal entanglement of the IF is sufficiently low. We illustrate the versatility of the IF approach by analyzing several models that exhibit a range of dynamical behaviors, from thermalizing to many-body localized, in both Floquet and Hamiltonian settings. The IF approach offers a new lens on many-body non-equilibrium phenomena, both in ergodic and non-ergodic regimes, connecting the theory of open quantum systems theory to quantum statistical physics.

DY 5.5 Mon 11:00 H20

Transition from localized to uniform scrambling in locally hyperbolic systems — •MATHIAS STEINHUBER, JUAN-DIEGO URBINA, and KLAUS RICHTER — University of Regensburg, Regensburg, Germany

A major signature of Quantum Chaos is the fast scrambling of quantum correlations, quantified by the exponential initial (pre-Ehrenfest time) growth of out-of-time-order correlators (OTOCs) and by their later saturation. As previously shown by [1] and [2], there is a significant difference in the short time dynamics of the OTOCs in integrable systems around hyperbolic fixed points depending on the initial state being localized or uniform (high-temperature). In these cases, the exponential regime is given respectively by twice the instability-exponent 2λ or only once the stability-exponent λ of the hyperbolic fixed point. We show that a local wave-packet can have a clear dynamical transition between these two reported exponential-regions within the pre-Ehrenfest-time regime. Thus, the question arises on how to decide, based on the properties of the hyperbolic fixed point which of the two scenarios applies in each particular situation.

[1] Hummel, Q., Geiger, B., Urbina, J. D. & Richter, K. Reversible Quantum Information Spreading in Many-Body Systems near Criticality. Phys. Rev. Lett. 123, 160401 (2019).

[2] Xu, T., Scaffidi, T. & Cao, X. Does Scrambling Equal Chaos? Phys. Rev. Lett. 124, 140602 (2020).

15 min. break

DY 5.6 Mon 11:30 H20

Optimal route to quantum chaos in the Bose-Hubbard model — LUKAS PAUSCH^{1,2}, EDOARDO CARNIO^{1,2}, ANDREAS BUCHLEITNER^{1,2}, and •ALBERTO RODRÍGUEZ³ — ¹Physikalisches Institut, Albert-Ludwigs-Universität Freiburg, Hermann-Herder-Straße 3, D-79104, Freiburg, Germany — ²EUCOR Centre for Quantum Science and Quantum Computing, Albert-Ludwigs-Universität Freiburg, Hermann-Herder-Straße 3, D-79104, Freiburg, Germany — ³Departamento de Física Fundamental, Universidad de Salamanca, E-37008 Salamanca, Spain

The dependence of the chaotic phase of the Bose-Hubbard Hamiltonian [1,2] on particle number N , system size L and particle density is investigated in terms of spectral and eigenstate features. We analyze the development of the chaotic phase as the limit of infinite Hilbert space dimension is approached along different directions, and show that the fastest route to chaos is the path at fixed density $n \leq 1$ [3]. The limit $N \rightarrow \infty$ at constant L leads to a slower convergence of the chaotic phase towards the random matrix theory benchmarks. In this case, from the distribution of the eigenstate generalized fractal dimensions, the ergodic phase becomes more distinguishable from random matrix theory for larger N , in a similar way as along trajectories at fixed density.

[1] L. Pausch *et al.*, Phys. Rev. Lett. 126, 150601 (2021)

[2] L. Pausch *et al.*, New J. Phys. 23, 123036 (2021)

[3] L. Pausch *et al.*, arxiv:2205.04209

DY 5.7 Mon 11:45 H20

Observation of phase synchronization and alignment during free induction decay of quantum spins with Heisenberg interactions — •JÜRGEN SCHNACK¹, HEINZ-JÜRGEN SCHMIDT², CHRISTIAN SCHRÖDER³, and PATRICK VORNDAMME¹ — ¹Universität Bielefeld — ²Universität Osnabrück — ³Fachhochschule Bielefeld

Equilibration of observables in closed quantum systems that are described by a unitary time evolution is a meanwhile well-established phenomenon apart from a few equally well-established exceptions. Here we report the surprising theoretical observation that integrable as well as non-integrable spin rings with nearest-neighbor or long-range isotropic Heisenberg interaction not only equilibrate but moreover also synchronize the directions of the expectation values of the individual spins (New J. Phys. 23 (2021) 083038). We highlight that this differs from spontaneous synchronization in quantum dissipative systems. In our numerical simulations, we investigate the free induction decay (FID) of an ensemble of up to $N = 25$ quantum spins with $s = 1/2$ each by solving the time-dependent Schrödinger equation numerically exactly. Our findings are related to, but not fully explained by conservation laws of the system. The phenomenon very robust

against for instance random fluctuations of the Heisenberg couplings. Synchronization is not observed with strong enough symmetry-breaking interactions such as the dipolar interaction and is also not observed in closed-system classical spin dynamics.

DY 5.8 Mon 12:00 H20

Long-lived coherence in driven spin systems: from two to infinite spatial dimensions — •WALTER HAHN^{1,2,3} and VIATCHESLAV DOBROVITSKI^{2,4} — ¹Fraunhofer IAF, Fraunhofer Institute for Applied Solid State Physics, Freiburg, Germany — ²QuTech, Delft University of Technology, Lorentzweg 1, 2628 CJ Delft, The Netherlands — ³Institute for Quantum Optics and Quantum Information of the Austrian Academy of Sciences, Innsbruck, Austria — ⁴Kavli Institute of Nanoscience, Delft University of Technology, Lorentzweg 1, 2628 CJ Delft, The Netherlands

Long-lived coherences, emerging under periodic pulse driving in the disordered ensembles of strongly interacting spins, offer immense advantages for future quantum technologies but the physical origin and the key properties of this phenomenon remain poorly understood. We theoretically investigate this effect in ensembles of different spatial dimensionality, and predict existence of the long-lived coherences in all such systems, from two-dimensional to infinite-dimensional, which are of particular importance for quantum sensing and quantum information processing. We explore the transition from two to infinite dimensions and show that the long-time coherence dynamics in all dimensionalities is qualitatively similar, although the short-time behavior is drastically different exhibiting dimensionality-dependent singularity

DY 5.9 Mon 12:15 H20

A Flow Equation Approach to Many-Body Localisation — •STEVEN THOMSON — Dahlem Centre for Complex Quantum Systems, Freie Universität Berlin

Many-body localisation is a fascinating example of a scenario in which interacting quantum systems isolated from their environments can fail to thermalise, usually due to some form of disorder. Key to our understanding of this enigmatic phase of matter are emergent conserved quantities known as local integrals of motion (LIOMs, or I-bits), which prevent thermalisation from occurring. In

this talk, I will present a powerful new numerical method known as the tensor flow equation technique ideally suited for computing LIOMs.

I will demonstrate how this method can be used to compute the integrals of motion in a variety of different systems, including disorder-free potentials and models of spinful fermions. I will show how this method gives an insight into the nature of many-body localisation in these different models, with LIOMs that retain a strong 'fingerprint' of the underlying potential, and will show that in some cases the method can also predict the onset of a delocalised phase. I will end by outlining promising future applications of the method, including to periodically driven and dissipative systems.

DY 5.10 Mon 12:30 H20

Towards a dictionary between JT gravity and periodic orbit theory — •TORSTEN WEBER, FABIAN HANEDER, JUAN-DIEGO URBINA, and KLAUS RICHTER — University of Regensburg, Germany

Periodic orbit theory is a far reaching development of the semiclassical methods where the most fundamental signatures of the quantum nature of closed systems, like the discreteness of their energy spectrum, emerges from interference between amplitudes constructed from the classical properties of periodic solutions [1]. This conceptual basis, leading to the celebrated Gutzwiller trace formula, has provided impressive achievements from quantum transport to atomic physics and multi-particle scattering. In particular, together with the necessary existence of periodic orbit bunching in ergodic systems, it has led to an understanding of the emergence of universal spectral correlations in chaotic systems, the BGS conjecture [2].

We report our progress in studying how a loss of information (characterized by a coarse graining of classical bunches of orbits) at the level of the trace formula implies the emergence of genus-like expansions with formally the same structure as the solution of JT quantum gravity found in [3]. Our work thus gives convincing hints toward a possible dictionary between quantum-gravitational and periodic orbit objects and concepts.

[1] See e.g. F. Haake, *Quantum Signatures of Chaos*, Springer, 2000

[2] S. Müller et al., *Phys. Rev. E* 72, 046207 (2005)

[3] P. Saad, S. Shenker, D. Stanford, arXiv:1903.11115

DY 6: Active Matter 1 (joint session BP/PP/DY)

Time: Monday 10:30–12:45

Location: H16

See BP 4 for details of this session.

DY 7: Statistical Physics of Biological Systems 1 (joint session BP/DY)

Time: Monday 15:00–17:15

Location: H16

See BP 6 for details of this session.

DY 8: Data Analytics for Complex Systems (joint session DY/SOE)

Time: Monday 15:00–17:45

Location: H18

DY 8.1 Mon 15:00 H18

Estimating covariant Lyapunov vectors from data — •NAHAL SHARAFI, CHRISTOPH MARTIN und SARAH HALLERBERG — Hamburg University of Applied Sciences, Hamburg, Germany

Covariant Lyapunov vectors characterize the directions along which perturbations in dynamical systems grow. They have also been studied as predictors of critical transitions and extreme events. For many applications, it is necessary to estimate these vectors from data since model equations are unknown for many interesting phenomena. We propose a novel approach for estimating covariant Lyapunov vectors based on data records without knowing the underlying equations of the system. In contrast to previous approaches, our approach can be applied to high-dimensional datasets. We demonstrate that this purely data-driven approach can accurately estimate covariant Lyapunov vectors from data records generated by low and high-dimensional dynamical systems. Additionally we test for the robustness against noise in a low-dimensional dynamical system.

DY 8.2 Mon 15:15 H18

Extending the limits of Electrochemical Impedance Spectroscopy with Machine Learning and Digital Twins — •LIMEI JIN^{1,2}, FRANZ P. BERECK², CHRISTIAN H. BARTSCH², JOSEF GRANWEHR², RÜDIGER-A. EICHEL², KARSTEN REUTER¹, and CHRISTOPH SCHEURER¹ — ¹Fritz-Haber-Institut der MPG, Berlin, Germany — ²IEK-9, Forschungszentrum Jülich, Jülich, Germany

Electrochemical impedance spectroscopy (EIS) is widely used to characterize electrochemical energy conversion systems. The traditional analysis with equiv-

alent circuit models (ECM) has recently been augmented by a transform based distribution of relaxation times (DRT) analysis which allows one to reduce the ambiguity in the construction of ECMs and thus overfitting. Yet, DRT, just like most traditional analyses, is firmly based in the linear response regime as well as based on frequency sweeps on a logarithmic scale. The latter makes these approaches time-consuming, the first limits their scope severely. To develop novel experimental spectroscopic excitation schemes that address these limitations, a model space of sufficiently realistic systems is required that substitutes for time-consuming measurements in terms of a digital twin. We present a joint experimental and theoretical approach for the construction of such a target space for the case of battery cell performance and ageing behaviour.

DY 8.3 Mon 15:30 H18

Bayesian approach to anticipate critical transitions in complex systems — •MARTIN HESSLER^{1,2} and OLIVER KAMPS² — ¹Westfälische Wilhelms-Universität Münster, 48149 Münster — ²Center for Nonlinear Science, Westfälische Wilhelms-Universität Münster, 48149 Münster

Complex systems in nature, technology and society can undergo sudden transitions between system states with very different behaviour. In order to avoid undesired consequences of these tipping events, statistical measures as variance, autocorrelation, skewness and kurtosis have been proposed as leading indicators based on time series analysis. Under favourable conditions they can give a hint of an ongoing bifurcation-induced destabilization process. However, they suffer from their loose connection to complex system dynamics, sensitivity to noise

and sometimes misleading trends. Therefore, we want to present an alternative approach assuming the dynamical system being described by a Langevin equation. Starting from this stochastic description, we combine MCMC sampling, rolling window methods and Bayesian reasoning to derive the drift slope as an alternative early warning sign. The Bayesian approach enables us to define credibility bands which make it easier to distinguish random fluctuations from real trends that imply a less resilient system. Our investigations suggest that the estimation procedure is rather robust even under strong noise. Besides, the noise level of the system is computed to get insights into the probability of a noise induced transition. We want to present some of the results and discuss possible limitations and tasks of future research.

DY 8.4 Mon 15:45 H18

Stochastic Interpolation of Sparsely Sampled Time Series by a Superstatistical Random Process and its Synthesis in Fourier and Wavelet Space — •JEREMIAH LÜBKE¹, JAN FRIEDRICH², and RAINER GRAUER¹ — ¹Institute for Theoretical Physics I, Ruhr-University Bochum, Universitätsstr. 150, 44801 Bochum, Germany — ²ForWind, Institute of Physics, University of Oldenburg, K pkersweg 70, 26129 Oldenburg, Germany

A novel method is presented for stochastic interpolation of a sparsely sampled time signal based on a superstatistical random process generated from a Gaussian scale mixture. In comparison to other stochastic interpolation methods such as kriging, this method possesses strong non-Gaussian properties and is thus applicable to a broad range of real-world time series. A precise sampling algorithm is provided in terms of a mixing procedure that consists of generating a field $u(\xi, t)$, where each component $u_\xi(t)$ is synthesized with identical underlying noise but covariance $C_\xi(t, s)$ parameterized by a log-normally distributed parameter ξ . Due to the Gaussianity of each component $u_\xi(t)$, standard sampling algorithms and methods to constrain the process on the sparse measurement points can be exploited. The scale mixture $u(t)$ is then obtained by assigning each point in time t a $\xi(t)$ and therefore a specific value from $u(\xi, t)$, where $\log \xi(t)$ is itself a realization of a Gaussian process with a correlation time large compared to the correlation time of $u(\xi, t)$. Finally, a wavelet-based hierarchical representation of the interpolating paths is introduced, which is shown to provide an adequate method to locally interpolate large datasets.

DY 8.5 Mon 16:00 H18

Global sensitivity analysis of Monte Carlo models using Cramer-von Mises distance — •SINA DORTAJ^{1,2} and SEBASTIAN MATERA^{1,2} — ¹Fritz-Haber-Institut der Max-Planck-Gesellschaft, Faradayweg 4-6, 14195 Berlin, Germany — ²Institute for Mathematics, Freie Universit t Berlin, Arnimallee 6, 14195 Berlin, Germany

Typically, the parameters entering a physical simulation model carry some kind of uncertainty, e.g. due to the intrinsic approximations in a higher fidelity theory from which they have been obtained. Global sensitivity analysis (GSA) targets quantifying which parameters uncertainties impact the accuracy of the simulation results, e.g. to identify which parameters need to be determined more accurately.

We present a GSA approach on basis of the Cramers-von Mises distance. Unlike prevalent approaches it combines the following properties: i) it is equally suited for deterministic as well as stochastic model outputs, ii) it is free of gradients, and iii) it can be estimated from any suitable numerical quadrature (NQ) without further numerical tricks. Using Quasi-Monte Carlo for NQ and prototypical first-principles kinetic Monte Carlo models (kMC), we examine the performance of the approach. We find that the approach typically converges in a modest number of NQ points. Furthermore, it is robust against even extreme relative noise. All these properties make the method particularly suited for expensive (kinetic) Monte Carlo models, because we can reduce the number of simulations as well as the target variance of each of these.

15 min. break

DY 8.6 Mon 16:30 H18

Reproducible and transparent research software pipelines using semantic research data management and common workflow language — •ALEXANDER SCHLEMMER^{1,2,5}, INGA KOTTLARZ^{1,3}, BALTASAR R CHARDT^{1,5}, ULRICH PARLITZ^{1,3,5}, and STEFAN LUTHER^{1,4,5} — ¹Max Planck Institute for Dynamics and Self-Organization, G ttingen — ²IndiScale GmbH, G ttingen — ³Institute for the Dynamics of Complex Systems, Georg-August-Universit t G ttingen — ⁴Institute of Pharmacology and Toxicology, University Medical Center G ttingen — ⁵German Center for Cardiovascular Research (DZHK), Partner Site G ttingen

Sustainable and well-documented scientific software is essential for effectiveness and reproducibility in data-intensive research. In practice, incompletely documented software hinders in many cases replicability, reproducibility and method comparison. In our terminology, documentation includes method and algorithm descriptions as well as human- and machine-readable representations of parameters, initial conditions and data, versions and dependencies and a well-defined software execution environment. We present an approach combining

semantic data management with CaosDB and processing pipelines with Common Workflow Language (CWL), showing use cases from dynamical systems research. The CWL-based environment provides a transparent description of the process and includes metadata that can be searched within CaosDB. Input/output-data and parameters can be directly linked to algorithms and software snapshots. The employment of containers simplifies reproducibility and interoperability.

DY 8.7 Mon 16:45 H18

MDSuite: A post-processing engine for particle simulations — •FABIAN ZILLS¹, SAMUEL TOVEY¹, FRANCISCO TORRES-HERRADOR², CHRISTOPH LOHRMANN¹, and CHRISTIAN HOLM¹ — ¹Institute for Computational Physics, University of Stuttgart, Stuttgart, Germany — ²von Karman Institute for Fluid Dynamics, Rhode-St-Genese, Belgium

Particle-based simulations are experiencing a rapid growth wherein system sizes in the hundreds of thousands or even millions are becoming commonplace. With this growth in system size comes the additional challenge of post-processing the simulation data.

In this talk, we introduce the Python package MDSuite. MDSuite is designed for the post-processing of particle-based simulation in an efficient manner and on modern hardware. Built on top of TensorFlow, MDSuite calculators are fully parallelised, gpu-enabled, and, due to the use of modern data pipe-lining methods, completely memory safe. Furthermore, the use of HDF5 and SQL database structures enables effective tracking of calculation parameters as well as a compressed trajectory storage medium. We present MDSuite as a standalone package for the storage, analysis, and comparison of large-scale simulation studies.

DY 8.8 Mon 17:00 H18

Distinguishing noise from high-dimensional chaos — •INGA KOTTLARZ^{1,2} and ULRICH PARLITZ^{1,2} — ¹Max Planck Institute for Dynamics and Self-Organization, G ttingen, Germany — ²Institute for Dynamics of Complex Systems, Georg-August-Universit t G ttingen, G ttingen, Germany

The ordinal pattern-based Complexity-Entropy Plane is a popular tool in non-linear dynamics for distinguishing noise from chaos. While successful attempts to do so have been documented for low-dimensional maps and continuous-time systems, high-dimensional systems have been somewhat neglected so far. To address the question in which way time series from highdimensional chaotic attractors can be characterized by their location in the Complexity-Entropy Plane we analyze data from the high-dimensional continuous-time Lorenz-96 system, the discrete generalized H non map and the Mackey-Glass equation as a delay system and discuss the crucial role of the lag and the pattern length or the ordinal pattern, and the length of the available time series.

DY 8.9 Mon 17:15 H18

The impact of the UEFA European Football Championship on the spread of COVID-19 — •JONAS DEHNING¹, SEBASTIAN B. MOHR¹, SEBASTIAN CONTRERAS¹, PHILIPP D NGES¹, EMIL IFTEKHAR¹, OLIVER SCHULZ², PHILIP BECHTLE³, and VIOLA PRIESEMAN^{1,4} — ¹MPI for Dynamics and Self-Organization, 37077 G ttingen — ²MPI for Physics, 80805 M nchen — ³Physikalisches Institut, University of Bonn — ⁴Institute for the Dynamics of Complex Systems, University of G ttingen

Large-scale international events like the UEFA Euro 2020 football championship offer a unique opportunity to quantify the impact of match-related social gatherings on COVID-19, as the number of matches played by participating countries resembles a randomized trial. Moreover, soccer-related activities have a marked gender-imbalance that we can exploit for inference. In our work, we build a differentiable Bayesian SEIR-like model. Its parameters are inferred with Hamiltonian Monte-Carlo using the PyMC3 package. Our model simulates COVID-19 spread in each country using a discrete renewal process and gender-resolved case numbers. On average, 3.2% (95% CI: [1.3%, 5.2%]) of new cases in the 12 analyzed countries can be associated with the match-related social gatherings throughout our analysis period. Individually, England, the Czech Republic and Scotland showed a significant effect. Besides these insights on the spread of COVID-19 during large-scale events, our approach is an example of how modern Bayesian tools can be leveraged to gain insights on a complex dynamic process.

DY 8.10 Mon 17:30 H18

Recurrence-based analysis of instantaneous fractal characteristics of geomagnetic variability — •REIK V. DONNER^{1,2}, TOMMASO ALBERTI³, and DAVIDE FARANDA⁴ — ¹Hochschule Magdeburg-Stendal, Magdeburg, Germany — ²Potsdam Institute for Climate Impact Research, Potsdam, Germany — ³National Institute for Astrophysics, Rome, Italy — ⁴LSCE, Universit  Paris-Saclay, Gif-sur-Yvette, France

We employ two complementary approaches based on the concept of recurrences in phase space to quantify the local (instantaneous) and global fractal dimensions of the temporal variations of a suite of low (SYM-H, ASY-H) and high latitude (AE, AL, AU) geomagnetic indices and discuss similarities and dissimilarities of the obtained patterns for one year of observations during a solar activity maximum. Subsequently, we introduce bivariate extensions of both approaches,

and demonstrate their capability of tracing different levels of interdependency between low and high latitude geomagnetic variability during periods of magnetospheric quiescence and along with perturbations associated with geomagnetic storms and magnetospheric substorms, respectively. Our results open new

perspectives on the nonlinear dynamics and intermittent mutual entanglement of different parts of the geospace electromagnetic environment, including the equatorial and westward auroral electrojets, in dependence of the overall state of the geospace system affected by temporary variations of the solar wind forcing.

DY 9: Invited Talk Ralf Stannarius

Time: Monday 15:00–15:30

Location: H19

Invited Talk

DY 9.1 Mon 15:00 H19

Granular matter composed of non-convex grains — •RALF STANNARIUS — Otto-von-Guericke-Universität Magdeburg

The majority of granular matter studies so far has been devoted to hard, spherical grains. Recently, efforts have been increasingly focused on the investigation of shape-anisotropic and soft particle systems. We report experimental inves-

tigations of granular matter composed of non-convex particles. The random packing and orientational short-range order of flat crosses is studied in a two-dimensional geometry, and the influence of the aspect ratio (arm length divided by arm length) is analyzed. With spatial crosses (hexapods), we perform shear experiments and report an unexpected phenomenon in split-bottom containers, a 'reversed Weissenberg effect' of granular matter. Secondary flow leads to convection rolls normal to the shear direction.

DY 10: Modeling and Simulation of Soft Matter (joint session CPP/DY)

Time: Monday 15:00–17:45

Location: H39

See CPP 9 for details of this session.

DY 11: Granular Matter and Contact Dynamics

Time: Monday 15:30–18:00

Location: H19

DY 11.1 Mon 15:30 H19

Measuring the coarsening dynamics of ferromagnetic granular networks under impact of a vertical magnetic field — MATTHIAS BIRSACK¹, OKSANA BILOUS², PEDRO SANCHEZ², SOFIA KANTOROVICH², and •REINHARD RICHTER¹ — ¹University of Bayreuth, Experimental Physics V, 95447 Bayreuth, Germany — ²Computational Physics, University of Vienna, 1090 Vienna, Austria

We are exploring in experiments the aggregation process in a shaken granular mixture of glass and magnetized steel beads, occurring in a horizontal vessel after the shaking amplitude is suddenly decreased. Then the magnetized beads form a transient network that coarsens in time into compact clusters, following a viscoelastic phase separation [1]. A homogeneous magnetic field oriented parallel to the system plane has been observed to "unknot" network structures orthogonal to the field [2]. Here we focus on the impact of a homogeneous magnetic field oriented in vertical direction. For certain field amplitudes we observe a three-phase state, namely mobile glass beads, a grid of isolated steel beads and the coarsening network. Our results demonstrate that via dipole-dipole repulsion the field reduces the mobility of isolated steel beads, thus hindering the growth of the networks. The experimental results are compared with those of numerical simulations.

[1] A. Kögel, et al. *Soft Matter*, 14 (2018) 1001.

[2] P. A. Sánchez, J. Miller, S. S. Kantorovich, R. Richter, *J. Magn. Magn. Mater.*, 499 (2019) 166182.

DY 11.2 Mon 15:45 H19

Dynamic light scattering from single macroscopic particles — •PHILIP BORN and LISA DOSSOW — Institut für Materialphysik im Weltraum, Deutsches Zentrum für Luft- und Raumfahrt (DLR), 51170 Köln, Germany

Here we present a methodology to extract information from the light intensity fluctuations that arise from motion of single granular particles. We first describe the experimental setup for dynamic light scattering measurements and the associated theoretical framework required to isolate contributions from the translational motion and from the rotational motion to the intensity autocorrelation function [1]. We subsequently present an approach to extract the angular velocity and the translational speed of the granular particles from the intensity autocorrelation. The approach is applied to a small ensemble of granular particles in an hour-glass-like experiment to determine the granular temperature with a dynamic light scattering measurement. The results indicate the next steps to be taken to eventually develop a thermometer for fluidized granular media based on dynamic light scattering.

[1] L. Dossow, R. Kessler, M. Sperl & P. Born, *Dynamic light scattering from single macroscopic particles*. *Applied Optics*, 60(32), 10160-10167 (2021).

DY 11.3 Mon 16:00 H19

Structural Analysis of Disordered Dimer Packings — •ESMA KURBAN and ADRIAN BAULE — School of Mathematical Sciences, Queen Mary University of London, Mile End Road, London E1 4NS, UK

Jammed disordered packings of non-spherical particles show significant variation in the packing density as a function of particle shape for a given packing

protocol. Rotationally symmetric elongated shapes such as ellipsoids, spherocylinders, and dimers, e.g., pack significantly denser than spheres over a narrow range of aspect ratios, exhibiting a characteristic peak at aspect ratios of $\alpha_{\max} \approx 1.4 - 1.5$. However, the structural features that underlie this non-monotonic behaviour in the packing density are unknown. Here, we study disordered packings of frictionless dimers in three dimensions generated by a gravitational pouring protocol in LAMMPS. Focusing on the characteristics of contacts as well as orientational and translational order metrics, we identify a number of structural features that accompany the formation of maximally dense packings as the dimer aspect ratio α is varied from the spherical limit. Our results highlight that dimer packings undergo significant structural changes as α increases up to α_{\max} manifest in the reorganisation of the contact configurations between neighbouring dimers, increasing nematic order, and decreasing local translational order. Remarkably, for $\alpha > \alpha_{\max}$ our metrics remain largely unchanged, indicating that the peak in the packing density is related to the interplay of structural rearrangements for $\alpha < \alpha_{\max}$ and subsequent excluded volume effects with unchanged structure for $\alpha > \alpha_{\max}$.

15 min. break

DY 11.4 Mon 16:30 H19

The role of the particle aspect ratio in the discharge of a narrow silo — •BO FAN^{2,4}, TIVADAR PONGÓ^{1,2}, DARIEL HERNÁNDEZ-DELFIN^{1,5}, JÁNOS TÖRÖK³, RALF STANNARIUS⁶, RAÚL CRUZ-HIDALGO¹, and TAMÁS BÖRZSÖNYI² — ¹Universidad de Navarra, Pamplona, Spain — ²Wigner Research Centre for Physics, Budapest, Hungary — ³Budapest University of Technology and Economics, Budapest, Hungary — ⁴Wageningen University, Wageningen, The Netherlands — ⁵Basque Center for Applied Mathematics, Bilbao, Spain — ⁶Otto von Guericke University, Magdeburg, Germany

The time evolution of silo discharge is investigated for different granular materials made of spherical or elongated grains in laboratory experiments and with discrete element model (DEM) calculations. For spherical grains, we confirm the widely known typical behavior with constant discharge rate (except for initial and final transients). For elongated particles with aspect ratios between $2 < L/d < 6.1$, we find a peculiar flow rate increase for larger orifices, especially in the last third of the discharge process. While the flow field is practically homogeneous for spherical grains, it has strong gradients for elongated particles with a fast-flowing region in the middle of the silo surrounded by a stagnant zone. For large enough orifice sizes, the flow rate increase is connected to a gradual change in the character of the flow field, including a shrinkage of the stagnant zone and an increase in both the packing fraction and flow velocity near the silo outlet.

DY 11.5 Mon 16:45 H19

Excitation of Platonic bodies on a vibrating plate analyzed with smart IMUs — •TORSTEN TRITTEL, DMITRY PUZYREV, NIKLAS DIECKMANN, and RALF STANNARIUS — Otto-von-Guericke Universität Magdeburg

For the investigation of granular gases, i.e. large ensembles of macroscopic particles that interact via frequent mutual collisions, an initial or permanent exci-

tation of the ensembles is prerequisite. Typically, this excitation is realized by one or more vibrating plates (container walls). We investigate such a mechanical excitation of different Platonic bodies, e.g. icosahedra and cubes, and compare their dynamics with that of spherical particles. In earlier experiments with mechanically excited rods [1], the dynamic data were extracted from a huge amount of stereoscopic video data. This procedure is very complicated and time consuming. To overcome this problem, we equipped our particles with small IMUs (inertial measurement units) that are typically used for motion tracking [2]. From acceleration and rotation data, it is straightforward to calculate the rotational and translational energies of each jump. We present distributions of the energies on individual degrees of freedom and determine the efficiency of the excitation depending on vibration parameters. Finally, we compare the experimental findings with results obtained from numerical simulations.

[1] T. Trittel et al., Mechanical excitation of rodlike particles by a vibrating plate, *Phys. Rev. E* 95, 062904, (2017)

[2] M. Zenker, Dynamik platonischer Körper bei mechanischer Anregung, BA, Magdeburg (2021)

DY 11.6 Mon 17:00 H19

Rare Fluctuations in Sheared 2D LJ Fluids — •DANIEL DERNBACH and JÜRGEN VOLLMER — Institut für Theoretische Physik, Universität Leipzig, Brüderstr. 16, D-04103 Leipzig, Germany

A distinguishing feature of sheared particulate flows are very large fluctuations in the dissipation, i.e. the product of the local velocity gradient and the local shear stress. At times, it even takes negative values (rare fluctuations). Surprisingly, the probability of rare fluctuations vanishes close to jamming [1], a far-from-equilibrium critical point where fluctuations are expected to be large.

Here, we compare this setting to the motion of classical fluids with attractive, elastic interactions. Specifically, we consider the transition from fluid to plastic flow in a two-dimensional (2D) Lennard-Jones (LJ) fluid subjected to a Nosé-Hoover thermostat.

Close to its critical rigidity transition this time-reversible sheared dynamics also features a drop of the probability of rare fluctuations. We will scrutinize the analogies and differences between the emergence of rare fluctuations in irreversible particulate flow and in time-reversible classical dynamics.

[1] Rahbari, Saberi, Park, Vollmer, *Nat. Commun.* 8, 11 (2017)

DY 11.7 Mon 17:15 H19

Granular Gases of Mixtures of Rods in Microgravity — •KIRSTEN HARTH^{1,2}, DMITRY PUZYREV³, TORSTEN TRITTEL³, and RALF STANNARIUS³ — ¹Fachbereich Technik, TH Brandenburg, Brandenburg an der Havel, Deutschland — ²MARS und MRTM, Otto von Guericke Universität Magdeburg, Deutschland — ³Institut für Physik und MARS, Otto von Guericke Universität Magdeburg, Deutschland

Granular gases consist of macroscopic particles in erratic motion, rarely colliding among each other. They are a comparatively simple, yet illustrative example of a non-equilibrium dynamical system. Numerous theoretical and numerical studies deal with their dynamics, however, the realization of 3D experiments is rare. It usually requires microgravity. Typical experiments are either performed under continuous external energy supply or they consider the process of collective kinetic energy decay by dissipation (granular cooling). It has been recently

shown that both ensembles of rods and spheres follow the scaling predicted by Haff in 1983, however, with stark quantitative disagreement with the theory.

Here, we consider a bidisperse ensemble of 2 types of rods in a cuboid container. We track their positions and rotations in 3D. Experimental data will be compared to validated numerical simulations of frictional rods under similar conditions. We extract kinetic energies in individual degrees of freedom and other statistical quantities.

DY 11.8 Mon 17:30 H19

Pauling Structures in tribocharged Granular Media — JAN HAEBERLE, MATTHIAS SPERL, and •PHILIP BORN — Institut für Materialphysik im Weltraum, Deutsches Zentrum für Luft- und Raumfahrt (DLR), Köln, Germany

Crystal-like arrangements of granular particles had been studied in the past for their mechanical properties or as a model system to study structure formation of non-equilibrium systems. These studies were limited to the formation of either hcp or fcc densest arrangements of monodisperse spheres. However, in most situations the hard core and the frictional contacts of the granular particles stabilize less dense disordered packings. Here we show that binary packings of granular particles with strong tribocharging spontaneously take BCC-like packing structures under suitable conditions [1]. We use a version of the bond-order parameter which is robust against noise to identify crystalline structures x-ray tomography reconstructions [2]. The observed BCC-like packing structures formed in incommensurate containers are, to large extent, in agreement with the prediction of Pauling's rules for ionic crystals, i.e. equilibrium structures of thermal ions.

[1] J. Haeberle, J. Harju, M. Sperl and P. Born, "Granular ionic crystals in a small nutshell", *Soft Matter* 15, 7179-7186 (2019).

[2] J. Haeberle, M. Sperl and P. Born, "Distinguishing noisy crystalline structures using bond orientational order parameters", *EPJ E* 42, 1-7 (2019).

DY 11.9 Mon 17:45 H19

Visualization of flow dynamics for Poly-dispersed dense granular suspension in various sections of pipe — •HIMANSHU P PATEL and GÜNTER K AUERNHAMMER — Leibniz-Institut für Polymerforschung Dresden e. V., Germany

The study of flow dynamics in non-Newtonian media with polydispersed dense granular suspension, e.g., slurry, mud, concrete, still lacks quantification on the flow parameters linked to shear induced particle migration and insight about flow at center and at wall in closed pipes.

We developed transparent granular system that is a granular suspension of particles suspended in non-Newtonian media (particle volume fractions of 30% to 48%) [1]. The non-Newtonian granular system has yield stress and plastic viscosity and is well index matched. The rheological characteristics of the model system is tunable through its composition of additives.

We analyze gravity-assisted continuous flow of millimetric sized particles. We perform tracking of flow at different sections of pipe. The flow analysis reveals understanding on the relaxation of such flow and the development of velocity profile within the length of pipe, we observe this using camera at entry and exit of pipe and later a 3D setup to observe flow at near end of pipe. This gives quantitative values into the particle migration to understand the effect of polydispersity and particle flow.

[1] Auernhammer, Günter K., et al., *Materials & Design* (2020):108673

DY 12: Focus Session: Nonlinear Dynamics of Nanomechanical Oscillators

Time: Monday 15:30–17:45

Location: H20

Invited Talk

DY 12.1 Mon 15:30 H20

A phonic frequency comb from a single resonantly driven nanomechanical mode — •EVA WEIG — Department of Electrical and Computer Engineering, Technical University of Munich

Doubly-clamped nanostring resonators excel as high Q nanomechanical systems enabling room temperature quality factors of several 100,000 in the 10 MHz eigenfrequency range. Dielectric transduction via electrically induced gradient fields provides an integrated control scheme while retaining the large mechanical quality factor. Dielectrically controlled nanostrings are an ideal testbed to explore a variety of dynamical phenomena ranging from multimode coupling to coherent control. Here I will focus on the nonlinear dynamics of a single, resonantly driven mode. The broken time reversal symmetry gives rise to the squeezing of the string's fluctuations. As a result of the high mechanical Q factor, the squeezing ratio is directly accessible from a spectral measurement. It is encoded in the intensities of the two spectral peaks arising from the slow dynamics of the system in the rotating frame. For stronger driving, an onset of self-sustained oscillation is observed which leads to the generation of a nanomechanical frequency comb. The effect is a consequence of a resonantly induced negative effective friction force induced by the drive. This is the first observation of a frequency comb arising solely from a single mode and a single, resonant drive tone.

DY 12.2 Mon 16:00 H20

Fluctuations and strong nonlinear effects in nanomechanical resonators — •FAN YANG¹, MENGQI FU¹, YUXUAN JIANG², and ELKE SCHEER¹ — ¹University of Konstanz, Konstanz, Germany — ²Anhui University, Hefei, China

Membrane resonators are ideal model systems to investigate nonlinear dynamics. Membrane resonators operated in the nonlinear regime, far beyond the Duffing regime exhibit unusual dynamic behavior, including localized overtones of spatial modulation [1], parametric flexural mode coupling, and persistent response [2]. Our research focusing on revealing the microscopic origins, their characterization, local control, exploring the universality and fluctuations [3] of the nonlinear state.

[1] Yang, Fan, et al. "Spatial modulation of nonlinear flexural vibrations of membrane resonators." *Physical review letters* 122.15 (2019): 154301.

[2] Yang, Fan, et al. "Persistent Response in an Ultrastrongly Driven Mechanical Membrane Resonator." *Physical Review Letters* 127.1 (2021): 014304.

[3] Yang, Fan, et al. "Mechanically Modulated Sideband and Squeezing Effects of Membrane Resonators" *Physical Review Letters* 127 (18), 184301.

DY 12.3 Mon 16:15 H20

Tuning nonlinear damping in graphene nanoresonators by parametric-direct internal resonance — •ATA KEŞKEKLER¹, ORIEL SHOANI², MARTIN LEE¹, HERRE VAN DER ZANT¹, PETER STEENEKEN¹, and FARBOD ALIJANI¹ — ¹TU Delft, Delft, The Netherlands — ²Ben-Gurion University of Negev, Beersheba, Israel

Micro/Nano-mechanical systems are utilized in many technologies and often have been used for their sensing capabilities. An ideal framework for sensitive nanomechanical devices is 2-D materials, and especially graphene, due to its exceptional mechanical, electrical and thermal properties. By their atomically thin nature, these systems are fundamentally nonlinear. In addition to their geometric nonlinearities, graphene membranes have shown nonlinear energy decay mechanisms. Nonlinear damping in these devices is a fundamental limitation to their sensing capabilities yet its full understanding is an open question. Among different dissipation mechanisms, an important factor that is hypothesized to affect damping properties of graphene nanodrums is the intermodal couplings. In this work, we study the nonlinear dynamics of a nanomechanical graphene resonator near its internal resonance condition to amplify the intermodal effects and uncover the physics between nonlinear damping and mode coupling. We observe a massive increase in damping in the vicinity of internal resonance that is followed by a bifurcation causing a dramatic increase of amplitude and resonance frequency. Our study opens up a route towards utilizing modal interactions and parametric resonance to realize resonators with engineered nonlinear dissipation over wide frequency range.

Invited Talk

DY 12.4 Mon 16:30 H20

From period-doubling bifurcations to time crystals and coherent Ising machines — •ODED ZILBERBERG^{1,2}, TONI L. HEUGEL², JAN KOŠATA², JAVIER DEL PINO², R. CHITRA², and ALEXANDER EICHLER² — ¹Department of Physics, University of Konstanz, 78464 Konstanz, Germany — ²Department of Physics, ETH Zürich, CH-8093 Zürich, Switzerland

Networks of coupled parametric resonators (parametrons) hold promise for parallel computing architectures. These are classical systems with period-doubling bifurcations, where the logic information is stored in oscillation modes of the system. Such networks similarly realize the physics of so-called discrete time crystals (DTCs). The latter are a many-body state of matter whose dynamics are slower than the forces acting on it. I will report on our theoretical and experimental work on parametron networks, their relation to DTCs and their potential application for the realization of coherent Ising machines.

DY 12.5 Mon 17:00 H20

Sideband and noise squeezing effects in nonlinear mechanical membrane resonators — •MENGQI FU¹, FAN YANG¹, YUXUAN JIANG², and ELKE SCHEER¹ — ¹Fachbereich Physik, Universität Konstanz, 78457 Konstanz, Germany — ²Anhui University, Hefei, China

The nonlinearity of a mechanical system has been shown to squeeze the noise by redistributing it in two conjugates of the observables under certain conditions and therefore provides a way to break the sensing limit of mechanical systems. In this work, we develop a novel method to characterize the noise squeezing of a nonlinear mechanical system by the frequency response of the low-frequency modulation based on a suspended silicon nitride (Si-N) membrane (~ 500 nm thickness) structure [1]. We first demonstrate an antiresonance effect between the “quasi modes” of the nonlinear mechanical system in the sideband spectra through low-frequency two-tone probing measurements. Then a direct connection between the antiresonance frequency and the noise squeezing factor of the system can be established to characterize the noise squeezing factor in a simple and robust method.

[1] F. Yang et al., Phys. Rev. Lett., 127, 184301 (2021).

Invited Talk

DY 12.6 Mon 17:15 H20

2D membranes in motion — •HERRE VAN DER ZANT — Kavli Institute of Nanoscience, Department of Quantum Nanoscience, Delft University of Technology, The Netherlands

Atomically thin membranes are ideal building blocks for nanoelectromechanical systems (NEMS) because of their unique mechanical properties and their low mass. We make membranes by transferring atomically thin layers on top of silicon oxide substrates that are pre-patterned with circular or rectangular holes. The suspended membranes are characterized by a laser interferometer set-up that gives access to information on the dynamics in the frequency- and time-domain. The setup is equipped with a moveable x-y stage so that the membrane motion can be visualized; the nonlinear response of the motion is used to extract the mechanical parameters including the Young's modulus. Recently, it has become clear that nanomechanics can also probe thermodynamic properties such as thermal conductivity, specific heat, and thermal expansion [Dynamics of 2D material membranes, 2D Materials 8 (2021) 042001]. Specifically, phase transitions are typically accompanied by abrupt changes in the specific heat, resulting in accompanying changes in the strain of the material which are measured via mechanical resonances. In this way, we have detected the Néel temperature of antiferromagnetic FePS₃ membranes, their magnetic anisotropy and studied the nonlinear coupling between magnetic and elastic properties.

DY 13: Big Data and Artificial Intelligence (joint session SOE/DY)

Time: Monday 17:45–18:15

Location: H18

See SOE 7 for details of this session.

DY 14: Invited Talk Sabine Klapp

Time: Tuesday 9:30–10:00

Location: H18

Invited Talk

DY 14.1 Tue 9:30 H18

Non-Markovian Brownian systems: from single-particle thermodynamics to collective behavior — •SABINE KLAPP — Institut fuer Theoretische Physik, TU Berlin, Hardenbergstrasse 36, 10623 Berlin

Recently, the dynamical behavior and the thermodynamics of stochastic systems involving time-delay or, more generally, memory effects has become a focus of growing interest. Indeed, memory is essentially omnipresent in many complex fluids and biological systems, but may also arise, e.g., due to delayed feedback protocols or sensorial delay in active systems. The theoretical description of such systems is still challenging due to the non-Markovian nature of the underlying

Langevin equations, particularly in the case of discrete time delays. Here we present, first, recent research for Brownian particles subject to feedback with discrete or distributed time delay. We discuss peculiar thermodynamic features, such as delay-induced heat production, and the theoretical treatment based on the introduction of auxiliary variables with non-reciprocal coupling. Considering an ensemble of delayed Brownian particles we demonstrate the occurrence of new phases resembling active particles. Our second focus lies on systems with fractional Brownian motion (fBm). fBM is a well-established model for anomalous diffusion, where non-Markovianity arises through the noise correlation function. We discuss strategies how to treat this system thermodynamically and the role of memory for the collective behavior.

DY 15: Delay and Feedback Dynamics

Time: Tuesday 9:30–10:30

Location: H19

DY 15.1 Tue 9:30 H19

Emergence of collective motion in two-dimensional colloidal systems with delayed feedback — •ROBIN A. KOPP and SABINE H. L. KLAPP — ITP, TU Berlin, Berlin, Germany

In recent years, delayed feedback in colloidal systems has become an active and promising field of study [1], key topics being history dependence and the manipulation of transport properties. Here we study the dynamics of a two-

dimensional colloidal suspension, subject to time-delayed feedback. To this end we perform overdamped Brownian dynamics simulations, where the particles interact through a Weeks-Chandler-Andersen potential. Furthermore, each particle is subject to a Gaussian, repulsive feedback potential, that depends on the difference of the particle position at the current time, and at an earlier time. We observe and quantitatively study the emergence of collective motion characterized by a nonzero mean velocity and provide a possible explanation com-

binning single-particle and mean-field-like effects. Studying the corresponding one-particle system we obtain an understanding of the history dependence and the long-time behavior, in particular a nonzero stationary constant velocity state of the deterministic problem that translates to a constant average velocity magnitude in the stochastic system. By studying the mean square displacement we are able to point out how delayed feedback affects diffusion in the one-particle and the interacting system differently.

[1] S. A. M. Loos, S. Hermann, and S. H. L. Klapp, *Entropy* **23**, 696 (2021)

DY 15.2 Tue 9:45 H19

The role of the polarization dephasing time for stabilizing coupled nanolasers — •AYCKE ROOS¹, STEFAN MEINECKE¹, and KATHY LÜDGE² — ¹TU Berlin - Institut für Theoretische Physik, Hardenbergstraße 36, 10623 Berlin — ²TU Ilmenau - Institut für Physik, Fachgebiet Theoretische Physik 2, 98684 Ilmenau

As a prototypical model for on-chip laser networks, mutually coupled nanolasers attract attention in laser physics and dynamics. In the regime of small cavity lifetimes the carrier polarization essentially influences the dynamics of such lasers. We investigate the emission dynamics of two coupled lasers, modeled by Maxwell-Bloch type laser equations (class-C laser), and predict ways to optimize their stability, i.e., maximize their locking range. We find that tuning the cavity lifetime to the same order of magnitude as the dephasing time of the microscopic polarization yields optimal operation conditions, which allow for wider tuning ranges than usually observed in conventional semiconductor lasers. We present the steady state solutions and numerically characterize the emission dynamics via the underlying bifurcation structure. The dephasing time is found to be a crucial parameter, which impacts the observed dynamics in the parameter space spanned by frequency detuning, coupling strength and coupling phase.

DY 15.3 Tue 10:00 H19

Frequency combs and localized states in time-delayed Kerr-Gires-Tournois interferometers — •THOMAS G. SEIDEL^{1,2}, JULIEN JAVALOYES², and SVETLANA V. GUREVICH^{1,2} — ¹Institute for Theoretical Physics & Center for Nonlinear Science (CeNoS), University of Münster, Schlossplatz 2, 48149 Münster, Germany — ²Dpt. de Física, Universitat de les Illes Balears & IAC-3, Campus UIB, E-07122 Palma de Mallorca, Spain

We study theoretically the formation of phase-locked temporal localized states (TLSs) and frequency combs. Our system consists in an optically injected Fabry-

Perot micro-cavity containing a Kerr medium that is coupled to an external cavity. Using a first-principles model based on delay algebraic equations (DAEs) and applying a combination of direct numerical simulations and path continuation methods, we disclose sets of multistable dark and bright TLSs coexisting on their respective bistable homogeneous backgrounds. We show that the detuning of the injection with respect to the micro-cavity resonance controls the region of existence of TLSs and its change can lead to a period-doubling route to chaos. Understanding the influence of the system parameters on physical mechanisms such as group delay dispersion and third order dispersion do not appear so obvious in the DAE model. Therefore, we transform the DAE into a real order parameter equation by using a rigorous multiple time scale analysis applied at the onset of bistability. The normal form given by a real Ginzburg-Landau equation and the full DAE model exhibit excellent quantitative agreement in both one- and two-parameter bifurcation diagrams.

DY 15.4 Tue 10:15 H19

Dynamics of square waves in a vertical external-cavity delayed Kerr-Gires-Tournois interferometer — •ELIAS R. KOCH¹, THOMAS G. SEIDEL^{1,2}, JULIEN JAVALOYES², and SVETLANA V. GUREVICH^{1,2} — ¹Institute for Theoretical Physics & Center for Nonlinear Science (CeNoS), University of Münster, Schlossplatz 2, 48149 Münster, Germany — ²Dpt. de Física, Universitat de les Illes Balears & IAC-3, Campus UIB, E-07122 Palma de Mallorca, Spain

We study theoretically the mechanisms of square wave (SW) formation in a monomode micro-cavity, containing a nonlinear Kerr medium coupled to a long external feedback cavity under continuous wave injection. Employing a first-principle delay-algebraic equation (DAE) model in the long delay limit, we provide a simple analytical approximation of the SW's plateau intensities and the bifurcation points limiting the range of existence of the SWs. Using a combination of path-continuation techniques and direct numerical simulations, we show that depending on the system parameters SWs can exhibit homoclinic snaking leading to the formation of complex-shaped multistable SW solutions. Beyond that, more complex SW dynamics can be identified, including a period doubling route to chaos. The results obtained from the full DAE model and the simple analytical approximation are in excellent agreement. Furthermore, we demonstrate that SWs can be used as a platform to host other structures and we show that robust multiple bound states consisting of localized pulses can be formed on the SW plateaus.

DY 16: Active Matter 2 (joint session DY/BP/PPP)

Time: Tuesday 10:00–13:00

Location: H18

DY 16.1 Tue 10:00 H18

Density fluctuations in bacterial binary mixtures — •SILVIA ESPADA BURRIEL, VICTOR SOURJIK, and REMY COLIN — Max Planck Institute for Terrestrial Microbiology, Karl-von-Frisch-strasse 10, 35043 Marburg & Center for Synthetic Microbiology (SYNMIKRO), Karl-von-Frisch-strasse 14, 35043 Marburg

In wild environments, bacteria are found as mixtures of motile and sessile species, which interact physically and chemically to give rise to complex community organization. Very little is understood of the role of physical interactions in these processes: Numerical works on dry active matter and experiments on colloidal systems have shown that the activity of the active particles may affect the spatial distribution of passive particles with which they are mixed. However, the physical behavior of binary mixtures of bacteria remains largely unexplored. In our study, we present a novel phenomenon in which non-motile bacteria form large density fluctuations when mixed with motile bacteria, distinct from the aforementioned behaviors. We systematically explored the phase diagram of the mixtures in experiments combining microfluidics, fluorescence (confocal) microscopy, quantitative image analysis and parameter tuning by genetic engineering. Our experimental results show that the emergence of these large density fluctuations of the non-motile cells in presence of motile cells is controlled by hydrodynamic interactions between the motile and non-motile cells and by the sedimentation of the non-motile cells, possibly because it breaks the systems symmetry.

DY 16.2 Tue 10:15 H18

Pulsating Active Matter — •YIWEI ZHANG and ETIENNE FODOR — 0 Av. de la Faiencerie, 1511 Luxembourg

Active matter features the injection of energy at individual level keeping the system out of equilibrium, which leads to novel phenomenologies without any equilibrium equivalents. So far, most active matter models assign a velocity to each particle, whilst we herein consider a system of pulsating soft particles where the activity sustains particles' periodic deformation instead of spatial displacement. At sufficiently high density, we reveal the existence of wave propagation independent of any particle migration, and derive the corresponding phase diagram. We study the character of phase transitions, and investigate the underlying physical mechanisms, using both particle-based simulations and hydrodynamic analysis.

DY 16.3 Tue 10:30 H18

Long-Range Nematic Order in Two-Dimensional Active Matter — •BENOÎT MAHAULT¹ and HUGUES CHATÉ^{2,3} — ¹MPIDS, 37077 Göttingen, Germany — ²SPEC, CEA-Saclay, 91191 Gif-sur-Yvette, France — ³CSRC, Beijing 100193, China

Studies of active matter continue to flourish, exploring more and more complex situations in an increasingly quantitative manner. Evidence has accumulated that shows active matter exhibits properties that are impossible in thermal equilibrium or even in driven systems. In spite of all this progress, important fundamental questions remain open. Such a long-standing issue is whether true long-range nematic order can emerge in two space dimensions. In this talk, we will present theoretical and numerical results obtained from minimal models of self-propelled polar particles aligning nematically. Our study shows that the orientational order emerging from such systems is quasi-long-ranged beyond the scale associated to induced velocity reversals, which is typically extremely large and often cannot even be measured. On scales where particle motion is ballistic, nematic order appears truly long-range. A hydrodynamic theory for this de facto phase is derived, and we show that its structure and symmetries differ from conventional descriptions of both polar flocks and active nematics. Our analysis of this field theory predicts π -symmetric propagative sound modes and the scaling form of space-time fluctuations. Finally, numerical results confirm the theory and allow us to estimate all scaling exponents.

DY 16.4 Tue 10:45 H18

Collective behavior of repulsive chiral active particles with non-reciprocal couplings — •KIM L. KREIENKAMP and SABINE H. L. KLAPP — Technische Universität Berlin, Germany

Mixtures of chiral active particles [1] as well as non-reciprocal systems [2] show intriguing collective behavior like pattern formation and traveling waves. The combination of both – non-reciprocal couplings in mixtures of chiral active particles – promises a rich variety of collective dynamics.

Here, we investigate how non-reciprocal couplings and naturally occurring repulsive interactions due to finite particle sizes affect the collective behavior in a mixture of two species of particles. We analyze the effects due to non-reciprocity and finite size individually as well as their interplay based on a field description

of the system in terms of the particle concentration and director field, measuring the overall orientation of particles at a certain position.

We derive the field equations under the mean-field assumption by coarse-graining microscopic Langevin equations for individual chiral particles, which are modeled as self-propelling circle swimmers with soft repulsive forces, comprising the finite size effects. Particles of the two species rotate with different intrinsic frequencies and align with near-by particles. Focusing on non-reciprocity, we use a non-mutual alignment between the particles.

[1] D. Levis and B. Liebchen, *Phys. Rev. E* 100, 012406 (2019)

[2] M. Fruchart, R. Hanai, P. B. Littlewood, and V. Vitelli, *Nature* 592, 363-369 (2021)

DY 16.5 Tue 11:00 H18

Memory-induced chirality in self-freezing active droplets — •ARITRA K. MUKHOPADHYAY¹, KAI FENG², JOSÉ CARLOS UREÑA MARCOS¹, RAN NIU², QIANG ZHAO², and BENNO LIEBCHEN¹ — ¹Technische Universität Darmstadt, 64289 Darmstadt, Germany. — ²Huazhong University of Science and Technology, 430074 Wuhan, China.

We experimentally realize and numerically model a new type of self-propelled droplet swimmer which exhibits chiral motion due to self-induced memory effects without requiring any explicit symmetry breaking caused by specific droplet geometries or complex environments. The droplets are composed of a binary polymer mixture that solidifies over time, simultaneously emitting certain polymers into their environment. A spontaneous asymmetry of the emitted polymer concentration along the stationary droplet surface induces Marangoni flows which cause the droplet to initially self-propel ballistically. However, the emitted polymers diffuse slowly and form long-lived trails with which the droplet can self-interact in the course of time and this leads to a dynamical transition from ballistic to chiral motion. The droplets persistently exhibit chiral motion with the same handedness until at even later times a second transition occurs when the droplets confine themselves leading to self-trapping over the timescale of our experiments and simulations. Our results exemplify a new route to realizing synthetic active particles whose dynamics can be controlled via the pronounced self-induced memory effects.

15 min. break

DY 16.6 Tue 11:30 H18

Role of advective inertia in active nematic turbulence — •COLIN-MARIUS KOCH and MICHAEL WILCZEK — Theoretical Physics I, University of Bayreuth, Bayreuth

Suspensions of active agents with nematic interactions can exhibit complex dynamics such as mesoscale turbulence. Continuum descriptions for such systems are inspired by the hydrodynamic theory of liquid crystals and feature an advective nonlinearity which represents inertial effects. The typically low Reynolds number of such active flows raises the question whether and under which conditions the active stresses present in these systems can excite inertial flows. To address this question, we investigate mesoscale turbulence in a two-dimensional model for active nematic liquid crystals. In particular, we compare numerical simulations with and without nonlinear advection and frictional damping of the flow field. Studying the nondimensionalized equations of motion, we find that inertia can trigger large-scale motion even for small microscopic Reynolds numbers if the active forcing is sufficiently large and the Ericksen number is sufficiently low. Performing a spectral analysis of the energy budget, we identify an inverse energy transfer caused by inertial advection, whose impact is small in comparison to active forcing and viscous dissipation but accumulates over time. We additionally show that surface friction, mimicked by a linear friction term, dissipates the transported energy and suppresses the large-scale motion. We conclude that, without an a priori knowledge of model parameters matching experiments, including inertia and friction may be necessary for consistent modeling of active nematic turbulence.

DY 16.7 Tue 11:45 H18

Pumping in active microchannels — •GONCALO ANTUNES^{1,2,3}, PAOLO MALGARETTI^{1,2,3}, SIEGFRIED DIETRICH^{2,3}, and JENS HARTING^{1,4} — ¹Helmholtz-Institut Erlangen-Nürnberg für Erneuerbare Energien (IEK-11), Forschungszentrum Jülich, Erlangen, Germany — ²Max-Planck-Institut für Intelligente Systeme, Stuttgart, Germany — ³Universität Stuttgart, Stuttgart, Germany — ⁴Friedrich-Alexander-Universität Erlangen-Nürnberg, Nürnberg, Germany

Much attention is currently being given to the problem of manipulating fluids at the microscale, with successful applications to fields such as 3D fabrication and biomedical research. Often micropumps are a fundamental component of these microfluidic systems. An intriguing technique to manipulate fluid flows in a channel is diffusioosmosis. Fluid flow is obtained upon imposing an inhomogeneous concentration of some solute, which generates flow in a boundary layer around the channel walls. This inhomogeneity is the result of a spatially inhomogeneous production rate of solute inside the channel.

We show that a solute-producing, corrugated, active channel can act as a micropump even when it is fore-aft symmetric. This result is obtained by coupling

the Stokes equation with an advection-diffusion equation for the solute concentration, which we solve analytically in the limit of thin, weakly-corrugated channels. Lattice Boltzmann simulations further support the existence of the symmetry-breaking. Our calculations are also valid for left-right asymmetric channels, and provide a tool to optimize the pumping rate of an active microchannel by tuning its shape or its solute production rate.

DY 16.8 Tue 12:00 H18

Active Refrigerators Powered by Inertia — •LUKAS HECHT¹, SUVENDU MANDAL¹, HARTMUT LÖWEN², and BENNO LIEBCHEN¹ — ¹Institut für Physik kondensierter Materie, Technische Universität Darmstadt, Hochschulstr. 8, D-64289 Darmstadt, Germany — ²Institut für Theoretische Physik II - Soft Matter, Heinrich-Heine-Universität Düsseldorf, Universitätsstraße 1, D-40225 Düsseldorf, Germany

We present the operational principle for a refrigerator which uses inertial effects in active Brownian particles (ABPs) to locally reduce the (kinetic) temperature by two orders of magnitude below the environmental temperature. This principle requires two ingredients: First, we need the feature of inertial ABPs to undergo motility-induced phase separation into coexisting phases with different (kinetic) temperatures and second, a mechanism which localizes the dense phase in the targeted cooling domain is required.

Here, we exploit the peculiar but so-far unknown shape of the phase diagram of inertial ABPs to initiate motility-induced phase separation in the targeted cooling domain only. Remarkably, active refrigerators operate without requiring isolating walls separating the cooling domain from its environment. This feature opens the route towards using active refrigerators to systematically absorb and trap substances such as toxins or viruses from the environment.

DY 16.9 Tue 12:15 H18

The influence of motility on bacterial accumulation in a microporous channel — •CHRISTOPH LOHRMANN¹, MIRU LEE², and CHRISTIAN HOLM¹ — ¹Institute for Computational Physics, University of Stuttgart, Allmandring 3, 70569 Stuttgart, Germany — ²Institute for Theoretical Physics, Georg-August-Universität Göttingen, 37073 Göttingen, Germany

Swimming microorganisms are often encountered in confined geometries where also an external flow is present, e.g. in filters or inside the human body. To investigate the interplay between microswimmer motility and external flows, we developed a model for swimming bacteria based on point coupling to an underlying lattice Boltzmann fluid. Random reorientation events reproduce the statistics of the run-and-tumble motion of the bacterium *E. coli*. We present the application of the model to the study of bacterial dynamics in a channel with a single cylindrical obstacle. In accordance with experimental measurements, simulations show asymmetric accumulation behind the obstacle only when the bacteria are active and an external flow is present.

Lee, Miru *et al.*, *Soft Matter* 17, 893-902 (2021)

DY 16.10 Tue 12:30 H18

Inertial dynamics of an active Brownian particle* — •JONAS MAYER MARTINS and RAPHAEL WITTKOWSKI — Institut für Theoretische Physik, Center for Soft Nanoscience, Westfälische Wilhelms-Universität Münster, 48149 Münster, Germany

Active Brownian motion commonly assumes spherical overdamped particles. However, self-propelled particles are often neither symmetric nor overdamped yet underlie random fluctuations from their surroundings. Active Brownian motion has already been generalized to include asymmetric particles. Separately, recent findings have shown the importance of inertial effects for particles of macroscopic size or in low-friction environments. We aim to consolidate the previous findings into the general description of a self-propelled asymmetric particle with inertia. We derive the Langevin equation of such a particle as well as the corresponding Fokker-Planck equation. Furthermore, a formula is presented that allows to reconstruct the hydrodynamic resistance matrix of the particle by measuring its trajectory. Numerical solutions of the Langevin equation show that, independent of the particle's shape, the noise-free trajectory at zero temperature starts with an inertial transition phase and converges to a circular helix. We discuss this universal convergence with respect to the helical motion that many microorganisms exhibit.

Funded by the Deutsche Forschungsgemeinschaft (DFG) - Project-ID 433682494 - SFB 1459

DY 16.11 Tue 12:45 H18

Stochastic motion under active driving due to inverted dry (solid) friction — •ANDREAS M. MENZEL — Otto-von-Guericke-Universität Magdeburg, Magdeburg, Germany

It has become common to describe the motion of actively driven or self-propelled objects using a driving force of constant magnitude. We assume that this driving force always acts along the current velocity direction. Moreover, we consider objects featuring a nonpolar axis, along which driving and propagation occur [1].

In that case, spontaneous symmetry breaking decides on the heading of propagation, that is, "forward" or "backward" along the nonpolar axis. Stochastic

effects may reverse the velocity and thus the direction of the driving force.

As it turns out, active driving under these circumstances corresponds to inverted dry (solid) friction of the Coulomb type. Corresponding tools of theoretical analysis can thus be adopted, mapping the velocity spectrum to the one of a quantum-mechanical harmonic oscillator subject to a repulsive delta potential. In this way, the diffusion coefficient can be calculated analytically. We evaluate

velocity and displacement statistics. Outward propagating displacement maxima emerge under increased active driving. The trajectories feature pronounced cusps when velocity reversals occur.

Our results should apply, for instance, to certain types of vibrated nonpolar rods and swimming bacteria that may reverse their propagation direction.

[1] A. M. Menzel, submitted.

DY 17: Invited Talk Bernhard Mehlig

Time: Tuesday 10:30–11:00

Location: H19

Invited Talk

DY 17.1 Tue 10:30 H19

Caustics in turbulent aerosols — •BERNHARD MEHLIG — University of Gothenburg

Turbulent aerosols are suspensions of heavy particles in a turbulent fluid – such as water droplets in the turbulent air of a cumulus cloud, or dust grains in the turbulent gas around a growing star. The analysis of such highly non-linear and multi-scale problems poses formidable challenges. Experiments resolving the particle dynamics have only recently become possible, and direct numerical simulations of such systems are still immensely difficult.

Here I describe a different approach, to analyse the dynamics of turbulent aerosols in terms of synthetic turbulence models, using methods from non-equilibrium statistical physics and dynamical-systems theory. Although the models are highly idealised, their analysis has led to significant progress in understanding the mechanisms determining the particle dynamics. As an example I discuss the formation of mathematical catastrophes in the phase-space dynamics of turbulent aerosols, akin to caustics in geometrical optics. I describe where and how often these singularities form, and I explain their physical significance. I conclude with a discussion of successes and limitations of this statistical approach, and with a summary of open questions.

DY 18: Nonlinear Dynamics 1: Synchronization and Chaos (joint session DY/SOE)

Time: Tuesday 11:15–12:45

Location: H19

DY 18.1 Tue 11:15 H19

Stable Poisson chimeras in networks of two subpopulations — •SEUNGJAE LEE and KATHARINA KRISCHER — Technical University of Munich, Garching, Germany

In this talk, we introduce recent results on dynamical and spectral properties of chimeras in two-population network based on Kuramoto order parameter and Lyapunov stability analysis. In particular, we address two qualitatively different dynamics of incoherent oscillator populations according to the given initial conditions, and which led to the classification of Poisson and non-Poisson chimera states. We numerically calculate the Lyapunov exponents and covariant Lyapunov vectors to determine the spectral properties of the chimera states, and then expound the classification of the Lyapunov exponents. Our stability analysis also confirms that the chimera states of Kuramoto-Sakaguchi phase oscillators in two-population networks are neutrally stable in many directions. Furthermore, we demonstrate that two ‘perturbations’ of the phase model that reflect more realistic situations render Poisson chimeras stable. These models consider a nonlocal intra-population network and Stuart-Landau planar oscillators with amplitude degrees of freedom, respectively. Both these ‘perturbations’ might be considered a heterogeneity of the phase model and give rise to an asymptotically attracting Poisson chimera in two-population networks.

pacemaker and the driven units. Noise as well as a small back-coupling to the pacemaker facilitate synchronization. Units can be synchronously entrained to different temporal patterns, depending on the selected path in the hierarchical heteroclinic network. These locally generated temporal sequences of information items can be transferred over a spatial grid by entrainment to the pacemaker dynamics. Such spatiotemporal patterns are believed to code information in brain dynamics. Depending on the number and location of pacemakers on two-dimensional grids, synchronization can be maintained in the presence of a large number of resting state units and mediated via target waves when the pacemakers are concentrated to a small area of such grids. In view of brain dynamics, our results indicate a possibly ample repertoire for coding information in temporal patterns.

DY 18.4 Tue 12:00 H19

Suppression of quasiperiodicity in circle maps with quenched disorder — •DAVID MÜLLER-BENDER¹, JOHANN LUCA KASTNER¹, and GÜNTER RADONS^{1,2} — ¹Institute of Physics, Chemnitz University of Technology, 09107 Chemnitz, Germany — ²Institute of Mechatronics, 09126 Chemnitz, Germany

We show that introducing quenched disorder into a circle map leads to the suppression of quasiperiodic behavior in the limit of large system sizes. Specifically, for most parameters the fraction of disorder realizations showing quasiperiodicity decreases with the system size and eventually vanishes in the limit of infinite size, where almost all realizations show mode-locking. Consequently, in this limit, and in strong contrast to standard circle maps, almost the whole parameter space corresponding to invertible dynamics consists of Arnold tongues.

Details can be found in the preprint D. Müller-Bender, J. L. Kastner, and G. Radons, Suppression of quasiperiodicity in circle maps with quenched disorder, arXiv:2204.09392 [nlin.cd] (2022).

DY 18.2 Tue 11:30 H19

On rational reactions - and other ones - of overloaded magnetic gears — •INGO REHBERG and STEFAN HARTUNG — Universität Bayreuth

Experiments exploring the coupling of two rotating spherical magnets reveal a cogging-free coupling for two specific angles between the input and output rotation axes. The striking difference between these two phase-locked modes of operation is the reversed sense of rotation of the driven magnet. For other angles, the cogging leads to a more complex dynamical behaviour. The experimental results can be understood by a mathematical model based on pure dipole-dipole interaction, with the addition of adequate friction terms [1].

Like all magnetic couplings, the setup contains intrinsic overload protection. The dynamic answer of the gear with cogging to an overload shows a plethora of modes of the driven magnet.

[1] Dynamics of a magnetic gear with two cogging-free operation modes, Stefan Hartung & Ingo Rehberg, Archive of Applied Mechanics 91, 1423-1435 (2021).

DY 18.5 Tue 12:15 H19

Reservoir Computing and Nonlinear Dynamics — •ULRICH PARLITZ — Max Planck Institute for Dynamics and Self-Organization, Göttingen, Germany — Institute for the Dynamics of Complex Systems, Georg-August-Universität Göttingen, Göttingen, Germany

We discuss the interrelation between reservoir computing (RC) and nonlinear dynamics (NLD). On the one hand, the performance of RC can be characterized and improved by concepts from NLD such as generalized synchronization and delay embedding. On the other hand, RC can be used to predict and control dynamical systems, including hybrid architectures that employ physically informed machine learning. Various aspects of this mutual relationship between RC and NLD are illustrated using low-dimensional and spatially extended chaotic dynamical systems.

DY 18.3 Tue 11:45 H19

Heteroclinic units acting as pacemakers: Entrained dynamics for cognitive processes — •BHUMIKA THAKUR and HILDEGARD MEYER-ORTMANN — School of Science, Jacobs University Bremen, Campus Ring 1, 28759 Bremen, Germany Heteroclinic dynamics is a suitable framework for describing transient and reproducible dynamics such as cognitive processes in the brain. We demonstrate how heteroclinic units can act as pacemakers to entrain larger sets of units from a resting state to hierarchical heteroclinic motion that is able to describe fast oscillations modulated by slow oscillations, features which are observed in brain dynamics. The entrainment range depends on the type of coupling, the spatial location of the pacemaker and the individual bifurcation parameters of the

DY 18.6 Tue 12:30 H19

Chameleon attractors in deterministic and stochastic Lorenz-63 systems — •REIK V. DONNER^{1,2}, TOMMASO ALBERTI³, and DAVIDE FARANDA⁴ — ¹Hochschule Magdeburg-Stendal, Magdeburg, Germany — ²Potsdam Institute for Climate Impact Research, Potsdam, Germany — ³National Institute for Astrophysics, Rome, Italy — ⁴LSCE, Université Paris-Saclay, Gif-sur-Yvette, France

The dynamical characteristics of a trajectory on a chaotic or stochastic attractor undergo marked changes when successively eliminating the low-frequency variability components and focusing on the fast fluctuations only, motivating the new concept of Chameleon attractors. Here, we study the time scale dependent instantaneous and average fractal characteristics of partial sums of dynamical modes identified by means of empirical mode decomposition for the Lorenz-

63 system and two stochastic versions thereof with additive and multiplicative noise as obtained by exploiting recurrences in phase space using extreme value theory. While the average fractal dimensions converge to the expected values as more and more low-frequency modes are included, we find an excess dimension larger than 3 for higher frequency modes below the Lyapunov time scale resulting from the stochastic components.

DY 19: Many-Body Quantum Dynamics 2 (joint session DY/TT)

Time: Tuesday 11:30–13:00

Location: H20

DY 19.1 Tue 11:30 H20

Disorder-free localization transition in a two-dimensional lattice gauge theory — •NILOTPAL CHAKRABORTY¹, MARKUS HEYL^{1,2}, PETR KARPOV¹, and RODERICH MOESSNER¹ — ¹Max Planck Institute for physics of complex systems, Dresden — ²University of Augsburg, Augsburg

While the nature of the quantum localization transition (QLT) is still debated for conventional many-body localization, here we provide the first comprehensive characterization of the QLT in two dimensions (2D) for a disorder-free case. Disorder-free localization can appear in homogeneous 2D LGTs such as the U(1) quantum link model (QLM) due to an underlying classical percolation transition fragmenting the system into disconnected real-space clusters. Building on the percolation model, we characterize the QLT in the U(1) QLM through a detailed study of the ergodicity properties of finite-size real-space clusters via level-spacing statistics and localization in configuration space. We argue for the presence of two regimes - one in which large finite-size clusters effectively behave non-ergodically, a result naturally accounted for as an interference phenomenon in configuration space and the other in which all large clusters behave ergodically. As one central result, in the latter regime we claim that the QLT is equivalent to the classical percolation transition and is hence continuous. Utilizing this equivalence we determine the universality class and critical behaviour of the QLT from a finite-size scaling analysis of the percolation problem.

DY 19.2 Tue 11:45 H20

Quantifying local memory in disordered systems across the ETH-MBL transition — •SEBASTIAN WENDEROTH and MICHAEL THOSS — Physikalisches Institut, Albert-Ludwigs-Universität Freiburg, Freiburg

Thermalization describes the process of a system reaching thermal equilibrium with its environment. The asymptotic state solely depends on a few macroscopic parameters of the environment. Hence, the information about the initial state is lost during the process. Many-body localized systems fail to thermalize due to the absence of transport, and thus, some information about the initial state is retained in local observables at all times.

Based on the time-evolution of a subsystem, we present a concept which can be used to quantify the influence of the initial state on local observables. Using this approach, we investigate local memory in the XXZ Heisenberg spin chain with random local disorder, a paradigmatic model exhibiting a transition from thermalizing to localized dynamics. We discuss the loss of local information and identify different delocalization mechanisms.

DY 19.3 Tue 12:00 H20

Dynamically Induced Exceptional Phases in Quenched Interacting Semimetals — •CARL LEHMANN¹, JAN CARL BUDICH¹, and MICHAEL SCHÜLER² — ¹TU Dresden, Dresden, Germany — ²Paul Scherrer Institute, Villigen, Switzerland

We report on the dynamical formation of exceptional degeneracies in basic correlation functions of nonintegrable one- and two-dimensional systems quenched to the vicinity of a critical point. Remarkably, fine-tuned semimetallic points in the phase diagram of the considered systems are thereby promoted to topologically robust non-Hermitian (NH) nodal phases emerging in the coherent time evolution of a dynamically equilibrating system. Using nonequilibrium Greens function methods within the conserving second Born approximation, we predict observable signatures of these NH nodal phases both in equilibrated spectral functions and in the nonequilibrium dynamics of single-particle density matrix functions.

DY 19.4 Tue 12:15 H20

Nontrivial damping of quantum many-body dynamics — •TJARK HEITMANN¹, JONAS RICHTER², JOCHEN GEMMER¹, and ROBIN STEINIGEWEG¹ — ¹Department of Physics, University of Osnabrück, Germany — ²Department of Physics and Astronomy, University College London, UK

Understanding how the dynamics of a given quantum system with many degrees of freedom is altered by the presence of a generic perturbation is a notoriously difficult question. Recent works predict that, in the overwhelming majority of cases, the unperturbed dynamics is just damped by a simple function, e.g., ex-

ponentially. While these predictions rely on random-matrix arguments and typicality, they can only be verified for a specific physical situation by comparing to the actual solution or measurement. Crucially, it also remains unclear how frequent and under which conditions counterexamples to the typical behavior occur. Here, we discuss this question from the perspective of projection-operator techniques, where exponential damping of a density matrix occurs in the interaction picture but not necessarily in the Schrödinger picture. We show that a nontrivial damping in the Schrödinger picture can emerge if the dynamics in the unperturbed system possesses rich features, for instance due to the presence of strong interactions. This suggestion has consequences for the time dependence of correlation functions. We substantiate our theoretical arguments by large-scale numerical simulations of charge transport in the extended Fermi-Hubbard model with nearest-neighbor interactions as perturbations to the integrable reference system.

DY 19.5 Tue 12:30 H20

Effect of electron-electron interaction on the spectral statistics in circular sector graphene billiards — •XIANZHANG CHEN^{1,2} and LIANG HUANG¹ — ¹Lanzhou Center for Theoretical Physics, and Key Laboratory for Magnetism and Magnetic Materials of MOE, Lanzhou University, Lanzhou, Gansu 730000, China — ²Université de Strasbourg, CNRS, Institut de Physique et Chimie des Matériaux de Strasbourg, UMR 7504, F-67000 Strasbourg, France

The spectral statistics is a fundamental issue in quantum chaos and has been used widely as a measure to probe the complexity of the underlying quantum systems. In this work, we adopt the one-orbital mean-field Hubbard model to investigate the effect of many-body interactions on the spectral statistics of circular sector graphene billiards. It is found that the spectral statistics are insensitive to the Hubbard interaction U for most of the energy ranges, except for energies around the Dirac point. We choose two representative systems, whose spectral statistics follow Poisson and Gaussian orthogonal ensemble (GOE) when $U = 0$, respectively. As U increases, for both cases, the spectral statistics moves toward GOE. However, after passing a critical value U_c , the spectral statistics turns back toward Poisson as U is increased further, due to the emerging gap and henceforth distinct behaviors of the quasiparticles. In addition, the energies above and below the Dirac point may exhibit different spectral statistics. These results uncover the intriguing connection between Hubbard interaction and the spectral statistics in graphene sector billiards. A physical picture is provided to understand these effects.

DY 19.6 Tue 12:45 H20

Anisotropy-mediated localization — •IVAN KHAYMOVICH — Nordic Institute for Theoretical Physics, Stockholm, Sweden

Recently, the standard picture of Anderson localization transition in d -dimensional long-range (e.g. dipolar) systems has been argued due to several reported counterintuitive examples of (at least power-law) localization beyond the convergence of the perturbation theory. In addition, wave-function spatial decay rates obey a "mysterious" duality [1] mapping different powers 'a' of power-law bending symmetrically around the critical point $a=d$.

In my talk, I address this intriguing question, present a general approach applicable to all such models, and uncover the role of correlations and the origin of the above duality [2]. The phenomenon of the correlation-induced localization [2] is just the very peak of the iceberg in this field. Therefore I will focus on the effects of anisotropy [3] in dipolar system and show the reentrant localization governed by the anisotropy parameter given by the tilt of an electric field. Note that the range of systems is also not limited by the dipolar systems, but includes also the Weyl semimetals, ultracold atoms, Rydberg excitations in the optical traps and many others.

Literature: [1] X. Deng, V. E. Kravtsov, G. V. Shlyapnikov and L. Santos, Phys. Rev. Lett. 120, 110602 (2018). [2] P. Nosov, I. M. Khaymovich, V. E. Kravtsov, Correlation-induced localization Phys. Rev. B 99, 104203 (2019) [arXiv:1810.01492] [3] X. Deng, A. L. Burin, I. M. Khaymovich, Anisotropy-driven localization transition in quantum dipoles [arXiv:2002.00013]

DY 20: Complex Fluids and Colloids, Micelles and Vesicles (joint session CPP/DY)

Time: Tuesday 11:30–13:00

Location: H38

See CPP 18 for details of this session.

DY 21: Invited Talk Dirk Brockmann (joint session SOE/DY)

Time: Wednesday 9:30–10:15

Location: H11

See SOE 11 for details of this session.

DY 22: Active Matter 3 (joint session BP/ CPP/DY)

Time: Wednesday 9:30–12:30

Location: H16

See BP 14 for details of this session.

DY 23: Complex Fluids and Soft Matter 1 (joint session DY/ CPP)

Time: Wednesday 9:30–12:00

Location: H18

DY 23.1 Wed 9:30 H18

Writing in Water — •THOMAS PALBERG and NADIR MÖLLER — Institut für Physik, Johannes Gutenberg Universität Mainz

Writing is an ancient cultural technique, typically performed by leaving some trace in or on a solid surface. We here explore the possibilities of leaving the trace in a liquid medium close to a surface and obtain lines or letters with high contrast and durability. Ion exchange (IEX) resin beads are used as mobile proton or hydroxyl ion sources. Moving them across the substrate in low-salt water, leaves a pH trace. Added autonomously swimming particles are able to follow this trace, mimicking hunter and prey dynamics or mate tracing, but without leaving a visible testimony. Written lines are realized by adding larger amounts of micron-sized passive particles, which settle to the like-charged substrate. Being phoretically drawn to or repelled from the pH traces, they form a well-visible trail behind the source. Trails of cationic IEX are white on black, those of anionic IEX are black on white. Their diffusive fading is slowed by continued phoretic flows and trails are stable up to hours. Sources moving autonomously just scribble. Sources propelled straight by gravity leave high-contrast lines. Deliberate tilting sequences for the substrate, then, facilitate writing.

DY 23.2 Wed 9:45 H18

Composition Dependent Instabilities in Mixtures With Many Components

— •FILIPE THEWES, MATTHIAS KRÜGER, and PETER SOLLICH — Institut für Theoretische Physik, Georg-August-Universität Göttingen, Göttingen, Germany

Understanding the phase behavior of mixtures with many components is a key step towards a physics-based description of intracellular compartmentalization. We study the instabilities of a model where the interactions as quantified by the second virial coefficients are taken as random Gaussian variables. Using tools from free probability theory we obtain the spinodal curve and the nature of instabilities for an arbitrary distribution of components, thus lifting the drastic simplification of uniform composition that has been made in earlier work. We illustrate our results with examples and show that, by controlling the density of only a few components, one can systematically change the nature of instabilities and achieve demixing for realistic scenarios, which appeared to be ruled out by previous studies. Inspired by these results, we introduce an additive model taking into account also deterministic interactions. We show how this systematic interaction leads to a competition between different forms of instabilities that can be tuned by controlling the model parameters. Since most experimental protocols for complex mixtures rely on tuning either the composition or systematic interactions, we expect our results to significantly extend the range of mixtures that can be treated within the mean-field model.

DY 23.3 Wed 10:00 H18

Phase behaviour of mixtures of hard spheres and hard rods — •POSHIKA GANDHI¹, JOERI OPDAM², ANJA KUHNHOLD¹, TANJA SCHILLING¹, and REMCO TUINIER² — ¹Institute of Physics, Albert-Ludwigs-University Freiburg, Germany — ²Institute for Complex Molecular Systems, Eindhoven University of Technology, The Netherlands

Phase behaviours of complex mixtures are challenging to predict. A binary mixture of hard spherocylinders (HSC) and hard spheres (HS) is one such system. As rod-like particles have large excluded volume, a free volume theory (FVT) can be used to gain insights into demixing phenomenon and phase stability.

Vliegthart *et al*[1] modified an existing FVT for binary mixtures of HS to accommodate HSC. This FVT works well for the needle limit, i.e., weak excluded volume interactions between HSC. It, however, predicts the phase boundaries at too low HSC concentrations. Opdam *et al*[2] showed that by incorporating excluded volume interactions between the depletants even in the reservoir improves the FVT significantly.

We used the new FVT to predict phase boundaries of colloidal mixtures and compared them to MC simulations. The results show that accounting for all the excluded volumes of all the components may be pivotal in understanding phase behaviour of colloidal mixtures [3].

[1] G. A. Vliegthart *et al.*, *J. Chem. Phys.*, **111**, 4153 (1999).[2] J. Opdam, *et al.*, *J. Chem. Phys.*, **154**, 204906 (2021)[3] J. Opdam, *et al.*, *Phys. Chem. Chem. Phys.*, **24**, 11820 (2022)

DY 23.4 Wed 10:15 H18

Markov State Modelling of Self Assembling Colloidal Systems — •SALMAN FARIZ NAVAS and SABINE H.L. KLAPP — ITP, Technische Universität Berlin, Germany

Many colloidal particle systems display self-assembly phenomena yielding, e.g., clusters or gel-like materials. The current project focuses on the use of phase space discretization techniques towards developing a coarse-grained description of self-assembly processes in colloidal systems.

Specifically, we develop a corresponding Markov State Model from particle-resolved Brownian Dynamics simulations, wherein the Markov states are the various local structural configurations present in the system and the Markovian process describing the stochastic transition of particles from one structure to the other.

The specific self-assembly problem studied here involves the aggregation of colloidal particles with field-induced multipolar interactions [1]. We use bond orientational order parameters and the coordination number as parameters to define the discrete states. The number of particles in the largest cluster in the system (n) is used as a parameter to quantify the progress of the overall aggregation. Transition probability matrices (TPM) between the different states are then computed for each value of n . Information regarding relaxation times and pathways relevant to the aggregation process are extracted by analyzing changes in the TPM elements.

[1] Florian Kogler, Orlin D. Velez, Carol K. Hall and Sabine H. L. Klapp, *Soft Matter* **11**, 7356 (2015)

DY 23.5 Wed 10:30 H18

Repulsion of topological defects in quasi-2D liquid crystal films — •KIRSTEN HARTH^{1,2} and RALF STANNARIUS³ — ¹Fachbereich Technik, TH Brandenburg, Brandenburg an der Havel, Deutschland — ²MARS und MRTM, Otto von Guericke Universität Magdeburg, Deutschland — ³Institut für Physik und MARS, Otto von Guericke Universität Magdeburg, Deutschland

The dynamics of topological defects is of interest, e.g., in phase transitions, cosmology or structural organization of colloids and active matter. Liquid crystals are a straightforward system allowing optical characterization of defect motion. As anisotropic fluids, they are characterized by orientational order, introducing long-range elastic forces, in addition to liquid-like fluidity with viscosity coefficients related to, e.g., the local shear flow directions respective to the local orientational field. This causes intriguing effects and must not be neglected.

The comparison of recent experiments [1,2] in free-standing smectic C films to theoretical and numerical predictions [2,3] leaves a number of questions unanswered. A proper consideration of flow coupling and / or of an anisotropy of the elastic constants in a simulation with realistic boundary conditions may solve the issues. We explain why elastic anisotropy is particularly important here. Experimental and numerical data are compared to elucidate the effect of elastic constants and flow on the repulsion dynamics.

[1] A. Missaoui, *et al.*, *PR Research* **2** 013080 (2020). [2] R. Stannarius, K. Harth, *PRL* **117** 157801 (2016). [3] e.g. X. Tang, J. V. Selinger, *Soft Matter* **13** 5481 (2017) ; *Soft Matter*, **15** 587 (2019)

15 min. break

DY 23.6 Wed 11:00 H18

Incipient motion for 3d geometries — •DOMINIK GEYER, PAOLO MALGARETTI, OTHMANE AOUANE, and JENS HARTING — Helmholtz Institute Erlangen-Nürnberg for Renewable Energy (IEK-11), Cauerstr. 1, 91058 Erlangen, Germany

The incipient motion describes the threshold conditions between erosion and sedimentation. This natural process is relevant for a broad field of natural and industrial processes, for example, cell detachment, cleaning of surfaces, and transportation in pipelines. Our interest is in the incipient motion of a single particle on non-trivial geometries. The crucial parameter for describing incipient motion is the so-called Shields number which is the ratio between viscous forces and buoyancy. Interestingly, the incipient motion has been reported at values of the Shields number much smaller than unity ($\theta \approx 10^{-2}$) hence questioning whether the proposed Shields number is indeed capturing the relevant physical phenomena. In order to critically discuss this aspect, we perform lattice Boltzmann simulations of a solid particle on a substrate consisting of solid spheres taking into account the local fluid velocity and the particle size. Our numerical data will allow us to calculate the effective viscous force acting on the particle and hence to propose possible corrections to the Shields number which can better account for the experimental and numerical data.

DY 23.7 Wed 11:15 H18

Phase behaviour in a mono-layer colloidal membrane — •LÉA BEAULES, ANJA KUHNHOLD, and TANJA SCHILLING — Institute of Physics, Albert-Ludwigs-University Freiburg, Germany

Kosterlitz-Thouless-Halperin-Nelson and Young (KTHNY) theory predicted that the melting of a purely 2D hard disk system would be defect-mediated and occur via two continuous transitions: from the solid to the intermediate hexatic phase and, from the hexatic to the fluid phase. Since then phase behaviour of this system as well as closely related systems have been extensively investigated and debated, showing that the hexatic-liquid transition is of first order for purely hard system [1]. Additionally, upon increasing interaction range or adding dispersity in the system the transition can become continuous or the hexatic phase can vanish [2].

However a large number of real systems can be more accurately approximated as a quasi-2D system that exhibits out of plane interactions, e.g. biological membranes; therefore understanding their role in the phase behaviour is important. Thus to extend our understanding of these systems, we use Monte-Carlo simulations to study an infinite mono-layer membrane of hard rod-like particles. We investigate how the orientational degree of freedom of the rods, and the range of their out of plane interactions affect the phase behaviour of the system.

[1] E. P. Bernard and W. Krauth, *Phys. Rev. Lett.* **107**, p. 155704 (2011).[2] Y.-W. Li and M. P. Ciamarra, *Phys. Rev. E* **102**, p. 062101 (2020).

DY 23.8 Wed 11:30 H18

Particle-resolved topological defects of smectic colloidal liquid crystals in 2d confinement — •RENÉ WITTMANN¹, PAUL A. MONDERKAMP¹, LOUIS B. G. CORTES^{2,3}, DIRK G. A. L. AARTS³, FRANK SMALLENBURG⁴, and HARTMUT LÖWEN¹ — ¹Institut für Theoretische Physik II: Weiche Materie, Heinrich-Heine Universität Düsseldorf, Germany — ²School of Applied and Engineering Physics, Cornell University, USA — ³Department of Chemistry, Physical and Theoretical Chemistry Laboratory, University of Oxford, UK — ⁴Laboratoire de Physique des Solides, CNRS, Université Paris-Saclay, France

We present a general classification scheme [1] of the intrinsic structure of smectic colloidal liquid crystals in two spatial dimensions, dictated by the interplay between the intrinsic layering and the externally imposed boundary structure. Thereby, we demonstrate that topological defects emerge in the form of spatially extended grain-boundaries, which are characterized by coexisting nematic and tetratic orientational order. We examine these intriguing topological properties on the particle scale by means of Monte-Carlo simulations, fundamental-measure-based density functional theory and real-space microscopy of colloidal rods. The structural details agree on a quantitative level. In particular, we analyze the typical shape of grain-boundary networks in a large range of polygonal confinements [1] and the stability of different competing topological states in nontrivial domains with additional interior boundaries [2].

[1] P. A. Monderkamp et al., *Phys. Rev. Lett.* **127**, 198001 (2021).[2] R. Wittmann et al., *Nat. Commun.* **12**, 623 (2021).

DY 23.9 Wed 11:45 H18

Structure of nematic hard rod tactoids — •ANJA KUHNHOLD¹ and PAUL VAN DER SCHOOT² — ¹University of Freiburg, Freiburg, Germany — ²Eindhoven University of Technology, Eindhoven, The Netherlands

Droplets of ordered phases of anisotropic particles take on specific shapes and internal structures. Compared to droplets of spherical particles, tactoids are elongated with cusp-like tips. Several parameters dictate the overall shape and structure: density of the system, elastic constants of the particles, anchoring strength, interfacial tension, and volume of the tactoid. [1]

We compare Monte Carlo simulation results of hard rod tactoids in a bath of spherical ghost particles to predictions from a scaling theory. We focus on small tactoids where the macroscopic scaling description might break down. We find that smaller tactoids have a more uniform director field than larger tactoids. Also, the segment density increases towards the tactoid tips in agreement with the theory. In addition, we find further density modulations when the average density increases.

Besides, we test the effect of an aligning field on the shape and structure of the tactoids and find that the director field becomes more uniform and the aspect ratio increases, but not to a vast extent. [2]

[1] P. Prinsen, P. van der Schoot, *EPJ E* **13**, 35 (2004).[2] A. Kuhnhold, P. van der Schoot, *JCP* **156**, 104501 (2022).

DY 24: Stochastic Thermodynamics and Information Processing

Time: Wednesday 9:30–11:15

Location: H19

DY 24.1 Wed 9:30 H19

Optimising Energetics in Field Theories: Pareto Front and Phase Transitions — •ATUL TANAJI MOHITE and ETIENNE FODOR — University of Luxembourg, Department of Physics and Materials Science, L-1511, Luxembourg

Field theories have been extremely successful in characterizing the universal properties of various phase transitions, and in delineating a few canonical models which capture the essential Physics in a large class of systems. Interestingly, a generic framework for optimizing the energetic cost associated with the finite-time driving of such systems is still largely missing. Here, building on recent advances in stochastic thermodynamics and optimal transport theory, we show how to analytically derive the optimal driving protocols that minimise average stochastic work, which we apply to cases with either conserved or non-conserved scalar order parameter in the weak noise regime. Moreover, we formulate a numerical multi-optimization problem to simultaneously optimize the mean and fluctuations of stochastic work, leading to revealing a first-order phase transition in the corresponding Pareto front, which features the coexistence of multiple optimal protocols. Overall, our results elucidate how to drive field theories at a minimal energy cost, with the potential to be deployed to a broad class of systems.

DY 24.2 Wed 9:45 H19

Replica-Symmetry Breaking for Ulam's problem — •PHIL KRABBE¹, HENDRIK SCHAWÉ², and ALEXANDER K. HARTMANN¹ — ¹Institute of Physics, University of Oldenburg, Germany — ²LPTM, CY Cergy Paris Université, France

For a given sequence $X = x_1, x_2, \dots, x_n$ of numbers, an increasing subsequence (IS) is a subset of l elements $i(1) < i(2) < \dots < i(l)$ such that $x_{i(1)} < x_{i(2)} < \dots < x_{i(l)}$. The longest increasing subsequences (LIS) problem, i.e. to maximise

l , was considered numerically first by S. Ulam and is a well studied topic. Here we consider the length l as an energy and study the canonical ensemble of ISs controlled by temperature parameter T , which includes the LIS for $T \rightarrow 0$. We extended our algorithm from [1] such that we can draw ISs in perfect equilibrium in polynomial time. This allows us to study large sequences with up to $n = 8192$ numbers.

We studied the IS numerically [2] for sequences X being permutations of integers. As measurable quantities, we analysed the mean energy, the specific heat C and the overlap q between the drawn ISs. Our exact-sampling results indicate that the IS exhibits in the thermodynamic limit a complex energy landscape in the spirit of Replica Symmetry Breaking, characterised by a broad distribution $P(q)$ of overlaps and a hierarchical organization of the configuration space.

[1] P. Krabbe, H. Schawe and A.K. Hartmann, *Phys. Rev. E* **101**, 062109 (2020)[2] A.K. Hartmann, *Big Practical Guide to Computer Simulations*, World Scientific (2015)

15 min. break

DY 24.3 Wed 10:15 H19

Optimality of nonconservative driving for finite-time processes with discrete states — •BENEDIKT REMLEIN and UDO SEIFERT — II. Institut für Theoretische Physik, Universität Stuttgart, 70550 Stuttgart, Germany

An optimal finite-time process drives a given initial distribution to a given final one in a given time at the lowest cost as quantified by total entropy production. We prove that for a system with discrete states this optimal process involves nonconservative driving, i.e., a genuine driving affinity, in contrast to the case of a system with continuous states. In a multicyclic network, the optimal driving

affinity is bounded by the number of states within each cycle. If the driving affects forward and backwards rates nonsymmetrically, the bound additionally depends on a structural parameter characterizing this asymmetry [1]. [1] B. Remlein and U. Seifert, Phys. Rev. E 103, L050105 (2021)

DY 24.4 Wed 10:30 H19

Phase shift in periodically driven non-equilibrium systems: Its identification and a bound — •JULIUS DEGÜNTHER, TIMUR KOYUK, and UDO SEIFERT — II. Institut für Theoretische Physik, Universität Stuttgart, 70550 Stuttgart, Germany
Time-dependently driven stochastic systems form a vast and manifold class of non-equilibrium systems used to model important applications on small length scales such as bit erasure protocols or microscopic heat engines. One property that unites all these quite different systems is some form of lag between the driving of the system and its response. For periodic steady states, we quantify this lag by introducing a generalized phase difference. We prove two tight bounds for this generalized phase difference, which provide upper limits to the lag such systems can yield. The first and most general bound depends only on the relative speed of the driving. The second more detailed bound takes additional information about the rates into account. We show that both bounds can be saturated by an appropriate choice of parameters.

DY 24.5 Wed 10:45 H19

Thermodynamic inference in partially accessible Markov networks: A unifying perspective from transition-based waiting time distributions — •JANN VAN DER MEER, BENJAMIN ERTEL, and UDO SEIFERT — II. Institut für Theoretische Physik, Universität Stuttgart, 70550 Stuttgart, Germany
The inference of thermodynamic quantities from the description of an only partially accessible physical system is a central challenge in stochastic thermodynamics. A common approach is coarse-graining, which maps the dynamics of such a system to a reduced effective one. While coarse-graining states of the system into compound ones is a well studied concept, recent evidence hints at a complementary description by considering observable transitions and waiting times. We consider waiting time distributions between two consecutive transitions of a partially observable Markov network and their ratios to quantify irre-

versibility and entropy production. We formulate criteria whether this entropy estimator provides a lower bound or recovers the full physical entropy production. Additionally, we derive estimators for the topology of the network, i.e., the presence of a hidden cycle, its number of states and its driving affinity. From a different perspective, our results can be condensed into a fluctuation theorem for an equivalent semi-Markov process. This mathematical perspective provides a unifying framework to compare our and known estimators. The correct version of time-reversal is crucial to clarify the relationship of formal versus physical irreversibility. Numerical calculations illustrate our exact results and estimate the quality of our bounds.

DY 24.6 Wed 11:00 H19

Geometric Brownian Information Engine — •DEBASISH MONDAL, RAFNA RAFAEK, and SYED YUNUS ALI — Department of Chemistry, Indian Institute of Technology Tirupati, Andhra Pradesh, India
We design a geometric Brownian information engine by considering overdamped Brownian particles inside a 2-D monolobal confinement with irregular width. Under such detention, particles experience an effective entropic potential which has a logarithmic form. We employ a feedback control protocol as an outcome of error-free position measurement. We reposition the centre of the confinement to the feedback site (x_f) instantaneously when the position of the trapped particle crosses the measurement distance (x_m) for the first time. Then, the particle is allowed to thermal relaxation. We find the exact analytical value of the upper bound of extractable work as $(\frac{5}{3} - 2ln2)k_B T$. We introduce a constant force G downwards to the transverse coordinate. G tunes the entropic contribution in the effective potential and hence the standard deviation (σ) of the probability distribution. The upper bound of the achievable work shows a cross-over from $(\frac{5}{3} - 2ln2)k_B T$ to $\frac{1}{2}k_B T$ when the system changes from an entropy dominated regime to energy dominated one. Compared to an energetic analogue, the loss of information during the relaxation process is higher in the entropy-dominated region, which accredits the less value in achievable work. We recognize that the extracted work is maximum when $x_f = 2x_m$ with $x_m \sim 0.6\sigma$, irrespective of the extent of the entropic limitation. The average displacement increases with growing entropic control and is maximum when $x_m \sim 0.81\sigma$.

DY 25: General Session to the Symposium: Interplay of Substrate Adaptivity and Wetting Dynamics from Soft Matter to Biology (joint session CPP/DY)

Time: Wednesday 9:30–11:15

Location: H39

See CPP 20 for details of this session.

DY 26: Critical Phenomena and Phase Transitions

Time: Wednesday 10:00–11:30

Location: H20

DY 26.1 Wed 10:00 H20

Percolation properties of the Ising spin glass in two dimensions — •LAMBERT MÜNSTER and MARTIN WEIGEL — Institut für Physik, TU Chemnitz, 09107 Chemnitz, Germany

Cluster representations provide a framework to study critical phenomena from the geometrical perspective of percolation. Due to frustration the common Fortuin-Kasteleyn cluster representation of ferromagnets is not well suited to describe the spin-glass transition [1,2]. The order parameter of this transition is the overlap which is naturally defined with respect to two replicas. In the present work we hence study a two-replica cluster representation [3] of the two-dimensional Ising spin glass by performing Monte Carlo simulations at low temperatures. Our data is consistent with the existence of a zero-temperature percolation transition in agreement with the zero-temperature spin-glass transition in two dimensions. The overlap is proportional to the difference in density of the two largest clusters.

- [1] V. Cataudella, G. Franzese, M. Nicodemi, A. Scala, and A. Coniglio, Phys. Rev. Lett. **72**, 1541, (1994).
[2] H. Fajen, A. K. Hartmann, and A. P. Young, Phys. Rev. E **102**, 012131, (2020).
[3] J. Machta, C. M. Newman, and D. L. Stein, J. Stat. Phys. **130**, 113, (2008).

DY 26.2 Wed 10:15 H20

Replica-symmetry breaking for directed polymers in correlated random media — •ALEXANDER K. HARTMANN — Inst. of Physics, University of Oldenburg
The phase-space behavior of complex system can often be described by *replica-symmetry breaking* (RSB), as introduced by Giorgio Parisi for mean-field Ising spin glasses [1] and highlighted by the Nobel price 2021. Numerically, spin glasses and related problems are notoriously hard to study, such that models exhibiting RSB have been treated so far only for small sizes. Here, directed polymers on 1+1 dimensional lattices at temperature T are considered [2]. New ensembles with correlations of the disorder as well as fractal patterning are introduced [3].

This model allows for direct sampling in perfect thermal equilibrium for large system sizes of $N = L^2 = 32768 \times 32768 \approx 10^9$ sites. Fluctuations of the free energy and transverse extension are obtained and compared with the standard uncorrelated ensemble. The phase-space structure is studied via the distribution of overlaps, hierarchical clustering methods and analysis of ultrametricity. One ensemble shows a simple behavior like a ferromagnet. The other two ensembles exhibit indications for multiple RSB. In total, the present model ensembles offer convenient numerical access to comprehensively studying complex RSB-like behavior.

- [1] G. Parisi, Phys. Rev. Lett. **43**, 1754 (1979)
[2] A. K. Hartmann, Big Practical Guide to Computer Simulations, World-Scientific, Singapore (2015)
[3] A. K. Hartmann, Euro. Phys. Lett. **137**, 41002 (2022)

DY 26.3 Wed 10:30 H20

Interplay of disorder and flat band geometry for generalized Lieb models in 3D with correlated order — •JIE LIU¹, CARLO DANIELI², JIANXIN ZHONG¹, and RUDOLF A. RÖMER^{1,3,4} — ¹School of Physics and Optoelectronics, Xiangtan University, Xiangtan 411105, China — ²MPI-PaKS, Nöthnitzer Strasse, Dresden, Germany — ³Department of Physics, University of Warwick, Coventry, CV4 7AL, United Kingdom — ⁴CY Advanced Studies and LPTM (UMR8089 of CNRS), CY Cergy-Paris Université, F-95302 Cergy-Pontoise, France
Uniform Anderson disorder in generalized 3D Lieb models gives rise to the existence of bounded mobility edges and destroys the macroscopic degeneracy of the compactly-localized states. We now introduce correlated order such that this degeneracy remains and the compactly-localized states are preserved. We obtain the energy-disorder phase diagrams via transfer matrix methods, computing the localization lengths and via sparse-matrix direct diagonalization, using r -value energy-level statistics. For suitably large disorders, we can finite-size scale both quantities and identify mobility edges with critical properties close to the

standard Anderson transition in 3D. Intriguingly, the survival of the compactly-localized states lead to seemingly diverging mobility edges. For small disorder, however, a change from extended to localized behavior can be found upon decreasing disorder — leading to an unconventional "inverse Anderson" behavior.

DY 26.4 Wed 10:45 H20

Anomalous collective dynamics of auto-chemotactic populations — JASPER VAN DER KOLK¹, •FLORIAN RASSHOFFER¹, RICHARD SWIDERSKI¹, ASTIK HALDAR², ABHIK BASU², and ERWIN FREY^{1,3} — ¹Arnold Sommerfeld Center for Theoretical Physics and Center for NanoScience, LMU München, Theresienstraße 37, Munich, Germany — ²Theory Division, Saha Institute of Nuclear Physics, HBNI, 1/AF Bidhannagar, Calcutta 700 064, West Bengal, India — ³Max Planck School Matter to Life, Hofgartenstraße 8, Munich, Germany

While the role of local interactions in non-equilibrium phase transitions is well studied, a fundamental understanding of the effects of long-range interactions is lacking. In particular, we ask the question how long-ranged interactions can alter the universal behaviour close to an absorbing state. As a model system, we study the critical dynamics of reproducing agents subject to auto-chemotactic interactions and limited resources.

A renormalization group analysis reveals distinct scaling regimes for fast (attractive or repulsive) interactions; for slow signal transduction the dynamics is dominated by a diffusive fixed point. Further, we present a novel nonlinear mechanism that stabilizes the continuous transition against the emergence of a characteristic length scale due to a chemotactic collapse.

DY 26.5 Wed 11:00 H20

Population Annealing Monte Carlo Using the Rejection-Free n-Fold Way Update Applied to a Frustrated Ising Model on a Honeycomb Lattice — •DENIS GESSERT^{1,2}, MARTIN WEIGEL^{1,3}, and WOLFHARD JANKE² — ¹Centre for Fluid and Complex Systems, Coventry University, Coventry, CV1 5FB, United Kingdom — ²Institut für Theoretische Physik, Leipzig University, Postfach 100920, 04009 Leipzig, Germany — ³Institut für Physik, Technische Universität Chemnitz, 09107 Chemnitz, Germany

Population annealing (PA) is a Monte Carlo method well suited for problems with a rough free energy landscape such as glassy systems. PA is similar to re-

peated simulated annealing, with the addition of a resampling step at each temperature. While a large population may to some extent compensate for imperfect equilibration, it is clear that PA must fail if almost no spins are flipped during equilibration.

This is the case in systems with a phase transition at a very low temperature where a high Metropolis rejection rate makes sampling phase space near infeasible. To overcome this slow-down we propose a combination of the PA framework with the rejection-free "n-fold way" update and achieve an exponential speed-up at low temperatures as compared to Metropolis.

To test our method we study the Ising model with competing ferromagnetic ($J_1 > 0$) nearest and antiferromagnetic ($J_2 < 0$) next-to-nearest neighbor interactions on a honeycomb lattice. As T_c becomes arbitrarily small when approaching the special point $J_2 = -J_1/4$ with $T_c = 0$ we consider this a good choice to test the efficacy of our method.

DY 26.6 Wed 11:15 H20

Critical behavior of the three-state random-field Potts model in three dimensions — MANOJ KUMAR¹, VARSHA BANERJEE², SANJAY PURI³, and •MARTIN WEIGEL¹ — ¹Institut für Physik, Technische Universität Chemnitz, 09107 Chemnitz, Germany — ²Department of Physics, Indian Institute of Technology, Hauz Khas, New Delhi – 110016, India — ³School of Physical Sciences, Jawaharlal Nehru University, New Delhi – 110067, India.

Enormous advances have been made in the past 20 years in our understanding of the random-field Ising model, and there is now consensus on many aspects of its behavior at least in thermal equilibrium. In contrast, little is known about its generalization to the random-field Potts model which has a number of important experimental realizations. Here we start filling this gap with an investigation of the three-state random-field Potts model in three dimensions. Building on the success of ground-state calculations for the Ising system, we use a recently developed approximate scheme based on *graph-cut methods* to study the properties of the zero-temperature random fixed point of the system that determines the zero and non-zero temperature transition behavior. We find compelling evidence for a continuous phase transition. Implementing an extensive finite-size scaling (FSS) analysis, we determine the critical exponents and compare them to those of the random-field Ising model.

DY 27: Networks: From Topology to Dynamics (joint session SOE/BP/DY)

Time: Wednesday 10:15–12:45

Location: H11

See SOE 12 for details of this session.

DY 28: Extreme Events, Glasses and Miscellaneous

Time: Wednesday 11:15–13:00

Location: H19

DY 28.1 Wed 11:15 H19

Symmetries and zero modes in sample path large deviations — •TIMO SCHORLEPP¹, TOBIAS GRAFKE², and RAINER GRAUER¹ — ¹Institute for Theoretical Physics I, Ruhr-University Bochum, Bochum, Germany — ²Mathematics Institute, University of Warwick, Coventry, United Kingdom

Sharp large deviation estimates for stochastic differential equations with small noise, based on minimizing the Freidlin-Wentzell action functional under appropriate boundary conditions, can be obtained by integrating certain matrix Riccati differential equations along the large deviation minimizers or instantons, either forward or backward in time. Previous works in this direction often rely on the existence of isolated minimizers with positive definite second variation. By adopting techniques from field theory and explicitly evaluating the large deviation prefactors as functional determinant ratios using Forman's theorem, we extend the approach to general systems where degenerate submanifolds of minimizers exist. The key technique for this is a boundary-type regularization of the second variation operator. This extension is particularly relevant if the system possesses continuous symmetries that are broken by the instantons. We find that removing the vanishing eigenvalues associated with the zero modes is possible within the Riccati formulation and amounts to modifying the initial or final conditions and evaluation of the Riccati matrices. We apply our results in multiple examples including a dynamical phase transition for the average surface height in short-time large deviations of the one-dimensional Kardar-Parisi-Zhang equation with flat initial profile.

DY 28.2 Wed 11:30 H19

Diffusivity dependence of the transition path ensemble — LUKAS KIKUCHI, RONOJOY ADHIKARI, and •JULIAN KAPPLER — DAMTP, Cambridge University, Cambridge, UK

Transition pathways of stochastic dynamical systems are typically approximated by instantons. Here we show, using a dynamical system containing two com-

peting pathways, that at low-to-intermediate temperatures, instantons can fail to capture the most likely transition pathway. We construct an approximation which includes fluctuations around the instanton and, by comparing with the results of an accurate and efficient path-space Monte Carlo sampling method, find this approximation to hold for a wide range of temperatures. Our work delimits the applicability of large deviation theory and provides methods to probe these limits numerically.

DY 28.3 Wed 11:45 H19

Sampling Rare Event Energy Landscapes via a Birth-Death Process — •BENJAMIN PAMPEL¹, SIMON HOLBACH², LISA HARTUNG², and OMAR VALSSON^{1,3} — ¹Max-Planck-Institute für Polymerforschung, Ackermannweg 10, 55128 Mainz — ²Institut für Mathematik, Johannes Gutenberg-Universität Mainz, Staudingerweg 9, 55099 Mainz — ³Department of Chemistry, University of North Texas, Denton, TX, USA

We investigate a novel sampling algorithm that augments Langevin dynamics with birth-death moves. This is a modification of a previously proposed algorithm [arXiv:1905.09863] that provides an approximation of a stochastic birth-death process for a particle-based implementation. The method connects multiple parallel Langevin dynamics simulations of the same system with a birth-death scheme to facilitate global sampling according to the equilibrium distribution. We investigate the algorithm theoretically, implement it into a custom molecular simulation code, and test it via numerical simulations. We also examine the behavior of the algorithm under change of parameters. In this process, we observe the desired sampling for all tested systems. We find that the performance of the method is independent of the intrinsic time scales and barriers of the system, which is favorable for systems with processes on long time scales.

DY 28.4 Wed 12:00 H19

MD simulations of partially frozen water in silica nanopores — •SEBASTIAN KLOTH and MICHAEL VOGEL — TU Darmstadt, Institut für Physik kondensierter Materie, Hochschulstr. 6, 64289, Darmstadt, Germany

The properties of confined water are of enormous importance in nature and technology. In particular, the effects of partial freezing on structure and dynamics is highly relevant for, e.g. geology, cryopreservation and our understanding of the glass transition of water [1]. A powerful tool to study structural and dynamical properties of confined liquids are MD simulations [2]. We use this method to gain a better understanding of the effect of partial crystallization on the properties of confined water. A series of silica confinements with and without an artificially frozen crystalline core were prepared and the remaining liquid water layer was analyzed. Dynamics and structures of liquid layers with various thicknesses and their temperature dependencies are determined and compared to those with interfacial layers in the absence of a frozen crystalline core. We show that partial crystallization has substantial effects on the properties of confined water. Additionally the simulation results are used to calculate spectral densities of water dynamics for comparison with results of experimental studies. In particular, we explore which model for the functional form of the spectral density should be used in NMR spin-lattice relaxation studies on the dynamics of completely liquid or partially frozen water in nanopores.

[1] Cervený, S. et al., Chem. Rev., **2016**, *116* (13) 7608-7625

[2] Horstmann, R. et al., Langmuir, **2022**, 10.1021/acs.langmuir.2c00521

DY 28.5 Wed 12:15 H19

Driven aging dynamics on sparse networks — •BENEDIKT JOHANNES GRÜGER¹, DIEGO TAPIAS¹, and PETER SOLLICH^{1,2} — ¹Institute for Theoretical Physics, Georg-August-Universität Göttingen, 37077 Göttingen, Germany — ²Department of Mathematics, King's College London, London WC2R 2LS, UK

We investigate the interaction of two paradigmatic ways of being out of equilibrium, aging and driving, in simple models of glassy dynamics. We specifically consider the Bouchaud model, where a system jumps between the numerous minima of a rough energy landscape in configuration space. As the temperature decreases, the system undergoes a dynamical phase transition, at which the relaxation time diverges. With an additional field, we then drive the system by biasing its dynamics towards higher/lower jumping activity. We investigate the spectrum of the (biased) master operator in that framework, using a population dynamics algorithm based on cavity theory that allows us to deduce statements about the thermodynamic limit. Combining this with extensive diagonalization we identify novel regimes in the bias-temperature phase diagram that are distinguished by the occurrence of different kinds of eigenvector localization and are linked to the existence of a spectral gap. We also present methodological advances in the form of novel strategies for operating the population dynamics algorithm.

DY 28.6 Wed 12:30 H19

Moiré-pattern evolution couples rotational and translational friction at crystalline interfaces — •XIN CAO¹, ANDREA SILVA^{2,3}, EMANUELE PANIZON⁴, ANDREA VANOSSÌ^{2,3}, NICOLA MANINI⁵, ERIO TOSATTI^{2,3,4}, and CLEMENS BECHINGER¹ — ¹Fachbereich Physik, Universität Konstanz, 78464 Konstanz, Germany — ²CNR-IOM, Consiglio Nazionale delle Ricerche - Istituto Officina dei Materiali, c/o SISSA, Via Bonomea 265, 34136, Trieste, Italy — ³International School for Advanced Studies (SISSA), Via Bonomea 265, 34136 Trieste, Italy — ⁴The Abdus Salam International Centre for Theoretical Physics (ICTP), Strada Costiera 11, 34151 Trieste, Italy — ⁵Dipartimento di Fisica, Università degli Studi di Milano, Via Celoria 16, 20133 Milano, Italy

We experimentally and theoretically study the rotational dynamics and depinning of two-dimensional colloidal crystalline clusters on periodically corrugated surfaces under well-controlled torques. We demonstrate that the traversing of locally commensurate areas of the moiré pattern through the edges of clusters, which is hindered by potential barriers during cluster rotation, eventually controls its rotational depinning. The experimentally measured depinning thresholds as a function of cluster size strikingly collapse onto a universal theoretical curve which predicts a superlow-static-torque state for large clusters. We further reveal a cluster-size-independent rotation-translation depinning transition when lattice-matched clusters are driven jointly by a force and a torque. Our work provides guidelines to the design of nanomechanical devices that involve rotations on atomic surfaces.

DY 28.7 Wed 12:45 H19

Accurate dynamics from memory in chemical reactions with small copy numbers — •MOSHIR HARSH and PETER SOLLICH — Institut für Theoretische Physik, Georg-August-Universität Göttingen

Chemical reactions in the regime of small copy numbers of species such as *gene* regulation or *protein* interaction networks show large fluctuations, making mean field solutions as given by mass action kinetics unreliable. Accurate calculations of the one and two-time quantities of these stochastic processes remain a challenging problem; numerical solutions to the master equation or stochastic simulations can be deployed, but these are computationally intensive and do not allow likelihood inference from dynamical trajectories.

Here, we present a method that captures the fluctuations beyond mean field using self-consistently determined *memory*: by integrating information from the past we can systematically improve our approximation for the dynamics of chemical reactions. This memory is not added ad-hoc, but can be shown to arise naturally by considering the effective action of the Doi-Peliti field theory of chemical reactions. The effective action is treated perturbatively but we can self-consistently resum a very large class of diagrams resulting in a stable expansion. We demonstrate this method and its accuracy on single and multi-species binary reactions across a range of parameter values. We show how this approach also opens a route to making inferences from experimentally measured dynamics.

DY 29: Invited Talk Eric Bertin

Time: Wednesday 12:00–12:30

Location: H18

Invited Talk

DY 29.1 Wed 12:00 H18

Derivation of a continuum description of sheared jammed soft suspensions from particle dynamics — •ERIC BERTIN, NICOLAS CUNY, and ROMAIN MARI — Univ. Grenoble Alpes, CNRS, LIPhy, 38000 Grenoble, France

Jammed soft suspensions exhibit a rich phenomenology under deformation, including the existence of a yield stress and non-monotonous stress relaxations. Starting from the microscopic particle dynamics, we derive using a set of approximations a continuum description in terms of the macroscopic stress tensor (or more precisely, its traceless part) for given applied time-dependent defor-

mations. The coefficients appearing in this equation are expressed in terms of the packing fraction and of particle-level parameters. This constitutive equation rooted in the microscopic dynamics qualitatively reproduces a number of salient features of the rheology of jammed soft suspensions, including the presence of yield stresses for both the shear component of the stress and the normal stress difference. Time-dependent protocols like the relaxation after a preshear are also considered, showing that a stronger preshear eventually leads to a more relaxed stress. This new methodology opens avenues for future developments, and involves physically more transparent approximations than the Mode Coupling approach.

DY 30: Energy Networks (joint session SOE/DY)

Time: Wednesday 12:45–13:15

Location: H11

See SOE 13 for details of this session.

DY 31: Active Matter 4 (joint session DY/BP/PPP)

Time: Wednesday 15:00–17:30

Location: H18

DY 31.1 Wed 15:00 H18

Clusters and fractals in non-reciprocally interacting colloids — •SEBASTIAN FEHLINGER and BENNO LIEBCHEN — Institut für Physik kondensierter Materie, TU Darmstadt, Hochschulstraße 8, D-64289 Darmstadt, Germany

Non-reciprocal interactions are widespread in nature. For the specific case of a binary mixture of passive particles, the breaking of the action reaction principle can lead to formation of active colloidal molecules which are capable of self-propulsion. For small systems, such active molecules have already been realized in experiments based on phoretically interacting binary colloidal mixtures [1,2].

The focus of the present work is to understand the many body behaviour of active molecules. Using particle based simulations and continuum theory, we find that non-reciprocal attractions in a binary mixture of non-motile particles can destabilize the uniform disordered phase and lead to clusters which grow in time. Surprisingly, for a wide parameter range, the clusters only grow up to a certain size such that coarsening is arrested. We attribute this to an effective screening effect which hinges on the characteristic spatiotemporal organization of the two species within the clusters. In addition, remarkably, in a different parameter regime, we find porous macroclusters featuring significant holes and a fractal dimension which differs from the one expected for conventional diffusion limited aggregation.

[1]F. Schmidt et al. J. Chem. Phys. 150, 094905 (2019)

[2]J. Grauer et al. Nat. Commun. 12, 6005 (2021).

DY 31.2 Wed 15:15 H18

Analysis of transient dynamics of bioconvection in swimming algae — •ALEXANDER JAROSIK, FLORIAN VON RÜLING, and ALEXEY EREMIN — Otto-von-Guericke Universität, Magdeburg, Germany

Swimming unicellular algae *Chlamydomonas reinhardtii* exposed to light form intricate hydrodynamic instability patterns called bioconvection. High-density plumes of cells are formed in the top layer, descend to the container's bottom, and rise again to the top. This instability arises from coupling between the gyro- and phototactic behaviour of the cells, their physical properties and the flow. In this work, we analyse the microswimmer's dynamics as a function of the cell density, confinement of the environment and light. The transient behaviour of the plume formation is analysed using the Continuous Wavelet Transformation (CWT). We demonstrate that the plume formation can be controlled by local illumination.

DY 31.3 Wed 15:30 H18

Optimal turbulent transport in microswimmer suspensions — •HENNING REINKEN¹, SABINE H. L. KLAPP¹, and MICHAEL WILCZEK² — ¹Technische Universität Berlin — ²Universität Bayreuth

Microswimmer suspensions, a paradigmatic example of an active fluid, self-organize into complex spatio-temporal flow patterns, including regular vortex lattices and mesoscale turbulence. This work investigates the transport properties of these suspensions by tracking the diffusive motion of passive tracers in the turbulent flow. We apply a continuum model for the effective microswimmer velocity field [1,2], where the dynamics is governed by the competition between relaxation to a regular vortex lattice and destabilization by nonlinear advection. Varying the strength of nonlinear advection, we observe two qualitatively different regimes of flow transport that we distinguish with the help of the dimensionless Kubo number K , which compares different time scales. Right above the transition to turbulence, the flow field evolves very slowly ($K \gg 1$) and the spatial vortex structures lead to dominant trapping effects. In contrast, for large advection strength, much faster dynamics ($K \ll 1$) leads to transport properties completely determined by the temporal correlations of the flow. In between ($K \approx 1$), we observe a regime of optimal transport, where the diffusion coefficient reaches a maximum.

[1] Reinken, Klapp, Bär, Heidenreich, Phys. Rev. E **97**, 022613 (2018)

[2] James, Bos, Wilczek, Phys. Rev. Fluids **3**, 061101(R) (2018).

DY 31.4 Wed 15:45 H18

Interfacial activity dynamics of confined active droplets — •PRASHANTH RAMESH^{1,2}, BABAK VAJDI HOKMABAD¹, ARNOLD J.T.M. MATHIJSEN³, DMITRI O. PUSHKIN⁴, and CORINNA C. MAASS^{1,2} — ¹Max Planck Institute for Dynamics and Self-Organization — ²University of Twente — ³University of Pennsylvania — ⁴University of York

Active emulsions exhibit a complex hydrodynamic mode spectrum driven by chemical advection-diffusion instabilities. We study such an active emulsion consisting of oil droplets that dynamically solubilize in a supramolecular aqueous surfactant solution. It has been predicted that the interaction with self-generated chemical fields leads to multistable higher-mode flow fields and chemorepulsive phenomena. To investigate such chemodynamic effects, we study cylindrical droplets pinned between the top and bottom surfaces of a microfluidic reservoir, such that they only produce pumping flows, while we simultaneously quantify

the chemical concentration field and the hydrodynamic velocity field. With increasing droplet radius we observe: vortical structures generated by the droplet migrating around the interface, bistability between a dipolar and quadrupolar flow mode, and, eventually, a transition to multipolar modes. We further measured flow fields by particle image velocimetry and compared them to a hydrodynamic model based on a Brinkman squirmer. A simultaneous quantification of the flow fields and oil-filled micelle distribution suggests that a local buildup of chemical products leads to a saturation of the surface, which affects the propulsion mechanism and eventually suppresses all activity.

DY 31.5 Wed 16:00 H18

Hydrodynamics and fluctuations in bacterial models — •SUBHADIP CHAKRABORTI — Friedrich-Alexander-Universität Erlangen-Nürnberg, Erlangen, Germany — Max-Planck-Zentrum für Physik und Medizin, Erlangen, Germany

Motivated by a biological example of the persistent motion of bacteria, we propose two one-dimensional models of active lattice gases with hardcore interactions. Using macroscopic fluctuation theory (MFT), we analytically derive hydrodynamics for those models and calculate two density-dependent transport coefficients – the bulk-diffusion coefficient and the conductivity, and verify the Einstein relation (ER) by comparing the ratio of those transport coefficients with subsystem number fluctuation. The first model consisting of particles with competing mechanisms of short and long-range hopping obeys the Einstein relation, and exhibits, in the limit of infinite range hopping, upon tuning density (or activity), a 'superfluid' transition from a finitely conducting state to an infinitely conducting one. Interestingly, the bulk-diffusion coefficient remains constant throughout. The diverging conductivity induces 'giant' number fluctuations in the system. In the second model, consisting of hardcore run and tumble particles with persistent motion in one direction decided by an associated spin variable until the direction of spin is reversed, we perform a similar calculation and find that the Einstein relation is violated. This analytic framework could be useful for a better understanding of the collective behavior of many biological systems such as bacterial colonies and other multicellular aggregates, in the context of dynamics and transport properties.

15 min. break

DY 31.6 Wed 16:30 H18

Shearing an Active Glass — •RITUPARNO MANDAL and PETER SOLLICH — Institut für Theoretische Physik, Göttingen, Germany

Recent experiments and simulations have revealed glassy features of cytoplasm, tissues and dense assemblies of self propelled colloids. This prompts the fundamental question of whether non-equilibrium (active) amorphous materials are essentially equivalent to their passive counterparts, or whether they can present qualitatively different behaviour. To tackle this challenge we investigate the yielding and mechanical behaviour of a model active glass former, a Kob-Andersen glass in two dimensions where each particle is driven by a constant propulsion force whose direction varies diffusively over time. Using extensive Molecular Dynamics simulations, we focus in particular on the effects of the intermittent dynamics in the regime of highly persistent activity and reveal a novel type of shear induced orientational ordering in the system.

DY 31.7 Wed 16:45 H18

Active motion with varying self propulsion — LORENZO CAPRINI¹, ALEXANDER R. SPRENGER¹, UMBERTO M. B. MARCONI², HARTMUT LÖWEN¹, and •RENÉ WITTMANN¹ — ¹Institut für Theoretische Physik II: Weiche Materie, Heinrich-Heine Universität Düsseldorf, Germany — ²School of Sciences and Technology, University of Camerino, Italy

Active Brownian Particles (ABPs), commonly perceived as the standard model for (dry) active motion, are characterized by a constant self-propulsion velocity along the direction of a unit vector which performs rotational diffusion. In nature, however, the swim velocity is usually not a constant in time and space. Here, we present a generic form of the equations of motion of active particles, which account for two aspects of varying self propulsion. First, we introduce a general stochastic process with fluctuating modulus of the self-propulsion vector, which defines a parental active model (PAM). We argue that the two well-known models of ABPs and Active Ornstein-Uhlenbeck Particles (AOPUs) emerge as limiting cases of the PAM [1], i.e., they are rather sisters than cousins. Second, we demonstrate that a position-dependent swim-velocity field can be consistently introduced for any self-propulsion mechanism [2]. Finally, we discuss the effects of varying self propulsion in external confinement [1,3] and predict the stationary probability distributions in terms of effective interactions [3].

[1] L. Caprini et al., J. Chem. Phys. 156, 071102 (2022).

[2] L. Caprini et al., Soft Matter, 18, 1412 (2022).

[3] L. Caprini et al., arXiv:2203.00603 (2022).

DY 31.8 Wed 17:00 H18

Perturbing the athermal jamming transition by activity — •MICHAEL SCHMIEDEBERG — Friedrich-Alexander-Universität Erlangen-Nürnberg, Erlangen, Germany

By minimizing the interaction energy in a soft sphere system without crossing energy barriers the discontinuous athermal jamming transition can be observed at a packing fraction of about 0.64 in three dimensions [1]. We consider the jamming of active particles where the activity corresponds to a perturbation to the athermal jamming process. We find that due to the activity the transition becomes continuous and the transition packing fraction might occur at a different density [2]. The critical exponents agree to those of the universality class of directed percolation. As a consequence, athermal jamming of passive particles seems to be a (singular) limit of the jamming transition in an active system. Note that other perturbation like thermal fluctuations lead to a similar behavior [3]. Therefore, athermal active particles can be seen as a prototype system that leads to new insights how jamming with perturbations (as also studied in [2-5]) can be related to glassy dynamics.

[1] C.S. O'Hern et al., Phys. Rev. Lett. 88, 075507 (2002) and Phys. Rev. E 68, 011306 (2003).

[2] M. Maiti and M. Schmiedeberg, EPL 126, 46002 (2019).

[3] M. Maiti and M. Schmiedeberg, Scientific Reports 8, 1837 (2018); for 2D: Eur. Phys. J. E 42, 38 (2019).

[4] L. Milz and M. Schmiedeberg, Phys. Rev. E 88, 062308 (2013).

[5] S. Wilken et al., Phys. Rev. Lett. 127, 038002 (2021).

DY 31.9 Wed 17:15 H18

Non-equilibrium phase separation in mixtures of catalytically active particles: size dispersity and screening effects — •VINCENT OUAZAN-REBOUL¹, JAIME AGUDO-CANALEJO¹, and RAMIN GOLESTANIAN^{1,2} — ¹Max Planck Institute for Dynamics and Self-Organization, Am Fassberg 17, D-37077, Göttingen, Germany — ²Rudolf Peierls Centre for Theoretical Physics, University of Oxford, OX1 3PU, Oxford, UK

Biomolecular condensates in cells are often rich in catalytically active enzymes. This is particularly true in the case of the large enzymatic complexes known as metabolons, which contain different enzymes that participate in the same catalytic pathway. One possible explanation for this self-organization is the combination of the catalytic activity of the enzymes and a chemotactic response to gradients of their substrate, which leads to a substrate-mediated effective interaction between enzymes. These interactions constitute a purely non-equilibrium effect and show exotic features such as non-reciprocity. Here, we analytically study a model describing the phase separation of a mixture of such catalytically active particles. We show that a Michaelis-Menten-like dependence of the particles' activities manifests itself as a screening of the interactions, and that a mixture of two differently sized active species can exhibit phase separation with transient oscillations. We also derive a rich stability phase diagram for a mixture of two species with both concentration-dependent activity and size dispersity.

DY 32: Invited Talk Stephan Weiss

Time: Wednesday 15:00–15:30

Location: H19

Invited Talk

DY 32.1 Wed 15:00 H19

Large scale patterns in turbulent Rayleigh-Bénard convection — •STEPHAN WEISS — DLR Göttingen — MPI f. Dyn. & Self-Org.

Thermal convection is one of the most important heat transport mechanisms and the driving force behind large scale flows in geo- and astrophysics. It is mostly studied in the Rayleigh-Bénard (RB) setup, where a horizontal fluid layer is heated from below and cooled from above. RB convection is a model system not only to study transport phenomena in turbulent flows under strong driving, but also to study pattern formation as it exhibits regular laminar flow patterns under weak thermal driving. Turbulent RB convection is usually studied experimentally and numerically in containers of small aspect ratios between their lat-

eral size (L) and their height (H). Rather recently, however, investigations have also focused on RB convection in laterally extended systems, as it was found that the time-averaged mean velocity resembles the laminar pattern under weak driving. In my talk I will first discuss some recent developments in the research of large scale patterns in RB convection. Then I will present our own results from volumetric spatially velocity measurements in a rectangular RB cell with a square horizontal cross-section and an aspect ratio $\Gamma = L/H = 16$. Via Lagrangian particle tracking, we have measured the velocity and acceleration of up to 300,000 fluorescent microspheres simultaneously and have calculated the entire three-dimensional velocity field with a resolution of about the Kolmogorov length. From these data, we can determine the large scale patterns, as well as their morphology and follow their slow temporal evolution.

DY 33: Invited Talk Anatoli Polkovnikov

Time: Wednesday 15:00–15:30

Location: H20

Invited Talk

DY 33.1 Wed 15:00 H20

Detecting dynamical quantum phase transitions by string observables — •ANATOLI POLKOVNIKOV¹, AMIT DUTTA², and SOUVIK BANDYOPADHYAY² — ¹Boston University, Boston, USA — ²IIT Kanpur, India

Dynamical quantum phase transitions (DQPT) were proposed as singularities developing in time following a quantum quench in the return amplitude or

the Loschmidt echo. They have close connection with Fisher zeros of the partition function extended to imaginary temperatures (real time). Because the Loschmidt echo is hard to measure it is not easy to observe DQPT experimentally. In this talk I will explain how one can detect DQPT both as a function of time and as a function of quench amplitude in finite size string observables. These findings are in very good agreement with an experiment by J. Zhang et. al. Nature 551, 601 (2017) performed in a trapped ion simulator.

DY 34: Fluid Physics: Turbulence and Convection

Time: Wednesday 15:30–17:15

Location: H19

DY 34.1 Wed 15:30 H19

Ejection of marine microplastics by raindrops: A computational and experimental study — •MORITZ LEHMANN¹, LISA MARIE OEHLISCHLÄGEL², FABIAN HÄUSL¹, ANDREAS HELD², and STEPHAN GEKLE¹ — ¹Biofluid Simulation and Modeling - Theoretische Physik VI, Universität Bayreuth — ²Umweltchemie und Luftreinhaltung, Technische Universität Berlin

Raindrops impacting water surfaces such as lakes or oceans produce myriads of tiny droplets which are ejected into the atmosphere at very high speeds. Here we combine computer simulations and experimental measurements to investigate whether these droplets can serve as transport vehicles for the transition of microplastic particles with diameters of a few tens of micrometers from ocean water to the atmosphere. Using the Volume-of-Fluid lattice Boltzmann method, extended by the immersed-boundary method, we performed more than 1600 raindrop impact simulations and provide a detailed statistical analysis on the ejected droplets. Using typical sizes and velocities of real-world raindrops, we

simulate straight impacts with various raindrop diameters as well as oblique impacts. We find that a 4 mm diameter raindrop impact on average ejects more than 167 droplets. We show that these droplets indeed contain microplastic concentrations similar to the ocean water within a few millimeters below the surface. To further assess the plausibility of our simulation results, we conduct a series of laboratory experiments, where we find that microplastic particles are indeed contained in the spray. Based on our results and known data, we estimate the global relevance of this transport mechanism.

DY 34.2 Wed 15:45 H19

Transition between 2D and 3D rotating incompressible convection in direct numerical simulations — •KEVIN LÜDEMANN and ANDREAS TILGNER — Institute of Astrophysics and Geophysics, Göttingen, Germany

Direct numerical simulations of an incompressible fluid with a Prandtl number of 0.7 are used to investigate differences between exact 2D and 3D convection.

The fluid is rotating about a direction perpendicular to the direction of gravity (centrifugal gravity) and zonal flow is suppressed by horizontal walls in a container with an aspect ratio of 0.5. The convection is controlled by a Rayleigh number ranging from 10^4 to 10^9 and rotation is characterised by the Ekman number ranging from 10^{-1} down to 10^{-5} . Due to the Taylor-Proudman theorem, the convective flow will be restrained to the plane perpendicular to the direction of rotation at high rotation rates. This behaviour will break down once convective driving and therefore kinetic energy is large enough. Thermal transport and kinetic energy density show different scalings for the 2D and 3D flow. The stability theory of a vortex with elliptical streamlines is tailored to the geometry in order to explain the transition. Ultimately, a dependence of the Reynolds number on the Rossby number is found $Re \propto Ro^{-2}$ for small Rossby numbers. Both are based on the RMS velocity of the vortex.

15 min. break

DY 34.3 Wed 16:15 H19

The onset of non-Gaussian velocity gradient statistics in low-Reynolds number flows — •MAURIZIO CARBONE¹ and MICHAEL WILCZEK^{1,2} — ¹Max Planck Institute for Dynamics and Self-Organization, Am Faßberg 17, 37077 Göttingen, Germany — ²Theoretical Physics I, University of Bayreuth, Universitätsstr. 30, 95447 Bayreuth, Germany

The Reynolds number prescribes the range of active scales involved in a turbulent flow. Stirring a fluid through a Gaussian forcing at vanishingly small Reynolds produces a multi-point Gaussian field, while flows at higher Reynolds exhibit non-Gaussianity, cascades, anomalous scaling and preferential alignments. Recent works (Yakhot and Donzis, Phys. Rev. Lett. 2017) showed that low-Reynolds flows exhibit features of high-Reynolds turbulence.

We address the onset of turbulent features in low-Reynolds flows by combining a perturbation theory of the full Navier-Stokes equations (Wyld, Ann. Phys. 1961) with the Lagrangian modelling of velocity gradients along fluid particle trajectories (Meneveau, Annu. Rev. Fluid Mech. 2011). We construct a stochastic model for the velocity gradient in which all the model coefficients follow directly from the Navier-Stokes equations. The associated Fokker-Planck equation for the single-time velocity gradient probability density admits analytic solutions which show the onset of non-Gaussianity: skewness, intermittency and preferential alignments arise in the gradients statistics as the Reynolds number increases. The results are in excellent agreement with direct numerical simulations of low-Reynolds flows.

DY 34.4 Wed 16:30 H19

Temporal large-scale intermittency and its impact on flow statistics — •LUKAS BENTKAMP^{1,2} and MICHAEL WILCZEK^{1,2} — ¹Theoretical Physics I, University of Bayreuth, Universitätsstr. 30, 95447 Bayreuth — ²Max Planck Institute for Dynamics and Self-Organization, Am Faßberg 17, 37077 Göttingen

Turbulent flows in three dimensions are characterized by the transport of energy from large to small scales, the so-called energy cascade. Since the small scales are the result of the nonlinear dynamics across the scales of the energy cascade, they are often thought of as universal and independent of the large scales. However, as famously remarked by Landau in 1959, sufficiently slow variations of the large scales should nonetheless be expected to impact small-scale statistics. Such variations, often termed large-scale intermittency, are almost inevitable in experiments and even in simulations, while differing from flow to flow.

Here we evaluate the impact of temporal large-scale fluctuations on velocity,

velocity gradient, and acceleration statistics by introducing controlled variations of the energy injection rate into direct numerical simulations of turbulence. We find that slow variations can have a strong impact on flow statistics, amplifying the tails of the measured distributions. We also show that the stronger tails can be accounted for by superposing an ensemble of stationary flows such that the temporal variations of an appropriate flow measure such as the energy dissipation rate are matched. Overall, our work demonstrates that in order to ensure comparability of statistical results in turbulence, large-scale intermittency needs to be taken into account.

DY 34.5 Wed 16:45 H19

Towards an effective description of turbulent superstructures in simple shear flows — •FABIÁN ÁLVAREZ-GARRIDO and MICHAEL WILCZEK — Theoretical Physics I, University of Bayreuth, Bayreuth

Turbulent flows driven by large-scale forces such as convection, shear, or rotation may display large-scale coherent flows, namely turbulent superstructures, coexisting with fully developed turbulence on the small scales. A complete description of these flows involves innumerable degrees of freedom, yet turbulent superstructures seem to evolve according to a comparably lower-dimensional set of equations. In addition, despite the ubiquity of turbulent superstructures, their interplay with the smaller scales is not yet fully understood. We study a simple shear-driven flow, the three-dimensional Kolmogorov flow. The large scales in this flow feature the formation of large-scale vortex pairs. Moreover, the system exhibits permanent dynamics between states having a different number of vortex pairs. Employing amplitude equations, we characterize the dynamics of the large scales close to the onset of the vortex pairs. We show that the dynamics close to the onset correspond to the one of a two-dimensional flow. Furthermore, we show that far from the onset, the derived model captures the structure of the large-scale vortices. Based on data from direct numerical simulations, we introduce new stochastic terms to these amplitude equations to model the contribution of the small scales to the dynamics of the large ones. These modified amplitude equations can qualitatively reproduce the dynamics of these large-scale vortex pairs and shed light on the role of small-scale turbulence in the formation of turbulent superstructures.

DY 34.6 Wed 17:00 H19

3D simulation of convection patterns in dry salt lakes — •LUCAS GOEHRING¹, MATTHEW THREADGOLD², CÉDRIC BEAUME², and STEVE TOBIAS² — ¹Nottingham Trent University, Nottingham, UK — ²University of Leeds, Leeds, UK

Salt deserts are some of the most extreme and beautiful landscapes in the world—flat silver-white crystalline plains covered with bizarre and seemingly unnatural shapes. The most prominent feature of these fantastic landscapes is a characteristic tiling of polygons, formed by ridges in the salt-encrusted surface, and always a few meters across. Recently, a dynamical model has been proposed to explain their formation as the surface expression of buoyancy-driven convection happening in the wet salty soil beneath the desert surface. Here, we present a 3D numerical model of the salt lake problem, where a fluid-saturated porous medium is subject to a constant surface evaporation, mimicking the conditions of a desert with an underground aquifer near the surface. We look in turn at the initial instabilities expected in this system, and how they will evolve in time into a dynamical steady state. In this we focus on identifying the patterns that develop in the model, and exploring how the surface flux of salinity depends on the driving parameters.

DY 35: Quantum Chaos and Coherent Dynamics

Time: Wednesday 15:30–18:00

Location: H20

DY 35.1 Wed 15:30 H20

THz-induced high-order harmonic generation and nonlinear transport in graphene — •WENWEN MAO¹, ANGEL RUBIO^{1,2}, and SHUNSUKE A. SATO^{3,1} — ¹Max Planck Institute for the Structure and Dynamics of Matter, Luruper Chaussee 149, 22761 Hamburg, Germany — ²Center for Computational Quantum Physics (CCQ), Flatiron Institute, 162 Fifth Avenue, New York, NY 10010, USA — ³Center for Computational Sciences, University of Tsukuba, Tsukuba 305-8577, Japan

Employing the quantum master equation with phenomenological relaxation, we theoretically study the nonequilibrium dynamics of THz-induced high-order harmonic generation in graphene. We first performed fully dynamical simulation to investigate the high-order harmonic generation in graphene induced by THz laser fields. We found that the emitted harmonics is enhanced with the increase in the chemical potential, and this observation is consistent with the recent experiments. Then we introduce a quasi-static picture to develop the microscopic understanding of the THz-induced currents and the population distribution of conduction band in graphene from the viewpoint of a nonequilibrium picture of electron dynamics. The nonlinear electric conductivity of graphene is

also investigated under static electric fields for various field strength and chemical potential shifts. The impact of electron temperature change is also investigated to compare with the thermodynamic model in the previous work.

DY 35.2 Wed 15:45 H20

Explicit expressions for stationary states of the Lindblad equation for a finite state space — •BERND MICHAEL FERNENDEL — TU Darmstadt, Germany

The Gorini-Kossakowski-Sudarshan-Lindblad Equation describes the time evolution of the probabilities of and the coherences between the quantum mechanical states. It is often used to model open quantum systems. We give explicit expressions of stationary solutions of the Lindblad equation in the case of a finite state space, using the concept of state transition networks of Markov chains. Our treatment is based on the so-called quantum-jump unravelling, which is an ensemble of stochastic quantum trajectories, compatible with the Lindblad equation. A single such trajectory shows a continuous time evolution, which is interrupted by stochastic jumps. We discuss differences to the classical case and conditions, under which the Lindblad equation is asymptotically stable (also called 'relaxing').

DY 35.3 Wed 16:00 H20

Eigenstate entanglement in coupled kicked spin chains with chaotic dynamics — •TABEA HERRMANN, MAXIMILIAN F. I. KIELER, and ARND BÄCKER — TU Dresden, Institut für Theoretische Physik, Dresden, Germany

We study the behaviour of the eigenstate entanglement in two coupled quantum chaotic kicked spin chains in dependence on the coupling strength. It is demonstrated that a random matrix transition ensemble explains the transition from the uncoupled case to strong coupling. Remarkably, the numerical results can be described by an extended perturbation theory which was introduced for the case of two coupled chaotic one-body-systems.

DY 35.4 Wed 16:15 H20

Quantum chaos in microwave cavities with mixed dynamics — •LENNART ANDERSON and ANDREAS WIECK — Angewandte Festkörperphysik, Ruhr-Universität Bochum

Based on the analogy of the Schrödinger equation with Dirichlet boundary conditions and the Helmholtz equation for a flat resonator, it is possible to study the dynamical and statistical properties of quantum billiards experimentally in the quasi-classical limit. Billiards, i.e. dynamical systems in which a particle moves ballistically and gets reflected by hard walls, provide a very simple model system, since the entire dynamics only depends on the geometry of the boundary. We investigate Hamiltonian systems with divided phase space, i.e. systems enabling a continuous transition from completely regular to completely chaotic dynamics, like the mushroom billiard, introduced by L. Bunimovich, in the quantum regime. Generalizations of the mushroom billiard and further geometries, i.e. those ranging from convex to non-convex domains, are considered. We further discuss the experimental setup and the impact of parameters like the conductivity of the resonator.

15 min. break

DY 35.5 Wed 16:45 H20

NQCDynamics.jl: Nonadiabatic quantum classical dynamics in the Julia language — •JAMES GARDNER¹, OSCAR A. DOUGLAS-GALLARDO¹, WOJCIECH G. STARK¹, JULIA WESTERMAYR¹, SVENJA M. JANKE^{1,2}, SCOTT HABERSHON¹, and REINHARD J. MAURER¹ — ¹Department of Chemistry, University of Warwick, United Kingdom — ²Institute of Advanced Study, University of Warwick, United Kingdom

Accurate and efficient methods to simulate nonadiabatic and quantum nuclear effects in high-dimensional and dissipative systems are crucial for the prediction of chemical dynamics in the condensed phase. To facilitate effective development, code sharing, and uptake of newly developed dynamics methods, it is important that software implementations can be easily accessed and built upon. In this talk, I will present the NQCDynamics.jl package, which provides a Julia language framework for established and emerging methods for performing semiclassical and mixed quantum-classical dynamics in the condensed phase. The code provides several interfaces to existing atomistic simulation frameworks, electronic structure codes, and machine learning representations. In addition to the existing methods, the package enables the development and deployment of new dynamics methods for condensed phase quantum dynamics, which I will show using examples based on model Hamiltonians and full-dimensional ab-initio systems.

DY 35.6 Wed 17:00 H20

Metastability and quantum coherence-assisted sensing in interacting parallel quantum dots — •STEPHANIE MATERN¹, KATARZYNA MACIESZCZAK², SIMON WOZNY¹, and MARTIN LEIJNSE¹ — ¹NanoLund and Solid State Physics, Lund University, Box 118, 22100 Lund, Sweden — ²TCM Group, Cavendish Laboratory, University of Cambridge, J. J. Thomson Ave., Cambridge CB3 0HE, United Kingdom

We study the transient dynamics of two interacting parallel quantum dots weakly coupled to macroscopic leads to gain access to the non-equilibrium transport properties. The stationary state current of this quantum system is known to be

sensitive to perturbations much smaller than any other energy scale in the system, specifically compared to the system-lead coupling and the temperature. We show that this is due to a bistable point which leads to a regime in the dynamics where the system exhibits metastability and the dynamics is described as classical dynamics between two metastable phases. The competition of those two metastable phases explain the sensitive behaviour of the stationary current towards small perturbations. We show that this behaviour bears the potential of utilizing the parallel dot as charge sensor which makes use of the quantum coherence effects to achieve a high sensitivity that is not limited by temperature. We analyse the sensitivity in terms of the current signal to noise ratio and find that the parallel dots outperform an analogous single dot setup for a wide range of parameters.

DY 35.7 Wed 17:15 H20

Classical and Quantum Dynamics in Resonance Channels — •JAN ROBERT SCHMIDT, ARND BÄCKER, and ROLAND KETZMERICK — TU Dresden, Institut für Theoretische Physik, Dresden, Germany

In higher-dimensional Hamiltonian systems resonance channels play a prominent role for chaotic transport. It is typically slow due to Arnold diffusion, leading quantum mechanically to dynamical localization. Resonance channels widen as they approach the chaotic sea. We show that this geometry induces classically a drift. Quantum mechanically this leads to a transition from localization to delocalization if the drift is strong enough. This is quantified using a transition parameter depending on classical quantities only. Numerically this is confirmed for a 4D symplectic map.

DY 35.8 Wed 17:30 H20

Coupling in Optical Microcavity-Arrays — •TOM RODEMUND and MARTINA HENTSCHEL — Department of Physics, Technische Universität Chemnitz, Chemnitz, Germany

Optical microcavities capture light by total internal reflection in so-called whispering-gallery modes. Deformed disk-shaped microcavities, for example of Limaçon shape, allow one to keep high Q-factors while manipulating the far-field emission via the resonator geometry, thereby allowing for a wide range of applications from microlasers to sensors.

Coupling of several microdisk resonators enhances the possibilities to tame light considerably [1]. Depending on the number and distance of the coupled cavities, the far-field characteristics vary tremendously and can even be reversed [1]. Here, we investigate the underlying mechanisms. To this end we use phase-space methods and analyze the resonance wave functions in real space as well as the corresponding Husimi functions to characterize the coupling behavior. We employ ideas from ray-wave correspondence to deepen our insight by establishing a relation to the nonlinear light ray dynamics and its fingerprint in the Poincaré surface of section.

[1] J. Kreismann et al., Phys. Rev. Res. 1, 033171 (2019).

DY 35.9 Wed 17:45 H20

Time-dependent Redfield and Lindblad equations with effective time-dependent temperature — •NIKODEM SZPAK, LUKAS LITZBA, ERIC KLEINHERBERS, and JÜRGEN KÖNIG — Theoretische Physik, Universität Duisburg-Essen, Lotharstr. 1, 47048 Duisburg

For a quantum system coupled to environment we apply the first Markov approximation and write the Redfield equation at the first order in the system-environment coupling. Then, we evaluate the remaining time-dependent integral and approximate it uniformly for all times, temperatures and energies by one simple analytical function which corresponds to the Fermi-Dirac distribution with time-dependent effective temperature $T(t)$. Thus, we obtain a new Redfield equation with time-dependent effective temperature. A consecutive approximation brings it to the Lindblad equation with time-dependent Lindblad operators whose time-dependence enters solely via $T(t)$. The variation of the effective temperature $T(t)$ reflects the sudden switch-on of the system-environment interaction at the beginning and becomes high at early times to eventually fall to the true environment temperature T . We discuss possible physical effects and their measurability in some simple examples.

DY 36: Quantum Coherence and Quantum Information Systems (joint session TT/DY)

Time: Thursday 9:30–12:30

Location: H22

See TT 27 for details of this session.

DY 37: Invited Talk David Zwicker

Time: Thursday 9:30–10:00

Location: H20

Invited Talk

DY 37.1 Thu 9:30 H20

Controlled and robust phase separation in cells — •DAVID ZWICKER — MPI for Dynamics and Self-Organization, Göttingen, Germany

Phase separation is a key process for the spatiotemporal organization of biomolecules in cells. In particular, phase separation explains how droplets can form spontaneously to create subcellular compartments. However, traditional theories of phase separation cannot explain how cells control these droplets robustly. To elucidate this, I will discuss how droplets interact with the elastic cellular environment and how cells use driven chemical reactions to control droplets.

First, I will show how monodisperse emulsions form when droplets grow in a mesh that can break and re-arrange. We demonstrate that stiffness gradients cause elastic ripening, which biases droplets toward softer regions. These processes quantitatively explain experiments where oil droplets form in PDMS gels. The same physics applies to droplets interacting with the cytoskeleton in cells. In the second part, I will show how driven reactions control droplet size and position so that multiple droplets can coexist. Taken together, our models identify key physical processes that allow cells to control the phase separation of biomolecules.

DY 38: Complex Fluids and Soft Matter 2 (joint session DY/ CPP)

Time: Thursday 10:00–11:30

Location: H18

DY 38.1 Thu 10:00 H18

Underscreening in the Restricted Primitive Model — •ANDREAS HÄRTEL — Institute of Physics, University of Freiburg, Germany

Electric double layers occur where charges are screened by other charges, for instance, when charged surfaces of electrodes, colloids, or cells are exposed to electrolytes (mobile ions in a solvent). Increasing the concentration of mobile ions leads to more efficient screening, if concentrations are sufficiently low. At high concentrations, however, the screening by finite-sized ions becomes less efficient than those of point-like ions due to packing, an effect called underscreening. Some experiments report underscreening as a strong effect that follows some universal scaling [1], but the observation could not be explained by theoretical models yet. Conversely, independent theoretical studies actually ruled out the most important model for electrolytes of finite-sized ions as a candidate able to explain underscreening, namely the restricted primitive model [2]. In this talk I will discuss in which sense underscreening can and cannot be found in the restricted primitive model and in which sense the effect follows some universal scaling. I will support the discussion by recent theoretical results obtained from simulations and liquid state theories.

[1] Lee et al., Underscreening in concentrated electrolytes, *Faraday Discuss.* 199, 239 (2017).

[2] Cats et al., Primitive Model Electrolytes in the Near and Far Field: Decay Lengths from DFT and Simulations, *J. Chem. Phys.* 154, 124504 (2021).

DY 38.2 Thu 10:15 H18

Reciprocal and nonreciprocal eigenmodes of viscoelastic fluids — •JULIANA CASPERS¹, CLEMENS BECHINGER², NIKOLAS DITZ², MATTHIAS FUCHS², FELIX GINOT², KARTHIKA KRISHNA KUMAR², LUIS FRIEDER REINALTER², and MATTHIAS KRÜGER¹ — ¹Institute for Theoretical Physics, Georg-August Universität Göttingen, 37073 Göttingen, Germany — ²Fachbereich Physik, Universität Konstanz, 78457 Konstanz, Germany

Complex fluids such as wormlike micellar solutions are in general non-Markovian. In equilibrium, their behavior is often well approximated by a simple Maxwell model with one characteristic timescale [1]. Recoil experiments, after a colloidal probe has been sheared through the solvent, however, displayed a double-exponential relaxation [2]. We found excellent agreement of our measurements with a linear two-bath particle model. Depending on whether the optical trap which confines the probe is turned on or off, we find two sets of eigenmodes in our model, corresponding to either nonreciprocal (trap on) or reciprocal (trap off) forces. Using different recoil protocols as well as equilibrium mean square displacement measurements we confirmed the existence of these two different sets of timescales with experiments. Finally, for linear systems, we find a Volterra relation between two memory kernels, characterizing reciprocal and nonreciprocal forcing.

[1] F. Ginot, J. Caspers, M. Krüger, C. Bechinger. *Phys. Rev. Lett.* **128**, 028001 (2022)

[2] F. Ginot, J. Caspers, L. F. Reinalter, K. Krishna Kumar, M. Krüger, C. Bechinger. *arXiv:2204.02369* (2022)

DY 38.3 Thu 10:30 H18

Elastic Turbulence in von Kármán geometry — •REINIER VAN BUEL and HOLGER STARK — Institut für Theoretische Physik, Technische Universität Berlin, Hardenbergstr. 36, 10623 Berlin, Germany

Elastic turbulence, occurring in viscoelastic fluid flow at vanishing Reynolds numbers, is an interesting flow state [1-4] and has been experimentally studied in the von Kármán geometry [1]. Elastic turbulence is especially appealing for the mixing of fluids on the micron scale, which is extremely challenging in Newtonian fluids where transport relies on diffusion. Here, we present a fully three-dimensional numerical investigation of the von Kármán flow using the Oldroyd-B model [4]. We observe a non-axisymmetric mode with four-fold sym-

metry that drives the flow instability towards elastic turbulence and compare it to results obtained from a linear stability analysis. By analyzing the velocity fluctuations and defining an order parameter, we identify a bistable flow state above a sub-critical transition, which switches between a weakly chaotic flow state and elastic turbulence and exhibits hysteretic behavior. Furthermore, we reveal a sharp increase in the flow resistance at the transition to elastic turbulence, which we attribute to the elastic contribution of the work performed at the open side surface of the flow. Finally, an analysis of the spatial and temporal velocity power spectra confirms the turbulent nature of the flow.

[1] A. Groisman and V. Steinberg, *Nature* **405**, 53 (2000).

[2] R. Buel, C. Schaaf, H. Stark, *Europhys. Lett.* **124**, 14001 (2018).

[3] R. Buel and H. Stark, *Sci. Rep.* **10**, 1-9 (2020).

[4] R. Buel and H. Stark, *Phys. Fluids* **34**, 4 (2022).

DY 38.4 Thu 10:45 H18

Coarsening dynamics of quasi 2D emulsions in free-standing smectic films — •CHRISTOPH KLOPP, TORSTEN TRITTEL, and RALF STANNARIUS — Institute for Physics, Otto von Guericke University Magdeburg, Germany

Hydrodynamic phenomena in thin films play a crucial role in biological systems, in nature and modern technology. Various experimental and theoretical studies explored, e.g., the motion of objects in quasi two-dimensional films [1], the merging of inclusions [2-4] and the structural change of emulsions during long-term observations. Here, we demonstrate and describe the coarsening dynamics of emulsions formed by smectic islands (flat circular regions) on liquid crystal bubbles in microgravity at the International Space Station (ISS). The smectic islands form polydisperse, disordered arrangements representing quasi 2D emulsions. We analyze the time evolution of these ensembles that proceed through direct island coalescence or the exchange of material through the background film (Ostwald ripening). Coarsening is ubiquitous in liquid emulsions and foams, and important for their stability. We compare our results with such systems and analyze the dominant process for the 2D coarsening dynamics.

Acknowledgements: This study was supported by NASA, DFG and DLR within the OASIS and OASIS-Co projects.

References: [1] A. Eremin et al., *Phys. Rev. Lett.*, **107**, 268301 (2011) [2] N. S. Shuravin et al., *Phys. Rev. E*, **99**, 062702 (2019) [3] Z. H. Nguyen et al., *Phys. Rev. Research*, **3**, 033143 (2021) [4] C. Klopp et al., *Soft Matter* **16** 4607 (2020)

DY 38.5 Thu 11:00 H18

Phase transitions in the generalised chiral Lebwohl-Lasher model — •PHILIPP ELSÄSSER and ANJA KUHNHOLD — Institute of Physics, Albert-Ludwigs-University Freiburg, Germany

The behaviour of liquid crystals can be described by using the Lebwohl-Lasher (LL) model, where unit vectors that resemble nematic directors are positioned on a simple cubic lattice. Due to the interaction potential, which favours parallel orientations, this model is well suited to analyse isotropic-nematic (IN) phase transitions.

There exist several extensions to this model with which its applicability can get further enhanced. We use two combined extensions to obtain the generalised chiral Lebwohl-Lasher model: We apply a generalisation to tune the sharpness of the potential, as in the work of Fish and Vink [1] and add a chiral term which is based on the work of Memmer et al. [2]. In this system we study the phase transition properties with the help of Monte Carlo simulations. To identify characteristic properties of the transitions, we apply finite-size scaling. This allows us to determine chirality-sharpness parameter pairs with which we can manipulate the nature of the transition between ordered and disordered states [3].

[1] J. M. Fish, R. L. C. Vink, *PRE* **81**, 021705 (2010).

[2] R. Memmer, O. Fliegans, *PCCP* **5**, 558 (2003).

[3] P. Elsässer, A. Kuhnhold, *PRE* **105**, 054704 (2022).

DY 38.6 Thu 11:15 H18

Systematic parametrization of non-Markovian dissipative thermostats for coarse-grained molecular simulations with accurate dynamics — •VIKTOR KLIPPENSTEIN and NICO F. A. VAN DER VEGT — Eduard-Zintl-Institut für Anorganische und Physikalische Chemie, Technische Universität Darmstadt, 64287 Darmstadt, Germany

The Mori-Zwanzig theory, in principle, allows to derive an exact equation of motion for coarse-grained degrees of freedom based on the dynamics of an underlying fine-grained reference system.[1] Still, in practice the simultaneous representation of structural and dynamic properties in particle-based models poses a complicated problem, e.g. due to the non-linearity of the exact coarse-grained equation of motion.

A viable approximate approach is to start from a conservative coarse-grained force-field and to extend the standard Newtonian equation of motion used in molecular simulation with a linear generalized Langevin thermostat. We demonstrate how such a thermostat can be parametrized to correctly represent dynamic properties, both in a purely bottom-up approach[2,3] or by applying iterative optimization.[3] We consider the Asakura-Oosawa model as a test case.[3]

[1] V. Klippenstein, M. Tripathy, G. Jung, F. Schmid, and N. F. A. van der Vegt, *The Journal of Physical Chemistry B* 125, 4931 (2021).

[2] V. Klippenstein and N. F. A. van der Vegt, *The Journal of Chemical Physics* 154, 191102 (2021).

[3] V. Klippenstein and N. F. A. Van Der Vegt, *The Journal of Chemical Physics* under review (2022).

DY 39: Pattern Formation and Reaction-Diffusion Systems

Time: Thursday 10:00–12:15

Location: H19

DY 39.1 Thu 10:00 H19

Dynamics of tagged particles in a biased $A + A \rightarrow \emptyset$ system in one dimension: result for asynchronous and parallel updates — •RESHMI ROY¹, PARONGAMA SEN¹, and PURUSATTAM RAY² — ¹University of Calcutta, Kolkata, India — ²IMSC, Chennai, India

We have studied dynamical features of tagged particles in one dimensional $A + A \rightarrow \emptyset$ system, where the particles A have a bias ϵ such that they move towards their nearest neighbour with the probability $0.5 + \epsilon$ and move in the opposite direction with probability $0.5 - \epsilon$ and annihilate on contact. We found that for $\epsilon > 0$ when asynchronous dynamics is used to update the system, probability distribution $\Pi(x, t)$ of the particles shows a double peak structure with a dip at $x = 0$ and it assumes a double delta form at very late time regime. For any $\epsilon > 0$, there is a crossover at time t^* , below which the particle motions are highly correlated, and beyond t^* , the particles move as independent biased walkers. When we use parallel updating rule, $\Pi(x, t)$ shows a non-Gaussian single peaked structure and the fraction of surviving particle $\rho(t)$ shows a $\ln t/t$ variation. For the deterministic point $\epsilon = 0.5$, we found that an isolated pair of particles, termed as dimers, can survive indefinitely in the system which is exclusive for parallel dynamics. When ϵ is made negative, $\Pi(x, t)$ becomes Gaussian as found in $\epsilon = 0$. A comparative analysis for the relevant quantities using asynchronous and parallel dynamics shows that there are significant differences for $\epsilon > 0$ while the results are qualitatively similar for $\epsilon < 0$.

Journal Ref: J. Phys. A: Math. Theor. 53, 155002 (2020), J. Phys. A: Math. Theor. 53, 405003 (2020), Physica A 97569, 125754 (2021).

DY 39.2 Thu 10:15 H19

Wrinkling in Curved Films — •MEGHA EMERSE and LUCAS GOEHRING — Nottingham Trent University, Nottingham, United Kingdom

Thin films or sheets exposed to external forces can become unstable to drastic shape changes, often forming regular or periodic patterns like wrinkles, folds, creases, etc. This can be distinctly observed when one tries to wrap a world map onto a globe since it is unachievable without creating any wrinkles. Wrinkling is a self-initiated process, spontaneously generating periodic structures out of a uniformly smooth surface and represents a pathway for simply creating regular surface topography. Here, we study thin elastic membranes that form complex wrinkle patterns when put on substrates where there is a mismatch in their inherent shape. Using 3D-printed moulds, we prepare elastic membranes with different curvatures, including cases of positive and negative Gaussian curvature, and shapes with two distinct principal curvatures. Through these, we experimentally investigate the dependence of the amplitude and wavelength of the wrinkles that spontaneously form when these curved membranes are constrained by a flat fluid substrate. We also study how these properties change along the membrane, for example with distance from the film edges.

DY 39.3 Thu 10:30 H19

Exploring Bifurcations in Bose-Einstein Condensates via Phase Field Crystal Models — •ALINA B. STEINBERG¹, FABIAN MAUCHER², SVETLANA V. GUREVICH^{1,3}, and UWE THIELE^{1,3} — ¹Institut für Theoretische Physik, Westfälische Wilhelms-Universität Münster, Wilhelm-Klemm-Strasse 9, 48149 Münster, Germany — ²Departament de Física, Universitat de les Illes Balears \& IAC-3, Campus UIB, E-07122 Palma de Mallorca, Spain — ³Center of Nonlinear Science (CeNoS), Westfälische Wilhelms-Universität Münster, Corrensstrasse 2, 48149 Münster, Germany

To facilitate the analysis of pattern formation and phase transitions in Bose-Einstein condensates as well as to unravel analogies we present an explicit approximate mapping from the nonlocal Gross-Pitaevskii equation with cubic nonlinearity to a model of phase field crystal type. This approximation is valid close to the superfluid-supersolid phase transition and permits us to explore the phase transition through the corresponding bifurcation diagrams obtained via numerical path continuation. Additionally the effects of phenomenological

higher order nonlinearities are considered. In passing we discuss the importance of localized states as an indicator of a first order character of the phase transition. A. B. Steinberg, F. Maucher, S. V. Gurevich and U. Thiele, *Exploring Bifurcations in Bose-Einstein Condensates via Phase Field Crystal Models*, <http://arxiv.org/abs/2205.15194> (2022)

DY 39.4 Thu 10:45 H19

Phase Field Crystal model for particles with n -fold rotational symmetry in two dimensions — •ROBERT F. B. WEIGEL and MICHAEL SCHMIEDEBERG — Friedrich-Alexander-Universität Erlangen-Nürnberg, Erlangen, Germany

We introduce a Phase Field Crystal (PFC) model for particles with n -fold rotational symmetry in two dimensions [1]. The n -fold symmetry of the particles corresponds to the one that can be realized for colloids with symmetrically arranged patches, with the patches being either attractive or repulsive.

Our approach is based on a free energy functional that depends on the reduced one-particle density, the strength of the orientation, and the direction of the orientation, where all these order parameters depend on the position. The functional is constructed such that for particles with axial symmetry (*i. e.* $n = 2$) the PFC model for liquid crystals [2] is recovered. We explain how both, repulsive as well as attractive patches, are described in our model.

We discuss the stability of the functional and explore phases that occur for $1 \leq n \leq 6$. In addition to isotropic, nematic, stripe, and triangular order, we also observe cluster crystals with square, rhombic, honeycomb, and even quasicrystalline symmetry.

[1] arXiv:2204.00051 [cond-mat.soft]

[2] H. Löwen, *J. Phys.: Condens. Matter* 22, 364105 (2010)

15 min. break

DY 39.5 Thu 11:15 H19

Control-optimisation for spatiotemporal chaos in 2D excitable media through a genetic algorithm — •MARCEL ARON^{1,2,3}, THOMAS LILIENKAMP^{2,4}, STEFAN LUTHER^{1,2,3,5}, and ULRICH PARLITZ^{2,3,5} — ¹Institute of Pharmacology and Toxicology, University Medical Center Göttingen, Göttingen, Germany — ²Max Planck Institute for Dynamics and Self-Organization, Göttingen, Germany — ³Institute for the Dynamics of Complex Systems, Georg-August-Universität Göttingen, Göttingen, Germany — ⁴Computational Physics in den Life Sciences, Technische Hochschule Nürnberg, Nürnberg, Germany — ⁵German Center for Cardiovascular Research (DZHK), Partner Site Göttingen, Göttingen, Germany

The emergence of spatiotemporal chaos (*i. e.* fibrillation) in the cardiac muscle (an excitable medium) leads to loss of pumping function and sudden cardiac death. Clinically, such episodes are treated with high-energy electric shocks to control (terminate) the chaotic dynamics and restore a regular heart rhythm. However, high shock energies result in increased risk of tissue damage or worsening the overall prognosis. This motivates the search for alternatives, including periodic sequences of low-energy electric pulses of constant field strength, which has seen success in pre-clinical trials on pig hearts.

Here we show that non-uniform pulse energies and time intervals can be used to further optimise the control of spatiotemporal chaos in 2D simulations of homogeneous cardiac tissue. We use a simplified shock-application model and define control-performance metrics to employ a genetic algorithm in the search for more efficient control approaches.

DY 39.6 Thu 11:30 H19

The French flag problem revisited: Creating robust and tunable axial patterns without global signaling — •STEPHAN KREMSE¹, GABRIEL VERCELLI^{1,2}, and ULRICH GERLAND¹ — ¹Physics Department, Technical University of Munich — ²MIT Microbiology Program, Massachusetts Institute of Technology

Wolpert's French flag problem conceptualizes the task of forming axial patterns with broad regions in multicellular systems. Wolpert described two different so-

lutions to his problem, the balancing model and thresholding of a morphogen gradient, both of which require global, long-range signaling between cells. Since global signaling becomes challenging in large systems, we computationally explore alternative solutions, which use only local cell-cell signaling and are simple enough to potentially be implemented in natural or synthetic systems. We employ cellular automata rules to describe local signal processing logics, and search for rules capable of robust and tunable axial patterning with evolutionary algorithms. This yields large sets of successful rules, which however display only few types of different behaviors. We introduce a rule alignment and consensus procedure to identify patterning modules that are responsible for the observed behaviors. With these modules as building blocks, we then construct local schemes for axial patterning, which function also in the presence of noise and growth, and for patterns with a larger number of different regions. The regulatory logic underlying these modules could therefore serve as the basis for the design of synthetic patterning systems, and as a conceptual framework for the interpretation of biological mechanisms.

DY 39.7 Thu 11:45 H19

Coupling-Mediated Protein Waves in Mass-Conserved Pattern Forming Systems — •BENJAMIN WINKLER¹, SERGIO ALONSO MUÑOZ², and MARKUS BÄR^{1,3} — ¹Physikalisch-Technische Bundesanstalt — ²Universitat Politècnica de Catalunya — ³TU Berlin

The formation of protein patterns inside biological cells is of crucial importance for their spatial organization, growth and division. In many cases these dynamics can be described by coupled, mass-conserving reaction-diffusion equations [Brauns et al., PRX, 2020]. Motivated by the question how the generation of cell polarity is influenced by membrane heterogeneity, we study the behavior of the coupled dynamics of two well-known, mass-conserved systems. System A is therein given by a simplified model [Mori et al., Biophys.J., 2008] for the emer-

gence of cell polarity with a single pair of activated-inactivated proteins M and B. The inactive, fast-diffusing species (B) in the bulk of the cell becomes activated (M) when bound to the cell membrane. When endowed with a positive feedback on the membrane-mediated activation, the system exhibits inherent polarizability. System B is described by the Cahn-Hilliard equation, two membrane species demixing into a pattern of comparatively small, static droplets. We then consider a difference in interaction affinity for M with respect to the two phases of the cell membrane and an additional contribution in the chemical potential of the membrane, depending on the presence of M. In the so coupled system, the emergence of traveling waves can be observed above a finite threshold of coupling strength.

DY 39.8 Thu 12:00 H19

Robustness of *in vivo* Min patterns underlines complex protein interaction motives — •HENRIK WEYER, LAESCHKIR WÜRTHNER, and ERWIN FREY — Arnold Sommerfeld Center for Theoretical Physics and Center for NanoScience, Department of Physics, Ludwig-Maximilians-Universität München, Theresienstraße 37, D-80333 München, Germany

The Min protein system organizes the symmetric cell division of *E. coli* bacteria: Two proteins, MinD and MinE, undergo pole-to-pole oscillations via a reaction-diffusion mechanism, and guide the cell-division machinery towards midcell. In elongated, filamentous cells the pole-to-pole oscillations transition into a standing-wave pattern forming several stripes along the cell. We show that modeling of the latent MinE state, which allows for Min pattern formation over a large range of MinE densities, suppresses standing-wave patterns. This effect is explained to demonstrate a generic mechanism that latent states form a homogeneous reservoir in reaction-diffusion systems. We reason that the MinE-MinD interaction cannot be described as a single hydrolysis step, and that MinE plays a more complex role in the Min protein network, a finding supported by recent experimental evidence.

DY 40: Brownian Motion and Anomalous Diffusion

Time: Thursday 10:00–12:00

Location: H20

DY 40.1 Thu 10:00 H20

Depinning and structural transitions of confined colloidal dispersions under oscillatory shear — •MARCEL HÜLSBERG and SABINE H.L. KLAPP — ITP, Technische Universität Berlin, Germany

Strongly confined colloidal dispersions under shear exhibit a variety of dynamical phenomena, including a depinning transition, which is accompanied by lateral structural changes [1].

Here, we investigate the depinning behaviour of these systems under pure oscillatory shearing with shear rate $\dot{\gamma}(t) = \dot{\gamma}_0 \cos(\omega t)$, as it is a common scenario in rheological experiments [2].

The colloids' depinning behaviour is assessed from a microscopic level based on particle trajectories, which are obtained from overdamped Brownian Dynamics simulations. The numerical approach is complemented by an analytic one based on an effective single-particle model in the limits of weak and strong driving.

Investigating a broad spectrum of shear rate amplitudes $\dot{\gamma}_0$ and frequencies ω , we observe complete pinning as well as temporary depinning behaviour. We discover that temporary depinning occurs for shear rate amplitudes above a frequency-dependent critical amplitude $\dot{\gamma}_0^{\text{crit}}(\omega)$, for which we attain an approximate functional expression.

Above $\dot{\gamma}_0^{\text{crit}}(\omega)$, we further observe a variety of dynamical structures, whose stability exhibits an intriguing $(\dot{\gamma}_0, \omega)$ dependency. This might enable new perspectives for potential control schemes.

[1] S. Gerloff and S.H.L. Klapp, *Phys. Rev. E* **94**(6), 062605 (2016)[2] S.M. Fielding, *J. Rheol.*, **64**(3), 723-738 (2020)

DY 40.2 Thu 10:15 H20

Ballistic Hot Brownian Motion — •XIAOYA SU¹, FRANK CICHOS¹, and KLAUS KROY² — ¹Peter Debye Institute for Soft Matter Physics, University Leipzig, Leipzig, Germany — ²Institute of Theoretical Physics, University Leipzig, Leipzig, Germany

Brownian motion is the erratic motion of particles in a fluid due to the bombardment of the particle with solvent molecules providing thermal energy and viscous friction. It is fundamental for the dynamics of soft matter and defines the prototype of a fluctuation dissipation relation. While at long timescales the motion is purely stochastic, it is at shorter times influenced by hydrodynamic effects and even ballistic at ultrashort timescales. Yet, the ballistic motion, same as the stochastic motion, is still determined by the temperature of the system. Here we explore the transition to the ballistic regime for a hot Brownian particle, i.e. a microparticle which is heated by a laser in an optical trap. In this case the particle temperature is different from the solvent temperature and so far, only theoretical predictions exist for the relevant temperature determining the particle velocity.

We report the first measurements of the thermal non-equilibrium process in a

specially designed optical trap which is able to resolve particle displacements of about 20 pm with a time-resolution of 10ns. We show how the mean squared displacement of the particle from the nanosecond to the second timescale changes as a function of the surface temperature of the particle and discuss the model of a frequency dependent effective temperature of hot Brownian motion.

DY 40.3 Thu 10:30 H20

Stochastic action for tubes: Connecting path probabilities to measurement — •JULIAN KAPPLER¹, JANNES GLADROW^{2,3}, ULRICH F. KEYSER³, and RONOJOY ADHIKARI¹ — ¹DAMTP, Cambridge University, Cambridge, UK — ²Microsoft Research, Cambridge, UK — ³Cavendish Laboratory, University of Cambridge, Cambridge, UK

The trajectories of diffusion processes are continuous but nondifferentiable, and each occurs with vanishing probability. This introduces a gap between theory, where path probabilities are used in many contexts, and experiment, where only events with nonzero probability are measurable. We bridge this gap by considering the probability of diffusive trajectories to remain within a tube of small but finite radius around a smooth path. This probability can be measured in experiment, via the rate at which trajectories exit the tube for the first time, thereby establishing a link between path probabilities and physical observables. In my contribution I will show how this link can be used to both measure ratios of path probabilities [1], and to extend the theoretical stochastic action from individual paths to tubes [2]. I will furthermore relate our results to the usual path-integral formalism.

[1] J. Gladrow, U. F. Keyser, R. Adhikari, and J. Kappler. Experimental measurement of relative path probabilities and stochastic actions. *Phys. Rev. X* **11**, 031022 (2021). 10.1103/PhysRevX.11.031022[2] J. Kappler and R. Adhikari. Stochastic action for tubes: Connecting path probabilities to measurement. *Physical Review Research* **2**(2), 023407 (2020). 10.1103/PhysRevResearch.2.023407

DY 40.4 Thu 10:45 H20

Size matters for Bayesian chemotaxis — •JULIAN RODE¹, MAJA NOVAK^{1,2}, and BENJAMIN M. FRIEDRICH^{1,3} — ¹cfaed, TU Dresden, Germany — ²Department of Physics, University of Zagreb, Croatia — ³PoL, TU Dresden, Germany

Navigation by chemical cues, e.g., chemotaxis, is employed by single biological cells and animals. The size and speed of search agents dictate noise levels and thus optimal strategies to find a target.

Here, we address information theory of gradient sensing for an ideal agent and ask for optimal strategies as a baseline for real agents. We extend the seminal work on infotaxis [1], by applying its idea of maximizing information gain to agents of finite size. These agents can now measure gradients both by temporal comparison due to their active motion [1], and by spatial comparison across

their diameter, prompting an optimal weighting of both information sources [2].

In the absence of noise, trajectories show stereotypic behavior; the entropy of directional uncertainty collapses onto a master curve parameterized by a signal-to-noise ratio. Unlike [1], we account for rotational diffusion, which is prevalent for microscopic agents: Its competition with information gain due to spatial comparison sets an effective measurement time (given by the inverse geometric mean of a rate constant of information gain and the rotational diffusion coefficient), which is different from the typical bound argued by Howard Berg for bacterial chemotaxis (inverse rotational diffusion coefficient) [3].

[1] M. Vergassola et al, *Nature* (2007); [2] A. Auconi et al., *EPL*, in press (arXiv:2111.09630); [3] M. Novak et al., *New J Phys* (2021).

15 min. break

DY 40.5 Thu 11:15 H20

Superstatistics of protein diffusion dynamics in bacteria — •YUICHI ITO — Aichi Institute of Technology, Aichi, Japan — ICP, Universität Stuttgart, Stuttgart, Germany

In recent years, non-Gaussian normal/anomalous diffusion have experimentally been observed in a wide class of living cells. Superstatistics is a “statistics of statistics” with two largely separated time scales for treating nonequilibrium complex systems. Here, a superstatistical diffusion theory [1] is presented for obtaining a q-Gaussian displacement distribution decaying as a power law found for heterogeneous diffusion phenomenon of DNA-binding proteins in bacteria [2]. This theory takes into account the joint fluctuations of both the diffusion exponent and the (inverse) temperature, which are hierarchically combined with a fractional Brownian motion describing a local stochastic process of the proteins. Correlation between the fluctuations is also discussed and its weakness is shown to be essential. The results obtained are in a good agreement with the experimental data.

[1] Y. Ito and C. Beck, *J. R. Soc. Interface* 18, 20200927 (2021).

[2] A.A. Sadoon and Y. Wang, *Phys. Rev. E* 98, 042411 (2018).

DY 40.6 Thu 11:30 H20

Generalised master equation for diffusion and reaction problems in heterogeneous media — DANIELA FRÖMBERG¹ and •FELIX HÖFLING^{1,2} — ¹Department of Mathematics and Computer Science, Freie Universität Berlin — ²Zuse Institute Berlin

The kinetics of chemical reactions in a heterogeneous or crowded medium significantly deviates from that in a well-mixed, aqueous environment. One example is the partitioning of cell membranes and intracellular spaces, e.g., into cyto-

plasm and nucleus. For reaction–diffusion problems in such compartmentalised spaces, we extend a recently proposed generalised master equation (GME) for non-Markovian jump processes [1]. The GME governs the time evolution of the occupation probability of the spatial domains, its main ingredient are first-passage time densities encoding the transport behaviour in each domain. The domains can differ with respect to their diffusivity, geometry, and dimensionality, but can also refer to transport modes alternating between diffusive, driven, or anomalous motion. We discuss further the inclusion of barriers and the Markovian limit of the GME.

For a cherry-pit geometry with a reactive inner domain, we obtain the first-reaction time density and infer the effective reaction rate constant. This rate constant is timescale dependent and exhibits an enhancement at intermediate times by orders of magnitude and an algebraically slow convergence to the long-time limit. Our stochastic approach does not depend on the existence of a stationary distribution and thus overcomes a limitation of the classical Smoluchowski theory.

[1] D. Frömberg and F. Höfling, *J. Phys. A* 54, 215601 (2021).

DY 40.7 Thu 11:45 H20

Molecular dynamics simulations of supercooled water in silica pores — •MARKUS HANEKE, ROBIN HORSTMANN, and MICHAEL VOGEL — TU Darmstadt, Institut für Physik kondensierter Materie, Hochschulstr. 6, 64289, Darmstadt, Germany

Being highly relevant in biology as well as in technology and other areas, water is subject to extensive research. Especially its anomalies pose questions. Commonly, it is argued that the anomalies of water originate in the supercooled state, which is therefore regularly subject to exploration. To suppress freezing in experimental studies, confinements can be employed, where silica pores proved to be very useful.

Molecular dynamic simulations are a valuable tool to take a closer look. They allow analyses with high spatial and temporal resolution while making it easy to extract dynamic and static information. [1]

Here, we perform simulations to analyse the diffusion of water in silica pores. We want to find the influence of the pore on dynamics, as well as of the capping if the water outside of the pore freezes.

Results of our analysis are, that the diffusion inside of the pore is anomalous and slowed down. The systems show to be subdiffusive. Capping not only restricts diffusion but also slows down local relaxation and yields a nearly triangular probability density of propagation distance, contradicting free 1D-diffusion.

[1] R. Horstmann, L. Hecht, S. Kloth, and M. Vogel. "Structural and Dynamical Properties of Liquids in Confinements: A Review of Molecular Dynamics Simulation Studies". In: *Langmuir* 2022 38 (21), 6506-6522

DY 41: Nonequilibrium Quantum Many-Body Systems (joint session TT/DY)

Time: Thursday 15:00–18:15

Location: H22

See TT 33 for details of this session.

DY 42: Statistical Physics of Biological Systems 2 (joint session BP/DY)

Time: Thursday 15:00–16:30

Location: H16

See BP 27 for details of this session.

DY 43: Poster Session: Quantum Chaos and Many-Body Dynamics

Time: Thursday 15:00–18:00

Location: P2

DY 43.1 Thu 15:00 P2

Localization persisting under aperiodic driving — •HONGZHENG ZHAO^{1,2}, FLORIAN MINTERT², JOHANNES KNOLLE^{2,3,4}, and RODERICH MOESSNER¹ — ¹Max Planck Institute for the Physics of Complex Systems, Dresden, Germany — ²Imperial College London, London, United Kingdom — ³Technical University of Munich, Munich, Germany — ⁴Munich Center for Quantum Science and Technology, Munich, Germany

Localization may survive in periodically driven (Floquet) quantum systems, but is generally unstable for aperiodic drives. In this work, we identify a hidden conservation law originating from a chiral symmetry in a disordered spin-1/2 XX chain. This protects indefinitely long-lived localization for general—even aperiodic—drives. Therefore, rather counter-intuitively, adding further potential disorder which spoils the conservation law delocalizes the system, via a controllable parametrically long-lived prethermal regime. This provides a first example of persistent single-particle ‘localization without eigenstates’. Reference: arXiv:2111.13558

DY 43.2 Thu 15:00 P2

Prethermalization in confined spin chains — •STEFAN BIRNKAMMER, ALVISE BASTIANELLO, and MICHAEL KNAP — Technical University Munich, Germany

Unconventional nonequilibrium phases with restricted correlation spreading and slow entanglement growth have been proposed to emerge in systems with confined excitations, calling their thermalization dynamics into question. Here, we investigate the many-body dynamics of a confined Ising spin chain, in which domain walls in the ordered phase form bound states reminiscent of mesons. We show that the thermalization dynamics after a quantum quench exhibits multiple stages with well separated time scales. The system first relaxes towards a prethermal state, described by a Gibbs ensemble with conserved meson number. The prethermal state arises from rare events in which mesons are created in close vicinity, leading to an avalanche of scattering events. Only at much later times a true thermal equilibrium is achieved in which the meson number conservation is violated by a mechanism akin to the Schwinger effect.

DY 43.3 Thu 15:00 P2

Enhanced state transfer by complex instability in coupled tops — •MAXIMILIAN FRIEDRICH IRENÄUS KIELER and ARND BÄCKER — TU Dresden, Institut für Theoretische Physik, Dresden, Germany

By considering coupled tops we provide a mechanism for a fast transfer between two specific states representing bits. This crucially relies on that fact that the semiclassical limit corresponds to a higher-dimensional system which allows for more types of stability of fixed points than the two-dimensional case. Tuning the parameters, the coupled tops have fixed points with complex instability. Quantum mechanically this allows for a rapid transfer between coherent states located at these points, which is much faster than the coexisting dynamical tunneling.

DY 43.4 Thu 15:00 P2

Quantum signatures of partial barriers in 4D symplectic maps — •JONAS STÖBER, ARND BÄCKER, and ROLAND KETZMERICK — TU Dresden, Institut für Theoretische Physik, Dresden, Germany

Partial transport barriers in the chaotic sea of Hamiltonian systems restrict classical transport, as they only allow for a small flux between phase-space regions. Quantum mechanically for 2D symplectic maps one has a universal quantum localizing transition: quantum transport is suppressed if the Planck cell of size h is much greater than the flux Φ , while mimicking classical transport if h is much smaller. The scaling parameter is Φ/h .

In a higher-dimensional 4D map one would naively expect that the relevant scaling parameter is Φ/h^2 . However, we show that due to dynamical localization along resonance channels the localization length modifies the scaling parameter. This is demonstrated for coupled kicked rotors for a partial barrier that generalizes a cantorus to higher dimensions.

DY 43.5 Thu 15:00 P2

Metallicity in the Dissipative Hubbard-Holstein Model: Markovian and Non-Markovian Tensor-Network Methods for Open Quantum Many-Body Systems — •MATTIA MORODER¹, MARTIN GRUNDNER¹, FRANÇOIS DAMANET², ULRICH SCHOLLWÖCK¹, SAM MARDAZAD¹, THOMAS KÖHLER³, SEBASTIAN PAECKEL¹, and STUART FLANNIGAN⁴ — ¹Department of Physics, Ludwig-Maximilians-Universität München, München, Germany — ²Institut de Physique Nucléaire, Atomique et de Spectroscopie, CESAM, University of Liège, B-4000 Liège, Belgium — ³Department of Physics and Astronomy, Uppsala University, Uppsala, Sweden — ⁴Department of Physics & SUPA, University of Strathclyde, Glasgow G4 0NG, United Kingdom

We investigate the impact of dissipation on polarons and bipolarons in the paradigmatic Hubbard-Holstein model. We do so by combining the non-Markovian hierarchy of pure states (HOPS) method and the Markovian Quantum Jump (QJ) method with the newly-developed projected-purification (PP) method for matrix-product states (MPS).

By studying the system's dynamics after global quenches from different ground states, we show that dissipation reduces the polaron's mobility and the electron pairing.

We also find that PP gives a significant speedup (proportional to the phononic local Hilbert space dimension) and allows to systematically converge all observables to very high accuracy in an automated fashion.

DY 43.6 Thu 15:00 P2

Time evolution in the one-magnon subspace of the sawtooth chain at the quantum-critical point. — •JANNIS ECKSELER and JÜRGEN SCHNACK — Fakultät für Physik, Universität Bielefeld, Postfach 100131, D-33501 Bielefeld, Germany

It is known for the sawtooth chain to develop a flat band at the quantum-critical point of $J_1 = 2J_2$ [1]. We are looking at the time evolution of several observables in the one-magnon subspace of the sawtooth chain, especially near that point.

[1] J. Schulenburg, A. Honecker, J. Schnack, J. Richter, H.-J. Schmidt, Phys. Rev. Lett. 88 (2002) 167207

DY 43.7 Thu 15:00 P2

Nonequilibrium dynamics in quantum spin systems with neural quantum states — •DAMIAN HOFMANN¹, GIAMMARCO FABIANI², JOHAN MENTINK², GIUSEPPE CARLEO³, MARTIN CLAASSEN⁴, and MICHAEL SENTEF¹ — ¹Max Planck Institute for the Structure and Dynamics of Matter, Center for Free-Electron Laser Science (CFEL), Luruper Chaussee 149, 22761 Hamburg, Germany — ²Radboud University, Institute for Molecules and Materials, Heyendaalseweg 135, 6525 AJ Nijmegen, The Netherlands — ³Institute of Physics, École polytechnique fédérale de Lausanne (EPFL), 1015 Lausanne, Switzerland — ⁴Department of Physics and Astronomy, University of Pennsylvania, Philadelphia, PA 19104, USA

Neural quantum states (NQS) are a variational ansatz in which a neural network is used to parametrize the quantum state of a many-body system. NQS-based methods can be applied to learning both ground states and dynamics of quantum many-body systems by optimizing the network weights as variational parameters. In this poster, we present our current efforts in applying NQS methods to simulating strongly correlated quantum systems in and out of equilibrium. In particular, we highlight our recent work on understanding the stability properties of time-evolution algorithms for NQS based on the time-dependent variational Monte Carlo method (Hofmann et al., SciPost Phys. 12, 2022). Furthermore, we will present our ongoing research into the application of NQS to learning states in quantum spin liquid systems.

DY 43.8 Thu 15:00 P2

Source-driven optical microcavities — •LUKAS SEEMANN and MARTINA HENTSCHEL — TU Chemnitz

Optical microcavities – open billiards for light – are known to possess far field emission patterns that sensitively depend on their geometric shape: the geometry determines the light's nonlinear dynamics and, via the associated unstable manifold and invariant measure, the emission characteristics. However, this behavior might change, and new features can be added, when the microcavity is driven by a local internal light source [1]. Here, we investigate the properties of optical microcavities with sources both with ray and with wave methods. To this end we extend the ray picture by the phase information and collect the wavelength-dependent phase information along the ray trajectories. We use phase-space methods to analyze the source-induced time-dependent dynamics and compare the Poincaré surface of section for rays with phase to the Husimi function dynamics of wave solutions, thereby exploring chances and limitations of ray-wave correspondence.

[1] J.-K. Schrepfer, S. Chen, M.-H. Liu, K. Richter, and M. Hentschel, Phys. Rev. B 104, 155436 (2021)

DY 44: Poster Session: Statistical Physics and Critical Phenomena

Time: Thursday 15:00–18:00

Location: P2

DY 44.1 Thu 15:00 P2

How to distinguish between indistinguishable particles — •MICHAEL TE VRUGT — Institut für Theoretische Physik, Center for Soft Nanoscience, Philosophisches Seminar, 48149 Münster, Germany

Does exchanging two indistinguishable particles lead to a new physical state? While the answer appears to be clear in quantum mechanics (no), the situation in *classical* statistical mechanics is up to considerable debate. In this work [1], we show that order-preserving dynamics, a recently developed formalism that allows for an accurate treatment of single-file diffusion within dynamical density functional theory, provides a strong argument for haecceitism (the view that such an exchange does make a difference) since it requires treating observationally indistinguishable particle configurations as being different. This result turns out to have interesting consequences for the concept of thermodynamic equilibrium.

[1] M. te Vrugt, Br. J. Phil. Sci. (forthcoming), doi: 10.1086/718495

DY 44.2 Thu 15:00 P2

Operationally Accessible Uncertainty Relations for Thermodynamically Consistent Semi-Markov Processes — •BENJAMIN ERTEL, JANN VAN DER MEER, and UDO SEIFERT — II. Institut für Theoretische Physik, Universität Stuttgart, 70550 Stuttgart, Germany

Semi-Markov processes generalize Markov processes by adding temporal memory effects as expressed by a semi-Markov kernel. We recall the path weight for a semi-Markov trajectory and the fact that thermodynamic consistency in equilibrium imposes a crucial condition called direction-time independence for which we present an alternative derivation. We prove a thermodynamic uncertainty relation that formally resembles the one for a discrete-time Markov process. The result relates the entropy production of the semi-Markov process to mean and variance of steady-state currents. We prove a further thermodynamic uncertainty relation valid for semi-Markov descriptions of coarse-grained Markov processes that emerge by grouping states together. A violation of this inequality can be used as an inference tool to conclude that a given semi-Markov process cannot result from coarse-graining an underlying Markov one. We illustrate these results with representative examples [1].

[1] Benjamin Ertel, Jann van der Meer and Udo Seifert, Phys. Rev. E 105, 044113 (2022)

DY 44.3 Thu 15:00 P2

Lane formation of gravitationally driven model colloids in two-dimensional linear channels — •MARC ISELE, KAY HOFMANN, and PETER NIELABA — Physics Department, University of Konstanz, Konstanz, Germany

We conducted Brownian dynamics simulations to investigate the segregation phenomena of driven model colloids in two-dimensional linear channels. Two kinds of spherical particles of different sizes were driven in the same direction by a gravitational force. The difference in driving force acting on these particles creates a segregation similar to the lane formation of oppositely driven colloids. We had a closer look at parameter values facilitating lane formation and the resulting lanes were examined more closely. This approach creates a system which is easier to reproduce in experiments than the conventional oppositely driven setups by tilting a linear channel with two particle kinds of different size.

DY 44.4 Thu 15:00 P2

Geometric Brownian Information Engine : Essentials of optimal work and performance. — •RAFNA RAFEEK, SYED YUNUS ALI, and DEBASISH MONDAL — Department of Chemistry and Center for Molecular and Optical Sciences & Technologies, Indian Institute of Technology Tirupati, Yerpedu 517619, Andhra Pradesh, India

We investigate a Geometric Brownian Information Engine (GBIE) in the presence of an error-free feedback controller that transforms the information gathered on the state of particles entrapped in mono-lobal geometric detention into extractable work. We determine the benchmarks for utilizing the available information in an output work and the optimum operating requisites for best performance. Apart from a reference measurement distance x_m and feedback site x_f , upshots of the information engine also depend on the transverse constant bias force (G). G tunes the entropic contribution in the effective potential and the standard deviation (σ) of the equilibrium marginal probability distribution.

We find that the upper bound of the achievable work shows a crossover from $(5/3 - 2\ln 2)kBT$ to $1/2kBT$ when the system changes from entropy to an energy-dominated one. The higher loss of information during the relaxation process, accredits the lower value of work in entropic instances of GBIE. We recognize that the work extraction reaches a global maximum when $x_f = 2x_m$ with $x_m = 0.6\sigma$, irrespective of the extent of the entropic limitation. Also we explore the effect of entropic control on the unidirectional passage of the particle and efficacy of the GBIE.

DY 44.5 Thu 15:00 P2

Shear flow induced instability of a trapped colloidal particle in a complex medium — •LEA FERNANDEZ and SABINE H.L. KLAPP — Institute for Theoretical Physics, TU Berlin

The motion of a colloidal particle in a complex medium, bound by an optical trap and subjected to a shear flow can be modelled by the Langevin equations for an over-damped harmonic oscillator in n dimensions. Here we treat n_{obs} observed, physical variables, with $n = n_{obs} + n_{int}$, and n_{int} internal, auxiliary variables modelling a complex medium. Analytical and numerical results are presented for $n_{obs} = 2$ and $n_{int} = 1$, where the coupling between the observed variables is given by a plane Couette flow. We analyse the dynamics of averages, probability densities, and trajectories using Brownian dynamics and the Smoluchowski equation. Of special interest is the effect of the coupling with the auxiliary variable. The focus is on coupling parameters where the steady shear flow causes a transition from a stationary state to an in-stationary state, corresponding to a delocalisation of the particle, when the shear rate exceeded a critical value.

DY 44.6 Thu 15:00 P2

Quantifying the potential energy landscape within nanoconfinements by MD simulations — •SIMON HEFNER, ROBIN HORSTMANN, and MICHAEL VOGEL — TU Darmstadt, Institut für Physik kondensierter Materie, Hochschulstr. 6, 64289, Darmstadt, Germany

Nanoconfinements find applications in various fields from catalysis to electronics, [1] although the properties of confined systems are still not fully understood. For instance, the effects of different kinds of confinements on the dynamical and structural properties of confined liquids are still elusive. To obtain a better understanding of those effects MD simulations are well suited [2]. Here, we performed simulations for TIP4P/2005 water. Neutral pores of water were prepared. From the time-averaged static density profile in the pore the potential energy landscape was reconstructed and the energy barrier against water motion at the wall and in bulk were calculated and compared. We calculated the temperature and radial dependence of the energy barrier. The translational dynamics of water can be derived from the obtained energy landscape using the Arrhenius law. We further applied these methods to other kinds of pore systems and liquids and compared the results.

[1] Clancy, Adam J. et al. Chem. Rev., 2018, 118 (16), 7363-7408

[2] Horstmann, R. et al, Langmuir, <https://doi.org/10.1021/acs.langmuir.2c00521>

DY 44.7 Thu 15:00 P2

Fluctuations of work and heat in a driven entropic potential — •SYED YUNUS ALI, PRASHANTA BAURI, and DEBASISH MONDAL — Department of Chemistry and Center for Molecular and Optical Sciences & Technologies, Indian Institute of Technology Tirupati, Yerpedu 517619, Andhra Pradesh, India

We consider the motion of an over-damped Brownian particle in two-dimensional bilobal confinement driven by a periodic field in the presence of a transverse bias force. The confinement results in an entropic bistable potential in a reduced dimension. We calculate the work done and absorbed heat over a period and their mean and relative variance fluctuations in entropy and energy-dominated regimes. The average work done and absorbed heat over a period show turnover behavior as a function of noise strength and frequency input. Therefore, these observables can be considered potential quantifiers of the entropic stochastic resonance phenomena. We find that the heat fluctuations over a single period are always greater than the work fluctuations. We also discuss the applicability of steady-state fluctuation theorems in this system.

DY 44.8 Thu 15:00 P2

Exploiting Brownian motion and correlations for computing — •ALESSANDRO PIGNEDOLI¹ and KARIN EVERSCHOR-SITTE² — ¹Twist Group, Faculty of Physics, University of Duisburg-Essen — ²Twist Group, Faculty of Physics, University of Duisburg-Essen

Brownian motion is a natural phenomenon that can be exploited for computing [1]. Particle swarm optimization [2] based on the ideas of swarm intelligence is an example of this sort of computation. While the random motion of particles allows the exploration of the entire phase space of the system, interactions and driving forces break ergodicity. This allows for an efficient solution to an optimization problem, which can be identified by looking at the system's correlations and statistical observables. To accomplish Brownian computation, we employ a Langevin model to describe magnetic skyrmions [3], which are topologically stable magnetic whirls that have been shown to behave like interacting Brownian particles [4].

[1] C.H. Bennett, Int. J. Theor. Phys. 21, 905 (1982). [2] J. Kennedy and R. Eberhart, Proc. of ICNN'95 * Int. Conf. on Neural Networks, 4, 1942 (1995) [3] K. Everschor-Sitte, J. Masell, R. M. Reeve and M. Kläui, J. Appl. Phys. 124, 240901 (2018) [4] J. Zázvorka, et al. Nat. Nanotechnol. 14, 658 (2019)

DY 44.9 Thu 15:00 P2

Overload wave-memory induces amnesia of a self-propelled particle — •MAXIME HUBERT¹, STÉPHANE PERRARD², NICOLAS VANDEWALLE³, and MATTHIEU LABOUSSE⁴ — ¹PULS group, FAU Erlangen-Nürnberg, Erlangen, Germany — ²PMMH, ESPCI Paris and PSL University, Paris, France — ³GRASP, University of Liège, Liège, Belgium — ⁴Guliver, ESPCI Paris and PSL University, Paris, France

“Walking droplets” constitute a model system to investigate active transport dynamics driven by complex memory kernels. The droplet stores positional information in a wavefield at an oil interface that in return serves as a propulsive mechanism. The complexity of the wavefield and the amount of positional information are remotely controlled through a single scalar value, the memory of the system, which corresponds to the persistence time of the waves. In this study, we investigate the high-memory limit of both the droplet and the wavefield dynamics. We show that an overload of memory brings the droplet to a diffusive dynamics which cannot be distinguished from an active Markovian dynamics. The wavefield however contains all the correlations of the dynamics and exhibits an energy-minimization principle and equipartition of energy in the eigenmodes of the wavefield.

DY 44.10 Thu 15:00 P2

Coarse-graining of systems with discrete Markovian dynamics — STEFAN KLUMPP and •MIGUEL RODRÍGUEZ MARTÍN — Institute for the Dynamics of Complex Systems, University of Göttingen, Göttingen.

There exists a wide range of physical systems that can be described by discrete Markovian dynamics. In many cases it is desirable to reduce the number of states in order to lower the computational cost or obtain an effective description that captures the most relevant effects at a given scale. A steady state-conserving method of coarse graining based on merging adjacent states and obtaining new transition rates from the optimization of the Kullback-Leibler divergence is generalized by minimizing the Rényi divergence instead. The resulting transition rates depend on the quotients between the steady state probabilities of the merged states in the original system, so a method is developed to compute these transition rates without the need of finding the steady state probabilities. Making use of the similarities between the master equation and Schrödinger's equation, a formulation for classical discrete Markov processes analogous to quantum mechanics is developed, both in the frame of Schrödinger's formulation and second quantization. These are used to study coarse graining under the constraint that the steady state must be conserved.

DY 44.11 Thu 15:00 P2

Molecular dynamics simulations of binary mixtures in nanostructured pores — NIELS MÜLLER, MICHAEL VOGEL, and MARKUS HANEKE — TU Darmstadt, Institut für Physik kondensierter Materie, Hochschulstr. 6, Darmstadt, Germany

Water and its mixtures are fairly common in nature and technology. Here, we seek to understand the influence of solid surfaces with nanostructured porous confinements on binary aqueous mixtures. For this purpose, we exploit that MDS allow us to determine structural and dynamical properties in a spatially resolved manner. The inner surfaces and the aqueous mixtures of the simulated systems are made of differently polarized molecules. The composition and temperature are varied, approaching the regime of spinodal decomposition.

We find that the nanostructured surfaces impose a corresponding nanoscopic phase separation onto the confined mixtures. Explicitly, the concentration of the mixture components varies along the pore axis in phase with the surface patterning, where the effect is stronger near the pore walls. Moreover, the particle mobility differs between the components and depends on the position within the porous confinement. In particular, the imposed concentration fluctuations cause diffusion barriers.

DY 44.12 Thu 15:00 P2

Microcanonical analysis of model polymers interacting via many-body dispersion — BENEDIKT AMES, MARIO GALANTE, MATTEO GORI, and ALEXANDRE TKATCHENKO — Department of Physics and Materials Science, Université du Luxembourg

Non-covalent interactions play a crucial role in the energetics and structure formation of many systems of interest for physics, chemistry and biology.

Among computational methods which include van der Waals (vdW) interactions, the many-body dispersion framework (MBD) attains an excellent accuracy by accounting for all orders of the coupling. Its application has shown the importance of going beyond the pairwise (PW) approximation, for example to obtain the correct energy ordering of molecular crystals and for the adhesion of 2D structures. Nevertheless, the phenomena of MBD-driven dynamics remain largely unexplored.

Here, as a means to probe these dynamics, we study the phase transitions of a simplified model polymer via microcanonical inflection point analysis [1], a recent generalization of the notion of phase transitions from the thermodynamic limit to finite-size systems. By contrasting simulations using MBD and PW methods, we explore whether the different characteristics of each vdW model manifest themselves in distinct properties of the polymer's clustering transition.

[1] Koci, Qi and Bachmann, J. Phys.: Conf. Ser. 759, 012013 (2016).

DY 44.13 Thu 15:00 P2

Arcsine laws in non-equilibrium regime — AVIJIT KUNDU^{1,2}, RAUNAK DEY², BISWAJIT DAS², and AYAN BANERJEE² — ¹University of Bayreuth, Universitätsstrasse 30, 95447, Bayreuth, Germany — ²Indian Institute of Science Education and Research Kolkata, Mohanpur, Kalyani, 741246, India

Most of the processes in the mesoscopic world especially inside living cell are far from thermal equilibrium. The time evolution of such processes is important to study to characterize the processes. Remarkably, Paul Lévy defined arcsine laws for three variables related to the stochastic Wiener process. Here we have studied stochastically driven colloidal particle in a viscous fluid and observed the entropic current, work done on the system or dissipated by it, follow the Lévy arcsine laws in the large time limit. The significant lead of this work is to show the convergence of cumulative distribution to the arcsine law is faster for the case of near equilibrium system where the entropy production rate is smaller. We also have tested the convergence rates of cumulative distributions for different non-equilibrium systems by driving the optically trapped colloidal probe with external noise parameters and changing the flow field by introducing a microbubble in its vicinity.

DY 44.14 Thu 15:00 P2

Phase transition in clustering algorithms — JULIAN ZITTERICH and ALEXANDER K. HARTMANN — Institute of Physics, University of Oldenburg, Germany

A well known problem in data analysis and machine learning is the clustering problem. It consists of grouping a set of data vectors into subsets, such that *similar* vectors end up in the same subset. How to define similarity and how to find these subgroups depend much on the investigated problem, thus many algorithms and metrics exist. Also it may be that an algorithm is not able to successfully detect structure in the given data. Thus, we study here ensembles of artificially generated data controlled by parameters such that for some parameter values the clustering is *easy* or at least *possible* while for other values it is *hard* or *impossible*. Thus, from a statistical physics viewpoint we are interested in phase transitions of the clustering problem between such phases. Previously, the existence of such phase transitions was observed for a single ensemble in high-dimensional space by using the AMP algorithm [1]. Here, we investigate numerically [2] four different state-of-the-art cluster algorithms and analyse their behaviour for increasingly complex ensembles. Low complexity ensembles are realized by direct sampling of data vectors, while high complexity ensembles are implemented by short simulations of simple models of interacting particles.

[1] T. Lesieur et al., 54th Annual Allerton Conference on Communication, Control, and Computing (Allerton), arXiv:1610.02918 (2016)

[2] A.K. Hartmann, *Big Practical Guide to Computer Simulations*, World Scientific (2015)

DY 44.15 Thu 15:00 P2

Chemfiles: reading and writing atomistic modeling files — GUILLAUME FRAUX — Institute of Materials, EPFL, Lausanne, Switzerland

Running atomistic simulations produces enormous amounts of data, which has to be post-processed in order to extract scientifically relevant information. Unfortunately, this task is made much harder by the vast menagerie of existing file formats, all containing similar data in a different formatting.

Chemfiles is a software library providing a unified interface to these formats, allowing researchers to spend their time analyzing their data instead of writing file parsers over and over. Chemfiles is implemented in C++, and provides programming interfaces to most of the scientific languages: Python, Fortran, C, Rust and Julia. 21 different formats are currently supported, including both text and binary (i.e. XTC, TNG, DCD, ...) formats. All text formats can be read and written with multiple compression standards (gzip, xz, bzip2). Chemfiles also offers a comprehensive atom selection language, including the unique feature of simultaneous selection of multiple atoms (e.g. pairs: `name(#1) == H and name(#2) == O and distance(#1, #2) < 3.0`).

Overall, chemfiles is one of the fastest libraries for reading files used in atomistic simulation, being between 20% and 10 times faster than other commonly used libraries; while offering a simpler and easy to use programming interface; freeing up time for scientists working with these file formats.

DY 44.16 Thu 15:00 P2

Phase transitions for two-stage stochastic minimum spanning tree optimization problem — ROBERT STRASSEN and ALEXANDER K. HARTMANN — Institute of Physics, University of Oldenburg

Phase transitions in classical optimization problems have been studied extensively in statistical physics [1]. Here, we consider two-stage stochastic optimization problems, where the optimization is performed in two different stages, such that in the first stage not all information is available. In particular, we consider the two-stage stochastic minimum spanning tree (MST) problem for undirected graphs with given initial edge costs. In the second stage, one of a set of random scenarios is realized, involving different edge costs. In each stage, edges can be selected such that a spanning tree is finally formed, aiming at a minimum expected total costs. Unlike the conventional MST problem, the two-stage version is generally worse-case "hard" to solve, even though there are problem instances that are "easy". We investigate numerically [2] the problem by the calculation of bounds and applying several approximation algorithms, including one of Dhamdhere et al. [3] on various random ensembles of graphs. Our aim is to find out whether there are phase transitions between typical easy and hard problem phases.

[1] A.K. Hartmann and M. Weigt, *Phase Transitions in Optimization Problems*, Wiley-VCH, Berlin 2005

[2] A.K. Hartmann, *Big Practical Guide to Computer Simulations*, World-Scientific, Singapore, 2015

[3] K. Dhamdhere, R. Ravi, M. Singh, IPCO 2005, LNCS 3509, pp. 321-334, (2005)

DY 44.17 Thu 15:00 P2

Critical Casimir effect in the square-lattice Ising model with quenched surface disorder — LUCA CERVELLERA and ALFRED HUCHT — Theoretische Physik, Universität Duisburg-Essen and CENIDE, 47048 Duisburg, Germany

For the square-lattice Ising model, the critical Casimir amplitude and force can be calculated exactly for many geometries and boundary conditions. From a recent exact solution for the cylinder with length L , circumference M , and with arbitrary random boundary conditions at one boundary, we determine the full density of thermodynamic states $\omega(\delta F, m_B)$, with residual free energy δF and boundary magnetization m_B at criticality. From this quantity we can derive the disorder averaged Casimir potential for different aspect ratios and disorder ensembles.

DY 44.18 Thu 15:00 P2

Anomalous collective dynamics of auto-chemotactic populations — JASPER VAN DER KOLK¹, FLORIAN RASSHOFFER¹, RICHARD SWIDERSKI¹, ASTIK HALDAR², ABHIJIT BASU², and ERWIN FREY^{1,3} — ¹Arnold Sommerfeld Center for Theoretical Physics and Center for NanoScience, Department of Physics, Ludwig-Maximilians-Universität München, Munich, Germany — ²Theory Division, Saha Institute of Nuclear Physics, HBNI, 1/AF Bidhannagar, Calcutta 700 064, West Bengal, India — ³Max Planck School Matter to Life, Hofgartenstraße 8, 80539 Munich, Germany

While the role of local interactions in nonequilibrium phase transitions is well studied, a fundamental understanding of the effects of long-range interactions is lacking. We study the critical dynamics of reproducing agents subject to auto-chemotactic interactions and limited resources. A renormalization group anal-

ysis reveals distinct scaling regimes for fast (attractive or repulsive) interactions; for slow signal transduction the dynamics is dominated by a diffusive fixed point. Further, we present a novel nonlinear mechanism that stabilizes the continuous transition against the emergence of a characteristic length scale due to a chemotactic collapse.

DY 44.19 Thu 15:00 P2

Multifractality at the integer quantum Hall transition — •MARTIN PUSCHMANN¹, DANIEL HERNÁNDEZ-PÉREZ², BRUNO LANG³, SOUMYA BERA⁴, and FERDINAND EVERS¹ — ¹Institute of Theoretical Physics, University of Regensburg, D-93053 Regensburg, Germany — ²Department of Molecular Chemistry and Material Science, Weizmann Institute of Science, Rehovot 7610001, Israel — ³IMACM and Institute of Applied Computer Science, Bergische Universität Wuppertal, D-42119 Wuppertal, Germany — ⁴Department of Physics, Indian Institute of Technology Bombay, Mumbai 400076, India
The quantum Hall transitions are still one of the bigger mysteries of condensed matter theory. In the past twenty years several conjectures have been made as to what the field theory of the critical fixed point of the integer (class A) quantum Hall transition could be. The multifractal spectrum provides a characteristic fingerprint of the phase transition. Here, recent analytical work predicts a parabolic dependency of the anomalous dimension $\Delta_q = q(1-q)/4$, where the exponents $\tau_q = 2(q-1) + \Delta_q$ describe the system-size scaling of wavefunction moments $|\Psi|^{2q}$ [1]. In great analogy to our previous analysis on the spin (class C) quan-

tum Hall transition [2], we investigate the multifractal spectrum of the class A transition and similarly demonstrate the presence of quartic terms in Δ_q . Our findings are thus clearly inconsistent with the strict parabolicity predicted for "traditional" conformal field theories. [1] M. R. Zirnbauer, Nucl. Phys. B 941, 458 (2019) [2] M. Puschmann et al., Phys. Rev. B 103, 235167 (2021)

DY 44.20 Thu 15:00 P2

Detection of defects in soft quasicrystals with neural networks — •ALI DOENER and MICHAEL SCHMIEDEBERG — Theoretische Physik I, Erlangen, DE
The aim of this work is to construct and employ a neural network for the detection of topological defects in dodecagonal quasicrystalline patterns. Even though quasicrystals are aperiodic, they exhibit a long-range order. Furthermore, in principle any discrete rotational symmetry can occur.

In this work, dodecagonal quasicrystalline patterns in two-dimensions with a built-in dislocation are generated and employed as input images of the neural network. The network then should figure out not only the position but also the type of the Burgers vector of the defect.

Our trained neural network is able to recognize the type of the Burgers vector very good. The position of the dislocation is recognized up to a mean deviation from the real position that is much smaller than the small length scale in the quasicrystals. In future, we want to train the network with patterns that contain multiple dislocations as well as phasonic excitations.

DY 45: Poster Session: Nonlinear Dynamics, Pattern Formation, Data Analytics and Machine Learning

Time: Thursday 15:00–18:00

Location: P2

DY 45.1 Thu 15:00 P2

Influence of protective measures on rare-event behavior of the dynamics of the SIR model. — •TIMO MARKS, YANNICK FELD, and ALEXANDER K. HARTMANN — Institute of Physics, University of Oldenburg

Since the outbreak of the SARS-CoV-2 pandemic in early 2020, there has been a surge of interest in modeling disease spreading. The basis of many more complex models is the SIR model [1], in which the population is divided into a group of *Susceptible*, *Infected* and *Recovered* individuals.

Here, the SIR model is applied to a small-world ensemble that can model social interactions of a real population [2]. Using large-deviation methods and in particular the Wang-Landau algorithm, the distributions of quantities of interest can be calculated over basically the full support [3]. To include protective measures, once a predefined threshold of simultaneously infected nodes is reached, the transmission parameter is decreased. We compare the impact of these measures with unrestrained disease spreading on the level of the full probability distributions, which were obtained down to probabilities such as 10^{-50} . We thereby observe significant changes in the shape of the distributions.

[1] W. O. Kermack and A. G. McKendrick, Proc. R. Soc. Lond. A **115**, 700*721 (1927)

[2] S. Milgram, Psychology Today **1**, 60*67 (1967)

[3] Y. Feld, A. K. Hartmann, PhysRevE.105.034313 (2022)

DY 45.2 Thu 15:00 P2

Pattern Formation in non-ideal systems: From Turing patterns to active droplets — •LUCAS MENOUE and DAVID ZWICKER — Max Planck Institute für dynamik und selbstorganisation, Göttingen, Germany

Turing's seminal reaction-diffusion model explains how patterns form in non-equilibrium systems. Typical Turing models assume ideal diffusion, which implies dilute or ideal systems. In contrast, active droplets use chemical reactions to control phase separation emerging in strongly interacting systems. We unite both theories by combining the classical Cahn-Hilliard model, which describes non-ideal solutions, with the typical non-linear reactions responsible for Turing patterns. We find that interactions can promote or suppress the emergence of periodic patterns. Interestingly, patterns can form even when all species have equal diffusivity, which is impossible in traditional Turing models. Taken together, our theory shows a rich behavior that interpolates between the traditional Turing patterns and active droplets.

DY 45.3 Thu 15:00 P2

Chaotic Diffusion in Delay Systems: Giant Enhancement by Time Lag Modulation — •TONY ALBERS, DAVID MÜLLER-BENDER, LUKAS HILLE, and GÜNTER RADONS — Institute of Physics, Chemnitz University of Technology, Chemnitz, Germany

We consider a typical class of systems with delayed nonlinearity, which we show to exhibit chaotic diffusion. It is demonstrated that a periodic modulation of the time-lag can lead to an enhancement of the diffusion constant by several orders of magnitude. This effect is the largest if the circle map defined by the modula-

tion shows mode locking and more specifically, fulfills the conditions for laminar chaos. Thus we establish for the first time a connection between Arnold tongue structures in parameter space and diffusive properties of a delay system. Counterintuitively, the enhancement of diffusion is accompanied by a strong reduction of the effective dimensionality of the system.

Details can be found in: T. Albers, D. Müller-Bender, L. Hille, and G. Radons, Phys. Rev. Lett. **128**, 074101 (2022)

DY 45.4 Thu 15:00 P2

Bistable vortices formed by active particles with retarded interactions — XI-ANGZUN WANG¹, •PIN-CHUAN CHEN², KLAUS KROY², VIKTOR HOLUBEC³, and FRANK CICHOS¹ — ¹Peter Debye Institute for Soft Matter Physics, Leipzig University, Leipzig, Germany — ²Institute for Theoretical Physics, Leipzig University, Leipzig, Germany — ³Department of Macromolecular Physics, Faculty of Mathematics and Physics, Charles University, Prague, Czech Republic

In recent experiments done in the Molecular Nanophotonics Group in the Peter Debye Institute, thermophoretic microswimmers are observed to self-assemble into bi-stable rotational modes due to retarded attractive interactions.

For the particular case where a single swimmer is attracted to an immobilized target, we show how we can analytically understand such non-linear stochastic time-delayed system. This could be achieved by Taylor expanding the equation for small time delay. The system can then be described by an overdamped Langevin equation with a potential determined by time delay, and the transition in between the two stable modes is well predicted by Kramers' escape rate. However, expanding the delayed term in Taylor series is actually not as trivial as it seems to be, as instability would occur if we keep derivatives up to arbitrarily high orders.

For the case where multiple swimmers are present, the swimmers form a cluster with co-rotating and counter-rotating shells. We further discuss the competition between the time-delay and hydrodynamic effects, which result in this phenomenon.

DY 45.5 Thu 15:00 P2

Synchronizing Cells Based on Local Interactions — •STEPHAN KREMSER, MAREIKE BOJER, and ULRICH GERLAND — Physics Department, Technical University of Munich

Tissue-wide temporal synchronization of cellular processes is a desirable property for many systems in synthetic and developmental biology. Here, we look at a setting where cells have only limited information about the behavior of neighboring cells, receiving new information only after these neighbors change their internal state. Under these assumptions, we ask if global synchronization can be reached based on local (e.g. direct contact) interactions. We develop a conceptual model of the synchronization process and explore it computationally for different dimensions and interaction network topologies of the tissue. We show that temporal corrections to cellular processes based on magnitude ('proportional feedback control') or sign ('on-off feedback control') of local time differences are enough to conserve local synchronization and bound global asynchrony by a

constant independent of time for a long period of time. This allows us to establish a link to the physics of growing surfaces and to investigate the interplay of patterning and synchronization dynamics.

DY 45.6 Thu 15:00 P2

Network complexity versus network synchronicity: A case study of the Kuramoto model on complex networks — ARCHAN MUKHOPADHYAY and JENS CHRISTIAN CLAUSSEN — University of Birmingham, UK

During the last two decades, complexity measures for graphs and networks have gained significant attention (see [1] for a comparison), especially in the aim to distinguish "complex" topologies from regular lattices as well as random structures. However, what is the influence of topology on dynamics? Here we specifically analyze synchronization in a network of Kuramoto oscillators where the topology (between a high-complexity graph and a random graph) is parameterized by a complexity measure, as Offdiagonal Complexity [2] or one of the other graph complexity measures. This approach may provide a new light on both the influence of complexity on synchronization, as well as the complexity measures and which aspects of dynamical complexity these may predict.

[1] J. Kim, T. Wilhelm, *Physica A* 387, 2637 (2008)

[2] Jens Christian Clausen, *Physica A* 375, 365 (2007)

DY 45.7 Thu 15:00 P2

Quantum synchronization in a network of dissipatively coupled oscillators — JUAN NICOLAS MORENO, CHRISTOPHER W. WÄCHTLER, and ALEXANDER EISEL — Max Planck Institute for the Physics of Complex Systems, Dresden, Germany

Synchronization in classical systems has a long history and by now is a very well understood phenomenon. However, the question whether the classical notions of synchronization can be extended to the quantum regime has only recently been addressed in investigations of classically inspired models like quantum Van der Pol oscillators as well as models without classical analog. Inspired by the theoretical prediction that two-level atoms are able to synchronize even without interacting directly [1], we investigate a network of dissipatively coupled quantum harmonic oscillators. Within a mean-field approximation we find that the network is able to synchronize. For the fully quantum system described in terms of a Lindblad master equation we analyze various measures that have been proposed in the literature. Additionally, we investigate the Liouvillian spectrum in order to draw connections between the spectrum and the synchronization measures.

[1] PRA 101, 042121 (2020)

DY 45.8 Thu 15:00 P2

Neural Network-Based Approaches for Multiscale Modelling of Topological Defects — KYRA KLOS¹, KARIN EVERSCHOR-SITTE², and FRIEDERIKE SCHMID¹ — ¹Johannes Gutenberg University, Mainz, Germany — ²University of Duisburg-Essen, Duisburg, Germany

Topological defects and their dynamics are a heavily researched topic in a wide range of physics fields [1].

Due to the multiscale character of those defect structures, numerically simulating a large number of them in full microscopic detail gets highly computationally expensive, as the large size of associated deformation fields around each core leads to a complex interaction pattern.

To give a possible insight into the connection between the macroscopic (particle) description of a model with topological defects and the underlying microscopic structure, we propose the use of neural networks. With a spin-dynamic simulated microscopic model as training data, we use a conditional generative adversarial network system [2] with Wasserstein-loss [3] to generate reasonable spin-configurations from given defect configuration inputs. To guarantee the generation of realistic spin configuration, we also include additional physical constraints into our generator.

[1] Mermin N. D., *Rev. Mod. Phys.* 51, 591, (1979)

[2] Mirza M. ; Osindero S., arXiv:1411.1784v1, (2014)

[3] Arjovsky M. et al., *ICML, PMLR* 70, 214, (2017)

[4] Goodfellow I. et al., *NeurIPS*, (2014)

DY 45.9 Thu 15:00 P2

Characterizing quasicrystalline patterns with neural networks — JONAS BUBA and MICHAEL SCHMIEDEBERG — Friedrich-Alexander-Universität Erlangen-Nürnberg, Erlangen, Germany

There exist multiple ways to generate two dimensional quasicrystal patterns such as superpositions of plane waves [1-3] or projection methods [4], each using different parametrisations. A deep convolutional Autoencoder is utilized to determine whether an artificial neural network is capable of finding sufficient parametrisations for these patterns.

Furthermore another neural network was used to classify them by symmetry. Finally, deep dream methods [5] are employed to analyze which features the artificial intelligence bases its symmetry classification on. Currently we are trying to find out how the deep dream approach can be applied to modify existing patterns by enhancing features corresponding to specific symmetries.

[1] D.S. Rokhsar, N.D. Mermin, and D.C. Wright, *Acta Cryst.* A44, 197 (1988).

[2] S.P. Gorkhali, J. Qi, and G.P. Crawford, *J. Opt. Soc. Am. B* 23, 149 (2005). [3]

M. Schmiedeberg and H. Stark, *J. of Phys.: Cond. Matter* 24(28), 284101 (2012). [4] M. Duneau and A. Katz, *Phys. Rev. Lett.* 54, 2688 (1985). [5] A. Mordvintsev, C. Olah, and M. Tyka, "Inceptionism: Going Deeper into Neural Networks", Google AI Blog (2015).

DY 45.10 Thu 15:00 P2

Influence of delay-times on photonics reservoir computing performance — LINA JAURIGUE and KATHY LÜDGE — Institut f. Physik, Technische Universität Ilmenau, Weimarer Str. 25, 98684 Ilmenau, Germany

Reservoir computing is a machine learning approach that utilises the non-linear responses of dynamical systems to perform computational tasks. Due to the relative simplicity of this approach the implementation in hardware is practicable, particularly the delay-based reservoir computing paradigm. Delay-based reservoirs use a single non-linear node subject to self-feedback. The high-dimensional dynamics that arise due to the feedback are utilised by driving the reservoir with time-multiplexed inputs. There have been a number of successful implementations of delay-based reservoirs in electronic, opto-electronic and photonic systems, among others. However, a challenge that remains is the efficient optimisation of a reservoir for performance on a variety of tasks. To this end we explore the influence of the delay-time on the performance of time-series prediction tasks and compare the computational performance of different methods of including task specific delay-timescales in a photonic reservoir setup.

DY 45.11 Thu 15:00 P2

Reservoir computing with memory cells: Impact of perturbations and phase effects — NOAH JAITNER¹, ELIZABETH ROBERTSON³, LINA JAURIGUE², JANIK WOLTERS³, and KATHY LÜDGE² — ¹Institute of Theoretical Physics, Technische Universität Berlin, Hardenbergstr. 36, 10623 Berlin, Germany — ²Institut f. Physik, Technische Universität Ilmenau, Weimarer Str. 25, 98684 Ilmenau, Germany — ³Deutsches Zentrum für Luft- und Raumfahrt e.V. (DLR), Insitut für Optische Sensorsysteme, Rutherfordstr. 2, 12489 Berlin, Germany

Reservoir computing is a versatile, fast-trainable approach for machine learning that utilites the capabilities of dynamical systems. The common approach is to use a nonlinear element and a delay line to construct a virtual network. These virtual networks have limited topology. By utilizing cesium cells as coherent optical memory cells to create a hybrid architecture [1] the limitations of topology can be overcome and a more dynamically versatile virtual network can be created. The optical memory used in the corresponding experiment performs well in memory bandwidth but experiences high noise levels. [2] The dynamics and noise resistance of this approach is examined to find an optimal approach for different time series prediction tasks.

[1] L. C. Jaurigue, E. Robertson, J. Wolters and K. Lüdge *Entropy* 23, 1099-4300 (2021).

[2] L. Esguerra, L. Meßner, E. Robertson, N. V. Ewald, M. Gündoan and J. Wolters arXiv:2203.06151.

DY 45.12 Thu 15:00 P2

Reconstructing spatiotemporal chaos in three-dimensional excitable media based on surface data — INGA KOTTLARZ^{1,2}, SEBASTIAN HERZOG^{1,3}, ROLAND STENGER^{1,2}, BALASAR RÜCHARDT^{1,4}, STEFAN LUTHER^{1,4,5}, and ULRICH PARLITZ^{1,2,4} — ¹Max Planck Institute for Dynamics and Self-Organization, Göttingen, Germany — ²Institute for Dynamics of Complex Systems, Georg-August-Universität Göttingen, Göttingen, Germany — ³Department for Computational Neuroscience, Third Institute of Physics - Biophysics, University of Göttingen, Göttingen, Germany — ⁴German Center for Cardiovascular Research (DZHK), partner site Göttingen, Robert-Koch-Str. 42a, 37075 Göttingen, Germany — ⁵Institute of Pharmacology and Toxicology, University Medical Center Göttingen, Robert-Koch-Str. 40, 37075, Göttingen, Germany

The cardiac muscle is an excitable medium that can exhibit complex dynamics, including spatiotemporal chaos associated with (fatal) cardiac arrhythmias. While mechanical motion within the myocardium can be observed with ultrasound, there are no noninvasive techniques (to date) to measure the electrical state within the tissue. To overcome this limitation of observable quantities, we address the task of predicting the electrical state inside the heart from surface data using data-driven reconstruction by means of artificial neural networks. We study the feasibility of this approach in a homogenous and isotropic excitable medium with spatiotemporal dynamics in three spatial dimensions, applying and comparing different deep learning methods (i.e. LSTM, Convolutional Autoencoder, ...).

DY 45.13 Thu 15:00 P2

Ordinal Patterns as Robust Biomarkers in Multichannel EEG Time Series — INGA KOTTLARZ^{1,2}, SEBASTIAN BERG¹, DIANA TOSCANO-TEJEIDA³, IRIS STEINMANN³, MATHIAS BÄHR⁴, STEFAN LUTHER^{1,5,6}, MELANIE WILKE^{3,7}, ULRICH PARLITZ^{1,2,6}, and ALEXANDER SCHLEMMER^{1,6} — ¹Max Planck Institute for Dynamics and Self-Organization, Göttingen, Germany — ²Institute for Dynamics of Complex Systems, Georg-August-Universität Göttingen, Göttingen, Germany — ³Department of Cognitive Neurology, University Medical Center Göttingen, Göttingen, Germany — ⁴Department of Neurology, University Medical

Center Göttingen, Göttingen, Germany — ⁵Institute of Pharmacology and Toxicology, University Medical Center Göttingen, Göttingen, Germany — ⁶German Center for Cardiovascular Research (DZHK), Partner Site Göttingen, Göttingen, Germany — ⁷German Primate Center, Leibniz Institute for Primate Research, Göttingen, Germany

Neurobiological changes in healthy and pathological aging and their electrophysiological correlates (EEG) are still an important topic in the neuroscience

DY 46: Poster Session: Complex Fluids, Soft Matter, Active Matter, Glasses and Granular Materials

Time: Thursday 15:00–18:00

Location: P2

DY 46.1 Thu 15:00 P2

Analysis of liquid distribution in microchannel systems using the electrohydraulic analogy — •MARIUS PÄTZOLD¹, FELIX SENF¹, CARL E. KRILL III², and OTHMAR MARTI¹ — ¹Institut für experimentelle Physik, Universität Ulm — ²Institut für funktionelle Nanosystem, Universität Ulm

The research program investigates the calculation of leakages in hydraulic systems by modelling the latter using electric resistor networks as an alternative to simulations employing computational fluid dynamics.

Based on a rigid geometry that describes a network of channels having rectangular cross sections of constant height, the hydraulic properties of the network are examined. The system is then modelled using an electric resistor network that incorporates these hydraulic properties. For a given pressure drop between the inlet and outlets, the model can be solved and leakages can be calculated using a modified nodal analysis.

The results show that modelling the geometry in this manner can be an efficient alternative to simulations using computational fluid dynamics within the requirements set by the electric-hydraulic analogy. Modelling hydraulic networks that are not within these requirements, like those with very short channels or highly complex channel networks, leads to the propagation of errors through the network, resulting in significant differences between the modelling and simulation approach.

DY 46.2 Thu 15:00 P2

Topological fine structure of smectic grain boundaries and tetratic disclination lines within three dimensional smectic liquid crystals* — PAUL A. MONDERKAMP¹, RENÉ WITTMANN¹, •MICHAEL TE VRUGT², AXEL VOIGT³, RAPHAEL WITTKOWSKI², and HARTMUT LÖWEN¹ — ¹Institut für Theoretische Physik II: Weiche Materie, Heinrich-Heine-Universität Düsseldorf, Universitätsstraße 1, 40225 Düsseldorf, Germany — ²Institut für Theoretische Physik, Center for Soft Nanoscience, Westfälische Wilhelms-Universität Münster, 48149 Münster, Germany — ³Institut für Wissenschaftliches Rechnen, Technische Universität Dresden, 01062 Dresden, Germany

Based on recent insights into the orientational topology of smectic grain boundaries in two dimensions, we analyse boundaries in three-dimensional confined smectics from the perspective of tetratic symmetry. Monte-Carlo simulations show the emergence of orientational grain boundaries. Using a 3d tetratic order parameter constructed from the Nelson-Steinhardt invariants, we show that the orientational topological fine structure of the planar smectic grain boundaries can be interpreted as a pair of tetratic disclination lines that are located on the edges of the nematic domain boundary [1]. Thereby, we shed light on the fine structure of the orientational topology of grain boundaries in three-dimensional confined smectics.

[1] P. A. Monderkamp et al., Phys. Chem. Chem. Phys. (2022), <https://doi.org/10.1039/D2CP00060A>

*Funded by the Deutsche Forschungsgemeinschaft (DFG) – grants VO 899/19-2, WI 4170/3-1, and LO 418/20-2.

DY 46.3 Thu 15:00 P2

From a microscopic inertial active matter model to the Schrödinger equation* — •MICHAEL TE VRUGT^{1,2}, TOBIAS FROHOFF-HÜLSMANN¹, EYAL HEIFETZ³, UWE THIELE¹, and RAPHAEL WITTKOWSKI^{1,2} — ¹Institut für Theoretische Physik, Westfälische Wilhelms-Universität Münster, 48149 Münster, Germany — ²Center for Soft Nanoscience, Westfälische Wilhelms-Universität Münster, 48149 Münster, Germany — ³Porter School of the Environment and Earth Sciences, Tel Aviv University, 69978 Tel Aviv, Israel

Field theories for the one-body density of an active fluid, such as the paradigmatic active model B+, are simple yet very powerful tools for describing phenomena such as motility-induced phase separation. No comparable theory has been derived yet for the underdamped case. In our work [1], we introduce active model I+, an extension of active model B+ to particles with inertia. The governing equations of active model I+ are systematically derived from the microscopic Langevin equations. We show that, for underdamped active particles, thermodynamic and mechanical definitions of the velocity field no longer coincide and that the density-dependent swimming speed plays the role of an effective viscos-

ity. Moreover, active model I+ contains the Schrödinger equation in Madelung form as a limiting case, allowing to find analogs of the quantum-mechanical tunnel effect and of fuzzy dark matter in the active fluid. We investigate the active tunnel effect analytically and via numerical continuation. [1] M. te Vrugt et al., arXiv:2204.03018

*Funded by the Deutsche Forschungsgemeinschaft (DFG) – grant 283183152.

DY 46.4 Thu 15:00 P2

Inertial Active Particles in Unbiased ac Fields Sediment at the Top Wall — •JOSÉ CARLOS UREÑA MARCOS and BENNO LIEBCHEN — Institut für Physik Kondensierter Materie, Technische Universität Darmstadt, Darmstadt, Germany

A detailed understanding of the controllability of the swimming direction of active particles through external fields is crucial for many of their proposed future applications, from nanomedicine to bioapplications.

While such steering is often achieved with dc fields with a net gradient, we show in this work that the use of rapidly oscillating ac fields allows the steering of inertial active particles even in the absence of a net gradient. To demonstrate this, we develop an analytical framework which shows that fast ac fields can stabilise fixed points in the dynamics of active particles which would otherwise be unstable.

To exemplify the applicability of this scheme, we explore inertial active particles in a gravitational field and observe that, in the presence of a rapidly oscillating ac field, a substantial fraction of them persistently travel in the upward direction and sediment at the top wall of the simulation box.

DY 46.5 Thu 15:00 P2

Rheological properties of Stockmayer supracolloidal magnetic polymers under shear flow — •VLADIMIR ZVEREV¹, EKATERINA NOVAK¹, and IVAN NOVIKAU² — ¹UNIVIE, Vienna, Austria — ²Ekaterinburg, Russia

Supracolloidal magnetic polymers (SPMs) are polymer-like structures in which magnetic nanoparticles construction SPMs has recently been made possible. Their advantage is that they keep their structure independently from the temperature. SPMs can be potentially used as an alternative to nanoparticles in magnetic fluids to obtain a desired and easily controlled magnetic or rheological response.

We assume SMPs formed by monodisperse magnetic colloids, modeled as identical spherical beads. We consider SMPs of four different topologies: chain-, Y-, X- and ring-like ones. Using Langevin dynamics simulations, we pay our attention to solutions of filaments, the magnetic nanoparticles in which are not only interacting via dipole-dipole potential but also via short-range attractive forces (Van der Waals force). Such filaments tend to aggregate in dense spherical droplet-like clusters. The resulting composite soft colloid is placed in the microchannel, where its behavior in the shear flow under influence of an external field is investigated, varying a wide range of system parameters. It was found that clusters can demonstrate oscillating in time magnetic response and complex mutual influence of the flow and the magnetic field.

The work was supported by RSF 19-72-10033.

DY 46.6 Thu 15:00 P2

Experimental study of statistical structures and forces in granular matter — AMELIE MAYLÄNDER¹, CLARA C. WANJURA², LUKAS REITER¹, RAPHAEL BLUMENFELD^{3,2}, and •OTHMAR MARTI¹ — ¹Institute of Experimental Physics, Ulm University, D-89069 Ulm — ²Cavendish Laboratory, University of Cambridge, Cambridge, CB3 0HE, UK — ³Gonville & Caius College, University of Cambridge, Trinity Street, Cambridge CB2 1TA, United Kingdom

We investigated the structure-forces coevolution in rotational shear of a planar assembly of photo-elastic polyurethane-discs of four different sizes under constant confining stress. Disc positions and contacts were determined using unpolarized red light. A dark-field polariscope, using circularly polarized blue light, detected mechanical deformations and the force network. The experiment ran through: a de-correlation step, initial state preparation, steady-state dynamics.

Repeated measurements of the structure and cell order distribution of the geometric contact network were carried out, validating theoretical predictions of detailed balance [1] and maximum entropy [2]. Simultaneously detected force chain

networks had more cells of higher orders than the geometric network, providing less than maximum entropy. This is attributed to the sensitivity of force detection to low-force contacts. Characteristic differences also existed in the shapes of small cells.

[1] C. C. Wanjura et al., *Granular Matter* 22, 91 (2020).

[2] X. Sun et al., *Phys. Rev. Lett.* 125, 268005 (2020)

DY 46.7 Thu 15:00 P2

Ising-like critical behavior of vortex lattices in an active fluid — •HENNING REINKEN¹, SEBASTIAN HEIDENREICH², MARKUS BÄR², and SABINE H. L. KLAPP¹ — ¹Technische Universität Berlin — ²Physikalisch-Technische Bundesanstalt Berlin

Turbulent vortex structures emerging in bacterial active fluids can be organized into regular vortex lattices by weak geometrical constraints such as obstacles [1,2]. Here we show, using a continuum-theoretical approach [3], that the formation and destruction of these patterns exhibit features of a continuous second-order equilibrium phase transition, including long-range correlations, divergent susceptibility, and critical slowing down. The emerging vorticity field can be mapped onto a two-dimensional (2D) Ising model with antiferromagnetic nearest-neighbor interactions by coarse-graining. The resulting effective temperature is found to be proportional to the strength of the nonlinear advection in the continuum model [4].

[1] D. Nishiguchi, I. S. Aranson, A. Snezhko, and A. Sokolov, *Nat. Commun.* 9, 4486 (2018)

[2] H. Reinken, D. Nishiguchi, S. Heidenreich, A. Sokolov, M. Bär, S. H. L. Klapp, and I. S. Aranson, *Commun. Phys.* 3, 76 (2020)

[3] H. Reinken, S. H. L. Klapp, M. Bär, and S. Heidenreich, *Phys. Rev. E* 97, 022613 (2018)

[4] H. Reinken, S. Heidenreich, M. Bär, and S. H. L. Klapp, *Phys. Rev. Lett.* 128, 048004 (2022)

DY 46.8 Thu 15:00 P2

Cohesive rotation of particles with misaligned perception-dependent motility — •RODRIGO SAAVEDRA, GERHARD GOMPPER, and MARISOL RIPOLL — Institute of Biological Information and Institute for Advanced Simulation, Forschungszentrum Jülich, Germany

Systems of agents with discontinuous motility that activate according to visual perception rules have been found to aggregate into cohesive groups. Here we study the formation of rotating cohesive clusters by considering the particles' vision cone to have a fixed misalignment with respect to the self-propulsion direction. Together with the motility rule, we find this mechanism to facilitate both cohesion and rotation of the cluster. The presence of steric interactions translates into a compact cluster which might eventually be driven by particles in its outer layer. We systematically explore the effect of misalignment and perception on the cluster morphology by means of particle-based numerical simulations. We find good agreement of the results with a proposed coarse-grained model.

DY 46.9 Thu 15:00 P2

Diffusion in a sulfonated co-polynaphthoyleimide proton exchange membrane studied by NMR — •CELINE WOLTER, ALEXEI PRIVALOV, and MICHAEL VOGEL — TU Darmstadt, Institut für Physik kondensierter Materie, Darmstadt, Germany

Nowadays, most fuel cells are based on proton-exchange membranes such as Nafion, which contain fluorine and therefore have some disadvantages for disposal. One alternative are fluorine-free hydrocarbon-based polymers. Their respective characteristics for use in fuel cells are similar to Nafion membranes, but they are easier and cheaper to produce and recycle. An important parameter for these systems is the proton diffusion coefficient, since it is related to charge transfer across the membrane and removal of the resulting water. We investigated self-diffusion in a sulfonated co-polynaphthoyleimide proton exchange membrane using ¹H static field gradient (SFG) nuclear magnetic resonance (NMR). The polymer under study has a ratio of hydrophilic to hydrophobic groups of 60:40, and the saturation humidity of the samples varies from 31% to 100%. For this polymer, the magnetization transfer effects between protons in the membrane framework and water protons must be taken into account. To do this, we applied a model that accounts for such exchange phenomena and were able to determine the diffusion coefficients within a few percent uncertainty in the temperature range from 190 K to 365 K. We found a significant decrease in diffusion at low water concentrations and an increase in activation energy below 250 K, indicating a change in the diffusion mechanism.

DY 46.10 Thu 15:00 P2

Non-mechanical Electrowetting Pump On a Chip — •SEBASTIAN BOHM^{1,2}, HAI BINH PHI², LARS DITTRICH², and ERICH RUNGE¹ — ¹Technische Universität Ilmenau, Theoretische Physik 1, Weimarer Str. 25, 98693 Ilmenau — ²5microns GmbH, Ehrenbergstr. 11, 98693 Ilmenau

Numerical simulations suggests that by using the EWOD (electrowetting-on-dielectric) effect a micropump can be manufactured, that works completely without any moving components [1,2]. The volume stroke is generated by the periodic movement of liquid-vapor interfaces in a large number ($\approx 10^6$) of micro-

cavities ($\Delta V \approx 1$ pl per cavity). Passive Tesla-Diodes are used to rectify the resulting volume stroke to completely forgo any moving parts. Even though our simulation suggests a high efficiency comparable to that of conventional designs in particular for small pumps, the actual realization poses multiple challenges. In this work, first experimental results of the characterization of the micropump are presented. The manufacturing process is described, which is based on a smart combination of processes commonly used in microsystems technology. This enables a cost-effective manufacturing that can be carried out entirely on wafer level. In addition, the direct integration of the pump into wafer-based microfluidic or lab-on-a-chip applications is facilitated. Possible use cases are presented and discussed.

[1] Bohm, S., Dittrich, L., Runge, E.; COMSOL Conference 2020 Europe, 14-15. Oct. 2020 online

[2] Hoffmann et al.; patent DE 11 2011 104 467 (2012)

DY 46.11 Thu 15:00 P2

Collective Behaviour of Active Assemblies Induced by Internal Feedback — •LISA ROHDE and FRANK CICHOS — Molecular Nanophotonics Group, Peter Debye Institute for Soft Matter Physics, Leipzig University, Linnéstr. 5, 04103 Leipzig, Germany

Collective phenomena and self-organising processes in nature such as structure formation of cells or flocking of birds are generated by physical interactions between autonomous objects ruled by feedback, information processing or sensing. Recently there has been an increasing interest in studying the collective behaviour of artificial active particles that provide the basic functionality of self-propulsion on the microscale. Here, we introduce physical interactions between artificial microswimmers in a crowded environment by implementing feedback rules to mimic the self-organisation of their living counterparts. We use differently shaped Janus particles capped with a thin gold layer. They are driven by self-thermophoresis, which we control by heating the gold layer with a laser. Depending on the shape of the Janus particle we observe different clustering behaviour as a result of a positive feedback mechanism by which Janus particles are attracted due to a temperature increase of a growing cluster. Our system reacts on hydrodynamic flow fields that are internally induced by other components by showing for example, a polarised motion of particles when being subjected to the feedback loop. We investigate and quantify the role of shape dependent hydrodynamic flow fields on the feedback mechanism by dedicated experiments on the clustering of active assemblies.

DY 46.12 Thu 15:00 P2

Bacterial swimmers' motility under external and light-induced flows — •VALERIA MURAVEVA^{1,2}, ROBERT GROSSMANN¹, MAREK BEKIR², SVETLANA SANTER², and CARSTEN BETA¹ — ¹Biological Physics, University of Potsdam, Potsdam, Germany — ²Smart Soft Matter, University of Potsdam, Potsdam, Germany

We report on changes in the swimming strategy of rod-shaped bacteria under flow conditions.

To swim bacteria utilise lash-like organelles on the cell body, flagella. The model organism for this study is the soil bacterium *Pseudomonas putida*, which has a rod-shaped body and multiple flagella located at one pole of the cell, so they can act in concert to drive the bacterium in a single direction. The strategy of switching between different swimming modes in bulk was well described. Here, we study the cells' locomotion strategy under flow to better understand the processes of infection spreading and biofilm formation in a natural environment.

To create shear stress conditions hydrodynamic flows are used. For varying the geometry of flow patterns on the micron-scale we also use light-induced flow technics (in particular thermo-osmosis on a gold surface) to create flow locally and to advect or trap swimming bacteria.

To analyse the well-known "run-and-turn" strategy, we concentrate on characteristic features of the swimming pattern: changes in the run-time and turn angle distributions. We also study mutant cell lines under flow (cells with partial or total deficiency in motor function) to elucidate the role of the different components of the motility apparatus in this process.

DY 46.13 Thu 15:00 P2

Phase behaviour of mixtures of attractive rods and spheres — ANJA KUHN-HOLD and •ELEONORA FOSCHINO — Institute of Physics, Albert-Ludwigs-University Freiburg, Germany

The aim of this project is to study a mixture of anisotropic rod-shaped particles and spherical particles in a bulk by means of Monte Carlo simulations. The goal is to find regions in the parameter space that show stable de-mixed phases in three-dimensional systems and stable mixed phases in two-dimensional systems. This would be preliminary to the study of thickness-dependent de-mixing during film growth, which was observed and studied in experiments with blends of organic molecular semiconductors (JR. Banerjee et Al., "Evidence for Kinetically Limited Thickness Dependent Phase Separation in Organic Thin Film Blends", 2013).

The simulation is based on an implementation of the Metropolis algorithm in a box with periodic boundary conditions. Rod-shaped particles are modelled as hard spherocylinders and spherical particles as hard spheres, and the

spheres/rods composition is kept constant, as well as the volume of the simulation box. All particles interact through hard-body repulsion and an additional pair potential, to mimic van der Waals interactions between molecules in the mixture. The parameter space includes the rod-shaped particles' dimensions (the spherocylinders' diameter with respect to the spheres' diameter and the aspect ratio), as well as the strengths and ranges of the attractive interaction.

DY 46.14 Thu 15:00 P2

Electrophoretic mobility of liquid droplets — •ALEXANDER REINAUER and CHRISTIAN HOLM — Institute for Computational Physics, Stuttgart, Germany
Electrophoresis of liquid droplets displays many complex phenomena with applications for phase separation and transport in biological systems. It is significantly more complex than particle electrophoresis due to the mobility of the surface charges as well as the non-rigid nature of the fluid-fluid interface. To investigate the different contributions we conduct a lattice Boltzmann (LB) simulation study of freely suspended liquid droplets under application of an external electric field. We use the Color-Gradient multicomponent LB extension which is coupled to a lattice electrokinetics model for dissolved charged chemical species. Our ongoing study intends to quantify the influence of the viscosity ratio, the salt concentration as well as the charge of the droplet on the measured electrophoretic mobility.

DY 46.15 Thu 15:00 P2

Capacitive Density Functional Theory - C++ support for classical Density Functional Theory implementations — •MORITZ BÜLTMANN, PHILIPP PELAGEJCEV, and ANDREAS HÄRTEL — Institute of Physics, University of Freiburg, Germany

CapDFT is a C++ library and provides functional implementations and methods to implement classical Density Functional Theory (DFT) calculations. It is currently developed in our Statistical Physics of Soft Matter and Complex Systems group at the University of Freiburg and we would be happy to discuss ideas and concepts at our poster.

DY 46.16 Thu 15:00 P2

The Scallop Theorem and Swimming at the Mesoscale — •MAXIME HUBERT¹, OLEG TROSMAN¹, YLONA COLLARD², ALEXANDER SUKHOV³, JENS HARTING³, NICOLAS VANDEWALLE², and ANA-SUNČANA SMITH^{1,4} — ¹PULS group, FAU Erlangen-Nürnberg, Erlangen, Germany — ²GRASP, University of Liège, Liège, Belgium — ³Helmholtz Institute Erlangen-Nürnberg for Renewable Energy (IEK-11), Forschungszentrum Jülich, Nürnberg, Germany — ⁴Group for Computational Life Sciences, Ruder Bošković Institute, Zagreb, Croatia

By comparing theoretical modeling, simulations and experiments, we show that there exists a swimming regime at low-Reynolds number solely driven by the inertia of the swimmer itself. This is demonstrated by considering a dumbbell with an asymmetry in coasting time in its two spheres. Despite deforming in a reciprocal fashion, the dumbbell swims by generating a non-reciprocal Stokesian flow, which arises from the asymmetry in coasting times. This asymmetry acts as a second degree of freedom, which allows for recasting the scallop theorem at the mesoscopic scale at the lowest level of theory.

DY 46.17 Thu 15:00 P2

Fisher-Widom line for systems with competing repulsive and attractive interaction — •MATTHIAS GIMPERLEIN and MICHAEL SCHMIEDEBERG — FAU Erlangen-Nuremberg, Germany

We study colloid-polymer mixtures interacting via a Double-Square-Well potential (DSW-potential) consisting of hard core repulsion, short range attraction and longer range repulsive interaction. The Fisher-Widom line (FW-line) can be used as an indicator for the interplay between repulsion and attraction in the system. It separates regimes of monotonically (attraction dominates) or oscillatory (repulsion dominates) decaying pair correlation function in the phase diagram.

Solving the Ornstein-Zernike equation we find that the regime of monotonically decaying pair correlation function decreases. On the high density side of the phase diagram repulsion dominates (hard core interaction), but the introduction of the longer range repulsive step leads to a dominance of repulsion also on the low density side of the phase diagram. Only for intermediate densities and temperatures close to the critical temperature attraction dominates the system.

Further research includes a detailed check and analysis of the theoretical results by Brownian Dynamics simulations. The intersection of the binodal and the FW-line could be interesting for the structure of systems below the binodal line and eventually for gel network formation.

DY 46.18 Thu 15:00 P2

Self-propelled Ellipsoidal Swimmers — •GORDEI ANCHUTKIN¹, VIKTOR HOLUBEC², ARTEM RYABOV³, and GORDEI ANCHUTKIN¹ — ¹Molecular Nanophotonics Group, Peter Debye Institute for Soft Matter Physics, Leipzig University, 04103 Leipzig, Germany — ²Institute for Theoretical Physics, Leipzig University, 04103 Leipzig, Germany — ³Department of Macromolecular Physics, Faculty of Mathematics and Physics, Charles University, CZ-180 00 Praha, Czech Republic

The active motion of microswimmers has attracted broad interest for the last decades. A variety of active particles with different shapes and designs have been demonstrating various applications from biosensing to synergistic drug delivery most of them, though, with spherical particles involving a single orientational relaxation time. To generalize the complexity of active microswimmers* behavior, we investigate the fundamentals of active motion for microswimmers with multiple timescales of rotational diffusion. We investigate Janus ellipsoids thermophoretically propelled along the short axis of the ellipsoid. We report three different motion regimes of Janus ellipsoids: the active ballistic motion, run and tumble, and the diffusive regime. Using mean squared displacement analysis, we describe each regime and the corresponding time scales and show the coupling between translational and orientational motions. Our experimental results are compared to a theoretical model of an active ellipsoid motion. The different modes of active motion on different timescales deliver interesting perspectives to explore the interaction with obstacles and other particles at different densities.

DY 46.19 Thu 15:00 P2

Hyperspace-simulations of quasicrystalline structures on periodic substrates — •JOHANNES SCHÖTTNER and MICHAEL SCHMIEDEBERG — FAU, Erlangen, Deutschland

We perform Monte Carlo simulations a toy model where particles move on a hyperlattice. Therefore, jumps in hyperspace corresponding to phasonic flips are considered while phononic noise is not taken into account. Note that the interaction energy is determined after the particles have been projected onto the physical space. This approach can be used to learn about the stability and other physical properties of quasicrystals. Our work here is motivated by experiments [1] where quasi-crystalline structures grows self-organized on a crystalline surface. Therefore, we consider an external periodic potential that acts in our toy model. Our goal is to investigate how phasonic modes are influenced by the external periodic potential. A major advantage of our approach is that by construction we know all hyperspace positions of all particles. Furthermore, phasonic excitations due to the external potential can be determined without ambiguity. [1] Förster et al., Nature, 502:215*218, 10 (2013)

DY 46.20 Thu 15:00 P2

Theory of scanning gate Microscopy in graphene — •XIANZHANG CHEN^{1,2}, GUILLAUME WEICK³, DIETMAR WEINMANN³, and RODOLFO JALABERT² — ¹Lanzhou Center for Theoretical Physics, and Key Laboratory for Magnetism and Magnetic Materials of MOE, Lanzhou University, Lanzhou, Gansu 730000, China — ²Université de Strasbourg, CNRS, Institut de Physique et Chimie des Matériaux de Strasbourg, UMR 7504, F-67000 Strasbourg, France

The conductance of graphene nanoribbons and quantum point contacts under scanning gate microscopy tip has been systematically studied. The first- and second-order conductance corrections caused by the tip potential disturbance in armchair graphene are expressed in terms of the scattering states of the unperturbed structure using a scattering approach for a noninvasive probe. The second-order term prevails in the conductance plateaus for armchair graphene strips, but the first-order corrections dominate everywhere at the conductance steps for graphene shaped in quantum point contact. For the stronger tip, where the perturbation approach breaks down, we discovered that conductance corrections exhibit resonance effects at specific values of the tip potential width and strength, which can be regarded as carriers trapped below the tip. Additionally, the numerical results for zigzag graphene also follow the weak probe theory.

DY 46.21 Thu 15:00 P2

Characterization and control of traffic-jam transition for self-propelled particles with q -fold discrete symmetry: The restricted Active Potts Model — •SWARNAJIT CHATTERJEE¹, MINTU KARMAKAR², MATTHIEU MANGEAT¹, HEIKO RIEGER¹, and RAJA PAUL² — ¹Saarland University, Saarbrücken, Germany — ²Indian Association for the Cultivation of Science, Kolkata, India

We undertake comprehensive numerical simulations of the q -state active Potts model (APM) [EPL **130**, 66001 (2020); Phys. Rev. E **102**, 042601 (2020)] applying distinct volume exclusions to the self-propulsion of the active particles in the quest to explore the characteristics of the emerging phases, kinetic arrest, and jamming transitions. We broadly explore two scenarios where (a) the population of a lattice site is prearranged (hard-core restriction) and (b) particle movements are governed by a local repulsive field (soft-core restriction) and show that such effects lead to a surprisingly rich variety of self-organized spatial patterns. While bands and lanes of moving particles commonly occur without or under weak volume exclusion, strong volume exclusion along with low temperature, high activity, and large particle density facilitates traffic jams. Through a number of phase diagrams, we identify the phase boundaries separating the jammed and free-flowing phases and study the transition between these phases which provide us with both qualitative and quantitative predictions of how jamming might be delayed or dissolved. We further validate our numerical findings with a hydrodynamic model description.

DY 46.22 Thu 15:00 P2

Polar flocks with discretized directions: the active clock model approaching the Vicsek model — •MATTHIEU MANGEAT, SWARNAJIT CHATTERJEE, and HEIKO RIEGER — Universität des Saarlandes, Saarbrücken, Germany

We study the off-lattice two-dimensional q -state active clock model (ACM) as a natural discretization of the Vicsek model (VM) [Phys. Rev. Lett. **75**, 1226 (1995)] describing flocking. The ACM consists of particles able to move in the plane in a discrete set of q equidistant angular directions, as in the active Potts model (APM) [EPL **130**, 66001 (2020); Phys. Rev. E **102**, 042601 (2020)], with a local alignment interaction inspired by the ferromagnetic equilibrium clock model. A collective motion emerges at high densities and low noise. We compute

phase diagrams of the ACM and explore the flocking dynamics in the region, in which the high-density (polar liquid) phase coexists with the low-density (gas) phase. We find that for a small number of directions, the flocking transition of the ACM has the same phenomenology as the APM, including macrophase separation and reorientation transition from transversal to longitudinal band motion as a function of the particle self-propulsion velocity. For a larger number of directions, the flocking transition in the ACM becomes equivalent to the one of the VM and displays microphase separation and only transverse bands, i.e. no reorientation transition. Concomitantly also the transition of the $q \rightarrow \infty$ limit of the ACM, the active XY model (AXYM), is in the same universality class as the VM. We also construct a coarse-grained hydrodynamic description for the ACM and AXYM akin to the VM.

DY 47: Members' Assembly

Time: Thursday 18:30–19:15

Location: H19

All members of the Dynamics and Statistical Physics Division are invited to participate.

DY 48: Invited Talk Kathy Lüdge (joint session DY/SOE)

Time: Friday 9:30–10:00

Location: H19

Invited Talk

DY 48.1 Fri 9:30 H19

Photonic Reservoir Computing: Analytic insights and possibilities for optimization — LINA JAURIGUE¹, FELIX KÖSTER², and KATHY LÜDGE¹ — ¹Institute of Physics, Technische Univ. Ilmenau, Weimarer Str. 25, 98684 Ilmenau — ²Institute of Theoretical Physics, Technische Univ. Berlin, Hardenbergstr. 36, 10623 Berlin

Reservoir computing has gained a lot of attention because its relatively simple setup that can be easily implemented in hardware, specifically with optical devices. Using one nonlinear node, i.e., a laser with an optical feedback loop and time-multiplexed input, already allows to solve complex time-series prediction tasks after a proper training via linear regression. Nevertheless, the performance

depends on properly adjusted timescales and not every physical system is suitable for a given task [1].

We present ways to improve the computing performance of delay-based photonic reservoir computing systems using delay-time tuning, and we discuss to what extent delay-coupled laser-networks with more than one optical element can be beneficial to improve the overall performance. Furthermore, we discuss analytic insights into the information processing capacity of a reservoir computing system and its correlation to the linear system response of the reservoir as well as to the series expansion of a chosen task.

[1] T. Hülser, F. Köster, L. C. Jaurigue, and K. Lüdge, Opt. Mater. Express **12**, 1214 (2022).

DY 49: Statistical Physics: General

Time: Friday 9:30–12:15

Location: H20

DY 49.1 Fri 9:30 H20

Large-Deviation Properties of Non-equilibrium RNA Work Processes — •PETER WERNER and ALEXANDER K. HARTMANN — Institute of Physics, University of Oldenburg, Germany

The Higgs RNA model [1] is one of the few cases of a model with quenched disorder and complex free energy landscape, where *exact* partition function calculation and sampling can be done in polynomial time. Building on previous work [2], non-equilibrium properties of this model are investigated further. Here, we are interested in the case where, by applying an external force, RNAs are stretched or refolded, like it is also done in experiments with real RNA. Such processes are realized by first sampling an RNA secondary structure in equilibrium and subsequently performing a non-equilibrium MC Simulation during which the external force parameter is varied. The performed physical work W and secondary structures are measured during the processes.

By utilizing a *large-deviation algorithm* that is based on biasing random numbers [3], we are able to measure the work distributions $P(W)$ over a wide range of the support down to probabilities such as 10^{-40} . We show how work distributions and the corresponding *large-deviation rate function* behave under an appropriate length variations of various nucleotide sequences, specifically, whether the *large-deviation* principle holds.

[1] P. G. Higgs, Phys. Rev. Lett., **76**, 704 (1996)

[2] P. Werner and A. K. Hartmann, Phys. Rev. E **104**, 034407 (2021)

[3] A. K. Hartmann, Phys. Rev. E **89**, 052103 (2014)

DY 49.2 Fri 9:45 H20

Choosing the right event (in non-reversible event-chain Monte Carlo) — •PHILIPP HÖLLMER¹, NICOLAS NOIRAUT², BOTAO LI², A. C. MAGGS³, and WERNER KRAUTH² — ¹University of Bonn, Germany — ²École normale supérieure de Paris, France — ³ESPCI Paris, France

The general framework of event-chain Monte Carlo (ECMC) constructs non-reversible Markov chains for continuous statistical-physics models ranging from hard-disk systems to long-range interacting molecular systems. Over recent years, several algorithms from the family of ECMC have been proposed, which, in the event-driven formulation of ECMC, only differ in their treatment of events (e.g., of disk collisions in a hard-disk system). Still, we show that different vari-

ants can have widely different performances. As a first example, we consider locally stable sparse hard-disk packings. Using a scaling theory confirmed by simulation results, we obtain two classes for the escape from slightly relaxed hard-disk packings parameterized by a relaxation parameter. In one class, the escape time varies algebraically with the relaxation parameter. In the other class, the escape time only scales as the logarithm of the relaxation parameter. As a second example, we consider integrated autocorrelation times in dense systems of flexible extended hard-disk dipoles. Here, the ECMC variants show order-of-magnitude spreads. We expect the performance differences to carry over to long-range interacting molecular systems, where the choice of the optimal ECMC variant is thus highly important.

DY 49.3 Fri 10:00 H20

The GOE ensemble for quasiperiodic tilings without unfolding: r -value statistics — •RUDOLF A. RÖMER¹ and UWE GRIMM² — ¹University of Warwick, Coventry, UK — ²Open University, Milton Keynes, UK

We study the level-spacing statistics for non-interacting Hamiltonians defined on the two-dimensional quasiperiodic Ammann-Beenker (AB) tiling. When applying the numerical procedure of “unfolding”, these spectral properties in each irreducible sector are known to be well-described by the universal Gaussian orthogonal random matrix ensemble. However, the validity and numerical stability of the unfolding procedure has occasionally been questioned due to the fractal self-similarity in the density of states for such quasiperiodic systems. Here, using the so-called r -value statistics for random matrices, $P(r)$, for which no unfolding is needed, we show that the Gaussian orthogonal ensemble again emerges as the most convincing level statistics for each irreducible sector [1]. The results are extended to random-AB tilings where random flips of vertex connections lead to the irreducibility.

[1] U. Grimm, R. A. Römer, Phys. Rev. B **104**(6), L060201 (2021)

DY 49.4 Fri 10:15 H20

Classical density functional theory and the primitive model: beyond the standard mean-field approximation — •MORITZ BÜLTMANN and ANDREAS HÄRTEL — Albert-Ludwigs-Universität Freiburg, Physikalisches Institut

To understand the physics of electrolyte solutions one often uses the *primitive model*, where ions are represented by charged hard spheres in a dielectric back-

ground. The powerful theory of density functionals, which is widely known from quantum mechanics, can also be applied to such systems in the context of statistical physics. There, the first order of a functional perturbation yields the *mean-field electrostatic functional*, which also contributes at particle separations that are forbidden due to the hard-core interactions.

In this talk I summarize our findings from the article [J. Phys.: Condens. Matter **34** 235101], where we modified the mean-field functional such that the occurring pair potential is constant for distances smaller than hard-core contact. The resulting formalism involves weighted densities similar to the ones used in most hard-sphere functionals. Comparing different functionals and result from MD simulations, we analyze density profiles, direct and total correlation functions, and thermodynamic sum rules. Thereby, we found that the modifications improved the predictions compared to the standard mean-field functional significantly. Finally, I report on recent findings of the modified mean-field functional e.g. concerning the decay behavior of total correlation functions.

DY 49.5 Fri 10:30 H20

Recoil experiments determine the eigenmodes of viscoelastic fluids — KARTHIKA KRISHNA KUMAR¹, FÉLIX GINOT¹, JULIANA CASPERS², LUIS REINALTER¹, MATTHIAS KRÜGER², and CLEMENS BECHINGER¹ — ¹Fachbereich Physik, Universität Konstanz, Germany — ²Institute for Theoretical Physics, Georg-August Universität Göttingen, Germany

Probing viscoelastic media using colloidal particles reveals their complex relaxation processes at the microscopic level. Unlike Newtonian fluids, viscoelastic fluids can store and dissipate energy on much longer timescales because of their microstructure, therefore, these materials play a significant role in many technical applications. In this work, we perturb a viscoelastic fluid by driving a colloidal particle through the fluid using an optical tweezer. On deforming the viscoelastic matrix, the fluid tries to relax back by pushing the particle to recoil when the trap is turned off. The trajectory of such a recoiling particle exhibits a bi-exponential behavior indicating two distinct relaxation processes of the fluid. Detailed investigation shows that a microscopic model, with two fictitious bath particles connected to the probe particle via harmonic springs, explains the observed behavior. The analytical solution to the model also reveals two more timescales corresponding to the relaxation of the bath particles when the probe is fixed. The need for two bath particles to explain the results can be justified by considering the fluid as a glassy system, however, further experiments are required to confirm this.

15 min. break

DY 49.6 Fri 11:00 H20

FIPS: A generic framework for many-particle simulations focusing on efficiency and reliability* — JULIAN JEGGLE and RAPHAEL WITTKOWSKI — Institut für Theoretische Physik, Center for Soft Nanoscience, Westfälische Wilhelms-Universität Münster, 48149 Münster, Germany

Numerical calculation of particle trajectories in many-particle systems is an important class of molecular dynamics (MD) simulations that has been implemented in well-known MD packages such as GROMACS, HOOMD-blue, and LAMMPS. Recently, efforts have been made to develop more flexible data models for this task with the help of modern programming techniques. In this talk, we present further advancements into this direction in the form of FIPS, the *flexibly integrating particle simulator*. This tool enables the simulation of many-particle systems and their dynamics described by a domain specific language heavily inspired by GPU shaders. Unlike traditional MD packages, we utilize just-in-time compilation and shared-state concurrency to achieve a high degree of efficiency. To increase resilience towards programming errors, our implementation is tightly coupled to Rust, a novel systems programming language with a focus on reliability, in particular for concurrent applications.

*Funded by the Deutsche Forschungsgemeinschaft (DFG) – Project-ID 433682494 – SFB 1459

DY 49.7 Fri 11:15 H20

The reversible heat production during the electric double layer buildup: Analysis with an extension of the primitive model by hydration shells — PHILIPP PELAGEJCEV, FABIAN GLATZEL, and ANDREAS HÄRTEL — Albert-Ludwigs-Universität Freiburg

The reversible heat production during the electric double layer (EDL) buildup was measured experimentally [Janssen et al., Phys. Rev. Lett. **119**, 166002 (2017)] and in theoretical work [Glatzel et al., J. Chem. Phys. **154**, 064901 (2021)], it was found that steric interactions of ions with the flat electrodes, which result in the so-called Stern layer, are sufficient to explain the experimental results. In the latter only symmetric ion sizes in a restricted primitive model were examined.

In this work, I present the impact of ion asymmetry on the reversible heat production for each electrode separately. Additionally, an extension of the primitive

model where hydration shells of ions can evade in the vicinity of the electrodes is discussed. With this extended model one can describe situations where one electrode is heated and the other electrode is cooled simultaneously during charging, while both electrodes together behave similarly to the already mentioned experimental results.

Thus, in experiments the heat production should be measured for each electrode separately. By this, the importance of certain ingredients for a primitive model based electrolyte could be evaluated experimentally, finally leading to a deeper understanding of EDLs. (Reference: [Pelagejcev et al., J. Chem. Phys. **156**, 034901 (2022)])

DY 49.8 Fri 11:30 H20

Uncovering broken detailed balance hidden by unknown degrees — GABRIEL KNOTZ, TILL MORITZ MÜNCKER, TIMO BETZ, and MATTHIAS KRÜGER — Fakultät für Physik, Georg-August-Universität, Göttingen, Germany

The complex nature of non equilibrium systems remains a challenging task in statistical physics, but especially for living matter. A major experimental problem is, that often some relevant degrees cannot be observed (are hidden) which complicates theoretical analysis. We study a non-equilibrium model with two degrees of freedom. If both degrees are observed, the breaking of detailed balance can easily be quantified. However, by treating one of the degrees as hidden, the trajectory of the other is time reversal symmetric. To still detect the breakage of detailed balance we can use a new quantity, the mean backward relaxation (MBR), that measures the relaxation of displacements caused by the fluctuating forces. By deriving rigorous statements for equilibrium in general and calculating the MBR for the non-equilibrium system, we show that the MBR reveals that the system breaks detailed balance even though one degree is hidden. Further we are able to relate the deviation of the MBR compared to an equilibrium system to an effective energy. This analysis adds a new approach to systems that deal with unknown, but relevant non-equilibrium degrees of freedom.[1]

[1] Till M. Muenker, Gabriel Knotz, Matthias Krüger and Timo Betz. *On-sager regression characterizes living systems in passive measurements*. bioRxiv: 2022.05.15.491928

DY 49.9 Fri 11:45 H20

Generalized hydrodynamics description of the classical Toda lattice and high-low pressure domain wall initial conditions — CHRISTIAN MENDEL and HERBERT SPOHN — Technische Universität München (TUM)

We review and discuss generalized hydrodynamics applied to the classical Toda lattice, a paradigmatic example for an interacting integrable system. One first identifies the Lax matrix of the system, which is closely related to the microscopic conservation laws. For the Toda lattice, the free energy can be expressed in terms of the eigenvalue spectrum of the Lax matrix. One finally arrives at semi-analytic formulas for dynamical correlation functions in equilibrium, which show good agreement with molecular dynamic simulations.

In the second part, we focus on domain wall initial conditions, for which the left and right half lattice are in thermal equilibrium but with distinct parameters. The particular case of interest is a jump from low to high pressure at uniform temperature and zero mean velocity, whereby the scaling function for the average stretch is forced to change sign. The hydrodynamic equations seem to be singular at zero stretch, but nevertheless the self-similar solution exhibits smooth behavior.

[1] C. B. Mendl, H. Spohn, High-low pressure domain wall for the classical Toda lattice, SciPost Phys. Core **5**, 002 (2022)

[2] H. Spohn, Hydrodynamic equations for the Toda lattice, arXiv:2101.06528

[3] H. Spohn, Generalized Gibbs ensembles of the classical Toda chain, J. Stat. Phys. **180**, 4 (2020)

DY 49.10 Fri 12:00 H20

The square-lattice Ising model on the rectangle — FRED HUCHT — Universität Duisburg-Essen, Lotharstraße 1, 47048 Duisburg

For the square-lattice Ising model, the universal critical Casimir potential and force scaling functions can be calculated exactly for many geometries and boundary conditions. We present a recent exact solution of the square lattice Ising model on the $L \times M$ rectangle, with open boundary conditions in both directions [1], in terms of the determinant of a $M/2 \times M/2$ Hankel matrix \mathbf{H} . The $M - 1$ independent matrix elements of \mathbf{H} are Fourier coefficients of a certain symbol function, which is given by the ratio of two characteristic polynomials. These polynomials are associated to the different directions of the system, encode the respective boundary conditions, and are directly related through the symmetry of the considered Ising model under exchange of the two directions. This representation is a major simplification of earlier results [2,3].

[1] A. Hucht, *J. Phys. A: Math. Theor.* **54**, 375201 (2021). arXiv:2103.10776.

[2] A. Hucht, *J. Phys. A: Math. Theor.* **50**, 065201 (2017). arXiv:1609.01963, erratum [4].

[3] A. Hucht, *J. Phys. A: Math. Theor.* **50**, 265205, (2017). arXiv:1701.08722.

[4] A. Hucht, *J. Phys. A: Math. Theor.* **51**, 319601 (2018).

DY 50: Active Matter 5 (joint session DY/BP/PPP)

Time: Friday 10:00–12:45

Location: H18

DY 50.1 Fri 10:00 H18

Anomalous cooling and overcooling of active colloids — •FABIAN JAN SCHWARZENDAHL and HARTMUT LÖWEN — Institut für Theoretische Physik II: Weiche Materie, Heinrich-Heine-Universität Düsseldorf, 40225 Düsseldorf, Germany

The phenomenon that a system at a hot temperature cools faster than at a warm temperature, referred to as the Mpemba effect, has been recently realized for trapped colloids. Here, we investigate the cooling and heating process of a self-propelling active colloid using numerical simulations and theoretical calculations with a model that can directly be tested in experiments. Upon cooling activity induces a Mpemba effect and the active particle escapes an effective temperature description. At the end of the cooling process the notion of temperature is recovered and the system can exhibit even smaller temperatures than its final temperature, a surprising phenomenon which we refer to as activity-induced overcooling.

DY 50.2 Fri 10:15 H18

Active Ornstein-Uhlenbeck model for self-propelled particles with inertia — •GIA HUY PHILIPP NGUYEN, RENÉ WITTMANN, and HARTMUT LÖWEN — Institut für Theoretische Physik II: Weiche Materie, Heinrich-Heine-Universität Düsseldorf, Germany

Self-propelled particles, which convert energy into mechanical motion, exhibit inertia if they have a macroscopic size or move inside a gaseous medium, in contrast to micron-sized overdamped particles immersed in a viscous fluid. We have studied an extension of the active Ornstein-Uhlenbeck model, in which the self-propulsion is described by colored noise, to access these inertial effects affecting their translational motion [1]. In this talk, analytical solutions of the mean displacement, mean-squared displacement and velocity autocorrelation function will be discussed for a free active particle and in more general settings including an active dimer, a time-dependent mass and various external forces.

[1] G. H. P. Nguyen, R. Wittmann, H. Löwen, J. Phys.: Condens. Matter 34, 035101 (2021)

DY 50.3 Fri 10:30 H18

A quantitative scattering theory of active particles — •THOMAS IHLE¹, RÜDIGER KÜRSTEN¹, and BENJAMIN LINDNER² — ¹Institute for Physics, University of Greifswald, Greifswald — ²Institute for Physics, Humboldt University of Berlin, Berlin

We consider a particular model of self-propelled particles with Kuramoto-type alignment interactions. Starting from the N -particle Fokker-Planck equation we observe that the usual factorization Ansatz of the probability density, often called Molecular Chaos approximation, predicts a relaxation behavior which qualitatively disagrees with agent-based simulations. Therefore, we develop a scattering theory which resolves the time-evolution of the two-particle correlation function, i.e. goes beyond the mean-field approximation. The theory does not require input from agent-based simulations; it is self-consistent and leads to analytical expressions. We show that this theory predicts the relaxation behavior of the system and the transport coefficients with high precision in certain parameter ranges.

DY 50.4 Fri 10:45 H18

Hierarchical self-organization in communicating polar active matter — •ALEXANDER ZIEPKE¹, IVAN MARYSHEV¹, IGOR S. ARANSON², and ERWIN FREY¹ — ¹Ludwig-Maximilians-Universität München, München, Germany — ²Pennsylvania State University, University Park PA, USA

Self-organization in active matter plays an important role for various biological and artificial systems. In numerous cases, inter-agent communication is a key mechanism for the formation and localization of critical structures, such as the fruiting body in *Dictyostelium discoideum* or aggregation clusters in quorum-sensing bacteria. Despite its importance, the specific role of communication and its interplay with self-propulsion remains largely unexplored.

We propose a model for communicating active matter that endows self-propelled polar agents with information processing and signal relaying capabilities. We show that information processing greatly enriches the ability of these systems to form complex structures, allowing them to self-organize through a range of different collective dynamical states at multiple hierarchical levels. This provides insights into the role of self-sustained signal processing for self-organization in biological systems and opens pathways for applications using chemically driven colloids or microrobots.

DY 50.5 Fri 11:00 H18

Collective transport of microparticles by active cells — •ROBERT GROSSMANN¹, KEVIN MEISSNER¹, FERNANDO PERUANI², and CARSTEN BETA¹ — ¹University of Potsdam, Potsdam, Germany — ²CY Cergy Paris Université, Cergy-Pontoise, France

Motivated by the challenge of targeted delivery of micron-sized objects, we investigate a novel type of bio-hybrid active matter, composed of motile cells acting as autonomously moving agents that transport passive cargoes. The transport process is a collective phenomenon: a bead can be lost by one cell and may be picked up by another one, or multiple cells transport one bead together, thereby giving rise to an intermittent, stochastic stop-and-go dynamics. Combining experiment and active matter theory, we investigate the emerging transport properties of this system. We first deduce the waiting time distributions of active and passive transport episodes from experiments with the amoeba *Dictyostelium discoideum*: whereas the duration of actual transport phases – determined by the time that cells and cargoes are in contact – are exponentially distributed, the waiting time distribution for passive periods exhibits power-law characteristics which results from the search of cells looking for immobile colloids. We predict displacement distributions and the mean-squared displacement of colloids based on the statistics of waiting times and particularly point out a crossover from normal to sub-diffusive scaling. These results provide the basis for the future design of cellular micro-carriers and for extending our findings to more advanced transport tasks in complex, disordered environments, such as tissues.

DY 50.6 Fri 11:15 H18

Odd viscosity and active turbulence of hydrodynamic microrotors — •JOSCHA MECKE¹, YONGXIANG GAO², DIRK G.A.L. AARTS³, ALBERTO MEDINA¹, GERHARD GOMPPER¹, and MARISOL RIPOLL¹ — ¹Institute of Biological Information Processing, Forschungszentrum Jülich, Germany — ²Institute for Advanced Study, Shenzhen University, China — ³Department of Chemistry, University of Oxford, UK

Suspensions of rod-like silica colloids with a ferromagnetic head are considered in a rotating magnetic field applied parallel to a substrate. The magnetic moment is oriented perpendicular to the rod axis which implies a non-equilibrium vertical orientation to the substrate and synchronous spinning in the rotating field. We combine experiments and simulations to study the collective properties of these rotors. The hydrodynamic flows generated by the colloid rotations induce a cascade of translational motions in the neighbouring colloids. Thus, the rotors can be regarded as active matter with transport coefficients varying with local configuration and thus rotor density. The competition between hydrodynamic and steric interactions renders the translational dynamics non-monotonous in rotor density. The ensemble dynamics shows the emergence of eddies of various sizes reminiscent of turbulence. Furthermore, the rotor fluid is a realisation of a chiral active fluid with odd viscosity, that manifests itself in stress forces orthogonal to the direction of shear. In vortex flow, the stress acts like an effective pressure leading to density-vorticity correlations. Our experimental and numerical results are found to be in agreement.

DY 50.7 Fri 11:30 H18

Two-temperature activity drives liquid-crystal and crystalline order in soft repulsive spherocylinders — •JAYEETA CHATTOPADHYAY, SINDHANA PANNIR-SIVAJOTHI, KAARTHIK VARMA, SRIRAM RAMASWAMY, CHANDAN DASGUPTA, and PRABAL K. MAITI — Centre for Condensed Matter Theory, Department of Physics, Indian Institute of Science, Bangalore 560012, India

We study the scalar activity induced phase separation and liquid crystal ordering in a system of Soft Repulsive Spherocylinders (SRS) of various aspect ratios (L/D). Activity was introduced by increasing the temperature of half of the SRS (labeled 'hot') while maintaining the temperature of the other half constant at a lower value (labeled 'cold'). The difference between the two temperatures scaled by the lower temperature provides a measure of the activity. We find that activity drives the cold particles through a phase transition to a more ordered state and the hot particles to a state of less order compared to the initial equilibrium state. For $L/D = 5$, the cold components of a homogeneous isotropic (I) structure acquire nematic (N) and, at higher activity, crystalline (K) order. Similarly, the cold zone of a nematic initial state undergoes smectic (Sm) and crystal ordering while the hot component turns isotropic. Interestingly, we observe liquid crystal ordering for the spherocylinders having aspect ratio below Onsager's limit. The hot particles occupy a larger volume and exert an extra kinetic pressure, confining, compressing and provoking an ordering transition of the cold-particle domains.

Ref: Phys. Rev. E104, 054610 (2021).

DY 50.8 Fri 11:45 H18

Spontaneous trail formation in populations of communicating active walkers — ZAHRA MOKHTARI¹, ROBERT I. A. PATTERSON², and •FELIX HÖFLING^{1,3} — ¹Dept. Mathematics and Computer Science, Freie Universität Berlin — ²WIAS Berlin — ³Zuse Institute Berlin

How do ants form long stable trails? Despite abundant evidence that trail formation in colonies of insects or bacteria originates in their sensing of and responding to the deposits of chemicals that they produce, there is no consensus on the minimum required ingredients for this phenomenon. To address this

issue, here, we develop an agent-based model in terms of active random walkers communicating via pheromones, which can generate trails of agents from an initially homogeneous distribution [1]. Based on extensive off-lattice computer simulations we obtain qualitatively the non-equilibrium state diagram of the model, spanned by the strength of the agent-chemical interaction and the number density of the population. In particular, we demonstrate the spontaneous formation of persistent, macroscopic trails, and highlight some behaviour that is consistent with a dynamic phase transition. We also propose a dynamic model for few macroscopic observables, including the sub-population size of trail-following agents, which captures the early phase of trail formation. At high densities and for strong alignment, we observe that rotating clusters (“ant mills”) are more stable than trails and can swallow them up.

[1] Z. Mokhtari, R. I. A. Patterson & F. Höfling, *New J. Phys.* **24**, 013012 (2022).

15 min. break

DY 50.9 Fri 12:00 H18

Dynamics of microalgae in a porous environment — •FLORIAN VON RÜLING, LIUBOV BAKHCHOVA, DMITRY PUZYREV, ULRIKE STEINMANN, and ALEXEY EREMIN — Otto von Guericke University Magdeburg, Germany

The navigation through complex environments is a task the microalgae *Chlamydomonas reinhardtii* are frequently confronted with in their natural habitats, where they encounter suspended and sedimented particles as well as rough surfaces. To investigate the motion in heterogeneous surroundings, we observe dilute and crowded active colloidal suspensions of *Chlamydomonas* in quasi-two-dimensional microstructured PDMS-channels. Arrays of cylindrical or elongated pillars with varying lattice spacing and obstacle orientation serve as artificial porous environments. The swimmer behaviour is characterised by means of velocity and orientation autocorrelation functions, trajectory straightness, velocity distributions and the reflection/transmission coefficients for the porous segments.

DY 50.10 Fri 12:15 H18

Extending the active Phase Field Crystal model to describe motility-induced condensation and crystallization — •MAX PHILIPP HOLL¹ and UWE THIELE^{1,2} — ¹Institut für Theoretische Physik, Universität Münster — ²Center for Nonlinear Science, Universität Münster

The passive conserved Swift-Hohenberg equation (or phase-field-crystal [PFC] model) corresponds to a gradient dynamics for a single order parameter field related to density [1]. It provides a microscopic continuum description of the thermodynamic transition between liquid and crystalline states. A recent extension allows one to investigate both, vapour-liquid and liquid-solid transitions [3]. We first discuss the bifurcation and phase structure of this passive, i.e., thermodynamic model. Our subsequently introduced extension of the standard active PFC model [2] is able to describe passive and active (motility-induced) vapour-liquid and liquid-solid transitions. This is shown through a bifurcation and phase analysis based on path continuation supplemented by time simulations.

[1] H. Emmerich, H. Löwen, R. Wittkowski, T. Gruhn, G. I. Tóth, G. Tegze, and L. Gránásy. Phase-field-crystal models for condensed matter dynamics on atomic length and diffusive time scales: an overview. *Adv. Phys.*, 61:665-743, 2012 [2] A. M. Menzel and H. Löwen. Traveling and resting crystals in active systems. *Phys. Rev. Lett.*, 110:055702, 2013 [3] Z.-L. Wang, Z. Liu, Z.-F. Huang, and W. Duan. Minimal phase-field crystal modeling of vapor-liquid-solid coexistence and transitions. *Phys. Rev. Materials*, 4:103802, 2020

DY 50.11 Fri 12:30 H18

Engines driven by active fields — •PATRICK PIETZONKA¹ and MICHAEL E. CATES² — ¹Max Planck Institute for the Physics of Complex Systems, Dresden, Germany — ²Department of Applied Mathematics and Theoretical Physics, University of Cambridge, United Kingdom

On macroscopic scales, where trajectories of individual particles cannot be observed, active matter may appear like matter in thermal equilibrium. We discuss how the non-equilibrium character of active matter can nonetheless be revealed by using it as a working medium of engines delivering mechanical work in an isothermal environment. We focus on scalar active field theories such as the active model B as minimal continuum models for active matter undergoing a phase separation. The shape and chemical potential of droplets can be controlled through external potentials and activity patterns. We show how an asymmetric periodic activity pattern can drive a flow of active matter against an external force, thus acting as an autonomous engine. Moreover, we calculate and optimise the work that can be extracted by a cyclic engine that manipulates the activity and the potential landscape.

DY 51: Machine Learning in Dynamics and Statistical Physics (joint session DY/SOE)

Time: Friday 10:00–11:15

Location: H19

DY 51.1 Fri 10:00 H19

Reinforcement learning of optimal active particle navigation — •MAHDI NASIRI and BENNO LIEBCHEN — Institut für Physik kondensierter Materie, Technische Universität Darmstadt, Hochschulstraße 8, D-64289 Darmstadt, Germany

In sufficiently complex environments, there is no simple way to determine the fastest route of an active particle that can freely steer towards a given target. In fact, while classical path planning algorithms (e.g. A*, Dijkstra) tend to fail to reach the global optimum, analytical approaches are incapable of handling generic complex environments. To overcome this gap in the literature, in the present work, we develop a policy gradient-based deep reinforcement learning method that employs a hybrid continuum-based representation of the environment and allows, for the first time, to determine the asymptotically optimal path in complex environments. Our results provide a key step forward towards a universal path planner for future intelligent active particles and nanorobots with potential applications in microsurgery as well as in drug and gene delivery.

DY 51.2 Fri 10:15 H19

Deep reinforcement learning for chemotactic active particles — •EDWIN LORAN, MAHDI NASIRI, and BENNO LIEBCHEN — Institute of Condensed Matter Physics, Technische Universität Darmstadt, D-64289 Darmstadt, Germany

Throughout evolution, microorganisms have developed efficient strategies for locating nutrients and avoiding toxins in complex environments. Understanding their adaptive policies can provide new key insights for the development of smart artificial active particles. Here, we use a machine learning approach, namely deep reinforcement learning, to develop smart foraging strategies for chemotactic active particles which consume nutrients for their survival. Our method is able to devise efficient chemotactic navigation strategies guaranteeing “survival” inside unknown and complex landscapes while only having access to local sensory data. Our approach is based on deep Q-learning and uses the particle’s observation of its surrounding chemical (nutrient) concentration as the input. The presented method highlights the extent of the capabilities of reinforcement learning approaches in mimicking (and going beyond) the evolutionary strategies learned by microorganisms.

DY 51.3 Fri 10:30 H19

Machine Learning the 2D percolation transition — •DJÉNABOU BAYO^{1,2}, ANDREAS HONECKER³, and RUDOLF A. RÖMER¹ — ¹Departement of Physics, University of Warwick, Coventry, CV47AL, United Kingdom — ²Laboratoire de Physique Théorique et Modélisation (LPTM) (CNRS UMR8089), CY Cergy Paris Université, 95302 Cergy-Pontoise, France

The percolation model is one of the simplest models in statistical physics displaying a phase transition. A classical lattice is occupied randomly with a given probability at each site (or bond). A phase transition from a non-percolating to a percolating state appears around the so-called percolation threshold. Machine Learning (ML) and Deep Learning (DL) techniques are still relatively new methods when applied to physics. Recent work shows that ML/DL techniques seemingly detect the percolation transition from images of percolation clusters. We employ such supervised learning techniques, i.e., classification and regression for 2D site percolation. We find that the identification of spanning clusters provided by such methods does not fully correlate with their existence. Rather, the identification seems to rely on proxy measures such as the site occupation density. Furthermore, constructing challenging cluster distributions show scope for much misclassification when using even highly trained DL networks. Unsupervised ML strategies, such as variational autoencoders, might be able to reconstruct percolation clusters with acceptable spatial resolution, but in many cases struggle to reproduce the geometry of spanning clusters faithfully. Our work uses Python and the ML/DL libraries of PyTorch.

DY 51.4 Fri 10:45 H19

Exploring structure-property maps with kernel principal covariates regression — •GUILLAUME FRAUX, BENJAMIN HELFRECHT, ROSE CERSONSKY, and MICHELE CERIOTTI — Institute of Materials, EPFL, Lausanne, Switzerland

Data analyses based on linear methods constitute the simplest, most robust, and transparent approaches to the automatic processing of large amounts of data for building supervised or unsupervised machine learning models. Principal covariates regression (PCovR) is an underappreciated method that interpolates between principal component analysis and linear regression and can be used conveniently to reveal structure-property relations in terms of simple-to-interpret, low-dimensional maps. We introduce a kernel version of PCovR (KPCovR),

and demonstrate the performance of this approach in revealing and predicting structure-property relations in chemistry and materials science.

For large datasets, interactive exploration of the resulting map is a great tool to extract understanding. To this end, we introduce chemscope, an open source software able to display and explore maps with hundred of thousands of points together with the corresponding molecular or crystal structure. Chemscope is usable as an online tool, or locally through jupyter notebooks.

DY 51.5 Fri 11:00 H19

Investigation of plasticity in off-resonant delay-coupled reservoir computing — •JONAS NAUJOKS¹, FELIX KÖSTER¹, and KATHY LÜDGE² — ¹Institute for Theoretical Physics, Technische Universität Berlin, 10559 Berlin, Germany — ²Institute of Physics, Technische Universität Ilmenau, Weimarer Str. 25, 98693 Ilmenau, Germany

We analyse the effect of neuronal plasticity on the performance of a delay-based reservoir computer modelled by a generic oscillator with self-feedback. The memory capacity and task-specific performance are investigated in the case of non-resonant delay-clock-cycle configurations. By modifying the temporal multiplexing of the input, the responsiveness of the virtual nodes is maximised while promoting individual decorrelation. The training is done in an unsupervised manner. The effect on the task-specific performance is investigated, while we additionally demonstrate that the memory capacity can be tuned.

DY 52: Nonlinear Dynamics 2: Stochastic and Complex Systems, Networks (joint session DY/SOE)

Time: Friday 11:30–12:45

Location: H19

DY 52.1 Fri 11:30 H19

Thermodynamic uncertainty relations for many-body systems with fast jump rates and large occupancies — •OHAD SHPIELBERG¹ and ARNAB PAL² — ¹University of Haifa, Haifa, Israel. — ²Department of Physics, Indian Institute of Technology, Kanpur, India

The thermodynamic uncertainty relations constitute an important inequality, bounding the entropy production through current fluctuations. The results have been successfully applied, in particular for single body dynamics. Here we present uncertainty relations and other useful inequalities for the many body systems, in the limit of highly occupied systems. The resulting coarse grained theory also accounts for tighter inequalities than the single body case.

DY 52.2 Fri 11:45 H19

Effects of measures on phase transitions in two cooperative susceptible-infectious-recovered dynamics — ADIB KHAZAEI¹ and •FAKHTEH GHANBARNEJAD^{1,2} — ¹Sharif University of Technology, Tehran, Iran — ²Chair for Network Dynamics, Institute for Theoretical Physics and Center for Advancing Electronics Dresden (cfaed), Technical University of Dresden, 01062 Dresden, Germany

In recent studies, it has been shown that a cooperative interaction in a co-infection spread can lead to a discontinuous transition at a decreased threshold. Here, we investigate effects of immunization with a rate proportional to the extent of the infection on phase transitions of a cooperative co-infection. We use the mean-field approximation to illustrate how measures that remove a portion of the susceptible compartment, like vaccination, with high enough rates can change discontinuous transitions in two coupled susceptible-infectious-recovered dynamics into continuous ones while increasing the threshold of transitions. First, we introduce vaccination with a fixed rate into a symmetric spread of two diseases and investigate the numerical results. Second, we set the rate of measures proportional to the size of the infectious compartment and scrutinize the dynamics. We solve the equations numerically and analytically and probe the transitions for a wide range of parameters. We also determine transition points from the analytical solutions. Third, we adopt a heterogeneous mean-field approach to include heterogeneity and asymmetry in the dynamics and see if the results corresponding to homogeneous symmetric case stand. (Physical Review E 105 (3), 034311)

DY 52.3 Fri 12:00 H19

ANDOR and beyond: Dynamically switchable logic gates as modules for flexible information processing in biochemical regulatory networks — •MOHAMMADREZA BAHADORIAN^{1,2} and CARL D. MODES^{1,2,3} — ¹Max Planck Institut for Molecular Cell Biology and Genetics (MPI-CBG), 01307 Dresden, Germany — ²Center for Systems Biology Dresden (CSBD), 01307 Dresden, Germany — ³Cluster of Excellence Physics of Life, TU Dresden, 01069 Dresden, Germany

Understanding how complex (bio-)chemical regulatory networks may be capable of processing information in flexible, yet robust ways is a key question with implications in biology and dynamical systems theory. Considerable effort has been focused on identification and characterization of structural and dynamical motifs of biological information processing, but a framework for studying flexibility and robustness of the motifs is lacking. We here propose a small set of effective modules capable of performing different logical operations based on the basin of attraction in which the system resides. These dynamically switchable logic gates require fewer components than their traditional analogs where static, separate gates are used for each desired function. We demonstrate the applicability and limits of these circuits by determining a robust range of parameters over which they correctly operate and then characterize their resilience against intrinsic noise of the constituent reactions using the theory of large deviations. Trade-offs between multi-functionality and robustness against various types of noise are shown.

DY 52.4 Fri 12:15 H19

Memory formation in adaptive networks — •KOMAL BHATTACHARYYA¹, DAVID ZWICKER¹, and KAREN ALIM^{1,2} — ¹Max Planck Institute for Dynamics and Self-Organization, 37077 Göttingen, Germany — ²Physik-Department, Technische Universität München, Garching, Germany

Continuous adaptation of networks like our vasculature ensures optimal network performance when challenged with changing loads. Here, we show that adaptation dynamics allow a network to memorize the position of an applied load within its network morphology. We identify that the irreversible dynamics of vanishing network links encode memory. Our analytical theory successfully predicts the role of all system parameters during memory formation, including parameter values which prevent memory formation. We thus provide an analytically tractable theory of memory formation in disordered systems.

DY 52.5 Fri 12:30 H19

Inference of fractional nonlinear models from temperature time series and application to predictions — •JOHANNES A. KASSEL and HOLGER KANTZ — MPI for the Physics of Complex Systems, Dresden, Germany

We introduce a method to reconstruct macroscopic models of one-dimensional nonlinear stochastic processes with long-range correlations from sparsely sampled time series by combining fractional calculus and discrete-time Langevin equations. We reconstruct a model for daily mean temperature data recorded at Potsdam (Germany) and use it to predict the first frost date. Including the Arctic Oscillation Index as an external driver into our model, we predict extreme temperatures for several European weather stations, illustrating the potential of long-memory models for predictions in the subseasonal-to-seasonal range.

[1] Johannes A. Kassel and Holger Kantz, Phys. Rev. Research 4, 013206

Semiconductor Physics Division Fachverband Halbleiterphysik (HL)

Axel Lorke
University Duisburg-Essen
Lotharstr. 1
47048 Duisburg
axel.lorke@uni-due.de

Overview of Invited Talks and Sessions

(Lecture halls H31, H32, H33, H34, and H36; Poster P2 and P2)

Invited Talks

HL 2.1	Mon	9:30–10:00	H31	Observation of quantum Zeno effects for localized spins — •ALEX GREILICH, NIKITA V. LEPPENEN, VITALIE NEDELEA, EIKO EVERS, DMITRY S. SMIRNOV, MANFRED BAYER
HL 3.1	Mon	9:30–10:00	H32	Pushing the limits in real-time measurements of quantum dynamics — •ERIC KLEINHERBERS, PHILIPP STEGMANN, ANNIKA KURZMANN, MARTIN GELLER, AXEL LORKE, JÜRGEN KÖNIG
HL 6.1	Mon	9:30–10:00	H36	g-factors in van der Waals heterostructures: revealing signatures of interlayer coupling — •PAULO E. FARIA JUNIOR
HL 8.1	Mon	15:00–15:30	H32	Crux of Using the Cascaded Emission of a Three-Level Quantum Ladder System to Generate Indistinguishable Photons — •EVA SCHÖLL, LUCAS SCHWEICKERT, LUKAS HANSCHKE, KATHARINA D. ZEUNER, FRIEDRICH SBRESNY, THOMAS LETTNER, RAHUL TRIVEDI, MARCUS REINDL, SAIMON FILIPE COVRE DA SILVA, RINALDO TROTTA, JONATHAN FINLEY, JELENA VUČKOVIĆ, KAI MÜLLER, ARMANDO RASTELLI, VAL ZWILLER, KLAUS D. JÖNS
HL 9.1	Mon	15:00–15:30	H33	Exceptional points in optics: From bulk materials to one-dimensional confined systems — •CHRIS STURM
HL 9.2	Mon	15:30–16:00	H33	Complex Skin Modes in Non-Hermitian Coupled Laser Arrays — •MERCEDEH KHAJAVIKHAN, YUZHOU LIU
HL 9.3	Mon	16:15–16:45	H33	Non-Hermitian effects in exciton polaritons — •ELIEZER ESTRECHO
HL 9.4	Mon	16:45–17:15	H33	Nonlinear dynamics and exceptional points in exciton-polariton condensates — •STEFAN SCHUMACHER
HL 12.1	Tue	9:30–10:00	H32	Wafer-Scale Epitaxial Modulation of Quantum Dot Density — •NIKOLAI BART, CHRISTIAN DANGEL, PETER ZAJAC, NIKOLAI SPITZER, MARCEL SCHMIDT, KAI MÜLLER, ANDREAS D. WIECK, JONATHAN FINLEY, ARNE LUDWIG
HL 14.1	Tue	9:30–10:00	H34	Materials and Device Engineering for Gallium Oxide-based Electronics — NIDHIN KURIAN KALARICKAL, SUSHOVAN DHARA, ASHOK DHEENAN, •SIDDHARTH RAJAN
HL 14.2	Tue	10:00–10:30	H34	Ferroelectric two-dimensional electron gases for oxide spin-orbitronics — •JULIEN BRÉHIN
HL 14.8	Tue	12:15–12:45	H34	Strain-driven dissociation of water on (incipient) ferroelectrics — JOSHUA L. BATES, •CHIARA GATTINONI
HL 15.1	Tue	9:30–10:00	H36	Ultrafast all-optical modulation and frequency conversion in 2D materials — •SEBASTIAN KLIMMER, ARTEM SINELNIK, ISABELLE STAUDE, GIANCARLO SOAVI
HL 19.1	Wed	9:30–10:00	H34	Quantum Interference of Identical Photons from Remote GaAs Quantum Dots — •GIANG NAM NGUYEN, LIANG ZHAI, CLEMENS SPINNLER, JULIAN RITZMANN, MATTIAS C. LÖBL, ANDREAS D. WIECK, ARNE LUDWIG, ALISA JAVADI, RICHARD J. WARBURTON
HL 27.1	Thu	9:30–10:00	H33	What limits state-of-the-art chalcopyrite solar cells? — •SUSANNE SIEBENTRITT
HL 27.2	Thu	10:00–10:30	H33	Approaches to improve CIGS absorber quality and the CIGS/buffer interface to reach 24% efficiency and beyond — •WOLFRAM WITTE
HL 33.6	Thu	16:30–17:00	H32	Ultrastrong light-matter coupling in materials — •NICLAS S. MUELLER, EDUARDO B. BARROS, FLORIAN SCHULZ, HOLGER LANGE, STEPHANIE REICH
HL 34.1	Thu	15:00–15:30	H33	Super-high efficiency CIGS devices: current status and pathways forward — •ROMAIN CARRON
HL 34.2	Thu	15:30–16:00	H33	Highlights from the development of the world record Cd-free CIGS_{Se} 30x30cm² solar module — •ANASTASIA ZELENINA

HL 34.5	Thu	17:00–17:30	H33	Digital Twins - a simulation model for Cu(In,Ga)Se₂ solar cells of high and moderate efficiency — •MATTHIAS MAIBERG, CHANG-YUN SONG, MARCIN MORAWSKI, FELIX NEDUCK, JOSHUA DAMM, HEIKO KEMPA, DIMITRIOS HARISKO, WOLFRAM WITTE, ROLAND SCHEER
HL 40.5	Fri	10:45–11:15	H33	Ultrafast subcycle dynamics of deep-strong light-matter coupling — •JOSHUA MORNHINWEG, MAIKE HALBHUBER, LAURA DIEBEL, VIOLA ZELLER, JOSEF RIEPL, CRISTIANO CIUTI, DOMINIQUE BOUGEARD, RUPERT HUBER, CHRISTOPH LANGE

Invited Talks of the joint Symposium **Frontiers of Orbital Physics: Statics, Dynamics, and Transport of Orbital Angular Momentum (SYOP)**

See SYOP for the full program of the symposium.

SYOP 1.1	Mon	9:30–10:00	H1	Orbital degeneracy in transition metal compounds: Jahn-Teller effect, spin-orbit coupling and quantum effects — •DANIEL KHOMSKII
SYOP 1.2	Mon	10:00–10:30	H1	Orbital magnetism out of equilibrium: driving orbital motion with fluctuations, fields and currents — •YURIY MOKROUSOV
SYOP 1.3	Mon	10:30–11:00	H1	Orbitronics: new torques and magnetoresistance effects — •MATHIAS KLÄUI
SYOP 1.4	Mon	11:15–11:45	H1	Orbital and total angular momenta dichroism of the THz vortex beams at the antiferromagnetic resonances — •ANDREI SIRENKO
SYOP 1.5	Mon	11:45–12:15	H1	Observation of the orbital Hall effect in a light metal Ti — •GYUNG-MIN CHOI

Invited Talks of the joint Symposium **SKM Dissertation Prize 2022 (SYSD)**

See SYSD for the full program of the symposium.

SYSD 1.1	Mon	10:15–10:45	H2	Charge localisation in halide perovskites from bulk to nano for efficient optoelectronic applications — •SASCHA FELDMANN
SYSD 1.2	Mon	10:45–11:15	H2	Nonequilibrium Transport and Dynamics in Conventional and Topological Superconducting Junctions — •RAFFAEL L. KLEES
SYSD 1.3	Mon	11:15–11:45	H2	Probing magnetostatic and magnetotransport properties of the antiferromagnetic iron oxide hematite — •ANDREW ROSS
SYSD 1.4	Mon	11:45–12:15	H2	Quantum dot optomechanics with surface acoustic waves — •MATTHIAS WEISS

Invited Talks of the joint Symposium **From Physics and Big Data to the Design of Novel Materials (SYNM)**

See SYNM for the full program of the symposium.

SYNM 1.1	Mon	15:00–15:30	H1	How to tackle the "I" in FAIR? — •CLAUDIA DRAXL
SYNM 1.2	Mon	15:30–16:00	H1	Beyond the average error: machine learning for the discovery of novel materials — •MARIO BOLEY, SIMON TESHUVA, FELIX LUONG, LUCAS FOPPA, MATTHIAS SCHEFFLER
SYNM 1.3	Mon	16:00–16:30	H1	The Phase Diagram of All Inorganic Materials — •CHRIS WOLVERTON
SYNM 1.4	Mon	16:45–17:15	H1	Automated data-driven upscaling of transport properties in materials — •DANNY PEREZ, THOMAS SWINBURNE
SYNM 1.5	Mon	17:15–17:45	H1	Data-driven understanding of concentrated electrolytes — •ALPHA LEE

Invited Talks of the joint Symposium **High Yield Devices for Photonic Quantum Implementations (SYPQ)**

See SYPQ for the full program of the symposium.

SYPQ 1.1	Tue	9:30–10:00	H1	Designing driving protocols for high-fidelity quantum devices using numerically exact predictions — •MORITZ CYGOREK, ERIK M. GAUGER
SYPQ 1.2	Tue	10:00–10:30	H1	Challenges towards high efficiency quantum dot single photon sources — •ARNE LUDWIG
SYPQ 1.3	Tue	10:30–11:00	H1	Organic Molecules in photonic quantum technologies — •COSTANZA TONINELLI
SYPQ 1.4	Tue	11:15–11:45	H1	Quantum-dot single-photon sources for quantum photonic networks — •PETER MICHLER
SYPQ 1.5	Tue	11:45–12:15	H1	Quantum light sources: entanglement generation in semiconductor nanostructures — •ANA PREDOJEVIC

Invited Talks of the joint Symposium Entanglement Distribution in Quantum Networks (SYED)

See SYED for the full program of the symposium.

SYED 1.1	Wed	9:30–10:00	H1	A multi-node quantum network of remote solid-state qubits — •RONALD HANSON
SYED 1.2	Wed	10:00–10:30	H1	Quantum key distribution with highly entangled photons from GaAs quantum dots — •ARMANDO RASTELLI, SANTANU MANNA, SAIMON COVRE DA SILVA, GABRIEL UNDEUTSCH, CHRISTIAN SCHIMPF
SYED 1.3	Wed	10:30–11:00	H1	Entanglement distribution with minimal memory requirements using time-bin photonic qubits — •JOHANNES BORREGAARD
SYED 1.4	Wed	11:15–11:45	H1	Quantum photonics: interference beyond HOM and quantum networks — •STEFANIE BARZ
SYED 1.5	Wed	11:45–12:15	H1	Photonic cluster-state generation for memory-free quantum repeaters — •TOBIAS HUBER

Invited Talks of the joint Symposium United Kingdom as Guest of Honor (SYUK)

See SYUK for the full program of the symposium.

SYUK 1.1	Wed	9:30–10:00	H2	Structure and Dynamics of Interfacial Water — •ANGELOS MICHAELIDES
SYUK 1.2	Wed	10:00–10:30	H2	A molecular view of the water interface — •MISCHA BONN
SYUK 1.3	Wed	10:30–11:00	H2	Motile cilia waves: creating and responding to flow — •PIETRO CICUTA
SYUK 1.4	Wed	11:00–11:30	H2	Cilia and flagella: Building blocks of life and a physicist's playground — •OLIVER BÄUMCHEN
SYUK 1.5	Wed	11:45–12:15	H2	Computational modelling of the physics of rare earth - transition metal permanent magnets from SmCo₅ to Nd₂Fe₁₄B — •JULIE STAUNTON
SYUK 2.1	Wed	15:00–15:30	H2	Hysteresis Design of Magnetic Materials for Efficient Energy Conversion — •OLIVER GUTFLEISCH
SYUK 2.2	Wed	15:30–16:00	H2	Non-equilibrium dynamics of many-body quantum systems versus quantum technologies — •IRENE D'AMICO
SYUK 2.3	Wed	16:00–16:30	H2	Quantum computing with trapped ions — •FERDINAND SCHMIDT-KALER
SYUK 2.4	Wed	16:45–17:15	H2	Breaking the millikelvin barrier in cooling nanoelectronic devices — •RICHARD HALEY
SYUK 2.5	Wed	17:15–17:45	H2	Superconducting Quantum Interference Devices for applications at mK temperatures — •SEBASTIAN KEMPF

Invited Talks of the joint Symposium Complexity and Topology in Quantum Matter (SYQM)

See SYQM for the full program of the symposium.

SYQM 1.1	Fri	9:30–10:00	H1	The role of crystalline symmetries in topological materials: the topological materials database — •MAIA VERGNIORY
SYQM 1.2	Fri	10:00–10:30	H1	Microwave Bulk and Edge Transport in HgTe-Based 2D Topological Insulators — •ERWANN BOCQUILLON, MATTHIEU C. DARTAILH, ALEXANDRE GOURMELON, HIROSHI KAMATA, KALLE BENDIAS, SIMON HARTINGER, JEAN-MARC BERROIR, GWENDAL FÈVE, BERNARD PLAÇAIS, LUKAS LUNCZER, RAIMUND SCHLERETH, HARTMUT BUHMANN, LAURENS MOLENKAMP
SYQM 1.3	Fri	10:30–11:00	H1	Spectral Sensitivity of Non-Hermitian Topological Systems — •JAN CARL BUDICH
SYQM 1.4	Fri	11:15–11:45	H1	Topological photonics and topological lasers with coupled vertical resonators — •SEBASTIAN KLEMBT
SYQM 1.5	Fri	11:45–12:15	H1	Spectroscopic Studies of the Topological Magnon Band Structure in a Skyrmion Lattice — •MARKUS GARST

Sessions

HL 1.1–1.4	Sun	16:00–18:20	H2	Tutorial: 2D Quantum Materials and Heterostructures: From Fabrication to Applications (joint session HL/TUT)
HL 2.1–2.5	Mon	9:30–11:00	H31	Spin Phenomena in Semiconductors
HL 3.1–3.11	Mon	9:30–13:00	H32	Quantum Dots and Wires 1: Transport and Electronic Properties
HL 4.1–4.11	Mon	9:30–12:45	H33	Semiconductor Lasers
HL 5.1–5.11	Mon	9:30–12:45	H34	Perovskite and Photovoltaics 1 (joint session HL/PPP/KFM)
HL 6.1–6.10	Mon	9:30–12:45	H36	2D Materials 1 (joint session HL/PPP/DS)
HL 7.1–7.10	Mon	15:00–18:00	H31	(Quantum) Transport Properties
HL 8.1–8.10	Mon	15:00–18:15	H32	Quantum Dots and Wires 2: Optics 1

HL 9.1–9.5	Mon	15:00–17:30	H33	Focus Session: Exceptional Points and Non-Hermitian Physics in Semiconductor Systems
HL 10.1–10.13	Mon	15:00–18:30	H34	Nitrides
HL 11.1–11.12	Mon	15:00–18:30	H36	2D Materials 2 (joint session HL/ CPP/ DS)
HL 12.1–12.10	Tue	9:30–12:45	H32	Quantum Dots and Wires 3: Growth
HL 13.1–13.10	Tue	9:30–12:15	H33	Ultra-Fast Phenomena
HL 14.1–14.8	Tue	9:30–12:45	H34	Focus Session: Quantum Properties at Functional Oxide Interfaces (joint session HL/ DS)
HL 15.1–15.8	Tue	9:30–12:00	H36	2D Materials 3 (joint session HL/ CPP/ DS)
HL 16.1–16.4	Wed	9:30–11:00	H17	Focus Session: Quantum Properties at Functional Oxide Interfaces (joint session DS/ HL)
HL 17.1–17.10	Wed	9:30–12:30	H32	Quantum Dots and Wires 4: Devices
HL 18.1–18.11	Wed	9:30–12:30	H33	Oxide Semiconductors (joint session HL/ KFM)
HL 19.1–19.11	Wed	9:30–13:00	H34	Materials and Devices for Quantum Technology 1
HL 20.1–20.9	Wed	9:30–12:00	H36	2D Materials 4 (joint session HL/ CPP/ DS)
HL 21.1–21.12	Wed	15:00–18:30	H32	Optical Properties 1
HL 22.1–22.10	Wed	15:00–18:00	H33	Heterostructures, Interfaces and Surfaces
HL 23.1–23.11	Wed	15:00–18:15	H34	Perovskite and Photovoltaics 2 (joint session HL/ CPP/ KFM)
HL 24.1–24.12	Wed	15:00–18:30	H36	Functional Semiconductors for Renewable Energy Solutions (joint session HL/ KFM)
HL 25.1–25.98	Wed	18:00–20:00	P2	Poster 1
HL 26.1–26.11	Thu	9:30–12:45	H32	Quantum Dots and Wires 5: Optics 2
HL 27.1–27.4	Thu	9:30–11:00	H33	Focus Session: Perspectives in Cu(In,Ga)Se 1
HL 28.1–28.8	Thu	9:30–11:45	H34	Organic Semiconductors 1
HL 29.1–29.6	Thu	9:30–11:00	H36	2D Materials: Graphene
HL 30.1–30.51	Thu	11:00–13:00	P3	Poster 2
HL 31.1–31.4	Thu	11:15–12:15	H36	2D Materials 5 (joint session HL/ CPP/ DS)
HL 32.1–32.6	Thu	15:00–16:30	H31	Perovskite and Photovoltaics 3 (joint session HL/ CPP/ KFM)
HL 33.1–33.10	Thu	15:00–18:00	H32	Optical Properties 2
HL 34.1–34.7	Thu	15:00–18:00	H33	Focus Session: Perspectives in Cu(In,Ga)Se 2
HL 35.1–35.4	Thu	15:00–16:00	H34	Acoustic Waves and Nanomechanics
HL 36.1–36.10	Thu	15:00–17:45	H36	Materials and Devices for Quantum Technology 2
HL 37.1–37.3	Thu	16:30–17:15	H34	Thermal Properties
HL 38	Thu	18:00–19:00	H34	Members' Assembly
HL 39.1–39.5	Fri	9:30–10:45	H32	Quantum Dots and Wires 6: II-VI and related
HL 40.1–40.7	Fri	9:30–11:45	H33	THz and MIR Physics in Semiconductors
HL 41.1–41.5	Fri	9:30–10:45	H34	Organic Semiconductors 2
HL 42.1–42.9	Fri	9:30–12:00	H36	2D Materials 6 (joint session HL/ CPP/ DS)

Members' Assembly of the Semiconductor Physics Division

Donnerstag 18:00–19:00 H34

- Bericht
- Informationen zu Dresden 2023
- Verschiedenes

Sessions

– Invited Talks, Tutorials, Contributed Talks, and Posters –

HL 1: Tutorial: 2D Quantum Materials and Heterostructures: From Fabrication to Applications (joint session HL/TUT)

Due to the atomic thickness of 2D materials, stacking of different monolayers has opened the door for artificial van der Waals heterostructures. By exploiting the strongly different nature of the individual layers (semiconducting, metallic, magnetic, superconducting, etc.) and rotating them from layer to layer, heterostructures with unique physical properties and functionalities can be envisioned for novel electronic or optical devices. The tutorial will cover the fabrication of these heterostructures and their potential use in applications ranging from electronic to optical devices, operating at the quantum level.

Time: Sunday 16:00–18:20

Location: H2

Tutorial HL 1.1 Sun 16:00 H2
Discovering, Creating, and Exploring Novel Atomically-Thin Materials and Heterostructures — •JOSHUA ROBINSON — The Pennsylvania State University, University Park, PA, USA

The last decade has seen an exponential growth in the science and technology of two-dimensional materials. Beyond graphene, there is a huge variety of layered materials that range in properties from insulating to superconducting. Furthermore, heterogeneous stacking of 2D materials also allows for additional dimensionality for band structure engineering. In this talk, I will discuss recent breakthroughs in two-dimensional atomic layer synthesis and properties, including novel 2D heterostructures and realization of unique 2D allotropes of 3D materials (e.g. 2D metals and oxides). Our recent works demonstrate that the properties and doping of 2D materials, especially synthetic 2D materials, are extremely sensitive to the substrate choice. I will discuss substrate impact on 2D layer growth and properties, doping of 2D materials, selective area synthesis of 2D materials, and creating 2D allotropes from traditionally 3D materials for photonic and quantum applications. Our work and the work of our collaborators has lead to a better understanding of how substrate not only impacts 2D crystal quality, but also doping efficiency in 2D materials, and stabilization of 3D materials at their quantum limit.

Tutorial HL 1.2 Sun 16:35 H2
Non-identical moire twins in bilayer graphene — •REBECA RIBEIRO-PALAU¹, EVERTON ARRIGHI¹, VIET-HUNG NGUYEN², MARIO DI LUCA¹, GAIA MAFFIONE¹, KENJI WATANABE³, TAKASHI TANIGUCHI³, DOMINIQUE MAILLY¹, and JEAN-CHRISTOPHE CHARLIER² — ¹Universite Paris-Saclay, CNRS, Centre de Nanosciences et de Nanotechnologies (C2N), 91120 Palaiseau, France — ²Institute of Condensed Matter and Nanosciences, Universite catholique de Louvain (UCLouvain), 1348 Louvain-la-Neuve, Belgium — ³National Institute for Materials Science, 1-1 Namiki, Tsukuba, Japan

I will present recent results which demonstrate that the moire superlattice formed by a bilayer graphene aligned with BN, is present every 60 deg, but the symmetry is broken between the 0 deg and 60 deg alignments, creating non-identical "moire twins" with different electronic properties. In particular, electron transport measurements display a fully developed valley Hall effect at 0 deg while on the contrary, it is completely absent at 60 deg. We explain this effect by performing numerical simulations, which highlight the central role of the atomic-scale structural relaxation of the second graphene layer. This in-plane atomic relaxation, different for the two alignments, impacts on the electronic band structure of our system. Our results demonstrate that in situ control of the rotational order provides a unique insight on the interplay between mechanical and electronic properties, and increases the possibilities for band-structure engineering on van der Waals heterostructures.

Tutorial HL 1.3 Sun 17:10 H2
Single-photon emitters in 2D materials — •STEFFEN MICHAELIS DE VASCONCELLOS — University of Münster, Institute of Physics and Center for Nanotechnology, Wilhelm-Klemm-Str. 10, 48149 Münster, Germany

Single-photon sources are key components for quantum technologies, such as communications, cryptography, computation, and metrology. Recently, the family of solid-state quantum light emitters was joined by single-photon sources in atomically thin materials [1]. Compared to 3D bulk materials, the 2D host crystals with their high structural flexibility allow for a high photon extraction efficiency, new methods for the deterministic creation, and convenient integration with photonic circuits.

In this tutorial, I will introduce the basic properties of single-photon emitters in different 2D van der Waals material systems and discuss present experimental methods for their creation, control, and coupling to photonic nanostructures.

[1] S. Michaelis de Vasconcellos et al., "Single-Photon Emitters in Layered Van der Waals Materials," *Phys. Status Solidi B* **2022**, 259, 2100566

Tutorial HL 1.4 Sun 17:45 H2
Introduction to 2D superconducting spintronics — •ELKE SCHEER — Department of Physics, University of Konstanz, Konstanz

The proximity effect between a conventional (s-wave) 3D superconductor (S) and a ferromagnet (F) can lead to the formation of Cooper pairs with parallel-spin (spin-triplet) alignment instead of the conventional antiparallel-spin (spin-singlet) state. The demonstration of spin-triplet generation in S/F systems [1,2] has inaugurated the field of superconducting spintronics aiming at developing energy-efficient spintronic devices [3]. Both superconductivity and ferromagnetism depend on the dimensionality of the system, but have been shown to exist in 2D or quasi-2D systems [4,5]. The possibility to exfoliate layered van der Waals (vdW) materials down to the few-layer limit [6] in combination with the existence of S and of F vdW materials makes this material basis in particular promising to explore triplet S in 2DS/2DF heterostructures. In this tutorial talk I will briefly recall the physics of SF spintronics in 3D, before I will describe the particular properties and challenges in the investigation of 2D-SF hybrid systems and give an overview over the so far best-studied material combinations and target devices.

[1] R. Keizer et al., *Nature* **95**, 825 (2006)

[2] A. Buzdin, *Rev. Mod. Phys.* **77**, 935 (2005)

[3] J. Linder & J. Robinson, *Nature Phys.* **11**, 307 (2015)

[4] B. Huang et al., *Nature* **546**, 270 (2017)

[5] M. Smidman et al., *Rep. Prog. Phys.* **80**, 036501 (2017)

[6] A. K. Geim & I. V. Grigorieva, *Nature* **499**, 419 (2013).

HL 2: Spin Phenomena in Semiconductors

Time: Monday 9:30–11:00

Location: H31

Invited Talk HL 2.1 Mon 9:30 H31
Observation of quantum Zeno effects for localized spins — •ALEX GREILICH¹, NIKITA V. LEPPENEN², VITALIE NEDELEA¹, EIKO EVERS¹, DMITRY S. SMIRNOV², and MANFRED BAYER¹ — ¹Experimentelle Physik 2, Technische Universität Dortmund, 44221 Dortmund, Germany — ²St. Petersburg, Russia

One of the main dephasing mechanisms for the localized carrier spins in semiconductors is the coupling to the fluctuating nuclear spin environment. Here we present an experimental observation on the effects of the quantum back action

under pulsed optical measurements and demonstrate that the nuclei-induced spin relaxation can be influenced. We show that the fast measurements freeze the spin dynamics and increase the effective spin relaxation time, the so-called quantum Zeno effect. Furthermore, we demonstrate that if the measurement rate is comparable with the spin precession frequency in the effective magnetic field, the spin relaxation rate increases and becomes faster than in the absence of the measurements, an effect known as the quantum anti-Zeno effect.

HL 2.2 Mon 10:00 H31

Interplay of spin-orbit coupling and spin diffusion on spin helices lifetime in GaAs quantum wells — •SERGIU ANGHEL¹, KARL SCHILLER¹, GO YUSA^{2,3}, TAKA AKI MANO⁴, TAKESHI NODA⁴, and MARKUS BETZ¹ — ¹Experimentelle Physik 2, Technische Universität Dortmund, Otto-Hahn-Straße 4a, D-44227 Dortmund — ²Department of Physics, Tohoku University, Sendai 980-8578, Japan — ³Center for Spintronics Research Network, Tohoku University, Sendai 980-8578, Japan — ⁴National Institute for Materials Science, Tsukuba, Ibaraki 305-0047, Japan

This work reveals the dependence of the persistent spin helix (PSH) lifetime on spin diffusion coefficient and the electron density, by employing time-resolved magneto-optical Kerr effect microscopy to study the spin polarization evolution in low-dimensional GaAs QWs. It is shown that for the achieving the longest PSH lifetime, the variation of scattering rate with the electron density is of higher importance than the fulfilling of the persistent spin helix condition when the Rashba α and Dresselhaus β parameters are balanced (suppression of D'yakanov-Perel spin dephasing mechanism). More specifically, the PSH relaxation rate is determined mostly by the spin diffusion coefficient that depends on electron density nonmonotonously. The longest experimentally observed PSH lifetime occurs at an electron density, corresponding to the transition from Boltzmann to Fermi-Dirac statistics - several times higher than that when the persistent spin helix is expected. These facts highlight the role the electron density may play when considering applications for spintronic devices.

HL 2.3 Mon 10:15 H31

Selective optical charging and spin preparation of a single quantum dot molecule — •C. THALACKER¹, F. BOPP¹, A. AHMADI¹, N. REVENGA¹, F. VÖGL¹, C. CULLIP¹, K. BOOS¹, F. SBRESNY¹, N. BART², A. WIECK², A. LUDWIG², D. REUTER³, J. SCHALL⁴, S. REITZENSTEIN⁴, H. RIEDL¹, K. MÜLLER¹, and J. J. FINLEY¹ — ¹Walter Schottky Institut und Physik Department, TU München, Garching, Germany — ²Ruhr-Universität Bochum, Bochum, Germany — ³Universität Paderborn, Paderborn, Germany — ⁴Technische Universität Berlin, Berlin, Germany

Coherence, ease of control and scalability lie at the heart of hardware for distributed quantum technologies. Spin-photon interfaces based on III-V semiconductor quantum dots (QDs) combine properties such as strong light-matter interactions, robust spin-photon selection rules and ease of integration into opto-electronic devices. Two vertically stacked QDs, a so-called QD-molecule (QDM) are expected to exhibit enhanced coherence times (T_2^*) due to the formation of singlet-triplet (S-T) qubits. We embed a single QDM into an ultralow capacitance p-i-n diode that allows for ultrafast electrical tuning (>500 MHz). Photon extraction efficiencies are improved to >20% by deterministically placing a circular Bragg grating around the QDM. Using our device we demonstrate all optical control of the charge state, as well as optical spin pumping. Our results form the basis of an optically active S-T spin-qubit with enhanced coherence.

HL 2.4 Mon 10:30 H31

Resonant spin amplification in Faraday geometry — •NEDELEA VITALIE¹, PHILIPP SCHERING², DMITRY SMIRNOV³, EIKO EVERS², EVGENY ZHUKOV^{1,3}, DMITRI YAKOVLEV^{1,3}, MANFRED BAYER^{1,3}, UHRIG GÖTZ², and ALEX GREILICH¹ — ¹Experimental Physics 2, TU Dortmund University, Dortmund, Germany — ²Condensed Matter Theory, TU Dortmund University, Dortmund, Germany — ³St. Petersburg, Russia

The possibility to use the spin degree of freedom for quantum information continues to drive research on semiconductor nanostructures. The main characteristic in this field is defined by the lifetime of the information or the spin coherence time. One of the most basic parameters of the spin dynamics is the g factor, which is often anisotropic in semiconductor nanostructures. Its transverse component can be measured very precisely when a magnetic field is applied in Voigt geometry by means of the resonant spin amplification effect (RSA).

Model consideration predict [1] that the realization of the RSA effect in Faraday geometry, where a magnetic field is applied parallel to the optically induced spin polarization, can be realized for a central spin interacting with a fluctuating spin environment. To confirm theory, we chose an ensemble of singly-charged (In,Ga)As/GaAs quantum dots, where the resident electron spin interact with the surrounding nuclear spins. The observation of RSA in Faraday geometry requires intense pump pulses with a high repetition rate and can be enhanced by means of the spin-inertia effect. Potentially, it provides the most direct and reliable tool to measure the longitudinal g factor of the charge carrier.

HL 2.5 Mon 10:45 H31

Cavity-enhanced single-shot readout of a quantum dot spin within 3 ns — •NADIA OLYMPIA ANTONIADIS¹, MARK RICHARD HOGG¹, WILLY FREDERIK STEHL¹, ALISA JAVADI¹, NATASHA TOMM¹, RÜDIGER SCHOTT², SASCHA RENÉ VALENTIN², ANDREAS DIRK WIECK², ARNE LUDWIG², and RICHARD JOHN WARBURTON¹ — ¹Department of Physics, University of Basel — ²Lehrstuhl für Angewandte Festkörperphysik, Ruhr-Universität Bochum

Rapid, high-fidelity single-shot readout of quantum states is a ubiquitous requirement in quantum information technologies. Readout of spin states in optically active emitters can be achieved by driving a spin-preserving optical transition and detecting the emitted photons. The speed and fidelity of this approach is typically limited by a combination of low photon collection rates and measurement back-action. Here, we demonstrate single-shot optical readout of a semiconductor quantum dot spin state, achieving a readout time of only a few nanoseconds. Our approach embeds a gated InAs quantum dot device into an open microcavity architecture. The Purcell enhancement generated by the microcavity selectively increases the readout transition emission rate, as well as efficiently channelling the emitted photons into a well-defined detection mode. We achieve single-shot readout of an electron spin state in 3 ns with a fidelity of (95.85±0.71)%, and observe quantum jumps using repeated single-shot measurements. Our work reduces the spin readout-time to values well below both the achievable spin T1 and T2* times in InAs quantum dots, opening up new possibilities for their use in quantum technologies.

HL 3: Quantum Dots and Wires 1: Transport and Electronic Properties

Time: Monday 9:30–13:00

Location: H32

Invited Talk

HL 3.1 Mon 9:30 H32

Pushing the limits in real-time measurements of quantum dynamics — •ERIC KLEINHERBERS¹, PHILIPP STEGMANN², ANNIKA KURZMANN³, MARTIN GELLER¹, AXEL LORKE¹, and JÜRGEN KÖNIG¹ — ¹Faculty of Physics and CENIDE, University Duisburg-Essen, 47057 Duisburg, Germany — ²Department of Chemistry, Massachusetts Institute of Technology, Cambridge, Massachusetts 02139, USA — ³2nd Institute of Physics, RWTH Aachen University, 52074 Aachen, Germany

Time-resolved studies of quantum systems are the key to understand quantum dynamics at its core. The real-time measurement of individual quantum numbers as they switch between certain discrete values, well known as random telegraph signal, is expected to yield maximal physical insight. However, the signal suffers from both systematic errors, such as a limited time resolution and noise from the measurement apparatus, as well as statistical errors due to a limited amount of data. Here we demonstrate that an evaluation scheme based on factorial cumulants can reduce the influence of such errors by orders of magnitude [1]. The error resilience is supported by a general theory for the detection errors as well as experimental data of single-electron tunneling through a self-assembled quantum dot. Thus, factorial cumulants push the limits in the analysis of random telegraph data which represent a wide class of experiments in physics, chemistry, engineering and life sciences.

[1] E. Kleinherbers et al., Phys. Rev. Lett. 128, 087701 (2022)

HL 3.2 Mon 10:00 H32

Creating and detecting poor man's Majorana bound states in interacting quantum dots — •ATHANASIOS TSINTZIS¹, RUBÉN SEOANE SOUTO^{1,2}, and MARTIN LEIJNSE^{1,2} — ¹Division of Solid State Physics and NanoLund, Lund University, S-221 00 Lund, Sweden — ²Center for Quantum Devices, Niels Bohr Institute, University of Copenhagen, DK-2100 Copenhagen, Denmark

We theoretically study a system of two quantum dots (QDs) coupled via a third (coupler) QD which is additionally proximitized by an s-wave superconductor. For a wide parameter range, the system can be tuned to sweet spots with a doubly-degenerate ground state, as switches between even- and odd-parity ground states are found to be ubiquitous. The necessary ingredients are a) a finite magnetic field to break the spin degeneracy and b) spin-orbit interaction to mix the spin species. The sweet spots harbor poor man's Majorana bound states (Phys. Rev. B 86, 134528, 2012) whose quality is quantified by calculating the Majorana polarizations of the degenerate ground states (Phys. Rev. B 101, 125431, 2020). The QDs' electrochemical potentials are the control knobs utilized to reach the sweet spots and local and non-local conductance calculations provide a useful map for experimentalists navigating the parameter space. The above system can be realized in a semiconductor 2D electron gas or nanowire with gate- or epitaxially defined QDs coupled to a grounded superconductor. This work provides a path towards near-future demonstration of nonabelian and non-local Majorana properties, with possible (more long-term) applications in topologically protected quantum computing.

HL 3.3 Mon 10:15 H32

Interference and parity blockade in transport through a Majorana box — •MAXIMILIAN NITSCH¹, RUBÉN SEOANE SOUTO^{1,2}, and MARTIN LEIJNSE^{1,2} — ¹Division of Solid State Physics and NanoLund, Lund University, S-22100 Lund, Sweden — ²Center for Quantum Devices, Niels Bohr Institute, University of Copenhagen, DK-2100 Copenhagen, Denmark

A Majorana box - two topological superconducting nanowires coupled via a trivial superconductor - is a building block in devices aiming to demonstrate nonabelian physics, as well as for topological quantum computer architectures. We theoretically investigate charge transport through a Majorana box and show that current can be blocked when two Majoranas couple to the same lead, fixing their parity. In direct analogy to Pauli spin blockade in spin qubits, this parity blockade can be used for fast and high-fidelity qubit initialization and readout, as well as for current-based measurements of decoherence times. Furthermore, we demonstrate that transport can distinguish between a clean Majorana box and a disordered box with additional unwanted Majorana or Andreev bound states.

HL 3.4 Mon 10:30 H32

Wave-function mapping of excited quantum dot states — •DANIEL HECKER¹, JENS KERSKI¹, NELSON CREUTZBURG¹, ARNE LUDWIG², ANDREAS D. WIECK², MARTIN GELLER¹, and AXEL LORKE¹ — ¹Faculty of Physics and CENIDE, University of Duisburg-Essen, Germany — ²Chair of Applied Solid State Physics, Ruhr-University Bochum, Germany

Self-assembled quantum dots (QDs) are promising candidates for quantum information technologies, quantum sensing and various electro-optical applications. They are often approximated as two-dimensional harmonic oscillators. Although this approximation of electron states in a harmonic oscillator is very successful, the influence of the electron-electron interaction on the excited few-particle wave-functions and their dynamics into equilibrium has not been studied in detail.

We investigate an ensemble of InAs/GaAs QDs, embedded in a high-electron-mobility transistor with a two-dimensional electron gas (2DEG) as conductive channel. By applying a gate voltage to the transistor, the QDs can be selectively occupied with electrons tunneling from the 2DEG, and the time-resolved transconductance of the 2DEG can be measured. A rate equation based evaluation of the transconductance allows us to determine the tunneling rates of the QD states. In combination with a magnetic field that tunes the wave function-dependent tunneling probability, this enables us to investigate the shape and dynamics of the (excited) few-electron states.

HL 3.5 Mon 10:45 H32

Charge tuning of GaAs quantum dots using Schottky diode structure — •NAND LAL SHARMA¹, GHATA SATISH BHAYANI¹, OLIVER G. SCHMIDT², and CASPAR HOPFMANN¹ — ¹Institute for Integrative Nanosciences, IFW Dresden, Helmholtzstrasse 20, 01069 Dresden, Germany — ²Material Systems for Nanoelectronics, Technical University Chemnitz, 09107 Chemnitz, Germany

Semiconductor quantum dots (QDs) are promising candidates for high quality photon sources and the biexciton-exciton cascade in these structures is one of the most advanced techniques for generation of entangled photon pairs. In this work droplet etched GaAs/AlGaAs QDs [1] are embedded in Schottky diode structures within nanomembranes. The membranes are transferred to Au coated substrates via selective etching. The Au coated substrate facilitates the back while the Si-doped GaAs acts as the top contact. The QD photoluminescence from different charge states is controlled by application of an external bias. The effects of quantum dot charging, quantum confined Stark effect, exciton fine structure and photon coherence are investigated as a function of bias voltage.

[1] Keil et. al. Nat. comm. 8, 15501 (2017)

30 min. break

HL 3.6 Mon 11:30 H32

Modeling and simulation of the electric control of quantum dot photodiodes — •DUSTIN SIEBERT¹, ALEX WIDHALM^{1,2}, SEBASTIAN KREHS², NAND LAL SHARMA², TIMO LANGER², BJÖRN JONAS², DIRK REUTER², ANDREAS THIEDE¹, ARTUR ZRENNER², and JENS FÖRSTNER¹ — ¹Paderborn University, Electrical Engineering Department, Warburger Straße 100, 33098 Paderborn, Germany — ²Paderborn University, Physics Department, Warburger Straße 100, 33098 Paderborn, Germany

Optoelectronic devices like photodiodes based on single quantum dots are one of the new major fields of research for quantum computing, communication and sensing. In our work, we present our theoretical model and approaches using optoelectronic Bloch simulations to reproduce experimental results considering influences of a timing jitter between optical and electric pulses. Further, we use our model to validate quantum sensing methods and we show low frequency field simulations to estimate the electric properties of photodiodes, especially the RC-characteristics, to obtain a better understanding of the quantum dynamic and its electric control.

[1] Amlan Mukherjee, Alex Widhalm, Dustin Siebert, Sebastian Krehs, Nand Lal Sharma, Andreas Thiede, Jens Förstner, and Artur Zrenner, APL, Vol.116,

251103 (2020)

[2] Alex Widhalm, Sebastian Krehs, Dustin Siebert, Nand Lal Sharma, Timo Langer, Björn Jonas, Dirk Reuter, Andreas Thiede, Jens Förstner, and Artur Zrenner, APL, Vol. 119, 181109 (2021)

HL 3.7 Mon 11:45 H32

Electrostatic coupling of double layer self-assembled quantum dots — •LUKAS BERG¹, LAURIN SCHNORR¹, THOMAS HEINZEL¹, ARNE LUDWIG², and ANDREAS DIRK WIECK² — ¹Heinrich-Heine Universität, Düsseldorf, Germany — ²Ruhr-Universität, Bochum, Germany

The electron capture- and emission dynamics of two layers of self-assembled quantum dots in large distance to each other as well as to their reservoirs is studied by time resolved capacitance spectroscopy. The occupation dynamics of the individual layers can be well separated at certain bias voltages. Additionally, an interaction of the electrostatic character is observed in terms of a shift of emission lifetimes and the extracted binding energies. To model this effect, the corresponding system of rate equations is solved.

HL 3.8 Mon 12:00 H32

Temperature-dependence of current peaks in InAs double quantum dots — •OLFA DAN¹, ROBERT HUSSEIN², JOHANNES C. BAYER¹, SIGMUND KOHLER³, and ROLF J. HAUG¹ — ¹Institut für Festkörperphysik, Leibniz Universität Hannover, Hanover, Germany — ²Institut für Festkörpertheorie und -optik, Friedrich-Schiller-Universität Jena, Jena, Germany — ³Instituto de Ciencia de Materiales de Madrid, CSIC, Madrid, Spain

We investigate electron transport through asymmetrically coupled InAs double quantum dots. Measurements of the resonances of single-electron tunneling shows a quite strong temperature dependence of those coherent current peaks. Their width and background increase with temperature in the range of 1.5-21 K, which indicates an influence of the substrate phonons. The broadening of such peaks can be modeled with rather good precision and can be fully explained with quantum dissipation [1] modeled by two baths, the one coupling to the dot occupation, the other to the inter-dot current. Application of magnetic fields helps us to identify the different quantum dot states. [1] Olfa Dani, Robert Hussein, Johannes C. Bayer, Sigmund Kohler, Rolf J. Haug, Temperature-dependent broadening of coherent current peaks in InAs double quantum dots, arXiv:2204.06333 (2022)

HL 3.9 Mon 12:15 H32

Heterogeneous III-V nanowire quantum emitters on silicon photonic circuits — •HYOWON JEONG¹, AKHIL AJAY¹, NITIN MUKHUNDHAN¹, MARCUS DÖBLINGER², JONATHAN J. FINLEY¹, and GREGOR KOBLMÜLLER¹ — ¹Walter Schottky Institute & Physics Department, Technische Universität München, Garching, Germany — ²Department of Chemistry, Ludwig-Maximilians-Universität München, Munich, Germany

III-V quantum dots (QDs) act as naturally bright and highly efficient quantum emitters that can generate deterministic single or entangled photons pairs. QDs embedded in a nanowire (NW) serve as a scalable platform for site-selective and geometry-controlled in-situ heterogeneous integration onto photonic waveguides (WG) - a crucial milestone for the realization of a Quantum Photonic Integrated Circuit.

In the first part, we show by numerical modelling how geometrical parameters of a NW and Si-WG design influence the spontaneous emission enhancement of the QD emitter and the in-coupling efficiencies at the NW-WG interface [1]. Preliminary experiments towards the development of an integrated III-V NW-QD system are then presented. Here, we demonstrate a droplet-free site-selective epitaxy of NWs, where first data of GaAsSb/InGaAs axial heterostructures and their distinct luminescence features will be shown. Furthermore, we discuss control of Indium incorporation into the InGaAs axial segment, in order to tune the emission wavelength before optimizing the axial size, progressing towards an axial QD.

[1] N. Mukhundan, et al., Opt. Express 29, 43068 (2021).

HL 3.10 Mon 12:30 H32

Optoelectronic properties of GaAs(Sb)-AlGaAs core-shell NW diodes on silicon — •TOBIAS SCHREITMÜLLER, PATRICK JONG, DANIEL RUHSTORFER, AKHIL AJAY, ANDREAS THURN, JONATHAN FINLEY, and GREGOR KOBLMÜLLER — Walter Schottky Institute, Technical University of Munich, 85748 Garching, Germany

The ability to integrate III-V semiconductor nanowires (NW) on the silicon (Si) platform opens many perspectives for advanced nanoelectronic and optoelectronic device applications on-chip. However, for energy-efficient device performance, the design of axial or radial heterostructures, the control of accurate doping properties and the formation of low-resistance ohmic contacts are crucial. In this contribution, we present ongoing developments of radial n-i-p core-multishell NW heterostructures monolithically integrated on the n-Si (111) platform. The NW structure is designed to host n-type doped GaAs(Sb) cores, while the shell is composed of either GaAs homojunctions or (In,Al)GaAs(Sb)-based heterojunctions that define intrinsic and p-type doped regions. We show that

n-type conduction is feasible in the Si-doped core by pioneering a novel catalyst-free, vapor-solid growth process of Si-doped GaAs NWs using molecular beam epitaxy (MBE). The n-doped NW cores were then implemented into radial n-i-p NW homo-junction devices to establish electrical contact formation and perform first electroluminescence (EL) experiments. The EL measurements illustrate successful diode characteristics, with luminescence features that are typical for the underlying material properties.

HL 3.11 Mon 12:45 H32

Band structure and end states in InAs/GaSb core-shell-shell nanowires — •FLORINDA VIÑAS BOSTRÖM^{1,2}, ATHANASIOS TSINTZIS², MICHAEL HELL², and MARTIN LEIJNSE² — ¹Institute for Mathematical Physics, TU Braunschweig, Braunschweig, Germany — ²Division of Solid State Physics and NanoLund, Lund University, Lund, Sweden

Heterostructures made from the III-V semiconductors InAs and GaSb have been studied mainly for their bulk broken band gap alignment, meaning that the va-

lence band of GaSb is higher in energy than the conduction band in InAs, in bulk. In addition, the materials are nearly lattice matched, leading to structures with almost no strain. In two dimensions, the InAs/GaSb quantum well is a topological insulator, exhibiting a hybridization gap in the topologically non-trivial regime where quantum spin Hall edge states are present. We have calculated the non-trivial band structures and wave functions of InAs/GaSb core-shell-shell nanowires, using $\mathbf{k} \cdot \mathbf{p}$ theory. For hollow core-shell-shell InAs/GaSb nanowires, we also calculate the wave functions for a finite system with wire ends, using a BHZ model with parameters taken from the resulting $\mathbf{k} \cdot \mathbf{p}$ calculations. We establish that there are localized end-states, with energies inside the bulk gap. However, in contrast to the topological edge states in two dimensions, these end states are fourfold degenerate, and split into two Kramers pairs under potential disorder along the nanowire growth direction. Nevertheless, the end states are robust against potential disorder applied in the angular direction, as long as the bulk band gap is not closed.

HL 4: Semiconductor Lasers

Time: Monday 9:30–12:45

Location: H33

HL 4.1 Mon 9:30 H33

Spin lasing in bimodal quantum dot micropillar cavities — •NIELS HEERMEIER¹, TOBIAS HEUSER¹, JAN GROSSE¹, NATALIE JUNG², MARKUS LINDEMANN², NILS GERHARD², MARTIN HOFMANN², and STEPHAN REITZENSTEIN¹ — ¹Institut für Festkörperphysik, Technische Universität Berlin, D-10623 Berlin, Germany — ²Lehrstuhl für Photonik und Terahertztechnologie, Fakultät für Elektrotechnik und Informationstechnik, Ruhr-Universität Bochum, D-44780 Bochum

Spin-controlled lasers have been shown to provide ultra-fast polarization dynamics in excess of 200 GHz. In contrast to conventional semiconductor lasers their temporal properties are not limited by the intensity dynamics, but are governed primarily by the birefringent mode splitting that determines the polarization oscillation frequency. Another class of modern semiconductor lasers are high-beta emitters which benefit from enhanced light-matter interaction due to strong mode confinement in low-mode-volume microcavities. In such structures, the emission properties can be tailored by the resonator geometry to realize for instance bimodal emission behavior in slightly elliptical micropillar cavities. We utilize this feature to demonstrate and explore spin-lasing effects in bimodal high-beta quantum dot micropillar lasers. The studied microlasers show spin laser effects with polarization oscillation frequencies up to 15 GHz controlled by the ellipticity of the resonator. Our results reveal appealing prospects for very compact and energy-efficient spin lasers and can pave the way for future purely electrically injected spin lasers enabled by short injection path lengths. Laser and Photonics Reviews 2022, 16, 2100585.

HL 4.2 Mon 9:45 H33

Temperature-dependent lasing operation of hybrid semiconductor nanowire-metal grating plasmonic nanolasers — •FRANCESCO VITALE¹, DANIEL REPP², THOMAS SIEFKE³, UWE ZEITNER², THOMAS PERTSCH², and CARSTEN RONNING¹ — ¹Institut für Festkörperphysik, Friedrich-Schiller-Universität Jena, Max-Wien-Platz 1, D-07743 Jena — ²Institut für Angewandte Physik, Friedrich-Schiller-Universität Jena, Albert-Einstein-Straße 15, D-07745 Jena

Nanowire(NW)-based semiconductor-insulator-metal (SIM) plasmonic structures represent a benchmark platform for the next generation of hybrid nanolasers, capable of sustaining sub-wavelength hybrid lasing modes, which, in turn, lead to an overcoming of diffraction-limited mode footprints and an acceleration of the lasing dynamics, when compared to their photonic counterparts. In this work, we report on the realization and optical investigation of hybridized SIM platforms, in which single ZnO NWs are deterministically overlaid onto metal gratings (MGs), FIB-milled into a 70 nm Al layer with a nanometric Al₂O₃ spacer on top. By performing ns-excitation steady-state micro-PL, we study the spectral and temporal properties of such hybrid platforms, as a function of the cavity geometry (i.e. NW size, grating period and NW-trench orientation) and temperature. We report about room-temperature lasing in some of these hybrid NW-MG structures and lowering of the lasing threshold compared to the planar SIM plasmonic nanolasers.

HL 4.3 Mon 10:00 H33

Field-resolved high-order sub-cycle nonlinearities in a terahertz quantum cascade laser — •JOSEF RIEPL¹, JÜRGEN RAAB¹, PAVEL ABAJYAN², HANONG NONG², JOSHUA FREEMAN³, LIANHE H. LI³, EDMUND H. LINFIELD³, A. GILES DAVIES³, ANDREAS WACKER⁴, TIM ALBES⁵, CHRISTIAN JIRAUSCHEK⁵, CHRISTOPH LANGE⁶, SUKHEEP S. DHILLON², and RUPERT HUBER¹ — ¹University of Regensburg, Germany — ²Université de Paris, France — ³University of Leeds, UK — ⁴Lund University, Sweden — ⁵Technical University of Munich, Germany — ⁶TU Dortmund University, Germany

Employing ultrafast electron dynamics in quantum cascade lasers (QCLs) holds enormous potential for intense, compact mode-locked terahertz (THz) sources, squeezed THz light, frequency mixers, and comb-based metrology systems. Yet the important sub-cycle dynamics have been notoriously difficult to access in operational THz QCLs. Here, we perform the first ultrafast two-dimensional high-field spectroscopy of a free running THz QCL. The detected strong incoherent and coherent nonlinearities up to eight-wave mixing do not only reveal extremely short gain recovery times, but also reflect the nonlinear polarization dynamics of the QCL laser transition for the first time. A density-matrix approach reproducing all nonlinearities and their ultrafast evolution, allows us to map the coherently induced trajectory of the Bloch vector. The observed nonlinearities benefit from resonant enhancement in a regime of negative absorption and bear potential for various future applications, ranging from efficient intracavity frequency conversion and mode proliferation to passive mode locking.

HL 4.4 Mon 10:15 H33

Tuning nanowire lasers via hybridization with two-dimensional materials — •EDWIN EOBALDT¹, FRANCESCO VITALE¹, MAXIMILIAN ZAPP¹, MARGARITA LAPTEVA¹, CHRISTOF NEUMANN², ANDREY TURCHANIN^{2,3}, GIANCARLO SOAVI^{1,3}, and CARSTEN RONNING^{1,3} — ¹Institute of Solid State Physics, Friedrich Schiller University Jena, 07743 Jena, Germany — ²Institute of Physical Chemistry, Friedrich Schiller University Jena, 07743 Jena, Germany — ³Abbe Center of Photonics, Friedrich Schiller University Jena, 07745 Jena, Germany

Semiconductor nanowires have attracted great scientific attention due to their remarkable waveguiding properties and their intrinsic capability to lase under sufficiently high excitation, thus, paving the way towards nanoscaled coherent light sources and the realization of all-optical circuits. After the spectral and temporal characteristic of single nanowire lasers have been extensively studied during the past decade, today's research focuses on their effective integration into functional and nanoscaled environments. In this regard, the hybridization of semiconductor nanowire lasers with two-dimensional materials could offer new capabilities for a dynamical emission tuning enabled by charge transfer processes at the heterointerface. As a proof of concept, hybrids systems containing ZnO nanowires on top of MoS₂ monolayers were investigated by micro-photoluminescence measurements. By further adopting a deterministic transfer approach, it was possible to study hybridization-related changes of the lasing emission on one and the same nanowire.

HL 4.5 Mon 10:30 H33

Generalization of the Siegert relation — •MONTY LEON DRECHSLER^{1,2}, FREDERIK LOHOF^{1,2}, and CHRISTOPHER GIES^{1,2} — ¹Institute for Theoretical Physics, University of Bremen, Bremen, Germany — ²Bremen Center for Computational Materials Science, University of Bremen, Bremen, Germany

The Siegert relation connects the first- and second-order coherence properties of light. While it is valid for thermal light, this relation is routinely extended also to the partially coherent regime of high- β nanolasers, where it aids in the identification of the lasing threshold [1]. We test the validity of this extension by introducing a generalized Siegert relation. Based on the cluster expansion method we derive a full two-time quantum optical theory and combine it with our new approach, allowing us to revise the Siegert relation in different device regimes. We find that correlations lead to deviations from the Siegert relation and in particular highlight the influence correlations related to sub- and super-radiance [2].

[1] Kreinberg et al., Laser & Photonics Reviews 14, 2000065 (2020)

[2] Drechsler et al., arXiv:2204.02747v2 (accepted for publication in Appl. Phys. Lett.)

HL 4.6 Mon 10:45 H33

Development of a 850 nm VCSEL array for real world QKD via the BB84 and decoy state protocol — •MORITZ BIRKHOFF, MICHAEL ZIMMER, SERGEJ VOLLMER, MICHAEL JETTER, and PETER MICHLER — Institut für Halbleitertechnik und Funktionelle Grenzflächen, Universität Stuttgart, Allmandring 3, 70569 Stuttgart

Quantum key distribution offers fundamental advantages over classical key distribution. If done correctly a perfectly private key (e.g. a one time pad) can be exchanged between two parties and any eavesdropping attack will be detected. This could be an interesting feature for e.g. worldwide financial applications but the technological hurdles to overcome are numerous.

Here we show the advances towards a complete eight VCSEL array with an integrated polarization grating in the light emission window, to create quantum states and transmit the quantum key. The basic structure is grown by metal-organic vapor-phase epitaxy (MOVPE). Then this structure is processed to allow data transmission in the GHz regime. Various methods including a co-planar contact geometry are used to achieve this. A vector network analyzer is then used to measure the scattering parameter as well as the transmission bandwidth. Finally a eye diagram is recorded to determine the data rate. The polarization grating is defined by an electron beam lithography and etched with an ICP machine to allow light output in four different polarizations. The pulses of the eight different VCSEL are evaluated for indistinguishability.

30 min. break

HL 4.7 Mon 11:30 H33

Investigations on high- β silver-coated InP-based metallic nanolasers and their spectral line shape behavior — •MONTY LEON DRECHSLER¹, J. BUCHGEISTER¹, A. KOULAS-SIMOS², K. LAIHO², G. SINATKAS², T. ZHANG³, J. XU³, F. LOHOF¹, F. JAHNKE¹, C. GIES¹, W. W. CHOW⁴, C.-Z. NING³, and S. REITZENSTEIN² — ¹University of Bremen, Bremen, Germany — ²Technical University of Berlin, Berlin, Germany — ³Tsinghua University, 1303 Beijing 100084, China — ⁴Sandia National Laboratories, Albuquerque, New Mexico, USA

We investigate a silver-coated InP-based metallic nanolasers with a diameter of several 100 nm and β -factor close to unity, pushing the device in the regime of quantum optics. We use a quantum optical semiconductor laser model utilizing an equation of motion approach together with the cluster expansion technique to analyze the device. Photon correlations quantified by $g^{(1)}(\tau)$ and $g^{(2)}(\tau)$ are an essential tool for this research. Information about the energy spectrum and the detection characteristics of photons is encoded in them. In this study, an unconventional behavior of the spectral line shape was found. We observe that the line shape takes a Gaussian profile above the laser threshold. The exciting question arises whether the Gaussian line shape can be used as an indicator of laser activity. In previous works, a similar behavior has been reported, but no explanation was given. We provide an explanation for this behavior of the line shape in the framework of an open-cavity multimode model.

HL 4.8 Mon 11:45 H33

Extraction of silver losses at cryogenic temperatures through optical characterization of Ag-coated plasmonic nanolasers — •ARIS KOULAS-SIMOS¹, GEORGIOS SINATKAS^{1,2}, TAIPING ZHANG³, JIA-LU XU³, WILLIAM E. HAYENGA⁴, QIANG KAN⁵, RUIKANG K. ZHANG⁵, MERCEDEH KHAVAVIKHAN^{4,6}, CUN-ZHENG NING^{3,7}, and STEPHAN REITZENSTEIN¹ — ¹Institut für Festkörperphysik, Technische Universität Berlin, Hardenbergstr. 36, 10623 Berlin, Germany — ²Institute of Integrated Photonics, RWTH Aachen University, Campus Blvd. 73, Aachen 20 52074, Germany — ³Department of Electronic Engineering, Tsinghua University, Beijing, 100084, China — ⁴CREOL, The College of Optics and Photonics, University of Central Florida, Orlando, FL, USA — ⁵Institute of Semiconductors, Chinese Academy of Sciences, Beijing, 100083, China — ⁶Ming Hsieh Department of Electrical and Computer Engineering, University of Southern California, Los Angeles, CA, USA — ⁷School of Electrical, Computer and Energy Engineering, Arizona State University, Tempe, 85287, Arizona, USA

We present a rigorous method for the extraction of silver losses at temperatures T from 10 K to 180 K at NIR wavelengths through T-dependent μ PL studies on silver-coated InP-based nanolasers in conjunction with cavity simulations. The numerical algorithm maps the changes of the Q-factor, estimated at transparency, into the imaginary part of silver permittivity. The results are in good agreement with theoretical predictions estimating a drop of one order from room

to cryogenic temperatures. This data is long missing from the literature and sets a pathway for the optimization of plasmonic nanolasers.

HL 4.9 Mon 12:00 H33

Quantum-optical study of an InGaAsP metallic cavity nanolaser: A systematic approach to the identification of lasing — •J. BUCHGEISTER¹, M. L. DRECHSLER¹, F. LOHOF¹, C. GIES¹, A. KOULAS-SIMOS², K. LAIHO², G. SINATKAS², T. ZHANG⁴, J. XU⁴, Q. KAN⁶, R. K. ZHANG⁶, C.-Z. NING^{4,5}, S. REITZENSTEIN², W. W. CHOW³, and F. JAHNKE¹ — ¹Universität Bremen, Germany — ²Technische Universität Berlin, Germany — ³Sandia National Laboratories, USA — ⁴Tsinghua University, China — ⁵Arizona State University, USA — ⁶Institute of Semiconductors, China

Semiconductor nanolasers as small-scale sources of coherent light have become increasingly important for applications in the data industry for their size, power-efficiency, and modulation speed. Determining the presence of lasing, however, is challenging due to the near-thresholdless behaviour of ultra-efficient devices, which requires going beyond I/O characteristics. The research presented here focuses on a quantum-optical study of a silver-coated InGaAsP nanolaser by means of a full quantum-mechanical semiconductor laser theory. We calculate the time-resolved single- and two-photon correlation function, allowing us to identify the onset of coherent emission with confidence. Our theoretical model can match the experimentally obtained data using a single set of realistic parameters and hence presents a comprehensive strategy for the identification of lasing while being extensible to those gain materials requiring a more pronounced focus on quantum-material aspects, like TMDCs.

HL 4.10 Mon 12:15 H33

Random Lasing with Dye-doped Fluorescent Aerogels — •MATTHIAS KESTLER, THEOBALD LOHMÜLLER, and JOCHEN FELDMANN — Chair for Photonics and Optoelectronics, Nano-Institute Munich and Department of Physics, Ludwig-Maximilians-Universität (LMU), Königinstr. 10, 80539 Munich, Germany

Aerogels are a translucent, amorphous network of colloidal particles, which scatter light at visible wavelengths. Doping an aerogel matrix with fluorescent dyes or nano-particles enables their wider use for optical applications, including random lasing. Here, we report on the synthesis of fluorescent silica aerogels by supercritical drying of dye-doped silica gels. By our refined process, we obtain large, porous samples, where scattering events lead to closed photon paths that act as optical oscillators in the micrometer range. We analyze the corresponding photo-luminescence, amplified stimulated emission and random lasing spectra that are obtained for different dye-loaded aerogel samples. Random lasing is confirmed by different characteristic features like a lasing threshold, bandwidth narrowing and strongly fluctuating Anderson localized modes. Furthermore, we find that the extraordinary thermal stability of aerogels enables the use of high laser pumping energies without visible sample degradation.

HL 4.11 Mon 12:30 H33

Towards a novel vertical external-cavity surface-emitting laser based on a grating waveguide structure — •PETER GIERSS¹, ANA ČUTUK¹, MAXIM LEYZNER², UWE BRAUCH², MARWAN ABDU AHMED², MICHAEL JETTER¹, THOMAS GRAF², and PETER MICHLER¹ — ¹Institut für Halbleitertechnik und Funktionelle Grenzflächen, Center for Integrated Quantum Science and Technology (IQST) and SCoPE, University of Stuttgart, Allmandring 3, 70569 Stuttgart — ²Institut für Strahlwerkzeuge, University of Stuttgart, Pfaffenwaldring 43, 70569 Stuttgart

Vertical external-cavity surface-emitting lasers (VECSELs) provide favorable properties compared to other laser systems. The external cavity allows for incorporation of additional optical elements like birefringent filters or absorbers for passive mode-locking which makes it very attractive for various applications. While the possibility of band-gap engineering and a broad gain spectrum are also advantageous, the heat dissipation from the active region due to the thick distributed Bragg reflector (DBR) is a drawback.

A novel approach is a VECSEL based on a grating waveguide structure (GWS) paired with a low-refractive-index heat-spreader below the active region. The absence of a DBR improves the heat removal while the guided-mode resonances from the GWS should provide good coupling of the pump and laser field as well as the high reflectivity necessary for the laser operation. We present the progress towards the realization of an AlGaInP-based GWS-VECSEL for laser emission in the red spectral range.

HL 5: Perovskite and Photovoltaics 1 (joint session HL/CPP/KFM)

Time: Monday 9:30–12:45

Location: H34

HL 5.1 Mon 9:30 H34

The Electronic Structure of $\text{Cs}_2\text{AgBiBr}_6$ at Room Temperature — •JULIAN GEBHARDT^{1,2} and CHRISTIAN ELSÄSSER^{1,2,3} — ¹Fraunhofer Institute for Mechanics of Materials IWM, 79108 Freiburg — ²Cluster of Excellence livMatS at FIT - Freiburg Center for Interactive Materials and Bioinspired Technologies, Albert-Ludwigs-University Freiburg, 79104 Freiburg — ³Freiburg Materials Research Center (FMF), Albert-Ludwigs-University Freiburg, 79104 Freiburg

$\text{Cs}_2\text{AgBiBr}_6$ is a stable halide double perovskite with a band gap of about 2.2 eV. Therefore, it is intensively studied as possible lead free alternative to hybrid perovskite solar cell absorber materials such as methylammonium-lead iodide. However, power conversion efficiencies of solar cells with this material have not yet exceeded 3%. A detailed understanding of the electronic structure of this material is difficult, due to the variance of reported data and experimental as well as theoretical difficulties that occur in going beyond a qualitative understanding of such an indirect semi-conductor at device operation temperature. Here we combine self-energy corrected electronic-structure theory including spin-orbit coupling and structural dynamics at room temperature to model and understand this compound in a quantitative manner, and we compare our theoretical findings with experimental ones. Based on an achieved good agreement, we propose that the observed low power conversion efficiencies can be attributed to the density of states in the conduction band region. From the relation between dimensionality and electron conductivity, we suggest a general design principle for absorber material search.

HL 5.2 Mon 9:45 H34

Photon-echo spectroscopy of a $\text{CH}_3\text{NH}_3\text{PbI}_3$ perovskite single crystal — •STEFAN GRISARD¹, ARTUR V. TRIFONOV^{1,2}, ALEKSANDR N. KOSAREV^{1,3}, ILYA A. AKIMOV^{1,3}, DMITRII R. YAKOVLEV^{1,3}, JULIAN HÖCKER⁴, VLADIMIR DYAKONOV⁴, and MANFRED BAYER^{1,3} — ¹Experimentelle Physik 2, Technische Universität Dortmund — ²Spin Optics Laboratory, St. Petersburg State University, Russia — ³St. Petersburg, Russia — ⁴Experimental Physics 6, Julius-Maximilian University of Würzburg

Lead halide perovskites such as $\text{CH}_3\text{NH}_3\text{PbI}_3$ (MAPbI₃) show outstanding characteristics important for photovoltaic and optoelectronic applications. However, the peculiarities of light-matter interactions in these materials are far from being fully explored. Here, we applied time-resolved photon echo spectroscopy to a high quality MAPbI₃ single crystal highlighting the importance of inhomogeneous broadening of excitonic transitions even at cryogenic temperatures. Furthermore, we developed an experimental photon-echo polarimetry method that unambiguously identifies contributions from exciton and biexciton to the coherent optical response. Most importantly, our method allows to accurately extract the biexciton binding energy of 2.4 meV, even though the period of the observed quantum beats exceeds the coherence times of exciton and biexciton.

HL 5.3 Mon 10:00 H34

Structural properties of (hot-)pressed MAPbI₃ films revealed by detailed temperature-dependent optical analyses — •CHRISTINA WITT¹, KONSTANTIN SCHÖTZ¹, NICO LEUPOLD², SIMON BIBERGER¹, PHILIPP RAMMING¹, RALF MOOS², and FABIAN PANZER¹ — ¹Soft Matter Optoelectronics, University of Bayreuth, Bayreuth 95440, Germany — ²Department of Functional Materials, University of Bayreuth, Bayreuth 95440, Germany

Halide perovskites attracted much attention in recent years, due to the remarkable increase in corresponding solar cell efficiencies. More recently, hot-pressing has emerged as attractive method for manufacturing and post-treatment of perovskite films [1, 2]. However, a detailed understanding regarding the role of temperature during hot-pressing on resulting film properties is still missing. Thus, we use temperature-dependent PL and absorption measurements of MAPbI₃ thin films pressed with different temperatures and in detail analyze their optical properties. This allows us to draw conclusions about structural and optoelectronic properties, revealing that an increased temperature improves film morphology, structural and optoelectronic film properties.

[1] Witt, C. et al. Impact of Pressure and Temperature on the Compaction Dynamics and Layer Properties of Powder-Pressed Methylammonium Lead Halide Thick Films. ACS Appl. Electron. Mater. 2020, 2 (8), 2619–2628.

[2] Pourdavoud, N. et al. Room-Temperature Stimulated Emission and Lasing in Recrystallized Cesium Lead Bromide Perovskite Thin Films. Adv. Mater. 2019, 31, 1903717.

HL 5.4 Mon 10:15 H34

Application of atomic layer deposition and x-ray photoelectron spectroscopy in perovskite solar cells — •MAŁGORZATA KOT¹, CHITTARANJAN DAS², LUKAS KEGELMANN³, HANS KOEBLER³, MIKHAILO VOROKHTA⁴, CARLOS ESCUDERO⁵, STEVE ALBRECHT³, ANTONIO ABATE³, and JAN INGO FLEGE¹ — ¹BTU Cottbus-Senftberg, Cottbus, Germany — ²KIT, Eggenstein-Leopoldshafen, Germany

— ³HZB, Berlin, Germany — ⁴Charles University, Prague, Czech Republic — ⁵ALBA Synchrotron, Cerdanyola del Vallès, Spain

In this work we have utilized near-ambient pressure and ultra-high vacuum X-ray photoelectron spectroscopy as well as atomic layer deposition to investigate perovskite solar cells (PSCs). We have demonstrated that ultrathin room temperature atomic layer-deposited aluminium oxide on the perovskite surface very effectively suppresses iodine migration [1] and improves the long term stability and efficiency of PSCs [2,3]. Furthermore, exposure to light proves more detrimental to the perovskite film than exposure to water vapor. [2] Absorbed photons create Frenkel defects in the perovskite crystal and their number strongly depends on the used illumination. The higher the photon flux, the higher the concentration of Frenkel defects, and thus the stronger the degradation of power conversion efficiency and the stronger the hysteresis in the J-V characteristics. [1] C. Das, M. Kot et al., Cell Reports Physical Science 2020, 1, 100112. [2] M. Kot et al., ChemSusChem 2020, 13, 5722. [3] M. Kot et al., ChemSusChem 2018, 11, 3640.

HL 5.5 Mon 10:30 H34

Chemical Engineering of Ferroelastic Twin Domains in MAPbI₃ Thin Films — •YENAL YALCINKAYA¹, ILKA HERMES¹, TOBIAS SEEWALD², KATRIN AMANN-WINKEL¹, LOTHAR VEITH¹, LUKAS SCHMIDT-MENDE², and STEFAN A.L. WEBER¹ — ¹Max Planck Institute for Polymer Research, Ackermannweg 10, 55128 Mainz, Germany — ²Department of Physics, University of Konstanz, Universitätsstr. 10, 78464, Germany

In this study, we introduce a new chemical method for controlling the strain in methylammonium lead iodide (MAPbI₃) perovskite crystals by varying the ratio of Pb(Ac)₂ and PbCl₂ in the precursor solution. We used a combination of piezoresponse force microscopy (PFM) and X-ray diffraction (XRD) to observe the effect on crystal strain. We observed larger ferroelastic twin domains upon increasing the PbCl₂ content, indicating increased crystal strain via PFM images. We confirmed the increased crystal strain via the XRD patterns with strong crystal twinning features. We suggest that this behaviour is caused by different evaporation rates of methylammonium acetate and methylammonium chloride which led to a strain gradient during the crystallization as revealed by time-of-flight secondary ion mass spectroscopy (ToF-SIMS) and grazing incidence x-ray diffraction (GIXRD) measurements. We observed films with larger twin domain structures show an increased carrier via time-resolved photoluminescence (TRPL). The results demonstrate the potential of chemical strain engineering as an easy method for controlling strain-related effects in lead halide perovskites.

HL 5.6 Mon 10:45 H34

Inspecting the local structure of cubic phase halide perovskites from first-principles — •XIANGZHOU ZHU, SEBASTIÁN CAICEDO-DÁVILA, CHRISTIAN GEHRMANN, and DAVID A. EGGER — Department of Physics, Technical University of Munich, Garching, Germany

Halide perovskites (HaPs) have been identified as one of the most promising optoelectronic materials in recent years. Different from the conventional inorganic semiconductors, HaPs exhibit profound deviations from their average atomic structure at finite temperature, which have important consequences for their optoelectronic properties. However, a detailed understanding of these local structural fluctuations, the underlying physical mechanisms as well as their consequences is far from complete. Here, we perform molecular dynamics (MD) calculations based on density functional theory (DFT) to investigate the local structure and anharmonic dynamics of CsPbBr₃ in the cubic phase at T=425 K and 525K. We find that motions of neighboring Cs-Br atoms interlock within a nominal cubic unit cell. This manifests in the most likely Cs-Br distance being significantly shorter than what is inferred from an ideal cubic structure. Furthermore, we use the statistical information on the dynamic atomic distributions to quantify the effective potential associated with certain atomic motions at two temperatures. We find that Br motions occur in a dynamically disordered potential energy landscape and relate the Cs motion as well the Cs-Br coupling to PbBr₆ octahedral rotations.

30 min. break

HL 5.7 Mon 11:30 H34

Distinct Resonances in Absorption Spectra of Lead Halide-based Quantum Dots — •ANJA BARFÜSSER, QUINTEN A. AKKERMAN, SEBASTIAN RIEGER, AMRITA DEY, AHMET TOSUN, TUSHAR DEBNATH, and JOCHEN FELDMANN — Chair for Photonics and Optoelectronics, Nano-Institute Munich and Department of Physics, Ludwig-Maximilians-Universität (LMU), Königinstr. 10, 80539 Munich, Germany

In recent years, perovskite nanocrystals have attracted much attention for their unique optical properties. Here, we discuss sphere-like lead halide-based quan-

tum dots with diameters in the range of 4.5-12 nm featuring a multitude of distinct resonances in their absorption spectra. We have investigated the nature of these resonances by comparing experimental data with model calculations based on weak and strong confinement. In transient absorption experiments, bleaching and induced absorption signals are observed, which we discuss in terms of confined excitons and biexcitonic contributions.

HL 5.8 Mon 11:45 H34

Revealing the doping density in perovskite solar cells and its impact on device performance — •FRANCISCO PEÑA-CAMARGO and MARTIN STOLTERFOHT — Physik weicher Materie, Institut für Physik und Astronomie, Universität Potsdam, Karl-Liebknecht-Str. 24-25, 14776 Potsdam, Germany

Inorganic semiconductors can be electronically doped with high precision. Conversely, there is still conjecture regarding the assessment of the electronic doping density in metal-halide perovskites, not to mention of a control thereof. This study presents a multifaceted approach to determine the electronic doping density for a range of different lead-halide perovskite systems. Optical and electrical characterisation techniques comprising intensity-dependent and transient photoluminescence, AC Hall effect, transfer-length-methods, and charge extraction measurements were instrumental in quantifying an upper limit for the doping density. The obtained values are subsequently compared to the electrode charge per cell volume at short-circuit conditions (CU_{bi}/eV), which amounts to roughly 10^{16} cm^{-3} . This figure of merit represents the critical limit below which doping-induced charges do not influence the device performance. The experimental results demonstrate consistently that the doping density is below this critical threshold ($< 10^{12} \text{ cm}^{-3}$ which means $\ll CU_{bi}/eV$) for all common lead-based metal-halide perovskites. Nevertheless, although the density of doping-induced charges is too low to redistribute the built-in voltage in the perovskite active layer, mobile ions are present in sufficient quantities to create space-charge-regions in the active layer.

HL 5.9 Mon 12:00 H34

Ground-state structures, electronic structure, transport properties and optical properties of anion-ordered anti-Ruddlesden-Popper phase oxide perovskites — •DAN HAN, SHIZHE WANG, THOMAS BEIN, and HUBERT EBERT — Department Chemie, Ludwig-Maximilians-Universität München, Germany

Anti-Ruddlesden-Popper (ARP) phase oxide perovskites Ca_4OA_2 ($A = \text{P, As, Sb, Bi}$) have recently attracted great interest in the field of ferroelectrics and thermoelectrics, while their optoelectronic application is dominantly limited by their indirect band gaps. In this work, we consider A-site anion ordering in Ca_4OA_2 ($A = \text{P, As, Sb, Bi}$), and find that it induces an indirect-to-direct band gap transition. Using first-principles calculations, we study the ground-state structures, electronic structure, transport properties and optical properties of anion-ordered ARP phase oxide perovskites Ca_4OAA . Based on an analysis of the lattice dynamics, the ground-state structures of Ca_4OAsSb , Ca_4OAsBi , Ca_4OPSb and Ca_4OPBi are identified. In contrast to the Ruddlesden-Popper (RP) phase oxide and halide counterparts, Ca_4OAA show larger band dispersion along the out-of-plane direction, smaller band gaps and highly enhanced out-of-plane mobilities, which is ascribed to the short interlayer distances and enhanced covalency of the pnictides. Although the out-of-plane mobilities of these $n = 1$ ARP phase perovskites highly increase, comparatively strong polar optical phonon (POP)

scattering limits the further enhancement of their mobilities. This work shows that these anion-ordered Ca_4OAA exhibit the potential for optoelectronic applications.

HL 5.10 Mon 12:15 H34

Including light management concepts in performance prediction modelling of perovskite-silicon tandem solar cells by implementing transfer matrix method — AMINREZA MOHANDÉS^{1,2}, PEYMANEH RAFIEIPOUR^{1,2}, MOHAMMAD MOADDELI¹, and •MANSOUR KANANI¹ — ¹Department of Materials Science and Engineering, School of Engineering, Shiraz University, Shiraz, Iran — ²Department of Physics, Shiraz University, Shiraz, Iran

The 2-T monolithic perovskite-silicon tandem design holds a record efficiency of 29.80%, recently. To perform more accurate, complete and experimentally reliable modelling of tandem solar cell, we adopt the transfer matrix method (TMM) which incorporates the interfacial reflections, light scattering and parasitic absorption losses in the calculation of the light transmitted from the top perovskite solar cell. The results reveal that the light scattering and interfacial reflection losses cannot be ignored and the previously used Beer-Lambert exponential relation is insufficient for studying tandem configuration. Including TMM method in the performance optimization of the tandem solar cells lets to consider light management concepts more extensively. Therefore, identifying and reducing optical losses in each layer/interface and designing appropriate anti-reflection coatings in a multilayer tandem simulation can be achieved. In this study, standalone and tandem devices have been analyzed and the effect of absorber layer thickness variation, J-V curves, external quantum efficiency (EQE), filtered spectra, current matching, and tandem performance parameters on the cell efficiency is considered.

HL 5.11 Mon 12:30 H34

Highly Efficient Perovskite-on-Silicon Tandem Solar Cells on Planar and Textured Silicon — •CHRISTIAN M. WOLFF¹, XIN YU CHIN², KEREM ARTUK¹, DENIZ TÜRKAY¹, DANIEL JACOBS¹, QUENTIN JEANGROS², and CHRISTOPHE BALLIF^{1,2} — ¹École polytechnique fédérale de Lausanne, STI IEM PVLAB, Rue de la Maladière 71b, 2000 Neuchâtel — ²Centre Suisse d'Electronique et de Microtechnique, Rue Jaquet-Droz 1, 2002 Neuchâtel

Multi-junction devices offer the possibility to harness the sun's light beyond the limitations of single-junction solar cells. Among the different combinations perovskite-on-silicon (Pk/Si) tandems hold the great promise of high efficiencies $>30\%$, while maintaining low cost. I will report on our latest progress in the development of Pk/Si tandems comparing our efforts on single-side and double-side textured Pk/Si tandems, reaching a V_{OC} up to 1.95V, summed short-circuit currents above 41 mA/cm^2 , and certified efficiencies $>29\%$, on an active area of 1 cm^2 . We achieved these results by dedicated electrical and optical optimizations of all layers within the stack. Specifically, we reduced recombination and transport losses in the Pk absorbers through process and additive engineering for both solution-processed one-step and hybrid two-step deposited Pks, and improved the transparency of the front stack electrodes and contacts through simulation-guided optimizations of the front grid and layer thicknesses. Furthermore, we investigated the stability of single-junction Pk and tandem devices under reverse-bias and standardized accelerated aging conditions.

HL 6: 2D Materials 1 (joint session HL/CPP/DS)

Time: Monday 9:30–12:45

Location: H36

Invited Talk HL 6.1 Mon 9:30 H36
g-factors in van der Waals heterostructures: revealing signatures of interlayer coupling — •PAULO E. FARIA JUNIOR — University of Regensburg, Regensburg, Germany

The interplay of the spin and the orbital angular momenta of electrons in semiconductors governs the observed Zeeman splitting, often described by the effective g-factors. In the realm of 2D materials, transition metal dichalcogenides (TMDCs) are ideal candidates to explore the manifestation of coupled spin and orbital degrees of freedom under external magnetic fields. In this talk, I will cover the basic physics behind the Zeeman splitting and effective g-factors, emphasizing the recent first-principles developments in monolayer TMDCs that nicely reproduce the available experimental data. These new theoretical insights demystify the valley-Zeeman physics in TMDCs and finally establish a connection to the vast existing knowledge in the area of III-V materials. Beyond monolayers, I will discuss TMDC-based van der Waals heterostructures, particularly $\text{MoSe}_2/\text{WSe}_2$ and $\text{WS}_2/\text{graphene}$ systems, in which the spin-valley physics and g-factors encode valuable information about the interlayer coupling.

HL 6.2 Mon 10:00 H36
Optical Properties of Encapsulated Transition-Metal Dichalcogenide Monolayers, Bilayers, and Heterostructures — •MANAN SHAH¹, PHILIP KLEMENT¹, SANGAM CHATTERJEE¹, KYUNGNAM KANG², EUI-HYEOK YANG², and ARASH RAHIMI-IMAN¹ — ¹I. Physikalisches Institut und Zentrum für Materialwissenschaften, Justus-Liebig Universität Gießen, D-35392, Germany — ²Department of Mechanical Engineering, Stevens Institute of Technology, Hoboken, NJ, 07030, USA

Van-der-Waals heterostructures (vdW-HSs) based on 2D-layered materials have received unrivaled attention among nanomaterials due to their promising optoelectronic properties induced by moiré potential landscapes; secondly, their strong light-matter interactions; and third, the promise of bandgap engineering capabilities. The optical properties of transition-metal dichalcogenides (TMDs) depend considerably on the substrate, stacking configuration, interface quality, and encapsulation. As more and more layered materials have come into the focus, the demand for a comprehensive understanding of their optical, optoelectronic, and vibronic properties is increasing drastically.

We focus on the discussion of photoluminescence and the Raman response of tungsten-based TMD monolayers and stacks thereof [1, 2], as well as encapsulated configurations. We further aim at unraveling structural alterations and emission properties by monitoring the temporal behavior in their responses.

[1] Semiconductors 2019, 53, 2140. [2] Sci. Rep. 2022, 12, 6939.

HL 6.3 Mon 10:15 H36

Electrically Tunable Photoluminescence in Monolayer MoS₂ and graphene/MoS₂ Heterostructures — •TARLAN HAMZAYEV and GIANCARLO SOAVI — Institute of Solid-State Physics, Friedrich Schiller University Jena, Germany

The optical response of monolayer (ML) transition metal dichalcogenides (TMDs) is dominated by the co-existence, even at room temperature, of excitons, bi-excitons, and trions.

The photoluminescence (PL) emission of these quasi-particles can be modulated via external knobs, such as doping, pressure and strain. In particular, the PL emission from the neutral exciton is greatly modulated during the crossover from the undoped to the highly doped regime [1]. In the latter case, PL emission is mainly suppressed due to the presence of trions, which have a fast non-radiative decay.

In this work, we study the gate dependence of the PL emission in encapsulated ML MoS₂ and ML graphene/MoS₂ heterostructures (HS). We show that in the HS region the PL emission mainly comes from neutral excitons even at large values of external gate voltage, thus confirming that graphene is an efficient filter for PL emission [2]. This work clarifies the interplay between charge transfer and PL filtering in graphene/TMD layered HS.

[1] Mak, K. F. et al. Nature materials 12, 207-211 (2013).

[2] Lorchat, E. et al. Nature Nanotechnology 15, 283-288 (2020).

15 min. break

HL 6.4 Mon 10:45 H36

Integration of Transferable Organic Semiconductor Nanosheets with 2D Materials for van der Waals Heterojunction Devices — •SIRRI BATUHAN KALKAN¹, EMAD NAJAFIDEHAGHANI², ZIYANG GAN², FABIAN ALEXANDER CHRISTIAN APFELBECK¹, UWE HÜBNER³, ANTONY GEORGE², ANDREY TURCHANIN², and BERT NICKEL¹ — ¹Faculty of Physics and CeNS, Ludwig-Maximilians-Universität, Geschwister-Scholl-Platz 1, Munich, Germany — ²Institute of Physical Chemistry and Abbe Center of Photonics, Friedrich Schiller University Jena, Lessingstr. 10, Jena, Germany — ³Leibniz Institute of Photonic Technology (IPHT), Albert-Einstein-Str. 9, 07745, Jena, Germany

Evaporation of organic semiconductors (OSC) on atomically thin transition metal dichalcogenides (TMD) for van der Waals (vdW) heterojunctions is limited by obstructed growth of the organic small molecules on the TMD surface. For the realization of such vdW heterojunction devices, we have established a transfer technique that allows for wafer-scale fabrication of 50 nm OSC nanosheets on TMDs. A key feature of this transfer is the controlled release of the ultrathin OSC film from a water-soluble sacrificial film by a suited wetting geometry. We demonstrate functional and highly ordered OSC nanosheets on prefabricated electrodes and TMD monolayers. Devices fabricated this way include unipolar, ambipolar and anti-ambipolar field-effect transistors [1].

References: [1] Kalkan et al., Wafer scale synthesis of organic semiconductor nanosheets for van der Waals heterojunction devices, npj 2D Materials and Applications 5, 92 (2021)

HL 6.5 Mon 11:00 H36

Non-resonant and resonant low-frequency Raman scattering in twisted TMDC bilayers at millikelvin temperatures — •HENDRIK LAMBERS¹, NIHIT SAIGAL¹, TORSTEN STIEHM¹, FLORIAN SIGGER², LUKAS SIGL², MIRCO TROUE², JOHANNES FIGUEIREDO², ALEXANDER HOLLEITNER², and URSULA WURSTBAUER¹ — ¹Institute of Physics, University of Münster, Münster, Germany — ²Walter Schottky Institute and Physics Department, TU Munich, Garching, Germany

Twisted TMDC bilayers are subject of many current studies because they can host many body physics and correlated phases such as superconductors and Mott insulators.[1] The moiré potential evolving with a twist angle or lattice constant mismatch could also be exploited to simulate Mott-Hubbard physics. The interlayer coupling within the bilayer correlates with the interlayer breathing mode and the shear mode, which can be characterized by low frequency Raman spectroscopy.[2] We study TMDC heterobilayers of WSe₂ and MoSe₂ by resonant and non-resonant Raman spectroscopy at millikelvin temperatures. The shear mode is resonant with the exciton transitions in both monolayers and its line-shape and transition energy are modified due to coupling to the exciton continuum. In addition, several sharp and highly resonant modes are observed in the high frequency Raman spectrum. We acknowledge financial support via DFG WU 637/7-1 and SPP2244. [1] L. Sigl et al., Phys. Rev. Research 2, 042044(R) (2020) [2] J. Holler et al., Appl. Phys. Lett. 117, 013104 (2020)

HL 6.6 Mon 11:15 H36

Investigating Twist Angle Dependence of Exciton Resonances in WSe₂/MoSe₂ Heterostructures — •CHIRAG PALEKAR, TOBIAS MANTHEI, BÁRBARA ROSA, and STEPHAN REITZENSTEIN — Institute of Solid State Physics, Technische Universität Berlin, D-10623 Berlin, Germany

Artificially produced TMDC heterostructures (HS) realized by stacking two different TMDC monolayers (ML) are a new class of promising semiconducting

heterostructures. Due to their type-II band alignment, TMDC HSs tend to host the spatially indirect interlayer excitons (IX) where electrons and holes are located in conduction and valence bands, respectively, of the different layers. Here we study the twist angle dependence of IX resonances employing micro-photoluminescence excitation (PLE) measurements on twisted WSe₂/MoSe₂ heterobilayer. PLE measurements reveal anti-correlation between linewidth and emission energy of IX. Resonant excitation at intralayer exciton energies of constituent ML yields high emission intensity of the IX with linewidth narrowing above 10 meV. We measure a drastic reduction in PL emission from IX for twist angles in the range of 10° - 50° due to large interlayer separation. Moreover, we show a noticeable IX exciton resonance separation which increases as function of twist angle i.e. from 0° (67 meV) to 24° (96 meV) along with observable red shift in IX emission energy. This fundamental study of excitons resonances deepens the current understanding of physics of twisted TMDC heterostructures and paves the way for future experiments and theoretical work.

HL 6.7 Mon 11:30 H36

Counterintuitive electric-field dependence of weak antilocalization in a bilayer graphene/WSe₂ heterostructure — JULIA AMANN¹, TOBIAS VÖLKL¹, TOBIAS ROCKINGER¹, DENIS KOCHAN², KENJI WATANABE³, TAKASHI TANIGUCHI³, JAROSLAV FABIAN², DIETER WEISS¹, and •JONATHAN EROMS¹ — ¹Institute of Experimental and Applied Physics, University of Regensburg, Regensburg, Germany — ²Institute of Theoretical Physics, University of Regensburg, Regensburg, Germany — ³National Institute for Materials Science, Tsukuba, Japan

Heterostructures of bilayer graphene (BLG) and transition metal dichalcogenides (TMDC) were recently proposed as a means of generating a gate-tunable, proximity-induced spin-orbit coupling (SOC) in graphene. Total SOC splitting of the band structure increases monotonically with the out-of-plane electric field, as confirmed by recent charge transport experiments. To elucidate the spin relaxation caused by SOC, weak antilocalization (WAL) experiments are frequently employed. Contrary to the naïve expectation of a monotonic increase of the WAL effect strength with electric field D , we observe a maximum of WAL visibility around $D = 0$. This counterintuitive behaviour originates in the intricate dependence of WAL in graphene on two different spin lifetimes τ_{sym} and τ_{asy} , which are due to spin relaxation caused by the valley-Zeeman and Rashba terms, respectively. Our calculations, based on modeling spin precession by an 8×8 Hamiltonian of BLG with one-sided TMDC show the same non-monotonic dependence on D as the experimental data.

15 min. break

HL 6.8 Mon 12:00 H36

Millikelvin Spectroscopy on Degenerate Exciton Ensembles in van der Waals Bilayers — •NIHIT SAIGAL¹, TORSTEN STIEHM¹, HENDRIK LAMBERS¹, FLORIAN SIGGER², LUKAS SIGL², MIRCO TROUE², JOHANNES FIGUEIREDO², ALEXANDER HOLLEITNER², and URSULA WURSTBAUER¹ — ¹Institute of Physics, University of Münster, Münster, Germany — ²Walter Schottky Institute and Physics Department, TU Munich, Garching, Germany

Homo- and hetero-bilayers of transition metal dichalcogenides host a rich variety of interlayer exciton (IX) species where the electrons and holes reside in different monolayers. [1] This leads to enhanced lifetimes of IXs and also imparts them with a permanent dipole moment. [1,2] Such IXs provide an ideal platform for exploring many body physics such as dipole-dipole interactions and Bose-Einstein condensation. [2] We have investigated IXs in a heterobilayer of MoSe₂ and WSe₂ encapsulated in hBN, using temperature, laser power and time dependent photoluminescence (PL) spectroscopy down to millikelvin temperatures. At lowest temperatures and exciton densities, we observe a single low energy peak in the IX PL spectrum which has been attributed to be a signature of degenerate exciton gas. [2] We observe an unexpected nearly excitation power-independent IX energies at lowest temperatures (10 mK to ~10K) that converts into the well-known dipolar blue-shift at elevated temperatures. We acknowledge financial support by DFG via WU 637/4-2 and No. HO 3324/9-2 and SPP2244.

[1] B. Miller et al., Nano Lett. 17, 5229 (2017). [2] L. Sigl et al., Phys. Rev. Research 2, 042044 (R) (2020).

HL 6.9 Mon 12:15 H36

Infrared photocurrent in transition-metal dichalcogenide heterostructures — JEONG WOO HAN¹, PEIZE HAN², YIJING LIU², PAOLA BARBARA², THOMAS E. MURPHY³, and •MARTIN MITTENDORFF¹ — ¹Universität Duisburg-Essen, Fakultät für Physik, 47057 Duisburg, Germany — ²Georgetown University, Department of Physics, Washington, 20057 DC, USA — ³University of Maryland, Institute for Research in Electronics and Applied Physics, College Park, 20740 MD, USA

Heterostructures of transition metal dichalcogenites (TMDCs) have characteristic optical properties like the interlayer excitons due to the band offset between two adjacent TMDC layers. Such heterostructures are promising candidates for photodetectors with higher efficiencies compared to a single TMDC layer, furthermore, the interlayer excitation enables photocurrents at photon energies be-

low the direct bandgap of each of the layers. Here we present measurements on a MoS_2/WS_2 heterostructure at photon energies of around 800 meV, which is significantly below the interlayer exciton. The cross-shaped structure of our samples allows measurements of the heterostructure as well as each individual layer. While at high photon energies photocurrents are observed in each of the layers, the low photon energy only leads to a photocurrent when the heterostructure is illuminated. We interpret this effect to be caused by intraband absorption and subsequent interlayer tunneling.

HL 6.10 Mon 12:30 H36

Strong exciton-plasmon coupling in hybrids of 2D semiconductors and metal supercrystals — •LARA GRETEN, ROBERT SALZWEDEL, MALTE SELIG, and ANDREAS KNORR — Institut für Theoretische Physik, Nichtlineare Optik und Quantenelektronik, Technische Universität Berlin, Hardenbergstr. 36, 10623 Berlin, Germany

Monolayers of transition metal dichalcogenides (TMDC) are direct semiconductors that exhibit tightly bound excitons with uniquely large optical amplitudes.

Thus, they are promising for optoelectronic applications and a prime example to investigate excitonic effects.

Complementary, plasmonic supercrystals, that are arrays of metal nanoparticles, support collective plasmon modes. They facilitate an impressive amplification of the electric near-field which allows to tailor electric fields on the nano-scale.

In the presented work, we theoretically consider exciton-plasmon coupling in a hybrid structure of a TMDC layer interacting with a single metal nano-particle or a two-dimensional supercrystal. For this purpose, we develop a Maxwell-Bloch theory where the excitons are described within the Heisenberg equation of motion framework and the metal nano-particles are treated as coupled dipoles in Mie theory.

Our studies reveal new "plexcitonic" eigenstates of the hybrid system. Furthermore, we are able to compute the scattered light in the near- and far-field explicitly and identify signatures of strong exciton-plasmon coupling featuring a Rabi splitting of tens of meV.

HL 7: (Quantum) Transport Properties

Time: Monday 15:00–18:00

Location: H31

HL 7.1 Mon 15:00 H31

A new Time-Domain Approach for Linear Responses and Electrical Conductivity — •MICHEL PANHANS^{1,2} and FRANK ORTMANN^{1,2} — ¹Department of Chemistry, TU München — ²Center for Advancing Electronics Dresden, TU Dresden

Linear-response theory is a powerful theoretical framework to investigate, e.g., electrical and magnetic transport and to compare theory with experiments. Many intriguing quantum-transport phenomena such as quantum Hall effects, spin Hall effects, and quantum spin Hall effects have been derived within this framework. Beyond the general theory, strong efforts have been spent in the last decade to develop efficient and accurate computational methods to calculate charge transport in condensed matter. [1] In our recent work, we present a new time-domain approach to calculate arbitrary linear responses, which is based on a decomposition of the general Kubo formula into time-symmetric and time-antisymmetric parts. [2] The new algorithm is at least 1000 times faster compared to former time evolution schemes. [3] As a showcase, we have investigated the quantum anomalous Hall effect of the disordered Haldane model, where the quantum dynamics of the topological state have been analyzed. The proposed theory and the computational method provide a promising route to access transport phenomena in complex and topological systems.

[1] Z. Fan et al., *Physics Reports*, 903, 1-69 (2021)

[2] M. Panhans and F. Ortmann, *Phys. Rev. Lett.* 127, 016601 (2021)

[3] F. Ortmann et al., *Phys. Rev. B* 91, 165117 (2015)

HL 7.2 Mon 15:15 H31

Anomalous photo-Nernst currents in HfTe_5 — •WALDEMAR SCHMUNK, MAANWINDER SINGH, ALEXANDER HOLLEITNER, and CHRISTOPH KASTL — Walter Schottky Institut

Recently, strong evidence of a quasi-quantized 3D quantum Hall effect in non-magnetic semimetals HfTe_5 and ZrTe_5 has been reported by various groups. Plateau-like features in the Hall conductivity of HfTe_5 and ZrTe_5 point towards unconventional Hall physics in these 3D semimetals. Additionally, in high-density HfTe_5 crystals, an anomalous, but non-hysteretic, Hall conductivity has been reported as well, which points to a non-zero Berry curvature. Here, we present photocurrent measurements of thin HfTe_5 films in an external magnetic field. We find a localized edge photo response with opposite polarity at opposite edges. We interpret these edge photocurrents in terms of an anomalous Nernst current arising from the local excitation, the symmetry breaking at the edges, and the anomalous Hall conductivity. Such local photocurrents open the possibility to image anomalous Hall responses and possible related edge state physics in layered quantum materials.

HL 7.3 Mon 15:30 H31

Aharonov-Bohm oscillations and phase-coherence analysis in selectively grown topological-insulator rings — •GERRIT BEHNER, DENNIS HEFFELS, JONAS KÖLZER, KRISTOFF MOORS, ABDUR REHMAN JALIL, ERIK ZIMMERMANN, GREGOR MUSSLER, DETLEV GRÜTZMACHER, HANS LÜTH, and THOMAS SCHÄPERS — Peter Grünberg Institut (PGI-9), Forschungszentrum Jülich, 52425 Jülich, Germany

The study of quantum-interference effects in 3D topological insulators is crucial for understanding their transport properties. We present low-temperature magneto-transport measurements on selectively-grown Sb_2Te_3 ring structures. Pronounced Aharonov-Bohm oscillations in the conductance are observed with a major contribution of surface-state transport. The surface contributions are determined from magnetotransport under the application of an in-plane magnetic

field. Furthermore we determine the phase-coherence length by analysing universal conductance fluctuations. Finally, we perform quantum transport simulations based on tight-binding calculations using KWANT. The simulations allow us to reproduce the predominant features of the experimental data and further deepen the understanding of the underlying physical effects.

HL 7.4 Mon 15:45 H31

Tunneling spectroscopy simulations of topological insulator (TI) nanoribbons — •DENNIS HEFFELS¹, DECLAN BURKE², MALCOLM R. CONNOLLY², PETER SCHÜFFELGEN¹, KRISTOF MOORS¹, and DETLEV GRÜTZMACHER¹ — ¹PGI-9, FZ Jülich — ²IC London

TI nanoribbons with proximity-induced superconductivity have been proposed as a possible platform for the realization of Majorana bound states (MBS). Attempts to detect these MBS have received much attention in solid-state physics in recent years. A major goal is to exploit their unusual non-Abelian statistics for topologically protected quantum computing. A very common method for the detection of MBS is tunneling spectroscopy. Implementing this experimental scheme with TI nanoribbons is very challenging, due to stringent requirements on the interfaces of the required heterostructure. Similar experiments on semiconductor nanowires have shown that careful interpretation of the measured data is of prime importance. Here, we present simulations that are tailored to support such tunneling spectroscopy experiments on TI nanoribbons that are proximitized via the top surface with a superconductor. We show that a 3D simulation of the TI-based tunnel junction device is essential to properly describe the proximity effect and disorder, which plays a crucial role. Interestingly, the absence or presence of a zero-bias conductance peak does not always reveal whether the system is in the trivial or the topological regime. We obtain a phase diagram of subgap features in the tunneling conductance as a function of magnetic field and Fermi level.

HL 7.5 Mon 16:00 H31

Transport in high mobility HgTe heterostructures — •MICHAEL KICK, LENA FÜRST, JOHANNES KLEINLEIN, SAQUIB SHAMIM, HARTMUT BUHMANN, and LAURENS W. MOHLENKAMP — Experimentelle Physik III, Physikalisches Institut, Universität Würzburg, Am Hubland, 97074

The Fractional Quantum Hall Effect (FQHE) has not yet been observed in the material system of HgTe. Due to recent progress in MBE growth, routinely charge carrier mobilities of HgTe heterostructures of over $\mu > 1 \cdot 10^6 \text{ cm}^2/\text{Vs}$ are obtained which is in the same order of magnitude as in the first reported experimental observation of the FQHE in GaAs/GaAlAs heterostructures. This opens up new prospects for transport investigations into the long time still open question of fractional states in this material system.

In 2-dimensional HgTe quantum wells, transport measurements show well pronounced quantum Hall plateaus for all filling factors, but no indication of any fractional state. High magnetic field measurements show a prolonged $\nu = 1$ plateau and a transition to an insulating state. Intriguingly, the $\nu = 1$ plateau exhibits a transition to an insulating state for filling factor $\nu = 1/2$.

Another possibility to observe the FQHE in HgTe is provided by the 2D surface states of a 3D topological insulator. High mobility layers, $\mu > 2 \cdot 10^6 \text{ cm}^2/\text{Vs}$, of tensile strained HgTe are subject of extensive magneto-transport investigations. First results reveal so far unresolved features predicted by recent band structure calculations, while the search for FQHE states is still on.

30 min. break

HL 7.6 Mon 16:45 H31

Structure-imposed electronic topology in cove-edged graphene nanoribbons — •FLORIAN ARNOLD¹, TSAI-JUNG LIU¹, AGNIESZKA KUC², and THOMAS HEINE^{1,2,3} — ¹Technische Universität Dresden, Dresden, Germany — ²HZDR, Leipzig, Germany — ³Yonsei University, Seoul, Republic of Korea

Cove-edged zigzag graphene nanoribbons (ZGNR-C) take their name from a regular pattern of coves which is formed by removing one terminal CH group per length unit on each zigzag edge. Based on three structural parameters that unambiguously characterize the atomistic structure of ZGNR-C, we present a scheme that classifies their electronic state, i.e., if they are metallic, topological insulators or trivial semiconductors, for all possible widths N , unit lengths a and cove position offsets at both edges b , thus showing the direct structure-electronic structure relation. We further present an empirical formula to estimate the band gap of the semiconducting ribbons from N , a , and b . Finally, we show possible ribbon terminations, which should give guidance for future synthetic efforts to realize new topological ZGNR-C with large band gap and to realize topologically protected edge states in these systems.

HL 7.7 Mon 17:00 H31

Temperature and magnetic field-dependent noise measurements in GaAs/AlGaAs quantum rings — •BIRKAN DÜZEL¹, OLIVIO CHIATTI¹, SVEN S. BUCHHOLZ¹, ANDREAS D. WIECK², DIRK REUTER³, and SASKIA F. FISCHER¹ — ¹Novel Materials Group, Humboldt-Universität zu Berlin, 10099 Berlin, Germany — ²Angewandte Festkörperphysik, Ruhr-Universität Bochum, 44780 Bochum, Germany — ³Optoelektronische Materialien und Bauelemente, Universität Paderborn, 33098 Paderborn, Germany

Nanostructured materials offer a way to investigate phase-coherent transport of electrons and the resulting interference effects in systems. Measurements of the white noise have been used to determine system properties such as the electron temperature T_e . Recently noise measurements in quantum ring structures have revealed white noise exceeding the expected thermal noise [1].

This work investigates the dependence of the excess noise in quantum rings on the bath temperature and applied magnetic field. Noise measurements in $\text{Al}_x\text{Ga}_{1-x}\text{As}/\text{GaAs}$ -based etched quantum rings are performed in equilibrium with bath temperatures ranging from 15 mK to 4.2 K and magnetic fields ranging from -50 mT to 50 mT. Additionally, magnetotransport measurements are performed at 1 K with magnetic fields ranging from 0 T to 12 T.

[1] C. Riha *et al.*, Appl. Phys. Lett. **117**, 063102 (2020).

HL 7.8 Mon 17:15 H31

Coplanar waveguides for electronic measurements at terahertz frequencies — •SERGEY LAVRENTYEV¹, JOHANNES GRÖBMEYER¹, GERHARD HUBER², and ALEXANDER HOLLEITNER¹ — ¹Walter Schottky Institut and Physics Department, TU Munich — ²Walther-Meißner-Institut and Physics Department, TU Munich

We explore the usability of gold coplanar waveguides on a sapphire substrate as contacts for electronic transport measurements on 2D and topological mate-

rials in the terahertz regime. Our simulations reveal different modes with low attenuation. For the coplanar waveguide, we find the lowest attenuation in even modes compared to the predominance of odd modes in coplanar strip geometries. Moreover, our results show a frequency dependent behavior of the complex refractive index of the modes at sub-millimeter wavelengths. We find that gold coplanar waveguides are well suited for electronic measurements at terahertz frequencies.

HL 7.9 Mon 17:30 H31

Influence of fixed scatterers of various sizes and densities on the giant negative magnetoresistance in two dimensional electron gases. — •JANUS LAMMERT¹, BEATE HORN-COSFELD¹, JAKOB SCHLUCK¹, MIHAI CERCHEZ¹, THOMAS HEINZEL¹, KLAUS PIERZ², HANS WERNER SCHUMACHER², and DOMINIQUE MAILLY³ — ¹Institut für Experimentelle Physik der kondensierten Materie, Heinrich-Heine-Universität, Universitätsstraße 1, 40225 Düsseldorf, Germany — ²Physikalisch-Technische Bundesanstalt, Bundesallee 100, 38116 Braunschweig, Germany — ³CNRS, Univ. Paris-Sud, Université Paris-Saclay, C2N Marcoussis, 91460 Marcoussis, France

The giant negative magnetoresistance (GNMR) in a 2DEG is studied through the effects produced by artificial scatterers (Lorentz arrays [1]) with varying scatterer density. The influence of the different types and ratios of scattering mechanisms shed light on both the temperature independent and the temperature dependent parts of the GNMR [2]. The effect of scattering on the shape and amplitude of the GNMR will be discussed. [1] H. A. Lorentz, Proc. R. Acad. Sci. Amsterdam **7**, 438, 1905, [2] B. Horn-Cosfeld et al. Phys. Rev. B **104**, 045306, 2021

HL 7.10 Mon 17:45 H31

First-principles calculations of temperature-dependent transport in semiconductors — DAN HAN, ANDREAS HELD, •MASAKO OGURA, and HUBERT EBERT — Ludwig-Maximilians-University Munich, Munich, Germany

The carrier mobility is one of the central properties of semiconductors. So far, most first-principles calculations of carrier mobilities for bulk semiconductors are based on the Boltzmann transport equation. In this contribution, we present an alternative scheme to evaluate temperature dependent carrier mobilities.

As a starting point, we calculate the electronic structures using the Korringa-Kohn-Rostoker (KKR) Green's function method in combination with the coherent potential approximation (CPA) alloy theory allowing for chemical as well as temperature induced disorder in the material. Dealing with undoped elemental or compound systems, we account this way for lattice vibrations, i.e. atom displacements depending on temperature, which affect the electronic structure and also cause a finite electric resistivity. The corresponding electric conductivity is calculated by means of the Kubo-Greenwood formula implemented on the basis of the KKR-CPA. The carrier mobility is evaluated from the resulting temperature-dependent conductivity and carrier concentration. Results for the intrinsic transport properties of undoped elemental and compound semiconductors will be presented.

HL 8: Quantum Dots and Wires 2: Optics 1

Time: Monday 15:00–18:15

Location: H32

Invited Talk

HL 8.1 Mon 15:00 H32

Crux of Using the Cascaded Emission of a Three-Level Quantum Ladder System to Generate Indistinguishable Photons — •EVA SCHÖLL^{1,2}, LUCAS SCHWEICKERT², LUKAS HANSCHKE^{1,3}, KATHARINA D. ZEUNER², FRIEDRICH SBRESNY³, THOMAS LETTNER², RAHUL TRIVEDI⁴, MARCUS REINDL⁵, SAIMON FILIPE COVRE DA SILVA⁵, RINALDO TROTTA⁶, JONATHAN FINLEY³, JELENA VUČKOVIĆ⁴, KAI MÜLLER³, ARMANDO RASTELLI⁵, VAL ZWILLER², and KLAUS D. JÖNS^{1,2} — ¹PhoQS, CeOPP, and Department of Physics, Paderborn University, Germany — ²KTH Stockholm, Sweden — ³WSI, MCQST and TUM Munich, Germany — ⁴Stanford University, California, USA — ⁵JKU Linz, Austria — ⁶Sapienza University Rome, Italy

Single and indistinguishable photons are basic building blocks for many quantum technology applications. Here (PRL, **125**, 233605 (2020)), we investigate the degree of indistinguishability of cascaded photons emitted from a three-level quantum ladder system; in our case the biexciton-exciton cascade of semiconductor quantum dots. Despite unprecedented single-photon purity, we theoretically show that the indistinguishability for both emitted photons is inherently limited by the ratio of the lifetimes of the excited and intermediate states. We confirm this finding both experimentally and with quantum optical simulations by comparing the quantum interference visibility of cascaded and noncascaded exciton emission of the same quantum dot. Based on our model, we propose photonic structures or stimulated emission (PRL, **128**, 093603, (2022)) from the excited to the intermediate state to increase the lifetime ratio and overcome the limited indistinguishability.

HL 8.2 Mon 15:30 H32

Carrier dynamics in quantum-dot tunnel-injection structures: microscopic theory and experiment — •MICHAEL LORKE¹, IGOR KHANONKIN², STEPHAN MICHAEL¹, JOHANN PETER REITHMAIER³, GADI EISENSTEIN², and FRANK JAHNKE¹ — ¹Institute for Theoretical Physics, University of Bremen, Otto-Hahn-Allee 1, Bremen, 28359, Germany — ²Electrical Engineering Department and Russel Berrie Nanotechnology Institute, Technion, Haifa, 32000, Israel — ³Technische Physik, Institute of Nanostructure Technologies and Analytics, Center of Interdisciplinary Nanostructure Science and Technology (CINSaT), University of Kassel, Kassel, 34132, Germany

Among the challenges for the next generation of semiconductor lasers is the enhancement of their modulation speed to satisfy the need for higher data transfer rates. For this purpose, tunnel injection lasers are an appealing concept, as they promise improved modulation rates and better temperature stability. Moreover, they eliminate a major detrimental effect of quantum dot lasers, which is the gain nonlinearity caused by hot carriers. It is shown in this work how the aforementioned improvements depend on the design of tunnel-injection devices. We perform a theory-experiment comparison on scattering times in tunnel injection devices to highlight the importance of alignment between the injector well and the quantum dot ensemble. It is shown how differences in the coupling to the injector quantum well caused by the alignment lead to scattering times into the quantum dot ensemble that vary by an order of magnitude.

HL 8.3 Mon 15:45 H32

Statistical limits for entanglement swapping with independent semiconductor quantum dots — •JINGZHONG YANG¹, MICHAEL ZOPF¹, PENGJI LI¹, NAND LAL SHARMA², WEIJIE NIE², FREDERIK BENTHIN¹, TOM FANDRICH¹, EDDY PATRIC RUGERAMIGABO¹, CASPAR HOPFMANN², ROBERT KEIL², OLIVER G. SCHMIDT^{2,3,4}, and FEI DING^{1,5} — ¹Institut für Festkörperphysik, Leibniz Universität Hannover, Appelstraße 2, 30167 Hannover, Germany — ²Institute for Integrative Nanosciences, Leibniz IFW Dresden, Helmholtzstraße 20, 01069 Dresden, Germany — ³Material Systems for Nanoelectronics, Technische Universität Chemnitz, 09107 Chemnitz, Germany — ⁴Nanophysics, Faculty of Physics and Würzburg-Dresden Cluster of Excellence ct.qmat, TU Dresden, 01062 Dresden, Germany — ⁵Laboratorium für Nano- und Quantenengineering, Leibniz Universität Hannover, Schneiderberg 39, 30167 Hannover, Germany

Semiconductor quantum dots are promising constituents for future quantum communication. Here we explore the limits for sources of polarization-entangled photons from biexciton-exciton cascade of the quantum dots. We stress the necessity of tuning the exciton fine structure, and explain why the time evolution of photonic entanglement in quantum dots is not applicable for large quantum networks. We identify the critical device parameters and present a numerical model for benchmarking the device scalability in order to bring the realization of distributed semiconductor-based quantum networks one step closer to reality.

HL 8.4 Mon 16:00 H32

Maximally entangled and GHz-clocked on-demand photon pair source — •CASPAR HOPFMANN¹, WEIJIE NIE¹, NAND LAL SHARMA¹, CARMEN WEIGEL¹, FEI DING², and OLIVER G. SCHMIDT^{1,3,4} — ¹Institute for Integrative Nanosciences, Leibniz IFW Dresden, Helmholtzstr. 20, 01069 Dresden, Germany — ²Institut für Festkörperphysik, Leibniz Universität Hannover, Appelstr. 2, 30167 Hannover, Germany — ³Material Systems for Nanoelectronics, Technische Universität Chemnitz, 09107 Chemnitz, Germany — ⁴Nanophysics, Faculty of Physics and Würzburg-Dresden Cluster of Excellence ct.qmat, TU Dresden, 01062 Dresden, Germany

We present a 1 GHz-clocked, maximally entangled and on-demand photon pair source based on droplet etched GaAs quantum dots using two-photon excitation. By employing these GaP microlens-enhanced devices in conjunction with their substantial brightness, raw entanglement fidelities of up to 0.95 and post-selected photon indistinguishabilities of up to 0.93, the suitability for quantum repeater based long range quantum entanglement distribution schemes is shown. Comprehensive investigations of a complete set of polarization selective two-photon correlations facilitate an innovative method to determine the extraction and excitation efficiencies directly - opposed to commonly employed indirect techniques. Additionally, time-resolved analysis of Hong-Ou-Mandel interference traces reveal an alternative approach to the investigation of pure photon dephasing.

HL 8.5 Mon 16:15 H32

Photoneutralization of charges in GaAs quantum dot based entangled photon emitters — JINGZHONG YANG¹, TOM FANDRICH¹, •FREDERIK BENTHIN¹, ROBERT KEIL², NAND LAL SHARMA², WEIJIE NIE², CASPAR HOPFMANN², OLIVER G. SCHMIDT^{2,3,4}, MICHAEL ZOPF¹, and FEI DING^{1,5} — ¹Institut für Festkörperphysik, Leibniz Universität Hannover, Germany — ²Institute for Integrative Nanosciences, Leibniz IFW Dresden, Germany — ³Material Systems for Nanoelectronics, Technische Universität Chemnitz, Germany — ⁴Nanophysics, Faculty of Physics and Würzburg-Dresden Cluster of Excellence ct.qmat, TU Dresden, Germany — ⁵Laboratorium für Nano- und Quantenengineering, Leibniz Universität Hannover, Germany

Semiconductor-based quantum dot emitters are an attractive source for generating pairwise photonic entanglement and a promising constituent of photonic quantum technologies. However, quantum dots typically suffer from luminescence blinking, lowering the efficiency of the source and hampering their scalable application in quantum networks. We investigate the spectral and quantum optical response of the quantum dot emission by introducing an additional wavelength tunable gate laser. Under two-photon resonant excitation of the neutral biexciton in a GaAs/AlGaAs quantum dot, the blinking of the neutral exciton emission was observed. Our finding demonstrates that the emission blinking can be actively suppressed by controlling the balance of free electrons and holes in the vicinity of the quantum dot thereby significantly increasing the quantum efficiency by 30%.

30 min. break

HL 8.6 Mon 17:00 H32

Franson interference on a resonantly driven biexciton cascade — •MARCEL HOHN¹, KISA BARKEMEYER², MATTHIAS KUNZ¹, ARSENY KAGANSKIY¹, SAMIR BOUNOUAR¹, ALEXANDER CARMELE², SVEN RODT¹, and STEPHAN REITZENSTEIN¹ — ¹Institut für Festkörper Physik, Technische Universität Berlin, 10623 Berlin, Germany — ²Institut für Theoretische Physik, Technische Universität Berlin, 10623 Berlin, Germany

The deterministic generation of entangled photon pairs is of special interest for applications in quantum communication and computation. As many experi-

ments focus on entanglement in the polarization base, energy-time entangled photons used for Franson interference offer the advantage of high robustness in long-distance fiber transmission. We report on Franson measurements performed in cw mode on the resonantly driven biexciton cascade of a deterministically fabricated quantum dot device. The two-photon visibility of such a three-level system crucially depends on the decay rates of the ideally long upper- and short living intermediate state [1]. A relation hard to achieve for the biexciton cascade, where the lifetime of the biexciton state is usually short compared to the exciton state. Nevertheless, our measurements yield a high two-photon visibility up to $(73 \pm 2)\%$, surpassing the CHSH inequality of 70.7% [2]. This result demonstrates the high potential of generating energy time entangled photons in a resonantly driven biexciton cascade.

[1] K. Barkemeyer, et al., Phys. Rev. A, 103, 62423 (2021)

[2] J. F. Clauser, et al., Phys. Rev. Lett. 23, 880 (1969)

HL 8.7 Mon 17:15 H32

Red Detuned Excitation of a Quantum Dot — •YUSUF KARLI¹, FLORIAN KAPPE¹, THOMAS BRACHT², JULIAN MÜNZBERG¹, TIM SEIDELMANN³, VOLLRATH MARTIN AXT³, SAIMON COVRE DA SILVA⁴, ARMANDO RASTELLI⁴, VIKAS REMESH¹, DORIS REITER⁵, and GREGOR WEIHS¹ — ¹Institute für Experimentalphysik, Universität Innsbruck, Innsbruck, Austria — ²Institut für Festkörpertheorie, Universität Münster, Münster, Germany — ³Theoretische Physik III, Universität Bayreuth, Bayreuth, Germany — ⁴Institute of Semiconductor and Solid State Physics, Johannes Kepler University Linz, Linz, Austria — ⁵Condensed Matter Theory, Department of Physics, TU Dortmund, Dortmund, Germany

Semiconductor quantum dots have emerged as promising sources of highly indistinguishable single photons. To operate as an on-demand photon source, a quantum dot must be prepared in its exciton state, for which, several protocols exist. A recent remarkable theoretical discovery, also presented at this conference, showed that the exciton state in a quantum dot can be efficiently populated by two red-detuned pulses in a swing-up mechanism. We demonstrate the experimental implementation of this mechanism relying on amplitude-shaping of a broadband laser pulse in a 4f shaper including a spatial light modulator. The decisive advantage of our scheme is that both pulses are red-detuned and therefore, no higher-lying states of the quantum dot will be directly addressed. Our results contribute towards an effortless method for generating high-purity single photons, yet most importantly, removing the need for stringent polarization filtering.

HL 8.8 Mon 17:30 H32

Dephasing mechanisms revealed by two-photon coincidence measurements — •JULIAN WIERCINSKI, MORITZ CYGOREK, and ERIK M. GAUGER — SUPA, Institute of Photonics and Quantum Sciences, Heriot-Watt University, Edinburgh, UK

Cooperative effects of entangled quantum emitters play a key role in quantum technologies like, e.g., quantum computing and are known to influence their light emission as well as absorption - a key ingredient for highly efficient quantum batteries and light harvesting complexes. Only recently, cooperative emission of two quantum dots has been observed experimentally.

Inspired by these results we use numerically complete methods to theoretically investigate the impact of different dephasing mechanisms on the cooperative emission of two quantum dots. We show that different dephasing mechanisms lead to severe qualitative differences in the two-photon coincidence signals. These can be explained by the influence of dephasing on the dynamics of the inter-emitter entanglement. Therefore, we argue, two-photon coincidence measurements make dephasing visible in the experiment acting as a probe for underlying dephasing mechanisms.

HL 8.9 Mon 17:45 H32

Bandwidth Limit in Optically Detected Single Electron Tunneling Events — •JENS KERSKI¹, HENDRIK MANNEL¹, PIA LOCHNER¹, ERIC KLEINHERBERS¹, ANNIKA KURZMANN², ARNE LUDWIG³, ANDREAS D. WIECK³, JÜRGEN KÖNIG¹, AXEL LORKE¹, and MARTIN GELLER¹ — ¹Faculty of Physics and CENIDE, University of Duisburg-Essen, Germany — ²2nd Institute of Physics, RWTH Aachen University, Germany — ³Chair of Applied Solid State Physics, Ruhr-University Bochum, Germany

Measurements of single quantum processes have recently attracted increasing attention. One example is the counting of single electron tunnel events in quantum dots. These individual quantum jumps are usually measured electrostatically. However, new optical detection methods have been developed that promise higher time resolution, although their potential has not yet been fully investigated. Here, we study the resonance fluorescence of the excitonic transition from a self-assembled quantum dot embedded in a tailored diode structure.

We detect the optical signal with single photon resolution and use a post-processing procedure to identify the optimal bandwidth for the analysis of our data. We demonstrate that we can evaluate our data with up to 175 kHz bandwidth and show how the chosen bandwidth affects the determined tunneling rates and the evaluation by full counting statistics. Using a simple model, we discuss how the Poisson distribution of the photons limits the time resolution

even in ideal measurements and propose how a time resolution of more than 1 MHz could be achieved.

HL 8.10 Mon 18:00 H32

The Origin of Antibunching in Resonance Fluorescence — •LUKAS HANSCHKE^{1,2}, LUCAS SCHWEICKERT³, JUAN CAMILO LÓPEZ CARREÑO⁴, EVA SCHÖLL^{1,3}, KATHARINA D. ZEUNER³, THOMAS LETTNER³, EDUARDO ZUBIZARRETA CASALENGUA⁴, MARCUS REINDL⁵, SAIMON FILIPE COVRE DA SILVA⁵, RINALDO TROTTA⁶, JONATHAN J. FINLEY², ARMANDO RASTELLI⁵, ELENA DEL VALLE^{4,7}, FABRICE P. LAUSSY^{4,8}, VAL ZWILLER³, KAI MÜLLER², and KLAUS D. JÖNS¹ — ¹PhoQS, CeOPP, and Department of Physics, Paderborn University, Germany — ²WSI, MCQST and TU Munich, Germany — ³KTH Stock-

holm, Sweden — ⁴University of Wolverhampton, UK — ⁵JKU Linz, Austria — ⁶Sapienza University Rome, Italy — ⁷Universidad Autónoma de Madrid, Spain — ⁸Moscow, Russia

We present measurements that prove that the simultaneous observation of sub-natural linewidth and antibunching of resonance fluorescence is not possible. High-resolution spectroscopy reveals the sharp spectral feature of the weak driving regime with a vanishing component of incoherently scattered light. Filtering the emission in the order of the Fourier limited linewidth leads to the loss of antibunching in the correlation measurement. Our theoretical model identifies two-photon interference between the coherent and incoherently scattered light as the origin of antibunching. This prefigures schemes to achieve a source of single photons with sub-natural linewidth [PRL 123, 170402 (2020)].

HL 9: Focus Session: Exceptional Points and Non-Hermitian Physics in Semiconductor Systems

The strong recent interest into nonconservative/non-Hermitian systems and their exotic degeneracies - so-called exceptional points - is driven by the occurrence of rather unconventional and fascinating physics and by potential applications such as ultrasensitive sensing, orbital angular momentum lasers, and topological energy transfer for mode and polarization conversion. This Focus Session aims at discussing the latest experimental and theoretical results in the rapidly developing field with special focus on semiconductor systems, where engineering the interplay of coupling, dissipation and amplification mechanisms offers novel opportunities. Moreover, we give an overview to young scientists of the exciting possibilities of interdisciplinary research in this field.

Organized by Sebastian Klemmt and Jan Wiersig

Time: Monday 15:00–17:30

Location: H33

Invited Talk HL 9.1 Mon 15:00 H33

Exceptional points in optics: From bulk materials to one-dimensional confined systems — •CHRIS STURM — Felix Bloch Institute for Solid State Physics, Universität Leipzig, Leipzig, Germany

The research of exceptional points (EP) was initiated by W. Voigt in 1902 when he discovered that for certain directions in orthorhombic crystals only one circular polarized eigenstate exists, as soon as absorption sets in [1]. These directions corresponds to EPs in the momentum space. The presence of such EP is not limited to orthorhombic crystals only and appears in many optical systems. Here we present an overview of the appearance and the properties of these EPs in bulk crystal and optically one-dimensional confined systems. We show that the properties of the EPs in bulk crystals are determined by the dielectric function and the symmetry of the crystal, which allows to distinguish between optically biaxial materials having triclinic, monoclinic or orthorhombic crystal symmetry. In the presence of an optical confinement, like in thin films or microresonators, EPs can even appear in systems consisting of optically uniaxial materials, which was recently observed experimentally (e.g. Ref. [2]). Furthermore, in contrast to bulk crystals, the properties of the EPs are determined not only by the dielectric function of the materials but depends also on the design of the system, e.g. film thickness and confinement properties.

[1] W. Voigt, Ann. Phys. **314**, 367 (1902).

[2] S. Richter, Phys. Rev. Lett. **123**, 227401 (2019).

Invited Talk HL 9.2 Mon 15:30 H33

Complex Skin Modes in Non-Hermitian Coupled Laser Arrays — •MERCEDEH KHAJAVIKHAN and YUZHOU LIU — 1002 Childs Way, Los Angeles, CA 90089

In the realm of non-Hermitian physics, the possibility of complex and asymmetric exchange interactions between a network of oscillators has been theoretically shown to lead to novel behaviors like delocalization, skin effect, and bulk-boundary correspondence. While the ramifications of these theoretical works in optics have been recently pursued in synthetic dimensions, the Hatano-Nelson model has yet to be realized in real space. In this work, by using active optical oscillators featuring non-Hermiticity and nonlinearity, we introduce an anisotropic exchange between the resonant elements in a lattice, an aspect that enables us to observe the non-Hermitian skin effect, phase locking, and near-field beam steering in a Hatano-Nelson laser array. This work can open up new regimes of phase-locking in lasers while shedding light on the fundamental physics of non-Hermitian systems.

15 min. break

Invited Talk HL 9.3 Mon 16:15 H33

Non-Hermitian effects in exciton polaritons — •ELIEZER ESTRECHO — ARC Centre of Excellence in Future Low-Energy Electronics Technologies and Department of Quantum Science and Technology, Research School of Physics, The Australian National University, Canberra, ACT 2601, Australia

I will present our experimental results highlighting non-Hermitian effects in exciton-polariton systems—quasiparticles arising from the strong coupling of

excitons in semiconductors and photons in a cavity. This hybrid system is naturally non-Hermitian due to inherent loss and gain. The former arises from photon leakage through the cavity mirrors and the short lifetime of excitons, while the latter arises from an external pump used to maintain the density, for example, in the creation of Bose-Einstein condensates.

Using exciton-polariton condensates, we demonstrate exceptional points in the deformation parameter space of a quantum billiard. In particular, we are able to trace the energy levels close to the exceptional point, observe the topological Berry phase, and demonstrate the chirality of the state.

We also observe exceptional points in momentum space. By studying the energy and pseudospin structure, we directly measured a novel non-Hermitian topological invariant and differentiated it from its Hermitian counterparts. Furthermore, we also observe an anomalous dispersion resulting from the dissipative coupling of excitons and photons. The resulting inverted dispersion leads to a negative-mass propagation where the particles move in the opposite direction to their momentum.

Invited Talk HL 9.4 Mon 16:45 H33

Nonlinear dynamics and exceptional points in exciton-polariton condensates — •STEFAN SCHUMACHER — Physics Department & CeOPP, Paderborn University, Germany

Non-Hermitian physics and exceptional points have attracted significant attention in the past two decades. Enormous progress has been made for example in non-Hermitian optics. Non-Hermitian degeneracies and exceptional points have also been demonstrated for exciton polaritons in semiconductor microcavities [1]. For non-resonant excitation, polaritons can spontaneously exhibit macroscopic coherence, known as polariton condensation. The non-equilibrium nature of polariton condensates makes them perfect for studies of non-Hermitian physics. The gain can be tailored by varying the spatial optical pump profile, for example allowing realization of PT-symmetric lattices [2]. The polariton-polariton interaction gives rise to inherently nonlinear phenomena such as vortex formation [3]. Recently, we reported the observation of an exceptional point in a double-well potential [4]. There, the polariton condensate can be localized in one well and switched off by an additional optical excitation in the other well that surprisingly induces additional loss [4]. The nonlinearity and related energy blueshift also allows to approach the exceptional point. This work paves the way to explore non-Hermitian physics in a system with strong nonlinearity and in tailored potential energy landscapes. [1] T. Gao et al., Nature **526**, 554-558 (2015). [2] X. Ma et al., New Journal of Physics **21**, 123008 (2019). [3] X. Ma et al., Nature Communications **11**, 897 (2020). [4] Y. Li et al., arXiv:2101.09478 (2021).

HL 9.5 Mon 17:15 H33

Exceptional points in anisotropic ZnO thin films — •SEBASTIAN HENN, EVGENY KRÜGER, CHRIS STURM, and MARIUS GRUNDMANN — 1 Universität Leipzig, Faculty of Physics and Earth Sciences, Felix Bloch Institute for Solid State Physics, Linnéstr. 5, 04103 Leipzig, Germany

In this talk we present findings regarding the existence of exceptional points in anisotropic thin films. Analogous to degeneracies of optic axes in absorptive bi-

axial materials, so-called singular optic axes [1], anisotropic transparent structures contain exceptional points in momentum space, where two orientation- and polarization-dependent modes are equal in resonance energy and lifetime. The latter is determined by dissipative photon loss at the interfaces, which renders the system non-Hermitian. This phenomenon has been observed in dielectric optical microcavities [2] and principally exists also in anisotropic thin films, where resonances correspond to well-known Fabry-Pérot modes. We show re-

sults of rigorous calculations for *m*-ZnO thin films, based on scattering matrices whose complex poles correspond to the resonance energies. This allows to find exceptional points in two-dimensional momentum space and we confirm important characteristics, such as a square-root topology and circularity.

[1] Grundmann et al., Phys. Status Solidi RRL 11.1 1600295 (2017)

[2] S. Richter et al., Phys. Rev. Lett. 123 227401 (2019)

HL 10: Nitrides

Time: Monday 15:00–18:30

Location: H34

HL 10.1 Mon 15:00 H34

Degradation of the electrooptical properties of UVB LEDs observed by temperature dependent electroluminescence spectroscopy — •JAKOB HÖPFNER¹, PRITI GUPTA¹, MARTIN GUTTMANN¹, JAN RUSCHEL², JOHANNES GLAAB², TIM KOLBE², ARNE KNAUER², TIM WERNICKE¹, MARKUS WEYERS², and MICHAEL KNEISSL^{1,2} — ¹Technische Universität Berlin, Institute of Solid State Physics, Berlin, Germany — ²Ferdinand-Braun-Institut, Berlin, Germany

The operation of UVB-LEDs induces changes in their electrooptical characteristics, especially a gradual reduction in the emission power. As the lifetime of a device is a key property for its application, it is important to understand the microscopic processes governing their degradation behavior. We report an investigation on UVB-LEDs emitting at 310 nm before and after aging for 1000 h at 100 mA (67 Acm⁻²) and a heatsink temperature of 70 °C using temperature(T)-dependent electroluminescence spectroscopy from 20 K - 340 K. Before aging, the external quantum efficiency (EQE) at 10 mA gradually increases with decreasing temperature from 0.8 % at 340 K to 1.8 % at 150 K and stays at that level for lower temperatures, indicating that EQE(T) is dominated by the radiative recombination efficiency. After 1,000 h of operation, the EQE has reduced to 0.45 % at 340 K and it shows a maximum of 1.4 % at 80 K. Also below 80 K, the EQE again decreases. These findings suggest a stress-induced reduction of both the radiative recombination efficiency and the carrier injection efficiency.

HL 10.2 Mon 15:15 H34

Short pulse operation of (Al,In)GaN laser diodes to increased linewidth and decreased coherence for laser displays — •JANNINA J. TEPASS¹, LUKAS UHLIG¹, DOMINIC KUNZMANN¹, GEORG BRÜDERL², and ULRICH T. SCHWARZ¹ — ¹Institute of Physics, Chemnitz University of Technology, 09126 Chemnitz, Germany — ²ams OSRAM Group, 93055 Regensburg, Germany

Red, green, and blue (RGB) laser diodes are used as the light source in laser displays in particular laser glasses for augmented, virtual, and mixed reality (AR/VR/MR). A narrow linewidth and corresponding high coherence will lead to speckles and non-uniform scattering at the gratings used for the projection into the eye box. Therefore, it is necessary to enhance the spectral linewidth of each laser diode to about 10 nm.

Mode competition causes a dynamic broadening of the laser spectrum already to about 1 nm. Here, we explore short pulse modulation to further increase the linewidth. A wavelength chirp at the beginning of each pulse is generating additional broadening at a pulse length of the order of a few nanoseconds. This chirp is the consequence of overshooting the carrier density above the threshold carrier density, resulting in a blue-shifted gain spectrum.

We investigate these broadening effects in blue and green (Al,In)GaN and red (Al,Ga)InP laser diodes with the help of a streak camera experiment. We took measurements for varying pulse length to analyse the spectral changes of those laser diodes and the behaviour with different pulse length.

HL 10.3 Mon 15:30 H34

Investigation of lateral charge carrier diffusion via micro-photoluminescence in InGaN MQWs and SQWs — •CONNY BECHT¹, ULRICH T. SCHWARZ¹, MICHAEL BINDER², BASTIAN GALLER², JÜRGEN OFF², MAXIMILIAN TAUER², ALVARO GOMEZ IGLESIAS², HENG WANG², and MARTIN STRASSBURG² — ¹Institute of Physics, Chemnitz University of Technology, 09126, Chemnitz, Germany — ²ams-OSRAM International GmbH, Leibnizstr. 4, 93053 Regensburg, Germany

InGaN multi-quantum well (MQW) structures are used to obtain highly efficient blue light emitting diodes (LED). After the injection of carriers into the active layer of blue LEDs, a part of the carriers diffuses laterally before recombining (non-)radiatively. The diffusion behaviour in InGaN MQWs is up to now poorly understood.

In this study InGaN MQWs and single QWs (SQW) are investigated by micro-photoluminescence at room temperature. To study the diffusion behaviour, the excitation spot is decoupled from the detection area, which we call a pinhole scan. With the size of the excitation spot known, conclusions about the diffusion length of the charge carriers after optical pumping can be drawn. For deeper analysis of the diffusion behaviour the excitation density is varied and an external bias can be applied in addition.

The results show a long-range diffusion up to several 10 μm's. The energy shows a increasing blue shift with higher excitation power at the center (i.e. excitation spot).

HL 10.4 Mon 15:45 H34

Threshold and gain measurements of AlGaIn-based UVC lasers — •MARKUS BLONSKI¹, GIULIA CARDINALI¹, BERND WITZIGMANN², NORMAN SUSILO¹, DANIEL HAUER VIDAL¹, MARTIN GUTTMANN¹, TIM WERNICKE¹, and MICHAEL KNEISSL¹ — ¹Technische Universität Berlin, Institute of Solid State Physics, Berlin, Germany — ²Department Elektrotechnik-Elektronik-Informationstechnik (EEI), University Erlangen-Nürnberg (FAU), Erlangen, Germany

Recently, first UVC laser diodes were demonstrated, with relatively high threshold current densities and pulsed operation. Critical parameters affecting the threshold are the electron and hole wavefunctions overlap and the optical confinement factor. While thicker quantum wells (QWs) yield higher confinement factors, the wavefunctions overlap in AlGaIn QWs thicker than 3 nm is reduced due to the quantum-confined Stark effect (QCSE). In this work, the influence of QW thickness on lasing threshold and optical gain in AlGaIn-based optically pumped lasers with SQWs between 3 nm and 12 nm emitting at 275 nm is studied. The lasing peak shifts to shorter wavelengths with respect to the spontaneous emission in thin wells, while the widest wells exhibit a red-shift. Similar lasing threshold power density was observed for all samples at around 1.4 MW cm⁻². Variable stripe length method measurements showed positive net gain in all the samples with comparable values of differential net gain. Simulations of the material gain show that higher energy states contribute to the gain in wider wells, whereas in the 3 nm AlGaIn QW the ground state provides the gain.

HL 10.5 Mon 16:00 H34

Drift-diffusion simulation of UVC-LEDs with varied emission wavelength — •F. BILCHENKO¹, A. MUHIN¹, M. GUTTMANN^{1,2}, T. WERNICKE¹, F. RÖMER³, B. WITZIGMANN³, and M. KNEISSL^{1,2} — ¹Technische Universität Berlin, Institute of Solid State Physics, Berlin, Germany — ²Ferdinand-Braun-Institut, Leibniz-Institut für Hochfrequenztechnik, Berlin, Germany — ³Friedrich-Alexander-Universität Erlangen-Nürnberg, Lehrstuhl für Optoelektronik, Erlangen, Germany

The external quantum efficiency (EQE) of AlGaIn-based deep ultraviolet (UVC) light emitting diodes (LEDs) decreases strongly for emission wavelengths (λ) below 240 nm by two orders of magnitude from 1% (240 nm) to 0.01% (217 nm). We showed that the light extraction efficiency (LEE) on wafer level decreases only by a factor of less than 3 from 4% (240 nm) to 1.5% (217 nm), leaving current injection efficiency (CIE) and radiative recombination efficiency (RRE) as possible major causes for the EQE decrease. In order to estimate the contribution of the CIE and RRE to the EQE we analyse measured electroluminescence characteristics by simulating an LED-series with nominally identical heterostructure but varying AlGaIn composition in the active region in order to achieve λ ranging from 217 nm to 263 nm. Our results suggest that, in this wavelength range, the change in CIE contributes greatly to the decrease in EQE. For devices emitting at 263 nm and 249 nm the CIE stays roughly constant at around ~50%, showing a significant decrease towards shorter λ, i.e. 48% at 240 nm and 2% at 217 nm. Based on these results, it appears that improvement of the CIE is paramount for achieving high-power UVC-devices.

HL 10.6 Mon 16:15 H34

Realizing tunnel junctions in AlGaIn-based UVC light emitting diodes emitting at 232 nm — •VERENA MONTAG¹, FRANK MEHNKE¹, MARTIN GUTTMANN², LUCA SULMONI¹, CHRISTIAN KUHN¹, JOHANNES GLAAB², TIM WERNICKE¹, MARKUS WEYERS², and MICHAEL KNEISSL^{1,2} — ¹Technische Universität Berlin, Institute of Solid State Physics, Hardenbergstraße 36, 10623 Berlin, Germany — ²Ferdinand-Braun-Institut, Gustav-Kirchhoff-Straße 4, 12489 Berlin, Germany

An ultraviolet C (UVC)-transparent p-AlGaIn layer is needed to overcome the strong absorption of p-layers in deep UV light emitting diodes (LEDs). However, transparent p-AlGaIn layers exhibit high sheet and contact resistances resulting in very large operating voltages. A promising alternative to standard p-contacts is the injection of holes into the AlGaIn quantum well by tunnel heterojunctions

(TJs). This allows for low resistivity n-layers and n-contacts on both sides of the device. We have successfully demonstrated fully transparent AlGaIn-based TJ-LEDs emitting at 232 nm grown entirely by metal-organic vapor phase epitaxy. A thin GaN interlayer was implemented to enhance carrier tunneling at the TJ interface. Typically, the operating voltages, the output powers and the external quantum efficiencies of a 0.15 mm² TJ-LED featuring a 8 nm thick GaN interlayer are 24 V, 77 μ W and 0.29%, respectively, measured on wafer at 5 mA in cw operation. This is the first reported TJ-LED in the wavelength range below 240 nm.

15 min. break

HL 10.7 Mon 16:45 H34

Influence of the AlGaIn MQW growth temperature on the performance characteristics of DUV-LEDs with emission at 235 nm — •MARCEL SCHILLING, NORMAN SUSILO, GIULIA CARDINALI, ANTON MUHIN, FRANK MEHNKE, TIM WERNICKE, and MICHAEL KNEISSL — Technische Universität Berlin, Institute of Solid State Physics, Hardenbergstraße 36, 10623 Berlin, Germany

The realization of efficient deep ultraviolet light emitting diodes (DUV-LEDs) with emission wavelength near 235 nm is very challenging as the photon energy is very close to the band gap of AlN. For AlGaIn layers with high Al mole fractions point defects like vacancies and impurities are easily incorporated during metal organic vapor phase epitaxy (MOVPE). Deep levels in the energy band gap associated with these point defects play a decisive role in non-radiative carrier recombination and consequently low internal quantum efficiency (IQE) of DUV-LEDs. Therefore, the understanding of the generation of point defects during the growth of high Al containing AlGaIn layers is crucial for the development of efficient DUV-LEDs. In this study the influence of the AlGaIn MQW growth temperature on the point defect density in 235 nm DUV-LEDs is investigated. DUV-LEDs were grown by MOVPE with MQW growth temperatures between 850 °C and 1100 °C. Temperature dependent PL measurements show that the point defect incorporation might be controlled with the MOVPE growth temperature. Electroluminescence measurements showed an increase in optical output power from 5 μ W up to 300 μ W at 20 mA for 235 nm DUV-LEDs for increasing MQW growth temperatures from 850 °C up to 1020 °C.

HL 10.8 Mon 17:00 H34

Temperature dependent electroluminescence spectroscopy on AlGaIn-based 235nm far-UVC LEDs with different active region growth temperature — •PAULA VIERCK, JAKOB HÖPFNER, MARTIN GUTTMANN, MARCEL SCHILLING, LUCA SULMONI, ANTON MUHIN, TIM WERNICKE, and MICHAEL KNEISSL — Technische Universität Berlin, Institute of Solid State Physics, Berlin, Germany Light emitting diodes (LEDs) emitting in the far ultraviolet-C (far-UVC) spectral range are promising for applications such as sensing and monitoring of gases, and skin safe disinfection. To improve their external quantum efficiency (EQE), it is crucial to understand the influence of growth parameters on their performance. In this paper, AlGaIn-based LEDs emitting around 235 nm were investigated, while their active region growth temperature (T_{growth}) was varied between 900 °C and 1100 °C. Temperature dependent light output power-current-voltage characteristics (LIV) and spectra were measured on-wafer for temperatures between 100 K and 340 K. An increasing EQE was observed for increasing T_{growth} up to 1060 °C with a maximum value of 0.25 % at room temperature. This increase in EQE is attributed to a reduced point defect incorporation at higher active region growth temperatures. This finding is supported by a shift of the EQE vs. temperature maximum from a sample stage temperature of 220 K for an active region growth temperature of 900 °C to 260 K for an active region growth temperature of 1060 °C indicating an increased radiative recombination efficiency as a consequence of reduced point defect incorporation.

HL 10.9 Mon 17:15 H34

UVC-LEDs grown on HTA-AlN templates with low dislocation densities and high Si doping for strain management — •SARINA GRAUPETER¹, MICHAEL GAIL¹, GIULIA CARDINALI¹, MASSIMO GRIGOLETTO^{1,2}, SYLVIA HAGEDORN², TIM WERNICKE¹, MARKUS WEYERS², and MICHAEL KNEISSL^{1,2} — ¹Technische Universität Berlin, Institute of Solid State Physics, Hardenbergstraße 36, 10623 Berlin, Germany — ²Ferdinand-Braun-Institut (FBH), Gustav-Kirchhoff-Straße 4, 12489 Berlin, Germany

High temperature annealing (HTA) of AlN layers reduces the threading dislocation density of such layers on sapphire substrates below 10⁹ cm⁻² enabling UVC-LEDs with improved efficiencies. However, the HTA AlN-layers are under high compressive strain after cooling down, which leads to strain relaxation and defect formation during further LED heterostructure growth. Growing Si-doped AlN layers on HTA-AlN can reduce the strain. In this work we investigate the influence of such an AlN:Si-interlayer on the growth of UVC-LEDs emitting at 265nm on HTA AlN/sapphire templates, with different thicknesses and offset angles. XRD measurements show a reduction of the compressive strain from 0.5% to 0.1% depending on layer thickness. Optical characterization with Photoluminescence and Cathodoluminescence shows, that depending on the layer thickness, defect formation in the form of Ga-rich plateaus occurs. Electro-

luminescence measurements of full UVC-LED structures shows emission powers around 0.75mW at 20mA for the templates with 350nm layer thickness, which is comparable to LEDs grown on more expensive standard templates.

HL 10.10 Mon 17:30 H34

Distributed polarization doping for 265 nm UVC LEDs — •MASSIMO GRIGOLETTO^{1,2}, SARINA GRAUPETER¹, ANTON MUHIN¹, FEDIR BILCHENKO¹, EVIATHAR ZIFFER¹, NORMAN SUSILO¹, TIM WERNICKE¹, and MICHAEL KNEISSL^{1,2} — ¹Technische Universität Berlin, Institute of Solid State Physics, 10623 Berlin, Germany — ²Ferdinand-Braun-Institut, 12489 Berlin, Germany

Distributed polarization doping (DPD) for optoelectronic devices with high aluminium mole fractions in AlGaIn alloys is a promising concept for achieving high hole densities and simultaneously minimize the light absorption on the p-side. A continuous grading downward from an higher to a lower aluminium mole fraction in the alloy composition of the AlGaIn layer, leads to a steady piezoelectric polarization change creating a negative net charge that is compensated by free holes. In this way, dopant-free without thermal activation is possible, which can exhibit orders of magnitude higher hole densities than comparable magnesium impurity doped AlGaIn layers.

In this study we investigate the influence of the DPD graded layer design on the electro optical properties and material properties of 265 nm AlGaIn-based LEDs by varying the thickness and aluminium gradient. The LED heterostructures with and without the different DPD-layers are grown by metal organic vapor phase epitaxy and analyzed by electroluminescence measurements, transmission spectroscopy, high resolution X-ray diffraction, atomic force microscopy, capacitance voltage spectroscopy and determination of sheet and contact resistance.

HL 10.11 Mon 17:45 H34

Temperature dependent photoluminescence spectroscopy of self-assembled InGaIn superlattices embedded in GaN Nanowires — •RUDOLFO HÖTZEL¹, MANUEL ALONSO ORTS¹, TIM GRIEB², JÖRG SCHÖRMANN¹, STEPHAN FIGGE¹, and MARTIN EICKHOFF¹ — ¹University of Bremen, Institute of Solid State Physics, 28359 Bremen, Germany — ²I. Physikalisches Institut, Justus-Liebig-Universität, Heinrich-Buff-Ring 16, 35392 Giessen, Germany

In this work, the structure and optical properties of single InGaIn/GaN Nanowires grown by plasma assisted molecular beam epitaxy have been analyzed by micro photoluminescence (PL), scanning transmission electron microscopy (STEM) and energy dispersive X-rayspectroscopy (EDX). These nanowires consist of an indium rich core that contains a self assembled InGaIn superlattice within a GaN shell. In order to understand the origin of their optical properties, PL was combined with STEM analysis to identify single nanowire structures. Temperature-dependent as well as polarized PL were conducted on isolated nanowires and revealed an emission consisting of broader bands at room temperature and multiple narrow peak superpositions at low temperatures. The overall emission ranges from 1,8 eV up to 2,9 eV. One contributing factor to their emission is the indium distribution within the superlattice, which was determined by EDX. A polarization dependence of the PL signal with respect to the growth direction was observed at 4K and room temperature and ascribed to the indium rich core (parallel contributions) and self assembled superlattice (perpendicular contributions).

HL 10.12 Mon 18:00 H34

Luminescence Characteristics of GaInN/GaN Multi Quantum Wells with Ga and N Polarity — •SAMAR HAGAG, MALTE SCHRADER, HEIKO BREMERS, UWE ROSSOW, and ANDREAS HANGLEITER — Institut f. Angewandte, TU Braunschweig, Germany

The optical properties of Ga- and N-polar GaInN/GaN Multi Quantum Wells (MQW) grown on sapphire and bulk N-polar GaN substrates, respectively, using metal-organic chemical vapor deposition were investigated using photoluminescence (PL) and time-resolved photoluminescence (TRPL) spectroscopy. The low temperature PL spectrum of N-polar GaInN/GaN MQW showed a reduced PL intensity and broad emission peak compared to their Ga-polar counterparts and shorter PL decay times of N-polar GaInN/GaN MQW were observed in low temperature TRPL measurements. Using non-resonant excitation, N-polar GaN PL spectra at low temperature have shown the presence of luminescence lines associated with structural defects of the type II basal-plane stacking faults. The low PL intensity and short PL decay time at low temperature of N-polar GaInN/GaN MQW indicate the existence of non-radiative recombination at low temperature likely caused by partial dislocations associated with the stacking faults. For the fabrication of pyramidal nanostructures serving as nanooptical light emitters, wet etching of N-polar GaInN/GaN MQW in KOH solution has been used. The etched N-polar samples have shown an improved luminescence and the absence of stacking fault-related luminescence lines. Optimization of the growth procedure for N-polar GaInN/GaN MQW is required in order to reduce structural defects.

HL 10.13 Mon 18:15 H34

Pump-probe studies with varying excitation wavelengths applied for GaInN/GaN single quantum wells — •MALTE SCHRADER, RODRIGO DE VASCONCELLOS LOURENCO, HEIKO BREMERS, UWE ROSSOW, and ANDREAS HANGLEITER — Institut für Angewandte Physik & Laboratory for Emerging Nanometrology, Technische Universität Braunschweig, Germany

The goal of this study is to characterize the ultra-fast carrier dynamics in c-plane GaInN/GaN single quantum wells (SQWs). To make transmission experiments possible the samples were grown on double-side polished sapphire by MOVPE. Furthermore we use time-resolved photoluminescence (TRPL) to measure the radiative and non-radiative carrier lifetimes of the samples from 5 K up to 300

K. By using a transmission-mode degenerate pump-probe technique at 300 K the generated state occupation in the SQW can be observed directly. Different excitation wavelengths produced using an optical parametric amplifier provided pulses of nominal 35 fs duration.

We observe carrier lifetimes at room temperature in the low ns range by TRPL, which are strongly impacted by nonradiative processes. Pump-probe at 300 K gives a fast characteristic relaxation time in the low ps range and a slower component associated with the decay observed in TRPL. This indicates that a fast initial non-equilibrium relaxation is followed by a component representing recombination of a quasi-equilibrium carrier ensemble. A surprising observation is the relatively slow relaxation time of a few ps, which one would rather expect to be in the femtosecond range.

HL 11: 2D Materials 2 (joint session HL/ CPP/DS)

Time: Monday 15:00–18:30

Location: H36

HL 11.1 Mon 15:00 H36

On-demand light emission from helium ion induced defects in atomically thin WS₂ — •NINA PETTINGER, ANA MICEVIC, ALEXANDER HÖTGER, CHRISTOPH KASTL, and ALEXANDER HOLLEITNER — TU Munich, Germany

Optically active defects created with a helium ion microscope (HIM) propose the possibility for structuring and tailoring quantum emitters on an atomistic scale [1]. We introduce the generation of positioned defects in encapsulated monolayer WS₂ with a HIM. The HIM induced defects exhibit sharp photoluminescence emission in the energy range of 1.55 to 1.79 eV.

[1] J. Klein and L. Sigl et al., ACS Photonics 8, 669 (2021).

HL 11.2 Mon 15:15 H36

Concept of an all-optical THz near-field microscope for flakes of 2D materials — •AHMAD-REZA ETEMADI, SEBASTIAN MATSCHY, AHANA BHATTACHARYA, and MARTIN MITTENDORFF — Department of physics, University of Duisburg-Essen, 47057 Duisburg, Germany

While THz spectroscopy is an excellent tool to investigate the free charge carriers in many semiconducting materials, the long-wavelength is an inherent feature linked to a large spot size in the millimeter range, and thus large samples are required. Small flakes of two-dimensional materials exfoliated from bulk crystals are usually much smaller than the spot size of a conventional THz spectrometer. The direct detection of the THz signal in the vicinity of the flake gains the phase and amplitude information with a higher spatial resolution. This is accessible by placing the sample directly on top of an electro-optic crystal. Sampling the THz field at the flake position gives access to the complex conductivity and thus the carrier density as well as the carrier mobility. A frequency-doubled fiber laser with a pulse duration of about 80 fs at 780 nm is exploited to generate and sample the THz field. GaSe, and ZnTe are employed as electro-optic crystals. Here we present the current state of the near-field microscope and the first measurements of the spatial resolution. The experimental results are accompanied by rigorous modeling of the THz propagation within the electro-optic crystal.

HL 11.3 Mon 15:30 H36

Ab initio description of valley-selective circular dichroism — •MAXIMILIAN SCHEBEK¹, YIMING PAN², CECILIA VONA¹, CLAUDIA DRAXL¹, and FABIO CARUSO² — ¹Institut für Physik and IRIS Adlershof, Humboldt-Universität zu Berlin, Berlin, Germany — ²Institut für Theoretische Physik und Astrophysik, Christian-Albrechts-Universität zu Kiel, Kiel, Germany

By enabling control of valley degrees of freedom, valley-selective circular dichroism (VSCD) has become a key concept in valleytronics. In this work, we present an *ab initio* many-body theory of VSCD based on the Bethe-Salpeter equation. Our approach provides a new route to accurately predict the degree of valley polarization upon absorption of circularly polarized light. With the example of monolayer transition-metal dichalcogenides, we further show that valley excitons - bound electron-hole pairs formed at either the K or \bar{K} valley upon absorption of circularly-polarized light - are chiral quasiparticles characterized by a finite orbital angular momentum (OAM). Beside governing the interaction with circularly polarized light, the OAM results in a finite magnetization of excitons, which in turn provides a route for the interaction of excitons with external magnetic fields and other spin-orbital degrees of freedom.

HL 11.4 Mon 15:45 H36

Dark and bright exciton dynamics probed by time-resolved photoluminescence in hBN-encapsulated MoWSe₂ monolayers — •JULIAN SCHRÖBER^{1,3}, JOANNA KUTROWSKA-GIRZYCKA², LESZEK BRYJA², JOANNA JADCAK², and JÖRG DEBUS¹ — ¹TU Dortmund, Experimentelle Physik 2, AG Debus — ²Wrocław University of Science and Technology, Department of Experimental Physics — ³Universität Rostock, Institut für Physik, AG Korn: Zweidimensionale Kristalle und Heterostrukturen

Semiconducting monolayers of ternary MoWSe₂ alloys combine the unique properties of the binary transition metal dichalcogenide (TMDC) materials

MoSe₂ and WSe₂. The alloying leads to, for example, brightening of the momentum- and spin-forbidden dark exciton states. Detailed studies on the dynamics of these brightened dark states are missing. We report on the exciton and trion formation lying in the 1-3 ps range, while the decay time approaches hundreds picoseconds. Additionally, strong dependences on the temperature and exciting laser light polarization are observed. In time-resolved and stationary photoluminescence measurements, we reveal the impact of the crystal disorder potential on the exciton properties. The polarization dynamics of the exciton and trion photoluminescence indicate possible contributions from chiral phonons as well as electrons and holes from different valleys of the Brillouin zone. Our work is a further step towards a deeper understanding of the dynamics of dark excitons in TMDC materials.

15 min. break

HL 11.5 Mon 16:15 H36

Signatures of a degenerate many-body state of interlayer excitons in a van der Waals heterostack — •JOHANNES FIGUEIREDO¹, LUKAS SIGL¹, FLORIAN SIGGER¹, JONAS KIEMLE¹, MIRCO TROUPE¹, URSULA WURSTBAUER², and ALEXANDER HOLLEITNER¹ — ¹Walter-Schottky-Institut, Technical University of Munich — ²Institute of Physics, Westfälische Wilhelms-Universität Münster

In atomistic van der Waals heterostacks of transition metal dichalcogenides, the reduced dimensionality and changing dielectric environment leads to the formation of strongly bound excitons. Optically generated interlayer excitons exhibit an additional spatial separation of the electron-hole pair with a reduced overlap of the electrons' and holes' wave-functions, evidenced through their long lifetimes. These long-lived, photogenerated composite bosons yield several signatures of a quantum degenerate many-body system at cryogenic temperatures. The emergence of this state is in accordance with theoretical predictions of a critical condensation temperature above 10K. We present new insights into the phase-diagram of such interlayer exciton ensembles. [1]

[1] L. Sigl et al., Phys. Rev. Research 2, 042044(R) (2020)

HL 11.6 Mon 16:30 H36

exciton species in highly doped WS₂ monolayers — DAVID TIEDE, •HOSSEIN OSTOVAR, HENDRIK LAMBERS, NIHIT SAIGAL, and URSULA WURSTBAUER — Institute of Physics, University of Münster, Münster, Germany

Semiconducting two-dimensional transition metal dichalcogenides such as WS₂ excel due to their exciton dominated light-matter interaction even at room temperature (RT) that is highly tunable by external stimuli such as doping, light excitation, dielectric environment, or strain [1]. In this work, an optimized field effect structure utilizing a polymer electrolyte top gate electrode is employed to study the evolution of the optical response in monolayer WS₂ at RT in dependence of doping by means of photoluminescence and spectroscopic imaging ellipsometry measurements. The huge geometrical gate capacitance enables capacitance spectroscopy of the conduction band as well as valence band edge yielding a gap energy of 2.6eV in agreement with the determination from the exciton Rydberg series. The gate allows the injection of large electron and hole densities exceeding 10^{14} cm^{-2} , sufficient to enable the exciton Mott transition. The obtained doping dependent emission and absorption spectra also facilitate the identification of phonon activated, neutral and charged exciton species as well as dressed excitons in a fermi sea. We acknowledge financial support via DFG WU 637/7-1 and SPP2244. [1] U. Wurstbauer et al. J. Phys. D: Appl. Phys. 50, 173001 (2017).

HL 11.7 Mon 16:45 H36

Pump probe signatures of interlayer excitons in TMDC heterostructures — •HENRY MITTENZWEY, MANUEL KATZER, ANDREAS KNORR, and MALTE SELIG — Institut für Theoretische Physik, Nichtlineare Optik und Quantenelektronik, Technische Universität Berlin, Hardenbergstr. 36, 10623 Berlin, Germany

TMDC heterobilayers are promising candidates for novel optoelectronic applications, since they exhibit long-lived excitonic states with spatially separated electrons and holes located in different layers. The relaxation dynamics of these interlayer excitons and their interplay with intralayer excitons are still under investigation.

Here, we present a microscopic description for the phonon and tunneling induced formation and relaxation of intra- and interlayer excitons in a $\text{MoSe}_2/\text{WSe}_2$ stack. Based on the microscopic dynamics we calculate the pump probe signal for intra- and interlayer transition and their population dynamics including hot exciton bottleneck effects.

HL 11.8 Mon 17:00 H36

Angle- and polarization-resolved luminescence from suspended and hBN encapsulated MoSe_2 monolayers — •BO HAN¹, SVEN STEPHAN¹, JOSHUA J.P. THOMPSON², MARTIN ESMANN¹, CARLOS ANTÓN-SOLANAS¹, HANGYONG SHAN¹, SAMUEL BREM³, CHRISTOPH LIENAU¹, KENJI WATANABE⁴, TAKASHI TANIGUCHI⁴, MARTIN SILIES¹, ERMIN MALIC^{2,3}, and CHRISTIAN SCHNEIDER¹ — ¹Carl von Ossietzky Universität, Oldenburg, Germany. — ²Philipps Universität, Marburg, Germany. — ³Chalmers University of Technology, Gothenburg, Sweden. — ⁴National Institute for Materials Science, Tsukuba, Japan.

We apply combined angle- and polarization-resolved spectroscopy to explore the interplay of excitonic physics and phenomena arising from the commonly utilized encapsulation on the optical properties of atomically thin transition metal dichalcogenides. In our study, we probe MoSe_2 monolayers which are prepared in both a suspended and an encapsulated manner. We show that the hBN encapsulation significantly enhances the linear polarization of exciton PL at large emission angles. This degree of linear polarization of excitons can increase up to 17% in the hBN encapsulated samples. As confirmed by finite-difference time-domain simulations, it can be directly connected to the optical anisotropy of the hBN layers. In comparison, the linear polarization at finite exciton momenta is significantly reduced in suspended MoSe_2 monolayer, and only becomes notable at cryogenic conditions. This phenomenon strongly suggest that the effect is rooted in the k -dependent anisotropic exchange coupling inherent in 2D excitons.

15 min. break

HL 11.9 Mon 17:30 H36

Photonic and Phononic Couplings in Hybrid High-Q Nanocavities with Encapsulated MoS_2 Monolayer — •CHENJIANG QIAN¹, VIVIANA VILLAFANE¹, PEDRO SOUBELET¹, ALEXANDER HÖTGER¹, TAKASHI TANIGUCHI², KENJI WATANABE², NATHAN WILSON¹, ANDREAS STIER¹, ALEXANDER HOLLEITNER¹, and JONATHAN FINLEY¹ — ¹Walter Schottky Institut und Physik Department, Am Coulombwall 4, 85748 Garching, Germany — ²National Institute for Materials Science, 1-1 Namiki, Tsukuba 305-0044, Japan

Monolayer TMDs are ideal active materials for solid-state cQED. However, the direct coupling of TMDs to 0D nanocavities whilst preserving pristine excitonic properties and large cavity-TMD overlap remains a challenge. Most commonly, non-encapsulated TMDs are stacked on top of prefabricated photonic structures using pick-and-place assembly. In this case, environmental disorders strongly perturb the excitonic properties. Whilst disorder can be mitigated by full hBN encapsulation, this approach moves the TMD away from the cavity field, thereby, trading spatial coupling for homogeneous linewidth. Here, we integrate hBN/ MoS_2 /hBN heterostructures to Si_3N_4 nanobeams as hybrid nanocavities. Our approach solves the trade-off problem by making the unpatterned heterostructure a functional part of the cavity field. Therefore, the pristine excitonic quality, high cavity mode Q-factor > 10000, and the strong cavity- MoS_2 overlap are achieved simultaneously. We study the coupling of MoS_2 excitons to the cavity optical and vibrational modes using PL and Raman spectroscopy, and novel coupling phenomena are observed based.

HL 11.10 Mon 17:45 H36

Terahertz free carrier absorption to modulate the optical properties of nanometer-thick van der Waals semiconductors — •TOMMASO VENANZI^{1,2}, MALTE SELIG³, ALEXEJ PASHKIN², STEPHAN WINNERL², MANUEL KATZER³, HIMANI ARORA², ARTUR ERBE², AMALIA PATANE⁴, ZAKHAR R. KUDRYNSKYI⁴,

ZAKHAR D. KOVALYUK⁵, LEONETTA BALDASSARRE¹, ANDREAS KNORR³, MANFRED HELM², and HARALD SCHNEIDER² — ¹Sapienza University of Rome, 00185 Rome, Italy — ²Helmholtz-Zentrum Dresden-Rossendorf, 01328 Dresden, Germany — ³Technical University Berlin, 10623 Berlin, Germany — ⁴University of Nottingham, Nottingham NG7 2RD, UK — ⁵The National Academy of Sciences of Ukraine, 58001 Chernivtsi, Ukraine

Free carriers in doped semiconductors absorb terahertz radiation when the frequency of the electromagnetic field is lower or comparable to the plasma frequency of the system. This phenomenon can be used to manipulate the optical response of the material. We present here the results of two different experiments performed at the infrared free-electron laser FELBE on atomically-thin van der Waals semiconductors. In MoSe_2 monolayers, we observe a terahertz-induced redshift of the trion resonance. Terahertz absorption induces an average high momentum to the carriers and this momentum gets transferred during the trion formation, resulting in a net redshift in the absorption. In few-layer InSe, the terahertz pulses induce a transient quenching of the photoluminescence emission. In both cases, a microscopic study of the hot carrier distribution cooling is also presented.

HL 11.11 Mon 18:00 H36

Theory of Exciton-Phonon Interaction for Stationary State Experiments in Atomically Thin Semiconductors — •MANUEL KATZER, ANDREAS KNORR, and MALTE SELIG — Nichtlineare Optik und Quantenelektronik, Technische Universität Berlin, Hardenbergstr. 36, 10623 Berlin, Germany

Atomically thin semiconductors exhibit tightly bound electron hole pairs which stimulated exciton research in recent years [1]. While typical experimental techniques include the cw excitation of the material, only few are known theoretically about the related exciton dynamics and the formation of non-equilibrium steady states. Based on excitonic Boltzmann scattering equations, we demonstrate that the formation of such stationary states is also accompanied with the formation of phonon replica in the photoluminescence excitation spectrum [2], in agreement with available experiments [3]. So far, many studies focused on the understanding of exciton dynamics in the limit of weak excitation. Above this limit, we find both bosonic but also fermionic contributions to the thermalization, due to the co-bosonic nature of excitons. Based on a Heisenberg equation of motion ansatz [4], we discuss the first order of non-linear exciton-phonon interaction exceeding the classical Boltzmann scattering limit, in order to analyze the exciton thermalization at elevated excitation densities.

[1] Wang et al. RMP, 90, 021001 (2018). [2] Selig et al. arXiv:2201.03362 (2022). [3] Chow et al., Nano Lett. 17, 1194 (2017); Shree et al. PRB 98, 035302 (2018). [4] Selig et al. PRR, 1, 022007 (2019); Katsch et al., PRL 124 25 257402 (2020).

HL 11.12 Mon 18:15 H36

Ultrafast control of spins in transition metal dichalcogenides — •ABHIJEET KUMAR¹, DENIS YAGODKIN¹, DOUGLAS J. BOCK¹, NELE STETZUHN^{1,2}, SVIATOSLAV KOVALCHUK¹, ALEXEY MELNIKOV³, PETER ELLIOTT², SANGEETA SHARMA², CORNELIUS GAHL¹, and KIRILL I. BOLOTIN¹ — ¹Department of Physics, Freie Universität Berlin, 14195 Berlin, Germany — ²Max-Born-Institut für Nichtlineare Optik und Kurzzeitspektroskopie, Max-Born Straße 2a, 12489 Berlin, Germany — ³Institute for Physics, Martin Luther University Halle, 06120 Halle, Germany

Control and manipulation of the coupled spin/valley degrees of freedom in transition metal dichalcogenides (TMDs) are essential for their applications in spin/valleytronics. Here, we achieve ultrafast control of spins in TMDs via two distinct approaches, namely, proximity-coupling to another TMD and strain. First, we use a type-II heterostructure $\text{MoS}_2 - \text{MoSe}_2$ to enable directional optical pumping of spin-polarized carriers. We find that the photoexcited carriers conserve their spin for both tunneling directions across the interface. We observe dramatic differences in the spin/valley depolarization rates for electrons and holes, 30 and <1 ns⁻¹, respectively, which relates to the disparity in the spin-orbit splitting in conduction and valence bands of TMDs. Second, by applying biaxial strain (exceeding 2%) in monolayer WSe_2 , we evidence the hybridization of the conduction bands with the in-gap localized defects that brightens the lowest-lying dark excitons. This novel hybrid state exhibits unique spin/valley signatures which are strongly manipulated on picosecond-timescale by strain and doping.

HL 12: Quantum Dots and Wires 3: Growth

Time: Tuesday 9:30–12:45

Location: H32

Invited Talk

HL 12.1 Tue 9:30 H32

Wafer-Scale Epitaxial Modulation of Quantum Dot Density — •NIKOLAI BART¹, CHRISTIAN DANGEL², PETER ZAJAC¹, NIKOLAI SPITZER¹, MARCEL SCHMIDT¹, KAI MÜLLER^{2,3}, ANDREAS D. WIECK¹, JONATHAN FINLEY², and ARNE LUDWIG¹ — ¹Ruhr-Universität Bochum, Lehrstuhl für Angewandte Festkörperphysik, Universitätsstraße 150, 44801 Bochum, Germany — ²Walter

Schottky Institut und Physik Department, Technische Universität München, Am Coulombwall 4, 85748 Garching, Germany — ³Walter Schottky Institut und Department of Electrical and Computer Engineering, Technische Universität München, Am Coulombwall 4, 85748 Garching, Germany

The effect of nanoscale surface roughness on the nucleation of self-assembled InAs quantum dots (QD) is investigated with photoluminescence (PL) spec-

troscopy and atomic force microscopy. We show in-situ control of the roughness modulation by common epitaxial layer-by-layer growth, leaving alternating atomically smooth (rough) surfaces for integer (fractional) completion of a monolayer. We report significant differences in both PL intensity and QD surface density at the critical threshold of nucleation. By varying the underlying GaAs thickness gradients, we create and control 1- and 2-dimensional density modulation patterns on entire 3-inch wafers with modulation periods between a few mm and down to hundreds of μm and densities between 1 and 10 QDs/ μm^2 . Bart, N., Dangel, C. et al. Wafer-scale epitaxial modulation of quantum dot density. *Nat Commun* **13**, 1633 (2022).

HL 12.2 Tue 10:00 H32

Full Wafer Property Control of Local Droplet Etched GaAs Quantum Dots — •HANS-GEORG BABIN, NIKOLAI BART, MARCEL SCHMIDT, NIKOLAI SPITZER, ANDREAS D. WIECK, and ARNE LUDWIG — Ruhr-Universität Bochum, Deutschland

Local droplet etched GaAs quantum dots (LDE-QDs) are a promising candidate for excellent single and entangled photon sources [1]. It is important that the carefully developed and highly complex structures are matched perfectly with the embedded QDs [2]. In this submission, we show a way to control QD properties during molecular beam epitaxy on a single wafer, which opens the opportunity to find optimally fitting QDs for the desired experiments by just changing the position on the wafer.

We induce flux gradients by stopping sample rotation and using the parallax of the effusion-cells, resulting in a gradual change of deposited material and cell flux. By this we can vary properties of the QDs like density and emission wavelength on a single wafer. In this work, the widest achieved wavelength shift of the ground state emission energy at 100 K extends over the range of 795 nm to 737 nm [3]. The induced surface roughness modulation additionally induces a stripe-patterned modulation, which was shown before only with Stranski-Krastanov QDs [4].

- [1] Huber, D. et al., *Nat. Commun.* 8 (1), S. 15506 (2017).
- [2] Zhai, L. et al., *Nat. Commun.* 11 (1), S. 4745 (2020).
- [3] Babin, H.G. et al., *J. Cryst. Growth* 591, S. 126713 (2022).
- [4] Bart, N.; Dangel, C.; et al., *Nat. Commun.* 13, 1663 (2022).

HL 12.3 Tue 10:15 H32

Towards MOVPE-grown c-band emitting InAs quantum dots on a Si (001) substrate based on heterogeneous integration of membrane and epitaxial regrowth — •PONRAJ VIJAYAN, ROBERT SITTIG, SIMONE LUCA PORTALUPI, MICHAEL JETTER, and PETER MICHLER — Institut für Halbleitertechnik und Funktionelle Grenzflächen, Center for Integrated Quantum Science and Technology (IQST) and SCoPE, Universität Stuttgart, Germany

Silicon photonics for telecommunications applications has garnered much attention in recent decades. The optical transparency and the large refractive index contrast of silicon in the telecommunication wavelengths allow the implementation of high-density photonic integrated circuit. The drawback of silicon photonics is that there is no native light source due to the indirect band-gap nature of silicon. Integration of III-V material, which offers outstanding optical emission properties, on silicon provides a potential solution. The monolithic integration i.e. the direct growth of III-V materials on silicon is the most desired approach. However, it is very challenging because of large lattice mismatch and material polarity difference between the III-V materials and silicon. An alternate monolithic approach is through heterogeneous integration of thin III-V membrane using direct bonding techniques followed by epitaxial regrowth. Our group has previously developed InAs QD/InGaAs MMB/GaAs substrate structures for long-distance optical fiber applications. Here, we report on the route to monolithically integrate the telecom C-band emitting InAs QD on a wafer bonded GaAs/Si substrate using MOVPE.

HL 12.4 Tue 10:30 H32

Non-vapor-liquid-solid selective area epitaxy of GaAs1-xSbx nanowires on silicon — AKHIL AJAY¹, HYOWON JEONG¹, •HAITING YU¹, NITIN MUKHUNDHAN¹, TOBIAS SCHREITMÜLLER¹, MARKUS DÖBLINGER², and GREGOR KOBLMÜLLER¹ — ¹Walter Schottky Institute & Physics Department Technical University of Munich, Garching, Germany — ²Ludwig-Maximilians-University, Munich, Germany

Epitaxial growth of semiconductor nanowires (NWs) is generally known to proceed via a vapor-liquid-solid (VLS). However, an absence of the liquid droplet would be ideal for III-V NW integration on Si and the exploration of atomically abrupt NW heterostructures. In this work, we report a novel non-VLS growth mechanism for the selective area growth of GaAs_{1-x}Sb_x NWs on Si(111) substrates using molecular beam epitaxy. Non-VLS NWs are known to have many structural defects and poor aspect ratios. Surprisingly, we observe an increased axial growth and aspect ratio in these NWs by adding low concentrations of Sb. This also contrasts the commonly believed enhancement in radial growth for VLS growth claimed to be due to the surfactant effect of Sb. We report on realizing control over aspect ratio and yield by optimizing SiO₂ mask hole diameter, growth time and growth temperature. In this process we observe

a hitherto unreported dynamic growth rate that increases with time. We also investigate the initial growth of such non-VLS NWs forming inside the SiO₂ mask opening, describing the facets and morphology. We also explore n-doping in these NWs with Si which also helps in realizing nearly unity yield and homogeneity.

HL 12.5 Tue 10:45 H32

Epitaxial growth and characterization of multilayer site-controlled InGaAs quantum dots based on the buried stressor method — •IMAD LIMAME, CHING-WEN SHIH, ALEXEJ KOLTCHANOV, MORITZ PLATTNER, JOHANNES SHALL, SVEN RODT, and STEPHAN REITZENSTEIN — Institute for Solid State Physics, Technical University of Berlin, Germany

The buried-stressor epitaxial growth concept is a prim approach for the realization of site- and number- controlled quantum dots (QDs) with optical high quality. This advanced technique has a wide application spectrum including nanophotonics devices such as single-photon sources (SPSs), microlasers, and emitter-arrays for neuromorphic photonic computing. Here, we report on the development of multi-layer site-controlled QDs (ML-SCQDs) integrated in micropillar laser arrays with low threshold pump power. The buried-stressor technique utilizes a partially oxidized buried AlAs aperture to engineer the strain profile in the following GaAs capping layer and control the position and number of the QDs at the GaAs surface. Thanks to the unetched GaAs surface, the buried-stressor SCQDs exhibits excellent optical properties in comparison to other SCQDs growth approaches, using for instance nano-hole arrays as nucleation centers. Additionally, after integration into micropillar cavities the partially oxidized aperture results in additional confinement of the optical mode in lateral direction, leading to lower mode volume and higher Q-factor for a given micropillar geometry. The grown ML-SCQDs are investigated using atomic force microscopy, micro-photo- and cathodoluminescence spectroscopy.

30 min. break

HL 12.6 Tue 11:30 H32

Growth of shallow GaAs quantum dots and investigation of their optical properties — •MORITZ LANGER¹, NAND LAL SHARMA¹, GHATA SATISH BHAYANI¹, ANKITA CHOUDHARY¹, OLIVER G. SCHMIDT², and CASPAR HOPFMANN¹ — ¹Institute for Integrative Nanoscience - IFW Dresden, Dresden, Germany — ²Center for Materials, Architectures, and Integration of Nanomembranes (MAIN), TU Chemnitz, Chemnitz, Germany

In recent years local droplet etching developed into an attractive growth process for strain-free semiconductor quantum dots. Typically, conical nanoholes etched into Al_{0.15}Ga_{0.85}As buffer layer by the droplet etching process using molecular beam epitaxy machine [1], have a width of about 50 nm and a depth of 15 nm. By using migration enhanced epitaxy, these nanoholes filled with GaAs and capped with an Al_{0.15}Ga_{0.85}As layer, buried around 6 nm high quantum dot structures of high optical quality are obtained. For enhanced interaction of quantum dots with external stimuli e.g. magnetic fields of thin films -, it is desirable to produce quantum dots close to the surface. Consequentially, the nature of the sample surface and the electronic and optical properties the quantum dot cannot be considered independently. For this purpose, the influence of capping layer thickness on the optical properties of GaAs/Al_{0.15}Ga_{0.85}As quantum dots are investigated using photoluminescence spectroscopy.

- [1] Xiaoying Huang et al, 2020 *Nanotechnology* 31 495701 (2020)

HL 12.7 Tue 11:45 H32

Local droplet etching on InAlAs/InP surfaces with InAl droplets — •YITENG ZHANG¹, XIN CAO¹, CHENXI MA¹, YINAN WANG¹, BENEDIKT BRECHTKEN², ROLF J. HAUG², EDDY P. RUGERAMIGABO¹, MICHAEL ZOPF¹, and FEI DING¹ — ¹Institut für Festkörperphysik, Leibniz Universität Hannover, Hannover, Germany — ²Laboratorium für Nano- und Quantenengineering, Leibniz Universität Hannover, Hannover, Germany

GaAs quantum dots (QDs) grown by local droplet etching (LDE) have been studied extensively in recent years. The LDE method allows for high crystallinity, as well as precise control of the density, morphology, and size of QDs. These properties make GaAs QDs an ideal candidate as single photon and entangled photon sources at short wavelengths (<800 nm). For technologically important telecom wavelengths, however, it is still unclear whether LDE grown QDs can be realized. In this work, we study Indium-Aluminum (InAl) droplet etching on ultra-smooth In_{0.55}Al_{0.45}As surfaces on InP substrates, with a goal to lay the foundation for growing symmetrical and strain-free telecom QDs using the LDE method. We report that both droplets start to etch nanoholes at a substrate temperature above 415 °C, showing varying nanohole morphology and rapidly changing density (by more than one order of magnitude) at different temperatures. Al and In droplets are found to not intermix during etching, and instead etch nanoholes individually. The obtained nanoholes show a symmetric profile and very low densities, enabling infilling of lattice-matched InGaAs QDs on InAlAs/InP surfaces in further works.

HL 12.8 Tue 12:00 H32

Influence of miscut angle on the exciton fine structure in GaAs/AlAs(111) and InAs/GaAs(111) quantum dots — •GEOFFREY PIRARD¹ and GABRIEL BESTER^{1,2} — ¹Physical Chemistry and Physics Departments, University of Hamburg, Luruper Chaussee 149, D-22761 Hamburg, Germany — ²The Hamburg Centre for Ultrafast Imaging, University of Hamburg, Luruper Chaussee, 149, D-22761 Hamburg, Germany

Self-assembled quantum dots (QDs) grown on (111) surfaces constitute, in principle, excellent solid-state quantum emitters of polarized-entangled photon pairs making them promising candidates for quantum information processing applications. However, in practice, the growth on such substrates introduces limitations on the growth rate hindering the generation of sufficiently intense signal for such applications. One potential solution to address this problem is to grow these systems on misoriented substrates.

Using atomistic, million-atom screened pseudopotential theory together with configuration interaction, we perform numerical calculations and analyze the influence of the miscut on the exciton fine structure (FS) of GaAs/AlAs(111) and InAs/GaAs(111) QDs. We show that the presence of the miscut modifies the spatial distribution of the electron and hole wave functions, which elongate along the [110] crystal axis. In turn, the polarization of the excitonic states acquires a clear preferential orientation and this effect is strongly enhanced in strained systems. Finally, the FS splitting increases with the miscut within a range depending on the material and the amplitude of the miscut.

HL 12.9 Tue 12:15 H32

Controlled MOF growth on functionalized carbon nanotubes — •MARVIN J. DZINNIK¹, NECMETTIN E. AKMAZ¹, ADRIAN HANNEBAUER², PETER BEHRENS², and ROLF J. HAUG¹ — ¹Leibniz Universität Hannover, Institut für Festkörperphysik, 30167 Hannover — ²Leibniz Universität Hannover, Institut für Anorganische Chemie, 30167 Hannover

The class of metal organic frameworks (MOFs) is continuously growing. These materials consist of inorganic building blocks, held together by organic linker molecules. Schulze *et al.* [1] showed that adding functionalized multi-walled carbon nanotubes (MWCNTs) to a UiO-66 synthesis drastically decreased the nucleation time. The MOFs preferably grow on the MWCNT until they fully

encapsulate it. We demonstrate a mechanism to spacially control the UiO-66 MOF growth on individual carbon nanotubes and deplete the encapsulation. The MWCNTs are drop-casted on a silicon dioxide surface and then locally modified. The samples are then submerged in the synthesis solution. This process leads to a growth of MOF crystals on the MWCNT surface leaving the modified areas depleted. With this method we are able to define lines free of MOF on the length of a single MWCNT down to several hundred nanometres for example to electrically contact the tubes ends.

[1] Schulze, H. A., *et al.* Electrically Conducting Nanocomposites of Carbon Nanotubes and Metal-Organic Frameworks with Strong Interactions between the two Components. *ChemNanoMat*, 5(9), (2019), 1159-1169.

HL 12.10 Tue 12:30 H32

Surface quantum dots with pure, coherent, and blinking-free single photon emission — •MICHAEL ZOPF¹, XIN CAO¹, JINGZHONG YANG¹, PENGJI LI¹, TOM FANDRICH¹, EDDY P. RUGERAMIGABO¹, CHENXI MA¹, ROBERT KEIL², FREDERIK BENTHIN¹, BENEDIKT BRECHTKEN¹, ROLF J. HAUG^{1,4}, YITENG ZHANG¹, SUSANNE WOCHE³, ZHAO AN¹, CONSTANTIN SCHMIDT¹, and FEI DING^{1,4}

— ¹Institut für Festkörperphysik, Leibniz Universität Hannover, Germany — ²Fraunhofer-institut für Angewandte Festkörperphysik IAF, Freiburg, Germany — ³Institut für Bodenkunde, Leibniz Universität Hannover, Germany — ⁴Laboratorium für Nano- und Quantenengineering, Leibniz Universität Hannover, Germany

The surface of semiconductor micro- and nanostructure-based devices has a major impact on their performance. Disorder and defects in the crystal typically lead to electronic states in the bandgap, degrading charge carrier transport and radiative recombination. In next generation semiconductor devices such as single or entangled photon sources, surface effects lead to low efficiency, photon dephasing, blinking or spectral jittering. Here we show unprecedented optical quality of GaAs quantum dots that are grown directly on an AlGaAs surface and passivated with 1-Octadecanethiol. Single photons are generated with 98.8% purity, 78% indistinguishability and narrow linewidths down to 7 μeV , close to the radiative limit. The emission is unaffected by the surface and shows no blinking over more than 12 orders of magnitude in time, yielding an on-fraction of 99.7%. These results are likely to stimulate new fundamental studies and quantum applications.

HL 13: Ultra-Fast Phenomena

Time: Tuesday 9:30–12:15

Location: H33

HL 13.1 Tue 9:30 H33

Ultrafast hot charge carrier transport across graphene nano-gaps — •JOHANNES GRÖBMEYER, PHILIPP ZIMMERMANN, and ALEXANDER HOLLEITNER — Walter Schottky Institute and Physics Department, Technical University of Munich, Germany

We study the hot charge carrier transport across nanoscale junctions for ultrafast electric pulse generation on the nanometer scale. To avoid laser ablation problems common to metal based photoemission devices, we investigate the possibility of graphene nanojunctions positioned on a sapphire substrate. We create the emitter-collector structure by bisecting a graphene strip utilizing a helium ion beam to create a ~30 nm wide nano-gap. Due to substrate interaction with the helium ion beam this gap is filled by a bulge of highly defected sapphire. Measuring the ultrafast and time-integrated charge carrier transport, we find evidence of an ultrafast photoemission across this gap. Our work demonstrates that graphene based nano-gaps have the potential of replacing photoconductive switches at low temperatures.

HL 13.2 Tue 9:45 H33

Studying hot electron transport in bismuth with transient all optical pump-probe spectroscopy — •FABIAN THIEMANN¹, GERMÁN SCIAINI², ALEXANDER KASSEN¹, and MICHAEL HORN-VON HOEGEN¹ — ¹University of Duisburg-Essen, Lotharstr. 1, 47057 Duisburg, Germany — ²University of Waterloo, 200 University Avenue West, Waterloo, ON N2L 3G1, Canada

Bismuth as a Peierls-Jones distorted semimetal is famous for its photoexcited coherent optical phonon modes and its delicate interplay with the electron dynamics. Especially the A_{1g} phonon mode at ≈ 3 THz and its characteristic softening upon photoexcitation is easily accessible and can be studied with all optical pump-probe spectroscopy, solely by monitoring the change in reflectivity $\Delta R/R_0$. The number of excited carriers in bismuth influences the atomic potential energy surface and thus the mode's softening. Therefore, in turn, we employed the redshift of the A_{1g} mode as a robust quantity to determine the spatial distribution of excited carriers and the absorbed energy density in the carrier system. A homogenous distribution due to ultrafast transport of hot carriers was observed, limited by an effective carrier penetration depth that is way beyond the optical skin depth.

HL 13.3 Tue 10:00 H33

Ultrafast Dynamics of Inter- and Intraband Transitions in GaP Investigated by fs-Time Resolved Ellipsometry — •RÜDIGER SCHMIDT-GRUND¹, NOAH STIEHM¹, ERICH RUNGE¹, MARTIN ZAHRADNÍK², SHIRLY ESPINOZA², MATEUSZ REBARZ², JAKOB ANDREASSON², and STEFAN KRISCHOK¹ — ¹TU Ilmenau, Technische Physik I and Theoretische Physik I, Weimarer Straße 32, 98693 Ilmenau, Germany — ²ELI Beamlines, Fyzikální ústav AV ČR, Za Radnici 835, 25241 Dolní Břežany, Czech Republic

We discuss the ultrafast dynamics of the dielectric function after excitation with a high-power laser pulse of the semiconductor GaP in the spectral range around the fundamental absorption edge, measured by pump-probe fs-time resolved spectroscopic ellipsometry [1,2]. The excited hot carriers cause several effects: we observe in different regions of the Brillouin zone both, Pauli-blocking of valence-to-conduction-band transitions and arising of new intra-conduction and -valence-band transitions, enabled by carrier scattering within the Brillouin zone and in particular tunnelling to the indirect minimum. We understand our observations with the help of density functional theory from which we derived band structure, transition matrix elements and the joint density of states between bands energetically relevant in our study. Our results show long lasting non-equilibrium phenomena (> ns), probably due to carrier trapping processes.

[1] S. Richter *et al.*, *Rev. Sci. Instrum.* **92**, 033104 (2021).

[2] S. Richter *et al.*, *New J. Phys.* **22**, 083066 (2020).

HL 13.4 Tue 10:15 H33

Multiparameter determination of time-resolved photoluminescence measurements — •SEBASTIAN BOHM¹, MAX GROSSMANN¹, STEFAN HEYDER¹, KLAUS SCHWARZBURG², PETER KLEINSCHMIDT¹, ERICH RUNGE¹, and THOMAS HANNAPPEL¹ — ¹Fakultät für Mathematik und Naturwissenschaften, Technische Universität Ilmenau, Ehrenbergstraße 29, 98693 Ilmenau — ²Institut Solare Brennstoffe, Helmholtz-Zentrum Berlin für Materialien und Energie, Hahn-Meitner-Platz 1, 14109 Berlin

Accurate knowledge of radiative, non-radiative, and trapping photoluminescence lifetimes is crucial for the understanding and improvement of semiconductor devices. In principle, these parameters can be obtained from time-resolved photoluminescence spectroscopy (TRPL) measured at different excitation level, see, e.g., M. W. Gerber and R. N. Kleiman, *J. Appl. Phys.* **122**,

095705 (2017), DOI 10.1063/1.5001128. We show that a full multi-parameter estimation based on a suitable maximum likelihood estimator and state-of-the-art non-linear multi-parameter optimization yields superior results compared to conventional data analysis.

HL 13.5 Tue 10:30 H33

Strategies for Automating Femtosecond Time-Resolved Ellipsometry Data Analysis — •NOAH STIEHM¹, YIXUAN ZHANG², ERICH RUNGE³, STEFAN KRISCHOK¹, HONGBIN ZHANG², and RÜDIGER SCHMIDT-GRUND¹ — ¹Technische Universität Ilmenau, Fachgebiet Technische Physik I, Weimarer Straße 32, 98693 Ilmenau, Germany — ²Technische Universität Darmstadt, Research Group Theory of Magnetic Materials, Otto-Berndt-Straße 3, 64287 Darmstadt — ³Technische Universität Ilmenau, Fachgebiet Theoretische Physik I, Weimarer Straße 32, 98693 Ilmenau, Germany

With the recently developed experimental method of femtosecond time-resolved spectroscopic ellipsometry [1], it is possible to obtain the transient dielectric function of a sample after excitation in a pump-probe scheme. However, modeling the experimental data manually with established ellipsometry modeling workflows is cumbersome and significantly reduces the throughput of the experiment. Here we present strategies I) to formalize the experience and physical intuition usually entering modeling strategies, II) to reduce computational costs by application of dimensionality reduction techniques, especially in the additionally required ab-initio theory calculations, and III) to improve stability, to enable an automated modeling pipeline with minimal human intervention.

[1] S. Richter *et al.*, Rev. Sci. Instrum. 92, 033104 (2021).

15 min. break

HL 13.6 Tue 11:00 H33

Coherent Dynamics of Charge-Transfer Excitons — •MARKUS STEIN¹, MELANIE FEY¹, CHRISTIAN FUCHS², WOLFGANG STOLZ², KERSTIN VOLZ², and SANGAM CHATTERJEE¹ — ¹Institute of Experimental Physics I and Center for Materials Research, Justus-Liebig-University Giessen, Heinrich-Buff-Ring 16, D-35392 Giessen, Germany — ²Department of Physics and Material Sciences Center, Philipps-Universität Marburg, Renthof 5, 35032 Marburg, Germany

Charge carrier transport phenomena through internal interfaces in semiconductor heterostructures are currently in the spotlight of scientific research due to the advancing miniaturization of devices. However, how internal interfaces in semiconductor heterostructures affect the coherent dynamics, i.e., the transition from a coherent polarization to a population, is largely unexplored. To shed some light on the subject, we use a GaInAs/GaAs/GaAsSb type-II like double quantum well structure which, due to its design, exhibits a charge-transfer exciton resonance in the linear absorption. This allows us to study the coherent dynamics of charge-transfer excitons and excitons that can relax across the internal interface into a charge-transfer state by means of degenerate four-wave-mixing. Furthermore, adding an optical prepulse, the phase relaxation of charge-transfer excitons subjected to collisions with either free carriers or incoherent excitons is investigated.

HL 13.7 Tue 11:15 H33

Intense terahertz radiation via the transverse thermoelectric effect — •TIM PRIESSNITZ^{1,2}, PETAR YORDANOV¹, MIN-JAE KIM^{1,2,3}, GEORG CRISTIANI¹, GENNADY LOGVENOV¹, BERNHARD KEIMER¹, and STEFAN KAISER^{1,2,3} — ¹Max-Planck Institute for Solid State Research, 70569 Stuttgart, Germany — ²4th Physics Institute and Research Center SCoPE, University of Stuttgart, 70569 Stuttgart, Germany — ³Institute of Solid State and Materials Physics, Technical University Dresden, 01069 Dresden, Germany

Terahertz (THz) radiation became a powerful tool with widespread applications ranging from imaging and spectroscopy to nonlinear optical control of materials. However, efficient and scalable THz sources remain rare. Here, we present a novel approach to generate powerful THz radiation making use of an ultrafast current induced via the transverse thermoelectric effect (TTE). We realize this in off-cut grown thin films of the delafossite PdCoO₂ and the cuprate La_{1.84}Sr_{0.16}CuO₄ driven by femtosecond laser pulses resulting in an ultrafast transient diffusion of charge carriers. Characterizing the resulting THz radiation, we find it comparable in power and spectral bandwidth to standard emitters based on nonlinear crystals. A first basic model including the Seebeck anisotropy, electrical and thermal conductivities and the transient diffusivity allows materials based predictions. Due to its simplicity and potential for scalability in terms of multiple tunable material parameters, THz generation based

on the TTE opens a new avenue for high-field THz generation and novel cost-efficient emitters.

HL 13.8 Tue 11:30 H33

Clocking the dynamics of correlated Bloch electrons on an attosecond time scale — •JOSEF FREUDENSTEIN¹, MARKUS BORSCH², MANUEL MEIERHOFER¹, DMYTRO AFANASIEV¹, CHRISTOPH PETER SCHMID¹, FABIAN SANDNER¹, MARLENE LIEBICH¹, ANNA GIRNGHUBER¹, MATTHIAS KNORR¹, MACKILLO KIRA², and RUPERT HUBER¹ — ¹University of Regensburg, 93051 Regensburg, Germany — ²University of Michigan, Ann Arbor, Michigan 48109, USA

Delocalized Bloch electrons and the low-energy correlations between them determine key properties of solids. To directly capture how many-body correlations affect the actual motion of Bloch electrons, sub-femtosecond temporal precision is desirable. Here, we study attosecond shifts in the dynamics of charge carriers at the Fermi level, combining sub-fs resolution with meV energy selectivity. Coherent excitons are injected in bulk and monolayer tungsten diselenide and subsequently accelerated by multi-terahertz light fields. Quasiparticle collisions lead to the emission of high-order sidebands, which contain key information about the ballistic dynamics of the charge carriers. We show how the excitonic binding energy, the strength of the driving field, the valley polarization and Pauli blocking influence these dynamics on an attosecond time scale and faithfully reproduce these results with quantum-dynamic many-body computations in a Wigner-function representation. This opens a new pathway to understanding emergent quantum dynamics and phases and sets a corner stone for future optoelectronics and quantum-information processing.

HL 13.9 Tue 11:45 H33

Time-resolved ellipsometry on CuI thin films — •CAROLA EMMINGER^{1,2}, EVGENY KRÜGER¹, MICHAEL BAR¹, SHIRLY ESPINOZA³, MARTIN ZAHRADNIK³, MATEUSZ REBARZ³, FELIX-FLORIAN DELATOWSKI³, JAKOB ANDREASSON³, MICHAEL SEIFERT⁴, SILVANA BOTTI⁴, CHRIS STURM¹, and MARIUS GRUNDMANN¹ — ¹Felix-Bloch Institut für Festkörperphysik, Universität Leipzig, Germany — ²Institut für Physik, Humboldt-Universität zu Berlin, Germany — ³ELI Beamlines, Czech Republic — ⁴Institut für Festkörpertheorie und Optik, Friedrich-Schiller-Universität Jena, Germany

We report the impact of the carrier dynamics on the dielectric function of CuI thin films by means of femtosecond pump-probe spectroscopic ellipsometry. As expected, we observe a strong decrease of the exciton peak due to the pump pulse, which starts to recover after 200-300 fs. Interestingly, we notice a small increase in absorption below the band gap after a delay time of about 400 fs, which might be explained by valence- to valence-band transitions resulting from the laser-induced increased carrier density. At about 10 ps, the dielectric function has almost fully recovered. We analyze the delay-time dependent dielectric function and discuss possible explanations for the changes related to the carrier density.

HL 13.10 Tue 12:00 H33

Gain recovery dynamics after stimulated emission in type-II semiconductor laser materials — •MARKUS STEIN¹, FELIX SCHÄFER¹, JANINE LORENZ¹, JOHANNES STEINER², JÖRG HADER³, JERRY MOLONEY³, TORSTEN MEIER², STEPHAN W. KOCH⁴, and SANGAM CHATTERJEE¹ — ¹Institute of Experimental Physics I and Center for Materials Research, Justus-Liebig-University Giessen, Heinrich-Buff-Ring 16, D-35392 Giessen, Germany — ²Department of Physics, Paderborn University, Warburger Strasse 100, D-33098 Paderborn, Germany — ³Wyant College of Optical Sciences, University of Arizona, 1630 East University Boulevard, Tucson, Arizona 85721, USA — ⁴Department of Physics and Material Sciences Center, Philipps-Universität Marburg, Renthof 5, 35032 Marburg, Germany

Type-II active devices combine the advantages of spectrally broad, temperature-stable efficient gain with the potential for electrical injection pumping. Intrinsic charge-carrier relaxation dynamics limit the feasible repetition rates beyond constraints of cavity design and heat removal. Here, we investigate the recovery of material gain after a stimulated emission process in an InGaAs/GaAs/GaAsSb heterostructure, experimentally simulating the operation condition of a pulsed laser system. In an optical pump - optical probe setup, a first optical pulse injects hot charge carriers. Subsequently, a second pulse tuned to the broad spectral region in which gain is observed is used to stimulate emission. A detailed analysis of the dynamics after stimulated emission reveals that the physical limit for the highest possible laser repetition rate for this material system is in the range of 100 GHz.

HL 14: Focus Session: Quantum Properties at Functional Oxide Interfaces (joint session HL/DS)

Modern oxide materials exhibit a rich variety of physical properties that lead to potential applications such as sensors and detectors, solar energy harvesting, transparent and power electronics. Understanding their quantum properties at surfaces and interfaces may play a decisive role for functionalities in high-electron-mobility transistors, quantum electronics or topological quantum computation. These typically require homo- or heteroepitaxial layers of high crystallinity and investigation methods designed to reveal the fascinating physics at (complex) oxide interfaces. This session sets a focus on growth of oxide interfaces, the experimental and theoretical investigation of their novel physical, in particular quantum properties as well as fabrication and characterization of demonstrator devices.

Organized by Martin Albrecht, Oliver Bierwagen, and Saskia F. Fischer

Time: Tuesday 9:30–12:45

Location: H34

Invited Talk

HL 14.1 Tue 9:30 H34

Materials and Device Engineering for Gallium Oxide-based Electronics — NIDHIN KURIAN KALARICKAL¹, SUSHOVAN DHARA¹, ASHOK DHEENAN¹, and •SIDDHARTH RAJAN^{1,2} — ¹ECE Department, The Ohio State University — ²MSE Department, The Ohio State University

This presentation will discuss our recent work on epitaxy, heterostructure design, and electrostatics to achieve high-performance β -Ga₂O₃ lateral and vertical electronic devices. We will discuss some key results in materials growth and device design for lateral structures, including the first β -(Al,Ga)₂O₃/ β -Ga₂O₃ modulation-doped structures with excellent transport properties, double-heterostructure modulation-doped structures, and scaled delta-doped transistors with cutoff frequency of 27 GHz, and self-aligned lateral field effect transistors with > 900 mA/mm current density. We will discuss the use of a new damage-free epitaxial etching technique using Ga atomic flux that enables highly precise fabrication of 3-dimensional structures, and applications of this etching to realize field termination in vertical diodes, and lateral FINFETs with enhanced performance. Extreme-permittivity dielectrics provide unique opportunities to create devices that can sustain extreme fields without premature breakdown of metal-semiconductor and dielectric-semiconductor interfaces. We will discuss promising results of electrostatic engineering using BaTiO₃/Ga₂O₃ heterojunctions that enable high fields to be sustained within Gallium Oxide diodes and transistors.

Invited Talk

HL 14.2 Tue 10:00 H34

Ferroelectric two-dimensional electron gases for oxide spin-orbitronics — •JULIEN BRÉHIN — Unité Mixte de Physique CNRS/Thales

Just as the apparent incompatibility between ferroelectricity and magnetism prompted the renaissance of multiferroics, the research on ferroelectric metals conjectured in the 1960s by Anderson and Blount was recently revitalized. Yet, their experimental demonstration remains very challenging due to the contradiction between the presence of free charge carriers and switchable electric dipoles. In this talk we will report on two-dimensional electron gases (2DEGs) formed on Ca-substituted SrTiO₃ (STO). Signatures of the ferroelectric phase transition near 30 K are visible in the temperature dependence of the sheet resistance RS and in a strong, reproducible hysteresis of RS with gate voltage. In addition, spectroscopic measurements of the 2DEG region indicate the presence of switchable ionic displacements. Beyond their fundamental interest in materials physics, ferroelectric 2DEGs offer opportunities in spin-orbitronics: we will show how their spin-charge conversion properties, caused by the inverse Rashba-Edelstein effect, can be electrically tuned in amplitude and sign in a non-volatile way. These results open the way to a whole new class of ultralow-power spin-orbitronic devices operating without the need for magnetization switching. Finally, we will describe how one can introduce magnetism into such systems to achieve multiferroic 2DEGs displaying magnetoelectric coupling.

HL 14.3 Tue 10:30 H34

Electron transport of the two-dimensional electron gas in polar-discontinuity doped LaInO₃/BaSnO₃ heterostructure — GEORG HOFFMANN¹, FAZEEL ZOHAI¹, MARTINA ZUPANCIC², MARTIN ALBRECHT², and •OLIVER BIERWAGEN¹ — ¹Paul-Drude-Institut für Festkörperelektronik Leibniz-Institut im Forschungsverbund Berlin e.V., Hausvogteiplatz 5-7, D-10117 Berlin, Germany — ²Leibniz-Institut für Kristallzüchtung im Forschungsverbund Berlin e.V., Max-Born-Straße 2 D-12489 Berlin, Germany

Transparent semiconducting oxides (TSOs) are key players for new (opto-)electronic devices and two-dimensional electron gases (2DEGs) are relevant for high-frequency applications. Polar-discontinuity doping (interfacing a polar material with a nonpolar one), has been demonstrated to provide a 2DEG at the interface between the perovskites LaAlO₃ and SrTiO₃ with a high electron concentration but suffers from low room-temperature (RT) electron mobilities of SrTiO₃. In this contribution we demonstrate polar-discontinuity doped 2DEG at the interface between the perovskites LaInO₃ and BaSnO₃, grown by plasma-assisted molecular beam epitaxy. While the individual, undoped oxide layers were found to be insulating, the formation of the polar-discontinuity

doped 2DEG at their interface is confirmed by capacitance-voltage (CV) and van der Pauw-Hall measurements. The extracted sheet electron concentrations >2e13cm⁻² and RT electron mobilities above >50cm²/Vs are promising for device applications. The transport properties of the 2DEG are compared to those of La-doped BaSnO₃ layers.

HL 14.4 Tue 10:45 H34

Non-Abelian braiding of phonons in monolayer oxides — •BO PENG¹, ADRIEN BOUHON¹, BARTOMEU MONSERRAT^{1,2}, and ROBERT-JAN SLAGER¹ — ¹TCM Group, Cavendish Laboratory, University of Cambridge, J. J. Thomson Avenue, Cambridge CB3 0HE, United Kingdom — ²Department of Materials Science and Metallurgy, University of Cambridge, 27 Charles Babbage Road, Cambridge CB3 0FS, United Kingdom

Non-Abelian braiding of quasiparticles can encode quantum information immune from environmental noise with the potential to realize topological quantum computation. Here we propose that phonons, a bosonic excitation of lattice vibrations, can carry non-Abelian charges in their band structures that can be braided using external stimuli. Taking some earthly abundant materials such as silicates [1] and aluminium oxide [2] as representative examples, we demonstrate that an external electric field or electrostatic doping can give rise to phonon band inversions that induce the redistribution of non-Abelian charges, leading to non-Abelian braiding of phonons. We show that phonons can be a primary platform to study non-Abelian braiding in the reciprocal space, and we expand the toolset to study such braiding processes.

References: [1] Bo Peng, Adrien Bouhon, Bartomeu Monserrat & Robert-Jan Slager. Nature Communications 13, 423 (2022). [2] Bo Peng, Adrien Bouhon, Robert-Jan Slager & Bartomeu Monserrat. Physical Review B 105, 085115 (2022).

30 min. break

HL 14.5 Tue 11:30 H34

Shift of the absorption onset in corundum-like α -(Ti_xGa_{1-x})₂O₃ — •ELIAS KLUTH¹, MICHAEL FAY², CHRISTOPHER PARMENTER³, JOSEPH ROBERTS⁴, FABBIEN MASSABU⁵, RÜDIGER GOLDHAHN¹, and MARTIN FENEBERG¹ — ¹Institut für Physik, Otto-von-Guericke-Universität Magdeburg, Germany — ²Advanced Materials Research Group, Faculty of Engineering, University of Nottingham, NG7 2RD, UK — ³Nottingham Nanotechnology and Nanoscience Centre, University of Nottingham, University Park, Nottingham NG7 2RD, UK — ⁴School of Engineering, The University of Liverpool, Liverpool L69 3GH, UK — ⁵Department of Physics, SUPA, University of Strathclyde, Glasgow G4 0NG, UK

Corundum-like α -Ga₂O₃ is a metastable phase of the polymorphic ultra-wide band gap semiconductor Ga₂O₃. While previous research has mostly focused on the stable β -phase the α -phase is less discussed, but interesting as well as it allows bandgap-engineering by alloying e.g. with α -Al₂O₃ (sapphire) or In₂O₃.

Since the transition metal oxide Ti₂O₃ as well, has a corundum-like phase (α -phase), with a small lattice mismatch of about 3.5% to α -Ga₂O₃, we investigate here (0001) α -Ga₂O₃ thin films alloyed with Ti, grown by ALD (atomic layer deposition).

We use spectroscopic ellipsometry in ultraviolet range to obtain the complex dielectric function (DF) of α -(Ti_xGa_{1-x})₂O₃ up to $x = 0.61$. We find a clear red shift of the absorption onset with increasing Ti content, as well as an increase of the amplitude of the DF.

HL 14.6 Tue 11:45 H34

Optical signatures of polarons trapped at ferroelectric domain walls in bismuth ferrite — •SABINE KÖRBELE — Institute of Physics of the Czech Academy of Sciences, Prague, Czech Republic — Friedrich Schiller University Jena, Germany
Ferroelectric domain walls are atomically narrow planes that can behave very differently from the surrounding bulk ferroelectric material. For example, the domain walls in many ferroelectrics can collect and conduct charge carriers despite the insulating nature of the host material. Domain walls can be created,

moved, and removed again in a controlled way, thus they can be used to alter the electronic properties of the ferroelectric as desired. Charge carriers that accumulate at domain walls may induce metallic or semiconducting behavior depending on whether they are delocalized or form self-trapped small polarons. The latter may be detected, for example, as deep levels within the band gap in absorption or photoluminescence spectra. Here we predict optical signatures of charge carriers trapped as small polarons at ferroelectric domain walls in BiFeO₃, using first principles calculations.

HL 14.7 Tue 12:00 H34

Anharmonicity of lattice vibrations in α -Ga₂O₃ investigated by temperature dependent Raman spectroscopy — •JONA GRÜMBEL¹, RÜDIGER GOLDHAHN¹, DAE-WOO JEON², and MARTIN FENEBERG¹ — ¹Otto-von-Guericke Universität, Magdeburg, Germany — ²Korea Institute of Ceramic Engineering and Technology, Jinju, Republic of Korea

We investigate the Raman excitations of a corundum-like α -Ga₂O₃ thin film under temperature variation from 80K up to 790K. This yields detailed information about anharmonic processes in the crystal. For the two dominant phonon modes for each of the two Raman-active phonon mode symmetries (A_{1g} and E_g) model calculations are performed in order to quantify the contributions of different decay mechanisms. It is shown, that our experimental data can be well described by the applied theoretical models. The determined coefficients of cubic and quartic decay for both, phonon energy and linewidth, are compared with those from

hexagonal GaN and AlN as well as with those from α -Al₂O₃. We observe, that for the two selected phonon modes of α -Ga₂O₃ the quartic decay processes are negligible for the phonon frequencies, but not for the phonon linewidths behavior under temperature variation. A quantitative description within the model parameters is presented.

Invited Talk

HL 14.8 Tue 12:15 H34

Strain-driven dissociation of water on (incipient) ferroelectrics — JOSHUA L. BATES and •CHIARA GATTINONI — Department of Chemical and Energy Engineering, London South Bank University, London, UK

Functional materials have great promise in catalysis, and especially within dynamic catalytic cycles, where the “functional” properties are used to cyclically modify the local environment of a surface to enhance turnover frequency. In particular, strain-driven mechanisms exploiting the properties of piezo- and ferroelectric materials, are of great interest.

In this work we focus on (incipient) ferroelectric nanomaterials BiFeO₃, BaTiO₃, KTaO₃ and SrTiO₃, perovskites presenting a wide range of bulk properties and behaviours. We uncover how interplay between these properties (such as the spontaneous polarization) and nanoscale effects (such as the depolarizing field and the surface structure), affect the strain-driven water-splitting abilities of these nanoscale functional materials. Finally, we identify the most desirable properties for a highly efficient ferroelectric material for dynamic catalysis.

HL 15: 2D Materials 3 (joint session HL/ CPP/DS)

Time: Tuesday 9:30–12:00

Location: H36

Invited Talk

HL 15.1 Tue 9:30 H36

Ultrafast all-optical modulation and frequency conversion in 2D materials — •SEBASTIAN KLIMMER¹, ARTEM SINELNIK^{1,2}, ISABELLE STAUBE^{1,2}, and GIAN-CARLO SOAVI¹ — ¹Institute of Solid State Physics, Friedrich Schiller University Jena, Jena, Germany — ²Institute of Applied Physics, Friedrich Schiller University Jena, Jena, Germany

Large efforts have been devoted in the last years to realizing nonlinear integrated devices for frequency conversion, sensing, signal modulation and quantum optics. Two-dimensional (2D) materials, such as graphene and transition metal dichalcogenides (TMDs), provide distinct advantages in this respect thanks to their ease of integration on photonic platforms[1] and their atomically thin nature, which relaxes phase matching constraints and thus offers a practically unlimited bandwidth for nonlinear optical effects [2]. In this seminar I will present our recent results in the field of nonlinear optics with 2D materials, including ultra-broadband four-wave mixing in the telecom range, ultrafast all-optical modulation of second- and third-harmonic generation in TMDs[3] and graphene and ultrafast polarization-resolved second-harmonic spectroscopy to probe the valley degree of freedom in TMDs.

[1] He, J. *et al.*, *Nano Lett.* **21**, 7, 2709-2718 (2021)

[2] Trovatiello, C. *et al.*, *Nat. Photonics.* **15**, 6-10 (2021)

[3] Klimmer, S. *et al.*, *Nat. Photonics.* **15**, 837-842 (2021)

HL 15.2 Tue 10:00 H36

strain tuning of exciton and trion dynamics in monolayer WSe₂ at cryogenic temperatures — •ZHAO AN¹, PEDRO SOUBELET², ANDREAS V. STIER², MICHAEL ZOPF¹, YAROSLAV ZHUMAGULOV³, JAROSLAV FABIAN³, PAULO E. FARIA JUNIOR³, JONATHAN J. FINLEY², and FEI DING^{1,4} — ¹Institut für Festkörperphysik, Leibniz Universität Hannover, Appelstraße 2, 30167 Hannover, Germany — ²Walter Schottky Institut and Physik Department, Technische Universität München, 85748 Garching, Germany — ³Institute for Theoretical Physics, University of Regensburg, 93040 Regensburg, Germany — ⁴Laboratorium für Nano- und Quantenengineering, Leibniz Universität Hannover, Schneiderberg 39, 30167 Hannover, Germany

Transition metal dichalcogenides (TMD) receive increasing attention these years. In TMD monolayers, the light-matter interaction is driven by strong excitonic effects. Additional to neutral excitons, singlet/ triplet trions are observed, in which the additional charge is either in the same or opposite valley with respect to excitons. We apply dynamic strain at cryogenic temperatures to investigate the exciton dynamics of monolayer WSe₂. Biaxial strain is electrically controlled via a piezoelectric actuator and transferred to the hBN/WSe₂/hBN. We find that next to changes in the emission energy and intensity, the singlet-triplet trion fine structure is affected. Polarization-resolved PL spectroscopy reveals that biaxial strain alters the polarizations of trions, which is attributed to changes in the pumping of resident electrons and the intervalley scattering of excitons and electrons.

HL 15.3 Tue 10:15 H36

Optical nonlinearities in the excited carrier density of 2d TMDs — •DANIEL ERBEN¹, ALEXANDER STEINHOFF¹, MICHAEL LORKE^{1,2}, and FRANK JAHNKE¹ — ¹Institute for Theoretical Physics, University of Bremen — ²Bremen Center for Computational Materials Science, University of Bremen

The prospects of using 2d transition metal dichalcogenides (TMDs) in future optoelectronic device application requires insight in the excitation dynamics of photoexcited charge carriers and the resulting optical nonlinearities. Utilizing ab-initio electronic-state calculations combined with many-body treatment of optical excitation, we calculate the excited carrier dynamics and the nonlinear absorption in MoS₂, MoSe₂, WS₂, and WSe₂ under various excitation conditions.

We find, that the increase of the carrier density with excitation strength deviates from a linear behaviour. Based on this, the validity range of a linear approximation for the excited carrier density as function of the pump fluence is determined. The use of a linear absorption coefficient of the unexcited system can significantly underestimate the achievable carrier density for strong pump fields. Furthermore, we study the excitation-induced many-body effects of excited charge carriers like band-gap renormalization, dephasing, screening, and scattering processes, that are mediated by the strong Coulomb interaction. Additional contributions to optical nonlinearities originate from phase space filling.

15 min. break

HL 15.4 Tue 10:45 H36

Second order coherence of a condensate of exciton-polaritons in an atomically thin crystal — •JENS-CHRISTIAN DRAWER¹, HANGYONG SHAN¹, SVEN HÖFLING², CARLOS ANTON-SOLANAS³, MARTIN ESMANN¹, and CHRISTIAN SCHNEIDER¹ — ¹Universität Oldenburg, Germany — ²Universität Würzburg, Germany — ³Universidad Autónoma de Madrid, Spain

We study the second order coherence of a condensate of exciton-polaritons emerging in a microcavity loaded with an atomically thin MoSe₂ crystal. Under cryogenic temperatures, angle-resolved PL and reflectivity measurements reveal the formation of two polariton resonances, as the hallmark of the strong coupling regime. The characteristic condensation threshold manifests via the nonlinear input-output-characteristics of the emission. In order to gain deeper information about the photon statistics emitted from the cavity, we perform the Hanbury Brown- and Twiss experiment as a function of the polariton occupation in the effective ground state. While the emission features a bunching effect below threshold, hinting at a thermal contribution of the polariton emission, above threshold the second order correlation transits towards $g^{(2)}(\tau = 0) = 1$, which is indicative for the formation of a coherent state in the quantum optical sense.

HL 15.5 Tue 11:00 H36

Theoretical description of moiré excitons in twisted MoSe₂ homobilayers — •RUVEN HÜBNER¹, MALTE KREMSE², VIVIANA VILLAFANE², MARKO M. PETRIĆ³, MATTHIAS FLORIAN⁴, ALEXANDER STEINHOFF¹, MACKILLO KIRA⁴, NATHAN P. WILSON², ANDREAS V. STIER², KAI MULLER³, and JONATHAN J.

FINLEY² — ¹Institut für Theoretische Physik, Universität Bremen, Bremen, Germany — ²Walter Schottky Institut und Physik Department, Technische Universität München, Garching, Germany — ³Walter Schottky Institut und Department of Electrical and Computer Engineering, Technische Universität München, Garching, Germany — ⁴University of Michigan, Dept. of Electrical Engineering and Computer Science, Ann Arbor, MI, USA

By introducing a twist between multiple monolayers of transition metal dichalcogenides we can observe superstructures with a new periodicity - namely the moiré lattice. Its size depends on the twist angle and therefore offers the possibility to modify properties like exciton energies as a function of the twist angle. We demonstrate, how DFT calculations of an untwisted MoSe₂ bilayer allow us to locally model the band variation inside the moiré unit cell at all dominant high symmetry points of the Brillouin zone. The resulting model provides access to arbitrary moiré potentials experienced by different exciton species and allows us to calculate their twist angle dependent spectra. For all twist angles we assign the lowest energy to interlayer excitons formed between the Γ - and K-valley. The twist angle dependent shift of 5 meV per degree for small angles is in good agreement with experiment.

HL 15.6 Tue 11:15 H36

Dielectric screening effects on the exciton binding-energy and exciton diffusion in a 2D material — •LUKAS GÜMBEL, PHILIP KLEMENT, and SANGAM CHATTERJEE — Institute of Experimental Physics I and Center for Materials Research (ZfM/LaMa), Justus Liebig University Giessen, Heinrich-Buff-Ring 16, Giessen D-35392, Germany

Two-dimensional semiconductors have proven to be candidates for numerous applications in the field of optoelectronics. Especially transition-metal dichalcogenides such as WS₂ have attracted extensive research due to the direct band-gap emerging in the monolayer limit. The optoelectronic properties are dominated by tightly-bound excitons denoted as A, B, and C. As the electric field lines of the excitonic states extend into the surrounding material, the energy states are subject to dielectric screening effects. Here we show that stronger dielectric screening equally shifts the excitonic ground state energies of the A-, B-, and C-excitons in WS₂ to lower energies. We find a shift of 20 meV in monolayers encapsulated in hBN and observe a non-hydrogenic Rydberg-series yielding a quasiparticle band-gap energy of 2.33 eV with an 1s excitonic binding energy of 0.30 eV. Additionally, we study exciton diffusion in different dielectric environments yielding a diffusion coefficient of 9 cm²/s. These results complement the underlying theory and may pave the way to a deeper understanding of screening effects in various 2D-Materials.

HL 16: Focus Session: Quantum Properties at Functional Oxide Interfaces (joint session DS/HL)

Time: Wednesday 9:30–11:00

Location: H17

See DS 14 for details of this session.

HL 17: Quantum Dots and Wires 4: Devices

Time: Wednesday 9:30–12:30

Location: H32

HL 17.1 Wed 9:30 H32

Highly Pure and Bright Emission of a Telecom C-Band Quantum Dot in a Circular Bragg Grating Cavity — •RAPHAEL JOOS, CORNELIUS NAWRATH, SASCHA KOLATSCHKEK, STEPHANIE BAUER, PASCAL PRUY, ROBERT SITTING, PONRAJ VIJAYAN, JIASHENG HUANG, MICHAEL JETTER, SIMONE L. PORTALUPI, and PETER MICHLER — Institut für Halbleitertechnik und Funktionelle Grenzflächen (IHFG), Center for Integrated Quantum Science and Technology (IQST) and SCoPE, Universität Stuttgart

Quantum communication schemes, which can prospectively guarantee secure communication by physical laws, rely on the availability of single-photons utilized as flying qubits. For this purpose, InAs quantum dots (QDs) can be employed as single-photon source, particularly, providing access to emission at telecom wavelengths which is highly sought-after for fiber-based applications and will, thus, most probably be the operating regime for real-world applications. However, simple planar QD structures suffer from a low collection efficiency due to the high refractive index contrast at the semiconductor/air interface. This issue can be tackled by the application of photonic nanostructures. This contribution deals with the optical and quantum optical investigation of telecom C-band QDs embedded in circular Bragg grating cavities, which allow for strongly increased light collection in a broad range of wavelengths as well as Purcell enhanced emission of the QDs. In this way, QD emission with a near perfect single-

HL 15.7 Tue 11:30 H36

Brightening of a dark monolayer semiconductor via strong light-matter coupling in a cavity — •HANGYONG SHAN¹, IVAN IORSH², BO HAN¹, FALK EILENBERGER⁴, MARTIN ESMANN¹, SEBASTIAN KLEMBT³, SVEN HÖFLING³, CARLOS ANTÓN-SOLANAS¹, IVAN A. SHELYKH², and CHRISTIAN SCHNEIDER¹ — ¹Oldenburg University, Oldenburg, Germany. — ²St. Petersburg, Russia — ³Universität Würzburg, Würzburg, Germany — ⁴Friedrich Schiller University, Jena, Germany

We study the modification of the material properties via strong coupling and demonstrate an effective inversion of the excitonic band-ordering in a monolayer of WSe₂ with spin-forbidden, optically dark ground state. In our experiments, we harness the strong light-matter coupling between cavity photon and the high energy, spin-allowed bright exciton, and thus creating two bright polaritonic modes in the optical bandgap with the lower polariton mode pushed below the WSe₂ dark state. We demonstrate that in this regime the commonly observed luminescence quenching stemming from the fast relaxation to the dark ground state is prevented, which results in the brightening of this intrinsically dark material. We probe this effective brightening by temperature-dependent photoluminescence, and we find an excellent agreement with a theoretical model accounting for the inversion of the band ordering and phonon-assisted polariton relaxation.

HL 15.8 Tue 11:45 H36

Broadband pump-probe microscopy at 1.5 MHz repetition rate — •DEVAPRIYO MITHUN¹, MICHAEL FROSZ², and GIANCARLO SOAVI¹ — ¹Institute of Solid State Physics, Friedrich Schiller University Jena, Jena, Germany — ²Max Planck Institute for the Science of Light, Erlangen, Germany

Ultrafast pump-probe spectroscopy is one of the most commonly used techniques to resolve photoinduced excited states dynamics: a pump pulse excites the system under investigation, which is then monitored by measuring the changes in the differential reflection ($\Delta R/R$) of a temporally delayed probe pulse. Here, we discuss the realization of a pump-probe setup, which exhibits high sensitivity operating with a temporal resolution of ≈ 100 fs and spatial resolution of ≈ 3 μ m with 515 nm pump and a broadband probe spectrum in the range 650-1000 nm, generated with a photonic crystal fiber.

We modulate the pump pulse at 1.5 MHz using an acousto-optic modulator. By doing this, we achieve a sensitivity, defined as the minimum detectable $\Delta R/R$, of 10^{-7} at 10 ms integration time. Finally, we implemented a Fourier transform based interferometric detection scheme to achieve a fast measurement of $\Delta R/R$ over the entire broadband spectrum.

Our pump-probe setup provides a powerful tool for broadband pump-probe microscopy with high sensitivity and high temporal resolution, which is ideal for the study of nanostructures such as carbon nanotubes and layered materials.

photon purity as well as very high collection efficiency is achieved leading to megahertz count rate of actual single-photons available for further applications.

HL 17.2 Wed 9:45 H32

Realization of Gaussian-shaped micro-cavities for Quantum Dots emitting in the telecom C-band — •JENS JAKSCHIK — Institut für Halbleitertechnik und funktionelle Grenzflächen, Center for Integrated Quantum Science and Technology (IQST) and SCoPE, University of Stuttgart, Germany

Semiconductor quantum dots (QDs) are a prime candidate for the generation of efficient single, indistinguishable photons. When utilizing these QDs for e.g. long-distance quantum communication, it is important to operate at the transmission loss minimum of the existing global optical fiber network. Therefore, the QDs have to emit in the telecom C-Band (~ 1550 nm). To keep the advantages of the mature GaAs technology, the QDs are grown on an InGaAs metamorphic buffer (MMB) layer with high In-content on GaAs. The emission of QDs can be optimized by confining them into cavities. In this work novel Gaussian-shaped micro-cavities based on high-reflective DBRs are used. To reach high quality factors and increase the extraction efficiency in Gaussian-shaped cavities, the radial symmetry given by the wet-chemically etched Gaussian-shaped microlens, forming the center of the cavity has to be preserved over multiple layers of top DBR growth. This has to be realized despite the varying growth rates of

InGaAs along different crystal axes. In this contribution, we present the results of the optical simulations for optimizing these cavities for the telecom C-Band, as well as the effect of different growth conditions on the overgrowth of InGaAs on wet-chemically pre-structured substrates to enable the fabrication of novel Gaussian-shaped micro-cavities.

HL 17.3 Wed 10:00 H32

Optically induced in-situ strain-tuning of InGaAs quantum dots for nanophotonic devices — •CHING-WEN SHIH¹, MARCO HOLZER², IMAD LIMAME¹, LASSE KOSIOL¹, SOURISH BANERJEE², ARIS KOULAS-SIMOS¹, VEERESH DESHPANDE², CATHRINE DUBOURDIEU^{2,3}, and STEPHAN REITZENSTEIN¹ — ¹Institut für Festkörperphysik, Technische Universität Berlin, Berlin, Germany — ²Helmholtz-Zentrum Berlin für Materialien und Energie GmbH, Berlin, Germany — ³Freie Universität Berlin, Physical Chemistry, Berlin, Germany

Self-assembled semiconductor quantum dots (QDs) have been widely incorporated in solid-state cavities to enable quantum technologies. However, the nature of self-assembled QDs poses a big challenge to achieving controlled emitter-cavity and emitter-emitter coupling as it not only requires an accurate spatial positioning, but also a precise spectral matching of the system. Here, we report on the MOCVD growth and fabrication of micropillar-like nanophotonic light sources consisting of strain-tunable InGaAs QDs with ALD-deposited HfO₂ thin film cladding. We show that the emission energy of QDs can be in-situ tuned by thermally annealing the HfO₂ film with a focused laser beam integrated in a μ -photoluminescence setup under cryogenic temperature. We demonstrate a tunability up to 2 meV without QDs degradation. Furthermore, we successfully tuned two separated QD emission peaks from the same structure into resonance. The developed technique paves the path for scaling up the number of coupled QDs in semiconductor nanophotonic devices.

HL 17.4 Wed 10:15 H32

Optical properties of In(Ga)As QDs emitting in the telecom C-band grown on a non-linear metamorphic buffer layer — •PASCAL PRUY, CORNELIUS NAWRATH, ROBERT SITTIG, SIMONE LUCA PORTALUPI, MICHAEL JETTER, and PETER MICHLER — Institut für Halbleitertechnik und Funktionelle Grenzflächen, Center for Integrated Quantum Science and Technology (IQST) and SCopE, University of Stuttgart, Allmandring 3, 70569 Stuttgart

Semiconductor Quantum Dots (QDs) are excellent structures for the generation of non-classical light states with outstanding performance regarding single-photon purity, photon indistinguishability and entanglement fidelity, making them promising sources for currently researched subjects such as quantum computation and quantum communication. The telecom C-band (1530-1565 nm) spectral regime is especially sought-after for fiber-based implementations of these applications due to the absorption minimum in the globally used silica fiber network. On the mature and promising GaAs material platform, the telecom C-band can be reached using a metamorphic buffer (MMB) layer and the recent progress on such QDs has attracted great interest.

While so far MMBs with a thickness of 1080nm have been employed resulting in a nominal 3λ cavity, a 1λ cavity would be greatly beneficial for more elaborate photonic structures regarding brightness and coherence. Here we report on the optical properties such as brightness, coherence and purity of In(Ga)As Quantum Dots emitting in the telecom C-band spectral regime on a novel metamorphic buffer layer compatible with 1λ cavities.

HL 17.5 Wed 10:30 H32

Optical properties of semiconductor quantum dots embedded in an open, fiber-based cavity emitting in the telecom regime — •JULIA WECKER¹, THOMAS HERZOG¹, JONAS GRAMMEL², PONRAJ VIJAYAN¹, ROBERT SITTIG¹, MICHAEL JETTER¹, SIMONE LUCA PORTALUPI¹, DAVID HUNGER², and PETER MICHLER¹ — ¹Institut für Halbleitertechnik und Funktionelle Grenzflächen, Center for Integrated Quantum Science and Technology (IQST) and SCopE, University of Stuttgart, Germany — ²Physikalisches Institut, Karlsruher Institut für Technologie (KIT), Karlsruhe, Germany

Enhancing the brightness of quantum emitters can be achieved by coupling them to optical microcavities. Together with an enhanced light extraction, shortening of the spontaneous emission rate can be achieved via the Purcell effect. In this work, we investigate In(Ga)As quantum dots embedded in an open fiber-based Fabry-Pérot cavity. On the bottom distributed Bragg reflector, quantum dots operating at the telecom O- and telecom C-Band are grown, while the top mirror is deposited on a silica fiber which can be moved with nanometric precision across the sample. Therefore, the cavity mode can be tuned in order to achieve spatial and spectral matching with the investigated emitter. The emitted photons are then directly coupled into the telecom fiber, making this fiber-coupled single-photon source promising for quantum communication applications.

30 min. break

HL 17.6 Wed 11:15 H32

GaSb quantum dots surrounded by AlGaSb with indirect-direct bandgap crossover at telecom range — •LUCIE LEGUAY and ANDREI SCHLIWA — Institut für Festkörperphysik, Technische Universität Berlin

We report the modeling and theoretical characterization of a new type-I semiconductor material based on GaSb quantum dots embedded into AlGaSb with GaSb as substrate. The calculations are performed by the nextnano++ solver, using both the effective mass and the 8-band k-p method.

Experimental work shows the formation of nano-holes with a wide range of tunability in depth and density by the local droplet etching of a surface of AlGaSb by liquid gallium [1]. Then, optically active quantum dots are obtained by filling those nano-holes with GaSb and by the deposition of a GaSb quantum well on top [2].

Our calculations demonstrate an indirect-direct bandgap crossover as the thickness of the quantum well increases, which allows control of the system's luminescence. In the direct bandgap regime, the quantum dots emit narrow excitonic spectral lines in the telecom wavelength range. These properties, as well as the low density of the quantum dots, show a lot of promise for applications in the field of infrared quantum optics.

[1] J. Hilska, A. Chellu, T. Hakkarainen, Cryst. Growth Des. 2021, 21, 1917-1923

[2] A. Chellu, J. Hilska, J-P Penttinen, T. Hakkarainen, APL Mater. 9, 051116 (2021)

HL 17.7 Wed 11:30 H32

Coherent Spin Control in InAs Quantum Dots Emitting in the Telecom C-Band — •JOHANNES MICHL¹, ŁUKASZ DUSANOWSKI^{1,3}, CORNELIUS NAWRATH², MICHAEL JETTER², SIMONE L. PORTALUPI², TOBIAS HUBER¹, PETER MICHLER², and SVEN HÖFLING¹ — ¹Technische Physik, Julius-Maximilians University of Würzburg — ²Institut für Halbleitertechnik und Funktionelle Grenzflächen (IHFG), University of Stuttgart — ³Princeton University

Semiconductor quantum dots can be used as spin-photon interfaces, enabling the preparation of photonic cluster states with a single spin in the quantum dot acting as the entangler. This leads the way towards memory-less quantum repeater protocols for quantum network applications. InAs quantum dots can be grown on metamorphic buffer layers, leading to strain relaxed growth and therefore light emission directly into the telecom C-band. Here we show magneto and polarization resolved photoluminescence experiments conducted to characterize the different charge complexes in a single quantum dot. Furthermore, we implement laser pulse sequences to gain full coherent control over a hole qubit.

HL 17.8 Wed 11:45 H32

Quantum Dot Localization Methodology based on Imaging — •MARC SARTISON, EVA SCHÖLL, LUKAS HANSCHKE, IOANNIS CALTZIDIS, OSCAR CAMACHO IBARRA, and KLAUS D. JÖNS — PhoQS, CeOPP, and Department of Physics, Paderborn University, Germany

Since the discovery of the triggered generation of single photons in 2000, quantum dots have proven to be one of the most versatile quantum light sources for pure, indistinguishable, entangled photons while maintaining high brightness. Before developing deterministic integration techniques, high yield in device fabrication remained elusive due to the statistical growth properties in high-quality self-assembled growth modes. Several methods have been developed, providing the quantum dot location and its spectral information, namely in-situ optical lithography, in-situ electron beam lithography, and quantum dot localization using quantum dot imaging. Our work describes a methodological workflow using computational, and image processing approaches in python to precisely determine the quantum dot position concerning pre-deposited metal marker structures. Here, we investigate different hardware, marker geometries, and software methods. Furthermore, we quantify the expectable upper bound accuracy for device integration. Importantly, our presented methods are not developed for a fixed emitter wavelength or type. With the right choice of optical elements within the setup, it is possible to cover the wavelengths from the visible up to the telecom C-band. The presented technique can, in principle, be applied to any type of solid-state quantum emitters.

HL 17.9 Wed 12:00 H32

Fabrication and Electrical Characterisation of Junctionless Nanowire Transistors for Detection of Atmospheric Radicals and Other Gases — •SAYANTAN GHOSH¹, MUHAMMAD BILAL KHAN¹, VAISHALI VARDHAN², ULRICH KENTSCH¹, SLAWOMIR PRUCNAL¹, SUBHAJIT BISWAS², JUSTIN HOLMES², ARTUR ERBE¹, and YORDAN M. GEORGIEV^{1,3} — ¹Institute of Ion Beam Physics and Materials Research, Helmholtz-Zentrum Dresden-Rossendorf, Dresden, Germany — ²School of Chemistry, University College Cork, Cork, Ireland — ³Institute of Electronics, Bulgarian Academy of Sciences, Sofia, Bulgaria

Silicon junctionless nanowire transistors (JNTs) have shown excellent sensitivity to record-low concentrations of the protein streptavidin in liquid phase. However, JNTs have not yet been tested for sensing in gas phase. Here we present the fabrication and initial electrical characterisation of JNT-based electronic sensors for detection of atmospheric free radicals such as hydroxyl (*OH) and nitrate

(*NO₃), which are the main drivers of chemical processes in the atmosphere. The aim of this work is to develop small, low-cost JNT-based nanosensors for radical detection. Silicon-on-insulator wafers were doped by ion implantation and flash-lamp annealing. Device patterning was based on electron beam lithography, inductively-coupled reactive ion etching, metal deposition and lift-off. Initial electrical characterisation and gas sensing experiments on fabricated devices proved their good performance and potential suitability for detection of atmospheric free radicals.

HL 17.10 Wed 12:15 H32

Single photons from Semiconductor Quantum Dots in Circular Bragg Gratings for Quantum Cryptography — •DANIEL VAJNER, LUCAS RICKERT, TIMM GAO, KORAY KAYMAZLAR, JAN-NIKLAS DONGES, JOHANNES SCHALL, SVEN RODT, STEPHAN REITZENSTEIN, and TOBIAS HEINDEL — Institut für Festkörperphysik, Technische Universität Berlin, 10623 Berlin, Germany

Semiconductor quantum dots are an excellent source of single photons for future quantum networks [1]. In order to enhance their properties they are typically incorporated into photonic structures. Among these, circular bragg gratings (CBG) are a promising way to further enhance the outcoupling efficiency [2]. Additionally, they are especially suited for fiber-coupling to achieve more compact plug-and-play single photon sources [3]. In this work we deterministically integrate single InGaAs quantum dots in CBG structures, which have been numerically optimized beforehand. We characterize the properties of the CBGs and quantify the purity and indistinguishability of the emitted photons. Finally, we aim for the implementation of cryptographic primitives such as strong quantum coin flipping using single photons.

[1] D. Vajner et al., Adv. Quantum Technol. 2100116 (2022)

[2] L. Rickert et al., Optics Express 27.25 (2019)

[3] T. Gao et al., Applied Physics Reviews 9.1 (2022)

HL 18: Oxide Semiconductors (joint session HL/KFM)

Time: Wednesday 9:30–12:30

Location: H33

HL 18.1 Wed 9:30 H33

Heavily doped Zinc Oxide with plasma frequencies in the telecommunication wavelength range — •ALEXANDER KOCH¹, HONGYAN MEI², JURA RENSBERG¹, MARTIN HAUFERMANN¹, JAD SALMAN², CHENGHAO WAN^{2,5}, RAYMOND WAMBOLD², DANIEL BLASCHE³, HEIDEMARIE SCHMIDT³, JÜRGEN SAALFELD⁴, SEBASTIAN GEBURT⁴, MIKHAIL KATS^{2,5,6}, and CARSTEN RONNING¹ — ¹Institute for Solid State Physics, Friedrich Schiller University Jena, 07743 Jena, Germany — ²Department of Electrical and Computer Engineering, University of Wisconsin Madison, Madison, Wisconsin 53706, USA — ³Leibniz Institute of Photonic Technology, 07745 Jena, Germany — ⁴Innovavent GmbH, 37077 Göttingen, Germany — ⁵Department of Materials Science and Engineering, University of Wisconsin Madison, Madison, Wisconsin 53706, USA — ⁶Department of Physics, University of Wisconsin Madison, Madison, Wisconsin 53706, USA

We demonstrate high doping of ZnO by a combination of Ga ion implantation using a focused ion beam (FIB) system and post-implantation laser and flash lamp annealing. While ion implantation allows for the incorporation of impurities with nearly arbitrary concentrations, the additional optical annealing processes enable dopant activation close to the solid-solubility limit of Ga in ZnO. By this means, we achieved highly-doped ZnO:Ga with free-carrier concentrations of $9.5 \cdot 10^{20} \text{ cm}^{-3}$, which results in a plasma wavelength shorter than the telecommunication wavelength of $1.55 \mu\text{m}$. Thus, ZnO:Ga is a very promising plasmonic material for optical applications in the near-infrared spectral region.

HL 18.2 Wed 9:45 H33

Side-by-side display of optical and resistive H₂S gas sensing properties of pristine and gold functionalized ZnO nanowires — •ANGELIKA KAISER¹, TANJA MAURITZ¹, JOACHIM BANSMANN³, ULRICH HERR¹, and KLAUS THONKE² — ¹Institute of Functional Nanosystems, University Ulm, 89081 Ulm, Germany — ²Institute of Quantum Matter, Semiconductor Physics Group, University Ulm, 89081 Ulm, Germany — ³Institute for Surface Chemistry and Catalysis, University Ulm, 89081 Ulm, Germany

We investigate the mechanism of hydrogen sulfide (H₂S) gas sensing in pristine and gold functionalized zinc oxide (ZnO) nanowires (NW), two potent nanomaterial systems with an enlarged surface-area-to-volume ratio for medical breath analysis in the sub-ppm regime through the "electronic nose" approach. Pristine ZnO NWs (ZnO(NM)) are grown by high-temperature chemical vapor deposition (CVD) and functionalized with gold (Au) nanoparticles by magnetron sputtering (ZnO(Au)). The sensor response is studied by photoluminescence (PL) and electrical conductivity measurements of as-grown ZnO NWs and open gate ZnO NW ChemFET structures. A systematic side-by-side comparison of PL-intensity-time measurements and current-time measurements reveal a two-step detection process between 1 ppm of H₂S and ZnO(NM)/ZnO(Au) NWs. Temperature series hints at underlying gas adsorption/desorption processes. Additional X-ray photoelectron spectroscopy (XPS) confirms the beneficial gas-sensitive affinity between Au functionalization and H₂S gas, which leads to a significant improvement of the sensitivity for H₂S detection.

HL 18.3 Wed 10:00 H33

Growth window of α -Ga₂O₃ on m-plane sapphire by pulsed laser deposition — •C. PETERSEN, S. VOGT, M. KNEISS, H. VON WENCKSTERN, and M. GRUNDMANN — Universität Leipzig, Felix Bloch Institute for Solid State Physics, Semiconductor Physics Group, Leipzig, Germany

Due to its high bandgap of 4.6–5.3 eV and high predicted breakdown field of 8 MV/cm [1], much attention is drawn to the wide bandgap semiconductor Ga₂O₃ for applications in high-power devices. However, besides the well-studied thermodynamically stable monoclinic β -phase of Ga₂O₃, the metastable

α -polymorph with corundum structure is gaining scientists' interest. Since it is isostructural to Al₂O₃, miscibility over the entire composition range of α -(Al_xGa_{1-x})₂O₃ can be achieved [2] and the growth on cost-effective sapphire substrates becomes feasible. Thereby m-plane sapphire facilitates the growth of the corundum phase [3] and allows for thin films with electron mobilities as high as $65 \text{ cm}^2 (\text{Vs})^{-1}$ [4]. We present phase-pure α -Ga₂O₃ thin films grown on m-plane sapphire over a wide temperature range of 565 °C up to 750 °C with high crystallinity and surface roughnesses as low as 0.7 nm (RMS). We further demonstrate that for oxygen partial pressures above 0.001 mbar the formation of the monoclinical β -phase and spinel-defective γ -phase occurs and provide a corresponding phase diagram. Resulting samples were investigated employing X-ray diffraction, reciprocal space maps and atomic force microscopy. [1] Higashiwaki, Sc. Sci. Tech., 034001, 2016. [2] Hassa, pss-b, 2000394, 2020. [3] Kneiß, jmr, 4816-4831, 2021. [4] Akaiwa, pss-a, 1900632, 2020.

HL 18.4 Wed 10:15 H33

Simulation of Switching Processes Inside Bilayer Valence Change Memory Cells by a Drift-Diffusion Model — •NILS SOMMER¹, STEPHAN MENZEL¹, and RAINER WASER^{1,2} — ¹Peter Grünberg Institut 7, Forschungszentrum Jülich, Germany — ²Institut für Werkstoffe der Elektrotechnik 2, RWTH Aachen, Germany

Valence change memory (VCM) cells are promising candidates for future non-volatile storage devices [1]. VCM cells are characterized by their ability to switch between at least two stable resistance states by applying suitable bias voltages. A special structure of VCM cells are bilayer cells consisting of two semiconducting oxide layers, with one oxide serving as a tunnel barrier. Experiments show that a change in resistance of the cell can be caused by the exchange of oxygen between the two oxide layers [2]. However, the processes taking place are not yet well understood. We use a drift-diffusion model to simulate the movement of oxygen inside the semiconductor to gain a better understanding of the exchange process between the layers. We investigate the internal electric fields acting as a driving force on the oxygen, as well as the oxygen diffusion process that causes it to return to an equilibrium state. We show that an oxygen exchange deforms the shape of the tunnel barrier and by this changing the resistance of the cell. Further, we show that the change in resistance depends on the permittivity of the oxides.

[1] R. Waser, R. Dittmann, G. Staikov, K. Szot, Adv. Mater. 2009, 21, 2632 [2] A. Gutsche, S. Siegel, J. Zhang, S. Hamsch, R. Dittmann, Frontiers in Neuroscience, 2021, 15, 661261

HL 18.5 Wed 10:30 H33

Phonons, Isotope Effects, and Point Defects in β -Ga₂O₃ — •BENJAMIN M. JANZEN¹, PIERO MAZZOLINI^{2,3}, ROLAND GILLEN⁴, ANDREAS FALKENSTEIN⁵, VIVIAN F. S. PELTASON¹, HANS TORNATZKY¹, DANIEL CIERPINSKY¹, ANDREA ARDENGHI², MANFRED MARTIN⁵, JANINA MAULTZSCH⁴, ROBERTO FORNARI^{2,3}, ZBIGNIEW GALAZKA⁶, OLIVER BIERWAGEN², and MARKUS R. WAGNER¹ — ¹Technische Universität Berlin, Institute of Solid State Physics, Berlin, Germany — ²Paul-Drude-Institut für Festkörperelektronik, Leibniz-Institut im Forschungsverbund Berlin e.V, Germany — ³Department of Mathematical, Physical and Computer Sciences, University of Parma, Italy — ⁴Chair of Experimental Physics, Friedrich-Alexander-Universität Erlangen-Nürnberg, Germany — ⁵Institute of Physical Chemistry, RWTH Aachen University, Germany — ⁶Leibniz-Institut für Kristallzüchtung, Berlin, Germany

We present a combined experimental and theoretical study of lattice vibrations in a homoepitaxial β -Ga₂O₃ thin film grown by MBE with different oxygen isotopes (16O, 18O). Using polarized first- and second order micro-Raman spectroscopy, we identified all 15 first-order Raman modes of β -Ga₂O₃. In combi-

nation with density functional perturbation theory calculations, we identify the atomistic origins (Ga-Ga, Ga-O or O-O) of all Raman active phonon modes in β -Ga₂O₃ by quantifying the isotopically-induced relative frequency shifts of the individual Raman modes and investigate the presence of point defects on specific lattice sites.

HL 18.6 Wed 10:45 H33

Epitaxial ZnO thin films and NWs — •MAXIMILIAN KOLHEP¹, MARGIT ZACHARIAS¹, and JÜRGEN BLÄSING² — ¹Laboratory for Nanotechnology, Department of Microsystems Engineering (IMTEK), University of Freiburg, Freiburg 79110, Germany — ²Otto-von-Guericke-University Magdeburg, Institute of Physics, Magdeburg, Germany

Due to its high piezoelectric coefficient and direct band gap of 3.37 eV, ZnO and especially ZnO nanowires are of interest for numerous future applications. We demonstrate the epitaxial growth of ZnO on Si(111) substrates using an AlN buffer layer by atomic layer deposition (ALD). ALD is a promising technique as it allows the deposition of extremely thin films with precise thickness control and excellent conformality over large areas. The crystalline quality of ZnO thin films determined by XRD increases with increasing deposition temperature and an additional post-annealing step. These thin films have a great potential as a substrate for the subsequent catalyst-free and epitaxial growth of ZnO NWs by CVD. The influence of growth parameters on the morphology of ZnO NWs will be discussed.

15 min. break

HL 18.7 Wed 11:15 H33

Investigation of CuBr_xI_{1-x} thin films and CuI bulk material — •MICHAEL BAR¹, EVGENY KRÜGER¹, STEFFEN BLAUROCK², STEFAN MERKER², HOLGER VON WENCKSTERN¹, HARALD KRAUTSCHEID², and MARIUS GRUNDMANN¹ — ¹Universität Leipzig, Felix-Bloch Institute, Germany — ²Universität Leipzig, Institute of Inorganic Chemistry, Germany

Oxide based wide-bandgap materials with suitable transparency in the visible range are typically unipolar, such that heterostructures are needed for complementary devices. The search for a suitable p-type candidate has led to copper iodide (CuI), which unites transparency in the visible spectral range with exceptional hole mobility, therefore sharing and yet complementing typical properties of oxides. Fabrication methods include sputtering, spin coating and molecular beam epitaxy. [1,2] We present structural, electrical and optical properties of CuI bulk material, and thin films which were grown by pulsed laser deposition (PLD). Furthermore, alloyed thin films of CuBr_xI_{1-x} were deposited with a segmented target PLD approach and investigated using x-ray diffraction, transmission and photoluminescence measurements. This PLD approach allows for deposition of thin films in the full composition range using only a single target without the need of sintering. [3] A systematic shift of lattice constants as well as the excitonic features can be observed as function of alloy composition.

[1] C. Yang *et al.*, Proc. Natl. Acad. Sci. USA, **113**(46), 12929, (2016).

[2] S. Inagaki *et al.*, Appl. Phys. Lett., **116**(19), 192105, (2020).

[3] H. Wenckstern *et al.*, Phys. Stat. Sol. (b), **257**(7), 1900626, (2020).

HL 18.8 Wed 11:30 H33

A Koopman's compliant exchange correlation potential for semiconductors — •MICHAEL LORKE¹, PETER DEAK², and THOMAS FRAUENHEIM² — ¹Institute for Theoretical Physics, University of Bremen, Germany — ²BCCMS, University of Bremen, Germany

Density functional theory is the workhorse of theoretical materials investigations. Due to the shortcoming of (semi-)local exchange correlation potentials, hybrid functionals have been established for practical calculations to describe surfaces, molecular adsorption, and defects. These functionals operate by mixing between semi-local and Hartree-Fock exchange semi-empirically. However, their parameters have to be optimized for every material separately. To treat materials with a more physics driven approach and without the need of parameter optimization is possible with many-body approaches like GW, but at an immense increase in computational costs and without the access to total energies and hence geometry optimization.

We propose a novel exchange correlation potential[1] for semiconductor materials, that is based on physical properties of the underlying microscopic screening. We demonstrate that it reproduces the low temperature band gap of several materials. Moreover it respects the required linearity condition of the total energy with the fractional occupation number, as expressed by the generalized

Koopman's theorem. We also show that this novel functional can be used as a kernel in linear response TDDFT to reproduce excitonic effects in optical spectra

[1] Physical Review B 102 (23), 235168 (2020)

HL 18.9 Wed 11:45 H33

The role of defects in polaron hopping transport in epitaxial BiVO₄ for solar water splitting — •MALTE LUCA WEBER, VIKTORIA FRANZISKA KUNZELMANN, and IAN SHARP — Walter Schottky Institute, TUM, Am Coulombwall 4, 85748 Garching, Germany

Use of green hydrogen as a fuel, energy storage medium, and reactant in chemical industry is one of the key strategies on the way to a sustainable economy. In this regard, solar driven water splitting using semiconductor photoelectrodes is a promising approach for sustainable production of hydrogen. Among various investigated semiconductor photoelectrodes, BiVO₄ offers several desirable characteristics, including favourable band edge energetics, high carrier separation efficiency, and potential for stable operation under photoelectrochemical conditions. However, the material is characterised by very low carrier mobilities due to self-trapping formation of small polarons. Here, the effect of intentionally introduced defects on charge carrier mobility is investigated. Using a novel solution-based synthesis technique, high-quality epitaxial BiVO₄ thin films were grown on YSZ (001). Post-synthetic vacuum annealing enables tuneable introduction of tuneable concentrations of oxygen vacancy defects. Optical characterisation by photothermal deflection spectroscopy clearly indicates an increase of the sub-bandgap absorption for an increasing defect concentration, leaving unaltered the bandgap. Temperature-dependent electrical conductivity measurements indicate a thermally-activated hopping behaviour, which is characterised by higher conductivities and lower hopping behaviours with increasing native point defect concentrations.

HL 18.10 Wed 12:00 H33

Conduction channels in polycrystalline copper iodide thin films — •TILLMANN STRALKA — Universität Leipzig, Felix Bloch Institute for Solid State Physics, Linnéstr. 5, 04103 Leipzig, Germany

The search for high-performance, transparent p-type conductive materials has been a major challenge for decades [1]. Copper iodide (CuI) or alloys based on CuI [2] could offer a solution, since CuI does outperform all other known p-type TCMs, concerning transmittance in the visible spectrum as well as electrical conductivity at room temperature [3]. In this contribution polycrystalline CuI thin films, grown by sputtering, are investigated. Hereby we try to understand and differentiate the contribution of grains and grain boundaries (GBs) to electrical transport. Extended structural defects such as GBs lead to a depletion of majority charge carriers in their vicinity and even a localised inversion (two dimensional electron gas) within GBs was reported [4]. To acquire morphological (grain and GBs) and electrical properties with a high spatial resolution we employ current probe atomic force microscopy and Kelvin probe force microscopy. We evaluate these measurements with a novel approach that offers the possibility to correlate topographic and electrical properties over a whole series of scans in dependence on an externally applied voltage [5], measuring temperature, probe force, plasma treatment and degradation over time.

[1] M. Grundmann *et al.*, J.Phys.D.Apps.Phys., 49(213001), 2016 [2] T. Jun *et al.*, Adv. Mater., 30(1706573), 2018 [3] C. Yang *et al.*, PNAS 113(412929), 2016 [4] M. Kneiß *et al.*, Adv. Mater. Interfaces, 5(6), 2018 [5] I. Visoly-Fisher *et al.*, Adv. Funct. Mater., 16(649), 2016

HL 18.11 Wed 12:15 H33

First-Principles Studies of Defects in Bismuth Vanadate — •NICKLAS ÖSTERBACKA¹, FRANCESCO AMBROSIO², and JULIA WIKTOR¹ — ¹Chalmers University of Technology, Gothenburg, Sweden — ²University of Salerno, Fisciano, Italy

Bismuth vanadate, a transition-metal oxide semiconductor with a bandgap of 2.4 eV, has shown great promise as a water-splitting photocatalyst. Its practical performance remains limited due to slow hole transfer, high charge recombination rates, and low conductivity, however. An atomistic understanding of the relationship between the material's structure and its properties is key to solving these issues. To this end, we have performed first-principles calculations on the native defects of bismuth vanadate, revealing their structural complexity and highlighting the importance of taking charge localization into account for this class of materials. Additionally, we show that oxygen vacancy-induced distortions in the material complicates phase identification of synthesized samples by making powder X-ray diffraction ambiguous.

HL 19: Materials and Devices for Quantum Technology 1

Time: Wednesday 9:30–13:00

Location: H34

Invited Talk

HL 19.1 Wed 9:30 H34

Quantum Interference of Identical Photons from Remote GaAs Quantum Dots — •GIANG NAM NGUYEN¹, LIANG ZHAI¹, CLEMENS SPINLER¹, JULIAN RITZMANN², MATTIAS C. LÖBL¹, ANDREAS D. WIECK², ARNE LUDWIG², ALISA JAVADI¹, and RICHARD J. WARBURTON¹ — ¹Department of Physics, University of Basel — ²Lehrstuhl für Angewandte Festkörperphysik, Ruhr-Universität Bochum

Efficient generation and detection of coherent single photons are key to advances in photonic quantum technologies such as quantum computation, quantum simulation, and quantum communication. For applications, a significant roadblock is the poor quantum coherence upon interfering single photons created by independent emitters.

Here, we present near-unity two-photon interference visibilities from two separate GaAs quantum dots [1]. This high visibility (~93%) is achieved under rigorous conditions: there is no Purcell enhancement, no temporal post-selection, no narrow spectral-filtering, nor frequency stabilization. Using photons emitted from two remote quantum dots, we demonstrate a photonic CNOT gate. Interfering photons in this quantum logic gate, we generate an entangled two-photon state using photons from separate semiconductor chips. We obtain an entanglement fidelity of (85 ± 1)%, exceeding the CHSH threshold for violating Bell inequalities. This result highlights the importance of the high two-photon visibility for high fidelity entanglement operations.

[1] L. Zhai et al., Nature Nanotechnol. (2022)

HL 19.2 Wed 10:00 H34

Optimizing quantum teleportation with imperfect quantum dot sources — •FRANCESCO SALUSTI¹, FRANCESCO BASSO BASSET², LUCAS SCHWEICKERT³, MICHELE B. ROTA², DAVIDE TEDESCHI², SAIMON FILIPE COVRE DA SILVA⁴, EMANUELE ROCCIA², VAL ZWILLER³, KLAUS D. JÖNS¹, ARMANDO RASTELLI⁴, and RINALDO TROTTA² — ¹Department of Physics, Paderborn University, Paderborn, Germany — ²Department of Physics, Sapienza University of Rome, Rome, Italy — ³Department of Applied Physics, Royal Institute of Technology, Stockholm, Sweden — ⁴Institute of Semiconductor and Solid State Physics, Johannes Kepler University, Linz, Austria

All-optical quantum communication protocols such as teleportation and entanglement swapping require the generation of entangled photons. Quantum dots, with their on-demand generation and low unwanted multi-photon emission are excellent candidates to realize these protocols. However, finding quantum dots with near-perfect quantum optical properties remains challenging. Instead, in our work we demonstrate that it is possible to improve a quantum teleportation protocol by acting exclusively on the experimental setup. [1] Despite selecting a source with non-ideal figures of merit, we have been able to enhance the overall protocol fidelity. The obtained values agree with our developed model, taking the quantum dot properties into account. Our model provides predictive power for future source optimization. Reference: [1] F. Basso Basset, F. Salusti et al., npj Quantum Information 7, 7 (2021)

HL 19.3 Wed 10:15 H34

Time Dependent Redfield Dynamics of Semiconductor Quantum-Dot Molecules — •STEFFEN WILKSEN, ISABELL HÜLLEN, FREDERIK LOHOF, and CHRISTOPHER GIES — Institute for Theoretical Physics, University of Bremen, Bremen, Germany

Semiconductor quantum dots provide a promising platform for applications in quantum information technologies, like quantum repeaters, which enable secure quantum communication over long distances. Two quantum dots, separated by a small tunneling layer, can be combined into so-called quantum dot molecules (QDMs) which exhibit properties similar to classical molecules. These properties can be tuned by applying an external electric field, which allows to perform switching operations on QDM-based qubits.

The QDM can not be treated in isolation, since the electron-phonon interaction plays a crucial role in the systems dynamics. We thus treat the QDM as an open quantum system coupled to the external phonon reservoir. The application of a time-dependent electric field not only changes the QDM's properties, but also the form of the electron-phonon interaction, which allows for a time dependent tuning of dissipative effects.

We investigate the behaviour of the system for different switching speeds of the electric field using a time-dependent Redfield master equation approach. Slow switching leads to predictable and controlled adiabatic behaviour but limits the clock rate of the quantum repeater, whereas fast switching allows for higher clock rates but leads to non-adiabatic behaviour.

HL 19.4 Wed 10:30 H34

Three-dimensional electrical control of the excitonic fine structure for a quantum dot in a cavity — •MARTIN ESMANN^{1,2}, HÉLÈNE OLLIVIER¹, PRIYA PRIYA¹, ABDELMOUNAIM HAROURI¹, ISABELLE SAGNES¹, ARISTIDE LEMAÎTRE¹, OLIVIER KREBS¹, LOIC LANCO¹, DANIEL LANZILLOTTI-KIMURA¹, and PASCALE SENELLART¹ — ¹Université Paris-Saclay, CNRS, Centre de Nanosciences et de Nanotechnologies (C2N), Palaiseau, France — ²Institut für Physik, Universität Oldenburg, Germany

The excitonic fine structure plays a key role for the quantum light generated by semiconductor quantum dots, both for entangled photon pairs and single photons [1]. Controlling the excitonic fine structure has been demonstrated using electric, magnetic, or strain fields, but not for quantum dots in optical cavities, a key requirement to obtain high source efficiency and near-unity photon indistinguishability [2]. Here, we demonstrate the control of the fine structure splitting for quantum dots embedded in micropillar cavities. We propose and implement a scheme based on remote electrical contacts connected to the pillar cavity through narrow ridges. Numerical simulations show that such a geometry allows for a three-dimensional control of the electrical field. We experimentally demonstrate tuning and reproducible canceling of the fine structure, a crucial step for the reproducibility of quantum light source technology.

[1] P. Senellart, G. Solomon, and A. White, Nature Nanotechnology 12, 1026 (2017). [2] R. Trotta et al. PRL 114, 150502 (2015). [3] H. Ollivier et al. arXiv:2112.00400.

HL 19.5 Wed 10:45 H34

Design study of electrically contacted quantum dot circular Bragg gratings — •QUIRIN BUCHINGER, TOBIAS HUBER, and SVEN HÖFLING — Technische Physik, Universität Würzburg, 97074 Würzburg, Germany

Recently, photonic quantum networks receive a lot research interest. Semiconductor quantum dots offer a local memory, utilizing single spins and are highly efficient single or entangled photon sources. Therefore, they are among suitable candidates for a scalable hardware platform for quantum networks. To enhance brightness and extraction efficiency the quantum dots are typically embedded into microcavities, here circular Bragg gratings. By incorporating the quantum dots into a diode structure they can be charged with a single electron or hole and thus generate a ground state spin qubit [1]. This provides opportunity for spin photon coupling [2]. To apply voltage to the quantum dot inside of a circular Bragg grating, bridges through the etched rings have to be leaved unetched as a path for the current to the central disc of the microcavity. We discuss different layouts of these bridges and their influence on cavity wavelength, quality factor and polarisation.

[1] Warburton, R., Nature Mater 12, 483-493 (2013)

[2] De Greve, K., et al. Nature 491, 421-425 (2012)

30 min. break

HL 19.6 Wed 11:30 H34

Influence of extended defects on the formation energy, hyperfine structure, and zero-field splitting of NV centers in diamond — WOLFGANG KÖRNER¹, •DANIEL URBAN¹, and CHRISTIAN ELSÄSSER^{1,2} — ¹Fraunhofer Institute for Mechanics of Materials IWM, Wöhlerstr. 11, 79108 Freiburg, Germany — ²University of Freiburg, Freiburg Materials Research Center (FMF), Stefan-Meier-Straße 21, 79104 Freiburg, Germany

We present a density-functional theory analysis of nitrogen-vacancy (NV) centers in diamond, which are located in the vicinity of extended defects, namely, intrinsic stacking faults, extrinsic stacking faults, and coherent twin boundaries on 111 planes in diamond crystals [1]. Several sites for NV centers close to the extended defects are energetically preferred with respect to the bulk crystal. This indicates that NV centers may be enriched at extended defects. We report the hyperfine structure and zero-field splitting parameters of the NV centers at the extended defects, which typically deviate by about 10% but in some cases up to 90% from their bulk values. Furthermore, we find that the influence of the extended defects on the NV centers is of short range: NV centers that are about three double layers (corresponding to ~ 6 Å) away from defect planes already show bulklike behavior.

[1] W. Körner, D. F. Urban, and C. Elsässer, Phys. Rev. B 103, 085305 (2021).

HL 19.7 Wed 11:45 H34

Topological insulator based axial DC SQUID quantum interferometer structure — •ERIK ZIMMERMANN^{1,2}, BENEDIKT FROHN^{1,2}, JAN KARTHEIN^{1,2}, GERIT BEHNER^{1,2}, ABDUR REHMAN JALIL^{1,2}, TOBIAS SCHMITT^{2,3}, MICHAEL SCHLEENVOIGT^{1,2}, GREGOR MUSSLER^{1,2}, PETER SCHÜFFELGEN^{1,2}, HANS LÜTH^{1,2}, DETLEV GRÜTZMACHER^{1,2,3}, and THOMAS SCHÄPERS^{1,2} — ¹Peter Grünberg Institut (PGI-9), Forschungszentrum Jülich, 52425 Jülich, Germany — ²JARA-Fundamentals of Future Information Technology, Jülich-Aachen Re-

search Alliance, Forschungszentrum Jülich and RWTH Aachen University, Germany — ³Peter Grünberg Institut (PGI-10), Forschungszentrum Jülich, 52425 Jülich, Germany

Three-dimensional topological insulators (TIs) form a new material class that may enable robust topological quantum computing when combining them with a superconductor by using so-called Majorana zero modes. Recently, Josephson junctions and SQUIDs using a TI as a weak link are investigated for interface characterization. We present the in-situ fabrication of an interferometer structure formed by an axial DC SQUID that is based on a ternary TI with a $\text{Bi}_{0.18}\text{Sb}_{1.82}\text{Te}_3$ composition. For the in-situ fabrication shadow mask techniques and selective area growth by molecular beam epitaxy are used. Furthermore, magnetotransport measurements are shown, revealing induced superconductivity in both Josephson junctions and an in-plane magnetic field dependent interference pattern corresponding to SQUID oscillations. Lastly, the Shapiro response of the device is investigated.

HL 19.8 Wed 12:00 H34

Top-down nanofabrication of silicon nanopillars hosting telecom photon emitters — •NAGESH S. JAGTAP^{1,2}, MICHAEL HOLLENBACH^{1,2}, CIARÁN FOWLEY¹, JUAN BARATECH¹, VERÓNICA GUARDIA-ARCE¹, ULRICH KENTSCH¹, ANNA EICHLER-VOLF¹, NIKOLAY V. ABROSIMOV³, ARTUR ERBE¹, CHAEHO SHIN⁴, HAKSEONG KIM⁴, MANFRED HELM^{1,2}, WOO LEE⁴, GEORGY V. ASTAKHOV¹, and YONDER BERENCÉN¹ — ¹Helmholtz-Zentrum Dresden-Rossendorf, Institute of Ion Beam Physics and Materials Research, Bautzner Landstrasse 400, 01328 Dresden, Germany — ²Technische Universität Dresden, 01062 Dresden, Germany — ³Leibniz-Institut für Kristallzüchtung, 12489 Berlin, Germany — ⁴Korea Research Institute of Standards and Science, 34113 Daejeon, Republic of Korea

Silicon, a ubiquitous material in modern computing, is an emerging platform for realizing a source of indistinguishable single-photons on demand. The integration of recently discovered single-photon emitters in silicon into photonic structures is advantageous to exploit their full potential for integrated photonic quantum technologies [1] [2]. Here, we show the integration of an ensemble of telecom photon emitters in a two-dimensional array of silicon nanopillars. We developed a top-down nanofabrication method, enabling the production of thousands of individual nanopillars per square millimeter with state-of-the-art photonic-circuit pitch, all the while being free of fabrication-related radiation damage defects. We found a waveguiding effect of the 1278 nm G-center emission along individual pillars accompanied by improved brightness, compared to that of bulk silicon.

HL 19.9 Wed 12:15 H34

Large hBN single-photon emitter arrays fabricated by capillary assembly — •JOHANN ADRIAN PREUSS, EDUARD RUDI, JOHANNES KERN, ROBERT SCHMIDT, RUDOLF BRATSCHITSCH, and STEFFEN MICHAELIS DE VASCONCELLOS — University of Münster, Institute of Physics and Center for Nanotechnology, Wilhelm-Klemm-Str. 10, 48149 Münster, Germany

Convenient and readily available quantum light sources are a crucial building block for quantum photonic technologies. Recently, single-photon emitters have been discovered in hexagonal boron nitride (hBN), which efficiently emit single

photons even at room temperature. Controlling the positioning of nanocrystals hosting these light emitters is an important technique for the bottom-up fabrication of functional nanostructures. Here, we demonstrate the fabrication of mm^2 -sized rectangular arrays formed by tens of thousands of hBN nanoplatelets [1]. Using capillary assembly, we arrange commercially available hBN nanopowder. Positioning yields of >95% are achieved on individual fields. We find stable and spectrally narrow quantum optical light emitters in 16% of the positions. Our preparation method opens the way for the combination of quantum light emitters in hBN with further fabrication steps for integrated photonic chips, which can provide thousands of single-photon sources at different emission energies.

[1] J. A. Preuß et al., 2D Materials 8, 035005 (2021)

HL 19.10 Wed 12:30 H34

Single-electron shuttling by Si/SiGe Quantum Bus — •RAN XUE, INGA SEIDLER, TOM STRUCK, SIMON HUMPHOL, TOBIAS HANGLEITER, HENDRIK BLUHM, and LARS R. SCHREIBER — JARA-FIT Institute for Quantum Information, Forschungszentrum Jülich GmbH and RWTH Aachen University, Aachen, Germany

The electron-spin in gate-defined quantum dots in a Si/SiGe heterostructure is one of the most promising qubits for scalable quantum computing. Qubit gates beyond the error-correction threshold have been widely investigated, however, the long range coupling of qubits remains challenging. Here we study the feasibility of single electron shuttling by forming a propagating sinusoidal potential in a gate-defined 1-dimensional channel. A $99.42 \pm 0.02\%$ high single-electron shuttle fidelity over a distance of 420 nm has been demonstrated in our recent research. [1] It provides adiabatic movement of a quantum dot filled by a single electron representing the qubit. An extension to 10 μm long devices is in progress. The number of control lines is intrinsically independent from the shuttle length, therefore, no additional scalability complexity regarding signal generation and wiring is expected. Our concept is compatible with industrial CMOS fabrication lines and ultimately might lead to transport spin qubit information without much loss of spin-coherence.

[1] Seidler, I. et al., Conveyor-mode single-electron shuttling in Si/SiGe for a scalable quantum computing architecture. arXiv:2108.00879 (2021).

HL 19.11 Wed 12:45 H34

Device-Scale Modeling and Simulation of Solid State Spin-Qubit-Shuttles —

•LASSE ERMONEIT, MARKUS KANTNER, and THOMAS KOPRUCKI — Weierstrass Institute for Applied Analysis and Stochastics (WIAS), 10117 Berlin, Germany
We develop a theoretical model and a numerical simulation framework for a spin-qubit shuttling device for coherent transfer of quantum information between remote arrays of gate-defined quantum dots. The goal is to provide a device-scale simulation environment that solves the Schrödinger wave packet propagation problem in the presence of specific disorder potentials inside the shuttling device. Time-dependent electrostatic potentials of the gate electrodes and perturbations are obtained as solutions of Poisson's equation. We present our modeling approach together with first simulations results and outline how methods of model order reduction and optimal control theory can be employed to find a solution that ensures a high transmission fidelity in the presence of dephasing.

HL 20: 2D Materials 4 (joint session HL/ CPP/DS)

Time: Wednesday 9:30–12:00

Location: H36

HL 20.1 Wed 9:30 H36

Dark exciton anti-funneling in monolayer transition metal dichalcogenides — •ROBERTO ROSATI¹, ROBERT SCHMIDT², SAMUEL BREM¹, RAÜL PEREA-CAUSÍN³, IRIS NIEHUES⁴, JOHANNES KERN², JOHANN ADRIAN PREUSS², ROBERT SCHNEIDER², STEFFEN MICHAELIS DE VASCONCELLOS², RUDOLF BRATSCHITSCH², and ERMIN MALIC^{1,3} — ¹Philipps-Universität Marburg — ²University of Münster — ³Chalmers University of Technology — ⁴CIC nanoGUNE BRTA

Current nanoelectronics relies on transport. While charged carriers can be controlled by electric fields, atomically thin semiconductors are governed by excitons, which are neutral electron-hole pairs. Recently, strain engineering has been introduced to manipulate exciton diffusion [1] and propagation [2] in monolayer transition metal dichalcogenides. Strain-induced energy gradients give rise to exciton funneling up to a micrometer range. Combining spatiotemporal photoluminescence measurements with microscopic theory, here we track the way of excitons in time, space and energy. Surprisingly we find that in WS_2 excitons move away from high-strain regions, contrary to what we observe in MoSe_2 [2]. This anti-funneling behavior can be ascribed to dark excitons, whose strain-induced energy variations are opposite compared to bright excitons. Our findings open new possibilities to control transport in exciton-dominated materials.

[1] R. Rosati et al., 2D Mater. 8, 015030 (2021).

[2] R. Rosati, R. Schmidt et al., Nat. Commun. 12, 7221 (2021).

HL 20.2 Wed 9:45 H36

Ultrafast nanoscopy of a Mott transition in twisted bilayer WSe_2 — •SVENJA NERRETER¹, THOMAS SIDAY¹, FABIAN SANDNER¹, SAMUEL BREM^{2,3}, MARTIN ZIZLSPERGER¹, FELIX SCHIEGL¹, RAUL PEREA-CAUSIN³, MARKUS PLANKL¹, PHILIPP MERKL¹, FABIAN MOOSHAMMER^{1,4}, MARKUS A. HUBER¹, ERMIN MALIC^{2,3}, and RUPERT HUBER¹ — ¹Department of Physics and Regensburg Center for Ultrafast Nanoscopy, University of Regensburg, Germany — ²Department of Physics, Philipps-Universität Marburg, Germany — ³Department of Physics, Chalmers University of Technology, Gothenburg, Sweden — ⁴Department of Physics, Columbia University, New York, USA

The density-driven transition of an exciton gas into a Fermi liquid of unbound electron-hole pairs has formed a compelling testing ground of many-body physics. Layered transition metal dichalcogenides feature advantageous conditions, yet nanoscale inhomogeneities have complicated quantitative studies of this elusive transition. Here, we use ultrafast polarization nanoscopy to trace optically bright and dark electron-hole pairs during an exciton Mott transition in a twisted homobilayer of WSe_2 . At elevated densities, initially monomolecular recombination dynamics of optically dark excitons continuously evolve into the bimolecular recombination of unbound electron-hole pairs. We directly reveal how the Mott transition varies over nanometer length scales, evidencing strong spatial disorder in stacked monolayers and demonstrating the capabilities of our technique to resolve the local interplay of strong electronic correlations.

HL 20.3 Wed 10:00 H36

Rashba excitons in the 2D Ruddlesden-Popper perovskite (BA)MAPI — •PHILIPP MOSER¹, MARTIN SCHALK¹, ATSUSHIKO MIYATA², JOACHIM WOSNITZ², ANDREAS STIER¹, and JONATHAN FINLEY¹ — ¹Walter Schottky Institute, Garching, Germany — ²Helmholtz-Zentrum Dresden-Rossendorf, Dresden, Germany

Two-dimensional organic-inorganic perovskites have emerged as remarkable materials for energy conversion, optoelectronic and spintronic applications. Recently, the role of spin-orbit (SO) coupling and the resulting effects on the band-structure and dark/bright optical transitions has become a key topic of interest. The necessary structural inversion asymmetry for SO-coupling is predicted to stem from the organic cations comprising the crystals. As a result, dark excitons, red detuned from the bright exciton, have been discussed in this material system. Here, we investigate the exciton physics of the 2D Ruddlesden-Popper perovskite (BA)MAPI. By performing one-photon absorption, -PL and two-photon PLE spectroscopy, we investigate the optical transitions close to the R-point of the Brillouin zone and find distinct 2-photon transitions blue detuned from the ground state exciton that can be explained by a Rashba-split band-structure. Utilizing high-field magneto-spectroscopy up to $B=60$ T, we determine that these absorption features are due to Wannier excitons. We determine the size and binding energy from the diamagnetic shift of the features and obtain evidence that 2D (BA)MAPI hosts strongly bound Rashba excitons.

HL 20.4 Wed 10:15 H36

Ultrafast pseudospin quantum beats in multilayer WSe₂ and MoSe₂ — •SIMON RAIBER¹, PAULO E. FARIA JUNIOR², DENNIS FALTER¹, SIMON FELDL¹, PETTER MARZENA¹, KENJI WATANABE³, TAKASHI TANIGUCHI⁴, JAROSLAV FABIAN², and CHRISTIAN SCHÜLLER¹ — ¹Institut für Experimentelle und Angewandte Physik, Universität Regensburg, D-93040 Regensburg, Germany — ²Institut für Theoretische Physik, Universität Regensburg, D-93040 Regensburg, Germany — ³Research Center for Functional Materials, NIMS, Tsukuba, Japan — ⁴International Center for Materials Nanoarchitectonics, NIMS, Tsukuba, Japan

We present investigations of excitonic transitions in mono- and multilayer WSe₂ and MoSe₂ materials by time-resolved Faraday ellipticity (TRFE) with in-plane magnetic fields, of up to $B = 9$ T. In monolayer samples, the measured TRFE time traces are almost independent of B , which confirms a close to zero in-plane exciton g factor, consistent with first-principles calculations. In stark contrast, we observe pronounced temporal oscillations in multilayer samples for $B > 0$. Remarkably, the extracted in-plane g factors are very close to reported out-of-plane exciton g factors of the materials, namely $|g_{< 1s}| = 3.1 \pm 0.2$ and 2.5 ± 0.2 for the $1s$ A excitons in WSe₂ and MoSe₂ multilayers, respectively. Our first-principles calculations nicely confirm the presence of a non-zero in-plane g for the multilayer samples. We propose that the oscillatory TRFE signal in the multilayer samples is caused by pseudospin quantum beats of excitons, which is a manifestation of spin- and pseudospin layer locking in the multilayer samples.

HL 20.5 Wed 10:30 H36

Nonlinear Exciton Dynamics in Layered Heterostructures — •VIPIN KRISHNA¹, XIAO CHEN², TARLAN HAMZAYEV¹, SILVANA BOTTI², and GIANCARLO SOAVI¹ — ¹Institute of Solid state Physics, Friedrich-Schiller-University, Jena — ²Institute of Theoretical Solid State Theory and Optics, Friedrich-Schiller-University, Jena

Transition-metal-dichalcogenides and related heterostructures (HS) are promising candidates for photonic and optoelectronic applications owing to strong light-matter coupling and electrically-tunable carrier dynamics. However, the presence of intense nonlinear effects such as Exciton-Exciton Annihilation (EEA) [1] limits the maximum realizable exciton-density, and is particularly efficient for interlayer-excitons (IL) due to their out-of-plane dipole nature [2]. In this work, we systematically study the onset of EEA in type-II WS₂/WSe₂ HS by steady-state and nonlinear time-resolved PL. We infer that in HS the generation-rate is at least one order of magnitude larger for interlayer compared to intralayer-excitons for a given excitation-fluence, as expected from the ultrafast interlayer-charge-transfer and consequent IL formation. However, we do not observe stronger EEA for interlayer compared to intralayer-excitons and observe that for HS the recombination-dynamics are identical for both, suggesting that the EEA mechanism is dominated by the total excitonic-density via intra and interlayer-exciton interactions. Our work provides new insights on EEA mechanism, which is of paramount importance for optoelectronic-devices and study of excitonic-condensates with layered-materials. [1] Kuechle et al. J.OMX (2021), 12. [2] Sigl et al. Phys. Rev. B 105, 035417.

15 min. break

HL 20.6 Wed 11:00 H36

Tunable exciton-polaritons emerging from WS₂ monolayer excitons in a photonic lattice at room temperature — •LUKAS LACKNER¹, MARCO DUSEL², OLEG EGOROV³, BO HAN¹, HEIKO KNOPF³, FALK EILENBERGER³, CARLOS ANTON-SOLANAS¹, SVEN HÖFLING², and CHRISTIAN SCHNEIDER¹ — ¹University of Oldenburg, Oldenburg, Germany — ²University of Würzburg, Würzburg, Germany — ³Friedrich Schiller University Jena, Jena, Germany

The engineering of non-linear light-matter states in optical lattices has emerged as a key research strategy for the exploration of Hamiltonians in the spirit of ultrafast- and possibly quantum-simulation. It furthermore has revealed its potential to probe non-trivial topology phenomena. Excitons in atomically thin crystals have emerged as an ideal active medium for such purposes, since they couple strongly with light, and bear the potential to harness giant non-linearities and interactions.

In this work, we present an experiment conducted at room temperature in an open optical cavity of high quality, with an implemented one-dimensional photonic lattice. In our present work we integrate an atomically thin layer of WS₂ in such a device. We discuss the emergence and tunability of a lattice-band-structure in the tight-binding configuration at room temperature, fuelled by the emission from monolayer excitons [1].

References

[1] L. Lackner et al., *Nat Commun* 12, 4933 (2021).

HL 20.7 Wed 11:15 H36

Optical Spectroscopy of Colloidal Transition Metal Dichalcogenides — •ANDRÉ PHILIPP FRAUENDORF¹, ANDRÉ NIEBUR², JENS HÜBNER¹, JANNIKA LAUTH^{2,3}, and MICHAEL OESTREICH¹ — ¹Institut für Festkörperphysik, Leibniz Universität Hannover — ²Institut für Physikalische Chemie und Elektrochemie, Leibniz Universität Hannover — ³Institut für Physikalische und Theoretische Chemie, Universität Tübingen

Atomically thin transition metal dichalcogenides (TMDs) are at the forefront of a new generation of two-dimensional semiconductor systems and experience an increasing research interest due to their unique optical properties. As an additional fabrication approach the wet-chemical synthesis has emerged as a promising method for the straightforward solution-processing of these materials. [1] Nevertheless, the optical properties of colloidal TMD mono- and few-layer structures have been sparsely studied.

Here, we demonstrate room-temperature micro-photoluminescence of colloidal TMD nanosheets. Both, mono- and multilayer photoluminescence are observed rendering these delicate structures fully competitive with conventionally fabricated TMDs. [1] In addition temperature-dependent transient absorption measurements are presented as a convincing technique for the exploration of the ultra-fast recombination dynamics of two-dimensional materials. [2]

[1] A. Frauendorf et al., *J. Phys. Chem. C* 125, 18841 (2021).

[2] A. Frauendorf et al., Manuscript in preparation (2022).

HL 20.8 Wed 11:30 H36

Capacitively and inductively coupled excitons in bilayer MoS₂ — •LUKAS SPONFELDNER¹, NADINE LEISGANG¹, SHIVANGI SHREE², IOANNIS PARADISANOS², KENJI WATANABE³, TAKASHI TANIGUCHI⁴, CEDRIC ROBERT², DELPHINE LAGARDE², ANDREA BALOCCHI², XAVIER MARIE², IANN C. GERBER², BERNHARD URBASZEK², and RICHARD J. WARBURTON¹ — ¹Department of Physics, University of Basel — ²Université de Toulouse, INSA-CNRS-UPS, LPCNO — ³Research Center for Functional Materials, National Institute for Materials Science — ⁴International Center for Materials Nanoarchitectonics, National Institute for Materials Science

Exciton-exciton couplings in semiconductors lead to a plethora of phenomena such as nonlinear optical effects and quantum condensation. Transition-metal dichalcogenides constitute a versatile platform to study these effects as the excitons are very robust and their couplings can be controlled by exploiting their spin and valley properties.

Here, we probe exciton-exciton couplings in gated-homobilayer MoS₂. Using a driven-coupled oscillator model it is shown that the measured optical susceptibility reveals both the magnitude and the phase of the coupling constants. The interlayer excitons (IE) and intralayer B-excitons couple via a 0-phase (capacitive) coupling; the IE and the intralayer A-excitons couple via a π -phase (inductive) coupling. Using the IE as a sensor, the A-B intravalley exchange coupling is determined, a result which is also relevant for a monolayer. Finally, we realize a bright and highly tunable lowest-energy momentum-direct exciton at high electric fields.

HL 20.9 Wed 11:45 H36

Controlling the non-linearity in two dimensional materials — •MATHIAS FEDEROLF and SVEN HÖFLING — Technische Physik, Universität Würzburg, 97074 Würzburg, Germany

Recently Datta et al. [1] have shown that exciton-polaritons in bilayer MoS₂ experience a blueshift due to interacting with other exciton-polaritons. The observed blueshift is non-linear with respect to the laser power used for excitation.

Due to the bilayer's nature interlayer-excitons can occur, which exhibit an out of plane dipole moment. Using an electric field along the out of plane axis those dipoles can be aligned and used to influence the exciton-exciton interaction. By using a varying electric field, we map the parameter space to gain deterministic

control over the blueshift. Understanding and controlling the system allows us to tune the polariton-polariton interaction such that they can be used in future application i.e., single-photon sources.

[1] Datta, Biswajit, et al. arXiv preprint arXiv:2110.13326 (2021).

HL 21: Optical Properties 1

Time: Wednesday 15:00–18:30

Location: H32

HL 21.1 Wed 15:00 H32

Dynamics of exciton-polariton emission in CuI — •E. KRÜGER¹, M. BAR¹, S. BLAUROCK², L. TREFFLICH¹, R. HILDEBRANDT¹, A. MÜLLER¹, O. HERRFURTH^{1,3}, G. BENNDORF¹, H. VON WENCKSTERN¹, H. KRAUTSCHEID², M. GRUNDMANN¹, and C. STURM¹ — ¹Universität Leipzig, Felix-Bloch-Institut für Festkörperphysik, Germany — ²Universität Leipzig, Institut für Anorganische Chemie, Germany — ³now at: Active Fiber Systems GmbH, Germany

Copper iodide (CuI) is a promising candidate for transparent optoelectronic applications due to its large band gap of 3.1 eV and high exciton binding energy of 62 meV [1]. Here we present spectral- and time-resolved measurements of the near-band-edge luminescence of CuI bulk crystals for temperatures between 10 K and 250 K. The line shape of the emission lines at low temperatures is interpreted in terms of defect-bound excitons and exciton-polaritons [2]. The different decay characteristics of free and localized exciton states are explained by their coupled interaction. Based on the rise time of bound excitons, the defect density is estimated to be about $1 \times 10^{17} \text{ cm}^{-3}$, which is in good agreement with the density of free holes at room temperature. The decay times of the free exciton polaritons increase with increasing temperature up to 360 ps. For the emission of bound excitons, decay times between 180 ps and 380 ps are observed at low temperatures.

[1] M. Grundmann et al., *pss* (a) **210**, 1671 (2013)

[2] E. Krüger et al., *APL Mater.* **9**, 121102 (2021)

HL 21.2 Wed 15:15 H32

Coherent phonon oscillations and transient critical-point parameters in femtosecond pump-probe ellipsometry spectra — •S. ZOLLNER¹, C. EMMINGER^{1,2,3,4}, S. ESPINOZA⁵, S. RICHTER^{3,5,6}, M. REBARZ⁵, O. HERRFURTH^{3,7}, M. ZAHRADNIK⁵, R. SCHMIDT-GRUND⁸, and J. ANDREASSON⁵ — ¹NMSU, Las Cruces, NM, USA — ²Masaryk University, Brno — ³Uni Leipzig — ⁴Humboldt Universität, Berlin — ⁵ELI Beamlines, Dolní Břežany, Czech Republic — ⁶Lund University — ⁷Active Fiber Systems GmbH, Jena — ⁸TU Ilmenau

Spectroscopic ellipsometry measures the dielectric function of materials, which is related to the electronic band structure of semiconductors, and allows the study of critical points and their parameters (energy, broadening, amplitude, phase angle). At ELI Beamlines, femtosecond pump probe ellipsometry measurements can be performed with a white-light continuum probe beam, resulting in a time resolution of 120 fs. We report the transient dielectric function of Ge as a function of delay time between the pump and probe beams near the E_1 and $E_1 + \Delta_1$ critical points. The changes of the critical-point amplitudes are attributed to band filling at the L -point, intervalley scattering, carrier diffusion, lattice heating, and recombination. We also calculate the derivatives of these spectra using a novel Fourier analysis technique and determine the critical point parameters. We find oscillations of the critical-point energies with a period of 11 ps, related to the propagation of coherent acoustic phonons (strain waves) generated by the pump pulse. The amplitude of these oscillations shows that the strain is hydrostatic (isotropic) and has a magnitude of 0.1%.

HL 21.3 Wed 15:30 H32

Temperature dependence of the mid-infrared dielectric function of InSb from 80 to 800 K — MELISSA RIVERO ARIAS¹, CESH ZAMARRIPA¹, JADEN LOVE¹, CAROLA EMMINGER^{1,2,3,4}, and •STEFAN ZOLLNER¹ — ¹New Mexico State University, Las Cruces, NM, USA — ²Masaryk University, Brno, Czech Republic — ³Uni Leipzig — ⁴Humboldt Universität, Berlin

We describe measurements of the mid-infrared dielectric function of bulk InSb near the direct band gap using Fourier-transform infrared spectroscopic ellipsometry from 80 to 800 K in an ultra-high vacuum cryostat. Indium antimonide is the zinc blende compound semiconductor with the smallest direct band gap ($E_0=0.18$ eV at 300K) due to its heavy elements, the large resulting spin-orbit splitting and Darwin shifts. It has a low melting point of 800 K. Previously, the band gap of InSb has only been measured up to room temperature and estimated from Hall effect measurements of the effective mass up to 470 K. Calculations indicate that InSb should undergo a topological phase transition from semiconductor to semi-metal at 600 K. It is interesting to see in the data if this transition occurs below the melting point of InSb.

HL 21.4 Wed 15:45 H32

Ultra-fast change of the absorption onset in undoped cubic GaN — •ELIAS BARON¹, MARTIN FENEBERG¹, RÜDIGER GOLDHAHN¹, MICHAEL DEPPE², DONAT J. AS², SHIRLY ESPINOZA³, and MARTIN ZAHRADNIK³ — ¹Institut für Physik, Otto-von-Guericke-Universität Magdeburg, Germany — ²Department Physik, Universität Paderborn, Germany — ³ELI Beamlines, Institute of Physics, Czech Academy of Science, Dolní Břežany, Czech Republic

Nitride semiconductors are essential for modern applications, which means that an example for nitride research is necessary. For this, the cubic zincblende phase is predestined on account of isotropic properties. We present our investigation of thin film zincblende GaN, deposited by plasma-assisted molecular beam epitaxy on 3C-SiC/Si substrates in (001) orientation, by time-resolved spectroscopic ellipsometry, based on a pump-probe approach in the visible and ultra violet spectral range. The 266nm pump beam excites the cubic GaN far above the band gap and therefore creates up to $\approx 5 \times 10^{20} \text{ cm}^{-3}$ electron-hole pairs, which influence the dielectric function due to many-body effects like band gap renormalization and Burstein-Moss shift. By varying the delay time between pump and probe beam from femto- to nanoseconds, a time-resolved change of the absorption onset due to the relaxation and recombination of electron-hole pairs in the context of many-body effects is observed and concur with comparable steady-state measurements of highly n-type doped GaN.

15 min. break

HL 21.5 Wed 16:15 H32

Strain-induced bandgap transition in III-V semiconductors — •BADAL MONDAL and RALF TONNER-ZECH — Wilhelm-Ostwald-Institut für Physikalische und Theoretische Chemie, Universität Leipzig, 04103 Leipzig, Germany

In the interest of a deep and thorough understanding of the effect of strain on the electronic properties, we have developed a systematic strategy for the analysis of composition-strain-bandgap relationship in III-V semiconductors. Using the tool of computational method, modern *ab-initio* density functional theory (DFT), we have shown that depending on the nature and strength of applied strain in the system the material behavior can change substantially. Namely, a direct bandgap semiconductor can transform to an indirect bandgap semiconductor and vice versa. This ultimately enables us to construct the 'bandgap phase diagram' [1] by mapping the different direct-indirect transition points with composition and strain. By combining the advanced tools of machine learning with DFT, we have further developed an efficient approach to extend the scope in multinary systems. In combination with the thermodynamic phase diagram, we have shown that this new way of mapping the effect of strain will significantly improve the future developments in terms of strategic choice of certain application-oriented best-suited material systems or vice versa.

[1] <https://bmondal94.github.io/Bandgap-Phase-Diagram/>, 2022

Acknowledgments: This work is supported by the German Research Foundation (DFG) in the framework of the Research Training Group "Functionalization of Semiconductors" (GRK 1728).

HL 21.6 Wed 16:30 H32

Probing free carrier and exciton dynamics in bulk gallium selenide with two-dimensional electronic spectroscopy — •JONAS ALLERBECK^{1,2}, THOMAS DECKERT², LAURENS SPITZNER³, and DANIELE BRIDA² — ¹nanotech@surfaces Laboratory, Empa, Überlandstrasse 129, 8600 Dübendorf, Switzerland — ²Department of Physics and Materials Science, Université du Luxembourg, 162a Avenue de la Faiënerie, L-1511 Luxembourg, Luxembourg — ³Department of Physics, University of Konstanz, Universitätsstrasse 10, 78457 Konstanz, Germany

Multidimensional optical spectroscopy employing a sequence of three or more pulses is a powerful technique to disentangle energetic correlations. While the technique has been used to study molecular systems, its application to femtosecond dynamics in solid state materials remains new. In this work, we investigate the ultrafast response of excitons and free carriers in the technologically important semiconductor gallium selenide (GaSe) with 10 fs temporal and 1 THz (4 meV) spectral resolution. 2D spectra resolve the excitation energy of broadband pulses and reveal strong bleaching at the exciton resonance, which is hidden by the free carrier response in standard pump-probe measurements, allowing to extract an exciton relaxation time of 112 fs at room temperature. Our quantitative

mapping of carrier thermalization shows the interplay of spectral diffusion, induced absorption and dephasing, motivating ongoing theoretical investigation and paving the way for future investigation of quasiparticle correlations in functional material systems.

HL 21.7 Wed 16:45 H32

Multistable, co- and counterflowing currents of polariton condensates in concentric ring-shaped and elliptical potentials — •FRANZISKA BARKHAUSEN, MATTHIAS PUKROP, XUEKAI MA, and STEFAN SCHUMACHER — Department of Physics and CeOPP, Paderborn University, Germany

Vortices occur in a broad range of nonlinear systems. They have been widely investigated in many physical systems and different materials for their fundamental interest and for applications in data storage and information processing. In polariton condensates in semiconductor microcavities vortices can be supported and trapped by including a ring-shaped potential, for example optically induced using spatially structured non-resonant excitation [1]. Here we theoretically study vortices excited non-resonantly in different fabricated ring-shaped and elliptical external potentials. These kinds of potentials trap the polariton condensate such that different steady-state solutions, oscillating or co- and counterrotating solutions can be formed, depending on the size and number of the potential wells. A single ring potential can stabilize multistable solutions carrying different orbital angular momenta (OAM) which can lead to the beating of different modes and spatially rotating solutions. A concentric arrangement of many rings enables the excitation of Bessel-like solutions [2]. Embedding a standard ring potential in an elliptical one gives rise to phase differences of the condensates in the two rings and to counterflowing condensate currents.

[1] X. Ma, et al., Nat Commun 11, 897 (2020).

[2] F. Barkhausen, et al., Phys. Rev. B 103, 075305 (2021).

HL 21.8 Wed 17:00 H32

Optical properties of transition metal oxide perovskites by the Bethe-Salpeter equation — •LORENZO VARRASSI¹, PEITAO LIU², ZEYNEP ERGÖNENC YAVAS³, MENNO BOKDAM⁴, GEORG KRESSE², and CESARE FRANCHINI^{1,2} — ¹Department of Physics, University of Bologna — ²Faculty of Physics, University of Vienna — ³Turkish Aerospace Industries- Department of Materials Engineering — ⁴University of Twente, Faculty of Science and Technology

The accurate account of optical spectra of semiconductors and insulators requires the explicit treatment of the electron-hole (e-h) interaction. This talk will present a systematic investigation of the role of excitonic effects on the optical properties of transition metal oxide perovskites. A representative set of fourteen compounds has been selected, including 3d, 4d, and 5d perovskites. Optical conductivities and exciton binding energies are calculated through the Bethe-Salpeter equation (BSE) based on G0W0 approximation. Results are compared with the experimental data.

The origin of spectra's main peaks are investigated through the analysis of the e-h coupling coefficients. A particular emphasis in our analysis was placed on how differences between the electronic bandstructures of the studied compounds impact the optical properties and e-h coupling coefficients.

A computationally cheaper model-BSE approach, based on a model dielectric screening, was employed for the calculations of the excitonic binding energies. The quality and validity of the approach was assessed through a comparison with reference G0W0+BSE values.

15 min. break

HL 21.9 Wed 17:30 H32

Dynamics of phase defects trapped in optically imprinted or-bits in dissipative binary polariton condensates — •JAN WINGENBACH, MATTHIAS PUKROP, STEFAN SCHUMACHER, and XUEKAI MA — Physics Department and CeOPP, Paderborn University, Germany

Polaritons are quasiparticles, formed due to the strong coupling of photons and excitons in planar semiconductor microcavities. In polariton condensates, quantized vortices can form, which makes them promising candidates for novel quantum technological devices [1]. By nonresonant excitation of the condensate, periodic potentials can be generated, which can be used to trap vortices and stabilize phase defects, so-called dark solitons [2]. We study the dynamics of phase defects trapped in a finite, optically imprinted ring lattice in binary polariton condensates. Depending on their topological charge a Magnus force leads to the circulation of vortices in these orbits. This is investigated considering the cross interaction (CI) between the condensates in different spin components and the spin-orbit interaction (SOI). We observe elongated vortices and frozen phase defects, which resemble dark solitons showing finite size in both spin components. When the entire orbit is occupied, a snake instability is triggered, leading to the decay of the dark ring solution. In our system, the motion of vortex constel-

lations is affected by the SOI. [1] X. Ma, et al., Nature Communications 11, 1 (2020). [2] X. Ma, et al., Phys. Rev. Lett. 118, 157401 (2017).

HL 21.10 Wed 17:45 H32

Optimization of Silicon Nanoantenna for Optical Phased Arrays — •ANDREAS STRAUCH, HENNA FARHEEN, VIKTOR MYROSHNYCHENKO, and JENS FÖRSTNER — University Paderborn - Department of Electrical Engineering and Information Technology, Paderborn, Germany

The classical microwave phased array is a proven antenna technology since the beginning of the last century. Among other things, it leads to significant improvements in radar technology as well as mobile, radio and satellite communications. Beyond that, this principal is not limited to the microwave band and can transfer into the optical spectrum, such as for light detection and ranging (LIDAR). The specific, technical features of the optical phased array (OPA) are the fast, non mechanical variation of directional characteristic (beam steering) during the operation and the great beam focusing through an ensemble of sophisticatedly, interacting single antennas. Besides them, the usage of several single antennas increases the redundancy and gives a high operational reliability and signal-to-noise ratio.

We designed, numerically analyzed, and optimized an efficient Silicon on Insulator (SOI) based photonic light transmitter, working in the infrared band, with high antenna gain and sidelobe attenuation (super resolution in principle), high redundancy and noise robustness and most important an electronically, configurable farfield characteristic. In comparison to a reference design, we increased the radiation efficiency from 2.66 to 9% by numerical optimization using evolutionary and natural analogue approaches.

HL 21.11 Wed 18:00 H32

Spatially Resolved Dynamics of Intra 3d Luminescence of Co in ZnO Nanowires Revealed by Nanoscale X-ray Analysis — •CHRISTIAN PLASS¹, VALENTINA BONINO², MAURIZIO RITZER¹, LUKAS JÄGER¹, JAIME SEGURA-RUIZ², GEMA MARTINEZ-CRIADO², and CARSTEN RONNING¹ — ¹Institut für Festkörperphysik, Friedrich-Schiller-Universität Jena, Max-Wien-Platz 1, 07743, Jena — ²ESRF - The European Synchrotron, 71 Avenue des Martyrs, 38043 Grenoble, France

Color centers in semiconductors have drawn a lot of interest in recent years. They are able to provide high quality single photon sources. Such color centers can for example be obtained by doping ZnO with Co. The underlying emission processes have to be determined in order to achieve quantum emission by such a system. Hence, there is a strong need to evaluate how the dynamics of the luminescence is influenced by elemental composition and local environment of the color centers. High resolution synchrotron based methods like X-ray fluorescence (XRF) and X-ray excited optical luminescence (XEOL) enable insight into such compositional and functional variations. Simultaneous XRF and XEOL measurements of Co doped ZnO nanowires were conducted: The highly focused X-ray nanobeam at the ID16B-NA station of the European Synchrotron Radiation Facility scanned the nanowire and by analyzing the emitted X-ray fluorescence radiation together with the corresponding optical luminescence correlating maps were obtained. As the spatial resolution is about 50nm, we can show how the local composition influences the spectral dynamics of the obtained emission.

HL 21.12 Wed 18:15 H32

Fröhlich polarons in cubic materials — •B. GUSTER¹, P.M.M.C. MELO², B.A.A. MARTIN³, V. BROUSSEAU-COUTURE⁴, J.C. DE ABREU², A. MIGLIO¹, M. GIANTOMASSI¹, M. CÔTÉ⁴, J.M. FROST³, M.J. VERSTRAETE², and X. GONZE^{1,5} — ¹UCLouvain(UCL), IMCN, Louvain-la-Neuve, Belgium — ²NanoMat/Q-Mat/CESAM, Université de Liège, Liège, Belgium — ³Department of Physics, Imperial College London, London, UK — ⁴Département de Physique, Université de Montréal, Montréal, Canada — ⁵Moscow, Russia

Most works on polaron models, to understand their characteristics such as radius, effective mass, mobility and energy dispersion, have focused on the original Fröhlich model. Real cubic materials have electronic band extrema that are often degenerate, or anisotropic. In this work, we keep the continuum hypothesis inherent to large polaron models, but go beyond the existing isotropic and non-degeneracy hypotheses, and also include multiple phonon modes. For polaron effective masses, we provide (i) the analytical result for the case of anisotropic electronic energy dispersion, with two distinctive effective masses (uniaxial), (ii) an approximate expression for the case of three distinctive axes (ellipsoidal), (iii) numerical simulations for the 3-band degenerate case, typical of III-V and II-VI semiconductor valence bands. We also deal with the strong-coupling limit, using a variational treatment: we propose trial wavefunctions for the three above-mentioned cases as well, providing polaron radii and energies. We gauge such approaches for the case of a dozen of II-VI and III-V semiconductors, and oxides.

HL 22: Heterostructures, Interfaces and Surfaces

Time: Wednesday 15:00–18:00

Location: H33

HL 22.1 Wed 15:00 H33

Band-gap and strain engineering in GeSn alloys using post-growth pulsed laser melting — •O. STEUER¹, D. SCHWARZ², M. OEHME², J. SCHULZE³, H. MACZKO⁴, R. KUDRAWIEC⁴, I. FISCHER⁵, R. HELLER¹, R. HÜBNER¹, M. KHAN¹, Y. GEORGIEV¹, S. ZHOU¹, M. HELM¹, and S. PRUCNAL¹ — ¹Helmholtz-Zentrum HZDR, GER — ²University of Stuttgart, GER — ³Fraunhofer IIS, GER — ⁴Wrocław University, POL — ⁵TU Cottbus-Senftenberg, GER

Alloying Ge with Sn enables effective band-gap engineering and improves significantly the charge carrier mobility. The pseudomorphic growth of Ge_{1-x}Sn_x on Ge causes in-plane compressive strain, which degrades the superior properties of the Ge_{1-x}Sn_x alloys. Therefore, efficient strain engineering is required. In this talk, we will present strain and band-gap engineering in GeSn alloys grown on a Ge virtual substrate using post-growth nanosecond pulsed laser melting (PLM). Micro-Raman spectroscopy and X-ray diffraction show that the initial in-plane compressive strain is removed. Moreover, for PLM energy densities higher than 0.5 J cm⁻², the Ge_{0.89}Sn_{0.11} layer becomes tensile strained. Simultaneously, as revealed by Rutherford Backscattering spectrometry, cross-sectional transmission electron microscopy investigations and X-ray diffraction, the crystalline quality and Sn-distribution in PLM-treated Ge_{0.89}Sn_{0.11} layers are only slightly affected. Additionally, the change of the band structure after PLM is confirmed by low-temperature photoreflectance measurements. The presented results prove that post-growth ns-range PLM is an effective way for band-gap and strain engineering in highly-mismatched alloys.

HL 22.2 Wed 15:15 H33

Reconfigurable Complementary and Combinational Logic based on Monolithic and Single-Crystalline Al-Si Heterostructures — •RAPHAEL BÖCKLE¹, MASIAR SISTANI¹, MARTINA BAŽÍKOVÁ¹, LUKAS WIND¹, ZAHRA SADRE-MOMTAZ², MARTIEN I. DEN HERTOEG², CORBAN G.E. MURPHEY³, JAMES F. CAHOON³, and WALTER M. WEBER¹ — ¹Institute of Solide State Electronics, TU Wien, Vienna, Austria — ²Institut Néel, CNRS, Grenoble, France — ³Department of Chemistry, University of North Carolina, Chapel Hill, North Carolina, United States

Overcoming the difficulty in reproducibility and deterministically defining the metal phase of metal-Si heterostructures is among the key prerequisites to enable next-generation nanoelectronic devices. Here, the formation of monolithic Al-Si-Al heterostructures obtained from Si nanowires and Al contacts is presented. Transmission electron microscopy and energy-dispersive X-ray spectroscopy confirmed both the composition and crystalline nature of the presented Al-Si-Al heterostructures, with no intermetallic phases formed during the exchange process in contrast to state-of-the-art metal silicides. In this context, reconfigurable field-effect transistors (RFET), capable of dynamically altering the operation mode between n- or p-type are realized. Having devised symmetric on-currents as well as threshold voltages for n- and p-type operation as a necessary requirement to exploit complementary reconfigurable circuits, selected implementations of logic gates such as inverters and combinational wired-AND gates are built from single elementary RFETs.

HL 22.3 Wed 15:30 H33

Investigations on graphene-oxide-silicon structures for field emission — •ALEXANDER MAI¹, FLORIAN HERDL², SIMON EDLER¹, ANDREAS SCHELS², MICHAEL BACHMANN¹, FELIX DÜSBERG¹, ANDREAS PAHLKE¹, and GEORG DUESBERG² — ¹Ketek GmbH, Hofer Str. 3, 81737 Munich, Germany — ²University of the Bundeswehr Munich, Institute of Physics, Werner-Heisenberg-Weg 39, 85577 Neubiberg, Germany

In field emission (FE) electrons can tunnel through a potential barrier by applying a large electric field (> 1 V/nm), which is required to obtain a reasonable current. Therefore, often high voltages (> 300 V) and sharp tip geometries are used. However, a high sensitivity to poor vacuum makes these emitters unsuitable for many applications. Planar devices like graphene-oxide-semiconductor (GOS) structures are promising candidates as they are independent on the ambient pressure level. The necessary electric fields are achieved by applying a low operation voltage (< 20 V) on a thin oxide barrier (5 - 20 nm). The maximum emission to tunnel current ratio (efficiency) achieved in a GOS structure to this date is 48.5%. In this presentation, results of recent measurements and simulations on GOS structures are shown. The measured structures show efficiencies between 0.1 and 23%, mainly depending on the thickness of the gate electrode, while an emission current of at least about 1 nA was achieved in most samples. Simulations show a voltage drop near the contact pad resulting from the sheet resistance of the gate electrode, which limits the maximum tunnel current in the GOS structure.

HL 22.4 Wed 15:45 H33

Topological photonics for optoelectronic sensing — •JAKOB LINDENTHAL^{1,2}, JOHANNES BENDUHN¹, and KARL LEO^{1,2} — ¹Institute of Applied Physics, Technische Universität Dresden — ²ct.qmat - Würzburg-Dresden Cluster of Excellence

Topological properties of photonic systems are a quickly emerging research field. The physical realisation of topological invariants allows the creation of photonic states with strong protection of the state's existence against perturbation. The energy levels of topological states can be made highly sensitive to external influences, enabling the design of novel optoelectronic sensing devices. Theoretical concepts of different topological photonic systems are discussed, and experimental systems are showcased. The presentation reports about an optoelectronic pressure sensor developed at the Institute of Applied Physics at TU Dresden and other devices fabricated by partnering organisations. Key concepts and technological advantages of topological systems are summarised, highlighting the prospects for incorporating topology in optoelectronic sensing devices.

HL 22.5 Wed 16:00 H33

Interplay of anomalous strain relaxation and minimization of polarization changes at nitride semiconductor heterointerfaces — YUHAN WANG^{1,2}, •MICHAEL SCHNEDLER^{1,2}, QIANQIAN LAN^{1,2}, FENGSHAN ZHENG^{1,2}, LARS FRETER^{1,2}, YAN LU^{1,2}, UWE BREUER³, HOLGER EISELE⁴, JEAN-FRANÇOIS CARLIN⁵, RAPHAËL BUTTE⁵, NICOLAS GRANDJEAN⁵, RAFAL E. DUNIN-BORKOWSKI^{1,2}, and PHILIPP EBERT^{1,2} — ¹Peter Grünberg Institut, Forschungszentrum Jülich GmbH, 52425 Jülich, Germany — ²Ernst Ruska Centrum, Forschungszentrum Jülich GmbH, 52425 Jülich, Germany — ³Zentralinstitut für Engineering, Elektronik und Analytik (ZEA-3), Forschungszentrum Jülich GmbH, 52425 Jülich, Germany — ⁴Institut für Festkörperphysik, Technische Universität Berlin, Hardenbergstrasse 36, 10623 Berlin, Germany — ⁵Institute of Physics, Ecole Polytechnique Fédérale de Lausanne, 1015 Lausanne, Switzerland

Polarization and electron affinity changes at Al_{0.06}Ga_{0.94}N/GaN and In_{0.05}Ga_{0.95}N/Al_{0.06}Ga_{0.94}N interfaces are quantified by combining off-axis electron holography in transmission electron microscopy, scanning tunneling microscopy, and simulations of the electrostatic potential and electron phase maps. The In_{0.05}Ga_{0.95}N/Al_{0.06}Ga_{0.94}N interface reveals, as expected, biaxial relaxation as well as polarization and electron affinity changes. However, at the Al_{0.06}Ga_{0.94}N/GaN interface anomalous lattice relaxations and vanishing polarization and electron affinity changes occur, whose underlying physical origin is anticipated to be total energy minimization by the minimization of Coulomb interactions between the polarization-induced interface charges.

30 min. break

HL 22.6 Wed 16:45 H33

Determination of relaxation in thin InGaAs-films by Raman spectroscopy — •JOHANN FRIEDEMANN SCHULZ¹, TOBIAS HENKSMEIER², MARTIN FENEBERG¹, ELIAS KLUTH¹, DIRK REUTER², and RÜDIGER GOLDHAHN¹ — ¹Otto von Guericke University, Institute of Physics, Universitätsplatz 2, 39106 Magdeburg, Germany — ²Paderborn University, Department of Physics, Warburger Str. 100, 33089 Paderborn, Germany

Semiconductor heterostructures suffer inherently from differences in their lattice parameters. This causes strain and, in the worst case, crystal defects in the material, rendering it potentially unusable for electronic or optical devices. The relaxation of thin mismatched films is therefore important for assessing the crystal quality. One possibility to experimentally access the degree of relaxation is to accurately determine the phonon frequencies of the strained material, as Phonon frequencies depend on composition and lattice parameters. Such measurements can be carried out quickly and easily using Raman spectroscopy. Here, we present results on In_xGa_{1-x}As grown on GaAs-substrates by molecular beam epitaxy. We investigate different strained films with varied composition and several different film thicknesses. We find Raman spectroscopy a viable tool to determine the degree of relaxation even in films which are too thin for usual reciprocal space map experiments.

HL 22.7 Wed 17:00 H33

Time-resolved measurement of propagating exciton-polariton condensates in confined systems using a streak camera — •CHRISTIAN MAYER, SIMON BETZOLD, PHILIPP GAGEL, TRISTAN H. HARDER, MONIKA EMMERLING, ADRIANA WOLF, FAUZIA JABEEN, SVEN HÖFLING, and SEBASTIAN KLEMBT — Technische Physik, RCCM and Würzburg-Dresden Cluster of Excellence ct.qmat, University of Würzburg, Germany

Strong coupling between photons and excitons in an optical microcavity leads to the formation of hybrid light-matter quasiparticles called exciton-polaritons. In the low-density regime, these particles follow bosonic statistics and can therefore

undergo dynamical condensation above a critical particle density by stimulated relaxation to the ground state. The low effective mass of polaritons compared to excitons, which results from the photonic fraction, leads to comparatively long diffusion lengths. The excitonic fraction, on the other hand, is responsible for relevant polariton-polariton interaction, which leads to a repulsive behavior. Exciting non-resonantly with a pulsed laser results in an additional repulsive force at finite wavevector due to the exciton reservoir. These factors can lead to a significant propagation of the polariton condensate, with relevant effects already taking place on the time scale of a few picoseconds.

Here, we utilize electron beam lithography and etching techniques to form potential landscapes such as coupled resonator lattices and waveguides. We use a streak camera to resolve and visualize the propagation of polaritons in these systems.

HL 22.8 Wed 17:15 H33

Towards predictive modeling of optical properties of quantum dots under externally applied stress — •PETR KLENOVSKY^{1,2}, XUEYONG YUAN³, SAIMON FILIPE COVRE DA SILVA³, and ARMANDO RASTELLI³ — ¹Department of Condensed Matter Physics, Faculty of Science, Masaryk University, Brno, Czech Republic — ²Czech Metrology Institute, Brno, Czech Republic — ³Institute of Semiconductor and Solid State Physics, Johannes Kepler University Linz, Austria

GaAs quantum dots (QDs) have been found in the past to be an exceptionally good platform for construction of the light emitters. They have also advantageous properties for spin physics because of the absence of strain and strain inhomogeneity. Still, strain is important to achieve quadrupolar splitting, e.g., to build up a quantum register with nuclear spins. Understanding and quantitative prediction of strain-induced effects will be important to guide future optimization, since a trial and error procedure is not acceptable in view of the huge parameter space available for GaAs QDs (e.g. WL thickness tunable at will). Former attempts have qualitatively reproduced results but failed to achieve the quantitative agreement, e.g., bright-dark exciton splitting or used unphysical assumptions. That was further exacerbated by the lack of knowledge of the exact applied strain configuration.

Here we go beyond by combining precisely determined strain and QD properties with dedicated calculations using $\mathbf{k} \cdot \mathbf{p}$ and correlated configuration interaction (CI) methods. We show for the first time quantitative agreement between experiment and theory for strained GaAs QDs.

HL 22.9 Wed 17:30 H33

Growth of epitaxial GaN by reactive magnetron sputtering — •RALF BORGMANN, FLORIAN HÖRICH, JÜRGEN BLÄSING, ARMIN DADGAR, ANDRÉ STRITTMATTER, ANJA DEMPEWOLF, FRANK BERTRAM, JÜRGEN CHRISTEN, and GORDON SCHMIDT — Otto-von-Guericke-Universität Magdeburg, Universitätsplatz 2, 39106 Magdeburg, Germany

For high power transistors GaN is an excellent base material semiconductor with a high bandgap and a high breakdown field which is often realized on Si substrates. A specific buffer arrangement is needed for MOVPE grown structures, to achieve these properties. Especially doping with Fe or C is essential for insulating sheets. In comparison with reactive magnetron sputtering uses pure metal targets and does not necessarily require Fe or C doping to achieve highly insulating GaN. We investigated growth parameters like growth temperature and reactive gas flow on various templates. An important parameter determining the material quality is the reactive gas. Ga droplets occur on the wafer surface, when using nitrogen. Investigations on growth temperature reveal a narrow growth window. An optimum growth temperature was by around 715 °C. With low ammonia gas flow the AFM measurement shows a grainy surface. By using a higher ammonia gas flow, the growth rate decreases and a closed meandering surface structure appears. Full sputtered undoped layers show a vertical breakdown field strength of > 2.5 MV/cm for 200 nm AlN 2x 200 nm transition layer AlGaIn and 820 nm GaN.

HL 22.10 Wed 17:45 H33

Ultrafast transient spectroscopy of Cu(In,Ga)Se₂ coupled to different buffer layers. — •PIRMIN SCHWEIZER, RICARDO ROJAS-AEDO, ALICE DEBOT, PHILIP DALE, and DANIELE BRIDA — Department of Physics and Materials Science, University of Luxembourg, 162a avenue de la Faiënerie, L-1511 Luxembourg, Luxembourg

The dynamic parameters of photo-induced electron-hole pairs, such as recombination time and charge conductivity, play a major role in the efficiency of photovoltaic devices. Among thin film materials for photovoltaics, one of the most interesting is the p-type Cu(In,Ga)Se₂ alloy (CIGS) on which an n-type buffer layer is deposited, forming the initial part of the device p-n junction. The inter-material transport dynamics strongly depend on how the band structure is affected by the buffer layer, and also on the quality of the CIGS / buffer layer interface which may contain defects. In our experiments we have compared the ultrafast transient reflectivity on CIGS epitaxially grown on a GaAs substrate. New Cd free buffer layers In₂S₃ and band offset tunable Zn(O,S), are compared to the most commonly used buffer layer, CdS. The transient reflection measurements allow for the extraction of the electronic transport dynamics at the interface with the buffer. This study allows us to draw conclusions about the pair formation capacity mediated by the transport properties between the CIGS and the buffer layer. The results can guide the development of Cd free buffer layers thus reducing the environmental impact caused by CdS in traditional CIGS solar cells.

HL 23: Perovskite and Photovoltaics 2 (joint session HL/PPP/KFM)

Time: Wednesday 15:00–18:15

Location: H34

HL 23.1 Wed 15:00 H34

Electronic structure analysis of the interface of a TiO₂ electron-transport layer with a perovskite CsPbI₃ photovoltaic absorption layer — •AMIRHOSSEIN BAYANI¹, JULIAN GEBHARDT¹, and CHRISTIAN ELSÄSSER^{1,2} — ¹Fraunhofer Institute for Mechanics of Materials IWM, Wöhlerstrasse 11, 79108 Freiburg, Germany — ²Freiburg Materials Research Center (EMF), Albert-Ludwigs-University Freiburg, 79104 Freiburg, Germany

Lead-based hybrid perovskite halides are currently the most promising light absorbing materials to supplement or even replace Si in next generation solar cells. With intensive research of the bulk material properties in recent years, a strong interest emerges in studying the interfaces to the contact layers in order to reach the final boost of solar efficiency in devices. Here, we study the interface of CsPbI₃ with TiO₂ as model interface for a perovskite with an electron transport layer. In particular, we investigate the rutile-TiO₂(001)[001] / CsPbI₃(001)[100] interface using self-energy corrected density functional theory. By this state-of-the-art modeling technique, we analyze the alignment of work-functions and investigate the band alignment at the interface.

HL 23.2 Wed 15:15 H34

Influence of the Ionic Liquid BMIMBF₄ on the film formation and optoelectronic properties of MAPbI₃ — •SIMON BIBERGER, KONSTANTIN SCHÖTZ, PHILIPP RAMMING, NICO LEUPOLD, RALF MOOS, ANNA KÖHLER, HELEN GRÜNINGER, and FABIAN PANZER — University of Bayreuth, Bayreuth, Germany Today, metal halide perovskite solar cells (PSCs) are one of the most promising emerging photovoltaic technologies. However, their still limited stability is a main hurdle for their successful commercialization. In the past, various approaches have been developed to improve the long-term stability and performance of PSCs. Here ionic liquids (IL) as additives have attracted much attention

as they passivate defects and suppress ion migration. In this work, we investigate the effect of the IL BMIMBF₄ on the film formation and optoelectronic properties of the model halide perovskite MAPbI₃. By multimodal in situ optical spectroscopy, we investigate the formation of the perovskite film during solution processing via one-step spin coating and a solvent engineering approach and how the film formation alters when the IL is added to the precursor solution. We find that the IL does not impact the formation of perovskite-solvent complexes, but the perovskite growth rate decreases with increasing IL content in the precursor solution. Additionally, we reveal that the IL already interacts with precursor materials and changes the evolution of the PbI_4^{2-} properties. Thus, our work provides important insights into how decisive ILs impact the sensitive interconnection between precursor properties, film formation process and final optoelectronic functionality of perovskite thin films.

HL 23.3 Wed 15:30 H34

Transversal halide motion enables sharp optical absorption profiles in halide perovskites — •SEBASTIÁN CAICEDO-DÁVILA, CHRISTIAN GEHRMANN, XIANGZHOU ZHU, and DAVID A. EGGER — Department of Physics, Technical University of Munich, Garching, Germany

Despite their strong vibrational anharmonicity, halide perovskites (HaPs) exhibit favorable optoelectronic properties, which facilitate their outstanding performance in solar cells, comparable to high-quality inorganic semiconductors. In this contribution, we explore the mechanisms and consequences of dynamic structural flexibility in CsPbBr₃ using first-principles molecular dynamics based on density-functional theory. We show that large Br displacements occur on planes that are transversal to the Pb-Br-Pb bonding axis. This transversality is concurrent with vibrational anharmonicity, results in short-ranged disorder correlations, and sharpens the joint-density of states rise at finite temperature.

Finally, we contrast these results to the case of PbTe, which shares key properties with CsPbBr₃ but cannot exhibit any *transversality*, to show that this system features wider band-edge distributions and longer-ranged disorder correlations. These findings are relevant for connecting the structural flexibility and bonding of the halide perovskite structure with the sharp optical absorption of these materials.

HL 23.4 Wed 15:45 H34

Investigating underlying mechanisms of K doping on stability of single- and mixed-cation perovskite solar cells with experimental and computational informed modelling — SAIED MOLLAVALI, MOHAMMAD MOADDELI, and •MANSOUR KANANI — Department of Materials Science and Engineering, School of Engineering, Shiraz University, Shiraz, Iran

Recent studies revealed that the interstitial occupancy of potassium in single/mixed-cation based perovskite structures could hinder the ion migration mechanisms near interfaces, and therefore leads to a better structural stability. However, the underlying stability enhancement mechanisms and probable side effects of additional K atoms in incorporate with other organic/inorganic constituents, with a long-range electronic bonding character, is not clear completely. In this study, the effect of doping K on the structural, morphological, electronic, and optical properties of different perovskite structures is investigated experimentally and computationally. The beneficial effect of interstitial K atom on long-range bonding of I atoms with organic molecules is observed. Furthermore, no degradation from additional K is detected for specific range of doping. This result opens a new insight on constructive impact of inorganic dopant on stability issue in perovskite solar cells. SEM, XRD, Photoluminescence and optical absorbance analysis were performed on the perovskite layer. The one layer-based experimental data incorporation with DFT based results were informed into the SCAPS-1D solar cell simulator package to predict cell efficiency, systematically.

HL 23.5 Wed 16:00 H34

Revealing efficiency losses due to mobile ions in perovskite solar cells — •SAHIL SHAH, JARLA THIESBRUMMEL, and JONAS DIEKMANN — University of Potsdam, Germany

Perovskite semiconductors are distinct from most other semiconductors due to a large number of mobile ions in the active layer (e.g., iodide and methylammonium ions and vacancies, and others). Thus, ion dynamics have a critical impact on the performance and stability of perovskite-based applications.

In this work, we will show how the ionic density and induced losses change with device degradation under elevated temperatures and continuous light illumination. This is investigated via a simple and newly developed method *fast-hysteresis* which is a JV scan at a faster rate (~1000 Vs-1) which prevents the perturbation of mobile ions and we get the true ion free potential of the device. The fast-hysteresis measurements are corroborated by transient charge extraction and capacitance measurements as well as numerical simulations, which provide important insights into the dynamics of free electronic charges and mobile ions. We will then demonstrate how the mobile ions affect a range of commonly used mixed cation metal halide perovskite compositions and how the ionic losses vary with the charge transport layer.

Overall, the proposed methods quantify the ion-induced field screening, shed light on the complex device degradation process and PCE losses allow for a better understanding of several key phenomena in perovskite solar cells, and open up a large range of future experiments.

HL 23.6 Wed 16:15 H34

Dissecting Ultrafast Polarization Responses in Lead Halide Perovskites via the THz-induced Kerr Effect — •MAXIMILIAN FRENZEL¹, MARIE CHERASSE^{1,2}, JOANNA URBAN¹, FEIFAN WANG³, BO XIANG³, LEONA NEST¹, LUCAS HUBER³, MARTIN WOLF¹, X.-Y. ZHU³, and SEBASTIAN F. MAEHRLEIN¹ — ¹Fritz Haber Institute of the Max Planck Society, Department of Physical Chemistry, Berlin, Germany — ²LSI, CEA/DRF/IRAMIS, CNRS, Ecole Polytechnique, Institut Polytechnique de Paris, Palaiseau, France — ³Columbia University, Department of Chemistry, New York City, USA

The microscopic origin of the surprising optoelectronic properties of lead halide perovskite (LHP) semiconductors is still under debate. One hypothesis is that the highly polar and anharmonic lattice of LHPs influences their optoelectronic properties through dynamic charge carrier screening. We therefore study the ultrafast polarization response of the hybrid LHP MAPbBr₃ when exposed to transient electric fields in the form of intense, single-cycle THz pulses. By probing the THz-induced Kerr effect (TKE), we observe strong THz polarizability and complex ultrafast polarization dynamics. We perform 4-wave-mixing simulations, which show that it is crucial to account for anisotropic and dispersive light propagation for the correct interpretation of the measured TKE signals. Finally, we unveil a coherent phonon response in MAPbBr₃, which we assign to the inorganic cage and conclude to be the dominating polarizable mode in this material. This finding highlights the role of the inorganic lattice for dynamic carrier screening and the related mechanism of charge carrier protection.

30 min. break

HL 23.7 Wed 17:00 H34

Calculating the temperature-dependent band gap of the halide perovskite CsPbBr₃ — •STEFAN SEIDL, CHRISTIAN GEHRMANN, XIANGZHOU ZHU, SEBASTIAN CAICEDO DAVILA, and DAVID A. EGGER — Department of Physics, Technical University of Munich, Garching, Germany

Theoretical calculations based on density functional theory (DFT) can predict thermal effects in the electronic structure by considering important phenomena, such as thermal lattice expansion and electron-phonon coupling. The latter can be calculated using a Monte-Carlo (MC) sampling approach that is formally rooted within the harmonic approximation, which has recently been shown to yield accurate temperature-dependent band gaps for inorganic semiconductors [1]. A complementary approach to predict thermal effects in the electronic structure is first-principles molecular dynamics (MD), which can account for vibrational anharmonicity that is an important effect for certain technologically relevant materials. Here, we assess the temperature-dependent band gap of the halide perovskite CsPbBr₃ in the cubic and orthorhombic phases employing the two different methods, MC and MD, and compare our findings with experimental results. This includes a discussion about the role of anharmonicity and the contributions from spin-orbit coupling and thermal lattice expansion.

[1] F. Karsai et al, New J. Phys. 20, 123008 (2018)

HL 23.8 Wed 17:15 H34

Electronic structure prediction of hybrid organic-inorganic metal halide perovskites using cost-effective DFT-1/2 method — MOHAMMAD MOADDELI und •MANSOUR KANANI — Department of Materials Science and Engineering, School of Engineering, Shiraz University, Shiraz, Iran

Hybrid organic-inorganic metal halide perovskites (OIHPs) have attracted much attention in the last decade because of tunable photovoltaic performance and low fabrication cost. Regarding the tunable parameters for controlling the fundamental properties of OIHPs, recent computational and data-driven based approaches can accelerate new material prediction procedure significantly. Density functional theory (DFT) is considered as fundamental block of many multiscale, high-throughput and data-driven approaches typically. However, because of complexity of electronic orbital in OIHP as well as high sensitivity of regarding properties to atomistic configuration, employing conventional computational approaches faces many obstacles or needs very expensive corrections. Underestimation of routine functionals used in DFT calculations push people apply expensive approaches such as hybrid functionals and GW approximation. Here, DFT-1/2 method with a normal computational cost has been used for determining not only the band gap but also the true form of valence and conduction bands of OIHPs. The results showed that, the method could preserve the known Rashba band splitting in the conduction band of mixed-cation perovskites, which is the source of longer carrier lifetime behavior.

HL 23.9 Wed 17:30 H34

Phonon Signatures for Polaron Formation in an Anharmonic Semiconductor — •FEIFAN WANG^{1,2}, WEIBIN CHU³, JIN ZHAO³, and X.-Y. ZHU¹ — ¹Columbia University, New York, NY, 10027 USA — ²Dept. of Materials, ETH Zurich, Switzerland — ³University of Science and Technology of China, Hefei, Anhui 230026, China

Polaron formation, in which charge carriers are dressed by a cloud of lattice distortions, is partially responsible for the long carrier lifetimes and diffusion lengths in the lead halide perovskite (LHP), a superior optoelectronic material. Considerations of ferroelectric-like phonon anharmonicities of this system lead to the recent proposal of ferroelectric large polarons, which attributes efficient charge-carrier screening to the extended ordering of dipoles associated with inversion-symmetry-breaking unit cells. Here, we study electron-phonon coupling in Bi₂O₂Se, a semiconductor which bears resemblance to LHPs in ionic bonding, band transport with long carrier diffusion lengths, and dynamical phonon disorder as revealed by low-frequency Raman spectroscopy. Using coherent phonon spectroscopy, we show the strong coupling of an anharmonic phonon mode to photo-excited charge carriers, while the Raman excitation of this mode is symmetry-forbidden in the ground-state. Density functional theory calculations verify that the phonon mode originates from the symmetry reduction after charge injection and indicate the local dipole ordering induced by photo-excited electrons. This study provides an initial attempt to generalize the proposed charge-carrier screening model to account for the outstanding optoelectronic properties of defect-tolerant semiconductors.

HL 23.10 Wed 17:45 H34

Tuning Perovskite Crystallization in the Hybrid Route — •MOHAMED MAHMOUD, PATRICIA SCHULZE, ANDREAS BETT, and OUSSAMA ER-RAJI — Fraunhofer ISE

In 2009, perovskite solar cells were discovered in the solid-state that can be used not only as a single junction absorber but also in tandem configuration thanks to their bandgap tunability. It is a combination of organic and inorganic lead halide materials and they have the advantage of a strong absorption edge, defect tolerance and potential cheap production due to easy production methods such as spin coating or slot-die coating as a highly scalable production method. In the

industry, double-sided textured silicon (DSTS) is commonly produced to overcome the reflection losses at surfaces. Spin coating of perovskite on top of DSTS resulted in low conformality which resulted in shunts and non-working solar cells. To overcome this issue, the hybrid route was developed, in which inorganic materials are co-evaporated using the thermal vapour deposition technique and then organic materials are spin-coated. By doing that, the high conformality of the thin film on top of the c-Si is achieved. However, the resulting perovskite grain size is in the nanometer scale. To increase the grain size - which results in higher short circuit current, lower grain boundaries and thus a more stable device - thermodynamics of the crystallization process need to be studied. In this work, using the thermodynamics fundamentals of crystallization, we tune the grain size of perovskite deposited via the hybrid route. In addition, we study the consequences of different grain sizes on the efficiency of the solar cell and especially on the stability.

HL 23.11 Wed 18:00 H34

Dynamic nuclear spin polarization in lead halide perovskites — •NATALIA KOPTVA¹, DENNIS KUDLACIK¹, MAREK KARZEL¹, MLADEN KOTUR¹, DMITRI YAKOVLEV¹, OLEH HORDIICHUK², OLGA NAZARENKO², DMITRY DIRIN²,

MAKSYM KOVALENKO^{2,3}, and MANFRED BAYER¹ — ¹Experimentelle Physik 2, TU Dortmund, 44221 Dortmund, Germany — ²Laboratory of Inorganic Chemistry Department of Chemistry and Applied Biosciences, ETH Zürich, CH-8093 Zürich, Switzerland — ³Laboratory for Thin Films and Photovoltaics Empa-Swiss Federal Laboratories for Materials Science and Technology, CH-8600 Dübendorf, Switzerland

Lead halide perovskites are promising for applications in spintronics due to the nanosecond coherence time of the resident carriers [1]. The primary source of losing spin coherence is the interaction with the fluctuating nuclear spin environment [2]. Optically oriented carrier spins polarize nuclei, which create an Overhauser field. Due to the different strengths of the hyperfine interaction with the nuclear spins, the electron and hole experience different magnitude and directions of the Overhauser field. To study the degree of nuclear spin polarization and fluctuation, we investigate the interaction of resident and optically created carrier spins with nuclei using the Hanle effect in the tilted magnetic field in bulk formamidineum caesium lead iodine bromide.

[1] V. V. Belykh et al., Nat. Commun. 10, 673 (2019)

[2] I. A. Merkulov et al., Phys. Rev. B 65, 205309 (2002)

HL 24: Functional Semiconductors for Renewable Energy Solutions (joint session HL/KFM)

Time: Wednesday 15:00–18:30

Location: H36

HL 24.1 Wed 15:00 H36

A facile freeze-thaw ultrasonic assisted circulation method of graphite flakes prepared by anode graphite from spent lithium-ion batteries — •YU QIAO^{1,2}, ZHONGHAO RAO^{3,4}, HUAPING ZHAO¹, and YONG LEI¹ — ¹Fachgebiet Angewandte Nanophysik, Institut für Physik & IMN MacroNano, Technische Universität Ilmenau, 98693 Ilmenau, Germany — ²School of Electrical and Power Engineering, China University of Mining and Technology, 221116, Xuzhou, China — ³School of Energy and Environmental Engineering, Hebei University of Technology, 300401, Tianjin, China — ⁴Hebei Key Laboratory of Thermal Science and Energy Clean Utilization, Hebei University of Technology, 300401, Tianjin, China

Lithium-ion batteries (LIBs) have been widely employed in fast-growing mobile devices, stationary storage devices and electric vehicles. However, limited by particular service life, the booming increase in LIBs production will result in a large retirement wave. As the most common anode material in LIBs, waste graphite has also developed into a mode of high production capacity with the retirement of spent LIBs. Anode graphite (AG) of spent LIBs has the characteristics of large layer spacing and ease of being intercalated due to the reduced interlamination force after repeated charge and discharge cycles. This study presents a facile freeze-thaw ultrasonic-assisted circulation method to prepare two-dimensional low-layer graphite flakes (GFs) using AG from spent LIBs. The results indicate that the freeze-thaw ultrasonic-assisted circulation method is feasible for preparing two-dimensional laminar materials.

HL 24.2 Wed 15:15 H36

How could the heating process reduce the crystal damage of semiconductors? — •KHALID LAHMIDI, JALE SCHNEIDER, ANDREAS BRAND, SEBASTIAN RODER, and ANDREAS BETT — Fraunhofer Institute for Solar Energy Systems, Heidenhofstr. 2, 79110 Freiburg, Germany

Laser material processing can no longer be imagined away from the production chains in semiconductor industries. While being a precise, fast and wear-free processing tool, high intensity laser irradiation can also induce damage within the material, e.g. crystal damage, compromising the device quality. However, this damage can partly be healed or even prevented by an accompanying (laser) heating process.

In our laser lab, we built up a flexible laser heating setup with a spatial light modulator (SLM) as the core element. The setup allows to locally heat work pieces with different beam shapes with an intensity up to 220 W/cm² employing a cw-infrared laser source. Current research focuses on the temperature distribution in dependence of beam shape and beam dwell time on a specific position. Comsol based simulations support the experiments. Eventually, the heating beam will be overlaid to the process beam in use cases such as laser contact opening at lowered ablation thresholds or laser metal bonding for solar cell manufacturing. The damage after laser process with and without heating will be analyzed via microscopy.

HL 24.3 Wed 15:30 H36

Energy landscape of the Boron and Indium single-atom defects in Silicon calculated by DFT — •AARON FLÖTOTTO, WICHARD BEENKEN, and ERICH RUNGE — Institut für Physik, Technische Universität Ilmenau, Weimarer Str. 32, 98693 Ilmenau, Germany

The III group elements Boron and Indium form not only substitutional defects, which are important as electron acceptors, but also interstitial defects. Differ-

ent configurations are possible for a single impurity atom: (i) the impurity atom on an interstitial site, (ii) a substitutional impurity near a single interstitial Si atom, or (iii) the impurity and one Si atom form a pair of interstitials around an empty lattice point. We calculated within DFT the stable configurations of these defects for the Si:B and the Si:In system. We utilized the Nudged Elastic Band algorithm for finding minimal paths between these energetic minima in order to explore the energy landscape and to derive transition probabilities. The results are discussed with respect to the dynamical model suggested by K. Lauer et al. [1] for the explanation of PL-spectra of In-doped Si. [1] Lauer, K.; Möller, C.; Schulze, D. & Ahrens, C.; AIP Adv. 5 (2015) 017101

HL 24.4 Wed 15:45 H36

Effects of Defects on the Optoelectronic Properties of Ta₃N₅ Thin Films — •LUKAS M. WOLZ, GABRIEL GRÖTZNER, LAURA I. WAGNER, IAN D. SHARP, and JOHANNA EICHHORN — Walter Schottky Institut, Technische Universität München

For photoelectrochemical energy conversion, metal nitride semiconductors have the potential to overcome several limitations associated with the more intensively investigated class of metal oxides. Among these materials, Ta₃N₅ is especially promising, possessing a bandgap of ~2.2 eV and effective long-range charge transport. However, the (opto)electronic and photoelectrochemical properties of Ta₃N₅ photoelectrodes are often dominated by defects, such as oxygen impurities, nitrogen vacancies, and low-valent Ta cations. To identify the impact of such defects on the material properties, we prepare Ta₃N₅ via two different synthetic routes. As precursor, Ta_xN_y and Ta_xO_y thin films were deposited by magnetron sputtering and were subsequently annealed at high temperatures in NH₃ to form Ta₃N₅. Both films are homogenous and reveal the formation of phase-pure orthorhombic Ta₃N₅. Compared to nitride-derived Ta₃N₅, the oxide-derived films are characterized by higher structural disorder as well as higher oxygen and lower nitrogen concentrations. Despite these higher defect concentrations, the oxide-derived Ta₃N₅ films exhibit improved stability under photoelectrochemical operation conditions, though both films show similar photoelectrochemical performance. The improved understanding of defect properties and their impact on PEC stability provides a path to tailored optimization of photoelectrode properties.

HL 24.5 Wed 16:00 H36

Investigation of various quenching materials on the P-line — •DOMINIK BRATEK, KATHARINA PEH, KEVIN LAUER, AARON FLÖTOTTO, DIRK SCHULZE, and STEFAN KRISCHOK — Institut für Physik, Technische Universität Ilmenau, Weimarer Str. 32, 98693 Ilmenau, Germany

Solar-grade Si shows degradation effects and a lowering of the charge carrier lifetimes after illumination [1]. For In implanted Si this effect was shown to be connected to the P-line in photoluminescence spectra [2]. This P-line can furthermore be influenced by applying a strong quenching after an anneal. The intensity of the P-line increases by several orders of magnitude depending on the cooling rate [3]. In this contribution we investigate the influence of four different quenching liquids on the P-line. From an experimental point of view we discuss the applicability of each used liquid in consideration of P-Line intensity and probe integrity. [1] C. Möller and K. Lauer, Physica Status Solidi (RRL) 7, 461 (2013). [2] K. Lauer, C. Möller, D. Schulze, and C. Ahrens, AIP Advances 5, 017101 (20125). [3] M. L. W. Thewalt, U. O. Ziemelis, and P. R. Parsons, Solid State Communications 39, 27 (1981).

HL 24.6 Wed 16:15 H36

Simulation of the reaction kinetics of the A_{Si} - Si_i -defect — •KEVIN LAUER^{1,2}, KATHARINA PEH², WICHARD BEENKEN², ERICH RUNGE², and STEFAN KRISCHOK² — ¹CIS Forschungsinstitut für Mikrosensorik GmbH, Konrad-Zuse-Str. 14, 99099 Erfurt, Germany — ²TU Ilmenau, Institut für Physik und Institut für Mikro- und Nanotechnologien, 98693 Ilmenau, Germany

Light-induced degradation (LID) is a severe problem for silicon photo-sensitive devices like solar cells and photo detectors. LID reaction kinetics may be explained by the A_{Si} - Si_i -defect model. [1] This model consists of seven states. The transitions between these states are assumed to be first order equilibrium reactions, which can be mathematically treated by a system of linear differential equation. [1] This is numerically solved and compared to the LID cycle using well-known together with some estimated reaction constants.

[1] K. Lauer, C. Möller, C. Tessmann, D. Schulze, and N. V. Abrosimov, "Activation energies of the In_{Si} - Si_i defect transitions obtained by carrier lifetime measurements", *physica status solidi (c)*, vol. 14, no. 5, p. 1600033, 2017.

30 min. break

HL 24.7 Wed 17:00 H36

Exploring Zirconium-doped Tantalum Nitride as a Photoanode for Solar Energy Conversion — •OLIVER BRUNE, LAURA I. WAGNER, VERENA STREIBEL, and IAN D. SHARP — Walter Schottky Institut und Physics Department, Technical University of Munich, Am Coulombwall 4, 85748 Garching, Germany

Solar water splitting could pave the way to carbon-free hydrogen production as it allows for direct transformation of sunlight into chemical energy. While the oxygen evolution reaction is a crucial step in generating green hydrogen, there remains a lack of semiconductor photoanode materials that can simultaneously fulfill three key requirements: long-term chemical stability, high photocarrier extraction efficiencies, and appropriate bandgap for harvesting solar radiation. Nevertheless, among the various materials that have been investigated, the transition metal nitride Ta₃N₅ offers significant promise as an efficient n-type photoanode. Building upon this established material, we use reactive co-sputtering and subsequent ammonia annealing to introduce Zr into Ta₃N₅, with the aim of investigating how the ternary nitride character of Zr-Ta-N(O) enables tuning of key semiconductor properties. Using a range of complementary characterization methods, we show that synthesis parameters and Zr content have a significant influence on the crystal structure, morphology, and optoelectronic properties of this ternary compound. Based on these insights, we optimize the composition and synthesis processes to achieve a highly stable and efficient photoanode material, which is a key requirement for solar water splitting.

HL 24.8 Wed 17:15 H36

Defect-Engineered Atomic Layer Deposited TaO_x Protection Layers for Photoelectrochemistry — •TIM RIETH, CLARA SCHERM, and IAN SHARP — Walter Schottky Institute and Physics Department, Technical University of Munich, Am Coulombwall 4, 85748 Garching, Germany

Photoelectrochemical (PEC) energy conversion provides a viable route to the generation of chemical fuels from solar light. In this approach, charge carriers generated within a semiconductor light absorber immersed in an electrolyte are used to drive water splitting or carbon dioxide reduction reactions. A particularly relevant PEC configuration uses photovoltaic absorbers coated with transparent and conductive protection layers that prevent chemical corrosion of the semiconductor components. However, ensuring that the protection layer simultaneously fulfills the criteria for chemical stability, electronic conductivity, and optical transparency remains a challenging task. Here, we utilize plasma enhanced atomic layer deposition (PE-ALD) to create defect engineered and ultrathin tantalum oxide (TaO_x) protection layers for PEC applications. In addition to their optical transparency, the TaO_x films form continuous coatings on the photoabsorber and provide improved chemical stability compared to titanium dioxide. A sufficiently high film conductivity is obtained by intentionally introducing electronic defects from hydrogen plasma sub-cycles during the ALD process. The demonstrated defect engineering mechanism and achieved TaO_x protection layers represent an advance towards efficient and stable PEC devices.

HL 24.9 Wed 17:30 H36

Exploring novel ternary nitride semiconductor photoabsorbers for solar energy conversion applications — •LAURA I. WAGNER¹, ELISE SIROTTI¹, JOHANNA EICHHORN¹, CHANG-MING JIANG¹, MATTHIAS KÜHL¹, VERENA STREIBEL¹, DAVID EGGER², and IAN D. SHARP¹ — ¹Walter schottky Institut und TUM, München, Germany — ²TUM, München, Germany

Solar water splitting offers the possibility to harvest the sunlight and store it in the chemical bonds of hydrogen. Exploratory research has revealed several possible photoanode materials, but until now no material meets the core requirements for photochemical stability, carrier extraction efficiency, and moderate band gap in the visible range. In this context, transition metal nitride semiconductors are

underexplored and offer promise as new photoanode materials candidates. As a non-equilibrium synthesis approach, reactive magnetron co-sputtering enables the synthesis of novel ternary nitride photoabsorbers. In this work, a new ternary metal nitride photoanode material, cubic bixbyite-type ZrTa₃N₃, is presented. We observe the reactively sputtered ZrTa₃N₃ thin films to exhibit an optical bandgap at 2.4 eV and n-type behavior. Most importantly, the resulting polycrystalline films exhibit appreciable photoactivity when implemented as a photoanode in a photoelectrochemical cell. Benefiting from the tunability of cation (Ta,Zr) ratio of reactive sputtering and anion (N,O) ratio with post annealing treatments, the solid solution of ZrxTa_{2-x}N₃(O) offers a large parameter space to tune and optimize optoelectronic properties for various applications, including for PEC applications.

HL 24.10 Wed 17:45 H36

Electrical transport across catalyst/defect-engineered titania corrosion protection layer interfaces for light-driven CO₂ reduction — •JULIUS KÜHNE, OLIVER BIENEK, TIM RIETH, and IAN D. SHARP — Walter Schottky Institute and Physics Department, Technical University of Munich, Am Coulombwall 4, 85748 Garching, Germany

Producing value-added products via light-driven CO₂ reduction represents a promising approach to sustainably address increasing CO₂ emissions and meet the growing global energy demand. However, such solar fuels systems require passivating layers to chemically protect semiconductor light absorbers from harsh reaction environments. Despite great progress in the development of atomic layer deposited (ALD) protection layers, the factors governing efficient charge injection into the catalytic component are not yet well understood. Here, the charge transport characteristics between various defect-engineered TiO₂ protection layers grown with ALD and metal catalyst layers including Ag, Au, Pt, Ni and Ti are analyzed. This work aims to get a deeper understanding of the interface between catalyst and protection layer in terms of contact resistivity, carrier transport, and interface kinetics. Additionally, results of EC and PEC measurements are compared to assess the stability and activity of these systems under CO₂ reduction conditions in a two-compartment cell with ion exchange membrane. The selectivity of selected catalyst layers is evaluated by gas chromatography of the reaction products, thereby enabling a quantification of their overall performance characteristics.

HL 24.11 Wed 18:00 H36

Finite supercell charge correction for electronic transitions in defects including electronic and ionic screening — •CHRISTOPH FREYSOLDT¹, BAOYING DOU¹, STEFANO FALLETTA², and JÖRG NEUGEBAUER¹ — ¹Max-Planck-Institut für Eisenforschung GmbH, Max-Planck-Str. 1, 40237 Düsseldorf — ²Ecole Polytechnique Fédérale de Lausanne (EPFL), CH-1015 Lausanne, Switzerland

Charged point defects play an important role in the function of (opto)electronic devices. Theoretical investigations have proven valuable to understand quantitatively their stability, electrical and optical properties, and hence their beneficial or detrimental role in device performance. Electronic transitions involving localized defect states have recently moved into the focus. Similar to formation energies, also the transition energies suffer from artifacts due the long-range Coulomb interactions and the artificial periodicity in supercell models of defects. While the initial charge state is subject to full electronic and ionic screening, the changes upon the transition are screened by electrons only. Yet, the required charge corrections cannot be derived by cleverly combining traditional corrections for formation energies of initial and final state. I will present an overview of how these artifacts can be understood and corrected for. I will show applications for vertical transitions and non-radiative carrier capture.

HL 24.12 Wed 18:15 H36

Influence of Sr concentration on atomic, magnetic, and electronic structure of Ruddlesden-Popper oxide La_{2-x}Sr_xCo_{1-y}Fe_yO₄ — •DINA I. MAZITOVA¹, DEBALAYA SARKER^{1,2}, and SERGEY V. LEVCHENKO¹ — ¹Moscow, Russia — ²UGC-DAE CSR, Indore, India

Ruddlesden-Popper oxides were demonstrated to be promising catalysts for oxygen evolution reaction. There are numerous attempts in the literature to find descriptors for predicting a catalytic activity. However, the descriptors may depend on the distribution of ions of different types in these multi-component systems.

We calculated atomic, electronic, and magnetic structure of La₂Co_{0.5}Fe_{0.5}O₄, LaSrCo_{0.5}Fe_{0.5}O₄ (LSCFO), and Sr₂Co_{0.5}Fe_{0.5}O₄ for different distributions of iron and cobalt using all-electron DFT in GGA and GGA+*U* approximations. Our calculations show that the favorable distribution of transition metal cations depends on the amount of Sr substituted in the A site. The electronic and magnetic structures depend strongly on the Fe/Co distribution. For example, GGA-RPBE calculations in LSCFO showed charge-ordered ferromagnetic structure in the Co layer and antiferromagnetic structure in the Fe layer when Co and Fe layers interchange with one another, but for uniform distribution of iron and cobalt ions, LSCFO becomes ferromagnetic.

HL 25: Poster 1

Topics:

- 2D semiconductors and van der Waals heterostructures
- Acoustic waves and nanomechanics
- Focus Session: Perspectives in Cu(In,Ga)Se₂: How to go beyond 23.4 percent
- Focus Session: Quantum Properties at Functional Oxide Interfaces
- Functional semiconductors for renewable energy solutions
- Heterostructures, interfaces and surfaces
- Optical properties
- Organic semiconductors
- Quantum dots and wires
- Quantum transport and quantum Hall effects
- Semiconductor lasers
- Spin phenomena in semiconductors
- Thermal properties
- THz and MIR physics in semiconductors
- Transport properties

Time: Wednesday 18:00–20:00

Location: P2

HL 25.1 Wed 18:00 P2

A versatile transfer printing toolbox for 2D material stacking — •IOANNIS CALTZIDIS, MAJA GROLL, JULIUS BÜRGER, MARC SATISON, JÖRG K. N. LINDNER, and KLAUS D. JÖNS — Institute for Photonic Quantum Systems, Center for Optoelectronics and Photonics Paderborn, and Department of Physics, Paderborn University, 33098 Paderborn, Germany

2D materials are of great interest to scientists due to the versatile integration with other materials into, for example, Van-der-Waals heterostructures. The resulting nanoscale Moiré superlattices have applications in electronic and photonic quantum technologies. In 2D materials, the electronic band structure is generally determined by the number of layers, species of materials, as well as their angular and relative translational orientation. Transfer printing 2D materials on top of each other or onto different platforms is a frequently used fabrication method for 2D devices in state-of-the-art laboratories worldwide. Here we show how our transfer printing apparatus can be used to deterministically transfer tungsten diselenide (WSe₂) on transmission electron microscope (TEM) grids for high-resolution differential phase contrast measurements, revealing the electronic field distribution. We employ water-assisted and dry transfer methods with WSe₂ on a polyvinylalcohol (PVA) - polymethylmethacrylate (PMMA) or polydimethylsiloxane (PDMS) polymer substrate. The transfer stage's translational, rotational, and azimuthal degrees of freedom enable deterministic positioning and control in the fabrication process.

HL 25.2 Wed 18:00 P2

Enhancement of Raman and Defect Photoluminescence Emission in Hexagonal Boron Nitride (h-BN) — •FELIX SCHAUMBURG, MARCEL ZÖLLNER, VASILIS DERGAINLIS, AXEL LORKE, MARTIN GELLER, and GÜNTHER PRINZ — Faculty of Physics and CENIDE, University Duisburg-Essen, Germany

Optical spectroscopy, especially Raman- and photoluminescence (PL)-spectroscopy, is commonly used to study the optical properties of two-dimensional materials. In order to obtain the highest Raman/PL-signals, it is important to reduce the reflection of the excitation laser. We studied a number of exfoliated h-BN flakes with different thicknesses on a Si substrate with a 300 nm SiO₂ top-layer. By changing the h-BN layer-thickness, we found a specific thickness, where all Raman signals showed maximum intensity, whereas the backscattered laser light was almost completely suppressed. To explain the increased intensities, we calculated the reflectivity of the layer system (air, h-BN, SiO₂, Si) for different h-BN layer thicknesses and used the transfer-matrix-algorithm. For our 532 nm excitation laser, the minimum reflectivity was found for a h-BN flake thickness of about 160 nm. Using AFM measurements, we were able to confirm that the thickness of the h-BN flakes having the strongest Raman signals correspond almost exactly to the calculated thickness. Our results suggest, that the PL from defects will also be strongly enhanced for an h-BN thickness of 160 nm and an excitation laser wavelength of 532 nm. This optimal thickness for the defect state PL emission can easily be calculated for other excitation laser wavelengths, as well as for other materials.

HL 25.3 Wed 18:00 P2

Surface acoustic wave modulation of optical and electrical properties in TMDC monolayers — •CLEMENS STROBL, BENJAMIN MAYER, HENDRIK LAMBERS, URSULA WURSTBAUER, and HUBERT KRENNER — Institute of Physics, University of Münster, Germany

Two-dimensional transition metal dichalcogenides (TMDCs) such as WSe₂ exhibit large exciton binding energies combined with a high sensitivity of their bandgap energy to mechanical stimuli [1]. Excitons in these materials can be generated either optically by above band-gap illumination or via two electrodes. Similarly, excitons in TMDCs can be studied optically via photoluminescence and absorption spectroscopy, electrically by detecting a photocurrent or via the interaction with surface acoustic waves (SAWs).

The aim of this project is to investigate SAW-dependent photoconductance in exfoliated monolayers [2] and to determine the influence of SAWs on the optical and optoelectronic properties in TMDCs. We study the SAW-driven exciton transport in monolayers and thus the change in the exciton decay rate [1]. For all experiments lithium niobate (LiNbO₃) substrates and interdigitated electrodes (IDTs) operating at a frequency range from 300MHz up to 1GHz are used.

[1] Datta et al. Nat. Photon. 16, 242-247 (2022). [2] Preciado, E., Schülein, F., Nguyen, A. et al. Nat Commun 6, 8593 (2015).

HL 25.4 Wed 18:00 P2

Raman fingerprint of twisted TMDC bilayers — •SINA BAHMANYAR, NIHIT SAIGAL, HENDRIK LAMBERS, LAURA SCHUSSER, CLEMENS STROBL, and URSULA WURSTBAUER — Institute of Physics, University of Münster, Münster, Germany

The discovery of superconductivity and other correlated phases in twisted bilayer graphene opened up a new field of research aimed at understanding the many body physics and strong electronic interactions in twisted van der Waals bilayers. [1] Such bilayer systems provide an ideal platform for simulation of Hubbard model physics and its control using the relative twist angle between the layers [2] in order to tune interlayer interaction and electronic correlations. [1,2] We have fabricated twisted WSe₂ bilayers with various twist angles between the monolayers and characterized them using low and high energy Raman spectroscopy and photoluminescence spectroscopy. The low-frequency Raman spectra shows the shear modes that are highly sensitive to the twist angle and interlayer coupling between the monolayers. Our measurements establish Raman spectroscopy as a non-destructive way to characterize the interlayer coupling in twisted TMDC bilayers to study electronic and excitonic correlation physics [3]. We acknowledge financial support via WU 637/7-1 and SPP2244. [1] Y. Cao et al., Nature 556, 23 (2018). [2] Y. Tang et al., Nature 579, 353 (2020) [3] L. Sigl. et al. Phys. Rev. Res. 2, 042044(R) (2020)

HL 25.5 Wed 18:00 P2

Nonlinear spectroscopy of valley polarization in transition metal dichalcogenides — •PAUL HERRMANN¹, SEBASTIAN KLIMMER¹, and GIANCARLO SOAVI^{1,2} — ¹Institute of Solid State Physics, Friedrich Schiller University Jena, Jena, Germany — ²Abbe Center of Photonics, Friedrich Schiller University Jena, Jena, Germany

Valleytronics is the branch of science that aims at controlling the valley (i.e., local maximum/minimum in the valence/conduction bands) degree of freedom to store, manipulate and read information. Monolayer transition metal dichalcogenides (TMDCs) are promising candidates for valleytronic applications their hexagonal symmetry in the real and reciprocal space leads to the appearance of two energetically degenerate but non-equivalent valleys at the K and -K points. In addition, their direct bandgap nature in the monolayer limit enables direct optical excitation into these valleys, which can be achieved in a highly selective fashion by means of circularly polarized light [1]. All-optical control of the valley population would enable information processing at optical frequencies, thus over-

coming by three to six orders of magnitude the speed of current electronic devices [2]. Here, we perform non-linear and time-resolved optical spectroscopy to study the purity and temporal evolution of the valley population in TMDs. In particular, we combine 2-photon-photoluminescence and time-resolved second harmonic measurements to investigate the impact of intra-valley relaxation and inter-valley scattering on the degree of valley polarization.

[1] Xu X. *et al.*, NPhys 10, 5 (2014) 343-350

[2] Mitchell Waldrop M. *et al.* Nature 530, (2016) 144-147

HL 25.6 Wed 18:00 P2

Charge carrier dependent Raman response in WS₂ monolayers — •HENDRIK LAMBERS, NIHIT SAIGAL, and URSULA WURSTBAUER — Institute of Physics, University of Münster, Münster, Germany

Semiconducting transition metal dichalcogenides such as WS₂ and MoS₂ are among the most widely studied 2D materials due to their unique optical and electronic properties. Monolayers of these materials show a large exciton dominated light matter coupling. Exciton-phonon and electron-phonon interaction effects are prone to modification of the charge carrier density and impacts the optical and electronic behavior of the atomically thin semiconductors [1]. Here we report on a detailed Raman study of the charge carrier dependent evolution of the phonon modes in WS₂ monolayer embedded in a field effect structure using a solid-state electrolyte [2]. The optimized field effect structure using a polymer electrolyte top gating allows tuning the fermi-energy cross the band gap and hence enables ambipolar doping.

We acknowledge financial support via DFG WU 637/7-1 and SPP2244.

[1] B. Miller *et al.*, Nat Commun 10, 807 (2019).

[2] B. Miller *et al.*, APL 106, 122103 (2015).

HL 25.7 Wed 18:00 P2

Tuning exciton recombination rates in doped transition metal dichalcogenides — •THERESA KUECHLE, SEBASTIAN KLIMMER, MARCO GRUENEWALD, and GIANCARLO SOAVI — Institute of Solid State Physics, Friedrich Schiller University Jena, Helmholtzweg 5, 07743 Jena, Germany

Monolayer transition metal dichalcogenides (TMDs) are direct gap semiconductors that hold great promise for advanced applications in photonics and optoelectronics such as integrated, flexible and high-speed light emitting devices [1]. Understanding the interplay between their radiative and non-radiative recombination pathways is thus of crucial importance not only for fundamental studies but also for the design of future nanoscale on-chip devices. Here, we investigate the interplay between doping and exciton-exciton annihilation (EEA) and their impact on the photoluminescence quantum yield in different TMD samples and related heterostructures. We demonstrate that the EEA threshold increases in highly doped samples, where the radiative and non-radiative recombination of trions dominates [2]. The results are interpreted with a rate equation model that takes into account all radiative and non-radiative recombination pathways of excitons and trions in TMDs as a function of doping (*i.e.*, trion concentration) and generation rate (*i.e.*, photoexcited carrier concentration).

[1] Wang *et al.*, Nanoscale Adv. 2, 4323 (2020)

[2] Kuechle *et al.*, Opt. Mat.: X 12, 100097 (2021)

HL 25.8 Wed 18:00 P2

Destructive Photon Echo Formation in Six-Wave Mixing Signals Induced by Local Field Effects — •THILO HAHN¹, JACEK KASPRZAK², TILMANN KUHN¹, and DANIEL WIGGER³ — ¹Institute of Solid State Theory, University of Münster, Germany — ²Université Grenoble Alpes, CNRS, France — ³School of Physics, Trinity College Dublin, Ireland

The optical properties of transition metal dichalcogenides have emerged as an outstanding topic in nanoscience. In these materials, tightly bound excitons dominate the optical response. Ultrafast nonlinear spectroscopy is an ideal tool to study the excitonic properties and their dynamics. To model the dynamics of excitonic transitions we use a few-level system with an additional local field (LF) effect to describe exciton-exciton interaction [1]. Effectively, the LF shifts the transition energy depending on the exciton occupation, which is directly visible in pump-probe experiments [2]. In this contribution we consider six-wave mixing spectroscopy [3], where we discover a new destructive photon echo effect, that is produced by the LF contribution. In contrast to the traditional echo formed by constructive interference [4], the signal is temporarily suppressed due to destructive quantum interference.

[1] T. Hahn, *et al.*, New J. Phys. 23, 023036 (2021), [2] A. Rodek *et al.*, Nanophotonics 10, 2717 (2021), [3] T. Hahn, *et al.*, Adv. Sci. 9, 2103813 (2021), [4] E. L. Hahn, Phys. Rev. 80, 580 (1950)

HL 25.9 Wed 18:00 P2

Signature of lattice dynamics in twisted 2D homo/hetero-bilayers — •YANG PAN^{1,2}, SHUTONG LI³, MAHFUJUR RAHAMAN^{1,2}, ILYA MILEKHIN^{1,2}, and DIETRICH R. T. ZAHN^{1,2} — ¹Semiconductor Physics, Institute of Physics, Chemnitz University of Technology, Chemnitz, Germany — ²Center for Materials, Architectures, and Integration of Nanomembranes (MAIN), Chemnitz, Germany — ³Department of Chemical Engineering and Materials Science, University of Minnesota, Minneapolis, Minnesota, USA

Twisted 2D bilayer materials are created by artificial stacking of two monolayer crystal networks of 2D materials with a desired twisting angle θ . The material forms a moiré superlattice due to the periodicity of both top and bottom layer crystal structure. The optical properties are modified by lattice reconstruction and phonon renormalization, which makes optical spectroscopy an ideal characterization tool to study novel physics phenomena. Here, we report a Raman investigation on a full period of the twisted bilayer (tB) WSe₂ moiré superlattice (*i.e.* $0^\circ \leq \theta \leq 60^\circ$). We observe that the intensity ratio of two Raman peaks, B_{2g} and E_{2g}/A_{1g} correlates with the evolution of moiré period. Using a series of temperature-dependent Raman and photoluminescence (PL) measurements as well as *ab initio* calculations, the intensity ratio $I_{B_{2g}}/I_{E_{2g}/A_{1g}}$ is explained as a signature of lattice dynamics in tB WSe₂ moiré superlattices. By further exploring different material combinations of twisted hetero-bilayers, the results are extended for all kinds of Mo- and W-based TMDCs.

HL 25.10 Wed 18:00 P2

Transport Measurements on Twisted Graphene Heterostructures around Magic Angle — •BEI ZHENG, XIAO YUE ZHANG, JUN HUI HUANG, LINA BOCKHORN, and ROLF J. HAUG — Institut für Festkörperphysik, Leibniz Universität Hannover, 30167 Hannover, Germany

The twisting of graphene layers opens up a whole new field of rich physics [1]. Especially, the electronic properties of twisted (double Bernal-stacked) bilayer graphene layers depend strongly on the twist angle, owing to the energy band modulation from the corresponding Moiré superlattice [2,3]. Furthermore, twisted graphene structures around the magic angle were the first systems that show new many-body phases, as e. g. superconductivity or Mott insulator phases [4].

We fabricated twisted graphene heterostructures around the magic angle encapsulated in hexagonal boron via 'tear and stack' method and investigated their transport characteristics at low temperature down to 1.5 K. The longitudinal resistance was observed to periodically change with charge carrier concentration. The periodicity is relative to the superlattice density n_s , and depends on how the degenerated superlattice sub-bands are filled.

[1] H. Schmidt *et al.*, Nat. Commun. 5, 5742 (2014)

[2] J. C. Rode *et al.*, 2D Mater. 3, 035005 (2016)

[3] S. J. Hong *et al.*, 2D Mater. 8, 045009 (2021)

[4] Y. Cao *et al.*, Nat. 556, 43-50 (2018)

HL 25.11 Wed 18:00 P2

Rashba Splitting Modulated by Tuned Intrinsic Dipole Moment in MoSSe/WSSe Heterostructures — •HAMID MEHDIPOUR and PETER KRATZER — Faculty of Physics, University of Duisburg-Essen, Lotharstrasse 1, 47057 Duisburg, Germany

First-principles calculations in the framework of the density-functional theory are performed to study the van der Waals heterostructures of two Janus transition metal dichalcogenide (TMDC) monolayers, MoSSe and WSSe. Sixteen possible heterostructures of the two monolayers and their associated stackings (AA, AB) are studied. Thermal stability and electric and optical properties of all possible heterostructure configurations are investigated and compared. Owing to the lack of structural mirror symmetry in this class of TMDCs, a non-zero electric dipole moment exists for each Janus monolayer. The intrinsic dipole moments of the monolayers could build up an inter-monolayer coupling, which varies in magnitude across the possible heterostructure configuration spectrum. The total electric moment modulated by stacking could impact the overall stability of the heterostructures and their electronic and linear optical responses. Most intriguing for this class of material is the Rashba splitting of band structures for each Janus monolayer, which strongly depends on the intrinsic electric field associated with the non-zero electric moment due to the lack of mirror symmetry. By combining the DFT calculation and charge analysis, we quantify the Rashba effect for each heterostructure of MoSSe/WSSe and bring into the spotlight the role the stacking plays in modulating this effect.

HL 25.12 Wed 18:00 P2

Valley dynamics in WSe₂ monolayers and MoSe₂-WSe₂ heterobilayers — •PHILIPP PARZEFALL, MATTHIAS BREM, and CHRISTIAN SCHÜLLER — Institut für Experimentelle und Angewandte Physik, Universität Regensburg, Deutschland

We have performed an in depth study of the valley coherence and polarization in hBN-encapsulated WSe₂ monolayers, which shall be extended to WSe₂-MoSe₂ heterostructures.

Therefore, we investigate first the excitonic properties and possible exciton-phonon coupling in hBN-encapsulated WSe₂ monolayers via micro-photoluminescence and resonant Raman spectroscopy measurements with excitation energies close to the A-exciton's fine-structure. Hereby, the valley polarization and -coherence are of special interest as possible resonant phonon excitation influences the valley dynamics behavior tremendously.

Afterwards, the resulting understanding is used to investigate interlayer excitons and trions on MoSe₂-WSe₂ heterobilayers with 0° or 60° relative twist between the layers, similarly, with an excitation energy close to the resonances of the WSe₂'s A-exciton.

HL 25.13 Wed 18:00 P2

Electrical control of orbital and vibrational interlayer coupling in bi- and trilayer 2H-MoS₂. — JULIAN KLEIN^{1,2}, JAKOB WIERZBOWSKI¹, PEDRO SOUBELET¹, THOMAS BRUMME^{3,4}, LORENZO MASCHIO⁵, AGNIESZKA KUC^{6,7}, KAI MÜLLER¹, ANDREAS V. STIER¹, and JONATHAN J. FINLEY¹ — ¹Walter Schottky Institut, TU München, Germany — ²Department of Materials Science and Engineering, MIT, USA. — ³Wilhelm-Ostwald-Institute for Physical and Theoretical Chemistry, Leipzig University, Germany. — ⁴Faculty for Chemistry and Food Chemistry, TU Dresden, Germany. — ⁵Dipartimento di Chimica and Centre of Excellence NIS, Università di Torino, Italy. — ⁶Helmholtz-Zentrum Dresden-Rossendorf, Abteilung Ressourcenökologie, Forschungsstelle Leipzig, Germany — ⁷Department of Physics and Earth Sciences, Jacobs University Bremen, Germany.

Manipulating electronic interlayer coupling in layered vdW materials is essential for designing optoelectronic devices. Here, we control vibrational and electronic interlayer coupling in bi- and trilayer 2H-MoS₂ using large external electric fields in a microcapacitor device. The electric field lifts Raman selection rules and activates phonon modes in excellent agreement with ab initio calculations. Through polarization-resolved photoluminescence spectroscopy, we observe a strongly tunable valley dichroism. By modeling our result using rate equations, we have explained the valley dichroism tunability using realistic material parameters.

HL 25.14 Wed 18:00 P2

Assigning excitonic transitions in reconstructed MoSe₂-WSe₂ heterostacks — CHRISTOS PASPALIDES¹, MIRCO TROUE¹, LUKAS SIGL¹, JOHANNES FIGUEIREDO¹, MANUEL KATZER², MALTE SELIG², FLORIAN SIGGER¹, ROLAND GILLEN³, JONAS KIEMLE¹, ANDREAS KNORR², URSULA WURSTBAUER⁴, and ALEXANDER HOLLEITNER¹ — ¹TU Munich — ²Technische Universität Berlin — ³Friedrich-Alexander-Universität Erlangen-Nürnberg — ⁴University of Münster

Transition metal dichalcogenide monolayers exhibit strong light-matter interactions, which promotes them as ideal candidates for novel 2D optoelectronic applications. The vertically stacked Van der Waals heterostacks facilitate the emergence of a type-II band alignment, which leads to the formation of long-lived interlayer excitons. We present g-factors for three distinct interlayer exciton emissions in MoSe₂-WSe₂ heterostacks measured up to 9T. Theoretical considerations including density functional theory lead to the assignment of the characteristic emission lines to optical transitions inside an atomically reconstructed H-type heterostack with a near-zero twist-angle. Here, the H_n^i atomic registry is able to fill sizable commensurate domains within the reconstructed lattice while the corresponding selection rules are found to govern the optical response of the system.

Following the attribution of the interlayer exciton emissions, we provide a deeper insight into the effect of atomic reconstruction in MoSe₂-WSe₂ heterostacks and discuss the possibility for a macroscopic occupation of the ground-state leading to unique many-body effects of interlayer excitons in such systems.

HL 25.15 Wed 18:00 P2

Fabrication and Characterization of Twisted TMDC Bilayer — LAURA NICOLLETTE SCHUSSER, SINA BAHMANYAR, NIHIT SAIGAL, HENDRIK LAMBERS, HOSEIN OSTOVAR, and URSULA WURSTBAUER — Institute of Physics, University of Münster, Münster, Germany

Semiconducting 2D materials such as transition metal dichalcogenides (SC-TMDCs) excel due to their strong exciton dominated light matter interaction [1]. Van der Waals (VdW) heterobilayers prepared from SC-TMDCs are ideal systems for the realization and study of dense exciton ensembles [2,3] and correlated phases of matter [4]. We are working to improve the fabrication protocol for high-quality twisted TMDC bilayers. We obtain monolayers by micro-mechanical exfoliation along with a deterministic pick-up and dry transfer using a viscoelastic stamp and to create vdW heterostacks with several layers. The twist angle between the layers is precisely controlled by using a rotation stage. We use hexagonal boron nitride (hBN) as an encapsulating material. Photoluminescence (PL) spectroscopy combined with Raman spectroscopy is utilized for characterization. While the former technique probes the intralayer and interlayer exciton transitions, the latter one is used for the investigation of the phonon fingerprints of the system. [1] [1] U. Wurstbauer et al. J. Phys. D: Appl. Phys. 50, 173001 (2017). [2] L. Sigl et al. Physical Review Research 2, 042044(R) (2020). [3] J. Kiemle et al. Phys. Rev. B 101, 121404(R) (2020). [4] Y. Tang et al., Nature 579, 353 (2020).

HL 25.16 Wed 18:00 P2

Optical characterization of van der Waals WS₂ Monolayer- Pyrenemethylammonium chloride few-layer vertical heterointerfaces — MOHAMMED ADEL ALY^{1,2}, HILARY MASENDA^{1,3}, ARSLAN USMAN^{1,4}, BETTINA WAGNER⁵, JOHANNA HEINE⁵, MARINA GERHARD¹, and MARTIN KOCH¹ — ¹Department of Physics and Materials Sciences Center, Philipps-Universität, Marburg, 35032 Germany — ²Department of Physics, Faculty of Science, Ain Shams University, Cairo, 11566 Egypt — ³School of Physics, University of the Witwatersrand, Johannes-

burg, 2050 South Africa — ⁴Department of Physics, COMSATS University Islamabad - Lahore Campus, Lahore, 54000 Pakistan — ⁵Department of Chemistry and Material Sciences Center, Philipps-Universität Marburg, 35043 Marburg, Germany

Van-der-Waals transition metal dichalcogenides (vdW-TMDCs) layered materials have received huge attention due to their strong light-matter interaction. Moreover, combining 2D TMDCs with different organic materials opened a new line in heterostructure(Hs) research, providing unprecedented tunability for heterostructure(Hs) engineering. Few layers Pyrenemethylammonium chloride (PyMACL) is an emerging exfoliable organic material that offers distinct properties and could be attractive for photonic and optoelectronic applications. Here, we present our work on WS₂/PyMACL vdW-HS. We have investigated our specimen using micro-photoluminescence and time-resolved photoluminescence shedding light on exciton dynamics in such structures, and possible recombination channels. Moreover, investigating possible charge transfer between the different layers of the Hs.

HL 25.17 Wed 18:00 P2

Modification of charge transport in single layer MoS₂ — ZAHRA FEKRI¹, PHANISH CHAVA¹, GREGOR HLAWACEK¹, VIVEK KOLADI², TOMMASO VENANZI³, WAJID AWAN¹, ANTONY GEORGE⁴, ANDREY TURCHANIN⁴, KENJI WATANABE⁵, TAKASHI TANIGUCHI⁵, MANFRED HELM¹, and ARTUR ERBE¹ — ¹Helmholtz Zentrum Dresden Rossendorf, Dresden, Germany — ²Imec, Leuven, Belgium — ³Sapienza University of Rome, Rome, Italy — ⁴Friedrich Schiller University, Jena, Germany — ⁵National Institute for Materials Science, Tsukuba, Japan

Ion beam irradiation is a technique that can be used to alter the electrical and optical properties of two-dimensional (2D) materials through defect creation. In this work, we used 5-7.5 keV helium and neon ions to modify charge transport in monolayer molybdenum disulfide (MoS₂). Electrical characterization was performed in-situ immediately after ion beam irradiation. Raman and photoluminescence spectroscopy were implemented to further characterize the effect of ion irradiation on MoS₂. Our experiments show that the electrical properties of MoS₂-based transistors strongly depend on the nature of the substrate and the specific ion and dose used. Although 10¹²-10¹³ helium ions/cm² contribute to the increase in the current level, a similar dose of neon ions deteriorates the channel. To examine the role of the substrate, few-layer hexagonal boron nitride (h-BN) was used as an intermediate layer between MoS₂ and the Si/SiO₂ substrate. MoS₂ samples on h-BN show different electrical behaviour during ion irradiation as compared to the MoS₂ flakes which were directly placed on SiO₂.

HL 25.18 Wed 18:00 P2

Tunable THz-absorption and gain in transition metal dichalcogenides — JOSEFINE NEUHAUS, TINEKE STROUCKEN, and STEPHAN W. KOCH — Philipps University, Marburg, Germany

Exhibiting linear optical spectra that are dominated by strongly bound excitonic features, transition metal dichalcogenides have attracted considerable interest in the past decade. In a properly pre-excited system, it is possible to study intra-excitonic transitions between optically bright *s*- and dark *p*-type excitons by their THz-absorption. In particular, as *p*-type states lie energetically below *s*-type states of equal main quantum number, not only absorptive but also gain features can be observed. Furthermore, the application of an external magnetic field perpendicular to the sample results in a shift of the various excitonic resonances. As the induced Zeeman shift depends on the angular momentum quantum number, the magnetic field induced shift differs for *s*- and *p*-type excitonic states, enabling a tunability of the intra-excitonic transitions. Here, we study the tunability of the intra-excitonic absorption and gain spectra upon the interplay of an applied magnetic field, the dielectric environment and the material parameters by means of a combined approach based on DFT and a Semiconductor-Bloch equation approach.

HL 25.19 Wed 18:00 P2

Contact engineering of black phosphorus field-effect transistors — YAGNIKA VEKARIYA¹, PHANISH CHAVA¹, ZAHRA FEKRI¹, KENJI WATANABE³, TAKASHI TANIGUCHI³, SIBYLLE GEMMING², and ARTUR ERBE¹ — ¹Helmholtz Zentrum Dresden Rossendorf, 01328 Dresden, Germany — ²Technische Universität Chemnitz, 09126 Chemnitz, Germany — ³National Institute for Materials Science, Tsukuba 305-0044, Japan

Black phosphorus (BP) has recently emerged as new semiconducting two-dimensional (2D) material because of its unique properties such as tunable direct bandgap, high field-effect mobility, and good on/off ratio. In this work, we fabricated and characterized field-effect transistors (FETs) based on a few layers of black phosphorus, in order to evaluate the performance of devices using different contact materials like Graphene, Nickel (Ni), Titanium (Ti), and Chromium (Cr). We observed that the polarity and mobility value of transistors strongly depend on the contact material.

HL 25.20 Wed 18:00 P2

Single photon emitters study in hBN via low power implantation approach — •RENU RANI¹, MINH BUI^{1,2}, BILAL MALIK^{1,2}, MANUEL AUGÉ³, THORSTEN BRAZDA¹, HANS HOFSSÄSS³, DETLEV GRÜTZMACHER^{1,2}, and BEATA KARDYNAŁ^{1,2} — ¹Peter Grünberg Institut-9, Forschungszentrum Jülich, Jülich — ²Department of Physics, RWTH Aachen, Aachen — ³II. Physikalisches Institut, Georg-August-Universität Göttingen

A discovery of quantum emitters in hexagonal boron nitride (hBN) has recently incited immense interest in the field of quantum technologies. It offers not only a platform for fundamental science but is of interest for applications in quantum photonics owing to its robust single photon emission at room temperature. Recent studies have suggested that these SPEs are associated with intrinsic defects, which led to efforts to engineer the SPE in hBN by various such as plasma treatment, annealing, laser, e-beam and ion irradiation methods. Despite these efforts, the origin of single photon emission and the correlation of emission with particular defects still need to be scrutinized. Here we propose to use low-energy ion implantation to introduce the different defects in hBN. We will show results of optical characterization of hBN implanted with various noble gas ions with different energies, which depending on their atomic mass generate different vacancies and at different depths. We will discuss the viability of creating localized emitters throughout the surface, not only edges or grain boundaries. We will use Raman spectra to show that implanted material is free of contamination and damage associated with energetic particle beams.

HL 25.21 Wed 18:00 P2

Twist angle dependent proximity induced spin-orbit coupling in graphene/WSe₂/hBN heterostructures — •TOBIAS ROCKINGER¹, ANTONY GEORGE², ANDREY TURCHANIN², ZIYANG GAN², KENJI WATANABE³, TAKASHI TANIGUCHI³, DIETER WEISS¹, and JONATHAN EROMS¹ — ¹University of Regensburg, DE-93040 Regensburg, Germany — ²Friedrich-Schiller-Universität, DE-07743 Jena, Germany — ³NIMS, Tsukuba 305-0044, Japan

Recently, theoretical calculations predicted a strong dependence of the proximity-induced SOC on the twist angle between SLG and TMDCs [1]. To prove this, we fabricated SLG/WSe₂/hBN heterostructures with well-defined twist angles between the SLG and WSe₂ layers in two ways. For the first type, we exfoliated SLG and WSe₂ which often break along zigzag or armchair edges [2]. This was used to align and estimate the rotation angles between the flakes (zigzag/armchair edges not distinguishable). For the other type of samples, we used CVD-grown WSe₂ on anisotropically etched SLG to align and determine the twist angles exactly (zigzag/armchair edges distinguishable) [3]. Strong SOC causes weak anti-localization, which we used to determine the strength of the Rashba type SOC (λ_R) and the valley-Zeeman type SOC (λ_{VZ}). We found that samples with an angle around 15° or 22° show a much stronger SOC in both cases, for λ_R as well as for λ_{VZ} , compared to samples, with twist angles around 0°/30° or 11°. This is in qualitative agreement with theoretical predictions [1]. [1]Y. Li and M. Koshino, *Phys. Rev. B* **99**, (2019) 075438; [2]Y. Guo *et al.*, *ACS Nano* **10**, (2016) 8980; [3]P. Ince *et al.*, *Nano Res* **3**, (2010) 110

HL 25.22 Wed 18:00 P2

Nucleation of hBN on HOPG in conventional MBE — •CONSTANTIN HILBRUNNER, JULI ZHANG, JOERG MALINDRETOS, and ANGELA RIZZI — IV. Physikalisches Institut - Georg-August-Universität Göttingen

Due to its large bandgap of around 5.9 eV and due to its high breakdown voltage as well as its natural inertness, hexagonal boron nitride (hBN) is a promising substrate and encapsulation material to study the intrinsic properties of two-dimensional materials. Due to thermodynamics, the growth of hBN requires very high substrate temperatures. At present, the hBN films grown by molecular beam epitaxy (MBE) on non-metallic substrates with highest structural quality were fabricated using substrate temperatures between 1300°C and 1600°C not achievable using conventional systems.

In a different approach, we intend to utilize laser assisted heating during MBE. Here, we report on our preliminary results concerning the nucleation of hBN on HOPG at conventional substrate temperatures for varying B fluxes and the heating characteristic of the substrate surface in response to ns laser pulses.

HL 25.23 Wed 18:00 P2

Ultra-sensitive extinction measurements of optically active defects in monolayer MoS₂ — •INES AMERSDORFFER¹, FLORIAN SIGGER², ALEXANDER HÖTGER², MANUEL NUTZ¹, ALEXANDER HÖGELE¹, DAVID HUNGER³, THOMAS HÜMMER¹, and CHRISTOPH KASTL² — ¹Faculty of physics, Ludwig-Maximilians-Universität Munich, Germany — ²Walter Schottky Institute and Physics Department, Technical University of Munich, Germany — ³Physikalisches Institut, Karlsruhe Institute of Technology, Germany

Measurements of the marginal absorption of nanomaterials are challenging. One way to address this issue is the use of an optical resonator in which the light passes the sample multiple times and thereby enhances the absorption of nanoscale objects to a measurable amount. Here, we demonstrate how a high-finesse microcavity can be exploited in order to measure the extinction by defects in monolayer MoS₂. Such atomistic defects embedded in nanomaterials are a promising

candidate for single-photon sources. However, to make them optically accessible, it is beneficial to know their absorption properties. To this end, we performed wavelength-dependent extinction measurements. The absolute values of extinction were recorded with a detection limit of down to 0.01% and agree in the order of magnitude with theoretical predictions. In case of neglectable scattering, the extinction values can be interpreted as absorption. The results show advances towards routine hyperspectral absorption measurements on the nanoscale.

HL 25.24 Wed 18:00 P2

Electrical tuning of excitonic complexes in twisted van-der-Waals heterostructures — •BARBARA ROSA, CHIRAG PALEKAR, and STEPHAN REITZENSTEIN — Institute of Solid State Physics, Technische Universität Berlin, D-10623 Berlin, Germany

Moiré excitons arising from transition metal dichalcogenides (TMDs) bilayers are directly controlled by the twist angle between the monolayers[1]. Noteworthy features of that new class of excitons, such as their ultrafast formation and charger transfer, long population recombination lifetimes, and binding energy of ~150 meV[2,3], turn TMD heterostructures into an attractive device for the study and manipulation of optical and transport properties via electrical fields. Here, we explore the ability to modulate interlayer exciton states in homo- and heterobilayers (HB) throughout electrical tuning. By fabricating TMD heterostructures using CVD and exfoliated monolayers, we study the effects of an out-of-plane applied electrical field in heterostructures with distinct twist angles. Our work aims to achieve control of optical and transport properties of interlayer excitons, which have shown energy tunability that ranges over several hundreds of meV[2,3]. Furthermore, we intend to discuss our first results in exploring light-matter interaction of an HB embedded in a photonic microcavity by electrically manipulating the Moiré excitonic response.

[1] K. L. Seyler *et al.*, *Nature* **567**, 66-70 (2019)[2] A. Ciarrocchi *et al.* *Nature Photon.* **13**, 131 (2019)[3] H. Baek *et al.* *Science Advances* **6**, 37 (2020)

HL 25.25 Wed 18:00 P2

Optical excitations in 2D material heterostructures under pressure — •DEVIKA SVANKUTTY, PAUL STEEGER, JOHANN PREUSS, ROBERT SCHMIDT, STEFFEN MICHAELIS DE VASCONCELLOS, and RUDOLF BRATSCHITSCH — University of Münster, Institute of Physics and Center for Nanotechnology, Wilhelm-Klemm Str. 10, 48149 Münster

Heterostructures of transition metal dichalcogenides (TMDCs) have attracted a lot of attention due to their unique optical and electronic properties and easy fabrication by stacking distinct TMDC monolayers on top of each other. Depending on the material choice, the heterostructures can also exhibit interlayer excitons, where the hole resides in one layer and the electron in the other. The coupling between the layers, and thereby the optical and electronic properties of the heterostructure, are expected to be strongly dependent on the interlayer distance, which can be tuned by applying pressure to the heterostructure. Here, we investigate the optical properties of TMDC heterostructures under high pressure in a diamond anvil cell. We use a home-built stamping setup to fabricate the heterostructures and perform optical spectroscopy at various pressure values to investigate the excitonic resonances.

HL 25.26 Wed 18:00 P2

Optical properties of multilayer MoS₂ under high pressure — •PAUL STEEGER¹, ROBERT SCHMIDT¹, ILYA KUPENKO², CARMEN SANCHEZ-VALLE², STEFFEN MICHAELIS DE VASCONCELLOS¹, and RUDOLF BRATSCHITSCH¹ — ¹University of Münster, Institute of Physics and Center for Nanotechnology, Wilhelm-Klemm-Str. 10, 48149 Münster, Germany — ²University of Münster, Institute for Mineralogy, Corrensstr. 24, 48149 Münster, Germany

Vertically stacked homo- and heterostructures of 2D semiconductors have recently attracted a lot of attention. One of the most critical parameters affecting their optical and electronic properties is the interlayer coupling. Controlling the distance between the layers by applying pressure to the sample allows to tune the interlayer interaction in-situ and opens up new ways to investigate its influence on the physical properties of multi-layered 2D materials. Here, we use a diamond anvil cell to measure how absorption and emission properties of multilayer MoS₂ crystals change under pressure, highlighting the differences between inter- and intralayer excitons.

HL 25.27 Wed 18:00 P2

Deterministic creation of strain gradients in 2D materials — •ROBERT SCHMIDT, JOHANNES KERN, JANNIS BENSMANN, PAUL STEEGER, ROBERT SCHNEIDER, HELGE GEHRING, WOLFRAM H. P. PERNICE, STEFFEN MICHAELIS DE VASCONCELLOS, and RUDOLF BRATSCHITSCH — University of Münster, Institute of Physics and Center for Nanotechnology, Wilhelm-Klemm-Str. 10, 48149 Münster, Germany

Strain is a powerful tool to modify the optical and electrical properties of 2D materials. While the controlled application of homogeneous strain to 2D materials is feasible, the creation of deterministic strain gradients over distances of several micrometers is still challenging. Commonly, monolayers or few-layers

are manually transferred onto a pre-patterned substrate, which often results in strain gradients differing from sample to sample.

In this work, we imprint structures into 2D materials. Using a homebuilt nanoimprint setup and SiO₂ stamps produced by reactive ion etching, we print into 2D materials with lateral precision below one micrometer. The strain fields induced by this deformation are analyzed using optical absorption mapping.

HL 25.28 Wed 18:00 P2

"Ghupft und Gschobm": An ab initio multi-scale approach to bands and electron-phonon coupling in twisted WSe₂ bilayers — •MICHAEL WINTER and TIM WEHLING — I. Institute of Theoretical Physics, Universität Hamburg
Transition metal dichalcogenide bilayers host electron correlation effects like superconductivity, exciton condensation, and Mott insulation. These phenomena are tuneable via charge doping, optical excitation, dielectric environment, and twist angle. The complex interplay of Coulomb and electron-phonon interactions with multi-orbital and multi-valley physics behind the aforementioned correlation effects remains to be understood.

We study the twisted homo-bilayer of tungsten diselenide by construction of many-body quantum lattice models describing the electronic and phonon degrees of freedom as well as their coupling. From ab initio DFT and DFPT calculations with subsequent Wannier constructions on untwisted snapshots of commensurate structures corresponding lattice models are compiled. With an automated interpolation we are able to address twisted systems.

HL 25.29 Wed 18:00 P2

Ultrafast dynamics of dark states in photocurrent of TMD heterostructures — •DENIS YAGODKIN, ELIAS ANKERHOLD, ABHIJEET KUMAR, JOHANNA RICHTER, FIRAS BEN MOUSSA, CORNELIUS GAHL, and KIRILL BOLOTIN — Freie Universität Berlin

We study the photocurrent response of TMD heterostructures MoS₂/MoSe₂ with 150 femtosecond time resolution. In order to study the dynamics of transport at the interface of the heterostructure, we tune one pulse to MoS₂ excitation resonance and the second, time-delayed pulse, to that of MoSe₂. We find stark asymmetry between negative and positive delays. We attribute this asymmetry to the formation of interlayer excitons. Using a simple model of charge carriers decaying in optically dark states we successfully describe both time-resolved reflectivity and photocurrent response of heterostructures. Extracted formation time of interlayer excitons is similar to that observed in ARPES and TR-THz at room temperature. Strong response to interlayer excitons shows the potential of our technique in detecting other dark states promising for information storing and processing.

HL 25.30 Wed 18:00 P2

Charge carrier localization in nanobubbles of atomically thin TMD semiconductors — CHRISTIAN CARMESIN¹, MICHAEL LORKE^{1,2}, MATTHIAS FLORIAN¹, •DANIEL ERBEN¹, and FRANK JAHNKE¹ — ¹Institute for Theoretical Physics, University of Bremen — ²Bremen Center for Computational Materials Science, University of Bremen

Atomically thin transition metal dichalcogenides on nanostructured substrate like nanopillar arrays have gained attention as they show single photon emission. In contrast to a prestructured substrates, we investigate TMD nanobubbles that form naturally during stacking processes. Upon optical excitation these bubbles also exhibit quantum light emission, which indicates strong charge carrier confinement.

Starting from atomistic modelling of the strain field and electronic confinement potential of the nanobubble structure, we calculate the excitation spectrum for different bubble geometries. The microscopic origin of this carrier confinement lies in the bending rigidity of these materials leading to wrinkling of the surface. The resulting strain field facilitates nanoscale carrier localization due to its pronounced influence on the band gap. This localization mechanism is supported by local changes of the dielectric environment. As a result, strongly localized states are formed that lead to emission sites around the periphery of the nanobubble. A specific localization signature allows for experimental identification of this mechanism, which has also been demonstrated in spatially resolved photoluminescence experiments.

HL 25.31 Wed 18:00 P2

Tunable 2D phononic crystals — •YUEFENG YU, JAN KIRCHHOF, BIANCA HOFER, OGUZHAN YÜCEL, and KIRILL BOLOTIN — Department of Physics, Freie Universität Berlin, 14195 Berlin, Germany

In the field of phononics, periodic patterning controls vibration and thereby flow of heat and sounds based on its phononic band structure. This kind of structures name as phononic crystals (PnCs). Bandgaps of PnCs arise their potentials in low-dissipation mechanical states towards efficient waveguide and stable mechanical qubit. By combining highly flexible suspended two-dimension (2D) materials and PnCs into 2D-capacitor framework, applying pressure through voltage and thereby changing the unit size of periodic pattern to tune the phononic bandgap is accomplishable. For now, we are playing the PnCs in graphene and 2D MoS₂ with hexagonal lattice and microscale cavity. From

cavity interferometric measurement, the periodic pattern can effectively block a frequency-range of vibration modes and establish the 1.5MHz-wide phononic bandgap of 2D-MoS₂ PnCs. By varying the incident-laser power and gating voltage, position of bandgap moves in MHz-frequency-range. With the supporting of simulation, graphene shows a much higher tunability of the width and position in frequency of phononic bandgap than MoS₂. All of these suggests a potential playground for quantum information and phase transition in mechanical.

HL 25.32 Wed 18:00 P2

Effect of gallium content on the grain boundary properties of polycrystalline Cu(In,Ga)Se₂ absorber layers in thin-film solar cells — •SINJU THOMAS¹, WOLFRAM WITTE², DIMITRIOS HARISKOS², STEFAN PAETEL², CHANG-YUN SONG³, HEIKO KEMPA³, NORA EL-GANAINY⁴, and DANIEL ABOU-RAS¹ — ¹Helmholtz Zentrum Berlin für Materialien und Energie (HZB) — ²Helmholtz Zentrum Berlin für Materialien und Energie GmbH, Hahn-Meitner-Platz 1, 14109 Berlin, Germany — ³Martin-Luther-Universität Halle-Wittenberg, Institut für Physik, Fachgruppe Photovoltaik — ⁴Competence Centre Photovoltaics Berlin (PVcomB)/(HZB)

In the present work, we apply several scanning electron microscopy techniques in a correlative manner on five solar cells with different ([Ga]/([Ga]+[In])) GGI (0.13, 0.34, 0.51, 0.67, and 0.83) in the Cu(In,Ga)Se₂ photoabsorbers, in addition to time-resolved photoluminescence and quantum-efficiency measurements. Grain sizes, electron lifetimes, grain-boundary (GB) recombination velocities, elemental distributions within the absorber layer, as well as luminescence emission distributions were assessed for all five samples. Owing to much reduced grain size at a GGI of 0.83, there is a high density of GBs that serve as active recombination centers. At this GGI, Voc losses via non-radiative recombination deteriorates the device efficiency. However, the effective GB recombination velocity does not vary linearly with the increasing GGI. Distribution of the recombination velocities at individual GBs suggests that upward and downward band bending at GBs is independent of the Ga concentration

HL 25.33 Wed 18:00 P2

Phonon Transport in Thin Homoepitaxial β -Ga₂O₃ Films — •ROBIN AHRING¹, OLIVIO CHIATTI¹, RÜDIGER MITTDANK¹, ZBIGNIEW GALAZKA², ANDREAS POPP², and SASKIA F. FISCHER¹ — ¹Novel Materials Group, Humboldt-Universität zu Berlin, 10099 Berlin, Germany — ²Leibniz Institute for Crystal Growth, 12489 Berlin, Germany

As a wide-band gap semiconductor with a high breakthrough field, gallium oxide (Ga₂O₃) has shown to be a promising material for applications in high power electronics. However, due to the materials low thermal conductivity [1,2] heat dissipation is a challenge for future device applications. By photolithography, magnetron sputtering and subsequent liftoff we prepare structures for investigating the thermal transport in the bulk Ga₂O₃ substrate and the thin homoepitaxial β -Ga₂O₃ films by applying the 2- ω and 3- ω measurement techniques.

For the substrate, we observe a dominance of phonon-phonon Umklapp scattering for high temperatures (>90 K) and a combination of point defect scattering and boundary effects for low temperatures. The phonon mean free path reaches a limit for low temperatures that can be explained with the crystal thickness. We aim to investigate the thermal transport exclusively in the thin films by producing sub- μ m heater widths using electron beam lithography and performing measurements at higher frequencies.

[1] M. Handweg *et al.*, *Semicond. Sci. Technol.* **30**, (2015) 024006

[2] M. Handweg *et al.*, *Semicond. Sci. Technol.* **31**, (2016) 125006

HL 25.34 Wed 18:00 P2

Towards Heat Transport in Exfoliated β -Ga₂O₃ Flakes — •SAKHIR SHIBLI¹, ROBIN AHRING¹, OLIVIO CHIATTI¹, RÜDIGER MITTDANK¹, ZBIGNIEW GALAZKA², and SASKIA F. FISCHER¹ — ¹Novel Materials Group, Humboldt-Universität zu Berlin, 10099 Berlin, Germany — ²Leibniz Institute for Crystal Growth, 12489 Berlin, Germany.

Heat transport is known as a diffusive process that is characterized as a slow process compared to other physical processes. Nevertheless, heat transport can also occur ballistically in the speed of sound within a material over distances comparable to the phonon's mean free path, known as Casimir limit [1]. Therefore, thin-layer materials are of interest for detecting ballistic heat transport [2]. As a model system with large potential of application, e.g. in power electronics, we are investigating exfoliated thin-layer flakes of β -Ga₂O₃ single crystal [3][4]. As a wide-band gap semiconductor with a high-breakthrough field, β -Ga₂O₃ has shown to be a promising material for applications in high power electronics [5]. In this work, we fabricate and pattern micro-heater lines in order to employ the 3 ω - and 2 ω - methods [3].

[1] Casimir, H.B.G. (1938) *Physica*, **5**, 495-500.

[2] T. Yamada *et al.* **61** (2013) 287*292.

[3] M. Handweg, *Sci. Technol.* **30** (2015) 024006.

[4] Galazka, Zbigniew *et al.* **45** (2010): 1229-1236.

[5] J. Boy *et al.*, *APL Mater.* **7**, 022526 (2019).

HL 25.35 Wed 18:00 P2

Investigation of pinhole defects in ALD TiO_{2-x} corrosion protection layers on III-V semiconductor photocathodes — •NICOLA TAFFERTSHOFER, TIM RIETH, and IAN SHARP — Walter Schottky Institute and Physics Department, Technical University of Munich, Am Coulombwall 4, 85748 Garching, Germany

The application of semiconducting photoabsorbers for photoelectrochemistry (PEC) provides a relevant path to solar fuel generation. However, a major challenge is the chemical instability of many potentially suitable semiconductors in PEC applications. Titania (TiO_{2-x}) protection layers with defined properties can be conformally deposited by atomic layer deposition (ALD) and have been shown to improve chemical stability of photoelectrodes in PEC cells. Despite these benefits, TiO_{2-x} ALD protection layers exhibit structural imperfections, including pinholes, that limit the long-term stability of underlying semiconductor photoelectrodes under PEC conditions. In our work, we quantify the pin-hole density in TiO_{2-x} ALD protection layers, synthesized under different growth conditions, by combining controlled etching experiments with inductively coupled plasma mass spectrometry (ICP-MS). Using the high sensitivity of ICP-MS, the unprotected substrate area associated with existing and emerging pinholes can be deduced by an increase of the substrate elements concentrations dissolved in liquid. Overall, this method provides crucial information for the development of pinhole mitigation strategies in the TiO_{2-x} ALD growth process and, hence, is an important step towards an increased lifetime of photoelectrodes.

HL 25.36 Wed 18:00 P2

Investigation of Electrically-Active Dopants in Sulfur-Hyperdoped Silicon Using Resistance Measurements — •SKROLLAN DETZLER, CHRISTOPH FLATHMANN, and MICHAEL SEIBT — 4th Institute of Physics - Solids and Nanostructures, University of Goettingen, Friedrich-Hund-Platz 1, 37077 Göttingen, Germany

Due to its abundance and particularly adjustable electric properties, silicon has become the dominating material in solar cell fabrication as of today. One approach to further increase the efficiency of silicon solar cells is to introduce an intermediate band into the band gap, allowing for broader absorption of the sunlight spectrum. This could be realized by doping the material with deep-level impurities far beyond its equilibrium solubility limit. In this study, we analyze sulfur-hyperdoped silicon, produced by femtosecond pulsed laser annealing, resulting in inhomogeneous regions reaching from the surface into the bulk material. To gain information on electrically-active dopants across different regions, resistance measurements using micromanipulators and scanning electron microscopy imaging were performed.

HL 25.37 Wed 18:00 P2

Automation of band structure simulations to determine Si-dopant efficiency in AlGaAs — •MAXIMILIAN KRISTO, NICO BROSDA, ANDREAS D. WIECK, and ARNE LUDWIG — Lehrstuhl für Angewandte Festkörperphysik, Ruhr-Universität Bochum, D-44801 Bochum, Germany

The potential landscape for electrons in semiconductor heterostructures is represented by its band structure. Their simulations can significantly help in the design of devices with new functionality. In order to systematically evaluate the doping efficiency in heterostructure samples, we automatized band structure calculations in a feedback loop with experimentally determined Hall parameters. These were determined by Van der Pauw measurements at 4.2 K.

The effective dopant concentration in the simulations was adapted to fit the experimental results and thus allowed to determine the effective dopant efficiency of Si doped AlGaAs HEMT structures to be compared with the dopant efficiency in Si doped GaAs samples. A majority of the dopant atoms are present in AlGaAs (with an aluminium concentration above 20 %) as deep impurities (Donor Complex (DX) centers), which do not contribute to the electrical conductivity at 4.2 K if cooled in dark without bias. Therefore, these DX centers in Si doped AlGaAs lower the doping efficiency compared to Si doped GaAs. For AlGaAs with an aluminium concentration of 34 %, an average dopant efficiency of 14 ± 3 % and a negative correlation of -0.83 with the thickness of the doped layer could be found this way.

HL 25.38 Wed 18:00 P2

Electrochemical epitaxial (200) PbSe submicron plates on single layer graphene for ultrafast infrared response — •CHAN YANG, SHUANGLONG FENG, YINYE YU, JUN SHEN, XINGZHAN WEI, and HAOFEI SHI — Chongqing Institute of Green and Intelligent Technology, Chinese Academy of Sciences

Highly efficient near and medium-wave infrared detection at room temperature is considered one of the most intensive studies due to their robust detection in foggy weather or other low visibility conditions. 2D atomic layer graphene has an unconventional broad optical spectrum and high carrier mobility properties for the next generation electronics and optoelectronics device. The single-layer graphene has a lower quantum efficiency, and the PbSe has a direct narrow bandgap with a highly sensitive infrared response. Here, we examine the growth mechanism of high quality-oriented (200) PbSe crystals on a single atomic layer graphene using the electrochemical atomic layer epitaxy growth method in an

aqueous electrolyte. The crystalline phase and density of nucleating seeds controlled by changing electrodeposition parameters are crucial for determining the submicron-crystal geometry. It is revealed that the controllable growth orientation and nucleation of PbSe crystals are realized by combining underpotential deposition of Pb and overpotential deposition of Se. The PbSe crystals/graphene hybrid photodetector indicates the benefit of infrared absorption. The extraordinary response speed of 1.8 ms, photo-responsivity in exceeding 36 AW^{-1} , and figure-of-merit detectivity $D^* > 2.7 \times 10^9$ Jones have been demonstrated in $2.7 \mu\text{m}$ at room temperature.

HL 25.39 Wed 18:00 P2

Reconstructions of the As-terminated GaAs(001) surface exposed to atomic hydrogen — MARSEL KARMO¹, ISAAC AZAHEL RUIZ ALVARADO², WOLF GERO SCHMIDT², and •ERICH RUNGE¹ — ¹Technische Universität Ilmenau — ²Universität Paderborn

We explore the atomic structures and electronic properties of the As-terminated GaAs(001) surface in the presence of hydrogen based on ab-initio density functional theory. We calculate a phase diagram dependent on the chemical potentials of As and H, showing which surface reconstruction is the most stable for a given set of chemical potentials. The findings are supported by the calculation of energy landscapes of the surfaces, which indicate possible H bonding sites as well as the density of states, which show the effect of hydrogen adsorption on the states near the fundamental band gap [1]. Extension to the GaAs_xP_{1-x}(001) surfaces are presented.

[1] M. Karmo et al., ACS Omega 7, 5064-5068 (2022), <https://doi.org/10.1021/acsomega.1c06019>

HL 25.40 Wed 18:00 P2

Remote Heteroepitaxy of In(x)Ga(1-x)As on Graphene Covered GaAs(001) Substrates — •TOBIAS HENKSMEIER¹, FRIEDEMANN SCHULZ², ELIAS KLUTH², MARTIN FENEBERG², RÜDIGER GOLDHAHN², and DIRK REUTER¹ — ¹Paderborn University, Warburger Str. 100, 33089 Paderborn, Germany — ²Otto von Guericke University, Magdeburg, Universitätsplatz 2, 39106 Magdeburg, Germany

Recently, remote epitaxy on monolayer graphene covered substrates has attracted considerable attention as a way to improve lattice mismatched growth. It was reported that placing a monolayer graphene on a substrate offers a relaxation pathway different to the creation of crystal defects. Here, we present a study on solid source molecular beam epitaxy of In(x)Ga(1-x)As-layers ($0 < x < 0.5$) on chemical vapor deposition monolayer-graphene covered GaAs-(001) substrates. We show detailed investigations on the low temperature In(x)Ga(1-x)As nucleation and on the strain relaxation of 200 nm thick In(x)Ga(1-x)As-layers on graphene covered GaAs and for comparison on bare GaAs. The samples were analyzed by atomic force microscopy (AFM), scanning electron microscopy (SEM), Raman-spectroscopy and high-resolution X-ray diffraction measurements (HRXRD). We see the same crystal orientation and similar root-mean-square roughness for films grown on graphene and on bare GaAs substrates. Further, the layers grown on graphene show a more symmetric strain relaxation and a larger degree of strain relaxation compared to films grown on bare GaAs where the strain relaxation is larger along [110].

HL 25.41 Wed 18:00 P2

Nonlinear dynamics of Dirac fermions in topological HgTe structures — •TATIANA AURELIA UAMAN SVETIKOVA¹, ALEXEY PASHKIN¹, THALES OLIVEIRA¹, FLORIAN BAYER², CHRISTIAN BERGER², LENA FÜRST², HARTMUT BUHMANN², LAURENS W. MOLENKAMP^{2,3}, MANFRED HELM¹, TOBIAS KIESSLING², STEPHAN WINNERL¹, SERGEY KOVALEV¹, and GEORGY V. ASTAKHOV¹ — ¹HZDR, Dresden, Germany — ²Physikalisches Institut (EP3), Universität Würzburg, Würzburg, Germany — ³Institute for Topological Insulators, Würzburg, Germany

High harmonic generation has applications in various fields, including ultrashort pulse measurements, material characterization and imaging microscopy. Strong THz nonlinearity and efficient third harmonic generation (THG) were demonstrated in graphene [1], therefore it is natural to assume the presence of the same effect in other Dirac materials, such as topological insulators (TI)[2].

We used a series of HgTe samples corresponding to three qualitatively different cases: 2D trivial and topological structures and 3D TIs. By using moderate THz fields, the presence of highly efficient THG was measured at different temperatures and THz powers. This provides insight into physical mechanisms leading to THG in TIs. For in-depth understanding of Dirac fermions dynamics and dominating scattering mechanisms in HgTe TI, we conducted THz pump-probe experiments that reveal several relaxation time scales.

[1] Hafez, H. A. et al., Nature 561, 507 (2018).

[2] Kovalev, S. et al., Quantum Mater. 6, 84 (2021)

HL 25.42 Wed 18:00 P2

Graphitic Carbon Nitride/Semiconductor Quantum Dots 2D/0D Heterostructures — •THUY LINH NGUYEN THI, OLEKSANDR SELYSHCHEV, and DIETRICH R.T. ZAHN — Semiconductor Physics, TU Chemnitz, Chemnitz D-09107, Germany

The 2D semiconductor graphitic carbon nitride (g-C₃N₄) is of great interest due to its photocatalytic properties and potential application in optoelectronic devices. However, a relatively large bandgap of 2.7 eV [1] requires its additional sensibilization to extend the photosensitivity to entire visible range. Here, we investigate heterostructures of n-type g-C₃N₄ and p-type semiconductor quantum dots (QDs), e.g. AgInS₂. The single-layered g-C₃N₄ flakes exfoliated from bulk material using tetraethylammonium hydroxide (TEA-OH) ligands [1] and AgInS₂ QDs with a size of ~3.5 nm [2] were used in aqueous solutions. X-ray Diffraction (XRD) indicates the intercalation of TEA-OH ligands between the flakes of g-C₃N₄. The thickness of the carbon nitride flakes of 0.3 +/- 0.1 nm, corresponding to a monolayer, and lateral sizes in the range of 35 - 55 nm are confirmed by Atomic Force Microscopy (AFM). Photoluminescence (PL) quenching of both g-C₃N₄ and QDs indicates an electronic interaction. A model photodetector device based on a thin film of a g-C₃N₄ and QD mixture, a TiO₂ transport layer, indium-tin-oxide and gold electrodes was utilized for investigating the photoconductivity.

[1] O. Stroyuk et al., Phys. Status Solidi B, 2018, 256, 2, 1800279.

[2] A. Raevskaya et al., J. Phys. Chem. C, 2017, 121,16, 9032.

HL 25.43 Wed 18:00 P2

Contactless mapping of the sheet resistance of GaAs samples — •TIMO A. KURSCHAT, ARNE LUDWIG, and ANDREAS D. WIECK — Angewandte Festkörperphysik, Ruhr-Universität Bochum, Universitätsstraße 150, D-44780 Bochum
Measurements of the sheet resistance without the need to break the sample and integrate electrical contacts enable the evaluation of the homogeneity and quality of samples before further processing. Spatially resolved maps can be created without destroying or modifying the wafer.

The sheet resistance is measured by placing the sample on top of two circular electrodes. These couple capacitively with the conducting layer through the substrate. When applying a high frequency alternating voltage at one electrode, a signal can be measured at the other one. The sheet resistance is measured by sweeping the frequency from 1 MHz to 400 MHz and applying a fit. The setup works for sheet resistances between 300 Ω/□ and 50 kΩ/□.

The measured resistance and the coupling capacitances depend on the geometry of the sample and the electrodes. The changes at the edges of a sample are shown with line scans across a quarter 3" wafer and across a 5 mm wide sample. To show the effect of changes in the sheet resistance, the conducting layer was partly removed by etching. This shows artifacts especially if one electrode is completely below an isolating region. The spatial resolution depends strongly on the orientation of the electrodes.

HL 25.44 Wed 18:00 P2

GW benchmarks — •MARYAM AZIZI, MATTEO GIANTOMASSI, and XAVIER GONZE — Université Catholique de Louvain, Louvain-la-Neuve, Belgium

GW is presently the best available first-principles methodology for the prediction of electronic structure, including band gaps. However, dealing with GW calculations is always challenging, not simply due to unfavorable scaling with system size, or possible lack of symmetry, but also due to the large number of parameters of such calculations. As a consequence, systematic GW benchmarks for large sets of materials are much more limited than for density-functional theory.

In the present work, we pave the way beyond the study of Van Setten and coworkers, who examined 70 materials, however aiming to a limited target accuracy. Indeed we consider a convergence criterion of 0.02 eV in the GW band gap, more stringent than the 0.05 eV target of this previous study. Moreover, the latter relied on a plasmon-pole model, while the present analysis also focus on contour-deformation and analytic continuation methodologies which are computationally more expensive and theoretically better justified. Like Van Setten et al, we use ABINIT, and stay at the non-self-consistent G_0W_0 level. Besides, the parallel speedup and efficiency of the implementation have been investigated.

HL 25.45 Wed 18:00 P2

Two-Photon Absorption Induced Photoluminescence in CuI Single Crystals — •ANDREAS MÜLLER¹, EVGENY KRÜGER¹, LUKAS TREFFLICH¹, STEFFEN BLAUROCK², HARALD KRAUTSCHEID², MARIUS GRUNDMANN¹, and CHRIS STURM¹ — ¹Felix-Bloch-Institut für Festkörperphysik, Universität Leipzig — ²Institut für Anorganische Chemie, Universität Leipzig

The intrinsically p-type copper iodide (CuI) with a direct band gap of 2.95 eV at 300 K [1] and high exciton binding energy is a promising material for transparent semiconductor devices. The photoluminescence (PL) emission properties of CuI crystals have been recently reported [2]. However, the PL emission induced by two-photon absorption (TPA-PL) has not been discussed in detail, so far.

We report on TPA-PL phenomena in CuI single crystals. A redshift compared to the conventional PL emission was observed. The TPA-PL spectrum can be nicely described by means of a simplified approach which takes into account the internal emission spectrum at the focal point, the propagation of the emitted photons inside the crystal and the absorption coefficient of CuI (determined by ellipsometry and taken from [2]). For the entire TPA-PL intensity we observed a non-linear power dependence, namely $I \propto P^\gamma$. The exponent γ depends on the excitation wavelength and ranges from 2 (expected for TPA-PL excitation via a

virtual state) down to 1.5. The latter value was justified by a two-step TPA-PL process via a real state i.e. defect level.

[1] M. Grundmann et al., Phys. Status Solidi A 210, 1671 (2013)

[2] E. Krüger et al., APL Mater. 9, 121102 (2021)

HL 25.46 Wed 18:00 P2

Time-Resolved Nanoscale X-ray Analysis to Investigate Luminescence Dynamics of Co in ZnO-Material Systems — •ADRIAN NOWOTNICK¹, CHRISTIAN PLASS¹, VALENTINA BONINO², MAURIZIO RITZER¹, LUKAS JÄGER¹, JAIME SEGURA-RUIZ², GEMA MARTINEZ-CRIADO², and CARSTEN RONNING¹ — ¹Institut für Festkörperphysik, Friedrich-Schiller-Universität Jena, Max-Wien-Platz 1, 07743, Jena — ²ESRF - The European Synchrotron, 71 Avenue des Martyrs, 38043 Grenoble, France

High resolution synchrotron based methods like X-ray fluorescence (XRF) and X-ray excited optical luminescence (XEOL) are well established characterization techniques. A highly focused X-ray nanobeam at the ID16B-NA station of the European Synchrotron Radiation Facility provides an excellent spatial resolution of about 50nm. This enables compositional mapping of nanomaterials. Uniquely, the beam line was equipped with a streak camera allowing analysis of the spectral dynamics of optical luminescence. Consequently, one can investigate the influence of elemental compositions and local environments on the emission properties of e.g. color centers in semiconductor nanomaterials. These are able to provide high quality single photon emitters, which have drawn a lot of interest in recent years. Simultaneous XRF and XEOL measurements of Co in ZnO systems were conducted and by analyzing the emitted X-ray fluorescence radiation together with the corresponding optical luminescence correlating maps were obtained. Additionally, the dynamic of the luminescence could be determined depending on the Cobalt concentration and the system morphology.

HL 25.47 Wed 18:00 P2

Photoluminescence observation of Erbium implanted semiconductor nanostructures — •NICO BROSDA, CRISTIAN DÜPUTELL, ARNE LUDWIG, and ANDREAS WIECK — Lehrstuhl für angewandte Festkörperphysik, Ruhr-Universität Bochum, D-44801 Bochum, Germany

The rare earth element Erbium is known for its spectral transitions around 1.5 μm. This wavelength region coincides with the absorption minimum of optical fibers. How to maximize the photoluminescence of Er doped semiconductor nanostructure is therefore a reasonable research topic.

The doping of GaAs semiconductor structures was achieved with focussed ion beam implantation. To recover the crystal structure and activate the Er atoms the samples are thermally annealed. Finding the optimal annealing parameters requires PL measurements in the near-infrared regime. A suitable PL setup was build around an InGaAs detector and a He-flow cryostat, allowing to measure the PL signal of Er. A 805 nm laser diode was used for the excitation. Optical parts in the setup were chosen with an antireflection coating for light around 1.5 μm.

The comparison between different annealing respectively implantation parameters allowed to identify values resulting in a brighter PL spectrum of the Er.

HL 25.48 Wed 18:00 P2

Semiclassical and quantum optical field dynamics in an optical cavity with a finite number of quantum emitters — •KEVIN JÜRGENS¹, FRANK LENGERS¹, DANIEL GROLL¹, DORIS E. REITER^{1,2}, DANIEL WIGGER³, and TILMANN KUHN¹ — ¹Institute of Solid State Theory, University of Münster, Germany — ²Condensed Matter Theory, Technische Universität Dortmund, Germany — ³School of Physics, Trinity College Dublin, Ireland

Ensembles of quantum emitters (QE) coupled to the quantized light field inside a photonic cavity are promising building blocks in quantum technologies. Due to the interaction of several QEs with a single light mode, the emitters can produce interesting collective behavior. We calculate the spectra and dynamics of such an ensemble with up to $N = 60$ emitters after excitation by a short external laser pulse within the Tavis-Cummings model and compare the findings with those obtained in the semiclassical limit ($N \rightarrow \infty$) [1]. When increasing the pulse amplitude we find a sharp transition in the semiclassical limit from exciton-polariton-like behavior to Rabi oscillations. The full quantum calculations reproduce such a transition behavior independent of N , but in particular for smaller N the transition between these regimes is broadened over a certain range of pulse amplitudes.

Wigner functions are calculated to investigate the properties of the light field and show the emergence of quantum features [1]. On longer time scales we see the formation of $N + 1$ quasi coherent states with Schrödinger-cat-like interferences between each pair.

[1] Jürgens et al., Phys. Rev. B 104, 205308 (2021)

HL 25.49 Wed 18:00 P2

Temperature dependence of phonons of CuI — •R. HILDEBRANDT¹, M. SEIFERT², S. BOTTI², C. STURM¹, and M. GRUNDMANN¹ — ¹Universität Leipzig, Felix Bloch Institute for Solid State Physics, Germany — ²Friedrich-Schiller-Universität Jena, Institute of Condensed Matter Theory and Optics, Germany

Cuprous iodide (CuI) is unique as intrinsic transparent p-type semiconductor with high figure of merit regarding various optical and electrical properties [1]. Properties and processes like thermal conductivity, electron-phonon coupling, phonon scattering, phonon-decay and elastic constants are influenced or mediated by different types of phonons. Their characteristics will be investigated here by Raman scattering.

We present temperature dependent Raman scattering spectra for CuI by using a 532nm incident laser source on solution grown single crystals. The allowed TO and LO modes are observed as well as the weaker second order Raman spectrum, which contains the full information of CuI's phonon dispersion [2]. It is used to determine the energy of the - usually forbidden - acoustic and optic zone boundary phonons by modeling the two-phonon sum spectrum [3].

Up to about 170 K the temperature dependence of the acoustic phonons could be tracked and compared with computational as well as other experimental results [3]. All results are in agreement and provide high accuracy information for the phonon dispersion of CuI.

[1] M. Grundmann *et al.*, Phys. Stat. Sol. (a), **210**, 1671, 2013.

[2] J. Birman, J., Phys. Rev., **131**, 1489, 1963.

[3] Z. Vardeny *et al.*, Phys. Rev. B, **18**, 44876, 1978.

HL 25.50 Wed 18:00 P2

Manipulating light-emission in direct band gap hexagonal Silicon Germanium nanowire arrays — •DAVID BUSSE¹, VICTOR VAN LANGE², ELHAM FADALY², WOUTER PEETERS², MARCO VETTORI², JOS HAVERKORT², ERIK BAKKERS², GREGOR KOBLMÜLLER¹, and JONATHAN FINLEY¹ — ¹Walter Schottky Institut, Garching near Munich, Germany — ²Eindhoven University of Technology, Eindhoven, Netherlands

We present results on the redistribution and enhancement of light within a 2D photonic crystal array formed by a hexagonal array of standing $Si_{1-x} - Ge_x$ nanowires (NWs). It was previously shown that these NWs are direct bandgap semiconductors when the crystal lattice has a hexagonal crystal structure. Fully 3D FDTD-simulations were performed to calculate the frequency of the photonic bands and their dependence on the lattice pitch and radius of the NW array. Essentially, the peak of the photoluminescence (PL) emission from the $Si_{1-x} - Ge_x$ NWs at 0.352eV, can be continuously tuned through the dielectric and air photonic band edges by changing lattice pitch and radius. For NW radius $r=210\text{nm}$, length $l=6\mu\text{m}$ and variable distance between the NWs (pitch $a=0.8\mu\text{m}$ up to $1.95\mu\text{m}$) we tune the photonic band edges through NW PL emission. Crucially, for situations close to resonance we observe an increase in the time-integrated PL intensity and transient carrier recombination dynamics measured using time-resolved pump-probe reflectance spectroscopy.

HL 25.51 Wed 18:00 P2

Influence of encapsulation material on organic magnetoconductance effect in organic light emitting diodes (OLED) — •ANNIKA MORGENSTERN¹, DOMINIK WEBER², APOORVA SHARMA¹, DANIEL SCHONDELMAIER², DIETRICH R.T. ZAHN^{1,3}, and GEORGETA SALVAN^{1,3} — ¹Semiconductor Physics, TU Chemnitz, 09107 Chemnitz, Germany — ²Nanotechnology and Functionalized Surfaces, Westsächsische Hochschule Zwickau, 08056 Zwickau, Germany — ³Center of Materials, Architectures and Integration of Nanomembranes, TU Chemnitz, 09126 Chemnitz, Germany

Organic semiconductors are the basic building block of organic light-emitting diodes (OLED). It was reported that certain OLEDs based on Alq₃, P3HT, etc. when exposed to an external magnetic field show a change in the electrical resistance. This phenomenon is called the organic magnetoconductance (OMC) effect, which stems from the influence of the magnetic field on the charge carrier density and/or mobility. OLEDs are also known to degrade due to the infiltration of oxygen and moisture into the constituting layers. In this work, we present a systematic study of the influence of polymethyl methacrylate (PMMA) and soda-lime glass encapsulation layer on the OMC effect, using a homebuilt electrical test bench based on a magnetic field modulation technique to remove the time-dependent change in the current. Additionally, we compare the passivation efficacy of the investigated encapsulation material on the lifetime of OLEDs. The lifetime of the studied OLEDs were measured using a test setup equipped with a photodiode, allowing to record the OLED light output over time.

HL 25.52 Wed 18:00 P2

The Impact of Mechanical Stress on Structural, Morphological and Electrical Properties of Transferable Organic Semiconductor Nanosheets — •VERONIKA REISNER, SIRRI BATUHAN KALKAN, and BERT NICKEL — Faculty of Physics and CeNS, Ludwig-Maximilians-Universität, Geschwister-Scholl-Platz 1, 80539 Munich, Germany

Recently, we presented a technique to transfer organic small-molecule nanosheets using a sacrificial water-soluble polymer layer. This approach enables

the transfer of highly ordered organic films on substrates, which are unfavorable for direct growth by physical vapor deposition. However, the transferable nanosheets experience a considerable amount of mechanical stress during the release and transfer process. Here, we investigate the structural and morphological changes induced in the transferable nanosheets to optimize the transfer technique. For this purpose, we use pentacene films as stress sensors. Pentacene films show a distinct response to the mechanical stress by an irreversible phase change from the thin-film phase to the Campbell bulk phase. To reveal these structural and morphological changes, we employ X-ray diffraction analysis and atomic force microscopy technique. We find that thinner pentacene nanosheets show a lower Campbell bulk phase contribution after the transfer process. Finally, we use an optimized transfer technique to fabricate transistors based on the transferable organic small-molecule DNTT. DNTT nanosheets are more brittle compared to pentacene nanosheets but exhibit superior device performance.

HL 25.53 Wed 18:00 P2

Damping and detecting vibrational modes in organic semiconductors with tunable graphene cavities — •LUKAS RENN and THOMAS WEITZ — I. Physical Institute, Georg-August-University, Friedrich-Hund-Platz 1, 37077, Göttingen

The true nature of charge transport in organic semiconductors (OSC) is still not fully understood. A novel picture to describe the charge transport is the so-called transient localization, where the charge transport is intrinsically limited by inter- and intramolecular vibrations, which are a direct consequence of the weak van der Waals interactions in OSCs. Recently it was discovered that the mobility in OSCs is mainly hampered by single low-frequency sliding modes, which in some molecules contribute more than 80% of the total thermal disorder. (1) The aim of this work is to first detect the lattice vibrations in OSCs and subsequently manipulate them using 2D cavities. To this end, we deposit monolayer thin, highly crystalline OSC films (PDI1MPCN2) from solution onto graphene flakes, which should result in quenching of a broad spectral range of IR-active vibrational modes in the OSC. First measurements show that we are able to detect the vibrational modes via Raman and a SNOM-based Nano-FTIR measurement setup. One step further, we want to tune the plasmon frequencies of the graphene cavities via lithography-patterning and thereby selectively couple to molecular vibrations in this frequency range and measure their relative impact on the charge carrier mobility. (1) Schweicher *et al.*, Adv. Mat. 1902407 (2019)

HL 25.54 Wed 18:00 P2

Towards charge-carrier transport studies in organic semiconductors strongly coupled to the electromagnetic vacuum field — •DANIEL VITROLER^{1,2}, JAMES W. BORCHERT¹, and R. THOMAS WEITZ¹ — ¹Universität Göttingen, Göttingen, Deutschland — ²LMU München, München, Deutschland

Strong coupling between the vacuum field and an excitonic transition in a semiconductor using plasmonic resonators or optical cavities leads to the formation of exciton polaritons [1]. Among the many prospective uses of strong coupling, recent studies have demonstrated that the formation of polaritons is an intriguing potential approach for improving charge transport in e.g. organic semiconductors [2]. However, there have so far been limited experimental demonstrations of strongly-coupled organic transistors [3], leaving many questions about the detailed physics of charge-carrier transport in these devices. In this work, we investigate light-matter coupling in thin films based on a perylene diimide derivative (PDI1MPCN2) which has previously shown electron mobilities as high as $4\text{cm}^2/\text{Vs}$ in organic transistors [4]. Tuned Fabry-Pérot cavities were implemented to achieve strong coupling to an excitonic transition of PDI1MPCN2 dispersed in a polymer matrix.

[1] Garcia-Vidal, F. J. *et al. Science*. **373**, eabd0336 (2021).

[2] Hagenmüller, D. *et al. Phys. Rev. Lett.* **119**, 223601 (2017).

[3] Orgiu, E. *et al. Nature Mater.* **14**, 1123-1129 (2015).

[4] Vladimirov, I. *et al. Nano Lett.* **18**, 9-14 (2018).

HL 25.55 Wed 18:00 P2

Influence of the probe-to-semiconductor contact on the electrical characterization of nanowire structures — •JULIANE KOCH¹, LISA LIBORIUS², PETER KLEINSCHMIDT¹, NILS WEIMANN², WERNER PROST², and THOMAS HANNAPPEL¹ — ¹Fundamentals of energy materials, Ilmenau University of Technology, Germany — ²Components for high frequency Electronics (BHE), University of Duisburg-Essen, Germany

For the purpose of well-defined III-V semiconductor junctions, various sophisticated tip-based methods such as multi-tip scanning tunnelling microscopy (MTSTM) can be employed to study the electrical behaviour with high spatial resolution. We investigated a variety of upright, freestanding GaAs-based axial as well as co-axial nanowires on the growth substrates covered with native oxide. Based on our studies with MTSTM, we demonstrate that in tip-based measurement methods, the probe-to-semiconductor contact is essential for interpreting the properties of the sample. Our investigation reveals charging currents at the interface between the measuring tip and the semiconductor via the native insulating oxide, which acts as a MIS-capacitor in the operating voltage range. All the samples investigated displayed a strong dependency of the overall electrical behaviour on the condition of the tip-to-semiconductor contact. We analyse in

detail the observed I-V characteristics and propose a strategy to achieve an optimized measuring tip-to-semiconductor junction which minimizes the influence of the native oxide layer on the overall electrical measurements.

HL 25.56 Wed 18:00 P2

Efficient spectral separation of single and entangled photons — •PATRICIA KALLERT, LUKAS HANSCHKE, EVA SCHÖLL, BJÖRN JONAS, and KLAUS D. JÖNS — Institute for Photonic Quantum Systems, Center for Optoelectronics and Photonics Paderborn, and Department of Physics, Paderborn University, 33098 Paderborn, Germany

Experiments and protocols based on single-photons with different properties are crucial to develop photonic quantum technologies. Semiconductor quantum dots are a promising platform for the emission of single, indistinguishable, and entangled photons. The efficient routing and filtering of frequency-mismatched photons, for example, from the biexciton-exciton cascade, is crucial to facilitate the full potential of quantum dots. The separation of photons of different energies allows for efficient entanglement swapping and teleportation experiments, which rely on multiphoton coincidences. Spectral separation and simultaneous detection of adjacent wavelengths are complex to realise. Here we exploit a strategy to build a blaze grating-based transmission spectrometer with outstanding figures of merit. We shed light on the basic principle and the pitfalls that lead to a severe decrease of the efficiency or deterioration of the resolution and how to overcome them. Balancing the main properties, our overall efficiency exceeds 66 %, and our resolution is 21 GHz. Simultaneously, wavelengths distanced by 0.2 nm can be separated. Our self-built setup offers all functionalities to characterise single-photon sources and efficiently incorporate them in modern quantum optics experiments.

HL 25.57 Wed 18:00 P2

Telecom wavelength InP based quantum dots: Growth and characterization — •RANBIR KAUR, MOHANAD ALKAALES, JOHANN PETER REITHMAIER, and MOHAMED BENYOUCEF — Institute of Nanostructure Technologies and Analytics, University of Kassel, Kassel, Germany

InP-based semiconductor quantum dots (QDs) represent an attractive light source for quantum communication applications due to their ability to emit photons at the telecom C-band. Self-assembled low-density QDs can be realized by careful control of the growth conditions. Here, we investigate the effect of different growth parameters to optimize telecom wavelengths

InP-based QD structures using molecular beam epitaxy with controlled properties in photonic and pin-diode structures. The QDs structures with and without doping were grown on distributed Bragg reflectors to enhance the light emission. Using proper doping levels, high-quality QDs can be embedded in pin-diode structures. Low-temperature μ -PL measurements show bright single QD emission around 1.55 μ m with narrow linewidth and low fine-structure splitting. Furthermore, studies related to doped QD structures and fabrication of pin-diode structures emitting at telecom wavelength are presented.

HL 25.58 Wed 18:00 P2

Energy dependent tunnel coupling of QDs to a reservoir at elevated temperatures — •ISMAIL BÖLÜKBASI¹, İBRAHİM ENGİN¹, PATRICK LINDNER², ARN BAUDZUS¹, ANDREAS D. WIECK¹, BJÖRN SOTHMANN³, and ARNE LUDWIG¹ — ¹Ruhr-Universität Bochum, D-44780 Bochum, Germany — ²TU Dortmund, D-44221, Dortmund, Germany — ³Theoretische Physik, Universität Duisburg-Essen and CENIDE, D-47048 Duisburg, Germany

Quantum dots have interesting physical properties and allow research in zero dimensional systems. They are used in modern displays and are highly efficient sources of high-fidelity single photons [1]. For their applicability, it is advantageous to understand the electrical properties and tunnelling behaviours of QDs coupled to a charge reservoir. Capacitance-voltage spectroscopy is used to characterize quantum dots by electronically accessing the quantized states. A resonance shift with temperature in the ground-state charging peaks, the s-type states [2] originates from the degeneracy of the one- and two electron quantum states. An approach to model these measurements with a master equation [3] can describe these shifts including excitonic and non-equilibrium states. It is however limited to constant tunnel-coupling. We present experimental observations like frequency dependent peak shifts that need an extended model and propose an improved master equation approach to address this behaviour.

[1] Tomm et al. (2021) Nat. Nanotechnol. 16(4) [2] Brinks et al. (2016) New Journal of Physics, 18(12). [3] Valentin et al. (2018) Physical Review B, 97(4).

HL 25.59 Wed 18:00 P2

Auger Recombination Rate: Magnetic Field Dependence in a Self-Assembled Quantum Dot — •FABIO RIMEK¹, HENDRIK MANNEL¹, MARCEL ZÖLLNER¹, ARNE LUDWIG², ANDREAS D. WIECK², AXEL LORKE¹, and MARTIN GELLER¹ — ¹Faculty of Physics and CENIDE, University Duisburg-Essen, Germany — ²Chair of Applied Solid State Physics, Ruhr-University Bochum, Germany

A quantum dot (QD) is an ideal system to study electron-electron interaction in a confined nanostructure [1]. The Auger recombination is a special case, where the recombination energy is transferred to a third charge carrier that leaves the dot

[2] or is excited to a higher energy level. Therefore, the Auger effect destroys the radiative recombination of the charged exciton (trion) - an effect, which should be minimized for future applications of QDs that use spin states as stationary qubits, which can be transferred to photons via the trion transition.

In this work, we investigate how the Auger rate is affected by an external magnetic field, applied perpendicular to the plane of the dots. In the magnetic field, the trion transition of a QD is no longer spin degenerate and splits up. We use two-color, time-resolved resonance fluorescence to investigate the quenching of the trion recombination by the Auger effect. Two-color excitation allows us to excite two quantum dot transitions and neglect spin relaxation as well as spin-flip Raman scattering. This ensures that we can directly measure the Auger and the tunneling rate of an electron into the dot.

[1] A. Kurzmann et al., Nano Lett. 16, 3367-3372 (2016)

[2] P. Lochner et al., Nano Lett. 20, 1631-1636 (2020)

HL 25.60 Wed 18:00 P2

Effects of bias-cooling on charge noise in gated Si/SiGe quantum dots — •JULIAN FERRERO¹, DANIEL SCHROLLER¹, THOMAS KOCH¹, VIKTOR ADAM¹, RAN XUE², INGA SEIDLER², LARS SCHREIBER², HENDRIK BLUHM², and WOLFGANG WERNSDORFER¹ — ¹Physikalisches Institut, KIT Karlsruhe — ²II. Physikalisches Institut, RWTH Aachen

Electron spins in gated Si/SiGe quantum dots provide a great potential in scalable quantum-computing platforms due to their long coherence times and wide tunability. However, charge noise in the vicinity of the qubit region decreases the two-qubit gate fidelities that are needed for up-scaled error correction. Furthermore, the devices drift to different working points and need to be retuned regularly. The source of fast charge noise is thought to arise from twolevel fluctuators in the aluminium oxide dielectric, whereas the drift can be caused by slow charging of the silicon cap. A feasible possibility to suppress such noise and drift is the application of a bias voltage on all gates during cool down. This project strives to investigate the effects of different bias-coolings on charge noise using simultaneous current spectroscopy and peak tracking of two single electron transistors. Since the involved processes range on a wide time scale, the noise spectrum is investigated between 50 microhertz and 1 kilohertz.

HL 25.61 Wed 18:00 P2

Characterization of InGaAs quantum dots as active region for edge emitting laser with emission in the telecom O-band — •PHILIPP NOACK — Institut für Halbleitertechnik und funktionelle Grenzflächen, Universität Stuttgart, Deutschland

Generally, laser diodes with quantum dots as active region are superior to quantum well laser diodes in terms of threshold current and temperature stability. Additionally, stacking of quantum dot layers can provide a broad gain spectrum, which can be ideally used for the fabrication of tunable laser devices with large bandwidth.

To this end, indium gallium arsenide quantum dots with emission in the telecom O-band wavelength range around 1300nm are grown at high densities with MOVPE and characterized with photoluminescence and atomic force microscopy measurements. We have designed edge emitting structures with waveguide simulations and characterized them using the segmented contact method. Parameters for the growth, like the V/III material ratio, were adjusted to create high density InGaAs quantum dots in a single layer. The emission intensity was further enhanced by the incorporation of a dots in well structure, an arsine interruption during growth and vertical stacking of quantum dot layers.

Following the design of the laser device, characterizations of edge emitting structures with one and multiple QD layer with regards to absorption characteristics were performed, which allowed for the characterization of the intrinsic losses of differently structured devices.

HL 25.62 Wed 18:00 P2

Wavelength tuning mechanisms in GaAs based-photonics integrated circuits — •ULRICH PFISTER¹, FLORIAN HORNING¹, STEPHANIE BAUER¹, ERIC REUTTER², MICHAEL JETTER¹, SIMONE L. PORTALUPI¹, JÜRGEN WEIS², and PETER MICHLER¹ — ¹Institut für Halbleitertechnik und Funktionelle Grenzflächen (IHFG), Center for Integrated Quantum Science and Technology (IQST) and SCoPE, Universität Stuttgart — ²Max-Planck-Institut für Festkörperforschung (MPI)

InGaAs quantum dots (QDs) grown in GaAs-based photonic integrated circuits are promising candidates to fulfill the requirements for basic on-chip photonic quantum computing gates. The necessary optical elements like beam splitters, on-chip detectors and waveguide structures have already been realized. An important step towards more complex experiments is to control the emission wavelength of the QDs. Recently, we matched the emission wavelength of a QD with a cavity-waveguide mode by applying strain with piezo electric actuators, resulting in Purcell enhancement [1]. Additionally, we discuss other tuning mechanisms like the crystallization of HfO₂ which has been already demonstrated for self-standing GaAs waveguides [2].

[1] Hepp, Stefan et al. Appl. Phys. Lett. 117, 254002 (2020)

[2] Grim, Joel Q. et al. Nat. Mater. 18, 963-969 (2019)

HL 25.63 Wed 18:00 P2

High-resolution spectroscopy of single photons from a self-assembled quantum dot — •LUCAS STAHL¹, HENDRIK MANNEL¹, FABIO RIMEK¹, MARCEL ZÖLLNER¹, ANDREAS WIECK², ARNE LUDWIG², MARTIN GELLER¹, and AXEL LORKE¹ — ¹Faculty of Physics and CENIDE, University of Duisburg-Essen, Duisburg, Germany — ²Chair of Applied Solid State Physics, Ruhr-University Bochum, Germany

Self-assembled quantum dots (QD) are highly promising as building blocks for applications in future quantum information technologies, where single confined spin states can form a qubit that can be transferred to a single photon. This requires long spin and photon coherence times [1], which have been demonstrated to be limited by spin- and charge-noise as well as co-tunneling with a reservoir [1]. These dephasing mechanisms affect the linewidth of the emitted photons.

In order to study various dephasing processes that occur on the exciton and trion transition in resonance fluorescence on a single dot, we set up a laser-stabilized high-finesse Fabry-Perot-interferometer. By using a single-photon detector in combination with a picosecond time-tagger and a newly-developed post-processing method for stabilization, we obtained an interferometer resolution of 8 MHz.

This high-resolution enables us to detect dephasing mechanisms in the linewidth of the dot and to understand the influence of the Auger-scattering [2] of the trion transition in resonance fluorescence.

[1] G. Gillard et al., Quant. Inf. 7, 43 (2021). [2] A. Kurzman et al., Nano Lett. 16, 5, 3367-3372 (2016).

HL 25.64 Wed 18:00 P2

Growth and characterisation of local droplet etched InAs quantum dots in an InGaAs matrix — •NIKOLAI SPITZER, ARNE LUDWIG, and ANDREAS WIECK — Ruhr-Universitaet Bochum, Lehrstuhl fuer Angewandte Festkoerperphysik, Universitaetsstraße 150, 44801 Bochum, Germany

We present a new local droplet etching (LDE) method for selforganized InGaAs quantum dots (QDs). We use gallium droplets to etch on an InGaAs matrix layer and fill the nanoholes with InAs. The impact of the indium concentration in the InGaAs-layer and of the deposited InAs amount after etching is investigated by atomic force microscopy and photoluminescence spectroscopy.

HL 25.65 Wed 18:00 P2

Three-photon excitation of InGaN quantum dots — •VIVIANA VILLAFANE¹, BIANCA SCAPARRA¹, MANUEL RIEGER¹, STEPHAN APPEL¹, RAHUL TRIVEDI², TONGTONG ZHU³, JOHN JARMAN³, RACHEL OLIVER³, ROBERT TAYLOR⁴, JONATHAN FINLEY¹, and KAI MUELLER¹ — ¹Walter Schottky Institut, TUM, Garching, Germany — ²Max-Planck-Institute for Quantum Optics, Garching, Germany — ³Department of Materials Science, University of Cambridge, UK — ⁴Clarendon Laboratory, University of Oxford, UK

Solid-state quantum emitters are prominent examples of systems showing excellent agreement between theoretical predictions and experimental measurements, being commonly taken as evidence that the fundamental physics of quasi two-level quantum emitters is almost fully understood. In our work, we explore multi-photon absorption selection rules in semiconductor quantum dots within the dipole approximation. It can be proven that given a two-level quantum system, if the excitation scheme involves N-photons of the same energy and polarization, either all even or odd resonances are enhanced, based on the parity of the ground and excited states. We demonstrate that semiconductor quantum dots can be excited efficiently in a resonant three-photon process, whilst resonant two-photon excitation is highly suppressed. Time-dependent Floquet theory is used to quantify the strength of the multi-photon processes and model the experimental results. Our resonant three-photon excitation scheme allows us to measure directly the radiative lifetime of InGaN QDs and obtain a greater degree of linear polarization.

HL 25.66 Wed 18:00 P2

Lattice thermal expansion of as-grown GaAs nanowires due to optical excitation measured by X-ray pump probe experiment — •TASEER ANJUM^{1,2}, FRANCISCA LARGO², WAHEED SALEHI¹, MATTHIAS RÖSSLE³, OLIVER BRANDT², LUTZ GEELHAAR², and ULLRICH PIETSCH¹ — ¹Festkörperphysik, Universität Siegen, Siegen, Germany — ²Paul-Drude-Institut für Festkörperelektronik, Leibniz-Institut im Forschungsverbund Berlin e.V., Berlin, Germany — ³Helmholtz-Zentrum Berlin für Materialien und Energie, Wilhelm-Conrad-Röntgen Campus, BESSY II, Berlin, Germany

We investigated the transient structural response in the ensemble of AlIn_xAs/GaAs core-shell NWs, grown on Si (111) substrate when irradiated with femtosecond laser pulses via x-ray pump-probe experiment at KMC3-XPP & P08 beamlines of Bessy II & PETRA III respectively. Femtosecond laser irradiation of solids excites photoelectrons from valance band to conduction and triggers a cascade of fundamental dynamical processes that occur on the picosecond to nanosecond time scales such as excitation and thermal equilibration of phonons. We observe a linear behavior of strain and temperature for the first few hundreds of picoseconds followed by the thermal relaxation up to few ns. Thinner NWs cool down slowly in comparison to thicker NWs which suggests a direct depen-

dence of thermal conductivity on the diameter. Through time-resolved x-ray pump-probe experiments we identified the thermal relaxation processes and the dynamics of the structural response of two NW samples.

HL 25.67 Wed 18:00 P2

Investigation of the Correlation between Quantum Dot Density and Photoluminescence Intensity — •SIMON SCHLOMBS, NIKOLAI SPITZER, NIKOLAI BART, ANDREAS WIECK, and ARNE LUDWIG — Angewandte Festkörperphysik, Ruhr-Universität Bochum, Universitätsstraße 150, D-44780 Bochum

Semiconductor devices based on quantum dots (QDs) require good knowledge of the QD density. Capacitance voltage spectroscopy (C(V)) enables the measurement of buried QDs; however, it requires extensive prior processing of the samples and only allows small areas to be measured. In this work the correlation between QD density and photoluminescence (PL) intensity is investigated. For this purpose, the quantum dot density along a density gradient has been determined and compared to PL measurements. The measured intensity is strongly dependent on the sample structure (absorption, thin-film interference). Because of this the intensity is corrected by an experimentally determined factor. The results allow for an optical determination of the QD density of entire wafers for an arbitrary sample structure.

HL 25.68 Wed 18:00 P2

Metallic nanowires assembled by DNA Origami — •BORJA RODRÍGUEZ-BAREA¹, SHIMA JAZAVANDI-GHAMSARI¹, ARCHA JAIN¹, TÜRKAN BAYRAK¹, JINGJING YE², RALF SEIDE², ENRIQUE SAMANO³, and ARTUR ERBE¹ — ¹Institute of Ion Beam Physics and Material Science, Helmholtz-Zentrum Dresden-Rossendorf, Germany — ²Peter Debye Institute for Soft Matter Physics, Universität Leipzig, Germany — ³Centro de Nanociencias y Nanotecnología-UNAM, Ensenada, B.C., México

In the pursuing to increase the processing power, electronic circuits look for new bottom-up strategies. Namely, (DNA) nanotechnology has shown valuable tools for the creation of nanostructures of arbitrary shape that can be used as templates. Here we demonstrate the formation of 1D Au nanostructures based on DNA Origami templates. DNA nanomolds are employed, inside which gold deposition is employed by site-specific attached seeds. To prove their metallic nature, top-down approach allows us to perform temperature-dependent charge transport measurements along the nanostructures. Transport through these assemblies is strongly nonlinear and shows a decrease in conductance towards low temperatures. Thanks to the converging of both fabrication approaches, the shape of the nanowires can be controlled and measured. We use DNA-origami templates which are functionalized on their surface in order to create desired shapes of the metallic nanostructures and the nanoparticles show temperature dependent charge transport measurements reveal the dominating charge transport mechanisms along these wires.

HL 25.69 Wed 18:00 P2

Multi-Orbital Kondo Effect in Few-Electron Quantum Dots — •OLFA DANI¹, JOHANNES BAYER¹, TIMO WAGNER¹, GERTRUD ZWICKNAGL², and ROLF J. HAUG¹ — ¹Institut für Festkörperphysik, Leibniz Universität Hannover, Germany — ²nstitut für Mathematische Physik, Technische Universität Braunschweig, Germany

The Kondo effect is a many particle entangled system, that involves the interaction between a localized spin in the quantum dot and free electrons in the electron reservoirs. This entanglement can be calculated using simplifying assumptions concerning the electronic structure of the quantum dot.

We investigate a lateral quantum dot with a small number of electrons, formed electrostatically in a two-dimensional electron gas using top-gates. A quantum point contact was operated as a sensitive charge detector allowing the detection of single-electron tunneling through the system, which enables us to know the exact number of electrons N in the quantum dot. The latter is varied by changing the applied gate voltage.

For a strong coupling to the leads and possible symmetrical tunnel barriers, a Zero-bias anomaly (ZBA) is observed. This Kondo resonance appears for successive N showing a deviation from the conjectured odd-even behavior. The observed ZBA is strongest for N=9 and displays a particle-hole symmetry for N=7,...,11. It is absent for N=6 and N= 12. This observations indicate the influence of the shell structure of the electronic states in the quantum dot where orbital degeneracy is present.

HL 25.70 Wed 18:00 P2

Grating Couplers on a III-V Semiconductor Platform for Single-Photon Applications — •VALENTINO MERKL, STEPHANIE BAUER, ROBERT SITTING, SIMONE LUCA PORTALUPI, MICHAEL JETTER, and PETER MICHLER — Institut für Halbleitertechnik und Funktionelle Grenzflächen, Center for Integrated Quantum Science and Technology (IQST) and SCoPE, University of Stuttgart, Allmandring 3, 70569 Stuttgart

Photonic quantum computing is one of the most studied fields of the 21st century, with the potential to revolutionize computation as we know it today. Using integrated quantum photonics to miniaturize setups, it is possible to increase

the computation complexity drastically. For this purpose a III-V semiconductor platform is highly advantageous, as it enables the possibility of integrating quantum dots as single photon sources, which cannot be done on silicon based platforms. They utilize the beneficial aspects of non-classical light for the computation. In some applications it is necessary to couple light from a chip into single mode fibers or vice versa. For this purpose, grating couplers, which demonstrated high coupling efficiencies of up to 89% on the silicon platform, are a highly versatile and promising method. In this contribution, we will present simulation results, fabrication steps and measurements on grating couplers constructed on the GaAs/AlO_x platform. Using 2D and 3D FDTD simulations, these structures are optimized to have high coupling efficiencies in the near infrared regime and common telecom frequencies matching the emission wavelength of the QDs.

HL 25.71 Wed 18:00 P2

Heat Radiation of Semiconductor Wafers — •BASTIAN SCHMÜLLING, TIMO KRUCK, ANDREAS D. WIECK, and ARNE LUDWIG — Lehrstuhl für Angewandte Festkörperphysik, Ruhr-Uni Bochum

This work is about the struggles of pyrometer measurements of substrate temperature during molecular beam epitaxy (MBE) growth. During the growth of a typical GaAs wafer, a substrate temperature of 300 to 650 degree celsius is required. In our setup, a wafer is mounted in front of a radiation heater. To measure the substrate temperature, a pyrometer measures the thermal radiation. During growth, the substrate temperature is of utmost importance. However, the reflectivity and thus the emissivity changes with each additional layer deposited and the temperature measured by the pyrometer varies accordingly. These pyrometer measurements can be used to measure the growth rate. We plan to combining reflectometry and pyrometry during growth, to determine the actual temperature of the wafer.

HL 25.72 Wed 18:00 P2

Density Modulation of InAs/GaAs Quantum Dots and Pre Dots — •PETER ZAJAC¹, NIKOLAI BART¹, CHRISTIAN DANGEL², KAI MÜLLER³, ANDREAS D. WIECK¹, JONATHAN FINLEY², and ARNE LUDWIG¹ — ¹Ruhr-Universität Bochum, Universitätsstraße 150, 44801 Bochum, Germany — ²Walter Schottky Institut and Physik Department, Technische Universität München, Am Coulombwall 4, 85748 Garching, Germany — ³Walter Schottky Institut and Department of Electrical and Computer Engineering, Technische Universität München, Am Coulombwall 4, 85748 Garching, Germany

Epitaxial layer-by-layer growth without rotation of the substrate creates a thickness gradient along the surface with alternating smooth and rough layer areas. InAs quantum dots (QDs) grown on top of a GaAs gradient layer exhibit a density modulation along this gradient, which is studied with macro photoluminescence spectroscopy and atomic force microscopy (AFM). The periodicity of the modulation can be varied from a few hundred microns to several millimeters, depending on the thickness of the underlying gradient layer. Automated AFM measurements, covering multiple modulation periods along the gradient allow the investigation of wetting layer roughness, QD density and density of a smaller species of QDs, termed pre dots. AFM data analysis and extraction of parameters such as QD and monolayer step density is presented.

Bart, N., Dangel, C. et al. Wafer-scale epitaxial modulation of quantum dot density. *Nat Commun* **13**, 1633 (2022).

HL 25.73 Wed 18:00 P2

Calibrating Photoluminescence Yield for Quantum Emitters in Planar Photonic Heterostructures — •TIMO KRUCK, HANS-GEORG BABIN, DANIAL KOHMINAEI, SAYED SADAT, ANDREAS D. WIECK, and ARNE LUDWIG — Ruhr-Universität-Bochum; Lehrstuhl für angewandte Festkörperphysik, Bochum, Deutschland

When performing photoluminescence (PL) measurements, the spectral intensity of the emitted radiation strongly depends on the dielectric structure surrounding the quantum emitter. Here we show a method for calibrating PL measurements to obtain the unaltered spectrum of the optically active medium. For this purpose, the spectral reflectivity and the wavelength dependent standing wave field are used. The reflectivity is determined by reflectometer measurements and a simulation based on the transfer matrix method are used to compensate for the true layer thickness. This is then used to calculate the standing wave field, the outcoupling efficiency and the quantum yield. To validate the method, the calibrated spectra are compared with cleaved-edge PL measurements where the QDs are excited from the side and the light is also collected from the side.

HL 25.74 Wed 18:00 P2

Development of deterministic fabrication of quantum systems for single photon delay at Cesium wavelength — •AVIJIT BARUA¹, MONICA PENDERLA¹, LUCAS BREMER¹, LUCAS RICKERT¹, JIN-DONG SONG², and STEPHAN REITZENSTEIN¹ — ¹Technische Universität Berlin, Berlin, Germany — ²Korea Institute of Science and Technology, Seoul, Republic of Korea

Semiconductor QDs are extensively investigated as single-photon sources for photonic quantum technology. The information that is encoded in single pho-

tons may be used as quantum interfaces between stationary and flying qubits. Here, we develop bright and strain-tunable QD single-photon sources at the Cs D1 transition wavelength (894 nm) to explore the storage ability of semiconductor QD in atomic quantum memories. The devices are designed and numerically optimized to maximize the extraction efficiency using the FEM solver JCMSuite. By considering circular Bragg resonators with up to 2 rings with integrated QDs and an Au-backside mirror we numerically demonstrate a photon extraction efficiency as high as 65% (NA = 0.4) and a Purcell factor of 0.72. In the experimental development, we realized hybrid CBGs which facilitate Piezo-strain tuning of the QD device. We then implement in-situ electron-beam lithography to precisely integrate the selected single QD at 894 nm in such a structure to create bright single-photon sources. Furthermore, the emission from the developed structures is studied by means of photon autocorrelation measurements, and light-matter interaction with Cs vapor is investigated.

HL 25.75 Wed 18:00 P2

Purcell enhanced two indistinguishable emissions from two separated quantum dots for on-chip complex photonics quantum circuits — •YUHUI YANG¹, SHULUN LI^{1,2}, JOHANNES SCHALL¹, SVEN RODT¹, ZHICHUAN NIU², and STEPHAN REITZENSTEIN¹ — ¹Institut für Festkörperphysik, TU Berlin, Berlin, Germany — ²State Key Laboratory for Superlattice and Microstructures, Institute of Semiconductors, Chinese Academy of Sciences, Beijing, China

Quantum dots (QDs) are excellent single-photon emitters with a close to ideal quantum nature of emission. For large-scale integrated photonic quantum circuits, indistinguishable and bright single photons emitted by independent QDs are required. In this regard, QDs integrated into nanocavities that are compatible with on-chip waveguide systems are highly interesting since they have a small footprint while providing strong Purcell enhancement.

Here, we demonstrate the deterministic integration of two spectrally similar single QDs in separate, one-dimensional photonic crystal nanobeam cavities with significant Purcell enhancement. Our flexible and accurate deterministic fabrication concept allows us to combine the nanobeam waveguides with integrated QDs into a 2x2 on-chip multimode interferometer (MMI) beam splitter with a 50/50 splitting ratio to perform on-chip Hanbury Brown and Twiss (HBT) and Hong-Ou-Mandel (HOM) measurements. The obtained results demonstrate that our approach is very promising toward two-photon interference from monolithic independent single-photon emitters, and fully integrated photonic quantum circuits.

HL 25.76 Wed 18:00 P2

Experimental and numerical investigation of the evanescent coupling between an integrated micropillar laser and a ridge waveguide — •LÉO ROCHE¹, IMAD LIMAME¹, CHING-WEN SHIH¹, YUHUI YANG¹, SHULUN LI^{1,2}, and STEPHAN REITZENSTEIN¹ — ¹Institut für Festkörperphysik, Technische Universität Berlin, Hardenbergstraße 36, 10623 Berlin, Germany — ²State Key Laboratory for Superlattice and Microstructures, Institute of Semiconductors, Chinese Academy of Sciences, Beijing 100083, China

Integrated Quantum Photonic Circuits (IQPCs) are very promising candidates for scalable and flexible on-chip quantum computation and quantum communication hardware. One critical requirement for their realization is the scalable integration of on-demand indistinguishable single-photon emitters. This is potentially possible through the resonant excitation of an integrated QD in a waveguide by means of an on-chip integrated coherent light microlaser. Towards this goal, we investigate the coupling and lasing properties of coherent light laterally emitted from a whispering gallery mode (WGM) type micropillar laser evanescently coupled to a single mode ridge waveguide. Using finite element method (FEM) simulations, we investigate the coupling efficiency and the Q-factor of the pillar-waveguide system for different angular mode number and various pillar-waveguide air gap distances. The III-V semiconductor type nanostructures composed of a GaAs cavity with InAs QDs and distributed Bragg reflectors are carefully processed using electron beam lithography and then measured using micro-photoluminescence spectroscopy.

HL 25.77 Wed 18:00 P2

Building charge detection in indium antimonide nanowires for scanning tunneling microscopy using gate-defined quantum dots — •KANJI FURUTA¹, FELIX JEKAT¹, BENJAMIN PESTKA¹, SASA GAZIBEGOVIC², DIANA CAR², SEBASTIAN HEEDT³, MARCUS LIEBMAN¹, THOMAS SCHÄPERS³, ERIK BAKKERS², and MARKUS MORGENSTERN¹ — ¹II. Phys. Inst. B, RWTH Aachen Univ, Germany — ²Dept. of Appl. Phys., Eindhoven Univ., The Netherlands — ³PGI-9, FZ Jülich, Germany

InSb nanowires are investigated with respect to suitability as a charge detector to be combined with scanning tunneling microscopy. Mechanically exfoliated hexagonal boron nitride (h-BN) as a dielectric is placed onto bottom finger gates (50 nm wide, 30 nm spacing). The nanowires are then aligned and placed mechanically onto h-BN. We present transport measurements on gate-defined quantum dots at temperatures down to 300 mK. Due to the dielectric, the time stability of our device improved to around 5 μ eV/h. The charge stability diagram shows Coulomb diamonds with a charging energy of 2.5 meV and an orbital en-

ergy of 0.3 meV. Depending on the gate and magnetic field, additional transport channels are occasionally observed, causing additional lines in the charge stability diagram and a shift of the Coulomb peak pattern around a magnetic field of ≈ 400 mT. This points to the presence of an unintentional second quantum dot in the gate region. Different configurations are discussed in terms of their coupling to the leads and the main dot, and their effects on charge detection.

HL 25.78 Wed 18:00 P2

Coherent manipulation of GaAs quantum dot spin qubits using microwaves — ANKITA CHOUDHARY¹, NAND LAL SHARMA¹, MORITZ LANGER¹, GHATA SATISH BHAYANI¹, URI VOOL², and CASPAR HOPFMANN¹ — ¹Leibniz Institute for Solid State and Materials Research, Dresden — ²Max Planck Institute for Chemical Physics of Solids, Dresden

Spin qubits in semiconductor quantum dots are attractive resources for performing quantum computations. In these systems single optically addressable spin qubits can be realized by single confined charge carriers, electrons, heavy holes, and their excited states. The quantum dot spin qubit coherence is however limited due to their semiconductor environment due to spin-orbit coupling to the magnetic moments of the atomic nuclei. Our goal is to facilitate the heralded and deterministic spin state preparation as well as to minimize the decoherence. While the all-optical heralded preparation of spin states in GaAs quantum dots has been demonstrated by us [1], the latter may be achieved by coherent manipulation of the spin states using the spin echo technique [2]. Our immediate goal is therefore to enable coherent manipulation of quantum dot spin qubits via injection of microwave pulses by superconducting co-planar waveguide structures. This technique will allow us to achieve full manipulation of the quantum dot and we expect to be able to achieve strong interaction between microwaves and quantum dot spin qubits, which could enable the coherent coupling between superconducting and quantum dot qubits. [1] C. Hopfmann et al, PRB 104, 75301 (2021). [2] F. H. L. Koppens et al, PRL 100 (2008).

HL 25.79 Wed 18:00 P2

Synthesis of ZnS nanoparticles investigated by in-situ X-ray scattering and spectroscopy — LARS KLEMEYER, TJARK GROENE, OLGA VASYLIEVA, FRANCESCO CADDEO, SANI HAROUNA-MAYER, and DOROTA KOZIEJ — Universität Hamburg, Institut für Nanostruktur- und Festkörperphysik, Center for Hybrid Nanostructures, Luruper Chaussee 149, 22761 Hamburg

Transition metal sulfides are promising materials for a variety of applications. Especially the electronic configuration of the d-orbitals leads to unique electronic properties of transition metals and their compounds. Zinc sulfide (ZnS) is one of the most widely used transition metal sulfide due to its broad availability and relatively low toxicity as well as saturated d-orbitals. However, the synthesis approaches of ZnS nanoparticles in solution are not fully understood. We show complementary analysis with in-situ pair distribution function (PDF) and in-situ X-ray spectroscopy of the solvothermal synthesis of ZnS for a comprehensive picture of the nucleation and growth from precursors to nanoparticles.

HL 25.80 Wed 18:00 P2

Efficient frequency filtering of quantum dot photons using a self-constructed transmission grating monochromator — MORITZ MEINECKE, SVEN HÖFLING, and TOBIAS HUBER — Lehrstuhl für Technische Physik, Universität Würzburg, 97074 Würzburg, Germany

Many spectroscopic measurements for characterizing quantum dot emission lines require spectral signal filtering that is narrower or matched to the expected line widths to analyze photons from different single excitonic charge complexes. Furthermore, to use the quantum dot photons for applications, this filtering should be efficient. A classical reflection monochromator is not ideal for this purpose, since it often comes with a low filter efficiency when the light is coupled to fiber, which is required for photon detection with superconducting nanowire detectors and for usage in any application. Furthermore, a reflection monochromator is strongly polarization dependent, which limits its use to non-polarization sensitive measurements, or requires polarization projection before frequency filtering. Alternative filter optics, like bandpass filters, have low flexibility and often need time consuming adjustments.

Here, we present a self-constructed transmission grating monochromator. It allows efficient, frequency filtering of quantum dot emission lines in the near infrared region. It is fully automatized and precise in approaching any filter position. Furthermore, the nearly polarization independent performance allows for polarization sensitive measurements.

HL 25.81 Wed 18:00 P2

Establishment of a method to make PL measurements on optically active layers in different dielectric structures comparable — SAYED SHKEEBULLAH SADAT, DANIAL KOHMINAEI, TIMO KRUCK, HANS-GEORG BABIN, ANDREAS WIECK, and ARNE LUDWIG — Ruhr-Universität Bochum, Bochum, Deutschland To improve extraction of photoemission from optically active layers such as quantum dots (QDs) or quantum wells (QWs) one can e.g. grow them inside dielectric structures (DBR - distributed Bragg reflector). However, the emerging wavelength-dependent standing wave field alters the spectral intensity of the

quantum emitters, which means straightforward comparisons of photoluminescence (PL) measurements are no longer possible. Therefore we present a method by which you can obtain the unaltered spectrum. To calculate the standing field we determine the specific reflectivity first and adjust it to the true thickness of the layers. From here it is possible to determine the efficiency of the photon extraction and thus the quantum yield, which allows us to calibrate and transfer the spectra back to its unmodified form. Since this can be performed on any dielectric structure it now is possible to compare the calibrated spectra with each other. Furthermore there is a possibility to automate this process, allowing the instantaneous comparison of PL measurements on optically active layers in DBR surroundings. To verify the validity of this method the calibrated spectrum is compared to the spectra of cleaved-edge probes, where the DBR has no notable influence since the photons are detected from the side here.

HL 25.82 Wed 18:00 P2

Quantum efficiency boost by photoneutralization of charges in GaAs quantum dots based entangled photon emitters — JINGZHONG YANG¹, TOM FANDRICH¹, FREDERIK BENTHIN¹, ROBERT KEIL², NAND LAL SHARMA², WEIJIE NIE², CASPAR HOPFMANN², OLIVER G. SCHMIDT^{2,3,4}, MICHAEL ZOPF¹, and FEI DING^{1,5} — ¹Institut für Festkörperphysik, Leibniz Universität Hannover — ²Institute for Integrative Nanosciences, Leibniz IFW Dresden — ³Material Systems for Nanoelectronics, Technische Universität Chemnitz — ⁴Nanophysics, Faculty of Physics and Würzburg-Dresden Cluster of Excellence ct.qmat, TU Dresden — ⁵Laboratorium für Nano- und Quantenengineering, Leibniz Universität Hannover

Single- and entangled-photon sources are a key component of photonic applications in i.e. quantum communication. GaAs quantum dots are very promising candidates because of their compatibility to integrated photonic structures and the ability to generate photons on demand with low multiphoton emission, near-unity entanglement fidelity and high indistinguishability. One limiting factor is the emission blinking of the resonance fluorescence. This reduces the efficiency and limits the scalability in quantum networks. The neutral biexciton is resonantly excited via two-photon excitation displaying such blinking behavior. By introducing an additional weak off-resonant excitation, the balance of free charges close to the quantum dot was controlled. This leads to a reduction of blinking caused by the intrinsic Coulomb blockade due to captured charges. This method increases the excitation efficiency by 30% while maintaining the fidelity of the entangled-photon pairs.

HL 25.83 Wed 18:00 P2

Frequency Shift of Electronic Resonances in Self Assembled InAs Quantum Dots — IBRAHIM AZAD ENGIN¹, ISMAIL BÖLÜKBASI¹, ARN BAUDZUS¹, PATRICK LINDNER², ANDREAS WIECK¹, BJÖRN SOTHMANN³, and ARNE LUDWIG¹ — ¹Lehrstuhl für Angewandte Festkörperphysik, Ruhr-Universität Bochum, 44801 Bochum — ²Experimentelle Physik 2, Technische Universität Dortmund, 44227 Dortmund — ³Fakultät für Physik, Universität Duisburg-Essen, 47048 Duisburg Self-assembled InAs quantum dots (SAQD) proved to be promising semiconductor structures for applications as single-photon sources [1]. Especially, charge stabilization by coupling to a reservoir is important for quantum memory resources [2].

In this contribution, we investigate InAs SAQDs in a diode structure coupled to an electron reservoir by capacitance-voltage-spectroscopy to electrically probe QD energy levels and vary parameters like ac-frequency and bath temperature. For the lowest energy s-states a thermal shift in equilibrium has been reported [3]. Non-equilibrium coupling has been observed and described with a master equation [4], where resonance shifts at higher frequencies and temperature remain unexplored. We rectify this here by proposing a more elaborated model and experimental data interpretation.

[1] Tomm, N. et al., Nat. Nanotechnol. 16, 399-403 (2021). [2] Prechtel, J. et al., Nat. Mater. 15, 981-986 (2016) [3] Brinks, F. et al., New J. Phys. 18, 123019 (2016). [4] Valentin, S. et al., Phys. Rev. B 97, 045416 (2018).

HL 25.84 Wed 18:00 P2

Droplet epitaxy of InGaAs quantum dots for spin-photon interface devices — XUELIN JIN^{1,2}, DAVID FRICKER^{1,2}, NILS VON DEN DRIESCH^{1,3}, ALEXANDER PAWLIS^{1,3}, RENU RANI^{1,3}, MINH BUI^{1,3}, DETLEV GRÜTZMACHER^{1,2}, and BEATA KARDYNAL^{1,2} — ¹PGI 9, Forschungszentrum Jülich, 52425 Jülich, Germany — ²Department of Physics, RWTH Aachen, 52074 Aachen, Germany — ³PGI 10, Forschungszentrum Jülich, 52425 Jülich, Germany

Abstract. Quantum networks use photonic qubits to send information, that means photonic qubits need to be converted into stationary qubits at the network nodes. A transfer information from a photonic to a spin qubit has been already demonstrated. Here we study the possibility of transferring photonic qubits into spin qubits which offer a potential of scaling into quantum processors, ones in gate-defined quantum dots in GaAs. Since gate-defined quantum dots do not confine holes, a direct conversion of photon qubits into spin qubits in these quantum dots is not possible. Here, we explore the possibility of using self-assembled InGaAs quantum dots grown by droplet epitaxy as an optical interface to the gated quantum dots defined in GaAs. We will discuss the con-

ditions that the heterostructure has to fulfil to facilitate tunable tunnel coupling between the two quantum dots and we will show the progress in its growth and characterisation. In order to maintain the stable operation of the gated quantum dots, we use droplet epitaxy to grow InGaAs QDs. We will show that this method allows us to create quantum dots with energies suitable for tunnel coupling and minimize the impact of the wetting layer on the two-dimensional electron gas.

HL 25.85 Wed 18:00 P2

Deterministic Coupling of Gold Nanorods with GaAs Quantum Dots — •YINAN WANG¹, PENGJI LI¹, CHENXI MA¹, ANDREAS SCHELL^{1,2}, MICHAEL ZOPF¹, and FEI DING^{1,2} — ¹Institut für Festkörperphysik, Leibniz Universität Hannover, Appelstraße 2, 30167 Hannover, Germany — ²Laboratorium für Nano- und Quantenengineering, Leibniz Universität Hannover, Schneiderberg 39, 30167 Hannover, Germany

Coupling single-photon sources with metal nanoparticles is an emerging topic in quantum optics. Thus the deterministic fabrication of metal nanoantennas is crucial. Here we report our recent efforts on coupling single gold nanorods to single GaAs quantum dots. Two different techniques were investigated: (1) drop-casting a gold nanorod containing solution on the quantum dot sample, and (2) deterministic nano-manipulation of gold nanorods via Pick-and-Place functionalities of an atomic force microscope. We observed the modified photoluminescence of quantum dots, due to their coupling to the localized surface plasmons of the gold nanoparticles. The experimental details and also kinetic modeling will be also shown in detail.

HL 25.86 Wed 18:00 P2

Measurement and calculation of spectral emissivity of semiconductor quantum emitters in dielectric environments — •DANIAL KOHMINAEI, SAYED SHKEBULLAH SADAT, TIMO KRUCK, HANS-GEORG BABIN, ANDREAS D. WIECK, and ARNE LUDWIG — Ruhr-Universität Bochum; Lehrstuhl für angewandte Festkörperphysik, Deutschland

Quantum dots (QDs) emit light divergently. For improved outcoupling of this photon emission, QDs are grown above so-called distributed Bragg reflectors (DBRs), which have a maximum reflectivity at the wavelength of the light of the QDs. Reflection also occurs unwantedly at the interface of the semiconductor to the vacuum. Therefore, when performing photoluminescence (PL) measurements, the measured spectral intensity of the emitted radiation strongly depends on the (dielectric) structure of the sample. Here we show a method for calibrating PL measurements to obtain the unaltered spectrum of the optically active medium. First, the spectral reflectivity is determined by reflectometer measurements, and compared to a simulation based on the transfer matrix method for the true layer thickness. This is then used to calculate the wavelength dependent standing wave field, the outcoupling efficiency and the quantum yield. Furthermore, the influence of the absorption of the exciting laser light in the semiconductor, on the overall spectrum will be analyzed. To validate the method, the calibrated spectra are compared with cleaved-edge PL measurements, where the QDs are excited from the side and the light is also collected from the side.

HL 25.87 Wed 18:00 P2

Fabrication & Electrical Characterization of Silicon-Germanium Nanowire Schottky Barrier Transistors — •MUHAMMAD MOAZZAM KHAN¹, OLIVER STEUER¹, SLAWOMIR PRUCNAL¹, and YORDAN M GEORGIEV^{1,2} — ¹Institute of Ion Beam Physics and Materials Research, Helmholtz-Zentrum Dresden-Rossendorf, Bautzner Landstraße 400, D-01328 Dresden, Germany — ²Institute of Electronics at the Bulgarian Academy of Sciences, 72, Tzarigradsko chaussee blvd, 1784-Sofia, Bulgaria

CMOS scaling is reaching physical limits in near future. Therefore, new approaches are required to continue achieving high speed and high performance devices. Replacing silicon with silicon-germanium alloy as a channel material having higher mobility contributes to faster and energy-efficient devices. In this work, we are investigating the transistor properties built from silicon germanium based nanowire channel. Schottky Barrier Field Effect Transistors are fabricated, which also have an additional functionality of re-configurability. This means that a single device can be operated as an N or P channel just by controlling the electric potential applied at the gate terminals. The devices are fabricated by top-down approach with nickel metal pads on both sides of the silicon-germanium nanowire. To form schottky junctions, flash lamp annealing is performed to diffuse metal into the nanowires. The schottky junctions formed at the interface between nickel-germano-silicide and nanowire are electrically controlled to operate the device. Transfer characteristics of these devices are measured to investigate the transistor properties.

HL 25.88 Wed 18:00 P2

realization of on-chip wavelength multiplexing with self-assembly InGaAs quantum dot in telecom C-band — •DONGZE WANG, STEPHANIE BAUER, MICHAEL JETTER, SIMONE PORTALUPI, and PETER MICHLER — Institut für Halbleitertechnik und Funktionelle Grenzflächen, Stuttgart, Germany

Photonic integrated circuits (PIC) are a highly appealing platform for the realization of quantum photonic devices on a scalable dimension. The technol-

ogy of PIC has enabled the generation, processing, and detection of the quantum state of light. Several different material platforms for the realization of PIC were proposed and are currently under intense investigation. Gallium arsenide-based (GaAs) PIC provides a straightforward combination with a self-assembled quantum dot (QD), which can serve as an efficient on-demand single-photon source with high purity and indistinguishability. In this work, we present a wavelength-division multiplexing system based on indium gallium arsenide (InGaAs) waveguides containing self-assembled InGaAs QDs located at the telecom C-band. The waveguide core is deposited on aluminum gallium arsenide (AlGaAs), which provides large refractive index contrast resulting in good confinement for the propagating photons. The dimensional parameters of the single-mode waveguide were simulated by a finite-difference time-domain method. Afterwards, standard semiconducting nanofabrication processes including electron beam lithography and inductively coupled plasma-reactive ion etching technology were used to fabricate the InGaAs photonic chip.

HL 25.89 Wed 18:00 P2

Magnetotransport in narrow-gap semiconductors with nanostructured constrictions — •OLIVIO CHIATTI¹, JOHANNES BOY¹, CHRISTIAN RIHA¹, CHRISTIAN HEYN², WOLFGANG HANSEN², and SASKIA F. FISCHER¹ — ¹Novel Materials Group, Humboldt-Universität zu Berlin, 10099 Berlin, Germany — ²Institut für Nanostruktur- und Festkörperphysik, Universität Hamburg, 20355 Hamburg, Germany

Measurements in magnetic fields are an effective tool to investigate transport properties of low-dimensional electron systems. We investigate the magnetotransport of semiconductor heterostructures and nanostructures with spin-orbit interaction (SOI), under the influence of in-plane and out-of-plane electric fields. The nanostructures are quantum point contacts (QPCs) etched in Hall-bars with in-plane gates. The Hall-bars and the constrictions were defined by micro-laser photolithography and wet-chemical etching from an InGaAs/InAlAs quantum well with an InAs-inserted channel [1]. We have performed transport measurements at low temperatures in the combined QPC and Hall-bar structures in magnetic fields. We can tune the gate-voltages to control the filling-factor mismatch between bulk Hall-bar and QPC. We observe a crossover from reflection to transmission of the quantum Hall edge channels at the QPC and a tunneling across the QPC between reflected edge states, which depends on the magnitude and direction of the in-plane electric field.

[1] Chiatti *et al.*, Appl. Phys. Lett. **106**, 052102 (2015).

HL 25.90 Wed 18:00 P2

Acquisition and analysis of photocurrent spectra for 850 nm oxide-confined vertical-cavity surface-emitting lasers — ARNDT JAEGER¹, MARWAN BOU SANAYEH², HELMUT MEINERT¹, •MANUEL HAERER¹, OLEG YU. MAKAROV², ILYA E. TITKOV², NIKOLAY LEDENTSOV JR.², and NIKOLAY N. LEDENTSOV² — ¹Esslingen University of Applied Sciences, Flandernstrasse 101, 73732 Esslingen, Germany — ²VI Systems GmbH, Hardenbergstrasse 7, 10623 Berlin, Germany

Vertical-cavity surface-emitting lasers (VCSELs) are of utmost importance as key components for high-speed datacom, sensor and free-space applications. Therefore, for a successful further optimization of their performance, understanding their aging behavior is of crucial importance. The 850 nm oxide-confined VCSELs used in this study were intentionally operated at extreme conditions to accelerate their degradation until reaching optical damage. For monitoring operation-induced changes, a photocurrent spectroscopy (PCS) setup was established and applied before and after accelerated aging. The PCS results at different reverse biases reveal changes that can be explained by non-radiative recombination centers generated during accelerated aging. This finding contributes to the understanding of the aging mechanisms in these tiny devices.

HL 25.91 Wed 18:00 P2

Polariton condensation with extreme confinement of light — •MARIA VITORIA GURRIERI¹, PHILIP KRISTENSEN¹, JESPER MØRK¹, and EMIL DENNING² — ¹Department of Electrical and Photonics Engineering, Technical University of Denmark, 2800 Kgs. Lyngby, Denmark — ²Nonlinear Optics and Quantum Electronics, Technical University of Berlin, 10623 Berlin, Germany

Strong coupling between light and electronic excitations mixes the constituent eigenstates into hybrid polaritonic quasiparticles. Under certain conditions it is possible to predict the formation of a polariton condensate with macroscopic occupation number and spontaneous coherence in the ground state. This condensate is a source of coherent matter waves and photons.

In this work we theoretically investigate the possibility of achieving polariton condensation in an extended sheet of 2D semiconductor coupled to a novel dielectric nanocavity with deep subwavelength confinement and featuring a spectrally isolated mode. Such coupling leads to the formation of a spatially localized polariton state, which interacts with the continuum of excitons through Coulomb interaction. The system is modelled by a Born-Markov master equation for the polariton subsystem, where the exciton continuum is traced out. This enables the derivation of a rate equation model to describe the dynamics of the lower polariton population.

HL 25.92 Wed 18:00 P2

Time resolved spin dynamics in lead halide hybrid organic perovskite $\text{Fa}_{0.9}\text{Cs}_{0.1}\text{PbI}_{2.8}\text{Br}_{0.2}$ — •ERIK KIRSTEIN¹, EIKO EVERS¹, VASILII V. BELYKH^{1,2}, EVGENY A. ZHUKOV¹, DENNIS KUDLACIK¹, INA V. KALITUKHA³, OLGA NAZARENKO⁴, MAXIM V. KOVALENKO^{4,5}, DMITRI R. YAKOVLEV^{1,3}, and MANFRED BAYER^{1,3} — ¹Experimentelle Physik 2, Technische Universität Dortmund, D-44227 Dortmund, Germany — ²Moscow, Russia — ³St. Petersburg, Russia — ⁴Laboratory of Inorganic Chemistry, ETH Zürich, CH-8093 Zürich, Switzerland — ⁵Laboratory for Thin Films and Photovoltaics, Empa-Swiss Federal Laboratories for Materials Science and Technology, CH-8600 Dübendorf, Switzerland

Lead halide hybrid organic perovskites attract increased attention due their promising applications, related to their high quantum efficiency and easy synthesis. The spin dynamics in perovskite materials is not studied in detail so far, but shows promising results. The studied $\text{Fa}_{0.9}\text{Cs}_{0.1}\text{PbI}_{2.8}\text{Br}_{0.2}$ bulk sample was grown out of solution of respective ions in polar solvents. Its bandgap of 1.51 eV makes this material well-suited for the resonant excitation with Ti:Sapphire laser. We study the coherent spin dynamics of electrons and holes by means of time-resolved pump-probe Kerr rotation technique at cryogenic temperatures and magnetic fields up to 6 T. We measure longitudinal spin relaxation times T_1 , transverse dephasing times T_2^* , g-factor values and their spread Δg .

HL 25.93 Wed 18:00 P2

Temperature dependence of the bandgap of ^{28}Si and its use as time-resolved, high precision thermometer — EDUARD SAUTER¹, NICOLAY V. ABROSIMOV², •JENS HÜBNER¹, and MICHAEL OESTREICH¹ — ¹Institut für Festkörperphysik, Leibniz Universität Hannover, Appelstraße 2, 30167 Hannover, Germany — ²Leibniz-Institut für Kristallzüchtung, Max-Born-Straße 2, 12489 Berlin, Germany

We measure by high resolution absorption spectroscopy of the extremely narrow donor bound trion $^{28}\text{Si:P}$ transition the precise temperature dependence of the indirect bandgap of isotopically purified ^{28}Si in helium exchange gas in the regime from 0.1 K to 2 K. The measurements evidence that the trion frequency can be used as an efficient, contactless, local temperature sensor with a demonstrated time-resolution of a few microseconds. Furthermore, the all-optical sensor is also quite sensitive to changes of the local electric field and of the helium cooling gas pressure allowing detailed studies of the complex $^{28}\text{Si:P}$ system dynamics after perturbations.

[1] M. Beck, N. V. Abrosimov, J. Hübner, and M. Oestreich, Phys. Rev. B, **99**, 245201 (2019).

[2] E. Sauter, N. V. Abrosimov, J. Hübner, and M. Oestreich, Phys. Rev. Lett. **126**, 137402 (2021).

HL 25.94 Wed 18:00 P2

Spin noise spectroscopy of a single InGaAs quantum dot at high magnetic fields — •KAI HÜHN, PAVEL STERIN, JENS HÜBNER, and MICHAEL OESTREICH — Institut für Festkörperphysik, Leibniz Universität Hannover, Appelstraße 2, 30167 Hannover, Germany

Single holes in InGaAs quantum dots hold great promise as potential qubits due to the slow relaxation of selected spin degrees of freedom. However, the impact of phonon induced spin relaxation and occupancy noise for high magnetic fields remained unclear so far. Here, we use the method of spin noise spectroscopy (SNS) to gain a detailed insight into such mechanisms and measure the spin and charge dynamics for magnetic fields up to 4T and temperatures between 1.8K and 10K. Here, we combine, the quasi non-disturbant measurement scheme of SNS with an extrapolation to truly zero disturbance of the QD system. We find that the total noise power originates not just only from the hole-spin but from several processes including the relaxation of the hole spin and the charge state dynamics of the QD due to Auger recombination. In addition, our measurements indicate a long term stability of the intrinsic hole spin life time on the order of months. We compare our results with theoretical calculations which explicitly address one and two phonon processes as the limiting mechanism of the intrinsic hole spin relaxation.

HL 25.95 Wed 18:00 P2

Thermal Transport in c-plane GaN Membranes Characterized by Raman Thermometry — •WILKEN SEEMANN¹, JOACHIM CIERS², ISABELL HÜLLEN¹, MAHMOUD ELHAJHASAN¹, JEAN-FRANÇOIS CARLIN³, NICOLAS GRANDJEAN³, ÅSA HAGLUND², and GORDON CALLEN¹ — ¹Institute of Solid State Physics, University of Bremen, Germany — ²Department of Microtechnology and Nanoscience, Chalmers University of Technology, Gothenburg, Sweden — ³Institute of Physics, École Polytechnique Fédérale de Lausanne (EPFL), Switzerland

Excess heat often limits the lifetime or stability of semiconductor devices, like laser structures, e.g. by affecting the refractive index or defect formation. It

is therefore vital to understand how thermal energy is dissipated from the active region. In this contribution, we analyze the in-plane thermal transport in GaN-based membranes which can be applied in UV-visible light emission. The temperature of the material is probed by the shift and width of Raman modes under heating with a UV laser. This method allows for a contactless characterization without the need for additional processing steps often needed for alternative thermometry. We find, that the thermal conductivity, κ , is significantly reduced compared to bulk GaN due to the finite thickness of the analyzed membranes. Phonon scattering due to roughness and porosity of the membrane is found to further reduce κ . Studying in-plane thermal transport lays the foundation for subsequent thermal studies on entire device structures; exploiting a subtle balance of in- and cross-plane thermal transport which could improve device designs.

HL 25.96 Wed 18:00 P2

A ultrafast Optical-pump/THz-probe spectrometer based on sub-diffraction field confinement — •JULIA A. LANG, MICHAEL SEIDEL, and GEORG HERINK — Experimental Physics VIII, University of Bayreuth, Germany

Time-resolved THz spectroscopy is a powerful tool for characterizing transient carrier dynamics in electronic materials and devices. In this contribution, we present an optical-pump/THz-probe spectrometer based on a high-repetition rate femtosecond fiber laser and photoconductive antennas combined with resonant microstructures for signal amplification. In particular, this approach exploits sub-diffraction Terahertz confinement in metallic microstructures to reduce the large mismatch between optical and THz foci. We demonstrate local spectroscopy of carrier dynamics in a semiconductor material inside a single resonator and corroborate our findings with finite-element simulations.

HL 25.97 Wed 18:00 P2

In depth comparison of Raman and Hall measurements for the determination of the electrical transport parameters of N-doped 4H-SiC — •HANNES HERGERT^{1,2}, MATTHIAS T. ELM^{1,2,3}, and PETER J. KLAR¹ — ¹Institute of Experimental Physics I, Giessen, Germany — ²Center for Materials Research, Giessen, Germany — ³Institute of Physical Chemistry, Justus Liebig University, 35392 Giessen, Germany

A precise characterisation of the impact of doping on the electronic transport properties is necessary for the application of silicon carbide (SiC) in semiconductor devices. Hall effect measurements yield reliable results for mobility and carrier density but electrical contacts are needed. These are often not desired. An alternative approach is the analysis of the longitudinal optical phonon electron plasma coupled (LOPC) mode using Raman spectroscopy. This approach also delivers non-invasively information about the charge carrier density and the electron mobility. In this work, we compare the results obtained by Hall and Raman measurements. We show that the effective carrier density and the mobility obtained by Hall measurements deviate from those determined using Raman spectroscopy. The deviations arise as only electrons in the conduction band couple to the LO mode, while electrons in the impurity band do not, but still contribute to the electrical transport. To extract the charge carrier density in the conduction band from Hall measurements, a three-band model is employed. In addition, the two measurement methods yield different values of the mobility due to its frequency-dependence.

HL 25.98 Wed 18:00 P2

Electrical characterization of core/shell GaAs/InAs/Al nanowire-based Josephson junctions — •FARAH BASARIC¹, ANTON FAUSTMANN¹, MARVIN M. JANSEN¹, ALEXANDER PAWLIS^{1,2}, ERIK ZIMMERMANN¹, HANS LÜTH^{1,2}, DETLEV GRÜTZMACHER^{1,2}, and THOMAS SCHÄPERS^{1,2} — ¹Peter Grünberg Institut (PGI-9), Forschungszentrum Jülich, 52425 Jülich, Germany — ²JARA-Fundamentals of Future Information Technology, Jülich-Aachen Research Alliance, Forschungszentrum Jülich and RWTH Aachen University, Germany

Epitaxially grown phase-pure GaAs/InAs core/shell nanowires offer uniformity in their electrical, mechanical and optical properties. High electron mobility, large g-factor and strong Rashba spin-orbit coupling in combination with phase-pure wurtzite GaAs core offer heterostructure with transport properties governed by the presence of confined states in the InAs shell. A Josephson junction was realized by wet chemical etching of an *in-situ* deposited Al half-shell. Clean semiconductor-superconductor interface by such deposition was important for obtaining high critical current and good electrical transport control. The nanowire system was fabricated fully *in-situ* in a state-of-the-art nanofabrication clustertool, enabling precisely defined interfaces. Magnetotransport measurements at variable temperature regime were carried out for structures with normal and superconducting contacts under applied in-plane magnetic field, with varying gate potential. Such hybrid structure represents a promising candidate in realizing superconducting qubits and Majorana circuits.

HL 26: Quantum Dots and Wires 5: Optics 2

Time: Thursday 9:30–12:45

Location: H32

HL 26.1 Thu 9:30 H32

All-optical polarization control of single photons emitted by a quantum dot — •BYÖRN JONAS, DIRK HEINZE, EVA SCHÖLL, PATRICIA KALLERT, TIMO LANGER, SEBASTIAN KREHS, ALEX WIDHALM, KLAUS D. JÖNS, DIRK REUTER, STEFAN SCHUMACHER, and ARTUR ZRENNER — Paderborn University, Physics Department, Warburger Straße 100, 33098 Paderborn, Germany

In our work we employ an all-optical approach based on nonlinear principles to control the polarization of single photon emission from a single quantum dot. To achieve this, we make use of a nonlinear down-conversion process from the biexciton to the ground state [1]. This opens an alternative decay path in addition to the biexciton cascade. Previous theoretical work suggests the possibility to manipulate the properties of the emitted photons by tuning the respective properties of a control laser [2].

By exploiting this mechanism, we were able to demonstrate polarization control of the emitted photons for linear and circular polarization. Our findings show no influence of the fine-structure splitting on the polarization of the emitted photons. We furthermore present a theoretical model to describe our results and we find excellent agreement between experiment and theory.

[1] B. Jonas et al., *Nature Communications* **13**, 1387 (2022)

[2] D. Heinze et al., *Nature Communications* **6**, 8473 (2015)

HL 26.2 Thu 9:45 H32

Temporal evolution of line broadening in charge controlled quantum dots — •TIM STROBEL¹, JONAS H. WEBER¹, MARCEL SCHMIDT², LUKAS WAGNER¹, ANDREAS D. WIECK², MICHAEL JETTER¹, SIMONE L. PORTALUPI¹, ARNE LUDWIG², and PETER MICHLER¹ — ¹Institut für Halbleitertechnik und Funktionelle Grenzflächen, Center for Integrated Science and Technology (IQST¹) and SCoPE, University of Stuttgart, Allmandring 3, 70569 Stuttgart, Germany — ²Lehrstuhl für Angewandte Festkörperphysik, Ruhr-Universität Bochum, D-44780 Bochum, Germany

Self-assembled semiconductor quantum dots (QDs) present themselves as an attractive platform for the implementation of scalable hybrid quantum-information schemes. On-demand emission of high-quality single photons demonstrates the potential of such systems. Sources of noise, caused by the interaction with the solid-state environment can lead to an inhomogeneous broadening of the emission line. The magnitudes and timescales of such dephasing mechanisms vary strongly with the material composition and heterostructure of a sample. Here, we employ Photon-correlation Fourier spectroscopy as a powerful experimental method to study the spectral dynamics of single emitters, with high spectral and temporal resolution. In particular, the broadening mechanisms of QDs embedded in a novel type of gated structure, based on a n-i-n-diode are investigated.

HL 26.3 Thu 10:00 H32

High-quality single-photons from hybrid MOVPE/MBE grown n-i-n quantum-dot structures — •LUKAS WAGNER¹, TIM STROBEL¹, MARCEL SCHMIDT², JONAS H. WEBER¹, LENA ENGEL¹, ANDREAS D. WIECK², MICHAEL JETTER¹, SIMONE L. PORTALUPI¹, ARNE LUDWIG², and PETER MICHLER¹ — ¹Institut für Halbleitertechnik und Funktionelle Grenzflächen (IHFG), Center for Integrated Quantum Science and Technology (IQST) and SCoPE, University of Stuttgart, Allmandring 3, 70569 Stuttgart, Germany — ²Lehrstuhl für angewandte Festkörperphysik, Ruhr-Universität Bochum, Universitätsstraße 150, 44801 Bochum, Germany

Photonic quantum operations require sources of photons with Fourier-limited linewidth and high brightness. Stark-shift tuning of the emission wavelength can be of interest in upscaling the complexity, employing multiple quantum dots (QDs) tuned at the same emission wavelength. QDs in gated structure can provide a stabilization of the electric field environment, pushing the photon linewidth close to the Fourier limit. In addition, the embedding diode structure can be used to electrically tune the emission wavelength. The growth of self-assembled semiconductor QDs is usually carried out via metal-organic vapor-phase epitaxy (MOVPE) or molecular-beam epitaxy (MBE). This work combines MOVPE and MBE techniques for hybrid growth of gated semiconductor QD samples. This provides spectrally tunable InAs QDs with narrow emission linewidth. High single-photon purity and indistinguishability are proven via Hanbury-Brown and Twiss, and Hong-Ou-Mandel experiments in resonant excitation.

HL 26.4 Thu 10:15 H32

Ultrafast electric control of cavity mediated photons from a semiconductor quantum-dot — •DAVID BAUCH¹, DIRK HEINZE¹, JENS FÖRSTNER¹, KLAUS D. JÖNS¹, and STEFAN SCHUMACHER^{1,2} — ¹Department of Physics and CeOPP, Paderborn University, Germany — ²College of Optical Sciences, University of Arizona, Tucson, USA

On demand sources for single photon and photon pairs are essential for quantum communication protocols. Exciton and cascaded biexciton-exciton transitions in semiconductor quantum dots offer the potential for optically controlled generation of a single photon [1] and polarization-entangled twin photons [2]. In addition to pure optical control, externally applied time-dependent electric fields enable control of the (bi-)exciton resonance through the quantum confined Stark effect, resulting in changes of the (bi-)exciton dynamics and the resulting photon emission. Here we investigate theoretically the optical excitation of the (bi-)exciton state off-resonant to a cavity mode followed by ultrafast control of the states, which then allows for cavity-resonant emission of the photons. Our scheme allows for high preparation fidelities followed by the generation of highly indistinguishable single photons and polarization entangled twin-photons via the biexciton-exciton cascade and biexciton two-photon emission with high emission probabilities [3].

[1] D. Heinze, D. Breddermann, A. Zrenner, S. Schumacher, *Nat. Commun.* **6**, 8473 (2015). [2] D. Heinze, A. Zrenner, S. Schumacher, *Phys. Rev. B* **95**, 245306 (2017). [3] D. Bauch, D. Heinze, J. Förstner, K. D. Jöns, S. Schumacher, *Phys. Rev. B* **104**, 085308 (2021).

HL 26.5 Thu 10:30 H32

Sub- and Superradiant Effects in Bimodal Quantum-Dot Microcavity Lasers — •ISA HEDDA GROTHE and JAN WIERSIG — Institut für Physik, Otto-von-Guericke-Universität Magdeburg, Germany

In standard nanolasers with a single cavity mode a strong influence of inter-emitter correlations on the input-output dynamics as well as the statistical properties of the emitted light has been described [1]. Below threshold subradiant emission emerges with superthermal values of the autocorrelation function $g^{(2)}(0)$, which is associated with strong bunching of the emitted photons. Similarly high values of $g^{(2)}(0)$ have also been found for the weak mode in micropillar lasers with two orthogonally polarized modes [2,3]. Here, however, this phenomenon is rooted in the interaction of both modes with a common gain medium which leads to gain competition between the two modes.

Making use of a theoretical semiconductor laser model based on the cluster-expansion method, we include correlations between the emitters in the description of bimodal microcavity lasers. This enables us to compare the influence of sub- and superradiant effects on the emission of bimodal lasers to that on lasers with a single mode. Additionally, we are able to distinguish features of the statistical properties of the emitted light that characterize either subradiance or gain competition as the source of superthermal photon bunching in bimodal lasers.

[1] H. A. M. Leymann et al., *Phys. Rev. Applied* **4**, 044018 (2015).

[2] H. A. M. Leymann et al., *Phys. Rev. A* **87**, 053819 (2013).

[3] M. Schmidt et al., *Phys. Rev. Research* **3**, 013263 (2021).

HL 26.6 Thu 10:45 H32

GaAs Droplet Epitaxy Quantum Dots as Deterministic Single Photon Sources for Entangling SiV-Centers in Diamond — •MANUEL RIEGER¹, VIVIANA VILLAFANE¹, ANDREAS NICKL¹, CHRISTIAN DANGEL¹, HANS-GEORG BABIN², TIM SCHRÖDER³, ARNE LUDWIG², ANDREAS WIECK², KAI MÜLLER¹, and JONATHAN FINLEY¹ — ¹Walter Schottky Institut/Physik Department, TUM, 85748 Garching, Germany — ²Physik Department, RU Bochum, Universitätsstraße 150, 44801 Bochum, Germany — ³Physik Department, HU Berlin, Newtonstraße 15, 12489 Berlin, Germany

Quantum algorithms promise acceleration of tasks like computational chemistry and machine learning. In this context, diamond-based quantum hardware capable of interfacing spins and photons in a scalable network [1] is particularly advantageous since it combines excellent coherence times, gate fidelities and the possibility for on-chip integration. We demonstrate GaAs based quantum dot (QD) deterministic single photon sources grown using droplet epitaxy (DE) and resonant with the SiV⁻ center in diamond at 737nm. By characterizing single dots using low temperature optical spectroscopy, we measure a non-classical second order photon intensity correlation function ($g^{(2)}(0) < 0.3$), demonstrate electrical tunability of the charge occupancy and show wide tunability of the emission frequency over 250GHz. Furthermore, we show that the optical lifetimes of the DE-QDs lie in the range 1-1.5ns, similar to those of SiV⁻ (1-2ns), a prerequisite for high-fidelity photon mediated entanglement [1,2]. [1] K. Nemoto et al., *Phys. Rev. X* (2014). [2] C. Dangel et al., arXiv preprint (2022).

30 min. break

HL 26.7 Thu 11:30 H32

To boldly excite where no one has excited before — THOMAS K. BRACHT¹, YUSUF KARL², FLORIAN KAPPE², VIKAS REMESH², TIM SEIDELMANN³, ARMANDO RASTELLI⁴, GREGOR WEIHS², VOLLRATH MARTIN AXT³, and •DORIS E. REITER^{1,5} — ¹Institut für Festkörpertechnik, Universität Münster, 48149 Münster, Germany — ²Institute für Experimentalphysik, Universität Innsbruck,

Innsbruck, Austria — ³Institute of Semiconductor and Solid State Physics, JKU Linz, Linz, Austria — ⁴Theoretische Physik III, Universität Bayreuth, 95440 Bayreuth, Germany — ⁵Condensed Matter Theory, TU Dortmund, 44221 Dortmund, Germany

In the Rabi scheme, off-resonant excitations of a two-level system do not lead to a full inversion, when no further auxiliary particles are participating. Surprisingly, the Swing-UP of the quantum Emitter population (SUPER) scheme uses off-resonant excitations to fully bring a two-level system from the ground to excited state [PRX Quantum 2, 040354 (2021)]. The scheme relies on a gradual swing-up, which can be achieved by modulation of the excitation frequency or amplitude. Here, we discuss the theory of the SUPER scheme and how it can be implemented for a semiconductor quantum dot by using a two-color excitation with pulses detuned by several meV. Due to the electron-phonon interaction, the SUPER scheme results in the emission of phonon wave packets [psb, 2100649 (2022)], but overall the phonon influence is rather small. The experimental realization of SUPER scheme [arXiv:2203.00712 (2022)], as will be presented in a different contribution, shows great agreement with the theoretical prediction.

HL 26.8 Thu 11:45 H32

Internal Photoeffect from a Single Quantum Emitter — PIA LOCHNER¹, JENS KERSKI¹, ANNIKA KURZMANN², HENDRIK MANNEL¹, MARCEL ZÖLLNER¹, ANDREAS D. WIECK³, ARNE LUDWIG³, MARTIN P. GELLER¹, and AXEL LORKE¹ — ¹University of Duisburg-Essen and CENIDE, Germany — ²RWTH Aachen University, Germany — ³Ruhr-University Bochum, Germany

As quantum information technologies require long spin coherence times in qubits and highly indistinguishable photons [1], we present a new and mostly neglected mechanism in self-assembled quantum dots that fundamentally limits the coherence times in optical quantum devices. By time-resolved resonance fluorescence (RF) measurements on a single quantum dot, we demonstrate an internal photoeffect [2] that emits electrons from the dot by an intra-band excitation. While the tunneling rate of an electron into the quantum dot is constant for increasing non-resonant laser intensity, the emission rate by the photoeffect increases linearly with increasing excitation intensity. This way, the emission rate is tunable over several orders of magnitude by adjusting the non-resonant laser excitation intensity.

Our findings show that a process, which is well known in single atom spectroscopy (i.e. photo ionization) can also be observed for a solid-state quantum emitter and has to be avoided or reduced to push the limits towards long qubit coherence times.

[1] T. D. Ladd et al., Nature 464, 45-53 (2010)

[2] P. Lochner et al., Phys. Rev. B 103, 075426 (2021)

HL 26.9 Thu 12:00 H32

Nuclear Spin Polarization by Electron Spin Mode Dragging in an Ensemble of (In,Ga)As Quantum Dots — •EIKO EVERS¹, NATALIA E. KOPTEVA^{1,2}, IRINA A. YUGOVA^{2,3}, DMITRI R. YAKOVLEV^{1,4}, MANFRED BAYER¹, and ALEX GREILICH¹ — ¹Experimentelle Physik 2, TU Dortmund, 44221 Dortmund, Germany — ²Spin Optics Laboratory of St. Petersburg State University, 198504 St. Petersburg, Russia — ³St. Petersburg, Russia — ⁴St. Petersburg, Russia

The electron-nuclear spin system in singly charged (In,Ga)As quantum dots (QDs) promises to combine the efficient optical electron spin (ES) orientation with the long coherence time in the nuclear spin (NS) system [1]. To come closer

to a state of large NS polarization, we synchronize an ensemble of QDs, inhomogeneous in size, g factor, and resident ES precession frequency in a transverse external field, to a laser with a pulse repetition frequency of 1 GHz. As a result, the ensemble of ESs is homogenized by focusing it on a single precession mode by nuclei-induced frequency focusing [2]. In a substantial external field range, the single mode is fixed by a simultaneous build-up of an anti-parallel Overhauser field B_N caused by the polarization of NSs. The Overhauser field achievable in each QD differs and leads to the surprising emergence of equally spaced ES precession components in the ensemble.

[1] D. Gangloff et al., Science 364, 62 (2019)

[2] A. Greilich et al., Science 317 1896 (2007)

HL 26.10 Thu 12:15 H32

Auger-assisted electron spin-flips in a single quantum dot — •HENDRIK MANNEL¹, JENS KERSKI¹, PIA LOCHNER¹, MARCEL ZÖLLNER¹, FABIO RIMEK¹, ARNE LUDWIG², ANDREAS WIECK², AXEL LORKE¹, and MARTIN GELLER¹ — ¹Faculty of Physics and CENIDE, University of Duisburg-Essen, Duisburg, Germany — ²Chair of Applied Solid State Physics, Ruhr-University Bochum, Germany

A long electron spin coherence lifetime is the key requirement for future solid-state spin qubits. However, for instance, in self-assembled quantum dots the coupling to nuclei, co-tunneling with a nearby reservoir, and spin-orbit coupling limit the spin-lifetime.

Using resonance fluorescence, we here demonstrate an additional fundamental process that can lead to a single electron spin-flip via an Auger recombination [1]. The quantum dot is placed in a magnetic field in Faraday geometry and charged with one (spin-up or spin-down) electron [2]. In time-resolved resonant fluorescence measurements and using a rate equation model, we can determine the Auger and spin-flip rates in a magnetic field.

Our results reveal an additional, so far neglected Auger-assisted spin-flip process: Auger recombination with subsequent electron tunneling from the reservoir. The present dot is weakly coupled to an electron reservoir. A strong coupling will enhance this Auger-assisted spin-flip rate and thus reveal an important mechanism limiting the spin lifetime due to a strong coupling to a nearby reservoir.

[1] A. Kurzmann et al., Nano Lett. 16, 3367 (2016). [2] J. Dreiser et al., Phys. Rev. B 77, 075317 (2008).

HL 26.11 Thu 12:30 H32

Spin control of single spins in semiconductor quantum dots placed in a microcavity — •MARCO DE GREGORIO, TOBIAS HUBER, and SVEN HÖFLING — Technische Physik, Julius-Maximilians-Universität, Würzburg, Deutschland

Implementation of secure communication with entangled photons is a continuously evolving field. Different platforms have been investigated during the last decades and quantum dots have been proven to be a promising candidate as source for entangled photons. Despite their deterministic photon creation and excellent multi-photon suppression, quantum dot sources suffer from outcoupling efficiencies, when not embedded into photonic structures. Here, we present a low quality factor micropillar cavity, which is broadband, but still enhances the photon extraction efficiency. Analysis of deterministically placed low-q micropillars, characterization and optimization of the emission behavior and control of the spin are necessary steps paving the way towards the generation of a quantum repeater.

HL 27: Focus Session: Perspectives in Cu(In,Ga)Se 1

The chalcopyrite Cu(In,Ga)Se₂ is currently one of the few photovoltaic materials with an active participation in the market share of thin-film technologies, offering also the advantage of having a low production carbon footprint. After a rapid increase in its record power conversion efficiency during the last decade, the technology seems to have stagnated at 23.4 percent, a record achieved in 2019. Several strategies, which have been partially responsible of the newest record efficiencies, have been developed in order to push Cu(In,Ga)Se₂ further by targeting the improvement of the bulk properties and the interfaces: post-deposition treatments with heavy alkali metal fluorides, incorporation of other metals like silver and the mixture with other chalcogens like sulfur, are just some examples. The aim of this focus session is to bring Cu(In,Ga)Se₂ experts together in order to discuss the current limitations and propose new routes and concepts that could lead to a further improvement in this technology.

Organized by AK-jDPG (Aubin Prot, Omar Ramirez and Taowen Wang)

Time: Thursday 9:30–11:00

Location: H33

Invited Talk

HL 27.1 Thu 9:30 H33

What limits state-of-the-art chalcopyrite solar cells? — •SUSANNE SIEBENTRITT — Laboratory for Photovoltaics, Department of Physics and Materials Science, University of Luxembourg

Chalcopyrite solar cells have reached 23.4% efficiency, less than Si solar cells. Why are chalcopyrite solar cells not better? State of the art chalcopyrite solar cells

are based on an absorber with a band gap gradient in depth, to keep electrons from the back contact and to reduce non-radiative recombination at the back contact. However, this graded band gap profile can decrease the short circuit current because of a rather low absorbance near the absorption edge. Additionally, the gradual increase of the absorbance leads to radiative loss in the open circuit voltage (VOC). Additional fluctuations and disorder lead to exponential

band tails and to radiative and non-radiative VOC losses. These Urbach tails are larger in polycrystalline films than in epitaxial films, indicating a contribution of grain boundaries, however, the difference is only a few meV in Urbach energy, indicating a common source independent of grain boundaries. The dependence of the Urbach energy on the net doping level hints to electrostatic fluctuations as a main source of tail states. In addition to these limitations of the short circuit current and the open circuit voltage, the diode factor of most chalcopyrite solar cells is high, implying a low fill factor. It became only recently clear, that metastable defects contribute massively to the increased diode factor of these solar cells.

Invited Talk

HL 27.2 Thu 10:00 H33

Approaches to improve CIGS absorber quality and the CIGS/buffer interface to reach 24% efficiency and beyond — •WOLFRAM WITTE — Zentrum für Sonnenenergie- und Wasserstoff-Forschung Baden-Württemberg (ZSW), Stuttgart, Germany

Cu(In,Ga)Se₂ (CIGS) thin-film solar cells with polycrystalline absorber layers exhibit high power conversion efficiencies above 23% for small-area devices. The bandgap energy (E_g) of CIGS is tunable and the material can be used either as bottom cell within a tandem device, e. g. in combination with perovskite as a top cell or the CIGS cell can be applied as wide-bandgap top cell and combined with e. g. a silicon bottom cell. In spite of their excellent photovoltaic (PV) performance, it is apparent, when comparing the PV parameters of record single junction CIGS devices with the theoretical radiative limit, that various loss mechanisms are present in the devices. As few examples, the open-circuit voltage (V_{oc}) and the fill factor (FF) are limited by non-radiative recombination and additional parasitic absorption takes place in the buffer and adjunct high-resistive (HR) layer, which can limit the short-circuit current (J_{sc}).

This contribution gives an overview on approaches to improve CIGS single-junction solar cells beyond 24%. Increasing grain size and/or eliminate the Ga/(Ga+In) grading in the absorber can reduce V_{oc} losses and alloying of silver to CIGS can increase FF values.

To overcome parasitic absorption of the standard buffer system CdS/i-ZnO, the application of wide-bandgap buffer or HR materials such as Ga₂O₃ with $E_g > 4$ eV can be an option to increase J_{sc} further.

HL 27.3 Thu 10:30 H33

Role of Na in interconnection between chemical composition and electrical properties of grain boundaries in Cu(In,Ga)Se₂ — •AZAM KARAMI¹, MARCIN MORAWSKI², HEIKO KEMPA², ROLAND SCHEER², and OANA COJOCARU-MIRÉDIN¹ — ¹RWTH Aachen University, Aachen, Germany — ²Martin-Luther-Universität Halle-Wittenberg, Halle, Germany

Nowadays, the polycrystalline Cu(In,Ga)Se₂ thin-film solar cells have attained increased interest due to their lower costs and higher cell efficiency in energy conversion. These polycrystalline absorbers contain a large ratio of grain boundaries which can be detrimental (increase in recombination activity compared to the bulk), neutral (no change in electrical properties relative to grains) or benign (increase in electrical properties) for the cell performance. In the present work, different techniques such as atom probe tomography and electron backscattered diffraction are used to investigate different grain boundaries in order to illustrate the relation between the chemical composition and the electrical properties of the grain boundaries. It is shown that the elemental changes at the grain boundaries such as Cu depletion, In enrichment and segregation of alkali dopants like Na, can directly affect their beneficial behavior in favor of cell performance. The experimental findings prove the significant role of Na addition in improving the cell parameters such as open circuit voltage and fill factor. Although it is also shown that the excessive addition of Na dopant can have a detrimental effect on the cell efficiency by increasing the density of dislocations and interference of deep defects with dopants.

HL 27.4 Thu 10:45 H33

Electronic properties of the back contact in Cu(In,Ga)Se₂ solar cells — TORSTEN HÖLSCHER, THOMAS SCHNEIDER, MERVE DEMIR, JULIA HORSTMANN, MELINA KRISTEN, HEIKO KEMPA, and •ROLAND SCHEER — Martin-Luther-Universität Halle/Wittenberg, Naturwissenschaftliche Fakultät II, Institut für Physik, Fachgruppe Photovoltaik, Von-Danckelmann-Platz 3, 06120 Halle/Saale
Cu(In,Ga)Se₂ solar cells are interesting for single junction and multi-junction (tandem) photovoltaic energy conversion. Although not being ideal, their back contact may exhibit a secondary junction. This is the case for low bandgap Cu(In,Ga)Se₂ with a molybdenum back contact. Here, the secondary junction leads to a certain admittance step, a saturation in the $V_{oc}(T)$ plot, but has little impact on the device performance for thick Cu(In,Ga)Se₂ layers: The barrier typically is small enough to allow for majority carrier transport and sufficiently far away from the main junction to impede minority carrier recombination. Only for ultrathin Cu(In,Ga)Se₂ solar cells, the barrier can limit the device performance. For wide bandgap Cu(In,Ga)Se₂ on molybdenum, the barrier appears to be even smaller. The situation is much less clear for Cu(In,Ga)Se₂ on a transparent ITO back contact for tandem applications. For low bandgap Cu(In,Ga)Se₂, no barrier is to be detected by admittance and $V_{oc}(T)$ experiments. For widegap Cu(In,Ga)Se₂, the barrier formation in addition depends on the type of dopant. In this contribution, we used different experimental techniques in order to develop electronic models for opaque (Molybdenum) and transparent (ITO) back contacts.

HL 28: Organic Semiconductors 1

Time: Thursday 9:30–11:45

Location: H34

HL 28.1 Thu 9:30 H34

Dual-color organic LEDs for on demand activation and inhibition of cellular activity — •GIUSEPPE CICCONE¹, ILENIA MELONI², RODRIGO GASTON FERNANDEZ LAHORE³, HANS KLEEMAN¹, PETER HEGEMANN³, KARL LEO¹, and CAROLINE MURAWSKI² — ¹Dresden Integrated Center for Applied Physics and Photonic Materials (IAPP) and Institute for Applied Physics, Technische Universität Dresden, Dresden, Germany. — ²Kurt-Schwabe-Institut für Mess- und Sensortechnik Meinsberg e.V., Waldheim, Germany — ³Institute for Biology, Experimental Biophysics, Humboldt-Universität zu Berlin, Berlin, Germany

Optical stimulation of light sensitive proteins in neurons allows optogenetics to stimulate and probe cellular activity with high spatial and temporal resolution. Multiple light sources with different wavelengths are usually required to stimulate light-sensitive proteins that combine a cation-conducting and an anion-conducting channel. Here, we present two stacked OLED architectures that can emit light with two different emission colors from the same pixel, addressing the single domains of bidirectional ion channels expressed in *Drosophila melanogaster* larvae and ND7/23 cells with one single, organic device. Tuning of microcavities allowed us to well match the OLED emission spectra to the activation spectra of the combined photo-sensitive proteins BiPOLES and BiPOLES-ChRmine. Our work shows that OLEDs can provide narrowband light emission with minimal crosstalk between sub-pixels, enabling us to switch between optogenetic activation and inhibition of living systems with a single device.

HL 28.2 Thu 9:45 H34

Revealing the origin of short channel effects in organic electrochemical transistors — •ANTON WEISSBACH¹, HSIN TSENG¹, LAURIE E. CALVET², HANS KLEEMANN¹, and KARL LEO¹ — ¹Technische Universität Dresden, Germany — ²Université Paris-Saclay-CNRS, Palaiseau, France

Organic electrochemical transistors (OECTs) emerged as promising building blocks for brain-inspired hardware. Several studies demonstrated the synaptic-like properties of OECTs. However, the fabrication of integrated hardware with OECTs is hampered by the nature of the electrolyte. In particular, liquid electrolytes are prone to evaporation and cover multiple devices. Here, we present an OECT with photopatternable solid electrolyte that we structure down to 10 micrometer resolution. The patternability of the electrolyte allows us to integrate OECTs in circuitry without crosstalk between devices. On the single-device-level, it exhibits an on-off ratio of 10^6 , and a subthreshold swing of 61 mV/dec, close to the thermodynamic minimum.

Moreover, we show that these devices exhibit short channel effects, even at large channel lengths up to 100 micrometers. We reveal that the origin lies in the capacitive coupling of the drain electrode with the electrolyte. We then quantify and systematically study the strength of the coupling and show that it can be altered by the overlap of the semiconductor with the drain electrode. Our results reveal that the capacitive drain coupling can be more than 50 % compared to the gate coupling. Based on that, we provide a design principle for diminishing the detrimental short channel effect in OECTs.

HL 28.3 Thu 10:00 H34

Laser induced fluorescence spectroscopy of TIPS pentacene attached to rare gas cluster — •MICHELBACH MORITZ, DEMIANENKO ALEXANDER, HARTWEG SEBASTIAN, and STIENKEMEIER FRANK — Institute of Physics, University of Freiburg, Germany

In the recent years bis(triisopropylsilyl)ethynyl (TIPS)) pentacene has gained interest in the field of singlet fission. Originally developed for field-effect transistors, the TIPS side groups of the pentacene lead to favourable intermolecular orientation, high hole mobility in thin films and better solubility in organic solvents [1]. We present a comparison study of the pentacene and its derivative, in which we cover the energetic structure of the excited states, the influence of the

surrounding medium and the effect of neighbouring molecules. Especially the collective effects are investigated with a lifetime analysis and give a direct hint for lifetime reducing effects like superradiance and singlet fission [2], [3].

[1] Giri et al., Nature 480, 504-508 (2011)

[2] Bohlen, M. et al., J. Chem. Phys. 156, 034305 (2022)

[3] Izadnia, S. et al., J. Phys. Chem. Lett. 8, 2068*2073 (2017)

HL 28.4 Thu 10:15 H34

Heterostructure photodiodes of PbS nanocrystals with different types of ligands — •SHAIMAA ABDALBAQI¹, FLORIAN GRASSL¹, ALEXANDER HOFMANN¹, AHMED MANSOUR², ALADIN ULLRICH¹, NORBERT KOCH², ANDREAS OPITZ², MARCUS SCHEELE³, and WOLFGANG BRÜTTING¹ — ¹Institut für Physik, Universität Augsburg, Germany — ²Institut für Physik & IRIS Adlershof, Humboldt-Universität zu Berlin, Berlin, Germany — ³Institut für Physikalische und Theoretische Chemie, Universität Tübingen, Tübingen, Germany

The influence of the ligands in coupled organic-inorganic nanostructures (COINs) on the performance of optoelectronic devices is investigated. We fabricate photodiodes based on pentacene and PbS nanocrystals coupled to organic ligands like 1,2-ethanedithiol (EDT) and tetrabutylammonium iodide (TBAI) and a combination of both as a heterostructure. These ligands were first separately used to fabricate a single ligand-type of organic-inorganic device and later compared with a heterostructure of PbS-EDT and PbS-TBAI. To tune the optical energy gap of COINs to align with the triplet level of pentacene, it was necessary to choose the suitable particle size. For this purpose, ultraviolet photo-emission spectroscopy (UPS) was used to determine the energy of the highest occupied molecular orbital (HOMO) and the work function of COINs. Devices with heterostructure COINs achieve a higher short circuit current than COINs with a single type of ligands. Incident photon to current efficiency (IPCE) shows different excitonic absorption peaks in the visible range for different stacks.

15 min. break

HL 28.5 Thu 10:45 H34

Development of an OLED as excitation light source for photocatalytic active materials — •DOMINIK WEBER¹, DANIEL SCHONDELMAIER¹, DIETRICH R.T. ZAHN², TERESA ISABEL PICOTO PENA MADEIRA², SALVAN GEORGETA², and ANNIKA MORGENSTERN² — ¹Westfälische Hochschule Gelsenkirchen, Faculty of Physical Engineering and Computer Sciences/ Nanotechnology, Gelsenkirchen, Deutschland — ²Technische Universität Chemnitz, Physics Department / Semiconductor Physics, Chemnitz, Deutschland

Since its first publication in 1987 by Tang and VanSlyke, organic light-emitting diodes (OLEDs) have been in the focus of science for more than 3 decades and have been continuously improved. Especially in the field of RGB OLEDs, substantial progress has been achieved in terms of lifetime and efficiency, which is why they are used today in particular in the display and solid-state lighting technology.

The work presented focuses on the optimization of UV-to-blue OLEDs for use as an illumination source and a source of excitation for photocatalytic active layers. Therefore, an OLED with a suitable characteristic (wavelength, lifetime, efficiency) is developed, by studying the influences of different materials, layer systems, and the integration of nanostructures. Additionally, the photocatalytic active layer titanium dioxide is generated and optimized (absorption behavior, effectiveness), which can be realized by thermally excited phase conversion. The relationship between photocatalytic activity and the phase composition will be investigated here.

HL 28.6 Thu 11:00 H34

Photoexcited charge carrier and spin dynamics in methylammonium lead bromide doped by magnetic transition metals — •STANISLAV BODNAR¹, JONATHAN ZERHOCH^{1,2}, ANDRII SHCHERBAKOV^{1,2}, SHANGPU LIU^{1,2}, LISSA EYRE¹, and FELIX DESCHLER^{1,2} — ¹Walter Schottky Institut, Physik Department, Technische Universität München, Garching, Germany — ²Heidelberg University, Heidelberg, Germany

One of the most challenging tasks for LED applications is emitting 100% polarized light from the device. Typically, this is achieved by introducing an additional layer of polarization filter which leads to losing half of the light intensity. To overcome this issue, one has to find a system with a high degree of photoluminescence (PL) polarization. A promising approach here is using magnetic metal doping in combination with a highly efficient semiconductor. We have chosen to use transient absorption (TA) spectroscopy at cryogenic temperatures to investigate changes in the optical properties induced by magnetic metal doping in CH₃NH₃PbBr₃ since it gives spectral information about the energies of electronic states and dynamic properties of the photoexcited carriers. We find a change in the main ground state bleach (GSB) peak position in doped CH₃NH₃PbBr₃, which depends on the transition metal used. The main GSB peak of pure CH₃NH₃PbBr₃ at 4 K is at 2.32 eV. Doping CH₃NH₃PbBr₃ with Mn leads to a shift of the main peak to lower energies by 0.04 eV and 0.08 eV, respectively. The modifications of the TA spectra are associated with changes in the bandgap energy, which is the result of doping-induced lattice expansion.

HL 28.7 Thu 11:15 H34

Ultrastrong light-matter interaction of J-aggregated squaraine in an open cavity for polariton lattices — •CHRISTOPH BENNENHEI¹, LUKAS LACKNER¹, MORITZ GITTINGER¹, HEIKO KNOPF², FALK EILENBERGER², JENNIFER ZABLOCKI³, ARNE LÜTZEN³, CHRISTOPH LIENAU¹, MARTIN SILIES¹, MARTIN ESMANN¹, and CHRISTIAN SCHNEIDER¹ — ¹Institute of Physics, University of Oldenburg — ²Institute of Applied Physics, Abbe Center of Photonics, Friedrich Schiller University, Jena — ³Kekulé Institute of Organic Chemistry and Biochemistry, University of Bonn

Organic molecule exciton-polaritons in artificial lattices are an emerging platform to emulate complex electronic Hamiltonians at ambient conditions. We present J-aggregated squaraine dye (SQ) thin films [1] as a promising candidate for exciton-polaritons in optical cavities due to its high oscillator strength and tunable resonance. Using white light reflection spectroscopy, we demonstrate tunable ultrastrong coupling of light to the SQ thin film in an open cavity at room temperature [2], which we support by transfer matrix calculations. In ongoing experiments, we introduce structured photonic lattices to the open cavity to investigate the coupling of the polaritons to tailored potential landscapes.

[1] M. Schulz, et al., Nat Commun 9, 2413 (2018).

[2] L. Lackner, et al., Nat Commun 12, 4933 (2021).

HL 28.8 Thu 11:30 H34

Exploring the Device Physics of Photomultiplication in Organic Photodetectors — •LOUIS CONRAD WINKLER, JONAS KUBLITSKI, JOHANNES BENDUHN, and KARL LEO — TU Dresden, Germany

Recently, photomultiplication (PM) in organic photodetectors has been achieved, but working mechanism and physics are not fully understood. Contrary to inorganic photodiodes, impact ionization and avalanche breakdown cannot be achieved in organic semiconductors. Instead, the accumulation of one charge carrier type close to an electrode leads to a strong energy level bending, which increases the tunnelling probability of the opposite charge carrier type under reverse bias from the metal contact into the device. In this contribution, we investigate the well-known donor-acceptor system ZnPc:C60, using the acceptor as an electron trapping state to inject holes into the donor phase. Since the effective electron mobility is strongly decreased, we investigate whether shifting the generation location influences the device operation, e.g. the response speed and external quantum efficiency. Furthermore, a gradient donor-acceptor mixing ratio is introduced to increase both response speed and free charge carrier generation efficiency via an enlarged donor-acceptor interface. We also investigate the effect of trapping time being larger than the carrier transit time, leading to reduced cut-off frequencies.

HL 29: 2D Materials: Graphene

Time: Thursday 9:30–11:00

Location: H36

HL 29.1 Thu 9:30 H36

Twist angle engineering of proximity exchange in graphene/Cr₂Ge₂Te₆ bilayers — •KLAUS ZOLLNER and JAROSLAV FABIAN — Institute for Theoretical Physics, University of Regensburg, 93053 Regensburg, Germany

Van der Waals heterostructures composed of twisted monolayers promise great tunability of electronic, optical, and magnetic properties. The most prominent example is twisted bilayer graphene, exhibiting magnetism and superconductivity due to strong correlations [1]. In addition, twistronics has already demonstrated its potential in tuning proximity spin-orbit coupling in graphene/TMDC heterostructures [2]. In this talk, we present the twist-angle and gate depen-

dence of the proximity exchange coupling in graphene/Cr₂Ge₂Te₆ bilayers from first principles [3]. The proximitized Dirac band dispersions of graphene show a continuous tunability of the ferromagnetic exchange from 4 to -4 meV, when twisting from 0° to 30°. Remarkably, at 19.1° the induced exchange coupling becomes even antiferromagnetic. Further tuning is provided by a transverse electric field and the interlayer distance.

This work was supported by DFG SFB 1277, DFG SPP 2244, and the EU Horizon 2020 Research and Innovation Program (Graphene Flagship).

[1] X. Lu et al., Nature 574, 653 (2019). [2] T. Naimer et al., Phys. Rev. B 104, 195156 (2021). [3] K. Zollner and J. Fabian, arXiv:2108.03984 (2021).

HL 29.2 Thu 9:45 H36

Direct observation of ultraclean tunable band gaps in bilayer graphene — •EIKE THOMAS ICKING^{1,2}, LUCA BANSZERUS^{1,2}, PHILIPP SCHMIDT^{1,2}, CORINNE STEINER^{1,2}, FREDRIKE WÖRTCHE¹, FRANK VOLMER¹, STEPHAN ENGELS^{1,2}, JONAS HESSELMANN¹, MATTHIAS GOLDSCHÉ^{1,2}, KENJI WATANABE³, TAKASHI TANIGUCHI⁴, CHRISTIAN VOLK^{1,2}, BERND BESCHOTEN¹, and CHRISTOPH STAMPFER^{1,2} — ¹RWTH Aachen University, Germany — ²Forschungszentrum Jülich, Germany — ³Research Center for Functional Material, Japan — ⁴International Center for Materials Nanoarchitectonics, Japan

Control over the charge carrier density and the band gap size of a semiconductor paves the way for a wide range of applications, such as highly-tunable transistors, photodetectors, and lasers. Bernal-stacked bilayer graphene (BLG) allows tuning the band gap by an out-of-plane electric displacement field. The first evidence of this unique band gap tunability was found ten years ago, but it took until recently to fabricate sufficiently clean heterostructures to use the band gap to suppress electric current or confine charge carriers. We present a detailed study of the tunable band gap in gated BLG characterized by temperature-activated transport and finite-bias spectroscopy measurements. The latter method allows comparing different gate materials and device technologies that directly affect the effective disorder potential. We show that in graphite-gated BLG there are as good as no sub-gap states resulting in ultraclean band gaps with values in good agreement with theory, allowing to achieve band gaps up to 120 meV.

HL 29.3 Thu 10:00 H36

Domain determination of rhombohedral multilayer graphene devices for magnetotransport measurements — •CHRISTIAN ECKEL, ANNA SEILER, FRANCESCA FALORSI, NIKLAS KOHLRAUTZ, and THOMAS WEITZ — 1. Physikalisches Institut, Universität Göttingen, Friedrich-Hund Platz 1 37077 Göttingen

Graphene as the most prominent example of a 2D-material exhibits relatively different electronic band properties compared to its bulk counterpart. For monolayer, bi-layer or tri-layer the electronic properties have already been explored by multiple groups in the past. However, studies on higher layer number rhombohedral graphene (5 layers in this work) with respect to magnetoelectrical transport measurement are still pending. Finding and determining the rhombohedral domains in mechanically exfoliated flakes is the first bottleneck in the fabrication procedure. Raman spectroscopy is a well-established technique for layer number determination but often lacks a high lateral resolution. Kelvin-probe-force-microscopy (KPFM) allows a lateral resolution of the domains where the different stackings exhibit a distinguishable 15meV work function difference. Additionally, a cryogenic scanning near field optical microscopy (Cryo-SNOM) allows to depict the domains in a temperature dependent manner. The combination of all measurements will be discussed on the poster. A second challenge is the fabrication process of high quality devices for magnetotransport measurements in the milli Kelvin regime. Therefore, encapsulation in hexagonal Boron Nitride (hBN) together with graphite contacts and gates are necessary.

HL 29.4 Thu 10:15 H36

All-optical modulation of third harmonic generation in graphene — •OMID GHAEBI¹, SEBASTIAN KLIMMER¹, HABIB ROSTAMI², and GIANCARLO SOAVI¹ — ¹Institute of Solid-State Physics, Friedrich Schiller University, Jena, Germany — ²Nordita, KTH Royal Institute of Technology and Stockholm University, Sweden

Graphene is a unique platform for non-linear optics thanks to its linear band dispersion that allows gate tunable resonant light-matter interactions [1]. While the gate tunability of THG have been investigated in recent years [1], less is known about the possibility to realize all-optical nonlinear modulators, which could provide higher modulation speed (THz) compared to electrical modulators (GHz) [2]. In this work, we show all-optical TH modulation in graphene at

different values of the Fermi level and with a modulation depth up to 85%. First, we demonstrate that it is possible to actively control the THG recombination dynamics by tuning the graphene Fermi level. This is due to phase-space filling and quenching of the scattering between hot electrons and optical phonons [3]. In addition, we reveal the interplay between TH modulation due to increase in the electronic temperature and due to Pauli blocking at different values of the Fermi level. This work offers new insights for the understanding of TH all-optical modulation and thus for the realization of ultrafast frequency converters and nonlinear modulators. [1] Soavi, G. et al. *Nature Nanotechnology* 13, 583-588 (2018). [2] Cheng, Y. et al. *Nano Letters* 20, 8053-8058 (2020). [3] Pogna, E. A. et al. *ACS Nano* 15, 11285-11295 (2021).

HL 29.5 Thu 10:30 H36

Anisotropic transport in 1D graphene superlattices — •JULIA AMANN¹, KENJI WATANABE², TAKASHI TANIGUCHI², DIETER WEISS¹, and JONATHAN EROMS¹ — ¹Institute of Experimental and Applied Physics, University of Regensburg, Regensburg, Germany — ²National Institute for Materials Science, Tsukuba, Japan

One-dimensional superlattices (1DSL) in graphene were predicted to show intriguing effects, such as anisotropy in transport, additional Dirac points and a distorted Fermi contour. In contrast to two-dimensional graphene superlattices, which have been widely studied, only very few experiments on graphene 1DSLs have been reported. We use a patterned few-layer graphene gate underneath an encapsulated monolayer graphene to create a 1DSL. With the combined action of a global silicon backgate and the patterned bottom gate we are able to control superlattice potential strength and charge carrier density independently. We show low temperature transport measurements on a gate tunable 1DSL in graphene with a period of 50 nm in directions parallel and perpendicular to the modulation as we use an L-shaped Hall bar. The typical Dirac cone shape gets distorted, and we observe anisotropic transport in x and y direction. We observe the emergence of multiple Dirac points in modulation direction due to band flattening with increasing superlattice potential. These extra Dirac points are represented as additional Landau fans in magnetotransport. Further, Weiss oscillations can be observed which confirm the 1D superlattice modulation and the anisotropy.

HL 29.6 Thu 10:45 H36

Topological Phenomena in Self Assembled Folded Graphene — •LINA BOCKHORN¹, SUNG JU HONG², BEI ZHENG¹, JOHANNES C. RODE¹, and ROLF J. HAUG¹ — ¹Institut für Festkörperphysik, Leibniz Universität Hannover, 30167 Hannover, Germany — ²Division of Science Education, Kangwon National University, Chuncheon, 24341, Republic of Korea

The stacking- and folding angle of 2D materials to 3D structures has emerged as an important, novel tuning parameter for the tailoring of optical, mechanical, electronic and magnetic properties. Here, we investigate the final interlayer configurations of self-assembled folded graphene structures generated via atomic force microscopy technique [1, 2] and its electronic properties [3, 4].

Self-assembled folded graphene shows not only the typical electronic properties of twisted graphene layers but also phenomena due to the folded region [3, 4]. In our magnetotransport measurements, we observe e.g. an additional peak next to the charge neutrality peak which is independent of the magnetic field. This peak at a certain charge carrier density is attributed to the compressive strain due the folded edge [3].

[1] J. C. Rode et al., *2D Mater.* 6, 015021 (2018)[2] L. Bockhorn et al., *Appl. Phys. Lett.* 118, 173101 (2021)[3] S. J. Hong et al., *2D Materials*, 8, 045009 (2021)[4] S. J. Hong et al., *Phys. Rev. B*, 105, 205404 (2022)

HL 30: Poster 2

Topics:

- Materials and devices for quantum technology
- Nitrides: Devices
- Nitrides: Preparation and characterization
- Oxide semiconductors
- Perovskite and photovoltaics
- Ultra-fast phenomena

Time: Thursday 11:00–13:00

Location: P3

HL 30.1 Thu 11:00 P3

NV⁻ center in the vicinity of linear defects in diamond — •REYHANEH GHASSEMIZADEH¹, WOLFGANG KRÖRNER¹, DANIEL URBAN¹, and CHRISTIAN ELSÄSSER^{1,2} — ¹Fraunhofer Institute for Mechanics of Materials IWM, Wöhlerstr. 11, 79108 Freiburg, Germany — ²University of Freiburg, Freiburg Materials Research Center (FMF), Stefan-Meier-Straße 21, 79104 Freiburg, Germany

The NV⁻ center is a point-defect complex in the diamond crystal with an excellent potential for implementing qubits in future quantum computing hardware. However, the structuring of point defects on the atomic scale remains an experimental challenge. Here we study theoretically the interaction between dislocations and the NV⁻ center. We evaluate to which extent dislocation lines that are naturally present in the diamond crystal may be used for structuring NV⁻ center as a first step towards a NV-based quantum register. Using density functional theory (DFT) we model NV⁻ centers in the vicinity of the most common dislocations in diamond and calculate the defect formation energy, structural geometry, defect levels and zero-field (ZFS) parameters. Our simulations reveal that dislocations potentially trap the NV⁻ with an energy release of up to 3 eV. Although the analysis of geometry, defect levels and ZFS parameters of NV⁻ centers being close to dislocations in general show strong deviations from their values in the perfect bulk structure, the lowest energy configuration of a NV⁻ center at the reconstructed dislocation cores have ZFS values with less than 5% deviation from their NV⁻ bulk values. Our results opens new insights for the design of NV-based quantum computing devices.

HL 30.2 Thu 11:00 P3

Quantifying Quantum Coherence in Polariton Condensates — •CAROLIN LÜDERS¹, MATTHIAS PUKROP², ELENA ROZAS¹, CHRISTIAN SCHNEIDER³, SVEN HÖFLING⁴, JAN SPERLING⁵, STEFAN SCHUMACHER^{2,6}, and MARC ASSMANN¹ — ¹Experimentelle Physik 2, TU Dortmund, Germany — ²Department of Physics and Center for Optoelectronics and Photonics Paderborn (CeOPP), Universität Paderborn, Germany — ³Institute of Physics, University of Oldenburg, Germany — ⁴Technische Physik, Physikalisches Institut und Würzburg-Dresden Cluster of Excellence ct.qmat, Universität Würzburg, Germany — ⁵Integrated Quantum Optics Group, Institute for Photonic Quantum Systems (PhoQS), Paderborn University, Germany — ⁶Wyant College of Optical Sciences, University of Arizona, USA

We theoretically and experimentally investigate quantum features of an interacting light-matter system from a multidisciplinary perspective, unifying approaches from semiconductor physics, quantum optics, and quantum information science. As an example of a hybrid light-matter interface, we drive a polariton microcavity across the condensation threshold and observe the transition from an incoherent thermal state to a coherent state in the emission. By analyzing the phase-space distributions of the emitted light, we quantify the amount of quantum coherence that results from the quantum superposition of Fock states, constituting a measure of the resourcefulness of the produced state for modern quantum protocols.[1]

[1] C. Lüders et al., PRX Quantum 2, 030320 (2021)

HL 30.3 Thu 11:00 P3

Machine Learning enhanced in-situ electron beam lithography of photonic nano-structures — •JAN DONGES, MARVIN SCHLISCHKA, CHING-WEN SHIH, MONICA PENDERLA, IMAD LIMAME, JOHANNES SCHALL, LUCAS RICKERT, SVEN RODT, and STEPHAN REITZENSTEIN — Technische Universität Berlin, Hardenbergstr. 36, 10623 Berlin, Germany

The unique in-situ electron beam lithography (iEBL) nanotechnology concept enables us to embed single quantum emitters into photonic nano-structures with a 34nm precision. To obtain the fitted position of the quantum emitter with high accuracy, the signal-to-noise ratio of their catholuminescence (CL) needs to be well above unity even for ms integration times. Here we show that for samples with dark quantum emitters, such as telecom quantum dots or low planar photon-extraction efficiency, machine learning (ML) is very well suited to drastically improve the performance of iEBL at low CL intensities. The machine learning software utilizes computer algorithms, which were trained through data samples to denoise data with a barely visible quantum dot emission. We present

experimental results for InGaAs quantum dots, which could be successfully embedded into circular Bragg grating structures with the assistance of machine learning. Our experimental results yield that by using ML, the CL sensitivity and the alignment accuracy could be increased by more than an order of magnitude compared to standard iEBL.

HL 30.4 Thu 11:00 P3

Photon propagation between quasinormal mode cavities — •ROBERT FUCHS, SEBASTIAN FRANKE, ANDREAS KNORR, and MARTEN RICHTER — Technische Universität Berlin, Berlin, Germany

Quasinormal modes (QNMs) provide a useful and intuitive way to define modes for open cavities. They have been utilized for a variety of problems both in classical electrodynamics, and recently used in a fully quantized description for three dimensional geometries.

We show that a multi-cavity extension of the QNM quantization is possible if the cavities are far away from each other so that retardation effects are important. However, this quantization approach leads to a set of non-bosonic operators with a continuous spectrum. In the multi-cavity theory, this continuum serves as a bath which can be used to describe photon propagation between the separately quantized cavities.

Using a fourth-order Nakajima-Zwanzig equation, we point out how to get equations of motion for the system density matrix that include dissipation as well as inter-cavity transfer terms with significant retardation delays described by microscopic QNM parameters.

HL 30.5 Thu 11:00 P3

Sionludi - A table-top dilution refrigerator — •VIKTOR ADAM, ALEXANDER ZILZ, and WOLFGANG WERNSDORFER — KIT, Wolfgang-Gaede-Str. 1, 76131 Karlsruhe

Dilution cryostats are the only technology that provides continuous cooling performance from room temperature down to several mK. These devices utilize the endothermic process of diluting liquid He³ into liquid He⁴, which occurs even at 0 K. By evaporating He³ from this mixture and returning it to the mixing chamber, the refrigerator can be operated continuously.

The Sionludi dilution refrigerator is a unique platform for low-temperature research. The table-top design combined with its small dimensions of approximately 25 cm in diameter and 50 cm in height allow for comfortable mounting of experiments and periphery to the cryostat. The key advancement of this cryostat is the fast injection line, which allows direct cooling of the dilution stage of the cryostat by the circulation of 4 K cold mixture during precooling without affecting the operation at lowest temperatures. As a result, the Sionludi features fast cool-down and warm-up times of less than 3 and 1.5 hours, respectively, while providing cooling powers of up to 200 μ W at 100 mK as well as base temperatures of below 20 mK. The fast turnaround time can accelerate sample throughput and thus progress in many research applications such as quantum sensing or quantum computing.

HL 30.6 Thu 11:00 P3

Telecom-band single photons from functionalized carbon nanotubes coupled to an open cavity — •LUKAS HUSEL¹, JULIAN TRAPP¹, XIAOJIAN WU², MANUEL NUTZ³, THOMAS HÜMMER³, YUHUANG WANG², DAVID HUNGER⁴, and ALEXANDER HÖGELE^{1,5} — ¹Ludwig-Maximilians-Universität, 80539 München — ²University of Maryland, 20742 Maryland, USA — ³Qlibri GmbH, 80337 München — ⁴Karlsruher Institut für Technologie, 76131 Karlsruhe — ⁵Munich Center for Quantum Science and Technology, 80799 München

Quantum light at telecom wavelengths is of fundamental relevance in science and technology. A promising room temperature source of telecom single photons are functionalized carbon nanotubes (CNTs). In this system, dephasing and spectral diffusion limit spectral purity and indistinguishability of the generated photons, which can in principle be overcome by coupling the emitters to a cavity. Here, we demonstrate spectrally narrow single photon emission at wavelengths around 1460 nm from single CNT defects coupled to a fiber-based Fabry-Pérot resonator. We operate the cavity at ambient conditions and in the regime of low Purcell enhancement. By changing the cavity length, we tune the

emission wavelength over a range of tens of nm, and the power spectral density by a factor of six. The coherence time of the generated photons matches the cavity linewidth, which constitutes an increase compared to the expected dephasing-limited free-space linewidth. Our results represent a step towards CNT-based sources of telecom-band single photons with high purity and indistinguishability.

HL 30.7 Thu 11:00 P3

Bright Electrically Controllable Quantum-Dot-Molecule Devices Fabricated by In Situ Electron-Beam Lithography — •JOHANNES SCHALL¹, MARIELLE DECONINCK¹, NIKOLAI BART², MATTHIAS FLORIAN³, MARTIN VON HELVERSEN¹, CHRISTIAN DANGEL⁴, RONNY SCHMIDT¹, LUCAS BREMER¹, FREDERIK BOPP⁴, ISABELL HÜLLEN³, CHRISTOPHER GIES³, DIRK REUTER⁵, ANDREAS D. WIECK², SVEN RODT¹, JONATHAN J. FINLEY⁴, FRANK JAHNKE³, ARNE LUDWIG², and STEPHAN REITZENSTEIN¹ — ¹IFKP, TU Berlin, Germany — ²LS AFP, Ruhr-Universität Bochum, Germany — ³ITP, University of Bremen, Germany — ⁴WSI, TU München, Germany — ⁵Department Physik, Universität Paderborn, Germany

In quantum repeater networks it is of central importance to temporarily store and retrieve quantum information. Concepts based on quantum dot molecules (QDMs) promise storage times in excess of 1 ms. To make use of QDM based quantum memories, efficient coupling to flying qubits needs to be realized while maintaining precise electrical control. We report on the development of electrically tunable single-QDM devices with strongly enhanced broadband photon extraction efficiency. The quantum devices are based on stacked quantum dots in a pin-diode structure underneath a deterministically defined circular Bragg grating using in situ electron beam lithography. We determine the photon extraction efficiency, demonstrate bias voltage dependent spectroscopy and measure excellent single-photon emission properties. The metrics make the developed QDM device an attractive building block for use in future photonic quantum networks.

HL 30.8 Thu 11:00 P3

Machine Learning-Based Optimization of Chiral Photonic Nanostructures: Evolution- and Neural Network-Based Designs — •OLIVER MEY¹, •MANAN SHAH², and ARASH RAHIMI-IMAN² — ¹Fraunhofer IIS/EAS, Fraunhofer Institute for Integrated Circuits, Division Engineering of Adaptive Systems, Dresden — ²1. Physikalisches Institut und Zentrum für Materialwissenschaften, Justus-Liebig Universität Gießen, D-35392, Germany

Machine learning (ML) techniques such as deep learning (DL) and evolutionary algorithms (EA) exhibit unprecedented capabilities in the scientific ML realm. DL uses artificial neural networks to infer unintuitive solutions for complicated design requirements and specific functionalities. Likewise, the EA attempts to find the optimized solution by utilizing principles such as mutation of parameters and extinction of less promising solutions. These approaches are faster and more effective in the inference of nanostructure design parameters for desired properties, such as wavelength coverage and peculiar response functions, compared to conventional numeric simulations.

We present a nano-patterned GaP dielectric substrate that favors single-handed circularly polarized light (CPL) in reflection or transmission [1]. The optimization in chiral dichroism (CD) by neural networks is compared with the evolutionary algorithm. The increased CD in simulated spectra for designs with stronger reflectivity of right CPL and lower transmissivity of left CPL makes the ML techniques effective to optimize a myriad of properties for metamaterials and photonic nanostructures. [1] Phys. Status Solidi RRL 2022, 16, 2100571.

HL 30.9 Thu 11:00 P3

Strain-tunable GaAs quantum dot-based circular Bragg gratings towards entangled photon pairs with high indistinguishability — •CHENXI MA¹, JINGZHONG YANG¹, CONSTANTIN SCHMIDT¹, XIN CAO¹, YITENG ZHANG¹, MAXIMILIAN HELLER¹, JÜRGEN BECKER², EDDY P. RUGERAMIGABO¹, MICHAEL ZOPP¹, and FEI DING^{1,3} — ¹Institut für Festkörperphysik, Leibniz Universität Hannover, Hannover, Germany — ²Institut für Mikroproduktionstechnik, Leibniz Universität Hannover, Garbsen, Germany — ³Laboratorium für Nano- und Quantenengineering, Leibniz Universität Hannover, Hannover, Germany

The on-demand generation of bright entangled photon pairs is an attractive goal for the realization of quantum communication networks. Epitaxial GaAs quantum dots (QDs), grown via local droplet etching and nanohole infilling, are promising candidates because they are symmetric and strain-free. This leads to small exciton fine structures and high entanglement fidelities of photons emitted from the biexciton-exciton cascade. However, the photon indistinguishability is intrinsically limited in this scheme. GaAs QDs also suffer from inefficient photon extraction, which was addressed by embedding QDs in circular Bragg gratings. Here, we propose to engineer the cavity mode to match the biexciton transition with the assistance of strain-tuning techniques. The resulting asymmetric Purcell enhancement will increase the decay rate of the biexciton transition and consequently improve the photon indistinguishability. This heterogeneous photonic nanostructure can serve as a blueprint for future quantum communication devices.

HL 30.10 Thu 11:00 P3

GaAs heterostructures for coupling of spin qubits to self-assembled quantum dots — •SELMA DELIĆ^{1,2}, PRIYABRATA MUDI^{1,2}, SEBASTIAN KINDEL², PAOLA ATKINSON³, DETLEV GRÜTZMACHER¹, and BEATA KARDYNAL^{1,2} — ¹Peter Grünberg Institute 9, Forschungszentrum Jülich, 52425 Jülich, Germany — ²Department of Physics, RWTH Aachen University, 52074 Aachen, Germany — ³Institut des Nano Sciences de Paris, CNRS UMR 7588, Sorbonne Université, 75005 Paris, France

Operation of quantum networks relies on encoding qubits on photons. These photons can be converted into spin qubits in many material systems. Yet, in order to take full advantage of the electrons with information encoded in their spins, the spin qubits should be scalable or the spin should be transferred to spin qubits that can be scaled into quantum processors. Here, we use singlet-triplet (S-T) qubits defined in a GaAs/AlGaAs gate-defined quantum (double-) dot (GDQD) as a scalable qubit. While GaAs is suitable for a qubit exchange with photons due to its direct bandgap, the GDQD does not confine holes. Therefore, we use a GaAs droplet dot (QD) to achieve a coherent transfer of information between a photon and a spin of an electron before the electron is transferred to the S-T qubit. In this contribution, we show the design of heterostructure that can be used to fabricate S-T qubit coupled to epitaxial GaAs QD. We further report on the progress in optical and electrical characterisation of the device in gated structures aligned to the GaAs QD.

HL 30.11 Thu 11:00 P3

GaN/AlGaIn/GaN solution gate field effects transistors as pH- and enzymatic sensors — •GENRIETTA STEINGELB, ALEXANDER HINZ, STEPHAN FIGGE, and MARTIN EICKHOFF — Institute of Solid State Physics, University of Bremen, Otto-Hahn-Allee 1, 28359 Bremen, Germany

A GaN/AlGaIn/AlGaIn-heterostructure solution gate field effect transistors (SGFETs) as pH-sensors will be presented. We discuss the performance of differential sensors realized by one SGFET with passivated gate and one with a bare GaN cap layer as a gate on one chip. The compensation of drift-effects such as like persistent photocurrent and temperature dependence will be discussed.

We have used such devices to study the time-dependent response of covalently immobilized enzymes on the gate surface towards the presence of their specific substrate molecules with acetylcholinesterase and penicillinase as examples.

HL 30.12 Thu 11:00 P3

Impact of GaN barrier thickness on indium incorporation in GaInN/GaN multiple quantum wells grown via MBE — •FAROUK ALJASEM, HEIKO BREMERS, UWE ROSSOW ROSSOW, and ANDREAS HANGLEITER — Institut für Angewandte Physik & Laboratory for Emerging Nanometrology, Technische Universität Braunschweig, Germany

The internal quantum efficiency (IQE) of optical devices based on GaInN is highly sensitive to the thickness of GaInN quantum well. The main way to increase the emission wavelength of GaInN quantum wells is to increase the indium content in the quantum well by enhancing the incorporation rate of indium. We grew fivefold GaInN MQWs at a substrate temperature of 580°C and the GaN barrier layer was grown in two steps. The first step is at the same growth temperature of GaInN quantum wells (580°C), called the low-temperature GaN (LT-GaN) layer and the second step is the high-temperature GaN (HT-GaN), which was grown after the ramping of the substrate temperature up to 725°C. From high-resolution XRD and high-resolution TEM measurements, we found that the thickness of the GaInN wells increased significantly with the increase of the growth time of the LT-GaN layer. The effects of changing the growth time of the LT-GaN layer include changing the indium content of the GaInN well and the thickness of the barrier layer. The analysis of GaInN/GaN MQWs samples using different characterization methods such as HR-XRD, HR-TEM, AFM, and PL provides a detailed understanding of the role of the indium adlayer and its impact on the growth mechanism at low temperatures.

HL 30.13 Thu 11:00 P3

Aging of GaN-based laser diodes investigated by micro-EL and micro-PL spectroscopy — •LUKAS UHLIG¹, CONNY BECHT¹, ERIK FREIER², JI-HYE KANG², VEIT HOFFMANN², CHRISTOPH STRÖLMACKER², SVEN EINFELDT², and ULRICH T. SCHWARZ¹ — ¹Institut für Physik, Technische Universität Chemnitz, 09126 Chemnitz, Germany — ²Ferdinand-Braun-Institut gGmbH, Leibniz-Institut für Höchstfrequenztechnik, 12489 Berlin, Germany

For the work towards long-time reliable GaN-based ridge waveguide laser diodes it is essential to understand the specific degradation effects that occur after some time of operation. Among the reported aging mechanisms are the generation of point defects in the active layer and a decrease in p-side conductivity.

To clarify this, we compare a previously stressed device with a similar but unstressed laser diode using micro-electroluminescence (EL) and confocal micro-photoluminescence (PL) spectroscopy. The devices are mounted p-side-down and the metal layer on the n-side is polished away to allow optical characterization in the plane of the quantum wells.

In contrast to the homogeneous EL-emission from the non-stressed device, the stressed laser diode exhibits bright and dark areas along the ridge on the scale

of few 10 μm . The systematic correlation of high intensity with a spectral blue-shift and vice versa indicates local changes in the charge carrier density that we attribute to inhomogeneous electrical pumping. The micro-PL-measurements show an increased defect density in the active region.

HL 30.14 Thu 11:00 P3

Spectral and temporal behavior of the near field of 10 μm broad area blue laser diodes — •DOMINIC J. KUNZMANN¹, LUKAS UHLIG¹, JANNINA J. TEPASS¹, ANNA KAFAR^{2,3}, SZYMON STANCZYK^{2,3}, PIOTR PERLIN^{2,3}, and ULRICH T. SCHWARZ¹ — ¹University of Technology Chemnitz, 09126 Chemnitz, Germany — ²Institute of High Pressure Physics PAS, Warsaw, Poland — ³TOP-GAN Ltd., Warsaw, Poland

We investigate the near field for the laser diodes driven in pulsed conditions with pulse lengths in the range of a few 10 ns up to 100 ns and currents from 1.5 I_{th} to 4 I_{th} . A streak camera image and a high resolved longitudinal mode spectrum are taken at each point of a near field scan for blue laser diodes with a 10 μm broad ridge.

The combination of the streak camera setup and the high resolution spectrometer allows us to investigate: the spectral-lateral-temporal behavior with complex dynamics due to lateral-longitudinal mode competition, the wavelength shift at the lasing onset and on the other hand to get the longitudinal mode spectrum. Different mode combs are interacting in this longitudinal mode spectrum and the predominating mode comb changes for different parts of the spectrum.

An increasing laser current leads to a broadening of the spectrum as well as to the filling of the gain volume, while for higher currents the lateral distribution seems to be similar across the whole spectrum. Comparing these results to previously measured devices with a 40 μm broad ridge, we observe a less homogeneous near field distribution with a slight systematic asymmetry.

HL 30.15 Thu 11:00 P3

Molecular beam epitaxy of ScGaN on 6H-SiC — •AARON GIESS, FABIAN ULLMANN and STEFAN KRISCHOK — Institut für Mikro und Nanotechnologien, Institut für Physik, TU Ilmenau

Group III-nitrides are well-suited semiconductors for optoelectronic and sensor devices. Among them, Sc-containing nitrides are of recent interest as well. In this contribution we report on our present progress in ScGaN PAMBE growth. We grow ScGaN using plasma-assisted molecular beam epitaxy on Si-faced 6H-SiC. Prior growth the SiC-surface is cleaned by a HF-Dip and a gallium anneal. Compared to GaN growth the implementation of scandium poses significant challenges: (i) ScN inclines to cubic growth and (ii) Gallium tends to form liquid droplets. In order to find optimal growth conditions, parameters such as substrate-temperature and nitrogen as well as Sc and Ga flux have been systematically varied. During growth, reflection high-energy electron diffraction (RHEED) diffraction patterns have been monitored. Further characterization has been performed by X-Ray photoelectron spectroscopy (XPS) and scanning electron microscopy (SEM). In future we plan systematic studies on the electronic properties of high quality epitaxial ScGaN thin films as well as their interaction with molecules.

HL 30.16 Thu 11:00 P3

MOVPE-grown optoelectronic devices with GaN:Mg/GaN:Ge tunnel junctions — •CHRISTOPH BERGER, ARMIN DADGAR, JÜRGEN BLÄSING, GORDON SCHMIDT, HANNES SCHÜRMAN, PETER VEIT, FRANK BERTRAM, JÜRGEN CHRISTEN, and ANDRÉ STRITTMATTER — Otto-von-Guericke-Universität Magdeburg, Deutschland

We report on low resistive GaN-based tunnel junctions (TJ) and TJ optoelectronic devices grown by metalorganic vapor phase epitaxy. Very high donor concentrations, which are mandatory for low-resistive TJs, are achieved by using germanium instead of commonly used silicon. For efficient activation of GaN:Mg, a growth process was developed that includes an in-situ activation step and overgrowth of the p-type GaN with GaN:Ge in nitrogen ambient to prevent the repassivation of the buried p-type layer. Electrical and optical characterization of the fabricated LEDs shows that GaN:Mg is efficiently activated and additional ex-situ activation is expendable. Tunnel-junction LEDs show an improved light output by approximately 20 % in comparison to conventional LEDs with semitransparent contacts and exhibit a comparable differential resistance of $1.2 \times 10^{-2} \Omega \text{cm}^2$ at a current density of 100 Acm^{-2} without voltage penalty. Such tunnel-junctions were implemented in laser diode structures and were used to realize cascaded LEDs with up to three pn-junctions stacked on top of each other. We will present our latest results on the growth, the challenges and the characteristics of these sophisticated optoelectronic devices.

HL 30.17 Thu 11:00 P3

object detection of patterned GaN using convolutional neural networks and synthetic data — •MAHDI KHALILI HEZARJARIBI, UWE ROSSOW, MARKUS ETZKORN, HEIKO BREMERS, and ANDREAS HANGLEITER — Institut für Angewandte Physik, Technische Universität Braunschweig

Employing a practical object detection algorithm, we have developed a process to detect GaN pyramid structures, extracted from SEM images. A procedure has been developed to generate synthetic images for training the algorithm instead of

the drudgery of multiple imaging of samples. These synthetic data include noise, blurring, and other contributing factors in order to realize images that are accurate enough to train an object detection algorithm. A MobileNet algorithm has been employed for the Object detection process. The synthetic database proved pragmatic leading to a promising confidence value of 75% for detecting real objects.

HL 30.18 Thu 11:00 P3

Nominally identical GaInN/GaN single quantum wells : variations of optical and structural properties — •RODRIGO DE VASCONCELOS LOURENCO^{1,2}, MALTE SCHRADER^{1,2}, UWE ROSSOW¹, HEIKO BREMERS^{1,2}, and ANDREAS HANGLEITER^{1,2} — ¹Institute of Applied Physics, Technische Universität Braunschweig, Germany — ²Laboratory for Emerging Nanometrology, Braunschweig, Germany

We have unexpectedly observed differences in luminescence and structural properties in GaInN/GaN single quantum wells (SQW), grown under nominally identical conditions. This may be related to specific growth condition such as variation in substrate temperature or doping level; or substrate characteristics, e.g. bowing and offset; as well as the status of the growth system. The samples were grown in low-pressure metalorganic vapour-phase epitaxy (MOVPE) on c-plane sapphire substrate. The differences in emission wavelength of the SQWs suggest that either there is a discrepancy in In content or in doping level. From the reference multiple quantum wells samples, a variation of 5 % in In concentration was observed. This fluctuation in In content may explain variations in the lattice constants of the SQWs measured by high-resolution X-ray diffraction (HRXRD). We aim to understand how the In content and among other attributes could influence the internal quantum efficiency at room temperature of GaInN/GaN SQWs ranging from 0.6 to 47%.

HL 30.19 Thu 11:00 P3

Skull-melting technique for the crystal growth of high-melting oxides — •DEMIAN RANFTL, KLAUS-DIETER LUTHER, and CORNELIUS KRELLNER — Physikalisches Institut, Goethe-Universität Frankfurt, 60438 Frankfurt/Main, Germany

For growing high melting oxide single crystals a quasi crucible-free induction melting technique can be used. Within a so-called skull-oven a high frequency electric field is applied to a powdered sample. A metallic part in the center of the powder will absorb the field and increase in temperature while also increasing the temperature of the oxides surrounding it. By cooling the outer sections of the sample it is possible to create a melt of a semiconductor in a crucible made out of its own sintered material, thus avoiding integration of unwanted crucible elements and enabling melts even at temperatures where no crucible material exist. This method was developed for the growth of, for example, ZrO_2 crystals with a melting temperature of 2700 °C [1].

In this contribution we will present the working principles of the skull-oven built at the Physikalisches Institut (Goethe Universität, Frankfurt) together with a brief introduction to skull-melting and its features. Additionally, we will present first attempts of the single crystal growth of pure titanium(IV) oxide using this skull-melting technique.

[1] Assmus, W. and Whippey, N. Ueber das Skull-Schmelzen. Chem.-Ing.-Tech. 55, 716-717 (1983).

HL 30.20 Thu 11:00 P3

Investigation into the electric properties of α -Ga₂O₃ based Schottky diodes with various Schottky metals — •S. KÖPP, C. PETERSEN, H. VON WENCKSTERN, and M. GRUNDMANN — Universität Leipzig, Felix Bloch Institute for Solid State Physics, Semiconductor Physics Group, Leipzig, Germany

We present current-voltage measurements of α -Ga₂O₃:Sn based Schottky diodes with various Schottky metals and show on/off current ratios of up to 8 orders of magnitude. We thereby evaluate the effective Schottky barrier height by temperature dependent measurements in the range of 40K up to 400K.

Due to its possible applications in high-power electronics, a great deal of attention has been drawn to the wide bandgap semiconductor Ga₂O₃. In recent years, in addition to the well-researched thermodynamically stable monoclinic polymorph β -Ga₂O₃ the metastable corundum-structured α -phase of Ga₂O₃ has shown to have promising physical properties. With a bandgap of 5.0-5.3 eV [1] and a predicted breakdown field of 8 MV/cm [2] it surpasses the theoretical limits of β -Ga₂O₃ in terms of Baliga's figure of merit [1]. Further, α -Ga₂O₃ is isostructural to α -Al₂O₃ and hence epitaxial growth on cost-efficient sapphire substrates is possible.

[1] Yang, D. *et al.*, El. Mat. Letters 18.2 p. 113-118 (2022)

[2] Higashiwaki, M. *et al.*, Semicond. Sci. Technol, 034001, (2016)

HL 30.21 Thu 11:00 P3

Copper tin oxide: An amorphous ternary oxide with tunable optical and electrical properties — •ARNE JÖRNS, HOLGER VON WENCKSTERN, and MARIUS GRUNDMANN — University of Leipzig, Felix Bloch Institute for Solid State Physics, Semiconductor Physics Group

Due to the mismatching crystal structures of copper oxide (CuO) and stannic oxide (SnO₂) an amorphous alloy can form when these materials are combined. Few reports show that the resulting alloy exhibits *p*-type behavior, but low hole mobility results in unreliable Hall measurements [1]. Nevertheless, optical and electrical properties can be tuned by the alloy composition.

In this work we investigated copper tin oxide thin films deposited by pulsed laser deposition of ceramic CuO and SnO₂ targets at room temperature and in oxygen atmosphere. The resulting samples are highly disordered and *n*-type semiconducting with room temperature mobilities up to 11 cm²V⁻¹s⁻¹. Optical and electrical properties can be tuned in a wide range by varying composition ratio and chamber pressure. Temperature dependent Hall-measurement for different cation contents and a first approach on Schottky diodes will be reported.

[1] P. J. M. Isherwood *et al.*, *J. Appl. Phys.*, **118**, 105702, 2015

HL 30.22 Thu 11:00 P3

Indium oxide metal-semiconductor field-effect transistors — •FABIAN SCHÖPPACH, HOLGER VON WENCKSTERN, and MARIUS GRUNDMANN — Felix Bloch Institute for Solid State Physics, Universität Leipzig, Germany

Indium oxide (In₂O₃) combines promising physical properties such as high carrier mobility and transparency in the visible. However, In₂O₃ is generally challenging to use in active devices. This is mainly due to its tendency to form an electron accumulation layer on its surface (SEAL) which is reported to be caused by surface near oxygen vacancies [1]. Both, compensating Mg doping and oxygen plasma treatment can be used to suppress the SEAL formation [2,3]. Moreover, as a sesquioxide, In₂O₃ is a very robust material that resists classical patterning processes and cannot be patterned by wet chemical processes.

In this work, In₂O₃ films grown by pulsed laser deposition are structured via dry-etching techniques. With that field-effect transistors were fabricated for the first time, reaching on-off ratios of over 5 orders of magnitude and low sub-threshold swings of about 110 mV/dec. For the source and drain contacts, gold was deposited by inert ambient sputtering. Schottky gate diodes were fabricated in a reactive sputtering process, which is a prerequisite for obtaining electrically rectifying contacts to In₂O₃ [4].

[1] KING, *et al.* *Physical Review B* 80.8, 081201 (2009)

[2] SCHMIDT, *et al.* *physica status solidi (b)* 252.10, 2304–2308 (2015)

[3] MICHEL, *et al.* *ACS Appl. Mater. Interf.* 11, 27073–27087 (2019)

[4] VON WENCKSTERN, *et al.* *APL Materials* 2.4, 046104 (2014)

HL 30.23 Thu 11:00 P3

Electrical transport properties of Sn, Si and Ge doped α -Ga₂O₃ — •THORBEN SLOTSCH, CLEMENS PETERSEN, HOLGER VON WENCKSTERN, and MARIUS GRUNDMANN — Universität Leipzig, Felix Bloch Institute for Solid State Physics, Semiconductor Physics Group, Leipzig, Germany

We present Schottky barrier diodes based on PLD-grown α -Ga₂O₃ thin films, doped with the effective mass donors Sn, Si and Ge. By employing temperature dependent current-voltage measurements, Hall-effect measurements and thermal admittance spectroscopy of the space charge region we investigate the electric transport properties of α -Ga₂O₃ in relation to the doping levels provided by the combinatorial PLD method.

Materials with large bandgaps (> 3.4 eV) have attracted scientist's interest more and recently. With its high bandgap of 4.6-5.3 eV Ga₂O₃ is well suited for applications in high-power devices [1]. Numerous studies have already reported on the thermodynamically stable monoclinic β -phase of gallium oxide. However the metastable α -polymorph has gained scientist's attention. Its corundum structure allows α -Ga₂O₃ to form alloys with other corundum-structured materials like α -Al₂O₃ over the whole composition range to tune the bandgap energy up to 8.75 eV [2]. In order to grow α -Ga₂O₃ combinatorial pulsed laser deposition can be employed, which offers the advantage of a precise dopant incorporation and lateral continuous doping gradients [3].

[1] M. Higashiwaki, *apl*, 013504, 2012. [2] A.Hassa, *pss-b*, 2000394, 2020. [3] H. v. Wenckstern, *pss-b*, 1900626, 2020.

HL 30.24 Thu 11:00 P3

Characterization and optimization of MgZnO thin films with steep lateral composition gradient — •LAURENZ THYEN, MAX KNEISS, HOLGER VON WENCKSTERN, and MARIUS GRUNDMANN — Universität Leipzig, Felix-Bloch-Institut für Festkörperphysik, Linnéstraße 5, 04103 Leipzig, Germany

The materials magnesium- and zinc-oxide have been widely investigated in the past. Corresponding step graded ternary alloy thin films of Mg_xZn_{1-x}O have been of great interest [1]. Pulsed laser deposition (PLD) has been used to grow laterally and vertically graded thin films [2]. The precise control of its chemical composition is of great importance for possible applications. Additionally, in the course of miniaturization of electrical devices like wavelength-selective multi-channel UV photodetectors, a well-defined steep slope of the material gradient will be beneficial [3,4].

In this contribution the properties of Mg_xZn_{1-x}O thin films with lateral compositional gradient grown by pulsed laser deposition will be discussed. In order to obtain information about the material composition of the thin films, energy-dispersed X-ray spectroscopy, spatially resolved ellipsometry and micro-

photoluminescence spectroscopy measurements have been conducted. Moreover, steep lateral gradients with a slope of up to 20 % Mg content per millimeter were realised.

[1] Z. Zhang, *et al.* *IEEE Journal Quantum Elec.* 20.6, 106-111, (2014)

[2] H. v. Wenckstern, *et al.* *physica status solidi (b)* 257.7 (2020)

[3] M. Grundmann, *IEEE Transact. Elec. Dev.* 66.1 (2018): 470-477

[4] M. Kneiß, *et al.* *ACS combinatorial science* 20.11 (2018): 643-652.

HL 30.25 Thu 11:00 P3

Characterization of Schottky barrier contacts on a (Mg,Zn)O thin film with lateral composition gradient — •MAURICIO BASSALLO, LAURENZ THYEN, MAX KNEISS, HOLGER VON WENCKSTERN, and MARIUS GRUNDMANN — Universität Leipzig, Felix-Bloch-Institut für Festkörperphysik, Linnéstraße 5, 04103 Leipzig, Germany

A lateral chemical gradient composition structure based on (Mg,Zn)O is a promising material that allows a spectrally resolved detection of UV photons due to a systematic shift of the absorption edge with the position. In that sense, N different photodetectors, fabricated at different positions of the gradient, would be sensitive to specific photon energies [1]. Due to the challenges of stable *p*-type (Mg,Zn)O fabrication with high conductivity and mobility, metal-semiconductor-metal (MSM) structures are preferentially chosen for (Mg,Zn)O-based photodetectors [2]. These consist of two small interdigitated coplanar Schottky contacts, which are 10 μ m wide and 10 μ m apart and whose simplicity in fabrication makes the MSM structure promising for photodetection. In this contribution the electrical properties of the Schottky contacts in such MSM structures are discussed using the current-voltage measurements. Additionally, the influence of the surface characteristics on the contacts are discussed using Atomic Force Microscopy measurements.

[1] M. Grundmann, *IEEE Transact. Electr. Dev.* **2019**, 66, 470.

[2] S. Liang, H. Sheng, Y. Liu, Z. Hou, Y. Lu, and H. Shen, *J. Cryst. Growth* **225**, 110 (2001).

HL 30.26 Thu 11:00 P3

Porosity Analysis of Mesoporous Silicon by SEM Images of Polished Cross Sections — •STEFANIE LAWUNDY^{1,2}, WALDEMAR SCHREIBER¹, and STEFAN JANZ¹ — ¹Fraunhofer ISE, Freiburg i. Br., Germany — ²University of Freiburg, Germany

Porous silicon fabricated by electrochemical etching is a material known for decades with a wide field of applications ranging from photovoltaics to medicine. Nevertheless, the determination of its key property porosity is still an issue that is to be refined.

Especially, the spatially resolved porosity analysis of layered mesoporous silicon stacks are challenging due to the small structures of only about 10 nm. Current measurement techniques as gas adsorption are not appropriate for such structures since they cannot fully penetrate the pores, cannot resolve the porosity profile over layer depth and lead to no information about the pore morphology.

In order to account for these challenges a new approach has been developed. It is based on the analysis of SEM cross section images where contrast and homogeneity are enhanced by a preceding polishing procedure. Pores are defined by using an image processing software and porosity profiles are calculated.

Results of this procedure are assumed to be an important step towards an accurate description of the etching process.

HL 30.27 Thu 11:00 P3

Temperature dependent light beam induced current (LBIC) investigation of PCMO-STNO interfaces — •SOPHIE SCHAIBLE¹, TOBIAS WESTPHAL¹, FELIX MÜLLER¹, STEPHAN MELLES², CHRISTIAN JOOSS², and MICHAEL SEIBT¹ — ¹IV. Physical Institute, University of Goettingen, Göttingen, Germany — ²Institute for Materials Physics, University of Goettingen, Göttingen, Germany

Pn-heterojunctions of calcium doped praseodymium manganite Pr_{0.66}Ca_{0.34}MnO₃ and niobium doped strontium titanate SrTi_{0.998}Nb_{0.002}O₃ (PCMO-STNO) are used as a model system to investigate next generation solar cells going beyond the Shockley-Queisser limit by harvesting hot polaron-type charge carriers. In order to study the photovoltaic response in combination with the temperature and wavelength dependent generation of charge carriers, LBIC is used on a specially grown wedge-shaped PCMO thin film. A position dependent signal is obtained, which translates into the variation of the absorber thickness. PCMO has a perovskite structure and exhibits strong electron-phonon coupling leading to stable polarons. At the charge ordering temperature (*T*_{CO} \approx 230 K) PCMO undergoes a phase transition from the semiconducting paramagnetic to the charge ordered phase [1]. Liquid nitrogen cooling of the LBIC setup enables temperature dependent LBIC measurements below room temperature and thus gives insights into this transition. Comparison with temperature dependent electron beam induced current (EBIC) measurements highlights differences between photon and electron excitation. [1] L. Wu *et al.*, *Phys. Rev. B* 76, 174210 (2007)

HL 30.28 Thu 11:00 P3

Mapping Excitonic and Ionic Dynamics in Lead Halide Perovskite Thin Films — •YENAL YALCINKAYA¹, PASCAL ROHRBECK¹, EMILIA SCHÜTZ², LUKAS SCHMIDT-MENDE², and STEFAN A.L. WEBER¹ — ¹Max Planck Institute for Polymer Research, Ackermannweg 10, 55128 Mainz, Germany — ²Department of Physics, University of Konstanz, Universitätsstr. 10, 78464, Germany

Understanding the dynamics of excitons and ions is crucial for improving the lead halide perovskites and related devices. In this study, we fabricated triple cation lead halide perovskite half cells (ITO/SnO₂/Perovskite) with small and large grain sizes. We obtained nearly 100 μm large grains by heat treating perovskite films under methylamine gas atmosphere. Since the grain boundaries are known to be the main source of defects and ion migration in lead halide perovskites, a certain change between charge carrier and defect behaviour between these two types of films is expected. Therefore, we utilized Time-resolved Kelvin Probe Force Microscopy (Tr-KPFM) for mapping the recombination of free charge carriers and ion migration in triple cation lead halide perovskite films with varying grain sizes. Mapping these excitonic and ionic components of photovoltage allowed us to map the defects within the perovskite films. Our results showed a significant increase in free electron-hole lifetimes in large grained perovskite films. Furthermore, we demonstrate the ion migration was suppressed by having fewer grain boundaries within the film. Our study shows how grain sizes affect the free charge carrier movements and how we can track these changes on nanoscale via KPFM.

HL 30.29 Thu 11:00 P3

The Effects of Residual Lead Iodide on the Stability of Perovskite Solar Cells — •XIONGZHUO JIANG and PETER MÜLLER-BUSCHBAUM — TU München, Physik-Department, Lehrstuhl für Funktionelle Materialien, 85748 Garching, Deutschland

Over the past few years, hybrid organic-inorganic lead halide perovskite materials have attracted tremendous interest as its excellent photovoltaic properties in perovskite solar cells (PSCs) with record power conversion efficiency. The residual lead iodide is easy to form during the fabrication of perovskite layer, especially for the two-step deposition method. In addition, residual lead iodide has been universally used in the state-of-the-art devices to boost the device performance. However, the effects of residual lead iodide on the stability of PSCs has not been fully understood and, therefore, needs to be deeply investigated for further improvement of device performance. Herein, it is shown that residual lead iodide exhibits insufficient stability under continuous light radiation and heating. The photodecomposition products (lead and iodine) of lead iodide pose a threat to the efficiency and stability of devices. Thus, unstable lead iodide under light radiation and heating is one of the main reasons for the degradation of perovskite device. Therefore, carefully controlling or eliminating the residual lead iodide in perovskite film is one of the critical methods to improve the long-term stability of PSCs.

HL 30.30 Thu 11:00 P3

Multi-photon induced ultrafast absorption dynamics of optical excitons in 2D inorganic-organic hybrid semiconductor — •MOHAMMAD ADNAN^{1,2}, RUDOLF BRATSCHITSCH², and GADDAM VIJAYA PRAKASH¹ — ¹Nanophotonics Lab, Department of Physics, Indian Institute of Technology Delhi, Hauz Khas, New Delhi 110016 India — ²Institute of Physics, University of Münster, Wilhelm-Klemm-Straße 10 48149 Münster, Germany

Two-dimensional inorganic-organic (IO) hybrid semiconductors have attracted prodigious attentions due to unique crystal structural packing and tunable exciton characteristics and exhibit strong optical exciton features at room temperature due to their large exciton binding energies (200-250 meV) [1]. These optical excitons are highly sensitive to the layer thickness and demonstrate distinct excitonic behaviors from surface and bulk regions. Multi-photon absorption spectroscopy is a novel probing tool which can monitor excitons from the deeper energy levels [1]. Nonlinear one-photon (3.54 eV), two-photon (1.55 eV) and three-photon (1.21 eV) transient absorption studies have been carried out to have better understanding of hot-carrier relaxations from different lower lying exciton energy levels. Fluence-dependent studies clearly demonstrate various nonlinear effects such as hot phonon bottleneck effect, exciton-exciton annihilation and Auger processes at higher fluences [2]. The results presented here may find interesting applications in developing advanced optoelectronic devices.

1. Adnan et al., *Sci. Rep.*, 2019, 10, 2615.
2. Adnan et al., *J. Phys. Chem. C.*, 2021, 125, 12166.

HL 30.31 Thu 11:00 P3

Electron Beam Induced Current (EBIC) Investigations of Femtosecond Laser Sulfur Hyperdoped Silicon — •MENGROU SUN¹, TOBIAS WESTPHAL¹, SIMON PAULUS², SÖREN SCHÄFER², STEFAN KONTERMANN², and MICHAEL SEIBT¹ — ¹University of Goettingen, IV. Physical Institute, Göttingen, Germany — ²Institute for Microtechnologies (IMTech), University of Applied Sciences Rhein-Main, Rüsselsheim, Germany

S hyperdoped Si formed by fs-laser irradiation improves the absorption of the Si-based optoelectronic devices to infrared wavelengths. A p-n junction is cre-

ated between the B doped p-type Si wafer and the S hyperdoped n-type region produced as a result of fs-laser pulse irradiation of the Si wafer surface under SF₆ atmosphere. The structural and electronic properties of the fs-laser hyperdoped S depend strongly on the laser-processing parameters such as the number of pulses per spot and laser fluence. In this contribution, we focus on S hyperdoped Si fabricated via fs-laser irradiation at 800nm wavelength and various laser processing parameters. Electron Beam Induced Current (EBIC) performed in plan-view and cross-section geometry is used for characterizing the electronic properties of the sample like excess minority carrier diffusion length. Combining EBIC with SEM images, the correlations between electronic properties and the surface textures can be observed. The results of this work show the important role of processing parameters on the surface macro- and microstructure. EBIC data further indicates the different behaviors of the excess carriers within the ridges and the valleys at the surface.

HL 30.32 Thu 11:00 P3

Spin Polarization Dynamics of Photo-excited Carriers in CsPbX₃ Nanocrystals — •AHMET TOSUN, SIMONE STROHMAYER, ANJA BARFÜSSER, QUINTEN AKKERMAN, TUSHAR DEBNATH, AMRITA DEY, and JOCHEN FELDMANN — Chair for Photonics and Optoelectronics, Nano-Institute Munich and Department of Physics, Ludwig-Maximilians-Universität (LMU), Königinstr. 10, 80539 Munich, Germany

We present results on spin relaxation dynamics of photoexcited carriers in CsPbX₃ nanocrystals by employing time-resolved differential transmission spectroscopy. After photoexcitation with circularly polarized light we observe a pronounced spin polarization in CsPbI₃ nanocrystals. This spin-polarization is caused by selectively exciting spin-allowed transitions and is lost during thermalization and cooling of the photoexcited charge carriers. From temperature-dependent experiments we conclude that carrier-spin relaxation in CsPbI₃ nanocrystals is predominantly caused by carrier-LO phonon scattering and can be described by the Elliot-Yafet mechanism.

HL 30.33 Thu 11:00 P3

Characterizing the conductive channels of 2D perovskite field-effect transistors with Kelvin probe force microscopy — •KONSTANTINOS BIDINAKIS, SHUANGLONG WANG, PAUL W.M. BLOM, WOJCIECH PISULA, TOMASZ MARSZALEK, and STEFAN A.L. WEBER — Max Planck Institute for Polymer Research, Ackermannweg 10, 55128 Mainz, Germany

Perovskite-based field-effect transistors (FETs) are a promising class of electronic materials, which also provide a basis for understanding the lateral charge transport within perovskites. Specifically, FETs of 2D perovskite materials exhibit diminished ion migration and improved stability against moisture compared to their 3D counterparts, due to their specific structure. The performance of the transistors is strongly influenced by the nanoscale morphology of the perovskite film. We used Kelvin probe force microscopy (KPFM) to correlate the local morphology and crystallinity with the potential distribution across a bottom-gate top-contact perovskite FET channel under operating conditions. The measured potential distribution from source to drain can indicate unwanted losses, e.g. at grain boundaries or at the electrodes.

In order to increase the crystalline quality of a Sn-based perovskite film, an additive with high Lewis alkalinity is used in the precursor solution, which coordinates with the Sn cation and retards crystallization. Using KPFM, we examined devices with and without such an additive and correlated the measured potential profiles with the charge transport characteristics, as well as ion migration and behavior at the perovskite grain boundaries.

HL 30.34 Thu 11:00 P3

Cross linkable hole transport materials for p-i-n perovskite solar cells — •MOHSEN HOSSEINI FARD, MANUEL NEUBAUER, ERVIN ALJIC, SIMON EWERTOWSKI, SELINA OLTHOF, DIRK HERTEL, and KLAUS MEERHOLZ — Department of Chemistry, University of Cologne, Germany

The use of hole transport materials (HTMs) in perovskite solar cells (PSCs) is indispensable. Many reports illustrate the importance of layer thickness, energy level alignment, doping and mobility of HTMs on PSCs performance. However, there are ambiguities regarding the properties of HTMs, which invoke further fundamental studies. Here, we investigate a series of cross-linkable hole transport materials (x-HTMs), TPD and TAPC derivatives, with different HOMO and LUMO energy positions. The advantage of HOMO and LUMO tunability of the above-mentioned compounds by exchanging molecular substituents is applied to investigate their hole extraction and electron blocking abilities. J-V characterization was used to investigate changes in the device characteristics. Major improvement in fill factor and Voc of MAPbI₃ based solar cells was demonstrated by adjusting the thickness of x-HTMs. As a result, large improvements were observed in power conversion efficiency (PCE). A thin layer application of x-HTMs showed competitive results in PCE performance compared to the commonly used, commercially available materials like PTAA. Nevertheless, the application of a thin layer of QUPD (less than 5 nm) leads to high-efficient PSCs with a shown record PCE up of 19.56% using MAPbI₃ as absorber, similar to the performance of a PTAA-based device.

HL 30.35 Thu 11:00 P3

Effect on Surface Morphology on 1.7eV-GaInAsP-layers on GaAs by surfactant-assisted MOVPE growth — •IVO RAHLFF, PATRICK SCHYGULLA, JENS OHLMANN, and DAVID LACKNER — Fraunhofer ISE, Freiburg i. B., Germany

III-V-compound multi junction solar cells hold record efficiencies since many decades. Recently, we have demonstrated a GaInP(1.9eV)/AlGaAs(1.44eV)//GaInAsP(1.09eV)/GaInAs(0.74eV) 4-junction wafer bonded solar cell that reaches 47.6% under a concentration of 665 suns (AM1.5d). All subcells are epitaxially deposited by MOVPE. To further increase the realistic efficiency potential above 50% a 6-junction device with the following bandgaps (1.94eV/1.71eV/1.42eV//1.19eV/0.98eV/0.74eV) is suggested. One promising candidate for the 1.71eV junction is GaInAsP. The challenge for this material system lies in the compositional regime between 1.60eV and 1.75eV, where phase separation has been reported.

In this work we investigate the effect of surfactant-assisted growth of GaInAsP alloys on the surface morphology during MOVPE growth. It is found that the GaInAsP growth without surfactant leads to severe surface roughening which is believed to be due to the onset of phase separation. XRD measurements revealed further decreasing tensile strain with increasing TMSb/III ratios which is expected, since the surfactant alters the atomic incorporation. Further investigations on the effect of the opto-electrical quality of the surfactant on the GaInAsP 1.7eV material is currently in progress.

HL 30.36 Thu 11:00 P3

Getting started in Perovskite Solar Cells - The little complications that are unmentioned — •MAXIMILIAN SPIES, SIMON BIBERGER, and FABIAN PANZER — University of Bayreuth, Bayreuth, Germany

Due to the current interest in highly efficient perovskite solar cells (PSCs), many groups are attempting to produce such PSCs based on published recipes. Since these recipes often assume a lot of prior knowledge or do not consider environmental conditions in sufficient detail, resulting efficiencies are low. This work shows some of the complications one faces when attempting to build a PSC in n-i-p-structure, considering especially the transport layers. Starting from low single digit power conversion efficiency (PCE), we exceeded PCEs of 12% due to modifications of the production process. We tested different variations of the hole transport layer "on device", including a relatively new approach of solution-based CO₂-doping. With the detrimental factor of humidity to perovskite being known, we show systematically the impact of in-glovebox-processing on PCE and V_{OC}. Further, we found that surface properties of the bottom electrode critically influence the fillfactor.

HL 30.37 Thu 11:00 P3

First-principles study of perovskite/halide interfaces — •SAMUELE SPREAFICO and BERND MEYER — Interdisciplinary Center for Molecular Materials and Computer Chemistry Center, FAU Erlangen-Nürnberg, Germany

Lead halide perovskites are a promising new class of semiconductors, which are easy and cheap to process and show high efficiency in optoelectronic applications. Photovoltaic engineering requires a controlled integration of the photoactive perovskite into a multi-layer heterostructure or quantum dot composite [1]. However, the interfaces in these devices unavoidably affect their optical response, for example the photoluminescence quantum yield. Here we present a density-functional theory investigation on the properties of the interfaces in a composite of CsPbBr₃ quantum dots embedded in a CsBr or NaBr matrix. First we performed a systematic screening of the structure and chemical composition of the interfaces. For the most stable configurations we determined the band alignments and we show how the band offsets at these interfaces depend on the interface structure, which can be tuned by changing synthesis conditions.

[1] B. Chaudhary, Y.K. Kshetri, H.S. Kim, S.W. Lee, T.H. Kim, *Nanotechnology* **32** (2021) 502007

HL 30.38 Thu 11:00 P3

Energy Transfer in Stability-Optimized Perovskite Nanocrystals — •MICHÈLE G. GREINER, ANDREAS SINGLDINGER, NINA HENKE, CAROLA LAMPE, ULRICH LEO, MORITZ GRAMLICH, and ALEXANDER S. URBAN — Nanospectroscopy Group and Center for Nanoscience (CeNS), Nano-Institute Munich, Department of Physics, Ludwig Maximilians University Munich, Koeniginstr. 10, 80539 Munich, Germany

Halide perovskites nanocrystals (NCs) are auspicious materials for low-cost, high efficient photovoltaic and light-emitting devices. Nevertheless, the fast degradation in contact with moisture is one critical issue. Another problem constitutes the inefficient charge transfer between different layers. To counteract both problems, we employ micelles made of diblock copolymers filled with methylammonium lead bromide (MAPbBr₃) NCs. With this approach, we bypass the charge transfer issue by exploiting energy transfer (ET) between CsPbBr₃ nanoplatelets and the MAPbBr₃ micelles. We chose micelles with different diameters to find the best balance between protection and ET efficiency. As a result, we found an increase in stability by around 56% from the smallest to the thickest shell and a transfer efficiency up to 73.6% for the smallest mi-

celle. These findings could help improve different optoelectronic devices, such as perovskite-based solar cells or light-emitting devices.

HL 30.39 Thu 11:00 P3

Probing structural dynamics in optically excited 2D heterostructures by Ultrafast Electron Diffraction — •MASHOOD TARIQ MIR, ARNE UNGEHEUER, AHMED HASSANIEN, LUKAS NÖDING, ARNE SENFTLEBEN, and THOMAS BAUMERT — University of Kassel, 34132 Kassel, Germany

Layered transition metal dichalcogenides (TMDs) host a rich collection of physical properties, opening many different applications with atomically thin films such as sensors, electronic switching, or energy storage. Among those materials, 1T-TaS₂ exhibits a complex phase diagram depending on temperature encompassing charge density waves (CDW) with diverse commensurabilities. New phenomena have been observed and are further expected from combining different materials to 2D heterojunctions. We aim to use femtosecond laser pulses to induce rapid structural changes and probe them with ultrafast electron diffraction (UED). In this work, free-standing single-crystalline heterostructure samples were prepared down to a few nanometre thicknesses to allow electron diffraction in transmission mode. The preparation method was optimized using atomic force microscopy and optical microscopy to isolate atomically thin flakes. In addition, we present an initial UED study of CDW heterostructure (1T-TaS₂ / Graphite). Upon lattice heating, the CDW material undergoes several phase transitions. We focus on the reversible phase transition of 1T-TaS₂ from the nearly commensurate to the incommensurate phase and study the effect of interlayer coupling of stacked 1T-TaS₂ / Graphite heterostructures.

HL 30.40 Thu 11:00 P3

Theory of non-integer high-harmonic generation in a topological surface state — •MAXIMILIAN GRAML¹, MAXIMILIAN NITSCH^{1,2}, ADRIAN SEITH¹, FERDINAND EVERS¹, and JAN WILHELM¹ — ¹Institute of Theoretical Physics, University of Regensburg — ²NanoLund and Solid State Physics, Lund University, Sweden

High-harmonic emission from a topological insulator has been observed recently [1] opening a platform to explore topology and relativistic quantum physics using strong laser fields. Strikingly, the higher order resonance frequencies can be continuously shifted to non-integer multiples of the driving frequency by varying the carrier-envelope phase (CEP) of the driving field. Based on a semiclassical model we explain this finding as a characteristic property of the Dirac dispersion. We complement analytical results with numerical simulations based on the semiconductor Bloch equations.[2]

[1] C.P. Schmid, et al.: Tunable non-integer high-harmonic generation in a topological insulator, *Nature* **593**, 385-390 (2021).

[2] M. Graml, et al.: Theory of non-integer high-harmonic generation in a topological surface state, arXiv:2205.02631 (2022)

HL 30.41 Thu 11:00 P3

Ultrafast spectroscopy of single quantum dots utilizing synchronized GHz-Oscillators — •VALENTIN DICHTL, MICHAEL SEIDEL, GERHARD SCHÄFER, and MARKUS LIPPITZ — Experimental Physics III, University of Bayreuth, Germany

Ultrafast transient absorption or reflection spectroscopy of single semiconductor quantum dots is a well established technique, typically based on laser oscillators with about 80 MHz repetition rate. The excited state lifetime of the emitter is however much shorter than the pulse separation in these experiments. Most of the time one thus waits for the next laser pulse.

Here we present a modified setup based on two synchronized Ti:Sa lasers operating at 1 GHz repetition rate and a line camera with a spectral rate of 127 kHz. Noise suppression is accomplished via double modulation using a field programmable gate array (FPGA) for synchronizing AOMs with the line camera.

We demonstrate the perturbed free induction decay of single AlGaAs quantum dots at temperatures below 20 K. The total integration time is less than three minutes – currently software limited.

HL 30.42 Thu 11:00 P3

Non-linear optimization and error estimation for the dynamical modelling of photoluminescence spectra — •SEBASTIAN BOHM¹, MAX GROSSMANN¹, STEFAN HEYDER¹, KLAUS SCHWARZBURG², PETER KLEINSCHMIDT¹, ERICH RUNGE¹, and THOMAS HANNAPPEL¹ — ¹Fakultät für Mathematik und Naturwissenschaften, Technische Universität Ilmenau, Ehrenbergstraße 29, 98693 Ilmenau — ²Institut Solare Brennstoffe, Helmholtz-Zentrum Berlin für Materialien und Energie, Hahn-Meitner-Platz 1, 14109 Berlin

Modern compute power and improved algorithms allow to determine, e.g., the parameters of a kinetic model of time-resolved photoluminescence spectroscopy (TRPL) via the simultaneous fit of many excitation-dependent TRPL spectra. Since our method is based on a maximum likelihood estimator, we obtain information on the reliability of the derived values as well. As example, we use a TRPL model of M. W. Gerber and R. N. Kleiman [*J. Appl. Phys.* **122**, 095705 (2017), URL 10.1063/1.5001128].

HL 30.43 Thu 11:00 P3

Pulse-driven non-adiabatic tunneling in nanocontacts: quasiclassical approach — SANGWON KIM¹, TOBIAS SCHMUDE², GUIDO BURKARD², and •ANDREY S. MOSKALENKO¹ — ¹KAIST, Daejeon, Korea — ²University of Konstanz, Konstanz, Germany

We develop a general quasiclassical theory for the description of the tunneling through time-dependent barriers induced by ultrashort light pulses and apply it to the tunneling induced by such pulses in nanocontacts [1]. In particular, we analyze the situation when the tunneling is driven by ideal half-cycle pulses. Among the numerous solutions that contribute to the tunneling probability, we choose two main solution branches with the largest contributions: The 1st solution exhibits the "tunneling" behavior of a wave packet whereas the 2nd solution exhibits the "evanescent-wave" behavior. For a large enough intercontact distance, the 1st solution dominates in terms of the tunneling probability. However, for minute distances and small field strengths, when the electron does not manage to escape from the classically forbidden region, the 2nd solution starts to dominate. Finally, we study a situation when the tunneling is driven by realistic few-cycle pulses. We see that the direction of the electron transport in the nanocontacts may be altered in dependence on the carrier-envelope phase of the driving pulse. We also find that the time when the electron effectively emerges from under the barrier does not necessarily exactly coincide with one of the peaks of the driving electric field.

[1] Sangwon Kim et al., *New J. Phys.* 23, 083006 (2021).

HL 30.44 Thu 11:00 P3

Time-resolved broadband transient reflectivity studies in ultrathin bismuth films — •ALEXANDER KASSEN¹, FABIAN THIEMANN¹, GERMÁN SCIAN², and MICHAEL HORN-VON HOEGEN¹ — ¹University of Duisburg-Essen, Lotharstr. 1, 47057 Duisburg, Germany — ²University of Waterloo, 200 University Avenue West, ON N2L 3G1, Canada

Bismuth, through its Peierls-Jones distorted lattice, offers the possibility to excite coherent phonon modes upon irradiation with ultra-short laserpulses. The optical A_{1g} mode at ≈ 3 THz is triggered by the displacive excitation mechanism due to transient changes of the atomic potential energy surface. These changes arise from optical excitation of the electron system and thus lead to a strong coupling between the phonons and charge carriers. The density of excited charge carriers, which depends on the incident fluence and film thickness, alters the equilibrium position of the atoms and softens the potential energy surface, leading to a redshift of the A_{1g} mode. Conversely, in an all optical pump-probe experiment with a measurement of the relative change of reflectivity $\Delta R/R_0$, we utilized the redshift of the A_{1g} mode to determine the level of excitation of the electron system. In the next step, this allowed us to compare the relaxation behavior and transient optical properties of films with different thicknesses leading to a broader insight in the phonon and carrier excitation mechanisms.

HL 30.45 Thu 11:00 P3

Dimensionality Reduction Techniques in Femtosecond Time-Resolved Ellipsometry Data Analysis and Theory — •NOAH STIEHM¹, YIXUAN ZHANG², ERICH RUNGE³, STEFAN KRISCHOK¹, HONGBIN ZHANG², and RÜDIGER SCHMIDT-GRUND¹ — ¹Technische Universität Ilmenau, Fachgebiet Technische Physik I, Weimarer Straße 32, 98693 Ilmenau, Germany — ²Technische Universität Darmstadt, Research Group Theory of Magnetic Materials, Otto-Berndt-Straße 3, 64287 Darmstadt — ³Technische Universität Ilmenau, Fachgebiet Theoretische Physik I, Weimarer Straße 32, 98693 Ilmenau, Germany

Physical modeling and interpretation of the transient dielectric function obtained from femtosecond time-resolved spectroscopic ellipsometry [1] poses a significant challenge, as it consists of many temporally and spectrally overlapping processes that need to be reliably separated to obtain stable and physically meaningful fit results. Ab-initio theory can help to separate these processes, but is not available for the whole time scale (≈ 100 fs to several ns) of the experiment, due to the associated computational costs.

To help overcome these challenges we investigate the use of dimensionality reduction techniques like dynamic mode decomposition and manifold learning methods like locally-linear embeddings and autoencoders to be applied I) in model approximation of the experimental data and II) on ab-initio results from time-dependent density functional theory to cover larger time scales. By this we identify strategies for a reliable modeling pipeline with minimal human intervention.

[1] S. Richter et al., *Rev. Sci. Instrum.* 92, 033104 (2021).

HL 30.46 Thu 11:00 P3

Numerically exact simulations of quantum devices coupled to arbitrary environments using tensor networks — •MORITZ CYGOREK¹, VOLLRATH MARTIN AXT², BRENDON W. LOVETT³, JONATHAN KEELING³, and ERIK M. GAUGER¹ — ¹Heriot-Watt University, Edinburgh, UK — ²Universität Bayreuth, Germany — ³University of St Andrews, UK

Reliable predictions of the dynamics in nanoscale quantum devices with applications in photonics, transport, quantum information and communication require a careful consideration of environment effects. Here, we present the novel

numerical method Automated Compression of Environments (ACE): The open quantum systems dynamics is expressed in terms of a tensor network, where the influence of the environment is incorporated into a matrix product operator in time, the so-called process tensor. ACE provides a direct way to calculate this process tensor numerically exactly with numerical errors originating only from time discretization and matrix product operator compression. As the numerical procedure starts directly from the microscopic Hamiltonian, no problem-specific derivations are required. Thus, as we show on a series of examples, one and the same computer code can be used to simulate the dynamics of open quantum systems with environments as diverse as photons, phonons, electrons, and spins, as well as combinations of multiple environments. This proof of principle demonstrates the tremendous potential of tensor network approaches as one-size-fits-all solutions to open quantum systems dynamics.

HL 30.47 Thu 11:00 P3

Transient negative thermal expansion in HgTe/CdTe heterostructures by heating of transverse phonons — •MATTHIAS RÖSSLE¹, MARC HERZOG², JAN PUDELL^{1,3}, WOLFRAM LEITENBERGER², MAXIMILIAN MATTERN², LUKAS LUNCZER⁴, CLAUS SCHUMACHER⁴, HARTMUT BUHMANN⁴, LAURENS MOLENKAMP⁴, and MATIAS BARGHEER^{1,2} — ¹Helmholtz-Zentrum Berlin, Germany — ²Institut für Physik und Astronomie, Universität Potsdam, Germany — ³European XFEL Facility GmbH, Schenefeld, Germany — ⁴Physikalisches Institut EP3, Universität Würzburg, Germany

We investigate the transient negative thermal expansion of semimetallic HgTe and semiconducting CdTe by using synchrotron-based time-resolved X-ray diffraction. At $T = 20$ K, far below the Debye temperature of both materials, the selective optical excitation of the HgTe top layer with an ultrashort near-infrared laser pulse leads to a rapid expansion of HgTe that is followed by a long lasting contraction. The CdTe substrate is compressed by the HgTe thin film expansion, and subsequently CdTe contracts due to thermally excited transverse phonon modes. This shows that negative thermal expansion is manifest on ultrafast timescales, consistent with the negative Grüneisen coefficient for transverse phonons in semiconducting materials with sphalerite crystal structure. At $T = 200$ K, far above the Debye temperature of both materials, the expansion driven by longitudinal acoustic phonons is prevalent. We simulate the lattice dynamics in an elastic model where transient thermal stresses are calculated via heat diffusion based on equilibrium thermoacoustic properties.

HL 30.48 Thu 11:00 P3

Resonant and phonon-assisted ultrafast coherent control of a single hBN color center — •DANIEL GROLL¹, JOHANN A. PREUSS², ROBERT SCHMIDT², THILO HAHN¹, PAWEŁ MACHNIKOWSKI³, RUDOLF BRATSCHITSCH², TILMANN KUHN¹, STEFFEN MICHAELIS DE VASCONCELLOS², and DANIEL WIGGER^{3,4} — ¹Institute of Solid State Theory, University of Münster, Germany — ²Institute of Physics, University of Münster, Germany — ³Department of Theoretical Physics, Wrocław University of Science and Technology, Poland — ⁴School of Physics, Trinity College Dublin, Ireland

For the development of scalable quantum technologies, reliable single-photon emitters in solid state systems are required. In this context, promising candidates are the recently discovered color centers in the van der Waals insulator hBN. These single photon emitters are attracting increasing attention due to their quantum performance at room temperature and wide range of transition energies. Here we report on our recent results on the ultrafast optical coherent state manipulation of a single hBN color center [1]. By combining experiment and theory we achieve a sound understanding of the impact of environment noise and the coupling to phonons on the emitter's coherence. Specifically, we detect the decoherence of optical phonon-assisted transitions, stemming in part from the finite lifetime of these phonons. The creation of acoustic phonons manifests in a rapid decrease of the emitter coherence during their emission and can lead to an ultrafast beat of the coherent control signal.

[1] J. Preuss, D. Groll, et al., *Optica* 9, 522-531 (2022)

HL 30.49 Thu 11:00 P3

Coherent acoustic phonons in a Graphite-hBN heterostructure observed by ultrafast electron diffraction — •ARNE UNGEHEUER¹, NORA BACH², AHMED HASSANIEN¹, MASHOOD MIR¹, LUKAS NÖDING¹, SASCHA SCHÄFER², THOMAS BAUMERT¹, and ARNE SENFTLEBEN¹ — ¹University of Kassel, Institute of Physics, Kassel, Germany — ²University of Oldenburg, Institute of Physics, Oldenburg, Germany

We investigate the dynamics of photoexcited coherent acoustic phonon modes in a graphite-hexagonal boron nitride (hBN) heterostructure. Since the hBN layer is transparent at our excitation central wavelength of 785 nm we assume that the optically induced stress pulse occurs mainly in the graphite layer. Subsequent lattice coupling to the hBN layer depends on the coupling strength at the bilayer interface and determines the nanomechanical resonance frequencies of the system. Observation of specific coherent acoustic phonon modes in the individual layers is interpreted within the framework of ultrafast electron diffraction [1] and experimental results are compared with numerical simulations based on a discrete numerical linear chain model [2].

[1] Gerbig, C., et al. *New Journal of Physics* 17.4 (2015): 043050. [2] Bach, N., and S. Schäfer, *Structural Dynamics* 8.3 (2021): 035101.

HL 30.50 Thu 11:00 P3

Unraveling electron-phonon and exciton-phonon couplings in transition metal dichalcogenides. — •AHMED HASSANIEN, ARNE UNGEHEUER, MASHOOD TARIQ MIR, LUKAS NÖDING, ARNE SENFTLEBEN, and THOMAS BAUMERT — University of Kassel, Institute of Physics and Center for Interdisciplinary Nanostructure Science and Technology (CINSA-T), D - 34132 Kassel, Germany
The observation of coherent phonons following resonant electronic excitation is a clear sign of the coupling between the electronic and the lattice degrees of freedom [1]. Using a highly compact femtosecond electron diffractometer developed in our group [2], we were able to differentiate between the electron-phonon and exciton-phonon couplings in mechanically exfoliated few-layers WSe₂. Based on our results, both free and bound charge carriers couple to the interlayer vibrational modes. Further analysis of our results unveiled the specific modes coupled to either type of charge carrier.

[1] Jeong, Tae Young, et al. *ACS Nano* 10.5 (2016): 5560-5566

[2] Gerbig, C., et al. *New J. Phys.* 17.4 (2015):043050.

HL 30.51 Thu 11:00 P3

Measuring ultrashort electron pulse durations by streaking with free electrons — •LUKAS NÖDING, ARNE UNGEHEUER, AHMED HASSANIEN, MASHOOD TARIQ MIR, ARNE SENFTLEBEN, and THOMAS BAUMERT — Institute of Physics; Experimental Physics III, Kassel University

Ultrafast electron diffraction is a well-known method for time-resolved measurements on molecules and condensed matter. The duration of the electron pulse directly determines the temporal resolution of the UED setup as it works like the shutter speed of a camera. A streaking setup utilizing free electrons is implemented to measure the duration of the electron pulse. For this, a new measurement device was designed. It consists of an aperture and a metal surface behind the aperture, parallel to the path of the electron pulse. A femtosecond laser pulse is focused onto the metal surface. As the beam incides, electrons are released from the metal surface. Because of their momentum at first, they separate from the surface, create an electric field perpendicular to the surface and then recombine. This short-lived electric field is used to streak the electron pulse. The electron pulse at the front of the pulse should experience a different field strength than the electrons at the end. By that the duration of the pulse is mapped into a spatial extension of the pulse. The spatial and temporal overlap for the electron pulse and the laser beam had to be set exactly. The results are shown with their evaluation and compared to simulations.

HL 31: 2D Materials 5 (joint session HL/CPP/DS)

Time: Thursday 11:15–12:15

Location: H36

HL 31.1 Thu 11:15 H36

Generating extreme electric fields in 1 2D materials by dual ionic gating — •BENJAMIN ISAAC WEINTRUB¹, YU-LING HSIEH^{1,2}, JAN N. KIRCHHOF¹, and KIRILL I. BOLOTIN¹ — ¹Department of Physics, Freie Universität Berlin, Berlin, Germany — ²Department of Mechanical Engineering, National Central University, Taoyuan City, Taiwan

We demonstrate a new type of dual gate transistor to induce record electric fields through two-dimensional materials (2DMs). At the heart of this device is a 2DM suspended between two volumes of ionic liquid (IL) with independently controlled potentials. The potential difference between the ILs falls across an ultrathin layer consisting of the 2DM and the electrical double layers above and below it, thereby producing an intense electric field across the 2DM. We determine the field strength via i) electrical transport measurements and ii) direct measurements of electrochemical potentials of the ILs using semiconducting 2DM, WSe₂. The field strength across a bilayer WSe₂ sample reaches ~2.5 V/nm, the largest static electric field through the bulk of any electronic device to date. Additionally, we create electric fields strong enough to close the bandgap of 3-layer and 4-layer WSe₂ (~1.4 V/nm and ~0.9 V/nm respectively). Our approach grants access to previously-inaccessible phenomena occurring in ultrastrong electric fields.

HL 31.2 Thu 11:30 H36

Tip-enhanced Raman spectroscopy combined with other Scanning Probe Microscopy Methods: Focus on 2D Materials — •JANA KALBACOVA — HORIBA Jobin Yvon GmbH, Neuhofstr. 9, Bensheim 64625, Germany

New two dimensional materials are on the rise. After the wonder material graphene, new materials such as MoS₂, MoSe₂, WSe₂ have an intrinsic bandgap and as such are opening new doors for semiconductor applications. Raman spectroscopy offers information on the chemical structure of materials but cannot provide information on the electronic properties such as surface potential or photocurrent of our sample. Co-localized measurements combining scanning probe microscopy (SPM) with Raman spectroscopy can already bring a wealth of information; however, further improvements can be obtained by a tip that will act as an antenna and amplify the Raman signal and thus breaking the diffraction limit in a method called Tip-enhanced Raman spectroscopy (TERS). Typically spatial resolution of 10 - 20 nm can be achieved. In this contribution, we investigate different 2D materials by a combination of TERS, tip-enhanced photoluminescence, Kelvin probe microscopy, and other SPM methods to show very locally for example doping variations or defects that would otherwise go unnoticed with other macro- and microscopic techniques.

HL 31.3 Thu 11:45 H36

Defects in 2D WS₂ monolayers — ASWIN ASAITHAMBI¹, ROLAND KOZUBEK¹, FRANCESCO REALE², ERIK POLLMANN¹, MARCEL ZÖLLNER¹, CECILIA MATTEVI², MARIKA SCHLEBERGER¹, AXEL LORKE¹, and •GÜNTHER PRINZ¹ — ¹Fakultät für Physik und CENIDE, Universität Duisburg-Essen, Germany — ²Department of Materials, Imperial College London, UK

In this presentation, we report about optical characterization and manipulation of defects in tungsten disulfide (WS₂) monolayers. WS₂ is one prominent member of the 2D transition metal dichalcogenides (TMDC). In these materials, defects and adsorbates can easily modify e.g., conductivity, optical properties, or even create single photon emitters. For this study we used high quality WS₂ CVD-grown monolayers to purposely introduce defects via irradiating them with Xe³⁰⁺ ions with different fluences [1]. Low temperature photoluminescence (PL) spectra of these irradiated WS₂ monolayers show two defect related broad bands, beside the excitonic contribution. By exposing these flakes to laser light with powers up to 1.5mW, the intensity of these two PL bands can be reduced. By comparing the intensity of the excitonic contribution before and after this laser processing, we don't observe an increase in intensity, leading us to conclude, that the defects aren't getting healed. If the samples are heated to room temperature, the defect luminescence recovers. To interpret our observation, we suggest that the defects might be attributed to vacancy defects together with adsorbates at different defect sites.

[1] A. Asaithambi et al., *Phys. Status Solidi RRL* 2021, 15, 2000466

HL 31.4 Thu 12:00 H36

Large perpendicular field in bilayer TMD via hybrid molecular gating — •SVIATOSLAV KOVALCHUK¹, ABHIJEET KUMAR¹, SIMON PESSEL¹, KYRYLO GREBEN¹, DOMINIK CHRISTIANSEN², MALTE SELIG², ANDREAS KNORR², and KIRILL BOLOTIN¹ — ¹Department of Physics, Quantum Nanoelectronics of 2D Materials, Freie Universität Berlin, Arnimallee 14, 14195 Berlin, Germany — ²Institut für Theoretische Physik, Nichtlineare Optik und Quantenelektronik, Technische Universität Berlin, Hardenbergstr. 36, 10623 Berlin, Germany

We consider structures in which bilayer TMDs are sandwiched between a layer of molecules and Si gate. We show that these structure allow increasing, by a factor of 2, maximum electric field achievable in this 2D material. This in turn, allows reaching electric field >0.2 V/nm. In MOS₂ this is sufficient to bring interlayer excitons IX into resonance with either A or B intralayer excitons. We study coupling between these excitons, and give an outlook on the new technique to achieve large perpendicular electric fields detectable in optical measurements.

HL 32: Perovskite and Photovoltaics 3 (joint session HL/ CPP/KFM)

Time: Thursday 15:00–16:30

Location: H31

HL 32.1 Thu 15:00 H31

Atomically Thin Sheets of Lead-Free 1D Hybrid Perovskites Feature Tunable White-Light Emission from Self-Trapped Excitons — •PHILIP KLEMENT¹, NATALIE DEHNHARDT², CHUAN-DING DONG³, FLORIAN DOBENER¹, JULIUS WINKLER², SAMUEL BAYLIFF⁴, DETLEV M. HOFMANN¹, PETER J. KLAR¹, STEFAN SCHUMACHER^{3,5}, SANGAM CHATTERJEE¹, and JOHANNA HEINE² — ¹Institute of Experimental Physics I and Center for Materials Research (ZfM), Justus Liebig University Giessen, Giessen, Germany — ²Department of Chemistry and Material Sciences Center, Philipps-Universität Marburg, Marburg, Germany — ³Department of Physics and Center for Optoelectronics and Photonics Paderborn (CeOPP), Paderborn University, Paderborn, Germany — ⁴Department of Chemistry and Biochemistry, University of Oklahoma, Norman, OK, USA — ⁵College of Optical Sciences, The University of Arizona, Tucson, AZ, USA

One of the major current challenges in 2D materials' synthesis is the intentional design of building blocks to introducing superior chemical and physical properties. The limiting factor in this approach is the commonly-believed paradigm that in-plane covalent interactions are strictly necessary to form 2D materials, limiting the number of candidates. Here, we go beyond the paradigm that atomically thin materials require in-plane covalent bonding and report single layers of the one-dimensional organic-inorganic perovskite [C₇H₁₀N]3[BiCl₅]Cl. Its unique 1D-2D structure enables single layers and the formation of self-trapped excitons which show white-light emission.

HL 32.2 Thu 15:15 H31

Multiple spin-flip Raman scattering in bulk lead halide perovskites — •MAREK KARZEL¹, DENNIS KUDLACK¹, NATALIA E. KOPTOVA¹, INA KALITUKHA², MAKSYM V. KOVALENKO³, DMITRI R. YAKOVLEV¹, and MANFRED BAYER¹ — ¹Experimentelle Physik 2, Technische Universität Dortmund, 44227 Dortmund, Germany — ²St. Petersburg, Russia — ³Laboratory of Inorganic Chemistry, ETH Zürich, 8093 Zürich, Switzerland

Lead halide perovskites like FACs are promising competitors for conventional semiconductors in spintronics due to their highly efficient light absorption and emission properties. We study spin-flip Raman scattering (SFRS) of resident carriers and investigate possible carrier exchange interactions. The measurements are performed at low temperatures around 1.6 K and external magnetic fields up to 10 T in Faraday and tilted geometries. This method allows us to observe Raman shifts in high magnetic fields which according to [1] are attributed to the g-factors of resident electrons and holes. The SFRS efficiency significantly increases for resonant probing of the free exciton resonances. We conduct from our measurements, that the creation of the free exciton is the essential requirement for observation of multiple spin-flip Raman scattering.

[1] E. Kirstein et al., Adv. Mater. 34, 2105263 (2022).

HL 32.3 Thu 15:30 H31

Stability Enhancement of perovskite nanoplatelets via crosslinking of ligands — •MAXIMILIAN GRUBER, ULRICH LEO, NINA HENKE, PATRICK GANSWINDT, MICHAEL LICHTENEGGER, CONNOR HEIMIG, and ALEXANDER URBAN — Nanospectroscopy Group and Center for Nanoscience (CeNS), Nano-Institute Munich, Department of Physics, Ludwig-Maximilians-Universität München, Königstr. 10, 80539 Munich, Germany

In recent years lead halide perovskite nanoplatelets (NPL) have attracted a lot of attention due to low-cost production and excellent spectral tuning. Additionally, perovskite NPLs exhibit the benefit of exciton energy tunability via quantum confinement as well as large photoluminescence quantum yield. The high surface to volume ratio of the NPLs, however, makes them susceptible to degradation by water, air and ion migration.

One solution to these issues of degradation investigated here is a process called crosslinking. Hereby the exposure of a film of NPLs to a dose of electron radiation induces intermolecular bonds between the organic ligands attached to the individual nanocrystals, hence forming a protective matrix around a film of pristine perovskite NPLs.

Varying dosages of irradiation of three monolayer CsPbBr₃ NPLs were investigated followed by an exposure to other halides, NPLs with a different halide composition as well as different solvents, showing a drastic increase in stability of the crosslinked compared to untreated NPLs. This enables the possibility of a future application of lead halide perovskite NPLs under ambient conditions.

HL 32.4 Thu 15:45 H31

Enhancing the optical performance of perovskite nanoplatelets — •STEFAN MARTIN¹, CAROLA LAMPE¹, NINA HENKE¹, IOANNIS KOUROUDIS², MILAN HARTH², ALESSIO GAGLIARDI², and ALEXANDER URBAN¹ — ¹LMU Munich, Nanospectroscopy Group — ²TU Munich

Lead halide perovskites have been drawing a lot of interest during the last few years due to their unique properties. Their excellent optical performance combined with easy and cost-efficient production are interesting for both light-emitting devices and solar cells. Perovskite nanoplatelets are furthermore convincing with high photoluminescence quantum yields and narrow emission linewidths tunable from 430 to 505 nm. The thickness of these nanoplatelets can be tuned with a monolayer precision and determines the absorption and emission profile of the sample.

By using different machine learning approaches the synthesis parameters were investigated and optimized based on the emission spectrum. With this method, the emission properties of nanoplatelets with thicknesses reaching from 2 to 8 monolayers were enhanced. Additionally, the emission wavelengths can be fine-tuned using a post-synthetic enhancement treatment comprising a lead halide ligand solution. Depending on the time interval between synthesis and enhancement, a redshift of controllable extent can be introduced while further reducing the emission linewidth. With these strategies, a narrow and symmetric emission peak can be achieved at any desired wavelength. This is particularly interesting for the implementation in optoelectronic devices.

HL 32.5 Thu 16:00 H31

Extensive study on sequential physical vapor deposition of mixed-cation perovskite (Cs,FA)PbI₃ — •KARL HEINZE¹, TOBIAS SCHULZ¹, ROLAND SCHEER¹, and PAUL PISTOR² — ¹Institute of Physics, Martin-Luther-University Halle-Wittenberg, von-Danckelmann-Platz 3, 06120 Halle (Saale), Germany — ²Universidad de Pablo Olivade, Carretera de Utrera 1, 41013, Sevilla, Spain

Sequential deposition via physical vapor deposition (PVD) is underexplored, even though it offers precise adjustment of components and composition and a variety of routes to investigate the optimization of perovskite growth. We combine in situ XRD and in situ laser light scattering to monitor phase evolution of (Cs,FA)PbI₃ during PVD. We study the influence of deposition sequence of the components PbI₂, FAI and CsI on CsFAPbI₃ growth. Noticeably, the sequence strongly influences the orientation of deposited components. Similarly, diffusion before and during annealing as well as resulting alpha phase share depend on the evaporation sequence. When depositing PbI₂ first, conversion to the perovskite phase was not achieved, unless an over stoichiometric share of FAI was deposited. Depositing FAI first and PbI₂ later resulted in a high probability of layer conversion to the perovskite phase without secondary phases being detected. A striking feature during our investigation was the absence of the delta phase during deposition and annealing, seemingly caused solely by the preparation method. We deliver important insight into this poorly investigated preparation path and provide a foundation for further research based on our detailed study of sequence-dependent crystalline growth.

HL 32.6 Thu 16:15 H31

Ultrafast transient spectroscopy of Cu(In,Ga)Se₂ coupled to different buffer layers. — •PIRMIN SCHWEIZER, RICARDO ROJAS-AEDO, ALICE DEBOT, PHILIP DALE, and DANIELE BRIDA — Department of Physics and Materials Science, University of Luxembourg, 162a avenue de la Faïencerie, L-1511 Luxembourg, Luxembourg

The dynamic parameters of photo-induced electron-hole pairs, such as recombination time and charge conductivity, play a major role in the efficiency of photovoltaic devices. Among thin film materials for photovoltaics, one of the most interesting is the p-type Cu(In,Ga)Se₂ alloy (CIGS) on which an n-type buffer layer is deposited, forming the initial part of the device p-n junction. The inter-material transport dynamics strongly depend on how the band structure is affected by the buffer layer, and also on the quality of the CIGS \ buffer layer interface which may contain defects. In our experiments we have compared the ultrafast transient reflectivity on CIGS epitaxially grown on a GaAs substrate. New Cd free buffer layers In₂S₃ and band offset tunable Zn(O,S), are compared to the most commonly used buffer layer, CdS. The transient reflection measurements allows for the extraction of the electronic transport dynamics at the interface with the buffer. This study allows us to draw conclusions about the pair formation capacity mediated by the transport properties between the CIGS and the buffer layer. The results can guide the development of Cd free buffer layers thus reducing the environmental impact caused by CdS in traditional CIGS solar cells.

HL 33: Optical Properties 2

Time: Thursday 15:00–18:00

Location: H32

HL 33.1 Thu 15:00 H32

Implementation of the Bethe-Salpeter Equation using Crystal Symmetries — •JÖRN STÖHLER^{1,2}, DMITRII NABOK¹, STEFAN BLÜGEL¹, and CHRISTOPH FRIEDRICH¹ — ¹Peter Grünberg Institut and Institute for Advanced Simulation, Forschungszentrum Jülich, Germany — ²RWTH Aachen University, Germany

The Bethe-Salpeter equation (BSE) and *GW* approximation are two many-body perturbation theory techniques that together form the state-of-the-art method to include electron-hole interaction in periodic systems. The BSE has proven to be the most accurate tool to compute optical absorption for the valence and core energy region, as well as electron energy loss.

We have implemented the BSE in the SPEX code, a full-potential linearized augmented plane-wave (FLAPW) code that supports Green-function based methods including the *GW* approximation, optical spectra in the random phase approximation, and more. We use crystal symmetries to achieve a significant computational speedup for the construction and diagonalization of an effective electron-hole Hamiltonian in the Tamm-Dancoff approximation, from which we obtain symmetric exciton wavefunctions and energies.

Our code is parallelized and has been tested for various bulk, layered and monolayer semiconductors, among them LiF and MoS₂, and includes spin-orbit coupling. The results agree with available theoretical and experimental spectra from the literature.

HL 33.2 Thu 15:15 H32

The Berry dipole photovoltaic demon and the thermodynamics of photocurrent generation within the optical gap of metals — LI-KUN SHI¹, OLES MATSYSHYN^{2,1}, JUSTIN C. W. SONG², and •INTI SODEMANN VILLADIEGO^{3,1} — ¹Max-Planck-Institut für Physik komplexer Systeme — ²Division of Physics and Applied Physics, Nanyang Technological University, Singapore — ³Institut für Theoretische Physik, Universität Leipzig

Berry phase driven photo-voltaic effects offer novel mechanisms that could allow to engineer a new generation of opto-electronic technologies.

We will show that there is a large class of bulk photovoltaic mechanisms that make possible to produce a net rectified photo-voltaic current even when the impinging radiation has a frequency that resides within the optical gap of the material, in contrast to previous claims. We will describe the thermodynamics of these in-gap rectification effects and show that most of these mechanisms are necessarily accompanied by a small but finite irreversible photon absorption in order for them to be consistent with the laws of thermodynamics. There is, however, one remarkable exception: the intra-band non-linear Hall effect arising from the anomalous velocity induced by the Berry curvature. This non-linear Hall effect allows to have a photovoltaic mechanisms whose maximum allowed efficiency can be 100% for the conversion of circularly polarized light onto electricity. More remarkably, because it is a reversible process, this same mechanism can be conversely used as a highly efficient electrical amplifier of circularly polarized light.

HL 33.3 Thu 15:30 H32

Nonlinear photocurrents induced by terahertz radiation in twisted bilayer graphene — •STEFAN HUBMANN¹, PHILIPP SOUL¹, GIORGIO DI BATTISTA², MARCEL HILD¹, KENJI WATANABE³, TAKASHI TANIGUCHI³, DMITRI EFETOV², and SERGEY GANICHEV¹ — ¹Terahertz Center, University of Regensburg, 93040 Regensburg, Germany — ²ICFO, Castelldefels, Barcelona 08860, Spain — ³National Institute for Materials Science, 1-1 Namiki, Tsukuba 305-0044, Japan

We report on the observation of nonlinear photocurrent and photoconductivity in twisted bilayer graphene (tBLG) with twist angles below 1°. We show that excitation of the tBLG bulk causes a photocurrent, whose sign and magnitude are controlled by the orientation of the radiation electric field and the photon helicity. The developed theory shows that the current is formed by asymmetric scattering in gyrotropic tBLG. For the observed photocurrents, we demonstrate the emergence of pronounced oscillations upon variation of the gate voltage, which correlate with the oscillations of the sample resistance. These photocurrent oscillations originate in interband transitions between a multitude of subbands in tBLG. Furthermore, at higher radiation intensities, we detected a nonlinear intensity dependence of bulk photogalvanic current and photoconductivity. These nonlinear photoresponses are caused by the interplay between interband, inter-subband, and intraband transition. This interplay is controlled by the Fermi level position with respect to the Moiré subbands. We show that the photosignals saturate with rising intensity, while contributions from different transitions differ in their respective saturation behavior.

HL 33.4 Thu 15:45 H32

Dielectric function of CuBr_xI_{1-x} thin films — •E. KRÜGER¹, M. SEIFERT², M. BAR¹, S. MERKER³, P. BISCHOFF¹, H. KRAUTSCHEID³, S. BOTTI², M. GRUNDMANN¹, and C. STURM¹ — ¹Universität Leipzig, Felix-Bloch-Institut für Festkörperphysik, Germany — ²Friedrich-Schiller-Universität Jena, Institut für

Festkörpertheorie und -optik, Germany — ³Universität Leipzig, Institut für Anorganische Chemie, Germany

Copper halides such as CuI and CuBr are promising p-type semiconductors for transparent optoelectronic devices, especially due to the recently proposed hole density tunability [1]. Here, we present the dielectric function of CuBr_xI_{1-x} thin films (0 ≤ x ≤ 1) determined by spectroscopic ellipsometry in the spectral range from 0.7 eV to 6.5 eV at room temperature. The observed features in the dielectric function are attributed to various electronic transitions in the Brillouin zone [2]. Non-monotonic behavior is observed for the band gap energy as a function of alloy composition revealing a quadratic bowing parameter of 0.5 in good agreement with literature [3]. The spin-orbit splitting decreases linearly from 650 meV for CuI to 150 meV for CuBr. The experimental results are compared with DFT-calculated band structures for different alloy compositions. The effects of bond length mismatches, chemical disorder, and different contributions of metal and halogen atoms to the upper valence bands are discussed in detail.

[1] Yamada et al., Adv. Funct. Mater. **30**, 2003096 (2020)[2] Krüger et al., APL **113**, 172102 (2018)[3] M. Cardona, Phys. Rev. **113**, 69 (1963)

HL 33.5 Thu 16:00 H32

Neutralisation of detrimental effects on the Rydberg exciton absorption spectrum — •KATHARINA BRÄGELMANN, MARIAM HARATI, BINOD PANDA, JULIAN HECKÖTTER, and MARC ASSMANN — Experimentelle Physik II, Technische Universität Dortmund, 44225 Dortmund

We report on the neutralisation of charged impurities by excitation of Rydberg excitons with surprisingly small laser powers. Rydberg excitons are highly excited states in Cu₂O with principal quantum numbers of up to $n = 30$ [1] with extensions in μm range. The wellknown theories propose an n^{-3} scaling for both oscillator strengths and linewidths of the excitons. Usually the highest states ($n = 16$ and above) show some deviation from those theories, as oscillator strengths are smaller and linewidths are wider than expected, which leads to an reduced absorption of these states. Those deviation are known to stem from the presence of charged impurities in the material [2]. Here, we show a way to increase the absorption and to minimize the deviations mentioned above. This increase of absorption happens when the system is pumped in an extremely narrow energy region around the band gap (less than 1 meV) with very small powers of only 0.1 – 10 μW . This effect indicates a 'purification' of the illuminated volume as the naturally charged impurities have less detrimental impact on the high excitonic states. This research contributes to a deeper understanding of impurity - exciton interactions.

¹ M. A. M. Versteegh et al., Phys. Rev. B **104**, 245206 (2021).² S. O. Krüger et al., Phys. Rev. B **101** (2020).

15 min. break

HL 33.6 Thu 16:30 H32

Invited Talk Ultrastrong light-matter coupling in materials — •NICLAS S. MUELLER^{1,2}, EDUARDO B. BARROS³, FLORIAN SCHULZ⁴, HOLGER LANGE⁴, and STEPHANIE REICH¹ — ¹Department of Physics, Freie Universität Berlin, Berlin, Germany — ²Present address: NanoPhotonics Centre, Cavendish Laboratory, University of Cambridge, United Kingdom — ³Department of Physics, Universidade Federal do Ceara, Fortaleza, Ceara, Brazil — ⁴Department of Physical Chemistry, University of Hamburg, Hamburg, Germany

Driven by the field of cavity quantum electrodynamics there is an ever-growing quest for systems with extreme light-matter coupling. In the regimes of ultra- and deep strong coupling the coupling strength becomes comparable to the bare excitation energy, leading to exotic phenomena like virtual photons in the ground state and the breakdown of the Purcell effect. Here, we discuss how ultrastrong coupling is systematically achieved in materials, without the need for external cavities. We introduce densely packed supercrystals of gold nanoparticles as an artificial material where the coupling strength can be tuned from ultra- to deep strong coupling. Using a unified theory of dipole-active material excitations, we show that light-matter coupling gets maximized in three-dimensional materials, setting an upper limit for the coupling strength in cavities. From a large set of experimental data, we identify phonons in ferroelectrics, excitons in molecular crystals, and plasmons in metallic supercrystals as excitations where light-matter coupling is so strong that it affects the material ground state, eventually leading to phase transitions and changing the mechanical properties.

HL 33.7 Thu 17:00 H32

Optical Characterization of Phase-Pure Wurtzite GaAs/II-VI Core/Shell Nanowires — •MIKE KÜLKENS, MARVIN MARCO JANSEN, DETLEV GRÜTZMACHER, and ALEXANDER PAWLIS — Peter-Grünberg-Institut (PGI-9), Forschungszentrum Jülich GmbH, Germany

Self-catalysed III/V semiconductor core/shell nanowires (NWs) grown by molecular beam epitaxy (MBE) provide enormous potential to develop miniatur-

ized electronic and optoelectronic devices. Following our recent demonstration of WZ-phase-pure GaAs NW growth we investigated a novel type of hybrid NWs composed of a WZ-type GaAs core with various WZ-type II/VI-semiconductor shells. The shell provides excellent confinement and passivation of the GaAs core due to the large bandgap energy difference between the two materials and allows to tune the optical bandgap of the GaAs core by tensile strain within a range of several 100 meV.

Here we report on the structural and optical properties of WZ-phase-pure grown GaAs/Zn_{1-x}Mg_xSe core/shell NWs. μ -PL investigations reveal the presence of tensile strain in the GaAs core induced by the Zn_{1-x}Mg_xSe shell, which can be engineered via the magnesium concentration and the shell thickness. The measured redshift of the near-band emission from the GaAs core was verified by evaluation of the strain and its effect on the GaAs bandgap, using a hydrostatic strain model. The results presented here pave the way for applications of WZ-phase-pure GaAs/II-VI core/shell NWs for optoelectronic devices with tunable wavelength in the infrared spectral range.

HL 33.8 Thu 17:15 H32

ZnSe-Based Microdisk Resonators in Novel Supported Geometry — •WILKEN SEEMANN¹, CHRISTIAN TESSAREK¹, SIQI QIAO², NILS VON DEN DRIESCH², ALEXANDER PAWLIS², GORDON CALLEN¹, and JÜRGEN GUTOWSKI¹ — ¹Institute of Solid State Physics, University of Bremen, Germany — ²Peter Grünberg Institute (PGI-9), Forschungszentrum Jülich, Germany

Microdisk resonators often suffer from thermal problems due to the limited contact of the underetched structure to the substrate. In order to circumvent this, ZnSe-based microdisks were fabricated in a supported geometry, i.e., in contact to the substrate over their whole bottom facet. This is achieved by growing a ZnSe:Cl quantum well (QW) encapsulated in ZnMgSe barriers on an AlAs underlayer. Oxidation of the underlayer to Al₂O₃ after disk fabrication increases the refractive index difference between the resonator and the substrate.

Scanning electron microscopy reveals a high structural quality of the fabricated microdisks. Micro-photoluminescence measurements show that the resulting resonators support high-Q resonances near the band edge emission of the ZnSe:Cl QW and a large number of whispering gallery modes on the defect emission band. The latter can be reproduced using a plane-wave model. Raman measurements of microdisks, as well as the as-grown ZnSe-based structure on the oxidized and non-oxidized AlAs underlayer, are used to analyze the mechan-

ical properties of the disk and the influence of the oxidation process on the strain in the QW structure.

HL 33.9 Thu 17:30 H32

Enhancing directivity in optical waveguide antennas — •HENNA FARHEEN¹, LOK-YEE YAN², TILL LEUTERITZ², SIQI QIAO², FLORIAN SPREYER¹, CHRISTIAN SCHLICKRIEDE¹, VIKTOR QUIRING¹, CHRISTOF EIGNER¹, THOMAS ZENTGRAF¹, STEFAN LINDEN², VIKTOR MYROSHNYCHENKO¹, and JENS FÖRSTNER¹ — ¹Paderborn University, Paderborn, Germany — ²Universität Bonn, Germany

We show the numerical and experimental realization of optimized broadband optical traveling-wave antennas made from low-loss dielectric materials. The antennas are composed of a director and reflector placed over a glass substrate and a dipole emitter located in the feed gap between them serves as an internal source of excitation. Our studies reveal that the highly directive nature of our antennas comes from two dominant guided TE modes excited in the waveguide-like director of the antenna, in addition to the leaky modes. Furthermore, our numerical results are in excellent agreement with the experimental measurements of the antennas that were fabricated using a two-step electron beam lithography. Compared to the previously studied plasmonic antennas for photon emission, our all-dielectric approach demonstrates a new class of highly directional, low loss, and broadband optical antennas.

[1]Farheen, Henna, et al. Optimization of optical waveguide antennas for directive emission of light. JOSA B 39.1 (2022): 83-91.

[2]Farheen, Henna, et al. Broadband optical Ta2O5 antennas for directional emission of light. Optics Express 30.11 (2022): 19288-19299.

HL 33.10 Thu 17:45 H32

First-principles study of momentum-forbidden excitons in bulk 2H-MoX₂ (X= S, Se) — •RAVI KAUSHIK^{1,2} and SERGEY ARTYUKHIN¹ — ¹Italian Institute of Technology, Genova, Italy — ²University of Genova, Genova, Italy

Coulomb-bound electron-hole pairs (excitons) dominate the optical response of atomically thin transition metal dichalcogenide (TMD) semiconductors. While Mo-based TMDs monolayers have a direct gap, bulk MoS₂ and MoSe₂ possess an indirect gap, with momentum-forbidden lowest energy excitonic transitions. Here we study how the effects of translational symmetry breaking by thermal phonons and in scanning spectroscopies can lead to a violation of the usual optical selection rules.

HL 34: Focus Session: Perspectives in Cu(In,Ga)Se 2

Time: Thursday 15:00–18:00

Location: H33

Invited Talk

HL 34.1 Thu 15:00 H33

Super-high efficiency CIGS devices: current status and pathways forward — •ROMAIN CARRON — Laboratory for Thin Films and Photovoltaics, Empa, Dübendorf, Switzerland

In this contribution, we discuss the limitations to the photovoltaic performance of Cu(In,Ga)Se₂ (CIGS) devices, and possible pathways to boost cell efficiencies towards 25% and beyond. Starting from a comparison of record CIGS cells to other photovoltaic technologies, we evaluate the potential for improvement of each of the individual parameters Voc, Jsc, and FF towards the Shockley-Queisser limit. Then we walk through the main causes for losses for each of the individual parameters, connect them to the last decade's progress, and suggest pathways for future improvements. The open-circuit voltage is discussed in particular depth, including the prediction of its value, the role of impurities and alkali elements in high-efficiency devices, the impact of other absorber modifications, and of advanced optical management. Finally, we discuss how the layer sequence of a CIGS solar cell differs from its functional structure. On this basis, we describe potentially advantageous modifications to the device architecture and the related challenges.

Invited Talk

HL 34.2 Thu 15:30 H33

Highlights from the development of the world record Cd-free CIGSSE 30x30cm² solar module — •ANASTASIA ZELENINA — AVANCIS GmbH, Otto-Hahn-Ring 6, 81739 Munich, Germany

In this contribution, the R&D process of 30x30 cm² CIGSSE solar modules will be discussed [1]. One of the main advantages of the process is the application of an environmentally friendly dry Zn(O,S) buffer, which is applied as an alternative to the widely used CdS chemical bath deposition (CBD) process. Over the past few years, our development of the 30x30 cm² CIGSSE modules has been focused on the optimization of the absorber properties. An increased absorber thickness has been applied, with the aim to increase absorption and increase the short circuit current density (JSC). The Jsc-improvement was combined with enhancing the absorber quality through the optimization of the elemental absorber depth profile. The enhanced absorber quality lead to better diode parameters and higher JSC*VOC product values. Furthermore, the absorber surface homogeneity was improved for this increased absorber thickness leading to an enhancement of the Fill Factor (FF) values. The improved absorber homogeneity results

mostly from tuning the rapid thermal annealing (RTP) process. The combination of these development steps lead to the achievement of a world record efficiency of 19.8% [2]. This new process developments on 30x30cm² sized modules will also be the basis for the power development on production-sized modules and will be used for further production upgrades.

[1] "Absorber optimization in CIGSSE modules with a sputtered Zn(O,S) buffer layer at 19% Efficiency", M. Stölzel et al., Proceedings of 36th EU PVSEC, Marseille (2019), p. 590-596, DOI: 10.4229/EUPVSEC20192019-3AO.7.1

[2] NREL Champion Photovoltaic Module Efficiency Chart <https://www.nrel.gov/pv/module-efficiency.html>

HL 34.3 Thu 16:00 H33

Overcoming current limitations of Cu(In,Ga)Se₂ photovoltaic devices — •DANIEL ABOU-RAS — Helmholtz-Zentrum Berlin für Materialien und Energie GmbH, Hahn-Meitner-Platz 1, 14109 Berlin, Germany

Recently, a review paper entitled "CIGS photovoltaics: reviewing an evolving paradigm" (Stanbery et al 2022 J. Phys. D: Appl. Phys. 55 173001, doi: 10.1088/1361-6463/ac4363) has provided an overview of various issues to be improved in Cu(In,Ga)Se₂ (CIGS) thin-film solar cells to reach power-conversion efficiencies of 25% and beyond. The authors of this contribution highlight the necessity of implementing device concepts already in use for the established Si and GaAs photovoltaic technologies also for CIGS devices. Possible ways of enhancing the collection and reducing nonradiative recombination in CIGS solar cells are described. I intend to give a brief insight into the main aspects of this review paper in the planned Focus Session.

HL 34.4 Thu 16:15 H33

Identification of nonradiative recombination centers in CuInSe₂ and Cu-GaSe₂ — •BAOYING DOU¹, STEFANO FALLETTA², CHRISTOPH FREYSOLDT¹, and JÖRG NEUGEBAUER¹ — ¹Max-Planck-Institut für Eisenforschung GmbH — ²Ecole Polytechnique Fédérale de Lausanne

Cu(In,Ga)Se₂ is a promising solar absorber for thin-film solar cell applications. Nonradiative carrier recombination is one of the key processes that limits the device efficiency. To achieve high performance, it is crucial to identify the critical defects and quantify their induced nonradiative recombination rates. Prior first-principle calculations proposed that the antisites InCu and GaCu, are donors

with a transition levels in the band gap, so they may act as nonradiative recombination centers. However, the existence of transition levels in the band gap does not necessarily trigger nonradiative recombination. Using first-principles methods, we quantitatively show that internal conversion in the neutral charge state to the distorted DX center configuration plays a crucial role in carrier recombination by opening an efficient hole capture pathway. The positive charge state returns to the anti-site configuration without barrier to complete the entire recombination cycle. However, our calculations show that the DX center is only stable in CuGaSe₂, not in CuInSe₂. We discuss the consequences of these findings for defect engineering in CuInSe₂, CuGaSe₂, and its alloys.

30 min. break

Invited Talk

HL 34.5 Thu 17:00 H33

Digital Twins - a simulation model for Cu(In,Ga)Se₂ solar cells of high and moderate efficiency — •MATTHIAS MAIBERG¹, CHANG-YUN SONG¹, MARCIN MORAWSKI¹, FELIX NEDUCK¹, JOSHUA DAMM¹, HEIKO KEMPA¹, DIMITRIOS HARISKO², WOLFRAM WITTE², and ROLAND SCHEER¹ — ¹Institute of Physics, Martin-Luther-University Halle-Wittenberg, von-Danckelmann-Platz 3, 06120 Halle (Saale), Germany — ²Zentrum für Sonnenenergie- und Wasserstoffforschung Baden-Württemberg, Meitnerstraße 1, 70563 Stuttgart, Germany

To overcome the current record efficiency of Cu(In,Ga)Se₂ (CIGSe) solar cells, loss mechanisms need to be identified through comprehensive device models. The development of such models, however, is hampered by the complex film microstructure of CIGSe as well as its multi-component device structure. In the first part of our talk, we present one-dimensional models for CIGSe solar cells with high efficiency at around 19 % and moderate efficiency at around 16 %. These models have been obtained by a fitting routine for a set of experimental data which calls the simulation tool Synopsys TCAD as the subprogram. As an outcome, we obtain material parameters of CIGSe. The minority carrier lifetime, for example, exhibits values of >15 ns in the highly efficient cells while it is only 3 ns in the moderately efficient device. In the second part of our talk, we use such digital twin in order to identify loss mechanisms in the solar cells. Here, we address the non-radiative recombination as origin of electronic losses as well as the band gap grading and the window layers as origins for optical losses.

HL 34.6 Thu 17:30 H33

Analysis of the diode factor in CIGSe solar cells — •VALENTINA SERRANO ESCALANTE and THOMAS PAUL WEISS — University of Luxembourg

In previous work [1] we suggest there is a link between metastable defects and the diode factor. Changes in doping density after light soaking are observed when

measuring CV profiles. Those changes are caused by metastable transitions, accounted by the shift of the majority fermi level upon illumination, which in turn increases the diode factor. There are several methods to determine this parameter, namely, from an analysis of the current-voltage curves (JV) [2], using the diode equation or from the slope of the Voc dependence with illumination intensity: Jsc-Voc [3]. Within this work, those methods are tested in a set of CIGSe, Cu poor samples, grown with the three-stage process, with good efficiencies (without any post-deposition treatment) in the range from 15% to 17%. For the analysis of the JV curves under dark, the two-diode model [4] is implemented. Using a 1-diode fit always results in a high value (>1.5), indicating dominant recombination in the space charge region. We use a 2-diode fit to obtain information on the diode factor originating from recombination in the quasi-neutral zone, which is affected by the metastable effects. In the case of JV under illumination, the extraction of the diode factor seems to be hampered by the cross-over between light and dark JV characteristics, which in CIGSe cells might be due to a change in an energetic barrier under light [5]. Therefore, the diode factor under illumination is determined more reliably from Jsc-Voc measurements.

HL 34.7 Thu 17:45 H33

Exact determination of Quasi-Fermi Level splitting from absolute photoluminescence and absorbance spectra — •SEVAN GHARABEIKI, TAOWEN WANG, AJAY SINGH, ALEX REDINGER, and SUSANNE SIEBENTRITT — Department of Physics and Materials Science, University of Luxembourg, 4422 Belvaux, Luxembourg

Photoluminescence (PL) is a powerful tool to investigate the Quasi-Fermi level splitting (QFLS) in absorbers and hence the upper limit of the open-circuit voltage (Voc) in a solar cell. Planck's generalized law and external radiative (ERE) method are the two most common ways to determine the QFLS. Planck's generalized law uses a high energy slope of the PL spectrum and assumes the absorbance (A) to be unity for the photons with energy sufficiently higher than the absorber bandgap. However, in CIGSe solar cells, which employ a graded bandgap, and poly-crystalline perovskite solar cells, the assumption A=1 is no more valid. On the other hand, the ERE method makes use of the radiative bandgap. Many studies consider the PL emission peak position to be the radiative bandgap which is not accurate. Herein, we present a combination of PL and absorbance measurements to accurately determine the QFLS in the CIGSe and methylammonium tin-triiodide Perovskite (MASI) absorbers. Then, we compare our QFLS values from the Planck's generalized law and the ERE method. We emphasize that the radiative bandgap and PL maximum are not the same, and using the PL maximum as a radiative bandgap can result in errors in QFLS extraction.

HL 35: Acoustic Waves and Nanomechanics

Time: Thursday 15:00–16:00

Location: H34

HL 35.1 Thu 15:00 H34

A hybrid (Al)GaAs-LiNbO₃ surface acoustic wave resonator for cavity quantum dot optomechanics — •EMELINE NYSTEN¹, ARMANDO RASTELLI², and HUBERT KRENNER¹ — ¹Physikalisches Institut, WWU Münster, Germany — ²Institute of Semiconductor and Solid-State Physics, Johannes Kepler Universität Linz, Austria

Surface acoustic waves (SAW) are a useful tool to control the emission of quantum dots (QDs). In particular, SAWs enable the modulation of their energy levels through the deformation potential coupling [1]. Here, we explore the possibility to enhance the interaction between the SAW and the QDs by transferring them on a strong piezoelectric LiNbO₃ substrate by epitaxial lift-off [2,3]. Additionally, the membrane is transferred inside a SAW resonator confining the acoustic field inside the cavity. High acoustic quality factors of $Q > 4000$ are demonstrated for the SAW resonator for an operation frequency of $f = 300$ MHz and stay high even after the hybridization. The frequency and position dependent optomechanical coupling of single quantum dots with the resonator modes is recorded and quantified. A possible non-linear coupling between the QDs and the resonator modes is also observed [4]. [1] Appl. Phys. Lett. 93, 081115 (2008) [2] Phys. Rev. B 88, 085307 (2013) [3] J. Phys. D: Appl. Phys. 50, 43LT01 (2017) [4] Appl. Phys. Lett. 117, 121106 (2020)

HL 35.2 Thu 15:15 H34

Determining Amplitudes of Standing Surface Acoustic Waves via Atomic Force Microscopy — •JAN HELLEMANN¹, FILIPP MÜLLER¹, MADELEINE MSALL², PAULO V. SANTOS¹, and STEFAN LUDWIG¹ — ¹Paul-Drude-Institut für Festkörperelektronik, Berlin, Deutschland — ²Bowdoin College, Maine, USA

Our aim is the realization of strong coupling between cavity phonons and a few electron double quantum dot as an on-chip hybrid system for quantum information applications. For this purpose, we develop radio frequency surface-phonon cavities containing a double quantum dot laterally defined in a GaAs/AlGaAs heterostructure. To characterize a phonon cavity we generate standing surface

acoustic waves (SSAW) by driving the cavity defining interdigital transducers and image the SSAW using atomic force microscopy (AFM), which is able to resolve submicron wavelengths of the SSAW at a few GHz. Alternative techniques are discussed in a related contribution by N. Ashurbekov.

Here, we focus on the AFM cantilever deflection, which substantially overestimates the SSAW amplitude because the cantilever with an eigenfrequency in the kHz range is driven by energy transfer from the much faster oscillating surface. We demonstrate a method to nevertheless determine the actual SSAW amplitude by comparing the hystereses of force curve measurements with model predictions based on solving the equation of motion of the driven cantilever [1]. Finally we present our first characterization measurements of a double quantum dot coupled to a phonon cavity.

[1] J. Hellemann et al, PRApplied 17, 044024 (2022)

HL 35.3 Thu 15:30 H34

Radio Frequency Surface Acoustic Wave Cavities near 6 GHz — •NAZIM ASHURBEKOV¹, MICHAEL HANKE¹, EDOARDO ZATTERIN², MADELEINE MSALL³, JAN HELLEMANN¹, PAULO SANTOS¹, TOBIAS SCHULLI², and STEFAN LUDWIG¹ — ¹Paul-Drude-Institut, Berlin, Germany — ²European Synchrotron, Grenoble, France — ³Bowdoin College, Maine, USA

Aiming at strong coupling between confined phonons and confined electrons in hybrid quantum circuits, we develop radio frequency (rf) surface-phonon cavities. The cavities are defined by focusing surface gate Bragg mirrors. They also serve as interdigital transducers, which we use to generate standing surface acoustic waves (SSAWs) for characterizing the cavities. At frequencies >3 GHz corresponding to wavelengths <1 μm most methods to measure the SSAWs become increasingly difficult.

Here, we explore two experimental methods with superior resolutions, scanning X-ray diffraction microscopy (SXDM) and atomic force microscopy (AFM). We present AFM measurements of focused rf SSAWs near 6 GHz and compare them with SXDM measurements. While AFM provides a basic char-

acterization of the SSAW, SXDM in addition yields its complete 3D strain field, relevant for the electron-phonon coupling.

Finally, comparing our experimental results with finite elements method simulations allows us to explore design variations for future optimizations of the electron-phonon coupling in quantum devices.

HL 35.4 Thu 15:45 H34

A quantum dot coupled to a mechanical resonator — •CLEMENS SPINNLER¹, GIANG NAM NGUYEN¹, LIANG ZHAI¹, ALISA JAVADI¹, ANDREAS D. WIECK², ARNE LUDWIG², YING WANG³, PETER LODAHL³, LEONARDO MIDOLO³, and RICHARD J. WARBURTON¹ — ¹Department of Physics, University of Basel — ²Lehrstuhl für Angewandte Festkörperphysik, Ruhr-Universität Bochum — ³Niels Bohr Institute, University of Copenhagen

Coupling a single-photon emitter to a mechanical resonator is a promising route towards operations involving a single photon and a single phonon. Semiconduc-

tor quantum dots (QDs) are bright sources of coherent single-photons, and their optical two-level transition can be coupled to mechanical motion via deformation-potential coupling.

Here, we present a membrane-design resonator: a cantilever with a fundamental in-plane mode at 3.1 MHz with a quality factor as high as 22'000. The membrane design hosts a heterostructure diode for stabilising the QD's charge state. This results in narrow optical linewidths and a high mechanical sensitivity. We probe the Brownian motion at low temperature, 4 K, of the mechanical resonator via the resonance fluorescence from a single quantum dot. The mechanical noise imprinted on the QD's photons is extracted via an autocorrelation measurement. A single photon coupling strength of around 100 kHz is estimated. The in-plane mechanical motion probed here, together with the membrane design, allows a translation to higher frequencies using phononic-crystal resonators for which operation in the resolved-sideband regime becomes viable.

HL 36: Materials and Devices for Quantum Technology 2

Time: Thursday 15:00–17:45

Location: H36

HL 36.1 Thu 15:00 H36

Influence of (N,H)-terminated surfaces on stability, hyperfine structure, and zero-field splitting of NV centers in diamond — WOLFGANG KÖRNER¹, •REYHANEH GHASSEMIZADEH¹, DANIEL URBAN¹, and CHRISTIAN ELSÄSSER^{1,2} — ¹Fraunhofer Institute for Mechanics of Materials IWM, Wöhlerstr. 11, 79108 Freiburg, Germany — ²University of Freiburg, Freiburg Materials Research Center (FMF), Stefan-Meier-Straße 21, 79104 Freiburg, Germany

We present a density functional theory analysis of the negatively charged nitrogen-vacancy (NV⁻) defect complex in diamond located in the vicinity of (111)- or (100)-oriented surfaces with mixed (N,H)-terminations [1]. We assess the stability and electronic properties of the NV⁻ center and study their dependence on the H:N ratio of the surface termination. The formation energy, the electronic density of states, the hyperfine structure and zero-field splitting parameters of an NV⁻ center are analyzed as function of its distance and orientation to the surface. We find stable NV⁻ centers with bulk-like properties at distances of at least ~ 8 Å from the surface provided that the surface termination consists of at least 25% substitutional nitrogen atoms. The studied surface terminations have a minor effect on the ground state whereas the NV orientation has major effects. Our results show that axial NV centers near a flat 100% N-terminated (111) surface are the optimal choice for NV-based quantum sensing applications as they are the least influenced by the proximity of the surface.

[1] W. Körner, R. Ghassemizadeh, D. F. Urban, and C. Elsässer, arXiv:2109.12557

HL 36.2 Thu 15:15 H36

Quantum optimal control for conveyor-mode single-electron shuttling in Si/SiGe — •ALESSANDRO DAVID¹, VEIT LANGROCK², JULIAN D. TESKE³, LARS R. SCHREIBER³, HENDRIK BLUHM³, TOMMASO CALARCO¹, and FELIX MOTZOI¹ — ¹Institute of Quantum Control (PGI-8), Forschungszentrum Jülich, Germany — ²Institute of Theoretical Nanoelectronics (PGI-2), Forschungszentrum Jülich, Germany — ³JARA-FIT Institute of Quantum Information, Forschungszentrum Jülich and RWTH Aachen, Germany

An electron shuttling device is a promising candidate for the scalability of spin-qubits quantum computers. We consider a gated Si/SiGe quantum well capable of shuttling electrons smoothly by a translating confining potential (conveyor-mode). Dephasing coupling with valley degree of freedom and geometry of the quantum well dictate a maximum shuttling speed to keep the electron state adiabatically in the ground state and avoid excitation of the valley state. In this work we use the position of the electron as a control parameter and we optimise the trajectory of the electron to show how the electron can be shuttled faster and with lower infidelity compared to the adiabatic regime.

HL 36.3 Thu 15:30 H36

Optimizing Diamonds for the Electrical Readout of Nitrogen-Vacancy Centers in Diamond — •LINA MARIA TODENHAGEN, HAMZA OUERFELLI, and MARTIN STEFAN BRANDT — Walter Schottky Institut, Technische Universität München, Garching

The nitrogen-vacancy (NV) center in diamond is one of the most attractive quantum systems used in practical applications. Owing to its exceptionally stable spin state, it can be easily initialized, manipulated and read out even at room temperature. However, the widely used optical readout (ODMR) of the NV center is not easily miniaturized, since it requires an extensive optical setup. Alternatively, we can directly read out the spins electrically by generating a spin-dependent photocurrent (EDMR). However, compared to the traditional optical readout, EDMR of NV centers has been investigated in much less detail up to now.

The present work addresses the optimization of the diamond host material for the electrical readout and compares the results to the optical analogue. The

investigated substrates cover type IIa CVD diamonds as well as type Ib HPHT diamonds, both in their as-grown state and after different post-treatments, including electron irradiation and annealing. We focus on the effects of other defects such as substitutional nitrogen present in the samples on the spin-dependent photocurrent and the achievable contrast. Our results indicate that the choice of diamond material is a lot more critical for EDMR than for ODMR and may serve as a guideline for the further development of highly integrated NV sensors based on electrical readout.

HL 36.4 Thu 15:45 H36

Superconducting single-photon detectors made of NbTiN using a novel method to characterize the timing jitter — •LUCIO ZUGLIANI¹, RASMUS FLASCHMANN¹, STEFAN STROHAUER², CHRISTIAN SCHMID¹, FABIAN WIETSCHORKE¹, STEFANIE GROTHOWSKI², SVEN ERNST², SIMONE SPEDICATO², MIRCO METZ¹, BJÖRN JONAS¹, JONATHAN FINLEY², and KAI MÜLLER¹ — ¹Walter Schottky Institute and Department for Electrical and Computer Engineering, Technical University of Munich, Germany — ²Walter Schottky Institute and Physics Department, Technical University of Munich, Germany

In recent years, superconducting single-photon detectors (SSPDs) have raised tremendous attention as a key technology for optical quantum processing and faint light detection. With their unparalleled performances to detect single photons, further investigation of these detectors is of high interest [1, 2].

Here, we present our recent progress on NbTiN SSPDs measured at 4.5K. We discuss our approaches to improve the most important figures of merit (dark count rate, dead time, timing jitter, efficiency) including an optimization of the quality of the superconducting NbTiN films and the integration of the detector in a broad-band cavity.

In particular, we focus on the impact of the substrate material on the resulting parameters such as the detected voltage pulse. We investigate the characteristic of pulse height, rise time and timing jitter, finding a relation between the timing jitter and the pulse properties.

[1]*C. Natarajan et al., Sup. Sci. and Tech. 25, 063001 (2012)

[2]*I. Zadeh, Appl. Phys. Lett. 118, 190502 (2021)

HL 36.5 Thu 16:00 H36

Focused ion beam implantation and luminescence of erbium ions in semiconductor nanostructures — •CHRISTIAN DÜPOTEL¹, PATRICK LINDNER², VARVARA FOTEINO³, YUJIAO LI⁴, JÖRG DEBUS², ARNE LUDWIG¹, and ANDREAS D. WIECK¹ — ¹Lehrstuhl für Angewandte Festkörperphysik, Ruhr-Universität Bochum — ²Experimentelle Physik 2, TU Dortmund — ³RUBION, Ruhr-Universität Bochum — ⁴ZGH, Ruhr-Universität Bochum

We report on focused ion beam (FIB) implantation of erbium ions in semiconductor nanostructures. Semiconductor nanostructures have attracted a lot of attention due to their unique optical, electrical and mechanical properties. Focused ion beam is an elegant method to tune these specific properties. This contribution lines out the implantation processes and the methods used to characterize the samples after implantation. Erbium is implanted in various semiconductor nanostructures in its 3+ state using an alloy liquid metal ion source. Furthermore, a sputter cathode source is used to implant erbium(III) oxide. Implantation is done at room temperature as well as at elevated temperatures to reduce radiation damage. The implanted ion distribution is simulated by SRIM and measured by atom probe tomography. After the implantation, the samples are annealed under nitrogen gas using a rapid thermal annealing technique. Photoluminescence measurements on erbium luminescence are carried out at cryogenic temperatures (10 K) as a function of the annealing and implantation parameters. The quality of the samples is then rated according to emission intensity of the important telecom-C-band wavelength of 1.54 μm.

15 min. break

HL 36.6 Thu 16:30 H36

Searching for signatures of magnetism and induced superconductivity in magnetic topological insulator-superconductor hybrid devices —

•MAX VASSEN-CARL, MICHAEL SCHLEENVOIGT, BENEDIKT FROHN, DETLEV GRÜTZMACHER, and PETER SCHÜFFELGEN — Peter Grünberg Institute 9, Forschungszentrum Jülich GmbH, 52425 Jülich, Germany

Topological materials harbor great possibilities for the future of quantum computation. In theory, when quasi-1D topological isolators (TIs) are coupled to superconductors localized Majorana zero modes (MZM) arise at the end of the quasi-1D hybrid structure. However, quasi-1D TIs require a certain in-plane magnetic field, which depends on the cross-section area of the TI, to retrieve the topological properties lost by confinement. Deviations of said TI cross-section change the penetrating flux and can lead to additional opening and closing of the topological gap, creating unwanted MZMs. One possible solution is to integrate magnetism directly into the TI, creating so-called magnetic topological insulators (MTIs), which retain their topological properties even when confined. In this work Chromium is used to magnetically dope (BixSb1-x)2Te3, by means of MBE. First, ex-situ fabricated MTI-Nb Josephson Junctions (JJ) showed no supercurrent, but instead an increase of resistance for low bias voltages. To gain further insights on the interplay between SC and MTI a new sample layout was designed which allows for Josephson and Hall bar measurements in one device. In order to obtain highest S-MTI interface quality those hybrid devices are fully fabricated under UHV conditions.

HL 36.7 Thu 16:45 H36

Coherent interactions between confined fluids of light and GHz-phonons —

•ALEXANDER KUZNETSOV, KLAUS BIERMANN, and PAULO SANTOS — Paul-Drude-Institut für Festkörperelektronik in Forschungsverbund Berlin, e. V., Berlin, Germany

Microcavity exciton-polaritons are at the heart of an emerging field of polaromechanics, which studies coupling between polariton and mechanical degrees of freedom and promises unit quantum cooperativity. One challenge is to reach the regime of coherent interactions, when the polariton decoherence rate is smaller than mechanical frequency.

We reached this milestone by coupling polariton fluids of light (macroscopic quantum state) to GHz phonons. High-resolution optical spectroscopy revealed ns-long coherence time reaching $\tau = 2ns$. Monochromatic $\Omega_M = 7GHz$ phonons were injected into a trap using acoustic transducers. Since $1/\tau < \Omega_M$, the interaction resulted in the appearance of well-resolved phonon sidebands in the emission – an optical frequency comb. We demonstrated tuning of the sidebands by the phonon amplitude, which was controlled by the radio-frequency power applied to the transducer.

The demonstrated coherent polaromechanical device is a building block for a bi-directional interface between microwave and optical domains, atomic clocks, and is useful to study rich physics of sideband cooling and amplification.

HL 36.8 Thu 17:00 H36

A solid-state source of single and entangled photons at diamond SiV-center transitions operating at 80 K —•EDDY P. RUGERAMIGABO¹, XIN CAO¹, JINGZHONG YANG¹, TOM FANDRICH¹, YITENG ZHANG¹, BENEDIKT BRECHTKEN¹, ROLF J. HAUG^{1,2}, MICHAEL ZOPF¹, and FEI DING^{1,2} — ¹Institut für Festkörperphysik, Leibniz Universität Hannover, Germany — ²Laboratorium für Nano- und Quantenengineering, Leibniz Universität Hannover, Germany

Epitaxially grown quantum dots (QDs) hold great potential for the generation of 'flying' qubits. Coupling these emitters to quantum memories with long co-

herence times enables the development of hybrid nanophotonic devices incorporating the advantages of both systems. GaAs/AlGaAs QDs based on droplet etching and nanohole infilling exhibit tunable, well-defined optical properties, with emission typically reported at around 780nm. Silicon-vacancy (SiV) centers in diamond show long coherence times and strong interactions with single photons via their zero phonon line (ZPL) at around 737 nm. Here we report the first quantum dot containing material emitting nonclassical light that matches the SiV ZPL. Careful adjustments of the GaAs thickness in the QDs lead to a narrow wavelength distribution (736.2 ± 1.7 nm) and small exciton fine structures (7.0 ± 4.6 eV). Polarization entangled photons are generated via the biexciton-exciton cascade decay with a fidelity of 0.727 ± 0.092 . High single photon purity is maintained from 4 K ($g^{(2)}(0) = 0.07 \pm 0.02$) up to 80 K ($g^{(2)}(0) = 0.11 \pm 0.01$), therefore, paving the way towards cost-efficient applications in quantum repeaters and quantum memories.

HL 36.9 Thu 17:15 H36

Electric field-induced exciton darkening and fine structure vanishing in GaAs/AlGaAs coneshell quantum structures —•GEOFFREY PIRARD¹ and GABRIEL BESTER^{1,2} — ¹Physical Chemistry and Physics Departments, University of Hamburg, Luruper Chaussee 149, D-22761 Hamburg, Germany — ²The Hamburg Centre for Ultrafast Imaging, University of Hamburg, Luruper Chaussee, 149, D-22761 Hamburg, Germany

Electronic and optical properties of coneshell quantum structures (CSQS) are investigated via a combination of the empirical pseudopotential and the configuration interaction methods. It is found that the application of a vertical electric field onto CSQS can provoke a darkening of the exciton bright doublet accompanied by the suppression of its fine structure. The existence of such a four-fold degenerate exciton state finds its origins in the carriers' localization: one type of carrier is strongly confined at the bottom of the nanostructure whereas its counterpart is pulled apart in such a way that its probability density acquires a delocalized ring-like nature. The separation between carriers' wave functions leads to a vanishing exchange interaction and reduces the values of the direct Coulomb integrals, giving rise to a tunable long-lived degenerate dark exciton. These properties make the CSQS promising candidates to construct the building blocks of quantum memories.

HL 36.10 Thu 17:30 H36

Bright InAs quantum dot based single-photon sources at telecom wavelengths —•MONICA PENGERLA¹, ALKAALES MOHANAD², RANBIR KAUR², JAN DONGES¹, LUCAS BREMER¹, JOHANNES SCHALL¹, SVEN RODT¹, MOHAMED BENYOUCEF², and STEPHAN REITZENSTEIN¹ — ¹Institut für Festkörperphysik, Technische Universität Berlin, Hardenbergstraße 36, D-10623 — ²Institute of Nanostructure Technologies and Analytics (INA), Center for Interdisciplinary Nanostructure Science and Technology (CINSA-T), University of Kassel, Heinrich-Plett-Str. 40, 34132 Kassel, Germany

Quantum dot (QD) based single-photon sources are key elements of photonic quantum networks. Most interesting are sources emitting at telecom wavelengths to enable long distance quantum communication. Here, we report on deterministically fabricated single-photon sources based on InAs QDs grown on InP substrate. Numerical simulations of such QD heterostructures with backside distributed Bragg reflector and reveal photon extraction efficiency exceeding 50% when integration the QD into mesa or circular Bragg grating structures. The numerical designs are implemented by deterministic device processing using machine learning enhanced in-situ electron beam lithography. Micro-photoluminescence studies reveal the excellent optical and quantum optical properties of the fabricated quantum devices.

HL 37: Thermal Properties

Time: Thursday 16:30–17:15

Location: H34

HL 37.1 Thu 16:30 H34

Thermal characterization of semiconductor membranes by Raman thermometry —•ISABELL HÜLLEN¹, MAHMOUD ELHAJHASAN¹, WILKEN SEEMANN¹, MARKUS R. WAGNER², and GORDON J. CALLEN¹ — ¹Institut für Festkörperphysik, Universität Bremen, Germany — ²Institut für Festkörperphysik, Technische Universität Berlin, Germany

Photonic structures like nanolasers are often based on freestanding semiconductor membranes comprising hole lattices. As a result, a high number of interfaces limits the thermal conductivity and consequently the overall device performance under high injection conditions. Thus, it remains an open task to correlate the thermal and optical characterization of photonic membranes often based on III-V semiconductors. In this contribution we follow a careful step-by-step approach to attest the suitability of Raman thermometry (RT) for a precise determination of the thermal conductivity κ . First, we analyse a well-studied bulk material like Ge to not only extract κ , but also to assess underlying errors and experimental limitations. Consequently, the RT technique is applied to Ge membranes, in

preparation of the subsequent thermal characterization of photonic membranes. Here, we characterize a 250-nm-thick c-plane GaN membrane, which forms the basis for state-of-the-art nanobeam lasers. RT reveals that κ is reduced by up to one order of magnitude in comparison to bulk values. The pronounced Photoluminescence signal of our GaN membrane directly enables an alternative optical and thermal characterization, which we link to RT, aiming to bridge optical and thermal material characterization.

HL 37.2 Thu 16:45 H34

Can group IV alloys compete in thermoelectrics? —•OLIVER KRAUSE¹, ADA CHIMENTI², OMAR CONCEPCIÓN¹, THORSTEN BRAZDA¹, STEFANO RODDARO², DETLEV GRÜTZMACHER¹, and DAN BUCA¹ — ¹Peter-Grünberg-Institute 9 (PGI-9), Forschungszentrum Jülich, 52428 Jülich, Germany — ²Dipartimento di Fisica "E. Fermi", Università di Pisa, Largo Bruno Pontecorvo 3, 56127 Pisa, Italy

The thermoelectric effect allows the conversion of heat into electricity. A material suited for efficient thermoelectric power generation using small temperature

differences with a base at room temperature is of outmost interest. The figure of merit in thermoelectrics is ZT , indicating how suited a material is for thermoelectric applications. It can be optimized by reducing the thermal conductivity k and increasing the electrical conductivity σ of a material with a large Seebeck coefficient α . Here, we investigate the potential of group-IV alloys GeSn and SiGeSn, a material system compatible to standard Si technology.

We present a study of k of crystalline GeSn alloys deposited by chemical vapor deposition. The differential 3ω technique was used to determine k electrically. Our preliminary data shows that k strongly decreases with increasing the Sn content, reaching values as low as $5 \frac{\text{W}}{\text{m}\cdot\text{K}}$ at room temperature. The data are compared with previous reports of the same material using Raman thermometry. Using data of the electrical conductivity and modelling of Seebeck coefficient, ZT values for both p and n type GeSn layers are calculated.

HL 37.3 Thu 17:00 H34

Anisotropy in the c-plane thermal conductivity of Gallium Nitride — •MAHMOUD ELHAJHASAN¹, ISABELL HÜLLEN¹, WILKEN SEEMANN¹, IAN ROUSSEAU², NICOLAS GRANDJEAN², and GORDON CALLEN¹ — ¹Institute of

Solid State Physics, University of Bremen, Germany — ²Institute of Solid State Physics, École Polytechnique Fédérale de Lausanne (EPFL), Switzerland

The thermal characterization of modern semiconductor membranes commonly employed for photonic devices like nanobeam lasers (1D) or photonic crystals (2D), often lacks spatial resolution and appropriate quantification. However exactly these two points are relevant for the detection of e.g., thermal anisotropies, heat spots, and interfaces providing thermal resistance.

In this contribution, Raman thermometry employing one laser beam (1LRT) is used to quantify the thermal conductivity κ of 250-nm-thick state-of-the-art, c-plane GaN membranes. The same membranes are then probed by two laser Raman thermometry (2LRT) to map the temperature distribution caused by a heating laser via a second probe laser. As a result, κ is determined for all in-plane crystal directions. A particular thermal anisotropy is revealed in c-plane GaN via this direct thermal imaging technique with sub- μm spatial resolution, which compares well to ab-initio calculations.

Consequently, we outline first potential routes towards thermal optimizations of photonic nanostructures.

HL 38: Members' Assembly

Themen unter anderem:

- Bericht
- Informationen zu Dresden 2023
- Verschiedenes

Time: Thursday 18:00–19:00

Location: H34

All members of the Semiconductor Physics Division are invited to participate.

HL 39: Quantum Dots and Wires 6: II-VI and related

Time: Friday 9:30–10:45

Location: H32

HL 39.1 Fri 9:30 H32

Raman and X-ray photoemission study of thin films of binary and ternary semiconductor quantum dots — •OLEKSANDR SELYSHCHEV^{1,2}, VOLODYMYR DZHAGAN^{3,4}, and DIETRICH R.T. ZAHN^{1,2} — ¹Semiconductor Physics, TU Chemnitz, Germany — ²Center for Materials, Architectures, and Integration of Nanomembranes (MAIN), TU Chemnitz, Germany — ³Institute of Semiconductors Physics, NAS of Ukraine, Kyiv, Ukraine — ⁴Taras Shevchenko National University of Kyiv, Ukraine

Quantum dots (QDs) of ternary semiconductor chalcogenides MInS_2 ($M = \text{Cu, Ag}$) attract attention as environment friendly alternatives to toxic cadmium and lead chalcogenides. Even though both ternary and binary QDs exhibit size dependent absorption and photoluminescence spectra, the properties of ternary compounds additionally depend on composition, variety of crystalline phases, and defects. Here, we present a comparative Raman and X-ray photoemission spectroscopic (XPS) study of thin films of binary CdS and ternary MInS_2 QDs to examine their structural and electronic properties. Raman results show that MInS_2 QDs co-exist in chalcopyrite and Cu-Au type phases. XPS study revealed indium-rich surface deviating from ideal stoichiometry. Auger parameters confirm metal ions in the expected oxidation states, while the boundary states of sulfur indicate surface passivation through the thiolate group of thioglycolate ligands. The ionization potentials of binary and ternary QDs are found to be the same as those for the bulk indicating that the bandgap increase is due to quantum confinement of electrons in the conduction band.

HL 39.2 Fri 9:45 H32

Collective Properties of CdSe-CdS giant-shell Quantum Dots — •YANNIC STÄCHELIN¹, ARTUR FELD¹, AGNES WEIMER¹, MICHAEL DEFFNER^{2,3}, SONJA KROHN⁴, JAN STEFFEN NIEHAUS⁴, and HOLGER LANGE^{1,3} — ¹Institut für Physikalische Chemie, Universität Hamburg, Hamburg, Germany — ²Institut für Anorganische und Angewandte Chemie, Universität Hamburg, Hamburg, Germany — ³The Hamburg Centre for Ultrafast Imaging, Hamburg, Germany — ⁴Fraunhofer IAP-CAN, Hamburg, Germany

CdSe-CdS core-giant-shell QDs are nowadays available with near-unity quantum yields, which makes them interesting candidates for lasing or display applications. Bright, high-PLQY QDs might also contribute to photonic quantum technologies as building blocks. QDs can realize deterministic photon-emitters and enable key quantum photonic resources and functionalities. Interaction of densely packed QDs can lead to collective phenomena like excitonic and pho-

tonic coupling, superfluorescence and enhanced quantum coherence. Incoherent dephasing processes may deteriorate the inherent quantum properties of QDs. We investigate dependencies of exciton formation in CdSe-CdS giant-shell QDs and interaction in dense ensembles of QDs via ultrafast THz and transient absorption spectroscopy. Polymer-micelles are used to produce dense ensembles containing a variable amount of QDs. In dense ensembles, we observe the onset of a collective dynamic depending on the excitation conditions, which are thus a means of controlling the dynamics.

HL 39.3 Fri 10:00 H32

Excitonic fine structure of epitaxial Cd(Se,Te) on ZnTe type-II quantum dots — •PETR KLENOVSKY^{1,2}, PIOTR BARANOWSKI³, and PIOTR WOJNAR³ — ¹Department of Condensed Matter Physics, Faculty of Science, Masaryk University, Kotlářská 267/2, 61137 Brno, Czech Republic — ²Czech Metrology Institute, Okružní 31, 63800 Brno, Czech Republic — ³Institute of Physics, Polish Academy of Sciences, Al Lotników 32/46, PL-02-668 Warsaw, Poland

The structure of the ground state exciton of Cd(Se,Te) quantum dots embedded in ZnTe matrix is studied experimentally using photoluminescence spectroscopy and theoretically using $\mathbf{k} \cdot \mathbf{p}$ and configuration interaction methods. The experiments reveal a considerable reduction of fine-structure splitting energy of the exciton with increase of Se content in the dots. That effect is interpreted by theoretical calculations to originate due to the transition from spatially direct (type-I) to indirect (type-II) transition between electrons and holes in the dot induced by increase of Se. The trends predicted by the theory match those of the experimental results very well.

The theory identifies that the main mechanism causing elevated fine-structure energy in particular in type-I dots is due to the multipole expansion of the exchange interaction. Moreover, the theory reveals that for Se contents in the dot > 0.3 , there exist also a peculiar type of confinement showing signatures of both type I and type II and which exhibits extraordinary properties, such as almost purely light hole character of exciton and toroidal shape of hole states.

HL 39.4 Fri 10:15 H32

Polarized emission with sub-meV linewidth from single, two-dimensional PbS nanoplatelets — •PENGJI LI¹, LARS KLEPZIG^{2,3}, JINGZHONG YANG¹, MICHAEL ZOPF¹, JANNIKA LAUTH^{2,3,4}, and FEI DING¹ — ¹Institut für Festkörperphysik, Leibniz Universität Hannover, 30167 Hannover, Germany — ²Institute of Physical Chemistry and Electrochemistry, Leibniz Universität Hannover, 30167 Hannover, Germany — ³Cluster of Excellence PhoenixD, Welfen-

garten 1A, D-30167 Hannover, Germany — ⁴Universität Tübingen, Institute of Physical and Theoretical Chemistry, Auf der Morgenstelle 18, D-72076 Tübingen, Germany

In the past few decades, the tunability and strong light-matter coupling in nanometer-sized colloidal systems promotes their potential use in novel applications such as quantum metrology, quantum imaging or quantum communication. Two-dimensional (2D) nanoplatelets (NPLs) have recently moved into focus due to their controllable photoluminescence properties. In this work, the optical properties of single colloidal 2D PbS NPLs are explored at cryogenic temperature ($T=4$ K). Stable and narrow-band excitonic emission of single PbS NPL near 1.8 eV is observed with linewidths down to 0.6 meV. The prominent exciton-phonon interaction are detected. The emission features a strongly polarized emission with a degree of polarization up to 77%. These findings denote the first observation of narrow-band polarized photoluminescence (PL) from 2D PbS nanoplatelets, which were believed to suffer from broad PL due to complex band-edge exciton states evolving from the 64-fold degeneracy in PbS.

HL 40: THz and MIR Physics in Semiconductors

Time: Friday 9:30–11:45

Location: H33

HL 40.1 Fri 9:30 H33

Generation of intense sub-half-cycle terahertz pulses from spatially indirect interband transitions — •CHRISTIAN MEINEKE¹, MICHAEL PRAGER¹, JOHANNES HAYES¹, QIANNAN WEN², LUKAS KASTNER¹, DIETER SCHUH¹, KILIAN FRITSCH³, OLEG PRONIN³, MARKUS STEIN⁴, SANGAM CHATTERJEE⁴, MACKILLO KIRA², RUPERT HUBER¹, and DOMINIQUE BOUGEARD¹ — ¹University of Regensburg, 93040 Regensburg — ²University of Michigan, Ann Arbor, MI 48109 — ³Helmut Schmidt University, 22043 Hamburg — ⁴Justus Liebig University, 35392 Giessen

Ultimately short phase-stable terahertz (THz) pulses form the bedrock of THz lightwave electronics, where the carrier field creates a transient bias to control electrons on sub-cycle time scales. Here, we introduce a fully scalable high-repetition-rate THz source generating intense phase-locked and strongly asymmetric sub-cycle field transients. The key idea is to engineer electronic wavefunctions in type-II aligned semiconductor quantum wells such that resonant interband photoexcitation induces an ultrafast charge separation over several nanometers even without any bias. Our detailed quantum mechanical analysis reveals that local charging dynamics lifts the spatial separation of electrons and holes, leading to an abrupt decrease of the dipole moment, generating one single pronounced positive field peak. The THz bandwidth is scalable up to the mid-infrared by reducing the pump pulse duration. The versatility of our emitter allows adjusting waveforms, spectra, and field strengths to many applications, such as ultrabroadband spectroscopy and femtosecond nanoscopy.

HL 40.2 Fri 9:45 H33

Exploring mid-infrared transient gain in graphene — •KALLIOPI MAVRIDOU^{1,2}, ANGELIKA SEIDL^{1,2}, RAKESH RANA¹, ALEXEY PASHKIN¹, MANFRED HELM^{1,2}, and STEPHAN WINNERL¹ — ¹Institute of Ion Beam Physics and Materials Research, Helmholtz-Zentrum Dresden-Rossendorf, Bautzner Landstraße 400, Dresden 01328, Germany — ²Faculty of Physics and Center for Advancing Electronics Dresden, Technische Universität Dresden, Dresden 01062, Germany

In our study we employ a powerful method, namely a three-pulse pump-probe technique, that was first suggested by Kim *et al.*¹, to explore the possibility to achieve transient gain photon energies below the optical phonon energy (~200 meV) in graphene. Intriguingly, this technique is not widely established and to our knowledge has never been used in the mid- or far-infrared spectral range. The principle behind this method relies on the effect of a strong pre-pump pulse of 1.55 eV photons, which can cause a transient population inversion at lower energies. This population inversion is evidenced by a sign flip of the mid-infrared (86 meV photon energy) pump-probe signal that is related to either absorption or stimulated emission of mid-infrared photons of the pump beam. We present the results on multilayer graphene obtained under various experimental configurations. Our findings shed light into the completion of rapid thermalization via Coulomb scattering and carrier cooling via optical phonons.

1. Kim, K.; Urayama, J.; Norris, T.; Singh, J.; Phillips, J.; Bhattacharya, P. *Appl. Phys. Lett.*, **2002**, *81*, 670–672.

HL 39.5 Fri 10:30 H32

Exciton recombination dynamics and polarization properties in CsPbI₃ perovskite nanocrystals — •GANG QIANG¹, DMITRI R. YAKOVLEV^{1,2}, ELENA V. SHORNIKOVA¹, DANIL O. TOLMACHEV¹, MIKHAIL A. PROSNIKOV³, ELENA V. KOLOBKOVA⁴, PETER C. M. CHRISTIANEN³, and MANFRED BAYER^{1,2} — ¹Experimentelle Physik 2, Technische Universität Dortmund, D-44221 Dortmund, Germany — ²St. Petersburg, Russia — ³High Field Magnet Laboratory (HFML-EMFL), Radboud University, 6525 ED Nijmegen, The Netherlands — ⁴St. Petersburg, Russia

We synthesized CsPbI₃ NCs in fluorophosphate glass matrix and investigated the optical properties at various temperatures down to 4.2 K and in external magnetic fields up to 30 T. Recombination dynamics demonstrate clearly two-exponential decay characteristic for exciton emission with the dark exciton as a ground state. An anomalous polarization properties is observed at low temperature (e.g. 4.2 K), i.e. with the increasing of magnetic field, the degree of circular polarization (DCP) increases smoothly, while at ~21 T a 'hump' shows up. Higher temperature blurs this behavior, and it can not be clearly observed at 20 K. Moreover, for the spin dynamics, at low temperature (4.2 K) and high magnetic field (> 8 T), after reaching the maximum, the time resolved DCP tends to decrease and slowly relaxes to at a constant level, which is quite different from the observations in III-V and II-VI NCs.

HL 40.3 Fri 10:00 H33

Elastic and inelastic exciton scattering in InGaAs multi-quantum wells — •DANIEL ANDERS, MARKUS STEIN, and SANGAM CHATTERJEE — Institute of Experimental Physics I and Center for Materials Research (LAMA), Justus-Liebig-University Giessen, Heinrich-Buff-Ring 16, D-35392 Giessen, Germany

The interaction of optically injected excitons amongst each other as well as with electrons is one of the most fundamental questions in semiconductor physics. In the past, scattering processes in semiconductors between charge carriers and excitons have been studied intensively using a wide variety of experimental methods, e.g., four-wave-mixing spectroscopy, time-resolved photoluminescence spectroscopy, or optical pump - optical probe spectroscopy. In contrast to the aforementioned methods optical pump - terahertz probe spectroscopy allows to distinguish between elastic and the destructive inelastic scattering processes of excitons. While the linewidth of the intraexcitonic resonance provides a measure for the total scattering rate of all scattering processes, the change of the intraexcitonic oscillator strength is only sensitive to inelastic scattering processes. In this work, we compare exciton-electron and exciton-exciton scattering and determine the respective contributions of elastic and inelastic scattering processes.

HL 40.4 Fri 10:15 H33

Highly superlinear terahertz photoconductance in GaAs quantum point contacts in the deep tunneling regime — •MAXIMILIAN OTTENEDER¹, MARCEL HILD¹, ZE-DON KVON^{2,3}, EKATERINA E. RODYAKINA^{2,3}, MIKHAIL M. GLAZOV⁴, and SERGEY D. GANICHEV^{1,5} — ¹Terahertz Center, University of Regensburg, Regensburg, Germany — ²Novosibirsk, Russia — ³Novosibirsk, Russia — ⁴St. Petersburg, Russia — ⁵CENTERA, Institute of High Pressure Physics, Warsaw, Poland

A highly superlinear in radiation intensity photoconductance induced by continuous wave terahertz laser radiation with low intensities has been observed in quantum point contacts made of GaAs quantum wells operating in the deep tunneling regime. For very low values of the dark conductance $G_{\text{dark}}/G_0 \approx 10^{-6}$, with the conductance quantum $G_0 = 2e^2/h$, the photoconductance scales exponentially with radiation intensity and increases by almost four orders of magnitude at already 100 mW/cm². This effect is observed for a radiation electric field oriented along the source drain direction. We provide model considerations of the effect and attribute it to the variation of the tunneling barrier height by the radiation field due to local diffraction effects. We also demonstrate that cyclotron resonance due to an external magnetic field manifests itself in the photoconductance, completely suppressing the photoresponse.

15 min. break

HL 40.5 Fri 10:45 H33

Ultrafast subcycle dynamics of deep-strong light-matter coupling — •JOSHUA MORNHINWEG¹, MAIKE HALBHUBER¹, LAURA DIEBEL¹, VIOLA ZELLER¹, JOSEF RIEPL¹, CRISTIANO CIUTI², DOMINIQUE BOUGEARD¹, RUPERT HUBER², and CHRISTOPH LANGE³ — ¹Universität Regensburg, Germany — ²Université de Paris, France — ³TU Dortmund, Germany

Subcycle interactions of strong light fields and electric charges lead to multi-octave spanning dynamics such as high-harmonic generation. In optical microcavities, even vacuum field fluctuations can drive non-perturbative light-matter

coupling. Once the rate of energy exchange between the cavity and the matter mode becomes of the order of the carrier frequency of light, ultrastrong coupling (USC) emerges, and the profound modification of the vacuum ground state gives rise to novel phenomena such as cavity-mediated superconductivity. Here, we explore intriguing subcycle effects of USC including non-adiabatic dynamics occurring during quasi-instantaneous switch-off of the coupling, for which we observe sub-polariton-cycle polarization oscillations. Additionally, we drive USC with strong coherent THz fields to reveal nonlinear interactions between the polariton states, breaking the normal-mode approximation. Finally, we present deep-strong coupling (DSC) of multiple light and matter modes, creating a spectrum of Landau magneto-polaritons which covers 6 optical octaves, a coupling strength of $\Omega_R/\omega_c \approx 3.0$, and a record virtual ground state population exceeding 1 photon. Our results open up new avenues for dynamically tailoring of USC and DSC on strongly subcycle timescales.

HL 40.6 Fri 11:15 H33

Probing Free Electrons in InSb with Terahertz Shockwave Spectroscopy — •PETER FISCHER, GABRIEL FITZKY, DAVIDE BOSSINI, ALFRED LEITENSTORFER, and RON TENNE — Department of Physics and Center for Applied Photonics, University of Konstanz, D-78457 Konstanz, Germany

The Auger process, a non-radiative three-particle recombination, is critical especially in narrow-band semiconductors where it sets a fundamental efficiency limit for optoelectronic applications. Since their characteristic response frequencies fall within a broadband interval in the terahertz and mid-infrared range, quantitative studies of the electron dynamics in these materials remain challenging. Here, we demonstrate a new pump-probe technique able to monitor the free carrier plasma by observing its signature in the transient terahertz reflectivity spectrum. A broadband terahertz source, providing at the same time maximum temporal resolution, emerges from slicing the electric-field transient on a subcycle time scale, effectively generating a shockwave. Applying this tran-

sient to InSb after interband excitation, we find that the Auger-recombination coefficient increases by a factor of two from room temperature to 4.2 K. Furthermore, the importance of electron trapping to accurately model carrier dynamics is illustrated. Our approach exclusively targets the response of free charge carriers, disentangled from other contributions by e.g. bound excitons. Therefore, it offers a tool complementary to established time-resolved techniques.

HL 40.7 Fri 11:30 H33

Nonlinear photocurrents induced by terahertz radiation in twisted bilayer graphene — •STEFAN HUBMANN¹, PHILIPP SOUL¹, GIORGIO DI BATTISTA², MARCEL HILD¹, KENJI WATANABE³, TAKASHI TANIGUCHI³, DMITRI EFETOV², and SERGEY GANICHEV¹ — ¹Terahertz Center, University of Regensburg, 93040 Regensburg, Germany — ²ICFO, Castelldefels, Barcelona 08860, Spain — ³National Institute for Materials Science, 1-1 Namiki, Tsukuba 305-0044, Japan

We report on the observation of nonlinear photocurrent and photoconductivity in twisted bilayer graphene (tBLG) with twist angles below 1°. We show that excitation of the tBLG bulk causes a photocurrent, whose sign and magnitude are controlled by the orientation of the radiation electric field and the photon helicity. The developed theory shows that the current is formed by asymmetric scattering in gyrotropic tBLG. For the observed photocurrents, we demonstrate the emergence of pronounced oscillations upon variation of the gate voltage, which correlate with the oscillations of the sample resistance. These photocurrent oscillations originate in interband transitions between a multitude of subbands in tBLG. Furthermore, at higher radiation intensities, we detected a nonlinear intensity dependence of bulk photogalvanic current and photoconductivity. These nonlinear photoresponses are caused by the interplay between interband, inter-subband, and intraband transition. This interplay is controlled by the Fermi level position with respect to the Moiré subbands. We show that the photosignals saturate with rising intensity, while contributions from different transitions differ in their respective saturation behavior.

HL 41: Organic Semiconductors 2

Time: Friday 9:30–10:45

Location: H34

HL 41.1 Fri 9:30 H34

Understanding structure-to-property relationships for phonons and thermal transport in hydrogen-bonded organic semiconductors. — •LUKAS LEGENSTEIN, LUKAS REICHT, TOMAS KAMENECZK, SANDRO WIESER, and EGBERT ZOJER — Institute of Solid State Physics, Graz University of Technology, Graz, Austria

Research on organic semiconductors (OSC) has primarily focused on their (opto-)electronic properties. The understanding of phonons in these materials is, however, still rather poorly developed, despite their crucial role for charge and heat transport processes. Of central importance in this context are lattice phonons dominated by translations and rotations of entire molecules, which are coupled through non-covalent interactions. To elucidate how non-covalent bonding types such as H-bonding and π - π interactions affect phonons in otherwise vdW-stacked OSCs, we simulate the phonon bands of crystalline quinacridone (QA), as a prototypical H-bonded OSC. Notably, QA forms polymorphs with fundamentally different crystal structures, which strongly impact the observed phonons. The obtained phonon bands show complex dispersions with avoided crossings and mode hybridisations due to a mixing of inter- and intra-molecular vibrations. The phonons are simulated combining the phonopy package with density-functional theory employing the FHI-aims and VASP codes. The calculated phonon band structures are also used for benchmarking on-the-fly trained machine learning force fields calculated with VASP, which are then employed for modelling thermal transport within the Green-Kubo formalism.

HL 41.2 Fri 9:45 H34

Regiochemistry of Donor-Dendrons Controls the Performance of TADF Dendrimer based OLEDs — •RISHABH SAXENA¹, DIANMING SUN², STAVROS ATHANASOPOULOS¹, ELI ZYSMAN-COLMAN², and ANNA KÖHLER¹ — ¹University of Bayreuth, Germany — ²University of St. Andrews, UK

The potential of dendrimers exhibiting thermally activated delayed fluorescence (TADF) as emitters in solution-processed organic light-emitting diodes (OLEDs) has to date not yet been realized. This in part is due to a poor understanding of the structure-property relationships in dendrimers where reports of detailed photophysical characterization and mechanism studies are lacking. In this study, we investigated dendrimers with multiple dendritic electron-donating moieties connected to a central electron-accepting core via a para- or a meta-phenylene bridge. Characterization of host-free OLEDs revealed the superiority of meta-dendrimers as compared to the already reported para-analogue. Photophysical investigations in the films showed that, although all the dendrimers possess similar singlet-triplet energy gap, normally implying similar reverse intersystem crossing (RISC) rate, better TADF properties are obtained for meta-dendrimers when compared to para-dendrimers. In this regard, what this study reveals is

that the reorganization energy can play an important role in enhancing RISC rate and that this can be modulated as a function of the regiochemistry of donor dendron about the acceptor. This is a heretofore unexploited strategy and can be used as a general chemical design principle, especially in the case of bulky dendrimers.

HL 41.3 Fri 10:00 H34

Optical Vortices in Hemispherical Organic Microcavities — •JOHANNES DÜRETH¹, SIMON BETZOLD¹, MARCO DUSEL¹, MONIKA EMMERLING¹, JÜRGEN OHMER², UTZ FISCHER², CHRISTIAN SCHNEIDER³, SVEN HÖFLING¹, and SEBASTIAN KLEMBT¹ — ¹Technische Physik, RCCM and Würzburg-Dresden Cluster of Excellence ct.qmat, University of Würzburg, Germany — ²Department of Biochemistry, University of Würzburg, Germany — ³Institute of Physics, University of Oldenburg, Germany

Light can carry two different kinds of angular momentum: spin angular momentum (SAM), which is associated with polarization, and orbital angular momentum (OAM), which occurs in light with spiral phase fronts. In recent years, it has been shown that rotational symmetry of a microcavity systems leads to an effective spin-orbit coupling of the SAM and the OAM of photons, resulting in new polariton eigenstates.

Here, we study helical Laguerre-Gaussian modes $LG_{0\pm 1}^{\sigma_{\pm}}$ formed in such systems. For a total angular momentum of $J = 0$, both eigenstates are radially and azimuthally polarized, respectively. Due to the spatial dependence of the linear polarization, we measure spin vortices for these modes. In contrast, the energetically degenerate modes with $J = 2$ exhibit opposite circular polarization and carry an optical OAM with opposite chirality. Accordingly, phase vortices with opposite sign were measured by polarization-dependent interference measurements.

Moreover, we show that the preservation of pump polarization allows selection of the optical OAM of ± 1 .

HL 41.4 Fri 10:15 H34

Experimental and theoretical studies of the occupied density of states distribution of charge carriers at low temperatures in disordered organic semiconductors — •ANDREI STANKEVYCH, RISHABH SAXENA, HEINZ BÄSSLER, ANDREY KADASHCHUK, and ANNA KÖHLER — Soft Matter Optoelectronics and Bavarian Polymer Institute (BPS), Universitätsstrasse 30, 95448 Bayreuth, Germany

The thermally-stimulated luminescence (TSL) technique has been applied to determine the width of density of state (DOS) distribution σ_{DOS} in pristine amorphous films of 18 common OLED materials. The high-temperature wing of the TSL curve in amorphous materials is an exact replica of the deeper portion of the DOS distribution and yields the effective DOS width. In addition, we mea-

sured the width of the TSL curves σ_{TSL} and found that it scales linearly with σ_{DOS} parameter, suggesting an existence of a universal ratio $\sigma_{TSL} / \sigma_{DOS} \approx 2/3$ observed for a large set of organic materials. The low-temperature energy relaxation of photogenerated carriers within a Gaussian DOS implies a significant narrowing of the ODOS distribution. In order to gain a deeper insight into this effect, we performed extensive Monte-Carlo simulations of charge-carrier energetic relaxation process and found that such "spectral narrowing" effect is a genuine property of the hopping carrier relaxation at low temperature within a Gaussian DOS. Moreover, we found that spatial energy correlation effects, which are indeed present in organic media, must be considered for the quantitative description of experimental observations.

HL 41.5 Fri 10:30 H34

Exploring the interplay of oriented molecules and device performance by post-annealing studies of organic light-emitting diodes — •DINARA SAMIGULINA, CHRISTIAN HÄNISCH, KARL SEBASTIAN SCHELLHAMMER, and SEBASTIAN REINEKE — Dresden Integrated Center for Applied Physics and Photonic Materials (IAPP) and Institute of Applied Physics, Technische Universität Dresden, Germany

HL 42: 2D Materials 6 (joint session HL/CPP/DS)

Time: Friday 9:30–12:00

Location: H36

HL 42.1 Fri 9:30 H36

THz conductivity of nanograined Bi₂Te₃ pellets with varying Te doping — •AHANA BHATTACHARYA¹, JEONGWOO HAN¹, SEPIDEH IZADI², SARAH SALLOUM³, STEPHAN SCHULZ³, GABI SCHIERNING², and MARTIN MITTENDORFF¹ — ¹Universität Duisburg-Essen, Fakultät für Physik, 47057 Duisburg, Germany — ²Universität Bielefeld, Fakultät für Physik, 33615 Bielefeld, Germany — ³Universität Duisburg-Essen, Fakultät für Chemie, 45141 Essen, Germany

The topological insulator Bi₂Te₃ hosts surface states with a high carrier mobility as back scattering of charge carriers is suppressed due to the spin-momentum locking. While in large crystals the electronic properties are dominated by the bulk states, hot-pressed pellets of nanograined Bi₂Te₃ offer a high surface-to-volume ratio, which provides a platform to exploit the surface carriers even in extended samples. Here we employ THz time-domain spectroscopy to disentangle the contribution of surface and bulk carriers to the transport properties. Even at room temperature the THz reflection is determined by characteristic features of the high-mobility surface carriers, i.e. Drude conductivity but also plasmonic contributions. The latter are caused by confinement of the surface carriers due to the mechanical structure of the sample. Variations of the Te content allows to shift the Fermi energy and thus strongly influences the resulting THz spectra.

HL 42.2 Fri 9:45 H36

Direct growth of monolayer MoS₂ on nanostructured silicon waveguides — •A KUPPADAKKATH¹, E NAJAFIDEHAGHANI², Z GAN², A TUNIZ³, G NGO¹, H KNOPF¹, F LÖCHNER¹, F ABTAHI¹, T BUCHER^{1,5}, S SHRADHA¹, T KÄSEBIER¹, S PALOMBA³, N FELDE⁴, P PAUL¹, T ULLSPERGER¹, S SCHRÖDER⁴, A SZEGHALMI^{1,4}, T PERTSCH^{1,4}, I STAUDE^{1,5}, U ZEITNER^{1,4}, A GEORGE², A TURCHANIN², and F EILENBERGER¹ — ¹Institute of Applied Physics (FSU), Jena, Germany — ²Institute of Physical Chemistry (FSU), Jena, Germany — ³Sydney Nano, Camperdown, Australia — ⁴Fraunhofer IOE, Jena, Germany — ⁵Institute of Solid State Physics (FSU), Jena, Germany

We report for the first time the direct growth of Molybdenum disulfide (MoS₂) monolayers on nanostructured silicon-on-insulator waveguides. Our results indicate the possibility of utilizing the Chemical Vapour Deposition (CVD) on nanostructured photonic devices in a scalable process. Direct growth of 2D material on nanostructures rectifies many drawbacks of the transfer-based approaches. We show that the van der Waals materials grow conformally across the curves, edges, and the silicon-SiO₂ interface of the waveguide structure. Here, the waveguide structure used as a growth substrate is complex not just in terms of its geometry but also due to the two materials (Si and SiO₂) involved. A transfer-free method like this yields a novel approach for functionalizing nanostructured, integrated optical architectures with an optically active direct semiconductor.

HL 42.3 Fri 10:00 H36

Atomic layer deposition of ternary MoWS₂ — •CHRISTIAN TESSAREK, TIM GRIEB, ANDREAS ROSENAUER, and MARTIN EICKHOFF — Institut für Festkörperphysik, Universität Bremen

Two-dimensional (2D) monolayers of binary molybdenum disulfide (MoS₂) and tungsten disulfide (WS₂) belong to the transition metal dichalcogenide (TMDC) material family and are direct band gap semiconductors. The optical band gap of monolayer MoS₂ and WS₂ is ~1.9 and 2.0 eV, respectively. Ternary Mo_xW_{1-x}S₂ enables tuning of excitonic transition energy dependent on the concentration x .

Atomic layer deposition (ALD) is used to deposit MoWS₂ in the whole composition range between pure MoS₂ and WS₂. The concentration x is determined

by the frequency position of the A_{1g} Raman mode. The distribution of W and Mo atoms in the crystal lattice of MoWS₂ is studied by high resolution scanning transmission electron microscopy. Additional annealing is performed to improve structural and optical properties. Photoluminescence spectroscopy measurements show concentration dependent spectral position of A and B excitonic emission.

HL 42.4 Fri 10:15 H36

Epitaxial growth of post transition metal chalcogenides: From standard approaches to new capabilities — •EUGENIO ZALLO^{1,2}, MICHELE BISSOLO¹, MARCO DEMBECKI¹, GREGOR KOBLMÜLLER¹, and JONATHAN J. FINLEY¹ — ¹Walter-Schottky-Institut und Physik Department, Technische Universität München, Am Coulombwall 4, 85748, Garching, Germany — ²Paul-Drude-Institut für Festkörperelektronik, Leibniz-Institut im Forschungsverbund Berlin e.V., Hausvogteiplatz 5-7, 10117, Berlin, Germany

Van der Waals (vdW) materials grown epitaxially are an urgent challenge for the development of scalable and high-crystalline-quality semiconductor films that can be exploited for novel device technologies. 2D materials "beyond graphene" have sparked immense interest in recent years, due to their excellent physical properties. Among them, post transition metal chalcogenides (PTMC, M={In,Ga} and C={S,Se,Te}) are vdW semiconductor materials with extraordinary photoresponsivity, a quasi-direct gap with a Mexican hat valence band and promising thermoelectric properties but they suffer from fast layer oxidation. In this presentation, the molecular beam epitaxy (MBE) growth of large-area PTMC is demonstrated on 3D and 2D bonded substrates by means of encapsulation strategies and careful microscopic and spectroscopic characterizations supported by density functional theory calculations. In order to study the pristine information of air sensitive materials, we present a cutting edge UHV cluster tool for the synthesis of ultrapure 2D-PTMCs and their heterostructures. The potential directions will be described.

HL 42.5 Fri 10:30 H36

Fabrication of Dielectric Mirrors and Microcavity Configurations for Light-Matter Coupling with Transition-Metal Dichalcogenides Heterostructures — •CHIRAG PALEKAR¹, MANAN SHAH², FYNN KUNZE², PETER KLAR², STEPHAN REITZENSTEIN¹, and ARASH RAHIMI-IMAN² — ¹Institute of Solid State Physics, Technische Universität Berlin, D-10623, Germany. — ²I. Physikalisches Institut und Zentrum für Materialwissenschaften, Justus-Liebig Universität Gießen, D-35392, Germany

15 min. break

HL 42.6 Fri 11:00 H36

Selective area growth of MoS₂ via CVD on patterned GaN-AIO_x substrates — •SIMON WÖRLE, THERESA GRÜNLEITNER, ALEX HENNING, and IAN SHARP — Walter Schottky Institute and Physics Department, Technical University of Munich, Garching, Germany

Two-dimensional (2D) transition metal dichalcogenides have attracted considerable attention due to their unique optoelectronic properties. For the application of 2D materials in semiconductor devices, the controlled and scalable synthesis of high-quality 2D materials is critical.

Here, we demonstrate the selective area growth of MoS₂ by chemical vapor deposition (CVD) on GaN substrates that were patterned with ultrathin aluminum oxide coatings created by low-temperature atomic layer deposition. Optical and scanning electron microscopy images show that mono- and few-layer

MoS₂ flakes preferentially nucleate and grow directly on the (uncoated) GaN. Atomic force microscopy and Raman measurements further reveal the formation of triangular and star-like shaped multilayer MoS₂ crystals at the interfaces between GaN and AlO_x. Moreover, the observed fixed orientation of the triangular MoS₂ flakes with respect to the GaN substrate lattice indicates van der Waals epitaxy. By altering the CVD growth conditions, the density of deposited MoS₂ flakes can be tuned, resulting in the growth of either isolated MoS₂ nanosheets or continuous films, in the latter of which the individual flakes have coalesced.

The presented results mark an important step towards integrated MoS₂ based heterostructures for semiconductor device applications.

HL 42.7 Fri 11:15 H36

Patterned growth of transition metal dichalcogenides monolayers and multilayers for electronic and optoelectronic device application — •SEUNG HEON HAN¹, ZIYANG GAN¹, EMAD NAJAFIDEHAGHANI¹, FATEMEH ABTAHI², CHRISTOF NEUMANN¹, JULIAN PICKER¹, TOBIAS VOGEL², UWE HÜBNER³, FALK EILENBERGER², ANTONY GEORGE¹, and ANDREY TURCHANIN¹ — ¹Institute of Physical Chemistry, Friedrich Schiller University Jena, Jena, Germany — ²Institute of Applied Physics, Friedrich Schiller University Jena, Jena, Germany — ³Leibniz Institute of Photonic Technology (IPHT), Jena, Germany

We present a simple, large area, cost effective soft lithographic method for growth of high-quality two-dimensional transition metal dichalcogenides (TMDs). Initially, a liquid precursor (Na₂MoO₄ in aqueous solution) is patterned on the growth substrate using micro-molding in capillaries (MIMIC) technique. Subsequently, a chemical vapor deposition (CVD) step is employed to convert the precursor patterns to monolayer, few layers, or bulk TMDs, depending on the precursor concentration. The grown patterns were characterized using optical microscopy, atomic force microscopy, Raman spectroscopy, X-ray photoelectron spectroscopy, scanning electron microscopy, and photoluminescence spectroscopy to reveal their morphological, chemical, and optical characteristics. The applicability of the grown patterned TMDs were tested for application such as field effect transistors, photodetectors, and memtransistor devices.

HL 42.8 Fri 11:30 H36

Conductive 2D MOFs in van-der-Waals heterostructures — •JONAS PÖHLS¹, ZHIYONG WANG², RENHAO DONG², and THOMAS WEITZ¹ — ¹I. Physical Institute University of Göttingen, Göttingen, Germany — ²Technical University of Dresden, Dresden, Germany

In conventional three-dimensional (3D) Metal-Organic Frameworks (MOFs) the electric conductivity is limited by the large separation of the metal centers by the

organic ligands. Recent advantages in the synthesis of layered two-dimensional conjugated MOFs (2D c-MOFs) lead to a large improvement of the electronic properties, these materials allow a charge transfer along both interlayer (π - π -stacking) and intralayer (basal plane) directions [1]. In order to elucidate the underlying charge transport mechanisms in the 2D c-MOFs, we perform electronic characterizations of the films implemented in field-effect transistors under varying conditions. In addition to the improved properties of the 2D c-MOFs themselves, their 2D nature make them also a promising candidate for the fabrication of van-der-Waals heterostructures with other 2D materials like graphene, which could give access to a variety of interaction-driven effects. We present first results on the charge transport of 2D c-MOFs down to the size of single crystals as well as implemented in van-der-Waals heterostructures.

[1] Z. Wang et al. "Interfacial Synthesis of Layer-Oriented 2D Conjugated Metal*Organic Framework Films toward Directional Charge Transport", J. Am. Chem. Soc. (2021)

HL 42.9 Fri 11:45 H36

Controlled Encapsulation of Monolayer MoS₂ with Ultrathin Aluminium Oxide for Tunnel Contacts — •SERGEJ LEVASHOV, CHENJIANG QIAN, THERESA GRÜNLEITNER, JON J. FINLEY, ALEX HENNING, and IAN D. SHARP — Walter Shottky Institut, TUM, München, Deutschland

Two-dimensional (2D) semiconductors have unique optoelectronic properties that provide the opportunity to overcome current scaling and performance limits of semiconductor devices. To harness the full of potential of 2D materials, requires their seamless integration with bulk materials. In particular, contacting mono- and few-layer 2D semiconductors with metals is challenging since the deposition process may introduce defects impeding interfacial charge transport. Here we use low-temperature atomic layer deposition to encapsulate monolayer MoS₂ with a van der Waals bonded and ultrathin aluminium oxide (AlO_x) layer. The 18 Å thin AlO_x coating introduces additional charge carriers ($\sim 5 \cdot 10^{12} \text{ cm}^{-2}$), while it also protects monolayer MoS₂ from defect creation during metallization. Microscratching of the AlO_x adlayer by contact mode atomic force microscopy and subsequent spectroscopic analysis demonstrate the reversibility of the charge transfer doping effect, indicating weak interaction. Importantly, current voltage measurements yielded a two-fold reduction in the contact resistance for MoS₂ field-effect transistors contacted with AlO_x interlayer. Overall, this work demonstrates the beneficial effect of the AlO_x adlayer for improving 2D device contacts and provides a scalable route to the damage-free integration of 2D semiconductors.

Crystalline Solids and their Microstructure Division

Fachverband Kristalline Festkörper und deren Mikrostruktur (KFM)

Prof. Dr. Theo A. Scherer
 Karlsruher Institut für Technologie (KIT) IAM-AWP
 Hermann-von-Helmholtz-Platz 1
 D-76344 Eggenstein-Leopoldshafen
 theo.scherer@kit.edu

Overview of Invited Talks and Sessions

(Lecture halls H5 and H7; Poster P2)

Invited Talks

KFM 2.1	Mon	9:30–10:00	H5	Domain-wall engineering in multiferroic materials — •GUILLAUME NATAF
KFM 2.5	Mon	11:15–11:45	H5	Charged Higher Order Topologies in Room Temperature Magnetoelectric Multiferroic Thin Films — •SHELLY CONROY, KALANI MOORE, SINEAD GRIFFIN, LYNETTE KEENEY, EOGHAN O'CONNELL
KFM 7.1	Mon	15:00–15:30	H5	Multiferroic coupling on the level of domain walls — •MADS C. WEBER, YANNIK ZEMP, MARCELA GIRALDO, EHSAN HASSANPOUR, QUINTIN MEIER, YUSUKE TOKUNAGA, YOSHINORI TOKURA, SANG-WOOK CHEONG, NICOLA N. SPALDIN, THOMAS LOTTERMOSER, MANFRED FIEBIG
KFM 10.2	Tue	10:00–10:30	H5	Negative capacitance and voltage amplification in ferroelectric heterostructures — •JORGE INIGUEZ
KFM 10.4	Tue	11:15–11:45	H5	Magnetization processes in SmFeO₃ — •THOMAS SCHREFL, ALEXANDER KOVACS, ROMAN BEIGELBECK, HUBERT BRÜCKL, SHIXUN CAO, WEI REN
KFM 18.1	Wed	15:00–15:30	H5	Deep understanding of advanced optical and dielectric materials for fusion diagnostic applications — •ANATOLI I. POPOV, E KOTOMIN, V KUZOVKOV, A LUSHCHIK, THEO A SCHERER

Invited Talks of the joint Symposium **Frontiers of Orbital Physics: Statics, Dynamics, and Transport of Orbital Angular Momentum (SYOP)**

See SYOP for the full program of the symposium.

SYOP 1.1	Mon	9:30–10:00	H1	Orbital degeneracy in transition metal compounds: Jahn-Teller effect, spin-orbit coupling and quantum effects — •DANIEL KHOMSKII
SYOP 1.2	Mon	10:00–10:30	H1	Orbital magnetism out of equilibrium: driving orbital motion with fluctuations, fields and currents — •YURIY MOKROUSOV
SYOP 1.3	Mon	10:30–11:00	H1	Orbitronics: new torques and magnetoresistance effects — •MATHIAS KLÄUI
SYOP 1.4	Mon	11:15–11:45	H1	Orbital and total angular momenta dichroism of the THz vortex beams at the antiferromagnetic resonances — •ANDREI SIRENKO
SYOP 1.5	Mon	11:45–12:15	H1	Observation of the orbital Hall effect in a light metal Ti — •GYUNG-MIN CHOI

Invited Talks of the joint Symposium **SKM Dissertation Prize 2022 (SYSD)**

See SYSD for the full program of the symposium.

SYSD 1.1	Mon	10:15–10:45	H2	Charge localisation in halide perovskites from bulk to nano for efficient optoelectronic applications — •SASCHA FELDMANN
SYSD 1.2	Mon	10:45–11:15	H2	Nonequilibrium Transport and Dynamics in Conventional and Topological Superconducting Junctions — •RAFFAEL L. KLEES
SYSD 1.3	Mon	11:15–11:45	H2	Probing magnetostatic and magnetotransport properties of the antiferromagnetic iron oxide hematite — •ANDREW ROSS
SYSD 1.4	Mon	11:45–12:15	H2	Quantum dot optomechanics with surface acoustic waves — •MATTHIAS WEISS

Invited Talks of the joint Symposium United Kingdom as Guest of Honor (SYUK)

See SYUK for the full program of the symposium.

SYUK 1.1	Wed	9:30–10:00	H2	Structure and Dynamics of Interfacial Water — •ANGELOS MICHAELIDES
SYUK 1.2	Wed	10:00–10:30	H2	A molecular view of the water interface — •MISCHA BONN
SYUK 1.3	Wed	10:30–11:00	H2	Motile cilia waves: creating and responding to flow — •PIETRO CICUTA
SYUK 1.4	Wed	11:00–11:30	H2	Cilia and flagella: Building blocks of life and a physicist's playground — •OLIVER BÄUMCHEN
SYUK 1.5	Wed	11:45–12:15	H2	Computational modelling of the physics of rare earth - transition metal permanent magnets from SmCo₅ to Nd₂Fe₁₄B — •JULIE STAUNTON
SYUK 2.1	Wed	15:00–15:30	H2	Hysteresis Design of Magnetic Materials for Efficient Energy Conversion — •OLIVER GUTFLEISCH
SYUK 2.2	Wed	15:30–16:00	H2	Non-equilibrium dynamics of many-body quantum systems versus quantum technologies — •IRENE D'AMICO
SYUK 2.3	Wed	16:00–16:30	H2	Quantum computing with trapped ions — •FERDINAND SCHMIDT-KALER
SYUK 2.4	Wed	16:45–17:15	H2	Breaking the millikelvin barrier in cooling nanoelectronic devices — •RICHARD HALEY
SYUK 2.5	Wed	17:15–17:45	H2	Superconducting Quantum Interference Devices for applications at mK temperatures — •SEBASTIAN KEMPF

Sessions

KFM 1.1–1.3	Sun	16:00–18:15	H3	Tutorial: Functional Ferroics (joint session KFM/TUT)
KFM 2.1–2.7	Mon	9:30–12:25	H5	Focus Session: Defects and Interfaces in Multiferroics 1
KFM 3.1–3.4	Mon	9:30–10:50	H7	Microscopy and Tomography with X-ray, Photons, Electrons, Ions and Positrons
KFM 4.1–4.11	Mon	9:30–12:45	H34	Perovskite and Photovoltaics 1 (joint session HL/PPP/KFM)
KFM 5.1–5.9	Mon	10:30–13:00	S053	New Methods and Developments: Scanning Probe Techniques 1 (joint session O/KFM)
KFM 6.1–6.4	Mon	11:05–12:25	H7	Instrumentation and Methods for Micro- and Nanoanalysis
KFM 7.1–7.6	Mon	15:00–17:25	H5	Focus Session: Defects and Interfaces in Multiferroics 2
KFM 8.1–8.6	Mon	15:00–17:15	H7	Crystallography in Materials Science, Microstructure and Dielectric Properties
KFM 9.1–9.5	Mon	15:00–16:15	S053	New Methods and Developments: Scanning Probe Techniques 2 (joint session O/KFM)
KFM 10.1–10.6	Tue	9:30–12:25	H5	Focus session: Polar Materials Meet Energy demands
KFM 11.1–11.5	Tue	9:30–11:10	H7	Crystal Structure Defects / Real Structure / Microstructure
KFM 12.1–12.12	Tue	9:30–12:45	H37	Skyrmions 1 (joint session MA/KFM)
KFM 13.1–13.5	Tue	10:15–11:30	H46	Materials for Storage and Conversion of Energy (joint session MM/KFM)
KFM 14.1–14.7	Wed	9:30–12:05	H5	Ferroics – Domains and Domain Walls 1
KFM 15.1–15.7	Wed	9:30–12:05	H7	Materials for Energy Storage (joint session KFM/PPP)
KFM 16.1–16.11	Wed	9:30–12:30	H33	Oxide Semiconductors (joint session HL/KFM)
KFM 17.1–17.10	Wed	15:00–18:30	H3	Focus Session: Surfaces and Interfaces of (Incipient) Ferroelectrics (joint session O/KFM)
KFM 18.1–18.5	Wed	15:00–16:50	H5	Focus Session: Diamond and related dielectric materials
KFM 19.1–19.3	Wed	15:00–16:00	H7	Ferroics – Domains and Domain Walls 2
KFM 20.1–20.11	Wed	15:00–18:15	H34	Perovskite and Photovoltaics 2 (joint session HL/PPP/KFM)
KFM 21.1–21.12	Wed	15:00–18:30	H36	Functional semiconductors for renewable energy solutions (joint session HL/KFM)
KFM 22	Wed	17:00–18:00	H5	Members' Assembly
KFM 23.1–23.13	Thu	9:30–12:45	H37	Skyrmions 2 (joint session MA/KFM)
KFM 24.1–24.7	Thu	10:30–12:30	H6	New Methods and Developments: Spectroscopies, Diffraction and Others (joint session O/KFM)
KFM 25.1–25.21	Thu	15:00–18:00	P2	Poster
KFM 26.1–26.8	Thu	15:00–18:30	H10	Focus Session: Topological Devices (joint session TT/KFM)
KFM 27.1–27.6	Thu	15:00–16:30	H31	Perovskite and Photovoltaics 3 (joint session HL/PPP/KFM)
KFM 28.1–28.10	Thu	15:00–17:45	H37	Topological Insulators (joint session MA/KFM)
KFM 29.1–29.7	Thu	15:00–16:45	H47	Multiferroics and Magnetoelectric Coupling (joint session MA/KFM)
KFM 30.1–30.13	Fri	9:30–12:45	H37	Skyrmions 3 (joint session MA/KFM)
KFM 31.1–31.4	Fri	11:30–12:30	H38	Electrical, Dielectrical and Optical Properties of Thin Films (joint session PPP/KFM)

Members' Assembly of the Crystalline Solids and their Microstructure Division

Wednesday 17:00–18:00 H5

Sessions

– Invited Talks, Prize Talks, Topical Talks, Tutorials, Contributed Talks, and Posters –

KFM 1: Tutorial: Functional Ferroics (joint session KFM/TUT)

Chair: Dr. Jan Schultheiß (Augsburg University / NTNU Trondheim)

Time: Sunday 16:00–18:15

Location: H3

Tutorial

KFM 1.1 Sun 16:00 H3

Domains and domain walls in functional ferroics — •DENNIS MEIER — Department of Materials Science and Engineering, Norwegian University of Science and Technology — Center for Quantum Spintronics, Department of Physics, Norwegian University of Science and Technology, Trondheim, Norway

Ferroic materials with spontaneous magnetic or electric long-range order are a rich source for functional phenomena. Ferromagnets, for example, are used in hard discs and read heads, whereas ferroelectrics find application as capacitors, energy harvesters, and in tunnel junctions. The rich functionality of ferroic materials is closely linked to their domain structures and the responses of the domains to external stimuli.

In this tutorial, I will give an introduction to the fundamentals that underpin the domain formation in ferroics and discuss different microscopy techniques that allow for imaging electric and magnetic domains. Furthermore, we will talk about more exotic systems, such as improper ferroelectrics and multiferroics, where the interplay of coexisting order parameters gives rise to completely new domain and domain wall properties at the nanoscale. Open experimental challenges will be addressed, as well as future application and research opportunities.

Tutorial

KFM 1.2 Sun 16:45 H3

Theory and simulations of ferroelectrics and related materials — •JORGE INIGUEZ — Luxembourg Institute of Science and Technology — University of Luxembourg

In this tutorial I will introduce the theoretical and simulation methods most frequently employed to investigate ferroelectrics and related materials (antiferroelectrics, multiferroics). I will start from the general electronic-structure methods that permit predictive calculations at the atomic scale, and introduce successive simplifications to eventually reach continuum field schemes that give us access to the mesoscale. I will illustrate the specificity and usefulness of the dif-

ferent approaches by presenting, for each of them, one or two classic examples of application. In passing, this will allow me to emphasize the key role that simulation has played in our field, and to touch upon interesting possibilities for application in energy-related problems.

Jorge Íñiguez's work on ferroelectrics and related materials is mainly funded by the Luxembourg National Research Fund, currently through projects FNR/C18/MS/12705883/REFOX/Gonzalez, INTER/NWO/20/15079143, and C21/MS/15799044.

Tutorial

KFM 1.3 Sun 17:30 H3

Atomic scale analysis of ferroic domain walls — •SHELLY CONROY — Department of Materials, London Centre of Nanotechnology, Imperial College London, United Kingdom

The dynamic interfaces of ferroic materials known as domain walls by-pass the static limitations of traditional nano-device designs. In contrast to hetero-interfaces between different materials, domain walls can be created, moved and removed via an applied stimulus. By combining multiple ferroic properties such as electricity and magnetism, new multi-functional interactive device applications are possible. As these mobile walls can be atomically sharp, it is essential to have physical characterisation at this scale spatially and time-resolved. In this tutorial, I will give an introduction to electron microscopy techniques starting with how to identify domain patterns in the bulk samples, and the most appropriate electron microscopy techniques to use with increasing magnification, leading to pico-meter characterisation. We will discuss some of the most recent advances in electron microscopy characterisation methods for ferroelectrics such as visualising electric charge density at sub-angstrom resolution, and the benefits of coupling polarisation characterisation with electron energy loss spectroscopy band structure analysis. We will then talk about how one can probe multiferroic properties such as magnetic field, strain and phonon modes. As one of the most exciting aspects of ferroic domain walls is their mobility, the various in situ options to investigate their dynamics will be detailed.

KFM 2: Focus Session: Defects and Interfaces in Multiferroics 1

The focus session is dedicated to advanced nano scale-characterization, property-engineering, and modelling methods of multiferroic materials focusing on defects and interfaces. Typical examples may include ferroic domain walls, microstructural levers, or strain effects. Further, applications in novel nanoelectronic devices and nano-related engineering concepts of macroscopic properties of multiferroics are of interest.

Organizers: Dr. Jan Schultheiß (Augsburg University, NTNU Trondheim) and Dr. Marion Höfling (DTU Copenhagen)

Chair: Dr. Marion Höfling (DTU Copenhagen)

Time: Monday 9:30–12:25

Location: H5

Invited Talk

KFM 2.1 Mon 9:30 H5

Domain-wall engineering in multiferroic materials — •GUILLAUME NATAF — GREMAN UMR7347, CNRS, University of Tours, INSA Centre Val de Loire, 37000 Tours, France

Ferroelectric and ferroelastic domain walls are two-dimensional topological defects with thicknesses approaching the unit cell level that can move in response to an electric-field or an applied stress. They exhibit emergent functional properties, such as polarity in non-polar systems or electrical conductivity in otherwise insulating materials, and due their complex strain profiles they interact with phonons as 'defects' would.

In this talk I will: (1) Show how to characterize domain walls with optical techniques (polarized light optical microscopy, liquid crystal decoration, Raman spectroscopy); (2) Discuss how domain walls move in response to an electric field or an applied stress, through discrete impulsive jumps, indicators of avalanches on a broad range of scales; (3) Show that domain walls can be used to induce large thermal conductivity variations in materials.

KFM 2.2 Mon 10:00 H5

Engineering of improper ferroelectric vortex- and stripe-like domains in polycrystalline ErMnO_3 — •MAX HAAS, JAN SCHULTHEISS, and DENNIS MEIER — Norwegian University of Science and Technology (NTNU), 7034 Trondheim, Norway

The functionality and physical properties of ferroelectric materials are intimately coupled to their domain structure. An exciting recent discovery are topologically protected vortex domains in hexagonal manganites, which are of interest for different fields ranging from nanoelectronics to cosmology-related questions. A key characteristic of the domain structure is the vortex density, that can readily be tuned via the cooling rate across the ferroelectric phase transition.

Here, we explore the effect of cooling rate variations in combination with three-dimensional spatial confinement in high-quality ErMnO_3 polycrystals. Utilizing piezoresponse force microscopy, we demonstrate a propensity for the formation of stripe-like domains. Analogous to the vortex-like domains observed in ErMnO_3 single crystals, we find that the periodicity of the stripe-like domains depends on the cooling rate through the Curie temperature. For cooling rates in the range of 10^{-2} to 10^1 K/min, the periodicity of the stripe-domains increases

logarithmically. This scaling behavior is explained based on the interplay between cooling rate and long-ranging strain fields, offering new possibilities for the engineering of domains and domain walls in polycrystalline improper ferroelectrics.

KFM 2.3 Mon 10:20 H5

Tuning multiferroic properties in hexagonal YMnO_3 by manipulation of the structural order — •M. GIRALDO¹, H. SIM², A. SIMONOV¹, M. LILIENBLUM¹, A. SAMIR¹, E. GRADAUSKAITE¹, Y. HEO¹, M. ROSSELL³, M. TRASSIN¹, J.-G. PARK², TH. LOTTERMOSER¹, and M. FIEBIG¹ — ¹Department of Materials, ETH Zurich — ²Department of Physics and Astronomy, Seoul National University — ³Electron Microscopy Center, EMPA

We investigate the enhancement and suppression of the structural distortion (Q) in hexagonal YMnO_3 upon substituting Mn by Al and Ga. We demonstrate its consequences on the electric and magnetic long-range order. We deploy various techniques for a systematic investigation. We observe a progressive decrease in the structural order. This behaviour is caused by the chemical pressure induced by the ionic size of Al and Mn. On the level of the ferroelectric domains, the suppression of the structural order manifests in a progressive size decrease upon increased Al concentration. We do not observe a domain size variation upon Ga substitution. Our experiments suggest that, surprisingly, the progressive reduction on the structural distortion is not directly proportional to a decrease in ferroelectric polarization. On the magnetic level, we find a progressive decrease of the ordering temperatures. This is due to the direct perturbation of the magnetic sublattices formed by the Mn^{3+} moments and the progressive dilution of the magnetic long-range order. By tracing changes in the inherent properties of these systems, we aim to broaden the understanding for new routes in the manipulation of ferroic properties in these compounds.

KFM 2.4 Mon 10:40 H5

Strain-induced multiferroic ribbons in non-multiferroic phase of MnWO_4 — •LEA FORSTER¹, SHINGO TOYODA², MANFRED FIEBIG^{1,2}, TAKA-HISA ARIMA^{2,3}, YOSHINORI TOKURA^{2,4,5}, and NAOKI OGAWA^{2,5,6} — ¹Department of Materials, ETH Zurich, Switzerland — ²RIKEN CEMS, Saitama, Japan — ³Department of Advanced Materials Science, University of Tokyo, Kashiwa, Japan — ⁴Tokyo College, University of Tokyo, Tokyo, Japan — ⁵Department of Applied Physics, University of Tokyo, Tokyo, Japan — ⁶PRESTO, JST, Kawaguchi, Japan

Local structures, such as structural defects, interfaces, and domain walls have the potential to exhibit different physical properties than the bulk. The occurrence of magnetic and electric orders in a confined area may be of particular interest for technological applications, for example, to electrically control the magnetization in memory devices. However, probing local multiferroic structures is challenging caused by a lack of experimental techniques. In this study, we demonstrate a ribbon-shaped, spatially confined multiferroic phase in a non-multiferroic environment in MnWO_4 . We use optical second harmonic generation imaging to show that a multiferroic phase can be generated by local strain within a non-multiferroic bulk structure. Furthermore, we reveal within the confined multiferroic regions domains with different electric polarization directions and demonstrate deterministic writing of a multiferroic state by the application of strain.

15 min. break

Invited Talk

KFM 2.5 Mon 11:15 H5

Charged Higher Order Topologies in Room Temperature Magnetoelectric Multiferroic Thin Films — •SHELLY CONROY^{1,2}, KALANI MOORE², SINEAD GRIFFIN³, LYNETTE KEENEY⁴, and EOGHAN O'CONNELL² — ¹Imperial College London, London, United Kingdom — ²University of Limerick, Limerick, Ireland — ³Lawrence Berkeley National Laboratory, Berkeley, USA — ⁴Tyndall National Institute, Cork, Ireland

Multiferroic topologies are an emerging solution for future low-power magnetic nanoelectronics due to their combined tuneable functionality and mobility. Here, we show that in addition to being magnetoelectric multiferroic at room temperature, thin film Aurivillius phase $\text{Bi}_6\text{TixFeyMnzO}18$ is an ideal material platform for both domain wall and vortex topology based nanoelectronic devices. Utilising atomic resolution electron microscopy and atom probe tomography, we reveal the presence and structure of 180 type charged head-to-head and tail-to-tail domain walls passing throughout the thin film. Theoretical calculations confirm the sub-unit cell cation site preference and charged domain wall energetics for $\text{Bi}_6\text{TixFeyMnzO}18$. Finally, we show that polar vortex type topologies also form at out-of-phase boundaries of stacking faults when interlaminar strain and electrostatic energy gradients are altered. This study could pave the way for controlled polar vortex topology formation via strain engineering in other multiferroic thin films. Moreover, these results confirm the sub-unit-cell topological features play an important role in controlling the charge and spin state of Aurivillius phase films and other multiferroic heterostructures.

KFM 2.6 Mon 11:45 H5

X-ray investigation of a multiferroic YBaCuFeO_5 single crystal — •ARKADY SIMONOV¹, MARISA MEDARDE², and RUGGERO FRISON³ — ¹ETH Zürich, Zürich, Switzerland — ²Paul Scherrer Institut (PSI), Willigen, Switzerland — ³University of Zürich, Zürich, Switzerland

Recent reports have shown that type-II multiferroic materials can be created using chemical disorder. Disorder frustrates magnetic interaction and induces a magnetic spiral state which breaks the inversion symmetry of the crystal [1]. Such a mechanism is robust since it involves only nearest-neighbor magnetic exchanges and can stabilize the spiral state almost up to room temperature in materials like YBaCuFeO_5 . However, due to the complexity of characterizing and controlling chemical disorder, this mechanism is rarely used in practice to design novel multiferroic materials.

In this work we propose single-crystal x-ray diffuse scattering as a method for characterizing disorder. Using YBaCuFeO_5 as our model system, we show that diffuse scattering can efficiently probe the local structure induced by chemical disorder. Moreover, when measured at sufficiently high resolution, diffuse scattering is also sensitive to the magnetic phase transition from antiferromagnetic to spiral state of the YBaCuFeO_5 . This is unusual, and likely indicates that atomic relaxations induced by this transition are larger than the values observed in typical type-II multiferroics.

[1] M. Morin et al. Nat. Comms. 7, (2016): 133758.

KFM 2.7 Mon 12:05 H5

A phase-field model for ferroelectrics with local chemical defects — •DILSHOD DURDIEV¹, FRANK WENDLER¹, TAKAHIRO TSUZUKI², SHUJI OGATA², RYO KOBAYASHI², MASAYUKI URANAGASE², and HIKARU AZUMA² — ¹Friedrich-Alexander University Nuremberg-Erlangen, Fürth, Germany — ²Nagoya Institute of Technology, Nagoya, Japan

In this work, an electromechanical fully coupled phase-field model (PFM) is developed, based upon the approach [1], to study domain evolution and polarization switching under the combined influence of the mechanical and electrical loads and local chemical defects in a BaTiO_3 single crystal. The free energy density of the system includes the Landau potential, gradient, mechanical, piezoelectric and electrical energy, respectively. We apply a Fourier spectral method to solve the coupled constitutive equations. Molecular dynamics simulations with core-shell potentials are conducted to capture the domain wall dynamics including vacancies and cation-anion vacancy dipoles [2]. We develop procedures to obtain kinetic and energetic parameters of the PFM from these simulations. Scaling relations are applied to transfer local fields (of vacancies and aliovalent dopants) as well as local bond effects (from vacancies) from the micro- to the continuum scale.

[1] D. Schrade, et al., Arch. Appl. Mech., 83,1393–1413 (2013).

[2] T. Tsuzuki, et al., Appl. Phys. 131, 194101 (2022).

KFM 3: Microscopy and Tomography with X-ray, Photons, Electrons, Ions and Positrons

Time: Monday 9:30–10:50

Location: H7

KFM 3.1 Mon 9:30 H7

Small-Angle X-ray Scattering: Characterization of arbitrarily shaped nanoparticles using the Debye equation — •JÉRÔME DEUMER¹, BRIAN RICHARD PAUW², SYLVIE MARGUET³, DIETER SKROBLIN¹, OLIVIER TACHÉ³, MICHAEL KRUMREY¹ and CHRISTIAN GOLLWITZER¹ — ¹Physikalisch-Technische Bundesanstalt, Abbestr. 2-12, 10587 Berlin — ²Federal Institute for Materials Research and Testing (BAM), Unter den Eichen 87, 12205 Berlin — ³Université Paris-Saclay, CEA, CNRS, NIMBE, 91191 Gif-sur-Yvette, France

We propose a versatile software package in the form of a Python extension, named CDEF (Computing Debye's scattering formula for Extraordinary Form-factors), to approximately calculate scattering profiles of arbitrarily shaped na-

noparticles for small-angle X-ray scattering (SAXS). CDEF generates a quasi-randomly distributed point cloud in the desired particle shape and then applies the open source software DEBYER for efficient evaluation of Debye's scattering formula to calculate the SAXS pattern. The usage of the software is demonstrated for the evaluation of scattering data of Au nanocubes with rounded edges, which were measured at the four-crystal monochromator beamline of PTB at the synchrotron radiation facility BESSY II in Berlin. Our implementation is fast enough to run on a single desktop computer and perform model fits within minutes. The accuracy of the method was analyzed by comparison with analytically known form factors.

KFM 3.2 Mon 9:50 H7

Flat-field correction of highly-dynamic processes — •THEA ENGLER¹, JOHANNES HAGEMANN¹, CHRISTIAN SCHROER¹, and MATHIAS TRABS² — ¹Deutsches Elektronen-Synchrotron DESY, Hamburg, Germany — ²Karlsruhe Institute of Technology KIT, Germany

Using hard coherent x-rays, as produced in PETRA III at DESY and in the European XFEL, objects with a size of μm to nm can be imaged with full-field phase-contrast imaging. With single-pulse imaging, specifically dynamic processes on the nanosecond-timescales can be investigated. A recorded single-pulse hologram of the object under investigation in a lens-less imaging setup is disturbed by illumination artifacts. The origin of these artifacts are aberrations in the optics, such as figure errors and surface roughness. For further analysis, the illumination artifacts have to be removed, which is achieved by a flat-field correction. Therefore, the x-ray image of the object of interest is divided by an empty-beam image. This approach assumes temporal stability of both illumination and object. In the case of XFEL experiments, the pulse-to-pulse fluctuations stemming from the SASE process violate this assumption. For the imaging conducted at PETRA III, in addition to vibrations in the beamline's optical components, the object itself incorporates dynamic movements. The common case of the flat-field correction can be improved by recording an empty-beam image-series. With principal component analysis (PCA) of the image series and a careful selection of the principal components, a synthetic flat-field can be reconstructed for each object-image.

KFM 3.3 Mon 10:10 H7

Formation and time dynamics of hydrogen-induced vacancies in nickel — •MAIK BUTTERLING¹, LUCA CHIARI², MASANORI FUJINAMI², MACIEJ OSKAR LIECKE¹, ERIC HIRSCHMANN¹, AHMED GAMAL ATTALLAH¹, and ANDREAS WAGNER¹ — ¹Institute for Radiation Physics, Helmholtz-Zentrum Dresden-Rossendorf, Dresden, Germany — ²Department of Applied Chemistry and Biotechnology, Chiba University, 1-33 Yayoi, Inage, Chiba 263-8522, Japan

The formation of hydrogen-induced defects in nickel was investigated by positron annihilation lifetime spectroscopy and the time dynamics of those defects during room temperature aging was tracked with an unprecedented time resolution of the order of minutes using an ultrahigh-flux slow positron beam. Those measurements showed the formation of a large number of atomic vacan-

cies simply by hydrogen addition at room temperature. It could be proved that they were monovacancy-level defects and that hydrogen was trapped and bound to those vacancies during the hydrogen charge. Room temperature aging, i.e. below the stage III temperature in Ni, and the concomitant hydrogen desorption induced the agglomeration of those monovacancies into large vacancy clusters which remained even after all the hydrogen had desorbed and hydrides had disappeared. These results constitute the first empirical evidence that vacancy-hydrogen complexes are induced in Ni only by hydrogen charging and demonstrate that hydrogen has a primary role in the formation and stabilization of vacancies even at room temperature.

KFM 3.4 Mon 10:30 H7

Stereo X-Ray Microscopy: Seeing the nanocosm in 3D — •SINA RÖPER^{1,2}, KAROLINA STACHNIK², LUKAS GROTE², MATTIAS ÅSTRAND³, HANNA OHLIN³, MARTIN SEYRICH¹, SARAH-ALEXANDRA HUSSAK², THOMAS FRISK³, ANDREAS SCHROPP¹, ULRICH VOGT³, DOROTA KOZIEJ², and CHRISTIAN SCHROER^{1,2} — ¹Deutsches Elektronen-Synchrotron DESY, Hamburg, Germany — ²University of Hamburg, Hamburg, Germany — ³KTH Royal Institute of Technology, Stockholm, Sweden

Understanding the nucleation and growth mechanisms involved in the synthesis of nanomaterials is a key factor in determining their performance and functionality. In many cases, these processes are still not well understood in particular, due to the difficulty of observing them *in situ* or *operando*. Scanning hard X-ray microscopy offers the potential for *in situ* nanoimaging of complex chemical systems under relevant environmental conditions. However, standard X-ray tomography relies on the rotation of the sample with respect to the X-ray beam. This is typically not possible for the synthesis of nanoparticles in solution, which requires an extended reaction cell.

We have developed a new stereoscopic X-ray imaging technique with improved depth resolution to overcome these challenges. By simultaneously illuminating the sample with two nanofocused X-rays at different angles, we increased the effective numerical aperture and improved the spatial resolution along the X-ray beam path. This provides a significant gain in depth-sensitivity in ptychography with multi-slicing and allows us to obtain 3D structural information from 2D scans.

KFM 4: Perovskite and Photovoltaics 1 (joint session HL/PPP/KFM)

Time: Monday 9:30–12:45

Location: H34

See HL 5 for details of this session.

KFM 5: New Methods and Developments: Scanning Probe Techniques 1 (joint session O/KFM)

Time: Monday 10:30–13:00

Location: S053

See O 7 for details of this session.

KFM 6: Instrumentation and Methods for Micro- and Nanoanalysis

Time: Monday 11:05–12:25

Location: H7

KFM 6.1 Mon 11:05 H7

Sub-nm Control of Radioactive Isotope Incorporation at Surfaces and Interfaces using Ultra-Low Energy Ion Implantation: The ASPIC and ASCII Vacuum Chambers — •KOEN VAN STIPHOUT, LEONARD-ALEXANDER LIESKE, MANUEL AUGÉ, and HANS HOFSSÄSS — Georg-August-Universität Göttingen, Friedrich-Hund-Platz 1, 37077 Göttingen, Germany

The use of radioactive tracer isotopes has a long history of providing unique insights into magnetic interactions, electric environments and crystal structures of materials at the atomic scale. Experimental techniques such as perturbed γ - γ angular correlations or emission Mössbauer spectroscopy require the incorporation of radioactive isotopes into the crystal lattice. However, as more research focuses on ever-smaller nano-scaled systems such as atomically thin 2D materials, precise and reproducible incorporation becomes challenging. One way of overcoming these difficulties is the introduction of ultra-low energy (ULE) ion implantation (10 - 100 eV), which enables sub-nm control of the implanted probe's location at the first few monolayers of the sample.

We present the refurbishment, design and application of two vacuum chambers that will soon be installed in the ISOLDE experimental hall of CERN: the *apparatus for surface physics and interfaces at CERN(ASPIC)*, an experienced ultra-high vacuum chamber dedicated to surface characterization and modification, and the new *ASPIC's ion implantation (ASCII)* chamber, designed for ULE ion implantation of radioactive probes.

KFM 6.2 Mon 11:25 H7

Combined X-ray Raman Scattering Spectroscopy and X-Ray Diffraction on Shock-Compressed Vitreous SiO₂ — •LENA BUSSMANN¹, MIRKO ELBERS³, CHRISTIAN ALBERS², JOHANNES KAA², MARTIN SUNDERMANN⁴, HLYNUR GRETARSSON⁴, NICOLA THIERING², CHRISTIAN STERNEMANN², SINDY FUHRMANN¹, THOMAS SCHLOTHAUER¹, and GERHARD HEIDE¹ — ¹TU Bergakademie Freiberg, Institut für Glas und Glastechnologie/Institut für Mineralogie, D-09599 Freiberg — ²TU Dortmund, Fakultät Physik/DELTA, D-44221 Dortmund — ³Universität Potsdam, Institut für Geowissenschaften, D-14467 Potsdam-Golm — ⁴DESY, D-22609 Hamburg

Vitreous SiO₂ is a suitable model material for dynamic compression experiments: Many of its pressure-related properties are fairly well known, yet, several questions remain unsolved. Vitreous silica has been shock-compressed in the "Reiche Zeche" mine in Freiberg and investigated at the P01 beamline of PETRA III at DESY via X-ray Raman spectroscopy (XRS) and X-ray diffraction (XRD). XRS allows to classify the shock effects on a short scale, while XRD reflects the intermediate-range structure. Results are compared to crystalline SiO₂ modifications. The combination of both methods hence allows to analyse the samples in terms of the effective shock pressure achieved. Furthermore, time-resolved XRD acquisition revealed a structural 'relaxation' process in the shock-compressed samples induced by the X-ray irradiation. This process is studied for different heat-treated glass samples as a function of time and temperature, and characterized by collating the XRD and XRS results.

KFM 6.3 Mon 11:45 H7

X-ray diffraction with micrometer spatial resolution for highly absorbing samples — PRERANA CHAKRABARTI^{1,2}, ANNA WILDEIS¹, MARKUS HARTMANN¹, ROBERT BRANDT¹, GIOVANNI FEVOLA², CHRISTINA OSSIG^{2,3}, MICHAEL STUCKELBERGER², JAN GARREVOET⁴, KEN VIDAR FALCH⁴, VANESSA GALBIERZ⁴, GERALD FALKENBERG⁴, and •PETER MODREGGER^{1,2} — ¹Universität Siegen — ²CXNS, DESY, Hamburg — ³Universität Hamburg — ⁴DESY, Hamburg

We report on a novel goniometer-based setup for X-ray diffraction at high photon energies with micrometer spatial resolution, which was implemented at the P06 beamline of PETRA III. The 6-axes goniometer features 3 translations with 1 nm accuracy and 3 rotations with 0.1 μ rad accuracy and allows for 5D scans: 2 in direct and 3 in reciprocal space. Utilizing X-ray focus sizes of 1 μ m at a photon energy of 35 keV provided by P06, enables us to characterize the strain field of a 1 mm thick, poly-crystalline martensitic steel sample with micrometer spatial resolution. Further, we experimentally demonstrate the assessment of elemental distribution by fluorescence simultaneous with diffraction for high-Z materials in a ACIGS thin film solar cell. Future plans include the extension of multimodal

experiment including ptychography or XBIC and improving spatial resolutions to 200 nm.

KFM 6.4 Mon 12:05 H7

How Silicon Crystals are Used to Disseminate the SI Base Units Mole and Kilogram — •AXEL PRAMANN and OLAF RIENITZ — Physikalisches-Technische Bundesanstalt, Bundesallee 100, 38116 Braunschweig, Germany

It is explained how the SI base units mol and kilogram are disseminated in practice using the X-ray-crystal-density (XRCD) method *counting* silicon atoms in single-crystalline silicon spheres [1-3]. Few practical examples and the status are given how the revision of the SI base units impacts the application of such quantities in chemistry and physics. In case of the XRCD method, the availability of macroscopic single crystalline silicon spheres highly enriched in ²⁸Si is emphasized and the method of the dissemination is shown in detail with regard to the experimental mass spectrometric procedures. [1] K. Fujii et al., *Metrologia*, 53, A19 (2016). [2] B. Guettler, O. Rienitz, A. Pramann, *Annalen der Physik*, 1800292 (2018). [3] R. J. C. Brown, P. J. Brewer, A. Pramann, O. Rienitz, and B. Guettler, *Anal. Chem.* 93, 12147 (2021).

KFM 7: Focus Session: Defects and Interfaces in Multiferroics 2

The focus session is dedicated to advanced nano scale-characterization, property-engineering, and modelling methods of multiferroic materials focusing on defects and interfaces. Typical examples may include ferroic domain walls, microstructural levers, or strain effects. Further, applications in novel nanoelectronic devices and nano-related engineering concepts of macroscopic properties of multiferroics are of interest.

Organizers: Dr. Jan Schultheiß (Augsburg University, NTNU Trondheim) and Dr. Marion Höfling (DTU Copenhagen)

Chair: Dr. Jan Schultheiß (Augsburg University, NTNU Trondheim)

Time: Monday 15:00–17:25

Location: H5

Invited Talk

KFM 7.1 Mon 15:00 H5

Multiferroic coupling on the level of domain walls — •MADS C. WEBER^{1,2}, YANNIK ZEMP¹, MARCELA GIRALDO¹, EHSAN HASSANPOUR^{1,3}, QUINTIN MEIER¹, YUSUKE TOKUNAGA⁴, YOSHINORI TOKURA^{4,5}, SANG-WOOK CHEONG⁶, NICOLA N. SPALDIN¹, THOMAS LOTTERMOSER¹, and MANFRED FIEBIG¹ — ¹ETH Zurich — ²Le Mans University — ³University of Bern — ⁴University of Tokyo — ⁵RIKEN — ⁶Rutgers University

Multiferroic materials are of interest for the coupling of different ferroic properties on the level of the domains. However, this coupling is not only limited to the bulk but concerns the domain walls too. Here, we show on the example of three different multiferroic systems, that the multi order-parameter coupling on the domain wall level leads to a wide variety of intrinsic domain wall phenomena. In (Dy,Tb)FeO₃, we demonstrate that the interaction of two independent magnetic sublattices gives rise to a polar, multiferroic domain wall in a non-multiferroic environment. The crosstalk of ferroelectricity, structural distortions and magnetic order in hex-ReMnO₃ leads to spin rotations of 60°, 120° or 180° about the magnetic domain walls. Depending on the position of the magnetic domain walls with respect of the ferroelectric domain walls, these walls can exchange their rotational character. In the last example, we show that the interplay of two structural distortions in hybrid improper ferroelectrics induces head-to-head and tail-to-tail orientations of the polarization of adjacent ferroelectric domains. These examples illustrate the wide variety of domain wall phenomena thanks to (multi)ferroic coupling effects on the nanoscale.

KFM 7.2 Mon 15:30 H5

3D imaging of multiferroic (LuFeO₃)₉/(LuFe₂O₄)₁ superlattices by atom probe tomography — •KASPER HUNNESTAD¹, HENA DAS², CONSTANTINOS HATZOGLOU¹, MEGAN HOLTZ³, CHARLES BROOKS³, ANTONIUS T. J. HELVOORT¹, DARRELL SCHLON^{3,4}, JULIA MUNDY⁵, and DENNIS MEIER¹ — ¹Norwegian University of Science and Technology, Norway — ²Tokyo Institute of Technology, Japan — ³Cornell University, USA — ⁴Kavli Institute at Cornell for Nanoscale Science, USA — ⁵Harvard University, USA

Oxide interfaces are a rich source for novel physical phenomena, ranging from interfacial superconductivity to unusual (multi-)ferroic effects. Over the last decade, significant progress has been made in both the understanding and engineering of oxide interfaces, propelled by the ongoing progress in the development of atomic-scale characterization techniques.

Here, we introduce atom probe tomography (APT) as versatile tool for studying oxide interfaces, investigating the 3D atomic-scale structure and chemical composition of multiferroic (LuFeO₃)₉/(LuFe₂O₄)₁ superlattices. Our APT measurements reveal a substantial accumulation of oxygen vacancies at the LuFe₂O₄ layers. Based on the data, we quantify the vacancy concentration and discuss their accumulation in relation to calculated defect formation energies

and the multiferroic domain structure. In general, this research establishes a new pathway for studying the interaction of interfaces and point defects in oxides, expanding related atomic-scale investigations into 3D.

KFM 7.3 Mon 15:50 H5

Electric-field control of oxygen defects and local transport properties in ErMnO₃ — •JIALI HE¹, URSULA LUDACKA¹, DONALD M. EVANS¹, THEODOR S. HOLSTAD¹, ERIK D. ROEDE¹, KASPER A. HUNNESTAD¹, KONSTANTIN SHAPOVALOV², ZEWU YAN^{3,4}, EDITH BOURRET⁴, ANTONIUS T. J. VAN HELVOORT¹, SVERRE M. SELBACH¹, and DENNIS MEIER¹ — ¹NTNU Norwegian University of Science and Technology, Norway — ²Institute of Materials Science of Barcelona, Spain — ³ETH Zurich, Switzerland — ⁴Lawrence Berkeley National Laboratory, USA

The electronic properties of complex oxides can be tuned via oxygen defects, offering intriguing opportunities for controlling conductivity. Recently, anti-Frenkel defects moved into focus for minimally invasive property engineering, and their creation makes it possible to adjust the electronic properties without long-range ionic migration or stoichiometry changes. Here, we present a detailed analysis of the electric-field-driven formation and time-voltage-dependent evolution of anti-Frenkel defects in hexagonal ErMnO₃. By combining atomic force microscopy and scanning electron microscopy, we investigate the local electronic transport properties associated with the written defects, complemented by numerical simulations. The study reveals that oxygen interstitial - vacancy pairs can be split under an applied electric field. This splitting leads to spatially separated and well-defined vacancy- and interstitial-rich regions, forming a bipolar nanoscale junction. The results provide new insight into the electric-field-driven ionic migration in ErMnO₃ and defects physics in functional oxides.

15 min. break

KFM 7.4 Mon 16:25 H5

Deep learning evaluation of conductive atomic force microscopy data — LORENZ GLÜCK^{1,2}, •MANUEL ZAHN^{1,3}, LUKAS PUNTIGAM¹, DONALD M. EVANS¹, SOMNATH GHARA¹, MICHAEL HEIDER², and STEPHAN KROHNS¹ — ¹Experimental Physics V, University of Augsburg, 86159 Augsburg — ²Organic Computing Group, University of Augsburg, 86159 Augsburg — ³Institut für Angewandte Physik, Technische Universität Dresden, 01069 Dresden

Machine learning has gained an enormous interest in the past decade to boost data evaluation in many fields of applied physics. For example, feature recognition in high dimensional datasets in scanning probe microscopy (SPM) can be improved and hidden effects resolved. However, the physical relevance of resolved features is normally still determined by humans.

In this work, we investigate if the regularization of a deep learning (DL) neural network, composed of long-short term memory and temporal convolu-

tional network based layers inside an autoencoder architecture, can be utilized to characterize physical significance. We do this on a conductive atomic force microscopy dataset, collected on ferroelectric GaV4S8, as the general properties have already been identified and there are emergent traits at the domain walls. The resolved features from the DL approach are compared to those derived from classical clustering algorithms and classically resolved local material properties. This set up is the first steps to automatic evaluation of physically significant properties in GaV4S8, and is expected to be applicable to other ferroelectric systems.

KFM 7.5 Mon 16:45 H5

Oxygen off-stoichiometry and domain wall conductance in ErMnO₃ — •LEONIE RICHARZ¹, JAN SCHULTHEISS¹, EDITH BOURRET^{2,3}, ZEWU YAN³, ANTONIUS T.J. VAN HELVOORT¹, and DENNIS MEIER¹ — ¹NTNU Norwegian University of Science and Technology, Trondheim, Norway — ²ETH Zurich, Switzerland — ³Lawrence Berkeley National Laboratory, Berkeley, CA, USA

Ferroelectric domain walls are natural interfaces, separating volumes with different orientation of the spontaneous polarization. Due to their symmetry, electrostatics, and strain, the walls can develop completely different electronic properties than the surrounding domains. In ferroelectric oxides, oxygen off-stoichiometry is an additional versatile control parameter. This is reflected by the neutral ferroelectric domain walls in hexagonal manganites: Depending on the oxygen content, their conduction behavior varies from insulating to highly conducting.

In this work, we monitor the electronic transport properties at the domain walls as a function of temperature and oxygen partial pressure with nanoscale spatial resolution. Conductive atomic force microscopy measurements on high-quality ErMnO₃ single crystals show anomalous conductance at the domain walls within the whole temperature range of 25 to 300°C. Furthermore, we find

that by annealing the sample in nitrogen, the domain wall conductance can be enhanced. Our results provide new insight into the impact of environmental parameters on the electronic domain wall properties. This is of interest for the development of atmospheric sensors, adding a new direction to the field of domain wall nanotechnology.

KFM 7.6 Mon 17:05 H5

Manipulation of improper ferroelectric domains in Gd₂(MoO₄)₃ using temperature, electric fields, and mechanical stress — •IVAN USHAKOV¹, THEODOR HOLSTAD¹, DIDIER PERRODIN², EDITH BOURRET^{2,3}, THOMAS TYBELL¹, and DENNIS MEIER¹ — ¹Norwegian University of Science and Technology (NTNU), Norway — ²Lawrence Berkeley National Laboratory, USA

In improper ferroelectrics, the spontaneous polarization arises as a byproduct of magnetic or structural order, promoting the formation of domains and domain walls with unusual electronic transport phenomena and scaling behavior. Gd₂(MoO₄)₃ is a classical example of an improper ferroelectric material where a structural instability leads to the formation of a polar axis.

Here, we expand previous mesoscale microscopy studies of the domain structure to the nanoscale. By using piezoresponse force microscopy, we image the patterns of ferroelectric and structural anti-phase domains in Gd₂(MoO₄)₃. In addition to the established domain patterns, we resolve so far unexplored stripe-like nanodomains with a periodicity of about 60 nm. Temperature-dependent measurements show that the nanodomains are stable up to 70°C. Furthermore, we demonstrate reversible switching of these nanodomains by local electric fields and their control via mechanical stress. Our findings provide new insight into the nanoscale domain-physics of Gd₂(MoO₄)₃ and introduce novel opportunities for domain engineering in improper ferroelectrics.

KFM 8: Crystallography in Materials Science, Microstructure and Dielectric Properties

Time: Monday 15:00–17:15

Location: H7

KFM 8.1 Mon 15:00 H7

In Situ Structural and Optical Characterization of Laser Recrystallization in an Ultrafast TEM — •JAKOB HAGEN, MURAT SIVIS, and CLAUS ROPERS — Max-Planck-Institute for Multidisciplinary Sciences, Göttingen, Germany
Surface-plasmon resonances (SPR) have gained increasing attention due to their widespread use in various scientific fields [1]. These resonantly excited collective free-electron oscillations are able to localize and enhance electromagnetic fields beyond the diffraction limit [2]. To this date, the fabrication of such structures with high optical quality remains challenging, since in general, bottom-up approaches suffer from the poly-crystallinity of the metal which counteracts the plasmon propagation by damping at grain boundaries [3]. In this study, we created plasmonic nanodiscs by electron beam lithography (EBL) and subsequently performed in situ annealing with a pulsed laser source in an ultrafast transmission electron microscope (TEM). This method allows for live-tracking of the boundary migration and also for characterization of SPRs by photon-induced near-field electron microscopy (PINEM) [4]. Upon illumination, the number of grains reduces drastically leading to almost perfect mono-crystals while preserving the shape. Our approach combines the benefits of mono-crystalline plasmonics [5] with nanometrically precise positioning from EBL.

[1] S. Lal et al., Nat. Photonics 1, 641-648 (2007), [2] K. B. Crozier et al., J. Appl. Phys., 94, 4632 (2003), [3] M. Bosman et al., Sci. Rep. 4, 5537 (2014), [4] L. Piazza et al., Nat. Commun. 6, 6407 (2015), [5] J.-S. Huang, Nat. Commun., 1:150 (2010)

KFM 8.2 Mon 15:20 H7

Impact of the stacking sequence on the stability of transition-metal diborides — •THOMAS LEINER¹, NIKOLA KOUTNÁ², PAUL H. MAYRHOFFER², and DAVID HOLEC¹ — ¹Department of Materials Science, Montanuniversität Leoben, Austria — ²Institute of Materials Science and Technology, TU Wien, Austria
Transition-metal diborides are a very hard and brittle type of materials, which, among others, find their use as protective coatings, because of their excellent heat conductivity, oxidation stability and wear resistance.

The investigated diborides XB₂ X=(Cr, Hf, Mn, Mo, Nb, Re, Ta, Ti, V, Zr) occur in three different known stackings, the A-A-A stacking of e.g. TiB₂, the A-B-A-B stacking of ReB₂ and the A-B-B-A stacking of WB₂.

In this work, the impact of the stacking sequence on the stability of diborides is investigated via *ab initio* methods (VASP) and phonon analysis. The energy levels and the energy barriers for the different structures of the transition-metal diborides is calculated and evaluated. The stability of observed local and global energy minima are further investigated by assessing their phonon density of states and their phonon frequencies.

Predictions about a possible stability of certain stackings are made and the behaviour of different diborides was compared to each other.

KFM 8.3 Mon 15:40 H7

Pressure-driven insulator-to-metal transition and superconductivity in one-dimensional transition-metal-trichalcogenide microstructures — •CHIN SHEN ONG¹, L. F. SHI^{2,3}, JIN-GUANG CHENG^{2,3}, IRINA GORLOVA⁴, SERGEY ZYBTSEV⁴, LINGYI AO⁵, JUNWEI HUANG⁵, HONGTAO YUAN⁵, RAMAN THIYAGARAJAN⁶, VADIM POKROVSKI⁴, OLLE ERIKSSON^{1,7}, and MAHMOUD ABDEL-HAFIEZ¹ — ¹Uppsala University, Uppsala, Sweden — ²Chinese Academy of Sciences, Beijing, China — ³University of Chinese Academy of Sciences, Beijing, China — ⁴Moscow — ⁵Nanjing University, Nanjing, China. — ⁶Indian Institute of Technology Madras, Chennai, India — ⁷Örebro University, Örebro, Sweden

Transition metal trichalcogenides exhibit large tunability of nontrivial electronic states by modifying chemical composition, temperature, and pressure. Despite great interest in TMTCs, very little information exists on how their electronic properties change with compression. Here, we systematically investigate the high-pressure behavior of n-type semiconducting TiS₃ of one-dimensional microstructural form. High-pressure electrical resistance measurements up to 98 GPa identify an exotic sequence of transitions from being a semiconductor to insulator, then metal and finally, a hitherto undiscovered superconducting phase at pressures above 70 GPa. The experimental results are supported by first-principles theoretical calculations.

KFM 8.4 Mon 16:00 H7

Impact of point defects on the ferroelectric phase diagram: a molecular dynamics study on the defect arrangements — •SHENG-HAN TENG and ANNA GRÜNEBOHM — Interdisciplinary Centre for Advanced Materials Simulation (ICAMS) and Center for Interface-Dominated High Performance Materials (ZGH), Ruhr-University Bochum, Germany

Ferroelectric perovskites usually host imperfections and defects that affect their functional properties. Aging and fatigue are often related to the redistribution of these defects [1-3]. Microscopic insights are therefore needed to better apply these materials to different applications. In this study, we use the first-principle based effective Hamiltonian method [4] to screen the impact of distribution and agglomeration of point defects on the phase diagrams of BaTiO₃-based materials. With this approach, we can simulate up to 10⁶ unit cells and efficiently investigate different defect arrangements. We find that the local fields induced by the defect dipoles play a key role in ferroelectric phase stability and the optimization of functional properties.

[1] Yuri A. Genenko, Julia Glaum, Michael J. Hoffmann, and Karsten Albe. *Mater. Sci. Eng. B*, **192**, 52-82 (2015)

[2] D. Lupascu and J. Rödel. *Adv. Eng. Mater.* **7**(10), 882-898 (2005)

[3] Xiaobing Ren. *Nat. Mater.* **3**(2), 91-94 (2004)

[4] T. Nishimatsu, A. Grünebohm, U. V. Waghmare, M. Kubo, *J. Phys. Soc. Jpn.* **85**, 114714 (2016)

15 min. break

KFM 8.5 Mon 16:35 H7

Strain-Induced Collapse of Landau Levels in TaAs — •YANG-JUN LEE^{1,2,3}, CHEOL-HWAN PARK^{1,2,3}, and MARIA A.H VOZMEDIANO⁴ — ¹Center for Correlated Electron Systems, Institute for Basic Science, Seoul 08826, Korea — ²Department of Physics and Astronomy, Seoul National University, Seoul 08826, Korea — ³Center for Theoretical Physics, Seoul National University, Seoul 08826, Korea — ⁴Instituto de Ciencia de Materiales de Madrid, CSIC, Cantoblanco, Madrid 28049, Spain

A Weyl semimetal, which has a topologically protected conic electronic structure, hosts interesting phenomena such as Fermi arc surface states and chiral anomaly. Recently, the deformation-driven pseudo gauge fields in strained Weyl semimetals have received attention. Among such examples is the collapse of strain-induced Landau levels in Weyl semimetal. In this study, we establish the theory for the effect of strain-induced gauge fields on realistic Weyl semimetals, and based on first-principles calculations, we investigate the conditions on the external strain for the collapse of Landau levels in TaAs.

KFM 8.6 Mon 16:55 H7

Hidden order in ferroelectric oxide thin films — •JOOHEE BANG¹, NIVES STRKALJ², MARTIN SAROTT¹, MORGAN TRASSIN¹, and THOMAS WEBER¹ — ¹Department of Materials Science, ETH Zurich, Zurich, Switzerland — ²Department of Materials Science and Metallurgy, Cambridge University, Cambridge, United Kingdom

Nontrivial polar topologies such as flux-closure, vortex-antivortex pair, and skyrmions in ferroelectric thin films have recently garnered much interest as they have implications for the creation of new states of matter and hold promise for alternative device configurations for microelectronics [1]. These observations called for an in-depth structural investigation of the material as the polarization states such as orientation and domain architecture define the macroscopic ferroelectric properties in ferroelectric thin films. In fact, characterization of local order in such films using noninvasive probes is important as it not only allows access to the polarization states in the bulk, but also tracks structural local order. Here, we present a newly discovered local order state on ferroelectric lead titanate and dielectric strontium titanate superlattices from a comprehensive reciprocal space investigation analyzed with three-dimensional delta pair distribution function (3D- Δ PDF) method [2]. The structural analysis was performed by collecting a complete three-dimensional diffuse X-ray scattering data, which, to the best of our knowledge, was used for the first time to study local order in single-crystalline thin films.

[1]Yadav, A., et al. 2016

[2]Weber and Simonov 2012

KFM 9: New Methods and Developments: Scanning Probe Techniques 2 (joint session O/KFM)

Time: Monday 15:00–16:15

Location: S053

See O 14 for details of this session.

KFM 10: Focus session: Polar Materials Meet Energy demands

Polar materials, in particular in (anti-) ferroelectrics, play an important role in future energy storage and energy harvesting devices and have a high potential for ultra-low power memory and logic devices as well as energy efficient cooling technologies. The aim of this focus-session is to bring together scientists from theory and experiment to improve the fundamental understanding and optimization of the underlying material properties and microstructures in a multiphysics and multidisciplinary scenario.

Organizers: Prof. Dr. Anna Grünebohm (Bochum) and Prof. Dr. Bai-Xiang Xu (TU Darmstadt)

Chair: Prof. Dr. Anna Grünebohm (Bochum University)

Time: Tuesday 9:30–12:25

Location: H5

Prize Talk

KFM 10.1 Tue 9:30 H5

Einfluss des Sauerstoffgehalts auf das Koerzitivfeld für die Polarisationsumschaltung in HfO₂ aus der Dichtefunktionaltheorie — •LUIS AZEVEDO ANTUNES — Hochschule für angewandte Wissenschaften München — Laureate of the Georg-Simon-Ohm-Prize 2022

Die fortschreitende Miniaturisierung in der Mikroelektronik stößt beim Thema Energieeffizienz zunehmend an ihre Grenzen. Der Grund sind die Speicher- und Schaltkonzepte, welche auf dem Schalten von elektrischen Strömen basieren. Einen Ausweg könnte hier der ferroelektrische Feldeffekt-Transistor (FeFET) bieten, welcher stromsparend und ohne Kondensator viel besser skalierbar ist. Mit dem vor 15 Jahren in einem Industrielabor in Dresden gefundenen ferroelektrischen HfO₂ und ZrO₂ gibt es ein Material, welches die Anforderungen bei sehr kleinen Bauelementen zu erfüllen scheint. Die Fluorit-strukturierte ferroelektrische Phase des HfO₂ weist im Vergleich zu den Perowskit-basierten Ferroelektrika jedoch ein höheres Koerzitivfeld auf, welches die Zuverlässigkeit einschränkt. Derzeit wird der Einfluss von Dotierstoffen sowie von Sauerstoff auf die Eigenschaften des Koerzitivfeldes und weiterer Eigenschaften untersucht. In dem Vortrag wird über First-Principle-Berechnungen dieser Eigenschaften berichtet, welches Übergangszustände in den kristallinen Materialien betrachtet. Die Ergebnisse führen zu einem grundlegenden Verständnis von Sauerstoffdefekten auf die Bindungsstruktur und weiterführend auf das Koerzitivfeld. Die Ergebnisse werden mit experimentell gemessenen Koerzitivfeldern verglichen.

Invited Talk

KFM 10.2 Tue 10:00 H5

Negative capacitance and voltage amplification in ferroelectric heterostructures — •JORGE INIGUEZ — Luxembourg Institute of Science and technology — University of Luxembourg

My group is interested in the behavior of ferroelectric materials that present nontrivial polar orders (vortexes, skyrmions) and properties (chirality, negative capacitance) in situations of reduced dimensionality (ultra-thin layers or films)

and/or subject to suitable electrostatic boundary conditions. In this talk I will review our most recent theoretical results for one of the model systems in the field, the PbTiO₃/SrTiO₃ ferroelectric/dielectric superlattices where many of the above effects were first demonstrated. In particular, I will discuss the negative-capacitance response of such materials, with an emphasis on the attendant voltage amplification. I will show that this anomalous behavior is actually quite frequent, occurring in regular multi-domain structures as well as in novel topological states. Further, I will explain its atomistic underpinnings and show how it can be optimized (to obtain voltage amplifications beyond x10) if the polar layers are tuned to display an incipient ferroelectric state.

Most of the work done in collaboration with M. Graf and H. Aramberri (postdocs at the Luxembourg Institute of Science and Technology) and funded by the Luxembourg National Research Fund through Grants INTER/RCUK/18/12601980 and C18/MS/12705883/REFOX. Other key contributors include P. Zubko (UC London), J. Junquera (U. Cantabria), R. Ramesh (UC Berkeley), etc.

Topical Talk

KFM 10.3 Tue 10:30 H5

Advanced Phase-field Simulation of Ferroelectrics and Antiferroelectrics — •BAI-XIANG XU — Division Mechanics of Functional Materials, Institute of Materials Science, TU Darmstadt

Featured by high power density and high cyclic stability, ferroelectric (FE) and antiferroelectric (AFE) perovskites are distinct type of materials for energy storage and conversion particularly in pulse power equipment, miniaturized electronic devices and electronic control system in electric vehicles. The key issue is to increase the energy storage density, which is strongly related to ferroelectric domain structure in the materials and its interaction with defects.

In this talk I will present advanced phase-field simulations on the domain scale of such energy materials. In the first part, by combining phase-field simulations with dislocation mechanics and driving force theory (Zhou et al. IJSS

2021; Höfling et al. Science, 2021), I will show simulation results and mechanistic understanding on domain wall-dislocation interaction in mechanically hardened ferroelectrics and its impact on properties. In the second part, a high order gradient phase-field model for antiferroelectrics will be presented (Liu and Xu, Script Mat. 2020). It enables simulations of the newly observed incommensurate modulations of (anti-)ferroelectric polarization configuration, which goes beyond the capability of the established models like the Kittel sublattice model. Simulations on the domain structure, hysteresis, and temperature induced FE-AFE phase transition will be shown, along with the comparison to experimental results.

15 min. break

Invited Talk

Magnetization processes in SmFeO₃ — •THOMAS SCHREFL¹, ALEXANDER KOVACS¹, ROMAN BEIGELBECK¹, HUBERT BRÜCKL¹, SHIXUN CAO², and WEI REN² — ¹Department for Integrated Sensor Systems, Danube University Krems, Viktor Kaplan Straße 2E, 2700 Wiener Neustadt, Austria — ²Department of Physics, Shanghai University, China

SmFeO₃ is an antiferromagnet with a canted spin structure. We analyzed the basic magnetic properties of monocrystalline SmFeO₃ samples through magnetic measurements and micromagnetic simulations. The measurements of the temperature dependent magnetization confirm a spin reorientation at 181 °C. Hysteresis properties were found to depend on the magnetic history. We observed exchange bias at room temperature whereby the bias field is sensitive on and increases with the field which is applied after field cooling. Using the double sublattice weak ferromagnetic model we derived effective intrinsic material properties for micromagnetic simulations. The simulations show the existence of metastable multidomain states. In SmFeO₃ ferroelectricity is believed to arise from antiferromagnetic domain walls. In a phenomenological model, in which the electric polarization arises from the noncollinear magnetization distribution in the domain walls, the average electric polarization is directly proportional to the total number of domain walls. We show how the number of antiferromagnetic domain walls and the electric polarization changes with the applied magnetic field.

Work supported by The Austrian Research Promotion Agency (FFG) project 20087207, MagnifiSense.

KFM 10.4 Tue 11:15 H5

KFM 10.5 Tue 11:45 H5

A first-principles study of electronic properties of lead iron niobate — •MADHURA MARATHE¹, ANNA GRUNEBOHM², DORU LUPASCU³, and VLADIMIR SHVARTSMAN³ — ¹Department of Physics and Astronomy, Uppsala University, 75120 Uppsala, Sweden. — ²Interdisciplinary Center for Advanced Materials Simulations (ICAMS), Ruhr-University Bochum, 44801 Bochum, Germany — ³Institute for Materials Science and Center for Nanointegration Duisburg-Essen (CENIDE), University of Duisburg-Essen, 45141 Essen, Germany

Efficient and cost-effective photovoltaic devices require materials which have optimal band gaps for absorption in the visible spectrum. Several ferroelectric perovskite materials have been investigated for their photovoltaic performance, but have too large band gaps. One promising candidate is multiferroic lead iron niobate Pb(Fe,Nb)O₃ (PFN) which has a narrower band gap [1].

We study the electronic and magnetic properties of PFN using density functional theory calculations. We explore how magnetic ordering and structure (ground-state rhombohedral versus high temperature cubic phases) influence the electronic structure and can thus be used to improve material performance.

References 1. N. Bartek, *et al.*, Materials, **14**, 6841 (2021).

KFM 10.6 Tue 12:05 H5

Lead-free Barium Zirconium Titanate-Based Ceramics for Energy Storage — •EVA KRÖLL, VLADIMIR SHVARTSMAN, and DORU LUPASCU — Institute for Materials Science and Center for Nanointegration Duisburg-Essen (CENIDE), University of Duisburg-Essen, Universitätsstr. 15, 45141 Essen, Germany

The growing world population and new technical developments request advanced energy storage systems which offer long life time, high power and energy densities. Relaxor ferroelectrics promise to provide these requirements for new energy storage systems due to their high dielectric permittivity and low hysteresis losses. In this work we added bismuth compounds, Bi(Zn_{2/3}Nb_{1/3})O₃ and Bi(Zn_{2/3}Ta_{1/3})O₃, to the ferroelectric barium zirconium titanate to induce a relaxor state. The heterovalent substitution at the A- and B-sites interrupts the long-range ferroelectric order. Concurrently, Bi³⁺ and Nb⁵⁺ as ferro active ions improve the polarizability of the materials. The addition of Ta⁵⁺ should increase the breakdown strength of the ceramic which is crucial to withstand high electric fields and to increase the stored energy density. We used X-ray diffraction for the phase characterization and scanning electron microscopy for the microstructure analysis. The dielectric spectroscopy and polarization measurement show that small amounts of 1.5 mol% BZNb and BZTa induce relaxor behavior in Ba(Ti_{0.85}Zr_{0.15})O₃. With increasing content of dopants, the polarization loops become linear. The samples with 2 mol% BZNb and BZTa show the highest energy storage performance with 0.417 J/cm³ and 0.423 J/cm³ at 100 kV/cm, respectively.

KFM 11: Crystal Structure Defects / Real Structure / Microstructure

Time: Tuesday 9:30–11:10

Location: H7

KFM 11.1 Tue 9:30 H7

HRTEM study of nanoparticle precipitation in additively manufactured 1.2709 maraging steel — •ANNA BENEDIKTOVÁ¹, DAGMAR JANDOVÁ¹, JIŘÍ BENEDIKT², ROSTISLAV MEDLÍN¹, and JÁN MINÁR¹ — ¹New Technologies - Research Center, University of West Bohemia, Pilsen, Czech Republic — ²Faculty of Applied Sciences, University of West Bohemia, Pilsen, Czech Republic

Maraging steels are known for their excellent properties, such as high strength and toughness, which are mainly due to the precipitation of intermetallic compounds during heat treatment. Up to now, mainly precipitation hardening from a temperature of about 500 °C has been studied, however, the hardening effect begins to show clearly at lower temperatures, even from 250 °C.

The HRTEM study was performed on maraging steel samples without tempering as well as after tempering at 350 °C and 490 °C, and the results were compared with simulations. Besides other relatively coarse precipitates, a high density of globular coherent nanoparticles with a superlattice was found in samples tempered at 350 °C. While the sample tempered at 490 °C contained slightly larger globular and rod-shaped Ni₃Mo particles.

KFM 11.2 Tue 9:50 H7

Tuning local structure in Prussian Blue Analogues — •YEVHENIIA KHOLINA and ARKADIY SIMONOV — ETH Zurich, Switzerland

Prussian Blue analogues, M[M'(CN)₆]_{1-x}·nH₂O, which we abbreviate here as M[M'] (M and M' = transition metal ions), is a diverse family of cyanide materials, which is intensely investigated for its potential application for hydrogen storage, as catalysts and as electrode materials. Applications that require efficient mass transport utilize the ability of the structure to accommodate a large number of M'(CN)₆ vacancies, which create a highly connected porous network. It was theoretically shown that the connectivity and the accessible volume of such a network depend on the local structure[1]. Therefore, to optimize mass transport properties not only the number of vacancies but also their distribution must

be precisely controlled. In this work we show how to tune the local structure of Mn[Co] Prussian Blue analogues grown in gel by varying the crystallization parameters: the type of gel, the crystallization temperature, the concentration of reactants, and the concentration of chelating agents. We probe the defect distribution by single-crystal x-ray diffuse scattering, which allows quantitative characterization of the local structure. All of the above-mentioned parameters allow smooth continuous control of diffuse scattering and thus of the local order in Mn[Co] crystals.

[1] Simonov, Arkadiy, et al. "Hidden diversity of vacancy networks in Prussian blue analogues." Nature 578.7794 (2020): 256-260.

KFM 11.3 Tue 10:10 H7

Electronically driven anharmonicities in low-energy lattice models: Affordable molecular dynamics of charge-density-wave systems — ARNE SCHOBERT¹, •JAN BERGES¹, MICHAEL SENTEF², MARIANA ROSSI², ERIK VAN LOON³, SERGEY BRENER⁴, and TIM WEHLING⁴ — ¹University of Bremen, Bremen, Germany — ²Max Planck Institute for the Structure and Dynamics of Matter, Hamburg, Germany — ³Lund University, Lund, Sweden — ⁴University of Hamburg, Hamburg, Germany

Charge-density waves (CDWs) occupy an important position in the phase diagram of low-dimensional systems such as the transition metal dichalcogenide monolayers. Although a CDW can often be identified already from the undistorted structure in linear response, anharmonic effects are eventually responsible for the stabilization of the distorted phase and its precise properties. To study the mechanisms responsible for the anharmonicity, we build an ab-initio low-energy lattice model, which reproduces Born-Oppenheimer potential surfaces from density-functional-theory (DFT). The ab-initio low-energy lattice model is used for molecular dynamics in the CDW phase of 1H-TaS₂.

KFM 11.4 Tue 10:30 H7

Ab Initio Thermodynamics for Surface Motifs of the M1 Selective Oxidation Catalyst — •K. NAM¹, Y. LEE¹, L. MASLIUK², T. LUNKENBEIN², A. TRUNTSCHKE², C. SCHEURER¹, and K. REUTER¹ — ¹Theory Dept., Fritz-Haber-Institut der MPG, Berlin — ²Inorganic Chemistry Dept., Fritz-Haber-Institut der MPG, Berlin

The activity and selectivity of heterogeneous catalysts can be altered noticeably by small changes in different factors such as bulk composition, dopants, defects, reaction conditions, etc. The effects of these factors are furthermore interrelated in non-trivial ways. As an important first step to rationally disentangle them, we here aim to understand their influences on the local atomic-scale structural motifs offered by the catalyst. Specifically, we do this for the M1 structural modification of (Mo,V)O_x and (Mo,V,Te,Nb)O_x as an active catalyst for the oxidative dehydrogenation reaction of ethane to ethylene.

The large primitive cell of this M1 catalyst challenges a detailed study by means of predictive-quality first-principles calculations. To this end, we deconstruct the primitive cell into 'rod-like structures' of surface motifs with various oxygen content, faithfully modeling reported data from electron microscopy [1]. *Ab initio* thermodynamics then allows us to explore the effect of varying reaction conditions on the stability of these motifs and thus on M1 catalyst surfaces. Exploiting the data thus generated to train a machine-learn potential we can specifically rationalize the influence of vanadium and niobium doping on the active surface structure.

[1] L. Masliuk *et al.*, J. Phys. Chem. C **121**, 24093 (2017).

KFM 11.5 Tue 10:50 H7

Raman spectroscopic structure analysis of colloidal semiconductor core-shell quantum dots for the achievement of near-unity quantum efficiency — •SANDRA HINZ^{1,2}, SONJA KROHN^{2,3}, HANNES VAN AVERMAET⁴, ZEGGER HENS⁴, JAN STEFFEN NIEHAUS³, JANINA MAULTZSCH¹, and HOLGER LANGE² — ¹Department of Physics, Friedrich-Alexander-Universität Erlangen-Nürnberg, Erlangen, Germany — ²Institute of Physical Chemistry, University of Hamburg, Hamburg, Germany — ³Fraunhofer IPA - Center for Applied Nano-Technology CAN, Hamburg, Germany — ⁴Physics and Chemistry of Nanostructures, Ghent University, Ghent, Belgium

State of the art applications of quantum dots (QDs) require near-unity photoluminescence quantum yield (PLQY). This demand is rarely achieved and therefore the synthesis process is under constant optimization and nanocrystals consisting of a core with one or more shells of different materials are paving the way to achieve high PLQY. As those components have diverse lattice parameters, the induction of strain within the QDs is inevitable. Recently, we applied Raman spectroscopy for in depth structure characterization and a strain minimization approach to optimize the synthesis of InP/ZnSe/ZnS QDs towards near-unity PLQY. A similar effect plays a role in CdSe/CdS QDs when aiming for high PLQY. In these QDs, the formation of an alloyed interface between the CdSe core and CdS shell is assumed. By Raman spectroscopy, we are able to monitor the formation of these alloyed domains for different QD parameters and correlate it with the PLQY.

KFM 12: Skyrmions 1 (joint session MA/KFM)

Time: Tuesday 9:30–12:45

Location: H37

See MA 12 for details of this session.

KFM 13: Materials for Storage and Conversion of Energy (joint session MM/KFM)

Time: Tuesday 10:15–11:30

Location: H46

See MM 14 for details of this session.

KFM 14: Ferroics – Domains and Domain Walls 1

Chair: Dr. Donald Evans (Augsburg University)

Time: Wednesday 9:30–12:05

Location: H5

KFM 14.1 Wed 9:30 H5

Strain driven conducting domain walls in a Mott insulator — •LUKAS PUNTIGAM¹, DONALD EVANS¹, MARKUS ALTHALER¹, SOMNATH GHARA¹, LILIAN PRODAN¹, VLADIMIR TSURKAN^{1,2}, STEPHAN KROHNS¹, and ISTVAN KEZSMARKI¹ — ¹Universität Augsburg, 86159, Augsburg, Deutschland — ²Institute of Applied Physics, MD 2028 Chisinau, Moldova

Ferroelectric domain walls, which can be written, tuned or erased, are being considered as functional building blocks for nanoelectronics. Especially, conducting domain walls are of high interest to achieve this functionality. To date, the origin for increased conductivity in ferroelectrics domain walls has been typically attributed to the formation of screening charges driven by polar discontinuities.

Here, we establish that for the template system, the lacunar spinel GaV₄S₈ also strain can enhance the conductivity of specific domain walls. This system exhibits ferroelectric domain pattern below a Jahn-Teller transition at 42K. At this temperature a change in its crystal structure can result in mechanical stress at domain walls. Piezoresponse force microscopy revealed an interesting ferroelectric pattern. Each ferroelectric domain can be identified by structural considerations to be one of the four possible polar direction. In case of domain walls between structural incompatible domains measurements with conductive atomic force microscopy show strongly enhanced conductivity denoting an additional twist highly conductive domain walls. Further, spatially resolved IV spectroscopy enable the investigation of the underlying conductivity mechanism at the tip-sample interface.

KFM 14.2 Wed 9:50 H5

In-situ tracking of the evolution of polarization during the growth of layered-ferroelectric Aurivillius phases — •IPEK EFE, ELZBIETA GRADAUSKAITE, MANFRED FIEBIG, and MORGAN TRASSIN — Department of Materials, ETH Zürich, Switzerland

The highly anisotropic nature of layered oxides is key to exotic functionalities such as superconductivity, magnetoresistance, and ferroelectricity, which are promising for applications. However, their integration in epitaxial design is chal-

lenging due to the complexity of the unit cell, which makes precise monitoring of the growth a necessity. Here, we directly access the polarization dynamics of the model system Aurivillius Bi₅FeTi₃O₁₅ films during the epitaxial growth using in-situ optical second harmonic generation (ISHG). We identify an oscillating intensity of the ISHG signal during two-dimensional layer-by-layer growth. We correlate these oscillations with the periodical evolution of the polarization of ferroelectric film dictated by the chemistry of the planes in the unit-cell, which consists of alternating positively charged fluorite-like (Bi₂O₂)²⁺ layer and negatively charged (Bi₃FeTi₃O₁₃)²⁻ perovskite blocks. In combination with reflection high-energy electron diffraction, we show how polarization of the films consistently switches from an out-of-plane orientation during the perovskite blocks growth, to a fully-in-plane orientation with the completion of the unit-cell termination and the (Bi₂O₂)²⁺ capping. Our findings reveal previously hidden polarization dynamics during the epitaxial design and bring new insights in the sub-unit cell control of layered oxide films properties for the development of energy efficient oxide electronics.

KFM 14.3 Wed 10:10 H5

Continuous polarization control at nanoscopic dimensions — •MARTIN F. SAROTT¹, MARTA D. ROSSELL², MANFRED FIEBIG¹, and MORGAN TRASSIN¹ — ¹Department of Materials, ETH Zurich, Switzerland — ²Electron Microscopy Center, Empa Swiss Federal Laboratories for Materials Science and Technology, Switzerland

The switchable bistable polarization in ferroelectrics allows for the binary control of optical, electronic, and catalytic properties. Going beyond the limitation of a binary remanent polarization holds great promise for emerging neuromorphic concepts. Here, we demonstrate that we can arbitrarily set the magnitude of the remanent ferroelectric polarization at the nanoscale in epitaxial PbZr_{0.52}Ti_{0.48}O₃ thin films with a single DC bias. By approaching the PZT morphotropic phase boundary, we achieve a high degree of control over this unusually susceptible system via epitaxial strain. We employ this to accomplish the formation of decoupled nanometric 180° domains with a broad coercive field dis-

tribution. Using in-situ optical second harmonic generation and X-ray diffraction, we study the emergence of the nanoscopic domain configuration. We then use piezoresponse force microscopy to demonstrate the ability to locally and reversibly modulate the remanent polarization *continuously* between depolarized and saturated, while preserving the nanoscopic length scale of the domains. We highlight the technological relevance of nanoscale non-binary polarization switching, by showing (i) the voltage-controlled tunability of the nonlinear optical response and (ii) the quasi-continuous tunability of the tunnel electroresistance in ferroelectric tunnel junctions.

KFM 14.4 Wed 10:30 H5

Impact of strontium on domain wall mobility in barium titanate — •ARIS DIMOU¹, PIERRE HIREL², and ANNA GRÜNEBOHM¹ — ¹Ruhr-Uni. Bochum, Interdisciplinary Centre for Advanced Materials Simulation (ICAMS), Bochum, Germany — ²Univ. Lille, Unité Matériaux et Transformations (UMET), Lille, France

Solid solutions of barium-strontium titanate are widely used, environmentally friendly ferroelectric materials that are important for a plethora of applications [1,2]. The presence of domain walls are known to change the properties of a material, and its mobility is of key interest in contemporary electronic devices [3]. Surprisingly little attention has so far been paid to the impact of Sr on the domain wall mobility in barium titanate.

Here we present a microscopic study on the case of Sr inclusions in barium titanate. Our simulations reveal an increase in the activation energy for domain wall movement at the Sr inclusion. Suggesting that a thin Sr plane is enough to pin the domain wall.

[1] Acosta et al., BaTiO₃-based piezoelectrics: Fundamentals, current status, and perspectives. *Applied Physics Review*, **4**, 2017.

[2] Grünebohm et al., Interplay of domain structure and phase transitions: theory, experiment and functionality. *J. Phys. L Condens. Matter*, **34**, 2022.

[3] Sharma et al., Functional ferroic domain walls for nanoelectronics. *Currently. Open. Solid State Mater. Sci.*, **9**, 2005.

15 min. break

KFM 14.5 Wed 11:05 H5

Stability of enhanced domain wall conductivity in single-crystalline lithium niobate — •AHMED SAMIR LOTFY^{1,2}, MANUEL ZAHN¹, MICHAEL RÜSING¹, and LUKAS ENG¹ — ¹Institute of Applied Physics, Technische Universität Dresden, Dresden, Germany — ²Department of materials, ETH Zürich, Zürich, Switzerland

Domain-wall conductivity (DWC) in ferroelectrics has emerged as a key functionality for developing nanoelectronic devices. In this regard, lithium niobate (LNO) is a promising candidate as previous studies have shown the capability to significantly enhance its DWC by making use of head-to-head and tail-to-tail DW configurations, and DW inclination angles under voltage treatments. However, understanding of the temporal and temperature-dependent stability of the enhanced DWC is lacking, limiting further steps of device implementation. For this, we performed a series of conductive atomic force microscopy and macroscopic electrometer measurements on single crystalline LNO samples. We show a characteristic conductance trend during voltage-induced enhancement which provides insights into the temporal stability of DWC. Moreover, our temperature-dependent measurements between 100 K and 300 K reveal

the transport mechanism along the walls, pointing to the role of bound polarons. This is confirmed by the calculation of the activation energy. These results provide key insights into the stability of DWC in LNO for applications in practical devices.

KFM 14.6 Wed 11:25 H5

Electron scattering signatures of ferroelectric domains — •URSULA LUDACKA¹, JIALI HE¹, EMIL FRANG CHRISTIANSEN¹, SHUYU QIN², ZEWU YAN^{3,4}, EDITH BOURRET⁴, ANTONIUS VAN HELVOORT¹, JOSHUA AGAR², and DENNIS MEIER¹ — ¹NTNU Norwegian University of Science and Technology, Trondheim, Norway — ²Department of Materials Science and Engineering, Lehigh University, Bethlehem, PA 18015, USA — ³ETH Zurich, Zurich, Switzerland — ⁴Lawrence Berkeley National Laboratory, Berkeley, USA

The emergence of ferroelectricity originates from polar displacements of lattice atoms, connotating a one-to-one correlation between electronic and structural properties at the atomic level. An established approach that allows for determining associated structural variations is scanning electron diffraction (SED). In SED, a focused electron beam is scanned over the specimen, probing diffracted electrons at each position of the raster scan. The corresponding patterns represent unique fingerprints of the probed areas, containing structural information. We demonstrate the potential and opportunities of this innovative 4D-STEM approach using improper ferroelectric ErMnO₃, an ideal model system as its basic ferroelectric properties and atomic-scale structure are well understood. In the ferroelectric state, the Er ions exhibit characteristic up-up-down and down-down-up patterns, corresponding to ferroelectric 180° domains with positive and negative polarization, respectively. These shifts cause different Bragg scattering conditions for the electrons and, hence, specific diffraction patterns that we utilize for domain imaging assisted by machine learning algorithms.

KFM 14.7 Wed 11:45 H5

Oxygen vacancies nucleate domain walls in ferroelectrics — •URKO PETRALANDA¹, MADDS KRUSE¹, HUGH SIMONS², and THOMAS OLSEN¹ — ¹CAMD, Department of Physics, Technical University of Denmark, 2800 Kgs. Lyngby, Denmark — ²Department of Physics, Technical University of Denmark, 2800 Kgs. Lyngby, Denmark

Domain walls are topological defects which emerge spontaneously in ferroelectrics [1]. At charged domain walls (CDW), free charge from the bulk is promoted to the conduction band through a band-bending mechanism, to compensate their local bound charge [2]. This creates highly conductive embedded mobile 2D nanosheets, suitable for nanoelectronics related applications [2]. Oxygen vacancies are believed to play a role in helping CDW overcome their strong electrostatic interaction. In this work [3], by means of density functional theory calculations in BaTiO₃ we clarify the screening mechanism of CDW charge in both pristine and oxygen vacancy aided cases, and we propose that, beyond the commonly accepted view of oxygen vacancies as CDW stabilizers, they can actually ignite the formation of CDW. We explain the experimentally observed difference in electronic conductivity of the positively and negatively charged CDW in BaTiO₃, as well as the generic prevalence of CDW in ferroelectrics. Such a vacancy driven CDW formation implies that specific charged domain wall configurations may be realized by bottom-up design.

[1] G. Catalan et al, *Rev. Mod. Phys.* **84**, 119 (2012)

[2] T. Sluka et al, *Nat. Commun.* **4**, 1808 (2013).

[3] U Petralanda et al, *Phys. Rev. Lett.* **127**, 117601 (2021)

KFM 15: Materials for Energy Storage (joint session KFM/PPP)

Chair: Prof. Dr. Theo Scherer (KIT, Karlsruhe)

Time: Wednesday 9:30–12:05

Location: H7

KFM 15.1 Wed 9:30 H7

Hybrid CuCo₂O₄ nanosheets as binder-free supercapacitor electrodes — •ZIDONG WANG^{1,2}, YUDE WANG², HUAPING ZHAO¹, and YONG LEI¹ — ¹Fachgebiet Angewandte Nanophysik, Institut für Physik & IMN MacroNano, Technische Universität Ilmenau, 98693 Ilmenau, Germany — ²School of Materials and Energy, Yunnan University, 6500504 Kunming, Peoples Republic of China

CuCo₂O₄ is one kind of pseudocapacitive materials and it has a high theoretical capacitance, but it suffers from poor electrical conductivity. In this work, CuCo₂O₄ nanosheets were directly grown on a conductive skeleton to significantly enhance the conductivity and at the same time reduce the agglomeration of CuCo₂O₄ nanosheets. In addition, the hybrid nanosheet structures also expand the interface and provide more active electrochemical sites, facilitating kinetic processes and electrochemical reactions. The as-prepared CuCo₂O₄ nanosheets on a conductive skeleton were studied as binder-free electrode and exhibited outstanding electrochemical performance with the specific capacitance of 1595 F g⁻¹ at a current density of 1 A g⁻¹ and 85.1% capacitance retention after

4600 cycles. These results indicated that hybrid CuCo₂O₄ nanosheets has great application potential as binderfree electrode in supercapacitors.

KFM 15.2 Wed 9:50 H7

Investigation of K-ion Intercalation and Conversion in Layer Transition Metal Disulfide anode: The case of MoS₂ and WS₂ — •YULIAN DONG, HUAPING ZHAO, and YONG LEI — Fachgebiet Angewandte Nanophysik, Institut für Physik & IMN MacroNano, Technische Universität Ilmenau, 98693 Ilmenau, Germany

Two-dimensional transition metal dichalcogenides (2D-TMDs) have a unique layered structure characterized by weak interlayer van der Waals interaction and strong in-plane covalent bonding. The structure allows the intercalation of guest species in the interlayer space, which shows impressive properties in potassium-ion batteries (PIBs). Thus, various 2D TMDs, including sulfides (MoS₂, SnS₂, WS₂) and selenide (MoSe₂ and VSe₂), have been studied as potential anode materials for PIBs. This work compares the intercalation and conversion of K in MoS₂ and WS₂. Intercalation and conversion process is observed during potassium in MoS₂ in a voltage range of 3.0-0.5V and 0.5-0.01V, respectively. By con-

trolling cut-off voltage, the investigation demonstrated high capacities derived from the conversion, but it destroys the 2D diffusion pathways leading to an unstable cycling span. While the K⁺ storage in WS₂ is governed by the intercalation reaction rather than the conversion reaction. It exhibited a low capacity decay rate at both low and high current densities as well as great rate capability.

KFM 15.3 Wed 10:10 H7

Elucidation of the Pore Formation Mechanism in Hard-Carbon Microspheres — •MARTIN WORTMANN¹, WALDEMAR KEIL², MICHAEL WESTPHAL¹, ELISE DIESTELHORST³, JAN BIEDINGER¹, BENNET BROCKHAGEN³, GÜNTER REISS¹, CLAUDIA SCHMIDT², KLAUS SATTLER⁴, and NATALIE FRESE¹ — ¹Bielefeld University, Bielefeld, Germany — ²Paderborn University, Paderborn, Germany — ³Bielefeld University of Applied Sciences, Bielefeld, Germany — ⁴University of Hawaii, Honolulu, USA

Micro-spherical hydrochar can be carbonized by pyrolysis to produce hard-carbon microspheres with excellent electrochemical properties for the application as anode material in batteries. In this contribution, a temperature-resolved study of the chemical and morphological evolution of saccharide-derived hydrochar during pyrolysis up to 1000°C is presented. By combining a wide range of characterization methods all aspects of the structural transition are examined. The chemical processes occurring both in the bulk and at the surface of the carbon spheres are shown to affect the transition from an amorphous-polymeric to a nanocrystalline carbon-structure. The study focuses on the pore formation mechanism, which is driven by the aggregation of nanometer-sized oxygen-rich clusters at the sphere surface, which disintegrate in a narrow temperature range, leaving behind a mesoporous structure. The revealed molecular mechanisms provide key insights into the pyrolysis of carbonaceous materials.

KFM 15.4 Wed 10:30 H7

Hydrogenation of Pd nanoparticles at the nanoscale with in-situ TEM — •SVETLANA KORNEYCHUK^{1,2}, STEFAN WAGNER¹, GEORGIAN MELINTE², DARIUS ROHLEDER³, PHILIPP VANA³, and ASTRID PUNDT¹ — ¹IAM-WK, Karlsruhe Institute of Technology, Karlsruhe, Germany — ²INT, Karlsruhe Institute of Technology, Karlsruhe, Germany — ³Institute of Physical Chemistry Georg-August-University Göttingen, Göttingen, Germany

Palladium-based nanomaterials play an important role in hydrogen technology. Extreme affinity of palladium to hydrogen is very attractive for various applications. Besides catalysis, Pd nanoparticles can assist in hydrogen delivery into other materials for hydrogen storage through a spill-over process. Pd-based materials are also used as hydrogen purification membranes and hydrogen detectors. The hydrogenation and dehydrogenation process of Pd nanoparticles is hence of high interest in the applications mentioned above. Nanoscale systems reveal significant thermodynamic deviations from the bulk due to higher surface to volume ratio, absence of grain boundaries, different behavior of defects and mechanical stress. In this work, we investigate the behavior of Pd nanoparticles and formation of PdH_x in real time with in-situ H₂-gas TEM. Many applications require operation at elevated temperatures. With the special gas holder from Protochips it is possible to reach pressures up to 1 atmosphere and study the particles at elevated temperatures with the limit of 1000°C. We can observe the local phase change at different temperatures and pressures with the help of spectroscopic and diffraction techniques at the nanoscale.

15 min. break

KFM 15.5 Wed 11:05 H7

Mild-temperature solution-assisted encapsulation of phosphorus into ZIF-8 derived porous carbon as lithium-ion battery anode — •CHENGZHAN YAN¹, SHUN WANG², and YONG LEI¹ — ¹Fachgebiet Angewandte Nanophysik, Institut für Physik & IMN MacroNano, Technische Universität Ilmenau, 98693 Ilmenau, Germany. — ²Key Laboratory of Carbon Materials of Zhejiang Province, Institute of Materials and Industrial Technologies, Wenzhou University, Wenzhou, Zhejiang, 325027, China.

The high theoretical capacity of red phosphorus (RP) makes it a promising anode material for lithium-ion batteries (LIBs). However, the large volume change of RP during charging/discharging imposes an adverse effect on the cyclability, and the rate performance suffers from its low conductivity. Herein, a facile solution-based strategy is proposed to incorporate phosphorus into the pores of MOF-derived carbon hosts under a mild temperature. With this method, the blocky RP is etched into the form of polyphosphides anions (PP, mainly P₅-), making it easily diffuse into the pores of porous carbon hosts. Especially, the indelible crystalline surface phosphorus could be effectively avoided, which is generated in the conventional vapor condensation encapsulation method. Moreover, highly-conductive ZIF-8 derived carbon hosts with any pore smaller than 3 nm are efficient for loading PP and these pores can well alleviate the volume change. Finally, the composite of phosphorus encapsulated into ZIF-8 derived porous carbon exhibits a significantly improved electrochemical performance as LIBs anode.

KFM 15.6 Wed 11:25 H7

Study on Li Ion Diffusion in Li_xV₂O₅ using First Principle Calculations and Kinetic Monte Carlo Simulations — •FABIAN DIETRICH¹, EDUARDO CISTERNAS¹, MARCELO PASINETTI², and GONZALO DOS SANTOS^{2,3} — ¹Universidad de La Frontera, Temuco, Chile — ²Universidad Nacional de San Luis, CONICET, San Luis, Argentina — ³Universidad de Mendoza, Mendoza, Argentina

We study the Li diffusion in Li_xV₂O₅ (0 < x ≤ 1) - a potential cathode material for Lithium ion batteries. Different diffusion pathways in this material in dependence on the Li ion concentration are investigated by applying first-principles calculations. The results are used to obtain the corresponding diffusion coefficients by employing two complementary methodologies: Kinetic Monte Carlo (KMC) simulations and a statistical thermodynamics approach. The KMC simulations for two different crystal planes give new evidence that the diffusion occurs mainly along the [010] direction, while the corresponding diffusion coefficients show a temperature dependence obeying the Arrhenius' Law. The necessity of the consideration of concentration-dependent barrier heights in the KMC simulations are demonstrated by looking at the significant changes of the concentration-dependence of the diffusion coefficients. The simulated diffusion coefficients of the combined approach show a good quantitative agreement with experimental data reported previously.

KFM 15.7 Wed 11:45 H7

NMR studies of sintering effects on the lithium ion dynamics in Li_{1.5}Al_{0.5}Ti_{1.5}(PO₄)₃ — •PHILIPP SEIPEL¹, EDDA WINTER¹, MICHAEL VOGEL¹, TATIANA ZINKEVICH², SYLVIO INDRIS², BAMBAR DAVASSUREN³, and FRANK TIETZ³ — ¹AG Vogel, Institute for Condensed Matter Physics, Technische Universität Darmstadt, Germany — ²Karlsruhe Institut of Technology, IAM-ESS, Karlsruhe, Germany — ³Forschungszentrum Jülich GmbH, IEK-1, Jülich, Germany

Various NMR methods are combined to study the structure and dynamics of Li_{1.5}Al_{0.5}Ti_{1.5}(PO₄)₃ samples, which were obtained from sintering at various temperatures between 650 °C and 900 °C and show high bulk conductivities up to 5 mS/cm. We use ⁷Li NMR to study the transport mechanism in these glass ceramics [1]. Analysis of ⁷Li spin-lattice relaxation and line-shape changes indicates the existence of two species of lithium ions with clearly distinguishable jump dynamics, which can be attributed to crystalline and amorphous sample regions. An increase of the sintering temperature leads to higher fractions of the fast lithium species with respect to the slow one, but hardly affects the jump dynamics in either of the phases. ⁷Li field-gradient diffusometry reveals that the long-range ion migration is limited by the sample regions featuring slow transport. The high spatial resolution available from the high static field gradients of our setup allows us to observe also the lithium ion diffusion inside the small (< 100 nm) LATP crystallites, yielding a high self-diffusion coefficient of D=2 x 10⁻¹² m²/s at room temperature. [1]Winter et al., ZPCH, DOI:10.1515/zpch-2021-3109

KFM 16: Oxide Semiconductors (joint session HL/KFM)

Time: Wednesday 9:30–12:30

Location: H33

See HL 18 for details of this session.

KFM 17: Focus Session: Surfaces and Interfaces of (Incipient) Ferroelectrics (joint session O/KFM)

Ferroelectricity is a property of materials that allows spontaneous, switchable electric polarization. Recently, many surface-related applications have been proposed where ferroelectric or incipient-ferroelectric materials exhibit superior properties. These include catalysis, electron-hole separation in light harvesting, unique electronic properties such as a negative capacitance in heterostructures of ferroelectric materials, to name just a few. While (incipient) ferroelectrics clearly perform well in the aforementioned applications, there is very limited fundamental understanding of the processes involved on the surfaces of these materials.

Organizers: Martin Setvin (Charles University, Prague), Chiara Gattinoni (London South Bank University), and Michele Reticioli (University of Vienna)

Time: Wednesday 15:00–18:30

Location: H3

See O 44 for details of this session.

KFM 18: Focus Session: Diamond and related dielectric materials

This focus session contains basic diamond research due to optical and dielectric properties for applications in low and high power electronics. High frequency and high microwave power applications are discussed. The use of diamond material in GHz up to THz range is the main purpose of this session.

Organizer: Prof. Dr. Theo Scherer (KIT, Karlsruhe)

Time: Wednesday 15:00–16:50

Location: H5

Invited Talk

KFM 18.1 Wed 15:00 H5

Deep understanding of advanced optical and dielectric materials for fusion diagnostic applications — •ANATOLI I. POPOV¹, E KOTOMIN¹, V KUZOVKOV¹, A LUSHCHIK², and THEO A SCHERER³ — ¹Institute of Solid State Physics, University of Latvia, 8 Kengaraga str., LV-1063 Riga, Latvia — ²Institute of Physics, University of Tartu, W. Ostwald Str. 1, 50411, Tartu, Estonia — ³Karlsruhe Institute of Technology, Hermann-von-Helmholtz-Platz 1, D-76344 Eggenstein-Leopoldshafen, Germany

In this talk, I will give a short overview of the most interesting results obtained in the framework of two EUROfusion Enabling Research projects - Advanced experimental and theoretical analysis of defect evolution and structural disordering in optical and dielectric materials for fusion applications (AETA) (2019-2020) and Investigation of defects and disorder in nonirradiated and irradiated Doped Diamond and Related Materials for fusion diagnostic applications (DDRM) Theoretical and Experimental analysis (2021-2023).

In a series of joint works by ISSP UL (Latvia), UT (Estonia), and KIT (Germany), radiation damage of some promising functional materials (Al₂O₃, MgAl₂O₄, SiO₂, and diamond) from the priority list of the EUROfusion consortium was studied under neutron, proton, heavy-ion. Their optical, dielectric, vibrational & magnetic properties were carefully studied. Based on this study, we developed new theoretical methods able to evaluate and predict some important properties of these materials as well as their radiation damage evolution under extreme reactor conditions.

KFM 18.2 Wed 15:30 H5

Physics of natural and artificial diamond gemstones — •THEO SCHERER — Karlsruhe Institut of Technology (KIT-IAM-AWP)

Diamond gemstones were very well appreciated in the antique world. Independent on the purpose of jewelry, diamond is a crystalline solid state material with excellent physical and chemical properties as a high Young modulus or a very high thermal conductivity. By doping the material with boron, electrical conductivity can be observed. This is important for electronic devices. In this talk the wide range of production of gemstones and technical applications like high frequency high power microwave transmission diamond windows for nuclear fusion power plants will be presented. Different diamond classifications, cuts and colors by impurities will be shown. A comparison of natural diamonds and artificial produces ones are topic of the discussion.

KFM 18.3 Wed 15:50 H5

Basic considerations for fracture toughness measurements of MPA CVD diamond to be used in nuclear fusion — •GAETANO AIELLO, THEO SCHERER, ANDREAS MEIER, SABINE SCHRECK, and DIRK STRAUSS — Karlsruhe Institute of Technology, Institute for Applied Materials, D-76344 Eggenstein-Leopoldshafen, Germany

In nuclear fusion, Microwave Plasma Assisted (MPA) Chemical Vapour Deposition (CVD) polycrystalline diamond is the only material allowing for transmission of high power microwave beams (1-2 MW) in long-pulse gyrotron operations. The reason lies in the combination of extraordinary thermal, mechanical

and optical properties of diamond, which is used in the shape of disks having thickness of 1 to 2 mm for windows. Being diamond a brittle material, failure to fracture is the main failure mode. Accordingly, an appropriate mechanical characterization is required as diamond plays a major safety role in fusion machines. Due to limited body of work in literature, fracture toughness measurements have to be first carried out for this material and then a design criterion for structural integrity assessment has to be applied. In this work, the preliminary activities aiming to define the optimum experimental measurement method of fracture toughness for thin diamond samples are shown and discussed. An outlook to the next steps is also given.

KFM 18.4 Wed 16:10 H5

Development diamond based Kinetic Inductance Detectors — •FRANCESCO MAZZOCCHI, DIRK STRAUSS, and THEO SCHERER — Karlsruhe Institute Of Technology

Kinetic Inductance Detectors (KIDs) have proven themselves as a very versatile cryogenic detector technology capable of applications in various fields due to their flexibility of design, sensibility and ease of production. We have recently proposed a polarization sensitive Lumped Elements KID as sensor for an innovative polarimetric diagnostics based on quantum cascade lasers (QCL) for application in the nuclear fusion. Each detector unit is composed by 4 pixels arranged at the vertices of a square, each pixels being sensible to only one polarization direction. The current system is based on niobium nitride (NbN) superconductor over High Resistivity Silicon (HRSi) substrate. Such material delivers good performances but its relatively high dielectric constant and loss tangent lead to increased substrate losses. Using a transparent substrate may improve this aspect and also the radiation resistance of such devices. Diamond is the substrate of choice, being a material already widely studied and used in the fusion environment as high power microwave window, due to its outstanding optical and mechanical performances. In this work we present the preliminary design study for a diamond based Kinetic Inductance Detector and subsequent characterization measurements of the first prototypes.

KFM 18.5 Wed 16:30 H5

Characterization of - A survey of electrical and dielectric properties — •THEO SCHERER — Karlsruhe Institute of Technology (KIT-IAM-AWP)

p-Boron-doped polycrystalline CVD diamond samples were produced and delivered by the German company Diamond Materials in Freiburg (Germany). In a first step, main properties of this candidates for diagnostic and/or heating windows in future nuclear fusion reactors were investigated. By a special measurement technique, it was possible to determine the Boron doping concentration in Diamond by measurement of the resistive properties by using the van der Pauw method. So prepared, an irradiation campaign with neutrons and/or heavy ions on these samples will follow. The second material investigated, was r-plane single crystalline sapphire. For the first characterization the dielectric properties of a 3*-wafer in dependency of the frequency in a FABRY-PEROT resonator setup was performed. Also, this is the preparation for the next irradiation experiments in this project.

KFM 19: Ferroics – Domains and Domain Walls 2

Chair: Dr. Jan Schultheiß (Augsburg University, NTNU Trondheim)

Time: Wednesday 15:00–16:00

Location: H7

KFM 19.1 Wed 15:00 H7

Phase Field Simulations of the Dipolar Interaction in Hexagonal Manganites — •AARON MERLIN MÜLLER, AMADÉ BORTIS, MANFRED FIEBIG, and THOMAS LOTERMOSER — Department of Materials, ETH Zurich, 8093 Zurich, Switzerland

We introduce a phase-field method that allows simulation of dipolar interaction in thin-film hexagonal manganites and investigate its effect on the unconventional ferroelectric vortex domain pattern of the material. Dipolar interactions are assumed to have negligible influence because of the improper nature of the ferroelectric order. Hence, dipolar interactions are commonly neglected when modeling such systems. Efficiently incorporating dipolar interactions of out-of-plane-oriented dipoles in phase-field methods is challenging as they represent a nonlocal Coulomb contribution to the free energy. In addition, the Coulomb interaction of a polarization field diverges at zero distance, unlike for atomistic dipole models. In our work, we show that including the dipolar interaction in the phase-field method results in more regular shaped domains in comparison to simulations that ignore the dipolar interaction, with lower variance in domain size. The ferroelectric domains of our revised approach resemble the experimentally observed patterns more closely. Hence, our work gives insights on the often neglected effects of dipolar interaction and the resulting depolarizing field on ferroelectric domains in an important class of improper ferroelectric materials.

KFM 19.2 Wed 15:20 H7

Dynamics of the electrocaloric effect in ferroelectric materials — •JAN FISCHER, DANIEL HÄGELE, and JÖRG RUDOLPH — Ruhr-Universität Bochum, Faculty of Physics and Astronomy, Experimental Physics VI (AG), Germany

The electrocaloric effect (ECE) in ferroelectrics is a promising candidate for energy efficient cooling technologies. The ECE leads to a reversible adiabatic temperature change ΔT of a ferroelectric material upon a change of an external electric field. The reliable determination of the adiabatic ΔT is, however, experimentally challenging and most studies use either indirect methods which are prone to artifacts, or comparably slow direct methods. The dynamics of the ECE has therefore not been systematically studied so far. Here, we introduce a direct

and contactless method to study the full dynamics $\Delta T(t)$ of the ECE with μK temperature resolution and μs temporal resolution via the infrared emission of the sample. The simultaneous recording of transients for $\Delta T(t)$, applied electric field $E(t)$, and induced polarization $P(t)$ gives the opportunity to correlate the caloric properties with the dielectric properties thus opening perspectives for a fundamental understanding of the ECE also in complex materials like relaxor ferroelectrics. Our techniques allows also for high-frequency measurements as needed for adiabatic measurements in thin films.^{1,2} We will discuss several examples ranging from bulk materials to thin films.

¹ J., Döntgen, *et al.*, Applied Physics Letters 106, 3 (2015)² J., Döntgen, *et al.*, Energy Technology 6, 8 (2018)

KFM 19.3 Wed 15:40 H7

Interfacial Stabilization of Homochiral Ferroelectric Domain Walls in BiFeO₃ — •ELZBIETA GRADAUSKAITE¹, QUINTIN N. MEIER², NATASCHA GRAY¹, MARCO CAMPANINI³, MARTA D. ROSSELL³, MANFRED FIEBIG¹, and MORGAN TRASSIN¹ — ¹Department of Materials, ETH Zurich, Switzerland — ²CEA Grenoble, LITEN, Grenoble, France — ³Electron Microscopy Center, Empa, Switzerland

Chirality is a concept central to all molecular interactions in biological systems. In the last decade its importance was also highlighted in condensed-matter physics, where spin textures at the homochiral ferromagnetic domain walls were shown to enable their deterministic current-driven motion. Nevertheless, only a few reports on polar chirality exist to this date, prompting increased research efforts on this important issue. Here, we report the stabilization of net chirality in BiFeO₃ ferroelectric films grown on a fully in-plane-polarized ferroelectric layer of the Aurivillius phase. By introducing an in-plane-polarized epitaxial buffer we create polarization continuity and provide a symmetry breaking at the interface with the out-of-plane polarized BiFeO₃. Scanning probe microscopy uncovers the stabilization of conceptually novel 251° domain walls in BiFeO₃. Their unusual chirality is likely associated with the ferroelectric analog to the Dzyaloshinskii-Moriya interaction in magnets. Thus, we demonstrate a simple design combining perpendicular polar anisotropies for the effective stabilization of homochiral textures in ferroelectric thin films.

KFM 20: Perovskite and Photovoltaics 2 (joint session HL/PPP/KFM)

Time: Wednesday 15:00–18:15

Location: H34

See HL 23 for details of this session.

KFM 21: Functional semiconductors for renewable energy solutions (joint session HL/KFM)

Time: Wednesday 15:00–18:30

Location: H36

See HL 24 for details of this session.

KFM 22: Members' Assembly

Annual KFM Meeting with elections of the spokespersons.

Time: Wednesday 17:00–18:00

Location: H5

All members of the Crystalline Solids and their Microstructure Division are invited to participate.

KFM 23: Skyrmions 2 (joint session MA/KFM)

Time: Thursday 9:30–12:45

Location: H37

See MA 27 for details of this session.

KFM 24: New Methods and Developments: Spectroscopies, Diffraction and Others (joint session O/KFM)

Time: Thursday 10:30–12:30

Location: H6

See O 63 for details of this session.

KFM 25: Poster

Time: Thursday 15:00–18:00

Location: P2

KFM 25.1 Thu 15:00 P2

Ferroelectric properties of $(\text{Na}_{0.5}\text{Bi}_{0.5})\text{TiO}_3$ -BaTiO₃ perovskite ceramics modified by LiF additives — •SOBHAN M. FATHABAD¹, VLADIMIR V. SHVARTSMAN¹, EKATERINA D. POLITOVA², GALINA M. KALEVA², and DORU C. LUPASCU¹ — ¹Institute for Materials Science and Center for Nanointegration Duisburg-Essen (CENIDE), University of Duisburg Essen, Essen, Germany — ²Moscow

The system of $(\text{Na}_{0.5}\text{Bi}_{0.5})\text{TiO}_3$ -BaTiO₃ solid solutions has attracted considerable interest due to its promising electromechanical, electrocaloric, and energy storage properties. In this work, the effect of LiF additive on the ferroelectric properties of $0.8(\text{Na}_{0.5}\text{Bi}_{0.5})\text{TiO}_3$ -0.2BaTiO₃ ceramics is investigated. The samples were prepared by the conventional solid state synthesis technology. The LiF content varied from 0 to 15 mol

KFM 25.2 Thu 15:00 P2

Strain and defect location in the cross-section of laterally aligned SnO₂ NWs — •JASMIN-CLARA BÜRGER, SEBASTIAN GUTSCH, and MARGIT ZACHARIAS — Laboratory for Nanotechnology, Department of Microsystems Engineering - IMTEK, University of Freiburg, Georges-Köhler-Allee 103, 79110 Freiburg, Germany

The 1D structure and the high surface-to-volume ratio of SnO₂ nanowire-based devices allow for high sensitivities in gas- and biosensing. By their self-alignment towards the substrate edge and by the self-alignment of the SnO₂ nanowire crystal lattice towards the atomic arrangement on the substrate surface[1], laterally aligned SnO₂ NWs are superior to freestanding NWs as a basic structure for a single-NW-based sensor. However, up to now, only little is known about their crystal quality compared to the excellent material quality of freestanding NWs. Hence, here, laterally aligned SnO₂ NWs on r-plane sapphire substrates were grown by the vapor-liquid-solid mechanism and morphologically analyzed by scanning electron microscopy. By focused-ion beam preparation, cross-sectional TEM lamellas of the laterally aligned SnO₂ NWs on r-plane sapphire were prepared. For analysis of the NW defect density, post-processed strain maps were computed of atomically resolved TEM images. The theoretical background for the experimentally observed location of the lowest strain density close to the substrate-NW interface and the highest defect density close to the NW surface will be discussed.

[1] J.-C. Bürger et al., Cryst. Growth Des. (2021), 21 (1), 191-199

KFM 25.3 Thu 15:00 P2

Influence of sulfur doping on the creation yield of near-surface nitrogen vacancy centers and their charge state ratio — •SVEN GRAUS¹, ULRICH KÖHLER¹, TOBIAS LÜHMANN², and JAN MEIJER² — ¹Lehrstuhl für Experimentalphysik IV, Ruhr-Universität Bochum — ²Felix-Bloch-Institut für Festkörperphysik, Angewandte Quantensysteme, Universität Leipzig

The negative charge state of nitrogen vacancy (NV) centers presents an extremely attractive candidate for a number of applications in quantum information technology and magnetometry. However, the implantation of near-surface NV centers shows a low yield and they have the tendency to convert into the neutral charge state. Recently, a significant increase in the creation yield of negative NV centers in the bulk of the diamond has been achieved by prior local doping of sulfur. We report on the in-situ implantation of sulfur and subsequent nitrogen implantation at energies of up to 5 keV while the sample is heated to temperatures of up to ~800 °C under UHV conditions. Our setup presents a unique method for the implantation of near surface NV centers in small laboratories. First results on how these parameters influence the creation yield of negative NV centers close to the surface are presented.

KFM 25.4 Thu 15:00 P2

Improved thermoelectric properties of SnSe through forming a phase employing metavalent bonding — •NAN LIN, YUAN YU, OANA COJOCARU-MIRE DIN, and MATTHIAS WUTTIG — I.Physikalisches Institut IA, RWTH Aachen, Sommerfeldstraße 14, 52074 Aachen, Germany

SnSe only shows high ZT values above 750 K when the structure transforms from the asymmetrical Pnma phase to the higher symmetrical Cmcm phase. As a typical IV-VI compound bonded by p-state electrons, the Cmcm phase SnSe with an improved symmetry is expected to show the same chemical bonding with other rock-salt IV-VI compounds, which could be responsible for its excellent thermoelectric performance. Yet, it is challenging to stabilize the Cmcm phase at room temperature to characterize the bonding indicators. We successfully obtained the high-symmetry rock-salt SnSe phase by growing $(\text{SnSe})_{0.67}(\text{AgSbTe})_{0.33}$, $(\text{SnSe})_{0.67}(\text{AgBiTe})_{0.33}$, $(\text{SnSe})_{0.67}(\text{AgBiSe})_{0.33}$, and $(\text{SnSe})_{0.5}(\text{AgSbSe})_{0.5}$ alloys in a Bridgman oven. All cubic SnSe alloys show a unique portfolio of properties including a high optical dielectric constant, a large Born effective charge, and abnormal bond-breaking behavior in laser-assisted atom probe tomography. All these characteristics are indicative of

the metavalent bonding mechanism while are not found in the pristine SnSe. Concomitantly, zT increases from near 0.1 for the Pnma SnSe to about 1.0 for all the Fm-3m SnSe phases. Our work demonstrates that metavalent bonding could be the origin of many special properties of SnSe including the excellent thermoelectric performance.

KFM 25.5 Thu 15:00 P2

Real space texture analysis using the 3D pair distribution function on a Pt thin film — •SANI Y. HAROUNA-MAYER^{1,2}, ZIZHOU GONG³, MARTIN V. ZIMMERMANN⁴, ANN-CHRISTIN DIPPEL⁴, SIMON J.L. BILLINGE², and DOROTA KOZIEJ^{1,2} — ¹Institute for Nanostructure and Solid-State Physics, Center for Hybrid Nanostructures (CHyN), University of Hamburg, Hamburg, Germany — ²The Hamburg Center for Ultrafast Imaging, Hamburg, Germany — ³Department of Applied Physics and Applied Mathematics, Columbia University, New York, USA — ⁴Deutsches Elektronen-Synchrotron DESY, Hamburg, Germany

An approach is described for studying texture in nanostructured materials. It is demonstrated on a fiber textured polycrystalline Pt thin film. The approach uses 3D PDF methods to reconstruct the orientation distribution function (ODF) of the powder crystallites from a set of diffraction patterns taken at different tilt angles of the substrate with respect to the incident beam directly from the 3D PDF of the sample. A real space equivalent of the reciprocal space pole figure is defined in terms of interatomic vectors in the PDF and computed for various interatomic vectors in the Pt film. Further, it is shown how a valid isotropic PDF may be obtained from a weighted average over the tilt series. Finally, we describe an open source Python software package, FouriGUI, that may be used to help in studies of texture from 3D reciprocal space data, and indeed for Fourier transforming and visualizing 3D PDF data in general.

KFM 25.6 Thu 15:00 P2

An X-ray diffraction studies on AlCrVY(O)N thin films. — •ERIC SCHNEIDER¹, MICHAEL PAULUS¹, NELSON FILIPE LOPES DIAS¹, DAVID KOKALJ², DOMINIC STANGIER², and WOLFGANG TILLMANN² — ¹Fakultät Physik/DELTA TU Dortmund University, 44221 Dortmund, Germany — ²Institute of Materials Engineering, Dortmund, Germany

The aim of this project is to gain a fundamental understanding of the dependence between deposition parameters, layer structure and oxidation behavior of AlCrVY(O)N coatings. For this purpose, the coating systems were deposited on a WC-Co composite substrate by DC sputtering and high-energy pulse magnetron sputtering (HiPIMS). In addition to this, individual process parameters such as BIAS voltage and substrate temperature are varied to determine their influence on the thin films structure. For the investigation of the samples we used synchrotron radiation at beamline BL9 of the synchrotron radiation source DELTA (Dortmund, Germany) to perform XRD measurements. The samples were heated in an heating cell to temperatures up to 1000 °C to study their oxidation behavior. Depending on the process parameters, different oxidation behaviour and residual stresses present in the samples were observed. We thank DELTA for providing synchrotron radiation. This work was supported by the DFG via TO 169/21-1.

KFM 25.7 Thu 15:00 P2

Hydrostatic high-pressure cells for X-ray scattering applications — •KEVIN LEHNINGER¹, CHRISTIAN STERNEMANN¹, MICHAEL PAULUS¹, BRIDGET MURPHY¹, METIN TOLAN¹, and LUTZ FELDMANN² — ¹Fakultät Physik/DELTA TU Dortmund, 44221 Dortmund, Deutschland — ²Fakultät Physik/Konstruktionsbüro TU Dortmund, 44221 Dortmund, Deutschland

Small angle and wide angle X-ray scattering (SAXS/WAXS) at moderate pressures are of increasing relevance for the study of e.g. protein denaturation and stimuli responsive materials, respectively. One of the experimental challenges here is the precise pressure control in the pressure range up to 10 kbar while separating the sample volume from the pressure transmitting medium. For this purpose, we present two dedicated hydrostatic high pressure cells designed for use at beamlines BL2 and BL9 of the DELTA synchrotron radiation source that use water for pressure transmission. The WAXS cell with an opening angle of 60 degrees allows a sample volume with a cross-sectional area of one square millimeter that can be exposed to a maximum pressure of 5000 bar. The sample volume is enclosed in a flexible capillary tube which is placed between two diamond windows and can have a maximum diameter of 1.5 mm. The SAXS cell can be operated up to a pressure of 10000 bar providing an opening angle 20 degrees. Here the sample volume is contained in a cylinder sealed by polyimide film which is screwed into the high pressure cell by a slide system.

KFM 25.8 Thu 15:00 P2

Entwicklung von Herstellungsverfahren für koordinatenbasierte 3D Mikro-Standarts — •CELINA HELLMICH¹, SEBASTIAN BÜTEFISCH¹, THOMAS WEIMANN¹, STEFANIE KROKER^{1,2} und MATTHIAS HEMMLEB³ — ¹Physikalisch-Technische Bundesanstalt Braunschweig, Bundesallee 100, 38116 Braunschweig, Deutschland — ²Technische Universität Braunschweig, Institut für Halbleitertechnik, LENA Laboratory for Emerging Nanometrology, Hans-Sommer-Str. 66, 38106 Braunschweig, Deutschland — ³point electronic GmbH Erich-Neuß-Weg 15 D-06120 Halle (Saale) Deutschland

3D-Normale vereinen die Eigenschaften der üblichen Normale und die Kalibrierfaktoren für alle Achsen und die Kopplungsfaktoren zwischen ihnen können in einem Mess- und Auswertungsschritt ermittelt werden können. Mit diesem alternativen Kalibrieransatz können geometrische Verlagerungen über 3D-Referenzstrukturen mit bekannten Objektkoordinaten bestimmt werden. Die derzeit verwendeten 3D-Normale werden mit FIB hergestellt. Jedes Normal ist daher eine kostenintensive Sonderanfertigung, die zudem eine zeitaufwendige Kalibrierung erfordert. Daher sollen waferbasierte Maskenprozesse zur Herstellung von 3D-Standarts entwickelt werden, mit denen viele Strukturen reproduzierbar hergestellt und an das jeweilige zu kalibrierende Gerät angepasst werden können. Erste Ergebnisse wurden durch den schrittweisen Aufbau von Siliziumoxidschichten in Kombination mit einem Trockenätzverfahren erzielt. Auf diese Weise können zweistufige Pyramidenstrukturen hergestellt werden, auf die der Marker für die Kalibrierung mit Hilfe von Lift-off aufgebracht werden kann.

KFM 25.9 Thu 15:00 P2

The Relation between Electrocaloric Effect and Non-Collinear Electric Fields: A Coarse-Grained Case Study of BaTiO₃ — •LAN-TIEN HSU^{1,2}, FRANK WENDLER¹, and ANNA GRÜNEBOHM² — ¹Institute of Materials Simulation (WW8), Friedrich-Alexander University of Erlangen-Nürnberg, Dr.-Mack-Str. 77, 90762 Fürth, Germany — ²Interdisciplinary Centre for Advanced Materials Simulation (ICAMS) and Center for Interface-Dominated High Performance Materials (ZGH), Ruhr-University Bochum, Universitätsstr 150, 44801 Bochum, Germany

Ferroelectric perovskites are promising candidates for future electrocaloric cooling devices due to their adiabatic temperature changes in varying external electric fields.[1,2] Recently, the origin of the inverse electrocaloric effect (ECE) has been discussed.[2,3,4] In this work, we do coarse-grained molecular dynamic simulation using feram[5] to explore the phase stability and calorimetric responses of BaTiO₃ over a wide temperature range including fields in low-symmetry directions. We observe large inverse ECEs close to high-symmetry directions where the applied fields stabilize phases outside the zero-field coexistence temperature range. We believe this finding can provide general insights into the anisotropic nature of the ECE of ferroelectric perovskites.

- [1] A. Torelló and E. Defay, Adv. Electron. Mater. (2022)
- [2] A. Grünebohm, et al., Energy Technol. 6 (2018)
- [3] H. H. Wu and R. E. Cohen., J. Phys.: Condens. Matter 29 (2017)
- [4] M. Marathe, et al., Phys. Rev. B 96 (2017)
- [5] T. Nishimatsu, et al., Phys. Rev. B 78 (2008)

KFM 25.10 Thu 15:00 P2

Dielectric loss measurements of CVD diamond disks for ITER windows — •SABINE SCHRECK¹, GAETANO AIELLO¹, PABLO ESTEBANEZ², ANDREAS MEIER¹, DIRK STRAUSS¹, and THEO SCHERER¹ — ¹Karlsruhe Institute of Technology, Institute for Applied Materials, Hermann-von-Helmholtz-Platz 1, 76344 Eggenstein-Leopoldshafen, Germany — ²F4E, Josep Pla 2, Torres Diagonal Litoral B3, 08019 Barcelona, Spain

Diamond disks manufactured by chemical vapor deposition (CVD) are essential elements of windows of the Electron Cyclotron Heating and Current Drive systems of fusion reactors like ITER. Diamond is selected as window material because of its high mechanical stability, high thermal conductivity and low dielectric loss. Only diamond disks with a low loss tangent guarantee a high transmission, i.e. a low absorption of microwave power in the disk. The latter results in moderate window temperatures and therefore in low thermal stresses. Hence, the measurement of the loss tangent is essential for the qualification of diamond disks for high-power windows. Dedicated measurement facilities (Fabry-Perot resonators) at KIT allow a high resolution measurement of the loss tangent at the disk centre (spherical set-up) as well as a mapping over the disk area to estimate its homogeneity (hemispherical set-up). Within a contract between F4E and KIT more than 60 diamond disks (D=70mm, t=1.11mm) produced similarly by MPA-CVD need to be qualified for their application in the ITER EC-system. The development of a dedicated test plan as well as initial results for the first disks delivered to KIT will be presented.

KFM 25.11 Thu 15:00 P2

X-ray emission spectroscopy at DELTA — •NICOLA THIERING, CHRISTIAN ALBERS, ROBIN SAKROWSKI, MICHAEL PAULUS, METIN TOLAN, and CHRISTIAN STERNEMANN — Fakultät Physik/DELTA, Technische Universität Dortmund, D-44221 Dortmund, Germany

The analysis of the electronic and structural properties of transition metals is of enormous importance for a variety of research fields and applications. At beam-

line BL2 of the DELTA synchrotron radiation source (Dortmund, Germany) we used a hardened white beam of a bending magnet for efficient excitation to conduct X-ray emission spectroscopy experiments. The emission spectra were measured using a von Hámos spectrometer equipped with four cylindrically bent analyzer crystals in combination with a Pilatus 100K area detector. In order to demonstrate the capabilities of this setup, we present $K\alpha$, $K\beta$, and valence-to-core spectra of selected transition-metal bearing compounds.

KFM 25.12 Thu 15:00 P2

Phase retrieval for X-ray in-line holographic imaging: beyond the homogeneous object assumption — •JENS LUCHT¹, SIMON HUHN¹, LEON MERTEN LOHSE^{1,2}, and TIM SALDITT¹ — ¹Institut für Röntgenphysik, Universität Göttingen — ²Deutsches Elektronen-Synchrotron DESY

X-ray lensless near-field holographic imaging offers high resolution 3d imaging with spatial resolution down to the nanometer scale with wide applicability in biomedical imaging and material sciences. To access quantitative images, phase retrieval has to be performed on the recorded Fresnel diffraction patterns. This constitutes an ill-posed inverse problem where several reconstruction methods have been developed. For high resolution synchrotron experiments, computationally efficient algorithms are needed. Widely employed is the computationally efficient contrast transfer function (CTF) method proposed by P. Cloetens two decades ago [P. Cloetens et al., Appl. Phys. Lett. 75, 2912 (1999)], besides more demanding nonlinear Fresnel propagation based methods. The CTF relies upon linearization of the Fresnel propagation. Notwithstanding its tremendous success, CTF-based methods often assume a homogeneous or low absorbing object a priori. We propose a CTF-based scheme that could relax these restriction to applicability while keeping reconstruction stability and computational requirements comparable. First experiments indicate very promising results.

KFM 25.13 Thu 15:00 P2

X-ray emission setup to study electronic structure of iron bearing compounds in situ at high pressure and high temperature — •NICOLA THIERING¹, CHRISTIAN ALBERS¹, ROBIN SAKROWSKI¹, MAX WILKE², JOHANNES KAA^{1,4}, HLYNUR GREYARSSON^{3,5}, MARTIN SUNDERMANN^{3,5}, METIN TOLAN^{1,6}, and CHRISTIAN STERNEMANN¹ — ¹Fakultät Physik/DELTA, Technische Universität Dortmund, Dortmund, Germany — ²Institut für Geowissenschaften, Universität Potsdam, Potsdam, Germany — ³Deutsches-Elektronen-Synchrotron DESY, Hamburg, Germany — ⁴European XFEL, Schenefeld, Germany — ⁵Max Planck Institute for Chemical Physics of Solids, Dresden, Germany — ⁶Universität Göttingen, Göttingen, Germany

The determination of iron-bearing compounds' electronic structure under high pressure and temperature (HPHT) conditions is pivotal to understand the chemistry, physics and dynamics of the Earth's interior [1]. We present a setup for investigating the electronic structure of such compounds *in situ* at HPHT up to 80 GPa and 3000 K, achieved by using diamond anvils cells in combination with a double-sided laser heating setup [2,3] using (resonant) X-ray emission spectroscopy ((R)XES) and show results for α -Fe₂O₃ and FeCO₃. (R)XES spectra were acquired utilizing a wavelength-dispersive von Hámos spectrometer in combination with a Pilatus 100K area detector [4] at PETRA III. [1] B. Orcutt et al. Deep Carbon (2019) [2] C. Albers et al. PRB 105 085155 (2022) [3] G. Spiekermann et al. JSR, 27, 414 (2020) [4] C. Weis et al. JAAS 34, 384 (2019)

KFM 25.14 Thu 15:00 P2

X-ray off-axis holography using iterative phase retrieval and waveguide beam splitters — •PAUL MEYER and TIM SALDITT — Institute for X-ray Physics, Georg August University of Göttingen, Germany

Propagation based phase contrast imaging (PB-PCI) with hard X-rays has become a powerful technique to study weakly absorbing specimen. Iterative algorithms can for example make single cells in a hydrated environment visible by retrieving the phase shift induced by the sample [1].

As image contrast in PB-PCI data arises from phase curvature, the reconstruction of low-frequency signals is challenging. In practice, it often requires support constraints on the sample. This problem does not arise with off-axis holography. Here, information of the phase image is extracted through interference with an additional reference beam that can for example be generated by a beamsplitting waveguide [2].

We observed that introducing such a reference beam in simulations for PB-PCI accelerates convergence and improves accuracy of the iterative phase retrieval (RAAR). We aim to transfer the observed advantage to the practical application of off-axis holography at synchrotron imaging facilities.

[1] Krenkel et al. Three-dimensional single-cell imaging with X-ray waveguides in the holographic regime. Acta Cryst A 73, 282-292 (2017). [2] Fuhse et al. Waveguide-Based Off-Axis Holography with Hard X Rays. Phys. Rev. Lett. 97, 254801 (2006).

KFM 25.15 Thu 15:00 P2

Hierarchically Porous Carbon Derived from the Activation of Waste Chestnut Shells as High Performance Electrode Materials for Supercapacitor — •PING HONG^{1,2}, YUDE WANG², HUAPING ZHAO¹, and YONG LEI¹ — ¹Fachgebiet Angewandte Nanophysik, Institut für Physik & IMN MacroNano, Technische Universität Ilmenau, 98693 Ilmenau, Germany — ²School of Materials Science and Engineering, Yunnan University, Kunming, People's Republic of China

3D hierarchically porous carbon consisting of micropores, mesopores and macropores was successfully prepared through the activation of chestnut shell with potassium bicarbonate (KHCO₃). The influence of KHCO₃/chestnut shell ratio on the textural properties was carefully investigated. By optimizing the amount of KHCO₃, 3D hierarchically porous carbon with high specific pore surface area (2298 m² g⁻¹) and high total pore volume (1.51 cm³ g⁻¹) were achieved. When applying the as-prepared 3D hierarchical porous carbon as electrode materials for supercapacitors, a high specific electric capacity of 387 F g⁻¹ was reached at a current density of 2 A g⁻¹. The remarkable electrochemical performances are mainly attributed to the hierarchical porous structure with the high specific surface area and the eminent total pore volume. It suggests that this hierarchical porous carbon prepared by activated by using KHCO₃ would have more promising foreground in the field of energy storage.

KFM 25.16 Thu 15:00 P2

Ni-SnO₂ nanopore arrays as potassium-ion battery anodes — •MO SHA, HUAPING ZHAO, and YONG LEI — Fachgebiet Angewandte Nanophysik, Institut für Physik & IMN MacroNano, Technische Universität Ilmenau, 98693 Ilmenau, Germany

Sodium-ion batteries (SIBs) represent an effective energy storage technology with potentially lower material costs than lithium-ion batteries. Here, we show the electrochemical performance of SIBs with electrode design at the nanoscale. Highly ordered three-dimensional (3D) selfsupported Ni-TiO₂ nanopore arrays (NiNPA@TiO₂) with highly oriented nanoporous structures are fabricated using nanoimprinted AAO templating technique and applied as nanostructured anodes for SIBs applications. Their large specific surface area can ensure a high capacity, and their highly oriented and stable nanoporous structure can facilitate ion transport. The NiNPA@TiO₂ nanoarrays delivered a reversible capacity of 240 mAh g⁻¹ after 100 cycles at the current density of 50 mAh g⁻¹ and were able to retain a capacity of 105 mAh g⁻¹ at the current density as high as 5 A g⁻¹. Their large active sites, high ion accessibility, fast electron transport, and excellent electrode integrity were shown as great merits to obtain the presented electrochemical performance. Not limited to the SIBs electrodes, the highly ordered 3D heterostructured nanoarrays as a promising electrode design for other electrochemical energy conversion and storage devices.

KFM 25.17 Thu 15:00 P2

Enhanced efficiency of graphene-silicon Schottky junction solar cell through inverted pyramid arrays texturation — •JIAJIA QIU^{1,2}, HUAPING ZHAO¹, WENHUI MA², and YONG LEI¹ — ¹Fachgebiet Angewandte Nanophysik, Institut für Physik & IMN MacroNano, Technische Universität Ilmenau, 98693 Ilmenau, Germany — ²State Key Laboratory of Complex Nonferrous Metal Resources Clean Utilization, Kunming University of Science and Technology, Kunming 650093, China

Nanostructures of silicon are gradually becoming hot candidate due to outstanding capability for trapping light and improving conversion efficiency of solar cell. In this work, silicon nanowires (SiNWs) and silicon inverted pyramid arrays (SiIPs) were introduced on surface of graphene-silicon (Gr-Si) solar cell through silver and copper-catalyzed chemical etching, respectively. The effects of SiNWs and SiIPs on carrier lifetime, optical properties and efficiency of Gr-SiNWs and Gr-SiIPs solar cells were systematically analyzed. The results show that the inverted pyramid arrays have more excellent ability for balancing antireflectance loss and surface area enlargement. The power conversion efficiency (PCE) and carrier lifetime of Gr-SiIPs devices respectively increase by 62% and 34% by comparing with that of Gr-SiNWs solar cells. Finally, the Gr-SiIPs cell with PCE of 5.63% was successfully achieved through nitric acid doping. This work proposes a new strategy to introduce the inverted pyramid arrays for improving the performance of Gr-Si solar cells.

KFM 25.18 Thu 15:00 P2

Structural behavior of delithiated Li_xNi_{0.8}Co_{0.15}Al_{0.05}O₂ (0 < x < 1) battery cathodes — •TOBIAS HÖLDERLE^{1,2}, PETER MÜLLER-BUSCHBAUM^{1,2}, and ANATOLIY SENYSHYN² — ¹Lehrstuhl für funktionelle Materialien, Technische Universität München, Garching, Germany — ²Heinz Maier-Leibnitz Zentrum (MLZ), Technische Universität München, Garching, Germany

The development of portable electronic devices up to electric vehicles powered with lithium-ion batteries led to an increased demand for lithium-ion batteries with higher capacities, energy/power densities, and cycling life. One of the most encouraging and state of the art commercial cathode materials are mixed lithium Ni, Co, Al metal oxides, e.g. in the form of high nickel content LiNi_{0.8}Co_{0.15}Al_{0.05}O₂ (NCA) cathodes possessing high energy and power densities at lower costs. Besides advantages, NCA materials possess several essential drawbacks. For example, NCA cathode materials are known to suffer from poor

thermal stability, pronounced capacity as well as power density fading, and anti-site disorder in NCA materials [1]. In the current contribution, a systematic *ex-situ* neutron powder diffraction study on differently electrochemically delithiated NCA cathode materials is presented. A set of structural parameters was obtained using full-profile Rietveld refinement. The lithium occupations reflect the increasing state-of-charge whilst the occupations of transition metals do not change, indicating the absence of antisite defects (cation mixing) in the NCA material. [1] C. Xu, P. J. Reeves, Q. Jacquet and C. P. Grey, *Adv. Energy Mater.*, 11, 2003404 (2021).

KFM 25.19 Thu 15:00 P2

Dense binary Fe-Cu sites promoting CO₂ utilization to enable highly-reversible hybrid Na-CO₂ battery — •CHANGFAN XU — Fachgebiet Angewandte Nanophysik, Institut für Physik & IMN MacroNano, Technische Universität Ilmenau, 98693 Ilmenau, Germany — School of Metallurgy and Environment, Central South University, Changsha 410083, China — Faculty of Metallurgical and Energy Engineering, Kunming University of Science and Technology, Kunming 650093, China

A well-defined morphology of nitrogen-rich graphitic carbon framework with dense bimetallic active sites (Fe-Cu-N-C) was facilely prepared by introducing Fe³⁺ and Cu²⁺ to regulate in-situ grown carbon nanotubes as an advanced catalyst toward hybrid Na-CO₂ batteries. Through metal content-tuning and carbon architecture-altering, the Fe-Cu-N-C was proved to be dramatically more effective than Cu-N-C and Fe-N-C. As the cathodic catalyst of a hybrid Na-CO₂ battery, Fe-Cu-N-C can facilitate the fast evolution and degradation of flocculent discharge products and achieve an excellent long-term cyclability up to 1550 cycles (over 600 h). The outstanding performance is attributed to the cross-linked conductive framework affording a highway for accelerating electron transport and Na⁺/CO₂ diffusion. Besides, the synergistic effects among defect-rich interfaces, Fe/Fe₃C nanocrystals, Fe-N_x, and Cu-N_x sites derived from nitrogen doping enhance the catalytic activity. The possible growth and decomposition mechanisms of NaHCO₃ products were also presented and discussed.

KFM 25.20 Thu 15:00 P2

Dynamics of lithium-distribution in 18650-type LFP|C lithium-ion batteries during electrochemical cycling — •DOMINIK PETZ^{1,2}, PETER MÜLLER-BUSCHBAUM^{1,2}, and ANATOLIY SENYSHYN¹ — ¹Heinz Maier-Leibnitz Zentrum (MLZ), Garching, Germany — ²Lehrstuhl für Funktionelle Materialien, Technische Universität München, Garching, Germany

The electrochemical cycling of lithium-ion batteries is characterized by an active transport of lithium ions and electrons, which are exchanged between the cathode and anode materials. Ionic exchange influences structural and chemical properties of electrode materials, which, in turn, affects electrode dimensions and geometry, current density, temperature, pressure, reaction rate, etc. Such parameters are in general neither uniformly nor statically distributed and therefore serve as stabilizing factor for heterogeneous states in lithium-ion batteries, which are typically reflected in the lithium concentration distribution in the electrodes. In most of the studies reported in literature, the lithium distribution has typically been examined in static equilibrium (e.g. in fully charged state), neglecting the evolution of the distribution under real charging conditions like the influence of C-rates, etc.

In this work the evolution of the lithium-ion distribution in the graphite anode was investigated in-operando by spatially-resolved neutron powder diffraction. Neutron data were supplemented by diffraction studies with high-energy photons. The occurrence of lithium inhomogeneities on different length scales was observed and will be presented in the current contribution.

KFM 25.21 Thu 15:00 P2

Strong electron-phonon coupling in EuPd₂Si₂ — •MAI YE¹, MARK JOACHIM GRAF VON WESTARP¹, SOFIA-MICHAELA SOULIOU¹, MARIUS PETERS², ROBERT MÖLLER², KRISTIN KLIEMT², CORNELIUS KRELLNER², and MATTHIEU LE TACON¹ — ¹Institute for Quantum Materials and Technologies, Karlsruhe Institute of Technology, 76021 Karlsruhe, Germany — ²Institute of Physics, Goethe-University Frankfurt, 60438 Frankfurt am Main, Germany

Mixed-valence metal EuPd₂Si₂ exhibits a valence transition from Eu²⁺ to Eu³⁺ with the crossover temperature T_v around 140 K [*Jpn. J. Appl. Phys.* 50 (2011) 05FD03]. On cooling, the tetragonal crystal symmetry is unchanged, with the a-axis length decreasing and the c-axis length essentially unchanged [arXiv:2203.05136]. We study the phonon modes of this material by Raman spectroscopy to explore the effect of valence transition and electron-phonon coupling. The Raman-active A_{1g} phonon mode shows Fano-type asymmetric line-shape, indicating interaction between the phonon mode and underlying continuum of electronic excitations. This mode also exhibits large frequency hardening on cooling: the frequency at 25 K is around 30% larger than that at 300 K. Such a large frequency change cannot be solely explained by the change of lattice parameters, which is only 2%, and points to the role played by electron-phonon interaction. Moreover, the frequency and linewidth of other Raman-active phonon modes show anomalies at T_v. We also present Raman spectra of EuPd₂(Si_{0.94}Ge_{0.06})₂ for comparison.

KFM 26: Focus Session: Topological Devices (joint session TT/KFM)

The properties of topological phases of matter give rise to unique phenomena, such as edge or surface transport, spin-momentum locking, or topological protection against perturbations. Many years after their conception, several topological platforms have reached maturity, and research interests have shifted towards mesoscopic devices unveiling rich and new topological physics, driven in part by the perspectives of novel topological quantum computation. Within this Focus Session, recent examples of devices exploring or exploiting the topological properties of various phases of matter shall be discussed.

Organizers: Erwann Bocquillon, Oliver Breunig, Yoichi Ando (all Universität zu Köln)

Time: Thursday 15:00–18:30

Location: H10

See TT 32 for details of this session.

KFM 27: Perovskite and Photovoltaics 3 (joint session HL/ CPP/KFM)

Time: Thursday 15:00–16:30

Location: H31

See HL 32 for details of this session.

KFM 28: Topological Insulators (joint session MA/KFM)

Time: Thursday 15:00–17:45

Location: H37

See MA 31 for details of this session.

KFM 29: Multiferroics and Magnetoelectric Coupling (joint session MA/KFM)

Time: Thursday 15:00–16:45

Location: H47

See MA 33 for details of this session.

KFM 30: Skyrmions 3 (joint session MA/KFM)

Time: Friday 9:30–12:45

Location: H37

See MA 37 for details of this session.

KFM 31: Electrical, Dielectrical and Optical Properties of Thin Films (joint session CPP/KFM)

Time: Friday 11:30–12:30

Location: H38

See CPP 48 for details of this session.

Magnetism Division Fachverband Magnetismus (MA)

Heiko Wende
Universität Duisburg-Essen
Fakultät für Physik
Lotharstr. 1
D-47048 Duisburg
heiko.wende@uni-due.de

Overview of Invited Talks and Sessions

(Lecture halls H37, H43, H47, and H48; Poster P2 and P4)

Invited Talks

MA 10.1	Mon	15:00–15:30	H47	Magnetic vortices: into the third dimension — •SEBASTIAN GLIGA
MA 12.1	Tue	9:30–10:00	H37	Topological spin structures at surfaces — •STEFAN HEINZE
MA 14.1	Tue	9:30–10:00	H47	Overriding universality of ferromagnetic phase transitions through nano-scale materials design — •ANDREAS BERGER
MA 17.1	Tue	15:00–15:30	H43	Ultimately fast, small and energy-efficient magnetism: fundamentals and prospects — •JOHAN MENTINK
MA 17.2	Tue	15:30–16:00	H43	From spintronics at limiting temporal and spatial scales in antiferromagnets to an emerging altermagnetic phase — •TOMAS JUNGWIRTH
MA 17.3	Tue	16:00–16:30	H43	An electronic structure viewpoint on candidate van der Waals ferromagnets — •PHIL KING, MATT WATSON, BRENDAN EDWARDS, AKHIL RAJAN, JIAGUI FENG, DEEP BISWAS, MONICA CIOMAGA HATNEAN, AMELIA HALL, GEETHA BALAKRISHNAN, GIOVANI VINAI, DAVID BURN, THORSTEN HESJEDAL, GERRIT VAN DER LAAN, OLIVER DOWINTON, SAEED BAHRAMY
MA 17.4	Tue	16:30–17:00	H43	Nano-scale skyrmions and atomic-scale spin textures studied with STM — •KIRSTEN VON BERGMANN
MA 20.1	Wed	9:30–10:00	H37	Recent developments in X-ray three-dimensional magnetic imaging — •VALERIO SCAGNOLI
MA 20.2	Wed	10:00–10:30	H37	Magnetic depth profiling with x-ray resonant magnetic reflectivity (XRMR) — •TIMO KUSCHEL
MA 20.3	Wed	10:30–11:00	H37	Magnetic Bragg Ptychography Studies of Spin Caloritronic — •DINA CARBONE, PENG LI, STEPHAN GEPRÄGS, RUDOLF GROSS, PAUL EVANS, VIRGINIE CHAMARD, DAN MANNIX
MA 20.4	Wed	11:15–11:45	H37	Imaging the 3D magnetic texture of skyrmion tubes and approaches towards determining their Hall signature — •B. RELLINGHAUS, S. SCHNEIDER, D. WOLF, U.K. RÖSSLER, M. SCHMIDT, A. KOVÁCS, R.E. DUNIN-BORKOWSKI, D. POHL, A. THOMAS, D. KRIEGER, B. BÜCHNER, A. LUBK
MA 20.5	Wed	11:45–12:15	H37	Determination of spin chirality and helicity angle by circular dichroism in soft x-ray absorption and resonant elastic scattering — •GERRIT VAN DER LAAN
MA 20.6	Wed	12:15–12:45	H37	Identification of complex spin-textures by novel Hall effects — •JUBA BOUAZIZ, HIROSHI ISHIDA, SAMIR LOUNIS, STEFAN BLÜGEL
MA 31.1	Thu	15:00–15:30	H37	Neutron scattering on magnetic topological materials: From topological magnon insulators to emergent many-body effects — •YIXI SU

Invited Talks of the joint Symposium **Frontiers of Orbital Physics: Statics, Dynamics, and Transport of Orbital Angular Momentum (SYOP)**

See SYOP for the full program of the symposium.

SYOP 1.1	Mon	9:30–10:00	H1	Orbital degeneracy in transition metal compounds: Jahn-Teller effect, spin-orbit coupling and quantum effects — •DANIEL KHOMSKII
SYOP 1.2	Mon	10:00–10:30	H1	Orbital magnetism out of equilibrium: driving orbital motion with fluctuations, fields and currents — •YURIY MOKROUSOV
SYOP 1.3	Mon	10:30–11:00	H1	Orbitronics: new torques and magnetoresistance effects — •MATHIAS KLÄUI

SYOP 1.4	Mon	11:15–11:45	H1	Orbital and total angular momenta dichroism of the THz vortex beams at the antiferromagnetic resonances — •ANDREI SIRENKO
SYOP 1.5	Mon	11:45–12:15	H1	Observation of the orbital Hall effect in a light metal Ti — •GYUNG-MIN CHOI

Invited Talks of the joint Symposium SKM Dissertation Prize 2022 (SYSD)

See SYSD for the full program of the symposium.

SYSD 1.1	Mon	10:15–10:45	H2	Charge localisation in halide perovskites from bulk to nano for efficient optoelectronic applications — •SASCHA FELDMANN
SYSD 1.2	Mon	10:45–11:15	H2	Nonequilibrium Transport and Dynamics in Conventional and Topological Superconducting Junctions — •RAFFAEL L. KLEES
SYSD 1.3	Mon	11:15–11:45	H2	Probing magnetostatic and magnetotransport properties of the antiferromagnetic iron oxide hematite — •ANDREW ROSS
SYSD 1.4	Mon	11:45–12:15	H2	Quantum dot optomechanics with surface acoustic waves — •MATTHIAS WEISS

Invited Talks of the joint Symposium United Kingdom as Guest of Honor (SYUK)

See SYUK for the full program of the symposium.

SYUK 1.1	Wed	9:30–10:00	H2	Structure and Dynamics of Interfacial Water — •ANGELOS MICHAELIDES
SYUK 1.2	Wed	10:00–10:30	H2	A molecular view of the water interface — •MISCHA BONN
SYUK 1.3	Wed	10:30–11:00	H2	Motile cilia waves: creating and responding to flow — •PIETRO CICUTA
SYUK 1.4	Wed	11:00–11:30	H2	Cilia and flagella: Building blocks of life and a physicist's playground — •OLIVER BÄUMCHEN
SYUK 1.5	Wed	11:45–12:15	H2	Computational modelling of the physics of rare earth - transition metal permanent magnets from SmCo₅ to Nd₂Fe₁₄B — •JULIE STAUNTON
SYUK 2.1	Wed	15:00–15:30	H2	Hysteresis Design of Magnetic Materials for Efficient Energy Conversion — •OLIVER GUTFLEISCH
SYUK 2.2	Wed	15:30–16:00	H2	Non-equilibrium dynamics of many-body quantum systems versus quantum technologies — •IRENE D'AMICO
SYUK 2.3	Wed	16:00–16:30	H2	Quantum computing with trapped ions — •FERDINAND SCHMIDT-KALER
SYUK 2.4	Wed	16:45–17:15	H2	Breaking the millikelvin barrier in cooling nanoelectronic devices — •RICHARD HALEY
SYUK 2.5	Wed	17:15–17:45	H2	Superconducting Quantum Interference Devices for applications at mK temperatures — •SEBASTIAN KEMPF

Sessions

MA 1.1–1.1	Sun	16:00–17:30	H1	Tutorial: Careers in Science (joint session MA/TUT)
MA 2.1–2.4	Mon	9:30–10:30	H37	Magnetic Imaging Techniques
MA 3.1–3.3	Mon	9:30–10:15	H43	Spin-Dependent Phenomena in 2D
MA 4.1–4.4	Mon	9:30–10:30	H47	Disordered Magnetic Materials
MA 5.1–5.4	Mon	9:30–10:30	H48	Magnetic Instrumentation and Characterization
MA 6.1–6.4	Mon	11:00–12:00	H37	Complex Magnetic Oxides
MA 7.1–7.4	Mon	11:00–12:00	H43	Magnetic Relaxation and Gilbert Damping
MA 8.1–8.12	Mon	15:00–18:00	H37	Ultrafast Magnetization Effects 1
MA 9.1–9.4	Mon	15:00–17:00	H43	INNOMAG e.V. Prizes 2022 (Diplom-/Master and Ph.D. Thesis)
MA 10.1–10.6	Mon	15:00–16:45	H47	Non-Skyrmionic Magnetic Textures
MA 11.1–11.8	Mon	15:00–17:00	H48	Computational Magnetism 1
MA 12.1–12.12	Tue	9:30–12:45	H37	Skyrmions 1 (joint session MA/KFM)
MA 13.1–13.12	Tue	9:30–12:30	H43	Magnonics 1
MA 14.1–14.9	Tue	9:30–12:00	H47	Cooperative Phenomena: Spin Structures and Magnetic Phase Transitions
MA 15.1–15.8	Tue	9:30–11:30	H48	Computational Magnetism 2
MA 16.1–16.11	Tue	15:00–17:45	H37	Frustrated Magnets
MA 17.1–17.4	Tue	15:00–17:00	H43	PhD Focus Session: The Hitchhiker's Guide to Spin Phenomena at the Space and Time Limit
MA 18.1–18.9	Tue	15:00–17:15	H47	Spintronics
MA 19.1–19.64	Tue	17:30–20:00	P2	Poster 1
MA 20.1–20.7	Wed	9:30–13:00	H37	Focus Session: Revealing Multidimensional Spin Textures and their Dynamics via X-rays and Electrons
MA 21.1–21.11	Wed	9:30–12:15	H43	Terahertz Spintronics

MA 22.1–22.9	Wed	9:30–11:45	H47	Thin Films: Magnetic Coupling Phenomena / Exchange Bias / Magnetic Anisotropy
MA 23.1–23.5	Wed	9:30–10:45	H48	Magnetic Domain Walls
MA 24.1–24.12	Wed	15:00–18:00	H37	Spin Transport and Orbitronics, Spin-Hall Effects
MA 25.1–25.8	Wed	15:00–17:00	H43	Ultrafast Magnetization Effects 2
MA 26.1–26.4	Wed	15:00–16:00	H48	Molecular Magnetism
MA 27.1–27.13	Thu	9:30–12:45	H37	Skyrmions 2 (joint session MA/KFM)
MA 28.1–28.13	Thu	9:30–12:45	H43	Magnonics 2
MA 29.1–29.9	Thu	9:30–11:45	H47	Caloric Effects in Magnetic Materials
MA 30.1–30.8	Thu	9:30–11:30	H48	Surface Magnetism
MA 31.1–31.10	Thu	15:00–17:45	H37	Topological Insulators (joint session MA/KFM)
MA 32.1–32.8	Thu	15:00–17:00	H43	Bulk Materials: Soft and Hard Permanent Magnets
MA 33.1–33.7	Thu	15:00–16:45	H47	Multiferroics and Magnetoelectric Coupling (joint session MA/KFM)
MA 34.1–34.7	Thu	15:00–16:45	H48	Functional Antiferromagnetism
MA 35.1–35.76	Thu	16:00–18:00	P4	Poster 2
MA 36	Thu	18:00–19:00	H37	Members' Assembly
MA 37.1–37.13	Fri	9:30–12:45	H37	Skyrmions 3 (joint session MA/KFM)
MA 38.1–38.7	Fri	9:30–11:15	H43	Electron Theory of Magnetism and Correlations
MA 39.1–39.6	Fri	9:30–11:00	H47	Magnetic Particles / Clusters
MA 40.1–40.5	Fri	9:30–10:45	H48	Weyl Semimetals
MA 41.1–41.5	Fri	11:30–12:45	H47	Micro- and Nanostructured Magnetic Materials
MA 42.1–42.5	Fri	11:30–12:45	H48	Magnetic Heuslers

Members' Assembly of the Magnetism Division

Thursday 18:00–19:00 H37

Sessions

– Invited Talks, Tutorials, Contributed Talks, and Posters –

MA 1: Tutorial: Careers in Science (joint session MA/TUT)

Time: Sunday 16:00–17:30

Location: H1

Tutorial

MA 1.1 Sun 16:00 H1

Careers in science: "To boldly go where no one has gone before" — •MANFRED FIEBIG — Department of Materials, ETH Zurich

What does it take to do a career in science and become a university professor? An obvious answer is: you have to do outstanding research. But just doing great science plays a surprisingly small part — and what defines scientific work as outstanding anyway? Then, you also need to communicate your findings well. The best result is worth little if you present it in an awful talk or manuscript. You also need to be "good with people", may these be your students or your colleagues.

Even luck can play an important role in a successful scientific career, but is very important to distinguish luck from "luck". I will refer to all these points and analyze what "being lucky" has actually to do with luck. I will present a list of points that I consider essential for a prosperous start into a scientific career. Some of these points are surprisingly unnoticed, so following them may put you ahead of the crowd.

Questions and discussion

MA 2: Magnetic Imaging Techniques

Time: Monday 9:30–10:30

Location: H37

MA 2.1 Mon 9:30 H37

High resolution magnetic imaging with holography-aided phase retrieval — •RICCARDO BATTISTELLI¹, SERGEY ZAYKO², MICHAEL SCHNEIDER³, CHRISTIAN M. GÜNTHER⁴, KATHINKA GERLINGER³, DANIEL METTERNICH¹, LISAMARIE KERN³, KAI LITZIUS⁵, STEFAN EISEBITT^{3,4}, BASTIAN PFAU³, and FELIX BÜTTNER¹ — ¹Helmholtz-Zentrum Berlin, Berlin, Germany — ²University of Göttingen, Göttingen, Germany — ³Max Born Institute, Berlin, Germany — ⁴Technische Universität Berlin, Berlin, Germany — ⁵Max-Planck-Institut für Intelligente Systeme, Stuttgart, Germany

In the fields of magnetism and spintronics, magnetic multilayers continue to thrive as pivotal structures to functionalize magnetic interactions and to engineer complex non-trivial spin textures. Despite the intense research on this topic, relatively little is known about 3D magnetic textures in multilayers and their interaction with local defects, despite the expected richer physics and potential in information technologies. The experimental challenges of studying such systems can be met by merging Fourier Transform Holography with phase retrieval algorithms for coherent diffractive imaging, obtaining high throughput, high resolution and high contrast images of magnetic materials. Here we present 5 nm resolution X-ray images of magnetic multilayers in which the presence of 3D magnetic defects can be inferred thanks to the high sensitivity of the technique. The interaction of magnetic domains with these defects favors the presence of domain walls, reducing the average domain size with respect to the pristine material.

MA 2.2 Mon 9:45 H37

Using electron microscopic methods to evaluate the magnetic proximity effect — •DANIELA RAMERMANN^{1,3}, INGA ENNEN¹, DOMINIK GRAULICH¹, TREVOR ALMEIDA², STEPHEN MCVITIE², BJÖRN BÜKER¹, TIMO KUSCHEL¹, and ANDREAS HÜTTEN¹ — ¹Universität Bielefeld, Dünne Schichten und Physik der Nanostrukturen, Universitätsstr. 25, 33615 Bielefeld, Germany — ²University of Glasgow, School of Physics and Astronomy, Glasgow G12 8QQ, UK — ³Max Planck Institute for Chemical Energy Conversion, Stiftstraße 34-36, 45470 Mülheim an der Ruhr

Magnetic proximity effects are part of spintronic, superconducting, excitonic and topological phenomena which can induce desired or parasitic effects in measurements and devices. They are induced by a ferromagnet in a layer of a material close to the Stoner criterion in proximity to the ferromagnet. Usually magnetic proximity effects are studied by X-ray techniques. Modern analytical electron microscopy can be used to analyse the same underlying effects as well as electronic structure properties of materials. Therefore, it can be used to investigate the proximity effect in thin film systems.

As a model system a V/Fe thin film sample has been chosen. The techniques of electron energy loss magnetic chiral dichroism (EMCD) and differential phase contrast (DPC) have been used in combination. EMCD is used to show the presence of a magnetic moment on the material and DPC to locate the magnetic induction with high accuracy. Thus, we were able to observe a magnetic proximity effect of about 1.5 nm in V, which is in agreement with X-Ray measurements.

MA 2.3 Mon 10:00 H37

Coherent Correlation Imaging: Resolving fluctuating states of matter — •CHRISTOPHER KLOSE¹, FELIX BÜTTNER^{2,3,4}, WEN HU³, CLAUDIO MAZZOLI³, KAI LITZIUS², RICCARDO BATTISTELLI⁴, IVAN LEMESH², JASON M. BARTELL², MANTAO HUANG², CHRISTIAN M. GÜNTHER⁵, MICHAEL SCHNEIDER¹, ANDI BARBOUR³, STUART B. WILKINS³, GEOFFREY S.D. BEACH², STEFAN EISEBITT^{1,5}, and BASTIAN PFAU¹ — ¹Max Born Institute, Berlin — ²Massachusetts Institute of Technology, Cambridge, MA, USA — ³National Synchrotron Light Source II, Upton, NY, USA — ⁴Helmholtz-Zentrum Berlin — ⁵Technische Universität Berlin

Fluctuations and stochastic transitions are ubiquitous in nanometer-scale systems, especially in the presence of disorder. However, their direct observation has so far been impeded by a seemingly fundamental, signal-limited compromise between spatial and temporal resolution.

Here, we develop coherent correlation imaging (CCI) — a high-resolution, full-field imaging technique that realizes multi-shot, time-resolved imaging of stochastic processes. The key of CCI is the classification of camera frames that correspond to the same physical state by combining a correlation-based similarity metric with powerful classification algorithm developed for genome research.

We apply CCI to study previously inaccessible magnetic fluctuations in a highly degenerate magnetic stripe domain state with nanometer-scale resolution. The spatiotemporal imaging reveals the transition network between the states and details of the magnetic pinning landscape which have been inaccessible so far.

MA 2.4 Mon 10:15 H37

Charge State Instabilities of shallow Nitrogen-Vacancy Centers in Diamond at Cryogenic Ultra-High-Vacuum Conditions — DOMENICO PAONE^{1,2,5}, •TONI HACHE^{1,5}, JEFFREY N. NEETHIRAJAN^{1,2,5}, DINESH PINTO^{1,3}, ANDREJ DENISENKO², RAINER STÖHR², PÉTER UDVARHELYI⁴, ÁDÁM GALI⁴, APARAJITA SINGHA¹, JÖRG WRACHTRUP^{1,2}, and KLAUS KERN^{1,3} — ¹Max Planck Institute for Solid State Research — ²3rd Institute of Physics and Research Center SCoPE, University of Stuttgart — ³Institute de Physique, École Polytechnique Fédérale de Lausanne — ⁴Wigner Research Centre for Physics, Institute for Solid State Physics and Optics, Hungarian Academy of Sciences — ⁵Equal contribution.

Nitrogen-vacancy (NV) centers in diamond have attracted an immense interest for non-invasive magnetic imaging and quantum sensing. All NV based magnetic sensing protocols rely on the negative charge state of this quantum sensor (NV⁻). In this work we demonstrate dramatic charge state conversions within individual NV centers at cryogenic (4.7 K) and $2 \cdot 10^{-10}$ mbar ultra-high-vacuum (UHV) conditions. The NV centers are characterized based on autocorrelation measurements, ODMR contrast and emission spectra. Under these extreme conditions, each of these measurements indicate a significant decrease of the relative occupancy of the NV⁻ charge state. Furthermore, we note a slight recovery of the NV⁻ charge state by dosing water (H₂O) on top of the diamond surface under UHV conditions. These results indicate that controlled surface treatments are essential for implementing NV center based quantum sensing protocols at cryogenic-UHV conditions.

MA 3: Spin-Dependent Phenomena in 2D

Time: Monday 9:30–10:15

Location: H43

MA 3.1 Mon 9:30 H43

Noncollinear magnetism in a monolayer of two-dimensional CrTe₂ — •NIHAD ABUAWWAD^{1,2}, MANUEL DOS SANTOS DIAS^{2,1}, HAZEM ABUSARA³, and SAMIR LOUNIS^{1,2} — ¹Peter Grünberg Institut and Institute for Advanced Simulation, Forschungszentrum Jülich & JARA, 52425 Jülich, Germany — ²Faculty of Physics, University of Duisburg-Essen, 47053 Duisburg, Germany — ³Department of Physics, Birzeit University, PO Box 14, Birzeit, Palestine

The discovery of two-dimensional (2D) van der Waals magnets opened unprecedented opportunities for the fundamental exploration of magnetism in quantum materials. Recently, thin CrTe₂ films were demonstrated to be ferromagnetic up to room temperature, with an intriguing dependence of the easy axis on the thickness of the material [1,2]. Using first principles, we show that the charge-density waves characterizing a single CrTe₂ give rise to spiral magnetism through the emergence of the Dzyaloshinskii-Moriya interaction (DMI). Utilizing atomistic spin dynamics, we perform a detailed investigation of the complex magnetic properties pertaining to this 2D material impacted by the presence of various types of charge density waves. Also, we study the electronic and magnetic properties of heterostructures consisting of a single CrTe₂ monolayer interfaced with either Graphene or hBN.

–Work funded by the Palestinian-German Science Bridge (BMBF–01DH16027) and SPP 2244 (project LO 1659/7-1).

[1] Zhang *et al.*, Nat. Commun. **12**, 2492 (2021); [2] Meng *et al.*, Nat. Commun. **12**, 809 (2021).

MA 3.2 Mon 9:45 H43

Electric-field control of the DMI in magnetic heterostructures — •DONYA MAZHJOO, GUSTAV BIHLMAYER, and STEFAN BLÜGEL — Peter Grünberg Institut and Institute for Advanced Simulation, Forschungszentrum Jülich, Germany

The use of external electric fields can extend the exploration of spintronic devices with a tunable Dzyaloshinskii-Moriya interaction (DMI) by allowing control of the interfacial DMI. Moreover, the magnetocrystalline anisotropy energy (MAE) changes as function of electric field intensity. By using density functional theory as implemented in the FLEUR-code [1], we investigated the electric field effects on graphene (Gr) covered Co/Pt(111) heterostructures. Experiments show evidence of a sizable DMI at the Gr/Co interface which partially compensates

the spin-orbit coupling induced DMI at the Co/Pt interface [2], which could make these structures susceptible to electric fields. To stimulate their influence, we sandwiched the film between two electrodes of opposite polarity. The self-consistent spin-spiral calculations were performed with these changed boundary conditions and spin-orbit effects were included in first order perturbation theory for the DMI and self-consistently for the MAE. We demonstrate that external fields lead to modulation of the spin-orbit induced quantities that allow a tuning of properties like domain wall widths or skyrmion radii. Support from the FLAG-ERA JTC 2019 grant SOgraphMEM is gratefully acknowledged.

[1] <https://www.flapw.de>

[2] F. Ajejas *et al.* Nano Lett. 2018, **18**, 5364-5372

MA 3.3 Mon 10:00 H43

Spinon induced drag in quantum spin liquid heterostructures — •RAFFAELE MAZZILLI¹, ALEX LEVCHENKO², and ELIO KOENIG¹ — ¹Max-Planck-Institut für Festkörperforschung, 70569 Stuttgart, Germany — ²Department of Physics, University of Wisconsin-Madison, Madison, Wisconsin 53706, USA

Several quantum spin liquid candidate materials, such as α -RuCl₃ and 1T-TaSe₂, are exfoliable, so that it is possible to investigate 2D samples which avoid the manifestation of bulk properties that might disrupt the quantum spin liquid phase. In this phase the material is a Mott insulator and therefore it is impenetrable to direct electric probes such as charge currents. Despite this, in this work we propose an experimental setup that will allow to use non-local electrical probes to gain information on the transport properties of a gapless quantum spin liquid. The proposed setup is a spinon induced drag experiment, that consists in interfacing two metallic films separated by a layer of a quantum spin liquid. A current is injected in one of the two layers (active layer) and a voltage is measured on the second (passive) metallic film. The overall momentum transfer mechanism is a two-step process mediated by the Kondo interaction between the local moments in the quantum spin liquid and the spins of the electrons. We calculate, both for a U(1) and a Z₂ spin liquids, the drag resistivity in the framework of the linearized quantum Boltzmann equation derived from the Keldysh formalism. In this framework the three layers are out of thermodynamic equilibrium. We further confront the results obtained with the equilibrium case and with the results of standard Coulomb drag.

MA 4: Disordered Magnetic Materials

Time: Monday 9:30–10:30

Location: H47

MA 4.1 Mon 9:30 H47

Destruction of long-range magnetic order in the Cu₂GaBO₅ ludwigite in a magnetic field — A. KULBAKOV¹, R. SARKAR¹, O. JANSON², S. DENGRE¹, E. M. MOSHKINA³, P. Y. PORTNICHENKO¹, H. LUETKENS⁴, F. YOKAICHIYA⁵, A. S. SUKHANOV^{1,6}, R. M. EREMINA⁷, A. SCHNEIDEWIND⁸, H.-H. KLAUSS¹, A. KORSHUNOV⁹, and •D. S. INOSOV¹ — ¹TU Dresden, Germany — ²IFW Dresden, Germany — ³Krasnoyarsk, Russia — ⁴PSI, Villigen, Switzerland — ⁵HZB, Berlin, Germany — ⁶MPI CPFS, Dresden, Germany — ⁷Kazan, Russia — ⁸JCNS @ MLZ, Forschungszentrum Jülich, Germany — ⁹ESRF, Grenoble, France

The quantum spin system Cu₂GaBO₅ with the ludwigite structure consists of a structurally ordered Cu²⁺ sublattice interpenetrated by a disordered sublattice with a random site occupation by magnetic Cu²⁺ and nonmagnetic Ga³⁺. In zero magnetic field, antiferromagnetic long-range order with the propagation vector $q_m = (0.45, 0, 0.7)$ sets in below $T_N = 4.1$ K, corresponding to a complex non-collinear structure with a large magnetic unit cell. Gapless spin dynamics in the form of a diffuse quasielastic peak is evidenced by neutron scattering. Remarkably, a magnetic field of ~ 1 T destroys the static long-range order, which is manifested in the gradual broadening of magnetic Bragg peaks. Such a crossover to a spin-glass regime may result from orphan spins on the structurally disordered magnetic sublattice, which are polarized in magnetic field and act as a tuning knob for field-controlled magnetic disorder. For details, see Phys. Rev. B **103**, 024447 (2021).

MA 4.2 Mon 9:45 H47

Transport properties of FeAl under ion irradiation — •SERHI SOROKIN¹, GREGOR HLAWACEK¹, SHADAB ANWAR¹, JOÃO SALGADO-CABAÇO¹, RICHARD BOUCHER², KAY POTZGER¹, JÜRGEN FASSBENDER¹, JÜRGEN LINDNER¹, and RANTEJ BALI¹ — ¹Institute of Ion Beam Physics and Materials Research, HZDR, Dresden, Germany — ²Institute for Materials Science, TU Dresden, Germany

In Fe₆₀Al₄₀ ion irradiation can be used to control the saturation magnetization (M_s) due to the gradual transition from paramagnetic (ordered B2-phase) to ferromagnetic (disordered A2-phase) as a function of ion fluence. The corresponding changes to the transport properties occurring during this phase transition are

less known. Here we track the variation of electronic transport properties in parallel with gradual ion irradiation. A sample is inserted into a He/Ne-ion microscope on top of a permanent magnet and contacted with feedthrough probes to enable step-wise measurements during Ne⁺-irradiation. The variation of the resistance and the Hall voltage are tracked as a function of the Ne⁺-fluence, as the ordered B2 structure transforms into a disordered A2 structure. Peaks in the electrical resistance and the Hall voltage are observed corresponding to the existence of a partial B2/A2 state, thereby hinting at the important role of the induced ferromagnetic clusters and their distribution on the transport properties. The state of disorder is reversible by annealing with higher electric current.

Project funded by the DFG - 322462997 (BA 5656/1-2 | WE-2623/14-2).

MA 4.3 Mon 10:00 H47

Magnetostructural phase transition in Fe₆₀V₄₀ alloy thin films — •MD SHADAB ANWAR^{1,2}, HAMZA CANSEVER¹, BENNY BOEHM³, RUDOLFO GALLARDO⁵, RENÉ HÜBNER¹, SHENGQIANG ZHOU¹, ULRICH KENTSCH¹, BENEDIKT EGGERT⁴, SIMON RAULS⁴, HEIKO WENDE⁴, KAY POTZGER¹, JÜRGEN FASSBENDER¹, KILLIAN LENZ¹, JÜRGEN LINDNER¹, OLAV HELLWIG^{1,3}, and RANTEJ BALI¹ — ¹HZDR, Germany — ²TU Dresden, Germany — ³TU Chemnitz, Germany — ⁴UDE Duisburg, Germany — ⁵UTF Santa Maria, Chile

Ferromagnetism can be induced in non-ferromagnetic alloys such as B2 Fe₆₀Al₄₀ [1] and B2 Fe₅₀Rh₅₀ [2] through lattice disordering. Here we study a magnetostructural transition in Fe₆₀V₄₀ thin films using ion-irradiation. We show that the as-grown films possess an M_s of 17 kA/m and irradiation with 25 keV Ne⁺-ions at a fluence of 5×10^{15} ions/cm² leads to an increase of M_s to ~ 750 kA/m. A structural short-range order is observed in the as-grown films that transforms to A2 phase via ion-irradiation. Mössbauer spectroscopy and Ferromagnetic Resonance have been applied to track the variation of local magnetic ordering and dynamic behaviour respectively.

Financial support by DFG grants BA 5656/1-2 and WE 2623/14-2 is acknowledged.

[1] Ehrler, J. *et al.*, New J. Phys., **22**, 073004 (2020)

[2] Eggert, B. *et al.*, RSC Adv., **10**, 14386 (2020)

MA 4.4 Mon 10:15 H47

Understanding the ion induced reordering of amorphous Fe₆₀V₄₀ thin films — •SIMON RAULS¹, BENEDIKT EGGERT¹, SHADAB ANWAR², DAMIAN GÜNZING¹, PHILIPP KLASSEN¹, ALEXANDER HERMAN¹, RANJEJ BALI², and HEIKO WENDE¹ — ¹Faculty of Physics and CENIDE, University of Duisburg-Essen — ²Interface Magnetism, Helmholtz-Zentrum Dresden-Rossendorf

For efficient spintronic devices, magnetic materials possessing both low moment and low Gilbert damping are highly demanded [1]. In this field, binary alloys consisting of Fe and easily polarizable elements like V are promising candidates, as they are reported to have a Gilbert damping parameter of $\alpha \sim 0.001$ which is about one order of magnitude lower as compared to the much-used permalloy [2]. Additionally, FeV can be grown as amorphous, paramagnetic thin films

which reorder to the A2 structure upon ion irradiation. This can be exploited in such a way that ferromagnetic nanostructures can be written into the paramagnetic template in a single ion irradiation step using focussed ion beams or broad ion beams with masks.

Using Mössbauer spectroscopy and EXAFS, we will provide further insights into the reordering mechanics of amorphous Fe₆₀V₄₀ thin films by comparing the evolution of short range order and the hyperfine fields across the ion irradiation- and annealing-induced phase transition.

Funding by the Deutsche Forschungsgemeinschaft (DFG) - 322462997 (BA5656/1-2 WE 2623/14-2) is acknowledged.

- [1] A. Barman et al. *J. Phys.: Condens. Matter* **33** 413001 (2021)
[2] D. Smith et al., *Phys. Rev. Applied* **14**, 034042 (2020)

MA 5: Magnetic Instrumentation and Characterization

Time: Monday 9:30–10:30

Location: H48

MA 5.1 Mon 9:30 H48

Cubic magneto-optic Kerr effect in Ni(111) thin films with and without twinning — •MAIK GAERNER¹, ROBIN SILBER², TOBIAS PETERS¹, JAROSLAV HAMRLE³, and TIMO KUSCHEL¹ — ¹Bielefeld University, Germany — ²IT4Innovations, VŠB - Technical University of Ostrava, Czech Republic — ³Charles University, Prague, Czech Republic

In most studies utilizing the magneto-optic Kerr effect (MOKE), the detected change of polarized light upon reflection from a magnetized sample is supposed to be proportional to the magnetization M . However, MOKE signatures quadratic in M have also been identified and utilized, e.g., to sense the structural order in Heusler compounds [1].

In our study, we employ the eight-directional method [2] to separate different MOKE contributions in Ni(111) thin films. We observe a strong anisotropic longitudinal MOKE contribution of third order in M which we attribute to a cubic magneto-optic tensor proportional to M^3 [3]. We further show that the angular dependence of cubic MOKE (CMOKE) is affected by the amount of structural domain twinning (two structural (111) phases with 60° in-plane rotation) in the sample [3]. Our detailed study on CMOKE for two selected photon energies will open up new opportunities for CMOKE applications with sensitivity to twinning properties of thin films, e.g. CMOKE spectroscopy and microscopy or time-resolved CMOKE.

- [1] R. Silber et al., *Appl. Phys. Lett.* **116**, 262401 (2020)
[2] K. Postava et al., *J. Appl. Phys.* **91**, 7293 (2002)
[3] M. Gaerner et al., arXiv: 2205.08298 (2022)

MA 5.2 Mon 9:45 H48

A cryogen-free 10T asymmetric neutron scattering magnet with 50mm sample space and temperature range from 300mK to 375K — •TOM RITMAN-MEER, MARC SAVEY-BENNETT, and ROGER MITCHELL — Cryogenic Ltd, 6 Acton Park Estate, The Vale, London, W3 7QE, United Kingdom

Cryogenic Ltd has built and delivered a Cryogen-Free ring-separated magnet for polarised neutron scattering experiments with 10T central field and integral VTI cooled from a single 1.8W cryocooler.

The magnet has a novel dual power-supply control unit to provide an asymmetric field when required, allowing the twin requirements of minimal depolarisation and maximum homogeneity to be managed. The magnet consists of inner and outer pairs which are separately controlled to minimise the impact of the asymmetry. The zero field point can be shifted by up to 20mm from the central plane.

The system has a sample space of 50mm diameter, housed within a closed-cycle refrigeration system, offering a temperature controlled environment of 1.5K-375K. Sample exchange is into an inner *static column* eliminating the risk of accidental blockage.

The system includes a specially designed helium-3 insert with >40mm working space inside an aluminium IVC of just 1mm thick allowing continuous operation at 280mK for 76 hours within the main VTI space. Total aluminium in

the beam path is limited to just 15mm (sample to outer wall).

The system also includes an automated z-axis and rotation manipulator stage for both the He-3 unit and standard sample probes.

MA 5.3 Mon 10:00 H48

Detection of nanowire vibrations with a co-resonantly coupled cantilever system — •MANEESHA SHARMA, ANIRUDDHA SATHZADHARMA PRASAD, BERND BÜCHNER, and THOMAS MÜHL — Leibniz Institute for Solid State and Materials Research, IFW Dresden, Germany

Nanowires can constitute the basis for high-sensitivity sensing of masses and magnetic properties of nanoparticles. We report a novel and efficient yet simple method for detecting nanowire flexural vibrations. In this work we present a co-resonantly coupled cantilever system consisting of a microcantilever and a nanocantilever. Achieving co-resonance involves matching the resonance frequencies of the individual systems. It allows us to measure the coupled system's eigenmodes at the microcantilever. In the co-resonant state weak force gradients acting at the nanowire end have a considerable impact on the eigenmodes of the coupled system and thus can be easily sensed at the microcantilever.

We analyze mechanical properties of the nanowire subsystem and of the coupled system by exploiting thermally induced fluctuations which are measured by recording time-resolved secondary electron signals when using an electron beam and, in case of the microcantilever, by optical laser deflection. Finally, we discuss applications of the coupled cantilever sensor for high-sensitivity magnetometry.

MA 5.4 Mon 10:15 H48

A Ti/Pt/Co Multilayer Stack for Transfer Function Based Magnetic Force Microscopy Calibrations — •BAHA SAKAR¹, SIBYLLE SIEVERS¹, OSMAN ÖZTÜRK², and HANS WERNER SCHUMACHER¹ — ¹Physikalisch-Technische Bundesanstalt, Braunschweig, Germany — ²Gebze Technical University, Kocaeli, Turkey

Magnetic force microscopy (MFM) is a widespread technique for imaging magnetic structures with a resolution of some 10 nanometers. MFM can be calibrated to obtain quantitative (qMFM) spatially resolved magnetization data in units of A/m by determining the calibrated point spread function of the instrument, its instrument calibration function (ICF), from a measurement of a well-known reference sample. Beyond quantifying the MFM data, a deconvolution of the MFM image data with the ICF also corrects the smearing caused by the finite width of the MFM tip stray field distribution. However, the quality of the calibration depends critically on the calculability of the magnetization distribution of the reference sample. Here, we discuss a Ti/Pt/Co multilayer stack that shows a stripe domain pattern as a suitable reference material. A precise control of the fabrication process, combined with a characterization of the sample micromagnetic parameters, allows reliable calculation of the sample's magnetic stray field, proven by a very good agreement between micromagnetic simulations and qMFM measurements. A calibrated qMFM measurement using the Ti/Pt/Co stack as a reference sample is shown and validated, and the application area for quantitative MFM measurements calibrated with the Ti/Pt/Co stack is discussed.

MA 6: Complex Magnetic Oxides

Time: Monday 11:00–12:00

Location: H37

MA 6.1 Mon 11:00 H37

Polaronic behavior in La_{1.2}Sr_{1.8}Mn₂O₇ — •DANIEL JOST¹, MATTEO ROSSI¹, HSIAO-YU HUANG², AMOL SINGH², DI-JING HUANG², YONGHUN LEE^{1,3}, BRIAN MORITZ¹, JOHN MITCHELL⁴, ZHI-XUN SHEN^{1,3,5,6}, THOMAS DEVEREAUX^{1,7}, and WEI-SHENG LEE¹ — ¹Stanford Institute for Materials and Energy Sciences, Menlo Park, USA — ²National Synchrotron Radiation Research Center, Hsinchu, TW — ³Department of Physics, Stanford University, Stanford, USA

— ⁴Materials Science Division, ANL, Lemont, USA — ⁵Department of Applied Physics, Stanford University, USA — ⁶Geballe Laboratory for Advanced Materials, Stanford University, USA — ⁷Department of Materials Science and Engineering, Stanford University, USA

The microscopic mechanism driving colossal magneto-resistance (CMR) remains controversial. In La_{1.2}Sr_{1.8}Mn₂O₇, CMR is most pronounced at its insu-

lator to ferromagnetic-metal transition at $T_c = 120$ K. In this compound, initial ARPES studies revealed the abrupt formation of quasi-particles having a strong mass renormalization below T_c , subsequently interpreted as the condensation of localized polarons into a coherent polaronic liquid. Yet, conflicting results showing finite quasi particle spectral weight above T_c cast doubt on this scenario. Here we use resonant inelastic X-ray scattering (RIXS) to investigate this controversy. In contrast to ARPES which measures the single particle spectral function, RIXS probes collective excitations directly and is thus especially suitable for the investigation of charge-lattice coupled phenomena. In this presentation, I will discuss the RIXS signatures of polarons in $\text{La}_{1.2}\text{Sr}_{1.8}\text{Mn}_2\text{O}_7$.

MA 6.2 Mon 11:15 H37

Magneto-optic Kerr effect in ferromagnetic manganite multilayers — •JÖRG SCHÖPF, PAUL H.M. VAN LOOSDRECHT, and IONELA LINDFORS-VREJOIU — Universität zu Köln, II. Physikalisches Institut, Zùlpicherstr. 77, 50937 Köln (DE) Magnetic functional oxide epitaxial thin films and heterostructures offer a rich variety of physical properties due to lattice mismatch induced strain, interfacial effects and interlayer coupling between different ferromagnetic (FM) layers. The magneto-optic Kerr effect (MOKE) can be used as an indirect probe of the magnetization of a sample. The MOKE of a material is wavelength dependent, and is non-monotonic in the vicinity of MO-active transitions, where the Kerr rotation can change sign and even vanish at particular wavelengths. Knowledge of the wavelength dependence can help to distinguish the contributions of different FM layers within a multilayer to the total measured Kerr effect. Here we present a study on the MOKE of a heterostructure of 10% Ru-doped $\text{La}_0.7\text{Sr}_0.3\text{MnO}_3$ (LSMRO), where the layers are of different thickness (30 nm bottom layer and a 10 nm top layer), and separated by a NdNiO_3 spacer. We found that the measured Kerr hysteresis loops of the heterostructure have an anomalous shape originating from a different sense of rotation of the MOKE from the different LSMRO layers. This can readily be described by Kerr-loops measured on reference samples using the additivity of the MOKE in multilayer systems.

MA 6.3 Mon 11:30 H37

Strain-induced ferromagnetism in LaCoO_3 thin film — •FARZIN ABADIZAMAN, MICHAL KIABA, and ADAM DUBROKA — Department of Condensed Matter Physics, Faculty of Science, Masaryk University, Kotlářská 2, 611 37 Brno, Czech Republic.

Ellipsometry measurements were performed on unstrained, tensile strained, and compressive strained LaCoO_3 thin films. Only the tensile strained sample shows ferromagnetism, which has a Currie temperature of about 85 K. Using the differential optical conductivity, $\delta\sigma_1 = \sigma_1(T) - \sigma_1(T = 7\text{K})$, we find that in the tensile strain sample, while the spectral weight $N_{\text{eff}} = 2mV/\pi e^2 \int \sigma_1(\omega) d\omega$ below 3.5 eV decreases with decreasing temperature in the paramagnetic phase, it starts increasing in the ferromagnetic phase below the transition temperature. This is the first time that the ferromagnetism in this material is observed via optical measurements, and we interpret the results as stabilization of the high-spin state in the ferromagnetic phase associated with transition of spectral weight from higher to lower energy region.

MA 6.4 Mon 11:45 H37

Spin-Orbit Excitations in a Strongly Correlated 4d-Metal Studied by Resonant Inelastic X-ray Scattering — •VALENTIN ZIMMERMANN¹, DENIZ WONG², CHRISTIAN SCHULZ², MACIEJ BARTKOWIAK², KLAUS HABICHT², ARVIND YOGI³, MASAHIKO ISOBE¹, LICHEN WANG¹, MATTEO MINOLA¹, GINIYAT KHALLIULIN¹, BERNHARD KEIMER¹, and MATTHIAS HEPTING¹ — ¹Max-Planck-Institute for Solid State Research, Stuttgart, Germany — ²Helmholtz-Zentrum Berlin für Materialien und Energie, Berlin, Germany — ³UGC-DAE-Consortium for Scientific Research, Indore, India

Spin-orbit coupling (SOC) is an important player determining the electronic and magnetic properties of 4d and 5d transition metal oxides. The 5d compound Sr_2IrO_4 is an antiferromagnetic Mott insulator, where SOC leads to a splitting of the t_{2g} manifold into bands with effective total angular momentum $J_{\text{eff}} = 3/2$ and $1/2$. This electronic structure gives rise to low-energy excitations with excitonic character, which were recently studied by resonant inelastic X-ray scattering (RIXS) and assigned to the transition of holes across the spin-orbit split states. Here, we use RIXS at the oxygen K-edge to investigate the isovalent 4d compound Sr_2RhO_4 , which is a paramagnetic, strongly correlated metal. We observe similar spin-orbit excitons as in Sr_2IrO_4 , however, on a smaller energy scale and with a distinct dispersion, which we attribute to a reduced SOC strength and the metallic ground state, respectively. In addition, we explore whether the solid-solution $\text{Sr}_2\text{Rh}_{1-x}\text{Ir}_x\text{O}_4$ is a viable platform to tune the effective strength of SOC.

MA 7: Magnetic Relaxation and Gilbert Damping

Time: Monday 11:00–12:00

Location: H43

MA 7.1 Mon 11:00 H43

Strong photon-magnon-coupling between superconducting niobium lumped-element-resonators and micron sized magnets — •PHILIPP GEYER¹, PHILIP TREMPER¹, KARL HEIMRICH¹, and GEORG SCHMIDT^{1,2} — ¹Institut für Physik, Martin-Luther-Universität Halle-Wittenberg, Von-Danckelmann-Platz 3, 06120 Halle (Saale), Germany — ²Interdisziplinäres Zentrum für Materialwissenschaften, Martin-Luther-Universität Halle-Wittenberg, Nanotechnikum Weinberg, 06120 Halle (Saale), Germany

Since quantum computing plays a more and more important role in information technology hybrid quantum magnonics emerge as a promising research field. Here, the coupling between different quantum states like microwave photons and magnons at cryonic temperatures is in focus [1]. We investigate the coupling between superconducting niobium Lumped-Element-Resonators and thin micron-sized magnetic structures. Therefore, we use the magnetic material permalloy and yttrium-iron-garnet (YIG). Permalloy was structured by optical lithography and grown by argon-ion sputtering at room-temperature. YIG was grown as free standing structure [2] or commercial LPE film and further processed and placed on the cavity by focused-ion-beam technique. We detect strong coupling as avoided crossing in the transmission related S-Parameter measured by a vector-network-analyzer. For validation of our experimental results, we perform electromagnetic simulations with CST Studio Suite and micromagnetic simulations with MuMax3. [1] H. Huebl et al. Phys. Rev. Lett. 111, 127003 (2013) [2] P. Trempler et al. Appl. Phys. Lett. 117, 232401 (2020) 401 (2020)

MA 7.2 Mon 11:15 H43

Magnetization dynamics affected by phonon pumping — •RICHARD SCHLITZ¹, LUISE SIEGL², TAKUMA SATO³, WEICHAO YU⁴, GERRIT E. W. BAUER³, HANS HUEBL⁵, and SEBASTIAN T. B. GOENNENWEIN² — ¹Department of Materials, ETH Zürich, 8093 Zürich, Switzerland — ²Department of Physics, University of Konstanz, 78457 Konstanz, Germany — ³Tohoku University, Sendai 980-8577, Japan — ⁴State Key Laboratory of Surface Physics and Institute for Nano-electronic Devices and Quantum Computing, Fudan University, Shanghai 200433, China — ⁵Walther-Meißner-Institute, Bayerische Akademie der Wissenschaften, 85748 Garching, Germany

Coupling magnetic and acoustic excitations enables novel functionalities for magnonic devices. We explore broadband ferromagnetic resonance (FMR) in

a $\text{Y}_3\text{Fe}_5\text{O}_{12}$ film on a $\text{Gd}_3\text{Ga}_5\text{O}_{12}$ substrate. At low frequencies, the Kittel mode hybridizes with standing ultrasound waves that form across the layer stack resulting in a characteristic modification of the magnetic susceptibility. At higher frequencies, the individual phonon resonance overlap, leading to a permanent emission of phonons and thus an enhanced relaxation of the FMR. The broadband frequency dependence of the magnetoelastic coupling and thus the phonon pumping follows theoretical predictions. We additionally find substantial magnon-phonon coupling of a perpendicular standing spin wave mode. This evidences the importance of the mode overlap between the acoustic and magnetic modes and thus paves the way to tailoring the magnetoelastic mode coupling.

[1] R. Schlitz et al., arxiv:2202.03331 (2022)

MA 7.3 Mon 11:30 H43

Gilbert damping in the real-space KKR method — BALÁZS NAGYFALUSI¹, LÁSZLÓ SZUNYOGH², and KRISZTIÁN PALOTÁS^{1,2} — ¹Wigner Research Center for Physics, Budapest, Hungary — ²Institute of Physics, Budapest University of Technology and Economics, Budapest, Hungary

The ab-initio determination of Gilbert damping parameters is an important issue for accurate atomistic spin dynamics calculations. Going beyond presently available methods of calculating the Gilbert damping scalar parameter in bulk materials, we implemented the torque-torque correlation formula [1] into the real-space Korringa-Kohn-Rostoker (KKR) method [2] using the Budapest SKKR code to be able to treat chemically inhomogeneous systems. This enables the ab-initio determination of spatially resolved on-site and non-local Gilbert damping tensors [3] in atomic nanostructures. After performing extensive tests for metallic bulk materials to identify the relevant parameter settings of the calculations, we show some examples of inhomogeneous Gilbert damping results in various metallic atomic (nano-)structures.

[1] H. Ebert et al., Phys. Rev. Lett. 107, 066603 (2011). [2] B. Lazarovits et al., Phys. Rev. B 65, 104441 (2002). [3] D. Thonig et al., Phys. Rev. Mater. 2, 013801 (2019).

MA 7.4 Mon 11:45 H43

Bath-induced spin inertia — MARIO A. GASPARGUARENTA¹, •TIM LUDWIG¹, HUAIYANG YUAN¹, and REMBERT A. DUINE^{1,2} — ¹Institute for Theoretical Physics, Utrecht University, Princetonplein 5, 3584 CC Utrecht, The Netherlands — ²Department of Applied Physics, Eindhoven University of Technology, P.O. Box 513, 5600 MB Eindhoven, The Netherlands

In spintronics, magnetization dynamics is often described by the Landau-Lifshitz-Gilbert equation, where Gilbert damping is included phenomenologically to account for dissipation. In microscopic models, dissipation can be described by coupling the magnetization to a bath that can absorb energy and angular momentum. Gilbert damping is then obtained if one assumes the bath to

be Ohmic; that is, if one assumes the bath spectral density to be linear in frequency. Real baths, however, can be Ohmic only at low frequencies and, as we will argue, the baths' high-frequency modes induce magnetization inertia. Explicitly, we show for a macrospin coupled linearly to a bath of harmonic oscillators (Caldeira-Leggett model) that the low-frequency bath modes (if Ohmic) lead to Gilbert damping while the high-frequency bath modes universally lead to macrospin inertia. We expect our results to give new insights into recent experiments on magnetization nutation. But our results might prove to be relevant in general, as they indicate that a Gilbert-damping term should always be accompanied by a term accounting for bath-induced spin inertia.

MA 8: Ultrafast Magnetization Effects 1

Time: Monday 15:00–18:00

Location: H37

MA 8.1 Mon 15:00 H37

Spectrally resolved spin dynamics of 3d transition metals in EUV T-MOKE — •HENRIKE PROBST¹, CHRISTINA MÖLLER¹, MARIANA BREDE¹, MAREN SCHUMACHER¹, KAREN STROH¹, MARCEL REUTZEL¹, G. S. MATTHIJS JANSSEN¹, SANGEETA SHARMA², DANIEL STEIL¹, and STEFAN MATHIAS¹ — ¹I. Physikalisches Institut, University of Göttingen — ²Max-Born-Institute for Non-linear Optics and Short Pulse Spectroscopy, Berlin

Light in the extreme ultraviolet (EUV) range has found increasing application in the field of magneto-optical spectroscopy. It allows to get new insights in light-matter interaction processes, as EUV spectroscopy provides the potential to investigate energy- and element-resolved spin dynamics [1-2].

Here, we carry out a comprehensive study of spectrally resolved spin dynamics of the 3d transition metals Co, Fe and Ni using EUV transverse magneto-optical Kerr spectroscopy (T-MOKE) [3]. Covering the *M*-edges in the 30-72 eV energy window, this allows to resolve spin dynamics at specific energies around the Fermi-level. We discuss different processes leading to energy dependent changes in the magnetic asymmetry at early times after the optical excitation, i.e. charge excitation and band renormalization.

[1] Hofherr et al., Sci. Adv. 6.3 (2020): eaay8717.

[2] Tengdin et al., Sci. Adv. 6.3 (2020): eaaz1100.

[3] Möller et al., Rev. Sci. Instrum., 92(6) (2021): 065107.

MA 8.2 Mon 15:15 H37

Ultrafast element- and depth-resolved magnetization dynamics probed by transverse magneto-optical Kerr effect spectroscopy in the soft x-ray range —

•MARTIN HENNECKE¹, DANIEL SCHICK¹, THEMISTOKLIS SIDIROPOULOS¹, FELIX WILLEMS¹, ANKE HEILMANN¹, MARTIN BOCK¹, LUTZ EHRENTRAUT¹, DIETER ENGEL¹, PIET HESSING¹, BASTIAN PFAU¹, MARTIN SCHMIDBAUER², ANDREAS FURCHNER^{3,4}, MATTHIAS SCHNUEERER¹, CLEMENS VON KORFF SCHMISING¹, and STEFAN EISEBITT^{1,5} — ¹Max-Born-Institut, Berlin, Germany — ²Leibniz-Institut für Kristallzüchtung, Berlin, Germany — ³Helmholtz-Zentrum Berlin, Berlin, Germany — ⁴Leibniz-Institut für Analytische Wissenschaften, Berlin, Germany — ⁵IOAP, Technische Universität Berlin, Berlin, Germany

Understanding the light-driven spin dynamics occurring at buried interfaces of complex magnetic heterostructures as used in today's opto-spintronics applications requires direct experimental access to the nonlocal magnetic order on sub-ps time scales. Here, we report on broadband time- and angle-resolved transverse magneto-optical Kerr effect spectroscopy probing the Gd N_{5,4} resonance (~150 eV) of a ferrimagnetic GdFe nanostructure with fs soft x-ray pulses provided by a laboratory-scale light source based on high-harmonic generation. Employing a pump-probe technique, we follow the fs laser-induced demagnetization of the GdFe layer. Analyzing the fs time-resolved spectra via magnetic scattering simulations allows a quantitative determination of the transient magnetization depth profiles evolving within the magnetic film due to strongly layer-dependent photoexcitation.

MA 8.3 Mon 15:30 H37

Table-top X-ray magnetic circular dichroism at the Fe *L* edges — •MARTIN BORCHERT^{1,2}, DANIEL SCHICK¹, CLEMENS V. KORFF SCHMISING¹, DENNY SOMMER¹, DIETER ENGEL¹, BASTIAN PFAU¹, and STEFAN EISEBITT^{1,2} — ¹Max-Born-Institut, Berlin — ²TU Berlin

Time-resolved X-ray magnetic circular dichroism (XMCD) is a powerful tool to directly probe the element-specific magnetization in multi-component heterostructures.

Due to the lack of laboratory-scale light sources with sufficient brightness and control over the light's polarization, static and time-resolved XMCD studies in the higher soft X-ray photon energy range have so far been limited to large-scale facilities such as synchrotrons and free-electron lasers.

Here, we present first XMCD spectroscopy data recorded at the Fe L_{3,2} resonances employing a laboratory-scale soft X-ray source utilizing a magnetic thin-film polarizer to circularly polarize the soft X-rays from the continuous, broad-

band (50–1500 eV) emission of a laser-driven plasma source with <10 ps pulse duration. A reflection zone plate (RZP) is used as the single optical element to collect, disperse and focus the full spectrum across the Fe *L* edges through a thin-film sample, to which an external magnetic field can be applied to observe the resulting asymmetry spectrum, as well as hysteresis loops.

Utilizing different RZPs, this setup enables the first laboratory-based white-light XMCD spectroscopy with picosecond time resolution, covering the full spectrum of the magnetically relevant resonances from the transition metal *M* and *L* edges up to the rare earth *M* edges.

MA 8.4 Mon 15:45 H37

Temperature dependence of spin interaction parameters in two-sublattice ferrimagnets — •LEVENTE RÓZSA¹, SEVERIN SELZER¹, NIKLAS WINDBACHER¹, ULRICH NOWAK¹, and UNAI ATXITIA² — ¹University of Konstanz, Konstanz, Germany — ²Instituto de Ciencia de Materiales de Madrid, Madrid, Spain

Ferrimagnets consist of two antiferromagnetically coupled sublattices with different magnetic moments, thereby possessing a finite magnetization like ferromagnets. The ferrimagnet magnetite has been known since ancient times, yet ferrimagnets continue to attract research interest in various areas of spintronics from magnons to skyrmions. The properties of ferrimagnets may be tuned between those of ferromagnets and antiferromagnets by changing the temperature. Therefore, determining the temperature dependence of model parameters of ferrimagnets is essential for their accurate description.

Here we present an analytical method for describing the temperature dependence of spin interactions in ferrimagnets, based on Callen's Green's function formalism [1]. The temperature dependence of the Heisenberg and Dzyaloshinsky-Moriya interactions, as well as of the anisotropy terms are derived and compared to known expressions in ferromagnets [2,3]. The role of spin correlations is highlighted in reduced dimensions. The results are compared to numerical simulations of the magnon frequencies and of reversal times of nanoparticles.

[1] H. B. Callen, Phys. Rev. 130, 890 (1963).

[2] L. Rózsa et al., Phys. Rev. B 96, 094436 (2017).

[3] R. F. L. Evans et al., Phys. Rev. B 102, 020412(R) (2020).

MA 8.5 Mon 16:00 H37

Electron-Magnon Scattering Dynamics in a two-band Stoner Model — •FÉLIX DUSABIRANE, KAI LECKRON, SANJAY ASHOK, BÄRBEL RETHFELD, and HANS CHRISTIAN SCHNEIDER — Physics Department & Research Center OPTIMAS, University of Kaiserslautern, Germany

We use a microscopic model to study carrier dynamics in ferromagnets due to electron-magnon scattering on ultrafast timescales. We employ a simple model band structure (Stoner model), for which the electron magnon-interaction is formally obtained as coupling to a Heisenberg spin system in the Hamiltonian. We compute the dynamics of momentum resolved electron and magnon distributions due to electron-magnon and statically screened electron-electron scattering, which are treated at the level of Boltzmann scattering integrals. We find that electron-magnon scattering leads to a pronounced non-equilibrium for magnon modes that couple directly to Stoner transitions. The spin-flip scattering with electrons results in a transient electron spin polarization, which is similar for excitations either within the minority or the majority band. The influence of model parameters such as band filling and exchange coupling strengths will be discussed.

MA 8.6 Mon 16:15 H37

Ultrafast optical generation of antiferromagnetic spin texture — •SUMIT GHOSH^{1,2}, STEFAN BLÜGEL¹, and YURIY MOKROUSOV^{1,2} — ¹PGII, Forschungszentrum Jülich, Germany. — ²Institute of Physics, Johannes Gutenberg-University Mainz, Germany.

We present here an unified picture of ultrafast manipulation of collinear antiferromagnetic order by combining both electronic and magnetic degrees of freedom via a hybrid quantum classical evolution scheme. Our approach allows us to

probe slow magnetic relaxation for several picoseconds with a sub-femtosecond resolution and thus allows us to identify the emergent interactions driving the formation of nontrivial textures which remains hidden from classical magnetisation dynamics. In case of a one dimensional spin chain this mechanism can lead to the formation of spin spirals [1] where the induced chirality can be tuned with the laser parameter. In case of two dimensional antiferromagnets this mechanism can lead to more exotic outcome - generation of a texture and anti-texture which can survive for 100ps [2] and is fairly robust against impurity. Our results thus opens new possibilities to generate higher order nontrivial magnetic texture with ultrafast laser.

[1] S. Ghosh, et al. *Communications Physics*, 5(1), 69, 2022. <https://doi.org/10.1038/s42005-022-00840-3>

[2] S. Ghosh, S. Blügel and Y. Mokrousov. arXiv:2205.12100. <http://arxiv.org/abs/2205.12100>

MA 8.7 Mon 16:30 H37

Polarized phonons carry the missing angular momentum in femtosecond demagnetization — •HANNAH LANGE¹, MARTIN EVERS¹, ANDREAS DONGES¹, SONJA TAUCHERT^{1,2}, MIKHAIL VOLKOV^{1,2}, PETER BAUM^{1,2}, and ULRICH NOWAK¹ — ¹University of Konstanz, Fachbereich Physik, 78464 Konstanz — ²LMU Munich, Am Coulombwall 1, 85748 Garching

When a thin nickel film is subjected to ultrashort laser pulses, it can lose its magnetic order almost completely on within hundreds of femtoseconds. This phenomenon offers opportunities for rapid information processing or ultrafast spintronics. However, a crucial question has remained elusive: Where is the angular momentum transferred to in such short time? Here we use molecular dynamics simulations to investigate the role of phonon angular momentum. When exciting a rotational lattice motion which carries the amount of angular momentum corresponding to the demagnetization, we observe an anisotropy of the atoms' velocities which violates the equipartition theorem. When calculating the corresponding electron diffraction pattern, this results in an anisotropy of normally equivalent Bragg spots. This is in line with ultrafast electron diffraction which show an almost instantaneous, long-lasting, non-equilibrium population of phonons. Theory and experiment hence indicate the formation of polarized phonons that take up the missing angular momentum [1] before the onset of a macroscopic Einstein-de Haas rotation [2].

[1] Tauchert et al. *Nature* 602, 73-77 (2022).

[2] Dornes et al. *Nature* 565, 209-212 (2019).

MA 8.8 Mon 16:45 H37

Does the orbital angular momentum of light affect ultrafast demagnetization? — •EVA PRINZ¹, BENJAMIN STADTMÜLLER^{1,2}, and MARTIN AESCHLIMANN¹ — ¹Department of Physics and Research Center OPTIMAS, TU Kaiserslautern, Germany — ²Institute of Physics, Johannes Gutenberg University Mainz, Germany

Optical fields can carry an orbital angular momentum (OAM) in helical beams with an azimuthal phase dependence. Since its discovery in 1992 [1], there has been a variety of applications of light with additional OAM, such as quantum entanglement, micro manipulation, communication, and microscopy [2].

Our research is focused on exploring the potential effects of the OAM of light on laser-induced ultrafast demagnetization. In this field, the question of how the angular momentum is conserved during spin-flips is not fully answered. Pumping the system with photons carrying OAM offers the potential to provide new insights, not only into the dissipation of angular momentum in the material but also into the interaction of photonic OAM with matter in general.

We investigate ultrafast demagnetization of ferromagnetic thin films induced by OAM light with time-resolved magneto-optic Kerr-effect measurements. We observed peculiar demagnetization dynamics that have so far not been observed for light without OAM.

[1] Allen et al., *Phys. Rev. A* 45 (1992)

[2] Shen et al., *Light: Science & Applications* 8 (2019)

MA 8.9 Mon 17:00 H37

Role of diffusive transport in ultrafast demagnetization dynamics — •SANJAY ASHOK, SEBASTIAN T. WEBER, CHRISTOPHER SEIBEL, JOHAN BRIONES, and BÄRBEL RETHFELD — Fachbereich Physik and OPTIMAS Research Center, TU Kaiserslautern, Kaiserslautern, Germany

Ultrafast demagnetization dynamics in thick metallic magnetic films is greatly influenced by transport processes. In this contribution we present the space-resolved magnetization dynamics in a thick Nickel film induced by a femtosecond laser pulse [3]. Starting from the thermodynamic μ T-model [1], we explicitly include diffusive heat transport, spin-resolved charge transport, as well as Seebeck and Peltier effects.

Our results show that the spatial dependence of maximal magnitude of quenching is induced by a depth-dependent energy deposition and is only moderately equilibrated by transport processes. We reveal a stronger influence of transport on the time of quenching which becomes nearly independent of depth

[3]. Additionally, we present the influence of pump-wavelength [2] on spatially resolved magnetization dynamics.

[1] B.Y. Mueller and B. Rethfeld, *Phys. Rev. B*, 90, 144420 (2014)

[2] U. Bierbrauer et al., *JOP Cond. Mat.*, 29 (24), 244002 (2017)

[3] S. Ashok et al., *Appl. Phys. Lett.* 120, 142402 (2022)

MA 8.10 Mon 17:15 H37

Spin fluctuations around a reorientation transition in $\text{Sm}_{0.7}\text{Er}_{0.3}\text{FeO}_3$ — •JULIUS SCHLEGEL¹, MARTIN EVERS¹, TOBIAS DANNEGGER¹, ANDREAS DONGES¹, MARVIN WEISS¹, TAKAYUKI KURIHARA², SEBASTIAN T.B. GOENNENWEIN¹, and ULRICH NOWAK¹ — ¹Department of Physics, University of Konstanz — ²ISSP, University of Tokyo

The competition between thermal fluctuations, spin-spin interactions and magnetic anisotropies can lead to various magnetic phase transitions. For example the antiferromagnetic orthoferrite $\text{Sm}_{0.7}\text{Er}_{0.3}\text{FeO}_3$ undergoes a reorientation transition at approximately room temperature. On the basis of an atomistic spin model and the LANDAU-LIFSHITZ-GILBERT equation of motion we numerically calculate the time evolution of the magnetization around the reorientation transition on a timescale from picoseconds up to one nanosecond and investigate the thermal fluctuations of the magnetization. By FOURIER-transforming the time dependent magnetization we find that the spectra of the noise are temperature dependent and change significantly while going through the reorientation. We also observe several resonances in the spectra. By means of analytical calculations based on linear spin wave theory these peaks can be assigned to the different modes of a model with four sublattices.

Finally, these results are compared to current experimental data from spin noise measurements.

MA 8.11 Mon 17:30 H37

Ultrafast spin dynamics: complementing theoretical analyses by quantum state measures — FRANZISKA ZIOLKOWSKI, •OLIVER BUSCH, JÜRGEN HENK, and INGRID MERTIG — Institut für Physik, Martin-Luther-Universität, D-06099 Halle

In theoretical studies of ultrafast spin dynamics, one usually analyses and discusses observables — such as magnetization. On top of this, quantum state (QS) measures defined for density matrices may provide additional valuable insights into the dynamics [1].

We report on a study on QS measures that complement simulations of ultrafast spin dynamics [2]. For a Co/Cu heterostructure which is excited by a femtosecond laser pulse and coupled to a bosonic heat bath, we discuss the time dependence of QS measures, in particular distances in Hilbert space and degree of purity in the density matrix [3].

We identify observables and modifications of the investigated system to which both the distance and the purity measures are in particular sensitive: the polarization of the laser pulse and the composition of the sample. In contrast, temperature and photon energy affect the QS measures mildly. Our study shows that QS measures are complementary and beneficial quantities for spin dynamics simulations.

[1] S. Barnett, *Quantum Information* (Oxford University Press, Oxford, 2009)

[2] F. Töpler *et al.*; *New Journal of Physics* 23, 033042 (2021)

[3] R. Jozsa, *Fidelity for Mixed Quantum States*, *Journal of Modern Optics* 41, 2315 (1994)

MA 8.12 Mon 17:45 H37

Tuning all-optical magnetization switching efficiency by laser pulse wavelength variation — •MARCEL KOHLMANN¹, LUCAS VOLLROTH¹, KRISTÝNA HOVOŘÁKOVÁ², EVA SCHMORANZEROVÁ², ROBIN JOHN¹, DENISE HINZKE⁴, PETER OPPENEER³, ULRICH NOWAK⁴, MARKUS MÜNZENBERG¹, and JAKOB WALOWSKI¹ — ¹Greifswald University, Greifswald, Germany — ²Charles University, Prague, Czech Republic — ³Uppsala University, Uppsala, Sweden — ⁴Konstanz University, Konstanz, Germany

Heat-assisted magnetic recording (HAMR) presents a promising candidate for high data density devices. Leaving investigation of magnetization manipulation a topic of interest for research and development. We study all-optical helicity-dependent switching of FePt granular HAMR media [2] as an alternative writing mechanism. The latest perception of interaction of heating and ultra fast excitation suggests the contribution of magnetic dichroism and the inverse Faraday effect as interchanging driving forces behind the magnetization reversal. The switching rates for individual FePt nano particles from ab-initio calculations of the inverse Faraday effect and magnetic dichroism induced heating provide a model to describe the switching as a stochastic process. We extend the study to wavelength dependent switching experiments from 800 nm up to 1550 nm for all-optical writing experiments on FePt granular media evaluating the writing efficiency.

We greatly acknowledge the DFG funding within the project "Fundamental aspects of all-optical single pulse switching in nanometer-sized magnetic storage media.

MA 9: INNOMAG e.V. Prizes 2022 (Diplom-/Master and Ph.D. Thesis)

Die Arbeitsgemeinschaft Magnetismus der DPG hat einen Dissertationspreis und einen einen Diplom-/Masterpreis ausgeschrieben, welche auf der Tagung der DPG 2022 in Regensburg vergeben werden. Ziel der Preise ist die Anerkennung herausragender Forschung im Rahmen einer Diplom-/Masterarbeit beziehungsweise einer Promotion und deren exzellente Vermittlung in Wort und Schrift. Im Rahmen dieser Sitzung tragen die besten der für ihre an einer deutschen Hochschule durchgeführten Diplom-/Masterarbeit beziehungsweise Dissertation Nominierten vor. Im direkten Anschluss entscheidet das Preiskomitee über den Gewinner des INNOMAG e.V. Diplom-/Masterpreises und des Dissertationspreises 2022. Talks will be given in English!

Time: Monday 15:00–17:00

Location: H43

MA 9.1 Mon 15:00 H43

Magnetoelastic coupling and uniaxial pressure dependencies in the honeycomb quantum magnets CrI_3 and $\text{Na}_2\text{Co}_2\text{TeO}_6$ — •JAN ARNETH¹, MARTIN JONAK¹, MAHMOUD ABDEL-HAFIEZ², KWANG-YONG CHOI³, and RÜDIGER KLINGELER¹ — ¹Kirchhoff-Institute for Physics, Heidelberg University, Germany — ²Dep. of Physics and Astronomy, Uppsala University, Sweden — ³Dep. of Physics, Sungkyunkwan University, Republic of Korea

Due to their layered structure, competing magnetic interactions, and magnetic anisotropy, quasi-2D honeycomb systems are promising quantum materials featuring fundamentally and technologically relevant phenomena. Often, relevant materials are at the verge of the desired properties, and strain has been proven to be a tuning parameter. Strain engineering of the critical temperature in 2D ferromagnetic semiconductors such as CrI_3 [1] towards room temperature or driving the quantum magnet $\text{Na}_2\text{Co}_2\text{TeO}_6$ into the Kitaev spin-liquid phase are illustrative examples. The precise determination of uniaxial strain effects is hence a mandatory step towards new applications and phenomena. We report dilatometric studies on the honeycomb quantum magnets CrI_3 and $\text{Na}_2\text{Co}_2\text{TeO}_6$ at low temperatures and high magnetic fields. Our data enable us to quantify magnetoelastic coupling and the uniaxial pressure dependencies of the respective ordering temperatures. Additionally, the magnetic phase diagrams are constructed, including structural response of the surface phase in CrI_3 and signatures of competing degrees of freedom in $\text{Na}_2\text{Co}_2\text{TeO}_6$.

[1] J. Arneth et al., Phys. Rev. B 105, L060404 (2022)

MA 9.2 Mon 15:20 H43

Magnetisation dynamics in epitaxial Co_2Mn -based Heusler thin films with ultralow damping for thicknesses below 50 nm — •ANNA M. FRIEDEL^{1,2}, CLAUDIA DE MELO², VICTOR PALIN^{2,3}, SÉBASTIEN PETIT-WATELOT², STÉPHANE ANDRIEU², and PHILIPP PIRRO¹ — ¹Fachbereich Physik and Landesforschungszentrum OPTIMAS, Technische Universität Kaiserslautern, Kaiserslautern, Germany — ²Institut Jean Lamour, UMR CNRS 7198, Université de Lorraine, Nancy, France — ³Synchrotron SOLEIL-CNRS, L'Orme des Merisiers, Gif-sur-Yvette, France

For future applications of magnetisation dynamics, materials with low Gilbert damping are indispensable. Co_2Mn -based Heusler compounds are considered excellent candidates as they combine high saturation magnetisation, high Curie temperature, half-metallicity and ultralow Gilbert damping, especially when grown epitaxially with decent control over stoichiometry to ensure the desired chemical ordering [1]. However, downscaling towards microstructures is a challenge in which the fabrication of high-quality ultrathin films with consistent excellent properties is a crucial step. We succeeded in the epitaxial growth of high-quality Co_2MnSi Heusler films in the thickness range of 4–44 nm for all of which the half-metallicity was confirmed [2]. Consequently, an ultralow Gilbert damping was obtained for the whole series reaching down to 7.8×10^{-4} for the 8 nm film. Coupling effects and magnetisation dynamics in heterostructures are currently under investigation.

[1] C. Guillemard, et al., J. Appl. Phys. 128, 241102 (2020)

[2] C. de Melo, et al., Appl. Mater. Today 25, 101174 (2021)

MA 9.3 Mon 15:40 H43

ΔE -Effect Magnetic Field Sensors — •BENJAMIN SPETZLER, ELIZAVETA GOLUBEVA, PATRICK WIEGAND, ROBERT RIEGER, JEFFREY MCCORD, and FRANZ FAUPEL — Kiel University, Kiel, Germany

Many conceivable biomedical and diagnostic applications require the detection of small-amplitude and low-frequency magnetic fields. Against this background, we investigate a magnetometer concept based on the magnetoelastic ΔE effect. The ΔE effect causes the resonance frequency of a magnetoelastic resonator to detune in the presence of a magnetic field, which can be read out electrically with an additional piezoelectric phase. Various microelectromechanical resonators are experimentally analyzed in terms of the ΔE effect and signal-and-noise response, and models are developed and extended where necessary to identify current limitations. Although a large ΔE effect is confirmed in the shear modulus, the sensitivity of classical cantilever resonators does not benefit from this effect. An approach utilizing surface acoustic shear waves provides a solution and can detect small signals over a large bandwidth. Comprehensive analyses of the quality factor and piezoelectric material parameters indicate methods to increase sensitivity and signal-to-noise ratio significantly. The latter is currently limited by the loss of the magnetic material. First exchange-biased ΔE -effect sensors pave the way for compact setups and arrays with a large number of sensor elements. The insights gained lead to a new resonator and processing concept that can circumvent several previous limitations with prospects for sensor improvements in the future.

MA 9.4 Mon 16:05 H43

High-contrast mapping of atomic-scale spin-textures — •LUCAS SCHNEIDER, PHILIP BECK, JENS WIEBE, and ROLAND WIESENDANGER — Department of Physics, University of Hamburg, D-20355 Hamburg, Germany

A scanning tunneling microscope (STM) with a magnetic tip that has a sufficiently strong spin polarization can be used to map the sample's spin structure down to the atomic scale [1] but usually lacks the possibility to absolutely determine the value of the sample's spin polarization. Magnetic impurities in superconducting materials give rise to pairs of perfectly, i.e., 100%, spin-polarized subgap resonances. In this talk, I will present a method exploiting this effect by functionalizing the apex of a superconducting Nb STM tip with such impurity states [2]. These tips can be used to probe the spin polarization of atom-manipulated Mn nanomagnets on a Nb(110) surface. By comparison with spin-polarized STM measurements of the same nanomagnets using conventional Cr bulk tips, we demonstrate an extraordinary spin sensitivity and the possibility to measure the sample's spin-polarization values close to the Fermi level quantitatively with the new functionalized probes.

[1] R. Wiesendanger, Rev. Mod. Phys. 81, 1495 (2009)

[2] L. Schneider et al., Sci. Adv. 7, eabd7302 (2021)

30 min. discussion break and bestowal of INNOMAG e.V. Diplom-/Master Prize and Ph.D. Thesis Prize

MA 10: Non-Skyrmionic Magnetic Textures

Time: Monday 15:00–16:45

Location: H47

Invited Talk

MA 10.1 Mon 15:00 H47

Magnetic vortices: into the third dimension — •SEBASTIAN GLIGA — Swiss Light Source, Paul Scherrer Institute, 5232 Villigen PSI, Switzerland

Vortices are familiar phenomena in fluids and gases. In ferromagnets, they are naturally forming flux-closure states characterized by a curling of the magnetization around a very stable and narrow core. Over the past decades, vortex structures have been extensively studied in laterally confined thin-film elements owing to their rich dynamics [1].

Recently, non-destructive imaging of three-dimensional magnetic structures at the nanoscale has become possible. Using hard X-ray tomography [2], we

have uncovered three-dimensional structures forming closed vortex loops in a bulk magnet. Based on magnetic vorticity (a quantity analogous to hydrodynamic vorticity), we identified these configurations as magnetic vortex rings [3]. In contrast to theoretical predictions, the observed vortex rings exist as static configurations, rather than purely dynamic states.

Our results open possibilities for further studies of complex three-dimensional solitons.

[1] R. Hertel, S. Gliga, M. Fähnle, and C. M. Schneider, Phys. Rev. Lett. 98, 117201 (2007)

[2] C. Donnelly, M. Guizar-Sicairo, V. Scagnoli, S. Gliga, M. Holler, J. Raabe, L.

J. Heyderman, *Nature* **547**, 328-331 (2017)

[3] C. Donnelly, K. L. Metlov, V. Scagnoli, M. Guizar-Sicairos, M. Holler, N. S. Bingham, J. Raabe, L. J. Heyderman, N. R. Cooper, S. Gliga, *Nature Physics* **17**, 316-321 (2021)

MA 10.2 Mon 15:30 H47

High-Resolution Magnetic Imaging of Surface Magnetic Textures in Synthetic Antiferromagnets Using SEMPA — •MONA BHUKTA, TAKA AKI DOHI, M-A. SYSKAKI, ROBERT FRÖMTER, and MATHIAS KLÄUI — Institut für Physik, Johannes Gutenberg-Universität Mainz, Staudingerweg 7, Mainz, Germany
Magnetic skyrmions[1] are twisted spin configurations, which shows a non-zero skyrmion Hall angle when driven by current due to their topological nature[2], which is detrimental for applications. Skyrmions in synthetic antiferromagnet(SAFs), could suppress this effect owing to an overall zero topological charge. Recent observations of skyrmions in SAFs have opened the possibility for using skyrmions as a candidate for logic operations, data storage devices[3]. Here, we investigate different, more exotic spin textures in a SAF consisting of (CoFeB/Ir/CoFeB)*n* by using scanning electron microscopy with polarization analysis (SEMPA). The unique feature of SEMPA is especially effective on a SAFs enabling us to investigate the topological spin textures even in a fully compensated composition. We report high-resolved vortex-antivortex pairs in the SAF that are stable at zero magnetic fields and room temperature. Micromagnetic simulations of the investigated SAF stacks have been carried out to understand the way stabilize for these exotic spin textures as well as to explore the possible emergence of three-dimensional (3D) spin structures in the SAF multilayer system. [1] K. Everschor-Sitte et al., *J. Appl. Phys.* **124**, 240901 (2018) [2] K. Litzius et al., *Nat. Phys.* **13**, 170 (2017). [3] T. Dohi et al, *Nat. Commun.* **10**, 5153 (2019).

MA 10.3 Mon 15:45 H47

Effects of static magnetic fields in antiferromagnetic ring-shaped spin chains — •YELYZAVETA A. BORYSENKO^{1,2,3}, DENIS D. SHEKA¹, JÜRGEN FASSBENDER², JEROEN VAN DEN BRINK³, DENYS MAKAROV², and OLEKSANDR V. PYLYPOVSKYI^{2,4} — ¹Taras Shevchenko National University of Kyiv, Kyiv, Ukraine — ²Helmholtz-Zentrum Dresden-Rossendorf e.V., Dresden, Germany — ³IFW Dresden, Dresden, Germany — ⁴Kyiv Academic University, Kyiv, Ukraine
While antiferromagnets with the easy axis of anisotropy are considered to be robust against external magnetic fields of a moderate strength, strong-field-driven spin reorientations provide an insight into subtle properties of the material usually hidden by the high symmetry of the ground state. Here, we address theoretically the effects of curvature in the curvilinear antiferromagnetic achiral anisotropic ring-shaped spin chains in strong magnetic fields. We identify the geometry-driven helimagnetic phase transition above the spin-flop field between the vortex and onion states. The spin-flop transition is of the first- or second-order depending on the ring curvature, which is influenced by the geometry-induced Dzyaloshinskii-Moriya interaction. Inhomogeneity of the Néel vector distribution in spin-flop phase generates weakly ferromagnetic response, which lies in the plane perpendicular to the applied magnetic field. Our findings provide an understanding of complex responses of curvilinear antiferromagnets on magnetic fields and allow further experimental study of geometrical effects relying on spin-chain-based nanomagnets.

MA 10.4 Mon 16:00 H47

Screw dislocations in chiral magnets — •MARIA AZHAR¹, VOLODYMYR KRAVCHUK^{1,2}, and MARKUS GARST¹ — ¹Karlsruhe Institute of Technology, Germany — ²Bogolyubov Institute for Theoretical Physics of National Academy of Sciences of Ukraine, Kyiv, Ukraine
The Dzyaloshinskii-Moriya interaction stabilizes helimagnetic order in cubic chiral magnets for a large range of temperatures and applied magnetic field. In

this helimagnetic phase the magnetization varies only along the helix axis, that is aligned with the applied field, giving rise to a one-dimensional periodic magnetic texture. This texture shares many similarities with generic lamellar order like cholesteric liquid crystals, for example, it possesses disclination and dislocation defects [1]. Here, we investigate both analytically and numerically screw dislocations of helimagnetic order. Whereas the far-field of these defects is universal, we find that various core structures can be realized even for the same Burgers vector of the screw dislocation. In particular, we identify screw dislocations with smooth magnetic core structures, that close to the transition to the field-polarized phase continuously connect either to vortices of the XY-order parameter or to skyrmion strings. In addition, close to zero fields we find singular core structure comprising a chain of Bloch points with alternating topological charge [2].

[1] P. Schoenher et al. *Nature Physics* **14**, 465 (2018).

[2] M. Azhar, V. Kravchuk, and M. Garst, *Physical Review Letters* **128**, 157204 (2022).

MA 10.5 Mon 16:15 H47

Chiral response of spin spiral states as the origin of chiral transport fingerprints of spin textures — •JONATHAN KIPP^{1,2}, FABIAN LUX³, and YURIY MOKROUSOV^{2,3} — ¹Department of Physics, RWTH Aachen University, 52056 Aachen, Germany — ²Peter Grünberg Institut and Institute for Advanced Simulation, Forschungszentrum Jülich and JARA, 52425 Jülich, Germany — ³Institute of Physics, Johannes Gutenberg University Mainz, 55099 Mainz, Germany

To extend the commonly accepted yet simplifying and approximate picture of transport effects taking place in systems with spatially varying magnetization such as skyrmions, domain walls and multi-q states, it is important to understand the transport properties of the homochiral spin-spiral states, which are building blocks for these more advanced textures of different nature and dimensionality. In this work, by referring to phenomenological symmetry arguments based on gradient expansion and explicit calculations within the Kubo framework, we study transport properties of various types of spin-spirals in a two-dimensional model with strong spin-orbit interaction. Specifically, we focus on the contributions to the magnetoconductivity, planar Hall effect and anomalous Hall effect, which are sensitive to the sense of chirality of the spiral states. In particular, we analyze the emergence, symmetry, and microscopic properties of the resulting chiral magnetoconductivity, chiral planar Hall effect and chiral Hall effect in terms of spin-spiral propagation direction, cone angle, spiral pitch and disorder strength.

MA 10.6 Mon 16:30 H47

Single-crystal growth and low temperature properties of ErB₂ — •CHRISTOPH RESCH¹, ANDREAS BAUER¹, GEORG BENKA², and CHRISTIAN PFLEIDERER¹ — ¹TU München Physik-Department, 85748 Garching, Germany — ²Kiutra GmbH, 81369 München, Germany

Single crystals of the hexagonal rare-earth diboride ErB₂ were synthesized by means of the self-adjusted flux travelling solvent optical floating zone technique and metallurgically characterized. The magnetic phase diagram of single crystalline ErB₂ was inferred from measurements of the specific heat, the magnetisation, the ac susceptibility, and the electrical transport for fields applied along major crystallographic axes. We find behavior characteristic of an easy-plane antiferromagnet below $T_N = 14$ K. For magnetic fields applied along the hard out-of-plane axis we observe a spin-flip transition at $B_N = 12$ T. Most notably, the Hall resistivity below T_N for fields applied along the hard axis exhibits a large anomalous contribution that does not scale with the uniform magnetization. Possible origins include spin-chirality mechanisms and large Berry curvatures associated with a canted spin structure, or more exotic types of magnetic order.

MA 11: Computational Magnetism 1

Time: Monday 15:00–17:00

Location: H48

MA 11.1 Mon 15:00 H48

Monte Carlo modeling of magnetic crystals from graphical input — MICHAEL GIGER, •AMADÉ BORTIS, MANFRED FIEBIG, and THOMAS LOTTERMOSER — Department of Materials, ETH Zurich

Magnetism in crystals can be described by a spin Hamiltonian which contains all the magnetic interactions between spins. The resulting magnetic properties of the material, like the spin-ordering or the critical behavior, can be derived from Monte Carlo simulations. The correct and efficient implementation of such a Hamiltonian into a computer program for the simulation is error-prone and time-consuming. Here, we present a tool where the magnetic interactions can be defined by connecting atoms in a three-dimensional visualization of a crystal. Our software then automatically generates an efficient code for the Monte Carlo simulations. All simulation parameters can be set in a graphical user interface. We will showcase our software by reproducing the magnetic order in the proto-

typical antiferromagnet Cr₂O₃ as an example. Our tool thus makes Monte Carlo simulations of complex spin systems more accessible to non-specialist users.

MA 11.2 Mon 15:15 H48

AiiDA-UppASD: Automatic workflow engine for high-throughput magnetic simulations and machine learning — •QICHEN XU^{1,2,3}, JONATHAN CHICO⁴, MANUEL PEREIRO², DANNY THONIG⁵, ERIK SJÖQVIST², OLLE ERIKSSON², ANDERS BERGMAN², and ANNA DELIN^{1,3} — ¹KTH Royal Institute of Technology, Stockholm, Sweden — ²Uppsala University, Uppsala, Sweden — ³Swedish e-Science Research Center, Stockholm, Sweden — ⁴Sandvik Coromant, Stockholm, Sweden — ⁵Örebro University, Örebro, Sweden

The ever-raising theoretical peak performance and accessibility of supercomputer resources bring automated simulations to a more important position for studies of magnetic materials properties. Recently, Huber et al. developed the

AiiDA framework. In order to perform high-throughput atomic spin dynamics (ASD) simulations and take advantage of AiiDA platform and its build-in DFT plugins, we introduce the AiiDA-UppASD plugin which allows users to access to the majority of the functionalities of the UppASD code within the AiiDA framework via a Python package. In addition, several robust built-in workflows are also provided for managing ASD simulations, handling possible errors, and providing common modular workchains. With these workflows, complex tasks like high-throughput simulations of magnetodynamic properties as well as the determination of spin-wave excitation spectra and magnetic phase diagrams can be performed in a very efficient manner. Meanwhile, a machine learning (ML) prepared data generation workflow is also designed in order to offer ASD-related databases for the ML community to benchmark and develop methods.

MA 11.3 Mon 15:30 H48

Calculation of magnetic properties using Green's functions in the LAPW basis — •HENNING JANSSEN^{1,2}, STEFAN BLÜGEL¹, GUSTAV BIHLMAYER¹, and ALEXANDER SHICK³ — ¹Forschungszentrum Jülich, Jülich, Germany — ²RWTH, Aachen, Germany — ³Czech Academy of Sciences, Prague, Czech Republic

Green's functions are a powerful tool for understanding responses and interactions, including the magnetic properties, in materials.

A method for calculating Green's functions utilizing the Kramers-Kronig transformation is presented. The implementation of this method in the linearized augmented plane-wave basis, as implemented in the Fleur code [1], is especially suited for orbitals mainly localized inside the muffin-tin regions around the atoms. These Green's functions are used to calculate magnetic properties including the Heisenberg exchange constants J_{ij} or the Dzyaloshinskii-Moriya Interaction (DMI) using force-theorem methods [2] and non-collinear torques. Results for these calculations are shown for bulk systems of iron and Co/Pt films.

The authors gratefully acknowledge the computing time granted by the JARA Vergabegremium and provided on the JARA Partition part of the supercomputer CLAX at RWTH Aachen University.

[1]: www.flapw.de

[2]: A. I. Liechtenstein, et al. *J. Magn. Magn. Mater.* **67**, 65 (1987)

MA 11.4 Mon 15:45 H48

Ab initio study of exchange interactions at planar defects of crystal lattices — •MARTIN ZELENÝ¹, MONIKA VŠIANSKÁ², DENIS LEDUE³, RENAUD PATTE³, MIROSLAV ČERNÝ⁴, LADISLAV STRAKA⁵, and OLEG HE CZKO⁵ — ¹Institute of Materials Science and Engineering, Faculty of Mechanical Engineering, Brno University of Technology, Brno, Czech Republic — ²Department of Chemistry, Faculty of Science, Masaryk University, Brno, Czech Republic — ³Normandie Université, UNIROUEN, INSA Rouen, CNRS, GPM, Saint Étienne du Rouvray, France — ⁴Central European Institute of Technology, Brno University of Technology, Czech Republic — ⁵FZU - Institute of Physics of the Czech Academy of Sciences, Czech Republic

Planar defects play an important role in crystalline magnetic materials, because they serve as obstacles to magnetic domain wall motion. Atomistic description of the magnetic properties requires knowledge of exchange interaction parameters J_{ij} between two atomic sites. These parameters can be found in literature for many bulk magnetic materials. However, very little is known about J_{ij} in the vicinity of planar defects where the symmetry of crystal lattice is reduced and atoms have different chemical environment. We provide deep analysis of J_{ij} obtained from ab initio calculations in the vicinity of the clean $\Sigma 5(310)$ grain boundary in bcc Fe as well as grain boundary with segregated P impurities. We analyze also J_{ij} parameters in the vicinity of twin boundaries and antiphase boundaries in Ni_2MnGa magnetic shape memory alloys. Our results show strong influence of planar defects on exchange interactions.

MA 11.5 Mon 16:00 H48

Computationally Driven Evaluation of Magnetocrystalline Anisotropy — •SIMONE KÖCHER^{1,2} and STEFANO SANVITO¹ — ¹School of Physics / CRANN, Trinity College Dublin, Ireland — ²IEK-9 - Fundamental Electrochemistry, Forschungszentrum Jülich, Germany

Custom-tailored magnetic materials are a crucial component in numerous modern technologies. The experimental search for new high-performance magnets can profit considerably from guidance by computational screening approaches, which however depend on reliable first-principle methods for calculating the key physical properties which underlie the magnetism of the material. One of them is the magnetocrystalline anisotropy (MCA), which contributes to the magnetic hardness.

For the well-studied $X(\text{acac})_3$ (X = transition metal) coordination complexes we specifically explore and compare different methods for calculating the MCA: the finite energy difference approach (force theorem) within periodic boundary conditions and all-electron, full-potential perturbative approaches ranging from PT2 on PBE DFT to CASSCF-PT2 and NEVPT2. We explicitly study the influence of cluster geometry and various computational parameters at different levels of theory. Finally, we address the challenges involved in high-throughput MCA calculations for material screening applications.

MA 11.6 Mon 16:15 H48

Functional RG for Rydberg Array Spin Hamiltonians — •BENEDIKT SCHNEIDER — Physics Department, Arnold Sommerfeld Center for Theoretical Physics, and Center for NanoScience, Ludwig Maximilian University Munich, 80333, Germany

Rydberg-Atom arrays are a versatile platform to simulate strongly correlated phenomena from spin liquids to lattice gauge theories. We develop a functional renormalization group approach based on Kitaev's pseudo-Majorana spin representation that produces quantitative accurate results for Rydberg array Hamiltonians at finite temperature. A special feature of our approach is that implementation of infinite lattices with long-range interactions and complicated lattice geometries is straightforward.

MA 11.7 Mon 16:30 H48

Hubbard interactions in 2D magnetic FeP_3 and CrI_3 — •FATEMEH HADDADI¹, EDWARD LINS COTT¹, MARCO GIBERTINI², IURI TIMROV¹, and NICOLA MARZARI¹ — ¹THEOS and MARVELL, EPFL, Lausanne, Switzerland — ²University of Modena and Reggio Emilia, Modena, Italy

Hubbard-corrected density-functional theory has proven to be successful in addressing self-interaction errors in 3D magnetic materials. However, the effectiveness of this approach for magnetic 2D materials has remained elusive. Here, we use PBEsol+U and its extensions to investigate the electronic, structural, and vibrational properties of two 2D magnets: antiferromagnetic FeP_3 and ferromagnetic CrI_3 . Hubbard parameters are computed from first-principles using density-functional perturbation theory (DFPT) [PRB 98, 085127 (2018)], thus avoiding any empiricism. First, we show that for FeP_3 , the Hubbard corrections are crucial for obtaining the experimentally observed insulating state with the correct crystal symmetry. While empirical U can lead to instabilities, the Hubbard parameters from DFPT stabilize the ground state. We show that Hubbard-corrected vibrational frequencies are in good agreement with Raman experiments. Finally, we discuss 2D CrI_3 , and the requirements it elicits in correcting separately the majority and minority bands.

MA 11.8 Mon 16:45 H48

Magnetism in strongly correlated twisted bilayers from first principles — •ADITYA PUTATUNDA and SERGEY ARTYUKHIN — Italian Institute of Technology, Genova, Italy

Twisted bilayer structures of van der Waals materials attract experimental and theoretical interest because of easy single layer exfoliation and processing and a variety of correlated states. 1,2 Magnetic twisted bilayers hosting skyrmions have recently been demonstrated. 3 Within first-principles approach, large supercells and tight convergence are required to compute magnetic interactions. Here we combine DFT and model simulations of Wannier function based tight-binding Hamiltonian to study the states in the twisted bilayer of CrI_3 .

[1] Xu et al., *Nature Nanotechnology* **17**, 143-147 (2022) [2] N. Sivasdas., *Nano Lett.* **18**, 7658-7664 (2018) [3] Shang et al., *ACS Appl. Nano Mater.* **3**, 1282-1288 (2020)

MA 12: Skyrmions 1 (joint session MA/KFM)

Time: Tuesday 9:30–12:45

Location: H37

Invited Talk

MA 12.1 Tue 9:30 H37

Topological spin structures at surfaces — •STEFAN HEINZE — Institute of Theoretical Physics and Astrophysics, University of Kiel, Germany

Magnetic skyrmions are of great interest for future applications ranging from data storage to neuromorphic computing [1]. Fundamental insight into the properties of skyrmions and the underlying microscopic interactions can be obtained by studying them at surfaces [2,3]. Here, I will discuss the stabilization, creation, and annihilation mechanisms of nanoscale topological spin structures based on density functional theory and atomistic spin simulations [4-8]. A novel

skyrmion annihilation mechanism, the Chimera collapse [4], is presented which has been confirmed by direct comparison with scanning tunneling microscopy (STM) experiments [5]. It is further shown that skyrmion stability can be tuned via applied electric fields [6] allowing writing and deleting of skyrmions. Higher-order exchange interactions (HOI) beyond Heisenberg exchange also play a role since they can stabilize skyrmion lattices [2] as well as isolated skyrmions or antiskyrmions [7]. Unexpectedly, HOI can induce not only non-collinear but also collinear two-dimensional multi-Q states observed via spin-polarized STM [8].

[1] A. Fert et al., *Nat. Rev. Mater.* **2**, 1 (2017), [2] S. Heinze et al., *Nat. Phys.* **7**,

713 (2011), [3] N. Romming *et al.*, *Science* **341**, 639 (2013), [4] S. Meyer *et al.*, *Nat. Commun.* **10**, 3823 (2019), [5] F. Muckel *et al.*, *Nat. Phys.* **17**, 395 (2021), [6] S. Paul *et al.*, *npj Comput. Mater.* **8**, 105 (2022), [7] S. Paul *et al.*, *Nat. Commun.* **11**, 4756 (2020), [8] M. Gutzeit *et al.*, arxiv:2204.01358 (2022).

MA 12.2 Tue 10:00 H37

Controlling Magnetic Skyrmion Nucleation and Motion — •LISA-MARIE KERN¹, VICTOR DEINHART^{1,4}, KATHINKA GERLINGER¹, MICHAEL SCHNEIDER¹, DIETER ENGEL¹, CHRISTIAN GÜNTHER^{2,3}, KATJA HÖFLICH^{4,5}, RICCARDO BATISTELLI⁴, DANIEL METTERNICH⁴, FELIX BÜTTNER⁴, BASTIAN PFAU¹, and STEFAN EISEBITT^{1,3} — ¹Max-Born-Institut, Berlin, Germany — ²Zentraleinrichtung für Elektronenmikroskopie (ZELMI), Technische Universität, Berlin, Germany — ³Institut für Optik und Atomare Physik, Technische Universität, Berlin, Germany — ⁴Helmholtz Zentrum für Materialien und Energie, Berlin, Germany — ⁵Ferdinand-Braun-Institut, Berlin, Germany
Magnetic skyrmions are topological quasiparticles, stabilized in out-of-plane magnetized multilayers. Great advances have been reported in generating, annihilating and shifting skyrmions via spin-orbit torque from spin-polarized currents. Optical nucleation with single laser pulses offers a possibly faster and more energy-efficient alternative. While the underlying mechanisms of the nucleation are different, both methods suffer from a certain stochasticity in the spatial distribution of the skyrmions nucleated. However, in view of scientific and practical applications, a controllable localization of the skyrmion's nucleation site is typically required. Nanopatterning of a tailored magnetic anisotropy landscape using He⁺-ions provides a promising platform for enhanced control of skyrmions in thin films. Based on this technique, we have recently demonstrated reproducible skyrmion nucleation and motion - a prerequisite for any fundamental or applied research on topological structures.

MA 12.3 Tue 10:15 H37

Current-Induced H-Shaped Skyrmion Creation and Their Dynamics in the Helical Phase — •ROSS KNAPMAN^{1,4}, DAVI R RODRIGUES², JAN MASELL³, and KARIN EVERSCHOR-SITTE^{4,5} — ¹Institute of Physics, Johannes Gutenberg University Mainz, 55128 Mainz, Germany — ²Department of Electrical and Information Engineering, Politecnico di Bari, 70126 Bari, Italy — ³RIKEN Center for Emergent Matter Science (CEMS), Wako 351-0198, Japan — ⁴Faculty of Physics, University of Duisburg-Essen, 47057 Duisburg, Germany — ⁵Center for Nanointegration Duisburg-Essen, University of Duisburg-Essen, 47057 Duisburg, Germany

A potential application of magnetic skyrmions is in racetrack memory devices. [1] While efforts have often been concentrated on the use of ferromagnetic and antiferromagnetic racetracks, previous work has suggested that the use of helimagnets could be more effective. [2] Here, the helices provide a means to naturally confine the skyrmions to quasi-1D channels, mitigating the skyrmion Hall effect. They additionally allow for high-speed skyrmion motion. Moreover, inspired by previous works which demonstrated electric-current-controlled skyrmion injection at magnetic impurities, [3] we propose a method of creating skyrmions in a helical background. [4]

[1] Fert, A. *et al.*, *Nat. Nanotechnol.* **8**, 152-156 (2013)

[2] Müller, J. *et al.*, *Phys. Rev. Lett.* **119**, 137201 (2017)

[3] Everschor-Sitte, K. *et al.*, *New J. Phys.* **19**, 092001 (2017)

[4] Knapman, R. *et al.* *J. Phys. D: Appl. Phys.* **54**, 404003 (2021)

MA 12.4 Tue 10:30 H37

Skyrmion automotion in confined geometries for applications — •KILIAN LEUTNER¹, THOMAS BRIAN WINKLER¹, HANS FANGOHR^{2,3}, and MATHIAS KLÄUI¹ — ¹Johannes Gutenberg University, Institute for Physics, Staudinger Weg 7, 55128 Mainz, Germany — ²Max-Planck Institute for the Structure and Dynamics of Matter, Luruper Chaussee 149, 22761 Hamburg, Germany. — ³University of Southampton, SO17 1BJ, Southampton, United Kingdom
Magnetic skyrmions are promising candidates for energy-efficient applications due to their quasi-particle nature and their topological stabilization. We present here a new concept for a multi-turn sensor-counter based on skyrmions. The skyrmion-boundary force in confined geometries leads with the topology-dependent dynamics to the effect of automotion in certain cases. Automotion describes the movement of magnetic structures without the supply of external energy. For our case, we describe and investigate this effect with micromagnetic simulations and the coarse-grained Thiele equation. Automotion has already been demonstrated for domain walls [1], but is not well explored in skyrmionic systems yet.

[1] M.-A. Mawass *et al.*, *Phys. Rev. Applied* **7**, 044009, 2017

MA 12.5 Tue 10:45 H37

Walking Skyrmions — •ALLA BEZVERSHENKO and ACHIM ROSCH — Institute for Theoretical Physics, University of Cologne, 50937 Cologne, Germany
We study the pinning - unpinning transition of the skyrmion lattice in bulk MnSi under applying a slowly oscillating transverse magnetic field. We model the system using an elastic model for skyrmion strings in the presence of pinning forces. With this effective model we show that the presence of a transverse magnetic field reduces the critical current density needed to depin the skyrmion lattice,

reaching zero at the critical magnetic field value. Further, the complete phase diagram of this model will be discussed. Below the threshold amplitude, the skyrmion lines stay fully pinned. Upon increasing the amplitude, a so-called "walking" phase starts, where the skyrmion lines start to unpin. If in this phase a sufficiently large electric current is being applied, the skyrmion lattice starts to move. Obtained results are compared to the experimental data on the transverse susceptibility measurements for this system.

MA 12.6 Tue 11:00 H37

Small-angle neutron scattering of kinetically driven skyrmion lattice motion — •DENIS METTUS¹, ALFONSO CHAGON¹, ANDREAS BAUER¹, SEBASTIAN MÜLBAUER², and CHRISTIAN PFLEIDERER¹ — ¹Physik-Department, Technische Universität München, D-85748 Garching, Germany — ²Heinz Maier-Leibnitz Zentrum (MLZ), Technische Universität München, Garching, Germany
Skyrmions are topologically non-trivial spin textures that exhibit an exceptionally efficient coupling to spin currents, notably spin-polarized charge currents and magnon currents as observed in MnSi, FeGe, and Cu₂OSeO₃. This raises the question for the microscopic mechanisms that control the pinning of the skyrmion lattice, and how they depend on the topology, electronic structure, and disorder. We report neutron scattering measurements of kinetically driven skyrmion lattice unpinning and motion by means of Time-Involved Small Angle Neutron scattering Experiment (TISANE). In our study we examined the unpinning process under changing field orientation for different materials including the metallic systems Mn_{1-x}Fe_xSi and the insulator Cu₂OSeO₃. We discuss our results in the light of methodological aspects of the TISANE technique and recent theoretical predictions of walking skyrmions.

MA 12.7 Tue 11:15 H37

Spin Wave Driven Skyrmions in Antiferromagnets — •MICHAEL LAU¹, WOLFGANG HÄUSLER², and MICHAEL THORWART¹ — ¹I. Institut für Theoretische Physik, Universität Hamburg — ²Institute of Physics, University of Augsburg
In a two-dimensional lattice of antiferromagnetically coupled classical magnetic moments of unit length it is theoretically possible to stabilize Skyrmions when appropriately adjusting the Dzyaloshinskii-Moriya interaction (DMI) and a uniaxial anisotropy. We present simulations on a discrete lattice which reveal that these Skyrmions can be moved by spin waves injected at one edge of the lattice. It is known that in ferromagnets spin waves are scattered by Skyrmions, imposing a driving force on them. In antiferromagnets, we find similar scattering of spin waves by Skyrmions, exerting a net driving force. However, contrary to ferromagnets, the driving force acts in the direction of spin wave propagation and the Skyrmion accelerates like a classical particle with finite mass, as typically found for antiferromagnetic solitons. Additionally, we exploit the fact that antiferromagnetic spin waves can appear left- or right handed and study the impact of spin waves of different polarizations on the Skyrmion. It turns out that chirality, frequency and amplitude of the spin waves all significantly influence the Skyrmion motion.

MA 12.8 Tue 11:30 H37

Skyrmion lattice dynamics — •DANIEL SCHICK, MARKUS WEISSENHOFER, LEVENTE RÓZSA, and ULRICH NOWAK — Universität Konstanz, Konstanz, Germany
We investigate the movement of skyrmions in lattices by performing molecular dynamics simulations based on the Thiele equation [1], using different effective skyrmion-skyrmion interactions. We compare mean-square displacement and the dynamical orientational correlation function $g_6(t)$ for different values of damping α and different topological charges and find the topological charge to change the effect of damping on the examined quantities. Furthermore, we find that for finite topological charge, the mean-square displacement in low-density skyrmion lattices increases compared to free diffusion. By comparing to trivial topology, we can demonstrate the increase in mean-square displacement to be the result of the gyrocoupling of skyrmions.

[1] A.A. Thiele, *Phys. Rev. Lett.* **30**, 6 (1973)

MA 12.9 Tue 11:45 H37

Skyrmion Pinning Energetics in Thin Film Systems — RAPHAEL GRUBER¹, JAKUB ZÁZVORKA¹, •MAARTEN A. BREMS¹, DAVI R. RODRIGUES¹, TAKAOKI DOHI¹, NICO KERBER¹, BORIS SENG¹, MEHRAN VAFAEE-KHANJANI¹, KARIN EVERSCHOR-SITTE², PETER VIRNAU¹, and MATHIAS KLÄUI¹ — ¹Institute of Physics, Johannes Gutenberg-Universität Mainz, 55099 Mainz, Germany — ²CENIDE, University of Duisburg-Essen, 47057 Duisburg, Germany
Magnetic skyrmions in thin films have been shown to exhibit thermal diffusion, making them a promising system for applications in probabilistic computing [1] as well as Brownian computing [2]. In such applications, pinning effects are of crucial importance as the pinning strength is often comparable to thermal excitations and thus impacts the operation of skyrmion-based devices. Using thermal skyrmion dynamics, we characterize the pinning in a sample and ascertain the spatially resolved energy landscape [3]. To understand the mechanism of pinning, we image the skyrmion pinning details and find a strong size-dependence. We observe that the skyrmion is pinned at its boundary (domain wall) and not as previously considered at its core. As a consequence, we find that the size-

dependence follows from different favorable overlaps of the skyrmion boundary with the pinning regions, which is supported by micromagnetic simulations. This allows us to switch pinning sites on and off by small tuning of external fields. [1] J. Zázvorka et al., *Nat. Nanotechnol.* 14, 658 (2019). [2] M. A. Brems et al., *Appl. Phys. Lett.* 119, 132405 (2021). [3] R. Gruber et al., under review (2021).

MA 12.10 Tue 12:00 H37

Coexistence of topologically distinct spin textures — •BÖRGE GÖBEL¹, JAGANNATH JENA², STUART PARKIN², and INGRID MERTIG¹ — ¹Institut für Physik, Martin-Luther-Universität Halle-Wittenberg — ²Max-Planck-Institut für Mikrostrukturphysik, Halle

Over the last decade, the field of skyrmionics has attracted great research interest, as skyrmions (small, whirl-like spin textures) possess a topologically-induced stability that allows to consider them as the carriers of information in future data storage devices. However, due to their integer topological charge there are two major shortcomings of skyrmion-based racetrack storages: The skyrmions do not move parallel to a current and multiple skyrmions attract and repel each other.

A solution to these problems is the utilization of alternative magnetic nano-objects that go beyond conventional skyrmions; see review [1]. In this talk, we show via simulations, Lorentz transmission electron microscopy measurements [2,3] and Hall transport measurements [4] that skyrmions, antiskyrmion and topologically trivial bubbles [5] can coexist in Heusler materials. They can even appear fractionally near the sample's edges [6]. We propose an advanced version of the racetrack storage device based on these results.

[1] BG et al. *Physics Reports* 895, 1-28 (2021), [2] Jena, BG et al. *Nat. Com.* 11, 1115 (2020), [3] Jena, BG et al. *Science Advances* 6, eabc0723 (2020), [4] Sivakumar, BG et al. *ACS Nano* 14, 13463 (2020), [5] BG et al. *PRAppl.* 15, 064052 (2021), [6] Jena, BG et al. *Nat. Com.* 13, 2348 (2022)

MA 12.11 Tue 12:15 H37

Topological magnetism in multiferroic lacunar spinels — •VLADISLAV BORISOV¹, PATRIK THUNSTRÖM¹, ANNA DELIN², and OLLE ERIKSSON^{1,3} — ¹Ångström Laboratory, Uppsala University, Uppsala, Sweden — ²Department of Applied Physics, School of Engineering Sciences, KTH Royal Institute of Technology, Stockholm, Sweden — ³Örebro University, Örebro, Sweden

Several skyrmionic magnetic systems have been discovered since the first observation of skyrmions in a B20 compound MnSi. Only a few of them host not just

magnetism but also ferroelectricity and prominent examples are lacunar spinels GaV₄S₈ and GaV₄Se₈. These bulk systems are rather unique, because they host Neel skyrmions, which are otherwise only observed in metallic multilayers. Detailed description of magnetic phenomena in the multiferroic spinels is challenging for theory due to correlations within the V₄ clusters.

We study the role of the magnetic state of these clusters and electronic correlations for the Heisenberg and Dzyaloshinskii-Moriya interactions in V- and Mo-based lacunar spinels. The character of magnetic interactions is discussed in relation to the crystal symmetry and electronic properties derived from the V₄ molecular orbitals. Based on micromagnetic simulations, we determine the role of different interactions for the formation of magnetic textures.

This work was supported by the Knut and Alice Wallenberg Foundation, the Swedish Research Council and the Swedish National Infrastructure for Computing.

MA 12.12 Tue 12:30 H37

Systematic identification and assessment of topological spin textures via saddle point searches — •HENDRIK SCHRAUTZER^{1,2}, GRZEGORZ KWIATKOWSKI¹, HANNES JÓNSSON¹, PAVEL F. BESSARAB^{1,3}, and STEFAN HEINZE² — ¹University of Iceland, Reykjavik, Iceland — ²Christian-Albrechts-University, Kiel, Germany — ³Linnaeus University, Kalmar, Sweden

Magnetic systems hosting topological textures such as skyrmions have been of great technological and fundamental interest in recent years. The growing zoo [1] of co-existing meta-stable states makes investigation of such systems challenging. Here, we present a methodology combining global optimization based on recursive traversing between energy minima via saddle points on the energy surface [2,3], and harmonic transition state theory. The methodology provides a systematic approach to predict previously unknown metastable states, identify their lifetime at a given temperature and compute kinetics of their mutual transformations. We apply the method to the widely studied Pd/Fe/Ir(111) skyrmionic system, parametrized using density functional theory, and predict a variety of new transition mechanisms and spin textures including skyrmions with chiral kinks [1], which have been unknown so far in this system.

1: V. M. Kuchkin, *et al.*, *Phys. Rev. B* 102.14 (2020): 144422.

2: A. Pedersen, *et al.*, *International Workshop on Applied Parallel Computing* (pp. 34-44) (2010). Springer, Berlin, Heidelberg.

3: G. P. Müller *et al.*, *Phys. Rev. Lett.* 121.19 (2018): 197202

MA 13: Magnonics 1

Time: Tuesday 9:30–12:30

Location: H43

MA 13.1 Tue 9:30 H43

Topology induced spin-wave modes in curved surfaces — •MICHAEL VOGEL¹, TIM MEWES², and CLAUDIA MEWES² — ¹Institute of Physics and Center for Interdisciplinary Nanostructure Science and Technology (CINSA-T), University of Kassel, Kassel, Germany — ²Department of Physics and Astronomy, University of Alabama, Tuscaloosa, USA

Extending the research of magnetization dynamics from planar two-dimensional structures into the third dimension [1] promises rich physics from theoretically predicted fast domain wall velocities beyond the walker breakdown [2] to Cherenkov-like effects for magnons[3]. Here we investigate the effects of curvature in soft-magnetic hemispheres by means of micromagnetic simulation. The resonant spin-wave spectrum is calculated for different geometries and the power-spectral density is evaluated. The interplay of the local curvature and the external field gives rise to new spin-wave modes at relatively high frequencies located at the edge of the three-dimensional objects.

1. R. Kandori et al., *J. Phys. D Appl. Phys. J. Phys. D Appl. Phys.* 49, 45 (2016). 2. M. Yan, A. Kákay, S. Gliga, R. Hertel, *Phys. Rev. Lett.* 104, 057201 (2010). 3. M. Yan, A. Kákay, C. Andreas, R. Hertel, *Phys. Rev. B - Condens. Matter Mater. Phys.* 88, 20412 (2013).

MA 13.2 Tue 9:45 H43

Propagating Spin-Wave Spectroscopy Studies in a Millikelvin Temperature Environment — •DAVID SCHMOLL, SEBASTIAN KNAUER, ROSTYSLAV SERHA, QI WANG, and ANDRII CHUMAK — University of Vienna, Faculty of Physics, Boltzmannngasse 5, A-1090 Vienna, Austria

Technological advancements in the access to millikelvin temperatures, combined with high-frequency microwave technology, allow first steps towards the investigation of individual magnons, as the corresponding quasi-particles of spin waves, in the field of quantum magnonics. Such experiments require millikelvin base temperatures, to ensure a thermal magnon-free system. We measured spin-wave propagation for external bias magnetic fields in the range of 300 mT to -300 mT at room temperature and at a base temperature of 45 mK. The results were obtained in a cryogenic propagating spin-wave spectroscopy setup, comprising a dilution refrigerator, a 9-1-1 T vector magnet, and a 65 GHz-rated VNA mea-

surement system. The spin-wave transmission was measured in a 70 mm × 2 mm × 5.65 μm yttrium-iron-garnet (YIG) film on a 500 μm-thick gadolinium-gallium-garnet (GGG) substrate in the Magnetostatic Surface Spin-Wave Configuration (MSSW), using a microstrip antenna PCB. The demonstration of spin-wave propagation at cryogenic temperatures, provides the technical capabilities and the platform for future investigations of individual magnons. Moreover, direct optical access to the dilution refrigerator allows millikelvin experiments in the field of hybrid opto-magnonic quantum systems.

MA 13.3 Tue 10:00 H43

Finite-element micromagnetic modeling of spin-wave propagation with the open-source package TetraX — •LUKAS KÖRBER^{1,2}, GWENDOLYN QUASEBARTH^{1,2}, ALEXANDER HEMPEL^{1,2}, ANDREAS OTTO², JÜRGEN FASSBENDER^{1,2}, and ATTILA KÁKAY¹ — ¹Helmholtz-Zentrum Dresden - Rossendorf, Dresden Germany — ²Fakultät Physik, Technische Universität Dresden

We present a finite-element-method (FEM) dynamic-matrix approach to efficiently calculate the dispersion and spatial mode profiles of spin waves propagating in waveguides with arbitrary cross section, where the equilibrium magnetization is invariant along the propagation direction. This is achieved by solving numerically a linearized version of the equation of motion of the magnetization only in a single cross section of the waveguide at hand. To compute the dipolar field, we present an extension of the well-known Fredkin-Koehler method to plane waves. The presented dynamic-matrix approach is implemented within our recently published open-source micromagnetic modeling package TetraX [1] which aims to provide user friendly and versatile FEM workflows for the magnonics community (not only for magnonics community, but FEM simulations in general), covering several classes of sample geometries and, in the near future, also antiferromagnets. As a brief introduction, this talk will include a short live-demo of TetraX.

[1] <https://gitlab.hzdr.de/micromagnetic-modeling/tetrx>

MA 13.4 Tue 10:15 H43

Magnons in antiferromagnets: tools for transport and processing of information — •OLENA GOMONAY — 1Institute of Physics, Johannes Gutenberg University Mainz, Staudingerweg 7, 55128 Mainz, Germany

Magnonics as a concept of information processing with magnon spins is a promising alternative to spintronics, which manipulates electron-mediated spin currents. Magnons in antiferromagnets have further advantages of high limiting velocities and long propagation length compared to their ferromagnetic counterparts. Moreover, magnon currents in antiferromagnets, in contrast to ferromagnets, can carry both spin orientations and thus can be used for manipulation of the magnetic states. In my talk I discuss different aspects of magnon-mediated transport in antiferromagnets and possible applications to information processing. I compare two mechanisms of the nonlocal spin transport observed in easy-plane and easy-axis antiferromagnets via spin-polarised eigenmodes and via magnon birefringence. Magnon birefringence effect can be also observed in the multidomain antiferromagnets with the pronounced magnetostriction. Interaction of magnons in such a case results in a paramagnetic downconversion and resonance excitation of different magnon modes. I show further how the spin-polarised magnons can be used for manipulation of the magnetic states in multilayered films.

MA 13.5 Tue 10:30 H43

A bifid theoretical approach to spin transport in 2D easy axis and easy plane antiferromagnets — •VERENA BREHM and ALIREZA QAIUMZADEH — QuSpin, NTNU Trondheim, Norway

Due to their terahertz excitation spectrum and the absence of stray fields, antiferromagnetic insulators are great candidates for magnonic applications [1].

We model an antiferromagnet with homogenous DMI inspired by hematite α - Fe_2O_3 , that undergoes two phase transitions: For very low temperatures, there is no magnetization as the Néel vector lies in the plane, which corresponds to an easy axis anisotropy. At the Morin temperature, the Néel vector rotates out of plane, leading to a finite DMI-induced magnetization with the system being in an easy plane phase, until at the Néel temperature magnetic order is lost. Spin transport measurements across the Morin temperature [2] are exciting, since the magnonic modes show an anisotropy-dependent polarization [3], which has an impact on the transported angular momentum [4].

In this talk, we demonstrate both analytically and numerically (micromagnetic simulations [5]), how the magnon polarization impacts the spin transport signal across the Morin transition, in connection to Néel vector dynamics and dispersion relation analysis.

[1] Rezende, White. *Phys. Rev. B* **14** (1976)

[2] Ross et al. *J. Mag. Magn. Mat.* **453** (2022); arXiv:2106.12853

[3] Rezende et al. *J. Appl. Phys.* **126** (2019)

[4] Lebrun, Kl'aui et al. *Nat. Comm.* **11** 6332 (2020)

[5] Lepadatu. *J. Appl. Phys.* **128** 243902 (2020)

MA 13.6 Tue 10:45 H43

Employing magnons for generating multi-qubit entangled states for quantum error correction — IDA SKOGVOLL¹, JONAS LIDAL¹, JEROEN DANON¹, and •AKASHDEEP KAMRA^{2,1} — ¹Center for Quantum Spintronics, Norwegian University of Science and Technology, Trondheim, Norway — ²Condensed Matter Physics Center (IFIMAC) and Departamento de Física Teórica de la Materia Condensada, Universidad Autónoma de Madrid, Madrid, Spain

The ongoing rapid progress towards quantum technologies relies on new hybrid platforms optimized for specific quantum computation and communication tasks, and researchers are striving to achieve such platforms. We study theoretically a spin qubit exchange-coupled to an anisotropic ferromagnet that hosts magnons with a controllable degree of intrinsic squeezing. We find this system to physically realize the quantum Rabi model from the isotropic to the Jaynes-Cummings limit with coupling strengths that can reach the deep-strong regime. We demonstrate that the composite nature of the squeezed magnon enables concurrent excitation of three spin qubits coupled to the same magnet. Thus, three-qubit Greenberger-Horne-Zeilinger and related states needed for implementing Shor's quantum error-correction code can be robustly generated. Our analysis highlights some unique advantages offered by this hybrid platform, and we hope that it will motivate corresponding experimental efforts.

I. C. Skogvoll, J. Lidal, J. Danon, and A. Kamra, *Phys. Rev. Applied* **16**, 064008 (2021).

MA 13.7 Tue 11:00 H43

Long-range quantum entanglement between two distant ferromagnets mediated by dipol-dipol interaction — •DENNIS WUHRER, NIKLAS ROHLING, and WOLFGANG BELZIG — Universität Konstanz, D-78457 Konstanz, Germany

Recently the quantum states of an antiferromagnet in the spin wave approximation have been identified as two-mode squeezed sublattice-magnon states. The massive sublattice entanglement leads to a non-trivial structure of the two-mode squeezed vacuum in the magnetic Brillouin Zone.

Further the entanglement in synthetic antiferromagnets became of interest. It can be tuned by an applied magnetic field, but an extraction of squeezing pa-

rameters is difficult. In this talk we regard a system consisting of two distant 2D ferromagnets coupled via dipol-dipol interaction. The Bogoliubov transformation will be interpreted in terms of inter-/intra-layer squeezing and hybridisation parameters. Using the logarithmic negativity we derive an analytic formula to quantify the degree of entanglement for which we investigate the distance dependence due to the long-range interaction. Using the distance and an external field the entanglement can be manipulated from zero to large values and maintained over large distances. The prospect to transfer massive entanglement over large distances is discussed.

MA 13.8 Tue 11:15 H43

Control of the Magnon Bose-Einstein Condensation by the Spin Hall Effect — •MICHAEL SCHNEIDER¹, DAVID BREITBACH¹, ALEXANDER A. SERGA¹, ANDREI N. SLAVIN², VASYL S. TYBERKEVICH², BJÖRN HEINZ¹, BERT LÄGEL¹, CARSTEN DUBS³, PHILIPP PIRRO¹, BURKARD HILLEBRANDS¹, and ANDRII V. CHUMAK⁴ — ¹Fachbereich Physik und Landesforschungszentrum OPTIMAS, Technische Universität Kaiserslautern, D-67663 Kaiserslautern, Germany — ²Department of Physics, Oakland University, Rochester, Michigan 48326, USA — ³INNOVENT e.V. Technologieentwicklung, D-07745 Jena, Germany — ⁴Faculty of Physics, University of Vienna, A-1090 Vienna, Austria

Generally, magnon Bose-Einstein condensation (BEC) is achieved by increasing the particle density. Previously, it was shown that the rapid cooling of yttrium-iron garnet/Pt nanostructures, preheated by an electric current passed through the Pt layer, leads to an imbalance between the magnon and the phonon system. Consequently, magnon BEC is triggered by the excess of magnons.

We report on the additional contribution of the spin Hall effect (SHE), generating a spin current in the Pt layer. Depending on the orientation of the electric current and the applied field, the SHE injects or annihilates magnons. We find that the SHE contribution prevents or promotes the rapid-cooling induced magnon BEC, changing the BEC threshold by -8% to +6% depending on the current polarity. These results demonstrate a new method for controlling macroscopic quantum states and pave the way for its application in spintronic devices.

MA 13.9 Tue 11:30 H43

Confinement of Bose-Einstein magnon condensates in adjustable complex magnetization landscapes — •MATTHIAS R. SCHWEIZER, ALEXANDER J.E. KREIL, GEORG VON FREYMAN, ALEXANDER A. SERGA, and BURKARD HILLEBRANDS — Fachbereich Physik and Landesforschungszentrum OPTIMAS, TU Kaiserslautern, Kaiserslautern, Germany

We demonstrate the capability to control a room-temperature magnon Bose-Einstein condensate (BEC) by spatial modulation of the saturation magnetization. We use laser heating in combination with a phase-based wavefront modulation technique to create adjustable temperature patterns in an yttrium-iron-garnet film. The increase in temperature leads to a decrease of the local saturation magnetization and in turn to the modification of the corresponding BEC frequency. Over time, a phase accumulation between different BEC-areas arises, leading to phase-driven magnon supercurrents.

The BEC is created by microwave parametric pumping and probed by Brillouin light scattering spectroscopy. We observe a strong magnon accumulation effect caused by magnon supercurrents for several distances between heated regions. This accumulation effect manifests in the confinement of the magnon BEC, which exhibits an enhanced lifetime due to the continuous influx of magnons. The experimental results are supported by a numerical model, based on the hydrodynamic approximation of the Gross-Pitaevskii equation.

Funded by the Deutsche Forschungsgemeinschaft (DFG, German Research Foundation) – TRR 173 – 268565370 (project B04).

MA 13.10 Tue 11:45 H43

New magnetostatic modes in biaxial magnets — •YUE SUN^{1,2}, CHANGMIN LEE², LINDA YE³, SHINGO TOYODA^{1,2}, VERONIKA SUNKO^{1,2}, JOSEPH CHECKELSKY⁴, and JOSEPH ORENSTEIN^{1,2} — ¹University of California, Berkeley, Berkeley, California, USA — ²Lawrence Berkeley National Laboratory, Berkeley, California, USA — ³Stanford University, Stanford, California, USA — ⁴Massachusetts Institute of Technology, Cambridge, Massachusetts, USA

Easy-plane antiferromagnets have been demonstrated to have long-distance magnon propagation and flexible control of ultrafast magnetic dynamics. However, exact XY systems are rare, and it is common to have a small in-plane crystalline easy-axis, which leads to the great interest in biaxial magnets. Spin superfluidity has been predicted in biaxial antiferromagnet in an applied magnetic field. Here, we discover new magnetostatic modes in both biaxial ferromagnet and antiferromagnet, where the interesting biaxial anisotropy opens new ranges for magnon frequency. We observe the new magnetostatic modes in biaxial ferromagnet Fe_3Sn_2 , and the prediction of the magnetostatic modes in biaxial antiferromagnet matches with the experimental observations in CrSBr. Comparing to the spin wave induced by the exchange interaction, the magnetostatic modes dominate in the long wavelength limit and offer a unique possibility to observe magnon Bose-Einstein condensation in biaxial antiferromagnet.

MA 13.11 Tue 12:00 H43

Features of magnon spectra in conductive altermagnet: ab initio calculations — •ALBERTO MARMODORO¹, ONDŘEJ ŠÍPR^{1,2}, and TOMAS JUNGWIRTH¹ — ¹Institute of Physics (FZU) of the Czech Academy of Sciences, Prague, Czech Republic — ²New Technologies Research Centre, University of West Bohemia, Pilsen, Czech Republic

Altermagnets [1] are materials with zero net magnetization, alike traditional antiferromagnets, as well as a characteristic alternation of spin polarization for the electronic structure in reciprocal space, due to the relative orientation for anisotropic crystal field effects on different magnetic sublattices in direct space. This may have significant implications for possible spintronics and nano-electronics applications. We report on ongoing work for the ab initio study of transverse magnon excitations in the case of the conducting, colinear antiferromagnetic altermagnet material RuO₂

[1] arXiv 2105.05820v2

MA 13.12 Tue 12:15 H43

Beating Fabry-Pérot interference pattern in a magnonic scattering junction in the graphene quantum Hall ferromagnet — •JONATHAN ATTEIA^{1,2}, FRANÇOIS PARMONTIER³, PREDEEN ROULLEAU³, and MARK-OLIVER GOERBIG² — ¹Faculty of Physics, University of Duisburg-Essen, 47057 Duisburg, Germany — ²Laboratoire de Physique des Solides, Université Paris Saclay, CNRS UMR 8502, F-91405 Orsay Cedex, France — ³SPEC, CEA, CNRS, Université Paris-Saclay, CEA Saclay, F-91191 Gif sur Yvette Cedex, France

At filling factor $\nu = 0, \pm 1$, the ground state of graphene is a particular SU(4) ferromagnet which hosts a rich phase diagram along with several spin, pseudospin or “entanglement” magnon modes. Motivated by recent experiments, we study a $\nu = -1|0| - 1$ Fabry-Pérot magnonic junction. If the ground state at $\nu = 0$ is spin polarized, there exist two spin modes which interfere and create a beating pattern, while pseudospin modes are reflected. The same scenario occurs for pseudospin magnon if the $\nu = 0$ ground state is pseudospin polarized. The observation of such an interference pattern would provide information on the low-energy anisotropies and thus on the ground state.

MA 14: Cooperative Phenomena: Spin Structures and Magnetic Phase Transitions

Time: Tuesday 9:30–12:00

Location: H47

Invited Talk

MA 14.1 Tue 9:30 H47

Overriding universality of ferromagnetic phase transitions through nano-scale materials design — •ANDREAS BERGER — CIC nanoGUNE BRTA, E-20018 San Sebastian, Spain

In recent years, significant interest has developed in magnetic thin films, in which the exchange coupling strength is ferromagnetic everywhere, but locally varying by means of nano-scale materials design. This interest is associated with the fact that such designed materials profiles translate into strongly varying magnetization states down to the 1-2 nm length scale, which is somewhat surprising, given that ferromagnetism is a collective phenomenon [1]. Correspondingly, such exchange-graded magnetic materials have shown themselves to be a very efficient way of modifying magnetic properties of otherwise rather conventional materials [1]. The most impressive result is hereby the possibility to tune critical exponents, in particular the magnetization onset exponent β in an extremely wide parameter range, which represents a unique way to override the universality usually associated with phase transitions of ferromagnets [2]. The same approach also enabled a complete separation of the temperature dependent onset of ferromagnetism at the Curie temperature from the onset of hysteresis, even in anisotropic materials [3], and it allowed for an enhancement of magnetocaloric properties [4]. Thus, exchange-graded materials are an extremely promising way to design the thermal evolution of magnetic properties and adapt it to device requirements. [1] Phys. Rev. B 98, 064404 (2018); [2] Phys. Rev. Lett. 127, 147201 (2021); [3] Phys. Rev. Appl. 16, 034038 (2021); [4] J. Phys. D 54, 304003 (2021).

MA 14.2 Tue 10:00 H47

Poisson-Dirichlet distributions and weakly first-order spin-nematic phase transitions — •NILS CACI¹, PETER MÜHLBACHER², DANIEL UELTSCHI², and STEFAN WESSEL¹ — ¹RWTH Aachen University, Aachen, Germany — ²University of Warwick, Coventry, United Kingdom

Weakly first-order transitions, i.e. discontinuous phase transitions with very large correlation lengths, have become a vivid subject in condensed matter research and beyond in recent years. Therefore, establishing quantum systems in which weakly first order phase transitions can be robustly demonstrated is of great interest. We present a quantitative characterization of generic weakly first-order thermal phase transitions out of planar spin-nematic states in three-dimensional spin-one quantum magnets, based on calculations using Poisson-Dirichlet distributions (PD) within a universal loop model formulation, combined with large-scale quantum Monte Carlo calculations. In contrast to earlier claims, the thermal melting of the nematic state is not continuous, instead we identify a weakly first-order transition. Furthermore, we obtain exact results for the order parameter distribution and cumulant ratios at the melting transition. Our findings establish the thermal melting of planar spin-nematic states as a generic platform for quantitative approaches to weakly first-order phase transitions in quantum systems with a continuous SU(2) internal symmetry.

MA 14.3 Tue 10:15 H47

Derivation of Spin Hamiltonian by Algebraic Methods — •HIROSHI KATSUMOTO¹, FABIAN LUX^{1,2}, YURIY MOKROUSOV^{1,2}, and STEFAN BLÜGEL¹ — ¹Peter Grünberg Institute and Institute for Advanced Simulation, Forschungszentrum Jülich and JARA, 52425 Jülich, Germany — ²Institute of Physics, Johannes Gutenberg University Mainz, 55099 Mainz, Germany

Complex magnetism is known to emerge from competing Heisenberg interactions and higher-order spin interactions [1]. In addition, previously unknown interactions such as the Chiral-Chiral interaction due to topological orbital magnetism turn also out to be essential to explain the magnetic properties [2]. How-

ever, a method for uniquely deriving spin Hamiltonians that captures the spin interactions of a given system has not yet been established. In this presentation, we give rigorous spin Hamiltonians for isotropic spin interactions for a given total localized spin S and the number of magnetic sites. The derivation of the spin Hamiltonian is based on the algebraic structure that the spin operators follow for arbitrary spin magnitude. By organizing the algebraic structure obeyed by the general spin operators, we discuss the construction of the exact spin Hamiltonian and the higher-order terms of interactions, especially for the cases $S = 1/2$ and 1.

We acknowledge funding from the European Research Council grant 856538 (project “3D MAGIC”); and Deutsche Forschungsgemeinschaft (DFG) through SPP-2137 and SFB-1238 (project C1).

[1] M. Hoffmann *et al.*, Phys. Rev. B **101**, 024418 (2020).[2] S. Grytsiuk *et al.*, Nat. Commun. **11**, 511 (2020).

MA 14.4 Tue 10:30 H47

Ab initio approach to compute magnetic Gibbs free energies and phase transitions using magnetically constrained supercells — •EDUARDO MENDIVE TAPIA^{1,2,3}, NICOLAS ESSING¹, RUDOLF ZELLER¹, STEFAN BLÜGEL¹, JÖRG NEUGEBAUER², and TILMANN HICKEL² — ¹Forschungszentrum Jülich and JARA, 52425 Jülich, Germany — ²Max-Planck-Institut für Eisenforschung, 40237 Düsseldorf, Germany — ³Universitat de Barcelona, D-08028 Barcelona, Spain

We present a first-principles approach for the computation of the magnetic Gibbs free energy of materials using magnetically constrained supercell calculations [1]. Our approach, based on an adiabatic approximation for the local moment orientations [2], describes magnetic phase transitions and how electronic and magnetovolume mechanisms generate a discontinuous (first-order) character. Results obtained for bcc Fe and the triangular antiferromagnetic state of Mn₃AN (A = Ga, Ni) [3] will be presented and used to explain their negative volume expansion and the first-order nature observed experimentally. The performance of two different density functional theory codes, the Vienna Ab Initio Simulation package (VASP) and the linear-scaling KKR-nano code suitable for thousands of atoms (<https://jukkr.fz-juelich.de>), will be shown.

[1] E. Mendive-Tapia, J. Neugebauer, T. Hickel, Phys. Rev. B **105**, 064425 (2022).[2] B. Gyroffy *et al.*, J. Phys. F: Met. Phys. **15** 1337 (1985).[3] D. Boldrin *et al.*, Phys. Rev. X **8** 041035 (2018).

MA 14.5 Tue 10:45 H47

spin-reorientation in CuCr₂S₄ from muSR — •ELAHEH SADROLLAHI¹, JOCHEN LITTERST², LILIAN PRODAN^{3,4}, VLADIMIR TSURKAN^{3,4}, and ALOIS LOIDL³ — ¹Institut für Festkörper- und Materialphysik, Technische Universität Dresden, Germany — ²Institut für Physik der kondensierten Materie, Technische Universität Braunschweig, Germany — ³Institute of Physics, University of Augsburg, 86135 Augsburg, Germany — ⁴Institute of Applied Physics, MD 2028, Chisinau, Republic of Moldova

Muon Spin Relaxation and Rotation (muSR) experiments have been performed on the thio spinel CuCr₂S₄ for further clarifying the long-standing controversy regarding its electronic and magnetic states [1,2]. Long regarded as ferromagnet (T_c=378 K) with magnetic moments residing only on Cr, CuCr₂S₄ is nowadays considered a ferrimagnetic with small magnetic moments on the Cu sites [3]. In addition to the transition at T_c, our muSR data reveal transitions around 50 K and 100 K with changes in spontaneous rotation signals and in relaxation behaviour. There is a close resemblance between these muSR results with those found for Fe_{1-x}Cu_xCr₂S₄ with high Cu concentrations [4]. We interpret the

transitions with spin re-orientations and will discuss the Jahn-Teller effect as a possible reason.[1] F. K. Lotgering et al., *J. Phys. Chem. Solids* 30, 799 (1969) and *Solid State Commun.* 2, 55 (1964). [2] J. B. Goodenough, *Solid State Commun.* 5, 577 (1967) and *J. Phys. Chem. Solids* 30, 261 (1969).[3] A. Kimura et al., *Phys. Rev. B* 63,224420 (2001).[4] E. Sadrollahi, Doctoral Thesis (2018): https://publikationsserver.tu-braunschweig.de/receive/dbbs_mods_00066058.

MA 14.6 Tue 11:00 H47

identification of a new hidden-order phase in the magnetic phase diagram of $\text{Ce}_3\text{Pd}_{20}\text{Si}_6$ — •F. MAZZA¹, P. Y. PORTNICHENKO², P. STEFFENS³, M. BOEHM³, E. S. CHOI⁴, M. NIKOLO⁵, S. PASCHE¹, and D. S. INOSOV² — ¹TU Wien, Austria — ²TU Dresden, Germany — ³ILL, Grenoble, France — ⁴Florida State University, Tallahassee, USA — ⁵St. Louis University, USA

Magnetically hidden order is a hypernym for electronic ordering phenomena whose microscopic symmetry cannot be revealed with conventional neutron or x-ray diffraction. In a handful of *f*-electron systems, the ordering of odd-rank multipoles leads to order parameters with a vanishing neutron cross-section. Among them, $\text{Ce}_3\text{Pd}_{20}\text{Si}_6$ is known for its unique phase diagram exhibiting two distinct multipolar-ordered ground states (phases II and II'), separated by a field-driven quantum phase transition. Using torque magnetometry at subkelvin temperatures, here we find another phase transition at higher fields above 12 T, which appears only for low-symmetry magnetic field directions. While the order parameter remains unknown, this discovery renders $\text{Ce}_3\text{Pd}_{20}\text{Si}_6$ the first known material with two metamultipolar phase transitions. They are both clearly manifested in the magnetic-field dependence of the field-induced (111) Bragg intensities measured with neutron scattering for $\mathbf{B} \parallel [11\bar{2}]$. Furthermore, the magnetic excitation spectrum suggests that the new phase II'' may have a different propagation vector in the vicinity of $\mathbf{Q} = (010)$, revealed by the minimum in the dispersion representing the Goldstone mode of this hidden-order phase.

MA 14.7 Tue 11:15 H47

Magnetic and thermodynamic properties of van-der-Waals CuCrP_2S_6 — •KRANTHI KUMAR BESTHA^{1,2}, LAURA TERESA CORREDOR BOHORQUEZ¹, VILMOS KOCSIS¹, SEBASTIAN SELTER¹, SAICHARAN ASWARTHAM¹, BERND BUECHNER^{1,2}, and ANJA U. B. WOLTER¹ — ¹Institute for Solid State Research, Leibniz IFW Dresden, 01069, Dresden, Germany — ²Institute of Solid State and Materials Physics and Wuerzburg-Dresden Cluster of Excellence ct.qmat, Technical University Dresden, 01062 Dresden, Germany

Two-dimensional van-der-Waals materials with intrinsic multiferroic properties are advantageous over 3D multiferroic materials for next generation nanoscale magnetic and electric devices. CuCrP_2S_6 is a quasi-2D vdW multiferroic candidate with magnetic and ferroelectric polarization arising from Cr and Cu sublattices, respectively. CuCrP_2S_6 exhibits intralayer ferromagnetic and interlayer antiferromagnetic interactions. $M(T)$ and $C_p(T)$ on single crystal CuCrP_2S_6 reveal antiferromagnetic ordering at $T_N=31.5$ K. Our magnetic data reveal predominant ferromagnetic interactions below the ordering temperature and short-range ferromagnetic correlations above T_N . Magnetic fields applied in the ab-plane exhibit a spin-flop transition at a relatively small magnetic field of 4.3 kOe with weak anisotropy in the ab-plane. For a clear understanding of the magnetic anisotropy of this material, in-plane and out-of-plane angular-dependent

dc magnetic studies were performed. Different symmetries are observed for both the in- and out-of-plane angular-dependent data. Our results are summarized in H-T phase diagrams for different main directions.

MA 14.8 Tue 11:30 H47

Probing magneto-elastic coupling in the quasi-2D van der Waals ferromagnet $\text{Cr}_2\text{Ge}_2\text{Te}_6$ — •LAURA T. CORREDOR¹, BASTIAN RUBRECHT^{1,2}, TAKAHIRO SAKURAI³, HITOSHI OHTA⁴, ALEXEY ALFONSOV¹, SEBASTIAN SELTER¹, SAICHARAN ASWARTHAM¹, VLADISLAV KATAEV¹, ANJA U. B. WOLTER¹, and BERND BÜCHNER⁵ — ¹Institute for Solid State Research, Leibniz IFW Dresden, 01069 Dresden, Germany — ²Institute for Solid State and Materials Physics, TU Dresden, 01062 Dresden, Germany — ³Research Facility Center for Science and Technology, Kobe University, Kobe 657-8501, Japan — ⁴Molecular Photoscience Research Center, Kobe University, Nada, Kobe 657-8501 Japan — ⁵Institute of Solid State and Materials Physics and Würzburg-Dresden Cluster of Excellence ct.qmat, Technische Universität Dresden, 01062 Dresden, Germany

The first 2D uniaxial ferromagnetic semiconductor $\text{Cr}_2\text{Ge}_2\text{Te}_6$ -with a layered structure-is promising for exciting new applications such as ultra-compact spintronics or magnonic devices, which need 2D long-range magnetic order as crucial feature. Since magnetocrystalline anisotropy is essential for the stabilization of magnetic order in 2D spin systems, the possibility to control it via a tunable external parameter-such as pressure or strain-can provide useful hints for the engineering of magneto-electric heterostructures with strained architectures. With this motivation, magnetization and ferromagnetic resonance (FMR) experiments under hydrostatic pressure on $\text{Cr}_2\text{Ge}_2\text{Te}_6$ single crystals were performed. Insights on the magneto-elastic coupling and magnetic interactions with the increase of pressure are discussed.

MA 14.9 Tue 11:45 H47

Spin structure of Frenkel excitons on Cu^{2+} -ions in the antiferromagnet CuB_2O_4 revealed by magneto-absorption spectroscopy — •DENNIS KUDLACIK¹, NATALIA E. KOPEVA¹, DIMITRI R. YAKOVLEV¹, MIKHAIL V. EREMIN³, ALEXEY R. NURMUKHAMEDOV³, MANFRED BAYER¹, and ROMAN V. PISAREV² — ¹Experimentelle Physik 2, Technische Universität Dortmund, 44221 Dortmund, Germany — ²St. Petersburg, Russia — ³Kazan, Russia

Frenkel excitons in magnetic insulators have attracted considerable interest in recent years as they allow the migration or transmission of a localized excitation. We have investigated this property which is reflected in the Davydov splitting of the exciton in the antiferromagnet copper metaborate, CuB_2O_4 [1]. This magnetic insulator consists of two weakly interacting sublattices of Cu^{2+} ions. Below the Neel temperature of $T_N = 21$ K its magnetic structure is dominated by the antiferromagnetic order of the 4b sublattice which comprises 4 Cu^{2+} ions twice degenerate in spin resulting in the formation of 8 collective charge-spin Frenkel-Davydov excitations. From a comparison of the experimental data with the results of the theoretical model we define the parameters of Frenkel exciton states, determine the electron-energy transfer between antiferromagnetically coupled copper spins as well as the anisotropic Cu^{2+} g-factors of ground and excited states.

[1] N. E. Kopteva et al., *Phys. Rev. B* 105, 024421 (2022).

MA 15: Computational Magnetism 2

Time: Tuesday 9:30–11:30

Location: H48

MA 15.1 Tue 9:30 H48

An *ab initio* study of temperature effects on the optical and magneto-optical properties of ferromagnetic BCC Fe — •KISUNG KANG, DAVID G. CAHILL, and ANDRÉ SCHLEIFE — Department of Materials Science and Engineering, University of Illinois at Urbana-Champaign, Urbana, Illinois 61801, USA

This work investigates the temperature-dependent optical properties of ferromagnetic BCC Fe in terms of electron, lattice, and magnetic temperatures. With the supercell approach, lattice and magnetic temperature is portrayed by the perturbed atomic and magnetic structures at finite temperature. In imaginary optical conductivity spectra at finite temperature, a large signal at low energy range is induced by phonon and magnon-assisted intraband transitions. We identify that this surging signal originates from the change of the dipole transition matrix elements. Magnetic temperature provokes a unique spectral change which is a redshift of the peak near 2.8 eV in the imaginary optical conductivity spectrum. From band unfolding analysis, it turns out that thermal demagnetization induces the reduction of exchange splitting in the electronic band structure, leading to the electron excitation with a smaller energy transition and explaining the peak redshifting. **Illinois MRSEC NSF DMR-1720633 Kisung Kang's present address: The NOMAD laboratory, Fritz-Haber-Institut der Max-Planck-Gesellschaft, Faradayweg 4-6, 14195 Berlin, Germany

MA 15.2 Tue 9:45 H48

An *ab-initio* parameterised spin model of hematite — •TOBIAS DANNEGGER¹, ANDRÁS DEÁK², SHUBHANKAR DAS³, E. F. GALINDEZ RUALES³, EUNCHONG BAEK³, MATHIAS KLÄUI³, LÁSZLÓ SZUNYOGH^{2,4}, and ULRICH NOWAK¹ — ¹Department of Physics, University of Konstanz — ²Department of Theoretical Physics, Institute of Physics, Budapest University of Technology and Economics — ³Institute of Physics, Johannes Gutenberg University Mainz — ⁴MTA-BME Condensed Matter Research Group, Budapest University of Technology and Economics

The canted antiferromagnetic insulator hematite, known for motivating the theory of the Dzyaloshinskii-Moriya interaction [1, 2] as well as the first description of the Morin transition [3], is of interest in modern antiferromagnetic spintronics because of its long-distance spin transport properties [4]. We present an *ab-initio* parameterised atomistic spin model of hematite that accurately reproduces its magnetic properties and phase transitions, and shows how dipole-dipole interactions play an important role in determining the transition between the antiferromagnetic and weak ferromagnetic phase. We compare our model's predictions with extensive experimental measurements on a hematite single crystal and find good quantitative agreement across a wide range of temperatures.

[1] I. Dzyaloshinskii, *J. Phys. Chem. Solids* 50, 241 (1958).

[2] T. Moriya, *Phys. Rev.* 120, 91 (1960).

[3] F. J. Morin, *Phys. Rev.* 78, 819 (1950).

[4] R. Lebrun et al., *Nature* 561, 222 (2018).

MA 15.3 Tue 10:00 H48

The pyrochlore $s = 1/2$ Heisenberg antiferromagnet at finite temperature — •ROBIN SCHÄFER¹, IMRE HAGYMÁSI^{1,2}, RODERICH MOESSNER¹, and DAVID LUITZ¹ — ¹Max Planck Institute for the Physics of Complex Systems, Dresden, Germany — ²Strongly Correlated Systems *Lendület* Research Group, Budapest, Hungary

We use state-of-the-art computational methods to investigate a frustrated three-dimensional quantum spin liquid candidate, the pyrochlore $s = 1/2$ antiferromagnet at finite temperature.

Using a systematic cluster expansion based on tetrahedra, including clusters up to 25 lattice sites with nontrivial hexagonal and octagonal loops, we gain access to various thermodynamic properties in the thermodynamic limit at finite temperature. We found a pronounced maximum in the specific heat at $T = 0.57J$ that is stable across finite size clusters and converged in the series expansion. At $T \approx 0.25J$ (the limit of convergence of our method), the residual entropy per spin is $0.47k_B \log(2)$, which is relatively large compared to other frustrated models at this temperature.

The generality of this algorithm allows us to investigate realistic compounds: Using recent experimental data on the dipolar-octopolar pyrochlore $\text{Ce}_2\text{Zr}_2\text{O}_7$, we were able to determine possible regions for the exchange parameters which give an accurate description of the high temperature regime.

MA 15.4 Tue 10:15 H48

Stabilisation of external-magnetic-field-induced magnetisation switching with respect to thermal fluctuations — •GRZEGORZ J. KWIATKOWSKI¹, MOHAMMAD H. A. BADARNEH¹, and PAVEL F. BESSARAB^{1,2} — ¹Science Institute of the University of Iceland, Reykjavík, Iceland — ²Department of Physics and Electrical Engineering, Linnaeus University, Kalmar, Sweden

As magnetic memory devices are the cornerstone of data storage, rapid global growth of information transfer creates a pressing need for faster and more energy-efficient memory devices. One of the important directions of research is focused on optimizing the magnetization switching protocols [1,2] showing that both the amplitude of the external pulse as well as the switching time can be significantly reduced in comparison to currently used ones. Before those ideas are implemented one needs to test reliability of the designed optimal pulses when thermal fluctuations are present.

We present the effect of thermal fluctuations on the success rate of magnetization switching induced by an optimized external magnetic field pulse [1]. Furthermore, using perturbation theory and direct numerical simulations we systematically study how to increase the probability of switching by modifying the external pulse depending on the system parameters, temperature and chosen switching time.

[1] Kwiatkowski, G. J. et al. Phys. Rev. Lett., 126(17), 177206

[2] Badarneh, M. H. A. et al. F. Nanosyst.: Phys. Chem. Math., 11(3), 294-300

MA 15.5 Tue 10:30 H48

Energy-efficient control of magnetization reversal in nanoparticles — •MOHAMMAD BADARNEH¹, GRZEGORZ KWIATKOWSKI¹, and PAVEL BESSARAB^{1,2} — ¹Science Institute of the University of Iceland, 107 Reykjavík, Iceland — ²Department of Physics and Electrical Engineering, Linnaeus University, Kalmar, Sweden

Control of magnetization switching is of critical importance for the development of novel technologies based on magnetic materials. Here we identify by means of optimal control theory energy-efficient protocols for magnetization switching in nanoparticles with uniaxial and biaxial anisotropy [1]. Optimal control paths minimizing the energy cost of magnetization reversal are calculated as functions of the switching time and materials properties, and used to derive energy-efficient switching pulses of external magnetic field. Hard-axis anisotropy reduces the minimum energy cost of magnetization switching due to activation of the internal torque in the desired switching direction. Analytical estimates quantifying this effect are obtained based on the perturbation theory. The optimal switching time providing a tradeoff between fast switching and energy efficiency is obtained. The energy cost of switching and the energy barrier between the stable states can be tuned independently in a biaxial nanomagnet. This provides a solution for the dilemma between energy-efficient writability and good thermal stability of magnetic memory elements.

This work was funded by the Icelandic Research Fund (Grant No. 217813-052). [1] G.J. Kwiatkowski et al., Phys. Rev. Lett. 126, 177206 (2021).

MA 15.6 Tue 10:45 H48

Exchange striction from first principles: how electron-phonon coupling modifies magnetic exchange — •RYOTA ONO and SERGEY ARTYUKHIN — Italian Institute of Technology, Via Morego, 30, 16163 Genoa, Italy

Electron-phonon coupling refers to interactions between electrons and lattice distortions. We investigate how such coupling affects interactions between spins in solids. Ionic displacements from equilibrium positions modify overlap integrals between magnetic ions and ligands and thus modulate magnetic exchange. By extracting the self-consistent potential in the first-order in ionic displacements within the Born-Oppenheimer approximation, we obtain a general formula of the change in the one-electron Hamiltonian (electron-phonon coupling). The realistic electron-phonon coupling parameters entering a model Hamiltonian are accessible through the constrained density functional perturbation theory [1]. Using the obtained parameters, we construct a multi-band Hubbard-like model. Finally, realistic magnetic interactions are obtained through Anderson's superexchange theory.

[1] Y. Nomura and R. Arita, Phys. Rev. B 92, 245108 (2015)

MA 15.7 Tue 11:00 H48

First principles theory of electron-magnon scattering and the spin polarized electron energy loss spectroscopy — •SEBASTIAN PAISCHER¹, PAWEŁ BUCZEK², MIKHAIL KATSNELSON³, and ARTHUR ERNST¹ — ¹JKU Linz — ²HAW Hamburg — ³Radboud University Nijmegen

Magnetic solids constitute a very important class of materials as they are extensively used in everyday life and are essential to many new technologies currently under development. In spite of their high relevance, some of the basic properties, like the interaction between electronic and magnetic degrees of freedom still remain a mystery. It leads to spin dependent lifetimes of electronic states and inelastic electron transport to name but a few. In our current study we investigate the impact of magnetic excitations on the electronic spectrum of solids as well as the scattering of high energy electrons with magnetic materials to formulate an ab initio theory for the spin polarized electron energy loss spectroscopy (SPEELS). Our approach is formulated in the framework of the formally exact many body GW theory. The novelty in our approach is that quantities from linear response time dependent density functional theory (LRTDDFT) calculations will be used to approximate an effective interaction between electrons and magnons. As our LRTDDFT calculations are based upon the Korringa-Kohn-Rostocker method, bulk systems as well as complex geometries can be accounted for. In this presentation, we sketch the theoretical basis of the electron-magnon scattering as well as the SPEELS theory and show several results.

MA 15.8 Tue 11:15 H48

The Complex Magnetic Structure and Giant Topological Hall Conductivity in Kagome Metal YnMn_6Sn_6 — •HAO WANG¹, STEFAN BLÜGEL¹, and YURIY MOKROUSOV^{1,2} — ¹Peter Grünberg Institut and Institute for Advanced Simulation, Forschungszentrum Jülich and JARA, Jülich, Germany — ²Institute of Physics, Johannes Gutenberg University Mainz, Mainz, Germany.

The discovery of topological Kagome magnets attracts enormous research interest in recent years. The typical band structure of a Kagome lattice includes a flat band and a Dirac point. The high localized electrons induced strong many-body interactions in the flat bands and the linear dispersion of the Dirac point could lead to many intriguing physical phenomena, such as the quantum anomalous Hall effects, superconductivity, and the non-Fermi liquid behavior. Furthermore, the relationship between the complex noncolinear magnetic structures and band topology of the Kagome magnets also deserves further exploration. In this work, using first-principles calculation and spin Hamiltonian analysis, we investigated the complex magnetic structures, phase transition, and topological Hall conductivity of the Kagome metal YMn_6Sn_6 . We confirm that the ground state of this material is a double flat-spiral structure, and we demonstrate the important role of thermal fluctuation in the origin of the giant Hall conductivity. This work provides a platform to understand the complex magnetic structure and topological properties of Kagome magnets for future spintronic devices.

MA 16: Frustrated Magnets

Time: Tuesday 15:00–17:45

Location: H37

MA 16.1 Tue 15:00 H37

Another Exact Ground State of a 2D Quantum Antiferromagnet — •PRATYAY GHOSH, TOBIAS MÜLLER, and RONNY THOMALE — Institut für Theoretische Physik und Astrophysik und Würzburg-Dresden Cluster of Excellence ct.qmat, Universität Würzburg, Am Hubland Campus Süd, Würzburg 97074, Germany

We present the exact dimer ground state of a quantum antiferromagnet on

the maple-leaf lattice. A coupling anisotropy for one of the three inequivalent nearest-neighbor bonds is sufficient to stabilize the dimer state. Together with the Shastry-Sutherland Hamiltonian, we show that this is the only other model with an exact dimer ground state for all two-dimensional lattices with uniform tilings.

MA 16.2 Tue 15:15 H37

Pseudo-Majorana approach to Spin-Systems: Advanced Diagrammatics and Applications — •BJÖRN SBIERSKI — LMU München, Germany

Frustrated three-dimensional quantum magnets bear a rich phenomenology but are notoriously hard to treat theoretically. We show how a $SO(3)$ Majorana representation of spin operators, in combination with advanced diagrammatic techniques like the functional renormalization group or the parquet approximation allows for quantitative simulations at finite temperatures. We apply our method on various frustrated Heisenberg magnets. On the cubic lattice, we study magnetic phase transitions via finite-size scaling and we also present results for the Pyrochlore lattice. We also show how the method can be applied to meet some challenges of long-range interacting spin Hamiltonians arising in the context of Rydberg atom array quantum simulators.

Based on: [1] PRB 103.104431 (2021) [2] SciPost Phys. 12, 156 (2022)

MA 16.3 Tue 15:30 H37

Dynamical Spin Structure Factor of the spin- $\frac{1}{2}$ $J_1 - J_2$ Heisenberg Model on the Triangular Lattice — •MARKUS DRESCHER¹, LAURENS VANDERSTRAETEN², RODERICH MOESSNER³, and FRANK POLLMANN^{1,4} — ¹TU München, 85748 Garching, Germany — ²University of Ghent, 9000 Ghent, Belgium — ³Max-Planck-Institut für Physik komplexer Systeme, 01187 Dresden, Germany — ⁴Munich Center for Quantum Science and Technology, 80799 Munich, Germany

The spin- $\frac{1}{2}$ Heisenberg model with antiferromagnetic nearest and next-to-nearest neighbour interactions on a triangular lattice exhibits—driven by the highly frustrated spins—a rich phase diagram and is relevant for various two-dimensional quantum materials. Using large-scale density matrix renormalization group simulations and time evolution algorithms for matrix product states, we obtain the dynamical spin structure factor of the triangular $J_1 - J_2$ Heisenberg model depicting the low-energy excitations both in the 120° -ordered phase at $J_2 = 0$ and the spin liquid phase at $J_2/J_1 = 0.125$. This method allows us to compare the low-energy properties of the isotropic Heisenberg model with previous analytical and numerical approaches.

In the ordered phase, we observe avoided decay of the lowest magnon branch. Our findings in the spin-liquid phase support the field-theoretical predictions by Song *et al.* [1,2], in particular the emergence of low-lying monopole excitations at the corners of the Brillouin zone. [1] X.-Y. Song *et al.*, Nat. Comm. **10**, 4254 (2019).

[2] X.-Y. Song *et al.*, Phys. Rev. X **10**, 011033 (2020).

MA 16.4 Tue 15:45 H37

An Exact Chiral Amorphous Spin Liquid — •PERU D'ORNELLAS¹, TOM HODSON¹, GINO CASSELLA¹, JOHANNES KNOLLE^{1,2,3}, and WILLIAN NATORI⁴ — ¹Blackett Laboratory, Imperial College London, London SW7 2AZ, United Kingdom — ²Department of Physics TQM, Technische Universität München, James-Frank-Straße 1, D-85748 Garching, Germany — ³Munich Center for Quantum Science and Technology (MCQST), 80799 Munich, Germany — ⁴Institut Laue-Langevin, BP 156, 41 Avenue des Martyrs, 38042 Grenoble Cedex 9, France

The conventional wisdom has been that amorphous lattice structure would provide an obstacle to the formation of a long-range entangled ground states because of the inherent geometric disorder. Recently, symmetry protected topological phases have been proposed in non-interacting amorphous systems, raising the question of whether it is possible to construct a topologically ordered quantum many-body phase on an amorphous lattice. Here we provide such an example. We extend the Kitaev honeycomb Hamiltonian to amorphous lattices, constructed using the Voronoi method on a set of random points. The resulting model retains its exact solubility, displaying Abelian as well as a non-Abelian quantum spin liquid phases. However, the presence of plaquettes with an odd number of sides leads to a spontaneous breaking of time reversal symmetry, opening a gap in the non-Abelian phase. Furthermore, we show that the system undergoes a finite-temperature phase transition to a conducting thermal metal state. Possible experimental realisations in metal-organic frameworks are discussed.

MA 16.5 Tue 16:00 H37

Hole Spectral Function of a Chiral Spin Liquid in the Triangular Lattice Hubbard Model — •WILHELM KADOW^{1,2}, LAURENS VANDERSTRAETEN³, and MICHAEL KNAP^{1,2} — ¹Department of Physics, Technical University of Munich, 85748 Garching, Germany — ²Munich Center for Quantum Science and Technology (MCQST), Schellingstr. 4, 80799 München, Germany — ³Department of Physics and Astronomy, Ghent University, B-9000 Ghent, Belgium

Quantum spin liquids are fascinating phases of matter, hosting fractionalized spin excitations and unconventional long-range quantum entanglement. These exotic properties, however, also render their experimental characterization challenging and finding ways to diagnose quantum spin liquids is therefore a pertinent challenge. Here, we numerically compute the spectral function of a single hole doped into the half-filled Hubbard model on the triangular lattice using techniques based on matrix product states. At half filling the system has been proposed to realize a chiral spin liquid at intermediate interaction strength, surrounded by a magnetically ordered phase at strong interactions and a supercon-

ducting/metallic phase at weak interactions. We find that the spectra of these phases exhibit distinct signatures. By developing appropriate parton mean-field descriptions, we gain insight into the relevant low energy features. Our results suggest that the hole spectral function, as measured by Angle-Resolved Photoemission Spectroscopy (ARPES), provides a useful tool to characterize quantum spin liquids.

MA 16.6 Tue 16:15 H37

The nature of visons in the perturbed ferromagnetic and antiferromagnetic Kitaev honeycomb models — CHUAN CHEN¹ and INTI SODEMANN VILLADIEGO^{2,3} — ¹Institute for Advanced Study, Tsinghua University, 100084 Beijing, China — ²Institut für Theoretische Physik, Universität Leipzig, 04103 Leipzig, Germany — ³Max-Planck Institute for the Physics of Complex Systems, 01187 Dresden, Germany

The Kitaev honeycomb model hosts a fascinating fractionalized state of matter that features emergent Majorana fermions and a vison particle that carries the flux of an emergent gauge field. In the exactly solvable limit, these visons are static, but perturbations can induce their motion.

We show that the nature of the vison motion is sharply distinct in the ferromagnetic vs the anti-ferromagnetic Kitaev models. Namely, in the ferromagnetic model the vison has a trivial non-projective translational symmetry, whereas in the anti-ferromagnetic Kitaev model it has a projective translational symmetry with π -flux per unit cell. The visons of the FM case have zero Berry curvature, and no associated intrinsic contribution to the Thermal Hall effect. In contrast, in the AFM case and under a Zeeman perturbing field, there are two gapped vison bands with opposite Chern numbers and an associated intrinsic vison contribution to the Thermal Hall effect. We will comment on other results in the literature that are in disagreement with ours (arXiv:2109.00250, 2021) and discuss the potential connections of our findings to the physics of the spin liquid candidate α -RuCl₃.

MA 16.7 Tue 16:30 H37

Magnetism in a distorted kagome lattice: the case of Y-kapellasite — •ALEKSANDAR RAZPOPOV¹, MAX HERRING², FRANCESCO FERARRI¹, IGOR MAZIN³, ROSER VALENTI¹, HARALD JESCHKE⁴, and JOHANNES REUTHER² — ¹Goethe University, Frankfurt, Germany — ²Free University of Berlin, Berlin, Germany — ³George Mason University, Washington DC, United States — ⁴Okayama University, Okayama, Japan

Compounds like the well-known Herbertsmithite are examples of the ideal spin-1/2 antiferromagnetic (AFM) kagome lattice which has one of the most interesting magnetic phase diagrams. However, while the perfect AFM kagome lattice has been extensively investigated, less is known about distorted kagome lattices.

Here we focus on an unexplored distorted spin-1/2 kagome lattice with three symmetry-inequivalent nearest-neighbor AFM Heisenberg couplings. The recently synthesized Y-kapellasite $Y_3Cu_9(OH)_{19}Cl_8$ is a realization of such a distorted lattice. First, we analyse the classical magnetic phase diagram using analytical arguments and numerical methods, and find a rich classical phase diagram with a $Q=0$ magnetic phase, $Q=(1/3,1/3)$ non-collinear coplanar magnetic phases and a classical spin liquid regime. In a second step we estimate the effective magnetic Heisenberg Hamiltonian by total-energy mapping analysis within the FPLO framework. Using the extracted Heisenberg Hamiltonian we predict Y-kapellasite to be localized in the $Q=(1/3,1/3)$ phase which is stable after inclusion of quantum effects.

MA 16.8 Tue 16:45 H37

Thermodynamic and magnetic properties of the rare-earth delafossite NaGdS₂ — •JUSTUS GRUMBACH¹, MATHIAS DOERR¹, ELLEN HAEUSSLER², and SERGEY GRANOVSKY¹ — ¹Institut für Festkörper- und Materialphysik, Technische Universität Dresden, 01062 Dresden, Germany. — ²Fakultät für Chemie und Lebensmittelchemie, Technische Universität Dresden, 01062 Dresden, Germany

Rare-earth delafossites are materials containing ideal triangular magnetic planes which are frustrated. Due to their properties, rare-earth delafossites are promising candidates for a QSL ground state. In recent years, research has focused on $S = \frac{1}{2}$ delafossites where either QSL or AFM ground states occur, with transitions in the mK range (e.g. [1] vs. [2]).

Now a number of new measurements have been made on NaGdS₂ single crystals with the pure spin moment $J = S = \frac{7}{2}$ of the Gd³⁺ magnetic ion. Measurements of several thermodynamic and magnetic properties were performed on very small samples (size $\sim \mu\text{m}$) down to 40 mK. Essential physical data could be extracted which consistently show a magnetic ordered AFM ground state below ~ 200 mK.

[1] G. Bastien *et al.*, SciPost Phys. **9**, 041 (2020)

[2] M. Baenitz *et al.*, Phys Rev B **98**, 220409(R) (2018)

MA 16.9 Tue 17:00 H37

Single crystal study of the magnetic phase diagrams in $\text{BaCo}_2(\text{PO}_4)_2$ — •XIAO WANG¹, ROHIT SHARMA¹, PETRA BECKER-BOHATÝ², LADISLAV BOHATÝ², and THOMAS LORENZ¹ — ¹II. Physikalisches Institut, Universität zu Köln, Zùlpicher Straße 77, Köln, Germany — ²Abteilung Kristallographie, Institut für Geologie und Mineralogie, Universität zu Köln, Zùlpicher Straße 49b, Köln, Germany

The study of the Kitaev materials has been an active area in the past decades, mainly motivated by their novel physical properties such as topological order, exotic excitations and potential application for quantum computing. Motivated by recent theoretical proposals that Kitaev model might be realized in 3d transition-metal compounds, we have successfully synthesized single crystal samples of $\text{BaCo}_2(\text{PO}_4)_2$. Our work on the high-quality $\text{BaCo}_2(\text{PO}_4)_2$ sample unveils a sharp phase transition at $\sim 3.5\text{K}$ which signals the evolution of antiferromagnetic long-range order in zero magnetic field. Such a transition is not observed in previous studies on polycrystalline $\text{BaCo}_2(\text{PO}_4)_2$ [3], while for a $T_N = 5.4\text{K}$ is reported for $\text{BaCo}_2(\text{AsO}_4)_2$ [4]. Here we present a comprehensive study of the magnetic phase transitions by magnetization, specific heat and thermal expansion measurements and construct the magnetic phase diagram of $\text{BaCo}_2(\text{PO}_4)_2$. This work is funded by the DFG via CRC 1238 Projects A02 and B01.

[1] A. Kitaev, Ann. Phys. (N. Y.), 321, 2 (2006) [2] H. Liu, et al. Phys. Rev. Lett. 125, 3 (2020) [3] H. S. Nair, et al. Phys. Rev. B 97, 1 (2018) [4] R. Zhong, et al. Sci. Adv. 6, 1 (2020)

MA 16.10 Tue 17:15 H37

Resonant X-ray and neutron investigation of the double perovskite $\text{Nd}_2\text{ZnIrO}_6$ — •FABIAN STIER, MAREIN RAHN, and JOCHEN GECK — Institut für Material- und Festkörperphysik, TU Dresden, Deutschland

We present a study of the magnetic order in the double perovskite $\text{Nd}_2\text{ZnIrO}_6$ as a function of temperature and magnetic field. This material contains Ir with a formal valence of 4+, which is very often described in terms of localized $j=1/2$

states. The magnetism of such $j=1/2$ states has attracted much attention, especially in relation to the possible formation of quantum spin liquids in actual materials. In order to elucidate the magnetism of the Nd 4f- and the Ir 5d-electrons in $\text{Nd}_2\text{ZnIrO}_6$, we performed resonant magnetic x-ray scattering and neutron powder diffraction. Below $T_N=15\text{K}$ we observe magnetic order with propagation vector (0.5 0.5 0) and moments in the ab plane. The temperature dependence reveals the Ir moment as the driving force of the magnetic ordering below T_N . Applying a magnetic field along the crystallographic a-direction at $T=5\text{K}$ causes a metamagnetic transition to a phase with a propagation vector (0 0 0). Interestingly, applying the magnetic field along the crystallographic c-direction shows a linear field dependence.

MA 16.11 Tue 17:30 H37

Pressure induced multicritical behaviour in a kagome ferromagnet — •ARVIND MAURYA — Max Planck Institute for Solid State Research, Heisenbergstrasse 1, 70569 Stuttgart, Germany

We report high quality single crystal growth of ferromagnet URhSn , crystallizing in ZrNiAl -type hexagonal structure in which the magnetic U-atoms form potentially frustrated quasi-kagome two-dimensional net. Our measurements of electrical transport under hydrostatic pressures up to 11 GPa reveals two bicritical points concurrent at $P_C = 6.25\text{GPa}$ corresponding to its successive double phase transitions ($T_O = 54\text{K}$, $T_C = 18\text{K}$ at ambient). Remarkably, the intermediate phase remains hidden as local probes like neutron scattering and Mössbauer spectra do not capture any new feature across the T_O . Our low temperature resistivity data under pressure points out a Fermi surface reconstruction across the P_C , corresponding to an unconventional class of quantum phase transition involving multicritical points. This picture is further ascertained by gradual development of $-\ln T$ behavior in 5f-derived electrical resistivity and appearance of $T^{5/3}$ dependence in the pressure induced phase.

MA 17: PhD Focus Session: The Hitchhiker's Guide to Spin Phenomena at the Space and Time Limit

The growing hunger of society for fast data storage and processing, together with the end of Moore's law, demand the development of new technologies to implement smaller, faster and more power-efficient devices. Research in magnetic materials has shown the potential of spin-based devices in this regard. Pushing for 'More than Moore' devices, space and time limits need to be tackled. At the heart of this research are three fundamental operations: Control of magnetic order, spin transport and efficient monitoring of spin angular momentum in space and time. Topical clusters ranging from ferro- to antiferromagnets up to 2D materials, magnetic-organic interfaces and heterostructures are extensively studied. New materials and concepts are being developed rapidly which can appear very complex to someone new to the field. Young researchers often manage to get an overview of their own specific field but lack the big picture. For this reason, this PhD symposium will focus on talks in mostly tutorial-like style, yet will also include recent highlights. In addition, the symposium aims to exchange ideas and foster discussions on a broad range of spin phenomena.

Organizers: Yannic Behovits (Physics, Freie Universität Berlin and Fritz Haber Institute of the MPS), Mona Bhukta (Physics, Johannes Gutenberg University Mainz), Bikash Das Mohapatra (Physik, Martin-Luther-Universität Halle-Wittenberg), Oliver Gueckstock (Physics, Freie Universität Berlin and Fritz Haber Institute of the MPS), Hendrik Meer (Physics, Johannes Gutenberg University Mainz), Maximilian Paleschke (Physik, Martin-Luther-Universität Halle-Wittenberg), Eva S. Walther (Physics, Technische Universität Kaiserslautern).

Time: Tuesday 15:00–17:00

Location: H43

Invited Talk

MA 17.1 Tue 15:00 H43

Ultimately fast, small and energy-efficient magnetism: fundamentals and prospects — •JOHAN MENTINK — Radboud University, Nijmegen, The Netherlands

Findings ways to switch between magnetically ordered states at the smallest possible length and time scale, while simultaneously dissipating the least amount of energy is a major challenge in magnetism. One of the most appealing routes to achieve this goal is by bringing a magnetic system strongly out of equilibrium, after which the dynamics is driven by exchange interaction, the strongest force in magnetism. Although this has been extensively discussed in ferrimagnetic systems, harnessing such exchange-driven dynamics in ferromagnets is fundamentally limited by angular momentum conservation. We will discuss basic models of magnetism that can be solved even under strongly nonequilibrium conditions and have been key to identify the mechanisms for ultrafast switching. We will exemplify this for chiral ferromagnets as studied by recent XFEL experiments. For this case, the nonequilibrium dynamics is driven by an additional antisymmetric exchange interaction, resulting in ultrafast nucleation of nanoscale magnetic skyrmions. This opens a new path for switching that is not only fast, but also can operate at the nanoscale. By comparing with the fundamental energy-speed limits for switching between physically distinct states, we will argue that such

exchange-driven dynamics can be key to achieve even faster, smaller and much more energy-efficient switching than demonstrated so far.

Invited Talk

MA 17.2 Tue 15:30 H43

From spintronics at limiting temporal and spatial scales in antiferromagnets to an emerging altermagnetic phase — •TOMAS JUNGWIRTH — Institute of Physics, Czech Academy of Sciences and University of Nottingham, UK

Magnetically ordered crystals are traditionally divided into two basic phases – ferromagnetism and antiferromagnetism. In the first part of the talk, we will recall that the ferromagnetic order offers a range of phenomena and existing device applications, while the vanishing net magnetization in antiferromagnets is potentially favorable for temporal and spatial scalability of spintronic devices. In the second part of the talk we will move on to the recent predictions of instances of strong time-reversal symmetry breaking and spin splitting in electronic bands, typical of ferromagnetism, in crystals with antiparallel compensated magnetic order, typical of antiferromagnetism. This apparent fundamental conflict in magnetism is resolved by symmetry considerations that allow us to classify and describe a third basic magnetic phase. Its alternating spin polarizations in both crystal-structure real space and electronic-structure momentum space suggest a term altermagnetism. We will demonstrate that altermag-

nets combine merits of ferromagnets and antiferromagnets, that were regarded as principally incompatible, and have merits unparalleled in either of the two traditional basic magnetic phases. We will show that they underpin a development of a new avenue in spintronics based on strong non-relativistic spin-conserving phenomena, without magnetization imposed scalability limitations, and with complex logic-in-memory functionalities.

Invited Talk

MA 17.3 Tue 16:00 H43

An electronic structure viewpoint on candidate van der Waals ferromagnets

— •PHIL KING¹, MATT WATSON¹, BRENDAN EDWARDS¹, AKHIL RAJAN¹, JIAGUI FENG¹, DEEP BISWAS¹, MONICA CIOMAGA HATNEAN², AMELIA HALL², GEETHA BALAKRISHNAN², GIOVANI VINAI³, DAVID BURN⁴, THORSTEN HESJEDAL⁵, GERIT VAN DER LAAN⁴, OLIVER DOWINTON⁶, and SAEED BAHRAMY⁶ — ¹Univ. St Andrews — ²Univ. Warwick — ³ Elettra synchrotron — ⁴Diamond Light Source — ⁵Univ. Oxford — ⁶Univ. Manchester

Control over materials thickness down to the single-atom scale has emerged as a powerful tuning parameter for manipulating both single-particle band structures and collective states of solids. Magnetism is a new frontier in the study of 2d materials. Here, I will show how direct measurement of the electronic structure using angle-resolved photoemission (ARPES) can lead to valuable insight not only into whether a 2d material exhibits long-range magnetic order, but also on its microscopic mechanisms. I will consider monolayer VSe₂, where a putative magnetic order is destabilised by the formation of a robust charge density wave,^{1,2} but can be re-established via proximity coupling,³ V_{1/3}NbS₂, where proximity coupling to the surface layer can lead to a modulation of spin-valley locking, and CrGeTe₃, an established van der Waals ferromagnet, where band structure measurements provide important microscopic insights even in a local

moment system.⁴ ¹Rajan et al., Phys. Rev. Materials 4 (2020) 014003; ²Feng et al., Nano Lett. 18 (2018) 4493; ³Vinai et al., Phys. Rev. B 101 (2020) 035404; ⁴Watson et al., Phys. Rev. B 101 (2020) 205125.

Invited Talk

MA 17.4 Tue 16:30 H43

Nano-scale skyrmions and atomic-scale spin textures studied with STM

— •KIRSTEN VON BERGMANN — Department of Physics, University of Hamburg, Germany

Non-collinear magnetic order arises due to the competition of different magnetic interactions. Often the dominant interaction is the isotropic pair-wise exchange between neighboring atomic magnetic moments. An additional sizable contribution from anisotropic exchange (Dzyaloshinskii-Moriya-Interaction) typically leads to spin spiral ground states in the absence of magnetic fields. In applied magnetic fields such systems can transition into skyrmion lattices or isolated skyrmions with diameters down to a few nanometers.

In zero magnetic field single skyrmions can arise as metastable states, stabilized by frustrated exchange interactions, which originate from competing non-negligible exchange interaction to more distant magnetic moments [1]. Periodic two-dimensionally modulated magnetic states on the atomic scale can arise due to higher-order magnetic interactions. Such higher-order interactions can favor superpositions of spin spirals, so called multi-q states. Depending on the sample system atomic scale non-collinear magnetic lattices of different symmetry and size can form [2]. Higher-order interactions can also determine the type and width of domain walls in antiferromagnets [3].

[1] S. Meyer et al., Nature Commun. 10, 3823 (2019).

[2] M. Gutzeit et al., arXiv:2204.01358.

[3] J. Spethmann et al., Nature Commun. 12, 3488 (2021).

MA 18: Spintronics

Time: Tuesday 15:00–17:15

Location: H47

MA 18.1 Tue 15:00 H47

Multilayer on-chip spintronic THz emitters

— •WOLFGANG HOPPE¹, MOHAMED AMINE WAHADA², STUART S. P. PARKIN², and GEORG WOLTERS DORF¹ — ¹Institute of Physics, Martin Luther University Halle-Wittenberg, Von-Dankelmann-Platz 3, 06120 Halle, Germany — ²Max Planck Institute for Microstructure Physics, Weinberg 2, 06120 Halle, Germany

Nanometer thin ferromagnet/heavy metal bilayers illuminated by intense, short laser pulses have proven to be a reliable source for THz emission [1]. When integrated into a gold waveguide structure, the bilayer can be used as an on-chip source for ultrafast current pulses, ranging from the GHz to the THz regime [2]. One possible application is the switching of the magnetization of an adjacent magnetic layer [3]. A way to achieve the needed threshold current density is by increasing the amplitude of the current-pulses. This can be accomplished by stacking the bilayers, each separated by a thin MgO interlayer impeding the formation of any spin-currents in between the individual bilayers [4]. Here, the charge current in all bilayers can add, leading to an enhanced signal. We demonstrate an increase by a factor of three for the optimal stacking configuration. The multilayers are investigated by electro-optic sampling.

[1] Seifert et al. Nature Photon 2016, 10, 483-488

[2] W. Hoppe et al. ACS Appl. Nano Mater. 2021, 4, 7, 7454-7460

[3] Y. Yang et al. Sci. Adv. 2017, 3, 11

[4] M. A. Wahada et al. ACS Nano Lett. 2022, 22, 9, 3539-3544

MA 18.2 Tue 15:15 H47

Ab initio studies of chiral crystals for generalized linear response transport and x-ray absorption spectroscopy

— •ALBERTO MARMODORO¹, HUBERT EBERT², and ONDŘEJ ŠÍPR^{1,3} — ¹Institute of Physics (FZU) of the Czech Academy of Sciences, Prague, Czech Republic — ²Department of Chemistry, Ludwig-Maximilians-University (LMU), Munich, Germany — ³New Technologies Research Centre, University of West Bohemia, Pilsen, Czech Republic

Materials with a chiral atomic arrangement exhibit specific electronic structure features [1]. The clock-wise or anti-clock-wise winding of sublattices has been associated with a radial spin texture of the Fermi surface in reciprocal space [2]. This provides interesting consequences for the response [3] to e.g. an applied electric field, for instance in terms of Edelstein effect and particularly its dependence on the sign of the perturbation. We report generalized linear response predictions [3] and theoretical x-ray spectroscopy cross-sections [4] for inorganic bulk crystals from first-principles studies performed within the frameworks of a spin-polarized relativistic Korringa, Kohn, Rostoker (SPRKKR) treatment.

[1] <http://dx.doi.org/10.7566/JPSJ.83.061018>

[2] <http://dx.doi.org/10.1103/physrevlett.127.126602>, <http://dx.doi.org/10.1038/s42005-021-00564-w>

[3] <http://dx.doi.org/10.1103/PhysRevB.91.165132>

[4] <http://dx.doi.org/10.1107/S090904959801680X>

MA 18.3 Tue 15:30 H47

Studying Spin Dynamics of Thin Cr₂Ge₂Te₆, using Superconducting Resonators

— •CHRISTOPH W. ZOLLITSCH¹, SAFE KHAN¹, NAM VU THANH TRUNG², DIMITRIOS SAGKOVITS¹, IVAN VERZHBITSKIY², GOKI EDA², and HIDEKAZU KUREBAYASHI¹ — ¹London Centre for Nanotechnology, University College London, London WC1H 0AH, United Kingdom — ²Department of Physics, National University of Singapore, 2 Science Drive 3, Singapore 117551

Two-dimensional van der Waals material systems gained an increased interest in the field of spintronics, as they can maintain ferromagnetic order even down to the few monolayer regime. These materials naturally permit device miniaturization. An ideal test bed for new spintronics applications in the 2D limit is the ferromagnetic semiconductor Cr₂Ge₂Te₆, where intrinsic ferromagnetism has been discovered for atomic bilayers [1].

We investigate the spin dynamics of thin exfoliated flakes (11 - 150 nm) of Cr₂Ge₂Te₆, using superconducting lumped element resonators made of NbN. The flakes are transferred directly on top of several superconducting resonator structures, featuring resonance frequencies from 12 GHz to 18 GHz. We perform ferromagnetic resonance (FMR) at a temperature of 1.8 K and can easily resolve the response from the flakes, even down to a thickness of 11 nm. With our multi-resonator approach, can confirm a Kittel FMR behaviour for the full thickness range. The FMR data can very well be described with bulk values of the magnetic parameters.

[1] Cheng Gong et al., Nature 546, 265-269 (2017)

MA 18.4 Tue 15:45 H47

Spin wave spectrum asymmetry from nonlocal chiral renormalization of gyromagnetic ratio

— •IVAN ADO^{1,2} and MIKHAIL TITOV² — ¹Institute for Theoretical Physics, Utrecht University, 3584 CC Utrecht, The Netherlands — ²Institute for Molecules and Materials, Radboud University, 6525 AJ Nijmegen, The Netherlands

We present a new potential source of the spin wave spectrum asymmetry in metallic and semiconducting magnets. Such an asymmetry is often used to experimentally measure the Dzyaloshinskii-Moriya interaction (DMI) strength using Brillouin light scattering (BLS). We argue that there exists an additional contribution to the asymmetry that originates in coupling between magnetic moments and charge carriers. Moreover, this contribution is sensitive to electron scattering by impurities and depends on the parameters of the electron diffusive motion. We address the corresponding mechanism as "nonlocal chiral renormalization of gyromagnetic ratio". We analyze it both microscopically and using symmetry arguments, for a prototypical 2D metallic ferromagnet. The resulting contribution to the asymmetry scales quadratically with the scattering time and thus can be particularly strong in sufficiently clean systems. We suggest that experimental measurements of DMI by means of BLS may be inaccurate if one does not take this effect into account.

MA 18.5 Tue 16:00 H47

Influence of dusting layers on the magneto-ionic response of Ta/X/CoFeB/Y/MgO/HfO₂ thin film stacks — •TANVI BHATNAGAR-SCHÖFFMANN¹, AURÉLIE SOLIGNAC², DJOUDI OURDANI³, ROHIT PACHAT¹, MARIA-ANDROMACHI SYSKAKI⁵, YVES ROUSSIGNÉ³, SHIMPEI ONO⁶, DAFINÉ RAVELOSONA⁴, JÜRGEN LANGER⁵, MOHAMED BELMEGUENAI³, and LIZA HERRERA DIEZ¹ — ¹Centre de Nanosciences et de Nanotechnologies, CNRS, Université Paris-Saclay, 91120 Palaiseau, France — ²Université Paris-Saclay, CEA, CNRS, SPEC, 91191, Gif-sur-Yvette, France — ³Laboratoire des Sciences des Procédés et des Matériaux, CNRS-UPR 3407, Université Paris 13, Sorbonne Paris Cité, 93430 Villetaneuse, France — ⁴Spin-Ion Technologies, C2N, 10 Boulevard Thomas Gobert, 91120 Palaiseau, France — ⁵Singulus Technologies AG, Hanauer Landstrasse 103, 63796 Kahl am Main, Germany — ⁶Central Research Institute of Electric Power Industry, Yokosuka, Kanagawa 240-0196, Japan

Here, we present the room temperature magneto-ionic control of magnetic anisotropy, coercivity and DMI in Ta/X/CoFeB/Y/MgO/HfO₂, where X and Y are dusting layers of heavy metal elements (Pt, W) sharing different interfaces with CoFeB. Dusting layers at the bottom interface (Y) can define a system locked in a PMA state allowing for a reversible magneto ionic control of coercivity, while samples with dusting layers at the top interface (X) can allow for a full and reversible spin-reorientation transition. The intercalation of dusting layers of heavy metal elements in Ta/CoFeB/MgO stacks has the potential to fine tune magnetic properties.

MA 18.6 Tue 16:15 H47

Anisotropic magnetoresistance in systems with non-collinear magnetic order — •PHILIPP RITZINGER and KAREL VYBORNÝ — Institute of Physics of the Czech Academy of Sciences, Na Slovance 1999/2, 182 21 Prague 8, Czech Republic

Since its discovery in 1857 by William Thomson, the anisotropic magnetoresistance (AMR) has been in focus of many theoretical studies seeking to understand the microscopic mechanisms of this effect. Most attention has been paid to ferromagnets (FMs) and recently, the scope of research on AMR is extended to include also antiferromagnets (AFMs). AMR can be due to anisotropic scattering (extrinsic) or an anisotropic Fermi surface (intrinsic). Here we focus on the latter, much less investigated intrinsic mechanism, which is achieved by considering non-collinear magnetic order inspired by real materials such as CrSe, delta-FeMn, Mn₃Ge or RbFe(MoO₄)₂. We explore various types of lattices on toy model level amongst which are trigonal, tetrahedral or Kagome lattice. Magnetic moments can be arranged in many different ways on such lattices and seemingly small changes alter the Fermi surface symmetry, spin texture and transport properties. We have investigated systematically the influence of magnetic ordering on these properties which allows to predict general features of spin texture and transport by only considering the symmetry of the underlying system. As an example of these effects we have shown that AFM systems without spin-orbit coupling on Kagome lattices can develop anisotropy in the electric conductivity under applied in-plane magnetic field. This does not occur in FMs without spin-orbit coupling.

MA 18.7 Tue 16:30 H47

Spin-split collinear antiferromagnets: a large-scale ab-initio study — •YAQIAN GUO¹, HUI LIU^{1,2}, OLEG JANSON¹, COSMA FULGA^{1,2}, JEROEN VAN DEN BRINK^{1,2}, and JORGE I. FACIO^{1,3,4} — ¹Leibniz Institute for Solid State and Mate-

rials Research, IFW Dresden, 01069 Dresden, Germany — ²Würzburg-Dresden Cluster of Excellence ct.qmat, Technische Universität Dresden, 01062 Dresden, Germany — ³Centro Atómico Bariloche and Instituto Balseiro, CNEA, 8400 Bariloche, Argentina — ⁴Instituto de Nanociencia y Nanotecnología CNEA-CONICET, Argentina

Collinear antiferromagnetic (cAFM) materials can break the spin degeneracy in momentum space based on their magnetic symmetry, giving rise to the so called AFM-induced spin splitting. In this mechanism, spin splitting originates neither from a non-zero net magnetization (Zeeman effect) nor spin-orbit coupling (SOC) in noncentrosymmetric materials (Rashba-Dresselhaus effect), but from the magnetic symmetries. In this work, we performed a systematic analysis for 62 cAFM compounds and investigated the AFM-induced spin splitting without considering SOC. We established three measures to analyze the average spin splitting. Based on our measures, we identified the compounds with sizable spin splitting, such as CoF₂ and FeSO₄F, and analyzed their electronic structure in detail. A similar analysis was performed for particular low-dimensional magnets, e.g. LiFe₂F₆ and antiferromagnetic metals with spin splitting, e.g. RuO₂, CrNb₄S₈ and CrSb.

MA 18.8 Tue 16:45 H47

Superparamagnetic tunnel junctions for neuromorphic computing — •LEO SCHNITZSPAN^{1,2}, GERHARD JAKOB^{1,2}, and MATHIAS KLÄUI^{1,2} — ¹Institut für Physik, Johannes Gutenberg Universität Mainz — ²Max Planck Graduate Center, Mainz

Superparamagnetic tunnel junctions (SMTJ) are promising candidates for the implementation of neuromorphic computing. In a SMTJ, the magnetic free layer can switch its orientation induced by thermal activation, leading to a random two-level resistance fluctuation with relaxation times in the order of a few nanoseconds [1]. Their intrinsic stochastic behaviour and additional tunability by external magnetic fields, Spin Transfer Torques (STT) or Spin Orbit Torques (SOT) are key ingredients for low-energy artificial neurons in neural networks. Non-conventional computing, like inverse logic for integer factorization already has been demonstrated based on SMTJs [2]. Measurements of the characteristic stochastic switching behaviour are highlighted and the quality of randomness (according to NIST Statistical Test Suite) for a SMTJ as a potential true random number generator is evaluated. New possible implementation ideas of a stochastic neural network based on SMTJs are proposed and their efficiency is studied in detail.

[1] Hayakawa, K. et al., Phys. Rev. Lett. 126, 117202 (2021). [2] Borders, W. A. et al., Nature 573, 390-393 (2019).

MA 18.9 Tue 17:00 H47

Simulation of Polymer Spintronics — •SHIH-JYE SUN — National University of Kaohsiung, Kaohsiung, Taiwan

We proposed a two-level model to simulate the spin-polarization current and the mobility in a field-effect transistor constructed by an antiferromagnetic-coupling polymer chain connected with the source, drain electrodes, and the oxide gate. This model is beyond the single-level model because of considering the inducing states in the polymer host by adding the magnetic functional side groups. We found that the double Coulombic excitations sensitively depend on the inducing states in the model significantly influencing the spin-polarization current and the mobility. Eventually, the workable organic spintronics can be realized based on our simulations.

MA 19: Poster 1

Topics: Skyrmions (MA 19.1-19.8), Non-Skyrmionic Magnetic Textures (MA 19.9-19.10), Caloric Effects in Ferromagnetic Materials (MA 19.11-19.15), Spin Calorics (general)(MA 19.16-19.17), Molecular Magnetism (19.18-19.22), Biomagnetism, Biomedical Applications (MA 19.23), Electron Theory of Magnetism and Correlations (MA 19.24), Magnetic Imaging Techniques (MA 19.25-19.29), Neuromorphic Magnetism / Magnetic Logic (MA 19.30-19.31), Computational Magnetism (MA 19.32-19.38), Spin Transport and Orbitronics, Spin-Hall Effects (MA 19.39-19.45), Terahertz Spintronics (MA 19.46-19.54), Spin-Dependent Phenomena in 2D (MA 19.55-19.56), Spintronics (other effects) (MA 19.57-19.61), Functional Antiferromagnetism (MA 19.62-19.64).

Time: Tuesday 17:30–20:00

Location: P2

MA 19.1 Tue 17:30 P2

Magnetic states in the FeGe nanocylinder — •ANDRII SAVCHENKO^{1,2}, FENGSHAN ZHENG^{3,4}, NIKOLAI KISELEV¹, LUYAN YANG³, FILIPP RYBAKOV⁵, STEFAN BLÜGEL¹, and RAFAL DUNIN-BORKOWSKI³ — ¹Peter Grünberg Institute and Institute for Advanced Simulation, Forschungszentrum Jülich and JARA, 52425 Jülich, Germany — ²Donetsk Institute for Physics and Engineering, NAS of Ukraine, 03028 Kyiv, Ukraine — ³Ernst Ruska-Centre for Microscopy and Spectroscopy with Electrons and Peter Grünberg Institute, Forschungszentrum Jülich, 52425 Jülich, Germany — ⁴Spin-X Institute, School of Physics and

Optoelectronics, State Key Laboratory of Luminescent Materials and Devices, Guangdong-Hong Kong-Macao Joint Laboratory of Optoelectronic and Magnetic Functional Materials, South China University of Technology, Guangzhou 511442, China — ⁵Department of Physics and Astronomy, Uppsala University, SE-75120 Uppsala, Sweden

Magnetic states in a nanocylinder of B20-type FeGe are studied using off-axis electron holography and micromagnetic simulations [1]. Considering the presence of a damaged layer on the surface of the nanocylinder, which results from focused ion beam milling during sample preparation, we achieved a quantita-

tive agreement between experimental and theoretical images. Remarkably, we identified one of the experimentally observed states as a dipole string composed of two Bloch points of opposite topological charge. 1. A.S. Savchenko et al., arXiv:2205.05753.

MA 19.2 Tue 17:30 P2

Imaging magnetization dynamics in ferromagnetic multilayer systems with Dzyaloshinskii-Moriya interaction, modified by local He⁺ irradiation — •ARNE VEREIJKEN¹, SAPIDA AKHUNDZADA¹, FLORIAN OTT¹, MAXWELL LI², TIM MEWES³, ARNO EHRESMANN¹, VINCENT SOKALSKI², and MICHAEL VOGEL¹ — ¹Institute of Physics and Center for Interdisciplinary Nanostructure Science and Technology (CINaT), University of Kassel, Kassel, Germany — ²Department of Materials Science and Engineering, Carnegie Mellon University, Pittsburgh, USA — ³Department of Physics and Astronomy, University of Alabama, Tuscaloosa, USA

The Dzyaloshinskii-Moriya interaction (DMI) is an asymmetric exchange interaction[1,2] promoting chiral coupling between spins, giving rise to robust, chiral, topological spin textures, e.g., skyrmions with outstanding properties for information storage and processing[3]. DMI may originate, e.g., from the interface between a ferromagnet and a heavy metal. Recently it has been demonstrated that the DMI at such interfaces can be tuned by irradiation with keV He⁺ ions[4]. In a systematic study, we investigated the influence of local He⁺ ion irradiation on the magnetization dynamics in a perpendicularly magnetized ferromagnetic/heavy metal multilayer system by high-resolution magneto-optical Kerr microscopy. [1] T. Moriya, Phys. Rev. Lett. 4, 228 (1960) [2] I. E. Dzyaloshinskii, J. Phys. Chem. Solids 4(4), 241-255 (1958) [3] C. Back et al, J. Phys. D: Appl. Phys. 53 363001 (2020) [4] H. T. Nembach, et al., Int. J. Appl. Phys. 131, 143901 (2022)

MA 19.3 Tue 17:30 P2

Limits of skyrmion detection — •HAUKE LARS HEYEN¹, JAKOB WALOWSKI¹, MALTE RÖMER-STUMM², MARKUS MÜNZENBERG¹, and JEFFREY MCCORD² — ¹Institut für Physik, Universität Greifswald, Felix-Hausdorff-Straße 6, 17489 Greifswald, Germany — ²Christian-Albrechts-Universität zu Kiel, Institute for Materials Science, Nanoscale Magnetic Materials and Magnetic Domains, 24143 Kiel, Germany

Skyrmion detection is an important feature for the implementation in storage media like e.g. racetrack memory. Kerr microscopy is well suited for the detection of skyrmions on the micrometer scale, but can not be miniaturised down to the nanometer scale. To compete with established storage media methods, miniaturisation of detection methods is essential. Magnetic tunnel junctions (MTJ) are a promising tool to detect small magnetisation changes.

The selected Ta/CoFeB/MgO material system allows to build MTJs integrated into tracks in which skyrmions can be generated and moved along using current pulses. This integration of MTJs into skyrmion racetracks remains challenging, even though they work fine independently. We employ Kerr microscopy to investigate the influence of MTJs on the skyrmion generation and propagation.

MA 19.4 Tue 17:30 P2

Exchange- and Dzyaloshinskii-Moriya interactions in magnetic multilayers at surfaces — •TIM DREVELOW, MARA GUTZEIT, and STEFAN HEINZE — Institute of Theoretical Physics and Astrophysics, University of Kiel, Leibnizstraße 15, 24098 Kiel, Germany

The coupling of magnetic skyrmions in synthetic antiferromagnets leads to a significant reduction of skyrmion Hall effect and therefore enhanced transports properties [1]. We investigate antiferromagnets based on Rh/Fe and Rh/Co bilayers on an Ir(111) surface, which have previously been grown on this surface [2,3]. With an additional magnetic layer of Fe or Co, we find that these systems realize a synthetic antiferromagnet as a potential host for magnetic skyrmions. Considerations on the symmetry of magnetic states in multilayer systems allow to compute both exchange and Dzyaloshinskii-Moriya interactions within and in between the magnetic layers with *ab initio* calculations using density functional theory.

[1] Zhang *et al.* Nat. Com. 7, 10293 (2016)

[2] Romming *et al.* Phys. Rev. Lett. 120, 207201 (2018)

[3] Meyer *et al.* Nat. Com. 10, 3823 (2019)

MA 19.5 Tue 17:30 P2

High-resolution in-situ mapping of magnetization dynamics — •ARSHA THAMPI^{1,2}, FELIX LUCAS KERN¹, YEJIN LEE¹, DANIEL WOLF¹, ANDY THOMAS^{1,2}, and AXEL LUBK^{1,2} — ¹Leibniz IFW Dresden, D-01069 — ²Institute for Solid State and Materials Physics, TU Dresden, D-01069

Mapping of magnetization dynamics at the nanometer scale, which includes domain wall motion and also study on magnetic textures like skyrmions, is performed with time resolved measurements using transmission electron microscopy (TEM). On-chip micro-sized magnetic charged particle optical elements were developed for spatiotemporal electron beam modulation. The employed micro-coils with a diameter of about 80 μm are combined with soft-magnetic cores and arranged as dipoles and quadrupoles. These micro-electromagnets can generate alternating magnetic fields of about ± 100 mT up

to hundred MHz. They supply sufficiently large optical power and high-frequency beam manipulation to perform stroboscopic imaging. We discuss stroboscopic magnetization dynamics measurement employing either fast beam blanking or fast focusing. In order to study dynamics of magnetic structures, short electric pulses are applied by means of a sample holder that passes high frequencies. Current driven domain wall motion by spin torque effect is observed in a Nickel system by Lorentz TEM. The shift in domain walls is quantitatively analyzed depending on the current density and the heat deposited on the system. High-resolution mapping of magnetization dynamics can open the way to understand more on defects or pinning sites of domain wall.

MA 19.6 Tue 17:30 P2

Spin dynamics of skyrmion lattices in a chiral magnet resolved by micro-focused Brillouin light scattering — PING CHE¹, •RICCARDO CIOLA², MARKUS GARST², ARNAUD MAGREZ¹, HELMUTH BERGER¹, THOMAS SCHÖNENBERGER¹, HENRIK RØNNOW¹, and DIRK GRÜNDLER¹ — ¹École Polytechnique Fédérale de Lausanne, Lausanne (CH) — ²Karlsruhe Institute of Technology, Karlsruhe (DE) Chiral magnets provide an innovative framework to study non-collinear spin textures and their associated magnetization dynamics. They include helical and conical magnetic textures that are spatially modulated with a wavevector k_h , as well as the topologically non-trivial skyrmion lattice (SkL) phase. So far, different techniques have been used to probe the magnetization dynamics of the latter SkL phase both in the small wavevector limit, $k \ll k_h$, as well as for $k > k_h$. Here, we show that Brillouin light scattering (BLS) is ideally suited to probe the complementary range of wavevectors $k \lesssim k_h$. We study both theoretically and experimentally BLS from bulk spin waves in the SkL phase of Cu_2OSeO_3 . We provide parameter-free predictions for the BLS cross section and compute both the resonances and their spectral weight. The theoretical results are compared to BLS experiments in the backscattering geometry that probe magnons with a wavevector $k = 48/\mu\text{m} < k_h = 105/\mu\text{m}$. The clockwise, counterclockwise and breathing modes are clearly resolved. Due to the finite wavevector of the magnon excitations, finite spectral weight is theoretically predicted also for other resonances. Experimentally, at least one additional resonance can be identified.

MA 19.7 Tue 17:30 P2

Interplay of moderate magnetocrystalline anisotropies and skyrmion lattice order in $\text{Fe}_{1-x}\text{Co}_x\text{Si}$ — •DENIS METTUS¹, GRACE CAUSER¹, ALFONSO CHACON¹, ANDREAS BAUER¹, CHRISTIAN FRANZ¹, ANNA SOKOLOVA², SEBASTIAN MÜHLBAUER³, and CHRISTIAN PFLIEDERER¹ — ¹Physik-Department, Technische Universität München, D-85748 Garching, Germany — ²Australian Nuclear Science and Technology Organisation (ANSTO), Lucas Heights NSW 2234, Australia — ³Heinz Maier-Leibnitz Zentrum (MLZ), Technische Universität München, Garching, Germany

Cubic chiral magnets exhibit a universal magnetic phase diagram due to a hierarchy of energy scales comprising exchange interactions, Dzyaloshinsky-Moriya spin-orbit coupling and magnetocrystalline anisotropies (MCAs). In MnSi thermal Gaussian fluctuations stabilize a skyrmion lattice phase near T_c for all magnetic field orientations reflecting very weak MCAs [1,2]. In Cu_2OSeO_3 , an additional skyrmion lattice phase stabilizes in the low temperature limit due to strong MCAs for magnetic field parallel $\langle 100 \rangle$ [3]. We report a study of the interplay of moderate MCAs and disorder in $\text{Fe}_{1-x}\text{Co}_x\text{Si}$. Combining magnetometry and small-angle neutron scattering we observe a wide parameter range in which the effects of thermal fluctuations, MCAs and disorder stabilize skyrmion lattice order over an exceptionally wide parameter range depending on field orientation.

[1] S. Mühlbauer *et al.*, Science 323 915 (2009); [2] T. Adams *et al.*, Phys. Rev. Lett. 121 187205 (2018); [3] A. Chacon *et al.*, Nat. Phys. 14 936 (2018).

MA 19.8 Tue 17:30 P2

Interactions between magnetic skyrmions — •LÁSZLÓ UDVARDI^{1,2} and MÁTYÁS TÖRÖK¹ — ¹Budapest University of Technology and Economics, Budapest Hungary — ²MTA-BME Condensed Matter Research Group, Budapest, Hungary

Recently magnetic skyrmions received considerable attention due to their potential in spintronic devices. Magnetic properties of skyrmions are often described by a classical Heisenberg model with tensorial couplings. We have developed a conjugate gradient method to find the local minima of the energy of a classical spin system. By analyzing the energy of an isolated skyrmion and of pair of skyrmions in the case of FePd bilayer on Ir(111) substrate¹ interactions can be derived as a function of the separation of the skyrmions. The knowledge of the pair interactions permits us to perform Monte Carlo simulations treating skyrmions as quasi particles.

1. Phys. Rev. B 93, 024417 (2016)

MA 19.9 Tue 17:30 P2

Realization of Shankar Skyrmions in magnetically frustrated platforms. — •STEVEN SCHOENMAKER, RICARDO ZARZUELA, and JAIRO SINOVA — Johannes Gutenberg University, Mainz, Germany

Three-dimensional magnetic solitons are gathering momentum in the last few years due to their intrinsic complexity and their potential use in topological com-

puting and high-density memory storage. For instance, recent advances have led to the experimental observation of hopfions [1] and skyrmion strings [2] in collinear magnets. Shankar skyrmions [3], the condensed matter realization of skyrmions present in baryonic matter and of which magnetic skyrmions are a two-dimensional analog, can emerge in spin systems described by a SO(3)-order parameter, such as frustrated magnets (namely, magnetic systems with frustrated interactions dominated by isotropic exchange) [4]. Motivated by this possibility, we propose phenomenological and exactly solvable models for Shankar skyrmions in magnetically frustrated spintronic platforms and we also explore whether these topological textures form a crystal phase.

[1] N. Kent et al., Nat. Comms. 12, 1562 (2021).

[2] T. Yokouchi et al., Sci. Adv. 4, eaat1115 (2018);

S. Seki et al., Nat. Comms. 11, 256 (2020).

[3] R. Shankar, J. Physique 38, 1405 (1977).

[4] R. Zarzuela, H. Ochoa and Y. Tserkovnyak, Phys. Rev. B 100, 054426 (2019).

MA 19.10 Tue 17:30 P2

Exploring the limitations of the micromagnetic framework with a stable Bloch point — •THOMAS BRIAN WINKLER¹, MARIJAN BEG², MARTIN LANG^{3,4}, MATHIAS KLÄUI¹, and HANS FANGOHR^{3,4} — ¹Institut für Physik, JGU Mainz — ²Department of Earth Science and Engineering, Imperial College London — ³Faculty of Engineering and Physical Sciences, University of Southampton — ⁴Max Planck Institute for the Structure and Dynamics of Matter Hamburg

Bloch points [1,2] are well-known magnetisation configurations that often occur in transient processes. However, recent simulations have shown that opposing chiralities of layers in a thin-film geometry can stabilise such magnetic Bloch points and make them equilibrium states [3], potentially opening the door towards Bloch point based spintronic applications [4]. An open question, from a methodological point of view, is whether the Heisenberg model approach (atomistic model) must be used to study such systems or if the – computationally more efficient – micromagnetic models can be used as well. In this work, we are investigating and comparing the energetics and dynamics of a stable Bloch point [3,4] obtained using both Heisenberg and micromagnetic approaches.

[1] Ricardo Gabriel Elias et al., Eur. Phys. J. B 82, 159-166 (2011). [2] Oleksandr V. Pylypovskyi et al., Phys. Rev. B 85, 224401 (2012). [3] Marijan Beg et al., Scientific Reports 9, 7959 (2019). [4] Martin Lang et al., Bloch points in nanostrips, arxiv:2203.13689 (2022).

MA 19.11 Tue 17:30 P2

Magnetocaloric effect in (La, Ce)(Fe, Si, Mn)₁₃ with tunable, low transition temperature — •M. STRASSHEIM^{1,2}, C. SALAZAR MEJIA¹, J. WOSNITZA^{1,2}, and T. GOTTSCHALL¹ — ¹Hochfeld-Magnetlabor Dresden (HLD-EMFL), HZDR, Dresden, Germany — ²Technische Universität Dresden, Dresden, Germany

The La(Fe, Si)₁₃ family is one of the most promising group of magnetocaloric materials due to their overall good cost-benefit ratio in comparison to alloys based on scarce rare-earths such as Gd or Ho. By partly substituting La with Ce and Fe with Mn, the point of the metamagnetic transition can be tuned down to at least 40 K, while maintaining a rather sharp transition to enable a notable magnetocaloric effect. Tuning the magnetocaloric effect down to these temperatures opens up large-scale applications such as the magnetic liquefaction of hydrogen. In this work, we synthesized (La_{1-z}Ce_z)(Fe_{0.88-y}Mn_ySi_{0.12})₁₃ with z = 0 ... 0.4, y = 0 ... 0.04 and determined the adiabatic temperature change in pulsed magnetic fields. For some samples, we calculated the magnetic entropy change using isothermal magnetization measurements.

MA 19.12 Tue 17:30 P2

Chemical Ordering and Phase Transition in all-d-metal Heusler alloy NiCoMnTi — •DAVID KOCH¹, BENEDIKT BECKMANN¹, OLGA MIROSHKINA², NUNO M. FORTUNATO¹, MARKUS GRUNER², HONGBIN ZHANG¹, OLIVER GUTFLEISCH¹, and WOLFGANG DONNER¹ — ¹Institute of Material Science, Technical University of Darmstadt, 64287 Darmstadt Germany — ²Faculty of Physics and Center of Nanointegration, University of Duisburg-Essen, 47057 Duisburg Germany

Chemical ordering in NiMn-based Heusler alloys with magnetostructural phase transition is crucial for understanding the physics of the phase transition and is known for influencing the properties of the alloys. In the new field of all-d-metal Ni(Co)MnTi Heusler alloys, the experimental determination of chemical order is challenging due to the low difference in scattering power of the different elements. Here we report a combined approach of neutron and x-ray diffraction for an analysis of chemical order in Ni(Co)MnTi alloys and show that no Heusler-typical L21 order between Ti and Mn is present. Furthermore, Co and Ni atoms do not exhibit order among them; however, the martensitic phase transition and Curie temperature of Co containing samples can be shifted significantly by changing the degree of B2 order with a proper heat treatment. Using first-principles calculations, we reveal how the structural and magnetic sub-systems depend on the degree of B2 disorder. An outlook to further experiments on single crystals is given.

MA 19.13 Tue 17:30 P2

Simultaneous measurements of magnetocaloric materials in pulsed magnetic fields — •TINO GOTTSCHALL¹, EDUARD BYKOV^{1,2}, MARC STRASSHEIM¹, TIMO NIEHOFF^{1,2}, CATALINA SALAZAR-MEJIA¹, and JOCHEN WOSNITZA^{1,2} — ¹Dresden High Magnetic Field Laboratory (HLD-EMFL), HZDR, Dresden — ²Institut für Festkörper- und Materialphysik, TU Dresden, Germany

The direct determination of the adiabatic temperature change as a function of magnetic field and starting temperature is of central importance for a profound characterization of magnetocaloric materials. Recently, we developed a technique to measure the temperature change in pulsed magnetic fields directly and simultaneously also other properties such as strain and magnetization can be determined. In this work, we give an overview of the most recent results that have been obtained in pulsed fields at the Dresden High Magnetic Field Laboratory. This work was supported by HLD at HZDR, member of the European Magnetic Field Laboratory (EMFL) and the Helmholtz Association via the Helmholtz-RSF Joint Research Group Project No. HRSF-0045.

MA 19.14 Tue 17:30 P2

Tuning the magnetocaloric phase transition of La(Fe,Si)₁₃ by rare earth doping — •JOHANNA LILL¹, BENEDIKT EGGERT¹, BENEDIKT BECKMANN², OLGA N. MIROSHKINA¹, ILIYA RADULOV², KONSTANTIN SKOKOV², JOSE R. LINARES MARDEGAN³, SONIA FRANCOUAL³, RICHARD BRAND¹, KATHARINA OLLEFS¹, MARKUS E. GRUNER¹, OLIVER GUTFLEISCH², and HEIKO WENDE¹ — ¹University of Duisburg-Essen, Duisburg, Germany — ²TU Darmstadt, Darmstadt, Germany — ³DESY, Hamburg, Germany

Magnetocaloric (MC) materials are promising environmentally friendly candidates to replace gas-compression refrigerants. There are many MC systems possessing a high MC effect by showing high adiabatic temperature or isothermal entropy changes, but goals are still to minimize hysteresis and to tune the phase transition (PT) temperature to room temperature (RT). Therefore, knowledge of electronic and magnetic interactions in different magnetic phases are essential, as these determine the PT properties. One promising MC material is La(Fe,Mn,Si)₁₃H, which has its PT temperature around RT after hydrogenation, stabilized by Mn-doping which increases thermal hysteresis. To tune its thermal hysteresis, we study the effect of rare earth doping in the (La,Ce,Nd)(Fe,Si)₁₃ system and systematically investigate local electronic and magnetic properties in the different magnetic states utilizing e.g. XMCD and Mössbauer spectroscopy. With this study we present a deepened understanding of tuning local properties which may open new ways for tailoring hysteresis of MC materials. We acknowledge financial support from DFG through TRR270 HoMMage.

MA 19.15 Tue 17:30 P2

Insights into the magnetic structure of Mn-doped La(Fe,Si)₁₃ — •BENEDIKT EGGERT¹, JOHANNA LILL¹, OLGA N. MIROSHKINA¹, KONSTANTIN SKOKOV¹, KATHARINA OLLEFS¹, MARKUS E. GRUNER¹, OLIVER GUTFLEISCH², and HEIKO WENDE¹ — ¹Faculty of Physics and CENIDE, University of Duisburg-Essen — ²Functional Materials, TU Darmstadt

Magnetic cooling has the potential to replace conventional gas compression refrigeration. Here, materials such as FeRh, NiMn-based Heusler alloys or La(Fe,Si)₁₃ exhibit a sizeable first-order magnetocaloric effect. To further optimize the efficiency, it is necessary to tune the phase transition close to room temperature and reduce the thermal hysteresis. For La(Fe,Si)₁₃, it was shown that it is possible to tailor the phase transition towards room temperature by interstitial H-doping, while maintaining first-order character. In addition, Mn doping allows fine tuning of T_c to enlarge to temperature window of operation, inducing also second-order features. We discuss variations of the electronic and geometric structure in La(Fe,Si)₁₃ with increasing Mn content by means of Mössbauer spectroscopy. Mössbauer measurements reveal a reduction of the Fe magnetic moment with increasing Mn concentration. A reduction and broadening of the hyperfine field distribution occurs for higher Mn-content, while in-field measurements indicate a non-collinear spin structure for high Mn-concentrations. We acknowledge the financial support through the Deutscheforschungsgemeinschaft within the framework of the CRC/TRR270 HoMMage.

MA 19.16 Tue 17:30 P2

Thermally generated spin transport in Fe₃O₄/NiO/Pt trilayers — •JOHANNES DEMIR¹, STEFAN BECKER¹, PAULA BUNTE¹, LENNART SCHWAN², OLGA KUSCHEL³, JOACHIM WOLLSCHLÄGER³, and TIMO KUSCHEL¹ — ¹Bielefeld University, Germany — ²Bielefeld University of Applied Sciences, Germany — ³Osnabrück University, Germany

We investigate the spin Seebeck effect (SSE) in Fe₃O₄/NiO/Pt trilayers by varying the thickness of the antiferromagnetic NiO layer from 0 to 20 nm. Furthermore, we compare the SSE voltage normalized to the temperature difference to literature [1] and to the experimentally detected heatflux [2]. The Fe₃O₄/NiO bilayer is grown in situ by molecular-beam epitaxy, while the Pt layer is deposited ex situ by DC sputtering. We see an enhanced spin current signal in 0.5 and 1.1 nm NiO on 48 nm Fe₃O₄ for both normalizations. Moreover, we recognize a deviation from the simple exponential behaviour above 9.5 nm NiO thickness indicating a generation of spin current in NiO detectable for larger NiO thickness. Addi-

tionally, we simulate the temperature gradient in Fe_3O_4 in an equivalent circuit model depending on the NiO thermal conductivity and the interface thermal conductances to examine the influence of the thermal depth profile of the NiO layer on the thermally induced spin current.

[1] L. Baldrati et al., Phys. Rev. B 98, 014409 (2018)

[2] A. Sola et al., Sci. Rep. 7, 46752 (2017)

MA 19.17 Tue 17:30 P2

Systematic variation of NiFe_2O_4 thin film lattice parameters by post-annealing in oxygen atmosphere — •JULIAN STRASSBURGER, JAN BIEDINGER, OLIVER RITTER, TOBIAS PETERS, LUCA MARNITZ, KARSTEN ROTT, and TIMO KUSCHEL — Center for Spinelectronic Materials and Devices, Bielefeld University, Germany

Nickel ferrite (NFO) is a ferrimagnetic insulator and a promising material for spin caloric applications [1,2,3]. In this study, twin samples of NFO thin films (45nm thick) were prepared on MgAl_2O_4 substrates by reactive DC magnetron sputter deposition. The samples were in-situ post-annealed in oxygen atmosphere at different temperatures. After cooling down to room temperature, one sample of each pair was capped by 3nm of Pt for future spin Seebeck effect studies. It was shown by x-ray diffraction analysis that the in-plane and out-of-plane lattice constants change systematically by varying the post-annealing temperature. A possible change of oxygen content in the samples was investigated by determining the unit cell volume and Possion's ratio from the lattice parameters as well as the optical band gap energy from optical spectroscopy data [4,5]. In a next step, the influence of systematically modified lattice parameters on thermally induced spin transport will be investigated.

[1] D. Meier et al., Phys. Rev. B 87, 054421 (2013)

[2] C. Klewe et al., J. Appl. Phys. 115, 123903 (2014)

[3] D. Meier et al., Nat. Commun. 6, 8211 (2015)

[4] P. Bougiatioti et al., Phys. Rev. Lett. 119, 227205 (2017)

[5] P. Bougiatioti et al., J. Appl. Phys. 122, 225101 (2017)

MA 19.18 Tue 17:30 P2

The origin of S-shaped magnetizations and why the connection to toroidal moments is misleading — •DENNIS WESTERBECK, DANIEL PISTER, and JÜRGEN SCHNACK — Universität Bielefeld, D-33501 Bielefeld, Deutschland

Recent studies for toroidal molecules suggest a connection between low-lying toroidal states and an S-shaped magnetization [1]. We show that for theoretical models the S-shape neither is an evidence for a toroidal moment nor do all toroidal systems form S-shaped magnetizations [2]. Instead, the shape of magnetization curve is a result of a combination of strong anisotropies with spin-spin interactions blocking a spin flip for weak magnetic fields. The phenomenon also strongly depends on the spin quantum numbers. Toroidal moments even can be transformed to zero, if no additional anisotropic interactions between spins are taken into account.

[1] K. R. Vignesh, Nat. Commun. 8, 1023 (2017)

[2] J. M. Ashtree, Eur. J. Inorg. Chem. 2021 (5), 435 (2021)

MA 19.19 Tue 17:30 P2

X-ray absorption and differential reflectance spectroscopies of spin-crossover molecules on HOPG — •JORGE TORRES¹, SASCHA OSSINGER², SANGEETA THAKUR¹, CLARA W.A. TROMMER², MARCEL WALTER¹, IVAR KUMBERG¹, RAHIL HOSSEINIFAR¹, EVANGELOS GOLIAS¹, SEBASTIEN HADJADJ¹, JENDRIK GÖRDES¹, PIN-CHI LIU¹, CHEN LUO³, LALMINTHANG KIPGEN¹, TAUQIR SHINWARI¹, FLORIN RADU³, FELIX TUCZEK², and WOLFGANG KUCH¹ — ¹Freie Universität Berlin, Institut für Experimentalphysik, Berlin, Germany — ²Christian-Albrechts-Universität zu Kiel, Institut für Anorganische Chemie, Kiel, Germany — ³Helmholtz-Zentrum Berlin für Materialien und Energie, Berlin, Germany

In order to use visible light to observe the switching between the high spin (HS) and low spin (LS) state of a $[\text{Fe}\{\text{H}_2\text{B}(\text{pzpy})_2\}_2]$ [1] spin-crossover molecule (SCM), a sub-monolayer was deposited on highly oriented pyrolytic graphite (HOPG) and the sample temperature varied from 120 to 350 K. The difference in light reflection between the pristine HOPG and the SCM sub-monolayer was analyzed by differential reflectance spectroscopy (DRS). Furthermore, the total HS fraction obtained from X-ray absorption spectroscopy (XAS) at temperatures ranging from 10 to 350 K was compared to the DRS absorption spectra. A systematic absorption in the UV region shows that the intensity is proportional to the temperature. Here, the ligand-centered absorption is stronger than the metal-to-ligand charge transfer, making this SCM a promising candidate for optically switched storage devices at room temperature. [1] S. Ossinger, Inorg. Chem., 2020, 59, 7966-7979

MA 19.20 Tue 17:30 P2

Spin-phonon interaction and tunnel splitting in single-molecule magnets — •KILLIAN IRLÄNDER¹, JÜRGEN SCHNACK¹, and HEINZ-JÜRGEN SCHMIDT² — ¹Fakultät für Physik, Universität Bielefeld, Postfach 100131, D-33501 Bielefeld, Germany — ²Fachbereich Physik, Universität Osnabrück, D-49069 Osnabrück, Germany

Quantum tunneling of the magnetization is a phenomenon that impedes the use of small anisotropic spin systems for storage purposes even at the lowest tem-

peratures. Phonons, usually considered for relaxation of the magnetization over the anisotropy barrier, also contribute to magnetization tunneling for integer spin quantum numbers. In this context, it is not viable to consider phonons perturbatively but to treat spins and phonons on the same footing by performing quantum calculations of a Hamiltonian where the single-ion anisotropy tensors are coupled to harmonic oscillators.

We demonstrate the ability of phonons to induce a tunnel splitting of the ground doublet which then reduces the required bistability due to Landau-Zener tunneling of the magnetization [1]. We also present the unexpected observation that certain spin-phonon Hamiltonians are robust against the opening of a tunneling gap, even for strong spin-phonon coupling. The key to understanding this phenomenon is provided by an underlying supersymmetry that involves both spin and phonon degrees of freedom [2].

[1] K. Irländer, and J. Schnack, Phys. Rev. B 102, 054407 (2020).

[2] K. Irländer et al., Eur. Phys. J. B 94, 68 (2020).

MA 19.21 Tue 17:30 P2

⁵⁷Fe Mössbauer spectroscopy on FePcF_{16} and its μ -Oxo dimer in catalysis reaction — •FELIX SEEWALD¹, FLORIAN PULS², HANS-JOACHIM KNÖLKER², and HANS-HENNING KLAUSS¹ — ¹Institute of Solid State and Materials Physics, TU Dresden, D-01069, Germany — ²Department Chemie, Technische Universität Dresden, Bergstraße 66, D-01069 Dresden, Germany

Iron-hexadecafluorophthalocyanine (FePcF_{16}) is used as an oxidation catalyst. Understanding its catalysis mechanism is part of current research. The Fe atom is square planar coordinated by four nitrogen atoms. Both FePcF_{16} and its μ -Oxo dimer ($[\text{FePcF}_{16}]_2\text{O}$) are already identified as steps of the oxidation cycle.

The Mössbauer spectra of $[\text{FePcF}_{16}]_2\text{O}$ can be described by two sites at room temperature, both exhibiting quadrupole splitting. A temperature dependent reversible transition between both sites can be observed. Below 30 K the onset of a magnetic hyperfine field is observed obtaining a value of $B_{\text{Hyp}} = 48.77(12)$ T at 4.2 K.

The FePcF_{16} spectra show one additional third site with a considerable quadrupole splitting and an electric field gradient largest principle component of $V_{zz} = 154(2)$ V/Å². This site stays paramagnetic down to 4.2 K.

First measurements of the frozen reaction solution unveil an additional fourth site in a characteristic Fe(II) charge and high spin (S=2) state. We will discuss the implications of these findings on the catalysis process.

MA 19.22 Tue 17:30 P2

Approaches towards observing toroidal magnetic moments in Dy-based molecular nanomagnets with Inelastic Neutron Scattering techniques. — •DENNY LAMON¹, JULIUS MUTSCHLER¹, THOMAS RUPPERT², CHRISTOPHER E. ANSON², ANNIE K. POWELL², and OLIVER WALDMANN¹ — ¹Physikalisches Institut, Universität Freiburg, Germany — ²Institut für anorganische Chemie, Universität Karlsruhe, KIT, Germany

Single-molecule toroids (SMT) have been a subject of increasing interest both for their fundamental physics properties and for the potential applications in quantum computers or information storage. In fact the associated vortex arrangement of magnetic moments leads to weaker dipolar interactions and to a lack of interaction with a possible external magnetic field. A particular class of these molecules, which incorporate a triangle of exchange coupled magnetic Dy ions, can support a toroidal magnetic moment; in this work a class of Me_2Dy_3 molecules, where Me = Al, Cr, Fe, is investigated. The available experimental data for magnetic susceptibility and magnetization curves are fitted and simulated using full and effective Hamiltonian models in order to extract the model parameters, especially the tilt angles of the anisotropy axes. The inelastic neutron scattering spectra are simulated in order to develop experimental schemes for directly observing toroidal magnetic moments in SMTs.

MA 19.23 Tue 17:30 P2

Synthesis, optical and magnetic properties of Au-Fe₃O₄ nanohybrids — •TATIANA SMOLIAROVA, MARINA SPASOVA, ULF WIEDWALD, and MICHAEL FARLE — Faculty of Physics, University of Duisburg-Essen, Duisburg, 47057, Germany

Gold-magnetite nanohybrids composed of Fe_3O_4 and Au nanoparticles (NPs) have attracted large attention due to the evident advantages of Au nanoparticles such as unique biocompatibility, facile surface modification, and high catalytic properties. Herein, we report on the facile room-temperature synthesis approach for Au- Fe_3O_4 nanohybrids preparation and their optical and magnetic properties investigation.

Au- Fe_3O_4 nanohybrids were synthesized by chemical precipitation with a chemisorption process of Au nanoparticles (NPs) to the Fe_3O_4 surface using polyvinylpyrrolidone (PVP) coverage. Prepared NPs were studied by transmission electron microscopy (TEM), UV-vis spectroscopy and magnetometry. The obtained results seem to be the promising step for the core-shell Au- Fe_3O_4 NPs preparation, in the case of Au NPs will be considered as the seeds for the complete Au shell growth.

This work was supported by European Union's Horizon 2020 research and innovation program under grant agreement No 857502 (MaNaCa).

MA 19.24 Tue 17:30 P2

Chern insulators at finite magnetic fields in twisted bilayer graphene. — •MIGUEL SÁNCHEZ¹, TOBIAS STAUBER^{1,2}, and JOSÉ GONZÁLEZ³ — ¹ICMM CSIC Madrid — ²University of Augsburg — ³IEM CSIC Madrid

We calculate the topological properties (Chern numbers) of the correlated insulator states of magic angle twisted bilayer graphene (TBG) observed at integer number of electrons per Moiré unit cell.

Using the periodic Landau gauge to make manifest the magnetic translation symmetry and the Peierls' substitution, we obtain the Landau levels and Hofstadter butterfly of TBG. Via a self-consistent Hartree-Fock method we study electron correlations and the Chern insulator states at finite magnetic fields in our atomistic tight-binding description. Also, recent discoveries drive our attention to spontaneous translation symmetry breaking at half-integer fillings.

MA 19.25 Tue 17:30 P2

Differential Phase Contrast and Lorentz microscopy — •JUDITH BÜNTE, BJÖRN BÜKER, DANIELA RAMERMANN, INGA ENNEN, and ANDREAS HÜTTEN — Universität Bielefeld, Dünne Schichten und Physik der Nanostrukturen, Universitätsstr. 25, 33615 Bielefeld, Germany

Differential Phase Contrast (DPC) and Lorentz microscopy are two well-known techniques for analyzing magnetic structures in the transmission electron microscope (TEM). The Lorentz force inside the magnetic domain of a specimen deflects the transmitted electron beam depending on the orientation of the corresponding magnetic field. This deflected beam then results in a different intensity distribution in the recorded image which can be analyzed. In this contribution we present DPC and Lorentz transmission electron microscope (LTEM) images of a specimen consisting of a CoFe membrane with structured holes. These different kinds of holes inside the magnetic material of the specimen yield interesting domain structures. The focus is on the analysis of these magnetic domain structure and the impact of changing external magnetic fields. For this, a hysteresis loop inside the TEM is recorded. Furthermore, the two different techniques are compared giving the possibility to confirm the resulting domain structure.

MA 19.26 Tue 17:30 P2

Kerr microscopy for all-optical helicity-dependent magnetization switching — •LUCAS VOLLROTH¹, MARCEL KOHLMANN¹, KRISTÝNA HOVOŘÁKOVÁ², EVA SCHMORANZEROVÁ², MARKUS MÜNZENBERG¹, and JAKOB WALOWSKI¹ — ¹Greifswald University, Greifswald, Germany — ²Charles University, Prague, Czech Republic

The ever growing demand for data storing capacities requires the development of high bit density data storage devices with fast read and write capabilities. New generation heat assisted magnetic recording devices (HAMR) emerging the market are promising candidates decreasing bit sizes. Simultaneously, the recording media based on nanometer sized FePt grains are suitable for other writing approaches like the all-optical helicity-dependent switching (AOHDS) [1]. We investigate this method for potential future applications of HAMR media. Wide field Kerr-microscopy is a well suited method to explore and analyze the outcome of our AOHDS experiments. We present a build from scratch and cost efficient Kerr microscope for the observation of magnetic domains. The setup can be implemented in pump-probe experiments to investigate magnetization changes after the deposition of ultrashort laser pulse energies in magnetic thin films. Besides measurements on hard drive media, the microscope can also be used for the observation of skyrmions.

[1] John, R. et al. Magnetisation switching of FePt nanoparticle recording medium by femtosecond laser pulses. *Sci Rep* 7, 4114 (2017)

MA 19.27 Tue 17:30 P2

Magnetic proximity effect in V uncovered by TEM techniques — •INGA ENNEN¹, DANIELA RAMERMANN¹, DOMINIK GRAULICH¹, TREVOR ALMEIDA², STEPHEN McVITIE², BJÖRN BÜKER¹, TIMO KUSCHEL¹, and ANDREAS HÜTTEN¹ — ¹Universität Bielefeld, Dünne Schichten und Physik der Nanostrukturen, Universitätsstr. 25, 33615 Bielefeld, Germany — ²University of Glasgow, School of Physics and Astronomy, Glasgow G12 8QQ, UK

Thin film structures consisting of magnetic and non-magnetic materials are of great technical interest, due to their special magnetic and electronic characteristics. These characteristics were influenced e.g. by the interface quality and the magnetic proximity effect. Here, the penetration depth of magnetism in non-magnetic films adjacent to ferromagnetic layers is investigated, usually by employing X-ray techniques such as XRMR. In this contribution, we demonstrate the opportunities of modern transmission electron microscopy techniques for the investigation of the magnetic proximity effect in a V/Fe thin film system as a model sample. Here, a combination of magnetic differential phase contrast (DPC) and electron energy loss magnetic chiral dichroism (EMCD) has been employed. The basic idea is that DPC measures the presence of a magnetic induction into V and EMCD shows that there is a magnetic moment present. In this way, a magnetic proximity effect of about 1.5nm in V has been observed, which is in accordance to corresponding measurements with X-rays.

MA 19.28 Tue 17:30 P2

Imaging the coherent spin dynamics of nitrogen vacancies coupled to CrTe₂ at room temperature — •RICCARDO SILVIOLI¹, MARTIN SCHALK¹, KARINA HOUSKA¹, DOMINIK BUCHER², ZDENEK SOFER³, ANDREAS V. STIER¹, and JONATHAN J. FINLEY¹ — ¹WSI, TUM — ²Chemie, TUM — ³UCT Prague

Magnetic resonance imaging of coupled spin-systems is a technique capable of rendering highly accurate descriptions of magnetic fields even at room temperature, and is therefore lying at the heart of various applications in medicine, chemistry and physics. We present coherent wide-field imaging of a 100 x 100 μm sized region of interest implanted with nitrogen vacancy centers (NVs) in diamond coupled to a 50 nm thick flake of the in-plane van der Waals ferromagnet CrTe₂. We can quantitatively probe the stray magnetic field of the material with the NVs' electron spin signal. First, we combine the nano-scale sample shapes measured by atomic force microscope with the magnetic resonance imaging data for accurate reconstruction of the sample's magnetization. We then map out the coherent dynamics of the colour centers coupled to the van der Waals ferromagnet using pixel-wise coherent Rabi and Ramsey imaging of the NV sensor layer. We find that the spin coherence of the ensemble is strictly correlated with the variation in the magnetic field generated by the sample. What results is an enhanced detection of the magnetic field where we describe its variation in three dimensions, improving the reconstruction of the magnetization. Finally, we infer the quantum dynamics using a neural network to speed up the convergence of the pixel-wise Hamiltonian fitting.

MA 19.29 Tue 17:30 P2

Ultrafast Lorentz microscopy with magnetic field excitation at microwave frequencies — JONATHAN TILMAN WEBER, NIKITA PORWAL, •ANDREAS WENDELN, MICHAEL WINKLHOFFER, and SASCHA SCHÄFER — Carl von Ossietzky Universität, Oldenburg, Deutschland

Recent progress in the development of laser-driven, high brightness photocathodes offers a path to investigate magnetization dynamics with high spatial and temporal resolution, utilizing a Lorentz imaging approach in ultrafast transmission electron microscopy (UTEM) [1]. In particular, non-optical excitation schemes, such as current or field excitation provide pathways for a selective triggering of magnetic dynamics. Extending the available frequencies in such experiments [2], we developed a TEM sample holder based on a two-dimensional microwave cavity, with which we can excite ferromagnetic resonances in magnetic nanostructures. The microwave excitation signals are phase-locked to the nanolocalized photoemission of ultrashort electron pulses from a Schottky field emitter, using high harmonics of the amplified laser system as a master clock for their synchrotronization [3]. With this advanced excitation and measurement scheme we aim to image ferromagnetic resonance modes with high spatial and temporal resolution and to further establish ultrafast Lorentz microscopy as a powerful tool to characterize magnetization dynamics on the nanoscale.

[1] N. R. da Silva et al. *Phys. Rev. X* 8, 031052 (2018).

[2] M. Möller et al. *Commun Phys* 3, 36 (2020).

[3] M.R. Otto et al. *Struct. Dyn.* 4, 051101 (2017).

MA 19.30 Tue 17:30 P2

Brownian reservoir computing realized using geometrically confined skyrmions — •KLAUS RAAB¹, MAARTEN A. BREMS¹, GRISCHA BENEKE¹, TAKAOKI DOHI¹, JAN ROTHÖRL¹, FABIAN KAMMERBAUER¹, JOHAN H. MENTINK², and MATHIAS KLÄUI^{1,3} — ¹Institut für Physik, Johannes Gutenberg-Universität Mainz, Staudingerweg 7, 55128 Mainz, Germany — ²Radboud University, Institute for Molecules and Materials, Heyendaalseweg 135, 6525 AJ Nijmegen, The Netherlands — ³Graduate School of Excellence Materials Science in Mainz, Staudingerweg 9, 55128 Mainz, Germany

We demonstrate experimentally [1] a conceptionally new approach for reservoir computing (RC), that leverages the thermally activated diffusive motion of magnetic skyrmions in a confined, triangular geometry. The combination of gated and thermal skyrmion motion of a single skyrmion already suffices to realize all Boolean logic gate operations including the non-linearly separable XOR operation that cannot be realized using a conventional single layer perceptron. An effective potential well created by the confinement allows for a natural, energy efficient reset mechanism enabled by the thermal fluctuations of the skyrmions. We show that the output training costs using linear regression are low and that our ultra-low power operation using current densities orders of magnitude smaller than used in existing spintronic reservoir computing demonstrations. Our concept can be easily extended by linking multiple confined geometries for scalable and low-energy reservoir computing. [1] K. Raab et al. *Brownian reservoir computing with geometrically confined skyrmions* - arXiv:2203.14720

MA 19.31 Tue 17:30 P2

FD micromagnetic solver for inverse-design magnonics — •ANDREY VORONOV¹, QI WANG¹, DIETER SUESS², ANDRII CHUMAK¹, and CLAAS ABERT² — ¹Nanomagnetism and Magnonics, Faculty of Physics, University of Vienna, Austria — ²Physics of Functional Materials, Faculty of Physics, University of Vienna, Austria

The idea of utilizing a collective excitation of the electron spin system in magnetic solids, so-called spin-waves, for data processing has been developing in recent

years. However, the design of complex data-processing units requires elaborate and complicated investigations.

Recently, the concept of inverse-design magnonics, in which any functionality can be specified first and a feedback-based computational algorithm is used to obtain the device design, has been demonstrated numerically [1]. The same algorithm was used to design a magnonic (de-)multiplexer, a nonlinear switch, and a circulator [1].

One of the next challenges for inverse design is the computation of universal Boolean logic gates NAND and NOR. However, such gates require increasing the complexity of the structure used in [1] and the combination of the MuMux3 simulations with the direct binary search algorithm (DBS) is no longer applicable. Here I report on the use of finite difference (FD) micromagnetic solver based on the Pytorch open source machine learning framework for inverse design. The proposed algorithm greatly facilitates the design of the applied devices and is a useful tool especially for spin-wave computing elements.

[1] Wang, Q., et al (2021). Nature Communications, 12(1), 1-9.

MA 19.32 Tue 17:30 P2

Efficiency and Comfort Optimization of Induction Hobs Through Appropriate Materials Selection — •LENNART SCHWAN^{1,2}, SONJA SCHÖNING¹, and ANDREAS HÜTTEN² — ¹Bielefeld Institute for Applied Materials Research (BIFAM), Bielefeld University of Applied Sciences, Department of Engineering Sciences and Mathematics — ²Thin Films & Physics of Nanostructures Bielefeld University, Department of Physics

Inductive power transfer is nowadays a widely used technology, e.g. for inductive heating in industrial applications and household appliances like inductions hobs. An inductive heating system usually consists of a coil (transmitter) which is powered by an alternating current and a ferromagnetic material (receiver), for example a pot. The ferromagnetic material is heated by induced eddy currents and hysteresis losses. Regarding to energy efficiency and comfort, it is desirable to minimize the parasitic losses which do not contribute to the heating of the cooking good and to homogenize the temperature distribution within the cooking container. As a future basis for the development of novel cooking containers, we use FEM simulations to investigate the influence of the material parameters of the ferromagnetic material on the efficiency and temperature distribution. In addition to the simulations, parts of the results are verified by experimental investigations.

MA 19.33 Tue 17:30 P2

Moments and multiplets in moiré materials: A pseudo-fermion functional renormalization group for spin-valley models — •LASSE GRESISTA, DOMINIK KIESE, and SIMON TREBST — Institute for Theoretical Physics, University of Cologne, Germany

The observation of strongly-correlated states in moiré systems has renewed the conceptual interest in magnetic systems with higher SU(4) spin symmetry, e.g. to describe Mott insulators where the local moments are coupled spin-valley degrees of freedom. In addition to possible geometrical or interaction induced frustration, the enhanced quantum fluctuations in these systems are expected to counteract the formation of magnetic order, making them prime candidates to host exotic quantum spin-valley or spin-orbital liquid ground states. A method that has demonstrated its potential to distinguish between magnetically ordered and disordered states, even in the presence of frustration and in three dimensions, is the pseudo-fermion function renormalization group (pf-FRG). In our work we generalize this method from conventional SU(2) spin models to very general spin-valley Hamiltonians, showing that it can indeed be applied to study the magnetic behavior of moiré materials. We present the quantum phase diagram of $SU(2)^{\text{spin}} \otimes U(1)^{\text{valley}}$ symmetric spin-valley models relevant for the strong coupling description of trilayer graphene on hexagonal boron nitride (TG/h-BN) and twisted bilayer graphene (TBG).

MA 19.34 Tue 17:30 P2

Calculation of the temperature-dependent exchange stiffness from Domain Wall modelling — •FELIX SCHUG^{1,2}, NILS NEUGEBAUER^{2,3}, MICHAEL CZERNER^{1,2}, and CHRISTIAN HEILIGER^{1,2} — ¹Institute for Theoretical Physics, Justus Liebig University Giessen, Heinrich-Buff-Ring 16, 35392 Giessen, Germany — ²Center for Materials Research (LaMa), Justus Liebig University Giessen, Heinrich-Buff-Ring 16, 35392 Giessen, Germany — ³Institute of Experimental Physics I, Justus Liebig University Giessen, Heinrich-Buff-Ring 16, 35392 Giessen, Germany

Understanding the different influences on the macroscopic magnetic properties of a material at finite temperatures is of great interest from the theoretical point of view. As macroscopic magnetic properties, such as anisotropies or the exchange stiffness, are related to the quantum nature of electrons and thus to the most fundamental level of solids, the atomic level, atomistic modelling of a magnetic material may promote a more profound understanding of the microscopic processes. Performing the corresponding numerical simulations at various temperatures from 0 K to the Curie-temperature T_C , the temperature dependence of the associated macroscopic properties may be modelled. These modelled material parameters can then be used to simulate magnetic properties on the next higher

hierarchy to the microscopic scale, leading to the so-called multi-scale modelling approach. Here the approach of simulating Bloch walls of a finite cobalt stripe at different temperatures is demonstrated to extract the macroscopic crystalline anisotropy constant K_C and the exchange stiffness parameter A_{exc} .

MA 19.35 Tue 17:30 P2

Multiconfigurational approach to XAS applied to Co- and Ni-doped magnetite — •FELIX SORGENFRET¹, JOHANN SCHÖTT¹, M'EBAREK ALOUANI², PATRIK THUNSTRÖM¹, and OLLE ERIKSSON¹ — ¹Department of Physics and Astronomy, Uppsala University, Box-516, Uppsala SE-751 20 Sweden — ²Université de Strasbourg, IPCMS UMR 7504, 67034 Strasbourg, France

L-edge X-ray absorption spectroscopy (XAS) is an important tool to extract element-specific information about the electronic structure, magnetism and in particular electronic correlation effects. Ab initio calculations typically struggle to reproduce the 2p to 3d excitation, in particular for materials with strong electron correlations and significant core-hole effects. The combination of density functional theory and multiplet ligand field theory is applied to fill this gap. Here, parameters are calculated from first principles and used to construct a single-impurity Anderson model by projecting the local Hamiltonian and hybridization function onto the 3d states. In this talk, this method is applied to NiFe₂O₄, CoFe₂O₄ and Fe₃O₄. We find systematically good agreement with experiment for both XAS and XMCD spectra.

MA 19.36 Tue 17:30 P2

Finite-element dynamic-matrix approach for propagating spin waves: Extension to mono- and multilayers of arbitrary spacing and thickness — •ALEXANDER HEMPEL^{1,2}, LUKAS KÖRBER^{1,2}, ANDREAS OTTO², RODOLFO GALLARDO^{3,4}, YVES HENRY⁵, and ATTILA KÁKAY¹ — ¹Helmholtz-Zentrum Dresden - Rossendorf, Germany — ²Technische Universität Dresden, Germany — ³UTFSM, Chile — ⁴CEDEENNA, Chile — ⁵IPCMS, France

Over the last few years micromagnetic simulations became an important tool in the field of magnonics. In a recent work Körber et al. [1] presented an efficient method to numerically determine the dispersion and the spatial mode profiles of spin-waves propagating in waveguides with arbitrary cross section, if the equilibrium magnetization is invariant along the propagation direction. In this work their finite-element dynamic-matrix approach is used as a starting point to develop a tool to investigate propagating spin waves in mono- and multilayers. This approach has the advantage, that the linearized equation of motion is solved in just a section of the layers, and has therefore a comparatively low numerical complexity. Nevertheless the dipolar interaction still requires special care and we show how an extension of the Fredkin-Koehler method can be used to handle this problem. As a validation of the method, which is implemented into the open source FEM micromagnetic package TetraX [2], we present a variety of simulation results and compare them with analytics and other numerical approaches.

[1] Körber et al., AIP Advances 11, 095006 (2021). [2] TetraX - DOI: 10.14278/rodare.1418

MA 19.37 Tue 17:30 P2

Predictive Design of Induction Coil Geometries using Neural Networks — •SIMON BEKEMEIER¹, SVEN GEHLE¹, and CHRISTIAN SCHRÖDER^{1,2} — ¹Bielefeld Institute for Applied Materials Research (BIfAM), Computational Materials Science and Engineering (CMSE), Bielefeld University of Applied Sciences, Department of Engineering Sciences and Mathematics, Interaktion 1, 33619 Bielefeld, Germany — ²Faculty of Physics, Bielefeld University, Universitätsstraße 25, 33615 Bielefeld, Germany

Nowadays, inductive power transfer is an established technology with its most common application in induction hobs. Such appliances usually use planar coils with homogeneous winding distances. With regard to energy efficiency, comfort and electromagnetic compatibility it is desirable to start from an optimal magnetic field distribution and derive the necessary coil geometry from it.

Unknown, highly non-linear functional relations can be modelled using neural networks with relative ease. In this contribution, we use a deep convolutional auto-encoder to predict the relationship between coil geometries and the respective magnetic fields. To achieve this, the current-path and the coil's magnetic field are presented to the neural network in spatially discretized form. By using the current-path as input and the magnetic field as output, the neural net is trained to find coil geometries, which produce a desired magnetic field. In this contribution we present our results of predicted coil designs for magnetic fields, which require coil geometries ranging from simple linear wires to more complex spiral geometries.

MA 19.38 Tue 17:30 P2

First-principles local interactions extracted from non-collinear magnetic states — MIKLÓS SALÁNKI¹, BENDEGÚZ NYÁRI¹, ANDRÁS LÁSZLÓFFY², and •LÁSZLÓ SZUNYOGH¹ — ¹Department of Theoretical Physics, Budapest University of Technology and Economics, Hungary — ²Wigner Research Centre for Physics, Institute for Solid State Physics and Optics, Hungary

The local Dzyaloshinskii-Moriya interactions (DMI) derived from first principles in non-collinear magnetic configurations in the absence of spin-orbit cou-

pling [1] became recently the subject of an intense discussion [2,3,4]. On the one hand, the local DMI has been explained due to charge and spin currents emerging in non-collinear spin-configurations [1,3], on the other hand, it was shown to be a consequence of fourspin (or higher-order multispin) interactions [2].

As in Ref. [1] we perform calculations of the local interaction parameters for a Cr trimer on Au(111) in terms of the multiple scattering Green's function technique. We use two alternative formalisms that lead to different local parameters. We show that this ambiguity occurs due to longitudinal terms in the corresponding expressions. We find that the formalism based on the structural Green's-function matrices provides local interactions being consistent with a spin model including fourspin interactions calculated on the same basis.

- [1] R. Cardias *et al.*, arXiv:2003.04680; Sci. Rep. 10, 20339 (2020).
- [2] M. dos Santos Dias *et al.*, Phys. Rev. B 103, L140408 (2021).
- [3] R. Cardias *et al.*, Phys. Rev. B 105, 026401 (2022).
- [4] M. dos Santos Dias *et al.*, Phys. Rev. B 105, 026402 (2022).

MA 19.39 Tue 17:30 P2

Anomalous and spin Hall effect in chiral antiferromagnets Mn_3X ($X=Ir, Sn, \dots$) — •OLIVER BUSCH, BÖRGE GÖBEL, and INGRID MERTIG — Institut für Physik, Martin-Luther-Universität, D-06099 Halle

Recently, large anomalous Hall effects (AHEs) have been measured in the non-collinear kagome antiferromagnets (AFMs) Mn_3Sn [1] and Mn_3Ge [2] and large spin Hall effects (SHEs) were predicted in such compensated Mn_3X systems [3].

We discuss the intrinsic contributions to both Hall effects of kagome AFMs via tight-binding calculations. We describe a microscopic mechanism for the occurrence of the AHE: within this model, spin-orbit coupling (SOC) is equivalent to an out-of-plane tilting of the magnetic texture [4]. Thus, the AHE can be interpreted as a topological Hall effect generated by the opening angle of the virtually tilted texture.

Besides, we find that the main contribution to the SHE in Mn_3X is a pure spin current originating from the non-collinear magnetic texture and it occurs even without SOC when the AHE is absent [5]. In addition to that, SOC gives rise to the AHE and reduces the SHE effectively which gives rise to spin-polarized currents.

- [1] S. Nakatsuji, N. Kiyohara, T. Higo; Nature 527, 212 (2015)
- [2] A. K. Nayak *et al.*; Science Advances 2, e1501870 (2016)
- [3] Y. Zhang *et al.*; New Journal of Physics 20, 073028 (2018)
- [4] O. Busch, B. Göbel, I. Mertig; Phys. Rev. Research 2, 033112 (2020)
- [5] O. Busch, B. Göbel, I. Mertig; Phys. Rev. B 104, 184423 (2021)

MA 19.40 Tue 17:30 P2

Vertical Pt| $Y_3Fe_5O_{12}$ |Pt heterostructures for magnon mediated magnetoresistance measurements — •PHILIPP SCHWENKE^{1,2}, MANUEL MÜLLER^{1,2}, ANDREAS HASLBERGER^{1,2}, STEPHAN GEPRÄGS¹, and RUDOLF GROSS^{1,2,3} — ¹Walther-Meißner-Institut, Bayerische Akademie der Wissenschaften, 85748 Garching, Germany — ²Physik-Department, Technische Universität München, 85748 Garching, Germany — ³Munich Center for Quantum Science and Technology (MCQST), 80799 München, Germany

Spin currents and their generation (detection) via the (inverse) spin Hall effect in heavy metal (HM)|ferrimagnetic insulator (FMI) heterostructures gain increasing attention in the field of spintronics. In particular, spin current valves in HM|FMI|HM trilayers such as Pt|YIG|Pt heterostructures are of great interest to enable device miniaturization and the implementation of three-dimensional spintronic devices. In this work we optimize the fabrication of these vertical Pt|YIG|Pt heterostructures. We study the interface quality between Pt and YIG by performing angle dependent magnetoresistance measurements on the Pt layers. We observe a good top YIG|Pt interface quality and find an improvement of the bottom Pt|YIG interface by introducing a Ru buffer layer, which reduces the intermixing of Pt and YIG. Furthermore, we observe a finite magnon mediated magnetoresistance and spin Seebeck effect signal in our heterostructures demonstrating the possibility of HM|FMI trilayers as spin current valve devices.

MA 19.41 Tue 17:30 P2

Investigation of Quasiparticle Spin Transport in Superconductors/Ferrimagnet Heterostructures — •YUHAO SUN^{1,2}, MANUEL MÜLLER^{1,2}, JANINE GÜCKELHORN^{1,2}, MATTHIAS GRAMMER^{1,2}, HANS HUEBL^{1,2,3}, RUDOLF GROSS^{1,2,3}, and MATTHIAS ALTHAMMER^{1,2} — ¹Walther-Meißner-Institut, Bayerische Akademie der Wissenschaften, Garching, Germany — ²Physik-Department, Technische Universität München, Garching, Germany — ³Munich Center for Quantum Science and Technology, München, Germany

Magnon based spintronics is intensely researched as it enables alternative information processing schemes and additional functionalities compared to charge based counterparts. Recent studies suggest that the interplay of superconductivity and magnetism can enhance spin-related effects, such as the interfacial spin injection efficiency [1]. The present assumption is that magnetic excitation or magnons interact with the quasiparticles of the superconducting phase. To test this conjecture, we investigate magnon injection and transport using the ferrimagnetic insulator $Y_3Fe_5O_{12}$ as magnetic system. In detail, we use a superconducting niobium nitride (NbN) strip as the detector. A heater structure on top

of the NbN allows to apply thermal gradient. A spatially separated heavy metal platinum strip acts as the injector of thermal magnon spin-currents. We present temperature dependent data to access the influence of superconducting quasiparticles on our transport signal.

[1] Jeon *et al.*, ACS Nano 14, 15874, (2020).

MA 19.42 Tue 17:30 P2

Nonrelativistic spin currents in altermagnets — •RODRIGO JAESCHKE-UBIERGO, LIBOR ŠMEJKAL, and JAIRO SINOVA — Institut für Physik, Johannes Gutenberg Universität Mainz, Germany

Altermagnetism has emerged recently as a third basic collinear magnetic phase [1], in addition to ferromagnets and antiferromagnets. Conventional antiferromagnets exhibit two sublattices with opposite magnetic moment related by translation or inversion. In altermagnets the magnetic sublattices are connected by a rotation or a mirror operation. The particular symmetry causes that altermagnets display time-reversal (\mathcal{T}) symmetry breaking and spin split band structure even in absence of spin-orbit coupling [2].

In this work, we study the spin conductivity tensor in altermagnets by using spin group theory formalism [1]. We also use Kubo's linear response to calculate the spin conductivity tensor in all the altermagnetic spin point groups models. Additionally, we identify and sort 200 altermagnetic candidates into spin conductivity tensor classes. We will discuss some spin point groups that allow for a transverse spin current in detail. This is the case of spin splitter current in RuO_2 [3,4], which is a nonrelativistic effect that conserves spin unlike in general magnetic spin Hall effect in noncollinear magnets. Moreover, the spin conductivity tensor is symmetric and \mathcal{T} -odd, which makes it different to the conventional spin Hall effect.

[1] Šmejkal, *et al.* arXiv preprint arXiv:2105.05820, 2021. [2] Šmejkal, *et al.* Sci. Adv. 2020. [3] Gonzalez-Hernandez, *et al.* PRL 2021. [4] Šmejkal, *et al.* PRX 2022.

MA 19.43 Tue 17:30 P2

Spin-orbit torques in ferromagnetic heterostructures — •MISBAH YAQOUB¹, FABIAN KAMMERBAUER², VITALIY VASYUCHKA¹, GERHARD JAKOB², MATHIAS KLÄUI², and MATHIAS WEILER¹ — ¹Fachbereich Physik und Landesforschungszentrum OPTIMAS, TU Kaiserslautern, Kaiserslautern, Germany — ²Institut für Physik, Johannes Gutenberg-Universität Mainz, Mainz, Germany

Spin-orbit torques (SOTs) can be used to electrically control the spin dynamics, while inverse SOTs enable the electrical detection of spin dynamics. Here, based on theoretical predictions [1], we study the spin-to-charge conversion in ferromagnetic materials with high spin-orbit interaction. In particular, we chose the perpendicular magnetic anisotropy (PMA) multilayers CoNi and CoPt. We investigate the spin dynamics and SOTs of corresponding purely metallic ferromagnetic thin film in-plane anisotropy (IPA) / PMA hybrid systems using an inductive technique based on vector network analysis [2].

We observe substantial damping-like SOTs generated in the PMA layers. The SOTs in CoNi/Cu/CoFeB are comparable to those observed in Pt/CoFeB [3] and Pt/NiFe [4] heterostructures using the same technique and similar layer thicknesses.

- [1] A. Davidson *et al.*, Phys. Lett. A 384, 126228 (2020).
- [2] A. J. Berger *et al.*, Phys. Rev. B 97, 94407 (2018).
- [3] M. Meinert *et al.*, Phys. Rev. Applied 14, 064011 (2020).
- [4] A. J. Berger *et al.*, Phys. Rev. B 98, 024402 (2018).

MA 19.44 Tue 17:30 P2

Current-induced interlayer DMI in synthetic antiferromagnets — •FABIAN KAMMERBAUER¹, WON-YOUNG CHOI¹, FREIMUTH FRANK², KYUJOON LEE³, ROBERT FRÖMTER¹, YURIY MOKROUSOV^{1,2}, and MATHIAS KLÄUI¹ — ¹Institute of Physics, Johannes Gutenberg University, Staudingerweg 7, 55128 Mainz, Germany — ²Peter Grünberg Institut and Institute for Advanced Simulation, Forschungszentrum Jülich and JARA, 52425 Jülich, Germany — ³Division of display and semiconductor physics, Korea University, Sejong-ro 2511, Sejong, Republic of Korea

There is rising interest in 3D magnetism and magnetic textures, such as hopfions. Stabilizing 3D magnetic textures is in need of additional interactions favoring the canting of spins in the lateral direction. Layered synthetic antiferromagnets coupled by the symmetric interlayer exchange can additionally display an antisymmetric interlayer exchange, henceforth called interlayer DMI, which exerts such canting. Here, we report the effect of an electrical current on the antisymmetric interlayer DMI by employing anomalous Hall effect measurements with an additional applied in-plane field. In order to quantify the current dependence of the antisymmetric interlayer exchange interaction, an interlayer DMI field is introduced. Using a model of two superimposed cosine functions accounting for current-dependent and static contributions, we demonstrate that the current-dependent interlayer DMI field increases linearly with current and maximal along the direction of current flow. Thus, we demonstrate the possibility to control the interlayer DMI directly by electrical currents.

MA 19.45 Tue 17:30 P2

Spin current transmission in LaSrMnO / NiO / Pt layers — •EVANGELOS TH. PAPAIOANNOU¹, CAMILLO BALLANI¹, PHILIPP GEIER¹, PHILIP TREMPLE¹, CHRISTOPH HAUSER¹, OLENA GOMONAY², and GEORG SCHMIDT¹ — ¹Institute of Physics, Martin-Luther University Halle-Wittenberg, 06120 Halle, Germany — ²Institute of Physics, Johannes Gutenberg University Mainz, 55128 Mainz, Germany

We investigate the effect of spin pumping and inverse spin-Hall effect (ISHE) in trilayers composed of a ferromagnetic half-metal/ antiferromagnetic oxide/non-magnetic layer in the form of La_{0.7}Sr_{0.3}MnO₃/ NiO (x nm) / Pt. The generated spin current is pumped through the antiferromagnetic NiO layer and is detected via ferromagnetic resonance and ISHE measurements at low temperatures down to 10K. We refine two competing mechanisms of spin transport whose contribution to spin transport and supremacy is temperature dependent. The mechanism arising from the direct exchange coupling between FM and AFM dominates below the blocking temperature, while the spin pumping mechanism dominates above the blocking temperature and shows to be more efficient spin current transport through NiO layers.

MA 19.46 Tue 17:30 P2

THz-2D Scanning Spectroscopy — •FINN-FREDERIK STIEWE, TOBIAS KLEINKE, TRISTAN WINKEL, ULRIKE MARTENS, JAKOB WALOWSKI, CHRISTIAN DENKER, and MARKUS MÜNZENBERG — Institute of Physics, University Greifswald, Germany

THz-spectroscopy offers attractive imaging capabilities for scientific research, especially in life science. Its low photon energies lead to non-destructive interaction with matter. In our study, we investigate THz-pulses generated by fs-laser excitations in CoFeB/Pt heterostructures (STE), based on spin currents together with a LT-GaAs Auston switch as detector. The spatial resolution is tested by applying a 2D scanning technique with motorized stages allowing scanning steps in the sub-micrometer range. By applying an external magnetic field, the spin alignment in the CoFeB layer can be changed and the influence on the THz emission can be studied. For determining the spatial resolution, the STE is directly evaporated on a gold-test pattern separated by a several hundred nanometer thick insulating spacer layer. We observe a THz beam FWHM of 4.86 * 0.37 μm at 1 THz by using near-field imaging, which are in the dimension of the laser spot [1]. Our phase sensitive detection allows to image the magnetic alignment of the CoFeB layer. For this purpose, the STE's are patterned in micrometer sized geometric shapes on a glass substrate and scanned by our 2D scanning technique. Due to its simplicity, our technical approach offers a large potential for wide-ranging applications. [1] F.-F. Stiewe et al., Appl. Phys. Lett. 120, 32406 (2022).

Funding by: MetaZIK PlasMark-T (FKZ:03Z22C511), BMBF

MA 19.47 Tue 17:30 P2

Spatially Resolved Terahertz Spectroscopy using Spintronic-Terahertz-Emitter — •BRUNO ROSINUS SERRANO^{1,2}, ALEX CHEKHOV^{1,2}, YANNIC BEHOVITS^{1,2}, and TOBIAS KAMPFRATH^{1,2} — ¹Freie Universität Berlin — ²Fritz-Haber-Institut Berlin

New efficient laser-driven sources provide high THz fields suitable for excitation of ultrafast spin dynamics in various materials. These intense THz pulses are often characterized with a use of infrared and THz cameras also known as focal plane arrays (FPA). Since the FPA output strongly depends on its spectral sensitivity, it is often important to know the transfer function of a given FPA in the corresponding THz range. Here, we develop a table-top technique, which allows one to separate and spatially resolve spectral contributions to the FPA image in the THz range. Our results indicate that the FPA sensitivity can be quite resonant at different frequencies.

MA 19.48 Tue 17:30 P2

Identification and characterization of plastics using THz-spectroscopy — •TOBIAS KLEINKE, FINN-FREDERIK LIETZOW, ULRIKE MARTENS, JAKOB WALOWSKI, and MARKUS MÜNZENBERG — Institute of Physics, University Greifswald, Germany

THz-spectroscopy is an attractive tool for scientific research, especially in life science, offering non-destructive interaction with matter due to its low photon energies [1]. Current research investigates the impact of plastic nanoparticles on cell tissue in several aspects, because those particles are highly abundant in the environment and also enter the human body potentially causing harmful interactions [2].

THz spectroscopy offers the opportunity to discover and study the influence of microplastics in living human cells. Our project aims to identify and characterize different types of plastics in the human body or even in cells. Therefore it is necessary to set up a database with THz-spectra of the most abundant polymers. We analyse transmission spectra of several plastics with a commercial THz spectrometer (bandwidth from 0.1 to 6 THz) and identified specific absorption peaks for the individual studied materials. Furthermore, by determining the refractive index and the absorption coefficient, specific polymers can be characterized and identified.

[1] W. Shi et al., Journal of Biophysics, Vol. 14, 2021

[2] A. Ragusa et al., Environment International, Vol. 146, 2021

MA 19.49 Tue 17:30 P2

Spin-Hall-Angle measurements on magnetic heterostructures with bismuth alloys using THz-spectroscopy — •TRISTAN WINKEL¹, FINN-FREDERIK STIEWE¹, JAKOB WALOWSKI¹, CHRISTIAN DENKER², and MARKUS MÜNZENBERG¹ — ¹Institute of Physics, University Greifswald, Germany — ²EMCC DR. RASEK, Ebermannstadt, Deutschland

Spin Hall angle measurements are important for spin device design. THz spectroscopy provides effective means to measure spin Hall angles. In our study, we investigate THz pulses generated by fs laser excitations in magnetic heterostructures based on spin currents, together with an LT-GaAs Auston switch as a detector. The magnetic heterostructures consist of a CoFeB layer and a heavy metal layer such as bismuth alloys [1]. From the THz measurement, we can extrapolate the spin Hall angle of the heavy metal. The data is then used to build optimized spin Hall nano-oscillators for the fabrication of a neuromorphic computer chip [2]. Our technical approach offers great potential for wide-ranging applications due to its simplicity.

[1] Caiyun Hong et al., Advanced Electronic Materials. 10.1002/aelm.201700632 (2018)

[2] M. Zahedinejad et al., Appl. Phys. Lett. 112, 132404 (2018)

MA 19.50 Tue 17:30 P2

Formation and decay dynamics of the perpendicular standing spin-wave (PSSW) mode following the ultrafast demagnetization of an ultrathin permalloy film — •ANULEKHA DE¹, AKIRA LENTFART¹, LAURA SCHEUER¹, BENJAMIN STADTMÜLLER^{1,2}, PHILIPP PIRRO¹, GEORG VON FREYMAN^{1,3}, and MARTIN AESCHLIMANN¹ — ¹Department of Physics and Research Center OPTIMAS, University of Kaiserslautern, Germany — ²Institute of Physics, Johannes Gutenberg University Mainz, Germany — ³Fraunhofer Institute for Industrial Mathematics ITWM

One of the most thoroughly explored spin-wave modes in ferromagnetic films is the perpendicular standing spin wave (PSSW) mode, the coherent excitation of which require nonuniform excitation or pinning of the magnetization. By tuning the film thickness, it is possible to shift this mode to the sub-THz regime due to the increased exchange contribution quantized over the thickness. Here, we demonstrate the formation of the first PSSW mode on the ps timescale following the optically induced ultrafast demagnetization of the thin Py film using fs-light pulses in an all-optical, time-resolved magneto-optical Kerr effect (tr-MOKE) technique. For the excitation of coherent spin waves using ultrashort laser pulses, the magnetization of the samples was canted in OOP direction with an external field. The observed time-dependent behavior of the first PSSW mode gives an insight into the role of spin waves during the ultrafast demagnetization and remagnetization process. This research was supported by the DFG through No. TRR 173-268565370 (B11).

MA 19.51 Tue 17:30 P2

Characterizing electro-optic terahertz analyzers using a polarization-tunable spintronic terahertz emitter — •GENARO BIERHANCE^{1,2}, OLIVER GUECKSTOCK^{1,2}, and TOBIAS KAMPFRATH^{1,2} — ¹Department of Physical Chemistry, Fritz Haber Institute of the Max Planck Society, 14195 Berlin, Germany — ²Department of Physics, Freie Universität Berlin, 14195 Berlin, Germany

One goal of current spintronics research is to push the speed of spin torques, transport and their detection to terahertz (THz) frequencies. Here, THz spectroscopy is a powerful tool that provides immediate access to the femtosecond time scales of spin dynamics. The toolbox of THz spectroscopy was recently extended by spintronic emitters (STEs), which provide efficient, spectrally broad and gapless emission in the THz frequency range.

Here, we show that the emitted THz field has a linear polarization with a high intensity purity. The polarization axis can easily be set by an external magnetic field. Subsequently, we use this property to quantify the capability of the electro-optic crystals ZnTe and GaP as THz polarization analyzers in the context of electro-optic THz detection. We find excellent performance with frequency-resolved intensity extinction ratios up to 40,000:1.

MA 19.52 Tue 17:30 P2

Orbitronic influences on spintronic THz emitters — •JULIEN SCHÄFER, LAURA SCHEUER, PHILIPP PIRRO, and BURKARD HILLEBRANDS — TU Kaiserslautern, Kaiserslautern, Deutschland

Magnetic / non-magnetic thin film bilayers were recently introduced as novel sources of THz radiation: A fs laser pulse generates a spin current in the ferromagnetic layer which diffuses into the non-magnetic layer. Usually, the non-magnetic layer is chosen to exhibit a high spin-orbit coupling in order to efficiently transform the spin current into a charge current via the inverse spin-Hall effect. The accelerated electrons of the transient charge current then emit a broadband radiation in the THz regime.

The orbital Hall effect is reported to be remarkably long-ranged in ferromagnets and to generate considerable spin-orbit torques on CuO_x/Pt interfaces [1]. Therefore, we investigated Co/Pt-emitters in various combinations with CuO_x

and Al₂O₃ as an insulator barrier to extract the influence of a potential inverse orbital Hall effect on the THz emission. The exploitation of the inverse orbital Hall effect opens new perspectives in terms of material choices for the next generation of spintronic THz emitters.

[1]: D. Go *et al.*: *Long-Range Orbital Transport in Ferromagnets*, arXiv:2106.07928 [cond-mat.mes-hall] (2022)

MA 19.53 Tue 17:30 P2

Enhancement of THz emission from Fe/LI₀-FePt/Pt spintronic emitters — •LAURA SCHEUER¹, MORITZ RUHWEDEL¹, DOMINIK SOKOLUK³, GARIK TOROSYAN⁴, MARCO RAHM³, BURKARD HILLEBRANDS¹, THOMAS KEHAGIAS², RENÉ BEIGANG¹, and EVANGELOS PAPAIOANNOU⁵ — ¹Department of Physics and Landesforschungszentrum OPTIMAS, TU Kaiserslautern, Kaiserslautern, Germany — ²Department of Physics, Aristotle University of Thessaloniki, Thessaloniki, Greece — ³Fachbereich Elektro-Informationstechnik und Landesforschungszentrum OPTIMAS, University of Kaiserslautern, Kaiserslautern, Germany — ⁴Photonic Center Kaiserslautern, Kaiserslautern, Germany — ⁵Institute for Physics, Martin-Luther University Halle Wittenberg, Halle, Germany

The development of thin film multilayers composed of a ferromagnetic metal (FM) layer and a non-magnetic metal (NM) layer as sources for THz emission opened a new direction in physics.

In this presentation we concentrate on the impact of the FM/NM interface on the THz emission. We intentionally modify the Fe/Pt interface by manipulating the Pt growth temperature to achieve the formation of an ordered LI₀-FePt alloy interlayer. Subsequently, we find a Fe/LI₀-FePt (2nm)/Pt configuration to be significantly superior to a Fe/Pt bilayer structure, regarding THz emission amplitude and bandwidth. Both can be controlled by the extent of alloying on either side of the interface [1].

[1] L. Scheuer *et al.*: *THz emission from Fe/Pt spintronic emitters with LI₀-FePt alloyed interface*, *iScience*, Volume 25, Issue 5, 2022

MA 19.54 Tue 17:30 P2

Spectral characteristics of microstructured spintronic THz emitters — •RIEKE VON SEGGERN¹, CHRISTOPHER RATHJE¹, LEON GRÄPER¹, JANA KREDL², JAKOB WALOWSKI², MARKUS MÜNZENBERG², and SASCHA SCHÄFER¹ — ¹Institute of Physics, University of Oldenburg, Germany — ²Institute of Physics, University of Greifswald, Germany

The introduction of spintronic terahertz emitters (STE) opened up a new class of terahertz (THz) sources with useful properties for spectroscopy applications, such as an ultrabroad and gapless emission spectrum and high THz peak field strengths [1].

Here, a resonator-grafted STE bilayer (CoFeB/Pt) is illuminated by a focused optical excitation pulse (780-nm central wavelength, 70-fs pulse duration, 16-µm FWHM spot size) to generate a micrometer-scale broadband THz source. The radiated THz field coupled to the adjacent resonator is recorded via electro-optic sampling, dependent on the excitation location. Remarkably, the emitted THz signal changes drastically due to the coupling of the local dipole to the microresonators [2]. The spectral influence of different resonator geometries is experimentally demonstrated, and the underlying physical mechanisms are discussed based on detailed numerical simulations of the phenomenon. Special emphasis is placed on the interplay between intrinsic resonator characteristics and angular THz emission distributions.

[1] Seifert *et al.*, *Nat. Photonics* 10, 483 (2016)

[2] Rathje, von Seggern *et al.*, manuscript in preparation

MA 19.55 Tue 17:30 P2

Domain structure of few-layer Fe₃GeTe₂ microflakes — •HONEY BOBAN¹, KEDA JIN², TOBIAS WICHMANN², ANNA MANDZIAK³, EWA MADEJ³, JOSE MARTINEZ CASTRO², VITALIY FEYER⁴, IULIA COJOCARIU⁴, DANIEL BARANOWSKI⁴, FELIX LUPKE², CLAUDIUS MICHAEL SCHNEIDER¹, and LUKASZ PLUCINSKI¹ — ¹PGI-6, Forschungszentrum Juelich — ²PGI-3, Forschungszentrum Juelich — ³SOLARIS Centre, Krakow — ⁴Elettra Synchrotron, Trieste

Fe₃GeTe₂ is a ferromagnetic 2D metal with a bulk transition temperature of 220K[1]. Monolayer FGT is inversion asymmetric, whereas in the bulk inversion symmetry is recovered because of the AB stacking. FGT exhibits stripe domain patterns with an average width of 140 nm at 110K[1]. Within each layer a combination of inversion asymmetry with ferromagnetism gives rise not only to a finite spin polarization but also to energy shifts of spectral features between K and K' momenta[2].

To study the spin polarized bands in FGT, we shall probe a single terrace with domain larger than the photon beamspot. We exfoliated FGT flakes of 4-5 monolayer thickness on graphite/Au/SiO₂ in a glovebox and encapsulated them with graphene, since thin FGT flakes degrade rapidly in ambient conditions[3]. Dichroic PEEM measurements on these flakes showed single domains of sizes up to 4 x 3 µm, when cooled down to <100K. The thin flakes with 4 x 3 µm single domain can be used to demonstrate the predicted asymmetries at the K and K' points.

[1] Nano Lett. 18, 5974(2018), [2] Nature Physics 10, 387(2014), [3] npj 2D Materials and Applications 4, 33(2020)

MA 19.56 Tue 17:30 P2

Exchange interactions in monolayers of the MnBi₂Te₄ family — •DONYA MAZHJOO, GUSTAV BIHLMAYER, and STEFAN BLÜGEL — Peter Grünberg Institute and Institute for Advanced Simulation, Forschungszentrum Jülich, D-52425 Jülich, Germany

Due to their novel properties, two-dimensional magnetic materials are highly desirable for spintronic applications. An interesting material is MnBi₂Te₄ [1]. Of substantial interest is the relating of the intrinsically topological properties of MnBi₂Te₄ and the magnetic interactions and the impact of the alteration of their chemical constitution. The question can be resolved by density functional theory (DFT), which enables the calculation of the magnetic interaction directly from the electronic structure.

By using the full-potential linearized augmented planewave method (FLAPW) as implemented in the FLEUR-code [2], we analyzed the exchange interaction in septuple layers of MnBi₂Te₄ type. Mapping our results on the extended Heisenberg model, we disentangle different exchange interactions, spin-orbit coupling effects like the magnetocrystalline anisotropy, and higher-order interactions [3]. Also, applying an external electric field breaks the inversion symmetry and allows for a strong DMI that may lead to the realization of metastable topological magnetic structures [4].

[1] M. Otrokov *et al.*, *Nature* 576, 416 (2019).

[2] <https://www.flapw.de>

[3] M. Hoffmann *et al.*, *Phys. Rev. B* 101, 024418 (2020).

[4] D. Mazhjo *et al.*, *Proc. SPIE* 11470, 114702S (2020).

MA 19.57 Tue 17:30 P2

Investigation of the surface structure of Y₃Fe₅O₁₂ thin films by X-ray photoelectron spectroscopy and diffraction (XPS and XPD) — •THOMAS RUF¹, PHILIP TREMPER², GEORG SCHMIDT², and REINHARD DENECKE¹ — ¹Wilhelm-Ostwald-Institut, Universität Leipzig — ²Institut für Physik, Martin-Luther-Universität Halle-Wittenberg

Y₃Fe₅O₁₂ (YIG) is a ferrimagnetic and insulating material with low ferromagnetic resonance (FMR) linewidth and damping constant. High surface quality and complete epitaxial growth are important for YIG thin films. High-quality YIG thin films are good candidates for integrated magnonics and spin injection in YIG/metal bilayers.

XPD measurements for assignment of the surface structure of pulsed laser deposited, high quality and pseudomorphic YIG(100) on Gd₃Ga₅O₁₂(100) and YIG(111) on Gd₃Ga₅O₁₂(111) 50 nm thin films were conducted. XPS angular intensity anisotropies for high kinetic energy lines Y 3d (E_{kin} = 1329 eV), Fe 3p (E_{kin} = 1430 eV) and O 1s (E_{kin} = 957 eV) of the thin films can be interpreted in the forward focusing regime as a bulk-like (SG Ia3d) surface structure. Simplifying the interpretation to forward focusing allows for interpretation as a real space scan. The normalized intensity for Y 3d and Fe 3p lies in the range of 0.85 to 1.2 and approx. 0.9 to 1.1 for O 1s. This confirms epitaxial coherence reaching to the film surface, as XPD effects are restricted to few atomic layers. The measured XPS quantification ratios of 1.1 and 1.2 for [Y]/[Fe], compared to nominally 0.6, can only be partly explained by those XPS angular intensity anisotropies.

MA 19.58 Tue 17:30 P2

Ti, V, Ta, Nb as a boron sink in crystalline CoFeB/ MgO/ CoFeB Magnetic Tunnel Junctions — •TOBIAS PETERS, LAILA BONDZIO, INGA ENNEN, and GÜNTER REISS — Center for Spinelectronic Materials and Devices, University of Bielefeld, Germany

We investigated the tunnel magnetoresistance (TMR) in CoFeB/MgO/ CoFeB Magnetic Tunnel Junctions (MTJs) and studied the use of Ti, V, Ta and Nb as a boron getter during thermal annealing. Exchange bias MTJs were deposited by sputtering deposition. The basic TMR stack was modified by inserting an additional ultrathin layer into the CoFeB bottom electrode and changing the capping layer with the stated materials. TMR measurements have been performed for samples post-annealed at temperatures from 270°C to 420°C for 1h. The boron diffusion was observed via Electron Energy Loss Spectroscopy and Transmission Electron Microscopy. Nb-samples show the highest TMR for post-annealing temperatures smaller than 360°C. For higher temperatures we found even higher TMR for a Ta-sample. However, the insertion of Ta in the CoFeB electrode leads to a severe loss of pinning.

MA 19.59 Tue 17:30 P2

Magnetization dynamics in hybrid ferromagnetic / antiferromagnetic systems — •HASSAN AL-HAMDO¹, YARYNA LYTUVYENKO², GUTENBERG KENDZO¹, MISBAH YAQOOB¹, MORITZ RUHWEDEL¹, PHILIPP PIRRO¹, OLENA GOMONAY², VITALIY I. VASYUCHKA¹, MATHIAS KLÄUI², MARTIN JOURDAN², and MATHIAS WEILER¹ — ¹Fachbereich Physik und Landesforschungszentrum OPTIMAS, Technische Universität Kaiserslautern, 67663 Kaiserslautern, Germany — ²Institute of Physics, Johannes Gutenberg-University Mainz, 55128 Mainz, Germany

While typical antiferromagnetic magnons are in the THz range at zero external magnetic field, ferromagnetic magnons are gapless. A ferromagnet/antiferromagnet bilayer is thus expected to host hybrid spin excitations. We

study the magnetization dynamics of $\text{Mn}_2\text{Au}/\text{Ni}_{80}\text{Fe}_{20}$ thin film bilayers. This system allows us to control the Mn_2Au Néel vector orientation with moderate external magnetic fields [1]. Mn_2Au furthermore shows strong spin-orbit torque efficiency [2] making this system intriguing for all-electrical control of magnetization direction. By varying the thickness of $\text{Ni}_{80}\text{Fe}_{20}$, we investigated the effect of the $\text{Mn}_2\text{Au}/\text{Ni}_{80}\text{Fe}_{20}$ interface on $\text{Ni}_{80}\text{Fe}_{20}$ spin dynamics. Broadband ferromagnetic resonance and Brillouin light scattering experiments reveal that interfacial exchange coupling causes an increase in the resonance frequency of $\text{Ni}_{80}\text{Fe}_{20}$. Reference(s): [1] Bommanaboyena et al., Nature Communications 12, 6539 (2021) [2] Bodnar et al., Nature Communications 9, 348 (2018)

MA 19.60 Tue 17:30 P2

Imaging the magnetic structure of antiferromagnetic PtMn — •BEATRICE BEDNARZ, CHRISTIN SCHMITT, HENDRIK MEER, ADITHYA RAJAN, MATHIAS KLÄUI, and GERHARD JAKOB — Institut für Physik, Johannes Gutenberg-Universität Mainz, Staudingerweg 7, 55128 Mainz, Germany

Antiferromagnetic materials (AFM) are gaining increasing interest in the recent years because of their high potential for new spintronic devices with very high bit packing densities and ultrafast dynamics. [1] PtMn is widely used, especially to pin ferromagnetic layers in magnetic devices. [2] $\text{Pt}_{50}\text{Mn}_{50}$ has a CuAu-I type structure with a high bulk Néel temperature of 975 K. [3] THz spin dynamics [4] and periodic chiral structures [5] have been predicted in PtMn. However, to use it as the active layer of spintronic devices, the first crucial step is to read out its magnetic state. This was achieved now by imaging the domains with x-ray magnetic linear dichroism (XMLD). Additionally, the domain size was determined from a Fourier transform of the XMLD images for 40 nm PtMn grown on MgO (001) and capped with 1.6 nm Al. It shows a distinct ring, corresponding to an average domain periodicity of approximately 650 nm.

[1] V. Baltz et al., Rev. Mod. Phys. 90, 015005 (2018). [2] G.W. Anderson et al., J. Appl. Phys. 87, 5726 (2000). [3] L. Pál et al., J. Appl. Phys. 39, 538 (1968). [4] K. Kang et al., ArXiv:2112.13954 [Cond-Mat] (2021). [5] Md.R.K. Akanda et al., Phys. Rev. B 102, 224414 (2020).

MA 19.61 Tue 17:30 P2

Ultrafast Magnetization Dynamics in spin Hall nano-oscillators layer-stacks with different heavy metals — •TAHEREH SADAT PARVINI, JAKOB WALOWSKI, and MARKUS MUENZENBERG — Institut für Physik, Universität Greifswald, Greifswald, Germany

We employed an all-optical time-resolved magneto-optical Kerr effect (TRMOKE) microscope for an unambiguous determination of oscillation frequency and Gilbert damping of spin Hall nano-oscillators. The structures of the stacks are $W\text{Ta}(5)/\text{Py}(7)/\text{Pt}(2)/\text{HfO}_x$, $W(5)/\text{Py}(7)/\text{Pt}(2)/\text{HfO}_x$, $\text{Py}(7)/\text{PtCu}(5)/\text{HfO}_x$, and $\text{Py}(7)/\text{PtCr}(5)/\text{HfO}_x$ (thicknesses are in nm). The oscillation frequency and effective damping parameters are investigated as a function of the intensity and direction of the external magnetic field, the intensity of the pump, and cap layer thicknesses. Our results show stacks with PtCr and PtCu cap layers have smaller Gilbert damping than stacks with Pt cap layers. This study paves the way for developing ultrafast spintronic devices for data storage and information processing.

MA 19.62 Tue 17:30 P2

Direct imaging of current-induced antiferromagnetic switching in NiO revealing a pure thermomagnetoelastic switching mechanism — •HENDRIK MEER¹, FELIX SCHREIBER¹, CHRISTIN SCHMITT¹, RAFAEL RAMOS^{2,3}, EIJI SAITOH^{2,4}, OLENA GOMONAY¹, JAIRO SINOVA¹, LORENZO BALDRATI¹, and MATHIAS KLÄUI¹ — ¹Institute of Physics, Johannes Gutenberg-University Mainz, Mainz, Germany — ²CIQUS, Departamento de Química-Física, Uni-

versidade de Santiago de Compostela, Santiago de Compostela, Spain — ³WPI-Advanced Institute for Materials Research, Tohoku University, Sendai, Japan — ⁴Department of Applied Physics, The University of Tokyo, Tokyo, Japan

Antiferromagnetic spintronics is considered as a disruptive approach, enabling scalable ultrafast and efficient spintronic devices. We observe current-induced magnetic switching of insulating antiferromagnet/heavy metal bilayers. Previously, different reorientations of the Néel order for the same current direction were reported for different device geometries and different switching mechanisms were proposed. Here, we combine concurrent electrical readout and optical imaging of the switching of antiferromagnetic domains with simulations of the current-induced temperature and strain gradients. By comparing the switching in specially engineered NiO/Pt device and pulsing geometries, we can rule out dominating spin-orbit torque based mechanisms and identify a thermomagnetoelastic mechanism to switch the antiferromagnetic domains, reconciling previous reports.

MA 19.63 Tue 17:30 P2

Spin Hall magnetoresistance effect in orthoferrites/Pt heterostructures. — S. BECKER¹, •E.F. GALINDEZ-RUALES¹, A. ROSS¹, E. POMJAKUSHINA², F. SCHREIBER¹, R. LEBRUN^{1,3}, G. JAKOB¹, O. GOMONAY¹, and M. KLÄUI¹ — ¹Institute of Physics, Johannes Gutenberg University Mainz, 55099 Mainz, Germany. — ²Laboratory for Multiscale Materials Experiments, PSI, 5232, Villigen PSI, Switzerland — ³Unité Mixte de Physique CNRS-Thales, Palaiseau, France Although there are advantages of antiferromagnetic systems [1], there are some limitations in the length of the spin transmission distance that only recently have been tackled using orthoferrites [2]. TmFeO_3 (TFO), a rare earth orthoferrite, possesses both collinear antiferromagnetic ordering and a net canted ferromagnetic moment. That is due to the bulk Dzyaloshinskii-Moriya interaction (DMI), which leads to a canting of the four magnetic iron sublattices [3]. Spin Hall magnetoresistance (SMR) is used to investigate the magnetic properties of a bulk sample [4]. We can identify the onset of the spin reorientation transition (SRT) as well as the spin-flop field, which changes approximately linearly with temperature around the SRT. We observe differences between the different devices likely stemming from the symmetry breaking at the TFO/Pt interface due to interfacial DMI.

[1] Lebrun, R., et al. Nat. Commun 11, 6332 (2020). [2] S. Das, et. al. ArXiv:2112.05947 [cond-mat.str-el] [3] S. Becker, et.al. Phys. Rev. B103, 024423 (2021). [4] R. Lebrun, et. al. Commun. Phys. 2, 50 (2019).

MA 19.64 Tue 17:30 P2

Structure and magnetism of hematite nanodiscs — •MARYNA SPASOVA and MICHAEL FARLE — Faculty of Physics and Center of Nanointegration (CENIDE), University of Duisburg-Essen, Germany

Hexagonal shaped, single crystal hematite nanodiscs with thickness of 20 nm and different lateral sizes from 110 nm up to 250 nm were synthesized by an alcohol-thermal reaction. High Resolution Transmission Electron Microscopy reveals a very high crystallinity with (0001) basal planes and (101-2) side surfaces. The temperature of the Morin transition (MT) decreases for smaller diameters of the nanodiscs. The magnetization above the MT, however, does not depend on the particle size. It is close to the bulk value ($M = 0.3 \text{ Am}^2/\text{kg}$) whereas the coercivity decreases with increasing diameter from 55 kA/m (110 nm) to 37 kA/m (250 nm). Below the MT the nanodiscs are ferromagnetic due to uncompensated surface magnetic moments which are perpendicular to the (0001) crystal plane. The magnetization measured at 10K is proportional to the surface area of the sample. The coercivity at 10 K increases with increasing particle diameter, i.e. 50 kA/m for 110 nm up to 550 kA/m for 250 nm. A very high irreversibility field of 3000 kA/m indicates a high magnetic anisotropy of the sample.

MA 20: Focus Session: Revealing Multidimensional Spin Textures and their Dynamics via X-rays and Electrons

Non-collinear spin textures in magnetic materials and excitations within such spin arrangements moved into the focus of research. These system host topological spin states and unique excitations providing access to versatile future spintronic applications. The imaging of such complex internal magnetic orders of materials is a fundamental problem of extreme importance for the successful implementation of these applications. Characterizing the electronic, magnetic and transport properties of structures such as vortices, magnetic singularities or hopfions lead to the development of novel experimental and theoretical techniques. For instance, magnetic hopfions have been unveiled via a combination of X-ray photoemission electron microscopy and soft X-ray transmission microscopy using element-specific X-ray magnetic circular dichroism effects. Recently, time-resolved magnetic laminography enabled access to the temporal evolution of three-dimensional (3D) magnetic microdiscs with nanoscale resolution, while quantitative reconstruction of the 3D spintexture of skyrmions with sub-10 nm resolution was demonstrated by holographic vector field electron tomography or soft x-ray vector ptychography. Pivotal to these experimental developments are theoretical proposals for the detection and manipulation protocols. Although making a strong impact in the field of magnetism, this area of research calls for an in-depth exchange between experts of different techniques, experimental and theoretical, to unravel many of the open questions and puzzling behavior discovered within the last couple of years. This motivates the present focus session as an opportunity for discussions and to attract more researchers to this fascinating field.

Organizers: Samir Lounis (Uni.Duisburg-Essen and FZ-Jülich), Matthias Althammer, Stephan Geprägs (Walther-Meißner-Institut, Bayerische Akademie der Wissenschaften, Garching), Gisela Schütz (MPI-Intelligent systems, Stuttgart), Stefan Blügel (FZ-Jülich)

Time: Wednesday 9:30–13:00

Location: H37

Invited Talk

MA 20.1 Wed 9:30 H37

Recent developments in X-ray three-dimensional magnetic imaging —

•VALERIO SCAGNOLI — ETHZ - PSI

Three dimensional magnetic systems hold the promise to provide new functionality associated with greater degrees of freedom. Over the last years we have worked towards developing methods to fabricate and characterize three dimensional magnetic structures. Specifically, we have combined X-ray magnetic imaging with new iterative reconstruction algorithms to achieve X-ray magnetic tomography and laminography [1-4]. In a first demonstration, we have determined the three-dimensional magnetic nanostructure within the bulk of a soft GdCo₂ magnetic micropillar and we have identified the presence of Bloch points of different types [1] as well as three-dimensional structures forming closed vortex loops [3]. Subsequently, we have used the flexibility provided by the laminography geometry to perform time resolved measurements of the magnetization dynamics in a two-phase micrometer size GdCo disk. Therefore, X-ray magnetic three-dimensional imaging, with its recent extension to the soft X-ray regime [5], has now reached sufficient maturity that will enable to unravel complex three-dimensional magnetic structures for a range of magnetic systems.

[1] C. Donnelly et al., Nature 547, 328 (2017)

[2] C. Donnelly et al., New J. Phys. 20, 083009 (2018)

[3] C. Donnelly et al., Nat. Phys. 17, 316 (2021)

[4] C. Donnelly et al., Nat. Nanotechnol. 15, 356 (2020)

[5] K. Witte et al., Nano Letters 20, 1305 (2020)

Invited Talk

MA 20.2 Wed 10:00 H37

Magnetic depth profiling with x-ray resonant magnetic reflectivity (XRMR)

— •TIMO KUSCHEL — Department of Physics, Bielefeld University, 33615 Bielefeld, Germany

Magnetic depth profiling is one of the important thin-film characterization techniques in today's condensed matter physics and, in particular, in the spintronic research field. The interference of reflected light from the interfaces of a magnetic thin-film system depends on its magnetic state. Thus, the detected reflectivity of typically circularly polarized light provides information on the depth profile of the sample's magnetization. By the use of synchrotron x-rays, this dependence becomes element-selective as long as the absorption energy of a specific chemical element is used as photon energy. Therefore, the analysis of the x-ray resonant magnetic reflectivity (XRMR) separates the individual magnetic depth profiles of different chemical elements [1].

In my contribution, I will introduce this experimental technique and emphasize advantages over standard x-ray magnetic circular dichroism detection [2]. I will discuss the quantitative comparability of XRMR with other experimental techniques [3] and present recent results on the magnetic proximity effect in platinum (Pt), palladium (Pd) and vanadium (V). Finally, I will highlight the cation- and lattice-site sensitivity of XRMR for the study of Fe₃O₄ and its interfaces [4].

[1] S. Maske, E. Goering, J. Phys. Cond. Matter 26, 363201 (2014)

[2] T. Kusche et al., Phys. Rev. Lett. 115, 097401 (2015)

[3] D. Graulich, TK et al., Appl. Phys. Lett. 118, 089901 (2021)

[4] T. Pohlmann, TK et al. Phys. Rev. B. 102, 220411(R) (2020)

Invited Talk

MA 20.3 Wed 10:30 H37

Magnetic Bragg Ptychography Studies of Spin Caloritronic —

•DINA CARBONE¹, PENG LI², STEPHAN GEPRÄGS³, RUDOLF GROSS^{3,4}, PAUL EVANS⁵, VIRGINIE CHAMARD⁶, and DAN MANNIX⁷ — ¹MAX IV Laboratory, Lund SE — ²Diamond Light Source, Didcot UK — ³Walther-Meißner-Institut, BADW, Garching DE — ⁴Physik-Department, TUM, Garching DE — ⁵Univ. of Wisconsin, Madison USA — ⁶Institut Fresnel, Marseille FR — ⁷ESS, Lund SE & Institut Néel, Grenoble FR

Spin-caloritronics refer to a class of materials in which spin, charge and heat currents can be interconverted. This gives rise to diverse functional properties that offer a great potential towards a new generation of fast and low power consumption electronics. Advances in the design and understanding of future spintronic nanotechnologies require the development of state-of-the-art 3D magnetic characterisation tools. In particular, for crystalline magnetic materials grown at nanoscales, understanding the interdependence of their magnetic properties with crystal structure and strain is crucial.

We have developed a magnetic and structural microscopy based on scanning diffraction, by combining circular polarisation and focussing of the X-ray beam. This has revealed spin texture in prototype spin caloritronics device structures and its relation with crystal orientation down to micron resolution [1]. New results obtained with coherent X-rays, using magnetic Bragg ptychography, push this technique towards a 3D spin microscopy with a resolution of few tens of nm.

[1] Evans et al., Sci. Adv. 6, eaba935, 2020

15 min. break

Invited Talk

MA 20.4 Wed 11:15 H37

Imaging the 3D magnetic texture of skyrmion tubes and approaches towards determining their Hall signature —

•B. RELLINGHAUS¹, S. SCHNEIDER^{1,2}, D. WOLF², U.K. RÖSSLER², M. SCHMIDT³, A. KOVÁCS⁴, R.E. DUNIN-BORKOWSKI⁴, D. POHL¹, A. THOMAS², D. KRIEGER², B. BÜCHNER², and A. LUBK² — ¹DCN, caed, TU Dresden, Germany — ²IFW Dresden, Germany — ³MPI CPFS, Dresden, Germany — ⁴FZ Jülich, Germany

Despite the large interest in magnetic skyrmions, their 3D magnetic texture when being extended to skyrmion tubes (SkTs) in volume samples is largely unknown. We have therefore determined the magnetic structure of SkTs using low temperature holographic vector field electron tomography in an external magnetic field [1]. The resulting high-resolution 3D magnetic images reveal deviations from a homogeneous Bloch character, a collapse of the skyrmion texture near surfaces, the coexistence of longitudinal and transverse skyrmion textures, and a correlated axial modulation of the SkTs. Spatially resolved energy density maps calculated from the experimental magnetic induction data prove that these magnetic solitons are stabilized by the Dzyaloshinskii-Moryia interaction, which overcompensates the exchange energy in the centers of the tubes. In order to correlate the occurrence of skyrmionic structures with anomalies in their magneto-transport properties, we have devised a setup for the in-situ measurement of the Hall effect in a transmission electron microscope, first results of which will be highlighted. The work is gratefully supported by DFG within SPP 2137.

[1] D. Wolf et al., Nature Nanotechnology 17 (2021) 250.

Invited Talk

MA 20.5 Wed 11:45 H37

Determination of spin chirality and helicity angle by circular dichroism in soft x-ray absorption and resonant elastic scattering — •GERRIT VAN DER LAAN — Diamond Light Source, Didcot, UK

The depth profile of the full 3D spin structure of magnetic skyrmions below the surface of bulk Cu₂OSeO₃ was obtained using the polarization dependence of resonant elastic x-ray scattering (REXS) [AIP Advances 11, 015108 (2021)]. While the bulk spin configuration showed the anticipated Bloch type structure, the skyrmion lattice changes to a Néel twisting (i.e., with a different helicity angle) at the surface within a distance of several hundred nm. The experimental penetration length of the Néel twisting is 7x longer than the theoretical value given by the ratio of J/D. This indicates that apart from the considered spin interactions, i.e., Heisenberg exchange interaction J and Dzyaloshinskii-Moriya interaction D, as well as the Zeeman interaction, other effects must play an important role.

A new rule for the rotational symmetry invariance of the XMCD signal is presented [PRB 104, 094414 (2021)]. A threefold symmetric kagome lattice with negative spin chirality can give a nonzero x-ray magnetic circular dichroism (XMCD), despite a total spin moment of zero. A necessary condition is the existence of an anisotropic XMCD signal for the local magnetic atom. The maximum dichroism is not aligned along the spin direction but depends on the relative orientation of the spin with respect to the atomic orientation.

Invited Talk

MA 20.6 Wed 12:15 H37

Identification of complex spin-textures by novel Hall effects — •JUBA BOUAZIZ¹, HIROSHI ISHIDA², SAMIR LOUNIS¹, and STEFAN BLÜGEL¹ — ¹Peter Grünberg Institut and Institute for Advanced Simulation, Forschungszentrum Jülich & JARA, D-52425 Jülich, Germany — ²College of Humanities and Sciences, Nihon University, Sakurajosui, Tokyo 156-8550, Japan

Chiral magnetic phases of matter are commonly found in non-centrosymmetric materials. The complex magnetic order is stabilized by the Dzyaloshinskii-Moriya interaction, which promotes topologically non-trivial spin textures such as skyrmions. These entities imprint a characteristic signature on the Hall signal known as the topological Hall effect, allowing their detection employing

magneto-transport measurements. In this talk, relying on perturbation theory, we disentangle the multiple contributions to the Hall signal originating from non-collinear magnetism and relativistic effects. We unveil a new contribution, the non-collinear Hall effect (NHE) [1], whose angular form is determined by the magnetic texture, the spin-orbit field of the electrons, and the underlying crystal structure. The NHE together with other components of the Hall resistivity enables the decoding of exotic non-collinear magnetic textures that have been observed in itinerant magnets [1,2]. The impact of the NHE on the Hall signal of several two and three-dimensional spin textures such as magnetic hopfions is examined. [1] J. Bouaziz et al. PRL 126, 147203 (2021), [2] A. Neubauer et al. PRL 102, 186602 (2009).

MA 20.7 Wed 12:45 H37

All-electron holography of hopfions enabled by magneto-induced charges — •MORITZ WINTEROTT^{1,2} and SAMIR LOUNIS^{1,2} — ¹Peter Grünberg Institut and Institute for Advanced Simulation, Forschungszentrum Jülich & JARA, D-52425 Jülich, Germany — ²Faculty of Physics, University of Duisburg-Essen and CENIDE, 47053 Duisburg, Germany

In recent years, far-reaching progress has been made in the field of topological particles. In addition to the well-known skyrmions, three-dimensional topological particles such as hopfions, bobbers and cocoons, are also becoming increasingly interesting. Thereby, a major challenge is the visualisation and recognition of such topological particles hidden in bulk materials. An intuitiv approach is to resolve their magnetic contrast, which is highly non-trivial, especially for antiferromagnetic textures where the overall signals are expected to vanish. Here we demonstrate that the charge carried by such topological objects carries specific dependencies on the misalignment of the magnetic moments, which enable their identification without the need for spin-resolved measurements. We utilize multiple-scattering theory and address the case of ferro- and anti-ferromagnetic hopfions. We identify the achiral and chiral-induced charges. Spin-orbit interaction (SOI) gives rise to the latter in 1st order similarly to the Dzyaloshinskii-Moriya interaction and to anisotropic terms, 2nd order in SOI. We proceed to a systematic electron holography of the distinct magneto-induced charges, which provide a direct link to experiments.

MA 21: Terahertz Spintronics

Time: Wednesday 9:30–12:15

Location: H43

MA 21.1 Wed 9:30 H43

Spintronic THz emitters for lightwave-driven scanning tunneling microscopy at MHz repetition rates — •ALKISTI VAITSIS¹, VIVIEN SLEZIONA¹, FABIAN SCHULZ², LUIS ENRIQUE PARRA LOPEZ¹, TOM SEBASTIAN SEIFERT^{1,3}, MARTIN WOLF¹, and MELANIE MÜLLER¹ — ¹Fritz Haber Institute of the Max Planck Society, Berlin, Germany — ²CIC NanoGUNE BRTA, San Sebastian, Spain — ³Freie Universität Berlin, Germany

Attaining simultaneous high temporal resolution and signal-to-noise ratio in THz lightwave-driven scanning tunneling microscopy (THz-STM) requires broadband single-cycle THz pulses at high repetition rates and electric field strength. In this context, we report on the operation of ultrabroadband spintronic THz emitters (STE) at MHz repetition rates and pump powers of several Watts. We discuss saturation mechanisms which can reduce THz emission efficiency, such as steady-state and transient heating, limiting the usable fluence at the STE. Furthermore, to maximize the THz field in the STM junction, we analyze and optimize THz propagation into the STM, which due to the ultrabroadband spectrum of the STE requires careful consideration of pump spot sizes in combination with the limitations arising from pump fluence and average pump power density. We present detailed experimental and theoretical analysis of the ideal excitation geometry, which allows STE operation up to 10 W average powers at 2 MHz repetition rate at optimized fluence and THz propagation into the STM.

MA 21.2 Wed 9:45 H43

Investigation of THz electromagnetic response in nanopatterned magnetic heterostructures by current confinement — •BIKASH DAS MOHAPATRA¹, REZA ROUZEGAR³, EVANGELOS PAPAIOANNOU¹, TOBIAS KAMPFRATH³, and GEORG SCHMIDT^{1,2} — ¹Institut für Physik, Martin-Luther-Universität Halle-Wittenberg, Von-Danckelmann-Platz 3, D-06120 Halle, Germany — ²Interdisziplinäres Zentrum für Materialwissenschaften, Martin-Luther-Universität Halle-Wittenberg, Heinrich-Damerow-Straße 4, D-06120 Halle, Germany — ³Department of Physical Chemistry, Fritz Haber Institute, Faradayweg 4-6, 14195 Berlin, Germany

STEs (Spintronic Terahertz Emitters) are novel THz radiation sources. Many studies have demonstrated that the STEs when illuminated with fs-laser pulse, ultrafast spin current is produced which leads to ultrafast transverse charge current by Inverse Spin Hall Effect, resulting in THz electromagnetic pulses. We were able to fabricate THz emitters into arrays of various squares and rectangles

of micron or sub-micron size, using Sputter deposition and e-beam lithography. These emitters generate a different emission spectrum than large area reference emitters when irradiated with a fs laser. We propose that the confinement due to small size induces local charge buildup, which leads to additional currents that counterbalance the original charge current due to the Inverse Spin Hall Effect.

MA 21.3 Wed 10:00 H43

Coupling of a local broadband THz emitter to a 2D micro-resonator — •CHRISTOPHER RATHJE¹, RIEKE VON SEGGERN¹, LEON GRÄPER¹, JANA KREDL², JAKOB WALOWSKI², MARKUS MÜNZENBERG², and SASCHA SCHÄFER¹ — ¹Institut für Physik, Universität Oldenburg — ²Institut für Physik, Universität Greifswald

Recently, the advent of spintronic terahertz emitters (STE) has introduced a simple approach to generate broadband radiation in the terahertz (THz) spectral domain [1].

In this contribution, we utilize a resonator-grafted STE bilayer illuminated by a focused optical excitation pulse for the generation of a micrometer-scaled broadband THz emitter with a source size far below the THz diffraction limit [2]. The near-field of this localized transient electric dipole is coupled to a bow-tie antenna structure in direct proximity to the emitter. Depending on the position of the excitation focus, we detect the emitted THz time-domain signal in the far-field.

Our results show pronounced changes of the emission characteristics of the excited STE layer for a dipole positioned in the bow-tie gap, demonstrating the capability to tailor the emission spectrum including resonant enhancement of certain frequency components and increase of the overall bandwidth. We discuss the influence of different resonator designs and provide a model of the coupling process supported by numerical simulations. Further results for different isolated resonators and periodically structured metasurfaces are presented.

[1] Seifert et al., Nat. Photonics, 10, 483 (2016)

[2] Rathje et al., manuscript in preparation

MA 21.4 Wed 10:15 H43

Spin pumping in noncollinear antiferromagnets — •MIKE ALEXANDER LUND, AKSHAYKUMAR SALIMATH, and KJETIL MAGNE DØRHEIM HALS — University of Agder, Norway

The spin pumping and spin-transfer torque mechanisms in antiferromagnets have been theoretically and experimentally investigated in recent years. How-

ever, most of these works have concentrated on collinear antiferromagnets, leaving the spin dynamics of the more complex noncollinear antiferromagnets largely unexplored. Apart from a few works on spin-transfer torque, there has been no thorough investigation of the spin pumping process in noncollinear antiferromagnets.

In this talk, I will present our latest work on ac spin pumping in noncollinear antiferromagnets. Starting from an effective action description of the spin system, we derive the Onsager coefficients connecting the spin pumping and spin-transfer torque associated with the dynamics of the SO(3)-valued antiferromagnetic order parameter. Our theory is applied to a kagome antiferromagnet resonantly driven by a uniform external magnetic field. We demonstrate that the reactive (dissipative) spin-transfer torque parameter can be extracted from the pumped ac spin-current in phase (in quadrature) with the driving field. Furthermore, we find that the three spin-wave bands of the kagome antiferromagnet generate spin currents with mutually orthogonal polarization directions. This offers a unique way of controlling the spin orientation of the pumped spin current by exciting different spin-wave modes.

MA 21.5 Wed 10:30 H43

THz spin dynamics in antiferromagnetic Mn₂Au — •YANNIC BEHOVITS^{1,2}, ALEXANDER CHEKHOV^{1,2}, STANISLAV BODNAR³, MATHIAS KLÄUI³, MARTIN JOURDAN³, and TOBIAS KAMPFRATH^{1,2} — ¹Freie Universität Berlin, Institut für Experimentalphysik, 14195 Berlin, Germany — ²Fritz-Haber-Institut der Max-Planck-Gesellschaft, Abteilung Physikalische Chemie, 14195 Berlin, Germany — ³Johannes-Gutenberg-Universität, Institut für Physik, 55122 Mainz, Germany
In metallic antiferromagnets, intrinsic terahertz (THz) magnons may allow high-speed spin information processing. For CuMnAs and Mn₂Au, switching of the Néel vector has been demonstrated by using pulsed electrical currents and free-space THz pulses [1,2]. The switching was attributed to the current-induced Néel spin-orbit torque (NSOT)[3]. However, the underlying spin dynamics have not been observed on picosecond timescales. Here, we employ a THz-pump optical-probe setup to investigate dynamics of antiferromagnetic order induced by NSOT in Mn₂Au. We observe a signal proportional to the driving THz field, which is consistent with NSOT-driven spin dynamics both in frequency and symmetry. Our results indicate a strongly damped magnon mode at 0.6 THz. By using a simple model, we can extract material properties and estimate the field strengths required for picosecond rotation of the antiferromagnetic order.

[1] K. Olejnik et al., *Sci. Adv.*, 4(3): p. eaar3566 (2018) [2] S. Yu. Bodnar et al., *Nat. Commun.*, 9(1): p. 348. (2018) [3] J. Zelezny et al., *PRL*, 113(15): p. 157201 (2014)

MA 21.6 Wed 10:45 H43

Spin-orbit interaction at terahertz rates — •TOM S. SEIFERT and TOBIAS KAMPFRATH — FU Berlin

Spintronics aims at implementing the spin degree of freedom into conventional electronics. To be compatible and competitive, spintronic functionalities thus need to keep pace with the ever-increasing speeds of electronic devices that are foreseen to enter the terahertz range eventually [1]. Therefore, one needs to study fundamental spintronic phenomena at terahertz frequencies. Following this approach, one might not only hope to reveal new physics but also to apply these novel insights in terms of innovative terahertz photonic applications. Here, I will discuss our recent experimental efforts to study a central spintronic effect, the anomalous Hall effect (AHE) [2] in metallic magnets from DC to 40 THz. We find a largely frequency-independent AHE in DyCo₅, Gd₂₇Fe₇₃ and Co₃₂Fe₆₈, which we attribute to the large Drude scattering rate in metallic thin films. The gained knowledge could further enhance the efficiency of a novel ultrafast spintronic application, namely the spintronic terahertz source [3].

[1] Walowski, J., et al., *J. Appl. Phys.* 120 (2016). [2] Seifert, T. S., et al. *Adv. Mat.* 33 (2021). [3] Seifert, T. S., et al. *Appl. Phys. Lett.* 120 (2022).

MA 21.7 Wed 11:00 H43

Spin-orbit torque mediated coupling of terahertz light with magnon modes in heavy-metal/ferromagnet heterostructures — •RUSLAN SALIKHOV¹, IGOR ILYAKOV¹, LUKAS KÖRBER¹, ATTILA KÁKAY¹, KILIAN LENZ¹, JÜRGEN FASSBENDER¹, STEFANO BONETTI^{2,3}, OLAV HELLOWIG^{1,4}, JÜRGEN LINDNER¹, and SERGEY KOVALEV¹ — ¹Helmholtz-Zentrum Dresden-Rossendorf, Dresden, Germany — ²Stockholm University, Stockholm, Sweden — ³University of Venice, Venice, Italy — ⁴Chemnitz University of Technology, Chemnitz, Germany

Nonvolatile and energy-efficient spin-based technologies call for new prospects to realize computation and communication devices that are able to operate at terahertz (THz) frequencies. In particular, the coupling of electro-magnetic radiation to a spin system is a general requirement for future communication units and sensors. Here we propose a layered metallic system, based on a ferromagnetic film sandwiched in between two heavy metals that allows a highly effective coupling of millimeter wavelength THz light to nanometer-wavelength magnon modes. Using single-cycle broadband THz radiation we are able to excite spin-wave modes with a frequency of up to 0.6 THz and a wavelength as short as 6 nm. Our experimental and theoretical studies demonstrate that the coupling

originates solely from interfacial spin-orbit torques. These results are of general applicability to magnetic multilayered structures, and offer the perspective of coherent THz excitation of exchange-dominated nanoscopic magnon modes.

MA 21.8 Wed 11:15 H43

Laser-induced charge and spin photocurrents in BiAg₂ surface from first-principles — •THEODOROS ADAMANTOPOULOS^{1,2}, MAXIMILIAN MERTE^{1,2,3}, FRANK FREIMUTH^{1,3}, DONGWOOK GO^{1,3}, STEFAN BLÜGEL¹, and YURIY MOKROUSOV^{1,3} — ¹Peter Grünberg Institut and Institute for Advanced Simulation, Forschungszentrum Jülich and JARA, 52425 Jülich, Germany — ²Department of Physics, RWTH Aachen University, 52056 Aachen, Germany — ³Institute of Physics, Johannes Gutenberg University Mainz, 55099 Mainz, Germany

The physics of photo-induced effects in interfacial systems is intensively researched these days owing to numerous potential applications. Owing to the complexity of the problem, a comprehensive theoretical picture of photogalvanic effects is still lacking. Here we perform first-principles calculations of laser-induced currents in a BiAg₂ surface alloy, which is a well-known material realization of the Rashba model [1, 2]. Our results confirm the emergence of very large in-plane photocurrents as predicted by the Rashba model and establish a benchmark picture of photocurrents at Rashba-like surfaces and interfaces [3]. This work contributes to the study of the role of the interfacial Rashba spin-orbit interaction as a mechanism for the generation of in-plane photocurrents, which are of great interest in the field of ultrafast and terahertz spintronics.

[1] F. Freimuth et al., *Phys. Rev. B* **103**, 075428 (2021). [2] F. Freimuth et al., *Phys. Rev. B* **94**, 144432 (2016). [3] T. Adamantopoulos et al., arXiv:2201.07122 (2022).

MA 21.9 Wed 11:30 H43

Transition of laser-induced terahertz spin currents from torque-to conduction-electron-mediated transport — •OLIVER GUECKSTOCK¹, PILAR JIMENEZ-CAVERO^{1,2}, LUKAS NADVORNIK¹, IRENE LUCAS², TOM S. SEIFERT¹, LUIS MORELLON², and TOBIAS KAMPFRATH¹ — ¹FU Berlin, Germany — ²Universidad de Zaragoza, Spain

Transport of spin angular momentum is a fundamental operation required for future spin-electronic devices. To be competitive with other information carriers, it is required to push the bandwidth of spin transport to the terahertz (THz) frequency range [1]. Here, we use femtosecond laser pulses to excite prototypical F|N bilayers consisting of a ferrimagnetic metal F and a nonmagnetic metal N [2,3]. Following absorption of the pulse, a spin current in F is launched and converted into a transverse charge current in N, giving rise to the emission of a THz electromagnetic pulse [2]. Depending on the conductivity of F, two driving mechanisms of the spin current can occur: (i) the ultrafast spin Seebeck effect [3] generating magnons and (ii) a spin voltage, generating a spin current carried by conduction electrons [4]. Remarkably, in the half-metallic ferrimagnet Fe₃O₄, we observe the coexistence of these contributions and disentangle them based on their distinctly different ultrafast dynamics. Our results shed new light on the magnetic structure of this mature material. References: [1] Vedmedenko et al., *J. Phys. D: Appl. Phys.* 53 453001 (2020), [2] T. Seifert et al., *Nat. Phot.* 10, 483 (2016), [3] T. Seifert et al., *Nat. Comm.* 9, Article No: 2899 (2018), [4] R. Rouzegar et al., arXiv:2103.11710 (2021)

MA 21.10 Wed 11:45 H43

Ultrafast spintronic THz emission of thin CoFe/Pt films — •JANNIS BENSMANN¹, ROBERT SCHNEIDER¹, MARIO FIX², STEFFEN MICHAELIS DE VASCONCELLOS¹, MANFRED ALBRECHT², and RUDOLF BRATSCHITSCH¹ — ¹University of Münster, Institute of Physics and Center for Nanotechnology, 48149 Münster, Germany — ²University of Augsburg, Institute of Physics, 86159 Augsburg, Germany

THz radiation has great potential for spectroscopy, security and quality control applications. Recently, ultrafast spintronic THz emitters gained a lot of interest, as they are easy to handle and show high power and broadband emission. In these emitters, an ultrafast laser pulse launches a spin-polarized current from a nanometer-thin magnetic film into a non-magnetic metal layer. Due to the inverse spin Hall effect and the conversion to an ultrafast charge current, THz radiation is created. The THz emission of spintronic emitters can be tuned by the material compositions of the layers.

Here we present our recent results on THz emission spectroscopy of ultrathin Co_xFe_{1-x}/Pt bilayers with varying Co content x. The THz amplitude changes only slightly with x, leading to the conclusion that both Fe and Co have a similar contribution to the THz generation process [1]. Moreover, we were able to boost the THz emission by using multilayer stacks of the mentioned structure.

[1] R. Schneider et al., "Composition-dependent ultrafast THz emission of spintronic CoFe/Pt thin films", *Appl. Phys. Lett.* 120, 042404 (2022)

MA 21.11 Wed 12:00 H43

Ultrafast coherent THz lattice dynamics coupled to spins in a van der Waals antiferromagnetic flake — •FABIAN MERTENS¹, DAVID MÖNKEBÜSCHER¹, EUGENIO CORONADO², SAMUEL MAÑAS-VALERO², CARLA BOIX-CONSTANT², ALBERTA BONANNI³, MARGHERITA MATZER³, RAJDEEP ADHIKARI³, ALEXANDRA M. KALASHNIKOVA⁴, UMUT PARLAK¹, DAVIDE BOSSINI^{1,5}, and MIRKO CINCHETTI¹ — ¹Department of Physics, TU Dortmund University, Otto-Hahn-Straße 4, 44227 Dortmund, Germany — ²Instituto de Ciencia Molecular (ICMol) Universidad de Valencia, Spain — ³Institute of Semiconductor and Solid State Physics, Johannes Kepler University Linz, Austria — ⁴alexandra.kalashnikova@gmail.com — ⁵Department of Physics and Center for Applied Photonics, University of Konstanz, Germany

We used the setup described in [1] to study the laser driven lattice and spin dynamics of a 380 nm thick flake of the antiferromagnetic van der Waals semiconductor FePS₃ as a function of excitation photon energy and sample temperature. We found evidence of a coherent optical lattice mode at a frequency of 3.2 THz. The amplitude of the phononic signal vanishes as the phase transition to the paramagnetic phase occurs, revealing its close connection to the long-range magnetic order. These findings open a pathway towards the coherent manipulation of the magneto-crystalline anisotropy in a van der Waals antiferromagnet, scalable down to thinner flakes.

[1] F. Mertens et al., *Review of Scientific Instruments* **91** (2020)

MA 22: Thin Films: Magnetic Coupling Phenomena / Exchange Bias / Magnetic Anisotropy

Time: Wednesday 9:30–11:45

Location: H47

MA 22.1 Wed 9:30 H47

Spin dynamics in coupled ferrimagnetic heterostructures — •FELIX FUHRMANN¹, SVEN BECKER¹, AKASHDEEP AKASHDEEP¹, ZENGYAO REN^{1,2}, MATHIAS WEILER³, GERHARD JAKOB^{1,2}, and MATHIAS KLÄUI^{1,2,4} — ¹Institute of Physics, University of Mainz, Germany — ²Graduate School of Excellence "Materials Science in Mainz" (MAINZ), Germany — ³Fachbereich Physik and Landesforschungszentrum OPTIMAS, Technische Universität Kaiserslautern, Germany — ⁴Center for Quantum Spintronics, Norwegian University of Science and Technology, Trondheim, Norway

With growing demand for more energy efficient information technology, the utilization of magnons as information carriers entails potential advantages [1]. To successfully develop magnon-based devices, there are several requirements for the applied materials to meet. The insulating ferrimagnet Yttrium Iron Garnet (Y₃Fe₅O₁₂, YIG) and related garnets are good candidates with an outstanding low damping and large magnon propagation lengths [1]. Our heterostructures of YIG and Gadolinium Iron Garnet (Gd₃Fe₅O₁₂, GIG) were grown by pulsed laser deposition. We observe a ferromagnetic coupling between the Fe sublattices of the two layers, leading to complex magnetic response to external magnetic fields and a nontrivial temperature dependence [2]. We investigate the spin dynamics by broadband ferromagnetic resonance (FMR) experiments. Our observations are corroborated by measurements of SQUID magnetometry, spin Hall magnetoresistance and spin Seebeck effect [2]. [1] A. Chumak et al., *Nat. Phys.*, **11**, 453 (2015). [2] S. Becker et al., *Phys. Rev. Appl.*, **16**, 014047(2021).

MA 22.2 Wed 9:45 H47

Optical detection of magnon-phonon coupling using μ FR-MOKE technique — •MANUEL MÜLLER^{1,2}, LUKAS LIENSBERGER^{1,2}, MATHIAS WEILER³, MATTHIAS ALTHAMMER^{1,2}, RUDOLF GROSS^{1,2,4}, and HANS HUEBL^{1,2,4} — ¹Walther-Meißner-Institut, Bayerische Akademie der Wissenschaften, Garching, Germany — ²Physik-Department, Technische Universität München, Garching, Germany — ³Technische Universität Kaiserslautern, Kaiserslautern, Germany — ⁴Munich Center for Quantum Science and Technology (MCQST), München, Germany

Magnetoelastic coupling between wave-like excitations of the spin system (spin waves) and the lattice (elastic waves) can result in a hybridization of both modes. This coupling can reach the strong-coupling regime, which is of interest for future (quantum) applications, such as microwave-to-optics transducers and phononic spin valve devices.

We here present an experimental approach to investigate magnon-phonon coupling for the YIG layers in a YIG/GGG/YIG trilayer on an individual basis using the microfocused frequency-resolved magneto-optic Kerr effect (μ FR-MOKE) technique [1]. We discuss the magnetization dynamics recorded individually for the top and bottom YIG layer with those acquired using broadband ferromagnetic resonance. This data gives further insight to the involved modes as well as their coupling. As a longterm perspective, we expect that this technique will allow the investigation of microstructures with enhanced coupling rates via their optimized geometry.

[1] L. Liensberger et al., *IEEE Magn. Lett.* **10**, 5503905 (2019).

MA 22.3 Wed 10:00 H47

Experimental tests of the accuracy of the reflection matrix description in linear magneto-optics — •CARMEN MARTÍN VALDERRAMA, MIKEL QUINTANA, and ANDREAS BERGER — CIC nanoGUNE BRTA, E-20018 Donostia-San Sebastián, Spain

Magneto-Optical (MO) Kerr Effect (MOKE) techniques are frequently utilized to monitor magnetization M reversal, and even its vector information, in a non-destructive way [1]. The assumption is hereby that the Jones-formalism reflection matrix R, including 1st order MOKE, is given as $R = \begin{pmatrix} r_s & \alpha(m_x) + \gamma(m_z) \\ -\alpha(m_x) + \gamma(m_z) & r_p + \beta(m_y) \end{pmatrix}$, with $m_{x,y,z}$ being the M components in

Cartesian coordinates, r_s and r_p as Fresnel coefficients and α , β and γ being MOKE coefficients for longitudinal, transverse and polar effects. Recently, however, there have been reports of linear MOKE that is independent of a sample's magnetization [2]. Thus, it is important to verify the above R expression experimentally, which to our knowledge has not been done rigorously. For this, we utilized a sample with uniform M, which can be precisely rotated by an applied field, thus systematically varying the MOKE coefficients, while monitoring all of them simultaneously by means of General MO Ellipsometry. For the pure in-plane magnetization case, for instance, the α vs. β relation will lead to an ellipse equation, $\alpha^2/\alpha_0^2 + \beta^2/\beta_0^2 = 1$, if R is correct. We have confirmed this behavior experimentally with a very high degree of precision. However, we also discovered deviations from it in cases where samples exhibit MO anisotropy. [1] *Appl. Phys. Lett.* **71**, 965 (1997), [2] *Phys. Rev. B* **102**, 140408(R) (2020)

MA 22.4 Wed 10:15 H47

XMCD investigation on Sm-Co magnetic thin films: strong orbital pinning on Co and the role of Sm — •DAMIAN GÜNZING¹, GEORGIA GKOUZIA², RUIWEN XIE², TERESA WESSELS¹, HONGBIN ZHANG², LAMBERT ALFF², ALPHA T. N'DIAYE³, HEIKO WENDE¹, and KATHARINA OLLEFS¹ — ¹Faculty of Physics, University of Duisburg-Essen — ²Institute of Materials Science, Technical University of Darmstadt — ³Advanced Light Source, Lawrence Berkeley National Lab Berkeley

We present the investigation of crystalline Sm-Co thin films manufactured via MBE on an Al₂O₃ substrate without additional buffer layers [1] by soft X-ray magnetic circular dichroism (XMCD). We use XMCD to investigate the element-specific spin and orbital moments of the individual elements, here Sm and Co. Often, with soft X-rays only the first few nm are probed via electron yield detection, leading to significant surface effects. In contrast, here, we use the luminescence of the substrate and are able to study the entire sample over the whole film thickness. We see a surprisingly strong orbital pinning on the Co sites in applied fields up to 2T. From element-specific hysteresis curves we find that the Sm atoms are coupled to Co, but with spectroscopic features saturating different in high fields. We compare the experimental results obtained by XMCD with multiplet calculations using Quanty, which suggest an exchange field present at the Sm site. (Financially supported by the DFG Project-ID 405553726*CRK 270). [1] S. Sharma et al., *ACS Appl. Mater. Interfaces* (2021) **13**, 27, 32415-32423

MA 22.5 Wed 10:30 H47

Temperature independent coercivity by means of nanoscale materials design — •MIKEL QUINTANA¹, ADRIÁN MELÉNDEZ^{1,2}, CARMEN MARTÍN VALDERRAMA¹, LORENZO FALLARINO¹, and ANDREAS BERGER¹ — ¹CIC nanoGUNE BRTA, E-20018 Donostia-San Sebastián, Spain — ²UPV/EHU, E-48940 Bizkaia, Spain

Thin film materials, in which the exchange coupling strength is designed to be depth-dependent, behave at each depth as if their properties were controlled by a "local" Curie temperature T_c^{loc} , down to the 1-2 nm length-scale [1]. This phenomenon enables the control and design of ferromagnetic (FM) magnetization profiles as a function of temperature T . For instance, it allows one to engineer films exhibiting FM exchange-coupling everywhere, but which can split into separate multilayers exhibiting seemingly isolated FM states in certain T -ranges. Here, we present a multilayer system composed by two CoRu films separated by a graded Co_{1-x(z)}Ru_{x(z)} spacer layer with varying Ru concentration x along the depth z of the film. The spacer layer is such that an effective-PM-state thickness dividing two FM films decreases when reducing T . This specific materials design allows us to obtain a coercive field H_c plateau in an extended temperature range, in which H_c changes less than 2% between 150 K and 225 K, while conventional films exhibit a change of 20% in the same T -range. The stable coercivity plateau can be designed at any temperature by means of an adapted $T_c^{loc}(z)$ design, enabling T -independent operation points for technological applications. [1] L. Fallarino et al., *Materials* **11**, 251 (2018).

MA 22.6 Wed 10:45 H47

Influence of adhesion layer and sputter gas pressure on structural and magnetic properties of Co/Pt multilayers — •RICO EHRLER¹, TINO UHLIG¹, and OLAV HELLWIG^{1,2} — ¹Chemnitz University of Technology, D-09107 Chemnitz, Germany — ²Helmholtz-Zentrum Dresden-Rossendorf, D-01328 Dresden, Germany

Co/Pt multilayers (MLs) are standard systems for perpendicular anisotropy layered thin films. The use of a specific underlayer, sometimes in combination with additional, very thin adhesion layers, is a common practice to define a crystalline texture for the ML on amorphous substrates. In addition, the sputter gas pressure during deposition can be used to tune the lateral heterogeneity and laminate order, which strongly affect the magnetic behavior of the system. However, the precise interplay between adhesion and sputter gas pressure, especially for the seed layer, is often neglected.

In this context, we will discuss the impact of the underlayers on the structural and magnetic properties of the Co/Pt ML system. We will emphasize the influence of an adhesion layer on the whole system and combine this with a systematic and separate variation of the sputter deposition pressure of Pt seed and Co/Pt ML. Carefully tuning these parameters enables us to exert a high degree of control on the structure of these systems, with characteristics ranging from continuous thin films to isolated grain structures.

MA 22.7 Wed 11:00 H47

Evidence for perpendicular anisotropy gradients in Co thin films on Pt seeds — •GAURAVKUMAR PATEL¹, SVEN STIENEN¹, RUSLAN SALIKHOV¹, RODOLFO GALLARDO², LORENZO FALLARINO^{1,3}, KILIAN LENZ¹, JÜRGEN LINDNER¹, and OLAV HELLWIG^{1,4} — ¹Helmholtz-Zentrum Dresden-Rossendorf, 01328 Dresden — ²Universidad Tecnica Federico Santa Maria, Valparaiso, Chile — ³CIC energiGUNE BRTA, 01510 Vitoria-Gasteiz, Spain — ⁴Chemnitz University of Technology, 09107 Chemnitz

Tailoring the magnetization dynamics and anisotropy in ferromagnetic thin films by different seed layers is of great fundamental and practical importance, e.g., different seed layer materials lead to different microstructure and magnetocrystalline anisotropy energy. We have used Ta and Pt as seed layers for thin Co films and studied their broadband ferromagnetic resonance (FMR) in out-of-plane saturation as a function of Co thickness and determined the respective perpendicular magnetic anisotropy. For Ta seeds, the magnetic anisotropy decreases and shows an inverse thickness dependence. In contrast for Pt seeds the magnetic anisotropy is no longer monotonous with thickness, but shows an initial thickness dependent decrease with a distinct minimum and subsequently a steady increase again. XRD measurements show that for Pt seeds, the Co develops a well-defined hcp texture with a thickness dependent strain relaxation. As a result of this structural evolution for Co on Pt seeds our FMR measurements reveal a strong anisotropy gradient in growth direction for this system.

MA 22.8 Wed 11:15 H47

Magnetization reversal of Co/Pt multilayer systems with weak perpendicular magnetic anisotropy — •PETER HEINIG^{1,2}, RUSLAN SALIKHOV¹, FABIAN SAMAD^{1,2}, LORENZO FALLARINO^{1,3}, ATTILA KAKAY¹, and OLAV HELLWIG^{1,2} — ¹Helmholtz-Zentrum Dresden-Rossendorf — ²Chemnitz University of Technology — ³CIC energiGUNE

Perpendicular anisotropy thin film systems are well known for their highly periodic magnetic stripe domains. Here we study $[\text{Co}(3.0 \text{ nm})/\text{Pt}(0.6 \text{ nm})]_X$ multilayers in the regime of transitional in-plane to out-of-plane anisotropy. For this we vary the number of repeats X in order to tune the remanent state from purely in-plane (IP) via tilted stripe domains (tilted), i.e. with significant out-of-plane as well as in-plane magnetization component, to fully out-of-plane stripe domains (OOP). Vibrating Sample Magnetometry and Magnetic Force Microscopy are used to investigate three characteristic samples with $X = 6, 11$ and 22 , which represent the three above mentioned remanent states, respectively. In contrast to fully in-plane or fully out-of-plane systems experimental data and corresponding micromagnetic simulation of the tilted magnetization regime ($X = 11$) reveals fully reversible field regions as well as distinct points of irreversibility during an external field sweep. This collective reversal behavior seems at first sight somewhat counter intuitive for a macroscopic system and has qualitative similarities with microscopic systems, such as the Stoner Wohlfarth particle and the vortex reversal in an in-plane magnetized disk, which both show as well distinct points of irreversibility.

MA 22.9 Wed 11:30 H47

Magnetic anisotropy and magnetic ordering of transitionmetal phosphorus trisulfides — •TAE YUN KIM^{1,2} and CHEOL-HWAN PARK^{1,2} — ¹Center for Correlated Electron Systems, Institute for Basic Science, Seoul, Korea — ²Department of Physics and Astronomy, Seoul National University, Seoul, Korea

Transition-metal phosphorus trisulfides (TMPS₃'s) — a family of antiferromagnetic materials to which FePS₃, the first discovered two-dimensional magnetic material [1], belongs — have been regarded as an ideal testbed for studying the strong influence of low dimensionality on the existence of magnetic order. We developed anisotropic magnetic models for TMPS₃'s from first-principles calculations; the bulk magnetic properties, including the critical temperatures (T_N 's), reported from previous experiments were explained very well [2]. Remarkably, it was predicted by applying our magnetic models to the few-layer cases that monolayer NiPS₃ exhibits a fairly high T_N , which is in contrast with the conclusion from a recent Raman study that the T_N is largely suppressed in monolayer NiPS₃ [3]. We discuss how the degeneracy in the magnetic ground state of monolayer NiPS₃ changes significantly its polarized Raman spectra, which provides a reconciliation between our theoretical predictions and the previous experimental results as to the existence of magnetic order in monolayer NiPS₃.

[1] J.-U. Lee et al., Nano Lett. 16, 7433 (2016)

[2] T. Y. Kim and C.-H. Park, Nano Lett. 21, 10114 (2021)

[3] K. Kim et al., Nat. Commun. 10, 345 (2019)

MA 23: Magnetic Domain Walls

Time: Wednesday 9:30–10:45

Location: H48

MA 23.1 Wed 9:30 H48

Atomic-scale Insights to Design of High-Performing SmCo based Sintered Permanent Magnets gained by Atom Probe Tomography — •NIKITA POLIN¹, STEFAN GIRON², ESMAEL ADABIFIROOZJAEI², YANGYIWEI YANG², ALAUKIK SAXENA¹, OLIVER GUTFLEISCH², and BAPTISTE GAULT^{1,3} — ¹Max-Planck-Institut für Eisenforschung GmbH, Düsseldorf 40237, Germany — ²Institute of Materials Science, Technische Universität Darmstadt, 64287 Darmstadt, Germany — ³Department of Materials, Royal School of Mines, Imperial College, Prince Consort Road, London SW7 2BP, United Kingdom

Hard disc drives, electric cars and wind turbines - in all these devices permanent magnets are key components to translate mechanical into electrical energy and vice versa. Enhancing performance of permanent magnets thus contributes to energy transition and sustainability. However, practically the performance of permanent magnets only reaches 20% of the possible maximum (called Brown's paradox). This is related to imperfect nanostructure and nanocomposition where atom probe tomography is a suitable tool to gain atomic-scale insights.

In this talk I will present a structural and magnetical investigation of high-end production-grade Sm₂(Co,Fe,Cu,Zr)₁₇ permanent magnets which show unusual regions leading to suboptimal performance. Local differences of nanostructure and nano-composition between both regions are studied by atom probe tomography and transmission electron microscopy combined with micromagnetic simulations. These findings suggest design rules for higher performance of Sm₂Co₁₇ magnets.

MA 23.2 Wed 9:45 H48

Magneto-Optic Effects and Domain Imaging in EuO/Co Heterostructure — •SEEMA SEEMA¹, HENRIK JENTGENS¹, PAUL ROSENBERGER^{1,2}, and MARTINA MÜLLER¹ — ¹Fachbereich Physik, Universität Konstanz, 78457 Konstanz, Germany — ²Fakultät Physik, Technische Universität Dortmund, 44221 Dortmund, Germany

Ferromagnetic semiconductors and stable half-metallic ferromagnets with Curie temperatures (T_c) equal to or more than room temperature have been sought for their applications in novel spintronic devices. Europium oxide (EuO) is one of the potential candidates as it possesses strong ferromagnetism of $7 \mu_B/\text{Eu}$ atom with a T_c of 69 K. The present work focuses on the magnetization reversal mechanisms and domain images in EuO probed using magneto-optic Kerr microscopy. We aimed to visualize magnetic proximity effect induced changes in magnetic domains and T_c of EuO in a EuO/Metal heterostructure. We synthesized EuO/Co thin film using molecular beam epitaxy and observed differences in the domain saturation behavior as well as the Kerr rotation below T_c . This had been performed by magnetic hysteresis measurement along with simultaneous domain imaging to explore the temperature-dependent magneto-optic effects in EuO in the proximity of Co. This study of magnetic domains in EuO/Co heterostructure can provide insights into achieving room-temperature ferromagnetism in EuO.

MA 23.3 Wed 10:00 H48

Direct observation of bulk-DMI-stabilized Néel-type domain walls in ferromagnetic rare-earth transition-metal alloys — •DANIEL METTERNICH¹, RICCARDO BATTISTELLI¹, CHEN LUO¹, FLORIN RADU¹, SEBASTIAN WINTZ¹, KAI LITZUS², MARCEL MÖLLER³, JOHN GAIDA³, CLAUS ROPERS³, MANUEL

VALVIDARES⁴, PIERLUIGI GARGIANI⁴, ANDRADA-OANA MANDRU⁵, YAOXUAN FENG⁵, HANS JOSEF HUG⁵, and FELIX BÜTTNER¹ — ¹Helmholtz-Zentrum Berlin, Berlin, Germany — ²Max Planck Institute for Intelligent Systems, Stuttgart, Germany — ³Georg-August-Universität Göttingen, Göttingen, Germany — ⁴ALBA Synchrotron, Barcelona, Spain — ⁵Empa, Dübendorf, Switzerland

Since the discovery of bulk DMI within rare-earth transition-metal alloys, the possibility of bulk-DMI-stabilized skyrmions within these materials is an enticing prospect for potential spintronics applications. However, so far, no direct observation of any bulk-DMI-induced chiral spin textures has been reported in this material class.

We present our study on 50-nm-thick DyCo films, which we imaged with transmission X-ray microscopy. We found domain walls and skyrmions, both of which exhibit strong local variations of the chirality up to pure Néel-type. Due to the large film thickness, we attribute the formation of such Néel walls to the presence of significant bulk DMI in our sample. Moreover, we attribute the strong variations of the chirality to lateral changes of the material composition. Lorentz transmission electron microscopy and magnetic force microscopy measurements support our observations.

MA 23.4 Wed 10:15 H48

Electrostatic shaping of magnetic transition regions in La_{0.7}Sr_{0.3}MnO₃ — •QIANQIAN LAN¹, MICHAEL SCHNEDLER¹, LARS FRETER¹, LEI JIN¹, XIAN-KUI WEI¹, THIBAUD DENNEULIN¹, ANDRÁS KOVÁCS¹, PHILIPP EBERT¹, XIAOYAN ZHONG², and RAFAL E. DUNIN-BORKOWSKI¹ — ¹Ernst Ruska-Centre for Microscopy and Spectroscopy with Electrons (ER-C 1) and Peter Grünberg Institut (PGI-5), Forschungszentrum Jülich GmbH, 52425 Jülich, Germany — ²Department of Materials Science and Engineering, City University of Hong Kong, Kowloon 999077, Hong Kong SAR, People's Republic of China

Ferroelectric domain walls with no rotation of polarization but a change of magnitude of polarization were reported theoretically and experimentally. However, magnetic domain walls with a similar configuration have not been observed experimentally yet to our knowledge. Here, we report an experimental example

of a magnetic transition region in La_{0.7}Sr_{0.3}MnO₃ films where the magnitude of magnetization gradually changes without rotation even well below T_c. The magnetic and electrostatic characterization reveals that a charge redistribution governs the shape, magnitude, and extent of the corresponding magnetic transition region. The charge redistribution is caused by the equilibrium between carrier diffusion and drift in the electrostatic field at an interface with sharp Mn compositional change in LSMO. Thus, our results demonstrate a case of the electrostatic shaping of magnetic transition regions, which can be expected to be a general property of complex oxide materials.

MA 23.5 Wed 10:30 H48

Strain-controlled Domain Wall injection into nanowires for sensor applications — •GIOVANNI MASCIOCCHI^{1,2}, MOUAD FATTOUHI³, ANDREAS KEHLBERGER², LUIS LÓPEZ DÍAZ³, and MATHIAS KLÄUI¹ — ¹Institute of Physics, Johannes Gutenberg University Mainz, 55099 Mainz, Germany — ²Sensitec GmbH, 55130 Mainz, Germany — ³Department of Applied Physics, Universidad de Salamanca, E-37008 Salamanca, Spain

In this study, we address a well-known challenge in magnetic sensor development, which is the effect of packaging-induced strain on the sensor properties. While previously the field operation window has only been studied in idealized operation conditions, in real devices further external factors such as strain play a role.

In this experimental work, we investigate the injection of a 180° domain wall from a nucleation pad into a nanowire, as typically used for domain wall-based sensors, while straining the device along selected directions. Combining our experimental measurements by Kerr microscopy with micromagnetic simulations, we find that strain, regardless of its direction, increases the domain wall injection field due to the magnetoelastic coupling of the magnetic material. The above-described observations can be explained by an effective strain-induced anisotropy in the device.

We find additionally that a careful material preparation, comprising of an annealing step, can reduce the effective anisotropy caused by the strain in the magnetic layer. With this we show that a device free of magnetostrictive behavior can be achieved.

MA 24: Spin Transport and Orbitronics, Spin-Hall Effects

Time: Wednesday 15:00–18:00

Location: H37

MA 24.1 Wed 15:00 H37

Interplay between ferroelectricity and orbital angular momentum in a two-dimensional SnTe monolayer — •DIMOS CHATZICHRYSAFIS^{1,2}, DONGWOOK GO^{1,3}, and STEFAN BLÜGEL¹ — ¹Peter Grünberg Institut and Institute for Advanced Simulation, Forschungszentrum Jülich and JARA, 52425 Jülich, Germany — ²Physics Department, RWTH-Aachen University, 52062 Aachen, Germany — ³Institute of Physics, Johannes Gutenberg University Mainz, 55099 Mainz, Germany

Recent work on Orbitronics has shown that the orbital angular momentum (OAM) plays an important role in transport phenomena. A question that has arisen concerns the exploration of physical mechanisms that can serve as a control knob for the OAM. For that, ferroelectrics comprise the perfect playground. In this talk, we theoretically investigate the interplay between the electrical polarization in 2D SnTe monolayer, the OAM, and its transport effects. Using a tight-binding model we analyze the influence of the ferroelectric polarization on the electronic structure and the OAM texture. Based on this, we show that electric responses of the OAM and its current can be modulated by a ferroelectric order parameter. We believe that our work provides a novel route to controlling the OAM in 2D materials

MA 24.2 Wed 15:15 H37

Spin and orbital transport in rare earth dichalcogenides: The case of EuS₂ — •MAHMOUD ZEER^{1,2}, DONGWOOK GO^{1,3}, JOHANNA P CARBONE^{1,2}, TOM G SAUNDERSON³, MATTHIAS REDIES^{1,2}, MATHIAS KLÄUI³, JAMAL GHABBOUN⁴, WULFHEKEL WULF³, STEFAN STEFAN BLÜGEL^{1,2}, and YURIY MOKROUSOV^{1,3} — ¹Peter Grünberg Institut and Institute for Advanced Simulation, Forschungszentrum Jülich and JARA, Jülich, Germany — ²Department of Physics, RWTH Aachen University, Aachen, Germany — ³Institute of Physics, Johannes Gutenberg-University Mainz, Mainz, Germany — ⁴Department of Physics, Bethlehem University, Bethlehem, Palestine

With first principles the electronic, magnetic and transport properties of rare-earth dichalcogenides taking a monolayer of the H-phase EuS₂ as a representative. We predict that the H-phase of the EuS₂ monolayer exhibits a half-metallic behaviour upon doping with a very high magnetic moment.

We find the EuS₂ is very sensitive to the value of Coulomb repulsion U . We further predict that the non-trivial electronic structure of EuS₂ directly results in a pronounced anomalous Hall effect with non-trivial band topology. Moreover, while we find that the spin Hall effect closely follows the anomalous Hall

effect in the system, the orbital complexity of the system results in a very large orbital Hall effect, whose properties depend very sensitively on the strength of correlations. Our findings thus promote rare earth based dichalcogenides as a promising platform for topological spintronics and orbitronics.

Work funded by MMBF 01DH16027.

Zeet et al., arXiv:2201.11017

MA 24.3 Wed 15:30 H37

Differences between magnetotransport properties of doped alloys and doped crystals via ab-initio calculations — •ONDREJ ŠÍP^{1,2}, SERGEY MANKOVSKY³, and HUBERT EBERT³ — ¹Institute of Physics, Czech Academy of Sciences, Praha — ²New Technologies Research Centre, University of West Bohemia, Plzeň — ³Ludwig-Maximilians-Universität München

The description of magnetotransport has so far focused on how doping influences clean crystals. However, interest is turning also to substitutional alloys as hosts. Our aim is to investigate to what extent the approaches that proved to be useful for doped crystals can be applied to doped alloys. Calculations are performed for permalloy Fe₁₉Ni₈₁ doped with V, Co, Pt, and Au impurities, relying on the Kubo-Bastin equation implemented using the KKR-Green function method.

The dependence of the anomalous Hall and spin Hall conductivities σ_{xy} and σ_{xy}^z on the dopant concentration is nonmonotonic and strongly influenced by the temperature. The fact that the host is disordered and not crystalline has profound influence on how σ_{xy} and σ_{xy}^z depend on the dopant concentration. In particular, σ_{xy} and σ_{xy}^z are not proportional to σ_{xx} for low dopant concentrations. Consequently, the dependence of the anomalous Hall effect and spin Hall effect on the dopant concentration cannot be ascribed unambiguously to skew scattering, side-jump scattering, or intrinsic contributions in the same way as it can be done when investigating the effect of doping for a crystalline host, i.e., the standard scaling laws do not apply.

MA 24.4 Wed 15:45 H37

Atomic scale control of spin current transmission at interfaces — •MOHAMED AMINE WAHADA¹, ERSOY SASIOGLU², WOLFGANG HOPPE³, XILIN ZHOU¹, HAKAN DENIS¹, REZA ROUZEGAR⁴, TOBIAS KAMPFRATH⁴, INGRID MERTIG², STUART PARKIN¹, and GEORG WOLTERS DORF³ — ¹Max Planck Institute of Microstructure Physics, Weinberg 2, 06120 Halle(Saale) — ²Institute of Physics, Martin Luther University Halle-Wittenberg, Von-Seckendorff-Platz 1, 06120

Halle, Germany — ³Institute of Physics, Martin Luther University Halle-Wittenberg, von Danckelmann Platz 3, 06120 Halle, Germany — ⁴Department of Physics, Freie Universität Berlin, Arnimallee 14, 14195 Berlin, Germany

Ferromagnet (FM)/heavy metal (HM) bilayers are a fundamental building block in the field of spintronics. Exciting such bilayers with a femtosecond laser pulse can trigger ultrafast spin current (SC) from the FM to the HM layer. In the HM layer, the spin Hall effect converts the SC pulse into a charge current pulse, enabling efficient spintronic THz emitters. Equally as important as the SC generation process is the efficiency of the SC transmission across the FM/HM interface. We show experimentally that the SC transmission is partially suppressed when Ta is interfaced directly with 3d FM materials while this effect is absent when Pt is used as a HM. Based on theoretical calculations, we show that this is due to 3d-5d hybridization effects causing a significant moment reduction at the interface. This effect is expected for all 5d elements with less than half-filled 5d shell. Furthermore, we show that this effect can be eliminated by atomic scale oxide interlayers.

MA 24.5 Wed 16:00 H37

Spin Dynamics in Magnetic Nanojunctions — •RUDOLF SMORKA¹, MARTIN ŽONDA², and MICHAEL THOSS^{1,3} — ¹Institute of Physics, Albert-Ludwigs-Universität Freiburg — ²Department of Condensed Matter Physics, Faculty of Mathematics and Physics, Charles University Prague — ³EUCOR Centre for Quantum Science and Quantum Computing, Albert-Ludwigs-Universität Freiburg

Recent experimental advances of atomic and nanoscale magnetism motivate the study of spin dynamics on ultrafast time scales. In this contribution, we use a quantum-classical hybrid approach to study current-driven magnetization dynamics in systems consisting of tight-binding electrons and localized classical spins. Using this approach, we show that both the electronic structure of the central system and the self-consistent feedback of spin and electron dynamics play a significant role in the dynamical properties of magnetic nano-junctions driven by a dc voltage. Specifically, relaxation dynamics can be enhanced by tuning the dc voltage in resonance with electronic levels of the central system. We analyze this characteristic in nano-junctions containing a single classical Kondo impurity. Furthermore, we investigate current-induced spin-transfer torques in a ferromagnetic spin valve far away from equilibrium and show that electronic levels in the bias window lead to an enhancement of the spin-transfer torques.

MA 24.6 Wed 16:15 H37

Spin and orbital Edelstein effects in a bilayer system with Rashba interaction — •SERGIO LEIVA¹, INGRID MERTIG¹, and ANNIKA JOHANSSON² — ¹Martin Luther University Halle-Wittenberg, Institute of Physics, 06099 Halle, Germany — ²Max Planck Institute of Microstructure Physics, Halle, Germany

The spin Edelstein effect has proved to be a promising phenomenon to generate spin polarization from a charge current in systems without inversion symmetry. In recent years, current-induced orbital magnetization, also called the orbital Edelstein effect, has also been predicted for various systems with broken inversion symmetry [1-7].

In the present work, we calculate the current-induced spin and orbital magnetization for a bilayer system with Rashba interaction, using Boltzmann transport theory with a constant relaxation time. We compare the magnitudes of the spin and orbital Edelstein effects and find that their dependencies on model parameters such as effective mass, spin-orbit coupling, or energy, differ qualitatively, and they can even exhibit opposite signs.

- [1] T. Koretsune *et al.*, Phys. Rev. B, **86**, 125207 (2012).
- [2] T. Yoda *et al.*, Sci. Rep., **5**, 12024 (2015).
- [3] D. Go *et al.*, Sci. Rep., **7**, 46742 (2017)
- [4] T. Yoda *et al.*, Nano Lett., **18**, 916 (2018).
- [5] L. Salemi *et al.*, Nat. Commun., **10**, 5381 (2019)
- [6] D. Hara *et al.*, Phys. Rev. B, **102**, 184404 (2020).
- [7] A. Johansson *et al.*, Phys. Rev. Research, **3**, 013275 (2021).

MA 24.7 Wed 16:30 H37

Dynamic and static detection of current-induced spin-orbit magnetic fields — •LIN CHEN¹, MATTHIAS KRONSEDER², DIETER SCHUH², DOMINIQUE BOUGEARD², JAROSLAV FABIAN², DIETER WEISS², and CHRISTIAN BACK¹ — ¹Department of Physics, Technical University of Munich, Garching bei Munich, Germany — ²Institute of Experimental and Applied Physics, University of Regensburg, Regensburg

Quantifying current-induced effective spin-orbit magnetic-fields (SOFs) accurately is a central task for spin-orbitronics. Several methods, e.g., spin-transfer torque ferromagnetic resonance or second harmonic Hall measurements, have been frequently used in the past 10 years. However, most methods show weaknesses, and are not ideal to determine SOFs. Here, we will show two new approaches in this regard. Firstly, we show that it is possible to quantify the SOFs through an analysis of the shape of standing spin-wave patterns, which are probed by time-solved magneto-Kerr microscopy in a laterally confined Fe/GaAs system. This method, which is conceptually different from previous approaches based on lineshape analysis, is phase independent and self-calibrated. Secondly,

we show that one can simultaneously quantify the SOFs and the unidirectional magnetoresistance (UMR) by measuring the second harmonic longitudinal resistance in Co/Pt bi-layers. From these measurements, we can: I) establish a connection between SOFs and UMR, and II) discuss the origin of SOFs.

- L. Chen *et al.*, Phys. Rev. B **104**, 014425 (2021).
L. Chen *et al.*, Phys. Rev. B **105**, L020406 (2022).

MA 24.8 Wed 16:45 H37

Hidden current-induced spin and orbital torques in bulk Fe₃GeTe₂ from first-principles — •TOM G. SAUNDERSON^{1,2}, DONGWOOK GO^{1,2}, STEFAN BLÜGEL², MATHIAS KLÄUI^{1,3}, and YURIY MOKROUSOV^{1,2} — ¹Institute of Physics, JGU, 55099 Mainz, Germany — ²PGI and IAS, Forschungszentrum Jülich, Germany — ³Centre for Quantum Spintronics, NTNU, 7491 Trondheim, Norway

Within the field of spintronics, the two dimensional (2D) van der Waals (vdW) material Fe₃GeTe₂ has been in the spotlight in the last few years for exciting characteristics such as nodal line semimetallicity [1], highly efficient spin-orbit torque switching [2] and skyrmion formation [3]. In a recent collaboration [4] we found that spin-orbit torques were observed within the bulk, yet the clean crystal's bilayer system is centrosymmetric. Whilst this leads to overall vanishing spin-orbit torques, strong 'hidden' current-induced torques are harvested by each of the two-dimensional FGT layers separately. We demonstrate, from first principles [5], that an interplay of spin and orbital degrees of freedom has a profound impact on spin-orbit torques in this prototype material. We uncover a drastic difference in the behavior of the conventional spin flux torque and so-called orbital torque as the magnetization is varied resulting in a non-trivial evolution of switching properties. Our findings promote the design of non-equilibrium orbital properties as the guiding mechanism for crafting the properties of spin-orbit torques in layered vdW materials. [1] Nat. Mater. **794**, 17 (2018) [2] Nano Lett. **4400**, 19 (2019) [3] Nano Lett. **868**, 20 (2020) [4] arXiv:2107.09420 [5] arXiv:2204.13052

MA 24.9 Wed 17:00 H37

Modeling spin transport through thin antiferromagnetic insulators — •NIKLAS ROHLING¹ and ROBERTO E. TRONCOSO^{2,3} — ¹Department of Physics, University of Konstanz, D-78457 Konstanz — ²Center for Quantum Spintronics, Department of Physics, Norwegian University of Science and Technology (NTNU), NO-7491 Trondheim — ³Department of Mechanical and Industrial Engineering, NTNU

Experiments have shown spin transport enhancement by a thin antiferromagnetic insulator between a metal and a ferromagnetic insulator [1]. While previous theoretical work [2] was able to reproduce some of the features of those experiments, the interface is typically described by a single parameter only. We consider a model of a thin layer NiO oriented in (111) direction, sandwiched between a metal and a ferromagnetic insulator. We take into account nearest and next-nearest neighbor exchange coupling at the interfaces as well as different magnetic order. We compute the spin current through this system using Fermi's Golden Rule [3]. We find a sensitive dependence on the magnetic configuration as well as on the interface parameters.

- [1] Wang *et al.*, Phys. Rev. Lett. **113**, 097202 (2014), Phys. Rev. B **91**, 220410(R) (2015); Lin *et al.* Phys. Rev. Lett. **116**, 186601 (2016).
- [2] Khymyn *et al.*, Phys. Rev. B **93**, 224421 (2016); Rezende *et al.*, Phys. Rev. B **93**, 054412 (2016).
- [3] Bender *et al.*, Phys. Rev. Lett. **108**, 246601 (2012).

Financial support by the German Research Foundation (DFG), project No. 417034116 and by the Research Council of Norway through its Centres of Excellence funding scheme, project No. 262633, "QuSpin"

MA 24.10 Wed 17:15 H37

Unified theory of itinerant transport in magnetic platforms based on the slave-boson formalism — •RICARDO ZARZUELA¹ and JAIRO SINOVA^{1,2} — ¹Institut für Physik, Johannes Gutenberg Universität Mainz, D-55099 Mainz, Germany — ²Institute of Physics Academy of Sciences of the Czech Republic, Cukrovarnická 10, 162 00 Praha 6, Czech Republic

The slave-boson formalism, rooted in the idea that electron hopping in the lattice is accompanied by a backflow of spin excitations, has been widely used in the field of strongly correlated systems to describe metal-insulator transitions and high-Tc superconductivity, to name a few. It is also well suited to explore transport phenomena in spintronic platforms, since the spin exchange with the magnetic background can be easily incorporated into the representation of the electron operators. We show that the slave-boson approach to the Hubbard model for conduction electrons (near half filling) yields an effective low-energy long-wavelength theory for the itinerant transport in magnetic conductors. In particular, an emergent coupling between the magnetization current and the itinerant spin current is responsible for the spin-transfer physics as well as the topological Hall effect observed in magnetic systems. Our slave-boson approach does not require the adiabatic dynamics of the itinerant carriers, so our findings hold for any itinerant spin polarization. We also show that topological defects (e.g., magnetic vortices and magnetic disclinations) mediate both spin-transfer and topological Hall responses in the magnetic medium, which have not been observed experimentally yet.

MA 24.11 Wed 17:30 H37

Non-Collinear Spin Current for Switching of Chiral Magnetic Textures — •DONGWOOK GO^{1,2}, MORITZ SALLERMANN^{1,3}, FABIAN R. LUX², STEFAN BLÜGEL¹, OLENA GOMONAY², and YURIY MOKROUSOV^{1,2} — ¹Peter Grünberg Institut and Institute for Advanced Simulation, Forschungszentrum Jülich and JARA, 52425 Jülich, Germany — ²Institute of Physics, Johannes Gutenberg University Mainz, 55099 Mainz, Germany — ³Science Institute and Faculty of Physical Sciences, University of Iceland, VR-III, 107 Reykjavík, Iceland

We propose a concept of non-collinear spin current, whose spin polarization varies in space even in non-magnetic crystals. While it is commonly assumed that the spin polarization of the spin Hall current is uniform, asymmetric local crystal potential generally allows the spin polarization to be non-collinear in space. Based on microscopic considerations we demonstrate that such non-collinear spin Hall currents can be observed for example in layered Kagome Mn₃X (X = Ge, Sn) compounds. Moreover, by referring to atomistic spin dynamics simulations we show that non-collinear spin currents can be used to switch the chiral spin texture of Mn₃X in a deterministic way even in the absence of an external magnetic field. Our theoretical prediction can be readily tested in experiments, which will open a novel route toward electric control of complex spin structures in non-collinear antiferromagnets. Reference: Go *et al.* arXiv:2201.11476

MA 24.12 Wed 17:45 H37

Theory of charge and spin pumping in atomic-scale spiral magnets — DAICHI KUREBAYASHI^{1,2}, YIZHOU LIU¹, •JAN MASELL^{1,3}, and NAOTO NAGAOSA^{1,4} — ¹RIKEN CEMS, Wako, Japan — ²University of New South Wales, Sydney, Australia — ³Karlsruhe Institute of Technology (KIT), Karlsruhe, Germany — ⁴University of Tokyo, Tokyo, Japan

An Archimedean screw is a classical pump that exploits the equivalence of rotation and translation in helices. Similarly, a spin spiral texture can pump charge and spin by rotating at a frequency. We study these pumping phenomena within a microscopic quantum model by both perturbation theory and numerical simulations. Inside the spiral region, the spin polarization and charge current are linear in the frequency whereas the spin current scales with its square. We find that the charge current is related to the mixed momentum-phason Berry phase which can be viewed as a novel approximate realization of a Thouless pump. It is nearly quantized in spirals with short pitch but decays with $1/\lambda$ for longer pitches unlike true Thouless pumps or Archimedean screws. Moreover, we study the onset of non-adiabaticity, the impact of attached non-magnetic or magnetic contacts, the real-time evolution of the transport observables, and the effects of disorders which, surprisingly, might enhance the spin current but suppress the charge current.[1]

[1] D. Kurebayashi, Y. Liu, J. Masell, and N. Nagaosa, <https://doi.org/10.48550/arXiv.2201.05446>

MA 25: Ultrafast Magnetization Effects 2

Time: Wednesday 15:00–17:00

Location: H43

MA 25.1 Wed 15:00 H43

Light-induced magnetization dynamics in a ferromagnetic semiconductor — •JINGWEN LI¹, MASAKAZU MATSUBARA², KRISTIN KLIEMT³, NAZIA KAYA³, ISABEL REISER³, CORNELIUS KRELLNER³, JOHANN KROHA⁴, SHOYON PAL⁵, and MANFRED FIEBIG¹ — ¹ETH Zurich, Switzerland — ²Tohoku University, Japan — ³Goethe University Frankfurt, Germany — ⁴Bonn University, Germany — ⁵NISER Bhubaneswar, India

Ferromagnetic semiconductors are a rare class of materials that can provide a new platform with spin degrees of freedom in electronic and optical devices. All-optical control of the magnetic order is a demanding task, however. As one prototype example, EuO is intriguing for its high Curie Temperature ($T_c = 69$ K) induced by the indirect exchange interactions between the Eu atoms. The interactions can be enhanced by photo-doping in an ultrafast non-thermal way, strengthening the ferromagnetic order. This was verified in the ferromagnetic phase of the material [1], but evidence for an enhancement of the magnetic order around or above T_c is still lacking. In this contribution, we show the photo-induced presence of magnetic ordering even at temperatures higher than T_c by making use of the temperature-dependent spectral shift accompanying the magnetically ordered states using optical pump-probe spectroscopy. In optical reflection experiments, we observe two distinct types of ultrafast processes related to the optically driven magnetic order that show different relaxation rates. Our results provide clear evidence of short-range magnetic order above T_c , originating from the so-called exciton magnetic polarons.

MA 25.2 Wed 15:15 H43

Non-thermal optical generation of non-collinear magnetic phase in insulating ferrimagnetic iron garnet — •SERGIY PARCHENKO¹, ANTONI FREJ², HIROKI UEDA¹, ROBERT CARLEY¹, LAURENT MERCADIER¹, NATALIA GERASIMOVA¹, GIUSEPPE MERCURIO¹, JUSTINE SCHLAPPA¹, ALEXANDER YAROSLAVTSEV¹, NAMAN AGARWAL¹, ANDREAS SCHERZ¹, ANDRZEJ STUPAKIEWICZ², and URS SERGIJ³ — ¹European Free Electron Laser, Schenefeld, Germany — ²University of Białystok, Białystok, Poland — ³Paul Scherrer Institute, Villigen, Switzerland

For a long time, nearly all experimental examples of magnetic switching by femtosecond pulses were demonstrated on metals and relied on mechanisms directly related to laser-induced heating close to the Curie temperature. The discovery of all-optical magnetization switching in Co: doped iron garnets via photomagnetic effect opened a new approach for magnetization control and raised a question about the microscopic nature of photo-magnetic spin dynamics. In order to reveal the magnetization dynamic of individual sublattices after excitation with NIR ultrashort laser pulses, we implement time-resolved XMCD techniques in a soft x-ray regime. We found that the dynamics of two antiferromagnetically coupled magnetic moments are drastically different during the first picosecond after the NIR excitation. The dynamics of Fe in tetrahedral oxygen surroundings showed a fast component lasting for about a picosecond. We state that the observed photoinduced noncollinear magnetic phase might be crucial for the all-optical magnetization switching in this material.

MA 25.3 Wed 15:30 H43

Spin-dependent carrier dynamics in antiferromagnetic model systems — •MARIUS WEBER¹, KAI LECKRON¹, BENJAMIN STADTMÜLLER^{1,2}, BAERBEL RETHFELD¹, and HANS CHRISTIAN SCHNEIDER¹ — ¹Department of Physics and Research Center OPTIMAS, TU Kaiserslautern — ²Institute of Physics, Johannes Gutenberg University Mainz

The Elliott-Yafet mechanism for the relaxation of an electronic spin polarization was originally derived for the electron-phonon scattering in degenerate bands in semiconductors [1]. Recently, we investigated how the concept of Elliott-Yafet spin-flip scattering can be applied to a microscopic treatment of carrier scattering in ferromagnetic metals including a ferromagnetic splitting and spin-orbit coupling [2].

Here we use the microscopic approach of [2], which utilizes the equation of motion formalism for the k-resolved reduced spin density matrix, to calculate the electronic dynamics in antiferromagnets such as the minimal model system discussed in [3]. The band structure of this model is anisotropic with two twofold degenerate bands and pronounced spin mixing. We investigate the spin-resolved electronic dynamics for different scenarios of spin-polarized anisotropic excitation, such as spin injection and k-selective spin flips.

[1] R. J. Elliott; *Physical Review* 96, 266, (1954).

[2] K. Leckron et al.; *Phys. Rev. B* 96, 140408 (2017).

[3] L. Smejkal et al.; *Phys. Status Solidi RRL*, 11 (2017).

MA 25.4 Wed 15:45 H43

Spectroscopic Analysis of the Ultrafast Non-Equilibrium Dynamics in Nickel at the European X-Ray Free-Electron Laser — •T. LOJEWSKI¹, M. F. ELHANOTY², N. ROTHENBACH¹, Y. KVASHNIN², L. LE GUYADER³, B. VAN KUIKEN³, R. CARLEY³, J. SCHLAPPA³, R. GORT³, G. MERCURIO³, A. YAROSLAVTSEV^{2,3}, N. GERASIMOVA³, M. TEICHMANN³, L. MERCADIER³, R. Y. ENGEL⁴, P. MIEDEMA⁴, L. SPIEKER¹, F. DÖRING⁵, B. RÖSNER⁵, F. DE GROOT⁶, P. THUNSTRÖM², O. GRÄNÄS², J. JÖNSSON², C. LAMBERT⁷, I. PRONIN⁸, J. REZVANI⁹, M. PACE¹⁰, C. BOEGLIN¹⁰, C. STAMM^{7,11}, M. BEYE⁴, C. DAVID⁵, O. ERIKSSON², A. SCHERZ³, U. BOVENSIEPEN¹, H. WENDE¹, K. OLLEFS¹, and A. ESCHENLOHR¹ — ¹Univ. Duisburg-Essen — ²Uppsala Univ. — ³European XFEL — ⁴DESY — ⁵PSI — ⁶Utrecht Univ. — ⁷ETH Zürich — ⁸ITMO Univ. — ⁹INFN — ¹⁰Univ. of Strasbourg — ¹¹FHNW

X-ray absorption spectroscopy is a powerful technique to investigate non-equilibrium dynamics combining a sensitivity to electron and lattice dynamics with element specificity. We report the time-resolved, spectroscopic analysis of Nickel-metal L_{2,3}-edge X-ray absorption spectra and their pump-induced changes measured at the SCS instrument of the European XFEL with unprecedented energy resolution and dynamic range. In addition, *ab initio* DFT and TD-DFT calculations connect the pump-induced changes to modifications of the electronic DOS. We find pump-induced redshifts and reduced absorption at the L_{2,3}-edges, which we explain by a loss of magnetic moment, changes in the electronic correlations and redistribution of electron population.

MA 25.5 Wed 16:00 H43

Indirect optical manipulation of the antiferromagnetic order of insulating NiO by ultrafast interfacial energy transfer — •STEPHAN WUST¹, CHRISTOPHER SEIBEL¹, HENDRIK MEER², PAUL HERRGEN¹, CHRISTIN SCHMITT², LORENZO BALDRATI², RAFAEL RAMOS³, TAKASHI KIKKAWA⁴, EIJI SAITOH⁴, OLENA GOMONAY², JAIRO SINOVA², YURIY MOKROUSOV², HANS CHRISTIAN SCHNEIDER¹, MATHIAS KLÄUT², BAERBEL RETHFELD¹, BENJAMIN STADTMÜLLER^{1,2}, and MARTIN AESCHLIMANN¹ — ¹Department of Physics and Research Center OPTIMAS, Technische Universität Kaiserslautern, 67663 Kaiserslautern, Germany — ²Institute of Physics, Johannes Gutenberg-University Mainz, 55128 Mainz, Germany — ³CIQUS, Departamento de Química-Física, Universidade de Santiago de Compostela, Santiago de Compostela, Spain — ⁴Department of Applied Physics, The University of Tokyo, Tokyo 113-8656, Japan

Antiferromagnets are promising candidates for improved future spintronic devices in terms of robustness and speed. Here, we report the ultrafast, (sub)picosecond reduction of the antiferromagnetic order of the insulating NiO thin film in a Pt/NiO bilayer. This reduction of the antiferromagnetic order is not present in pure NiO thin films after a strong optical excitation. This ultrafast phenomenon is attributed to an ultrafast and highly efficient energy transfer from the optically excited electron system of the Pt layer into the NiO spin system. We propose that this energy transfer is mediated by a stochastic exchange scattering of hot Pt electrons at the Pt/NiO interface.

MA 25.6 Wed 16:15 H43

Heat-conserving three-temperature model for ultrafast demagnetisation simulations of nickel and iron — •MARYNA PANKRATOVA¹, IVAN MIRANDA¹, DANNY THONIG^{2,1}, MANUEL PEREIRO¹, ERIK SJÖQVIST¹, ANNA DELIN³, OLLE ERIKSSON^{1,2}, and ANDERS BERGMAN¹ — ¹Department of Physics and Astronomy, Uppsala University, Box 516, Uppsala, Sweden — ²School of Science and Technology, Örebro University, Örebro, Sweden — ³Department of Applied Physics, School of Engineering Sciences, KTH Royal Institute of Technology, AlbaNova University Center, Stockholm, Sweden

In this work, we introduce a new heat-conserving three temperature model (HC3TM) for calculations of spin, electron, and lattice temperatures during ultrafast magnetisation dynamics simulations.

The proposed HC3TM has several advantages in comparison with the three-temperature model (3TM), proposed by Beurepaire. It reduces the reliance on heat transfer parameters, such as electron-spin, electron-lattice, and spin-lattice. These parameters are often hard to estimate which impedes the comparison with experimental data.

We apply HC3TM for the simulations of ultrafast demagnetisation of nickel and iron and compare the results with 3TM. HC3TM gives a demagnetisation rate during the first picoseconds after the absorption of a laser pulse which is in line with experiments. Overall, the proposed HC3TM reproduces experimental observations for nickel and iron better than most existing 3TM while it reduces the number of required parameters.

MA 25.7 Wed 16:30 H43

X-ray absorption spectroscopy on spin-crossover molecules — •LEA SPIEKER¹, TOBIAS LOJEWSKI¹, CAROLIN SCHMITZ-ANTONIAK², FLORIN RADU³, TORSTEN KACHEL³, LAURENT MERCADIER⁴, ANDREAS SCHERZ⁴, LOÏC LE GUYADER⁴, MARTIN TEICHMANN⁴, ROBERT CARLEY⁴, GIUSEPPE MERCURIO⁴, NATALIA GERASIMOVA⁴, BENJAMIN VAN KUIKEN⁴, CAMMILLE CARINAN⁴, DAVID HICKIN⁴, DAMIAN GÜNZING¹, SOMA SALAMON¹, GÉRALD KÄMMERER¹, PETER KRATZER¹, KLAUS SOKOLOWSKI-TINTEN¹, MANUEL GRUBER¹, ANDREA ESCHENLOHR¹, KATHARINA OLLEFS¹, SENTHIL KUMAR KUPPUSAMY⁵, MARIO RUBEN^{5,6}, UWE BOVENSIEPEN¹, and HEIKO WENDE¹ — ¹University of Duisburg-Essen and CENIDE — ²University of Applied Science Wildau — ³Helmholtz Center Berlin — ⁴European XFEL — ⁵Karlsruhe Institute of Technology — ⁶CNRS-University of Strasbourg

Spin-crossover molecules with abrupt spin-state switching in the room temperature regime are of great interest for future device applications. With X-ray absorption spectroscopy (XAS), it is possible to investigate their temperature-, visible light-, or X-ray induced spin-state switching. Recently, we performed static, temperature-dependent XAS measurements to study X-ray induced switching behavior as well as ultrafast time-resolved XAS measurements to analyze light-induced spin-state switching. We acknowledge European XFEL in Schenefeld, Germany, for the provision of X-ray free-electron laser beamtime at the SCS instrument. The financial support by CRC 1242 Projects A05, A07, B02, and C01 (Project-ID 278162697) is gratefully acknowledged.

MA 25.8 Wed 16:45 H43

Ultrafast magnetization dynamics in heterogeneous material compositions — •SEBASTIAN T. WEBER¹, CHRISTOPHER SEIBEL¹, MARIUS WEBER¹, MARTIN STIEHL¹, SANJAY ASHOK¹, SIMON HÄUSER¹, MARTIN AESCHLIMANN¹, HANS CHRISTIAN SCHNEIDER¹, BENJAMIN STADTMÜLLER^{1,2}, and BAERBEL RETHFELD¹ — ¹Department of Physics and Research Center OPTIMAS, TU Kaiserslautern — ²Institute of Physics, Johannes Gutenberg University Mainz

Ultrafast magnetization dynamics plays a key role in the development of spintronic devices. The dynamics are influenced by the composition of material systems as well as the wavelength of the optical excitation. The latter can create spatially inhomogeneous excitation profiles in thick nickel films [1,2] or Ni|Au heterostructures [3].

In this contribution, we compare results of the thermodynamic μ T-model with kinetic Boltzmann calculations and MOKE-measurements to investigate the influence of the wavelength on magnetization dynamics in different compositions. Our results show that laser and material parameters can enhance or hinder the interplay of relaxation processes, leading to different laser-induced magnetization dynamics.

[1] U. Bierbrauer *et al.*, JOP: Cond. Mat. 29, 244002 (2017)[2] S. Ashok *et al.*, Appl. Phys. Lett. 120, 142402 (2022)[3] C. Seibel *et al.*, arXiv:2112.04780 (2021)

MA 26: Molecular Magnetism

Time: Wednesday 15:00–16:00

Location: H48

MA 26.1 Wed 15:00 H48

Density functional theory studies of a Fe(II) spin-crossover complex — •GERALD KÄMMERER and PETER KRATZER — University Duisburg-Essen, Duisburg, Germany

We investigate the spin-state switching of a Fe(II) spin-crossover complex ($[\text{Fe}(\text{1-bpp} - \text{COOC}_2\text{H}_5)_2](\text{BF}_4)_2\text{CH}_3\text{CN}$) from a diamagnetic low-spin ($S=0$) to a paramagnetic high-spin ($S=2$) state in the framework of density functional theory (DFT). The calculations were carried out with FHI-Aims code using PBE and B3LYP functionals. Due to the switching, the bond length Fe-N increases by up to 20%. In addition, calculations for Raman spectra were done for both spin-states and compared to temperature-dependent Raman measurements. This allows us the analysis of a unique fingerprint of the molecular bondings as well as the assignment of specific Raman modes. The financial support by DFG within CRC 1242 (Project B 02) and computation time on the MagnitUDE supercomputer system are gratefully acknowledged.

MA 26.2 Wed 15:15 H48

Inelastic Neutron Scattering and Magnetic Studies on Families of 3d-4f Heterometallic M_2Ln_2 Single-Molecule Magnets — •JULIUS MUTSCHLER¹, THOMAS RUPPERT², YAN PENG², JACQUES OLLIVIER³, QUENTIN BERROD³, JEAN-MARC ZANOTTI³, CHRISTOPHER E. ANSON², ANNIE K. POWELL², and OLIVER WALDMANN¹ — ¹Physikalisches Institut, Universität Freiburg, D-79104 Freiburg, Germany — ²Institut of Inorganic Chemistry, Karlsruhe Institute of Technology (KIT), D-76131 Karlsruhe, Germany — ³Institut Laue-Langevin, F-38042 Grenoble Cedex 9, France

MA 26.3 Wed 15:30 H48

Study of VOPc/TiOPc layers on Ag(100) using X-ray absorption spectroscopy — •JAEHYUN LEE^{1,2}, STEFANO REALE^{1,2}, KYUNGJU NOH^{1,2}, LUCIANO COLAZZO¹, DENIS KRYLOV¹, CHRISTOPH WOLF¹, ANDRIN DOLL³, ANDREAS HEINRICH^{1,2}, YUJEONG BAE^{1,2}, and FABIO DONATI^{1,2} — ¹Center for Quantum Nanoscience — ²Ewha Womans University, Seoul, Republic of Korea — ³Swiss Light Source, Paul Scherrer Institut (PSI), Villigen Switzerland

Vanadyl Phthalocyanine (VOPc) shows spin 1/2 and long coherence time of almost 1 microsecond up to room temperature [M. Atzori *et al.*, J. Am. Chem. Soc. 138, 2154 (2016)]. Investigating the orbital splitting when absorbed on a surface

and the interactions between the molecular spin and the supporting substrate is crucial to optimize their quantum coherence properties. Here, we use x-ray absorption spectroscopy to investigate the spin properties of VOPc on Ag(100) and on TiOPc/Ag(100). To interpret our data, we simulate x-ray spectra combining machine learning with multiplet calculations. We find that the interaction with the metal surface changes the orbital structure of VOPc when directly on the Ag(100). Decoupling from the metal using a TiOPc layer is sufficient to restore the spin and orbital structure of the free standing VOPc, which shows no changes upon annealing up to 450K. This robust molecular spin architecture shows the potential in quantum computing technology.

MA 26.4 Wed 15:45 H48

High-frequency EPR studies on monomeric 4f complexes — LENA SPILLECKE, CHANGHYUN KOO, and RÜDIGER KLINGELER — Kirchhoff Institute for Physics, Heidelberg University, Germany

Tuning of magnetic anisotropy by appropriate design of crystal fields in 4f monomeric complexes is guided by experimental determination of relevant parameters – here by high-frequency electron paramagnetic resonance (HF-EPR)

studies – and by numerical results. Our recent study on pentagonal-bipyramidal Er(III) [1] complexes is motivated by a reported difference in relaxation behavior [2]. Evaluating the data in a $S = 1/2$ pseudo spin approximation for each Kramers doublet (KD) results in the precise determination of the crystal field splitting energies and effective g-values of the three lowest KDs. Relaxation behaviour is directly traced back to changes in electronic structure, induced by the crystal field and are attributed to a pronounced non-axiality of the ground-state g-tensor promoting a fast QTM magnetic relaxation. Another confirmation of a guided approach is provided by recent data on a set of [Ln(III)L12]-complexes (Ln = Dy, Tb) involving tetradentate ligands [3] as well as by studies of a novel nonadentate bispidine-based ligand where the experimentally determined relaxation barrier of 46 cm^{-1} is rather modest but in excellent agreement with that predicted by ab-initio calculations [4].

[1] L. Spillecke et al., Dalton Transactions 50, 18143 (2021) [2] T.A. Bazhenova et al., Molecules 26, 6908 (2021) [3] P. Comba et al., Chemistry-Eur. J. 24, 5319 (2018) [4] P. Cieslik et al., J of Inorg. Gen. Chem. (Z. Anorg. Allg. Chem.) 647, 843 (2021)

MA 27: Skyrmions 2 (joint session MA/KFM)

Time: Thursday 9:30–12:45

Location: H37

MA 27.1 Thu 9:30 H37

Complementary investigations of magnetic textures in the antiskyrmion compound $\text{Mn}_{1.4}\text{PtSn}$ with REXS and LTEM — M. WINTER^{1,2,3,4}, M. RAHN⁴, D. WOLF³, S. SCHNEIDER², M. VALVIDARES⁵, C. SHEKAR¹, P. VIR¹, B. ACHINUQ⁶, H. POPESCU⁷, N. JAOUEN⁷, G. VAN DER LAAN⁸, T. HESJEDAL⁶, B. RELLINGHAUS², and C. FELSER¹ — ¹MPI CPfS, Dresden, Germany — ²DCN, TU Dresden, Germany — ³IFW Dresden, Germany — ⁴IFMP, TU Dresden, Germany — ⁵ALBA Synchrotron, Barcelona, Spain — ⁶Clarendon Laboratory, University of Oxford, UK — ⁷Synchrotron SOLEIL, Saint-Aubin, France — ⁸Diamond Light Source, UK

The Heusler compound $\text{Mn}_{1.4}\text{PtSn}$ is known to host multiple non trivial magnetic textures like antiskyrmions (aSKs). Its phase diagram depends not only on temperature and sample shape, but also on strength and orientation of an external magnetic field as well as on the history of its application. In order to better understand the formation of aSKs, we have conducted complementary experiments of resonant elastic x-ray scattering (REXS) and Lorentz transmission electron microscopy (LTEM) on an identical lamella of $\text{Mn}_{1.4}\text{PtSn}$. Our complementary approach allows for the first time to directly relate the REXS patterns to the underlying magnetic phase as determined from LTEM. Along this approach, LTEM has proven an ideal pre-characterization tool to navigate the high-dimensional parameter space and subsequently take advantage of the better control of magnetic field directions, temperature as well as of energy resolved measurements as provided by REXS. Part of this work is gratefully supported by DFG within SPP 2137.

MA 27.2 Thu 9:45 H37

Doping control of magnetic anisotropy for stable antiskyrmion formation in schreibersite (Fe,Ni)3P with S4 symmetry — KOSUKE KARUBE¹, LICONG PENG¹, JAN MASELL^{1,2}, MAMOUN HEMMIDA³, HANS-ALBRECHT KRUG VON NIDDA³, ISTVÁN KÉZSMÁRKI³, XIUZHEN YU¹, YOSHINORI TOKURA^{1,4}, and YASUJIRO TAGUCHI¹ — ¹RIKEN CEMS, Wako, Japan — ²Karlsruhe Institute of Technology (KIT), Karlsruhe, Germany — ³University of Augsburg, Augsburg, Germany — ⁴University of Tokyo, Tokyo, Japan

Recently, growing attention has also been paid to antiskyrmions emerging in non-centrosymmetric magnets with D2d or S4 symmetry. [1] In these magnets, complex interplay among anisotropic Dzyaloshinskii-Moriya interaction, uniaxial magnetic anisotropy, and magnetic dipolar interactions generates a variety of magnetic structures. We control the uniaxial magnetic anisotropy of schreibersite (Fe,Ni)3P with S4 symmetry by doping and investigate its impact on the stability of antiskyrmions. With magnetometry, supported by ferromagnetic resonance spectroscopy, Lorentz transmission electron microscopy, and micro-magnetic simulations, we quantitatively analyze the stability of antiskyrmion as functions of uniaxial anisotropy and demagnetization energy, and demonstrate that subtle balance between them is necessary to stabilize antiskyrmions.

[1] K. Karube, L. C. Peng, J. Masell, X. Z. Yu, F. Kagawa, Y. Tokura, and Y. Taguchi, Nat. Mater. 20, 335-340 (2021) [2] The authors, Adv. Mater. 34 (11), 2108770 (2022)

MA 27.3 Thu 10:00 H37

Magnetic and Morphological Phases in the 2D van der Waals Magnet FexGeTe_2 — KAI LITZIUS¹, MAX BIRCH^{1,5}, LUKAS POWALLA^{2,3,5}, SEBASTIAN WINTZ¹, FABIAN ALTEN¹, MICHAEL MILLER¹, MARKUS WEIGAND⁴, KLAUS KERN^{2,3}, MARKO BURGHARD², and GISELA SCHÜTZ¹ — ¹Max-Planck-Institute for Intelligent Systems, 70569 Stuttgart, Germany — ²Max-Planck-Institute

for Solid State Research, 70569 Stuttgart, Germany — ³Institut de Physique, École Polytechnique Fédérale de Lausanne, CH-1015 Lausanne, Switzerland — ⁴Helmholtz-Zentrum Berlin für Materialien und Energie GmbH, 12489 Berlin, Germany — ⁵These authors contributed equally to the work

Recently, observations of magnetic skyrmions in 2-dimensional (2D) itinerant ferromagnets opened many possibilities for technological implementation of 2D van der Waals structures in spintronics. However, the stability of the different magnetic states and morphological phases in FexGeTe_2 remains an unresolved issue. In this work, we utilize real-space imaging to determine magnetic phase diagrams of exfoliated FexGeTe_2 films. Our findings show besides complex, history-dependent magnetization states also that changes in the crystalline structure significantly alter the magnetic behavior. Ultimately, the choice of material and a proper nucleation mechanism result in the stabilization of a variety of (meta-) stable magnetic configurations, including skyrmions. These findings open novel perspectives for designing van der Waal heterostructure-based devices incorporating topological spin textures.

MA 27.4 Thu 10:15 H37

Antiskyrmions in B20-type FeGe — NIKOLAI S. KISELEV¹, FENGSHAN ZHENG^{2,3}, LUYAN YANG², VLADYSLAV M. KUCHKIN¹, FILIPP N. RYBAKOV^{4,5}, STEFAN BLÜGEL¹, and RAFAL E. NIKOLAI² — ¹Peter Grünberg Institute and Institute for Advanced Simulation, Forschungszentrum Jülich and JARA, 52425 Jülich, Germany — ²Le Brandst. 1 — ³Spin-X Institute, School of Physics and Optoelectronics, State Key Laboratory of Luminescent Materials and Devices, Guangdong-Hong Kong-Macao Joint Laboratory of Optoelectronic and Magnetic Functional Materials, South China University of Technology, Guangzhou 511442, China — ⁴Department of Physics and Astronomy, Uppsala University, SE-75120 Uppsala, Sweden — ⁵Department of Physics, KTH-Royal Institute of Technology, SE-10691 Stockholm, Sweden

We report the highly reproducible observations of statically stable antiskyrmion [1] – skyrmion antiparticle in thin plates of B20-type FeGe chiral magnet where only skyrmions were observed earlier. Using Lorentz TEM and electron holography, we showed that skyrmions and antiskyrmions could coexist in a wide range of fields and temperatures. These findings are entirely consistent with micro-magnetic simulations and prior theoretical studies of two-dimensional systems [2]. The mechanism of antiskyrmion stability, nucleation, and annihilation with ordinary skyrmions is discussed in detail.

[1] F. Zheng et al., Nat. Phys. (2022) accepted.

[2] V. M. Kuchkin, N. S. Kiselev, Phys. Rev. B 101, 064408 (2020).

MA 27.5 Thu 10:30 H37

Asymmetric magnetization reversal in perpendicularly magnetized micro stripes induced by exchange-bias effect and Dzyaloshinskii-Moriya interaction — SAPIDA AKHUNDZADA¹, PIOTR KUŚWIK², CHRISTIAN JANZEN¹, ARNO EHRESMANN¹, and MICHAEL VOGEL¹ — ¹Institute of Physics and Center for Interdisciplinary Nanostructure Science and Technology (CINaT), University of Kassel, Kassel, Germany — ²Institute of Molecular Physics, Polish Academy of Sciences, Poznań, Poland

In a systematic study, the magnetization reversal in exchange-biased Ti/Au/Co/NiO/Au micro stripes with perpendicular magnetic anisotropy is characterized using high-resolution magneto-optical Kerr microscopy. Thereby, the remagnetization process is observed to be asymmetric with respect to the two branches of the hysteresis loop, being quantified as a higher nucleation density formed along one field branch with decreasing structure width. Additionally, a

local asymmetry in the domain nucleation and domain wall movement within the stripe geometry is observed. The influence of the exchange bias effect and the Dzyaloshinskii-Moriya interaction is investigated by field-cooling and the application of additional in-plane magnetic fields during the magnetization reversal process. XMCD and XMLD experiments reveal the corresponding domain texture in the ferromagnetic and antiferromagnetic layers. These experiments show how the interplay between chiral Dzyaloshinskii-Moriya interaction and the unidirectional anisotropy modify the magnetic domain texture and the resulting magnetization reversal in microstructures.

MA 27.6 Thu 10:45 H37

Magnetic skyrmion braids — •NIKOLAI S. KISELEV¹, FENGSHAN ZHENG², FILIPP N. RYBAKOV³, DONGSHENG SONG², ANDRÁS KOVÁCS², HAIFENG DU⁴, STEFAN BLÜGEL¹, and RAFAL E. DUNIN-BORKOWSKI² — ¹Peter Grünberg Institute and Institute for Advanced Simulation, Forschungszentrum Jülich and JARA, 52425 Jülich, Germany — ²Ernst Ruska-Centre for Microscopy and Spectroscopy with Electrons and Peter Grünberg Institute, Forschungszentrum Jülich, 52425 Jülich, Germany — ³Department of Physics, KTH-Royal Institute of Technology, Stockholm, SE-10691 Sweden — ⁴The Anhui Key Laboratory of Condensed Matter Physics at Extreme Conditions, High Magnetic Field Laboratory, Chinese Academy of Science (CAS), Hefei, Anhui Province 230031, China In cubic chiral magnets, the magnetization of skyrmions resembles a string-like or filamentary texture. Skyrmion strings are naturally expected to interwind and form complex three-dimensional superstructures by analogy to elastic strings. We found that skyrmion strings in cubic crystals of chiral magnets can form braids – statically stable configurations where skyrmion strings wind around one another [1]. This finding is confirmed by direct observations of skyrmion braids in B20-type FeGe using transmission electron microscopy. The theoretical analysis predicts that the discovered phenomenon is general for a wide family of chiral magnets and can be observed in thick plates and bulk crystals.

[1] F. Zheng, et al., *Nature Commun.* 12, 5316 (2021).

MA 27.7 Thu 11:00 H37

Tunable ellipticity of Bloch skyrmions in antiskyrmion-hosting materials — SEBASTIAN SCHNEIDER^{1,2}, •JAN MASELL^{1,3}, FEHMI S. YASIN¹, LICONG PENG¹, KOSUKE KARUBE¹, YASUJIRO TAGUCHI¹, DARIUS POHL², BERND RELLINGHAUS², YOSHINORI TOKURA^{1,4}, and XIUZHEN YU¹ — ¹RIKEN CEMS, Wako, Japan — ²TU Dresden, Dresden, Germany — ³Karlsruhe Institute of Technology (KIT), Karlsruhe, Germany — ⁴University of Tokyo, Tokyo, Japan Magnetic skyrmions are usually stabilized and studied in materials with isotropic Dzyaloshinskii-Moriya interaction (DMI). In materials with D2d or S4 symmetry, however, the sign of the DMI is exactly opposite in two orthogonal directions such that it favors antiskyrmions instead of skyrmions. [1,2] Yet, uniaxial anisotropy and dipolar interactions can also help stabilizing skyrmions in such materials which, as a consequence of the anisotropic DMI, are rendered elliptical. We quantify the elliptical distortion of skyrmions in an S4 symmetric material as function of magnetic field and temperature using LTEM holography. Our micromagnetic simulations and simple analytical modelling explain the experimentally observed behavior and provide a technique to quantitatively estimate the DMI.

[1] K. Karube, L. C. Peng, J. Masell, X. Z. Yu, F. Kagawa, Y. Tokura, and Y. Taguchi, *Nat. Mater.* 20, 335-340 (2021) [2] K. Karube, L. C. Peng, J. Masell, M. Hemmida, H.-A. Krug von Nidda, I. Kézsmárki, X. Z. Yu, Y. Tokura, and Y. Taguchi, *Adv. Mater.* 34 (11), 2108770 (2022) [3] In preparation.

MA 27.8 Thu 11:15 H37

Long-range non-collinearity and spin reorientation in the centrosymmetric hexagonal magnet NiMnGa — •PARUL DEVI¹, SANJAY SINGH², THOMAS HERMANNSDÖRFFER¹, and JOACHIM WOSNITZA^{1,3} — ¹Dresden High Magnetic Field Laboratory, HZDR, Germany — ²Institut für Festkörper und Materialphysik, TU Dresden, Germany — ³School of Materials Science and Technology, Indian Institute of Technology (BHU), Varanasi-221005, India

The recent discovery of biskyrmions and skyrmions in globally centrosymmetric crystals has raised questions about the role of the Dzyaloshinskii-Moriya interactions (DMI) in causing the topologically stable spin vortex textures, since DMI vanishes in such crystal structures. Here, we present a detailed crystal and magnetic structure investigation of the non-collinear hexagonal magnetic material NiMnGa exhibiting biskyrmions [1]. We show an investigation on the nature of the phase transitions, evidence of magnetoelastic coupling and anomalous thermal expansion in hexagonal, centrosymmetric NiMnGa using combined studies of magnetization and high-resolution synchrotron x-ray powder diffraction data. Magnetization data exhibits spin reorientation transition * 200 K. By means of powder neutron diffraction data, we investigate the change of the magnetic structure in NiMnGa. This study will help to understand the origin of biskyrmions in the absence of Dzyaloshinskii-Moriya interaction in magnetic materials.

[1] Yu et al., *Nat. Comm.* 5, 3198 (2014).

MA 27.9 Thu 11:30 H37

Zero-field skyrmionic states and in-field edge-skyrmions induced by boundary tuning — •JONAS SPETHMANN, ELENA Y. VEDMEDENKO, ROLAND WIESEN-DANGER, ANDRÉ KUBETZKA, and KIRSTEN VON BERGMANN — Universität Hamburg, Hamburg, Germany

When magnetic skyrmions are moved via currents, they do not strictly travel along the path of the current, instead their motion also gains a transverse component. This so-called skyrmion Hall effect can be detrimental in potential skyrmion devices because it drives skyrmions towards the edge of their hosting material where they face potential annihilation. To mitigate this problem it was proposed to create a potential well within the skyrmion hosting material and thereby guide the skyrmions along a desired pathway[1]. Here we have experimentally modified a skyrmion model system—an atomic Pd/Fe bilayer on Ir(111)[2]—by growing a self-assembled ferromagnetic Co/Fe bilayer adjacent to it. Employing spin-polarized scanning tunneling microscopy, we demonstrate that this ferromagnetic rim has an immediate effect on the spin spiral ground state of the Pd/Fe bilayer, stabilizes skyrmions and target states in zero field and prevents skyrmion annihilation at the film edge. Furthermore we show that in applied magnetic fields the Co/Fe gives rise to edge-skyrmions pinned to the Pd/Fe island rim. Finally we have performed spin dynamics simulations to investigate the role of different magnetic parameters in causing these edge effects.

[1] I. Purnama *et al.*, *Scientific Reports* 5, 10620 (2015).

[2] N. Romming *et al.* *Science* 341, 636-639 (2013).

MA 27.10 Thu 11:45 H37

Real-space determination of the isolated magnetic skyrmion deformation under electric current flow — FEHMI S. YASIN¹, •JAN MASELL^{1,2}, KOSUKE KARUBE¹, AKIKO KIKKAWA¹, YASUJIRO TAGUCHI¹, YOSHINORI TOKURA^{1,3}, and XIUZHEN YU¹ — ¹RIKEN CEMS, Wako, Japan — ²Karlsruhe Institute of Technology (KIT), Karlsruhe, Germany — ³University of Tokyo, Tokyo, Japan

The effect of electric current on topological magnetic skyrmions, such as the current-induced deformation of isolated skyrmions, is of fundamental interest. The deformation has consequences ranging from perturbed dynamics to modified packing configurations. [1] We measure the current-driven real-space deformation of isolated, pinned skyrmions within CoZn at room temperature. We observe that the skyrmions are surprisingly soft, readily deforming during electric current application into an elliptical shape with a well-defined deformation axis. We find that this axis rotates towards the current direction, in agreement with our simply Thiele-based theoretical analysis. We quantify the average eccentricity and how the skyrmion size expands during current application. This first evaluation of in-situ electric current-induced skyrmion deformation paints a clearer picture of spin-polarized electron-skyrmion interactions and may prove essential when designing spintronic devices.

[1] J. Masell, D.R. Rodrigues, B.F. McKeever, and K. Everschor-Sitte, *Phys. Rev. B* 101, 214428 (2020). [2] Under review.

MA 27.11 Thu 12:00 H37

Magnetocrystalline anisotropy in cubic chiral magnets — •VIVEK KUMAR¹, ANDREAS BAUER¹, SCHORSCH MICHAEL SAUTHER¹, MICHELLE HOLLRICHER¹, MARKUS GARST², MARC ANDREAS WILDE¹, and CHRISTIAN PFLEIDERER¹ — ¹Physik-Department, Technische Universität München, D-85748 Garching, Germany — ²Institut für Theoretische Festkörperphysik, Karlsruhe Institute of Technology, D-76131 Karlsruhe, Germany

Magnetocrystalline anisotropy plays an important role in the stabilization, orientation and manipulation of exotic spin textures like skyrmions in cubic chiral magnets [1-3]. Here, we report the determination of the fourth and sixth order anisotropy constants of MnSi as a function of temperature and field using the cantilever torque magnetometry option in a physical property measurement system. Torque curves were recorded by rotating the single-crystalline spherical sample in the field polarized state. This allows us to extract anisotropy constants by fitting the experimental data to the theoretical expressions of torques belonging to the symmetry class ($P2_13$). In addition, we discuss technical issues in measurement related to sample shape and geometry. The present technique is used to obtain the anisotropy constants of other cubic chiral magnets including Cu_2OSeO_3 , $\text{Mn}_{1-x}\text{Fe}_x\text{Si}$ and $\text{Fe}_{1-x}\text{Co}_x\text{Si}$ series.

[1] Chacon *et al.*, *Nat. Phys.* 14, 936 (2018).

[2] Bauer *et al.*, *Phys. Rev. B* 95, 024429 (2017).

[3] Adams *et al.*, *Phys. Rev. Lett.* 121, 187205 (2018).

MA 27.12 Thu 12:15 H37

Change of electronic Chern number induced by phase shifts in multiple-Q textures — •PASCAL PRASS¹, FABIAN R. LUX¹, DUCCO VAN STRATEN², and YURIY MOKROUSOV^{1,3} — ¹Institute of Physics, Johannes Gutenberg University Mainz, Germany — ²Institute of Mathematics, Johannes Gutenberg University Mainz, Germany — ³Peter Grünberg Institut and Institute for Advanced Simulation, Forschungszentrum Jülich and JARA, Germany

A multiple-Q spin texture is given by the superposition of multiple spin spirals and gives rise to a periodic array of topological spin structures, such as skyrmions. Using the emergent magnetic field formalism [1] the topological Hall current in the texture is proportional to the real-space winding number of its

spin vector field. In recent articles [2,3], it was illustrated how tuning the relative phase shifts of the spin waves as well as the textures' net magnetization leads to topological phase transitions in the spin texture, i.e. integer jumps of its winding number. Combining these ideas implies the existence of significant discontinuous jumps in the topological Hall current and its associated Chern numbers in the underlying electronic spectrum. In this work, we directly investigate the spin textures' electronic band topology to determine the relationship between its real-space winding number and quasi-momentum space Chern numbers. Understanding the electronic behaviour during these transitions will have far-reaching implications for developing tunable topological Hall devices. [1] T. Schulz et al. *Nat. Phys.* 8, 301-304 (2012). [2] K. Shimizu et al. *arXiv:2201.03290* (2022). [3] S. Hayami et al. *Nat. Commun.* 12, 6927 (2021).

MA 27.13 Thu 12:30 H37

Audio Recognition with Skyrmion Mixture Reservoirs — •ROBIN MSISKA¹, JAKE LOVE¹, JONATHAN LELLAERT², JEROEN MULKERS², GEORGE BOURIANOFF³, and KARIN EVERSCHOR-SITTE¹ — ¹University of Duisburg-Essen, Duisburg, Germany — ²Ghent University, Ghent, Belgium — ³Senior Principle Engineer, Intel Corp. (Retired)

Physical reservoir computing is an information processing scheme that enables energy efficient temporal pattern recognition to be performed directly in physical matter [1]. Previously, random topological magnetic textures have been shown to have the characteristics necessary for efficient reservoir computing [2] and allowed for simple pattern recognition with two input channels [3].

We propose a skyrmion mixture reservoir computing model with multi-dimensional inputs. Through micro-magnetic simulations, we show that our implementation can solve audio classification tasks at the nanosecond timescale to a high degree of accuracy. Due to the quality of the results shown and the low power properties of magnetic texture reservoirs, we argue that skyrmion magnetic textures are a competitive substrate for reservoir computing.

Funding from the Emergent AI Centre (Carl-Zeiss-Stiftung), DFG (320163632), FWO-Vlaanderen and computer resources by VSC (Flemish Supercomputer Center) are gratefully acknowledged.

[1] G. Tanaka et al., *Neural Networks* 115, 100 (2019). [2] D. Prychynenko et al., *Physical Review Applied* 9, 014034 (2018) [3] D. Pinna et al., *Phys. Rev. Applied* 14, 054020 (2020)

MA 28: Magnonics 2

Time: Thursday 9:30–12:45

Location: H43

MA 28.1 Thu 9:30 H43

Imaging and phase-locking of non-linear spin waves — •ROUVEN DREYER¹, ALEXANDER F. SCHÄFFER¹, HANS G. BAUER², NIKLAS LIEBING¹, JAMAL BERAKDAR¹, and GEORG WOLTERS DORF¹ — ¹Martin Luther University Halle-Wittenberg, Institute of Physics, Von-Danckelmann-Platz 3, 06120 Halle (Saale), Germany — ²Jahnstrasse 23, 96050 Bamberg, Germany

Non-linear processes are a key feature in the emerging field of spin-wave based information processing since they allow to convert uniform spin-wave excitations into propagating modes at different frequencies. Typically, non-linear spin-wave generation is well described by three and four-magnon scattering processes in the small modulation limit. Recently, the existence of non-linear magnons at odd half-integer multiples of the driving frequency (such as $3/2 f_{rf}$, $5/2 f_{rf}$, etc.) has been predicted for $\text{Ni}_{80}\text{Fe}_{20}$ at low bias fields [1]. However, it is an open question under which conditions these non-linear spin waves emerge coherently and how they can be manipulated in devices. Using super-Nyquist sampling MOKE [2] we directly image these non-linear spin waves in the strong modulation regime. The spatially-resolved investigation of such excitations in $\text{Ni}_{80}\text{Fe}_{20}$ elements reveals two distinct phase states [3]. Moreover, we use phase-locking to an external 'seed' frequency to actively manipulate the phase state. These results open new possibilities for spin-wave sources and phase-encoded information processing with magnons.

[1] H. G. Bauer et al., *NC* 6:8274 (2015) [2] R. Dreyer et al., *PRM* 5(6):064411 (2021) [3] T. Makiuchi et al., *APL* 118, 022402 (2021)

MA 28.2 Thu 9:45 H43

Frequency multiplication by collective nanoscale spin wave dynamics — •CHRIS KÖRNER¹, ROUVEN DREYER¹, MARTIN WAGENER², NIKLAS LIEBING¹, HANS G. BAUER³, and GEORG WOLTERS DORF¹ — ¹Department of Physics, Martin Luther University Halle-Wittenberg, Von-Danckelmann-Platz 3, 06120 Halle, Germany — ²Institute for Quantum Electronics, ETH Zürich, Otto-Stern-Weg 1, 8093 Zürich, Switzerland — ³Jahnstrasse 23, 96050 Bamberg, Germany

We observe all-magnetic frequency multiplication and the generation of a 6-octave spanning frequency comb within an extended polycrystalline NiFe layer [1]. We investigate this process by means of super Nyquist sampling MOKE microscopy [2] and diamond NV center spectroscopy. Our experimental observations in conjunction with micromagnetic simulations reveal the mechanism of this unexpected phenomenon.

At low bias fields the magnetization locally tilts due to a magnetic ripple effect in the NiFe film. Driving the magnetization with frequencies far below ferromagnetic resonance, i.e. in the MHz range, causes rapid synchronous switching. These switching processes lead to high harmonic spin wave emission. The spin waves emitted by multiple switching events across the film interfere and form a phase stable coherent spin wave frequency comb extending into the GHz regime.

[1] Koerner et al. *Science*, 375 (6585), 1165-1169 (2022) [2] Dreyer et al. *Phys. Rev. Materials* 5, 064411 (2021)

MA 28.3 Thu 10:00 H43

Hybridization Induced Spin-Wave Stop Band — •CHRISTIAN RIEDEL, TAKUYA TANIGUCHI, and CHRISTIAN H. BACK — Technische Universität München

We present complex spin-wave diffraction patterns in the near-field diffraction limit by using a custom-made time-resolved magneto-optical Kerr effect (TR-MOKE) microscope for visualizing the local and time-resolved dynamic magnetization, i.e. propagating spin-waves. To investigate magnonic interference

behaviors, we fabricate a diffraction grating in a 200 nm thick ferrimagnetic YIG film by argon ion-beam etching. A coplanar waveguide (CPW) located parallel to the grating, is used to coherently excite spin-waves. Our results represent the experimental realization of complex spin-wave interference patterns arising from various diffraction gratings, as preliminary investigated by Mansfeld et al.. We further demonstrate that the interference pattern behind the diffraction grating can be tuned through careful selection of the external magnetic field strength. A reduction in the effective magnetic field between the grating antidots can lead to a hybridization of two spin-wave modes and with this to a spin-wave transmission stop-band. This work contributes to the understanding of spin-wave interference behaviors for enhancing the performance of future magnonic devices.

MA 28.4 Thu 10:15 H43

Investigation of Spin Wave Caustics Phenomena — •FRANZ VILSMEIER¹, ALEXIS WARTELLE², TAKUYA TANIGUCHI¹, and CHRISTIAN BACK¹ — ¹Technische Universität München — ²Grenoble Institute of Technology

We present a systematic survey of caustic spin wave beams and their properties in an anisotropic magnetic environment.

Based on the theory from Kalinikos and Slavin for spin waves in soft films [*Journal of Physics C: Solid State Physics*, 1986, 19, 7013-7033], an anisotropic dispersion relation allows caustic points to exist. Here, several wavevectors with the same group velocity direction can be excited over a broad angular range within the sample plane. These caustic points result in nondiffractive spin wave beams and are characterised by their propagation direction, wavefront angle and wavelength.

Experimentally, we excite the caustic points in 200 nm thick Yttrium Iron Garnet by sending an rf current through a bow-shaped antenna. Time Resolved Kerr Microscopy is used to investigate the propagation behaviour both, spatially, as well as time resolved. We are able to access one caustic pocket and detect caustic-like beams over a range of different rf frequencies and external magnetic field values. Furthermore, the caustic-like beams are used to directly observe anisotropic reflection phenomena and steering of the beams with rotation of the externally applied field. The findings are compared to micromagnetic simulations with the help of Mumax3.

MA 28.5 Thu 10:30 H43

The Optimization of Yttrium Iron Garnet Spin-wave Lenses for Amplification of Spin Waves — •STEPHANIE LAKE¹, PHILIPP GEYER¹, ROUVEN DREYER¹, NIKLAS LIEBING¹, PHILIP TREMPER¹, EVANGELOS PAPAIOANNOU¹, GEORG WOLTERS DORF¹, and GEORG SCHMIDT^{1,2} — ¹Institut für Physik, Martin-Luther-Universität Halle-Wittenberg, 06120 Halle, Germany — ²Interdisziplinäres Zentrum für Materialwissenschaften, Martin-Luther-Universität Halle-Wittenberg, 06120 Halle, Germany

Exciting magnons in magnetic materials for high-frequency applications is inefficient; one way to improve the process is to focus a manifold of spin waves. Following this idea, we create a magnon counterpart to the nonimaging Fresnel lens concentrator called a "spin-wave lens."

We simulate spin-wave (SW) propagation through funnel-like SW lenses based on the material Yttrium Iron Garnet (YIG) using Mumax [1]. When a frequency of 3.25 GHz and field of 51.62 mT are applied, SW modes with wavelengths 9.4 μm are excited, and furthermore, have a 384-fold increase in their intensity relative to the structure's start.

To test the simulation's accuracy, we fabricate SW lenses out of YIG [2] and measure the precession of excited SWs by a magneto-optic Kerr effect (MOKE) measurement scheme. We conduct several parameter sweeps of geometric characteristics and experimental conditions and currently attain a 51-fold increase in intensity near the funnel's exit for a frequency of 3.68 GHz and magnetic field of 66.15 mT.

[1] A. Vansteenkiste, et al., *AIP Adv.* **4**, 107133 (2014).

[2] F. Heyroth, et al., *Phys. Rev. Appl.* **12**, 054031 (2019).

MA 28.6 Thu 10:45 H43

Exchange spin waves excitation in nanoscale magnonic waveguides using deeply nonlinear phenomena — •QI WANG^{1,2}, ROMAN VERBA³, BJÖRN HEINZ⁴, MICHAEL SCHNEIDER⁴, ONDŘEJ WOJEWODA⁵, CARSTEN DUBS⁶, NORBERT NORBERT², MICHAL URBÁNEK⁵, PHILIPP PIRRO⁴, and ANDRII CHUMAK¹ — ¹Faculty of Physics, University of Vienna, Vienna, Austria — ²Wolfgang Pauli Institute c/o Faculty of Mathematics, University of Vienna, Vienna, Austria — ³Institute of Magnetism, Kyiv, Ukraine — ⁴Fachbereich Physik und Landesforschungszentrum OPTIMAS, Technische Universität Kaiserslautern, Kaiserslautern, Germany — ⁵CEITEC BUT, Brno University of Technology, Brno, Czech Republic — ⁶INNOVENT e.V., Technologieentwicklung, Jena, Germany High-speed and ultrashort waves with pronounced nonlinear phenomena are an ideal medium for wave-based computing. Spin waves, and their quanta magnons, meet all the requirements and are prospective data carriers in future signal processing systems. However, an efficient method for the excitation of short-wavelength spin waves is still an unsolved problem and a major obstacle for broadband spin-wave applications. Here, we present a universal approach to excite spin waves with wavelengths from micrometers down to tens of nanometers in nanoscale waveguides by exploiting deep nonlinear phenomena and validate it experimentally by microfocused Brillouin light scattering spectroscopy. The novel excitation method removes the wavelength limitations imposed by the antenna size, increases the excitation efficiency of short spin waves, and enables direct on-chip integration.

MA 28.7 Thu 11:00 H43

Symmetry of the magnetoelastic interaction of Rayleigh- and shear horizontal-magnetoacoustic waves — •MATTHIAS KÜSS¹, MICHAEL HEIGL¹, LUIS FLACKE^{2,3}, ANDREAS HEFELE¹, ANDREAS HÖRNER¹, MATHIAS WEILER^{2,3,4}, MANFRED ALBRECHT¹, and ACHIM WIXFORTH¹ — ¹University of Augsburg, Experimental Physics I and IV — ²Walther-Meißner-Institut, Bayerische Akademie der Wissenschaften — ³Physics-Department, Technical University Munich, 85748 Garching, Germany — ⁴Fachbereich Physik und Landesforschungszentrum OPTIMAS, Technische Universität Kaiserslautern Surface acoustic waves (SAWs) have made their way into many everyday devices. These "nano earthquakes" can be efficiently launched and detected on piezoelectric substrates with periodic metallic gratings. Resonant coupling of SAWs with spin waves (SWs) is the basis for an energy-efficient approach towards SW manipulation. In addition, magnetoacoustic interaction affects the properties of the SAW, which in turn can be used to devise new types of microwave devices. However, SAW-SW coupling is limited to certain experimental geometries, defined by the orientation of the static magnetization with respect to the SW wave vector. This orientation dependence is caused by the SAW mode-specific symmetry of the magnetoelastic driving fields. In this contribution, we demonstrate how the SAW mode-shape determines the symmetry of the magnetoelastic interaction and its nonreciprocal behavior, caused by the SAW-SW helicity mismatch effect [M. Küß et al., *Phys. Rev. Applied* **15**, 034046 (2021)].

MA 28.8 Thu 11:15 H43

Direct maskless magnetic patterning using a cobalt focused ion beam — JAVIER PABLO-NAVARRO¹, •KILIAN LENZ¹, NICO KLINGNER¹, GREGOR HLAWACER¹, RYSZARD NARKOWICZ¹, LOTHAR BISCHOFF¹, RENE HÜBNER¹, WOLFGANG PILZ², FABIAN MEYER², PAUL MAZAROV², and JÜRGEN LINDNER¹ — ¹Institut für Ionenstrahlphysik und Materialforschung, Helmholtz-Zentrum Dresden-Rossendorf, 01328 Dresden — ²Raith GmbH, Konrad-Adenauer-Allee 8, 44263 Dortmund We present direct maskless magnetic patterning of ferromagnetic nanostructures using a novel liquid metal alloy ion source for focused ion beam systems (FIB). We used a Co₃₆Nd₆₄ alloy as the FIB source. A Wien mass filter allows for quick switching between the ion species in the alloy without changing the source. A single 5 × 1 × 0.05 μm³ permalloy strip served as the sample. Using the FIB we implanted a 300 nm wide track with Co ions. We observed the Co-induced changes by measuring the sample with microresonator ferromagnetic resonance before and after the implantation. Structures as small as 30 nm can be implanted up to a concentration of 10 % at the surface. Such lateral resolution is hard to reach for other lithographic methods. In contrast to electron beam lithography with broad beam ion implantation, the maskless FIB process does not require the complicated and difficult removal of the ion-hardened resist if optical measurements like BLS or MOKE are needed.

MA 28.9 Thu 11:30 H43

Experimental Detection of Magnon Noise Enhancement near Spin Reorientation in Sm_{0.7}Er_{0.3}FeO₃ — •MARVIN WEISS¹, ANDREAS HERBST¹, JULIUS SCHLEGEL¹, MARTIN EVERS¹, TOBIAS DANEGGER¹, ANDREAS DONGES¹, MAKOTO NAKAJIMA², SEBASTIAN T. B. GOENNENWEIN¹, ALFRED LEITENSTORFER¹, ULRICH NOWAK¹, and TAKAYUKI KURIHARA^{1,3} — ¹Department of Physics, University of Konstanz — ²ILE, Univ. Osaka — ³ISSP, Univ. Tokyo

Disentangling intrinsic quantum mechanical interactions and thermal fluctuations is especially important for understanding and controlling magnetic phase transitions. In solids, the dynamics of thermal fluctuations of elementary excitations typically proceed on a picosecond timescale. Although optical pump-probe experiments give access to this range, the experimental detection of ultrafast spin fluctuations remains largely unexplored due to their incoherent character. We investigate the elementary dynamics of thermally excited incoherent magnons in the time domain with femtosecond resolution. The experiments are enabled by a novel setup that allows for extracting the correlation of the pulse-to-pulse polarization fluctuations between two temporally and spectrally separated femtosecond probe pulses that transmit through the sample. As a proof-of-principle demonstration, we study the critical phenomena around the spin reorientation transition (SRT) of the orthoferrite Sm_{0.7}Er_{0.3}FeO₃. Distinct changes of magnon noise amplitude and dynamics are mapped out around the SRT.

MA 28.10 Thu 11:45 H43

Lattice-driven femtosecond magnon dynamics in α-MnTe — •KIRA DELTENRE¹, DAVIDE BOSSINI², MIRKO CINCHETTI¹, GÖTZ S. UHRIG¹, and FRITHJOF B. ANDERS¹ — ¹Department of Physics, TU Dortmund University, D-44227 Dortmund — ²Department of Physics and Center for Applied Photonics, University of Konstanz, D-78457 Konstanz

The femtosecond dynamics of the sublattice magnetizations in the antiferromagnetically ordered phase of α-MnTe is investigated theoretically with linear spin wave theory as a function of an external drive [1]. We assume that collective coherent lattice vibrations generated by laser pulses induce an oscillating Heisenberg coupling thus inducing the driving. The calculated dynamics of the antiferromagnetic order parameter exhibits damped coherent longitudinal oscillations, which decay due to dephasing. The frequency of the oscillations is determined by the external driving phonon. We make contact to experiments [2] by analyzing the spin dynamics for realistic parameters and discussing the effect of oscillating Heisenberg couplings between different types of (next-)nearest neighbors.

[1] K. Deltenre, D. Bossini, F. B. Anders, and G. S. Uhrig, *Phys. Rev. B* **104**, 184419 (2021)

[2] D. Bossini, S. D. Conte, M. Terschanski, G. Springholz, A. Bonanni, K. Deltenre, F. Anders, G. Uhrig, G. Cerullo, and M. Cinchetti, *Phys. Rev. B* **104**, 224424 (2021)

MA 28.11 Thu 12:00 H43

Hybrid magnon-quantum spin defects system in SiC — •MAURICIO BEJARANO^{1,2}, FRANCISCO J. T. GONCALVES³, TONI HACHE⁴, MICHAEL HOLLENBACH^{1,2}, CHRISTOPHER HEINS¹, TOBIAS HULA^{1,5}, YONDER BERENCÉN¹, GEORGY V. ASTAKHOV¹, and HELMUT SCHULTHEISS¹ — ¹Helmholtz-Zentrum Dresden-Rossendorf, Dresden, Germany — ²Technische Universität Dresden, Dresden, Germany — ³X-Fab, Dresden, Germany — ⁴Max Planck Institute for Solid State Research, Stuttgart, Germany — ⁵Technische Universität Chemnitz, Chemnitz, Germany

Hybrid magnon-quantum spins systems have been gathering scientific interest in the last years due to their increased coupling strength, scalability down to the nanoscale regime and their potential as energy efficient quantum buses. While magnon-mediated control of quantum spins has been demonstrated with NV-centers in diamond, it has remained elusive on the silicon carbide (SiC) platform mainly due to the absence of a resonance overlap between the magnetic system and the spin-defect center. Here we circumvent this challenge by harnessing non-linear magnon scattering processes taking place in a magnetic vortex to access spin-wave eigenmodes that overlap with the intrinsic resonance of silicon vacancy defect centers in 4H-SiC. Our results offer a route to develop hybrid magnon-quantum spins systems that benefit from the electrical and optical properties of SiC for future quantum computing applications. This work was supported in part by the German Research Foundation under Grants SCHU 2922/4-1 and AS 310/9-1.

MA 28.12 Thu 12:15 H43

Topological magnons driven by the Dzyaloshinskii-Moriya interaction in the centrosymmetric ferromagnet Mn₅Ge₃ — •MANUEL DOS SANTOS DIAS^{1,2}, NIKOLAOS BINISKOS³, FLAVIANO JOSÉ DOS SANTOS⁴, KARIN SCHMALZ⁵, JÖRG PERSSON⁶, NICOLA MARZARI⁴, STEFAN BLÜGEL², THOMAS BRÜCKEL⁶, and SAMIR LOUNIS^{1,2} — ¹Peter Grünberg Institut and Institute for Advanced Simulation, FZ Jülich & JARA, Jülich, DE — ²Faculty of Physics, University of Duisburg-Essen and CENIDE, Duisburg, DE — ³FZ Jülich, Jülich Centre for Neutron Science at MLZ, Garching, DE — ⁴Theory and Simulation of Materials and National Centre for Computational Design and Discovery of Novel Mate-

rials, EPFL, Lausanne, CH — ⁵FZ Jülich, Jülich Centre for Neutron Science at ILL, Grenoble, FR — ⁶FZ Jülich, Jülich Centre for Neutron Science and Peter Grünberg Institut, JARA-FIT, Jülich, DE

The Berry phase of electrons and magnons can lead to various unique transport effects and protected edge states of topological nature. Here, we show theoretically and via inelastic neutron scattering experiments that bulk ferromagnetic Mn_5Ge_3 hosts topological Dirac magnons. Although inversion symmetry prohibits a net Dzyaloshinskii-Moriya interaction in the unit cell, it is locally allowed and is responsible for the gap opening in the magnon spectra. This gap is predicted and experimentally verified to close by rotating the magnetization from being parallel to being perpendicular to the c -axis. The tunability of Mn_5Ge_3 by chemical doping or by thin film nanostructuring makes it an exciting new platform to explore and design topological magnons.

MA 28.13 Thu 12:30 H43

Electric field control of magnons in magnetic thin films: Ab initio predictions for two-dimensional metallic heterostructures — •ALBERTO MARMODORO¹, SERGIY MANKOVSKY², HUBERT EBERT², JAN MINÁR³, and ONDŘEJ ŠIPR^{1,3} — ¹Institute of Physics (FZU) of the Czech Academy of Sciences, Prague, Czech Republic — ²Department of Chemistry, Ludwig-Maximilians-University (LMU), Munich, Germany — ³New Technologies Research Centre, University of West Bohemia, Pilsen, Czech Republic

We report on a possible venue to control magnons in 2D heterostructures by an external electric field acting across a dielectric barrier [1]. By performing ab initio 2D TB-KKR calculations for a Fe monolayer and Fe bilayer, both suspended in vacuum and deposited on Cu(001), we demonstrate that external electric field can significantly modify magnon lifetimes and that these changes can be related to field-induced changes in layer-resolved electronic Bloch spectral function. Further changes appear in cases with more than a single magnetic layer, and are strongly dependent on the presence of the substrate.

[1] Phys.Rev. B 105, 174411 (2022)

MA 29: Caloric Effects in Magnetic Materials

Time: Thursday 9:30–11:45

Location: H47

MA 29.1 Thu 9:30 H47

"Giant" magnetocaloric effects for 2nd order phase transition near 20 K: a study on rare-earth Laves phases for hydrogen liquefaction — •WEI LIU¹, FRANZISKA SCHEIBEL¹, TINO GOTTSCHALL², EDUARD BYKOV², KONSTANTIN SKOKOV¹, and OLIVER GUTFLEISCH¹ — ¹Funktionale Materialien, Technische Universität, TU Darmstadt, Germany — ²Hochfeld- Magnetlabor Dresden, Helmholtz-Zentrum Dresden-Rossendorf, Germany

Hydrogen will play a key role for building a climate-neutral society, where renewables are the major energy sources [1]. Liquid hydrogen is essential for efficient storage and transport of hydrogen, but expensive due to the low efficiency of traditional gas-compression refrigeration [2]. As an emerging and energy-saving technology, magnetocaloric gas liquefaction can be an a "game-changer". Here we report a noticeable, but unaddressed feature for magnetocaloric hydrogen liquefaction using rare-earth-based intermetallic alloys: magnetocaloric effect of a 2nd order magnetocaloric materials can become "giant" when the Curie temperature T_C is near the hydrogen boiling point of 20 K. Based on our study on rare-earth Laves phases for hydrogen liquefaction and a comprehensive literature review, we summarized two phenomenological rules for a rare-earth-based intermetallic series: (1) magnetic entropy change increases with decreasing T_C ; (2) adiabatic temperature change decreases firstly with decreasing T_C but increases in cryogenic temperature range. These findings are well interpreted by a mean-field approach. Our studies can guide the materials design for hydrogen liquefaction.

MA 29.2 Thu 9:45 H47

Magnetocaloric effect in Tb_3Ni studied in high magnetic fields for cryogenic applications — •T. NIEHOFF^{1,2}, T. GOTTSCHALL¹, C. SALAZAR MEJIA¹, A. HERRERO³, A. OLEAGA³, A.F. GUBKIN⁴, and J. WOSNITZA^{1,2} — ¹Dresden High Magnetic Field Laboratory (HLD-EMFL), HZDR, Dresden, Germany — ²Technische Universität Dresden, Dresden, Germany — ³Universidad del País Vasco, Bilbao, Spain — ⁴Ekaterinburg, Russia

Tb_3Ni exhibits a large variety of temperature and magnetic-field dependent phase transitions in a temperature range of 3 to 90 K. This gives rise to a very competitive conventional magnetocaloric effect and an inverse magnetocaloric effect at very low temperature. These properties make this material an interesting candidate for magnetic refrigeration applications in the gas liquefaction temperature range. In this work, we present a comprehensive analysis of the magnetocaloric effect in a Tb_3Ni single crystal in pulsed magnetic fields up to 50 T and by heat capacity measurements in static fields.

MA 29.3 Thu 10:00 H47

Direct measurements of the adiabatic temperature change of holmium for cryogenic applications — •E. BYKOV^{1,2}, T. GOTTSCHALL¹, Y. SKOURSKI¹, C. SALAZAR MEJIA¹, J. WOSNITZA^{1,2}, M. D. KUZ'MIN³, Y. MUDRYK⁴, D. L. SCHLAGEL⁴, and V. PECHARSKY^{4,5} — ¹Hochfeld-Magnetlabor Dresden (HLD-EMFL), HZDR, Dresden, Germany — ²Technische Universität Dresden, Dresden, Germany — ³Aix-Marseille Université, IM2NP, Marseille, France — ⁴Ames Laboratory, U.S. Department of Energy, Iowa State University, Ames, USA — ⁵Department of Materials Science and Engineering, Iowa State University, Ames, USA

Rare-earth elements and their intermetallic compounds are interesting candidate materials for magnetic cooling at and below room temperature. Holmium demonstrates one of the largest magnetic moment in the lanthanide series and possesses other unusual magnetic properties. This metal exhibits numerous magnetic phase transitions as the temperature and/or magnetic field vary. Its

Néel temperature accounts for $T_N = 132$ K, and its Curie temperature is $T_C = 20$ K resulting in a strong magnetocaloric effect in a large temperature window. This fact makes holmium a promising single-stage refrigerator material in an AMR (active magnetic regenerator) scheme for the liquefaction of natural gas and hydrogen. In this work, we present a comprehensive analysis of the magnetocaloric effect in a holmium single crystal in high magnetic fields up to 60 T.

MA 29.4 Thu 10:15 H47

Anomalous Nernst effect in ferromagnetic τ -MnAl thin films — •DANIEL SCHEFFLER¹, HELENA REICHOVA¹, SEBASTIAN BECKERT¹, TORSTEN MIX², THOMAS G. WOODCOCK², SEBASTIAN T. B. GOENNENWEIN³, and ANDY THOMAS^{1,2} — ¹Technische Universität Dresden — ²Leibniz Institute for Solid State and Materials Research Dresden (IFW Dresden) — ³University of Konstanz

τ -MnAl is a ferromagnetic compound with high uniaxial magnetocrystalline anisotropy. In single crystalline films, the anomalous Hall effect and the tunnel magnetoresistance effect have been investigated, the magneto-thermal transport properties of τ -MnAl films are unknown. Given the unique anisotropy, this material could allow for a robust spontaneous anomalous Nernst effect generated by a thermal gradient applied in the film plane.

We have successfully grown single crystalline τ -MnAl thin films via co-sputtering. X-ray diffraction and DC magnetometry confirm a good structural quality and strong perpendicular magnetic anisotropy. We observe a robust anomalous Hall effect with a coercivity of 1 T in magneto-transport measurements. In the same device, a defined thermal gradient can also be applied in the sample plane, resulting in a clear anomalous Nernst effect response.

We will present results from our magneto-transport and magneto-thermopower experiments, which in particular allow to quantify the anomalous Nernst effect coefficient. Our results show that τ -MnAl in thin film form is an interesting material for spin-caloritronic research and devices.

MA 29.5 Thu 10:30 H47

Magnonic to electronic spin current conversion in a quantum dot hybrid system with magnetic insulator — •EMIL SIUDA and PIOTR TROCHA — Faculty of Physics, Institute of Spintronics and Quantum Information, Adam Mickiewicz University, ul. Uniwersytetu Poznańskiego 2, 61-614 Poznań, Poland

One of the challenges of further miniaturization of electronic components is managing heat generated due to the Joule heating and other effects. While magnonics offers a way to reduce generation of the waste heat in the device it is still impossible to get rid of it entirely. Hence a way of converting heat to useful electric power is desirable.

We investigate a hybrid system which utilizes a temperature gradient to produce a magnon current and converts it to a spin electronic current. The considered system consists of a quantum dot coupled to the two ferromagnetic insulators or one ferromagnetic insulator and one ferromagnetic metal. This work focuses on the influence of energy-dependent density of states and many-body magnon interactions in the magnonic reservoir on the thermally induced spin transport through the system. Energy-dependent density of states is crucial for boson-like particles, especially in the low energy limit where the lowest momentum states dominate the transport. Thus, in the present work we consider explicit energy dependence of the density of states for the magnonic reservoirs. Moreover, taking into account many-body magnon interactions leads to a temperature-dependent density of states of magnons which results in temperature-dependent couplings of the dot to the magnonic reservoirs.

MA 29.6 Thu 10:45 H47

Magneto-thermal transport in non-collinear antiferromagnetic thin films — •SEBASTIAN BECKERT¹, JOÃO GODINHO^{2,4}, FREYA JOHNSON³, JOZEF KIMÁK⁴, EVA SCHMORANZEROVÁ⁴, ZBYNĚK ŠOBÁŇ², KAMIL OLEJNÍK², JAN ZEMEN⁵, JOERG WUNDERLICH⁶, PETR NĚMEC⁴, DOMINIK KRIEGER^{1,2}, LESLEY F. COHEN³, ANDY THOMAS^{1,7}, SEBASTIAN T. B. GOENNENWEIN⁸, and HELENA REICHLÓVÁ^{1,2} — ¹TU Dresden — ²IoP ASCR Prague — ³Imperial College London — ⁴Charles University — ⁵Czech TU — ⁶University of Regensburg — ⁷IFW Dresden — ⁸University of Konstanz

Understanding the interplay between topological properties and transport phenomena in non-collinear antiferromagnets is important for exploiting their unconventional characteristics in spintronics. Non-collinear antiferromagnets can exhibit phenomena previously known to be exclusive to ferromagnets, such as the anomalous Hall Effect (AHE) or the anomalous Nernst effect (ANE).

We experimentally study magneto-thermal transport in a Mn₃NiN thin film antiferromagnet. In our films the spins are arranged in the (111) plane, resulting in a component of the Hall vector in both out-of-plane and in-plane direction. This makes Mn₃NiN an ideal candidate for a systematic study of magneto-thermal transport phenomena. We will present measurements of ANE, AHE, magnetoresistance and magneto-Seebeck effect measured in a single device. We will compare the amplitudes of the magneto-thermal transport coefficients and discuss them in context of the Mott relation.

MA 29.7 Thu 11:00 H47

Multicaloric all-d-metal Ni-Co-Mn-Ti Heusler alloys: Heat treatment optimization and arrested martensitic transformations — •BENEDIKT BECKMANN¹, ANDREAS TAUBEL¹, LUKAS PFEUFFER¹, DAVID KOCH¹, TINO GOTTSCHALL², FRANZISKA SCHEIBEL¹, KONSTANTIN P. SKOKOV¹, and OLIVER GUTFLEISCH¹ — ¹TU Darmstadt, Institute of Material Science, 64287 Darmstadt, Germany — ²Dresden High Magnetic Field Laboratory (HLD-EMFL), Helmholtz-Zentrum Dresden-Rossendorf, Dresden 01328, Germany

Ni-Mn-based Heusler alloys display precisely tunable first-order martensitic transformations and are promising candidates for multicaloric cooling applications [1]. In our work, all-d-metal Ni_{50-x}Co_xMn_{50-y}Ti_y Heusler alloys, showing an enhanced mechanical stability, are analyzed in detail [2]. A systematic heat treatment optimization results in a tailored microstructure and leads to large isothermal entropy changes up to 38 J(kgK)⁻¹ and adiabatic temperature changes up to -3.8 K for the first field application in moderate magnetic field changes of 2 T. The contradictory role of the magnetic entropy contribution [3], which leads to arrested martensitic transformations in Ni_{50-x}Co_xMn_{50-y}Ti_y inverse magnetocaloric Heusler alloys, is discussed in detail.

MA 30: Surface Magnetism

Time: Thursday 9:30–11:30

Location: H48

MA 30.1 Thu 9:30 H48

Interplay of magnetic states and hyperfine fields of iron dimers on MgO(001) — •SUFYAN SHEHADA^{1,2,3}, MANUEL DOS SANTOS DIAS^{4,1}, MUAYAD ABUSAA³, and SAMIR LOUNIS^{1,4} — ¹Peter Grünberg Institut and Institute for Advanced Simulation, Forschungszentrum Jülich & JARA, 52425 Jülich, Germany — ²Department of Physics, RWTH Aachen University, 52056 Aachen, Germany — ³Department of Physics, Arab American University, Jenin, Palestine — ⁴Faculty of Physics, University of Duisburg-Essen, 47053 Duisburg, Germany

Individual nuclear spin states can have very long lifetimes and could be useful as qubits. Progress in this direction was achieved on MgO/Ag(001) via detection of the hyperfine interaction (HFI) of Fe, Ti and Cu adatoms using scanning tunneling microscopy (STM)[1,2]. Previously, we systematically quantified from first-principles the HFI for the whole series of 3d transition adatoms (Sc-Cu) deposited on various ultra-thin insulators, establishing the trends of the computed HFI with respect to the filling of the magnetic s- and d-orbitals of the adatoms and on the bonding with the substrate[3]. Here we take one step further by investigating the impact of the magnetic coupling between the dimer atoms on the HFI of Fe dimers on MgO(001) and its dependence on where the Fe atoms are located on the surface[4]. –Work funded by (BMBF-01DH16027).

[1] Willke *et al.*, *Science* **362**, 336 (2018); [2] Yang *et al.*, *Nat. Nano.* **13**, 1120 (2018); [3] Shehada *et al.*, *Npj Comput. Mater.* **7**, 87 (2021). [4] Shehada *et al.*, *arXiv*. **2202.00336** (2022).

MA 30.2 Thu 9:45 H48

Low-energy end states in proximitized antiferromagnetic nanowires — •LUCAS SCHNEIDER¹, PHILIP BECK¹, THORE POSSKE^{2,3}, LEVENTE RÓZSA⁴, JENS WIEBE¹, and ROLAND WIESENDANGER¹ — ¹Department of Physics, Universität Hamburg, D-20355 Hamburg, Germany — ²I. Institute for Theoretical Physics, Universität Hamburg, D-20355 Hamburg, Germany — ³The Hamburg Centre for Ultrafast Imaging, Luruper Chaussee 149, 22761 Hamburg, Germany — ⁴Department of Physics, University of Konstanz, D-78457 Konstanz, Germany

We acknowledge financial support from DFG (CRC/TRR 270) and ERC (Adv. Grant No. 743116).

[1] T. Gottschall *et al.*, *Nat. Mater.* **17**, 929-934 (2018)

[2] A. Taubel *et al.*, *Acta Mater.* **201**, 425-434 (2021)

[3] T. Gottschall *et al.*, *Phys. Rev. B* **93**, 184431 (2016)

MA 29.8 Thu 11:15 H47

Magnetocaloric effect of Gd - an realistic ab-initio study — •RAFAEL VIEIRA^{1,2}, OLLE ERIKSSON^{1,3}, TORBJÖRN BJÖRKMAN², and HEIKE C. HERPER¹ — ¹Department of Physics and Astronomy, Uppsala University, Box 516, SE-75120 Uppsala, Sweden — ²Physics, Faculty of Science and Engineering, Åbo Akademi University, FI-20500 Turku, Finland — ³School of Science and Technology, Örebro University, SE-701 82 Örebro, Sweden

We present a computational approach to evaluate field-dependent entropy of magnetocaloric materials from ab-initio calculations. Taking hcp Gd as a test system, we fully characterize the entropy associated with the magnetocaloric effect by including the entropy's electronic, lattice, and magnetic contributions.

The 2nd order nature of the ferromagnetic (FM)→paramagnetic (PM) transition in Gd implies considering intermediate states of magnetic disorder. We describe the properties of these intermediate states as weighted averages of the properties of the FM and PM phases, with mixing weights defined by the magnetization of the system at a given temperature, to which we use the results from the Monte Carlo simulations. This approach allows a realistic system description, bringing the total entropy variation in agreement with reported measurements.

We find, as expected that the magnetic entropy is the dominant entropy. However, we also observe that the lattice contribution has a role in total entropy variation.

MA 29.9 Thu 11:30 H47

Electrochemical corrosion study of La(FeSi)13Hf1,5 in diverse chemical environments — •ULYSSE ROCABERT¹, FALK MUNCH², MAXIMILIAN FRIES², BENEDIKT BECKMANN¹, KONRAD LOEWE³, HUGO VIEYRA³, MATTHIAS KATTER³, ALEXANDER BARCZA³, WOLFGANG ENSINGER¹, and OLIVER GUTFLEISCH¹ — ¹Technische Universität Darmstadt — ²MagnTherm Solutions GmbH — ³Vacuumschmelze GmbH & Co

Hydrogenated La(FeMnSi)13 alloys represent a promising material class for magnetocaloric cooling at ambient temperatures, but contain highly oxophilic elements and are chemically sensitive. The development of protection strategies ensuring long-term stability is required and so analysis focused on Linear sweep voltammetry as the main analytical tool were performed in preferably buffered electrolytes with pH values reaching from moderately acidic to strongly alkaline to study different passivation strategies.

Magnetically ordered nanowires coupled to a superconducting surface have been proposed to host Majorana modes (MMs) at their ends, which form a single, highly non-local fermionic state together. While multiple experiments claim the observation of MMs via a zero-bias resonance in tunneling conductance at the ends of nanowires, this is not a unique signature of MMs. In this work, we study the emergence of low-energy end states in artificially crafted antiferromagnetic nanowires on two different superconducting surfaces using scanning tunneling spectroscopy. While some of the end states are observed close to zero energy, we find that they can be split into two non-degenerate components localized on the left and right ends by local defects - in clear contrast to expectations for a single non-local state. The phenomenology of these trivial bound states can be explained by simple toy-model calculations. We propose that similar perturbations by local defects could be used on other sample systems to probe the stability of candidate topological edge modes against local disorder.

MA 30.3 Thu 10:00 H48

Spin-resolved Fermi Surface of "Half-Metallic" FePd Alloy Monolayers — •XIN LIANG TAN^{1,2}, KENTA HAGIWARA^{1,2}, YING-JIUN CHEN^{1,2}, VITALIY FEYER¹, CLAUD M. SCHNEIDER^{1,2}, and CHRISTIAN TUSCHE^{1,2} — ¹Forschungszentrum Jülich, Peter Grünberg Institut, Jülich — ²Fakultät für Physik, Universität Duisburg-Essen, Duisburg

Magnetism in reduced dimensions is one of the preconditions for the realization of nanoscale spintronics. Despite the recent discovery of ferromagnetism in monolayers of two-dimensional materials, tunability and engineering on such systems are challenging. Here we present the electronic structure of ultrathin ferromagnetic iron-palladium alloy films using spin-resolved momentum microscopy. Momentum microscopy enables the two-dimensional detection of photoelectrons with an in-plane crystal momentum over the full Brillouin zone. By employing an imaging spin filter, spin-resolved momentum maps of the iron-palladium alloy were acquired. Breaking of time reversal symmetry by the remanent magnetization of the film manifests in a pronounced anisotropy of the elec-

tron states in the Fermi surface. In particular, the competition between exchange interaction and strong spin-orbit coupling in the FePd alloy leads to the formation of wave-vector dependent local gaps in the Fermi surface. Moreover, the spin-resolved maps recorded by the momentum microscope give evidence for a non-collinear spin texture of the electron states at the Fermi surface, where the local spin polarization vector points orthogonal to the remanent magnetization of the sample.

MA 30.4 Thu 10:15 H48

Real-time MOKE measurements of CoTMPP on magnetic Ni/Cu(110)-(2x1)O — •GIZEM MENDIREK¹, ALEKSANDER BROZYNIAK², MICHAEL HOHAGE¹, ANDREA NAVARRO-QUEZADA¹, and PETER ZEPPENFELD¹ — ¹Institute of Experimental Physics, Johannes Kepler University Linz, Altenberger Str. 69, 4040 Linz, Austria — ²Christian Doppler Laboratory for Nanoscale Phase Transformations, Johannes Kepler University Linz, Altenberger Str. 69, 4040 Linz, Austria

In this work, we report the detailed analysis employing a fitting algorithm on a setup consisting of a combination of a sinusoidal modulation of the magnetic field with the synchronous detection of the reflectance difference spectroscopic MOKE (RD-MOKE) signal. This setup allows recording hysteresis loops continuously revealing relevant magnetic properties like magnetization amplitude, remanent magnetic signal and coercive field as a function of coverage, time or temperature with high precision in real-time. The capabilities of our setup and our analysis algorithm is demonstrated for Ni thin films grown on a Cu(110)-(2x1)O reconstructed surface with a sharp spin reorientation transition at 9 ML. Subsequently, the deposition of cobalt tetramethoxyphenylporphyrin (CoTMPP) thin films on the Ni/Cu(110)-(2x1)O system is investigated. The adsorption of the molecules induces characteristic changes in the magnetic properties such as the decrease of the Curie temperature of the Ni thin films upon CoTMPP deposition with different thicknesses.

MA 30.5 Thu 10:30 H48

Thermally-induced magnetic order from glassiness in elemental neodymium — BENJAMIN VERLHAC¹, •LORENA NIGGLI¹, ANDERS BERGMANN², UMUT KAMBER¹, ANDREY BAGROV^{1,2}, DIANA IUŞAN², LARS NORDSTRÖM², MIKHAIL I. KATSNELSON¹, DANIEL WEGNER¹, OLLE ERIKSSON^{2,3}, and ALEXANDER A. KHAJETOORIAN¹ — ¹Institute for Molecules and Materials, Radboud University, Nijmegen, The Netherlands — ²Department of Physics and Astronomy, Uppsala University, Uppsala, Sweden — ³School of Science and Technology, Örebro University, SE-701 82 Örebro, Sweden

While traditional spin glasses are characterized by randomness and frustration, elemental neodymium shows glassy behavior as a result of competing interactions, particularly without extrinsic disorder [1]. Adding to the list of intriguing effects found in spin glasses, e.g. aging and memory, we observe an unconventional magnetic phase transition from a glassy to a long-range ordered phase in Nd as temperature is increased [2]. To characterize the spatially varying magnetization patterns, we employ temperature-dependent spin-polarized scanning tunnelling microscopy between 5-15K along with atomistic spin dynamics simulations that support our findings. A new analysis method allows us to extract the phase transition temperature directly by evaluating our experimental data. Notably, such an unusual magnetic phase transition serves as a counterexample to the common thermodynamic understanding of temperature and disorder being synonymous.

[1] U. Kamber et al., *Science* **368** (2020).

[2] B. Verlhac et al., arXiv:2109.04815, accepted at Nat. Phys.

MA 30.6 Thu 10:45 H48

Distorted 3Q state driven by topological-chiral magnetic interaction — •SOUMYAJYOTI HALDAR¹, SEBASTIAN MEYER², ANDRÉ KUBETZKA³, and STEFAN HEINZE¹ — ¹Institute of Theoretical Physics and Astrophysics, University of Kiel, Leibnizstr. 15, 24098 Kiel, Germany — ²Nanomat/Q-mat/CESAM, Université de Liège, B-4000 Sart Tilman, Belgium — ³Department of Physics, University of Hamburg, 20355 Hamburg, Germany

Non-collinear spin structures are of fundamental interest in magnetism since they allow to obtain insight into the underlying microscopic interactions and are promising for spintronic applications [1,2]. Here, we demonstrate that recently proposed topological-chiral magnetic interactions [3] can play a key role for magnetic ground states in ultrathin films at surfaces [4]. Using density functional theory we show that significant chiral-chiral interactions occur in hexagonal Mn monolayers due to large topological orbital moments which interact with the emergent magnetic field. Superposition states of spin spirals such as the 2Q state or a distorted 3Q state arise due to the competition with biquadratic and four-spin interactions. Simulations of spin-polarized scanning tunneling microscopy images suggest that the distorted 3Q state could be the magnetic ground state of a Mn monolayer on Re(0001).

[1] A. Fert *et al.*, Nat. Rev. Mater. **2**, 17031 (2017). [2] J. Grollier *et al.*, Nat. Electron. **3**, 360 (2020). [3] S. Grytsiuk *et al.*, Nat. Commun. **11**, 511 (2020). [4] S. Haldar *et al.*, Phys. Rev. B **104** L180404 (2021).

MA 30.7 Thu 11:00 H48

The mutual impact of magnetism on proximity-induced superconductivity — •URIEL ACEVES^{1,2}, FILIPE GUIMARAES³, and SAMIR LOUNIS^{1,2} — ¹Peter Grünberg Institut and Institute for Advanced Simulation, Forschungszentrum Jülich & JARA, 52425 Jülich, Germany — ²Faculty of Physics & CENIDE, University of Duisburg-Essen, 47053 Duisburg, Germany — ³Jülich Supercomputing Centre, Forschungszentrum Jülich & JARA, 52425 Jülich, Germany

In a conventional superconductor (SC), vibrations on the crystal lattice can cause electrons to attract mutually and bind in the so-called Cooper pairs. At the interface of a normal metal (NM), Cooper pairs can wander from SC to NM resulting in a proximity induced gap. Electrons from NM can also travel into SC by normal transport or Andreev reflection. This exchange of electrons can impact the properties of both materials. Moreover, if the NM is magnetic new and exciting physics appears. In this work, we explore NM/SC interface phenomena by introducing a method to extract the tensor of magnetic exchange interactions within the framework of the Bogoliubov-de Gennes equations where superconductivity is induced via an effective electron-phonon coupling constant λ and accounting for spin-orbit coupling. Based on a realistic description of the electronic structure, we analyze the behaviour of the isotropic exchange and the Dzyaloshinskii-Moriya interaction as a function of λ on a Mn monolayer on top of a superconducting Nb (110) slab. Additionally, we investigate the impact of λ on the proximity-induced gap as a function of the direction of the magnetic moment in Mn.

MA 30.8 Thu 11:15 H48

Observation of spin-correlated exciton-polaritons in a van der Waals magnet — •FLORIAN DIRNBERGER¹, REZLIND BUSHATI^{1,2}, BISWAJIT DATTA¹, AJESH KUMAR³, ALLAN H. MACDONALD³, EDOARDO BALDINI³, and VINOD M. MENON^{1,2} — ¹Department of Physics, City College of New York, New York, NY 10031, USA — ²Department of Physics, The Graduate Center, City University of New York, New York, NY 10016, USA — ³Department of Physics, University of Texas at Austin, Austin, TX 78712, USA

The recent discovery of optically active excitons in magnetic van der Waals crystals offers extraordinary opportunities to study collective phenomena in quantum materials via light-matter interactions. A prime candidate in this endeavor is nickel phosphorus trisulfide (NiPS₃), a van der Waals antiferromagnet with highly correlated magnetic and electronic degrees of freedom. By coupling optical fields to its excitonic excitations, we demonstrate a previously unobserved class of polaritons with unique signatures of excitons, photons and spins. A detailed spectroscopic analysis of these newly formed quasiparticles in conjunction with our microscopic theory shows that magnetically coupled excitations can have an origin and interactions that are distinct from those of excitons in conventional band semiconductors.

MA 31: Topological Insulators (joint session MA/KFM)

Time: Thursday 15:00–17:45

Location: H37

Invited Talk

MA 31.1 Thu 15:00 H37

Neutron scattering on magnetic topological materials: From topological magnon insulators to emergent many-body effects — •YIXI SU — Jülich Centre for Neutron Science JCNS at MLZ, Forschungszentrum Jülich, 85747 Garching, Germany

Recent theoretical predictions and experimental realizations of exotic fermions and topologically protected phases in condensed matter have led to tremendous research interests in topological quantum materials. Especially, magnetic topological materials, such as magnetic Dirac and Weyl semimetals, and intrinsic

magnetic topological insulators etc., in which non-trivial topology of single-electron band structures and electronic correlation effects are often intertwined, have emerged as an exciting platform to explore novel phenomena. Here I will present our recent neutron scattering studies. In the Dirac semimetal EuMnBi₂, the evidence for the possible impact of magnetism on Dirac fermions is obtained via a detailed neutron diffraction study of the spin-flip transition [1]. Based on our inelastic neutron scattering study and theoretical analysis of spin-wave excitations, the exotic topological magnon insulators, the bosonic analogs of topological insulators, have been experimentally realized in the two-dimensional van

der Waals honeycomb ferromagnets CrSiTe₃ and CrGeTe₃ [2]. Furthermore, in the magnetic Weyl semimetal Mn₃Sn, an unusual magnetic phase transition that is driven by emergent many-body effects is revealed via a combined neutron scattering study and band-structure calculations [3].

[1] F. Zhu, et al., Phys. Rev. Research 2, 043100 (2020). [2] F. Zhu, et al., Sci. Adv. 7, eabi7532 (2021). [3] X. Wang (unpublished)

MA 31.2 Thu 15:30 H37

Tuning the magnetic gap of a topological insulator — •MARCUS LIEBMANN¹, PHILIPP KÜPPERS¹, JANNIK ZENNER¹, STEFAN WIMMER², GUNTHER SPRINGHOLZ², OLIVER RADER³, and MARKUS MORGENSTERN¹ — ¹II. Phys. Inst. B, RWTH Aachen Univ., Germany — ²Inst. Halbleiter- u. Festkörperphysik, Johannes Kepler Univ., Linz, Austria — ³Helmholtz-Zentrum Berlin f. Mater. u. Energie, Germany

Mn-rich MnSb₂Te₄ is a ferromagnetic topological insulator with yet the highest Curie temperature $T_C = 45 - 50$ K. It exhibits a magnetic gap at the Dirac point of the topological surface state that disappears above T_C . We probe the gap size by scanning tunneling spectroscopy, varying in-plane magnetic field $B_{||}$ and temperature. We demonstrate shrinkage of the average gap size with $B_{||}$ revealing that the gap opening originates from out-of-plane magnetization. In line, the gap does not close completely up to $B_{||} = 3$ T as the magnetization is only partially rotated in-plane. In addition, we demonstrate significant spatiotemporal fluctuations of the gap size at temperatures as low as $T_C/2$, above which the remanent magnetization indeed decays. Thus, the gap is tightly bound to the out-of-plane magnetization, as expected theoretically but not demonstrated experimentally yet. The partial in-plane rotation at $B_{||} = 3$ T and the low temperature onset of fluctuations stress the important role of competing magnetic orders in the formation of the favorable ferromagnetic topological insulator in Mn-rich MnSb₂Te₄, providing insight into the complex magnetic gap opening that is decisive for quantum anomalous Hall devices.

MA 31.3 Thu 15:45 H37

Local magnetic and electronic properties of the intrinsic magnetic topological insulator MnBi₆Te₁₀ — •ABDUL-VAKHAB TCAKAEV¹, VOLODYMYR ZABOLOTNYI¹, BASTIAN RUBRECHT², LAURA CORREDOR², JORGE FACIO², LAURA FOLKERS³, ANJA WOLTER², ANNA ISAEVA², and VLADIMIR HINKOV¹ — ¹Experimentelle Physik IV and Röntgen Research Center for Complex Materials (RCCM), Fakultät für Physik und Astronomie, Universität zu Würzburg, Am Hubland, D-97074 Würzburg, Germany — ²Leibniz IFW Dresden, Helmholtzstraße 20, D-01069 Dresden, Germany — ³Faculty of Physics, Technische Universität Dresden, D-01062 Dresden, Germany

The recent observation of novel phenomena in the intrinsic magnetic topological insulator MnBi₆Te₁₀, such as the quantum anomalous Hall effect and the topological magnetoelectric effect has prompted research of the higher- n members of the (MnBi₂Te₄)(Bi₂Te₃) _{n} family. Here we combine x-ray absorption spectroscopy, and x-ray circular and linear dichroism at the Mn $L_{2,3}$ edges, with density-functional (DFT) and multiplet ligand-field (MLFT) theory to investigate the ground state of Mn in MnBi₆Te₁₀ single crystals. Our magnetometry data reveal FM state with finite remanence consistent with the spectroscopy data. Our spectroscopy results together with DFT and *ab initio* MLFT calculations allow us to determine in full detail the local magnetic and electronic properties of the Mn ions in the bulk and near the surface, and deliver important microscopic physical parameters, including Mn $3d$ -shell occupation, the spin and orbital magnetic moments.

MA 31.4 Thu 16:00 H37

Probing the Superconductor / Quantum Anomalous Hall Interface — •ANJANA UDAY¹, GERTJAN LIPPERTZ^{1,2}, ANDREA BLIESENER¹, ALEXEY TASKIN¹, and YOICHI ANDO¹ — ¹University of Cologne, Cologne, Germany — ²KU Leuven, Leuven, Belgium

Recently, crossed Andreev conversion was reported in a hybrid quantum Hall (QH) / Superconductor (SC) system [1]. The evidence was based on the observation of a negative downstream resistance R_D in a three-terminal measurement of a Hall-bar device with respect to the grounded SC electrode. Similar experiments would be of great interest in the quantum anomalous Hall (QAH) / SC hybrid system, where superconductivity can be suppressed for control experiments by applying a magnetic field while keeping the 1D edge state unchanged. We fabricated Hall-bar devices from V-doped (Bi _{x} Sb _{$1-x$})₂Te₃ thin films contacted with Nb electrodes having various widths. We found a finite positive R_D which increases with decreasing the widths of the SC electrode due to the QAH breakdown mechanism [2]. We also found a clear increase in R_D upon killing the superconductivity with a magnetic field for Nb electrodes narrower than 200 nm; this can be attributed to either non-local Andreev reflections on top of the breakdown-induced finite R_D or local Andreev reflections on the 2D normal metal/SC interface, which can be created by the charge transfer from the Nb electrode to the gapped VBST surface state. In both cases our observation implies a high transparency of the SC/QAH interface.

[1] G.-H. Lee et al., Nat. Phys. 13, 693-698 (2017)

[2] G. Lippertz et al., arXiv:2108.02081 (2021)

MA 31.5 Thu 16:15 H37

Magnetotransport Properties of MnSb₂Te₄ — •MICHAEL WISSMANN^{1,2,3}, JOSEPH DUFOULEUR², ANNA ISAEVA⁴, BERND BÜCHNER^{2,3}, and ROMAIN GIRAUD^{1,2} — ¹Université Grenoble-Alpes, CNRS, CEA, SPINTEC, F-38000 Grenoble, France — ²Leibniz Institute for Solid State and Materials Research IFW Dresden, 01069 Dresden, Germany — ³Institute of Solid State Physics, TU Dresden, 01069 Dresden, Germany — ⁴Department of Physics and Astronomy, University of Amsterdam, 1098 XH Amsterdam, Netherlands

The new family of intrinsically magnetic van-der-Waals layered topological insulators Mn(Bi,Sb)Te, with strong spin-orbit coupling, is of great interest to investigate the interplay between topology and magnetic order in electronic band structures. When introducing magnetism into a 3D topological insulator, this interplay can generate topological quantum states like the quantum anomalous Hall effect (QAH) or the axion insulator, which can be modified by tuning the magnetization.

Our recent studies consider the MnSb₂Te₄ compound, a ferromagnet with a perpendicular-to-plane anisotropy and a critical Curie-Weiss temperature as high as 50K. MnSb₂Te₄ has been controversially discussed to be a magnetic Weyl semimetal or a candidate to realize the axion insulator. We investigated the thickness-dependent properties of exfoliated nanoflakes using magnetotransport, revealing the change in important parameters such as the resistivity, the Curie temperature and the magnetic coercive field. The influence of both the intrinsic electrical doping and disorder in magnetic topological insulators is considered as well.

MA 31.6 Thu 16:30 H37

Investigation of the magnetic and electronic properties of topological insulator/ferromagnet heterostructures — •SIMON MAROTZKE^{1,2}, ANDRÉ PHILIPPI-KOBS^{1,2}, LEONARD MÜLLER^{1,3}, MATTHIAS KALLÄNE², JENS BUCK², WOJCIECH ROSEKER¹, NILS WIND³, SANJOY MAHATHA⁴, NILS HUSE⁴, GERHARD GRÜBEL^{1,3}, MARTIN BEYE¹, and KAI ROSSNAGEL^{1,2} — ¹Deutsches Elektronen-Synchrotron DESY, Hamburg, Germany — ²Christian-Albrechts-Universität zu Kiel, Germany — ³Universität Hamburg, Germany — ⁴Thapar Institute of Engineering and Technology, Patiala, India

Heterostructures of the design Bi₂Se₃/X/Co/Pt, with X = None, Pt, B₄C or B₄C/Pt as separation layer between the topological insulator (TI) and the ferromagnetic overlayer are studied. By means of magneto-optical Kerr effect, the magnetic behaviour is characterised, showing that perpendicular magnetic anisotropy can be achieved in the overlayer and minutely tuned by changing layer properties. In X-ray photoemission spectroscopy measurements, two Bi phases are identified in the heterostructures. By systematically varying the photon energy, the depth, in which the two Bi phases are located, is analysed. Significant differences of the chemical properties at the interface to the TI are found for heterostructures consisting of Bi₂Se₃ with a metallic or insulating overlayer, respectively. Finally, a scheme to invert the heterostructures is presented, potentially enabling angle-resolved photoemission spectroscopy measurements on the TI's surface in future in order to study the influence of the magnetisation state on the TI's surface states.

MA 31.7 Thu 16:45 H37

Current-induced breakdown of the quantum anomalous Hall effect — •GERTJAN LIPPERTZ^{1,2}, ANDREA BLIESENER¹, ANJANA UDAY¹, LINO M.C. PEREIRA², ALEXEY TASKIN¹, and YOICHI ANDO¹ — ¹University of Cologne, Cologne, Germany — ²KU Leuven, Leuven, Belgium

The quantum anomalous Hall (QAH) effect is characterised by zero longitudinal resistivity and quantized Hall resistance without the need of an external magnetic field. However, when reducing the device dimensions or increasing the current density, an abrupt breakdown of the dissipationless state occurs. In this talk, the mechanism of breakdown will be addressed, and the electric field created between opposing chiral edge states will be shown to lie at its origin. Electric-field-driven percolation of two-dimensional charge puddles in the gapped surface states of compensated topological-insulator films is proposed as the most likely cause of the breakdown [1].

Moreover, it was recently reported that the interplay between the 1D chiral edge state and the 2D surface state can give rise to nonreciprocity in the longitudinal resistance [2]. In this talk, it will be shown that the onset of 2D conduction due to breakdown is sufficient to create the nonreciprocal effect, allowing for efficient switching between the dissipationless and nonreciprocal transport regime of the QAH state.

[1] G. Lippertz et al., arXiv:2108.02081 (2021)

[2] K. Yasuda et al., Nat. Nanotechnol. 15, 831-835 (2020)

MA 31.8 Thu 17:00 H37

Thermal Hall Effect of Magnons in Collinear Antiferromagnets: Signatures of Magnetic and Topological Phase Transitions — •ROBIN R. NEUMANN¹, ALEXANDER MOOK², JÜRGEN HENK¹, and INGRID MERTIG¹ — ¹Institut für Physik, Martin-Luther-Universität Halle-Wittenberg, Halle (Saale), Germany — ²Department of Physics, University of Basel, Basel, Switzerland

While chiral edge states of topological bosons lack clear hallmarks and are difficult to detect, topological electrons can directly be identified by means of the

quantized transverse conductivity intrinsic to the quantum anomalous Hall effect. In this talk I consider magnons, the bosonic quanta of collective spin excitations, in a collinear antiferromagnet that is driven from its antiferromagnetic phase via a spin-flop phase to the field-polarized phase by an external magnetic field. Besides the magnetic phase transitions, topological phases occur in the spin-flop and field-polarized phases. To identify these phase transitions, the thermal Hall effect (THE), i. e. the transversal heat transport induced by a longitudinal temperature gradient, is studied across the phase transitions. It is demonstrated that the THE exhibits pronounced signatures of the phase transitions and the temperature tunes the sensitivity to these phase transitions oppositely, allowing for their distinction in transport experiments.

MA 31.9 Thu 17:15 H37

Topology, Colossal Magnetoresistance, and Complex Magnetic Domains in Eu5In2Sb6 — •MAREIN RAHN^{1,2}, MURRAY N. WILSON³, PRISCILA F. S. THOMAS², TOM LANCASTER³, FILIP RONNING², and MARC JANOSCHEK^{4,5} — ¹IFMP, TU Dresden, 01062 Dresden, Germany — ²LANL, Los Alamos, New Mexico 87545, USA — ³Department of Physics, Durham University, Durham, DH1 3LE, UK — ⁴Laboratory for Neutron and Muon Instrumentation, Paul Scherrer Institute, CH-5232 Villigen, Switzerland — ⁵Physik-Institut, U. Zürich, Winterthurerstrasse 190, CH-8057 Zürich, Switzerland

The axion insulating state is a paradigm of topological correlated matter which has been particularly difficult to demonstrate in real materials. Using neutron scattering, resonant elastic x-ray scattering, muon spin-rotation and bulk mea-

surements, we demonstrate how the combination of co-planar glide symmetries and large Eu²⁺ magnetic moments in the Zintl phase Eu₅In₂Sb₆ produces an unusual two-step ordering process. At 14 K, Eu₅In₂Sb₆ first forms a complex non-collinear weak Ising-ferrimagnet, which we identify as a trivial insulator. Below 7.5 K, this phase is continuously displaced by a growing volume fraction of a compensated antiferromagnetic arrangement that may have axion insulating character. This discovery also implies the presence of a solitonic antiferromagnetic domain structure on the mesoscale, which demonstrably couples to charge transport and, due to the net magnetization of some domains, should be highly susceptible to manipulation. This may open up a platform to engineer interfaces of trivial and non-trivial insulators on the mesoscale.

MA 31.10 Thu 17:30 H37

Invisible flat bands on a topological chiral edge — •YOUJIANG XU, IRAKLI TITVINIDZE, and WALTER HOFSTETTER — Institut für Theoretische Physik, Goethe-Universität, 60438 Frankfurt am Main, Germany

We prove that invisible bands associated with zeros of the single-particle Green's function exist ubiquitously at topological interfaces of 2D Chern insulators, dual to the chiral edge/domain-wall modes. We verify this statement in a repulsive Hubbard model with a topological flat band, using real-space dynamical mean-field theory to study the domain walls of its ferromagnetic ground state. Moreover, our numerical results show that the chiral modes are split into branches due to the interaction, and that the branches are connected by invisible flat bands. Our work provides deeper insight into interacting topological systems.

MA 32: Bulk Materials: Soft and Hard Permanent Magnets

Time: Thursday 15:00–17:00

Location: H43

MA 32.1 Thu 15:00 H43

High-Entropy/Compositionally-Complex B2 Heusler alloy — •ASLI ÇAKIR^{1,2}, MEHMET ACET², and MICHAEL FARLE² — ¹Department of Metallurgical and Materials Engineering, Mugla University, 48000, Mugla, Turkey — ²Fakultät für Physik, Universität Duisburg-Essen, Forsthausweg 2, 47057 Duisburg, Germany
High entropy alloys (HEAs) emerge as a new alloy concept contrary to conventional alloy design that includes one or two main elements with additional amounts of property-tuning elements. It has been established that the general physical properties of 3d-metallic HEAs can be understood within the known valence-electron-concentration scheme. Using this scheme alloys with particular physical properties can be designed. Here, we present a compositionally-complex alloy consisting of a HEA-component, MnFeCoNiCu, with 25 at% added Al. The resulting material is identical to a stoichiometric B2-Heusler alloy (HEA)50(HEA)25Al25. We have performed X-ray diffraction, energy-dispersive x-ray spectroscopy studies, and magnetization measurements. The alloy exhibits the ordered B2 structure with saturation-magnetization of 1.3 Bohr magneton and Curie temperature of 550 K.

MA 32.2 Thu 15:15 H43

Magnetic-field-, temperature- and time-dependence of structural and magnetic properties of shell-ferromagnets — •NICOLAS JOSTEN¹, STEFFEN FRANZKA², MEHMET ACET¹, FRANZISKA SCHEIBEL³, ASLI ÇAKIR⁴, FRANZISKA STAAB⁵, and MICHAEL FARLE¹ — ¹Faculty of Physics and Center for Nanointegration (CENIDE), University Duisburg Essen, Duisburg, 47057, Germany — ²Interdisciplinary Center for Analytics on the Nanoscale (ICAN), Carl-Benz-Straße 199, 47057 Duisburg, Germany — ³Functional Materials, Institute of Materials Science, Technical University of Darmstadt, Alarich-Weiss-Str. 16, 64287 Darmstadt, Germany — ⁴Department of Metallurgical and Materials Engineering, Mugla University, 48000 Mugla, Turkey — ⁵Physical Metallurgy, Institute of Materials Science, Technical University of Darmstadt, Alarich-Weiss-Str. 2, 64287 Darmstadt, Germany

The strong pinning of magnetic moments in off-stoichiometric Ni₅₀Mn₄₅X₀₅ (X= Al, Ga, In, Sn, Sb) Heusler alloys after magnetic annealing at 650K is known as the shell-ferromagnetic effect. This pinning leads to coercive fields larger than 6 Tesla and is interesting for the development of novel ultrahard permanent magnets. We report on the optimization of the strength of this effect by varying the annealing field, time, and temperature. The origin of the effect is discussed based on these results combined with magnetic force microscopy images.

Funded by the Deutsche Forschungsgemeinschaft (DFG, German Research Foundation) * Project-ID 405553726 * TRR 270.

MA 32.3 Thu 15:30 H43

Effects of disorder on the magnetic properties of L1₀-FeNi — ANKIT IZARDAR and •CLAUDE EDERER — ETH Zürich, Switzerland
L1₀-ordered FeNi is a promising candidate for cheap mid-range permanent magnets. However, since the synthesis of fully ordered samples is very challenging, it is important to understand how deviations from perfect chemical order affect the magnetic properties of FeNi, in particular the magneto-crystalline anisotropy

and Curie temperature. We use DFT in combination with a sampling over different supercell configuration to address effects of chemical disorder in FeNi. Our results show that a decrease in chemical order of up to 25 % does not cause a significant reduction of the magneto-crystalline anisotropy, and that the anisotropy can even be increased for Fe-rich compositions. We also show that the dominant magnetic coupling is strongly dependent on the specific chemical environment and vary drastically in the partially disordered system. We discuss these results in relation to alternative approaches to disorder, such as, e.g., the coherent potential approximation.

MA 32.4 Thu 15:45 H43

Influence of filler morphology, arrangement and filling fraction on the magnetic properties of polymer-bonded magnets produced by laser powder bed fusion — •KILIAN SCHÄFER¹, TOBIAS BRAUN¹, STEFAN RIEGG¹, JENS MUSEKAMP², and OLIVER GUTFLEISCH¹ — ¹Functional Materials, Institute of Materials Science, Technical University Darmstadt, Darmstadt — ²Institute for Materials Technology (MPA-IfW), Technical University Darmstadt, Grafenstraße 2, D-64283 Darmstadt

Bonded permanent magnets are key components in many energy conversion, sensor and actuator devices. These applications need high magnetic performance, customizability, and freedom of shape. With additive manufacturing processes, for example laser powder bed fusion (LPBF), it is possible to produce bonded magnets with tailored stray field distribution.

Up to now, most studies use spherical powders as magnetic fillers due to their good flowability. Here, the behavior of large SmFeN platelets with a high aspect ratio as filler material and its influence on the arrangement and the resulting magnetic properties were examined. To study the distribution and orientation of the magnetic filler in 3D, computed tomography measurements were conducted and analyzed with the open-source software ImageJ. It is shown that the platelet-shaped particles align themselves perpendicular towards the buildup direction during the process. In addition, the effect of filling fraction on the magnetic properties of the composites is investigated.

MA 32.5 Thu 16:00 H43

magnetocrystalline anisotropy in easy-plane kagomé ferromagnet Fe₃Sn — •LILIAN PRODAN¹, VLADIMIR TSURKAN^{1,2}, and ISTVÁN KÉZSMÁRKI¹ — ¹Experimental Physics V, Institute of Physics, University of Augsburg, D-86159 Augsburg, Germany — ²Institute of Applied Physics, MD 2028, Chisinau, Republic of Moldova

Kagomé magnets are expected to host exotic magnetic and electronic properties due to possible interplay of spin-orbit coupling (SOC) and specific topology of the energy band structures [1,2,3]. Here, we present the field-dependent and angular-dependent magnetization studies of the kagomé -lattice easy-plane ferromagnet Fe₃Sn. The SOC is probed by the measurements of the magnetocrystalline anisotropy in high-quality bulk single crystals. Measurements in high fields reveal the difference in the saturation magnetization along the *a* and the *c* axes, which does not vanish up to the highest applied field of 14 T. The anisotropy evidenced in the saturation moment indicates a possible contribution

of the orbital moment. The temperature dependence of the magnetocrystalline anisotropy constants K_1 and K_2 was determined. [1] L. Ye et al., *Nature* 555, 638 (2018), M. Althaler et al., *Phys. Rev. Research* 3, 043191 (2021), J. Watanabe, et al., arXiv:2202.06665 (2022).

MA 32.6 Thu 16:15 H43

First principles study of the complex magnetism in $\text{Ce}_2\text{Fe}_{17}$ — ALENA VISHINA¹, OLLE ERIKSSON^{1,2}, ANDERS BERGMAN¹, and HEIKE C. HERPER¹ — ¹Department of Physics and Astronomy, Uppsala University, Uppsala, Sweden — ²School of Science and Technology, Örebro University, Örebro, Sweden

With its comparably low cost and high magnetization the intermetallic $\text{Ce}_2\text{Fe}_{17}$ has potential to become a candidate for permanent magnets. Problems arising from the in-plane magnetocrystalline anisotropy and the low T_C could be overcome by doping with light elements. Despite that, there is an ongoing debate regarding the magnetic phases in $\text{Ce}_2\text{Fe}_{17}$. While a large number of partially seemingly contradicting experimental findings have been reported, only few theoretical studies exist and they do not capture the experimental findings. Performing a comprehensive study of the magnetic properties of $\text{Ce}_2\text{Fe}_{17}$ we applied various approaches for the exchange-correlation functional to identify the best theoretical treatment of the system. To account for the mixed valent nature of $\text{Ce}_2\text{Fe}_{17}$ we tested several approximations including an analysis of the hybridization function. We used a combination of ab initio methods (VASP, FP-LMTO RSPt) to obtain geometrical and magnetic data including magnetic exchange parameters.

Our results [1] clearly show that the ground state is non-collinear with a strong FM component which explains the low magnetic moment reported in experiment. At 93 K the FM component vanishes and we observe correctly the transition to the helical state.

[1] A. Vishina et al., *JALCOM* 888, 161521 (2021)

MA 32.7 Thu 16:30 H43

High-throughput and data-mining search for novel rare-earth-free permanent magnets — ALENA VISHINA¹, HEIKE HERPER¹, and OLLE ERIKSSON^{1,2} — ¹Department of Physics and Astronomy, Uppsala University, Se-75120 Uppsala, Sweden — ²School of Science and Technology, Örebro University, SE-701 82 Örebro, Sweden

Rare-earth (RE) magnetic materials dominate the market when high-performance permanent magnets are needed (e.g. the area of 'green' energy

technology, such as electric vehicles and windmills). At the same time, there is a growing interest in RE-free alternatives, since the heavier RE elements are quite expensive and are often mined with methods that leave an environmental footprint. We propose to use the data-mining approach to search for high-performance RE-free/lean magnetic materials. Filtering through a large number of known structures from ICSD database, we are looking for materials with high magnetization $M > 1$ T, uniaxial MAE > 1 MJ/m³, and $T_C > 300$ K. Sometimes, additional elements alterations are attempted to make the material more cost-effective. Two searches have already been performed. New magnetic material has been found and consequently synthesized by experimental collaborators - $\text{Co}_3\text{Mn}_2\text{Ge}$. From the ab-initio calculations, the defect-free material was predicted to have the saturation magnetization of 1.71 T, the uniaxial magnetocrystalline anisotropy of 1.44 MJ/m³, and the Curie temperature of 700 K. Its magnetism depends critically on the amount of disorder of the Co and Ge atoms, a further improvement of the magnetism is possible.

MA 32.8 Thu 16:45 H43

MAELAS: Magneto-ELAStic properties calculation via computational high-throughput approach — PABLO NIEVES¹, SERGIU ARAPAN¹, SHIHAO ZHANG², ANDRZEJ KADZIELAWA¹, RUIFENG ZHANG², and DOMINIK LEGUT¹ — ¹IT4Innovations, VSB-TU Ostrava, Ostrava, Czech Republic — ²School of Mat. Sci. and Eng., Beihang University, Beijing, China

Magnetostriction is a physical phenomenon in which the process of magnetization induces a change in the shape or dimension of a magnetic material. Nowadays, materials with large magnetostriction are used in many electromagnetic microdevices as actuators and sensors. By contrast, magnetic materials with extremely low magnetostriction are required in applications such as electric transformers. In this work, we present the program MAELAS[1,2] to calculate anisotropic magnetostriction coefficients and magnetoelastic constants in an automated way by quantum-mechanical calculations. The behavior of the magnetocrystalline anisotropy energy and magnetostrictive coefficients under a general external magnetic field could be visualized as a relative length change using our MAELASviewer tool[3]. To verify accuracy and our approach in general we present a number of examples of each crystal symmetry class with calculated magnetostriction and magnetoelastic constants and compare them with recorded data.

References:[1-3] www.md-esg.eu/software and references therein

MA 33: Multiferroics and Magnetolectric Coupling (joint session MA/KFM)

Time: Thursday 15:00–16:45

Location: H47

MA 33.1 Thu 15:00 H47

Fast non-volatile electrical switching of the magnetolectric domain states in the cubic spinel Co_3O_4 — MAXIMILIAN WINKLER, SOMNATH GHARA, KORBNIAN GEIRHOS, LILIAN PRODAN, VLADIMIR TSURKAN, STEPHAN KROHNS, and ISTVAN KEZSMARKI — Universität Augsburg, Augsburg, Deutschland

Here, we investigate the magnetolectric effect of Co_3O_4 at temperatures far below the Neel-temperature of $T_N = 30$ K. A large magnetolectric coefficient of up to 14ps/m is achieved if the system is cooled through TN while magnetic and/or electric fields are applied. According to these poling procedures we provide a systematic analysis of how the magnetolectric domain state can be controlled and even in situ switched by reversing the direction of either the electric or the magnetic field. The complete switching of the antiferromagnetic state is found to be faster than microseconds. Altogether, the control of the magnetolectric domains and the fast switching dynamics makes the linear magnetolectric coupling of Co_3O_4 highly interesting for spintronics.

MA 33.2 Thu 15:15 H47

Contribution of charge and strain coupling in artificial multiferroic $\text{Fe}_3\text{O}_4/\text{PMN-PT}$ heterostructures — PATRICK SCHÖFFMANN^{1,2}, ANIRBAN SARKAR², MAI H. HAMED², TANVI BHATNAGAR-SCHÖFFMANN³, SABINE PÜTTER⁴, PHILIPPE OHRESSER¹, BRIAN J. KIRBY⁵, ALEXANDER J. GRUTTER⁵, JURI BARTHEL⁶, EMMANUEL KENTZINGER², ANNIKA STELLHORN², MARTINA MÜLLER⁷, and THOMAS BRÜCKEL² — ¹Synchrotron SOLEIL, France — ²Forschungszentrum Jülich GmbH, JCNS-2 and PGI-4, JARA-FIT, Germany — ³Centre de Nanoscience et de Nanotechnologies, CNRS, Université Paris-Saclay, France — ⁴Forschungszentrum Jülich GmbH, JCNS@MLZ, Germany — ⁵NIST Center for Neutron Research, USA — ⁶Forschungszentrum Jülich GmbH, ER-C-2, Germany — ⁷Fachbereich Physik, Universität Konstanz, Germany

To be able to develop denser and faster data storage and computing solutions artificial multiferroic heterostructures are a promising approach, as they enable direct switching of magnetic states with voltage. We grow ferrimagnetic Fe_3O_4 thin films on ferroelectric PMN-PT substrates to study the effect of strain and polarisation induced by the substrate onto the magnetic properties of the film. We found that the coupling due to strain and charge is strongly dependent on the orientation of the sample in an external magnetic field as well as the sub-

strate cut. We will present a simple model to explain the contribution of strain and charge for different substrate and magnetic field orientations.

MA 33.3 Thu 15:30 H47

Microscopic theory of the THz modes and their nonreciprocal directional dichroism in the antiferromagnet $\text{Fe}_2\text{Mo}_3\text{O}_8$ — KIRILL VASIN^{1,2}, ALEXEY NURMUKHAMEDOV², MIKHAIL EREMIN², ANNA STRINIC¹, LILIAN PRODAN¹, VLADIMIR TSURKAN¹, ISTVÁN KÉZSMÁRKI¹, and JOACHIM DEISENHOFER¹ — ¹Augsburg University, Augsburg, Germany — ²Kazan, Russia

In the present work, the transmission measurements of a polar dielectric $\text{Fe}_2\text{Mo}_3\text{O}_8$ were performed by THz time-domain spectroscopy. The origin of the low-lying excitations is not clear, but they were assigned to electromagnons and magnons due to their appearance below TN.

Our microscopic model successfully describes the origin of the optical excitation spectrum in a broad frequency range from the THz to the near-infrared frequency range and the observed dichroism of the low-lying optical modes because of the on-site excitations of the Fe^{2+} ions in this material. We used the technic of the effective Hamiltonian, including the effects of the crystal field, superexchange interaction and spin-orbit coupling, to model the level schemes of Fe ions projected on the ground configuration of 3d6 electrons.

The directional dichroism in $\text{Fe}_2\text{Mo}_3\text{O}_8$ can be described by the interference of magnetic and electric-dipole matrix elements, which depend on the applied magnetic field. Our modelled results agrees to the acquired experimental data.

MA 33.4 Thu 15:45 H47

Magnetization reversal through an antiferromagnetic state — SOMNATH GHARA¹, EVGENII BARTS², KIRILL VASIN¹, DMYTRO KAMENSKYI¹, LILIAN PRODAN¹, VLADIMIR TSURKAN¹, MAXIM MOSTOVOY², ISTVAN KEZSMARKI¹, and JOACHIM DEISENHOFER¹ — ¹Experimentalphysik V, University of Augsburg, Augsburg, Germany — ²University of Groningen, Groningen, The Netherlands

The polar magnet $\text{Fe}_2\text{Mo}_3\text{O}_8$ has recently attracted tremendous interests due its versatile properties, such as magnetolectric effect and giant thermal hall effect. This compound has a polar hexagonal (space group $P6_3mc$) structure at room temperature and undergoes a collinear antiferromagnetic ordering of Fe^{2+} moments below $T_N = 60$ K, accompanied by a large electric polarization

besides that of the structural origin. Upon application of (high) magnetic field, a metamagnetic transition from the antiferromagnetic to a ferrimagnetic state takes place. The ferrimagnetic state can also be stabilized by partially substituting Fe^{2+} ions by Zn^{2+} ions. The magnetic symmetry ($6m'$) of the ferrimagnetic state is compatible with a linear magnetoelectric effect. In this talk, I will show that at the coercive field of the isothermal reversal of a ferrimagnetic state in $\text{Fe}_{1.86}\text{Zn}_{0.14}\text{Mo}_3\text{O}_8$ the pristine antiferromagnetic state re-emerges as a metastable state. The reappearance of the antiferromagnetic state, supported by the theoretical calculations, is reflected in a large change of electric polarization and directly established by the reoccurrence of the characteristic low-energy THz excitation of the AFM state.

MA 33.5 Thu 16:00 H47

Transfer of a domain pattern between ferroic orders — •YANNIK ZEMP¹, EHSAN HASSANPOUR¹, YUSUKE TOKUNAGA², YASUJIRO TAGUCHI³, YOSHINORI TOKURA³, THOMAS LOTTERMOSER¹, MANFRED FIEBIG¹, and MADS C. WEBER^{1,4} — ¹Department of Materials, ETH Zurich — ²University of Tokyo — ³Riken CEMS, Japan — ⁴IMMM, Université Le Mans

In multiferroic materials with two ferroic orders, the order parameters and their respective domain patterns may be rigidly coupled or completely independent, with both of these cases having their merits. We show that in materials with three ferroic order parameters, unusual combinations of coupling and independence are possible. One such material is $\text{Dy}_{0.7}\text{Tb}_{0.3}\text{FeO}_3$. Here, an antiferromagnetic order of the rare earth ions (L) and a ferromagnetic order of the iron ions (M) induce an electric polarisation (P) and a trilinear coupling term $M \cdot L \cdot P$ contributes to the free energy. This coupling term dictates that a reversal of one order parameter needs to be compensated by the product of the other two order parameters to minimise the free energy. Using this fact, we show that a domain pattern in M can be transferred to P while erasing it in the original order parameter, and vice versa, by the application of magnetic and electric fields. We measure the P and M patterns independently by optical second harmonic generation imaging and Faraday rotation microscopy, respectively. The third order parameter L acts as the "memory buffer" for the transfer. The presented work demonstrates the significance of exploration in multiferroics beyond a bilinear coupling.

MA 33.6 Thu 16:15 H47

Magnetoelectric domains and topological defects in hexagonal manganites — •M. GIRALDO, Q. N. MEIER, A. BORTIS, D. NOWAK, N. A. SPALDIN, M. FIEBIG, M. C. WEBER, and TH. LOTTERMOSER — Department of Materials, ETH Zurich

Domains and domain walls reflect the different interdependence of magnetic and electric order in multiferroics. For example, in type-II multiferroics, magnetic and electric domain patterns are one-to-one linked, whereas in type-I multiferroics, magnetic and electric domain morphologies can be different, and their coupling no longer mandatory. We show – using experiment and theory – that multiferroics with separately emerging magnetic and electric order can have a strong bulk magnetoelectric coupling even though the leading magnetoelectric cross-coupling is symmetry-forbidden. We show, taking ErMnO_3 as example, that the structural distortions that lead to the ferroelectric polarization also break the balance of the competing superexchange contributions. The resulting bulk coupling leads to novel types of topological defects, like magnetoelectric domain walls and multifold vortex-like singularities. We argue that the apparent independence of magnetic and electric orders in type-I multiferroics leads to uncommon phenomena, not open to the type-II class, which can open additional degrees of freedom for the future control of their magnetoelectric functionality [1].

[1] M. Giraldo, Q.N. Meier, A. Bortis et al. Magnetoelectric coupling of domains, domain walls and vortices in a multiferroic with independent magnetic and electric order. *Nat Commun* 12, 3093 (2021).

MA 33.7 Thu 16:30 H47

Measuring Antiferromagnets with a SQUID Setup in Magnetically Shielded Environments — •MICHAEL PAULSEN¹, JÖRN BEYER¹, MICHAEL FECHNER², RALF FEYERHERM³, KLAUS KIEFER³, BASTIAN KLEMKE³, JULIAN LINDNER³, and DENNIS MEIER⁴ — ¹Physikalisch-Technische Bundesanstalt, Berlin, Germany — ²Max Planck Institute for the Structure and Dynamics of Matter, CFEL, Hamburg, Germany — ³Helmholtz-Zentrum Berlin, Berlin, Germany — ⁴Norwegian University of Science and Technology, Trondheim, Norway

Antiferromagnets possess zero net dipole magnetization. While predictions of higher order magnetizations have been made for Cr_2O_3 , few confirmed measurements exist. In this contribution, we present low-temperature measurements gained on different systems with antiferromagnetic order in very low magnetic backgrounds using a dedicated SQUID setup. In particular, we discuss our results on exterior quadrupolar magnetic fields and relate the distinct quadrupolar magnetic signals to the microscopic spin arrangement in our model systems.

MA 34: Functional Antiferromagnetism

Time: Thursday 15:00–16:45

Location: H48

MA 34.1 Thu 15:00 H48

Giant and tunneling magnetoresistance in unconventional compensated magnets with nonrelativistic d-wave spin-momentum couplings — LIBOR ŠMEJKAL^{1,2}, •ANNA B. HELLENES¹, RAFAEL GONZÁLEZ-HERNÁNDEZ³, JAIRO SINOVA^{1,2}, and TOMAŠ JUNGWIRTH^{2,4} — ¹Johannes Gutenberg Universität Mainz, Germany — ²Czech Academy of Sciences, Prague, Czech Republic — ³Universidad del Norte, Barranquilla, Colombia — ⁴University of Nottingham, United Kingdom

The magnetoresistance effects used in commercial spintronics devices rely on spin current generated by the time-reversal broken band structure of ferromagnets. Realizing counterpart effects with all-antiferromagnetic electrodes has remained experimentally elusive, as conventional compensated antiferromagnets exhibit symmetries combining time-reversal with translation or inversion and thus prohibit nonrelativistic spin-polarized bands and spin currents. Recently, we have predicted large magnetoresistance effects in multilayers with an unconventional compensated magnetic phase [1]. It is characterized by zero magnetization and a time-reversal broken band structure [2], with d-wave spin-momentum coupling and alternating spin polarization [1,3] (thus also referred to as alternating magnetism [3]). In the present contribution, we will describe mechanisms for giant and tunneling magnetoresistance relying on the anisotropic and valley-dependent forms of the d-wave spin-momentum coupling [1]. [1] L. Šmejkal, A. B. Hellenes et al., *Phys. Rev. X* 12, 011028, 2022. [2] L. Šmejkal et al., *Sci. Adv.* 6, eaaz8809, 2020. [3] L. Šmejkal et al., arXiv:2105.05820v2, 2021.

MA 34.2 Thu 15:15 H48

Exploring the magnetic ground states in different layers of Mn on Ir (111) by SP-STM — •VISHESH SAXENA, ARTURO RODRIGUEZ SOTA, ROLAND WIESEN-DANGER, and KIRSTEN VON BERGMANN — Institut für Nanostruktur- und Festkörperphysik, Hamburg

Conventional magnetic skyrmions are susceptible to unwanted phenomena such as the skyrmion Hall effect. This is a highly undesirable effect that hinders the application of such skyrmions in spintronic devices. An alternative are antiferromagnetic skyrmions which do not show a skyrmion Hall effect [1]. In the quest to explore systems that can host antiferromagnetic skyrmions, we have studied

the magnetism of Mn on Ir (111) using spin-polarized scanning tunneling microscopy (SP-STM). Having an antiferromagnetic spin order on a periodic lattice can induce magnetic frustration. It has already been shown that the magnetic ground states of Mn monolayers on Re (0001) can be the row-wise antiferromagnetic state or the 3Q state depending on the stacking of Mn [2]. In the present work, the magnetic behavior of the monolayer, double layer, and the triple layer of Mn on Ir(111) is studied. Different magnetic ground states are observed depending on the Mn layer thickness.

[1] X. Zhang, Y. Zhou, and M. Ezawa, *Antiferromagnetic Skyrmion: stability, creation and manipulation*, Scientific Reports 6, 1 (2016). [2] J. Spethmann, S. Meyer, K. von Bergmann, R. Wiesendanger, S. Heinze, and A. Kubetzka, *Discovery of magnetic single- and triple-q states in Mn/Re(0001)*, *Physical Review Letters* 124, 227203 (2020).

MA 34.3 Thu 15:30 H48

Identification of Néel vector orientation in antiferromagnetic NiO thin films

— •CHRISTIN SCHMITT¹, LUIS SANCHEZ-TEJERINA², RAFAEL RAMOS³, EJI SAITOH^{3,4}, GIOVANNI FINOCCHIO², LORENZO BALDRATI¹, and MATHIAS KLÄUI¹ — ¹Institute of Physics, Johannes Gutenberg-University Mainz, Germany — ²Department of Mathematical and Computer Sciences, Physical Sciences and Earth Sciences, University of Messina, Italy — ³WPI-AIMR, Tohoku University, Japan — ⁴Department of Applied Physics, The University of Tokyo, Japan

Spintronics using antiferromagnets (AFM) is promising due to intrinsic dynamics in the THz range and the absence of stray fields. However, efficient writing and reading is necessary in terms of applications. Recently, current-induced writing of the Néel order in AFMs has been reported and different switching mechanisms have been put forward [1,2]. The mechanisms depend on the type of domains present. Here, we focus on antiferromagnetic NiO/Pt thin films, and image reversible electrical switching by photoemission electron microscopy (PEEM) employing the x-ray magnetic linear dichroism (XMLD) effect. By varying the x-ray polarization and sample azimuthal angle, we identify the crystallographic orientation of the domains that can be switched and quantify the Néel vector direction, showing that the switching occurs between different T-domains [3]. Finally, we characterize the domain walls showing that they are non-chiral

and reveal a large anisotropy in the NiO thin films. [1] T. Moriyama, et al., *Sci. Rep.* 8, 14167 (2018). [2] P. Zhang, et al., *Phys. Rev. Lett.* 123, 247206 (2019). [3] C. Schmitt, et al., *Phys. Rev. Appl.* 15, 034047 (2021).

MA 34.4 Thu 15:45 H48

Magnon Hanle effect in easy-plane antiferromagnets — •JANINE GÜCKELHORN^{1,2}, AKASHDEEP KAMRA³, TOBIAS WIMMER^{1,2}, MATTHIAS OPEL¹, STEPHAN GEPRÄGS¹, RUDOLF GROSS^{1,2,4}, HANS HUEBL^{1,2,4}, and MATTHIAS ALTHAMMER^{1,2} — ¹Walther-Meißner-Institut, BAdW, 85748 Garching, Germany — ²Physik-Department, TUM, 85748 Garching, Germany — ³IFIMAC and Departamento de Física Teórica de la Materia Condensada, Universidad Autónoma de Madrid, 28049 Madrid, Spain — ⁴Munich Center for Quantum Science and Technology, 80799 München, Germany

Antiferromagnets have drawn much attention due to their unique properties and potential for interesting device applications. In analogy to a spin-1/2 system, antiferromagnetic magnon pairs can be described in terms of a magnonic pseudospin. Recently, first experimental observations of the associated dynamics and the magnon Hanle effect have been reported and described using a 1D pseudospin transport model. Here, we discuss the effects of dimensionality on the magnon spin signal by studying insulating hematite (α -Fe₂O₃) films with varying thickness [1]. For both a thin and a thick film, we find a pronounced signal caused by the magnon Hanle effect. However, the magnonic spin signal exhibits clear differences in both cases. We extend the theoretical description by taking into account low-energy finite-spin magnons and use it to explain our observations. This provides deeper insight into the detailed understanding of magnonic pseudospin dynamics.

[1] J. Gückelhorn *et al.*, *Physical Review B* 150, 094440 (2022)

MA 34.5 Thu 16:00 H48

Role of substrate clamping on anisotropy and domain structure in the canted antiferromagnet α -Fe₂O₃ — •ANGELA WITTMANN¹, OLENA GOMONAY¹, KAI LITZIUS², ALEXANDRA CHURIKOVA³, NORMAN BIRGE⁴, FELIX BÜTTNER⁵, SEBASTIAN WINTZ², MOHAMAD MAWASS⁵, MARKUS WEIGAND⁵, FLORIAN KRONAST⁵, JAIRO SINOVA¹, GISELA SCHÜTZ², and GEOFFREY BEACH³ — ¹Johannes Gutenberg Universität Mainz, Germany — ²Max Planck Institute for Intelligent Systems, Stuttgart, Germany — ³Massachusetts Institute of Technology, Cambridge, USA — ⁴Michigan State University, East Lansing, USA — ⁵Helmholtz-Zentrum für Materialien und Energie GmbH, Berlin, Germany

Antiferromagnets are at the forefront of research in spintronics and demonstrate high potential for revolutionizing memory technologies. For this, understanding the formation and driving mechanisms of the domain structure is paramount. In this work, we investigate the domain structure in a thin-film canted antiferromagnet α -Fe₂O₃ using x-ray linear dichroism (XMLD) and spin Hall magnetoresistance (SMR) measurements. We find that the internal destressing fields driving the formation of domains do not follow the crystal symmetry of α -Fe₂O₃ but fluctuate due to substrate clamping. This leads to an overall isotropic distribution of the Néel order with locally varying effective anisotropy in antiferromagnetic thin films. The insights gained from our work serve as a foundation for further studies of electrical and optical manipulation of the domain structure of antiferromagnetic thin films.

MA 34.6 Thu 16:15 H48

Correlation of Atomic Disorder and Anomalous Hall Effect in a Non-Collinear Antiferromagnet — •BERTHOLD H. RIMMLER¹, BINOY K. HAZRA¹, HOLGER L. MEYERHEIM¹, ARTHUR ERNST², and STUART S. P. PARKIN¹ — ¹Max Planck Institute for Microstructure Physics, Weinberg 2, 06120 Halle, Germany — ²Johannes Kepler University, Altenbergerstraße 69, Linz 4040, Austria

Non-collinear antiferromagnets (NCAFs) such as the well-studied alloy Mn₃Sn have compensated triangular magnetic structures with vanishing net magnetization. Due to magnetic symmetry breaking, they can display a large Anomalous Hall Effect (AHE). Measurement of the AHE requires an imbalance of antiferromagnetic domains. Domain structure control by magnetic field or spin torques is possible in Mn₃Sn, because crystalline anisotropy induces weak canted moments. In contrast, these moments are not intrinsic to cubic NCAFs. In this work, we investigate the crystallographic, magnetic and magneto-transport properties of thin films of the cubic NCAF Mn₃SnN. We find that the manganese atoms can be displaced from their high-symmetry positions. This atomic site disorder correlates with a finite AHE. We employ ab-initio calculations to show that the manganese site displacement can induce canting. In analogy to Mn₃Sn, these canted moments may allow for domain structure control leading to the observed AHE. This work provides new insight into the microscopic origin of canted moments in cubic NCAFs and their correlation with the AHE. Our findings have implications for other magneto-transport effects such as the anomalous Nernst effect or the spin Hall effect.

MA 34.7 Thu 16:30 H48

Spontaneous anomalous Hall effect arising from antiparallel magnetic order in a semiconductor — •RUBEN DARIO GONZALEZ BETANCOURT^{1,2,3,4}, JAN ZUBÁČ^{3,4}, RAFAEL JULIAN GONZALEZ HERNANDEZ⁵, KEVIN GEISHENDORF³, ZBYNEK ŠOBÁŇ³, GUNTHER SPRINGHOLZ⁶, KAMIL OLEJNÍK³, LIBOR ŠMEJKAL³, TOMAS JUNGWIRTH^{3,7}, SEBASTIAN TOBIAS BENEDIKT GOENNENWEIN^{1,8}, ANDY THOMAS^{1,2}, HELENA REICHOVÁ³, JAKUB ŽELEZŇÝ³, and DOMINIK KRIEGNER^{1,3} — ¹IFMP, TU Dresden — ²IFW Dresden — ³Institute of Physics, AV ČR, Prague — ⁴Charles University, Prague — ⁵Universidad del Norte, Barranquilla — ⁶Semiconductor Physics, JKU Linz — ⁷University of Nottingham — ⁸University of Konstanz

It is known that collinear antiferromagnets cannot host a spin split band structure and therefore not show any anomalous Hall effect. Following the recent theory development [1], we experimentally show that this paradigm needs to be revised. We theoretically identify and experimentally confirm the symmetry components of the longitudinal and transversal anisotropic magnetoresistance in thin films of the compensated collinear antiferromagnet MnTe. We experimentally find a hysteretic signal odd in magnetic field in the transversal magnetoresistance, i.e. spontaneous anomalous Hall effect [2]. This effect can be rationalized considering nonmagnetic atoms at non-centrosymmetric lattice sites which break additional symmetries and cause a spin splitting in certain parts of the Brillouin zone.

[1] L. Šmejkal *et al.*, *Sci. Adv.* 6, aaz8809(2020)

[2] R. D. Gonzalez Betancourt *et al.*, (2021) *arXiv:2112.06805*

MA 35: Poster 2

Topics: Magnonics (35.1-35.14), Magnetic Domain Walls (non-skyrmionic) (MA 35.15-35.17), Ultrafast Magnetization Effects (MA 35.18-35.33), Magnetic Relaxation and Gilbert Damping (MA 35.34-35.36), Magnetic Semiconductors (MA 35.37-35.38), Magnetic Heuslers (MA 35.39-35.40), Complex Magnetic Oxides (MA 35.41), Frustrated Magnets (MA 35.42-35.44), Thin Films: Magnetic Coupling Phenomena / Exchange Bias (MA 35.45-35.48), Thin Films: Magnetic Anisotropy (MA 35.49-35.51), Bulk Materials: Soft and Hard Permanent Magnets (MA 35.52), Magnetic Instrumentation and Characterization (MA 35.53-35.59), Magnetic Particles / Clusters (MA 35.60-35.61), Magnetic Information Technology, Recording, Sensing (MA 35.62), Micro- and Nanostructured Magnetic Materials (MA 35.63-35.65), Multiferroics and Magnetoelectric Coupling (MA 35.66-35.67), Surface Magnetism (MA 35.68-35.71), Cooperative Phenomena: Spin Structures and Magnetic Phase Transitions (MA 35.72), Topological Insulators (MA 35.73-35.75), Weyl Semimetals (MA 35.76).

Time: Thursday 16:00–18:00

Location: P4

MA 35.1 Thu 16:00 P4

Magnetic Coupling in Y₃Fe₅O₁₂/Gd₃Fe₅O₁₂ Heterostructures — SVEN BECKER¹, ZENGYAO REN^{1,2,3}, •AKASHDEEP AKASHDEEP¹, and GERHARD JAKOB^{1,2} — ¹Institute of Physics, Johannes Gutenberg-University Mainz, Staudingerweg 7, Mainz 55128, Germany — ²Graduate School of Excellence *Materials Science in Mainz* (MAINZ), Staudingerweg 9, Mainz 55128, Germany — ³School of Materials Science and Engineering, University of Science and Technology Beijing, Beijing 100083, China

Ferrimagnetic Y₃Fe₅O₁₂ (YIG) is the prototypical material for studying magnonic properties due to its exceptionally low damping. By substituting the yttrium with the temperature-dependent magnetic moment of gadolinium, we can introduce an additional spin degree of freedom in form of a magnetic compensation point. Here, we study the magnetic coupling in epitaxial Y₃Fe₅O₁₂/Gd₃Fe₅O₁₂ (YIG/GIG) heterostructures grown by pulsed laser deposition. The XRD patterns show Laue oscillations and a narrow rocking curve indicating a smooth surface and interface. From bulk sensitive magnetometry and surfacesensitive spin Seebeck effect and spin Hall magnetoresistance mea-

surements, we determine the alignment of the heterostructure magnetization as a function of temperature and external magnetic field. We show that we can control the magnetic properties of the heterostructures by tuning the thickness of the individual layers. These bilayer devices could potentially control the magnon transport analogously to electron transport in giant magnetoresistive devices [1].

[1] H. Wu et al.; Phys. Rev. Lett. 120, 097205 (2018).

MA 35.2 Thu 16:00 P4

GHz frequency layered antiferromagnets for novel Magnonic computing applications — •SALLY LORD and JOHN GREGG — Clarendon Laboratory, Department of Physics, University of Oxford, Parks Road, Oxford, OX1 3PU, United Kingdom

Magnonic computing is a novel computing paradigm that exploits the unusual behaviour of magnons to develop faster, more efficient devices, that have the potential to rival existing CMOS technologies. Antiferromagnetic materials are a prime candidate for such applications, primarily due to their typical THz resonant frequencies, which offer the possibility of creating devices with faster operating speeds. However, studying the THz frequencies of these materials, using conventional electronic methods, is challenging. Layered antiferromagnetic materials offer a promising solution to this challenge, since the weak interlayer coupling results in resonant frequencies that exist in the easily accessible microwave range. Furthermore, these materials can be artificially created by coupling two ferromagnetic layers via a non-magnetic spacer layer to create synthetic antiferromagnet. In this contribution, we report on the experimental setup designed to explore the magnetic properties of such materials.

MA 35.3 Thu 16:00 P4

Towards Integration: On-chip Excitation of Spin Waves using Meander Antennas tailored to practical Applications — •JOHANNES GREIL¹, MARTINA KIECHLE¹, MATTHIAS GOLIBRZUCH¹, ÁDÁM PAPP², GYÖRGY CSABA², and MARKUS BECHERER¹ — ¹Technical University of Munich (TUM), Germany — ²Pázmány Peter Catholic University, Budapest, Hungary

Albeit spin-wave (SW) computation principles are understood well, integrating SW-based devices makes an efficient excitation of SWs inevitable. Electrical measurements are performed most conveniently with inductive antennas that transfer radio frequency (RF) power into the SW system and pick up the output signals.

We demonstrate the realization of broadband efficient excitation of SWs with meander antennas in a chip-on-platform system. The platform is a PCB that carries the RF signal to a 100nm thin YIG film with metallized bond pads and meander antennas on top. Despite the lower spectral bandwidth of meander antennas compared to CPW structures they have better impedance matching over a wide frequency range and thus provide efficient SW excitation.

We also demonstrate a new design for a dual-wavelength spin wave antenna that consists of a meander structure with two linewidths and gap sizes. Feeding the antenna with two RF frequencies enables for simultaneous excitation of SWs with two wavelengths at one magnetic bias field. Thus, it can be seen as a first realization of purely SW frequency modulation or as the basis for SW-based frequency-division multiplexing (FDM) with two sub-bands.

MA 35.4 Thu 16:00 P4

Non-linear spin waves at low bias fields in Ni₈₀Fe₂₀ elements — •MATTHIAS VOLZ, ROUVEN DREYER, and GEORG WOLTERS DORF — Martin Luther University Halle-Wittenberg, Institute of Physics, Von-Danckelmann-Platz 3, 06120 Halle (Saale), Germany

Magnetic rf fields can be used to excite non-linear spin waves in Ni₈₀Fe₂₀ elements at low bias fields. At a certain rf threshold field, spin waves oscillating at odd half-integer multiples of the driving frequency can be excited [1]. Here, the $\frac{3}{2}\omega$ mode is investigated with frequency resolved magneto-optical Kerr microscopy [2]. Specifically we determine the dynamical response at $\frac{3}{2}$ multiple of the driving frequency. By simultaneously detecting real and imaginary parts of the response at $\frac{3}{2}$ of the driving frequency, we reveal phase stable regimes for these $\frac{3}{2}\omega$ non-linear spin wave modes. These modes are investigated as a function of the pump power level, the bias field, and the Ni₈₀Fe₂₀ element thickness. We show that a phase stable non-linear regime can be established for Ni₈₀Fe₂₀ thicknesses between 10 nm and 20 nm.

[1] H. G. Bauer et al., Nat. Commun. 6:8274 (2015)

[2] R. Dreyer et al., Phys. Rev. Materials 5.6 (2021)

MA 35.5 Thu 16:00 P4

Sensing of magnetic excitations in 2D-materials with NV-spins — •HOSSEIN MOHAMMADZADEH, DOMINIK MAILE, and JOACHIM ANKERHOLD — ICQ and IQST, University of Ulm, Ulm, Germany

Magnetism in two-dimensional (2D) van der Waals (vdW) materials has recently emerged as one of the most promising areas in condensed matter research, with many exciting emerging properties and significant potential for applications ranging from topological magnonics to low-power spintronics, quantum computing, and optical communications [1]. The nitrogen-vacancy (NV) center in diamond is an excellent platform to detect nanoscale signatures in magnetic

materials [2]. The spin state of the NV center can be easily initialized and read out in the optical domain and coherently manipulated with microwave fields. Motivated by and in collaboration with recent experimental activities in this direction [3], in this poster we describe the general strategy and first theoretical results. The latter is based on a description of low energy magnetic excitations in terms of a Kitaev-Heisenberg model and the coupling of magnons in the trivial and in the topological phase to single NV-electronic spins.

[1] Qing Hua Wang et al., ACS Nano, 16, 5, 6960-7079 (2022)

[2] Francesco Casola, Toeno van der Sar, and Amir Yacoby. Nat Rev Mater 3, 17088 (2018)

[3] Jörg Wrachtrup et al. Nat Commun 12, 1989 (2021)

MA 35.6 Thu 16:00 P4

Microwave Control of Magnon Transport in Nanostructures — •FRANZ WEIDENHILLER^{1,2}, JANINE GÜCKELHORN^{1,2}, MANUEL MÜLLER^{1,2}, HANS HUEBL^{1,2,3}, MATTHIAS ALTHAMMER^{1,2}, and RUDOLF GROSS^{1,2,3} — ¹Walther-Meißner-Institut, Bayerische Akademie der Wissenschaften, Garching, Germany — ²Physik-Department, Technische Universität München, Garching, Germany — ³Munich Center for Quantum Science and Technology, München, Germany

Magnon transport in magnetically ordered insulators is of great interest for the implementation of magnonic devices. We here present our results on the diffusive magnon transport signal in yttrium iron garnet (YIG) due to the simultaneous excitation of magnons with electromagnetic microwaves. Using E-beam lithography, we pattern two platinum strips on top of the YIG for the injection and detection of magnons. The Pt strips are electrically insulated from an aluminum microwave antenna, which covers both strips and the gap in between. Via the antenna, microwave driven generation of magnons in the active device area through ferromagnetic resonance is possible. We investigate how these microwave injected magnons affect the magnon transport between the two Pt strips. We compare these results to spin pumping experiments using the two Pt strips as electrical detectors. Finally, we discuss relevant magnon relaxation mechanisms in our experiments.

MA 35.7 Thu 16:00 P4

Unidirectional spin wave propagation mediated by Co₂₅Fe₇₅-nanogratings — •CHRISTIAN MANG^{1,2}, MONIKA SCHEUFELE^{1,2}, MANUEL MÜLLER^{1,2}, JOHANNES WEBER^{1,2}, VINCENT HAUEISE^{1,2}, HANS HUEBL^{1,2,3}, MATTHIAS ALTHAMMER^{1,2}, STEPHAN GEPRÄGS¹, and RUDOLF GROSS^{1,2,3} — ¹Walther-Meißner-Institut, Bayerische Akademie der Wissenschaften, Garching, Germany — ²Physik-Department, Technische Universität München, Garching, Germany — ³Munich Center for Quantum Science and Technology (MCQST), München, Germany

Unidirectional spin wave propagation adds additional functionalities to magnonic devices and their potential application in communication technology. We report the fabrication of Co₂₅Fe₇₅-nanogratings via electron beam lithography and DC magnetron sputtering on yttrium iron garnet (YIG) thin films. The dipolar magnetic interactions between the Co₂₅Fe₇₅-nanogratings and the YIG-film give rise to a finite non-reciprocity of the spin wave propagation in the YIG-film for a collinear magnetization configuration of the Co₂₅Fe₇₅-gratings and the YIG-film [1]. By performing spin wave spectroscopy, we study the coupled spin wave modes of the Co₂₅Fe₇₅-nanogratings and the YIG thin films in the Damon-Eshbach geometry using a vector network analyzer.

[1] J. Chen et al., Phys. Rev. B 100, 104427, (2019)

MA 35.8 Thu 16:00 P4

Spontaneous emergence of spin-wave frequency combs mediated by vortex gyration — •CHRISTOPHER HEINS¹, KATRIN SCHULTHEISS¹, LUKAS KÖRBER^{1,2}, ATTILA KÁKAY¹, TOBIAS HULA^{1,3}, MAURICIO BEJARANO^{1,2}, VADYM IURCHUK¹, JÜRGEN LINDNER¹, JÜRGEN FASSBENDER^{1,2}, and HELMUT SCHULTHEISS^{1,2} — ¹Helmholtz-Zentrum Dresden-Rossendorf, Dresden, Germany — ²Fakultät Physik, Technische Universität Dresden, Dresden, Germany — ³Institut für Physik, Technische Universität Chemnitz, Chemnitz, Germany

We present experimental investigations of the spin-wave frequency comb formation in a confined system, a magnetic vortex. The magnetic vortex shows rich spin-wave dynamics like the formation of whispering gallery magnons and non locally induced three-magnon scattering, all with frequencies in the GHz range. Additionally, there is the low frequency gyration of the vortex core itself. The combination of these dynamics on two different time scales inside magnetic vortices, results in the generation of spin-wave frequency combs with their spacing given by the vortex gyration frequency.

Using Brillouin light scattering microscopy, we show that large amplitude excitations of spin waves purely in the GHz range can induce a gyration of the vortex core, which leads to the formation of frequency combs. Analyzing the mode profiles of the sidebands by micromagnetic simulations, shows that the comb is generated via three magnon scattering under conservation of energy and angular momentum.

The authors acknowledge financial support from the Deutsche Forschungsgemeinschaft within program SCHU 2922/1-1.

MA 35.9 Thu 16:00 P4

Magneto-optical Investigation of non-reciprocal Phonon-Magnon interaction — •YANNIK KUNZ¹, MICHAEL SCHNEIDER¹, MORITZ GEILEN¹, TORBEN PFEIFER¹, MATTHIAS KÜSS², MANFRED ALBRECHT², PHILIPP PIRRO¹, and MATHIAS WEILER¹ — ¹Fachbereich Physik und OPTIMAS, TU Kaiserslautern — ²Institut für Physik, Universität Augsburg

Surface acoustic waves (SAWs) are employed to achieve miniaturization of telecommunication devices, as they live in the Gigahertz-regime with wavelengths on the micrometre scale. The coupling of SAWs with spin waves (SWs) leads to nonreciprocal SAW-propagation, induced by symmetry breaking coupling mechanisms [1]. We investigated the coupling of SAWs, excited by Interdigital Transducers (IDTs), with SWs in a LiNbO₃/Co₄₀Fe₄₀B₂₀ (10 nm)/SiN(5 nm)-structure using well-established micro-focused Brillouin Light Scattering Spectroscopy and the novel micro-focused frequency-resolved magneto-optical Kerr effect with phase resolution, empowered by vector network analysis [2]. We model the magnetic field and angle-dependent SAW-SW-coupling using an extended theoretical model for continuous, viscoelastic Rayleigh-mode SAWs [3] as well as a theoretical model to describe the magneto-elastic coupling [4]. We acknowledge the funding by DFG via project No. 492421737.

[1] M. Küß et al., Phys. Rev. Lett. 125, 217203 (2020).

[2] L. Liensberger et al. IEEE Magn. Lett. 10, 5503905 (2019).

[3] P.K. Currie et al., Q. Appl. Math. 35, (1977).

[4] M. Küß et al., Phys. Rev. Applied 15, 034060 (2021).

MA 35.10 Thu 16:00 P4

Magnon Bose-Einstein condensates in microscopic thermal landscapes — •FRANZISKA KÜHN, MATTHIAS R. SCHWEIZER, GEORG VON FREYMAN, ALEXANDER A. SERGA, and BURKARD HILLEBRANDS — Fachbereich Physik and Landesforschungszentrum OPTIMAS, TU Kaiserslautern, Kaiserslautern, Germany

This contribution is focused on the behavior of a magnon Bose-Einstein condensate (BEC) in artificial magnetization landscapes at the scale of the wavelengths of condensed magnons. In our work, the magnon condensate is created by overpopulation of a magnon gas using microwave parametric pumping. By combining a heating laser with a microscopic phase-based wave front modulation technique, a temperature pattern is imprinted on the yttrium-iron-garnet film sample. Accordingly, the saturation magnetization, on which the dispersion relation of the magnons depends, is shifted. The corresponding spatial variation of the condensate frequency, acting as an artificial potential for the BEC, affects its dynamics and propels magnon supercurrents and Bogoliubov waves. Since the size of these patterns is small compared to the area of BEC formation, it is possible to investigate the BEC in two-dimensional thermal landscapes. In the experiment, by utilizing microfocused Brillouin light scattering spectroscopy, we study the anisotropy of the two-dimensional density distribution of a magnon BEC and the possibility of interference effects between Bogoliubov waves.

Funded by the Deutsche Forschungsgemeinschaft (DFG, German Research Foundation) – TRR 173 – 268565370 (project B04).

MA 35.11 Thu 16:00 P4

Optical characterisation of direct write 3D nanoarchitectures for magnonics — •SEBASTIAN LAMB-CAMARENA^{1,2}, SABRI KORALTAN³, QI WANG¹, FABRIZIO PORRATI⁴, SVEN BARTH⁴, MICHAEL HUTH⁴, MICHAEL URBANEK⁵, DIETER SUESS³, ANDRII CHUMAK¹, and OLEKSANDR DOBROVOLSKIY¹ — ¹University of Vienna, Nanomagnetism and Magnonics, Boltzmannngasse 5, 1090 Vienna, Austria — ²University of Vienna, Vienna Doctoral School in Physics, Boltzmannngasse 5, 1090 Vienna, Austria — ³University of Vienna, Physics of Functional Materials, Boltzmannngasse 5, 1090 Vienna, Austria — ⁴Physikalisches Institut, Goethe-Universität, Max-von-Laue-Str. 1, 60438 Frankfurt am Main, Germany — ⁵CEITEC BUT, Brno University of Technology, Brno 61200, Czech Republic Major directions in magnonics are the extension of magnonic conduits into the third dimension, and operations with short wavelength, fast moving exchange magnons. Both are addressed by direct write nanoarchitectures fabricated by focused electron beam induced deposition (FEBID). Characterisation results of 2D and 3D magnetic FEBID nanostructures by Brillouin light scattering (BLS) spectroscopy and ferromagnetic resonance (FMR) measurements are presented, including a structure with 3D hemicylindrical protrusion along the top face of the rectangular waveguide. The FEBID nanostructures exhibit strong magnetic response to quasi-static and dynamic external magnetic stimuli. Further characterisation of the material properties is foundational for advancing research into spin wave dynamics and geometric curvature induced effects on signal propagation.

MA 35.12 Thu 16:00 P4

VSM and EPR characterization of GGG at ultralow temperatures — •R. O. SERHA¹, S. KNAUER¹, D. SCHMOLL¹, K. DAVIDKOVA³, Q. WANG¹, B. BUDINSKÁ¹, O. V. DOBROVOLSKIY¹, V. E. DEMIDOV², M. URBANEK³, S. O. DEMOKRITOV², and A. V. CHUMAK¹ — ¹University of Vienna, Faculty of Physics, Boltzmannngasse 5, A-1090 Vienna, Austria — ²Boltzmannngasse 5 Institute for Applied Physics and

Center for Nonlinear Science, University of Muenster, Corrensstrasse 2-4, D-48149 Muenster, Germany — ³CEITEC BUT, Brno University of Technology, Purkynova 123, 612 00 Brno, Czech Republic

Magnons, the quanta of spin-waves, also exist in paramagnetic materials and are known as paramagnons. Paramagnon properties are governed by the exchange interactions, which do not vanish above Curie/Neel temperature and the dipolar interactions. Here we present our results on the investigation of electron paramagnetic resonance (EPR) spectroscopy in gadolinium gallium garnet (GGG) and DPPH bulk slabs in a wide range of temperatures down to 20 mK. GGG is one of the materials of choice, as Gd³⁺ ions have a large spin $S = 7/2$ and its saturation magnetization is about $M_s = 800$ kA/m. Millikelvin temperatures allow reaching the saturation of the GGG magnetization, by applying magnetic fields of hundreds mT. However, the EPR linewidth of GGG is strongly influenced by the phenomenon of dipolar broadening, while DPPH is known to have a very narrow resonance line. These studies form an initial step toward investigations of long-propagating paramagnons.

MA 35.13 Thu 16:00 P4

Aharonov-Casher effect in spin-wave refraction — •ANDRII SAVCHENKO^{1,2}, VLADIMIR KRIVORUCHKO², and STEFAN BLÜGEL¹ — ¹Peter Grünberg Institut and Institute for Advanced Simulation, Forschungszentrum Jülich, D-52425 Jülich, Germany — ²Donetsk Institute for Physics and Engineering, National Academy of Sciences of Ukraine, 03028 Kyiv, Ukraine

It has been shown that in a homogeneous magnetic film there is a possibility of electric field control on the reflection and refraction of spin waves at the interface formed by regions under the effect of different electric fields. Under these conditions, the critical angles for Snell's law, the positive or negative refraction of the spin waves, and their non-reciprocity with respect to the incident angle are determined by the electric field. This is possible due to the electrically induced Aharonov-Casher phase shift of the spin-wave phase, that is equivalent to adding a Dzyaloshinskii-Moriya-like interaction between the spins of neighboring ions.

MA 35.14 Thu 16:00 P4

Ring-shaped multi-bandpass spin wave filter — •TAKUYA TANIGUCHI, MICHAEL LINDNER, CHRISTIAN RIEDEL, and CHRISTIAN BACK — Technische Universität München

Spin waves (SWs) are fundamental collective excitations of magnetic order and their wave character makes it possible to potentially realize next generation logic devices. As one of the possible logic devices, multi-bandpass filters are desired in order to forbid certain frequency bands of SWs. In this work, we design a SW wave-guide, which has a ring shape attached to the middle of a stripe. In the device, SWs (SW1s) travel through the stripe part and are split to the ring part and the stripe part at the middle of the stripe. The SWs traveling through the ring (SW2s) interfere with the SW1s after traveling one round and SW1s are suppressed when the phase difference between SW1s and SW2s is π . We fabricate devices from 200-nanometer-thick YIG films and observe SW propagation using Brillouin light scattering (BLS). Since the phase difference depends on the wavelength of the SWs, we control the wavelength by varying the SW excitation frequency and evaluate the filtering effect. In the presentation, we report the efficiency of the ring-shaped SW filter and provide some key parameters for determining the forbidden frequencies of SWs.

MA 35.15 Thu 16:00 P4

Orientation and Shape of 180° Magnetoelastic Domain Walls in Antiferromagnets — •BENNET KARETTA, OLENA GOMONAY, and JAIRO SINOVA — Institut für Physik, Johannes Gutenberg Universität Mainz, D-55099 Mainz, Germany

Antiferromagnets are potential candidates to be used in the future for active spintronics elements as they are faster and more stable than the ferromagnets in recent devices. However, without a net magnetization it is more difficult to manipulate their magnetic state. Recent studies suggested that the magnetoelastic coupling can be used to overcome this problem. Thus, it is essential to understand the interaction between the strains in the antiferromagnet and the Néel vector. In this study, we investigate the 180° antiferromagnetic domain wall and the influence on it from the strains. It is known that non-180° domain walls have preferred alignments in antiferromagnets since strains in the respective domains are incompatible for certain orientations. We show, that there is a similar anisotropy for the orientation of 180° domain walls, which now is induced by incompatibilities at the domain wall itself. We further investigate this anisotropy to determine how magnetoelasticity affects the shape of the closed 180° domain wall loop in the antiferromagnet. With this, we demonstrate that the shape of the loop significantly changes in comparison to a purely magnetic system and thus verify the strong influence of the magnetoelastic coupling on the equilibrium domain structure.

MA 35.16 Thu 16:00 P4

Current-induced Creation of domain walls in synthetic antiferromagnets — ROBIN MSISKA¹, •OMER FETAI¹, RAPHAEL KROMIN², DAVI RODRIGUES³, and KARIN EVERSCHOR-SITTE^{1,4} — ¹Faculty of Physics, University of Duisburg-Essen, Duisburg, Germany — ²Institute of Physics, Johannes Gutenberg Uni-

versity Mainz, Mainz — ³Politecnico di Bari, Bari, Italy — ⁴Center for Nanoin-
tegration Duisburg- Essen (CENIDE)

Improvements in the storage capacity of modern-day memory devices are slow-
ing down and new concepts for storing data are required. A suggestion for a
three-dimensional data storage is the racetrack memory which stores informa-
tion in terms of magnetic domains. The use of synthetic antiferromagnets (SAF),
i.e., antiferromagnetically coupled ferromagnetic bilayer systems, accelerates the
information access time because the domain walls can be moved up to ten times
faster [1]. To obtain a market-ready device, many challenges must be overcome,
one of which is integrating a controlled domain wall write process into SAFs. We
study the controlled creation of domain walls in SAFs by electrical means. In the
case of spin-transfer torques, we find a critical current strength above which anti-
ferromagnetic domain walls are created from an inhomogeneity. In contrast to
the ferromagnetic case[2] we show that the critical current density is an order of
magnitude higher.

[1] S. Parkin, S.-H. Yang, Nat. Nanotechnol. 10, 195 (2015)

[2] M. Sitte et al. Phys. Rev. B 94, 064422 (2016)

MA 35.17 Thu 16:00 P4

**Magnetization patterns in biaxial Fe₃₂Co₆₈ core-shell nanostructures with
hexagonal cross-section** — •ANASTASHA KORNIENKO¹, ALEXIS WARTELLE²,
MATTHIAS KRONSEDER³, MICHAEL FOERSTER⁴, MIGUEL ÁNGEL NIÑO⁴, SAN-
DRA RUIZ-GOMES⁴, MUHAMMAD WAQAS KHALIQ^{4,5}, and CHRISTIAN H. BACK¹
— ¹Technical Univ. of Munich, Garching, Germany — ²Univ. Grenoble Alpes,
Grenoble, France — ³Univ. of Regensburg, Regensburg, Germany — ⁴Alba
Synchrotron Light Facility, CELLS, Barcelona, Spain — ⁵Univ. of Barcelona,
Barcelona, Spain

We fabricate nanostructures with a Fe₃₂Co₆₈ shell on GaAs nanorods with
hexagonal cross-section. Such a FeCo alloy, deposited on the (110) GaAs planes
(the rod's facets), shows a thickness-dependent spin-reorientation transition [1].
At a thickness of 32 monolayers, we expect our tube walls to feature a biaxial
behavior, with distinct azimuthal components of magnetization. Here we use
Photoemission Electron Microscopy in combination with X-ray Magnetic Cir-
cular Dichroism (XMCD-PEEM) to image the magnetic configuration of indi-
vidual nanostructures [2]. The XMCD-PEEM imaging was done at remanence,
between applications of magnetic fields and for different angles between the x-
rays and the tube axis. Some of our nanostructures feature a large number of
unexpectedly persistent magnetic domains. We observed a switching between
almost longitudinal and azimuthal magnetization for some domains, confirm-
ing system's biaxial behavior.

[1] Muermann et al., J. Appl. Phys., 103, 07B528 (2008).

[2] Wyss et al., PRB 96, 024423 (2017).

MA 35.18 Thu 16:00 P4

Exploring transient ferromagnetism in La_{0.9}Sr_{0.1}MnO₃ thin films — •KAREN
P. STROH, TIM TITZE, HENRIKE PROBST, STEFAN MATHIAS, DANIEL STEIL,
and VASILY MOSHNYAGA — I. Physikalisches Institut, Georg-August-Universität
Göttingen

In perovskite manganites such as La_{1-x}Sr_xMnO₃ (LSMO), complex phase dia-
grams with different magnetic, electric, and structural phases are obtained as a
function of chemical doping. Whilst $x = 0.33$ is referred to as optimal doping,
underdoped LSMO with $x \sim 0.1 - 0.15$ is close to a PM-I/FM-M phase boundary
for $T > T_C$ [1] and thus a suitable candidate for photo-induced transitions. Ultra-
fast laser pulses may photoionize electrons from Mn³⁺ to Mn⁴⁺, establishing a
double exchange interaction and a FM state, so that the compositional phase
boundary might temporarily also be crossed via “optical” doping [2].

Underdoped LSMO/SrTiO₃(100) thin films were epitaxially grown by met-
alorganic aerosol deposition (MAD) and investigated by time-resolved magneto-
optical Kerr effect (MOKE) and pump-probe reflectivity (PPR). Temperature-,
fluence-, and magnetic field-dependent measurements have been performed on
timescales from femtoseconds to nanoseconds using a pulsed fs laser setup. Our
results indicate a possibility to optically drive a paramagnetic-insulating LSMO
into a transient ferromagnetic state above T_C on a sub-ps timescale.

Financial support by the DFG via Project 399572199 and within the SFB 1073
(TP A02) is acknowledged.

[1] Hemberger et al., Physical Review B 66, 094410 (2002)

[2] Matsubara et al., Physical Review Letters 99(20), 207401 (2007)

MA 35.19 Thu 16:00 P4

Influence of metallic substrates on the OISTR effect in permalloy thin films
— •MARTIN ANSTETT¹, SIMON HÄUSER¹, JONAS HOEFER¹, LAURA SCHEUER¹,
PHILIPP PIRRO¹, BURKARD HILLEBRANDS¹, BENJAMIN STADTMÜLLER^{1,2}, and
MARTIN AESCHLIMANN¹ — ¹Department of Physics and Research Center OP-
TIMAS, TU Kaiserslautern, 67663 Kaiserslautern, Germany — ²Institute of
Physics, Johannes Gutenberg University Mainz, 55128 Mainz, Germany

Optical manipulation of magnetic materials on extremely short, sub-100 fs
timescales can be achieved either by generation and injection of optically in-
duced (ballistic) spin currents or by direct excitation of the spin system, for in-
stance by the optically induced spin transfer (OISTR) effect as shown in [1, 2].

In this work, we aim to reveal the mutual interplay of these spin-transfer ef-
fects on ultrafast timescales. Therefore, we investigate the ultrafast demagne-
tization of a thin Fe₂₀Ni₈₀ alloy on a non-magnetic Au substrate and how it is
influenced by the spin-dependent charge transport into the Au substrate. As
an element-resolved probe of the spin dynamics, we employ time-resolved Kerr
spectroscopy with fs-XUV radiation in transversal geometry to disentangle the
spectroscopic signatures of the OISTR and ballistic spin transport in this materi-
al. Our results will be compared to the magnetization dynamics of a Fe₂₀Ni₈₀
film on an insulating substrate.

References: [1] Dewhurst et al.; Nano Lett., 2018; 18: 1842*1848 [2] Hofherr
et al., Sci. Adv., 2020; 6: eaay8717

MA 35.20 Thu 16:00 P4

Ultrafast magnetization dynamics in perovskite manganites — •MAREN
SCHUMACHER, HENRIKE PROBST, MARIANA BREDE, CHRISTINA MÖLLER,
KAREN STROH, TIM TITZE, CINJA SEICK, SABINE STEIL, MARCEL REUTZEL, G.
S. MATTHIJS JANSEN, DANIEL STEIL, VASILY MOSHNYAGA, and STEFAN MATH-
IAS — I. Physikalisches Institut, Göttingen, Germany

Correlated manganese oxides are promising materials to realize new function-
alities in spintronic applications, which are enabled by strong correlations be-
tween electrons, lattice, and spins. Femtosecond time-resolved spectroscopy has
proven to be a powerful probe of these interactions. Here, we study demagne-
tization dynamics in thin-film perovskite manganites using magneto-optical
Kerr spectroscopy (MOKE) in the visible and extreme ultraviolet (XUV) range
of the spectrum. This allows us to study the samples as a function of temper-
ature ($T=10 - 400$ K), magnetic field (up to $B=1$ T), and, in the case of using
XUV probe light, with element-specificity. We will show first results of element-
specific HHG-MOKE data on high-quality manganite thin film of LSMO and
compare it to standard visible-MOKE.

MA 35.21 Thu 16:00 P4

**Wide spectral range ultrafast pump-probe magneto-optical spectrometer at
low temperature, high-magnetic and electric fields** — •FABIAN MERTENS¹,
MARC TERSCHANSKI¹, DAVID MÖNKEBÜSCHER¹, STEFANO PONZONI¹, DAVIDE
BOSSINI^{1,2}, and MIRKO CINCHETTI¹ — ¹Department of Physics, TU Dortmund
University, Otto-Hahn-Straße 4, 44227 Dortmund, Germany — ²Department of
Physics and Center for Applied Photonics, University of Konstanz, Germany.

We developed a table-top setup to perform magneto-optical pump-probe mea-
surements with the possibility to independently tune the photon-energy of both
pump and probe beams in the 0.5 eV - 3.5 eV range[1]. Our apparatus relies on
a commercial turn-key amplified laser system, able to generate light pulses with
duration shorter than or comparable to 100 fs throughout the whole spectral
range. The repetition rate of the source can be modified via the computer in the
1 kHz - 1 MHz range. A commercial balanced detector is connected to a high-
frequency digitizer, allowing for a highly-sensitive detection scheme: rotations
of the probe polarization as small as $70 \mu\text{deg}$ can be measured. Additionally, a
DC magnetic field as high as 9 T and voltages in the kV regime can be applied on
the sample. A cryostat allows us to precisely set the temperature of the sample
in the 4 K - 420 K interval. We test the performance of our setup by measuring
the ultrafast demagnetization of a cobalt crystal as a function of a wide variety
of experimental parameters.

[1] F. Mertens et al., *Review of Scientific Instruments* 91 (2020)

MA 35.22 Thu 16:00 P4

**Integration of a supercontinuum probe line in a setup for time-resolved
magneto-optical spectroscopy** — •SOPHIE BORK, RICHARD LEVEN, MARC TER-
SCHANSKI, FABIAN MERTENS, UMUT PARLAK, and MIRKO CINCHETTI — Depart-
ment of Physics, TU Dortmund University, Otto-Hahn-Straße 4, 44227 Dort-
mund, Germany

We have recently developed a setup for wide spectral range ultrafast pump-probe
magneto-optical spectroscopy at low temperature, high-magnetic and electric
fields [1]. Here we present an upgrade of this setup that allows to measure the
transient reflectivity ($\Delta R/R$) in a broad spectral range and with femtosecond
time-resolution. To this end, we have generated a broadband supercontinuum
(white light) probe beam that covers the wavelengths from the near UV to the
near IR region. The detection of the white light spectrum reflected or transmit-
ted from the sample is achieved by a 1D-array of CMOS detectors that allow for
simultaneous data acquisition of all available wavelengths. This upgraded setup
can work at high repetition rates (< 100 kHz) and allows to perform measure-
ments with high temporal and spectral resolution. This is particularly useful,
for example, to fully map the photo-driven transient evolution of the band gap
energy in magnetically ordered semiconducting systems and to assess whether
it is linked to the magnetization dynamics [2]. In this poster contribution we
will present all technical details of the setup together with first characterization
measurements to specify its performance.

[1] Mertens et al., Rev. Sci. Instrum. 91, 113001 (2020)

[2] Bossini et al., Phys. Rev. B 104, 224424 (2021)

MA 35.23 Thu 16:00 P4

All-optical switching of magnetically hard CoPt and L₁₀-FePt in contact with a Gd-layer — •JOHANNES SEYD¹, JULIAN HINTERMAYR², MANFRED ALBRECHT¹, and BERT KOOPMANS² — ¹Institute of Physics, University of Augsburg, 86159 Augsburg, Germany — ²Department of Applied Physics, Eindhoven University of Technology, 5600 MB Eindhoven, The Netherlands

All-optical switching (AOS) by single femtosecond laser pulses promises to be an ultrafast, energy-efficient alternative to conventional writing in magnetic recording using magnetic fields. L₁₀-FePt is a magnetic material with high perpendicular magnetic anisotropy (PMA), which makes it an interesting candidate for future ultrahigh-density magnetic recording applications, and for which helicity-dependent multi-shot AOS has already been confirmed [1].

Thermally-induced single-shot AOS is not only possible in ferrimagnetic alloys with a compensation temperature near room temperature, but also in synthetic ferrimagnets consisting of a ferromagnetic (multi-) layer in contact with a Gd layer, as shown for Co and Co/Ni [2]. These results suggest the possibility of reproducing the same kind of switching in other magnetic thin films, which in the case of L₁₀-FePt would circumvent the problem of writing the magnetically hard material in magnetic recording applications.

We show the most recent results on the thermally-induced AOS behaviour of thin CoPt and L₁₀-FePt films in contact with a Gd layer.

[1] R. John et al., Scientific Reports 7, 4114 (2017)

[2] M. Beens et al., Physical Review B 100, 220409(R) (2019)

MA 35.24 Thu 16:00 P4

Magnetic field-dependent ultrafast control of an antiferromagnet — •A. ARORA^{1,4}, Y.W. WINDSOR⁶, S.E. LEE¹, J. SARKAR¹, K. KLIEMT³, CH. SCHÜSSLER-LANGEHEINE², N. PONTIUS², C. KRELLNER³, D.V. VYALIKH⁵, and L. RETTIG¹ — ¹FHI der MPG, Berlin — ²HZB für Materialien und Energie GmbH, Berlin — ³Phy. Inst., Goethe-Uni., Frankfurt am Main — ⁴Fach. Phys., FU Berlin — ⁵DIPC, Basque, Spain — ⁶IOAP, TU Berlin

Antiferromagnets, due to their zero net magnetization, offer faster manipulation of spins and more robust devices. But this also makes the interaction with magnetic order challenging. One way to achieve this is to utilize the magnetic anisotropy to manipulate the spin arrangement which we demonstrated recently using ultrafast optical excitation [1]. For practical applications, understanding the interaction of this effect with external magnetic fields is of strong interest. To this end, we perform time-resolved resonant soft X-ray diffraction in the prototypical A-type antiferromagnet GdRh₂Si₂. Consistent with our previous study, we observe a coherent rotation of the antiferromagnetic (AF) arrangement of Gd 4f spins followed by oscillations of the AF order as a consequence of a light-induced change in the anisotropy potential. Surprisingly, upon increasing magnetic field, the frequency of the oscillations as well as the extent of demagnetization upon photoexcitation increases. These observations indicate a change in the magnetic anisotropy potential and may offer a new way towards deterministic control of spin order using combined electromagnetic and magnetic fields. [1] Windsor et al. Commun Phys 3, 139 (2020)

MA 35.25 Thu 16:00 P4

Studying double pulse toggle switching of GdFe — •RAHIL HOSSEINIFAR¹, IVAR KUMBERG¹, SANGEETA THAKUR¹, EVANGELOS GOLIAS¹, SEBASTIEN HADJADJ¹, JENDRIK GÖRDES¹, JORGE TORRES¹, FLORIAN KRONAST², MARIO FIX³, MANFRED ALBRECHT³, and WOLFGANG KUCH¹ — ¹Institut für Experimentalphysik, Freie Universität Berlin, Arnimallee 14, 14195 Berlin, Germany — ²Helmholtz-Zentrum Berlin, Albert-Einstein-Straße 15, 12489 Berlin, Germany — ³Institut für Physik, Universität Augsburg, Universitätsstraße 1, 86159 Augsburg, Germany

Switching of magnetization without the help of a magnetic field by using an ultrafast laser pulse is a popular topic for both applied and fundamental research. We study the effect of double-pulse optical excitation on all-optical toggle switching in Gd₂₆Fe₇₄ ferrimagnetic alloys with perpendicular magnetic anisotropy by X-ray magnetic circular dichroism photoelectron emission microscopy. Varying the temporal separation of the two pulses and their intensities reveals a lowering threshold for toggle switching compared to a single pulse, and the formation of three areas in the footprint of the laser pulses for time delays below 1 ps. First, an area is located at lower fluences that does not switch. The second area is at higher fluences where multi-domain nucleation is observed, and the third area is in between and switches deterministically. The experiment is done starting from either a saturated state or in presence of magnetic domains. In both cases, a deterministically switching area is observed which would be desirable for many applications.

MA 35.26 Thu 16:00 P4

Magneto-optical study of proximity effects at the EuO/Co interface — •DAVID MÖNKEBÜSCHER¹, PAUL ROSENBERGER^{1,2}, DAVIDE BOSSINI^{1,2}, Umut PARLAK¹, MARTINA MÜLLER², and MIRKO CINCHETTI¹ — ¹Department of Physics, TU Dortmund University, Germany — ²Department of Physics, University of Konstanz, Germany

Europium monoxide has shown great potential as a magnetic insulator and was successfully employed in various spintronic applications as a spin filter with nearly

100% spin polarized currents [1]. For the use in practical applications, an increase of its relatively low Curie temperature ($T_C = 69$ K) is necessary. One approach relies on proximity effects, i.e. the coupling with a high T_C ferromagnetic layer [2]. Following this approach, we prepared YSZ/EuO/Co multilayers using molecular beam epitaxy (MBE) [3], and studied them using the magneto-optical setup described in Ref. [4]. First, we measured static hysteresis to gain insight about the nature of the proximity-induced coupling of the two magnetic sublattices. Then we used that the pump-probe experimental scheme to manipulate this coupling by varying the pump laser fluence and the delay between the pump and the probe beam.

[1] T. Santos et al., Phys. Rev B 69, 241202 (2004)

[2] S. Pappas et al. Sci Rep 3, 1333 (2013).

[3] P. Rosenberger et al. Phys. Rev. Mater. 6, 044404 (2022).

[4] F. Mertens et al. Rev. Sci. Instrum. 91, 113001 (2020).

MA 35.27 Thu 16:00 P4

Wavelength-dependent magnetization dynamics in Ni|Au heterostructures

— •STEPHANIE RODEN¹, CHRISTOPHER SEIBEL¹, MARIUS WEBER¹, MARTIN STIEHL¹, SEBASTIAN T. WEBER¹, MARTIN AESCHLIMANN¹, BENJAMIN STADTMÜLLER^{1,2}, HANS CHRISTIAN SCHNEIDER¹, and BAERBEL RETHFELD¹ — ¹Department of Physics and Research Center OPTIMAS, TU Kaiserslautern, Kaiserslautern, Germany — ²Institute of Physics, Johannes Gutenberg University Mainz, Mainz, Germany

For a long time, the ultrafast magnetization dynamics of ferromagnets has predominantly been studied for optical excitation using only one photon energy. However, recent experiments have shown that the dynamics of the demagnetization and remagnetization process can be altered by the wavelength of the exciting laser pulse [1, 2].

In this contribution, we extend the temperature-based μT -model to investigate the ultrafast magnetization dynamics of Ni|Au heterostructures. Our model is based on realistic densities of states of both materials and includes energy and spin transfer at the interface. Thereby, we explicitly consider the wavelength- and layer-dependent absorption profile within multilayer structures. This allows us to show the influence of the wavelength-dependent excitation on the magnetization dynamics [3], which is also affected by the substrate thickness.

References:

[1] V. Cardin et al., Phys. Rev. B 101, 054430 (2020)

[2] U. Bierbrauer et al., JOP: Cond. Mat. 29, 244002 (2017)

[3] C. Seibel et al., arXiv:2112.04780 (2021)

MA 35.28 Thu 16:00 P4

Optical manipulation of the antiferromagnetic order in a Pt/NiO bilayer system by ultrafast energy transfer — •PAUL HERRGEN¹, STEPHAN WUST¹, CHRISTOPHER SEIBEL¹, HENDRIK MEER², CHRISTIN SCHMITT²,

LORENZO BALDRATI², RAFAEL RAMOS³, TAKASHI KIKKAWA⁴, EIJI SAITOH⁴, OLENA GOMONAY², JAIRO SINOVA², YURIY MOKROUSOV², HANS CHRISTIAN SCHNEIDER¹, MATHIAS KLÄU², BAERBEL RETHFELD¹, BENJAMIN STADTMÜLLER^{1,2}, and MARTIN AESCHLIMANN¹ — ¹Department of Physics and Research Center OPTIMAS, Technische Universität Kaiserslautern, 67663 Kaiserslautern, Germany — ²Institute of Physics, Johannes Gutenberg-Universität Mainz, 55128 Mainz, Germany — ³CIQUS, Departamento de Química-Física, Universidade de Santiago de Compostela, Santiago de Compostela, Spain — ⁴Department of Applied Physics, The University of Tokyo, Tokyo 113-8656, Japan

Antiferromagnets are promising materials for future spintronic devices due to their resilience against external magnetic fields and their high frequency magnon modes. Here, we explore the subpicosecond magnetization dynamics of the antiferromagnet NiO after strong optical excitation with fs light pulses. We find a clear reduction of the magnetic order for a Pt/NiO bilayer systems on subpicosecond timescales. Our observations are discussed in the framework of an extended μT model. We conclude that the ultrafast loss of antiferromagnetic order in the Pt/NiO bilayer system is mediated by a highly efficient energy transfer between the hot Pt electrons and the NiO spins.

MA 35.29 Thu 16:00 P4

Spin-transport-driven ultrafast magnetization dynamics in a ferrimagnetic Gd/Fe bilayer — •HUIJUAN XIAO, BO LIU, and MARTIN WEINELT — Fachbereich Physik, Freie Universität Berlin, Arnimallee 14, 14195, Berlin

Laser-induced spin transport has been proven to be a key ingredient in ultrafast spin dynamics, such as femtosecond demagnetization and all-optical switching (AOS). We use time- and spin-resolved photoemission spectroscopy of the gadolinium surface state to study spin dynamics in a ferrimagnetic Gd/Fe bilayer. This prototype system for AOS was epitaxially grown on W(110). Our findings suggest that spin transport between the antiferromagnetically coupled gadolinium and iron layers leads to an ultrafast drop of the spin polarization and an increased exchange splitting at the Gd surface. The Gd surface state shows an ultrafast decrease of the spin polarization by 20% within the first ~ 100 fs and a subsequent slower decrease by about 5% on the picosecond timescale. The increase of the exchange splitting counterbalances the overall demagnetization of

the Gd layer. In contrast, the pure Gd/W(110) film shows a constant spin polarization and a reduced exchange splitting of the surface state upon optical excitation. These findings are corroborated by the transient electron temperature. Our results provide clear evidence that magnetization dynamics in the Gd/Fe bilayer can be driven by spin transport. We see distinct signatures in the spin-dependent electronic structure that allow us to gain microscopic insights into ultrafast spin dynamics (supported by SFB/TRR 227 Ultrafast Spin Dynamics).

MA 35.30 Thu 16:00 P4

Ultrafast demagnetization of 2d ferromagnets — •NELE STETZUHN^{1,2}, FELIX STEINBACH¹, MARTIN BORCHERT¹, ABHIJEET KUMAR², DENIS JAGODKIN², CLEMENS VON KORFF SCHMISING¹, STEFAN EISEBITT¹, and KIRILL BOLOTIN² — ¹Max-Born-Institut, Max-Born-Straße 2 A, 12489 Berlin — ²Fachbereich Physik der Freien Universität Berlin, Arnimallee 14, 14195 Berlin

Two-dimensional ferromagnets are one of the latest additions to the family of 2d materials and offer a new platform to study ultrafast magnetic phenomena. When combining 2d ferromagnets with other 2d materials such as transition metal dicalchogenides (TMDs), the absence of lattice mismatch between layers also makes the resulting heterostructures promising for high-performance spintronic devices. Here, we measure the ultrafast demagnetization of 2d ferromagnets with the structure Fe_xGeTe_2 ($x = 3, 5$) after excitation by a pump laser using time-resolved MOKE. The usually low Curie temperature of Fe_xGeTe_2 ($x = 3, 5$) can be increased above room temperature, e.g. by doping with Ni, allowing us to do element-resolved demagnetization measurements at the free-electron laser facility FERMI. This can give insight into effects such as optical inter-site spin transfer (OISTR) in the material.

MA 35.31 Thu 16:00 P4

Heat capacities and Curie curve in the Stoner and Heisenberg models — •NABIL MAKADIR, STEPHANIE RODEN, SANJAY ASHOK, SEBASTIAN T. WEBER, FELIX DUSABIRANE, H. CHRISTIAN SCHNEIDER, and BAERBEL RETHFELD — Department of Physics and Research Center OPTIMAS, TU Kaiserslautern, Germany

The excitation of a metallic ferromagnet with an ultrashort laser pulse leads to a demagnetization on the femtosecond timescale. The response of the material is governed by macroscopic properties, like the heat capacities and the equilibrium magnetization (Curie curve). They can be calculated for instance with either the Stoner model or the Heisenberg model. The former attributes the change of magnetization to the shifting of the spin-resolved density of states. The latter describes the reduction of the magnetization through collective angular oscillation of the individual magnetic moments.

In this contribution, we derive the temperature-dependent heat capacities and the Curie curves for Nickel. We compare the results of the Stoner and the Heisenberg model and analyze the advantages and drawbacks of both approaches. Finally, we investigate the transition between Stoner and Heisenberg excitations.

MA 35.32 Thu 16:00 P4

Hybrid simulation tracing non-equilibrium spin-dynamics and -transport — •LUKAS JONDA, JOHAN BRIONES, SEBASTIAN T. WEBER, CHRISTOPHER SEIBEL, SANJAY ASHOK, and BAERBEL RETHFELD — Department of Physics and Research Center OPTIMAS, TU Kaiserslautern, Germany

We simulate the complex phenomena arising in a magnetic film after femtosecond laser irradiation with help of a hybrid model. This model consists of a combination of two methods: The μT model [1] and a kinetic Monte Carlo method [2]. The former treats the low-energetic electrons as an ensemble, tracing spin resolved temperatures and chemical potentials, as well as their gradients [3]. The latter traces individual high-energetic non-equilibrium electrons, including spin-dependent scattering processes and spin-flip probabilities. We present first investigations of how non-equilibrium electrons influence the magnetization dynamics for Nickel.

The long-term perspective of this project is to develop a model that can describe both the transport of the electron ensemble and individual high-energetic super-diffusive electrons. This allows to study the different types of non-equilibrium transport and their effects on magnetization dynamics.

[1] B. Y. Mueller and B. Rethfeld, *Phys. Rev. B*, **90**, 144420 (2014).

[2] J. Briones, H.C.Schneider, B.Rethfeld, *J. Phys.*, **6**, 035001 (2022).

[3] S. Ashok et al., *Appl. Phys. Lett.*, **120**, 142402 (2022).

MA 35.33 Thu 16:00 P4

Ultrafast Tunnel Magnetoresistance — •THOMAS JAUK¹, KAZUMA KOMATSU¹, HANA K. HAMPEL¹, JANA KREDL², JAKOB WALOWSKI², FLORIAN LACKNER¹, SANGEETA SHARMA³, MARKUS MÜNZENBERG², and MARTIN SCHULTZE¹ — ¹Institute of Experimental Physics, Graz University of Technology, Graz, Austria — ²Institute of Physics, University of Greifswald, Greifswald, Germany — ³Max Born Institute, Berlin, Germany

Magnetic tunnel junctions (MTJ) have been arousing ongoing interest due to their peculiar spin-transfer mechanism since the discovery of the large tunnel magnetoresistance. However, a complete microscopic understanding of the underlying physics is still lacking. We put the spotlight on the interface between

a MgO-based tunnel barrier and a CoFeB wedge-like electrode in order to disentangle intertwined phenomena which come along with ultrafast demagnetization. By employing circularly-polarized visible light pulses and utilizing magnetic circular dichroism in a two-photon-photoemission (2PPE) experiment we establish a direct route to the buried interface, providing insight into the spatial arrangement and the electronic behaviour of the magnetic pattern near the Fermi level. Beside the typical demagnetization curve we observe a light-induced increase in magnetic moment for specific energy/momentum intervals. Together with DFT calculations we try to shed light on the microscopic processes involved in the ultrafast demagnetization and, especially, emphasize on the peculiarity of MTJs acting as an energy- and spin-filter.

MA 35.34 Thu 16:00 P4

Ferromagnetic resonance study of spin pumping in epitaxial Fe/Rh bilayers — •JONAS WIEMELER, ALI CAN ACTAS, MICHAEL FARLE, and ANNA SEMISALOVA — Faculty of Physics and CENIDE, University of Duisburg-Essen, 47057 Duisburg, Germany

The alloy FeRh has been studied extensively for structural, electrical and magnetic properties. On the other hand spin dynamics in a Fe/Rh thin film bilayer system in detail has not been addressed yet. In this work, 5 nm Fe films capped with Rh of thicknesses (0, 1, 2, 3, 5, 10, 15) nm were grown on GaAs(100) substrates using molecular beam epitaxy (MBE). Ferromagnetic resonance (FMR) experiments at room temperature, utilising both angular X-Band and frequency dependence (1-40GHz), were used to characterise the magneto dynamic properties of these bilayers. The growth characteristics of Rh on a 5 nm substrate Fe layer have been investigated using Auger electron spectroscopy (AES) measurements during the Rh growth. It was found, that Rh grows epitaxially on Fe in a layer-by-layer manner. The thickness dependence of the magnetisations precession damping, measured using FMR, shows an exponential behaviour which was analysed in terms of a spin pumping effect. We found, that the spin pumping efficiency of Rh is comparable to Pt, while the spin flip rate compares to that of Pd.

Funding by DFG Project No. 392402498 (SE 2852/1-1 | AL 618/37-1) and helpful discussion with R. Meckenstock and T. Strusch are acknowledged.

MA 35.35 Thu 16:00 P4

Magnetization dynamics of γ -Fe₂O₃ thin films with reduced effective magnetization — •MONIKA SCHEUFELE^{1,2}, MANUEL MÜLLER^{1,2}, JANINE GÜCKELHORN^{1,2}, LUIS FLACKE^{1,2}, ANDREAS HASLBERGER^{1,2}, MATTHIAS WEILER³, HANS HUEBL^{1,2,4}, STEPHAN GEPRÄGS¹, RUDOLF GROSS^{1,2,4}, and MATTHIAS ALTHAMMER^{1,2} — ¹Walther-Meißner-Institut, Bayerische Akademie der Wissenschaften, Garching, Germany — ²Physik-Department, Technische Universität München, Garching, Germany — ³Fachbereich Physik und Landesforschungszentrum OPTIMAS, Technische Universität Kaiserslautern, Kaiserslautern, Germany — ⁴Munich Center for Quantum Science and Technology (MCQST), München, Germany

Magnetic insulators (MI) are of key importance in the emerging fields of magnonics and spin-caloritronics. In this respect, the room-temperature MI γ -Fe₂O₃ is a promising candidate offering a variety of application perspectives. Here, we report on the static and dynamic magnetic properties of pseudomorphic-grown γ -Fe₂O₃ thin films on MgO (001). We find a strain-induced small effective magnetization M_{eff} , showing a sign change at 200 K. In addition, we also observe the impact of slowly relaxing impurities to the ferromagnetic resonance (FMR) field and the linewidth as a function of temperature. Moreover, above 150 K we detect an increase of the FMR linewidth, which we attribute to valence-exchange damping induced by Fe²⁺-ions in γ -Fe₂O₃ [1].

[1] M. Müller *et al.*, arXiv:2204.11498.

MA 35.36 Thu 16:00 P4

Spin pumping in embedded lateral nanostructures in Fe60Al40 — TANJA STRUSCH¹, RALF MECKENSTOCK¹, RANTEJ BALI², JONATHAN EHRLER², KAY POTZGER², KILIAN LENZ², JÜRGEN LINDNER², MICHAEL FARLE¹, and •ANNA SEMISALOVA¹ — ¹Faculty of Physics and CENIDE, University of Duisburg-Essen, Duisburg, Germany — ²Helmholtz-Zentrum Dresden-Rossendorf, Institute of Ion Beam Physics and Materials Research, Dresden, Germany

The magnetic properties of an Fe60Al40 (FeAl) alloy are tailorable from paramagnetic (PM) to ferromagnetic (FM) state by variation of the structure through ion beam irradiation, making it a promising material for the fabrication of magnetic landscapes and magnonic crystals. Here, we report on ferromagnetic resonance (FMR) detected spin pumping in FeAl/Pd and Py/FeAl bilayers and laterally patterned nanostructures and show that FeAl can be used as spin source and as spin sink. Using FMR, we estimate the spin pumping efficiency and find a spin-mixing conductance of $g_{\text{FeAl}}=2.1(+/-0.2) \text{ nm}^{-2}$ and a spin diffusion length of $\lambda_{\text{FeAl}}=11.9(+/-0.2) \text{ nm}$ for paramagnetic FeAl, and $g_{\text{Pd}}=3.8(+/-0.5) \text{ nm}^{-2}$ and $\lambda_{\text{Pd}}=9.1(+/-2.0) \text{ nm}$ for Pd. Further, we investigate the spin pumping in laterally patterned FeAl nanostructures representing 500 nm wide FM strips separated by PM strips of different width (100-400 nm) produced in a 40 nm thick FeAl film. We find an enhancement of the damping parameter with decreasing width of the PM FeAl areas due to an increase of the number

of FM/PM interfaces. Financial support from DFG is gratefully acknowledged (project No. 392402498 (SE 2852/1-1 | AL 618/37-1)).

MA 35.37 Thu 16:00 P4

Growth optimization of ferromagnetic gadolinium nitride (GdN) thin films for magnon transport phenomena — •RAPHAEL HOEPFL^{1,2}, MANUEL MÜLLER^{1,2}, MATTHIAS OPEL¹, STEPHAN GEPRÄGS¹, HANS HUEBL^{1,2,3}, RUDOLF GROSS^{1,2,3}, and MATTHIAS ALTHAMMER^{1,2} — ¹Walther-Meißner-Institut, Bayerische Akademie der Wissenschaften, Garching, Germany — ²Physik-Department, Technische Universität München, Garching, Germany — ³Munich Center for Quantum Science and Technology (MCQST), München, Germany

Ferromagnetic (FM) semiconductors are of great interest for spintronics devices. Gadolinium nitride (GdN) is one candidate for a semiconducting ferromagnet with a Curie temperature T_C of 65-70 K [1]. In this study, we investigate the static and dynamic properties of FM GdN thin films by SQUID magnetometry and broadband ferromagnetic resonance experiments in a cryogenic environment. In detail, we prepare tantalum nitride (TaN)/GdN/TaN thin films on thermally oxidized Si substrates using DC magnetron sputtering, where the TaN is used as seed and protective top layer. Here, we discuss the impact of the various deposition parameters, such as deposition pressure, temperature, rate and reactive N_2 gas flow on the static and dynamic magnetic properties of GdN.

[1] W. B. Mi *et al.*, *Appl. Phys. Lett.* **102**, 222411 (2013).

MA 35.38 Thu 16:00 P4

Spin polarized band engineering for spin-photocatalyst in ZnO nanowires — HUA SHU HSU¹, JUN-XIAO LIN¹, JUTATHIP THAOMONPUN¹, WEI-JHONG CHEN¹, SHIH JYE SUN², and ZDENEK REMES³ — ¹No. 4-18, Minsheng Road, Pingtung City, 90044, Taiwan (R.O.C.) — ²700, Kaohsiung University Rd., Nanzih District, Kaohsiung 811, Taiwan (R.O.C.) — ³Na Slovance 1999/2, Praha 8, Czech Republic

Transition metal-doped oxides with spin-polarization energy bands have been expected as potential materials for semiconductor spintronics applications. In our work, we found that through surface-doped Co/ZnO nanowires (NWs), the generation of spin-polarized energy bands can be confirmed in the ultraviolet (UV) region by magnetic circular dichroism measurements. Because ZnO itself can be applied in the UV photocatalytic material. Therefore, the magnetic field-enhanced photocurrent and magnetic field-enhanced photocatalytic effect due to modulation of the spin-polarized energy band can be observed. And spin-polarized energy band engineering can be extended to non-magnetic ion-doped ZnO NWs. The realization of these spin photocatalytic effects will also provide new opportunities for the study of spin-polarized energy bands in semiconductors.

MA 35.39 Thu 16:00 P4

Electric transport properties of Ni-Mn-In alloy exposed to external stimuli — •SERGIY KONOPLYUK¹ and ALEXANDR KOLOMIETS² — ¹Institute of magnetism of NASU and MESU, Kyiv, Ukraine — ²Department of Physics, Lviv Polytechnic National University, Lviv, Ukraine

The polycrystalline Ni_{45.4}Mn₄₀In_{14.6} Heusler alloy was studied to find dominant factors affecting its electric transport behavior in austenitic and martensitic phases. Analysis of three main contributions into temperature dependent resistivity has shown that prevalent mechanisms of carrier scattering in the austenitic phase are scattering on structural and magnetic disorders rather than on thermal fluctuations.

In spite of the small transformation volume effect of 0.09 %, application of hydrostatic pressure of 2 GPa results in almost threefold rise in the longitudinal resistivity and twofold rise in the Hall resistivity due to the pressure-induced martensitic transformation. The measurements of the ordinary Hall resistivity have shown that main charge carriers in both phases are holes whose mobility is ten times as high in the austenitic phase as in the martensitic one.

The anomalous Hall resistivity (AHE) of the Ni_{45.4}Mn₄₀In_{14.6} reaches significant magnitude of 20 microOhm*cm in the martensitic phase. Unusual scaling relation between AHE and the longitudinal resistivity is discussed.

MA 35.40 Thu 16:00 P4

Magnetometry of Buried Co-based Nanolayers by Hard X-ray Photoelectron Spectroscopy — •ANDREI GLOSKOVSKI¹, CHRISTOPH SCHLUETER¹, and GERHARD FECHER² — ¹Photon Science / DESY, Hamburg — ²Max Planck Institute for Chemical Physics of Solids, Dresden

The intensity and shape of photoelectron lines of magnetic materials depend on the relative orientation of the sample magnetization, the X-ray beam polarization and the spectrometer axis, i.e. the electron emission direction. In the hard X-ray regime, the beam polarization can be conveniently modified utilizing the phase shift produced by a diamond phase plate in the vicinity of a Laue or Bragg reflection. A single-stage in-vacuum phase retarder is installed and commissioned in 2020 at the HAXPES beamline P22 at PETRA III (Hamburg) [1].

The electronic and magnetic properties of CoFe and Co-based Heusler nanolayers were studied using the linear and circular magnetic dichroism in the angular distribution of photoelectrons. The layers were remanently magnetized in-situ and Co 2p_{1/2} and 2p_{3/2} core levels were probed at room temperature [2-

3]. Both the polarization-dependent spectra and the dichroism indicate that the lines of the multiplet extend over the entire spectral range. In particular, the dichroism does not vanish between the two main parts of the spin-orbit doublet.

References [1] C. Schlueter *et al.*, AIP conference proceedings 2054(1), 040010 (2019). [2] G.H. Fecher *et al.*, *SPIN* **04**, 1440017 (2014). [3] P. Swekis *et al.*, *Nano-materials* **11**, 251 (2021).

MA 35.41 Thu 16:00 P4

Ultrafast optical Spectroscopy of LaMnO₃/SrMnO₃ Superlattices — •TIM TITZE, LEONARD SCHUELER, JANNIK BRUMM, VITALY BRUCHMANN-BAMBERG, VASILY MOSHNYAGA, DANIEL STEIL, and STEFAN MATHIAS — I. Physikalisches Institut, Goettingen, Germany

We investigate photoinduced dynamics of a LaMnO₃/SrMnO₃ superlattice, using transient reflectivity $\Delta R/R$ at various temperatures. The superlattice exhibits a low- T_C ferromagnetic (FM) phase below $T_{C,LMO} = 200$ K with a bulk-LMO-like behavior. Further, Keunecke *et al.* reported on a high- T_C interfacial quasi-2D FM phase below $T_{C,2D} = 350$ K that results from an LMO to SMO charge transfer during sample growth [1].

By studying the system response on timescales from fs to ns we aim to determine whether the 2D interfacial phase shows a distinctly different response to an ultrafast optical stimulus than the bulk FM phase. We find that on the sub-ps timescale the T-dependent dynamics mimic the static M(T)-curve, i.e., both ferromagnetic phases seem to contribute to the ultrafast system response. On the 100 ps timescale spin-phonon coupling leads to an additional component in $\Delta R/R$ within the bulk FM phase, which is not observed for the high- T_C quasi-2D FM phase. An additional signature in the T-dependent relaxation time on a ns timescale around 300 K is tentatively attributed to the vanishing of the 2D FM phase already below its $T_{C,2D}$ due to optical excitation.

Financial support by the DFG within the CRC 1073 is acknowledged.

Ref.: [1] M. Keunecke *et al.*, doi: 10.1002/adfm.201808270

MA 35.42 Thu 16:00 P4

Frustrated triangular magnetism in new copper based single crystals. — •ASWATHI MANNATHANATH CHAKKINGAL¹, CHLOE FULLER², DMITRY CHERNYSHOV², MAXIM AVDEEV³, MAREIN CHRISTOPHER RAHN¹, FALK PABST⁴, YIRAN WANG⁴, DARREN PEETS¹, and DMYTRO INOSOV¹ — ¹IFMP, TU Dresden, Germany — ²ESRF, Grenoble, France — ³ANSTO, Sydney, Australia — ⁴Professur f. Anorganische Chemie II, TU Dresden, Germany

The hydrothermal technique is an efficient strategy to synthesize mineralogically inspired structures, including natural and synthetic cuprate minerals with a variety of exciting frustrated magnetic lattices. We report the hydrothermal synthesis of single crystals of a new material Cu₄(SO₄)(OH)₆. Single-crystal x-ray and neutron diffraction studies performed to determine the crystal structure reveal the presence of three copper layers which stack in an ABACABAC pattern in the crystal, which results in a large *b* lattice constant of 25Å. Seemingly-distorted and -expanded SO₄²⁻ tetrahedra in the system are likely attributable to vacancies and structural disorder. The Cu²⁺ copper ions are arranged in buckled sheets consisting of ribbons of edge-sharing and corner-sharing octahedra, and form a heavily distorted triangular lattice. Diffuse scattering measured with synchrotron x-rays also reveals strong stacking-fault disorder in this system. We report details of the crystal structure and its low temperature magnetic properties.

MA 35.43 Thu 16:00 P4

High-pressure crystal growth and the magnetic phase diagram of hexagonal GdInO₃ — •NING YUAN, AHMED ELGHANDOUR, LUKAS GRIES, WALDEMAR HERGETT, and RÜDIGER KLINGELER — Kirchhoff Institute for Physics, Heidelberg University, Germany

GdInO₃ is hexagonal structured system which exhibits strong geometrical frustration and improper geometric ferroelectricity [1,2]. We report the growth of macroscopic GdInO₃ single crystals which are used to study magnetization, specific heat, and thermal expansion in magnetic field up to 16 T. The data are used to construct the magnetic phase diagram. Anomalies in the specific heat confirm the evolution of long-range magnetic order at $T_N = 2.1$ K. At the antiferromagnetic phase boundary, anomalies in thermal expansion and magnetostriction imply significant spin-lattice coupling. A modest net magnetic moment points along the crystallographic *c* axis in the ground state. The magnetic phase diagrams for B||*c* and B||*ab* are presented for temperatures down to 400 mK and magnetic fields up to 14 T. Isothermal magnetization curves indicate a narrow 1/3 magnetization plateau as well as a sharp anomaly at about 5 T.

[1] Y. Li *et al.*, *J. Mater. Chem. C* **6**, 7024 (2018).

[2] X. Q. Yin *et al.*, *Phys. Rev. B* **104**, 134432 (2021).

MA 35.44 Thu 16:00 P4

Spin Excitations, Accidental Soft Modes, and Phase Diagram of the Triangular-Lattice $t-t'-U$ Hubbard Model — •JOSEF WILLSHER¹, HUI-KE JIN¹, and JOHANNES KNOLLE^{1,2,3} — ¹TUM, Munich, Germany — ²MCQST, Munich, Germany — ³Imperial College London, London, UK

The structure factor is an important probe of quantum magnets but due to numerical limitations it remains a challenge to make theoretical predictions beyond linear spin wave calculations of Heisenberg-like models. In this work we

study the excitation spectrum of the triangular lattice Hubbard model including next-nearest neighbour hopping within a self-consistent random phase approximation. Starting from the 120-degree and stripe magnetic orders we compute the relevant magnon spectra and discuss connections to recent experiments on triangular lattice compounds. In addition, we show that the condensation of accidental soft-modes allows us to construct the phase diagram of the model, which is consistent with previous results of the variational cluster approximation. We discuss the implications of our findings for unconventional magnon spectra and even for the presence of quantum disordered phases without long range order.

MA 35.45 Thu 16:00 P4

Exchange Enhancement of Ferromagnetic Resonance in Mn₂Au/Py — •TOBIAS WAGNER and OLENA GOMONAY — Johannes Gutenberg-University Mainz, Germany

In the future, AFMs as active components will bring favourable advantages to spintronics: Robustness to external magnetic fields, temperature stability of the Néel ordered state and lack of stray fields. Therefore, AFMs are suitable for ultrafast and ultra high density spintronics. Recently, strong exchange coupling between Mn₂Au and thin layers of Permalloy (Ni₈₀Fe₂₀) has been shown [1]. As a consequence, the coercive field of Mn₂Au/Py was reported to be 5000 Oe, which is high compared to 200 Oe in CuMnAs/Fe [1]. High coercive fields lead to long term stability at room temperature. Due to strong exchange coupling, the AFM Néel vector and the FM magnetisation rotate coherently, when an external field is applied to the FM. Ferromagnetic resonance spectroscopy revealed two distinct frequencies for the coupled bilayer system, both of which lie above the resonance frequency of Permalloy. We model these findings using a phenomenological model. Our model enables us to demonstrate how the interfacial exchange coupling enables tuning of the ferromagnetic resonance frequency by variation of the thickness of the ferromagnetic layer.

References: [1] Bommanaboyena, S. P. et al., Nat. Comm. 12, 6539 (2021), [2] Al-Hamdo, H. et al., to be released (2022)

MA 35.46 Thu 16:00 P4

Voltage induced magneto-ionic interactions controlling magnetic properties of synthetic antiferromagnets — •MARIA-ANDROMACHI SYSKAKI^{1,2}, TAKAOKI DOHI², JÜRGEN LANGER¹, MATHIAS KLÄUI², and GERHARD JAKOB² — ¹Singulus Technologies AG, 63796 Kahl am Main, Germany — ²Institut für Physik, Johannes Gutenberg-Universität Mainz, Staudingerweg 7, 55128 Mainz, Germany Voltage control of magnetic properties in spintronic devices is one of the most promising device-compatible and energy-efficient ways for future storage applications [1]. This approach can be ideally realized with the advantages of a synthetic antiferromagnet (SAF) system, which provides higher thermal stability and a wide dynamic range, e.g. high domain wall velocities for nearly compensated SAFs [2] when integrated into MRAM devices. In our work, we have grown a SAF stack by magnetron sputtering consisting of two ferromagnetic layers coupled by a non-magnetic spacer layer. A thermodynamically stable skyrmion state at elevated temperatures is achievable in this stack [3]. With room temperature voltage-controlled magneto-ionic effects, we focus on the modulation of the magnetic properties in this system, i.e., the voltage control of the compensation ratio between the layers, the perpendicular magnetic anisotropy, and the antiferromagnetic RKKY coupling strength. [1] T. Nozaki et al., Micromachines 10(5), 327 (2019). [2] Y. Guan et al., Nat. Commun. 12, 5002 (2021). [3] T. Dohi, et al., Nat. Commun 10, 5153 (2019).

MA 35.47 Thu 16:00 P4

Micromagnetic simulation of magnetic reversal processes in exchange biased micro stripes — •LUKAS PAETZOLD, SAPIDA AKHUNDZADA, CHRISTIAN JANZEN, MICHAEL VOGEL, and ARNO EHRESMANN — Institute of Physics and Center for Interdisciplinary Nanostructure Science and Technology (CINSaT), University of Kassel, Heinrich-Plett-Strasse 40, 34132 Kassel, Germany

Exchange bias, being first observed by Meiklejohn and Bean [1] and described as a unidirectional anisotropy, is a well-known interface effect between antiferromagnetic and ferromagnetic thin films. Initiated by field cooling [1], sputter deposition [2], or light-ion bombardment [3] the effect appears as a shift of the hysteresis loop and increased coercive fields [4]. Micromagnetic simulations [5,6] are presented for investigating the magnetic reversal processes in exchange biased micro stripes with a polycrystalline uncompensated antiferromagnetic layer. Special focus is put on the nucleation processes occurring in the microscopic range depending on the stripe width.

- [1] W. H. Meiklejohn et al., Phys. Rev. 105, 904 (1956)
- [2] A. E. Berkowitz et al., J. Magn. Magn. Mater. 200, 552-570 (1999)
- [3] D. Engel et al., J. Magn. Magn. Mater. 293, 849-853 (2005)
- [4] J. Nogués et al., J. Magn. Magn. Mater. 192(2), 203-232 (1999)
- [5] A. Vansteenkiste et al., AIP Advances 4, 107133 (2014)
- [6] J. De Clercq et al., J. Phys. D: Appl. Phys. 49, 435001 (2016)

MA 35.48 Thu 16:00 P4

Exchange-spring behavior at magnetic perovskite oxide interfaces —

•ANTONIA RIECHE, MARTIN MICHAEL KOCH, MICHAEL ENDERS, AURORA DIANA RATA, and KATHRIN DÖRR — Martin-Luther-Universität Halle-Wittenberg Advances in ultrathin film deposition allow the investigation of exceptional properties at interfaces which significantly differ from those of bulk materials. A particular kind of interface coupling between magnets is the exchange spring, whose magnetic switching is distinctly different from that of exchange-bias coupling. To explore exchange springs in oxides, high quality SrRuO₃/La_{0.7}Sr_{0.3}MnO₃ (SRO/LSMO) and La_{0.7}Sr_{0.3}CoO₃ (LSCO/LSMO) bilayers were grown by pulsed laser deposition on different substrates with systematically varied layer thicknesses. Strong antiferromagnetic Mn-O-Ru or ferromagnetic Mn-O-Co exchange coupling connects the magnetic moments at the interface. An exchange spring resembling a Bloch wall is formed in the hard magnet due to a striking reduction of the magnetocrystalline anisotropy near the interface and return to bulk behavior further away from the interface. The thickness-dependent switching is analyzed to derive the exchange and anisotropy energies of the spring, its length and field-temperature „phase diagram“. We discuss the impact of such interfacial spin textures on magnetic switching as well as on further properties which are important for spintronics applications.

MA 35.49 Thu 16:00 P4

Effect of laser annealing on the magnetic properties of Co/Pt based multilayers — •LOKESH RASABATHINA¹, APOORVA SHARMA¹, SANDRA BUSSE³,

BENNY BÖHM¹, FABIAN SAMAD^{1,2}, GEORGETA SALVAN¹, ALEXANDER HORN³, and OLAV HELLWIG^{1,2,4} — ¹Institute of Physics, Chemnitz University of Technology, 09107 Chemnitz, Germany — ²Institute of Ion Beam Physics and Materials Research, Helmholtz-Zentrum Dresden-Rossendorf, Bautzner Landstraße 400, 01328 Dresden, Germany — ³Laserinstitut Hochschule Mittweida, Schillerstraße 10, 09648 Mittweida, Germany — ⁴Center for Materials, Architectures and Integration of Nanomembranes (MAIN), Chemnitz University of Technology, 09107 Chemnitz, Germany

Two modes of laser annealing, namely, Continuous Wave (CW) and Pulsed Wave (PW) mode, are used for modifying the magnetic properties of perpendicular magnetic anisotropy (PMA) multilayers in a controlled manner. For this we compare two types of samples - a PMA (Co/Pt)₁₀ multilayer and an antiferromagnetically interlayer exchange coupled PMA (Co/Pt)₂/Co/Ir/(Co/Pt)₅ multilayer. Room temperature hysteresis loops using polar MOKE magnetometry are measured for the different laser annealing modes. Thus, a relationship between the applied laser parameters and the magnetic properties is extracted, which provides an opportunity to alter magnetic properties of PMA multilayer systems locally with high spatial resolution on demand.

MA 35.50 Thu 16:00 P4

Anisotropic spin dynamics in Mn₂Au/Ni₈₀Fe₂₀ thin-film bilayers —

•GUTENBERG KENDZO¹, HASSAN AL-HAMDO¹, VITALIY VASYUCHKA¹, PHILIPP PIRRO¹, YARYNA LYTUVYENKO², OLENA GOMONAY², MATHIAS KLÄUI², MARTIN JOURDAN², and MATHIAS WEILER¹ — ¹Fachbereich Physik and Landesforschungszentrum OPTIMAS, Technische Universität Kaiserslautern, Kaiserslautern, Germany — ²Institut für Physik, Johannes Gutenberg-Universität Mainz, Mainz, Germany

Ferromagnets and antiferromagnets host qualitatively different spin dynamics. At the ferromagnet/antiferromagnet interface we thus expect coupled spin dynamics of hybrid character. We experimentally investigate the anisotropic coupling of spin dynamics in antiferromagnetic/ferromagnetic (Mn₂Au/Ni₈₀Fe₂₀) thin-film heterostructures by ferromagnetic resonance spectroscopy. To this end, we carried out measurements on two samples Mn₂Au(40nm)/Ni₈₀Fe₂₀(10nm; 7,5nm) as a function of the orientation of the static external magnetic field. For each orientation, the ferromagnetic resonance frequency at fixed magnetic field magnitude was measured. We find a pronounced anisotropy of the Ni₈₀Fe₂₀ ferromagnetic resonance. This finding is attributed to coupling of the Ni₈₀Fe₂₀ magnetization to the Mn₂Au Néel vector in conjunction with the Mn₂Au crystalline anisotropy. Funding by DFG via CRC/TRR 173 "Spin+X", projects A01, A05, B12 & B13 is gratefully acknowledged.

[1] S. P. Bommanaboyena et al., Nat. Commun. 12, 6539 (2021).

MA 35.51 Thu 16:00 P4

Magnetic Anisotropies and Large Exchange Bias of Ultrathin Ni_{0.95}Fe_{0.05}/NiFeO Multilayers —

DIMITRIOS ANYFANTIS¹, CAMILLO BALLANI², NIKOLAOS KANISTRAS², ALEXANDROS BARNASAS¹, GEORG SCHMIDT², •EVANGELOS TH. PAPAIOANNOU², and PANAGIOTIS POULOPOULOS¹ — ¹Department of Materials Science, University of Patras, 26504 Rio, Patras, Greece — ²Institute of Physics, Martin-Luther University Halle-Wittenberg, 06120 Halle, Germany

Magnetic anisotropy at metal/oxide interfaces has played a significant role in the development of technological applications in recording, spintronics, sensors and actuators over the years[1]. In this work we present a novel method to produce

high quality Ni(0.95)Fe(0.1)/NiFeO multilayers with the aid of the natural oxidation procedure and with the help of a single magnetron sputtering head [2]. Doping of Ni by only 5% Fe results in enhanced layering quality as X-ray reflectivity reveals. Due to magnetostatic anisotropy, the multilayers were found to be in-plane magnetized. Mild thermal annealing ($T = 525$ K) results in the enhancement of perpendicular magnetic anisotropy, mainly due to an increase in the uniaxial volume anisotropy term. Temperature-dependent hysteresis measurements between 4–400 K revealed considerable enhancement of coercivity and appearance of strong exchange bias effect.

[1] Dieny, B.; Chshiev, M., *Rev. Mod. Phys.* 2017, 89, 025008. [2] D. Anyfantis et al., *Coatings* 2022, 12, 627.

MA 35.52 Thu 16:00 P4

Additive Manufacturing of (Pr,Nd)-Fe-Cu-B Permanent Magnets using functionalized microparticles — •JIANING LIU¹, LUKAS SCHÄFER¹, HOLGER MERSCHROTH², JANA HARBIG², YING YANG³, ANNA ZIEFUS³, MATTHIAS WEIGOLD², STEPHAN BARCIKOWSKI³, OLIVER GUTFLEISCH¹, and KONSTANTIN SKOKOV¹ — ¹Functional Materials, Technical University of Darmstadt, Germany — ²Alarich-Weiss-Str. 16 — ³Technical Chemistry I, University of Duisburg-Essen, Germany

Additive Manufacturing (AM) of permanent magnets is an upcoming and challenging task in material science and engineering. A microstructure with engineered grain boundaries and grain sizes necessary for high coercivity is not easily obtainable, especially when using Laser Powder Bed Fusion (L-PBF) to obtain fully dense magnets. In order to achieve the desired microstructure and hard magnetic properties after printing, we proposed Pr-Fe-Cu-B based alloy as a useful alloy system and compare this with its Nd-based counterpart. Our studies describe the Pr-Fe-Cu-B alloys and their annealing optimization for L-PBF. In order to achieve an improved flowability and refined microstructure, the grain boundary engineering with nanoparticles shows great potential. The nanoparticle functionalized Pr-Fe-Cu-B powder was being validated as a precursor for AM. During L-PBF, the hypothesis of heterogeneous nucleation induced by NP inoculums during resolidification is explored with the goal of grain refinement and realizing more uniaxial growth. We acknowledge the support of the Collaborative Research Centre/Transregio 270 HoMMage.

MA 35.53 Thu 16:00 P4

In-situ rotation of sample in the magnet with a rotator — •M. SAFIRI, P. Y. PORTNICHENKO, M. SIEGEL, and D. S. INOSOV — TU Dresden, Germany

Field-induced collective excitations in f-electron systems with multipolar order parameters were recently shown to exhibit significant anisotropy in field space even in structurally cubic systems, such as CeB₆ [P. Y. Portnichenko et al., *Phys. Rev. X* 10, 021010 (2020)]. However, following such changes in the excitation spectrum in a neutron scattering experiment currently requires a tedious and time-consuming sample realignment for every field direction. To enable a much faster in-situ rotation of the sample inside a cryomagnet, we have designed and manufactured a compact piezo-driven rotator with a diameter of 32 mm that is compatible with cryomagnets used on the time-of-flight or triple-axis neutron spectrometers, up the maximum field of 10 T. This new piece of sample environment will allow us to change the sample orientation within 360° by rotating it precisely around the momentum transfer **Q** at low temperatures, which corresponds to a rotation of magnetic field in the vertical plane orthogonal to **Q**. This is supposed to add a new dimension to neutron-spectroscopy measurements, facilitating continuous scans vs. magnetic field angle that contain crucial information about magnetic anisotropy and other spin-orbit coupling effects.

MA 35.54 Thu 16:00 P4

MIASANS at the longitudinal neutron resonant spin echo spectrometer RESEDA — •JONATHAN LEINER^{1,2}, CHRISTIAN FRANZ^{1,2,3}, JOHANNA JOCHUM^{1,2}, and CHRISTIAN PFLEIDERER¹ — ¹Technical University of Munich, Garching, Germany — ²Heinz Maier-Leibnitz Zentrum (MLZ), Garching, Germany — ³JCNS at MLZ, FZ Jülich GmbH, Garching, Germany

The RESEDA (Resonant Spin-Echo for Diverse Applications) instrument has been optimized for neutron scattering measurements of quasi-elastic and inelastic processes over a wide parameter range. One spectrometer arm of RESEDA is configured for the MIEZE (Modulation of Intensity with Zero Effort) technique, where the measured signal is an oscillation in neutron intensity over time prepared by two precisely tuned radio-frequency (RF) flippers. With MIEZE, all of the spin-manipulations are performed before the beam reaches the sample, and thus the signal from sample scattering is not disrupted by any depolarizing conditions there (i.e. magnetic materials and fields). The MIEZE spectrometer is being further optimized for the requirements of small-angle neutron scattering (MIASANS), a versatile combination of the spatial and dynamical resolving power of both techniques. We present the current status of (i) newly installed superconducting solenoids as part of the RF flippers to significantly extend the dynamic range and (ii) development and installation of a new detector on a translation stage within a new larger SANS-type vacuum vessel for flexibility with angular coverage and resolution.

MA 35.55 Thu 16:00 P4

An Efficient Magnetic Hyperthermia Setup for Controlled Nanoparticle Heating — •DANIEL KUCKLA, JULIA-SARITA BRAND, VINZENZ JÜTTNER, and CORNELIA MONZEL — Heinrich-Heine-University, Düsseldorf, Germany

Magnetic hyperthermia is a promising approach to enable a remote and localized heating of magnetic nanoparticles (MNPs) with various applications in condensed matter or biomedical physics. The MNPs may be positioned precisely in space and act as hot spots by increasing the temperature in the nanometer vicinity of the particle while causing minimal effects on the macroscopic environment. The heat dissipation arises from energy delivered to the nanoparticle in the form of an alternating magnetic field with ~100kHz frequency and 50mT magnetic flux density. A particular challenge is to realize an efficient magnetic hyperthermia setup and to image the localized heating. Here, we present such setup consisting of an electromagnet in a resonance circuit and exhibiting a small form factor to be implemented under a microscope. We provide a profound characterization of the different components of this setup - the electromagnet and electric circuit, essential improvements to reduce power loss arising from electromagnetic induction as well as strategies to directly record thermal changes. We demonstrate efficient heating/cooling cycles using well-defined MNP samples in suspension and create MNP lithographically structured substrates. Our setup may be used to create localized hot spots in condensed matter samples, to create thermofunctional switches or to study heat-sensitive molecules in biophysics, among other examples.

MA 35.56 Thu 16:00 P4

Investigation of de Haas-van Alphen oscillations under temperature modulation in Bi — •MICHELLE HOLLRICHER, CHRISTIAN PFLEIDERER, and MARC A. WILDE — Physik-Department, Technical University of Munich, D-85748 Garching, Germany

The properties of Bi have become the drosophila of studies of the electronic structure and the Fermi surface of metals [1-4]. An inherent constraint of present-day detection techniques of quantum oscillations concerns the separation of signal components associated with large differences of the effective charge carrier masses. We report the development of a detection technique for measurements of the de Haas-van Alphen (dHvA) effect by means of an inductive signal pickup that is driven by temperature oscillations of the sample [1]. Resulting in an effective convolution of the oscillatory signal components with the derivative of the effective charge carrier mass with respect to temperature, our setup permits to discriminate elegantly light from heavy masses, and allows in-situ determination of the charge carrier effective masses. We have revisited the dHvA effect in Bi, focusing on the nature and character of the electron pockets.

[1] D. Shoenberg, *Magnetic oscillations in metals*, Cambridge Monographs in Physics.

[2] V.S. Edel'man, *Adv. Phys.* **25**, 555 (1976).

[3] K. Behnia *et al.*, *Science* **317**, 1729 (2007).

[4] Z. Zhu *et al.*, *J. Phys.: Condens. Matter* **309**, 313001 (2018).

MA 35.57 Thu 16:00 P4

Visualization of Exchange Spin Coupling Constants — •LAWRENCE RYBAKOWSKI^{1,2}, TORBEN STEENBOCK², and CARMEN HERRMANN¹ — ¹Institut für Inorganische und Angewandte Chemie, Luruper Chaussee 149, Hamburg, Germany — ²Institut für Physikalische Chemie, Luruper Chaussee 149, Hamburg, Germany

Most current methods for calculating the magnetic exchange interactions can calculate coupling constants for two and multi-spin systems, but a single number, the exchange spin coupling constant, is often poorly informative about the origins of the coupling. With our method, footing on nonrelativistic first-principle electronic structure calculations, the coupling constant can be decomposed into atomic and basis function contributions, which allows to plot a three-dimensional density distribution of the coupling constant weighted by the atomic orbital basis contributions and thus to analyze the influences of ligands and coordinations on the coupling behavior of different magnetic ions. In addition, exchange-correlation functional dependencies and influences of structure distortions on the strength and character of the exchange coupling constant can be investigated.

We can show that in complex compounds with competing exchange pathways, individual ligand classes can be associated with characteristic contributions to the total coupling constant. Furthermore, the inclusion and enhancement of exact exchange in the exchange-correlation functional induces an alternating contribution of neighboring atomic orbitals, having a direct impact on the calculated exchange coupling constants.

MA 35.58 Thu 16:00 P4

A Sacrificial Magnet System for Flux Dependent Surface Science Studies — •DANYANG LIU¹, JENS OPLIGER¹, ALEŠ CAHLÍK¹, CATHERINE WITTEVEEN^{1,2}, FABIAN O. VON ROHR², and FABIAN DONAT NATTERER¹ — ¹Department of Physics, University of Zurich, Winterthurerstrasse 190, CH-8057 Zurich, Switzerland — ²Department of Quantum Matter Physics, University of Geneva, 24 Quai Ernest-Ansermet, CH-1211 Geneva, Switzerland

Here we describe the design and characterization of a NbFeB permanent magnet system that can be retrofitted to the sample holders of existing STM. Our design produces a magnetic field of up to 400 mT that is compatible with high temperature sample cleaning routines above the Curie point of the magnet frequently used in UHV experiments. We characterize the flux density using superconducting vortices in NbSe₂ and BSCCO and demonstrate the life-cycle of the magnet from sample preparation to characterization. Our magnet is an accessible way to flux-dependent surface science, ranging from vortices in high-temperature superconductors to STM-enabled electron spin resonance.

MA 35.59 Thu 16:00 P4

DC-Mode Background Subtraction for the MPMS3 SQUID Magnetometer by Quantum Design — •BÖRGE MEHLHORN¹, ANJA WOLTER¹, and BERND BÜCHNER^{1,2} — ¹Leibniz IFW Dresden, D-01069 Dresden, Germany — ²Institute for Solid State and Materials Physics and Würzburg-Dresden Cluster of Excellence ct.qmat, TU Dresden, D-01062 Dresden, Germany

Due to vibrating-sample SQUID magnetometry becoming more common in magnetization studies, the software satisfying the needs of slow linear DC mode became rather sparse. As one example raw-voltage background subtraction software is no longer supplied with the instruments, but is needed, whenever the background signal becomes large compared to the intrinsic magnetization signal of the sample.

As a response a handful of scientists began developing their own solutions. Most commonly known is the open source software published by M. J. Coak et al.¹ at the universities of Warwick and Cambridge free for academic use and based on *MathWorks MATLAB*.

The solution presented here is an independent work published as free (as in freedom) open source software. It is founded on the ecosystem of scientific software in the Python programming language. Therefore, it does not only allow frictionless future contributions by the scientific community, but also makes use of the countless human hours invested in that open source ecosystem in the past.

As an interesting scientific example the software will be demonstrated on a low-moment small-size 2D van-der-Waals crystal mounted on a horizontal rotator.

MA 35.60 Thu 16:00 P4

Mössbauer study of anisotropic magnetic nanoparticle systems — •JURI KOPP¹, JOACHIM LANDERS¹, SOMA SALAMON¹, ROBERT MÜLLER², SARAH ESSIG³, SILKE BEHRENS³, and HEIKO WENDE¹ — ¹Faculty of Physics and Center for Nanointegration Duisburg-Essen (CENIDE), University of Duisburg-Essen — ²Leibniz Institute of Photonic Technology — ³Institute of Catalysis Research and Technology (IKFT), Karlsruhe Institute of Technology

Liquid crystalline (LC) systems have a wide range of applications as they combine the properties of a liquid and orientability in electric fields. In turn, if magnetic nanoparticles are added to such systems, we obtain magneto-responsive liquid crystals. Barium ferrite particles can be considered as possible candidates for use in such magneto-responsive LC systems. Accordingly, this work is geared towards the study of doped and undoped anisotropic barium ferrite nanoparticles using magnetic field and temperature dependent Mössbauer spectroscopy. In pure barium ferrite samples, the five different sublattice positions could be resolved and reorientation in magnetic fields was observed. In the doped samples an asymmetry in the Mössbauer lines as well as partial overlap of the individual sublattices' contributions was visible, which points towards altered environments of the iron atoms. In particular, the 2b site with its relatively high quadrupole level shift provides information about the magnetic orientation relative to the crystal structure. These results enable us to analyze orientation phenomena in future barium ferrite based magnetic liquid crystalline systems.

MA 35.61 Thu 16:00 P4

Fe₃N nanoparticles as alternative material for magnetic fluid hyperthermia — •YEVHEN ABLETS, IMANTS DIRBA, and OLIVER GUTFLEISCH — Technical University of Darmstadt, Darmstadt, Germany

Magnetic fluid hyperthermia (MFH) is one of the modern individual and adjuvant methods for cancer treatment. Usually, iron oxide nanoparticles (IONP) are used for this purpose due to their chemical stability, non-toxicity, well-established and cost-effective production, well-known metabolism of iron in the human body. However, the heating performance of IONP is limited due to moderate values of saturation magnetization and magnetocrystalline anisotropy. Using particles with enhanced magnetic properties will enable more effective tumor treatment, and within AC magnetic field amplitude (H) and frequency (f) conditions of the so-called Brezovich-Atkinson criteria ($H \cdot f = 5 \times 10^8$ A/m²s), which leads to less discomfort for the patients.

In this work, a new synthesis method of crystalline Fe₃N nanoparticles is demonstrated. Metal-organic compound iron pentacarbonyl is thermally decomposed in the presence of polyisobutylene succinimide under continuous ammonia flow. Varying gas flow concentrations and type of surfactant (oleic acid, oleylamine) Fe₃O₄ and Fe homogeneous spherical particles were obtained with an average diameter of 14 nm. Fe₃N particles show better magnetic properties and heating performance than Fe₃O₄ and better chemical stability compared to Fe particles. First stage biocompatible studies are ongoing.

MA 35.62 Thu 16:00 P4

Origin of magnetic loss and noise in magnetoelastic magnetic field sensors — •ELIZAVETA GOLUBEVA¹, BENJAMIN SPETZLER², FRANZ FAUPEL¹, and JEFFREY McCORD¹ — ¹Kiel University, Kiel, Germany — ²Technical University Ilmenau, Ilmenau, Germany

Magnetoelastic magnetic field sensors based on the delta-E effect have proven their high potential for detecting small-amplitude and low-frequency magnetic fields. The concept of such sensors evolves from the dependency of the stiffness tensor on the applied magnetic field and can be utilized in various device configurations, including surface acoustic wave sensors and composite cantilevers. Previous research has shown that the main factor limiting the performance of such sensors comes from the sensor's intrinsic noise. However, the challenge of quantifying different noise sources has not been resolved yet. In this work, we suggest a general methodology for estimating the magnetic noise in magnetoelastic delta-E-effect sensors. Here, we present a complete physical device model and experimental analysis at the example of a millimeter-sized cantilever sensor. In this case, the magnetic noise associated with the hysteresis loss dominates the sensor performance and determines a minimal detectable field for the sensor of about 300 pT/Hz^{1/2} @ 10 Hz. The described principles can also be applied to other magnetoelastic magnetic field sensors.

This work was funded by the German Research Foundation (DFG) through the Collaborative Research Centre CRC 1261 "Magnetoelastic Sensors - From Composite Materials to Biomagnetic Diagnostics" and the Carl-Zeiss Foundation via the Project MemWerk.

MA 35.63 Thu 16:00 P4

Giant and Tunneling Magnetic Resistance sensor elements based on Focused Ion Beam methods and chemical synthesis — •LAILA BONDZIO, BjÖRN BÜKER, NADINE FOKIN, PIERRE PIEL, and ANDREAS HÜTTEN — University of Bielefeld, Germany

Common GMR and TMR sensors are based on sputter deposited multilayer stacks. Structuring these thin films using lithography can be expensive and time consuming, thus alternative ways of structuring are explored such as nanoparticle synthesis or high-precision milling via ion beam.

A dual-beam Focused Ion Beam (FIB) microscope can be used for Focused Electron Beam Induced Deposition (FEBID) to deposit small Co dots as nanoparticles, which are afterwards covered with a slightly conductive material to fill the gaps, so that a granular highly ordered, 2 dimensional GMR array is created in a bottom-up method. Alternatively, the ion beam can be used for a top-down approach by milling grid-like structures into a deposited magnetic layer to create rectangular particles. In spite of successful proof of concept measurements, higher particle densities are needed to produce a sufficiently high effect for sensor applications.

With chemical nanoparticle synthesis arrays of randomly arranged nanoparticles can be created representing the ferromagnetic layers. The organic ligand shells of e.g. oleic acid create the isolated TMR barrier between the particles. Measurements on these otherwise untreated random, 3 dimensional particle arrays have shown a broad TMR curve for high fields.

MA 35.64 Thu 16:00 P4

Two-photon lithography as a fabrication tool for 3D curved magnetic thin film arrays — •CHRISTIAN JANZEN¹, SAPIDA AKHUNDZADA¹, ARNE VEREIJKEN¹, MICHAŁ MATCZAK², PIOTR KUŚWIK², ARNO EHRESMANN¹, and MICHAEL VOGEL¹ — ¹Institute of Physics and Center for Interdisciplinary Nanostructure Science and Technology (CINSaT), University of Kassel, Heinrich-Plett-Str. 40, 34132 Kassel, DE — ²Institute of Molecular Physics, Polish Academy of Science, ul. Mariana Smoluchowskiego 17 60-179 Poznań, PL

Fabrication of 3D magnetic nanostructures of complex geometry is a challenging task not easily achievable by standard lithography techniques. Two-photon lithography exploits the non-linear absorption properties of the utilized resist to initialize its polymerization at the volume of highest intensity, called voxel. By manipulating the three-dimensional position of the voxel, it is possible to prepare microstructures with varying Gaussian curvature (e.g., torus), being used as templates for the deposition of magnetic thin films. For preparing high-quality thin films, minimal surface roughness is required. Hence, the latter was investigated by atomic force microscopy depending on process parameters. By spatially separating the curved template from the substrate surface with an additional spacer, the magnetostatic interaction between the magnetic cap and the flat full film becomes negligible. Individual template structures are written with variable spacing to their nearest neighbors, enabling the magnetostatic interaction via strayfields as a tunable parameter of the interaction within the magnetic array.

MA 35.65 Thu 16:00 P4

Applications of 3D Nano-Lithography in Magnetism — •JANA KREDL¹, CHRISTIAN DENKER¹, CORNELIUS FENDLER², ROBIN SILBER³, HAUKE HEYEN¹, TRISTAN WINKEL¹, FINN-F. STIEWE¹, NINA MEYER¹, TOBIAS TUBANDT¹, NEHA JHA¹, JAKOB WALOWSKI¹, MARCEL KOHLMANN¹, JULIA BETUNE¹, CHRIS BADENHORST¹, ALENA RONG¹, MARK DOERR¹, RAGHVENDRA PALANKAR¹, MI-

HAELA DELCEA¹, UWE T. BORNSCHEUER¹, ROBERT BLICK², SWADHIN MANDAL⁴, ALEXANDER PAARMANN⁵, and MARKUS MÜNZENBERG¹ — ¹University of Greifswald, Germany — ²Universität Hamburg, Germany — ³VŠB-Technical University of Ostrava, Czech Republic — ⁴Indian Institute of Science Education and Research Kolkata, India — ⁵Fritz Haber Institute of the Max Planck Society, Berlin, Germany

3D 2-Photon-Lithography, originally developed for 3D photonic crystals, opens a wide range of new possible applications in many fields, e.g. life sciences, micro-optics and mechanics. We will present our recent applications of 3D 2-Photon-lithography and show 3D evaporation masks for in-situ device fabrication using different deposition angles, infra-red laser light focusing lenses directly fabricated on optical fibers, tunnel structures for guiding growth of neurons [1], pillars for investigation of cell mechanics and master-mold fabrication for Polydimethylsiloxane (PDMS) micro-fluidic channels. Based on our experience we will discuss possible applications in magnetism. [1] C. Fendler et al., Adv. Biosys. 5 (2019) doi: 10.1002/adbi.201970054

MA 35.66 Thu 16:00 P4

Monte-Carlo study of commensurate-incommensurate phase transition of YBaCuFeO5 — •MUKESH SHARMA and TULIKA MAITRA — Indian Institute of Technology Roorkee, Roorkee Uttarakhand, India

Type-II multiferroic materials where ferroelectricity is driven by magnetic order are highly sought after these days. Intense research is being carried out to increase the transition temperature of multiferroicity to near room temperature. YBaCuFeO5 (YBCFO) is one such rare material where it has been reported that incommensurate spiral magnetic ordering is stable up to temperatures higher than room temperature even though the presence of ferroelectricity is still debated. Motivated by the recent experimental evidence of tuning commensurate-incommensurate magnetic phase transition temperature in this system via Fe-Cu disorder, we have studied the role of anisotropic exchange and Fe-Cu site disorder on this transition. Using various exchange interactions obtained from density functional theory, our Monte-Carlo simulations show that both anisotropic exchange and site disorder play significant roles in giving rise to spiral magnetic ordering at lower temperatures.

MA 35.67 Thu 16:00 P4

Formation, effects and suppression of M-Type hexaferrite in barium titanate-spinell ferrite multiferroic composites — •DANIL LEWIN, SOFIA SHAMSULBAHRIN, VLADIMIR V. SHVARTSMAN, and DORU C. LUPASCU — Institute for Materials Science and Center for Nanointegration Duisburg-Essen (CENIDE), University of Duisburg-Essen, Germany

The combination of a ferroelectric barium titanate-based perovskite with a magnetic ferrite is a common approach for creating multiferroic composites. In some cases, however, a hexagonal phase, usually identified as barium ferrite (BaFe12O19, BaM), appears during sintering. As a noticeable difference exists in the optimal sintering temperature for both phases, it may become a challenge to create an electrically well insulating ceramic. Confronted with strong formation of BaM at high sintering temperatures (1270 °C), we investigate efficient ways to suppress its formation for combinations of barium titanate with cobalt ferrite or nickel ferrite. We show that by using a reducing atmosphere, the formation of BaM is heavily suppressed, while addition of extra cobalt oxide or nickel oxide during the synthesis can further improve the magnetoelectric coefficient while minimizing the remaining amount of BaM. A clear correlation between the amount of BaM and the polarizability and magnetoelectric coupling of the composites is established.

MA 35.68 Thu 16:00 P4

Transport properties of systematically disordered Cr₂AlC films — •JOAO S. CABACO¹, ULRICH KENTSCHE¹, JURGEN LINDNER¹, JURGEN FASSBENDER¹, CHRISTOPH LEYENS^{2,3}, RANTEJ BALI¹, and RICHARD BOUCHER² — ¹Institute of Ion Beam Physics and Materials Research, Helmholtz Zentrum, Dresden-Rossendorf, Germany — ²Institute for Materials Science, TU Dresden, Germany — ³Fraunhofer Institute for Material and Beam Technology IWS, Dresden, Germany

Nano-lamellar composite materials, known as MAX-phases, can possess a combination of ceramic and metallic properties. A prototype compound is Cr₂AlC, formed from a unit cell of Cr₂C sandwiched between atomic planes of Al.

In this work we study the modifications to the structural, transport and magnetic behavior of 500 nm thick Cr₂AlC after irradiation with Co⁺ ions, and Ar⁺ noble gas ions as control. X-ray diffraction shows that ion-irradiation induces a suppression of the 0002 reflection, indicating a deterioration of the crystal structure. Increasing the ion fluence leads to an increase of the saturation magnetization at 1.5 K, whereby both Ar⁺ and Co⁺ cause an increased magnetization, respectively to 150 kA.m⁻¹ and 190 kA.m⁻¹, for the highest fluences used. At Co⁺ fluences of 5×10¹³ ions.cm⁻² the magnetoresistance (MR) shows a 2-order of magnitude increase, up to 3% (10 T) at 100 K. A similar effect also occurs for 5×10¹² ions.cm⁻² Ar⁺ irradiated films, however, with a smaller MR-increase. The disordering of MAX phase films may reveal interesting spin-related transport phenomena.

MA 35.69 Thu 16:00 P4

A Floquet Green's Function technique to study ESR spectra — •JOSE REINA GALVEZ — Center for Quantum Nanoscience, Ewha University, Seoul, Republic of Korea

This poster presents a theoretical framework to describe experiments directed to controlling single-atom spin dynamics by electrical means using a scanning tunneling microscope. The model consists of a quantum impurity connected to electrodes while an electrical time-dependent bias is applied. The quantum impurity consists of a localized electronic state, with a Coulomb repulsion U term, connected magnetically to a localized spin S.

Applying the Heisenberg picture, in the limit of weak coupling between the impurity and the electrodes, Born-Markov approximation, a quantum master equation can be obtained. The rates in this equation are derived by the non-equilibrium Green's function formalism. The Floquet theorem is used to transform the differential equation into algebraic one.

We show results in two cases. The first case is just a single atomic orbital subjected to a time-dependent electric field, and the second case consists of a single atomic orbital coupled to a second spin-1/2. This first case reproduces the main experimental features Ti atoms on MgO/Ag (100) but in a sequential tunneling regime and for different U values. The second case directly addresses the experiments on two Ti atoms.

These calculations permit us to explore the effect of different parameters to reproduce experimental fingerprints of the ESR technique.

MA 35.70 Thu 16:00 P4

Characterization of thin MgO layers grown on Fe(100) and Fe(100)-p(1x1)O — •MIRA ARNDT, DAVID JANAS, GIOVANNI ZAMBORLINI, and MIRKO CINCHETTI — Department of Physics, TU Dortmund University, Otto-Hahn-Straße 4, 44227 Dortmund, Germany

In the field of spintronics, thin magnesium oxide (MgO) interlayers play a major role as dielectric tunneling barriers in magnetic tunnel junctions. As the most prominent example, MgO enhances the tunneling magnetoresistance of Fe/MgO/Fe heterolayers. Crucially, exposing Fe to oxygen results in rapid oxidation of the surface, which in turn highly influences the MgO growth process and makes it less reproducible, eventually, changing the device performances. This problem can be overcome by controlled passivation of the Fe surface with oxygen prior to MgO deposition. In this contribution we present the characterization of the growth of MgO layers with variable thickness on the clean Fe(100) and the passivated Fe(100)-p(1x1)O surface. The studies have been performed by employing various surface sensitive techniques, such as Auger electron spectroscopy, low energy electron diffraction (LEED), reflective medium energy electron diffraction (MEED), and photoelectron spectroscopy (PES). Our data show that, despite evident differences in the growth behavior, the electronic properties of the two interfaces are very similar.

MA 35.71 Thu 16:00 P4

Correlation of Magnetism and Disordered Shiba bands in Fe Monolayer Islands on Nb(110) — JULIA J. GOEDECKE¹, LUCAS SCHNEIDER¹, YINGQIAO MA³, •KHAH TON THAT¹, DONGFEI WANG², JENS WIEBE¹, and ROLAND WIESENDANGER¹ — ¹Department of Physics - University of Hamburg, Hamburg, Germany — ²CIC Nanogune, Donostia - San Sebastian, Spain — ³Institute of Chemistry - Chinese Academy of Sciences, Beijing, China

Two-dimensional (2D) magnet-superconductor hybrid systems are intensively studied due to their potential for realizing 2D topological superconductors with Majorana edge modes. It is theoretically predicted that this quantum state can occur in spin-orbit coupled ferromagnetic or skyrmionic 2D layers in proximity to an s-wave superconductor. However, recent examples suggest, that the requirements for topological superconductivity are complicated by the multi-orbital nature of the magnetic components and disorder effects.

Here, we investigate Fe monolayer islands grown on a surface of the s-wave superconductor with the largest gap of all elemental superconductors, Nb, with respect to magnetism and superconductivity using spin-resolved scanning tunneling spectroscopy. We find three types of Fe monolayer islands which significantly differ by their reconstruction, by the magnetism and the disordered Shiba bands, without any signs of topological gaps or edge states.

Our work illustrates, that a reconstructed growth mode of magnetic layers on superconducting surfaces is detrimental for the formation of 2D topological superconductivity.

MA 35.72 Thu 16:00 P4

Suppression of Weak Ferromagnetic Order in SrRuO₃ under Pressure — •ANH TONG¹, PAU JORBA¹, MARC SEIFERT¹, STEFAN KUNKEMÖLLER², KEVIN JENNI², MARKUS BRADEN², JAMES S. SCHILLING¹, and CHRISTIAN PFLEIDERER¹ — ¹Technical University of Munich, Garching bei München, Germany — ²University of Cologne, Cologne, Germany

In the Ruddlesden-Popper perovskite series, Sr_{n+1}Ru_nO_{3n+1}, intense experimental and theoretical efforts have been dedicated to unravel the nature of unconventional superconductivity in single-layer Sr₂RuO₄ (n = 1) as well as a putative electronic nematic phase masking the quantum critical endpoint in the double-

layer itinerant metamagnet $\text{Sr}_3\text{Ru}_2\text{O}_7$ ($n = 2$). We report an experimental study of the zero temperature ferromagnetic-to-paramagnetic transition under pressures up to 20GPa in high quality single crystals of the infinite layer itinerant ferromagnet SrRuO_3 ($n = \infty$). Electrical transport measurements in Bridgman anvil high pressure cells, as well as neutron depolarization measurements in diamond anvil cells were performed on SrRuO_3 . Our study aims to investigate quantum criticality in SrRuO_3 and reconcile the properties of $\text{Sr}_3\text{Ru}_2\text{O}_7$ and Sr_2RuO_4 with the generic temperature-pressure-magnetic field phase diagram of itinerant ferromagnets.

- [1] M. Brando et al., *Rev. Mod. Phys.* **88**, 2 (2016).
 [2] J. J. Hamlin et al., *Phys. Rev. B* **76**, 1 (2007).
 [3] G. Cao et al., *Phys. Rev. B* **56**, 1 (1997).

MA 35.73 Thu 16:00 P4

Magneto-transport in (Bi,Sb)Te nanostructures — •TITOUAN CHARVIN^{1,2}, FELIX HANSEN², SILKE HAMPEL², JOSEPH DUFOULEUR², BERND BÜCHNER^{2,3}, and ROMAIN GIRAUD^{1,2} — ¹Université Grenoble Alpes, CNRS, CEA, IRIG/Spintec, F-38000 Grenoble, France — ²Leibniz Institute for Solid State and Materials Research Dresden, Helmholtzstrasse 20, D-01069 Dresden, Germany — ³Institut für Festkörperphysik, TU Dresden, D-01062 Dresden, Germany

The investigation of Dirac fermions surface states in binary 3D topological insulators, such as Bi_2Te_3 or Sb_2Te_3 , is limited by their large bulk-carrier densities. This shift of the Fermi level, away from the bulk band gap, is caused by a high density of point defects, acting as donors or acceptors. With the aim to achieve a bulk-charge compensation, we grew $(\text{Bi}_x\text{Sb}_{1-x})_2\text{Te}_3$ nanostructures by chemical vapor transport, with different stoichiometries, in order to vary both the band structure and the relative contributions of different types of point defects. From magneto-transport measurements, we infer the bulk and surface carrier densities and mobilities. Although the bulk contribution to the conductivity can be reduced for some stoichiometries, all samples show a metallic-like behavior of their conductivities, with coexisting bulk and surface states contributions.

MA 35.74 Thu 16:00 P4

Electrical and thermal hall transport in compensated topological insulator BiSbTeSe₂ — •ROHIT SHARMA, MAHASWETA BAGCHI, OLIVER BREUNIG, YOICHI ANDO, and THOMAS LORENZ — II. Physikalisches Institut, Universität zu Köln, Zùlpicher Straße 77, D-50937 Köln, Germany

The existence of puddles in BiSbTeSe_2 at low temperature ($T < 50\text{K}$) has been detected using optical conductivity measurements, where DC electrical conductivity data shows an insulating behaviour, but above 50K, optical and transport results agree well with each other due to evaporation of charge puddles with increasing T [1]. By comparing thermal conductivity κ_{xx} and thermal hall effect κ_{xy} data with the electrical counterparts (σ_{xx} & σ_{xy}), we study a possible influence of charge puddles on thermal transport. Electrical hall conductivity (σ_{xy}) shows hole like (p-type) behaviour at elevated T , which changes to multi-band behaviour at low T . From the electrical transport data electronic contribution to thermal transport κ_e was calculated by using Wiedemann-Franz law and then compared with the measured thermal transport data where it was found that both κ_{xx} and κ_{xy} shows phonon dominated behaviour. When compared κ_{xy} and κ_e , data matches well with each other above 50K. In contrast, below 50K κ_{xy} shows a sign change and evolves to a large thermal hall signal, whereas κ_e has

no sign change and smoothly decreases. Possible reason for large thermal hall effect in BiSbTeSe_2 will be discussed.

Funded by the DFG via CRC 1238 Projects A04 and B01

- [1] N. Borgwardt et al. *Phys. Rev. B* **93**, 245149 (2016)

MA 35.75 Thu 16:00 P4

Topology and DC quantum transport in Floquet-driven systems — •AYA ABOUELELA and JOHANNES KROHA — University of Bonn

Recently, several works have investigated the topological properties emerging in periodically driven systems, where a periodic drive is used to engineer the band structure such as to support topologically stabilized edge modes. The topological phases of periodically driven systems have been classified across all dimensions in the periodic table of Floquet topological insulators. The Floquet multiplicity of bands implies the emergence of anomalous edge states which cross bulk gaps that do not occur in static systems. Here, we present our studies on the non-interacting topological Qi-Wu-Zhang (QWZ) model under the influence of a periodic drive, and analyze its drive-induced edge modes, using the Floquet formalism. Investigating two regimes of the driving frequency, higher or lower than the static bandwidth, the latter is shown to support anomalous edge modes. For the experimental detection of edge states, we calculate the dI/dV spectra at non-zero DC bias voltage V , using the Keldysh-Floquet formalism. We predict quantized conductance plateaus when the transport voltage is within a normal gap (V centered around $V = 0$, normal edge mode) or within an anomalous gap (V centered around $V = \pm\Omega/2$, anomalous edge mode). We also perform a spatially resolved computation of the chiral transmission channels of the finite-size system with finite bias applied, showing that the transport is along an edge and that it is spatially modulated corresponding to the wave number π of the (anomalous) edge mode.

MA 35.76 Thu 16:00 P4

Effects of the chiral anomaly on charge and heat transport in Weyl semimetals — •ALINA WENZEL^{1,2}, ANNIKA JOHANSSON¹, and INGRID MERTIG² — ¹Max Planck Institute of Microstructure Physics, Halle, Germany — ²Martin Luther University Halle-Wittenberg, Halle, Germany

The chiral anomaly in Weyl semimetals, which corresponds to nonconservation of chiral charge if a magnetic field is applied nonorthogonal to an electric field or a temperature gradient, leads to unconventional contributions to longitudinal charge and thermal transport, strongly depending on the external magnetic field [1-3]. We calculate the thermoelectric transport properties for Weyl systems by solving the semiclassical Boltzmann equation including a temperature gradient. To analytically calculate the transport coefficients the Sommerfeld expansion is used. The isotropic Weyl Hamiltonian [2] and an anisotropic, more realistic model to describe pairs of Weyl points [4,5] are discussed. Using the latter, Weyl semimetals with either broken time reversal or inversion symmetry are simulated and the influence of symmetry on the electric and thermal transport properties is discussed.

- [1] H. B. Nielsen and M. Ninomiya, *Phys. Lett. B* **130**, 389 (1983)
 [2] D. T. Son and B. Z. Spivak, *Phys. Rev. B* **88**, 104412 (2013)
 [3] K. Kim, *Phys. Rev. B* **90**, 121108(R) (2014)
 [4] S. Murakami *et al.*, *Phys. Rev. B* **78**, 165313 (2008)
 [5] R. Okugawa *et al.*, *Phys. Rev. B* **89**, 235315 (2014)

MA 36: Members' Assembly

Time: Thursday 18:00–19:00

Location: H37

All members of the Magnetism Division are invited to participate.

MA 37: Skyrmions 3 (joint session MA/KFM)

Time: Friday 9:30–12:45

Location: H37

MA 37.1 Fri 9:30 H37

Emergence of zero-field non-synthetic single and catenated antiferromagnetic skyrmions in thin films — •AMAL ALDARAWSEH^{1,2}, IMARA LIMA FERNANDES¹, SASCHA BRINKER¹, MORITZ SALLERMANN¹, MUAYAD ABUSAA³, STEFAN BLÜGEL¹, and SAMIR LOUNIS^{1,2} — ¹Peter Grünberg Institute and Institute for Advanced Simulation, Forschungszentrum Jülich and JARA, D-52425 Jülich, Germany — ²Faculty of Physics, University of Duisburg-Essen and CENIDE, 47053 Duisburg, Germany — ³Department of Physics, Arab American University, Jenin, Palestine

Antiferromagnetic (AFM) skyrmions are envisioned as ideal topological magnetic bits in future information technologies. In contrast to ferromagnetic (FM) skyrmions, they are immune to the skyrmion Hall effect, might offer potential terahertz dynamics [1] while being insensitive to external magnetic. Although observed in synthetic AFM structures [2], their realization in non-synthetic

AFM films has been elusive. Here[3], we unveil their presence in a row-wise AFM Cr film deposited on PdFe bilayer grown on fcc Ir(111) surface. Using first-principles, we demonstrate the emergence of single and catenated AFM skyrmions, which can coexist with the rich inhomogeneous exchange field, including that of FM skyrmions, hosted by PdFe. Besides the identification of an ideal platform of materials for intrinsic AFM skyrmions, we anticipate the uncovered solitons to be promising building blocks in AFM spintronics. - Work funded by (BMBF-01DH16027) [1] Gomony et al., *Nat. Physics* **14**, 213 (2018). [2] Legrand et al., *Nat. Materials* **19**, 34 (2020). [3] Aldarawsheh et al., *ArXiv:2202.12090* (2022).

MA 37.2 Fri 9:45 H37

Chiral standing spin waves in 3D skyrmion lattice — •ANDRII SAVCHENKO^{1,2}, VLADYSLAV KUCHKIN¹, FILIPP RYBAKOV^{3,4}, STEFAN BLÜGEL¹, and NIKOLAI KISELEV¹ — ¹Peter Grünberg Institut and Institute for Advanced Simulation, Forschungszentrum Jülich and JARA, D-52425 Jülich, Germany — ²Donetsk Institute for Physics and Engineering, National Academy of Sciences of Ukraine, 03028 Kyiv, Ukraine — ³Uppsala University, SE-75120 Uppsala, Sweden — ⁴KTH Royal Institute of Technology, SE-10691 Stockholm, Sweden

The resonance excitations of the three-dimensional skyrmions lattice in the finite thickness plate of an isotropic chiral magnet were studied using spin dynamics simulations. We calculated the absorption spectra and resonance mode profile configurations for the cases of in-plane and out-of-plane excitations. These results differ from those predicted by the two-dimensional model and the model of the unconfined bulk crystal. In the case of in-plane excitation, absorption spectra dependencies on film thickness have the periodic zones with fading intensity. This effect can be explained by the formation of chiral standing spin waves, which, contrary to conventional standing spin waves, are characterized by the helical profile of dynamic magnetization of fixed chirality defined by the Dzyaloshinskii-Moriya interaction [1]. The chiral standing spin waves are localized in the inter-skyrmion area or the skyrmion core. Under out-of-plane excitation, the absorption spectrum also demonstrates the appearance of standing spin waves, which are localized in the skyrmion shell. 1. A.S. Savchenko et al, arXiv:2205.05466

MA 37.3 Fri 10:00 H37

Generalization of the collective variables approach for skyrmion strings. — •VOLODYMYR KRAVCHUK^{1,2} and MARKUS GARST¹ — ¹Karlsruhe Institute of Technology, Germany. — ²Bogolyubov Institute for Theoretical Physics, Kyiv, Ukraine

In a bulk saturated chiral magnet, the skyrmion core penetrates the ferromagnet volume forming a string-like object [1]. Here we describe the small-amplitude dynamics of the string, applying the generalized collective variable approach. For the collective variables, we use the coordinate- and time-dependent string position defined as the first moment of topological charge calculated for the continuously stacked horizontal cross-sections perpendicular to the applied magnetic field. The simplest "plane-wave" solution corresponds to the helix-shaped deformation of the string. In a nonlinear regime, this solution is unstable due to the Lighthill criterion, that results in a self-modulation of the wave. Using a multiscale analysis both in space and time, we show that this modulation is captured by a non-linear Schrödinger equation of focusing type. Two classes of non-linear periodic waves of skyrmion string (so-called dc- and cn-waves) are analytically predicted and numerically verified. The separatrix soliton solution just corresponds to the solitary wave found previously [1]. The developed approach is generalized for the case of arbitrary meaning of the collective variables. The latter enables us to describe the string excitations of various symmetries, e.g. breathing and elliptical modes in a nonlinear regime.

[1] V. Kravchuk, U. Rößler, J. van den Brink, M. Garst, PRB, 102, 220408(R) (2020).

MA 37.4 Fri 10:15 H37

Fermi-surface origin of helical single Q-state and skyrmion lattice in centrosymmetric Gd compounds — •JUBA BOUAZIZ¹, EDUARDO MENDIVE-TAPIA¹, STEFAN BLÜGEL¹, and JULIE STAUNTON² — ¹Forschungszentrum Jülich, Germany — ²University of Warwick, Coventry CV4 7AL, United Kingdom

We show from first principles that cylindrical structures within the Fermi surface are the origin of the single-Q helical state in the GdRu₂Si₂ and Gd₂PdSi₃ intermetallic compounds. The geometry of the Fermi surface nesting describes the strength and sign of the underlying pairwise Ruderman-Kittel-Kasuya-Yosida interactions between the Gd moments as the main mechanism. These interactions are quasi-two-dimensional, isotropic within the Gd layers, and provide a transition temperature and helix period in very good agreement with experiment. Using atomistic spin-dynamical simulations, we investigate the effects of magnetic anisotropy and construct a general magnetic phase diagram that explains the stabilization of the 2Q-skyrmion lattice observed in experiment with applied magnetic fields.

Funding: ERC Grant No. 856538 (project "3D MAGIC"), SPP 2137 "Skyrmionics" (Project No. BL 444/16), UK EPSRC Grant No. EP/M028941/1.

MA 37.5 Fri 10:30 H37

Non-Abelian Vortices in Magnets — •FILIPP RYBAKOV¹ and OLLE ERIKSSON^{1,2} — ¹Uppsala University, Sweden — ²Örebro University, Sweden

The non-Abelian (non-commutative) topological states in ordered media may exhibit interesting physics emerging from purely topological arguments [1].

Here we show that non-Abelian vortices also can exist in magnets [2]. We give a topological classification of these vortices and reveal their connection with Abelian topological structures, such as usual vortices, merons, skyrmions. We analyze the potential of non-Abelian magnetic vortices for memory devices and emphasize their advantage, since they provide topological protection of all information, rather than individual bits, as in Abelian cases.

[1] N. D. Mermin, Rev. Mod. Phys. 51, 591 (1979).

[2] F. N. Rybakov and O. Eriksson, arXiv:2205.15264 (2022).

MA 37.6 Fri 10:45 H37

Thermal properties of magnetic skyrmions — •BALÁZS NAGYFALUSI¹, LÁSZLÓ UDVARDI^{2,3}, and LÁSZLÓ SZUNYOGH^{2,3} — ¹Wigner Research Center for Physics, Institute for Solid State Physics and Optics, Budapest, Hungary — ²Budapest University of Technology and Economics, Budapest Hungary — ³MTA-BME Condensed Matter Research Group, Budapest, Hungary

We have recently implemented metadynamics in Monte Carlo simulation code¹, which has been modified to use the topological charge Q of magnetic skyrmions as collective variable. The free energy can thus be determined as a function of Q and its equilibrium value can be explored as a function of temperature. The knowledge of the free energy $F(Q; T)$ also permits to evaluate the chemical potential μ of the skyrmions.

We investigated the thermal evolution of magnetic skyrmions in a Pt₉₅Ir₅/Fe bilayer on Pd(111) and an FePd bilayer on Ir(111) substrate in the presence of a normal-to-plane external magnetic field. The equilibrium number of skyrmions and the phase boundaries are in good agreement with previous studies^{2,3}. For the former system we found that Q has a maximum around 60 K and below this temperature this number drops rapidly, while for the later system it freezes in as the skyrmion lattice is a ground state of the system. The slope of $\mu(T)$ also distinguishes the different ground states of the two system.

1. Nagyfalusi *et al.*, Phys. Rev. B 100, 174429 (2019)2. Rózsa *et al.*, Phys. Rev. B 93, 024417 (2016)3. Schick *et al.*, Phys. Rev. B 103, 214417 (2021)

MA 37.7 Fri 11:00 H37

Constructing coarse-grained skyrmion potentials from experimental data with Iterative Boltzmann Inversion — •JAN ROTHÖRL, YUQING GE, MAARTEN A. BREMS, NICO KERBER, RAPHAEL GRUBER, FABIAN KAMMERBAUER, TAKAOKI DOHI, MATHIAS KLÄUI, and PETER VIRNAU — Institut für Physik, Johannes Gutenberg-Universität, Staudinger Weg 9, D-55099 Mainz, Germany

In an effort to understand skyrmion behavior like skyrmion lattice formation [1] or commensurability effects [2], skyrmions are often described as 2D quasi particles on a coarse-grained level evolving according to the Thiele equation. In particular, the interaction potentials are the key missing parameters for predictive modeling of experiments. We apply the Iterative Boltzmann Inversion technique commonly used in soft matter simulations to construct potentials for skyrmion-skyrmion and skyrmion-magnetic material boundary interactions from a single experimental measurement without any prior assumptions of the potential form. We find that the two interactions are purely repulsive and can be described by an exponential function for experimentally relevant micrometer-sized skyrmions. This captures the physics on experimental time and length scales that are of interest for most skyrmion applications and typically inaccessible to atomistic or micromagnetic simulations. [3]

[1] J. Zázvorka *et al.*, Adv. Funct. Mater. 30, 2004037 (2020). [2] C. Song *et al.*, Adv. Funct. Mater. 2010739 (2021) [3] Y. Ge *et al.*, arXiv:2110.14333 [cond-mat.mtrl-sci] (2021)

MA 37.8 Fri 11:15 H37

Development of a current solver for studying non-linear skyrmion dynamics — •THORBEN PÜRLING^{1,2}, DANIELE PINNA³, FABIAN LUX⁴, JONATHAN KIPP^{1,3}, STEFAN BLÜGEL^{1,3}, ABIGAIL MORRISON^{2,5}, and YURIY MOKROSOV^{3,4} — ¹Department of Physics, RWTH Aachen University, Aachen, Germany — ²Institute of Neuroscience and Medicine 6 and Institute for Advanced Simulation 6 and JARA BRAIN Institute I, Jülich Research Centre, Jülich, Germany — ³Peter Grünberg Institute 1 and Institute for Advanced Simulation 1, Forschungszentrum Jülich and JARA, Jülich, Germany — ⁴Institute of Physics, Johannes Gutenberg University Mainz, Mainz, Germany — ⁵Computer Science 3 - Software Engineering, RWTH Aachen University, Aachen, Germany

Transport phenomena in skyrmionic textures have recently gained attention owing to possible applications in spintronics and in cognitive computing. While the reservoir computing aspect of skyrmions relies heavily on their nonlinear response properties, little is known about the real-space distribution of the current density that reflects the non-trivial structure of the local conductivity tensor of these complex objects. Here we report on the development of a method that provides the local current distribution for arbitrary spin textures under bias, and apply that method to study the current distribution of isolated skyrmions. We address the importance of diagonal and Hall components of the conductivity tensor for the current distribution and discuss possible relevance of our findings to reservoir computing applications.

MA 37.9 Fri 11:30 H37

Atomistic spin simulations of electric-field assisted nucleation and annihilation of magnetic skyrmions — •MORITZ A. GOERZEN¹, STEPHAN V. MALOTTKI^{1,4}, GRZEGORZ J. KWIAKOWSKI², PAVEL F. BESSARAB^{2,3}, and STEFAN HEINZE¹ — ¹Institute of Theoretical Physics and Astrophysics, University of Kiel, Germany — ²University of Iceland, Reykjavík, Iceland — ³St. Petersburg, Russia

— ⁴Thayer School of Engineering, Dartmouth College, Hannover, USA

We demonstrate electric-field assisted thermally activated writing and deleting of magnetic skyrmions in ultrathin transition-metal films. We apply an atomistic spin model which is parameterised from density functional theory (DFT) calculations for a Pd/Fe bilayer on the Ir(111) surface for electric fields of $\mathcal{E} = 0, \pm 0.5$ V/Å. Based on harmonic transition-state theory [1,2], we calculate the transition rates for skyrmion nucleation and annihilation. Using these rates we quantify the probability for electric-field assisted deleting and writing of skyrmions by means of Master equations. The magnetic-field dependent skyrmion probability can be directly related to the free energy differences of the skyrmion and the ferromagnetic state and resembles a Fermi-Dirac distribution function. The obtained probability function at opposite electric fields is in striking agreement with experimental results [3].

[1] Bessarab *et al.*, *Sci. Rep.* **8**, 3433 (2018)

[2] von Malottki *et al.*, *Phys. Rev. B* **99**, 060409 (2019)

[3] Romming *et al.*, *Science* **341**, 636 (2013)

MA 37.10 Fri 11:45 H37

Strain and electric field control of magnetic skyrmions in Fe₃GeTe₂ van der Waals heterostructures — •DONGZHE LI¹, SOUMYAJYOTI HALDAR², and STEFAN HEINZE² — ¹CEMES, Université de Toulouse, CNRS, 29 rue Jeanne Marvig, F-31055 Toulouse, France — ²Institute of Theoretical Physics and Astrophysics, University of Kiel, Leibnizstrasse 15, 24098 Kiel, Germany

Magnetic skyrmions are topologically protected chiral spin structures with particle-like properties, which are often induced by the Dzyaloshinskii-Moriya interaction (DMI). The recent discovery of truly two-dimensional (2D) magnetic materials opened up new opportunities for exploring magnetic skyrmions in atomically thin vdW materials. Here, using density functional theory and atomistic spin simulations, we predict the emergence of a large DMI in 2D vdW heterostructures where a 2D ferromagnetic metal Fe₃GeTe₂ monolayer is deposited on a nonmagnetic vdW layer. In particular, the DMI turns out to be highly tunable by strain and electric-field, leading to giant DMI comparable to that of ferromagnetic/heavy metal interfaces, which have been recognized as prototype multilayer systems to host skyrmion states. Our atomistic spin simulations further show that the efficient control of the DMI, the exchange coupling, and the magnetic anisotropy energy by strain, lead to the stabilization of isolated skyrmions.

MA 37.11 Fri 12:00 H37

Resonant optical Hall conductivity from skyrmions — •SOPHEAK SORN¹, LUYI YANG², and ARUN PARAMAKANTI³ — ¹Institute for Quantum Materials and Technologies, Karlsruhe Institute of Technology, Karlsruhe, Germany — ²Department of Physics, Tsinghua University, Beijing, China — ³Department of Physics, University of Toronto, Toronto, Canada

Metallic magnets hosting topological skyrmions exhibit the topological Hall effect, which arises from a real-space Berry-phase mechanism, and it has been used as an indirect signature of skyrmions in transport experiments. This talk will focus on the less explored impact of skyrmions on optical Hall conductivity which is studied using a two-dimensional model of conduction electrons coupled to a background skyrmion spin texture via an effective Hund's coupling. For a skyrmion crystal, a Kubo-formula calculation reveals a resonant feature in the optical Hall response at a frequency set by the Hund's coupling. A linear relation between the area under the Hall resonant curve and the skyrmion den-

sity is discovered numerically and is further elucidated in a gradient expansion analysis. The presence of the resonance is robust, persisting in a system with an isolated skyrmion and even in a three-site system hosting a trimer of noncoplanar spins, which implies the indispensable role of the local noncoplanarity. Our results suggest that the resonance can be used as a basis for a magneto-optical Kerr microscopy for visualizing skyrmions.

MA 37.12 Fri 12:15 H37

Artificial neuron based on a magnetic biskyrmion — •ISMAEL RIBEIRO DE ASSIS, BÖRGE GÖBEL, and INGRID MERTIG — Institut für Physik, Martin-Luther-Universität Halle-Wittenberg

Skyrmionics and neuromorphics are among the most promising fields of physics with the perspective of creating future devices and technologies. Magnetic skyrmions are extremely stable and can be moved by currents which has led to the prediction of a skyrmion-based artificial neuron [1]: When a skyrmion is pushed by current pulses, it will eventually reach a designated location and can be detected electrically. This resembles the excitation process of a neuron that fires ultimately. However, a realistic refractory process has not been achieved, so far, for such a device. The skyrmion-based neuron would keep on firing when more current pulses are applied which renders this device not useful.

In this talk we suggest that a biskyrmion solves this major issue. The attractive interaction of the two partially overlapping skyrmions and their skyrmion Hall effects lead to a unique trajectory when they are driven by current pulses: The two sub-skyrmion move along opposite directions to the two designated detection areas where they reverse their direction of motion until they come back and eventually reestablish the biskyrmion. During the second period the skyrmion cannot fire again. Our suggested device resembles the response of a biological neuron better than all existing skyrmion-based devices so far.

[1] S. Li *et al.*, *Nanotechnology* **28**, 31LT01 (2017)

MA 37.13 Fri 12:30 H37

Magnetoelastic surface states of skyrmion textures — •LARS FRANKE and MARKUS GARST — Institute for Theoretical Solid State Physics, Karlsruhe Institute for Technology, Germany

At the surface of chiral magnets uncompensated Dzyaloshinskii-Moriya interaction modifies the boundary conditions for the magnetization resulting in a so-called a surface twist. Consequently, skyrmions are expected to change their helicity from Bloch-like within the bulk of the chiral magnet to Néel-like close to the surface [1]. Resonant elastic X-ray scattering experiments [2] have confirmed this predicted change of helicity close to the surface, but the experimentally observed penetration depth was found to be an order of magnitude larger than theoretically expected. In order to account for this discrepancy, we investigate theoretically the influence of a magnetoelastic coupling on the surface twist. Analytical calculations are complicated by broken translational invariance and non-trivial boundary conditions at the surface. However, as in the uncoupled system the length scale for helicity variations is already encoded in the bulk equation. We demonstrate how to extract the length scale from a perturbative approach. The validity of these calculations is checked using micromagnetic simulations, extended with magnetoelastic coupling, of the complete surface state including boundary conditions.

[1] Three-dimensional skyrmion states in thin films of cubic helimagnets, F. N. Rybakov *et al.* *Phys. Rev. B* **87**, 094424 (2013).

[2] Reciprocal space tomography of 3D skyrmion lattice order in a chiral magnet, S. Zhang *et al.* *PNAS* **201803367** (2018).

MA 38: Electron Theory of Magnetism and Correlations

Time: Friday 9:30–11:15

Location: H43

MA 38.1 Fri 9:30 H43

Magnetic torque and DMI-like spin-lattice-coupling parameters from first principles — •S. MANKOVSKY¹, H. LANGE¹, S. POLESYA¹, M. WEISSENHOFER², U. NOWAK², and H. EBERT¹ — ¹Dept. Chemistry, LMU Munich, Germany — ²Fachbereich Physik, Uni. Konstanz, Germany

Magneto-elastic couplings can play a crucial role both for ground state magnetic properties of materials giving rise to modified forms of the magnetic ground state accompanied by a spontaneous lattice deformation, as well as for spin-lattice dynamics, e.g. having a leading role for Gilbert damping in insulators.

As the magneto-elastic properties are fully determined by the electronic structure, the corresponding spin-lattice coupling (SLC) parameters can be calculated at a first-principles level. Aiming at that, we start with the phenomenological atomistic spin-lattice Hamiltonian which can be seen as an extension of the standard Heisenberg spin Hamiltonian. Focusing on the SOC-driven SLC effects, we discuss the torque on the magnetic moment as well as the modification of the Dzyaloshinskii-Moriya interaction (DMI) induced by an atomic displacement, giving access to corresponding SLC parameters. The expressions for these SLC parameters have been worked out based on the fully-relativistic KKR Green functions formalism. Corresponding calculations have been done

for different two-dimensional and three-dimensional systems. Their properties as well as possible impact on the magnetic structure are discussed in comparison with the ordinary MCA and DMI parameters.

MA 38.2 Fri 9:45 H43

Angular momentum transfer via relativistic spin-lattice coupling from first principles — •HANNAH LANGE¹, SERGIY MANKOVSKY¹, SVITLANA POLESYA¹, MARKUS WEISSENHOFER², ULRICH NOWAK², and HUBERT EBERT¹ — ¹Dept. Chemistry, LMU Munich, Butenandtstr. 11, 81377 Munich — ²Dept. Physics, Uni Konstanz, 78457 Konstanz

The transfer and control of angular momentum is a key aspect for spintronic applications. Only recently, it was shown that it is possible to transfer angular momentum from the spin system to the lattice on ultrashort time scales [1]. Hence, combined molecular-spin dynamics simulations using first-principles parameters might give access to the central aspects of the underlying mechanisms.

To contribute to the understanding of angular momentum transfer between spin and lattice degrees of freedom we present a scheme to calculate fully-relativistic spin-lattice coupling parameters from first-principles. By treating changes in the spin configuration and atomic positions at the same level, closed

expressions for the atomic spin-lattice coupling parameters can be derived in a coherent manner up to any order. Analyzing the properties of these parameters, in particular their dependence on spin-orbit coupling, we find that even in bcc Fe the leading term for the angular momentum exchange between the spin system and the lattice is a Dzyaloshinskii-Moriya-type interaction, which is due to the symmetry breaking distortion of the lattice.

[1] Tauchert et al. Nature 602, 73 (2022).

MA 38.3 Fri 10:00 H43

Double-Exchange Enhanced Magnetic Blue-Shift of Mott Gaps — •MOHSEN HAFEZ-TORBATI¹, DAVIDE BOSSINI², FRITHJOF B. ANDERS¹, and GOETZ S. UHRIG¹ — ¹Technical University of Dortmund, Dortmund, Germany — ²University of Konstanz, Konstanz, Germany

Strong correlations in Mott insulators induce a substantial charge excitation energy known as the Mott gap. We study how the Mott gap is affected by long-range antiferromagnetic ordering upon reducing the temperature below the Néel temperature. Our finding is that the Mott gap is increased by the magnetic ordering: a magnetic blue-shift (MBS) occurs. We unveil the origin of the MBS of the Mott gap by analyzing the Hubbard model and the Hubbard-Kondo model and clarify the subtle differences. We show that in the Hubbard model the MBS is determined by the magnetic exchange coupling. In the Hubbard-Kondo model an additional contribution proportional to the hopping is induced by the double-exchange mechanism. We describe the magnetic contribution to the band gap blue-shift observed in the optical conductivity of α -MnTe and pinpoint a hopping contribution of 64% and a magnetic exchange contribution of 36%. A MBS with the energy scale of the hopping and the exchange interaction bears the potential to enable spin-to-charge conversion on extreme time scales, highly promising for spintronic and magnonic applications.

MA 38.4 Fri 10:15 H43

A Theory for Colors of Strongly Correlated Electronic Systems — •SWAGATA ACHARYA¹, CEDRIC WEBER², DIMITAR PASHOV², MARK VAN SCHILFGAARDE³, ALEXANDER I LICHTENSTEIN⁴, and MIKHAIL I KATSNELSON¹ — ¹Radboud University, Nijmegen, The Netherlands — ²King's College London, London, UK — ³National Renewable Energy Laboratory, Colorado, US — ⁴Institute of Theoretical Physics, University of Hamburg, Germany

Many strongly correlated transition metal insulators are colored, even though they have large fundamental band gaps and no quasi-particle excitations in the visible range. We pick two archetypal cases as examples: NiO with green color and MnF₂ with pink color. We show that a perturbative theory based on low-order extensions of the GW approximation is able to explain the color in NiO, and indeed well describe the dielectric response over the entire frequency spectrum, while the same theory is unable to explain why MnF₂ is pink. We show its color originates from higher order spin-flip transitions that modify the optical response. This phenomenon is not captured by low-order perturbation theory, but is contained in dynamical mean-field theory (DMFT), which has a dynamical spin-flip vertex that contributes to the charge susceptibility. Within our combined self-consistent GW-BSE approximation and DMFT approach we can describe the peaks in subgap charge susceptibilities in both NiO and MnF₂. As a secondary outcome of this work, we establish that the one-particle properties of paramagnetic NiO and MnF₂ are both well described by an adequate single Slater-determinant theory and do not require a dynamical vertex.

MA 38.5 Fri 10:30 H43

Electron-plasmon and electron-magnon scattering in ferromagnets from first principles by combining GW and GT self-energies — DMITRII NABOK, •STEFAN BLÜGEL, and CHRISTOPH FRIEDRICH — Peter Grünberg Institut and Institute for Advanced Simulation, Forschungszentrum Jülich and JARA, 52425 Jülich, Germany

This work combines two powerful self-energy techniques: The well-known GW method and a self-energy recently developed by us [1] that describes the renor-

malization caused by the scattering of electrons with magnons and Stoner excitations. This GT self-energy, which is fully \mathbf{k} dependent and contains infinitely many spin-flip ladder diagrams, was shown to have a profound impact on the electronic band structure of Fe, Co, and Ni. For example, it predicted a band anomaly in iron that was later confirmed experimentally. In the present work [2], we refine the method by combining GT with the GW self-energy. The resulting GWT spectral functions exhibit strong lifetime effects and emergent dispersion anomalies. They are in a better agreement with experimental spectra than those obtained with GW or GT alone, even showing partial improvements over local-spin-density approximation dynamical mean-field theory. The shape of the iron band anomaly improves, too. We acknowledge the Center of Excellence MaX Materials Science at the Exascale (EU H2020-INFRAEDI-2018) for financial support.

[1] M.C.T.D. Müller, S. Blügel, and C. Friedrich, Phys. Rev. B **100**, 045130 (2019)

[2] D. Nabok, S. Blügel, and C. Friedrich, Npj Comput. Mater. **7**, 178 (2021)

MA 38.6 Fri 10:45 H43

Effective exchange interaction in non-collinear states from electronic structure theory — •SIMON STREIB¹, RAMON CARDIAS², MANUEL PEREIRO¹, ANDERS BERGMAN¹, ERIK SJÖQVIST¹, CYRILLE BARRETEAU³, ANNA DELIN², OLLE ERIKSSON^{1,4}, and DANNY THONIG^{4,1} — ¹Department of Physics and Astronomy, Uppsala University, Sweden — ²Department of Applied Physics, School of Engineering Sciences, KTH Royal Institute of Technology, Sweden — ³SPEC, CEA, CNRS, Université Paris-Saclay, France — ⁴School of Science and Technology, Örebro University, Sweden

The determination of exchange parameters in non-collinear magnetic configurations directly from the electronic structure has been a challenge since the initial development of the Lichtenstein-Katsnelson-Antropov-Gubanov (LKAG) formalism for collinear configurations. Usually, the isotropic exchange interaction between two magnetic moments is only taken into account to bilinear order (Heisenberg exchange). We introduce instead a generalized isotropic two-spin exchange interaction, which takes all orders into account, and from which we derive an effective exchange interaction. We demonstrate how in an arbitrary non-collinear configuration this effective exchange interaction can be extracted from the energy curvature tensor, which describes the local energy curvature with respect to the directions of two magnetic moments. We apply our formalism to examples from tight-binding electronic structure and demonstrate strong fluctuations of the effective exchange interaction during spin dynamics simulations [1].

[1] S. Streib et al., arXiv:2203.11759.

MA 38.7 Fri 11:00 H43

Electric-field control of the exchange interactions — •SVITLANA POLESYA¹, SERGIY MANKOVSKY¹, ESZTER SIMON¹, ALBERTO MARMODORO², and HUBERT EBERT¹ — ¹Dept. Chemistry, LMU Munich, Butenandtstrasse 11, D-81377 Munich, Germany — ²Inst. of Physics, Czech Academy of Sciences, Cukrovarnicka 10, 162 00 Praha 6, Czech Republic

The impact of an applied electric field on the exchange coupling parameters has been investigated based on first-principles electronic structure calculations by means of the KKR Green function method. The calculations have been performed for a Fe monolayer (ML) and for deposited Fe films on different substrates, i.e., metallic (Pt) and semiconducting (GaAs). We analyze the origin of the field-induced change of the exchange interactions J_{ij} and the features of their field-dependent behavior specific for the studied systems. In particular, rather pronounced changes of J_{ij} have been found for the Fe/Pt(111) system due to the localized electronic states at the Fe/Pt interface. In the case of Fe/GaAs(001) films we discuss also the dependence of the field-induced modification of J_{ij} on the thickness of the Fe film. For all studied systems, a strong impact of surface relaxation is found both for the ground-state exchange parameters as well as for their field induced modification.

MA 39: Magnetic Particles / Clusters

Time: Friday 9:30–11:00

Location: H47

MA 39.1 Fri 9:30 H47

Direct determination of magnetic properties from energy landscapes around trapped magnetic beads — FLORIAN OSTERMAIER, MORITZ QUINCKE, BENJAMIN RIEDMÜLLER, MENG LI, MANUEL HERSCHEL, and •ULRICH HERR — Institut für Funktionelle Nanosysteme, Universität Ulm

Many Lab-on-Chip applications make use of micrometer sized polystyrene beads containing superparamagnetic iron oxide nanoparticles. Precise knowledge of magnetic properties is important for well-controlled manipulation by magnetic fields. We present a study of pairs of magnetic beads trapped in a current-carrying micro ring structure combined with a superimposed homogeneous field [1]. The trapped particles interact via repulsive dipole-dipole interaction. From

analysis of the Brownian motion of the trapped particles we can extract information about the trap stiffness as well as the magnetic moments of the beads. The trap stiffness obtained in this way is compared to analytical and numerical calculations of the magnetic field distribution in the vicinity of the micro ring structure. We find that the restricted movement of the two interacting beads in the trap structure leads to a faster and more accurate measurement of the beads compared to observations made on single beads trapped in the same structure.

[1] F. Ostermaier, M. Quincke, B. Riedmüller, M. Li, M. Herschel, U. Herr, J. Phys. Chem. C **2022**, 126, 7272-7280, DOI 10.1021/acs.jpcc.2c00759

MA 39.2 Fri 9:45 H47

Room-temperature synthesis of AuFe solid solution nanoparticles and their transformation to Au/Fe Janus nanostructures — MARIA V. EFREMOVA¹, MARINA SPASOVA², MARKUS HEIDELMANN³, MICHAEL FARLE², and ULF WIEDWALD² — ¹Department of Applied Physics, Eindhoven University of Technology, Netherlands — ²Faculty of Physics and Center for Nanointegration Duisburg-Essen, University of Duisburg-Essen, Germany — ³ICAN - Interdisciplinary Center for Analytics on the Nanoscale and Center for Nanointegration Duisburg-Essen, University of Duisburg-Essen, Germany

AuFe solid solution nanoparticles (NPs) are synthesized in ambient conditions by colloidal chemistry previously established for a Fe₃O₄ – Au core-shell morphology [1]. These AuFe NPs preserve the fcc structure of Au with paramagnetic Fe ions incorporated. Interestingly, the solid solution is metastable at room temperature forming Fe-rich regions in the Au matrix during storage. In situ annealing experiments up to 700°C in a transmission electron microscope and vibrating sample magnetometer leads to segregation of metallic Fe from the AuFe solid solution finally forming Au/Fe Janus NPs. The ferromagnetic bcc Fe grows epitaxially on low index fcc Au planes. The study facilitates the reassessment of possible applications of such NPs leading to a new material for magnetoplasmonics. First tests for biomedical applications are presented.

[1] M.V. Efremova, M. Spasova, M. Heidelmann, et al., *Nanoscale* 13, 10402 (2021).

MA 39.3 Fri 10:00 H47

Structural, chemical and magnetic properties of iron-oxide core-shell nanocubes — ALADIN ULLRICH, MICHAEL KÜHN, and MANFRED ALBRECHT — Institut für Physik, Universität Augsburg, 86159 Augsburg, Germany

Iron oxide nanoparticles in the size range from 8 to 17 nm were synthesized by thermal decomposition of iron oleate precursor in a high-boiling solvent with Na-oleate as surfactant to produce cubic nanoparticles. The structural composition of the nanoparticles was investigated by transmission electron microscopy and electron energy loss spectroscopy, revealing a core-shell structure with a wustite like structure in the core and a spinel like structure in the shell [1]. Changes in the oxidation state of the iron as well as the core/shell ratio were determined. The core/shell ratio was tuned by successive oxidation until the core had disappeared completely. A sample series consisting of 8 different core/shell ratios was produced during the oxidation process. The magnetic properties of this antiferromagnetic core - ferrimagnetic shell system like exchange bias, coercivity, and blocking behaviour were investigated. With decreasing core/shell ratio the blocking temperature, the coercivity, as well as the exchange anisotropy decreased. Besides this, the influence of the particle size on the magnetic properties was studied as well. Here, for rising particle size an increasing blocking temperature, as well as an increasing exchange anisotropy in the blocked state at low temperatures was found.

[1] A. Ullrich, et al., *Sci. Rep.* 9, 19264 (2019).

MA 39.4 Fri 10:15 H47

Effect of laser treatment on catalyst materials investigated by Mössbauer spectroscopy — SOMA SALAMON¹, JOACHIM LANDERS¹, SWEN ZEREBECKI², SVEN REICHENBERGER², STEPHAN BARCIKOWSKI², and HEIKO WENDE¹ — ¹Faculty of Physics and CENIDE, University of Duisburg-Essen — ²Institute for Technical Chemistry I and CENIDE, University of Duisburg-Essen

Mössbauer spectroscopy is utilized as a non-destructive, element-specific measurement method to probe hyperfine interactions in spinels that are promising candidates for application in electrocatalysis. By recording low temperature (4.3 K) high field (5-10 T) spectra, it is possible to discern individual contributions from tetrahedrally and octahedrally coordinated crystallographic sites found in the spinel lattice of materials such as CoFe₂O₄, enabling access to the

degree of inversion. Latter provides the distribution of Fe ions across these sites, while also allowing insight regarding the displacement of other ions within the lattice. This enables us to correlate changes in ion distribution in the lattice with improvements in catalytic activity, also giving clues about which ions on which positions serve as active sites during catalysis. Our results show that single-pulse laser excitation can selectively modify the ion distribution, while leaving the particles and their morphology largely intact. Further experiments also include tests of laser-induced diffusion of Fe into Co₃O₄ particles, with the use of isotope-pure ⁵⁷Fe allowing Mössbauer experiments to be performed on samples that do not normally contain any Fe. Funding by the DFG via the CRC/TRR 247 (ID 388390466, Projects B2, C5) is acknowledged.

MA 39.5 Fri 10:30 H47

Towards FeRh nanoparticles for printable magnetocaloric media — JOACHIM LANDERS¹, SOMA SALAMON¹, RUKSAN NADARAJAH², SHABBIR TAHIR², BENEDIKT EGGERT¹, BILAL GÖKÇE², and HEIKO WENDE¹ — ¹Faculty of Physics and CENIDE, University of Duisburg-Essen — ²Materials Science and Additive Manufacturing, University of Wuppertal

Magnetocaloric (MC) materials are promising candidates for energy efficient cooling applications. Here, FeRh nanoparticles prepared via laser ablation in liquids (LAL) are studied as possible means towards printable MC media. First experiments focused on how to minimize surface oxidation during nanoparticle preparation in solution. After ensuring low oxidation levels, our main interest was to find a method to regain the FeRh B2 structure and its MC properties during further processing. For that purpose, extensive studies via magnetometry, XRD and Mössbauer spectroscopy were performed to analyze magnetic structure and phase composition when exposing the particles to elevated temperatures, as would occur during laser printing of MC structures. We observed a transition from the predominant γ -FeRh-phase formed during laser particle synthesis to the B2-phase we aimed for, constituting a maximum B2-fraction of ca. 90 % of the material. Ongoing studies are currently searching for optimum processing parameters for laser-sintering of the FeRh-NP-based inks in an approach to form 2D magnetocaloric structures, with first results indicating the presence of the field-induced B2-phase antiferro- to ferromagnetic transition. This work is supported by the DFG through CRC/TRR 270.

MA 39.6 Fri 10:45 H47

Drifting inwards in protoplanetary discs: The role of hydrogen on planetesimal formation — CYNTHIA PILLICH¹, JANOSCH TASTO¹, TABEA BOGDAN², JOACHIM LANDERS¹, GERHARD WURM², and HEIKO WENDE¹ — ¹Faculty of Physics and Center for Nanointegration Duisburg-Essen (CENIDE), University of Duisburg-Essen, Lotharstr. 1, 47057 Duisburg, Germany — ²Faculty of Physics, University of Duisburg-Essen, Lotharstr. 1, 47057 Duisburg, Germany

Dust particles in protoplanetary discs, which can be seen as building blocks for planetesimals, are coupled to gas, mostly hydrogen. Due to this coupling, those particles may drift towards the inner part of the disc and are therefore exposed to very high temperatures, allowing for compositional and structural changes. To simulate the conditions at the early phase of planetary formation, two chondrites were milled to dust and subjected to temperatures up to 1400 K in a hydrogen atmosphere of approximately 1 mbar. The changes in composition were then studied by the means of ⁵⁷Fe Mössbauer spectroscopy and magnetometry. Comparing these results to vacuum tempered dust, we observe an influence of the heating atmosphere on compositional changes in the meteorites. At very high temperatures (>1200 K), Fe silicates are mostly reduced to metallic FeNi, altering adhesive properties of protoplanetary dust and therefore the potential for planetesimal growth.

Funding by the DFG (projects WE 2623/19-1 and WU 321/18-1) is gratefully acknowledged.

MA 40: Weyl Semimetals

Time: Friday 9:30–10:45

Location: H48

MA 40.1 Fri 9:30 H48

Magneto-optical detection of topological contributions to the anomalous Hall effect — FELIX SCHILBERTH^{1,2}, NICO UNGLERT³, LILIAN PRODAN¹, CHRISTINE KUNTSCHER⁴, LIVIU CHIONCEL³, and SÁNDOR BORDÁCS² — ¹Experimentalphysik V, Augsburg University, Augsburg, Germany — ²Department of Physics, BME Budapest, Hungary — ³Theoretische Physik III, Augsburg University, Augsburg, Germany — ⁴Experimentalphysik II, Augsburg University, Augsburg, Germany

The anomalous Hall effect (AHE) is a profound manifestation of non-trivial band structure topology in magnetic materials. The ambiguous separation of its intrinsic and extrinsic contributions leads to a fundamental limitation in identifying topological states based on common magnetotransport experiments. Here we demonstrate, via a case study on the prominent topological kagome magnet Fe₃Sn₂, that the intrinsic contribution to AHE can be determined un-

ambiguously from the broadband spectrum of the optical Hall effect, obtained by energy-resolved magneto-optical Kerr-effect (MOKE) measurements. Using MOKE spectroscopy complemented with material-specific theory, we identified the interband excitations responsible for the intrinsic AHE. We found that low-energy transitions, tracing "helical volumes" in momentum space reminiscent of the formerly predicted helical nodal lines, substantially contribute to the AHE, which is further increased by contributions from multiple higher-energy interband transitions. Our calculation also shows that local Coulomb interactions lead to important band reconstructions near the Fermi level.

MA 40.2 Fri 9:45 H48

Magnetic and transport properties of Mn₃Sn and Fe doped Mn₃Sn Weyl semimetal — •SUBHADIP JANA — Jülich Centre for Neutron Science (JCNS-2) and Peter Grünberg Institute (PGI-4), JARA-FIT, Forschungszentrum Jülich GmbH, D-52425 Jülich, Germany

A large Anomalous Hall Effect (AHE) has been found in Mn₃Sn due to the non-vanishing Berry flux emerging from the Weyl points. This compound draws enormous interest due to the complicated magnetic structure and its correlation with the transport properties. We observed AHE from 420 K ($T_N = 420$ K) down to 5 K for Mn_{3.17}Sn. From single-crystal neutron diffraction, we conclude that the magnetic structure is commensurate with magnetic moments in the hexagonal basal plane between 420 K (T_N) < T < 5 K. An additional incommensurate phase appears below 250 K. The presence of AHE in the whole temperature range is consistent with the commensurate magnetic structure. Fe doping influences the nearest-neighbor exchange energy, thereby changing the magnetic and transport properties. The Néel temperature was found to be 405 K for Mn_{3.02}Fe_{0.08}Sn, slightly lower than the parent compound. The commensurate magnetic structure has been observed between 210 K < T < 405 K from neutron powder diffraction. An incommensurate magnetic phase was observed below 210 K. The electro-transport study of Fe-doped sample shows vanishing AHE below 207 K. Therefore, we conclude that Fe doping significantly influences the magnetic structure in the commensurate region and that AHE completely vanishes in the incommensurate region.

MA 40.3 Fri 10:00 H48

Anomalous transport properties of the topological (Weyl) semimetal: Hexagonal - (Mn_{1- α} Fe _{α})₃Ge — •VENUS RAI¹, SHIBABRATA NANDI¹, ANNE STUNAU², WOLFGANG SCHMIDT³, SUBHADIP JANA¹, JIAN-RUI SOH⁴, JÖRG PERSSON¹, and THOMAS BRÜCKEL¹ — ¹Jülich Centre for Neutron Science (JCNS-2) and Peter Grünberg Institute (PGI-4), JARA-FIT, Forschungszentrum Jülich, Germany — ²Institut Laue-Langevin, 71 avenue des Martyrs, CS20156, Grenoble, France — ³Forschungszentrum Jülich GmbH, Jülich Centre for Neutron Science at ILL, 71 Avenue des Martyrs, Grenoble, France — ⁴Institute of Physics, Ecole Polytechnique Fédérale de Lausanne (EPFL), CH-1015 Lausanne, Switzerland

Weyl semimetal (WS) - Mn₃Ge displays a large anomalous Hall effect (AHE), which originates from the non-zero Berry curvature. The location and separation of the Weyl nodes can be tuned using a suitable dopant. So, we have studied the evolution of transport properties of single-crystal (Mn_{1- α} Fe _{α})₃Ge. We observed that the strength of AHE and chiral anomaly weakens drastically with an increase in Fe doping and vanishes beyond $\alpha = 0.22$. Polarized and unpolarized neutron diffraction of $\alpha = 0.22$ showed that the magnetic structure of the compound remains the same as that of the parent compound, only in the

temperature regime where AHE and the chiral anomaly are observed. These observations suggest the location of Weyl points and separation between a pair of Weyl points change significantly with Fe doping. Therefore, suitable dopants can be used to tune the transport properties of the WS.

MA 40.4 Fri 10:15 H48

Prediction of a new type-I Weyl semimetal in a full-Heusler compound — •DAVIDE GRASSANO and NICOLA MARZARI — Theory and Simulations of Materials (THEOS) and National Center for Computational Design and Discovery of Novel Materials (MARVEL), Ecole Polytechnique Fédérale de Lausanne, CH-1015 Lausanne, Switzerland

Weyl semimetals are a class of topological semimetals with linear band crossings close to the Fermi level with non-trivial chirality, the existence of which gives rise to several exotic physical properties [1,2]. In order for such crossings to exist, either time-reversal or inversion symmetry must be broken [3]. Here we identify a new inversion-breaking Weyl semimetal. This material shows several features that are comparatively more intriguing with respect to other known inversion-breaking Weyl semimetals. The distance between two neighboring nodes is large enough to observe a wide range of linear dispersion in the band and only one kind of nodes can be identified. Finally, the lack of other trivial points insures that the low-energy properties of the material can be directly related to the presence of the Weyl nodes.

[1] Murakami S., New Journal of Physics 9.9 (2007):356

[2] Armitage NP, Mele EJ, Vishwanath A. - Rev. Mod. Phys. 90.1 (2018):015001

[3] Wan, Xiangang, et al. Phys. Rev. B 83.20 (2011): 205101

MA 40.5 Fri 10:30 H48

Multifold Hopf semimetals — •ANSGAR GRAF and FRÉDÉRIC PIÉCHON — Université Paris-Saclay, CNRS, Laboratoire de Physique des Solides, 91405, Orsay, France

Three-dimensional (3D) topological semimetals exhibit linear energy band crossings that act as monopole sources of Berry curvature. Here, we introduce *multifold Hopf semimetals (MHSs)*, which feature linear N -fold crossing points each of which acts as a *Berry dipole*. We construct models with $N = 3, 4, 5$ bands and show that their physical properties are crucially affected by the Berry dipole: First, it makes the Landau level spectrum strongly dependent on the orientation of an external magnetic field. Second, it causes an anomalous Hall effect and weak field magnetoconductivities resembling the chiral anomaly, chiral magnetic and magnetochiral effects familiar from a pair of coupled Weyl nodes. Gapping up MHSs, we obtain multiband Hopf insulators (MHIs) with Hopf numbers up to $\mathcal{N}_{\text{Hopf}} = 10$. MHSs and MHIs provide a fertile playground to explore delicate topology and exhibit analogies to 2D Dirac semimetals and Chern insulators.

MA 41: Micro- and Nanostructured Magnetic Materials

Time: Friday 11:30–12:45

Location: H47

MA 41.1 Fri 11:30 H47

Dynamic properties of magnetic Nanoparticles: arrangement-, distance- & frequency-dependent properties — •NILS NEUGEBAUER^{1,2}, HELMUT SCHULTHEISS³, XINGCHEN YE⁴, and PETER KLAR^{1,2} — ¹Institute of Experimental Physics I, Justus Liebig University Giessen, Heinrich-Buff-Ring 16, 35392 Giessen, Germany — ²Center for Materials Research (LaMa), Justus Liebig University Giessen, Heinrich-Buff-Ring 16, 35392 Giessen, Germany — ³Helmholtz-Center Dresden-Rossendorf, Institute of Ion Beam Physics and Materials Research, Bautzner Landstraße 400, 01328 Dresden, Germany — ⁴Department of Chemistry, Indiana University, Bloomington, 47405 Indiana, United States

Investigations focusing on the mutual dipolar interactions of magnetic nanoparticles (MNPs) are presented. As nanoparticles may be arranged into highly ordered, crystal-like structures, so called mesocrystals, novel properties may arise due to the introduction of an additional degree of freedom in manipulating the magnetic properties of a material. Manipulating the interparticle distance, distinct spectral features related to the dipole-dipole interaction can be observed. Based on these nano-building blocks, assemblies of MNPs of well-defined size and shape can be constructed. Such assemblies show distinct collective properties, e.g. well-localized magnetic vibrational modes, frequency- and field-dependent characteristics. The experiments are supported by utilizing numerical simulations of corresponding model systems to underline the observed characteristics.

MA 41.2 Fri 11:45 H47

Quantitative analysis of magnetic states in an artificial spin ice by off-axis electron holography — •TERESA WESSELS^{1,2}, SEBASTIAN GLIGA³, SIMONE FINIZIO³, ANDRAS KOVACS², and RAFAL DUNIN-BORKOWSKI² — ¹Faculty of Physics and Center for Nanointegration Duisburg-Essen (CENIDE), Univer-

sity Duisburg-Essen, 47057 Duisburg, Germany — ²Ernst Ruska-Centre for Microscopy and Spectroscopy with Electrons and Peter Grünberg Institute, Forschungszentrum Jülich, 52425 Jülich, Germany — ³Swiss Light Source, Paul Scherrer Institut, 5232 Villigen PSI, Switzerland

The study of emergent phenomena in artificial spin ices (ASIs) consisting of patterned nanomagnets is presently the focus of intense research. We used off-axis electron holography in the transmission electron microscope to quantitatively measure the magnetic phase shift induced by ASI with chiral geometry. The phase shift of the electron wave was measured using an electron biprism and interpreted using a model-based iterative reconstruction algorithm to retrieve the projected in-plane magnetization. The permalloy nanomagnets were patterned on a SiN membrane using lift-off lithography. Magnetic interactions within individual arrays were studied by applying in-plane magnetic fields to the sample. The reconstructed magnetization shows a single-domain state of the nanomagnets with an average magnetic polarization of 0.73 T. The low magnetic polarization value may result from a combination of the microstructure, composition, and oxidation. The project received funding from the ERC (856538) and the DFG (392476493, 405553726).

MA 41.3 Fri 12:00 H47

Monolayer MnX and Janus XMnY (X, Y = S, Se, Te): A New Family of 2D Antiferromagnetic Semiconductors — •SHAHID SATTAR, MD FHOKRUL ISLAM, and CARLO MARIA CANALI — Department of Physics and Electrical Engineering, Linnaeus University, Kalmar SE-39231, Sweden

We present first-principles results on the structural, electronic, and magnetic properties of a new family of two-dimensional antiferromagnetic (AFM) manganese chalcogenides, namely monolayer MnX and Janus XMnY (X, Y = S, Se, Te). By carrying out calculations of the phonon dispersion and ab-initio molec-

ular dynamics simulations, we first confirmed that these systems, characterized by an unconventional strongly-coupled-bilayer atomic structure (consisting of Mn atoms buckled to chalcogens forming top and bottom ferromagnetic (FM) planes with antiparallel spin orientation) are dynamically and thermally stable. The analysis of the magnetic properties shows that these materials have robust AFM order, whereas electronic structure calculations reveal that pristine MnX and their Janus counterparts are indirect-gap semiconductors, covering a wide energy range and displaying tunable band gaps by the application of biaxial tensile and compressive strain. Interestingly, owing to the absence of inversion and time-reversal symmetry, and the presence of an asymmetrical potential in the out-of-plane direction, Janus XMnY become spin-split gapped systems, presenting a rich physics yet to be explored. Our findings provide novel insights in this physics, and highlight the potential of two-dimensional manganese chalcogenides in AFM spintronics.

MA 41.4 Fri 12:15 H47

Magnetic properties of cobalt - nanomagnets: towards spin qubit control — •LIZA ZAPER^{1,2}, PETER RICKHAUS², ALEXANDER STARK², FLORIS BRAAKMAN¹, and MARTINO POGGIO¹ — ¹University of Basel, Basel, Switzerland — ²Qnami AG, Muttentz, Switzerland

A promising platform to realise quantum computation uses the spin states of confined electrons to define the qubit. In order to achieve reliable control and high integration of spin qubit devices on a chip, we aim to pattern nanometer-scale magnets that have large magnetic field gradients at the position of the confined electron. We fabricate highly magnetic cobalt nanostructures using focused-electron-beam-induced deposition. We characterize the magnetization

properties of the nanomagnets by NV scanning microscopy, as well as magnetotransport. The scanning probe images indicate the structure of the magnetic domains and the profile of the magnetic stray fields, which can be further used as a guideline for qubit device optimisation.

MA 41.5 Fri 12:30 H47

Cellulose nanocomposite with SrFe₁₂O₁₉ nanoparticles as a novel magnetic nanopaper coating — •ANDREI CHUMAKOV¹, KORNELIYA GORDEYEVA², CALVIN J. BRETT^{1,2}, ANASTASIA V. RIAZANOVA², DIRK MENZEL³, DANIEL SOEDERBERG², and STEPHAN V. ROTH^{1,2} — ¹DESY, Hamburg, Germany — ²KTH Royal Institute of Technology, Stockholm, Sweden — ³TU Braunschweig, Braunschweig, Germany

The possibility of the coating by a new magnetic nanocomposite based on negatively charged cellulose colloids (1360 μmol/g) and positively charged hard magnetic hexaferrite (SrFe₁₂O₁₉) nanoparticles with a large permanent magnetic moment was demonstrated. Thin nanofilms of magnetic cellulose composite were obtained by spray deposition on a silicon substrate and studied by microscopic imaging, surface-sensitive X-ray scattering, and magnetic determining techniques. Ferromagnetic nanoparticles are uniformly distributed in the cellulose matrix and form a nanocomposite due to the opposite charges of the initial components. Magnetic nanoplates show a predominant orientation parallel to the plane of the substrate and the resulting nanocomposite has the highest intrinsic coercivity field inherent in the properties of individual nanoparticles. Coatings of magnetic nanopaper with a large coercive field can be widely used from catalysis to promising nanoelectronic devices.

MA 42: Magnetic Heuslers

Time: Friday 11:30–12:45

Location: H48

MA 42.1 Fri 11:30 H48

First-principles study of magnetic tunnel junctions based on half-metallic and spin-gapless semiconducting Heusler compounds: Reconfigurable diode and inverse TMR effect — •THORSTEN AULL, ERSOY SASIOGLU, and INGRID MERTIG — Martin-Luther-Universität Halle-Wittenberg, Institut für Physik, 06120 Halle (Saale)

Magnetic tunnel junctions (MTJs) based on half-metallic magnets (HMMs) and spin-gapless semiconductors (SGSs) exhibit unique properties, such as current rectification, i.e., diode effect, and reconfigurability in addition to a tunnel magnetoresistance (TMR) effect [1]. We investigate from first-principles MTJs based on SGS and HMM quaternary Heusler compounds [2]. Our quantum transport calculations have demonstrated that these MTJs exhibit current rectification with high on/off ratios. Moreover, depending on the relative orientation of the magnetization of the electrodes, the MTJ allows the electrical current to pass either in one or the other direction, which leads to an inverse TMR effect. We show that, in contrast to conventional semiconductor diodes, the rectification bias voltage window of the MTJs is limited by the spin gap of the HMM and SGS Heusler compounds. The combination of nonvolatility, reconfigurable diode functionality, and high Curie temperatures of the electrode materials makes the proposed MTJs very promising for room temperature spintronic applications and opens new ways to magnetic memory and logic concepts.

[1] N. Maji and T. Nath, *Appl. Phys. Lett.* **120**, 072401 (2022).

[2] T. Aull *et al.*, arXiv:2202.06752 (2022).

MA 42.2 Fri 11:45 H48

Exploring all 3d-metal Heusler alloys for functional properties: density functional theory + Monte Carlo study — •MADHURA MARATHE and HEIKE C. HERPER — Department of Physics and Astronomy, Uppsala University, 75120 Uppsala, Sweden.

The search for cost-effective and rare-earth metal free permanent magnets is essential for various applications. In this study, we explore a novel class of Heusler alloys consisting of all 3d-metals. We do high-throughput studies using an electronic structure database to search for X₂YZ-type Heuslers (X = Fe, Ni) with tetragonal symmetry and high magnetic moments. We perform density functional theory calculations to obtain the ground state structure, magnetic anisotropy energy (MAE) as well as the exchange interaction parameters J_{ij} for selected materials. Using the calculated J_{ij} 's, we map our system on a Heisenberg model and perform Monte Carlo simulations to calculate the Curie temperature. Through such multiscale modeling, we aim to identify potential candidates for permanent magnets. We find that for these systems J_{ij} 's have oscillations over a long range with both ferromagnetic and antiferromagnetic interactions, and it is essential to include these in the model to capture correct transition.

MA 42.4 Fri 12:15 H48

Tuning of the effective magnetic decoupling in Ni-Mn-(In,Sn) Heusler alloys — •OLGA N. MIROSHKINA¹, FRANCESCO CUGINI^{2,3}, SIMONE CHICCO², FABIO ORLANDI⁴, GIUSEPPE ALLODI², PIETRO BONFÀ², VINCENZO VEZZONI², LARA RIGHI^{2,3}, FRANCA ALBERTINI³, ROBERTO DE RENZI², MASSIMO SOLZI^{2,3}, and MARKUS E. GRUNER¹ — ¹Department of Physics and CENIDE, University of Duisburg-Essen, Duisburg, Germany — ²University of Parma, Parma, Italy — ³IMEM-CNR, Parma, Italy — ⁴Rutherford Appleton Laboratory, Chilton, Didcot, Oxfordshire, United Kingdom

The magnetocaloric effect at first-order phase transitions is considered as an efficient and ecologically friendly alternative to conventional compressor cooling. This contribution is devoted to the complex magnetic ordering mechanisms in magnetocaloric Ni-Mn-(In,Sn) Heusler alloys, which we explore by means of density functional theory. The calculations accompany extensive experimental investigations, which reveal a non-monotonic trend in the Curie temperature and an effective magnetic decoupling of 4a and 4b sublattices [1]. Our first-principles calculations confirm a composition-dependent competition of the effective ferromagnetic and antiferromagnetic coupling between the sublattices, which can be directly controlled by electron doping in terms of In/Sn substitution. This result shows the possibility of fine-tuning of Heusler materials via exchanging the main-group element increasing the range of their potential applications. This work is funded by DFG within CRC/TRR 270 (project no. 405553726).

[1] F. Cugini *et al.*, *Phys. Rev. B* **105**, 174434 (2022).

MA 42.5 Fri 12:30 H48

Noncollinear magnetic order in epitaxial thin films of the MnPtGa hard magnet — •REBECA IBARRA^{1,2}, ÉDOUARD LESNE¹, BACHIR OULADDIAF³, KETTY BEAUVOIS³, ALEXANDR SUKHANOV², RAFAL WAWRZYŃCZAK¹, WALTER SCHNELLE¹, ANTON DEVISHVILI³, DMYTRO INOSOV², CLAUDIA FELSER¹, and ANASTASIOS MARKOU¹ — ¹Max-Planck-Institute für Chemische Physik fester Stoffe, D-01187 Dresden, Germany — ²Institut für Festkörper- und Materialphysik, Technische Universität Dresden, D-01069 Dresden, Germany — ³Institut Laue-Langevin, CS20156, 38042 Grenoble Cedex 9, France

Noncollinear magnetism has attracted great attention in the recent years and promise rich exotic properties with potential for spintronic applications. In

this work, we present a detailed analysis of the structural and magnetic properties of high-quality thin films of the hexagonal MnPtGa hard magnet grown on Al₂O₃(0001) substrates. The films crystalize in the $P6_3/mmc$ space group, with an ordering temperature of $T_C = 263$ K into a ferromagnetic (FM) state, followed by a spin reorientation transition at $T_{sr} \sim 160$ K. A large uniaxial magnetic anisotropy is observed in this centrosymmetric compound. We further investigate the magnetic transitions by single-crystal neutron diffraction at zero applied magnetic field. The emergence of the structurally forbidden (001) Bragg reflection for $T < 160$ K, unequivocally determines a transition to a spin canted state, where the Mn magnetic moments align ferromagnetically along the c -axis and antiferromagnetically in the basal plane, resulting in a spin canting angle of 20° respect to the c -axis.

Metal and Material Physics Division Fachverband Metall- und Materialphysik (MM)

Astrid Pundt
Institut für Angewandte Materialien-Werkstoffkunde (IAM-WK)
Karlsruher Institut für Technologie (KIT)
Kaiserstraße 12
76131 Karlsruhe
astrid.pundt@kit.edu

Overview of Invited Talks and Sessions

(Lecture halls H44, H45, and H46; Poster P2)

Invited Talks

MM 1.1	Mon	9:30–10:00	H44	A novel mechanism to generate metallic single crystals — •CAROLIN KÖRNER, JULIAN PISTOR, JOHANNES BÄREIS, MATTHIAS MARKL
MM 11.1	Tue	9:30–10:00	H44	Fast calorimetry: studying phase transitions in slow motion — •JÖRG F. LÖFFLER
MM 19.1	Wed	9:30–10:00	H44	High-Entropy Alloys: Materials design in high dimensional chemical space from ab initio thermodynamics — •FRITZ KÖRMANN
MM 27.1	Thu	9:30–10:00	H44	Crystal rotation kinematics during the tribological loading of high-purity copper — •CHRISTIAN GREINER

Invited Talks of the joint Symposium SKM Dissertation Prize 2022 (SYSD)

See SYSD for the full program of the symposium.

SYSD 1.1	Mon	10:15–10:45	H2	Charge localisation in halide perovskites from bulk to nano for efficient optoelectronic applications — •SASCHA FELDMANN
SYSD 1.2	Mon	10:45–11:15	H2	Nonequilibrium Transport and Dynamics in Conventional and Topological Superconducting Junctions — •RAFFAEL L. KLEES
SYSD 1.3	Mon	11:15–11:45	H2	Probing magnetostatic and magnetotransport properties of the antiferromagnetic iron oxide hematite — •ANDREW ROSS
SYSD 1.4	Mon	11:45–12:15	H2	Quantum dot optomechanics with surface acoustic waves — •MATTHIAS WEISS

Invited Talks of the joint Symposium From Physics and Big Data to the Design of Novel Materials (SYNM)

See SYNM for the full program of the symposium.

SYNM 1.1	Mon	15:00–15:30	H1	How to tackle the "I" in FAIR? — •CLAUDIA DRAXL
SYNM 1.2	Mon	15:30–16:00	H1	Beyond the average error: machine learning for the discovery of novel materials — •MARIO BOLEY, SIMON TESHUVA, FELIX LUONG, LUCAS FOPPA, MATTHIAS SCHEFFLER
SYNM 1.3	Mon	16:00–16:30	H1	The Phase Diagram of All Inorganic Materials — •CHRIS WOLVERTON
SYNM 1.4	Mon	16:45–17:15	H1	Automated data-driven upscaling of transport properties in materials — •DANNY PEREZ, THOMAS SWINBURNE
SYNM 1.5	Mon	17:15–17:45	H1	Data-driven understanding of concentrated electrolytes — •ALPHA LEE

Invited Talks of the joint Symposium United Kingdom as Guest of Honor (SYUK)

See SYUK for the full program of the symposium.

SYUK 1.1	Wed	9:30–10:00	H2	Structure and Dynamics of Interfacial Water — •ANGELOS MICHAELIDES
SYUK 1.2	Wed	10:00–10:30	H2	A molecular view of the water interface — •MISCHA BONN
SYUK 1.3	Wed	10:30–11:00	H2	Motile cilia waves: creating and responding to flow — •PIETRO CICUTA

SYUK 1.4	Wed	11:00–11:30	H2	Cilia and flagella: Building blocks of life and a physicist's playground — •OLIVER BÄUMCHEN
SYUK 1.5	Wed	11:45–12:15	H2	Computational modelling of the physics of rare earth - transition metal permanent magnets from SmCo₅ to Nd₂Fe₁₄B — •JULIE STAUNTON
SYUK 2.1	Wed	15:00–15:30	H2	Hysteresis Design of Magnetic Materials for Efficient Energy Conversion — •OLIVER GUTFLEISCH
SYUK 2.2	Wed	15:30–16:00	H2	Non-equilibrium dynamics of many-body quantum systems versus quantum technologies — •IRENE D'AMICO
SYUK 2.3	Wed	16:00–16:30	H2	Quantum computing with trapped ions — •FERDINAND SCHMIDT-KALER
SYUK 2.4	Wed	16:45–17:15	H2	Breaking the millikelvin barrier in cooling nanoelectronic devices — •RICHARD HALEY
SYUK 2.5	Wed	17:15–17:45	H2	Superconducting Quantum Interference Devices for applications at mK temperatures — •SEBASTIAN KEMPF

Invited Talks of the joint Symposium Frontiers of Electronic-Structure Theory: Focus on Artificial Intelligence Applied to Real Materials (SYES)

See SYES for the full program of the symposium.

SYES 1.1	Thu	15:00–15:30	H1	Machine-learning-driven advances in modelling inorganic materials — •VOLKER L. DERINGER
SYES 1.2	Thu	15:30–16:00	H1	Machine-Learning Discovery of Descriptors for Square-Net Topological Semimetals — •EUN-AH KIM
SYES 1.3	Thu	16:00–16:30	H1	Four Generations of Neural Network Potentials — •JÖRG BEHLER
SYES 1.4	Thu	16:30–17:00	H1	Using machine learning to find density functionals — •KIERON BURKE
SYES 1.5	Thu	17:00–17:30	H1	Coarse graining for classical and quantum systems — •CECILIA CLEMENTI

Sessions

MM 1.1–1.1	Mon	9:30–10:00	H44	Invited Talk Carolin Körner
MM 2.1–2.10	Mon	10:15–13:00	H44	Computational Materials Modelling: Energy Materials
MM 3.1–3.9	Mon	10:15–12:45	H45	Microstructures and Phase Transformations: Metals & Alloys
MM 4.1–4.10	Mon	10:15–13:00	H46	Structural Materials
MM 5.1–5.1	Mon	15:00–15:30	H44	Non-equilibrium Phenomena in Materials Induced by Electrical and Magnetic Fields 1
MM 6.1–6.10	Mon	15:45–18:30	H44	Computational Materials Modelling: Defects / Alloys
MM 7.1–7.5	Mon	15:45–17:00	H45	Microstructures and Phase Transformations: Oxides & Perovskites
MM 8.1–8.10	Mon	15:45–18:30	H46	Materials for Storage and Conversion of Energy
MM 9.1–9.4	Mon	17:15–18:30	H45	Non-equilibrium Phenomena in Materials Induced by Electrical and Magnetic Fields 2
MM 10.1–10.30	Mon	18:00–20:00	P2	Poster Session 1
MM 11.1–11.1	Tue	9:30–10:00	H44	Invited Talk Jörg F. Löffler
MM 12.1–12.10	Tue	10:15–13:00	H44	Computational Materials Modelling: Physics of Ensembles 1
MM 13.1–13.7	Tue	10:15–13:00	H45	Non-equilibrium Phenomena in Materials Induced by Electrical and Magnetic Fields 3
MM 14.1–14.5	Tue	10:15–11:30	H46	Materials for Storage and Conversion of Energy (joint session MM/KFM)
MM 15.1–15.5	Tue	11:45–13:00	H46	Hydrogen in Materials: Hydrogen Effects
MM 16.1–16.4	Tue	14:00–15:00	H44	Mechanical Properties
MM 17.1–17.5	Tue	14:00–15:15	H46	Hydrogen in Materials: Hydrogen Storage
MM 18.1–18.43	Tue	17:30–20:00	P2	Poster Session 2
MM 19.1–19.1	Wed	9:30–10:00	H44	Invited Talk Fritz Körmann
MM 20.1–20.10	Wed	10:15–13:00	H44	Computational Materials Modelling: HEA, Alloys & Nanostructures
MM 21.1–21.10	Wed	10:15–13:00	H45	Transport in Materials: Thermal transport
MM 22.1–22.8	Wed	10:15–13:00	H46	Data Driven Materials Science: Experimental Data Treatment and Machine Learning
MM 23.1–23.10	Wed	15:45–18:30	H44	Computational Materials Modelling: Magnetic & Electrical Properties
MM 24.1–24.7	Wed	15:45–18:30	H45	Non-equilibrium Phenomena in Materials Induced by Electrical and Magnetic Fields 4
MM 25.1–25.8	Wed	15:45–18:30	H46	Data Driven Materials Science: Computational Frameworks / Chemical Complexity
MM 26	Wed	18:45–20:15	H44	Members' Assembly
MM 27.1–27.1	Thu	9:30–10:00	H44	Invited Talk Christian Greiner

MM 28.1–28.5	Thu	10:15–11:30	H44	Transport in Materials: Diffusion / Electrical Transport & Magnetism
MM 29.1–29.5	Thu	10:15–11:30	H45	Data Driven Materials Science: Design of Functional Materials
MM 30.1–30.10	Thu	10:15–13:00	H46	Liquid and Amorphous Metals
MM 31.1–31.5	Thu	11:45–13:00	H44	Computational Materials Modelling: Physics of Ensembles 2
MM 32.1–32.5	Thu	11:45–13:00	H45	Nanomaterials: Surface Effects
MM 33.1–33.10	Thu	15:45–18:30	H44	Computational Materials Modelling: Process Schemes / Oxides
MM 34.1–34.10	Thu	15:45–18:30	H45	Data Driven Materials Science: Interatomic Potentials / Reduced Dimensions
MM 35.1–35.10	Thu	15:45–18:30	H46	Nanomaterials: Structure & Properties

Members' Assembly of the Metal and Material Physics Division

Wednesday 18:45–20:15 H44

Room	Montag, 5.9.		Dienstag, 6.9.		Mittwoch, 7.9.		Donnerstag, 8.9.					
	H44	H45	H46	H44	H45	H46	H44	H45	H46			
08:30	Plenary Talk			Plenary Talk			Plenary Talk					
08:45												
09:00												
09:15	Invited Talk Carolín Körner			Invited Talk Jörg Löffler			Invited Talk Fritz Körmann					
09:30												
09:45												
10:00												
10:15	Computational Energy materials I MM2	Phase Transf. Metals & alloys I MM3	Structural Materials I MM4	Computational Ensembles I MM12	Topical: Non-equ. Metal-based oxides Graeve Müller MM13	Energy Materials III MM14	transport Thermal transport MM20	Topical: data driven Data treatment & machine learning Koch MM22	transport Diffusion, electrical transport & magnetism MM28	Topical data drive Design of functional material materials MM29	Liquid and Amorphous Met. I MM30	
10:30												
10:45												
11:00												
11:15												
11:30												
11:45	Computational Energy materials II MM2	Phase Transf. Metals & alloys II MM3	Structural Materials II MM4	Computational Ensembles II MM12	Topical: Non-equ. Magnetism Maccari MM13	Hydrogen Effects MM15	transport Grain boundaries, diffusion & phase transitions MM21	Topical: data driven Data treatment & machine learning Hébert MM22	Computational Ensembles III MM31	Nanomaterials Surface effects MM32	Liquid and Amorphous Met. II MM30	
12:00												
12:15												
12:30												
12:45												
13:00	Prize Talk			Prize Talk			Prize Talk					
13:15												
13:30												
13:45												
14:00	Plenary Talk			Mechanical Properties MM16	Hydrogen Storage MM17		Plenary Talk					
14:15												
14:30												
14:45												
15:00	Topical: Non-equ. Kirchheim MM5											
15:15												
15:30												
15:45	Computational Defects MM6	Phase Transf. Oxides & perovskite MM7	Energy Materials I MM8				Computational Magnetic & electric properties MM23	Topical: Non-equ. Crystal structures Urban MM24	Topical: data driven Computational frameworks / chemical complexity Janssen MM25	Computational Process schemes MM33	Topical: data driver Interatomic potentials / reduced dimensions MM34	Nanomaterials Structure and properties I MM35
16:00												
16:15												
16:30												
16:45												
17:00												
17:15	Computational Alloys MM6	Topical: Non-equ. Material modification Choi MM9	Energy Materials II MM8				Computational electrical properties MM23	Topical: Non-equ. Sintering technique Luo MM24	Topical: data driven Computational frameworks / chemical complexity Sandfeld MM25	Computational Oxides MM33	Topical: data driver Interatomic potentials / reduced dimensions MM34	Nanomaterials Structure and properties I MM35
17:30												
17:45												
18:00												
18:15												
18:30												
18:45												
19:00												
19:15												
19:30												
19:45												
20:00												

Sessions

– Invited Talks, Topical Talks, Contributed Talks, and Posters –

MM 1: Invited Talk Carolin Körner

Time: Monday 9:30–10:00

Location: H44

Invited Talk

MM 1.1 Mon 9:30 H44

A novel mechanism to generate metallic single crystals — •CAROLIN KÖRNER, JULIAN PISTOR, JOHANNES BÄREIS, and MATTHIAS MARKL — Friedrich-Alexander Universität Erlangen-Nürnberg, Germany

Single crystals are used for high strength materials with high creep resistance such as turbine blades from nickel-base superalloys. The fabrication techniques applied to produce single crystals involve highly controlled and therefore relatively slow crystallization. For turbine blades, the Bridgman technique, i.e. investment casting combined with direction solidification, is the standard. The single crystal either develops starting from a single crystalline seed or by a geometric grain selection process. Microstructure evolution is determined by the

solidification conditions resulting in a dendrite arm spacing of several hundreds of microns. This contribution shows how single crystals from nickel-base superalloys develop without seed during layer by layer metal additive manufacturing (AM) in the powder bed. These AM single crystals develop under rapid and directional solidification conditions with solidification microstructures one or two orders of magnitude finer than in the conventional Bridgman process. In addition, the underlying mechanism to generate the single crystal is based on thermo-mechanical provoked texture formation. The latter allows a very precise orientation of the single crystal. A manipulation of the orientation is possible by applying adequate process strategies. The basis mechanisms leading to the single crystal and the implications on the resulting properties are discussed.

MM 2: Computational Materials Modelling: Energy Materials

Time: Monday 10:15–13:00

Location: H44

MM 2.1 Mon 10:15 H44

Importance of electronic correlations in exploring the exotic phase diagram of Li ion battery cathodes — •HRISHIT BANERJEE^{1,2}, CLARE P. GREY¹, and ANDREW J. MORRIS² — ¹Department of Chemistry, University of Cambridge, UK — ²School of Metallurgy and Materials, University of Birmingham, UK.

We explore electronic and magnetic states of layered Li_xMnO_2 , a well known cathode material for Li ion batteries, as a function of states of charge x , using *ab-initio* dynamical mean-field theory. Projecting onto low-energy subspace of Mn $3d$ states, and solving a multi-impurity problem, we find that an antiferromagnetic insulating state appears in LiMnO_2 , with a moderate Néel temperature in agreement with experimental studies. As the system is delithiated we find various exotic states emerge such as ferrimagnetic correlated metals, charge ordered ferromagnetic correlated metals with large quasiparticle weight, ferromagnetic metals with small quasiparticle weight, as a function of various states of delithiation of LiMnO_2 and finally an antiferromagnetic insulator for the fully delithiated state, which is albeit unstable. At moderate states of charge, $x=0.67-0.33$, a mix of +3/+4 formal oxidation states of Mn is observed, while its overall nominal oxidation state changes from +3 in LiMnO_2 to +4 in MnO_2 . In all these cases the high-spin state emerges as the most likely state. The quasiparticle peaks in the correlated metallic states could be attributed to polaronic states. We explore the temperature vs. state of charge phase diagram and conclude that the state of charge is a key ingredient for the emergence of the exotic correlated phase transitions in this material.

MM 2.2 Mon 10:30 H44

Quantum-mechanical characterization of sulfur/carbon co-polymer cathodes for Li-S batteries — •POUYA PARTOVI-AZAR — MLU Halle-Wittenberg, Germany

Lithium-sulfur (Li-S) batteries are among the candidates for next-generation energy-storage systems thanks to their high energy density which arises from a high lithium capacity of elemental sulfur. However, cycling performance of Li-S batteries is drastically declined by a reversible capacity fade which is brought about by the diffusion of soluble Li-polysulfides through the electrolyte.^[1,2]

It has been recently shown that polymeric sulfur cathodes exhibit a promising performance in limiting the shuttle effect during the discharge.^[2] However, a clear atomistic picture on the favorable structures and their lithiation mechanism is still not fully established.

Here, we report our recent works on structural and electronic properties as well as finite-temperature vibrational spectra of polymeric sulfur cathodes, namely sulfur/1,3-diisopropenylbenzene^[3] and sulfur/polyacrylonitrile-based nanofiber^[4] co-polymers obtained through quantum-mechanical calculations.

[1] Qing Zhang *et al.*, *Adv. Sci.* 2103798 (2021); [2] G. Bieker *et al.*, *Commun. Mater.* 2, 37 (2021); [3] R. Kiani *et al.*, *ChemPhysChem*, doi: 10.1002/cphc.202100519; [4] P. Partovi-Azar *et al.*, *Phys. Rev. Applied* 1, 014012 (2018); P. Partovi-Azar, *under review* (2022)

MM 2.3 Mon 10:45 H44

Si nanostructure formation in quenched AlSi μ -droplets for application as anode material in lithium-ion-batteries — •DAVID TUCHOLSKI and KARL-HEINZ HEINIG — Helmholtz-Center Dresden-Rossendorf, Dresden, Germany

We report on 3D lattice kinetic Monte Carlo (3DlKMC) simulation of nanostructure formation during rapid quenching in gas-atomization (up to 10^8K/s) of droplets of AlSi alloy melt. The nanostructured Si particles (with the Al selectively etched away) promise to enable about 10x the capacity of the current state-of-the-art graphite in lithium-ion batteries by mitigating Si pulverization.

This work reproduces the experimentally found nanosponge and core-shell particles and reveals heteronucleation at Al_2O_3 sites resulting from trace oxygen at the surface as the formation mechanism for core-shell particles.

The computer simulation uses a memory-efficient bit-encoded lattice, enabling large scale atomistic calculations, while kinetics is implemented via CPU-efficient bit-manipulation for atom jumps between lattice sites. The jump probabilities are described by the metropolis algorithm with a look-up-table of energies calculated with an angular dependent potential for the Si-Al-Au system in LAMMPS.

This work is supported by the federal ministry for economic affairs and climate protection under grant number 01221755/1.

MM 2.4 Mon 11:00 H44

Tackling structural complexity in $\text{Li}_2\text{S-P}_2\text{S}_5$ solid-state electrolytes using Machine Learning — •TABEA HUSS, CARSTEN STAACKE, JOHANNES MARGRAF, KARSTEN REUTER, and CHRISTOPH SCHEURER — Fritz-Haber-Institut der MPG The lithium thiophosphate (LPS) material class provides promising candidates for solid-state electrolytes (SSE) in lithium ion batteries due to high lithium ion conductivities, non-critical elements, and low material cost. LPS materials are characterized by complex thiophosphate microchemistry and structural disorder influencing the material performance. *Ab-initio* studies probing lithium ion conductivity are constrained in system size and simulated time scales. This limits the transferability of computational results to industrial applicable LPS materials. Therefore, we present the development of a data efficient training protocol for the LPS material class using the Gaussian Approximation Potential (GAP). The GAP model can likewise describe crystal and glassy materials and different P-S connectivities P_mS_n . We apply the GAP model to probe lithium ion conductivity and discuss the influence of poly-anions on the latter. The sampling approach allows for a variety of extension and transferability to other SSE.

MM 2.5 Mon 11:15 H44

Exploration of cathode-stable layered solid-state electrolytes — •SINA ZIEGLER, CHRISTOPH SCHEURER, and KARSTEN REUTER — Fritz-Haber-Institut der MPG, Berlin, Germany

Promising higher safety and capacity, all-solid-state lithium batteries are envisioned to replace standard lithium-ion batteries in the future. Lithium thiophosphates achieve the highest Li ion conductivities of SSEs to date exceeding liquid electrolytes at 10 mS/cm [1].

Until now, the instability of most SSEs towards high-performance electrodes remains a critical challenge, with hardly any known SSE withstanding the reducing/oxidizing conditions at the lithium metal anode and/or high-voltage cathodes or forming electrochemically benign interfaces with the electrode active materials.

To address this issue, we investigate the concept of rare earth lithium halides as a material-efficient, nm thick cathode coating in contact with thiophosphate

electrolytes as they provide wide electrochemical stability windows (0.36-6.71 V vs Li/Li^+) as well as good chemical and thermodynamic stability [2,3].

In order to validate this approach, the thermodynamic stabilities of the emerging SSE / halide interfaces are examined by ab initio thermodynamics to screen reaction free enthalpies of possible interface reactions. Furthermore, (stable) products of selected material combinations are surveyed for sufficient lithium ion mobility.

[1] C. Wang et al., Energy Environ. Sci., 2021, 14, 2577 [2] J. Liang et al., Acc. Chem. Res. 2021, 54, 1023-1033 [3] K. Kim et al., Chem. Mater. 2021, 33, 10, 3669-3677

15 min. break

MM 2.6 Mon 11:45 H44

Ab-initio core spectroscopy of LiCoO₂ and CoO₂ — DANIEL DUARTE RUIZ and •CATERINA COCCHI — Carl von Ossietzky Universität Oldenburg, Institut für Physik, Oldenburg, Deutschland

X-ray absorption spectroscopy (XAS) is one of the most widely used technique to study the electronic structure of cathode active materials in operando conditions. From a theoretical point of view, many-body perturbation theory on top of density-functional theory [1] is the state of the art in the prediction of XAS and in the interpretation of corresponding experimental results. In this work, we investigate core spectroscopy in LiCoO₂ and CoO₂, considering excitations from the Co K- and L23-edges as well as from the O K-edge. Our results, in agreement with experimental data, indicate that excitonic effects are negligible for the absorption spectra. The spectral fingerprints are well reproduced already by the independent particle approximation and, on a qualitative level, by the atomic, orbital features in the projected density states. These findings suggest that monitoring the electronic structure of LiCoO₂ during the delithiation process is sufficient to capture the evolution of XAS signatures even in a possible high-throughput fashion.

[1] C. Vorwerk et al. Electron. Struc. 1, 037001 (2019)

MM 2.7 Mon 12:00 H44

High-throughput computational screening of fast Li-ion conductors — •TUSHAR THAKUR, LORIS ERCOLE, and NICOLA MARZARI — THEOS, EPFL, Switzerland

We present a high-throughput computational screening to find fast Li-ion conductors to identify promising candidate materials for application in solid-state electrolytes. Starting with ~30,000 experimental structures sourced from COD, ICSD and MPDS repositories, we performed highly automated calculations using AiiDA at the level of Density Functional Theory (DFT) to identify electronic insulators and to estimate lithium ion diffusivity using the pinball model [1] which describes the potential energy landscape of diffusing lithium at near DFT level accuracy while being orders of magnitude faster. We present the workflow where the accuracy of the pinball model is improved self-consistently and which is necessary in automatically running the thousands of required calculations and analysing their results. Promising conductors are further studied with first principles Molecular Dynamics simulations.

[1] Kahle, L. et al Modeling lithium-ion solid-state electrolytes with a pinball model. Phys. Rev. Mater. 2, 65405 (2018)

MM 2.8 Mon 12:15 H44

Adaptive kinetic Monte Carlo driven by local environment recognition — •KING CHUN LAI, SEBASTIAN MATERA, CHRISTOPH SCHEURER, and KARSTEN REUTER — Fritz Haber Institute of the Max Planck Society, Berlin, Germany
Efficient lattice kinetic Monte Carlo (kMC) simulation generally relies on a complete prior-understanding of the possible elementary processes and their corresponding energy barriers. Adaptive kMC (akMC) overcomes this limitation

by searching for those kinetics during the simulation, but the transition state searches (TSSs) become a bottleneck. To address this, we augment akMC with machine learning on local atomistic environments. Assigning a Smooth Overlap of Atomic Positions vector to each found process, we build up a database during simulation. This database is used to propose initial guesses for TSSs on basis of the proximity of the current local environments and the database entries. This proximity measure is self-adjusted based on statistics from TSSs on-the-fly. As the database fills, the proposed guesses from the database become close to the true transition states. These high quality TSS guesses improve simulation efficiency in two ways. First, the number of TSSs per kMC step gets significantly reduced by avoiding unsuccessful or repeating random TSSs. Second, damped Newton-Raphson becomes practical, which completes a proposed TSS in only a handful iterations. Taking a Pd surface as an illustrative example, we demonstrate the performance of the approach and also discuss how clustering and proximity learning can improve the TSS guesses further.

MM 2.9 Mon 12:30 H44

Atomistic Simulation Study of Li-Aluminosilicate Glass Scintillators — •EL MEHDI GHARDI, PRINCE RAUTIYAL, FIONA PEARCE, ANITA CROMPTON, LEE EVITS, SIMON MIDDLEBURGH, WILLIAM LEE, and MICHAEL RUSHTON — Nuclear Futures Institute, Bangor University, Gwynedd, LL57 2DG, United Kingdom

Radiation sensors are an important enabling technology in a number of fields, such as medicine, research, energy, military and homeland security. Glass base scintillators have been in use for more than 50 years and offer some benefits including their ability to respond to different types of radiation, and to be formed into various shapes. There is, however the possibility to discover and improve glass scintillators. With this in mind, this work provides insight from atomic scale simulations on the cerium doped Li-Aluminosilicate ($\text{SiO}_2\text{-Al}_2\text{O}_3\text{-MgO-Li}_2\text{O-Ce}_2\text{O}_3$) glass scintillators. Three glass compositions were studied using Molecular Dynamics (MD) and Density functional Theory (DFT) to investigate the effect of the ratio $R = ([\text{Al}_2\text{O}_3])/([\text{MgO}] + [\text{Li}_2\text{O}])$ (with $R = [0.3, 0.8$ and $2]$) on structural, electronic and optical properties. The effect of R on the complex structure of the system of interest was mainly associated to the increase of Q₄ population that replaced Q₃'s within the network, while electronic mid gap defects were found to be present when $R < 1$. The optical properties including absorption coefficients and energy loss spectra are calculated and analysed based on the electronic structures.

MM 2.10 Mon 12:45 H44

Bonding descriptor based approach for analysing and finding new Photo-voltaic absorbers — •JAKOB JOHANNES LÖTFERING and MATTHIAS WUTTIG — RWTH Aachen University, Aachen, Germany

The discovery of Halide Perovskites as good Photovoltaic absorbers and their rapid optimization lead to the question whether there are other materials yet undiscovered for Photovoltaic applications. In order to find new Photovoltaic absorbers, many approaches focus on structural data. We propose a bonding descriptor based approach using two quantities called electrons shared (ES) and electrons transferred (ET), which can be calculated using Density Functional Theory (DFT) calculations. ES and ET are derived from the Quantum Theory of Atoms in Molecules (QTAIM). The first quantity we employ is twice the delocalization index ($\delta(\Omega', \Omega)$) between neighboring atoms. The second one is the number of electrons transferred to/from an atom compared to the unbonded atom. $\delta(\Omega', \Omega)$ is a measure for the number of electron pairs shared between two atoms. It can be obtained by integrating the exchange-correlation pair density over two domains Ω and Ω' , which correspond to the two atoms. ES and ET have already shown to be good bonding descriptors and property predictors, e.g. for Halide Perovskites and Phase Change Materials. We propose that these quantities can also be used to analyse chemical bonding in Photovoltaic absorbers and predict novel materials in this category.

MM 3: Microstructures and Phase Transformations: Metals & Alloys

Time: Monday 10:15-12:45

Location: H45

MM 3.1 Mon 10:15 H45

Analysis of the precipitates in rapidly quenched Al-Cu alloys obtained in a magnetic pulse weld and through a melt spinning process — •DAVID STEIN, MAXIMILIAN GNEDEL, and FERDINAND HAIDER — Universität Augsburg, Institut für Physik, Universitätsstraße 1, 86159 Augsburg, Germany
Magnetic pulse welding (MPW) is a collision welding technique, where a flyer is accelerated towards a target using induced magnetic fields. This technique enables the welding of dissimilar metals. The microstructure of the interface is well described in the literature and typically displays a wave like structure. In the eye and wake of these waves an area of intermetallic phases can be found, depending on the materials and welding parameters. In this case an Al 1050 flyer and Cu DHP target were used. The structure of the interface has given strong indications

of melting. Atomic resolution HAADF STEM was performed on this part and GP I and GP II Zones and disc shaped Θ' phases were found in the same area. The latter typically only form after longer heat treatments at elevated temperature. Albeit the theoretically predicted shape of Θ' Phases is disc shaped with very large diameter to thickness ratio, in the case studied here, they are much more compact and have a far smaller diameter to thickness ratio. The current working hypothesis is, that in the MPW process rapid solidification of the melt occurs, which leads to a high density of excess vacancies in the crystal structure, allowing for higher atom mobility. In an ongoing study we follow the precipitation process in rapidly quenched Al-Cu alloys obtained through a melt spinning process.

MM 3.2 Mon 10:30 H45

Crystal nucleation in undercooled Cu-Ge melts — •MANOEL W. DA SILVA PINTO, MARTIN PETERLECHNER, and GERHARD WILDE — Institut für Materialphysik, WWU Münster

Experimental calorimetric data obtained by differential thermal analysis on the nucleation of undercooled Cu-Ge melts are presented. Deep undercooling levels have been reached throughout the entire composition range of this binary alloy in an experimental setup using an inorganic glass as an embedding medium. The heating and cooling cycles are statistically analyzed and lead to quantitatively determining nucleation rates independent of a specific nucleation kinetics model. Parameters of the classical nucleation theory, such as the kinetic pre-factor and nucleation work, are extracted. We further discuss the data using different solution models for the alloy melts and consider their impact on nucleation kinetics. Thus, the nucleation kinetics parameters for the binary alloy system have been determined as a function of composition throughout the entire composition range and allow comparison with simplified models for concentration-dependent nucleation kinetics.

MM 3.3 Mon 10:45 H45

Experimental investigation of the early stage precipitation reactions in Al-Cu alloys — •JOHANNES BERLIN, TOBIAS STEGMÜLLER, and FERDINAND HAIDER — Chair for Experimental Physics I, University of Augsburg, Universitätsstraße 1, 86159 Augsburg

Due to their superior strength to weight ratio heat treatable Al-Cu alloys (2XXX-Series) are widely used particularly in aerospace industry. Although the hardening precipitates in these alloys are well-known, the very early stages of decomposition are still topic of ongoing research. Based on state-of-the-art scanning transmission electron microscopy, single Cu atoms can be imaged and natural ageing in form of Guinier*Preston zone formation accelerated by excess vacancies can be investigated, which was possible before only by diffraction experiments. Scanning transmission electron microscopy is used to investigate the influence of different parameters, such as thermal history, on early-stage precipitation in Al. The growth of GP I Zones is followed by ex-situ recording of a detailed time series during natural aging. In addition, resistivity and hardness measurements are performed to evaluate the temper state of the specimens. The results are compared to numerical simulations. A better understanding of the mechanisms leading to precipitate formation in these alloys for light-weight construction could be tuned more precisely regarding their intended use.

MM 3.4 Mon 11:00 H45

2D precipitate growth in a 3D matrix – Revealing the kinetics of Guinier-Preston zone formation in Al-Cu from atomic Monte Carlo — •TOBIAS STEGMÜLLER and FERDINAND HAIDER — University of Augsburg, Universitätsstr. 1, 86159 Augsburg, Germany

Guinier-Preston zones (GPZ) in Al-Cu, constituting the precipitate phase that was already responsible for the hardness increase in the first age-hardenable Al-alloy about 115 years ago, still attract attention first because of their special atomic mono- up to multilayer structure of Cu atoms and second due to their even at room temperature occurring formation, requiring an unexpected fast Cu diffusion.

To understand the origin of the GPZ structure, we performed Monte Carlo (MC) simulations mimicking precipitate growth by applying a Cluster Expansion (CE) for Al-Cu. From this we were able to identify an energy barrier above and below the layers of GPZ that is hardly overcome by migrating Cu. With this barrier we are able to explain the morphology of GPZ from a perspective focussing on the growth kinetics. On the one hand, the barrier guides migrating Cu to the layers' edges, supporting 2D growth. On the other hand, Cu atoms moving towards the layers' faces are stopped by the barrier, leading to nucleation of further Cu layers and explaining the multilayer shape.

To study the origin of the high Cu mobility, we recently included vacancies into simulations by switching from the CE based rigid lattice MC to a MC method allowing lattice relaxations by using a neural network interatomic potential. We present first results from this approach with regard to the interaction of vacancies with GPZ.

MM 3.5 Mon 11:15 H45

Atomic-scale observation of silver segregation in a high angle grain boundary in copper — •LENA FROMMEYER, TOBIAS BRINK, GERHARD DEHM, and CHRISTIAN LIEBSCHER — Max-Planck-Str. 1, 40213 Düsseldorf

Although it is well recognized that segregation to grain boundaries (GBs) influences mechanical and electrical properties of materials, the impact of segregation on individual GB phases is poorly understood on the atomic level. Thermodynamic models are established to describe equilibrium segregation, but the atomistic origins and direct observation of solute segregation inside the GB core structure are seldomly investigated since high resolution imaging and spectroscopy are required.

Lately, we were able to resolve the atomic structure of a symmetric Σ 37c <111> {3 4 7} tilt GB in a Cu thin film using aberration-corrected high angle annular dark field scanning transmission electron microscopy (HAADF-STEM). By

depositing a 100 nm thin Ag layer on top of our 2 μ m-thick Cu thin film and subsequent annealing at 600°C, we could investigate the effect of Ag segregation on these GBs. Interestingly, the structure of the GB remains unchanged. Ag atoms solely substitute specific sites in the GB. If the Ag content in the GB is increased, one atomic column in the GB structure is filled up first, followed by four other columns. A combination of atomic resolution energy dispersive X-ray spectrometry, HAADF-STEM experiments and atomistic simulations were used to explore the underlying mechanisms leading to the observed Ag segregation pattern.

15 min. break

MM 3.6 Mon 11:45 H45

Grain boundary phase transitions and patterning in a copper tilt grain boundary — •TOBIAS BRINK¹, LENA FROMMEYER¹, RODRIGO FREITAS², TIM OFEY FROLOV³, CHRISTIAN H. LIEBSCHER¹, and GERHARD DEHM¹ — ¹Max-Planck-Institut für Eisenforschung GmbH, Germany — ²MIT, USA — ³LLNL, USA

The atomic structure of grain boundaries (GBs) can exhibit different “phases” (also called complexions), which undergo thermodynamic phase transitions, but which have been observed in just a few simulation studies. Experimental confirmation often remains indirect. Here, we report on such a transition investigated by molecular dynamics computer simulations and supported by direct evidence from STEM imaging [1]. Two distinct atomistic structures could be found in a Σ 37c [111] tilt GB by a search with an evolutionary algorithm. Free energy calculations using the quasi-harmonic approximation predict a GB phase transition at 460 K. In the experiment, both phases also occur, but exhibit a pattern at room temperature in which the two phases alternate. We present a hypothesis to explain this thermodynamically unexpected phenomenon by elastic interactions of the phase junctions, which are line defects with partial dislocation character.

Acknowledgment: This result is part of a project that has received funding from the ERC under the European Union's Horizon 2020 research and innovation programme (Grant agreement No. 787446).

[1] Frommeyer, Brink et al., “Dual phase patterning during a congruent grain boundary phase transition in elemental copper” Nat. Commun. (accepted, 2022)

MM 3.7 Mon 12:00 H45

Structural and thermal characterisation of a AuGe alloy via electron microscopy and fast differential scanning calorimetry — •STEFAN STANKO¹, JÜRGEN SCHAWÉ^{1,2}, and JÖRG LÖFFLER¹ — ¹Laboratory of Metal Physics and Technology, Department of Materials, ETH Zurich, 8093 Zurich, Switzerland — ²Mettler-Toledo GmbH, Analytical, 8606 Nänikon, Switzerland

A device combining scanning electron microscopy (SEM) and fast differential scanning calorimetry (FDSC) was developed to perform *in situ* characterisation of metastable phase transformations. The potential of this device is demonstrated on the example of a AuGe eutectic alloy. Upon rapid cooling, the alloy forms the metastable crystalline phases β and γ and an amorphous phase. A thin lamella for transmission electron microscopy (TEM) was produced from a sample prepared in FDSC to further characterise the microstructure of the alloy beyond the capabilities of the *in situ* device. *Ex situ* FDSC experiments were performed using cooling and heating rates of several 1000 K/s to characterise the thermal behaviour of the β and γ phase. The transformation kinetics of the metastable phases was investigated. Finally, we show that we can prepare the glassy phase in FDSC and determine its thermophysical properties.

MM 3.8 Mon 12:15 H45

Phase decomposition in nanoporous Au-Pt — •MAOWEN LIU^{1,2} and JÖRG WEISSMÜLLER^{1,2} — ¹Institute of Materials Mechanics, Helmholtz-Zentrum Hereon — ²Institute of Materials Physics and Technology, Hamburg University of Technology

Nanostructured Au-Pt system has attracted great attention for its broad applications in catalysis. Due to the miscibility gap for a large range of composition and temperature in bulk Au-Pt system, a comprehensive understanding of the structure transformation at various temperatures is necessitated. In the present work, nanoporous Au-Pt prepared by dealloying is selected for the investigation of the microstructure evolution during annealing. Dealloying transforms the homogeneous, ternary bulk solid solution Ag-Au-Pt into a nanoporous Au-Pt solution that would be immiscible at thermodynamic equilibrium. Remarkably, in view of the substantial atomic-scale rearrangement at the dissolution front, our experiments confirm a homogeneous Au-Pt solid solution. Upon annealing-induced coarsening, the phase structure evolves to semicoherent two-phase by way of an intermediate, coherent two-phase state.

MM 3.9 Mon 12:30 H45

Microstructural characteristics of lean magnesium alloys — •TATIANA AKHMETSHINA, LEOPOLD BERGER, SAMUEL MONTIBELLER, ROBIN E. SCHÄUBLIN, and JÖRG F. LÖFFLER — Laboratory of Metal Physics and Technology, Department of Materials, ETH Zurich, 8093 Zurich, Switzerland

Lean magnesium alloys with less than 1 at.% of alloying elements are of high interest for biodegradable implant applications, where the implant remains only

temporarily in the body, but degrades after it has fulfilled its task. With a specific combination of requirements, such as biocompatibility, appropriate mechanical properties and low degradation rate, such alloy development is still challenging. Here, we tailored the mechanical properties of lean Mg-Ca alloys by hot extrusion. The optimal alloying range was obtained via thermodynamic calculations using Pandat. The alloys were cast and extruded at the same ratio with different speeds and temperatures. A tensile toughness of up to 76 MJ/m³ was obtained, indicating a superior combination of strength and ductility. Depending on the

extrusion parameters, the alloys exhibit a tensile strength of more than 420 MPa or, alternatively, a high ductility of up to 35% elongation at fracture. To obtain a clear understanding of the relationship between mechanical properties and microstructure, the latter was investigated by SEM, TEM and EBSD, focusing on precipitation, grain morphology, and dislocation structure. The grain size varied from submicrometer to several tens of micrometers. Apart from weak texture, the most ductile materials revealed an intriguing activation of <c+a> pyramidal slip.

MM 4: Structural Materials

Time: Monday 10:15–13:00

Location: H46

MM 4.1 Mon 10:15 H46

Nanoscale analysis of Ti-modified Mo-Si-B alloy to elucidate solid solution and particle strengthening — •RESHMA SONKUSARE¹, TORBEN BOLL¹, JULIA BECKER², MARTIN HEILMAIER¹, and MANJA KRÜGER² — ¹Institute of Applied Materials and Karlsruhe Nano Micro Facility, Karlsruhe Institute of Technology, Germany — ²Institut für Werkstoff- und Fügetechnik, Otto-von-Guericke-Universität Magdeburg, Germany

Mo-Si-B alloys are attractive high-temperature structural materials due to their high melting point (>2000C), high-temperature strength and good oxidation resistance. We found that small additions of Ti to multi-phase Mo-Si-B lead to strengthening of alloy at intermediate and high temperatures. To understand the effect of Ti on microstructure and thus mechanical properties, we investigated powder metallurgically processed Mo-7.2Si-9.7B-1.7Ti. The microstructure consists of Mo solid solution phase, intermetallic silicide phases, nanoscale oxide and silicide particles. To analyze the composition of these nanoscopic particles, atom probe tomography is required. APT reveals Ti to cause an unexpected compositional change of Mo(SS) phase. This change and an analysis of the composition and distribution of other phases combined with an investigation of the particles and elemental segregations at the grain boundaries and inside the grains improve the understanding of the solid solution and particle strengthening in the alloy and hence the mechanical behavior.

MM 4.2 Mon 10:30 H46

Intrinsic room temperature ductilisation of lean rare-earth free ternary Mg alloys — •WASSILIOS DELIS¹, PIA HUCKFELDT¹, BENGT HALLSTEDT², PEI-LING SUN¹, DIERK RAABE³, SANDRA KORTE-KERZEL¹, and STEFANIE SANDLÖBESHAUT¹ — ¹Institute for Physical Metallurgy and Materials Physics, RWTH Aachen, 52074 Aachen, Germany — ²Institute for Materials Applications in Mechanical Engineering, RWTH Aachen, 52062 Aachen, Germany — ³Max-Planck Institut für Eisenforschung, Max-Planck-Straße 1, 40237 Düsseldorf, Germany

Mg is a lightweight structural material with a good specific strength. Unfortunately, it lacks good room temperature formability and therefore a wider commercial use of Mg is hindered. The preferred basal slip and strong basal-type texture were found to be the main reasons for the poor room temperature formability. For basal slip the von Mises' criterion is not fulfilled. Recent experimental and simulative studies tried to activate more slip systems without changing the mechanical properties with alloying approaches. Alloys containing Y and rare-earth elements showed a highly increased room-temperature ductility. Since Y and rare-earth elements are costly further research has been carried out to identify similar acting alloy systems. For this purpose, the parameter II SFE has been used and the system Mg-Al-Ca was identified to have a similar II SFE. In experiments the system indeed showed the expected increased room temperature ductility. Further research of the effects of the chemical composition on the ductilisation has now been performed.

MM 4.3 Mon 10:45 H46

PT phase transitions and spectral structure of the interacting Hatano-Nelson model — •SONGBO ZHANG — Stetthachrain 20, Zurich, Switzerland

In this talk, I will discuss the Hatano-Nelson model, i.e., a one-dimensional non-Hermitian chain of spinless fermions with nearest-neighbour nonreciprocal hopping, in the presence of repulsive nearest-neighbour interactions. At half-filling, I will show two PT transitions, as the interaction strength increases. The first transition is marked by an exceptional point between the first and the second excited state in a finite-size system and is a first-order symmetry-breaking transition into a charge density wave regime. Persistent currents characteristic of the Hatano-Nelson model abruptly vanish at the transition. The second transition happens at a critical interaction strength that scales with the system size and can thus only be observed in finite-size systems. It is characterized by a collapse of all energy eigenvalues onto the real axis. I will also show that in a strong interaction regime, but away from half-filling, the many-body spectrum shows point gaps with nontrivial winding numbers, akin to the topological properties of the single-particle spectrum of the Hatano-Nelson chain.

MM 4.4 Mon 11:00 H46

Novel CDB Data Processing and Evaluation Software — •LEON CHRYSOS, VASSILY VADIMOVITCH BURWITZ, LUCIAN MATHES, and CHRISTOPH HUGENSCHMIDT — Heinz Maier-Leibnitz Zentrum (MLZ), Technical University of Munich, Lichtenbergstr. 1, 85748 Garching, Germany

The Coincidence Doppler-Broadening (CDB) spectrometer at NEPOMUC has recently been upgraded with six additional HPGe Detectors, bringing the total number of detectors to ten. To take full advantage of the even more capable instrument a novel data evaluation software package (STACS) is currently under development. The software can already handle and visualize the data generated by Coincidence Doppler-Broadening Spectroscopy (CDBS) and provides a wide range of tools to analyze such data. Some of the main functions include the extraction of the electron-positron annihilation photo peak from CDB spectra as well as a simple background subtraction algorithm that is able to increase the peak-to-noise ratio of the extracted photo peak further. This combined with a new multi detector CDB function, which enables the combination of the data from all 10 detectors, provides detailed information about the chemical environment of the positron annihilation site. The software capabilities were tested on W samples, to demonstrate the sensitivity for high Doppler shifts. Measurements on the precipitation hardening properties of Al alloy samples were subsequently performed and will be shown.

MM 4.5 Mon 11:15 H46

Plasticity of the Ca(Al,Mg)₂ phase with variable temperature and composition — •MARTINA FREUND¹, DOREEN ANDRE¹, PEI-LING SUN¹, NICOLAS J. PETER², and SANDRA KORTE-KERZEL¹ — ¹Institut für Metallkunde und Materialphysik, RWTH Aachen University — ²Max-Planck-Institut für Eisenforschung GmbH, Düsseldorf

Magnesium is a promising lightweight material, but its application as cast alloys at elevated temperature is limited because of its low creep resistance. By alloying with Al and Ca different Laves phases form, which improve creep strength. While investigating largely unknown properties with respect to composition and temperature changes, a challenge is to physically relate and represent such results. Here, we explore - in addition to the specific findings - how this may be done in terms of defect phase diagrams. Due to their complex packing, Laves phases are brittle at low temperatures. In order to overcome this restriction and to study their mechanical properties and mechanisms of plasticity, we used nanomechanical testing. For the cubic CaAl₂ phase, nanoindentation tests revealed a constant hardness of 5.9 ± 1.2 GPa and indentation modulus of 120.3 ± 17.9 GPa. Slip traces and cracks in the vicinity of indents were correlated with the crystal orientation and mostly corresponded to the {111} and {112} planes. Microcompression revealed deformation on {111} and {112} planes in <1-10> direction and the CRSS has been calculated as 0.97 ± 0.03 GPa and 0.96 ± 0.03 GPa, respectively. These planes and Burgers vectors were also confirmed by TEM using the g*b criterion.

15 min. break

MM 4.6 Mon 11:45 H46

Ab initio study of magneto-chemo-structural coupling at FeMn grain boundaries — •OMKAR HEGDE, JÖRG NEUGEBAUER, and TILMANN HICKEL — Max-Planck-Institut für Eisenforschung, Max-Planck-Strasse 1, 40227 Düsseldorf, Germany

Mn segregation at Fe grain boundaries is known to be a precursor for a variety of phenomena such as embrittlement, spinodal decomposition, phase transformation, etc [1,2]. Therefore, various heat treatments are performed in experiments to control Mn decoration at grain boundaries for *segregation engineering* [1], which could alter the local magnetic state. In this direction, a thorough understanding of the connection between the local magnetic state and segregation remains elusive. In the present work, we tackle this issue by studying segregation in both the ferromagnetic state (low-temperature) and paramagnetic state (high-temperature) using ab initio-based approaches [3]. We demonstrate that the Mn segregation profile is mainly modulated by local magnetic interactions, providing new opportunities for grain boundary segregation engineering. Finally, we

show that the formation of grain boundary and Mn segregation can, in turn, tune the local magnetic transition temperature, thereby revealing a complex coupling of structure, chemistry, and magnetism.

[1] D Raabe et al., *Current Opinion in Solid State and Materials Science*, 18, 253-261 (2014).

[2] AK Da Silva et al., *Nature communications*, 9, 1-11 (2018).

[3] O Hegde et al., *Physical Review B*, 102, 144101 (2020).

MM 4.7 Mon 12:00 H46

Sulphation kinetics of chloride particles, corrosion potential and effect of reactive additives — •SEBASTIAN PENTZ and FERDINAND HAIDER — Universität Augsburg, Institut für Physik, 86135 Augsburg

Chlorine induced high temperature corrosion leads to massive problems especially in waste-to-energy-plants, but also in biomass combustion. During the combustion process chloride containing particles are released and deposited on heat exchanger surfaces. There chlorides get converted into sulphates with a release of chlorine species which then lead to severe corrosion. In laboratory experiments we study the conversion kinetics under various conditions like temperature, particle size or gas composition. Both the sulphation reaction and the rate of subsequent corrosion show an Arrhenius dependency on temperature, a linear dependence on time, on particle surface and on partial pressure of SO₂. The addition of reactive additives can strongly influence this reaction and consequently the release of chlorine species: Adding iron oxide (e.g. Fe₂O₃) results in a strong acceleration of the sulphation process due to catalysis of the reaction from SO₂ to SO₃. On the other hand, a reduction of the sulphur content in the reaction atmosphere by desulphurising species like calcium oxide slows down the sulphation reaction and reduces the amount of released chlorine compounds. In lab experiments, chlorides (mixed with additives) are applied to 16Mo3 steel samples and exposed to a flowing reaction atmosphere in a tube furnace. Support by Federal Ministry for Economic Affairs and Climate Action on the basis of a decision by the German Bundestag.

MM 4.8 Mon 12:15 H46

Influence of oxygen and carbon on the chemistry at the niobium/alumina interface in a refractory composite material — •MICHAEL EUSTERHOLZ¹, TORBEN BOLL¹, ALEXANDER KAUFFMANN¹, RESHMA SONKUSARE¹, VINCENT OTT¹, JULIAN GEBAUER¹, BASTIAN KRAFT¹, ANJA WEIDNER², MICHAEL STÜBER¹, SVEN ULRICH¹, and MARTIN HEILMAIER¹ — ¹Karlsruhe Institute of Technology (KIT) — ²TU Bergakademie Freiberg (TUBAF)

High-temperature processes such as steel casting impose harsh conditions on materials, which thus require excellent properties, including creep strength and resistance to thermal shock. Composites based on coarse-grained refractory metals and refractory ceramics promise superior performances due to adjustable mechanical and electrical properties.

Conventionally sintered composites from technical grade raw materials of α -Al₂O₃ and Nb include impurity elements that form carbides alongside oxides during synthesis. To understand the principles of formation, we investigate α -Al₂O₃ substrates sputter-coated with Nb as model materials beside the technical grade material. As the latter is subjected to carbon and oxygen containing gases during sintering, we compare the effect of oxygen and carbon overexposure on the ceramic-metal interface and contrast these results with a heat treatment with

unaffected interface. Electron microscopy techniques elucidate the microstructure, while atom probe tomography advances the understanding of nano-scale phase formation at the phase boundary which are decisive for the material properties and corrosion resistance.

MM 4.9 Mon 12:30 H46

Oxidation mechanisms of SMART alloys and MAX phases — •ANICHA REUBAN^{1,2}, JESUS GONZALEZ-JULIAN^{1,2}, IVAN POVSTUGAR¹, ANDREY LITNOVSKY^{1,3}, and CHRISTIAN LINSMEIER¹ — ¹Forschungszentrum Jülich GmbH, 52425 Jülich, Germany — ²Institute of Mineral Engineering, RWTH Aachen University, 52064 Aachen, Germany — ³Moscow

Concentrated Solar Power (CSP) is a sustainable energy technology where sunlight is focused on a solar receiver and the thermal energy is used to generate electricity. The receiver must withstand temperatures greater than 1000 °C, be resistant to oxidation by air and/or corrosion by molten salts and maintain its properties over time. Self-passivating SMART alloys, originally designed for the fusion reactor, are resistant to plasma sputtering and can suppress oxidation in case of an accident with air ingress, up to 1000 °C. MAX phases, a bridge between metals and ceramics, are lightweight, easily machinable materials, oxidation- and corrosion-resistant up to 1400 °C. To understand the oxidation mechanisms in these materials, it is important to obtain nanoscale information using advanced characterization techniques such as Atom Probe Tomography (APT). According to the APT analysis of the SMART alloy W-Cr-Y, Y segregates at oxide grain boundaries while in the alloy it forms Y-O precipitates. Further analyses are being performed to get more information about the role of Y in the oxidation process. Electron microscopy is used along with APT for a correlative approach to nanoscale characterization.

MM 4.10 Mon 12:45 H46

Development of Tungsten fiber reinforced tungsten (Wf/W) using yarn based textile preforms — •ALEXANDER LAU¹, JAN WILLEM COENEN¹, DANIEL SCHWALENBERG¹, YIRAN MAO¹, ALEXIS TERRA¹, LEONARD RAUMANN^{1,2}, MICHAEL TREITZ^{1,4}, JOHANN RIESCH³, HANNS GIETL^{3,4}, BEATRIX GÖHTS¹, CHRISTIAN LINSMEIER¹, KATHARINA THEIS-BRÖHL², TILL HÖSCHEN³, and PHILLIP HUBER⁵ — ¹Forschungszentrum Jülich GmbH, Institut für Plasma-physik, 52425 Jülich — ²Hochschule Bremerhaven, 27568 Bremerhaven — ³Max-Planck-Institute for Plasma Physics, 85748 Garching b. München — ⁴Technische Universität München, 85748 Garching — ⁵RWTH Aachen University, 52062 Aachen, Germany

The focus of this work is the development of a new composite material, that has to withstand the immense heat and particle fluxes in future fusion reactors. The wall material is based on the element tungsten, which already shows a very high compliance with the requirement profile in its pure form. Pure tungsten is inherently brittle below the DBTT and cracks could lead to a complete failure of the wall material. To counter this problem, extrinsic strengthening mechanisms were tested with new fabric types, based on radially braided yarns with seven core- and 16 sleeve filaments. These yarns were coated with an Yttriumoxide interface by Magnetron-sputtering and then further processed with chemically vapor deposited tungsten in a six-layer structure to form a solid composite material. This sample was analysed optically and got mechanically tested in a three-point bending test.

MM 5: Non-equilibrium Phenomena in Materials Induced by Electrical and Magnetic Fields 1

Time: Monday 15:00–15:30

Location: H44

Topical Talk

MM 5.1 Mon 15:00 H44

Vacancy transport in oxides exposed to high electric fields — •REINER KIRCHHEIM — University of Goettingen, Goettingen, Germany — Max-Planck-Institute for Iron Research, Duesseldorf, Germany — I2CNER, Fukuoka, Japan Internal electrochemical redox reactions and accumulation of charge in oxides are treated. Internal reactions shall lead to electronic conduction in the reduced and oxidized regions near cathode and anode respectively. Several scenarios for the generation and transport of charged oxygen vacancies and the attainment of steady state are discussed. It will be shown that at high cell voltages the characteristic time for reaching steady state, also called incubation time, is smaller

than the characteristic time for the growth of reacted regions. Then the incubation time is inverse proportional to the squared cell voltages or the voltage drop across the oxide, respectively. Examples where this relation is fulfilled are given for electromigration in integrated circuits, formation of memristors, flash sintering of ceramics and degradation of high-k materials. In addition, diffusion coefficients for vacancies evaluated from incubation times of yttria stabilized zirconia (YSZ) agree with extrapolated measured values. Internal reactions will also play a role in solid oxide fuel cell (SOFC) and solid oxide electrolysis cells (SOEC), where current densities may exceed the reaction rates with gases at the porous electrodes.

MM 6: Computational Materials Modelling: Defects / Alloys

Time: Monday 15:45–18:30

Location: H44

MM 6.1 Mon 15:45 H44

Unveiling the mechanisms of motion of synchro-Shockley dislocations in Laves phases — •ZHUOCHENG XIE¹, DIMITRI CHAURAUD^{2,3}, ACHRAF ATILA^{2,3}, ERIK BITZEK^{2,3}, SANDRA KORTE-KERZEL¹, and JULIEN GUÉNOLE⁴ — ¹Institute of Physical Metallurgy and Materials Physics, RWTH Aachen University, 52056 Aachen, Germany — ²Max-Planck-Institut für Eisenforschung GmbH, Max-Planck-Str. 1, 40237 Düsseldorf, Germany — ³Institute I: General Materials Properties, Friedrich-Alexander-Universität Erlangen-Nürnberg, 91058 Erlangen, Germany — ⁴Université de Lorraine, CNRS, Arts et Métiers ParisTech, LEM3, 57070 Metz, France

In Laves phases, synchroshear is the dominant basal slip mechanism. It is accomplished by the glide of synchro-Shockley dislocations. However, the atomic-scale mechanisms of motion of such zonal dislocations are still not well understood. In this work, using atomistic simulations, two 30° synchro-Shockley dislocations with different Burgers vectors and core structures and energies are identified. We demonstrate that nucleation and propagation of kink pairs is the energetically favorable mechanism for the motion of the synchro-Shockley dislocation. Vacancy hopping and interstitial shuffling are identified as two key mechanisms related to kink propagation and we investigated how vacancies and antisite defects assist kink nucleation and propagation, which is crucial for kink mobility. These findings provide insights into the dependency on temperature and chemical composition of plastic deformation induced by zonal dislocations in topologically close-packed phases.

MM 6.2 Mon 16:00 H44

Macroscopic characteristics of plastic deformation described through dislocation mobility properties — •SERGEI STARIKOV, ANTOINE KRAYCH, and MATOUŠ MROVEC — Ruhr University Bochum, ICAMS, Germany

Plastic deformation of bcc metals is a complicated phenomenon that links a behaviour of crystal defects with the macroscopic change of a sample shape. It is known that one of the basic mechanisms of plasticity is a motion of dislocations under applied stress. In this work, on the example of Mo and Nb, the study of plastic deformation in bcc metals was carried out with large-scale atomistic modelling. The temperature-dependent mobility functions of screw and edge dislocations were calculated from molecular dynamics simulation. The simulations of screw dislocation movement under applied shear stress revealed that the process can proceed in two different regimes: through thermally activated motion and athermal motion. Hence, the dislocation velocity depends on the shear stress in a non-trivial way. The calculated data provide a way to evaluate the basic macroscopic characteristics of plastic deformation at various temperatures and strain rates.

MM 6.3 Mon 16:15 H44

Analytic description of grain boundary segregation, tension, and formation energy in the copper-nickel system — TAMARA KRAUSS, FELIX FISCHER, and •SEBASTIAN EICH — Institut für Materialwissenschaft — Lehrstuhl für Materialphysik, Universität Stuttgart

In this atomistic study, a recently proposed segregation model [1] is applied to segregation data of an exemplary $\Sigma 5$ grain boundary (GB), which is investigated using a copper-nickel embedded-atom method potential. Segregation in the semi-grandcanonical ensemble is systematically studied by varying the chemical potential in order to explore the full composition range for temperatures from 500 K to 1000 K. As a major thermodynamic feature, the mentioned segregation model avoids the usage of *interface compositions*, for which an arbitrary volume must be defined, but rather models the thermodynamically unambiguous solute excess. It was shown that the solute excess and the interface formation energy could be described very accurately over a wide range of temperatures and over the entire composition. Since the model was initially derived for systems without lattice mismatch, the copper-nickel system with a mismatch of roughly 2.7% is chosen in this study to further extend the segregation model by a linear-elastic theory to also account for the interface tensions. Using this extended model, it will be shown that the solute excess, GB tensions, and GB formation energies can be derived from an effective energy of segregation for all temperatures and over the whole composition range [2].

[1] T. Krauß, S. M. Eich, Acta Mater. 187, 73 (2020)

[2] F. Fischer, S. M. Eich, Acta Mater. 201, 364 (2020)

MM 6.4 Mon 16:30 H44

Impurity segregation at grain boundaries in bcc iron: large scale models based on machine learned interatomic potentials — •PETR ŠESTÁK¹, MONIKA VŠIANSKÁ^{1,2}, PAVEL LEJČEK^{1,3}, and MIROSLAV ČERNÝ¹ — ¹Central European Institute of Technology, CEITEC BUT, Brno University of Technology, Purkyňova 123, CZ-616 69 Brno, Czech Republic — ²Department of Chemistry, Faculty of Science, Masaryk University, Kotlářská 2, CZ-611 37 Brno, Czech Republic — ³Institute of Physics of the Czech Academy of Sciences, Na Slovance 2, CZ-182 21 Prague 8, Czech Republic

In this work, we employed on the fly machine learning (ML) as it is implemented in the current version of the VASP to study segregation of Sn, P and Ge atoms at selected GBs (e.g. $\Sigma 3(112)$, $\Sigma 3(111)$, $\Sigma 5(310)$, $\Sigma 5(210)$, $\Sigma 13(510)$, $\Sigma 13(320)$, etc.) in bcc iron. Segregation energies were obtained using small supercells (<100 atoms), medium cells (~400 atoms) and also larger cells (>1000 atoms). Data obtained from the small and medium cells were compared with results of ab initio calculations as well as with available experimental data and predictions. This comparison serves as a benchmark of the interatomic potentials received from ML. The comparison shows that the segregation energies and some other GBs characteristics obtained for small cells are very consistent with ab initio simulations which bring a proof of reliability of interatomic potentials. The obtained results revealed that using small simulation cells (leading to high concentrations of impurity atoms), typical for ab initio simulations, might not be sufficient to predict correct segregation energies.

MM 6.5 Mon 16:45 H44

An efficient method to access the grain boundary parameter space with atomistic simulations — •TIMO SCHMALOFSKI¹, MARTIN KROLL², REBECCA JANISCH¹, and HOLGER DETTE² — ¹ICAMS, Ruhr-University Bochum, 44780 Bochum, Germany — ²Department of Mathematics, Ruhr-University Bochum, 44780 Bochum, Germany

A grain boundary (GB) is a two dimensional defect in solids with significant influence on different material properties. It describes the interface between two grains with different orientations and is thus defined by five macroscopic degrees of freedom (DOF), 2 from the rotation axis, 1 from the misorientation angle and 2 from the grain boundary normal vector. The GB energy as a function of the DOF can be obtained e.g. by atomistic simulations. However, a systematic sampling of the 5D grain boundary parameter space, or even lower-dimensional subspaces of it, comes with several challenges. To overcome them, a sampling method is needed, which only needs a small number of data points and can automatically find the cusps (deep minima) in the energy while sampling. Recently we introduced a sequential sampling technique which fulfills both [1] in the 1D subspace of symmetrical tilt grain boundaries. Now this sequential sampling technique will be evaluated for a 2D analysis of the energy as a function of GB plane inclination for fixed misorientations. [1] Kroll, M., Schmalofski, T., Dette, H. and Janisch, R. (2022), Efficient Prediction of Grain Boundary Energies from Atomistic Simulations via Sequential Design. Adv. Theory Simul. 2100615.

15 min. break

MM 6.6 Mon 17:15 H44

Electronic band gap of $\text{Al}_x\text{Sc}_{1-x}\text{N}$: a comparison of CPA and SQS — •JAN M. WAACK^{1,2}, MARKUS KREMER^{1,2}, MICHAEL CZERNER^{1,2}, and CHRISTIAN HEILIGER^{1,2} — ¹Institut für theoretische Physik, Justus-Liebig-Universität Gießen, Germany — ²Center for Materials Research (LaMa), Justus-Liebig-Universität Gießen, Germany

Calculating physical properties of random substitutional solid solutions such as $\text{Al}_x\text{Sc}_{1-x}\text{N}$ requires specific methods such as the coherent potential approximation (CPA)[1] and special quasi-random structures (SQS)[2]. We compare the CPA in the framework of the atomic sphere approximation (ASA) Korringa-Kohn-Rostoker (KKR) density functional theory (DFT) with the SQS using the plane-wave pseudopotential DFT to calculate the lattice parameters and electronic band structures of the face-centered cubic phase of $\text{Al}_x\text{Sc}_{1-x}\text{N}$ (with $0 \leq x \leq 1$).

Using the low-computational-cost LDA-1/2 quasiparticle method[3] to calculate the electronic band structures within SQS and CPA, we present the first implementation of LDA-1/2 within the KKR DFT. We find that both the lattice parameter and the indirect band gap satisfy Vegard's law including a bowing parameter.

[1] C. Franz, M. Czerner, and C. Heiliger, Phys. Rev. B 88, 94421 (2013). <https://doi.org/10.1103/PhysRevB.88.094421>[2] A. Zunger, S.-H. Wei, L. G. Ferreira, and J. E. Bernard, Phys. Rev. Lett. 65, 353 (1990). <https://doi.org/10.1103/PhysRevLett.65.353>[3] L. G. Ferreira, M. Marques, and L. K. Teles, Phys. Rev. B 78, 125116 (2008). <https://doi.org/10.1103/PhysRevB.78.125116>

MM 6.7 Mon 17:30 H44

Using MD simulations to better understand and control self-propagating reactions in Al-Ni multilayers — •FABIAN SCHWARZ and RALPH SPOLENAK — Laboratory for Nanometallurgy, Department of Materials, ETH Zürich, CH-8093 Zürich, Switzerland

Reactive multilayers are capable of releasing large amounts of heat in a short time, making them a possible tool for energy storage or joining applications. Molecular Dynamics (MD) simulations can be used as a tool to study the front propagation, while varying certain system parameters. We study the influence

of the crystal structure on the reaction front propagation in Al-Ni multilayers by looking at various microstructures, such as amorphous, single crystal or different grain structures. We found that crystallinity has a significant impact on the front propagation speed, which is likely related to different diffusion mechanisms. The more disordered the individual layers become, e.g., by increasing the grain boundary density, the higher is the resulting propagation speed. Furthermore, we study the influence of a premixed interlayer at the interface on the reaction propagation. For this, premixed interlayers with different, namely homogeneous, gradient and s-shaped profiles are studied and compared to existing experimental results. Beyond better understanding of the premixed interlayer, we show that it can be used to control the front propagation speed in reactive multilayers. Furthermore, we show that the heat of crystallization of amorphous AlNi to B2-AlNi alone is high enough for a self-propagating reaction to occur.

MM 6.8 Mon 17:45 H44

strong impact of spin fluctuations on the antiphase boundary energies of weak ferromagnetic Ni₃Al — •XIANG XU^{1,2}, XI ZHANG², ANDREI RUBAN^{3,4}, SIEGFRIED SCHMAUDER¹, and BLAZEJ GRABOWSKI² — ¹Institute for Materials Testing, Materials Science and Strength of Materials, University of Stuttgart, Germany — ²Institute for Materials Science, University of Stuttgart, Germany — ³KTH Royal Institute of Technology, Stockholm, Sweden — ⁴Materials Center Leoben Forschung GmbH, Leoben, Austria

The antiphase boundary (APB) was believed to be crucial for explaining the anomalously increased yield stresses of L1₂ Ni₃Al. However, an accurate temperature-dependent APB energy is still missing and the magnetic effect was often underestimated or even neglected. In this work, the influence of longitudinal spin fluctuations (LSF) as well as other thermal mechanisms were considered within the ab-initio framework up till the melting point. We found that the calculated *T*-dependent APB energies show a remarkable agreement with the experimental data despite the large discrepancy between different works. The LSF effect was determined to crucially increase APB energies, especially for (100)APB with a maximum of 50% over the nonmagnetic data. This significant contribution prompts to take serious consideration of LSFs when studying the paramagnetism, even for weak itinerant ferromagnetic materials. The accurate APB energy acquired in this work can be used to set up quantitative models for simulating dislocation motions and the elastic-plastic behavior for Ni-based superalloys on the macro scale.

MM 6.9 Mon 18:00 H44

Ab initio study on the phase stabilities of multi-component carbides in high-Mn steels — LEKSHMI SREEKALA¹, JÖRG NEUGEBAUER¹, and •TILMANN HICKEL^{1,2} — ¹Max-Planck-Institut für Eisenforschung, Düsseldorf, Germany — ²BAM Bundesanstalt für Materialforschung und -prüfung, Berlin, Germany

The high strength and ductility of advanced high Mn steels makes them suitable for lightweight applications in the transportation sector. A modification of their properties can be achieved by intentional or unintentional addition of further alloying elements, which is often connected with the formation of secondary phases. In particular, Cr addition improves corrosion resistance and, at the same time, inadvertently yields a substantial increase in the number of carbides precipitated, such as Fe₃C and Fe₂₃C₆. Therefore, in the present work, we use density functional theory to determine the thermodynamic driving force for the formation of these multicomponent carbides by evaluating their phase stabilities. We study the free energy of formation at finite temperatures by considering the vibrational, electronic and magnetic contributions. While both Cr and Mn stabilize Fe-carbides, we found that the impact of Cr is higher than that of Mn for a typical host matrix composition of Fe, Cr and Mn. Further, we analyze the critical role of magneto-structural coupling for the phase stability of these compositionally complex carbides. Through this study, we demonstrate the predictive capability of ab initio thermodynamics to accurately describe the phase stabilities of chemically complex secondary phases in metallic alloys.

MM 6.10 Mon 18:15 H44

Atomistic simulation of diffusion in γ' -strengthened Co-based superalloys — •LIN QIN¹, JUTTA LOGAL^{2,3}, DOROTA KUBACKA⁴, and RALF DRATZ¹ — ¹ICAMS, Ruhr University Bochum, Bochum, Germany — ²Department of Chemistry, New York University, New York, United States — ³Department of Physics, Free University of Berlin, Berlin, Germany — ⁴Institute of Micro- and Nanostructure Research, FAU, Erlangen, Germany

The suppressed diffusion of Al in the strengthening γ' precipitates in Co-based superalloys is suspected to be one plausible reason to cause the selective formation of alumina in the early stage of oxidation above 900°C. In order to validate this assumption, the diffusion properties of Al, Co and W in a prototype structure of γ' phase, i.e. L1₂-Co₃ (Al, W), are investigated with Density Functional Theory (DFT) and Kinetic Monte Carlo (KMC) simulations. DFT calculations reveal that the migration barrier of each element in Co sublattice is comparable with its respective barrier in pure Co. However, the crossover barriers of Al and W from their original positions to Co sublattice are much higher than the barriers for the reverse process. This large discrepancy in barriers constrains the site fraction of Al and W in Co sublattice, and therefore significantly suppresses the long-distance diffusion of Al and W in γ' phase. KMC results show that Al diffusivity in γ' phase is over two order of magnitudes lower than that in a solute γ phase (Co₇₅Al_{12.5}W_{12.5}) at 900°C, suggesting that the sluggish diffusion of Al in γ' can be a possible reason to cause the selective formation of alumina in Co-based superalloys.

MM 7: Microstructures and Phase Transformations: Oxides & Perovskites

Time: Monday 15:45–17:00

Location: H45

MM 7.1 Mon 15:45 H45

Evolution of a particle in twisted bilayer optical potentials — •GANESH C. PAUL¹, PATRIK RECHER^{1,2}, and LUIS SANTOS³ — ¹Institut für Mathematische Physik, Technische Universität Braunschweig, 38106 Braunschweig, Germany — ²Laboratory for Emerging Nanometrology, 38106 Braunschweig, Germany — ³Institut für Theoretische Physik, Leibniz Universität Hannover, Germany

Very recently few theoretical proposals have been put forward to simulate twisted bilayers using cold atoms in state-dependent optical lattices, which can be used as an alternative platform to investigate twisted bilayers in solid-state experiments. We study the band structure of both square and hexagonal geometries in an optical lattice set-up, where the band structure can be tuned to be almost flat by proper implementation of interlayer Gaussian-type coupling. We examine the evolution of a particle in the twisted bilayer square-like potential, and find that the particle follows specific paths forming channels when the interlayer hopping is much stronger than the intralayer hopping strength. Due to the flexibility of controlling the inter- and intralayer coupling in optical lattices, our proposals should be easy to be realised in a cold atom set-up.

MM 7.2 Mon 16:00 H45

Phase transitions and phonon renormalization in CsPbBr₃ via a machine learning interatomic potential — •ERIK FRANSSON¹, FREDRIK ERIKSSON¹, PETER ROSANDER¹, TERUMASA TADANO², and PAUL ERHART¹ — ¹Chalmers University of Technology, Gothenburg, Sweden — ²National Institute for Materials Science, Tsukuba, Japan

Here, we present a study on phase-transition and phonon renormalization in the metal halide perovskite CsPbBr₃ using a machine learning (ML) interatomic potential. The ML potential is a neuroevolution-potential constructed using the GPUMD software and is trained on atomic forces, energies and stresses obtained from DFT calculations. We find that the ML potential captures the correct phase-

transition from the orthorhombic phase to tetragonal phase and from tetragonal to cubic phase. The phase transition temperatures obtained are slightly underestimated compared to experimental studies, but in good qualitative agreement. These phase-transitions are connected to the so called tilt-modes at the R and M point in the Brillouin zone, which corresponds to tilting of the PbBr₆ octahedra. The dynamics of these modes are studied with MD simulations and mode projections, and we find that they have a strongly anharmonic and overdamped character. Furthermore, we investigate and benchmark how different self-consistent phonon methods work for these strongly anharmonic modes.

MM 7.3 Mon 16:15 H45

A particular EFG temperature dependence for 181-Ta(TiO₂): An electron-gamma TDPAC study — •IAN CHANG JIE YAP¹, JULIANA SCHELL^{2,3}, THIEN THANH DANG³, CORNELIA NOLL⁴, REINHARD BECK⁴, ULLI KÖSTER⁵, RONALDO MANSANO⁶, PETER BLÖCHL^{1,7}, and HANS CHRISTIAN HOFSSÄSS¹ — ¹Georg-August Universität Göttingen — ²European Organization for Nuclear Research (CERN) — ³Institute for Materials Science and Center for Nanointegration Duisburg-Essen (CENIDE), University of Duisburg-Essen — ⁴Helmholtz-Institut für Strahlen- und Kernphysik, University of Bonn — ⁵Institut Laue-Langevin — ⁶Escola Politécnica, Universidade de São Paulo — ⁷Technische Universität Clausthal, Institute of Theoretical Physics

In this work, we report on the hyperfine parameters of the implanted 181Ta probe in the rutile structure of the single crystal TiO₂ using the $e - \gamma$ time differential perturbed angular correlation ($e - \gamma$ TDPAC) technique. The experiments were performed under vacuum within the temperature range of 50 K - 427 K. The hyperfine parameters that are obtained from the $e - \gamma$ TDPAC spectroscopy agrees with that of the $\gamma - \gamma$ TDPAC spectroscopy at room temperature, apart from a calibration factor, both from our experiments and literature. Surprisingly, we have detected a parabolic increase of V_{zz} with a concave curvature at the low-

temperature regime (50 K - 427 K), as opposed to the linear increase at the high-temperature regime (600 K - 1200 K) as found in the literature. Hence, we are performing DFT calculations on Ta-doped TiO₂ over a broad temperature range to obtain deeper insights.

MM 7.4 Mon 16:30 H45

Hidden charge order in square-lattice Sr₃Fe₂O₇ — •DARREN C. PEETS^{1,2,3}, JUNG-HWA KIM¹, MANFRED REEHUIS⁴, PETER ADLER⁵, ANDREY MALJUK^{1,6}, TOBIAS RITSCHHEL², MORGAN C. ALLISON², JOCHEN GECK^{2,7}, JOSE R. L. MARDEGAN⁸, PABLO J. BERECIARTUA PEREZ⁸, SONIA FRANCOUAL⁸, ANDREW C. WALTERS^{1,9}, THOMAS KELLER^{1,10}, PAULA M. ABDALA¹¹, PHILIP PATTISON^{11,12}, PINDER DOSANJH¹³, and BERNHARD KEIMER¹ — ¹MPI-FKE, 70569 Stuttgart — ²IFMP, TU Dresden, 01069 Dresden — ³NIMTE CAS, Ningbo, 315201 China — ⁴HZB, 14109 Berlin — ⁵MPI-CPfS, 01187 Dresden — ⁶IFW, 01171 Dresden — ⁷ct.qmat, TU Dresden, 01062 Dresden — ⁸DESY, Hamburg 22603 — ⁹Diamond, Didcot OX11 0DE, UK — ¹⁰MPI Outstation at MLZ, 85748 Garching — ¹¹SNBL at ESRF, 38042 Grenoble, France — ¹²EPFL, BSP-Dorigny, CH-1015 Lausanne, Switzerland — ¹³UBC, Vancouver, V6T 1Z1 Canada

Since the discovery of charge disproportionation in Sr₃Fe₂O₇ by Mössbauer spectroscopy >50 years ago, the spatial ordering pattern of the disproportionated charges has stayed “hidden” to conventional diffraction, despite numerous x-ray and neutron studies. Our neutron Larmor diffraction and Fe K-edge resonant x-ray scattering demonstrate checkerboard charge order in the FeO₂ planes that vanishes at a sharp second-order phase transition at 332 K. Stacking disorder of the checkerboard pattern due to frustrated interlayer interactions broadens their superstructure reflections, greatly reducing their amplitude, explaining the dif-

ficulty to detect them. We discuss implications of these findings for research on “hidden order” in other materials.

MM 7.5 Mon 16:45 H45

Band structure effects of a current-induced Mott-insulator to metal transition in Ca₂RuO₄ — •D. CURCIO¹, C. E. SANDERS², A. CHIKINA¹, M. BIANCHI¹, H. E. LUND¹, V. GRANATA³, M. CANNAVACCIULO³, P. DUDIN⁴, J. AVILA⁴, C. POLLEY⁵, B. THIAGARAJAN⁵, A. VECCHIONE⁶, and P. HOFMANN¹ — ¹Department of Physics and Astronomy, Aarhus University, Denmark — ²STFC Central Laser Facility, Harwell Campus, United Kingdom — ³Dipartimento di Fisica *E.R. Caianiello*, Università degli Studi di Salerno, Italy — ⁴Synchrotron SOLEIL, Gif-sur-Yvette, France — ⁵MAX IV Laboratory, Lund University, Lund, Sweden — ⁶CNR-SPIN, c/o Università degli Studi di Salerno, Italy

The Mott insulator Ca₂RuO₄ can be turned into a metal by the application of a weak electric field and a corresponding transport current. This transition affects the optical and magnetic properties of the material. However, because of the electric field's presence and the field-induced energy broadening, it is challenging to determine the electronic structure in the metallic state by angle-resolved photoemission spectroscopy (ARPES). Making use of the recently introduced approach to enable ARPES measurements of current-carrying devices by using a nano-scale light spot [1], we are able to measure ARPES data that tracks the current-induced phase transition in Ca₂RuO₄ simultaneously with the electrical transport, revealing the spectral function of the current-induced state along with a potential map of the sample's surface.

[1] D. Curcio *et al.* Phys. Rev. Lett. 125, 236403 (2020).

MM 8: Materials for Storage and Conversion of Energy

Time: Monday 15:45–18:30

Location: H46

MM 8.1 Mon 15:45 H46

Atomistic analysis of Li migration in Li_{1+x}Al_xTi_{2-x}(PO₄)₃ (LATP) solid electrolytes — •DANIEL PFALZGRAF^{1,2}, DANIEL MUTTER², DANIEL URBAN^{1,2}, and CHRISTIAN ELSÄSSER^{1,2} — ¹Freiburg Materials Research Center (FMF), University of Freiburg, Stefan-Meier-Straße 21, 79104 Freiburg, Germany — ²Fraunhofer IWM, Wöhlerstraße 11, 79108 Freiburg, Germany

We present an examination of the ionic migration of Li in LATP [Li_{1+x}Al_xTi_{2-x}(PO₄)₃] solid electrolytes from an atomistic viewpoint based on density functional theory calculations [1]. In our study, we vary the Al content and investigate its effects on the crystal structure of LATP and on the migration energy landscape of interstitial Li ions. The energy profiles governing the Li diffusion are found to be systematically influenced by the position of Al ions in direct vicinity of the migration path, and we derive a simplified classification scheme of three universal energy profile shapes. The overall influence of the Al/Ti-ratio on the Li migration is analyzed by a separation into chemical and geometrical aspects. This work provides a solid basis for a resource-efficient computational examination of the ionic conductivity of Li in LATP with varying Al/Ti concentrations.

[1] D. Pfalzgraf, D. Mutter, and D.F. Urban, Solid State Ionics 359, 115521 (2021)

MM 8.2 Mon 16:00 H46

Diffraction tomography studies of lithium distribution in 18650-type Li-ion cells — •ANATOLIY SENYSHYN¹, VLADISLAV KOCHETOV², DOMINIK PETZ³, and MARTIN MÜHLBAUER⁴ — ¹Forschungsneutronenquelle Heinz Maier-Leibnitz, Technische Universität München, Garching, Germany — ²Institut für Physik, Universität Rostock, Rostock, Germany — ³Physik Department, Technische Universität München, Garching, Germany — ⁴Institute for Applied Materials, Karlsruhe Institute of Technology, Karlsruhe, Germany

At the moment Li-ion batteries are dominating in the segment of energy storage for portable electronics and electric drivetrains. Despite its overall popularity and widespread, the Li-ion technology has a high improvement potential, especially in the aspects concerning power and energy density, power fading, safety etc. Besides the variety of different factors, the chemical, mechanical and morphological uniformity of the cell components is one of the aspects crucial for optimization, estimation and prediction of cell parameters and cell behavior during standard operation and misuse. In the current contribution a series of diffraction-based methods (spatially resolved diffraction using radial oscillating collimators and/or conical slits as well as X-ray and neutron diffraction tomography) applied to probe inner structure of samples (either on example of dedicated phantom sample or cylinder-type Li-ion battery) will be briefly introduced and reviewed.

MM 8.3 Mon 16:15 H46

Li diffusion in perovskite materials for battery applications — •WEI WEI¹, JULIAN GEBHARDT^{1,2}, DANIEL URBAN^{2,3}, and CHRISTIAN ELSÄSSER^{1,2,3} — ¹Cluster of Excellence livMatS, University of Freiburg, Germany — ²Fraunhofer Institute for Mechanics of Materials IWM, Freiburg, Germany — ³Freiburg Materials Research Center (FMF), University of Freiburg, Germany

Metal halide perovskites are promising photovoltaic (PV) absorber materials, with the highest power conversion efficiency values currently exceeding 22%. Furthermore, unlike most of the traditional PV materials, hybrid perovskites have a strong ionic character. Therefore, these materials have recently been reported to have good ionic conductivity and lithium storage potential,^[1] allowing in principle the combination of a solar cell and a Li-ion battery in a single device. Here, we investigate this possibility by a Li-CsPbI₃ model system. By means of density-functional-theory calculations, we consider two scenarios: 1) Li in the rigid cubic perovskite structure, and 2) Li in the perovskite structure with flexible tilted bonds, which is the more realistic scenario at room temperature. The results of our simulations show that in the less symmetric structure the interstitial Li sites become nondegenerate and Li ions migrate along more complicated paths and have to overcome higher barriers than in the cubic structure. Nevertheless, diffusing Li ions have to overcome only moderate energy barriers of 0.16-0.33 eV, corroborating the potential use of metal-halide perovskites as Li-ion conducting PV materials.

[1] Zhen Li *et al.* Energy Environ. Sci.10 (2017) 1234

MM 8.4 Mon 16:30 H46

Analytical TEM studies of LiCoO₂ thin film electrode for Li-ion batteries — •ARDAVAN MAKVANDI¹, SANDRA LOBE², MICHAEL WOLFF², MARTIN PETERLECHNER¹, CHRISTOPH GAMMER³, SVEN UHLENBRUCK², and GERHARD WILDE¹ — ¹Institute of Materials Physics, University of Münster, Münster, Germany — ²Institute of Energy and Climate Research, Materials Synthesis and Processing (IEK-1), Forschungszentrum Jülich GmbH, Jülich, Germany — ³Erich Schmid Institute of Materials Science, Austrian Academy of Sciences, Leoben, Austria

LiCoO₂ is the mostly used cathode material in commercial Li-ion batteries. However, only half of its theoretical capacity can be used due to the structural and chemical instability of its surface at charge voltages higher than 4.2 V. In general, interfaces (e.g. active material/coating, electrode surface/electrolyte) determine the local Li-ion transport kinetics and finally the electrochemical performance. Therefore, it is necessary to study the structure and chemistry of electrodes and electrode/electrolyte interfaces. In this work, the structure and chemistry of the bulk and surface regions of LiCoO₂ thin film before and after cycling are studied using transmission electron microscopy (TEM). In this case, the effect of an Al-doped ZnO-coating layer on the stability of the electrode surface upon cycling at high charge voltage has been studied.

MM 8.5 Mon 16:45 H46

Investigation of volume changes in the colquirite structure due to Li insertion from first principles — •ALJOSCHA BAUMANN^{1,2}, DANIEL MUTTER², DANIEL URBAN^{1,2}, and CHRISTIAN ELSÄSSER^{1,2} — ¹Freiburger Materialforschungszentrum, Stefan-Meier-Straße 21, 79104 Freiburg — ²Fraunhofer IWM, Wöhlerstraße 11, 79108 Freiburg

The long-term stability of lithium-ion batteries (LIB) is often negatively affected by mechanical stresses in the cathode material during charge/discharge cycles. Materials that show a zero-strain (ZS) behavior, i.e. their volume changes hardly during insertion or extraction of Li ions, are therefore of great interest. For individual compounds of the material class of colquirites, $\text{LiA}^{\text{II}}\text{M}^{\text{III}}\text{F}_6$, ZS behavior has already been predicted theoretically and observed experimentally, e.g. for $\text{Li}_{1-x}\text{CaFeF}_6$, which exhibited a volume change of less than 0.5 % upon insertion of lithium ions up to $x=0.8$.

In order to identify the mechanism responsible for the ZS behavior we calculated the variation of the equilibrium volume due to varying Li concentration using density-functional theory (DFT). The analysis of the electronic and magnetic structure and local structure parameters at equilibrium volumes indicates that the total volume is influenced by a combination of expanding fluorine octahedra around the transition-metal ions due to the changing oxidation state, the distortion of octahedra around the Ca ions, and a decrease of repulsion between fluorine anions due to the inserted Li ions.

15 min. break

MM 8.6 Mon 17:15 H46

Cu²⁺ Intercalated Vanadium Pentoxide Grown on Carbon Cloth as Binder-Free Cathodes for Reversible Aqueous Zinc Ion Batteries — •PING HONG^{1,2}, YUDE WANG², HUAPING ZHAO¹, and YONG LEI¹ — ¹Fachgebiet Angewandte Nanophysik, Institut für Physik & IMN MacroNano, Technische Universität Ilmenau, 98693 Ilmenau, Germany — ²School of Materials Science and Engineering, Yunnan University, Kunming, People's Republic of China

Aqueous zinc batteries (ZIBs) with low cost, safety, environmentally friendly, and high theoretical capacity are a promising electrochemical energy storage technology. Vanadium based materials have been widely studied as cathode materials for ZIBs because of their safety, diverse crystal structure, abundant resources, low cost and high theoretical capacity. In the reported cathode materials, the mass loading of the cathode is usually less than 4 mg/cm² is not sufficient enough for practical applications. Herein, Cu²⁺ intercalated vanadium pentoxide (CVOH@CC) with high loading (~7 mg/cm²) were directly grown on carbon cloth via hydrothermal method. The as-prepared CVOH@CC has a distinct 3D interconnected nested structure. When applying as binder-free cathode for ZIBs, CVOH@CC electrodes exhibited a high capacity of 223.4 mAh/g at 1.0 A/g and a long cycling performance of over 2000 cycles. The intercalation resulted in a better capacitive response and faster diffusion rate for the cathode compared to pure vanadium pentoxide (VOH@CC), which means better rate performance and cycling stability, providing a viable design proposal for the production of industrial grade ZIBs.

MM 8.7 Mon 17:30 H46

Reversible hybrid Na-CO₂ batteries with low charging voltage and long-life — •CHANGFAN XU — Fachgebiet Angewandte Nanophysik, Institut für Physik & IMN MacroNano, Technische Universität Ilmenau, 98693 Ilmenau, Germany — School of Metallurgy and Environment, Central South University, Changsha 410083, China — Faculty of Metallurgical and Energy Engineering, Kunming University of Science and Technology, Kunming 650093, China

A reversible and long-life hybrid Na-CO₂ battery was proposed by using Na₃Zr₂Si₂PO₁₂ solid electrolyte as a separator, the saturated NaCl solution as an aqueous electrolyte, and nitrogen-rich graphitic carbon framework with well-defined morphology and dense bimetallic Fe-Cu sites (Fe-Cu-N-C) as cathodic catalyst. Besides having high Na⁺ ion conductivity, Na₃Zr₂Si₂PO₁₂ solid electrolyte also can prevent potential contamination from H₂O and CO₂ to sodium anode and avoid the internal short-circuit touch of Na dendrite with the cathode, thus improving the battery safety. The aqueous electrolyte can facilitate the dissolution of insulated discharge products, which overwhelmingly improves the reaction kinetics. The Fe-Cu-N-C cathodic catalyst can facilitate the fast evolution and degradation of flocculent discharge products. Finally, the hybrid Na-CO₂ battery exhibited an excellent long-term cyclability with up to 1550 cycles (over 600 h). The reaction mechanism of Na-CO₂ battery was revealed by in-situ Raman, SEM and XRD analyses.

MM 8.8 Mon 17:45 H46

Revisiting the storage capacity limit of graphite battery anodes: spontaneous lithium overintercalation at ambient pressure — CRISTINA GROSU^{1,2}, •CHIARA PANOSSETTI¹, STEFFEN MERZ², PETER JAKES², SEBASTIAN MATERA¹, RÜDIGER-A. EICHEL², JOSEF GRANWEHR², and CHRISTOPH SCHEURER¹ — ¹Fritz-Haber-Institut, Berlin, Germany — ²IEK-9, Forschungszentrum Jülich, Germany

The market quest for fast-charging, safe, long-lasting, and performant batteries drives the exploration of new energy storage materials, but also promotes fundamental investigations of those already widely used. Presently, revamped interest in anode materials is observed – primarily graphite electrodes for Li-ion batteries. We focus on the upper intercalation limit in the morphologically quasi-ideal highly oriented pyrolytic graphite (HOPG), with a LiC₆ stoichiometry corresponding to 100% state of charge (SOC). We prepared a sample by immersion in liquid lithium at ambient pressure. Investigation by static ⁷Li nuclear magnetic resonance (NMR) resolves unexpected signatures of superdense intercalation compounds, LiC_{6-x}. These were ruled out for decades, since the highest geometrically accessible composition, LiC₂, can only be prepared under high pressure. We thus challenge the widespread notion that any additional intercalation beyond LiC₆ is not possible under ambient conditions. We monitored the sample upon calendaric aging and employed *ab initio* calculations to rationalise the NMR results. The computed relative stabilities of different superdense configurations reveal that non-negligible overintercalation does proceed spontaneously beyond the currently accepted capacity limit.

MM 8.9 Mon 18:00 H46

The dielectric behaviour of Lithium intercalated graphite anodes as a function of the state of charge — •SIMON ANNIÉS^{1,2}, CHIARA PANOSSETTI², MARIA VORONENKO¹, and CHRISTOPH SCHEURER² — ¹Theoretical Chemistry, Technical University Munich, Germany — ²Fritz Haber Institut, Berlin, Germany

The dielectric behaviour of battery materials is a crucial piece of information for understanding atomistic mechanics and modelling diffusion and charging processes. However, for the most common anode material in today's Lithium ion batteries (Lithium intercalated graphite), literature results regarding this property are sparse, conflicting and only available for the empty state of charge (SOC).

Utilizing our recently developed DFTB parametrization (based on a machine-learned repulsive potential), we are - for the first time - able to compute the dielectric behaviour of Lithium intercalated graphite for the entire range of charge from 0% to 100%. Our results agree with experiments for 'empty' graphite, as well as for (bilayer-) graphene, which we use for an additional benchmark of our approach.

With increasing state of charge, we find a linear dependency of the dielectric constant, growing from around 7 at 0% SOC to around 29 at 100% SOC. With this, we lay an important piece of foundation for the understanding and multi-scale modelling of entire charging and discharging processes of Li-ion batteries.

MM 8.10 Mon 18:15 H46

In-situ analysis of SEI formation and cycle behavior on Sn by combined QCM-CV — •KE WANG and GUIDO SCHMITZ — Chair of Materials Physics, Institute for Materials Science, University of Stuttgart, Heisenbergstr. 3, 70569 Stuttgart, Germany

Sn (Tin) could in principle be a promising candidate for a lithium-ion battery anode since it offers larger capacity than commercially graphite. But, researchers are still confused about the capacity fade especially caused by the formation of solid electrolyte interface (SEI). Here, we perform an in-situ characterization to clarify the mechanisms of SEI formation. Cyclic voltammetry has been conducted in combination with a quartz crystal microbalance to measure the growth of the SEI. Beside the overall mass increase, evaluating the mass change per charge (MPE) even enables identification of the ab/desorbed species. In advanced analysis, we combine three different characteristics including mass spectra, real-time MPE and average MPE, for the different stages of the long-term SEI formation. Except the SEI layer formed in first cycle, the SEI is continuously affected by the formation of Li₂O during lithiation and the oxidation of Sn during de-lithiation. In addition, the influence of the voltage window and the thickness of the electrodes on SEI formation are investigated. Remarkably, the SEI thickness reveals a linear relation to the electrode thickness which is linked to continuous cracking and major oxidation of Sn bulk. Particularly, the inorganic part of the SEI formed during lithiation in the specific voltage range of 0.36 - 0.27 V plays an important role on the microstructure of electrode and stabilizing the electrode.

MM 9: Non-equilibrium Phenomena in Materials Induced by Electrical and Magnetic Fields 2

Material modification

Time: Monday 17:15–18:30

Location: H45

Topical Talk

MM 9.1 Mon 17:15 H45

Design of corrosion-free and highly active electrocatalysts and photocatalysts via combinations of ab initio calculations and electrodynamics — •HEECHAE CHOI — Institute of Inorganic Chemistry, University of Cologne, Greinstr. 6, 50939, Cologne, Germany

Long enough lifetime of a catalyst is a very important, and frequently overlooked issue in catalyst design and development. For catalytic materials used in extreme conditions, corrosion resistance is the key factor to determine the lifetime and the steady performances over time. However, the theoretical design principle for the corrosion resistance of catalytic materials is lacking compared to the performance descriptor, which can give accurate predictions of catalytic activities of metallic materials. Recently, using the combinations of ab initio calculations and electrodynamics model, we proposed a new theoretical scheme to improve the catalytic activity and corrosion resistivity. Under the hypothesis that the resistance of corrosion is a function of adsorption energy of corrosive ions in aqueous phases, we attempted to install built-in electric fields on heterogeneous catalyst surfaces. As the results, the performances of TiO₂ photoanode, Co/graphene Zn-air battery, and the water splitting by metal/carbon heterojunctions were highly improved. In this talk, I will introduce the procedures of such materials design theory developments and the experimental verifications.

MM 9.2 Mon 17:45 H45

Understanding DC-induced abnormal grain growth in FeC-thin films — •THOMAS BREDE, MICHEL KUHFUSS, REINER KIRCHHEIM, and CYNTHIA VOLKERT — Institut für Materialphysik, Universität Göttingen, Deutschland

The field of processing materials with magnetic or electric fields and currents is steadily growing, since it opens the door to more efficient ways of material treatment and former not achievable material modifications. In this scope, it was shown recently, that high DC electric current densities up to 4 MA/cm² can be used at elevated temperatures of 550°C to produce elongated ferrite grains with high aspect ratios in an otherwise nanocrystalline iron-carbon thin film. To understand the underlying mechanism we will present experiments in a wide range of process parameters. The samples were characterized by SEM and EBSD in different stages of the experiment. The results shown allow a detailed description of the underlying mechanism of the evolution of the abnormal grown structures. In addition they reveal a threshold linked to the electromigration-induced C-flux, below which no changes occur. A purely kinetic model will be presented to describe the observed behaviour and allow the prediction of similar effects at different process parameters and material systems.

MM 9.3 Mon 18:00 H45

Cavity induced and influenced phases of matter — •CHRISTIAN J. ECKHARDT^{1,2}, GIACOMO PASSETTI², MARIOS MICHAEL¹, FRANK SCHLAWIN¹, DANTE M. KENNES^{2,1}, and MICHAEL A. SENTEF¹ — ¹Max Planck Institute for the Structure and Dynamics of Matter, Hamburg, Germany — ²RWTH Aachen University, Aachen, Germany

An optical cavity may be used to influence or induce phases of matter. We discuss how a charge-density wave phase in a 1-dimensional chain of spinless fermions is enhanced through the coupling to the quantized photon field. At the critical point between the Luttinger liquid and the charge-density wave, we find strong light-matter entanglement. Additionally, we ask in what ways photons can be used as pairing glue for superconductivity (SC). We show that a fingerprint feature of such cavity-induced SC is the pickup of a k-dependence of the gap in the electronic spectrum on the Fermi-surface.

MM 9.4 Mon 18:15 H45

Floquet engineering the band structure of materials with optimal control theory — •ALBERTO CASTRO^{1,2}, UMBERTO DE GIOVANNINI^{3,4}, SHUNSUKE SATO^{5,4}, HANNES HÜBENER⁴, and ANGEL RUBIO^{4,6} — ¹ARAID Foundation, Zaragoza (Spain) — ²Institute for Biocomputation and Physics of Complex Systems, University of Zaragoza, Spain — ³Università degli Studi di Palermo, Dipartimento di Fisica e Chimica - Emilio Segrè, Palermo, Italy — ⁴Max Planck Institute for the Structure and Dynamics of Matter, Hamburg, Germany — ⁵Center for Computational Sciences, University of Tsukuba, Tsukuba, Japan — ⁶Center for Computational Quantum Physics (CCQ), The Flatiron Institute, New York NY

We demonstrate that the electronic structure of a material can be deformed into Floquet pseudo-bands with tailored shapes. We achieve this goal with a novel combination of quantum optimal control theory and Floquet engineering. We illustrate this framework utilizing a tight-binding description of graphene. We show several examples focusing on the region around the K (Dirac) point of the Brillouin zone: creation of a gap with opposing flat valence and conduction bands, creation of a gap with opposing concave symmetric valence and conduction bands, or closure of the gap when departing from a modified graphene model with a non-zero gap. We employ time periodic drives with several frequency components and polarizations, in contrast to the usual monochromatic fields, and use control theory to find the optimal amplitudes of each component that optimize the shape of the bands as desired.

MM 10: Poster Session 1

Time: Monday 18:00–20:00

Location: P2

MM 10.1 Mon 18:00 P2

Training Gaussian Approximation Potentials for Aqueous Systems — •NIKHIL BAPAT, MARTIN VONDRÁK, JOHANNES T. MARGRAF, HENDRIK H. HEENEN, and KARSTEN REUTER — Fritz-Haber-Institut der MPG, Berlin, Germany

An accurate and efficient description of aqueous systems via atomistic computer simulations is of high relevance for many applications. Machine learning potentials (MLPs) trained on first principles data have demonstrated promising accuracy and computational efficiency for the length and time scales critical to the description of water. But even with the compelling advancements in MLPs, building a successful data-efficient atomistic model for complex aqueous systems remains a challenging task. The training of such MLPs can be notoriously difficult and so far required either negligence of chemical reactivity in the MLP or excessive amounts of training data.

In this work we propose an efficient training procedure specifically designed for aqueous systems. To that end, we employ the widely applicable Gaussian approximation potential MLP and leverage it with a workflow for generating training data which ensures systematic inclusion of the bulk water configuration space. We calculate and compare ensemble properties of bulk water like its equilibrium density and diffusion coefficient to validate the MLP. The resulting model, when coupled with an added stimuli from a solid surface, can provide insights into many technologically important solid-liquid systems which are difficult to simulate otherwise.

MM 10.2 Mon 18:00 P2

Transfer learning on organic/inorganic interfaces for different substrates — •ELIAS FÖSLEITNER, JOHANNES CARTUS, LUKAS HÖRMANN, and OLIVER T. HOFMANN — Graz University of Technology, Graz, Austria

Performing structure search of organic molecules on metallic surfaces requires finding the structure with the lowest energy. Using conventional density functional codes this proves to be a time-consuming task, since the number of possible configurations is large and individual calculations are expensive. For all-electron approaches, this becomes even more problematic when calculating molecules on metal substrates of higher nuclear charge number, e.g. on gold. To circumvent the computation of all possible configurations, machine learning techniques such as Gaussian process regression proved to be a useful tool to reduce the amount of calculated data.

In our work we further reduce the data requirements by using transfer learning from one substrate to another. To this end, we first train the system on substrate A, and use this information to accelerate the learning process of the system on another substrate B. This is done by using the energy predictions of substrate A as a prior for the machine learning model imposed on system B. By doing so, we can reduce the data requirements for the training of expensive systems to an extent that makes the investigation computationally feasible.

MM 10.3 Mon 18:00 P2

Large-scale molecular dynamics simulations using fourth generation neural network potentials — •EMIR KOCER¹, ANDREAS SINGRABER², TSZ WAI KO¹, JONAS FINKLER³, PHILIPP MISOF², CHRISTOPH DELLAGO², and JÖRG BEHLER¹ — ¹Georg-August University, Göttingen, Germany — ²University of Wien, Vienna, Austria — ³University of Basel, Basel, Switzerland

In the last decade, their proven success in bridging the gap between ab initio and classical molecular dynamics made machine learning potentials (MLP) very attractive. However, many MLPs are short-ranged and unable to capture interactions beyond a certain cutoff, which leads to inaccurate forces and energies

in systems where long-range interactions are important. While MLPs including long-range electrostatic interactions based on local charges have been available for some years, only recently fourth generation MLPs have emerged that can take also global phenomena like non-local charge transfer into account. An example is the fourth generation high dimensional neural network potential (4G-HDNNP), which utilizes a global charge equilibration step. This study presents a modified version of 4G-HDNNPs, in which the matrix solution is replaced by a function minimization algorithm for an enhanced scalability on multi-core systems. The new potential has been implemented into the LAMMPS software and tested in large-scale molecular dynamics simulations.

MM 10.4 Mon 18:00 P2

Interatomic Potential Fitting in pyiron — •MARVIN POUL¹, NIKLAS LEIMERO², ALEXANDER KNOLL³, MARIUS HERBOLD³, and JOERG NEUGEBAUER¹ — ¹Max-Planck-Institut fuer Eisenforschung — ²Universitaet Goettingen — ³TU Darmstadt

Interatomic potentials have a key role in computational materials science bridging the gap between Ab-Initio methods and large-scale engineering applications. pyiron[1] is an IDE for computational materials science that allows for reproducible yet easy to write simulation protocols. Within its framework we have developed tools that allow for semi-automatic fitting and verifying of potentials. This includes wrappers for AtomicRex[2] (for classical potentials) and as well the machine-learned Moment Tensor Potentials (MTP[3]), high-dimensional neural network potentials (HDNNP[4]), and ACE potentials. In this work we introduce the facilities offered by our code on the examples of an Magnesium MTP and an EAM potential for Copper.

[1]: <https://doi.org/10.1016/j.commatsci.2018.07.043>

[2]: <https://doi.org/10.1088/1361-651X/aa6ecf>

[3]: <https://doi.org/10.1088/2632-2153/abc9fe>

[4]: <https://doi.org/10.1103/PhysRevLett.98.146401>

MM 10.5 Mon 18:00 P2

Effect of temperature pre-treatments on atomic dynamics in PdNiP studied with ECM — •OLIVIA VAERST, MARTIN PETERLECHNER, and GERHARD WILDE — Institute of Material Physics, University of Münster, Germany

Pre-treatments on amorphous PdNiP, such as annealing and treatments of thermo-mechanical kind, significantly influence the local structure, kinetic stability, and mechanical properties of this bulk metallic glass (BMG).

In the present work, Pd₄₀Ni₄₀P₂₀ samples are pre-treated thermally by annealing them at different temperatures below the glass transition temperature. The resulting well-defined states are investigated via transmission electron microscopy (TEM) with electron correlation microscopy (ECM) at room temperature. ECM is used to study atomic rearrangements and dynamics in the material at nanometer spatial resolution [1,2]. The effect of thermal pre-treatments on ECM evaluation parameters is discussed. Such investigations of the atomic mobility in pre-treated PdNiP give further insight into underlying mechanisms and properties of the amorphous phase as well as on the local relaxation dynamics of a bulk metallic glass.

[1] L. He et al., *Microsc. and Microanal.* 21 (2015) 1026-1033.

[2] K. Spangenberg et al., *Adv. Funct. Mater.* 31 (2021) 2103742.

MM 10.6 Mon 18:00 P2

Investigating the short-range order of amorphous GeTe upon structural relaxation obtained by TEM diffractometry and RMC methods — •CHRISTIAN STENZ¹, JULIAN PRIES¹, T. WESLEY SURTA², MICHAEL W. GAULTOIS², and MATTHIAS WUTTIG¹ — ¹Institute of Physics IA, RWTH Aachen University, 52074 Aachen, Germany. — ²Faculty of Chemistry, University of Liverpool, Liverpool L7 3NY, United Kingdom.

New experimental insights into the structural changes during resistance drift in amorphous GeTe are presented. Selected area electron diffraction is performed on a-GeTe in five different annealing states to compute the pair distribution functions upon relaxation. Examination of the short-range order based on the order parameters $S(q_2)/S(q_1)$ and r_2/r_1 implies a continuous increase in the most prominent average bond angle by 1° towards 104.5°. This is consistent with the analysis of the bond angle distribution (RMC simulations) which reveals a shift of the main contribution (~ 103.5°) towards larger angles. A concomitant increase of intermediate geometries between tetrah. and octah. (~ 140°) is observed. Applying three different techniques to estimate the fraction of tetrahedral Ge atoms the three measures coherently suggest a decrease in tetrahedrality. We conclude that an enhancement of Peierls-like distorted/pyramidal motifs, i.e. an increase in the PD-ratio r_1/r_5 , causes the increase of the average bond angle, resulting in a widening of the band gap. This structural relaxation ultimately leads to the resistance drift.

MM 10.7 Mon 18:00 P2

Influence of swift heavy ion irradiation on Pd-based metallic glasses — •SABA KHADEMOREZAIAN¹, MAXIMILIAN DEMMING¹, MARILENA TOMUT^{1,2}, SERGIY DIVINSKI¹, and GERHARD WILDE¹ — ¹Institute of Materials Physics, University of Münster, Wilhelm-Klemm-Str. 10, 48149 Münster — ²GSI Helmholtz Zentrum für Schwerionenforschung, 64291 Darmstadt, Germany

Bulk and ribbon samples of Pd₄₀Ni₄₀P₂₀ in as-quenched and relaxed states were room-temperature irradiated with 4.8 MeV/u 179Au ions at the UNILAC accelerator. Ion beam-induced surface patterning associated with irradiation masks and smoothening of the surface were studied by laser scanning microscope and profilometry. Irradiation induces an out-of-plane swelling step of approximately 100 nm as measured at the boundary between the irradiated and non-irradiated areas and can be explained by additional free volume creation in the solidified ion tracks. The swelling and plastic flow mechanisms are analyzed. Changes in the relaxation enthalpy have been investigated using differential scanning calorimetry. Low-temperature heat capacity measurements substantiate prominent irradiation-induced changes of the Boson peak. Furthermore, changes in diffusivity with increasing fluence was found by post-irradiation tracer diffusion measurements. The evolution of mechanical properties was probed by nanoindentation measurements and the changes induced by irradiation are compared with those caused by mechanical rejuvenation.

MM 10.8 Mon 18:00 P2

Investigations on the relaxation of metallic glasses using fast scanning calorimetry — •MAXIMILIAN DEMMING, MARK STRINGE, MARTIN PETERLECHNER, and GERHARD WILDE — Institut für Materialphysik, Westfälische Wilhelms-Universität Münster, 48149 Münster

During isothermal annealing below the glass transition, all glasses, and thus also metallic glasses, show relaxation effects that resemble the underlying trajectory in phase space towards metastable equilibrium. Using fast scanning calorimetry (FSC) it becomes feasible to investigate such phenomena over a wide range of rates and at very high controlled heating or cooling rates. The tremendous advantage of FSC in comparison to a conventional differential scanning calorimeter (DSC) is, that here one can reach cooling and heating rates up to several 10000 K/s, which makes in-situ quenching possible. Another advantage is that a large number of measurements can be performed in small time intervals. This makes the FSC quite interesting for experiments in thermic cycling with controlled heating and cooling rates. One special method is the so-called cryogenic cycling, which means, that a sample is periodically quenched and reheated between room and a cryogenic temperature. According to literature, this treatment, that has been termed as *cryogenic rejuvenation* could lead to markedly changed properties of the metallic glass. The materials investigated here are Au-CuSiAg and PdNiS due to their low glass transition temperature and melting point. In this work different relaxation states achieved by in-situ quenching via FSC are examined and compared to the relaxation behavior observed at conventional rates.

MM 10.9 Mon 18:00 P2

Investigation of thermoelectric transport through infrared spectroscopy of Heusler and Heusler-like compounds based on Fe₂VAL — •SAHRA BLACK, MICHAEL PARZER, FABIAN GARMROUDI, ERNST BAUER, ANDREI PIMENOV, and EVAN CONSTABLE — Institute of Solid State Physics, Vienna University of Technology, 1040 Vienna, Austria

Thermoelectric materials have attracted much interest in recent years for their ability to convert a thermal gradient into an electric current, thereby acting as an electric power generator. Full and half Heusler compounds have attracted special interest in the growing field of thermoelectricity for several members with a high thermoelectric performance. One Heusler compound in particular Fe₂VAL was under investigation for its high power Factor *PF* and its high thermoelectric figure of merit *ZT*. And recently the element doped thin film Fe₂V_{0.8}W_{0.2}Al broke the world record for the highest thermoelectric figure of merit of roughly 5 ever recorded.

The purpose of the project was to investigate the dielectric response of the thermoelectric material class Fe₂VAL under different manufacturing methods with the usage of Fourier-transformed infrared (FTIR) spectroscopy. This led to a better understanding of the different contribution to the thermoelectric figure of merit *ZT*.

MM 10.10 Mon 18:00 P2

Atom probe tomography study of diffusion in Al-TiB₂ and Al₃Ta-TiB₂ systems — •EVGENIA VOLOBUEVA, PATRICK STENDER, JIEHUA LI, and GUIDO SCHMITZ — University of Stuttgart, Institute of Material Science, Heisenbergstr. 3, 70569, Stuttgart, Germany

To improve the quality of castings, grain refinement is a technique that can improve the overall qualities and properties of the material. For grain refinement in aluminum casting processes, TiB₂ and Ta are added. It is well known, that Al and Ta form an Al₃Ta phase inside the Al-based alloy. In order to gain insight into the process of grain refinement, the diffusion of Al₃Ta and Al in TiB₂ crystals was analyzed via Atom Probe Tomography (APT) in detail.

In this project, single crystals of TiB₂ were used as raw material, glued on top of tungsten posts. Both pure aluminum layers and stoichiometric Al₃Ta layers were deposited by sputter deposition on these crystals with a layer thickness of 200 nm. Subsequent annealing treatments were carried out to investigate segregation and diffusion phenomena at the crystal interface. To use the high spatial and chemical resolution of APT, the samples were sharpened to a final apex ra-

dus of 50 nm by azimuthal milling using a Focused Ion Beam Instrument (FIB). Observed segregation and determined diffusion coefficients will be presented.

MM 10.11 Mon 18:00 P2

Highly conductive Graphite Intercalated Compounds — •LEONHARD NIE-MANN — Robert Bosch GmbH

Since its discovery, graphene has been a material of great research interest due to its promising properties of high electron mobility and electrical conductivity. However, the proposed applications have not yet been realized due to the complexity of fabricating high-quality, defect-free, large-area graphene films. Graphite, which consists of stacked graphene layers, does not have the same promising properties but is easier to fabricate. By intercalating Lewis acids between the graphene layers of graphite, the layers decouple and graphene like behaviour is achieved. The conductivity of these graphite intercalated compounds (GIC) is increased. Here, we report a gas-phase intercalation method for graphite films with AlCl_3 , resulting in GICs with 20 MS/m. These films exhibit good long-term thermal stability. It is noted that the final conductivity depends on the electrical conductivity of the untreated graphite films which is affected by defects in single graphene flakes and the flake size. Studies to increase the conductivity of non-intercalated graphite films are necessary to increase the conductivity of GICs. Therefore, further studies on graphenization of graphite films and defect healing are conducted and the results are presented.

MM 10.12 Mon 18:00 P2

Flatbands and Nonlinear Transport in Nodal Line Semimetals — •THOMAS BÖMERICH, JINHONG PARK, and ACHIM ROSCH — Institute for Theoretical Physics, University of Cologne, Germany

Ohm's law describes the linear dependence of the current on the electric field. Although deviations from this relation are quite small for usual metals we present a model of a semimetal with large non-ohmic conductivity. Motivated by recent experiments on ZrTe_5 , we study a low-energy Hamiltonian consisting of a single Dirac point which gets deformed into a nodal line by mirror symmetry breaking. Upon Landau quantization a zero energy state for a wide range of momenta emerges. For small densities the lowest Landau level can be reached at feasible magnetic fields making it possible to investigate the properties of the flatband.

While flatbands have generated growing interest because of their large density of states and the importance of interactions, we instead focus on their impact on nonlinear transport. Using the Boltzmann equation we obtain higher order conductivities and compare our results to a Dirac semimetal. We show that in the quantum limit, the nonlinear signal of the nodal line semimetal is five orders of magnitude larger than the Dirac semimetal. This enhancement of the nonlinear properties originates from the emergence of the flat bands in the nodal line semimetal. Additionally we investigate the influence of disorder on the linear conductivity.

MM 10.13 Mon 18:00 P2

Towards an efficient formalism to calculate Electron-Phonon-coupling Self Energies and Transport properties from MD Simulation — •MARKUS KREMER^{1,2}, MICHAEL CZERNER^{1,2}, and CHRISTIAN HEILIGER^{1,2} — ¹Institut für Theoretische Physik, Heinrich-Buff-Ring 16, 35392 Gießen, Germany — ²Zentrum für Materialforschung Justus-Liebig-Universität Gießen, Heinrich-Buff-Ring 16, 35392 Gießen, Germany

Calculating transport properties for finite temperature systems has been a concern of research for a long time, with the semiclassical Lowest-order-variational approximation to the Boltzmann-equation (LOVA) being the most commonly used. Recently it was presented that within the KKR formalism more accurate results can be obtained for some materials by using a quantum mechanical Landauer-Büttiker approach incorporating phase-breaking scattering.

Here we want to investigate the possibility of obtaining transport properties at finite temperatures by using a classical MD Simulation and carrying out a transport calculation in the KKR formalism of a certain amount of randomly picked MD screenshots. This procedure is repeated for different lengths of the device to verify that the cell shows ohmic behaviour and obtain its specific resistance. Afterwards we can map this specific resistance to a self-energy.

MM 10.14 Mon 18:00 P2

Determination of interdiffusion coefficients for Pt-Pd binary system by Atom Probe Tomography and DFT calculations — •YOONHEE LEE¹, XI ZHANG², SEBASTIAN MANUEL EICH¹, PATRICK STENDER¹, BLAZEJ GRABOWSKI², and GUIDO SCHMITZ¹ — ¹Department for Materials Physics, Institute for Materials Science, University of Stuttgart, Heisenbergstr. 3, 70569 Stuttgart, Germany — ²Department of Materials Design, Institute for Materials Science, University of Stuttgart, Pfaffenwaldring 55, 70569 Stuttgart, Germany

Understanding the diffusion behavior of different alloy components is fundamental and many systems are well evaluated with distinct diffusivities. However, despite its significant usage as a catalyst for many applications, the interdiffusion behavior of the Pt-Pd binary system has not yet been fully uncovered due to the remarkably slow atomic migration. In this work, interdiffusion coefficients have been determined from experimental data and compared with the results of DFT

simulations. For the temperature range between 400 and 700 °C, nano-sized multilayer samples were created by Ion-Beam Sputtering (IBS). After heat treatment, the samples are analyzed by Atom Probe Tomography (APT). Obtained composition profiles are fitted by a Fourier series approach and the respective interdiffusion coefficients are determined. For the temperature range between 800 and 970 °C, micron-sized Pt/Pd diffusion couples are used and analyzed using EDX. The respective interdiffusion coefficients are determined by the Boltzmann-Matano method. All interdiffusion coefficients are compared with DFT simulations.

MM 10.15 Mon 18:00 P2

Imbibition- and Drying-Induced deformation of Nanoporous Solids — •JUAN SANCHEZ¹, PATRICK HUBER¹, HOWARD STONE², LARS DAMMANN¹, and ZHUO-QUING LI¹ — ¹Hamburg University of Technology (TUHH), Hamburg, Germany — ²Princeton University, NJ, USA

We present time-dependent macroscopic dilatometry experiments on the deformation of nanoporous monoliths (Vycor glass) upon spontaneous, capillarity-driven infiltration of water as well as drying. We find two distinct dynamical regimes. One of them can be quantitatively traced to deformation originating in changes in the surface stress at the inner pore walls (dynamic Bangham's regime), whereas the second results from Laplace pressure effects. The interplay of both strain-inducing regimes allows to infer the water content in the pore space.

The theoretical framework used to describe our experimental data combines simple continuum mechanics and fluid dynamics on the macroscopic porous-solid scale, supported by molecular dynamics simulations on the single-nanopore scale. Our study demonstrates that it is possible to monitor imbibition and drying dynamics by simple dilatometry measurements, offering multiple potential applications.

MM 10.16 Mon 18:00 P2

The Interplay of Spreading, Imbibition and Evaporation of Droplets at Nanoporous Surfaces — •LAURA GALLARDO^{1,2,3}, JUAN SANCHEZ^{1,2,3}, OLIVIER VINCENT⁴, and PATRICK HUBER^{1,2,3} — ¹Institute for Materials and X-Ray Physics, Hamburg University of Technology, 21073 Hamburg, Germany — ²Center for X-Ray and Nano Science CXNS, Deutsches Elektronen-Synchrotron DESY, 22607 Hamburg, Germany — ³Center for Hybrid Nanostructures CHyN, University of Hamburg, 22607 Hamburg, Germany — ⁴CNRS & Univ. Lyon 1, Institute for Light and Matter (ILM), Villeurbanne, France

The dynamics of a droplet deposited on a porous substrate is a combination of three phenomena: spreading, imbibition and evaporation. Here we present a study on the interactions of droplets on nanoporous silicon prepared by electrochemical etching as a function of time. The evolution of the droplet volume is analyzed theoretically and experimentally considering the evaporation and the imbibition of the liquid into the porous substrate. Water is employed to illustrate the case of an evaporation-dominated regime [1]. For an imbibition-dominated regime squalane is employed. The very low vapor pressure of this fluid allows for the analysis of the imbibition process of a droplet into a porous substrate without the contribution of evaporation. The agreement between the experimental data and the theoretical predictions deepens the understanding of the structure of HF-etched porous silicon substrates and provides new insights into the fundamentals of fluid transport in nanoporous media.

[1] Seker, Erkin, et al. APL 92.1 (2008): 013128

MM 10.17 Mon 18:00 P2

Kinetic trapping in brittle crack opening — •TOBIAS MÜLLER and BERND MEYER — Interdisciplinary Center for Molecular Materials and Computer Chemistry Center, FAU Erlangen-Nürnberg, Germany

In the 1920s, Griffith introduced his continuum approach for fracture. Since then great efforts were made to describe crack propagation more precisely within continuum mechanics. Nevertheless, it is evident that the atomic structure of the crack tip itself plays a major role in crack advancement, thus making it necessary to extend the concept of Griffith to the discrete atomic level. This enables the possibility to investigate essential and material-specific processes, such as local bond rearrangements and path-dependent activation barriers. In general, crack opening is a complex chemical process on a multi-dimensional potential energy surface with many local minima and saddle points. The complexity even increases if parameters such as temperature, pressure or chemical environments are included. Here we discuss first DFT-based geometry optimizations for silicon to study brittle fracture mechanics. We show that cracks can propagate via a multitude of local energy minimum configurations connected by a variety of energy barriers. We highlight the complex nature of crack advancement and the complexity of modelling and finding the correct fracture pathway even for a material with a simple crystal structure such as silicon.

MM 10.18 Mon 18:00 P2

Comparison of Crack - Dislocation Interactions in fcc and bcc Metals — •BENEDIKT EGGLE-STEVERS and ERIK BITZEK — Max-Planck-Institut für Eisenforschung GmbH, Max-Planck-Straße 1, 40237 Düsseldorf

The Interactions between Cracks and Dislocations are investigated by means of large scale atomistic simulations with EAM-potentials. Dislocations of differ-

ent character and Burgers vector are placed in the vicinity of a strain-controlled crack, resulting either in an attraction or repulsion of the dislocation. In the former case further interactions can be observed in the course of the simulation, e.g. dislocation emission or crossslipping of screw parts. Dependencies on the stress state, the crack system, dislocation character and distance between dislocation and crack tip are investigated in fcc and bcc crystals. The results are discussed in the framework of resolved shear stresses acting on the dislocations in the near field of the crack tip and for different dislocations characteristics in fcc and bcc.

MM 10.19 Mon 18:00 P2

Molecular dynamics analysis of point defects in ferroelectrics — •TAKAHIRO TSUZUKI¹, DILSHOD DURDIEV², FRANK WENDLER², RYO KOBAYASHI¹, MASAYUKI URANAGASE¹, HIKARU AZUMA¹, and SHUJI OGATA¹ — ¹Nagoya Institute of Technology, Nagoya, Japan — ²Friedrich-Alexander University of Erlangen-Nürnberg, Fürth, Germany

Ferroelectrics are used in many devices such as capacitors. Pb(Zr, Ti)O₃ is the most used material in piezoelectric devices but it contains lead which is gradually prohibited using these days because lead is poisonous to human health. BaTiO₃, which is a very famous classical ferroelectric and lead-free, is newly focused on because its characteristics improve treated by containing defects. But the mechanism of the effects of the defects is not well understood.

We investigated the effects of point defects, monovacancies, and first and second neighbor divacancies on the domain growth of BaTiO₃ with an applied electric field by molecular dynamics simulation using core-shell inter-atomic potential. We found that the first neighbor Ba-O divacancy is the most effective on the domain growth [1]. The sum of the electric field from the divacancy dipole and applied electric field, when they are in the same direction, strongly assist the domain growth.

Phase-field models are powerful tools to investigate ferroelectrics in mesoscale simulation. We obtained parameters, which contain the effect of vacancies mentioned above, for a phase-field model from the molecular dynamics simulation.

[1] Tsuzuki T. et al., J. Appl. Phys. 131, 194101(2022).

MM 10.20 Mon 18:00 P2

Effect of increasing Mn content on generalized planar fault energies of Ni-Mn-Ga alloys — •MARTIN HE CZKO¹, PETR ŠESTÁK², and MARTIN ZELENÝ¹ — ¹Institute of Materials Science and Engineering, Faculty of Mechanical Engineering, Brno University of Technology, Brno, Czech Republic — ²Institute of Physical Engineering, Faculty of Mechanical Engineering, Brno University of Technology, Brno, Czech Republic

Giant magnetic field induced strain (MFIS) in martensitic phase of Ni-Mn-Ga ferromagnetic shape memory alloy makes this alloy promising for various applications. The reasons for existence of MFIS are the high mobility of twin boundaries combined with large magneto-crystalline anisotropy. We performed our calculations using the spin-polarized DFT method implemented in the Vienna Ab Initio Simulation Package (VASP) to reveal the effect of increasing concentration of excess Mn on formation and propagation of twin boundaries, which can be characterized by changes in generalized planar fault energy (GPFE) curves. Effects of excess Mn local arrangement in Ga sublattice on GPFE curves has been considered as well.

Our results show that the barriers for nucleation and grow of a twin rise with increasing content of Mn. It results in more difficult twin formation and propagation in compositions far from stoichiometry. This effect is even more enhanced if excess Mn atom in Ga sublattice is located exactly in the planar fault.

MM 10.21 Mon 18:00 P2

Influence of Twin Boundaries on the Mechanical Behavior of Nanowires Subjected to Bending — •SABA KHADIVIANAZAR^{1,2}, JONAS SCHICKEL¹, and ERIK BITZEK^{1,2} — ¹Friedrich-Alexander-Universität Erlangen-Nürnberg, Chair of General Materials Properties, Institute I, Martensstr. 5, Erlangen 91058, Germany — ²Max-Planck-Institut für Eisenforschung GmbH, Max-Planck-Straße 1, Düsseldorf 40237, Germany

Metallic nanowires (NWs) display superior mechanical properties compared to their bulk counterparts and are regarded as promising building blocks for a variety of application such as touchscreen displays, flexible and stretchable electronic devices. Recently it has been observed that the multi twinned nanowires show higher yield stress and enhanced localized deformation compared to the single crystalline nanowires. Despite the importance of characterizing the deformation behavior under bending loads, most studies of metallic twinned NWs to date have been performed under tensile testing conditions.

Here we present recent results of atomistic simulations on bi-crystalline twinned nanowires under bending. Atomistic simulations allow for controlled variation of the material, size, morphology, the location of the twin boundary (TB), and loading conditions. We show that the presence of a TB not only influences the plastic deformation but also affects the stress state of nanowires. The critical resolved shear stress for dislocation nucleation was determined and the interactions of dislocations with TBs was studied in detail for varying twin boundary location and bending directions.

MM 10.22 Mon 18:00 P2

Benchmarking a Machine-Learning Enhanced Dimer Method for Transition State Search — •NILS GÖNNHEIMER, KING CHUN LAI, KARSTEN REUTER, and JOHANNES T. MARGRAF — Fritz-Haber-Institut der Max-Planck-Gesellschaft, Berlin, Germany

The implementation of Machine-Learning (ML) surrogate models into established atomistic simulation types (e.g. molecular dynamics or geometry optimizations) offers the opportunity of significantly lowering their computational cost. The Dimer method for finding saddle points on high-dimensional potential surfaces is a prime example of this. This method is an important tool for locating transition states and exploring reaction mechanisms in heterogeneous catalysis, but applications are limited by its large computational cost. Jacobsen et al. recently showed that this can be overcome by combining Dimer search with a Gaussian Process Regression surrogate model in the Artificial Intelligence-Driven dimer (AID-TS) algorithm. To better understand the role of the ML surrogate in this method, we compare accuracy, efficiency and diversity of the found states, for AID-TS and conventional dimer search, using surface self-diffusion of Pd(100) as an example.

MM 10.23 Mon 18:00 P2

Al-Ge solid solubility prediction using machine-learned forcefield potentials and phonon calculations — •ONDŘEJ FÍKAR and MARTIN ZELENÝ — Institute of Materials Science and Engineering, Faculty of Mechanical Engineering, Brno University of Technology, Brno, Czech Republic

This work is focused on a theoretical study of the phase stability of Al rich solid solution in Al-Ge alloy. The solubilities of the solid solution were first determined using temperature-dependent free energies of pure elements and solid solutions of various chemical compositions obtained from ab initio calculations based on density functional theory. All total energy calculations were performed by Vienna Ab initio Simulation Package (VASP) with the help of Projector Augmented-wave potentials. Contributions of vibrational free energy and electron free energy were obtained from Phonopy package. Subsequently, a forcefield potential for Al-Ge alloy using machine learning routines as implemented in the VASP package was created. The trained forcefield potential was then used to again carry out phonon calculations. The results were compared to the previous phonon calculations carried out without machine learning.

MM 10.24 Mon 18:00 P2

Simulation of long-term diffusion-based processes in Al and Ni — •DARIA SMIRNOVA¹ and ERIK BITZEK^{1,2} — ¹Max-Planck-Institut für Eisenforschung GmbH, Düsseldorf, Germany — ²Friedrich-Alexander-Universität Erlangen-Nürnberg, Erlangen, Germany

The study of coupled diffusive-displacive processes like dislocation climb at the atomic scale is inherently challenging due to the vastly different time scales involved in the individual processes. One way to address this challenge is to extend the possible simulation timescales while keeping proper atomistic description of a system by using diffusive molecular dynamics (DMD). The method combines classical atomistic interaction potentials in the variational Gaussian method with a numerical solver for the diffusion equation on a variable grid given by the atom positions. Recently, various computational implementations of DMD were presented. Here we describe in detail the different implementations of DMD and provide benchmarks for their efficiency using vacancy diffusion at defects in Al and Ni as model systems.

MM 10.25 Mon 18:00 P2

Ab initio study on novel precipitate-matrix interfaces in Al-Sc based alloys — •UJJAL SAIKIA¹, TILMANN HICKEL^{1,2}, SANKARAN SHANMUGAM³, SERGIY V. DIVINSKI⁴, and GERHARD WILDE⁴ — ¹Department of Computational Materials Design, Max-Planck-Institut für Eisenforschung GmbH — ²BAM Bundesanstalt für Materialforschung und -prüfung — ³Indian Institute of Technology Madras — ⁴Institute of Materials Physics, University of Münster

The cube-on-cube orientation relationship (OR) with the Al matrix has been accepted as the orientation relationship for the coherent nano-scaled Al₃Sc-based particles in Al. Recently, in a severely cold-rolled and subsequently annealed Al-Sc-Zr-Ti alloy, atomic-scale investigations using high resolution scanning transmission electron microscopy (HRSTEM) reveals a novel type of precipitate/matrix coherency.

We performed density functional theory (DFT) based total energy calculations to understand the mechanism of formation of this new type of precipitate/matrix coherency between Al₃Sc and Al matrix and to compare it with the established interfaces. Our DFT results reveal that the newly observed interface corresponds to a local minimum of energy and there is an energy penalty for the interface boundary to 'escape' the particle. We also studied segregation behavior of Sc atoms to probe the initial stage of formation of the observed novel Al₃Sc/Al interface.

MM 10.26 Mon 18:00 P2

Ab initio study of point defects in disordered systems — •PAVEL PAPEZ¹, MARTIN FRIÁK², and MARTIN ZELENÝ¹ — ¹Institute of Materials Science and Engineering, Faculty of Mechanical Engineering, Brno University of Technology, Brno, Czech Republic — ²Institute of Physics of Materials, v.v.i., Czech Academy of Sciences, Brno, Czech Republic

This work is focused on a theoretical study of the influence of N and C interstitials in the equiatomic medium entropy alloy CoCrNi. These interstitials can be found in the alloy as contamination after preparation by powder-metallurgy techniques. The study was done by employing ab initio calculations based on the density functional theory and was performed by Vienna Ab initio Simulation Package (VASP) using the projector-augmented-wave formalism. The calculations were done on 6x6x2 supercells generated by using the special quasi-random structures approach (SQS) consisting of 216 atoms. The supercell consisted of 6 lattice planes {1 1 1} along the z-axis. The hcp structures were made from the fcc cells by moving the planes to create the hcp ABABAB stacking. Our results have shown which interstitial positions result in the lower enthalpy of formation. They are characterized by a higher amount of Cr and lower amount of Ni in their nearest neighbours (NN) shell with the most stable being the one with 2 Co, 3 Cr, and 1 Ni in its 1st NN shell. The stacking fault energy (SFE) was calculated using the first-order axial Ising model and by explicit stacking-fault calculations in two times larger fcc supercell. The results shown that interstitials always increase the SFE.

MM 10.27 Mon 18:00 P2

Charge distribution and electronic structure of ZIF-8 and its derivatives from first principles — •JOSHUA EDZARDS¹, HOLGER-DIETRICH SASSNICK¹, ANA MARIA VALENCIA^{1,2} und CATERINA COCCHI^{1,2} — ¹nstitut für Physik, Carl von Ossietzky Universität Oldenburg, 26129 Oldenburg — ²nstitut für Physik and IRIS Adlershof, Humboldt-Universität zu Berlin, 12489 Berlin

Metal organic frameworks are novel materials with high potential in many fields of applications, ranging from gas storage and catalysis to optoelectronics. In spite of their growing popularity, there is still a lack of fundamental understanding of the physico-chemical properties of these materials, even in the most established subgroups such as the zeolitic imidazolate frameworks (ZIFs). To shed light into the nature of the chemical bonds in these systems, we performed a first-principles study based on density-functional theory investigating the charge distribution in ZIF-8 and its derivatives with Br, Cl, and H terminations replacing CH₃. Our results indicate the presence of an ionic bond connecting the Zn atom to the organic scaffold, which is held together by covalent bonds. Control calculations performed on the building blocks of ZIF-8 indicate that the aforementioned characteristics are quantitatively influenced by the extended nature of the framework. The presence of halogen substituents, carrying around an excess of negative charge, leads only to a negligible redistribution of the charge density. On the other hand, the electronic structures computed for these systems indicate a reduction of about 0.5 eV of the band-gap in the Br- and Cl-terminated systems with respect to ZIF-8.

MM 10.28 Mon 18:00 P2

Recent progress in ICET — J. MAGNUS RAHM, •ERIK FRANSSON, PERNILLA EKBERG-TANNER, JOAKIM BRORSSON, MATTIAS ÅNGQVIST, and PAUL ERHART — Department of Physics, Chalmers University of Technology, Gothenburg, Sweden

Alloy cluster expansions (CEs) provide an accurate and computationally efficient mapping of the potential energy surface of multi-component systems that enables comprehensive sampling of the many-dimensional configuration space. In this contribution, we provide an update regarding recent developments and new features in the integrated cluster expansion toolkit (ICET). We have im-

plemented a version of the constituent strain formalism in ICET, which enables treatment of long-ranged strain contributions. This approach is demonstrated for the Pd-H system in order to study coherent phase transitions via constrained Monte Carlo simulations. Furthermore, in CEs of low-dimensional systems, lack of symmetry leads to large numbers of independent effective cluster interactions (ECIs). We have made it possible to merge orbits, i.e., reduce the number of independent ECIs by considering local symmetries and merging parameters that are similar. This approach enables training of accurate models while requiring significantly fewer DFT calculations. This approach is employed to study surface segregation in AuPd and CuPd in environments ranging from vacuum to high pressures of hydrogen. Finally, we have added a number of additional features, including Wang-Landau sampling and extraction of long-range order parameters, and the code has undergone a thorough review that has resulted in a significant performance boost.

MM 10.29 Mon 18:00 P2

Molecular dynamics simulations of porous silica networks — •HEMANGI PATEL¹, BARBARA MILOW^{1,2}, and AMEYA REGE¹ — ¹Institut für Werkstoff-Forschung, Abteilung Aerogele und Aerogelverbundwerkstoffe, Deutsches Zentrum für Luft- und Raumfahrt e.V. (DLR), Cologne, Germany — ²Nanostructured Cellular Materials, Institut of Inorganic Chemistry, University of Cologne, Cologne, Germany

Molecular dynamics (MD) simulations offer a significant advantage over experimental procedures to investigate the nanoporous structure in silica-based systems because they present a detailed insight into the atomic-scale phenomena that underlie the formation of the materials* network. In this work, porous silica networks are modelled using MD simulations. α - quartz form of SiO₂ is subjected to high temperature and equilibration followed by quenching to obtain amorphous silica structure α - quartz form of SiO₂ is subjected to high temperature and equilibration followed by quenching to obtain amorphous silica structure. The negative pressure rupturing approach is then used to obtain a fractal structure. Local minimum energy configuration is obtained using the conjugate gradient scheme for the formation of a stable porous network. The structural evolution of the silica backbone in the network is investigated. This technique is used to obtain porous networks of varying densities. The resulting model systems are investigated for their structural and mechanical properties. Uniaxial tensile and compressive simulations will be presented, and properties such as their Young's modulus will be quantified.

MM 10.30 Mon 18:00 P2

Magnetotransport properties of coupled nanowire arrays in LAO/STO — •RANJANI RAMACHANDRAN¹, DENG YU YANG¹, MUQING YU¹, ADITI NETHWEWALA¹, PATRICK IRVIN¹, JEREMY LEVY¹, and KI-TAE EOM² — ¹University of Pittsburgh, Pittsburgh, USA — ²University of Wisconsin-Madison, Madison, WI, USA

The ability to create and characterise an array of coupled nanowires is an important step towards understanding the physics of systems like stripe phase superconductors, sliding Luttinger liquids, anisotropic materials made up of quasi-1D chains, etc. Here, we create nanowire arrays using Ultra Low voltage Electron beam lithography. ULVEBL has been shown to create conducting nanostructures in the 2D electron system at the LAO/STO interface. We study the transport properties of this system at low temperatures and high magnetic fields. We show that it is possible to reversibly tune the interwire coupling using a back gate voltage and magnetic field. This can act as a tool to study the dimensionality cross over from 1D to 2D. This can potentially be extended further to create more complicated structures using ULV-EBL that can model the behaviour of other materials and lattice models.

MM 11: Invited Talk Jörg F. Löffler

Time: Tuesday 9:30–10:00

Location: H44

Invited Talk

MM 11.1 Tue 9:30 H44

Fast calorimetry: studying phase transitions in slow motion — •JÖRG F. LÖFFLER — Laboratory of Metal Physics and Technology, Department of Materials, ETH Zurich, 8093 Zurich, Switzerland

Studying the details of phase transitions and metastable phase formation is generally difficult for metallic materials because of their rapid nucleation and growth kinetics. Bulk metallic glasses (BMGs), on the other hand, show very sluggish crystallization kinetics. By applying fast calorimetry to slowly transforming BMG-forming systems at heating and cooling rates of several 10,000 K/s, we are able to determine phase transitions more or less in slow motion. In this way, we can explore novel glass states [1], determine their stochastics of nucleation, and study metastable phase formation. During heating at low temperatures, BMGs

generally form metastable crystals that transform into more stable modifications at higher temperatures. The classical interpretation is a direct solid-to-solid transformation, but by fast calorimetry we can show that this transition occurs via metastable melting [2]. Furthermore, while with classical calorimetry it is not possible to sufficiently characterize metastable phases owing to their structural changes upon slow heating, fast calorimetry allows for detailed measurements of their heat capacity and melting temperatures [3]. In this way, we are able to verify the existence of monotropic polymorphism and validate Ostwald's phase rule for many metastable phases. [1] J. E. K. Schawe, J. F. Löffler, Nat. Commun. 10, 1337 (2019). [2] S. Pogatscher et al., Nat. Commun. 7, 11113 (2016). [3] J. E. K. Schawe, J. F. Löffler, Acta Mater. 226, 117630 (2022).

MM 12: Computational Materials Modelling: Physics of Ensembles 1

Time: Tuesday 10:15–13:00

Location: H44

MM 12.1 Tue 10:15 H44

Pinpointing Hubbard corrections to tackle inhomogeneous n_l subshells: The DFT+U(m) method — •ERIC MACKE¹, IURI TIMROV², LUCIO COLOMBI CIACCHI¹, and NICOLA MARZARI² — ¹Hybrid Materials Interfaces Group and Bremen Center for Computational Materials Science, MAPEX, University of Bremen, Am Fallturm 1, 28359 Bremen, Germany — ²Theory and Simulation of Materials (THEOS) and National Centre for Computational Design and Discovery of Novel Materials (MARVEL), Ecole Polytechnique Federale de Lausanne (EPFL), CH-1015 Lausanne, Switzerland

DFT+U remains a key tool in computational material science as it mitigates the DFT self-interaction error. While this simplistic approach often provides electronic and magnetic properties in fair agreement with literature, recent investigations revealed that DFT+U massively over-stabilizes high spin configurations of transition metal elements surrounded by strong ligand fields. In such compounds, the projection of occupied Kohn-Sham states onto the atomic basis frequently yields occupation numbers $n_m^\sigma \approx 0.5$ for certain magnetic quantum numbers m , so that the penalizing Hubbard term $E_U = \sum_{m,\sigma} U/2 [n_m^\sigma(1 - n_m^\sigma)]$ is maximized. We argue that if the occupation of a magnetic (spin-) orbital is dominated by the effect of hybridization with a ligand, Hubbard corrections should not be applied in the same way as for unaffected orbitals. To account for such inhomogeneous bonding regimes, we propose a more flexible scheme that enables the use of distinct Hubbard parameters $U(m)$ for the same species, computable by means of *ab initio* methods.

MM 12.2 Tue 10:30 H44

Efficient computation of optical properties of large-scale heterogeneous systems — •JOSEPH C. A. PRENTICE¹ and ARASH A. MOSTOFI² — ¹Department of Materials, University of Oxford, UK — ²Departments of Physics and Materials, Imperial College London, UK

The optical properties of large-scale (>1000 atoms) heterogeneous systems are of interest in several fields, from photovoltaics to biological systems. Computing such properties accurately from first principles, however, is challenging; even if only a small region is optically active, quantum mechanical environmental effects must often be included, and the cost of applying a quantitatively accurate level of theory is prohibitive. Here, I present recent work demonstrating how such calculations can be performed efficiently from first principles via two methods: an extension of the spectral warping method of Ge et al., and a novel combination of quantum embedding (specifically embedded mean-field theory) and linear-scaling (time-dependent) density functional theory. The accuracy and utility of these methods is demonstrated by applying them to systems including the molecular crystal ROY, chromophores in solution, and pentacene-doped p-terphenyl. The results pave the way for quantitatively accurate calculations to be performed on previously inaccessible large-scale systems.

MM 12.3 Tue 10:45 H44

Converging tetrahedron method calculations for non-dissipative parts of spectral functions — •MINSU GHIM^{1,2,3} and CHEOL-HWAN PARK^{1,2,3} — ¹Center for Correlated Electron Systems, Institute for Basic Science, Seoul 08826, Korea — ²Department of Physics and Astronomy, Seoul National University, Seoul 08826, Korea — ³Center for Theoretical Physics, Seoul National University, Seoul 08826, Korea

Integrations in k space are used to calculate many of the physical quantities in solid-state physics. Examples include various static or dynamical conductivity, self-energy of an electron, and electric polarizability. The integral usually takes the form of a product of proper matrix elements and $1/[\hbar\omega - (\epsilon_{mk} - \epsilon_{nk}) + i\eta]$, which is decomposed into the real part and the imaginary part, $\text{P}\{1/[\hbar\omega - (\epsilon_{mk} - \epsilon_{nk})]\}$ and $-i\pi\delta[\hbar\omega - (\epsilon_{mk} - \epsilon_{nk})]$, respectively. Here, ω is the frequency, ϵ_{mk} and ϵ_{nk} are the energies of the valence and conduction electronic bands with Bloch wavevector \mathbf{k} , respectively, and $\eta = 0^+$. Although the delta-function part has been widely calculated by the tetrahedron method, the non-dissipative principal value integral part has not. Tools to obtain matrix elements and energy eigenvalues from first principles have been actively developed, but there are technical difficulties in the tetrahedron method for the non-dissipative part. In this talk, we introduce an easy-to-implement, stable method to overcome those obstacles. Furthermore, our method is tested by calculating the spin Hall conductivity of fcc platinum.

MM 12.4 Tue 11:00 H44

Self-consistency in GW formalism leading to quasiparticle-quasiparticle couplings — •CARLOS MEJUTO-ZAERA¹ and VOJTECH VLČEK² — ¹Scuola Internazionale Superiore di Studi Avanzati SISSA, Trieste, Italy — ²University of California Santa Barbara UCSB, USA

Many-body perturbation theory (MBPT) has become a tool of choice for the description of materials. Traditionally tied to the weakly-interacting limit, e.g. through the GW approximation, its expansion towards higher interactions is a

fundamental goal in the field. Existing attempts can rely on selected diagram resummation or downfolding, which involve some choice of expansion parameters typically reducing the approach's generality and flexibility. Despite this apparently intrinsic price, MBPT provides through Hedin's equations a formally exact path to describe any dynamically correlated system, regardless of interaction strength. We revisit this framework to disentangle how to systematically extend its practical validity beyond weak interactions, focusing on the structure of the interaction vertex Γ within self-consistent implementations. Using the Hubbard dimer at half-filling, we unveil the role of Γ 's functional derivative with respect to the Green's function, hitherto typically neglected, in generating diagrams that can extend the reliability of MBPT towards high interactions [1].

[1] arXiv:2203.05029

MM 12.5 Tue 11:15 H44

Automated Corrections for Materials Design of Ionic Systems: AFLOW-CCE — •RICO FRIEDRICH^{1,2}, MARCO ESTERS¹, COREY OSSES¹, STUART KI¹, MAXWELL J. BRENNER¹, DAVID HICKS¹, MICHAEL J. MEHL¹, CORMAC TOHER¹, and STEFANO CURTAROLO^{1,3} — ¹Center for Autonomous Materials Design, Duke University, USA — ²Helmholtz-Zentrum Dresden-Rossendorf, Dresden — ³Materials Science, Electrical Engineering, and Physics, Duke University, USA

Materials databases such as AFLOW [1] leverage *ab initio* calculations for autonomous materials design. The predictive power critically relies on accurate formation enthalpies — quantifying the thermodynamic stability of a system. For ionic materials such as oxides and nitrides, standard DFT leads to errors of several hundred meV/atom [2,3].

We have recently developed the "coordination corrected enthalpies" (CCE) method yielding highly accurate room temperature formation enthalpies with mean absolute errors down to 27 meV/atom [3]. Here, we introduce AFLOW-CCE [4] — our implementation of CCE into the AFLOW framework. It provides a tool where users can input a structure file and receive the CCE corrections, or even the CCE formation enthalpies if pre-calculated LDA, PBE or SCAN values are provided. The implementation features a command line tool, a web interface, and a Python environment.

[1] S. Curtarolo *et al.*, *Comput. Mater. Sci.* **58**, 218 (2012).[2] V. Stevanović *et al.*, *Phys. Rev. B* **85**, 115104 (2012).[3] R. Friedrich *et al.*, *npj Comput. Mater.* **5**, 59 (2019).[4] R. Friedrich *et al.*, *Phys. Rev. Mater.* **5**, 043803 (2021).

15 min. break

MM 12.6 Tue 11:45 H44

Revealing the ambient and high-pressure phases of group IV monochalcogenides and monoxides with an evolutionary algorithm — •LONG NGUYEN and GUY MAKOV — Department of Materials Engineering, Ben-Gurion University of the Negev, Beer-Sheva, Israel

Group IV chalcogenides and oxides are candidates for incorporation into optoelectronic and thermoelectric conversion devices. These functional materials are mostly p-type semiconductors that provide low-cost, environmentally friendly, abundant, and high-efficiency. To expand the possible phases and study their stability upon compression, a combination of DFT modelling with evolutionary algorithm (EA) is applied to extensively investigate across the group IV monochalcogenides and oxides. We will report our results from the implementation of the EA to search for stable phases. In group IV monoxides, our results include multiple structural transitions of SnO and PbO upon compression. Two new high-pressure polymorphs are predicted, the orthorhombic Pbcm SnO and the octahedral monoclinic C2/m PbO. Weakening of the lone pairs and elastic instability are the main drivers for the structural transitions. Among the monochalcogenides, SnS and GeS phase families are examined together with their electronic and optical properties. At ambient conditions, GeS and SnS can present several polymorphs with bandgaps in the range from 0.3 to 1.6 eV, which can be attractive for a variety of optoelectronics applications. Upon compression, we found a similar convergence of SnS and GeS into the Cmcm and later the Pm3m phase. The transition mechanism is discussed through the lone pairs' influence on the structural distortion.

MM 12.7 Tue 12:00 H44

An Open-source Interface to MP2 and Coupled-Cluster Methods for Solids for Localized Basis Set Codes — •EVGENY MOERMAN¹, FELIX HUMMEL², ANDREAS IRMLER², ANDREAS GRÜN-EIS², and MATTHIAS SCHEFFLER¹ — ¹The NOMAD Laboratory at the FHI-MPG, Berlin — ²Inst. for Th. Phys., TU Wien, Vienna

Coupled cluster (CC) theory is often considered the gold standard of quantum-chemistry. For solids, however, the available software is scarce ([1] and references therein). We present CC-aims[2], which can interface *ab initio* codes with

localized atomic orbitals and the CC for solids (CC4S) code by the group of A. Grüneis. CC4S features a continuously growing selection of wave function-based methods including perturbation and CC theory. The CC-aims interface was developed for the FHI-aims code[2] but is implemented such that other codes may use it as a starting point for corresponding interfaces. As CC4S offers treatment of both molecular and periodic systems, the CC-aims interface is a valuable tool, where DFT is either too inaccurate or too unreliable, in theoretical chemistry and materials science alike. In this talk we describe the CC-aims interface, the CC4S code, and demonstrate the application of CC and MP2 by investigating the relative stability of boron nitride phases. - This work received support from the European Union's Horizon 2020 research and innovation program under Grant Agreement No. 951786 (The NOMAD CoE).

[1] Q. Sun *et al.*, J. Chem. Phys. 153:024109 (2020)

[2] E. Moerman *et al.* to be published, J. Open Source Software

[3] The FHI-aims web page: <https://fhi-aims.org>

MM 12.8 Tue 12:15 H44

Wannier function perturbation theory: localized representation and interpolation of wavefunction perturbation — •JAE-MO LIHM and CHEOL-HWAN PARK — Department of Physics, Seoul National University, Seoul, Korea

Wannier functions provide a localized representation of the electronic structure of solids and are thus finds wide application in condensed matter physics. However, the Wannier function method is limited in that it cannot be used to represent the change of the wavefunctions due to perturbations. In this work, we introduce Wannier function perturbation theory (WFPT) [1], which overcomes this limitation by providing a localized representation of wavefunction perturbation which we term “Wannier function perturbation.” Among the diverse possible applications of WFPT, we provide three examples. First, we calculate the temperature dependence of the indirect optical absorption spectra of silicon. Our calculation differentiates phonon-absorption and phonon-emission processes and includes the band-gap renormalization without arbitrary temperature-dependent shifts in energy at the same time, which is beyond reach of existing methods. Second, we develop a theory for calculating the shift spin current without any band-truncation error and apply it to monolayer WTe_2 . Third, we apply WFPT to calculate the spin Hall conductivity of the same material, again without any band-truncation error. WFPT will open up a new way for studying the response properties of the electron states in real materials.

[1] J.-M. Lihm and C.-H. Park, Phys. Rev. X, 11, 041053 (2021)

MM 12.9 Tue 12:30 H44

Boosting first-principles molecular dynamics with orbital-free density functional theory — •LENZ FIEDLER¹, ZHANDOS A. MOLDABEKOV¹, XUECHENG SHAO², KAILI JIANG², TOBIAS DORNHEIM¹, MICHELE PAVANELLO², and ATTILA CANGI¹ — ¹Helmholtz-Zentrum Dresden-Rossendorf / CASUS — ²Rutgers University Newark

Kohn-Sham density functional theory (KS-DFT) is one of the most important simulation methods in materials science and quantum chemistry. Yet, standard DFT codes exhibit scaling behaviors in terms of system size and temperature that prohibit extended dynamical investigations of materials using DFT driven molecular dynamics simulations (MD), especially towards the warm dense matter regime (WDM). We present a practical hybrid approach that combines orbital-free density functional theory (DFT) with Kohn-Sham DFT for speeding up first-principles molecular dynamics simulations. Equilibrated atomic configurations are generated using orbital-free DFT for subsequent Kohn-Sham DFT molecular dynamics. This leads to a massive reduction of the simulation time without any sacrifice in accuracy. We show results across systems of different sizes and temperature, up to the warm dense matter regime. To that end, we use the cosine distance between the time series of radial distribution functions representing the ionic configurations. Likewise, we show that the equilibrated ionic configurations from this hybrid approach significantly enhance the accuracy of machine-learning models that replace Kohn-Sham DFT.

MM 12.10 Tue 12:45 H44

First-principles calculations of plasma frequency in an all-electron full-potential framework — •MARIA K. POGODAEVA, SERGEY V. LEVCHENKO, and VLADIMIR P. DRACHEV — Moscow, Russia

We present a first-principles methodology to calculate plasma frequency of using density-functional theory in an all-electron full-potential framework implemented in FHI-aims. The results are compared to the results obtained with pseudopotential approaches and experimental data from photo-emission, absorption, and electron energy loss spectra. We test the approach on seven elemental metals: gold, silver, sodium, copper, palladium, platinum, and aluminum. Our results reproduce experimental values for plasma frequency within 0.1-0.3 eV accuracy compared to experiment for all metals except sodium. Calculated plasma frequency for sodium is consistently overestimated by 0.5 eV by VASP and FHI-aims. For other metals except gold FHI-aims and VASP are in a perfect agreement with each other and with experiment. For gold VASP underestimates plasma frequency by 0.6 eV compared to experiment, but FHI-aims calculates the value within 0.2 eV. Overall, the agreement between the two codes and the experiment is good. This validates our all-electron implementation and allows for further applications of the methodology to more complex systems

MM 13: Non-equilibrium Phenomena in Materials Induced by Electrical and Magnetic Fields 3

Time: Tuesday 10:15–13:00

Location: H45

Topical Talk

MM 13.1 Tue 10:15 H45

Supercompatibility in ceramic micropillars of lanthanum niobate — •OLIVIA A. GRAEVE and HAMED HOSSEINI-TOUDESHPKI — University of California San Diego, La Jolla, CA, USA

Superelastic materials represent a distinct family of compounds with the ability to manifest reversible deformation in response to an applied stress. Generally, superelastic materials are metallic in nature, and only very few ceramics have been shown to fully or partially display this response. Here, we describe exceptional superelasticity and enhanced reversibility on micropillars of $LaNbO_4$ ceramic in response to compressive stresses up to 1100 MPa without fracture. The micropillars were prepared by focused ion beam machining from specimens consolidated by spark plasma sintering. The material response to stress is consistent with the theory of supercompatibility (cofactor theory) that has been reported to address the enhanced reversibility and low-hysteresis behavior (i.e., improved superelasticity) of certain shape memory metallic alloys. This makes $LaNbO_4$ a unique addition to the germane family of smart materials for applications as long-lived actuators impacting the automotive, energy and aerospace sectors, among many other technologically significant fields, especially in extreme conditions (i.e., higher temperatures or pressures) under which ceramics excel compared to metals.

Topical Talk

MM 13.2 Tue 10:45 H45

X-Ray Spectro(micro)scopy as analytics for field assisted deposition processes — •DAVID N. MUELLER — Peter Grünberg Institut, Forschungszentrum Jülich

X-Ray absorption spectroscopy (XAS) is element specific, sensitive to the electronic structure around the Fermi level, and provides information about the short-range order in a material, and can be tuned to be surface sensitive. It therefore represents a versatile tool to assess the impact of external fields during synthesis of functional materials on the structure property relations required for

optimizing functionalization. Providing spatial resolution on the sub micrometer scale with X-Ray photoemission electron microscopy (XPEEM) additionally allows identification of phase inhomogeneities and their peculiarities with respect to chemistry and structure.

In this presentation, we will use 3d transition metal based oxides of varying complexity to showcase how XAS and XPEEM can give valuable insights into the atomic and electronic structure and how those can be improved towards use in e. g. catalysis by using external fields during synthesis. It will furthermore be discussed how numerical methods such as principal component analysis can help analyzing spectromicroscopic data to unambiguously identify subtle lateral inhomogeneities in the spectroscopic signatures, providing information about phase formation and decomposition processes.

MM 13.3 Tue 11:15 H45

Magnetic Field-assisted Chemical Vapor Deposition of $MgFe_2O_4$ Films for Photoelectrochemical Water Splitting — HYENKWON LEE¹, •ZIYAAD TALHA AYTUNA¹, AMAN BHADRAWJ¹, MICHAEL WILHELM¹, KHAN LE¹, BENJAMIN MAY², DAVID MÜLLER², and SANJAY MATHUR¹ — ¹GreinstraÙe 6, 50939 Köln — ²Wilhelm-Johnen-StraÙe, 52438 Jülich

Single-phase magnesium ferrite films ($MgFe_2O_4$) were grown by magnetic field-assisted chemical vapor deposition (CVD) of mixed-metal precursor $[MgFe_2(OtBu)_8]$ as a function of the applied field strength ($B = 0.0, 0.5$ and 1.0 T). The formation of monophase $MgFe_2O_4$ deposits was confirmed by X-ray diffraction and photoelectron spectroscopy. The cross-sectional analysis (FIB-SEM) of the film revealed an increased densification and crystal growth, upon application of the magnetic field when compared to zero-field deposition. The $MgFe_2O_4$ films deposited under zero-field and field-assisted conditions were used as electrodes in a photoelectrochemical (PEC) water-splitting reaction. All the three samples showed a stable performance and photocurrent values, however, the photocurrent was found to gradually decrease with increasing applied

magnetic field (0 T: 5.74 $\mu\text{A}/\text{cm}^2$, 0.5 T: 2.33 $\mu\text{A}/\text{cm}^2$, and 1 T: 1.33 $\mu\text{A}/\text{cm}^2$ at 1.23 V (vs. RHE)), which is possibly due to change in absorption properties and crystal orientation, decreasing photo absorption intensity provided by the UV-vis results and the latter being evident in the disappearance of (220) peak in MgFe₂O₄ films grown under the influence of the external magnetic field.

15 min. break

MM 13.4 Tue 11:45 H45

PECVD carbon-coated electrospun vanadium pentoxide nanofibers as cathode material for photoresponsive batteries — •MICHAEL WILHELM, RUTH ADAM, AMAN BHARDWAJ, and SANJAY MATHUR — University of Cologne, Cologne, Germany

Harvesting and converting sunlight as the most sustainable energy source on earth is still challenging. Photo-rechargeable batteries represent a synergistic concept that integrates both energy harvesting and energy storage modalities based on dual-functional materials. Vanadium pentoxide nanofibers (VNF) as photoresponsive material was synthesized by electric field-assisted spinning technique and used as dual-action cathode material for photo-rechargeable lithium-ion batteries. A high discharge capacity was delivered, which could be increased under light illumination confirming the photoresponsive behavior. To minimize side reactions and to increase the stability of the electrodes, the VNF were carbon-coated by plasma-enhanced chemical vapor deposition (PECVD). Long-term stability tests showed that besides being a conductive shell, the carbon coating is also essential in retaining the structural instability of VNF. Higher capacity retention upon cycling compared to the non-carbon-coated VNF (after 300 cycles: 43.85 % capacity retention VNF and 61.13 % capacity retention for carbon-coated VNF). Further, the rechargeability of the material by light was demonstrated by illuminating with a UV lamp and afterward discharging the electrode material in the dark which delivered a photoconversion efficiency of 4.24 % for VNF and 5.07 % for carbon-coated VNF.

MM 13.5 Tue 12:00 H45

Structure and Morphology Engineering of Hexagonal Boron Nitride (h-BN) using Magnetic Field assisted CVD — •ANJA SUTORIUS, MICHAEL WILHELM, KHAN LÊ, ZIYAAD AYTUNA, and SANJAY MATHUR — University of Cologne, Cologne, Germany

The aim for two dimensional materials namely graphene, MoS₂ and borophene has become a high interest due to their amazing properties (e.g. conductivity, flexibility, dimensionality) and demand for innovative electronic device applications. The large band gap material h-BN catches the attention of latest research due to its non-toxicity, environmentally friendly and chemical stability as well as its dielectric properties. The commonly preparation of h-BN often requires a gas phase deposition on catalytic metals at very high temperatures and is despite intense research very challenging. A new opportunity is provided using an external magnetic field during synthesis. Precursor molecules like amino borane (NH₃BH₃) or dimethyl amino borane (CH₃)₂NBH₂ and h-BN itself exhibit a charge distribution and thus can be influenced by an applied field. Here, we

would like to report about the thin film formation of h-BN with and without an external magnetic field on a variety of substrates ranging from catalytic metal substrates to non-catalytic dielectric silicon substrates. Results from infrared and x-ray photoelectron spectroscopy, as well as transmission and scanning microscopy.

MM 13.6 Tue 12:15 H45

Nanocrystalline CoCrFeNiGax (x = 0.5, 1.0) high entropy alloys: structural and magnetic features — •NATALIA SHKODICH, MARINA SPASOVA, and MICHAEL FARLE — Faculty of Physics and Center of Nanointegration (CENIDE), University of Duisburg-Essen, Duisburg, 47057 Germany

Nanocrystalline single fcc phase CoCrFeNiGax (x = 0.5, 1.0) high entropy alloy (HEA) powder particles with good structural and compositional homogeneity were successfully fabricated by high energy ball milling (HEBM). Characterization by XRD, SEM/EDX, and TEM/EDX shows that the fcc phase with the refined microstructure of nanosized grains (~10 nm) could be obtained after 190 min of HEBM at 900 rpm. We used HEBM powders to fabricate homogeneous nanocrystalline bulk HEAs by spark plasma sintering (SPS). SPS at 1073 K of the CoCrFeNiGa_{0.5} HEA powder increases the crystallinity of the fcc phase, while for the equiatomic CoCrFeNiGa powder a partial transformation of the fcc into the bcc phase is observed. The nanocrystalline HEA CoCrFeNiGax (x = 0.5, 1.0) powders show a paramagnetic behavior at room temperature and a Curie temperature (T_c) is of 127K-130K. After SPS, the CoCrFeNiGa bulk material is ferromagnetic up to T_c = 775K. Its saturation magnetization M_s (300K) increases by a factor of 10 as compared to the HEA powder. The SPS of the CoCrFeNiGa_{0.5} HEA powder, however, does not change its paramagnetic nature at ambient temperature. This work has been supported by the Deutsche Forschungsgemeinschaft (DFG) within CRC/TRR 270, project S01 (project ID 405553726).

Topical Talk

MM 13.7 Tue 12:30 H45

Field-assisted processing of magnetic materials — •FERNANDO MACCARI and OLIVER GUTFLEISCH — Technical University of Darmstadt, 64287 Darmstadt, Germany

Optimization of materials requires a precise control of processing parameters to achieve a desired combination of phases and microstructural features. The application of an external fields during synthesis, going beyond the classical use of only temperature and time, can be used as additional degree of freedom to promote densification, solid state phase transformation, intermetallic compounds and precipitates formation. This combination opens new possibilities to obtain highly tailored microstructures and improved properties.

Focusing on magnetic materials, this talk will provide an overview on how different length scales can be manipulated using external magnetic and electric field assisted processing techniques to create materials with enhanced functional properties. Aspects related to induced magnetic anisotropy and phase formation in soft and hard magnetic materials will be covered. Additionally, field driven coupled magnetic and phase transition is going to be addressed and exemplified in ferromagnetic shape memory Ni-Mn-Ga Heusler compound.

MM 14: Materials for Storage and Conversion of Energy (joint session MM/KFM)

Time: Tuesday 10:15–11:30

Location: H46

MM 14.1 Tue 10:15 H46

How Important are Long-Range Electrostatics in Machine-Learning Potentials for Battery Materials? — •CARSTEN STAACKE¹, HENDRIK HEENEN¹, CHRISTOPH SCHEURER¹, GABOR CSANYI², KARSTEN REUTER¹, and JOHANNES MARGRAF¹ — ¹Fritz Haber Institut, Berlin, Germany — ²Engineering Department, Cambridge University, UK

All-solid-state Li-ion batteries promise gains in safety and durability by combining high Li-ion conductivity and mechanical ductility. In this respect, solid-state electrolytes (SSE) such as the Li₇P₃S₁₁ glass-ceramic have gained much attention. Modern machine learning (ML) potentials are increasingly being adopted as a tool for modeling SSEs at the atomistic level. However, the local nature of these ML potentials typically means that long-range contributions arising, e.g., from electrostatic interactions are neglected. To this end, we have combined short-ranged machine-learning potentials based on the Gaussian Approximation Potential (GAP) approach with a classical electrostatic model in the long-range (ES-GAP). We will present a first-principles validation of both, the pure GAP potential and the new ES-GAP for the LPS SSE. In particular, the role of Coulomb interactions in isotropic vs. non-isotropic system simulations will be evaluated. In standard isotropic simulation tasks, such as determining ionic conductivities, both GAP and ES-GAP yield similar results. In contrast, simulations on non-isotropic systems show the importance of ES contributions and provide new insights into interface stability of Li₇P₃S₁₁.

MM 14.2 Tue 10:30 H46

Oxygen Hole Formation Controls Stability in LiNiO₂ Cathodes: DFT Studies of Oxygen Loss and Singlet Oxygen Formation in Li-Ion Batteries — •ANNALENA GENREITH-SCHRIEVER^{1,3}, HRISHIT BANERJEE^{1,2,3}, CLARE P. GREY^{1,3}, and ANDREW J. MORRIS^{2,3} — ¹Yusuf Hamied Department of Chemistry, University of Cambridge, Cambridge, United Kingdom — ²School of Metallurgy and Materials, University of Birmingham, Birmingham, United Kingdom — ³The Faraday Institution, Harwell Science and Innovation Campus, Didcot, United Kingdom

Ni-rich cathode materials achieve both high voltages and capacities in Li-ion batteries but are prone to structural instabilities and oxygen loss via the formation of singlet oxygen. Using ab initio molecular dynamics simulations, we observe spontaneous O₂ loss from the (012) surface of delithiated LiNiO₂, singlet oxygen forming in the process. We find that the origin of the instability lies in the pronounced oxidation of O during delithiation, i.e., O plays a central role in Ni-O redox in LiNiO₂, as analysed with density-functional theory and dynamical mean-field theory calculations based on maximally localised Wannier functions. The O₂ loss route observed here consists of 2 surface O⁻ radicals combining to form a peroxide ion, which is oxidised to O₂, leaving behind 2 O vacancies and 2 O²⁻ ions: effectively 4 O⁻ radicals disproportionate to O₂ and 2 O²⁻ ions. Singlet oxygen formation is caused by the singlet ground state of the peroxide ion, with spin conservation dictating the preferential release of ¹O₂.

MM 14.3 Tue 10:45 H46

Defects and Phase Formation in Non-Stoichiometric LaFeO₃: A Combined Theoretical and Experimental Study — •DANIEL MUTTER¹, ROLAND SCHIERHOLZ², DANIEL URBAN¹, SABRINA HEUER^{2,3}, THORSTEN OHLERTH^{2,3}, HANS KUNGL², CHRISTIAN ELSÄSSER^{1,4}, and RÜDIGER-A. EICHEL^{2,3} — ¹Fraunhofer IWM, Freiburg — ²Forschungszentrum Jülich, IEK-9 — ³RWTH Aachen, Institute of Physical Chemistry — ⁴FMF, Universität Freiburg

Defect engineering of perovskite compounds has become increasingly popular as it offers the possibility to influence their catalytic properties for applications in energy storage and conversion devices such as solid-oxide fuel- and electrolyser cells. We present results of a combined theoretical and experimental study exploring the feasibility for an active manipulation of the La stoichiometry, and thereby the valence state of Fe, in LaFeO₃, which can be regarded as a base compound of the family of catalytically active La_{1-x}A_xFe_{1-y}B_yO_{3-δ} compounds. Concentrations of point defects are presented, derived from formation energies which were calculated by first-principles DFT+U calculations as a function of experimental processing conditions, resulting in predictions of achievable stoichiometry ranges. In the experimental part, LFO was synthesized with a targeted La-site deficiency, and we analyzed the phases in detail by X-ray diffraction and various electron microscopy methods (STEM, EDS, EELS). Instead of a variation of the La/Fe ratio, a mixture of two phases, Fe₂O₃/LaFeO₃, was observed, resulting in an invariant charge state of Fe, which is in line with the theoretical results.

MM 14.4 Tue 11:00 H46

Can we improve thermoelectric properties by microstructural manipulations? — •LEONIE GOMELL¹, TOBIAS HAEGER², MORITZ ROSCHER¹, HANNA BISHARA¹, RALF HEIDERHOFF², THOMAS RIEDL², CHRISTINA SCHEU¹, and BAPTISTE GAULT¹ — ¹Max-Planck-Institut für Eisenforschung GmbH, Düsseldorf, Deutschland — ²Institute of Electronic Devices, University of Wuppertal, Deutschland

Thermoelectric (TE) materials convert (waste) heat into electrical energy. Several material properties determine TE performance, with the influence of microstructure being the least understood. However, the microstructure plays a crucial role in the performance of TE materials.

We present microstructural investigations of Fe₂VAL, synthesized via laser surface remelting. Scanning electron microscopy and atom probe tomography were used to bridge the scale from nanometer to micrometer. The local electrical resistivity was analyzed by an in-situ four-probe technique and the thermal conductivity by scanning thermal microscopy.

We observed a high dislocation density in the order of 10¹³ m⁻² and small grains separated by low-angle grain boundaries. Segregation of V and N was found at grain boundaries and dislocations, observed by atom probe tomography. These defects scatter electrons and phonons, influencing their transport within the material.

We conclude that by manipulating the microstructure, we were able to improve the properties of Fe₂VAL. The combination of detailed microstructural analysis and local measurement of properties offers the possibility of understanding the microstructure-property relationship.

MM 14.5 Tue 11:15 H46

Enhanced efficiency of graphene-silicon Schottky junction solar cell through inverted pyramid arrays texturation — •JIAJIA QIU^{1,2}, HUAPING ZHAO¹, WENHUI MA², and YONG LEI¹ — ¹Fachgebiet Angewandte Nanophysik, Institut für Physik & IMN MacroNano, TU Ilmenau, 98693 Ilmenau, Germany — ²State Key Laboratory of Complex Nonferrous Metal Resources Clean Utilization, Kunming University of Science and Technology, Kunming 650093, China

Recently, a growing interest of incorporating graphene (Gr) with silicon (Si) to develop Gr-Si Schottky junction solar cells is considered as a potential low-cost alternative to the conventional p-n junction silicon solar cells. In this work, silicon nanowires (SiNWs) and silicon inverted pyramid arrays (SIIPs) were introduced on surface of Gr-Si solar cell through silver and copper-catalyzed chemical etching, respectively. The effects of SiNWs and SIIPs on carrier lifetime, optical properties and efficiency of Gr-SiNWs/SIIPs solar cell were systematically analyzed. The results show that the inverted pyramid arrays have ability of balance of antireflectance and surface area simultaneously. Compared to the Gr-SiNWs solar cells, power conversion efficiency (PEC) and carrier lifetime of Gr-SIIPs devices increase by 62% and 34%, respectively. Finally, the Gr-SIIPs cell with efficiency of 5.63% was successfully achieved through doping nitric acid. This work proposes a new strategy to introduce the inverted pyramid arrays for improving the performance of Gr-Si solar cells.

MM 15: Hydrogen in Materials: Hydrogen Effects

Time: Tuesday 11:45–13:00

Location: H46

MM 15.1 Tue 11:45 H46

Atomistic study of hydrogen behavior in bcc and fcc Fe in presence of crystal defects — •DARIA SMIRNOVA¹, SERGEI STARIKOV², TAPASWANI PRADHAN², RALF DRAUTZ², and MATOUS MROVEC² — ¹Max-Planck-Institut für Eisenforschung GmbH, Düsseldorf, Germany — ²Ruhr University Bochum, ICAMS, Bochum, Germany

We apply atomistic simulations to consider hydrogen behavior in Fe in presence of the given lattice distortions, namely, crystal defects or lattice expansion/compression due to applied stresses. Simulations are based on a new interatomic potential developed by the authors of current work. Firstly, we consider segregation of hydrogen on typical defects of different complexity: from vacancies to grain boundaries (GBs). Estimated segregation energies obtained for different types of GBs generally agree with the existing DFT data. Moreover, performed classical atomistic simulations give information on several types of GBs, which, due to their complex structure and considerable model size, are inaccessible for ab initio modeling. High-temperature simulations of H diffusion in the presence of GBs also show that for bcc Fe hydrogen diffusion coefficient in the GB is much lower than in bulk. The same type of study is carried out for fcc Fe. Also, we discuss variations in zero-temperature hydrogen migration barriers in bulk bcc Fe with applied stress and compare them with the results of the finite-temperature H diffusion simulations. We see that while the variations in the lattice parameter change hydrogen migration barrier, they give no significant impact on the finite-temperature hydrogen diffusion.

MM 15.2 Tue 12:00 H46

Interplay of hydrogen with defects in Al alloys — •POULAMI CHAKRABORTY¹, HUAN ZHAO¹, BAPTISTE GAULT^{1,2}, TILMANN HICKEL^{1,3}, and JÖRG NEUGEBAUER¹ — ¹Max-Planck-Institut für Eisenforschung, Düsseldorf, Germany — ²Department of Materials, Royal School of Mines, Imperial College London, United Kingdom — ³BAM Federal Institute for Materials Research and Testing, Berlin, Germany

Al alloys are used as major structural material in the aviation and more recently, automobile industries. This demands detail research of microstructural defects generated while usage. We have performed density functional theory calculations to study the competition of microstructural features including grain boundaries and second phase particles. The results reveal second phases as better

trapping sites since H has a higher solubility compared to the GBs. However, it is seen that certain solutes such as Mg enhances the chance of HE at the forming surface during crack initiation. This is further supported by experimental data where a high strength 7xxx Al alloy is charged by deuterium using atom probe tomography (APT). Subsequently, we have extended our study to several other alloying elements such as Sc, Sn and Zr, at the GB which are inevitably present as impurities in technical alloys. Interestingly, it is seen that Sn strongly binds with H at the GB without increasing the embrittling tendency. Based on these insights, effective alloying strategies can be developed to improve the resistance to hydrogen embrittlement.

MM 15.3 Tue 12:15 H46

Impact of H on Fe and Cr diffusion in pure Fe and FeCr alloy — •OLGA LUKIANOVA¹, ANTON CHYRKIN², VLADISLAV KULITCKII¹, JAN FROITZHEIM², SERGEI STARIKOV³, GERHARD WILDE¹, RALF DRAUTZ³, and SERGIY DIVINSKI¹ — ¹Institute of Materials Physics, University of Münster, Münster, Germany — ²Chalmers University of Technology, Department of Chemistry and Chemical Engineering, Division of Energy and Materials, Gothenburg, Sweden — ³ICAMS, Ruhr-Universität Bochum, Bochum, Germany

The impact of hydrogen on the tracer diffusion of the Fe and Cr in pure iron and Fe-18wt.%Cr alloy was measured at 873 K. The annealing treatments were performed in purified argon (H-free) and Ar+H₂ atmospheres. Volume diffusion of Cr was found not to be affected by the presence of H in both alpha-Fe and the FeCr alloy whereas volume diffusion of Fe was enhanced by an order of magnitude. On the contrary, grain boundary diffusion of Cr in the FeCr alloy was retarded, while it was not affected by hydrogen in pure iron. Grain boundary diffusion of Fe remains practically unchanged in both materials. The tracer data are compared with the predictions from atomistic simulations.

MM 15.4 Tue 12:30 H46

Correlation of hydrogen diffusion behavior and in situ micromechanics during hydrogen charging of bcc Fe-Cr alloys — •MARIA JAZMIN DUARTE CORREA, JING RAO, and GERHARD DEHM — Max-Planck-Institut für Eisenforschung, Düsseldorf, Germany

Hydrogen (H) is a strong candidate as energy carrier but it might cause material degradation through hydrogen embrittlement. Individual hydrogen-

microstructure interactions, can be studied by targeting analyses at the nano-/microscale during H exposure. We will present our novel "back-side" electrochemical H charging approach for nanoindentation related techniques. Hydrogen diffusion from the charged back-side towards the testing (front) surface is quantified by Kelvin probe permeation tests and unwanted corrosion is avoided. Our unique method allows differentiating between the effects of trapped and mobile H, and performing well controlled measurements with different H levels monitored over time to consider H absorption, diffusion and release through the metal. These aspects will be presented by nanoindentation and micropillar compression tests during H charging of Fe-Cr alloys (8-20 wt.%Cr). An enhanced dislocation nucleation is shown consistent with the defect theory, and a hardening effect while increasing the Cr content and the H entry. The mechanical data is finally analyzed in terms of the diffusion behavior and used to develop a nanohardness-based H diffusion coefficient approach.

MM 15.5 Tue 12:45 H46

Role of hydrogen on the relative stability of the phases in steels — •ALI TEHRANCHI, TILMANN HICKEL, and JÖRG NEUGEBAUER — Max Planck institute for Iron research, Max Planck Straße 1, 40237 Düsseldorf

Hydrogen embrittlement (HE) is a persistent mode of failure in high-strength steels. During the service life of these steels phase transformations occur and are a key element that determines their response to the service loads. Thus the investigation of the role of H atoms in the relative stability of the phases present and forming in steels is of great interest. In this work, we studied the role of H on the relative stability of the fcc/bcc/hcp phases using the ab initio thermodynamics. The results indicate that at low hydrogen chemical potentials the stability of the fcc phase, which can be representative of retained austenite (RA) in steels, is slightly enhanced by the presence of H atoms. In contrast, at high hydrogen chemical potentials the bcc phase is stabilized by H. Moreover, since the excess volume of the hydrogen-rich bcc phase is significantly larger than that of the fcc phase, the presence of a stress field can change the relative stability of these phases in the coexistence regions of the phase diagram. This feature is particularly important for cyclic loading conditions: during loading cycles forward and reverse phase transformations occur and the H released by these transformations can damage the material.

MM 16: Mechanical Properties

Time: Tuesday 14:00–15:00

Location: H44

MM 16.1 Tue 14:00 H44

co-electrodeposition of compositionally complex co-cr-fe-mo-ni alloy thin films — •HONGSHUAI LI, MARTIN PETERLECHNER, and GERHARD WILDE — Institute of Materials Physics, University of Münster, Wilhelm-Klemm-Str. 10, 48149 Münster, Germany

Co-Cr-Fe-Mo-Ni, a compositionally complex alloy with a face-centered cubic structure, was successfully obtained by electrochemical deposition. To achieve a smooth morphology, an aqueous electrolyte with several additives was used as the solution for electrodeposition. Since the characterization of the sample requires a certain thickness, the electrodeposition time was set to 10 min. Characterization of the film deposited under a constant current density reveals the deposit is metallic with a face-centered cubic structure. The adhesion properties as well as the effective mechanical performance have also been tested by nano-scratch experiments, indicating a microscopically ductile behavior. The electrolytes developed in this study may be a promising approach for the electrodeposition of Co-Cr-Fe-Mo-Ni medium entropy alloys.

MM 16.2 Tue 14:15 H44

orientation dependence of the deformation mechanisms of cocrfeni high entropy alloys — •HAIHONG JIANG, MARTIN PETERLECHNER, and GERHARD WILDE — Westfälische Wilhelms-Universität Münster, Institut für Materialphysik, Wilhelm-Klemm-Str. 10, D-48149 Münster, Germany

The mechanical behavior of CoCrFeNi high entropy alloys in different deformation states have been analyzed by nanoindentation. Microhardness and Young's modulus values were determined at high accuracy as a function of the specified crystallographic orientations, which were measured by electron backscatter diffraction (EBSD). Modulus and Poisson's ratio values of polycrystalline CoCrFeNi were calculated from experimentally determined ultrasonic velocities for comparison. This approach allows for in-depth analysis and comparison of the mechanical properties as function of the local orientations of the crystal lattice in dependence of the thermo-mechanical history.

MM 16.3 Tue 14:30 H44

Influence of crack tip radius on fracture toughness: an atomistic study — •TARAKESHWAR LAKSHMIPATHY¹ and ERIK BITZEK^{1,2} — ¹Department of Materials Science and Engineering, Institute I, Friedrich-Alexander-Universität

Erlangen-Nürnberg (FAU), Germany — ²Department Computational Materials Design, Max-Planck-Institut für Eisenforschung, Germany

In fracture mechanics, initial cracks are typically assumed to be infinitely sharp, leading to a singularity in the crack tip stress field. However, on the atomic scale, crack tips have a radius of at least one atomic distance, which removes the singularity and leads to high, but finite stresses directly at the crack tip. Furthermore, cracks may blunt due to various reasons which leads to an increase in the macroscopic stress to reinitiate a sharp crack. Using harmonic "snapping spring" nearest-neighbor potentials which provide the closest match to linear elastic fracture mechanics (LEFM) on a discrete lattice, we show that the LEFM model for sharp cracks is insufficient to describe the boundary value problem (BVP) of blunted cracks at the atomic scale. We also show that the LEFM-based equations for blunted cracks are insufficient to describe the stress distribution ahead of atomically blunted cracks. We develop a semi-empirical scaling relation for blunted cracks using the LEFM-based equations for elliptical cracks by introducing a factor to account for the deviations. Furthermore, we identify a lower bound for the maximum crack tip radius at which this factor stops playing a role and a scaling model from the unmodified LEFM-based equations for elliptical cracks can be used.

MM 16.4 Tue 14:45 H44

Interplay of Cottrell atmosphere formation and carbon ordering in ferrite — •SAM WASEDA, TILMANN HICKEL, and JÖRG NEUGEBAUER — Max-Planck-Institut für Eisenforschung, Düsseldorf, Germany

In common steels, carbon atoms are purportedly or unintentionally added and alter mechanical properties of the steels. In ferrite, it is proposed that much of them does not stay as solid solution and ends up in the following possibilities: 1, segregate to structural defects; 2, make an elastically favorable ordered structure (Zener-ordering); 3, diffuse to other phases or form a precipitate (austenite, cementite etc.). While they are individually well studied, the interplay between these different scenarios is hardly studied. In this work, we present a density-based diffusion model to study the chemical and elastic interactions between Fe and C as well as among C, in order to understand the interplay between the formation of Cottrell atmospheres and the Zener-ordering.

MM 17: Hydrogen in Materials: Hydrogen Storage

Time: Tuesday 14:00–15:15

Location: H46

MM 17.1 Tue 14:00 H46

Open system mechanical behavior of nanoporous palladium-platinum-hydrogen solid solution near critical point — •SAMBIT BAPARI and JÖRG WEISSMÜLLER — Werkstoffphysik und technologie, Technische Universität Hamburg

Bulk nanoporous palladium is an ideal system for studying open system elasticity as palladium with randomly oriented nanometer size ligaments affords rapid equilibration of hydrogen between an environment and the materials bulk [1]. In this work, nanoporous palladium-platinum (5 at%) alloy was prepared by electrochemical dealloying. Transmission electron microscopy, oxygen adsorption-desorption methods were used to characterize the morphology and

structure of the nanoporous alloy. The average ligament size of the as dealloyed nanoporous palladium-platinum alloy is 4 nm compared to 20 nm for nanoporous palladium. Hydrogen solubility isotherms show near critical point behavior in palladium-platinum-hydrogen solid solution at room temperature. Solute susceptibility and concentration-strain coefficient were determined to estimate the difference in compliance between open and closed systems. In situ quasistatic mechanical tests and strain rate jump tests were conducted to analyze the open system elastic and plastic deformations at near critical point.

[1] S Shi, J Markmann, J Weissmüller. Verifying Larché-Cahn elasticity, a milestone of 20th-century thermodynamics, PNAS, 2018,115 (43) 10914-10919

MM 17.2 Tue 14:15 H46

Metal-organic frameworks for hydrogen isotope separation — •MICHAEL HIRSCHER — Max-Planck-Institut für Intelligent Systeme, Stuttgart, Germany
One of the important operations in chemical industry is separation and purification of gaseous products. Especially H_2/D_2 isotope separation is a difficult task since its size, shape and thermodynamic properties resemble each other. Porous materials offer two different mechanisms for separating hydrogen isotopes, either confinement in small pores, i.e., *kinetic quantum sieving*, or adsorption on strong binding sites, i.e., *chemical affinity quantum sieving*. The new class of metal-organic frameworks (MOFs) allows the exact tailoring of pore size and aperture as well as including open metal sites into the framework. Furthermore, if MOFs consist not of a static, but flexible framework, they can reversibly respond to external stimuli, which may even enhance the separation selectivity.

Experimentally, the measurement of the selectivity for hydrogen isotope separation is very challenging, since it requires low temperatures near the boiling point of the gases. Using low-temperature thermal desorption spectroscopy (TDS), we have developed a method for measuring directly the isotope selectivity after exposure to H_2/D_2 mixtures.

Exemplarily, this talk will present experimental results on hydrogen isotope separation in MOFs.

MM 17.3 Tue 14:30 H46

Microstructural study of MgB_2 in the $LiBH_4$ - MgH_2 composite by TEM — •OU JIN¹, YUANYUAN SHANG², XIAOHUI HUANG¹, XIAOKE MU¹, DOROTHÉE VINGA SZABÓ¹, THI THU LE², STEFAN WAGNER¹, CHRISTIAN KÜBEL³, CLAUDIO PISTIDDA², and ASTRID PUNDT¹ — ¹Karlsruhe Institute of Technology, Karlsruhe, Germany — ²Helmholtz-Zentrum hereon GmbH, Geesthacht, Germany — ³Technical University of Darmstadt, Darmstadt, Germany

The $LiBH_4$ - MgH_2 composite is known as Reactive Hydride Composite for hydrogen storage that has an exceptional hydrogen storage capacity (up to ~ 12 wt% H_2) and enhanced thermodynamic properties (down to ~ 45 kJ/mol H_2). The main challenge that limits the extensive application of this material is its sluggish kinetic performance, which is primarily ascribed to the hampered nucleation of MgB_2 during decomposition. It was found that transition metal-based additives could facilitate the formation of MgB_2 and accelerate the decomposition of $LiBH_4$ - MgH_2 . However, the additive effect on the kinetic improvement had not been fully understood until now. To unravel the uncertainties, the formation of MgB_2 in the decomposed $LiBH_4$ - MgH_2 with and without the additive $3TiCl_3$ - $AlCl_3$ was studied using manifold transmission electron microscopy techniques. Varied MgB_2 morphologies have been determined, originating from different nucleation centers. Given the heterogeneous nucleation, the crystallographic orientation relationship of the relevant phases is in depth discussed. It turns out that atomic misfit plays a dominant role and directly affects the in-plane strain energy density, leading to varied kinetic performance.

MM 17.4 Tue 14:45 H46

ETEM studies on hydride precipitation and growth in Mg films — MAGNUS HAMM¹, MARIAN DAVID BONGERS¹, VLADIMIR RODATIS¹, STEFAN DIETRICH², KARL-HEINZ LANG², and •ASTRID PUNDT² — ¹Göttingen University, Institute of Materials Physics (IMP), Göttingen, Germany — ²Karlsruhe Institute of Technology (KIT), Institute for Applied Materials - Materials Science and Engineering (IAM-WK), Karlsruhe, Germany

Understanding solute-induced phase transformations is crucial in a variety of research fields such as catalysis, memory switching or energy storage. We present solute-induced phase transformations studied on the model system magnesium-hydrogen (MgH) which provides high lattice expansion during the phase transformation. In situ precipitation and growth of MgH_2 is studied in an environmental transmission electron microscope (ETEM), combining electron energy loss spectroscopy (EELS) and various imaging techniques. We observe that the Mg -hydride (MgH_2) formation proceeds through the formation of nanocrystals that are separated by low-angle grain boundaries. We attribute this microstructural change to large strains and stresses between the matrix and the MgH_2 created during the transformation. [1] M. Hamm et al., Int. J. Hydr. Energy 44 (2019) 32112.

MM 17.5 Tue 15:00 H46

Recycling as the key for developing sustainable hydrogen storage materials — •CLAUDIO PISTIDDA¹, YUANYUAN SHANG¹, THI THU LE¹, GOKHAN GIZER¹, HUJUN CAO¹, NILS BERGEMANN¹, RIFAN HARDIAN¹, MARTIN DORNHEIM¹, and THOMAS KLASSEN^{1,2} — ¹Department of Materials Design, Institute of Hydrogen Technology, Helmholtz-Zentrum hereon GmbH, 21502, Geesthacht, Germany — ²Helmut Schmidt University, Holstenhofweg 85, 22043, Hamburg, Germany
Metals play a crucial role in supporting the global economy and the wellbeing of humankind. Supported by the constantly increasing demand for metal-based products, the extraction of mineral resources has increased, over the last decades, at a faster rate than economic growth. This trend is forecasted to steadily increase in the near future, thus leading to concerns over the exploitation of the Earth's natural resources and the environmental impact that the extraction of metals will have. In this scenario, finding new ways to recycle metals and metal alloys, even those of low purity, is mandatory.

To reduce the carbon footprint and environmental impact that the mining of metals for hydrogen storage purposes entails and to reduce their cost, at the Helmholtz-Zentrum Hereon we pursue the possibility of obtaining high-quality hydride-based materials from industrial metal waste. A complete overview of recent scientific breakthroughs in the synthesis and characterization of hydrogen storage materials made from recovered metal wastes will be presented.

MM 18: Poster Session 2

Time: Tuesday 17:30–20:00

Location: P2

MM 18.1 Tue 17:30 P2

Thermal transport properties of sodium superionic conductors from molecular dynamics simulations — •INSA DE VRIES, FREYA HALLFARTH, HELENA OSTHUES, and NIKOS DOLTSINIS — Institut für Festkörpertheorie, Westfälische Wilhelms-Universität Münster, Germany

Improvements of energy storage systems include the usage of sustainable and low-cost materials. In the case of electrolytes for solid state batteries, this is true for sodium superionic conductors due to the high availability of sodium especially compared to lithium based systems. A proper and safe integration of the electrolyte into battery cells also requires taking into account its thermal properties. Due to the ionic motion enabled by the open crystal structure of the electrolyte, in addition to electronic and phononic parts, a diffusive part also contributes to thermal transport. It is thus important to determine activation barriers for ionic motion and diffusion mechanisms, as they affect the thermal properties.

Equilibrium atomistic molecular dynamics simulations were performed of $NaZr_2P_3O_{12}$ and $Na_3Zr_2Si_2PO_{12}$ using a pair potential by Kumar and Yashonath [1]. Besides identifying ionic diffusion pathways, diffusion constants and thermal transport properties were calculated for various temperatures and compared to results from first principles molecular dynamics.

[1] P. P. Kumar and S. Yashonath, J. Am. Chem. Soc. **124**, 3828 (2002)

MM 18.2 Tue 17:30 P2

hiphive - Constructing and sampling higher order force constants for strongly anharmonic materials — •ERIK FRANSSON¹, FREDRIK ERIKSSON¹, JOAKIM BRORSSON¹, ZHEYONG FAN², and PAUL ERHART¹ — ¹Chalmers University of Technology, Gothenburg, Sweden — ²Aalto, University Helsinki Finland
Higher order force constants (FCs) play a key role in lattice dynamics and are

crucial for the analysis of many thermodynamic materials properties. Typically FCs have been extracted using the finite displacement method, which suffers, however, from poor scaling with order and system size. In this contribution we present updates to and applications of the python package hiphive, a tool that allows the efficient extraction of FCs via a regression approach, both up to high order and for low symmetry systems. Higher order FCs can be used to directly run molecular dynamics (MD) simulations, however for strong anharmonic materials these models can become unstable. To overcome this obstacle, we present a self-consistent (iterative) approach for training higher order FCs and demonstrate its effectiveness for multiple strongly anharmonic materials. We have furthermore interfaced hiphive with the GPUMD software, which enables large scale molecular dynamics simulations using FC expansion potentials. This allows for sampling of, e.g., thermal conductivity via Green-Kubo techniques. This approach of extracting higher order FCs and sampling thermal conductivity is demonstrated for two very anharmonic materials, SnSe and BaGaGe. Lastly, we also demonstrate the application of this approach to study the complex dynamics of inorganic halide perovskites.

MM 18.3 Tue 17:30 P2

High-throughput calculations for property maps of solids — •DANIELA IVANOVA¹, DANIEL WORTMANN¹, STEFAN BLÜGEL¹, and MATTHIAS WUTTIG² — ¹Peter Grünberg Institut and Institute for Advanced Simulation, Forschungszentrum Jülich, Germany — ²Department of Physics, RWTH Aachen University, Aachen, Germany

Over the last two decades, high-throughput computation has become a vital pillar of the scientific research and development process in the field of computational science. In order to forecast material properties for a larger sets of atomic configurations, Density Functional Theory (DFT) as a widely utilized and high-

predictive-power first-principles approach, has become increasingly frequent to be used robust and automated. In this work, the DFT open-source of an integrated suite of codes for electronic-structure calculations, Quantum ESPRESSO is used as connected and deployed through the open source Automated Interactive Infrastructure and Database for Computational Science AiiDA framework to achieve automation. Aside from the existence of (1) covalent, (2) metallic, and (3) ionic bonding, as well as the two weaker forms of (4) hydrogen and (5) van der Waals bonding, compelling evidence has been found that a new bonding mechanism prevails in crystalline phase change materials, termed as $^{*}(6)$ 'metavalend bonding'. The materials data set chosen for high-throughput computing and calculation of the relevant materials properties supplies essential data for mapping distinctions between the bonding mechanisms. Such property maps can also lead to the conjecture of a sixth bonding mechanism (MVB).

MM 18.4 Tue 17:30 P2

High Performance Computing as enabler for condensed matter research — •ANDREAS STRAUCH, JENS FÖRSTNER, THOMAS KÜHNE, and CHRISTIAN PLESSL — Paderborn University, Paderborn, Germany

The availability of High Performance Computing resources has enabled a wide range of high-impact science in the field of condensed matter physics in the last decades. We review the numerical research performed at the Paderborn Center for Parallel Computing (PC²) ranging from atomistic ab-initio-calculations to electromagnetic, optoelectronic, and quantum dynamical simulations. Combining in-depth knowledge on high performance computing and on heterogeneous hardware architectures with topical research has led to the development of high-level hardware-agnostic parallel-computing frameworks like HighPerMeshes [1] and to research on novel numerical methods, e.g. for molecular dynamics simulations [2,3].

[1] S. Alhaddad et al, "The HighPerMeshes framework for numerical algorithms on unstructured grids", *Concurrency and Computation: Practice and Experience* (2021), pp. e6616, DOI: 10.1002/cpe.6616 (2022)

[2] R. Schade et al, "Towards electronic structure-based ab-initio molecular dynamics simulations with hundreds of millions of atoms", *Parallel Computing* 111, doi:10.1016/j.parco.2022.102920 (2022)

[3] R. Schade et al, "Breaking the Exascale Barrier for the Electronic Structure Problem in Ab-Initio Molecular Dynamics", arXiv:2205.12182 (2022)

MM 18.5 Tue 17:30 P2

Computational studies of liquid chromophores — •ERIC LINDGREN — Department of Physics, Chalmers University of Technology, Gothenburg, Sweden

Liquid chromophores such as perylene and its derivatives constitute an important class of materials, with applications ranging as solvent-free dyes to increasing the efficiency of solar cells via photon conversion. Their structural and in particular dynamical behaviour on the molecular level is not very well known, yet crucial for their optical properties. In this work, we use molecular dynamics (MD) simulations to investigate the structural and dynamical properties of perylene and two of its derivatives (perylene-ethyl and perylene-diimide). Specifically, we extract the static and dynamical structure factors and the current correlation functions for various temperatures as well as for two different initial structural models of the systems, which in principle allows us to establish a direct link to experimental studies. Motivated by recent experimental work by Hultmark et al. (*Science Advances* 7.29 (July 2021)), we consider two structural models that differ with respect to the relative orientation of the molecules. Whereas in model 1 the molecules are more or less randomly oriented, model 2 features domains with pronounced pi-pi stacking. The latter configuration corresponds to a simplified representation of the supramolecular aggregates that some extended perylene derivatives have been observed to form experimentally. At the moment we have established our simulation protocol and verified the basic premise of this project. Next we will extend our study to derivatives with larger sidegroups and mixtures thereof.

MM 18.6 Tue 17:30 P2

Edge states in proximitized graphene ribbons and flakes in a perpendicular magnetic field: Emergence of lone pseudohelical pairs and pure spin-current states — •YAROSLAV ZHUMAGULOV, TOBIAS FRANK, and JAROSLAV FABIAN — Institute for Theoretical Physics, University of Regensburg, 93040 Regensburg, Germany

Graphene influenced by the valley-Zeeman intrinsic spin-orbit coupling through proximity effects provides signatures of pseudohelical edge states. Analyzing the band structure of a zigzag graphene nanoribbon in the presence of proximity induced spin-orbit interaction and an external magnetic field, we have discovered the effect of stabilization of intervalley edge states and removal intravalley edge states by the external magnetic field. Stabilization of states is associated with the closing/reopening of the bulk bandgap between nonzero Landau levels. The magnitude of the external magnetic stabilization field was estimated both numerically and analytically. Finally, we have found that stabilized intervalley edge states in the presence or in the absence of a spin-flip hopping through the armchair edge form pseudohelical states or pure spin current states, respectively. The states of pure spin current are formed in wide graphene flakes and are protected

from scattering by defects on the zigzag edges of graphene flakes. This work was supported by DFG SPP 2244, DFG SFB 1277 and EU Graphene Flagship.

MM 18.7 Tue 17:30 P2

Modelling mechanical bond scission of amine cured Epoxy resins under stress — •SAMPANNAI PAHI¹, MATTIA LIVRAGHI¹, CHRISTIAN WICK^{1,2}, and ANA-SUNCANA SMITH^{1,3} — ¹PULS Group, Institute for Theoretical Physics and Interdisciplinary Center for Nanostructured Films (IZNF), Friedrich-Alexander Universität Erlangen-Nürnberg (FAU), 91058 Erlangen, Germany — ²Competence Unit for Scientific Computing (CSC), FAU, 91058 Erlangen, Germany — ³Group of Computational Life Sciences, Division of Physical Chemistry, Ruder Bosković Institute, 10000 Zagreb, Croatia

Epoxy resins are widely used thermoset polymers in manufacturing processes. Understanding of fracture propagation in cured epoxy resins is pivotal in determining the bulk level properties of the material. In this paper, a scale-bridging approach that links atomistic molecular dynamics (MD) simulations with DFT based Quantum Mechanical (QM) criterions has been implemented to model bond breakage in Quantum level. In our approach, we create smaller model systems for each bond and implement COGEF procedure to determine optimal bond breakage criterion. Furthermore, a hybrid on-the-fly QM/MM method is described and its ability to capture bond scission on cross linked polymer system with no predetermined fracture site is demonstrated. Using QM bond breakage criterion, bond scission in MD run is identified and checked using presence of spin contamination. Our study provides insights into the molecular mechanisms governing the fracture mechanism of epoxy resins and demonstrates the success of utilising atomistic molecular simulations towards predicting bulk properties.

MM 18.8 Tue 17:30 P2

Solvation effects on proton irradiation of DNA — •DANIEL MUÑOZ-SANTIBURCIO¹, BIN GU², and JORGE KOHANOFF¹ — ¹Instituto de Fusión Nuclear "Guillermo Velarde", Universidad Politécnica de Madrid, Spain — ²Department of Physics, Nanjing University of Information Science and Technology, China

Proton irradiation of DNA is of utmost importance for many fields, from radiation damage in space to medical applications for cancer treatment. Ab initio simulations are highly valuable tools for understanding such process, but they are cumbersome due to the required level of theory. These involve simulating the non-adiabatic propagation of the electronic subsystem of the target material, and to date have been restricted to DNA systems in absence of water, or at most with few solvating molecules. Here we present the results of large-scale ab initio (RT-TDDFT) simulations of proton irradiation of a realistic DNA system in bulk water, where we have determined different important aspects of the proton irradiation process such as the stopping power of the system, the spacial distribution of the holes in terms of the depopulations of the maximally localized Wannier functions, and more importantly the influence of the surrounding water. We will show that water is neither a mere spectator on the process nor a simplistic reducing or enhancing agent of the excitation process. Instead, water qualitatively changes the excitation landscape of the proton-irradiated DNA, making the hole population on the different atoms and bonds qualitatively different in the solvated vs. the dry DNA case.

MM 18.9 Tue 17:30 P2

Resistometric determination of GP-zone formation and growth — •FABIAN MILLER, JOHANNES BERLIN, TOBIAS STEGMÜLLER, and FERDINAND HAIDER — Universität Augsburg, Institut für Physik, 86135 Augsburg, Deutschland

Aluminium alloys are of crucial importance in today's economy, therefore the deeper understanding of their mechanical and electrical properties is important. These properties can be influenced by precipitate formation. In this work we focused in the Al³Cu system with samples containing around 4 wt.% of Cu. They were homogenized at the eutectic temperature and rapidly quenched to ambient temperature. Afterwards 4-point-resistance measurements were conducted during natural and artificial aging. Due to formation of Guinier Preston zones, the resistivity first increases, then slowly decreases, allowing to monitor the unmixing for different temperatures and for different quenching conditions. Further experiments with other alloying metals than Cu will be conducted and variations of the homogenisation temperature are planned to be inspected.

MM 18.10 Tue 17:30 P2

Dealloying and nanoscale structure formation at crystal-melt coexistence — •ZHONGYANG LI¹, NINA PETERSEN¹, LUKAS LÜHR¹, and JÖRG WEISSMÜLLER^{1,2} — ¹Institute of Materials Physics and Technology, Hamburg University of Technology — ²Institute of Materials Mechanics, Hybrid Materials Systems, Helmholtz-Zentrum Hereon

Recent work on Ti-Ag alloy has shown that a bicontinuous microstructure can be formed via peritectic melting, which could further transform to open porous Ti or Ag networks through selective etching. Several factors including the large solubility difference of two alloy elements in liquid phase, large composition difference and the volume fraction of the solid and liquid phases are considered to be criteria for this phenomenon. However, the formation mechanism of this particular microstructure during peritectic dealloying is still not fully known.

In this work, alloy systems including Bi-Ni, Fe-Sn and Mn-Sn, are chosen, which satisfy part or all of the aforementioned criteria. With SEM and diffraction experiments of these samples after peritectic melting, we investigate the morphology of different phases, and discuss the dominant factor for the formation of bicontinuous structure. The effect of parameters for thermal treatment, including temperature and duration of heat treatment, are also studied using SEM, in order to find the optimized combination that could produce finer microstructure. With the research in these two aspects, we discuss the possibility of broadening the application of this new dealloying method from peritectic dealloying to dealloying at liquid-solid coexistence state.

MM 18.11 Tue 17:30 P2

Structural and Textural Transitions of Discotic Ionic Liquid Crystals in Nanoporous Solids — •ZHUOQING LI¹, PATRICK HUBER¹, SABINE LASCHAT², AILEEN RAAB², ANDREAS SCHÖNHALS³, and MOHAMED A. KOLMANGADI³ — ¹Institute for Materials and X-Ray Physics, Technische Universität Hamburg, Hamburg, Germany — ²Institut für Organische Chemie, Universität Stuttgart, Stuttgart, Germany — ³Bundesanstalt für Materialforschung und -prüfung (BAM), Berlin, Germany

Discotic ionic liquid crystals (DILCs) derived from 3,4-dihydroxyphenylalanine (DOPA) have synergetic properties of liquid crystals and ionic liquids. Driven by the $\pi^*\pi$ interactions among the aromatic cores, DILCs may self-organize, leading to a hexagonal ordered columnar liquid crystalline mesophase. Embedding of DILCs in nanoporous solids allows one to design hybrid materials with 1-D ionic conductivity pathways on the single-nanopore scale and tailorable photonic properties. The structural organization of confined DILCs is determined by an interplay of geometrical constraints and interfacial interactions at the pore wall and thus depends on pore size, temperature treatment and molecular wall anchoring. The optical birefringence experiments and small angle X-ray scattering results indicate ordered liquid crystalline mesophases of different collective orientations as a function of anchoring of the DILC discs at the pore surface. In particular, these experiments suggest that depending on the pore size a transition from the formation of circular concentric ring structures to an arrangement, where the columns are aligned parallel to the pore axis occurs.

MM 18.12 Tue 17:30 P2

Laughlin topology on fractal lattices without area law entanglement — •MANI CHANDRA JHA — MPI-PKS

Laughlin states have recently been constructed on fractal lattices, and the charge and braiding statistics of the quasiholes were used to confirm that these states have Laughlin type topology. Here, we investigate density, correlation, and entanglement properties of the states on a fractal lattice derived from a Sierpinski triangle with the purpose of identifying similarities and differences compared to two-dimensional systems and with the purpose of investigating whether various probes of topology work for fractal lattices. Similarly to two-dimensional systems, we find that the connected particle-particle correlation function decays roughly exponentially with the distance between the lattice sites measured in the two-dimensional plane, but the values also depend on the local environment. Contrary to two-dimensional systems, we find that the entanglement entropy does not follow the area law if one defines the area to be the number of nearest neighbor bonds that cross the edge of the selected subsystem. Considering bipartitions with two bonds crossing the edge, we find a close to logarithmic scaling of the entanglement entropy with the number of sites in the subsystem. This also means that the topological entanglement entropy cannot be extracted using the Kitaev-Preskill or the Levin-Wen methods. Studying the entanglement spectrum for different bipartitions, we find that the number of states below the entanglement gap is robust and the same as for Laughlin states on two-dimensional lattices.

MM 18.13 Tue 17:30 P2

A study of the local fields in bismuth ferrite by using different radioactive tracer ions — •THANH T. DANG¹, JULIANA SCHELL^{1,2}, MARIANELA E-CASTILLO¹, DANIL LEWIN¹, ASTITA DUBEY¹, ANDREA G. BOA^{2,3}, REINHARD BECK⁴, CORNELIA NOLL⁴, JOÃO N. GONÇALVES⁵, DMITRY ZYABKIN⁶, KONSTANTIN GLUKHOV⁷, IAN C. J. YAP⁸, ADELEH M. GERAMI^{2,9}, KOEN V. STIPHOUT¹⁰, GEORG MARSCHICK¹¹, EDGAR M. S. D. REIS^{1,2}, SOBHAN M. FATHABAD¹, and DORU C. LUPASCU¹ — ¹University of Duisburg-Essen — ²European Organization for Nuclear Research — ³Technical University of Denmark — ⁴University of Bonn — ⁵Universidade de Aveiro — ⁶TU Ilmenau — ⁷Uzhhorod National University — ⁸Universität Göttingen — ⁹School of Particles and Accelerators — ¹⁰Georg-August-Universität Göttingen — ¹¹Vienna University of Technology

This work presents the study of the local electric and magnetic fields in multiferroic bismuth ferrite using Time Differential Perturbed Angular Correlation spectroscopy. The measurements were carried out at a wide range of temperatures up to 850°C, after the implantation of various radioactive tracer ions: 181Hf, 111In and 111mCd. The experimental results reflect the obedience to Landau theory and Brillouin-Weiss equation of local electric polarization and magnetization, respectively. Particularly, a huge coupling between local electric and magnetic

fields has been investigated in anti-ferromagnetic order. With the support of ab-initio DFT simulations, we can conclude that 111mCd is located at Bi-atom, 181Hf and 111In substitute Fe-atom.

MM 18.14 Tue 17:30 P2

Partitioning of transition metals to the γ and γ' phase of Co-based superalloys — •ISABEL PIETKA¹, ANDREAS FÖRNER², MANUEL KÖBRICH², STEFFEN NEUMEIER², RALF DRAUTZ¹, and THOMAS HAMMERSCHMIDT¹ — ¹Ruhr-Universität Bochum, Interdisciplinary Centre for Advanced Materials Simulation (ICAMS) — ²Friedrich-Alexander-Universität Erlangen-Nürnberg, Department of Materials Science & Engineering

Single-crystal Co-base superalloys are a promising class of materials in high-pressure high-temperature applications such as blades of gas turbines or jet engines. The superior mechanical properties at high temperatures are a consequence of the underlying γ/γ' microstructure. The improvement of the mechanical properties of these alloys is therefore closely tied to an understanding of the influence of alloying elements on the microstructure. In this work, we describe the γ/γ' partitioning of different alloying elements, i.e. their preference for the γ matrix or the γ' particles of the microstructure. In particular, we determine the energy difference of nearly all 3d, 4d, 5d transition metals (TMs) in $\text{Co}_3(\text{Al/W})$ by density functional theory calculations. In very good agreement with results from wavelength-dispersive X-ray spectroscopy and atom probe tomography, we find a preference of early TMs for the γ' phase while mid to late TMs show no clear preference. We demonstrate that the findings can be rationalized in terms of band-filling and atomic size differences by moment analysis from bond order potential theory.

MM 18.15 Tue 17:30 P2

The oxidation of TNM alloy at 700°C and 760°C — •HENG ZHANG^{1,2} and YONGFENG LIANG² — ¹Institute of Materials Physics, University of Münster, Germany — ²State Key Laboratory for Advanced Metals and Materials, University of Science and Technology Beijing, Beijing, China

The TNM sample morphology and components of the oxides are measured with SEM, EDS and XPS after oxidation until 200 hours at 700°C and 760°C respectively. Al_2O_3 is the main oxides at 700°C combined with a little TiO_2 , MoO_2 and MoO_3 , while the oxides are TiO_2 , MoO_2 and MoO_3 at 760°C, exhibiting a good oxidation resistance under 700°C.

MM 18.16 Tue 17:30 P2

Reactive Surface Corrosion of Stainless Steel studied with Atomic Force Microscopy and Kelvin Probe Force Microscopy — •JULIAN CREMER¹, SINAN KIREMIT², BERNHARD KALTSCHMIDT³, THOMAS KORDISCH², ANDREAS HÜTTEN³, and DARIO ANSELMETTI¹ — ¹Experimental Biophysics and Applied Nanoscience (BINAS), Bielefeld University — ²Bielefeld Institute for Applied Materials Research, Bielefeld University of Applied Sciences — ³Thin Films & Physics of Nanostructures, Bielefeld University

The pitting surface corrosion of three different stainless steels (1.4016, 1.4510 and 1.4301) used for industrial applications was investigated by exposition to oxidative liquids. Here, we focus on the investigation of the origin of the pitting using Kelvin probe force microscopy (KPFM) and on the prevention of corrosion by surfactants using high-resolution atomic force microscopy (AFM). KPFM allows to determine the work function of a sample with high spatial resolution. We found that the initiation of a pit can be caused by an abnormal anodic site (low work function) surrounded by a normal surface which acts as a cathode, or by the presence of an abnormal cathodic site (high work function) surrounded by a normal surface. In order to test whether KPFM can predict where and why pitting corrosion occurs, we use a micro corrosion liquid cell that allows live observation of the previously scanned area during corrosion. Additionally, we study the surface activity of surfactants acting as corrosion inhibitors on stainless steels regarding adsorption dynamics and layer thickness in different temperature-controlled solutions.

MM 18.17 Tue 17:30 P2

Reactive Surface Corrosion of Polypropylene studied with Atomic Force Microscopy — •JULIAN CREMER¹, BERNHARD KALTSCHMIDT², ANDREAS HÜTTEN², and DARIO ANSELMETTI¹ — ¹Experimental Biophysics and Applied Nanoscience (BINAS), Bielefeld University — ²Thin Films & Physics of Nanostructures, Bielefeld University

The surface corrosion of various polypropylene samples used for industrial applications was investigated by exposition to oxidative liquids. The samples are formulated by different additive packages and include fillers such as talc or glass fibers for reinforcement. In particular, we study the aging and corrosion of these polypropylene samples in oxidative liquid media, analyzing the influence of temperature and oxidants. Contrary to aging induced by UV radiation, aging in oxidative liquids is rarely studied. Shedding some light on this research area, we placed the polypropylene samples in an oxidative test solution at 95°C, which was constantly renewed. In total, the samples were examined after ten different time steps up to 4000h. Mainly, we used atomic force microscopy (AFM) to image the samples and to determine the Young's modulus, which is a decisive

parameter for the age of plastic materials. In some cases, we observe a growth of a fibrous structure on the surface covering nearly the whole sample. To determine the chemical composition of the bloomed structure and follow the aging on a chemical level, attenuated total reflection infrared spectroscopy was performed (ATR-FTIR). We present structural and chemical changes of aged industrial polypropylene as well as the consequence of additive blooming.

MM 18.18 Tue 17:30 P2

High-Pressure Torsion Deformed Magnesium: Microstructure Evolution and Hydrogen Diffusion — •SABINE SCHLABACH^{1,2,3}, BINGYU WU¹, GIORGIA GUARDI¹, STEFAN WAGNER¹, JULIA IVANISENKO^{2,3}, and ASTRID PUNDT¹ — ¹Karlsruhe Institute of Technology, Institute for Applied Materials, Karlsruhe, Germany — ²Karlsruhe Institute of Technology, Institute of Nanotechnology, Karlsruhe, Germany — ³Karlsruhe Institute of Technology, Karlsruhe Nano Micro Facility, Karlsruhe, Germany

Magnesium (Mg) is one of the materials considered as a solid state storage material for Hydrogen (H) as it is capable of storing up to 7.6 wt.% of H while forming magnesium hydride (MgH₂). However, the volume diffusion rate of H in MgH₂ is low, and thus the sorption rate of H is rather slow. As grain boundaries are suggested as fast diffusion paths, an increasing volume fraction of grain boundaries by reducing the grain size is aimed. Starting from polycrystalline bulk Mg, this can be done, e.g., by high-pressure torsion, one method of severe plastic deformation. The deformation induced microstructure evolution is investigated by using electron backscatter diffraction depending on different process parameters like imposed pressure and number of revolutions. Special attention is taken on local misorientations as a measure of dislocation density and their possible influence on H-diffusion. The related H loading capability of the deformed Mg samples is tested at room temperature utilizing gas volumetry. In a first step, H-diffusion in the α -Mg phase is assessed as model system. Thus, the maximum H concentration is kept below the solid solution limit.

MM 18.19 Tue 17:30 P2

Co(OH)₂@FeCo₂O₄ as high-performance electrode material for supercapacitors — •ZIDONG WANG^{1,2}, YUDE WANG², HUAPING ZHAO¹, and YONG LEI¹ — ¹Fachgebiet Angewandte Nanophysik, Institut für Physik & IMN MacroNano, Technische Universität Ilmenau, 98693 Ilmenau, Germany — ²School of Materials and Energy, Yunnan University, 6500504 Kunming, Peoples Republic of China

Spinel-type MCo₂O₄ (M = Zn, Ni, Fe, *) are regarded as a partial replacement of Co₃O₄ without crystal structure changes, and they provide advantages of lower cost and improved performance compared with Co₃O₄. Particularly, the variable valence of Fe in FeCo₂O₄ benefits the energy storage capability. However, previous works indicate that the attainable performance of FeCo₂O₄ is still limited. Herein, a 2D planar morphology design is proposed to optimize the performance of FeCo₂O₄ as active materials of supercapacitors. In this work, nano-sized Co(OH)₂ were composited on FeCo₂O₄ nanosheets skeleton by a simple one-step hydrothermal process. Due to the synergistic effect, the sample achieves outstanding performances with the specific capacitance of 1173.43 F g⁻¹ at a current density of 1 A g⁻¹ and 95.4% capacitance retention after 5000 cycles. It indicates that nanostructured Co(OH)₂@FeCo₂O₄ would have hopeful prospects in energy storage applications.

MM 18.20 Tue 17:30 P2

Quantitative investigation of reversible Li₂O formation on Germanium battery anodes — •KE WANG and GUIDO SCHMITZ — Chair of Materials Physics, Institute for Materials Science, University of Stuttgart, Heisenbergstr. 3, 70569 Stuttgart, Germany

Lithium-ion batteries (LIB) serves as efficient energy storage devices in many aspects of our life. Anodes belonging to the Group IV (Si, Ge and Sn) are promising candidates to replace commercially applied graphite (372 mAh g⁻¹) owing to their high theoretical capacity (3850 mAh g⁻¹ for Si, 1570 mAh g⁻¹ for Ge, and 990 mAh g⁻¹ for Sn). But, the respective mechanisms of Li storage and the formation of solid electrolyte interface (SEI) are still not clearly. In this work, cyclic voltammetry has been conducted in combination with a quartz crystal microbalance to measure the SEI mass, and the amount of eventual reversibly processed species. Similar to Si and Sn, also with Ge anodes, the QCM mass spectroscopy identifies Li₂O as a reversibly processed species that contributes a significant part to the electrochemical capacity. The amount of reversibly stored Li₂O decreases weakly with increasing cycling rate, but increases significantly with the thickness of the Ge anodes. Interestingly, the amount of Li₂O decreases if pronounced anode cracking appears, which is probably attributed to the fact that the fracture introduces short circuit transport paths deep into the volume of the Ge which accelerates lithiation. Thermodynamically, Li₂O should form before Li is inserted. But in the experiment simultaneously formation of Li₂O and Li_xSny is observed on Sn, probably attributed to lateral heterogeneity introduced by surface roughness.

MM 18.21 Tue 17:30 P2

Recycling of anode graphite from spent lithium-ion batteries and reused in heat transfer medium — •YU QIAO^{1,2}, ZHONGHAO RAO^{3,4}, HUAPING ZHAO¹, and YONG LEI¹ — ¹Fachgebiet Angewandte Nanophysik, Institut für Physik & IMN MacroNano, Technische Universität Ilmenau, 98693 Ilmenau, Germany — ²School of Electrical and Power Engineering, China University of Mining and Technology, 221116, Xuzhou, China — ³School of Energy and Environmental Engineering, Hebei University of Technology, 300401, Tianjin, China — ⁴Hebei Key Laboratory of Thermal Science and Energy Clean Utilization, Hebei University of Technology, 300401, Tianjin, China

Lithium-ion batteries (LIBs) have been widely employed in fast-growing mobile devices, stationary storage devices and electric vehicles. However, LIBs face a large wave of retirement because of a certain life. Graphite is the most common anode material in LIBs, amount of waste graphite will also be produced with the retirement of spent LIBs. Anode graphite (AG) from spent LIBs has the characteristics of large layer spacing and ease of being intercalated due to reducing the interlamination force after repeated charge and discharge cycles. In this study, two-dimensional graphite flakes (GFs) were prepared from spent AG through a freeze-thaw ultrasonic-assisted circulation method. The heat transfer ability of as-obtained GFs dispersed in ethylene glycol was investigated experimentally. The results indicated that GFs could enhance the heat transfer coefficient and the maximum enhancement is about 30%.

MM 18.22 Tue 17:30 P2

Mild-temperature solution-assisted encapsulation of phosphorus into ZIF-8 derived porous carbon as lithium-ion battery anode — •CHENGZHAN YAN¹, SHUN WANG², and YONG LEI¹ — ¹Fachgebiet Angewandte Nanophysik, Institut für Physik & IMN MacroNano, Technische Universität Ilmenau, 98693 Ilmenau, Germany. — ²Key Laboratory of Carbon Materials of Zhejiang Province, Institute of Materials and Industrial Technologies, Wenzhou University, Wenzhou, Zhejiang, 325027, China.

Phosphorus in the form of polyphosphides anions (PP) is encapsulated into ZIF-8 derived porous carbon through a solution-assisted etching diffusion process under a mild temperature, and the composites with a high phosphorous content of 30 wt% exhibit a high capacity, improved cycling stability as well as a good rate performance as a lithium-ion battery anode. Herein, a series of morphological and structural characterizations are applied to analyze the differences between individual MOF-derived carbon hosts with the whole body that has PP inside the pore. Subsequently, their electrochemical performance is also compared. The results of the above-mentioned material analysis and application practices jointly confirmed the superiority of this mild temperature solution-assisted encapsulation of phosphorus method. In summary, this work provides a new strategy to design and fabricate phosphorus-based electrodes for batteries beyond lithium-ion batteries.

MM 18.23 Tue 17:30 P2

Optimization of flash sintering input parameters for obtaining 8YSZ dense samples — •FÁBULO R. MONTEIRO¹, GUSTAVO C. DACANAL¹, JOÃO V. CAMPOS², LILIAN M. JESUS², ADILSON L. CHINELATTO³, and ELIRIA M. J. A. PALLONE¹ — ¹University of São Paulo, Pirassununga, Brazil — ²Federal University of São Carlos, São Carlos, Brazil — ³University of Ponta Grossa, Ponta Grossa, Brazil

Flash sintering has been widely investigated due to its technological potential, since it allows very rapid densification of different ceramic materials. The literature still lacks studies assessing how the electrical parameters of the technique (electric field and current density) involved in the process affect material densification since these parameters may vary depending on furnace type and, especially, sample geometry. Thus, this study used the response surface technique to analyze and relate, in a multivariate way, a few flash sintering variables. A mathematical model was proposed to optimize the densification of 8YSZ cylindrical and dog-bone samples. For this, a complete second order factorial planning with three central points was used in combination with the response surface methodology. The results obtained allowed us to predict electric field and electric current density values to optimize the densification of 8YSZ samples in the two geometries used and to understand how electric field and electrical current density values affected onset and sample temperatures (estimated by the black body radiation model).

MM 18.24 Tue 17:30 P2

The effect of crystallinity of layered transition metal disulfide on the performance of potassium-ion batteries: The case of molybdenum disulfide — •YULIAN DONG, HUAPING ZHAO, and YONG LEI — Fachgebiet Angewandte Nanophysik, Institut für Physik & IMN MacroNano, Technische Universität Ilmenau, 98693 Ilmenau, Germany

Layer-structured transition metal dichalcogenides (LS-TMDs) are being studied in potassium-ion batteries owing to their structural uniqueness and electrochemical mechanisms. In this work, the dependence of electrochemical performance on the crystallinity of LS-TMDs has been investigated. Taking MoS₂ as an example, lower crystallinity can alleviate diffusional limitation in 0.5*3.0 V, where intercalation reaction takes charge in storing K-ions. Higher crystallinity

can ensure the structural stability of the MoS₂ layers and promote surface charge storage in 0.01*3.0 V, where conversion reaction mainly contributes. The low-crystallized MoS₂ exhibits an intercalation capacity (118 mAh/g) and great rate capability (41 mAh/g at 2 A/g), and the high-crystallized MoS₂ delivers a high capacity of 330 mAh/g at 1 A/g and retains 161 mAh/g at 20 A/g. It shows that when intercalation and conversion reactions both contribute to store K-ions, higher crystallinity ensures the structural stability of the exfoliated MoS₂ basal layers and promotes surface-controlled charge storage.

MM 18.25 Tue 17:30 P2

Magnetic Hardening of Nd-Fe-B Permanent Magnets — •LUKAS SCHÄFER¹, KONSTANTIN SKOKOV¹, FERNANDO MACCARI¹, ILIYA RADULOV¹, DAVID KOCH², and OLIVER GUTFLEISCH¹ — ¹Functional Materials, Institute of Material Science, Technical University of Darmstadt, 64287, Darmstadt, Germany — ²Strukturforschung, Institute of Material Science, Technical University of Darmstadt, 64287, Darmstadt, Germany

Nd-Fe-B alloys used for permanent magnets provide highest performance and energy density and are therefore used in numerous energy and high-tech applications. The superior intrinsic properties of the hard magnetic Nd₂Fe₁₄B phase are translated by a controlled production processes leading to a specific micro- and grain boundary structure and high coercivity. In this work, we take a different approach and show a novel magnetic hardening mechanism in such materials. This mechanism has the potential to be incorporated into existing manufacturing processes and to be adapted to novel production routes for Nd-Fe-B permanent magnets such as Additive Manufacturing. As an example, we demonstrate how the microstructural transformation from metastable Nd₂Fe₁₇B_x phase to the hard magnetic Nd₂Fe₁₄B phase by controlled annealing leads to a significant increase in coercivity from 250 kAm⁻¹ to 700 kAm⁻¹ in Nd₁₆Fe_{bal-x-y-z}Co_xMo_yCu_zB₇ alloys. This approach offers also a promising opportunity for the fabrication of nano composite magnets.

MM 18.26 Tue 17:30 P2

Spin fluctuations and Wigner thermal transport in thermoelectric skutterudites — •ENRICO DI LUCENTE¹, MICHELE SIMONCELLI², and NICOLA MARZARI¹ — ¹Theory and Simulation of Materials (THEOS) and National Centre for Computational Design and Discovery of Novel Materials (MARVEL), École Polytechnique Fédérale de Lausanne, Lausanne 1015, Switzerland — ²TCM Group, Cavendish Laboratory, University of Cambridge, 19 JJ Thomson Avenue, Cambridge, CB3 0HE UK

Skutterudites are highly promising functional materials due to their peculiar thermoelectric and magnetic properties. We elucidate the complex phenomenology that takes place in these materials both in terms of spin fluctuations and in the crossover from a Peierls-Boltzmann to a Wigner thermal transport regime, where tunneling of phonon wavepackets emerges. We first study the electronic structure using the state-of-the-art DFT+Hubbard theory to uncover multiple self-consistent magnetic and charge disproportionated configurations. While the lowest energy state is antiferromagnetic but metallic, paramagnetic fluctuations captured through a special quasi random structure open a small gap of 61 meV, in good agreement with experiments. Moreover, in going from the parent compound to the related filled skutterudite, a transition from a Peierls-Boltzmann to a Wigner thermal transport regime arises, where, at working temperature of the devices, the tunneling of phonon wavepackets becomes as relevant as the drifting diffusion.

MM 18.27 Tue 17:30 P2

Freezing and melting of water in nanopores: A temperature-dependent X-ray scattering study — •LARS DAMMANN^{1,2}, STELLA GRIES^{1,2}, MILENA LIPPMANN¹, and PATRICK HUBER^{1,2} — ¹Deutsches Elektronen-Synchrotron DESY, Notkestr. 85, Hamburg 22607, Germany — ²Hamburg University of Technology, Institute for Materials and X-Ray Physics, Eißendorfer Straße 42, Hamburg 21073, Germany

The crystallization of water in extreme spatial confinement of nanoporous media plays a pivotal role in many natural and technological processes, ranging from frost heave to modern materials processing. However, the induced interfacial stresses in the porous medium during melting and crystallization and the crystalline structures of nanoconfined water are still subject of scientific discussions. Here we present simultaneous temperature dependent small and wide angle X-ray scattering (SAXS/WAXS) measurements of water in ordered silica nanopores of diameters around 3 nm and 7-8 nm in a temperature range from 300 K to 150 K. With SAXS we investigate the crystallization induced strain on the pore network and with WAXS the structure of water ice in nanoconfinement. A complete analysis of the measurements is yet to be conducted, however, promising first results of the SAXS measurements show a strong dependence of pore strain on freezing in the pores especially for the smaller pores. As a next step we aim to compare the SAXS data to the measured WAXS signal to investigate the structure of the crystallized confined water.

MM 18.28 Tue 17:30 P2

Liquids in Atom Probe Tomography — •TIM MAXIMILIAN SCHWARZ, HELENA SOLODENKO, JONAS OTT, GUIDO SCHMITZ, and PATRICK STENDER — University of Stuttgart, Institute for Materials Science, Chair of Materials Physics, Heisenbergstr. 3, 70569 Stuttgart, Germany

Frozen liquids are challenging and rather new in the investigation by atom probe tomography. However, recent progress in instrumentation, especially the introduction of cryo transfer shuttles, and the development of the required preparation routes to shape nanometric needles of frozen liquids enable measurements of sufficient quality and size of data sets to discover the typical features of this material class. The field evaporation of liquids resembles more the behaviour of weakly cross-linked polymers than that of metals. So frozen liquids, stabilized by weak hydrogen or van der Waals bonds, typically evaporate in large molecular fragments which raises general questions about spatial resolving power and chemical sensitivity of the atom probe tomography. At the example of saturated glucose solutions, we investigate the accuracy of the chemical analysis and the spatial resolution in localizing dissolved molecules. The direct comparison to the field evaporation of solid bulk glucose demonstrates in water a matrix-assisted field desorption that enables the detection of the chemical structure of larger organic molecules. One step further natural honey, which is a supersaturated solution consisting of a mixture of different monosaccharides and higher sugars in water, can be investigated on the nanoscale.

MM 18.29 Tue 17:30 P2

Fractal abnormal grain growth in nanocrystalline Pd-Au at the atomistic level — •JOHANNES WILD¹, TORBEN BOLL¹, JULES DAKE², DOROTHÉE VINGA SZABÓ¹, STEFAN WAGNER¹, CARL E. KRILL², and ASTRID PUNDT¹ — ¹Karlsruhe Institute of Technology (KIT), Institute for Applied Materials - Materials Science and Engineering (IAM-WK), Karlsruhe, Germany — ²University of Ulm, Institute of Functional Nanosystems, Ulm, Germany

Nanocrystalline (NC) Pd-10 at.% Au (PdAu) prepared by inert gas condensation (IGC) shows an unconventional manifestation of abnormal grain growth upon heat treatment. This unusual growth mode leads to complex and highly convoluted boundaries resembling those of fractal shapes. Furthermore, the microstructure shows a bimodal grain size distribution with regions of NC grains bordering grains in the micron range. This phenomenon is unique to this NC PdAu as conventionally prepared samples showed normal grain growth for the same heat treatment. In this study, we investigate the abnormal grain boundaries of heat-treated IGC PdAu using atom probe tomography (APT) and field ion microscopy (FIM). The position-specific APT samples are produced by targeted sample preparation with focused ion beam lift-out methods at chosen regions of interest that are identified beforehand by high-resolution electron backscatter diffraction imaging. We also use FIM, which has a higher lateral resolution than APT. This research is financially supported by the Deutsche Forschungsgemeinschaft (DFG) via project number 461632490, DFG PU131/18-1, DFG KR1658/10-1 and Karlsruhe Nano Micro Facility (KNMF).

MM 18.30 Tue 17:30 P2

Formation porous metal nanosystems under near-equilibrium condensation conditions in plasma-condensate system — •ANNA KORNUSHCHENKO^{1,2}, VYACHESLAV PEREKRESTOV¹, and GERHARD WILDE² — ¹Sumy State University, Laboratory of Vacuum Nanotechnologies, Sumy, Ukraine — ²Westfälische Wilhelms-Universität, Institute of Materials Physics, Münster, Germany

It is known, that porous structures depending on morphology can possess unique physical properties which can determine areas of their application. In the proposed work a new technique for synthesizing metal porous micro- and nanostructures has been developed. This approach is based on the phase transition of sputtered substances into the condensed state under conditions close to thermodynamic equilibrium. The low dimensional metal systems (Cr, Zn, Cu, Ti, Ni, Al) have been obtained in the different morphological forms, such as network structures, nanowires, agglomerations of weakly-bound crystals, columnar structures consisting of prolonged crystals with approximately identical habitus, etc. The results confirm the important new opportunities for size, shape and physical property tuning of nanostructured materials that are given by deposition near thermodynamic equilibrium conditions. It has been established that the growth mechanism under conditions close to thermodynamic equilibrium possesses principally new peculiarities and possibilities in comparison with traditional methods of condensation from vapor state and consequently can contribute to a new zone in the structure zone model.

MM 18.31 Tue 17:30 P2

Self-detachment and sub-surface densification of dealloyed nanoporous thin films — •GIDEON HENKELMANN¹, DIANA WALDOW¹, MAOWEN LIU¹, LUKAS LÜHRS¹, and JÖRG WEISSMÜLLER^{1,2} — ¹Institute of Materials Physics and Technology, Hamburg University of Technology, Hamburg, Germany — ²Institute of Materials Research, Materials Mechanics, Helmholtz-Zentrum Geesthacht, Geesthacht, Germany

This work highlights experimental observations showing microstructural gradients at interfaces in nanoporous gold, and it explains those observations as

a consequence of gradients in a laterally averaged mean curvature of the pore surfaces. Nanoporous gold can be covered by a densified layer at its external surfaces. Furthermore, as we report, thin films of the material often spontaneously detach from massive gold base layers that are intended to enhance adhesion to the substrate. Those phenomena appear intrinsic to the material, as they are naturally reproduced by our kinetic Monte Carlo (KMC) simulation of dealloying and of the subsequent microstructure evolution. Our results suggest that spontaneous densification or decohesion at interfaces may be generic features of nanoscale porous network materials that evolve by curvature-driven surface diffusion.

MM 18.32 Tue 17:30 P2

Structural-mechanical property correlation in hierarchical nanoporous gold — •LUKAS RIEDEL¹, SHAN SHI^{1,2}, JÜRGEN MARKMANN¹, and JÖRG WEISSMÜLLER^{1,2} — ¹Institute of Materials Mechanics, Helmholtz-Zentrum Hereon, Geesthacht, Germany — ²Institute of Material Physics and Technology, Hamburg University of Technology, Hamburg, Germany

Implementing a structural hierarchy in nanoporous metals has been demonstrated as an efficient way to achieve lightweight and enhanced mechanical performance. So far, several aspects of the correlation between structure and mechanical behavior are not clearly proven. Here, hierarchical nanoporous gold (HNPG) with tunable ligament size at each hierarchy level is synthesized out of Ag₉₀Au₁₀ via a dealloying-coarsening-dealloying strategy. The structural analysis is conducted with scanning electron microscopy, small-angle X-ray scattering (SAXS) and ultra small-angle X-ray scattering (USAXS). We demonstrate that SAXS and USAXS are valued as advantageous methods for the determination of the structural size of HNPG. In particular, USAXS is very useful for the description of nanoporous structures with a ligament size of several hundred nanometers. It is observed that the mechanical behavior of HNPG is highly dependent on the ligament size at both the upper and the lower hierarchy level. Moreover, HNPG made out of Ag₉₀Au₁₀ shows improved stiffness in comparison to HNPG made out of Ag₉₃Au₇ even though they have similar feature sizes. The results represent an evidence for the development of the connectivity during coarsening in relation to the solid fraction.

MM 18.33 Tue 17:30 P2

Hierarchical-structural effect on creep of nanoporous gold — •HANSOL JEON¹, SHAN SHI^{1,2}, JÜRGEN MARKMANN^{1,2}, and ERICA LILLEODDEN³ — ¹Helmholtz-Zentrum Hereon, Institute of Materials Mechanics, 21502 Geesthacht — ²Hamburg University of Technology, Institute of Materials Physics and Technology, 21073 Hamburg — ³Fraunhofer Institute for Microstructure of Materials and Systems, 06120 Halle (Saale)

Nanoporous gold (NPG), a bi-continuous structure composed of ligaments and pores, is highly attracting attention in application fields due to its high surface area and chemical inertness. In addition, hierarchical nested-network nanoporous gold (N3PG) has been developed as an even lighter and faster functional material. With respect to mechanical properties, the research on the time-dependent deformation as called creep for NPG and N3PG is scarce while there have many studies of tension, compression, and nanoindentation. In this study, we performed compressive creep tests for NPG and N3PG pillars in order to investigate the creep behavior under control of the electrochemical potential. We prepared N3PG samples with the same higher-level ligament size and with different lower-level ligament-sizes and a non-hierarchical NPG sample according to the higher-level ligament size so that we analyzed the effect of lower-level ligament-size on N3PG as well as the effect of the hierarchical structure itself on creep. In addition, by controlling the electrochemical potential, we controlled the surface status in order to check on the size effect of the relationship between creep behavior and surface state.

MM 18.34 Tue 17:30 P2

Fabrication of hierarchical porous silicon and amorphous silica by means of silver nanoparticle catalyzed chemical etching — •STELLA GRIES^{1,2,3}, MANUEL BRINKER^{1,2,3}, and PATRICK HUBER^{1,2,3} — ¹Institute for Materials and X-Ray Physics, Hamburg University of Technology, 21073 Hamburg, Germany — ²Center for X-Ray and Nano Science CXNS, Deutsches Elektronen-Synchrotron DESY, 22607 Hamburg, Germany — ³Center for Hybrid Nanostructures CHyN, University of Hamburg, 22607 Hamburg, Germany

Many biological tissues and materials exhibit a multiscale porosity with small, often nanoscale pores as well as large, macroscopic pores or capillaries in order to achieve simultaneously large inner surfaces in combination with an optimized mass transport capability. Achieving such a hierarchical porosity in artificial porous media is a very active research field. Here we present a novel approach based on silver nanoparticle-assisted chemical etching (MACE) of electrochemically fabricated macroporous silicon for the synthesis of wafer-scale, single-crystalline silicon with a bimodal pore size distribution. With MACE macroporous silicon membranes can be porosified into hierarchical porous silicon (hp-Si). The resulting semiconducting material offers good hydraulic permeabilities and simultaneously a large inner surface for potential applications in energy harvesting or conversion or for on-chip sensorics and actuators. Finally, the hp-

Si membranes can be transformed by thermal oxidation at temperatures above 800°C to hierarchical porous amorphous silica a material that could be of particular interest for opto-fluidic and photonic applications in the visible.

MM 18.35 Tue 17:30 P2

In situ X-ray spectroscopic and scattering studies on the emergence of CoO nano-assemblies in solution — •CECILIA ZITO¹, LUKAS GROTE^{1,2}, KILIAN FRANK³, ANN-CHRISTIN DIPPEL², PATRICK REISBECK³, KRZYSZTOF PITALA⁴, KRISTINA KVASHNINA⁵, STEPHEN BAUTERS⁵, BLANKA DETLEFS⁵, OLEH IVASHKO², PALLAVI PANDIT², MATTHIAS REBBER¹, SANI HAROUNA-MAYER¹, BERT NICKEL³, and DOROTA KOZIEJ¹ — ¹University of Hamburg, Germany — ²Deutsches Elektronen-Synchrotron, Hamburg, Germany — ³Ludwig-Maximilians-Universität München, Germany — ⁴AGH, University of Science and Technology, Faculty of Physics and Applied Computer Science, Krakow, Poland — ⁵European Synchrotron Radiation Facility ESRF, Grenoble, France

The key to fabricating complex, hierarchical materials is the control of chemical reactions at various length scales. The classical crystallization theory is insufficient to properly describe the chemical reaction leading to monomer formation, the evolution of small primary particles, and how they assemble into superstructures. Here, we illustrate how the combination of advanced X-ray spectroscopic and scattering in situ studies probe length scales all the way from atomic to macroscopic, and shed light on the formation mechanism of CoO nanocrystal assemblies in solution. Utilizing HERFD-XANES, we directly access the molecular level of the nanomaterial synthesis. We reveal that initially Co(acac)₃ rapidly reduces to square-planar Co(acac)₂ and coordinates to two solvent molecules. Furthermore, we track subsequent structural changes with in situ total X-ray scattering and atomic pair distribution function analysis, pinning down the transition from the dissolved Co complex to crystalline CoO. Ultimately, SAXS uncovers the assembly process of the crystallites into distinct spherical superstructures. The concomitant growth and assembly of crystallites into a superstructure differentiates the investigated pathway from a classical mechanism. The combination of X-ray spectroscopy and scattering can elucidate the emergence of assemblies in solution with a broad perspective.

MM 18.36 Tue 17:30 P2

Hierarchical materials mimicking mechanical behaviour of human bone synthesized by additive manufacturing and dealloying. — •ALEKSANDR FILIMONOV¹, LUTZ MÄDLER^{1,2}, and ILYA OKULOV^{1,2} — ¹Faculty of Production Engineering, University of Bremen, Badgasteiner Str. 1, 28359 Bremen, Germany — ²Leibniz Institute for Materials Engineering-IWT, Badgasteiner Str. 3, 28359 Bremen, Germany

The close match between the elastic properties of an implant material and bone is crucial to avoid the stress-shielding effect. Therefore, low modulus biomaterials are desirable for biomedical implants that ensure rapid healing of hard tissue. Due to its complex hierarchical structure, bone features moderate strength similar to some metals and low elastic modulus like polymers. Implant materials for bone fixation should be several times stronger compared with that of bone. However, the general relation between strength and elastic modulus of man-made materials suggest that stronger materials typically possess higher elastic modulus including metals - usual candidates for bone fixation. In this work, novel hierarchical metal-polymer composite materials "breaking" the general trend between strength and elastic modulus were synthesized by additive manufacturing and liquid metal dealloying. The large digital porosity of metallic scaffold was synthesized by additive manufacturing and its fine porosity is a result of materials self-organization upon dealloying. The results suggest that these novel composite materials mimicking the structure and mechanical behaviour of bone are potential candidates for biomedical applications.

MM 18.37 Tue 17:30 P2

Peculiarities of electron transport and resistive switching in point contacts on TiSe₂ and TiSe. — DMYTRO BASHLAKOV¹, •OKSANA KVITNITSKAYA¹, YULIA SHERMERLUK², SAICHARAN ASWARTHAM², DMITRI EFREMOV², BERND BÜCHNER^{2,3}, and YURI NAIDYUK¹ — ¹B. Verkin Institute for Low Temperature Physics and Engineering, NAS of Ukraine, Kharkiv, Ukraine — ²Institute for Solid State Research, IFW Dresden, Dresden, Germany — ³Institut für Festkörper- und Materialphysik und Würzburg-Dresden Cluster of Excellence ct.qmat, Technische Universität Dresden, Dresden, Germany

We report resistive switching in voltage biased point contacts (PCs) based on the transition metals chalcogenides TiSe₂ and TiSe. The switching is taking place between a low resistive *metallic-type* state and a high resistive *semiconducting-type* state by applying bias voltage (<0.4V), while reverse switching takes place by applying voltage of opposite polarity. The difference in resistance between these two states can reach of about two orders of magnitude at helium temperature. The origin of the effect can be attributed to the electric field induced change of stoichiometry in PC core due to drift of Se vacancies. Additionally, we demonstrated, that heating takes place in PC core, which can facilitate the electric field induced effect. At the same time we did not find any evidence for CDW spectral features in our PC spectra for TiSe₂. The observed resistive switching allows to propose TiSe₂ and TiSe as the promising materials,

e.g., for non-volatile resistive random access memory (ReRAM) engineering.

MM 18.38 Tue 17:30 P2

Electron-phonon interaction and point contact enhanced superconductivity in trigonal PtBi₂ — DMYTRO BASHLAKOV¹, OKSANA KVITNITSKAYA¹, GRIGORY SHIPUNOV², SAICHARAN ASWARTHAM², OLEG FEYA^{2,3}, DMITRI EFREMOV², and BERND BÜCHNER^{2,4} — ¹B. Verkin Institute for Low Temperature Physics and Engineering, NAS of Ukraine, Kharkiv, Ukraine — ²Institute for Solid State Research, IFW Dresden, Dresden, Germany — ³Kyiv Academic University, Kyiv, Ukraine — ⁴Institut für Festkörper- und Materialphysik and Würzburg-Dresden Cluster of Excellence ct.qmat, Technische Universität Dresden, Dresden, Germany

PtBi₂ is a Weyl semimetal, which demonstrates superconductivity with low critical temperature $T_c \sim 0.6$ K in the bulk. Here, we report our study of electron-phonon interaction (EPI) in trigonal PtBi₂ by the Yanson point contact (PC) spectroscopy and presenting the observation of PC enhanced superconductivity. We show, that the Yansons PC spectra display a broad maximum around 15 meV, indicating, apparently, EPI mechanism of Cooper pairing in PtBi₂. Moreover, we discovered a substantial increase of T_c up to ~ 3.5 K in PCs. The observed T_c is sufficiently higher than the bulk value, as well as detected at hydrostatic pressure. We calculated the phonon density of states and Eliashberg EPI function in PtBi₂ within the framework of the density functional theory. A comparison of experimental data with theoretical calculations showed acceptable agreement. The theoretical T_c is 3.5 K, which corresponds to the experimental value.

MM 18.39 Tue 17:30 P2

Quantification of intrinsic surface charges on MgO nanocubes using off-axis electron holography — YAN LU^{1,2}, FENGSHAN ZHENG¹, QIANQIAN LAN¹, MICHAEL SCHNEDLER¹, PHILIPP EBERT¹, and RAFAL E. DUNIN-BORKOWSKI¹ — ¹Ernst Ruska-Centre for Microscopy and Spectroscopy with Electrons (ER-C 1) and Peter Grünberg Institute (PGI 5), Forschungszentrum Jülich, Jülich, Germany — ²Beijing Key Lab and Institute of Microstructure and Properties of Advanced Materials, Beijing University of Technology, Beijing, China

Metal oxide nanoparticles exhibit outstanding catalytic properties, believed to be related to the presence of oxygen vacancies at the particle surface. However, little quantitative is known about concentrations of point defects inside and on surfaces of these nanoparticles due to the challenges in achieving an atomically resolved experimental access. By employing off-axis electron holography, we demonstrate exemplarily using MgO nanoparticles as a methodology, which allows us to discriminate between mobile charges induced by electron beam irradiation and immobile charges associated with deep traps induced by point defects as well as distinguish between bulk and surface point defects. Counting the immobile charges provides a quantification of the concentration of F^{2+} centers induced by oxygen vacancies at the MgO nanocube surfaces.

MM 18.40 Tue 17:30 P2

3D Printed One Piece Surface Alteration Sensor with Galvanic Isolation — MICHAEL FEIGE and SONJA SCHÖNING — Bielefeld Institute for Applied Materials Research (BIFAM), Bielefeld University of Applied Sciences, Department of Engineering Sciences and Mathematics

More recently it is possible to combine conductive and non-conductive materials in one 3D print process. This allows printing of complex structures like PCBs, 3D coils, transformers, capacitors or high frequency components like antennas or transmission lines. Furthermore it is possible to combine those components to build highly specialized sensors in one production step.

We developed a concept for a sensor which, in its specialized form, could be used for detection of mechanical, chemical or biological alteration of surfaces such as abrasion, material degradation or separation. The detection method is based on an electrical, inductive readout while maintaining a sufficient galvanic isolation between the sensing area and the readout circuit.

In this contribution an actual sensor device capable of detecting corrosion is presented, which was designed, printed and tested with successful results. The sophisticated design outweighs the lack of high electrical conductivity and high magnetic permeability within the range of printable materials by the ability of the printer to precisely integrate the conductive material into the insulating material.

MM 18.41 Tue 17:30 P2

A first study on the current-controlled flash sintering experiments on 3YSZ-Ni composites — PRANAV RAI and DEVINDER YADAV — Department of Metallurgical and Materials Engineering, Indian Institute of Technology Patna, Bihta, Patna 801106, India

Flash sintering involves densification of ceramic bodies in few seconds at relatively low furnace temperatures. The normal flash sintering experiments are characterized by a non-linear rise in the electrical conductivity of the sample. In the present work, flash sintering experiments were conducted in the current-controlled mode where the current is made to increase linearly through the sample at a constant rate. The sample sinters progressively as the current increases. Composites of 3YSZ and Ni, with different Ni contents (5wt.%, 10wt.%, and 20wt.%) were flash sintered at a constant current rate of 600 mA/min with a target current density of 100 mA/mm², at a furnace temperature of 900°C. The total span of the experiments was 50 s. The extent of densification decreased with increase in Ni content. In addition, the samples with higher Ni content started to densify at a higher current density. XRD revealed oxidation of Ni in all the samples, post flash sintering. However, complete oxidation of Ni to NiO in conventional sintering of the same composites occurred at 1450°C after a hold time of 2 hours. The flash sintered microstructure of 3YSZ phase was characterized by relatively fine grains with narrow grain size distribution. The 3YSZ-20Ni samples exhibited a microstructure with percolating network of the NiO phase. The processed samples can have possible applications in designing the anode materials for solid oxide fuel cells.

MM 18.42 Tue 17:30 P2

Electrospun Electroluminescent CsPbBr₃ Fibers: Flexible Perovskite Networks for Light-Emitting Application — KHAN LÊ¹, FLORIAN VON TOPERCZER², FERAY ÜNLÜ¹, THOMAS FISCHER¹, KLAS LINDFORS², and SANJAY MATHUR¹ — ¹Institute of Inorganic Chemistry, University of Cologne, Greinstr. 6, 50939 Cologne, Germany — ²Institute of Physical Chemistry, University of Cologne, Greinstr. 4-6, 50939 Cologne, Germany

Organic-inorganic and all-inorganic lead halide perovskites (APbX₃) have continuously attracted research interest and went through significant improvements towards highly efficient photovoltaic technologies and LEDs. Most lead-halide perovskite devices are based on thin films or quantum dots while reports on alternative morphologies are scarce. We prepared CsPbBr₃@polymer composite nanofibers by one-step electrospinning and characterized them by scanning electron microscopy, transmission electron microscopy, X-ray diffractometry, UV/vis and photoluminescence spectroscopy. As a proof-of-concept, we subsequently integrated the fiber mats as active layers in electrically driven light emitting devices. While the synthesis of perovskite nanofibers is not new, to the best of our knowledge we would be the first to report on electroluminescence of such fibers. In addition, all preparations were conducted under ambient atmosphere and the perovskite precursor ink was prepared with low toxicity solvents (H₂O/EtOH/ionic liquid). This work could pave the way towards cost effective and flexible optoelectronic fiber- or yarn-based lead-halide perovskite devices by an up-scalable method.

MM 18.43 Tue 17:30 P2

Raman spectra of Arsenopyrite: Experiment and Theory — NEBAHAT BULUT¹, AYBERK ÖZDEN¹, CAMELIU HIMCINSCHI¹, ESTEBAN ZUNIGA PUELLES², ROMAN GUMENIUK², and JENS KORTUS¹ — ¹TU Bergakademie Freiberg, Institute of Theoretical Physics — ²TU Bergakademie Freiberg, Institute for Experimental Physics, Germany

Arsenopyrite (FeAsS) is a semiconductor with a small bandgap and a common source for arsenic (As) mineral. Chemical and structural information on this material is still of interest. The crystal structure is, monoclinic with space group $P2_1/c$, derived from orthorhombic marcasite (FeS₂) [1]. Here we present a combined experimental and theoretical study on the vibrational properties of arsenopyrite, which have to our knowledge not yet been reported. Raman spectra have been recorded experimentally by means of a LabRam HR800 spectrometer from HORIBA Jobin Yvon using 633 nm laser as the excitation source. Additionally, Raman spectra were calculated using Quantum Espresso [2] with norm-conserving pseudopotential and PZ exchange-correlation functional. The comparison of experimental and theoretical data shows good agreement and allows for symmetry assignment of the Raman peaks.

[1] Bindi, L.; Moelo, Y.; Leone, P.; Suchaud, M. *Can. Mineral.* 50, 471*479 (2012).

[2] P. Giannozzi et al., *J.Phys. Condens. Matter* 21, 395502 (2009)

MM 19: Invited Talk Fritz Körmann

Time: Wednesday 9:30–10:00

Location: H44

Invited Talk

MM 19.1 Wed 9:30 H44

High-Entropy Alloys: Materials design in high dimensional chemical space from ab initio thermodynamics — •FRITZ KÖRMANN — Max-Planck-Institut für Eisenforschung GmbH, D-40237 Düsseldorf, Germany — Materials Science and Engineering, Delft University of Technology, 2628 CD, Delft, The Netherlands

A well-targeted design of modern alloys such as high entropy alloys (HEAs) is extremely challenging due to their immense composition space. In this talk I will discuss recent advances in fully parameter-free ab initio calculations combining advanced statistical concepts and machine learning techniques. These novel techniques allow to computationally identify favorable composition islands in the high dimension chemical phase space solely on the computer. Using this ap-

proach, various mechanisms and concepts proposed in the literature have been tested: Besides lattice distortions, stacking-fault energies (SFEs) have been successfully used as a descriptor to link atomistic simulations to the macroscopic deformation mechanisms that are behind the superior mechanical performance. Interstitial alloying with C reveals, e.g., large fluctuations in solution energies depending on the specific local chemical environment and its impact on SFEs can be even qualitatively different depending on alloy composition. We also discuss BCC-HCP stability as promising descriptor to identify mechanically appealing refractory HEAs and the critical role of lattice distortions therefore. Based on these computationally highly expensive computations easy-to-use materials design rules will be derived and discussed for the various examples.

MM 20: Computational Materials Modelling: HEA, Alloys & Nanostructures

Time: Wednesday 10:15–13:00

Location: H44

MM 20.1 Wed 10:15 H44

Microstructural evolution of severely deformed nanocomposite high entropy alloys irradiated by swift heavy ions — •SHABNAM TAHERINIYA¹, CHRISTIAN GADELMEIER², HARALD RÖSNER¹, MARTIN PETERLECHNER¹, CHRISTOPH GAMMER³, MARILENA TOMUT^{1,4}, SERGIY V. DIVINSKI¹, UWE GLATZEL², and GERHARD WILDE¹ — ¹Institute of Materials Physics, University of Münster, Germany — ²Metals and Alloys, University of Bayreuth, Bayreuth, Germany — ³Erich Schmid Institute of materials Science, Austrian Academy of Science, Leoben, Austria — ⁴GSI Helmholtz Center for Heavy Ion Research, Darmstadt, Germany

Structural modifications induced by the processing of high entropy alloys (HEAs) under non-equilibrium conditions are investigated to shed light into the stability of such advanced materials. The nanocomposite HEAs are produced by the room-temperature high pressure torsion (HPT) of stacked single-phase equiatomic FCC CoCrFeMnNi (Cantor) and BCC HfNbTaTiZr (Senkov) alloys. Solely Cantor and Senkov alloys were HPT-processed under the similar conditions, too. Cross-sections of the HPT-processed disks were subjected to high fluences of Au swift-heavy-ion irradiation at ambient and cryogenic temperatures. Deformation and irradiation-induced microstructural changes were examined in detail applying scanning and transmission electron microscopies with respect to evolution of chemical composition and local microstructure. A combination of nano-beam diffraction with angular correlation was utilized to provide information about the resolved crystal structures and strain fields in the different HEA phases.

MM 20.2 Wed 10:30 H44

Impact of high-pressure torsion and post-deformation annealing on CoCrFeMnNi high-entropy alloy with carbon content — •SANDRA HECHT, SERGIY V. DIVINSKI, and GERHARD WILDE — Institute of Materials Physics, University of Münster, Münster, Germany

The well-known Cantor alloy CoCrFeMnNi provides attractive mechanical properties and strength-ductility combinations, which can be improved by further alloying of small amounts of carbon.

In the present work, the impact of high-pressure torsion (HPT) and post-deformation annealing on equiatomic Cantor alloy and nearly-equiatomic (C alloyed (4.4 at.)) Cantor alloy, produced via arc-melting and subsequent homogenization at 1373 K for 3 days under pure Ar, is examined. The thermal, mechanical and microstructural properties of the initially coarse-grained samples were investigated before and after deformation at room temperature (5 rotations at 8 GPa) and afterwards post-deformation annealing treatments using differential-scanning calorimetry (DSC), X-ray diffraction (XRD), scanning and transmission-electron microscopy (SEM & TEM) as well as micro-hardness measurements. Impact of the interstitial carbon and in particular the carbides Cr₂₃C₆ on the mechanical response and microstructure evolution is examined.

MM 20.3 Wed 10:45 H44

Phase Stability and Ordering in Ta-Mo-Cr-Ti-Al Refractory High Entropy Alloys — •YILUN GONG¹, ALEXANDER SHAPEEV², FRITZ KOERMANN^{1,3}, and JOERG NEUGEBAUER¹ — ¹Max-Planck-Institut für Eisenforschung GmbH, Germany — ²Skolkovo — ³Delft University of Technology, The Netherlands

Predictive capabilities of phase stability and ordering in multi-component systems are critical to designing better alloys. This is particularly important for properties which are difficult to be quantified by traditional experimental techniques.

In the present work, a class of body-centered-cubic (bcc) refractory high en-

trophy alloys was studied. In contrast to its superior high-temperature behaviour, it shows less-satisfying ductility below 600 °C. As origin of the poor mechanical performance long-range B2-ordering at low temperatures has been proposed but is still controversially discussed due to contradicting experimental findings. To predict and to quantify the temperature-dependent stable structure, we employed on-lattice machine-learning interatomic potentials (namely low-rank potentials). This type of potentials is capable of accurately describing chemical interactions in multi-component systems used in subsequent Monte Carlo simulations. Systematic studies of training qualities, statistical uncertainties and impact of local lattice distortions were conducted. Computed ordering sequence, site occupancies, short-range order parameters and alloying with interstitial O will be discussed.

MM 20.4 Wed 11:00 H44

Stabilities and Mechanical Properties of Mg-based Light Metal Multi-Principal Alloys — •WERNFRIED MAYR-SCHMÖLZER¹, JOHANNES KIRSCHNER², CLEMENS SIMSON⁴, CHRISTOPH EISENMENGER-SITTNER², JOHANNES BERNARDI³, and GREGOR VONBUN-FELDBAUER¹ — ¹Institute of Advanced Ceramics, TU Hamburg — ²Institute of Solid State Physics, TU Vienna — ³USTEM, TU Vienna — ⁴LKR, Austrian Institute of Technology GmbH

Compositionally Complex Alloys (CCAs) consist of four or more elements alloyed in approximately equal fractions and often crystallize in a simple crystal lattice. In many cases, their mechanical properties like structural stability or ductility exceed that of common modern alloys. Usually, they mainly contain heavy d-Orbital metals, and investigations into low density light metal CCAs have been rare due to the complex binding modes of their constituents.

We use both a Cluster Expansion approach with stochastic prescreening steps and neural network based pair potentials to scan the large configuration space of the Mg-Al-Cu-Zn system for stable phases. Training data was generated using DFT calculations implemented in the VASP code. In conjunction with experiments, we find that addition of Cu into the Al-Mg-Zn system inhibits phase separation by formation of a stable cubic phase, reflected in an increase of the calculated bulk modulus. Furthermore, we evaluate the predictive power of these screening methods and their ability to provide insights into simulation of physical properties of these complex multicomponent alloys.

MM 20.5 Wed 11:15 H44

In-situ Nanoalloying by Laser Powder Bed Fusion: Molecular Dynamics Simulations of Cantor-Alloy Formation in a Powder Blend — •YULIA KLUNNIKOVA¹, ARNE J. KLOMP², and KARSTEN ALBE³ — ¹klunnikova@mm.tu-darmstadt.de — ²klomp@mm.tu-darmstadt.de — ³albe@mm.tu-darmstadt.de

Laser powder bed fusion (LPBF) is an additive manufacturing technology involving a gradual build-on of layers to form a complete component typically starting with prealloyed particles. Alternatively, one can also start with a powder blend and initiate in-situ alloying by the laser beam. In this context, multi-component systems, including high entropy alloys, are of particular interest. In this contribution we show results of molecular dynamics simulations of high-entropy nanoalloys formed by LPBF. We use the Cantor alloy as model system and explore the possibility to create the FeCrCoMnNi alloy from powder blends under far-from-equilibrium conditions and compare to the case of pre-alloyed nanopowders. By varying parameters (temperature field, melt pool, substrate type, etc.) we explore the correlation to microstructural features. In the case of the powder blend the elemental components mix in the liquid phase and solidify partially in crystalline and glassy states. Depending on the parameters of the laser (irradiation temperature, laser spot size) we see varying amounts of crystal defect, such as stacking faults, twinning, and vacancies. The results show that the result-

ing structures are delicately depending on the interplay of laser parameters, heat transport, interdiffusion and geometric factors. We acknowledge the NHR4CES for the computing time.

15 min. break

MM 20.6 Wed 11:45 H44

Phase stability and formation energies of stacking faults in intermetallic $Mg_xAl_{2-x}Ca$ Laves phases — •ALI TEHRANCHI, TILMANN HICKEL, and JÖRG NEUGEBAUER — Max Planck institute for Iron research, Max Planck Straße 1, 40237 Düsseldorf

The intermetallic Laves phases that form in Mg-based alloys at higher alloying concentrations have a significant impact on their mechanical properties. For example, they can enhance the creep resistance of the alloys and extend their application to higher temperature domains. However, the mechanisms of deformation of these phases are not fully understood. In this work, at first the formation energies of the different realizations of C14, C15, and C36 Laves phases in the composition domain, Mg_xAl_{2-x} with $0 < x < 2$, using the ab initio simulations is calculated. Using these formation energies, the phase diagram of the phases of interest is constructed. The effect of the strain fields on the relative stability of these phases is included. In addition, using the analytic Axial-Nearest Neighbor Ising (ANNNI) type model, the basal stacking faults in each phase and composition are calculated. The results of the analytic models are in good accordance with the results of the direct DFT simulations of the stoichiometric stacking faults. The gamma surface of certain realizations of the C36 phase is also investigated and explain the experimentally observed planar defects in the C36 phase.

MM 20.7 Wed 12:00 H44

Rational design of bimetallic nanoparticles — •SAMUEL BALTAZAR^{1,2}, JAVIER ROJAS^{1,2}, PAMELA SEPULVEDA², and RAFAEL FREIRE² — ¹Physics Department, Universidad de Santiago de Chile, Chile — ²Center for the development of Nanoscience and Nanotechnology, Universidad de Santiago de Chile, Chile

The study of bimetallic nanoparticles (BNP) has recently attracted increasing attention from researchers worldwide due to their potential for technological applications in the electronic and environment fields. This study will be carried out through a theoretical framework to identify the fundamental atomic-scale mechanisms for BNP such as FeCu, AgCu, and FeNi. It is therefore necessary to determine the structural, electronic, and magnetic properties of the nanostructures with two or more elements, where the interplay between both metallic elements can be used to limit the oxidation of iron or the electron transfer between elements. This can be done based on some of the characteristics of these systems, such as (i) the surface-volume ratio, (ii) the shape of nanoparticles as an interesting aspect due to the physico-chemical properties at their surface, (iii) Concentration and (iv) distribution of elements. We performed molecular dynamics simulations under the NVT canonical ensemble to further deepen our study. The results pointed out that AgCu and FeNi BNP with a core shell and janus like morphologies are some of the most stable configurations, with a competition between them for FeCu as a function of the concentration and size of each element. These results were compared with experimental data for BNP, evidencing a good agreement among these approaches.

MM 20.8 Wed 12:15 H44

Atomic cluster expansion for the Ag-Pd system — •YANYAN LIANG, MATOUS MROVEC, YURY LYSOGORSKIY, and RALF DRAUTZ — ICAMS, Ruhr-Universität Bochum, Germany

Alloys of noble metals, such as silver and palladium, have been regaining attention in recent years due to their importance in nanotechnology and cataly-

sis. However, for the binary Ag-Pd system reliable and efficient interatomic potentials that provide an accurate description of structural and thermodynamic properties are lacking. In this work, we developed a new atomic cluster expansion (ACE) parametrization for both elements Ag and Pd as well as their binary compounds by fitting to a large training set of ab initio data. The resulting ACE potential provides an accurate description for a wide range of fundamental properties, including the equations of states of various phases, elastic moduli, phonon frequencies, transformation paths, and defect energies. The excellent computer efficiency and linear scaling of ACE enable to carry out large-scale molecular dynamics and Monte Carlo simulations to evaluate complex phenomena, such as thermal expansion, melting, diffusion and phase diagrams. Examples of these simulations will be provided to demonstrate the outstanding predictive power of ACE.

MM 20.9 Wed 12:30 H44

Atomistic modelling of hybrid organic-inorganic nanocomposites — KAI SELLSCHOPP¹, WERNFRIED MAYR-SCHMÖLZER¹, ROBERT MEISSNER², and •GREGOR VONBUN-FELDBAUER¹ — ¹Institute of Advanced Ceramics, TU Hamburg, Germany — ²Institute of Polymers and Composites, TU Hamburg, Germany

Novel hybrid materials like supercrystalline nanocomposites from nano-building blocks promise excellent properties and functions for diverse applications. One realization are inorganic nanoparticles (NP) from transition-metal oxides which are functionalized with organic ligands and then assembled on different levels of hierarchy. In this contribution atomistic modelling based on density functional theory (DFT) calculations is used to shed light on the first level of hierarchy. Particularly, the interfacial properties of different ligands and effects in the interphase between the NP are addressed. For modelling interfaces, the configuration space is a challenge and here the program CodeRed (Configuration space determination and Reduction) is presented which allows to sample the adsorption configuration space and to select configurations as input for DFT calculations using unsupervised machine learning approaches. The results are further facilitated to obtain mechanical properties using DFT, and as input for molecular dynamics simulations as a first step towards multi-scale modelling to allow for an accurate description of larger and more complex systems.

MM 20.10 Wed 12:45 H44

Ab initio investigation of Mg alloy corrosion in water — •JING YANG, MIRA TODOROVA, and JÖRG NEUGEBAUER — Max-Planck-Institut für Eisenforschung GmbH, Düsseldorf, Germany

Magnesium alloys have great potential as structural materials for the automotive and aerospace industries, as well as bio-implants due to their low density and non-toxic nature. However, intrinsically poor ductility and poor corrosion resistance limit their practical application. In this work, we focus on the solid solution of Al and Ca in Mg, an alloying system which has shown improved ductility and corrosion resistance. In particular, we elucidate the effect of Al and Ca alloying on the aqueous corrosion process of Mg metal by ab initio molecular dynamics simulation of the metal/water system. We analyze the segregation behavior of the alloying elements, their impact on the interfacial water structure and dynamics, and the subsequent implication on corrosion kinetics. By combining our DFT calculations with thermodynamics, we construct interface phase diagrams for the Mg-Al-Ca system to elucidate the influence of the environment on surface structure and composition. We consider both implicit and explicit water calculations, which allows us to analyze the impact the water-modelling approach has on the constructed interface phase diagrams. We show that such ab initio molecular dynamics studies strongly improve our understanding on microscopic corrosion processes at realistic conditions.

MM 21: Transport in Materials: Thermal transport

Time: Wednesday 10:15–13:00

Location: H45

MM 21.1 Wed 10:15 H45

Computational modeling of extremely anisotropic van der Waals thermal conductors — SHI EN KIM¹, FAUZIA MUJID¹, AKASH RAI², •FREDRIK ERIKSSON³, JOONKI SUH¹, PREETI PODDAR¹, ARIANA RAY⁴, CHIBEOM PARK¹, ERIK FRANSSON³, YU ZHONG¹, DAVID A. MULLER⁴, PAUL ERHART³, DAVID G. CAHILL², and JIWOONG PARK¹ — ¹Uni. of Chicago, USA. — ²Uni. of Illinois UC, USA. — ³Chalmers, Sweden. — ⁴Cornell Uni., USA.

Materials with thermal conduction anisotropy can provide innovative thermal management strategies in integrated circuits. However, artificially engineered material lacks the anisotropy ratios seen in nature. Here, we report extremely anisotropic thermal conductors based on large-area van der Waals thin films with random interlayer rotations, which produce a room-temperature thermal anisotropy ratio close to 900 in MoS_2 , one of the highest ever reported. This is enabled by the interlayer rotations that impede the through-plane conductivity,

while the long-range intralayer crystallinity maintains high in-plane conductivity. In this contribution we will present the computational analysis of the measured ultralow thermal conductivities in the through-plane direction for MoS_2 (57 ± 3 mW m⁻¹ K⁻¹). Using molecular dynamics simulations we quantitatively explain these values and reveal a one-dimensional glass-like thermal transport. Conversely, the in-plane thermal conductivity in these MoS_2 films is close to the single-crystal value. Our work establishes interlayer rotation in crystalline layered materials as a new degree of freedom for engineering-directed heat transport in solid-state systems. Nature 597, 660-665 (2021)

MM 21.2 Wed 10:30 H45

Searching and Finding Thermal Insulators via ab initio Green-Kubo Simulations — •FLORIAN KNOOP^{1,2}, THOMAS A.R. PURCELL¹, MATTHIAS SCHEFFLER¹, and CHRISTIAN CARBOGNO¹ — ¹The NOMAD Laboratory at the FHI-MPG and HU, Berlin, Germany — ²Department of Physics, Chemistry and Biology (IFM), Linköping University, Sweden

We present a first-principles search for thermal insulators in material space, covering hundreds of compounds in seven space groups, including simple rock-salt and zinc blende structures up to complex perovskites. Using the high-throughput framework *FHI-vibes* [1] and a recently developed measure for the strength of anharmonicity, [2] we identify 120 experimentally known materials with potential for ultra-low thermal conductivity <2 W/mK at room temperature, i.e., comparable to those of thermoelectrics such as SnSe. For the 60 most promising candidates, we perform non-perturbative, fully anharmonic *ab initio* Green-Kubo simulations [3] to include all anharmonic effects. Besides revealing seven ultra-insulating compounds, these calculations shed light on the importance of strong anharmonic effects not accessible in perturbative phonon formalisms, e.g., short-lived metastable configurations and precursors of phase transitions.

[1] F. Knoop *et al.*, *J. Open Source Softw.* **5**, 2671 (2020).

[2] F. Knoop *et al.*, *Phys. Rev. Mater.* **4**, 083809 (2020).

[3] C. Carogno, R. Ramprasad, and M. Scheffler, *Phys. Rev. Lett.* **118**, 175901 (2017).

MM 21.3 Wed 10:45 H45

A spatially resolved optical method to measure thermal diffusivity — •FEI SUN¹, SIMLI MISHRA¹, PHILIPPA H MCGUINNESS¹, ZUZANNA H FILIPIAK¹, IGOR MARKOVIC¹, DMITRY A SOKOLOV¹, NAOKI KIKUGAWA², JOSEPH W ORENSTEIN^{3,4}, SEAN A HARTNOLL⁵, ANDREW P MACKENZIE^{1,6}, and VERONIKA SUNKO^{1,3} — ¹Max Planck Institute, CPfS, Dresden, Germany — ²NIMS, Ibaraki, Japan — ³UC Berkeley, California, USA — ⁴LBNL, California, USA — ⁵Univ. of Cambridge, Cambridge, UK — ⁶Univ. of St Andrews, St Andrews, UK

We introduce an optical method to directly measure thermal diffusivity across a broad range of temperatures. Two laser beams are used, one as a source to locally modulate the temperature, and the other as a probe of the reflectivity. Thermal diffusivity is obtained from the phase delay between two beams. Combining the technique with a microscope setup allows for spatially resolved measurements. The in-plane diffusivity can be obtained when overlapping the two laser beams instead of separating them in the traditional way, which further enhances the spatial resolution. We demonstrate on two rutherfates: Sr₃Ru₂O₇ and Ca₃Ru₂O₇. The spatial resolution allowed us to study the diffusivity in single domains of the latter, and we uncovered a temperature-dependent in-plane diffusivity anisotropy. Finally, we used the enhanced spatial resolution to study the Ti-doped Ca₃Ru₂O₇. We observed large variations of transition temperature over the same sample, originating from doping inhomogeneity, and pointing to the power of spatially resolved techniques in accessing inherent properties.

MM 21.4 Wed 11:00 H45

Investigation of temperature dependent thermal transport in Sr₂RuO₄ and Sr₃Ru₂O₇ over a wide temperature range — FEI SUN¹, •SIMLI MISHRA¹, ULRIKE STOCKERT¹, RAMZY DAOU², NAOKI KIKUGAWA³, ROBIN S PERRY⁴, SEAN A HARTNOLL⁵, ANDREW P MACKENZIE^{1,6}, and VERONIKA SUNKO^{1,7} — ¹Max Planck Institute - CPfS, Dresden, Germany — ²CRISMAT, ENSICAEN, UNICAEN, Normandie Université, Caen, France — ³NIMS, Ibaraki, Japan — ⁴LCN, University College London, London, UK — ⁵DAMTP, University of Cambridge, Cambridge, UK — ⁶School of Physics and Astronomy, University of St. Andrews, UK — ⁷Department of Physics, University of California, Berkeley, USA

We use optics to study thermal transport by modifying a typical laser pump-probe technique. A direct measurement of thermal conductivity is very challenging at high temperatures. In contrast, our method measures temperature dependent diffusivity over a wide range of temperature (10K up to 330K). As thermal diffusivity is the ratio of the thermal conductivity to the heat capacity, we can access the higher temperature thermal conductivity by an optical measurement of diffusivity and standard heat capacity measurement. We have used this technique to measure thermal diffusivity of two strongly correlated metals, Sr₂RuO₄ and Sr₃Ru₂O₇. This temperature dependent thermal transport combined with the resistivity measurements offers an insight into the electronic and phononic contributions to the quasiparticle scattering.

MM 21.5 Wed 11:15 H45

Simultaneous measurement for the complete characterization of thermoelectric materials - real experiment and its digital twin — •SEVERIN KOPATZ¹, ECKHARD MÜLLER^{1,2}, and PAWEŁ ZIOLKOWSKI¹ — ¹Institute of Materials Research, German Aerospace Center, Cologne, Germany — ²Institute of Inorganic and Analytical Chemistry, Justus Liebig University Gießen, Gießen, Germany

Thermoelectric (TE) materials directly convert thermal energy into electric energy. Their efficiency depends on the figure of merit zT ($zT = S^2\sigma/\kappa$). Commonly, the individual transport properties, mainly the electrical conductivity (σ), the Seebeck coefficient (S), and the thermal conductivity (κ) are measured in

separate measurement set-ups. Here, we report on the 'Combined ThermoElectric Measurement' (CTEM) apparatus, which provides temperature-dependent measurements of the aforementioned transport properties on a single TE sample such as Co-doped FeSi₂ simultaneously. The measurements are carried out in a temperature range between room temperature and 600 °C. Since experimental CTEM results deviate from reference values, we introduce a digital twin of the CTEM. In combination with the real experiment, the numerical model allows to study possible error sources. One of the examples discussed in this talk concerns radiative effects which have to be considered especially at high temperatures above 300 °C and affect the measurement of the thermal conductivity in particular.

15 min. break

MM 21.6 Wed 11:45 H45

Appearance of non-equilibrium grain boundaries in additively manufactured high-entropy CoCrFeMnNi alloy — •NURI CHOI^{1,2}, VLADISLAV KULITCKII¹, JOSUA KOTTKE¹, BENGÜ TAS¹, JUNGHO CHOE³, JI HUN YU³, SANG-SUN YANG³, JOO HYUN PARK², JAI SUNG LEE², GERHARD WILDE¹, and SERGIY DIVINSKI¹ — ¹Institute of Material Physics, University of Münster, Germany — ²Dep. of Mat. Sci. & Chem. Eng., Hanyang University, South Korea — ³Center for 3D Printing Materials Research, KIMS, South Korea

Additive manufacturing process with laser melting includes the repetitive melting/solidification, which generates residual thermal stresses in the bulk material, alongside with creation of various defects, including point defects, dislocations and numerous grain boundaries. How far the kinetic properties of these interfaces are modified by the processing remains an open issue, that is of fundamental importance for such phenomena as creep, phase transformation and precipitation. In the present study, grain boundary diffusion in additively manufactured CoCrFeMnNi high-entropy alloys is measured using the radiotracer technique. Since the additive manufacturing results in a hierarchical microstructure, grain boundary diffusion is examined in different samples prepared via different scan/build strategies. A non-equilibrium state of a fraction of high-angle grain boundaries is discovered. The non-equilibrium state is shown to relax after annealing at low temperatures without measurable microstructural changes. The grain boundary diffusivities of the 3D printed alloys are discussed with respect to those for fully homogenized cast or severe plastically deformed alloys.

MM 21.7 Wed 12:00 H45

Grain boundary diffusion and segregation of Cr in high-purity Ni bi-crystals with a $\Sigma 11$ grain-boundary — •D. GAERTNER¹, S. V. SEVLIKAR¹, G. M. MURALIKRISHNA¹, D. COZLIN², D. IRMER², D. SCHREIBER³, B. TAS¹, M. VAIDYA¹, T. BRINK⁴, V. E. ESIN², C. DUHAMEL², G. DEHM⁴, V. RAZUMOSKI³, G. WILDE¹, and S. V. DIVINSKI¹ — ¹Institute of Materials Physics, University of Münster, Münster, Germany — ²MINES ParisTech, PSL University, Centre des Matériaux, Evry, France — ³Materials Center Leoben Forschung GmbH (MCL), Austria — ⁴Max-Planck-Institut für Eisenforschung GmbH, Düsseldorf, Germany

Grain-boundary diffusion of Cr in a Ni near $\Sigma 11(113)[110]$ bi-crystal is measured in an extended temperature interval between 503 K and 1303 K using the radiotracer technique. The grain boundary diffusion coefficients, D_{gb} , and the triple products, P are determined in the C- and B-type kinetic regimes, observing a strong deviation from the otherwise linear Arrhenius-type temperature dependence above 1000 K. The present results substantiate that the segregation factor of Cr in Ni is about unity, being in agreement with the preliminary findings in polycrystalline counterparts measured by SIMS and are fully supported by DFT-based calculations. Extensive MD simulations with empirical interatomic potentials substantiate an extreme stability of the $\Sigma 11$ grain-boundary structure in Ni from 0 K up to melting point. The non-linear Arrhenius temperature dependence is interpreted in terms of pronounced anharmonic contributions to defect formation at elevated temperatures.

MM 21.8 Wed 12:15 H45

grain boundary melting phase transition in Ni-Bi system — •BAIXUE BIAN¹, BORIS STRAUMAL², SERGIY DIVINSKI¹, and GERHARD WILDE¹ — ¹Institute of Materials Physics, University of Münster, Wilhelm-Klemm-Str. 10, 48149 Münster, Germany — ²Chernogolovka

Grain boundary segregation may drastically decrease the strength of structural materials. The intermediate temperature embrittlement of Ni-based alloys is a classical example of a catastrophic matrix degradation caused by solute segregation, in particular by Bi. In this work, the impact of grain boundary segregation of Bi in dilute polycrystalline Ni-Bi alloys on Ni grain boundary diffusion was systematically studied as function of temperature and composition. The radiotracer technique was used applying the ⁶³Ni radioisotope and measuring grain boundary diffusion in both B- and C-type kinetic regimes after Harrison's classification. An abrupt increase of the grain boundary diffusivities by about two orders of magnitude was observed at certain Bi contents which are unequivocally in the single-phase region of the corresponding bulk phase diagram. The present results unambiguously prove the occurrence of a pre-melting grain boundary

phase transition in the Ni-Bi system.

MM 21.9 Wed 12:30 H45

Investigation of Phase Transitions in Polycrystalline Tungsten Trioxide Films during Ion Insertion and Extraction by in Situ Transmission and Raman Spectroscopy — •MARKUS S. FRIEDRICH^{1,2}, ALEXANDER G. STRACK^{1,2}, PAUL K. TUCHECKER^{1,2}, JAN L. DORNSEIFER^{1,2}, and PETER J. KLAR^{1,2} — ¹Institute of Experimental Physics I, Giessen, Germany — ²Center for Materials Research, Giessen, Germany

The International Energy Agency stated in its "European Union 2020 Energy Policy Review" that in 2016 in the European Union alone 152 TWh were consumed for air conditioning (AC), despite only six percent of the global stock of AC units is operated in the EU. So called "smart windows", e.g. windows based on electrochromic materials, such as tungsten trioxide, are promising candidates to reduce this kind of energy consumption. The coloration and bleaching of the EC material is based on the reversible insertion and extraction of small ions inside the material. Ion diffusion plays a key role in this process and therefore needs to be understood in depth in order to enable the optimization of future devices. Burkhardt et al. found, that the diffusion coefficient in this material is dependent on the concentration of already incorporated ions. We suggest, that this originates from changes in the crystal structure of the thin films. To substantiate this suggestion spatially and temporally resolved in situ transmission and

Raman spectroscopic experiments were performed during potentiostatic ion insertion and extraction to correlate the diffusion of small ions inside the material with changes of its crystal structure.

MM 21.10 Wed 12:45 H45

Self-diffusion in ge2sb2te5 thin films — •QINGMEI GONG, SERGIY DIVINSKI, and GERHARD WILDE — University of Münster, Institute of Materials Physics, Wilhelm-Klemm-str. 10, 48149 Münster, Germany

Phase change memory devices (PCM) are considered as one of the most mature technologies among the emerging non-volatile memories and are based on the reversibility of the amorphous-to-crystalline transition within a nanosecond timescale. Ge₂Sb₂Te₅ is the most widely studied composition. In this work, the self-diffusion in Ge₂Sb₂Te₅ thin films is measured using secondary ion mass spectroscopy (SIMS) and applying the highly enriched natural ¹²²Te isotope. A 200 nm thick layer of Ge₂Sb₂Te₅ was deposited on a Si substrate by DC magnetron sputtering at room temperature. Subsequently, a thin layer of ¹²²Te was deposited on as-prepared Ge₂Sb₂Te₅/Si samples using physical vapor deposition. In the as-deposited state, Ge₂Sb₂Te₅ was amorphous as confirmed by XRD and transmission electron microscopy. The Te diffusion coefficients in Ge₂Sb₂Te₅ were estimated from SIMS measurements after annealing at different temperatures below crystallization onset.

MM 22: Data Driven Materials Science: Experimental Data Treatment and Machine Learning

Time: Wednesday 10:15–13:00

Location: H46

Topical Talk

MM 22.1 Wed 10:15 H46

Ingredients for effective computer-augmented experimental materials science — •CHRISTOPH T. KOCH, MARKUS KÜHBACH, SHERJEEL SHABIH, BENEDIKT HAAS, and SANDOR BOCKHAUSER — Humboldt-Universität zu Berlin, Department of Physics & IRIS Adlershof, Berlin, Germany

Experimentally exploring the properties and uses of materials and improving them for particular purposes has been a major driving force for advancing the way people live over the last millennia. Experimental materials characterization techniques have now reached the level of detail that makes them converge with ab-initio computations based on fundamental building blocks: atoms and the electrons they share. During the last decades computers have surpassed the capacity of humans in the extraction of patterns in large amounts of data. It is thus a very natural consequence to involve their strengths also in further accelerating experimental materials science. In this talk we will use modern transmission electron microscopy as an example to illustrate current and future ways of how the process of linking the properties of materials to their fundamental structure can be supported computationally and by the availability of FAIR experimental and theoretical data sets. Along the way the contributions of the NFDI-project FAIRmat to this process will be highlighted, illustrating the importance of defining well-documented metadata catalogues, as well as providing community-specific online data processing capabilities.

MM 22.2 Wed 10:45 H46

A materials informatics framework to discover patterns in atom probe tomography data — •ALAUKE SAXENA, NIKITA POLIN, BAPTISTE GAULT, CHRISTOPH FREYSOLDT, and JÖRG NEUGEBAUER — Max-Planck-Institut für Eisenforschung GmbH, Düsseldorf 40237, Germany.

Atom probe tomography (APT) is a unique technique that provides 3D elemental distribution with near-atomic resolution for a given material. However, the large amount of data acquired during the experiment and the complexity of the 3D microstructures poses a challenge to fully quantify APT data. Here, taking APT measurements corresponding to a Fe-doped Sm-Co alloy as an example, we present an approach based on unsupervised machine learning to extract different phases in the data. On top of this method, we have built a PCA-based workflow to reduce secondary phase precipitates with complex morphology into simpler plate-like morphologies thus enabling the quantification of in-plane compositional and thickness fluctuations, and relative orientations of the precipitates. The labeled data acquired from the PCA-based approach is used to train a U-NET to perform the same task on different APT samples of the same material automatically. The composition and thickness-related insights are expected to help understand the contribution of the particles to the confinement of the magnetic domains of the dominant 2:17 bulk phase, providing further indications to guide the design of future permanent hard magnets.

MM 22.3 Wed 11:00 H46

Corrected density artifacts in Atom Probe reconstructions: A tip shape-corrected volume reconstruction approach — •PATRICK STENDER¹, DANIEL BEINKE¹, FELICITAS BÜRGER², and GUIDO SCHMITZ¹ — ¹Institute for Materials Science, University of Stuttgart — ²Fakultät für Mathematik, Universität Regensburg, D-93040 Regensburg, Germany

Atom Probe Tomography enables the chemical investigation of nanometric volumes with single atomic sensitivity in 3D. The tip shape sample is evaporated atom by atom. From the obtained data sequence, the respective volume is reconstructed.

Conventionally, this reconstruction is performed with the assumption of a hemispherical tip apex. This practice can lead to serious volume distortions (local-magnification effect). Instead of using in-situ correlative microscopy to discover the evolution of the tip shape during the measurement, we extract the emitter shape numerically from the event statistics on the 2D detector plane.

The method is based on the fundamental postulate that the detected density of events is linked to the local Gaussian curvature of the tip apex. Knowing the variation of this curvature, the surface profile is determined by a finite difference scheme. Except for convexity, no further restriction is imposed on the possible tip shapes.

Different simulated and experimental data sets of complex tip shapes will be discussed and compared. The method largely suppresses the local magnification effects appearing at interfaces between materials of contrasting evaporation thresholds.

MM 22.4 Wed 11:15 H46

Neural networks trained on synthetically generated crystals can classify space groups of ICSD powder X-ray diffractograms — •HENRIK SCHOPMANS^{1,2}, PATRICK REISER^{1,2}, and PASCAL FRIEDRICH^{1,2} — ¹Institute of Theoretical Informatics, KIT, Karlsruhe, Germany — ²Institute of Nanotechnology, KIT, Eggenstein-Leopoldshafen, Germany

Machine learning techniques have successfully been used to extract structural information such as the crystal space group from powder X-ray diffraction (XRD) patterns. However, training directly on simulated patterns from databases like the ICSD is problematic due to its limited size, class-inhomogeneity, and bias toward certain structure prototypes. We propose an alternative approach of generating random crystals with random coordinates by using the symmetry operations of each space group. Based on this approach, we present a high-performance distributed python framework to simultaneously generate structures, simulate patterns, and perform online learning. This allows training on millions of unique patterns per hour. For our chosen task of space group classification, we achieve a test accuracy of 60.4% on new ICSD structure prototypes not included in the statistics dataset guiding the random generation. Instead of space group classification, the developed framework can also be used for other common tasks, e.g. augmentation and mixing of patterns for phase fraction determination. Our results demonstrate, using the domain of X-ray diffraction, how state-of-the-art models trained on large, fully synthetic datasets can be used to guide the analysis of physical experiments.

15 min. break

Topical Talk

MM 22.5 Wed 11:45 H46

Physics guided machine learning tools in analytical transmission electron microscopy — •CECILE HEBERT^{1,3}, HUI CHEN¹, and ADRIEN TEURTRIE^{1,2} — ¹LSME - IPHYS Ecole Polytechnique Fédérale de Lausanne, Lausanne, Switzerland — ²Unité Matériaux et Transformations, Université de Lille, France — ³Institut de Matériaux, Ecole Polytechnique Fédérale de Lausanne, Lausanne, Switzerland

Modern transmission electron microscopes are capable of recording large datasets containing both structural and chemical information on a scale ranging from sub-micrometer to atomic resolution. Operated in scanning TEM mode, two kind of chemical information can be obtained: either via energy dispersive X-Ray spectroscopy or via electron energy loss spectroscopy. On modern instruments, both signals can be acquired at the same time. Turning this huge amount of information (datasets can weight up to several Gb) into segmented quantitative information representing the different phases of the specimen is a real challenge. Pure statistical analysis like principal component analysis generally fails because of two main reasons: artifacts linked to the detection chain and/or non uniqueness of a statistical decomposition. The task is generally complicated by the overlap of phases in the specimen thickness and the presence of the same elements in different phases

With the introduction of physical constraints, like a modelling of the spectrum based on prior knowledge, both on the specimen and on the physical process leading to the spectra, it is possible to obtain a physically meaningful spatial segmentation of the data and to proceed with chemical analysis.

MM 22.6 Wed 12:15 H46

Motif Extraction from Crystalline Images in Real Space — •AMEL SHAMSELDEEN ALI ALHASSAN and BENJAMIN BERKELS — AICES Graduate School, RWTH Aachen University, Germany

Using modern transmission and scanning transmission electron microscopes (S)TEM, atomic resolution images are readily available. In particular, the amount of data produced is so large that automatic analysis tools are needed.

During the last decade, automatic data analysis methods concerning different aspects of crystal analysis have been developed, for example, unsupervised primitive unit cell extraction and automated crystal distortion and defects detection. However, an automatic, dedicated motif extraction method is still called for by experimentalists. While previous works on motif extraction did good work in, for example, finding the plane symmetries and restoring smeared out features or finding positions in atomic columns, they were either not automated enough, not applicable to atomic scale images, or required special calibration.

Here, we propose and demonstrate a novel method for automatic direct mo-

tif extraction from crystalline images based on variational methods. Given an atomic resolution crystalline image, our method employs unit cell extraction to find the atomic structure then solves a minimization problem involving the unit cell projection operator to find the motif. The method was tested on various synthetic and experimental data sets. The results are a representation of the motif in form of an image, primitive unit cell vectors and a denoised reconstruction of the input image.

MM 22.7 Wed 12:30 H46

Analysis of acoustic emission spectra for structural health monitoring — •KLAUS LUTTER, VIKTOR FAIRUSCHIN, and THORSTEN UPHUES — Institute for Sensor and Actuator Technology, Coburg, Germany

Today, the analysis of vibration and acoustic emission spectra is routinely used for health monitoring of gears in industrial production. Recent developments of extended IIoT networks provide even fleet comparison and optimization of required field service.

Here, we present an extended approach to utilize acoustic emission spectra to monitor the structural health of machining tools like mills or drills to extract degradation and lifetime information from the acoustic emission. A successful application of a spectral analysis will provide a huge impact on production quality as well as tool quality according to different production parameters which are transferred into related spectral properties. Furthermore we follow an experimental approach using contact microphones. Our diagnostic approach is a detailed analysis of the corresponding frequency spectra and in particular the existing harmonic frequencies during milling processes.

We demonstrate the classification of different process parameter sets according to different dominant frequencies via classification algorithms. The retrieved classes of spectra are used for a classical regression model assisted by neural networks to analyse characteristics changes over time. From an industrial perspective this type of analysis is a non-invasive and versatile approach and easily implementable, even in existing production machinery.

MM 22.8 Wed 12:45 H46

Optimizing laser powder bed fusion by machine learning methods — •DMITRY CHERNYAVSKY — IFW Dresden, Germany

Additive manufacturing (AM) is a revolutionary manufacturing technique, providing design freedom and environmental advantages. Each newly AM processed material usually requires the identification of the optimal parameter set, a cost and time-consuming process, mostly conducted by trial and error. Here we discuss a machine learning approach for AM process parameter optimization on an example of a Zr-based alloy.

MM 23: Computational Materials Modelling: Magnetic & Electrical Properties

Time: Wednesday 15:45–18:30

Location: H44

MM 23.1 Wed 15:45 H44

Electronic structure of the non-centrosymmetric antiferromagnetic delafossite AgCrSe₂ — •SEO-JIN KIM¹, HAIJING ZHANG¹, MARCUS SCHMIDT¹, MICHAEL BAENITZ¹, GESA SIEMANN², CHIARA BIGI², PHIL D. C. KING², and HELGE ROSNER¹ — ¹Max Planck Institute for Chemical Physics of Solids, D-01187 Dresden, Germany — ²School of Physics and Astronomy, University of St. Andrews, St. Andrews KY16 9SS, United Kingdom

We present the theoretical studies of the electronic structure and the anomalous Hall effect in AgCrSe₂ based on density functional theory together with experimental results. AgCrSe₂ is a layered triangular lattice system that lacks inversion symmetry, and exhibits a ferromagnetic coupling in layer and an antiferromagnetic coupling between Cr adjacent layers. The comparison of the Cr partial DOS determined from the photoemission measurements and the magnetic LDA+U calculations with a value of $U = 0.75$ eV shows a good agreement, revealing that this compound is weakly correlated due to a strong hybridization with the ligands. The Se 4p states are dominating near the Fermi energy, resulting the sizeable band split of the order of 300 meV induced by the SOC. Our recent work demonstrates that this system shows an unconventional anomalous Hall effect driven by the Rashba-like spin-orbit coupling due to the non-centrosymmetric structure. The anomalous Hall conductivity was calculated based on the Berry curvature using an effective tight-binding model constructed by the Wannier function approach. The calculated σ_{xy} shows a good agreement to the experimental measurement.

MM 23.2 Wed 16:00 H44

Atomistic simulations of electrocaloric effects in ferroelectric-paraelectric superlattices — •DIANA ELISA MURILLO NAVARRO^{1,2}, HUGO IMANOL ARAMBERRI DEL VIGO¹, and JORGE ÍÑIGUEZ^{1,2} — ¹Materials Research and Technology Department, Luxembourg Institute of Science and Technology, Luxembourg — ²Department of Physics and Materials Science, University of Luxembourg

Electrocaloric effects (i.e., the temperature change caused by the application or

removal of an electric field) in ferroelectric materials could provide us with an alternative to current polluting cooling technologies. Ferroelectric/paraelectric superlattices, such as the PbTiO₃/SrTiO₃ system, usually present partly-disordered phases of high entropy (e.g., the so-called domain liquid state¹) whose polarization can be condensed (frozen) under the application of an electric field, potentially triggering a large change in temperature. Here we present our latest theoretical results on such electrocaloric effects obtained from second principles simulations².

Work funded by the Luxembourg National Research Fund through project C18/MS/12705883 *REFOX*.

1 P. Zubko et al., Nature 534, 524 (2016).

2 J.C. Wojdel et al., J. Phys.: Condens. Matt. 25, 305401 (2013).

MM 23.3 Wed 16:15 H44

Magnetically-textured superconductivity in elemental Rhenium — GABOR CSIRE¹, JAMES F ANNETT², •JORGE QUINTANILLA³, and BALAZS ÚJFALUSSY⁴ — ¹ICN2, Barcelona, Spain — ²University of Bristol, Bristol, United Kingdom — ³University of Kent, Canterbury, United Kingdom — ⁴Wigner Research Centre for Physics, Budapest, Hungary

Recent μ SR measurements revealed remarkable signatures of spontaneous magnetism coexisting with superconductivity in elemental rhenium. Here we provide a quantitative theory that uncovers the nature of the superconducting instability by incorporating every details of the electronic structure together with spin-orbit coupling and multi-orbital physics. We show that conventional s-wave superconductivity combined with strong spin-orbit coupling is inducing even-parity odd-orbital spin triplet Cooper pairs, and in presence of a screw axis Cooper pairs* migration between the induced equal-spin triplet component leads to an exotic magnetic state.

MM 23.4 Wed 16:30 H44

Magnetic bond-order potential for iron-cobalt alloys — •ALEKSEI EGOROV, APARNA SUBRAMANYAM, RALF DRAUTZ, and THOMAS HAMMERSCHMIDT — ICAMS, Ruhr-Universität Bochum, Bochum, Germany

We present a general-purpose analytic bond-order potential for large-scale simulations of magnetic FeCo alloys. The model is based on a d -valent orthogonal tight-binding Hamiltonian in two-center approximation and an embedding term to account for the s electrons. The BOP is a physical model and therefore requires only a comparably small set of reference data and only a small number of parameters to be optimized. It still provides good transferability to properties of FeCo that we did not include in the fit. We demonstrate the transferability of the FeCo BOP for defect formation energies, vibrational properties, and elastic constants. Due to the explicit treatment of magnetism, our BOP can reproduce the main features of the electronic structure of magnetic and nonmagnetic phases. The predictive power of the FeCo BOP yields a reasonable estimate of the order-disorder transition temperature of magnetic B2-FeCo. Our FeCo BOP also reproduces the dense sequence of stable structures for Fe-rich FeCo compounds.

MM 23.5 Wed 16:45 H44

Ab-initio High-Throughput Screening for Magnetic MAX Phases — •ALI MUHAMMAD MALIK, JOCHEN ROHRER, and KARSTEN ALBE — Materials Modelling, Technical University of Darmstadt, Germany

MAX phases are layered ternary transition metal carbides and nitrides that combine both metallic and ceramic properties such as high toughness and strength at elevated temperatures. So far about ~80 single-M containing MAX phases have been synthesised. But very few of these phases, have long-range magnetic order and are mostly based on Cr and/or Mn. It is expected that magnetically ordered MAX phases will be promising in spintronics and magnetocaloric applications. In this work, we systematically search for stable MAX phases with a focus on magnetic properties, by screening about 1200 potential compositions. The thermodynamic stability is based on relative formation enthalpy compared to known competing phases that are present in M-A-X ternary phase diagram obtained from online databases e.g. Materials Project. Based on the evaluation of relative formation enthalpy, we have predicted around ~170 new MAX phases that are potentially synthesizable. However, out of these predicted phases, only 2 in total, based on Cr or Mn, were found to have long-range magnetic order. Finally, it is concluded that the incorporation of a late-transition metal into the MAX structure by alloying or unconventional post-synthesis routes, is the way forward for achieving magnetic long-range order.

15 min. break

MM 23.6 Wed 17:15 H44

Energetic and electronic properties of CsK₂Sb surface facets: An *ab initio* study — •RICHARD SCHIER^{1,2}, HOLGER-DIETRICH SASSNICK², and CATERINA COCCHI^{2,1} — ¹Humboldt-Universität zu Berlin and IRIS Adlershof — ²Carl von Ossietzky Universität Oldenburg

For the efficient generation of ultra-bright electron beams, the microscopic understanding of the electronic structure of the photoemitting materials is crucial. Ternary alkali antimonides have been proposed as a promising class of photocathodes [1-4]. However, still little is known about their surface properties. We fill this gap with an *ab initio* study of the energetic and electronic properties of 7 CsK₂Sb surface facets of low Miller index. We investigate formation energies as a function of chemical potential to quantify the stability of these systems at varying concentration of the atomic species. We find that the (111)-surfaces terminated with K on top of Sb are generally the most stable, except for very high (low) concentrations of Cs (K). Calculated values for the work functions range from 2.33 eV for (100)-surfaces to 3.50 eV for (111)-surfaces terminated with a Sb layer. From the analysis of the band structures we find 4 out of 7 surfaces to be semiconducting. Metallic surfaces are formed upon an excess of metal atoms at the interface with vacuum.

[1] Schmeißer et al., PRAB 21, 113401 (2018). [2] Cocchi et al., JPCM 31, 014002 (2019). [3] Cocchi et al., Sci. Rep. 9, 18276 (2019). [4] Amador & Cocchi, JPCM 33, 365502 (2021).

MM 23.7 Wed 17:30 H44

Modeling Temperature-Dependent Electronic Structure of Semiconductors with a Dynamic Tight-Binding Approach — •MARTIN SCHWADE, MAXIMILIAN SCHILCHER, and DAVID EGGER — Department of Physics, Technical University of Munich, Garching, Germany

For theoretical calculations of large-scale system sizes or longer time-scale phenomena the computational costs of typical density functional theory can present a steep barrier, which needs to be tackled by development of alternative approaches. Here, we propose an extension of the tight-binding (TB) formalism

which allows for the calculation of macroscopic and temperature-dependent properties of semiconductors with little computational effort. In contrast to previous formulations, we fit TB parameters to first-principles energy eigenvalues using machine learning techniques. Furthermore, our TB approach employs hybrid orbital basis functions and addresses the problem of distance-dependent matrix elements by numerical integration of these orbitals. With this, we can maintain the average symmetry of the system as best as possible but still account for dynamic changes to that symmetry, e.g., by lattice distortions and other thermal effects. Our method is particularly helpful for getting an accurate solution of the electronic-structure problem for semiconductors at finite temperatures.

MM 23.8 Wed 17:45 H44

Coupled electronic and lattice degrees of freedom in excitonic insulator candidate Ta₂NiSe₅ and Ta₂NiS₅ — •BANHI CHATTERJEE, JERNEJ MRAVLJE, and DENIS GOLEŽ — Jozef Stefan Institute, Jamova 39, SI 1000, Ljubljana, Slovenia

The origin of phase-transition from a high temperature orthorhombic phase to a low temperature monoclinic phase in Ta₂NiSe₅ is debatable. There are two competing scenarios, namely, a structural instability with a B_{2g} zone center optical phonon and electronic order parameter of excitonic nature breaking the discrete set of lattice symmetries [1-3]. We defined a theoretical description which takes both scenarios on equal footings based on realistic modeling using DFT as a starting point and describe electronic and lattice correlation on a Hartree Fock level. We have identified both excitonic instability and the B_{2g} phonon mode in our calculations and investigate the effect of electron-phonon coupling. Within our methods we have further identified spectroscopic signatures showing the lack of excitonic ordering in the auxiliary compound Ta₂NiS₅ which is in agreement with the experimental ARPES observations [4].

[1] A. Subedi, Phys. Rev. Mater. 4, 083601 (2020). [2] L. Windgätter, M. Rösner, G. Mazza, H. Hübener, A. Georges, A. J. Millis, S. Latini, and A. Rubio, Angel,npj Comp. Mat 7, 14 (2021) [3] G. Mazza, M. Rösner, L. Windgätter, S. Latini, H. Hübener, A. J. Millis, A. Rubio, and A. Georges, Phys. Rev. Lett. 124, 197601 (2020) [4] K. Mu, H. Chen, Y. Li, Y. Zhang, P. Wang, B. Zhang, Y. Liu, G. Zhang, Li. Song, and Z. Sun, J.of Mat. Chem. C, 6, 3981 (2018)

MM 23.9 Wed 18:00 H44

Supermetal-insulator transition in a non-Hermitian network model — •HUI LIU¹, JHIIH-SHIH YOU², SHINSEI RYU³, and ION COSMA FULGA¹ — ¹IFW Dresden and Würzburg-Dresden Cluster of Excellence ct.qmat, Helmholtzstrasse 20, 01069 Dresden, Germany — ²Department of Physics, National Taiwan Normal University, Taipei 11677, Taiwan — ³Department of Physics, Princeton University, Princeton, New Jersey, 08540, USA

We study a non-Hermitian and non-unitary version of the two-dimensional Chalker-Coddington network model with balanced gain and loss. This model belongs to the class D^{\uparrow} with particle-hole symmetry† and hosts both the non-Hermitian skin effect as well as exceptional points. By calculating its two-terminal transmission, we find a novel contact effect induced by the skin effect, which results in a non-quantized transmission for chiral edge states. In addition, the model exhibits an insulator to "supermetal" transition, across which the transmission changes from exponentially decaying with system size to exponentially growing with system size. In the clean system, the critical point separating insulator from supermetal is characterized by a non-Hermitian Dirac point that produces a quantized critical transmission of 4, instead of the value of 1 expected in Hermitian systems. This change in critical transmission is a consequence of the balanced gain and loss. When adding disorder to the system, we find a critical exponent for the divergence of the localization length $\nu = 1$, which is the same as that characterizing the universality class of two-dimensional Hermitian systems in class D.

MM 23.10 Wed 18:15 H44

Dynamical mean-field theory on the high-temperature superconductivity for cerium hydrides under extreme pressure — •YAO WEI and CEDRIC WEBER — King's College London, London, UK

Hydrogen-rich superhydrides are promising high-T_csuperconductors, with superconductivity experimentally observed near room temperature, as shown in recently discovered lanthanide superhydrides at very high pressures, e.g. LaH₁₀ at 170 GPa and CeH₉ at 150 GPa. Superconductivity is believed to be closely related with the high vibrational modes of the bound hydrogen ions. Here we study the limit of extreme pressures (from 200 to 500 GPa or higher) where lanthanide hydrides with large hydrogen content have been observed. We focus on CeH₁₀, the prototype candidate for achieving a large electronic contribution from hydrogen in the electron-phonon coupling. In this work, we use a first-principles calculation platform with the inclusion of many-body corrections to evaluate the detailed physical properties of the Ce-H system and to understand the structure, stability and superconductivity of these systems at ultra-high pressure. We provide a DMFT approach to further investigate conventional superconductivity in hydrogen rich superhydrides.

MM 24: Non-equilibrium Phenomena in Materials Induced by Electrical and Magnetic Fields 4

Crystal structures

Time: Wednesday 15:45–18:30

Location: H45

Topical Talk

MM 24.1 Wed 15:45 H45

Electromigration effects on the atomic ordering process in hard magnetic $L1_0$ intermetallic phases — •DANIEL URBAN^{1,2} and CHRISTIAN ELSÄSSER^{1,2} — ¹Fraunhofer-Institut für Werkstoffmechanik IWM, Wöhlerstraße 11, 79108 Freiburg — ²Freiburger Materialforschungszentrum, Stefan-Meier-Straße 21, 79104 Freiburg

High-performance permanent magnets are needed for many applications in energy and information technology. The $L1_0$ phase of FeNi is a promising candidate for a sustainable material that is free of rare-earth elements. However, on earth FeNi can only be found in the disordered A1 crystal structure, although the layered $L1_0$ structure is lower in energy. By contrast, the latter was found in meteorites, proving the astronomical long timescales required for the dynamical ordering of the material.

We investigate the atomic migration processes in binary intermetallic $L1_0$ phases within the framework of density functional theory. Our main objectives are (i) to develop a thorough understanding of the possibilities to enhance the thermally activated diffusion processes at the atomic scale by electric fields and currents and (ii) an assessment in how far electromigration effects can be effective in processing hard magnetic materials. We extend the scope to the hard magnetic $L1_0$ phases of FePt, FePd, MnAl and MnGa as well as ternary Fe(Pt,Ni). These alloys cover a wide range of thermal ordering time scales and related experimental feasibilities.

MM 24.2 Wed 16:15 H45

Deriving Macroscopic Diffusivity from a Microscopic Master Equation Approach — •DANIEL PFALZGRAF^{1,2}, DANIEL URBAN^{1,2}, and CHRISTIAN ELSÄSSER^{1,2} — ¹Freiburg Materials Research Center (FMF), University of Freiburg, Stefan-Meier-Straße 21, 79104 Freiburg, Germany — ²Fraunhofer IWM, Wöhlerstraße 11, 79108 Freiburg, Germany

We present our generalisation of a model formalism that allows the derivation of macroscopic diffusion properties of a crystalline material from jump rates of individual atoms or ions. This work is based on a mathematical formalism modelling the uncorrelated motion of particles on a lattice by a Markov chain, from which a master equation in time and space is constructed. This approach is discussed, reformulated, and generalised to be applicable to any three-dimensional crystal system. Specifically, it is capable of describing the diffusion and drift of particles in a tilted potential landscape, as e.g. induced by electric fields. We sketch multiple use cases for systems involving point defects and grain boundaries and use the derived framework to discuss the diffusion of oxygen vacancies in strontium titanate.

MM 24.3 Wed 16:30 H45

Atomistic calculations of charged point defects at grain boundaries in $SrTiO_3$ — •CONG TAO¹, DANIEL MUTTER¹, DANIEL URBAN¹, and CHRISTIAN ELSÄSSER^{1,2} — ¹Fraunhofer IWM, Freiburg, Germany — ²University of Freiburg, FMF, Germany

Oxygen vacancies have been identified to play an important role in accelerating grain growth in polycrystalline perovskite-oxide ceramics. To advance the fundamental understanding of growth mechanisms at the atomic scale, we performed classical atomistic simulations to investigate the atomistic structures and oxygen vacancy formation energies at grain boundaries in the prototypical perovskite-oxide material $SrTiO_3$ [1]. We focus on two symmetric tilt grain boundaries, namely $\Sigma 5(310)[001]$ and $\Sigma 5(210)[001]$. Electrostatic potentials are present in supercells containing alternatingly charged lattice planes and grain boundaries. We derive analytic solutions for these potentials for both open and periodic boundary conditions and apply them to our atomistic model structures. In this way, simulation artifacts resulting from the interaction of the electrostatic potential with charged point defects can be corrected, leading to physically reasonable defect energies. We report calculated formation energies of oxygen vacancies on all possible sites across boundaries between the two misoriented grains, and we analyze the values with respect to local charge densities at the vacant sites. The developed calculation procedure can be transferred to more complicated interfaces such as asymmetric tilt grain boundaries [2].

[1] C. Tao, et. al., Phys. Rev. B 104, 054114 (2021).

[2] C. Tao, et. al., arxiv.org/abs/2110.02118.

MM 24.4 Wed 16:45 H45

Field assisted sintering of piezoelectric-bioactive scaffolds for bone tissue engineering — •ABDULLAH RIAZ¹, CHRISTIAN POLLEY¹, EBERHARD BURKEL², and HERMANN SEITZ¹ — ¹Chair of Microfluidics, Faculty of Mechanical Engineering and Marine Technology, University of Rostock, Rostock, Germany — ²Institute of Physics, University of Rostock, Rostock, Germany

The treatment of critical size bone defects is still a challenge. The external ma-

terial is often needed to support bone and guide tissue regeneration by physical stimulation. Promising effects of electrical stimulation on bone cell growth have led to an interest in using piezoelectric ceramics for tissue repair. Nevertheless, it is still concerning due to the toxicity of ceramics, which exhibit ion dissolution in biological fluids. In this study, nanostructured pure and doped calcium titanate is prepared by sol-gel synthesis and field assisted sintering. The piezoelectric behaviour is observed in calcium titanate, which is also a non-cytotoxic compound. This behaviour is referred to as pseudo-piezoelectricity since it is generated by the distorted structure which is formed during densification by field assisted sintering. Additionally, piezoelectric barium titanate-45S5 bioactive glass composites are combined with titanium alloy Ti6Al4V for the potential implantation of piezoelectric-bioactive scaffolds in load-bearing areas. For the engineering of these bulk scaffolds, electron beam melting is utilized for manufacturing metallic load-bearing lattice structures and combined with piezoelectric-bioactive composites for the joint processing via field assisted sintering.

15 min. break

MM 24.5 Wed 17:15 H45

Microstructure and hardness of self-passivating SMART alloys manufactured via field assisted sintering technology — •JIE CHEN¹, ANDREY LITNOVSKY¹, XIAOYUE TAN², and CHRISTIAN LINSMEIER¹ — ¹Forschungszentrum Jülich GmbH, IEK-4, 52425 Jülich, Germany — ²School of Materials Science and Engineering, Hefei University of Technology, 230009 Hefei, China

Self-passivating Metal Alloys with Reduced Thermo-oxidation (SMART) with a composition of W-11.4wt%Cr-0.6Y% is a promising candidate for plasma facing material of a future fusion power plant. In addition to sputtering resistance under plasma exposure, the laboratory-made bulk SMART system has exhibited excellent antioxidation performance at 1273K in humid environment relevant to accident conditions. The field assisted sintering technology is applied to manufacture SMART alloy. The microstructure of SMART alloy is intimately related to production parameters including heating ramp, sintering temperature, thermal holding time and applied pressure. Heating rate and appropriate sintering temperature are considered important to obtain ultrafine or nanosized grain. The machinability of sintered SMART alloy is under investigation in which hardness and thermal conductivity are of particular interest. The as-sintered SMART alloy with 1217 HV0.5 is obtained by heating at a rate of 200K/min to 1460°C and applying pressure of 50 MPa. There is an attempt to reduce the material's hardness to facilitate its application in fusion reactor. Details of the work are presented in the contribution.

Topical Talk

MM 24.6 Wed 17:30 H45

From Uncovering the Mechanisms of Flash Sintering to Realizing Ultrafast Sintering without Electric Fields and Discovering Electrochemically Driven Microstructural Evolution — •JIAN LUO — University of California San Diego, U.S.A.

This talk will first review our recent studies on understanding the scientific questions and technological opportunities of flash sintering [Scripta 146: 260 (2018); MRS Bulletin 46: 26 (2021)]. We originally proposed that flash sintering generally starts a thermal runaway [Acta 94:87 (2015)], but it can also be activated by bulk phase and grain boundary complexion transitions [Acta 181:544 (2019)]. We further proved that ultrafast densification is enabled by ultrahigh heating rates of ~100 K/s [Acta 125:465 (2017)]. Subsequently, a generic ultrafast high-temperature sintering was reported in a collaborative study [Science 368:521 (2020)]. Other related technologies include water-assisted flash sintering (WAFS) to flash ZnO at room temperature [Scripta 142:79 (2018)] and two-step flash sintering (TSFS) to densify ceramics with suppressed grain growth [Scripta 141:6 (2017)]. Recent research discovered electrochemically induced grain boundary transitions that can cause enhanced or abnormal grain growth [Nature Communications 12:2374 (2021)]. Subsequently, I will discuss a series of on-going studies to further investigate electrochemically controlled microstructural evolution and tailor the microstructural evolution with applied electric fields in various systems and schemes [Yan et al., unpublished work].

Topical Talk

MM 24.7 Wed 18:00 H45

Electric fields effects in ionic conductors during flash sintering and ion exchange — •MATTIA BIESUZ, GIAN DOMENICO SORARU, and VINCENZO MARIA SGLAVO — University of Trento, Trento, Italy

Electric fields can drive ceramic ionic conductors out of the equilibrium dictated by temperature, composition, and pressure. These phenomena can be used to promote ceramics sintering or ion exchange.

Herein, we explore flash sintering in oxygen ionic conductors (YSZ and GDC) evidencing the presence of some electrochemical effects producing alterations

of the defect chemistry and activating n-type electronic conductivity. This enhances the conductivity of the green sample, increases the electric power dissipation and contributes to the activation of the flash leading to sudden densification of ceramics. The pivotal role of electrochemical reduction during DC-flash sintering impacts the thermal history of the flashed samples generating strong thermal gradients between the cathode and anode which can be enhanced or removed by changing the quality and type of the used electrodes. The electro-

chemical description of flash sintering in oxygen ion conductors well explains the electrode configuration and atmosphere effects on the flash processes.

Electrochemical phenomena are, however, pivotal also in other ionic conductor systems subjected to flash-like processes. It is shown that the electrode material choice strongly affects the flash behavior and modifies the glass composition in the vicinity of electrodes. Hence, electric fields can be to modify the surface glass or ceramics composition improving mechanical and functional properties.

MM 25: Data Driven Materials Science: Computational Frameworks / Chemical Complexity

Time: Wednesday 15:45–18:30

Location: H46

Topical Talk

MM 25.1 Wed 15:45 H46

Automated atomistic calculation of thermodynamic and thermophysical data — •JAN JANSSEN^{1,2}, TILMANN HICKEL^{1,3}, and JÖRG NEUGEBAUER¹ — ¹Max-Planck-Institut für Eisenforschung, Düsseldorf, Germany — ²Los Alamos National Laboratory, Los Alamos, USA — ³Bundesanstalt für Materialforschung und -prüfung (BAM), Berlin, Germany

A major challenge in predicting the properties of materials at realistic conditions is the accurate inclusion of finite temperature effects. Doing this on an ab initio level often requires complex simulation protocols. These complex protocols, which often couple several specialized codes, make a quantitative description of error propagation and uncertainty quantification a critical issue.

To handle this high level of complexity we have developed an integrated development environment (IDE) called pyiron - <http://pyiron.org>. pyiron has been specifically designed to scale simulation protocols from the interactive prototyping level up to the high throughput level, all within the same software framework.

We highlight two recent success stories towards automated calculation of phase diagrams: We first discuss with the automated convergence for all key parameters in DFT codes, followed by the calculation of melting points with a guaranteed precision of better than 1K. These fully automated high-precision tools allow us to study trends over the periodic table in an efficient and systematic way. Examples how such high-throughput screenings allow to develop new strategies in designing materials will be given.

MM 25.2 Wed 16:15 H46

Efficient parameterization of the atomic cluster expansion — •ANTON BOCHKAREV, YURY LYSOGORSKIY, MATOUS MROVEC, and RALF DRAUTZ — Atomistic Modelling and Simulation, ICAMS, Ruhr-Universität Bochum, D-44801 Bochum, Germany

The atomic cluster expansion (ACE) is a machine learning model with a complete basis set representation that can be used for constructing interatomic potentials. These potentials can be both, general-purpose as well as potentials designed for a specific application. The former are usually more reliable and accurately describe materials in various conditions, but building such models often requires a materials specific expertise and extensive training datasets. Purpose-specific potentials have only limited ranges of applicability, but are also less demanding in terms of training data. Here we demonstrate a complete, efficient and largely automated framework for constructing quantum accurate ACE models for various applications. Our framework includes automated data generation, model parameterization and validation. Efficient implementations on CPU and GPU hardware enable large scale simulations.

MM 25.3 Wed 16:30 H46

Atomic cluster expansion for Mg: From defects to phase diagrams — •ESLAM IBRAHIM, YURY LYSOGORSKIY, MATOUS MROVEC, and RALF DRAUTZ — ICAMS, Ruhr Universität Bochum, 44780 Bochum, Germany

In this work, we developed a general-purpose parametrization of the atomic cluster expansion (ACE) for Mg. The model shows an outstanding transferability over a broad range of atomic environments and is able to capture physical properties of bulk as well as defective Mg phases in excellent agreement with reference first-principles calculations. We demonstrate the computational efficiency and the predictive power of ACE by calculating the phase diagram covering temperatures up to 3000 K and pressures up to 80 GPa using state-of-the-art thermodynamic integration techniques implemented in the CALPHY software package. The ACE predictions are compared with those of common interatomic potentials, such as the embedded atom method or the angular-dependent potential, as well as a recently developed neural network potential. The comparison reveals that ACE is the only model that is able to predict both qualitatively and quantitatively correctly the phase diagram in close experiment with experimental observations.

MM 25.4 Wed 16:45 H46

Learning design rules for selective oxidation catalysts from high-throughput experimentation and artificial intelligence — •LUCAS FOPPA¹, CHRISTOPHER SUTTON¹, LUCA M. GHIRINGHELLI¹, SANDIP DE², PATRICIA LÖSER³, STEPHAN SCHUNK^{2,3}, ANSGAR SCHÄFER², and MATTHIAS SCHEFFLER¹ — ¹The NOMAD Laboratory at the Fritz Haber Institute of the Max Planck Society, Germany — ²BASF SE, Germany — ³hte GmbH, Germany

The design of heterogeneous catalysts is challenged by the complexity of materials and processes that govern reactivity and by the very small number of good catalysts. Here, we show how the subgroup-discovery (SGD) artificial-intelligence *local* approach[1] can be applied to an experimental plus theoretical data set to identify constraints or *rules* on key physicochemical parameters that exclusively describe materials and reaction conditions with outstanding catalytic performance.[2] By using high-throughput experimentation, 120 SiO₂-supported catalysts containing Ru, W and P were synthesized and tested in propylene oxidation. As candidate descriptive parameters, the temperature and ten calculated parameters related to the composition and chemical nature of elements in the catalyst materials, were offered. The temperature, the P content, and the composition-weighted electronegativity are identified as key parameters describing high yields of value-added oxygenate products. The SG rules reflect the underlying processes associated to high performance, and guide catalyst design.

[1] B.R. Goldsmith, *et al.*, *New. J. Phys.* **19**, 013031 (2017).

[2] L. Foppa, *et al.*, *ACS Catal.* **12**, 2223 (2022).

15 min. break

Topical Talk

MM 25.5 Wed 17:15 H46

Understanding Dislocation Flow and Avalanches in High Entropy Alloys by Machine Learning-based Data Mining of In-Situ TEM Experiments — •STEFAN SANDFELD — FZJ/IAS-9, 52068 Aachen, Dennewartstr. 25-27

This talk will give an overview over recent developments in the field of material informatics and materials data science, in particular over current, state-of-the-art machine learning and data-mining techniques in the context of TEM experiments.

As a main example, the goal is to understand some of the many open questions concerning the underlying structure-property relations in High Entropy Alloys (HEAs). Although in-situ Transmission Electron Microscopy (TEM) allows high-resolution studies of the structure and dynamics of moving dislocations and – in a way – makes the local obstacle/energy "landscape" visible through the geometry of dislocations; a 3D analysis and high-throughput data-mining of the resulting data is still not possible.

We introduce a novel data-mining approach that is based on spatio-temporal coarse graining of TEM dislocation data, making ensemble averaging of a large number of snapshots in time possible. Using dislocations as "probes" we investigate the effect of pinning points on the dislocation glide behavior of CoCr-FeMnNi alloy during in-situ TEM straining. Additionally, we use our Deep Learning-based dislocation extraction and 3D reconstruction to analyze the strain avalanche statistics of in-situ TEM recordings and discuss the dependency of the power law exponent based on 3D dislocation dynamics simulations.

MM 25.6 Wed 17:45 H46

Phase stability and short range order in CrCoNi medium entropy alloy — •SHEULY GHOSH¹, VADIM SOTSKOV², ALEXANDER SHAPEEV², FRITZ KOERMANN^{1,3}, and JOERG NEUGEBAUER¹ — ¹Max-Planck-Institut für Eisenforschung GmbH — ²Skolkovo Institute of Science and Technology — ³Delft University of Technology

One of the key components in the design and exploration of multicomponent alloys is the knowledge about its phase stability. The solid solution of multicomponent alloys are often assumed to be ideally random. However, short-range order, which is challenging to quantify by experiments, is known to affect the mechanical properties of alloys. An important issue to address is therefore to quantify the degree of local chemical ordering as function of temperature and its chemical nature.

In the present work, we have investigated short-range order (SRO) and its impact on phase stability in CrCoNi medium entropy alloy. This alloy is known

for its cryogenic damage tolerance and general mechanical superiority. For this purpose, we have employed a recently proposed computationally efficient on-lattice machine-learning interatomic potential called low-rank potentials. These potentials are capable of accurately representing interactions in a system with many chemical components which is used in subsequent Monte Carlo simulations. The potentials are trained on DFT supercell calculations and thus allow to systematically include the impact of local lattice distortions. The computed short-range order parameters and observed ordering are discussed in view of recent simulation and experimental works.

MM 25.7 Wed 18:00 H46

Inverse Design of Multicomponent Crystalline Materials — TENG LONG^{1,2} and HONGBIN ZHANG¹ — ¹Institute of Materials Science, Technical University of Darmstadt, Darmstadt 64287, Germany — ²School of Materials Science and Engineering, Shandong University, Jinan 250061, China

Autonomous materials discovery with desired properties is one of the ultimate goals of materials science. In this work, we implement and apply constrained crystal deep convolutional generative adversarial networks to design unreported (meta-)stable crystal structures. The essential continuous latent space is obtained based on the voxel construction of crystal structures, resulting in an image-based latent space which is proven to be a robust descriptor for forward inference of various physical properties. This also allows prediction of new crystal structures based on generative adversarial network. Furthermore, taking the formation energy as an example, it is demonstrated how the physical properties can be optimized automatically in the latent space while exploring a big chemical space to

predict novel phases. Such an approach has been successfully applied on binary (e.g., Bi-Se) and multicomponent systems, which paves the way to achieve the inverse design of crystalline materials via multi-objective optimization.

MM 25.8 Wed 18:15 H46

Databases for Machine Learning of Grain Boundary Segregation — ALEXANDER REICHMANN¹, CHRISTOPH DÖSINGER¹, DANIEL SCHEIBER², OLEG PEIL², VSEVOLOD RAZUMOVSKIY², and LORENZ ROMANER¹ — ¹Department of Materials Science, Leoben, Austria — ²Materials Center Leoben Forschung GmbH, Leoben, Austria

The chemical and structural state of grain boundaries (GBs) is of great importance for the design and performance of many technologically relevant materials. On the basis of atomistic simulations, the relevant quantities of GB, in particular the segregation energy has been calculated for many materials. On the experimental side, the concentration of solute elements at the GBs can be measured with a variety of techniques including in particular Auger spectroscopy or Atom Probe Tomography. When comparing calculated segregation energies with segregation energy gained from experimental excess data, good agreement is not always observed. In this talk we will present our current and planned activities regarding creation of segregation databases and application of data driven models. One of these is the Bayesian inference framework, which we used in combination with Markov chain Monte Carlo simulations for uncertainty quantification and model evaluation. These activities shall lead to a better understanding of the deviation between DFT-calculated and experimentally determined GB excess.

MM 26: Members' Assembly

Time: Wednesday 18:45–20:15

Location: H44

All members of the Metal and Material Physics Division are invited to participate.

MM 27: Invited Talk Christian Greiner

Time: Thursday 9:30–10:00

Location: H44

Invited Talk

MM 27.1 Thu 9:30 H44

Crystal rotation kinematics during the tribological loading of high-purity copper — CHRISTIAN GREINER — Karlsruher Institut für Technologie (KIT), Kaiserstrasse 12, 76131 Karlsruhe

Friction, wear and the associated energy dissipation are major challenges from nanoelectromechanical systems, over hip implants to offshore wind turbines. Already in 1950, Bowden and Tabor pointed out that in metallic tribological contacts the majority of the dissipated energy is spent to change the contacting materials' microstructures. This - in part - explains why most metals show a highly dynamic subsurface microstructure under the shear load imposed by a sliding contact. In order to understand these processes, the elementary mechanisms accommodating the shear strain and acting in the material need to be revealed

and understood. One key process involved therein is the reorientation of the crystal lattice, or crystal rotation, due to the shear load imposed by the sliding contact. Our work sheds light on the early stage, fundamental mechanisms of tribologically induced lattice rotation kinematics. Using a high-purity copper bicrystal and a sapphire sphere, unlubricated, single-pass sliding tests were conducted. Electron backscatter diffraction (EBSD) performed directly on the wear track reveals a crystal rotation process around the transverse direction at the heart of tribologically induced lattice rotation, irrespective of sliding direction, grain orientation and normal load. A detailed analysis corroborates that surprisingly, changing the sliding direction merely alters the precise accommodation of crystal rotations, but not their fundamental nature.

MM 28: Transport in Materials: Diffusion / Electrical Transport & Magnetism

Time: Thursday 10:15–11:30

Location: H44

MM 28.1 Thu 10:15 H44

Electrical resistivity of magnetron-sputtered Fe_{1-x}O thin films — SIMON EVERTZ¹, NINA NICOLIN¹, DANIEL PRIMETZHOFFER², JAMES P. BEST¹, and GERHARD DEHM¹ — ¹Max-Planck-Institut für Eisenforschung GmbH, Max-Planck-Str. 1, 40237 Düsseldorf, Germany — ²Department of Physics and Astronomy, Uppsala University, S-75120 Uppsala, Sweden

Fe_{1-x}O (wüstite) is a critical phase for a number of applications in the future hydrogen economy, such as photochemical materials for H₂ production by water-splitting. Hence, charge transport is crucial for the applicability of Fe_{1-x}O in electrode materials. To probe the charge transport of close-to-stoichiometric Fe_{1-x}O, thin films were synthesized by reactive magnetron sputtering with systematically varied O₂ gas flow. The phase formation and chemical composition was correlated to the electrical resistivity and mechanical properties, as measured in a van-der-Pauw-setup and nanoindentation, respectively. The charge transport mechanism is shown to change from thermally activated hopping of charge carriers - typical for a semiconductor - to metallic-like behavior as a function of the phase purity of the films. By correlative analysis of phase purity, microstructure and mechanical properties, it is shown that already small amounts of Fe as impurity phase are decisive for changing the charge transport mechanism. These significant changes in charge transport are further compared to the hardness and Young's modulus of these films.

MM 28.2 Thu 10:30 H44

Electronic structure and transport properties of NdTe₃ — KIRSTINE J DALGAARD¹, SHIMING LEI¹, CLAUDIUS MÜLLER², STEFFEN WIEDMANN², MARTIN BREMHOLM³, and LESLIE M SCHOOP¹ — ¹Department of Chemistry, Princeton University, Princeton, NJ, USA — ²High Field Magnet Laboratory (HFML-EMFL), Radboud University, Nijmegen, Netherlands — ³Department of Chemistry, Aarhus University, Aarhus, Denmark

The delocalized, hypervalent bonding in some main group element square-net materials have been linked to fascinating phenomena, including band inversions with high charge carrier mobility, and topologically nontrivial band structures. The family of rare earth tritellurides crystalize in a van der Waals structure with double tellurium square-nets, where the tellurium p orbitals form the Fermi energy crossing bands, and the partly filled 4f orbitals give rise to a rich spectrum of magnetic properties. The tellurium square-nets also undergo incommensurate charge density wave transitions affecting the band structure in ways that are yet to be fully understood. In this work, we studied the electronic structure of neodymium tritelluride through quantum oscillation and transport measurements. A remarkably high electron mobility for a magnetic van der Waals material was found, suggesting steeply dispersed bands, along with thus far unreported deviations from conventional Lifshitz-Kosevich behavior.

MM 28.3 Thu 10:45 H44

Non-coplanar magnetism, topological density wave order and emergent symmetry at half-integer filling of moiré Chern bands — •PATRICK WILHELM¹, THOMAS LANG¹, MATHIAS SCHEURER¹, and ANDREAS LÄUCHLI^{1,2,3} — ¹Institut für Theoretische Physik, Universität Innsbruck, 6020 Innsbruck, Austria — ²Laboratory for Theoretical and Computational Physics, Paul Scherrer Institute, 5232 Villigen, Switzerland — ³Institute of Physics, École Polytechnique Fédérale de Lausanne (EPFL), 1015 Lausanne, Switzerland

We study the impact of Coulomb interactions at half-integer filling of the moiré Chern bands of twisted double-bilayer graphene and twisted mono-bilayer graphene, using unbiased exact diagonalization complemented by unrestricted Hartree-Fock calculations. For small intra-sublattice tunneling, w_{AA} , a non-coplanar magnetic state is found which has the same symmetries as the tetrahedral antiferromagnet of the triangular moiré lattice and can be thought of as a skyrmion lattice commensurate with the moiré scale. The antiferromagnetic order competes with a set of ferromagnetic, topological charge density waves, which are favored for larger w_{AA} and are associated with an approximate emergent $O(3)$ symmetry, 'rotating' the different charge density wave states into each other. Exhibiting a finite charge gap and Chern number $C=|1|$, the formation of charge density wave order which is intimately connected to a skyrmion lattice phase is consistent with recent experiments on these systems.

MM 28.4 Thu 11:00 H44

Interference effects in one-dimensional moiré crystals — •NILS WITTEMEIER¹, MATTHIEU J. VERSTRAETE^{2,4}, PABLO ORDEJÓN¹, and ZEILA ZANOLLI^{3,4} — ¹Catalan Institute of Nanoscience and Nanotechnology, ICN2 (CSIC, BIST), Bellaterra, Spain — ²NanoMat/Q-Mat/CESAM, Université de Liège (B5), Liège, Belgium — ³Chemistry Department & Debye Institute for Nanomaterials Science, Utrecht University, Utrecht, the Netherlands — ⁴ETSF

This work [1] investigates interference effects in finite sections of 1D moiré crystals using the Landauer-Büttiker formalism within the tight-binding approximation. We explain interlayer transport in double-wall carbon nanotubes and demonstrate that wave function interference is visible at the mesoscale: in the strong coupling regime, as a periodic modulation of quantum conductance and

emergent localized states; in the localized-insulating regime, as a suppression of interlayer transport, and oscillations of the density of states. The interlayer transmission between strongly coupled metallic nanotubes is limited to either $1G_0$ or $2G_0$. Our results could be exploited to design quantum electronic devices, e.g. nonelectric switches based on chiral nanotubes. Most importantly, we clarify the origin of the so-far unexplained $1G_0$ quantum conductance measured in multi-wall carbon nanotubes [2, 3].

[1] N. Wittemeier *et al.* Carbon **186**, 416 (2022)[2] S. Frank *et al.* Science **280** (1998)[3] W. A. de Heer & C. Berger, Phys. Rev. Lett. **93**, 259701 (2004)

MM 28.5 Thu 11:15 H44

On correlations between local chemistry, distortions and kinetics in high entropy nitrides: an ab initio study — •DAVID HOLEC¹, GANESH K. NAYAK¹, ANDREAS KRETSCHMER², PAUL H. MAYRHOFER², MARCUS HANS³, and JOCHEN M. SCHNEIDER³ — ¹Department of Materials Science, Montanuniversität Leoben, Leoben, Austria — ²Institute of Materials Science and Technology, TU Wien, Vienna, Austria — ³Materials Chemistry, RWTH Aachen University, Aachen, Germany

High entropy alloys (HEAs) have triggered significant scientific interest due to their unusual structural stability combined with excellent mechanical and other functional properties. Recently, exploration of materials used as protective coatings has also entered this room by exploring high entropy borides, oxides, carbides, and nitrides. These chemically complex systems provide huge combinatorial space for tuning the composition, hence making the experimental exploration tedious. High-throughput simulations based on unbiased ab initio calculations provide an ideal tool to guide the experiments.

We will show that for high entropy nitrides (HENs), strain is equally important for the stabilization as entropy. Our predictions were validated by experimental investigations on the thermal stability of selected HEN coatings. The predicted structures are further characterized in terms of their local distortions, one of the core effects of HEAs. Another core effect is sluggish bulk diffusion. Therefore, in the second part of the talk, we will explore correlations between migration barriers for bulk diffusion, local chemical compositions, and local distortions.

MM 29: Data Driven Materials Science: Design of Functional Materials

Time: Thursday 10:15–11:30

Location: H45

MM 29.1 Thu 10:15 H45

Investigations of the Polysulfide Conversion Mechanism via Gaussian Approximation Potentials — •XU HAN^{1,2}, CARSTEN G. STAACKE¹, HENDRIK H. HEENEN¹, XUEFEI XU², and KARSTEN REUTER¹ — ¹Fritz-Haber-Institut der MPG, Berlin, Germany — ²Tsinghua University, Beijing, China

Lithium-sulfur (Li-S) batteries have been regarded as promising energy storage systems with ultra-high theoretical energy density. During a charging cycle Li_2S is converted to S_8 and vice-versa, where intermediate Li polysulfides (LiPS) are formed in a complex reaction mechanism which is still under debate. The theoretical exploration of the involved Li-S chemistry is challenged by an extended reaction network making it intractable for first principles methods. In contrast, machine learning interatomic potentials (MLIPs) which potentially retain predictive accuracy at a fraction of the computational cost are ideally suited for this task.

Here, we establish a training protocol for a Gaussian approximation potential (GAP) to simulate the chemistry of LiPS. Our training is based on a constrained on-the-fly exploration of the LiPS chemical space. In that, we enumerate the connectivity of (poly)cyclic LiPS and explore their stability via global optimization procedures with iteratively refined MLIPs. We use the final, sufficiently accurate MLIP to sample the LiPS phase space and to compute charging/discharging curves which we can directly compare to experimental data. Our MLIP calculations are expected to provide more fundamental insights into the LiPS conversion mechanism in Li-S batteries.

MM 29.2 Thu 10:30 H45

Accelerating the High-Throughput Search for new Thermal Insulators with Symbolic Regression — •THOMAS PURCELL¹, MATHIAS SCHEFFLER^{1,2}, LUCA M. GHIRINGHELLI^{1,2}, and CHRISTIAN CARBOGNO¹ — ¹The NOMAD Laboratory at Fritz-Haber-Institut der Max-Planck-Gesellschaft — ²FAIRmat at Humboldt Universität zu Berlin, Berlin, Germany

Reliable artificial-intelligence models are key to accelerate the discovery of new functional materials for various applications. Here, we present a general, data-driven framework that combines symbolic regression with sensitivity analysis to create hierarchical workflows. We illustrate the power of this new framework by screening for new thermally insulating materials. We first use the sure-independence screening and sparsifying operator (SISSO) [1] to build an analytical model that describes the thermal conductivity of a material and then extract out the most important input properties using a variance-based sensitivity anal-

ysis [2]. Using the information gained from the analysis we screen over a set of 732 materials and find the region of space most likely to contain strong thermal insulators. Finally we confirm these predictions by calculating thermal conductivities using the *ab initio* Green-Kubo technique [3].

[1] R. Ouyang, *et al.* Phys. Rev. Mat. **2**, 083802 (2018)[2] S. Kucherenko, S. Tarantola, and P. Annoni. Comput. Phys. Commun. **183**, 937 (2012)[3] C. Carbogno, R. Ramprasad, and M. Scheffler. Phys. Rev. Lett. **118**, 175901 (2017)

MM 29.3 Thu 10:45 H45

Uncertainty Modelling for Property Prediction of Double Perovskites — •SIMON TESHUVA¹, MARIO BOLEY¹, FELIX LUONG¹, LUCAS POPPA², and MATTHIAS SCHEFFLER² — ¹Monash University, Melbourne, Australia — ²Fritz Haber Institute, Berlin, Germany

Statistical predictive models for double perovskite properties are of high interest, because the perovskite structure allows relatively accurate property prediction and at the same time provides enough flexibility to yield a huge number of different materials of which some are likely relevant for important applications. Existing results published for this class of materials typically refer only to the predictive performance as, e.g., measured by the root mean squared error. However, active learning strategies for effective materials screening also rely on adequate uncertainty estimates as provided by probabilistic models.

Here, we study the predictive performance of two popular machine learning models, Gaussian processes and random forests, together with the quality of their uncertainty estimates. This study is based on a dataset of over 800 single (ABO₃) and double (A₂B'B''O₆) cubic perovskite oxides with computed bulk modulus, cohesive energy, and bandgap. We show that Gaussian processes, while providing sound Bayesian uncertainty estimates, can have inferior performance when their assumption of isometric smoothness of the target property is not met. In this case, as exemplified by the double perovskite bandgaps, random forests provide a better alternative, despite their rather ad-hoc uncertainty estimates. Improving these estimates thus appears to be a promising direction for future research.

MM 29.4 Thu 11:00 H45

Automated effective Hamiltonian construction and active sampling of potential energy surface by Bayesian optimization — •MIAN DAI, YIXUAN ZHANG, and HONGBIN ZHANG — Institute of Materials Science, Technical University of Darmstadt, Darmstadt, 64287, Germany

A first-principles effective Hamiltonian method can be used to simulate the phase transition sequences. In practice it is quite tedious to express the total energy surfaces and estimate reasonable parameters for high-order polynomials. We implemented Bayesian optimization (BO) to sample the total energy surfaces based on active learning and fit the set of parameters for constructing the effective Hamiltonians. Taking BaTiO_3 as a case study, we found that less than 30 sampling configurations with automated generated structures by BO are enough to determine a new set of parameters. The hyperparameter in our BO process is tuned to show the improvement of the convergence for all fitted parameters. Using the new set of parameters, we perform Monte Carlo simulations which produce comparable phase transition temperatures with experimental values and previous results. Our BO algorithm has a great potential for future application in construction the effective Hamiltonians with more complicated subspace and effective atomic potentials describing the full lattice dynamics.

MM 29.5 Thu 11:15 H45

Predicting oxidation and spin states by high-dimensional neural networks — •KNUT NIKOLAS LAUSCH¹, MARCO ECKHOFF¹, PETER BLÖCHL², and JÖRG BEHLER¹ — ¹Georg-August-Universität Göttingen, Institut für Physikalische Chemie, Theoretische Chemie, Göttingen, Germany — ²Technische Universität Clausthal, Institut für Theoretische Physik, Clausthal-Zellerfeld, Germany

Machine learning potentials (MLP) such as high-dimensional neural network potentials (HDNNP) provide first-principles quality energies and forces enabling large-scale molecular dynamics simulations at low computational costs. However, most current MLPs do not provide any information about the electronic structure of the system, which is often important for a detailed understanding of complex systems such as transition metal oxides. The lithium intercalation compound $\text{Li}_x\text{Mn}_2\text{O}_4$ ($0 \leq x \leq 2$), a commercially used cathode material in lithium ion batteries, is such a system since the manganese ions adopt different oxidation states based on the lithium content and distribution. Here, we propose a high-dimensional neural network (HDNN) that can predict atomic oxidation and spin states as a function of the local atomic environments in $\text{Li}_x\text{Mn}_2\text{O}_4$. The HDNN can complement HDNNP-driven MD simulations giving insights into the underlying electronic processes that give rise to complex phenomena such as a charge ordering transition, and electrical conductance.

MM 30: Liquid and Amorphous Metals

Time: Thursday 10:15–13:00

Location: H46

MM 30.1 Thu 10:15 H46

Controlling the degree of rejuvenation and strain-hardening in metallic glasses — •DANIEL ŞOPU^{1,2}, XUDONG YUAN¹, and JÜRGEN ECKERT^{1,3} — ¹Erich Schmid Institute of Materials Science, Leoben, Austria — ²Technische Universität Darmstadt, Germany — ³Montanuniversität Leoben, Austria

The correlation between the degree of rejuvenation and strain-hardening in metallic glasses (MGs) is investigated using molecular dynamics simulations. By randomly removing atoms from the glass matrix, free volume is homogeneously generated and glassy states with different degrees of rejuvenation are designed and further mechanically tested. The highest rejuvenated state is defined by the dynamic balance between free volume generation and annihilation. The highest degree of rejuvenation correlates to the flow strain of the materials and the structure is similar to that found in shear bands. The free volume in the rejuvenated glasses can be annihilated under tensile or compressive deformation that consequently leads to structural relaxation and strain-hardening. Loading-unloading cycling tensile tests are simulated and the atomic-scale mechanism of strain-hardening in the highly rejuvenated MGs is highlighted.

MM 30.2 Thu 10:30 H46

Revealing the impact of Sulfur addition on the medium-range order and relaxation dynamics of metallic glasses — •HENDRIK VOIGT¹, NICO NEUBER², HARALD RÖSNER¹, MARTIN PETERLECHNER¹, RALF BUSCH², and GERHARD WILDE¹ — ¹Institut für Materialphysik, Westfälische Wilhelms-Universität Münster, Münster, Germany — ²Chair of Metallic Materials, Saarland University, Saarbrücken, Germany

The addition of Sulfur as an alloying element has been shown to enable or improve the glass forming ability of certain glasses drastically [1]. Despite growing knowledge of the impact that Sulfur has on the mechanical properties, the underlying structure and its dynamics are still not fully understood [2].

In this contribution the sample system $\text{Pd}_{31}\text{Ni}_{42}\text{S}_{27}$ has been investigated with respect to medium-range order (MRO). For the MRO analysis multiple series of nanobeam diffraction patterns with varying probe sizes were acquired in order to conduct variable resolution Fluctuation Electron Microscopy (FEM). Furthermore, Electron Correlation Microscopy (ECM) was employed to analyse relaxation dynamics by the acquisition of a tilted dark-field time series. By the combination of these two techniques it appears that the size of the regions displaying strongly decelerated dynamics at room temperature correlate with the detected MRO. The results are discussed with respect to current models.

[1] A. Kuball et al., Scripta Materialia (2018) 73-76 [2] H. Jiang et al., Scripta Materialia (2021) 116923

MM 30.3 Thu 10:45 H46

Glass Formation and Shear Banding in High-Entropy Metallic Glasses: A Molecular Dynamics Study — •MARIE J. CHARRIER, DANIEL T. UTT, ARNE J. KLÖMP, and KARSTEN ALBE — Fachgebiet Materialmodellierung, Institut fuer Materialwissenschaft, Technische Universität Darmstadt

Bulk metallic glasses (BMGs) and High-Entropy Alloys (HEAs) both comprise a large number of elements but deviate strongly in their mechanical properties. BMGs are strong but brittle and usually derived from crystalline binary subsystems with deep eutectics and intermetallic phases. HEAs, on the other hand, show remarkable ductility, a small heat of mixing, and are thus typically not glass formers. The open question is whether a classically crystalline random solid solution HEA can be transformed into a BMG using appropriate processing. In this work, we use atomistic computer simulations to study the combination of the two materials classes, HE-MGs. Here, we are able to kinetically suppress crystallization in the CrMnFeCoNi alloy, which in the real world remains a crystalline single-phase solid solution using conventional quench rates. First, we investigate the thermodynamics of the glass transition and its dependence on quench rate. Second, the phase stability of the HE-MG is compared to the crystalline HEA. Third, the atomic-level structure is characterized in terms of chemical and structural short- and medium-range order. Last, we perform compressive and tensile testing on HE-MG samples to assess failure by homogeneous deformation or shear localization and compare the mechanical properties against a CoCrFeMnNi nanocrystal.

MM 30.4 Thu 11:00 H46

Cyclical structural relaxation of PdNiP and micro-alloyed PdNiPFe and PdNiPCo glasses — •MANOEL W. DA SILVA PINTO, MARK STRINGE, KATHARINA SPANGENBERG, HARALD RÖSNER, and GERHARD WILDE — Institut für Materialphysik, WWU Münster

Relaxation phenomena in $\text{Pd}_{40}\text{Ni}_{40}\text{P}_{20}$ bulk metallic glasses (BMG) as well as in micro-alloyed forms of Co and Fe addition were investigated by calorimetry. The BMGs were submitted to different thermal treatments by varying temperatures and times. In order to identify distinct signatures of relaxation, the thermal and temporal evolution of enthalpic contributions to calorimetric signals were analyzed using different kinetic models. A possibility was found to control the formation and depletion of an endothermic signature before the glass transition by quenching and annealing procedures. From the evolution of the enthalpies with annealing time and from isothermal heat flow, time constants related to structural relaxation were obtained and supplemented by dynamical and structural TEM analyses. The obtained results are discussed with respect to existing models for glass relaxation.

MM 30.5 Thu 11:15 H46

Enhancing ductility and strain hardening by modulating residual stresses in metallic glasses — •XUDONG YUAN¹, DANIEL ŞOPU^{1,2}, and JÜRGEN ECKERT^{1,3} — ¹Erich Schmid Institute of Materials Science, Leoben, Austria — ²Technische Universität Darmstadt, Darmstadt, Germany — ³Montanuniversität Leoben, Leoben, Austria

The correlation between the deformation behavior and the residual stress modulation in metallic glasses (MGs) is investigated using molecular dynamics simulations. Particularly, the influence of residual compressive stress and stress

heterogeneity on the tensile deformation behavior of amorphous Cu₆₄Zr₃₆ alloys is investigated. Strain hardening together with enhanced tensile ductility in monolithic MGs can be attained by only modulating the internal stress without changing their local structure. The stress heterogeneity changes the shear band dynamics leading to the formation and interaction of multiple shear bands, which consequently enhances the macroscopic ductility. Additionally, the residual compressive stress offsets the external tensile stress, which delays shear band formation and enables strain hardening in uniaxial tensile tests.

15 min. break

MM 30.6 Thu 11:45 H46

Origin of the Invar effect in Fe-based bulk metallic glasses — •ALEXANDER FIRLUS¹, MIHAI STOICA¹, STEFAN MICHALIK², ROBIN E SCHÄUBLIN¹, and JÖRG F LÖFFLER¹ — ¹Laboratory of Metal Physics and Technology, Department of Materials, ETH Zurich, 8093 Zurich, Switzerland. ² — ²Diamond Light Source Ltd., Harwell Science and Innovation Campus, Didcot, Oxfordshire OX11 0DE, UK

Generally, metals, including most ferromagnetic ones, have a constant coefficient of thermal expansion (CTE). However, a few magnetic alloys show an anomalously low CTE below their Curie temperature. At the Curie temperature it increases abruptly by up to one order of magnitude. This effect is known as the Invar effect. While it is rare in crystalline alloys, it is universally observed in ferromagnetic Fe-based bulk metallic glasses (BMGs). To this day, it is still unclear in which way the amorphous atomic arrangement creates the Invar effect and how it manifests at the atomic scale.

In this work we studied BMGs with only one magnetic atom species, Fe, by in-situ high-energy X-ray diffraction. This allows us to measure the thermal expansion at the atomic scale and to associate it with specific atomic pairs. Fe-Fe pairs are found to be responsible for the Invar effect at the atomic scale. Moreover, also full atomic shells, which contain all atomic species, show an abrupt increase in their thermal expansion. This proves that the Invar effect is not just a macroscopic effect but has clear origins at the atomic scale.

MM 30.7 Thu 12:00 H46

Coupling deformation mechanisms in metallic glass-high entropy alloy nanolaminates — •QI XU¹, DANIEL ŞOPU¹, and JÜRGEN ECKERT^{1,2} — ¹Erich Schmid Institute of Materials Science, Leoben, Austria — ²Montanuniversität Leoben, Leoben, Austria

The uniaxial tensile deformation behavior of metallic glass (MG) - high entropy alloy (HEA) nanolaminates is explored through molecular dynamics simulations. The combination of glassy and crystalline nanolayers results in misfit stresses at the interface that drive the partial crystallization of amorphous phase and the nucleation of short dislocations. Upon loading, the further stress-induced crystallization facilitates the nucleation and growth of dislocations along the interfacial regions and across the HEA plate, which advances the yielding of MG-HEA nanolaminate. The dislocations are absorbed into the amorphous plate via slip transfer across glass-crystalline interface that in turn triggers the activation of homogeneously distributed STZs. The co-deformation mechanism suppresses the formation of critical shear bands and increases the resistance to dislocation motion that, consequently, promotes enhanced ductility in MG-HEA nanolaminate. The strength combination of HEA and MGs and the complex deformation behavior may overcome the typical strength-ductility trade-off and make MG-HEA laminates promising candidates for a variety of structural and functional applications.

MM 30.8 Thu 12:15 H46

Tracer diffusion of Fe and Zr in CuZr nanoglasses — •CHRISTIAN AARON RIGONI¹, HENDRIK VOIGT¹, EVGENIY BOLTJNYUK², BONNIE TYLER³, SERGIY DIVINSKI¹, HORST HAHN², and GERHARD WILDE¹ — ¹Institute of Materials Physics, University of Münster, Germany — ²Institute of Nanotechnology, Karlsruhe Institute of Technology, Germany — ³Physikalisches Institut, University of Münster, Germany

Metallic nanoglasses consist of nanometer-sized amorphous regions separated by amorphous interfaces. According to the current knowledge, the amorphous structure of these interfaces is different from that of the amorphous grains. This rather new class of material shows a different behaviour in comparison to conventional homogenous metallic glasses, e.g. a reduced density, a reduced number of nearest neighbor atoms, a different electronic structure, an increase in the ferromagnetic transition temperature and an increased thermal stability were reported. In the present work, tracer diffusion in CuZr nanoglasses and their homogenous amorphous counterparts is measured. For the investigation, a radiotracer technique via ion beam sputtering (⁸⁹Zr and ⁵⁵Fe radioisotopes) is applied as well as SIMS profiling using stable isotopes. The tracer diffusion measurements are demonstrated to represent a specific and sensitive probe of the structure modifications, and the results are compared to the observations made by TEM and APT.

MM 30.9 Thu 12:30 H46

Anomalous Liquids on a New Landscape: from Water to Phase-Change Materials — •SHUAI WEI — Aarhus University, Aarhus, Denmark

A liquid that is cooled below its melting temperature, referred to as a supercooled liquid, can solidify into an amorphous rigid state (i.e., glass), if cooling is fast enough and crystallization is avoided. The phenomenology of supercooled liquids has been in general established. However, there are pronounced exceptions (e.g., water) which do not fall into the class of "normal" liquids but exhibit a transition behavior in their liquid states. The latest advances connect the unusual aspect of liquids to the properties of Phase-Change Materials (PCMs) that are the basis for non-volatile memory and neuromorphic technologies. Here we demonstrate that the "water-like" liquid anomalies exist in many alloys based on group-IV, V, VI elements including technologically important PCMs. Heat capacity, density, and thermal expansivity maxima were observed in the (supercooled) liquid states of those alloys. Structural changes were monitored using in-situ X-ray scattering and femtosecond X-ray diffractions. Dynamic properties were characterized by quasi-elastic neutrons scattering. Their anomalous behaviors can be rationalized in terms of liquid-liquid (metal-semiconductor, and fragile-strong) transitions. These transition behaviors have important implications for understanding the unusual phase switching behaviors in PCMs, in which amorphous phase can crystallize rapidly within tens of nanoseconds at an elevated temperature, while it retains excellent amorphous stability for 10 years at room temperature.

MM 30.10 Thu 12:45 H46

Thermophysical study of anomalies and transitions in liquid Bi-Ga and Ga-In systems — •YURI KIRSHON¹, SHIR BEN-SHALOM¹, MORAN EMUNA², YARON GREENBERG², EYAL YAHEL², and GUY MAKOV¹ — ¹Department of Materials Engineering, Ben-Gurion University of the Negev, Beer-Sheva 84105, Israel — ²Physics Department, Nuclear Research Centre-Negev, Beer-Sheva 84190, Israel

Interest in the properties and applications of liquid metals has been reignited and leading to innovative new pathways. Work on low-melting alloys provided new products such as Galinstan liquid metal thermometers, self-healing electronic devices and cooling systems for high-temperature reactors. However, due to the experimental challenges, study of thermophysical properties of liquid binary systems remains limited. In particular, Bi-Ga and Ga-In alloys have attracted scientific interest due to possible changes in their liquid structure, reported recently [Q.Yu (2017), Z.Wang (2017), Y.Kirshon (2019)]. In the present contribution, we report on thermophysical measurements conducted on Bi-Ga and Ga-In alloys. Custom table-top resistivity and differential thermal analysis (DTA) setups are presented, including a demonstration of their capability to capture subtle transitions in the melts. We observed evidence of liquid-liquid crossover in the liquid Ga-In, measured both systems at a temperature range in good agreement with previous density measurements. In the Bi-Ga system, we probed the liquid-liquid miscibility gap and were able to obtain the latent heat and resistivity change during the liquid de-mixing process. Both results were in good agreement with previous reports.

MM 31: Computational Materials Modelling: Physics of Ensembles 2

Time: Thursday 11:45–13:00

Location: H44

MM 31.1 Thu 11:45 H44

Making low-scaling GW accurate — •JAN WILHELM¹ and DOROTHEA GOLZE² — ¹Institute of Theoretical Physics, University of Regensburg — ²Faculty of Chemistry and Food Chemistry, TU Dresden

In standard GW implementations, the computational cost is growing as $O(N^4)$ in the system size N , which prohibits their application to many systems of interest. I present a GW algorithm in a Gaussian-type basis with a computational cost that scales with N^2 to N^3 . It will be shown that large minimax grids and resolution of the identity with the truncated Coulomb metric improve the accuracy of

the low-scaling GW algorithm to < 0.01 eV for the GW100 test set. Large-scale applications of low-scaling GW will be discussed.

MM 31.2 Thu 12:00 H44

Atomic cluster expansion parametrization of carbon for a fast, accurate and transferable interatomic potential — •MINAAM QAMAR, MATOUŠ MROVEC, YURY LYSOGORSKIY, ANTON BOCHKAREV, and RALF DRAUTZ — Interdisciplinary Centre for Advanced Materials Simulation (ICAMS), Ruhr-University Bochum, Germany

We present a parametrization of the atomic cluster expansion (ACE) for carbon that can be employed in large-scale atomistic simulations of complex phenomena. The ACE model is parametrized over an exhaustive dataset of important carbon structures at extended volume and energy ranges, computed using highly accurate density functional theory (DFT). Dispersion corrections are explicitly added to properly account for long-ranged van der Waals interactions. A rigorous validation against DFT data reveals that ACE predicts accurately a broad range of properties of both crystalline and amorphous C phases while being significantly more computationally efficient than other popular machine learning models. We demonstrate the predictive power of ACE on two distinct applications: (1) brittle crack propagation in diamond at finite temperature, and (2) evolution of amorphous carbon structures at different densities and quench rates.

MM 31.3 Thu 12:15 H44

Design and analysis of scattering data driven molecular dynamics simulation on the example of water and selected crystals — •VERONIKA REICH¹, SEBASTIAN BUSCH¹, and MARTIN MÜLLER² — ¹German Engineering Materials Science Centre (GEMS) at Heinz Maier-Leibnitz Zentrum (MLZ), Helmholtz-Zentrum Hereon, Lichtenbergstr. 1, 85748 Garching bei München, Germany — ²Helmholtz-Zentrum Hereon, Max-Planck-Str. 1, 21502 Geesthacht, Germany

Molecular dynamics simulations are an indispensable tool to preinvestigate neutron scattering experiments. For many systems reliable force fields have been established and yield to significant simulations. On the other hand a lot of systems still don't have a satisfactory agreement between experiment and simulation.

In this work we compare experimental data to different liquid water model simulations and give an outline to crystal simulations.

We simulate the samples using molecular dynamics simulations using the program LAMMPS. Subsequently we calculate the coherent and incoherent scattering signals using the program SASSENA. Ensuing we compare the outcomes to already existing experimental data and evaluate changes in the underlying force fields in terms of their impact on the behaviour of the simulation. Finally we compare the incoherent calculations to mathematical models, which in turn we later fit to the simulation.

The aim of our work is to create a simple to use workflow of molecular dynamics simulations for scattering experiments.

MM 31.4 Thu 12:30 H44

Approximating nuclear quantum effects in solids by temperature remapping — •RAYNOL DSOUZA¹, LIAM HUBER¹, BLAZEJ GRABOWSKI¹, and JÖRG NEUGEBAUER¹ — ¹Max Planck Institut für Eisenforschung GmbH, 40237 Düsseldorf, Germany — ²University of Stuttgart, 70569 Stuttgart, Germany

The quantum nature of solids, which is especially important at low temperatures,

is often ignored in finite temperature atomistic simulations. Formulations to estimate quantum anharmonic effects precisely, such as the path integral method, are computationally demanding. Although various acceleration approaches allowing quantum effects to be fully accounted for in systems of hundreds of atoms have been proposed over the last two decades, they can fall short when it comes to modeling defects in solids, which can require significantly larger system sizes. We present a new approach for approximating nuclear quantum effects, exploiting a temperature map between the quantum system and its best classical surrogate. This map is constructed using the internal energies of classical and quantum harmonic oscillators within the Debye model. To a good approximation, our approach captures the impact of quantum effects on lattice constants, internal energies, and heat capacities with almost no additional cost compared to purely classical molecular dynamics simulations. Results for diamond cubic carbon and silicon are in good agreement with available literature values, which use full path integral Monte-Carlo simulations. We also show how this approach can be used to predict phase transition temperatures, e.g. the FCC to BCC transition for calcium.

MM 31.5 Thu 12:45 H44

Sharp phase-field modeling of isotropic solidification with a super efficient spatial resolution — •MICHAEL FLECK and FELIX SCHLEIFER — University of Bayreuth, 95447 Bayreuth, Germany

The phase-field method provides a powerful framework for microstructure evolution modeling in complex systems, as often required within the framework of integrated computational materials engineering. However, spurious grid friction, pinning and grid anisotropy seriously limit the resolution efficiency and accuracy of these models. The energetic resolution limit is determined by the maximum dimensionless driving force at which reasonable model operation is still ensured. This limit turns out to be on the order of 1 for conventional phase-field models. Grid friction and pinning can be eliminated by a the restoration of Translational Invariance (TI) in the discretized phase-field equation. This is called the sharp phase-field method, which allows to choose substantially coarser numerical resolutions of the diffuse interface without the appearance pinning. We propose an accurate scheme to restore TI locally in the local interface normal direction. The new model overcomes grid friction and pinning in three dimensional simulations, and can accurately operate at dimensionless driving forces up to the order of 10^4 . At one-grid-point interface resolutions, exceptional degrees of isotropy can be achieved, if further the inhomogeneous latent heat release at the advancing solid-liquid interface is mitigated. Imposing a newly proposed source term regularization the new model captures the formation of isotropic seaweed structures without spurious dendritic selection by grid anisotropy.

MM 32: Nanomaterials: Surface Effects

Time: Thursday 11:45–13:00

Location: H45

MM 32.1 Thu 11:45 H45

Effects of post anodization processes on the surface stability of anodic aluminum oxide — •LYDIA DAUM, STEFAN OSTENDORP, and GERHARD WILDE — Westfälische-Wilhelms-Universität, Münster, Germany

The wide spectrum of different aluminum alloys enables the industry an economically advantageous material with the desired mechanical properties. In contrast to high-purity aluminum, the formation of a thin protective alumina layer is suppressed, which leads to a lower chemical corrosion resistance. Here anodization and the generation of anodic aluminum oxides (AAOs) are mandatory to obtain a necessary protective coating. The participating alloying elements are obstacles for mechanical stresses inside the AAOs which promotes the formation of nano- and microcracks at the surface. Thus, chemical attacks of the aluminum alloy are more favorable.

The use of post anodization processes will densify the pores and flatten the surface, which enhances the chemical resistance. A combination of nanoindentation studies and electron microscopy measurements are analyzing the surface stability of AAOs. By varying the methods in duration and medium, different wear, hardness and ductility characteristics are visible.

MM 32.2 Thu 12:00 H45

Surfaces of nanoporous gold: rough and faceted? — •STEFAN A. BERGER¹, ULRIKE DETTE^{1,2}, LINGZHI LIU³, JÜRGEN MARKMANN^{1,2}, and JÖRG WEISSMÜLLER^{2,1} — ¹Helmholtz Zentrum Hereon — ²Technische Universität Hamburg — ³Shenyang National Laboratory for Materials Science

Nanoporous gold is an interesting model system for studying the impact of surfaces on the properties of nanomaterials. The surface morphology, faceted or rough, is of interest in that context. Scanning electron micrographs almost invariably show smoothly curved surfaces at the scale of the ligament size, suggesting roughness as opposed to faceting. Here, we show that proper imaging conditions to reveal facets, suggesting that the roughness may be an artifact of

imaging. We find that the roughness is most pronounced after annealing in oxygen atmosphere. While low index facets are expected to prevail on gold, we regularly also observe high index facets.

MM 32.3 Thu 12:15 H45

Understanding of the underlying field evaporation mechanism of pure water tips in high electric fields — •TIM MAXIMILIAN SCHWARZ¹, GUIDO SCHMITZ¹, NICO SEGRETO², JOHANNES KÄSTNER², and PATRICK STENDER¹ — ¹University of Stuttgart, Institute for Materials Science, Chair of Materials Physics, Heisenbergstr. 3, 70569 Stuttgart, Germany — ²University of Stuttgart, Institute for Theoretical Chemistry, Pfaffenwaldring 55, 70569 Stuttgart, Germany

Frozen liquids are challenging and rather new in the investigation by atom probe tomography. However, recent progress in instrumentation, especially the introduction of cryo transfer shuttles, and the development of the required preparation routes to shape nanometric needles of frozen liquids enable measurements of sufficient quality and size of data sets to discover the typical features of this material class. In this talk, we present the fragmentation behaviour of bulk frozen water as an important matrix for biomolecules or solvent of electrolytes. The obtained mass spectra are complex. However, this support of DFT calculations of the molecule stabilities, we identify a systematic series of protonated (H₂O)_nH₃O⁺ events that represent a clear "fingerprint" for the existence of water. Remarkably, tailing and the exact mass position of the two series differ, which provides evidence that the protonated fragments are permanently positively charged and therefore, slightly drawn out of the dielectric surface before the evaporation event.

MM 32.4 Thu 12:30 H45

Synthesis of superparamagnetic iron oxide nanoparticles by electron beam irradiation — •JOHANNES DIETRICH^{1,2} and STEFAN MAYR^{1,2} — ¹Leibniz-Institut für Oberflächenmodifizierung e.V. (IOM), Permoserstraße 15, 04318 Leipzig — ²Universität Leipzig, Fakultät für Physik und Geowissenschaften, Abteilung Oberflächenphysik, Linnéstraße 5, 04103 Leipzig

Nanoparticles based on iron oxides are a highly versatile material used in a broad range of applications, for instance embedding magnetic particles in polymer matrices to create ferrogels. A common procedure is to synthesize the particles in separate processes, add them to the gel and crosslink the polymer chains with nanoparticles by electron beam treatment. Combining synthesis and crosslinking would offer the possibility to create ferrogels by an one-step process.

In our work, we show a procedure to synthesize superparamagnetic nanoparticles with a narrow size distribution and an average size of approximately 5 nm directly by electron beam irradiation. The formation of small amounts of nanoparticles could already be observed for doses of 50 kGy, but these particles showed a low crystallinity and a higher percentage of amorphous particles. For higher doses increasing crystallinity and yield could be observed, which is also reflected in the higher saturation magnetization for samples irradiated with higher doses. Additionally, particles irradiated with doses starting from 150 kGy show a tendency to form bigger cluster with sizes from 34 nm to 73 nm.

MM 32.5 Thu 12:45 H45

Probing the oxide formation on Pt, Pd and Pt/Pd catalysts during NO oxidation by Atom Probe Tomography (APT) — •YOONHEE LEE¹, DANIEL DOBESCH¹, UTE TUTTLIES², PATRICK STENDER¹, ULRICH NIEKEN², and GUIDO SCHMITZ¹ — ¹Institute of Materials Science, University of Stuttgart, Heisenbergstr. 3, 70569 Stuttgart, Germany — ²Institute of Chemical Process Engineering, University of Stuttgart, Böblinger Str. 78, 70199 Stuttgart, Germany *Yoonhee.lee@mp.imw.uni-stuttgart.de

Inverse hysteresis behavior of Pt, Pd and PtPd alloy catalysts during NO conversion can be attributed to the formation of metal oxides. Even though there were many efforts to study the oxidation of these noble metals experimentally, still the surface change of the pure catalyst has not been observed yet. In this work, NO conversion measurements were carried out with nanoparticles of Pt, Pd and Pt/Pd alloy, produced by spark discharge method, in an isothermal flatbed reactor. The catalyst was subjected to alternating heating and cooling ramps in conditions prone to surface oxide formation. Besides, the oxygen content formed on the surface of catalyst was determined during Temperature-Programmed Reduction (TPR) in H₂ atmosphere. The same conditions (gas concentration, heating and cooling rate) of the NO conversion experiments have been achieved in a reaction chamber directly connected to the Atom Probe Tomography (APT) under ultra-high vacuum conditions. The samples were exposed to the gas and measured in APT. The 3D chemical structure was reconstructed and the effective thickness of formed oxides was determined.

MM 33: Computational Materials Modelling: Process Schemes / Oxides

Time: Thursday 15:45–18:30

Location: H44

MM 33.1 Thu 15:45 H44

How to Speed up First-Principles Based Geometry Optimization with Small Numerical Basis Sets — •ELISABETH KELLER, JOHANNES T. MARGRAF, and KARSTEN REUTER — Fritz-Haber-Institut der Max-Planck-Gesellschaft, Berlin, Germany

First-principles based geometry optimizations are often the most expensive part of high-throughput virtual screening studies for functional materials. This is particularly true for large systems, i.e. when studying complex surface reconstructions or nanoparticles. Here, the computational cost is strongly influenced by the size of the basis set. Large, converged basis sets result in precise equilibrium geometries, yet demand high computational cost and thus limit the simulation scale. Semiempirical methods using minimal basis sets offer a much lower computational cost, but may yield unacceptably large and uncontrolled errors. Furthermore, the availability of adequate parameterizations is rather sparse across the periodic table.

In this presentation, we will discuss the potential of using near-minimal basis sets for accelerating and enabling large-scale geometry optimizations at the DFT level. For this purpose, we studied how the size of the numeric atom-centered orbital (NAO) basis set in FHI-aims impacts the accuracy of bulk geometries. We recover equilibrium geometries at a nearly converged level with a highly compact basis by employing a simple short-ranged pair-potential correction. We show the scheme's ability to treat different systems across the periodic table ranging from small molecules and clusters to large-scale bulk and surface structures as well as complex molecule-surface interactions.

MM 33.2 Thu 16:00 H44

A machine-learned interatomic potential for crystalline and amorphous silica — •LINUS ERHARD¹, JOCHEN ROHRER¹, KARSTEN ALBE¹, and VOLKER DERINGER² — ¹Institute of Materials Science, Technische Universität Darmstadt, Otto-Berndt-Strasse 3, 64287 Darmstadt, Germany — ²Department of Chemistry, Inorganic Chemistry Laboratory, University of Oxford, Oxford OX1 3QR, United Kingdom

Fitting an interatomic potential for silicon oxide that can be used for both the amorphous and numerous crystalline phases has proven to be difficult. This is already shown by the large number of interatomic potentials published in the last decades. Here, we present a machine-learned interatomic potential for silica, which is highly transferable between different crystalline polymorphs and the amorphous phase. It predicts the thermodynamics of the system accurately and is able to generate low-defect amorphous models by melt and quench simulations. We also discuss the importance of choosing an appropriated exchange-correlation functional for density-functional data input, which is particularly

important for silica. Since the generation of realistic amorphous structure models by melt-quench simulations is highly dependent on the quench rate, we show new ways via hybrid simulations that combine the speed of classical interatomic potentials with the accuracy of machine-learning potentials. We also investigate the extrapolation behavior of our machine-learning potential using high-pressure simulations. Finally, we show first steps towards an interatomic potential for mixed Si-SiO₂ systems.

MM 33.3 Thu 16:15 H44

An all-functionals automatic workflow for IR and Raman spectra — •LORENZO BASTONERO¹ and LORENZO BASTONERO^{1,2} — ¹University of Bremen, Bremen, Germany — ²EPFL, Lausanne, Switzerland

IR and Raman spectroscopies are among the best methods for the characterization of materials at small scales, thanks to their fast measurement and high sensibility to local composition and configuration. Theoretical calculations are fundamental for the interpretation of experimental results and for the assessment of thermal properties. DFT has been employed in the last decades as a reliable tool for the analysis of these spectra, although the calculation of vibrational properties has been limited to the use of few functionals. Here, we devise an automatic user-friendly workflow for IR and Raman calculations within the AiiDA infrastructure, which exploits the finite displacements and finite fields to allow application to any complex functional. The package provides at the same time easy access and full customisability, relevant both for less experienced users and more elaborate purposes such as high-throughput searches.

MM 33.4 Thu 16:30 H44

A Workflow for Obtaining Robust Density Functional Tight Binding Parameters Across the Periodic Table — •MENGHAN CUI, JOHANNES T. MARGRAF, and KARSTEN REUTER — Fritz-Haber-Institut der MPG, Berlin, Germany

The Density Functional Tight Binding (DFTB) approach allows electronic structure based simulations at length and time scales far beyond what is possible with first-principles methods. This is achieved by using minimal basis-sets and empirical approximations. Unfortunately, the sparse availability of parameters across the periodic table is a significant barrier to the use of DFTB in many cases.

In this contribution, we therefore propose a workflow which allows the robust and consistent parameterization of DFTB across the periodic table. Importantly, the approach requires no element-pairwise parameters and can thus easily be extended to new elements. Specifically, the parameters defining the band energy and repulsive potential are obtained via Bayesian Optimization on a set of elemental solids. In this way, robust baseline parameters can be obtained for arbitrary element combinations. The transferability of the parameters and appli-

cations in hybrid DFTB/Machine Learning models will be discussed.

MM 33.5 Thu 16:45 H44

ChemiTEM - optimized solutions and workflows for electron microscopy in materials science and chemistry — •WALID HETABA^{1,2}, ROBERT IMLAU³, LISETH DUARTE-CORREA², MAXIMILIAN LAMOTH², STEPHAN KUJAWA³, and THOMAS LUNKENBEIN² — ¹Max-Planck-Institut für Chemische Energiekonversion, Mülheim/Ruhr, Deutschland — ²Fritz-Haber-Institut der MPG, Berlin, Deutschland — ³Thermo Fisher Scientific, Eindhoven, Niederlande

Transmission electron microscopy (TEM) is an important and versatile method for investigating materials on the nanoscale. Information about the elemental composition and electronic structure can be obtained while imaging the sample with atomic resolution. Such investigations are usually performed by TEM-experts. However, enabling non-expert TEM users to perform such measurements would tremendously improve the efficiency of TEM investigations in both, materials science and chemistry. We therefore developed ChemiTEM: a set of standardized workflows for data acquisition and analysis which are integrated in an app for tablets and smartphones to provide easy access for all TEM users, irrespective of their level of experience. We tested the ability of ChemiTEM in helping non-expert TEM users to collect high quality data by having non-expert and expert TEM users investigate the same sample. Using ChemiTEM, the data acquired by the non-expert users were of similar quality to that of the data recorded by the TEM-expert. Thus, we were able to show that using the ChemiTEM app, TEM can be made available to everyone working in materials science.

15 min. break

MM 33.6 Thu 17:15 H44

Determination of Formation Energies and Phase Diagrams of Transition Metal Oxides with DFT+U — •DANIEL MUTTER¹, DANIEL URBAN¹, and CHRISTIAN ELSÄSSER^{1,2} — ¹Fraunhofer IWM, Freiburg, Germany — ²Freiburger Materialforschungsinstitut (FMF), Freiburg, Germany

Knowledge about formation energies of compounds is essential to derive phase diagrams of multicomponent phases with respect to elemental reservoirs. The determination of formation energies using (semi-)local exchange-correlation approximations of the density functional theory exhibits well-known systematic errors if applied to oxide compounds containing transition metal elements. We generalize and reevaluate a set of approaches proposed and widely applied in the literature to correct for errors arising from the over-binding of the O₂ molecule and from correlation effects of electrons in localized transition-metal orbitals. The DFT+U method is exemplarily applied to iron oxide compounds, and a procedure is presented to obtain the U values, which lead to formation energies and electronic band gaps comparable to the experimental values. Using such corrected formation energies, we derive phase diagrams for LaFeO₃, Li₅FeO₄, and NaFeO₂, which are promising materials for energy conversion and storage devices. A scheme is presented to transform the variables of the phase diagrams from the chemical potentials of elemental phases to those of precursor compounds of a solid-state reaction, which represents the experimental synthesis process more appropriately. The workflow and methods can directly be applied to other transition metal oxides.

MM 33.7 Thu 17:30 H44

A comparative study of the bulk properties of iron oxides calculated using empirical potentials and ab-initio calculations — •AHMED ABDELKAWY, MIRA TODOROVA, and JÖRG NEUGEBAUER — Max-Planck-Institut für Eisenforschung, Max-Planck-Str.1, 40470 Düsseldorf

Striving toward a green economy requires re-evaluating industrial processes and looking for new routes to, e.g., obtaining iron from iron ore. This necessitates understanding the steps involved in the reduction of iron oxides and leading to several phase transitions the final product of which is iron. The optimization of the involved processes will hugely benefit from an atomistic level understanding. Atomistic simulation techniques are versatile but are dependent on the quality of the used underlying empirical potentials. We therefore first evaluate the applicability of interatomic potentials for this study by comparing them to ab initio calculations. Specifically, we focus on a reactive forcefield (ReaxFF) parametrized for these materials, which accounts for the different oxidation states of each species (Fe and O) and enables their variation depending on the local environment and coordination, bond breaking, and making. We assess the reliability of the force field by assessing various bulk properties of the relevant iron as compared to density functional theory calculations. We find that a universal force-

field that is able to accurately describe the three main iron oxides (Magnetite, Hematite, and Wüstite) is difficult to obtain.

MM 33.8 Thu 17:45 H44

Uncertainty in Predicting Thermodynamic Properties of TiO₂ Polymorphs — •OLGA VINOGRADOVA, PIN-WEN GUAN, SIYING LI, and VENKATASUBRAMANIAN VISWANATHAN — Carnegie Mellon University, Pittsburgh, USA

Polymorphism of crystals directly leads to materials with vastly different chemical and physical properties. However the lowest energy polymorphs often differ by only small amounts of energy. This makes it challenging to predict relative properties using first-principles density functional theory (DFT), which is significant in designing a material for the desired application. In this work we apply computational uncertainty within DFT to quantify the accuracy of stability and phase transition predictions under finite temperature and pressure. We study six polymorphs of TiO₂ using a set of six exchange-correlation functionals to present a detailed sensitivity analysis using uncertainty capabilities within the Bayesian Error Estimation Functional. We show that a prediction confidence metric is particularly important for comparing the stability of numerically close predictions. We show how the choice of functional significantly affects predictions of phase transitions and identify which structures and properties that have inherently large uncertainties. From the trends observed in stability, finite-temperature, and phase transition pressure predictions we propose that uncertainty quantification provides a valuable insight in problems where drawn conclusions are highly sensitive to the choice of the functional.

MM 33.9 Thu 18:00 H44

Self-consistent phonon calculations of lattice dynamical properties in cubic EuTiO₃ comparing with experimental thermal conductivity — •CHEN SHEN¹, WENJIE XIE¹, XINGXING XIAO¹, ANKE WEIDENKAFF¹, TERUMASA TADANO², and HONGBIN ZHANG¹ — ¹Institute of Materials Science, Technical University Darmstadt, Darmstadt 64287, Germany — ²Research Center for Magnetic and Spintronic Materials, National Institute for Materials and Science, Tsukuba, Japan

We investigate the role of the quartic anharmonicity in the lattice dynamics and thermal transport of the cubic EuTiO₃ by combining ab initio self-consistent phonon theory combined with compressive sensing techniques experimental thermal conductivity determination measurement. The antiferromagnetic G-type magnetic structure is used to mimic the para-magnetic EuTiO₃. We find that the strong quartic anharmonicity of oxygen atoms plays an essential role in the phonon quasiparticles free from imaginary frequencies in EuTiO₃, causing the hardening of vibrational frequencies soft modes. The hardened modes thereby affect calculated lattice thermal conductivity significantly, resulting in an improved agreement with experimental results, including the deviation from $\kappa_L \propto T^{-1}$ at high temperature. The calculated thermal conductivity of 8.2 W/mK at 300 K matched the experimental value of 6.1 W/mK. When considering the boundary scattering, the calculated thermal conductivity is reduced to 6.9 W/mK at 300 K, which agrees better with the experiment.

MM 33.10 Thu 18:15 H44

Simulated indentation on graphene oxide — •JAVIER ROJAS-NUNEZ¹, SAMUEL BALTAZAR¹, EDUARDO BRINGA², and ALEJANDRA GARCIA³ — ¹Physics Department and CEDENNA, Universidad de Santiago de Chile (USACH), Santiago, Chile — ²Laboratorio de síntesis y modificación de nanoestructuras y materiales bidimensionales, Centro de Investigación en Materiales Avanzados, Nuevo León, México — ³CONICET & Facultad de Ingeniería, Universidad de Mendoza, Mendoza, Argentina

The better understanding of nanomaterial properties will be a key factor to tailor and enhance properties of new materials. Graphene oxide in particular can be synthesized with different oxidation levels in order to gain similar properties to its deoxidized counterpart, graphene. Through the molecular dynamic simulations, the atomistic behavior of a tri-layer graphene membrane under mechanical indentation will be studied in this work.

This work will study a highly oxidized graphene oxide tri-layer that will be indented with a repulsive spherical indenter. The modeling of the membrane will generate single layer graphene oxide candidates to pick the lowest energy configuration and later stack this layer over itself. The final tri-layer was used for the indentation simulation, where the young modulus was reproduced with decent similarity to experimental results.

The atomistic analysis of the indentation process suggest an important role of epoxide groups in the mechanical deformation of the membrane.

MM 34: Data Driven Materials Science: Interatomic Potentials / Reduced Dimensions

Time: Thursday 15:45–18:30

Location: H45

MM 34.1 Thu 15:45 H45

Constructing Training Sets for Transferable Moment Tensor Potentials: Application to Defects in Bulk Mg — •MARVIN POUL, LIAM HUBER, ERIK BITZEK, and JOERG NEUGEBAUER — Max-Planck-Institut fuer Eisenforschung

Machine learned interatomic potentials promise to bring quantum mechanical accuracy to system sizes that are inaccessible with traditional QM approaches. Here, we present a set of unary Mg Moment Tensor Potentials[1] with different speeds and accuracies in the range of 100–5 meV/atom. We focus on understanding the role of the training data in the fitting process. We discuss several ways in which the structural complexity of the training structures and a physical understanding of them helps to design an efficient training set construction. The resulting potentials are verified on out-of-fold structures, like vacancies, surfaces, and high-symmetry grain boundaries. This work is implemented as a pyron[2] workflow and we identify challenges and opportunities of a fully automated setup to fit machine-learned potentials.

[1]: <https://doi.org/10.1088/2632-2153/abc9fe>[2]: <https://doi.org/10.1016/j.commatsci.2018.07.043>

MM 34.2 Thu 16:00 H45

Active learning and uncertainty quantification for atomic cluster expansion models — •YURY LYSOGORSKIY, ANTON BOCHKAREV, and RALF DRAUTZ — Atomistic Modelling and Simulation, ICAMS, Ruhr-University Bochum, D-44801 Bochum, Germany

Interatomic potentials (IP) are widely used in computational materials science, in particular for simulations that are too computationally expensive for density functional theory (DFT). Recently the atomic cluster expansion (ACE) was proposed as a new class of data-driven IP with basis set completeness. Development of any IP requires numerous iterations and careful selection of training data. Thus automation of both construction of training dataset as well as IP validation would significantly speed up the development process. In this work we apply the Maxvol algorithm for training dataset selection and study the extrapolation grade metric (Podryabinkin and Shapuev, 2017) in the context of ACE and compare it to the query-by-committee approach for uncertainty estimation. These methods allow us to introduce extrapolation control in ACE models and to design different exploration automated protocols for accurate interatomic potentials development.

MM 34.3 Thu 16:15 H45

Take Two: Δ -Machine Learning for Molecular Co-Crystals — •SIMON WENGERT^{1,2}, GÁBOR CSÁNYI³, KARSTEN REUTER¹, and JOHANNES T. MARGRAF¹ — ¹Fritz Haber Institut der MPG, Berlin, Germany — ²TU Munich, Germany — ³University of Cambridge, UK

Co-crystals are a highly interesting material class, as varying their components and stoichiometry in principle allows tuning supramolecular assemblies towards desired physical properties. The *in silico* prediction of co-crystal structures represents a daunting task, however, as they span a vast search space and usually feature large unit-cells. This requires theoretical models that are accurate and fast to evaluate, a combination that can in principle be accomplished by modern machine-learned (ML) potentials trained on first-principles data. Crucially, these ML potentials need to account for the description of long-range interactions, which are essential for the stability and structure of molecular crystals. In this contribution, we present a strategy for developing Δ -ML potentials for co-crystals, which use a physical baseline model to describe long-range interactions. The applicability of this approach is demonstrated for co-crystals of variable composition consisting of an active pharmaceutical ingredient and various co-formers. We find that the Δ -ML approach offers a strong and consistent improvement over the density-functional tight binding baseline. Importantly, this even holds true when extrapolating beyond the scope of the training set, for instance in molecular dynamics simulations at ambient conditions.

MM 34.4 Thu 16:30 H45

Magnetic Atomic Cluster Expansion and application to Iron — •MATTEO RINALDI, MATOUS MROVEC, and RALF DRAUTZ — Interdisciplinary Centre for Advanced Materials Simulation (ICAMS)

The atomic cluster expansion (ACE)^[1,2,3] has proven to be a valuable tool to parametrize complex energy landscapes of pure elements and alloys. However, its application to potential energy surfaces determined also by additional degrees of freedom, such as magnetic moments, has been still lacking. In particular, ferromagnetic materials cannot be tackled with the original ACE formalism, where the single-site energies depend parametrically only on interatomic distances and chemical species, since these descriptors cannot distinguish between atoms with different magnetic moments. The solution of this issue was given theoretically by Drautz^[4], where the ACE formalism was extended to take into account additional labels of the atomic sites of scalar, vectorial and tensorial nature by includ-

ing them in the definition of the atomic neighbor density. We have employed this formalism to parametrize a magnetic ACE for the prototypical ferromagnetic element Fe using a dataset of both collinear and non-collinear magnetic structures calculated with spin density functional theory. We will show that the new ACE model is able to describe correctly not only various magnetic phases of Fe at 0 K but also their finite temperature properties in good agreement with the reference *ab-initio* and experimental values.

[1] R. Drautz, Phys. Rev. B 99, 014104. [2] Y. Lysogorskiy et al., npj Comput Mater 7, 97 (2021). [3] A. Bochkarev et al., Phys. Rev. Materials 6, 013804. [4] R. Drautz, Phys. Rev. B 102, 024104.

MM 34.5 Thu 16:45 H45

Kernel Charge Equilibration: Learning Charge Distributions in Materials and Molecules — •MARTIN VONDRAK, NIKHIL BAPAT, HENDRIK H. HEENEN, JOHANNES T. MARGRAF, and KARSTEN REUTER — Fritz-Haber-Institut, Berlin, Germany

Machine learning (ML) techniques have recently been shown to bridge the gap between accurate first-principles methods and computationally cheap empirical potentials. This is achieved by learning a systematic relationship between the structure of molecules and their physical properties. However, the modern ML models typically represent chemical systems in terms of local atomic environments. This inevitably leads to the neglect of long-range interactions (most prominently electrostatics) and non-local phenomena (e.g. charge transfer), which can lead to significant errors in the description of polar molecules and materials (particularly in non-isotropic environments). To overcome these issues, we recently proposed a ML framework for predicting charge distributions in molecules termed Kernel Charge Equilibration (kQEq). Here, atomic charges are derived from a physical model using environment-dependent atomic electronegativities. These models can be trained to reproduce electrostatic properties (e.g. dipole moments) of reference systems, computed from first principles. The impact of different fitting targets on predicted charge distributions is compared. Furthermore, strategies for fitting to energies are discussed, including combination of Gaussian Approximation Potential (GAP) with kQEq.

15 min. break

MM 34.6 Thu 17:15 H45

Machine Learning of ab-initio grain boundary Segregation Energies — •CHRISTOPH DÖSINGER¹, DANIEL SCHEIBER², OLEG PEIL², VSEVOLOD RAZUMOVSKIY², ALEXANDER REICHMANN¹, and LORENZ ROMANER¹ — ¹Montanuniversität Leoben, Department of Materials Science, Leoben, Austria — ²Materials Center Leoben Forschung GmbH, Leoben, Austria

Grain-boundary (GB) segregation is an important phenomenon in alloys, where the resulting GB excess can strongly influence their properties, for example induce intergranular fracture or lead to phase transformations. A fundamental quantity that uniquely describes the propensity of a solute towards GB segregation is the segregation energy. It determines the tendency of a solute atom to enrich or deplete at the GB. This quantity can be directly calculated from first principles. However, such calculations are computationally expensive and can become computationally unfeasible as the complexity of the GB crystal structure increases. The aim of this work is to reduce the computational cost of GB segregation energies by applying machine learning methods trained at series of representative DFT calculations and expanding them to more complex GB structures. The atomic structure, together with the segregation energies are used to train a model, which then is employed to predict the segregation energy for arbitrary segregation sites and GB types. In our work we apply this method to tungsten alloys. The results show, that this approach indeed gives reliable results for the segregation energies and can be used to get a complete description of segregation profiles.

MM 34.7 Thu 17:30 H45

Stability of binary precipitates in Cu-based alloys investigated through active learning and quantum computing — •ANGEL DIAZ CARRAL¹, XIANG XU², AZADE YAZDAN YAR¹, SIEGFRIED SCHMAUDER², and MARIA FYTA¹ — ¹Institute for Computational Physics (ICP), Universität Stuttgart, Allmandring 3, 70569, Stuttgart, Germany — ²Institut für Materialprüfung, Werkstoffkunde und Festigkeitslehre (IMWF), Pfaffenwaldring 32 70569, Stuttgart, Germany

Understanding the structure of thermodynamically stable precipitates is of great interest in material science as they can affect the electrical conductivity and mechanical properties of the matrix to a great degree. In this work, we use a relaxation-on-the-fly active learning algorithm in order to scan all possible binary candidates, for different types and concentrations of alloy elements (mainly Cu, Si, and Ni). Quantum-mechanical calculations are performed on a small number of candidates to train and improve the machine-learned potential. The model is then used to predict the enthalpy of formation of all candidates. The

stability of binary precipitates, based on predicting the convex hull, is further assessed by the phonon density of states analysis calculated by classic and quantum computing.

MM 34.8 Thu 17:45 H45

How to teach my deep generative model to create new RuO₂ surface structures? — •PATRICIA KÖNIG, HANNA TÜRK, YONGHYUK LEE, CHIARA PANOSSETTI, CHRISTOPH SCHEURER, and KARSTEN REUTER — Fritz-Haber-Institut der MPG, Germany

Many widely used catalyst systems still hold complicated longstanding structural puzzles that hamper their full atomistic understanding and thus further knowledge based progress. Here, we address the well-known RuO₂ catalyst for the oxidative conversion of CO exhaust gases in combustion processes.

To explore the chemical space of RuO₂ surface structures, we trained a Generative Adversarial Network (GAN) that is capable of cheaply generating diverse structural guesses for novel surface structures. For the training set, 28,903 RuO₂ surface terminations were created with a grand-canonical basin hopping method. The atomic positions of these structures were mapped to Gaussian densities on a three-dimensional grid to generate the GAN input. We demonstrate how two-dimensional images of cuts through RuO₂ structures with inferred lattice lengths and energy conditioning can be created as a first step to realistic three-dimensional surface structures.

MM 34.9 Thu 18:00 H45

Data-Driven Design of Two-Dimensional Non-van der Waals Materials — •RICO FRIEDRICH^{1,2,3}, MAHDI GHORBANI-ASL¹, STEFANO CURTAROLO², and ARKADY V. KRASHENINNIKOV^{1,4} — ¹Helmholtz-Zentrum Dresden-Rossendorf, Dresden — ²Duke University, Durham, USA — ³TU Dresden — ⁴Aalto University, Aalto, Finland

Two-dimensional (2D) materials are traditionally associated with the sheets forming bulk layered compounds bonded by weak van der Waals (vdW) forces. The weak inter-layer interaction leads to a natural structural separation of the 2D subunits in the crystals, giving rise to the possibility of mechanical and liquid-phase exfoliation as well as enabling the formulation of exfoliability descriptors.

The unexpected experimental realization of non-vdW 2D compounds, for

which the previously developed descriptors are not applicable, opened up a new direction in the research on 2D systems [1]. Here, we present our recent data-driven search for representatives of this novel materials class [2]. By screening the AFLOW database according to structural prototypes, 28 potentially synthesizable candidates are outlined. The oxidation state of the surface cations is found to regulate the exfoliation energy with low oxidation numbers giving rise to weak bonding — thus providing an enabling descriptor to obtain novel 2D materials. The candidates showcase a diverse spectrum of appealing electronic, optical and magnetic features.

[1] A. Puthirath Balan *et al.*, Nat. Nanotechnol. **13**, 602 (2018).

[2] R. Friedrich *et al.*, Nano Lett. **22**, 989 (2022).

MM 34.10 Thu 18:15 H45

Robust recognition and exploratory analysis of crystal structures via Bayesian deep learning — •ANDREAS LEITHERER, ANGELO ZILETTI, and LUCA M. GHIRINGHELLI — The NOMAD Laboratory at the Fritz Haber Institute and at the Humboldt University of Berlin, Germany

Atomic-resolution studies are routinely being performed in modern materials-science experiments. Artificial-intelligence tools are promising candidates to leverage this valuable – yet underutilized – data in unprecedented, automatic fashion to discover hidden patterns and eventually novel physics. Here, we introduce ARISE (Nat. Commun. 2021, <https://doi.org/10.1038/s41467-021-26511-5>), a crystal-structure-identification method based on Bayesian deep learning. As a major step forward, ARISE is robust to structural noise and can treat more than 100 crystal structures, a number that can be extended on demand. While being trained on ideal structures only, ARISE correctly characterizes strongly perturbed single- and polycrystalline systems, from both synthetic and experimental sources. The probabilistic nature of the Bayesian-deep-learning model yields principled uncertainty estimates, which are found to be correlated with crystalline order of metallic nanoparticles in electron-tomography experiments. Application of unsupervised learning to the internal neural-network representations reveals grain boundaries and (unapparent) structural regions sharing interpretable geometrical properties. This work enables the hitherto hindered analysis of noisy atomic structural data from computations or experiments.

MM 35: Nanomaterials: Structure & Properties

Time: Thursday 15:45–18:30

Location: H46

MM 35.1 Thu 15:45 H46

Structural and Electronic Reconstruction of Hexagonal Boron Nitride Interlayers Steps — •SUBAKTI SUBAKTI^{1,2}, MOHAMMADREZA DAQIQSHIRAZI³, FELIX KERN^{1,2}, DANIEL WOLF¹, THOMAS BRUMME³, BERND BÜCHNER^{1,2}, and AXEL LUBK¹ — ¹Leibniz Institute for Solid State and Materials Research Dresden, Helmholtzstraße 20, 01069 Dresden, Germany — ²Institut für Festkörperphysik, TU Dresden, D-01062 Dresden, Germany — ³Chair of Theoretical Chemistry, Technische Universität Dresden, Bergstrasse 66, 01069 Dresden, Germany

The electrostatic potential of condensed matter provides not only atomic structure, but also the electronic structure that underlies the chemical bonding formation of atoms within one molecule. Off-axis electron holography (EH) technique allows us to probe the volume-averaged electrostatic potential (in crystalline materials over the unit cell) of the specimen with respect to a vacuum reference region. Therefore, a conjunction EH medium and high resolution data analysis and electrostatic potential based ab-initio calculation will be powerful for simultaneous atomic scale reconstruction and imaging. Visible projected potential jump at the edges of two adjacent monolayers hexagonal boron nitride (h-BN) will be addressed here as our data analysis suggest that it could be signature for the increased charge delocalization due to the formation of an additional covalent bond of the 2p orbitals in the rolled-up edge.

MM 35.2 Thu 16:00 H46

Atom Probe Study of self-assembled Monolayers — •HELENA SOLODENKO, PATRICK STENDER, and GUIDO SCHMITZ — University of Stuttgart, Institute for Materials Science, Heisenbergstr. 3, 70569 Stuttgart

Atom probe tomography is a well-established characterization technique for metals, semiconductors, oxides and minerals. However, measurement of organic matter and biological materials is still challenging. Field evaporation of organic species leads to detection of C_xH_y groups, instead of single atoms. The fragmentation of the molecules possibly depends on the applied electric field strength and the nature of chemical bonding. Self-assembled monolayers (SAMs) represent a suitable model system to study the fundamental questions about field evaporation of such systems, since they represent a well-defined molecular film with a limited number of possible molecular fragments. Furthermore, a chemical bond is formed between substrate surface and the headgroup the SAM. By variation of the field strength, we expect to learn more about the field evaporation process and thus about the binding energies of the SAMs. We present measurements

of alkane-thiolates on Pt and silanes on ZnO by laser-assisted APT. The backbone evaporates in the form of small hydrocarbon fragments consisting of one to four C atoms, while S evaporates exclusively as single ions. With increasing laser power, a significant trend towards larger fragment sizes is observed. Furthermore, comparison with liquid alkanes and cross linked alkane networks is insightful which demonstrates a continuous transition from evaporation of complete molecules to single atoms.

MM 35.3 Thu 16:15 H46

Tuning the Electronic Properties of Mesocrystals — •STEFAN MANUEL SCHUPP¹, CHRISTIAN JENEWEIN², BING NI², LUKAS SCHMIDT-MENDE¹, and HELMUT CÖLFEN² — ¹University of Konstanz, Department of Physics, Universitätsstraße 10, 78462 Konstanz, Germany — ²University of Konstanz, Department of Chemistry, Universitätsstraße 10, 78462 Konstanz, Germany

Colloidal crystals consisting of periodically aligned nanocrystalline building blocks, so-called mesocrystals, are promising candidates for nanostructured metamaterials. The high degree of order of the nanoparticles in the crystal results in a well-defined facet-to-facet distance which is determined by the used capping agents. In this work, we were able to grow micrometer-sized platinum nanocube-based mesocrystals with various capping agents and perform electrical measurements on individual crystals with a nanoprobe system. The extracted resistances increase with larger interparticle distances which can be attributed to the predominantly thermally activated tunneling mechanism in these superstructures. However, an additional annealing step leads to a decrease in resistance by seven orders of magnitude due to formed mineral bridges. After this treatment, the electronic properties are mainly determined by the nanomaterial itself. Finally, we were able to transfer these findings onto multi component superstructures consisting of platinum and iron oxide nanocubes. In these binary mesocrystals the ratio of the nanoparticle types can be varied to tune the electrical conductivity even further while simultaneously allowing to combine properties of both nanomaterials.

MM 35.4 Thu 16:30 H46

Direct Visualization of Ordered Mesoporous Silica Using Atom Probe Tomography — •KUAN MENG and GUIDO SCHMITZ — University of Stuttgart, Institute for Materials Science, Heisenbergstr. 3, 70569, Stuttgart, Germany

Inspired by enzyme catalytic reaction, heterogeneous catalysis with mesoporous support materials is considered as the fundamental for modern chemical syn-

thesis. However, the synergistic interplay between the catalysts and the pores is still unknown. To realize this, the structure of the mesoporous supports needs characterizing at first. Atom Probe Tomography, due to its subatomic resolution, strong chemical mapping power and direct visualization capability, is becoming a great candidate for mesoporous structure characterization. Yet to unfold its charm, pores must be filled.

In this work, Ordered Mesoporous Silica (OMS) filled with two different polymers, CDEAB and DCPD, was investigated. Firstly, both obtained mass spectra can be interpreted as a plausible combination of signature peaks between silica and polymers. Secondly, the porous network of OMS was visualized using neighboring analysis and the pore size turned out in the mesoporous range. Especially in the case of OMS filled with DCPD, the visualized network appeared to be regularly hexagonal, showing great resemblance with TEM images from similar pore orientations. Last, the obtained data were compared with the result of TAPsim simulations in order to understand the flaws in the visualization and to improve the understanding of the reconstructions.

MM 35.5 Thu 16:45 H46

plastic deformation of nanoporous gold modified with organic layers: a TEM study — •XIN ZHANG and NADIJA MAMEKA — Institute of Materials Mechanics, Helmholtz-Zentrum hereon, 21502 Geesthacht, Germany

As a result of their large specific surface area, strength of high-specific area materials must be sensitive to environment and surface chemistry. This notion is confirmed, e.g., by the enhanced flow stress found in single metal nanowires [1] and metallic networks like nanoporous metals when their surface is modified by adsorbed layers or surface coatings [2]. Yet, experimental studies of microstructural origins of the surface constraints impact on small-scale plasticity is still in its infancy. Here, we examine a defect structure of plastically deformed nanoporous gold (NPG) via ex-situ transmission electron microscopy. We exploit self-assembled monolayers (SAM) to modify a surface of NPG as inspired by a substantial flow stress increase due to SAM adsorption reported in [3]. In bare NPG deformed by rolling, we reveal higher density of twins consistent with [4]. In the deformed NPG with SAM, the formation of twins is strongly suppressed near the surface. Meanwhile, the existence of the organic layer apparently increases the density of twins in NPG. In the contribution, we discuss the TEM observations and link them to the findings from mechanical tests of the SAM-modified NPG. [1] Shin et al, Acta Mat. 166 (2019) 572e586. [2] Wu et al, Mater. Res. Lett. 6 (2018) 508. [3] Mameka et al, ACS Appl. Nano Mater. 1 (2018) 6613. [4] Liu, Weissmüller, Mater. Res. Lett. 9 (2021) 359.

15 min. break

MM 35.6 Thu 17:15 H46

Electrochemical actuation and tunable stiffness of hierarchical nanoporous gold via surface modification — •OLGA MATTS and NADIJA MAMEKA — Helmholtz-Zentrum Hereon, Geesthacht, Germany

Recently developed dealloying strategies towards nanoporous metals with structural hierarchy [1] open up new opportunities for functional behavior of this class of materials. The larger pores at the higher hierarchical level (characterized by diameters around 200 nm) of the hierarchical nanoporous metals (hc np) can promote fast mass exchange, while nanopores at the lower hierarchy level (below 30 nm) provide a large surface area. To explore the notion we employ electroactive self-assembled monolayers and conductive polymer polypyrrole for surface functionalization of hc np Au and np Au with unimodal pore size. Actuation and Young's modulus behavior of the hybrid materials were then analyzed in situ in a dynamical mechanical analyzer and dilatometer upon potential cycling in aqueous electrolytes. We revealed pronounced variations in the macroscopic length change as well as elastic modulus in response to the voltage-induced redox reactions of the organic films at the np electrodes. In the contribution, we discuss the origin of the observations and compare the functional performance of both types of the hybrids based on np Au.

[1] Shi et al., Science 371, 1026*1033 (2021).

MM 35.7 Thu 17:30 H46

Laser-Ultrasonics Reveals the Complex Mechanics of Nanoporous Silicon — •MARC THELEN¹, NICOLAS BOCHUD², MANUEL BRINKER¹, CLAIRE PRADA³, and PATRICK HUBER^{1,4,5} — ¹MXP, TUHH, Hamburg, Germany — ²MSME, CNRS UMR 8208, UPEC, Univ Gustave Eiffel, Creteil, France — ³Institut Langevin, ESPCI Paris, Université PSL, CNRS, Paris, France — ⁴CXNS, DESY, Hamburg, Germany — ⁵CHyN, UHH, Hamburg, Germany

Nanoporosity in silicon leads to completely new functionalities of this mainstream semiconductor with numerous discoveries in fields ranging from nanofluidics and biosensors to drug delivery, energy storage and photonics. Nevertheless, the mechanical properties, critical for a variety of applications, remain difficult to characterise comprehensively. The study presented here aims to address this problem by utilising laser-excited elastic guided waves, detected in dry and liquid-infused porous silicon. Among other things, the experiments reveal that the self-organised formation of 100 billions of parallel nanopores per square centimetre cross section results in an effective stiffness reduction of

about 80 %, a nearly isotropic elasticity perpendicular to the pore axes and a higher stiffness along the pore axis, altogether leading to significant deviations from bulk silicon. This thorough assessment of the wafer-scale mechanics of nanoporous silicon and recent breakthroughs in laser ultrasonics therefore open up entirely new frontiers for in-situ, non-contact and non-destructive mechanical characterisation of complex porous material systems [1].

[1] Thelen, M., Bochud, N. et al., Nat Commun., 12, 3597 (2021)

MM 35.8 Thu 17:45 H46

Fabrication and compressive behavior of monolithic nanoporous niobium at macroscale — •SEYUN SOHN^{1,2}, SHAN SHI^{2,1}, JÜRGEN MARKMANN^{1,2}, and JÖRG WEISSMÜLLER^{2,1} — ¹Institute of Materials Mechanics, Helmholtz-Zentrum hereon, Geesthacht, Germany — ²Institute of Materials Physics and Technology, Hamburg University of Technology, Hamburg, Germany

Studying the mechanical performance of nanoporous (np) metals allows us to understand nanoscale solids as well as to design functional applications. However, the majority of studies have been confined to face-centered cubic noble metals such as gold and palladium due to high electronegativity which facilitates preparation by dealloying. Since the electrochemical or chemical dealloying involves a selective dissolution of less noble constituent(s) in an electrolyte solution, the remaining constituent should be nobler to form a bicontinuous porous structure. Niobium (Nb) on the other hand is less noble than gold, has higher stiffness and lower ductility, and its crystal lattice is body-centered cubic. In this work, np Nb was fabricated out of Ni₇₅Nb₂₅ by liquid metal dealloying; the ligament size could be controlled from 400 nm to more than 1 μm by adjusting dealloying time and temperature. Each sample body is a few mm in size and freestanding, which allows us to perform conventional macro-compression tests to measure the strength and stiffness of the nano-ligament scaffold. Our observations support that the material strength is enhanced with smaller ligaments. More interestingly, our np Nb shows extremely anomalous compliance.

MM 35.9 Thu 18:00 H46

Maximal Anderson Localization and Suppression of Surface Plasmons in Two-Dimensional Random Au Networks — •JOHANNES SCHULTZ¹, KARL HIEKEL², PAVEL POTAPOV¹, PAVEL KHAVLYUK², ALEXANDER EYCHMÜLLER², and AXEL LUBK¹ — ¹Leibniz Institute for Solid State and Materials Research Dresden, Helmholtzstraße 20, 01069 Dresden, Germany — ²Chair of Physical Chemistry, TU Dresden, Zellescher Weg 19, 01069 Dresden, Germany

2D random metal networks possess unique electrical and optical properties, such as almost hundred percent optical transparencies and low sheet resistance, which are closely related to their disordered structure and may be exploited in various applications. Here we present a detailed experimental and theoretical investigation of their plasmonic properties, revealing Anderson (disorder-driven) localized surface plasmon (LSP) resonances of large quality factors and spatial localization close to the theoretical maximum. The LSPs typically consist of multiple field hotspots with a well-defined correlation distance. Moreover, they disappear above a geometry-dependent threshold at ca. 1.6 eV in the investigated networks, explaining their large transparencies in the optical spectrum. Electron energy loss spectroscopy in combination with scanning transmission electron microscopy was applied for the experimental studies. Both, the high spatial (≈1 nm) and spectral (≈50 meV) resolution allows to study the variety of LSP modes in terms of excitation energy and spatial localization. The theoretical study is based on a coupled dipole model, which allows modeling of large plasmonic systems by exploiting Babinet's principle.

MM 35.10 Thu 18:15 H46

Laterally aligned nanowires: Targeted process design and alignment control — •JASMIN-CLARA BÜRGER, SEBASTIAN GUTSCH, and MARGIT ZACHARIAS — Laboratory for Nanotechnology, Department of Microsystems Engineering - IMTEK, University of Freiburg, Georges-Köhler-Allee 103, 79110 Freiburg, Germany

For sensors, tin oxide nanowires (NWs) have shown superior properties due to their unique geometry, which allows for high sensitivities. NWs are often grown in freestanding mode for which metallization via standard lithography techniques is not applicable. In the production of single NW-based sensors, a multistep process has to be applied and an individual contacting of the NWs by, e.g., e-beam lithography becomes mandatory. Here, the use of planar NWs, i.e., laterally aligned NWs, is of advantage since the removal step from the growth substrate can be skipped and the NWs can be grown at defined positions. Due to their epitaxial contact with the monocrystalline growth substrate, the NWs are self-aligned towards the substrate lattice. However, the parameter space of these NWs is even smaller than for freestanding NWs. Based on finite element simulation and thermodynamic considerations, we developed a model for the growth of laterally aligned NWs.[1,2] The simulations and theory are supported by experimental results. Following, the preparation of longitudinal TEM lamella of individual NWs and AFM measurements allowed us for nanoscopic insight into the NW alignment on the growth substrate.[2]

[1] J.-C. Bürger et al., Beilstein J. Nanotechnol. (2020), 11, 843-853; [2] J.-C. Bürger et al., Cryst. Growth Des. (2021), 21 (1), 191-199

Surface Science Division Fachverband Oberflächenphysik (O)

Karsten Reuter
Fritz-Haber-Institut der MPG
Faradayweg 4-6
14195 Berlin
reuter@fhi.mpg.de

Overview of Invited Talks and Sessions

(Lecture halls H2, H3, H4, H6, S051, S052, S053, and S054; Poster P3 and P4)

Invited Talks

O 1.1	Mon	9:30–10:15	S054	Laser-excited electrons: how hot are they? — •BAERBEL RETHFELD
O 24.1	Tue	9:30–10:15	S054	Oxygen Evolution on Rutile Ruthenium and Iridium Dioxides — •YANG SHAO-HORN
O 36.1	Wed	9:30–10:15	S054	Heterogeneous chemistry of liquid-vapor interfaces investigated with X-ray photoelectron spectroscopy — •HENDRIK BLUHM
O 60.1	Thu	9:30–10:15	S054	Exciting states in atomically thin layers — •THORSTEN DEILMANN
O 77.1	Fri	9:30–10:15	S054	Sub-molecular fluorescence microscopy with STM — •GUILLAUME SCHULL
O 84.1	Fri	13:15–14:00	S054	Exploring the Mysteries of Topology in Quantum Materials — •CLAUS M. SCHNEIDER

Invited Talks of the joint Symposium **Frontiers of Orbital Physics: Statics, Dynamics, and Transport of Orbital Angular Momentum (SYOP)**

See SYOP for the full program of the symposium.

SYOP 1.1	Mon	9:30–10:00	H1	Orbital degeneracy in transition metal compounds: Jahn-Teller effect, spin-orbit coupling and quantum effects — •DANIEL KHOMSKII
SYOP 1.2	Mon	10:00–10:30	H1	Orbital magnetism out of equilibrium: driving orbital motion with fluctuations, fields and currents — •YURIY MOKROUSOV
SYOP 1.3	Mon	10:30–11:00	H1	Orbitronics: new torques and magnetoresistance effects — •MATHIAS KLÄUI
SYOP 1.4	Mon	11:15–11:45	H1	Orbital and total angular momenta dichroism of the THz vortex beams at the antiferromagnetic resonances — •ANDREI SIRENKO
SYOP 1.5	Mon	11:45–12:15	H1	Observation of the orbital Hall effect in a light metal Ti — •GYUNG-MIN CHOI

Invited Talks of the joint Symposium **SKM Dissertation Prize 2022 (SYSD)**

See SYSD for the full program of the symposium.

SYSD 1.1	Mon	10:15–10:45	H2	Charge localisation in halide perovskites from bulk to nano for efficient optoelectronic applications — •SASCHA FELDMANN
SYSD 1.2	Mon	10:45–11:15	H2	Nonequilibrium Transport and Dynamics in Conventional and Topological Superconducting Junctions — •RAFFAEL L. KLEES
SYSD 1.3	Mon	11:15–11:45	H2	Probing magnetostatic and magnetotransport properties of the antiferromagnetic iron oxide hematite — •ANDREW ROSS
SYSD 1.4	Mon	11:45–12:15	H2	Quantum dot optomechanics with surface acoustic waves — •MATTHIAS WEISS

Invited Talks of the joint Symposium **United Kingdom as Guest of Honor (SYUK)**

See SYUK for the full program of the symposium.

SYUK 1.1	Wed	9:30–10:00	H2	Structure and Dynamics of Interfacial Water — •ANGELOS MICHAELIDES
SYUK 1.2	Wed	10:00–10:30	H2	A molecular view of the water interface — •MISCHA BONN
SYUK 1.3	Wed	10:30–11:00	H2	Motile cilia waves: creating and responding to flow — •PIETRO CICUTA

SYUK 1.4	Wed	11:00–11:30	H2	Cilia and flagella: Building blocks of life and a physicist's playground — •OLIVER BÄUMCHEN
SYUK 1.5	Wed	11:45–12:15	H2	Computational modelling of the physics of rare earth - transition metal permanent magnets from SmCo₅ to Nd₂Fe₁₄B — •JULIE STAUNTON
SYUK 2.1	Wed	15:00–15:30	H2	Hysteresis Design of Magnetic Materials for Efficient Energy Conversion — •OLIVER GUTFLEISCH
SYUK 2.2	Wed	15:30–16:00	H2	Non-equilibrium dynamics of many-body quantum systems versus quantum technologies — •IRENE D'AMICO
SYUK 2.3	Wed	16:00–16:30	H2	Quantum computing with trapped ions — •FERDINAND SCHMIDT-KALER
SYUK 2.4	Wed	16:45–17:15	H2	Breaking the millikelvin barrier in cooling nanoelectronic devices — •RICHARD HALEY
SYUK 2.5	Wed	17:15–17:45	H2	Superconducting Quantum Interference Devices for applications at mK temperatures — •SEBASTIAN KEMPF

Invited Talks of the joint Symposium Frontiers of Electronic-Structure Theory: Focus on Artificial Intelligence Applied to Real Materials (SYES)

See SYES for the full program of the symposium.

SYES 1.1	Thu	15:00–15:30	H1	Machine-learning-driven advances in modelling inorganic materials — •VOLKER L. DERINGER
SYES 1.2	Thu	15:30–16:00	H1	Machine-Learning Discovery of Descriptors for Square-Net Topological Semimetals — •EUN-AH KIM
SYES 1.3	Thu	16:00–16:30	H1	Four Generations of Neural Network Potentials — •JÖRG BEHLER
SYES 1.4	Thu	16:30–17:00	H1	Using machine learning to find density functionals — •KIERON BURKE
SYES 1.5	Thu	17:00–17:30	H1	Coarse graining for classical and quantum systems — •CECILIA CLEMENTI

Sessions

O 1.1–1.1	Mon	9:30–10:15	S054	Overview Talk Bärbel Rethfeld
O 2.1–2.10	Mon	10:30–13:00	H3	Ultrafast Electron Dynamics at Surfaces and Interfaces 1
O 3.1–3.8	Mon	10:30–12:45	H4	Focus Session: Single Atom Catalysis 1
O 4.1–4.4	Mon	10:30–11:30	H6	Topology and Symmetry-Protected Materials
O 5.1–5.9	Mon	10:30–13:00	S051	Organic Molecules at Surfaces 1: Substrate Effects
O 6.1–6.10	Mon	10:30–13:00	S052	Nanostructures at Surfaces 1
O 7.1–7.9	Mon	10:30–13:00	S053	New Methods and Developments 1: Scanning Probe Techniques 1 (joint session O/KFM)
O 8.1–8.8	Mon	10:30–12:45	S054	Solid-Liquid Interfaces 1: Reactions and Electrochemistry
O 9.1–9.13	Mon	15:00–18:15	H3	Ultrafast Electron Dynamics at Surfaces and Interfaces 2
O 10.1–10.7	Mon	15:00–17:30	H4	Focus Session: Single Atom Catalysis 2
O 11.1–11.6	Mon	15:00–16:30	H6	Electronic Structure Theory
O 12.1–12.12	Mon	15:00–18:00	S051	Organic Molecules at Surfaces 2: Characterization of Organic Monolayers
O 13.1–13.10	Mon	15:00–17:30	S052	Nanostructures at Surfaces 2
O 14.1–14.5	Mon	15:00–16:15	S053	New Methods and Developments 2: Scanning Probe Techniques 2 (joint session O/KFM)
O 15.1–15.11	Mon	15:00–18:00	S054	Solid-Liquid Interfaces 2: Structure and Spectroscopy
O 16.1–16.12	Mon	18:00–20:00	P4	Poster Monday: Ultrafast Processes 1
O 17.1–17.12	Mon	18:00–20:00	P4	Poster Monday: Organic Molecules at Surfaces 1
O 18.1–18.28	Mon	18:00–20:00	P4	Poster Monday: 2D Materials 1
O 19.1–19.10	Mon	18:00–20:00	P4	Poster Monday: Scanning Probe Techniques 1
O 20.1–20.11	Mon	18:00–20:00	P4	Poster Monday: Solid-Liquid Interfaces
O 21.1–21.5	Mon	18:00–20:00	P4	Poster Monday: Topology and Symmetry-Protected Materials
O 22.1–22.8	Mon	18:00–20:00	P4	Poster Monday: Surface Structure, Epitaxy, Growth and Tribology
O 23.1–23.9	Mon	18:00–20:00	P4	Poster Monday: Nanostructures 1
O 24.1–24.1	Tue	9:30–10:15	S054	Overview Talk Yang Shao-Horn
O 25.1–25.7	Tue	10:30–13:00	H2	Focus Session: Atomic-Scale Characterization of Correlated Ground States in Epitaxial 2D Materials
O 26.1–26.9	Tue	10:30–12:45	H4	Surface Magnetism
O 27.1–27.5	Tue	10:30–11:45	H6	Electron-Driven Processes
O 28.1–28.9	Tue	10:30–12:45	S051	Organic Molecules at Surfaces 3: Theory
O 29.1–29.7	Tue	10:30–12:15	S052	Metal substrates 1
O 30.1–30.8	Tue	10:30–12:45	S053	Semiconductor Surfaces

O 31.1–31.7	Tue	10:30–12:30	S054	Solid-Liquid Interfaces 3: Reactions and Electrochemistry
O 32.1–32.9	Tue	11:00–13:00	P3	Poster Tuesday: Adsorption and Catalysis 1
O 33.1–33.11	Tue	11:00–13:00	P3	Poster Tuesday: Ultrafast Processes 2
O 34.1–34.10	Tue	11:00–13:00	P3	Poster Tuesday: Scanning Probe Techniques 2
O 35.1–35.8	Tue	11:00–13:00	P3	Poster Tuesday: Plasmonics and Nanooptics 1
O 36.1–36.1	Wed	9:30–10:15	S054	Overview Talk Hendrik Bluhm
O 37.1–37.8	Wed	10:30–12:45	H3	Plasmonics and Nanooptics 1
O 38.1–38.7	Wed	10:30–12:30	H4	Solid-Liquid Interfaces 4: Reactions and Electrochemistry
O 39.1–39.7	Wed	10:30–12:15	H6	Tribology
O 40.1–40.9	Wed	10:30–12:45	S051	Organic Molecules at Surfaces 4: Chemistry on Surfaces
O 41.1–41.8	Wed	10:30–12:30	S052	Graphene: Growth, Substrate Interaction, Intercalation, and Doping
O 42.1–42.5	Wed	10:30–11:45	S053	Metal substrates 2
O 43.1–43.10	Wed	10:30–13:00	S054	Frontiers of Electronic Structure Theory: Focus on Artificial Intelligence Applied to Real Materials 1
O 44.1–44.10	Wed	15:00–18:30	H3	Focus Session: Surfaces and Interfaces of (Incipient) Ferroelectrics (joint session O/KFM)
O 45.1–45.9	Wed	15:00–18:00	H4	Focus Session: Catalysis at Liquid Interfaces
O 46.1–46.8	Wed	15:00–17:00	H6	New Methods and Developments 3: Theory
O 47.1–47.10	Wed	15:00–18:00	S051	Focus Session: Atomic-Scale Studies of Spins on Surfaces with Scanning Tunneling Microscopy 1
O 48.1–48.10	Wed	15:00–17:30	S052	2D Materials 1: Electronic Structure of Transition Metal Dichalcogenides
O 49.1–49.10	Wed	15:00–17:30	S053	Oxide Surfaces 1
O 50.1–50.12	Wed	15:00–18:00	S054	Frontiers of Electronic Structure Theory: Focus on Artificial Intelligence Applied to Real Materials 2
O 51.1–51.10	Wed	18:00–20:00	P4	Poster Wednesday: Atomic-Scale Studies of Spins on Surfaces with Scanning Tunneling Microscopy
O 52.1–52.12	Wed	18:00–20:00	P4	Poster Wednesday: Adsorption and Catalysis 2
O 53.1–53.5	Wed	18:00–20:00	P4	Poster Wednesday: Spins and Magnetism
O 54.1–54.14	Wed	18:00–20:00	P4	Poster Wednesday: 2D Materials 2
O 55.1–55.16	Wed	18:00–20:00	P4	Poster Wednesday: Organic Molecules at Surfaces 2
O 56.1–56.6	Wed	18:00–20:00	P4	Poster Wednesday: Nanostructures 2
O 57.1–57.7	Wed	18:00–20:00	P4	Poster Wednesday: Electronic Structure
O 58.1–58.15	Wed	18:00–20:00	P4	Poster Wednesday: New Methods and Developments, Frontiers of Electronic Structure Theory
O 59.1–59.8	Wed	18:00–20:00	P4	Poster Wednesday: Plasmonics and Nanooptics 2
O 60.1–60.1	Thu	9:30–10:15	S054	Overview Talk Thorsten Deilmann
O 61.1–61.8	Thu	10:30–12:45	H2	Plasmonics and Nanooptics 2
O 62.1–62.9	Thu	10:30–12:45	H4	Surface Reactions and Heterogeneous Catalysis 1
O 63.1–63.7	Thu	10:30–12:30	H6	New Methods and Developments 4: Spectroscopies, Diffraction and Others (joint session O/KFM)
O 64.1–64.5	Thu	10:30–13:00	S051	Gerhard Ertl Young Investigator Award
O 65.1–65.8	Thu	10:30–12:30	S052	2D Materials 2: Growth, Structure and Substrate Interaction
O 66.1–66.9	Thu	10:30–13:00	S053	Oxide Surfaces 2
O 67.1–67.9	Thu	10:30–12:45	S054	Frontiers of Electronic Structure Theory: Focus on Artificial Intelligence Applied to Real Materials 3
O 68.1–68.10	Thu	15:00–18:30	H3	Focus Session: Time-Resolved Momentum Microscopy
O 69.1–69.10	Thu	15:00–17:45	H4	Surface Reactions and Heterogeneous Catalysis 2
O 70.1–70.10	Thu	15:00–17:45	H6	Supported nanoclusters: Structure, Reactions, Catalysis
O 71.1–71.10	Thu	15:00–18:00	S051	Focus Session: Atomic-Scale Studies of Spins on Surfaces with Scanning Tunneling Microscopy 2
O 72.1–72.8	Thu	15:00–17:00	S052	2D Materials 3: hBN and Electronic Structure
O 73.1–73.11	Thu	15:00–17:45	S053	Electronic Structure of Surfaces 1
O 74.1–74.12	Thu	15:00–18:00	S054	Organic Molecules at Surfaces 5: Molecular Switches
O 75	Thu	19:00–19:30	H1	Members' Assembly
O 76	Thu	19:30–20:30	H1	Post-Deadline Session
O 77.1–77.1	Fri	9:30–10:15	S054	Overview Talk Guillaume Schull
O 78.1–78.8	Fri	10:30–12:30	H3	Plasmonics and Nanooptics 3
O 79.1–79.8	Fri	10:30–12:45	H4	Surface Reactions and Heterogeneous Catalysis 3
O 80.1–80.7	Fri	10:30–12:15	S051	Focus Session: Atomic-Scale Studies of Spins on Surfaces with Scanning Tunneling Microscopy 3
O 81.1–81.6	Fri	10:30–12:00	S052	2D Materials 4: Heterostructures
O 82.1–82.7	Fri	10:30–12:15	S053	Electronic Structure of Surfaces 2

O 83.1–83.10	Fri	10:30–13:00	S054	Frontiers of Electronic Structure Theory: Focus on Artificial Intelligence Applied to Real Materials 4
O 84.1–84.1	Fri	13:15–14:00	S054	Overview Talk Claus M. Schneider (joint session O/CPP)

Members' Assembly of the Surface Science Division

Thursday 19:00–19:30 H1

- Report of the Chairman
- Presentation of the Gerhard Ertl Young Investigator Award
- Miscellaneous

Sessions

– Invited Talks, Topical Talks, Contributed Talks, and Posters –

O 1: Overview Talk Bärbel Rethfeld

Time: Monday 9:30–10:15

Location: S054

Invited Talk

O 1.1 Mon 9:30 S054

Laser-excited electrons: how hot are they? — •BAERBEL RETHFELD — Department of Physics and Research Center OPTIMAS, TU Kaiserslautern, Germany
Hot electrons play an important role in surface science. They are responsible for the functionalization of solar cells and the emission of intense THz beams, they drive chemical reactions at surfaces and are utilized in biosensing methods. Excitation and decay as well as transport of laser-excited electrons are fundamentally studied in pump-probe experiments using photoemission methods.

The term “hot electrons” is, however, not well-defined. It is used for single laser-excited electrons, for non-equilibrium electron distributions, and for Fermi distributions at elevated temperature. In all cases, the relaxation of such elec-

trons towards an equilibrated situation is of interest. Its dynamics may be complex, since several scattering mechanisms act on different timescales. Therefore, athermal electron distributions as well as highly excited electrons can exist much longer than the single-electron lifetime predicts.

In this presentation, I introduce the calculation method of Boltzmann collision integrals, allowing to study the effect and mutual influence of different scattering mechanisms. I further show how such intertwined relaxation processes affect measurable macroscopic quantities on ultrafast timescales, particularly in multiband materials. Examples include the electrical conductivity in highly excited noble metals, spin and charge transport in magnetically ordered systems and the nonthermal electron-phonon coupling strength in metals and dielectrics.

O 2: Ultrafast Electron Dynamics at Surfaces and Interfaces 1

Time: Monday 10:30–13:00

Location: H3

O 2.1 Mon 10:30 H3

Floquet Dressing and Multiphoton Photoemission on Metal Surfaces — •YUN YEN^{1,2} and MICHAEL SCHÜLER² — ¹Condensed Matter Theory Group, Paul Scherrer Institute, CH-5232 Villigen PSI, Switzerland — ²Ecole Polytechnique Fédérale de Lausanne (EPFL), CH-1015 Lausanne, Switzerland

Floquet engineering allows us to realize the control of quantum materials and explore exotic properties from light-matter interaction. Along with the development of various ultrafast experimental techniques, non-equilibrium quantum systems have gained more interests.

Metal surfaces such as Cu(111) or Ag(111) are considered as benchmarks for photoemission spectroscopy with nonlinear optical responses. The interplay between Shockley surface states (SS), image potential states (IP), and the related dressed bands can be studied with ultrafast pump-probe pulses. Starting from model potential, we utilize real space time-dependent surface flux method and non-equilibrium Green's function to simulate the non-equilibrium dynamics on the metal surfaces. We calculate the interferometric-time-resolved multiphoton photoemission (ITR-mPP) spectrum. The Fourier analysis of the simulated ITR-mpp spectrum shows the optical dressing of the surface electronic structures. Our approach successfully reproduce the previous experimental data, which allows us to investigate the origins of these signatures.

O 2.2 Mon 10:45 H3

Femtosecond orbital tomography of exciton dynamics in C₆₀ thin films — •G. S. MATTHIJS JANSEN¹, WIEBKE BENNECKE¹, RALF HEMM², ANDREAS WINDISCHBACHER³, DAVID SCHMITT¹, JAN PHILLIP BANGE¹, CHRISTIAN KERN³, DANIEL STEIL¹, SABINE STEIL¹, MARCEL REUTZEL¹, MARTIN AESCHLIMANN², PETER PUSCHNIG³, BENJAMIN STADTMÜLLER^{2,4}, and STEFAN MATHIAS¹ — ¹I. Physikalisches Institut, Georg-August-Universität Göttingen — ²Department of Physics and Research Center OPTIMAS, University of Kaiserslautern — ³Institute of Physics, University of Graz — ⁴Institute of Physics, Johannes Gutenberg-University Mainz

Time-resolved photoemission orbital tomography promises to be a unique probe of out-of-equilibrium electronic wavefunctions at the Ångström level and with femtosecond time resolution. Particularly interesting is the application to excitons, quasiparticles consisting of a bound electron and electron hole that govern the opto-electronic response of organic semiconductors. Here, we consider the prototypical organic semiconductor C₆₀, for which it has been proposed that the exciton cascade involves the two-step decay of a delocalized charge-transfer exciton into a localized Frenkel excitonic state. We will discuss how the combination of multi-dimensional photoemission spectroscopy with calculations within the many-body perturbation theory framework of the Bethe-Salpeter equation can shed light on the real-space femtosecond electron dynamics, and in particular show how the delocalization of excitons in C₆₀ evolves on the femtosecond timescale.

O 2.3 Mon 11:00 H3

Anisotropic carrier dynamics in a laser-excited Fe/(MgO)(001) heterostructure from real-time TDDFT — •ELAHEH SHOMALI, MARKUS ERNST GRUNER, and ROSSITZA PENTCHEVA — Department of Physics and Center for Nanointegration, CENIDE, University of Duisburg-Essen, Germany

The interaction of a femtosecond optical pulse with a Fe_n/(MgO)_m(001) (n=1,3,5 and m=3,5,7) metal/oxide heterostructure is addressed using time-dependent density functional theory (TDDFT) calculations in the real-time domain. We systematically study electronic excitations as a function of laser frequency (around and higher than the bulk MgO band gap). We find a marked anisotropy in the response to in- and out-of-plane polarized light, which changes its character qualitatively depending on the excitation energy: the Fe-layer is efficiently addressed at low frequencies by in-plane polarized light, whereas for frequencies higher than the MgO band gap, we find a particularly large sensitivity of MgO-layers to cross-plane polarized light. Moreover, the interface plays an important role, as it mediates transitions from the valence band of MgO into the 3d states of Fe closely above the Fermi-level and transitions from the Fe-states below the Fermi level into the conduction band of MgO. As these transitions can occur simultaneously without altering the charge balance of the layers, they could potentially lead to an efficient transfer of excited carriers into the MgO part [1]. Funding by SFB 1242, project C02, is gratefully acknowledged. [1] E. Shomali, M. E. Gruner, R. Pentcheva, Phys. Rev. B, in press, arXiv:2205.03178.

O 2.4 Mon 11:15 H3

Ultrafast electron transport across interfaces in Au/Fe/MgO(001) heterostructures — YASIN BEYAZIT¹, FLORIAN KÜHNE¹, MARKUS HECKSCHEN¹, BJÖRN SOTHMANN¹, ELAHEH SHOMALI¹, MARKUS GRUNER¹, ROSSITZA PENTCHEVA¹, PING ZHOU¹, DETLEF DIESING², and •UWE BOVENSIEPEN¹ — ¹Universität Duisburg-Essen, Fakultät für Physik, 47048 Duisburg — ²Universität Duisburg-Essen, Fakultät für Chemie, 45141 Essen

The dynamics of electronic excitations at buried interfaces is decisive in electron transfer and carrier multiplication in heterostructures. Following recent developments in time-resolved two-photon photoemission spectroscopy the relaxation dynamics of optically excited, hot electrons can be distinguished in the individual layers of Au/Fe/MgO(001) by analysis of the Au thickness dependent relaxation times [Beyazit et al., PRL **125**, 076803 (2020)]. Here we report on recent experimental results and the separation of the primary, optically excited electrons and the secondary, relaxed and propagating electron distribution. This study is complemented by calculations using the Boltzmann transport equation for the propagation through the Au layer and density functional theory calculations resolving the interface contribution.

Funding by the Deutsche Forschungsgemeinschaft through SFB 1242 is gratefully acknowledged.

O 2.5 Mon 11:30 H3

Non-equilibrium carrier dynamics of different surface reconstructions of Sn on SiC(0001) — •MAXIMILIAN STECHER¹, MARIA-ELISABETH FEDERL¹, NIKLAS HOFMANN¹, LEONARD WEIGL¹, JOHANNES GRADL¹, NEERAJ MISHRA^{2,3}, STIVEN FORTI², CAMILLA COLETTI^{2,3}, and ISABELLA GIERZ¹ — ¹Department of Physics, University of Regensburg, 93040 Regensburg, Germany — ²Center for Nanotechnology Innovation @NEST, Istituto Italiano di Tecnologia, 56127 Pisa, Italy — ³Graphene Labs, Istituto Italiano di Tecnologia, 16163 Genova, Italy
Sn on SiC(0001) forms different surface reconstructions in the monolayer coverage regime, among them a Mott insulating phase with a $(\sqrt{3}\times\sqrt{3})R30^\circ$ structure. We grow these structures and characterize them with low-energy elec-

tron diffraction (LEED), X-ray photoemission spectroscopy (XPS), and angle-resolved photoemission spectroscopy (ARPES). We then investigate their light-induced non-equilibrium carrier dynamics with time- and angle-resolved photoemission spectroscopy, looking for possible photo-induced phase transitions and metastable transient states. These preliminary studies then pave the way towards dynamical control of the electronic properties of Sn/SiC(0001) via resonant excitation of the IR-active phonon modes of the substrate that will modulate the atomic positions of the covalently bound Sn layer coherently.

O 2.6 Mon 11:45 H3

ultrafast carrier dynamics of graphene - 2D Sn van der Waals interface — •MARIA-ELISABETH FEDERL¹, NIKLAS HOFMANN¹, LEONARD WEIGL¹, JOHANNES GRADL¹, TIM WEHLING^{2,3}, NIKLAS WITT³, NEERAJ MISHRA⁴, CAMILLA COLETTI^{4,5}, STIVEN FORTI⁴, and ISABELLA GIERZ¹ — ¹Department of Physics, University of Regensburg, 93040 Regensburg, Germany — ²Institute for Theoretical Physics, University of Bremen, 28359 Bremen, Germany — ³Institute for Theoretical Physics, University of Hamburg, 22607 Hamburg, Germany — ⁴Center for Nanotechnology Innovation @NEST, Istituto Italiano di Tecnologia, Piazza San Silvestro 12, 56127 Pisa, Italy — ⁵Graphene Labs, Istituto Italiano di Tecnologia, 16163 Genova, Italy

The interface between epitaxial graphene and SiC(0001) is a confined space that allows for the growth of novel two-dimensional materials (2DMs) and thus graphene/2DM heterostructures. The electronic properties of these heterostructures are usually more complex than those expected from the sum of the individual layers as hybridization between the layers opens up band gaps in the electronic structure and produces electronic wavefunctions that are localized on both rather than individual layers of the heterostructure. We use time- and angle-resolved photoemission spectroscopy to reveal important differences between the non-equilibrium carrier dynamics of quasi-freestanding graphene and graphene proximity-coupled to a 2D metallic Sn layer that we interpret in terms of doping, scattering phase space, and ultrafast charge transfer with the help of ab initio band structure calculations.

O 2.7 Mon 12:00 H3

tr-ARPES experiment with mid-infrared excitation for dynamical band structure engineering — •LEONARD WEIGL¹, NIKLAS HOFMANN¹, JOHANNES GRADL¹, NEERAJ MISHRA^{2,3}, STIVEN FORTI², CAMILLA COLETTI^{2,3}, and ISABELLA GIERZ¹ — ¹Department of Physics, University of Regensburg, 93040 Regensburg, Germany — ²Center for Nanotechnology Innovation @NEST, Istituto Italiano di Tecnologia, 56127 Pisa, Italy — ³Graphene Labs, Istituto Italiano di Tecnologia, 16163 Genova, Italy

The band structure of a solid is mainly determined by the orbital overlap between neighboring atoms. Therefore, electronic properties are commonly controlled via the chemical composition that determines structural parameters such as bond angles and lengths. Recently, control of the effective orbital overlap has been achieved by periodic modulation of solids with strong mid-infrared (MIR) light fields. The ideal probe for investigating driving-induced band structure changes is time- and angle-resolved photoemission spectroscopy (tr-ARPES). We have built a tr-ARPES setup that combines a strong-field wavelength-tunable MIR pump source with extreme ultraviolet probe pulses providing access to the band structure of driven solids across the complete first Brillouin zone with sub 100meV energy and sub 250fs temporal resolution. We present first results on driven graphene, analyze the MIR pump-induced carrier dynamics, and discuss the possible formation of photon-dressed states. The excellent performance of the setup now paves the way for the future investigation of light-induced superconductivity as well as light-induced topological phase transitions.

O 2.8 Mon 12:15 H3

Anisotropic response to optical excitations in naturally layered delafossite PdCoO₂ from time-dependent DFT — •MIKE J. BRUCKHOFF, MARKUS E. GRUNER, and ROSSITZA PENTCHEVA — Faculty of Physics and Center of Nanointegration, CENIDE, University of Duisburg-Essen, 47048 Duisburg, Germany
In the framework of time-dependent density functional theory (TDDFT), we investigate the layer-resolved dynamics of the electronic structure of the metallic delafossite PdCoO₂ after optical excitations. PdCoO₂ can be conceived as a

natural multilayer system consisting of highly conductive Pd layers separated by insulating CoO₆ octahedra. We calculate the responses to optical pulses with two polarization directions, multiple frequencies, different pulse durations and laser fluences within the real-time approach (RT-TDDFT) and compare the results to optical absorption spectra obtained within the linear-response regime (LR-TDDFT). We observe a strong anisotropy of the electronic response to different polarization directions and particular frequencies of the incident electric field, which corresponds to the strong anisotropy visible in the absorption spectra. In particular, we see a significant charge redistribution and time-dependent changes of occupation numbers, which depend on the orbital character of the involved *d*-orbitals. Analogies to previous studies for a Fe₁/(MgO)₃(001) heterostructure [1] are discussed. Funding by DFG within SFB1242 is gratefully acknowledged.

[1]: M. E. Gruner and R. Pentcheva, Phys. Rev. B 99, 195104 (2019)

O 2.9 Mon 12:30 H3

Far-from-equilibrium electron-phonon interactions in optically-excited graphene — •MARCO MERBOLDT¹, MARTEN DÜVEL¹, JAN PHILIPP BANGE¹, MICHAEL STELLBRINK¹, HANNAH STRAUCH¹, KLAUS PIERZ², HANS WERNER SCHUMACHER², DAVOOD MOMENI², DANIEL STEIL¹, G. S. MATTHIJS JANSEN¹, SABINE STEIL¹, DINO NOVKO³, STEFAN MATHIAS¹, and MARCEL REUTZEL¹ — ¹I. Physikalisches Institut, Georg-August-Universität Göttingen, Göttingen, Germany — ²Physikalisch-Technische Bundesanstalt, Braunschweig, Germany — ³Institute of Physics, Zagreb, Croatia

Comprehending far-from-equilibrium many-body interactions is one major goal of current ultrafast condensed matter physics research. A particularly interesting but barely understood situation occurs during strong optical excitation, where electron and phonon systems are significantly perturbed from their equilibrium and cannot be described by Fermi-Dirac or Bose-Einstein distributions, respectively.

Here, we use time- and angle-resolved photoelectron spectroscopy (trARPES) to study such situation for the prototypical material graphene. We show that upon optical excitation, it exhibits a complex non-equilibrium many-body response by evaluating the Dirac state linewidth and thus the imaginary part of the quasiparticle self-energy $\text{Im}\Sigma$ from spectrally deconvoluted trARPES data. By employing first-principles theoretical modeling, we find that the observed experimental features are caused by ultrafast NEQ scatterings between optical phonons and photoexcited charge carriers, active on timescales well below 100 fs. Düvel, Merboldt *et al.*, Nano Letters, accepted.

O 2.10 Mon 12:45 H3

Coherent Time-Resolved Above-Threshold Plasmoemission from the Au(111) Shockley Surface State — •PASCAL DREHER, DAVID JANOSCHKA, ALEXANDER NEUHAUS, MICHAEL HORN-VON HOEGEN, and FRANK MEYER ZU HERINGDORF — Faculty of Physics, University of Duisburg-Essen, 47048 Duisburg, Germany

Strong nonperturbative interactions of an intense driving light field with the electronic band structure in a solid can result in exotic material properties that do not exist under equilibrium conditions. For suitable driving conditions, Floquet theory predicts that the originally unperturbed electronic structure is modified by the formation of light-dressed electron states in strong fields. Observing such dressing requires electronic state resolution as well as precise control over the intense periodic driving field to overcome intrinsic dissipation and decoherence in the solid.

Here, we explore nano-focusing of femtosecond surface plasmon polariton (SPP) pulses on flat surfaces as a possible route towards strong-field control over electronic states within a solid using time- and angle-resolved photoemission spectroscopy. We observe above-threshold electron emission from the Au(111) Shockley surface state by the absorption of up to seven SPP quanta. Two-dimensional time-resolved photoelectron spectroscopy using a birefringent delay line provides us with direct access to the coherent and incoherent dynamics of the electron emission process with attosecond precision. The presented results clearly indicate the coherent nature of the interaction of the intense SPP nano-focus with the band structure of the material.

O 3: Focus Session: Single Atom Catalysis 1

The field of single atom catalysis has emerged rapidly in recent years out of the desire to utilize less and less precious metals, and remarkable successes have been reported in thermo-, electro-, and photo-catalysis. While much of the early focus was on establishing synthesis routes to achieve atomic dispersion, it has become clear that "single atom" systems cannot be considered as the smallest possible nanoparticle. Because isolated adatoms are stabilized by chemical bonds to the support, they have much more in common with mononuclear complexes used in homogeneous catalysis. Thus, the focus has now changed towards understanding the role of coordination of the active site, and developing ways to tailor it toward specific processes. This has led to much interest in fundamental work, which opens up a tremendous opportunity for surface science to contribute to a hot topic in catalysis.

Organizer: Gareth Parkinson (Technical University Vienna), Matthias Meier (University of Vienna)

Time: Monday 10:30–12:45

Location: H4

Topical Talk

O 3.1 Mon 10:30 H4

Rational design of single atom electrocatalysts: handle with care — •GIANFRANCO PACCHIONI — Dipartimento di Scienza dei Materiali, Università Milano-Bicocca, Milano, Italy

One of the objectives of electronic structure theory is to predict chemical and catalytic activities. This is a challenging target due to the large number of variables that determine the performance of a heterogeneous catalyst. The complexity of the problem has reduced considerably with the advent of single atom catalysts (SAC) and, in particular, of graphene-based SACs for electrocatalytic reactions such as the oxygen reduction (ORR), the oxygen evolution (OER) and the hydrogen evolution (HER) reactions. In this context we assist to a rapidly growing number of theoretical studies based on density functional theory (DFT) and of proposals of universal descriptors that should provide a guide to the experimentalist for the synthesis of new catalysts. In this talk we critically analyze some of the current problems connected with the prediction of the activity of SACs based on DFT: accuracy of the calculations, neglect of important contributions in the models used, physical meaning of the proposed descriptors, inaccurate data sets used to train machine learning algorithms, not to mention some severe problems of reproducibility. It follows that the 'rational design' of a catalyst based on some of the proposed universal descriptors or of the DFT screening of large number of structures should be considered with great caution.

O 3.2 Mon 11:00 H4

Single atom co-catalyst dispersion on KTaO₃ (001) by surface polarity compensation. — •AJI ALEXANDER¹, JESÚS REDONDO¹, DOMINIK WRANA¹, LUKÁŠ FUSEK¹, VIKTOR JOHÁNEK¹, JOSEF MYSLIVEČEK¹, and MARTIN SETVIN^{1,2} — ¹Department of Surface and Plasma Science, Faculty of Mathematics and Physics, Charles University, Prague, Czech Republic — ²Institute of Applied Physics, TU Wien, Vienna, Austria

Redox chemistry on perovskite surfaces attracts attention due to these materials' promising catalytic properties, good ability to separate electron-hole pairs in light-harvesting, and the presence of ferroelectricity in many perovskites. This work focuses on enhancing catalytic activity achieved by activating the perovskite surface with extrinsic metals. Combined STM/AFM measurement together with XPS data shows the tendency of the cobalt atoms to disperse in the form of single adatoms on the polarity uncompensated KTaO₃ (001) surface [1]. The interaction of cobalt with KTO surfaces was studied under various reducing and oxidizing conditions, as well as a function of temperature. This, in turn, will allow characterization of the metallic, oxide, and hydroxide phases of cobalt in dependence on the environment. The work was supported by projects GACR 20-21727X and GAUK Primus/20/SCI/009. [1] M. Setvin, M. Reticioli, F. Poelzleitner et al., *Science* 359, 572 (2018)

O 3.3 Mon 11:15 H4

Comparison study of different transition metals on two TiO₂ model supports: anatase TiO₂(101) and rutile TiO₂(110) — •LENA PUNTSCHER¹, KEVIN DANINGER¹, PANUKORN SOMBUT^{1,2}, MATTHIAS MEIER², MICHAEL SCHMID¹, CESARE FRANCHINI², ULRIKE DIEBOLD¹, and GARETH S. PARKINSON¹ — ¹Institute of Applied Physics, TU Wien, Austria — ²Faculty of Physics, University of Vienna, Vienna, Austria

Single-atom catalysis (SAC) offers an opportunity to minimize the amount of precious catalyst material required for traditional heterogeneous catalysis and to heterogenize reactions presently requiring homogeneous catalysis. Unravelling how metal atoms bind to oxide supports is crucial for a better understanding of the SACs catalytic properties. Using STM and XPS, we compare the adsorption geometry and stability of several transition metals (Pt, Rh, Ir and Ni) on TiO₂ model supports: anatase TiO₂(101) and rutile TiO₂(110), and the influence of water on the dispersion of these systems. While most of the metals rapidly sinter on both surfaces, there are a few exceptions: Ir forms stable adatoms on the anatase support. Ni is much more dispersed when water vapor is added to the deposition and a very low coverage of Pt single atoms can be stabilized in oxygen vacancies formed on rutile (110), which are only stable in UHV conditions. This

study points out the importance of metal-support interaction and the surprisingly different behaviour of the transition metals on TiO₂ model supports.

O 3.4 Mon 11:30 H4

Methane Activation by Free Tantalum Cluster Cations: When the Atomic System is Different — •MARTIN TSCHURL, JAN ECKHARD, and UELI HEIZ — Physical Chemistry, Department of Chemistry and Catalysis Research Center, Technical University of Munich

The efficient conversion of methane into valuable chemicals represents a challenge in chemistry in general. It also carries the potential of becoming a key technological process, given the availability of the substance from fossil, as well as agricultural, sources. Despite decades of research, only steam reforming is used today on commercially relevant scales. Nevertheless, the interest in the topic remains steadily strong, in particular in heterogeneous catalysis. Studies of ion-molecule reactions have already provided substantial contributions to the field and enabled the identification of fundamental reaction pathways and key properties governing them. We use of this approach in order to reveal pathways and reaction kinetics in the C-H bond activation in methane. This way, we comprehensively elucidate the size-dependent reactivity of different cluster cations of tantalum - a metal, which has already been noted as a prospective candidate in the activation of C-H bonds. One of our main finding, in the combined experimental and theoretical study, reveals a significant difference in the reaction of single atoms compared to that of larger clusters. The single atom is the only size that facilitates an often-desired C-C coupling, which further suggests a possible intrinsic benefit of single atoms over clusters in the catalytic conversion of methane.

O 3.5 Mon 11:45 H4

Assessing the environmental benefit of palladium-based single-atom heterogeneous catalysts for Sonogashira coupling — •DARIO FAUST AKL¹, DARIO POIER^{1,2}, SHARON MITCHELL¹, ROGER MARTI², GONZALO GUILLÉN-GOSÁLBEZ¹, and JAVIER PÉREZ-RAMÍREZ¹ — ¹Institute of Chemical and Bioengineering, ETH Zurich, Switzerland — ²ChemTech, HEIA Fribourg, Switzerland

The Pd-Cu catalyzed Sonogashira coupling of terminal alkynes and aryl halides is a cornerstone organic transformation. A cradle-to-gate life cycle analysis (LCA) reveals a two orders of magnitude potential improvement in process footprint when replacing an organometallic Pd catalyst with a heterogeneous analogue. The latter could be easily separated permitting full Pd recovery and catalyst reuse. Heterogeneous catalysts based on isolated metal atoms (single-atom catalysts, SACs) demonstrate promising potential to synergize the benefits of solid and molecular catalysts for efficient Pd utilization. By anchoring Pd atoms on nitrogen-doped carbon we achieve full recovery of the metal, allowing catalyst reuse over multiple cycles. A hybrid process using the Pd-SAC with a homogeneous CuI cocatalyst is more productive than a fully heterogeneous bimetallic Pd-Cu SAC, which deactivates severely due to copper leaching. In some scenarios, the LCA-based metrics demonstrate the process footprint of the hybrid SAC system is leaner than the purely homogeneous counterpart already upon single reuse. Combining LCA with experimental evaluation could guide the design of reusable catalysts for more sustainable organic transformations.

O 3.6 Mon 12:00 H4

Nature of the active species in low-temperature CO oxidation over Pt-CeO₂ model catalysts — •ALEXANDER SIMANENKO¹, MAXIMILIAN KASTENMEIER¹, LESIA PILIAI², TOMÁŠ SKÁLA², YULIYA KOSTO², NATALIYA TSUD², SASCHA MEHL³, MYKHAILO VOROKHTA², IVA MATOLÍNOVÁ², YAROSLAVA LYKHACH¹, and JÖRG LIBUDA¹ — ¹Friedrich-Alexander-Universität Erlangen-Nürnberg, Erlangen, Germany — ²Charles University, Prague, Czech Republic — ³Elettra-Sincrotrone Trieste SCoA, Basovizza-Trieste, Italy

The low-temperature CO oxidation has wide applications in energy production and exhaust gas cleaning. Pt-CeO₂ catalysts with high Pt content allow achieving 100% CO conversion below room temperature. We investigated the nature of active sites on Pt-CeO₂ catalysts under the conditions of low-temperature CO oxi-

dition by means of synchrotron radiation photoelectron spectroscopy, resonant photoemission spectroscopy, and near ambient pressure XPS. Model Pt-CeO₂ systems were prepared by reactive physical vapor co-deposition and annealing in UHV or O₂ in order to obtain different types of platinum species on the surface. These included mainly Pt²⁺ species accompanied by a small number of Pt⁴⁺ species that were reduced to Pt²⁺ or metallic Pt during annealing. Exclusively, stable Pt⁴⁺ species were formed on a thick Pt-CeO₂ catalyst with high Pt content after annealing in oxygen at NAP conditions. The results of our study showed that there is no reduction or oxidation of the Pt-CeO₂ catalysts by CO below 450 K. These observations suggest that low-temperature CO oxidation on Pt-CeO₂ catalyst does not follow a Mars-Van Krevelen mechanism.

O 3.7 Mon 12:15 H4

Adsorption sites and thermal stability of Pt adatoms on Fe₂O₃(1102) — •ALI RAFSANJANI ABBASI, FLORIAN KRAUSHOFER, LENA HAAGER, MORITZ EDER, JIRI PAVELEC, GIADA FRANCESCHI, MICHELE RIVA, MICHAEL SCHMID, ULRIKE DIEBOLD, and GARETH S. PARKINSON — Institute of Applied Physics, TU Wien, Austria

Oxide-supported Pt catalysts offer superior performance because of their high activity and/or selectivity for many important chemical reactions. However, the high cost of Pt and its susceptibility to CO poisoning are two drawbacks to its role as a catalyst. Downsizing catalyst clusters to single atoms is an effective way to reach maximum efficiency, and so-called "single-atom catalysis" is now an important field of research [1]. Nevertheless, stabilizing single Pt atoms on oxide supports without compromising catalytic activity is still a key challenge. Here, we present a surface science study to investigate the local binding environment of Pt adatoms deposited on Fe₂O₃(1102) – (1 × 1) under UHV conditions. Ex-

tensive STM and XPS studies at different Pt surface coverages on Fe₂O₃(1102) revealed that Pt single atoms are highly stable at room temperature. STM images showed that Pt single atoms are adsorbing at two distinct sites with different apparent heights. Through an atom-by-atom analysis, the relative contributions of two types of Pt adsorption sites were determined for different surface coverages. Moreover, thermally induced sintering of the Pt single atoms is traced by means of XPS and STM.

[1] G. S. Parkinson, Catal. Lett. 149, 1137 (2019).

O 3.8 Mon 12:30 H4

Comparison of Single Metal Atoms on a Fe₂O₃ Model Support — •GARETH PARKINSON¹, ALI RAFSANJANI-ABBASI¹, LENA PUNTSCHER¹, FLORIAN KRAUSHOFER¹, PANUKORN SOMBUT¹, CHUNLEI WANG¹, MATTHIAS MEIER^{1,2}, MORITZ EDER¹, JIRI PAVELEC¹, GIADA FRANCESCHI¹, MICHELE RIVA¹, MICHAEL SCHMID¹, CESARE FRANCHINI^{2,3}, and ULRIKE DIEBOLD¹ — ¹TU Wien, Vienna, Austria — ²University of Vienna, Vienna, Austria — ³Università di Bologna, Bologna, Italy

Understanding how the local environment of a "single-atom" catalyst affects stability and reactivity remains a significant challenge. Fe₂O₃ is the most common iron-oxide support material utilized for SAC, but little is known about how metal adatoms bind at its surfaces. In this talk, I will compare and contrast the behavior of Pt, Rh, and Ir atoms on the flat, well-ordered (1x1) termination of Fe₂O₃(1-102). Using a combination of scanning probe microscopy and spectroscopic data, as well as theoretical calculations, I will demonstrate significant differences between the adsorption site and thermal stability of the metals, as well as differences in their interaction with water and CO.

O 4: Topology and Symmetry-Protected Materials

Time: Monday 10:30–11:30

Location: H6

O 4.1 Mon 10:30 H6

Tracing a Weyl Nodal Line in 3D-k-space via ARPES — •TIM FIGGEMEIER¹, MAXIMILIAN ÜNZELMANN¹, PHILIPP ECK², JAKUB SCHUSSER¹, JENNIFER NEU^{3,4}, THEO SIEGRIST^{3,5}, DOMENICO DI SANTE⁶, GIORGIO SANGIOVANNI², HENDRIK BENTMANN¹ and FRIEDRICH REINERT¹ — ¹EP VII, Universität Würzburg, Germany — ²TP I, Universität Würzburg, Germany — ³NHMFL, Tallahassee, FL, US — ⁴Nuclear Nonproliferation Division, ORNL, Oak Ridge, Tennessee 37831, US — ⁵FAMU-FSU, Tallahassee, FL, US — ⁶Center for Computational Quantum Physics, Flatiron Institute, New York 10010, US

In contrast to the more conventional Dirac nodal lines, Weyl nodal lines (WNL) are only twofold-degenerate and this degeneracy is robust against strong spin-orbit coupling [1]. The occurrence of WNL is guaranteed by the combination of a glide plane and time-reversal symmetry (TRS).

In this talk we will present a soft x-ray angle-resolved photoemission (ARPES) study where we will trace a WNL in 3D k-space throughout the Brillouinzone over a wide range of photon energies. The experimental results are compared to density functional and photoemission calculations. By utilizing dichroic ARPES experiments, we will moreover address the characteristics of the electronic wave functions around the WNL.

[1] M. Hirschmann et al., Symmetry-enforced band crossings in tetragonal materials: Dirac and Weyl degeneracies on points, lines, and planes; Phys. Rev. Mat 5; 054202 (2021)

O 4.2 Mon 10:45 H6

Momentum space signatures of Berry flux monopoles in a Weyl semimetal — •MAXIMILIAN ÜNZELMANN^{1,3}, TIM FIGGEMEIER^{1,3}, PHILIPP ECK^{2,3}, BEGMUHAMMET GELDIYEV^{1,3}, DOMENICO DI SANTE^{2,3}, GIORGIO SANGIOVANNI^{2,3}, HENDRIK BENTMANN^{1,3}, and FRIEDRICH REINERT^{1,3} — ¹Experimentelle Physik 7, Universität Würzburg — ²Theoretische Physik 1, Universität Würzburg — ³Würzburg-Dresden Cluster of Excellence ct.qmat

An intriguing property of Weyl semimetals (WSM) is that they feature topologically protected crossings of the spin-polarized valence and conduction bands in their three-dimensional bulk band structure. These crossing points – the Weyl points (WP) – can be considered as 'magnetic' monopoles, which, however, are not located in real space but rather in momentum space. The topological (monopole) character manifests itself in the momentum-dependence of the electronic wave functions, which is investigated in the paradigmatic WSM TaAs, using bulk-sensitive soft X-ray angle-resolved photoelectron spectroscopy combined with spin-resolved measurements and circular dichroism (CD) [1]. The latter addresses the local orbital angular momentum (OAM), which exhibits a non-trivial winding around the WP, similar to the Berry curvature, i.e., the k-space magnetic field. The momentum-dependent modulation of the OAM around the WP – observed in density functional theory calculations and CD-ARPES – thus denotes a direct signature for the Berry flux monopoles in TaAs.

[1] M. Ünzelmann et al., Nat. Commun., 12, 3650 (2021)

O 4.3 Mon 11:00 H6

Lifting the Spin-Momentum Locking in Ultra-Thin Topological Insulator Films — ARTHUR LEIS¹, JONATHAN HOFMANN¹, MICHAEL SCHLEENVOIGT², VASILY CHEREPANOV¹, FELIX LÜPKE¹, PETER SCHÜFFELGEN², GREGOR MUSSLER², DETLEV GRÜTZMACHER², •BERT VOIGTLÄNDER¹, and F. STEFAN TAUTZ¹ — ¹Peter Grünberg Institut (PGI-3), Forschungszentrum Jülich, 52425 Jülich, Germany — ²Peter Grünberg Institut (PGI-9), Forschungszentrum Jülich, 52425 Jülich, Germany

3D topological insulators are known to carry 2D Dirac-like topological surface states in which spin-momentum locking prohibits backscattering. When thinned down to a few nanometers, the hybridization between the topological surface states at the top and bottom surfaces results in a topological quantum phase transition, which can lead to the emergence of a quantum spin Hall phase. Here, the thickness-dependent transport properties are studied on the example of BiSbTe₃ films, with a four-tip scanning tunneling microscope. The findings reveal an exponential drop of the conductivity below the critical thickness. The steepness of this drop indicates the presence of spin-conserving backscattering between the top and bottom surface states, effectively lifting the spin-momentum locking and resulting in the opening of a gap at the Dirac point. Moreover, we probe the edge state conductance these films. The experiments provide a crucial step toward the detection of quantum spin Hall states in transport measurements.

O 4.4 Mon 11:15 H6

Simultaneous AFM and STM measurements of native point Defects in the topological insulator Bi₂Se₃ — •CHRISTOPH SETESCAK, ALEXANDER LIEBIG, ADRIAN WEINDL, and FRANZ J. GIESSBL — Institute of Experimental and Applied Physics, University of Regensburg, Regensburg, Germany

The main properties of topological insulators (TIs) can be derived from the fact that their band structure is "twisted" compared to normal insulators, leading to the creation of gapless states at the surface. To observe these states and make them viable for application in novel technologies it is crucial that the materials delicate electronic structure is not disturbed by defects. So far, experimental characterization of the native point defects relies on scanning tunneling microscopy (STM) and accompanying density functional theory [1]. Here, we present simultaneous atomic force microscopy (AFM) and STM measurements of surface and subsurface defects in Bi₂Se₃. We find not only rarely-observed single Se surface vacancies, but also larger defects that are composed of multiple surface vacancies. The AFM channel furthermore allows us to determine the relative relaxation of surface atoms in proximity of subsurface defects and to determine the polarity of surface defects by means of Kelvin probe force spectroscopy. This is especially valuable as surface Se vacancies contribute to unwanted charge doping of the TI. [1] J. Dai et al., PRL 117, 106401 (2016)

O 5: Organic Molecules at Surfaces 1: Substrate Effects

Time: Monday 10:30–13:00

Location: S051

Topical Talk

O 5.1 Mon 10:30 S051

Molecular nanostructures on metals vs. graphene — •MEIKE STÖHR — Zernike Institute for Advanced Materials, University of Groningen, Netherlands To preserve the (functional) properties of either individual adsorbates or well-ordered molecular assemblies upon adsorption on solid surfaces, the molecule substrate interactions have to be generally relatively weak. This can be achieved by introducing a decoupling layer between (metallic) surface and molecules. Among others, graphene has been shown to be a good choice towards this end due to its low density of states around the Fermi level [1]. For two different organic molecules, the similarities and changes will be discussed when adsorbed on metals and graphene, respectively [2]. In the second part, the formation of chevron-like graphene nanoribbons (GNRs) using Ullmann-type coupling will be presented in dependence of the substrate used. [3] While for Cu(111) and Ag(110) 1D metal-coordinated polymers were obtained GNR formation was successful on Au(111). The electronic properties of the GNRs were observed to display both a length and symmetry dependence. References: [1] S. Maier et al., *Beilstein J. Nanotechnol.* 12 (2021) 950. [2] J. Li et al., *J. Phys. Chem. C* 123 (2019) 12730; J. de la Rie et al., *J. Phys. Chem. C* accepted. [3] T.A. Pham et al., *Small* 13 (2017) 1603675; R.S.K. Houtsmma et al., submitted.

O 5.2 Mon 11:00 S051

Emergence of a singly-occupied state of *p*-terphenyl-based thiols bound to sulphur defects on MoS₂/Au(111) — •J. RIKI SIMON¹, DMITRII MAKSIMOV², JUAN PABLO GUERRERO FELIPE¹, PAUL WIECHERS¹, CHRISTIAN LOTZE¹, ANA M. VALENCIA^{3,4}, CATERINA COCCHI^{3,4}, BJÖRN KOBIN⁴, STEFAN HECHT⁴, MARIANA ROSSI², and KATHARINA J. FRANKE¹ — ¹Freie Universität Berlin, Germany — ²MPI for the Structure and Dynamics of Matter, Hamburg, Germany — ³Carl von Ossietzky Universität Oldenburg, Germany — ⁴Humboldt-Universität zu Berlin, Germany

The combination of transition-metal dichalcogenides (TMDCs) and organic molecules into hybrid inorganic-organic systems is a field gathering much interest in recent years. The use of submonolayers of the TMDC MoS₂ as a decoupling layer in an STM junction is already well established and allows highly resolved *dI/dV* spectra. But 2D materials also have drawbacks: Their properties are highly dependent on their local structure, because defects influence their properties severely. Here we utilise these defects by anchoring the thiol-based molecule CF3-3P-SH (trifluoromethyl-*p*-terphenyl-thiol) into purposely created top-layer sulphur point defects in MoS₂ on Au(111). One end-group of the anchored molecule is bound to the defect, allowing it to rotate around the anchoring point. On such molecules we observe a Kondo resonance. *Ab initio* molecular dynamics simulations show the emergence of a singly-occupied molecular state near E_F depending on the configuration of the molecule with respect to the surface, which in turn gives rise to the observed Kondo resonance.

O 5.3 Mon 11:15 S051

Electron spin resonance of iron-phthalocyanine molecules on a surface — •CHRISTOPH WOLF^{1,2}, XUE ZHANG^{2,3}, YU WANG^{1,2}, PHILIP WILLKE⁴, ANDREAS J. HEINRICH^{1,5}, and TAEYOUNG CHOI² — ¹Center for Quantum Nanoscience, Institute for Basic Science (IBS), Seoul, Republic of Korea — ²Ewha Womans University, Seoul, Republic of Korea — ³Institute of Spin Science and Technology, South China University of Technology Guangzhou, China — ⁴Physikalisches Institut, Karlsruhe Institute of Technology, Karlsruhe, Germany — ⁵Department of Physics, Ewha Womans University, Seoul, Republic of Korea.

The combination of the high energy resolution of electron spin resonance (ESR) and high spatial resolution of the scanning tunneling microscope (STM) resulted in a novel probe with unparalleled capabilities for the study of surface physics.

In this work, we present the first application of this tool to molecules by ESR-STM spectroscopy of iron-phthalocyanine (FePc) molecules on thin layers of the insulator magnesium-oxide deposited on silver. Here, I will focus on the insight gained by combining density functional theory (DFT) and ESR-STM experiment. I will highlight successes and shortcomings of DFT by discussing electronic states of single FePc molecules as well as the interaction between FePc dimers at the neV energy scale.

Finally, I will give an outlook on quantum coherent properties of FePc based on pulsed ESR measurements and a non-equilibrium Green's function model.

O 5.4 Mon 11:30 S051

Mapping of resonant excitation channels of C₆₀/Cu(111) sample system through multiphoton polychromatic momentum microscopy — •MARTIN MITKOV¹, RALF HEMM¹, TOBIAS FEUERBACH¹, AARON GEBERT¹, FLORIAN HAAG¹, KA MAN YU¹, MARTIN AESCHLIMANN¹, and BENJAMIN STADTMÜLLER^{1,2} — ¹TU Kaiserslautern and Research Center OPTIMAS, Erwin-Schrödinger Str. 46, 67663 Kaiserslautern, Germany — ²Institut für Physik, Johannes-Gutenberg-Universität Mainz, Mainz 55128, Germany

Mapping the excited states of organic molecular thin films is of crucial importance for understanding the optical and transport properties of organic materials. Here, we present a multiphoton photoemission study of the excited states of the C₆₀/Cu(111) interface for photon energies between 1.80 eV and 3.35 eV. Characteristic changes in the photoemission spectra for different photon energies allow us to determine the energetic positions of the excited states. In addition, we focus on the momentum-dependent photoemission pattern of the excited molecular states. The latter reveals distinct periodicities and symmetries based on the molecular orbitals involved in the optical excitation process. Altogether, this information will allow us to disentangle resonant intramolecular excitations from the Cu surface state. This allows us to uncover the photon energy-dependent excitation pathways of charge carriers at the C₆₀/Cu(111) interface.

O 5.5 Mon 11:45 S051

Disentangling the Complex Electronic Structure of an Adsorbed Nanographene: Cycloarene C108 — •JOSE MARTINEZ-CASTRO¹, RUSTEM BOLAT¹, QITANG FAN², SIMON WERNER², HADI AREFI¹, TANER ESAT¹, JÖRG SUNDERMEYER², CHRISTIAN WAGNER¹, J. MICHAEL GOTTFRIED², RUSLAN TEMIROV^{1,3}, MARKUS TERNES^{1,4}, and F. STEFAN TAUTZ¹ — ¹Peter Grünberg Institut (PGI-3), Forschungszentrum Jülich, 52425 Jülich, Germany — ²Department of Chemistry, Philipps-Universität Marburg, 35032 Marburg, Germany — ³II. Physikalisches Institut, Universität zu Köln, 50937 Köln, Germany — ⁴II. Institute of Physics, RWTH Aachen University, D-52074 Aachen, Germany.

We combine low-temperature scanning tunneling spectroscopy, CO functionalized tips and algorithmic data analysis to investigate the electronic structure of the molecular cycloarene C108 (graphene nanoring) adsorbed on a Au(111) surface. We demonstrate that CO functionalized tips enhance the visibility of molecular resonances, both in differential conductance spectra and in real-space topographic images. Comparing our experimental data with *ab-initio* density functional theory reveals a remarkably precise agreement of the molecular orbitals and enables us to disentangle close-lying molecular states only separated by 50 meV at an energy of 2 eV below the Fermi level. We propose this combination of techniques as a promising new route for a precise characterization of complex molecules and other physical entities which have electronic resonances in the tip-sample junction.

O 5.6 Mon 12:00 S051

Tuning of structure of cyano-porphyrin self-assemblies on surfaces: from metals to bulk insulators — MAXIMILIAN AMMON¹, MIRUNALINI DEVARAJULU¹, YI LIU¹, MARTIN GURRATH², DOMINIK LUNGERICH³, •BINBIN DA¹, NORBERT JUX³, BERND MEYER², and SABINE MAIER¹ — ¹Department of Physics, FAU Erlangen-Nürnberg, Erlangen, Germany. — ²Interdisciplinary Center for Molecular Materials and Computer Chemistry Center, FAU Erlangen-Nürnberg, Erlangen, Germany. — ³Lehrstuhl für Organische Chemie II, FAU Erlangen-Nürnberg, Erlangen, Germany.

We discuss the adsorption and binding motifs in self-assembled Zn-*p*CNTPP networks on Au(111), KBr(001), and MgO(001) using low-temperature STM and nc-AFM combined with DFT. Zn-CNTPPs adopt a planar adsorption geometry with the macrocycle parallel to the surface on all three surfaces and assemble in well-ordered islands. While a global minimum structure is found on KBr due to a strong CN···K interaction, multiple and energetically nearly equivalent adsorption sites occur on MgO and Au. Therefore, commensurate adsorption is suggested on KBr, while optimizing the molecule-molecule interactions over molecule-surface interactions is more important on MgO and Au, which the STM and nc-AFM data experimentally evidence.[1] However, since the interaction of porphyrins with Au(111) is stronger than on MgO(001), the phenyl rings are more inclined toward the surface, resulting in larger unit cells on Au(111) and also the binding motif of the cyanophenyl groups changes.

[1] Ammon, M. et al., *Surface Science*, 723, 122097, 2022.

O 5.7 Mon 12:15 S051

Comparing adsorption of triphenylene derivatives: metallic vs. graphitic surfaces — •JORIS DE LA RIE¹, MIHAELA ENACHE¹, QIANKUN WANG¹, WENBO LU¹, NICO SCHMIDT¹, MILAN KIVALA², and MEIKE STÖHR¹ — ¹Zernike Institute for Advanced Materials, University of Groningen — ²Institute of Organic Chemistry, University of Heidelberg

Thin films of organic molecules show great promise for applications in future (nano)electronic devices, such as solar cells, light emitting diodes and transistors. A major factor in the performance of these films is the interface between substrate and molecular film. The interfacial properties depend on the balance between intermolecular and molecule-substrate interactions. Herein, we present a comparative study on self-assembled monolayers (SAMs) of a triphenylene-based donor molecule (HAT) on three substrates: Ag(111), graphene/Ir(111)

and graphene/Ni(111). We studied the structure of the SAMs by means of scanning tunneling microscopy and low-energy electron diffraction, and their interaction with the substrates by X-ray and ultraviolet photoelectron spectroscopy. On each substrate, HAT formed a close-packed hexagonal network that is commensurate with the substrate. From the photoelectron spectroscopy measurements we only found a weak (physisorptive) interaction between molecules and substrates. This goes against the established belief for SAMs on metal surfaces, where commensurate networks are principally formed on strongly interacting surfaces where the molecules chemisorb.

O 5.8 Mon 12:30 S051

The Number of KCl layers counts:

Thickness dependent Growth of Quinacridone on KCl on the Ag(100) surface — •NIKLAS HUMBERG¹, RÉMI BRETTEL², and MORITZ SOKOLOWSKI¹ — ¹Institut für Physikalische und Theoretische Chemie der Universität Bonn, Germany — ²University of Paris-Saclay, Institut des Sciences Moléculaires D'Orsay, France

The epitaxial growth of the prochiral molecule quinacridone (QA) on an insulating KCl layer on the Ag(100) surface was investigated by STM. If QA is deposited onto a complete KCl layer, then the growth of QA structures is strongly dependent on the thickness of the KCl layer. For small amounts of QA on thin KCl layers small domains of parallel molecular chains were observed. The structure of these chains is identical to the chains that were previously observed on the Ag(100) surface. However, the repulsive substrate mediated interaction between neighboring chains that was observed on the Ag(100) surface cannot be observed on such KCl layers. Interestingly, depositing larger amounts of QA on such KCl layers leads to the formation of three-dimensional chain-like structures that show some similarities with the bulk crystal structures of QA.

Contrary to this, on thick KCl layers on the Ag(100) surface that are five or

more monolayers high dewetting of the molecules and a formation of three-dimensional QA clusters was already observed for very small amounts of QA. These effects are explained by the interaction between the QA molecules and the silver substrate which still plays a role for thin layers but is suppressed by thick KCl layers.

O 5.9 Mon 12:45 S051

Growth of chiral heptahelicene molecules on ferromagnetic Co and Fe thin-film substrates — •MOHAMMAD REZA SAFARI, FRANK MATTHES, DANIEL E. BÜRGLER, and CLAUD M. SCHNEIDER — Peter Grünberg Institut (PGI-6), Forschungszentrum Jülich, 52425 Jülich, Germany

The discovery of chirality-induced spin selectivity effects [1,2], which result from an interaction between the electron spin and the handedness of chiral molecules, has sparked interest in surface-adsorbed chiral molecules due to potential applications in spintronics, enantioseparation, and chemical sensing. Here, we report growth studies of chiral heptahelicene molecules on two monolayers Fe on W(110), Co bilayer nano-islands on Cu(111), and for comparison on Cu(111) by low-temperature spin-polarized scanning tunneling microscopy. In all cases, the molecules remain intact, adsorb in a flat configuration, and exhibit specific in-plane orientations that reflect the symmetry of the substrate lattices. The Co and Fe layers remain out-of-plane magnetized after molecular adsorption. In addition, we are able to determine the helicity of individual molecules adsorbed on the highly reactive Fe and Co surfaces in a similar manner as previously reported for the less reactive Cu(111) surface [3]. These observations pave the way for further investigations of CISS effects in well-defined molecule-substrate systems on the single-molecule scale as a basis for theoretical modeling.

[1] B. Göhler *et al.*, *Science* **331**, 894 (2011). [2] K. Banerjee-Ghosh *et al.*, *Science* **360**, 1331 (2018). [3] K.-H. Ernst *et al.*, *Nano Lett.* **15**, 5388 (2015).

O 6: Nanostructures at Surfaces 1

Time: Monday 10:30–13:00

Location: S052

O 6.1 Mon 10:30 S052

Autonomous non-contact molecular manipulation of nanocars based on reinforcement learning — •BERNHARD R. RAMSAUER¹, GRANT J. SIMPSON², LEONHARD GRILL², OLIVER T. HOFMANN¹, and ANDREAS JEINDL¹ — ¹Institute of Solid State Physics, NAWI Graz, Graz University of Technology, Petersgasse 16, 8010 Graz, Austria — ²Institute of Chemistry, NAWI Graz, University Graz, Heinrichstraße 28/IV, 8010 Graz, Austria

At the world's first race of nanocars at the CEMES-CNRS, in France, participants had to direct a nanocar across a specific *racetrack* [1]. In order to control their nanocar, they have to manipulate it via an STM-tip, without being in direct contact with the nanocar. The physics that govern the molecule's movement and rotation is complex and involves the interaction between the tip and the molecule as well as the molecule and the substrate [2]. Thus, it requires time and effort for humans to be able to maneuver a molecule with a reasonable success rate. However, predicting the outcome of a performed action is unintuitive and often hard to predict for humans. Therefore, we developed an artificial intelligence (AI) based on reinforcement learning (RL) and show how it can be implemented to manipulate single molecules. The AI utilizes an off-policy learning algorithm known as Q-Learning. Our results can be the basis for more sophisticated techniques of non-contact molecular manipulations. This allows to identify and manoeuvre single molecules at will, building the basis for future bottom-up constructions of nanotechnology. [1] G. Rapenne *et al.*, *Nature Rev. Mater.* **2**, 17040 (2017) [2] G. J. Simpson *et al.*, *Nature Nanotech.* **12**, 604 (2017)

O 6.2 Mon 10:45 S052

Constructing covalent organic nanoarchitectures molecule by molecule via scanning probe manipulation — QIGANG ZHONG^{1,2}, ALEXANDER IHLE^{1,2}, SEBASTIAN AHLES^{2,3}, HERMANN A. WEGNER^{2,3}, ANDRE SCHIRMEISEN^{1,2}, and •DANIEL EBELING^{1,2} — ¹Institute of Applied Physics, Justus Liebig University Giessen, Germany. — ²Center for Materials Research, Justus Liebig University Giessen, Germany. — ³Institute of Organic Chemistry, Justus Liebig University Giessen, Germany

Constructing low-dimensional covalent assemblies with tailored size and connectivity is challenging yet often key for applications in molecular electronics where optical and electronic properties of the quantum materials are highly structure dependent. We present a versatile approach for building such structures block by block on bilayer sodium chloride (NaCl) films on Cu(111) with the tip of an atomic force microscope, while tracking the structural changes with single-bond resolution. Covalent homo-dimers in *cis* and *trans* configurations and homo-/hetero-trimers were selectively synthesized by a sequence of dehalogenation, translational manipulation and intermolecular coupling of halogenated precursors. Further demonstrations of structural build-up include complex bonding motifs, like carbon-iodine-carbon bonds and fused carbon pentagons. This work paves the way for synthesizing elusive covalent nanoar-

chitectures, studying structural modifications and revealing pathways of intermolecular reactions.

Nature Chemistry **13**, 1133-1139 (2021)

O 6.3 Mon 11:00 S052

Electronic and magnetic properties of an on-surface synthesized 2D metal organic framework — •AMINA KIMOUCHE^{1,2}, ROBERTO ROBLES³, NOEMI CONTRERAS¹, DANIEL RUIZ¹, and AITOR MUGARZA^{1,4} — ¹Institut Català de Nanociència i Nanotecnologia, Barcelona, Spain — ²Institut für Physik und Astronomie, Universität Potsdam, Potsdam, Germany — ³Centro de Física de Materiales CFM/MPIC (CSIC-UPV/EHU), Donostia-San Sebastián, Spain — ⁴ICREA Institució Catalana de Recerca i Estudis Avançats, Barcelona, Spain

2D MOFs constitute a new class of designer materials where the coexistence of Dirac electrons and flat bands can lead to rich physical phenomena and to the realization of quantum phases such as topological or quantum anomalous Hall insulators.

Following the concepts of coordination chemistry, based on a surface-assisted self-assembly of the metal and organic components, we have carried out synthesis of Iron-hexaiminotriphenylene (HITP) MOFs on Au(111) substrate and characterized their electronic structure using scanning tunnelling spectroscopy (STS). On the other hand, ab-initio calculations of the observed structures indicate the presence of strong ferromagnetic interactions that persist under the influence of the Au substrate, indicating that the interaction with the Au substrate stabilizes even further the FM state on Fe3(HITP)2. We relate such strong magnetic interactions to the formation of a radical spin at the ligand that mediate the inter-ionic interactions.

O 6.4 Mon 11:15 S052

Host guest chemistry and supramolecular doping in triphenylamine-based covalent frameworks on Au(111) — CHRISTIAN STEINER¹, LUKAS FROMM², JULIAN GEBHARDT², YI LIU¹, ALEXANDER HEIDENREICH², NATALIE HAMMER², •HEXIA SHI¹, ANDREAS GÖRLING², MILAN KIVALA³, and SABINE MAIER¹ — ¹Department of Physics, Friedrich-Alexander Universität Erlangen-Nürnberg, Erlangen, Germany — ²Department of Chemistry and Pharmacy, Friedrich-Alexander Universität Erlangen-Nürnberg, Erlangen, Germany — ³Organisch-Chemisches Institut & Centre for Advanced Materials, Ruprecht-Karls-Universität Heidelberg, Heidelberg, Germany

We report the host-guest interaction in triphenylamine-based covalently-linked macrocycles and networks on Au(111) using low-temperature scanning tunneling microscopy in combination with density-functional theory. Triphenylamine precursors formed macrocycles and 2D networks featuring carbonyl- and hydrogen-functionalized pores, creating preferred adsorption sites for trimethylamine (TMA) and halogen atoms. TMA binds through hydrogen bonds to the carbonyl sites while halogens selectively adsorb between two carbonyl groups

at Au hollow sites. Band structure calculations reveal that TMA adsorption reduces the electronic band gap of the triphenylamine covalent frameworks due to charge transfer, while the interaction of the halogens leads to a slight downshift of the bands.^[1]

[1] Steiner, C. et al. *Nanoscale*, 2021, 13, 9798-9807.

O 6.5 Mon 11:30 S052

Carbon-carbon coupling on inert surfaces via a radical deposition source - proof-of-concept, challenges and perspective — •GIANLUCA GALEOTTI¹ and MARKUS LACKINGER^{1,2} — ¹Deutsches Museum, Museumsinsel 1, 80538 Munich, Germany — ²Technische Universität München, James-Franck-Str. 1, 85748 Garching, Germany

The realization of one-atom thin C-C-bonded nanostructures is an ongoing challenge of nanotechnology. Those are, however, almost exclusively synthesized on metal surfaces, taking advantage of the catalytic activity to lower the required temperature for monomer activation below the desorption threshold. The development of methods for the direct synthesis on inert and insulating surfaces would be a milestone in the field, enabling studies of nearly unperturbed covalent nanostructures with unique electronic properties, such as graphene nanoribbons and-conjugated 2D polymers. Here, we will describe the development of a Radical Deposition Source (RaDeS) for the direct deposition of radicals onto inert surfaces for subsequent coupling into C-C bonded polymers. The radicals are generated en route by indirect deposition of halogenated precursors through a heated reactive tube, where the dehalogenation reaction proceeds. As a model system for inert surfaces, we use Ag(111) passivated with a closed monolayer of chemisorbed iodine. We will first illustrate the proof-of-concept with the synthesis of poly-para-phenylene from iodinated terphenyl precursors. Subsequently, we show how this approach can be used to overcome limitations of the conventional on-surface synthesis imposed by desorption, opening additional pathways for the synthesis of nanostructures.

O 6.6 Mon 11:45 S052

Carbon-based low-dimensional materials from first principles — •NIKLAS ENDERLEIN, ROLAND GILLEN, SABINE MAIER, and JANINA MAULTZSCH — Friedrich-Alexander-Universität Erlangen-Nürnberg

Bottom-up synthesis of carbon-based networks from molecular precursors offers a promising path to material design, where the structural, electronic, optical and vibrational properties, in principle, can be tailored through the choice of the precursor structures and functionalization. Prominent examples for this method are chevron-type graphene nanoribbons with defined topology [1] and highly controllable nitrogen incorporation [2], or multifunctional nanoporous graphene [3]. Considering the vast number of possible carbon-based networks, density functional theory (DFT) is a powerful tool for the preselection and design of promising molecular precursors based on the computational prediction of their intrinsic physical properties.

In this spirit, we present the results of recent DFT simulations on potentially interesting carbon-based networks that lend themselves to on-surface bottom-up synthesis through Ullmann coupling of well-defined molecular precursors. We show how the electronic properties are significantly affected by the network topology and the structure of the molecular building blocks, potentially giving rise to novel phenomena. Our results inspire further efforts in the direction of molecular precursor design.

[1] Y. Lee et al., *Nano letters* 18.11, 7247-7253 (2018)

[2] C. Bronner et al., *Angewandte Chemie* 125.16, 4518-4521 (2013)

[3] C. Moreno et al., *Science* 360.6385, 199-203 (2018)

O 6.7 Mon 12:00 S052

Covalently linked molecules as 1D materials — •SAMUEL VASCONCELOS and MICHAEL ROHLFING — University of Münster

We performed first-principles calculations to address the problem of the formation and characterization of covalently linked structures with molecules as building blocks. We show that upon pressure a re-hybridization process takes place which leads to one-dimensional compounds resembling nanowires, in which carbon atoms are all 4-fold coordinated and possess remarkable mechanical properties. We show that for porphyrins, the resulting 1D nanostructures have metallic character. Moreover, in the case of porphyrin-metal complexes,

we find that the covalently linked structures may be a platform for the stabilization of straight metallic wires. We extend the methodology for the kekulene family, that throughout the same processes forms sp³ nanotubes.

O 6.8 Mon 12:15 S052

Peierls distortion and charge density waves in novel exfoliable 1D materials — •CHIARA CIGNARELLA¹, DAVIDE CAMPI², and NICOLA MARZARI¹ — ¹THEOS and MARVEL, EPFL, Lausanne, Switzerland — ²Universita di Milano Bicocca, Milano, Italy

One-dimensional materials are extremely attractive due to their unique electronic properties and potentialities in next-generation applications. A high-throughput screening has provided a portfolio of more than 800 novel 1D/quasi-1D materials exfoliable from the 3D Van der Waals compounds, out of which we select a dataset of metallic chains as possible candidates for vias and interconnects. Often, their low-dimensional nature leads to dynamical instabilities in the form of Peierls distortions or charge density waves (CDW), which drive structural phase transitions at finite wavevectors. Here, we analyse the stability of this novel class of materials, identifying the reconstructed stable superstructure from the phonon modes. In order to get more insight into the mechanism of the CDW, we then investigate the nesting function and the critical role of the electron-phonon coupling, still unexplored in real quasi-1D systems.

O 6.9 Mon 12:30 S052

Emulating organic molecular orbitals with artificial atoms on a surface — •E. SIERDA, D. BADRTDINOV, B. KIRALY, E. J. KNOL, X. HUANG, M. I. KATSNELSON, G. C. GROENENBOOM, D. WEGNER, M. RÖSNER, and A. A. KHAJETOORIANS — Institute for Molecules and Materials, Radboud University, Nijmegen, The Netherlands

Bottom-up strategies to emulate the orbital structure of organic compounds is an exciting prospect, especially for molecules that are complex, unstable or hard to isolate, e.g. cyclobutadiene or triangulene. A successful implementation of such an emulator requires creating and coupling artificial atoms with multi-orbital character and possibility for orbital hybridization, on a platform that does not couple to the emulated structure. We emulate the electronic structure of planar organic molecules, using coupled, bottom-up constructed quantum dots (QDs) composed of atomic ions. We illustrate that compact clusters of ions, created via atom manipulation, exhibit a well pronounced state, localized within the semiconductor bulk band gap. For a pair of such QDs, we observe two states and identify them as bonding and anti-bonding via spatial maps. Linear chains of QDs exhibit emulated linear combinations of atomic orbitals with both s- and p-like character. Furthermore, we construct artificial structures resembling sp²-hybridized organic molecules. A rich electronic structure with pronounced states is found in tunneling spectroscopy. By comparing their spatial maps with quantum-chemical simulations of the organic compound, we can identify the states as emulated organic orbitals, providing evidence for sp² hybridization present in the artificial structures.

O 6.10 Mon 12:45 S052

Substrate-mediated polymorphism in monolayer self-assembly at liquid-solid interfaces — •ARASH BADAMI BEHJAT¹, WOLFGANG HECKL^{1,2}, MICHAEL SCHMITTEL³, and MARKUS LACKINGER^{1,2} — ¹Technical University of Munich, James-Franck-Str. 1, 85748 Garching, Germany — ²Deutsches Museum, Museumsinsel 1, 80538 Munich, Germany — ³Universität Siegen, Adolf-Reichwein-Str. 2, 57068 Siegen, Germany

Scanning-Tunneling Microscopy (STM) studies of molecular self-assembly at liquid-solid interfaces require atomically flat, chemically inert, and electrically conductive substrates, hence are almost exclusively carried out on graphite. Here, we demonstrate that Au (111) passivated with a monolayer of chemisorbed iodine (I-Au(111)) constitutes a viable alternative for fundamental studies. By using aromatic homologues of tricarboxylic acids as a versatile model system, and by a direct comparison between graphite and I-Au (111), we experimentally study and demonstrate the decisive influence of molecule-surface interactions. We present three cases of a novel substrate-mediated polymorphism. On I-Au(111), we consistently find polymorphs with lower packing density and optimized intermolecular binding—a clear indication for diminished molecule-surface interactions. This hypothesis was corroborated by probing the monolayer's thermodynamic stability in variable temperature STM experiments.

O 7: New Methods and Developments 1: Scanning Probe Techniques 1 (joint session O/KFM)

Time: Monday 10:30–13:00

Location: S053

Topical Talk

O 7.1 Mon 10:30 S053

Identification of active electrocatalytic centers using EC- STM under reaction conditions — •ALIAXSANDR BANDARENKA — Technical University of Munich, Department of Physics, James-Franck-Str 1, 85748 Garching bei München, Germany

Identification of so-called active electrocatalytic centres can be very complicated under reaction conditions. In many cases, electrochemical scanning tunnelling microscopy can be efficiently used to do so by comparing the tunnelling noise in the presence and the absence of the electrocatalytic reactions. In the presentation, I will discuss examples, which deal with finding the active sites at the surface of

various electrodes for hydrogen evolution, oxygen reduction, and oxygen evolution reactions. Pt, HOPG, Pt-alloys, and transition metal oxides are used as the model systems.

O 7.2 Mon 11:00 S053

Coherent Noise Removal for Scanning Probe Microscopy — JENS OPPLIGER, DANYANG LIU, and FABIAN DONAT NATTERER — Department of Physics, University of Zurich, Winterthurerstrasse 190, CH-8057, Switzerland

Despite the best efforts to isolate the weak signals in scanning probe microscopes from sources of noise, white and coherent noise remain major nuisances. While the presence of Gaussian white noise can be handled with temporal averaging, the influence of high-Q coherent noise, such as coming from ground-loops or mechanical resonances, is less straightforward to delete when rastering along the surface. Such noise leads to characteristic streaks and spurious Bragg peaks in the Fourier transform of two-dimensional data. Here we demonstrate a straightforward method to remove coherent noise using data-labelling and exemplify its working for quasiparticle interference and topographic imaging.

O 7.3 Mon 11:15 S053

General, Strong Impurity-Strength Dependence of Quasiparticle Interference — SEUNG-JU HONG¹, JAE-MO LIHM^{1,2,3}, and CHEOL-HWAN PARK^{1,2,3} — ¹Department of Physics and Astronomy, Seoul National University, Seoul 08826, Korea — ²Center for Correlated Electron Systems, Institute for Basic Science, Seoul 08826, South Korea — ³Center for Theoretical Physics, Seoul National University, Seoul 08826, South Korea

Quasiparticle interference patterns induced by impurities contain information about electronic structures in momentum space. In this presentation, we show that the interpretation of quasiparticle interference patterns is not trivial and needs special care. Even in the simple case of a single-site impurity on the square lattice, the pattern is strongly dependent on the strength of impurity potential. For example, the wave vector with the strongest scattering differs by about 16% in spin-dependent JDOS and exact QPI computations. We also showed that this dependence can be analyzed by decomposing the pattern into the impurity-dependent T-matrix part and momentum-dependent Green function part. We applied our formalism to TaAs, an archetype Weyl semimetal with first-principles calculations. We find that the strong dependence on impurities is also present in TaAs. Thus, our work demonstrates that these quasiparticle interference patterns must be analyzed with care and needs more attention.

Reference [1] S.-J. Hong, J.-M. Lihm, and C.-H. Park, *J. Phys. Chem. C* 2021, 125, 13, 7488-7494

O 7.4 Mon 11:30 S053

Real-space sub-femtosecond imaging of quantum electronic coherences in molecules — MANISH GARG¹, ALBERTO MARTIN-JIMENEZ¹, MICHELE PISARRA², YANG LUO¹, FERNANDO MARTIN^{2,3,4}, and KLAUS KERN^{1,5} — ¹Max Planck Institute for Solid State Research, Stuttgart, Germany — ²Instituto Madrileño de Estudios Avanzados en Nanociencia (IMDEA Nano), Madrid, Spain — ³Universidad Autónoma de Madrid (UAM), Madrid, Spain — ⁴Condensed Matter Physics Center (IFIMAC), Universidad Autónoma de Madrid, Madrid, Spain — ⁵Institut de Physique, Ecole Polytechnique Fédérale de Lausanne, Lausanne, Switzerland

Tracking electron motion in molecules is the key to understand and control chemical transformations. Contemporary techniques in attosecond science have the capability to generate and trace the consequences of this motion in real time, but not in real space. Scanning tunnelling microscopy (STM), on the other hand, can locally probe the valence electron density in molecules, but cannot provide by itself dynamical information at this ultrafast time-scale. Here we show that, by combining STM and attosecond technologies, quantum electronic coherences induced in molecules by < 6 femtosecond long carrier-envelope-phase (CEP) stable near-infrared laser pulses can be directly visualized with angstrom-scale spatial and sub-femtosecond temporal resolutions. We demonstrate concurrent real-space and real-time imaging of coherences involving the valence orbitals of perylenetetracarboxylic dianhydride (PTCDA) molecules, and full control over the population of the involved orbitals.

O 7.5 Mon 11:45 S053

Femtosecond Tip-Enhanced Coherent Anti-Stokes Raman Spectroscopy of a Single Graphene Nanoribbon — YANG LUO¹, ALBERTO MARTIN-JIMENEZ¹, MANISH GARG¹, and KLAUS KERN^{1,2} — ¹Max Planck Institute for Solid State Research, Stuttgart, Germany — ²Institut de Physique, Ecole Polytechnique Fédérale de Lausanne, Lausanne, Switzerland

By integration of ultrashort laser pulses with a scanning tunneling microscope (STM) one can study the electronic and carrier dynamics with very high spatial and temporal resolution. Nevertheless, molecular vibrational modes at the single-molecule level are difficult to track, owing to the lack of energy resolution. To overcome this barrier, we have now integrated a local spectroscopic tool, combining ultrafast laser pulses with an STM-based tip-enhanced Raman spectroscopy (TERS). By performing TERS with femtosecond laser pulses, we have tracked vibrational coherences and phonon dephasing dynamics in a single graphene nanoribbon (7-GNR). The decoherence time ($T_2/2 \sim 440$ fs) of

the phonons in a GNR has been obtained from the time-resolved coherent anti-Stokes Raman spectra. Temporal evolution of vibrational coherences (beatings) between different phonon modes in the GNR has been measured, which evolve on time scales as short as ~ 100 fs. This work lays the foundation for investigating intramolecular vibrational coherences and vibronic dynamics with utmost spatial, temporal and energy resolutions, simultaneously.

O 7.6 Mon 12:00 S053

Coherent phonon spectroscopy on the nanoscale — SHUYI LIU¹, ADNAN HAMMUD¹, IKUTARO HAMADA², MARTIN WOLF¹, MELANIE MÜLLER¹, and TAKASHI KUMAGAI³ — ¹Fritz-Haber-Institut, Berlin, Germany — ²College of Materials Science and Engineering, Hunan, China — ³Institute for Molecular Science, Okazaki, Japan

Coherent phonon (CP) spectroscopy is a powerful tool to monitor ultrafast lattice dynamics under nonequilibrium conditions, providing insight into microscopic interactions that dictate macroscopic material properties. In imperfect crystals, the excitation and relaxation of CPs will be susceptible to the nanoscale environment, calling for real-space observation of ultrafast lattice dynamics. We demonstrate nanoscale coherent phonon spectroscopy by means of ultrafast laser-induced scanning tunneling microscopy (STM) in a plasmonic junction. Comparison of the CP spectra with tip-enhanced Raman spectroscopy allows us to identify the involved phonon modes. In contrast to the Raman spectra, the relative CP intensities exhibit strong nanoscale spatial variations, which correlate with changes in the local density of states recorded via scanning tunneling spectroscopy. Our work introduces a new approach to study the ultrafast structural response at solid surfaces using optical STM.

O 7.7 Mon 12:15 S053

Construction of a dry low temperature STM — SIMON GERBER¹ and WULF WULFHEKEL² — ¹Physikalisches Institut, Karlsruhe Institute of Technology — ²Physikalisches Institut, Karlsruhe Institute of Technology

Driven by rising helium prices, we design a dry, low temperature Scanning Tunneling Microscope with a closed helium cycle. We designed a compact dry four stage cryostat with an integrated dilution refrigerator which is cooled using helium from a 400 mW cold head. The STM is connected to the dilution refrigerator and allows measurements down to millikelvin temperatures. The system is mechanically decoupled at several points to minimize vibrations from the cold head reaching the STM. The microscope is positioned inside a split-coil magnet with magnetic fields up to 4T. Optical Access to the STM is possible in the parked position and allows fast tip and sample exchange. The tips and samples can then be prepared under UHV conditions. The complete cryostat and the STM are home-built.

O 7.8 Mon 12:30 S053

Probing tunneling processes into YSR states with microwaves — JANIS SIEBRECHT¹, HAONAN HUANG¹, PIOTR KOT¹, SUJOY KARAN¹, CIPRIAN PADURARIU², BJÖRN KUBALA², JOACHIM ANKERHOLD², ALFREDO LEVY YEYATI³, JUAN CARLOS CUEVAS³, and CHRISTIAN R. AST¹ — ¹Max-Planck-Institut für Festkörperforschung, Stuttgart, Germany — ²Institut für Komplexe Quantensysteme and IQST, Universität Ulm, Ulm, Germany — ³Departamento de Física Teórica de la Materia Condensada and Condensed Matter Physics Center (IFIMAC), Universidad Autónoma de Madrid, Madrid, Spain

Microwaves are an important tool in the manipulation of multi-level systems such as single spins on a surface, nitrogen vacancies in diamond or double quantum dots. Here we use a scanning tunneling microscope (STM) at a base temperature of 0.56 K to probe the intrinsic YSR states in a Vanadium tip in contact with a V(100) surface. The addition of an E-Band (60-90 GHz) microwave antenna at the junction opens the possibility to study the behavior of YSR states with AC driving - a scenario which has been subject to many theoretical but very few experimental studies. Using microwave-assisted tunneling, we gain insight into how the excited state participates in the tunneling process and how this is related to Andreev processes and parity conservation. Our results point at a new path, namely microwave manipulation of YSR states, which could be an important step towards using YSR states as qubits.

O 7.9 Mon 12:45 S053

Compressed fingerprint spectroscopy based on scanning microscopy — BERND KÄSTNER¹, MANUEL MARSCHALL¹, ARNE HOEHL¹, ANDREA HORNEMANN¹, GERD WÜBBELER¹, SELMA METZNER¹, PIOTR PATOKA², ECKART RÜHL², and CLEMENS ELSTER¹ — ¹Physikalisch-Technische Bundesanstalt, Berlin, Germany — ²Freie Universität Berlin, Germany

The infrared spectral region between 400 and 4000 cm^{-1} is called the fingerprint region, because the absorption features are unique to individual organic substances. Such a spectrum usually contains many peaks, making it difficult to link individual peaks to the substance. Consequently, the spatial mapping of substances requires spectral imaging, where at each point in space a complete spectrum needs to be recorded. Usually this can be achieved by spectrometers equipped with array detectors. Recently, scanning methods based on the optical nearfield and local thermal expansion with nanoscale spatial resolution have been developed allowing sub-diffraction spectral imaging. However, the inher-

ently serial recording severely limits their imaging application due to long acquisition times involved and the resulting stability issues. In this work we demonstrate different strategies to significantly reduce the measurement time in spec-

tral imaging measurement by compressing the measurement combined with a low-rank matrix reconstruction. Several examples from different fields of application will be discussed.

O 8: Solid-Liquid Interfaces 1: Reactions and Electrochemistry

Time: Monday 10:30–12:45

Location: S054

Topical Talk

O 8.1 Mon 10:30 S054

Dynamic structure changes of bare and modified Cu(111) during CO and water activation — •ANDREA AUER¹, NICOLAS HÖRMANN², MIE ANDERSEN³, KARSTEN REUTER², and JULIA KUNZE-LIEBHÄUSER¹ — ¹Institute of Physical Chemistry, University of Innsbruck, Austria — ²Fritz-Haber-Institut der Max-Planck-Gesellschaft, Berlin, Germany — ³Aarhus Institute of Advanced Studies, Denmark

CO is a key intermediate in the electro-oxidation of energy carrying fuels. Single-crystal Cu(111) model catalysts efficiently electro-oxidize CO in alkaline media, under strong and continuous surface structural changes that lead to simultaneous strengthening of the CO and weakening of the OH binding, which makes the observed high activity possible.

Cu(111) modified with Ni(OH)₂ and Co(OH)₂ reveals strong morphological changes upon adatom deposition, which lead to a significant enhancement in the rate of the alkaline hydrogen evolution reaction (HER), one of the most important processes in the development of hydrogen-based energy conversion devices. Adatom modification influences the charge distribution at the solid/liquid interface by a decrease of the electric field strength negative of the potential of zero charge. This implies an easier reorganization of the interfacial water molecules facilitating charge transfer through the double layer. The tendency of Cu(111) to restructure is found to dominate its electrochemical properties. The structural changes of the electrode surface are intimately related to the electric field at the solid/liquid interface and to its electrocatalytic activity, in general.

O 8.2 Mon 11:00 S054

Cu(111) reconstruction and oxidation imaged in oxygen free alkaline media with electrochemical scanning tunneling microscopy — •TONI MOSER, ANDREA AUER, and JULIA KUNZE-LIEBHÄUSER — Department of Physical Chemistry, University of Innsbruck, Innrain 52c, Innsbruck, Austria

Cu has recently gained attention due to its capability to efficiently oxidize CO at low overpotentials^[1]. However, the structural evolution of the surface at anodic potentials causing initiation of oxide formation under complete exclusion of oxygen has yet to be fully understood. While Cu(111) oxidation has previously been studied with electrochemical scanning tunneling microscopy (EC-STM), investigations without atmospheric oxygen and without contamination from dissolved glassware in alkaline media are sparse. Recent results indicate a significant delay in the anodic formation of Cu₂O in completely deaerated alkaline electrolyte, which indicates a significant impact of dissolved O₂ on the oxidation of copper surfaces. In this work, we focus on the in-situ investigation of hydroxide adsorption on and oxidation of Cu(111) via EC-STM, eliminating atmospheric oxygen by conducting the experiments inside an Ar-filled glove box. The delayed formation of an amorphous oxide layer at anodic potentials and subsequent reduction processes at cathodic potentials, where a smoothening of the surface can be observed, as well as new insights into the hydroxide adsorption structure are presented.

[1] A. Auer, M. Andersen, E.-M. Wernig, N. G. Hörmann, N. Buller, K. Reuter & J. Kunze-Liebhäuser, *Nat Catal* 3, 797–803 (2020).

O 8.3 Mon 11:15 S054

Enhanced Field Effects at Protruding Defect Sites in Electrochemistry? – A Theoretical Evaluation — •SIMEON D. BEINLICH^{1,2}, NICOLAS G. HÖRMANN¹, and KARSTEN REUTER¹ — ¹Fritz-Haber-Institut der Max-Planck-Gesellschaft, Berlin, Germany — ²Technical University of Munich, Munich, Germany

Does electrochemistry at protruding surface sites differ significantly from that at ideal low-index surfaces? Intuitively, classical electrostatics suggest a local field enhancement at protruding sites. In this case, a dipole-field-like picture would suggest a pronounced potential-dependence of adsorption energies at such sites.

Here, we evaluate these dependencies for various adsorbates on vicinal Pt(111) surfaces using first-principles calculations in combination with a fully grand canonical approach [1]. Our results show an enhancement of the local electric field at pristine surfaces. However, it is lifted upon adsorption and hence does not cause the anticipated stronger field-effects. Nevertheless, we observe dramatic variations in the potential-dependence which can be rationalized from the differences in surface dipoles that form upon adsorption. These correlate with site coordination showing a consistent trend across adsorbates and adsorption sites.

We rationalize these findings and discuss how the adsorption behavior changes on defect-rich, undercoordinated surfaces in an electrochemical environment.

[1] S.D. Beinlich *et al.*, *ACS Catal.* 12 6143–6148 (2022)

O 8.4 Mon 11:30 S054

Vapor adsorption on carbon nanomembranes (CNMs) — •EN-NEITA KHAYYA, PETR DEMENTYEV, and ARMIN GÖLZHÄUSER — Faculty of Physics, Bielefeld University, 33615 Bielefeld, Germany

Intrinsically porous carbon nanomembranes (CNMs) demonstrate promising mass transfer properties with respect to separation of liquids and gases. To complement the permeation studies with CNMs, we introduce a spectroscopic experiment for probing adsorption of vaporous substances on their surface under ambient conditions. Polarization-modulation infrared reflection absorption spectroscopy (PM IRAS) is used to quantify the number of adsorbed species with the help of innovative calibration approaches, including azeotropic mixtures and immobilization in a polymer matrix. Water and alcohols are found to readily condense on supported CNMs yielding liquid-like interfaces. The results are consistent with the vapor permeation rates measured in free-standing CNMs.

O 8.5 Mon 11:45 S054

Investigating Zirconium Nitride Cathodes for the Electrochemical Nitrogen Reduction Reaction — •TEODOR APETREI, SASWATI SANTRA, VERENA STREIBEL, and IAN D. SHARP — Walter Schottky Institut, Technische Universität München, Garching, Germany

The electrochemical nitrogen reduction reaction (NRR) can convert nitrogen to ammonia at ambient conditions. The most critical factor to activate N₂ is to cleave the N-N triple bond. Transition metal nitrides have been proposed as electrocatalysts for the NRR, with computational studies predicting that N-N bond cleavage can be facilitated via a Mars-van-Krevelen mechanism. Herein, we experimentally test this prediction by investigating sputter-deposited ZrN thin films for the NRR. Our investigations indicate that small amounts of ammonia are indeed produced when pristine ZrN thin films are used as NRR cathodes. However, we also observe nitrogen loss and electrochemical instabilities, which could indicate a sacrificial rather than catalytic role of ZrN. Hence, to accelerate the rate-limiting N-N bond splitting step and facilitate nitrogen replenishment, we anchor Fe SACs onto ZrN. Our preliminary results indicate that high-temperature attachment of Fe SACs leads to overall smaller current densities. However, electrochemical measurements and comparative XPS and XRD studies of the pre- and post-NRR samples suggest an increased nitrogen stability within the Fe-modified ZrN films and improved electrochemical stability. Whether this Fe-modification also facilitates N-N bond dissociation and boosts the NRR activity is currently investigated.

O 8.6 Mon 12:00 S054

Towards Understanding Platinum Degradation: Modelling the Growth of Nanoislands — •FRANCESCO VALLS MASCARO¹, MARC T.M. KOPER¹, and MARCEL J. ROST² — ¹Leiden Institute of Chemistry, Leiden University — ²Huygens-Kamerlingh Onnes Laboratory, Leiden Institute of Physics, Leiden University

Platinum is the catalyst of choice in many electrochemical energy conversion systems like fuel cells due to its superior activity. However, the stability of platinum catalysts is limited under fuel cell operation conditions. This degradation process has been extensively studied by cyclic voltammetry and inductively coupled plasma mass spectrometry (ICP-MS) [1, 2]. The origin of this degradation is most likely linked to the roughening of the surface due to the nucleation and growth of platinum nanoislands [3, 4, 5, 6]. In this work, we model, fully analytically and with the support from electrochemical data, the growth of these nanoislands on Pt(111) in perchloric acid. The model here presented successfully describes the surface growth taking place during the oxidation-reduction cycling. Different parameters such as the flux of adatoms and vacancies were obtained from the fittings between the model and the experimental data.

References: [1] Topalov, A. *et al.*, *Chem. Sci.*, 5, 631 (2014) [2] Sandbeck D.J.S. *et al.*, *ACS Appl. Mater. Interfaces*, 12, 25718 (2020) [3] Jacobse, L. *et al.*, *Nat. Mater.* 17, 277 (2018) [4] Jacobse, L. *et al.*, *ACS Cent. Sci.* 5 (12), 1920 (2019) [5] Rost, M.J. *et al.*, *Nat. Commun.* 10, 5233 (2019) [6] Ruge, M. *et al.*, *J. Am. Chem. Soc.*, 139, 4532 (2017)

O 8.7 Mon 12:15 S054

Exploring the Limits of Mean-Field Theory in Modeling Thermodynamic Cyclic Voltammograms — •NICOLAS BERGMANN, NICOLAS G. HÖRMANN, and KARSTEN REUTER — Fritz-Haber-Institut der Max-Planck-Gesellschaft, Berlin, Deutschland

Mean-field theory (MFT) is at the heart of many approaches to simulate materials. Recently, MFT has been used to model thermodynamic cyclic voltammo-

grams (CVs) [1], a standard electrochemical experiment. However, its accuracy limitations in this context remain unclear.

Here, we outline our general ansatz to derive mean field models for thermodynamic CVs based on *ab initio* DFT calculations of a wide variety of adsorbate configurations [1]. To derive continuous MFT expressions, we use nonparametric Gaussian process regression. We apply our method to assess the fingerprint CV of Cu(100) in iodine-containing, alkaline solutions. The simulations offer new insights into the competitive adsorption between I and OH. Additionally, we benchmark our method by comparing a mean-field model to grand canonical lattice Monte Carlo simulations for the well-studied system Ag(100) in Br-containing electrolyte [2,3].

We analyze in detail the respective (dis-)advantages of both methods.

[1] N.G. Hörmann *et al.*, *J. Chem. Theory Comput.* **2021**, 17, 1782

[2] M.T.M. Koper, *J. Electroanal. Chem.* **1998**, 450, 189-201

[3] M. Nakamura *et al.*, *Phys. Rev. B* **2011**, 84, 165433

O 8.8 Mon 12:30 S054

Neural network surrogates for kinetic Monte Carlo models of electrocatalytic surfaces — •YOUNES HASSANI ABDOLLAHI^{1,2}, JÜRGEN FUHRMANN³, and SEBASTIAN MATERA^{1,2} — ¹Institut f. Mathematik, Freie Universität Berlin, Arnimallee 6, 14195 Berlin, Germany — ²Fritz-Haber-Institut der Max-Planck-Gesellschaft, Faradayweg 4-6, 14195 Berlin, Germany — ³Weierstraß-Institut f. Angewandte Analysis u. Stochastik, Mohrenstr. 39 10117 Berlin, Germany

The kinetic Monte Carlo method (kMC) is the physically most sound approach for addressing the kinetic interplay of elementary processes at electrocatalytic surfaces but also comes at high computational costs. Therefore, computationally efficient surrogate models are highly desirable which allow the utilization of kMC simulation results in coarser scale simulations.

Using the oxygen reduction reaction on Pt(111) as a prototypical example, we investigate regression neural networks as surrogates to reproduce the stationary TOF as a function of all reaction conditions, i.e. electrostatic potential, concentrations, and temperature. We found that a relatively shallow perceptron with 2 layers of 32 and 32 neurons, respectively, and SiLU activation functions serve as an appropriate choice. We demonstrate the performance of this model with a varying number of kMC data points. Finally, we discuss how this model can be incorporated into a multiscale modeling approach, which addresses the interaction of transport and kinetics.

O 9: Ultrafast Electron Dynamics at Surfaces and Interfaces 2

Time: Monday 15:00–18:15

Location: H3

O 9.1 Mon 15:00 H3

Two distinct 4f states in mixed-valent TmSe_{1-x}Te_x — •CHUL HEE MIN¹, MICHAEL HEBER², SIMON MÜLLER³, LUKAS WENTHAUS², MARKUS SCHOZ², DMYTRO KUTNYAKHOV², LENART DUDY⁴, HENDRIK BENTMANN³, FEDERICO PRESSACCO², MATTHIAS KALLÄNE¹, WOJAE CHOI⁵, YONG SEUNG KWON⁵, FRIEDRICH REINERT³, and KAI ROSSNAGEL¹ — ¹IEAP, CAU Kiel, Germany — ²DESY, Hamburg, Germany — ³EP7 and ct.qmat, University of Würzburg, Germany — ⁴Synchrotron SOLEIL, Saint-Aubin, France — ⁵Dep. of EMS, DGIST, South Korea

From the strong electron correlation effects in rare earth compounds, rich phase diagrams emerge with tunable ground states, which underlie a series of unique physical phenomena and quantum states, including quantum criticality, topological Kondo insulators, and diverse charge-neutral quasiparticle formations. However, despite their importance, the nature of such composite quasiparticles is difficult to characterize because all coherent spectral features develop in a similar way. Using angle-resolved photoemission spectroscopy (ARPES) together with time-resolved PES, we have addressed distinct coherent 4f features in unique mixed-valence TmSe_{1-x}Te_x. Our findings open the path for future investigations of small energy-scale excitations and may provide a framework for understanding the dynamics and entangled nature of correlated electrons.

O 9.2 Mon 15:15 H3

Time- and angle-resolved photoemission study of magnetic topological insulators MnBi₂Te₄ and MnBi₄Te₇ — •PAULINA MAJCHRZAK¹, KLARA VOLCKAERT¹, DEEPNARAYAN BISWAS¹, DENNY PUNTEL², WIBKE BRONSCH², FEDERICO CILENTO², XING-CHEN PAN³, YONG CHEN^{1,3}, and SØREN ULSTRUP¹ — ¹Dept. of Physics and Astronomy, Aarhus University, DK — ²Elettra - Sincrotrone Trieste, IT — ³Advanced Institute for Materials Research, Tohoku University, JP

Van der Waals heterostructures comprising layers of intrinsically antiferromagnetic topological insulator (TI) MnBi₂Te₄ and non-magnetic TI Bi₂Te₃ offer a rich toolbox for engineering exotic quantum phenomena. Magnetic and transport properties of these materials are strongly affected by the interplay between bulk and surface states with divergent topologies resulting from hybridisation between the top layers.

Here, we disentangle those complex interactions in the time domain with TR-ARPES. We discuss the interband dynamics in bulk and surface states as a function of stacking and surface terminations for MnBi₂Te₄ and MnBi₄Te₇. Our results fill a knowledge gap in understanding of interlayer coupling in MnBi₂Te₄-based heterostructures.

O 9.3 Mon 15:30 H3

Electronic and phonon dynamics in 1T-TaS₂ with ultrafast core-level transient absorption spectroscopy in the extreme ultraviolet — •TOBIAS HEINRICH¹, HUNG-TZU CHANG¹, SERGEY ZAYKO¹, MURAT SIVIS^{1,2}, and CLAUD ROPERS^{1,2} — ¹Max Planck Institute for Multidisciplinary Sciences, Göttingen, Germany — ²4th Physical Institute - Solids and Nanostructures, University of Göttingen, Germany

Extreme ultraviolet (XUV) transient absorption spectroscopy with high harmonic sources is ideally suited to investigate the complex interplay between lat-

tice and electronic degrees of freedom on ultrafast timescale [1]. Here, we compare the experimental result of highly sensitive XUV transient absorption spectroscopy on the charge density wave (CDW) compound 1T-TaS₂ with density functional theory (DFT) simulations to disentangle electronic and phonon contributions to the transient absorption spectra. In addition to photo excited carriers we observe two coherently excited phonon modes that can be assigned to the A_{1g} optical mode (6 THz) and the A_{1g}* (3.3 THz) amplitude mode associated with the CDW formation [2]. The modes show distinct spectral fingerprints which are reproduced by DFT calculations such that their dynamics can be individually analyzed. It is found that only the amplitude mode vanishes at higher fluences, corroborating the proposed mechanism of non-thermal CDW melting [3].

- [1] A. R. Attar *et al.*, *ACS Nano* **14**, 11, 15829-15840 (2020)
[2] H. Hedayat *et al.*, *New J. Phys.* **23**, 033025 (2021)
[3] E. Möhr-Vorobeva *et al.*, *Phys. Rev. Lett.* **107**, 036403 (2011)

O 9.4 Mon 15:45 H3

Coherent phonon-driven transient modulation of a Dresselhaus-type spin splitting in Td-WTe₂ — PETRA HEIN¹, STEPHAN JAUERNIK¹, HERMANN ERK¹, LEXIAN YANG^{2,3}, YANGPEN QI^{4,5}, YAN SUN⁵, CLAUDIA FELSER⁵, and •MICHAEL BAUER¹ — ¹Institute of Experimental and Applied Physics, University of Kiel, Germany — ²State Key Laboratory of Low Dimensional Quantum Physics, Department of Physics, Tsinghua University, Beijing, China — ³Frontier Science Center for Quantum Information, Beijing, China — ⁴School of Physical Science and Technology, ShanghaiTech University, China — ⁵Max Planck Institute for Chemical Physics of Solids, Dresden, Germany

Time- and angle-resolved photoemission spectroscopy is used to study transient changes of the electronic structure in the Weyl-semimetal Td-WTe₂ in response to the excitation of coherent phonons. A Fourier-transform of the three-dimensional experimental data yields phonon-mode resolved insights into such coupling processes. Results of our analysis reveal a transient modulation of a Dresselhaus-type spin splitting of electronic bands that is selectively driven by the excitation of an interlayer shear mode of the layered compound [1]. The results provide real-time insights into electron-phonon coupled processes that are of vital importance for a light-driven topological phase transition in Td-WTe₂.

- [1] P. Hein, *et al.*, *Nat. Commun.* **11**, 2613 (2020).

O 9.5 Mon 16:00 H3

Coherent Control of a Metastable Hidden Phase — J. MAKLAR¹, S. DONG¹, J. SARKAR¹, Y. A. GERASIMENKO², T. PINCELLI¹, S. BEAULIEU¹, P. S. KIRCHMANN³, J. A. SABOTA³, S.-L. YANG^{3,4}, D. LEUENBERGER^{3,4}, R. G. MOORE³, Z.-X. SHEN^{3,4}, M. WOLF¹, D. MIHAILOVIC², R. ERNSTORFER^{1,5}, and L. RETTIG¹ — ¹Fritz-Haber-Institut der MPG, Berlin, DE — ²Jožef Stefan Institute, Ljubljana, SI — ³SLAC National Accelerator Laboratory, California, USA — ⁴Stanford University, California, USA — ⁵Technical University Berlin, DE

In materials with multiple competing orders, ultrashort light pulses can induce metastable states that are not accessible at thermodynamic equilibrium. One of such, the metallic hidden (H) phase of 1T-TaS₂, is of particular interest as it features an order-of-magnitude change in resistivity, promising for novel energy-efficient high-speed memory devices. We use time- and angle-resolved photoemission spectroscopy (trARPES) to investigate the electronic band structure and

formation dynamics of the metastable H-state in 1T-TaS₂. The band structure mapping of H-state reveals suppression of correlation effects and metallization, suggesting a critical role of interlayer stacking order of the TaS₂ sheets in the phase transition. The fluence-dependent dynamics provides strong evidence that the charge density wave amplitude mode governs a collective, ultrafast switching pathway to the H-state. This is further corroborated by demonstrating coherent control of the switching efficiency into the H-phase using a multi-pump-pulse excitation scheme.

O 9.6 Mon 16:15 H3

Influence of carbon buffer layer on non-equilibrium carrier dynamics of epitaxial graphene and WS₂/graphene heterostructures — •LUKAS BRUCKMEIER¹, NIKLAS HOFMANN¹, LEONARD WEIGL¹, JOHANNES GRADL¹, NEERAJ MISHRA^{2,3}, STIVEN FORTI², CAMILLA COLETTI^{2,3}, and ISABELLA GIERZ¹ — ¹Faculty for Physics, University of Regensburg, Regensburg, Germany — ²Center for Nanotechnology Innovation@NEST, Istituto Italiano di Tecnologia, Pisa, Italy — ³Graphene Labs, Istituto Italiano di Tecnologia, Genova, Italy The non-equilibrium photocarrier dynamics of epitaxial graphene on SiC(0001) have been studied in detail in the past. The fact that the graphene layer rests on a second two-dimensional carbon buffer layer (BL) - the well-known ($6\sqrt{3} \times 6\sqrt{3}$)R30° reconstruction - was believed to be of minor importance for the interpretation of the time-resolved data. We use time- and angle-resolved photoemission spectroscopy to show that photoexcitation of the graphene/BL heterostructure is followed by a short-lived transient decrease in binding energy of the Dirac cone indicating a transient charging of the graphene layer with excess electrons. We attribute the transient n-doping of the graphene layer to the resonant excitation of a direct electronic transition between the non-dispersive states of the BL located 0.5eV below the Fermi level and the Dirac cone. We further show that this direct electronic transition affects the charge transfer dynamics in epitaxial WS₂/graphene/BL heterostructures.

O 9.7 Mon 16:30 H3

Ultrafast phonon thermalization in a monolayer crystal — •HYEIN JUNG — Fritz-Haber-Institut der MPG Understanding energy flow in semiconductors following a perturbation is key for future applications. Observing dynamic processes on their fundamental time scales enables studying energy transfer processes between intrinsic subsystems, and subsequently understanding the coupling between them. Here we study ultrafast lattice dynamics in monolayer WSe₂, carried out using femtosecond (high-energy) electron diffraction (FED).

We studied the lattice response to laser excitation by probing laser-induced variations in Bragg peak intensities, which reflect changes in incoherent lattice vibrations (quantified by atomic mean squared displacements, MSD). We implement a novel approach to analyze such diffraction data, by which we disentangle element-specific vibrational responses in the sub-picosecond time domain.

Through this analysis, we observe a series of steps in the evolution of the lattice response through varying trends of the two elements (W, Se). These observations suggest a cascade of electron-phonon and phonon-phonon scattering processes occurring on short picosecond time scales. We interpret these by means of energy transfer between phonon groups using on ab-initio calculations of the partial phonon density of states phonon. These results demonstrate that our element-specific approach enables a deeper understanding of the cascade of e-ph and ph-ph energy transfer processes following excitation.

O 9.8 Mon 16:45 H3

k-dependent band gap renormalization in monolayer WS₂ revealed by ARPES — •NIKLAS HOFMANN¹, ALEXANDER STEINHOFF², LEONARD WEIGL¹, JOHANNES GRADL¹, TIM WEHLING^{2,3}, SIVAN REFAELY-ABRAMSON⁴, NEERAJ MISHRA^{5,6}, STIVEN FORTI⁵, CAMILLA COLETTI^{5,6}, and ISABELLA GIERZ¹ — ¹University of Regensburg, 93040 Regensburg, Germany — ²University of Bremen, 28359 Bremen, Germany — ³University of Hamburg, 22607 Hamburg, Germany — ⁴Weizmann Institute of Science, 7610001 Rehovot, Israel — ⁵Center for Nanotechnology Innovation @NEST, Istituto Italiano di Tecnologia, 56127 Pisa, Italy — ⁶Graphene Labs, Istituto Italiano di Tecnologia, 16163 Genova, Italy Monolayer transition-metal dichalcogenides show strong enhancement of Coulomb interactions due to their reduced dimensionality with immediate effects on both the optical as well as the single-particle band gap. Photogenerated electron-hole pairs have been shown to result in a giant band gap renormalization that has been attributed to efficient screening of the Coulomb interaction. The corresponding band structure changes are predicted to show a pronounced momentum dependence that we resolve using time- and angle-resolved photoemission spectroscopy on monolayer WS₂ supported by a graphene substrate. Excellent agreement with ab initio calculations allows us to disentangle the intricate interplay of different many-body contributions to the observed transient band structure renormalization with important implications for the optoelectronic properties of 2D semiconductors.

O 9.9 Mon 17:00 H3

Pump helicity-dependent anisotropic population dynamics in the topological insulator Sb₂Te₃ — •JAN BÖHNKE¹, HAYDAR ALTUG YILDIRIM^{1,3}, STEPHAN SCHMUTZLER¹, JAIME SÁNCHEZ-BARRIGA², OLIVER RADER², CORNELIUS GAHL¹, and MARTIN WEINELT¹ — ¹Fachbereich Physik, Freie Universität Berlin, Berlin, Germany — ²Helmholtz-Zentrum Berlin für Materialien und Energie GmbH, Berlin, Germany — ³Leibniz-Institut für Astrophysik, Potsdam, Germany

The specific spin texture of Dirac cone like topologically protected surface states (TSS) and the long electron mean free path allow for spin-polarized currents at the surface of topological insulators. Optical control of such currents has been discussed controversially.

We investigated the role of direct and indirect population channels for the unoccupied TSS on Sb₂Te₃ in 2D momentum space by time and angle-resolved two-photon photoemission spectroscopy. Excitation with 1.55 eV photons leads to an initially anisotropic population of the Dirac cone, dependent on the helicity of the excitation pulse and the azimuthal orientation of the sample. The strongest anisotropy is found in the energy range of the warped Dirac cone. It exhibits predominantly a 3-fold symmetry originating from the symmetry group of the bulk material. This contribution accordingly does not correspond to a macroscopic current in the TSS. On a time scale of 100 fs the population anisotropy is masked by electrons scattering from the bulk conduction band into the TSS.

O 9.10 Mon 17:15 H3

Spatio-temporal imaging of bright and dark excitonic quasiparticles in twisted TMD heterostructures — •JAN PHILIPP BANGE¹, DAVID SCHMITT¹, WIEBKE BENNECKE¹, ABDULAZIZ ALMUTAIRI², GIUSEPPE MENEGHINI³, DANIEL STEIL¹, R. THOMAS WEITZ¹, SABINE STEIL¹, G. S. MATTHIJS JANSEN¹, SAMUEL BREM³, ERMIN MALIC³, STEPHAN HOFMANN², MARCEL REUTZEL¹, and STEFAN MATHIAS¹ — ¹I. Physikalisches Institut, Georg-August-Universität Göttingen, Germany — ²Department of Engineering, University of Cambridge, U.K. — ³Fachbereich Physik, Philipps-Universität Marburg, Germany

In two-dimensional van-der-Waals semiconductors, the weak Coulomb screening of charge carriers leads to exciting new material properties, such as bright and dark excitons with large binding energies. Consequently, when creating a heterostructure from two transition-metal dichalcogenide (TMD) monolayers with a type II band alignment, interlayer excitons can be formed [1]. Because dark excitons are not directly accessible with optical techniques, the spatial and lateral dynamics on the fundamental nanometer length scale remain largely unexplored. How do dark and interlayer quasiparticles form, relax and diffuse in the presence of a heterojunction, stress fields and inhomogeneities? Here, we address this question using time-resolved momentum and dark-field photoemission microscopy which enables us to study the ultrafast formation dynamics of different excitonic species in twisted WSe₂/MoS₂ heterostructures. [1] Schmitt *et al.*, arXiv2112.05011 (2021).

O 9.11 Mon 17:30 H3

SHG imaging microscopy of ultrafast charge-transfer dynamics in twisted TMDC heterostructures — •MARLEEN AXT, JONAS E. ZIMMERMANN, GERSON METTE, and ULRICH HÖFER — Fachbereich Physik, Philipps Universität Marburg, Germany

Two-dimensional heterostructures of transition metal dichalcogenides (TMDC) represent very well-defined model systems of van-der-Waals interfaces. Many material combinations feature a type-II band alignment, which can separate photoexcited electrons and holes into different layers through ultrafast charge transfer leading to the formation of so-called interlayer excitons or interface excitons.

We investigate the ultrafast charge-transfer dynamics in TMDC heterostructures as a function of the stacking angle using time-resolved second-harmonic generation (SHG) imaging microscopy. This experimental technique combines the advantages of SHG with high temporal and spatial resolution. For differently twisted MoS₂/WSe₂ heterostructures the electron transfer from WSe₂ to MoS₂ after resonant excitation (1.70 eV) was found to depend considerably on the twist angle. The transfer time is reduced from 85 fs down to 12 fs when going from a larger rotational mismatch (16°) towards 2H-stacking (52°).

O 9.12 Mon 17:45 H3

Spin and charge carrier dynamics at a CuPc/WSe₂ heterostructure — •SEBASTIAN HEDWIG¹, GREGOR ZINKE¹, BENITO ARNOLDI¹, MARTIN AESCHLIMANN¹, and BENJAMIN STADTMÜLLER^{1,2} — ¹Department of Physics and Research Center OPTIMAS, TU Kaiserslautern, Erwin-Schroedinger-Str. 46, 67663 Kaiserslautern, Germany — ²Institute of Physics, Johannes Gutenberg University Mainz, Staudingerweg 7, 55128 Mainz, Germany

2D-Van-der-Waals systems are a highly intriguing class of low dimensional materials with promising spin functionalities for future nanoscale spintronic applications. Here, we show our approach to control the spin and charge carrier dynamics of the Van-der-Waals material WSe₂ by the adsorption of CuPc molecules. We conduct time-, angle- and spin-resolved photoemission experiments to investigate the optically excited carrier dynamics at the K- and Σ-

points of WSe_2 . After an initial spin-selective excitation at the K-point, depending on the pump light polarization [1], we observe that the subsequent intraband scattering from the K- to the Σ -point of the bare WSe_2 conduction band coincides with a change of the carriers spin polarization. Both, the optical excitation and the subsequent relaxation process can be actively modified by appropriate adsorption of CuPc. In particular, the dominant optical excitation at the K-point of WSe_2 is replaced by a direct interlayer excitation from the CuPc into the WSe_2 layer. We will show that the strength of the interlayer excitation can be tuned and controlled by the polarization of the exciting light field.

[1] Bertoni et al.; Phys. Rev. Lett. 117, 277201 (2016)

O 9.13 Mon 18:00 H3

Subcycle lightwave-ARPES in the strong-field regime — SUGURU ITO¹, MANUEL MEIERHOFER², JOSEF FREUDENSTEIN², DMYTRO AFANASIEV², JENS GÜDDE¹, RUPERT HUBER², and ULRICH HÖFER¹ — ¹Fachbereich Physik, Philipps-Universität Marburg, Germany — ²Fakultät für Physik, Universität Regensburg, Germany

Angle-resolved photoemission spectroscopy (ARPES) combined with THz excitation enables the investigation of lightwave-driven Dirac currents in the surface state of topological insulators with sub-cycle time resolution [1]. At low THz frequencies and moderate effective field strengths of a few kV/cm at the surface, we have shown that the current dynamics is dominated by intraband acceleration of the electrons within the surface band of Bi_2Te_3 .

Here, we will show how such experiments can be extended to the strong-field regime at driving frequencies of 25-40 THz. This is challenged by strong energy and momentum streaking of the photoelectrons after photoemission as well as the requirement of ultrashort pulses for photoemission which also introduce considerable energy broadening of the ARPES spectra. We will discuss how these challenges can be successfully overcome in order to enable lightwave-ARPES at field strength of ~ 1 MV/cm despite surface screening. This paves the way for visualizing strong-field phenomena such as high-harmonic generation (HHG) [2] and the emergence of Floquet-Bloch states directly in the band structure on a sub-optical-cycle time scale.

[1] J. Reimann *et al.*, Nature 562, 396 (2018).

[2] C. P. Schmid *et al.*, Nature 593, 385 (2021).

O 10: Focus Session: Single Atom Catalysis 2

Time: Monday 15:00–17:30

Location: H4

Topical Talk

O 10.1 Mon 15:00 H4

Atomically-precise design of low-nuclearity catalysts — SHARON MITCHELL and JAVIER PÉREZ-RAMÍREZ — ETH Zurich, Zurich, Switzerland

Nanostructured catalysts incorporating supported metal atoms or small clusters of defined size and chemical composition attract considerable attention because of their potential to maximize resource efficiency. When optimally assembled, all the metal nuclei can participate in the catalytic cycle with properties tailored to deliver high specific activity and stable performance. Over the past decade, the number and diversity of reported systems have exploded as researchers attempted to control the nanostructure with increasing atomic precision. Nonetheless, spatially resolving the architecture and properties of supported low-nuclearity catalysts using existing analytical methods remains challenging. This talk will discuss approaches to prepare and characterize catalytic materials integrating low-nuclearity metal species. Topical case studies will introduce recent achievements and challenges, including the synthesis of single-atom catalyst libraries with controlled density, the precision synthesis of low-nuclearity species, tools for metal speciation analysis in electron-beam-sensitive materials, and an automated image analysis approach for atom detection and classification.

O 10.2 Mon 15:30 H4

Synthesis of single-atom model catalysts via atomic layer deposition for CO oxidation — CHUNLEI WANG¹, HÉLOÏS TISSOT¹, JOAKIM HALLDIN STENLID², MARKUS SOLDEMO¹, SARP KAYA³, and JONAS WEISSENRIEDER¹ — ¹Materials and Nano Physics, KTH Royal Institute of Technology, SE-100 44 Stockholm, Sweden — ²Department of Physics, Stockholm University, SE-106 91 Stockholm, Sweden — ³Department of Chemistry, Koc University, 34450 Istanbul, Turkey

Single-atom model catalysts, with individual metal atoms anchored on well-defined single crystals under ultra-high vacuum conditions, can provide an atomic-scale insight into active sites and reaction mechanisms for applied catalysis, thus promoting the design of better industrial catalysts. The metal growth of model catalyst is usually synthesized by physical vapor deposition method. Here, we applied a novel atomic layer deposition strategy to model systems for the synthesis of single-atom FeOx catalysts on Cu₂O(100) and Pt(111). The coordination configuration was determined through a combination of scanning tunneling microscopy, synchrotron radiation X-ray photoelectron spectroscopy (XPS), and density functional theory calculations. The redox properties of single atoms were investigated using ambient-pressure XPS under mbar level of reactant gas.

O 10.3 Mon 15:45 H4

A Customized IRAS System for Investigations of Adsorbates on Metal-Oxide Single Crystals — DAVID RATH, JIRI PAVELEC, ULRIKE DIEBOLD, MICHAEL SCHMID, and GARETH S. PARKINSON — Institute of Applied Physics, TU Wien, Austria

The IRAS system GRISU (GRazing incident Infrared absorption Spectroscopy Unit) was developed to investigate adsorbates on metal oxide single crystals in the research field of single-atom catalysis [1]. It combines the commercially available FTIR spectrometer Bruker Vertex 80v with an UHV chamber [2]. The compact design requires only one CF150 port for the main optical components, features five mirrors for beam guidance placed in HV and UHV environment and optimises the system's performance, flexibility, and usability. The result is a small controllable focal-spot diameter (max. 3 mm) on the sample, motorised optical

components, and an aperture limiting the incidence angle range (variable, 49° to 85°) on the sample. The simulated system (done with a ray-tracing program and a simplified spectrometer model) shows an efficiency of 13 %, i.e., 13 % of the radiation passing through the first aperture (\varnothing 6 mm) after the IR source in the FTIR spectrometer reaches the detector after being reflected from the molecular beam spot (\varnothing 3.5 mm) on the sample. Compared to a commercially available system with two parabolic mirrors with a focal length of 250 mm, the efficiency is about 20× higher. First measurements demonstrate the performance of the system.

[1] G. S. Parkinson, Catal. Lett. 149, 1137 (2019)

[2] J. Pavelec, et al., J. Chem. Phys. 146, 014701 (2017).

Topical Talk

O 10.4 Mon 16:00 H4

Design of Model Single-Atom Catalysts: Metal Adatoms, Monomeric Oxide Units, and Mixed Surface Layers on Oxide Surfaces — ZDENEK DOHNALEK — Physical and Computational Sciences Directorate and Institute for Interfacial Catalysis, Pacific Northwest National Laboratory, Richland, WA 99354, USA

Single-atom catalysts have attracted significant attention due to their ultimate metal efficiency and the promise of novel properties. The sublimation of oxides and metals is employed to design monodispersed model systems with supported metal adatoms, monomeric oxide units, and ordered mixed oxide surfaces. Scanning tunneling microscopy, ensemble-averaged electron spectroscopies, and density functional theory are employed to achieve an atomic-level understanding. Specifically, the deposition of (MgO)₁ monomers and (MoO₃)_n oligomers is studied on anatase TiO₂(101) via direct evaporation of MgO and MoO₃ powders. While gas phase (MgO)₁ is readily immobilized at room temperature, (MoO₃)_n transiently diffuse, agglomerate, and spontaneously decompose into the (MoO₃)₁ monomers. The transient mobility of the oligomers is the key to the self-assembly of the ordered overlayers of (MoO₃)₁. Metal adatoms and mixed oxide surfaces are synthesized by the sublimation of Rh onto Fe₃O₄(001). Higher substrate temperatures facilitate Rh incorporation into the surface, leading to ordered mixed Rh-Fe₃O₄(001). Cryogenic deposition temperatures stabilize Rh on the surface and allow for the preparation of the pure Rh adatom phase. The effect of temperature and adsorbates on the stability of such model catalysts is explored.

O 10.5 Mon 16:30 H4

Rh and Ir single atoms on Fe₃O₄(001): local structure affecting catalytic properties — MATTHIAS MEIER^{1,2}, ZDENEK JAKUB¹, JIRI PAVELEC¹, MICHAEL SCHMID¹, ULRIKE DIEBOLD¹, CESARE FRANCHINI^{2,3}, and GARETH S. PARKINSON¹ — ¹Institute of Applied Physics, Technische Universität Wien, Vienna, Austria — ²Faculty of Physics and Center for Computational Materials Science, University of Vienna, Vienna, Austria — ³Department of Physics and Astronomy, Alma Mater Studiorum, Università di Bologna, Bologna, Italy

Single-atom catalysts are often supported by cheap oxides, such as iron oxides. As a model system [1], magnetite (Fe₃O₄), specifically its (001) facet has been used because it offers stable sites for single-atom adsorption up to high temperatures. Here, I will demonstrate how important the support is for the stability of single-atoms, as well as their catalytic properties. Rh and Ir [2] single atoms utilize Fe vacancies in the subsurface of the reconstructed Fe₃O₄(001) unit cell to incorporate into the surface layer. Changing the positions of Fe atoms in the support as part of the incorporation process enables the single atoms to be accommodated in a more favorable configuration than if they were adsorbing on top of the surface. Their catalytic properties are drastically affected by changes

in the atomic environment. Incorporation temperatures vary depending on both coverage and the presence or absence of adsorbates, such as CO.

[1] R. Bliem et al., *Science* **346**, 1215 (2014). [2] Z. Jakub et al., *Angew. Chemie Int. Ed.* **58**, 13961 (2019).

O 10.6 Mon 16:45 H4

Atomic-Level Studies of C₂H₄ on Clean and Rh₁ Single-Atom Decorated Fe₃O₄ (001) — •PANUKORN SOMBUT¹, LENA PUNTSCHER¹, CHUNLEI WANG¹, MANUEL ULREICH¹, JIRI PAVELEC¹, ALI RAFSANJANI-ABASSI¹, MATTHIAS MEIER², ULRIKE DIEBOLD¹, CESARE FRANCHINI^{2,3}, MICHAEL SCHMID¹, and GARETH S. PARKINSON¹ — ¹Institute of Applied Physics, TU Wien, Austria — ²Faculty of Physics, Center for Computational Materials Science, University of Vienna, Austria — ³Alma Mater Studiorum, Università di Bologna, Bologna, Italy

The local binding environment of metal-oxide supported single-atom catalysts (SACs) determines how reactants adsorb and therefore plays a decisive role in catalysis. Here, we study how Fe₃O₄(001)-supported Rh₁ adatoms interact with ethylene (C₂H₄) using DFT, combined with experimental surface science techniques (TPD, XPS, and STM). We show that C₂H₄ physisorbs on the clean Fe₃O₄(001). We also identify and model different molecule orderings at different coverages that agree nicely with STM images and TPD data. Then, we study C₂H₄ adsorption at 2- and 5-fold coordinated Rh sites at the Fe₃O₄(001) surface, and show that the local environment has a strong effect on the adsorption properties: 2-fold Rh can adsorb two C₂H₄ molecules, while 5-fold Rh can only host a single C₂H₄ molecule. Finally, we investigate coadsorption of C₂H₄ with

CO, a vital step towards enabling the hydroformylation reaction, and show that this is feasible only at 2-fold coordinated Rh sites.

Topical Talk

O 10.7 Mon 17:00 H4

Model catalysis of single atoms on ultrathin solid films — •KAI WU — College of Chemistry and Molecular Engineering, Peking University, Beijing 100871, China

Metal atoms at surfaces play a key role in catalysis and related disciplines. A new strategy is introduced to prepare ultrathin films like oxides on surfaces which are further utilized to prepare stabilized metal atoms. Since the surface free energy of a bulk oxide is much lower than the chemical potential or free energy of the metal atoms, one can play the game by reducing the thickness of the oxide film, even down to one atomic monolayer, which is grown on a bulk metal substrate. In such a way, the chemical potential of the oxide thin film can be tweaked by the underlying bulk metal substrate. Once the chemical potential or free energy of the ultrathin oxide support is tuned to such an extent that it becomes comparable with those of the metal atoms, can one then stabilize these metal atoms without additional measures. Such an approach may be termed as surface free energy strategy to prepare uncoordinated metal atoms at surfaces. Since the metal atoms are truly unprotected and therefore their physicochemical properties could be intrinsic, in sharp contrast to those of coordinated metal atoms prepared by surface coordination and crystal engineering strategies. In this presentation, several systems of the unprotected metal atoms including alkali and transition metal atoms on ultrathin films such as metallic oxides and carbides grown on bulk metal substrates are employed to explore surface catalysis.

O 11: Electronic Structure Theory

Time: Monday 15:00–16:30

Location: H6

O 11.1 Mon 15:00 H6

Quantum Nuclear Effects in Thermal Transport of Semiconductors and Insulators — •HAGEN-HENRIK KOWALSKI¹, MATTHIAS SCHEFFLER¹, MARIANA ROSSI², and CHRISTIAN CARBOGNO¹ — ¹The NOMAD Laboratory at the FHI-MPG and HU, Berlin, Germany — ²MPI for Structure and Dynamics of Matter, Hamburg, Germany

Accounting for the nuclear motion is essential for the prediction of various material properties, from thermal conductivity to the relative stability of different polymorphs. Often, it is assumed that quantum nuclear effects (QNEs) are decisive at low temperatures, but that anharmonic effects can be neglected in this limit. Conversely, it is often presumed that anharmonicity is influential at elevated temperatures, but that QNEs are not active in this limit. In this work, we investigate the interplay of QNEs and anharmonicity by extending a recently proposed anharmonicity metric [1] to path integral molecular dynamics (PIMD). Our *ab initio* MD and PIMD calculations for solid Argon, Silicon, Lithium Hydride, and Pentacene further substantiate that QNEs can have a massive impact even at room temperature and beyond, especially in weakly bonded systems [2]. Furthermore, we show that QNEs can induce strong anharmonic effects –beyond the applicability realm of perturbation theory– even at OK. We discuss the underlying microscopic mechanisms and hence elucidate why QNEs and strong anharmonicity often go hand in hand in real materials.

[1] F. Knoop, et al., *Phys. Rev. Mat.* **4**, 083809, (2020).

[2] M. Rossi, *J. Chem. Phys.* **154**, 170902 (2021)

O 11.2 Mon 15:15 H6

Volume Dependence of Excitation Energies of Sodium Clusters in GW — •ŠTĚPÁN MAREK and RICHARD KORYTÁR — Department of Condensed Matter Physics, Faculty of Mathematics and Physics, Charles University, Prague, Czech Republic

Prediction of molecular junction transport properties is a challenging task. One particularly complicated aspect of the problem is accurate description of binding between the molecule and the electrodes. Effect of image charges and non-ground state properties of the molecule-electrode system are expected to induce significant error when using DFT to evaluate the junction properties. GW is a post-DFT method that is assumed to fix some of the problems of bare DFT approach. In this contribution, we explore the (size) convergence properties of spectrum of sodium clusters using GW, and compare it to predictions by DFT and HF. We discuss the strategies to remove quasi-degeneracies induced by symmetries of the clusters, and their impact on critical properties of the spectrum, namely gap and average level spacing. Our analysis serves as a guide towards convergence studies of molecular junctions using GW.

O 11.3 Mon 15:30 H6

Ab initio phonon self-energies: To screen, or not to screen — •JAN BERGES¹, NINA GIROTTO², TIM WEHLING³, NICOLA MARZARI^{4,1}, and SAMUEL PONCÉ⁵ — ¹University of Bremen, Germany — ²Institute of Physics, Zagreb, Croatia — ³University of Hamburg, Germany — ⁴EPFL, Switzerland — ⁵UCLouvain, Belgium

First-principles calculations of phonons are often based on the adiabatic approximation and a Brillouin-zone sampling that is not sufficient to capture Kohn anomalies. These shortcomings can be remedied through corrections to the phonon self-energy arising from the low-energy electrons. A well-founded correction method exists [Calandra, Profeta, and Mauri, *Phys. Rev. B* **82**, 165111 (2010)], which only relies on readily available (adiabatically) screened quantities. However, many-body theory suggests to use one bare electron-phonon vertex in the phonon self-energy [Giustino, *Rev. Mod. Phys.* **89**, 015003 (2017)] to avoid double counting. This can be seen as a limiting case of downfolding to partially screened phonons and interactions [Nomura and Arita, *Phys. Rev. B* **92**, 245108 (2015)]. We compare these approaches using the examples of TaS₂, MgB₂, n-doped MoS₂, and p-doped diamond. We confirm the robustness of the former method, while the latter allows for systematic improvements to describe correlations or metal-insulator transitions.

O 11.4 Mon 15:45 H6

Implementation of DFT+U+J and the minimum-tracking linear response method for polaron formation modeling — •ZIWEI CHAI^{1,3}, KARSTEN REUTER³, HARALD OBERHOFER^{1,2}, and LIMIN LIU⁴ — ¹Chair for Theoretical Chemistry, Technische Universität München — ²Chair for Theoretical Physics VII, Universität Bayreuth, Germany — ³Fritz-Haber-Institut der Max-Planck-Gesellschaft — ⁴School of Physics, Beihang University

In many oxides charge carriers localize as small polarons. However, treating them with semi-local first-principles density-functional theory (DFT) tends to be a challenge usually addressed by hybrid DFT or Hubbard-corrected DFT+U. We present our implementation of DFT+U+J based on a "tensorial" representation of the subspace and the "minimum-tracking linear response method" which can determine U and J parameters from first-principles in the CP2K package. We performed systematic tests to prove the validity of the implementation.

Finally, the formation of polarons can be modeled by either breaking the symmetry of the initial structure or imposing an implicit or explicit constraining potential on the local orbital occupation. On top of our DFT+U+J implementation, we thus present the subspace occupancy-constraining potential (SOCP) approach to simulate the formation of polarons by constraining the occupancy number of the relevant local orbitals. Any polaronic configuration can thus straightforwardly be accessed without the need to explicitly break the system's symmetry.

O 11.5 Mon 16:00 H6

Signatures of molecular conformation in the evolution of DFT-based single molecule conductance — •HECTOR VAZQUEZ — Inst. of Physics, Czech Academy of Sciences

Single molecules placed between two nanoelectrodes represent the ultimate limit in downscaling of electronic components. Electron transport simulations based on DFT-NEGF have enabled the understanding of conducting junctions and the interpretation of experiments [1]. However, these computationally costly calculations are often carried out for a small number of representative junction structures. In contrast, in room temperature experiments, the geometry of the

molecule is expected to change significantly.

Here we describe and apply an approximate method to calculate molecular conductance within DFT for thousands of geometries. By combining it with room-temperature molecular dynamics (MD) simulations of the junction [2], we obtain the evolution of conductance for thousands of structure-conductance points. We analyze several geometric parameters and their effect on conductance, including quantum interference. This analysis on large datasets of DFT-based calculations reveals the signatures of molecular structure on junction conductance.

[1] F. Evers, R. Korytar, S. Tewari and J.M. van Ruitenbeek, *Rev. Mod. Phys.* 92, 35001 (2020)

[2] H. Vazquez, R. Skouta, S. Schneebeli, M. Kamenetska, R. Breslow, L. Venkataraman and M.S. Hybertsen, *Nature Nanotechnol.* 7, 663 (2012)

O 11.6 Mon 16:15 H6

Spectral properties and thermodynamics of correlated metals via the algorithmic inversion of dynamical potentials — •TOMMASO CHIAROTTI¹, ANDREA FERRETTI², and NICOLA MARZARI¹ — ¹Theory and Simulations of Materials (THEOS) and National Centre for Computational Design and Discovery

of Novel Materials (MARVEL), École Polytechnique Fédérale de Lausanne, 1015 Lausanne, Switzerland — ²Centro S3, CNR-Istituto Nanoscienze, 41125 Modena, Italy

Dynamical potentials are needed to predict accurate spectral, transport, and in general embedding properties of materials. The non-linearity introduced by the frequency changes at a fundamental level the problem to address, moving from the diagonalization of an operator, e.g., the Kohn and Sham Hamiltonian in density-functional theory, to the Dyson inversion of a self-energy. Here, we propose a novel treatment of frequency-dependence able to solve Dyson-like equations via an exact mapping to an effective non-interacting problem, extending to the non-homogeneous case the algorithmic inversion method (Chiarotti et al., PRR, 2022). A sum-over-poles representation for the self-energy, together with the static one-particle Hamiltonian, are used to build a (larger) effective Hamiltonian having the excitation energies of the system as eigenvalues and the Dyson orbitals as projections of the eigenvectors. As a case study, we consider the paradigmatic system of $SrVO_3$ to compute accurate spectra and energetics of the material.

O 12: Organic Molecules at Surfaces 2: Characterization of Organic Monolayers

Time: Monday 15:00–18:00

Location: S051

O 12.1 Mon 15:00 S051

Quantifying Interactions in Organic Monolayers — •PIERRE-MARTIN DOMBROWSKI, STEFAN RENATO KACHEL, LEONARD NEUHAUS, TOBIAS BREUER, J. MICHAEL GOTTFRIED, and GREGOR WITTE — Philipps-Universität Marburg, Germany

The formation of molecular nanostructures is determined by the interplay of intermolecular and molecule-substrate interactions, whose experimental determination is challenging. Temperature-programmed desorption (TPD) is a well-established technique capable of quantifying these interactions, but its analysis is by no means trivial and therefore rarely done quantitatively for large adsorbates. In the present study, we analyse the desorption kinetics of the two organic semiconductors pentacene and perfluoropentacene from Au(111) and MoS₂ surfaces to show the potential of TPD and highlight challenges for larger adsorbates. [1,2] Combining TPD with scanning tunnelling microscopy, work function measurements and theoretical modelling, we show that intermolecular interactions are dominated by the intramolecular charge distribution. We are further able to determine the coverage-dependent prefactor of desorption with unprecedented precision, which enables a correlation of the desorption signal with the activation of specific degrees of freedom of motion of adsorbed molecules. Lastly, we compare the differences in molecule-substrate interactions for the two substrates at hand, which reveals that entropy can stabilize organic monolayer films on MoS₂ despite a weak molecule-substrate bond.

[1] S. R. Kachel et al., *Chem. Sci.* (2021), 12, 2575-2585.

[2] P.-M. Dombrowski et al., *Nanoscale* (2021), 13, 13816-13826.

O 12.2 Mon 15:15 S051

Toward Understanding Thermal and Electric Properties of Single Molecular Junctions and Self-Assembled Monolayers — •MOHAMED IBRAHIM¹, PHILIPP WIESENER¹, LUKE O'DRISCOLL², MARTIN BRYCE², and ACHIM KITTEL¹ — ¹Oldenburg University, Oldenburg, Germany — ²Durham University, Durham, England

Over the last years, implanting organic molecules in devices is continuously attracting large attention because of their small size (nm scale), tunable electronic and thermal properties by manipulating individual atoms. Therefore, it is obvious to extend the field of thermoelectrics using molecules to cool devices and sensors very locally. A single layer of well organized molecules is formed and realized by the self assembly mechanism, which allows molecular moieties to be adsorbed spontaneously on a surface producing large domains. This motivated us to report here about the characterisation of selfassembled oligo phenylene ethynylene dithiol molecules (OPE3), and some specifically modified forms by mainly adding side groups to it on gold surfaces by means of X-ray photoelectron spectroscopy (XPS), reflected electron energy loss (REELS), and ultraviolet photoelectron spectroscopy (UPS). The results show that the unsubstituted OPE3 has a high densely packed SAM with a thickness 1.7 nm, while the presence of substituents, attached to the middle ring, led to variation of the SAM film thickness. This indicates changes in the geometric configuration of the π stacking of OPE3 especially, tilt angle and packing densities. Parent OPE3 REELS spectrum shows a band gap value of 2.01 eV which is totally different than the reported value in the literature.

O 12.3 Mon 15:30 S051

Molecular orientation and phase transitions of DHTAP — •CLAUDIA LÓPEZ-POSADAS¹, MICHAEL GYÖRÖK¹, ANTONY THOMAS², THOMAS LEONI², OLIVIER SIRI², CONRAD BECKER², and PETER ZEPPENFELD¹ — ¹Institute of Experimental Physics, Johannes Kepler University Linz, Altenberger Str. 69, 4040 Linz, Austria — ²Aix-Marseille University, CNRS, CINaM, UMR 7325, F-13288 Marseille, France

The structure and orientation of 5,14-dihydro-5,7,12,14-tetraazapentacene (DHTAP) layers deposited on Cu(110), Cu(110)-(2x1)O and the Cu(110)/Cu(110)-(2x1)O stripe phase was studied using reflectance difference spectroscopy (RDS), Scanning Tunneling Microscopy (STM) and Low Energy Electron Diffraction (LEED). The evolution of the RDS signal allows to identify the sequential formation of up to three monolayers as well as a phase transition upon completion of the first one. On Cu(110), DHTAP molecules in the first monolayer are always lying flat with their long molecular axis aligned parallel to the [-110]-direction of the Cu(110) surface. However, for subsequent layers the orientation critically depends on the deposition temperature T. At T=240K the DHTAP molecules are mostly aligned parallel to the ones in the first layer, whereas at room temperature and above their preferential orientation is orthogonal to the molecules in the first layer, the coexistence of the two orientations can be observed at a critical temperature of T=270K. Finally, the main optical transitions and the orientation of the transition dipole moments of the DHTAP layers were extracted from the RDS spectra.

O 12.4 Mon 15:45 S051

Nickel(II) Porphyrins on Metal Surfaces: Oxidation-State Tuning and Formation of a Supramolecular Mixed-Valence Adsorbate Structure — •JAN HERRITSCH, QITANG FAN, MARIE-IRÈNE ALBUS, LUKAS RUPPENTHAL, LUKAS J. HEUPLICK, LEONARD NEUHAUS, TOBIAS WASSERMANN, and J. MICHAEL GOTTFRIED — Philipps-Universität Marburg

Nickel tetrapyrrole complexes are structurally related to biologically relevant molecules (e.g., F430 cofactor, tunichlorin, nivalamine) and are promising precursors for novel functional interfaces. Here, we report on the influence of the interaction at the metal/organic interface on the electronic structure of a nickel octaethyl porphyrin (Ni(OEP)) monolayer on different coinage metal surfaces studied by XPS, UPS, STM, NEXAFS and LEED. On Ag(111), Ni(OEP) forms a mixed-valent adsorbate phase in which the Ni centers occur in two different oxidation states. The two separate peaks in the Ni 2p XP spectrum indicate that about 40% of the Ni centers are reduced. STM and LEED show an incommensurate superstructure with an ordered arrangement of the metal centers in different oxidation states. Further insights into the valence electronic structure were obtained by UPS and NEXAFS. On the more reactive Cu(111) surface, Ni(OEP) forms a long-range ordered structure in which nickel centers are uniformly reduced; whereas on the most inert Au(111) surface, the oxidation state of the Ni centers remains unaffected by adsorbate interactions.

O 12.5 Mon 16:00 S051

Electronic and structural properties at the NiTPP/O-Cu(100) interface — •JONAH ELIAS NITSCHKE¹, HENNING STURMEIT¹, IULIA COJOCARIU², VITALIY FEYER², ALESSANDRO SALA², ANDREAS WINDISCHBACHER³, PETER PUSCHNIG³, STEFANO PONZONI¹, GIOVANNI ZAMBORLINI¹, and MIRKO CINCHETTI¹ — ¹Department of Physics, TU Dortmund University, Germany — ²Peter Grünberg Institut (PGI-6), Forschungszentrum Jülich, Germany — ³Institute of Physics, University of Graz, Austria

Depending on the strength of the molecule-substrate interaction, charge transfer, chemical reactions or a redistribution of the electronic cloud may occur at organic-metal interfaces. Here, we investigate the structural and electronic properties of Nickel tetraphenylporphyrin molecules (NiTPP) deposited on oxygen-passivated Cu (100) surface. By using a multi-technique approach, which combines LEED and STM, we reveal a coverage dependent superstructure with multiple domains that ultimately reduces into a single unit cell.

In the latter configuration, STM measurements show that the NiTPP molecules adsorb either with the macrocycle planar to the surface on in a saddle-shape configuration, with the pairs of opposite pyrrole rings tilted upwards. STS and photoemission orbital tomo-graphy measurements show that, contrary to the NiTPP adsorbed on the bare Cu(100) surface, where a significant charge transfer is observed, the oxygen overlayer quenches the charge transfer at the interface, thus offering a simple approach to physically decouple of the molecular film from the underlying substrate.

O 12.6 Mon 16:15 S051

Surface Chemical Bond and Molecular Topology of Polycyclic Aromatic Systems — •LUKAS RUPPENTHAL¹, FLORIAN MÜNSTER¹, BENEDIKT P. KLEIN¹, JAN HERRITSCH¹, LEONARD NEUHAUS¹, STEFAN R. KACHEL¹, PENGCAI LIU², XING-YU CHEN², JIAWEN CAO², LARS E. SÄTTLER³, SEBASTIAN M. WEBER³, QI-TANG FAN¹, GERHARD HILT³, XIAO-YE WANG², and J. MICHAEL GOTTFRIED¹ — ¹Department of Chemistry, Philipps-University Marburg, Germany — ²College of Chemistry, Nankai University Tianjin, China — ³Institute of Chemistry, Carl von Ossietzky University Oldenburg, Germany

Metal/organic interfaces have a large impact on the performance of organic (opto-)electronic devices. Therefore, the detailed understanding of their chemical, electronic and geometric structure is important for the further technological development. Many common organic semiconductors contain π -electron systems with alternant topologies, whereas non-alternant alternatives have only recently found increasing attention due to their unusual electronic properties. Here, we compare the alternant polycyclic aromatic molecule pyrene with its non-alternant isomers acepleiadylene and azupyrene regarding their interaction with Cu(111) surface, using PES, NEXAFS, TPD and STM. The non-alternant isomers are also interesting as molecular models of graphene defects, e.g. azupyrene for the Stone-Wales defects. In all cases, the non-alternant isomers show increased metal/molecule-interaction due to their reduced HOMO-LUMO gap, which brings the LUMO energetically closer to the Fermi energy of the metal, causing stronger hybridization with electronic states of the metal surfaces.

O 12.7 Mon 16:30 S051

Tailoring the organic-semiconductor/metallic interface: From self-assembly to heteromolecular phases of carboxylic acids on Ag surfaces — •MATTHIAS BLATNIK, VERONIKA STARÁ, ANTON MAKOVEEV, JAKUB PLANER, THOMÁŠ KRAJČEK, PAVEL PROCHÁZKA, and JAN ČECHAL — CEITEC BUT, Brno, CZ

Atomic-level understanding of the metal/organic-semiconductor interface has become paramount in the strife for the development and fabrication of more efficient organic electronic devices in recent years. Interfacial properties are crucially linked to molecule-molecule and molecule-substrate interactions, molecular functionalization (e.g., deprotonation), a precise energy level alignment, substrate termination or the formation of multi- or heterolayers with a different organic compound. All these have to be well understood through the study of model systems in ultra-clean conditions before technological advances can be achieved. Here, we present a model system of self-assembled aromatic carboxylic acids (e.g., 4,4'-Biphenyl Dicarboxylic Acid, 1,3,5-Benzenetribenzoic Acid) on Ag surfaces (orientations (100) and (111)). We explore the effects of the metal substrate's orientation on formation and growth of single molecular phases, introduce a monolayer thick layer as a charge injection layer and study the formation of a heteromolecular compound with an additional organic material (e.g., pentacene). We employ low energy electron microscopy (LEEM) and diffraction (μ LEED), as well as STM and XPS to give a real-time view and detailed information on nucleation and growth of the molecular phases and transformations and the chemical composition.

O 12.8 Mon 16:45 S051

Highly ordered commensurate structures of merocyanines on Ag(100) — •ANNA JULIANA KNY¹, MAX REIMER², NOAH AL-SHAMERY¹, RITU TOMAR¹, THOMAS BREDOW¹, SELINA OLTHOFF², and MORITZ SOKOLOWSKI¹ — ¹Institut für Physikalische und Theoretische Chemie der Universität Bonn, Germany — ²Department für Chemie der Universität zu Köln, Germany

Vacuum deposited films of the merocyanine molecule 2-[5-(5-dibutylaminothiophen-2-yl-methylene)-4-*tert*-butyl-5H-thiazol-2-ylidene]-malononitrile (HB238) and its derivatives have been investigated in the context of organic solar cells [1].

Although the specific structural order in these films is important for the optical properties, only very little is known about the adsorption and ordering of merocyanines on surfaces. Therefore, we investigated monolayers of HB238 on a Ag(100) surface by SPA-LEED, STM, XPS, UPS, and DFT calculations.

Upon deposition onto the Ag(100) surface at room temperature the formation of a commensurate superstructure is observed. It is composed of homochiral HB238 aggregates of four molecules. We discuss the surface bonding and structure formation in dependence of the specific functional groups and, furthermore, the sterically demanding donor substituents. For the role of the latter one, we also investigated derivatives of HB238 on Ag(100). The merocyanines were synthesized and kindly provided by the group of Prof. K. Meerholz (Cologne).

Supported by the DFG through the research training group 2591. [1] JACS 137 (2015) 13524.

O 12.9 Mon 17:00 S051

Van der Waals Heteroepitaxy: Intrinsic Epitaxial Alignment of Perfluoropentacene Films on Transition Metal Dichalcogenides — •MAXIMILIAN DREHER, DARIUS GÜNDELER, and GREGOR WITTE — Philipps-University Marburg, Germany

In this work, we have studied the formation and azimuthal alignment of crystalline adlayers of the organic semiconductor (OSC) perfluoropentacene (PFP) on the basal plane of several transition metal dichalcogenides (TMDC) single crystals, which are further compared to graphite and hBN. The quite inert basal planes of TMDCs enable an unrestricted growth of OSCs without the requirement of relaxation in terms of commensurability at the interface, since molecules exhibit a stronger interaction among each other than with the substrate. Nevertheless, the crystalline PFP multilayers exhibit distinct azimuthal twist angles relative to the substrate surface, which we could rationalize by so called 'on-line coincidences' introduced by Forker et al. recently. [1] Here, the molecules do not favor a specific adsorption site at the interface as it is often described by commensurate superstructures. Instead the bulk crystal structure remains unperturbed down to the interface, but a specific twist angle is adopted, where molecules avoid unfavored adsorption sites. The extreme sensitivity of the resulting twist angles by small deviations in the crystal structure enabled us further to use the large thermal expansion of the OSC to control the twist angles by changing the substrate temperature during deposition. [1] Forker et al., Soft Matter 13, 1748-1758 (2017) [2] Dreher et al., Chem. Mater. 32, 20, 9034-9043 (2020)

O 12.10 Mon 17:15 S051

Steering Self-Assembly of Three-Dimensional Iptycenes on Au(111) by Tuning Molecule-Surface Interactions — LUKAS GROSSMANN^{1,2}, EVA RINGEL^{1,2}, WOLFGANG HECKL^{1,2}, and MARKUS LACKINGER^{1,2} — ¹Deutsches Museum, Museumsinsel 1, 80538 München — ²Technische Universität München, Physics Department, James-Frank-Strasse 1, 85748 Garching

Three-dimensional organic molecules have been neglected in studies on surfaces, even though their self-assemblies exhibit a far greater variability than their planar counterparts. While planar molecules adsorb mostly flat on surfaces, three-dimensional molecules can adopt vastly different adsorption geometries. This additional degree of freedom can result in self-assembly of entirely different supramolecular structures. Moreover, adsorption geometries can be steered by tuning molecule-surface interactions, thereby providing a new means for 2D crystal engineering. In this respect, iptycenes are highly stable, but currently underexplored model compounds. Here, we study self-assembly of three-fold symmetric triptycene derivatives with extended anthracene blades on Au(111) surfaces. Additionally, the influence of intrinsic dipole moments was investigated by comparing analogs with peripheral fluorine substitution. All structures were resolved by Scanning-Tunneling-Microscopy under ultra-high vacuum conditions. On pristine Au(111), the molecules maximize the area of contact, whereas iodine-passivation affords hexagonal porous structures that feature optimized molecule-molecule interactions through face-to-face stacking of all anthracene blades.

O 12.11 Mon 17:30 S051

Adsorption of Submonolayer Coverages of Phenylphosphonic Acid on Rutile TiO₂(110) — •ALEXANDER WOLFRAM¹, MAXIMILIAN MUTH¹, JULIA KÖBL¹, NATALIYA TSUD², SASCHA MEHL³, HANS-PETER STEINRÜCK¹, and OLE LYTKE¹ — ¹Friedrich-Alexander Universität Erlangen-Nürnberg, Lehrstuhl für Physikalische Chemie 2, Egerlandstr. 3, 91058 Erlangen, GER — ²Charles University, Faculty of Mathematics and Physics, Department of Surface and Plasma Science, Holešovičkách 2, Prague, 18000, Czech Republic — ³Elettra-Sincrotrone Trieste SCPA, Strada Statale 14, km 163.5, Trieste, Basovizza, 34149, Italy

The interfaces of oxide surfaces with organic molecules are crucial for the performance of devices, such as dye-sensitized solar cells, sensors and organic electronics. All these devices contain interfaces where organic molecules are bound to surfaces, often using covalent anchoring groups. These anchoring groups strongly influence the interface and thus the device performance. An interesting anchoring group is the phosphonic acid group, which is well known to bind strongly to oxide surfaces. At ELETTRA sincrotrone in Trieste we investigated submonolayer coverages of phenylphosphonic acid on a rutile TiO₂ (110) surface with high-resolution X-ray photoelectron spectroscopy (XPS) and near-edge X-ray absorption fine structure (NEXAFS) spectroscopy. Based on the changes in the O 1s and P 2p core levels, we are able to identify the different binding motifs

present on the surface at different temperatures, while the NEXAFS intensities gives us information about the orientation of the phenyl moiety.

O 12.12 Mon 17:45 S051

Accurate determination of adsorption-energy differences of metalloporphyrins on TiO₂(110) 1x1 — •MAXIMILIAN MUTH, ALEXANDER WOLFRAM, ELMAR KATAEV, JULIA KÖBL, HANS-PETER STEINRÜCK, and OLE LYTKEN — Univ. Erlangen-Nürnberg

A deeper knowledge of the behavior between porphyrin molecules and the rutile TiO₂(110) surface and is of crucial importance for the development of new applications. Especially the usage of such systems in photocatalysis or solar cells are promising possibilities. Therefore, we investigated the adsorption energy of three different metallo-tetraphenylporphyrins (MTPP M = Mg, Co, Zn). Un-

fortunately, temperature programmed desorption, a typical method for the determination of adsorption energies is not applicable for this particular system because of the irreversible adsorption of the monolayer in direct contact to the TiO₂-surface. For this reason, instead, we compared the adsorption-energy of the three MTPPs relatively to each other by using a layer exchange experiment. We adsorb mixtures of always two different MTPPs on top of each other and allow the molecules to diffuse during a heating ramp. Eventually, an equilibrium state forms in which the MTPP with the higher adsorption-energy will enrich in the monolayer in direct contact with surface while the weaker adsorbing MTPP will be enriched in the multilayer. After further heating for multilayer desorption we determine the concentrations of the MTPPs found in the remaining monolayer by using XPS and use them to calculate the difference in adsorption-energy of MTPPs via the equilibrium constant.

O 13: Nanostructures at Surfaces 2

Time: Monday 15:00–17:30

Location: S052

O 13.1 Mon 15:00 S052

A new setup for dimensional nanometrology using soft X-rays — •LEONHARD LOHR¹, RICHARD CIESIELSKI¹, ANALÍA FERNÁNDEZ HERRERO², ANDREAS FISCHER¹, ALEXANDER GROTHE¹, FRANK SCHOLZE¹, and VICTOR SOLTWISCH¹ — ¹Physikalisch-Technische Bundesanstalt (PTB), Abbestraße 2-12, 10587 Berlin, Germany — ²Helmholtz-Zentrum Berlin für Materialien und Energie, Albert-Einstein-Straße 15, 12489 Berlin, Germany

Measuring nanostructured surfaces on small test patterns on dies from semiconductor fabs is an important metrology challenge. The geometrical dimensions of metrology test structures, such as linear gratings, must be determined with uncertainties in the sub-nm range. By using methods such as small angle X-ray scattering or X-ray fluorescence under grazing incidence, the photon beam spot size becomes too large for sufficient accurate measurements.

We present a new setup, mounted on the soft X-ray beamline in PTB's laboratory at the electron storage ring BESSY II. This setup works with synchrotron radiation in an ultra-high vacuum and with lubricant-free mechanics. Its small and compact design enables to detect scattered monochromatic soft X-rays under angles of incidence up to 30 degrees. The setup reduces photon beam spot size and covers diffraction patterns like them from scattered hard X-rays under grazing incidence. Depending on the incident photon energy, fluorescence from small excited regions of the sample can be measured simultaneously.

We present first measurement results from small test patterns which are located by imaging the surface using a large photon beam.

O 13.2 Mon 15:15 S052

Synthesis of metal sulfide nanoribbons on graphene by self-assembly — •XUEJIAO ZHANG, KELVIN ANGGARA, VESNA SROT, XU WU, PETER A. VAN AKEN, and KLAUS KERN — Max Planck Institute for Solid State Research, 70569 Stuttgart, Germany

Bottom-up synthesis of nanostructures on surface have relied on the self-assembly of nanoscale building blocks. The diversity of accessible nanostructures however have been constrained by the limited choice of atomic and molecular building blocks that can be evaporated on surface. Here we bypass this limitation by using complex inorganic ions generated from electrospray ionization as building blocks to synthesize nanostructures on surfaces. We deposited HMonS_{3n+1}⁺ (n = 4-6) ions onto a freestanding single-layer graphene by Electro-spray Ion-Beam Deposition (ESIBD), and imaged the resulting nanostructures by aberration-corrected Scanning Transmission Electron Microscopy (STEM). The molecules were observed to form anisotropic, single-layered, crystalline MoS₂ nanoflakes (< 100 nm²), which in turn self-assembled into MoS₂ nanoribbons extending as far as 1 μm. The first observation of such nanostructures evidences the potential of this approach to prepare previously inaccessible nanomaterials on surfaces.

O 13.3 Mon 15:30 S052

Ni kagome lattice on Pb(111) — •GUSTAV BIHLMAYER¹, YEN-HUI LIN², STEFAN BLÜGEL¹, and PIN-JUI HSU² — ¹Peter Grünberg Institut und Institute for Advanced Simulation, Forschungszentrum Jülich, D-52425 Jülich, Germany — ²Department of Physics, National Tsing Hua University, Hsinchu, 30013, Taiwan

Deposition of atomically thin films on well-ordered surfaces sometimes allows realizing new structural motives that have no correspondence in the bulk phases. Here we observe that, at low temperatures, submonolayer growth of Ni on a Pb(111) substrate leads to well-ordered, hexagonal islands. In scanning tunneling microscopy (STM) two types of edges with very different apparent height and scattering properties are observed. From density functional theory (DFT) calculations and STM images with atomic resolution we conclude that the Ni atoms form a kagome lattice and the islands show saw-tooth edges. Comparison of STM and DFT data suggests that some Ni atoms are incorporated in the sub-surface layer and give rise to the low observed height of the islands and the strong

difference observed at their edges. From the DFT calculations we conclude that the Ni island is non-magnetic and the electronic structure shows some characteristics of the kagome lattice, i.e. flat bands also visible in scanning tunneling spectra.

O 13.4 Mon 15:45 S052

DNA origami as reference systems for nano-metrology — •ZIBA AKBARIAN^{1,2}, BIRKA LALKENS^{1,2}, MICHELLE WEINERT³, INGO BUSCH³, HARALD BOSSE³, and UTA SCHLICKUM^{1,2} — ¹Technische Universität Braunschweig, Braunschweig, Germany — ²Laboratory for Emerging Nanometrology (LENA), Braunschweig, Germany — ³Physikalisch Technische Bundesanstalt (PTB), Braunschweig, Germany

A key aspect of quantitative measurements is the traceability of all measurements to the international system of units (SI). DNA origami is capable of being traced back to SI units thanks to its precisely defined internal structures in 2D and 3D. Here, we will describe the possibilities of building reference systems for calibrating scanning probe instruments with μm resolution only that can be traced back to atomically precise structures. In order to accomplish this goal, we plan to fabricate DNA origami structures that include marks at well-defined positions to obtain measurable protrusions within the internal structures. The controlled fabrication of DNA origami structures that do not distort upon adsorption onto surfaces, in both liquid and air conditions will be surveyed as the first step in this research.

O 13.5 Mon 16:00 S052

How covalent chemistry affects the surface dipole of metallic nanostructures — RUSTEM BOLAT^{1,2}, •JOSE M. GUEVARA¹, MARVIN KNOL^{1,2}, PHILIPP LEINEN¹, RUSLAN TEMIROV^{1,2,3}, OLIVER T. HOFMANN⁴, REINHARD J. MAURER⁵, F. STEFAN TAUTZ^{1,2}, and CHRISTIAN WAGNER^{1,2} — ¹Forschungszentrum Jülich, Germany — ²RWTH Aachen University, Germany — ³Universität zu Köln, Germany — ⁴Graz University of Technology, Austria — ⁵University of Warwick, UK

Scanning probe experiments often encounter nanostructures of undercoordinated metal atoms, either as the investigated system or at the tip apex. While the electrostatic properties of extended planar surfaces are textbook material, the interaction of metal adatoms with the surface and with each other opens an interesting playground in which our intuition for the covalent chemistry of such metal structures is limited.

Here we investigate Ag and Au adatoms, monoatomic chains and small clusters, on the Ag (111) surface using quantum dot microscopy. We image the electrostatic potential above these nanostructures and quantify the respective surface dipoles. The two species of adatoms behave antagonistic, as the surface dipoles are positive for Ag and negative for Au structures. The measured dipoles are in excellent agreement with density functional theory calculations. We disentangle the influence of individual adatom-surface and adatom-adatom bonds down to individual atomic orbitals.

O 13.6 Mon 16:15 S052

Gold nanostructures with varying physicochemical surrounding examined with surface second harmonic generation circular dichroism spectroscopy — •NATALIE FEHN¹, EHSAN VAHIDZADEH², KARTHIK SHANKAR², UELI HEIZ¹, and ARAS KARTOUZIAN¹ — ¹Physical Chemistry, Department of Chemistry and Catalysis Research Center, Technical University of Munich — ²Electrical and Computer Engineering Department, Faculty of Engineering, University of Alberta

The sophisticated second-order spectroscopic methods of surface second harmonic generation (s-SHG) and s-SHG circular dichroism spectroscopies (s-SHG-CD) provide additional and complementary structural information in regards to their linear counterparts, absorbance and CD spectroscopy. Because of their surface sensitivity, s-SHG and s-SHG-CD represent an excellent choice for the investigation of molecular thin films and supported plasmonic structures,

such as nanoparticles and clusters. We are especially interested in the interaction of such nanostructures with their surroundings, e.g. chiral molecule adsorbates or oxide layers, with the goal of observing a chiral response from the originally achiral particles. Those particles may then serve as catalysts in asymmetric heterogeneous catalysis. This contribution will focus on our research with emphasis on supported gold nanostructures.

O 13.7 Mon 16:30 S052

Elucidating the chirality of polycrystalline films with fundamental and SHG-CD — •KEVIN LIANG¹, FLORIAN RISTOW², JAKOB SCHEFFEL², NATALIE FEHN¹, REINHARD KIENBERGER², UELI HEIZ¹, ARAS KARTOUZIAN¹, and HRISTO IGLEV² — ¹Physical Chemistry, Department of Chemistry and Catalysis Research Center, Technical University of Munich — ²Physics Department E11, Technical University of Munich

Preferential desorption of enantiomers of 1,1'-Bi-2-naphthol (BINOL) has been observed, depending on the handedness of circularly polarized light, which is of interest for enantioenrichment processes. Therefore, characterisation of the enantiomeric excess of the sample and the understanding of its chirality is key. However, that requires further studies and greater clarification to be carried out and obtained, respectively. This contribution discusses the optical properties of BINOL thin films with fundamental and second harmonic generation (SHG) circular dichroism spectroscopy (CD) with different sample preparation methods, enantiomeric compositions and under varying experimental conditions. Depending on the previous conditions mentioned, the observed CD and anisotropy (g) value can be even of opposite sign for the same thin film.

O 13.8 Mon 16:45 S052

AFM studies of ion-exchange treated glass surfaces — •FABIAN HÖHN^{1,3}, FABIAN ULLMANN^{1,3}, NORBERT ARNDT-STAUENBIEL², and STEFAN KRISCHOK^{1,3} — ¹Institute of Physics, TU Ilmenau, Weimarerstraße 25, Ilmenau, Germany — ²Fraunhofer Institute for Reliability and Microintegration, Gustav-Meyer-Allee 25, Berlin, Germany — ³Center of Micro- and Nanotechnologies, TU Ilmenau, Gustav-Kirchhof-Straße 7, Ilmenau, Germany

There is a big difference between the bond strength of glass and its respective tensile strength. The reason for this discrepancy is assumed to be so-called "microcracks", this surface damage is considered to massively reduce the tensile strength. We assume that these damages widen by stretching the surface and become thus more visible. Another point that will be investigated, regarding this matter, is micro waveguides in glass. These are created by silver ion exchange in glass. It is assumed that the mentioned surface damages are a cause for reduced quality of these waveguides. For this purpose, we examine the difference in topography between untreated Gorilla V1 glass from Corning, a sample stretched using the three-point method and a sample in which a silver ion exchange was carried out on the surface. The difference in topography is first described qualitatively and then determined quantitatively with roughness parameters. Finally, a comparison of the three samples should provide an insight into the topography of glasses under stress and a contribution to the optimization of the mentioned waveguides.

O 13.9 Mon 17:00 S052

Processing copper surfaces with ultrashort laser pulses to reduce secondary electron yield — •ELENA BEZ^{1,2}, MARCEL HIMMERLICH¹, ANA KAREN REASCOS PORTILLA¹, PIERRE LORENZ³, KLAUS ZIMMER³, MAURO TABORELLI¹, and ANDRÉ ANDERS^{2,3} — ¹CERN, European Organization for Nuclear Research, 1211 Geneva 23, Switzerland — ²University of Leipzig, Linnestr. 5, 04103 Leipzig, Germany — ³Leibniz Institute of Surface Engineering (IOM), Permoserstr. 15, 04318 Leipzig, Germany

Ultrashort-pulse laser processing in air is employed to engrave micro- and nanostructures on copper surfaces aiming to reduce secondary electron emission. Parameters such as the laser power and scanning speed are varied to investigate their influence on the resulting structures. The morphology, as well as the chemical composition of the laser-treated surfaces, are analyzed by scanning electron microscopy (SEM) and X-ray photoelectron spectroscopy (XPS), respectively. At low power and high scanning speed, only slight changes to the surface topography occur, whereas compact, cauliflower-like nanostructures and micrometer deep trenches are generated at high power and low scanning speed. The higher the accumulated laser fluence, the more material is ablated and the more oxidized particles are redeposited. A clear correlation exists between the accumulated fluence for processing with 355, 532 and 1064 nm photons, and the resulting secondary electron yield of the surface. Its maximum can be reduced from 2.2 to 0.7. Mastering these dependencies helps to develop a system that enables laser processing of beam pipes of selected magnets in the Large Hadron Collider.

O 13.10 Mon 17:15 S052

Highly ordered three-dimensional Ni-TiO₂ nanopore arrays as sodium-ion battery anodes — •MO SHA, HUAPING ZHAO, and YONG LEI — Fachgebiet Angewandte Nanophysik, Institut für Physik & IMN MacroNano, Technische Universität Ilmenau, 98693 Ilmenau, Germany

Sodium-ion batteries (SIBs) represent an effective energy storage technology with potentially lower material costs than lithium-ion batteries. Here, we show the electrochemical performance of SIBs with electrode design at the nanoscale. Highly ordered three-dimensional (3D) selfsupported Ni-TiO₂ nanopore arrays (NiNPA@TiO₂) with highly oriented nanoporous structures are fabricated using nanoimprinted AAO templating technique and applied as nanostructured anodes for SIBs applications. Their large specific surface area can ensure a high capacity, and their highly oriented and stable nanoporous structure can facilitate ion transport. The NiNPA@TiO₂ nanoarrays delivered a reversible capacity of 240 mAh g⁻¹ after 100 cycles at the current density of 50 mAh g⁻¹ and were able to retain a capacity of 105 mAh g⁻¹ at the current density as high as 5 A g⁻¹. Their large active sites, high ion accessibility, fast electron transport, and excellent electrode integrity were shown as great merits to obtain the presented electrochemical performance. Not limited to the SIBs electrodes, the highly ordered 3D heterostructured nanoarrays as a promising electrode design for other electrochemical energy conversion and storage devices.

O 14: New Methods and Developments 2: Scanning Probe Techniques 2 (joint session O/KFM)

Time: Monday 15:00–16:15

Location: S053

O 14.1 Mon 15:00 S053

The importance of the dipole at the metal tip apex when approaching closer with a CO tip — •SHINJAE NAM, OLIVER GRETZ, THOMAS HOLZMANN, ALFRED JOHN WEYMOUTH, and FRANZ J. GIESSIBLE — University of Regensburg, Regensburg, Germany

By functionalizing the tip with a single CO molecule, the resolution of atomic force microscope (AFM) can be drastically increased. The contrast enhancement produced by a CO tip has been explained in terms of strong Pauli repulsion and the associated tilting of the probe molecule. Although these two interactions play a dominant role at very close distances, recent experiments show that other interactions, especially electrostatic forces, are also important to understand the observed contrast. Here, we used Lateral Force Microscope, a variant of frequency modulation atomic force microscopy, to quantify the interaction between a CO tip and a CO on the Cu (111) surface. Interestingly, one more feature appeared in the measurement when we measured closer to the surface at the side of the surface CO. Following the results of other investigations, we include the electrostatic force in our simulations. We modeled our tip as a quadrupole, including a dipole at both the metal tip and on the CO molecules. We found that the dipole of the metal apex of the tip becomes a much greater influence as we approach closer to the surface.

O 14.2 Mon 15:15 S053

Chemical bond imaging using torsional and flexural higher eigenmodes of qPlus sensors — •DANIEL MARTIN-JIMENEZ¹, MICHAEL G. RUPPERT², ALEXANDER IHLE¹, SEBASTIAN AHLES³, HERMANN A. WEGNER³, ANDRÉ SCHIRMEISEN¹, and DANIEL EBELING¹ — ¹Institute of Applied Physics, Justus Liebig University Giessen, Heinrich-Buff-Ring 16, 35392 Giessen (Germany). — ²University of Newcastle, Callaghan, NSW, 2308 (Australia). — ³Institute of Organic Chemistry, Justus Liebig University Giessen, Heinrich-Buff-Ring 17, 35392 Giessen (Germany).

Non-contact atomic force microscopy (AFM) with CO-functionalized tips allows to visualize the chemical structure of adsorbed molecules and identify individual inter- and intramolecular bonds. Herein, we analyze the suitability of qPlus sensors, which are commonly used for bond imaging, for the application of modern multifrequency AFM techniques. Two different qPlus sensors were tested for submolecular resolution imaging via actuating torsional and flexural higher eigenmodes and via bimodal AFM. The torsional eigenmode of the first sensor is perfectly suited for performing lateral force microscopy (LFM) with single bond resolution. The advantage of using a torsional eigenmode is that the same molecule can be imaged either with a vertically or laterally oscillating tip without replacing the sensor simply by actuating a different eigenmode. Submolecular resolution is also achieved by actuating the 2nd flexural eigenmode of our second sensor. With laser Doppler vibrometry measurements and AFM simulations we can rationalize the image contrast mechanism of the 2nd eigenmode.

O 14.3 Mon 15:30 S053

3D Force mapping of single organic molecules at room temperature — •TIMOTHY BROWN, PHILIP BLOWEY, JACK HENRY, and ADAM SWEETMAN — University of Leeds, Leeds, UK

Scanning probe microscopy has established itself as a highly effective technique in the study of surfaces and molecules. In particular, non-contact atomic force microscopy has yielded enormous progress in our ability to characterise materials at the atomic scale, including the ability to resolve the chemical structure of individual molecules, and to acquire 3D force-maps with intramolecular resolution.

Intramolecular imaging is almost exclusively performed using qPlus sensors at cryogenic temperatures, as the functionalisation of the tip via a CO molecule (required for intra-molecular imaging) is only stable at near liquid helium temperatures. Although it has been shown that intramolecular imaging may be performed at higher temperatures, via use of semi-conducting, rather than metallic substrates, acquisition of high density 3D data sets generally requires long acquisition times. Hence the lack of thermal equilibrium between the tip and sample at room temperature makes acquisition of these datasets at elevated temperatures extremely challenging.

In this talk we present the first demonstration of high resolution 3D force mapping of a single organic molecule at room temperature using conventional silicon cantilevers. We show how the challenges of operating in a room temperature experimental environment can be overcome to acquire reproducible 3D force maps of a resolution and quality previously only demonstrated at low temperature.

O 14.4 Mon 15:45 S053

Monitoring of molecular configurations during manipulation with a scanning probe microscope — •JOSHUA SCHEIDT^{1,2}, ALEXANDER DIENER^{1,2}, MICHAEL MAIWORM³, ROLF FINDEISEN³, KURT DRIESSENS², F. STEFAN TAUTZ¹, and CHRISTIAN WAGNER¹ — ¹Peter Grünberg Institut (PGI-3), Forschungszentrum Jülich, Jülich, Germany — ²Maastricht University, Data Science and Knowledge Engineering, Maastricht, Netherlands — ³Control and Cyber-Physical Systems Laboratory, Technische Universität Darmstadt, Darmstadt, Germany

A bold vision of nanofabrication is the assembly of functional molecular structures with a scanning probe microscope (SPM). Such an approach allows the

quick variation of conformation and composition of (supra)molecular systems and an assessment of these parameters on the envisioned functionality. However, monitoring the molecular conformations during manipulations remain elusive due to the dual role of the SPM tip as an actuator and an imaging probe. We present an approach which enables monitoring based on continuously gathered force gradient data using a particle filter approach, which solves the inverse problem of conformation monitoring by comparing current force gradient data to a structured set of simulations stored in the form of a finite state automaton. This allows using molecular simulations with wall-times for completion much longer than the time scale of the experiments. Our proof-of-principle investigations are based on the vertical SPM manipulation of a PTCDA (3,4,9,10-perylene-tetracarboxylic dianhydride) molecule on the Au(111) surface.

O 14.5 Mon 16:00 S053

Real-space imaging of σ -hole by means of Kelvin probe force microscopy. — •AURELIO GALLARDO¹, BENJAMÍN MALLADA², BRUNO DE LA TORRE², and PAVEL JELÍNEK¹ — ¹FZU of the CAS, Prague, Czech Republic — ²RCPTM-CATRIN, Palacký University, Olomouc Czech Republic

Anisotropic charge distributions on individual atoms, such as σ -holes, are crucial for the structural properties of certain systems. Nevertheless, the existence of σ -holes has only been demonstrated indirectly, either observing the interaction between halogenated molecules or by theoretical calculations. However, there was no experimental technique that would allow the spatial resolution of anisotropic atomic charges.

To tackle this problem, we employed Kelvin probe force microscopy (KPFM) which imaging mechanism relies on the electrostatic tip-sample interaction. To achieve the requested resolution, we developed a theoretical description of the KPFM imaging mechanism on atomic scale, which enables optimize the experimental setup. Namely we demonstrated both theoretically and experimentally that probe tip functionalization by a single Xe atom enhances the spatial resolution to directly visualize the anisotropic charge of the σ -hole, as well as the quadrupolar character of the carbon monoxide molecule. [1]

We believe that this work large already outstanding imaging capabilities of scanning probe techniques. In particular, this KPFM technique will enable better description of charge distribution in molecular complexes as well as on surfaces.

References: [1] Mallada et al., Science 374, 863-867 (2021)

O 15: Solid-Liquid Interfaces 2: Structure and Spectroscopy

Time: Monday 15:00–18:00

Location: S054

Topical Talk

O 15.1 Mon 15:00 S054

Hydration Layer Mapping at Solid-Liquid Interfaces — •ANGELIKA KÜHNLE — Physical Chemistry I, Department of Chemistry, University Bielefeld, Universitätsstraße 25, 33615 Bielefeld, Germany

Solid-liquid interfaces are omnipresent in nature and technology. Under ambient conditions, the properties of many materials are governed by a thin layer of water at the interface. Understanding processes occurring at the solid-liquid interface thus almost always requires a detailed knowledge of the hydration structure at the interface. Recent improvements in atomic force microscopy (AFM) instrumentation now enable molecular-level insights into the three-dimensional (3D) solvation structure at the interface.

In this talk, the capability of 3D AFM will be presented by discussing the hydration structure at the gypsum-water interface. Gypsum, the dihydrate of calcium sulfate, is an abundant rock-forming mineral in the Earth's crust. It is composed of alternating bilayers of calcium sulfate and water. Upon cleavage, the crystal water is exposed. What is the fate of this crystal water at the aqueous interface? Comparing 3D AFM data with water density maps derived from molecular dynamics simulations allows for elucidating molecular-level details of the gypsum-water interface. Our findings indicate that the crystal water at the interface remains tightly bound, even when in contact with bulk water. Thus, the interfacial chemistry of gypsum is governed by the crystal water rather than the calcium or sulfate ions.

O 15.2 Mon 15:30 S054

Self-assembly and thin film growth dynamics of an ionic liquid on Au(111) investigated in real space — MANUEL MEUSEL¹, MATTHIAS LEXOW¹, AFRA GEZMIS¹, SIMON SCHÖTZ¹, MARGARETA WAGNER², •SIMON JAEKEL¹, ANDREAS BAYER¹, FLORIAN MAIER¹, and HANS-PETER STEINRÜCK¹ — ¹Chair of Physical Chemistry II, University of Erlangen-Nürnberg (FAU), Germany — ²Institute of Applied Physics, Technical University of Vienna, Austria

Ionic liquids (IL) are organic salts with low melting points, often at or even below room temperature. They have shown promise as solvents and electrolytes, but have also become part of novel catalytic concepts involving solid metal catalysts.

In this context, our group studied the self-assembly and growth dynamics of thin films of 1,3-dimethylimidazolium bis[(trifluoromethyl)sulfonyl]imide

([C₁C₁Im][Tf₂N]) on the model surface of Au(111) using scanning probe microscopy[1,2,3]. Our experiments show that the film undergoes distinct phases between the growth of the wetting layer and subsequent multilayers. Further, 2D film growth is shown to be in competition with the growth of a metastable 3D droplet phase, with the dominant growth mode determined by a combination of temperature and nucleus formation.

[1] Meusel et al. ACS Nano 14 (2020) 9000-9010

[2] Meusel et al. Langmuir 36 (2020) 13670-13681

[3] Meusel et al. J. Phys. Chem. C 125 (2021) 20439-20449

O 15.3 Mon 15:45 S054

Hydration layers at the graphite-water interface: Attraction or confinement?

— HAGEN SÖNGEN¹, YGOR MORAIS JAQUES², LIDIJA ZIVANOVIC², SEBASTIAN SEIBERT¹, •RALF BECHSTEIN¹, PETER SPIJKER², HIROSHI ONISHI³, ADAM S. FOSTER^{2,4}, and ANGELIKA KÜHNLE¹ — ¹Physical Chemistry I, Bielefeld University, Germany — ²COMP Centre of Excellence, Department of Applied Physics, Aalto University, Helsinki, Finland — ³Department of Chemistry, Kobe University, Japan — ⁴Division of Electrical Engineering and Computer Science, Kanazawa University, Japan

Water molecules at solid surfaces typically arrange in layers. The physical origin of the hydration layers is usually explained by (1) the attraction between the surface and the water and/or (2) the confinement of water due to the presence of the surface. While attraction is specific for the particular solid-solvent combination, confinement is a general effect at surfaces. A differentiation between the two effects is critical for interpreting hydration structures. At the graphite-water interface, the solid-solvent attraction is often considered to be negligible. Nevertheless, we observe hydration layers using three-dimensional atomic force microscopy at the graphite-water interface. We use Monte Carlo simulations to explain why confinement alone could cause the formation of hydration layers. With molecular dynamics simulations, we show that at ambient conditions, there is a significant graphite-water attraction which is pivotal for the formation of layers at the graphite-water interface.

[1] H. Söngen et al., Physical Review B, 100 (2019) 205410

O 15.4 Mon 16:00 S054

Investigation of the wetting layer of [ClC1Im][Tf2N] on Pt(111) by variable temperature scanning tunneling microscopy — •AFRA GEZMIS, SIMON JAEKEL, MANUEL MEUSEL, ANDREAS BAYER, FLORIAN MAIER, and HANS-PETER STEINRÜCK — Lehrstuhl für Physikalische Chemie II, Universität Erlangen-Nürnberg, Egerlandstr. 3, 91058 Erlangen, Germany

With the introduction of Ionic liquids (IL) novel catalytic concepts like the Solid Catalyst with Ionic Liquid Layer (SCILL) approach have emerged. In a SCILL system, a high surface area solid substrate is covered with a thin IL film, and this film modifies catalytically active surface sites at the support. In order to gain better insights in the underlying effects, it is crucial to obtain a detailed understanding of the IL/solid interface. Due to the low vapor pressure of ILs, these interfaces can be investigated in ultra-high vacuum by surface science methods. Herein, we present our first study on the adsorption behavior of 1,3-dimethylimidazolium bis[(trifluoromethyl)sulfonyl]imide ([ClC1Im][Tf2N]) on the reactive Pt(111) surface by variable-temperature scanning tunneling microscopy. We investigated the effect of temperature for coverages up to a closed wetting layer, in particular the formation of 2D islands and their temperature-dependent size. Interestingly, we were even able to detect mobile, single ion pairs on the surface, while for the 2D structures only limited mobility was seen.

Supported through an ERC Advanced Grant to H.P.S (#693398 ILID)

O 15.5 Mon 16:15 S054

bias-dependent switching of molecular nanostructures at the liquid-HOPG interface: the influence of concentration — •BAOXIN JIA¹, MIHAELA ENACHE¹, SANDRA MIGUEZ-LAGO², MILAN KIVALA², and MEIKE STÖHR¹ — ¹Zernike Institute for Advanced Materials, University of Groningen, Netherlands — ²Institute of Organic Chemistry, University of Heidelberg, Germany

Here we discuss the influence of concentration on the bias-dependent switching of a carboxy-functionalized triarylamine derivative at the nonanoic acid-HOPG interface studied by STM. For a fully saturated solution, a porous phase (chickenwire) was observed for negative sample bias and a close-packed phase for positive sample bias. For a 50% saturated solution, a second porous phase (flower) coexisted with the chickenwire phase at negative sample bias, while the close-packed phase was observed at positive sample bias. For a 20% saturated solution, the two porous phases and the close-packed phase coexisted at positive sample bias, while the two porous phases were observed at negative bias. For all concentrations investigated, a reversible phase transformation between the porous phases and the close-packed phase was accomplished by changing the bias polarity. Additionally, the switching behaviour for a 10:1 mixture of the triarylamine derivatives and 1,3,5-tris(4-carboxyphenyl) benzene molecules at the interface was studied. No intermixed structures were observed. Instead, both molecules formed networks separately but still showed a bias-induced phase transformation. However, the switching occurred for each molecule separately and no effect of cooperativity was detected.

O 15.6 Mon 16:30 S054

In-situ investigation of surface band-bending in the ZnO(0001)-OH/electrolyte interface via the excitonic response. — •LUIS ROSILLO-OROZCO, CHRISTOPH COBET, and KURT HINGERL — Johannes Kepler University, Linz, Austria

In recent years, the effects of adsorbates on the surface band-bending in ZnO have been studied in UHV and characterized by Valence-Band XPS [1],[2]; showing an alteration of the space-charge region due to the electron transfer that occurs in the absorption processes. In this work we aim to understand the surface optical properties of a hydroxide stabilized ZnO(0001)-OH surface, previously obtained by chemical etching by Valtiner et al. [3], in contact with 0.1M NaClO₄ as an electrolyte at a certain applied potential. By changing the cell applied potential, we can, in principle, produce any form of band bending at the semiconductor surface [4] including the flat-band condition. We use in-situ spectroscopic ellipsometry while varying the cell applied potential in order to study the response of the discrete excitons due to the inner electrical fields created by the band bending. We can identify the flat-band potential (V_{fb}) as the one where the imaginary part of the pseudo-dielectric function shows no change at the energy corresponding to the discrete exciton transition. By modulating the potential barrier at the interface we are able to investigate the response of the excitons at any given applied potential. Furthermore, given the significant sensibility of the band-bending to a surface dipole change, it is possible to use this technique to look into the effects of a modification of the surface such as adsorbates.

O 15.7 Mon 16:45 S054

Dynamic Polymorph Formation of a Trimesic Acid Derivative at Solid-Liquid Interface — •RICH A ARJARIYA¹, VIPIN MISHRA¹, GAGANDEEP KAUR¹, SANDEEP VERMA¹, MARKUS LACKINGER², and THIRUVANCHERIL G GOPAKUMAR¹ — ¹Department of Chemistry, Indian Institute of Technology Kanpur, Kanpur, UP-208016, India — ²Department of Physics, Technical University of Munich, James-Frank-Strasse 1, Garching 85748 and Deutsches Museum, Museumsinsel 1, Munich 80538, Germany

In this work we show the self-assembly of a tricarboxylic acid derivative of trimesic acid (BTA) at heptanoic acid-, nonanoic acid-graphite interface. At both

interfaces BTA forms a trimer based-self-assembly, super-flower (SF) pattern. The spontaneously formed SF pattern is observed to be dynamically converting to a dimer-based assembly, chicken-wire pattern (CW), at heptanoic acid-graphite interface while scanning. Interestingly, at nonanoic acid-graphite interface, SF pattern remains stable and not converted to CW pattern. We attribute that the formation energy of both SF and CW patterns is comparable. The difference in the stability of different patterns in heptanoic acid and nonanoic acid is most likely related to the solubility of BTA in these solvents.[1,2]

1) T. N. Ha, T. G. Gopakumar, M. Hietschold, J. Phys. Chem. C, 2011, 115, 21743.

2) M. Lackinger, S. Griessl, W. M. Heckl, M. Hietschold and G. W. Flynn, Langmuir, 2005, 21, 11, 4984-4988

O 15.8 Mon 17:00 S054

in-situ optical probe of chloride-induced surface states in Cu(110)/liquid interfaces — •SAUL VAZQUEZ-MIRANDA¹, KURT HINGERL¹, and CHRISTOPH COBET^{1,2} — ¹Johannes Kepler Universität Linz Altenberger Straße 69 4040 Linz, Austria — ²Johannes Kepler Universität, Linz School of Education, A-4040 Linz, Austria

While surface states (SSs) appearance and role in metal-electrolyte interfaces are still a controversial debate. The existence of SSs, permits control and tunability of electronic properties of metal-electrolyte interfaces. Resonant excitations among them could enhance, e.g. photocatalytic reactions. SSs and other properties are readily adjustable via an applied electrical potential that is, by promoting changes in the adsorption of ionic species. The electrolyte induces additional scattering and screening effects, so that the electron charge distributions can differ considerably in the presence of high electric fields. We report, by means of electrochemical impedance spectroscopy (EIS) jointly with in-situ reflectance anisotropy spectroscopy (RAS), which aimed to assess the evolution of surface properties and SSs occurring at Cu (110) in contact with an HCl solution. Thereafter, by modeling the RAS response and in comparison with EC-STM measurements, specific surface structures have been identified and ascribed to the optical response. In a specific potential range, three additional resonances are detected in RAS that can be explained by two-dimensional confined SSs.

O 15.9 Mon 17:15 S054

In-situ electrochemical X-ray photoelectron spectroscopy as laboratory technique to study the electrified interface — •CHRISTOPH GRIESSER, DANIEL WINKLER, TONI MOSER, and JULIA KUNZE-LIEBHÄUSER — Department of Physical Chemistry, University of Innsbruck, Innrain 52c, Innsbruck, Austria

The interface between a charged metal and an aqueous electrolyte is the most commonly studied in electrochemical surface science, as its properties determine the reactivity of many systems relevant for technological applications. More specifically, in the electrocatalytic conversion of energy, the activity, selectivity and efficiency are determined by the charge transfer between electrolyte and electrode, which is governed by the interfacial properties of the system. Therefore, a fundamental understanding of the interplay between applied potential and surface/interface chemistry is pivotal to further advance energy conversion and storage technologies. While there are several in-situ methods, to characterize the surface structure under reaction conditions, the surface chemistry (i.e. the elemental composition of the surface and the oxidation state of the components) itself is still most often investigated via ex-situ X-ray photoelectron spectroscopy (XPS). This work presents first in situ electrochemical XPS results obtained with a laboratory near ambient pressure (NAP-) XPS system. We show, that it is possible to track the oxidation state of a bulk gold (Au) electrode under reaction conditions, i.e. during anodic oxidation.

O 15.10 Mon 17:30 S054

Structure dependent product selectivity of the CO electroreduction on Au(111) electrodes modified with Cu adatoms — •DANIEL WINKLER, TONI MOSER, CHRISTOPH GRIESSER, MATTHIAS LEITNER, and JULIA KUNZE-LIEBHÄUSER — University of Innsbruck, Innrain 52c, 6020 Innsbruck, Austria

The efficient conversion of carbon dioxide (CO₂) into valuable hydrocarbons could be a promising solution for storage of excess energy and carbon neutral transportation. The electrochemical reduction of CO₂ has been extensively studied on different monometallic surfaces, where Cu remains the only metal providing a sufficient formation activity to value-added products, such as methane or ethylene. Despite this beneficial behavior, further strategies to increase the product selectivity must be found. This can be accomplished by understanding the exact CO₂ reduction reaction (CO₂RR) mechanism, which remains one of the most challenging problems. Here we focus on the carbon monoxide (CO) reduction on Au(111) electrodes modified with different coverages of Cu adatoms to address this issue. Differential electrochemical mass spectrometry (DEMS) shows an increase in selectivity for the formation of ethylene at low Cu coverages. *In situ* electrochemical scanning tunneling microscopy (EC-STM) and X-ray photoelectron spectroscopy results suggest that two different neighboring CO adsorption sites present at the interface between the metallic Cu islands and the Au(111) surface, which is maximized at low coverages, provide ideal conditions for a facilitated CO-CO coupling reaction resulting in an enhanced formation of ethylene.

O 15.11 Mon 17:45 S054

Electrochemical reflection anisotropy spectroscopy for time-resolved interface structures in aqueous and non-aqueous electrolytes — •MATTHIAS M. MAY^{1,2}, MARGOT GUIDAT^{1,2}, MARIO LÖW², FLORIAN KELLER², JUSTUS LEIST², and JONGMIN KIM^{1,2} — ¹Universität Tübingen, Institute of Physical and Theoretical Chemistry, Tübingen, Germany — ²Universität Ulm, Institute of Theoretical Chemistry, Ulm, Germany

The microscopic structure of electrochemical interfaces determines many properties that are decisive for the performance of applications in catalysis or batteries. Yet access to this solid-liquid interface at sufficient temporal and spatial

resolution is challenging and limits the understanding of this complex interface. Electrochemical reflection anisotropy spectroscopy (RAS) is a powerful emerging tool in spectroelectrochemistry [1], which we apply to a number of systems relevant for energy and matter conversion. Here, we present initial results on InP and Au in aqueous systems as well as select post-Li battery systems. For InP, we can directly observe stability windows with respect to applied potentials and electrolyte composition. We highlight the potential and challenges of electrochemical RAS from a perspective of both computational and experimental spectroscopy.

[1] May and Sprick, *New. J. Phys.* 20 (2018) 033031.

O 16: Poster Monday: Ultrafast Processes 1

Time: Monday 18:00–20:00

Location: P4

O 16.1 Mon 18:00 P4

Probing photo-induced, ultra-fast dynamics by time-resolved spectroscopic ellipsometry — •FELIX-FLORIAN DELATOWSKI^{1,3}, KRISHNA KHAKUREL¹, JÖRG RAPPICH², SHIRLY ESPINOZA¹, MATEUSZ REBARZ¹, MARTIN ZAHRADNIK¹, and JAKOB ANDREASSON¹ — ¹ELI Beamlines, Institute of Physics, Czech Academy of Sciences, Czech Republic — ²Institute Silicon Photovoltaics, Helmholtz-Zentrum Berlin für Materialien und Energie, Germany — ³Semiconductor Physics Group, Felix Bloch Institute for Solid State Physics, Universität Leipzig, Germany

Photo-induced phenomena, such as charge carrier and structural dynamics, charge transfer and relaxation processes on sub-picosecond time scales are of great interest for a profound understanding of light-matter interaction. Time-resolved spectroscopic ellipsometry is a promising surface sensitive tool to investigate these phenomena. In this work, we explore the potential of this measurement technique exemplarily on germanium and gold and present preliminary experimental results.

In addition to the experimental observations, we also present an approach to predict ellipsometry spectra through ab-initio DFT calculations using the program SIESTA. In order to extend this approach, some preliminary measurements of organic molecules (Pyrimidine) have been performed. We discuss the benefits that the synergy of ab-initio based spectrum predictions and experiments bring in the interpretation of the dynamics in the sample.

O 16.2 Mon 18:00 P4

Tailoring the carrier dynamics of WSe₂ by the adsorption of CuPc — •GREGOR ZINKE¹, SEBASTIAN HEDWIG¹, BENITO ARNOLDI¹, MARTIN AESCHLIMANN¹, and BENJAMIN STADTMUELLER^{1,2} — ¹Department of Physics and Research Center OPTIMAS, TU Kaiserslautern, Erwin-Schroedinger-Str. 46, 67663 Kaiserslautern, Germany — ²Institute of Physics, Johannes Gutenberg University Mainz, Staudingerweg 7, 55128 Mainz, Germany

Tailoring the electronic properties and carrier dynamics of 2D-Van-der-Waals materials is a highly promising way to design spin functionalities in low dimensions. This is often achieved by the formation of heterostructures with other Van-der-Waals materials.

Here, we functionalize the carrier dynamics of the prototypical Van-der-Waals material WSe₂ by the adsorption of the aromatic molecule CuPc. Using time- and angle-resolved photoemission with XUV-radiation, we investigate the temporal evolution of the excited states at the *K*- and Σ -points of WSe₂ after an optical excitation. For the bare WSe₂, we find a spin selective excitation at the *K*-point depending on the pump light polarization [1], which is followed by a spin-flip scattering from the *K*- to the Σ -point. After the adsorption of CuPc, the excitation scheme is completely altered. In particular, we uncovered a direct interlayer excitation from the CuPc into the WSe₂ layer that dominates the carrier dynamics of the CuPc/WSe₂ heterostructure.

Reference: [1] Bertoni et al.; *Phys. Rev. Lett.* 117, 277201 (2016)

O 16.3 Mon 18:00 P4

Numerous Improvements on Ultrafast Pump-Probe RHEED Experiment — •JONAS FORTMANN¹, CHRISTIAN BRAND¹, THORBEN GROVEN¹, MOHAMMAD TAJIK¹, MICHAEL HORN-VON HOEGEN¹, and THOMAS DUDEN² — ¹Department of Physics and Center for Nanointegration CENIDE, University of Duisburg-Essen, Lotharstraße 1, 47057 Duisburg — ²Construction office, Mustangweg 17, D-33649, Bielefeld

During the last year, major improvements have been made to our ultrafast time-resolved reflection high energy electron diffraction (tr-RHEED) experiment. In particular, the previous detection unit consisting of a multichannel plate and a cooled CCD camera has been replaced by a single electron sensitive CMOS based camera (TVIPS TemCam XF-416), which allows spot profile analysis with its superior resolution and signal-to-noise ratio and no blooming. Flatfielding of the detector is achieved with a home-built electron source at 20 keV accompanied by an external EM-deflection unit. In addition, the 80 fs-laser pump pulse ($\lambda = 800$ nm) has been upgraded with an optical parametric amplifier (Topas

Prime) that allows excitation of the sample's surface at 1.16–2.60 μm in future experiments. Re-routing of the beamline has shortened the beam paths by ~ 1.5 m and saved half of the mirrors, which provides higher beam stability. Also the third harmonic generation (THG) stage for electron generation in the Au film photocathode has been optimized. A new lab software has been established on the basis of TANGO controls. First experimental data with the new setup are shown.

O 16.4 Mon 18:00 P4

Ultrafast optical spectroscopy of few-layer TMDCs under ultrahigh-vacuum conditions — •MAXIMILIAN FRANZ, KILIAN KUHLEBRODT, JAN GERRIT HORSTMANN, and CLAUS ROPERS — Max-Planck-Institut für Multidisziplinäre Naturwissenschaften, Göttingen, Germany

Optical pump-probe spectroscopy (OPP) has enabled detailed investigations of the nonequilibrium optical properties of atomically thin materials, with prominent examples in graphene or transition metal dichalcogenide (TMDCs) heterostructures [1]. However, these materials are often susceptible to oxidation and contamination under atmospheric conditions, resulting in strongly altered physical and chemical properties [2]. Here, we present the development of an OPP setup for the investigation of dynamics in few-layer TMDCs and heterostructures under ultrahigh vacuum (UHV) conditions. We present first results on the ultrafast phase transition in 1T-TaS₂ samples using time-resolved reflectance and transmittance measurements with fs temporal and μm spatial resolutions. Furthermore, we discuss possible applications, e.g., layer-selective optical excitation of TMDC heterostructures, and the combination of OPP with structure-sensitive techniques like ultrafast low-energy electron diffraction [3].

[1] C. Jin et al., *Nature Nanotechnology* 13, 994-1003 (2018); [2] Y. Yu et al., *Nature Nanotechnology* 10, 270-276 (2015); [3] S. Vogelgesang et al., *Nature Physics* 14, 184-190 (2018)

O 16.5 Mon 18:00 P4

Description for the electronic non-equilibrium after ultrashort laser excitation of metals — •MARKUS UEHLEIN, SEBASTIAN T. WEBER, and BAERBEL RETHFELD — Department of Physics and Research Center OPTIMAS, TU Kaiserslautern, Germany

When a metal is excited by a femtosecond laser pulse in the visible range, electrons absorb the energy, resulting in a non-equilibrium energy distribution. This absorption behavior and the following thermalization to a hot Fermi distribution can be simulated using complex and numerically expensive Boltzmann collision integrals [1]. After the thermalization, the two-temperature model (TTM) can describe the relaxation of the heated electrons and the phonons in a simple way. It is, however, unable to trace non-thermal electrons.

We present an intermediate model, called extended TTM (eTTM). It was developed in Refs. [2, 3] and adds a system of non-equilibrium electrons to the TTM. Besides some improvements to the published versions, we compare the eTTM to the Boltzmann model as well as to the TTM [4]. In particular, we compare the spectral particle dynamics to a time-resolved two-photon photoemission measurement [5].

[1] B. Y. Mueller and B. Rethfeld; *PRB* 87, 035139 (2013)

[2] E. Carpene; *PRB* 74, 024301 (2006)

[3] G. D. Tsibidis; *Appl. Phys. A* 124, 311 (2018)

[4] M. Uehlein, S. T. Weber and B. Rethfeld; *Nanomaterials* 12, 1655 (2022)

[5] Y. Beyazit et al.; *Phys. Rev. Lett.* 125, 076803 (2020)

O 16.6 Mon 18:00 P4

A setup for interferometrically time-resolved multi-photon photoemission benchmarked on Ag(111) — •HANNAH STRAUCH, MARCO MERBOLDT, JAN PHILIPP BANGE, DANIEL STEIL, G. S. MATTHIJS JANSEN, SABINE STEIL, MARCEL REUTZEL, and STEFAN MATHIAS — I. Physikalisches Institut, Georg-August-Universität Göttingen, Göttingen, Germany

Time- and angle-resolved photoemission is the method of choice to directly study the electron dynamics of condensed matter systems with energy and mo-

mentum resolution. After the system is excited by a pump pulse, a delayed second pulse induces photoemission and thus probes the materials response. To complement the obtained insight with information on the coherence of the response, single-color phase-locked pulse pairs can be employed. Here, we present a setup for interferometric time-resolved multi-photon photoemission based on a passively stabilized Mach-Zehnder interferometer which produces phase-locked pulse pairs and provides an optical delay precision below 60 as. We show interferometric time- and angle-resolved multi-photon photoemission data from the Shockley surface state and the first image potential state of the Ag(111) surface as a benchmark for our setup. Supported by an optical Bloch equation model we explore possibilities to interpret such a data set.

A promising application of the interferometer is in combination a high harmonic generation EUV beamline. This enables double-pump-probe experiments with access to the full Brillouin zone, and allows a comprehensive investigation of optical excitations.

O 16.7 Mon 18:00 P4

Time-resolved ARPES probing Rabi Oscillations and Landau-Zener-Stückelberg Interferences in Graphene - a Proposal — •EDUARD MOOS, HAUKE BEYER, and MICHAEL BAUER — Institute of Experimental and Applied Physics, Kiel University, Germany

At sufficiently high intensities, the interaction of few-cycle laser fields with solids gives rise to strong-field effects envisioning novel and exciting strategies for controlling optical and electronic properties via the electric field waveform on sub-femtosecond timescales. A striking example is the CEP-control of light-field-driven currents in graphene due to Landau-Zener-Stückelberg (LZS) interferences [1] resulting from the complex interplay of field-driven adiabatic intraband and diabatic interband transitions. Simulations show that the LZS-interferences give rise to characteristic asymmetries in the momentum-distribution of the residual conduction band population in the Dirac cone on top of a symmetric quasi-periodic pattern indicative for Rabi oscillations. TRARPES using few cycle femtosecond pump laser pulses seems to be in ideal tool for the investigation of these processes and their dependence on parameters such as pulse peak electric field strength E_0 , laser polarization, and CEP phase. Based on preliminary results on graphite using 7 fs few-cycle NIR pump-pulses we will discuss in this presentation the prospects, but also the challenges that arise in such type of TRARPES experiment.

[1] T. Higuchi, *et al.*, Nature **550**, 224 (2017)

[2] G. Rohde, *et al.*, Phys. Rev. Lett. **121**, 256401 (2018)

O 16.8 Mon 18:00 P4

Laser-based low energy photoelectron diffraction of SnPc/graphite — •HERMANN ERK, STEPHAN JAUERNIK, PETRA HEIN, and MICHAEL BAUER — IEAP, CAU Kiel, Germany

Tin-phthalocyanine (SnPc) adsorbed on graphite has been studied using laser-based angle resolved photoemission spectroscopy (ARPES) at 5.9 eV photon energy and low energy electron diffraction (LEED). An ordered SnPc monolayer was prepared by thermal evaporation onto single crystalline graphite (SCG) flakes and subsequent annealing at 370 K. LEED data reveal an incommensurate ordered phase of the SnPc overlayer at room temperature. In the ARPES spectra the SnPc long-range order can be seen due to an adsorbate-induced backfolding of the band structure of graphite from the \bar{K} point to the center of the Brillouin zone. A comparison of ARPES spectra with simulations of the backfolded band structure under consideration of the LEED data will be discussed. First time-resolved ARPES measurements with the aim to address ultrafast changes in the SnPc long range order will be presented.

O 16.9 Mon 18:00 P4

Type II aligned TMD heterostructures: Probing moiré interlayer excitons with energy-, momentum-, and femtosecond time-resolution — •MARCEL REUTZEL¹, DAVID SCHMITT¹, JAN PHILIPP BANGE¹, WIEBKE BENNECKE¹, ABDULAZIZ ALMUTAIRI², GIUSEPPE MENEGHINI³, DANIEL STEIL¹, R. THOMAS WEITZ¹, SABINE STEIL¹, G. S. MATTHIJS JANSEN¹, SAMUEL BREM³, ERMIN MALIC³, STEPHAN HOFMANN², and STEFAN MATHIAS¹ — ¹I. Physikalisches Institut, Georg-August-Universität Göttingen, Göttingen, Germany — ²Department of Engineering, University of Cambridge, Cambridge CB3 0FA, U.K. — ³Fachbereich Physik, Philipps-Universität, 35032 Marburg, Germany

Transition metal dichalcogenides (TMDs) can be stacked into atomically thin p-n junctions, where an optically excited intralayer exciton can decay into interlayer excitons. Here, the electron and the hole contribution to the quasiparticle reside in the neighbouring TMD layers.

On this poster, we show our recent progress towards the identification and characterization of the ultrafast charge transfer process across a type II interface. Using femtosecond momentum microscopy, we identify the distinct momentum fingerprints of various excitonic states in this system, notably the bright and

dark intralayer excitons as well as the interlayer exciton. Most intriguingly, the momentum-resolved measurement provides quantitative access to the interlayer exciton wavefunction that is modulated within the moiré potential.

Schmitt *et al.*, *arXiv:2112.05011 (2021).

O 16.10 Mon 18:00 P4

Influence of the static dielectric permittivity on ultrafast quasiparticles dynamics in WS₂ monolayers — •SUBHADRA MOHAPATRA^{1,2}, STEFANO CALATI^{1,2}, QUIYANG LI³, XIAOYANG ZHU³, and JULIA STÄHLER^{1,2} — ¹Humboldt-Universität zu Berlin, Institut für Chemie, Berlin, Germany — ²Fritz-Haber-Institut der Max-Planck-Gesellschaft, Abt. Physikalische Chemie, Berlin, Germany — ³Columbia University, New York City, New York

In our recent fluence- and photon energy-dependent studies [1,2] of quasiparticle dynamics in WS₂ monolayers on fused silica (FS) and Si-SiO₂ substrates, we observed that excitonic screening solely reduces the binding energy of the excitons, leading to a transient blue-shift of the exciton resonance while quasi free carrier screening effectively shows a red shift, as the carrier-induced screening leads to a larger band gap renormalization than binding energy reduction. Further investigation of such fluence-dependent quasiparticle dynamics studies using a higher dielectric permittivity of a sapphire substrate, we found that scattering rates, relaxation time constants, and band gap renormalization are not influenced by the dielectric permittivity. On the contrary, the ratio of dynamic screening parameter of the excitons and their Bohr radius is approximately 4 times higher in sapphire than for FS, which must be a direct consequence of the increased dielectric permittivity likely leading to more localized excitons.

[1] Calati *et al.* PCCP **23**(39) (2021).

[2] Calati *et al.* arXiv:2204.02125 (2022).

O 16.11 Mon 18:00 P4

Ultrafast Transport and Energy Relaxation of Hot Electrons in Au/Fe/MgO(001) Investigated by Linear Time-resolved Photoelectron Spectroscopy — •FLORIAN KÜHNE¹, YASIN BEYAZIT¹, DETLEF DIESING², PING ZHOU¹, JESUMONY JAYABALAN¹, and UWE BOVENSIEPEN¹ — ¹University of Duisburg-Essen, Physics — ²University of Duisburg-Essen, Chemistry

Optically excited electrons and holes are of particular interest in solid-state physics because analysis of their dynamics allows a microscopic understanding of the interactions in non-equilibrium states. Here we want to discern the relaxation by such local inelastic processes and non-local transport effects. To analyze the ultrafast dynamics of charge carriers in the vicinity of the Fermi energy E_F , femtosecond time-resolved linear photoelectron spectroscopy was applied. We report on first experimental results obtained by using 1.55 eV pump and 6 eV probe photons on an Au/Fe/MgO(001) epitaxial heterosystem, complementary to previous work in Beyazit *et al.*, PRL **125**, 076803 (2020). By pumping the Fe side, hot electrons are excited in the Fe layer, and subsequently injected into the Au layer and propagate to the surface, where they are probed by photoelectron emission spectroscopy. In the Fe side pumped data, we observe thickness dependent differences in relaxation compared to the Au side pumped data. In Au side pumping we observe efficient transport into the Fe layer. We will present an energy E dependent analysis of the propagation and energy density $U(E, d_{Au})$ of electrons above E_F , which together with a two-temperature model shows a super diffusive transport limit.

O 16.12 Mon 18:00 P4

Investigations of polarons in hematite α -Fe₂O₃(1-102) by means of nc-AFM and KMC — •JESÚS REDONDO^{1,2}, VÍT GABRIEL¹, GIADA FRANCESCHI³, IGOR SOKOLOVIĆ³, DOMINIK WRANA¹, FLORIAN KRAUSHOFER³, ERIK RHEINFRANK³, MICHELE RIVA³, GARETH S. PARKINSON³, MICHAEL SCHMID³, ULRIKE DIEBOLD³, PAVEL KOCÁN¹, and MARTIN SETVIN^{1,3} — ¹Faculty of Mathematics and Physics, Charles University, Prague, Czech Republic — ²Faculty of Chemistry, University of the Basque Country, San Sebastián, Spain — ³Institute of Applied Physics, Vienna University of Technology, Vienna, Austria

Polarons are known to strongly influence the catalytic activity and the electronic, magnetic, and structural properties of transition metal oxides and halide perovskites. The study of polaron formation and dynamics is fundamental to understanding the actual mechanisms and yields of catalytic reactions in these materials. A new method for the investigation of electron and hole polarons is demonstrated. Charge carriers are injected with the AFM/STM tip into the surface of natural, Ti- and Ni-doped α -Fe₂O₃(1-102). The injected charges form a cloud of electrons or holes trapped in the lattice. This cloud expands due to electrostatic interactions and thermally activated polaron hopping. Controlled annealing of the sample and characterization by Kelvin probe force microscopy (KPFM) provides information on polaron dynamics; these results are compared to kinetic Monte Carlo (KMC) simulations and the dependence of the polaron hopping activation energy on the doping is shown.

O 17: Poster Monday: Organic Molecules at Surfaces 1

Time: Monday 18:00–20:00

Location: P4

O 17.1 Mon 18:00 P4

Influence of a BlueP interlayer on the properties of P2O on Au(111) — •FLORENTINE FRIEDRICH, MAXIMILIAN SCHAAL, FELIX OTTO, PHILIP GRIMM, MARCO GRUENEWALD, ROMAN FORKER, and TORSTEN FRITZ — Institute of Solid State Physics, Friedrich Schiller University Jena, Helmholtzweg 5, 07743 Jena, Germany

Two-dimensional (2D) materials have attracted much attention in solid state physics in recent years due to their unique properties. Amongst others, one novel representative is the phosphorus allotrope blue phosphorene (BlueP) with its high charge carrier mobility and suitable band gap, that is used here as an interlayer to obtain a decoupling of the functional organic molecule 6,13-pentacenequinone (P2O) from Au(111) surfaces. P2O is deposited in various film thicknesses (1 monolayer equivalent (MLE) up to 4-5 MLE) either on BlueP on Au(111) or directly on the metal substrate to investigate the influence of BlueP as an interlayer on the optical and structural properties of the P2O molecules. The film growth of P2O is monitored by in-situ differential reflectance spectroscopy (DRS), while the BlueP-Au substrate is kept at different temperatures. Further complementary experimental methods were low-electron energy diffraction (LEED), X-ray photoelectron spectroscopy (XPS), and low-temperature scanning tunneling microscopy (LT-STM). It turns out that the BlueP interlayer influences the monolayer structure as well as the growth mode. In contrast to previous studies on C_{60} , the BlueP interlayer stays intact.

O 17.2 Mon 18:00 P4

Navigating the Polymorph-Jungle with Optimal Control techniques — •SIMON HOLLWEGGER, ANNA WERKOVITS, RICHARD K. BERGER, and OLIVER T. HOFMANN — Institute of Solid State Physics, NAWI Graz, Graz University of Technology, Petersgasse 16, 8010 Graz, Austria

Properties of organic-inorganic interfaces are strongly dependent on the arrangement of the molecules on the surface. However, achieving a controlled growth of a polymorph with preferable physical properties is not straightforward at all - especially for metastable polymorphs.

In principle, starting from a thermodynamically easily accessible polymorph, kinetics can be utilized to stabilize a metastable polymorph. This can be done by promoting certain structural transitions by a-priori unknown sequentially changing growth conditions. Depending on the complexity of the transition network, often only a limited yield of the target polymorph can be reached during growth.

To computationally maximize the yield of the desired structure we use Optimal Control techniques. Therein, process parameters like temperature and pressure are varied to optimize parameter protocols. The transition network of our model system TCNE/Cu(111) is obtained via a combination of Transition State Theory and Density Functional Theory.

O 17.3 Mon 18:00 P4

Adsorption structure of mixed PTCDA derivatives on Ag(111) — •AMIN KARIMI¹, JOSE M. GUEVARA¹, VERONIKA SCHMALZ², ULRICH KOERT², F. STEFAN TAUTZ¹, and CHRISTIAN WAGNER¹ — ¹Peter Grünberg Institut (PGI 3), Forschungszentrum Jülich, Jülich, Germany — ²Chemistry Department, Philipps Universität Marburg, Marburg, Germany

For molecular manipulation and SPM tip functionalization, the mode of anchoring molecules to the tip is decisive. We recently found that PTCDA binds to a Ag tip with two oxygen-metal bonds after it is retracted from the surface. While this is crucial for its stabilization in a vertical state, the two bonds reduce the degrees of freedom during manipulation in the tip-molecule-surface junction. To overcome this problem, we synthesized a PTCDA derivative (reduced PTCDA), in which one carboxylic oxygen is replaced by two H atoms. For molecular manipulation, this allows choosing between one or two tip-oxygen bonds. Here we present a study on the adsorption structures formed by a mixture of PTCDA and reduced PTCDA on the Ag(111) surface with the help of low-temperature NC-AFM/STM. We observe that despite the minimal modification of reduced PTCDA compare to PTCDA, the mixture of both molecules exhibits a strongly different behaviour compared to the regular island growth of pure PTCDA. Particularly striking is the coexistence of zero-, one-, and two-dimensional structures. A likely explanation for such diverse structures is the influence of long-range electrostatic interactions related to the in-plane dipole moment of reduced PTCDA.

O 17.4 Mon 18:00 P4

Single-domain molecular layers on Ag (110) — •RAVI PRIYA, WEISHAN WU, and PETER JAKOB — Department of Physics, Philipps-Universität Marburg, Germany

Single domain molecular layers have been explored on the non-hexagonal Ag(110) substrate. The absence of rotational domains for fcc (110) metal substrates allows for growing layers with uniform azimuthal orientation of

deposited molecules. In our study we have investigated various molecules and configurations that may form single domain molecular layers (including mirror domains). Specifically, PTCDA, NTCDA, phthalocyanines (CuPc, SnPc, TiOPc) and regio-selectively substituted pentacene species (pentacene, pentacene-quinone, pentacene-tetrone, quinacridone) were deposited and examined in terms of their structure using SPA-LEED, and their vibrational signature using IR - spectroscopy. Amongst them, PTCDA, NTCDA and pentacene have been found to form single domain structures. In the case of PTCDA two prominent phases, the brick-wall (BW) and the herringbone (HB) phases exist, and they are readily distinguished not only by their LEED patterns but also from their vibrational signatures. Another finding refers to the increased molecule - metal interaction on Ag (110) vs. Ag (111) that leads to an extra energy (down)shift of the LUMO, thereby having a significant impact on interfacial dynamic charge transfer (IDCT) of vibrational modes [1].

[1] P. Jakob, S. Thussing, Phys. Rev. Lett. 126 (2021) 116801, DOI:10.1103/PhysRevLett.126.116801

O 17.5 Mon 18:00 P4

Generation of synthetic chiral structured images for computer vision applications — •JOHANNES TIM SEIFERT¹, PEER KASTEN¹, MANDY STRITZKE², BJÖRN MÖLLER³, TIMO DE WOLFF², TIM FINGSCHIEDT³, and UTA SCHLICKUM¹ — ¹Institut für Angewandte Physik, Technische Universität Braunschweig — ²Institut für Analysis und Algebra, Technische Universität Braunschweig — ³Institut für Nachrichtentechnik, Technische Universität Braunschweig

Scanning tunneling microscopy (STM) is a well-established tool to measure surface topographs with atomic precision. Since data generation is slow using STM, we present a tool to create synthetic images with realistic noise and defects, which provides labeled training data for neural networks. We compare two methods evaluating chiral structures in STM images using Deep Learning.

As one approach to classify structures, we are using semantic segmentation based on the U-Net architecture to create maps showing the distribution of both chiralities. Additionally, we use a faster R-CNN architecture for object detection to locate and classify each chiral structure individually.

Since the approaches serve different use cases, they also have separate label requirements. We show that models trained using only our synthetic images perform successfully for real STM Images.

O 17.6 Mon 18:00 P4

Ultrafast dynamics of quantum confined surface electrons in a T4PT-based metal-organic network on noble metals — •NILS BELLENBAUM¹, LU LYU¹, EVA WALTHER¹, TOBIAS EUL¹, BENITO ARNOLDI¹, MARTIN AESCHLIMANN¹, and BENJAMIN STADTMÜLLER^{1,2} — ¹Technische Universität Kaiserslautern and Research Center OPTIMAS, Erwin-Schrödinger Straße 46, 67663 Kaiserslautern, Germany — ²Institute of Physics, Johannes Gutenberg University Mainz, Staudingerweg 7, 55128 Mainz, Germany

Two-dimensional metal-organic networks have emerged as intriguing architectures to design and control quantum confinement of electrons at surfaces. In our work, we focus on the metal-organic network T4PT/Cu(111) comprised of triangular 2,4,6-tris(4-pyridine)1,3,5-triazine (T4PT) molecules adsorbed on a copper substrate. Using momentum-resolved photoemission, we demonstrate a spatial confinement of the free electron-like surface state of Cu(111) in the pores of the network structure. Similarly, the dispersion of the unoccupied image potential state (IPS) of Cu(111) is modulated by the network's periodic potential, leading to a severe increase of the effective band mass of the IPS. Finally, we discuss the influence of periodic modulation of the IPS on its energy and momentum-dependent population time using timeresolved two photon momentum microscopy. Our findings provide a first glimpse onto tunability of the electron dynamics at surfaces by spatial confinement in nanoporous metal-organic network structures.

O 17.7 Mon 18:00 P4

Organic Molecules on the Cu(110)-(2x1)O Striped Phase — •ILIAS GAZIZULLIN, CHRISTOPHE NACCI, and LEONHARD GRILL — Physical Chemistry Department, University of Graz, Heinrichstrasse 28, 8010 Graz, Austria

The deposition of molecules onto single-crystal surfaces allows their investigation at the single-molecule level by scanning tunneling microscopy (STM) and gives access to the controllable on-surface synthesis of 2D materials. Here, we have studied dibromo-p-terphenyl molecules on the Cu(110)-(2x1)O striped phase under ultra-high vacuum conditions with low-temperature STM. The Cu(110)-(2x1)O striped phase is of particular interest since it offers alternating stripes of (metallic) copper areas and of oxygen-covered areas where the adsorbed organic molecules are slightly decoupled from the metal substrate and hence have higher mobility.

Previously, the Cu(110)-(2x1)O striped phase was used as a template for the synthesis of organometallic structures having different sizes and shapes depend-

ing on the width of copper stripes [1]. The focus of our study is how annealing affects the molecular adsorption on the surface. It turns out that the molecules form organometallic chains on the copper areas, oriented in three surface directions. Increasing the sample temperature from 300 K to 450 K changes the orientation of the organometallic chains and the shape of the Cu-O areas. Possible interactions leading to such behaviour are discussed.

Reference: [1] Q. Fan, J. Dai, T. Wang, J. Kuttner, G. Hilt, J. M. Gottfried, and J. Zhu, ACS Nano, 3 (2016), 3747-3754

O 17.8 Mon 18:00 P4

Adsorption of phthalocyanine monolayers on Ag(110) — •GAANA KAINIKKARA, RAVI PRIYA, and PETER JAKOB — Phillips University of Marburg
Vibrational properties and long range ordering of TiOPc, CuPc and SnPc molecular layers on the non-hexagonal Ag(110) surface have been investigated using IR-spectroscopy and SPA-LEED. Special emphasis is put on a comparison with the related Ag(111) substrate surface that is characterized by a somewhat weaker molecule - metal interaction strength. This hypothesis is supported by distinct differences in the vibrational line shapes of modes associated with interfacial dynamical charge transfer [1], the primary cause being an extra shift in the energetic position of the former LUMO with respect to the Fermi energy for the Ag(110) substrate. Another objective in our study was to identify structural changes in the (layered) structural arrangement, both during the growth process, as well as annealing of the layers. Due to their only slightly different footprint, the molecules display similar long range ordered phases. Our primary focus thus concerned the identification of possibly inclined arrangements in the coverage range of 1-2 monolayers [1] P. Jakob, Peter and S. Thussing. "Vibrational Frequency Used as Internal Clock Reference to Access Molecule-Metal Charge-Transfer Times." Phys. Rev. Lett. 126, 116801 (2021).

Part-O: Surface Science Division Type-Poster Presentation Topic-Organic Molecules on Inorganic Substrates: Adsorption and growth

O 17.9 Mon 18:00 P4

Growth of organic crystals on nanoparticle precovered surfaces studied by PEEM — •KATHARINA ENGSTER¹, JÖRG HELLER¹, THORSTEN WAGNER², SYLVIA SPELLER¹, and INGO BARKE¹ — ¹University of Rostock, Institute of Physics, 18059 Rostock, Germany — ²Johannes Kepler University, Institute of Experimental Physics, 4040 Linz, Austria

Nanostructures can be used as plasmonic light sources [1] for local generation of excitons in organic semiconductors. This is a promising pathway to transfer energy in molecular aggregates from a defined starting point over longer distances via exciton propagation. In order to establish a suitable geometry of such a hybrid system, we are interested in the role of metallic clusters during subsequent molecular growth. Mass - selected silver nanoparticles are produced in a gas - phase cluster source and deposited onto a pristine HOPG surface. Afterwards, we use *in-situ* photoemission electron microscopy (PEEM) to monitor the physical vapour deposition of copper phthalocyanine (CuPc) molecules [2,3] on such surfaces. We observe a Stranski-Krastanov growth during deposition of CuPc and post - deposition further morphology changes of the nanocrystallites.

[1] K. Oldenburg et al., J. Phys. Chem. C 123, 1379 (2019).

[2] Y.-C. Chiu et al., Cryst. Res. Technol. 46, 295 (2011).

[3] T. Wagner et al., Ultramicroscopy 233, 113427 (2022).

O 17.10 Mon 18:00 P4

Visualizing self-assemblies of electrospayed complex molecules on surface: a non-contact force microscopy study — •GEMA NAVARRO¹, ANTOINE HINAUT¹, SEBASTIAN SCHERB¹, SHUYU HUANG¹, YIMING SONG¹, KLAUS MÜLLEN¹, THILO GLATZEL¹, AKIMITSU NARITA², and ERNST MEYER¹ — ¹Department of Physics, University of Basel, Klingelbergstrasse 82, 4056 Basel, Switzerland. — ²Max Planck Institute for Polymer Research, Ackermannweg 10, D-55128 Mainz, Germany.

Building up functional 2D supramolecular assemblies requires the unit blocks involved in their bottom up formation to be already complex. In the construc-

tion of the tailored nanostructures, different approaches can be adopted in order to circumvent the limitations of the traditional wet chemical methods [1,2]. Among them, specifically the Electro Spray Deposition (EDS) technique emerges as suitable pathway to explore the adsorption of organic compounds with higher structural complexity [3].

In the present work, we report the adsorption of complex molecules on a noble metal surface. Our study focus on the influence of intermolecular and surface-molecule interactions in the observed assemblies. The deposition of the molecules is carried out by HV-EDS. Furthermore, visualization of the molecules is achieved by means a home-made Atomic Force Microscopy (AFM) set-up, in non-contact operation mode.

[1] Z. Qiu, A. Narita, and K. Müllen, Faraday Discuss. 227,8 (2021).

[2] S. Scherb et al., Commun Mater 1, 1 (2020).

[3] I. C.-Y. Hou, A. Hinaut, Chem. Asian J., e202200220 (2022).

O 17.11 Mon 18:00 P4

C₆₀ - PEN Diels - Alder Cycloaddition Reaction on Ag(110) — •MOHAMMED SUHAIL ANSARI, RAVI PRIYA, and PETER JAKOB — Department of Physics, Philipps - Universität Marburg, Germany

Ultrathin films of C₆₀ and pentacene (PEN) have been prepared on Ag(110) and their vibrational properties, as well as thermal evolution investigated by IR spectroscopy. Monolayer species are found to display distinctly different vibrational signatures as compared to higher layers, so the characterization of the grown hetero layers is straightforward. Moreover, the excellent spectral resolution and chemical selectivity allowed us to unambiguously identify the C₆₀ - PEN Diels-Alder adduct [1]. In our thermal evolution study, the formation and decomposition of the C₆₀ - PEN reaction product as well as the abundances of the C₆₀ and PEN compounds have been examined. Production of the adduct species requires a weak thermal activation (annealing to 350 K) and proceeds largely independent of the C₆₀ / PEN stacking sequence. We find that this reaction occurs exclusively at the (abrupt) interface of C₆₀ and PEN for layered arrangements and is fully reversible, meaning that further annealing to 450 K (and higher) produces again C₆₀ and PEN, with the latter desorbing thermally and thus depleting the initial concentration of reactants.

[1] F. Cataldo, D. A. García-Hernández and A. Manchado, On the C₆₀ Fullerene Adduct with Pentacene: Synthesis and Stability, Fullerenes, Nanot. Carbon Nanostruct. 23 (2015) 818-823.

O 17.12 Mon 18:00 P4

First Steps Towards Carbon-Based Heisenberg Chains on Au(111) — •NILS KRANE¹, ELIA TURCO¹, ANNIKA BERNHARDT², MICHAL JURÍČEK², PASCAL RUFFIEUX¹, and ROMAN FASEL¹ — ¹nanotech@surfaces Laboratory, Empa - Swiss Federal Laboratories for Materials Science and Technology, Dübendorf, Switzerland — ²Department of Chemistry, University of Zurich, Zurich, Switzerland

Carbon based π -magnetism has been a growing field of interest in the recent years. By tailoring nanographenes with atomically precise shape and size it is possible to tune their electronic properties and create magnetically non-trivial groundstates. A recent study has demonstrated the formation of triangulene-based Haldene chains, consisting of spin-1 building blocks and featuring gapped spin excitation in the bulk [1]. On the other hand, a Heisenberg chain consisting of coupled spin-1/2 units is predicted to be gapless, due to a continuum of spin excitations above the ground state.

Here we present the first steps towards synthesizing all-carbon spin-1/2 chains. Phenalenyl-based precursors are used for a bottom-up approach to form oligomers of different lengths and spin-excitation gaps. The low activation barrier of hydrogen-passivated phenalenyl was found to be a potential inhibitor of the radical formation, which is required for the covalent coupling of the building blocks.

[1] S. Mishra et al., Nature 598, 287-292 (2021). <https://doi.org/10.1038/s41586-021-03842-3>

O 18: Poster Monday: 2D Materials 1

Time: Monday 18:00–20:00

Location: P4

O 18.1 Mon 18:00 P4

Scanning tunneling microscopy and spectroscopy of rubrene on clean and graphene-covered metal surfaces — •KARL ROTHE, ALEXANDER MEHLER, NICOLAS NÉEL, and JÖRG KRÖGER — TU Ilmenau, Institut für Physik

Rubrene (C₄₂H₂₈) was adsorbed with submonolayer coverage on Pt(111), Au(111) and graphene-covered Pt(111). Adsorption phases and vibronic properties of C₄₂H₂₈ consistently reflect the progressive reduction of the molecule-substrate hybridization. Separate C₄₂H₂₈ clusters are observed on Pt(111) as well as broad molecular resonances. On Au(111) and graphene-covered Pt(111) compact molecular islands with similar unit cells of the superstructure character-

ize the adsorption phase. The highest occupied molecular orbital of C₄₂H₂₈ on Au(111) exhibits weak vibronic progression while unoccupied molecular resonances appear with a broad line shape. In contrast, vibronic subbands are present for both frontier orbitals of C₄₂H₂₈ on graphene. They are due to different molecular vibrational quanta with distinct Huang-Rhys factors.

Financial support by the Deutsche Forschungsgemeinschaft through Grant No. KR 2912/12-1 is acknowledged.

O 18.2 Mon 18:00 P4

The effect of morphology of an intercalated Au layer on electronic properties of Graphene — •AMIRHOSSEIN BAYANI and KARIN LARSSON — Department of Chemistry-Ångström laboratory, Uppsala University, Uppsala, Sweden

Thermal Intercalation processes have recently made it possible to produce large quasi free-standing graphene layers on different substrates. One method, which is based on thermal annealing, uses a 4H-SiC (0001) substrate with an attached carbon buffer layer onto the Si-face of the substrate. Various types of metals have then been used with the purpose to intercalate these metal atoms between SiC and the buffer layers, thereby creating a monolayer (ML) of graphene with an intact Dirac point. Moreover, when positioning heavy metal atoms under graphene, the spin-orbit coupling will increase and thereby enhances the Rashba band splitting. This phenomenon comes from the breakage of a mirror symmetry due to interaction with the substrate. To the knowledge of the authors, the role of the morphology of the intercalated layer on the electronic properties of graphene has not yet been considered and it is worth considering this effect when electronic properties of graphene is wanted to be studied after intercalation. Here we show how the morphology of the intercalated Au layer will affect the electronic properties of a ML of graphene. The possibility to induce a band gap at the Dirac point of graphene by manipulating the staggered potential of a 4H-SiC/Au substrate, is thereby looked for. The calculations are based on density functional theory (DFT) + SOC.

O 18.3 Mon 18:00 P4

Intercalation of epitaxial graphene on SiC(0001) with sulfur — •SUSANNE WOLFF, NICLAS TILGNER, TASSILO RAUSCHENDORFER, FLORIAN SPECK, and THOMAS SEYLLER — Chemnitz University of Technology, 09126 Chemnitz, Germany

Epitaxial growth of graphene on SiC in argon atmosphere is a well-established method to produce high quality films. There, the first grown carbon layer is partially covalently bound to the substrate and lacks the graphene-like electronically properties. This so-called buffer layer can be decoupled from the substrate by intercalation. Furthermore, the choice of intercalant manipulates the electronic properties of the decoupled graphene.

We investigated the intercalation of a buffer layer with sulfur by X-ray photoelectron spectroscopy (XPS) and angle-resolved photoelectron spectroscopy (ARPES). The intercalation process was performed in a two-zone furnace where the Fe₂ precursor and the buffer layer can be heated separately. An argon gas flow transports the sublimated sulfur to the sample. Partial intercalated samples show two sulfur peaks at different binding energies in XPS. They can be attributed to intercalated sulfur and sulfur on top of the not intercalated buffer layer. ARPES measurement in the vicinity of the Dirac point showed that sulfur intercalation results in p-type doped decoupled graphene layers.

O 18.4 Mon 18:00 P4

twisted graphene on Ir(111) and SiC(0001) studied by SPA-LEED — •MOHAMMAD TAJIK¹, CHRISTIAN BRAND¹, BIRK FINKE¹, KARIM OMAMBAC¹, LAURENZ KREMEYER¹, FRANK MEYER ZU HERINGDORF^{1,2}, and MICHAEL HORN-VON HOEGEN^{1,2} — ¹Universität Duisburg-Essen — ²center for nanointegration duisburg-essen

when graphene is placed on a crystalline surface, the periodic structures within the layers superimpose and a moiré superlattices form. Small lattice rotations between the 2D-layer and the substrate strongly modify the moiré superlattice, upon which many electronic, vibrational, and chemical properties depend. Here we report on such structural modification of epitaxial graphene grown on metallic Ir(111) and semiconducting SiC(0001) surfaces. The spontaneous reorientation in the degree- and sub-degree-range of graphene on Ir(111) depends on the substrate temperature during growth. This effect is described by a 2D coincidence network favored by strain reduction together with the dissimilar thermal expansion of the substrate and graphene. For graphene on SiC(0001) only the oriented R0* phase is found due to the higher bonding strength to the substrate. Upon H and Sn intercalation this interaction can be reduced such that the graphene layer is lifted from the substrate. Finally, we present a detailed analysis of an unusually broad diffraction background found for graphene and hex-BN on both substrates.

O 18.5 Mon 18:00 P4

On the Way to Twisted Bilayer Graphene: Formation and Decoupling of 0°-Rotated Epitaxial Graphene — •HAO YIN^{1,2}, MIRIAM RATHS^{1,2}, MARK HUTTER^{1,2}, FRANÇOIS C. BOCQUET¹, and CHRISTIAN KUMPF^{1,2} — ¹Peter Grünberg Institute (PGI-3), Forschungszentrum Jülich and Jülich-Aachen Research Alliance (JARA), Fundamentals of Future Information Technology, Jülich, Germany — ²Experimentalphysik IV A, RWTH Aachen University, Aachen, Germany

On the way to twisted bilayer graphene with a twisting angle of 30°, we investigated the graphene growth on 6H-SiC(0001) using an unconventional epitaxial growth method named 'surfactant-mediated growth', which is based on annealing the SiC surface in borazine atmosphere. Here, we report a LEEM-based study on two different samples, on which we observed different surface mor-

phologies with varying numbers of stacked graphene layers. A large-scale uniform graphene R0° monolayer is found on the first sample that was annealed to 1330°C. This sample is a promising candidate for producing 30° TBG. Interestingly, some regions of the graphene R0° layer exhibit different brightness contrasts at specific start voltages, without showing significant differences in their LEEM-IV curves. The second sample was annealed 50°C higher, causing the formation of graphene multilayer domains. We utilized LEEM and LEEM-IV in order to determine the number of layers as well as the distribution of multilayer graphene domains. Furthermore, we discuss the influence of the annealing temperatures in terms of the formation and decoupling of the epitaxial graphene layers.

O 18.6 Mon 18:00 P4

Vertical structure of Sb-intercalated quasi-freestanding graphene on SiC(0001) — YOU-RON LIN^{1,2,3}, SUSANNE WOLFF^{4,5}, •MARK HUTTER^{1,2,3}, SERGUEI SOUBATCH^{1,2}, TIEN-LIN LEE⁶, F. STEFAN TAUTZ^{1,2,3}, THOMAS SEYLLER^{4,5}, CHRISTIAN KUMPF^{1,2,3}, and FRANÇOIS C. BOCQUET^{1,2} — ¹Peter Grünberg Institut (PGI-3), Forschungszentrum Jülich, Germany — ²Jülich Aachen Research Alliance (JARA) — ³Experimentalphysik IV A, RWTH Aachen University, Germany — ⁴Institute of Physics, Faculty of Natural Sciences, TU Chemnitz, Germany — ⁵Center for Materials, Architectures and Integration of Nanomembranes (MAIN), TU Chemnitz, Germany — ⁶Diamond Light Source Ltd., Didcot, Oxfordshire, UK

Using the normal incidence x-ray standing wave (NIXSW) technique, we have investigated the vertical structure of quasi-freestanding monolayer graphene (QFMLG) obtained by intercalation of antimony under the (6√3 x 6√3) R30° reconstructed graphitized 6H-SiC(0001) surface, also known as zeroth-layer graphene. We found that Sb intercalation decouples the QFMLG very well from the substrate. The distance from the QFMLG to the Sb layer almost equals the expected van der Waals bonding distance of C and Sb. The Sb-intercalation layer itself is mono-atomic, very flat, and located much closer to the substrate, at almost the distance of a covalent Sb-Si bond length. All data is consistent with Sb located on-top of the uppermost Si atoms of the SiC bulk.

O 18.7 Mon 18:00 P4

Bi(110) islands on epitaxial graphene — •SERGI SOLOGUB^{1,2}, JULIAN KOCH¹, CHITRAN GHOSAL¹, and CHRISTOPH TEGENKAMP¹ — ¹Institut für Physik, TU Chemnitz, Reichenhainerstr. 70, 09126 Chemnitz — ²Institute of Physics, NAS of Ukraine, Nauki avenue 46, 03028 Kyiv

The atomic structure and morphology of ultrathin epitaxial Bi islands grown on the graphene/SiC surface was examined by SPA LEED and STM. Bi films with an average height of a few bilayers were deposited at RT and annealed at 410 K for 30 min afterwards. A Volmer-Weber growth mode with a predominance of the Bi(110) orientation was found. LEED patterns show that the Bi(110) structure has three domains rotated by 60°, with each domain having two subdomains rotated by ±2° with the zig-zag direction of Bi parallel to the armchair direction of graphene and four (minority-)subdomains with the zig-zag direction of Bi parallel to the zig-zag direction of graphene. Moreover, STM investigations revealed an elongation of the islands in the zig-zag direction of Bi as well as preferential ("magic") thicknesses (even numbers of Bi monolayers).

Additionally, magneto transport measurements using a 4 T magnet were performed in order to investigate the influence of the Bi islands on the weak localization effect in graphene.

O 18.8 Mon 18:00 P4

Quantum well states in Bi(110) islands grown on epitaxial graphene — •CHITRAN GHOSAL and CHRISTOPH TEGENKAMP — Institut für Physik, TU Chemnitz

The semimetal Bi attracts a lot of interest because of its unique electronic properties such as a low carrier concentrations and large carrier mobilities coming along with mesoscopic Fermi wavelength giving rise to robust quantum confinement effects and spin polarized states in thin films [1]. In this work we studied the growth of Bi on n-type doped monolayer graphene (MLG) on SiC(0001) by means of STS and STM. While for low coverages Bi(110) islands are formed Bi(111) structures were found for higher coverages. This allotropic transition occurs at 10 monolayers (3.3nm) and is significantly larger than the critical coverage reported for Bi on Si(111) [2]. In contrast to Bi/MLG, the deposition of Bi on HOPG results in the formation of islands with an odd number of layers. These differences were attributed to different substrate screening effects. Irrespective of the interface, Bi seems to grow rather in a relaxed bilayers fashion, i.e. supporting the formation of black phosphorous structures [2]. Spectroscopy performed on islands of different heights revealed a large gap opening (750 meV) at the center of 4 ML islands. In addition, we found signatures of edge states, which might refer to a non-trivial topology within these QWS-stabilized nanostructures.

[1] T. Hirahara et al. Phys. Rev. B 75, 035422 (2007); [2] T. Nagao et al. Phys. Rev. Lett. 93, 105501 (2004).

O 18.9 Mon 18:00 P4

Identification of electronic structures and atomic configuration of Nitrogen defects on graphene/Pt(111) — •JEONG AH SEO^{1,2}, HYUNMIN KANG^{3,4}, YOUNG JAE SONG^{3,4}, JUNGSEOK CHAE¹, and ANDREAS J. HEINRICH^{1,2} — ¹Center for Quantum Nanoscience, Institute for Basic Science, Seoul, Korea — ²Department of Physics, Ewha Womans University, Seoul, Korea — ³Department of Nano Engineering, Sungkyunkwan University (SKKU), Suwon, Korea — ⁴SKKU Advanced Institute of Nano Technology (SAINT), Sungkyunkwan University (SKKU), Suwon, Korea

Nitrogen doped graphene is considered as an effective method for modulating the electronic states and properties of graphene. We have prepared nitrogen doped graphene on Pt(111) surface, grown by deposition of pyridine precursor molecules. We figured out there exist several types of defects including graphitic nitrogen and pyridinic nitrogen structure. The imaging of the defects is performed using low temperature scanning tunneling microscope (STM) and atomic force microscope (AFM). The defects preferred to have strong triangular shape features above certain bias voltage. To figure out the features of nitrogen dopant atom, we measured bias dependent STM images, scanning tunneling spectroscopy and AFM imaging. We have observed prominent difference in spectroscopic feature near the fermi energy between defects and pristine graphene. In addition, we also have observed atomic configuration of defect site using AFM. With the aid of STM simulation based on calculated results from the density functional theory, possible candidates of defect types will be provided.

O 18.10 Mon 18:00 P4

Bell-shaped Electron Diffraction Component in 2D Materials — •HANNAH KOHLER, FRANK MEYER ZU HERINGDORF, and MICHAEL HORN-VON HOEGEN — Faculty of Physics and Center for Nanointegration, Duisburg-Essen (CENIDE), University of Duisburg-Essen, 47048 Duisburg, Germany

In low energy electron diffraction a bell shaped component (BSC) is observed for graphene on SiC and Ir(111) and for hBN on Ir(111) [APL118 (2021) 241902]. The distinctiveness of this broad diffuse intensity appears to be indicative of a highly ordered 2D layer. Several attempts were made to explain the origin of the BSC, but the mechanism remains at large still unclear. In particular, a classification in which 2D systems a BSC exists is missing. Low energy electron microscopy (LEEM) combines the possibility to investigate the BSC with microdiffraction (μ -LEED) and *in-situ* imaging. It was found that the BSC can in fact be detected not only on graphene and hBN, but also on *ex-situ* chemical-vapor-deposition-grown MoS₂. In graphene on Ir(111) the full width at half maximum (FWHM) of the BSC decreases with an increase in rotational angle of the graphene. Measurements after Cs intercalation of the graphene show a smaller FWHM compared to the non-intercalated graphene layer.

O 18.11 Mon 18:00 P4

Buffer Layer Characterization of Epitaxial Graphene on Silicon Carbide with Scanning Tunneling Microscopy — •BENNO HARLING¹, ANNA SINTERHAUF¹, PETER RICHTER², PHILIP SCHÄDLICH², THOMAS SEYLLER², and MARTIN WENDEROTH¹ — ¹IV. Physikalisches Institut, Georg-August-Universität Göttingen, Germany — ²Institut für Physik, Technische Universität Chemnitz, Germany

In this contribution, we present a scanning tunneling microscopy study on the buffer layer of epitaxial graphene on 6H-silicon carbide (SiC) at 8 K and room temperature in UHV. The local configurations and properties of the buffer layer still leave many open questions concerning the interactions between graphene and substrate. Our goal is to disentangle the contributions of the graphene and the underlying buffer layer to the tunneling current on a local scale and to establish an understanding of the responsible mechanisms. We employ multibias imaging to investigate buffer layer contributions to the tunneling current. This measurement mode takes quasi-simultaneous STM images line per line at given bias voltages resulting in a connected stack of topography maps. This allows to observe the changes of the topography in dependency of the applied bias voltage, with much lower dependency on tip modifications while scanning. We connect local corrugation tendency to relative heights and the overall corrugation tendency within the stack. Financial support of the Deutsche Forschungsgemeinschaft (DFG) is given by project We 1889/13-1 and We 1889/14-1.

O 18.12 Mon 18:00 P4

Intercalation of Fe under graphene on Ir(110) — •JASON BERGELT, AFFAN SAFEER, STEFAN KRAUS, JEISON FISCHER, and THOMAS MICHELY — II. Physikalisches Institut, Universität zu Köln, Zùlpicher Str. 77, 50937 Köln, Germany

Graphene on Ir(110) is a single-crystal, where graphene is nearly strain free and the resulting moiré pattern consists of waves with crests and troughs along the [001]-Ir direction. Also it has been shown that the growth of graphene prevents the formation of nano-facets that are present in bare Ir(110) at room temperature. In this work, we intercalated several layers of Fe between Gr and unreconstructed Ir(110). By using scanning tunneling microscopy (STM) and low energy electron diffraction (LEED), we confirm that Fe grows pseudomorphic with respect to unreconstructed Ir(110). Due to strong adhesion of graphene to

Ir(110), deposition of Fe on a closed graphene layer results in the formation of clusters on the surface and negligible intercalation at temperatures where alloying of Fe with Ir(110) is absent. Therefore, we implemented a procedure to etch with molecular oxygen small holes of controlled size into graphene. Moreover, we investigated the temperature and evaporation flux dependence of intercalation. Furthermore, we discuss the limit of pseudomorphic growth in view of the formation of a reconstruction at thicker intercalated Fe films.

O 18.13 Mon 18:00 P4

Strongly correlated boundary states in topologically insulating chiral graphene nanoribbons tuned by contact potential — •LEONARD EDENS¹, FRANCISCO ROMERO¹, SOFIA SANZ², AMELIA DOMÍNGUEZ-CELORRIO⁵, MANUEL VILAS-VARELA³, JINGCHENG LI⁴, DAVID SERRATE⁵, DIEGO PEÑA³, and NACHO PASCUAL^{1,2} — ¹CIC nanoGUNE BRTA, San Sebastián, Spain — ²DIPC, San Sebastián, Spain — ³CIQUS and Departamento de Química Orgánica, Univ. de Santiago de Compostela, Spain — ⁴School of Physics, Sun Yat-sen University, Guangzhou, China — ⁵INMA, and Univ. de Zaragoza, 50009 Spain

Chiral graphene nanoribbons present a special class of nanographenes in that their distinct edge symmetry causes a topologically nontrivial band dispersion. Truncating such a ribbon results in a pair of symmetry-protected topological end states predicted to be spin-polarized. Metal substrates interact with the molecular orbitals, transferring charge and screening electron-electron correlations. We decouple the nanoribbons by dragging them onto an ultrathin large bandgap insulator using an STM, and also synthesize them on a low-work function surface. Scanning tunneling spectroscopy on the surface intermetallic GdAu2 reveals a near-neutral ribbon, showing its end state spin-split. On MgO/Ag(001), the ribbons are highly decoupled, leading a greatly enhanced tunneling lifetime, vibronic sidebands, a negative charge and an enhanced correlation gap of opening far in the quantized conduction band.

O 18.14 Mon 18:00 P4

Structural investigation of Pb intercalated graphene on SiC — •SHAISTA ANDLEEB, JULIAN KOCH, CHITRAN GHOSAL, and CHRISTOPH TEGENKAMP — Institut für Physik, TU Chemnitz, Reichenhainerstr. 70, 09126 Chemnitz

In order to modify the electronic properties of graphene, intercalation experiments have received a lot of attention recently. In this research, we examined the intercalation of Pb on carbon buffer layer on SiC(0001) using SPA-LEED and STM. The samples were prepared in UHV by several cycles of Pb deposition using MBE at RT followed by annealing at temperatures ranging from 500 to 900°.

In LEED the intercalated phase shows six characteristic spots around the (00)-spots, which we correlated with a striped phase in STM. The local structure on the stripes shows two honeycomb Pb layers with approximately twice the lattice constant of graphene and turned by $\pm 7.5^\circ$ with respect to graphene. The corresponding spots in LEED coincide with two buffer layer spots. Their energy dependent behavior was analyzed.

O 18.15 Mon 18:00 P4

Spectroscopic evidence of BCS-BEC crossover in FeSe monolayer — •WANTONG HUANG^{1,6}, HAICHENG LIN¹, GAUTAM RAI², YUGUO YIN¹, LIANYI HE¹, QI-KUN XUE^{1,5}, STEPHAN WOLFGANG HAAS^{2,3}, STEFAN KETTEMANN^{3,4}, XI CHEN^{1,5}, and SHUAI-HUA JI^{1,5} — ¹State Key Laboratory of Low-Dimensional Quantum Physics, Department of Physics, Tsinghua University, Beijing 100084, China — ²Department of Physics and Astronomy, University of Southern California, Los Angeles, CA 90089-0484, USA — ³Jacobs University, Campus Ring 1, 28759 Bremen, Germany — ⁴Division of Advanced Materials Science, POSTECH, San 31, Hoyoja-dong, Nam-gu, Pohang 790-784, South Korea — ⁵Frontier Science Center for Quantum Information, Beijing 100084, China — ⁶Karlsruhe Institute of Technology, 76131 Karlsruhe, Germany

It has been difficult to realize the crossover from Bardeen-Cooper-Schrieffer (BCS) to Bose-Einstein condensates (BEC) in solids. Here we report direct evidence of BEC in a FeSe monolayer. The Fermi energy of the FeSe film can be tuned by graphene/SiC substrate to realize a BCS-BEC crossover. As the Fermi energy drops, the local density of states measured by STM evolves continuously from a BCS gap to a step-like asymmetric spectrum of BEC state. The theoretical calculation based on a two-band model reproduces well the measured spectra and, in particular, identifies features in the quasi-particle density of states that indicate a transition from the BCS to the BEC regime. In addition, the Zeeman splitting of the quasi-particle states is found to be consistent with the characteristics of a condensate.

O 18.16 Mon 18:00 P4

Investigating the correlated ground state of metallic monolayer MoS₂ with scanning tunneling spectroscopy — •CAMIEL VAN EFFEREN, JEISON FISCHER, THOMAS MICHELY, and WOUTER JOLIE — II. Physikalisches Institut, Universität zu Köln, Germany

Using contactless chemical doping [1], we grow metallic monolayer 2H-MoS₂ on a graphene on Ir(111) substrate. Since this method leaves the surface accessible, we perform real space investigations of correlated behavior in metallic monolayer MoS₂ via scanning tunneling microscopy (STM) and spectroscopy (STS).

In STS, we find a broad depression in the density of states around the Fermi level, of about 100 meV. Upon closer inspection, the depression is revealed to consist of a series of small gaps and peaks, spaced by 26-28 meV. This interval corresponds to a flat band in the phonon dispersion of MoS₂. The appearance of the peaks can be explained by strong coupling between the MoS₂ electrons and phonons at the high-symmetry K-point of the Brillouin zone, and may point to the formation of Holstein polarons. The behavior of the polarons is studied near grain boundaries, edges and defects, where the polaron bands are surprisingly seen to bend under the influence of charge.

[1] C. van Efferen et al., 2D Mater. 9 025026 (2022)

O 18.17 Mon 18:00 P4

Artificial electronic lattices on InAs(111)A — •RIAN LIGTHART and INGMAR SWART — Condensed Matter and Interfaces, Debye Institute for Nanomaterials Science, Utrecht, The Netherlands

Artificial electronic lattices are a promising tool to elucidate novel effects in the quantum world. The Scanning Tunneling Microscope (STM) allows to build the lattices by manipulating atoms with nanoscale precision and to probe the electronic properties. The electronic lattices consist of artificial atoms on a metallic/semiconducting crystal with a surface state which acts as a 2D electron gas (2DEG). The 2DEG is patterned by scatterers on the surface creating artificial atoms. The versatile artificial atoms are used in lattices to study the effect of structure on electronic characteristics.

An already well-known system is CO on Cu(111), however, this system has a low energy resolution of 80 mV due to coupling of the surface state with bulk states. Here, the promising InAs(111)A surface with native In adatoms is studied since it has a higher energy resolution of around 5 meV. Vertical manipulation allows to place multiple In-adatoms in vicinity of each other. The In adatoms create a potential well that confines the surface state electrons of InAs. The artificial atom created can be coupled into dimers with different bond strengths by varying the distance or by introducing bridge sites. The artificial electronic lattices created on InAs(111)A can help to probe new characteristics in the lattices due to the vastly improved energy resolution.

O 18.18 Mon 18:00 P4

Resonant photoemission studies at the Fe 3p threshold on thin FeTe/Bi₂Te₃ and FeSe/Bi₂Se₃ — •MARTIN VONDRÁČEK¹, TOMÁŠ SKÁLA², KAREL CARVA², GUNTHER SPRINGHOLZ³, and JAN HONOLKA¹ — ¹Institute of Physics of the Czech Academy of Sciences, Prague, CZ — ²Charles University, Faculty of Mathematics and Physics, Prague, CZ — ³Johannes Kepler University, Institute of Semiconductor and Solid State Physics, Linz, AT

Monolayers (MLs) of tetragonal FeTe and FeSe grow on hexagonal Bi₂Se₃ (111) and Bi₂Te₃ (111) substrates as three 60°-rotated domains. In scanning tunnelling spectroscopy, a gap appears at the Fermi level of FeTe/Bi₂Te₃ suggesting interface-induced superconductivity below T_c ≈ 6 K [1]. FeSe/Bi₂Se₃ remains in a gapless state [2]. Unconventional superconductivity in Fe-chalcogenides (FeChs) is believed to be correlated to the texture of the Fermi surface at Γ - and M-points. However, ARPES data of FeCh MLs on Bi₂Ch₃ is complex due to the superposition of contributions from all three domains. Here we show photon energy dependent UPS data probing k_z dispersions along the Γ -Z direction. Fano-like modulations of valence band intensities are observed in the energy range 30-80 eV, indicative of a resonant photoemission effect at the Fe 3p edge around 55 eV. Our ML data is compared to previous bulk studies [3].

[1] A. Eich et al., Phys. Rev. B **94**, 125437 (2016). [2] S. Manna et al., Nat. Commun. **8**, 14074 (2017). [3] T. Yokoya et al., Sci. Technol. Adv. Mater. **13** (2012) 054403.

O 18.19 Mon 18:00 P4

Electron-stimulated photon emission on TMD defects — •LYSANDER HUBERICH¹, JONAS ALLERBECK¹, FEIFEI XIANG¹, RICCARDO TORSI², ANNE MARIE TAN³, PASCAL RUFFIEUX¹, ROMAN FASEL¹, OLIVER GRÖNING¹, RICHARD HENNIG³, YU-CHUAN LIN², JOSHUA ROBINSON², and BRUNO SCHULER¹ — ¹Empa - Swiss Federal Laboratories for Materials Science and Technology, Switzerland — ²Department of Materials Science and Engineering, The Pennsylvania State University, University Park, USA — ³Department of Materials Science and Engineering, University of Florida, USA

Due to their exceptionally long electron spin coherence and spin-selective optical readout nitrogen-vacancy centers in diamond are considered a key building block in quantum sensing and quantum-cryptography applications. However, defects in bulk materials suffer from limited tunability and placement control, poor photon extraction efficiency, and coherence degradation close to the surface. 2D materials such as monolayer transitional metal dichalcogenides (TMDs) are expected to overcome these challenges while offering new synthetic strategies for the bottom-up design of solid-state defects. Here we present an NV⁻ center analog in 2D; the dopant vacancy complex (Re_{M_o} + Vac_S)⁻ in MoS₂. We investigate its electronic states using scanning tunneling spectroscopy and present atomically-resolved photon emission maps of single TMD defects by means of STM luminescence.

O 18.20 Mon 18:00 P4

Electronic and structural properties of Fe-doped SnS van der Waals crystals — •DAMLA YESILPINAR^{1,5}, MARTIN VONDRÁČEK¹, ČESTMIR DRAŠAR², PATRIK ČERMAK², ONDŘEJ CAHA³, KAREL CARVA⁴, VÁCLAV HOLÝ⁴, JAN PROKLEŠKA⁴, HARRY MÖNIG⁵, and JAN HONOLKA¹ — ¹Institute of Physics, AV ČR, Na Slovance 1999/2 182 21 Praha 8, CZ — ²Faculty of Chemical Technology, University of Pardubice, Studentská 573, 532 10 Pardubice, CZ — ³Department of Condensed Matter Physics, Masaryk University, Žerotínovo nám. 617/9, 601 77 Brno, CZ — ⁴Department of Condensed Matter Physics, Charles University, Ke Karlovu 5, 121 16 Prague, CZ — ⁵Physikalisches Institute, Wilhelm-Klemm Str. 10, 48149 Münster, DE

We investigate the effect of low concentrations of iron on the physical properties of SnS van der Waals crystals grown from the melt. By means of scanning tunneling microscopy (STM) and photoemission spectroscopy we study Fe-induced defects and observe an electron doping effect in the band structure of the native p-type SnS semiconductor. Atomically resolved and bias dependent STM data of characteristic defects are compared to *ab initio* DFT simulations of vacancy (V_S and V_{Sn}), Fe substitutional (Fe_{Sn}) and Fe interstitial (Fe_{int}) defects. In line with our EXAFS data, we propose the importance of Fe_{int} and discuss possible pairing defects, e.g. with V_S.

O 18.21 Mon 18:00 P4

In Operando Soft X-Ray Photoemission Spectroscopy of TaS₂ and HfS₂ based memristive devices — •TAMMO ZIMMERMANN¹, ALENA NIERHAUVE^{1,2}, MATTHIAS KALLÄNE^{1,2}, JENS BUCK^{1,2}, ZHANGSONG GENG³, CHAO ZHANG³, FRANK SCHWIERZ², MARTIN ZIEGLER³, and KAI ROSSNAGEL^{1,2,4} — ¹Institut für Experimentelle und Angewandte Physik, Christian-Albrechts-Universität Kiel, 24098 Kiel, Germany — ²Ruprecht-Haensel-Labor, DESY and CAU Kiel, 22607 Hamburg and 24098 Kiel, Germany — ³Department of Electrical Engineering and Information Technology, TU Ilmenau, 98684 Ilmenau, Germany — ⁴Deutsches Elektronen-Synchrotron DESY, 22607 Hamburg, Germany

In neuromorphic engineering interface-based memristive devices (IMDs) are promising candidates to mimic synaptic behavior. A refined understanding of bias-induced changes in the band structure and the underlying transport mechanisms of layered transition-metal dichalcogenide-based IMDs will improve the development toward future applications, e.g., in artificial neural networks. Here, we show first *in operando* position- and momentum-resolved soft x-ray photoemission spectroscopy measurements obtained from transistor-like TaS₂- and HfS₂-based IMDs.

O 18.22 Mon 18:00 P4

Comparison of spin-crossover properties between thin film and bulk sample of a binuclear Fe(II) complex — •MARCEL WALTER¹, SANGEETA THAKUR¹, CLARA TROMMER², FELIX TUCZEK², SEBASTIEN ELIE HADJADJ¹, JORGE TORRES¹, and WOLFGANG KUCH¹ — ¹Institut für Experimentalphysik, Freie Universität Berlin, Arnimallee 14, 14195 Berlin — ²Institut für Anorganische Chemie, Christian-Albrechts-Universität zu Kiel, Max-Eyth-Straße 2, 24118 Kiel

Spin-crossover molecules (SCMs) are a promising material in the field of spintronics, due to the reversibility of switching between a high-spin and a low-spin state, which can be triggered by light and temperature [1]. The focus of our research is to deposit large SCMs to explore cooperativity in spin switching on surfaces. A pulsed-valve vapor deposition method is used for thin films. This has the advantage of depositing (sub-) monolayers of SCMs in an UHV environment without applying large amounts of thermal energy, which can decompose the large SCMs. We compare the spin-switching behavior of the dinuclear SCM [Fe(H₂B(pz)₂)₂]₂(μ-bipy-ac-bipy) as thin film on highly oriented pyrolytic graphite and as bulk sample using X-ray absorption spectroscopy. The spin-crossover properties were examined for thermal-induced spin state switching as well as for light-induced excited spin-state trapping. The results show that the thin films are locked in a mixed spin state while the bulk sample switches completely, although the equilibrium temperature of the spin states is comparable.

[1] L. Kipgen et al., Advanced Materials **33**, 24 (2021)

O 18.23 Mon 18:00 P4

Neutral and charged excitations in two-dimensional MoTe₂ from first principles — •FRANZ FISCHER^{1,2}, ABDERREZAK BESTER¹, and GABRIEL BESTER¹ — ¹University of Hamburg, Institute of Physical Chemistry, 22761 Hamburg, Germany — ²Max Planck Institute for the Structure and Dynamics of Matter, 22761 Hamburg, Germany

Atomically thin layers of transition metal dichalcogenides attract remarkable interest due to their extraordinary electronic and optical properties. The lack of inversion symmetry in their crystal structure combined with strong spin-orbit interaction caused by heavy metal atoms gives rise to an extra valley degree of freedom as well as large spin splittings in the Brillouin zone.

We present an effective first-principle formalism that is extendable to study any order of neutral or charged excitation [1]. Our formalism relies on configuration interaction and the GW-approximation and reduces in the case of excitons to the standard form of the BSE. We will present results of the excited states in

monolayer MoTe₂ and their emergence from the particular single-particle configurations. In the future we want to extend our methodology to the temporal domain in order to study dynamics of excited states in 2D materials.

[1] Phys. Rev. B. **100** 201403(R) (2019)

O 18.24 Mon 18:00 P4

Relaxation, the moiré potential and excited states for twisted TMDC bilayers — •CARL EMIL MØRCH NIELSEN, MIGUEL DA CRUZ, ABDERREZAK TORCHE, and GABRIEL BESTER — University of Hamburg, Institute of Physical Chemistry, 22761 Hamburg, Germany

In recent years, the research of transition metal dichalcogenides has amassed much attention due to interesting properties such as strong localisation of excited states. The field of twistronics emerged as twisting provides a new degree of freedom in engineering specific properties. However, the theoretical ab-initio approach shows an immediate challenge to overcome; large systems, where the moiré unit cell may hold thousands of atoms.

In this project, the aim is to theoretically study moiré confined optical excitations in twisted TMD vdW-homo and heterostructures. We have successfully integrated a force-field based method of relaxation using LAMMPS as suggested in a paper by Jain et. al. We have re-parameterized the SW and KC potentials seen in this paper and expanded the parameter set to include all possible bilayer TMD combinations. With these we can accurately model the associated local band gap variation, e.g. the moiré potential, taking into effect both lattice corrugation and atomic reconstruction. Our goal is now to investigate the excited state properties with our group-developed code from first-principles.

O 18.25 Mon 18:00 P4

Tip-induced excitonic luminescence of an atomically-resolved van der Waals heterostructure — •LUIS PARRA LOPEZ^{1,2}, ANNA ROSLAWSKA², FABRICE SCHEURER², STÉPHANE BERCIAUD², and GUILLAUME SCHULL² — ¹Department of Physical Chemistry, Fritz Haber Institute of the Max Planck Society, 14195 Berlin, Germany. — ²Université de Strasbourg, CNRS, IPCMS, UMR 7504, 67000 Strasbourg, France.

Van der Waals heterostructures (vdWH) made from stacks of transition metal dichalcogenides and other 2D-materials are appealing systems to investigate light-matter interaction. Their optical response is dominated by tightly bound excitons that are sensitive to the presence of atomic-scale inhomogeneities. These inhomogeneities lie at length-scales below the spatial resolution accessible with standard optical spectroscopies. Here, we present an approach using a scanning tunneling microscope to induce the luminescence of an MoSe₂/FL-graphene vdWH [1]. We correlate the atomic-scale landscape with the locally induced optical response and observe sizeable variations in the excitonic emission between different nm-sized areas. This study paves the way for novel investigations regarding the local properties of vdWH and highly localized excitons. To gain deeper insight into interlayer coupling mechanisms on the nanoscale, which occur on sub-ps timescales, requires additional high temporal resolution as well. I thus conclude with an outlook of an experimental setup capable of addressing ultrafast dynamics with fs-temporal and nm-spatial resolution [2]. [1] Parra et al, arXiv:2204.14022(2022). [2] Müller et al, ACS Photonics, 7(8), (2020).

O 18.26 Mon 18:00 P4

Changing structural and electronic properties of h-BN on Ir(111) by potassium intercalation — •PHILIP GRIMM, FRIEDRICH WANIERKE, FELIX OTTO, MAXIMILIAN SCHAAL, ROMAN FORKER, and TORSTEN FRITZ — Institute of Solid State Physics, Friedrich Schiller University Jena, Helmholtzweg 5, 07743 Jena, Germany

2D hexagonal boron nitride (h-BN) is applied in electronics components, e.g. in gate dielectrics for transistors. However, its insulating behaviour is strongly influenced by the growth on metal substrates. One possibility to restore the in-

ulating effect and to decouple h-BN is the intercalation of alkali metals due to their low ionization energies.

In this study, we use h-BN grown by CVD on Ir(111) while potassium is deposited by thermal evaporation. The samples are investigated at various temperatures, the lateral structure by means of LEED as well as the electronic properties by means of XPS and (AR)PES. A ($\sqrt{3} \times \sqrt{3}$)R30° superstructure of K and a decrease of the moiré pattern originating from h-BN/Ir(111) is observed. In addition, the core levels and the band structure shifts to higher binding energies whereas the work function decreases by the similar value. Another observation is a disappearing band folding of the σ -bands. Due to the metastability of the superstructure at room temperature, we switched to low temperature at 35 K and observed even larger shifts of the core levels as well as of the band-structure (≈ 3 eV). In conclusion, our results indicate an intercalation of K in the 2D-system and consequently h-BN is decoupled from Ir(111).

O 18.27 Mon 18:00 P4

Adsorption and Reaction of Bromine on h-BN/Rh(111) — •EVA MARIE FREIBERGER, NATALIE J. WALESKA, FELIX HEMAUER, VALENTIN SCHWAAB, HANS-PETER STEINRÜCK, and CHRISTIAN PAPP — Friedrich-Alexander-Universität Erlangen-Nürnberg, Erlangen, Germany

Due to their unique chemical and electronic properties, rendering them promising for many applications, numerous two-dimensional materials (2DM) have been predicted, synthesized and characterized. To tailor the properties of 2DM towards possible applications, their chemical modification is of special interest. Hexagonal boron nitride (h-BN), a graphene analogue, exhibits a so-called nanomesh on Rh(111), which can be used as a template enabling spatially defined modification of the 2DM. Using this template, we aim for selective functionalization of h-BN/Rh(111) with halogens, which lead to strong electronic doping. Here, we present a synchrotron radiation-based high-resolution X-ray photoelectron spectroscopy (XPS) study on the adsorption and thermally induced reaction of bromine on h-BN/Rh(111). The adsorption of different amounts of bromine was followed in situ at 170 K, confirming the template effect of the nanomesh for low coverages. Based on temperature-programmed XPS (TPXPS) experiments, we propose covalent functionalization of the pores and a thermally induced on-surface reaction of bromine. Furthermore, the adsorption is observed to be reversible upon heating to 800 K. By shedding light on their controlled chemical modification on the molecular scale, our work paves the way for purposeful tailoring of the properties of 2DM.

O 18.28 Mon 18:00 P4

Structural investigation of antimony monolayers on Ag(111) — •STEFANIE HILGERS¹, JULIAN A. HOCHHAUS^{1,2}, MALTE G. H. SCHULTE^{1,2}, and CARSTEN WESTPHAL^{1,2} — ¹TU Dortmund University, Department of Physics, Otto-Hahn-Str. 4a, 44227 Dortmund, Germany — ²DELTA, TU Dortmund, Maria-Goeppert-Mayer-Str. 2, 44227, Dortmund, Germany

Similar to graphene and further elements of the 4th main group, Group-V elements such as antimony are also predicted to have extraordinary electronic properties. Because of the strong spin-orbit coupling and the resulting topological properties, antimony monolayers are of great interest for future electronic applications. Since the structural configuration of 2D-materials has major influence on the electronic properties of the material, structural investigations are highly relevant. In the here presented research we report on the synthesis and structural investigation of antimony monolayers on Ag(111).

After several cleaning cycles in UHV, antimony is evaporated by a Kudsen cell to deposit monolayers on the Ag(111) surface. The well-known ($\sqrt{3} \times \sqrt{3}$)R30° superstructure can be identified by low-energy electron diffraction (LEED). In addition, a ($2\sqrt{3} \times 2\sqrt{3}$)R30° superstructure can be verified for higher coverages. Furthermore, the real space structure is investigated by scanning tunneling microscopy (STM).

O 19: Poster Monday: Scanning Probe Techniques 1

Time: Monday 18:00–20:00

Location: P4

O 19.1 Mon 18:00 P4

Quantifying Force and Energy in Single-Molecule Metalation — KARL ROTHE¹, •NICOLAS NÉEL¹, MARIE-LAURE BOCQUET², and JÖRG KRÖGER¹ — ¹Institut für Physik, Technische Universität Ilmenau, D-98693 Ilmenau, Germany — ²PASTEUR, Département de Chimie, École Normale Supérieure, PSL University, Sorbonne Université, CNRS, 75005 Paris, France

An atomic force microscope is used to determine the attractive interaction at the verge of adding a Ag atom from the probe to a single free-base phthalocyanine molecule adsorbed on Ag(111). The experimentally extracted energy for the spontaneous atom transfer can be compared to the energy profile determined by density functional theory using the nudged-elastic-band method at a defined probe-sample distance.

O 19.2 Mon 18:00 P4

Live demodulation of pseudo-heterodyne SNOM at kHz repetition rates — •PHILIPP SCHWENDKE¹, SAMUEL PALATO¹, NICOLAI GROSSE², and JULIA STÄHLER¹ — ¹PC dept., FHI of the MPG and HU Berlin — ²ELAB, FHI of the MPG

Scanning near-field optical microscopy (SNOM) allows the spectroscopic investigation of functional surfaces with spatial resolution beyond the diffraction limit. For the observation of electron dynamics on a femtosecond and nanometre scale, common setups rely on high repetition rate laser systems in order to avoid the Nyquist limit, imposed by signal modulation through the tapping AFM tip. Phase-domain sampling schemes allow sample rates below the Nyquist frequency, permitting the use of kHz-class optical amplifiers for tunable wavelengths down to the UV and femtosecond time resolution. We introduce quadra-

ture demodulation for a robust and fast signal demodulation, while also simplifying the experimental setup.

Here, we illustrate and evaluate different methods for signal modulation and data analysis, with the aim of increasing the signal to noise ratio while maintaining high spatial resolution. The near-field contribution is identified through retraction curves, while noise and overall performance is evaluated on real-space images of a Si test sample, showing a significant signal contrast at high harmonic orders of tapping modulation. The presented methods are straightforward to combine with established optical methods, paving the way towards time-resolved SNOM and nano-spectroscopy.

O 19.3 Mon 18:00 P4

Designing a Scanning Probe Microscope to quantify electron correlations in novel 2D materials — •NIKILH SEEJA SIVAKUMAR, HENNING VON ALLWÖRDEN, DANIEL WEGNER, ALEXANDER AKO KHAJETOORIANS, and NADINE HAUPTMANN — Institute for Molecules and Materials, Radboud University, Nijmegen, The Netherlands

Quantum phases in a single or few layers of van der Waal materials often exhibit novel types of charge and spin orders that are driven by electron correlations. To understand the role of electron-electron interactions, it is required to quantify the interplay between the geometric structure, charges and spins at the atomic scale. Scanning tunneling microscopy (STM) and its accompanying magnetic mode, spin polarized STM, are powerful techniques to study the geometric, electronic and magnetic structure, but their application is limited to metallic or semiconducting quantum phases. Here, we present the design and setup of a home-built scanning probe microscopy setup working at 1K based on a JT-stage with 4He, operating in a 3T out-of-plane magnetic field. The setup will combine STM with non-contact Atomic Force Microscopy, Kelvin Probe Force Microscopy, and Magnetic Exchange Force Microscopy to independently study the geometric, electronic and magnetic structure in insulating quantum phases of 2D materials, as well as at phase transitions to conducting phases. A gating stage will allow to study 2D materials in a device geometry.

O 19.4 Mon 18:00 P4

Nanoscale capacitance and dielectric permittivity measurements — •PASCAL ROHRBECK¹, LUKAS DRAGO CAVAR^{1,2}, PETER REICHEL², and STEFAN A. L. WEBER^{1,2} — ¹Max Planck Institute for polymer research, Department physics at interfaces, Ackermannweg 10, 55128 Mainz, Germany — ²Johannes Gutenberg University, Department of Physics, Staudingerweg 10, 55128 Mainz, Germany

The knowledge of capacitance and dielectric properties in the nanoscale is important to understand the basic physics of semiconductor materials, such as solar cells or battery materials.[1]

In this work, we demonstrate quantitative capacitance and dielectric constant measurements of individual nanostructures using an Atomic Force Microscope (AFM). The new Heterodyne Scanning Capacitance Microscopy (H-SCM) method is based on frequency mixing of two alternating current (AC)-voltages with frequencies in the MHz range. This new method enables quantitative measurements of tip-sample capacitance and local dielectric permittivity with the lateral resolution of the AFM. We can show that the H-SCM reduces the effect of stray capacitance and thereby yields superior lateral resolution.

References:

[1] Fumagalli, L.; Ferrari, G.; Sampietro, M.; Gomila, G. *Applied Physics Letters* 2007, 91(24), 236243110. doi:10.1063/1.2821119

O 19.5 Mon 18:00 P4

Sphere Probes for Scanning Thermal Microscopy — •SOPHIE RODEHUTSKORS, FRIDOLIN GEESMANN, PHILIPP THURAU, and ACHIM KITTEL — Institut für Physik, Carl-von-Ossietzky Universität Oldenburg

Scanning thermal microscopes based on STM and AFM have been used for years to observe near-field mediated heat transfer. Using custom-built coaxial thermocouple tips in an STM setup, spatially highly resolved heat transfer measurements are possible [1]. The total heat transfer between a spherically approximated tip and a sample is expected to depend on the square of the tip's radius [2]. By attaching a 20 μm borosilicate sphere to such a coaxial thermocouple sensor, heat flux sensitivity is further increased in distance-dependence measurements of the heat transfer between a cooled sample and a tip at room temperature for different materials. These sensors can be used for highly resolved radiative heat transfer measurements as well as for heat conduction measurements through self-assembled monolayers of organic molecules.

[1] K. Kloppstech et al., *Nat. Commun.*, 8, 14475 (2017)

[2] E. Rousseau et al., *Nat. Photonics* 3.9, 514-517 (2009)

O 19.6 Mon 18:00 P4

A New Sensor Concept for Scanning Thermal Microscopy — •MARVIN GLITZENBERG, PHILIPP WIESENER, and ACHIM KITTEL — Institut für Physik, Carl von Ossietzky Universität Oldenburg

Near-field mediated heat transfer (NFMHT) between two surfaces separated by a vacuum gap has become a widely investigated topic in the past decades. To measure this phenomenon, we are using a self-developed near-field scanning thermal microscope (NSThM) based on an STM. It is equipped with self-made

thermocouple tips consisting of a platinum wire molten into a borosilicate glass capillary which is then coated with gold. Since the gold layer can also be used as a tunneling electrode, we were able to measure the thermoelectric voltage and the tunneling current between the tip and sample simultaneously. However, the voltage drop due to the tunneling current interfered with the thermo voltage, making break junction experiments investigating heat and electrical conduction uninterpretable. In a new design of the tips for the NSThM, the thermocouple is covered first by an insulating silicon dioxide film and finally by a second gold film, which then acts as a tunneling electrode separate from the thermocouple and eliminates crosstalk. These tips are called PASA-tips due to the sequence of materials (platinum-gold-silicon dioxide-gold). Some example measurements of radiative heat transfer and heat conduction with these tips are shown to illustrate their capabilities.

O 19.7 Mon 18:00 P4

Implementation of a SPPX Setup and investigation of the delay-time modulation induced intensity modulation — •MARLO TEICHMANN, GEORG TRAEGER, and MARTIN WENDEROTH — V. Physical Institute, University of Göttingen, 37077, Göttingen, Germany

Shaken-pulse-pair-excited STM (SPPX-STM) successfully combines optical pump-probe techniques with STM to obtain high temporal and spatial resolution [1]. SPPX-STM achieves this by introducing a modulation of the delay time between pump- and probe pulses. The modulation of the delay time instead of the intensity leads to a constant thermal load and hence minimizes thermal effects. However, recent studies have shown that higher harmonics of this modulation causes additional undesirable signals in time resolved measurements [2].

In this study, we implemented a SPPX setup with two semiconductor lasers. These lasers can be triggered electronically which allows for delay times below 1ns between pump- and probe pulse. We implemented two different pump probe schemes to suppress the additional signals, caused by the SPPX-Method. By choosing an improved modulation scheme, we show that it is possible to suppress the contribution of the higher harmonic signals by more than one order of magnitude.

[1] Kloth et al. *Rev. Sci. Instrum.* 87 (2016)

[2] Takeuchi et al. 2019 *Jpn. J. Appl. Phys.* 58 S11A12

O 19.8 Mon 18:00 P4

Grating Coupled Illumination with Image Recognition for Scanning Tunneling Microscopy under Highly Stable and Truly Localized Optical Excitation — •GEORG A. TRAEGER¹, MARLO H. TEICHMANN¹, BENJAMIN SCHRÖDER^{1,2}, and MARTIN WENDEROTH¹ — ¹IV. Physikalisches Institut, Georg-August-Universität Göttingen, Germany — ²Max Planck Institute of Multidisciplinary Sciences, Göttingen, Germany

We present a versatile approach for a highly stable and localized optical excitation in a scanning tunneling microscopy (STM). Optical gratings on STM tips allow to excite a surface plasmon polariton (SPP), which travels to the tunneling junction and results in a highly confined optical excitation. Unfortunately, this technique comes with the drawback, that a much larger thermal load compared to the conventional direct illumination of the tunnel gap is introduced to the tip. This necessitates a high stability of the laser setup both in terms of long-term power stability and pointing[1]. The latter is limited by the mechanical decoupling of the STM from the environment, leading to independent movement of the microscope and the laser focus. We utilize an auto focus approach based on a CCD camera, which is aligned with the optical pathway of a fs-laser to achieve a active coupling between the laser and the STM. Studying ultrafast photo-currents in tunneling junctions we find that the new setup allows for STM operation under highly localized and background free illumination with a lateral resolution better than 2nm. [1] Kloth et al., *Rev. Sci. Instrum.* 87, (2016).

O 19.9 Mon 18:00 P4

Shot-noise measurements of single-atom Josephson junctions — •VERENA CASPARI, IDAN TAMIR, CHRISTIAN LOTZE, and KATHARINA J. FRANKE — Fachbereich Physik, Freie Universität Berlin, 14195 Berlin, Germany

Current passing through small constrictions fluctuates due to the discreteness of charge. Measuring this so-called shot noise in atomic-scale superconducting junctions can provide valuable information, from the quanta of charge transferred in multiple Andreev reflections to the correlations between the transmitted electrons in such processes. Here, we use a local shot-noise measurement apparatus, operating at low temperatures, to investigate shot noise in single-atom Pb-Pb junctions. We observe charge doubling inside the superconducting gap and an unexpected deviation from the thermal limit at zero bias voltage.

O 19.10 Mon 18:00 P4

Surface science with haptic feedback — •MAXIMILIAN KOALL¹, DENIS HEITKAMP², JACCOMO LORENZ², PHILIPP LENSING², and PHILIPP RAHE¹ — ¹Universität Osnabrück, BarbarasträÙe 7, 49076 Osnabrück, Germany — ²Hochschule Osnabrück, Albrechtstraße 30, 49076 Osnabrück, Germany

Modern scanning probe microscopy requires intuitive 3D tip positioning and direct access to 3D physical data for interpretation. Still, it is common practice

to rely on time-consuming 2D control protocols with only very few approaches involving 3D virtual reality methods [1].

Here, we employ a haptic device for moving the tip at the microscopic scale by hand. An immediate feedback from the measurement signals that reflect the interaction of the tip with the sample is provided, allowing for a quick and intuitive exploration of conductivity landscapes and force fields at surfaces as well as for atom manipulation and tip preparation procedures.

We present the *offline* implementation for recorded data of the well-studied

system PTCDA/Ag(111) in a virtual environment (Unity) for improved intuitive understanding of the physical properties. Furthermore, we discuss the approach to interface this system with the scan controller for *online* experiments. The 3D Systems Touch X is used to provide tip control and haptic feedback. The physical observable (tunneling current, frequency shift, damping, force or others) at the tip position in the recorded data is translated into haptic feedback.

[1] Leinen, P.; Green, M. F. B.; Esat, T.; Wagner, C.; Tautz, F. S.; Temirov, R. Beilstein J. Nanotechnol. 2015, 6, 2148

O 20: Poster Monday: Solid-Liquid Interfaces

Time: Monday 18:00–20:00

Location: P4

O 20.1 Mon 18:00 P4

Pd nanoparticles supported on ordered Co₃O₄(111): Particle size effects in electrochemical environment — •MAXIMILIAN KASTENMEIER¹, XIN DENG¹, TOMÁŠ SKÁLA², NATALIYA TSUD², LUKÁŠ FUSEK^{1,2}, VIKTOR JOHÁNEK², JOSEF MYSLIVĚČEK², YAROSLAVA LYKHACH¹, OLAF BRUMMEL¹, and JÖRG LIBUDA¹ — ¹FAU Erlangen-Nürnberg, Erlangen, Germany — ²Charles University, Prague, Czech Republic

Pd nanoparticles (NPs) are efficient electrocatalysts for oxidation of ethanol in alkaline direct ethanol fuel cells. We investigated the morphology and the oxidation state of Pd NPs supported on well-ordered Co₃O₄(111) films as a function of the particle size after treatment in ultrahigh vacuum and in alkaline electrolyte under potential control. We combined synchrotron radiation photoelectron spectroscopy and scanning tunneling microscopy. Electronic metal support interaction associated with the charge transfer at the Pd/Co₃O₄(111) interface yield partially oxidized ultra-small Pd^{δ+} aggregates and Pd²⁺ species at Pd coverages below 0.1 ML followed by the growth of two-dimensional metallic PdO NPs at higher coverages. The stabilities of ultra-small and conventionally-sized NPs supported on Co₃O₄(111) and HOPG were compared following an emersion from alkaline electrolyte at potentials between 0.5 and 1.5 VRHE. We observed different oxidation behavior related to two-dimensional and three-dimensional morphologies of supported Pd NPs on Co₃O₄(111) and HOPG, respectively. In sharp contrast, the oxidation state of the ultra-small Pd deposits remains unchanged between 0.5 and 1.5 VRHE.

O 20.2 Mon 18:00 P4

Film growth and stability of the ionic liquid [C₁C₁Im][Tf₂N] on Cu(111) — •TIMO TALWAR, STEPHEN MASSICOT, FLORIAN MAIER, and HANS-PETER STEINRÜCK — Lehrstuhl für Physikalische Chemie 2, Friedrich-Alexander-Universität Erlangen-Nürnberg, Egerlandstr. 3, 91058 Erlangen

Ionic liquids (ILs) are salts with melting points below 100°C and extremely low vapor pressure. These properties made them promising candidates for various new catalytic concepts like solid catalysis with Ionic Liquid Layer (SCILL). In this context, the interplay of ILs with metal surfaces is highly important.

In this study, the growth and thermal behavior of ultrathin films of 1,3-dimethylimidazolium bis[(trifluoromethyl)sulfonyl]imide [C₁C₁Im][Tf₂N] on Cu(111) are investigated under UHV conditions. The films are prepared in vacuum by physical vapor deposition and measured by angle-resolved and temperature-programmed X-ray photoelectron spectroscopy. Different film thicknesses are investigated to identify the underlying growth model, which is 2D growth up to 0.3 ML and 3D growth for higher coverages. Note that 1 ML corresponds to a bilayer of cations and anions irrespective of their arrangement. These films are stable up to 300 K. However above 300 K, the anion partly decomposes, and above 500 K, the remaining IL desorbs leaving a decomposed residual on the surface.

Supported through an ERC Advanced Investigator Grant (ILID 693398) to HPS and by the DFG (SFB 1452 CLINT).

O 20.3 Mon 18:00 P4

Influence of water in the electrolyte on the electrochromic characteristics of WO₃ — •SOPHIE GÖBEL, THI HAI QUYEN NGUYEN, and DERCK SCHLETTWEIN — Justus-Liebig-Universität Gießen, Institut für Angewandte Physik

In view of global warming, the reduction of CO₂ emissions in the energy sector, e.g. in private households is urgent. In this case, especially heat flow through windows has a main impact. With the help of so-called smart windows, the irradiation of sunlight can be controlled to decrease the energy consumption by air conditioning or heating systems. A possible approach to such switching is provided by electrochromic layers. One of the best observed materials for such smart windows is tungsten oxide WO₃. In this work, porous WO₃ films were prepared via a sol-gel process and spin-coating on fluorine-doped tin oxide (FTO). In order to achieve the porous structure, polymers (PEG400 and PIB₅₀-b-PEO₄₅) were added as additives in the precursor solution. To enhance the electrochromic characteristics of the WO₃ films in contact to an electrolyte consisting of LiClO₄ in propylene carbonate, addition of water into the electrolyte was studied. The amount of added water was varied while the influence on the electrochemical

and spectral properties was monitored by cyclic voltammetry and UV/Vis spectroscopy.

O 20.4 Mon 18:00 P4

In situ surface X-ray diffraction studies of Pt(110) — •JAN OLE FEHRS¹, TIMO FUCHS¹, JAKUB DRNEC², MARTA MIROLO², SERHIY CHEREVKO³, VALENTIN BRIEGA³, DAVID HARRINGTON⁴, CHENTIAN YUAN⁴, and OLAF MAGNUSSEN¹ — ¹Christian-Albrechts Universität zu Kiel, Germany — ²European Synchrotron Radiation Facility, Grenoble, France — ³Helmholtz Institute Erlangen-Nürnberg for Renewable Energy, Germany — ⁴University of Victoria, Canada

The surface oxidation of platinum is an important process in the degradation of platinum electrocatalysts in PEM fuel cells. Previously, the oxidation of the (111) and (100) surfaces of platinum was investigated by Fuchs et al. to understand the underlying mechanisms and growth of the oxide structures. In this work the (110) surface was studied by similar in situ high energy surface X-ray diffraction (HESXRD) at the ID31 beamline of the European Synchrotron Radiation Facility. Unreconstructed as well as (1x2)-reconstructed Pt(110) surfaces were prepared and their restructuring upon oxidation was examined. Distinct differences in this restructuring of the unreconstructed and the (1x2)-reconstructed surface were found. The changes in occupancy of the topmost surface layers after one oxidation/reduction cycle are greater for the unreconstructed surface than for the reconstructed surface, suggesting that the latter is more stable upon oxidation. In accordance with this result, it was also found that the missing row reconstruction of the surface was only lifted during the reduction of the surface oxide.

O 20.5 Mon 18:00 P4

Increase of the Spectroelectrochemical Performance of WO₃ Films by Using Additives During Film Growth — •THI HAI QUYEN NGUYEN¹, FLORIAN EBERHEIM¹, SOPHIE GÖBEL¹, PASCAL COP², MARIUS ECKERT¹, TIM P. SCHNEIDER¹, LUKAS GÜMBEL¹, BERND M. SMARSLY², and DERCK SCHLETTWEIN¹ — ¹Justus-Liebig-Universität Gießen, Institut für Angewandte Physik — ²Justus-Liebig-Universität Gießen, Physikalisch-Chemisches Institut Tungsten oxide (WO₃) is commonly used as an electrochromic material in smart windows. The electrochromic performance of WO₃ is highly influenced by the mixed electronic and ionic transport in the film and, thus, by the accessibility of the internal film volume. In this work, WO₃ thin films were prepared by spin-coating from a precursor solution based on peroxotungstic acid and different polymer additives such as polyethylene glycol (PEG), a block copolymer (PIB₅₀-b-PEO₄₅) and a combination thereof. The influence of the additives on the porosity and composition of WO₃ was studied by, e.g., scanning electron microscopy, X-ray photoelectron spectroscopy and atomic emission spectroscopy. Electrochromic characteristics of the films were measured with LiClO₄ in propylene carbonate as electrolyte. The intercalation of Li⁺ ions was analyzed by time-of-flight secondary ion mass spectrometry. The use of PEG provided microporous films leading to improved effective diffusion coefficients, transmittance modulations and response times compared to compact WO₃. Further improved characteristics were obtained for films with interconnected mesopores prepared with PEG and PIB₅₀-b-PEO₄₅.

O 20.6 Mon 18:00 P4

Visualizing electrochemical interfaces with combined AFM/STM — •ANDREA AUER, BERNHARD EDER, and FRANZ GRESSIBL — Institute of Experimental and Applied Physics, University of Regensburg, Germany Atomic force microscopy (AFM) that can be simultaneously performed with scanning tunneling microscopy (STM) modes using metallic tips attached to self-sensing quartz cantilevers (qPlus sensors) has advanced the field of surface science by allowing for unprecedented high spatial resolution under ultrahigh vacuum conditions. Applying a qPlus sensor-based AFM/STM setup to electrochemistry could offer new and groundbreaking possibilities to locally image both the 3D layering of the interfacial water and the lateral structure of the electrochemical double layer. In this work, a home-built AFM/STM instrument equipped with a qPlus sensor for operation under precise potential control in an electrochemical liquid cell is presented. Special care is taken in the preparation of etched Pt/Ir tips, which are attached to the qPlus sensor and subsequently

coated with insulating wax to allow for both AFM and STM measurements in the electrolyte with minimal leak currents. Ongoing work includes investigations of the potential-dependent structural interface organization of the electrochemical double layer on both highly oriented pyrolytic graphite (HOPG) and Au(111) electrodes in acidic media by means of (simultaneous) AFM/STM imaging and force spectroscopy.

O 20.7 Mon 18:00 P4

Phase-shifting electron holography in an environmental TEM — •ULRICH ROSS¹, JONAS LINDNER², TOBIAS MEYER², MICHAEL SEIBT¹, and CHRISTIAN JOOSS² — ¹IV. Physik Georg-August Universität Göttingen — ²IMP Georg-August Universität Göttingen

Off-axis electron holography is a phase reconstruction technique which enables access to the complex exit-wave of thin samples. Information on the phase and amplitude of the exit wave is useful in order to gain insight on nm-scale electromagnetic fields. In the field of catalyst research electrostatic surface fields are of particular interest, since the potential drop over the surface can be assumed to play a major role in the reaction mechanisms.

Conventional off-axis holography reconstruction operates via the Fourier domain. As a consequence, the accessible range of spatial frequencies is band-limited by the carrier frequency of the hologram. A trade-off is always necessary in order to optimize fringe frequency, visibility, phase-contrast transfer and instrument stability for a certain range of spatial frequencies. In contrast, we demonstrate the implementation of phase-shifting holography at sub-nm resolution combined with an advanced drift correction scheme, and successfully match the results to multislice image simulations as well as conventional defocus series. The method is added to the in-situ capabilities of a third-order aberration-corrected environmental TEM in order to investigate surface effects in catalytic platinum samples under low pressures of oxygen and water.

O 20.8 Mon 18:00 P4

Self-organized structures of peri-arylenes on electrode surfaces — •KRISTIN GRATZFELD¹, ANNA KNY¹, TOMASZ KOSMALA², RADOŚLAW WASIELEWSKI², MAREK NOWICKI², KLAUS WANDEL^{1,2}, and MORITZ SOKOŁOWSKI² — ¹Institut für Physikalische und Theoretische Chemie der Universität Bonn — ²Institute of Experimental Physics, University of Wrocław, Poland

We investigated self-ordered structures of 3,4,9,10-perylene-tetracarboxylic acid (PTCA) on the Au(111) electrode interface. In recent electrochemical studies, the protonation/ deprotonation process of PTCA was studied, however no structural data information was reported, yet [1]. To investigate the structures of PTCA at the Au(111) electrode interface we used cyclic voltammetry (CV) and electrochemical STM (EC-STM). For negatively charged surfaces, we observed stripe like phases of PTCA with an edge-on orientation of the molecules that transform into a less dense phase at more positive potential with flat-lying molecules. We suppose that this transition is correlated with a partial deprotonation of the PTCA. Acknowledgement: This work was supported by the DFG through the research training group 2591, the DAAD (Deutscher Akademischer Austauschdienst) program Ostpartnerschaften and the NAWA (National Agency for Academic Exchange) program. We thank H. Baltruschat for helpful discussions and experimental support. [1] J. Am. Chem. Soc., 138, 1493, 2016.

O 20.9 Mon 18:00 P4

DFT study of the interaction of Br and S adsorbates on the Ag(100) surface — •SÖNKE BUTTENSCHÖN and ECKHARD PEHLKE — Institut für Theoretische Physik und Astrophysik, Christian-Albrechts-Universität zu Kiel, 24098 Kiel, Germany

Adsorbate-adsorbate interactions on metal surfaces affect the adsorption and diffusion on surfaces and, in case of self-diffusion, the growth of surfaces. As

a model system, the diffusion of S adatoms on halogen-covered Cu and Ag electrodes at electrochemical interfaces has been studied by O. Magnussen and his group [1]. Prerequisite for a theoretical analysis is an accurate quantitative description of the adsorbate-adsorbate interactions of the species involved. To this end we have carried through density-functional total-energy calculations of the Br-Br and S-Br interaction on Ag(100) using the codes PWscf and PWneb from the Quantum ESPRESSO package [2]. We observe that additional contributions to the interaction energy beyond the dipole-dipole interaction [3] need to be included, which are due to electronic and elastic mechanisms [4].

[1] B. Rahn, O. M. Magnussen, ChemElectroChem 5, 3073 (2018).

[2] P. Giannozzi *et al.*, J. Phys. Condens. Matter 21, 395502 (2009), *ibid.* 29, 465901 (2017).

[3] T. Juwono *et al.*, J. Electroanal. Chem. 662, 130 (2011).

[4] K. H. Lau, W. Kohn, Surface Science 75, 69 (1978). K. H. Lau, W. Kohn, Surface Science 65, 607 (1977).

O 20.10 Mon 18:00 P4

The optical spectroscopy of InP(100) in contact with hydrochloric acid: A first-principles study — •JONGMIN KIM^{1,2}, MARGOT GUIDAT^{1,2}, MARIO LÖW¹, and MATTHIAS M. MAY^{1,2} — ¹Institute of Physical and Theoretical Chemistry, Universität Tübingen, D-72076 Tübingen, Germany — ²Institute of Theoretical Chemistry, Universität Ulm, Ulm, Germany

The III-V semiconductors, such as indium phosphide (InP), show highest solar energy conversion efficiencies, and are commonly used for a variety of applications, particularly high-performance opto-electronic devices. However, these semiconductors face fundamental challenges since they tend to corrode in aqueous electrolytes [1]. A passivation layer on their surface is the most efficient way to address this drawback. Studies have demonstrated that a system of the InP(100) in contact with hydrochloric acid exhibits high conversion efficiencies and reasonable stability. In this computational work, we investigate the interaction of InP(100) with hydrochloric acid by means of computational optical spectroscopy. Theoretically derived reflection anisotropy spectroscopy (RAS) is employed for the optical spectroscopy. According to our calculations, the RA spectra are significantly changed with probable surface geometries. A comparison of our results with experiment spectra reveals that the fully Cl-covered structure is the most reasonable surface. This verified structure can be used as a starting structure for further investigations of the InP(100)-electrolyte interface.

[1] O. Khaselev and J.A. Turner, Science 280, 425 (1998).

O 20.11 Mon 18:00 P4

Imaging and Illumination of Self-Assembled Molecules at Solid and Liquid Interfaces — •BENSU GÜNAY, •SHILPA PANCHAMI RAJ, CHRISTOPHE NACCI, and LEONHARD GRILL — University of Graz

Nanotechnological approaches for photochemical on-surface synthesis of covalently-bonded nanostructures have received recent attention at solid/air and solid/liquid interfaces. At the solid/liquid interface, there is in principle always a dynamic equilibrium between the molecules adsorbed on the surface and those still dissolved in the supernatant solution. Additionally, on-surface photochemical activation of chemical reactions provides new reaction pathways and enables the formation of long-range ordered covalent structures. The scanning tunneling microscope (STM) is a powerful tool for observing such structures at surfaces. In this study we present STM measurements under ambient pressure and at room temperature at the solid/liquid interface. In a first step for investigating photoactivated polymerisation under such conditions, 2,5-didodecyl-1,4-di-1-propenyl benzene was introduced onto a highly oriented pyrolytic graphite (HOPG) surface. We report on the self-assembled structures as well as attempts for photochemical activation using various wavelengths at room temperature.

O 21: Poster Monday: Topology and Symmetry-Protected Materials

Time: Monday 18:00–20:00

Location: P4

O 21.1 Mon 18:00 P4

Local manifestations of thickness dependent topology and axion edge state in topological magnet MnBi₂Te₄ — •FELIX LÜPKE^{1,2}, ANH PHAM², YI-FAN ZHAO³, LING-JIE ZHOU³, WENCHANG LU^{4,5}, EMIL BRIGGS⁴, JERZY BERNHOLC^{4,5}, MAREK KOLMER^{2,6}, WONHEE KO², CUI-ZU CHANG³, PANCHAPAKESAN GANESH², and AN-PING LI² — ¹Peter Grünberg Institut (PGI-3), Forschungszentrum Jülich, Germany — ²Center for Nanophase Materials Sciences, Oak Ridge National Lab, USA — ³Physics, The Pennsylvania State University, USA — ⁴Physics, North Carolina State University, USA — ⁵Computational Sciences and Engineering Division, Oak Ridge National Laboratory, Oak Ridge, Tennessee 37916, USA — ⁶Ames Laboratory, USA

The interplay of non-trivial band topology and magnetism gives rise to a series of exotic quantum phenomena, such as the emergent quantum anomalous Hall (QAH) effect. Many of these phenomena have local manifestations when the

global symmetry is broken. Here, we report local signatures of the thickness dependent topology in intrinsic magnetic topological insulator MnBi₂Te₄ (MBT), using scanning tunneling microscopy and spectroscopy on molecular beam epitaxy grown MBT thin films. A thickness-dependent band gap with an oscillatory feature is revealed, which we reproduce with theoretical calculations. At step edges, we observe localized electronic features, in agreement with topological phase transitions across the steps.

O 21.2 Mon 18:00 P4

Electronic Structure of the Weak 3D Topological Insulator Candidate Bi₁₂Rh₃Ag₆I₉ — •JOHANNES HESSDÖRFER^{1,2}, EDUARDO CARILLO-ARAVENA^{2,3}, ARMANDO CONSIGLIO^{2,4}, MICHAEL RÜCK^{2,3}, DOMENICO DI SANTE⁵, and FRIEDRICH REINERT^{1,2} — ¹Experimentelle Physik VII, Universität Würzburg, Würzburg, Germany — ²Würzburg-Dresden Cluster of Excellence ct.qmat,

Würzburg Dresden, Germany — ³Anorganische Chemie II, Technische Universität Dresden, Germany — ⁴Theoretische Physik I, Universität Würzburg, Würzburg, Germany — ⁵University of Bologna, Bologna, Italy

The electronic structure of $\text{Bi}_{12}\text{Rh}_3\text{Ag}_6\text{I}_9$, a weak topological insulator (TI) candidate, is investigated by means of angle-resolved photoelectron spectroscopy (ARPES) and density functional theory calculations. The compound consists of alternating layers of a 2D TI in a Kagome configuration, separated by insulating spacer layers. The Kagome net is formed by rhodium centered bismuth cubes, while the spacer consists of silver and iodine. The results are compared to the mother material $\text{Bi}_{14}\text{Rh}_3\text{I}_9$ [1], denoting the first experimentally observed weak TI. In particular, the influence of the silver substitution into the spacer layer and the potential modification of the coupling between the 2D TI layers is discussed.

[1] Rasche et al., *Nature Mater.*, 12, 422-425 (2013)

O 21.3 Mon 18:00 P4

Characterisation of Fe adsorbates and their effect on the local density of states on topological insulators TlBiSe_2 and Bi_2Se_3 by means of combined STM/STS and AFM — •ADRIAN WEINDL, CHRISTOPH SETESCAK, ALEXANDER LIEBIG, and FRANZ J. GIESSIBL — University of Regensburg, Germany

Can one tailor the properties of the topological surface state (TSS) of topological insulators (TIs) by magnetic doping of the TI material? Here, we study the effect of magnetic adatoms on TI surfaces by means of combined scanning tunneling microscopy (STM) and atomic force microscopy (AFM). Two archetypical TIs, Bi_2Se_3 and TlBiSe_2 , are studied, which both have relatively large band gaps with their Dirac points well isolated and far from bulk states. While the surface of Bi_2Se_3 is atomically flat, TlBiSe_2 exhibits a peculiar surface termination consisting of half a monolayer of thallium atoms sitting on top of a full selenium layer. Magnetic impurities, in this case single Fe adatoms, and their influence on the local density of states (LDOS) of the two TIs are investigated by means of scanning tunneling spectroscopy. We detect resonances in the LDOS for the Fe adatoms that arise due to the scattering of electrons in the TSS at these impurities. The position and shape of these resonances are a function of the exact adsorption position of the adatoms, which can be determined by means of atomically-resolved AFM measurements.

O 21.4 Mon 18:00 P4

Investigation of the V/TI interface by TEM and ARPES — •XIAO HOU¹, MAX VASSEN-CARL², MOHAMMED QAHOUSH¹, XIANKUI WEI³, PETER SCHÜFFELGEN², CLAUS MICHAEL SCHNEIDER¹, and LUKASZ PLUCINSKI¹ — ¹PGI-6, Forschungszentrum Jülich, Germany — ²PGI-9, Forschungszentrum Jülich, Germany — ³ERC-2, Forschungszentrum Jülich, Germany

Topological insulators (TIs) can host so-called Majorana zero modes (MZM) when proximitized with superconductors (SCs). Such a TI/SC system is a promising platform for realizing fault-tolerant quantum computers by employing braiding of the Majorana zero modes [1], in which a sharp interface between SC and TI is one of the prerequisites to realize the Majorana mode [2-3]. Here, vanadium(V) - $(\text{Bi}_{0.08}\text{Sb}_{0.92})_2\text{Te}_3$ is chosen as the SC/TI system.

We use advanced transmission electron microscopy (TEM) and angle-resolved photoemission spectroscopy (APRES) to study structural and electronic properties of the V/TI interfaces. High-resolution TEM and high-angle annular dark-field imaging provide details on crystallinity and atomic arrangements associated with various types of structural defects, while the energy-dispersive X-ray spectroscopy reveals the elemental distribution and also the interfacial interdiffusion. The band alignments between TI and V are studied using ARPES on ultrathin V films deposited on vacuum-transferred TI surfaces.

[1] B. Jäck et al. *Science* 364.6447 (2019). [2] P. Schüffelgen et al. *Journal of crystal growth* 477 (2017). [3] M. Bai et al. *Physical Review Materials* 4.9 (2020).

O 21.5 Mon 18:00 P4

Heterostructure engineering with the van der Waals topological insulator Bi_2Te_3 — M. DITTMAR^{1,2}, •E. MANTEL^{1,2}, P. KAGERER^{1,2}, C. I. FORNARI^{1,2}, H. BENTMANN^{1,2}, and F. REINERT^{1,2} — ¹Exp. Physik VII, Uni Würzburg — ²Würzburg-Dresden Cluster of Excellence ct.qmat

Recently, combining magnetism and topology has emerged as a promising research field spanning from topological insulator (TI)-superconductor interfaces to intrinsic magnetic systems [1]. In these systems exciting new phenomena such as Majorana modes are predicted to emerge. Here we present two approaches to study these promising structures.

The first focuses on the intrinsically ferromagnetic monolayer of MnBi_2Te_4 . In order to observe the predicted effects in this compound its Fermi level should be tuned inside the bulk band gap. Our approach to control the Fermi level position is to prepare a single layer of MnBi_2Te_4 on top of a p-n-junction of Sb_2Te_3 and Bi_2Te_3 grown by molecular beam epitaxy (MBE). In the second approach we investigate the preparation of thin films of the TI Bi_2Te_3 on superconductor substrates. In order to obtain more information about the crystalline structure and surface orientation, we use different characterization methods such as reflection high-energy electron diffraction, X-ray diffraction and low-energy electron diffraction. To investigate the impact on the electronic structures of these systems, angle resolved and X-ray photoemission spectroscopy are employed.

[1] M.M. Otrokov et al., *Nature* 576 (2019)

O 22: Poster Monday: Surface Structure, Epitaxy, Growth and Tribology

Time: Monday 18:00–20:00

Location: P4

O 22.1 Mon 18:00 P4

Ordering processes and phase transitions in amorphous carbon thin films induced by optical excitation — •CARL ARNE THOMANN¹, ADRIAN WITTRÖCK¹, ALEXANDRA WITTIG², FILIPE LOPES DIAS², DOMINIC STANGIER², WOLFGANG TILLMANN², and JÖRG DEBUS¹ — ¹Experimentelle Physik 2, TU Dortmund — ²Lehrstuhl für Werkstofftechnologie, TU Dortmund

Amorphous carbon is a metastable network of short-range ordered carbon atoms often used as protective coatings owing to their exceptional tribological properties. However, high temperatures in a tribological contact may cause considerable changes in the structural ordering, solid-to-solid phase transitions, and degradation of the film. In this work, we present an optical method to initiate and investigate the structural evolution including ordering processes of differently modified films. A pulsed pump laser with micrometer spot size introduces heat into the film, while a second laser probes the Raman scattering signatures. Increasing with laser power, five different stages of structural evolution are found: The first one is coined by thermally resistive amorphous carbon. It is followed by a continuous reduction in the number of lattice defects and non-sixfold aromatic rings. Further increasing pumping power induces a transition from a-C to defected graphite and eventually leads to graphite-dominant defect relaxation and an enhancement in hexagonal lattice areas. Our optical method provides a versatile tool to analyze temperature-induced structural surface changes in a controlled manner, which will improve the understanding about the conditions in tribological contacts.

O 22.2 Mon 18:00 P4

Interactions between bovine calf serum and metallic surface of hipimplant taper junctions — •ADRIAN WITTRÖCK¹, SASKIA HEERMANT¹, CHRISTIAN BECKMANN¹, MARKUS A. WIMMER², ALFONS FISCHER^{2,3}, and JÖRG DEBUS¹ — ¹Experimental Physics 2, TU Dortmund University, Dortmund, Germany — ²Department of Orthopedic Surgery, Rush University Medical Center, Chicago,

USA — ³Department Microstructure Physics and Alloy Design, Max-Planck-Institut für Eisenforschung GmbH, Düsseldorf, Germany

Within biomedical taper junctions metal surfaces interact with the human body fluid and sustain structural and chemical changes which are of particular interest from the medical and engineering point of view. To simulate the tribological contact of a hip implant taper junction, fretting tests of low-carbon CoCrMo alloys and high-nitrogen FeCrMnMoN steels are performed in bovine calf serum under different numbers of cycles. We investigate structural and chemical variations within the fretting contact by means of label-free and non-destructive Raman spectroscopy. A different absorption behavior of long-chained molecules is observed and the amide I band is shifted from 1655 cm^{-1} to about 1665 cm^{-1} , which indicates that once a protein is bound to the surface the conformation changes from α -helix to a random or β -sheet structure. A general denaturation of proteins occurs during the fretting experiment. At the heavily worn sample positions lipids are not detected, but sp^2 -hybridized amorphous carbon is sometimes measured. Our results contribute to a deeper understanding about structural and chemical properties of biomedical tribological surfaces.

O 22.3 Mon 18:00 P4

Distance dependence of local work function on Pb/Si(111) island — THOMAS SPÄTH¹, •DANIEL ROTHARDT², MANUEL SCHULZE², and REGINA HOFFMANN-VOGLE² — ¹Karlsruhe Institut Technology, D76131 Karlsruhe, Germany — ²University of Potsdam, Institute of Physics and Astronomy, Experimentelle Physik kondensierter Materie, D14469 Potsdam, Germany

In order to gain a better understanding of diffusion of Lead (Pb) islands on Si(111)-(7x7), it is extremely important to provide a complete description of the electronic properties and the forces acting on the system. Using a Scanning Force Microscope in non-contact mode with Pt coated Si-cantilever allows us to perform point bias-approach measurements at 115 K on Pb islands. We have investigated how the local work function changes as a function of tip-sample distance

and how the electrostatic force changes as a function of the applied bias between tip and sample. The resulting force was calculated from the frequency shift distance curves using Baratoﬀ's force inversion method. A significant change in the work function was found when the tip-sample distance was less than 1 nm, which could arise from the overlap of the tip wave functions and the sample wave functions.

O 22.4 Mon 18:00 P4

Epitaxial growth of gold films on elemental superconductors — •DONGFEI WANG¹, KATERINA VAXEVANI¹, JON ORTUZAR¹, STEFANO TRIVINI¹, DANILO LONGO¹, SAMUEL KERSCHBAUMER², MAXIM ILYN², CELIA ROGERO², and JOSÉ IGNACIO PASCUAL¹ — ¹CIC nanoGUNE-BRTA, 20018 Donostia-San Sebastian, Spain — ²Materials Physics Center (CSIC-UPV/EHU), San Sebastian 20018, Spain

In recent years, superconductivity proximity effect was employed in the designing of topological superconductors [1]. The basic principle in designing a topological superconductor is to introduce superconductivity, spin-orbital coupling and magnetism at the same time. Unfortunately, most of the available elemental superconductors shows less spin-orbital coupling. Gold (Au) is a material famous for its relatively large spin-orbital coupling strength. By placing Au on elemental superconductors, a superconducting system with strong spin-orbital coupling is expected [2]. In our research, Au films with different thickness were grown on elemental superconductors such as V(100) and Nb(110). The films quality were examined by STM as well as XPS technique. By placing magnetic molecules FeTPP on the surface Au/Nb(110), we demonstrate the tunability of magnetic exchange interaction between the molecule and the substrate with Yu-Shiba bound states. Moreover, great Kondo signal enhancements near the pyrolytic sites are observed.

[1] R. Lutchyn, et al., Phys. Rev. Lett. 105, 077001 (2010)

[2] A. Gupta, et al., Physical Review B 69, 104514 (2004)

O 22.5 Mon 18:00 P4

Preparation of highly pure Cu(110) surfaces — •MANUEL SEITZ, ANDREAS CHRIST, MARKUS LEISEGANG, and MATTHIAS BODE — Physikalisches Institut, Experimentelle Physik II, Universität Würzburg, Am Hubland, D-97074 Würzburg, Germany

Ballistic transport of hot charge carriers on the nanoscale becomes more and more important for the development of microelectronic components [1]. The molecular nanoprobe (MONA) technique [2] is a novel method to investigate ballistic charge transport which has already been applied to detect anisotropic transport on the Pd(110) surface [3]. For a more detailed understanding, a survey of other anisotropic fcc(110) surfaces, e.g. Cu(110), is aspired. To detect characteristics intrinsic to the Cu(110) surface, a highly clean and defect-free area of the surface is needed. However, cleaning (110) surfaces with such high purity has proven to be challenging. In this presentation, we summarize our experiences with the preparation of Cu(110) which are compared to similar experiments on Cu(111). While optimizing the preparation parameters, i.e., sputter and anneal cycles, we found a high mobility of surface atoms at room temperature on the Cu(110) surface. Furthermore, upon sputtering the Cu(111) surface, island formation is observed besides the expected vacancy islands [4].

[1] V. Sverdlov, et al., Sci. Eng. Rep. 58, 228 (2008).

[2] M. Leisegang, et al., Nano Lett. 18, 2165 (2018).

[3] M. Leisegang, et al., Phys. Rev. Lett. 126.14, 146601 (2021)

[4] T. Michely, et al., Phys. Rev. B 50.15, 11156 (1994).

O 22.6 Mon 18:00 P4

Nanotribological properties of Nitrogen doping-induced modification graphene in ultrahigh vacuum — •SHUYU HUANG^{1,2}, ANTOINE HINAUT¹, YIMING SONG¹, SEBASTIAN SCHERB¹, GEMA GNAVARRO¹, THILO GLATZEL¹, and ERNST MEYER¹ — ¹Department of Physics, University of Basel, 4056 Basel, Switzerland — ²Key Laboratory for Design and Manufacture of Micro-Nano Biomedical Instruments, School of Mechanical Engineering, Southeast University, Nanjing 211189, China

Graphene, as typical atomically-thin solid lubricant with potential applications in micro- and nano-electromechanical systems (MEMS/NEMS), has been extensively investigated on its nanotribological properties. In the present work, by using a novel experimental approach, for the first time we directly compare the frictional properties between pristine graphene and modified graphene on a single image, showing that atomic-scale friction can be significantly altered by Nitrogen doping-induced modification. Specifically, C60 nano-flakes are deposited as a mask on graphene/Ir (111) surface by thermal evaporation. The sample is then exposed to a nitrogen radical flux produced by a remote RF plasma source. After thermal annealing, to desorb C60 molecules, both nano-patterned modified graphene and pristine graphene, located below former C60 islands, surface is obtained simultaneously. By the means of high-resolution ultrahigh vacuum atomic force microscopy, the topography of surface with two different regions are characterized and discussed in non-contact mode and friction force variation is measured in contact mode.

O 22.7 Mon 18:00 P4

Investigation of indium fluctuation inside Al_{0.81}In_{0.19}N layers — •KEYAN JI¹, QIANQIAN LAN², YAN LU², MICHAEL SCHNEDLER¹, PHILIPP EBERT¹, and RAFAL E. DUNIN-BORKOWSKI² — ¹Peter Gruenberg Institut, Forschungszentrum Juelich, D-52425 Juelich, Germany — ²Ernst Ruska-Centre for Microscopy and Spectroscopy with Electrons, Forschungszentrum Juelich, D-52425 Juelich, Germany

We report on the characterization of Al_{0.81}In_{0.19}N/GaN heterostructures grown by Metalorganic Vapor Phase Epitaxy. The specimen was investigated by Electron Holography, High-angle annular dark-field (HAADF) imaging, Secondary-ion mass spectrometry, and Energy-dispersive X-ray spectroscopy. We reveal with different techniques that the Indium concentration gradually increases from 15% to the nominal value of 19% inside Al_{0.81}In_{0.19}N layers. We conduct quantitative analysis on experimental phase images from off-axis electron holography by comparing them with images calculated from the self-consistent electrostatic simulations. Our results illustrated that to accurately determine the electrostatic potential in semiconductor materials from electron holographic phase images, comprehensive knowledge of surface conditions, chemical compositions, and strains is required.

O 22.8 Mon 18:00 P4

Measuring energy dissipation on Si(111) with Lateral Force Microscopy (LFM) — •THOMAS HOLZMANN, SHINJAE NAM, OLIVER GRETZ, ALFRED JOHN WEYMOUTH, and FRANZ JOSEF GIESSBL — Universität Regensburg, Deutschland

In Lateral Force Microscopy (LFM), a cantilever is oscillated parallel to a sample surface at a set amplitude. The forces acting on such an oscillating cantilever are not necessarily conservative. The energy gain or energy loss can be position dependent, depending on the surface. We observed a strong lateral dependence of dissipation around adatoms of the 7x7-reconstruction of Si(111). We used LFM to measure this energy dissipation and applied different bias voltages between tip and sample, which changed the energy dissipation. Certain mechanisms, that contribute to energy dissipation, such as CO-bending (when using a CO-terminated tip) and chemical bonding should not be sensitive to changes in the bias voltage. Only the electrostatic part of the interaction should be influenced by a change in the bias voltage. We developed a model to simulate the energy dissipation due to electrostatic forces similar to that proposed in Ondracek et al. Nanotechnology 27, 274005 (2016). In this model, electrons tunnel to a local quantum dot on the tip or sample before diffusing to the bulk. It can predict the area where the dissipation occurs. But surprisingly the dissipation signal changes its sign, depending on which side of the quantum dot the tip is located. Following this observation we looked at possible explanations for this behaviour.

O 23: Poster Monday: Nanostructures 1

Time: Monday 18:00–20:00

Location: P4

O 23.1 Mon 18:00 P4

An Atomic Boltzmann Machine capable of Self-Adaption — BRIAN KIRALY¹, ELZE J. KNOL¹, •WERNER M.J. VAN WEERDENBURG¹, HILBERT J. KAPPEN², and ALEXANDER A. KHAJETOORIANS¹ — ¹Institute for Molecules and Materials, Radboud University Nijmegen, the Netherlands — ²Donders Institute for Neuroscience, Radboud University Nijmegen, the Netherlands

A grand challenge in creating materials with brain-like functionality is understanding multi-well systems. Such multi-well landscapes are linked to energy-based machine learning models, often based on Ising spins. However, the typi-

cal short-ranged exchange coupling of Ising spins in real materials prohibit the connectivity required for multi-well landscapes. Therefore, understanding how to create multi-well systems and link these to attractor network models is vital [1].

We present an atomic Boltzmann machine capable of self-adaption using single Co atoms on Black Phosphorus (BP). Using the concept of orbital memory in Co atoms [2], we design a tunable multi-well energy landscape by patterning atoms with atomic manipulation in a scanning tunneling microscope (STM). By electrically gating the structure with the STM tip, we allow the dynamical exploration

of its configurations. Due to the anisotropic BP, we find two different timescales that emulate a fast "neural" and a slow "synaptic" timescale. We demonstrate the self-adaptation of the synaptic weights to electrical stimuli and explore frequency-based input signals in new types of orbital memory.

[1] Kolmus et al., *New J. Phys.* 22 (2020);

[2] Kiraly et al., *Nat. Comm.* 9 (2018)

O 23.2 Mon 18:00 P4

Pulling individual polar molecular wires off of a surface — •CHRISTOPHE NACCI and LEONHARD GRILL — Department of Physical Chemistry, University of Graz, 8010 Graz, Austria

The frictional properties of individual nanostructures are strongly influenced by the reduced size and low dimensionality. Accordingly, challenging experiments are required to measure them. Probing the mechanical response of individual nanostructures on chemically different surfaces opens the possibility to explore how the static and dynamic friction depends on the interplay between structural commensurability and chemical composition. Here, we report the vertical pulling of DAD molecular wires [1] off metal surfaces by non-contact atomic force microscopy (AFM), performed under ultrahigh vacuum and at low temperatures. These are polar wires with alternating donor (D) and acceptor (A) groups incorporated in their chemical structure. The aim is to probe the mechanical response of individual molecular wires by force spectroscopy. To furthermore explore the role of structural commensurability between polymers and surface, the polar wires are grown on a variety of different surfaces, from stepped and corrugated surfaces to ultrathin insulating NaCl films on metal surfaces.

[1] C. Nacci et al., *Nature Comm.* 6, 7397 (2015)

O 23.3 Mon 18:00 P4

Efficient Sieving Performance with Carbon Nanomembranes (CNMs) — •YUBO QI, PETR DEMENTYEV, and ARMIN GÖLZHÄUSER — Bielefeld University, Bielefeld, Germany

Nanoporous membranes are promising candidates in ion transport and molecular separation; however, it is still a great challenge to achieve high permeability and selectivity. Carbon nanomembranes (CNMs) emerge as attractive materials for water purification, energy storage, and gas separation. In this work, we present facile CNMs fabrication from polycyclic aromatic hydrocarbons that are drop-cast onto arbitrary supports, including foils and metalized films. The electron-induced polymerization is shown to result in continuous sheets of various thickness, and the material is characterized by some spectroscopic and microscopic techniques. The permeation measurements with freestanding membranes reveal a high degree of porosity, and the water permeance ($\sim 10^{-4}$ mol m^{-2} s^{-1} Pa^{-1}) is four orders of magnitude higher than helium ($\sim 10^{-8}$ mol m^{-2} s^{-1} Pa^{-1}) with a membrane thickness of 3.0 nm. The ion transport properties were investigated via bias voltage applied across through CNMs. The nanomembrane showed the ability to sieve monovalent and divalent cations, selectivity of all cations follow the ordering $K^+ > Na^+ > Li^+ > Ca^{2+} > Mg^{2+}$. Functional CNMs fabricated from inexpensive precursors pave the way towards the rational design of 2D membranes for high efficient separation.

O 23.4 Mon 18:00 P4

Structure of NbO Nanocrystals on the Nb(110) Surface — •SAMUEL BERMAN¹, KUANYSH ZHUSSUPBEKOV¹, AINUR ZHUSSUPBEKOVA¹, BRIAN WALLS¹, KILLIAN WALSH¹, SERGEY I. BOZHKO^{1,2}, ANDREY IONOV², DAVID O. O'REGAN^{1,3}, and IGOR V. SHVETS¹ — ¹School of Physics and Centre for Research on Adaptive Nanostructures and Nanodevices (CRANN), Trinity College Dublin, Dublin 2, Ireland — ²Chernogolovka — ³AMBER, the SFI Research Centre for Advanced Materials and BioEngineering Research, Dublin 2, Ireland

The properties of Niobium based devices are greatly influenced by the presence of surface oxygen. The highly stable NbO(111) overlayer on the Nb(110) surface is known to host a distinctive nanocrystal structure, as observed by scanning tunnelling microscopy. However the exact structure of this surface has remained a mystery. In order to understand this surface structure, we carry out density functional theory calculations, along with scanning tunnelling microscopy/spectroscopy and X-ray/ultraviolet photoelectron spectroscopy experiments. We propose a new model, contrary to those previously proposed in the literature. The nanocrystal pattern is ascribed to a subtle reconstruction in the surface layer which locally breaks the hexagonal NbO(111) symmetry, giving rise to modulations in the local density of states. Excellent agreement is found between our model and the observed experimental data. We also investigate the underlying reasons that the surface adopts this unusual structure.

O 23.5 Mon 18:00 P4

Helium Ion Microscopy of insulating Materials using Charge Compensation — •MICHAEL WESTPHAL¹, NATALIE FRESE¹, YUBO QI¹, HIROYUKI TAKEI², PETR DEMENTYEV¹, ANDRÉ BEYER¹, and ARMIN GÖLZHÄUSER¹ — ¹Bielefeld University, Germany — ²Toyo University, Japan

Surface-sensitive imaging capabilities in nanotechnology have become increasingly important in recent years. While scanning electron microscopes (SEM) have become more powerful, they reach their limits when it comes to electri-

cally insulating samples. The accumulation of charge carriers on the sample surface can lead to severe imaging artifacts which necessitates the application of conductive coatings. Helium ion microscopes (HIM) have the possibility to stabilize electric charges by using an electron flood gun to reveal nanoscopic sample features that would otherwise be covered by a conductive coating. In this contribution, we show the benefits of charge-compensated HIM imaging over conventional SEM imaging using the examples of SARS-CoV-2 virus particles [1], carbon nanomembranes from Aromatic Precursors without Headgroups, metal coated SiO₂- and carbon micro-spheres [2]. [1] N. Frese et al., *Beilstein Journal of Nanotechnology* 12 172-179 (2021). [2] M. Wortmann et al., *Journal of Analytical and Applied Pyrolysis* Volume 161, January 2022, 105404.

O 23.6 Mon 18:00 P4

2D covalent organic frameworks from diboronic acids: the influence of the solvent — •WENBO LU, ETHAN MALONE, MIHAELA ENACHE, and MEIKE STÖHR — Zernike Institute for Advanced Materials, University of Groningen, Netherlands

Over the past years, two-dimensional (2D) covalent organic frameworks (COFs) have gained substantial interest for their use in nanopatterning, organic electronics, and as a basis for nanoreactors or molecular sieves. In particular, 2D COFs formed by polycondensation of boronic acids on surfaces have already yielded promising results [1, 2].

In this study, 2D COFs were synthesized by 1,4-benzenediboronic acid (BDBA) polycondensation on highly oriented pyrolytic graphite (HOPG) which resulted in the formation of a long-range ordered hexagonal molecular network. For the formation of the 2D COFs, a drop of BDBA solution was deposited onto HOPG, then placed in an autoclave and annealed at certain temperature. The structure and coverage of the 2D COFs was studied by scanning tunneling microscopy and atomic force microscopy under ambient conditions. In order to obtain both high quality as well as extended COFs, the influence of four solvents on the COF formation was studied. Our results provide guidance for obtaining high quality 2D COFs formed by boronic acid derivatives.

[1] S. Spitzer et al., *Chemical Communications* 53 (2017) 5147.

[2] J. F. Dienstmaier et al., *ACS Nano* 6 (2012) 7234.

O 23.7 Mon 18:00 P4

On-surface synthesis of narrow porous graphene nanoribbons — •CHRISTOPH DOBNER¹, MAMUN SARKER², ADRIAN EBERT¹, ALEXANDER SINITSKIY², and AXEL ENDERS¹ — ¹Physikalisches Institut, Universität Bayreuth, Universitätsstraße 30, 95447 Bayreuth, Germany — ²Department of Chemistry, University of Nebraska-Lincoln, Lincoln, NE68588, USA

Fueled by the technological necessity to induce semiconducting properties in graphenic nanostructures, the search for strategies to manipulate their electronic properties has become an active field of research. Common control parameters that determine the band gap of graphene nanoribbons (GNR) are structural width, edge design and heteroatom doping. It has also been theoretically predicted that periodic vacancies can open up a band gap in otherwise semimetallic 2D-graphene sheets. It is thus reasonable to expect that porosity could also contribute to the band structure of already semiconducting GNRs. In this work we present a strategy for the on-surface synthesis of porous GNRs using precursor. We will show that modified halogenation sites on the precursor molecules result in GNRs containing a periodic arrangement of vacancies along the ribbons backbones. Tunneling spectroscopy was used to determine the band edge locations and band gap width of such structures, revealing a increased band gap of 1.96 eV. Additional dI/dV mapping revealed that periodic electronic states are located at the edges and inside the backbone, induced by the porosity of the structures. Based on these findings a route towards considerably wider porous graphenic flakes will be discussed.

O 23.8 Mon 18:00 P4

Construction of a regular tessellation via bromine bond on a Ag(100) surface — •WENCHAO ZHAO, NAN CAO, BIAO YANG, and JOHANNES V BARTH — Physics Department E20, Technical University of Munich, D-85748 Garching, (Germany)

Engineering 2D surface tessellations at the molecular level attracted major interest with the development of nanoscience and technology. To this end supramolecular self-assembly exploiting tailored molecular species and programmed intermolecular interaction are widely employed. Halogen bonds are promising for potential application due to the σ -hole anisotropic charge distribution of halogen atoms 1,2,3. Herein, we address the behavior of ditopic bromine-terminated linear monomers on a Ag(100) surface at the molecular level, affording a tessellation guided by the surface symmetry. In the temperature range of 120 to 200 K, the building blocks form a porous nested grid structure stabilized by bromine bonds and molecule-substrate interactions. Two kinds of quad nodes are distinguished therein, involving a complex non-covalent bonding scheme. Interestingly, both nodes feature supramolecular chirality, entailing domains with both rectangular and trapezoid cavities. Our work introduces a new and complex surface tessellation scheme based on halogenated hydrocarbons on metal surfaces. References 1. G. Cavallo et al., *Chem. Rev.* 116, 2478-

2601 (2016). 2. Z. Han et al., *Science* 358, 206-210 (2017) 3. Mallada et al., *Science* 374, 863-867 (2021)

O 23.9 Mon 18:00 P4

Graphitic nitrogen substitution in graphene nanoribbons — •NICOLÒ BASSI¹, FEIFEI XIANG¹, PASCAL RUFFIEUX¹, AKIMITSU NARITA², KLAUS MÜLLEN², and ROMAN FASEL¹ — ¹Empa-Swiss Federal Laboratories for Materials Science and Technology, Dübendorf, Switzerland — ²Max Planck Institute for Polymer Research, 55124 Mainz, Germany

Graphene nanoribbons (GNRs), nanometer-wide strips of graphene, have attracted significant attention thanks to their tunable electronic properties originating from quantum confinement. A possible way to control these properties is through carbon substitution with heteroatoms, such as nitrogen. Despite a

large number of theoretical studies, there are few experiments where controlled N substitution has been achieved. We report the on-surface synthesis on Au of two different types of nanoribbons containing N atoms from specifically designed heteroaromatic precursors. The chemical structures of the resulting ribbons were characterized using scanning tunneling microscopy (STM) and non-contact atomic force microscopy (nc-AFM). We demonstrate the high quality ribbons growth, which involves a facile C-N bond formation at temperatures below typical C-C reactions. The electronic properties were further investigated by scanning tunneling spectroscopy (STS), which revealed unoccupied states localized on N atoms that are absent in the undoped sections. These results open new perspectives for growing and studying novel types of GNRs with the possibility to fine-tune electronic properties by controlled heteroatom substitution.

O 24: Overview Talk Yang Shao-Horn

Time: Tuesday 9:30–10:15

Location: S054

Invited Talk

O 24.1 Tue 9:30 S054

Oxygen Evolution on Rutile Ruthenium and Iridium Dioxides — •YANG SHAO-HORN — MIT, Cambridge, MA, USA

Rutile oxides have been studied intensively for water oxidation in acidic solutions. Unfortunately, atomic details of processes occurring at the electrified interface and active sites are not well understood. In this work, we combine in situ surface sensitive techniques, electrochemical mass spectrometry and density functional theory calculations to elucidate oxygen evolution reaction (OER) on ruthenium and iridium dioxides. Using synchrotron-based ambient pressure X-ray photoelectron spectroscopy and in situ surface diffraction on single crystal surfaces coupled with density functional theory calculations, we show that with increasing potential from 0.5 VRHE, adsorbed water on the coordina-

tively unsaturated sites (CUS) is successively deprotonated. Surface diffraction measurements and computation reveal what steps can be rate-limiting for OER. Such analyses are applied also to CUS sites on other surfaces as well as different IrO₂ surfaces, from which fingerprints of surface oxygen atoms are correlated with OER activity. In order to connect learnings from single-crystals with practical catalysts, electrochemical activity measurements were combined with highly sensitive electrochemical mass spectrometry to quantify the amount of evolved oxygen and reveal three Tafel regimes at different overpotentials, which was rationalized by the coverage of the reaction intermediates. In summary, by employing different experimental and theoretical techniques to model surfaces and practical catalysts, we discuss the nature of the active sites catalyzing OER on ruthenium and iridium dioxides.

O 25: Focus Session: Atomic-Scale Characterization of Correlated Ground States in Epitaxial 2D Materials

The rapid expansion of the family of two-dimensional (2D) materials led to the observation of various quantum phases with correlated ground states in the 2D limit, such as unconventional superconductivity, charge density waves, and novel magnetic phases. On the fundamental level, there are various open questions regarding the mechanisms that underlie these correlated ground states, as well as the understanding of the role of the interface and dimensionality. The epitaxial growth of 2D materials on inert substrates under ultrahigh vacuum conditions and respective in situ investigation allows direct and unambiguous comparison between experimental findings and first-principles calculations. Experimentally, scanning tunneling microscopy methods are ideal to explore the electronic structure and magnetic properties of emerging 2D quantum phases with ultimate real-space and energy resolution at ultra-low temperatures. Theoretically, the use of density functional theory calculations requires atomically well-defined unit cells to precisely predict the electronic and magnetic properties. Combining these complementary approaches helps to elucidate the role of the substrate, defects, and the coupling between quasiparticles in stacked heterostructures.

Organizers: Nadine Hauptmann (Radboud University, Nijmegen), Jeison Fischer (University of Cologne), and Wouter Jolie (University of Cologne)

Time: Tuesday 10:30–13:00

Location: H2

Topical Talk

O 25.1 Tue 10:30 H2

Designer electronic states in van der Waals heterostructures — •PETER LILJEROTH — Department of Applied Physics, Aalto University, PO Box 15100, 00076 Aalto, Finland

Van der Waals (vdW) heterostructures provide unique opportunities for engineering exotic quantum states not found in naturally occurring materials. I will highlight this approach by describing our recent results on realizing topological superconductivity [1,2] and artificial heavy fermion systems in vdW heterostructures [3]. We use molecular-beam epitaxy (MBE) and low-temperature scanning tunneling microscopy (STM) for the sample growth and characterization. Topological superconductivity can be realized by combining ferromagnetic CrBr₃ on a superconducting NbSe₂ substrate [1,2], which brings together the necessary ingredients for topological superconductivity (out of plane ferromagnetism, Rashba-type spin-orbit interactions and s-wave superconductivity). On the other hand, the building blocks of heavy fermion systems - Kondo coupling between a lattice of localized magnetic moments and mobile conduction electrons - can be mimicked in a 1T-TaS₂ / 1H-TaS₂ heterostructure. These examples highlight the versatility of vdW heterostructures in realizing quantum states that are difficult to find and control in naturally occurring materials.

[1] S. Kezilebieke et al. *Nature* 588, 424 (2020). [2] S. Kezilebieke et al. *Nano Lett.* 22, 328 (2022). [3] V. Vaňo et al. *Nature* 599, 582 (2021).

Topical Talk

O 25.2 Tue 11:00 H2

Magnetic order in a coherent Kondo lattice in the 1T/1H TaSe₂ heterostructure — WEN WAN¹, RISHAV HARSH¹, PAUL DREHER¹, SANDRA SAJAN¹, ANTONELLA MENINNO², ION ERREA², FERNANDO DE JUAN¹, and •MIGUEL UGEDA¹ — ¹Donostia International Physics Center (DIPC), Paseo Manuel de Lardizábal 4, 20018 San Sebastián, Spain — ²Centro de Física de Materiales (CSIC-UPV-EHU), Paseo Manuel de Lardizábal 5, 20018 San Sebastián, Spain

Kondo lattice systems are of fundamental importance for our understanding of quantum criticality and unconventional superconductivity. At the heart of their complexity lies the competition between the opposing forces of Kondo screening and magnetic interactions, which is revealed at very low temperatures as the moments start behaving coherently and eventually determines the fate of the ground state. While our understanding of Kondo lattices has traditionally relied on technically challenging strongly correlated bulk f-electron systems, new light is being shed on the problem thanks to heterostructures of 2D transition metal dichalcogenides, which realize a tunable Kondo lattice platform in a simple ma-

terial. Here, we study the 1T/1H-TaSe₂ heterostructure with high-resolution Scanning Tunneling Spectroscopy at 300 mK, and show a well resolved splitting of the Kondo peak, which increases monotonically in a non-linear fashion in the presence of an out-of-plane magnetic field. This behavior is unexpected for a fully screened Kondo lattice, and it originates instead from a ground state with residual magnetic order, consistent with a Kondo coupling much below the critical point in the Doniach phase diagram.

O 25.3 Tue 11:30 H2

Topological Surface State in epitaxial zz-GNRs — •M. GRUSCHWITZ¹, T.T.N. NGUYEN¹, N. DE VRIES², H. KARAKACHIAN³, J. APROJANZ¹, A.A. ZAKHAROV⁴, C. POLLEY⁴, T. BALASUBRAMANIAN⁴, U. STARKE³, C.E.J. FLIPSE², and C. TEGENKAMP¹ — ¹Technische Universität Chemnitz, Chemnitz, Germany — ²Eindhoven University of Technology, Eindhoven, The Netherlands — ³Max Planck Institute for Solid State Research, Stuttgart, Germany — ⁴MAX IV Laboratory and Lund University, Lund, Sweden

Protected and spin-polarized transport channels are the hallmark of topological insulators, coming along with an intrinsic strong spin-orbit coupling. Here we identified such corresponding chiral states in epitaxially grown zigzag graphene nanoribbons (zz-GNRs) on mesa-SiC(0001) templates, albeit with an extremely weak spin-orbit interaction. While the bulk of the monolayer zz-GNR is fully suspended across a SiC facet, the lower edge merges into the SiC(0001) substrate and reveals a surface state at the Fermi energy, which is extended along the edge and splits in energy toward the bulk. All of the spectroscopic details are precisely described within a tight binding model incorporating a Haldane term and strain effects. The concomitant breaking of time-reversal symmetry without the application of external magnetic fields is supported by ballistic transport revealing a conduction of $G = e^2/h$ [1,2].

[1] J. Baringhaus et al., Nature 506, 349 (2014)

[2] T.T.N. Nguyen et al. Nano Lett. 21, 2876 (2021)

Topical Talk

O 25.4 Tue 11:45 H2

Electronic-lattice correlations and charge order in two-dimensional materials — •TIM WEHLING — I. Institute of Theoretical Physics, Universität Hamburg, Germany

Electronic correlation phenomena in two-dimensional (2D) materials are often tightly linked to lattice degrees of freedom. Examples include superconductivity, periodic lattice distortions and charge density waves (CDWs), metal-insulator transitions, magnetic, *stripe,* or excitonic order across vastly different systems ranging from transition metal dichalcogenides to cuprate high-temperature superconductors. Here, we will address how to disentangle and eventually control the interplay of lattice and electronic degrees of freedom in 2D materials. We will discuss the concept of electron-phonon fluctuation diagnostics to identify the electronic processes behind phonon anomalies in materials like TaS₂ [1] and VS₂ [2]. We show how the coupling of low energy electrons and lattice degrees of freedom gives rise to anharmonicities and reveal an ultrastrong non-linear mode-mode coupling in VS₂.

[1] J. Berges et al., Phys. Rev. B 101, 155107 (2020).

[2] C. van Efferen et al., Nature Communications 12, 6837 (2021).

O 25.5 Tue 12:15 H2

Superconductivity of ultrathin crystalline Al films — •WERNER M.J. VAN WEERDENBURG¹, ANAND KAMLAPURE¹, NIELS P.E. VAN MULLEKOM¹, XIAOCHUN HUANG¹, MANUEL STEINBRECHER¹, PETER KROGSTROP², and ALEXANDER A. KHAJETOORIAN¹ — ¹Institute for Molecules and Materials, Radboud University Nijmegen, the Netherlands — ²Center for Quantum Devices, Niels Bohr Institute, University of Copenhagen, 2100 Copenhagen, Denmark

While bulk Al is one of the best known BCS superconductors (SC), it exhibits strange SC behavior in the thin film limit, e.g. a strong enhancement of the critical temperature T_c [1]. The transition from bulk to thin film can modulate the electronic structure and quasiparticle excitations, and the interface with the substrate becomes relevant [2]. Understanding the role of reduced dimensionality, screening and interface effects is important for SC quantum technology.

Here, we study epitaxially grown crystalline Al films on Si(111) as a function of film thickness. Using scanning tunneling microscopy / spectroscopy with temperatures down to 30 mK, we show a strong increase of both the SC gap size Δ and T_c for coverages between 4 and 35 monolayers. Remarkably, we find that Δ is threefold enhanced compared to the bulk value. We characterize the SC state of the thin films in (vector) magnetic field and find a new vortex structure.

[1] P.W. Adams et al., Phys. Rev. B 95, 094520 (2017)

[2] A. Kamlapure et al., arXiv:2109.08498 (2021)

O 25.6 Tue 12:30 H2

Realization of Pb honeycomb structures by intercalation of buffer layers on SiC(0001) — •CHITRAN GHOSAL, MARKUS GRUSCHWITZ, and CHRISTOPH TEGENKAMP — Institut für Physik, TU Chemnitz

The growth of 2D honeycomb lattices of group IV-elements has attracted a lot of interest during the last years. In contrast to graphene, the 2D analogues of Si and Ge can be stabilized on metals, while stanene and plumbene were recently prepared on compound crystals and magnetic substrates, respectively. Here we report on the intercalation of Pb using buffer layers (BL) on SiC(0001), resulting in the formation of freestanding and charge neutral graphene [1]. Depending on the bias voltage, scanning tunneling microscopy reveals complex Moiré structures, which are consistently explained in consideration of two plumbene lattices. These are rotated each by $\pm 7.5^\circ$ with respect to graphene and, thus, are commensurate with the former $6\sqrt{3} \times 6\sqrt{3}$ symmetry of the BL on SiC(0001). Locally, a (2×2) pattern becomes visible in STM and is expected since the lattice constant of plumbene is twice as large as for graphene. Local spectroscopy (STS) done at 4 K reveals an electronic gap of 30 meV and is in qualitative agreement with the band structure of low-buckeled and charge-neutral plumbene.

[1] M. Gruschwitz et al., Materials 14, 7706 (2021)

O 25.7 Tue 12:45 H2

Sn intercalation of the buffer layer/SiC(0001) interface studied by SPA-LEED and STM — •ZAMIN MAMIYEV, CHITRAN GHOSAL, and CHRISTOPH TEGENKAMP — Institut für Physik, Technische Universität Chemnitz, Chemnitz, Germany

Growth of graphene (Gr) with tailored properties and the simultaneous formation of an exotic 2D interface can be achieved by intercalation of different species below the buffer layer (BL) on SiC(0001). In this regard, Sn is interesting because of a potential Mott ground state imposed by the triangular lattice of Sn atoms at the interface and protected by the Gr layer. Therefore, we studied Sn-intercalation on BL/SiC(0001) by means of spot profile analysis low energy electron diffraction (SPA-LEED) and STM. Starting with a $6\sqrt{3} \times 6\sqrt{3}$ BL surface, we deposited monolayers of Sn at RT and annealed subsequently to higher temperatures. The formation of quasi-free standing monolayer graphene (QFMLG) is confirmed by an apparent 1×1 periodicity. Further insights for a successful decoupling of QFMLG were gained from inspecting the bell shape broadening of the diffraction spots, which is characteristic of weakly coupled 2D systems on surfaces. By further optimization of the post-intercalation treatment, a Sn-induced $\sqrt{3} \times \sqrt{3}$ reconstruction at the interface was achieved. Moreover, detailed studies showed a simultaneous transformation of $6\sqrt{3} \times 6\sqrt{3}$ periodicity into a $(\sqrt{39} \times \sqrt{39})R16.1^\circ$ reconstruction with corresponding domains. Interestingly, the new periodicities formed by the intercalant atoms are triggered by the former symmetry of the BL structure.

O 26: Surface Magnetism

Time: Tuesday 10:30–12:45

Location: H4

O 26.1 Tue 10:30 H4

Investigation of bubble domains in Fe₃GeTe₂ by spin-polarized scanning tunneling microscopy — •NAMRATA BANSAL¹, HUNG-HSIANG YANG¹, PHILIPP RUESSMANN², MARKUS HOFFMANN², LICHUAN ZHANG², DONGWOOK GO², AMIR-ABBAS HAGHIGHIRAD³, KAUSHIK SEN³, MATTHIEU LE TACON³, YURIY MOKROUSOV², and WULF WULFHEKEL¹ — ¹Physikalisches Institut, Karlsruhe Institute of Technology, 76131 Karlsruhe, Germany — ²Peter Gruenberg Institut (PGI-1) and Institute for Advanced Simulation (IAS-1) Forschungszentrum Juelich GmbH, D-52425 Juelich — ³Institute for Quantum Materials and Technologies, Karlsruhe Institute of Technology, 76131 Karlsruhe, Germany

We investigated the magnetic structure of the van der Waal material, Fe₃GeTe₂ (FGT), using a home-built low temperature (0.7 K) spin-polarized scanning tunneling microscope (SP-STM). Out-of-plane magnetic imaging with chromium-coated tungsten tip reveals bubble domains in FGT. When applying out-of-plane

magnetic fields, the domain shape transitioned from elliptical to circular and collapsed at around 0.32 T. We observed an inverse relation between the size of the bubble domains and the magnetic fields. Benefiting from the spatial resolution of the SP-STM, the domain wall widths were determined, which contains information about the exchange stiffness and the anisotropy constant of FGT.

O 26.2 Tue 10:45 H4

Magnetization switching on self-assembled structure of alpha-helix-polyalanine molecules observed by ambient STM — •NGUYEN T. N. HA¹, L. RASABATHINA², O. HELWIG², A. SHARMA³, G. SALVAN³, S. YOCHELIS⁴, Y. PALTIEL⁴, and C. TEGENKAMP¹ — ¹Solid Surface Analysis, Technische Universität Chemnitz, Germany — ²Functional Magnetic Materials, Technische Universität Chemnitz, Germany — ³Semiconductor Physics, Technische Universität Chemnitz, Germany — ⁴Department of Applied Physics, Hebrew University of Jerusalem, Israel

Polyalanine (PA) with an alpha-helix conformation has gathered recently a lot of interest as the propagation of electrons along the helical backbone structure comes along with spin polarization of the transmitted electron. The magnetization switching on self-assembly of PA molecules on Au(111)/Co/Au/Pt/Al₂O₃ substrate by an external magnetic field resulting the preferentially transmitted electrons depending on molecule's specific handedness and the direction of magnetization. The transmission of the electrons through this structure comes along with an quite high efficient spin polarization. The tip-sample distance variation due to magnetization switching on PA films has shown the jumping states between up and down magnetic direction, while on the bare substrate without PA film the stable tip-sample distance was observed. This observation is further confirmed the spin filter behavior of PA film on a magnetic substrate due to CISS effect at nanoscale.[1]N.T.N.Ha et al, J. Phys. Chem. C,124,10,5734-5739,2020.

O 26.3 Tue 11:00 H4

Inelastic Electron Tunneling through Nanomagnetic Structures — •DARIA MEDVEDEVA and JINDRICH KOLORENC — Institute of Physics (FZU), Czech Academy of Sciences

Inelastic electron tunneling spectroscopy (IETS) is a well-established technique used for investigation of vibrational spectra and, more recently, also for characterization of spin excitations in nanosystems probed in scanning tunneling microscopes (STM). If a magnetic molecule is attached to the STM tip, the possibilities of the probe are expanded [1], for instance, one can observe how excitations in the molecule are modified by exchange interactions with the magnetic nanosystem adsorbed on a surface. We use an in-house implementation of co-tunneling theory [2] to model IETS spectra of an STM tip decorated with nickelocene molecule (having spin 1) probing magnetic atoms with spins 3/2 and 2 subject to easy-axis anisotropy of varied direction. Experimentally, these situations were recently realized in an Fe adatom on Cu(100) [1] and in metal-organic chains, incorporating Co and Cr atoms, placed on Au(111) [3]. We discuss how accurate the theory is in reproducing the measured inelastic spectra, how the spectra depend on the direction of the magnetic anisotropy, and how important the appropriate alignment of the anisotropies of the probing molecule and the other spin is for efficient spin sensing.

* e-mail: medvedeva@fzu.cz, kolorenc@fzu.cz

[1] B. Verlhac *et al.*, Science **366**, 623 (2019); [2] F. Delgado and J. Fernández-Rossier, Phys. Rev. B **84**, 045439 (2011); [3] Ch. Wäckerlin *et al.*, to be submitted (2022).

O 26.4 Tue 11:15 H4

Magnetocrystalline anisotropy in two-dimensional EuAu₂ and GdAu₂: the role of band structure — •MARIA BLANCO-REY^{1,2}, RODRIGO CASTRILLO-BODERO³, KHADIZA ALI^{2,3}, POLINA SHEVERDYAEVA⁴, ENRIQUE ORTEGA^{1,3,2}, LAURA FERNANDEZ³, and FREDERIK SCHILLER^{3,2} — ¹Universidad del País Vasco UPV/EHU, Spain — ²Donostia International Physics Center, Spain — ³Centro de Física de Materiales CSIC-UPV/EHU-MPC, Donostia-San Sebastián, Spain — ⁴Instituto di Struttura della Materia ISM-CNR, Trieste, Italy

In rare earth (RE) intermetallic crystals, the magnetocrystalline anisotropy has a single-ion contribution from the *f* shell, often associated with a large orbital quantum number *L*, and an itinerant one, due to spin-orbit coupling effects in the band structure. As Eu and Gd are 4*f*⁷ RE atoms, *L* in 2D atom-thick EuAu₂ and GdAu₂ is essentially quenched. Therefore, these systems allow us to isolate the itinerant electron contribution in this 2D compound family. X-ray magnetic circular dichroism shows out-of-plane anisotropy in EuAu₂, in contrast to in-plane in GdAu₂. By means of angle-resolved photoemission and density-functional theory, we explain these behaviours in terms of the occupation of the spin-orbit-split dispersive RE(*d*)-Au(*s*) hybrid bands, which is ultimately dictated by the RE valence state (Eu²⁺ and Gd³⁺). In terms of energy, the itinerant electron contribution is ≈ 1 meV per unit cell, which may eventually compete with the single-ion contribution.

O 26.5 Tue 11:30 H4

Magnetic Domain Structures of Gd(0001)/W(110) Films — •PATRICK HAERTL, MARKUS LEISEGANG, and MATTHIAS BODE — Physikalisches Institut, Experimentelle Physik II, Universität Würzburg, Am Hubland, D-97074 Würzburg, Germany

Rare earth metal films are known to exhibit an extremely rich magnetic behavior. Depending on the sign of the RKKY coupling and details of the film preparation various domain structures have been observed, for example on Dy(0001)/W(110) films [1]. Here we report on experiments on Gadolinium (Gd) films epitaxially grown on W(110). Gd is a ferromagnetic metal with a Curie temperature of 293 K. Its half-filled 4*f* shell results in an almost spherical charge distribution which –in comparison to other rare earth metals– results in a very low magnetic anisotropy [2]. Our investigation on Gd(0001) films grown on W(110) indeed show a rather rich magnetic structure in spin-polarized STM studies. In agreement with earlier Kerr measurements [2], we find a thickness-dependent spin reorientation transition from in-plane at thin films to out-of-plane for films thicker than around 40 nm. The latter form up and down magnetized stripe domains which are tilted by ±30° with respect to the W[001] direction. With increasing coverage their periodicity increases from (50 ± 10) nm

up to (120 ± 40) nm and domain branching is observed. We will discuss the energetics of transition of the magnetic structure.

[1] L. Berbil-Bautista *et al.*, Phys. Rev. B **76**, 064411 (2007).

[2] A. Berger *et al.*, Phys. Rev. B **52**, 1078 (1995).

[3] P. Härtl *et al.*, Phys. Rev. B **105**, 174431 (2022).

O 26.6 Tue 11:45 H4

Tuning the electron spin-polarization via tunneling through image states — MACIEJ BAZARNIK^{1,2} and ANIKA SCHLENHOFF² — ¹Institute of Physics, Poznan University of Technology, Poland — ²Department of Physics, University of Hamburg, Germany

Image-potential states (IS) are unoccupied electronic states in front of polarizable surfaces. Towards step edges, IS energy bands bend [1], leading to laterally localized IS at the rim of nanoislands [2]. Our spin-resolved scanning tunneling microscopy (SP-STM) and spectroscopy experiments on nanomagnets reveal a spin-polarization of the IS rim state, causing a spatial modulation of the electron spin-polarization above uniformly magnetized nanoislands. An inversion of the electron spin-polarization is found at specific energies. When the electrons relax from the IS into the surface, a spin-transfer torque (STT) is exerted on the sample [3]. We show that according to the IS-induced inversion of the electron spin-polarization, the STT also changes its sign. Our findings indicate that the IS in front of the surface serves as a spin-filter that can tailor the spin-polarization of the resonant tunneling current. The existence of the rim state and its impact on the electron spin-polarization is expected at the step edge of any magnetic adlayer-substrate system. Hence, nanostructuring a magnetic surface enables tuning the local spin-polarization and thus tailoring the STT for current-induced magnetization switching.

[1] J.-F. Ge *et al.*, Phys. Rev. B **101**, 035152 (2020)

[2] S. Stepanow *et al.*, Phys. Rev. B **83**, 115101 (2011).

[3] A. Schlenhoff *et al.*, Phys. Rev. Lett. **109**, 097602 (2012).

O 26.7 Tue 12:00 H4

Circular dichroic UV-PEEM measurements of magnetic surfaces: From Magnetic Domain Imaging to Magnetoplasmonics — •MAXIMILIAN PALESCHKE and WOLF WIDRA — Martin-Luther-Universität Halle-Wittenberg, Halle (Saale), Germany

Over the last decades, the rapid progress in the ultrafast optical manipulation of magnetic materials has opened the development of several new methods for the investigation and control of spin and magnetization dynamics. Here, we investigate magnetic thin films and nanostructures on nanometer-femtosecond scales with a newly-designed experimental setup. We combine state-of-the-art time-resolved photoemission electron microscopy (PEEM) with circular dichroism imaging and normal incidence excitation via a tunable femtosecond fiber laser system.

In this talk, we report on two dichroism imaging techniques, namely magnetic circular dichroism (MCD) and the recently discovered plasmonic dichroism. The first is used to image magnetic in-plane and out-of-plane domains of ferromagnetic surfaces. The second was successfully used to image propagating surface plasmon polaritons (SPPs) on a ferromagnetic material in threshold photoemission for the first time [1]. With this, we show clear edge-induced SPPs with sub-micrometer wavelength and propagation length of about 3.5 μm on polycrystalline Ni₈₀Fe₂₀ microstructures. This finding extends experimental investigation of SPPs to materials with high plasma frequency and large damping.

[1] M. Paleschke *et al.*, New J. Phys. **23**, 093006 (2021)

O 26.8 Tue 12:15 H4

Chirality-induced electron spin polarization in chiral CuO and CoO_x catalyst surfaces — •PAUL VALERIAN MÖLLERS¹, JIMENG WEI², SUPRIYA GHOSH², SOMA SALAMON³, MANFRED BARTSCH¹, HEIKO WENDE³, DAVID WALDECK², and HELMUT ZACHARIAS¹ — ¹Center for Soft Nanoscience, WWU Münster, Germany — ²Department of Chemistry, University of Pittsburgh, Pittsburgh, USA — ³Faculty of Physics and Center for NanoIntegration Duisburg-Essen, Universität Duisburg-Essen, Germany

Spin-polarized catalytic surfaces can greatly enhance the selectivity of chemical reactions, e.g., in a photoinduced water splitting process. Here, we confirm that spin-polarized (photo)currents can be obtained from chiral cupric oxide¹ (CuO) and cobalt oxide² (CoO_x), and explore the underlying mechanism. Chiral oxide thin films were deposited using a method pioneered by Switzer *et al.*³ Photoelectrons were excited with deep-UV laser pulses and their average spin polarization (SP) was measured. For CuO thin films, correlating the SP values with electron energy spectra reveals that the measured SP values can be rationalized assuming an intrinsic SP in the chiral oxide layer and a chirality-induced spin selectivity (CISS)-related spin filtering of the electrons. On chiral CoO_x layers, the SP was found to depend on the Co oxidation state, which allows for reversible switching of the preferred spin orientation. The results support efforts towards a rational design of further spin-selective catalytic oxide materials.

¹ J. Phys. Chem. C **123**, 3024 (2019) ² J. Phys. Chem. C **124**, 22610 (2020) ³ Chem. Mater. **16**, 4232 (2004)

O 26.9 Tue 12:30 H4

A spin-polarized STM investigation of 3 AL Mn films on W(001) — •PAULA M. WEBER, JING QI, and MATTHIAS BODE — Physikalisches Institut, Experimentelle Physik II, Julius-Maximilians-Universität Würzburg, Germany
Spin spirals and dead magnetic layers in the antiferromagnetic transition metal Mn on the heavy bcc(001) surface of W have recently attracted considerable interest [1,2]. In this talk, we present a spin-polarized STM investigation of 2-4 atomic layer (AL) thick Mn films on W(001). For 3 AL Mn on W(001) it has been theoretically proposed that this system grows pseudomorphically while exhibiting an antiferromagnetic state [3]. Our topographic STM data confirm that

pseudomorphic growth even prevails up to a Mn film thickness of 4 AL. Spin-resolved data were acquired with W tips which had been magnetized on Mn layers by *in-situ* treatment on Mn/W(001). This allowed us to collect topographic and spin-resolved data on the same scanning area. Applying this method, we identify a magnetic zig-zag $2\sqrt{2} \times \sqrt{2}$ structure on 3 AL Mn and a strongly bias-dependent labyrinth overlay structure on 4 AL. Potential spin structures will be discussed.

[1] Ferriani *et al.*, Phys. Rev. Letters **101**, 027201 (2008).[2] Meyer *et al.*, Phys. Rev. Research **2**, 012075 (2020).[3] Dennler *et al.*, Phys. Rev. B **72**, 214413 (2005).

O 27: Electron-Driven Processes

Time: Tuesday 10:30–11:45

Location: H6

O 27.1 Tue 10:30 H6

Surprisingly fast adsorbate excitation: CO/Ru(0001) probed with X-ray absorption spectroscopy — •ELIAS DIESEN¹, HSIN-YI WANG², JOHANNES VOSS¹, ALAN C. LUNTZ¹, and ANDERS NILSSON² — ¹SUNCAT Center for Interface Science and Catalysis, SLAC National Accelerator Laboratory, Menlo Park, California, USA — ²Stockholm University, Sweden

Energy transfer between substrate excitations and adsorbate motion plays an essential role in determining chemical reactivity and selectivity on surfaces. Femtosecond pump-probe experiments, using an X-ray probe pulse from a free electron laser, give unique insights into such processes due to the short pulse duration and species-selective probing. We measure the time evolution of the C K-edge X-ray absorption spectrum from CO/Ru(0001) after excitation by a femtosecond high-intensity optical laser pulse, and use detailed spectrum simulations to distinguish excitations of different modes [1]. We find high excitation of the CO internal stretch and frustrated rotation modes within 200 fs of laser excitation - one order of magnitude faster than theoretical predictions. Consequences for our understanding of ultrafast adsorbate excitation will be discussed.

[1] Diesen *et al.*, Phys. Rev. Lett. **127**, 016802 (2021)

O 27.2 Tue 10:45 H6

Are vacancies in field ion microscopy artefacts? A DFT study — •SHYAM KATNAGALLU, JÖRG NÜEGEBAUER, and CHRISTOPH FREYSOLDT — Department of computational materials design, Max Planck Institut für Eisenforschung GmbH, Max-Planck-Str. 1, 40237, Düsseldorf, Germany.

Resolving the atomic structure of engineering materials in 3D continues to be an extensive research field. Field ion microscopy under evaporating conditions (3D-FIM) is one of the few techniques capable of delivering such atomic-scale information, allowing to even image vacancies and their interactions with solute atoms in alloys. However, the quantification of the observed vacancies and their origins are still a matter of debate. It was suggested that high electric fields (1-10 V/Å) used in FIM could introduce artefact vacancies. To investigate the possibility of this mechanism, we used density functional theory (DFT) simulations. Stepped Ni surfaces with kinks were modelled in the repeated slab approach with a (971) surface orientation. A field of up to 4 V/Å was introduced on one side of the slab using the generalized dipole correction. Contrary to conventional wisdom, we show that the reaction barrier to form vacancies on the electrified metal surface increases compared to the field-free case. We also find that the electric field can introduce kinetic barriers to a potential "vacancy-killing" mechanism. We compare these findings with field evaporation models proposed in the literature.

O 27.3 Tue 11:00 H6

Modeling electron beam damage in Gold nanoparticles and MoS₂ — •CUAUHTEMOC NÚÑEZ VALENCIA¹, MATTHEW HELMI LETH LARSEN¹, WILLIAM B. LOMHOLDT², PEI LIU², DANIEL KELLY², THOMAS W. HANSEN², and JAKOB SCHIØTZ¹ — ¹DTU Physics, Technical University of Denmark, Kgs. Lyngby, Denmark — ²DTU Nanolab, Technical University of Denmark, Kgs. Lyngby, Denmark

Beam damage in High-Resolution Transmission Electron Microscopy (HRTEM) is poorly understood theoretically, and not yet well described phenomenologically. The interaction between the specimen and the electron beam changes significantly depending on the material: semiconductors (like MoS₂) and metals (like Gold) have different lifetime excitations and beam damage can be triggered in different mechanism.

In this study, we investigate the beam damage in MoS₂ and Gold nanoparticles simulating the macroscopic timescale with a Kinetic Monte Carlo like algorithm, using different approaches: long Molecular Dynamics (MD) simulations for Gold and statistical model using different threshold energy (T_D) values for MoS₂ considering the thermal vibrations.

The second approach for modeling the beam damage in MoS₂ was through ab Initio Molecular dynamics the calculation of the threshold energies for the different scenarios. Where a Kinetic Monte Carlo simulation was implemented for study the dynamics of the defect production and the beam damage for MoS₂. Also, we studied the effect in the T_D when we remove or add electrons to the MoS₂.

O 27.4 Tue 11:15 H6

Electron-driven mobility of the hydrogen-bonded ammonia clusters — •PRASHANT SRIVASTAVA¹, DANIEL MILLER², and KARINA MORGENSTERN³ — ¹Chair of physical chemistry-I, Ruhr University Bochum, Germany — ²Department of Chemistry, Hofstra University, 106 Berliner Hall, Hempstead, New York 11549, United States — ³Chair of physical chemistry-I, Ruhr University Bochum, Germany

Electron-driven processes in polar solvents are of great interest to study, e.g., electron solvation in ammonia plays a vital role in ozone layer depletion. We study the impact of electrons on the ammonia clusters adsorbed on a copper surface using a combination of low-temperature scanning tunneling microscopy, femtosecond laser pulses, and ab-initio calculations. Photo-injected electrons from the copper surface lead to diffusion or desorption of the second layer of the clusters. Upward mass transport (UMT) and downward mass transport (DMT) also play an important role in modifying the hydrogen-bonded network of these clusters. Theoretical calculations confirm electron solvation into the second layer. We present a molecular-scale insight into the interactions of photo-injected electrons with the ammonia clusters in the second layer. Our results show that this interaction can modify an ammonia cluster and enhance its mobility.

O 27.5 Tue 11:30 H6

Distribution of Charge and Lattice Defects via Machine Learning. — VIKTOR BIRSCHITZKY¹, MICHAEL PREZZI¹, MARCO CORRIAS¹, LORENZO PAPA¹, IGOR SOKOLOVIC², ALEXANDER GORFER¹, MARTIN SETVIN^{2,3}, MICHAEL SCHMID², ULRIKE DIEBOLD², CESARE FRANCHINI^{1,4}, and •MICHELE RETICCIOLI¹ — ¹University of Vienna (Austria) — ²Institute of Applied Physics, TU Wien (Austria) — ³Charles University, Prague (Czech Republic) — ⁴University of Bologna (Italy)

Lattice defects and localized charge on oxide surfaces impact the properties of the material to a different degree depending on their spatial distribution. However, the high number of possible defect configurations poses practical challenges to first-principles studies. Here, we propose a machine-learning-accelerated approach to explore in the framework of density functional theory the spatial configurations of charge and lattice point defects. We apply this approach to analyze the distribution of surface oxygen vacancies on rutile TiO₂(110). The attractive interaction with small polarons (electrons localized on the Ti atoms) are revealed to weaken the repulsion between oxygen vacancies, favoring particular arrangements of the vacancies. The resulting distribution can be compared with the patterns identified by computer vision algorithms on scanning-probe microscopy images.

O 28: Organic Molecules at Surfaces 3: Theory

Time: Tuesday 10:30–12:45

Location: S051

O 28.1 Tue 10:30 S051

Switchable interfaces based on bistable molecules: tetrachloropyrazine on Pt(111) — •LUKAS HÖRMANN, ANDREAS JEINDL, and OLIVER T. HOFMANN — Institute of Solid State Physics, NAWI Graz, Graz University of Technology, Petersgasse 16, 8010 Graz, Austria

Organic/inorganic interfaces govern the properties of many organic electronic devices. To imbue devices with additional functionality, it would be useful to make these interface properties reversibly switchable by means of easily accessible external parameters, such as the temperature.

In this work, we realize such a switchable interface with tetrachloropyrazine (TCP) on Pt(111). TCP can either chemisorb or physisorb on the Pt(111) surface, forming a double-well potential with strongly differing adsorption geometries. These allow forming diverse interface structures with notably different work functions and coherent fractions (obtained by X-ray standing wave measurements).

We model this switchable interface using a machine learning algorithm, based on Gaussian process regression. This facilitates structure search for commensurate as well as higher-order commensurate adlayers. We find three different classes of interface structures with varying work functions and coherent fractions and demonstrate that external stimuli, such as temperature and pressure, allow to reversibly shift between these different classes. Based on our insights, we discuss how systems need to be constructed so that the switch between different states leads to an even larger change in their properties.

O 28.2 Tue 10:45 S051

Substrate enhanced Jahn-Teller effect in single molecule junctions — •MORITZ FRANKERL¹, LAERTE PATERA^{2,3}, THOMAS FREDERIKSEN⁴, JASCHA REPP³, and ANDREA DONARINI¹ — ¹Institute for Theoretical Physics, University of Regensburg — ²Catalysis Research Center, Technical University of Munich — ³Institute of Experimental and Applied Physics, University of Regensburg — ⁴Donostia International Physics Center (DIPC), Spain

The stabilization of several charge states of single molecules deposited on non-conductive NaCl films [1] allows to map out the electronic transition between different charge states by means of single-electron alternate-charging scanning tunneling microscopy [2]. Copper-phthalocyanine (CuPc) revealed a Jahn-Teller splitting (JTS) of its doubly degenerate LUMOs upon charging and, more surprisingly, the occupation of the same LUMO for both electrons upon double charging. We show by DFT calculations complemented by a group-theoretical analysis how the JTS for CuPc in gas phase is not sufficient to explain this behavior. We propose, instead, a cooperation between molecule and substrate deformation which enhances the strength of the JT coupling. The result is based on a microscopic model of the electron-phonon coupling between the molecule and the underlying thick layer of NaCl. The magnitude of the obtained substrate-induced JTS highlights the impact of the substrate on the electronic configuration of charged molecules, far beyond the mere charge stabilization. [1] Fatayer S. et al., Nature Nanotechnology 13, 376-380(2018) [2] Patera L.L. et al., Nature 566, 245-248(2019)

O 28.3 Tue 11:00 S051

Impact of electron-phonon interaction on metal-organic interface states — •LUKAS ESCHMANN, JAN NEUENDORF, and MICHAEL RÖHLFING — Institut für Festkörpertheorie, Westfälische Wilhelms-Universität Münster, 48149 Münster, Germany

We discuss electron phonon interaction (EPI) in the context of metal-organic adsorbate systems and the occurring nearly-free electron-like interface states (IS) whose energy E is strongly coupled to the vertical binding distance d with a coupling strength of $\lambda = \Delta E/\Delta d$ that is in the order of 1 eV/Å for several adsorbate systems.

We present an EPI model that is based on ab-initio data and uses the nearly-free electron-like character of the IS to obtain an analytic expression for the temperature induced renormalization of the latter^{1,2}. We find that the energy shift is dominated by the coupling to the out-of-plane phonon modes that change the average binding distance and scales quadratically with the coupling strength, i.e., $\sim \lambda^2$. Applied to the system of a NTCD layer adsorbed on Ag(111), our model predicts a renormalization of the IS onset energy through quantum mechanical coupling with the adsorbate phonons by -10 meV per 100 K. With this, we are able to explain the discrepancy between a classical lifting-effect and the experiment, thus revealing the important impact of EPI on spectroscopic states at metal-organic internal interfaces.

¹Eschmann, et al., Phys.Rev.B 104, L241102 (2021).²Eschmann, et al., Phys.Rev.B 104, 245403 (2021).

O 28.4 Tue 11:15 S051

X-ray spectroscopic fingerprints of chemical bonding at molecule-metal interfaces revealed by first-principles core-level simulation — •SAMUEL J. HALL¹, BENEDIKT P. KLEIN^{1,2}, and REINHARD J. MAURER¹ — ¹Department of Chemistry, University of Warwick, Coventry, UK — ²Diamond Light Source, Harwell Science and Innovation Campus, Didcot, UK

Characterisation of the chemical environment and electronic structure of organic materials and metal-organic interfaces can be carried out with x-ray photoelectron spectroscopy (XPS) and near-edge x-ray absorption fine structure (NEXAFS) spectroscopy. The adsorption of molecules onto surfaces has been shown to change various spectral features which have previously been connected to changes in chemical bonding and charge distribution. However, these can be difficult to interpret due to overlapping features of multiple species and widely broadened spectra. Through the use of density functional theory (DFT) calculations we study two molecular isomers, azulene and naphthalene, adsorbed onto three metal (111) surfaces of silver, copper, and platinum. Categorised into three regimes of molecule-metal chemical bonding, we connect the changes seen in the spectra to the chemical bonding behaviour and decompose the signatures into initial core-state and final valence-state contributions. We analyse the effect of charge transfer, electronic hybridisation and dispersion effects, and aim to provide guidance for experimental spectral analysis.

O 28.5 Tue 11:30 S051

The sensitivity of NMR chemical shifts to organic/inorganic interfaces — •VIVIANA PICCINI¹, EMMANOUIL VEROUTIS², KARSTEN REUTER¹, JOSEF GRANWEHR², and CHRISTOPH SCHEURER¹ — ¹Fritz Haber Institute of the Max Planck Society, Berlin — ²Forschungszentrum Jülich, IEK-9, Jülich

Composite polymer/ceramic solid electrolytes are promising materials for Li-ion batteries due to their high stability and safety. Yet, their organic/inorganic interface is believed to hinder the ionic conduction. NMR experiments on a poly(ethylene oxide)/Li_{1.5}Al_{0.5}Ti_{1.5}(PO₄)₃ electrolyte have shown that Li ions cross the interface on a timescale of seconds. To remedy the problem, mechanistic insights are required, but even the polymer/ceramic interface structure is unknown.

We therefore investigate representative potential binding situations between the two materials by computing the NMR shielding tensors, in order to verify whether there is a significant change in the chemical shifts depending on the interface structure. Due to the high computational cost, a simplified model exhibiting the same local chemical interactions is constructed, composed by an AlPO₄ slab and ethane-1,2-diol. NMR measurements on an AlPO₄/methanol system have also been carried out.

While the computed NMR properties are sensitive to changes in the interface structure, experiments reveal no chemical shifts variations in the ¹H NMR methanol/AlPO₄ spectra relative to neat methanol. This can be ascribed to the presence of surface water in AlPO₄, which would leave no available binding sites for methanol/AlPO₄ interactions.

O 28.6 Tue 11:45 S051

Classifying Chiral Structure by a Convolutional Neural Network — •PEER KASTEN¹, MANDY STRITZKE², JOHANNES TIM SEIFERT¹, Björn MÖLLER³, TIMO DE WOLFF², TIM FINGSCHIEDT³, and UTA SCHLICKUM¹ — ¹Institut für Angewandte Physik, Technische Universität Braunschweig — ²Institut für Analysis und Algebra, Technische Universität Braunschweig — ³Institut für Nachrichtentechnik, Technische Universität Braunschweig

Scanning tunneling microscopy (STM) is an important tool to image surfaces at atomic scale. To examine structures of molecules in STM images can be a difficult and time-consuming task. We present a method to recognize chirality within experimentally observed self-assembled molecular structures using the convolutional neural network (CNN) based object detection framework Faster R-CNN. Thereby we can classify unit cells in the image towards one of both chiral structures.

To train the neural network, a sufficient amount of correctly labeled images is necessary. To obtain such data and labels, we utilize a method to create realistic-looking, synthetic STM images in varying zoom-sizes containing lifelike properties such as noise and step edges along with corresponding labels.

Using this synthetic data, we trained a model capable of classifying synthetic images at sizes ranging from 8 nm to 100 nm with high performance. Evaluations of the CNN's predictions for real images show that this network trained on synthetic data can generalize towards inference on real images.

O 28.7 Tue 12:00 S051

Energy landscaping with external electric fields: Selective stabilization of interface polymorphs — JOHANNES CARTUS, ANDREAS JEINDL, •ANNA WERKOVITS, and OLIVER HOFMANN — Graz University of Technology, Graz, Austria

The polymorphs that inorganic/organic interfaces assume can have drastic consequences for the interface properties (such as, e.g., the work function). It is, therefore, of great relevance for applications in organic electronics to achieve precise control of the interface polymorphism. The stability of the respective polymorphs is determined by deposition conditions (e.g., temperature and pressure). In this contribution we investigate electric fields as an additional handle for better control over the polymorphism, thus selectively stabilizing polymorphs at conditions where they were previously inaccessible.

Using density functional theory calculations augmented by a smart-data machine learning approach (SAMPLE) we demonstrate how electric fields can be used to foster desired or even previously unseen polymorphs. Tetracyanoethylene (TCNE) on Cu(111) is an ideal test system because its work function can change by more than 3 eV for different polymorphs.

O 28.8 Tue 12:15 S051

Interlayer orbital overlap governing thin-film geometry: the role of interfacial charge transfer — •FABIO CALCINELLI, ANDREAS JEINDL, LUKAS HÖRMANN, and OLIVER HOFMANN — Institute of Solid State Physics, NAWI Graz, Graz University of Technology, Petersgasse 16, 8010 Graz, Austria

Organic thin films exhibit a large structural variability, and the substrate on which they grow has a relevant influence on their polymorphism. Predicting which structure a thin film will assume on a substrate is impossible through traditional first-principle modeling alone, because of the combinatorial explosion in the number of possible polymorphs. However, recent developments in machine-learning assisted structure search have made structure-to-property investigations accessible. Employing smart-data machine learning, we demonstrate the impact that different substrates can have on the geometry of the first two layers of a thin film. We identify the energetically most favourable geometries for ben-

zoquinone on silver and on graphene, and compare their electronic properties. While the polymorphs formed in the first layer of benzoquinone are very similar, for the second layer we find two significantly different structures. We explain this difference as an effect of the interplay between different charge transfer on the two substrates, and different interlayer orbital overlap for the two structures. Furthermore, we investigate the systematic impact of interlayer orbital overlap in defining the most stable polymorphs for different charge transfers.

O 28.9 Tue 12:30 S051

Polymorph trapping by optimized deposition conditions: A first-principles prediction for TCNE/Cu(111) — •ANNA WERKOVITS, ANDREAS JEINDL, LUKAS HÖRMANN, JOHANNES J. CARTUS, and OLIVER T. HOFMANN — Institute of Solid State Physics, NAWI Graz, Graz University of Technology, Petersgasse 16, 8010 Graz, Austria

Physical properties of small-molecule organic semiconductors are strongly determined by their polymorphs. Depending on the orientation in which molecules adsorb on the substrate, properties can significantly vary, as is the case, e.g. for tetracyanoethylene (TCNE) on Cu(111).

We propose conditions under which TCNE remains in the energetically less favorable lying position also for higher coverages. This requires fulfilling two prerequisites: To enable ordered growth, the temperature must be high enough to allow for sufficient diffusion of lying molecules, whereas the temperature must be low enough to inhibit the reorientation to the upright-standing position.

In this work, we utilize the nudged elastic band method and density functional theory to compute energy barriers. By means of the harmonic transition state theory temperature-dependent diffusion and reorientation rates are obtained for predicting a temperature range where the kinetic stabilization is attained.

O 29: Metal substrates 1

Time: Tuesday 10:30–12:15

Location: S052

O 29.1 Tue 10:30 S052

Controlling the translation of a single molecule — •GRANT J. SIMPSON¹, MATS PERSSON², and LEONHARD GRILL¹ — ¹University of Graz, Graz, Austria — ²University of Liverpool, Liverpool, UK

Controlling both of the orientation and the direction of translation of a single molecule is crucial to the understanding of molecular machines [1,2]. In addition, overcoming microscopic reversibility and realising unidirectional motion is a major criterion if a molecular machine is to do any meaningful work. Here, we report how single molecules can be translated in a directional manner over a metallic surface using voltage pulses from the tip of a scanning tunnelling microscope. Directionality of motion is possible due to translations occurring via an asymmetrically accessible intermediate state. The reaction pathway is discussed as well as how this molecular motion can be coupled to the motion of surface adsorbates.

[1] G. J. Simpson, V. García-López, A. D. Boese, J. Tour, L. Grill, *Nat. Commun.*, 10, 4631 (2019) [2] G. J. Simpson, V. García-López, P. Petermeier, L. Grill, J. Tour, *Nat. Nanotechnol.*, 12, 604 (2017)

O 29.2 Tue 10:45 S052

On-Surface Formation of Cyano-Vinylene Linked Chains by Knoevenagel Condensation — •KWAN HO AU-YEUNG¹, TIM KÜHNE¹, DIMITRY A. RYNDYK^{3,4}, GIANAURELIO CUNIBERTI³, THOMAS HEINE⁴, XINLIANG FENG², and FRANCESCA MORESCO¹ — ¹Center for Advancing Electronics Dresden (cfaed), TU Dresden, 01062 Dresden (Germany) — ²Institute of Molecular Functional Materials, Faculty of Chemistry and Food Chemistry, TU Dresden, 01062 Dresden (Germany) — ³Institute for Materials Science, TU Dresden, 01062 Dresden (Germany) — ⁴Theoretical Chemistry, TU Dresden, 01062 Dresden (Germany)

The incorporation of C=C bonds into conjugated nanostructures with additional functional groups (e.g. nitrogen substitution) has attracted extensive attention in recent years due to their intriguing electronic properties. However, the activation modes inside the toolbox of on-surface synthesis are still limited. We present the novel on-surface formation of CN-substituted phenylene vinylene chains on the Au(111) surface, thermally induced by annealing the substrate stepwise at temperatures between 220°C and 240°C. The reaction is investigated by scanning tunneling microscopy (STM) and density functional theory (DFT). Supported by the calculated reaction pathway, we assign the observed chain formation to a Knoevenagel condensation between an aldehyde and a methylene nitrile substituent.

O 29.3 Tue 11:00 S052

Self-assembly and on-surface Ullmann-type polymerisation of a DPP-based molecular wire on Au(111). — •MICHAEL CLARKE¹, ABIGAIL BELLAMY-CARTER², FERDINANDO MALAGRECA³, DAVID B. AMABILINO⁴, and ALEXANDER SAYWELL¹ — ¹School of Physics & Astronomy, University of Nottingham, NG7

2RD — ²School of Liberal Arts and Natural Sciences, University of Birmingham, Edgbaston, Birmingham, B15 2TT — ³School of Chemistry, University of Nottingham, NG7 2RD — ⁴ICMAB-CSIC, Campus de la UAB 08193 Bellaterra Barcelona, Spain

Diketopyrrolopyrrole (DPP) is a chemical moiety which may act as an electron acceptor within organic electronic-devices and exhibits a high charge carrier mobility. [1] Charge transport within such systems is affected by the local arrangement, and orientation, of molecules/domains; hence controlled formation of ordered structures is of interest. Self-assembly of functionalised DPP species is a route towards ordered structures [2], and on-surface protocols allow monomer units to be covalently coupled under appropriate reaction conditions (e.g. Ullmann-type reactions [3]). Here we study an alkyl chain functionalised DPP unit possessing aryl-hide groups to facilitate on-surface covalent coupling. The self-assembled structure of the monomer units is characterised and ordered polymers, formed via thermal treatment, are investigated using Scanning Tunneling Microscopy (STM). [1] Y. Li et.al, *Energy Environ. Sci.*, 2013, 6, 1684. Y. Zang et.al, *J. Am. Chem. Soc.*, 2018, 140, 13167. [2] A. Honda et.al, *Bull. Chem. Soc. Jpn.*, 2015, 88, 969. [3] L. Grill & S. Hecht, *Nat. Chem.*, 2020, 12, 115.

O 29.4 Tue 11:15 S052

Quantifying the diffusion of porphyrins on Au(111): A temperature-dependant STM study — •MATTHEW EDMONDSON and ALEX SAYWELL — School of Physics & Astronomy, University of Nottingham, Nottingham, UK

The diffusion of surface-confined molecules is a fundamental step within the formation of self-assembled structures and on-surface reactions. Scanning probe microscopies provide a route to characterising the diffusion pathways of these molecules, and allow a quantitative analysis of energetic barriers via Arrhenius-type rate analysis. (1) In particular, SPM allows the relationship between atomic-scale surface structures and molecular diffusion to be explored; a potential method for influencing on-surface reactivity. (2)

The Au(111) surface, frequently used as a substrate for on-surface coupling reactions (3), exhibits the well-known 'herringbone' reconstruction which may influence the diffusion of molecule species. In this work, we report on the diffusion of individual 2H-TTP on the Au(111) surface; characterising the diffusion rate via variable-temperature scanning tunnelling microscopy within specific regions of the reconstructed surface. The energy barrier to diffusion (obtained via Arrhenius analysis) was found to differ between the FCC and HCP regions of the herringbone reconstruction, indicating that local geometric/electronic surface-features play a role in on-surface diffusion.

1. H. Marbach, H.-P. Steinrück, *Chem. Commun.* 50, 9034 (2014).
2. S. Clair, D. G. de Oteyza, *Chem. Rev.* 119, 4717 (2019).
3. L. Grill et al., *Nat. Nanotechnol.* 2, 687 (2007).

O 29.5 Tue 11:30 S052

LT-STM induced reversible chiral switching of thiophene-based molecule on Au(111) — •SUCHETANA SARKAR^{1,2}, KWAN HO AU-YEUNG^{1,2}, TIM KUEHNE^{1,2}, DMITRY A. RYNDYK^{2,3}, ALBRECHT WAENTIG^{1,4}, XINLIANG FENG^{1,4}, and FRANCESCA MORESCO^{1,2} — ¹Center for Advancing Electronics Dresden, TU Dresden, 01062 Dresden, Germany — ²Institute for Materials Science, TU Dresden, 01062 Dresden, Germany — ³Theoretical Chemistry, TU Dresden, 01062 Dresden, Germany — ⁴Chair of Molecular Functional Materials and Faculty of Chemistry & Food Chemistry, TU Dresden, 01062 Dresden, Germany

In the ongoing quest for miniaturization of machines, single molecule machinery holds a plethora of possibilities. Advancements in nanoscale imaging techniques, such as Scanning Tunneling Microscopy and Spectroscopy (STM, STS), allows not only the addressing of single molecules individually but through tunneling electrons/electric field stimulation with an STM tip, one can experimentally study fundamental properties of molecules such as pi-conjugation and charge transfer to a surface, and the effect it has on the switching behavior. We present the design and synthesis of a nanoswitch which exhibits a reversible switching from achiral to chiral mode on Au(111). The electronic states of both conformations have been measured with a high degree of spatial resolution, thereby showing the pathways of the electron-induced isomerization. Furthermore, we demonstrate this effect being suppressed on Ag(111).

O 29.6 Tue 11:45 S052

Enravelling effects of dispersion interactions in enantioselective adsorption — •RAYMOND AMADOR^{1,2}, SAMUEL STOLZ³, NESTOR MERINO-DIEZ¹, OLIVER GROENING¹, ROLAND WIDMER¹, and DANIELE PASSERONE^{1,2} — ¹Empa - Dübendorf, Dübendorf, Switzerland — ²ETH Zürich, Zürich, Switzerland — ³Department of Physics, UC Berkeley, United States

van der Waals (vdW) interactions play a central role in a wide variety of systems. They are responsible for many natural processes, and thus, an accurate description of vdW forces is essential for improving our understanding phys-

ical phenomena. In this talk, we present our findings on the role of non-local vdW interactions in the enantioselective adsorption and debromination of the 10,10-dibromo-9,9'-bianthracene (DBBA) and 9-Phenanthracenylboronic acid (9PBA) molecules, as catalyzed by chiral surfaces of the palladium-gallium (PdGa) intermetallic compound. After a brief recapitulation on the framework of density-functional theory (DFT), we discuss its principle shortcomings within the context of many-body perturbation theory, and how our current calculations address and rectify these faults via higher-order treatments of the exchange integrals. We then present several figures of interest: adsorption configurations before and after geometry optimizations and charge localization plots of adsorption, and explore effects of both vdW interactions and the nonlocal exchange term via inclusion of hybrid functionals. In doing so, we provide the foundations for further study of non-local electronic correlation in chirality.

O 29.7 Tue 12:00 S052

The role of Adatoms for the Adsorption of F4TCNQ on Au(111) — •RICHARD BERGER, ANDREAS JEINDL, LUKAS HÖRMANN, and OLIVER HOFMANN — TU Graz Institut für Festkörperphysik, Graz, Österreich

Molecular adsorption on inorganic substrates often includes the incorporation of native adatoms within the adsorbate layer. The presence of the adatom in the adlayer causes significant changes in the electronic structure of the interface affecting properties such as the adsorption geometry, the bonding type, and the work function. Here we investigate the adsorption of F4TCNQ on Au (111), which is a prototypical system for the adsorption of an acceptor type molecule on a metallic substrate. Using density functional theory, we show that incorporating adatoms significantly changes the interface charge transfer and modifies the Fermi-level pinning mechanism for the adsorbed species. Furthermore, we find that the 5d orbitals of the Au adatom hybridize with the F4TCNQ molecular orbitals, introducing covalent coupling within the adlayer. The combination of this effect explains why the incorporation of adatoms, despite the high cost of extracting them from the bulk, is energetically favorable.

O 30: Semiconductor Surfaces

Time: Tuesday 10:30–12:45

Location: S053

Topical Talk

O 30.1 Tue 10:30 S053

Surface Phase Transitions in Atomistic Detail and with Femtosecond Resolution — •WOLF GERO SCHMIDT — Universität Paderborn

Ab initio molecular dynamics on ground and excited-state potential energy surfaces may be used to gain deep insight in the driving forces and mechanisms of surface phase transitions and can greatly assist the interpretation of experimental data. This is illustrated in my talk using two prominent examples: (i) Photoholes localized at the Brillouin zone boundary of the In/Si(111)(8x2) surface are shown to drive an ultrafast (8x2) → (4x1) phase change that is accompanied by an insulator-metal transition [1,2]. (ii) Thermal excitation of the Au/Si(553)(1x6) surface leads to soft Au chain vibrations that reduce transiently the Au electron affinity, which lowers the barrier for a $sp^2 + p \rightarrow sp^3$ hybridization change of Si step edge atoms. This leads eventually to an order-disorder phase transition and the formation of a two-dimensional spin liquid [3].

[1] T Frigge et al., Nature 544, 207 (2017).

[2] CW Nicholson et al., Science 362, 821 (2018).

[3] C Braun et al., PRL 124, 146802 (2020).

O 30.2 Tue 11:00 S053

Dimer coupling energies of the Si(001) surface examined by SPA-LEED — •CHRISTIAN BRAND, GIRIRAJ JNAWALI, JONAS FORTMANN, MOHAMMAD TAJIK, ALFRED HUCHT, PETER KRATZER, HAMID MEHDIPOUR, BJÖRN SOTHMANN, and MICHAEL HORN-VON HOEGEN — Department of Physics and Center for Nanointegration CENIDE, University of Duisburg-Essen, Lotharstraße 1, 47057 Duisburg

Though the surface of Si(001) belongs to the most famous in the world still some of its properties and phenomena are unrevealed. Si(001) exhibits buckled dimers in the topmost layer, arranged in dimer rows, and thus forming a (2×1) reconstruction at room temperature. Upon cooling the structure undergoes an disorder-order transition to the $c(4 \times 2)$ reconstructed ground state. High-resolution SPA-LEED (Spot Profile Analyzing - Low Energy Electron Diffraction) was used to quantify the structural change along the transition upon heating from low to high temperatures. Rapid cooling in the regime of critical slowing down formed a so-called domain structure with typical size of ~ 14 nm. The data is analyzed in the framework of the anisotropic 2D Ising model and complemented by density functional theory calculations. We determined a phase transition temperature of $T_c = 190.6$ K, critical exponents β , γ , and ν of the Ising model and the coupling constants $J_{\parallel} = (-24.9 \pm 1.3)$ meV and $J_{\perp} = (-0.8 \pm 0.1)$ meV of the Si dimers by solving Onsager's equation and evaluating the correlation length ratio of the two directions.

O 30.3 Tue 11:15 S053

Reduced contact resistance to gallium nitride by plasma-assisted atomic layer deposition — •MAXIMILIAN CHRISTIS — Walter Schottky Institut, Technische Universität München

Gallium nitride is an industrially relevant III-V semiconductor that draws significant attention for a range of both established and emerging applications, including for light emitting diodes, power electronics, photocatalysis, and sensing. Established contacting schemes for GaN rely on wet-chemical surface preparations and post-metallization high-temperature ($\geq 600^\circ\text{C}$) annealing processes, which complicate fabrication and may adversely affect device performance. Here, we present a low-temperature gas-phase process (200°C) that reduces the Schottky barrier height and the contact resistivity at the GaN/metal interface. In particular, we employ H₂ plasma-enhanced atomic layer deposition (ALD) that creates an ultimately thin, homogeneous AlO_x monolayer using oxygen from the native gallium oxide as oxidant. This AlO_x coating reduces the surface band bending and results in Ohmic current-voltage characteristics for n-doped GaN contacted by Ti metal. In ongoing work, we are also exploring how the monolayer AlO_x ALD approach can be applied to improve contacts to p-doped GaN in combination with high work function metals. Among the various applications that could benefit from this low thermal budget contact fabrication strategy, we are investigating how such metal/semiconductor structures impact the electrocatalytic performance of n-GaN/Pt cathodes for water splitting.

O 30.4 Tue 11:30 S053

Distance dependance and lateral change of electrostatic forces between Pb-islands and wetting layer on Pb/Si(111)-(7x7) — BEN LOTTENBURGER, •PAUL PHILIP SCHMIDT, DANIEL ROTHHARDT, MANUEL SCHULZE, and REGINA HOFFMANN-VOGEL — Universität Potsdam, Institut für Physik und Astronomie, Experimentelle Physik kondensierter Materie

Pb islands on silicon show a wide range of interesting properties, such as explosive island growth [1,2]. Previous work has already been able to explain some features, such as the unusual height distribution of the islands[3,4]. To understand this system in more detail, we have investigated the differences in the electrostatic interaction between the tip and the Pb islands on one side and the Pb-containing wetting layer on the other side. We have used scanning force microscopy in the non-contact frequency modulation mode and bias distance measurements in ultrahigh vacuum at ~ 120 K. The Si has been cleaned by direct current heating. Subsequently, Pb has been vapor deposited. The Frequency shift as a function of tip-sample distance has been measured on both Pb islands and the wetting layer. The differences in force and work function between have been investigated both.

[1] Hershberger et al, PRL 113, 236101 (2014). [2] Huang et al, PRL 108, 026101 (2012). [3] Hupaló et al, PRB 65, 115406 (2001). [4] Spáth et al, PRL 124, 016101 (2020)

O 30.5 Tue 11:45 S053

Growth of well-ordered K3C60 thin films on Bi2Se3 — •MICHAEL HERB and ISABELLA GIERZ — Department of Physics, University of Regensburg, 93040 Regensburg, Germany

The molecular solid K3C60 is a BCS-type superconductor with a critical temperature of 20K [1]. More intriguingly, K3C60 powder exposed to strong mid-infrared driving fields exhibits the optical properties of a transient superconductor [2] possibly up to room temperature [3] and with nanosecond lifetimes [4]. The microscopic mechanism behind these observations remains poorly understood. We want to shed light onto this issue by measuring the transient band structure of driven K3C60 using time- and angle-resolved photoemission spectroscopy (tr-ARPES). These experiments cannot be performed on the originally used K3C60 powder as they require large, well-ordered K3C60 single crystals. Therefore, we investigate the growth of K3C60 thin films on different substrates using low-energy electron diffraction (LEED) and ultraviolet photoemission spectroscopy (UPS). We provide evidence for well-ordered growth on Bi2Se3, enabling future tr-ARPES studies on the material.

O 30.6 Tue 12:00 S053

Structure and origin of antiphase domains and related defects in thin GaP epilayers on As-modified Si(100) — •FRANZ NIKLAS KNOOP¹, AGNIESZKA PASZUR², BENJAMIN BORKENHAGEN^{1,3}, OLIVER SUPPLIE^{2,4}, MANALI NANDY², GERHARD LILIENKAMP¹, PETER KLEINSCHMIDT², THOMAS HANNAPPEL², and WINFRIED DAUM¹ — ¹IEPT, TU Clausthal — ²Institute of Physics, TU Ilmenau — ³Fallstein Gymnasium Osterwieck — ⁴Physics Department, HU Berlin

The deposition of low-defect III-V-layers on Si(100) is impaired by the formation of antiphase domains (APDs) in the epilayer. We study the origin and formation of APDs and related defects in thin GaP buffer layers on nearly-single-domain, As-modified Si(100) substrates. By comparing results obtained by low energy electron microscopy (LEEM), AFM, STM and scanning Auger electron microscopy, we identify two different types of APD-related defects in the GaP layer and trace these defects back to residual minority (2x1) domains of the Si substrate. GaP growth on minority domain terraces with widths in the range 40-100 nm gives rise to APDs of comparable lateral dimensions. The observation of trench-like defects in the epilayer extending down to the surface of the substrate indicates that homogeneous layer-by-layer growth of GaP is impeded on narrow terraces (<20 nm) of the (2x1)-reconstructed minority domain of the substrate. We propose that insufficient nucleation of GaP on these terraces leads

to the formation of trenches, while on wider minority terraces APDs are formed by 3D-like growth.

O 30.7 Tue 12:15 S053

Adsorption of CO and CO₂ on the Y-stabilized ZrO₂(100) surface — •SHUANG CHEN, XIAOJUAN YU, ERIC SAUTER, ALEXEI NEFEDOV, STEFAN HEISSLER, CHRISTOF WÖLL, and YUEMIN WANG — Institute of Functional Interfaces (IFI), Karlsruhe Institute of Technology (KIT), 76344 Eggenstein-Leopoldshafen, Germany

Understanding the stabilization mechanism of the Y-stabilized zirconia (YSZ) (100) surface has triggered a great debate over the past 30 years. In this work, we focused on a fundamental study on the surface structure of YSZ(100) by polarization-resolved infrared reflection absorption spectroscopy (IRRAS), in combination with grazing-emission X-ray photoelectron spectroscopy (XPS). The combined IR and XPS results allowed to gain detailed insight into the adsorption of carbon monoxide and carbon dioxide on YSZ(100) over a large coverage range from submonolayer to multilayers. The experimental data were further analyzed based on the density functional theory (DFT) calculations.

O 30.8 Tue 12:30 S053

Starting from a Fixed Geometry: Real-Time XPS Investigation of a Surface Reaction with Controlled Molecular Configurations — •TIMO GLASER¹, CHRISTIAN LÄNGER¹, JULIAN HEEP¹, JANNICK MEINECKE², MATHIEU SILLY³, ULRICH KOERT², and MICHAEL DÜRR¹ — ¹Institut für Angewandte Physik und Zentrum für Materialforschung, Justus-Liebig-Universität Giessen, Germany — ²Fachbereich Chemie, Philipps-Universität Marburg, Germany — ³Synchrotron SOLEIL, 91192 Gif sur Yvette, France

The relative orientation between two reactants can have a major influence on the reactivity and on the products of a chemical reaction. In gas-surface chemistry with well-defined single-crystal surfaces, the orientation and configuration of one reactant is fixed by the surface, but still the reacting gas molecules can impact on the surface in all possible orientations. Here we show how to constrain the relative orientation of both reactants by attaching a reactive group (ether) via a linker (cyclooctyne) on a single crystal surface. This keeps the reacting group in a highly-constrained configuration close to the surface. We demonstrate this concept for ether cleavage on silicon (001), the surface analogue of an S_N2 reaction. The kinetics of the further reaction of the ether group with the silicon surface is studied by means of real-time XPS using synchrotron radiation. We find both a low-energy barrier and a low prefactor, which we discuss in terms of the constrained starting configuration of the ether group. As this configuration represents the starting point of a low-energy pathway, it gives direct experimental access to the underlying reaction mechanism.

O 31: Solid-Liquid Interfaces 3: Reactions and Electrochemistry

Time: Tuesday 10:30–12:30

Location: S054

Topical Talk

O 31.1 Tue 10:30 S054

Towards a realistic description of electrified solid-liquid interfaces — •NICOLAS G. HÖRMANN — Fritz-Haber-Institut der Max-Planck-Gesellschaft, Berlin, Germany

Atomistic modelling of electrified solid-liquid interfaces in the context of electrocatalytic and electrochemical transformations is a challenging task. This is in particular so as the description of many relevant processes involves the consideration of charge transfer, solvent reorganization and the long-range screening of the electrolyte. Many of these processes have been studied in the past using effective model hamiltonians and from a physical chemistry perspective, e.g. based on mean-field kinetic models. However, recent advances in the first-principles-based description have opened up pathways to study the involved phenomena with atomistic resolution and to gain new, fundamental insights.

In this talk, I will give a brief overview of such recent developments, concentrating mainly on the use of and results from DFT calculations in continuum solvation environments[1]. Without doubt, such calculations have had a tremendous impact on the community, as they paved the way to describe the interfacial energetics in a grand-canonical framework, aka at applied potential conditions[2]. In addition to discussing a range of results obtained on model systems, I will as well clarify the evident limitations and inaccuracies of such an approach and discuss briefly possible future pathways to improve upon those.

[1] S. Ringe *et al.*, Chem. Rev. (2021). [2] N.G. Hörmann *et al.*, JCP, **150**, 041730 (2019).

O 31.2 Tue 11:00 S054

Electrostatic potentials in molecular dynamics — •LUDWIG AHRENS-IWERS¹, GREGOR VONBUN-FELDBAUER¹, and ROBERT MEISSNER² — ¹Institute of Advanced Ceramics, Hamburg University of Technology, Hamburg, Germany — ²Institute of Polymers and Composites, Hamburg University of Technology, Hamburg, Germany

Molecular dynamics (MD) simulations in a constant potential ensemble are an increasingly important tool to investigate charging mechanisms in next-generation energy storage devices. The constant potential method (CPM) can be used in classical MD to model metallic electrodes at an electrostatic potential. In this method, charges of individual electrode atoms are set to meet the applied potential. Unfortunately, existing implementations are either highly specialized or not very performant.

As a new implementation of the CPM, the ELECTRODE package for the MD code LAMMPS is presented. This package integrates a particle-mesh solver to greatly reduce computation times of the long-range Coulomb interactions. Further, a dipole correction that is required for systems with a slab geometry is included. In addition to the CPM, the code features a constant charge method which distributes the charges within each electrode as well as a thermopotentialostat that utilizes the CPM algorithm. Moreover, the integration in LAMMPS allows the use of many tools from the base code and other packages.

O 31.3 Tue 11:15 S054

First-principles molecular dynamics simulations of electrified Pt(111)/H₂O interfaces — •LANG LI, NICOLAS G. HÖRMANN, and KARSTEN REUTER — Fritz-Haber-Institut der Max-Planck-Gesellschaft, Berlin, Germany

Metal-water interfaces play a fundamental role in electrochemistry. An accurate understanding of their properties is required in any attempt to describe electrochemical phenomena such as electrocatalytic reactions or charge transfer processes.

In this work, we benchmark the description of electrified Pt(111)/water interfaces based on first-principles molecular dynamics simulations at applied potential conditions using density functional theory. We apply the potential by introducing excess electrons that are counterbalanced by partially charged hydrogen atoms. This method is tested with a variety of slab setups and cell sizes. Additionally, we investigate different methods to determine the reference potential.

We analyze in detail the structure of the interface as well as the obtained capacitance vs. potential curves and compare these with published theoretical and experimental results [1]. Our results highlight the response of interfacial water to an applied potential and its importance for understanding the hump in the capacitance, observed at high electrolyte concentrations [2].

[1] L. Li, J.-B. Le, J. Cheng, *Cell Rep. Phys. Sci.*, 3, 100759 (2022). [2] J.B. Le, Q.Y. Fan, J.Q. Li, J. Cheng, *Sci. Adv.*, 6, eabb1219 (2020).

O 31.4 Tue 11:30 S054

First step of the oxygen reduction reaction on Au(111): An ab initio molecular dynamics study of the electrified metal/water interface — •ALEXANDRA M. DUDZINSKI, ELIAS DIESEN, HENDRIK H. HEENEN, VANESSA J. BUKAS, and KARSTEN REUTER — Fritz-Haber-Institut der MPG, Berlin, Germany

The oxygen reduction reaction (ORR) is a key electrocatalytic process for developing sustainable energy technologies. And yet, many aspects of the underlying reaction mechanism are still poorly understood at the molecular level. Especially at weak-binding electrode surfaces such as Au, even the ability to bind aqueous O₂ species as a first mechanistic step remain unclear. Resolving these questions requires going beyond the simplified thermodynamic models of charge-neutral reaction intermediates that have been commonly used in computational electrocatalysis so far. Here, we perform molecular dynamics simulations based on periodic density-functional theory (DFT) to investigate O₂ adsorption at an electrified Au(111)/water interface. We elucidate structural interfacial properties as a function of surface charge, and show that the latter can significantly alter the O₂ binding energy. Adsorption is specifically enhanced under electric fields that are realistic for ORR operation, suggesting this as a very possible first electrochemical, rather than purely chemical step of the mechanism and showing that field effects in corresponding DFT models cannot be neglected. The resulting dependence on (absolute) electrostatic potential may further explain the superior activity measured experimentally for this catalyst in alkaline vs. acidic media.

O 31.5 Tue 11:45 S054

Modeling varying potential conditions in electrochemical simulations: The case of O₂/Au(111) — •ELIAS DIESEN, ALEXANDRA M. DUDZINSKI, HENDRIK H. HEENEN, VANESSA J. BUKAS, and KARSTEN REUTER — Fritz-Haber-Institut der Max-Planck-Gesellschaft, Berlin

While significant insight has been gained in recent years by DFT-based simulations of electrochemical processes, crucial methodological challenges remain, especially for accurate determination of reaction energies under operando conditions. One open question is how to represent the constant electrode potential in simulations of an electrified water/metal interface, where the simulation setup requires a constant charge in the simulation cell throughout the reaction. Here we compare different levels of treatment of the electrochemical interface: explicit ab initio molecular dynamics, an implicit solvent model, and a sawtooth-potential electric field in vacuum, for the case of O₂ adsorption on Au(111). We characterize the dynamics near the surface and identify ways an applied electrode potential influences the adsorption. We find, in all methods, significantly

enhanced O₂ adsorption at more reducing conditions. However, we also show that certain aspects of the process can only be captured using a fully explicit treatment of the solvent.

O 31.6 Tue 12:00 S054

Understanding the Interfacial Capacitance of 2D Materials in an Implicit Water Environment — •HEDDA OSCHINSKI^{1,2}, NICOLAS G. HÖRMANN¹, and KARSTEN REUTER¹ — ¹Fritz-Haber-Institut der Max-Planck-Gesellschaft, Berlin, Germany — ²Technical University of Munich, Germany

The interfacial capacitance (*C*) is a central quantity in electrochemistry. For metal electrodes, *C* is dominated by the double layer capacitance that derives from the potential drop in the solvent. However, the finite density of states (DOS) in semiconducting 2D electrodes alters the picture and leads to a vanishing *C* around the point of zero charge. This entails a challenge in describing the energy-potential relation and the connected field effects when considering adsorbates.

To explore this challenge, we study the interfacial capacitance for 2D metal halides MX₂, using density-functional theory in a continuum solvent environment. We break down *C* into a DOS-filling-related quantum capacitance and the double layer capacitance. Our analysis demonstrates that such a separation into individual components is not straightforward. Nevertheless, the qualitative behavior of *C* can be rationalized, making this study a first step towards better understanding of 2D, in particular semiconducting, electrodes.

O 31.7 Tue 12:15 S054

Two-Dimensional 2D Materials interfacing liquid water : the new frontier from ab initio simulations — BENOIT GROSJEAN¹, FELIX MOUHAT¹, RODOLPHE VUILLEUMIER¹, FRANCOIS-XAVIER COUDERT², and •MARIE-LAURE BOCQUET¹ — ¹Ecole Normale Supérieure, PSL university and CNRS, Paris, France — ²Chimie Paris Tech, PSL university and CNRS, Paris, France

In spite of their computational cost, quantum dynamic insights open unprecedented avenues for the use of 2D materials for nanofluidics. In this talk, I will report on our recent theoretical findings on 2D materials like G (graphene), BN (boron nitride) and GO (graphene oxide) by means of Ab Initio Molecular Dynamics (AIMD) and their implications to rationalize their peculiar fluid transport and filtration properties. We demonstrate that the charging of pristine ideal 2D materials in aqueous conditions originate from the hydroxide anion and is crucially dependent of the electronic structure of the 2D layers ranging from chemisorption to physisorption. [1] We could pioneer the concept of static versus mobile extrinsic charges on prototypical 2D materials that have a huge impact on electro-kinetic transport.[2] We also predict that the water reactivity is further enhanced on hydrid sheets like planar G-BN heterostructure [3]. Finally, we explore the properties of various GO models in neutral water and we unveil several chemical processes [4].

[1] *Nat. Comm.* 10, 1656 (2019). [2] *J. Chem. Phys.* 156, 044703 (2022). [3] *Phys. Chem. Chem. Phys.* 22, 10710 (2020). [4] *Nat. Comm.* 11, 1566 (2020).

O 32: Poster Tuesday: Adsorption and Catalysis 1

Time: Tuesday 11:00–13:00

Location: P3

O 32.1 Tue 11:00 P3

Analysis of Electron-Transfer in Water-Based Dye-Sensitized Solar Cells — •DANIEL HOLZHACKER¹, ANDREAS RINGLEB¹, RAFFAEL RUESSE², and DERCK SCHLETTWEIN¹ — ¹Justus-Liebig-Universität Gießen, Institut für Angewandte Physik — ²Justus-Liebig-Universität Gießen, Physikalisches-Chemisches Institut

Dye-sensitized solar cells (DSSCs) present a possible low-cost technology for the conversion of sunlight into electrical energy. Most DSSCs are based on electrolytes with organic solvents. Due to environmental reasons it is attractive to replace organic solvents by water. In view of the damage typically caused to DSSCs by water contaminations, the use of water as contact solution represents a big challenge. Complete aqueous DSSCs were assembled with a combination of different organic dyes (D51, D35 and Y123) and organic redox mediators (TEMPO, AZADO and TEMPOL). The combination of Y123 and TEMPO yielded remarkable efficiencies of up to 4.4%. Although heavily limited in the fill factor, TEMPOL proved to be an interesting alternative, as its solubility in water is dramatically increased in comparison to TEMPO. Similar open circuit voltages and short circuit currents were reached but large overpotentials of electron transfer at the electrodes still limited TEMPOL-based cells. Subsequently, the electrolyte and electrode surfaces were modified in order to reduce the respective overpotentials.

O 32.2 Tue 11:00 P3

Novel corrugated geometric moiré pattern of a semi-periodically buckled, zebra-like topography of Xe on Ag(110) — •INGA CHRISTINA LANGGUTH and KARINA MORGENSTERN — Chair of Physical Chemistry I, Ruhr-Universität Bochum, Bochum, Germany

Solid rare gas films on metal single crystals are currently gaining interest due to their beneficial properties. As non-ionic, low interacting insulator surfaces they offer a potential application for unperturbed surface science studies. STM investigations of a thin xenon (Xe) film of several monolayers on Ag(110) reveal a novel corrugated structure of a semi-periodically buckled, zebra-like topography. The outstanding feature of this surface is a non-uniform distribution of buckled row orientations and distances. Instead of domain boundaries separating different phases, a gradual transition of row orientations is observed. The corrugated row pattern can be attributed to a geometric moiré pattern at the interface of the incommensurable Ag(110) and Xe(111) crystal lattices. A gradual change of the row orientation can further be explained by a gradually changing Xe-lattice orientation with respect to Ag(110) within a narrow angle regime. The stability of this semi-periodic structure against annealing reveals a remarkably flat potential energy surface for the turning of the Xe layer relative to the Ag(110) surface. The corrugated surface may serve as an interesting substrate for further studies of geometric confinement effects in an anisotropic environment.

O 32.3 Tue 11:00 P3

On-surface Synthesis of Naphthalocyanines with Extended π -Systems — •LUKAS J. HEUPLICK¹, QITANG FAN¹, DMITRIY A. ASHVATSUROV², DENNIS KÖRNER¹, TATIANA V. DUBININA², and J. MICHAEL GOTTFRIED¹ — ¹Fachbereich Chemie, Philipps-Universität Marburg, Marburg, Germany — ²Moscow

The distinct optical and electronic properties of phthalocyanines (Pc) make them interesting in a wide field of applications. Here we report the on-surface synthesis

of new naphthalocyanines with differently extended π -systems. This reaction in form of a cyclization is studied for different dicarbonitriles on the Ag(111) and Au(111) surfaces by scanning tunneling microscopy (STM) and X-ray photoelectron spectroscopy (XPS). 6,7-Diphenyl-2,3-naphthalenedicarbonitrile (DP-NDN) forms naphthalocyanines only with co-adsorbed Fe atoms on Ag(111) and Au(111). The larger 6,7-di(2-naphthyl)-2,3-naphthalenedicarbonitrile (DNNDN) can undergo this reaction directly on Ag(111) without co-adsorbed metal, resulting in the corresponding Ag-NPc.

O 32.4 Tue 11:00 P3

Adaptive training of a machine-learned model for nonadiabatic hydrogen chemistry on multiple facets of Copper. — •WOJCIECH G. STARK, JULIA WESTERMAYER, OSCAR A. DOUGLAS-GALLARDO, JAMES GARDNER, and REINHARD J. MAURER — University of Warwick, Coventry, United Kingdom

Traditionally, molecular dynamics methods utilise the Born-Oppenheimer approximation and dynamics are governed by a single potential energy surface. However, on metallic surfaces often the energy exchange between adsorbate and electronic excitations in the metal is significant and causes the breakdown of the Born-Oppenheimer approximation. There are multiple methods to include such nonadiabatic effects, with one of the most efficient being molecular dynamics with electronic friction (MDEF). MDEF introduces nonadiabatic effects via additional electronic friction forces, which can be calculated with time-dependent perturbation theory based on Density Functional Theory. However, a meaningful comparison between computational simulations and experiments demands the capability to run tens of thousands of MDEF trajectories. We present high-dimensional machine-learning based interatomic potential and electronic friction models that enable the simulation of nonadiabatic molecular dynamics of hydrogen scattering and associative desorption at different copper surfaces. We construct deep neural network representations via iterative adaptive sampling based on the target dynamical observables, namely the scattering and reaction probabilities.

O 32.5 Tue 11:00 P3

Adsorption and Diffusion of NH₃ on Rutile TiO₂(110): An STM Study — •HANNA BÜHLMAYER¹, KRAEN CHRISTOFFER ADAMSEN², TAO XU¹, LUTZ LAMMICH², JÖRG LIBUDA¹, STEFAN WENDT², and JEPPE VANG LAURITSEN² — ¹Interface Research and Catalysis, ECRC, Friedrich-Alexander-Universität Erlangen-Nürnberg, Egerlandstraße 3, 91058 Erlangen, Germany — ²Interdisciplinary Nanoscience Center, Aarhus University, Gustav Wieds Vej 14, 8000 Aarhus, Denmark

The adsorption of NH₃ on TiO₂ is an important step for many reactions in environmental catalysis such as the selective catalytic reduction (SCR) of NO_x over V₂O₅/TiO₂ and the removal of NH₃ from air and water over TiO₂. To obtain a detailed understanding of the surface chemistry of NH₃ on TiO₂, we investigated the adsorption of sub-monolayers of NH₃ on clean, hydroxylated, and O-precovered rutile TiO₂(110) surfaces by means of scanning tunneling microscopy (STM) under ultrahigh vacuum (UHV) conditions. We found that on the clean TiO₂(110) surface at 120 K, NH₃ adsorbs exclusively as monomers. On the hydroxylated TiO₂(110) surface at 160 K, we observe 2(NH₃) pairs and (NH₃)₂ dimers in addition to the majority of monomeric NH₃. At 270 K, monomeric NH₃ and surface hydroxyls diffuse together along the [001] direction. Additionally, NH₃ can also diffuse along the surface hydroxyl bridge in the [1-10] direction. On the surface precovered by O adatoms (Oot) at 160 K, we observe the formation of NH₂OH and 2(NH₂OH) species formed by the interaction of NH₃ monomers with Oot and Oot pairs.

O 32.6 Tue 11:00 P3

Real-space study of carbenes using a diazofluorene precursor adsorbed on a Cu(111) surface — •HUSSAIN MAZHAR¹, JULIEN ROWEN², WOLFRAM SANDER², and KARINA MORGENSTERN¹ — ¹Lehrstuhl für Physikalische Chemie I, Ruhr-Universität Bochum, 44801 Bochum, Germany — ²Lehrstuhl für Organische Chemie II, Ruhr-Universität Bochum, 44780 Bochum, Germany

Carbene is a reactive intermediate playing a vital role for many synthesis in the pharmaceutical industry [1]. Here, we study their properties on a metal substrate in real space using scanning tunnelling microscopy (STM) at 5 K. As carbenes are highly reactive species, they cannot be deposited directly on metal surfaces. The arrangement of their precursors on the surface is crucial for the carbene reactivity upon carbene formation. Diazofluorene molecules, already studied on the Ag(111) surface [2], are used as a precursor of the carbene to compare the influence of the surface on carbene reactivity. The STM study reveals dimer and cluster formation of the carbene precursor molecules on Cu(111) when de-

posited at 50 K and 100 K. While at 50 K more dimer formation occurs, at 100 K cluster formation is noticeable. An electrostatic surface potential map is used to determine charge distribution of the dimers. For carbene formation, a particular energy is required to cleave the diazo part from the molecule. In this study, we used STM manipulation to estimate the energy for the dissociation of the molecule. [1] Patil, Siddappa A, *Future Med. Chem.* 7. (2015) 1305-1333 [2] Mieres-Perez, Joel, *J. Am. Chem. Soc.* 143. (2021) 4653-4660

O 32.7 Tue 11:00 P3

Thickness-dependent energy level alignment of terrylene molecules on WS₂ monolayer — •QIANG WANG¹, SIFAN YOU³, BJÖRN KOBIN², PATRICK AMSALEM¹, LIFENG CHI³, STEFAN HECHT², and NORBERT KOCH¹ — ¹Institut für Physik & IRIS Adlershof Humboldt-Universität zu Berlin, Berlin, Germany — ²Department of Chemistry & IRIS Adlershof Humboldt-Universität zu Berlin, Berlin, Germany — ³Institute of Functional Nano and Soft Materials (FUNSOM), Soochow University, Suzhou, China

The exceptional large surface ratio makes 2D TMDC notably sensitive to extrinsic modification. In particular, we study the Van der Waals structure of WS₂ monolayers modified by the conjugated terrylene molecules. We show the terrylene/WS₂ heterostructures exist in different stacking configurations dependent on the layered coverage, revealed by photoemission spectroscopy and scanning tunnelling microscopy (STM). Electronically, the hybrid heterostructures exhibit type-II energy level alignment. It is further determined that the ionization potentials of terrylene, are reduced by 0.54 eV as the molecule switching from flat-lying to standing orientation. The adsorption behaviour is spatially resolved by STM, indicating two different atomic assembles. As determined by photophysical characterization, low energy electron-hole pairs are also populated upon molecule deposition. Meanwhile the external dielectric screening lowers the Rydberg states of WS₂. Our findings reveal the vertical 2D heterostructures enable effective tailoring of both electronic and photophysical properties, which can be applied for various optoelectronic devices.

O 32.8 Tue 11:00 P3

Nanocar Race II: How fast and how long can we drive nano-vehicles? — •TIM KÜHNE¹, KWAN HO AU YEUNG¹, SUCHETANA SARKAR¹, OUMAIMA AIBOUDI², SOYOUNG PARK², FRANZISKA LISSEL², and FRANCESCA MORESCO¹ — ¹Center for Advancing Electronics Dresden, TU Dresden, 01062 Dresden, Germany — ²Leibniz Institute of Polymer Research, 01062 Dresden, Germany

Scanning tunneling microscopy has progressed far beyond just being a probing technique. We can now address and manipulate single molecules and atoms with a great degree of precision and repeatability. The 2nd Nanocar Race saw surface science groups from across the globe design and synthesize molecules of at least 70 atoms with the intent of driving it on Au(111). The conversion of electric impulse from the tip to controllable translation of the nanocar along the FCC sites of Au(111) was demonstrated by each team, although the design philosophy and mediating physics theories varied across the board. Here, we present the TU Dresden nanocar. It was successfully manipulated via inelastic tunneling electrons for 290nm during the 24-hour race.

O 32.9 Tue 11:00 P3

First-Principles Study of Methanol and Benzene Adsorption on In₂O₃ (111) — •ANDREAS ZIEGLER¹, MARGARETA WAGNER², ULRIKE DIEBOLD², and BERND MEYER¹ — ¹Interdisciplinary Center for Molecular Materials and Computer Chemistry Center, FAU Erlangen-Nürnberg, Germany — ²Institute of Applied Physics, TU Wien, Austria

Indium oxide is widely used as transparent conductive oxide for electrodes in semiconductor devices, but it is also a promising new catalyst for hydrogenation and dehydrogenation reactions, e.g. methanol synthesis. To probe the reactivity of the most stable (111) termination of In₂O₃, we studied the adsorption of methanol and benzene, two prototypical polar and nonpolar molecules, by DFT geometry optimizations and Car-Parrinello molecular dynamics (CPMD) simulations. We find that the unit cell of the In₂O₃(111) surface is chemically quite heterogeneous: by searching for the most favorable configurations of methanol with increasing coverage from one to nine molecules per unit cell we find that the first three methanol molecules dissociate in one specific region of the unit cell, followed by molecular adsorption on neighboring sites, confirmed by TPD, XPS and ncAFM experiments. Also benzene prefers to adsorb at one specific site in the unit cell. Due to the large size of the unit cell, the benzene molecules are well separated. CPMD simulations show that the molecules can freely rotate and are well trapped at their adsorption site. However, rotation is suppressed for benzene derivatives with additional side groups.

O 33: Poster Tuesday: Ultrafast Processes 2

Time: Tuesday 11:00–13:00

Location: P3

O 33.1 Tue 11:00 P3

Anisotropic carrier dynamics in single crystalline graphite — •HAUKE BEYER, PETRA HEIN, KAI ROSSNAGEL, and MICHAEL BAUER — Institut für Experimentelle und Angewandte Physik, Christian-Albrechts-Universität zu Kiel, Germany

Time- and angle-resolved photoelectron spectroscopy at 35 fs time-resolution is employed to study the carrier dynamics in the Dirac cone of graphite upon excitation with linearly polarized light. Due to the pseudo spin degree of freedom, the nascent photogenerated carrier distribution exhibits a strong anisotropy in momentum space. We observe the formation of a quasi-thermalized distribution on ultrafast timescales (~ 10 fs) through e-e interactions exhibiting a clear azimuthal anisotropy similar to findings for graphene [1]. For the azimuthal thermalization our data reveal a characteristic time scale of 40 ± 10 fs. The residual non thermal part of the electron distribution shows a time-dependent shift in energy by ~ 150 meV, which we assign to the formation of a steplike distribution due to e-ph interactions. The results are in good qualitative agreement with calculations based on a model introduced in Ref. [2].

[1] S. Aeschlimann *et al.*, Phys. Rev. B **96**, 020301(R) (2017).

[2] E. Malic *et al.*, Phys. Rev. B **84**, 205406 (2011).

O 33.2 Tue 11:00 P3

High-harmonic generation from the surface state of Bi_2Se_3 with THz driving fields — •TIM BERGMEIER, SUGURU ITO, JENS GÜDDE, and ULRICH HÖFER — Fachbereich Physik, Philipps-Universität Marburg, Germany

The acceleration of charge carriers through the Dirac-point in the topologically protected surface state (TSS) of topological insulators (TIs) by strong electric fields with frequencies in the THz range gives rise to a nontrivial type of unusually efficient high-harmonic generation (HHG) as demonstrated for Bi_2Te_3 [1]. The long scattering times in the TSS resulting from spin-momentum locking are imprinted in the observation that the high-harmonic orders can be continuously shifted in frequency by varying the carrier-envelope phase of the driving field. This makes it possible to investigate the unusual transport properties in the TSS by this all optical method even at buried interfaces.

Here, we present first results for Bi_2Se_3 by using a newly developed setup that enables THz-HHG with a stable carrier-envelope phase at a repetition rate of 200 kHz reaching field strengths of up to 10 MV/cm in the frequency range of 12-90 THz. We show how the contribution of electrons in the TSS to the HHG spectra can be determined by measurements with varying field strengths and THz-frequencies above and below the bulk band gap, while analyzing the polarization of the high harmonic signal for different directions of the excitation in momentum space.

[1] C. P. Schmid *et al.*, Nature **593**, 385 (2021).

O 33.3 Tue 11:00 P3

Towards time-resolved photoemission orbital tomography on van-der-Waals heterostructures — •WIEBKE BENNECKE, DAVID SCHMITT, JAN PHILLIP BANGE, MATTIS LANGENDORF, KATHARINA D. FEESER, DANIEL STEIL, SABINE STEIL, MARCEL REUTZEL, G. S. MATTHIJS JANSEN, and STEFAN MATHIAS — I. Physikalisches Institut, Georg-August-Universität Göttingen

Heterostructures of two-dimensional van-der-Waals materials with molecular thin films provide an exceptional platform to tailor electronic energy level alignments that govern the optoelectronic response of such materials. In addition to the energy-level alignment, a detailed knowledge of the electronic wavefunctions in these systems would help to fundamentally understand optical excitations, exciton generation, charge-transfer and relaxation processes. Here, time-resolved orbital tomography is a promising method that potentially provides such information. On this poster, we show first results of femtosecond orbital tomography of PTCDA monolayers adsorbed on bulk as well as monolayer WSe_2 .

O 33.4 Tue 11:00 P3

Transient optical properties in non-equilibrium laser excited noble metals — •MARIUS WENK¹, PASCAL D. NDIONE¹, SEBASTIAN T. WEBER¹, DIRK O. GERICKE², and BAERBEL RETHFELD¹ — ¹Department of Physics and OPTIMAS Research Center, Technische Universität Kaiserslautern — ²CFSa, Department of Physics, University of Warwick

Ultrashort laser pulses can induce strong modifications of material properties of solids such as creating highly transient optical parameters. After excitation with lasers of high power, the conduction electrons thermalize quickly to a hot Fermi distribution. Yet, the band occupation numbers can still be far from equilibrium.

We study excitation of noble metals such as copper and gold with visible photons. We use a two-temperature model and construct electron density-resolved rate equations to simulate the non-equilibrium band occupation [1]. Applying the results of the simulation, particularly the occupation and temperature data, we compute the time-resolved dielectric function based on the Drude-Lorentz formalism. In order to compare the results with experimental data, we calculate

the transient optical properties such as probe reflectivity and transmissivity. Our predictions are compared with time-resolved measurements of optically excited metals, thus providing insights to electron dynamics on femto- and picosecond timescales.

[1] Pascal D. Ndione, Sebastian T. Weber, Dirk O. Gericke, and Baerbel Rethfeld. Scientific Reports, 12(1) 4693 (2022)

O 33.5 Tue 11:00 P3

LabVIEW based software solution for tr-ARPES experiments — •JOHANNES GRADL¹, NIKLAS HOFMANN¹, LEONARD WEIGL¹, YU ZHANG², CEPHISE CACHO³, NEERAJ MISHRA^{4,5}, STIVEN FORTI⁴, CAMILLA COLETTI^{4,5}, and ISABELLA GIERZ¹ — ¹Department of Physics, University of Regensburg, 93040 Regensburg, Germany — ²Central Laser Facility, STFC Rutherford Appleton Laboratory, Harwell Campus, Didcot OX11 0DE, United Kingdom — ³Diamond Light Source, Harwell Campus, Didcot OX11 0DE, United Kingdom — ⁴Center for Nanotechnology Innovation @NEST, Istituto Italiano di Tecnologia, 56127 Pisa, Italy — ⁵Graphene Labs, Istituto Italiano di Tecnologia, 16163 Genova, Italy

Time- and angle-resolved photoemission spectroscopy (tr-ARPES) is an experimental technique used for visualizing non-equilibrium carrier dynamics as well as transient band structures of photoexcited samples as a function of energy, momentum, and time. A tr-ARPES setup ideally includes femtosecond pump pulses with tunable photon energy, femtosecond extreme ultraviolet probe pulses an ultrahigh vacuum chamber equipped with a cryo-cooled sample manipulator and a photoelectron analyzer as well as additional features for in situ sample preparation and characterization. In addition to this hardware, the execution of tr-ARPES experiments requires a user-friendly software for hardware control, data acquisition, and real time data visualization. We will present our LabVIEW based software solution and demonstrate its successful implementation with a series of data sets from a $\text{WS}_2/\text{graphene}$ van der Waals heterostructure.

O 33.6 Tue 11:00 P3

Ultrabroadband THz-STM and its application to study hot electron dynamics in metals — NATALIA MARTÍN SABANÉS^{1,2}, FARUK KRECINIC¹, •VIVIEN SLEZIONA¹, TAKASHI KUMAGAI^{1,3}, FABIAN SCHULZ^{1,4}, LUIS ENRIQUE PARRA LOPEZ¹, ALKISTI VAITSI¹, MARTIN WOLF¹, and MELANIE MÜLLER¹ — ¹Fritz-Haber Institute of the Max-Planck Society, Berlin, Germany — ²IMDEA Nanoscience, Madrid, Spain — ³Institute of Molecular Science, 444-8585 Okazaki, Japan — ⁴CIC NanoGUNE BRTA, San Sebastian, Spain

Localized ultrafast currents across the junction of a scanning tunneling microscope (STM) can be generated by photo-assisted hot electron tunneling or *cold* lightwave-induced tunneling. In addition, but so far not considered, fs laser excitation can induce a transient thermalized electron distribution that can give rise to an ultrafast current component. Here we investigate the role of ultrafast thermionic tunneling for photoinduced hot electron tunneling from a photoexcited STM tip [1]. We access the dynamics of hot electron tunneling by phase-resolved sampling of ultrabroadband Terahertz (THz) waveforms inside the STM junction. Our results reveal the strong nonthermal character of photoinduced hot electron tunneling, and provide a new route to probe hot electron dynamics in metals using THz-STM. Furthermore, we report on the development of an ultrabroadband THz-STM with tunable optical excitation for the spatiotemporal investigation of photocarrier dynamics at metal-semiconducting interfaces. [1] N. Martín Sabanés *et al.*, 10.48550/arXiv.2205.08248

O 33.7 Tue 11:00 P3

Dark Exciton Formation Dynamics in TMDC Monolayers — •SARAH ZAJUSCH¹, LASSE MÜNSTER¹, RAUL PEREA-CAUSIN¹, SAMUEL BREM¹, KATSUMI TANIMURA¹, JENS GÜDDE¹, YAROSLAV GERASIMENKO², RUPERT HUBER², ERMIN MALIC¹, ULRICH HÖFER¹, and ROBERT WALLAUER¹ — ¹Fachbereich Physik, Philipps-Universität Marburg, Germany — ²Fachbereich Physik, Universität Regensburg, Germany

Charge transfer processes in two-dimensional TMDCs are governed by the formation of excitons. The excitonic landscape comprises optically accessible bright excitons as well as momentum- and spin-forbidden dark states. Our experimental setup combines time-resolved momentum microscopy with probe energies in the XUV regime which provides direct access to k-resolved exciton dynamics within the whole Brillouin zone on an ultrafast time scale.

Although structural features are very similar for different semiconductor TMDC materials, slight variations in both electronic band ordering and excitonic binding energy can drastically modify the excited population dynamics. We present a comparison of exciton formation in the two extreme cases of WS_2 and MoSe_2 monolayers after valley-sensitive excitation with circular polarized light. On the one hand, in MoSe_2 the bright KK'-exciton is the energetically most favorable state. On the contrary, in WS_2 , we additionally observe the ultrafast formation of energetically lower dark KK'- and K Σ -excitons. The microscopic understanding of these processes is crucial with regard to interlayer exciton formation in TMDC heterostructures.

O 33.8 Tue 11:00 P3

Time- and Angle-Resolved Photoelectron Spectroscopy with Nano-Focused Surface Plasmon Polaritons — •ALEXANDER NEUHAUS, PASCAL DREHER, DAVID JANOSCHKA, MICHAEL HORN-VON HOEGEN, and FRANK-J. MEYER ZU HERINGDORF — Faculty of Physics and Center for Nanointegration, Duisburg-Essen (CENIDE), University of Duisburg-Essen, 47048 Duisburg, Germany.

Non-perturbative interactions of intense light fields with the electronic band structure in a solid can result in transient electronic properties. The experimental conditions required to realize the necessary field strength can be realized in nano-optical systems, as these can be designed to provide tremendous enhancements of the local field amplitude. Ultimately, observing the non-equilibrium electron dynamics in such systems requires a combination of precise control over the local driving field, state resolution, and spatial selectivity.

Here, we explore electron emission from nano-focused femtosecond surface plasmon polariton (SPP) pulses, providing us with deep-subwavelength spatial selectivity. Time- and angle-resolved photoelectron spectroscopy with attosecond precision provides us access to the coherent and incoherent dynamics of the electron emission process. The technique is applied to the system Cs/Au(111), where we find a resonant enhancement of the electron emission by an image potential state.

O 33.9 Tue 11:00 P3

Ultra Fast Dynamics in Modified Thiophene based Conjugated Donor-Acceptor Organic Polymers — •TOBIAS REIKER^{1,2}, CARSTEN WINTER¹, DEB KUMAR BHOWMICK^{1,2}, NILS FABIAN KLEIMEIER^{1,2}, ZITONG LIU³, DEQING ZHANG³, and HELMUT ZACHARIAS^{1,2} — ¹Center for Soft Nanoscience, University of Münster, Germany — ²Physikalisches Institut, University of Münster, Germany — ³Institute of Chemistry, Chinese Academy of Science, Beijing, China

Thiophene-based polymers are promising candidates for solar cell, OLED or transistor applications. An internal donor - acceptor system is formed by coupling thiophene polymers with pyrrole chains. The charge transport behavior can be tuned by different alkyl side chains since they influence the electronic structure. A direct assessment of the intramolecular and intermolecular dynamics may guide synthesis routes. With pDPP4T, pDPP4T and pDPTT we investigated the electronic dynamics of verified high hole-mobility organic semiconductors. Either the backbone or the side chains were modified. In contrast, another polymer pF8T2 with bi-thiophene in the backbone was used, but with fluorene instead of pyrrole as acceptor. These different molecular configurations are intended to provide insights into the change in electron configuration due to both backbone modification and intermolecular packing. We report results of temporally resolved photoemission studies on thiophene polymers on silicon substrates.

O 33.10 Tue 11:00 P3

Density-dependent electron-phonon coupling in multiband systems. — •TOBIAS HELD, SEBASTIAN T. WEBER, and BAERBEL RETHFELD — Department of Physics and Research Center OPTIMAS, TU Kaiserslautern, Germany

If a solid is irradiated with a short-pulsed laser in the visible spectrum, the energy is almost entirely absorbed by the electrons while the lattice remains cold. The subsequent energy flow between electrons and phonons is usually described by the electron-phonon coupling parameter, which plays a central role in the Two-Temperature Model and most other temperature-based models. This coupling parameter depends on a multitude of observables. Most frequently a dependence on the electron temperature is considered.

In this work, we aim to investigate how a varying density distribution between different electron subsystems affects the coupling parameter. In gold, we distinguish between sp- and d-electrons and in magnetic nickel between majority and minority spins. Our results show that for gold, the total coupling strongly depends on the density distribution, while for nickel it is largely independent on the spin densities. In the latter case, the individual coupling contributions of the bands change significantly with density but mostly compensate each other in terms of the total coupling.

O 33.11 Tue 11:00 P3

Electron Dynamics of an intercalated Graphene Layer on Nickel — •KATHARINA HILGERT¹, CHRISTINA SCHOTT¹, EVA WALTHER¹, KAMAN YU¹, MARTIN AESCHLIMANN¹, and BENJAMIN STADTMÜLLER^{1,2} — ¹Department of Physics and Research Center OPTIMAS, University of Kaiserslautern, 67663 Kaiserslautern Germany — ²Institute of Physics, Johannes Gutenberg University Mainz, 55128 Mainz, Germany

One of the great challenges in information technology is to develop novel concepts for the realization of active functional units on ever smaller length scales. The simplest approach to reduce the size of any device structure is to employ atomically thin materials as graphene with their unique electronic and optical properties. However, these are often altered on surfaces due to strong chemical interaction with the substrate material. On this poster we present our approach to restore and design the electronic properties of graphene on a Ni(111) surface by intercalation of lead atoms. The changes in the electronic band structure of graphene on Ni(111) are monitored by angle resolved photoelectron spectroscopy with extreme ultra violet radiation. On the highly reactive Ni(111) surface, the linear dispersion of the Dirac cone of the free-standing graphene sheet is completely suppressed by the strong graphene surface interaction. This changes significantly after the intercalation of Pb. The band structure of the graphene/Pb/Ni(111) system reveals again the linear dispersion resembling the behavior in free-standing graphene. This has clear consequences on the carrier dynamics near the K-point as we will discuss in this contribution.

O 34: Poster Tuesday: Scanning Probe Techniques 2

Time: Tuesday 11:00–13:00

Location: P3

O 34.1 Tue 11:00 P3

Implementation of a Scanning Tunneling Microscope for Measurements in Electrochemical Environment — •FABIAN SCHRÖFEL, MATTHIAS GREVE, KARSTEN TARHOUNI, and OLAF MAGNUSSEN — Institute of Experimental and Applied Physics, Kiel University, Kiel, Germany

The atomic-scale understanding of processes at the interface between solid electrodes and liquid electrolytes is of high importance for electrochemical energy storage and conversion. Electrochemical scanning tunneling microscopy (ECSTM) is a key technique for the investigation of such interfaces. Operating an STM in an electrochemical environment requires special measures, as the potentials of both STM tip and sample need to be controlled and electrochemical currents at the tip need to be kept way below the tunneling current.

Here, we report details on a new ECSTM built in our group. It consists of a newly developed STM head that is optimized for studies in electrochemical environment, high scanning frequencies, and low thermal drift. The instrument is based on a commercial SPECS Nanonis STM controller that we equipped with a custom-build bipotentiostat and coarse-approach. A suitable control software for electrochemical studies, which we integrated into the Nanonis software, allows to perform cyclic voltammetry parallel and separate from the STM measurements. Characterization of the mechanical stability of the STM and first STM images and electrochemical data will be presented.

O 34.2 Tue 11:00 P3

Determining the phase transfer function of an STM for coherent spin operations — •EVERT STOLTE — TU Delft

Coherent control of single spin transitions in atoms on a surface has been achieved with electron spin resonance scanning tunnelling microscopy (ESR-STM).[1] Extending that control to a series of sequential gates on different transitions and developing more complex gates requires radio frequency (RF) pulses

at different frequencies with controlled relative amplitudes and phases, which are both affected by the transfer function of the power line to the tunnel junction. While the amplitude transfer function can be determined through a well-described rectification procedure [2], characterizing the phase transfer function remains challenging. Straightforward transmission or reflection measurements are excluded as it is not possible to separate phase rotations incurred on the way into the STM from those happening on the outward journey.

Here we report on the development of an in-situ method to determine the phase transfer function at radio frequencies that can be readily implemented to standard ESR-STM setups. The method is based on the envelope detection of the beat signal that is generated by adding two continuous wave RF signals separated by an audio frequency. The effectivity of the procedure is tested through pump-probe autocorrelation measurements with square pulses, which should show a reduced minimum width if the phase correction is successful.

[1] Yang, K. (2019). *Science*, 366(6464), 509-512.[2] Paul, W. (2016). *Review of Scientific Instruments*, 87(7).

O 34.3 Tue 11:00 P3

Performance of an electrically driven q-plus sensor in a commercial Joule Thomson STM — •HESTER VENNEMA, LAËTITIA FARINACCI, and SANDER OTTE — Delft University of Technology, Delft, The Netherlands

The q-plus sensor is a wide-spread tool for performing combined STM-AFM measurements in ultra-high vacuum at cryogenic temperatures. Here, we implement the use of q-plus sensors in a JT-STM. Contrary to other set-ups in which q-plus sensors are used, we do not drive our sensor mechanically, via an excitation of the Z-piezo, but electrically, with the excitation signal directly sent to the tuning fork.

In order to characterize the performance of our homemade q-plus sensors we develop a set-up to test their response to an electrical drive in ambient con-

ditions. Following M. Lee et al. [1], we can disentangle the mechanical and electrical response of the sensors to the driving signal. After transfer into the JT-STM, we demonstrate the possibility to use electrically driven q-plus sensors for combined STM-AFM measurements: with a Q factor around 20000 we can control the amplitude of the oscillation to be as low as 70 pm. Our first principle measurements are performed on a CuCl₂/Cu(100) surface [2]. We investigate with local contact potential difference measurements the local change of work function that leads to the confinement of field emission resonances above such vacancy patches.

[1] M. Lee et al., Appl. Phys. Lett. 91, 023117 (2007)

[2] R. Rejali et al., arXiv:2204.10559 (2022)

O 34.4 Tue 11:00 P3

Development of a compact millikelvin STM for single spin resonance — •DARIA SOSTINA¹, DAVID COLLOMB², WANTONG HUANG², MATE STARK², CHRISTOPH SÜRGER², PHILIP WILLKE², and WOLFGANG WERNSDORFER² — ¹Institute for Quantum Materials and Technologies (IQMT), Karlsruhe Institute of Technology, Karlsruhe, Germany — ²Physikalisches Institut (PHI), Karlsruhe Institute of Technology, Karlsruhe, Germany

In the last decade detection and manipulation of spins at the atomic scale has been achieved by combining techniques like electron spin resonance (ESR) with scanning tunneling microscopy (STM) [S. Baumann et al., Science 350 (6259), 417-420 (2015)]. However crucial properties of potential quantum spins such as the spin relaxation time T₁ and the phase coherence time T₂ remain short. Both T₁ and T₂ are affected by the proximity to the tip and substrate, which provide thermally excited electrons [P. Willke et al., Science Advances 4(2), 1543 (2018)]. A potential solution lies in lowering the temperatures utilizing dilution refrigerators (DR). Here, we present the design and implementation of a unique DR-STM optimized for ESR reaching millikelvin temperatures. Since the ground state population scales with the resonance frequency, better RF transmission at high frequencies is also desired for ESR-STM. In the compact dilution fridge, the RF line is optimized by a short total length of cables as well as using high-frequency cabling up until the tip. As a result, we believe that our compact DR-STM will help to improve ESR-STM paving the way for quantum information processing using single spin centers on surfaces.

O 34.5 Tue 11:00 P3

Design of a high-stability miniaturized scanning tunneling microscope for small-bore cryostats — •FELIX HUBER, STEPHAN SPIEKER, and SEBASTIAN LOTH — University of Stuttgart, Institute for Functional Matter and Quantum Technologies, Stuttgart, Germany

Low-temperature scanning tunneling microscopy (STM) setups are typically housed in large cryostats and require proportionally large vacuum chambers, as well as extensively shielded custom-built laboratories to reach the signal-to-noise ratios (SNR) desired for cutting-edge research. Yet, by miniaturizing the STM-head, the SNR can be significantly improved, due to the favorable scaling of resonance frequencies [1], thermal characteristics and the cryostat hold time. The STM design presented here, is optimized to work in noisy environments, provides optical access to the tunnel junction, and can be used in a standard-bore cryogenic dewar due to its small volume and dimensions [2]. This design could be used for experiments requiring long averaging times, and may serve as an easy upgrade to existing room-temperature setups.

[1] C.R. Ast, et al. Rev. Sci. Instrum. 79, 093704 (2008).

[2] R. Schlegel, et al. Rev. Sci. Instrum. 85, 013706 (2014).

O 34.6 Tue 11:00 P3

Functionalized Tips in low-temperature AFM/STM - Fabrication and Application — •LORENZ BRILL, MARCO GRÜNEWALD, ROMAN FORKER und TORSTEN FRITZ — Friedrich-Schiller-Universität, Jena, Germany

AFM with functionalized tips has been an emergent and fast growing field in the last couple of years. The chemical passivation of the metal tip achieved via functionalization allows for images with atomic or intramolecular resolution to be recorded.

In our contribution, we detail the fabrication of CO-functionalized tips with a commercial low-temperature STM/AFM by Specs Surface Nano Analysis GmbH and demonstrate atomic resolution on a Cu(111)-surface. Furthermore, we show structure elucidation of organic molecular islands on the Cu(111)-substrate via atomic resolution images.

This technique shows great promise for further investigations, especially in areas not accessible via conventional STM, e.g. detailed structure analysis of 1,4-benzoquinone on metal substrates.

O 34.7 Tue 11:00 P3

Inspecting non-linearities in scanning force microscopy — •LUKAS BÖTTCHER¹, ANNA DITTUS², JENS STARKE², INGO BARKE¹, and SYLVIA SPELLER¹ — ¹Institute of Physics, University of Rostock — ²Institute of Mathematics, University of Rostock

In dynamic force microscopy bistable states are often encountered. This includes two stable states at small and large amplitude flanking one unstable state at intermediate amplitude, separating two attracting regions. Our aim is to investigate the behavior of oscillating cantilevers in dynamic force microscopy [1,2]. We acquired distance dependent frequency sweeps of amplitude and phase. From this we determined saddle-node branches with cusps and compare the behavior with simulations.

[1] A.C. Boccaro et al., Applied Physics Letters 58 (1991).

[2] Robert W. Stark, Materials Today 13 (2010)

O 34.8 Tue 11:00 P3

Setup for laser-based time-resolved momentum microscopy — •FELIX PASSLACK, STEFANO PONZONI, GIOVANNI ZAMBORLINI, and MIRKO CINCHETTI — Department of Physics, TU Dortmund University, Otto-Hahn-Straße 4, Dortmund, Germany

In this work, we characterize the performance of a recently installed time-resolved angular-resolved photoemission spectroscopy (tr-ARPES) system. tr-ARPES is performed by coupling an optical beamline for pump-probe spectroscopy [1] to a state-of-the-art momentum-microscopy photoemission spectrometer (KREIOS MM, SPECS GmbH). This allows for an almost continuous tunability of the pump photon energy between 0.5 eV and 3.8 eV while capturing the full photoemission horizon of the 6 eV probe. The performance of the system is characterized through a set of measurements on the topological insulator Bi₂Se₃, for which both the static electronic structure and the out of equilibrium electron dynamics are already extensively studied in literature following the evolution of the electronic structure with an energy resolution in the order of 50 meV, a momentum resolution of 0.005 Å⁻¹ and a time resolution below 500 fs throughout the whole photoemission horizon. In particular, thanks to the ultimate angular acceptance of the photoemission microscope, we are able to track the dispersion of the photoexcited states in Bi₂Se₃ up to ±0.48 Å⁻¹ and 1 eV above the Dirac point, beyond the practical limitations of conventional high-resolution ARPES spectroscopy with 6 eV photons. [1] F. Mertens et al., Review of Scientific Instruments 91 (2020)

O 34.9 Tue 11:00 P3

Development and characterization of a Herriott-type multipass cell compression-setup for fs-pulses and variable repetition rates — •LASSE STERNEMANN¹, KARL SCHILLER¹, ALAN OMAR², MATIJA STUPAR¹, MIRKO CINCHETTI¹, and CLARA SARACENO² — ¹Department of Physics, TU Dortmund University, Otto-Hahn-Straße 4, 44227 Dortmund, Germany — ²Ruhr-Universität Bochum, Germany

We present development and characterization of a Herriott-style multipass cell aimed at achieving ultrashort pulses with high peak power. The setup is used as a driving laser for a high repetition rate HHG (High Harmonic Generation) source for time-resolved momentum microscopy.

The setup compresses the pulses generated by a commercial Ytterbium-based laser (Carbide, Light Conversion) with an average power of 50 W and a variable repetition rate between 100 kHz and 1 MHz. The pulses are first spectrally broadened by self-phase-modulation by passing through a non-linear χ⁽³⁾ medium multiple times. Then, a pair of negative group-dispersion-delay coated mirrors compress the pulse by dispersion correction. By moving the non-linear medium within the multipass cell we were able to compress the pulses from 242 fs to around 45 fs for different high repetition rates while keeping a transmission of over 90% and peak powers between 1 GW and 2 GW [1].

[1] A. Omar, et al. *Advanced Solid State Lasers*, OSA Technical Digest (Optical Society of America, 2021), paper JM3A.55

O 34.10 Tue 11:00 P3

Multispectral time-resolved energy-momentum microscopy using high-harmonic extreme ultraviolet radiation — •NILS WIND^{1,2}, MICHAEL HEBER³, DMYTRO KUTNYAKHOV³, FEDERICO PRESSACCO³, and KAI ROSSNAGEL^{2,4} — ¹Institut für Experimentalphysik, Universität Hamburg, 22761 Hamburg, Germany — ²Ruprecht-Haensel-Labor, Deutsches Elektronen-Synchrotron DESY, 22607 Hamburg, Germany — ³Deutsches Elektronen-Synchrotron DESY, 22607 Hamburg, Germany — ⁴Institut für Experimentelle und Angewandte Physik, Christian-Albrechts-Universität zu Kiel, 24098 Kiel, Germany

A 790-nm-driven high-harmonic generation source with a repetition rate of 6 kHz is combined with a toroidal-grating monochromator and a high-detection-efficiency photoelectron time-of-flight momentum microscope to enable time- and momentum-resolved photoemission spectroscopy over a spectral range of 23.6–45.5 eV with sub-100-fs time resolution. Three-dimensional (3D) Fermi surface mapping is demonstrated on graphene-covered Ir(111) with energy and momentum resolutions of ≤100 meV and ≤0.1 Å⁻¹, respectively. The table-top experiment sets the stage for measuring the k_z-dependent ultrafast dynamics of 3D electronic structure, including band structure, Fermi surface, and carrier dynamics in 3D materials as well as 3D orbital dynamics in molecular layers.

O 35: Poster Tuesday: Plasmonics and Nanoptics 1

Time: Tuesday 11:00–13:00

Location: P3

O 35.1 Tue 11:00 P3

Positioning of DNA origami based nanostructures on surfaces by lithographic patterning — ZHE LIU¹, ZUNHAO WANG², BIRKA LALKENS³, DAESUNG PARK², JANNIK GUCKEL², JULIANE BREITFELDER³, and MARKUS ETZKORN¹ — ¹Institute of Applied Physics, Technische Universität Braunschweig, 38106 Braunschweig, Germany — ²Physikalisch Technische Bundesanstalt, 38116 Braunschweig, Germany — ³Institute of Semiconductor Technology, Technische Universität Braunschweig, 38106 Braunschweig, Germany

Self-assembly protocols of functionalized DNA-origami structures can be used to create large amounts of identical hybrid nanostructures. We use this approach to create structures with tunable plasmonic properties. In our study, dimers of 15 nm gold nanoparticles with an average gap of 7 nm were self-assembled in solution. In order to control the positioning of such DNA-origami structures on surfaces, we created surface areas with hydrophobic/hydrophilic contrast by electron beam lithography and dry oxidative etching. This protocol offers positional control on the sub 10 nm scale. Here we will present results for hexamethyldisilazane (HDMS) covered silicon, but the approach can be utilized for various substrates and nanostructures. Our origami/dimer structure shows highly selective adsorption on different lithographically patterned structures. We achieve an efficiency in positioning, that is the ratio of origami in wanted to those in unwanted positions, of above 95%. Important parameters controlling the efficiency are discussed.

O 35.2 Tue 11:00 P3

Investigation of the plasmonic Phase-Change Materials AgSnTe₂ and In₃SbTe₂ for tuning nanoantenna resonances — KILIAN WILDEN, LUKAS CONRADS, ANDREAS HESSLER, MATTHIAS WUTTIG, and THOMAS TAUBNER — I. Institute of Physics (IA), RWTH Aachen University

Providing a high optical contrast between their amorphous and crystalline phases, phase-change materials (PCMs) can serve for many applications in nanophotonics. [1] Optical pulses can be used for switching between those two states. This enables the tunability of antenna resonances by changing the surrounding medium. Currently, a novel material class of switchable infrared plasmonic PCMs is rising, which is characterized by a negative permittivity and therefore a Drude-like behaviour in the crystalline. This plasmonic PCM In₃SbTe₂ (IST) offers resonance tuning by reconfiguring the antenna shapes of rod antennas and even more complex ones with magnetic resonances.[2] AgSnTe₂ (AST) is another plasmonic PCM with a smaller plasma frequency and higher plasmonic losses than IST. Here, we investigate directly optically written antenna structures of crystalline AST. The quality of the plasmonic resonances is compared to IST antennas. Furthermore, the well-established concepts of reconfiguring antenna geometries are applied to inverse antenna structures, in which amorphous holes are created in a crystalline plasmonic surrounding. Their resonance behavior can be described by Babinet's principle. [1] M. Wuttig, H. Bhaskaran and T. Taubner, *Nature Photonics* 11, 465-476 (2017). [2] A. Heßler et al., *Nature Communications* 12, 924 (2021).

O 35.3 Tue 11:00 P3

Large area writing of reconfigurable metasurfaces with the plasmonic PCM In₃SbTe₂ — NATALIE HONNÉ¹, LUKAS CONRADS¹, ANDREAS ULM², ANDREAS HESSLER¹, MATTHIAS WUTTIG¹, ROBERT SCHMITT², and THOMAS TAUBNER¹ — ¹I. Institute of Physics (IA), RWTH Aachen University — ²Fraunhoferinstitut für Produktionstechnologie

Phase-change materials (PCMs) are optimal candidates for optical components being non-volatile and reversibly switchable. Their amorphous and crystalline phases differ tremendously in their properties. Conventional PCMs exhibit a large contrast in their refractive index and can be used to tune antenna resonances by influencing their surrounding.[1] Recently, plasmonic PCMs, like In₃SbTe₂, has been introduced. They switch between a dielectric (amorphous) and a metallic (crystalline) phase in the complete IR and enable optical writing of metallic nanoantennas directly in a dielectric surrounding.[2] Large area writing of reconfigurable metasurfaces is a key feature for tuneable nanophotonic devices. Here, the Nanoscribe Photonic Professional GT is used, a femtosecond laser writer with an infrared wavelength. Large area direct laser crystallization is investigated to fabricate antenna arrays of several hundred micrometers. Finally, a beam steering device is designed and fabricated. This work paves the way towards large area fabrication of functional metasurfaces in the IR with the ability of rapid prototyping for IR nanophotonic devices.

1. Wuttig et al., *Nature Photonics* 11,465 (2017)2. Heßler et al., *Nature Communications* 12, 924 (2021)

O 35.4 Tue 11:00 P3

Direct Writing of Chiral and Nonlinear Plasmonic Devices — ALEKSEI TSARAPKIN¹, VICTOR DEINHART¹, THORSTEN FEICHTNER², and KATJA HÖFLICH¹ — ¹Ferdinand-Braun-Institut gGmbH, 12489 Berlin, Germany — ²University of Würzburg, 97074 Würzburg, Germany

The miniaturization of electrical and optical components allowed many technological and economic advancements over the last decades. Devices that permit control over the polarization of light are crucial in telecommunication and quantum optics but are usually realized as bulky optical systems and thus require further miniaturization. Here we aim at designing a uniquely compact converter and detector based on nanostructures. The device consists of a vertically oriented gold double helix coupled to a planar two-wire transmission line. The helix acts as a sensitive antenna for circularly polarized light, while the plasmonic transmission line guides plasmons on-chip. With numeric analysis we show that antisymmetric modes can be excited in both double helix and two-wire waveguide allowing spatial matching. Furthermore, one can match impedances of both components to maximize power transfer by adjusting their sizes. Finally, we developed fabrication protocols: while the helix can be directly written with an electron-induced deposition, the plasmonic waveguide can be cut from single-crystalline gold flake utilizing focused gallium-ion beam milling. We achieved high structuring resolution with both methods, allowing for efficient coupling to transform linear to circular polarization while retaining a device size of just a few microns.

O 35.5 Tue 11:00 P3

Transverse magnetic routing of light emission in hybrid plasmonic-semiconductor nanostructures: Grating period dependence — CAROLIN HARKORT¹, LARS KLOMPMAKER¹, ALEXANDER N. PODDUBNY², LEONID V. LITVIN³, RALF JEDE³, GRZEGORZ KARCEWSKI⁴, SERGIJ CHUSNUTDINOW⁴, TOMASZ WOJCIOWICZ⁵, DMITRI R YAKOVLEV^{1,2}, MANFRED BAYER^{1,2}, and ILYA A. AKIMOV^{1,2} — ¹Experimentelle Physik 2, Technische Universität Dortmund, 44221 Dortmund, Germany — ²St. Petersburg — ³Raith GmbH, Konrad-Adenauer-Allee 8, 44263 Dortmund, Germany — ⁴Institute of Physics, Polish Academy of Sciences, PL-02668 Warsaw, Poland — ⁵International Research Centre MagTop, PL-02668 Warsaw, Poland

We use plasmonic gratings to achieve transverse magnetic routing of the light emission of a nearby quantum well exciton via an external magnetic field. In a hybrid plasmonic-semiconductor (Cd,Mn)Te/(Cd,Mg)Te quantum well (QW) structure the effect of the plasmonic grating period on the directional emission spectra is measured using a Fourier imaging setup to obtain angular and energy resolved photoluminescence spectra for opposite transverse magnetic fields. We achieve a strong directionality of the QW emission of up to 15% at low temperature of about 5 K and magnetic fields of 500 mT with a grating period of 240 nm and demonstrate the effect of the changing SPP dispersion on the directional emission characteristics.

O 35.6 Tue 11:00 P3

Mapping Lamb, Stark and Purcell effects at a chromophore-picocavity junction with hyper-resolved fluorescence microscopy — ANNA ROSŁAWSKA¹, TOMÁŠ NEUMAN^{1,2,3}, BENJAMIN DOPPAGNE¹, ANDREI G. BORISOV³, MICHELANGELO ROMEO¹, FABRICE SCHEURER¹, JAVIER AIZPURUA², and GUILLAUME SCHULL¹ — ¹Université de Strasbourg, CNRS, IPCMS, UMR 7504, F-67000 Strasbourg, France — ²Center for Materials Physics (CSIC-UPV/EHU) and DIPIC, Paseo Manuel de Lardizabal 5, Donostia - San Sebastián 20018, Spain — ³Institut des Sciences Moléculaires d'Orsay (ISMO), UMR 8214, CNRS, Université Paris-Saclay, 91405 Orsay Cedex, France

Light-matter interaction plays a crucial role in the properties of light emission from single molecules. Here, we show that it can be probed with sub-molecular precision thanks to the atomically-confined electromagnetic field at the scanning tunneling microscope tip apex, which acts as a picocavity for localized plasmons. Such strong fields interact with the molecular exciton via Purcell, Lamb and Stark effects, which enable tuning the emission energy and line width. Hyper-resolved fluorescence maps of these two parameters can be understood as images of the static charge redistribution upon electronic excitation of the molecule, and the distribution of the dynamical charge oscillation associated with the molecular exciton, respectively [1].

[1] A. Rosławska et al., *Phys. Rev. X*, 12, 011012, 2022.

O 35.7 Tue 11:00 P3

Steps towards fluorescence detected two-dimensional electronic spectroscopy of a single molecule — SANCHAYEETA JANA and MARKUS LIPPITZ — Chair for Experimental Physics III, University of Bayreuth, Bayreuth, Germany

Two-dimensional electronic spectroscopy (2DES) is an ultrafast spectroscopic technique which gives information about the coupling between molecular energy levels. As spectroscopy of a single molecule by fluorescence detection is

a well established technique, we want to explore whether fluorescence-detected 2DES is possible at very low concentrations, ideally even on a single molecule. We use a sequence of four phase-modulated pulses to excite the molecules and collect the fluorescence by a high NA objective. The signal amplitude is demodulated at several mixing frequencies to extract the rephasing and nonrephasing contributions.

In this work, we study the 2D spectra measured from an ensemble of molecules in solution and discuss the challenges to experimentally measure 2D spectra from a single molecule.

O 35.8 Tue 11:00 P3

Coupling single epitaxial quantum dots to plasmonic waveguides — •MICHAEL SEIDEL¹, YUHUI YANG², SAIMON COVRE DA SILVA³, THORSTEN SCHUMACHER¹, ARMANDO RASTELLI³, STEPHAN REITZENSTEIN², and MARKUS LIPPITZ¹ — ¹Experimental Physics III, University of Bayreuth, Germany — ²Institute of Solid State Physics, TU Berlin, Germany — ³Institute of Semiconductor and Solid State Physics, Johannes Kepler University Linz, Austria

Integrated plasmonic nanocircuits are highly promising building blocks for future quantum optical applications. In combination with self-assembled epitaxially grown GaAs quantum dots as stable, bright and narrow-band single-photon sources, ultra-compact nanocircuits operating below the diffraction limit can be designed [1]. A crucial aspect is the coupling of the quantum dot emission into plasmonic waveguide modes. In this work, we demonstrate the coupling of a single near-surface GaAs quantum dot to a silver nanowire by introducing a 100nm thick dielectric spacer layer. We characterize the nanostructure by comparing different imaging methods involving low-temperature cathodoluminescence and photoluminescence as well as confocal laser reflection mapping. Supported by 3D numerical simulations, we find that resonant plasmonic wires can enhance the waveguide coupling efficiency.

[1] Wu et al., Nano Lett. 2017, 17, 7, 4291-4296

O 36: Overview Talk Hendrik Bluhm

Time: Wednesday 9:30–10:15

Location: S054

Invited Talk

O 36.1 Wed 9:30 S054

Heterogeneous chemistry of liquid-vapor interfaces investigated with X-ray photoelectron spectroscopy — •HENDRIK BLUHM — Fritz Haber Institute of the Max Planck Society, Berlin, Germany

Liquid-vapor interfaces drive numerous important processes in the environment and atmosphere, such as the sequestration of CO₂ by the oceans and the uptake

and release of trace gases by aerosol droplets. X-ray photoelectron spectroscopy is an excellent method for the investigation of liquid-vapor interfaces due to its interface sensitivity and chemical specificity. In this talk we will discuss the general approach in XPS experiments on liquid interfaces and present illustrative examples of the investigation of the heterogeneous chemistry of surfactants and ions at the interface of aqueous solutions.

O 37: Plasmonics and Nanooptics 1

Time: Wednesday 10:30–12:45

Location: H3

Topical Talk

O 37.1 Wed 10:30 H3

Merging integrated photonics with free-electron beams — •ARMIN FEIST — Max Planck Institute for Multidisciplinary Sciences, 37077 Göttingen, Germany The coherent coupling of electrons and light is at the heart of free-electron quantum optics [1]. However, fully exploring its capabilities requires supreme control over the electron beam and optical quantum states involved. This suggests combining integrated photonics with electron microscopy.

In this talk, I will briefly introduce the basic principles and selected applications of inelastic electron-light scattering in an ultrafast transmission electron microscope (UTEM) [2,3], including the nanoscale imaging of confined optical modes and shaping of electron beams in space and time [4].

Recent progress in coupling single electrons to high-Q integrated photonic microresonators will be discussed, enabling highly efficient continuous-wave optical phase modulation of electron beams and nanoscale- μeV spectroscopy of a photonic mode [5]. Furthermore, spontaneous scattering at the empty resonator modes creates electron-photon pair states [6], opening a pathway towards a new class of heralded single-electron or Fock-state photon sources.

[1] K. Wang *et al.*, Optics & Photonics News **31**, 35 (2020). [2] Barwick *et al.*, Nature **462**, 902 (2009). [3] A. Feist *et al.*, Nature **521**, 200 (2015). [4] F.J. Garcia de Abajo & V. Di Giulio, ACS Photonics **8**, 945 (2021). [5] J.W. Henke *et al.*, Nature **600**, 653 (2021). [6] A. Feist *et al.*, arXiv:2202.12821 (2022).

O 37.2 Wed 11:00 H3

Near-field spectroscopic predictions of low-temperature, gate-tunable plasmon-phonon coupling in the LaAlO₃/SrTiO₃ two-dimensional electron gas — •JULIAN BARNETT¹, YIGONG LUAN¹, FELIX GUNKEL², and THOMAS TAUBNER¹ — ¹I. Institute of Physics (IA), RWTH Aachen University — ²Peter Grünberg Institute, Forschungszentrum Jülich

Heterointerfaces of SrTiO₃ and LaAlO₃ give rise to a buried two-dimensional electron gas (2DEG) between polar insulators, that is very sensitive to local defects but difficult to characterize on the nanoscale. It was recently shown that scanning near-field optical microscopy (SNOM) enables the extraction of local 2DEG properties with nanoscale lateral resolution by using phonon-enhanced near-field spectroscopy. Interestingly, the 2DEG mobility increases strongly at low temperatures and the charge carrier concentration can be tuned via gating, allowing control over the electronic properties.

Here, we predict that the plasmon-phonon-coupled near-field response will undergo a transition from a phonon-dominated regime to a plasmon-dominated regime with rising 2DEG mobility, which translates to a fundamentally different near-field spectrum. Additionally, we show that the plasmon-dominated regime could allow for the extraction of the 2DEG depth distribution with nanoscale lateral resolution, potentially enabling its mapping around defects. These in-

sights can be directly transferred to the spectroscopic near-field investigation of 2DEGs, surface accumulation layers, and topologically protected surface states in a variety of bulk materials and heterostructures.

O 37.3 Wed 11:15 H3

Generation of Rotating Fields via Archimedean Spirals — •ESRA ILKE ALBAR, HEIKO APPEL, and FRANCO BONAFE — Max Planck Institute for the Structure and Dynamics of Matter, Center for Free Electron Laser Science, 22761 Hamburg, Germany

Twisted light (optical vortex), has the distinctive feature that it carries orbital angular momentum. This special type of electromagnetic field promises exciting opportunities for the interaction with matter, and it is expected to enhance spectroscopic techniques. Twisted light already has a vast potential of applications ranging from astronomy and optical tweezers to spintronics. Given this broad spectrum of applications and exciting prospects, it becomes worthwhile to investigate new and efficient methods to generate optical vortices. In this sense, metallic Archimedean spirals in the micro- and nanoscale are good candidates to produce such vortices. We design Archimedean spirals and test their performance in terms of generating field vortices. We perform numerical simulations with the Octopus code which employs the Riemann-Silberstein representation to propagate Maxwell's equations in real-time. Circularly-polarized light is passed through the designed structure, which is modeled both as a non-dispersive linear medium, and as Drude medium. We found that the out-coming field's angular momentum is altered by the structure. By using two different material models the effect of the materials' optical properties and the sole geometrical factors on the angular momentum outcome could be distinguished.

O 37.4 Wed 11:30 H3

Theory of radial oscillations in metal nanoparticles driven by optically induced electron density gradients — •ROBERT SALZWEDEL¹, ANDREAS KNORR¹, DOMINIK HÖING^{2,3}, HOLGER LANGE^{2,3}, and MALTE SELIG¹ — ¹Institut für Theoretische Physik, Nichtlineare Optik und Quantenelektronik, Technische Universität Berlin, 10623 Berlin, Germany — ²Institut für Physikalische Chemie, Universität Hamburg, 20146 Hamburg, Germany — ³The Hamburg Centre for Ultrafast Imaging, 22761 Hamburg, Germany

Upon optical excitation, metal nanoparticles oscillate in radial breathing modes. These oscillations are assumed to be driven mainly by the thermalization of hot electrons impulsively heating the lattice, which can be described classically [1,2]. Based on a combined approach of quantum hydrodynamics and Heisenberg equations of motion for the optical excitation of electron gas in metal nanoparticles and the associated electron-phonon interaction, we discuss the contribution of additional coherent sources to the radial breathing oscillations.

Our results reveal a more direct coupling mechanism between the field and phonons compared to the established interpretation of experiments: the optical pulse induces spatial gradients in the electron density that drive phonon oscillations coherently and directly on the time scale of the optical excitation. Therefore, thermal and coherent contributions must be considered in the early times of the oscillation.

- [1] Hartland, G. V. et al., *JCP*, **116**, 8048 (2002)
 [2] Hodak, J. H. et al., *JCP*, **111**, 8613 (1999)

O 37.5 Wed 11:45 H3

Near-field imaging of hyperbolic shear polaritons in gallium oxide — •SÖREN WASSERROTH¹, JOSEPH R. MATSON², XIANG NI³, GIULIA CARINI¹, KATJA DIAZ-GRANADOS², MAXIMILAN OBST⁴, ENRICO MARIA RENZI³, EMANUELLE GALIFI³, SUSANNE KEHR⁴, LUKAS M. ENG⁴, MARTIN WOLF¹, THOMAS G. FOLLAND⁵, ANDREA ALU³, JOSHUA D. CALDWELL², and ALEXANDER PAARMANN¹ — ¹Fritz-Haber-Institut der Max-Planck-Gesellschaft, Berlin, Germany — ²Vanderbilt University, Nashville, USA — ³City University of New York, New York, USA — ⁴Technische Universität Dresden, Dresden, Germany — ⁵University of Iowa, Iowa, USA

Controlling the propagation direction and other properties of light in a material and at an interface is a very active field in current research. Strong anisotropy in crystals can lead to a hyperbolic dispersion featuring coupled light-matter interactions known as polaritons with highly directional propagation. Recently [1], it was shown that the additional anisotropy in monoclinic crystals, such as beta phase gallium oxide (bGO), gives rise to tilted wave fronts and asymmetric responses, called hyperbolic shear polaritons (HShPs).

Here, we will show mid-infrared free electron laser based near-field imaging of HShPs in bGO. Gold discs are used as local emitters on the bGO substrate. By changing the IR wavelength we observe the rotation and asymmetry of the HShPs. We compare the obtained images to simulated near-field contributions.

- [1] Passler et al., *Nature* **602**, 595 (2022)

O 37.6 Wed 12:00 H3

Long-wave infrared super-resolution wide-field microscopy using sum-frequency generation — •RICHARDA NIEMANN¹, SÖREN WASSERROTH¹, GUANYU LU², CHRISTOPHER R. GUBBIN³, SIMONE DE LIBERATO³, JOSHUA D. CALDWELL², MARTIN WOLF¹, and ALEXANDER PAARMANN¹ — ¹Fritz Haber Institute of the Max Planck Society, Berlin, Germany — ²Vanderbilt University, Nashville, USA — ³University of Southampton, UK

We present our approach in infrared-visible (IR-VIS) sum-frequency generation (SFG) microscopy as a new tool for super-resolution imaging in the IR range.[1] Here, the imaging contrast in the microscope emerges from the IR resonances while the spatial resolution is provided by the SFG wavelength, i.e., well below the IR diffraction limit. As a proof of concept, we study localized phonon polaritons in sub-diffractive nanostructures made of Silicon Carbide.[2,3] A free electron laser as IR light source offers high-power laser pulses with tunable wavelengths.[4] We are able to resolve phonon polariton modes in individual sub-diffractive nanostructures and achieve a spatial resolution of $\sim 1.4 \mu\text{m}$ corresponding to $\lambda_{IR}/9$. [1] Full spectral mapping over the whole SiC Reststrahlenband allows the spectroscopic identification of the polariton resonances, while the high spatial resolution reveals the microscopic origin of the SFG emission.

O 38: Solid-Liquid Interfaces 4: Reactions and Electrochemistry

Time: Wednesday 10:30–12:30

Location: H4

Topical Talk

O 38.1 Wed 10:30 H4

Electrochemical Microcalorimetry — •ROLF SCHUSTER and MARCO SCHÖNIG — Institute of Physical Chemistry, Karlsruhe Institute of Technology, 76131 Karlsruhe, Germany

We investigate electrochemical reactions at single electrodes by measuring the accompanying heat changes. The heat reversibly exchanged during an electrode process is directly correlated to the reaction entropy of the half-cell reaction including all side reactions, e.g., ordering processes of the solvent or coadsorption processes of anions. Thus, measuring the heat exchange during an electrochemical process provides independent information on the ongoing reaction, which is complementary, e.g., to the potential-current relation, usually measured by cyclic voltammetry or impedance spectroscopy.

In this contribution we will briefly discuss some theoretical aspects of electrochemical microcalorimetry of single electrodes and present our strategy to measure the heat evolution upon surface electrochemical processes. With our setup we are sensitive to heat effects originating from minute conversions of a few percent of a monolayer of an electroactive species.

We will present examples for entropy changes upon anion adsorption and double layer charging on Au(111) and discuss the effect of configurational entropy of the adlayer. The hydrogen adsorption on Pt-films deals as an exam-

- [1] R. Niemann et al., *Appl. Phys. Lett.* **120**, 131102 (2022)

- [2] J.D. Caldwell et al., *Nanophotonics* **4**, 1 (2015)

- [3] I. Razzdolski et al., *Nano Letters* **16**, 6954 (2016)

- [4] W. Schöllkopf et al., *Proc SPIE* **9512**, 95121L (2015)

O 37.7 Wed 12:15 H3

Observation of Hyperbolic Shear Polaritons in Monoclinic Crystals — •GIULIA CARINI¹, NIKOLAI C. PASSLER¹, XIANG NI², GUANGWEI HU^{2,3}, JOSEPH R. MATSON⁴, MARTIN WOLF¹, MATHIAS SCHUBERT⁵, ANDREA ALU², JOSHUA D. CALDWELL⁴, THOMAS G. FOLLAND⁶, and ALEXANDER PAARMANN¹ — ¹FHI, Berlin, Germany — ²CUNY, NY, USA — ³NUS, Singapore, Singapore — ⁴Vanderbilt University, Nashville, TN, USA — ⁵University of Nebraska, Lincoln, NE, USA — ⁶University of Iowa, Iowa City, IA, USA

Surface phonon polaritons, light-matter coupled waves, have recently attracted much attention due to their versatility in nanophotonic applications in the infrared. In particular, highly anisotropic materials have been shown to support hyperbolic polaritons, which enable a deep sub-wavelength confinement of light [1,2].

In our contribution, we investigate the emergence of a new class of hyperbolic surface waves, that we call hyperbolic shear polaritons (HShPs), in the monoclinic β -gallium oxide (bGO) [3]. The symmetry breaking in the in-plane hyperbolic propagation is directly linked to the frequency dependence of the optical axis directions within the monoclinic plane, resulting in shear phenomena in the non-diagonalizable dielectric permittivity tensor. We experimentally demonstrate the hyperbolic in-plane dispersion of these new polariton modes by means of Otto-type prism coupling.

- [1] J. D. Caldwell, et al., *Nat. Commun.* **5**, 5221 (2014).

- [2] W. Ma, et al., *Nature* **562**, 557-562 (2018).

- [3] N. C. Passler, et al., *Nature* **602**, 595-600 (2022).

O 37.8 Wed 12:30 H3

Transverse magnetic routing of light emission in hybrid plasmonic-semiconductor nanostructures: Towards operation at room temperature —

•LARS KLOMPMAKER¹, ALEXANDER N. PODDUBNY², EYÜP YALCIN¹, LEONID V. LITVIN³, RALF JEDE³, GRZEGORZ KARCZEWSKI⁴, SERGIJ CHUSNUTDINOW⁴, TOMASZ WOJTCOWICZ⁵, DMITRI R. YAKOVLEV^{1,2}, MANFRED BAYER^{1,2}, and ILYA A. AKIMOV^{1,2} — ¹Experimentelle Physik 2, Technische Universität Dortmund, 44221 Dortmund, Germany — ²St. Petersburg — ³Raith GmbH, Konrad-Adenauer-Allee 8, 44263 Dortmund, Germany — ⁴Institute of Physics, Polish Academy of Sciences, PL-02668 Warsaw, Poland — ⁵International Research Centre MagTop, PL-02668 Warsaw, Poland

We studied the transverse magnetic routing of light emission from a hybrid plasmonic-semiconductor quantum well (QW) structure where the exciton emission from the QW is routed into surface plasmon polaritons propagating along a nearby semiconductor-metal interface. In our diluted magnetic semiconductor (Cd,Mn)Te/(Cd,Mg)Te QW structure the magnitude of routing is governed by the circular polarization of the exciton optical transitions, induced by the magnetic field. A strong directionality of emission of 15 % was measured at low temperatures of 20 K, but for increasing temperatures it decreases to 4 % at about 65 K due to the decreasing magnetic susceptibility. To avoid this strong temperature dependence we also suggest an alternative design based on a non-magnetic (In,Ga)As/(In,Al)As QW structure.

ple of a prototypical surface electrochemical reaction. Time-resolved studies of the heat evolution during Cu bulk deposition will demonstrate the implications from heat measurements on the subsequent reaction steps of this complex reaction.

O 38.2 Wed 11:00 H4

Direct Assessment of the Proton Affinity of Individual Surface Hydroxyls with AFM and DFT — •BERND MEYER¹, MARGARETA WAGNER², MARTIN SETVIN², MICHAEL SCHMID², and ULRIKE DIEBOLD² — ¹Interdisciplinary Center for Molecular Materials and Computer Chemistry Center, FAU Erlangen-Nürnberg, Germany — ²Institute of Applied Physics, TU Wien, Austria

The state of protonation/deprotonation of individual surface sites has far-ranging implications in all areas of chemistry. However, common experimental measurements of surface acidity are integral techniques which give only average quantities integrated over the whole surface. Here we show that an OH-functionalized tip of an atomic force microscope (AFM) can be used for quantitative insights into the acidity of individual surface OH groups [1]. The chosen model oxide, $\text{In}_2\text{O}_3(111)$, offers four types of surface O atoms with distinct properties, each giving rise to a characteristic force-distance curve after protonation. Density-functional theory (DFT) calculations demonstrate a linear correlation between

the force minimum and the proton affinity of the surface hydroxyls. By benchmarking the calculations to known proton affinities and pK_a values of gas-phase molecules, the force minima provide a direct measure of proton affinity distributions and pK_a differences at the atomic scale.

[1] M. Wagner, B. Meyer, M. Setvin, M. Schmid, U. Diebold, *Nature* **592** (2021) 722–725

O 38.3 Wed 11:15 H4

Revisiting the OH adsorption on Pt(111) in static water environments — •ALEXANDRA C. DÁVILA LÓPEZ, NICOLAS G. HÖRMANN, THORBEN EGGERT, and KARSTEN REUTER — Fritz-Haber-Institut der Max-Planck-Gesellschaft, Berlin, Germany

The partial solvation of adsorbates typically leads to altered adsorption energies at solid-liquid interfaces as compared to vacuum. While such solvation effects can be treated most accurately based on *ab initio* molecular dynamics simulations, an according description is hardly feasible for a large number of systems e.g. across different substrates, adsorbates and adsorbate coverages due to prohibitive computational costs. As a result, many studies rely on an approximate treatment based on static water environments. In this work, we study solvation effects based on our previously introduced method [1] to generate a wide range of different static water adlayers. In particular, we analyze the adsorption energy of solvated OH on Pt(111) for a variety of explicit solvation environments and OH configurations. The results are benchmarked against available theoretical and experimental literature data [2, 3], and they highlight prevailing uncertainties in the description of solvation effects.

[1] A. C. Dávila *et al.*, *J. Chem. Phys.* **155**, 194702 (2021).

[2] V. Tripković *et al.*, *Electrochim. Acta* **55**, 7975*7981 (2010).

[3] H. H. Kristoffersen *et al.*, *Chem. Sci.*, **9**, 6912–6921 (2018).

O 38.4 Wed 11:30 H4

Measuring the reaction volume of an electrochemical surface process: Cu underpotential deposition on Au(111) — •LISA HIRSCH, BIANCA KRUMM, TAMARA MEYER, and ROLF SCHUSTER — Karlsruhe Institute of Technology

Information about the reaction volume of electrochemical surface reactions is rather scarce [1-3] albeit this thermodynamic quantity would allow conclusions on solvent contribution and possible side processes. With a specifically designed electrochemical cell, we determined the variation of the cell potential of a (111)-textured Au-film in $\text{CuSO}_4 / \text{H}_2\text{SO}_4$ vs a Cu reference electrode, while applying pressure pulses of moderate amplitude (< 10 bar) and durations of several seconds, starting at different rest potentials. According to the pressure dependent potential variation, we calculated the reaction volume $\Delta_R V$ of the processes at the working electrode. For rest potentials in the Cu UPD region, $\Delta_R V$ varies only slightly ($\pm 8 \text{ cm}^3/\text{mol}$) around $\Delta_R V = 18 \text{ cm}^3/\text{mol}$, its value for Cu bulk deposition, moderately peaking upon formation of the ($\sqrt{3} \times \sqrt{3}$) Cu UPD structure. Positive of the Cu UPD, in the sulfate adsorption region, $\Delta_R V$ drops to smaller values. We check the integrity of the measured potential variations by their dependence on the pressure amplitude as well as by measuring the symmetrical $\text{Cu}|\text{Cu}^{2+}, \text{SO}_4^{2-}|\text{Cu}$ cells.

[1] Conway, B. E., Currie, J. C., *J. Chem. Soc.*, **74**, 1978, 1390-1402.

[2] Loewe, T., Baltruschat, H., *Phys. Chem. Chem. Phys.*, **7**, 2005, 379-384.

[3] Heusler, K. E., Gaiser, L., *Ber. Bunsenges. Phys. Chem.*, **73**, 1969, 1059-1068.

O 38.5 Wed 11:45 H4

Enter the Void: Cavity Formation at Metal-Water Interfaces — •THORBEN EGGERT^{1,2}, NICOLAS G. HÖRMANN¹, and KARSTEN REUTER¹ — ¹Fritz-Haber-Institut der Max-Planck-Gesellschaft, Berlin, Germany — ²Technical University of Munich, Munich, Germany

Time: Wednesday 10:30–12:15

O 39.1 Wed 10:30 H6

Automated calculation of surface energies of arbitrary crystals — •FIRAT YALCIN and MICHAEL WOLLOCH — Computational Materials Physics, Faculty of Physics, University of Vienna, Kolingasse 14-16, 1090 Vienna

The surface energy is one of the most fundamental properties of the surface facets of a crystal, determining the stability, equilibrium shape, catalytic activity, and other phenomena like surface segregation and roughening. In this work, we present a high-throughput workflow to calculate the surface energies of arbitrary crystals, accounting for all possible Miller indices and different terminations, using density functional theory (DFT). By employing available open-source libraries and custom-made tools, every step from querying bulk structures from various databases to the generation of slabs with precise geometries and subsequent DFT calculations is performed automatically and with minimal user input. Surface energies, Wulff shapes, as well as all in- and outputs, are automatically

Cavity formation is an important concept when rationalizing the solvation of ions. However, most studies analyze cavities only in bulk liquids, omitting that their properties may change dramatically at solid-liquid interfaces.

Here, we study cavities at interfaces, particularly their free energy of formation based on molecular dynamics simulations. Specifically, we use a particle insertion approach, as well as the Multistate Bennett Acceptance Ratio method. We demonstrate that cavity formation at interfaces is dependent on the substrate material, which can be partially rationalized by the substrate-specific interfacial water structure. Furthermore, we observe stabilized cavities behind the first solvation layer of water.

These results might on the one hand rationalize recent theoretical suggestions of a non-electrostatic, attractive force on ions near interfaces, and on the other hand enable the improvement of implicit solvation models, which typically neglect substrate-specificity in their description.

O 38.6 Wed 12:00 H4

Impact of confined water on solvation and adsorption/desorption energetics of charged ions at the electrified interface — •ZHENYU WANG, MIRA TODOROVA, and JÖRG NEUGEBAUER — Department of Computational Materials Design, Max-Planck-Institut für Eisenforschung, Max-Planck-Str.-1, D-40237, Düsseldorf, Germany

Understanding processes at electrified solid/liquid interfaces is crucial for many systems and a wide range of applications in electrochemical industry, catalytic sciences and biological engineering. Using a prototypical model system of a single ion in water confined between two charged electrodes, we perform nanosecond-scale atomistic molecular dynamics simulations to study the dielectric behavior of chemically pure water as well as the solvation of ions in the presence of an electric field. For weak electric fields we find that the screening charge density of water is proportional to the external electric intensity, in agreement with classical polarization theory. Probing the interface structure by the single Na^+/Cl^- ion we investigate the formation and evolution of the ion's solvation shell as function of the electrode-ion distance. Comparing potential profiles from Na^+/Cl^- calculations for different charge states and positions, we elucidate the role of screening and solvation shell size on reorganization energies and transmission barrier of the ions close to the interface.

O 38.7 Wed 12:15 H4

Are organic solvents key to enable CO_2 electro-reduction on Mo_2C as promised in theory? — •THOMAS MAIREGGER¹, CHRISTOPH GRIESSER¹, HAOBO LI², NICOLAS HÖRMANN³, KARSTEN REUTER³, and JULIA KUNZELIEBHÄUSER¹ — ¹Department of Physical Chemistry, Innsbruck, Austria — ²University of Adelaide, Adelaide, Australia — ³Fritz Haber Institute, Berlin, Germany

It has been proposed in active-site computational screening studies that Mo_2C is an effective electrocatalyst for the electrochemical CO_2 reduction reaction (CO_2RR) to valuable fuels, such as hydrocarbons and alcohols. However, the competing hydrogen evolution reaction (HER) has been found to exclusively take place.[1] Reason for this is the formation of a surface oxide film upon air exposure or immersion of Mo_2C into aqueous electrolytes that impedes the formation of the desired higher reduction products.[1]

Here we investigate the CO_2RR activity of polycrystalline hexagonal Mo_2C in non-aqueous electrolyte to avoid passivation of the electrode and circumvent the high HER activity. We show that Mo_2C is capable of reducing CO_2 in reasonable amounts in an acetonitrile electrolyte, with an onset at $-1.08 \text{ V}_{\text{SHE}}$. [1] The nature of the products, among them gaseous CO , depends on the concentration of water in the electrolyte. Furthermore, we show that the acetonitrile has a stronger impact on the CO_2 electro-reduction than previously believed.

[1] Griesser, C., et. al., *ACS Catalysis* **11**, 4920-4928 (2021).

O 39: Tribology

Location: H6

saved into an easily accessible, OPTIMADE compliant database. Example results are presented for some non-trivial surfaces with complex geometries to showcase the capabilities and validate our approach.

O 39.2 Wed 10:45 H6

High-throughput calculations of heterogeneous interfaces for tribology — •MICHAEL WOLLOCH^{1,2}, GABRIELE LOSI³, OMAR CHEHAIMI³, FIRAT YALCIN¹, MAURO FERRARIO⁴, and M. CLELIA RIGHI³ — ¹CMP, University of Vienna, Vienna, Austria — ²VASP software GmbH, Vienna, Austria — ³DIFA, University of Bologna, Bologna, Italy — ⁴FIM, UNIMORE, Modena, Italy

We have shown in the past that fundamental properties of sliding interfaces like adhesion, friction, and ultimate strength, are closely connected to one another and the re-arrangement of charge at the interface [1-3]. We extended the previously presented approach for homogeneous interfaces to nearly arbitrary in-

terfaces of crystalline surfaces, allowing us to treat heterogeneous interfaces of multi component systems [4].

In this talk we will present the fault tolerant and fully automatic workflow we developed, as well as initial results of the ongoing high-throughput studies we are conducting.

Part of this work was supported by ERC grant 865633 (SLIDE); [1] Wolloch et al. *Sci. Rep.* 9, 17062 (2019), [2] Restuccia et al. *Comput. Mater. Sci.*, 154:517-529 (2018), [3] Wolloch et al. *PRL* 121, 026804 (2018) [4] Wolloch et al. *Comput. Mater. Sci.*, 207:111302 (2022)

O 39.3 Wed 11:00 H6

The Influence of Temperature and Wear on Nanoscale Friction Anisotropy — •JENNIFER KONRAD, DIRK DIETZEL, and ANDRE SCHIRMEISEN — Institute of Applied Physics, Justus-Liebig University Giessen, 35392 Giessen, Germany

On atomically flat surfaces, the nanoscale friction force measured by atomic force microscopy shows a distinct variations dependent on the sliding direction of the AFM-tip. This anisotropy occurs as a consequence of the surface structure and is related to different energy barrier heights along different directions of the sample surface. In this work, this anisotropy of friction force is now analyzed as a function of temperature under UHV conditions on hexagonal lattices like HOPG or MoS₂ and also on ionic crystals with 90 degree symmetry like NaCl. At low sample temperatures, the friction force as deduced from the thermally activated Prandtl Tomlinson Model increases, and thermally activated random jumps become more unlikely, which direct influences the stability of the different sliding directions. This can be confirmed for HOPG and MoS₂, while, our results for the ionic crystals additionally show that the both the absolute friction and the anisotropy are not only influenced by temperature, but also reflect temperature dependent wear effects.

O 39.4 Wed 11:15 H6

Dissipative frictional mechanism over Moiré superstructure — •YIMING SONG¹, XIANG GAO², ANTOINE HINAUT¹, SEBASTIAN SCHERB¹, SHUYU HUANG¹, ODED HOD², MICHAEL URBAKH², and ERNST MEYER¹ — ¹Department of Physics, University of Basel, Basel, Switzerland — ²Department of Physical Chemistry, School of Chemistry, The Raymond and Beverly Sackler Faculty of Exact Sciences and The Sackler Center for Computational Molecular and Materials Science, Tel Aviv University, Tel Aviv, Israel.

Friction force microscopy experiments performed on graphene-coated platinum surfaces that exhibit a variety of moiré superstructures demonstrate that, in addition to the well-known atomic stick-slip dynamics, a new dominant energy dissipation mechanism emerges. The observed velocity dependence of friction displays two distinct regimes: (i) at low velocities, the friction force is small and nearly constant; whereas (ii) above some threshold, friction increases logarithmically with velocity. The threshold velocity, separating the two frictional regimes, decreases with increasing normal load and moiré superstructure period. Atomistic molecular dynamics simulations demonstrate that the main contribution to frictional energy dissipation results from the elastic deformation and subsequent relaxation of moiré ridges caused by the pushing action of the tip as it slides over the superstructure. Based on the simulation results we develop a semi-phenomenological model, which makes it possible to calculate friction under measurement conditions and provides excellent agreement with the experimental observations.

O 39.5 Wed 11:30 H6

Investigating thermal and directional motion in molecular friction processes by photonic force microscopy — •SUBHROKOLI GHOSH and ALEXANDER ROHRBACH — Lab for Bio- and Nano-Photonics, Department of Microsystems Engineering (IMTEK), University of Freiburg, Georges-Koehler-Allee 102, 79110 Freiburg, Germany

Friction of a moving particle is a complex process of energy dissipation to the environment, which is important on most length scales, time scales and across disciplines. Several theories approach the molecular origin of friction, but a com-

prehensive understanding is still missing. Usually, the relation between dynamic friction and velocity is quantified by a coefficient, which depends on various parameters. Two main routes to determine the friction coefficient can be addressed by either from a directed particle motion or from its thermal motion. In both cases, Photonic Force Microscopy (PFM) has proven to be one of the most elegant techniques that can be utilized to better understand friction on mesoscopic length scales, specially at soft (-bio) interfaces. Towards this aim, we employ PFM with high-frequency axial tracking for directed and frequency dependent measurements of different bead-surface model systems, starting from simple poly-styrene (PS) bead- glass surface. From Brownian dynamics simulations, in combination with experiments, we obtain better insights on the friction coefficient and its dependency on different system parameters. From this, we developed a theoretical model describing the microscopic origin of friction through molecular on- and off-binding processes.

O 39.6 Wed 11:45 H6

Single Asperity Sliding Friction across the Superconducting Phase Transition — WEN WANG, •DIRK DIETZEL, and ANDRÈ SCHIRMEISEN — Institute of Applied Physics, Justus Liebig University Giessen, Giessen, Germany

When analyzing sliding friction, it is usually an intriguing question to identify the different dissipation mechanisms contributing to friction. Usually, a number of different channels for dissipation are considered including phonon and electron systems, plastic deformation, and crack formation. Among these, especially the role of the electron system for energy dissipation often remains elusive. In this contribution, we now present experiments single asperity sliding friction monitored during AFM-measurements on a high- T_c BSCCO-superconductor. These measurements reveal a distinct temperature dependence of friction in a temperature range between 40 K and 300 K [1]. While the overall friction decreases with temperature as predicted by models about thermally activated friction, we find a distinct friction peak at about 95K. This peak can be explained by a superposition of different energy dissipation channels, where the influence of electronic contributions vanishes when cooling below the superconducting phase transition T_c . Our experiments thereby unambiguously link electronic friction effects to the number of normal state electrons in the superconducting phase below T_c . In addition, we analyze single asperity friction of BSCCO in the proximity of step-edges, where layer-defects reveal the potential influence of the topmost-layer on electronic friction contributions. [1] Wang, Dietzel, Schirmeisen, *Science Advances*, eaay0165 (2020)

O 39.7 Wed 12:00 H6

Fingerprint of a structural phase transition during superlubric sliding — •EBRU CIHAN^{1,2}, DIRK DIETZEL¹, and ANDRE SCHIRMEISEN¹ — ¹Institute of Applied Physics, Justus-Liebig University Giessen, 35392 Giessen — ²Institute for Materials Science, TU Dresden, 01062 Dresden

Although the fundamental concept of structural superlubricity (i.e. ultra-low friction observed between clean and atomically flat, incommensurate surfaces) is very straightforward, the effective energy barrier for lateral motion still depends on the exact structural dynamics at the sliding interface. In fact, it can be computationally predicted that the superlubricity of amorphous structures is less effective than that of crystalline structures, however this is not always easy to demonstrate experimentally. But we have now overcome this challenge by measuring the friction of antimony nanoparticles on highly oriented pyrolytic graphite in the high temperature regime, i.e. between 300 K and 750 K, where the interface can be restructured. At about 450 K, we trigger a phase transition in antimony nanoparticles, which also allows us to establish a direct link between friction and the interface structure. More specifically, our experiments reveal that the friction level decreases in the more crystalline state where the collective force cancellations are more effective. Due to the irreversible character of the phase transition, a reduced friction level can then also be observed after cooling back to room temperature. The reduction of friction can be associated with a decrease of the characteristic scaling factor of about 16%, as theoretically anticipated from the 'scaling law' for superlubricity.

O 40: Organic Molecules at Surfaces 4: Chemistry on Surfaces

Time: Wednesday 10:30–12:45

Location: S051

O 40.1 Wed 10:30 S051

On-surface synthesis of planar π -extended cycloparaphenylenes featuring an all-armchair edge topology — FEIFEI XIANG¹, SVEN MAISEL², SUMIT BENIWAL¹, VLADIMIR AKHMETOV^{2,3}, CORDULA RUPPENSTEIN³, MIRUNALINI DEVARAJULU¹, ANDREAS DÖRR¹, OLENA PAPAANINA³, ANDREAS GÖRLING², KONSTANTIN AMSHAROV^{2,3}, and •SABINE MAIER¹ — ¹FAU Erlangen-Nürnberg, Dept. of Physik — ²FAU Erlangen-Nürnberg, Dept. of Chemistry and Pharmacy — ³Institute for Chemistry, University Halle-Wittenberg

[n]cycloparaphenylenes ([n]CPPs) have attracted significant attention due to their unique cyclic structure and highly effective para-conjugation leading to

a myriad of fascinating (opto-)electronic properties. However, their strained topology prevents the π -extension of CPPs to convert them either into armchair nanobelts or planarized CPP macrocycles. We have successfully tackled this long-standing challenge and present the bottom-up synthesis and characterization of atomically precise in-plane π -extended [12]CPP on Au(111) by low-temperature scanning probe microscopy/spectroscopy combined with density functional theory.[1] The planar π -extended CPP represents the first nanographene with an all-armchair edge topology. The exclusive para-conjugation at the periphery yields delocalized electronic states and the planarization maximizes the overlap of p-orbitals, which both reduce the bandgap

compared to conventional CPP. Calculations predict ring currents and global aromaticity in the doubly charged system.

[1] F. Xiang et al., Nat. Chem. 2022, doi: 10.1038/s41557-022-00968-3.

O 40.2 Wed 10:45 S051

Electronic Properties of N-Heterotriangulene based Charge Transfer Complexes — •MOHSEN AJDARI¹, RONJA PAPPENBERGER¹, INA MICHALSKY², LEONIE PAP¹, CHRISTIAN HUCK¹, MARVIN HOFFMANN³, FRIEDRICH MAASS¹, MILAN KIVALA², ANDREAS DREUW³, and PETRA TEGEDER¹ — ¹Physikalisch-Chemisches Institut, Universität Heidelberg — ²Organisch-Chemisches Institut, Centre for Advanced Materials, Universität Heidelberg — ³Interdisziplinäres Zentrum für Wissenschaftliches Rechnen, Universität Heidelberg

N-heterotriangulenes (N-HTAs) are a class of organic electron-transporting semiconductors that belong to N-heteropolycyclic aromatic compounds, which are promising candidates for a variety of (opto) electronic applications. In this study, electronic high-resolution electron energy loss spectroscopy (HREELS) in combination with quantum-chemical theory are utilized to investigate the electronic properties of two N-HTA derivatives, N-HTA-550 and N-HTA-557 on Au(111). In addition, formation of charge transfer complexes (CTCs) with N-HTAs, acting as donor molecules in combination with two well-known cyano-based electron acceptor molecules, TCNQ and F4TCNQ is identified. Our findings indicate that formation of the 7-membered ring in N-HTA-557 by adding the -C=C- bridge leads to a narrowing of the optical gap size by 0.9 eV and a decrease in the first triplet state energy by 1.2 eV. Moreover, all donor/acceptor bilayer systems on Au(111) exhibit low-lying electronic transitions between 0.9 and 2.2 eV, which are attributed to the formation of CTCs.

O 40.3 Wed 11:00 S051

N-Heterotriangulenes Donors and Charge Transfer Complexes formed with strong Electron Acceptors investigated with Two-Photon Photoemission Spectroscopy — •JAKOB STEIDEL¹, INA MICHALSKY², MILAN KIVALA², and PETRA TEGEDER¹ — ¹Institute of Physical Chemistry, Heidelberg University, Im Neuenheimer Feld 253, 69120 Heidelberg — ²Institute of Organic Chemistry, Heidelberg University, Im Neuenheimer Feld 270, 69120 Heidelberg

Many opto-electronic devices such as organic photovoltaic cells or organic light emitting diodes utilize donor-acceptor-systems (D-A-systems). Triphenylamine derivatives are promising candidates for donors in D-A-systems. The introduction of an etheno-bridge in the planar triphenylamine derivative indolo[3,2,1-jk]carbazole (N-HTA-550) creates a seven membered antiaromatic ring in the resulting N-Heterotriangulene-557 (N-HTA-557). While the molecular geometry is mostly preserved, the electronic structure is strongly modified by this additional -C=C-moiety.

In the present contribution we study the electronic properties of N-HTA-550 and N-HTA-557 on a Au(111) surface using two-photon photoemission (2PPE) spectroscopy and temperature programmed desorption (TPD). Furthermore the formation of charge transfer complexes with strong electron acceptors (TCNQ and F4TCNQ) is investigated utilizing both 2PPE and TPD.

O 40.4 Wed 11:15 S051

Remarkably stable metal-organic networks on an inert substrate: Ni-, Fe-, and Mn-TCNQ on graphene — •ZDENĚK JAKUB¹, ANNA KUROWSKÁ¹, ONDŘEJ HERICH¹, LENKA ČERNÁ¹, LUKÁŠ KORMOŠ¹, AZIN SHAHSAVAR¹, PAVEL PROCHÁZKA¹, and JAN ČECHAL^{1,2} — ¹CEITEC, Brno University of Technology, Czechia — ²Faculty of Mechanical Engineering, Brno University of Technology, Czechia

Potential applications of 2D metal-organic frameworks (MOF) require the frameworks to be monophasic and well-defined at the atomic scale, to be decoupled from the supporting substrate, and to remain stable at the application conditions. Here, we present three systems meeting this elusive set of requirements: M-TCNQ (M = Ni, Fe, Mn) on epitaxial graphene/Ir(111). We study the systems experimentally by scanning tunneling microscopy, low energy electron microscopy and x-ray photoelectron spectroscopy. When synthesized on graphene, the 2D M-TCNQ MOFs are monophasic with M₁(TCNQ)₁ stoichiometry, and we demonstrate their remarkable chemical and thermal stability: All the studied systems survive exposure to ambient conditions, with Ni-TCNQ doing so without any significant changes to its atomic-scale structure or chemical state. Thermally, the most stable system is Fe-TCNQ which remains stable above 500 °C, while all the tested MOFs survive heating to 250 °C. Overall, the modular M-TCNQ/graphene system combines the atomic-scale definition required for fundamental studies with the robustness needed for applications, thus it presents an ideal model for research in single atom catalysis or spintronics.

O 40.5 Wed 11:30 S051

Control of overlayer-substrate coupling via alkali doping in two-dimensional metal-organic networks — •BILLAL SOHAIL¹, PHIL J. BLOWEY², TIEN-LIN LEE³, PAUL T. P. RYAN³, DAVID A. DUNCAN³, GIOVANNI CONSTANTINI¹, D. PHIL WOODRUFF¹, and REINHARD J. MAURER¹ — ¹University of Warwick — ²University of Leeds — ³Diamond Light Source

We characterise a two-dimensional donor-acceptor network formed by coadsorption of alkali atoms and the prototypical acceptor molecule TCNQ (7,7,8,8-

tetracyanoquinodimethane) at different orientations of Ag surfaces. We characterise the adsorption structure with a combination of normal incidence x-ray standing wave (NIXSW) measurements, Scanning Tunneling Microscopy, and dispersion-inclusive Density Functional Theory, which we find to be in excellent agreement with experiment. The adsorption structure sensitively depends on an interplay of molecule-metal charge transfer and long-range dispersion forces, which are influenced by the co-adsorption ratio between alkali atoms and TCNQ. In general, alkali atom co-adsorption reduces the molecule-substrate interaction strength, yet is energetically favoured compared to TCNQ co-adsorption with Ag adatoms. We show that the donor-acceptor ratio in the network is able to control the overlayer-substrate interaction, which strongly affects electronic properties such as the work function and the level alignment at the interface. Therefore, the concentration of alkali donor atoms can be used to tune electronic properties of the interface.

O 40.6 Wed 11:45 S051

Analysis of the 3-dimensional adsorption configuration of organic molecules by SPM manipulation and imaging — •ALEXANDER IHLE¹, DANIEL EBELING¹, DANIEL KOHRS², HERMANN A. WEGNER², and ANDRE SCHIRMEISEN¹ — ¹Institute of Applied Physics, Justus Liebig University Giessen — ²Institute of Organic Chemistry, Justus Liebig University Giessen

On-surface chemistry is a powerful tool for building covalent molecular structures such as chains, networks, or graphene nanoribbons (GNRs). In particular, the catalytic properties of the metal substrate as well as the 2D confinement facilitate the synthesis of new structures that are not accessible via solution chemistry. The Ullmann type coupling is one of the most frequently applied on-surface reaction for synthesizing C-C bonded structures. However, only limited information is available about the three dimensional adsorption conformation of the molecular educts and how this affects the reaction pathway. Here, we studied on-surface reactions of 9-X-10-(1,1':3',1''-terphenyl-5'-yl)anthracene (X= bromine, iodine) on Cu(111), Ag(111) and Au(111). Using low-temperature atomic force microscopy with CO-functionalized tips, we can identify the precise adsorption conformation of the pristine molecules as well as the intermediate and final products. In particular, the three dimensional conformation of the intermediates strongly inhibits the intermolecular coupling reaction between the educts on all surfaces. Instead, intramolecular bond formation is observed.

O 40.7 Wed 12:00 S051

STM growth studies of 5,14-ol-5,14-diborapentacyclo on low-index coinage metal surfaces — •WUN-CHANG PAN¹, JING QI¹, CARINA MÜTZEL², PAULA WEBER¹, FRANK WÜRTHNER², and MATTHIAS BODE¹ — ¹Physikalisches Institut, Experimentelle Physik II, Universität Würzburg, Am Hubland, D-97074 Würzburg, Germany — ²Institut für Organische Chemie & Center for Nanosystems Chemistry (CNC), Universität Würzburg, Am Hubland, D-97074 Würzburg, Germany

In recent studies [1, 2], heteroatoms-doped precursors have frequently been used to polymerize graphene nanoribbons with a large variety of structures or dopant heteroatoms. Using cryogenic scanning tunneling microscopy, we investigated the structure of self-assembled 5,14-ol-5,14-diborapentacyclo (CM218) on low-index coinage metal surfaces. The main focus of our study is on CM218 on Ag(111), where we find that molecular clusters and chains coexist with molecular islands. At low annealing temperature $T_{ann} < 100^\circ\text{C}$, the islands exhibit a rail track-like structure with a rhomboid-shaped unit cell. Besides, we find irregular clusters and molecular chains. At higher $T_{ann} \geq 180^\circ\text{C}$, islands with a honeycomb (HC) structure are observed. Topographic images of these HCs display a pronounced bias dependence. Molecule-functionalized tips allow for high-resolution images of these structures for which we suggest structural models.

[1] L. Grill and S. Hecht, Nature Chemistry 12, 115 (2020).

[2] Q. Zhong et al., Nature Chemistry 13, 1133 (2021).

O 40.8 Wed 12:15 S051

Surface chemistry of dibromoindigo - effects of temperature and type of surface — •MANUELA HOCKE^{1,2}, MICHAEL SCHMITTEL³, WOLFGANG HECKL^{1,2}, and MARKUS LACKINGER^{1,2} — ¹Deutsches Museum, 80538 München — ²Technische Universität München, Physics Department, 85748 Garching — ³Center of Micro and Nanochemistry, Universität Siegen, 57068 Siegen, Germany

Mother Nature offers a great variety of suitable halogenated compounds, which can readily be used as precursor for on-surface Ullmann couplings. Here, we study the thermally activated surface chemistry of the famous dye Tyrian purple (6,6'-dibromoindigo) comparatively on Ag(111) and Au(111) by Scanning-Tunneling-Microscopy. On Au(111) we observed two distinct self-assembled structures comprised of fully intact molecules. Covalent structures were obtained either by deposition onto hot surfaces or subsequent heating, where the heating rate is crucial. On Ag(111) only one self-assembled structure was observed. The organometallic structures obtained upon debromination rarely exhibited the anticipated linear structure. Instead, we find remarkably diverse structures. The additional functionalization of 6,6'-dibromoindigo with potent H-bond donor and acceptor groups renders the on-surface polymerization of this

compound particularly prone to additional influences of supramolecular bonds with a vivid contribution of the co-adsorbed dissociated bromine atoms. Moreover, the surprisingly large variation of the organometallic structures on Ag(111) and the profound dependence on preparation parameters indicate an unexpectedly large kinetic influence.

O 40.9 Wed 12:30 S051

Interface-driven Assembly of Pentacene/MoS₂ Lateral Heterostructures: A Combined STM and DFT Study — •SERGIO TOSONI¹, FRANCESCO TUMINO², ANDI RABIA², ANDREA LI BASSI², and CARLO CASARI² — ¹Dipartimento di Scienza dei materiali, Università di Milano-Bicocca, via Roberto Cozzi 55, I-20125 Milano, Italy — ²Dipartimento di Energia, Politecnico di Milano, via G. Ponzio 34/3, Milano, I-20133, Italy

Mixed-dimensional van der Waals heterostructures formed by molecular assemblies and 2D materials provide a novel platform for fundamental nanoscience

and future nanoelectronics applications. Here we investigate a hybrid heterostructure between pentacene molecules and 2D MoS₂ nanocrystals deposited on Au(111) by means of Scanning Tunneling Microscopy and Density Functional Theory calculations.

In the MoS₂/Au interface, the lattice mismatch leads to the growth of extended monolayer films displaying a non-commensurate lattice with the metal substrate and typical features of point defects, identified as single sulfur vacancies.

The formation of atomically thin pentacene/MoS₂ lateral heterostructures is observed on the Au substrate. Interestingly, the inner regions of the MoS₂ layer are not covered by pentacene. The density of states changes sharply across the pentacene/MoS₂ interface indicating a weak interfacial coupling, which leaves unaltered the electronic signature of MoS₂ edge states. This work unveils the growth of abrupt lateral heterostructures toward hybrid devices based on organic/inorganic one-dimensional junctions.

O 41: Graphene: Growth, Substrate Interaction, Intercalation, and Doping

Time: Wednesday 10:30–12:30

Location: S052

O 41.1 Wed 10:30 S052

Using polyaromatic hydrocarbons for graphene growth — •MATTHEW A. STOODLEY^{1,2}, BENEDIKT P. KLEIN^{1,2}, LUKE A. ROCHFORD², MATTHEW EDMONDSON³, MARC WALKER², TIEN-LIN LEE¹, ALEXANDER SAYWELL³, REINHARD J. MAURER², and DAVID A. DUNCAN¹ — ¹Diamond Light Source, Didcot, United Kingdom — ²University of Warwick, Coventry, United Kingdom — ³University of Nottingham, Nottingham, United Kingdom

Graphene, due to its widespread potential applications, has been one of the most studied materials this century. The most common approach to produce high quality graphene is through epitaxial growth utilising chemical vapour deposition (CVD) on copper surfaces. This method exploits the catalytic activity of copper to form highly crystalline, large area graphene. Traditionally, precursors used to grow graphene on Cu(111) require high pressures and elevated substrate temperatures, however, many cutting edge characterisation techniques cannot be used at such conditions. In this work, polyaromatic hydrocarbons (PAH) are used to grow high quality graphene on Cu(111) via CVD at relatively low surface temperatures. Furthermore, the low vapour pressure of the PAH permits us to synthesise graphene films in ultra-high vacuum conditions. We present a characterization of the grown graphene, by utilising a wide variety of techniques including Scanning Tunneling Microscopy, X-ray photoelectron spectroscopy, normal incidence x-ray standing waves, and near edge X-ray adsorption fine structure.

O 41.2 Wed 10:45 S052

Stone-Wales defect: molecular model system reveals increased interaction with Cu(111) surface — •BENEDIKT P. KLEIN^{1,2,3}, ALEXANDER IHLE⁴, STEFAN R. KACHEL¹, LUKAS RUPPENTHAL¹, SAMUEL J. HALL², DANIEL EBELING⁴, RALF TONNER-ZECH¹, REINHARD J. MAURER², ANDRE SCHIRMEISEN⁴, and J. MICHAEL GOTTFRIED¹ — ¹Philipps-Universität Marburg, Germany — ²University of Warwick, Coventry, UK — ³Diamond Light Source, Didcot, UK — ⁴Justus-Liebig-Universität Gießen, Germany

The properties of the graphene/metal interface are crucially influenced by the enhanced interaction of defects in the graphene layer with the metal substrate. However, due to experimental and computational constraints, it is difficult to investigate this interaction directly. We combine calculations with experimental analysis of large organic molecules adsorbed on metal surfaces as molecular model systems. We chose two model molecules, azupyrene and pyrene, which have the same aromatic topology as the prototypical Stone-Wales defect and the ideal graphene lattice, respectively. When adsorbed on the Cu(111) surface, we could show using TPD that the model defect binds much stronger to the surface. nc-AFM and NIXSW results furthermore prove a reduction in adsorption height while XPS, UPS, and NEXAFS show an increased electronic hybridisation between molecule and surface. DFT results agree with these findings and show a localized interaction with the metal surface, both for the molecular model systems and the defect embedded into the graphene layer.

O 41.3 Wed 11:00 S052

Determining the stability and catalytic formation of graphene on liquid Cu using machine-learning potentials — •HAO GAO¹, VALENTINA BELOVA², MACIEJ JANKOWSKI², HENDRIK H. HEENEN¹, GILLES RENAUD², and KARSTEN REUTER¹ — ¹Fritz-Haber-Institut der MPG, Berlin, Germany — ²ESRF, Grenoble, France

The recently discovered rapid, high-quality synthesis of graphene (Gr) on liquid Cu catalysts is microscopically still poorly understood. This is due to the difficult characterization of the Cu liquid surface. Especially in atomistic simulations, the large length and time scales necessary to reliably emulate the temporal evolution of the liquid are a major challenge. Corresponding molecular dynamics

simulations require large simulation cells and need to span well into the nanosecond regime – an endeavor presently intractable via first-principles methods. In this work we use computationally efficient machine-learning potentials (MLPs) trained to density-functional theory (DFT) data in order to extrapolate the first-principles predictive power to the required scales. Detailed benchmarking confirms that our MLP captures the involved physics well, accurately reproducing the experimentally determined Gr adsorption height. We apply the MLP to further study the catalytic mechanism of Gr synthesis in order to rationalize distinct reaction kinetics found experimentally. Our work draws a path for the use of reliably trained MLPs as a multiscale modeling technique to explore previously uncharted computational problems. In that we provide new insight into the domain of liquid metal catalysts which generally lack atomic-scale understanding.

O 41.4 Wed 11:15 S052

Properties of epitaxial graphene on various SiC terminations and polytypes investigated by low-energy electron microscopy — •PHILIP SCHÄDLICH^{1,2}, DAVOOD MOMENI PAKDEHI³, FLORIAN SPECK^{1,2}, KLAUS PIERZ³, and THOMAS SEYLLER^{1,2} — ¹Technische Universität Chemnitz, Chemnitz, Germany — ²Center for Materials, Architectures and Integration of Nanomembranes (MAIN), Chemnitz, Germany — ³Physikalisch-Technische Bundesanstalt, Braunschweig, Germany

The epitaxial growth of graphene on SiC has been improved from UHV growth to ambient pressure synthesis [1], and recently to the polymer-assisted sublimation growth (PASG) [2]. It results in an enhanced nucleation of the buffer layer and suppressed step bunching, which usually occurs upon the graphene formation by sublimation. Thus, PASG leads to homogeneous monolayer graphene with minimum step size equivalent to one or two SiC-bilayers. As a result of the latter, graphene on various surface terminations of the SiC substrate can now be systematically studied.

We utilize low-energy electron microscopy (LEEM) to identify the underlying substrate structure and to elucidate its delicate impact on the characteristic I(V) curves for different SiC polytypes. In addition, we investigate how the decoupling of the buffer layer from the substrate by hydrogen intercalation [3] influences the aforementioned effects.

[1] K. V. Emtsev et al., Nat. Mat. 8, 203 (2009). [2] M. Kruskopf et al., 2D Mater. 3 (4), 041002 (2016). [3] C. Riedl et al., PRL 103, 246804 (2009).

O 41.5 Wed 11:30 S052

Quasiparticle Interference Effects Revealed in Potassium-Intercalated Epitaxial Monolayer Graphene — TOBIAS HUEMPFNER, •FELIX OTTO, ROMAN FORKER, and TORSTEN FRITZ — Institute of Solid State Physics, Friedrich Schiller University Jena, Helmholtzweg 5, 07743 Jena, Germany

Epitaxial graphene is known for its fascinating physical properties, such as a linear dispersion at the K point, an anomalous quantum Hall effect and even superconductivity. These effects are based on the unique electronic structure of graphene, which can be tuned, e.g., by intercalation of metals. In this study, we scrutinize samples of epitaxial monolayer graphene (EMLG) on SiC(0001) intercalated with potassium by means of local and area-averaging experimental methods at low temperatures. For the highest accessible K concentration we find a highly ordered (2 × 2) superstructure that the K atoms form below the uppermost graphene layer. Further, we observe that the K atoms also reside below the buffer layer of the EMLG on SiC(0001) sample that is located between the quasi-freestanding graphene sheet and the SiC substrate. This causes an effective decoupling of the buffer layer and a transformation to K-intercalated epitaxial bilayer graphene (EBLG). This configuration promotes strong *n*-doping of the graphene sheets, where besides a rigid shift of the Dirac bands to higher binding energies also filling of two parabolic interlayer bands is observed.

O 41.6 Wed 11:45 S052

Structural and electronic properties of a van der Waals heterostructure of two-dimensional Pb and epitaxial graphene — •BHARTI MATTA, PHILIPP ROSENZWEIG, OLAF BOLKENBAAS, KATHRIN KÜSTER, and ULRICH STARKE — Max-Planck-Institut für Festkörperforschung, Heisenbergstraße 1, 70569 Stuttgart, Germany

Intercalation is an established technique for manipulating the electronic properties of epitaxial graphene. Moreover, it is a way to confine otherwise unstable two-dimensional (2D) layers of elements, leading to unique physical properties compared to their bulk counterparts due to quantum confinement. In this work, we show uniformly Pb-intercalated quasi-freestanding monolayer graphene on SiC, which turns out to be essentially charge neutral. Additional bands – some crossing the Fermi level – can be clearly discerned, demonstrating the metallic character of 2D Pb sandwiched within the graphene/SiC heterointerface. The band velocity of the graphene Dirac cone changes at binding energies of around 0.6 eV and 1.1 eV, which points towards hybridization with these Pb bands. Low-energy electron diffraction reveals a 10×10 Moiré periodicity with respect to graphene. This is consistent with a triangular lattice of intercalated Pb that is strained by less than 2% relative to bulk-truncated Pb(111) and of which a $(\sqrt{3} \times \sqrt{3})R30^\circ$ supercell matches 2×2 -SiC. However, finding direct signatures of the corresponding periodicities in the available band structure data is challenging. Our experimental results will provide a solid ground for further theoretical assessment of this system and better understanding of its properties.

O 41.7 Wed 12:00 S052

Surface Transport Properties of Pb- and Sn-intercalated Graphene — •M. GRUSCHWITZ, C. GHOSAL, Z. MAMIYEV, J. KOCH, S. WOLFF, T. SEYLLER, and C. TEGENKAMP — Institut für Physik, Technische Universität Chemnitz, Germany

Intercalation experiments on epitaxial graphene are attracting a lot of attention at present as a tool to boost further the electronic properties of 2D graphene. In this work we studied the intercalation of Pb using buffer layers on 6H-SiC(0001). Recent DFT calculations suggest Pb atoms to act as electron donors thus allowing the doping level of the quasi-freestanding graphene layer to be tuned by the amount of intercalated material [1].

In this work we present results about the large-area intercalation of Pb and Sn, investigated by means of electron diffraction, scanning tunneling microscopy,

photoelectron spectroscopy and in-situ surface transport. The intercalation of Pb and Sn results in formation of almost charge neutral graphene. In case of Pb, the intercalated layer consists of 2 ML and shows a strong structural corrugation. The epitaxial heterostructure provides an extremely high conductivity of $\sigma = 100$ mS/□. However, below 70 K we found a metal-insulator transition which we assign to the formation of minigaps in epitaxial graphene, possibly induced by a static distortion of graphene following the corrugation of the interface layer [2]. Sn intercalation does not cause such a transition while yielding a conductivity of $\sigma = 2.5$ mS/□.

[1] J. Wang et al., PRB 103, 085403 (2021); [2] M. Gruschwitz et al., Materials 14, 7706 (2021)

O 41.8 Wed 12:15 S052

Electron correlation effects in highly-doped single-layer graphene — •VIVIEN ENENKEL¹, PHILIPP ROSENZWEIG², HRAG KARAKACHIAN², FABIAN PASCHKE¹, ULRICH STARKE², and MIKHAIL FONIN¹ — ¹Fachbereich Physik, Universität Konstanz, 78457 Konstanz, Germany — ²Max-Planck-Institut für Festkörperforschung, Heisenbergstraße 1, 70569 Stuttgart, Germany

Electronic correlations in graphene are expected to be strongly enhanced when there is a very high density of states at the Fermi level, giving rise to many-body states such as superconductivity or charge density waves (CDW) [1]. While the latter have been reported for example in Ca-intercalated bilayer graphene [2,3], in case of epitaxial monolayer graphene no direct evidence of correlated electronic ground states has yet been reported. We investigate heavily n-doped monolayer graphene on SiC(0001), obtained by Yb intercalation underneath zero-layer graphene. Here, a van Hove singularity (VHS) is pushed to the Fermi level, giving rise to an extended VHS, effectively pinning an almost non-dispersive flat band at EF [4]. Low-temperature STM reveals several distinct structures of Yb-intercalated graphene, which we attribute to differing arrangements of the Yb at the interface. dI/dU spectra show a pronounced gap feature centered at EF, whose response to field and temperature variations allows the interpretation of the feature as a CDW state.

[1] M. L. Kiesel et al., Phys. Rev. B 86, 020507 (2012);
[2] R. Shimizu et al., Phys. Rev. Lett., 114, 146103 (2015);
[3] S. Ichinokura et al., ACS Nano 10, 2, 2761 (2016);
[4] P. Rosenzweig et al., Phys. Rev. B 100, 035445 (2019).

O 42: Metal substrates 2

Time: Wednesday 10:30–11:45

Location: S053

O 42.1 Wed 10:30 S053

Atomic structure determination of epitaxially grown tin perovskite CsSnBr₃ on gold surfaces — •MADAD ABBASLI¹, JENNY SCHRAGE¹, JIAQI CAI¹, JEREMY HIEULLE², ALEX REDINGER², CARSTEN BUSSE¹, and ROBIN OHMANN¹ — ¹University of Siegen, Department of Physics, Germany — ²University of Luxembourg, Department of Physics and Materials Science, Luxembourg

Tin perovskites can be efficient and environmentally friendly substitutions to lead perovskites, but they have a drawback due to oxidation from Sn^{2+} to Sn^{4+} . Here, we present an in-situ study of epitaxially grown CsSnBr₃ on Au(111) and Au(100) in ultrahigh vacuum (UHV) using scanning tunneling microscopy (STM), low energy electron diffraction (LEED) and x-ray photoelectron spectroscopy (XPS). By co-evaporation of the precursor molecules CsBr and SnBr₂ submonolayers up to a few monolayers are obtained. On Au(111), CsSnBr₃ grows in three differently oriented domains due to the hexagonal symmetry of the substrate. On Au(100), which has square symmetry, identical to CsSnBr₃, but with about half of the lattice constant of the perovskite, we observe a (2×2) superstructure. Chemical analysis shows no indication of tin oxidation, which demonstrates the importance of preparation of tin perovskites in vacuum using evaporation.

O 42.2 Wed 10:45 S053

Peculiar growth of Mn on Ir (111) investigated by SP-STM — •ARTURO RODRÍGUEZ SOTA, VISHESH SAXENA, ANDRÉ KUBETZKA, JONAS SPETHMANN, ROLAND WIESENDAINGER, and KIRSTEN VON BERGMANN — Institut für Nanostruktur- und Festkörperphysik, Universität Hamburg

The growth of metallic layers has been studied for many years, from single atom coverages via clusters and islands to extended films. The experimental parameters used during the growth, such as deposition temperature or amount of material, determine the resulting phase. Usually, only one phase is present for a given preparation, but for europium on graphene the coexistence of clusters and islands of has been documented. This was attributed to several effects including charge transfer from the metal clusters to the substrate in a precise window of coverage and temperature [1].

Here we study the growth of Mn on Ir(111) using spin polarized scanning tunneling microscopy (SP-STM). In this metallic system we have found the coexistence of clusters and islands for any Mn sub-monolayer coverage. We have

characterized the clusters in detail at low temperature and found several different configurations made out of three atoms. The Mn islands exhibit a reconstruction that disappears when the layer is completely closed. The monolayer presents the Néel state as its magnetic ground state.

[1] D. F. Förster et al., New J. Phys. 14, 023022 (2012).

O 42.3 Wed 11:00 S053

Breaking down of Stoner band ferromagnetism induced by interface formation — •DAVID JANAS¹, ANDREA DROGHETTI², IULIA COJOCARIU³, VITALI FEYER³, STEFANO PONZONI¹, MILOŠ RADONJIĆ⁴, IVAN RUNGGER⁵, LIVIU CHIONCEL⁶, GIOVANNI ZAMBORLINI¹, and MIRKO CINCHETTI¹ — ¹TU Dortmund University, Dortmund, Germany — ²Trinity College, Dublin, Ireland — ³Forschungszentrum Jülich, Jülich, Germany — ⁴University of Belgrade, Belgrade, Serbia — ⁵National Physics Laboratory, Teddington, United Kingdom — ⁶University of Augsburg, Augsburg, Germany

Interfaces between ferromagnetic transition metals and molecules or atoms display intriguing spin properties that have been invoked to explain the peculiar behavior of a variety of molecular spintronic and spin-optoelectronic devices [1]. Despite its relevance, a satisfying model for the hybridization occurring at such interfaces has not yet been presented. Experimentally, this is due to the lack of information on the interface band structure in the whole Brillouin zone, while, theoretically, the role of electron correlation has up to now mostly been neglected. Here, we overcome these limitations using state-of-the-art experimental and theoretical methods to explore the model interface between iron and an ordered oxygen layer. We use spin-resolved momentum microscopy to provide access to the complete spin-resolved interface band structure and explain our findings using DFT+ Σ_2 calculations that go beyond the one-electron approximation [2].

[1] Cinchetti, M. et al. *Nature Mater* 16, 507-515 (2017).
[2] Droghetti, A. et al. *Phys. Rev. B* 105, 115129 (2022).

O 42.4 Wed 11:15 S053

Computational screening of self-intercalated transition metal dichalcogenides for enhanced electrocatalytic activity — •STEFANO AMERICO and KRISTIAN S. THYGESEN — Center for Atomic-scale Materials Design, Department of Physics, Technical University of Denmark, DK - 2800 Kongens Lyngby, Denmark

Self-intercalation of metal atoms in bilayer transition metal dichalcogenides (TMD) has been recently realized experimentally through chemical vapor deposition (CVD) and molecular beam epitaxy (MBE), giving rise to completely new phases of the materials with controlled stoichiometry. However, little is known yet about the possible applications for this novel class of compounds. In this work, we use density functional theory to evaluate the catalytic activity towards electrochemical water splitting for 22 self-intercalated TMDs, including both metallic and semiconducting ones. We assess the thermodynamic and chemical stability of the compounds at different pH values and perform a systematic study of the hydrogen and oxygen adsorption energies at 33%, 66% and 100% intercalation degrees, identifying potential anode and cathode materials. Temperature-pressure phase diagrams are also calculated in order to guide the synthesis of compounds with the desired intercalation degree through CVD.

O 42.5 Wed 11:30 S053

A μ -Photoreactor for Investigating Planar Hydrogen Evolution Catalysts at Ambient Condition — •CLARA ALETSEE, MARTIN TSCHURL, and UELI HEIZ — Physical Chemistry, Department of Chemistry & Catalysis Research Center, Technical University of Munich

Photocatalytic water splitting and alcohol reforming offer promising alternatives for clean H₂ production, in contrast to the industrially applied steam reforming of fossil fuels. However, the understanding of the reaction mechanisms, which is indispensable for tailored performance improvement, is complicated by the structural complexity of powdered catalyst. In contrast, well-defined planar catalysts are already used for fundamental studies in ultra-high vacuum, but a simple extrapolation of the results to applied conditions is impractical due to a significant pressure difference.

Herein, we present a μ -photoreactor for the evaluation of planar model catalysts like single crystals or epitaxially grown semiconductors at ambient conditions in a continuous gas flow. In this system, the catalyst serves as the bottom of the reactor, while a 200 μ m O-ring on top defines the reactor volume of 12 μ L. It is sealed by a UV-vis transparent lid with lithographically implemented channels for the gas flow toward the quadrupole mass spectrometer for product analysis. The functionality is demonstrated by ethanol photoreforming over a Pt loaded TiO₂ catalyst. This concept will not only enable the evaluation of planar photocatalysts, but also the investigation of the transferability of UHV results to applied systems.

O 43: Frontiers of Electronic Structure Theory: Focus on Artificial Intelligence Applied to Real Materials 1

Time: Wednesday 10:30–13:00

Location: S054

O 43.1 Wed 10:30 S054

Structure of Amorphous Phosphorus from Machine Learning-Driven Simulations — •YUXING ZHOU, WILLIAM KIRKPATRICK, and VOLKER L. DERINGER — Department of Chemistry, Inorganic Chemistry Laboratory, University of Oxford Oxford OX1 3QR, UK

Amorphous phosphorus (a-P) has long attracted interest because of its complex atomic structure, and more recently as an anode material for batteries. However, accurately describing and understanding a-P at the atomistic level remains a challenge. In this talk, we show that a general-purpose Gaussian approximation potential (GAP) model for phosphorus can be created by machine learning (ML) from a suitably chosen ensemble of quantum-mechanical results. Its accuracy in describing the amorphous phase is demonstrated via large-scale molecular-dynamics simulations on the atomic structure of a-P: the calculated structure factors yield good agreement with earlier experimental evidence. Abundant five-membered rings are found in the structural model, which are the building block of more complex clusters. We provide new insights into the cluster fragments under pressure: an analysis of cluster fragments, large rings, and voids suggests that moderate pressure (up to about 5 GPa) does not break the connectivity of clusters, but higher pressure does. Changes in the simulated first sharp diffraction peak during compression and decompression indicate a hysteresis in the recovery of medium-range order. Our work provides a starting point for further computational studies of a-P, and more generally it exemplifies how ML-driven modeling can accelerate the understanding of disordered functional materials.

O 43.2 Wed 10:45 S054

Realistic Structural Properties of Amorphous SiN_x from Machine-Learning-Driven Molecular Dynamics — •GANESH KUMAR NAYAK¹, PRASHANTH SRINIVASAN², JURAJ TODT³, ROSTISLAV DANIEL¹, and DAVID HOLEC¹ — ¹Department of Materials Science, Montanuniversität Leoben, Leoben, Austria — ²Franz-Josef-Strasse 18 — ³Erich Schmid Institute of Materials Science of the Austrian Academy of Sciences, Jahnstrasse 12, Leoben, Austria

Machine-learning (ML)-based interatomic potentials can enable simulations of extended systems with an accuracy that is largely comparable to DFT, but with a computational cost, that is orders of magnitude lower. Molecular dynamics simulations further exhibit favorable linear (order N) scaling behavior.

Amorphous silicon nitride (a-SiN_x) is a widely studied noncrystalline material, and yet the subtle details of its atomistic structure and mechanical properties are still unclear. Due to the small sizes of representative models, DFT cannot reliably predict its structural properties and hence left an anisotropic order parameter. Here, we show that accurate structural models of a-SiN_x can be obtained using an ML-based inter-atomic potential. Our predictions of structural properties are validated by experimental values of mass density by X-ray reflectivity measurements and by radial distribution function measured by synchrotron X-ray diffraction.

Our study demonstrates the broader impact of ML potentials for elucidating structures and properties of technologically important amorphous materials.

O 43.3 Wed 11:00 S054

Combined experimental-computational directed sampling approach to modelling amorphous alumina — •ANGELA HARPER¹, STEFFEN EMGE², PIETER MAGUSIN^{2,3}, CLARE GREY², and ANDREW MORRIS⁴ — ¹Cavendish Laboratory, University of Cambridge — ²Department of Chemistry, University of Cambridge

— ³Institute for Life Sciences & Chemistry, Hogeschool Utrecht — ⁴School of Metallurgy and Materials, University of Birmingham

Understanding the electronic and atomic level structure of materials is imperative for discovering the next generation of solid state electronic devices. Yet for amorphous materials, it is non-trivial to determine the exact local ordering. In this talk, I outline a method for modelling disordered materials, using experimentally directed sampling of static configurations from *ab initio* molecular dynamics¹. We calculate experimentally relevant spectra and properties including X-ray absorption edges, nuclear magnetic resonance chemical shieldings, and the electronic density of states, with first principles accuracy. This model is validated on amorphous alumina, a widely used coating material in electronic devices, and identify two distinct five-fold coordinated geometries of AlO₅, as well as localised states at the conduction band minimum. By leveraging both experimental and computational data in our approach we highlight the need for experimentally informed calculations which lead to a more detailed understanding of complex materials, and develop an approach that is widely applicable to the modelling community.

¹Harper, AF et al., Under review (2021)
doi.org/10.33774/chemrxiv-2021-qjzjb

O 43.4 Wed 11:15 S054

Structural phases and thermodynamics of BaTiO₃ from an integrated machine learning model — •LORENZO GIGLI¹, MAX VEIT¹, MICHELE KOTIUGA², GIOVANNI PIZZI², NICOLA MARZARI², and MICHELE CERIOTTI¹ — ¹Laboratory of Computational Science and Modeling (COSMO), Institute of Materials, École Polytechnique Fédérale de Lausanne, CH-1015 Lausanne, Switzerland — ²Theory and Simulation of Materials (THEOS) and National Centre for Computational Design and Discovery of Novel Materials (MARVEL), École Polytechnique Fédérale de Lausanne, CH-1015 Lausanne, Switzerland

Modeling the ferroelectric transition of any given material requires three key ingredients: (1) a model of the potential energy surface, that describes the energetic response to a structural distortion; (2) the free energy surface sampled at the relevant, finite-temperature conditions; and; (3) the polarization of individual configurations that determines the observed polarization and the phase transitions. To this aim, we make use of an integrated machine-learning framework, based on a combination of an interatomic potential and a microscopic polarization model, which we use to run Molecular Dynamics simulations of ferroelectrics with the same accuracy of the underlying DFT method, on time and length scales that are not accessible to direct *ab-initio* modeling. This allows us to uncover the microscopic nature of the ferroelectric transition in barium titanate (BaTiO₃) and to identify the presence of an order-disorder transition as the main driver of ferroelectricity. The framework also allows us to reconstruct the temperature-dependent BaTiO₃ phase diagram, with first-of-its-kind accuracy.

O 43.5 Wed 11:30 S054

Dielectric properties of BaTiO₃ from an integrated machine-learning model — •MAX VEIT¹, LORENZO GIGLI¹, MICHELE KOTIUGA², GIOVANNI PIZZI², NICOLA MARZARI², and MICHELE CERIOTTI¹ — ¹Laboratory for Computational Science and Modeling (COSMO), Ecole Polytechnique Fédérale de Lausanne, Lausanne, CH — ²Laboratory for Theory and Simulation of Materials (THEOS), Ecole Polytechnique Fédérale de Lausanne, Lausanne, CH

Modeling the finite-temperature behavior of ferroelectric materials from first principles has always been challenging due to the large supercells and long simulation times required for adequate sampling. Here we demonstrate the use of an integrated machine learning (ML) model of the potential energy and polarization surfaces of barium titanate (BaTiO_3) to overcome these difficulties and run long MD simulations with DFT accuracy. We use these simulations to compute the frequency-dependent dielectric response function, finding a spectrum qualitatively similar that obtained with previous effective-Hamiltonian simulations as well as to experimentally measured profiles, with some remaining discrepancies that we trace back to the underlying DFT model. Finally, we discuss possible extensions of the model to explicitly include long-range interactions, previously included only in an implicit, emergent manner. We expect this integrated, generally applicable modeling technique to become a valuable tool for elucidating the ferroelectric behavior of a wide variety of materials.

O 43.6 Wed 11:45 S054

The first-principles phase diagram of monolayer nanoconfined water — •VENKAT KAPIL¹, CHRISTOPH SCHRAN¹, ANDREA ZEN², JI CHEN³, CHRIS PICKARD¹, and ANGELOS MICHAELIDES¹ — ¹University of Cambridge, UK — ²Università di Napoli Federico II, Italy — ³Peking University, Beijing, China

Water in nanoscale cavities is ubiquitous and of central importance to everyday phenomena in geology and biology, and at the heart of current and future technologies in nano-science. A molecular-level picture of the structure and dynamics of nano-confined water is a prerequisite to understanding and controlling the behavior of water under confinement. Here we explore a monolayer of water confined within a graphene-like channel using a framework that combines developments in high-level electronic structure theory, machine learning, and statistical sampling. This approach enables a treatment of nano-confined water at unprecedented accuracy. We find that monolayer water exhibits surprisingly rich and diverse phase behavior that is highly sensitive to temperature and the van der Waals pressure acting within the nano-channel. Monolayer water exhibits numerous molecular ice phases with melting temperatures that vary by over 400 degrees in a non-monotonic manner with pressure. In addition, we predict two unexpected phases: a *hexatic-like* phase, which is an intermediate between a solid and a liquid, and a superionic phase with a high electrical conductivity exceeding that of battery materials. Our work suggests that nano-confinement could be a promising route towards superionic behaviour at easily accessible conditions.

O 43.7 Wed 12:00 S054

Exploring amorphous graphene with empirical and machinelearned potentials — •ZAKARIYA EL-MACHACHI¹, MARK WILSON², and VOLKER L. DERINGER¹ — ¹Department of Chemistry, Inorganic Chemistry Laboratory, University of Oxford, Oxford OX1 3QR, UK — ²Department of Chemistry, Physical and Theoretical Chemistry Laboratory, University of Oxford, Oxford OX1 3QZ, UK

The structure of amorphous graphene (aG) lacks long range order whilst having short and medium range order yielding a rich and complex configurational space, which is yet to be fully understood. Here we report on an atomistic modelling study of aG using a machine learning (ML) based force field. ML force fields are typically “trained” on data from highly accurate but computationally costly density functional theory (DFT) computations. Atomistic models created by such ML methods can achieve near DFT accuracy at a fraction of the computational cost. One key assumption is that the global energy can be separated into sums of local energies. The physical interpretation of ML local energies is an interesting research question. We find that local and nearest neighbour (NN) ML energies can inform the generation of aG models from crystalline graphene via a Monte-Carlo bond switching algorithm. Bond switches are introduced as Stone-Wales defects, with the local energies of the defect pair and its NNs used in the acceptance criterion. Established empirical force fields are used in the same way and the resulting structures are studied. Our results provide insight into the modelling of amorphous graphene and into the nature of ML potential-energy models.

O 43.8 Wed 12:15 S054

Machine learning for estimation of spin models in undoped cuprates — •DENYS Y. KONONENKO¹, ULRICH K. RÖSSLER¹, JEROEN VAN DEN BRINK^{1,2}, and OLEG JANSON¹ — ¹Institute for Theoretical Solid State Physics, IFW Dresden, Dresden, Germany — ²Institute for Theoretical Physics, TU Dresden, Dresden, Germany

Undoped cuprates tailor a fascinating variety of low-dimensional and frustrated spin models, which can be indirectly characterized by the transfer integrals. The estimation of transfer integrals is related to a relatively complicated computational procedure which includes besides DFT calculation also a Wannierization. We propose a data-driven approach to replace this computationally demanding procedure.

We employ the Gaussian Process Regression model, trained on the results of high-throughput DFT calculations to estimate transfer integrals in undoped cuprates. The model learns from data the dependency between the local crystal environment of copper atoms pair and the corresponding value of transfer integral. The site position function of the local crystal environment is represented as a finite-dimensional vector composed of decomposition coefficients in the truncated basis of Zernike 3D functions [1]. The vector descriptor incorporates the spatial configuration and chemical composition of the local crystal environment. The proposed approach can be utilized for a rapid assessment of the spin models of new cuprates using structural information as the only input.

[1] M. Novotni and R. Klein, *Computer Aided Design* 36, 1047 (2004)

O 43.9 Wed 12:30 S054

Machine-learning Based Screening of Lead-free Perovskites for Photovoltaic Applications — •ELISABETTA LANDINI^{1,3}, HARALD OBERHOFER², and KARSTEN REUTER¹ — ¹Fritz-Haber-Institut der Max-Planck-Gesellschaft, Faradayweg 4-6, D-14195 Berlin, Germany — ²Chair for Theoretical Physics VII, Physikalisches Institut Universität Bayreuth, 95440, Bayreuth, Germany — ³Chair for Theoretical Chemistry, Technische Universität München, Lichtenbergstr. 4, D-85747 Garching, Germany

Lead-free halide double perovskites are promising stable and non-toxic alternatives to methylammonium lead iodide in the field of photovoltaics. In this context, the most commonly used double perovskite is $\text{Cs}_2\text{AgBiBr}_6$, due to its favorable charge transport properties [1]. However, the maximum power conversion efficiency obtained for this material does not exceed 3%, as a consequence of its wide indirect gap and its intrinsic and extrinsic defects [2]. On the other hand, the materials space that arises from the substitution of different elements in the 4 lattice sites of this structure is large and still mostly unexplored.

In this work a neural network is used to predict the band gap of double perovskites from an initial space of 7056 structures and select candidates suitable for visible light absorption. Successive hybrid DFT calculations are used to evaluate the thermodynamic stability and the power conversion efficiency of the selected compounds, and propose novel potential solar absorbers.

[1] E.T. McClure *et al.*, *Chemistry of Materials* 28, 1348 (2016).

[2] X. Yang *et al.*, *Energy & Fuels* 34, 10513 (2020).

O 43.10 Wed 12:45 S054

Equivariant graph neural network for linear scaling electron density estimation and applications in battery materials — •ARGHYA BHOWMIK and PETER JORGENSEN — 301 Anker Engelunds vej, Kgs. Lyngby, DK-2800

We present a machine learning framework for the prediction of $\rho(r)$ based on equivariant graph message passing neural networks. The electron density is predicted at special query point vertices that are part of the message passing graph, but only receive messages. The model is tested across multiple data sets of molecules (QM9), liquid ethylene carbonate electrolyte (EC) and $\text{Li}_x\text{Ni}_y\text{Mn}_z\text{Co}(1-y-z)\text{O}_2$ lithium ion battery cathodes (NMC). The model is used to explore large materials phase space for safer battery materials and uncovering new understanding how redox mediated diffusion occurs and battery materials.

O 44: Focus Session: Surfaces and Interfaces of (Incipient) Ferroelectrics (joint session O/KFM)

Ferroelectricity is a property of materials that allows spontaneous, switchable electric polarization. Recently, many surface-related applications have been proposed where ferroelectric or incipient-ferroelectric materials exhibit superior properties. These include catalysis, electron-hole separation in light harvesting, unique electronic properties such as a negative capacitance in heterostructures of ferroelectric materials, to name just a few. While (incipient) ferroelectrics clearly perform well in the aforementioned applications, there is very limited fundamental understanding of the processes involved on the surfaces of these materials.

Organizers: Martin Setvin (Charles University, Prague), Chiara Gattinoni (London South Bank University), and Michele Retliccioli (University of Vienna)

Time: Wednesday 15:00–18:30

Location: H3

Topical Talk

O 44.1 Wed 15:00 H3

In search of electrostatic happiness at surfaces — •NICOLA SPALDIN — Materials Theory, ETH Zurich

We review the concept of surface charge in ionic insulators, first, in the context of the polarization in ferroelectric materials (traditionally discussed in the ferroelectrics community) and, second, in the context of layers of charged ions (traditionally discussed in the surface science community). In both cases, the surface charge leads to an electrostatic instability if it is not compensated, which is usually detrimental for the development of electronic devices based on ferroelectrics, but favorable for applications such as catalysis where surface reactivity is desirable.

Using the prototypical multiferroic bismuth ferrite, BiFeO₃, as an example, we show how the spontaneous ferroelectric polarization and the charged ionic layers can in fact combine to yield stable, uncharged “happy” (100) surface geometries. Switching the polarization causes these (100) surfaces considerable electrostatic distress, which must be compensated by the introduction of charged point defects or adsorbates. We demonstrate that the relative happiness or unhappiness of the surfaces enables a cycle of alternating charged then neutral adsorbates on polarization switching, which can be exploited for water remediation and water splitting.

We close with a proposal that these physics can induce polarization in thin films of certain usually non-polar materials, and give a recipe for determining likely candidates.

In collaboration with Chiara Gattinoni, Ipek Efe and Marta Rossell

Topical Talk

O 44.2 Wed 15:30 H3

Synthesis and Characterisation of Ultra-thin Aurivillius Phase Multiferroics — •LYNETTE KEENEY — Tyndall National Institute, University College Cork, Lee Maltings Complex, Dyke Parade, Cork, Ireland, T12 R5CP

Multiferroic materials, possessing simultaneous ferroelectric and ferromagnetic memory states, have been road-mapped as promising multi-state architectures for memory scaling beyond current technologies. In recent years, my team reported the design of such a novel room temperature multiferroic material with an Aurivillius phase structure that could ideally be suited to future fabrication of revolutionary memory devices. Electrostatic strain and elastic energy variations close to defect regions increase the extent of magnetic partitioning and also influence the formation of exotic charged domain walls and polar vortices. This further initiates technology prospects in ultra-compact data storage, energy-efficient neuromorphic computing and ultrahigh speed data processing. As miniaturisation of electronic devices continues, a crucial requirement is the enhancement of their functional properties at very small dimensions. In this presentation, I will discuss how direct liquid injection chemical vapour deposition allows for frontier-development of ultra-thin films at fundamental thickness. Via a two-dimensional layer-by-layer growth mode, films equating to half of one unit-cell (2.5 nm) of the Aurivillius structure are grown. The persistence of stable ferroelectricity, even when pushed to ultra-thin thicknesses, demonstrates the recent progress in the optimisation of Aurivillius phase materials for utilisation in future miniaturised multiferroic-based devices.

O 44.3 Wed 16:00 H3

Influence of Nb dopants on the polarization and screening on cleaved SrTiO₃(001) surfaces — •IGOR SOKOLOVIĆ¹, ALEXANDER HOHENEDE¹, JESUS REDONDO², DOMINIK WRANA², MICHAEL SCHMID¹, ULRIKE DIEBOLD¹, and MARTIN SETVÍN² — ¹Institute of Applied Physics, TU Wien, Vienna, Austria — ²Faculty of Physics and Mathematics, Charles University, Prague, Czech Republic

The incipient ferroelectric SrTiO₃ can turn ferroelectric even at room temperature under the application of strain, and this quantum phase transition can be utilized to cleave SrTiO₃ single crystals that otherwise possess no preferable cleavage planes [1]. This cleaving procedure creates truly bulk-terminated SrTiO₃(001) surfaces that come the closest to being pristine [2]. In this talk, I will present how the SrO- and TiO₂-terminated surface domains of opposite polarity can be influenced by the small changes in the amounts of Nb doping. The cleaved SrTiO₃(001) surfaces with varying Nb doping levels were systematically studied

with atomic resolution using noncontact atomic force microscopy (ncAFM) and scanning tunneling microscopy (STM). It was observed that Nb doping does not affect the magnitude of the strain-induced polarization, yet still significantly affects the morphology, the electronic structure, and the domain-wall structure on cleaved SrTiO₃(001) surfaces. Beside demonstrating the interplay between the domain distribution and electrostatic screening, these results show how the properties of these heterogeneous surfaces can be tuned.

[1] Sokolović *et al.*, Phys. Rev. Mater. 3, 034407 (2019)

[2] Sokolović *et al.*, Phys. Rev. B 103, L241406 (2021).

O 44.4 Wed 16:15 H3

Polaronic Properties of the weakly-polar SrTiO₃(001) Surface — •FLORIAN ELLINGER¹, MICHELE RETICCIOLI¹, IGOR SOKOLOVIĆ², ULRIKE DIEBOLD², MARTIN SETVÍN³, and CESARE FRANCHINI^{1,4} — ¹University of Vienna — ²Technische Universität Wien — ³Charles University Prague — ⁴Università di Bologna

The SrTiO₃(001) surface shows ferroelectric-like distortions on the bulk-like termination, an out-of-plane dipole moment, and so-called “weak polarity”. Recent experiments propose that these effects are compensated by Sr-adatoms and -vacancies, stabilizing the unreconstructed surface. [1]

We investigate the 1 × 1 SrTiO₃(001) surface with TiO₂- and SrO-terminations by means of density functional theory (DFT) simulations. Our calculations confirm the experimental interpretation and show that these polarity-compensating surface defects introduce additional charge. Adsorbing Sr-adatoms and doping with Nb leads to excess electrons in the crystal, facilitating the formation of electron-polarons. On the other hand, by creating Sr-vacancies on the surface we introduce excess holes to the system, which can localize as hole-polarons. For both kinds of polarons we analyze their general properties, e.g., the preferred localization site or stability. Further, we compare results of different structural phases of this crystal to achieve a comprehensive understanding of mentioned physical phenomena.

[1] Sokolović *et al.*, *Incipient ferroelectricity: A route towards bulk-terminated SrTiO₃*, Phys. Rev. Materials 3, 034407 (2019)

O 44.5 Wed 16:30 H3

Ferroelectric domain imaging in barium titanate using infrared-visible sum-frequency generation microscopy — •DOROTHEE MADER¹, DANIEL LOURENS², MAARTEN KWAAITAAAL², RICHARDA NIEMANN¹, SÖREN WASSERROTH¹, SANDY GEWINNER¹, MARCO DE PAS¹, WIELAND SCHÖLLKOPF¹, MARTIN WOLF¹, ANDREI KIRILYUK², SEBASTIAN F. MAEHRLEIN¹, and ALEXANDER PAARMANN¹ — ¹Fritz Haber Institute of the Max Planck Society, Berlin, Germany — ²Radboud Universiteit, Nijmegen, The Netherlands

Phonons exhibit a mostly unexplored leverage on the mechanisms and dynamics of domain formation in ferroics. Here, a new method is employed combining resonant phonon excitation and ferroelectric domain imaging of barium titanate (BTO) using infrared-visible (IR-VIS) sum-frequency generation (SFG) microscopy [1]. BTO is a non-centrosymmetric perovskite oxide with a strong ferroelectric polarization in its tetragonal phase. Typically, BTO samples exhibit a multi-domain structure. In this contribution, SFG microscopy is shown to naturally provide domain contrast due to the polarization-induced local variation of the nonlinear susceptibility. Additionally, our spectral analysis of the SFG response reveals the domain-selective phonon resonances for all high-frequency phonons in the IR spectral range of 500–800 cm⁻¹. By locally mapping phonon resonances in domains and domain walls, this approach may enable in-depth understanding of the underlying physics of domain formation and its dynamics. [1] R. Niemann *et al.*, Appl. Phys. Lett. 120, 131102 (2022).

Topical Talk

O 44.6 Wed 16:45 H3

Water-oxidation catalysis on surfaces of ferroelectrics — •ULRICH ASCHAUER¹, NATHALIE VONRÜTI¹, ZHENYUN LAN², DIDRIK R. SMÅBRÄTEN¹, TEJS VEGGE², and IVANO E. CASTELLI² — ¹University of Bern, Bern, Switzerland — ²Technical University of Denmark, Kgs. Lyngby, Denmark

Surfaces of ferroelectrics have unique properties for catalysis since the binding strength of reaction intermediates can be modulated by switching the fer-

roelectric polarization. This could allow to overcome the limitations of the Sabatier principle and enable dynamical catalysts operation. In this talk, we will focus on the interplay between screening charge transfer to surfaces, the adsorbate coverage and the (photo)electrochemical water-oxidation activity of ferroelectric surfaces. We will compare different ferroelectric materials such as BaTiO₃, strained LaTiO₂N and the hexagonal improper ferroelectric oxy-nitride InSnO₂N. Our results indicate that ferroelectric switching can indeed provide an economically interesting route to enhance the catalytic activity but that material-specific intricacies of the surface adsorbate coverage need to be understood and controlled to exploit the full potential of ferroelectric switching in (photo)electrocatalysis.

O 44.7 Wed 17:15 H3

The polar KTaO₃ (001) surface: Electronic structure and CO adsorption — ZHICHANG WANG¹, MICHELE RETICCIOLI², ZDENEK JAKUB¹, MICHAEL SCHMID¹, GARETH PARKINSON¹, ULRIKE DIEBOLD¹, CESARE FRANCHINI², and MARTIN SETVIN³ — ¹TU Wien, Vienna, Austria — ²University of Vienna, Vienna, Austria — ³Charles University, Prague, Czech Republic

Polar surfaces offer intriguing physical and chemical properties applicable in electronics or catalysis. Cleaving the KTaO₃ perovskite along its polar (001) plane provides a well-defined, bulk-terminated surface with KO and TaO₂ terminations [1]. As-cleaved surfaces exhibit a high concentration of in-gap states; these electrons predominantly reside at the TaO₂-terminated parts of the surface. These electrons can affect surface chemistry, as is demonstrated for CO molecules. CO has two adsorption configurations on the TaO₂ termination, and the CO differs in how it couples to the excess electrons. DFT calculations indicate that CO preferentially couples to electron bipolarons.

The work was supported by FWF project P32148-N36, by GACR 20-21727X and GAUK Primus/20/SCI/009.

[1] M. Setvin, M. Reticcioli, F. Poelzleitner et al., *Science* 359, 572 (2018)

O 44.8 Wed 17:30 H3

Polarons and ferroelectricity: tip-induced phenomena on oxide perovskite surfaces — DOMINIK WRANA¹, IGOR SOKOLOVIĆ², JESUS REDONDO¹, PAVEL KOCÁN¹, AJI ALEXANDER¹, LORENÇ ALBONS¹, and MARTIN SETVIN¹ — ¹Department of Surface and Plasma Science, Charles University, Prague, Czech Republic — ²Institute of Applied Physics, TU Wien, Vienna, Austria

In this talk, I will present the similarities and differences between two representative perovskite oxide surfaces: KTaO₃(001) and BaTiO₃(001), showcasing the manifestation of the (incipient-) ferroelectricity on the atomic and electronic structure. Both surfaces were prepared by cleaving single crystals in situ and characterized by means of qPlus nc-AFM at temperatures ranging from 4K to 100K.

Bulk-terminated KTaO₃(001) develops two alternating domains of KO and TaO₂ [1]. Excess electrons injected from the AFM tip form quasiparticles called polarons (charges coupled with lattice distortions) which can be further shaped into 1D or 2D structures by emerging electric fields.

Different mechanism applies in the case of BaTiO₃(001), where at low temperatures titanium atoms can easily break the symmetry causing a spontaneous

polarization. Hence, a biased tip allows for reversible manipulation of individual atoms on the surface: writing and erasing polarized ferroelectric domains.

[1] Setvin, Martin, et al. *Science* 359.6375 (2018): 572-575

O 44.9 Wed 17:45 H3

Optimisation and miniaturisation of naturally-layered multiferroic thin films — LYNETTE KEENEY — Tyndall National Institute, University College Cork, Lee Maltings Complex, Dyke Parade, Cork, Ireland, T12 R5CP

Multiferroic materials, possessing simultaneous ferroelectric and ferromagnetic memory states, are road-mapped as promising multistate architectures for memory scaling beyond current technologies. In recent years, my team reported the design of such a novel room temperature multiferroic material with an Aurivillius phase structure that could ideally be suited to future fabrication of revolutionary memory devices. In this presentation, I will discuss how electrostatic strain and elastic energy variations close to bismuth oxide interfaces and defect regions are key to promoting magnetic cation partitioning and multiferroic behaviour. These also influence the formation of exotic charged domain walls and polar vortices, further initiating technology prospects in ultra-compact data storage. As miniaturisation of electronic devices continues, a crucial requirement is the enhancement of their functional properties at very small dimensions. Direct liquid injection chemical vapour deposition allows for frontier-development of ultra-thin films at fundamental thickness. Via a two-dimensional layer-by-layer growth mode, films equating to half of one unit-cell (2.5 nm) of the Aurivillius structure are grown. The persistence of stable ferroelectricity, even when pushed to ultra-thin thicknesses, demonstrates the recent progress in the optimisation of Aurivillius phase materials for utilisation in future miniaturised multiferroic-based devices.

Topical Talk

O 44.10 Wed 18:00 H3

Spin-orbitronics and superconductivity in KTaO₃ twodimensional electron gases — SRIJANI MALLIK¹, GERBOLD MÉNARD², GUILHEM SAIZ², HUGO WITT^{1,2}, SARA VAROTTO¹, LUIS M. VICENTE-ARCHE¹, JULIEN BRÉHIN¹, ANNIKA JOHANSSON³, BÖRGE GÖBEL⁴, RAPHAËL SALAZAR⁵, INGRID MERTIG⁴, LARA BENFATTO⁶, NICOLAS BERGEAL², and MANUEL BIBES¹ — ¹Unité Mixte de Physique CNRS/Thales, Palaiseau, France — ²LPEM ESCPI, Paris, France — ³MPI, Halle, Germany — ⁴Martin-Luther-Universität Halle-Wittenberg, Germany — ⁵Synchrotron SOLEIL, France — ⁶Sapienza University of Rome, Italy

Similar to SrTiO₃ (STO) recent research has shown that KTaO₃ (KTO) may also harbor a 2DEG at interfaces with several oxide materials. Due to the presence of Ta (5d element), it is expected that the Rashba spin-orbit coupling in KTO 2DEGs should be larger than in STO 2DEGs. Further, (110) and (111)-oriented KTO 2DEG show superconductivity at temperature a factor of ca. 10 higher than in STO 2DEGs. In this talk we will show that 2DEGs can be generated by the simple deposition of Al metal on KTO single crystals. We will report their electronic band structure by angle-resolved photoemission spectroscopy, evidencing a peculiar Rashba splitting. We will show that this Rashba state can be harnessed to achieve very efficient spin-charge interconversion. Finally, we will present microwave impedance spectroscopy measurements of the superconducting condensate and discuss the nature of superconductivity in these systems.

O 45: Focus Session: Catalysis at Liquid Interfaces

Catalysis at liquid Interfaces has emerged as novel approach to explore the highly dynamic, anisotropic environment of liquid interfaces to create, tailor, and stabilize catalytically active sites with unique reactivity and performance. With this concept, fundamental problems of catalyst science and technology can be addressed to develop novel catalytic materials that combine selectivity, productivity, robustness, and ease of processing at the highest possible level. Thus, the concepts of "Supported Catalytically Active Liquid Metal Solutions" (SCALMS), interface-enhanced "Supported Ionic Liquid Phase" (SILP) and advanced "Solid Catalysts with Ionic Liquid Layer" (SCILL) systems are of particular focus.

Organizers: Marcus Bär (Helmholtz-Zentrum Berlin), Jörg Libuda (FAU Erlangen-Nürnberg), Christian Papp (FAU Erlangen-Nürnberg)

Time: Wednesday 15:00–18:00

Location: H4

Topical Talk

O 45.1 Wed 15:00 H4

Addressing Electronic Effects in Catalysis by Intermetallic Compounds — MARC ARMBRÜSTER — Chemnitz University of Technology

The catalytic properties of materials are determined by their electronic and geometric structure. A reliable development addresses both influences separately and then combines the ideal electronic and structural properties resulting in superior catalytic materials.

Unfortunately, this is only straightforward on paper. The implementation faces hurdles concerning the control of the materials. E.g. the electronic modification of metallic materials by addition of a second metal with a different electron count can result in substitutional alloys with (in theory) random distribution of

the elements. However, the sought-for electronic modification is not reachable due to segregation. Another intrinsic challenge is the geometric and electronic entanglement, i.e. when substituting one element by another, the structure might change and with it, the electronic properties.

A new approach is the partial substitution of main group elements in isostructural intermetallic compounds, enabling excellent electronic control with minimal geometric variation. Taking InPd₂ and substituting In by Sn alters the valence electron count, while the distances are mostly not affected. Tuning the In/Sn ratio allows to address the electronic influence with very high resolution. Results in gas-phase hydrogenation and electrocatalysis are presented as examples of the broadly applicable approach.

O 45.2 Wed 15:30 H4

Gallium droplets on nanostructured surfaces as matrix material for supported liquid metal solutions — •ANDRÉ HOFER, NICOLA TACCARDI, PETER WASSERSCHIED, and JULIEN BACHMANN — FAU Erlangen, Germany

A large variety of organic compounds are produced industrially using a dehydrogenation reaction which removes H₂ from a molecule and hence converts it into a more reactive and valuable product. Usually, such a reaction is endothermic and needs to be catalysed or performed at elevated temperatures. Our approach for improving the availability of the catalyst is the utilization of supported catalytically active liquid metal solutions (SCALMS). Here, the catalytically active material is dissolved in a dynamic liquid matrix, protecting it from undesired deactivation. Ga is used in our approach as the matrix material due to its outstanding properties. So far, SCALMS catalysis has been performed with very limited control of particle sizes. Here, we present a model system to determine the fundamental kinetic parameters of SCALMS reactions. We fabricate highly ordered, nanostructured substrates by electrochemical anodization of Al, generating indentations in a hexagonal arrangement with a tunable diameter. These substrates are coated with acidic or alkaline metal oxides by ALD to affect the surface tension and wetting behaviour of the Ga droplets. Subsequently, a Ga complex is spin-coated from organic solution on the surfaces and the elementary Ga droplets are obtained upon thermal treatment. Parameters relevant to SCALMS application of the surface fabricated are investigated systematically as they depend on the preparative parameters.

O 45.3 Wed 15:45 H4

Extending the SCALMS catalytic concept to ternary systems — •MICHAEL MORITZ¹, SVEN MAISEL¹, NARAYANAN RAMAN², HAIKO WITTKÄMPER¹, CHRISTOPH WICHMANN¹, NICOLA TACCARDI², PETER WASSERSCHIED², ANDREAS GÖRLING¹, HANS-PETER STEINRÜCK¹, and CHRISTIAN PAPP¹ — ¹Friedrich-Alexander-Universität Erlangen-Nürnberg, Department Chemie und Pharmazie, Egerlandstraße 3, 91058 Erlangen, Germany — ²Friedrich-Alexander-Universität Erlangen-Nürnberg, Department Chemie- und Bioingenieurwesen, Egerlandstraße 3, 91058 Erlangen, Germany

Over the last few years, supported catalytically active liquid metal solutions (SCALMS) were shown to be remarkably efficient catalysts for alkane dehydrogenation. The active phase of these catalysts consists of a liquid metal matrix, in which catalytically active transition metals are dissolved. So far, only Gallium was used as a liquid matrix material, because of the low toxicity and low melting point. Since extensive research has already been made on Gallium-based SCALMS systems with different catalytically active transition metals, varying the matrix material is the logical next step to further improve the catalyst performance. These efforts are now extended to ternary systems such as GaInPt and GaSnPt. This extension opens up new questions as it increases the complexity, but also brings exciting new properties and insights into the dynamics of liquid SCALMS catalysts. In this talk, the most recent results regarding these ternary systems will be presented, with an emphasis on photoemission studies. Funded by SFB 1452.

O 45.4 Wed 16:00 H4

Investigation of Pt-Ga SCALMS model particles using photoelectron spectroscopy — •CHRISTOPH WICHMANN¹, HAIKO WITTKÄMPER¹, MICHAEL MORITZ¹, TZUNG-EN HSIEH², JOHANNES FRISCH², MINGJIAN WU³, MARCUS BÄR², ERDMANN SPIECKER³, HANS-PETER STEINRÜCK¹, and CHRISTIAN PAPP¹ — ¹Universität Erlangen, Physikalische Chemie II, Germany — ²Helmholtz-Zentrum Berlin, Germany — ³Universität Erlangen, Lehrstuhl für Werkstoffwissenschaften, Germany

Supported catalytically active liquid metal solutions (SCALMS) recently gained much attention as highly active and stable catalysts for the dehydrogenation of alkanes. SCALMS are metal solutions composed of low amounts of catalytically active transition metals like Rh, Pd, or Pt, alloyed with low melting metals like Ga, which act as matrix. Their stability is attested to a notable resistance against deactivation by coking, which is the prevalent deactivation route for dehydrogenation catalysts. To obtain a fundamental understanding, we make these complex materials systems accessible for a surface science approach. To gain insight in the catalytic properties of such nano-solutions, we work with supported PtGa particle systems. Herein, supported PtGa particle systems with low Pt content were investigated. The influence of the deposition sequence, the effects of annealing, and exposure to oxygen on the alloying and morphology of the resulting particle were studied with XPS using different excitation energies to obtain a depth-profile of the first few layers of the liquid.

Funded by SFB 1452.

Topical Talk

O 45.5 Wed 16:15 H4

Understanding liquid metal catalysts for graphene synthesis using machine learning interatomic potentials — •HENDRIK H. HEENEN — Fritz-Haber-Institut der MPG, Berlin, Germany

High-quality, near defect-free graphene can be synthesized on the levelled and uniform surfaces of liquid metal catalysts. This smoothness on the microscale is sometimes accompanied by seemingly different catalytic properties, the determination of which is, however, ambiguous. Assessing distinct catalytic proper-

ties of liquid metal catalysts by first principles atomistic simulations has so far been challenged due to the intractable long length and time scales necessary to model the liquid phase. Using computationally efficient machine learning interatomic potentials (MLIPs) trained to first principles data allows to extrapolate predictability to necessary scales and opens an avenue for obtaining the desired microscopic insight.

In this talk I will present strategies to train and employ MLIPs for the simulation of graphene synthesis on liquid metal catalysts. I will introduce the data-efficient training of MLIPs via fairly automatic workflows as a tool to extend the predictive accuracy of e.g. density functional theory to larger scales. On basis of these potentials, large-scale simulations can be performed to compute experimental observables and elucidate microscopic processes relevant to graphene synthesis. Further, one can identify trends between different metals and directly compare between the solid and liquid states of a catalyst. Findings based on these simulation approaches shed new light on the role of the liquid state of liquid metal catalysts.

Topical Talk

O 45.6 Wed 16:45 H4

Ionic liquids and deep eutectic solvents - sustainable media for selective molecular recognition and adsorption — •JAN BLASIUS, LEONARD DICK, and BARBARA KIRCHNER — Mulliken Center for Theoretical Chemistry, University of Bonn, Beringstrasse 4+6, D-53115 Bonn, Germany

The effective reduction of CO₂ emission and chemical waste production are key disciplines on our way towards a more sustainable future. Ionic liquids (ILs) and deep eutectic solvents (DESSs) offer new opportunities for addressing these challenges, as their properties can be adjusted in order to fulfill specific purposes. To efficiently optimize their usage for various applications, it is vital to understand the underlying molecular behavior and inherent structuring inside these liquids. Using state-of-the-art theoretical methods, we shed light on molecular adsorption and recognition mechanisms in ILs and DESSs. This enables us to determine the reasons for specific capacities and allows a theoretical design of solvents with precisely tuned geometric, energetic and kinetic parameters in order to enhance the processes of interest. In this presentation, we will highlight our most recent research concerning molecular recognition and adsorption in ILs and DESSs which can support the development of novel chemical processes that pave our way towards a more sustainable future.

O 45.7 Wed 17:15 H4

Surfaces of ionic liquids studied by ARXPS and UHV Pendant Drop — •ULRIKE PAAP, FLORIAN MAIER, and HANS-PETER STEINRÜCK — Chair of Physical Chemistry II, FAU Erlangen-Nürnberg, Egerlandstr. 3, Erlangen, Germany

Ionic liquids (ILs) are characterized by a low melting point, low vapor pressure and low surface tension. Many ILs exhibit high gas solubility along a high chemical and thermal stability. Such properties are beneficial in many areas such as gas absorbents, refrigerants, lubricants, antistatics and surfactants. In this work, we studied various imidazolium-based ILs with different functional PEG chains attached to the cation using angle-resolved X-ray photoelectron spectroscopy (ARXPS) and a new pendant drop setup, which enables to measure the surface tension also in ultrahigh vacuum (UHV). With ARXPS, we determine the surface composition of the topmost IL nanometers on the molecular level. We combine these results with our surface tensions studies in UHV and atmosphere. Our results allow for a deeper understanding of enrichment and molecular orientation processes at the outermost surface of these systems in a microscopic and macroscopic range.

This work was supported by the European Research Council (ERC) through an Advanced Investigator Grant (ILID 693398) to HPS and the Collaborative Research Center (CRC) 1452: Catalysis at Liquid Interfaces.

O 45.8 Wed 17:30 H4

Mixed Films of protic and non-protic Ionic Liquids on Metal Surfaces - on-surface metathesis on Ag(111) — •STEPHEN MASSICOT¹, TOMOYA SASAKI², MATTHIAS LEXO¹, SUNGHWAN SHIN¹, FLORIAN MAIER¹, SUSUMU KUWABATA², and HANS-PETER STEINRÜCK¹ — ¹Lehrstuhl für Physikalische Chemie 2, Friedrich-Alexander-Universität Erlangen-Nürnberg — ²Department of Applied Chemistry, Graduate School of Engineering, Osaka University

Ionic liquids (ILs) are salts that are composed of poorly coordinating ions and thus exhibit melting points typically well below 100°C. Thin films of ILs are of utmost interest in many applications such as in catalysis and electrochemistry. In this context, we investigate mixed ultrathin films of the protic IL diethylmethylammonium trifluoromethanesulfonate ([dema][TfO]) and the aprotic IL 1-methyl-3-octylimidazolium hexafluorophosphate ([C₈C₁Im][PF₆]) on a Ag(111) surface. The films are prepared by *in situ* physical vapor deposition in UHV. The molecular composition of the IL/solid and IL/vacuum interfaces is studied by angle-resolved and temperature-programmed X-ray photoelectron spectroscopy. We observe thermally induced phenomena of ion exchange and preferential enrichment at these interfaces. Furthermore, ions desorb selectively which leads to the on-surface formation of a new IL by metathesis at the IL/metal interface.

Supported through an ERC Advanced Investigator Grant (ILID 693398) to HPS and by the DFG through SFB 1452.

O 45.9 Wed 17:45 H4

SCILL model catalysis - butadiene hydrogenation studied with molecular beam techniques — •LEONHARD WINTER, STEPHEN MASSICOT, AFRA GEZMIS, FLORIAN MAIER, and HANS-PETER STEINRÜCK — Lehrstuhl für Physikalische Chemie II, Friedrich-Alexander-Universität Erlangen-Nürnberg (FAU), Egerlandstr. 3, 91058 Erlangen

Ionic Liquids (ILs) are low temperature melting salts, often liquid even below room temperature. In “Solid Catalyst with Ionic Liquid Layer (SCILL)” systems, IL thin films are used to coat the catalytically active metal and therefore, modify the reactivity and the selectivity of the catalyst. Selectivity is crucial e.g., in the

industrially important hydrogenation of 1,3-butadiene to butenes since further hydrogenation to *n*-butane must be suppressed.

We used a supersonic molecular beam to investigate the dynamical details of this reaction in a UHV model study. The method of King and Wells was used to measure sticking coefficients of 1,3-butadiene and 1-butene on bare Pt(111) and Pt(111) coated with ultrathin layers of the IL 1,3-dimethylimidazolium bis[(trifluoromethyl)sulfonyl]imide ([C₁C₁Im][Tf₂N]). The hydrogenation reaction was also modelled by pre-adsorbing and co-feeding hydrogen gas.

Supported by the DFG through the Collaborative Research Center (CRC)/Sonderforschungsbereich (SFB) 1452.

O 46: New Methods and Developments 3: Theory

Time: Wednesday 15:00–17:00

Location: H6

O 46.1 Wed 15:00 H6

Atomistic and coarse-grained modelling of liquid-liquid and liquid-gas interfaces — •JAKOB FILSER^{1,2}, KARSTEN REUTER^{1,2}, and HARALD OBERHOFER^{1,3} — ¹Chair of Theoretical Chemistry, TU Munich — ²Theory Department, Fritz Haber Institute Berlin — ³Chair for Theoretical Physics VII, University of Bayreuth

Modelling of dielectric interfaces remains a central challenge in computational chemistry. Liquid-liquid and liquid-gas interfaces have so far received relatively little attention, compared to solid surfaces. We present a new method to incorporate solvation effects into density-functional theory calculations of large organic adsorbates at liquid-liquid and liquid-gas interfaces. Simulating a large number of solvent molecules explicitly at this first-principles level is not computationally tractable. We therefore resort to an implicit solvation approach, treating the solvent as a structureless dielectric medium. Specifically, we advance the multipole-expansion method, in which we model the interface as the boundary of two semi-infinite media with different permittivity. Additionally, we introduce a piecewise expansion of the dielectric response. While the previous version of the MPE method could solve the electrostatic problem only for small solute molecules up to ≈ 10 non-hydrogen atoms, this development now allows us to simulate larger solutes with an overall non-convex hull, with electrostatic interaction energies converged up to few meV. Validating first results of our model for octanoic acid at a water-gas interface by explicit force-field level molecular dynamics simulation provides insight into the role of the atomistic structure of the solvent in the adsorption.

O 46.2 Wed 15:15 H6

Quantum feedback at the solid-liquid interface: flow-induced electronic current and negative friction — •BAPTISTE COQUINOT^{1,2}, LYDÉRIC BOCQUET¹, and NIKITA KAVOKINE² — ¹Laboratoire de Physique de l'École Normale Supérieure, ENS, Université PSL, CNRS, Paris, France — ²Center for Computational Quantum Physics, Flatiron Institute, New York, NY 10010, USA

An electronic current driven through a conductor can induce a current in another conductor through the famous Coulomb drag effect. Similar phenomena have been reported at the interface between a moving fluid and a conductor, but their interpretation has remained elusive. Here, we develop a quantum-mechanical theory of the intertwined fluid and electronic flows, taking advantage of the non-equilibrium Keldysh framework. We predict that a globally neutral liquid can generate an electronic current in the solid wall along which it flows. This hydrodynamic Coulomb drag originates from both direct Coulomb interactions and interactions mediated by the solid's phonons. We derive explicitly the Coulomb drag current in terms of the solid's electronic and phononic properties, as well as the liquid's dielectric response, a result which quantitatively agrees with recent experiments at the liquid-graphene interface. Furthermore, we show that the current generation counteracts momentum transfer from the liquid to the solid, leading to a reduction of the hydrodynamic friction coefficient through a quantum feedback mechanism. Our results provide a roadmap for controlling nanoscale liquid flows at the quantum level, and suggest strategies for designing materials with low hydrodynamic friction.

O 46.3 Wed 15:30 H6

A fully periodic treatment of the chemisorption function for the analysis of adsorbate-substrate interactions — •SIMIAM GHAN¹, KARSTEN REUTER¹, and HARALD OBERHOFER² — ¹Fritz-Haber-Institut der MPG, Berlin, Germany. — ²University of Bayreuth, Bayreuth, Germany

We discuss the extension of our improved Projection-Operator Diabatization scheme POD2GS[1] to the study of electronic coupling on surfaces within periodic density-functional theory (DFT) simulations. Using POD2GS, we calculate diabatic electronic couplings H_{ab} between adsorbate and surface bands throughout *k*-space. It becomes thus possible to directly calculate the chemisorption function of Newns and Anderson[2], a weighted density of states which appears often in the theoretical description of surface interactions.

Interpreting the chemisorption function within the Fermi Golden Rule yields ultrafast (spin)electron transfer lifetimes directly comparable to experiment, as we demonstrate for the case of core-excited Argon monolayers on ferromagnetic substrates Fe(110), Co(0001) and Ni(111)[3]. Our scheme reveals the importance of sampling the Brillouin zone to gain accurate and convergent electron transfer rates, and offers an array of further applications.

[1] J. Chem. Theory Comput. 2020, 16, 12, 7431-7443.

[2] Phys. Rev. 1969, 178, 1123.

[3] Phys. Rev. Lett. 2014, 112, 086801.

O 46.4 Wed 15:45 H6

A Revised Fourth-Generation Neural Network Potential for the Accurate Representation of Multiple Charge States — •ALEXANDER KNOLL, Tsz Wai KO, and JÖRG BEHLER — Georg-August-Universität Göttingen, Institut für Physikalische Chemie, Theoretische Chemie, Göttingen, Germany

Machine learning potentials (MLPs) have become a mature tool for large-scale atomistic simulations in chemistry and materials science. Recently, a fourth-generation high-dimensional neural network potential (4G-HDNNP) has been introduced, in which the atomic charges are determined in a charge equilibration step enabling the description of long-range charge transfer. The quality of the charge prediction depends on environment-dependent electronegativities expressed by atomic neural networks, which poses a challenge for structures with differing total charges but nearly-identical nuclear positions. Here, we propose a generalized method applicable to these situations, and for a series of model systems we demonstrate that this extension leads to additional flexibility of the atomic electronegativities, ultimately resulting in more accurate atomic charges, energies, and forces.

O 46.5 Wed 16:00 H6

Machine learning potentials for complex aqueous systems made simple — •CHRISTOPH SCHRAN¹, FABIAN L. THIEMANN^{1,2}, PATRICK ROWE¹, ERICH A. MÜLLER², ONDREJ MARSALEK³, and ANGELOS MICHAELIDES¹ — ¹University of Cambridge, UK — ²Imperial College London, UK — ³Charles University, Czech Republic

Simulation techniques based on accurate and efficient representations of potential energy surfaces are urgently needed for the understanding of complex systems such as solid-liquid interfaces. Here we present a machine learning framework that enables the efficient development and validation of models for complex aqueous systems. Instead of trying to deliver a globally optimal machine learning potential, we propose to develop models applicable to specific thermodynamic state points in a simple and user-friendly process. After an initial ab initio simulation, a machine learning potential is constructed with minimum human effort through a data-driven active learning protocol. Such models can afterward be applied in exhaustive simulations to provide reliable answers for the scientific question at hand or to systematically explore the thermal performance of ab initio methods. We showcase this methodology on a diverse set of aqueous systems. Highlighting the accuracy of our approach with respect to the underlying ab initio reference, the resulting models are evaluated in detail with an automated validation protocol that includes structural and dynamical properties and the precision of the force prediction of the models. Finally, we demonstrate the capabilities of our approach for providing insight into the solid-liquid interface for various systems.

O 46.6 Wed 16:15 H6

Quantifying the breakdown of electronic friction theory during molecular scattering of NO from Au(111) — •CONNOR L. BOX¹, YAOLONG ZHANG², RONGRONG YIN², BIN JIANG², and REINHARD J. MAURER¹ — ¹Department of Chemistry, University of Warwick, United Kingdom — ²Department of Chemical Physics, University of Science and Technology of China, Hefei, China

The Born-Oppenheimer approximation fails to capture the extent of multi-quantum vibrational energy loss recorded during molecular scattering from metallic

surfaces.[1] NO scattering on Au(111) has been one of the most studied examples in this regard, providing a testing ground for developing various nonadiabatic theories. The exact failings compared to experiment and their origin from theory are not established for any system, particularly since dynamic properties are affected by many compounding simulation errors, of which the quality of nonadiabatic treatment is just one. We use a high-dimensional machine learning representation of the energy and the electronic friction tensor to minimize errors that arise from quantum chemistry.[1,2] This allows us to perform a comprehensive quantitative analysis of the performance of molecular dynamics with electronic friction in describing state-to-state scattering. We find that electronic friction theory accurately predicts elastic and single-quantum energy loss, but underestimates multi-quantum energy loss and overestimates molecular trapping at high vibrational excitation. Our analysis reveals potential remedies to these issues. [1] C. L. Box & Y. Zhang et al, JACS Au, 2020 [2] R. Yin et al, J. Phys. Chem. Lett, 2019

O 46.7 Wed 16:30 H6

Accurate computation of chemical contrast in field ion microscopy — •SHALINI BHATT — Max Planck Institut für Eisenforschung GmbH Düsseldorf Germany

Field ion microscopy (FIM) was the first microscopy technique to image individual atoms on a metal surface with near atomic spatial resolution. In short an imaging gas (e.g. He, Ne) is ionized above a surface subject of a few field 10^{10} V/m. The imaging contrast is dominated by the ionization probability at 5-10 Å above the surface. To simulate this within density-functional theory (DFT), we adapt the Tersoff-Hamann theory known from scanning tunneling microscopy (STM).

The gigantic electric field leads to very fast decay of wavefunctions into the vacuum. At the ionization height, they run into a regime that is dominated by numerical noise. To address this noise challenge inherent to any global-scale Kohn-Sham solver employed in DFT codes, wavefunction tails must be recom-

puted. To solve 3D Schrödinger equation at local scale we develop the extrapolated tail via reverse algorithm (EXTRA). The decaying tails are obtained by reverse integration (from outside in) using a Numerov-like algorithm. The starting conditions are then iteratively adapted to match the values of planewave DFT wavefunctions close to the surface. We demonstrate chemical contrast for Ta and W at Ni surface using this new technique.

O 46.8 Wed 16:45 H6

Designing Covalent Organic Frameworks Through Active Machine Learning — •YUXUAN YAO^{1,2}, CHRISTIAN KUNKEL³, KARSTEN REUTER³, and HARALD OBERHOFER² — ¹Chair for Theoretical Chemistry and Catalysis Research Center, Technical University Munich — ²Fritz-Haber-Institut der Max-Planck-Gesellschaft — ³Chair for Theoretical Physics VII, University of Bayreuth

Covalent organic frameworks(COFs) are a class of materials with potential applications in many fields such as catalysis, sensing, or optoelectronics. It is well known that their design space is far too large to sample one by one. Focusing on their electronic properties, we modify an earlier active machine learning(AML) approach that explores the molecular design through the use of surrogate models for charge injection and transport descriptors. In this method, the Gaussian Process Regression(GPR) and AML are combined to train the molecular space. This way we ensure that only promising molecules or candidates that are very different from already explored ones have their descriptors evaluated on a comparatively expensive quantum mechanical level. Specifically, we modify molecular generation rules in order to produce three-fold rotational symmetric candidates molecules for use in COFs. In the future this approach can be generalized for any other symmetries, to potentially even allow for 3-dimensional network generation. The generation of a candidate space with well defined symmetries together with AML ensures a high efficiency in the detection of promising COFs with superior charge conduction properties and demonstrates the utility of this approach.

O 47: Focus Session: Atomic-Scale Studies of Spins on Surfaces with Scanning Tunneling Microscopy 1

Magnetic single atoms and molecules are intensively studied as the smallest building blocks for potential applications in spintronic devices and quantum information processing. Detecting and controlling single spin states and their spin interactions require both high energy resolutions and atomic scale imaging capability. Scanning tunneling microscopes provide not only the spatial resolutions but also the bottom up approach to build magnetic structures atom by atom. Recently, unprecedented spin sensitivities have been reached by functionalizing the STM tips or by combining STM with electron spin resonance. The goal of this symposium is to highlight the recent developments in the rapidly evolving field of atomic scale sensing and quantum control of spins on surfaces. Researchers that use STM to investigate atomic or molecular spins on surfaces will present their most recent results. Sharing technical advances and addressing current issues will create synergies to foster future progress in this field and a deeper understanding of the underlying physics.

Organizer: Andreas Heinrich (Center for Quantum Nanoscience, Seoul, Republic of Korea)

Time: Wednesday 15:00–18:00

Location: S051

Topical Talk

O 47.1 Wed 15:00 S051

Quantum control of multi-spin architectures on a surface — •YUJEONG BAE — Center for Quantum Nanoscience (QNS), Institute for Basic Science (IBS), 03760 Seoul, South Korea — Department of Physics, Ewha Womans University, Seoul 03760, South Korea

The spin-polarized scanning tunneling microscopy (STM) combined with electron spin resonance (ESR) [1] enables us to achieve single spin sensitivity with atomic precision. Employing ESR-STM, a single spin on a surface can be coherently probed and controlled [1,2], where the magnetic tip is positioned directly on the target spin. Here, we demonstrate a new approach to coherently control multi-electron spins in a quantum spin architecture crafted atom-by-atom. We found the remote spins, which are outside the tunnel junction, can be controlled by the local oscillating magnetic fields created by a single-atom magnet placed next to them in oscillating electric fields. The read-out of multi-electron spins is achieved by a sensor atom weakly coupled to them. The resonances of the sensor spin are separated in the frequency domain so that we can independently and simultaneously control the sensor and remote spins. Our work shows the enhanced coherent properties of the remote spins as well as fast controlled operations of multi-electrons in an all-electrical fashion. Our development widens the approaches to the multi-spin control in tailored spin structures on a surface.

[1] S. Baumann et al., Science, 350 (2015) 417.

[2] K. Yang et al., Science, 366 (2019) 509.

O 47.2 Wed 15:30 S051

Longitudinal and transverse electron paramagnetic resonance in a scanning tunneling microscope — •TOM S. SEIFERT¹, STEPAN KOVARIK², PIETRO GAMBARDIELLA², and SEBASTIAN STEPANOW² — ¹FU Berlin — ²ETH Zürich

Combining scanning tunneling microscopy (STM) with electron-paramagnetic resonance (EPR) allows for sensitive probing magnetic interactions at atomic scales [1]. However, the experimental requirements for driving the EPR transitions are not obvious [2,3]. In-depth understanding of what drives EPR-STM is mandatory to explore novel material systems with high sensitivity. Here, we acquire and model EPR spectra of single Fe and hydrogenated Ti atoms on bilayer MgO on Ag using a radio frequency (RF) antenna close to the STM junction [4]. We investigate in a systematic way the impact of RF excitation strength and tunneling parameters on the EPR signal and find strong evidence for a piezoelectric coupling mechanism [5]. Specifically, transverse magnetic field gradients drive the spin-1/2 hydrogenated Ti, whereas longitudinal magnetic field gradients drive the spin-2 Fe. Finally, we demonstrate how the choice of specific tip-sample distances allows one to minimize the impact of tip magnetic fields on the EPR-STM measurements thereby excluding a major experimental uncertainty when determining single-atom magnetic moments [6].

[1] S. Baumann et al., Science 350 (2015) [2] K. Yang et al., PRL 122 (2019) [3] P. Willke et al., Nano Lett. 19 (2019) [4] T.S. Seifert et al., PRR 2 (2020) [5] T.S. Seifert et al., Sci. Adv. 6 (2020) [6] T.S. Seifert et al., PRR 3 (2021)

O 47.3 Wed 15:45 S051

Experimental Determination of a Single Atom Ground State Orbital through Hyperfine Anisotropy — •LAËTTIA FARINACCI¹, LUKAS M. VELDMAN¹, PHILIP WILKE², and SANDER OTTE¹ — ¹Delft University of Technology, Delft, The Netherlands — ²Karlsruhe Institute of Technology, Karlsruhe, Germany

Electron spin resonance has long been a powerful tool for electronic analysis. Its recent combination with scanning tunneling microscopy [1] gives exceptional energy resolution for the investigation of the magnetism of single atoms in addition to a very good characterization of their spatial surroundings.

Here, we provide a full angle-dependent investigation of the anisotropy of the hyperfine splitting of single Ti atoms on MgO/Ag(100). We find that the anisotropy of the hyperfine splitting is related to that of the g factor: spin-orbit coupling leads to a partially unquenched angular momentum which couples to the electron spin and thereby affects its interaction both with an external magnetic field and the nuclear spin of the nucleus. Combining the symmetry properties of the atoms binding site with a simple point charge model, we provide a method to predict the shape of the ground state orbital of the Ti atom. Relying on experimental values only, this analysis paves the way for a new protocol for electronic structure analysis for spin centers on surfaces.

[1] Baumann et al., Science 350 (2015)

O 47.4 Wed 16:00 S051

Anisotropic hyperfine interaction of surface-adsorbed single atoms — •JINKYUNG KIM^{1,2}, KYUNGJU NOH^{1,2}, YI CHEN^{1,3}, CHRISTOPH WOLF^{1,3}, ANDREAS HEINRICH^{1,2}, and YUJEONG BAE^{1,2} — ¹Center for Quantum Nanoscience (QNS), Institute for Basic Science (IBS), Seoul 03760, South Korea — ²Department of Physics, Ewha Womans University, Seoul 03760, South Korea — ³Ewha Womans University, Seoul 03760, Republic of Korea

Hyperfine interactions between electron and nuclear spins provide sensitive probes to the chemical environment of atoms, molecules, and crystal defects as well as an alternative way to control the nuclear spins. While a variety of experimental techniques have been applied to the detection and control of single nuclear spins in various environments, simultaneous investigations of the single nuclear spin's resonance and the atomic scale imaging are more demanding. Using the electron spin resonance (ESR) technique in a scanning tunneling microscope (STM), we investigated hyperfine interaction of hydrogenated titanium (Ti) on MgO/Ag(100) and its local environment at the atomic scale. By means of atom manipulation in vector magnetic fields, we identified the hyperfine interaction of Ti along three principal axes, which shows a large anisotropy of hyperfine interaction. As a sensitive probe of chemical environment, the observed hyperfine interaction reflects the anisotropic orbital configuration of the electronic ground state, which is further supported by the density functional theory calculations.

O 47.5 Wed 16:15 S051

Electron Paramagnetic Resonance of individual Alkali Metal Atoms and Dimers on Ultrathin MgO — •STEPAN KOVARIK¹, ROBERTO ROBLES², RICHARD SCHLITZ¹, TOM SEBASTIAN SEIFERT^{1,3}, NICOLAS LORENTE^{2,4}, PIETRO GAMBARDELLA¹, and SEBASTIAN STEPANOW¹ — ¹Department of Materials, ETH Zurich, Switzerland — ²Centro de Física de Materiales, San Sebastian, Spain — ³Department of Physics, FU Berlin, Germany — ⁴Donostia International Physics Center, San Sebastian, Spain

Electron paramagnetic resonance (EPR) provides unique insight into the chemical structure and magnetic properties of dopants in oxide and semiconducting materials that are of interest for applications in electronics, catalysis, and quantum sensing. We demonstrate that EPR in combination with scanning tunneling microscopy (STM) [1, 2] allows for probing the spin and charge state of alkali metal atoms on an ultrathin magnesium oxide layer on a Ag(100) substrate. We identify a magnetic moment of $1 \mu_B$ for Li_2 , $LiNa$, and Na_2 dimers corresponding to spin radicals with a charge state of $+1e$ [3]. Individual alkali atoms have the same charge state and no magnetic moment. The ionization of the adsorbates is attributed to the charge transfer of one electron through the oxide to the metal substrate. Our work highlights the potential of EPR-STM to provide insight into dopant atoms, which are relevant for the control of the electrical properties of surfaces and represent a suitable platform for studying quantum nanomagnets.

[1] S. Baumann et al., Science 350 (2015) [2] T. S. Seifert et al., PRR 2 (2020) [3] S. Kovarik et al., Nano Lett. 22 (2022)

Topical Talk

O 47.6 Wed 16:30 S051

Free coherent evolution of a coupled atomic spin system initialized by electron scattering — •SANDER OTTE¹, LUKAS VELDMAN¹, LAËTTIA FARINACCI¹, RASA REJALI¹, RIK BROEKHOVEN¹, JEREMIE GOBEIL¹, DAVID COFFEY¹, and MARKUS TERNES^{2,3} — ¹Delft University of Technology, Delft, The Netherlands — ²RWTH Aachen University, Aachen, Germany — ³Forschungszentrum Jülich, Jülich, Germany

Full insight into the dynamics of a coupled quantum system depends on the ability to follow the effect of a local excitation in real-time. Here, we trace the free coherent evolution of a pair of coupled atomic spins by means of scanning tunneling microscopy. Rather than using microwave pulses, we use a direct-current

pump-probe scheme to detect the local magnetization after a current-induced excitation performed on one of the spins. By making use of magnetic interaction with the probe tip, we are able to tune the relative precession of the spins. We show that only if their Larmor frequencies match, the two spins can entangle, causing angular momentum to be swapped back and forth. These results provide insight into the locality of electron spin scattering and set the stage for controlled migration of a quantum state through an extended spin lattice.

O 47.7 Wed 17:00 S051

Controlled migration of a coherent spin excitation through atomically assembled nanomagnets — •LUKAS VELDMAN¹, LAËTTIA FARINACCI¹, RASA REJALI¹, RIK BROEKHOVEN¹, JEREMIE GOBEIL¹, DAVID COFFEY¹, MARKUS TERNES^{2,3}, and SANDER OTTE¹ — ¹TU Delft, Delft, The Netherlands — ²RWTH Aachen, Aachen, Germany — ³Forschungszentrum Jülich, Jülich, Germany

Tracing single coherent spin excitations in low dimensional nanomagnets has been a long standing goal in experimental solid state physics. Scanning tunneling microscopy offers a promising platform to chase this goal due to its capability to build nanomagnets atom-by-atom and address each atomic spin individually. Here, we show the possibility of inducing a single spin-flip excitation using electron scattering and the measurement of the resulting flip-flop interaction between two atomic spins [1]. Next, we use the same principle to observe coherent spin dynamics in multiple atomically assembled nanomagnets. By tuning the interaction between tip and nanomagnet, we are able to address different magnetic resonances in each atomic structure. In engineered branched structures, the spin excitation can be sent to different directions using the tip interaction. These techniques can serve as a platform for dynamical quantum simulation and can form a foundation for atomically assembled spintronic applications.

[1] Veldman, L. M., Farinacci, L., Rejali, R., ... & Otte, A. F. (2021) Science, 372

O 47.8 Wed 17:15 S051

Electric field control of spin transitions in a single molecule using ESR-STM — •MANEESHA ISMAIL, PIOTR KOT, and CHRISTIAN R. AST — Max-Planck-Institute for Solid State Research, Heisenbergstr. 1, 70569 Stuttgart, Germany

Since the demonstration of the control of spins on the atomic scale, the technique of ESR-STM has been used extensively to explore the field of spintronics. Here, we present an extension to the ESR-STM parameter space, which uses the bias voltage to tune the energy of the Zeeman transition. We demonstrate electronic control of spin resonance transitions in a single TiH molecule. We were able to observe a strong dependency of the g-factor along with a tip-field shift as function of the electric field. Finally, we manipulate a TiH dimer by continuously changing the bias voltage such that the dimer moves through an avoided crossing of the energy levels. This could be an important step towards pump-probe control of spin states through the bias voltage and opens new possibilities for coherent manipulation.

O 47.9 Wed 17:30 S051

Isotope detection inside single molecules in scanning-probe based electron spin resonance — •LISANNE SELLES, RAFFAEL SPACHTHOLZ, PHILIPP SCHEUERER, and JASCHA REPP — University of Regensburg, Regensburg, Germany

Electron spin resonance (ESR), a versatile technique to study materials with unpaired electrons, was recently combined with scanning tunneling microscopy (STM), bringing atomic-scale spatial resolution to ESR [1]. ESR-STM even allowed detecting strong hyperfine interactions between the single electron spin under study with the atom's nuclear spin [2], due to its largely improved energy resolution compared to conventional STM, reaching the nano-electron-volt regime. This energy resolution could even be improved further if the tunneling current as a read-out was avoided, since this current is the dominating decoherence source for the probed electron spin.

We propose, therefore, a new ESR scanning probe method based on atomic force microscopy (AFM). Since our technique does not rely on the tunneling current to read-out the ESR signal, we increase the coherence times of the electron spins and, consequently, the energy resolution. Therefore, we can resolve the hyperfine interaction inside organic molecules and distinguish molecules only differing in the isotopic composition. Thus, our technique allows the chemical fingerprinting of molecules and their surroundings.

References: [1] S. Baumann et al., Science 350, 417 (2015) [2] P. Willke et al., Science 362, 336 (2018)

O 47.10 Wed 17:45 S051

A home-built scanning tunneling microscope combined with electron spin resonance — •ANDREAS HEINRICH — Center for Quantum Nanoscience, Institute for Basic Science, Seoul, Korea

Scanning tunneling microscopy is a powerful tool to characterize the electronic and magnetic properties of atomic scale structures on a surface. Recently, improved spectral energy resolution has been achieved by functionalizing the STM tip with a well-characterized molecule at the apex [1,2] or by combining electron spin resonance with STM (ESR-STM) [3]. Here, we present the design and operation of an optimized, home-built ESR-STM with a specially designed me-

chanical damper, a Joule-Thomson refrigerator, and 2-axes vector magnets. This system provides outstanding performance of STM for nanoscale measurements. We further describe a new design of a microwave antenna to increase the transmission of RF voltages to the junction, which performs better than the direct connection to the tip. Applying RF power through the antenna terminated at

50 Ohm results in the reduction of standing waves and increases the available frequency range (5-40 GHz), which allows us to measure ESR of surface spins at elevated temperatures up to 10 K. References: [1] M. Ormaza et al., *Nano Lett.* 17, 1877-1882 (2017) [2] G. Czap et al., *Science*, 364, 670-673 (2019) [3] S. Baumann et al., *Science*, 350, 417-420 (2015)

O 48: 2D Materials 1: Electronic Structure of Transition Metal Dichalcogenides

Time: Wednesday 15:00–17:30

Location: S052

O 48.1 Wed 15:00 S052

the stability of point defects in 2D monolayer transition metal dichalcogenides and their impact on the electronic structure — •ALAA AKKOUSH^{1,2} and MARIANA ROSSI^{1,2} — ¹Fritz Haber Institute of the Max Planck Society, Faradayweg 4-6, Berlin — ²MPI for the Structure and Dynamics of Matter, Luruper Chaussee 149, 22765 Hamburg

Defects can strongly influence the electronic, optical and mechanical properties of 1D materials. However, their stability and distribution under different conditions of temperature, pressure and strain are not well characterized from an atomistic perspective. We have investigated the structural and electronic properties, as well as the thermodynamic stability of point defects (vacancies and adatoms) in monolayer transition metal dichalcogenides MX_2 with $\text{M}=\text{Mo}/\text{W}$ and $\text{X}=\text{S}/\text{Se}$, through density-functional theory (DFT) simulations with hybrid exchange correlation functional, as implemented in the all-electron package FHI-aims [1]. These calculations are carried out using a supercell approximation to model localised defects using periodic boundary conditions. We show quantitatively that X adatom is most favorable in rich X conditions while in poor X environment X monovacancy is most favorable. Interestingly, an interplay between adatom and divacancies takes place as temperature increases. To gauge the importance of vibrational free energy contributions on the engineering of gap states in the 2D monolayers, we compare the formation energies of point defects with an adsorbed F6TNAP at various thermodynamic conditions.

[1] S.V. Levchenko, et al., *Comp. Phys. Comm.* **192** 60-69 (2015)

O 48.2 Wed 15:15 S052

Non-linear optical response of TMD Nanotubes using Wannier interpolation — •JYOTI KRISHNA and JULEN IBAÑEZ-AZPIROZ — Centro de Física de Materiales (CSIC-UPV/EHU), Donostia-San Sebastian, Spain

Single crystals lacking an inversion center display a non-vanishing second-order response known as shift current- a dominant contribution to the bulk photovoltaic effect. There has been a renewed interest in novel materials with large non-linear absorption capabilities[1]. Here we focus on transition metal dichalcogenide nanotubes, which have recently exhibited a short-circuit intensity showing orders of magnitude enhancement over the monolayer value[2]. We systematically explore the implications of the different chiral indexes on both linear and quadratic optical responses for single-walled TMD NT employing the Wannier interpolation technique. We classify the allowed symmetry and calculate the dependence of the magnitude of the response as a function of NT diameter and chirality. Finally, we discussed our results in the context of the experimental measurements.

Funding provided by the European Union's Horizon 2020 research and innovation programme under the European Research Council (ERC) grant agreement No 946629. (1) L. Z. Tan, F. Zheng, F. Wang and A. M. Rappe, *npj Comput. Mater.* **2**, 16026 (2016). (2) Y. J. Zhang et. *Al Nature* **570**, 349 (2019). (3) G. Pizzi et. *Al, J. Phys. Cond. Matt* **32**, 165902 (2020).

O 48.3 Wed 15:30 S052

Structural, electronic and optical properties of strained MoS_2 — •JAN-HAUKE GRAALMANN and MICHAEL ROHLFING — Institute of Solid State Theory, University of Münster, 48149 Münster, Germany

Experimental and theoretical studies have shown that the spectrum of MoS_2 changes when the system gets strained. Stretching a monolayer leads to a shift of the optical absorption spectrum to lower energies. In case of the bilayer under hydrostatic stress, the interlayer interaction plays a major role.

In this talk we investigate the behaviour of a MoS_2 monolayer and bilayer theoretically using DFT, GdW and the Bethe-Salpeter equation. Our results show a transition of the monolayer from a direct semiconductor to an indirect one when the in-plane lattice constant is increased. Furthermore, the fundamental gap at the K point is reduced while the binding energies of the A and B excitons remain approximately constant. These effects lead to an effective shift of the excitation energies of both excitons towards lower energy with similar gauge factors.

We also find a significant influence of interlayer interaction within the bilayer. The effect of a decreasing gap by biaxial shrinking of each single layer under an external hydrostatic pressure gets counterbalanced by the reduction of the interlayer distance.

O 48.4 Wed 15:45 S052

Excitons in TMDC Bilayers — •JAN NELLESEN and MICHAEL ROHLFING — Westfälische Wilhelms-Universität, Münster, Germany

Semiconducting Transition-Metal-Dichalcogenides (TMDCs) have gained a lot of attention in the past few years due to possible new applications in optoelectronics. In particular, the excitonic properties of TMDC mono- and bilayers have been studied extensively.

This work focuses on interlayer excitons in TMDC heterostructures which combine large binding energies with relatively long lifespans. The exciton energies are investigated in different systems using the Bethe-Salpeter-Equation.

In order to describe excitons in twisted bilayers, which exhibit long-range moiré structures, *ab initio* approaches are no longer feasible because of their high computational demand. With the goal of studying excitons in such systems in mind, the TMDC bandstructure is modeled within a tight-binding approximation. For describing the electron-hole interaction, a model potential is used.

O 48.5 Wed 16:00 S052

Unoccupied electronic states of 1T-TiSe₂: Band dispersions and CDW-induced changes at $\bar{\Gamma}$ — •PATRICK GEERS, MARCEL HOLTSMANN, and MARKUS DONATH — University of Münster, Germany

The transition metal dichalcogenide 1T-TiSe₂ shows a phase transition into a charge density wave (CDW) below a critical temperature T_{CDW} [1]. This transition leads to a half-sized Brillouin zone and backfolded electronic bands. For the occupied electronic structure, photoemission results show a backfolding of $\text{Se-4p}_{x,y}$ valence bands below T_{CDW} from $\bar{\Gamma}$ to \bar{M} [2].

We present angle-resolved inverse-photoemission (IPE) measurements for the unoccupied electronic structure above and below T_{CDW} . Our data for the $\bar{\Gamma}\bar{M}$ azimuth resemble literature data for the energy vs. momentum dispersion of Ti-3d states as well as an image-potential-induced surface state [3]. In addition, we report on IPE measurements for the $\bar{\Gamma}\bar{K}$ azimuth. Finally, we give special attention to the changes in the electronic structure, which are caused by the CDW phase transition. Measurements around $\bar{\Gamma}$ below T_{CDW} show modifications in the spectra which are attributed to backfolded electronic bands from \bar{M} to $\bar{\Gamma}$ as a direct consequence of the CDW phase.

[1] Di Salvo *et al.*, *Phys. Rev. B* **14**, 4321 (1976).

[2] Watson *et al.*, *Phys. Rev. Lett.* **122**, 076404 (2019).

[3] Drube *et al.*, *J. Phys. C* **20**, 4201 (1987).

O 48.6 Wed 16:15 S052

Nontrivial Doping Evolution of Electronic Properties in Ising-Superconducting Alloys — •WEN WAN¹, DARSHANA WICKRAMARATNE², PAUL DREHER¹, RISHAV HARSH¹, IGOR I. MAZIN³, and MIGUEL UGEDA¹ — ¹Donostia International Physics Center (DIPC), Paseo Manuel de Lardizábal 4, 20018 San Sebastián, Spain — ²Center for Computational Materials Science, U.S. Naval Research Laboratory, Washington, DC 20375, USA — ³Department of Physics and Astronomy, George Mason University, Fairfax, VA 22030, USA

TMDs offer unprecedented versatility to engineer 2D materials with tailored properties to explore novel structural and electronic phase transitions. Here, we present the atomic-scale evolution of the electronic ground state of a monolayer of $\text{Nb1-}\delta\text{Mo}\delta\text{Se2}$ ($0<\delta<1$) using STM/STS measurements at 300 mK. We investigate the atomic and electronic structure of this 2D alloy throughout the metal to semiconductor transition (NbSe2 to MoSe2). Our measurements let us extract the effective doping of Mo atoms, the bandgap evolution and the band shifts, which are monotonic with δ . Furthermore, we demonstrate that collective phases (CDW and superconductivity) are remarkably robust against disorder. We further show that the superconducting TC changes non-monotonically with doping. This contrasting behavior in the normal and superconducting state is explained using first-principles calculations. We show that Mo doping decreases the DOS at EF and the magnitude of pair-breaking spin fluctuations as a function of Mo content. (1) W. Wan, et al. *Advanced Materials*, accepted (2022).

O 48.7 Wed 16:30 S052

Surface spin texture derived from a single mirror plane of WTe_2 — TRISTAN HEIDER¹, GUSTAV BIHLMAYER², JAKUB SCHUSSER^{3,4}, FRIEDRICH REINERT⁴, JAN MINAR³, STEFAN BLÜGEL², CLAUD M. SCHNEIDER¹, and •LUKASZ PLUCINSKI¹ — ¹PGI-6 Forschungszentrum Jülich — ²PGI-1 Forschungszentrum Jülich — ³University of West Bohemia, Pilsen, Czech Republic — ⁴Experimentelle Physik VII, Universität Würzburg

WTe₂ is an important semi-metallic quantum material that exhibits non-saturating magnetoresistance and potentially hosts Weyl type-II nodes [1]. Through the laser-driven spin-polarized ARPES Fermi surface mapping, we demonstrate highly asymmetric spin textures of electrons photoemitted from the surface states of WTe₂. Such asymmetries are not present in the initial state spin textures, which are bound by the time-reversal and crystal lattice mirror plane symmetries. The findings are reproduced qualitatively by theoretical modeling within the one-step model photoemission formalism, while a simple toy-model suggests that a similar effect shall be observed in other materials with low symmetry.

Our spin-polarized maps with detail comparable to the previous spin-integrated maps [2] have been measured using the newly developed high-resolution instrument at PGI-6 in Jülich that is based on a hemispherical analyzer with the scanning lens, an exchange-scattering spin detector, and a cw 6 eV laser.

[1] P. K. Das et al. Electron. Struct. 1, 014003 (2019) and refs. therein. [2] F. Y. Bruno et al., Phys. Rev. B 94, 121112 (2016).

O 48.8 Wed 16:45 S052

Effect of gold substrate on the excitonic properties of MoS₂: a final state sum frequency spectroscopy study — •TAO YANG, ERIK POLLMANN, STEPHAN SLEZIONA, MARIKA SCHLEBERGER, RICHARD KRAMER CAMPEN, and YUJIN TONG — Fakultät für Physik Universität Duisburg-Essen, Duisburg, Germany
Monolayer transition metal dichalcogenides (TMDCs) are promising candidates for applications in electronics, optoelectronics, and photocatalysts due to their good thermodynamic stability, ease of preparation, tunable bandgap in the visible region, and pronounced activity for photoelectrochemical water splitting. To take advantage of their excellent properties to build the devices and catalysts, a metallic surface is required to combine them. However, compared to the well-explored properties of monolayer TMDCs on dielectric substrates, less attention has been paid to these properties on metal substrates due to the challenges associated with linear spectroscopies probing, such as quenching. Here we use a final state sum frequency spectroscopy (FSSFG) to study the optical properties of MoS₂ exfoliated on a gold surface. Relative to the well-known six-fold symmetry of MoS₂ on SiO₂, the azimuthal dependent FSSFG show significantly different patterns at different polarization combinations. The current study provides important insights into the significant changes in electronic structure when MoS₂ comes into contact with gold, and the possibility to selectively switch resonance on and off through azimuthal tuning, as revealed by the robust FSSFG.

O 48.9 Wed 17:00 S052

Time-resolved momentum microscopy of moiré interlayer excitons in twisted TMD heterostructures — •DAVID SCHMITT¹, JAN PHILIPP BANGE¹, WIEBKE BENNECKE¹, ABDULAZIZ ALMUTAIRI², GIUSEPPE MENEGHINI³, DANIEL STEIL¹,

R. THOMAS WEITZ¹, SABINE STEIL¹, G. S. MATTHIJS JANSEN¹, SAMUEL BREM³, ERMIN MALIC³, STEPHAN HOFMANN², MARCEL REUTZEL¹, and STEFAN MATHIAS¹ — ¹I. Physikalisches Institut, Georg-August-Universität Göttingen, Friedrich-Hund-Platz 1, Göttingen, Germany — ²Department of Engineering, University of Cambridge, Cambridge CB3 0FA, U.K. — ³Fachbereich Physik, Philipps-Universität, 35032 Marburg, Germany

Transition metal dichalcogenides (TMDs) are extensively studied because of their exceptional material properties. The stacking of different TMDs can lead to even more intriguing electronic properties: In type-II band aligned TMD stacks, novel excitonic states can be created where the electron and the hole contribution to the exciton are separated between the van-der-Waals-coupled TMDs. A twist angle between these layers allows further manipulation of the electronic properties and gives rise to moiré-patterns which leads to distinct patterns in momentum space. Here, we make use of our setup for time-resolved momentum microscopy that is perfectly suited to probe these excitonic features with energy- and in-plane momentum resolution. We present femtosecond evaluation of the momentum-fingerprints of the excitonic features that are created on a type II aligned heterostructure. Schmitt *et al.*, arXiv:2112.05011 (2021).

O 48.10 Wed 17:15 S052

In Operando Soft X-Ray Photoemission Spectroscopy of 2D Material Devices — •ALENA NIERHAUVE^{1,2}, MATTHIAS KALLÄNE^{1,2}, TAMMO ZIMMERMANN¹, JENS BUCK^{1,2}, PHILIPP KAGERER³, ZHANSONG GENG⁴, CHAO ZHANG⁴, FRANK SCHWIERZ⁴, MARTIN ZIEGLER⁴, ROK VENTURINI⁵, and KAI ROSSNAGEL^{1,2,6} — ¹IEAP, CAU Kiel, 24098 Kiel, Germany — ²Ruprecht-Haensel-Labor, DESY and CAU Kiel, 22607 Hamburg and 24098 Kiel, Germany — ³Dep. of Exp. Physics VII, JMU Würzburg, 97074 Würzburg, Germany — ⁴Dep. of Electr. Engineering and Information Techn., TU Ilmenau, 98684 Ilmenau, Germany — ⁵Jožef Stefan Institute, 1000 Ljubljana, Slovenia — ⁶DESY, 22607 Hamburg, Germany
Layered transition-metal dichalcogenides (TMDCs) are a particularly promising platform for low-dimensional electronic devices due to their two-dimensional nature and richness regarding physical phenomena. This includes non-linear conductance behavior due to, e.g., metal-insulator transitions and memristive behavior, which is of particular interest to in-memory computing designs for neuromorphic systems. By combination of micrometer position- and angle-resolved photoemission spectroscopy (μ -ARPES) in the soft X-ray range with *in operando* electrical control, we attempt to study the electronic structure changes concomitant with thickness changes and non-equilibrium conditions in device-like structures based on TMDCs. A portrayal of conductance-governing mechanisms at a fundamental level could help to evolve towards the understanding and engineering of novel band structures, transport phenomena, and device functionality.

O 49: Oxide Surfaces 1

Time: Wednesday 15:00–17:30

Location: S053

O 49.1 Wed 15:00 S053

Revised Chen's derivative rule for efficient simulations of scanning tunneling microscopy: New results on surface oxides — •KRISZTIÁN PALOTÁS¹, YUNJAE LEE², TAEHUN LEE², and ALOYSIUS SOON² — ¹Wigner Research Center for Physics, Budapest, Hungary — ²Yonsei University, Seoul, Republic of Korea
Advanced simulation tools of scanning tunneling microscopy (STM) are vital for the proper understanding of various physical and chemical processes at material surfaces. For this reason Chen's derivative rule for electron tunneling has been revised [1] to build a computationally efficient STM simulation tool, based on ab initio electronic structure. This STM simulation method enables (i) the weighting of tunneling matrix elements of arbitrary tip-orbital composition, (ii) arbitrary tip geometrical orientations to mimic asymmetric tip-sample relations, and (iii) the possibility of quantitative analysis of tip-orbital interference contributions to the tunneling current. Recently, this method has been applied to diverse complex surface oxides [2,3,4], where a better agreement with STM experiments has been achieved than obtained with the Tersoff-Hamann (spherical tip orbital) model.

[1] G. Mándi and K. Palotás, Phys. Rev. B 91, 165406 (2015). [2] T. Lee et al., Nanoscale 11, 6023 (2019). [3] T. T. Ly et al., J. Phys. Chem. C 123, 12716 (2019). [4] Y.-J. Lee et al., Appl. Surf. Sci. 562, 150148 (2021).

O 49.2 Wed 15:15 S053

Hydrogen Atom Scattering at Aluminium Oxide — •MARTIN LIEBETRAU and JÖRG BEHLER — Universität Göttingen, Institut für Physikalische Chemie, Theoretische Chemie, Tammannstraße 6, 37077 Göttingen, Germany
The adsorption of atomic hydrogen is important in many fields, from heterogeneous catalysis via hydrogen storage to nuclear fusion. Here, we report molecular dynamics simulations of high-energy hydrogen atom scattering at the α -Al₂O₃(0001) surface. Employing a high-dimensional neural network potential,

which allows us to include the full-dimensional thermal motion of the surface atoms, we are able to calculate a large number of trajectories with the accuracy of density-functional theory at a small fraction of the computational costs. Investigating different kinetic energies, surface temperatures and incident angles, we are able to characterize the scattering process in detail.

O 49.3 Wed 15:30 S053

Adsorption of Gases on β -Ga₂O₃ Surfaces — •JONATHAN K. HOFMANN^{1,2}, CELINA S. SCHULZE¹, MARTIN FRANZ¹, NIPIN KOHLI¹, DOROTHEE ROSENZWEIG¹, ZBIGNIEW GALAZKA³, and HOLGER EISELE¹ — ¹Technische Universität Berlin, Institut für Festkörperphysik, Germany — ²Peter Grünberg Institut (PGI-3), Forschungszentrum Jülich, Germany — ³Institut für Kristallzüchtung, Germany

β -Ga₂O₃ is a wide band gap material, which is promising for high power and UV (opto-)electronics. The typical *n*-type doping is controllable via the growth parameters, intentional doping, or post-growth heat treatment. In this contribution, we address the question of its surface properties under typical ambient conditions, i. e., under H₂O and O exposure. The β -Ga₂O₃ single crystals were grown with the Czochralski method [1]. Using Auger electron spectroscopy (AES), and scanning tunnelling microscopy/spectroscopy (STM/STS), we show how the different adsorbed atoms/molecules change the structure and electronic properties of β -Ga₂O₃ (100) and (001) surfaces under UHV-conditions. On the (100) surface, large clusters of H₂O with an undisturbed surface in between were observed. However, STS showed no change in the electronic states. On the (001) surface, oxygen covered almost the complete surface. STS showed that O lifts the band bending inherent in clean β -Ga₂O₃ surfaces.

The project was supported by the Leibnitz Association, Leibnitz Science Campus GraFOX, project C2-3.

[1] Z. Galazka *et al.* ECS J. Solid State Sci. Technol. 6 (2017) Q3007

O 49.4 Wed 15:45 S053

Atomic scale studies of chromium species on Fe₃O₄(001) — •MORITZ EDER¹, PANUKORN SOMBUT¹, CHUNLEI WANG¹, MATTHIAS MEIER², JIRI PAVELEC¹, CESARE FRANCHINI^{2,3}, MICHAEL SCHMID¹, ULRIKE DIEBOLD¹, and GARETH PARKINSON¹ — ¹Institute of Applied Physics, TU Wien, Austria — ²Faculty of Physics and Center for Computational Materials Science, University of Vienna, Austria — ³Department of Physics and Astronomy, Alma Mater Studiorum, Università di Bologna, Bologna, Italy

Chromium (Cr) ferrite catalysts are industrially employed for the water gas shift reaction in order to provide large amounts of molecular hydrogen.[1] However, the European REACH legislation requires the removal of hexavalent Cr from all catalysts used in industrial processes due to its toxicity. Consequently, alternative metals are sought to fulfill the role of Cr species in the corresponding compounds.[2] To this end, one needs a fundamental understanding of Cr on iron oxides. We present the investigation of Cr species on Fe₃O₄(001) by means of STM and XPS at room temperature. We show the behavior during exposure to water gas shift reactants and upon high-temperature treatment. The results are compared to the behavior of other transition metals[3] and discussed with respect to implications for applied catalysis.

[1] Häussinger, Lohmüller, Watson, Hydrogen, 2. Production. In: Ullmann's Encyclopedia of Industrial Chemistry, 2011

[2] Glassner, Int. Surf. Technol.14, p. 36, (2021)

[3] Bliem et al., Phys. Rev. B 92, p. 075440 (2015)

O 49.5 Wed 16:00 S053

Adsorption and structural behaviour of thymine on Ce₂O₃ and Ce₆WO₁₂ — •SASCHA MEHL — Elettra Sincrotrone, Trieste, Italy

Reducible oxides are of particular interest in the field of biological systems and nanotechnology application for instance in biosensors, bio medicine and catalysis. The aim is to design novel nano-size structured thin cerium oxide films that possess bio recognition and bio catalytic properties to detect macro molecules e.g. nucleic acids. Model studies of simplified systems such as nucleobases on well-defined oxide surfaces play a major role for understanding and development of these highly promising bio analytical devices. We utilized synchrotron radiation photo electron spectroscopy (SRPES), resonant photo electron spectroscopy (RPES) and X-ray absorption spectroscopy (XAS) which provide ideal conditions to obtain oxidation states, structural and geometrical information on thin organic ad layers. Furthermore, the focus was on the adsorption behavior, electronic structure and thermal stability in the temperature range of 25 * 250 °C of thymine on reduced cerium oxide model systems: thymine/Ce₂O₃(111)/Cu(111) and thymine/Ce₆WO₁₂(100)/W(110). We distinguished two different adsorbed species of thymine on cerium oxide: one strongly bound chemisorbed type and a second weakly bound physisorbed species in the multi layer regime which desorbs at 75 °C. Further investigations have shown that chemisorbed thymine binds to the surface via N-atoms independent of elementary composition and stoichiometry of the substrate.

O 49.6 Wed 16:15 S053

Interaction of organic acids with magnetite surfaces - the DFT perspective — KAI SELLSCHOPP¹, WERNFRIED MAYR-SCHMÖLZER¹, SOMAK BANERJEE¹, JOHANN FLEISCHHAKER¹, ROBERT MEISSNER², and •GREGOR VONBUN-FELDBAUER¹ — ¹Institute of Advanced Ceramics, TU Hamburg, Germany — ²Institute of Polymers and Composites, TU Hamburg, Germany

Magnetite nanoparticles have a high potential for diverse applications like wastewater treatment, catalysis, and hybrid materials. Formic acid and phosphoric acid can be viewed as the smallest representatives of the acids, which are used to functionalize magnetite nanoparticles. Here, we present results from density functional theory (DFT) calculations on the adsorption of such acids on magnetite low index surfaces. For modelling the adsorption, the configuration space is a challenge and here an approach is presented which allows to sample the adsorption configuration space and to select configurations as input for DFT calculations using unsupervised machine learning approaches. The resulting structures allow for in-depth analyses of the systems including structural and electronic effects.

O 49.7 Wed 16:30 S053

Role of surface termination and orientation on the activity of CoFe₂O₄(001) and (100) surfaces for water oxidation — •SHOHREH RAFIEZADEH and ROSSITZA PENTCHEVA — Department of Physics and Center for Nanointegration Duisburg-Essen (CENIDE), University of Duisburg-Essen, 47057 Duisburg

CoFe₂O₄ plays an important role as an anode material for electrochemical water splitting, necessitating detailed understanding of the mechanism of oxygen evolution reaction (OER). This inverse spinel contains alternating layers of octahedral Co and Fe in the (001) direction and mixed Co and Fe layers along the (100) orientation. Here, we employ density functional theory calculations with an onsite Hubbard *U* term (DFT+*U*) to investigate the OER performance of CoFe₂O₄(100) and iron-rich (001) surfaces and compare to the cobalt-rich

(001) surface [1]. While the overpotentials of Fe reaction sites are above 0.44 V, octahedral Co shows the lowest overpotential: 0.38 V at the Co-rich (001) surface and even 0.20 V at the mixed Co-Fe (100) surface when terminated with an additional tetrahedral Fe-layer. This reduction of overpotential correlates with a Co²⁺ oxidation state at the surface and a stabilization of the *OOH intermediate due to hydrogen bonding to neighboring sites. Support by the German Science Foundation (DFG), CRC/TRR 247, project B04 and a computational grant at MagnitUDE are gratefully acknowledged.

[1] H. Hajiyani, R. Pentcheva, ACS Catalysis, 8, 11773-11782 (2018).

O 49.8 Wed 16:45 S053

Complexion Induced Active Phase Evolution in High-Temperature Solid Oxide Cells — •HANNA TÜRK, FRANZ-PHILIPP SCHMIDT, THOMAS GÖTSCH, ROBERT SCHLÖGL, AXEL KNOP-GERICKE, THOMAS LUNKENBEIN, CHRISTOPH SCHEURER, and KARSTEN REUTER — Fritz-Haber-Institut der MPG, Berlin, Germany

Solid oxide cells (SOCs) are among the most efficient technologies for energy-to-hydrogen conversion from fluctuating renewable electricity sources. While SOC are in principle well adapted to intermittent operation, cell performance and lifetime in electrolysis mode is severely limited by degradation of the anode. This degradation goes hand in hand with the oxygen evolution reaction (OER) taking place at the triple-phase boundary (TPB) between the anode, the solid electrolyte and the gas phase. Up to now, the atomistic structure of this active catalyst region is essentially unknown though, which prevents a detailed analysis of the actual degradation mechanisms.

Recently, we took the first step in elucidating the TPB structure by revealing a complexion at the underlying solid|solid interface of the sintered anode[1], featuring partial amorphization and varying elemental distributions deviating from the confining bulk phases. Based on this finding, we now expand our force field based Monte-Carlo simulations to the OER active site. Our experimentally validated results show unexpected compositional changes with respect to the thermodynamic equilibrium, that combined with a spatially resolved diffusion study indicate a hitherto unknown deactivation mechanism of the anode.

[1] H. Türk et al., Adv. Mater. Interfaces 8, 2100967 (2021).

O 49.9 Wed 17:00 S053

Synergistic Effects of Co and Fe on the Oxygen Evolution Reaction Activity of LaCo_xFe_{1-x}O₃ — •ACHIM FÜNGERLINGS and ROSSITZA PENTCHEVA — Universität Duisburg-Essen, Fakultät für Physik, Lotharstr. 1, 47057 Duisburg

The efficiency of the perovskite LaCo_xFe_{1-x}O₃ as a catalyst for the oxygen evolution reaction was investigated by DFT+*U* calculations. The overpotential required to drive the reaction is significantly reduced upon Co incorporation, with a subsequent nonmonotonic behaviour for larger amounts of Co. This is supported by electrocatalytic measurements of phase-pure LaCo_xFe_{1-x}O₃ samples [1]. With the deprotonation of adsorbed *OH being the potential determining step in all cases, the reason for the observed trend is twofold: Co turns out to be a more favorable reaction site than Fe, whereas the overpotential of the latter is decreased upon Co substitution. Variations of the magnetic moments of the Co and Fe cations during OER reveal the participation of several, particularly Co, cations up to several layers below the surface. This extends the concept of the active site.

[1] A. Füngrlings, A. Koul, M. Dreyer, A. Rabe, D. M. Morales, W. Schuhmann, M. Behrens, R. Pentcheva, Chem. Eur. J. 27, 17145-17158 (2021)

O 49.10 Wed 17:15 S053

Hydrophobic pockets on an oxide surface: In₂O₃(111) — HAO CHEN^{1,2}, MATTHIAS BLATNIK^{1,3}, MICHAEL SCHMID¹, BERND MEYER⁴, ULRIKE DIEBOLD¹, and •MARGARETA WAGNER^{1,3} — ¹TU Wien, Vienna, Austria — ²University of the Chinese Academy of Sciences, Beijing, China — ³CEITEC BUT, Brno, Czechia — ⁴FAU Erlangen-Nürnberg, Erlangen, Germany

Indium oxide, a transparent conductive oxide (TCO), is widely used in semiconductor industry but it also displays promising performance in electro- and photocatalytic reactions. In all applications, surrounding water molecules may influence chemical processes at the atomic scale, and understanding the interaction of water with In₂O₃ is important.

We focus on In₂O₃(111), which has an intrinsically large unit cell composed of a hydrophilic and a hydrophobic area. We test the reactivity of these areas by unraveling the interfacial water structures for the whole range of water coverages in UHV, from single dissociated molecules to multilayers, employing TPD, XPS, STM and AFM. Even at high coverages we clearly see hydrophilicity and hydrophobicity within the unit cell, both in experiments and calculations. Local accumulation and depletion of water is confirmed by DFT calculations and ab initio molecular dynamics (MD) simulations for ordered structures consisting of up to 18 water molecules per unit cell. This first water layer shows ordering into nanoscopic 3D water clusters separated by hydrophobic pockets. Going beyond UHV conditions, our MD simulations of a liquid layer show the robustness of the strongly hydrophobic area in the unit cell.

O 50: Frontiers of Electronic Structure Theory: Focus on Artificial Intelligence Applied to Real Materials 2

Time: Wednesday 15:00–18:00

Location: S054

O 50.1 Wed 15:00 S054

Automating the Generation of Linearized Augmented Planewave Basis Functions — •HANNAH KLEINE¹, SVEN LUBECK¹, ANDRIS GULANS², and CLAUDIA DRAXL¹ — ¹Humboldt-Universität zu Berlin — ²University of Latvia

The linearized augmented planewave (LAPW) and local orbitals (LO) method is known to be a highly precise scheme for solving the Kohn-Sham equations of density-functional theory (DFT) for solids. One drawback, however, is that the LAPW and LO basis functions depend on linearization energies which are material dependent. We propose an approach that allows us to compute the linearization energies from the number of nodes of the respective atomic function. It is implemented in the all-electron full-potential computer package exciting [1]. Following this prescription, we are able to automatize the generation of linearly independent basis functions for any material. This approach not only improves the usability of the method, it also leads to better reproducibility of results, and prepares the code for high-throughput calculations.

[1] A. Gulans et al., *J. Phys. Condens. Matter* **26**, 363202 (2014).

O 50.2 Wed 15:15 S054

Hybrid Density-Functional Theory at the Limit: All-electron Exact Exchange beyond 10,000 Atoms — FLORIAN MERZ¹, •SEBASTIAN KOKOTT², CHRISTIAN CARBOGNO², YI YAO³, MARKUS RAMPF⁴, MATTHIAS SCHEFFLER², and VOLKER BLUM³ — ¹Lenovo HPC Innovation Center, Stuttgart — ²The NOMAD Laboratory at the FHI-MPG and HU, Berlin — ³Duke University, North Carolina, USA — ⁴Max Planck Computing and Data Facility, Garching

The computational bottleneck of hybrid density functionals, such as HSE [1], is the evaluation of the exact exchange (EXX) contribution. In this work, we present algorithmic advances in the resolution-of-identity [2] based, real-space implementation of EXX in *FHI-aims* [3,4]. By exploiting MPI-3 intra-node shared memory and enhancing the parallelization scheme, scalability and workload distribution has been drastically improved, which results in memory efficiency and performance increases of up to two orders of magnitude compared to the original implementation, for both total energies and forces/stresses. [3,4] We discuss the details of our implementations and demonstrate the performance as well as scalability for a balanced test set covering inorganic solids, large molecules, and organic crystals with up to 10,000 atoms. Eventually, we show how these advancements enable insights for the design and optimization of hybrid organic/inorganic perovskites.

[1] Heyd, Scuseria, and Ernzerhof, *J. Chem. Phys.* **118**, 18, (2003).

[2] Ihrig et al., *New J. Phys.* **17**, 9, (2015).

[3] Levchenko et al., *Comp. Phys. Commun.* **192**, (2015).

[4] Knuth et al., *Comp. Phys. Commun.* **190**, (2015).

O 50.3 Wed 15:30 S054

Studying nuclear quantum effects on water splitting at a charged interface — •KAREN FIDANYAN and MARIANA ROSSI — Max Planck Institut for the Structure and Dynamics of Matter

Interfaces of water with charged metallic surfaces are relevant for multiple technological processes.¹ In particular, in electrolyzers, the water splitting reaction happens at charged metallic electrodes. The atomistic mechanisms of this fundamental reaction is determined not only by the surface charge induced by the potential bias, but also by nuclear quantum effects (NQE), which are known to impact such reactions strongly.² In this work, we present steps towards a framework for an *ab initio* evaluation of the interplay between these two effects. By making use of a new implementation of the nudged-elastic-band method in the *i-PI* software,³ we are able to calculate forces for this reaction from a variety of electronic-structure codes. At first, we approximate the electrode by a slab using density-functional theory with an applied homogeneous electric field and study how NQEs are changed through the water dissociation paths under different field strengths. Taking advantage of the capabilities of *i-PI* to connect to other codes, our framework can be extended to more accurate models of the potential bias, as for example grand-canonical electronic structure methods.

[1] G. Gonella et al., *Nat Rev Chem* **5**, 466–485 (2021).

[2] Y. Litman, D. Donadio, M. Ceriotti and M. Rossi, *J. Chem. Phys.* **148** 102320 (2018).

[3] V. Kapil et al., *Comp. Phys. Comm.* **236** 214–223 (2019).

O 50.4 Wed 15:45 S054

All-Electron BSE@GW Method for K-Edge Core Electron Excitation Energies — •YI YAO^{1,2}, DOROTHEA GOLZE^{3,4}, PATRICK RINKE⁴, VOLKER BLUM^{2,5}, and YOSUKE KANAI¹ — ¹Department of Chemistry, University of North Carolina at Chapel Hill, Chapel Hill, North Carolina 27599, United States — ²Thomas Lord Department of Mechanical Engineering and Materials Science, Duke University, Durham, North Carolina 27708, United States — ³Faculty of Chemistry

and Food Chemistry, Technische Universität Dresden, 01062 Dresden, Germany — ⁴Department of Applied Physics, Aalto University, P.O. Box 11100, FI-00076 Aalto, Finland — ⁵Department of Chemistry, Duke University, Durham, North Carolina 27708, United States

We present an accurate computational approach to calculate K-edge core electron excitation energies, achieved by combining all-electron GW and Bethe-Salpeter equation (BSE) methods. We assess the BSE@GW approach for calculating K-edge X-ray absorption spectra using a set of small organic molecules and also a medium-sized sulfur-containing molecule, which was used in a past benchmark of an equation-of-motion coupled-cluster (EOM-CC) method by Peng and coworkers [Peng et al., *J. Chem. Theory Comput.*, **11**, 4146 (2015)]. We present the influence of different numerical approximations. We assess the basis set dependence and convergence. We identify the importance of core-correlation basis functions as well as the augmenting basis functions. Compared to the experimental values, the predicted mean absolute error by BSE@GW is as low as 0.6-0.7 eV.

O 50.5 Wed 16:00 S054

Hybrid excitations at the interface between MoS₂ monolayer and organic molecules from first-principle calculation — •IGNACIO GONZALEZ OLIVA¹, FABIO CARUSO^{1,2}, PASQUALE PAVONE¹, and CLAUDIA DRAXL¹ — ¹Institut für Physik and IRIS Adlershof, Humboldt-Universität zu Berlin, 12489 Berlin, Germany — ²Institut für Theoretische Physik und Astrophysik, Christian-Albrechts-Universität zu Kiel, 24118 Kiel, Germany

Hybrid materials composed of organic and two dimensional (2D) inorganic semiconductors are receiving increasing attention due to the interesting physical processes happening at the interface. We present a first-principles investigation of the electronic and optical properties of hybrid organic-inorganic interfaces consisting of a MoS₂ monolayer and the π -conjugate molecules pyrene and pyridine. Employing the G_0W_0 approximation to obtain the quasi-particle band structures, and solving the Bethe-Salpeter equation, we compute the absorption spectra. The latter reveal intralayer excitons on the MoS₂ side, and also hybrid as well as charge-transfer excitons at the interface. Our findings indicate that hybrid systems consisting of semiconducting transition-metal dichalcogenides and organic π -conjugate molecules can host a rich variety of optical excitations and thus provide a promising venue to explore exciton physics in low dimensionality.

O 50.6 Wed 16:15 S054

Mott Metal-Insulator Transition from Steady-State Density Functional Theory — •DAVID JACOB^{1,2}, GIANLUCA STEFANUCCI³, and STEFAN KURTH^{1,2,4} — ¹Universidad del País Vasco UPV/EHU, San Sebastian, Spain — ²Ikerbasque Foundation, Bilbao, Spain — ³Università di Roma Tor Vergata, Rome, Italy — ⁴Donostia International Physics Center, San Sebastian, Spain

We present a computationally efficient method to obtain *many-body* spectral functions of bulk systems in a *density functional theory* framework [1]. To this end we generalize a recently developed method for computing many-body spectral functions of nanoscale systems [2], based on steady-state density functional theory (i-DFT) and using an idealized scanning tunneling microscope (STM) setup, to the case of bulk systems. In this setup the spectral function can be obtained from the finite-bias differential conductance of the current through the STM tip. The fictitious noninteracting system of i-DFT features an exchange-correlation (XC) contribution to the bias which guarantees the same current as in the true interacting system. Exact properties of the XC bias are established using Fermi-liquid theory and subsequently implemented to construct approximations for the Hubbard model. We show for two different lattice structures that our method captures the Mott metal-insulator transition.

References: [1] D. Jacob, S. Kurth, G. Stefanucci, *Phys. Rev. Lett.* **125**, 216401 (2020); [2] D. Jacob and S. Kurth, *Nano Lett.* **18**, 2086 (2018).

O 50.7 Wed 16:30 S054

Network of 1d edge channels and localized states emerging in moiré system — •JEYONG PARK, JINHONG PARK, and ACHIM ROSCH — Institute of theoretical physics, University of Cologne, Germany

For the general moiré system, we theoretically study the effective Hamiltonian for single layer considering the smooth periodic moiré potential induced by other layer, which appears because of distance difference between each pair of atoms located on different layer. For moiré potential larger than tunable moiré energy scale, we find the coexistence of 1D channels and localized state in real space. The 1D channels emerge along the three 1D lines where the mass gap of single layer coming from moiré potential becomes zero, which is showing that these channels are the edge states. Localized states emerge at the crossing point of three 1d lines. We construct the toy model which describes the coexistence of these states by symmetry analysis and consider the RKKY interaction between

localized states which is mediated by 1D channels by including whole spin and valley degrees of freedom. Expanding the effective action for the toy model and controlling chemical potential to suppress oscillation coming from fermi momentum gives three spin interaction $S \cdot (S \times S)$, which can give chiral spin liquid phase. We show how the analytical result can be seen in our model numerically and propose the graphene on top of AB stacking bilayer with twist as the candidate material for realization.

O 50.8 Wed 16:45 S054

Incorporating First-Principles Electronic Friction in Instanton Rate Theory — •YAIR LITMAN¹, ESZTER S. POS¹, CONNOR L. BOX², ROCCO MARTINAZZO³, REINHARD J. MAURER², and MARIANA ROSSI¹ — ¹MPI for the Structure and Dynamics of Matter, Hamburg, Germany. — ²Department of Chemistry, University of Warwick, Coventry, United Kingdom — ³Department of Chemistry, Università degli Studi di Milano, Milano, Italy

Reactions involving impurities in bulk metals are ubiquitous in a wide range of technological applications. The theoretical modelling of such reactions present a challenge for theory because nuclear quantum effects (NQE) can play a prominent role and the coupling of the atomic motion with the electrons in the metal gives rise to important non-adiabatic effects (NAEs). In this work, we present a theoretical framework for the calculation of reaction rates capable of capturing both NQEs and NAEs for high-dimension realistic systems [1,2]. This is achieved by combining the ring polymer instanton (RPI) formalism with *ab initio* electronic friction from Ref. [3]. We derive equations that incorporate the spatial and frequency dependence of electronic friction, and name the new method RPI with explicit friction (RPI-EF). We validate RPI-EF against numerically exact results and find, quantitatively, how the friction modifies reaction rates and tunnelling pathways. Finally, we present *ab initio* results for H-hopping in selected bulk metals. [1] Y. Litman, E. S. Pócs, C. L. Box, R. Martinazzo, R. J. Maurer, and M. Rossi, *JCP* **156**, 194106 (2022) [2] *id.* *JCP* **156**, 194107 (2022) [3] M. Head-Gordon, J. C. Tully, *JCP* **96**, 3939 (1992).

O 50.9 Wed 17:00 S054

Real-Time Time-Dependent Density Functional Theory within the FHI-aims code — JOSCHA HEKELE¹, YI YAO², VOLKER BLUM², YOSUKE KANAI³, and •PETER KRATZER¹ — ¹Faculty of Physics, University Duisburg-Essen, 47057 Duisburg, Germany — ²Thomas Lord Department of Mechanical Engineering and Materials Science, Duke University, Durham, North Carolina 27708, USA — ³Department of Chemistry, University of North Carolina, Chapel Hill, North Carolina 27599, USA

We present a high-precision all-electron RT-TDDFT implementation using numerical atom-centered orbital (NAO) basis functions into FHI-aims. First, RT-TDDFT results are validated against linear-response TDDFT results for the molecules of Thiel's test set and the importance of basis augmentation for adequate convergence is confirmed. Adopting a velocity-gauge formalism, dielectric properties of crystalline materials are calculated. Taking advantage of the all-electron full-potential implementation, we present applications to soft X-ray spectra of H₂O using hybrid functionals. Moreover, numerical performance tests are presented showing almost linear scaling on parallel computers.

O 50.10 Wed 17:15 S054

Ab initio study of many-body interacting nonlinear optical photoconductivity tensors — •PEIO GARCIA-GOIRICELAYA¹, JYOTI KRISHNA¹, and JULEN IBAÑEZ-AZPIROZ^{1,2} — ¹Centro de Física de Materiales, University of the Basque Country UPV/EHU, Spain — ²IKERBASQUE Basque Foundation for Science, Spain

We present a general scheme for calculating the many-body interacting second-order optical photoconductivity tensor from first-principles. Our practical implementation starts from the length-gauge formulation of the single-particle non-interacting second-order response tensor [1] that is efficiently calculated using Wannier interpolation [2]. In a second step, we make use of the TD-CDFT in

order to extract the many-body interacting response tensor, taking into account collective excitations, i.e. excitonic effects for semiconductors and plasmonic effects for metals. We employ this scheme to assess the impact of many-body excitations on second harmonic generation and benchmark our results with experiments on the semiconducting GaAs [3] and the semimetal TaAs [4], as well as with early calculations [5].

Funding provided by the European Union's Horizon 2020 research and innovation programme under the European Research Council (ERC) grant agreement No 946629.

- [1] J. E. Sipe and A. I. Shkrebtii, *Phys. Rev. B* **61**, 5337 (2000).
- [2] G. Pizzi *et al.*, *J. Phys. Cond.Matt.* **32**, 165902 (2020)
- [3] S. Bergfeld and W. Daum, *Phys. Rev. Lett.* **90**, 036801 (2003).
- [4] Shreyas Patankar *et al.*, *Phys. Rev. B* **98**, 165113 (2018).
- [5] E. Luppi *et al.*, *Phys. Rev. B* **82**, 235201 (2010).

O 50.11 Wed 17:30 S054

Electron-phonon drag in MgB₂ — •NAKIB PROTİK and CLAUDIA DRAXL — Institut für Physik and IRIS Adlershof, Humboldt-Universität zu Berlin, Berlin, Germany

MgB₂ is a well known phonon-mediated superconductor with a transition temperature around 40 K. The strong electron-phonon interactions present in the material also give rise to strong drag phenomena, as has been demonstrated experimentally in Refs. [1, 2]. While the measured thermopower in the normal phase shows hole-like transport, there is, however, no consensus regarding the sign and temperature dependence of the drag contribution. In this work, we carry out anisotropic and band-resolved *ab initio* transport calculations to investigate this puzzle. Our findings will shed light on the roles of the microscopic interactions on the strong drag behavior in metals.

[1] Schneider, Matthias, Dieter Lipp, Alexander Gladun, Peter Zahn, Axel Handstein, Günter Fuchs, Stefan-Ludwig Drechsler, Manuel Richter, Karl-Hartmut Müller, and Helge Rosner. "Heat and charge transport properties of MgB₂." *Physica C: Superconductivity* 363, no. 1 (2001): 6-12.

[2] Putti, M., E. Galleani d'Agliano, D. Marre, F. Napoli, M. Tassisto, P. Manfrinetti, A. Palenzona, C. Rizzuto, and S. Massidda. "Electron transport properties of MgB₂ in the normal state." *The European Physical Journal B-Condensed Matter and Complex Systems* 25, no. 4 (2002): 439-443.

O 50.12 Wed 17:45 S054

Ab initio simulations of vibrational sum frequency generation without molecular decomposition — •PAOLO LAZZARONI, ALAN LEWIS, and MARIANA ROSSI — Max Planck Institute for the Structure and Dynamics of Matter, Hamburg, Germany

Hydrogen evolution through heterogeneous catalysis is an increasingly popular solution for storage of energy generated from renewable sources, and as such is becoming a central part of green energy grids. Understanding the structure of water at solid interfaces is vital to find more efficient and cost-effective catalysts of this reaction, and sum-frequency generation spectroscopy provides a surface-specific method of investigating these structures [1]. In this work we present a new framework for *ab initio* calculations of the sum-frequency response which avoids the need for an arbitrary molecular decomposition of the polarizability and dipole moment. Within this approach, based on Density Functional Theory, the observables are evaluated using real space integrals directly on the whole system [2]. This allows us, for example, to unravel the effect of this decomposition on the sum-frequency response of the much-studied water/vacuum interface. This scheme also enables us, in the context of water-solid interfaces, to account explicitly for the contribution of the solid to the polarizability and dipole moment of the interface, which are commonly neglected.

- [1] A. Morita, J. Hynes, *J. Phys. Chem. B* **106**, 673 (2002)
- [2] H. Shang *et al.*, *New J. Phys.* **20**, 073040 (2018)

O 51: Poster Wednesday: Atomic-Scale Studies of Spins on Surfaces with Scanning Tunneling Microscopy

Time: Wednesday 18:00–20:00

Location: P4

O 51.1 Wed 18:00 P4

Nickelocene molecule as an STM magnetic sensor — •ANDRES PINAR SOLE, OLEKSANDR STETSOVYCH, PAVEL JELINEK, ALES CAHLIK, CHRISTIAN WAKERLIN, and JINDRICH KOLORENC — Czech Institute of Physics, Prague, Czech Republic, Email: pinar@fzu.cz

Functionalization of the scanning probe of a scanning tunnelling microscopy (STM) with metallocene molecule allows performing spin-sensitive measurements on magnetic systems. Here, we used a nickelocene molecule (NiCp₂), consisting of a Ni atom sandwiched between two cyclopentadienyl rings. As an S=1 system, it presents magnetic-induced spectral features due to the inelastic electron spin-flip.

First, we examined 1D metallorganic coordination polymers (2,5-diamino-1,4-benzoquinonediimines) on Au(111) with Co or Cr atoms as metal sites respectively. Nickelocene IETS conductance spectrum deformation was only sensitive to the out-of-plane magnetic anisotropy of the Cr.

Secondly, the Nc functionalized probe was also used to measure the magnetism emerging from the unpaired electron on the edge of a wave-like graphene nanoribbon (GNR) on Au(111). Here, we observed spectral convolution between a Kondo feature from the edge-state and the nickelocene spectrum.

To understand the IETS from the magnetic sensor, a many-body Hubbard model was proposed, and the system was simplified to a two-site model consisting of the partially filled 3d shell of the nickelocene and a 3d shell in the probed magnetic center.

O 51.2 Wed 18:00 P4

Yu-Shiba-Rusinov band dispersion of infinite Mn chains on top of a semi-infinite Nb(110) surface — •RIK BROEKHOVEN, ARTEM PULKIN, ANTONIO MANESCO, SANDER OTTE, ANTON AHKMEROV, and MICHAEL WIMMER — Delft University of Technology, Delft, The Netherlands

Chains of magnetic atoms on s-wave superconductors have been proposed to have a topological non-trivial phase, when the induced in-gap Yu-Shiba-Rusinov (YSR) bands are p-wave gapped by for example spin-orbit coupling. In order to determine the topological phase diagram, experiments were previously limited to probing local quantities of the chain. Recent improvements in STM methodology have made it possible however to now also probe the YSR band dispersion relation. It was found to be highly dependent on the chain spacing and orientation with respect to the superconductor lattice.

Motivated by this discovery, here we present a method to evaluate the in-gap dispersion relation of chains with different orientations and spacing. In contrast to previous works, we work with infinite chains on a semi-infinite surface to make sure the system is larger than the superconductor coherence length. We focus on Mn atoms on top of superconducting Nb(110). First, we derive an effective tight-binding model from ab initio calculation, and subsequently we use the multidimensional Green's function formalism to extend to a semi-infinite system and solve for the corresponding in-gap YSR bands.

O 51.3 Wed 18:00 P4

Unravelling the Magnetic Ground State of All-Organic Diradicals on Au Substrates — •ALESSIO VEGLIANTE¹, SALETA FERNANDEZ², RICARDO ORTIZ³, NIKLAS FRIEDRICH¹, ANDREA AGUIRRE¹, FRANCISCO ROMERO¹, DIEGO PEÑA², and THOMAS FREDERIKSEN³ — ¹CIC NanoGUNE, San Sebastian, Spain — ²CiQUS-USC, Santiago de Compostela, Spain — ³Donostia International Physics Center, San Sebastian, Spain

Open-shell organic molecules have received considerable interest as potential candidates for molecular spintronics. Magnetism can emerge in all-organic molecules due to the presence of one or more unpaired π -electrons. Organic diradicals, hosting two spin centers, are particularly interesting as model systems for investigating and manipulating magnetic interactions at the atomic scale.

Here we study the magnetic state of a Chichibabin's hydrocarbon diradical deposited on a gold substrate, by using scanning tunneling microscopy (STM) and spectroscopy (STS). We investigate the interaction between the two spin centers of the molecule, focusing on the influence of the molecular geometry. With the support of theoretical simulations, we show that the adsorption on the metal surface changes the ground state of the molecule from a triplet, expected in the gas phase, to a singlet state. Furthermore, we demonstrate that it is possible to modify the magnetic state of the diradical through conformational changes induced by the STM tip. These findings represent an important step towards the control of magnetic interactions within purely organic molecules.

O 51.4 Wed 18:00 P4

Quantifying the interplay between fine structure and geometry of an individual molecule on a surface — •MANUEL STEINBRECHER¹, WERNER M.J. VAN WEERDENBURG¹, ETIENNE F. WALRAVEN¹, NIELS P.E. VAN MULLEKOM¹, JAN W. GERRITSEN¹, FABIAN D. NATTERER², DANIS I. BADRTDINOV¹, ALEXANDER N. RUDENKO^{4,1}, VLADIMIR V. MAZURENKO³, MIKHAIL I. KATSNELSON¹, AD V.D. AVOIRD¹, GERRIT C. GROENENBOOM¹, and ALEXANDER A. KHAJETOORIAN¹ — ¹Institute for Molecules and Materials, Radboud University, Nijmegen, The Netherlands — ²Department of Physics, University of Zurich, Switzerland — ³Ekaterinburg — ⁴School of Physics and Technology, Wuhan University, China With spin-resolved scanning tunneling microscopy (SP-STM) and electron spin resonance (ESR) we have probed single TiH molecules deposited on a thin insulating MgO layer in a vector magnetic field at mK temperatures down to MHz frequencies. We find that the molecule retains a non-trivial orbital angular momentum resulting in a strongly renormalized and anisotropic g -tensor. As we prove, the latter does not stem from Kondo or Jahn-Teller effects. From quantum chemistry embedded cluster calculations we find an analytical expression for the g -tensor, which solely depends on the splitting of the ground states and the spin-orbit coupling. In a dynamic expansion of the model, the position of the H atom and rotational dynamics of the molecule were investigated. [1] Steinbrecher *et al.*, PRB 103, 155405 (2021) [2] v. Weerdenburg *et al.*, RSI 92, 033906 (2021)

O 51.5 Wed 18:00 P4

Magnetic molecule as a parity sensor in entangled spin and YSR excitation on a superconductor — •JON ORTUZAR¹, STEFANO TRIVINI¹, KATERINA VAXEVANI¹, JINGCHEN LI⁵, ANE GARRO¹, MIGUEL ANGEL CAZADILLA³, SEBASTIAN BERGERET^{2,3}, and JOSÉ IGNACIO PASCUAL^{1,4} — ¹CIC nanoGUNE-BRTA, San Sebastián, Spain — ²Centro de Física de Materiales (CFM-MPC), San Sebastián, Spain — ³Donostia International Physics Center (DIPC), San Sebastián, Spain — ⁴Ikerbasque, Bilbao, Spain — ⁵School of Physics, Sun Yat-sen University, Guangzhou, China

A magnetic molecule coupled to a superconductor induces Yu-Shiba-Rusinov (YSR) bound states, detected by tunneling spectroscopy as long-lived quasiparti-

cle excitations inside the superconducting gap [1]. The degeneracy of the system can be lifted by intrinsic magnetic anisotropy so that entangled spin and YSR excitations are possible [2]. We tune the exchange coupling between a FeTPP-Cl molecule and the proximitized Au(100)/V substrate to go through a Quantum Phase Transition from an unscreened half-integer spin (even parity) system to a screened integer spin (odd parity) system [3]. We use a single site superconductor model [4] to prove the capability to detect the parity of the system, getting fundamental insight into the interplay of YSR and spin excitation.

[1] B. W. Heinrich, *et. al.*, Prog. Surf. Sci.93, 1 (2018) [2] N. Hatter, *et. al.*, Nat. Commun.6, 8988 (2015) [3] S. Kezilebieke, *et. al.*, Nano Lett.19, 4614 (2019) [4] F. von Oppen and K. J. Franke, Phys. Rev. B103, 205424 (2021).

O 51.6 Wed 18:00 P4

Electronic Properties of Dysprosium-based Fe-Porphyrins Metal-Organic Coordination networks on Au(111) and Ag(100) Substrates — •SERIM JEON^{1,3}, LUKAS SPREE^{1,2}, CORINA URDANIZ^{1,2}, CAROLINE HOMMEL^{1,2}, ANDREAS HEINRICH^{1,2}, CHRISTOPH WOLF^{1,2}, and LUCIANO COLAZZO^{1,2} — ¹Center for Quantum Nanoscience, Institute for Basic Science, Seoul, Republic of Korea — ²Ewha Womans University, Seoul, Republic of Korea — ³Department of Physics, Ewha Womans University

Dy has become the cornerstone for many investigations on lanthanide-directed molecular-magnetism, thanks to its strong magnetic anisotropy. Iron Tetrapyrrole complexes, on the other hand, have shown promise as materials for quantum information processing. Creating a platform that incorporates both might have a way for the realization of multiqubit architectures. The presented study describes electronic properties within a metal-organic network MOF consisting of Iron-Tetrakis-(4-Cyanophenyl) Porphyrin Fe-TCPP and Dysprosium. Fe-TCPP was deposited on Au(111), Ag(100), and MgO/Ag(100). The deposition of Dy induces coordination between the cyano groups and the lanthanide atoms and gives rise to ordering and the formation of large islands of 2D MOF. The lanthanide-based organic network was examined by scanning tunneling microscopy STM on the substrates. Significant shifts in the energy of LUMO of the MOFs were observed via scanning tunneling spectroscopy STS after deposition of Dy. The results were combined with ab initio calculation to further elucidate the electronic structure of the deposited materials.

O 51.7 Wed 18:00 P4

Long-lived spin states of Fe atomic chains on Cu₂N via Hamiltonian engineering — ROBBIE J. G. ELBERTSE¹, •TAEHONG AHN^{2,3}, JIYOON HWANG^{2,3}, JEONGMIN OH^{2,3}, JORN C. RIETVELD¹, SANDER OTTE¹, ANDREAS J. HEINRICH^{2,3}, and UJUJEONG BAE^{2,3} — ¹Department of Quantum Nanoscience, Kavli Institute of Nanoscience, Delft University of Technology, Lorentzweg 1, Delft 2628 — ²Center for Quantum Nanoscience, Institute for Basic Science, Seoul, Korea — ³Department of Physics, Ewha Womans University, Seoul, Korea

A spin-polarized scanning tunneling microscope (STM) operating at various magnetic fields allows us to characterize the spin relaxation time of atomic structures on a surface, enabling Hamiltonian engineering. Here, we introduce 1D Fe atomic chains built on Cu₂N/Cu(100) using a home-built STM and the evolution of their spin lifetime depending on the length of chains and the direction and magnitude of magnetic fields. To measure the spin lifetime ranging from 10⁻⁶ to 10 seconds, we used two different detection schemes; pump-probe [Science 329, 1628-1630 (2010)] and two state switching [Science 335, 196-199 (2012)]. We observed the spin lifetime of Fe chains changes non-monotonically as passing through a diabolic point with varying magnetic fields changes the degree of superposition of the two Neél states in the lowest energy eigenstates. To control the spin lifetime of Fe chains, we use magnetic fields as a control knob. Our work shows a capability of the spin lifetime in a large time scale and the precise control of spin dynamics in engineered atomic structures.

O 51.8 Wed 18:00 P4

Local characterization of Yu-Shiba-Rusinov excitations in magnetic field — •NIELS P.E. VAN MULLEKOM¹, BENJAMIN VERLHAC¹, WERNER M.J. VAN WEERDENBURG¹, HERMANN OSTERHAGE¹, MANUEL STEINBRECHER¹, KATHARINA J. FRANKE², and ALEXANDER A. KHAJETOORIAN¹ — ¹Institute for Molecules and Materials, Radboud University Nijmegen, the Netherlands — ²Fachbereich Physik, Freie Universität Berlin, Germany.

An isolated spin, typically derived from an atomic or molecular adsorbate, can interact with a BCS superconductor leading to so-called Yu-Shiba-Rusinov (YSR) excitations. These excitations can be probed with scanning tunneling microscopy/spectroscopy (STM/STS), which are often characterized by resonances that reside in the superconducting gap and are linked to the excitation energies. These spin-based excitations to date have been poorly studied in magnetic fields, due to influence of magnetic fields on typical BCS superconductors. Here, utilizing STM/STS at milliKelvin temperatures, we report on a study of the YSR excitations of individual adsorbates in variable magnetic field.

O 51.9 Wed 18:00 P4

Extending the spin excitation lifetime of a magnetic molecule on a proximitized superconductor — •KATERINA VAXEVANI¹, STEFANO TRIVINI¹, JINGCHENG LI¹, JON ORTUZAR¹, DONGFEI WANG¹, DANILO LONGO¹, and JOSE IGNACIO PASCUAL^{1,2} — ¹CIC nanoGUNE-BRTA, 20018 Donostia-San Sebastian, Spain — ²Ikerbasque, Basque Foundation for Science, 48013 Bilbao, Spain

Magnetic molecules adsorbed on surfaces have been used as a platform to individually address and manipulate spins. Long spin-relaxation times are required in order to be able to use atomic spins in quantum information processing and data storage. Normally, coupling of the spin with the conduction electrons of metallic substrates can quench the excited state lifetime and lead to short relaxation times, but the presence of superconducting pairing effects in the metal substrate can protect the excited spin from relaxation[1]. Here, we use a substrate of a few monolayers of gold epitaxially grown on top of an oxygen reconstructed 1x5-V(100) surface to decouple the molecular spin of an iron-porphyrin-chloride from itinerant electrons. The gold film exhibits a proximitized superconducting gap with in-gap de Gennes-Saint James resonances, which protects molecular spin excited states and results into a lifetime of $\tau=80$ ns. The spin lifetime decreases with increasing the film thickness due to the gradual gap-closing by the in-gap states. Our results elucidate the use of proximitized gold electrodes for addressing quantum spins on surfaces, envisioning new routes for tuning the value of their spin lifetime.

[1] B. W. Heinrich et al., Nature Physics 9, 765 (2013).

O 51.10 Wed 18:00 P4

The Emergence of Magnetism in [5]-Aza-Triangulene — •LORENZ MEYER¹, FRANCISCO ROMERO LARA¹, NIKLAS FRIEDRICH¹, ALESSIO VEGLIANTE¹, MANUEL VILAS VARELA², UNAI URIARTE AMIANO¹, NATALIA KOVAL¹, EMILIO ARTACHO CORTÉS¹, DIEGO PEÑA GIL², and JOSE IGNACIO PASCUAL¹ — ¹CIC nanoGUNE, San Sebastian (Spain) — ²Centro Singular de Investigación en Química Biológica y Materiales Moleculares (CIQUS), Santiago de Compostela (Spain)

Zigzag-edged Graphene triangulenes are known to host a magnetic ground state due to sublattice imbalance. The magnetic properties of these structures can be tuned by the size of the triangulene or via heteroatom substitution. This makes them intriguing for future spintronic applications paving the way towards organic logical devices. So far, the influence of heteroatoms in larger triangulenes seems to be unknown. In our work, we report the bottom-up synthesis of [5] aza-Triangulene by means of surface-assisted cyclodehydrogenation on a Au(111) surface. Electronic transport measurements carried out with a scanning tunneling microscope reveal the high-spin ground state of this molecule via low energy phenomena. Additionally, we shine light on not only the influence of heteroatoms but also of additional Hydrogen atoms and defects which are able to tune the magnetic ground state. Density functional theory and Mean-Field-Hubbard calculations confirm the spin texture and the electronic structure of the observed molecules.

O 52: Poster Wednesday: Adsorption and Catalysis 2

Time: Wednesday 18:00–20:00

Location: P4

O 52.1 Wed 18:00 P4

Investigation of the influence of the spin in adsorption structures of oxygen on a cerium chloride catalyst surface in the Deacon process using computational methods — •KATHRIN NIESWIEC and FRANZISKA HESS — Technische Universität Berlin, Institut für Chemie, Straße des 17. Juni 124, 10623 Berlin, Germany

CeO₂-based catalysts in the HCl oxidation undergo reversible deactivation by forming CeCl₃. This work examines the interaction of the CeCl₃-(110)-surface with O₂ during the reoxidation of CeCl₃. CeCl₃ is an insulator, where Ce is 9-fold coordinated that exposes different adsorption sites at the surface. Different adsorption structures of atomic and molecular oxygen on the CeCl₃-(110)-surface are examined in terms of energy, electronic state and magnetization. Cerium-based catalyst systems are investigated by DFT calculations in the PAW approach with the PBE functional including Hubbard-U correction. Ab-initio thermodynamics are employed to analyze temperature and pressure-dependency of oxygen adsorption on the surface. Upon adsorption of oxygen on the surface, Ce³⁺ can be locally oxidized to Ce⁴⁺, resulting in different spin and charge density distributions. Consequently, the adsorption energies of oxygen can vary by over 1 eV, depending on the initial spin state. The ab-initio thermodynamics analysis based on the obtained oxygen adsorption energies suggests that the CeCl₃ surface is expected to be covered by oxygen due to the strong Ce-O bond. These results suggest that spin must be explicitly included when examining adsorption on CeCl₃ surfaces in order to obtain correct adsorption energies for catalysis applications.

O 52.2 Wed 18:00 P4

Influence of the Substrate Orientation Dependent Reactivity on the On-surface Ullmann Coupling Reaction of 2,2-Dibromobiphenyl Studied by XPS — •PAUL SCHWEER and KARINA MORGENSTERN — Chair of Physical Chemistry I, Ruhr-University of Bochum, Germany

The Ullmann coupling reaction is considered the leading approach for accessing low dimensional covalent organic structures in the context of on-surface synthesis. Despite extensive studies on the influence of the halogen substitution pattern of the halogen-aryl precursor on the reaction mechanism and product formation, the impact of ortho-substitution is barely investigated. Hence, this work aims to reveal the temperature-induced reaction steps for 2,2-dibromobiphenyl on low-index Cu surfaces. For this purpose, the precursor is deposited in ultra-high vacuum at 86 K and stepwise annealed to 600 K. By using X-ray photoelectron spectroscopy, chemical changes of the organic species and the bromine atoms are identified and assigned to the typical Ullmann reaction steps: dissociation of the halogen-carbon bond, surface bonding, and C-C coupling. Here, we further discuss different precursor reactivities on Cu(111) and Cu(110) and an additional binding energy shift on Cu(110), indicating a structural change of the surface bound biphenyl before C-C coupling at a higher temperature.

O 52.3 Wed 18:00 P4

Surface Chemistry of the MOST Energy Storage System 2-Carboethoxy-3-Phenyl-Norbornadiene/Quadricyclane — •FELIX HEMAUER, CORNELIUS WEISS, JOHANN STEINHÄUER, VALENTIN SCHWAAB, HANS-PETER STEINRÜCK, and CHRISTIAN PAPP — Friedrich-Alexander-Universität, Erlangen, Germany

The intermittent character of renewable energy sources gives the necessity for novel energy storage technologies. So-called molecular solar thermal (MOST) energy systems directly combine the light-harvesting process with storing the gained energy as molecular strain. In a photoconversion reaction, the energy-lean norbornadiene (NBD) is converted to its energy-rich valence isomer quadricyclane (QC). By derivatization of the molecular framework, the light-harvesting properties of the molecules are optimized.

The pair 2-carboethoxy-3-phenyl-NBD/QC was investigated as model system for heterogeneously catalyzed energy release. X-ray photoelectron spectroscopy was employed to study the adsorption and thermal evolution on a Ni(111) and Pt(111) surface, respectively. An unambiguous identification of the QC and NBD derivatives at low temperature was possible on both surfaces. In case of nickel, no cycloreversion of the QC derivative to NBD was found, but individual decomposition routes setting in at about 170 K. For platinum, the back conversion under energy release was found to start at 150 K and being completed at 230 K. Above 300 K, a fragmentation into carbonaceous species occurred. The work was supported by the DFG (Project No. 392607742) and the HZB for allocation of synchrotron radiation beamtime.

O 52.4 Wed 18:00 P4

Temperature-induced surface reactions of 1-cyclohexylethanol and acetophenone on Pt(111) — •VALENTIN SCHWAAB, FELIX HEMAUER, EVA MARIE FREIBERGER, NATALIE WALESKA, HANS-PETER STEINRÜCK, and CHRISTIAN PAPP — Friedrich-Alexander-Universität, Erlangen, Germany

1-Cyclohexylethanol (1-CHE) is an interesting candidate when it comes to molecular energy storage systems. Such secondary alcohols can function as electrofuel, whereby their oxidation over a platinum electrode yields the respective ketone together with two electrons and two protons. Additionally, 1-CHE and acetophenone (APH) represent an attractive liquid organic hydrogen carrier (LOHC) pair, as the complete dehydrogenation of the former leads to the release of four equivalents of H₂.

To gain fundamental insights into the surface reaction of both molecules, high-resolution temperature-programmed X-ray photoelectron spectroscopy experiments (HR-TPXPS) were carried out on a Pt(111) model catalyst. Based on the obtained C 1s and O 1s data, the dehydrogenation reaction of the alcohol and the formation of potential catalyst poisoning decomposition products are discussed.

We acknowledge financial support by the Bavarian Ministry of Economic Affairs, Regional Development and Energy, and by the DFG (Project No. 419654270). We thank HZB for the allocation of synchrotron radiation beamtime.

O 52.5 Wed 18:00 P4

Force-induced single-molecular switch of graphene-nanoribbon-fused helicene by atomic force microscopy — •AKITOSHI SHIOTARI^{1,2}, AYUMU ISHII¹, and YOSHIKI SUGIMOTO¹ — ¹The University of Tokyo, Kashiwa, Japan — ²Fritz-Haber Institute of the Max-Planck Society, Berlin, Germany

On-surface synthesis is an effective bottom-up method to fabricate nanocarbon materials, such as graphene nanoribbons (GNRs), in an atomically precise manner. In this study, using the on-surface method with multiple precursors, we successfully synthesized new helicene-derivative molecule fused by seven-atom-wide armchair GNRs on an Au(111) surface. Atomic resolution imaging with non-contact atomic force microscopy (AFM) identified the molecular structure and the helicity (i.e., chirality of the twisted terminal of the GNR). Although the helicities of individual GNRs on the surface remained stable during observation, the approach of the AFM tip to the helicene-type terminal caused repulsive interactions, leading to the inversion of the twisted structure in a selective and reversible manner. This finding would contribute to the advanced design of switchable molecules and control of chiral-molecule-based devices and machines.

O 52.6 Wed 18:00 P4

On-Surface Synthesis of Kekulene and Isokekulene — •TIM NAUMANN, QI-TANG FAN, LUKAS HEUPLICK, LUKAS RUPPENTHAL, SIMON WERNER, TOBIAS VOLLGRAFF, JÖRG SUNDERMEIER, and J. MICHAEL GOTTFRIED — Fachbereich Chemie, Philipps-Universität Marburg, Marburg (Germany)

The concept of aromaticity explains the exceptional stability of monocyclic, planar, conjugated molecules. When extending this concept on cycloarenes, however, the question arises whether the π -electron system is best described by the Clar model or rather by annulenic aromaticity, i.e. delocalization in the inner and outer annulene ring. This question has been discussed especially in the context of kekulene, an alternant benzenoid cycloarene. On-Surface techniques offer the possibility to synthesize kekulene and to investigate its resonance stabilisation. To create complete monolayers of kekulene for further spectroscopic studies, we developed a high-yield on-surface synthesis of kekulene on Cu(111) from vapor-deposited 1,4,7(2,7)-triphenanthrenacyclononaphane-2,5,8-triene, which undergoes cyclodehydrogenation upon annealing, resulting in extended (up to 100 nm) well-ordered domains of kekulene. While the reaction is highly selective towards kekulene on Cu(111), reaction on Cu(110) leads to an isomer of kekulene with a lower symmetry, named isokekulene. The precursor and the products were analyzed with scanning tunneling microscopy (STM), X-ray photoelectron spectroscopy (XPS) and other methods. Further annealing leads to peripheral C-H bond activation and linking towards chains and islands.

O 52.7 Wed 18:00 P4

2D arrays of reaction centers for CO oxidation over Pt/SiO₂/Si interface — •ARTUR BÖTTCHER¹, DAVID RETTINGER¹, JAKOB HAUNS¹, MANFRED KAPPES¹, DANIELA EXNER², RAHUL PARMER³, MATTEO AMATI³, and LUCA GREGORATTI³ — ¹Institute of Physical Chemistry, KIT, 76131 Karlsruhe, Germany — ²Institute for Applied Materials, KIT, 76344 Karlsruhe, Germany — ³Elettra - Sincrotrone Trieste ScPA, Area Science Park, 34149 Basovizza-Trieste, Italy

We created arrays of tailored reaction centers on the SiO₂/Si-wafer by annealing thin Pt layers deposited on He⁺-beam patterned Graphene/SiO₂/Si substrates.[1] The resulting spots have been identified as amorphous areas consisting of silicon carbides and silicon oxycarbides. These defected surface regions are expected to act as pinning sites for migrating Pt atoms. By thermally activating the surface diffusion of Pt adatoms (1h, 600 °C, UHV), the migrating atoms become immobilized thus forming chemical bonds with compounds created in the defected surface regions, resulting in 2D arrays of tailored Pt-based islands. The chemical state of individual islands has been studied by monitoring core level states (ESCA microscopy). The islands consist of Pt, PtSix and PtOx compounds and appear to be chemically resistant under exposure to molecular oxygen and carbon monoxide at T=550 °C, p= 0.4 mbar, 0.5 h. The CO₂-light-off curves enable to estimate the contribution of the artificial reaction centers to the total CO->CO₂ conversion yield.

[1] A. Böttcher et al. 2020 Nanotechnology 31 505302

O 52.8 Wed 18:00 P4

CO→CO₂ conversion over Pt/SiO₂/Si model catalyst — •ARTUR BÖTTCHER¹, PASCAL WEISENBURGER¹, DAVID RETTINGER¹, JAKOB HAUNS¹, RAHUL PARMER², MATTEO AMATI², LUCA GREGORATTI², and MANFRED KAPPES¹ — ¹Institute of Physical Chemistry, KIT, 76131 Karlsruhe, Germany — ²Elettra - Sincrotrone Trieste ScPA, Area Science Park, 34149 Basovizza-Trieste, Italy

We studied the thermal stability of the Pt/SiO₂/Si interface as the model catalyst for CO oxidation reaction. The 2D catalysts were prepared under UHV conditions by growing very thin Pt films on the SiO₂/Si wafer and subsequently performing a long-term annealing of the interface at elevated temperatures, T*(700-900K). Such a treatment results in the formation of the submicron-sized islands. The size/shape distribution of the islands scales primarily with the thickness of the Pt film. The chemical state of the islands as probed by ESCA microscopy (Elettra) evidences the formation of PtSinOm alloys as the dominating compo-

nent of the islands. The CO₂ light-off curves taken for Pt/SiO₂/Si interfaces fabricated at room temperature reveal the highest CO/CO₂ conversion yield, Y, and the lowest activation temperature, T_A ~400 K. Increasing alloying degree considerably quenches the conversion yield and shifts up the CO/CO₂ conversion onset.

O 52.9 Wed 18:00 P4

Adsorption and photocatalytic inactivation of Corona-virus like particles by anatase TiO₂(101) — •MONA KOHANTORABI, MICHAEL WAGSTAFFE, HESHMAT NOEI, and ANDREAS STIERLE — Centre for X-ray and Nano Science (CXNS), Deutsches Elektronen-Synchrotron (DESY), 22607 Hamburg, Germany

The adsorption of corona-virus like particles (VLPs), on the surface of the model catalyst TiO₂(101) was investigated using different spectroscopic and microscopic techniques.

Two different methods were employed to inactivate the virus after it was loaded on the surface of TiO₂: 1) UV light and 2) thermal treatment. The adsorbed virus morphology and virus particle arrangement on the surface of TiO₂ were investigated using grazing-incidence small-angle scattering. Microscopic studies demonstrate that the denatured spike proteins and other virus proteins dissociate from VLPs and adsorb on the surface of TiO₂.

Clarification of the interaction of the virus with the surface of semiconductor oxides will aid in obtaining a deeper understanding of the chemical processes involved in photo-inactivation of microorganisms which is important for the design of effective photocatalysts for air purification and self-cleaning materials.

O 52.10 Wed 18:00 P4

Calculation of XPS Core-Level Fingerprints of Intermediates in Methanol Synthesis on Cu Surfaces — •MATTIS GOSSLER, AZAD KIRSAN, and BERND MEYER — Interdisciplinary Center for Molecular Materials and Computer Chemistry Center, FAU Erlangen-Nürnberg, Germany

Cu/ZnO/Al₂O₃ is used as a highly efficient catalyst in industry for the synthesis of methanol from syn gas, i.e. H₂, CO and CO₂. Despite intensive research efforts over the past decades, the precise reaction pathway and the relevant intermediates in the synthesis process are still under debate. New insights can be provided by recently performed ambient pressure x-ray photoelectron spectroscopy (AP-XPS) measurements on ZnO-supported Cu clusters with well-defined crystal terminations [1]. In order to assist the interpretation of the measured AP-XP spectra, we determined the C-1s and O-1s core level shifts for a series of intermediates in the methanol synthesis process on a variety of Cu surfaces using DFT calculations. First, a careful search for the most stable structure of all intermediates on each surface was performed. Core-level shifts were then calculated by an ΔSCF approach after removing a core electron. This fingerprint data allows us to identify the most relevant intermediates present in the AP-XPS experiments and to assess the importance of different Cu surfaces for the overall reactivity.

[1] R. Gleissner, H. Noei, S. Chung, G.D.L. Semione, E.E. Beck, A.-C. Dippel, O. Gutowski, G. Gizer, V. Vonk, A. Stierle, J. Phys. Chem. C **125** (2021) 23561–23569

O 52.11 Wed 18:00 P4

The relation between structure sensitivity and doping of ceria(111) vs. ceria(100) — EMILIA POZAROWSKA¹, LINUS PLEINES², MAURICIO J. PRIETO³, LIVIU C. TĂNASE³, LUCAS DE SOUZA CALDAS³, AARTI TIWARI³, THOMAS SCHMIDT³, JENS FALTA², CARLOS MORALES¹, and •JAN INGO FLEGE¹ — ¹Applied Physics and Semiconductor Spectroscopy, BTU Cottbus-Senftenberg, Cottbus, Germany — ²Institute of Solid State Physics, University of Bremen, Bremen, Germany — ³Department of Interface Science, Fritz-Haber Institute, Berlin, Germany

CeO_x-Cu inverse catalysts have been shown to convert CO₂ into valuable chemicals through catalytic hydrogenation. The catalytic activity may further be enhanced by alloying ceria with trivalent, catalytically active metals, such as Sm, promoting the formation of Ce³⁺ active sites. In this work, the structural and chemical properties of (111)- and (100)- oriented CeO_x islands alloyed with samarium were explored by low-energy electron microscopy and X-ray photoemission electron microscopy. After Sm deposition on the as-grown CeO_x islands, the near-surface region of (100)-oriented CeO_x is reduced after exposure to H₂ at 470 °C, whereas the deeper layers as well as the whole (111)-oriented islands retain the Ce⁴⁺ state. Subsequent reoxidation with O₂ leads to the complete Ce⁴⁺ state recovery, suggesting the healing of oxygen vacancies. Additional annealing at 470 °C induces samarium diffusion into the ceria matrix. Yet, subsequent exposure to H₂ reduces neither the (111)- nor the (100)-oriented CeSmO_x islands, suggesting a quite unexpected stability of this system.

O 52.12 Wed 18:00 P4

Operando studies of CuZn catalysts for methanol synthesis — •DAVID KORDUS^{1,2}, NURIA JIMENEZ DIVINS², JANIS TIMOSHENKO¹, and BEATRIZ ROLDAN CUENYA¹ — ¹Departement of Interface Science, Fritz Haber Institute of the Max Planck Society — ²Departement of Physics, Ruhr University Bochum

Methanol is an essential feedstock for the chemical industry and may be a key component when switching to renewable resources. Industrially methanol pro-

duction uses a ternary Cu/ZnO/Al₂O₃ catalyst. Especially the interaction between Cu and ZnO is critical for a high activity of the catalyst. Multiple model catalysts were synthesized to target different aspects of this system, but particularly the Cu-ZnO interactions. In-situ and operando spectroscopy methods (XAS, XPS, Raman) together with microscopy and measurements of the catalytic performance allow us to follow the chemical and structural changes of the catalysts under reaction conditions. We investigated size-selected Cu and CuZn nanoparticles on multiple support materials (SiO₂, Al₂O₃ and ZnO/Al₂O₃) to

obtain a better insight into particle-support interactions. These studies show that the formation of metallic Zn for CuZn particles on SiO₂ is detrimental for the catalysts activity, as it coincides with a deactivation. On Al₂O₃ in contrast, ZnO is incorporated into the support and forms a spinel structure similar to ZnAl₂O₄. In another catalyst shaped Cu particles are used to create preferential facets on the surface of our catalysts. These unlike surface structures will then lead to different catalytic behavior. Here, a higher activity was observed for cubic particles.

O 53: Poster Wednesday: Spins and Magnetism

Time: Wednesday 18:00–20:00

Location: P4

O 53.1 Wed 18:00 P4

Ferroelectric BaTiO₃ (001): Atomic-level characterization and polarization by combined STM/AFM — •LORENÇ ALBONS CALDENTEY¹, DOMINIK WRANA¹, IGOR SOKOLOVIĆ², AJI ALEXANDER¹, and MARTIN SETVIN¹ — ¹Department of Surface and Plasma Science, Faculty of Mathematics and Physics, Charles University, 180 00 Prague 8, Czech Republic — ²Institute of Applied Physics, TU Wien, 1040 Vienna, Austria

Perovskites attract strong interest thanks to their catalytic properties, efficient electron-hole separation in light harvesting, or the frequent occurrence of ferroelectricity. In this work we show that BaTiO₃ single crystals can be cleaved along the (001) plane to obtain flat surfaces with domains of either BaO or TiO₂ termination. Using low temperature (4K) qPlus nc-AFM we have characterized the surface atomic structure and studied the tip-induced ferroelectric polarization of the material. The impact of ferroelectric poling on adsorbed species is discussed.

O 53.2 Wed 18:00 P4

DFT based analysis of surface reactions of stainless steels through degradation in aqueous media — •VAHID JAMEBOZORGI — Bielefeld University and Bielefeld University of applied science

Stainless steels (SSs) are widely used in industry due to their outstanding mechanical and physical properties plus their durability in corrosive media. The corrosion resistance of SSs is caused by the formation of a thin passive layer which mainly consists of chromium oxides. However, the passive layer makes SSs more vulnerable to localized corrosion including pitting corrosion. Pitting corrosion occurs when the passive layer interacts locally with bond-forming atoms and molecules dissolved in the aqueous media, e.g. halides or hydroxide. However, the process of bond formation, erosion of the passive layer, and consequently the degradation of SSs is still not completely understood. Amongst other parameters, the adsorption energy and work function seem to play a key role in pitting corrosion. The experimental determination of the work function is challenging since the surface texture, crystal defects and impurities can increase or decrease work function value significantly. Here, we show how density-functional theory (DFT) computation techniques can be used to obtain adsorption energies and work function values for different crystallographic orientations on the surfaces of Fe, Cr and Ni. As a result we will provide insight into the degradation mechanisms of SSs surfaces in aqueous media.

O 53.3 Wed 18:00 P4

Thermally-induced magnetic order from glassiness in elemental neodymium — •BENJAMIN VERLHAC¹, LORENA NIGGLI¹, ANDERS BERGMAN², UMUT KAMBER¹, ANDREY BAGROV^{1,2}, DIANA IUŞAN², LARS NORDSTRÖM², MIKHAIL I. KATSNELSON¹, DANIEL WEGNER¹, OLLE ERIKSSON^{2,3}, and ALEXANDER A. KHAJETOORIAN¹ — ¹Institute for Molecules and Materials, Radboud University, Nijmegen, The Netherlands — ²Department of Physics and Astronomy, Uppsala University, Uppsala, Sweden — ³School of Science and Technology, Örebro University, SE-701 82 Örebro, Sweden

In thermodynamic systems, temperature is synonymous with disorder as phase transitions between order to disorder occur when temperature is increased. Re-

cently, the first example of a spin-Q glass was found in elemental neodymium between 30mK and 4K(1). This phase originated from magnetic frustration within the dhcp lattice of neodymium. In this study, we show by means of spin-polarized scanning tunneling microscopy that neodymium undergoes an unusual magnetic transition, where long range multi-Q order emerges from the spin-Q glass phase as temperature is increased from 5 K to 15 K(2). We also developed a new analysis method, which analyzes the experimental data and extracts the phase transition temperature. These findings are supported by atomistic spin dynamics simulations, in which the phase transition is qualitatively explained by destroying spin frustration due to various exchange contributions of the different sublattices.

(1) Kamber, U. et al., *Science* **368** (2020)

(2) Verlhac, B. et al., arXiv:2109.04815

O 53.4 Wed 18:00 P4

Yu-Shiba-Rusinov states of Mn on Pb(110) — •BHARTI MAHENDRU, MARTINA TRAHMS, GAËL REECHT, and KATHARINA J. FRANKE — Fachbereich Physik, Freie Universität Berlin, Arnimallee 14, 14195 Berlin, Germany

Unpaired electron spins exchange coupled to a superconductor give rise to bound states inside the superconducting energy gap and are called Yu-Shiba-Rusinov (YSR) states. Previously, it has been shown that the crystal-field splits singly-occupied d levels of Mn atoms on Pb surfaces, which leads to distinct YSR states inheriting the symmetry of the spin-carrying orbital [1,2].

Here we investigate single atoms and chains of Mn on a Pb(110) surface using scanning tunneling microscopy and spectroscopy. We find different adsorption sites of the individual Mn atoms and chains, which can be distinguished by different YSR states. Some of the Mn sites show a bistability in the presence of the STM tip, while some of the YSR states are also influenced by the tip position.

[1] Michael Ruby, et al., *Phys. Rev. Lett.* **117**, 186801, 2016

[2] Michael Ruby, et al., *Phys. Rev. Lett.* **120**, 156803, 2018

O 53.5 Wed 18:00 P4

Imaging fast magnetization dynamics by Lorentz microscopy with event-based electron detectors — •ALEXANDER SCHRÖDER, CHRISTOPHER RATHJE, XINLAI XING, and SASCHA SCHÄFER — Institute of Physics, University of Oldenburg, Germany

In recent years, ultrafast transmission electron microscopy (UTEM) [1] has successfully enabled the imaging of ultrafast dynamics on the nanoscale by utilizing femtosecond electron pulses in an optical-pump/electron-probe approach. In a potentially more flexible approach, instead of femtosecond electron pulses, a continuous electron beam could be used to map the optically induced dynamics provided sufficiently fast, event-based electron detectors are employed.

Here, we present Lorentz microscopy of nanoscale magnetic dynamics observed with a Timepix3 hybrid pixel electron detector. In particular, we study the distortion of magnetic vortices triggered by femtosecond optical pulses, accessing reversible processes on time scales ranging from nanoseconds to milliseconds.

[1] A. Feist et al., *Ultramicroscopy* **176**, 63 (2017).

O 54: Poster Wednesday: 2D Materials 2

Time: Wednesday 18:00–20:00

Location: P4

O 54.1 Wed 18:00 P4

Mapping angle- and doping-dependent dispersion of bending graphene — •ZHIHAO JIANG¹, PAULINA MAJCHRZAK¹, BJARKE JESSEN², MAËLLE KAPFER², DEEPNARAYAN BISWAS¹, JOSE AVILA³, PAVEL DUDIN³, CORY DEAN², and SØREN ULSTRUP¹ — ¹Aarhus University — ²Columbia University — ³Synchrotron SOLEIL

The possibility to systematically engineer the interlayer rotation angle (θ) between two-dimensional (2D) materials stacked in heterostructures offers an in-

triguing means to tailor superlattices, electronic band structures and interactions. Here, we set out to perform a proof-of-principle nanoARPES experiment demonstrating the ability to continuously twist a graphene flake stacked on hexagonal boron nitride by tuning θ using a nano-rotation device engaged by the tip of an atomic force microscope (AFM). The overarching objective is thereby to capture the evolution of the θ -dependent electronic dispersion of graphene. Ultimately, these experiments are expected to pave the way for band structure measurements of systematically twisted heterostructures composed of bilayer graphene and monolayer dichalcogenides.

O 54.2 Wed 18:00 P4

Growth and characterization of WSe₂ on epitaxial graphene on SiC(0001) — •ADRIAN SCHÜTZE, PHILIP SCHÄDLICH, and THOMAS SEYLLER — Institute of Physics, TU Chemnitz, Chemnitz, Germany

2D materials such as, for example, graphene, hexagonal boron nitride or transition metal dichalcogenides have recently received much interest as building blocks for electronic devices. For a successful integration of these materials, scalable growth methods are essential. In this work we investigate the growth of WSe₂ by metal organic molecular beam epitaxy (MOMBE) [1] on epitaxial graphene on SiC(0001). In that process W(CO)₆ is used as a precursor in conjunction with selenium vapor produced by decomposition of SnSe₂ in a thermal evaporator. Using MOMBE we were able to grow ultra-thin films of WSe₂ on epitaxial graphene which were characterized by a combination of X-ray photoelectron spectroscopy (XPS), angle resolved photoemission spectroscopy (ARPES), low-energy electron diffraction and microscopy (LEED, LEEM) and atomic force microscopy (AFM). The films were observed to consist of triangular domains. We discuss the influence of the growth parameters such as the substrate temperature on the structural and electronic properties of the layers.

[1] S. Tiefenbacher et al., Surf. Sci. 318 (1994) L1161

O 54.3 Wed 18:00 P4

Vanadyl phthalocyanine: study of the formation of a characteristic molecular spin pattern on a diamagnetic template — •CORINA URDANIZ, KYUNGJU NOH, LUCIANO COLAZZO, JAEHYUN LEE, ANDREAS HEINRICH, CHRISTOPH WOLF, FABIO DONATI, and YUJEONG BAE — Center for Quantum Nanoscience (QNS), IBS, Ewha Womans University, Seoul, Republic of Korea

Achieving quantum coherent control of spins on surfaces at the atomic scale is the goal for quantum coherent nanoscience. A good surface spin system requires two components: a localized spin and a buffer layer to isolate that spin from the metallic substrate. The use of magnetic molecules as hosts for spin qubits is a promising pathway towards quantum information processing.

In this work, we used Vanadyl phthalocyanine (VOPc), a well-known spin = 1/2 molecule with long coherence times up to one microsecond in its crystalline form, and the non-magnetic Titanyl phthalocyanine (TiOPc) as a buffer layer from the metal. We found that TiOPc is an effective buffer layer, preserving vacuum-like electronic structure of VOPc. We present compelling arguments for using TiOPc as self-assembling templates with long-range order for adsorbed VOPc molecules. Our results suggest that the TiOPc/VOPc system is a potential candidate for long-lived molecular spin states on surfaces for the study of quantum information processing.

O 54.4 Wed 18:00 P4

Competing Processes as Quality Limitation: New Insights into Microscopic Growth Mechanism of hexagonal Boron Nitride on Ir(111) — •MARKO KRIEGEL¹, KARIM OMAMBAC¹, MARIN PETROVIC², BIRK FINKE¹, FRANK MEYER ZU HERINGDORF^{1,3}, and MICHAEL HORN-VON HOEGEN¹ — ¹Faculty of Physics, University of Duisburg-Essen, D-47057 Duisburg, Germany — ²Center of Excellence for Advanced Materials and Sensing Devices, Institute of Physics, HR-10000 Zagreb, Croatia — ³Interdisciplinary Center for Analytics on the Nanoscale (ICAN), D-47057 Duisburg, Germany

Despite the tremendous research effort targeting industrial growth of two-dimensional hexagonal boron nitride (hBN), especially on transition metal surfaces, until today no superior growth recipe was developed, promising large domain sizes, homogeneous lattice constants and a matching orientation of layer and substrate. Here we study single layer hBN grown on Ir(111) via conventional chemical vapor deposition (CVD) using borazine as precursor. We found two competing processes governing the density of hBN domains on a microscopic scale: Kinetic limitations at low T and the disintegration of B₃N₃ rings as well as the growth layer at high T. The interplay of both processes sets a fundamental limit to the achievable quality in this and other 2D material systems. Our study combines data from high-resolution reciprocal space mapping, using Spot Profile Analyzing Low Energy Electron Diffraction (SPA-LEED), allowing us to determine the complete distribution of domain orientations, and Low Energy Electron Microscopy (LEEM), for the measure of domain densities.

O 54.5 Wed 18:00 P4

Tuning MoS₂ doping by switching its support material — •MARCO BIANCHI¹, DANIEL LIZZIT⁴, PAOLO LACOVIG², CHARLOTTE SANDERS³, DAVIDE CURCIO¹, EZEQUIEL TOSI², MONIKA T. SCHIED², JILL MIWA¹, SILVANO LIZZIT², and PHILIP HOFMANN¹ — ¹Dep. of Physics and Astronomy, ASTRID2, iNANO, Aarhus University, DK. — ²Elettra Sincrotrone Trieste S.C.p.A., Trieste, IT — ³Artemis Program, UK Central Laser Facility, Harwell, STFC, UK — ⁴DPIA - University of Udine, IT

Tuning the electronic properties of a 2D crystal by the interaction with its support is the key to design well-controlled nanoelectronic devices based on transition metal dichalcogenides (TMDCs). In particular, the establishing of a low resistance between a metallic contact and the TMDC has been challenging and different strategies for this have been introduced. It was suggested that a low Schottky barrier could be achieved not only by choosing contact materials with

the suitable work function but also by introducing interface defects that can contribute independent of the metal contact work function.

Here we present a combined ARPES, STM, LEED and XPS study of MoS₂ grown on Au(111) using well established methods. After intercalation of Bi, which is semimetallic, and its further treatment we observe a doping consistent with what was inferred from recent transport measurements. The results shown here sheds light on a potential way for tuning the effects of contacts of a 2D layer and their influence on the TMDC electronic structure.

O 54.6 Wed 18:00 P4

Subnanoscale Engineering of 2D Magnetism in van der Waals Heterostructures — •KEDA JIN^{1,2}, JOSE MARTINEZ-CASTRO^{1,2}, STEFAN F. TAUTZ^{1,3}, and MARKUS TERNES^{1,2} — ¹Institute of Physics II B, RWTH Aachen University, 52074 Aachen, Germany — ²Peter Grünberg Institute (PGI-3), Forschungszentrum Jülich and Jülich-Aachen Research Alliance (JARA), Fundamentals of Future Information Technology, 52425 Jülich, Germany — ³Institute of Physics IV A, RWTH Aachen University, 52074 Aachen, Germany

The dry transferred method paves a way to investigate exotic properties and emerging new phenomena in van der Waals heterostructures. Polycarbonate (PC) is commonly used as a polymer for the dry transfer of 2D materials. A limitation of PC is the contamination of chemical residues on the surface and the difficulty to fabricate complex heterostructures. Here, we show the study of different polymers, including polyvinyl chloride (PVC) and nitrocellulose for an effective and clean way to assemble 2D heterostructures. In addition, based on our previous method of studying encapsulated air-sensitive 2D materials (Nano Lett. 18, 6696 (2018)), we show our current development in a new technique to study air-sensitive materials in heterostructures compatible with ultra-high vacuum: in-situ de-encapsulation. This technique aims to provide the required cleanliness of mechanically assembled air-sensitive van der Waals heterostructures for their study by scanning tunneling microscopy at ultra-high vacuum and low temperature.

O 54.7 Wed 18:00 P4

Growth and characterization of monolayer MnSe₂ on Au(111) — •SEBASTIEN ELIE HADJADI¹, EVANGELOS GOLIAS², JACK HAYES², MARCEL WALTER¹, CHRISTIAN LOTZE¹, SANGEETA THAKUR¹, IVAR KUMBERG¹, ISMET GELEN¹, JORGE TORRES¹, and WOLFGANG KUCH¹ — ¹Institut für Experimentalphysik, Freie Universität Berlin, Arnimallee 14, 14195 Berlin, Germany — ²MAX IV Laboratory, Lund University, Fotongatan 2, Lund, Sweden

During the last couple of years, there has been a rising interest in novel two-dimensional magnetic materials. Most recently, several groups have shown that magnetic order in two-dimensional materials can be stable. Among them, MnSe₂ is interesting, since it has shown magnetic properties at room temperature [1], making it an ideal candidate for applications. However, magnetic order so far has been reported for MnSe₂ grown on GaSe or SnSe₂, and the role of the interface in the stabilization of magnetic order is not yet clear. We use molecular beam epitaxy to co-deposit Se and Mn on Au(111) to ascertain if the magnetic ordering of monolayer MnSe₂ is an intrinsic effect of the material or an interface-induced phenomenon. We examine the films chemically by X-ray photoelectron spectroscopy (XPS) and X-ray absorption spectroscopy (XAS) as well as structurally by scanning tunneling microscopy (STM) and low-energy electron diffraction (LEED). The latter shows a near - 3 × 3 pattern. The XPS measurements show chemical shifts in the Mn and Se binding energies for the MnSe₂ sample in comparison to pure Mn and Se that confirm that the Mn has bonded to Se. [1] D. J. O'Hara et al., Nano Letters 18, 3125 (2018).

O 54.8 Wed 18:00 P4

Towards Shot-Noise Spectroscopy of Majorana Modes in 2D Systems — •JAN CUPERUS, FLORIS KOUIJ, and INGMAR SWART — Condensed Matter & Interfaces, Utrecht University, Utrecht, The Netherlands

The quasiparticles known as Majorana zero modes (MZMs) are particles that have the peculiar properties to be their own antiparticle and to obey non-Abelian statistics. Because of the latter, MZMs are predicted to be the building blocks of topological quantum computing. Over the past years, many signatures of what could be MZMs have been reported. Examples are the end modes of 1D atomic line defects in ML FeSe [1], or the edge modes found on CrBr₃ island grown on NbSe₂ [2]. Conclusive observations are however, still to be made. One reason for this is the similarity of MZMs to other (close-to-)zero-energy states, e.g. Yu-Shiba-Rusinov states or Andreev bound states. Scanning tunnelling microscopy (STM) has already shown to be a key tool in the field of condensed matter physics because of its extreme spatial resolution and spectroscopic abilities. Via a new STM-based tool, namely shot-noise spectroscopy, we aim to provide a new point of view onto the matter of MZMs.

References: [1]Chen et al., Nat. Phys., 16, 536-540 (2018) [2]Kezilebieke et al., Nature, 588, 424-428 (2020)

O 54.9 Wed 18:00 P4

The tellurization of Cu(111): From incorporated Te atoms via 1D-like surface reconstructions to closed films — •ANDREAS RAABGRUND, TILMAN KISSLINGER, MAXIMILIAN AMMON, LUTZ HAMMER, and M. ALEXANDER SCHNEIDER — Friedrich-Alexander-Universität Erlangen-Nürnberg, 91058 Erlangen, Germany

We investigated the tellurization of Cu(111) from low Te coverages up to thick films both structurally and electronically by STM, STS, LEED-IV structural analysis, and DFT. For $\Theta < 0.14$ ML Te forms a substitutional surface alloy with short-range ordered patches of a $(\sqrt{7} \times \sqrt{7})R19.1^\circ$ structure. Increasing the Te coverage leads to coexisting islands of a $(3 \times \sqrt{3})_{\text{rect}}$ superstructure which is well-ordered and fully developed at $\Theta = 0.33$ ML [1]. In the range $0.33 \text{ ML} < \Theta < 0.40 \text{ ML}$, the $(3 \times \sqrt{3})_{\text{rect}}$ structure coexists next to a well-ordered $(5 \times \sqrt{3})_{\text{rect}}$ phase which is completely developed at $\Theta = 0.40$ ML [2]. Our LEED-IV analyses reveal arrangements of Cu_2Te_2 chains, whereby for the $(5 \times \sqrt{3})_{\text{rect}}$ phase a substantial reorganization of the surface into troughs allows to incorporate more Te. STS finds an unoccupied chain state, that has lower energy on the $(3 \times \sqrt{3})_{\text{rect}}$ which we interpret as an indication of delocalization with decreasing interchain distance. By further tellurization beyond $\Theta = 1.1$ ML closed Cu_{2-x}Te films develop. For $\Theta > 4$ ML, a phase transition takes place below 300 K that results in a wrinkled appearance at low temperatures. On the surface two different reconstructions with distinct electronic fingerprint occur side-by-side.

[1] T. Kißlinger et al., Phys. Rev. B **102**, 155422 (2020)[2] T. Kißlinger et al., Phys. Rev. B **104**, 155426 (2021)

O 54.10 Wed 18:00 P4

Fabrication of nanostructured van der Waals heterostructures — •KHAIRI F. ELYAS¹, JOHANNA RICHTER³, KIRILL BOLOTIN³, HANNAH C. NERL², and KATJA HÖFLICH¹ — ¹Ferdinand Braun Institut gGmbH, Berlin, Germany — ²Humboldt Universität zu Berlin, Institute of Physics, Berlin, Germany — ³Freie Universität Berlin, Institute of Experimental Physics, Berlin, Germany

Two-dimensional (2D) materials can exhibit a significantly enhanced light-matter interaction making them interesting for highly-confined and low-loss light transport. When combining different 2D materials, the different polaritonic modes may hybridize to combine the strong localization of plasmonic excitations with the long propagation distances of phonon modes. Here we report on the fabrication of heterostructures of the (semi)metallic graphene and the wide-bandgap material hexagonal boron (hBN) nitride. The dry-release transfer of graphene and hBN makes use of polydimethylsiloxane (PDMS) and poly(propylene) carbonate (PPC) films. Due to the strong adhesion between PPC and 2D materials at room temperature, we show that single-layer to few-layer graphene as well as few-layer hBN can be produced on a spin coated PPC film/SiO₂/Si substrates by mechanical exfoliation. Using He ion beam patterning we further modify the geometry of the heterostructures on the nanoscale with the specific aim to tune hybrid polaritonic modes. The optical properties of the fabricated heterostructures are then mapped using monochromated low-loss scanning transmission electron microscopy (STEM) electron energy-loss spectroscopy (EELS) and outcomes compared to optical methods.

O 54.11 Wed 18:00 P4

Interlayer charge transport anomalies in 1T-TaS₂ and 2H-NbS₂ — EDOARDO MARTINO, LÁSZLÓ FORRÓ, and •KONSTANTIN SEMENIUK — Institute of Physics, École Polytechnique Fédérale de Lausanne (EPFL), CH-1015 Lausanne, Switzerland

Layered van der Waals materials, such as transition metal dichalcogenides, have emerged as promising platforms for realising functional materials for practical applications. Tuning interlayer coupling in these systems via twist, intercalation, exfoliation, etc. opens up a vast parameter space for inducing exploitable properties. Probing of the out-of-plane conduction is a useful tool for gauging the subtle interactions between the atomic planes, particularly in bulk crystals of TMDs.

We present comprehensive studies of charge transport anisotropies of bulk 1T-TaS₂ and 2H-NbS₂. The samples were tailored using focused ion beam in order to ensure homogeneous current flow across the principal crystallographic directions. We find that resistivity anisotropy of 1T-TaS₂ is, paradoxically, of the order of unity, with the out-of-plane conduction becoming more preferred at lower temperatures due to a formation of c-axis-oriented quasi-one-dimensional orbital chains. In 2H-NbS₂, we observe a pronounced upturn of the out-of-plane

resistivity upon cooling. We attribute the anomaly to a unidirectional Kondo scattering, caused by inherent inclusions of 1T-NbS₂ layers, which host a lattice of singly occupied orbitals.

[1] E. Martino et al., npj 2D Mater. Appl., **4**, 7 (2020).[1] E. Martino et al., npj 2D Mater. Appl., **5**, 86 (2021).

O 54.12 Wed 18:00 P4

STM studies of graphene encapsulated Fe₃GeTe₂ — •TOBIAS WICHMANN^{1,2,3}, FELIX LÜPKE^{1,2}, and F. STEFAN TAUTZ^{1,2,3} — ¹Peter-Grünberg-Institut (PGI-3), Forschungszentrum Jülich, Germany — ²Jülich Aachen Research Alliance (JARA) - Fundamentals of Future Information Technology, Germany — ³Institut für Experimentalphysik IV, RWTH Aachen, Germany

Fe₃GeTe₂ is a metallic 2D ferromagnet with a Curie Temperature of 130K, in which Kondo effect and skyrmions have been observed. These properties make it a promising candidate as a source of magnetic proximity effect in van der Waals heterostructures.

To examine its potential use in in van der Waals heterostructures we investigated the influence on adjacent layers of 2D materials through encapsulation with graphene. The resulting structure was characterized in a low temperature STM.

O 54.13 Wed 18:00 P4

Fabrication of nanostructured van der Waals heterostructures — •KHAIRI F. ELYAS¹, JOHANNA RICHTER³, KIRILL BOLOTIN³, HANNAH C. NERL², and KATJA HÖFLICH¹ — ¹Ferdinand Braun Institut gGmbH, Berlin, Germany — ²Humboldt Universität zu Berlin, Institute of Physics, Berlin, Germany — ³Freie Universität Berlin, Institute of Experimental Physics, Berlin, Germany

Two-dimensional (2D) materials can exhibit a significantly enhanced light-matter interaction making them interesting for highly-confined and low-loss light transport. When combining different 2D materials, the different polaritonic modes may hybridize to combine the strong localization of plasmonic excitations with the long propagation distances of phonon modes. Here we report on the fabrication of heterostructures of the singlecrystalline gold flakes or graphene and the wide-bandgap material hexagonal boron (hBN) nitride. Polydimethylsiloxane (PDMS) and poly(propylene) carbonate (PPC) films were used for the dry transfer of gold and hBN due to the strong adhesion between PPC and 2D materials at room temperature. Using this method, single-layer to few-layer hBN were successfully transferred. Using He ion beam patterning we further modify the geometry of the heterostructures on the nanoscale with the specific aim to tune hybrid polaritonic modes. The optical properties of the fabricated heterostructures are then mapped using monochromated low-loss scanning transmission electron microscopy (STEM) electron energy-loss spectroscopy (EELS) and outcomes compared to optical methods.

O 54.14 Wed 18:00 P4

Carbon Embedding of Pt Cluster Superlattices Templated by Hexagonal Boron Nitride on Ir(111) — •TOBIAS HARTL¹, MORITZ WILL¹, PANTELIS BAMPOULIS^{1,2}, VIRGINIA BOIX DE LA CRUZ³, PAOLO LACOVIG⁴, VEDRAN VONK⁵, SIMON CHUNG⁵, ANDREAS STIERLE⁵, JAN KNUDSEN³, SILVANO LIZZIT⁴, and THOMAS MICHELY¹ — ¹Universität zu Köln — ²University of Twente — ³MAX IV Laboratory and Division of Synchrotron Radiation Research — ⁴Eletra-Sincrotrone Trieste S.C.p.A — ⁵DESY Hamburg

With the goal to develop the fabrication of a new type of Pt-nanoparticle carbon support electrocatalyst, we investigate the carbon embedding of Pt cluster superlattices grown on the moiré of a monolayer of h-BN on Ir(111). Using STM and XPS we find that carbon embedding is conformal and does not deteriorate the excellent order of the clusters. The thermal and mechanical stability of the embedded clusters is greatly enhanced by the C forming a strong binding to the Pt clusters. Sintering as well as single cluster pick-up by the STM tip, are both suppressed. (Hartl, T. et al., J. Phys. Chem. C, 2021)

The only cluster decay path left takes place at an elevated temperature above 850 K. Cluster material penetrates through the h-BN sheet, whereby it becomes bound to the underlying metal. There are indications that while the a-C matrix and the Pt clusters bind strongly to each other, upon annealing both weaken their binding to h-BN.

We discuss how the binding between the membrane and the substrate can be weakened, such that it is possible to be split-off via a combination of hydrogen bubbling and dry transfer approaches.

O 55: Poster Wednesday: Organic Molecules at Surfaces 2

Time: Wednesday 18:00–20:00

Location: P4

O 55.1 Wed 18:00 P4

Self-assembly and debromination of a functionalized borazine on Ag(111) — •BIRCE SENA TÖMEKE¹, MARC G. CUXART¹, MARTINA CROSTA², MARCO FRANCESCHINI², DANIELE POLETTI², DAVIDE BONIFAZI², and WILLI

AUWÄRTER¹ — ¹Physics Department E20, Technical University of Munich, Germany — ²Institute of Organic Chemistry, University of Vienna, Austria

On-surface synthesis is a promising route towards the generation of doped graphene nanoarchitectures with tunable electronic properties [1]. To fabricate

atomically precise hybrid BNC materials, distinct precursors incorporating BN units can be used [2]. In this study, we employed a precursor with a borazine core and Br and OH functionalization. We report on a low-temperature scanning tunneling microscopy/spectroscopy and X-ray photoelectron spectroscopy characterization of well-ordered phases of this precursor on Ag(111). At low temperatures, the molecules adsorb intact. At moderate temperatures, debromination is activated and the self-assembly of a chiral kagomé lattice coexisting with a hexagonal packing is observed. At elevated temperatures, completion of cyclodehydrogenation leads to full planarization of the molecules, followed by covalent intermolecular coupling, thereby forming random BNC-based networks. We further investigated the electronic structure of the kagomé lattice on the single molecule level. Our findings constitute a step towards exploiting the structural and electronic properties of BNC architectures.

[1] R. Pawlak et al., *Angew. Chem. Int. Ed.* 2021, 60, 8370-8375

[2] C. Sánchez-Sánchez et al., *ACS Nano*. 2015, 9, 9228-9235

O 55.2 Wed 18:00 P4

The investigation of self-assembly molecule on metal substrate — •YONG-HE PAN and GERMAR HOFFMANN — Department of Physics, National Tsing Hua University

Field-effect transistors (FETs) made out of organic materials are lighter, mechanically more flexible, have lower costs and have higher field-effect mobility. For picene-(C₁₄H₂₉)₂ the highest field-effect mobility in all FETs was recorded. Here, phenacene-(C₁₄H₂₉)₂ is deposited on Au(111) by thermal evaporation and is investigated by STM and Scanning Tunneling Spectroscopy (STS) at 70 K under UHV conditions. The self-assembly molecule forms a rhombohedral unit cell with a two molecular basis, and the alkyl chain, flexible up to 15 degrees, is nearly parallel with the nearby molecules. Scanning close to the bandgap region of the phenacene(C₁₄H₂₉)₂ leads to imaging of the LUMO-state, which also shows the pronounced electronic state on the phenacene core and energetically broad state on the alkyl chain.

O 55.3 Wed 18:00 P4

adsorption structure and mechanical properties of single nonahelicene molecules on Ag(110) — •MAX HALBAUER^{1,2}, AKITOSHI SHIOTARI¹, TAKASHI KUMAGAI³, KYOKO NOZAKI², and MARTIN WOLF¹ — ¹Department of Physical Chemistry, Fritz-Haber-Institute of the Max-Planck-Society, Faradayweg 4-6, 14195 Berlin, Germany — ²Department of Chemistry and Biotechnology, School of Engineering, The University of Tokyo, 7-3-1 Hongo, Bunkyo-ku, 113-8656 Tokyo, Japan — ³Center for Mesoscopic Sciences, Institute for Molecular Science, 38 Nishigo-Naka, Myodaiji, 444-8585 Okazaki, Japan

Helicenes are a class of compounds that has received great attention due to their chiroptical properties, while the single-molecule mechanical behavior has often been overlooked. Scanning tunneling microscopy (STM) and atomic force microscopy (AFM) measurements of nonahelicene ([9]H) molecules on Ag(110) were performed in order to address this issue. The adsorption structure of isolated and aggregated [9]H molecules on the surface is revealed by high-resolution imaging. Interactions of the molecule with a probe tip are quantified by force curve measurements and a comparison with co-adsorbed coronene gives insights into the impact of the helical backbone on the mechanical properties.

O 55.4 Wed 18:00 P4

Changes in the coupling of a single-molecule magnetic moment to a Cooper pair condensate by the sequential removal of molecular moieties — •STEFAN SCHULTE¹, NICOLAS NÉEL¹, KRISZTIAN PALOTAS², and JÖRG KRÖGER¹ — ¹Institut für Physik, Technische Universität Ilmenau, Ilmenau, Germany — ²Institute for Solid State Physics and Optics, Wigner Research Center for Physics, Budapest, Hungary

Using the tip of a STM chemical reactions are induced in organic 5, 10, 15, 20-tetrakis(4-bromophenyl)-porphyrin-cobalt molecules adsorbed on superconducting Pb(111). Two chemical reactions, the dehalogenation and dephenylation of the molecules are presented. Yu-Shiba-Rusinov bound states occur in the superconductor energy gap only after the entire dephenylation of the molecule. The presence of the intragap resonances is related to an unoccupied molecular orbital that is confined to the atomic magnetic center (Co) of the porphyrin. From the energy position and spectral weight of these intragap resonances, a weak interaction between the molecular magnetic moment and the Cooper pair condensate is inferred. The electron-hole asymmetry of the bound states exhibits a spatial oscillation with a wavelength that evidences the exchange coupling of the molecular magnetic moment to the sp-sheet of the Fermi surface. The very low binding energy of the Yu-Shiba-Rusinov levels is consistent with the observed absence of the Kondo effect. Funding by the DFG through KR 2912/10-1 and KR 2912/10-3 is acknowledged.

O 55.5 Wed 18:00 P4

Pentacene on prototypical antiferromagnets: A photoemission study — •VALENTIN MISCHKE, DAVID JANAS, GIOVANNI ZAMBORLINI, JONAH E. NITSCHKE, and MIRKO CINCHETTI — Department of Physics, TU Dortmund University, Otto-Hahn-Straße 4, 44227 Dortmund, Germany

In the last years, so-called molecular spinterfaces have been intensively studied because of the novel spin properties raising from the molecule-metal hybridization [1]. Recently, antiferromagnets have been considered as an alternative to their ferromagnetic counterparts for the engineering of spinterfaces with novel spin properties. Here, we present the preliminary characterization of a single layer of pentacene atop two prototypical antiferromagnets, namely nickel oxide NiO(111) and iron oxide FeO(100). Both thin films have been grown in-situ, under UHV conditions, by depositing Ni and Fe in a O₂ background atmosphere onto Au(111) and oxygen-passivate Fe(100), respectively. The resulting interfaces have been characterized with low energy electron diffraction and momentum microscopy. In addition, photoemission tomography was employed to determine the energy level alignment of the molecular orbitals at the interface.

[1] Cinchetti, Dediu, Hueso, *Nature Materials* 16, 507 (2017)

O 55.6 Wed 18:00 P4

Systematically mapping the distance-dependent tip-sample interaction for the PTCDA/Ag(111) system — •TIM DIERKER and PHILIPP RAHE — Fachbereich Physik, Universität Osnabrück, BarbarasträÙe 7, 49076 Osnabrück, Germany Scanning probe microscopy (SPM) has been continually improved by establishing a number of controlled tip functionalizations [1]. In particular, the attachment of a single 3,4,9,10-perylene-tetracarboxylic-dianhydride (PTCDA) molecule to the apex of a metallic tip enables mapping of the electrostatic potential near sample surfaces by so called scanning quantum dot microscopy [2,3]. In order to reliably apply this technique, the expedient pick-up of a single molecule is required [4]. Here, the tip-molecule interaction between a metallic tip and surface-adsorbed molecules is investigated by means of systematic scanning tunneling (STM) and atomic force (AFM) microscopy measurements. In particular the vertical dependencies of the STM tunneling current and the AFM frequency shift are mapped along different axes of single PTCDA molecules embedded in the molecular film on Ag(111). Fingerprints for the dynamic behavior of the molecules are clearly revealed and guide the vertical manipulation for molecular pick-up.

[1] L. Gross, *Nat. Chem.* 3, 273 (2011)

[2] C. Wagner et al., *PRL* 115, 026101 (2015)

[3] M. F. B. Green et al., *JJAP* 55, 08NA04 (2016)

[4] M. F. B. Green et al., *Beilstein J. Nanotech.* 5, 1926 (2014)

O 55.7 Wed 18:00 P4

Photoemission and Raman Spectroscopic Studies of n-GaAs(100) Surface Passivation with Thioglycolic Acid — •ALEXANDER EHM, OLEKSANDR SELYSHCHEV, and DIETRICH R. T. ZAHN — Semiconductor Physics, TU Chemnitz, Chemnitz D-09107, Germany

Gallium arsenide is one of the most investigated inorganic semiconductors and used in a vast variety of applications and prospective for new high-performance devices. A challenge in constructing such devices is a surface of native oxides causing a high surface density of states, which leads to the mid-gap pinning of the surface Fermi level, band bending, and the formation of a surface depletion layer. Sulphur passivation yields a significant reduction of the depletion layer and related effects but requires several treatment steps [1].

We report a new simple approach utilizing thioglycolic acid (TGA) to provide a one-step effective removal of surface oxides and protection from reoxidation compared to etching with inorganic acids. This effect is confirmed by X-ray photoemission spectroscopy and the reduction of the depletion layer is confirmed by Raman spectroscopy results. n-GaAs(100)/poly(3,4-ethylenedioxythiophene) polystyrene sulfonate (PEDOT:PSS) solar cells show improved performance for such passivated n-GaAs(100) surfaces.

[1] V. N. Bessolov, M.V. Lebedev, D. R. T. Zahn: *J. Appl. Phys.* 82 (5) (1997)

O 55.8 Wed 18:00 P4

Vibrational quanta of single melamine on Cu(100) — •REBECCA CIZEK, NICOLAS NÉEL, and JÖRG KRÖGER — TU Ilmenau

Melamine adopts an up-standing adsorption geometry on Cu(100) and can be tautomerized by the local injection of electron from the tip of a scanning tunneling microscope [1]. Here, we compare inelastic electron tunneling spectroscopy (IETS) of intact and tautomerized melamine. Two low-energy vibrational quanta are observed for both molecules. The tautomer exhibits an energy shift and enhancement of one of the excitations. These findings are moreover complemented by IETS and tautomerization of the deuterated molecule.

[1] R.-P. Wang et al., *J. Phys. Chem. Lett.* 12, 1961 (2021)

O 55.9 Wed 18:00 P4

Photoemission orbital tomography of NiTPP molecules deposited on the passivated Fe(100)-p(1x1)O surface — •MICHAEL GUTNIKOV¹, DAVID JANAS¹, JONAH NITSCHKE¹, MIRA ARNDT¹, VITALIY FEYER², GIOVANNI ZAMBORLINI¹, and MIRKO CINCHETTI¹ — ¹Department of Physics, TU Dortmund University, Otto-Hahn-StraÙe 4, 44227 Dortmund, Germany — ²Peter Grünberg Institut (PGI-6), Forschungszentrum Jülich, Leo-Brandt-StraÙe, 52425 Jülich, Germany Recently, it was shown that a single layer of oxygen is sufficient to decouple nickel porphyrins from a ferromagnetic surface, thus, preserving most of the electronic

features of the pristine molecules [1]. However, distortions of the molecular structure, e.g. upward-bent phenyl-rings, can make the interpretation of surface imaging techniques like STM extremely challenging.

Additional information can be gained by photoemission tomography (PT), which combines angle-resolved photoelectron spectroscopy (ARPES) with ab-initio calculations of the gas phase molecules to interpret the orbital arrangement of thin molecular layers.

This work provides a characterization of NiTPP molecules on an oxygen passivated Fe(100)-p(1x1)O surface using PT, focusing not only on the energy level alignment but also on their azimuthal orientation with respect to the substrate. [1] G. Albani et al. *Micromachines* **12**, 191 (2021)

O 55.10 Wed 18:00 P4

Surface Chemical Bond of Alternant vs. Non-Alternant Aromatic Isomers — •FLORIAN MÜNSTER¹, LUKAS RUPPENTHAL¹, LEONARD NEUHAUS¹, JAN HERRITSCH¹, JON HENRICK BOTH¹, PENGCAI LIU², XING-YU CHEN², JIAWEN CAO², XIAO-YE WANG², and J. MICHAEL GOTTFRIED¹ — ¹Fachbereich Chemie, Philipps-Universität Marburg, Germany — ²College of Chemistry, Nankai University, Tianjin, China

The different effects of the topology of pyrene and cyclohepta[*fg*]acenaphthylene (acepleiadylene) on the occupied and the unoccupied electronic states as well as on the desorption process from the Cu(111) surface are studied using PES, NEX-AFS and TPD. Both molecules are aromatic but differ in their topology. While pyrene has an alternating structure, its constitutional isomer acepleiadylene has a non-alternating one. With TPD, we showed that the desorption of acepleiadylene begins at about 340 K, 40 K higher than for pyrene, indicating a stronger bond to the Cu(111) surface. Using the modified leading edge analysis we find a desorption energy of 152 kJ/mol for acepleiadylene compared to 108 kJ/mol for pyrene, each at monolayer coverage. Furthermore, combining PES and NEX-AFS, we were able to assess the energy needed in the excitation process of electrons originating from occupied valance orbitals into unoccupied ones. Here we find a 0.5 eV smaller energy difference for the non-alternating species in comparison to the alternating species.

O 55.11 Wed 18:00 P4

New Photon Scanning Tunnelling Microscope for studying electrically driven single photon emitters in the GHz range — •ANDREAS REUTTER^{1,2}, MIKE STUMMVOLL^{1,2}, NEDA NOEI¹, MARKUS ETZKORN^{1,2}, and UTA SCHLICKUM^{1,2} — ¹Institut für Angewandte Physik, Technische Universität Braunschweig, Mendelssohnstraße 2, 38106 Braunschweig — ²Laboratory for Emerging Nanometrology, Langer Kamp 6a/b, 38106 Braunschweig

Single atoms and molecules have always been an interesting research area. An important tool for investigating such is scanning tunnelling microscopy (STM) which has become a widely used method to characterize not only the surface density states and vibrational excitations but also electrical excitations and recombination processes of individual atoms and molecules by STM-induced luminescence (STML).

We would like to present a state-of-the-art, self-build, low-temperature, ultra-high vacuum STM with the possibility for STML measurements and for the time-resolved probing of electrically driven single photon emitters with a band width of up to around 20 GHz. This allows for instance the investigation of charge transfer in molecules below the nanosecond range and further insight into its exciton decay.

O 55.12 Wed 18:00 P4

Anchoring *p*-terphenyl-based thiols to top-layer sulphur defects on MoS₂/Au(111) — J. RIKA SIMON¹, DMITRII MAKSIMOV², •JUAN PABLO GUERRERO FELIPE¹, PAUL WIECHERS¹, CHRISTIAN LOTZE¹, ANA M. VALENCIA^{3,4}, CATERINA COCCHI^{3,4}, BJÖRN KOBIN⁴, STEFAN HECHT⁴, MARIANA ROSSI², and KATHARINA J. FRANKE¹ — ¹Freie Universität Berlin, Germany — ²MPI for the Structure and Dynamics of Matter, Hamburg, Germany — ³Carl von Ossietzky Universität Oldenburg, Germany — ⁴Humboldt-Universität zu Berlin, Germany Systems consisting of transition metal dichalcogenides (TMDCs) and organic molecules is a field gathering much interest in recent years. By using a scanning tunneling microscope (STM), it is possible to explore these systems in detail, where the TMDC layer works as a decoupling layer between the adsorbate and metal substrate. In our experiments, we investigate a monolayer of MoS₂ on Au(111) where interesting results occur once a sulphur defect on the top-layer is created. It gives rise to a localized resonance around the Fermi energy, not present in pristine MoS₂. Here we show experimental and theoretical comparisons where the thiol-based molecule CF₃-3P-SH (4⁺-(trifluoromethyl)-[1,1':4,1''-terphenyl]-4-thiol) is anchored to a sulphur top-layer defect, creating a chemical bond between the molecule and MoS₂. We observe a characteristic Kondo resonance due to the interaction between molecule and substrate. Additionally, we have mapped out the spatial distribution of the electronic states as well as explored the vibronic states of the molecule.

O 55.13 Wed 18:00 P4

On-Surface Transmetalation of a Lead-Porphyrin on the Cu(111) surface — •JAN HERRITSCH, STEFAN R. KACHEL, QITANG FAN, MARK HUTTER, LUKAS J. HEUPLICK, FLORIAN MÜNSTER, and J. MICHAEL GOTTFRIED — Philipps-Universität Marburg

Starting from porphyrin complexes, highly ordered nanostructures can be assembled on surfaces in which reactive metal centers are firmly anchored in a defined environment. Such structures have enormous potential in various areas of modern technology. A reaction in which there is an exchange of the central atom by another element leads to a drastic change in the properties of the functionalized surface. Here, we report on a thermally induced Pb/Cu metal exchange of lead(II)-tetraphenylporphyrin (Pb(TPP)) on the Cu(111) surface. Using temperature-dependent XPS, we were able to track this exchange reaction and the accompanying change of the Pb oxidation state by probing the Pb 4f level. The reaction starts already below 380 K and is completed at 600 K. In parallel, partial desorption of a monolayer occurs above 430 K. In a temperature-programmed reaction experiment (TPR), the desorbing species are unambiguously identified as the product, Cu(TPP), of the metal exchange by mass spectrometry. By STM, the adsorbate structure of Pb(TPP) on Cu(111) were revealed and individual free Pb atoms, which are formed in the course of the Pb/Cu metal exchange, were observed. Moreover, side-reactions of the peripheral phenyl substituents occur due to dehydrogenative coupling reactions.

O 55.14 Wed 18:00 P4

Tip-enhanced Raman Spectroscopy of a lifted single PTCDA molecule — •RODRIGO CEZAR DE CAMPOS FERREIRA¹, JIŘÍ DOLEŽAL^{1,2}, SOFIA CANOLA¹, PROKOP HAPALA¹, PABLO MERINO³, and MARTIN ŠVEC¹ — ¹Institute of Physics, Czech Academy of Science, Czech Republic — ²Faculty of Mathematics and Physics, Charles University, Czech Republic — ³Instituto de Ciencia de Materiales de Madrid; CSIC, Madrid, Spain

Advanced scanning probe techniques in the research of molecular adsorbates on surfaces have been instrumental in unveiling fundamental quantum phenomena with high sensitivity and spatial resolution at the nanoscale level. Such advances impact areas of molecular electronics, nanophotonics, and near-field spectroscopies. Tip-enhanced Raman spectroscopy (TERS) is a technique that provides access to vibrational modes of individual molecules via the extremely confined plasmonic field at the STM tip apex. This can be also used as a probe to chemically scrutinize single bonds with subnanometer precision. In this work, the STM-controlled TERS technique in a UHV environment at low temperature was performed for the perylene tetracarboxylic dianhydride molecule (PTCDA), in which we measured the Raman fingerprint for an array of PTCDA on Ag(111) as well as for a single molecule. Moreover, we were able to simultaneously follow the conductance spectrum of the system while lifting a single PTCDA from the surface. The observed transition in the Raman spectra correlates with the differential conductance showing the transition of the system from S=0 neutral to S=1/2 anion state.

O 55.15 Wed 18:00 P4

Electronic properties of CuPc/TiSe₂ heterostructures — •HIBIKI ORIO^{1,2}, KIANA BAUMGÄRTNER^{1,2}, CHRISTIAN METZGER^{1,2}, MARKUS SCHOLZ^{3,4}, KAI ROSSNAGEL^{4,5}, and FRIEDRICH REINERT^{1,2} — ¹Universität Würzburg Experimentelle Physik VII, Würzburg, Germany — ²Würzburg-Dresden Cluster of Excellence ct.qmat, Würzburg Dresden, Germany — ³European XFEL Facility, Schenefeld, Germany — ⁴Deutsches Elektronen-Synchrotron DESY, Hamburg, Germany — ⁵KiNSIS, Universität Kiel, Kiel, Germany

Transition metal dichalcogenides (TMDC) are a class of quasi-2D materials that exhibit a variety of electronic properties including superconductive, excitonic insulator, and charge-density wave (CDW) phases. TiSe₂ is one of the most prominent TMDC because it has intriguing CDW properties. The physical process of the CDW is not fully understood, however, and is attributed to either be purely electron-electron or jointly electron-electron and electron-phonon mediated. To gain more insight into the CDW buildup, modulating the intrinsic physical properties is useful [1]. For this purpose, we have used organic molecules as several interactions such as charge transfer or a rearrangement of the electron density can modulate the electronic properties at the organic/TMDC interface. We have evaporated copper phthalocyanine (CuPc) on TiSe₂ single crystals. We report the perturbed electronic characteristics of the resulting CuPc/TiSe₂ heterostructure examined with angle-resolved and X-ray photoelectron spectroscopy.

[1] K. Baumgärtner et al., submitted.

O 55.16 Wed 18:00 P4

Chirality-induced electron spin filtering in chiral helicene mono-, double- and multilayers — •RUWEN QUENTER¹, PAUL VALERIAN MÖLLERS¹, KARL-HEINZ ERNST², and HELMUT ZACHARIAS¹ — ¹Center for Soft Nanoscience, WWU Münster, Germany — ²Empa, Dübendorf, Switzerland

The transmission yield of electrons through molecules with chiral structure can depend on the electron spin. This phenomenon is established as chirality-induced spin selectivity (CISS).¹ While initial demonstrations of CISS were conducted with, e.g., short DNA strands,² studies with simpler molecules such as

helicene potentially allow for a better insight into the mechanism. Previous work³ on CISS in ordered monolayers of heptahelicene ([7]H) demonstrated that while the preferentially transmitted spin orientation depends on the helicity of the molecules, no major influence of the substrate is evident. Since the CISS increases with the number of helical turns, we investigate how it evolves for double and multilayers of [7]H adsorbed on a Cu(332) surface. Photoelectrons were excited from the substrate by deep-UV laser pulses and transmitted through [7]H

mono-, double or multilayers. Subsequently, the average spin polarization of the photoelectrons was measured via Mott scattering. With a [7]H monolayer a spin polarization of $P \approx 8\%$ was shown earlier³ and reproduced now. For the double and multilayers no increased spin polarization magnitude was found. ¹ D. H. Waldeck et al., *APL Mater.* **9**, 040902 (2021) ² B. Göhler et al., *Science* **331**, 894 (2011) ³ M. Kettner et al., *J. Phys. Chem. Lett.* **9**, 2025 (2018)

O 56: Poster Wednesday: Nanostructures 2

Time: Wednesday 18:00–20:00

Location: P4

O 56.1 Wed 18:00 P4

Pt Wedge on h-BN/Rh(111): Structural Analysis by HR-XPS — •NATALIE J. WALESKA, FABIAN DÜLL, FLORIAN SPÄTH, UDO BAUER, PHILIPP BACHMANN, JOHANN STEINHÄUER, and CHRISTIAN PAPP — Friedrich-Alexander-Universität, Erlangen, Germany

An approach to overcome the material gap to commercial catalysts is the investigation of metal nanoclusters on 2D materials (e.g. h-BN). To date, mostly 3D metal clusters with a narrow size distribution on such support materials were studied. However, the clusters' structure and thus the available adsorption sites, as well as the catalytic activity varies strongly from 3D to monolayer clusters or even single atoms.

To investigate the structural differences of clusters with varying sizes, a Pt wedge was prepared in a single preparation step on the h-BN/Rh(111) substrate, ranging from 0.21 to 0.001 ML Pt coverage. The analysis was performed using HR-XPS and CO as a probe molecule. From the data, we were able to determine the transition from monolayer to 3D cluster formation for the as-prepared Pt wedge. Upon heating to 550 K, structural changes of the Pt clusters were observed as a result of cluster ripening and sintering.

We thank Helmholtz-Zentrum Berlin for allocation of synchrotron-radiation beamtime and BESSY II staff for support during beamtime. This work was funded by the DFG within SFB 953 "Synthetic Carbon Allotropes" (Project #182849149).

O 56.2 Wed 18:00 P4

Charge effects on the (de-)Hydrogenation activity of Pt_n-clusters on *a*-SiO₂ thin films — •TOBIAS HINKE¹, ANDREW CRAMPTON¹, MARIAN RÖTZER¹, MAXIMILIAN KRAUSE¹, FLORIAN SCHWEINBERGER¹, BOKWOON YOON¹, UZI LANDMAN², and UELI HEIZ¹ — ¹Physical Chemistry, Department of Chemistry & Catalysis Research Center, Technical University of Munich, 85748 Garching, Germany — ²School of Physics Georgia Institute of Technology, Atlanta GA, U.S.A.

Catalytic model systems facilitate the gain of fundamental insights on molecular mechanisms and enable atom-precise manipulation of catalytic processes. Besides the size-effects of clusters with less than 100 atoms, the influence of the supporting material and the substrate are of special interest when steering reactivity. The catalyst's local electron density can be altered by varying the underlying metal. A high local work function of the substrate, Mo(112), yields clusters of positive charge while a low local work function, Pt(111), results in a negative charge. This allows for specifically altering the reactivity as well as the coking stability of the catalytic system.

In order to elucidate the impact of different support materials as well as cluster size-effects the change in activity of *a*-SiO₂ thin-film supported Pt_n-clusters towards ethylene (de-)hydrogenation was investigated.

The catalytic samples were characterized in a UHV setup with base pressures below $5 \cdot 10^{-10}$ mbar through IRRAS and electron spectroscopy (XPS, MIES, UPS), while reactivity was monitored with TPD and pulsed valve experiments (*p*-MBRS).

O 56.3 Wed 18:00 P4

Design of an Enhanced Ce-Evaporator for Ce_xO_y Thin Film Synthesis — •FLORA SIEGELE, KEVIN BERTRANG, TOBIAS HINKE, and UELI HEIZ — Physical Chemistry, Department of Chemistry and Catalysis Research Center, Technical University of Munich

In today's industry, the importance of sustainability regarding resource consumption and waste management is strongly increasing and hence, the contribution of catalysis-based processes is becoming more and more important. Substantial advances can be achieved by investigating catalytic model systems to facilitate the understanding of basic mechanisms on a molecular level. These model catalysts comprise a metal single crystal substrate with metal clusters (1-100 atoms), deposited on a metal oxide thin film (2-20 ML). Especially the Lewis acidic and basic properties of metal oxides showed promising results in terms of controlled tuning of the catalytic performance. However, the reducibility of thin film materials like CeO₂ offers an additional possibility of adjusting catalytic properties. Due to the lack of experimental results focusing on the influence of CeO₂ thin films on the reactivity and selectivity of clusters,

the poster presents the implementation of an optimized CeO₂ thin film generation procedure with a home-built ribbon evaporator. With this evaporator design, including a self-built quartz crystal microbalance, deposition rates of multiple monolayers per minute could be achieved and tracked with high accuracy. Electron emission spectroscopy (x-ray photoelectron spectroscopy and Auger electron spectroscopy) was performed to investigate the composition of the deposited film.

O 56.4 Wed 18:00 P4

CO Adsorption on PdPt Alloy Nanoparticles — •DANIEL SILVAN DOLLING^{1,2}, JAN-CHRISTIAN SCHÖBER^{1,2}, MARCUS CREUTZBURG¹, HESHMAT NOEI^{1,2}, and ANDREAS STIERLE^{1,2} — ¹Universität Hamburg — ²DESY

Platinum palladium alloy nanoparticles are of high interest because of their role as catalysts for different processes, including exhaust control and methane oxidation. Catalyst behavior is determined by the shape, structure and alloy composition of the particles. To enhance catalyst efficiency, it is thus necessary to improve our understanding of the structure of the nanoparticles and the active adsorption sites. In order to access detailed structural and morphological information, we employ the use of a model catalyst. In this work, platinum and palladium are co-deposited via molecular beam evaporation on α -Al₂O₃ (0001). The nanoparticles are grown epitaxially and have a well defined height to diameter ratio and alloy composition. By investigating the particle surface with the probe molecule CO using polarized infrared reflection absorption spectroscopy (IRRAS), we determined the surface species on top and side facets of the particles. The morphology was further identified with X-ray diffraction and X-ray reflectivity. The effect of the Pd/Pt alloy composition on the adsorption was investigated by comparing the IRRAS reflectivity. Moreover, the difference in the adsorption of CO was studied for samples annealed in hydrogen and oxygen.

O 56.5 Wed 18:00 P4

Methane activation with small Ta clusters — •KEVIN BERTRANG, TOBIAS HINKE, NIKITA LEVIN, MARTIN TSCHURL, and UELI HEIZ — Physical Chemistry, Department of Chemistry and Catalysis Research Center, Technical University of Munich

With the exhaustion of petroleum reserves, methane will become an important feedstock for the synthesis of fuels and fine chemicals. The challenge is to find an efficient way to activate the highly inert molecule under mild conditions and steer the reaction towards the formation of chemically precious products while preventing coking.

Studies of small cationic Ta-clusters in the gas phase and their oxides were found to exhibit high activity towards non-oxidative C-C-coupling of methane, yielding dehydrogenated carbohydrate species and ethane. The cluster charge was identified as a key parameter for activity. These studies are extended to their supported analogues. To replenish the cluster charge acidic (SiO₂) and reducible (CeO₂) thin metal-oxide films are employed and cluster oxygen content is tuned.

Characterization is performed by means of vibrational (IRRAS) and electron spectroscopy (XPS) and reactivity is studied via TPD and pulsed valves experiments.

[1] N. Levin et al. *J. Am. Chem. Soc.* **2020**, *142*, 12, 5862-5869

O 56.6 Wed 18:00 P4

3d-Nanoparticles on Graphene: Influence of Temperature — •KAI BESOCKE, MAHBOOBEH RAVANKHAH, and MATHIAS GETZLAFF — Institut für Angewandte Physik, Heinrich-Heine-Universität Düsseldorf

With its unique properties, such as high quality crystal structure, excellent electrical conductivity and high tensile strength, graphene is a promising substrate for fabricating nanocomposites. In this context we are investigating the influence of graphene as substrate for the deposition of metallic nanoparticles and the influence of subsequent heating. In this contribution we present our results concerning the mobility and distribution of Fe_{0.5}Ni_{0.5}-Nanoparticles on graphene surfaces.

A W(110) single crystal serves as the substrate being coated with a Co thin film of about 20 ML and annealed at temperatures up to 500 °C. Surfaces prepared in such a way exhibit elongated Co-islands with a width of several hundred

nm and height up to 10 nm, which are coated with graphene subsequently. For graphene synthesis the samples are heated in a Propene atmosphere of 10^{-6} mbar for several minutes. The nanoparticles are produced by means of Ar magnetron sputtering in a Haberland source and aggregation takes place in a He atmosphere.

The spherical particles under investigation have diameters of several nm. Particle distributions are analyzed via STM, both as-prepared as well as after heating. It will be discussed, whether the nanoparticles are more mobile on graphene compared to other surfaces.

O 57: Poster Wednesday: Electronic Structure

Time: Wednesday 18:00–20:00

Location: P4

O 57.1 Wed 18:00 P4

Josephson effect in the two-band superconductor Niobium Diselenide — •XIANZHE ZENG¹, HAONAN HUANG¹, SUJOY KARAN¹, KLAUS KERN^{1,2}, and CHRISTIAN AST¹ — ¹Max-Planck-Institut für Festkörperforschung, Heisenbergstraße 1, 70569 Stuttgart, Germany — ²Institut de Physique, Ecole Polytechnique Fédérale de Lausanne, 1015 Lausanne, Switzerland

Niobium Diselenide is a two-dimensional (2D) van der Waals s-wave superconductor that can be described by a two-band model. The Josephson effect between Niobium Diselenide and another known BCS superconductor is non-trivial since it involves Copper pair tunneling of two bands with different order parameters. Here, we measure quasiparticle tunneling as well as the Josephson current between a clean superconducting Niobium Diselenide surface and a superconducting Vanadium tip using low-temperature scanning tunneling microscopy and spectroscopy. We analyze our results with the McMillan formula for a two-band superconductor. Our observations present a first step towards understanding more complicated scenarios, such as the predicted p-wave triplet superconductivity in Chromium Tribromide islands on Niobium Diselenide.

O 57.2 Wed 18:00 P4

Bulk Ion Conductivity and Near Surface Composition of Ionic Liquid and Zwitterionic Salt Based Electrolytes for Lithium Battery Applications — •FABIAN ULLMANN, JOEL TAYO, ANNA DIMITROVA, and STEFAN KRISCHOK — Institut für Mikro und Nanotechnologien, Institut für Physik, TU Ilmenau

In this contribution we focus on the bulk conductivity and the near surface composition of several tertiary electrolytes which consist of Ionic Liquid (IL), Zwitterionic salt (ZwS) and lithium salt. Two ILs and ZwSs are chosen: IL: 1-ethyl-3-methyl-imidazolium bis-(trifluoromethylsulfonyl)imide - [EMIm][Tf2N] and 1-butyl-1-methylpyrrolidinium bis-(trifluoromethylsulfonyl)imide - [BMP][Tf2N]; ZwS: 3-(3-methylimidazolium-1-yl)Propane-1- sulfonate and 3-(3-vinylimidazolium-1-yl)Propane-1-sulfonate. As lithium precursor - bis(trifluoromethylsulfonyl)imide - Li[Tf2N] was used. Different Li[Tf2N]/ZwS ratios are considered and studied. Electrochemical Impedance Spectroscopy (EIS) enables us to determine the ion conductivity of the electrolytes. The results reveal that the presence of ZwSs enhances the ion conductivity, although they itself are not ion conductive. Further, by using X-Ray Photoelectron Spectroscopy (XPS) we analyze the near surface chemical composition at UHV-conditions. The XPS analysis displays a cation/anion/ZwS distribution as depended on the concentration of Li[Tf2N] and the type of IL and ZwS used. The spectroscopic results revealed solute-solvent interactions which modify the ion mobility.

O 57.3 Wed 18:00 P4

Line shape analysis of the resonant eigenstates in a quantum corral by means of tunneling spectroscopy and non contact AFM — •MARCO WEISS, MICHAEL ROESSNER, FABIAN STILP, and FRANZ J. GIESSIBL — Institute of Experimental and Applied Physics, University of Regensburg, Germany

Back in 1993 Crommie et al. [1] arranged 48 Fe adatoms on a Cu(111) surface in a circle with a diameter of 14.26 nm. This quantum corral confines surface electrons in a circular potential well. Past investigations with scanning tunneling microscopy revealed energetically discrete eigenstates that spatially appear as Bessel functions. But these studies on the Fe quantum corral showed unwanted movement of the corral walls during spectroscopic measurements. [1]

Instead of Fe, we used CO molecules to provide the corral with more stable walls. This permitted us to access a larger voltage window and allowed for a detailed line shape analysis of the corrals eigenenergy levels. Surprisingly, we discovered a large Gaussian broadening of the eigenstates.

We also acquired nc-AFM data of the corral. As we have previously done, we determined the occupation of electronic states that cross the Fermi level [2]. Similar to our previous work, we observed that the presence of the probe tip shifts the energy of the electronic states under study. In this work, we show that we can also use the AFM data to estimate the lifetime (i.e. the spectral width) of these states.

[1] M. F. Crommie et al., Science 262, 218-220 (1993)

[2] F. Stilp et al., Science 372, 1196-1200 (2021)

O 57.4 Wed 18:00 P4

Interaction between an artificial and a natural atom — •FABIAN STILP, MARCO WEISS, and FRANZ J. GIESSIBL — University of Regensburg, Regensburg, Germany

The surface state of Cu (111), a quasi-2-dimensional electron gas, is trapped to a small surface area of about $15 \times 15 \text{ nm}^2$ by placing 48 CO-molecules in a circular shape on the surface via atomic manipulation. By doing so, one creates a quantum corral with discrete electronic states forming an artificial atom. This structure can be described reasonably well by an infinitely high circular potential well leading to corral states with Bessel-type radial functions and an angular momentum normal to the surface. To investigate the interaction between this artificial atom and a natural atom we bring Fe atoms inside the corral and measure the response of the corral states.

Thanks to the large size, one can study the structure of the wave functions within that artificial atom by nc-AFM showing an angular dependence of the corral states after placing the atoms inside the corral. This change of the wave functions leads to an energy shift of a few meV confirmed by tunneling spectroscopy measurements. By investigating the change of the wave functions and the energies of the corral states when placing the adatom inside, one can draw conclusion about the interaction between this artificial atom and a natural atom. Here we expand the interpretation of the adatom acting repulsively on the corral states as stated by Stilp et al. [1].

[1] F. Stilp, A. Berezuk, J. Berwanger, N. Mundigl, K. Richter, F.J. Giessibl, Science 372, 1196-1200 (2021)

O 57.5 Wed 18:00 P4

Spontaneous Charge Localization on Polar Surfaces — •MICHELE RETICCIOLI¹, ZHICHANG WANG^{2,3}, ZDENEK JAKUB², IGOR SOKOLOVIC², MATTHIAS MEIER^{1,2}, GARETH S. PARKINSON², MICHAEL SCHMID², DOMINIK WRANA⁴, LYNN A. BOATNER⁵, ULRIKE DIEBOLD², MARTIN SETVIN^{2,4}, and CESARE FRANCHINI^{1,6} — ¹Faculty of Physics and Center for Computational Materials Science, University of Vienna, Austria — ²Institute of Applied Physics, TU Wien, Vienna, Austria — ³State Key Laboratory for Physical Chemistry of Solid Surfaces, Xiamen University, China — ⁴Department of Surface and Plasma Science, Faculty of Mathematics and Physics, Charles University, Prague, Czech Republic — ⁵Materials Science and Technology Division, Oak Ridge National Laboratory, Oak Ridge, USA — ⁶University of Bologna, Italy

Excess charge on polar surfaces of ionic compounds is commonly described by the two-dimensional electron gas (2DEG) model, a homogeneous distribution of charge confined in a few atomic layers. Conversely, our density functional theory calculations and scanning-probe microscopy measurements on $\text{KTO}_3(001)$ show spontaneous localization of the excess charge in the form of polarons, bipolarons and charge density waves. These electronic reconstructions form on the defect-free surface, and alter the material properties and functionalities to different degrees. Controlling the degree of charge ordering could be of great benefit for a wide range of applications: in our study, we analyze the impact on the surface reactivity by considering the interaction with CO molecules.

O 57.6 Wed 18:00 P4

Evolution of Property and Bonding Maps — •CARL-FRIEDRICH SCHÖN and MATTHIAS WUTTIG — RWTH Aachen University, Aachen, Germany

Since picking up the first tool, it has been the goal of mankind to create materials that best suit human needs. While for the longest time any development in this field was driven by an empirical approach, modern means of physics and chemistry gave rise to the concept of material and property maps based on chemical bonding. We have composed a database of elemental and binary compounds. For all compounds, the corresponding values of a set of properties were included, containing the conductivity, the Born Effective Charge, the Effective Coordination Number (ECoN) and the Bandgap, the melting point, the density and the atomic density. A Gaussian mixture algorithm was utilized to separate the compounds in the database into n clusters. With the number of allowed clusters set to 4, the algorithm nicely separates materials which employ metallic, ionic and covalent bonding. This implies that properties can be used to distinguish bonding mechanisms. Interestingly, a fourth class of materials is identified, characterized by a property portfolio neither found in metals, or materials employing ionic or covalent bonding. This is further support for the concept of metavalent bonding, a novel bond type characterized by the competition between localization and delocalization. This classification provides a close link between chemical bonding mechanisms and properties enabling novel routes to material's design with material maps.

O 57.7 Wed 18:00 P4

A theoretical investigation into gallic acid pyrolysis — •JAKOB KRAUS and JENS KORTUS — Institute of Theoretical Physics, TU Bergakademie Freiberg, Leipziger Str. 23, D-09599 Freiberg, Germany
Thermodynamical and kinetic information on the first two steps of gallic acid pyrolysis is calculated based on density functional theory and quantum chemistry. For the kinetics, transition states are identified with the help of the climb-

ing image nudged elastic band method. Both reactions exhibit two transition states. One of them is related to the rotation of OH groups, and the other one is related to the breaking and forming of bonds. The gallic acid pyrolysis as a whole is judged to be endothermic, and it changes from endergonic to exergonic between 500 K and 750 K. The second reaction step, the dehydrogenation of pyrogallol, is identified as the limiting step of gallic acid pyrolysis, with reaction rate constants below 1 s^{-1} for temperatures below 1250 K.

O 58: Poster Wednesday: New Methods and Developments, Frontiers of Electronic Structure Theory

Time: Wednesday 18:00–20:00

Location: P4

O 58.1 Wed 18:00 P4

Fully Atomistic Modelling of Tip-enhanced Raman Spectra from First Principles — •YAIR LITMAN, FRANCO BONAFE, ALAA AKKOUSH, HEIKO APPEL, and MARIANA ROSSI — MPI for the Structure and Dynamics of Matter, Hamburg, Germany.

Tip-enhanced Raman scattering (TERS) has emerged as a powerful tool to study surfaces with subnanometer spatial resolution [1]. In particular, single-molecule TERS studies have shown the capability to visualize high-resolution images of individual molecular normal modes in real space [2]. Theoretical simulations that can provide an unambiguous interpretation and atomic description of obtained TERS images often rely on crude approximations of the local electric field [3]. In this work, we present a novel method to compute TERS images by combining Time Dependent Density Functional Theory (TDDFT) and Density Functional Perturbation Theory (DFPT) to calculate Raman cross sections with realistic local fields. The new approach allows for a fully *ab initio* atomistic description of the tip-molecule-surface system, and naturally incorporates chemical effects arising from the molecule-surface interaction. We show results for benzene and pyridine and discuss the importance of a realistic description of the local field, and self-consistent evaluation of the electronic density response. Finally, we evaluate the use of 2D TERS imaging as an identification tool for defects in 2D materials. [1] M. Richard-Lacroix, *et al.*, Chem. Rev. 56, 3922 (2017) [2] L. Joonhee, *et al.*, Nature 568, 78 (2019) [3] P. Liu, X. Chen, H. Ye, and L. Jensen, ACS Nano 13, 9342 (2019)

O 58.2 Wed 18:00 P4

Deep learning based signal processing for touch-sensitive surfaces — •JAKOB ELSNER, VIKTOR FAIRUSCHIN, and THORSTEN UPHUES — Institute for Sensor and Actuator Technology, Coburg, Germany

Touch-sensitive surfaces enable intuitive and efficient operation of electronic devices and eliminate the need for external peripherals and mechanical components, making touch technology increasingly important in the modern society. However, conventional touch technologies, i.e. capacitive, resistive or optical, are usually limited to non-metallic materials that hardly meet the stringent requirements for robustness and hygiene in a medical environment. Stainless steel is one of the most commonly used materials in medical fields due to its high strength, chemical resistance and excellent hygienic properties. In this work, we present a novel approach based on Lamb wave technology and deep learning analytics, and apply this new principle to design a stainless steel touch-sensitive surface. Compared to Rayleigh wave-based touch technology, our approach requires no additional reflective structures and involves only a single piezoelectric transducer used to monitor the entire surface, while position-sensitive information is extracted from raw Lamb wave signals using a trained deep neural network.

O 58.3 Wed 18:00 P4

Enhanced Sampling of Surface Reactions Using Boltzmann Generators — •DAVID HERING, JOHANNES T. MARGRAF, and KARSTEN REUTER — FHI Theory Department, Berlin, DE

Computational surface science and catalysis research is still mainly conducted with static density functional theory (DFT) calculations. This approach is computationally convenient, but misses important aspects of surface chemistry, such as anharmonic free energy contributions. In principle, DFT-based molecular dynamics (MD) simulations (ideally combined with enhanced sampling algorithms) would allow a much more accurate description of these processes. Unfortunately, these are far too expensive to be routinely applied to complex surface/adsorbate systems. This is due to the fact that configurations in MD are generated sequentially. As a consequence, MD configurations are not statistically independent so that a very large number of samples is required to obtain converged ensemble properties. To overcome this limitation, Noé and co-workers recently proposed a generative machine learning model called the Boltzmann Generator, which was used to generate independent configurations of biomolecules. In this contribution, we explore how Boltzmann Generators can also be used to sample the free energy surface of surface/adsorbate systems relevant for heterogeneous catalysis. In particular, training protocols and validation metrics of generated ensembles will be discussed.

O 58.4 Wed 18:00 P4

theoretical and experimental investigation of Fe and Ni-TCNQ on graphene — •AZIN SHAHSAVAR, ZDENĚK JAKUB, ANNA KUROWSKÁ, JAKUB PLANER, ONDŘEJ HERICH, LENKA ČERNÁ, LUKÁŠ KORMOŠ, PAVEL PROCHÁZKA, and JAN ČECHAL — CEITEC Brno University of Technology Purkyňova 656/123 612 00 Brno, Czech Republic.

Due to the outstanding properties of the 2D metal-organic frameworks (MOF), intensive computational and experimental studies have been done. However, the lack of fundamental studies of MOFs on the graphene backbone is observed. This work studies Fe and Ni as metal and tetracyanoquinodimethane (TCNQ) with a high electron affinity as an organic linker functionalized on graphene. Here we present DFT calculations results to unveil the electronic and magnetic properties of iron and nickel-TCNQ physisorbed on graphene. Adsorption and Fermi energies, structural, and magnetic properties will be reported. Our experimental observations prove Fe- and NiTCNQ@Gr/Ir(111) are thermally highly stable up to 500 and 250 °C, respectively, making them promising materials for single-atom catalysts or high-density storage media [1]. [1] Z. Jakub *et al.*, Nanoscale, 1-9 (2022). DOI: 10.1039/d2nr02017c

O 58.5 Wed 18:00 P4

Assessment of Structural Descriptors for the Construction of High-Dimensional Neural Network Potentials — •MORITZ R. SCHÄFER¹, JONAS FINKLER², STEFAN GOEDECKER², and JÖRG BEHLER¹ — ¹Georg-August-Universität Göttingen, Institut für Physikalische Chemie, Theoretische Chemie, Tammannstraße 6, 37077 Göttingen, Germany — ²Basel University, Department of Physics and Astronomy, Klingelbergstrasse 82, 4056 Basel, Switzerland
High-dimensional neural network potentials (HDNNPs) can be used to efficiently compute close-to-*ab initio* quality energies and forces for performing large-scale molecular dynamics simulations of complex systems. In this method, the total energy is constructed as a sum of environment-dependent atomic energy contributions. Also electrostatic interactions based on environment-dependent charges can be included. Hence, a set of reliable structural descriptors for the atomic local environments is crucial to develop accurate potentials. Often, atom-centered symmetry functions (ACSFs) are used for this purpose in HDNNPs. In this work, we benchmark the accuracy and transferability of HDNNPs with respect to alternative descriptors like the recently proposed overlap matrix descriptor.

O 58.6 Wed 18:00 P4

Fortnet, a software package for training Behler-Parrinello neural networks — •TAMMO VAN DER HEIDE¹, JOLLA KULLGREN², PETER BROQVIST², VLADIMIR BAČIĆ³, THOMAS FRAUENHEIM^{4,5,1}, and BÁLINT ARADI¹ — ¹BCCMS, University of Bremen, Bremen, Germany — ²Dept. of Chemistry - Ångström Laboratory, Uppsala University, Uppsala, Sweden — ³Dept. of Physics and Earth Sciences, Jacobs University Bremen, Bremen, Germany — ⁴Beijing CSRC, 100193 Beijing, P. R. China — ⁵Shenzhen JL CSAR Institute, Shenzhen 518110, P. R. China
A new, open source, parallel, stand-alone software package (Fortnet) has been developed, which implements Behler-Parrinello neural networks. It covers the entire workflow from feature generation to the evaluation of generated potentials, coupled with higher-level analysis such as the analytic calculation of atomic forces. The functionality is demonstrated by driving the training for the fitted correction functions of the density functional tight binding (DFTB) method, which are commonly used to compensate the inaccuracies resulting from the DFTB approximations to the Kohn-Sham Hamiltonian. Their usual two-body form limits the transferability of parameterizations between very different structural environments. After investigating various approaches, we have found the combination of DFTB with a near-sighted artificial neural network, acting on-top of baseline correction functions, the most promising one. It allows to introduce many-body corrections on top of two-body parameterizations, while excellent transferability to deviating chemical environments could be demonstrated.

O 58.7 Wed 18:00 P4

Machine learning enhanced DFTB method for periodic systems — •WENBO SUN, GUOZHENG FAN, TAMMO VAN DER HEIDE, ADAM MCSLOY, THOMAS FRAUENHEIM, and BALINT ARADI — Bremen Center for Computational Materials Science, University of Bremen, Am Fallturm 1, Bremen 28359, Germany.

The Density Functional based Tight Binding (DFTB) is an approximative density functional based quantum chemical simulation method with low computational costs. In order to increase its accuracy, we have introduced a machine learning algorithm to optimize several parameters of the DFTB method, concentrating on solids with defects. The backpropagation algorithm was used to reduce the error between DFTB and DFT results w.r.t. the training dataset and to obtain adjusted DFTB Hamiltonian and overlap matrix elements. Afterwards, the generalization capability of the trained model was tested for geometries not being part of the training set. In the current work, we have focused on defective periodic silicon and silicon carbide systems as target materials and the density of states (DOS) as target property to demonstrate the feasibility of our approach. The trained model was able to reduce the differences between the DFTB and the DFT DOS significantly, while other derived properties (e.g. charge distribution, partial DOS) remained physically sound. Also, the transferability of the obtained model could be verified. Our method allows to carry out relatively fast simulations with high accuracy and only moderate training efforts, and represents a good compromise for cases, where long range effects make direct machine learning predictions difficult.

O 58.8 Wed 18:00 P4

Electronic properties of Density Functional Tight Binding by Machine Learning — •GUOZHENG FAN¹, ADAM MCSLOY¹, BALINT ARADI¹, CHI-YUNG YAM², and THOMAS FRAUENHEIM^{1,2} — ¹Bremen Center for Computational Materials Science (BCCMS), University of Bremen, Bremen, Germany — ²Beijing Computational Science Research Center (CSRC), Beijing, China

We have introduced a machine learning workflow, which could optimize electronic properties in density functional tight binding method. With this workflow, we can train and predict electronic properties in a cheap, accurate and transferable way. The implementation features of batch calculations greatly improve the calculation efficiency, especially for high throughput calculations. This workflow could optimize electronic properties by train basis functions or train a spline model to generate two center integrals for off-diagonal and onsite for diagonal Hamiltonian and overlap. The results show that compared with previous Slater-Koster parameters, the dipole moments, charges, the ratios of the on-site populations and the atomic numbers in charge population analysis method can be improved by both tuning basis function parameters or optimizing integrals in spline model directly. The training on basis functions could prevent the two center integrals go randomly and keep Hamiltonian and overlap in reasonable range. Besides, the multiple electronic properties could be improved simultaneously.

O 58.9 Wed 18:00 P4

Unsupervised regression-based measures for applications on atomistic features — •ALEXANDER GOSCINSKI¹, GUILLAUME FRAUX¹, GIULIO IMBALZANO¹, FÉLIX MUSIL^{1,2}, SERGEY POZDNYAKOV¹, and MICHELE CERIOTTI¹ — ¹Laboratory of Computational Science and Modeling, Institute of Materials, École Polytechnique Fédérale de Lausanne, 1015 Lausanne, Switzerland — ²National Center for Computational Design and Discovery of Novel Materials (MARVEL), Lausanne, Switzerland

The quality of the features as input for a machine learning model is a crucial factor for the prediction quality and the computational efficiency. Commonly, to assess the quality of features, they are compared by benchmarking the regression performance on several properties. Complementary to such a quality assessment, this work presents certain measures for direct feature-to-feature comparisons without the need of a target property. These measures are used to quantify the capacity of features representing geometrical space in atomistic applications and derive an understanding of the information encoded in features.

O 58.10 Wed 18:00 P4

Accelerating plane-wave-based *ab initio* molecular dynamics by optimization of Fast-Fourier transforms for modern HPC architectures — •CHRISTIAN RITTERHOFF, TOBIAS KLÖFFEL, SAGARMOY MANDAL, and BERND MEYER — Interdisciplinary Center for Molecular Materials and Computer Chemistry Center, FAU Erlangen-Nürnberg, Germany

The most important advantage of plane-wave basis sets is that wave functions can be transformed efficiently from reciprocal to real space and back by using the Fast-Fourier transform (FFT) algorithm. This allows to evaluate the kinetic and potential energy in reciprocal and real space, respectively, where both operators are diagonal. This reduces the computational cost for applying the Hamilton operator from N^2 to $N \log N$. However, the scalability of current FFT libraries is rather limited on today's HPC systems, which offer large numbers of compute nodes, each of them with many cores. Here we present our optimization of the FFTX library of the Quantum Espresso software package. Data distribution and communication patterns have been revised to make optimal use of combined

MPI and OpenMP parallelization. Scalability is further increased by combining FFTs into batches and by introducing overlapping computation and communication. We implemented the revised FFTX library in our optimized version of the CPMD code [1], and we demonstrate the achieved acceleration by a series of benchmark simulations.

[1] T. Klöffel, G. Mathias, B. Meyer, *Comput. Phys. Commun.* **260** (2021) 107745

O 58.11 Wed 18:00 P4

Surface tension measurement of pure water in vacuum — •PAUL T. P. RYAN, JIRI PAVELEC, JAN BALAJKA, MICHAEL SCHMID, and ULRIKE DIEBOLD — Institute of Applied Physics, TU Wien, Austria

Very little is known about the surface tension of pure liquids in contact with their pure gaseous phases, i.e. without the presence of other gases or liquid phase contaminants. This is surprising given that contaminants are known to greatly affect surface tensions values[1]. Recently we have developed a method to dose liquid water onto pristine surfaces in UHV using a small cryostat [2,3]. We combine this approach with the pendant drop method [4] to measure the surface tension of ultra-clean liquids in contact with their pure gaseous phases. The upgraded version of the small cryostat, replaces the syringe typically used in the pendant-drop method. The ultra-clean liquid is condensed onto a small cryostat placed in a vacuum chamber. A pendant drop is formed and carefully photographed allowing the surface tension of the liquid to be directly determined. The design of the apparatus will be discussed and preliminary measurements of ultra-clean water will be presented. [1] Yuki Uematsu, et. al., *Current Opinion in Electrochemistry*, Volume 13, (2019) [2] Jan Balajka, et. al., *Review of Scientific Instruments* 89, (2018) [3] Jan Balajka, et. al., *Science*, 361, (2018) [4] Berry, J. D. et. al., *J. Coll. Interface Sci.* 454, 226*237, (2015).

O 58.12 Wed 18:00 P4

Home-Built UHV Suitcase — •LUCA LEZUO¹, LUCIE DOCKALOVÁ², GARETH PARKINSON¹, ULRIKE DIEBOLD¹, and JIRI PAVELEC¹ — ¹Institute of Applied Physics, TU Wien, Wiedner Hauptstrasse 8-10/134, Vienna, Austria — ²Institute of Physical Engineering, Brno University of Technology

Due to their extreme sensitivity to adsorbing molecules, most surface experiments have to be carried out in ultra-high vacuum (UHV). Ideally, multiple different techniques are used to explain and understand the phenomena happening on an atomic scale. To this end, it is often necessary to transfer a sample from one chamber to another.

As a showcase, we discuss the analysis of perovskite oxides, produced by pulsed laser deposition (PLD) as thin films, in another UHV chamber that allows atomically resolved STM/AFM imaging with a Q+-sensor at liquid N_2/He - temperatures. The home built UHV suitcase consists of three stages divided by gate valves. It has a scroll pump for rough vacuum, a turbo pump to reach high vacuum, a NEG pump and a cryopump to ensure a clean transfer and an ION/NEG combination to provide UHV conditions long term in the storage stage, where the sample is transported.

O 58.13 Wed 18:00 P4

Wettability investigation of microscale water droplets on silicon substrate using atomic force microscopy — •MOHAMMADALI HORMOZI¹, MARVIN HOFFER^{1,2}, PAULINE BRUMM², and REGINE VON KLITZING¹ — ¹Soft Matter at Interfaces, Department of Physics, Technical University of Darmstadt, 64289 Darmstadt, Germany — ²Institute of Printing Science and Technology (IDD), Technische Universität Darmstadt, Magdalenenstraße 2, 64289 Darmstadt, Germany

The wettability of a particular substrate by a liquid drop is of interest in many scientific fields. This phenomenon is often described by the contact angle between the considered liquid and substrate. This parameter is an important boundary condition, especially for the wetting of mixtures and solutions. This study shows a methodology for evaluating the contact angle of different droplets with a base diameter down to 0.5 micrometers. 3D topography of water droplets - generated through condensation and Inkjet printing on a silicon substrate- has been determined using Atomic Force Microscopy. Also, the topography of printed mixture droplets including water-glycerol and water-glycerol-isopropanol has been measured. Different curves have been fitted to a 2D cross-section of each droplet, which provides information about their contact angle. The contact angle of the mixtures deviates from the macroscale contact angle at the vicinity of the three-phase contact line; however, this phenomenon cannot be seen in pure water droplets. While no effect of droplet diameter could be detected for diameters, ranging from 0.5 to 30 micrometers, the macroscopic contact angle of droplets is several degrees higher.

O 58.14 Wed 18:00 P4

High-frequency shot-noise STM to study correlated electron systems — •MAIALEN ORTEGO LARRAZABAL¹, JIASEN NIU², KOEN M BASTIAANS³, JIANFENG GE², TJERK BENSCHOP², MILAN P ALLAN², and INGMAR SWART¹ — ¹Debye Institute for Nanomaterials Science, Utrecht University, PO Box 80000, 3508 TA Utrecht, The Netherlands — ²Leiden Institute of Physics, Leiden University, Niels Bohrweg 2, 2333 CA Leiden, The Netherlands — ³Kavli Institute of Nanoscience, Delft University of Technology, 2628 CJ Delft, Netherlands

The fluctuations in time of a measured signal provide information that is not present in the time averaged value. For example, the discreteness of the electric charge leads to fluctuations in the tunneling current in an STM, known as shot-noise. Shot-noise measurements convey information about the correlations among the electrons in condensed matter systems, such as the effective charge of the carrier or their distribution in the tunneling process. However, other contributions to the measured noise, such as $1/f$ and thermal noise, make it difficult to isolate the shot-noise component. For this reason, we use custom-built electronics that allows us to read out the noise signal of the STM at high frequencies and cryogenic temperatures and that does not interfere with conventional STM measurements.

O 58.15 Wed 18:00 P4

Optimization of a Simple Electrospray Deposition Device — •KEN KOLAR¹, MIRIAM MEYER², HENRIK SIBONI¹, CHRISTOPHE NACCI¹, GRANT SIMPSON¹,

and LEONHARD GRILL¹ — ¹Institute for Chemistry, Department of Physical Chemistry, University of Graz, Austria — ²Institute for Ion Physics and Applied Physics, University of Innsbruck, Austria

A commercially available design of an electrospray deposition apparatus was optimized for cleaner and more controllable deposition in a high vacuum. The apparatus consists of a series of 5 differentially pumped chambers separated by skimmer cones or apertures. An angle-adjustable bellow was introduced between the second and third pumping chamber for better control over the alignment and, consequently, the ion beam flux reaching the final stage. Monitoring the flux/alignment was done by current measurements around the apertures and behind the last one with a conductive probe. Also, heating of the transfer capillary and enclosing the emitter-transfer capillary interface in a small transparent chamber (to allow different ambient gas environments) were introduced. The first depositions were done to test the performance of the improved design with some well-studied molecules.

O 59: Poster Wednesday: Plasmonics and Nanooptics 2

Time: Wednesday 18:00–20:00

Location: P4

O 59.1 Wed 18:00 P4

Quantum description of the optical response in metal nanoparticles — •JONAS GRUMM, ROBERT SALZWEDEL, MALTE SELIG, and ANDREAS KNORR — Institut für Theoretische Physik, Nichtlineare Optik und Quantenelektronik, Technische Universität Berlin, Berlin, Germany

The optical response of metal nanoparticles is dominated by the formation of collective electronic resonances, so-called plasmons.

Here, we present a microscopic approach for their temporal dynamics based on the self-consistent treatment of microscopic Boltzmann transport equations and macroscopic Maxwell equations for the electromagnetic fields. Numerical simulations describe the thermalization of the phonons and the relaxation of the electrons upon optical excitation and allow to include nonlinear optical processes in the description.

O 59.2 Wed 18:00 P4

Access to hot electron dynamics in a nanotip via ultrafast THz-streaking — •DOMINIK WEBER, FELIX SOMMER, MORITZ HEINDL, and GEORG HERINK — Experimental Physics VIII - Ultrafast Dynamics, University of Bayreuth

Field enhancement and localization of single-cycle Terahertz radiation at metallic nanotips forms the basis for a broad range of emerging ultrafast interactions - ranging from ultrafast nearfield and tunnelling microscopy, transient carrier dynamics to strong-field phenomena. We present an experimental access to ultrafast hot electron dynamics at the apex of a free-standing nanotip based on THz-nearfield streaking spectroscopy [1,2]. Using tunable fs-pulses, we induce non-equilibrium electron excitations and transient hot electron distributions. Access to local hot electron dynamics confined to the apex is provided via nonlinear sub-cycle field emission at the peak of the enhanced single-cycle THz-waveform. Based on experimental streaking waveforms, we discuss the impact of excitation conditions on hot electron relaxation and possibilities for external control of ultrafast carrier dynamics.

L. Wimmer et al., "Terahertz control of nanotip photoemission", *Nature Physics* 10 (2014)

G.Herink et al., "Field emission at terahertz frequencies: AC-tunneling and ultrafast carrier dynamics", *New Journal of Physics* 16 (2014)

O 59.3 Wed 18:00 P4

Near-field optical investigation of bandgap effects in SnTe — •CHRISTIAN JUSTUS, KONSTANTIN G. WIRTH, DARIO SIEBENKOTTEN, LUKAS CONRADS, SOPHIA WAHL, MATTHIAS WUTTIG, and THOMAS TAUBNER — I. Institute of Physics (IA), RWTH Aachen University

Phase change materials (PCMs) are prime candidates for non-volatile memory solutions [1]. Storage mediums with high memory density require a method for determining material properties with nanometer precision. One such tool to investigate the optical properties of nano-structures is scattering-type scanning near-field optical microscopy (s-SNOM). Thus far, bandgap effects in semiconductors have eluded experimental observation in s-SNOM. Specifically metavalently bonded materials may exhibit a bandgap shift by over a factor of three in reduced dimensions, such as in the case of Tin Telluride (SnTe) with a shift from 0.2 to 0.7 eV [2]. The primary goal of this work is to use s-SNOM to spectroscopically characterize bandgap effects in SnTe thin films. We find good agreement between Fourier-transform infrared spectroscopy (FTIR) and s-SNOM measurements over a spectral range spanning 0.3 to 0.9 eV and are able to identify a bandgap contribution to the spectral s-SNOM data. Our results may help to get a deeper insight into confinement effects on the optical properties of nano-scale PCM structures, such as PCM memory cells, and may provide a valuable tool for the analysis and characterization of PCM memory devices with high storage density.

O 59.4 Wed 18:00 P4

Energy and momentum distribution of surface plasmon-induced hot carriers — •CHRISTOPHER WEISS¹, EVA PRINZ¹, MICHAEL HARTELT¹, BENJAMIN STADTMÜLLER^{1,2}, and MARTIN AESCHLIMANN¹ — ¹Department of Physics and Research Center OPTIMAS, TU Kaiserslautern, Germany — ²Institute of Physics, Johannes Gutenberg University Mainz, Germany

Investigating the energy and momentum space signature of plasmon-induced hot electrons is essential for understanding novel plasmonic energy conversion schemes. The question remains, if plasmon-induced and photon-induced hot carriers are fundamentally different. For the bulk plasmon resonance, a fundamental difference is known, yet for the technologically important surface plasmons this is far from being settled. Just recently, we identified a similar characteristic signature in the surface plasmon polariton (SPP) emission that distinguishes them from photon-induced electrons [1].

To separate the energy and momentum distribution of the plasmon-induced hot electrons from those of the photoexcited electrons, we employ a two-colour femtosecond time-resolved 2-photon photoemission (2PPE) experiment. The spatial evolution of the photoemitted electrons was observed with energy-resolved photoemission electron microscopy (PEEM) and momentum microscopy during the propagation of an SPP pulse along a gold surface. Building on these findings, we extend this concept to SPPs of single crystalline silver surfaces to investigate the influence of the band structure and material properties.

[1] Hartelt et al., *ACS Nano* 15, 12 (2021), 19559–19569

O 59.5 Wed 18:00 P4

Near-field optical investigation of few layer graphene — •LINA JÄCKERING, KONSTANTIN WIRTH, CHRISTIAN JUSTUS, and THOMAS TAUBNER — I. Institute of Physics (IA), RWTH Aachen University

Few layer graphene (FLG) samples usually consist of various stacking orders, which show different optical and electronic properties. Direct imaging and characterization of stacking domains in FLG samples can be done with scattering scanning near-field optical microscopy (s-SNOM) [1]. s-SNOM is outstanding for its nanoscale resolution of about 20 nm and its capability to image buried structures [2]. Thus, it allows to characterize encapsulated FLG samples as they are used in transport devices. Previous s-SNOM investigations focussed on the excitation of free charge carriers in FLG at about 0.1 eV [3,4]. Recently, FLG stackings have been identified by exciting interband transitions (0.27 – 0.56 eV) [1,5]. Interband resonances of FLG have only been measured at punctual energies or small energy regimes. Here, we investigate trilayer graphene and bilayer graphene in the spectral range of 0.27 – 0.9 eV, providing a deeper understanding of their near-field optical response, particularly of their interband resonance. Furthermore, we identify different stacking domains in FLG samples encapsulated in hexagonal boron nitride. Our findings provide a promising technique to select stacking domains for fabrication of transport devices.

1. Kim et al., *ACS Nano*, 9, 7 (2005); 2. Jeong et al., *Nanoscale*, 9, 12 (2017); 3. Fei et al., *Nature* 487, 82 (2012); 4. Jiang et al., *Nat. Mater.* 15, 840 (2016); 5. Wirth et al., arXiv: 2203.07971v1 (2022)

O 59.6 Wed 18:00 P4

Photoemission electron microscopy of Ag nanostructures on silicon substrates — •MUHAMED SEWIDAN, KATHARINA ENGSTER, KEVIN OLDENBURG, SYLVIA SPELLER, and INGO BARKE — Rostock University, Rostock, Germany

We study electronic and optical coupling phenomena between plasmonic nano-objects, organic molecules, and the substrate. Localized plasmons created in metal nanostructures can lead to enhanced multiphoton photoelectron emission under pulsed light excitation. In a photoemission electron microscope (PEEM) individual particles of sub-15 nm size can be easily distinguished, providing ac-

cess to the single-particle plasmon properties for a large number of species simultaneously [1]. We present results on the spatially resolved photoemission dependence on wavelength, polarization, and the surface composition for size-selected Ag particles and nanostructure arrays prepared by nanosphere lithography on silicon. [1] K. Oldenburg et al., *J. Phys. Chem. C* 123, 1379 (2019)

O 59.7 Wed 18:00 P4

Inelastic electron-photon scattering with broadband optical pulses — •NIKLAS MÜLLER, RASMUS LAMPE, GERRIT VOSSE, CHRISTOPHER RATHJE, and SASCHA SCHÄFER — Institute of Physics, University of Oldenburg, 26129 Oldenburg, Germany

The inelastic scattering of fast electrons at spatially confined light fields has recently enabled new techniques in ultrafast transmission electron microscopy (UTEM) [1,2,3] but is typically performed with narrow bandwidth light pulses. Here, we study the interaction of fast electrons with broadband, strongly chirped light fields. Optical pulses are generated in a home-build noncollinear optical parametric amplifier (NOPA) [4] with a spectral width of up to 200 nm in the visible range. Light reflection at an aluminum coated silicon nitride membrane leads to an intense multicolor near-field at which we inelastically scatter femtosecond electron pulses forming photon sidebands in the electron energy spectrum. The spectral sideband position changes with the relative timing between electron and light pulse according to the instantaneous frequency of the driving laser field. Different parameter regimes of electron and light chirp and their impact on inelastic scattering patterns are discussed.

[1] G. De Abajo and M. Kociak, *New J. Phys.* 10, 073035 (2008) [2] Barwick et al., *Nature* 462, 902-906 (2009) [3] Feist et al., *Nature* 521, 200-203 (2015) [4] G. Cerullo and S. De Silvestri, *Rev. Sci. Instrum.* 74, 1 (2003)

O 59.8 Wed 18:00 P4

Probing Excitons-Photon interaction in WSe₂ beyond the Non-Recoil Approximation — •FATEMEH CHAHSHOURI, MASOUD TALEB, and NAHID TALEBI — Institute of Experimental and Applied Physics, Kiel University, 24118 Kiel, Germany

Cherenkov radiation from electrons propagating in materials with a high refractive index have applications in particle-detection mechanisms. However, the theory of the Cherenkov radiation has been treated up to now using the non-recoil approximation, which neglects the effect of electron deceleration in materials. Here, we report on the effect of the electron-beam deceleration on the radiated spectrum and exciton-photon interactions in nm-thick WSe₂ crystals beyond the non-recoil approximation. The calculation of the Cherenkov radiation is performed by simulating the energy distribution of an electron beam propagating inside a thick WSe₂ using the Monte Carlo method, and ascertaining the radiating power from electron beams with Liénard-Wiechert retarded potentials. Using this approach, we numerically demonstrate that in thick flakes the radiation due to the electron-beam deceleration is the dominating radiation mechanism. Our numerical findings agrees well with the experimental cathodoluminescence spectra. We further demonstrated that the captured CR in thick slabs could cause Fabry-Perot resonances that emerge as fine structures in the acquired CL spectra and demonstrate the fully coherent process of CR emission, happening due to its phase-matched excitation nature. Our findings pave the way for an accurate design of particle scintillators and detectors, based on the strong-coupling phenomenon.

O 60: Overview Talk Thorsten Deilmann

Time: Thursday 9:30–10:15

Location: S054

Invited Talk

O 60.1 Thu 9:30 S054

Exciting states in atomically thin layers — •THORSTEN DEILMANN — Institute of Solid State Theory, University of Münster, Germany

Monolayers of two-dimensional materials and its stacking unite the fascinating characteristics of the confined in-plane physics with novel features due to the interlayer interaction. Especially in semiconducting materials largely tunable band gaps and optical responses have been observed in various materials. Unraveling the corresponding excited states is a crucial challenge for basic research as well

as for possible applications in opto-electronic devices. Several external stimuli, e.g. doping, electric, or magnetic fields, can be applied to probe the response of many-particle states like excitons or trions, and thus also of its fundamental properties. Applying first-principles methods allows to predict, e.g., the quantum mechanical nature when an exciton is doped and becomes a trion, or its g factor due to the Zeeman effect. These calculations facilitate a connection of the experimental observations with the physical properties of the excited states. In the talk, several features in mono- and multilayer transition metal dichalcogenides and similar materials will be demonstrated.

O 61: Plasmonics and Nanoptics 2

Time: Thursday 10:30–12:45

Location: H2

Topical Talk

O 61.1 Thu 10:30 H2

Single Molecule Nonlinearity in a Plasmonic Waveguide — •MARKUS LIPPITZ — Experimental Physics III, University of Bayreuth

Plasmonic waveguides offer the unique possibility to confine light far below the diffraction limit. Past room temperature experiments focused on efficient generation of single waveguide plasmons by a quantum emitter. However, only the simultaneous interaction of the emitter with multiple plasmonic fields would lead to functionality in a plasmonic circuit. Here, we demonstrate the nonlinear optical interaction of a single molecule and propagating plasmons. An individual terrylene diimide (TDI) molecule is placed in the nanogap between two single-crystalline silver nanowires. A visible wavelength pump pulse and a red-shifted depletion pulse travel along the waveguide, leading to stimulated emission depletion (STED) in the observed fluorescence. The efficiency increases by up to a factor of 50 compared to far-field excitation. Our study thus demonstrates remote nonlinear four-wave mixing at a single molecule with propagating plasmons. It paves the way toward functional quantum plasmonic circuits and improved nonlinear single-molecule spectroscopy.

O 61.2 Thu 11:00 H2

Excitation of coherent phonon modes in plasmonic gold nanoparticles — •DOMINIK HÖING^{1,2}, ROBERT SALZWEDEL⁴, MALTE SELIG⁴, KARTIK AYYER^{2,3}, JOCHEN KÜPPER^{2,3}, ANDREAS KNORR⁴, and HOLGER LANGE^{1,2} — ¹Institute of Physical Chemistry, Universität Hamburg, Hamburg, Germany — ²The Hamburg Centre for Ultrafast Imaging, Hamburg, Germany — ³Center for Free-Electron Laser Science, Hamburg, Germany — ⁴Institut für Theoretische Physik, Technische Universität Berlin, Berlin, Germany

The plasmonic properties of gold nanoparticles (AuNP) have been widely studied, because of their exhibition of strong light-matter coupling and hot carrier generation. The carrier dynamics that follow the optical excitation are presently

understood as a series of events with increasing time-scales. Among them, the excitation of coherent acoustic phonon modes, also called breathing modes, is thought to result from the ultrafast heating of the lattice due to electron-phonon coupling. However, previous experimental studies were insufficient in detecting the onset of the breathing oscillation. Here, we use a combination of transient absorption spectroscopy, time-resolved X-ray scattering and a model combining quantum coherent and hydrodynamic theory to develop a different picture: We show that the gradient in electron density induced by the optical excitation instantaneously couples to coherent phonons, resulting in an immediate onset of the breathing oscillation with the optical excitation. Thus, the processes involved in the plasmon decay are more intertwined as previously assumed.

O 61.3 Thu 11:15 H2

Probing a plasmon-polariton quantum wave packet — SEBASTIAN PRES¹, BERNHARD HUBER¹, DANIEL FERSCH¹, ENNO SCHATZ², DANIEL FRIEDRICH², VICTOR LISINETSII¹, RUBEN POMPE³, •MATTHIAS HENSEN¹, BERT HECHT², WALTER PFEIFFER³, and TOBIAS BRIXNER¹ — ¹Institut für Physikalische und Theoretische Chemie, Universität Würzburg, Am Hubland, 97074 Würzburg, Germany — ²NanoOptics & Biophotonics Group, Experimental Physics 5, Universität Würzburg, Am Hubland, 97074 Würzburg, Germany — ³Fakultät für Physik, Universität Bielefeld, Universitätsstr. 25, 33615 Bielefeld, Germany

Beyond the classical picture, plasmon-polariton modes are treated as quasi-particles in quantum physics and they are considered essential for the realization of future nanoscale quantum functionality. Implementing and demonstrating such functionality requires local access to the quasi-particle's quantum state to monitor its corresponding quantum wave-packet dynamics. Here, we report the local probing of such an eigenstate superposition, linked to a nanoslit resonator, using plasmon-polariton-assisted electron emission as signal in coherent two-dimensional nanoscopy¹. We observe a quantum coherence oscillating

at the third harmonic of the plasmon-polariton frequency and identify it, using quantum dynamical simulations, to arise from the superposition of energetically non-adjacent plasmon-polariton occupation number states. The simulations also contain an improved model for plasmon-polariton-assisted electron emission processes.

[1] M. Aeschlimann et al., *Science* 333, 1723-1726 (2011)

O 61.4 Thu 11:30 H2

Modelling Plasmon-Exciton Interaction using a Coupled-Oscillator Approach — •SIMON DURST, CHRISTOPH SCHNUPPHAGN, and MARKUS LIPPITZ — Experimental Physics III, University of Bayreuth

Coupling effects between plasmonic and excitonic systems have attracted increasing interest in the last decade. In particular, Surface Lattice Resonances, diffractive modes supported by periodic arrays of metallic nanoparticles, allow for long-range coherent energy transfer and have been shown to strongly couple to interspersed excitonic emitters. Here, we will present experimental results showing strong coupling between Surface Lattice Resonances and the excitonic mode of a J-aggregate dye. The angle-resolved extinction spectra of this coupled system are modelled using a coupled oscillator model, which describes observed effects, such as a loss of contrast of the upper polariton branch or an asymptotic behaviour of the lower polariton branch well.

O 61.5 Thu 11:45 H2

Light emission from single self-decoupled molecules — •VIBHUTI RAI¹, LUKAS GERHARD¹, GABRIEL DERENBACH¹, NICO BALZER², MICHAL VALÁŠEK², MARCEL MAYOR², and WULF WULFHEKEL¹ — ¹Institute for Quantum Materials and Technologies, Karlsruhe Institute of Technology (KIT), D-76344 Eggenstein-Leopoldshafen, Germany — ²Institute of Nanotechnology, Karlsruhe Institute of Technology (KIT), D-76344 Eggenstein-Leopoldshafen, Germany

Realization of single molecules as electric light sources faces a dilemma: In order to emit light, they need to be decoupled from the metallic electrodes to prevent fluorescence quenching. To conduct, however, the molecular orbitals need to hybridize with the electrodes. This can be achieved by decoupling the molecular chromophore to a certain extent from the electrode via anchoring groups. In the past, such self-decoupled molecules often lacked reproducibility of the decoupling and energy of the emitted light. Here, we show reproducible and well defined electroluminescence of two different NDI chromophores linked to a gold substrate via a molecular tripod and via a vacuum barrier to the tip of a scanning tunnelling microscope [1]. The stability of the system allows to perform systematic experiments so far only possible for molecules decoupled via insulating layers.

[1] Edelmann, K. et al. *Rev. Sci. Instrum.* 89, 123107 (2018).

O 61.6 Thu 12:00 H2

Investigation of chemical interface damping on electrochemically functionalized flat gold and nanoporous gold surfaces — •MAURICE PFEIFFER¹, XINYAN WU¹, ALEXANDER PETROV^{1,2}, and MANFRED EICH^{1,2} — ¹Institute of Optical and Electronic Materials, Hamburg University of Technology, Germany — ²Institute of Photoelectrochemistry, Helmholtz-Zentrum Hereon, Geesthacht, Germany

The chemical interface damping (CID) effect occurs at metal surfaces when applying surface modifications, such as oxidation. It results in an increase of the electron collision frequency of the metal, thus altering its optical properties. Previous research showed that this effect may also enhance the efficiency of photocatalytic water splitting by visible light [1]. We investigate the CID effect on flat gold as well as nanoporous gold samples with the latter having the advantage

of a very high surface to volume ratio, making surface effects (like CID) more pronounced. Our experimental setup consists of a spectroscopic ellipsometer to investigate the optical properties. This device is equipped with an electrochemical cell in which we can reversibly oxidize the sample surface, allowing an in-situ study of the CID effect. Previous research investigated the CID effect on gold nanoparticles and observed an increase of the damping rate at the plasmon resonance [2]. Our results on flat gold reveal a similar increase of the damping, but additionally enable the investigation of broadband properties from which we expect further insights on the nature of the damping mechanism.

[1] Graf et al., *ACS Nano* 2021, 15, 2, 3188-3200 [2] Foerster et al., *Nano Lett.* 2020, 20, 5, 3338-3343

O 61.7 Thu 12:15 H2

Switching on the electroluminescence of single molecules adsorbed directly on a metal surface — VIBHUTI RAI¹, •LUKAS GERHARD¹, NICO BALZER², MICHAL VALÁŠEK², CHRISTOF HOLZER³, LIANG YANG², MARTIN WEGENER², CARSTEN ROCKSTUHL³, MARCEL MAYOR², and WULF WULFHEKEL¹ — ¹Institute for Quantum Materials and Technologies, Karlsruhe Institute of Technology (KIT), D-76344 Eggenstein-Leopoldshafen, Germany — ²Institute of Nanotechnology, Karlsruhe Institute of Technology (KIT), D-76344 Eggenstein-Leopoldshafen, Germany — ³Institute of Theoretical Solid State Physics, Karlsruhe Institute of Technology (KIT), D-76131 Karlsruhe, Germany

Exciting single molecules to emit light into the far-field requires them to be electronically decoupled from the contacting metallic leads. In the scanning tunnelling microscope (STM) geometry, typically this has been achieved by inserting insulating layers between the molecules and the metal substrate [1]. Here, we report our finding that it is possible to activate the electroluminescence (EL) of individual 2,6-core-substituted naphthalene diimide derivatives (Tpd-sNDI), adsorbed directly on a metal surface with the help of the STM tip. We observe that to emit light, both orbitals involved in the optical transition need to be electronically decoupled. The STM measurements were performed with a home-built, low temperature, ultra-high vacuum scanning tunnelling microscope (STM) with optical access [2].

[1] Zhang, Y. et al. *Nature* 531, 623 (2016).

[2] Edelmann, K. et al. *Rev. Sci. Instrum.* 89, 123107 (2018).

O 61.8 Thu 12:30 H2

First principles investigation of plasmonic hydrogen catalysis on metallic magnesium nanoparticles — •OSCAR A. DOUGLAS-GALLARDO, CONNOR L. BOX, and REINHARD J. MAURER — University of Warwick, Coventry, United Kingdom

Plasmon-induced hot-carrier photochemistry is currently a promising avenue to achieve highly selective and efficient chemical transformation on plasmonic metal surfaces. A new class of materials made up of Earth-abundant-elements has gained increasing interest in the plasmonic area, as an alternative to the oft studied late transition metals (Au, Ag and Cu).

Here, we will present our results on the optical and electronic properties of metallic magnesium nanoparticles and their potential use as plasmonic hydrogen catalysts. We explore the optical and electronic properties with time-dependent density functional tight-binding (TD-DFTB) and molecular dynamics with electronic friction (MDEF) simulations. Our results show that Mg nanoclusters can produce highly energetic hot-electrons and they energetically align with electronic states of physisorbed molecular hydrogen, the occupation of which by these hot electrons can promote hydrogen dissociation. The reverse reaction, hydrogen evolution on metallic Mg, may also be promoted by hot electrons, but following a different mechanism.

O 62: Surface Reactions and Heterogeneous Catalysis 1

Time: Thursday 10:30–12:45

Location: H4

O 62.1 Thu 10:30 H4

Gaussian Approximation Potentials for Surface Catalysis — •SINA STOCKER^{1,2}, GÁBOR CSÁNYI², KARSTEN REUTER¹, and JOHANNES T. MARGRAF¹ — ¹Fritz Haber Institut der Max Planck Gesellschaft, Berlin, Germany — ²Technische Universität München, Germany — ³University of Cambridge, United Kingdom

Predictive-quality first-principles based microkinetic models are increasingly used to analyze (and subsequently optimize) reaction mechanisms in heterogeneous catalysis. In full rigor, such models require the knowledge of all possible elementary reaction steps and their corresponding reaction barriers. Unfortunately, for complex catalytic processes (such as the generation of ethanol from syngas) the number of possible steps is so large that an exhaustive first-principles calculation of all barriers becomes prohibitively expensive.

To overcome this limitation, we develop machine learned (ML) interatomic potentials to model syngas conversion on Rhodium. These ML potentials can be used to determine free energy reaction barriers for a large number of adsorbates

at various CO coverages and at a fraction of the computational cost of the underlying first-principles method. Specifically, we use here the Gaussian Approximation Potential (GAP) framework and explore iterative training in combination with umbrella sampling.

O 62.2 Thu 10:45 H4

Hydrogen adsorption on Pd surfaces and its effect on CO₂ activation — •HERZAIN I. RIVERA-ARRIETA¹, IGOR KOWALEC², LUCAS FOPPA¹, ANDREW LOGSDAIL², DAVID WILLOCK², and MATTHIAS SCHEFFLER¹ — ¹The NO-MAD Laboratory at the Fritz Haber Institute of the Max Planck Society and the Humboldt-Universität zu Berlin, Germany — ²Cardiff Catalysis Institute, Cardiff University, UK

Understanding the reactivity of Pd-based catalysts in hydrogenation processes requires an accurate description of its surfaces at realistic temperature (T) and hydrogen pressure (p_{H_2}). Herein, by modeling the surface phase diagram of Pd (111) and (100) as a function of T , p_{H_2} via *ab initio* atomistic thermodynamics

[1], we predict 1 monolayer (ML) coverage of H as the most stable configuration under common experimental reaction conditions [2]. Taking a particular interest in the activation of CO₂, we performed simulations concerning the interaction of the molecule with the surfaces as the H-coverage increases from 0 to 1ML. Our results show how 1 ML of H inhibits the formation of chemisorbed CO₂^{δ-}, the initial intermediate in the CO₂ hydrogenation reaction. The generated data will be combined with information from other metal surfaces, and the subgroup-discovery artificial-intelligence approach [3] will be applied to identify which basic materials parameters correlate with indicators of CO₂ activation, e.g. the adsorption energy or the C-O bond elongation.

[1] C. Stampfl, *et al.*, *Appl. Phys. A*, **69**, 471 (1999).

[2] H. Bahruji, *et al.*, *J. Catal.*, **343**, 133 (2016).

[3] B. R. Goldsmith, *et al.*, *New J. Phys.*, **19**, 013031 (2017).

O 62.3 Thu 11:00 H4

Atomic steps as active sites in the Co-catalyzed Fischer-Tropsch synthesis: Evidence from an operando STM study on a stepped model catalyst — •KATHARINA GOLDBERGER and JOOST WINTERLIN — Ludwig-Maximilians-Universität München, Germany

Atomic steps are often assumed to represent the active sites on the surface of a heterogeneous catalyst. This assumption is based on turnover data that display a certain scaling of the activity with the particle sizes of the catalysts. However, this evidence is indirect and often controversial. We have recently shown that the activity of a Co(0001) single crystal surface in the Fischer-Tropsch synthesis of hydrocarbons is proportional to the density of atomic steps. This is a quite direct evidence for the activity of atomic steps, but it was obtained for a flat model system. Here we present results of investigations on a Co(101 $\bar{1}$ 5) surface that has a similar step density as the Co particles of the industrial Fischer-Tropsch catalyst. The experiments were performed with a scanning tunneling microscope (STM) at a syngas (2H₂+CO) pressure of ~1 bar and a temperature of 503 K. Hydrocarbon products were detected by a special gas chromatograph (GC). The STM data show that the morphology of the stepped surface is stable under operando conditions. The activity measured by GC is considerably higher than that of the Co(0001) sample. It is close to the activities reported for supported Co catalysts, a result that bridges the materials gap between model systems and the industrial Fischer-Tropsch catalysts.

O 62.4 Thu 11:15 H4

Predicting Binding Motifs of Complex Adsorbates Using Machine Learning with a Physics-inspired Graph Representation — •WENBIN XU¹, KARSTEN REUTER¹, and MIE ANDERSEN² — ¹Fritz-Haber-Institut der MPG, Berlin, Germany — ²Aarhus Institute of Advanced Studies and Department of Physics and Astronomy, Aarhus University, Denmark

Complex adsorbates are involved in many surface catalytic reactions such as Fischer-Tropsch, methanol, or higher oxygenate synthesis. The modeling of these species at transition metal catalysts must account for their ability to exhibit a wide range of adsorption motifs, including mono- and multi-dentate adsorption modes. Given the combinatorial explosion of possible adsorption motifs and the computational cost of density functional theory, it is desirable to develop machine learning (ML) models for predicting the binding motifs and their associated adsorption enthalpies. Most ML models to date are only applicable to simple adsorbates. In this work, we overcome this limitation and propose a kernelized ML model with a physics-inspired graph representation for the prediction of complex species. The model is data-efficient and its good extrapolation ability makes it promising for comprehensively exploring complex reaction networks on novel catalysts. Furthermore, we show that the outliers with large prediction errors can be reliably captured from an ensemble uncertainty prediction approach.

O 62.5 Thu 11:30 H4

Machine-Learning Driven Global Optimization of Surface Adsorbate Geometries — •HYUNWOOK JUNG, SINA STOCKER, KARSTEN REUTER, and JOHANNES T. MARGRAF — Fritz-Haber-Institut der MPG, Berlin, Germany

The adsorption energy is an essential descriptor for predicting catalytic activity in theoretical models of heterogeneous catalysis. Although established scaling relations facilitate the prediction of adsorption energies for small adsorbates like OH, they are not applicable to larger adsorbates that are frequently encountered in syngas chemistry. Such systems often feature complex potential energy surfaces due to their flexibility and the possibility of multidentate binding to the surface. Consequently, computing adsorption energies for such adsorbates implies a complex global optimization to find the ground state geometry. This is prohibitively expensive at the density functional theory (DFT) level for routine applications. To tackle this issue, we present a global optimization protocol for adsorbate geometries which trains a surrogate Gaussian Approximation Potential on-the-fly. The approach is applicable to generic surface models (i.e. without defining surface sites) and minimizes both user intervention and the number of DFT calculations by iteratively updating the training set with configurations explored by the algorithm. We demonstrate this approach for diverse adsorbates on the Rh (111) and (211) surfaces.

O 62.6 Thu 11:45 H4

New catalysts for oxidative-coupling of methane: theoretical search and experimental validation — •ALIAKSEI MAZHEIKA¹, MICHAEL GESKE¹, MATTHIAS MUELLER², STEPHAN SCHUNK², FRANK ROSOWSKI^{1,3}, and RALPH KRAEHNERT¹ — ¹Technische Universität, Berlin, DE — ²hte GmbH, Heidelberg, DE — ³BASF SE, Ludwigshafen, DE

Oxidative-coupling of methane (OCM) is a direct way for conversion of methane to higher hydrocarbons - ethane, ethylene. Despite many years spent for the search of an efficient catalyst, still a material which would satisfy industrial rentability has not been found. In our study we proceed from an experimentally observed volcano-like dependence of C₂-yields on formation energies of carbonates on oxide catalysts [1]. We developed a new method which allows to calculate carbonates formation energies from CO₂ adsorption energies on the surfaces of corresponding oxides. In combination with artificial intelligence methods (data mining and symbolic regression) this was used in the high-throughput screening. The latter is done in a way of active-learning, and we demonstrate its advantages compared to traditional scheme. Several catalysts obtained from the screening have been synthesized and experimentally tested together with less promising materials. Obtained C₂-yields follow the same volcano-type dependence that formed initial basis for the employed strategy. The best catalyst candidates reach maximum C₂-yields comparable to the well-known OCM catalysts and outperform them at lower temperatures.

[1] H. Wang *et al.*, <https://doi.org/10.26434/chemrxiv-2022-gxt5n>

O 62.7 Thu 12:00 H4

Finding catalyst genes with subgroup discovery — •ALIAKSEI MAZHEIKA¹, YANGGANG WANG², ROSENDO VALERO³, FRANCESC VINES³, FRANCESC ILLAS³, LUCA M. GHIRINGHELLI⁴, SERGEY V. LEVCHENKO⁵, and MATTHIAS SCHEFFLER⁴ — ¹Technische Universität, Berlin, DE — ²University of Science and Technology, Shenzhen, CN — ³Universitat de Barcelona, Barcelona, ES — ⁴The NOMAD Laboratory at the Fritz Haber Institute and Humboldt University, Berlin, DE — ⁵Moscow

Catalytic-materials design requires predictive modeling of the interaction between catalyst and reactants. This is challenging due to the complexity and diversity of structure-property relationships across the chemical space. Here, we report a strategy for a rational design of catalytic materials using the artificial intelligence approach (AI) subgroup discovery. We identify catalyst genes (features) that correlate with mechanisms that trigger, facilitate, or hinder the activation of carbon dioxide (CO₂) towards a chemical conversion. The AI model is trained on first-principles data for a broad family of oxides. We demonstrate that surfaces of experimentally identified good catalysts consistently exhibit combinations of genes resulting in a strong elongation of a C-O bond. The same combinations of genes also minimize the OCO-angle, the previously proposed indicator of activation, albeit under the constraint that the Sabatier principle is satisfied. Based on these findings, we propose a set of new promising catalyst materials for CO₂ conversion.—A. Mazheika *et al.* *Nature Comm.* 2022, 13, 419.

O 62.8 Thu 12:15 H4

Selectivity in single-molecule reactions by tip-induced redox chemistry — •FLORIAN ALBRECHT¹, SHADI FATAYER^{1,2}, IAGO POZO³, IVANO TAVERNELLI¹, JASCHA REPP⁴, DIEGO PENA³, and LEO GROSS¹ — ¹IBM Research - Zurich, 8803 Rüschlikon (Switzerland) — ²Physical Science and Engineering Division, King Abdullah University of Science and Technology (KAUST), 23955-6900 Thuwal (Saudi Arabia) — ³Centro Singular de Investigación en Química Biolóxica e Materiais Moleculares (CiQUS) and Departamento de Química Orgánica, Universidade de Santiago de Compostela, 15782 Santiago de Compostela (Spain) — ⁴Institute of Experimental and Applied Physics, University of Regensburg, 93053 Regensburg (Germany)

Since the first experiments by S.-W. Hla in 2000 [1], tip-induced on-surface synthesis is an active field. Not only in on-surface chemistry, selective control over the outcome of a reaction is a major quest. Here, we activate a molecule adsorbed on ultrathin insulating films by dehalogenation and perform selective constitutional isomerization reactions in a low temperature UHV combined STM and AFM. The selectivity is controlled by the polarity and amplitude of applied voltage pulses. The insulating films stabilize the isomers in different charge states and allow for their characterization. The importance of molecular charge state on the reaction is supported by DFT-derived isomerization energy landscape. [1] S.-W. Hla *et al.*, *Phys. Rev. Lett.* **85**, 2777 (2000).

O 62.9 Thu 12:30 H4

Abiotic Formation of an Amide Bond via Surface-Supported Direct Carboxyl-Amine Coupling — •BIAO YANG^{1,2}, KAIFENG NIU^{1,3}, FELIX HAAG², NAN CAO^{1,2}, JUNJIE ZHANG¹, HAIMING ZHANG¹, QING LI¹, FRANCESCO ALLEGRETTI², JONAS BJÖRK³, JOHANNES BARTH², and LIFENG CHI¹ — ¹Institute of Functional Nano and Soft Materials (FUNSOM), Soochow University, Suzhou 215123 (P. R. China) — ²Physics Department E20, Technical University of Munich, D-85748 Garching, (Germany) — ³Department of Physics, Chemistry and Biology, IFM, Linköping University, 58183 Linköping (Sweden)

Amide bond formation is one of the most important reactions in biochemistry,

notably being of crucial importance for the origin of life. Herein, we combine scanning tunneling microscopy and X-ray photoelectron spectroscopy studies to provide evidence for thermally activated abiotic formation of amide bonds between adsorbed precursors through direct carboxyl-amine coupling under ultrahigh-vacuum conditions by means of on-surface synthesis. Complementary insights from temperature-programmed desorption measurements and density

functional theory calculations reveal the competition between cross-coupling amide formation and decarboxylation reactions on the Au(111) surface. Furthermore, we demonstrate the critical influence of the employed metal support: whereas on Au(111) the coupling readily occurs, different reaction scenarios prevail on Ag(111) and Cu(111). [1] [1] Biao Yang⁺, Kaifeng Niu⁺, et al. *Angew. Chem. Int. Ed. anie*.202113590 (2021)

O 63: New Methods and Developments 4: Spectroscopies, Diffraction and Others (joint session O/KFM)

Time: Thursday 10:30–12:30

Location: H6

Topical Talk

O 63.1 Thu 10:30 H6

Element and Structure Analysis of Surfaces Using Positrons — •CHRISTOPH HUGENSCHMIDT — Forschungs-Neutronenquelle Heinz Maier-Leibnitz (MLZ), Technische Universität München, Lichtenbergstr. 1, 85748 Garching, Germany With the advent of bright low-energy positron beams novel analysis tools have been developed exploiting the unique properties of positron matter interaction such as repulsive crystal potential or positron trapping in surface states [1]. Positron annihilation is established for defect spectroscopy and the characterization of the free volume in amorphous matter. By applying a slow positron beam, however, defects near the surface can be specifically addressed, e.g. for the determination of the oxygen vacancy concentration in $\text{YBa}_2\text{Cu}_3\text{O}_{7-x}$ [2]. The positron counterparts of reflection high-energy electron diffraction (RHEED) and electron induced Auger-electron spectroscopy (AES) intrinsically exhibit superior surface sensitivity. In contrast to electrons, positrons show total reflection for small glancing angles. It was demonstrated that with reflection high-energy positron diffraction the structure of the topmost and the immediate subsurface atomic layer of surfaces are revealed with outstanding accuracy. The main advantages of positron annihilation induced AES are the missing secondary electron background and its topmost layer sensitivity for element analysis allowing, e.g. the *in-situ* observation of the Ni adatom migration from the Pd surface into the bulk [3]. [1] C. H.; *Surf. Sci. Reports* 71 (2016) 547; [2] M. Reiner et. al.; *Phys. Rev. B* 97 (2018) 144503; [3] S. Zimnik et. al.; *Surf. Sci.* 664 (2017) 61

O 63.2 Thu 11:00 H6

Active sample manipulation with electrostatic beams: a different way of bridging the high-voltage gap — •FRANCESCO GUATIERI, KILIAN BRENNER, and CHRISTOPH HUGENSCHMIDT — Heinz Maier-Leibnitz Zentrum (MLZ), Technical University of Munich, Lichtenbergstr. 1, 85748 Garching, Germany Most electrostatic positron beams used to perform surface studies are accelerated to the desired implantation energy by floating the target to a high electrostatic potential relative to ground. The presence of tens on kilovolts of electric potential makes the use of instrumentation attached directly to the sample inconvenient. The conventional solution to this hurdle consists in wiring insulated connections from the sample to a high-voltage galvanic decoupling placed outside of the experimental chamber far away from the sample holder. This solution carries limitations on the kind and amount of electrical connections employed. We will present, instead, a novel approach to in-operando sample manipulation that we have developed to be used at the Doppler broadening spectrometer installed on the NEPOMUC positron source, which implements the galvanic insulation in situ and removes many of the limitations imposed by conventional solutions.

O 63.3 Thu 11:15 H6

Advanced Kernel-Based NMR Cryoporometry Characterization of Mesoporous Solids — •HENRY R.N.B. ENNINFUL, DANIEL SCHNEIDER, RICHARD KOHNS, DIRK ENKE, and RUSTEM VALIULLIN — Leipzig University, Leipzig, Germany

NMR cryoporometry is a pore space characterization technique for industrial and natural materials such as catalysts, gas storage materials, cartilage, bones, rocks and many more. While gaining wide use, the fundamental phenomena underlying solid-liquid phase transitions in geometrically disordered porous materials is still not fully understood. This may lead to inaccurate pore size distributions from the NMR cryoporometry technique.

In this work, we have developed a new approach to NMR cryoporometry. Herein, it takes account of cooperativity effects in pores, the existence of a variable non-frozen layer (NFL) thickness between the frozen core and pore wall and the effect of curvature on thermal fluctuations in pores which hitherto are missing in the current approach. In the first place, we compile a family of transition curves characterizing the phase state in pores with different pore sizes, so called kernels. Thereafter, we apply a general framework for predicting phase equilibria in a collection of pores. Specifically, the proposed kernel-based approach is coupled with the serially-connected pore model (SCPM) to be able to predict phase behavior in independent pore systems as well as in pore networks. We demonstrate the new approach by applying it to ordered porous materials such as MCM-41 and SBA-15. Consequently, a more accurate pore size distribution (PSD) is obtained.

O 63.4 Thu 11:30 H6

Development of an electron spin resonance spectrometer in ultra-high vacuum for surface spins — •JUYOUNG PARK^{1,2}, FRANKLIN H. CHO^{1,2}, JISOO YU^{1,2}, LUCIANO COLAZZO^{1,2}, YEJIN JEONG^{1,2}, JUNJIE LIU³, ARZHANG ARDAVAN³, GIOVANNI BOERO⁴, ANDREAS HEINRICH^{1,2}, and FABIO DONATI^{1,2} — ¹Center for Quantum Nanoscience, Institute for Basic Science, Seoul, Republic of Korea — ²Ewha Womans University, Seoul, Republic of Korea — ³The Clarendon Laboratory, Department of Physics, University of Oxford, Oxford, UK — ⁴Ecole Polytechnique Fédérale de Lausanne, Laboratory for Microsystems, Lausanne, Switzerland

We present the development of an electron spin resonance (ESR) spectrometer operating in ultra-high vacuum (UHV) for studying surface-adsorbed molecular and atomic spin systems. Such surface spin systems are promising platforms for potential applications in quantum computing and information processing [*Science* 366, 509 (2019)]. Our spectrometer is capable of both continuous-wave and pulsed ESR measurement in the temperature range of 2.5 K to 300 K. The surface-sensitivity is attained using a surface-type microwave resonator with its resonance frequency in the X-band. The spectrometer is connected to a home-built in-situ preparation chamber which allows us to prepare and characterize surfaces with low-energy electron diffraction and Auger electron spectroscopy. We demonstrate that we are sensitive down to a monolayer of molecular film using organic radicals such as α,γ -Bisdiphenylene- β -phenylallyl, and metal phthalocyanine complexes such as vanadyl phthalocyanine.

O 63.5 Thu 11:45 H6

Unsupervised machine learning-assisted analysis of multidimensional ARPES data — •STEINN YMR AGUSTSSON¹, MOHAMMAD AHSANUL HAQUE², FATEMEH ZARDBANI², DAVIDE MOTTIN², PANAGIOTIS KARRAS², and PHILIP HOFMANN¹ — ¹Institute of Physics and Astronomy, Aarhus University, Denmark — ²Institute of Computer Science, Aarhus University, Denmark

In recent years, the size and complexity of experimental data sets has been dramatically growing in many fields of science. For photoemission spectroscopy, the development of novel detectors and multi-dimensional measurement modes (e.g., including a time dependence or spatial dependence), has lead to orders of magnitude more data being produced. Even after a necessary upgrade of the data management system, it remains highly challenging to visualize and superficially interpret the data fast enough to feed back into decisions about what to measure in an ongoing experimental run. A promising approach to address this is the application of machine learning tools. These have shown promising results when applied to data reduction and feature detection tasks in many fields of science. We have developed an unsupervised clustering method which is able to distinguish differences between ARPES spectra obtained from different spatial locations in nanoARPES measurements. This enables quick and automatic identification and classification of regions with different spectral features, allowing to invest more time in the collection of significant data.

O 63.6 Thu 12:00 H6

ViPerLEED: A modern all-in-one LEED I(V) package — •ALEXANDER M. IMRE¹, FLORIAN KRAUSHOFER^{1,2}, FLORIAN DOERR¹, TILMAN KISSLINGER³, MICHAEL SCHMID¹, ULRIKE DIEBOLD¹, LUTZ HAMMER³, and MICHELE RIVA¹ — ¹TU Wien, Vienna, Austria — ²TU Munich, Munich, Germany — ³FAU Erlangen-Nürnberg, Erlangen, Germany

Many surface science groups use Low-Energy Electron Diffraction (LEED) for quick, qualitative analysis of surface periodicity. Analysis of the beam intensities as a function of electron energy [LEED $I(V)$] is sensitive to surface atom positions at the picometer scale. Thus, comparison with calculated intensities can verify or reject structural models. Despite this, LEED $I(V)$ is currently rather unpopular, largely because the available software solutions are not sufficiently user-friendly. To greatly lower the barrier of entry into the field, we present the Vienna Package for TensErLEED (ViPerLEED) which provides a truly all-in-one package for LEED $I(V)$. ViPerLEED includes a freely available design for electronics that enable upgrading existing LEED setups for LEED $I(V)$ use. With sophisticated image acquisition and processing methods, as well as an automated spot-tracking tool for curve extraction, we greatly simplify the most tedious parts of the experiment. For the calculation of intensities, the pack-

age includes a user-friendly front-end and an extensive overhaul to the established TensErLEED package that only requires a few standardized input files. We further describe automated symmetry detection, improvements to the structure search algorithm, and a Python API.

O 63.7 Thu 12:15 H6

On-surface GNR fabrication via electrospray deposition of monomers and polymers from solution — •FELIX BAIER¹, CHRISTOPH DOBNER¹, MICHAEL BECKSTEIN¹, MAMUN SARKER², ALEXANDER SINITSKI², and AXEL ENDERS¹ — ¹Universität Bayreuth — ²University of Nebraska - Lincoln, USA

Strategies for depositing large organic molecules such as proteins, DNA or graphene nanoribbons (GNRs) are urgently needed because the conventional method of evaporation is impossible due to the size of the molecules. GNRs prepared in solution are of particular interest because they are longer compared to

those synthesized on the surface and can be produced in large quantities. Since GNRs form crystallites, they cannot be brought onto the surface by direct contact printing and characterized using STM. Therefore, a new electrospray setup was developed for the deposition of GNR precursor molecules, large precursor polymers, and GNR from a solution. The instrument consists of a heatable stainless steel capillary to which a high voltage in the range -8 to 8 kV, with respect to the sample can be applied. The assembly is placed in a glovebox which ensures the cleanliness of the working process. The characterization of the deposits was done with STM under ultra high vacuum after sample transfer. The deposition of TPTP monomers from solution onto Au(111) brought comparable results as other, established approaches were cGNR were formed after direct contact printing in UHV. Larger polymers were also deposited and completely cyclized on the surface after deposition, forming promising GNRs that have not been studied anywhere before.

O 64: Gerhard Ertl Young Investigator Award

Time: Thursday 10:30–13:00

Location: S051

O 64.1 Thu 10:30 S051

Gold-colored metallic water solution — •TILLMANN BUTTERSACK¹, PHILIP MASON², CHRISTIAN SCHEWE², RYAN MCMULLEN³, FLORIAN TRINTER^{1,4}, DANIEL NEUMARK⁵, STEPHAN THÜRMER⁶, ROBERT SEIDEL⁷, BERND WINTER¹, STEPHEN BRADFORTH³, and PAVEL JUNGWIRTH² — ¹Fritz-Haber-Institute, Berlin, GER — ²Czech Academy of Sciences, Prague, CZ — ³U Southern California, Los Angeles, USA — ⁴DESY, Hamburg, GER — ⁵UC Berkeley, USA — ⁶Kyoto U, JP — ⁷BESSY, Berlin, GER

Whereas tap water and common aqueous solutions conduct some electricity, pure water is an almost perfect insulator. The required pressures to transform water into a metallic state will not be achievable on Earth. Liquid Ammonia undergoes a gradual phase transition from a blue electrolyte solution to a bronze-colored metallic solution if the concentration of solvated alkali metal is enhanced. Water and alkali metals react vigorously, as the valence electrons of the alkali metal are transferred to the aqueous solution almost instantly, leading to a Coulomb explosion. Here, we demonstrate, that water from the gas phase adsorbs onto the surface of sodium-potassium alloy droplet leading to the formation of a thin shiny and golden layer. Characterization of the liquid with photoelectron and UV/Vis spectroscopy revealed a plasmon energy of 2.7 eV and signatures of liquid water. These observations are spectroscopic evidence for an aqueous solution with metallic properties. Its plasmon frequency is in the visible region of the spectrum and thus is the reason for the fascinating golden color.

O 64.2 Thu 11:00 S051

Standing molecules for quantum sensing — •TANER ESAT — Peter Grünberg Institute (PGI 3), Forschungszentrum Jülich, 52425 Jülich, Germany — Jülich Aachen Research Alliance (JARA), Fundamentals of Future Information Technology, 52425 Jülich, Germany

Artificial nanostructures, fabricated by placing building blocks like atoms and molecules in well-defined positions, are an almost universal playground where quantum effects can be studied and exploited on the atomic scale. In my talk, I will show that the manipulation capabilities of a scanning tunneling microscope (STM) allow the fabrication of metastable structures which do not form spontaneously in nature and that these structures offer attractive functionalities for quantum information and sensing. Specifically, I will demonstrate that a large planar aromatic molecule can be lifted into an upright standing geometry on a pedestal of two metal adatoms using the STM tip. This atypical and surprisingly stable upright orientation of the single molecule enables the system to function as a quantum dot and a coherent single-electron field emitter. Utilizing a novel homebuilt STM that uses adiabatic demagnetization refrigeration (ADR) to reach millikelvin temperatures, I will show that the standing molecule is weakly coupled to the surface and that it exhibits spin-flip excitations corresponding to a spin-1/2 system. If the standing molecule is fabricated on the tip, it can be used for the measurement of surface potentials and magnetic fields on the atomic scale at the same time - possibly even as an electron spin resonance sensor on the tip.

O 64.3 Thu 11:30 S051

On-surface synthesis and characterization of cyclo[18]carbon — •KATHARINA KAISER¹, LOREL SCRIVEN², FABIAN SCHULZ¹, PRZEMYSŁAW GAWEL², LEO GROSS¹, and HARRY ANDERSON² — ¹IBM Research - Zurich, Säumerstrasse 4, 8803 Rüschlikon, CH — ²Department of Chemistry, Oxford University, Chemistry Research Laboratory, Oxford, OX13TA, UK

Cyclo[*n*]carbons, purely *sp*-hybridized carbon allotropes with unique structural and electronic properties, have been predicted for decades to exist. Although a synthetic route was already elaborated in the 1980's, and glimpses of cyclo-carbons were detected in gas phase, they could never be stabilized long enough for characterization. A distinctive feature of cyclo[*n*]carbons is their two conju-

gated π -systems that can lead to the formation of two orthogonal ring currents and so-called double-aromatic stabilization. However, distortions in the geometry can lead to a lowering in ground state energy, and theoretically predicted ground state structures were found to depend on the level of theory. Consequently, cyclo[*n*]carbon's structures remained unknown.

AFM and STM at low temperatures allow triggering certain on-surface chemical reactions by atom manipulation and can thus facilitate the controlled formation of highly reactive molecules on inert surfaces from more stable precursors. Using this approach, we formed cyclo[18]carbon on a thin layer of NaCl. By comparing high-resolution AFM images with a functionalized tip and AFM simulations of different predicted resonance structures, we identified two possible ground state structures of cyclo[18]carbon adsorbed on bilayer NaCl.

O 64.4 Thu 12:00 S051

Correlative in situ microscopy of hydrogen oxidation on rhodium: from the meso- to the nanoscale — •JOHANNES ZEININGER — Institute of Materials Chemistry, TU Wien, Getreidemarkt 9, 1060 Vienna, Austria

Catalytic surface reactions, such as CO oxidation, may produce a variety of spatio-temporal effects on the catalyst surface. To reveal the mechanisms behind such spatio-temporal effects, it is advantageous to apply multiple techniques to the same samples, particularly at different length scales. In other research areas than catalysis this idea has led to the correlative microscopy approach. In catalysis, this approach is, if at all, used for sample characterization, often in two separate setups. In the present contribution, the correlative microscopy approach has been applied in situ to the catalytic hydrogen oxidation on rhodium to reveal the mechanism of multifrequent kinetic oscillations, a novel effect recently detected in this reaction. Such oscillations were first observed on a polycrystalline Rh foil, where the reaction oscillated in a self-sustained way between the states of high and low activity (a known behavior), but with different frequencies on adjacent domains (a new and unexpected behavior). Later on, such an effect was also observed on the nanofacets of a Rh tip modeling a single catalytic particle. Such behavior contradicts previous observations and expectations based on the known spatial coupling mechanisms and was never observed before, for any surface reaction.

O 64.5 Thu 12:30 S051

Efficient electronic passivation schemes for surface calculations of semiconductors exhibiting spontaneous polarization: Thermodynamic and electronic properties of GaN surfaces — •SU-HYUN YOO¹, MIRA TODOROVA¹, LIVERIOS LYMPERAKIS¹, CHRIS VAN DE WALLE², and JÖRG NEUGEBAUER¹ — ¹Department of Computational Materials Design, MPI für Eisenforschung, Germany — ²Computational Materials Group, Materials Department, UCSB, USA

Semiconductor surfaces play a central role in modern technology related to catalysis, electronics, and energy applications. The most widespread approach to study surfaces with density-functional theory calculations is to use slab geometries with periodic boundary conditions. A common strategy employed to avoid artificial charge transfer from one side of the slab to another, is to passivate the dangling bonds at its backside. Using the examples of wurtzite polar and semipolar surfaces, we demonstrate that the conventional passivation scheme using pseudo-H atoms fails to describe the electronic structure of low-symmetry semiconductors. We therefore developed an improved passivation method [npj Comp. Mater. 7, 58, 2021/PR Mater. 5, 044605, 2021] that takes the polarization effect and the concept of surface reconstructions into account. It accurately describes surface electronic properties and enables computationally efficient surface energy calculations. Using this novel approach we have studied the orientation-dependent thermodynamic stability and electronic properties of GaN surfaces. The resulting Wulff shape provides insight of how to avoid facet-related defects such as V-pits hampering GaN-based electronics.

O 65: 2D Materials 2: Growth, Structure and Substrate Interaction

Time: Thursday 10:30–12:30

Location: S052

O 65.1 Thu 10:30 S052

Segregation-enhanced epitaxy of borophene on Ir(111) by thermal decomposition of borazine — •KARIM OMAMBAC¹, MARKO KRIEDEL¹, MARIN PETROVIC^{1,2}, PANTELIS BAMPOULIS⁴, CHRISTIAN BRAND¹, PASCAL DREHER¹, DAVID JANOSCHKA¹, ULRICH HAGEMANN³, NILS HARTMANN³, PHILIPP VALERIUS⁴, THOMAS MICHELY⁴, FRANK-J. MEYER ZU HERINGDORF^{1,3}, and MICHAEL HORN-VON HOEGEN¹ — ¹Universität Duisburg-Essen, Germany — ²Institute of Physics, 10000 Zagreb, Croatia — ³Interdisciplinary Center for the Analytics on the Nanoscale, Germany — ⁴Universität zu Köln, Germany

While borophene is typically prepared by molecular beam epitaxy [1], we report here on an alternative way of synthesizing large single-phase borophene domains by segregation enhanced epitaxy. X-ray photoelectron spectroscopy shows that borazine dosing at 1100°C onto Ir(111) yields a boron-rich surface without traces of nitrogen. At high temperatures the borazine thermally decomposes, nitrogen desorbs, and boron diffuses into the substrate. Using time-of-flight secondary ion mass spectroscopy we show that during cooldown the sub-surface boron segregates back to the surface where it forms borophene. In this case electron diffraction reveals a (6x2) reconstructed borophene χ_6 -polymorph [1], and scanning tunneling spectroscopy suggests a Dirac-like behavior. Studying the kinetics of borophene formation in low energy electron microscopy shows elongated and extended borophene domains with exceptional structural order. [1] ACS Nano 13 (12), 14511-14518 (2019).

O 65.2 Thu 10:45 S052

Investigation of sub-monolayer Sn phases on Au(111) — •JULIAN ANDREAS HOCHHAUS^{1,2}, LUKAS KESPER^{1,2}, STEFANIE HILGERS¹, ULF BERGES^{1,2}, and CARSTEN WESTPHAL^{1,2} — ¹Technische Universität Dortmund, Fakultät Physik, Otto-Hahn-Str. 4, D-44227, Dortmund, Germany — ²DELTA, TU Dortmund, Maria-Goeppert-Mayer-Str. 2, D-44227, Dortmund, Germany

In this study we investigate the temperature and layer thickness dependence of sub-monolayer phases of Sn on Au(111). Stanene, the two-dimensional graphene analog of tin, is predicted to exhibit similar exceptional electronic properties. Since tin is one of the heavier elements in the carbon group, stanene exhibits topological properties even at RT due to its strong spin-orbit coupling. Therefore, stanene is a promising material for application in future two-dimensional topological devices.

Since the surface and interface structure of low-dimensional materials often influences their electronic properties, we focus on the structural and chemical analysis of the Sn/Au interface.

Here, we report a structural and chemical investigation of different sub-monolayer Sn phases on Au(111) by means of low energy electron diffraction (LEED) and photoelectron spectroscopy (XPS). Tin layers of different thicknesses were deposited gradually on the Au(111) surface by physical vapor deposition and subsequently heated. A strong dependence of the structural and chemical configuration of the tin atoms on the layer thickness and the post-deposition annealing temperature was observed.

O 65.3 Thu 11:00 S052

On the transition from MoS₂ single-layer to bilayer growth on the Au(111) surface — •MORITZ EWERT¹, LARS BUSS¹, FRANCESCA GENUZZIO³, TEVFIK ONUR MENTES³, ANDREA LOCATELLI³, JENS FALTA², and JAN INGO FLEGE¹ — ¹Applied Physics and Semiconductor Spectroscopy, Brandenburg University of Technology Cottbus-Senftenberg, Germany — ²Institute of Solid State Physics, University of Bremen, Germany — ³Elettra-Sincrotrone Trieste S.C.p.A., Basovizza, Trieste, Italy

MoS₂ is well known for changing from an indirect to a direct band-gap semiconductor as a single layer. Here, for the model system MoS₂/Au(111), we present in-situ studies of the continued growth of micron-size single-layer MoS₂ islands including the first formation of bilayer patches.

We have used angle-resolved photoemission spectroscopy from micrometer sized regions to investigate the local band structure of the islands' rims and centers, showing a prevalence for bilayer and single-layer formation at the rims and centers, respectively. The bilayer patches can clearly be identified locally on the few nanometer scale employing intensity-voltage low-energy electron microscopy as a fingerprinting method. Astonishingly, micro-spot low-energy electron diffraction hints toward the nucleation of the second layer of the MoS₂ between the single layer MoS₂ and the Au(111) substrate when the step bunches formed by the single-terrace growth mechanism become sufficiently high.

O 65.4 Thu 11:15 S052

Structural and electronic investigations of CVD-grown TMDs on Au(111) — •JULIAN PICKER¹, MAXIMILIAN SCHAAL², ZIYANG GAN¹, MARCO GRUENEWALD², CHRISTOF NEUMANN¹, ANTONY GEORGE¹, FELIX OTTO², TORSTEN FRITZ², and ANDREY TURCHANIN¹ — ¹Institute of Physical Chemistry, Friedrich Schiller University Jena, Lessingstraße 10, 07743 Jena, Ger-

many — ²Institute of Solid State Physics, Friedrich Schiller University Jena, Helmholtzweg 5, 07743 Jena, Germany

Transition metal dichalcogenides (TMDs) are layered two-dimensional (2D) materials which have come into the focus of research in recent years. Especially, the exciting change of properties when going from bulk to monolayer make them interesting for novel electronic applications. Here, we demonstrate the *ex-situ* growth of MoS₂ and MoSe₂ monolayers on Au(111) by chemical vapor deposition (CVD) in a two-zone furnace. Afterwards, the samples were analyzed in ultra-high vacuum (UHV) with the help of surface sensitive methods, including (low-temperature) scanning tunneling microscopy and spectroscopy (STM/STS), low-energy electron diffraction (LEED) as well as X-ray and angle-resolved ultra-violet photoelectron spectroscopy (XPS/ARPES). While we could confirm the growth of high-quality single crystalline TMDs, we also accessed the structural and electronic properties of these samples down to the atomic scale. Finally, the impact of annealing on the structure and properties of the TMDs was studied.

O 65.5 Thu 11:30 S052

Spectroscopic and microscopic study of carborane based 2D materials — •MARTHA FREY¹, JULIAN PICKER¹, JAKUB VIŠŇÁK², CHRISTOF NEUMANN¹, TOMÁŠ BAŠE², and ANDREY TURCHANIN¹ — ¹Friedrich Schiller University Jena, Institute of Physical Chemistry, Lessingstraße 10, 07743 Jena, Germany — ²The Czech Academy of Sciences, Institute of Inorganic Chemistry, 250 68 Husinec-Rez, c.p. 1001, Czech Republic

Carboranes are electron-delocalized molecular clusters containing boron, carbon and hydrogen. Because of their high stability and structural variability, they are interesting for a wide range of applications including nanoscale engineering, catalysis and boron neutron capture therapy. Here, we present the fabrication of a novel boron-based two-dimensional (2D) material *via* electron irradiation induced cross-linking of carborane self-assembled monolayers (SAMs) on silver or gold substrates. The SAMs, the cross-linking process and the resulting 2D nanosheets have been characterized with different complementary surface sensitive techniques including X-ray photoelectron spectroscopy (XPS), low-energy electron diffraction (LEED), scanning tunneling microscopy (STM) and scanning electron microscopy (SEM).

O 65.6 Thu 11:45 S052

Growth and Structural Properties of 2D Blue Phosphorene on Au(111) and on Au(100) — •MAXIMILIAN SCHAAL¹, JULIAN PICKER², FELIX OTTO¹, MARCO GRUENEWALD¹, ROMAN FORKER¹, and TORSTEN FRITZ¹ — ¹Institute of Solid State Physics, Friedrich Schiller University Jena, Helmholtzweg 5, 07743 Jena, Germany — ²Institute of Physical Chemistry, Friedrich Schiller University Jena, Lessingstraße 10, 07743 Jena, Germany

Blue phosphorene (BlueP) is a novel two-dimensional material that shares properties with black phosphorene and is potentially even more interesting for optoelectronic applications because of its layer dependent band gap of approx. 2 to 3 eV and superior charge carrier mobility [1]. Despite these promising properties, the growth of quasi-freestanding BlueP is still challenging.

In our contribution we will report on the structural and electronic properties of epitaxial BlueP on Au(111) and on Au(100) by means of scanning tunneling [hydrogen] microscopy (ST[H]M), distortion-corrected low-energy electron diffraction (LEED) as well as X-ray photoelectron spectroscopy and diffraction (XPS and XPD). It is already known that on Au(111) a network consisting of BlueP islands, which are connected by Au linker atoms, is formed [2]. In contrast, we demonstrate that on Au(100) quasi-free standing BlueP domains grow [3].

[1] Z. Zhu and D. Tománek, Phys. Rev. Lett. 112, 176802 (2014).

[2] H. Tian et al., Matter 2, 111 (2020).

[3] M. Schaal, J. Phys.: Condens. Matter 33, 485002 (2021).

O 65.7 Thu 12:00 S052

How the supple Pt(110) surface paves the way to single-domain h-BN growth. — •MARCO THALER¹, DOMINIK STEINER¹, FLORIAN MITTENDORFER², and ERMINDALD BERTEL¹ — ¹Department of Physical Chemistry, University of Innsbruck, Austria — ²Institute of Applied Physics and Center for Computational Materials Science, Vienna University of Technology, Austria

Its structural flexibility renders Pt(110) an extraordinary substrate for hexagonal boron nitride (h-BN) growth. Borazine-exposure at high temperature yields either an extended film or empty terraces depending on dosage. Annealing preadsorbed Borazine, in contrast, yields nuclei with a structure differing from the extended film. DFT modelling of the latter was carried out by starting with a stretched film, which ruptured upon relaxation into smaller h-BN islands. The Pt surface layer below them is severely disordered. Only after high-T annealing the islands relax into the final h-BN/Pt(110)-(1xn) missing-row configuration. Thus, this non-classical, two-step nucleation proceeds via a metastable transi-

tion structure. Under the conditions of high-T exposure the metastable nuclei are continuously dissolved by desorption and H-induced etching. Stochastic formation of a critical island size with the more stable (1x1)nm² structure requires a high supersaturation, but once formed, such an island grows explosively into an extended film. Hence, single-domain growth of h-BN on Pt(110) differs significantly from that on vicinal Cu(110), where (1-12) step edges act as nucleation sites giving rise to uniform nuclei capable of seamless coalescence.

O 65.8 Thu 12:15 S052

Development of strain- and gate-controllable STM sample holder — •JZ-YUAN JUO¹, BONG GYU SHIN¹, SOON JUNG JUNG¹, and KLAUS KERN^{1,2} — ¹Max-Planck-Institut für Festkörperforschung, Heisenbergstraße 1, DE-70569 Stuttgart, Germany — ²Institut de Physique, École Polytechnique Fédérale de Lausanne, CH-1015 Lausanne, Switzerland

An atomic-scale understanding of strain effects on electronic properties is essential for implementing two-dimensional materials into flexible electronics. The

scanning tunneling microscopy (STM) is an ideal method to advance this understanding. However, the combination of STM and strain-controllable devices remains challenging due to the high demand for compatibilities with limited STM space, ultrahigh vacuum, and mechanical stability. We have developed an indentation-based sample holder for STM measurements. A gearbox and a piezo stack were used to control the distance between the indenter and 2D materials transferred on the suspended polyimide. The gearbox has a travel range of ~120 μm and precision of ~1.4 μm; the piezo stack has a travel range of ~1.8 μm and precision of <1 nm. The combination of gearbox and piezo stack allowed us to tune the distance between indenter and sample continuously with nanometer precision, characterized by atomic force microscopy. Raman spectroscopy was used to measure strain distribution in monolayer MoS₂ at the indented area. The strain controllability is characterized by calculating graphene lattice constant changes in STM atomic-resolution images. Spectroscopic studies confirm the gate tunability by observing Dirac point shifts.

O 66: Oxide Surfaces 2

Time: Thursday 10:30–13:00

Location: S053

Topical Talk

O 66.1 Thu 10:30 S053

Charge-ordered states on incipient ferroelectric polar surfaces — •CESARE FRANCHINI — University of Vienna — University of Bologna

The precise atomic-scale knowledge of surface properties is mandatory for interpreting experimental data, optimizing (photo)catalytic processes, or predicting novel electronic phases. This is particularly challenging for perovskite materials, which typically show a variety of surface structural reconstructions that prevent a generally valid and transferable understanding of surface properties. However, recent experiments have shown that a novel cleavage protocol based on controlled exploitation of ferroelectric instabilities can generate well-defined bulk-terminated (001) surfaces, paving the way for a precise characterization of the surface electronic structure. This talk shall report first principles electronic structure calculations on polar KTaO₃(001), focusing on the dichotomy between charge localized/delocalized phases and their impact on surface reactivity. Our data, supported by experimental observations, show that polarity-induced uncompensated carriers in KTaO₃(001) exhibit charged-order patterns rather than common 2DEGs, manifested by charge-density wave and (bi)polaron states. Eventually, the trapped charge suppresses ferroelectric surface distortions, resulting in a binary CO adsorption process.

[1] M. Setvin et al. *Science* 359, 572 (2018). [2] M. Reticcioli et al., *Nat. Comm.* (2022). [3] Z. Wang et al., *Sc. Adv.* (2022).

O 66.2 Thu 11:00 S053

Surface phonons and their coupling to the 2D electron liquid at the CTO/STO surface — •M. DÖTTLING¹, E. B. GUEDES^{2,3}, T. P. VAN WAAS^{4,2}, S. PONCÉ^{4,5}, M. CAPUTO^{3,6}, N. C. PLUMB², N. MARZARI⁵, C. BERTHOD⁷, M. RADOVIĆ², J. H. DIL^{3,2}, and K. ZAKERI¹ — ¹PHI, Karlsruhe Institute of Technology — ²PSD, PSI — ³IPHYS, EPF Lausanne — ⁴IMCN, UC Louvain — ⁵THEOS, EPF Lausanne — ⁶Elettra, Trieste — ⁷DQMP, University of Geneva

Motivated by the recent discovery of a 2D electron liquid (2DEL) formed at the surface of CaTiO₃/SrTiO₃(001) heterostructure, we probed the phonon spectrum of the system by means of high-resolution electron energy-loss spectroscopy (HREELS). Our main aim was to address any possible interaction of 2DEL with phonons.

The HREELS measurements revealed the existence of the Fuchs-Kliewer (FK) phonon modes at the energies of 20, 60 and 93 meV. Interestingly, the Eliashberg-function $\alpha^2F(\omega)$ constructed based on the quasiparticle band dispersion, probed by angle-resolved photoemission experiments, exhibits peaks at energies of 20, 60 and 80 meV.

The apparent redshift of the highest energy peak in $\alpha^2F(\omega)$, compared to the 93 meV FK mode, can be attributed to the formation of band-gap states (BGS). Such states form upon photon irradiation at the same time as 2DEL is formed. This is shown by the simulated HREEL spectra including BGS. Our results demonstrate the importance of BGS and the necessity of their consideration in describing the properties of oxide heterostructures. Supported by DFG via Heisenberg Programme ZA 902/3-1, ZA 902/6-1 and ZA 902/5-1.

O 66.3 Thu 11:15 S053

Reversible switching of the 2D electron gas of SrTiO₃(001) studied by HREELS — •HANNES HERRMANN, FLORIAN SCHUMANN, and WOLF WIDDRA — Martin-Luther-Universität Halle-Wittenberg, Institute of Physics, 06120 Halle, Germany

The formation of a 2D electron gas (2DEG) gained high interest in surface science as it became accessible under oxygen-poor conditions at the TiO₂-terminated SrTiO₃(001) surface [1]. In this work, we follow the 2DEG formation by studying the SrTiO₃ surface plasmon polaritons (SPP) by high-resolution

electron energy loss spectroscopy (HREELS). The coupling of the SPP to the 2DEG leads to an asymmetric SPP line shape with extreme broadening. This strong electron-phonon coupling allows to quantify the 2DEG charge carrier density and is used to follow the reversible formation of the 2DEG by heating in UHV/O₂ atmosphere or by adsorbing molecular oxygen at 100 K.

The dielectric response will be discussed in terms of a two-layer model with a surface 2DEG which is modelled using a Drude-like response with a strongly frequency-dependent electronic mobility.

[1] A. F. Santander-Syro, O. Copie, A. Barthelemy, and M. J. Rozenberg, *Nature* 469, 189 (2011).

O 66.4 Thu 11:30 S053

Structure determination of a dodecagonal oxide quasicrystal — •SEBASTIAN SCHENK¹, OLIVER KRAHN¹, HOLGER L. MEYERHEIM², MARC DE BOISSIEU³, STEFAN FÖRSTER¹, and WOLF WIDDRA¹ — ¹Institute of Physics, Martin-Luther-Universität Halle-Wittenberg, 06120 Halle, Germany — ²Max-Planck-Institut für Mikrostrukturphysik, 06120 Halle, Germany — ³Université Grenoble Alpes, CNRS, SIMaP, St Martin d Heres, France

The dodecagonal symmetry and the general tiling motive of oxide quasicrystals (OQC) have been proven by electron diffraction (LEED) and scanning tunneling microscopy (STM) from their first observations [1,2]. However, the detailed atomic structure, which includes the decoration of individual tiling elements with metal and oxygen atoms, has been under debate for more than eight years.

In this talk we solve the atomic structure by combination of STM and surface x-ray diffraction (SXRD) of a quasicrystal approximant, which is derived from an ultrathin layer of SrTiO₃ on Pt(111). The derived structure model can be generalized for all related ternary oxide quasicrystals and their approximants. The measured diffraction intensities will be compared with calculated ones by lifting the atomic structure of the OQC into its four-dimensional periodic superlattice. These intensities will be compared to SXRD data obtained in synchrotron measurements.

[1] S. Förster et al., *Nature* 502, 215 (2013).

[2] S. Schenk et al., *J. Phys.: Condens. Matter* 29, 134002 (2017).

O 66.5 Thu 11:45 S053

Structural analysis of complex 2D Sr-Ti-O/Pd(111) films. — •MARTIN HALLER, SEBASTIAN SCHENK, STEFAN FÖRSTER, and WOLF WIDDRA — Martin-Luther-Universität Halle-Wittenberg, Institute of Physics, Von-Danckelmann-Platz 3, 06120 Halle, Germany

In 2013 the first 2D oxide quasicrystal (OQC) in thin Ba-Ti-O/Pt(111) films with astonishing structural properties has been discovered [1]. It features a twelve-fold rotational symmetry that is incompatible with lattice periodicity. Instead, it is described with a self-similar quasicrystalline structure that involves squares, triangles and rhombuses. In the wake of this discovery combinations of ternary oxide layers and different hexagonal substrates have been investigated to study the epitaxial preconditions for the formation of the OQC. In this contribution, we present a structural analysis for Sr-Ti-O on Pd(111). Globally, as seen from LEED, it forms a periodic structure with unit cell parameters $a = 1.32$ nm, $b = 2.96$ nm and $\alpha = 93.43^\circ$. However, locally a second phase has been identified in atomically-resolved STM data with twelvefold symmetric FFT and long range coherence in the 2D auto-correlation image. The analysis of the tiling statistics reveals a triangle: square: rhomb ratio of 2.84:1:0.39 which deviates slightly from the ideal OQC's ratio of 2.73:1:0.37 [2]. The given structure is discussed in terms of a disordered OQC which is further supported by a 4D hyperspace analysis.

[1] S. Förster et al., *Nature* 502, 215 (2013)

[2] S. Schenk et al., *J. Phys. Condens. Matter*, 29 (2017)

O 66.6 Thu 12:00 S053

Transformation from honeycomb binary oxide to quasicrystalline ternary oxide — •LOI V. TRAN, STEFAN FÖRSTER, and WOLF WIDDRA — Institute of Physics, Martin-Luther-University Halle-Wittenberg, Halle, Germany
Oxide quasicrystals (OQCs) are examples of aperiodically-ordered 2D materials. They have been found for 2D layers derived from BaTiO_3 on Pt(111) [1]. Their dodecagonal structure results from Ba decoration of a Ti_nO_n network where $n = 4$ (decorated with no Ba atom), 7 (decorated with one Ba atom) and 10 (decorated with two Ba and two additional O atoms). In contrast, periodic Ti_2O_3 honeycomb structures with Ti_6O_6 rings are well known in literature [2,3]. Here, we report on the transition of such honeycomb Ti_2O_3 structures to dodecagonal OQCs by adsorption of Ba and subsequent annealing. The structural transition is monitored with LEED and workfunction measurements. Upon room temperature Ba deposition, Ti_2O_3 honeycomb structure remains and Ti_6O_6 rings are decorated with Ba, reducing the workfunction from 5.12 to 2.97 eV. Annealing to 873 K in oxygen converts the honeycomb structure into a dodecagonal OQC, for which the workfunction increases to 3.85 eV. The workfunction changes associated with the transformation will be discussed in context of the height differences of Ba ions above the surface and the resulting dipole strength.

O 66.7 Thu 12:15 S053

Barium decorated Ti_2O_3 monolayers: a case study for Pd(111) substrates — •FRIEDRIKE WÜHRL, SEBASTIAN SCHENK, OLIVER KRAHN, STEFAN FÖRSTER, and WOLF WIDDRA — Institute of Physics, Martin-Luther-Universität Halle-Wittenberg, 06120 Halle, Germany

Oxides at the two-dimensional limit show a high flexibility in their structural properties ranging from hexagonal honeycomb structures to dodecagonal oxide quasicrystals (OQC) [1]. Recent work based on STM, surface x-ray diffraction (SXRD) and DFT calculations confirmed a structure model for oxide quasicrystals that explains this extraordinary structure as an aperiodically ordered Ti_2O_3 network with rings of different sizes on the metal support Pt(111), in which the largest rings are decorated with Ba ions [2]. The Ba ions form a self-similar tiling, which can be described through triangles, squares and rhombuses. In this contribution we report on a sequence of long-range ordered structures observed in $\text{Ba}_x\text{Ti}_2\text{O}_{3+y}$ on Pd(111) that are closely related to the OQC. We present a series of structures ranging from a $\text{Ba}_{0.66}\text{Ti}_2\text{O}_3$ to a $\text{BaTi}_2\text{O}_{3.5}$ stoichiometry. By varying the Ba content, we observe a transition from a triangle-square tiling via triangle-square-rhombus tilings to one consisting of triangles and rhombuses only [3]. It will be discussed how the Ba density sets the ratio of four to seven to ten membered rings in the Ti_2O_3 backbone.

[1] S. Förster *et al.*, Nature **502**, 215 (2013).[2] E. Cockayne *et al.*, Phys. Rev. B **93**, 020101(R) (2016).[3] F. E. Wühl *et al.*, Phys. Status Solidi B, 2100389 (2021).

O 66.8 Thu 12:30 S053

The (2x1) reconstruction of calcite(104) — JONAS HEGGEMANN¹, YASHASVI RANAWAT², ONDŘEJ KREJČÍ², ADAM S. FOSTER², and •PHILIPP RAHE¹ — ¹Fachbereich Physik, Universität Osnabrück, Barbarastr. 7, Osnabrück, Germany — ²Department of Applied Physics, Aalto University, Helsinki, Finland
Calcite is an abundant material in the Earth's crust, a central constituent of biominerals in living organisms [1], and currently investigated as a capture material for CO₂ [2]. Despite intensive studies, however, there is still serious ambiguity regarding the properties of this surface due to conflictive conclusions for the so-called row-pairing [3] and (2x1) reconstruction [4].

Here, we use a combination of non-contact atomic force microscopy (NC-AFM) with CO-functionalized tips at 5K, density functional theory with state-of-the-art dispersion corrections, and NC-AFM image simulations to clarify the microscopic geometry of calcite(104). A (2x1) reconstruction and a glide plane symmetry is consistently found in the NC-AFM data and DFT results. Most importantly, we identify two different adsorption positions for CO molecules within the (2x1) unit cell. These findings are most critical for future studies where processes on calcite(104)-(2x1) are influenced by the surface geometry.

[1] L. Addadi, S. Weiner, Angew. Chem. Int. Ed. Engl. **31**, 153 (1992). [2] P. A. E. Pogge von Strandmann, et al., Nat. Commun. **10**, 1983 (2019). [3] A. L. Rachlin, et al., Am. Mineral. **77**, 904 (1992). [4] S. L. S. Stipp, et al., Geochim. Cosmochim. Acta **58**, 3023 (1994).

O 66.9 Thu 12:45 S053

Growth of ultra thin Eu_xO_y films on Pt(001): A HREELS, XPS and LEED study — •ANNE OELSCHLÄGER, HANNES HERRMANN, STEFAN FÖRSTER, and WOLF WIDDRA — Martin-Luther-Universität Halle-Wittenberg, Institut of Physics, 06120 Halle, Germany

The gradually decreasing ionic radii along the series of lanthanides allow an exceptional fine tuning of lattice parameters, which makes this material class interesting for applications in epitaxial growth. In this contribution we report on the growth of thin Eu_xO_y films on Pt(001) and characterize the thin film oxidation upon annealing in various environments.

A 0.8 nm thin Eu layer has been deposited onto Pt(001) at room temperature in UHV conditions at a background pressure below $3 \cdot 10^{-10}$ mbar. By monitoring the surface phonons with HREELS and the valence state of Eu with XPS a continuous oxidation of Eu at room temperature by water from the residual gas as well as by molecular oxygen is observed as a transition from metallic Eu to Eu_2O_3 . The transition to Eu^{+} can be followed by increasing (decreasing) intensities for the surface phonon polariton at 364 cm^{-1} (525 cm^{-1}) in HREELS and the high binding energy component of the Eu3d core level at 1135 eV (1125 eV) in XPS. The long-range order starts to develop in the 0.8 nm thin layer upon annealing to 1000 K. LEED exhibits a complex twelve-fold diffraction pattern.

O 67: Frontiers of Electronic Structure Theory: Focus on Artificial Intelligence Applied to Real Materials 3

Time: Thursday 10:30–12:45

Location: S054

O 67.1 Thu 10:30 S054

Quantile Random Forest Model for Extrapolation to the Complete Basis Set Limit in Density Functional Theory Calculations — •DANIEL SPECKHARD¹, CHRISTIAN CARBOGNO², SVEN LUBECK², LUCA GHIRINGHELLI², MATTHIAS SCHEFFLER^{2,1}, and CLAUDIA DRAXL^{1,2} — ¹Humboldt-Universität zu Berlin, Physics Department and IRIS Adlershof, Berlin, Germany — ²The NOMAD Laboratory at the FHI-MPG and HU, Berlin, Germany

The precision of density-functional theory (DFT) calculations depends on a variety of computational parameters, the most critical being the basis-set size. With an infinitely large basis set, i.e., in the limit of a complete basis set (CBS), the result of the calculation is as precise as possible for the chosen exchange-correlation functional. Our aim in this work is to find a model that can extrapolate the result of an imprecise DFT calculation to the CBS limit. As a starting point, we use a dataset of 63 binary solids investigated with various basis-set sizes [1] with two all-electron DFT codes, `exciting` and `FHI-aims`, which use very different types of basis sets. A quantile random forest model is used to estimate the deviation of the total energy with respect to fully converged calculations as a function of the basis set size. The non-linear random forest model outperforms a previous approach that used a linear model. The quantile random forest model presented also provides prediction intervals which give the user an idea of the model's uncertainty.

[1] C. Carbogno *et al.*, npj Comput. Mater. **8**, 69 (2022).

O 67.2 Thu 10:45 S054

Symmetry and completeness in machine-learning models for atomistic simulations — •SERGEY POZDNYAKOV and MICHELE CERIOTTI — EPFL, Switzerland
During the last decade, machine learning methods have drastically changed atomistic simulations. On the one hand, they scale linearly with the size of the

system and thus, are significantly faster than the quantum mechanical calculations. On the other, they provide a functional form that is much more flexible than so-called classical force fields such as the Lennard Jones potential or embedded atom models. From one point of view, incorporating rotational symmetry is important for ML since it can make models more data-efficient and robust, but can also lead to incompleteness, limiting the ultimate accuracy of the model. I will discuss some examples of this and compare different types of models to show how one can find an optimal balance of the two effects.

O 67.3 Thu 11:00 S054

Fast, robust, interpretable machine-learning potentials — STEPHEN R. XIE^{1,2}, RICHARD G. HENNIG¹, and •MATTHIAS RUPP³ — ¹University of Florida, Gainesville, USA — ²KBR, NASA Ames Research Center, Mountain View, USA — ³University of Konstanz, Germany

Machine-learning potentials (MLPs) are increasingly successful in all-atom dynamics simulations where they act as surrogate models for ab-initio electronic structure methods. MLPs often result in two to three orders of magnitude improvements in the number of simulated atoms or duration of simulated time, enabling new insights and applications. Current limitations include data inefficiency, instabilities ("holes" in high-dimensional MLPs [2]), and lack of interpretability.

To address this challenge, we combine effective two- and three-body potentials in a cubic B-spline basis with second order-regularized linear regression. The resulting "ultra-fast potentials" are data-efficient, physically interpretable, sufficiently accurate for applications, can be parametrized automatically, and are as fast as the fastest traditional empirical potentials. [1] We demonstrate these qualities in retrospective benchmarks and present the prediction of thermal conductivities via the Green-Kubo formalism as a first application.

[1] Stephen R. Xie, Matthias Rupp, Richard G. Hennig, Ultra-fast interpretable machine-learning potentials. arXiv:2110.00624, 2021 [2] Jeffrey Li, Chen Qu, Joel M. Bowman: Diffusion Monte Carlo with fictitious masses finds holes in potential energy surfaces, *Mol. Phys.* 119(17–18): e1976426, 2021.

O 67.4 Thu 11:15 S054

Improving the transferability of high-dimensional neural network potentials by low-order terms — •ALEA MIAKO TOKITA and JÖRG BEHLER — Georg-August-Universität Göttingen, Institut für Physikalische Chemie, Theoretische Chemie, Tammannstraße 6, 37077 Göttingen, Germany

High-dimensional neural network potentials (HDNNPs) are able to provide accurate potential energy surfaces suitable for atomistic simulations of large systems. The key to this accuracy is the high flexibility of the atomic neural networks allowing to reproduce energies and forces from reference electronic structure calculations with very small errors. At the same time, this flexibility is limiting the transferability of HDNNPs to atomic configurations that are very different from the reference geometries. Here, we investigate possible improvements in transferability of HDNNPs by the explicit inclusion of low-order terms in the functional form of the potential. The performance is demonstrated for a series of molecular model systems.

O 67.5 Thu 11:30 S054

Predicting condensed-phase electron densities using machine learning — •ALAN LEWIS¹, ANDREA GRISAFI², MICHELE CERIOTTI², and MARIANA ROSSI¹ — ¹MPI for Structure and Dynamics of Materials, Hamburg, Germany — ²École Polytechnique Fédérale de Lausanne, Lausanne, Switzerland

The electron density is a fundamental quantity for understanding physical phenomena in materials, and is central to electronic structure theories such as density-functional theory. We present the SALTED machine learning method and demonstrate its ability to learn and predict the electronic densities of a range of materials from simple liquids and metals to hybrid organic-inorganic perovskites. This extends the framework presented in *ACS Cent. Sci.* 5, 57, 2019 to work with periodic boundary conditions and uses a resolution of the identity on a numeric atom-centered orbital basis to expand the all-electron periodic density. A Gaussian process regression model that makes use of local symmetry-adapted representations of the atomic structure is employed, making our method both data-efficient and highly transferable. [1] We also compare various methods of dealing with the non-orthogonality of the basis, accounting for correlations between pairs of off-centered density components, finding that the best compromise between accuracy and computational efficiency comes from approximating the density expansion coefficients by directly minimizing the loss function. The total energies derived from the densities obtained in this way present errors with respect to DFT of just 0.1 meV/atom.

[1] Lewis, Grisafi, Ceriotti, Rossi, *JCTC* 17, 11, 7203 (2021)

O 67.6 Thu 11:45 S054

Equivariant N-center representations for machine learning molecular Hamiltonians — •JIGYASA NIGAM, MICHAEL WILLATT, and MICHELE CERIOTTI — Laboratory of Computational Science and Modeling, Institute of Materials, Ecole Polytechnique Fédérale de Lausanne, 1015 Lausanne, Switzerland

Most of the widely used machine learning schemes that have been successful in predicting chemical and material properties rely on concise, symmetry-adapted descriptions of the underlying atomic structure. A class of these structural descriptions is built on hierarchical correlations of atom-centered densities (ACDC) [1]. These are subsequently used to model corresponding atomic properties or atomic contributions to a global observable. However, many quantum mechanical quantities, such as the effective single-particle Hamiltonian written on an atomic-orbital basis, are associated with multiple atom-centers. This effectively renders ACDCs inadequate to describe the additional degrees of freedom of such multicenter properties. We recently proposed an N-centered representation [2] that extends the ACDC framework to the case of targets that are simultaneously indexed by N atoms. I will demonstrate how devising a family of N-center representations opens avenues for new classes of machine learning models that are fully equivariant and describe their role in assisting electronic structure calculations.

[1] J. Nigam, S. Pozdnyakov, M. Ceriotti, *JCP* 153, 121101, 2020

[2] J. Nigam, M. Willatt, M. Ceriotti, *JCP* 156, 014115, 2022

O 67.7 Thu 12:00 S054

Similarity-of-materials analysis for reusability and interoperability of data in materials databases — •SIMON GABAJ, MARTIN KUBAN, SANTIAGO RIGAMONTI, and CLAUDIA DRAXL — Humboldt-Universität zu Berlin, Zum Großen Windkanal 2, 12489 Berlin, Germany

Large computational materials databases, such as NOMAD [1–2], make it possible to reuse already generated materials data. All these data typically come from different sources and have been created for a different purpose, be it geometry optimization, electronic structure, or alike. To support interoperability and thus reusability of such data, we devise a data-analysis workflow making use of similarity fingerprints. First, we encode the electronic density of states (DOS) in a vectorial representation [3] to obtain a descriptor. Then, we employ the Tanimoto coefficient to compute the similarity between all pairs of calculations. We demonstrate our workflow with selected materials, chosen from the NOMAD database. In the ideal case, all calculations of the same material in the same geometry should be identical. This is, however, not observed. Using our approach, we can uncover correlations between the DOS similarity and methodology as well as computational parameters. This way, we can also identify parameters that are relevant for the convergence of results.

[1] Draxl, C., Scheffler, M., *MRS Bulletin*, 43, 676, (2018)

[2] Draxl, C., Scheffler, M., *J. Phys. Mater.*, 2, 036001, (2018)

[3] Kuban, M., *et al.*, to be published

O 67.8 Thu 12:15 S054

Supervised and unsupervised deep Learning of topological phase transitions from entanglement aspect for one- and two-dimensional chiral p-wave superconductors — •MING-CHIANG CHUNG — Max-Planck-Institut für Physik komplexer Systeme, Dresden, Germany — National Chung-Hsing University, Taichung, Taiwan

The one-dimensional or two-dimensional chiral p-wave superconductor proposed by Kitaev has long become a classic example for understanding topological phase transitions through various methods, such as examining the Berry phase, edge states of open chains, and, in particular, aspects from quantum entanglement of ground states. In order to understand the amount of information carried in the entanglement-related quantities, here we study topological phase transitions of the model with emphasis of using the deep learning approach. Using both supervised or unsupervised ways, we feed different quantities, including Majorana correlation matrices (MCMs), entanglement spectra (ES) or entanglement eigenvectors (EE) originating from Block correlation matrices, into the deep neural networks for training, and investigate which one could be the most useful input format in this approach. We find that ES is information that is too compressed compared to MCM or EE. MCM and EE can provide us abundant information to recognize not only the topological phase transitions in the model but also phases of matter with different U(1) gauges, which is not reachable by using ES only. We also build a procedure for using unsupervised learning to find the phase transition points. We have used this method for other models.

O 67.9 Thu 12:30 S054

Machine Learning the Square-Lattice Ising Model — •BURAK ÇIVITCIOĞLU¹, ANDREAS HONECKER¹, and RUDOLF A. RÖMER² — ¹Laboratoire de Physique Théorique et Modélisation, CNRS UMR 8089, CY Cergy Paris Université *e, Cergy-Pontoise, France — ²Department of Physics, University of Warwick, Coventry, CV4 7AL, United Kingdom

Recently, machine-learning methods have been shown to be successful in identifying and classifying different phases of the square-lattice Ising model. We study the performance and limits of classification and regression models. In particular, we investigate how accurately the correlation length, energy and magnetisation can be recovered from a given configuration. We find that a supervised learning study of a regression model yields good predictions for magnetisation and energy, and acceptable predictions for the correlation length.

O 68: Focus Session: Time-Resolved Momentum Microscopy

Time-resolved momentum microscopy is a new experimental technique to study electron dynamics in momentum space. In momentum microscopy, the reciprocal image plane of photoemitted electrons is mapped onto a position-sensitive detector. In addition, the kinetic energy is extracted by energy dispersive elements, such as Time-of-Flight drift tubes or hemispherical analysers. Hereby, the complete information about the electronic structure of two-dimensional materials can be obtained (k_x , k_y , E). At the same time the signal can be restricted to micrometer-size spots, which is important for many types of quantum materials. By combining such electron spectrometers with pump-probe laser techniques, optical excitations, photo-induced phase transitions and charge transfer processes within the entire Brillouin zone can be imaged on ultrashort time scales. Several groups, with many of them in Germany, have established this technique during the last years in lab-based setups. In addition, first setups at large scale facilities, like ELI-ALPS or FLASH, are being commissioned or in operation. With higher photon energies available at free electron lasers, also structural dynamics will be observable through time-resolved electron diffraction.

Organizer: Robert Wallauer (Universität Marburg)

Time: Thursday 15:00–18:30

Location: H3

Topical Talk

O 68.1 Thu 15:00 H3

Exploring Excitonic Excitations in Momentum Space — •KESHAV DANI — Okinawa Inst. of Science and Technology, Graduate University, Onna-son, Japan
Optical techniques have provided us with rich information about the exciton * a two-particle photoexcited state in semiconductors and insulators. Yet, they have left a fundamental degree of freedom of the exciton inaccessible * its momentum! In this talk, I will discuss the application of time-resolved photoemission techniques to access the momentum coordinate of excitons in 2D semiconductors, thereby providing us with the formation pathways of momentum-forbidden dark excitons [1], an image of the electron around the hole in the exciton, the observation of the long-predicted anomalous dispersion of the exciton-bound electron [2], the momentum distribution of the exciton-bound hole, and the confinement of the interlayer exciton in a moiré cell [3].

References (*equal authors) [1] J. Madeo*, M. K. L. Man*, et al. *Science* 370, 1199 (2020). [2] M. K. L. Man*, J. Madeo*, et al. *Science Advances* 7, eabg0192 (2021). [3] O. Karni*, E. Barr*, V. Pareek*, J. D. Georganas*, M. K. L. Man*, C. Sahoo*, et al. *Nature* 603, 247 (2022).

Topical Talk

O 68.2 Thu 15:30 H3

Moiré interlayer and charge-transfer excitons in space and time: new experiments enabled by time-resolved momentum microscopy — •STEFAN MATHIAS — I. Physikalisches Institut, Georg-August-Universität Göttingen, Germany

In my talk, I introduce the time-resolved momentum microscopy setup that we developed in Göttingen (Germany) [1], which includes a MHz repetition rate extreme-ultraviolet beamline, and has recently been upgraded with a spin-imaging detector. In the following, I will discuss exemplary research projects that we cover with this new instrument. In particular, I will focus on the spatio-temporal identification and dynamics of moiré interlayer excitons in twisted WSe₂/MoS₂ heterostructures [2], and on an orbital-resolved study [3] of charge-transfer exciton dynamics in C60 thin films [4].

[1] Keunecke et al., *Rev. Sci. Instr.* 91, 063905 (2020)

[2] Schmitt et al., arXiv:2112.05011(2021)

[3] Jansen et al., *New Journal of Physics* 22, 063012 (2020)

[4] Stadtmüller et al., *Nature Communications* 10, 1470 (2019)

O 68.3 Thu 16:00 H3

The complete interface molecular movie: One-stop imaging of orbital, electronic, and structural dynamics — •MARKUS SCHOLZ¹, KIANA BAUMGÄRTNER², MARVIN REUNER³, CHRISTIAN METZGER², MICHAEL HEBER¹, DMYTRO KUTNYAKHOV¹, FRIEDRICH REINERT², DARIA POPOVA-GORELOVA³, MARTIN BEYE¹, and KAI ROSSNAGEL⁴ — ¹Deutsches Elektronen-Synchrotron DESY, Notkestrasse 85, 22607 Hamburg, Germany — ²Experimentelle Physik 7, Julius-Maximilians-Universität, Am Hubland, 97074 Würzburg, Germany — ³I. Institute for Theoretical Physics and Centre for Free-Electron Laser Science, Universität Hamburg, Luruper Chaussee 149, 22607 Hamburg, Germany — ⁴Institut für Experimentelle und Angewandte Physik, Christian-Albrechts-Universität zu Kiel, 24098 Kiel, Germany

Reactions of molecules on surfaces involve a complex interplay between electronic reorganization and the motion of atoms. The recent developments of higher-harmonics generation (HHG) and free-electron laser (FEL) based sources open up new opportunities for ultrafast spectroscopy toward simultaneously imaging subtle changes in the electronic structure and atomic positions on a femtosecond time scale and with sub-Ångström spatial resolution. Here, using a dual-electron messenger mode of momentum microscopy, we trace a photoinduced charge transfer process in energy-momentum space using valence electrons and, synchronously, at atomic sites using core electrons, in a single experimental setup for a molecule-2D material interface.

O 68.4 Thu 16:15 H3

Electron dynamics after a spin- and valley-polarized electronic excitation in WS₂ — •LASSE MÜNSTER¹, SARAH ZAJUSCH¹, RAUL PEREA-CAUSIN¹, SAMUEL BREM¹, KATSUMI TANIMURA¹, JENS GÜDDE¹, YAROSLAV GERASIMENKO², RUPERT HUBER², ERMIN MALIC¹, ULRICH HÖFER¹, and ROBERT WALLAUER¹ — ¹Fachbereich Physik, Philipps-Universität Marburg, Germany — ²Fachbereich Physik, Universität Regensburg, Germany

Atomically thin layers of TMDCs offer an ideal playground to study ultrafast electron dynamics. After optical excitation electrons scatter throughout the Brillouin zone to form a variety of excitonic states. We have shown that this formation process can be imaged by time-resolved momentum microscopy with tunable pump and high harmonic probe [1].

We recently incorporated a new pumping scheme, that allows us to excite the sample under an incident angle close to 0° with circularly polarized light. This results in an excitation, which is located purely within the K valley for one helicity and in the K' valley for the other helicity and provides access to all possible scattering processes. In the case of an excitation at K, electron scattering to K' and Σ is mediated by strong electron-phonon coupling with time constants of a few tens of femtoseconds. In addition, we observe the formation of spin-forbidden excitons in the K valley and electron scattering towards Σ . Both of these processes involve a spin-flip and are significantly slower (50 - 100 fs).

[1] R. Wallauer et al., *Nano Lett.* 21, 5867 (2021)

Topical Talk

O 68.5 Thu 16:30 H3

Momentum and energy dissipation of hot electrons in metals and metal-molecular heterostructures — •BENJAMIN STADTMÜLLER — Department of Physics and Research Center OPTIMAS, TU Kaiserslautern, 67663 Kaiserslautern, Germany — Institute of Physics, JGU Mainz, 55128 Mainz, Germany

The dynamics of optically excited carriers in condensed matter play a crucial role in many fundamental and device-relevant processes in materials. Here, I discuss the potential of time-resolved two-photon momentum microscopy (tr-2PMM) [1] to access the k-space signatures and the corresponding quasi-particle lifetimes of excited carriers in metals [2,3] and metal-molecular heterostructures. For metallic systems, I will demonstrate that tr-2PMM allows us to uncover anisotropies in the orientations of optical transition dipoles for highly free electron like noble metal surfaces [2] and to follow the ultrafast intra- and inter-band scattering processes of optically excited carriers in metallic quantum well systems [3] in real-time. In this context, I will also introduce two approaches to alter the electron dynamics of metal surfaces by the adsorption of molecular complexes or by periodically modulating the surface potential using porous molecular networks on surfaces. Finally, I will show our efforts to exploit the spatial resolution in tr-2PMM to disentangle the k-space signatures of photo- and plasmon-induced hot carriers at surfaces [4]. [1] F. Haag et al., *Rev. Sci. Instrum.* 90, 103104 (2019); [2] T. Eul et al. *Nat. Commun.* (2022); [3] F. Haag et al. *Phys. Rev. B* 104, 104308 (2021); [4] M. Hartelt et al. *ACS Nano* 15, 19559 (2021)

O 68.6 Thu 17:00 H3

Coherent response of the electronic system driven by non-interfering laser pulses — •TOBIAS EUL¹, EVA PRINZ¹, MICHAEL HARTELT¹, BENJAMIN FRISCH¹, MARTIN AESCHLIMANN¹, and BENJAMIN STADTMÜLLER^{1,2} — ¹Department of Physics and Research Center OPTIMAS, University of Kaiserslautern, Germany — ²Institute of Physics, Johannes Gutenberg University Mainz, Germany

The strength of light-matter interaction in condensed matter is fundamentally linked to the orientation and oscillation strength of the materials' optical transition dipoles. Structurally anisotropic materials, e.g. elongated molecules, exhibit optical transition dipoles with fixed orientations that govern the angular-dependent light-matter interaction. Contrary, free electron like metals should exhibit isotropic light-matter interaction with the light fields dictating the orien-

tation of the optical transition dipoles. Here, we demonstrate that an anisotropic direction of the optical transition dipoles even exists in highly free electron like noble metal surfaces. Our time- and phase-resolved photoemission experiment reveals coherent interference effects on the (110)-oriented silver surface after optical excitation with two non-interfering cross-polarized pulses. We explain this coherent material response within the density matrix formalism by an intrinsic coupling of the non-interfering light fields mediated by optical transition dipoles with fixed orientations in silver.

O 68.7 Thu 17:15 H3

Time-resolved photoemission orbital tomography of CuPc on Cu(001)-2O — •ALEXA ADAMKIEWICZ¹, MIRIAM RATHS², MONJA STETTNER², FRANCOIS C. BOCQUET², CHRISTIAN KUMPF², ROBERT WALLAUER¹, F. STEFAN TAUTZ², and ULRICH HÖFER¹ — ¹Fachbereich Physik, Philipps Universität Marburg, Germany — ²Peter Grünberg Institute (PGI-3), Jülich Research Centre, Germany Charge transfer across molecular interfaces is reflected in the population of electronic orbitals. For ordered organic layers, time-resolved photoemission orbital tomography (tr-POT) is capable of spectroscopically identifying the involved orbitals and deducing their population from the measured angle-resolved photoemission intensity with high temporal resolution. In a first example, we found that for PTCDA/ Cu(001)-2O, two distinct excitation pathways could be observed with visible light [1]. The parallel component of the electric field induces a direct HOMO-LUMO transition, the perpendicular component transfers a substrate electron into the molecular LUMO. While in this case, a distinct excitonic signature was not observed, changes in the momentum pattern can in general serve as a measure of detecting excitonic processes. Here, we show such time-dependent change of the pattern for CuPc/Cu(001)-2O. We demonstrate how the temporal evolution of the LUMO momentum distribution can be systematically disentangled from contributions of the projected HOMO. Moreover, we observe LUMO excitation of selected molecular orientation at normal incidence by aligning the pump polarization along the molecular axis. [1] R. Wallauer et al., *Science* 371, 1056 (2021).

Topical Talk

O 68.8 Thu 17:30 H3

Is there a perfect electron analyzer for time-resolved ARPES? — •LAURENZ RETTIG — Fritz-Haber-Institut der Max-Planck-Gesellschaft Recent years have seen a huge popularity of time-of-flight based momentum microscopes (MMs), which based on advanced electrostatic optics have revolutionized angle-resolved photoemission spectroscopy (ARPES). Compared to conventional hemispherical analyzers (HAs) with angle-dispersing electron lenses, which access only a small fraction of the reciprocal space at a given configuration, MMs allow for the simultaneous detection of multiple Brillouin zones without the need to rearrange the sample geometry. However, one drawback of such instruments, in particular in time-resolved studies, arises from the large energy and momentum range covered simultaneously, which in combination with detection limitations of delay-line detectors and space charge restrictions can severely reduce the effective detection rate for selected energy-momentum regions compared to conventional HAs.

In my talk I will discuss the advantages and limitations of both types of instruments for several application scenarios in time-resolved ARPES, and present some recent highlights in charge-density wave materials, which take advantage of the combination of both types of instruments.

O 68.9 Thu 18:00 H3

Developing a fs-XUV source for time-resolved momentum microscopy on 2D materials — •KARL SCHILLER¹, ALAN OMAR², LASSE STERNEMANN¹, MATIJA STUPAR¹, CLARA SARACENO², and MIRKO CINCHETTI¹ — ¹Department of Physics, TU Dortmund University, Germany — ²Ruhr-Universität Bochum, Germany

We introduce a newly developed setup for time-resolved momentum microscopy with femtosecond extreme ultraviolet (fs-XUV) radiation. The fs-XUV pulses with photon energy up to 30 eV are generated by high-harmonic generation in an Argon gas jet and are coupled to an energy-filtered momentum microscope (KREIOS MM, Specs GmbH). A commercial Ytterbium-based high-power laser system drives the generation with a variable high repetition rate between 100 kHz and 1 MHz (Carbide, Light Conversion). While this configuration allows for high energy resolution of 50 meV, a high temporal resolution can also be reached by coupling the laser to a tunable in-house build Herriot-type multipass cell compressor with peak powers up to 2 GW and pulse durations of ~45 fs [1]. In the talk, we will present the first characterization data of this setup and motivate its capability to examine few-layer 2D materials.

[1] A. Omar, et al. *Advanced Solid State Lasers*, OSA Technical Digest (Optical Society of America, 2021), paper JM3A.55

O 68.10 Thu 18:15 H3

FEL-based time-of-flight momentum microscopy: 3 time-resolved photoemission modalities in 1 experiment — •D. KUTNYAKHOV¹, R.P. XIAN², M. DENDZIK², M. HEBER¹, F. PRESSACCO³, S.Y. AGUSTSSON⁴, L. WENTHAUS¹, H. MEYER³, S. GIESCHEN³, K. BÜHLMAN⁵, S. DÄSTER⁵, R. GORT⁵, D. CURCIO⁶, K. VOLCKAERT⁶, M. BIANCHI⁶, CH. SANDERS⁶, J.A. MIWA⁶, S. ULSTRUP⁶, A. OELSNER⁷, C. TUSCHE^{8,9}, Y.-J. CHEN^{8,9}, D. VASILYEV⁴, K. MEDJANIK⁴, G. BRENNER¹, S. DZIARZHYTSKI¹, S. DONG², J. HAUER², L. RETTIG², J. DEMSAR⁴, H.-J. ELMERS⁴, PH. HOFMANN⁶, R. ERNSTORFER², G. SCHÖNHENSE⁴, Y. ACREMANN⁵, and K. ROSSNAGEL^{1,10} — ¹DESY, Hamburg — ²FHI Berlin — ³CFEL, Univ. Hamburg — ⁴Univ. Mainz — ⁵ETH Zürich — ⁶Univ. Aarhus — ⁷Surface Concept GmbH, Mainz — ⁸FZ Jülich GmbH — ⁹Univ. Duisburg-Essen — ¹⁰CAU Kiel

Time-resolved photoemission spectroscopy with ultrashort pump and probe photon pulses is an emerging technique with wide application potential. The ultimate combination of valence-band and core-level spectroscopy with photoelectron diffraction in a single experiment for electronic, chemical, and structural dynamics analysis specifically requires tunable monochromatic soft X-ray pulses at a high repetition rate as well as highly efficient single-shot electron detectors with increased multi-hit capabilities. We have realized such a 3-in-1 ultrafast photoemission experiment at FLASH/PG2, DESY merging free-electron laser capabilities with a multi-dimensional recording scheme.

O 69: Surface Reactions and Heterogeneous Catalysis 2

Time: Thursday 15:00–17:45

Location: H4

Topical Talk

O 69.1 Thu 15:00 H4

Theoretical Investigations of Size and Support Effects in Heterogeneous Catalysis — •FELIX STUDD — Institute of Catalysis Research and Technology, Karlsruhe Institute of Technology

Supported transition metal nanoparticles play an important role as catalysts in heterogeneous catalysis. The extend to which size, shape and metal support interaction influence a catalysts reactivity is still at the forefront of scientific research. Here we use density functional theory calculations on nanoparticles ranging from 0.5 to about 3.5 nm in size in order to gain insight into the particle size effect on a catalysts reactivity. We furthermore investigate how the interaction of nanoparticles with the support alters their reactivity with respect to the binding strength of adsorbates. Using computational models of particle-support interfaces we show how insight into changes in reactivity can be described.

O 69.2 Thu 15:30 H4

Why interlayer exchange is crucial for temperature programmed desorption — •TOBIAS DICKBREDER, RALF BECHSTEIN, and ANGELIKA KÜHNLE — Physical Chemistry I, Bielefeld University, Universitätsstraße 25, 33615 Bielefeld

Understanding the desorption of molecules from surfaces is fundamental for both natural and application-oriented processes such as dewetting, weathering and catalysis. A powerful method to investigate desorption processes is temperature programmed desorption (TPD) as it offers the possibility to gain mechanistic insights into the desorption kinetics. In the past, several analysis methods have been developed for TPD data. These methods have in common that

they rely on the Polanyi-Wigner equation, which requires proposing a desorption mechanism with a single (dominating) desorption path. For real systems, however, several coupled desorption paths can be easily envisioned. Here, we analyze the influence of exchange between the first and the second adsorbate layer on the desorption process. We show that considering this additional desorption pathway alters the desorption spectrum considerably. Thus, our study demonstrates that interlayer exchange can be crucial for the analysis of TPD data.

O 69.3 Thu 15:45 H4

CO oxidation on small size-selected Pt clusters supported on Fe₃O₄(001) — •JOHANNA PLANSKY¹, SEBASTIAN KAISER¹, FARAHNAZ MALEKI², KE ZHANG³, WOLFGANG HARBICH⁴, UELI HEIZ¹, SERGIO TOSONI², BARBARA A.J. LECHNER¹, GIANFRANCO PACCHIONI², and FRIEDRICH ESCH¹ — ¹Technical University of Munich, Garching, Germany — ²University of Milano-Bicocca, Milano, Italy — ³Technical University of Denmark, Kgs. Lyngby, Denmark — ⁴École Polytechnique Fédérale de Lausanne, Lausanne, Switzerland

Oxide-supported metal nanoparticles and clusters are common catalysts for heterogeneous reactions such as exhaust gas treatment. By studying supported size-selected clusters, we disentangle the influence of cluster size and support on reaction mechanisms. In the Pt_n/Fe₃O₄(001) model system, we observe a complicated interplay between lattice oxygen reverse spillover, cluster encapsulation and gas phase pressure dependence. Sophisticated pulsed-valve reactor experiments (Sniffer-MS) combined with variable temperature scanning tunneling microscopy (STM) reveal the reaction of CO with lattice oxygen occurs on the clus-

ter and not at the interface, but it is rapidly quenched by the strong metal-support interaction (SMSI). We will further demonstrate how UHV-based experiments can be quantified to provide turnover frequencies (TOFs) for comparison with real catalysts.

O 69.4 Thu 16:00 H4

A Model-Free Sparse Approximation Approach to Robust Formal Reaction Kinetics — •FREDERIC FELSEN, KARSTEN REUTER, and CHRISTOPH SCHEURER — Fritz-Haber-Institut der MPG, Berlin, Germany

Accurate and transferable models of reaction kinetics are of key importance for chemical reactors on both laboratory and industrial scale. Usually, setting up such models requires a detailed mechanistic understanding of the reaction process and its interplay with the reactor setup. We present a data-driven approach which analyzes the influence of process parameters on the reaction rate to identify effective rate laws without prior knowledge and assumptions. The algorithm we propose determines relevant model terms from a polynomial ansatz employing well established statistical methods. For the optimization of the model parameters special emphasis is put on the robustness of the results by taking not only the quality of the fit but also the distribution of errors [1] into account in a multi-objective optimization [2]. We demonstrate the flexibility of this approach based on synthetic kinetic data sets from microkinetic models. This way, we show that the kinetics of both the classical HBr reaction and a prototypical catalytic cycle are automatically reproduced. Further, combining our approach with experimental screening designs we illustrate how to efficiently explore kinetic regimes by using the example of the catalytic oxidation of CO.

[1] J. J. Filliben, *Technometrics*, 17, 111, 1975.

[2] K. Deb et al., *IEEE Trans. Evol. Comput.*, 6, 182, 2002.

O 69.5 Thu 16:15 H4

Combining Planar Laser-Induced Fluorescence with Stagnation Point Flows for Small Single-Crystal Model Catalysts: CO Oxidation on a Pd(100) — JIANFENG ZHOU¹, •SEBASTIAN MATERA^{2,4}, SEBASTIAN PFAFF¹, SARA BLOMBERG^{1,3}, EDVIN LUNDGREN¹, and JOHAN ZETTERBERG¹ — ¹Lund University, SE-22100 Lund, Sweden — ²Freie Universität Berlin, D-14195 Berlin, Germany — ³Lawrence Berkeley National Laboratory, Berkeley, CA 94720-8229, USA — ⁴Fritz-Haber-Institut der MPG, D-14195 Berlin, Germany

Mass transfer limitations can have a tremendous impact on catalysts characterization and must be accounted for by an appropriate modelling and, if possible, reactor design. We present a stagnation flow reactor for reaction product imaging by planar laser-induced fluorescence (PLIF), which is amenable to efficient low order modeling. Using CO oxidation over a Pd(100) single crystal as a showcase, we discuss the peculiarities for the case of small single-crystal model catalysts. While the ideal stagnation flow equations are not valid in this limit, a slightly modified theory can be derived, which exploits the information encoded in the PLIF signal. This combination of PLIF and half-theory/half-data driven modelling allows to efficiently analyze the experimental data and to estimate the turnover frequency and the CO₂, CO and O₂ concentrations at the surface from solely the CO₂ profile at some distance of the surface.

O 69.6 Thu 16:30 H4

On-surface collision reactions — •MATTHEW J. TIMM, KELVIN ANGGARA, LYDIE LEUNG, ZHIXIN HU, and JOHN C. POLANYI — Lash Miller Chemical Laboratories, Department of Chemistry, University of Toronto, 80 St. George Street, Toronto, Ontario M5S 3H6, Canada

Collisions between atoms and molecules are required for forming chemical bonds, thus they are central to any chemical reaction. The outcome of these collisions depends on the collision energy, geometry, and miss-distance between centers of the colliding reagents (called the impact parameter). As the incoming species - in general - randomly misses the target's center of mass, measurement of the impact parameter is a long-standing problem. Recently, a 'surface-molecular-beam' approach has been demonstrated that can allow for selection of impact parameter in a surface-reaction [1-3]. Energetic, oppositely-recoiling CF₂ or F-atom "projectiles" are formed on a Cu(110) surface by dissociation of chemisorbed CF₃ molecules with the tip of a Scanning Tunneling Microscope (STM). The inherent corrugation of Cu(110) leads to collimated trajectories of these projectiles, allowing them to be aimed to collide with nearby molecular "targets" at chosen impact parameters. The pattern of reactive and non-reactive scattering was then determined by STM with the dynamics of the collision elucidated by density functional theory calculations.

[1] Anggara, K.; Leung, L.; Timm, M. J.; Hu, Z.; Polanyi, J. C.; *Sci Adv.*, 2018, 4, eaau2821. [2] Anggara, K.; Leung, L.; Timm, M. J.; Hu, Z.; Polanyi, J. C.; *Faraday Discuss.*, 2019, 214, 89-103. [3] Leung, L.; Timm, M. J.; Polanyi, J. C.; *Chem. Commun.*, 2021, 57, 12647-12650.

O 69.7 Thu 16:45 H4

Faster oxygen adatom diffusion in a more densely packed CO adlayer on Ru(0001): A high-speed STM and DFT study — •HANNAH ILLNER¹, SUNG SAKONG², AXEL GROSS², and JOOST WINTERLIN¹ — ¹Ludwig-Maximilians-Universität München, Germany — ²Universität Ulm, Germany

Oxygen atoms on a Ru(0001) surface covered with 0.33 monolayers (ML) of coadsorbed CO travel through the CO layer by the so-called door opening mechanism. It is facilitated by structural fluctuations in the CO layer and leads to an enhanced diffusion constant [Henß et al., *Science* 363, 715 (2019)]. Expecting a lower diffusion constant on a more densely CO-covered surface we have investigated how this mechanism changes when the CO coverage is enhanced. The experiments were performed by means of a variable-temperature, high-speed STM. In the analyzed temperature range between 239 and 280 K the CO layer is disordered at a coverage of 0.47 ML. The obtained trajectories of the O atoms show that jumps occur in six equivalent directions with the same probability, in contrast to 0.33 ML, where three directions are preferred. Surprisingly, the Arrhenius plot of the hopping rates suggests a lower activation energy for the diffusion at the higher CO coverage than at 0.33 ML of CO. Density functional theory calculations suggest that at $\theta(\text{CO}) > 0.33$ ML clusters form at which the CO density is locally enhanced, and that the configurations of the O atoms with respect to CO molecules are modified. However, the door opening mechanism is still efficient. A weaker binding of the O atoms in the dense CO layer effectively leads to a lower diffusion barrier.

O 69.8 Thu 17:00 H4

Machine-learning Gaussian Approximation Potentials to solve a longstanding puzzle about RuO₂ surfaces — •YONGHYUK LEE, JAKOB TIMMERMANN, CHRISTOPH SCHEURER, and KARSTEN REUTER — Fritz-Haber-Institut der MPG, Berlin, Germany

Machine-learning Gaussian Approximation Potentials (GAPs) have recently evolved as a powerful class of surrogate models to computationally demanding first-principles calculations. Along with structure exploration techniques, they enable us to examine the potential energy surface of interest with a hitherto unforeseen combination of physical accuracy and computational efficiency and to achieve global surface structure determination (SSD) for increasingly complex systems. This can be leveraged e.g. to discover novel surface motifs which are critical in understanding the "living" state of heterogeneous catalysts and their degradation under dynamic operating conditions. In our preceding study, this versatility could be leveraged by a general and data-efficient iterative training protocol that allows for the on-the-fly generation of GAPs via the actual surface exploration process. The iterative refinement of GAPs identifies plenty of unknown low energy terminations of RuO₂ even within the restricted sub-space of (1 × 1) surface unit-cells. Moreover, by extending the protocol to larger surface unit-cells, we discovered new surface structures, which provide solutions to longstanding questions in heterogeneous catalysis.

[1] J. Timmermann et al., *Phys. Rev. Lett.* **125**, 206101 (2020)

[2] J. Timmermann et al., *J. Chem. Phys.*, **155**, 244107 (2021)

O 69.9 Thu 17:15 H4

Hydrogen cleaning induced surface changes of GaAs(110) — •DOROTHEE S. ROSENZWEIG¹, MORITZ N.L. HANSEMAN¹, PHILIPP EBERT², MICHAEL SCHNEDLER², HOLGER EISELE¹, and MARIO DÄHNE¹ — ¹Institut für Festkörperphysik, Technische Universität Berlin, 10623 Berlin, Germany — ²Forschungszentrum Jülich GmbH, Peter Grünberg Institut, 52425 Jülich, Germany

For the nanoscopic analysis of III/V nanowire (110) surfaces, hydrogen cleaning is a commonly used procedure. While hydrogen cleaning is reported to be destruction free [1] and to achieve clean, atomically flat surfaces—as they are present directly after growth—the actual processes and dynamics during cleaning are rarely examined. However, a detailed understanding of these issues is crucial for the interpretation of electronic surface properties, of the growth of Nanowires, as well as of built-in and distribution of dopants.

Here, we investigate the modifications of GaAs(110) as model system upon atomic hydrogen exposure at room temperature and under commonly used cleaning conditions at the atomic level. For depiction and measurement at the atomic scale, we used scanning tunneling microscopy and spectroscopy under UHV conditions. Using these methods we study the geometric arrangement of the adsorbed atoms as well as adsorption induced additional electronic states, band bending, defect states, and Fermi level pinning.

[1] Webb et al., *Nano Lett.* **15**, 8, 4865-4875 (2015)

O 69.10 Thu 17:30 H4

In-situ characterization of cyclic reduction and reoxidation of CeO_x(111) and CeO_x(100) islands on Cu(111) — •LINUS PLEINES¹, LARS BUSS², TEVFIK ONUR MENTEŞ³, FRANCESCA GENUZZO³, ANDREA LOCATELLI³, JENS FALTA^{1,4}, and JAN INGO FLEGE² — ¹Institute of Solid State Physics, University of Bremen, Germany — ²Applied Physics and Semiconductor Spectroscopy, Brandenburg University of Technology Cottbus-Senftenberg, Germany — ³Elettra-Sincrotrone Trieste S.C.p.A., Basovizza Trieste, Italy — ⁴MAPEX Center for Materials and Processes, Bremen, Germany

Cerium oxide (CeO_x) is of special interest due to its catalytic activity and various other electronic and optical applications. The inverse model catalyst CeO_x on Cu(111) has a high activity for methanol synthesis from H₂ and CO₂. For the activation of CO₂, Ce³⁺ sites have to be present at the surface, which means that

the CeO_x has to be reduced to some extent. This may be achieved by exposure to H_2 at elevated temperatures. We studied the interaction of H_2 and CO_2 with CeO_x islands on Cu(111) with low-energy electron microscopy (LEEM) and X-ray absorption spectroscopy (XAS). From earlier studies, the orientation of the CeO_x is known to be decisive for its catalytic activity. In our experiments (100)

and (111) CeO_x islands are grown side by side on the metal substrate, so that identical reaction conditions prevail during the experiment. At a high temperature of 550 °C, exposure to H_2 leads to partial reduction, and exposure to CO_2 leads to reoxidation of the CeO_x . The differences observed for the two island orientations regarding structure and composition will be discussed.

O 70: Supported nanoclusters: Structure, Reactions, Catalysis

Time: Thursday 15:00–17:45

Location: H6

Topical Talk

O 70.1 Thu 15:00 H6
Stability and dynamics of cluster catalysts and their supports — SEBASTIAN KAISER, JOHANNA PLANSKY, FABIAN KNOLLER, ALEXANDER BOURGUND, KE ZHANG, UELI HEIZ, FRIEDRICH ESCH, and BARBARA A. J. LECHNER — Department of Chemistry & Catalysis Research Center, Technical University of Munich, Germany

The intrinsic metastability of supported clusters can induce a vast range of dynamics that strongly influence their physical and chemical properties, while being experimentally highly challenging to investigate. Here, I will present a range of surface dynamics that occur in supported cluster dynamics, ranging from confined cluster diffusion, cluster encapsulation, support mobility and reactant spillover to lateral diffusion linked to reactivity. Our experimental approach is to combine static, statistically sound, and dynamic, time-resolved scanning tunneling microscopy (STM) to investigate the diffusion, sintering, and restructuring of size-selected clusters on weakly and strongly interacting supports.

O 70.2 Thu 15:30 H6
The role of water in oxidation of the Pt/Co3O4 interface — YAROSLAVA LYKHACH¹, LUKÁŠ FUSEK^{1,2}, MAXIMILIAN KASTENMEIER¹, TOMÁŠ SKÁLA², NATALIYA TSUD², VIKTOR JOHÁNEK², SASCHA MEHL³, JOSEF MYSLIVEČEK², OLAF BRUMMEL¹, and JÖRG LIBUDA¹ — ¹Friedrich-Alexander-Universität Erlangen-Nürnberg, Erlangen, Germany — ²Charles University, Prague, Czech Republic — ³Eletra-Sincrotrone Trieste SCPA, Basovizza-Trieste, Italy

Electronic metal-oxide interactions (EMSI) play a major role in the design of advanced functional materials for applications in catalysis. We investigated the influence of the EMSI on the oxidation state of ultra-small Pt particles supported on a well-ordered $\text{Co}_3\text{O}_4(111)$ substrate in the presence of co-adsorbates, i.e. hydroxyl groups and molecularly adsorbed water, by means of synchrotron radiation photoelectron spectroscopy and scanning tunnelling microscopy. The EMSI gives rise to charge transfer across the metal-oxide interface and results in partial oxidation of Pt deposits coupled with partial reduction of $\text{Co}_3\text{O}_4(111)$. We detected ultra-small $\text{Pt}^{\delta+}$ aggregates in combination with atomically dispersed $\text{Pt}^{2+/4+}$ species. While the oxidation degree of Pt deposits is not influenced by the presence of co-adsorbates, the magnitude of the charge transfer is enhanced in the presence of molecularly adsorbed water. Subsequent annealing in UHV leads to re-oxidation of $\text{Co}_3\text{O}_4(111)$ accompanied by an increase in the amount of Pt^{4+} species. This observation suggests the re-dispersion of $\text{Pt}^{\delta+}$ aggregates to Pt^{4+} species triggered by the dissociation of water.

O 70.3 Thu 15:45 H6
Ripening mechanism changes with cluster size: In situ observation of Pt cluster diffusion on $\text{Fe}_3\text{O}_4(001)$ — SEBASTIAN KAISER, JOHANNA PLANSKY, UELI HEIZ, BARBARA A. J. LECHNER, and FRIEDRICH ESCH — Technical University of Munich, Garching, Germany

Ripening of small oxide-supported metal clusters is a common deactivation mechanism in heterogeneous catalysis. We use scanning tunneling microscopy (STM) to follow the diffusion and ripening of size-selected Pt clusters on an $\text{Fe}_3\text{O}_4(001)$ support. Thanks to a strong cluster-support bonding, ripening and coalescence only set in at elevated temperatures. Particle size analysis of our STM images reveals that Pt_{19} exhibits Ostwald ripening at temperatures above 800 K, i.e. with cluster growth by atom diffusion. In contrast, the smaller Pt_5 and Pt_{10} clusters show Smoluchowski ripening, i.e. the diffusion of entire clusters, already in the temperature range of 600 to 800 K and Ostwald ripening >800 K. We not only observe the ripened clusters in STM, but could successfully follow the diffusion process *in situ* by STM movies. Surprisingly, temperature programmed desorption (TPD) measurements of CO molecules show that in this temperature range the clusters get concomitantly encapsulated by iron oxide via strong metal support interaction (SMSI). Cluster diffusion thus occurs despite a strong interaction with the magnetite support and the diffusing species is most likely a cluster with Fe and O atoms on top.

O 70.4 Thu 16:00 H6
Tuning SMSI Kinetics on Pt-loaded $\text{TiO}_2(110)$ by Choosing the Pressure — PHILIP PETZOLDT¹, MORITZ EDER¹, SONIA MACKEWICZ¹, MONIKA BLUM^{2,3}, TIM KRATKY⁴, SEBASTIAN GÜNTHER⁴, MARTIN TSCHURL¹, UELI HEIZ¹, and BARBARA LECHNER⁵ — ¹Physical Chemistry, Department of Chemistry and Catalysis Research Center, Technical University of Munich — ²Advanced Light

Source, Lawrence Berkeley National Laboratory — ³Chemical Sciences Division, Lawrence Berkeley National Laboratory — ⁴Physical Chemistry with Focus on Catalysis, Department of Chemistry and Catalysis Research Center, Technical University of Munich — ⁵Functional Nanomaterials, Department of Chemistry and Catalysis Research Center, Technical University of Munich

The encapsulation of noble metal particles on reducible supports due to a strong metal-support interaction (SMSI) has already been extensively studied. However, there is still an ongoing debate on important aspects such as the influence of oxygen or hydrogen treatments on the encapsulating overlayer. We have utilized synchrotron-based NAP-XPS in order to investigate the SMSI for Pt-loaded $\text{TiO}_2(110)$ single crystals under the influence of H_2 and O_2 at different pressures. In an O_2 atmosphere two different, pressure-dependent phenomena, namely, an oxidation of Pt particles and a loss of Pt signal intensity, are observed at 800 K. While the oxidation is partially reversed in vacuum, the intensity of the platinum signal cannot be recovered. H_2 annealing has no significant additional effect compared to vacuum annealing. In the presentation, we discuss possible origins of these observations.

O 70.5 Thu 16:15 H6
Deposition and annealing of FeNi nanoparticles on surfaces — MAHBOOBEH RAVANKHAH¹, MATHIAS GETZLAFF¹, GERHARD DEHM², and PHILIPP WATERMEYER² — ¹Institut für Angewandte Physik, Universität Düsseldorf — ²Max-Planck-Institut für Eisenforschung GmbH, Düsseldorf

3d bimetallic nanoparticles have received lots of attention due to their technological applications in ultrahigh density information storage, catalysis and biomedicine. The thermal stability and the magnetic properties of the *in vacuo* prepared bimetallic nanoparticles are shown to depend on the composition and their structure. Here we report on new findings of structure and composition of Fe-Ni nanoparticles, synthesized via a magnetron sputtering source and deposited on a Tungsten crystal surface. The elemental distribution of nanoparticles is determined by high resolution transmission electron microscopy (HRTEM) and electron energy loss spectroscopy (EELS). It is found that the nanoparticles have a shell formed by Fe atoms and a core composed of Fe and Ni with the gradient of composition from core to the surface. The melting behavior of nanoparticles was studied under UHV conditions by scanning tunneling microscopy (STM) as a function of heating temperature. The unrolling carpet, surface diffusion and anisotropy spreading are driving processes to form monolayer high islands above the melting point. The relevant result could be helpful for the design and preparation of stable and controllable bimetallic nanoparticles for technological applications.

O 70.6 Thu 16:30 H6
Reaction Pathways in Alcohol Photoreforming on Cluster Co-Catalyst Loaded $\text{TiO}_2(110)$ — SONIA MACKEWICZ, MORITZ EDER, PHILIP PETZOLDT, MARTIN TSCHURL, and UELI HEIZ — Physical Chemistry, Department of Chemistry and Catalysis Research Center, Technical University of Munich

Heterogeneous photocatalysis offers the prospect of utilizing solar energy for the environmentally benign production of chemical fuels such as hydrogen. State-of-the-art materials often comprise co-catalyst loaded semiconductors, but these systems are still limited in efficiency. In order to systematically optimize photocatalysts, a profound knowledge of reaction mechanisms is crucial, whose details are so far little understood. Alcohols are an ideal model system to investigate reaction mechanisms in photocatalysis. Furthermore, they may serve as renewable sources for hydrogen in the future. In this talk, we give insights into the mechanistic details of the alcohol photoreforming reaction on co-catalyst loaded $\text{TiO}_2(110)$. It is shown that semiconductor photocatalysis selectively enables new reaction pathways, which are not accessible by thermal or conventional chemical methods.

O 70.7 Thu 16:45 H6
Electron transfer reaction by time resolved (TRS) and core level spectroscopy (XPS) and STM on Au/ $\text{TiO}_2(110)$ single crystal systems. — HICHAM IDRISS — Institute of functional Interfaces, KIT, Karlsruhe

Charge transfer from or to a metal deposited on an oxide semiconductor are central to photocatalysis. In order to probe into this phenomenon, the effect of gold coverage on the chemical state of Ti cations, upon photoexcitation of rutile $\text{TiO}_2(110)$ single crystal, was investigated by X-ray photoelectron spec-

troscopy (XPS). Photocatalytic reaction of gas phase ethanol (a hole scavenger) on TiO₂(110) and Au/TiO₂(110) resulted in the formation of Ti³⁺ cations. Increasing the Au coverage resulted in the gradual decrease of these Ti³⁺ cations. The "quasi" total consumption of these reduced states was found at a ratio Au atoms to reacted Ti³⁺ close to one; this corresponded to about 0.50 at. % of Au. The relationship suggests that electron transfer occurs from the excited semiconductor to Au atoms during the catalytic reaction. In order to complement the work H₂ production rates of an electron donor, such as ethanol, over Au clusters with different sizes and coverage deposited on single crystal rutile TiO₂(110) were studied by scanning tunneling microscopy, online mass spectrometry and complemented by femto second pump probe spectroscopy. It was also found that there is a non-linear increase of the H₂ production rate with increasing gold coverage. The key determining factor appears to be the Au inter-particle distance. Increasing this distance resulted in an increase in the normalized reaction rate.

O 70.8 Thu 17:00 H6

Surface Ligand Infrared Spectroscopy: In-Situ Characterization of Noble Metal Clusters and Metal Oxides at Work — •ERIC SAUTER¹, DARIA GASHNIKOVA², FLORIAN MAURER², ALEXEI NEFEDOV¹, STEFAN HEISSLER¹, YUEMIN WANG¹, JAN-DIRK GRUNWALD², and CHRISTOF WÖLL¹ — ¹Institute of Functional Interfaces, KIT, Eggenstein-Leopoldshafen, Germany — ²Institute of Chemical Technology and Polymer Chemistry, KIT, Karlsruhe, Germany

To achieve a full understanding of chemical processes at exposed surfaces in-situ and operando investigations are required. For studies of catalytic processes under real conditions, IR spectroscopy offers a number of advantages. In the present study, surface ligand infrared spectroscopy was used to perform an in-situ investigation of the surface characteristics of cerium oxide single crystals as well as catalytic active NM-clusters on cerium oxide nanoparticles. Low temperature adsorption of carbon monoxide was used to identify the surface structure and morphology, visible through distinctive adsorption bands blue shifted in respect to the gas phase, which can be used as reference for the interpretation of more complicated spectra like powders or nanoparticles. Additionally, noble-metal clusters were investigated in pristine condition as well as in the reduced state. Upon heating, desorption of the probe molecule occurred and at higher temperatures deformation and sintering of the clusters was observed. The investigation shows the power of infrared spectroscopy as a tool for in-situ investigations and characterization of NM-clusters and metal oxides at work.

O 70.9 Thu 17:15 H6

AI with Experimental and Theoretical Data toward the Understanding CO₂ Hydrogenation Catalysis: The Role of the Support Materials — •RAY MIYAZAKI¹, KENDRA BELTHLE², HARUN TÜYSÜZ², LUCAS FOPPA¹, and MATTHIAS SCHEFFLER¹ — ¹The NOMAD Laboratory at the Fritz Haber Institute of the Max Planck Society, Germany — ²Max-Planck-Institut für Kohlenforschung, Germany

The genesis of organic molecules from CO₂ at a hydrothermal vent, which is a fissure on the seafloor, is one of the theories for the origin of life [1]. We focus on CO₂ hydrogenation catalyzed by cobalt nanoparticles supported on SiO₂, which mimic the environment of a hydrothermal vent. In particular, we investigate the role of support materials by using several amorphous SiO₂ supports incorporating different elements (e.g., Ti, Zr). In this study, the experimental selectivity toward organic molecules (e.g., methanol, formic acid) is modeled by the sure-independence screening and sparsifying operator (SISSO) AI approach [2]. Both experimental and theoretical data are adopted as the input features for SISSO, such as atomic-scale features calculated by density functional theory and experimental characterization data. Our approach identifies the key descriptive parameters correlated to the selectivity, which lead to a better understanding of the origin of life and to design of novel CO₂ hydrogenation catalysts.

[1] M. Preiner *et al.*, *Nat. Ecol. Evol.*, **4**, 534-542 (2020).

[2] R. Ouyang *et al.*, *Phys. Rev. Mater.*, **2**, 083802 (2018).

O 70.10 Thu 17:30 H6

Near-ambient pressure studies of size selected clusters on ultrathin silica films — •MATTHIAS KRINNINGER, FLORIAN KRAUSHOFER, FRIEDRICH ESCH, and BARBARA A.J. LECHNER — Department of Chemistry, Technical University of Munich, 85748 Garching, Germany

Silicon oxide is a widely used catalyst support material for clusters and nanoparticles. Understanding the relationship between these clusters and the support is challenging, however, because SiO₂ is insulating, and in most applications not crystalline, which limits the use of diffraction-based experimental techniques. Some progress has been made by growing ultrathin, quasi-2D silica bilayer films on a variety of metal supports [1], which can then be measured by scanning tunneling microscopy (STM). Here, we show first results for ultrathin silica films grown on Pt(111) and their interaction with deposited metal clusters, examined by near-ambient pressure (NAP) XPS and NAP-STM. We investigate the stability of the films, their ability to stabilize small clusters without sintering, and the dependence of this stability on the crystallinity of the film.

[1] C. Büchner, M. Heyde, Two-dimensional silica opens new perspectives, *Prog. Surf. Sci.*, **92** (2017) 341-374.

O 71: Focus Session: Atomic-Scale Studies of Spins on Surfaces with Scanning Tunneling Microscopy 2

Time: Thursday 15:00–18:00

Location: S051

Topical Talk

O 71.1 Thu 15:00 S051

Theory for Electron Spin Resonance based on electron transport — •NICOLAS LORENTE¹, JOSÉ REINA², and CHRISTOPH WOLF² — ¹Centro de Física de Materiales & DIPIC, Donostia, Spain — ²Center for Quantum Nano Science, Seoul, Korea

Recent progress in electron spin resonance with the scanning tunneling microscope (ESR-STM) [1] is greatly advancing the experimental possibilities of manipulating atomic spins by all-electrical means. Two-qubit operations have been made possible using a pulse-mode in the ESR-STM [2], and addressing remote qubits has been rendered possible by creating a new multi-frequency operational mode [3]. We aim at developing a computational tool that permits us to interpret and predict the outcome of experiments in ESR. The first results of such a simulation tool have addressed one and two spins under an STM current [4,5]. We use a non-equilibrium Green's function approach with Hubbard operators that allows us to write quantum adiabatic Markovian master equations in the presence of an electron current and under the driving of an external electric field. The results are enticing and the modelling is flexible enough to treat many different physical situations. References: [1] S. Baumann *et al.*, *Science* **350**, 417 (2015). [2] K. Yang *et al.*, *Science* **366**, 509 (2019). [3] S.-H. Phark *et al.*, *ArXiv:2108.09880*. [4] J. Reina *et al.*, *Phys. Rev. B* **100**, 035411 (2019). [5] J. Reina *et al.*, *Phys. Rev. B* **104**, 245435 (2021).

O 71.2 Thu 15:30 S051

Modeling the Electron Spin Resonance Spectrum in Scanning Tunneling Microscopy — •CHRISTIAN R. AST¹, PIOT KOT¹, MANEESHA ISMAIL¹, and JUAN CARLOS CUEVAS² — ¹MPI for Solid State Research, 70569 Stuttgart — ²Universidad Autónoma de Madrid, 28049 Madrid, Spain

The theory of electron spin resonance (ESR) spectroscopy in scanning tunneling microscopy (STM) has been debated for some time now with a number of

different proposals having different origin, but essentially leading to very similar results. While the focus so far has been on the ESR signal itself, the measured DC tunneling spectrum offers more details that allow for a more precise verification of the underlying theory. Here, we discuss the ESR signal from a theory point of view by allowing the tunneling electrons to interact with both the driven spin system and the incident microwave during the tunneling process. We find a more complete description of the whole tunneling current also going beyond the typical approximation of a constant density of states.

O 71.3 Thu 15:45 S051

A new view on the origin of zero-bias anomalies of Co atoms atop noble metal surfaces — JUBA BOUAZIZ¹, FILIPE S. M. GUIMARAES¹, and •SAMIR LOUNIS^{1,2} — ¹Peter Grünberg Institut and Institute for Advanced Simulation, Forschungszentrum Jülich & JARA, Jülich 52425, Germany — ²Faculty of Physics & CENIDE, University of Duisburg-Essen, 47057, Duisburg, Germany

Many-body phenomena are paramount in physics. In condensed matter, their hallmark is considerable on a wide range of material characteristics spanning electronic, magnetic, thermodynamic and transport properties. In this talk, we address systematically zero-bias anomalies detected by scanning tunneling spectroscopy on Co atoms deposited on Cu, Ag and Au(111) substrates, which remarkably are almost identical to those obtained from first-principles [1]. These features originate from gaped spin-excitations induced by a finite magnetic anisotropy energy, in contrast to the usual widespread interpretation relating them to Kondo resonances. Resting on relativistic time-dependent density functional and many-body perturbation theories, we furthermore unveil a new many-body feature, the spinaron, resulting from the interaction of electrons and spin-excitations localizing electronic states. Besides Co, we will show examples of anomalous spin-excitations characterising adatoms on Nb(110) surface [2,3].

[1] Bouaziz, Guimaraes, Lounis, Nat. Commun. 11, 6112 (2020); [2] Brinker, Küster, Parkin, Sessi, Lounis, Science Adv. 8, eabi7291 (2022); [3] Küster, Montero, Guimaraes, Brinker, Lounis, Parkin, Sessi, Nat. Commun. 12, 1108 (2021).

O 71.4 Thu 16:00 S051

Real-space observation of the Kondo effect in MoS₂ mirror twin boundaries — CAMIEL VAN EFFEREN¹, JEISON FISCHER¹, ACHIM ROSCH², THOMAS MICHEL¹, and WOUTER JOLIE¹ — ¹II. Physikalisches Institut, Universität zu Köln — ²Institut für Theoretische Physik, Universität zu Köln

Finite mirror twin boundaries in monolayer MoS₂ on graphene confine strongly correlated one-dimensional electronic states [1]. Using scanning tunneling microscopy and spectroscopy, we observe a resonance at the Fermi energy when the highest occupied confined state is filled with one electron. Magnetic field and temperature-dependence of the resonance unambiguously point to the Kondo effect, i.e., screening of the spin- $\frac{1}{2}$ confined state within the mirror twin boundary. Theoretical models for both Kondo resonance and spin- $\frac{1}{2}$ state are used to extract the Kondo coupling strength. Real-space mapping gives access to the correlated beating of both confined state and Kondo resonance along the boundary. Hence, our experiments reveal the behavior of the Kondo effect for a delocalized electronic state on the atomic scale.

[1] Jolie et al., Phys. Rev. X 9, 011055 (2019)

O 71.5 Thu 16:15 S051

Moiré tuning of spin excitations: individual Fe atoms on MoS₂/Au(111) — CHRISTIAN LOTZE¹, SERGEY TRISHIN¹, NILS BOGDANOFF¹, FELIX VON OPPEN², and KATHARINA J. FRANKE¹ — ¹Fachbereich Physik, Freie Universität Berlin, 14195 Berlin, Germany — ²Dahlem Center for Complex Quantum Systems and Fachbereich Physik, Freie Universität Berlin, 14195 Berlin, Germany

Magnetic adatoms have been investigated on various surfaces in regard to stabilizing, controlling and manipulating single quantum spins. Here, we study individual iron atoms adsorbed on a single layer of molybdenum disulfide (MoS₂) on a Au(111) crystal. MoS₂ has been recently reported as a well-suited system for decoupling molecules. We show that the Fe atoms are largely decoupled from the Au(111) substrate with the remaining coupling strength varying along the moiré structure. As a consequence, the spectroscopic fingerprints range from pure inelastic excitations to Kondo resonances. Moreover, we see spatial variations of those excitations over one atom, which result from the formation of Fe-S hybrid states and interference effects. In conclusion, our work establishes MoS₂ on Au(111) as a tuning layer for quantum spin properties. This tuning can be realized continuously.

O 71.6 Thu 16:30 S051

Spin excitations on hexagonal zinc oxide — LUKAS ARNHOLD, HENRIK LICHTL, LEON RULLKÖTTER, NICOLAJ BETZ, SUSANNE BAUMANN, and SEBASTIAN LOTH — University of Stuttgart, Institute for Functional Matter and Quantum Technologies, Stuttgart, Germany

Few-layer materials are widely used to tailor different electronic properties, down to the atomic level. We use a double layer of ZnO, a hexagonal wide bandgap semiconductor [1], to mitigate electron scattering between the Ag (111) substrate and Co atoms deposited on the ZnO surface. With low-temperature scanning tunneling microscopy we observe spin excitations and the ability to manipulate transition metal atoms on the surface into hexagonal arrangements. These findings make ZnO a viable candidate for resonant spin spectroscopy methods [2,3] and construction of geometrically frustrated magnetic structures.

[1] A. Shiotari et al., J. Phys. Chem. C 118, 27428 (2014). [2] S. Baumann et al., SCIENCE 350, 417 (2015). [3] M. Hänze et al., SCIENCE ADVANCES 7, eabg2616 (2021).

Topical Talk

O 71.7 Thu 16:45 S051

Stochastic resonance as a new tool to investigate spin dynamics — SUSANNE BAUMANN¹, NICOLAJ BETZ¹, MAX HÄNZE¹, GREGORY MCMURTRIE¹, SUSAN COPPERSMITH², and SEBASTIAN LOTH¹ — ¹University of Stuttgart, Institute for Functional Matter and Quantum Technologies, Stuttgart, Germany — ²School of Physics, University of New South Wales, Sydney, Australia

Stochastic resonance is an unusual phenomenon in which noise can be used as a resource to synchronize stochastic dynamics to a control signal [1,2]. In this talk, I will show how stochastic resonance can be induced in the spin switching of magnetic nanostructures on surfaces [3], and, more importantly, how we can use this as a tool to investigate the magnetization dynamics of these spin systems.

With this tool, one can get insight into the interaction of these structures with their environment. This also enables the observation of ultrafast dynamics of excited spin states that are not easily accessible to other scanning probe techniques. The new frequency resolved spectroscopy method allows for the broadband observation of spin dynamics with previously inaccessible bandwidth ranging from milliseconds to picoseconds.

References: [1] R. Benzi, J. Phys. A: Math. Gen 14, L453 (1981). [2] R. Löfstedt, S. N. Coppersmith, Phys. Rev. Lett. 72, 1947 (1994). [3] M. Hänze*, G. McMurtrie* et al. Science Adv. 7 eabg2616 (2021).

O 71.8 Thu 17:15 S051

Path-resolved measurement of ultrafast spin dynamics — NICOLAJ BETZ¹, MAX HÄNZE^{1,2}, GREGORY MCMURTRIE¹, SUSANNE BAUMANN¹, and SEBASTIAN LOTH^{1,2} — ¹University of Stuttgart, Institute for Functional Matter and Quantum Technologies, Stuttgart, Germany — ²Max Planck Institute for Solid State Research, Stuttgart, Germany

Transitions between quantum mechanical states are fundamentally random processes. While it is possible to directly observe individual quantum jumps [1] in a time resolved measurement [2], the dynamics of many systems exceed the resolution of real time measurements. This requires the use of time-averaged measurements such as pump probe experiments. These methods typically measure state occupation times and contain little information about the relaxation process itself. Here, we introduce a dynamic response measurement that is sensitive to the switching path between spin states and can be applied in scanning tunneling microscopy. By using stochastic resonance [3], this method resolves spin-switching dynamics of magnetic atoms and nanostructures ranging from milliseconds to picoseconds. Crucially, in more complex spin structures the measurement can distinguish multiple switching paths between higher excited states. This provides deeper insight into ultrafast spin dynamics than possible with relaxometry.

[1] Th. Sauter, et al. Phys. Rev. Lett. 57, 1696 (1986).

[2] M. Hänze, et al. Sci. Adv. 7, 33 (2021).

[3] R. Löfstedt, et al. Phys. Rev. Lett. 72, 1947 (1994).

O 71.9 Thu 17:30 S051

Growth and magnetic characterization of thermally robust cobalt islands on Cu₃Au(111) — ALEŠ CAHLÍK, DANYANG LIU, BERK ZENGİN, and FABIAN NATTERER — Institute of Physics, UZH, Zurich, Switzerland

Due to a larger tunability of the effective lattice parameter, bimetallic alloys can be an appealing choice as an alternative substrate for the growth of thin films and nanostructures. In this respect, we investigate Cu₃Au(111) as a platform for the growth of cobalt nano-islands. Using STM, we demonstrate unique thermal stability of Co/Cu₃Au(111) up to $\sim 340^\circ\text{C}$, compared to the fast intermixing of Co/Cu(111) at room temperature. We explore the structural and magnetic properties of the Co islands with spin-polarized and nickelocene functionalized tips. Finally, we find an effective method to produce spin-polarized tips by deliberately lifting off an entire island from the substrate and transferring it to the STM tip.

O 71.10 Thu 17:45 S051

Transport in the Rashba-split surface state of $(\sqrt{3} \times \sqrt{3})\text{Bi}/\text{Ag}(111)R30^\circ$ revealed by MONA — MARKUS LEISEGANG, PATRICK HÄRTL, and MATTHIAS BODE — Physikalisches Institut, Experimentelle Physik II, Universität Würzburg, Am Hubland, D-97074 Würzburg, Germany

Transport measurements that are sensitive to the band structure of a material require techniques that operate on the length scale of the charge carrier's mean free path. A novel method that fulfills this requirement is the molecular nanoprobe (MONA), which uses a single molecule to detect charge carriers [1].

In this study, we investigate the rotation and tautomerization of phthalocyanine molecules on the $(\sqrt{3} \times \sqrt{3})\text{Bi}/\text{Ag}(111)R30^\circ$ surface and utilize these excitations to investigate transport in the Rashba-split surface state characteristic for this surface [2]. We find that both excitation processes are driven by the N-H stretching mode and can be triggered by a single electron [3]. Our transport measurements prove the sensitivity to hot charge carriers which preferably propagate in the Rashba-split surface state of the BiAg₂ alloy. The expected impact of the spin-momentum-locking of this Rashba-split surface state on the surface transport is discussed and first experimental results obtained with spin-polarized tips will be presented.

[1] M. Leisegang et al., Nano Lett. 18, 2165–2171 (2018)

[2] C. R. Ast et al., Phys. Rev. Lett. 98, 186807 (2007)

[3] J. Kügel et al., Journ. Phys. Chem. C 121, 28204–28210 (2017)

O 72: 2D Materials 3: hBN and Electronic Structure

Time: Thursday 15:00–17:00

Location: S052

O 72.1 Thu 15:00 S052

Electronic Structure of Two-Dimensional CoO₂ — ANN JULIE U. HOLT¹, SAHAR PAKDEL¹, JONATHAN RODRÍGUEZ-FERNÁNDEZ², YU ZHANG³, DAVIDE CURCIO¹, ZHAOZONG SUN⁴, PAOLO LACOVIG⁵, YONG-XIN YAO^{6,7}, JEPPE V. LAURITSEN⁴, SILVANO LIZZIT⁵, NICOLA LANATA^{1,8}, PHILIP HOFMANN¹, MARCO BIANCHI¹, and •CHARLOTTE E. SANDERS³ — ¹Dept. of Physics and Astronomy, Interdisciplinary Nanoscience Center (iNANO), Aarhus Univ., 8000 Aarhus, DK — ²Dept. of Physics, Univ. of Oviedo, Oviedo 33007 ES — ³UK Central Laser Facility, RCaH, STFC RAL, Didcot, Oxfordshire OX11 0QX, UK — ⁴Interdisciplinary Nanoscience Center (iNANO), Aarhus Univ., 8000 Aarhus, DK — ⁵Elettra Sincrotrone Trieste S.C.p.A., AREA Science Park, Strada Statale 14, km 163.5, 34149 Trieste, IT — ⁶Ames Laboratory U.S.-DOE, Ames, IA 50011, USA — ⁷Dept. of Physics and Astronomy, Iowa State Univ., Ames, IA 50011, USA — ⁸Nordita, KTH Royal Institute of Technology and Stockholm Univ., Roslagstullsbacken 23, 10691 Stockholm, SE

The transition metal oxide CoO₂ forms bulk layered structures that exhibit complex correlated electronic states. However, little has been known about the electronic properties of the isolated single layer. We have now [1] studied CoO₂/Au(111), using angle-resolved photoemission spectroscopy, x-ray photoelectron diffraction, and density functional theory. The results of our study show single-layer CoO₂ to be metallic, with electronic correlations. They emphasize the interest of oxides as a new subject within two-dimensional materials research. [1] 2D Mater. 8 (2021) 035050.

O 72.2 Thu 15:15 S052

Unified Treatment of Magnons and Excitons in Monolayer CrI₃ from Many-Body Perturbation Theory — •THOMAS OLSEN — Technical University of Denmark

We present first principles calculations of the two-particle excitation spectrum of CrI₃ using many-body perturbation theory including spin-orbit coupling. Specifically, we solve the Bethe-Salpeter equation, which is equivalent to summing up all ladder diagrams with static screening, and it is shown that excitons as well as magnons can be extracted seamlessly from the calculations. The resulting optical absorption spectrum as well as the magnon dispersion agree very well with recent measurements, and we extract the amplitude for optical excitation of magnons resulting from spin-orbit interactions. Importantly, the results do not rely on any assumptions of the microscopic magnetic interactions such as Dzyaloshinskii-Moriya (DM), Kitaev, or biquadratic interactions, and we obtain a model independent estimate of the gap between acoustic and optical magnons of 0.3 meV. In addition, we resolve the magnon wave function in terms of band transitions and show that the magnon carries a spin that is significantly smaller than \hbar . This highlights the importance of terms that do not commute with S_z in any Heisenberg model description.

[1] T. Olsen, Phys. Rev. Lett. 127, 166402, (2021)

O 72.3 Thu 15:30 S052

Excitons in two-dimensional magnetic semiconductors — •MARIE-CHRISTIN HEISSENBÜTTEL, THORSTEN DEILMANN, PETER KRÜGER, and MICHAEL ROHLFING — Institute of Solid State Theory, University of Münster, Germany

Semiconducting two-dimensional magnets exhibit peculiar interrelation between magnetic properties and light-matter interaction. We will present and discuss ab-initio GW/Bethe-Salpeter equation calculations to examine excitonic states in different magnetic systems.

Due to the hexagonal crystal structure the out-of-plane ferromagnetic monolayer CrI₃ came to the fore for the construction of heterobilayers with transition-metal dichalcogenides [1]. Due to coupling effects the magnetic properties are transferred and can be observed in a splitting and a modified Zeeman effect of the excitons. On the other hand, CrSBr shows in-plane magnetization in combination with a large crystal anisotropy. This is reflected in the quasi-1D behavior of different opto-electronic properties [2].

[1] Nano Lett. Lett. 21, 5173-5178 (2021)

[2] <https://arxiv.org/abs/2205.13456>

O 72.4 Thu 15:45 S052

Nanoscale view of massive Dirac quasiparticles in lithographic superstructures — •ALFRED JONES¹, LENE GAMMELGAARD², DEEPNARYAN BISWAS¹, MIKKEL SAUER³, ROLAND KOCH⁴, CHRIS JOZWIAK⁴, ELI ROTENBERG⁴, AARON BOSTWICK⁴, KENJI WATANABE⁵, TAKASHI TANIGUCHI⁵, CORY DEAN⁶, THOMAS PEDERSEN³, ANTTI-PEKKA JAUHO², PETER BØGGILD², BJARKE JESSEN⁶, and SØREN ULSTRUP¹ — ¹Aarhus University, Denmark — ²Technical University of Denmark, Denmark — ³Aalborg University, Denmark — ⁴Advanced Light Source, USA — ⁵National Institute for Materials Science, Japan — ⁶Columbia University, USA

Massive Dirac quasiparticles play a central role in a number of emerging physical phenomena such as topological phase transitions and anomalous Hall effects.

Single-layer graphene appears to be an ideal platform to explore such properties, however engineering the transition from massless to massive Dirac quasiparticles in a controllable fashion remains a significant challenge. Here, we employ angle-resolved photoemission with a nanoscale light spot (nanoARPES) to directly measure the electronic structure modifications induced by lithographic patterning of an antidot superlattice onto a graphene device. We observe a transition from massless Dirac fermions in the pristine graphene to a massive character in patterned regions, and determine that the mass scales linearly with antidot diameter, consistent with theory. Gate-induced electron-doping of the patterned graphene produces an enhancement of the mass, highlighting the versatility of nanopatterned graphene as a platform for engineering such quasiparticles.

O 72.5 Thu 16:00 S052

Tuning lower dimensional superconductivity with hybridization at a superconducting-semiconducting interface — •ANAND KAMLAPURE¹, MANUEL SIMONATO¹, EMIL SIERDA¹, MANUEL STEINBRECHER¹, UMUT KAMBER¹, ELZE J. KNOL¹, PETER KROGSTRUP², MIKHAIL I. KATSNELSON¹, MALTE RÖSNER¹, and ALEXANDER A. KHAJETOORIAN¹ — ¹Institute for Molecules and Materials, Radboud University, 6525 AJ Nijmegen, the Netherlands — ²Center for Quantum Devices, Niels Bohr Institute, University of Copenhagen, 2100 Copenhagen, Denmark

Study of influence of interface electronic structure on the superconductivity (SC) in lower dimensions is important to tune SC in view of its applications to gated superconducting electronics, and superconducting layered heterostructures. Here, using ultra-low temperature scanning tunneling microscopy and spectroscopy, we demonstrate the formation of hybrid electronic structure at the interface between a lead film and black phosphorus. We show that interfacial hybridization weakly modifies the confinement potential and leads to a renormalization of the superconducting gap and a strong modification of the observed vortex structure. Using ab initio methods combined with analytical modeling, we link the renormalized gap to a weighting of the superconducting order parameter in reciprocal space. These results illustrate that interfacial hybridization can be used to tune SC in quantum technologies based on lower dimensional superconducting electronics. Reference: arXiv:2109.08498 (2021).

O 72.6 Thu 16:15 S052

Diversity of defect-related excitons in hBN from ab initio calculations — •ALEXANDER KIRCHHOFF, THORSTEN DEILMANN, PETER KRÜGER, and MICHAEL ROHLFING — Westfälische Wilhelms-Universität Münster, Institut für Festkörperteorie, Wilhelm-Klemm-Straße 10, 48149 Münster

While pristine hexagonal boron nitride (hBN) is an insulator with an optical gap of ~ 5 eV, point defects in this material are discussed as single-photon emitters in the visible optical spectrum. In this study, we examine different defects consisting of carbon or oxygen substitutions and vacancies in an hBN monolayer from an ab initio approach, via the GW/BSE approximation. Our results show deep defect states and defect-related excitations with energies in the visible regime. We present a detailed analysis of their structure and energetic composition and furthermore discuss the dependence of the excitonic spectrum on the geometry. Finally, we present a defect of two carbon substitutions adjacent to a divacancy, which shows an antiferromagnetic ground state.

O 72.7 Thu 16:30 S052

Engineering magnetic interactions in magnetic thin films with two-dimensional materials — •HANGYU ZHOU^{1,2}, MANUEL DOS SANTOS DIAS^{1,3,4}, WEISHENG ZHAO², and SAMIR LOUNIS^{1,3} — ¹Peter Grünberg Institut and Institute for Advanced Simulations, Forschungszentrum Jülich & JARA, 52425 Jülich, Germany — ²School of Integrated Circuit Science and Engineering, MIIT Key Laboratory of Spintronics, Beihang University, Beijing 100191, China — ³Faculty of Physics, University of Duisburg-Essen and CENIDE, 47053 Duisburg, Germany — ⁴Scientific Computing Department, STFC Daresbury Laboratory, Warrington WA4 4AD, United Kingdom

Two-dimensional (2D) materials have received great attention due to their unique physical and chemical properties and ease of integration in heterostructures, which can lead to improved magnetic properties. Here, we explore with density functional theory calculations the impact of monolayers of graphene and hexagonal boron nitride (h-BN) on the magnetism and structural properties of a Co monolayer placed on Pt(111) and Au(111) surfaces. In particular, we investigate how the magnetic interactions, such as the Heisenberg exchange interaction and the Dzyaloshinskii-Moriya interaction (DMI), are influenced by the 2D monolayer and by structural reconstructions, which in turn can be utilized to ignite complex spin-textures. These results may contribute to an enhanced tunability of skyrmion formation in such composite magnetic heterostructures.

O 72.8 Thu 16:45 S052

Threshold Energies for Defect Production in 2D Materials under Low Energy Ion bombardment: Insights from ab-initio Molecular Dynamics — •SILVAN KRETSCHMER, SADEGH GHADERZADEH, STEFAN FACSKO, and ARKADY V. KRASHENINNIKOV — Helmholtz-Zentrum Dresden-Rossendorf, Germany
Low energy ion implantation (LEII) provides a valuable tool to tune the mechanical, electronic and catalytic properties of 2D materials by the targeted implantation of impurities. In contrast to ion irradiation at higher energies the commonly applied binary collision formula fails to describe the outcome of the irradiation

process for ions close to the displacement energy, that is the minimum ion energy needed to displace the target atom. The dominating influence of the chemical interaction of projectile and target atoms and its effect on the displacement energy are addressed in this work. For that, we carried out ab-initio molecular dynamics (MD) simulations for a broad range of projectiles (elements Hydrogen to Argon) impacting on graphene and h-BN, and determined the energies needed to displace C, N and B atoms, respectively. We further present and validate a scheme to incorporate the effect of spin-polarization on the displacement process - as spin-polarized ab-initio MD runs tend to fail at bond-breaking.

O 73: Electronic Structure of Surfaces 1

Time: Thursday 15:00–17:45

Location: S053

O 73.1 Thu 15:00 S053

Rashba-split image-potential state at Re(0001) — •FABIAN SCHÖTTKE, SVEN SCHEMMELMANN, PETER KRÜGER, and MARKUS DONATH — Westfälische-Wilhelms-Universität Münster, Germany

Since image states are located mainly in the vacuum in front of the surface, the influence of spin-dependent interactions on these states is a topic of ongoing debate in the literature. In particular, calculations predict Rashba-type spin splittings for image states [1], but experimental results of small spin splittings are controversial [2,3]. In addition, these two-photon-photoemission results using circular dichroism provide only indirect information about the spin polarization of states.

We measured the unoccupied surface electronic structure of Re(0001) with spin- and angle-resolved inverse photoemission. This method allows to investigate the spin orientations directly. We identified the $n = 1$ image state at a binding energy of $E_V - E = 0.68 \pm 0.04$ eV and with an effective mass of $m^*/m_e = 1.2 \pm 0.1$. Careful spin-resolved measurements for several angles of electron incidence allowed us to detect Rashba-type spin-dependent energy splittings of this state with a Rashba parameter of $\alpha_R = 105 \pm 33$ meV Å [4].

[1] McLaughlan *et al.*, J. Phys.: Condens. Matter **16**, 6841 (2004).

[2] Tognolini *et al.*, Phys. Rev. Lett. **115**, 046801 (2015).

[3] Nakazawa *et al.*, Phys. Rev. B **94**, 115412 (2016).

[4] Schöttke *et al.*, Phys. Rev. B **105**, 155419 (2022).

O 73.2 Thu 15:15 S053

Rashba-split surface state and spin-dependent photon emission from Re(0001) at $\bar{\Gamma}$ — •SVEN SCHEMMELMANN¹, FABIAN SCHÖTTKE¹, PETER KRÜGER², and MARKUS DONATH¹ — ¹Physikalisches Institut, Westfälische Wilhelms-Universität, Münster — ²Institut für Festkörpertheorie, Westfälische Wilhelms-Universität, Münster

The unoccupied electronic structure of the Re(0001) surface around the center of the surface Brillouin zone was investigated by spin- and angle-resolved inverse photoemission [1]. The detected states were studied with respect to intrinsic and extrinsic spin-polarization effects. A surface state with Rashba-type spin splitting is detected close to the Fermi level, that disperses downward below the Fermi energy. Furthermore, for normal electron incidence, we observed spin-dependent photon emission from unpolarized bulk and surface states. The sign of the observed spin asymmetry varies for different states and depends on experimental parameters such as electron spin-polarization direction and photon-detection angle. Maximum spin asymmetry is observed if the electron spin polarization and the plane of photon emission are perpendicular. The asymmetry is zero if both are parallel [2]. The effect is traced back to the spin-orbit-induced hybridization of the involved states.

[1] S. Schemmelmann *et al.*, Physical Review B **104**, 205425 (2021)

[2] E. Tamura and R. Feder, Solid State Commun. **79**, 989 (1991)

O 73.3 Thu 15:30 S053

Distinct Tamm and Shockley surface states on Re(0001) - mixed by spin-orbit interaction — •MARCEL HOLTSMANN¹, PETER KRÜGER¹, KOJI MIYAMOTO², TAICHI OKUDA², PASCAL J. GRENZ¹, SHIV KUMAR², and MARKUS DONATH¹ — ¹Physikalisches Institut, Westfälische Wilhelms-Universität Münster, Wilhelm-Klemm-Straße 10, 48149 Münster, Germany — ²Hiroshima Synchrotron Radiation Center, Hiroshima University, 2-313 Kagamiyama, Higashi-Hiroshima 739-0046, Japan

Tamm and Shockley states - two paradigmatic concepts are used to describe surface states not only in electronic systems but also in photonic and phononic crystals. The Re(0001) surface hosts both types of electronic surface states in neighboring but qualitatively different energy gaps. Interestingly, spin-orbit interaction generates a double "W"-shaped energy vs. k_{\parallel} dispersion by mixing both types of states and lifting their spin degeneracy. By combining spin- and angle-resolved photoemission, tight-binding model calculations as well as density functional theory including the photoemission process, we develop verifiable criteria to distinguish between the two types of surface states and arrive at a consistent picture of the role of spin-orbit interaction in such a scenario.

O 73.4 Thu 15:45 S053

Electronic structure of a square Te adlayer on Au(100) surface — •BEGMUHAMMET GELDIYEV¹, TILMAN KISSLINGER², PHILIPP ECK³, MAXIMILIAN ÜNZELMANN¹, TIM FIGGEMEIER¹, JAKUB SCHUSSER¹, NIKOLAI TEZAK¹, LUTZ HAMMER², M. ALEXANDER SCHNEIDER², DOMENICO DI SANTE³, GIORGIO SANGIOVANNI³, HENDRIK BENTMANN¹, and FRIEDRICH REINERT¹ — ¹Experimentelle Physik 7 and Cluster of Excellence ct.qmat, Universität Würzburg — ²Lehrstuhl für Festkörperphysik, Universität Erlangen-Nürnberg — ³Institut für Theoretische Physik und Astrophysik und Cluster of Excellence ct.qmat, Universität Würzburg

In light of several theoretical predictions regarding the so-called square tellurene [1, 2], the growth and the electronic structure of Te deposited on a Au(100) surface is reported. At a coverage of 1/4 monolayer, Te forms a $p(2 \times 2)$ square lattice of adatoms on Au(100) as determined by a thorough LEED-IV characterization ($R_p = 0.085$) and STM. Utilizing angle-resolved photoemission spectroscopy and density functional theory an interface-like state with mixed $p_{x,y}$ and Au d orbital character is identified in addition to a complex multitude of backfolded bands of the substrate. Vastly differing Rashba parameters along the $\bar{X}\bar{G}$ and $\bar{X}\bar{M}$ lines cannot be explained within an (anisotropic) Rashba picture. The spin splitting rather depends on the momentum space texture of the atomic orbitals. Our work may stimulate further experimental explorations of symmetry and topology effects in 2D square-lattice systems. [1] Xian *et al.*, 2D Mater. **4**, 041003, (2017)

[2] Zhang *et al.*, Phys. Rev. B **98**, 115411, (2018)

O 73.5 Thu 16:00 S053

Interplay of exchange and spin-orbit interaction in ultrathin Ni films on W(110) — •PASCAL JONA GRENZ¹, PETER KRÜGER², and MARKUS DONATH¹ — ¹Physikalisches Institut, Westfälische Wilhelms-Universität Münster, 48149 Münster, Germany — ²Institut für Festkörpertheorie, Westfälische Wilhelms-Universität Münster, 48149 Münster, Germany

Ferromagnetic adsorbates on high- Z substrates are prototypical systems for studying the combined influence of spin-orbit and exchange interaction on electronic states [1,2]. The unoccupied electronic states of ultrathin Ni films on W(110) were investigated with spin- and angle-resolved inverse photoemission. Measurements were performed along $\bar{\Gamma}\bar{N}$ ($\bar{\Gamma}\bar{M}$ with respect to the Ni(111) surface Brillouin zone), where the quantization axis of the Rashba-spin component is collinear to the easy magnetization axis. Remarkably, the observed unoccupied Ni-derived exchange-split states change their energy-momentum dispersion upon magnetization reversal. Density functional theory calculations show that this phenomenon is a consequence of substrate-induced spin-orbit coupling within the Ni adlayers.

[1] P. Moras *et al.*, Phys. Rev. B **91**, 195410 (2015)

[2] P.J. Grenz *et al.*, J. Phys.: Condens. Matter **33**, 285504 (2021)

O 73.6 Thu 16:15 S053

ARPES studies of Hf(0001) monocrystal: experiment and theory — •SALEEM AYAZ KHAN¹, LAURENT NICOLAI¹, JEAN ZARAKET^{2,3}, MARIA CHRISTINE RICHTER^{2,3}, OLIVIER HECKMANN^{2,3}, LAXMAN NAGI REDDY^{2,3}, WALY NDIAYE^{2,3}, MAURO FANCIULLI^{2,3}, KAROL HRICOVINI^{2,3}, and JAN MINAR¹ — ¹NTC, University of West Bohemia, Plzeň, Czech Republic — ²LPMS, CY Cergy Paris University, France — ³DRE, IRAMIS, LIDYL, CEA Saclay, France

We present first ARPES studies of the electronic structure of the Hf(0001) surface. High- Z materials have attracted much interest, because the strong spin-orbit coupling in combination with the broken inversion symmetry and an important effective electric field at the surface results in a spin-momentum locking. Spin-polarized electrons at the surface are of interest in physics and novel applications in electronics and data processing. Extra sharp peaks observed in experiment are identified thanks to *ab-initio* calculations performed within the SPR-KKR package. These extra states come from oxygen contamination of the highly reactive surface of Hf(0001). Further comparison is done on the ARPES level, thanks to the one-step model which include all matrix elements effect, resulting in an excellent agreement.

O 73.7 Thu 16:30 S053

Establishing fundamentals of ARPES spin textures with model material PtTe₂ — •MOHAMMED QAHOSE, HONEY BOBAN, XIAO HOU, CLAUS-MICHAEL SCHNEIDER, and LUKASZ PLUCINSKI — Electronic Properties-Peter Grünberg Institute (PGI-6).

A novel quantum material PtTe₂ is used to establish the connection between ARPES spin textures and initial state spin textures. PtTe₂ is predicted to host Dirac type-II fermions and a number of application-relevant properties. The crystal structure of the most stable 1T-PtTe₂ polytype is trigonal, belongs to the space group 164 (P3m1), and exhibits 3-fold mirror planes and inversion symmetry. Since bulk 1T-PtTe₂ is both inversion-symmetric and non-magnetic, no bulk spin-polarized bands are allowed due to the Kramers degeneracy. At the surface, spin polarization is expected due to the broken inversion symmetry, however, it must obey the mirror and time-reversal symmetries.

We measured the dependence of spin-polarization on the symmetries of the ARPES experiment. This is performed in two geometries, with the reaction plane parallel to K-Γ-K and M-Γ-M reciprocal directions, i.e. either along or orthogonal to the crystal mirror plane. The measured spin texture is symmetric when the reaction plane is parallel to K-Γ-K. However, we could see asymmetries in the spin texture when the reaction plane is parallel to M-Γ-M. Such asymmetries are not allowed in the initial state and illustrate the mechanism of geometry-induced spin filtering in ARPES.

O 73.8 Thu 16:45 S053

Surface doping of the MnBi₂Te₄ family by rubidium deposition — •KLARA VOLCKAERT¹, PAULINA MAJCHRZAK¹, RAPHAËL DUBOURG¹, ZHIHAO JIANG¹, XING-CHEN PAN², YONG CHEN¹, and SØREN ULSTRUP¹ — ¹Department of Physics and Astronomy, Aarhus University, Denmark — ²Advanced Institute for Materials Research, Tohoku University, Japan

Intrinsic magnetic topological insulators, in the form of MnBi₂Te₄, have recently been realised as a remarkable platform to study quantised magnetoelectric phenomena. Here we look into the surface electronic structure during rubidium deposition in a combined angle-resolved photoemission and core level study. We find that for MnBi₂Te₄, the initial electron doping effect from the adsorbed rubidium atoms is small. However, deposition on the higher stoichiometry compound MnBi₄Te₇ leads to a dramatic modification of the electronic structure, which is different for the surface terminated by a Bi₂Te₃ quintuple layer compared to a MnBi₂Te₄ septuple layer. Additionally, high rubidium deposition rates lead to a change of the electronic structure including a shift of the valence bands towards the Fermi level for both compounds, presumably due to Rb-Te-Bi alloying. A distinct quantization of the valence states is simultaneously observed. These results are the first to explore the tunability of electronic states the surface terminations of MnBi₄Te₇ with in situ alkali doping and substitution, which could modify the surface magnetic ordering.

O 73.9 Thu 17:00 S053

Theoretical and experimental HARPES study of Weyl-semimetal TaAs: The application of machine-learning — •TRUNG-PHUC VO¹, ARIAN ARAB², SUNIL WILFRED D'SOUZA¹, LAURENT NICOLAÏ¹, TIEN-LIN LEE³, NITESH KUMAR⁴, CLAUDIA FELSER⁴, ALEXANDER GRAY², and JÁN MINÁR¹ — ¹New Technologies - Research Centre, University of West Bohemia, 301 00 Pilsen, Czech Republic — ²Department of Physics, Temple University, Philadelphia, Pennsylvania 19122, USA — ³Diamond Light Source Ltd., Didcot, Oxfordshire OX11 0DE, United Kingdom — ⁴Max Planck Institute for Chemical Physics of Solids, Nöthnitzer Str. 40, 01187 Dresden, Germany

The electronic structure properties of tantalum arsenide (TaAs), a Weyl semimetal, have been studied by soft and hard X-ray angle-resolved photoemis-

sion spectroscopy (ARPES) at energies of 440 eV and 2150 eV, respectively. For the first time, TaAs is experimentally investigated by the bulk sensitive photoemission in the hard X-ray regime. In order to interpret experimental data we performed one-step model of photoemission calculation which includes all matrix elements and final state effects. Due to the strong photon momentum effects and uncertainty in the tilt of experimental geometry we used a so-called machine learning algorithm combined with a free-electron final-state model to find best possible experimental parameters. Our findings re-emphasize the overwhelming accuracy of hard X-ray ARPES compared to the traditional ultraviolet and soft X-ray one in case of bulk electronic structure, motivating further material discoveries.

O 73.10 Thu 17:15 S053

Electron correlation in SrTiO₃ studied by double photoemission spectroscopy with a MHz high-order harmonics laser source — •ROBIN KAMRĀ¹, CHENG-TIEN CHIANG^{1,2}, FRANK OLIVER SCHUMANN³, and WOLF WIDDRA¹ — ¹Institute of Physics, Martin-Luther-Universität Halle-Wittenberg, Halle (Saale), Germany — ²Academia Sinica, Institute of Atomic and Molecular Sciences, Taiwan — ³Max Planck Institute of Microstructure Physics, Halle (Saale), Germany

Photoelectron spectroscopy (PES) has provided deep insights into the electronic structure of solids. However, correlation effects can only be addressed indirectly. To observe such phenomena directly, double photoemission (DPE) spectroscopy is able to detect pairs of correlated photoelectrons that are emitted upon absorption of a single photon. Upon surface near doping, SrTiO₃ (001) with a bandgap of 3.4 eV forms a two-dimensional electron gas (2DEG). In this contribution we present PES and DPE data for SrTiO₃ (001) with and without 2DEG states at the surface, obtained by a high-order harmonic (HHG) light source at 25.2 and 30.0 eV. PES reveals a change in spectral weight of the O2p states and a surface band bending of 250 meV upon flipping SrTiO₃ (001) into the 2DEG state and oxygen vacancy derived states emerging within the bandgap. In DPE, a band-bending induced shift of 500 meV, changes in the intensity of the O2p derived two hole states as well as emission from vacancy-valence pairs are identified via the two-electron sum energy spectrum. In addition, the role of Auger decays for the shallow Sr4p and O2s core level will be discussed.

O 73.11 Thu 17:30 S053

Doping of 1D topologically protected edge states on the (001) surface of the topological crystalline insulator (Pb,Sn)Se — •FLORIAN KELLER, ARTEM ODOBESKO, and MATTHIAS BODE — Physikalisches Institut, Experimentelle Physik II, Universität Würzburg, Am Hubland, 97074 Würzburg, Germany

Topological crystalline insulators (TCI) are a class of materials with topological protected surface states protected by crystalline symmetry. A particularly popular representative of this material class is (Pb,Sn)Se which exhibits four Dirac cones per Brillouin zone. It has been shown that surface step edges with a height equivalent to an odd number of atomic layers results in a topologically protected one-dimensional edge state which is characterized by a peak at the Dirac energy [1]. Theoretical analysis suggests that this state is caused by the broken translation-invariance at the step edge and originates from flat-dispersing bands which connect pairs of surface Dirac nodes [1]. Due to intrinsic doping, the energy of the edge modes of as-grown crystals is usually well separated from the Fermi level. Here we investigate the behavior of these one-dimensional edge modes during Fe surface doping. Since Fe donates charge to p-doped PbSnSe, it results in a downwards-bending of the surface band structure. We observe a peak splitting as the Dirac energy gets close to the Fermi level. We discuss the potential origins of this observation in terms of electron correlations.

[1] Sessi, Paolo, Science 354, 6317 (2016)

O 74: Organic Molecules at Surfaces 5: Molecular Switches

Time: Thursday 15:00–18:00

Location: S054

O 74.1 Thu 15:00 S054

Reprogrammable molecular memory array based on chemical switching — •TOBIAS BIRK¹, ANJA BAUER¹, FABIAN PASCHKE¹, RAINER WINTER², and MIKHAIL FONIN¹ — ¹Fachbereich Physik, Universität Konstanz, 78457 Konstanz, Germany — ²Fachbereich Chemie, Universität Konstanz, 78457 Konstanz, Germany

Technology on a molecular base promises highly interesting innovations for ultra-dense information storage devices and molecular electronics. Recently, a molecular three-state switch based on triazatruxene (TAT) on Ag(111) has been shown to have a great potential as data storage unit [1].

Here, we demonstrate the precise manipulation of the switching characteristics of individual TAT molecules within a 2D array using a low temperature scanning tunneling microscope (STM). By using the tip of the STM and the field applied within the contact, a successive pinning of the molecule via alkyl groups is achieved, leading to a gradual suppression of the current induced

molecular switching. The possibility to reversibly switch between differently pinned molecules in combination with the three-level switching of the unpinned molecule offers the possibility to realize 9 states on a single molecule. We also demonstrate that the intermolecular interaction between the switches within the 2D array leads to a strong increase of the number of states, which can be detected on a single TAT unit, yielding up to 24 distinguishable states.

[1] A. Bauer et al., Adv. Mater 32, 1907390 (2020)

O 74.2 Thu 15:15 S054

Uni-directional rotation of molecular motors on Cu(111) — •MONIKA SCHIED^{1,2}, DEBORAH PREZZI³, DONGDONG LIU⁴, PETER JACOBSON^{1,5}, ELISA MOLINARI³, JAMES M. TOUR⁴, and LEONHARD GRILL¹ — ¹University of Graz, Austria — ²Elettra Sincrotrone Trieste, Italy — ³Nanoscience Institute of CNR, Italy — ⁴Rice University, USA — ⁵The University of Queensland, Australia

Artificial molecular motors that convert external energy into controlled motion have seen great developments in the last decades [1]. While many studies exist

in solution, little is known how such functional molecules behave on a surface. However, such a solid support can be advantageous as it offers fixed points of reference as well as confinement in two dimensions, making it easier to study the directionality of their motion.

We have used low-temperature scanning tunnelling microscopy (STM) to study single molecules with a so-called Feringa motor [2,3] on a Cu(111) surface. It was found that rotations of individual molecules can be induced over rather long distances by voltage pulses with the STM tip. Importantly, these rotations show high directionality (clockwise or anticlockwise), which will be discussed in view of their specific chemical structure and adsorption.

[1] W. R. Browne and B. L. Feringa, *Nat. Nanotech.* 1, 25 (2006)

[2] T. Kudernac et al., *Nature* 479, 208 (2011)

[3] A. Saywell et al., *ACS Nano* 10, 10945 (2016)

O 74.3 Thu 15:30 S054

Precise control of single-molecule motion on Ag(111) — •DONATO CIVITA, GRANT SIMPSON, and LEONHARD GRILL — Department of Physical Chemistry, University of Graz, Austria

The motion of molecules adsorbed on metal single crystal surfaces is of fundamental importance in various fields such as heterogeneous catalysis, and on-surface polymerization. During diffusion, however, the motion of adsorbed molecules is characterised by random direction changes and thus control is limited. Moreover, adsorbates in the surroundings as well as substrate defects can strongly influence molecular motion.

With the use of a scanning tunnelling microscope (STM) at low temperature, we can control the motion of single di-bromo-ter-fluorene (DBTF) molecules on a Ag(111) surface over distances of more than 100 nm with picometric precision [1]. We find that a single molecule can move strictly along one atomic row across the surface. The molecule can be repelled or attracted by the STM tip, driven by an interplay of van der Waals and electrostatic interactions. The large spatial extension of the motion, and its unidimensional confinement allow the direct measurement of the molecular velocity. Ultimately, this system demonstrates the possibility of studying the influence of surrounding adsorbates, crystal defects, and STM tip on the molecular motion and velocity.

[1] D. Civita, M. Kolmer, G. J. Simpson, A.-P. Li, S. Hecht, L. Grill, *Control of long-distance motion of single molecules on a surface*, *Science*, Vol. 370, Issue 6519, pp. 957-960 (2020).

O 74.4 Thu 15:45 S054

Dynamics of a chiral molecular rotor under a scanning-tunneling microscope — •RICHARD KORYTÁR¹ and FERDINAND EVERS² — ¹Charles University, Prague — ²Universität Regensburg

Motivated by an experimentally realized chiral molecular switch, we devise a classical theory of the switching process, relevant for molecular electronics. The system of interest is a chiral molecular rotor in a scanning-tunneling setup, i.e. the switching occurs under the electric current. The molecule is modeled by a path in three dimensions. The path is massive and can rotate around a fixed axis. The incident electron traverses the path, inducing a torque on the path. We represent this two-body dynamics in a Lagrangian formalism. Switching mechanism and switching rates are discussed.

O 74.5 Thu 16:00 S054

Bipolar single-molecule electrofluorochromism — •TZU-CHAO HUNG¹, ROBERTO ROBLES², BRIAN KIRALY¹, JULIAN H. STRIK¹, BRAM A. RUTTEN¹, ALEXANDER A. KHAJETOORIAN¹, NICOLAS LORENTE², and DANIEL WEGNER¹ — ¹Institute for Molecules and Materials, Radboud University, Nijmegen, The Netherlands — ²Centro de Física de Materiales, CFM/MPC (CSIC-UPV/EHU), Paseo de Manuel de Lardizabal 5, 20018 Donostia-San Sebastián, Spain

The interplay between the charge state and the fluorescence of a molecule is not only important for the spectroscopic analysis of chemical reactions, but electrofluorochromic molecules can also be utilized in displays, sensors, and switches. To understand the fundamental mechanisms on the single-molecule level, we studied the transient charged state of zinc phthalocyanine (ZnPc) adsorbed on ultrathin NaCl films on Ag(111) by combining scanning tunneling microscopy (STM) and spectroscopy (STS) with STM-induced luminescence (STML). We found evidence for both cationic ([ZnPc]⁺) and anionic ([ZnPc]⁻) fluorescence, depending on the polarity of the tip-sample bias. By carefully mapping the molecular frontier orbitals over a wide energy range, correlating them with onset energies for light emission and comparing with results from DFT calculations, we propose an alternative charging and electroluminescence mechanism. Our study provides new insights into the tunability of molecular optical response, as well as novel aspects toward utilization of bipolar electrofluorochromism in devices.

O 74.6 Thu 16:15 S054

Electronic Motor Based on Single Tripodal Chiral Molecule — •JULIAN SKOLAUT¹, LUKAS GERHARD¹, NICO BALZER², MICHAL VALASEK², JAN WILHELM⁴, PHILIPP MARKUS⁵, MARCEL MAYOR^{2,3}, FERDINAND EVERS⁴, and WULF WULFHEKEL^{1,5} — ¹Institute for Quantum Materials and Technologies,

Karlsruhe Institute of Technology, Eggenstein-Leopoldshafen, Germany — ²Institute of Nanotechnology, KIT, Eggenstein-Leopoldshafen, Germany — ³Department of Chemistry, University Basel, Basel, Switzerland — ⁴Institute of Theoretical Physics, University of Regensburg, Regensburg, Germany — ⁵Physikalisches Institut, KIT, Karlsruhe, Germany

We present our results concerning a single molecular motor driven by the current in an STM. Three anchoring groups fix the molecules to a Au(111) surface. In specific ordered structures, the molecules adsorb such that the protruding head group is free to rotate. This chiral group is supposed to perform a rotation in a preferred direction, proposed to be driven based on the chiral-induced spin selectivity (CISS) effect. At fixed tip positions above the molecules, three distinguishable current levels can be observed. These are interpreted as metastable rotational states. That way, two rotation directions can be defined. Via binomial tests, we verify that the surplus of rotational switches in one direction compared to the other is statistically significant. In voltage and current dependent measurements, two interesting trends are observed. Firstly, the rate of events decreases with increasing current. Secondly, the asymmetry in the switching events shows non-monotonic behavior, depending on the voltage.

O 74.7 Thu 16:30 S054

Proton Transfer in Single Asymmetric Porphyrine Molecules — •SIMON JAEKEL^{1,2}, JACEK WALUK³, and LEONHARD GRILL¹ — ¹Department of Physical Chemistry, University of Graz, Austria — ²Chair of Physical Chemistry II, University of Erlangen-Nürnberg (FAU), Germany — ³Polish Academy of Science, Warsaw, Poland

Studying single molecular switches is of interest for a better understanding of fundamental physical and chemical processes, but also in view of their possible use in smart materials and nanoscale applications. It has been shown that switches based on tautomerization, i.e. hydrogen transfer, are especially suited for scanning tunneling microscopy (STM) studies, because the electronic states near the Fermi level are very sensitive to the position of the hydrogen atoms. Experiments on symmetric molecules such as naphthalocyanine [1], tetraphenylporphyrin [2], and porphycene [3] showed that the energies of the tautomers are degenerate, barring environmental modulation. Thus, if one is interested in switching processes with preferential switching directions between multiple states, structurally asymmetric molecules are of particular interest.

Here, we report STM results of the tautomerization properties of 22-Oxahemiporphycene, a derivative of porphycene with an asymmetric macrocycle, on a metal surface.

[1] Liljeroth et al. *Science*, 317 (2007), 1203-1206

[2] Auwärter et al. *Nature Nanotechnology*, 7 (2011), 41-46

[3] Kumagai et al. *Physical Review Letters* 111 (2013), 246101

O 74.8 Thu 16:45 S054

Tuning the chirality change of a single molecule by van der Waals interactions — •YUNJUN CAO and KARINA MORGENSTERN — Physical Chemistry I, Ruhr-Universität Bochum, Bochum, Germany

The chiral induction and control of molecules by non-covalent intermolecular interactions, like hydrogen bonding and van der Waals interactions, is crucial to understand the origin of homochirality in nature. However, it remains challenging to address these subtle intermolecular interactions at a single-molecular level, especially the weakest of them, the van der Waals interactions. Here, by adsorbing a specifically designed carbene molecule on a copper surface, we examine the influence of the van der Waals interactions on the chirality induction by scanning tunneling microscopy. While the strongly binding carbene center of this molecule suppresses any side-reactions upon excitation, its two low-interacting phenyl rings facilitate a chirality change induced by inelastically tunneling electrons. The potential energy of the chirality change is modified by the van der Waals interactions in the presence of a tip. A marginal change induces an asymmetric distribution of the carbene molecule between its two enantiomers during this chirality change. Our study shows how the weak van der Waals interactions alter the dynamics of chirality changes at the molecular level, enabling an in-depth understanding of the origin of homochirality in nature and providing new insights into the construction of homochiral supramolecular assemblies in solutions and on solid surfaces.

O 74.9 Thu 17:00 S054

Lateral Force Microscopy Reveals the Energy Barrier of a Molecular Switch — ALFRED JOHN WEYMOUTH, ELISABETH RIEGEL, •BIANCA SIMMET, OLIVER GRETZ, and FRANZ JOSEF GIESSBL — Universität Regensburg, Regensburg, Germany

Copper phthalocyanine (CuPc) is a small molecule often used in organic light emitting diodes where it is deposited on a conducting electrode. Previous scanning tunneling microscopy (STM) studies of CuPc on Cu(111) have shown that inelastic tunneling events can cause CuPc to switch between a ground state and two symmetrically equivalent metastable states in which the molecule is rotated. We investigated CuPc on Cu(111) and Ag(111) with STM and lateral force microscopy (LFM). Even without inelastic events, the presence of the tip can induce rotations and upon closer approach, causes the rotated states to be favored. Com-

binning STM measurements at various temperatures and LFM measurements, we show that the long-range attraction of the tip changes the potential energy landscape of this molecular switch. We can also determine the geometry of the rotated and ground states. We compare our observations of CuPc on Cu(111) to CuPc on Ag(111). On Ag(111), CuPc appears flat and does not rotate. Stronger bonding typically involves shorter bond lengths, larger shifts of energy levels, and structural stability. Although the binding of CuPc to Cu(111) is stronger than that on Ag(111), the nonplanar geometry of CuPc on Cu(111) is accompanied by two metastable states which are not present on the Ag(111) surface.

ACS Nano, 15, 3264 (2021)

O 74.10 Thu 17:15 S054

Evidence of trion-libron coupling in chirally adsorbed single molecules — •JIŘÍ DOLEŽAL^{1,2}, SOFIA CANOLA¹, PROKOP HAPALA¹, RODRIGO FERREIRA¹, PABLO MERINO³, and MARTIN ŠVEC¹ — ¹Institute of Physics, Czech Academy of Sciences; Cukrovarnická 10/112, CZ16200 Praha 6, Czech Republic — ²Faculty of Mathematics and Physics, Charles University; Ke Karlovu 3, CZ12116 Praha 2, Czech Republic — ³Instituto de Ciencia de Materiales de Madrid; CSIC, Sor Juana Inés de la Cruz 3, E28049 Madrid, Spain

Interplay between the motion of nuclei and excited electrons in molecules plays a key role both in biological and artificial nanomachines. Here we provide a detailed analysis of coupling between quantized librational modes (librons) and charged excited states (trions) on single phthalocyanine dyes adsorbed on a surface. By means of tunnelling electron-induced electroluminescence, we identify librational progressions on a μeV energy range in spectra of chirally adsorbed phthalocyanines, which are otherwise absent from spectra of symmetrically adsorbed species. Experimentally measured librational spectra match very well the theoretically calculated libron eigenenergies and peak intensities (Franck-Condon factors) and reveal an unexpected depopulation channel for the zero libron of the excited state that can be effectively controlled by tuning the size of the nanocavity. Our results showcase the possibility of characterizing the dynamics of molecules by their low-energy molecular modes using μeV -resolved tip-enhanced spectroscopy.

O 74.11 Thu 17:30 S054

Design Principles for Metastable Standing Molecules — HADI H. AREFI¹, MARVIN KNOL¹, DANIEL CORKEN², JAMES GARDNER², F. STEFAN TAUTZ¹, REINHARD J. MAURER², and •CHRISTIAN WAGNER¹ — ¹Peter Grünberg Institut (PGI-3), Forschungszentrum Jülich, Germany — ²Department of Chemistry, University of Warwick, Coventry, UK

Molecular nanofabrication with a scanning probe microscope is a promising route towards the prototyping of metastable functional molecular structures and devices which do not form spontaneously. The aspect of mechanical stability is crucial for such structures especially if they extend into the third dimension vertical to the surface. A prominent example are freestanding molecules on a metal which can function as field emitters or electric field sensors[1,2]. Improving the stability of such molecular configurations is an optimization task involving many degrees of freedom. Here, we present a combination of scanning probe experiments with ab initio potential energy calculations to investigate the stability of a prototypical standing molecule. We cast our results into a simple set of universal design principles for such metastable structures, the validity of which we demonstrate in two computational case studies. This offers the intuition needed to fabricate new devices without tedious trial and error.

[1] T. Esat, N. Friedrich, F. S. Tautz, R. Temirov, *Nature* **558**, 573 (2018)

[2] C. Wagner, M. F. B. Green, P. Leinen, T. Deilmann, P. Krüger, M. Rohlfing, R. Temirov, F. S. Tautz, *PRL* **115**, 026101 (2015)

O 74.12 Thu 17:45 S054

Improving the Switching Efficiency in Azobenzene Derivative Film on Graphite-Air Interface — •THIRUVANCHERIL G. GOPAKUMAR¹, KHUSHBOO YADAV¹, HARIOM BIRLA¹, SHOWKAT H. MIR^{1,2}, THOMAS HALBRITTER², ALEXANDER HECKEL², and JAYANT K. SINGH³ — ¹Department of Chemistry, Indian Institute of Technology Kanpur, Kanpur 208016, India — ²Institute for Organic Chemistry and Chemical Biology, Goethe-University Frankfurt, Max-von-Laue-Str. 9, 60438 Frankfurt, Germany — ³Department of Chemical Engineering, Indian Institute of Technology Kanpur, Kanpur 208016, India

The trans isomer of azobenzene (AB) and its derivatives is the most abundant under equilibrium-thermodynamical conditions and is known to switch between its trans and cis states when triggered by light and electrons/holes on graphite.[1] In this work, we show that AB derivatives are switching between two cis states (cis, cis') when electrons/holes induced switching is performed on a cis dominant non-equilibrium initial condition at HOPG-air interface. The switching efficiency in the cis adlayer is several folds higher than that in the trans adlayer. This is related to the low switching barrier for cis-cis' switching compared to that of trans-cis switching as revealed by density functional theory (DFT) calculations.

1) K. Yadav, S. Mahapatra, T. Halbritter, A. Heckel, T. G. Gopakumar, *J. Phys. Chem. Lett.*, 2018, 9, 6326-6333.

O 75: Members' Assembly

Topics: Report of the Chairman; Presentation of the Gerhard Ertl Young Investigator Award; Miscellaneous

Time: Thursday 19:00–19:30

Location: H1

All members of the Surface Science Division are invited to participate.

O 76: Post-Deadline Session

Time: Thursday 19:30–20:30

Location: H1

Contributed Post-Deadline Talks

O 77: Overview Talk Guillaume Schull

Time: Friday 9:30–10:15

Location: S054

Invited Talk O 77.1 Fri 9:30 S054
Sub-molecular fluorescence microscopy with STM — •GUILLAUME SCHULL — IPCMS - CNRS/Unistra - Strasbourg

The electric current traversing the junction of a scanning tunneling microscope (STM) may lead to a local emission of light that can be used to generate sub-molecularly resolved fluorescence maps of individual molecules [1]. Combined with spectral selection and time-correlated measurements, this hyper-resolved fluorescence microscopy approach allowed us to scrutinise the vibronic structure

of individual molecules [2] to characterise the emission properties of charged species [3], to track the motion of hydrogen atoms within free-base phthalocyanine molecules [4] and to follow energy transfers between multi-molecular architectures [5].

[1] A. Rosławska et al., *PRX* **12**, 011012 (2022)

[2] B. Doppagne et al., *PRL* **118**, 127401 (2017)

[3] B. Doppagne et al. *Science*, **361**, 251 (2018)

[4] B. Doppagne et al. *Nature Nanotechnol.* **15**, 207 (2020) .

[5] S. Cao et al. *Nature Chem.* **13**, 766 (2021)

O 78: Plasmonics and Nanoptics 3

Time: Friday 10:30–12:30

Location: H3

O 78.1 Fri 10:30 H3

Reconfiguring magnetic resonances with the plasmonic phase-change material In_3SbTe_2 — •LUKAS CONRADS, ANDREAS HESSLER, KONSTANTIN WIRTH, MATTHIAS WUTTIG, and THOMAS TAUBNER — I. Institute of Physics (IA), RWTH Aachen University

For miniaturized active nanophotonic components, resonance tuning of nanoantennas is a key ingredient. Phase-change materials (PCMs) have been established as prime candidates for non-volatile resonance tuning based on a change in refractive index [1]. Currently, a novel material class of switchable infrared plasmonic PCMs, like In_3SbTe_2 (IST), is emerging. Since IST can be locally optically switched between dielectric (amorphous phase) and metallic (crystalline phase) states in the whole infrared range, it becomes possible to directly change the geometry and size of nanoantennas to tune their infrared resonances [2]. Here, crystalline IST split-ring resonators (SRRs) are directly optically written and reconfigured in their arm size to continuously tune their magnetic dipole resonances over a range of $2.4 \mu\text{m}$ without changing their electric dipole resonances. The SRRs are further modified into crescents and J-antennas, which feature more complex resonance modes dependent on the polarization of the incident light [3]. Our concepts are well-suited for rapid prototyping, speeding up workflows for engineering ultrathin, tunable, plasmonic devices for infrared nanophotonics, telecommunications, or (bio)sensing.

[1] Wuttig et al., *Nat. Photon.* **11**, 465 (2017) [2] Heßler et al., *Nat. Commun.* **12**, 924 (2021) [3] Heßler, Conrads et al. *ACS Photonics* **9**, 5 (2022)

O 78.2 Fri 10:45 H3

Impact of atomistic structure and dynamics on inelastic light scattering in a plasmonic picocavity — •FRANCO BONAFÉ¹, SHUYI LIU², HEIKO APPEL¹, MARTIN WOLF², TAKASHI KUMAGAI^{2,3}, and ANGEL RUBIO¹ — ¹MPI for Structure and Dynamics of Matter, Hamburg, Germany — ²Dpmt. of Physical Chemistry, Fritz-Haber Institute, Berlin, Germany — ³Center for Mesoscopic Sciences, Institute for Molecular Science, Okazaki, Japan

Atomically sharp metallic tips can focus an electromagnetic field down to the sub-nanometer scale, leading to strong light-matter interactions in plasmonic “picocavities”. This atomic-scale field can be used in plasmon-enhanced spectroscopy, such as tip-enhanced Raman spectroscopy (TERS), which has enabled the visualization of optical properties at sub-molecular resolution. However, a full microscopic understanding of the interplay of structural relaxation, bonding, near-fields and vibrations has not been achieved.

In this work, we combine experimental observations of inelastic light scattering from a single silver adatom in a plasmonic picocavity controlled by a low-temperature scanning tunneling microscope (STM), with ab initio real-time electron dynamics simulations. The experiment demonstrates a dramatic enhancement of Raman scattering that occurs upon the formation of a quantum point contact. We model possible geometries for the plasmonic tips and compute the vibrational modes, electronic current and near-fields localized in the vicinity of the single adatom. These simulations reveal a crucial role of the atomistic structural relaxation in the optical response in a plasmonic nanocavity.

O 78.3 Fri 11:00 H3

Vector Polarimetry - Measuring Electrical Fields on Surfaces — •ALEXANDRA RÖDL¹, DAVID JANOSCHKA¹, PASCAL DREHER¹, ALEXANDER NEUHAUS¹, BETTINA FRANK², TIMOTHY DAVIS^{1,2,3}, MICHAEL HORN-VON HOEGEN¹, HARALD GIESSEN², and FRANK-J. MEYER ZU HERINGDORF¹ — ¹Faculty of Physics and Center for Nanointegration, Duisburg-Essen, University of Duisburg-Essen, 47048 Duisburg, Germany — ²4th Physics Institute, Research Center SCoPE, and Integrated Quantum Science and Technology Center, University of Stuttgart, 70569 Stuttgart, Germany — ³School of Physics, University of Melbourne, Parkville, Victoria 3010 Australia

Non-linear photoemission microscopy has been established as an excellent tool to investigate nano-optical fields at surfaces, in particular the fields of surface plasmon polaritons (SPPs). In a pump-probe experiment with femtosecond laser pulses we excite SPPs at grooves that are ion-milled into a Au platelet. The electric field of the probe-laser pulse interferes coherently with the electric field of the SPP and electrons are liberated through a nonlinear process by the combined field at the surface. The contrast depends on the alignment of the probe polarization and the orientation of the in-plane component of the SPP's electric field. Using a set of different polarizations for the probe laser pulse while keeping the same excitation conditions, one can reconstruct the in-plane component of the electric field of the SPP. The out-of-plane field component is calculated by Maxwell's equations to reconstruct the full electric vector field. Here, we measure and image complex electric vector fields of SPPs and analyze their topology.

O 78.4 Fri 11:15 H3

Spatially-resolved THz near-field spectroscopy — •MORITZ B. HEINDL¹, NICHOLAS KIRKWOOD², TOBIAS LAUSTER³, JULIA A. LANG¹, MARKUS RETSCH³, PAUL MULVANEY², and GEORG HERINK¹ — ¹Experimental Physics VIII, University of Bayreuth, Germany — ²ARC Centre of Excellence in Exciton Science, School of Chemistry, University of Melbourne, Australia — ³Physical Chemistry I, University of Bayreuth, Germany

Spectroscopic access to ultrafast electric waveforms is critical to the understanding of plasmonic and field-driven nonlinear phenomena, yet, microscopic measurements still present a grand challenge. Here, we present a fluorescence-based field microscope for imaging ultrafast THz near-field evolutions employing the quantum-confined Stark-effect in semiconductor quantum dots [1,2]. This Quantum-Probe Field Microscopy (QFIM) scheme [3] allows for detection of strongly confined near-fields in three-dimensional structures. Using QFIM, we demonstrate spatially-resolved near-field spectroscopy of single THz resonators and propagating THz excitations inside wave-guiding structures.

[1] Hoffmann, M. C. et al. *Appl. Phys. Lett.* **97**, 231108 (2010)

[2] Pein, B. C. et al. *Nano Lett.* **17**, 5375-5380 (2017)

[3] Heindl, M. B. et al. *Light Sci. Appl.* **11**, 5 (2022)

O 78.5 Fri 11:30 H3

Mode-selective imaging and control of nano-plasmonic near-fields — •MURAT SIVIS^{1,2}, HUGO LOURENÇO-MARTINS^{1,2}, ANDRE GEESE², TYLER R. HARVEY², THOMAS DANZ^{1,2}, RADWAN M. SARHAN³, MATIAS BARGHEER³, ARMIN FEIST^{1,2}, and CLAUS ROPERS^{1,2} — ¹Max Planck Institute for Multidisciplinary Sciences, Göttingen, Germany — ²4th Physical Institute - Solids and Nanostructures, University of Göttingen, Germany — ³Institut für Physik und Astronomie, Universität Potsdam, Potsdam, Germany

Electron energy-loss spectroscopy (EELS) in a transmission electron microscope allows for the study of optical excitations in plasmonic nanostructures with sub-nanometer spatial resolution. While EELS is a powerful tool, it can only provide information about the spontaneous losses in a system with limited spectral resolution (10-100 meV in the most advanced microscopes). Recent developments in ultrafast transmission electron microscopy overcome these limitations and enable the probing of laser-excited modes by using photon-induced near-field electron microscopy (PINEM). Here, we demonstrate how PINEM can be used to measure the modal structure of the optical response of individual plasmonic systems (metal nano-triangle-resonators) at the nanoscale. Using our boundary element method (BEM)-based data analysis, we extract the magnitude and relative phase of each plasmonic mode from optical near-field maps. This approach opens a route to study the influence of the laser polarization, wavelength and incidence angle on the population of each mode, as well as the control of complex mode patterns created by multicolor fields.

O 78.6 Fri 11:45 H3

Tailoring of nonlinear metasurfaces using sampling-based optimization — •DAVID HÄHNEL, JENS FÖRSTNER, and VIKTOR MYROSHNYCHENKO — Paderborn University, Theoretical Electrical Engineering, Warburger Str. 100, 33098 Paderborn, Germany

Various efficient methods for the design and optimization of linear metasurfaces have already been developed in the past [1]. Nowadays, attempts are being made to use these methods also for the design and optimization of nonlinear metasurfaces, which is a quite complex task due to the nonlinear processes involved. Here we present the design and optimization of all-dielectric nonlinear metasurfaces using a simple sampling method combined with Monte Carlo simulation, demonstrating that the use of sophisticated optimization methods is not necessarily required. Furthermore, this combination provides an effective approach in the optimization of nonlinear metasurfaces with a dynamic problem, such as a varying number of optimization parameters that are unknown in advance. We apply this method combination in the optimization of a nonlinear beam deflector metasurface for the third harmonic, which consist of an array of elliptical silicon disks and obtained a significant improvement in the radiated intensity compared to literature results [2]. [1] Chen, S. et al., *Advanced Optical Materials* **2018**, *6*, 1800104. [2] Lei Wang et al., *Nano Lett.* **2018**, *18*, *6*, 3978-3984.

O 78.7 Fri 12:00 H3

Polarization selective investigation of plasmonic Bloch modes with dark-field spectroscopy — •MAXIMILIAN JOHANNES BLACK and NAHID TALEBI — Institute for Experimental and Applied Physics, Kiel University, 24118 Kiel, Germany

Plasmonic and photonic crystals are widely used to mold the flow of light. Owing to its symmetry even the seemingly simple structure of a periodic square lattice of holes within a thin gold film shows a broad variety of plasmonic Bloch modes that are distinguished by the momenta and polarization. Therefore, the response of the system to the excitation is formed by a superposition of these modes. In this work we use polarization-selective optical dark-field microscopy

to decompose these modes. Dark-field microspectroscopy is used to enhance the resolution and to suppress the background illumination, whereas linear polarizers both in the illumination and the detection path enable the selection of Bloch modes by polarization. We find that the dominating signal is formed by the selective excitation and detection of radiating magnetic moments. These and a variety of other modes are visualized by hyperspectral imaging. In the far-field reciprocal space interference fringes are resolved, indicating the propagation of the observed modes along the surface of the plasmonic crystal. Our results prove the possibility to thoroughly investigate plasmonic Bloch modes using dark-field microscopy, adding its versatility to the range of methods for measuring light-matter interactions.

O 78.8 Fri 12:15 H3

A Ginzburg Landau model for femtosecond charge-density wave dynamics at the atomic scale — •KURT LICHTENBERG¹, MOHAMAD ABDO^{1,2}, SHAOXIANG SHENG¹, LUIGI MALAVOLTI^{1,2}, and SEBASTIAN LOTH^{1,2} — ¹University of Stuttgart, Institute for Functional Matter and Quantum Technologies, Stuttgart, Germany — ²Max Planck Institute for Solid State Research, Stuttgart, Germany

Charge-density waves (CDWs) feature collective excitations that can be observed as an oscillatory response of the electron system of a material to a fast optical stimulus [1]. At the same time, scanning tunneling microscopy (STM) measurements reveal highly localized interactions with atomic defects [2]. THz pump-probe spectroscopy in the STM reveals highly heterogeneous dynamics with spatial variations down one unit cell of the CDW. To improve the understanding of such local CDW dynamics, we developed an empirical model that is motivated by former approaches [3,4] and based on time-dependent Ginzburg Landau Theory. The combination of this theory with THz-STM measurements establishes a possibility to study the interplay between collective CDW dynamics with atomic pinning sites.

[1] M.-A. Méasson et. al, PRB 89, 060503(R) (2014)

[2] C. J. Arguello et. al, PRB 89, 235115 (2014)

[3] W. L. McMillan, PRB 12, 1187-1196 (4) (1975).

[4] G. Grüner, Density Waves in Solids. Perseus Publishing - Cambridge, Massachusetts, (2000).

O 79: Surface Reactions and Heterogeneous Catalysis 3

Time: Friday 10:30–12:45

Location: H4

Topical Talk

O 79.1 Fri 10:30 H4

Exploitation of Heterocycles for N-doped Graphene Nanomaterials — RÉMY PAWLAK¹, ULRICH ASCHAUER², SILVIO DECURTINS², JASCHA REPP³, PAVEL JELINEK⁴, ERNST MEYER¹, LAERTE L. PATERA⁵, and •SHI-XIA LIU² — ¹Department of Physics, University of Basel, Klingelbergstrasse 82, 4056 Basel, Switzerland — ²Department of Chemistry, Biochemistry and Pharmaceutical Sciences, University of Bern, 3012 Bern, Switzerland — ³Institute of Experimental and Applied Physics, University of Regensburg, 93053 Regensburg, Germany — ⁴Institute of Physics of Czech Academy of Sciences, 16200 Prague, Czech Republic — ⁵Department of Chemistry and Catalysis Research Center, Technical University of Munich, 85748 Garching, Germany

On-surface chemical reactions have been intensively investigated in order to obtain carbon-based functional nanomaterials which very often cannot be synthesized by wet chemistry. Thus, tailored heterocyclic precursors are becoming increasingly important for the development of highly symmetric 2D-conjugated porous architectures and 1D N-doped graphene nanoribbons (GNRs) with desired functions due to their intrinsic electronic properties. This presentation will focus on our collaborative work on C-C coupling reactions on various surfaces leading to the formation of a range of nanostructures, including molecular wires, fully fused porphyrin-GNR hybrids, as well as 1D- and 2D-conjugated porous networks. All of these atomically precise nanostructures can be directly visualized by STM and AFM. The fine-tuned electronic properties by chemical modification are discussed.

O 79.2 Fri 11:00 H4

On-surface cyclomerization of oxygen heterocycles: Controlling the ring size by tuning the molecule-surface interaction — •ANDREAS DÖRR¹, NEMANJA KOCIC¹, LUKAS FROMM², VLADIMIR AKHMETOV³, KONSTANTIN Y. AMSHAROV³, ANDREAS GÖRLING², and SABINE MAIER¹ — ¹Department of Physics, Friedrich-Alexander-Universität Erlangen-Nürnberg, 91058 Erlangen (Germany) — ²Department of Chemistry and Pharmacy, Chair of Theoretical Chemistry, Friedrich-Alexander-Universität Erlangen-Nürnberg, 91058 Erlangen (Germany) — ³Institute for Chemistry, Martin-Luther-University Halle-Wittenberg, 06099 Halle (Germany)

Heterocycles with nitrogen, oxygen, or sulfur atoms are the basic units that incorporate chemical functionalization into carbon scaffolds. For oxygen-doped nanographenes, furan and pyran, having five- and six-membered rings, respectively, are the most common ones. However, their on-surface synthesis via cyclomerization reactions has so far been elusive. Here, we present a low-temperature scanning tunneling microscopy study combined with density functional theory calculations to understand the on-surface synthesis of furan and pyran derivatives from ketone-functionalized precursors on metal surfaces. We first discuss the self-assemblies of the precursors, which are strongly influenced by molecule-surface interactions. Upon annealing, the different intermolecular binding motifs resulted in selective cyclomerization reactions toward furan and pyran moieties.

O 79.3 Fri 11:15 H4

Proximity-induced superconductivity in atomically precise nanographene — •JUNG-CHING LIU¹, RÉMY PAWLAK¹, XING WANG², PHILIPP D'ASTOLFO¹, CARL DRECHSEL¹, PING ZHOU², HONGYEN CHEN³, SILVIO DECURTINS², ULRICH ASCHAUER², SHI-XIA LIU², WULF WULFHEKEL³, and ERNST MEYER¹ — ¹Department of Physics, University of Basel, Klingelbergstrasse 82, CH-4056 Basel — ²Department of Chemistry, Biochemistry and Pharmaceutical Sciences,

University of Bern, Freiestrasse 3, CH-3012 Bern — ³Physikalisches Institut, Karlsruhe Institute of Technology, Wolfgang-Gaede-Str. 1, D-76131 Karlsruhe

Atomically precise nanographenes (NGs) can be efficiently synthesized through on-surface reactions. On such designed NGs, topological superconductivity could be fostered via proximity to a s-wave superconductor. However, on-surface synthesis of NGs is still missing on superconducting surfaces [1-3]. To fill the gap, we first fabricate a Ag buffer layer on the Nb(110) superconductor [4], and grow atomically precise NGs on the Ag/Nb substrate using DBBA as the precursor. Through the investigation of low temperature STM/AFM, we demonstrate successful synthesis of polymeric chains and NGs on the superconducting Ag/Nb(110) substrate. We believe our method provides a promising platform for studying the role of topology in the interaction between carbon magnetism and superconductivity [5]. [1]Cai et al., Nature 466, 470-473 (2010) [2]K. A. Simonov et al., Sci. Rep. 8, 3506 (2018) [3]M. Kolmer et al., Science 369, 571-575 (2020) [4]T. Tomanic et al., Phys. Rev. B 94, 220503 (2016) [5]J.-C. Liu et al., arXiv:2202.00460

O 79.4 Fri 11:30 H4

Real-space Imaging of Unprecedented Phenyl Group Migration Reaction on Metal Surfaces — •ZILIN RUAN^{1,2}, BAIJIN LI², SHIJIIE SUN², YONG ZHANG², LEI GAO³, JIANCHEN LU², MICHAEL GOTTFRIED¹, and JINMING CAI² — ¹Department of Chemistry, Philipps University Marburg, Hans-Meerwein-Straße 4, 35037 Marburg (Germany) — ²Faculty of Materials Science and Engineering, Kunming University of Science and Technology, Kunming, Yunnan 650093 (China) — ³Department of Chemistry, Philipps University Marburg, Hans-Meerwein-Straße 4, 35037 Marburg (Germany)

We report on-surface identification and visualization of an unprecedented and universal phenyl group migration reaction of 1,4-dimethyl-2,3,5,6-tetraphenyl benzene (DMTPB) precursor on Au(111), Cu(111) and Ag(110) substrates by a combination of bond-resolved scanning tunneling microscopy (BR-STM) and density functional theory (DFT) calculations. The phenyl group migration reaction of DMTPB precursor results in formations of variously unprecedented polycyclic aromatic hydrocarbons on the substrates. DFT calculations reveal that the multiple-steps phenyl group migration reactions are facilitated by the radical attack and rearomatization of the DMTPB precursor. Our study provides unprecedented insights into complex surface reaction mechanisms at the single molecule level, which may guide the design of chemical species.

O 79.5 Fri 11:45 H4

Deciphering the intramolecular C-C coupling mechanism of a model aryl radical via bond-level AFM imaging — •QIGANG ZHONG¹, JANNIS JUNG², DANIEL KOHRS³, DANIEL EBELING¹, DOREEN MOLLENHAUER², HERMANN A. WEGNER³, and ANDRÉ SCHIRMEISEN¹ — ¹Institute of Applied Physics, Justus-Liebig University Giessen (JLU), Germany — ²Institute of Physical Chemistry, JLU, Germany — ³Institute of Organic Chemistry, JLU, Germany

Although on-surface dehalogenative and dehydrogenative C-C coupling has proved to be a versatile and prevailing approach to constructing atomically precise carbon-based nanostructures, understanding of the reaction mechanisms remains limited by the elusive intermediates. Here, we studied the intramolecular cyclodehydrobromination of 1-bromo-8-phenylnaphthalene on Cu(111) and Ag(111) using bond-level atomic force microscopy (BL-AFM). The reaction occurs at room temperature on both metal surfaces, while the reaction rate on Cu(111) is much higher than that on Ag(111) presumably due to the higher catalytic activity of copper. Surface-bound radicals, cyclized intermediates and de-

hydrogenated product were captured by BL-AFM imaging and verified by DFT calculations, suggesting a multi-step reaction process, i.e. debromination, radical cyclization and dehydrogenation. The large proportion (up to 65 percent) of cyclized intermediates on Cu(111) indicates that dehydrogenation is the rate-determining step, which is corroborated by DFT calculations of activation barriers. To achieve a reasonable activation barrier for dehydrogenation, multiple pathways were theoretically evaluated.

O 79.6 Fri 12:00 H4

Interplay between π -conjugation and exchange magnetism in one-dimensional porphyrinoid polymers — •KALYAN BISWAS¹, MAXENCE URBANI¹, ANA SÁNCHEZ-GRANDE¹, DIEGO SOLER², KOEN LAUWAET¹, ADAM MATĚJ², PINGO MUTOMBO², JOSÉ M. GALLEGO¹, RODOLFO MIRANDA¹, DAVID ĚCJA¹, PAVEL JELÍNEK², TOMÁS TORRES¹, and JOSÉ I. URGEL¹ — ¹IMDEA Nanoscience, Madrid, Spain — ²CATRIN, Olomouc, Czech Republic

The field of carbon magnetism has gained an increased attention in view of the recent progress made in the synthesis and characterization of open-shell polycyclic aromatic hydrocarbons following a bottom-up synthetic approach. In this work, we introduce an exemplary approach toward the bottom-up fabrication of unprecedented magnetic porphyrinoid-based polymers homocoupled via surface-catalyzed [3 + 3] cycloaromatization of isopropyl substituents studied on Au(111) under ultra-high vacuum conditions. The chemical structure of the polymer, formed by thermal-activated intra- and intermolecular oxidative ring closure reactions followed by controlled tip-induced hydrogen dissociation from the porphyrinoid units, have been clearly elucidated by scanning tunneling microscopy and non-contact atomic force microscopy. Scanning tunneling spectroscopy, complemented by computational investigations reveals the anti-ferromagnetic singlet ground state (S=0), which display singlet-triplet inelastic excitations observed between spins of adjacent porphyrinoid units only along a specific π -conjugation pathway. We envision that our approach can be a highly relevant in nanoscale spintronic devices.

O 79.7 Fri 12:15 H4

Photoactivation of Azide in SURMOFs — •JIMIN SONG, XIAOJUAN YU, MANUEL TSOTSALAS, ALEXANDER KNEBEL, ALEXEI NEFEDOV, STEFAN HEISSLER, YUEMIN WANG, and CHRISTOF WÖLL — Institute of Functional In-

terfaces, Karlsruhe Institute of Technology, 76344, Eggenstein-Leopoldshafen, Germany

The ability to turn the surface activation of metal-organic frameworks (MOFs) is essential for developing advanced MOF applications. Here, we have successfully synthesized a surface-mounted MOF (SURMOF) model system with azide side groups in order to investigate the photoactivation of phenyl azide and its reaction pathways. In situ UHV infrared reflection absorption spectroscopy (IRRAS) was applied to precisely monitor the chemical changes taken place on the surface of highly oriented and crystalline SURMOFs under UV irradiation at different temperatures. Combining with in situ XRD, MS and XPS, a two-step mechanism is proposed including the activation and subsequent reaction of azide with adjacent C=C bonds yielding pyrrole species.

O 79.8 Fri 12:30 H4

Differences in the Intermolecular Interaction of Electron-rich Phosphines on a Metal and a Salt Surface — •VLADIMIR LYKOV¹, FLORENZ BUSS², MILICA FELDT³, KARINA MORGENSTERN¹, and FABIAN DIELMANN⁴ — ¹Chair of Physical Chemistry I, Ruhr Universität Bochum, Germany — ²Institute for Inorganic and Analytical Chemistry, Westphalian Wilhelms University of Münster, Germany — ³Leibniz-Institut für Katalyse e.V. (LIKAT), Rostock, Germany — ⁴Department of General, Inorganic and Theoretical Chemistry, University of Innsbruck, Austria

Electron-rich phosphines are attractive as capture molecules, for instance, for carbon dioxide (CO₂) and sulfur dioxide (SO₂) by forming zwitterionic Lewis base adducts with them [1]. The main focus of this project is understanding the interaction behind this capturing in real space. For this purpose, we use a low-temperature (7 K) scanning tunneling microscope (STM). To understand the influence of the metal surface on this capture process, we compare the molecules adsorbed on Ag(100) to those on NaBr(100). As a first step, the different interaction of phosphines with the salt multilayers and with the metal was investigated by step-wise heating from 43 K to 135 K. The difference in intermolecular interaction on these surfaces will be discussed in this presentation.

[1] Buß F, Röthel M.B., Werra J.A., Rotering P, Wilm L.F.B., Daniliuc C.G., Löwe P, Dielmann F, Chem. Eur. J. 10.1002/chem.202104021 (2021)

O 80: Focus Session: Atomic-Scale Studies of Spins on Surfaces with Scanning Tunneling Microscopy 3

Time: Friday 10:30–12:15

Location: S051

O 80.1 Fri 10:30 S051

Synthesis and Characterization of Triangulene: a novel concept of magnetic nanostructure made of carbon — •FRANCISCO R. LARA¹, SILVIA CASTRO², JEREMY HIEULLE¹, MANUEL VILAS-VARELA², ALESSIO VEGLIANTE¹, NIKLAS FRIEDRICH¹, LORENZ MEYER¹, UNAI URIARTE-AMIANO¹, SOFIA SANZ³, DULCE REY², NATALIA E. KOVAL¹, MARTINA CORSO^{4,3}, EMILIO ARTACHO^{1,5}, THOMAS FREDERIKSEN³, DIEGO PEÑA², and JOSE IGNACIO PASCUAL¹ — ¹CIC nanoGUNE BRTA, Donostia, Spain — ²Centro Singular de Investigación en Química Biolóxica e Materiais Moleculares, Santiago de Compostela, Spain — ³Donostia International Physics Center, Donostia, Spain — ⁴Centro de Física de Materiales, Donostia, Spain — ⁵Cavendish Laboratory, Cambridge, United Kingdom

In this talk, we present the synthesis and characterization of a [3]-triangulene ring of 6 units, the [3]-triangulene nanostar (TNS), and an aza-[5]-triangulene (A5T), on a Au(111) surface.

By means of scanning tunneling microscopy (STM) and spectroscopy (STS) the precise spin states of such carbon-based nanostructures have been studied. Such experimental findings, are supported by calculations from density functional theory (DFT), mean-field Hubbard model (MFH), and Heisenberg model.

Both nanostructures are achieved thanks to on-surface synthesis. TNS hosts antiferromagnetically coupled spin-1 showing a complex many-body inelastic excitation spectrum. A5T ground state has a spin larger than one. Here the presence of the N heteroatom substitution plays an important role in the spin state on surface.

O 80.2 Fri 10:45 S051

Local access to the Ln-Ln bonding orbital in dimetallofullerene molecular magnets — •FABIAN PASCHKE¹, TOBIAS BIRK¹, FUPIN LIU², STANISLAV M. AVDOSHENKO², ALEXEY A. POPOV², and MIKHAIL FONIN¹ — ¹Department of Physics, Universität Konstanz, 78457 Konstanz — ²Leibniz Institute for Solid State and Materials Research (IFW Dresden), 01069 Dresden

One of the key players in the single-molecule magnet community are members of the lanthanide (Ln) dimetallofullerene family that combine air-stable chemical robustness, easy functionalization, a large magnetic moment and slow magnetic relaxation up to 28 K [1]. Two Ln³⁺ ions are ferromagnetically coupled by a singly occupied Ln-Ln bonding orbital in the void of a C₈₀ fullerene cage.

In this talk I will first demonstrate the robust on-surface magnetism of {Ln₂} complexes that show outstanding magnetic blocking temperatures [2,3], an important prerequisite to address its molecular magnetism on a local scale. Subsequently, scanning tunneling spectroscopy unambiguously identifies the unoccupied component of the single-electron Ln-Ln bonding orbital in the spectrum of {Dy₂} on a graphene/Ir(111) surface [4]. This finding outlines a new route how to access the molecular spin dynamics of single {Ln₂} complexes and provides a working point for spin manipulation using chemical doping.

[1] F. Liu *et al.*, Nat. Commun. 10, 571 (2019). [2] F. Paschke *et al.*, Adv. Mater. 2102844 (2021). [3] L. Spree *et al.*, Adv. Funct. Mater. 2105516 (2021). [4] F. Paschke *et al.*, Small 2105667 (2022).

O 80.3 Fri 11:00 S051

Indirect spin-readout of rare-earth-based single-molecule magnet with STM — •HONGYAN CHEN¹, TIMO FRAUHAMMER¹, TIMOFEY BALASHOV², GABRIEL DERENBACH^{1,3}, SVETLANA KLYATSKAYA⁴, EUFEMIO MORENO-PINEDA⁵, MARIO RUBEN^{3,4,6}, and WULF WULFHEKEL^{1,3} — ¹Physikalisches Institut, Karlsruhe Institute of Technology (KIT), 76131 Karlsruhe, Germany — ²Physikalisches Institut, RWTH Aachen, 52074 Aachen, Germany — ³Institute for Quantum Materials and Technologies, KIT, 76021 Karlsruhe, Germany — ⁴Institute of Nanotechnology, KIT, 76021 Karlsruhe, Germany — ⁵Departamento de Química-Física, Escuela de Química, Facultad de Ciencias Naturales, Exactas y Tecnología, Universidad de Panamá 0824, Panamá — ⁶Centre Européen de Sciences Quantiques (CESQ) in the Institut de Science et d'Ingénierie Supramoléculaires (ISIS), 8 allée Gaspard Monge BP 70028, 67083 Strasbourg Cedex, France

Rare-earth based SMMs are promising candidates for magnetic information storage as their large magnetic moments are carried by localized 4f electrons. However, this in turn hampers a direct readout of the moment. Here, we present the indirect readout of the Dy moment in DyPc₂ molecules on Au(111) using mK-STM. Because of an unpaired electron on the Pc ligand, the molecules show a Kondo resonance that is, however, split by the ferromagnetic exchange interaction between the unpaired electron and the Dy spin. Using spin-polarized STS, we read out the Dy spin as a function of the applied magnetic field, exploiting the spin polarization of the exchange-split Kondo state.

O 80.4 Fri 11:15 S051

Yu-Shiba-Rusinov states of Fe dimers on NbSe₂ — •LISA M. RÜTTEN¹, EVA LIEBHABER¹, HARALD SCHMID¹, GAËL REECHT¹, KAI ROSSNAGEL^{2,3}, FELIX VON OPPEN¹, and KATHARINA J. FRANKE¹ — ¹Fachbereich Physik, Freie Universität Berlin, 14195 Berlin, Germany — ²Institut für Experimentelle und Angewandte Physik, Christian-Albrechts-Universität zu Kiel, 24118 Kiel, Germany — ³Ruprecht Haensel Laboratory, Deutsches Elektronen-Synchrotron DESY, 22607 Hamburg, Germany

Unpaired adatom spins on superconductors interact with the Cooper pairs of the substrate and induce Yu-Shiba-Rusinov (YSR) states inside the superconducting gap. These can be probed by scanning tunneling spectroscopy at the single-atom scale. 2H-NbSe₂ is a superconducting, layered van der Waals material, where the YSR wave functions of magnetic impurities extend over several nanometers. This provides a wide range of adatom spacings over which their interaction is sufficiently strong to be potentially observed as a splitting in the tunneling spectra. In addition to superconductivity, 2H-NbSe₂ hosts an incommensurate charge-density wave (CDW). The imposed variation of the local density of states leads to shifts in the energy of the YSR states and alters the spatial symmetry of YSR wave functions. Here, we arrange Fe atoms on 2H-NbSe₂ using the tip of a scanning tunneling microscope and realize dimers with different spacings and symmetries. We investigate the influence of spacing and position with respect to the CDW on the interaction between the YSR states.

O 80.5 Fri 11:30 S051

Atomic manipulation of spin structures on the β -Bi₂Pd Superconductor — CRISTINA MIER¹, DIVYA JYOTI^{1,2}, JIYOON HWANG³, JINKYUNG KIM³, YUJEONG BAE³, ANDREAS HEINRICH³, NICOLAS LORENTE^{1,2}, and •DEUNG-JANG CHOI^{1,2,4} — ¹Centro de Física de Materiales, CFM/MPC (CSIC-UPV/EHU), Paseo Manuel de Lardizabal 5, 20018 Donostia-San Sebastian, Spain — ²Donostia International Physics Center (DIPC), Paseo Manuel de Lardizabal 4, 20018 Donostia-San Sebastian, Spain — ³Center for Quantum Nanoscience (QNS), Institute for Basic Science (IBS), Seoul 03760, South Korea — ⁴Ikerbasque, Basque Foundation for Science, 48013 Bilbao, Spain

Recently, the introduction of impurity states in the superconducting gap has received a lot of attention. Indeed, the search of a new superconducting state called topological superconductivity is strongly based in the combination of doping classical (s-wave) superconductors with magnetic impurities that arrange spins in a chiral fashion. We present the first results of controlled single-atom manipulation to assemble a chain of Cr atoms on a β -Bi₂Pd superconductor [1,2]. Such magnetic impurities on different substrates allow us to explore many-body effects and exotic phenomena in different experimental spin systems giving an understanding on the parameters on each system.

[1] C. Mier et al., Atomic Manipulation of In-gap States on the β -Bi₂Pd Superconductors, Phys. Rev. B 104 (4), 045406 (2021). [2] Cristina Mier, Deung-Jang Choi and Nicolás Lorente, Phys. Rev. B 104 (24), 245415 (2021).

O 80.6 Fri 11:45 S051

Theory of transport between superconducting states bound to magnetic impurities — •CIPRIAN PADURARIU¹, HAONAN HUANG², BJÖRN KUBALA^{1,3}, CHRISTIAN R. AST², and JOACHIM ANKERHOLD¹ — ¹Institute for Complex Quantum Systems and IQST, Ulm University, Ulm, Germany — ²Max-Planck-Institut für Festkörperforschung, Stuttgart, Germany — ³Institute of Quantum Technologies, German Aerospace Center (DLR), Ulm, Germany

The realization of the Majorana chain [1], a 1D-chain of superconducting states bound to magnetic impurities, suggests that Majorana edge states can be probed using the superconducting tunneling microscope (STM). Recently, we have developed an ideal tool to probe and manipulate the edge states of a Majorana chain. It consists of a mK-STM with its own in-gap Yu-Shiba-Rusinov (YSR) state created by a magnetic impurity on the tip. With this device we have studied the sharp resonant transport between the YSR state on the tip and another YSR on the sample, and have developed the theory [2].

Here, we summarize and expand the theory of YSR-YSR tunneling to phenomena that occur when one YSR state is close to zero energy, near its quantum phase transition. If the zero-energy state sits at the edge of a Majorana impurity chain, theory predicts that the topological edge state will transfer from the chain to the tip.

[1] S. Nadj-Perge, *et al.*, "Observation of Majorana fermions in ferromagnetic atomic chains on a superconductor", Science **346**, 602 (2014).

[2] H. Huang, *et al.*, "Tunneling dynamics between superconducting bound states at the atomic limit", Nat. Phys. **16**, 1227 (2020).

O 80.7 Fri 12:00 S051

Many-body Excitations of a Quantum Spin on a Proximitized Superconductor — STEFANO TRIVINI¹, •JON ORTUZAR¹, KATERINA VAXEVANI¹, JINGCHEN LI², ANE GARRO¹, F. SEBASTIAN BERGERET³, MIGUEL.A CAZALILLA^{4,5}, and JOSÉ IGNACIO PASCUAL^{1,5} — ¹CICnanoGUNE, San Sebastian, Spain — ²School of Physics, Sun Yat-sen University, Guangzhou 510275, China — ³Centro de Física de Materiales (CFM-MPC), 20018 San Sebastian, Spain — ⁴Donostia International Physics Center (DIPC), 20018 San Sebastian, Spain — ⁵Ikerbasque, Basque Foundation for Science, 48013 Bilbao, Spain

In magnetic molecules intrinsic magnetic anisotropy breaks spin degeneracy, allowing inelastic spin excitations that can be protected by a superconducting gap. The coupling of the spin to the superconductor induces Yu-Shiba-Rusinov (YSR) states, detected by scanning tunneling microscopy (STM) as long-lived quasi-particles excitations inside the superconducting gap.

Here, we observe the signature of both described excitations in an Ferroporphyrin adsorbed on a Au/V(100) proximitized superconducting surface. We found that the STM tip affects in a similar way both in-gap and out-gap states, hint that they are correlated. Solving an effective Hamiltonian of the system, we describe the observed signals as multiple excitations of entangled states formed by the molecular spin and superconductor.

O 81: 2D Materials 4: Heterostructures

Time: Friday 10:30–12:00

Location: S052

O 81.1 Fri 10:30 S052

Sub-angstrom non-invasive imaging of microstructures in 2D hybrid perovskites — •SHAYAN EDALATMANESH^{1,3}, MYKOLA TELYCHKO², KAI LENG², IBRAHIM ABDELWAHAB^{2,4}, NA GUO⁵, CHUN ZHANG⁵, JESUS MENDIETA-MORENO¹, MATYÁŠ NACHTIGALL¹, JING LI⁴, KIAN PING LOH², PAVEL JELÍNEK^{1,3}, and JIONG LU^{2,4} — ¹Institute of Physics, The Czech Academy of Sciences, Prague, Czech Republic — ²Department of Chemistry, NUS, Singapore — ³RCPTM, Palacky University, Olomouc, Czech Republic — ⁴CA2DM, NUS, Singapore — ⁵Department of Physics, NUS, Singapore

Organic-inorganic hybrid two dimensional (2D) Ruddlesden-Popper perovskites (RPPs), made of soft insulating organic layers sandwiched between conducting inorganic frameworks, have recently gained a great deal of attention as candidates for the next generation of optoelectronic devices. To gain an understanding of the cooperative lattice relaxation governing the optoelectronic properties of 2D RPPs, we present sub-angstrom resolution imaging of both soft organic layers and inorganic framework in a prototypical 2D lead-halide RPP crystal using a tip-functionalized Scanning Tunneling Microscopy (STM), non-contact Atomic Force Microscope (ncAFM) and Kelvin Probe Force Microscopy (KPFM) corroborated by theoretical simulations, namely Density Functional Theory (DFT)[1]. We unveil the overall twin-domain composition of the RPP crystal, with alternating quasi-one-dimensional electron and hole-channels at neighboring twin-boundaries, possibly responsible for the long-distance exciton transport in RPPs. Reference: [1] <https://arxiv.org/abs/2109.05878>

O 81.2 Fri 10:45 S052

Electronic Structure of Quasi-Freestanding WS₂/MoS₂ Heterostructures — BORNA PIELIĆ¹, DINO NOVKO¹, IVA ŠRUT RAKIĆ¹, JIAQI CAI², MARIN PETROVIĆ¹, ALICE BREMERICH², ROBIN OHMANN², NATAŠA VUJIČIĆ¹, MARIO BASLETIĆ³, MARKO KRALJ¹, and •CARSTEN BUSSE² — ¹Institute of Physics, Zagreb, Croatia — ²Universität Siegen, Germany — ³University of Zagreb, Croatia

Quasi-freestanding heterostructures of semiconducting two-dimensional materials with sharp interfaces, large built-in electric field, and narrow depletion region widths are proper candidates for the future design of electronic and optoelectronic devices.

Here, we epitaxially grow lateral WS₂-MoS₂ and vertical WS₂/MoS₂ heterostructures on graphene under UHV conditions. By means of scanning tunneling spectroscopy (STS), we examine the electronic structure of monolayer MoS₂, WS₂, and WS₂/MoS₂ vertical heterostructure. Moreover, we investigate band bending in the vicinity of the narrow one-dimensional interface of the WS₂-MoS₂ lateral heterostructure. Density functional theory (DFT) is used for the calculation of the band structures, as well as for the density of states maps at the interfaces. For the WS₂-MoS₂ lateral heterostructure, we find type-II band alignment and determine the corresponding depletion regions, charge densities, and the electric field at the interface.

O 81.3 Fri 11:00 S052

Quantum spin Hall edge states and interlayer coupling in twisted bilayer WTe_2 — •FELIX LÜPKE¹, DACEN WATERS², ANH PHAM³, JIAQIANG YAN⁴, DAVID G. MANDRUS⁵, PANCHAPAKESAN GANESH³, and BENJAMIN M. HUNT⁶ — ¹Peter Grünberg Institut (PGI-3), Forschungszentrum Jülich, 52425 Jülich, Germany — ²Physics, University of Washington — ³Center for Nanophase Materials Sciences, Oak Ridge National Lab — ⁴Materials Science and Technology Division, Oak Ridge National Lab — ⁵Department of Materials Science and Engineering, University of Tennessee — ⁶Physics, Carnegie Mellon University

The quantum spin Hall (QSH) effect, characterized by topologically protected spin-polarized edge states, was recently demonstrated in monolayers of the transition metal dichalcogenide (TMD) WTe_2 . However, the robustness of this topological protection remains largely unexplored in van der Waals heterostructures containing one or more layers of a QSH insulator. In this work, we use scanning tunneling microscopy and spectroscopy (STM/STS), to study twisted bilayer (tBL) WTe_2 and compare it to topologically trivial natural bilayer. By comparing our experimental observations to first principles calculations, we conclude that the twisted bilayers are weakly coupled, preserving the QSH states and preventing back scattering.

O 81.4 Fri 11:15 S052

Real-time TD-DFTB simulations and modeling of Fano-induced transparency in molecular van der Waals Heterostructures — •CARLOS R. LIEN-MEDRANO¹, FRANCO P. BONAFÉ², CHI YUNG YAM³, CARLOS-ANDRES PALMA⁴, CRISTIÁN G. SÁNCHEZ⁵, and THOMAS FRAUENHEIM¹ — ¹BCCMS, Uni-Bremen, Germany — ²MPSD, Hamburg, Germany — ³CSAR, Shenzhen, P. R. China — ⁴IOP, Beijing, P.R. China — ⁵UNCuyo, Mendoza, Argentina

While gating and doping in two-dimensional (2D) materials is well-known, the physics of photosensitizing and advanced optical properties have not been fully investigated, especially in the context of molecular vdW heterostructures (MVHs), that is, regular monolayer stacks on 2D materials. In a recent work [1], we employed an adapted Gersten-Nitzan (two point dipoles) model and real time time-dependent density functional tight-binding to study the optoelectronics of self-assembled monolayers on graphene nanoribbons. We found Fano resonances that cause electromagnetic induced opacity and transparency and reveal an additional incoherent process leading to interlayer exciton formation with a characteristic charge transfer rate. These results showcase hybrid van der Waals heterostructures as paradigmatic 2D optoelectronic stacks, featuring tunable Fano optics and unconventional charge transfer channels. Our findings open a path for improved design of modular multilayer organic photovoltaic devices.

[1] Lien-Medrano, C. R., et al. Fano Resonance and Incoherent Interlayer Excitons in Molecular van der Waals Heterostructures. *Nano Letters* (2022), 22(3), 911-917.

O 82: Electronic Structure of Surfaces 2

Time: Friday 10:30–12:15

Location: S053

O 82.1 Fri 10:30 S053

Electron- and Hole-Like Transport in Shockley Type Surface States Detected by MONA — •ANDREAS CHRIST, MARKUS LEISEGANG, PATRICK HÄRTL, and MATTHIAS BODE — Physikalisches Institut, Experimentelle Physik II, Universität Würzburg, Am Hubland, D-97074 Würzburg, Germany

In recent years, we have established the STM-based molecular nanoprobe (MONA) technique to detect the transport of hot charge carriers over distances of a few nanometers [1,2]. In short, MONA uses a charge carrier-driven molecular switching events, such as a tautomerization or rotation, to detect currents injected a few nanometers away. Earlier experiments performed on Ag(111) showed that the surface state characteristic for fcc(111) surfaces facilitates effective charge transport between the charge injection point at the tip position and a single phthalocyanine (HPC) detector molecule [3]. Since, however, the energy threshold for tautomerization of HPC exceeds the energy onset of the Ag(111) surface state ($E = -63$ meV), hole transport remained inaccessible. In order to investigate the influence of the band structure on the propagation of hot charge carriers we compare results of MONA experiments performed on Ag(111) with the isoelectronic Cu(111) surface. Our results reveal that due to the lower surface state onset in Cu(111) at $E = -440$ meV hole-like charge transport can also be detected.

- [1] M. Leisegang *et al.*, *Nano Lett.* **18**, 2165-2171 (2018)
 [2] M. Leisegang *et al.*, *Phys. Rev. Lett.* **126**, 146601 (2021)
 [3] J. Kügel *et al.*, *Nano Lett.* **17**, 5106 (2017)

O 81.5 Fri 11:30 S052

High-throughput stacking reveals emergent and switchable properties of 2D van der Waals bilayers — •SAHAR PAKDEL, ASBJØRN RASMUSSEN, MAD S KRUSE, ALIREZA TAGHIZADEH, THOMAS OLSEN, and KRISTIAN SOMMER THYGESEN — CAMD, Computational Atomic-Scale Materials Design, Department of Physics, Technical University of Denmark, 2800 Kgs. Lyngby Denmark

Stacking atomically thin two-dimensional monolayers into van der Waals (vdW) heterostructures offer new opportunities to tune physical properties of 2D materials. Here we provide a systematic ab initio-based study of homo-bilayers created by stacking several hundreds of stable monolayers containing up to 10 atoms per unit cell. We investigate all configurations commensurate with the primitive cell and verify our approach by comparing our stacking orders with available bulk compounds. For the stable bilayers within a 3 meV/Å² binding energy distance from the most stable configuration, we calculate a range of electronic and magnetic properties. We explore switchable properties in bilayer pairs related with a slide vector. Our work is a step towards rational design of layered vdW materials and contributes to the systematization of 2D materials. Our results will be available online and integrated with the Computational 2D Materials Database (C2DB) which allows for comparison between mono- and bilayer properties.

O 81.6 Fri 11:45 S052

1D p-n junction electronic and optoelectronic devices from transition metal dichalcogenide lateral heterostructures grown by one-pot chemical vapor deposition synthesis — •E. NAJAFIDEHAGHANI¹, Z. GAN¹, A. GEORGE¹, T. LEHNERT², G. Q. NGO³, C. NEUMANN¹, T. BUCHER³, I. STAUBE³, D. KAISER¹, T. VOGL³, U. HÜBNER⁴, U. KAISER², F. EILENBERGER³, and A. TURCHANIN¹ — ¹Friedrich Schiller University Jena, Institute of Physical Chemistry, Germany — ²Ulm University, Central Facility of Materials Science Electron Microscopy, Germany — ³Friedrich Schiller University Jena, Institute of Applied Physics, Germany — ⁴Leibniz Institute of Photonic Technology (IPHT), Germany

Lateral heterostructures (LH) of dissimilar monolayer transition metal dichalcogenides provide great opportunities to build 1D in-plane p-n junctions for sub-nanometer thin low-power electronic, optoelectronic, optical, and sensing devices. Electronic and optoelectronic applications of such p-n junction devices fabricated using a scalable chemical vapor deposition process yielding MoSe_2 - WSe_2 LHs are reported here. Their growth is achieved by in situ controlling the partial pressures of the oxide precursors by a two-step heating protocol. The grown LHs are characterized structurally and optically using optical microscopy, Raman spectroscopy, and photoluminescence spectroscopy. High-resolution transmission electron microscopy further confirms the high-quality 1D boundary between MoSe_2 and WSe_2 in the LH. p-n junction devices are fabricated from these LH and their applicability solar cells, photodetectors, and electroluminescent emitters are demonstrated.

O 82.2 Fri 10:45 S053

Exploring polaron stability and defect structures at the $\text{Li}_4\text{Ti}_5\text{O}_{12}$ (LTO) surface: A combined theoretical and experimental approach — •YU-TE CHAN¹, MATTHIAS KICK², CRISTINA GROSU^{2,3}, CHRISTOPH SCHEURER¹, and HARALD OBERHOFER² — ¹Fritz-Haber-Institut — ²TU München — ³IEK-9, FZ Jülich

Spinel $\text{Li}_4\text{Ti}_5\text{O}_{12}$ (LTO) is a promising anode material for next-generation all-solid-state Li-ion batteries (ASSB) due to its "zero strain" charge/discharge behavior. Pristine, white LTO possesses poor ionic and electronic conductivity. Through tailoring the sintering protocol, one can produce oxygen vacancies, resulting in a performant, blue LTO material. Polarons induced by oxygen vacancies have been proposed as one of the origins of the higher electronic conductivity. However, detailed knowledge about polaron stability, distribution, and dynamics in LTO bulk and surface has been lacking. By performing *Hubbard corrected density functional theory* (DFT+U) calculations we are able to show that in fact polaron formation and a possible polaron hopping mechanism can not only play a significant role in enhancing electronic conductivity but boost Li^+ diffusion nearby through lowering the hopping barrier, in line with the experimentally observed improved conductivities.[1,2] In combination with positron lifetime spectroscopy data and theoretical positron lifetimes, we arrive at a rather complete picture of the bulk vs. surface defect chemistry in LTO particles and the resulting mixed ionic electronic conductivity.

- [1] M. Kick *et al.*, *J. Phys. Chem. Lett.* **11** (2020), 2535
 [2] M. Kick *et al.*, *ACS Appl. Energy Mater.* **4** (2021), 8583

O 82.3 Fri 11:00 S053

Spin-polarized VLEED from Au(111): Surface sensitivity of the scattering process — •CHRISTOPH ANGRICK¹, JÜRGEN BRAUN², and MARKUS DONATH¹ — ¹Westfälische Wilhelms-Universität Münster — ²Ludwig-Maximilians Universität München

Low-energy electron diffraction from Au(111) shows the well-known threefold symmetry of the diffracted electron beams despite the sixfold symmetry of the surface layer. This is due to the influence of the second and deeper layers and the probing depth of the electrons. In this work, we investigated Au(111) with spin-polarized very-low-energy electron diffraction (VLEED) [1,2] experimentally and theoretically. We monitor the reflected specular beam at a fixed polar angle of incidence of $\Theta = 45^\circ$ while the azimuthal orientation of the crystal is varied. This puts the surface sensitivity of the VLEED scattering process to a test.

Our results show that the electron reflection and the spin-orbit-induced reflection asymmetry along $\bar{\Gamma}\bar{M}$ and $\bar{\Gamma}\bar{M}'$ are equivalent. The observed sixfold symmetry suggests a sensitivity to one atomic layer only. At azimuth angles deviating from the high-symmetry directions $\bar{\Gamma}\bar{M}$ and $\bar{\Gamma}\bar{M}'$, however, the VLEED signal from Au(111) shows a threefold symmetry. To reveal the origin of this effect, we varied the parameters in the calculation. The results indicate a non-negligible influence of the second atomic layer in the VLEED scattering process.

[1] Burgbacher *et al.*, Phys. Rev. B **87**, 195411 (2013)

[2] Angrick *et al.*, J. Phys.: Condens. Matter **33**, 115001 (2020)

O 82.4 Fri 11:15 S053

The quantum corral: Perturbation by adatoms and bonding description by LCAO — •ANDREAS BEREZCUK¹, MARTIN STEINAU¹, FABIAN STILP², FRANZ JOSEF GIESSBIL², and KLAUS RICHTER¹ — ¹Institut of Theoretical Physics, University of Regensburg, Germany — ²Institute of Experimental and Applied Physics, University of Regensburg, Germany

The quantum corral, first investigated in 1993 [1] consists of a circle of 48 iron atoms placed on a copper surface and gives rise to a standing wave pattern of the local charge density (LDOS). Afterwards a plurality of different confinement shapes have been investigated [2,3]. We revisited this structure in [4] using atomic force microscope (AFM) and scanning tunneling microscopy (STM). A tight-binding model [5] provides a LDOS in consistency with STM measurements for the original and the perturbed quantum corral. We further consider weak bonds between the AFM tip and the artificial atom, indicated by a widely spread LDOS, by using linear combinations of atomic orbitals (LCAO).

[1] M. F. Crommie *et al.*, Science **262**, 218 (1993)

[2] M. Crommie *et al.*, Physica D: Nonlinear Phenomena **83**, 98 (1995)

[3] E. Heller *et al.*, Nature **369**, 464 (1994)

[4] F. Stilp *et al.*, Science **372**, 1196 (2021)

[5] C. W. Groth *et al.*, New J. Phys. **16**, 063065 (2014)

O 82.5 Fri 11:30 S053

Single-Molecule Ultrafast Fluorescence-Detected Pump-Probe Microscopy — •DANIEL FERSCH¹, PAVEL MALÝ^{1,2}, JESSICA RÜHE³, VICTOR LISINETSII¹, MATTHIAS HENSEN¹, FRANK WÜRTHNER^{3,4}, and TOBIAS BRIXNER^{1,4} — ¹Institut für Physikalische und Theoretische Chemie, Universität Würzburg, Am Hubland, 97074 Würzburg, Germany — ²Faculty of Mathematics and Physics, Charles University, Ke Karlovu 5, 121 16 Prague, Czech Republic — ³Institut für Organische Chemie, Universität Würzburg, Am Hubland, 97074 Würzburg, Germany — ⁴Center for Nanosystems Chemistry (CNC), Universität Würzburg, Theodor-Boveri-Weg, 97074 Würzburg, Germany

The spectroscopic signatures of bulk samples can differ vastly from those of the respective single molecules. In particular, access to the femtosecond dynamics of single molecules remains a large experimental challenge. Here, we present

a novel setup consisting of a spectrally tunable femtosecond laser source and a scanning confocal fluorescence microscope with fully reflective excitation geometry and single-molecule sensitivity. Using a phase-stable interferometer we create a pulse pair with variable time delay to measure the molecular fluorescence excitation spectrum by means of Fourier-transform spectroscopy. By exciting the molecule with an additional prior pump pulse, we gain access to the dynamics of the excited state as a function of the pump-probe delay, resulting in a fluorescence-detected pump-probe spectrum. We have obtained first results on single terrylene bisimide molecules and compare them to a spincoated thin film.

O 82.6 Fri 11:45 S053

Anomalies at the Dirac point in doped graphene (B, N, BN) — •SANGEETA THAKUR^{1,2}, ARINDAM PRAMANIK³, BAHADUR SINGH³, PHILIP WILLKE⁴, MARTIN WENDEROTH⁴, HANS HOFSSÄSS⁵, GIOVANNI DI SANTO¹, LUCA PETACCIA¹, and KALOBARAN MAITI³ — ¹Eletra Sincrotrone Trieste, Strada Statale 14 km 163.5, 34149 Trieste, Italy — ²Freie Universität Berlin, Institut für Experimentalphysik Arnimallee 14, 14195 Berlin, Germany — ³Department of Condensed Matter Physics and Materials Science, Tata Institute of Fundamental Research, Homi Bhabha Road, Colaba, Mumbai 400005, India — ⁴IV. Physikalisches Institut, Georg-August-Universität Göttingen, 37077 Göttingen, Germany — ⁵II. Physikalisches Institut, Georg-August-Universität Göttingen, 37077 Göttingen, Germany

The changes in the electronic properties of graphene on SiC, induced by different atomic species, B, N and BN, substituted, via low energy (25eV) ion bombardment were investigated via angle-resolved photoemission spectroscopy. The anomalies at the Dirac point for B, N, and BN doped graphene are attributed to the spectral width arising from the lifetime and momentum broadening in the experiments. An energy gap at the Dirac point of graphene is not observed even after 5 % of B and N substitution [1]. These results will provide new insight to tune the carrier properties of graphene while keeping the Dirac fermionic properties protected, which is important for exploring its technological applications. [1] A. Pramanik, Sangeeta Thakur *et al.* PRL **128**, 166401 (2022).

O 82.7 Fri 12:00 S053

Interplay of intrinsic and extrinsic states in pinning and passivation of *m*-plane facets of GaN *n-p-n* junctions — •LARS FRETER^{1,2}, YUHAN WANG^{1,2}, MICHAEL SCHNEDLER¹, JEAN-FRANÇOIS CARLIN³, RAPHAËL BUTTÉ³, NICOLAS GRANDJEAN³, HOLGER EISELE⁴, RAFAL EDWARD DUNIN-BORKOWSKI^{1,5}, and PHILIPP EBERT¹ — ¹Peter Grünberg Institut, Forschungszentrum Jülich GmbH, 52425 Jülich, Germany — ²Lehrstuhl für Experimentalphysik IV E, RWTH Aachen University, 52056 Aachen, Germany — ³Institute of Physics, Ecole Polytechnique Fédérale de Lausanne (EPFL), 1015 Lausanne, Switzerland — ⁴Technische Universität Berlin, Institut für Festkörperphysik, Hardenbergstr. 36, 10623 Berlin, Germany — ⁵Ernst Ruska-Centrum, Forschungszentrum Jülich GmbH, 52425 Jülich, Germany

Intrinsic and extrinsic pinning and passivation of *m*-plane cleavage facets of GaN *n-p-n* junctions were investigated by cross-sectional scanning tunneling microscopy and spectroscopy. On freshly cleaved and clean *p*-type GaN(10 $\bar{1}0$) surfaces, the Fermi level is found to be extrinsically pinned by defect states, whereas *n*-type surfaces are intrinsically pinned by the empty surface state. For both types of doping, air exposure reduces the density of pinning states and shifts the pinning levels toward the band edges. These effects are assigned to water adsorption and dissociation, passivating intrinsic and extrinsic gap states. The revealed delicate interplay of intrinsic and extrinsic surface states at GaN(10 $\bar{1}0$) surfaces is a critical factor for realizing flatband conditions at sidewall facets of nanowires exhibiting complex doping structures.

O 83: Frontiers of Electronic Structure Theory: Focus on Artificial Intelligence Applied to Real Materials 4

Time: Friday 10:30–13:00

Location: S054

O 83.1 Fri 10:30 S054

Alchemical machine learning for high entropy alloys — •NATALIYA LOPANITSYNA, GUILLAUME FRAUX, and MICHELE CERIOTTI — École Polytechnique Fédérale de Lausanne, Switzerland

High entropy alloys (HEAs) are a class of metallic materials composed of five or more principal elements. Interest in HEAs has grown over the last decades due to their exceptional structural and mechanical properties. HEAs are particularly challenging for atomistic modeling. Machine-learning (ML) models have emerged as a promising alternative to inaccurate empirical forcefields and very demanding first-principles simulations, with the ability to deliver the accuracy of first principle methods with lower computational resources. However, the complexity of ML models grows exponentially with the number of different elements due to the unfavourable scaling of their associated feature space sizes, limiting

the chemical diversity of the systems tackled thus far. To address the problems arising from the high feature space dimensionality, first, we propose a chemical embedding compression scheme to reduce the dimensionality of the feature space required for multi-component systems, based on the framework of Willatt *et al.* [Phys. Chem. Chem. Phys., 2018], and implemented in PyTorch. Second, we generate a dataset of several thousands configurations, assembled from 25 d-block elements, which aims to represent cross-elemental interactions, evaluating their energies and forces at the DFT level. We demonstrate the effectiveness of the alchemical ML model in learning the energetics of this extremely diverse dataset, and provide showcase calculations of the properties of some realistic HEA compositions.

O 83.2 Fri 10:45 S054

Stacking the odds: Distribution-biased generative deep learning for molecular design — •JOE GILKES^{1,2}, JULIA WESTERMAYR¹, RHYAN BARRETT³, and REINHARD J. MAURER¹ — ¹Department of Chemistry, University of Warwick, UK — ²HetSys CDT, University of Warwick, UK — ³Warwick Mathematics Institute, UK

Organic electronics applications pose a number of often competing requirements on molecular design that are hard to satisfy by conventional synthesis. Devices such as organic light-emitting diodes (OLEDs) must exhibit closely aligned optoelectronic properties, yet their component molecules must be easily synthesizable and stable. The odds of finding suitable molecules when drawing random samples from chemical space are still too low for targeted design of candidate systems for OLED devices. We develop an automated molecular design approach based on iterative biasing of a generative deep learning model. In successive iterations, the output of this model is filtered with a deep learning surrogate model of electronic structure and then used to retrain the generative model with a bias. This enables us to create models that are progressively biased towards, e.g., higher ionisation potentials, or smaller fundamental gaps. We also demonstrate how we can bias towards multiple properties simultaneously by filtering our results with the SCScore model for synthetic complexity. This creates more synthetically viable molecules while still meeting optoelectronic requirements. Our approach efficiently creates novel molecules with tuned optoelectronic properties. Clustering analysis reveals trends in bonding patterns which can be utilised in molecular design.

O 83.3 Fri 11:00 S054

Machine learning TCP phases with domain knowledge of the interatomic bond — •MARIANO FORTI, ALESYA BURAKOVSKAYA, RALF DRAUTZ, and THOMAS HAMMERSCHMIDT — ICAMS, Ruhr-Universität Bochum, Universitätsstr. 150, 44801 Bochum, Germany.

The understanding of the precipitation of topological close packed (TCP) phases in single-crystal superalloys is of central importance for the design of these materials for high-temperature applications. However, the structural complexity of these intermetallic compounds and the chemical complexity of the superalloys with typically N=5-10 elements hampers the exhaustive sampling of chemical space by density-functional theory (DFT) calculations. For example, the computation of the convex hull of the R phase with 11 inequivalent lattice sites would require N^{11} DFT calculations in an N-component system. We overcome this computational limitation by combining machine learning (ML) techniques with descriptors of the local atomic environment of the TCP phases. We present descriptors that are derived from bond order potential (BOP) theory which retain domain knowledge of the interatomic interaction from tight-binding Hamiltonians. We demonstrate that these descriptors enable us to predict the structural stability of TCP phases with simple regression algorithms. We apply this methodology to several systems with experimental evidence of R phase formation.

O 83.4 Fri 11:15 S054

Ab initio random structure search of organic molecules at substrates — •DMITRII MAKSIMOV^{1,2} and MARIANA ROSSI^{1,2} — ¹Fritz Haber Institute of the Max Planck Society, Berlin, Germany — ²Max Planck Institute for the Structure and Dynamics of Matter, Hamburg, Germany

Finding stable structures of molecular adsorbates (in isolation or forming layers) from calculations is challenging, exacerbated when the adsorbates are flexible. To make matters more complicated, in these situations, it is often difficult to find good and cheap potentials of such complex interfaces that allow a thorough and reliable global search of the structural space. To make this problem tractable with *ab initio* potentials, we present a random global geometry optimization package that can explicitly take into account the internal degrees of freedom of molecules, their position and orientation with respect to fixed surroundings, as well as periodic boundary conditions [1]. Electronic structure calculations and local geometry optimizations are performed through a connection to the ASE software [2], making it possible to interface this algorithm with various codes. To increase the efficiency of geometry optimizations, we introduce a framework to construct initial approximate Hessians for BFGS algorithms that are specially tailored to accelerate the relaxation of van der Waals bonded structures and handle large structural changes. We showcase the algorithm for the adsorption of di-L-alanine at Cu(110). [1] <https://github.com/sabia-group/gensec> [2] Larsen et. al., J. Phys.: Condens. Matter **29**, 273002 (2017).

O 83.5 Fri 11:30 S054

Active learning and element-embedding approach in neural networks for infinite-layer versus perovskite oxides — ARMIN SAHINOVIC and •BENJAMIN GEISLER — Fakultät für Physik, Universität Duisburg-Essen

The observation of superconductivity in NdNiO₂ films on SrTiO₃(001) by Li *et al.* [1] has sparked considerable interest in the materials class of infinite-layer oxides. Here we combine first-principles simulations and active learning of neural networks to explore formation energies of oxygen vacancy layers, lattice parameters, and their statistical correlations in infinite-layer versus perovskite oxides across the periodic table, and place the superconducting nickelate and cuprate

families in a comprehensive context. Neural networks accurately predict these observables, which act as a fingerprint of the complex reduction reaction, using only a fraction of the data for training. Unbiased by external knowledge, element embedding autonomously identifies chemical similarities between the individual elements in line with human knowledge. Active learning renders the training highly efficient, based on the physical concepts of entropy and information, and provides systematic accuracy control [2]. We recently applied this concept also to nitrides and fluorides [3]. This exemplifies how AI may assist on the quantum scale in discovering novel materials with optimized properties.

[1] D. Li *et al.*, Nature **572**, 624 (2019)[2] A. Sahinovic and B. Geisler, PR Research **3**, L042022 (2021)[3] A. Sahinovic and B. Geisler, J. Phys.: Condens. Matter **34**, 214003 (2022)

O 83.6 Fri 11:45 S054

Indirect learning interatomic potential models for accelerated materials simulations — •JOE D. MORROW and VOLKER L. DERINGER — Department of Chemistry, Inorganic Chemistry Laboratory, University of Oxford, Oxford OX1 3QR, United Kingdom

Machine learning (ML) based interatomic potentials are emerging tools for materials simulations but require a trade-off between accuracy and speed. We show how one ML potential can be used to train another: we use an existing, accurate, but more computationally expensive model to generate reference data (labels and locations) for a series of much faster “indirectly-learned” potentials. Extensive reference datasets can be easily generated without the need for quantum-mechanical reference computations at the indirect learning stage, and we find that the additional data significantly improve the predictions of fast potentials with less flexible functional forms.

We apply the technique to disordered silicon, including a simulation of vitrification and polycrystalline grain formation under pressure with a system size of a million atoms. When comparing indirectly learned potentials to models learned directly from a DFT-labelled database, the latter make unphysical predictions for large systems (10^5 atoms) that are not apparent in smaller simulations ($\leq 10^4$ atoms). This emphasises the importance of carefully validating ML potentials *chemically*, not only via numerical error measures. Our work provides conceptual insight into the machine learning of interatomic potential models, and it suggests a route toward accelerated simulations of nanostructured materials.

O 83.7 Fri 12:00 S054

Predicting hot electrons free energies from ground-state data — •CHIHEB BEN MAHMOUD, FEDERICO GRASSELLI, and MICHELE CERIOTTI — EPFL, Lausanne, Switzerland

Machine-learning potentials, while extremely successful in describing the stability of condensed phases, are usually trained on ground-state electronic-structure calculations depending exclusively on the atomic positions and ignoring the electronic temperature. Hence, they are limited in their ability to describe hot electrons. We introduce a rigorous framework to calculate the finite-temperature electron free energy based exclusively on ground-state total energy and electronic density of states, while allowing to sample on-the-fly the electronic free energy at any temperature [1]. Our physically-motivated approach facilitates modeling material properties in extreme conditions with a fraction of the usual cost. We demonstrate it by computing the equation of state and heat capacity of hydrogen in planetary conditions. This approach demonstrates the impact of a universal model describing structural and electronic properties inexpensively and its ability to enable more accurate and predictive materials modeling and design.

[1] C Ben Mahmoud, F Grasselli, M Ceriotti* - arXiv preprint 2205.05591, 2022

O 83.8 Fri 12:15 S054

Machine Learning the RPA density-density response function — •MARIO ZAUCHNER, JOHANNES LISCHNER, and ANDREW HORSFIELD — Imperial College London, London, United Kingdom

Clusters and nanoparticles are used in a variety of scientific and industrial applications, including optoelectronics, photocatalysis, single electron transistors and medical imaging, among others. Electronic excitations often play a key role in these applications, but theoretical techniques for calculating excited-state properties of materials, such as the first-principles GW/Bethe-Salpeter method, are typically limited to very small systems. A key bottleneck of such excited-state calculations of clusters and nanoparticles is the determination of the static density-density response function, which is often calculated using a sum-over-states technique. In this talk, we present a technique to decompose the density-density response function into atomic contributions. This can be achieved by exploiting the locality of the density-density response function in non-metallic systems. These atomic contributions can then be used to train a machine-learning model using a set of structural features with the same rotational symmetry as the atomic response functions, thus allowing direct prediction of the density-density response function using only structural information.

O 83.9 Fri 12:30 S054

MD-based Raman Spectra using Machine Learning — •MANUEL GRUMET¹, KARIN S. THALMANN¹, TOMÁŠ BUČKO^{2,3}, and DAVID A. EGGER¹ — ¹Department of Physics, Technical University of Munich, Garching, Germany — ²Comenius University in Bratislava, Slovakia — ³Slovak Academy of Sciences, Slovakia

Theoretical calculations of Raman spectra based on molecular dynamics (MD) trajectories allow to directly incorporate both anharmonic and temperature-dependent effects and thus yield more realistic spectra compared to a phonon-based approach [1]. The spectra can be calculated from the Fourier-transformed velocity correlation function of the polarizability tensor α . However, this requires evaluating α for a large number of MD configurations along each trajectory, which has high computational cost if done by ab-initio methods.

We therefore use kernel-based machine learning (ML) methods with density-based descriptors [2, 3] to predict α based on atomic positions. Ab-initio calculations are then only needed for obtaining a training data set, reducing the computational cost significantly. We use a number of test systems, including both solids and small molecules, to test and optimize several different variants of this approach and compare the achieved prediction performances. We also test transferability of the trained models to trajectories at different temperatures.

[1] M. Thomas et al., Phys. Chem. Chem. Phys. **15**, 6608 (2013)

[2] A. P. Bartók et al., Phys. Rev. B **87**, 184115 (2013)

[3] A. Grisafi et al., Phys. Rev. Lett. **120**, 036002 (2018)

O 83.10 Fri 12:45 S054

Thermal Transport via Green-Kubo Method and Message-Passing Neural-Network Potentials — MARCEL F. LANGER^{1,2}, FLORIAN KNOOP^{2,3}, CHRISTIAN CARBOGNO², MATTHIAS SCHEFFLER², and •MATTHIAS RUPP^{2,4} — ¹TU Berlin, Germany — ²The NOMAD Laboratory, FHI-MPG & HU Berlin, Germany — ³Theoretical Physics Division, Linköping U, Sweden — ⁴Konstanz U, Germany

Accurate, precise, and efficient computational access to thermal conductivities of materials is relevant for scientific understanding and industrial applications. The Green-Kubo method with first-principles calculations enables the determination of thermal conductivities, even for strongly anharmonic materials [1]. However, the high computational cost of long dynamics simulations of large supercells required for convergence limits applicability for large-scale, high-throughput materials discovery. Machine-learning potentials can reduce this cost [2].

Message passing neural networks (MPNNs) are a promising, but for this task yet untested, class of models due to their relational inductive bias, implicit long-range nature, and ability to incorporate directional information. We adapt the heat flux definition for MPNNs, investigate the impact of equivariance, present a systematic account of their convergence behavior and performance, and compare them to a simpler baseline model.

[1]: C. Carbogno, R. Ramprasad, and M. Scheffler, Phys. Rev. Lett. **118** 175901 (2017) [2]: P. Korotayev et al., Phys. Rev. B **100** 144308 (2019); C. Mangold et al., J. Appl. Phys. **127**, 244901 (2020); C. Verdi et al., NPJ Comput. Mat. **7** 156 (2021)

O 84: Overview Talk Claus M. Schneider (joint session O/PPP)

Time: Friday 13:15–14:00

Location: S054

Invited Talk

O 84.1 Fri 13:15 S054

Exploring the Mysteries of Topology in Quantum Materials — •CLAUS M. SCHNEIDER — Peter Grünberg Institut PGI-6, Forschungszentrum Jülich, 52425 Jülich

A characteristic feature of emergent or quantum materials is the competition of various spin-dependent interactions, such as spin-orbit coupling and exchange interaction. In addition, depending on the material system, there may be a breaking of time-reversal and/or inversion symmetries at play. As a consequence, topological materials may range from metals to insulators. In the vicinity of the Fermi level, this situation leads to peculiar electronic dispersions associated with Dirac and Weyl points, eventually also resulting in complex spin textures

in momentum space. The interplay of competing mechanisms often results in unusual charge and spin transport phenomena in such materials. In order to understand the physical properties of quantum materials on a fundamental level, we need to explore these electronic states in detail and disentangle the role of the various interactions. For this purpose, we employ electron spectroscopic approaches, which explicitly take the electron spin as an experimental quantity into account. In this contribution we discuss an avenue starting from simple single-crystalline systems (e.g. W(011), Fe(100) and Co(100)) to more complex 2D and 3D quantum materials and detail the role of the individual interactions and symmetry-breaking mechanisms by experimental examples.

Physics of Socio-economic Systems Division Fachverband Physik sozio-ökonomischer Systeme (SOE)

Jens Christian Claussen
School of Computer Science
University of Birmingham
Edgbaston
B15 2TT Birmingham, UK
j.c.claussen@bham.ac.uk

Marc Timme
Chair for Network Dynamics
cfaed & Institute of Theoretical
Physics,
TU Dresden, 01062 Dresden
marc.timme@tu-dresden.de

Jan Nagler
Frankfurt School of Finance &
Management
Adickesallee 32-34
60322 Frankfurt am Main
j.nagler@fs.de

Overview of Invited Talks and Sessions

(Lecture hall H11; Poster P2)

Plenary Talk Ricard Sole

PLV IX Thu 14:00–14:45 H1 **Evolutionary transitions: universality, complexity and predictability** — •RICARD SOLE

Lunch Talk Nicolas Wöhrl

PSV II Tue 13:15–13:45 H2 **Wissenschaftskommunikation - für wen eigentlich?** — •NICOLAS WÖHRL, PETER KOHL, AXEL LORKE

Invited Talks

SOE 2.1 Mon 9:30–10:15 H11 **Two-armed bandits versus Carnapian truth seekers and epistemic free riders with bounded confidence** — •RAINER HEGSELMANN
SOE 8.1 Tue 9:30–10:15 H11 **Musicians' Synchronization and the Enigma of Swing** — •THEO GEISEL
SOE 11.1 Wed 9:30–10:15 H11 **The Corona Data Donation Project - When Citizens Collaborate to Fight a Pandemic** — •DIRK BROCKMANN

Invited Tutorial Talks

SOE 1.1 Sun 16:00–16:50 H4 **Diffusion approximations for particles in turbulence** — •BERNHARD MEHLIG
SOE 1.2 Sun 16:50–17:40 H4 **Probabilities in physics, paradoxes and populations** — •TOBIAS GALLA
SOE 1.3 Sun 17:40–18:30 H4 **Risk Revealed: Cautionary Tales, Understanding and Communication** — •PAUL EMBRECHTS

Invited Talks of the joint Symposium SKM Dissertation Prize 2022 (SYSD)

See SYSD for the full program of the symposium.

SYSD 1.1 Mon 10:15–10:45 H2 **Charge localisation in halide perovskites from bulk to nano for efficient optoelectronic applications** — •SASCHA FELDMANN
SYSD 1.2 Mon 10:45–11:15 H2 **Nonequilibrium Transport and Dynamics in Conventional and Topological Superconducting Junctions** — •RAFFAEL L. KLEES
SYSD 1.3 Mon 11:15–11:45 H2 **Probing magnetostatic and magnetotransport properties of the antiferromagnetic iron oxide hematite** — •ANDREW ROSS
SYSD 1.4 Mon 11:45–12:15 H2 **Quantum dot optomechanics with surface acoustic waves** — •MATTHIAS WEISS

Invited Talks of the joint Symposium United Kingdom as Guest of Honor (SYUK)

See SYUK for the full program of the symposium.

SYUK 1.1 Wed 9:30–10:00 H2 **Structure and Dynamics of Interfacial Water** — •ANGELOS MICHAELIDES
SYUK 1.2 Wed 10:00–10:30 H2 **A molecular view of the water interface** — •MISCHA BONN
SYUK 1.3 Wed 10:30–11:00 H2 **Motile cilia waves: creating and responding to flow** — •PIETRO CICUTA

SYUK 1.4	Wed	11:00–11:30	H2	Cilia and flagella: Building blocks of life and a physicist's playground — •OLIVER BÄUM-CHEN
SYUK 1.5	Wed	11:45–12:15	H2	Computational modelling of the physics of rare earth - transition metal permanent magnets from SmCo₅ to Nd₂Fe₁₄B — •JULIE STAUNTON
SYUK 2.1	Wed	15:00–15:30	H2	Hysteresis Design of Magnetic Materials for Efficient Energy Conversion — •OLIVER GUTFLEISCH
SYUK 2.2	Wed	15:30–16:00	H2	Non-equilibrium dynamics of many-body quantum systems versus quantum technologies — •IRENE D'AMICO
SYUK 2.3	Wed	16:00–16:30	H2	Quantum computing with trapped ions — •FERDINAND SCHMIDT-KALER
SYUK 2.4	Wed	16:45–17:15	H2	Breaking the millikelvin barrier in cooling nanoelectronic devices — •RICHARD HALEY
SYUK 2.5	Wed	17:15–17:45	H2	Superconducting Quantum Interference Devices for applications at mK temperatures — •SEBASTIAN KEMPF

Invited Talks of the joint Symposium Collective Social Dynamics from Animals to Humans (SYSO)

See SYSO for the full program of the symposium.

SYSO 1.1	Thu	9:30–10:00	H1	Capturing group interactions: The next frontier of modeling social and biological systems — •FRANK SCHWEITZER
SYSO 1.2	Thu	10:00–10:30	H1	Modelling Individual Mobility Behavior — •LAURA MARIA ALESSANDRETTI
SYSO 1.3	Thu	10:30–11:00	H1	Validating argument-based opinion dynamics with survey experiments — •SVEN BANISCH
SYSO 1.4	Thu	11:15–11:45	H1	Self-organization, Criticality and Collective Information Processing in Animal Groups — •PAWEL ROMANCZUK
SYSO 1.5	Thu	11:45–12:15	H1	Collective dynamics and physiological interactions in bird colonies — •HANJA BRANDL

Sessions

SOE 1.1–1.3	Sun	16:00–18:30	H4	Tutorial: Stochastic Processes from Financial Risk to Genetics (joint session SOE/TUT/BP/DY)
SOE 2.1–2.1	Mon	9:30–10:15	H11	Invited Talk Rainer Hegselmann: Opinion Formation
SOE 3.1–3.5	Mon	10:15–11:45	H11	Economic Models
SOE 4.1–4.2	Mon	12:00–12:30	H11	Financial Risk
SOE 5.1–5.4	Mon	12:30–13:30	H11	Social Systems, Opinion and Group Dynamics
SOE 6.1–6.10	Mon	15:00–17:45	H18	Data Analytics for Complex Systems (joint session DY/SOE)
SOE 7.1–7.2	Mon	17:45–18:15	H18	Big Data and Artificial Intelligence (joint session SOE/DY)
SOE 8.1–8.1	Tue	9:30–10:15	H11	Invited Talk Theo Geisel: Human Synchronization in Music Performance
SOE 9.1–9.3	Tue	10:15–11:15	H11	Physics of Contagion Processes
SOE 10.1–10.6	Tue	11:15–12:45	H19	Nonlinear Dynamics 1: Synchronization and Chaos (joint session DY/SOE)
SOE 11.1–11.1	Wed	9:30–10:15	H11	Invited Talk Dirk Brockmann: Big Data in Epidemic Dynamics (joint session SOE/DY)
SOE 12.1–12.6	Wed	10:15–12:45	H11	Networks: From Topology to Dynamics (joint session SOE/BP/DY)
SOE 13.1–13.2	Wed	12:45–13:15	H11	Energy Networks (joint session SOE/DY)
SOE 14.1–14.5	Wed	15:00–16:45	H11	Computational Social Science
SOE 15.1–15.3	Wed	17:00–18:15	H11	Traffic Dynamics, Urban and Regional Systems
SOE 16	Wed	18:15–19:30	H11	Members' Assembly
SOE 17.1–17.6	Thu	15:00–18:00	P2	Poster
SOE 18.1–18.1	Fri	9:30–10:00	H19	Invited Talk Kathy Lüdge (joint session DY/SOE)
SOE 19.1–19.5	Fri	10:00–11:15	H19	Machine Learning in Dynamics and Statistical Physics (joint session DY/SOE)
SOE 20.1–20.5	Fri	11:30–12:45	H19	Nonlinear Dynamics 2: Stochastic and Complex Systems, Networks (joint session DY/SOE)

Members' Assembly of the Physics of Socio-economic Systems Division

Wednesday 18:15–19:30 H11

Agenda:

- Report on Activities
- Announcements
- Elections
- Miscellaneous

Sessions

– Invited Talks, Tutorials, Contributed Talks, and Posters –

SOE 1: Tutorial: Stochastic Processes from Financial Risk to Genetics (joint session SOE/TUT/BP/DY)

Macroscopic and microscopic models from Economy to Biology must account for stochasticity on various levels. While classical physics strives for deterministic descriptions through differential equations from fundamental level to thermodynamics, many physics-based models on higher level explicitly include stochasticity from various sources. Discrete and continuous stochastic processes then become the mathematical foundation of these models. This tutorial highlights classical as well as current methods and approaches of probabilistic models and stochastic processes in physics, biology as well as socio-economic systems, thereby bridging the risk to extinction in genetics with its economic counterpart. (Session organized by Jens Christian Clausen.)

Time: Sunday 16:00–18:30

Location: H4

Tutorial SOE 1.1 Sun 16:00 H4
Diffusion approximations for particles in turbulence — •BERNHARD MEHLIG — University of Gothenburg, Gothenburg, Sweden

The subject of this tutorial is the dynamics of particles in turbulence, such as micron-sized water droplets in the turbulent air of a cumulus cloud. The particles respond in intricate ways to the turbulent fluctuations. Non-interacting particles may cluster together to form spatial patterns – even though the turbulent fluid is incompressible [1]. In this tutorial I explain how to understand spatial clustering using diffusion approximations, highlighting an analogy with Kramers' escape problem [2]. I introduce/review the necessary elements of diffusion theory. My goal is to give a pedagogical introduction to diffusion approximations in non-equilibrium statistical physics, using particles in turbulence as an example.

[1] K. Gustavsson and B. Mehlig, Statistical models for spatial patterns of heavy particles in turbulence, *Adv. Phys.* 65 (2016) 57 (read Sections 1, 3.1, and 6.1).

[2] H. A. Kramers, Brownian motion in a field of force and the diffusion model of chemical reactions, *Physica* 7 (1940) 284 (read up to eq. (17)).

Tutorial SOE 1.2 Sun 16:50 H4
Probabilities in physics, paradoxes and populations — •TOBIAS GALLA — Instituto de Física Interdisciplinaria Sistemas Complejos, IFISC (CSIC-UIB), Campus Universitat Illes Balears, E-07122 Palma de Mallorca, Spain

It is notoriously hard for humans to develop a good intuition for probabilities and stochastic processes. Our brains are not able to do this naturally, and there

are numerous mistakes which are easy to make. These mistakes are in fact made regularly in the press (sometimes perhaps deliberately). More worrisome, decision makers such as judges, doctors or politicians are also prone to mishandling probabilities. In this tutorial I will outline a few of these traps, and how to avoid them. I will also discuss the nature of probabilistic models of physical processes – is there genuine randomness in the world around us? I will then present a number of instances in which physics approaches combined with stochastic modelling can make a difference. As one example, I will outline experimental and theoretical results which highlight the importance of stochastic processes in population dynamics. Other examples will include stochastic processes in genetics, the evolution of cancer and in game theory.

Tutorial SOE 1.3 Sun 17:40 H4
Risk Revealed: Cautionary Tales, Understanding and Communication — •PAUL EMBRECHTS — Department of Mathematics, ETH Zürich

The title of the tutorial refers to a forthcoming book, to be published by Cambridge University Press, co-authored with Valérie Chavez-Demoulin (Lausanne) and Marius Hofert (Waterloo). Extreme Value Theory (EVT) offers a mathematical tool for the modeling of so-called What-If events, or stress scenarios. I will present several examples of risk-based decision-making and show how EVT can be used as part of the solution. The current pandemic has clearly shown that the communication of scientific evidence has a difficult stand in the ubiquitous environment of social media. I will discuss some examples of this struggle.

SOE 2: Invited Talk Rainer Hegselmann: Opinion Formation

Time: Monday 9:30–10:15

Location: H11

Invited Talk SOE 2.1 Mon 9:30 H11
Two-armed bandits versus Carnapian truth seekers and epistemic free riders with bounded confidence — •RAINER HEGSELMANN — Frankfurt School of Finance & Management, Adickesallee 32-34, 60322 Frankfurt

In its original version, the so-called bounded confidence model only knows the exchange of opinions among individuals. The individuals may have formed their opinions beforehand through systematic experience (observation, experimentation), but no signal from the external world enters the modeled social exchange process. Later, Ulrich Krause and I extended the model to include a signal from the external world acting on the social exchange process. However, we put all details of this influence process into a black box.

In my talk I will present how this black box can be opened: The social exchange process of the bounded confidence model is linked to an explicitly modeled experimentation and evaluation of experimentally obtained data. The starting point is a community that has a choice between n strategies ($n = 2$), each leading to success with a constant but unknown probability. Such problems are known as n -armed-bandit-problems. It is further assumed that the community consists only partly of truth-seekers who 'conscientiously', following certain rules from Carnap's inductive logic, evaluate their experiences. Another part of the community consists of epistemic free riders, who do no statistics at all, but opportunistically follow their close-by neighbors. The talk will show that such a setting allows to answer questions about the efficiency of different epistemic policies.

SOE 3: Economic Models

Time: Monday 10:15–11:45

Location: H11

SOE 3.1 Mon 10:15 H11
Generic catastrophic poverty when selfish investors exploit a degradable common resource — •CLAUDIUS GROS — Institute for Theoretical Physics, Goethe University Frankfurt a.M.

The productivity of a common pool of resources may degrade when overly exploited by a number of selfish investors, a situation known as the tragedy of the commons. We examine the case that degradation is functionally dependent on total investments. The payoffs, which are independently optimized by each

agent, are given by the balance between the return from investing in the common resource and the investment costs, which are a function of the agent-specific per-unit costs. The payoffs of most agents are shown rigorously not to scale as $1/N$, the result for cooperating agents, but as $1/(N^2)$, where N is the number of agents. This scaling in the stationary state is denoted catastrophic poverty. A finite number of oligarchs may be present in addition, with the payoffs of the oligarchs remaining finite even in the large- N limit. The results hold under very general conditions for a wide class of models.

SOE 3.2 Mon 10:45 H11

Games in rigged economies — •LUIS F SEOANE — Systems Biology Department, Spanish National Center for Biotechnology (CNB-CSIC), C/ Darwin 3, Madrid, Spain.

Modern economies evolved from simpler material exchanges into very convoluted systems. Today, a multitude of aspects can be regulated, tampered with, or left to chance; these are economic degrees of freedom (DOF) which shape the flow of wealth. Economic actors can exploit them, at a cost, and bend that flow in their favor. If intervention becomes widespread, microeconomic strategies can collide or resonate, building into macroeconomic effects. How viable is a *rigged* economy? How do growing economic complexity and wealth affect it? We capture essential elements of rigged economies with a simple model. Nash equilibria in tractable cases show how increased intervention turns economic DOF from minority into majority games through a dynamical phase. This is reproduced by agent-based simulations of our model, which allow us to explore scenarios out of reach for payoff matrices. Increasing economic complexity appears as a mechanism to defuse cartels or consensus situations. But excessive complexity enters abruptly into a regime of large fluctuations (resulting from non-competitive intervention efforts coupled across DOF) that threaten the system's viability. Thus high economic complexity can result in negative spillover from non-competitive actions. Simulations suggest that wealth must grow faster than linearly with complexity to avoid this large fluctuations regime. Our model provides testable conclusions and phenomenological charts to guide policing of rigged economies.

SOE 3.3 Mon 11:00 H11

Risk Preferences in Time Lotteries — YONATAN BERMAN¹ and •MARK KIRSTEIN² — ¹King's College London — ²Max Planck Institute for Mathematics in the Sciences, Leipzig

An important but understudied question in economics is how people choose when facing uncertainty in the timing of events. Here we study preferences over time lotteries, in which the payment amount is certain but the payment time is uncertain. Expected discounted utility theory (EDUT) predicts decision makers to be risk-seeking over time lotteries. We explore a normative model of growth-optimality, in which decision makers maximise the long-term growth rate of

their wealth as suggested by the framework of ergodicity economics. Revisiting experimental evidence on time lotteries, we find that growth-optimality accords better with the evidence than EDUT. We outline future experiments to scrutinise further the plausibility of growth-optimality.

SOE 3.4 Mon 11:15 H11

Macroscopic approximation for an agent based socio-economic model — •SÖREN NAGEL¹, ECKEHARD SCHÖLL^{1,2}, and JOBST HEITZIG¹ — ¹Potsdam Institute for Climate Impact Research — ²Institut für Theoretische Physik, TU Berlin

We investigate an agent-based model for economic growth that contains an underlying social network in order to incorporate bounded rationality. To further extend the results presented in [1] we combine a moment closure approach for the economy and a stochastic differential equation approximation for the social choice. With this approach we can reproduce some characteristics of the original model like economic inequality, and we are able to link the business cycle oscillations to noise-induced excitation oscillations and coherence resonance.

[1] Yuki M Asano, Jakob J Kolb, Jobst Heitzig, and J Doyne Farmer. Emergent inequality and business cycles in a simple behavioral macroeconomic model. PNAS 118, e2025721118 (2021).

SOE 3.5 Mon 11:30 H11

Socioeconomic modeling of a fossil-fuel and renewable-energy based two-sector economy — •PHILIPPE LEHMANN¹, ECKEHARD SCHÖLL^{1,2}, and JOBST HEITZIG¹ — ¹Potsdam Institute for Climate Impact Research — ²Institut für Theoretische Physik, TU Berlin

We study a stylized economic model to capture the influence of social dynamics on investment decisions in a fossil-fuel and renewable energy based two-sector production economy. For this purpose the socioeconomic model in [1] is extended to two sectors. Although this model is based on simple assumptions, it shows extensive complex dynamics which we illustrate graphically to reveal the underlying mechanism. This empirical approach allows us to draw several analogies to patterns of our real economy that challenge current econometric models.

[1] Yuki M Asano, Jakob J Kolb, Jobst Heitzig, and J Doyne Farmer. Emergent inequality and business cycles in a simple behavioral macroeconomic model. PNAS 118, e2025721118 (2021).

SOE 4: Financial Risk

Time: Monday 12:00–12:30

Location: H11

SOE 4.1 Mon 12:00 H11

From many-body physics to financial markets: sparse modeling for inverse problems — •DANIEL GUTERDING — Fachbereich Mathematik, Naturwissenschaften und Datenverarbeitung, Technische Hochschule Mittelhessen, Wilhelm-Leuschner-Straße 13, 61169 Friedberg, Germany

The accurate valuation of plain-vanilla derivatives is one of the fundamental tasks of mathematical finance. In particular, arbitrage-free interpolations of market-quoted option prices or implied volatilities are needed for the pricing of most options. For this purpose, various standard interpolation techniques have been modified to accommodate the no-arbitrage conditions required by quantitative finance.

Despite this problem being so important for option pricing, the available approaches are quite involved and largely not stable against the noisy inputs that are often encountered in practical applications. Making use of recent progress on inverse problems in many-body physics [1], our method [2] is based on the relation between the terminal density of the underlying asset and plain-vanilla option prices.

We construct a few-parameter model for this relation using the singular value decomposition, which obviates the need to explicitly choose expansion or regression basis functions, such as they are encountered in many other methods. Furthermore, we show that our method by construction delivers arbitrage-free models even for inputs containing noise or severe arbitrage.

[1] Otsuki et al., J. Phys. Soc. Japan 89, 012001 (2020)

[2] Guterding, arXiv:2205.10865

SOE 4.2 Mon 12:15 H11

An ABM Marketmodel Study: Dynamics, Stochastics and Rule based Decisions — •MAGDA SCHIEGL — University of Applied Sciences Landshut, Am Lurzenhof 1, D-84036 Landshut

Riskmanagement is a main topic in insurance business with a variety of traditional methods. In recent years more and more methods of the field of complex systems as complex networks or ABMs play an important role. One of the first in the insurance mathematical literature published ABMs is by Ingram et al. [1]. The paper describes a model of a competitive (insurance and not only insurance) market that shows cyclical behavior.

We reformulate the above cited model in a form that makes it accessible for analytical as well as numerical treatment and discussion. We find three, interacting components of the model: the dynamics, the stochastics and the rule based decisions. The agents, insurance companies, play a rule based strategic game, competing with each other. The actions of the agents depend on both, the statistics of the single agent and the statistics of the market as a whole. We analyze the dynamics of the model being responsible for a parameter dependent, periodic behavior and investigate its stochastic and rule-based components. We implemented the model as a Monte Carlo simulation and examine the interactions of the model's different components.

[1] Ingram, D., Tayler, P., Thompson, M. (2012) Invited Discussion Paper: Surprise, Surprise From Neoclassical Economics To E-Life. ASTIN Bulletin 42(2): 389-411

SOE 5: Social Systems, Opinion and Group Dynamics

Time: Monday 12:30–13:30

Location: H11

SOE 5.1 Mon 12:30 H11

Bounded rational agents playing a public goods game — •PRAKHAR GODARA, TILMAN DIEGO ALEMAN, and STEPHAN HERMINGHAUS — Max Planck Institute for Dynamics and Self-Organization (MPIDS), 37077 Goettingen, Germany

An agent-based model for human behavior in the well-known public goods game (PGG) is developed making use of bounded rationality, but without invoking mechanisms of learning. The underlying Markov decision process is driven by a path integral formulation of reward maximization. The parameters of the model

can be related to human preferences accessible to measurement. Fitting simulated game trajectories to available experimental data, we demonstrate that our agents are capable of modeling human behavior in PGG quite well, including aspects of cooperation emerging from the game. We find that only two fitting parameters are relevant to account for the variations in playing behavior observed in 16 cities from all over the world. We thereby find that learning is not a necessary ingredient to account for empirical data.

SOE 5.2 Mon 12:45 H11

Social nucleation: Group formation as a phase transition — FRANK SCHWEITZER and •GEORGES ANDRES — ETH Zürich, Chair of Systems Design, Switzerland

The spontaneous formation and subsequent growth, dissolution, merger, and competition of social groups bear similarities to physical phase transitions in metastable finite systems. In this talk, I will examine three different scenarios, percolation, spinodal decomposition, and nucleation, to describe the formation of social groups of varying size and density. In an agent-based model, I will present a feedback between the opinions of agents and their ability to establish links. Groups can restrict further link formation, but agents can also leave if costs exceed the group benefits. I will show how to identify the critical parameters for costs and benefits and social influence to obtain either one large group or the stable coexistence of several groups with different opinions. Analytic investigations then allow to derive different critical densities that control the formation and coexistence of groups. This approach sheds light on the much-neglected early stage of network growth and the emergence of large connected components.

SOE 5.3 Mon 13:00 H11

Multiscale Causal Structure in Armed Conflict — •NIRAJ KUSHWAHA and EDWARD LEE — Complexity Science Hub Vienna, Josefstädter Straße 39, 1080 Vienna, Austria

Armed conflict is a major and ongoing problem around the world today. The very features of conflict that makes it important, its multiscale and multidimensional impact, render it difficult to understand quantitatively. Here, we introduce a first principles approach to conflict by clustering sequences of conflict events into causal conflict avalanches. We rely on armed conflict data from the ACLED

project, occurring from the years 1996-2021 in Africa. We investigate different spatial and temporal scales with a systematic coarse-graining procedure. For space, we tile the region with semi-regular bins that constitute our level of resolution, and for time we group days into discrete intervals. This formalism bridges the gap between microscopic and macroscopic descriptions of armed conflict. To infer causal relationships between different spatial bins we use a standard non-linear measure of statistical dependency called transfer entropy. Using transfer entropy, we extract a directed causal network that links adjacent geographic locations. We then leverage this causal structure to join two conflict events if they are adjacent in time and belong to adjacent and causally connected spatial bins. We call the resulting sequences of conflict events, conflict avalanches. Further statistical and dynamical analysis reveal that many conflict avalanche features follow power-law distributions. Our work paves way for future investigation on classes of models which can explain the emergence of scaling in conflict across different scales.

SOE 5.4 Mon 13:15 H11

Ordering dynamics and path to consensus in multi-state voter models — LUCÍA RAMÍREZ, MAXI SAN MIGUEL, and •TOBIAS GALLA — Instituto de Física Interdisciplinaria Sistemas Complejos, IFISC (CSIC-UIB), Campus Universitat Illes Balears, E-07122 Palma de Mallorca, Spain

We investigate the time evolution of the density of active interfaces and of the entropy of the distribution of agents among opinions in multi-state voter models. Individual realisations undergo a sequence of extinctions until consensus is reached. After each elimination the population remains in a meta-stable state. The density of active interfaces and the entropy in these states varies from realisation to realisation. Making some simple assumptions we are able to analytically calculate the average density of active interfaces and the average entropy in each of these states. We also show that, averaged over realisations, the density of active interfaces decays exponentially, with a time scale set by the size and geometry of the interaction graph, but independent of the initial number of opinion states. The decay of the average entropy is exponential only at long times when there are at most two opinions left in the network. Finally, we show how meta-stable states comprised of only a subset of opinions can be engineered as genuinely stationary states by introducing precisely one zealot in each of the prevailing opinions.

SOE 6: Data Analytics for Complex Systems (joint session DY/SOE)

Time: Monday 15:00–17:45

Location: H18

SOE 6.1 Mon 15:00 H18

Estimating covariant Lyapunov vectors from data — •NAHAL SHARAFI, CHRISTOPH MARTIN and SARAH HALLERBERG — Hamburg University of Applied Sciences, Hamburg, Germany

Covariant Lyapunov vectors characterize the directions along which perturbations in dynamical systems grow. They have also been studied as predictors of critical transitions and extreme events. For many applications, it is necessary to estimate these vectors from data since model equations are unknown for many interesting phenomena. We propose a novel approach for estimating covariant Lyapunov vectors based on data records without knowing the underlying equations of the system. In contrast to previous approaches, our approach can be applied to high-dimensional datasets. We demonstrate that this purely data-driven approach can accurately estimate covariant Lyapunov vectors from data records generated by low and high-dimensional dynamical systems. Additionally we test for the robustness against noise in a low-dimensional dynamical system.

SOE 6.2 Mon 15:15 H18

Extending the limits of Electrochemical Impedance Spectroscopy with Machine Learning and Digital Twins — •LIMEI JIN^{1,2}, FRANZ P. BERECK², CHRISTIAN H. BARTSCH², JOSEF GRANWEHR², RÜDIGER-A. EICHEL², KARSTEN REUTER¹, and CHRISTOPH SCHEURER¹ — ¹Fritz-Haber-Institut der MPG, Berlin, Germany — ²IEK-9, Forschungszentrum Jülich, Jülich, Germany

Electrochemical impedance spectroscopy (EIS) is widely used to characterize electrochemical energy conversion systems. The traditional analysis with equivalent circuit models (ECM) has recently been augmented by a transform based distribution of relaxation times (DRT) analysis which allows one to reduce the ambiguity in the construction of ECMs and thus overfitting. Yet, DRT, just like most traditional analyses, is firmly based in the linear response regime as well as based on frequency sweeps on a logarithmic scale. The latter makes these approaches time-consuming, the first limits their scope severely. To develop novel experimental spectroscopic excitation schemes that address these limitations, a model space of sufficiently realistic systems is required that substitutes for time-consuming measurements in terms of a digital twin. We present a joint experimental and theoretical approach for the construction of such a target space for the case of battery cell performance and ageing behaviour.

SOE 6.3 Mon 15:30 H18

Bayesian approach to anticipate critical transitions in complex systems — •MARTIN HESSLER^{1,2} and OLIVER KAMPS² — ¹Westfälische Wilhelms-Universität Münster, 48149 Münster — ²Center for Nonlinear Science, Westfälische Wilhelms-Universität Münster, 48149 Münster

Complex systems in nature, technology and society can undergo sudden transitions between system states with very different behaviour. In order to avoid undesired consequences of these tipping events, statistical measures as variance, autocorrelation, skewness and kurtosis have been proposed as leading indicators based on time series analysis. Under favourable conditions they can give a hint of an ongoing bifurcation-induced destabilization process. However, they suffer from their loose connection to complex system dynamics, sensitivity to noise and sometimes misleading trends. Therefore, we want to present an alternative approach assuming the dynamical system being described by a Langevin equation. Starting from this stochastic description, we combine MCMC sampling, rolling window methods and Bayesian reasoning to derive the drift slope as an alternative early warning sign. The Bayesian approach enables us to define credibility bands which make it easier to distinguish random fluctuations from real trends that imply a less resilient system. Our investigations suggest that the estimation procedure is rather robust even under strong noise. Besides, the noise level of the system is computed to get insights into the probability of a noise induced transition. We want to present some of the results and discuss possible limitations and tasks of future research.

SOE 6.4 Mon 15:45 H18

Stochastic Interpolation of Sparsely Sampled Time Series by a Superstatistical Random Process and its Synthesis in Fourier and Wavelet Space — •JEREMIAH LÜBKE¹, JAN FRIEDRICH², and RAINER GRAUER¹ — ¹Institute for Theoretical Physics I, Ruhr-University Bochum, Universitätsstr. 150, 44801 Bochum, Germany — ²ForWind, Institute of Physics, University of Oldenburg, Küppersweg 70, 26129 Oldenburg, Germany

A novel method is presented for stochastic interpolation of a sparsely sampled time signal based on a superstatistical random process generated from a Gaussian scale mixture. In comparison to other stochastic interpolation methods such as kriging, this method possesses strong non-Gaussian properties and is thus applicable to a broad range of real-world time series. A precise sampling algorithm is provided in terms of a mixing procedure that consists of generating a field

$u(\xi, t)$, where each component $u_\xi(t)$ is synthesized with identical underlying noise but covariance $C_\xi(t, s)$ parameterized by a log-normally distributed parameter ξ . Due to the Gaussianity of each component $u_\xi(t)$, standard sampling algorithms and methods to constrain the process on the sparse measurement points can be exploited. The scale mixture $u(t)$ is then obtained by assigning each point in time t a $\xi(t)$ and therefore a specific value from $u(\xi, t)$, where $\log \xi(t)$ is itself a realization of a Gaussian process with a correlation time large compared to the correlation time of $u(\xi, t)$. Finally, a wavelet-based hierarchical representation of the interpolating paths is introduced, which is shown to provide an adequate method to locally interpolate large datasets.

SOE 6.5 Mon 16:00 H18

Global sensitivity analysis of Monte Carlo models using Cramer-von Mises distance — •SINA DORTAJ^{1,2} and SEBASTIAN MATERA^{1,2} — ¹Fritz-Haber-Institut der Max-Planck-Gesellschaft, Faradayweg 4-6, 14195 Berlin, Germany — ²Institute for Mathematics, Freie Universität Berlin, Arnimallee 6, 14195 Berlin, Germany

Typically, the parameters entering a physical simulation model carry some kind of uncertainty, e.g. due to the intrinsic approximations in a higher fidelity theory from which they have been obtained. Global sensitivity analysis (GSA) targets quantifying which parameters uncertainties impact the accuracy of the simulation results, e.g. to identify which parameters need to be determined more accurately.

We present a GSA approach on basis of the Cramers-von Mises distance. Unlike prevalent approaches it combines the following properties: i) it is equally suited for deterministic as well as stochastic model outputs, ii) it is free of gradients, and iii) it can be estimated from any suitable numerical quadrature (NQ) without further numerical tricks. Using Quasi-Monte Carlo for NQ and prototypical first-principles kinetic Monte Carlo models (kMC), we examine the performance of the approach. We find that the approach typically converges in a modest number of NQ points. Furthermore, it is robust against even extreme relative noise. All these properties make the method particularly suited for expensive (kinetic) Monte Carlo models, because we can reduce the number of simulations as well as the target variance of each of these.

15 min. break

SOE 6.6 Mon 16:30 H18

Reproducible and transparent research software pipelines using semantic research data management and common workflow language — •ALEXANDER SCHLEMMER^{1,2,5}, INGA KOTTLARZ^{1,3}, BALTASAR RÜCHARDT^{1,5}, ULRICH PARLITZ^{1,3,5}, and STEFAN LUTHER^{1,4,5} — ¹Max Planck Institute for Dynamics and Self-Organization, Göttingen — ²IndiScale GmbH, Göttingen — ³Institute for the Dynamics of Complex Systems, Georg-August-Universität Göttingen — ⁴Institute of Pharmacology and Toxicology, University Medical Center Göttingen — ⁵German Center for Cardiovascular Research (DZHK), Partner Site Göttingen

Sustainable and well-documented scientific software is essential for effectiveness and reproducibility in data-intensive research. In practice, incompletely documented software hinders in many cases replicability, reproducibility and method comparison. In our terminology, documentation includes method and algorithm descriptions as well as human- and machine-readable representations of parameters, initial conditions and data, versions and dependencies and a well-defined software execution environment. We present an approach combining semantic data management with CaosDB and processing pipelines with Common Workflow Language (CWL), showing use cases from dynamical systems research. The CWL-based environment provides a transparent description of the process and includes metadata that can be searched within CaosDB. Input/output-data and parameters can be directly linked to algorithms and software snapshots. The employment of containers simplifies reproducibility and interoperability.

SOE 6.7 Mon 16:45 H18

MDSuite: A post-processing engine for particle simulations — •FABIAN ZILLS¹, SAMUEL TOVEY¹, FRANCISCO TORRES-HERRADOR², CHRISTOPH LOHRMANN¹, and CHRISTIAN HOLM¹ — ¹Institute for Computational Physics, University of Stuttgart, Stuttgart, Germany — ²von Karman Institute for Fluid Dynamics, Rhode-St-Genese, Belgium

Particle-based simulations are experiencing a rapid growth wherein system sizes in the hundreds of thousands or even millions are becoming commonplace. With

this growth in system size comes the additional challenge of post-processing the simulation data.

In this talk, we introduce the Python package MDSuite. MDSuite is designed for the post-processing of particle-based simulation in an efficient manner and on modern hardware. Built on top of TensorFlow, MDSuite calculators are fully parallelised, gpu-enabled, and, due to the use of modern data pipe-lining methods, completely memory safe. Furthermore, the use of HDF5 and SQL database structures enables effective tracking of calculation parameters as well as a compressed trajectory storage medium. We present MDSuite as a standalone package for the storage, analysis, and comparison of large-scale simulation studies.

SOE 6.8 Mon 17:00 H18

Distinguishing noise from high-dimensional chaos — •INGA KOTTLARZ^{1,2} and ULRICH PARLITZ^{1,2} — ¹Max Planck Institute for Dynamics and Self-Organization, Göttingen, Germany — ²Institute for Dynamics of Complex Systems, Georg-August-Universität Göttingen, Göttingen, Germany

The ordinal pattern-based Complexity-Entropy Plane is a popular tool in non-linear dynamics for distinguishing noise from chaos. While successful attempts to do so have been documented for low-dimensional maps and continuous-time systems, high-dimensional systems have been somewhat neglected so far. To address the question in which way time series from highdimensional chaotic attractors can be characterized by their location in the Complexity-Entropy Plane we analyze data from the high-dimensional continuous-time Lorenz-96 system, the discrete generalized Hénon map and the Mackey-Glass equation as a delay system and discuss the crucial role of the lag and the pattern length or the ordinal pattern, and the length of the available time series.

SOE 6.9 Mon 17:15 H18

The impact of the UEFA European Football Championship on the spread of COVID-19 — •JONAS DEHNING¹, SEBASTIAN B. MOHR¹, SEBASTIAN CONTRERAS¹, PHILIPP DÖNGES¹, EMIL IFTEKHAR¹, OLIVER SCHULZ², PHILIP BECHTLE³, and VIOLA PRIESEMANN^{1,4} — ¹MPI for Dynamics and Self-Organization, 37077 Göttingen — ²MPI for Physics, 80805 München — ³Physikalisches Institut, University of Bonn — ⁴Institute for the Dynamics of Complex Systems, University of Göttingen

Large-scale international events like the UEFA Euro 2020 football championship offer a unique opportunity to quantify the impact of match-related social gatherings on COVID-19, as the number of matches played by participating countries resembles a randomized trial. Moreover, soccer-related activities have a marked gender-imbalance that we can exploit for inference. In our work, we build a differentiable Bayesian SEIR-like model. Its parameters are inferred with Hamiltonian Monte-Carlo using the PyMC3 package. Our model simulates COVID-19 spread in each country using a discrete renewal process and gender-resolved case numbers. On average, 3.2% (95% CI: [1.3%, 5.2%]) of new cases in the 12 analyzed countries can be associated with the match-related social gatherings throughout our analysis period. Individually, England, the Czech Republic and Scotland showed a significant effect. Besides these insights on the spread of COVID-19 during large-scale events, our approach is an example of how modern Bayesian tools can be leveraged to gain insights on a complex dynamic process.

SOE 6.10 Mon 17:30 H18

Recurrence-based analysis of instantaneous fractal characteristics of geomagnetic variability — •REIK V. DONNER^{1,2}, TOMMASO ALBERTI³, and DAVIDE FARANDA⁴ — ¹Hochschule Magdeburg-Stendal, Magdeburg, Germany — ²Potsdam Institute for Climate Impact Research, Potsdam, Germany — ³National Institute for Astrophysics, Rome, Italy — ⁴LSCE, Université Paris-Saclay, Gif-sur-Yvette, France

We employ two complementary approaches based on the concept of recurrences in phase space to quantify the local (instantaneous) and global fractal dimensions of the temporal variations of a suite of low (SYM-H, ASY-H) and high latitude (AE, AL, AU) geomagnetic indices and discuss similarities and dissimilarities of the obtained patterns for one year of observations during a solar activity maximum. Subsequently, we introduce bivariate extensions of both approaches, and demonstrate their capability of tracing different levels of interdependency between low and high latitude geomagnetic variability during periods of magnetospheric quiescence and along with perturbations associated with geomagnetic storms and magnetospheric substorms, respectively. Our results open new perspectives on the nonlinear dynamics and intermittent mutual entanglement of different parts of the geospace electromagnetic environment, including the equatorial and westward auroral electrojets, in dependence of the overall state of the geospace system affected by temporary variations of the solar wind forcing.

SOE 7: Big Data and Artificial Intelligence (joint session SOE/DY)

Time: Monday 17:45–18:15

Location: H18

SOE 7.1 Mon 17:45 H18

Revealing interactions between HVDC cross-area flows and frequency stability with explainable AI — •SEBASTIAN PÜTZ^{1,2}, BENJAMIN SCHÄFER³, DIRK WITTHAUT^{1,2}, and JOHANNES KRUSE^{1,2} — ¹Forschungszentrum Jülich, Institute for Energy and Climate Research - Systems Analysis and Technology Evaluation (IEK-STE), 52428 Jülich, Germany — ²Institute for Theoretical Physics, University of Cologne, 50937 Köln, Germany — ³Karlsruhe Institute of Technology, Institute for Automation and Applied Informatics (IAI), 76344 Eggenstein-Leopoldshafen, Germany

The energy transition introduces more volatile energy sources into the power grids. In this context, power transfer between different synchronous areas through High Voltage Direct Current (HVDC) links becomes increasingly important. Such links can balance volatile generation by enabling long-distance transport or by leveraging their fast control behavior. Here, we investigate the interaction of power imbalances - represented through the power grid frequency - and power flows on HVDC links between synchronous areas in Europe. We use explainable machine learning to identify key dependencies and disentangle the interaction of critical features. Our results show that market-based HVDC flows introduce deterministic frequency deviations, which however can be mitigated through strict ramping limits. Moreover, varying HVDC operation modes strongly affect the interaction with the grid. In particular, we show that load-frequency control via HVDC links can both have control-like or disturbance-like impacts on frequency stability.

SOE 7.2 Mon 18:00 H18

From sample management to workflow integration: Semantic research data management in glaciology. — •FLORIAN SPRECKEISEN¹, DANIEL HORNING¹, and JOHANNES FREITAG² — ¹IndiScale GmbH, Göttingen — ²Alfred Wegener Institute, Helmholtz Centre for Polar and Marine Research, Bremerhaven

Organizing data from a diversity of sources, from acquisition to publication, can be a tough challenge. We present implementations with the flexible open-source research data management toolkit CaosDB in the glaciology department at the Alfred Wegener Institute (AWI) in Bremerhaven. CaosDB is used in a diversity of fields such as turbulence physics, legal research, animal behavior and glaciology. CaosDB links research data, makes it findable and retrievable, and keeps data consistent, even if the data model changes.

At AWI, CaosDB keeps track of ice core samples and to whom samples are loaned for analyses. It made possible additional features such as: A revision system to track all changes to the data and the sample state at the time of analysis. Automated gathering of information for the publication in FAIR-DO meta-data repositories, e.g. Pangaea. Tools for storing, displaying and querying geospatial information and graphical summaries of all analyses performed on each ice core. Automatic data extraction and refinement into data records in CaosDB to minimize manual users interaction. A state machine which guarantees certain workflows, simplifies development and can be extended to trigger additional actions upon transitions.

We demonstrate how CaosDB simplifies semantic data in science.

SOE 8: Invited Talk Theo Geisel: Human Synchronization in Music Performance

Time: Tuesday 9:30–10:15

Location: H11

Invited Talk

SOE 8.1 Tue 9:30 H11

Musicians' Synchronization and the Enigma of Swing — •THEO GEISEL — Max Planck Institute for Dynamics and Self-Organization & Bernstein Center for Computational Neuroscience Göttingen, Germany

It is a widespread opinion that musicians who are interacting together in a performance should perfectly synchronize their timing. This view was challenged for the swing feel, a salient feature of jazz, which has eluded scientific clarification for a century. For much of this period it was considered arcane, arguing that swing can be felt but not explained, until the theory of 'participatory discrepancies' raised the controversial claim that swing is caused by microtiming deviations between different participating musicians [1].

In several projects we have clarified the controversy on the central role of microtiming deviations for the swing feel using time series analysis and experiments with temporally manipulated MIDI-recordings, whose swing feel was measured through ratings of professional jazz musicians. We thereby showed that involuntary random microtiming deviations are irrelevant for swing, whereas a particular systematic microtiming deviation between musicians enhances the swing feel and is a key component of swing in jazz [2]. It consists in slightly delaying downbeats but not offbeats of soloists with respect to a rhythm section. This effect was unknown to professional jazz musicians, who are using it unconsciously but were unable to determine its nature.

[1] C. Keil, *Cultural Anthropology* 2, 275 (1987).

[2] C. Nelias et al., *Commun. Phys.*, to be publ.

SOE 9: Physics of Contagion Processes

Time: Tuesday 10:15–11:15

Location: H11

SOE 9.1 Tue 10:15 H11

Emergence of synergistic and competitive pathogens in a coevolutionary spreading model — •PHILIPP HÖVEL¹, ALESSIO CARDILLO², KAI SEEGER³, and FAKHTEH GHANBARNEJAD⁴ — ¹University College Cork, Ireland — ²Universitat Rovira i Virgili, Tarragona, Spain — ³Technische Universität Berlin, Germany — ⁴Sharif University of Technology, Iran

Cooperation and competition between pathogens can alter the amount of individuals affected by a coinfection giving rise to phenomena like comorbidity and cross-immunity. However, the evolution of the pathogens' behavior has been underexplored. We present a coevolutionary model where the simultaneous spreading is described by a two-pathogen susceptible-infected-recovered model in an either synergistic or competitive manner. At the end of each epidemic season, the pathogens species reproduce according to their fitness following a replicator equation. The fitness depends on the payoff accumulated during the spreading season in a hawk-and-dove game. We demonstrate that the proposed coevolutionary model displays a rich set of features and emergent behavior. For example, the evolution of the pathogens' strategy induces abrupt transitions in the epidemic prevalence. Furthermore, we observe that the long-term dynamics results in a single, surviving pathogen species, and that the cooperative behavior of pathogens can emerge even under unfavorable conditions.

SOE 9.2 Tue 10:45 H11

Assessing the effectiveness of COVID intervention measures in small communities using agent-based simulations — •JANA LASSER — Graz University of Technology, Graz, Austria — Complexity Science Hub Vienna, Vienna, Austria

The necessity of intervention measures like the wearing of masks, preventive testing and vaccinations to prevent the spread of COVID-19 have been vigorously in our societies. At the centre of these discussions is the effectiveness of these measures in suppressing large outbreaks. With our research, we contribute the necessary facts to the discussion by simulating the spread of COVID-19 using agent-based simulations that are calibrated to empirical outbreak data. Here we present three application cases of our simulations: (i) the development of a preventive testing strategy in nursing homes in a situation where no vaccinations are available yet, (ii) the assessment of the effectiveness of different combinations of measures in schools and (iii) an evaluation of the feasibility of preventing large outbreaks while requiring in-presence teaching in universities under the condition of community spreading of the Omicron variant.

SOE 9.3 Tue 11:00 H11

Epidemic processes on self-propelled particles — •JORGE P. RODRIGUEZ¹, MATTEO PAOLUZZI², DEMIAN LEVIS², and MICHELE STARNINI³ — ¹IMEDEA, CSIC-UIB, Esporles, Spain — ²Departament de Física de la Matèria Condensada, Universitat de Barcelona, Barcelona, Spain — ³ISI Foundation, Torino, Italy

Most spreading processes require spatial proximity between agents. The stationary state of spreading dynamics in a population of mobile agents thus depends on the interplay between the time and length scales involved in the epidemic process and their motion in space. We analyze the steady properties resulting from such interplay in a simple model describing epidemic spreading on self-propelled particles. The epidemic dynamics is described by a Susceptible-Infected-Susceptible model, while the movement of each particle is ruled by Run-and-Tumble motion. The interactions are given by the proximity between particles, with the particles'

movement modifying the relative distances between themselves. We analyze this problem from a continuum description of the system, and validate those results by numerical simulations of an agent-based model. Focusing our attention on the diffusive long-time regime, we find that the agents' motion changes qualitatively the nature of the epidemic transition characterized by the emergence of a

macroscopic fraction of infected agents. Indeed, the transition becomes of the mean-field type for agents diffusing in one, two and three dimensions, while, in the absence of motion, the epidemic outbreak depends on the dimension of the underlying static network determined by the agents' fixed locations.

SOE 10: Nonlinear Dynamics 1: Synchronization and Chaos (joint session DY/SOE)

Time: Tuesday 11:15–12:45

Location: H19

SOE 10.1 Tue 11:15 H19

Stable Poisson chimeras in networks of two subpopulations — •SEUNGJAE LEE and KATHARINA KRISCHER — Technical University of Munich, Garching, Germany

In this talk, we introduce recent results on dynamical and spectral properties of chimeras in two-population network based on Kuramoto order parameter and Lyapunov stability analysis. In particular, we address two qualitatively different dynamics of incoherent oscillator populations according to the given initial conditions, and which led to the classification of Poisson and non-Poisson chimera states. We numerically calculate the Lyapunov exponents and covariant Lyapunov vectors to determine the spectral properties of the chimera states, and then expound the classification of the Lyapunov exponents. Our stability analysis also confirms that the chimera states of Kuramoto-Sakaguchi phase oscillators in two-population networks are neutrally stable in many directions. Furthermore, we demonstrate that two 'perturbations' of the phase model that reflect more realistic situations render Poisson chimeras stable. These models consider a nonlocal intra-population network and Stuart-Landau planar oscillators with amplitude degrees of freedom, respectively. Both these 'perturbations' might be considered a heterogeneity of the phase model and give rise to an asymptotically attracting Poisson chimera in two-population networks.

SOE 10.2 Tue 11:30 H19

On rational reactions - and other ones - of overloaded magnetic gears — •INGO REHBERG and STEFAN HARTUNG — Universität Bayreuth

Experiments exploring the coupling of two rotating spherical magnets reveal a cogging-free coupling for two specific angles between the input and output rotation axes. The striking difference between these two phase-locked modes of operation is the reversed sense of rotation of the driven magnet. For other angles, the cogging leads to a more complex dynamical behaviour. The experimental results can be understood by a mathematical model based on pure dipole-dipole interaction, with the addition of adequate friction terms [1].

Like all magnetic couplings, the setup contains intrinsic overload protection. The dynamic answer of the gear with cogging to an overload shows a plethora of modes of the driven magnet.

[1] Dynamics of a magnetic gear with two cogging-free operation modes, Stefan Hartung & Ingo Rehberg, *Archive of Applied Mechanics* 91, 1423-1435 (2021).

SOE 10.3 Tue 11:45 H19

Heteroclinic units acting as pacemakers: Entrained dynamics for cognitive processes — •BHUMIKA THAKUR and HILDEGARD MEYER-ORTMANN — School of Science, Jacobs University Bremen, Campus Ring 1, 28759 Bremen, Germany
Heteroclinic dynamics is a suitable framework for describing transient and reproducible dynamics such as cognitive processes in the brain. We demonstrate how heteroclinic units can act as pacemakers to entrain larger sets of units from a resting state to hierarchical heteroclinic motion that is able to describe fast oscillations modulated by slow oscillations, features which are observed in brain dynamics. The entrainment range depends on the type of coupling, the spatial location of the pacemaker and the individual bifurcation parameters of the pacemaker and the driven units. Noise as well as a small back-coupling to the pacemaker facilitate synchronization. Units can be synchronously entrained to different temporal patterns, depending on the selected path in the hierarchical heteroclinic network. These locally generated temporal sequences of information items can be transferred over a spatial grid by entrainment to the pacemaker dynamics. Such spatiotemporal patterns are believed to code informa-

tion in brain dynamics. Depending on the number and location of pacemakers on two-dimensional grids, synchronization can be maintained in the presence of a large number of resting state units and mediated via target waves when the pacemakers are concentrated to a small area of such grids. In view of brain dynamics, our results indicate a possibly ample repertoire for coding information in temporal patterns.

SOE 10.4 Tue 12:00 H19

Suppression of quasiperiodicity in circle maps with quenched disorder — •DAVID MÜLLER-BENDER¹, JOHANN LUCA KASTNER¹, and GÜNTER RADONS^{1,2} — ¹Institute of Physics, Chemnitz University of Technology, 09107 Chemnitz, Germany — ²Institute of Mechatronics, 09126 Chemnitz, Germany

We show that introducing quenched disorder into a circle map leads to the suppression of quasiperiodic behavior in the limit of large system sizes. Specifically, for most parameters the fraction of disorder realizations showing quasiperiodicity decreases with the system size and eventually vanishes in the limit of infinite size, where almost all realizations show mode-locking. Consequently, in this limit, and in strong contrast to standard circle maps, almost the whole parameter space corresponding to invertible dynamics consists of Arnold tongues.

Details can be found in the preprint D. Müller-Bender, J. L. Kastner, and G. Radons, *Suppression of quasiperiodicity in circle maps with quenched disorder*, arXiv:2204.09392 [nlin.cd] (2022).

SOE 10.5 Tue 12:15 H19

Reservoir Computing and Nonlinear Dynamics — •ULRICH PARLITZ — Max Planck Institute for Dynamics and Self-Organization, Göttingen, Germany — Institute for the Dynamics of Complex Systems, Georg-August-Universität Göttingen, Göttingen, Germany

We discuss the interrelation between reservoir computing (RC) and nonlinear dynamics (NLD). On the one hand, the performance of RC can be characterized and improved by concepts from NLD such as generalized synchronization and delay embedding. On the other hand, RC can be used to predict and control dynamical systems, including hybrid architectures that employ physically informed machine learning. Various aspects of this mutual relationship between RC and NLD are illustrated using low-dimensional and spatially extended chaotic dynamical systems.

SOE 10.6 Tue 12:30 H19

Chameleon attractors in deterministic and stochastic Lorenz-63 systems — •REIK V. DONNER^{1,2}, TOMMASO ALBERTI³, and DAVIDE FARANDA⁴ — ¹Hochschule Magdeburg-Stendal, Magdeburg, Germany — ²Potsdam Institute for Climate Impact Research, Potsdam, Germany — ³National Institute for Astrophysics, Rome, Italy — ⁴LSCE, Université Paris-Saclay, Gif-sur-Yvette, France
The dynamical characteristics of a trajectory on a chaotic or stochastic attractor undergo marked changes when successively eliminating the low-frequency variability components and focusing on the fast fluctuations only, motivating the new concept of Chameleon attractors. Here, we study the time scale dependent instantaneous and average fractal characteristics of partial sums of dynamical modes identified by means of empirical mode decomposition for the Lorenz-63 system and two stochastic versions thereof with additive and multiplicative noise as obtained by exploiting recurrences in phase space using extreme value theory. While the average fractal dimensions converge to the expected values as more and more low-frequency modes are included, we find an excess dimension larger than 3 for higher frequency modes below the Lyapunov time scale resulting from the stochastic components.

SOE 11: Invited Talk Dirk Brockmann: Big Data in Epidemic Dynamics (joint session SOE/DY)

Time: Wednesday 9:30–10:15

Location: H11

Invited Talk

SOE 11.1 Wed 9:30 H11

The Corona Data Donation Project - When Citizens Collaborate to Fight a Pandemic — •DIRK BROCKMANN — Humboldt University of Berlin, Berlin, Germany

In response to the COVID-19 pandemic we launched the Corona Data Donation Project in April 2020. In this citizen science project participants donate physiological data on heart rate, sleep and physical activity measured by smart watches, fitness trackers and wearable devices on a daily bases. With more than

500,000 donors the project is the largest data donation project worldwide. Initially conceived as a tool for real-time syndromic surveillance of the Covid-19 pandemic and as a monitoring tool, it has evolved into a large scale experimental and exploratory technological framework that continues to reveal a number of fascinating insights concerning Covid-19 related topic such as Long-Covid, the

effects of vaccination, sleeping patterns but also insights with broader applications. The project now hosts physiological time-series that span over two years of over 200,000 individuals. I will discuss the promises and discoveries of citizen science and wearable devices from the perspective of digital epidemiology and illustrate what role "physics"-thinking plays in projects like this.

SOE 12: Networks: From Topology to Dynamics (joint session SOE/BP/DY)

Time: Wednesday 10:15–12:45

Location: H11

SOE 12.1 Wed 10:15 H11

Modeling tumor disease and sepsis by networks of adaptively coupled phase oscillators — •ECKEHARD SCHÖLL^{1,2,3}, JAKUB SAWICKI², RICO BERNER^{1,4}, and THOMAS LÖSER⁵ — ¹Institut für Theoretische Physik, TU Berlin, Germany — ²Potsdam Institute for Climate Impact Research — ³Bernstein Center for Computational Neuroscience Berlin — ⁴Institut für Physik, HU Berlin — ⁵Institut LOESER, Wettiner Straße 6, 04105 Leipzig

In this study, we provide a dynamical systems perspective to the modelling of pathological states induced by tumors or infection. A unified disease model is established using the innate immune system as the reference point. We propose a two-layer network model for carcinogenesis and sepsis based upon the interaction of parenchymal cells (organ tissue) and immune cells via cytokines, and the co-evolutionary dynamics of parenchymal, immune cells, and cytokines [1]. Our aim is to show that the complex cellular cooperation between parenchyma and stroma (immune layer) in the physiological and pathological case can be functionally described by a simple paradigmatic model of phase oscillators. By this, we explain carcinogenesis, tumor progression, and sepsis by destabilization of the healthy state (frequency synchronized), and emergence of a pathological state (multifrequency cluster). The coupled dynamics of parenchymal cells (metabolism) and nonspecific immune cells (reaction of innate immune system) are represented by nodes of a duplex layer. The cytokine interaction is modeled by adaptive coupling weights. [1] Sawicki, J., Berner, R., Löser, T., and Schöll, E., *Frontiers Netw. Physiology* 1,730385 (2022), arXiv:2106.13325v2.

SOE 12.2 Wed 10:45 H11

Analysis of the Football Transfer Market Network — •TOBIAS WAND — WWU Münster — CeNoS Münster

Football clubs buy and sell players for millions of Euros and until Covid, their combined transfer values were growing steadily at an impressive rate. Instead of analysing their aggregated transfer activities, one can take a look at the topology of the network of player transfers: complex networks have already been used in various sciences [1] including research on sports [2] and provide a novel approach to investigate the football transfer market network and in particular the impact of Covid on football clubs.

[1] G. Caldarelli and A. Vespignani, "Large Scale Structure and Dynamics of Complex Networks". World Scientific Publishing, 2007.

[2] Arriaza-Ardiles et al. "Applying graphs and complex networks to football metric interpretation". *Human Movement Science* 57, 2018.

SOE 12.3 Wed 11:00 H11

Variability in mesoscale structure inference using stochastic blockmodels — •LENA MANGOLD and CAMILLE ROTH — CNRS (Paris) / Centre Marc Bloch (Berlin)

Characterising the mesoscale structure of networks, in terms of patterns variously called communities, blocks, or clusters, has represented both a central issue and a key instrument in the study of complex systems. Clearly, distinct methods designed to detect different types of patterns may provide a variety of answers to the mesoscale structure. Yet, even multiple runs of a given method can sometimes yield diverse and conflicting results, posing challenges of model and partition selection. As an alternative to forcing a global consensus from a distribution of partitions (i.e. choosing one among many by maximising some objective), recent work has emphasised the importance of exploring the variability of partitions. Here we examine how a specific type of mesoscale structure (e.g. assortative communities or core-periphery) may be linked with more or less inconsistency in resulting partitions. We focus on Stochastic blockmodels (SBMs), initially proposed in mathematical sociology and increasingly used to infer mesoscale structure with a relatively general definition of similarity between nodes in the same group, and whose stochastic nature lends itself to the exploration of disagreement within populations of partitions. In particular, we generate families of synthetic networks in which we plant different types

of mesoscale structures and explore the transitions between consensus and disconsensus in the landscape of partitions over multiple SBM runs.

SOE 12.4 Wed 11:15 H11

Extracting signed relations from interaction data — •GEORGES ANDRES, GIONA CASIRAGHI, GIACOMO VACCARIO, and FRANK SCHWEITZER — ETH Zürich, Chair of Systems Design, Switzerland

Social relations influence human interactions and hence, help to explain individual behaviours. Moreover, humans perceive patterns of signed relations, either positive (e.g., friendship) or negative (e.g., enmity), and adapt to them. Data about signed relations are rare, despite their importance for understanding phenomena at the community level. Interaction data is, however, more abundantly available, for example, about proximity or communication events. Interactions and relations change on different time scales; interactions are more volatile and evolve faster than relations. Using this, I will present an ensemble-based approach to infer pair-wise signed relations from interaction data and consequently construct a signed network from them. By studying different datasets on interactions and relations, e.g. between students, I will further evaluate the quality of the inferred networks. Subsequently, I will study the presence of structural balance in the studied communities, describing the cognitive dissonance ensuing from particular triadic constellations of signed relations. Bearing similarities to frustrations in spin systems, structural balance can now be analysed solely from interaction data thanks to the presented method, a task which was previously out of reach.

SOE 12.5 Wed 11:45 H11

Disentangling homophily, community structure and triadic closure in networks — •TIAGO PEIXOTO — Central European University, Vienna, Austria

Network homophily, the tendency of similar nodes to be connected, and transitivity, the tendency of two nodes being connected if they share a common neighbor, are conflated properties in network analysis, since one mechanism can drive the other. Here we present a generative model and corresponding inference procedure that is capable of distinguishing between both mechanisms. Our approach is based on a variation of the stochastic block model (SBM) with the addition of a triadic closure dynamics, and its inference can identify the most plausible mechanism responsible for the existence of every edge in the network, in addition to the underlying community structure itself, based only on the final observation of the network. We show how the method can evade the detection of spurious communities caused solely by the formation of triangles in the network, and how it can improve the performance of link prediction when compared to the pure version of the SBM without triadic closure.

[1] Tiago P. Peixoto, Disentangling homophily, community structure and triadic closure in networks, *Phys. Rev. X* 12, 011004 (2022)

SOE 12.6 Wed 12:15 H11

Evolving networks towards complexity: an evolutionary optimization approach — ARCHAN MUKHOPADHYAY and •JENS CHRISTIAN CLAUSSEN — University of Birmingham, UK

Complexity measures for graphs have been proposed and compared [1,2] widely, but the question how to mathematically define complexity is less clear as for text strings where Lempel-Ziv and Kolmogorov complexity provide clear approaches. In complexity science, the notion of complexity implies distinction from regular structures (lattices) as well as from random structures (here: random graphs). This however has not lead to any constructive definition. Complexity measures therefore typically assess artefacts of complexity (in some cases quite successfully). Here we present a complementary computational approach: we utilize each complexity measure as a fitness function of an evolutionary algorithm, and investigate the properties of the resulting networks. The goal is a better understanding of the existing complexity measures, and to shed some light on (artificial) network evolution: what evolutionary goals lead to complexity?

SOE 13: Energy Networks (joint session SOE/DY)

Time: Wednesday 12:45–13:15

Location: H11

SOE 13.1 Wed 12:45 H11

Revealing drivers and risks for power grid frequency stability with explainable AI — •BENJAMIN SCHÄFER¹, JOHANNES KRUSE^{2,3}, and DIRK WITTHAUT^{2,3} — ¹Institute for Automation and Applied Informatics, Karlsruhe Institute of Technology, Eggenstein-Leopoldshafen, Germany — ²Forschungszentrum Jülich, Institute for Energy and Climate Research-Systems Analysis and Technology Evaluation (IEK-STE), Jülich, Germany — ³Institute for Theoretical Physics, University of Cologne, Köln, Germany

The transition to a sustainable energy system is challenging for the operation and stability of electric power systems as power generation becomes increasingly uncertain, grid loads increase, and their dynamical properties fundamentally change. At the same time, operational data are available at an unprecedented level of detail, enabling new methods of monitoring and control. To fully harness these data, advanced methods from machine learning must be used.

Here, we present explainable artificial intelligence (XAI) as a tool to quantify, predict, and explain essential aspects of power system operation and stability in three major European synchronous areas. We focus on the power grid frequency, which measures the balance of generation and load and thus provides the central observable for control and balancing. Combining XAI with domain knowledge, we identify the main drivers and stability risks, while our model and open dataset may enable further XAI research on power systems.

SOE 13.2 Wed 13:00 H11

Cascading Failures and Critical Infrastructures in Future Renewable Power Systems — FRANZ KAISER^{1,2}, JOHANNES KRUSE^{1,2}, •PHILIPP C. BÖTTCHER¹, MARTHA MARIA FRYSZTACKI³, TOM BROWN^{3,4}, and DIRK WITTHAUT^{1,2} — ¹IEK-STE Forschungszentrum Jülich, Jülich, Germany — ²THP Uni Köln, Köln, Germany — ³KIT-IAI, Karlsruhe, Germany — ⁴Institut für Energietechnik TU Berlin, Berlin, Germany

The world's power systems are undergoing a rapid transformation, shifting away from carbon-intensive power generation to renewable power sources. As a result, there is a growing importance of long-distance power transmission, while the intrinsic system inertia provided by thermal power plants decreases. This poses several challenges to the system such as accelerated dynamics and thus a higher control effort for transmission system operators. These developments make power grids more vulnerable to cascading failures, which may result in a splitting of the grid and eventually in a large-scale blackout. While large blackouts are rare but devastating events, several smaller splits were observed in recent years.

In this work, we use the state of the art open energy system model PyPSA to generate future energy systems and assess the risk of cascading failures and systems splits in the European power grid for different carbon reduction targets. We determine the likelihood of dangerous splits and discuss mitigation strategies.

SOE 14: Computational Social Science

Time: Wednesday 15:00–16:45

Location: H11

SOE 14.1 Wed 15:00 H11

Issue bundles: Understanding ideological patterns of polarization in political spaces. — •ECKEHARD OLBRICH¹ and SVEN BANISCH² — ¹Max Planck Institut für Mathematics in the Sciences, Leipzig, Germany — ²Institute of Technology Futures, Karlsruhe Institute of Technology, Germany

Many scholars of politics discuss the rise of the new populism in Western Europe and the US with respect to a new political cleavage related to globalization. In this contribution we empirically address this reconfiguration of the political space by comparing political spaces for Germany built using topic modeling with the spaces based on the content analysis of the Manifesto project and the corresponding categories of political goals. We find that both spaces have a similar structure and that the right-wing populist AfD appears on a new dimension. In order to characterize this new dimension we employ a novel technique to identify clusters of political goals, issue bundles, by maximizing the coherence of inter-issue consistency networks (IICN). These issue bundles allow to analyze the evolution of the correlations between the political positions on different issues over several elections. We find that the new dimension introduced by the AfD can be related to the split off of a new "culturally right" issue bundle from the previously existing center-right bundle.

E. Olbrich, and S. Banisch, The rise of populism and the reconfiguration of the German political space, *Frontiers in Big Data* 4, 731349 (2021).

SOE 14.2 Wed 15:30 H11

Quantifying the social dimension of citation behavior — •FRANK SCHWEITZER — Chair of Systems Design, ETH Zürich, Switzerland

Collaboration networks of scientists are a prime example of complex social systems. We study co-authorship networks to quantify the impact of social constituents, e.g. of previous co-authors, joint publications, on the success of publications as measured by their number of citations. This requires to solve different problems which are addressed in the talk: (i) to model growing networks with two coupled layers, the network of authors and the network of publications, (ii) to generate and test different hypotheses about the coupling between these two layers, (iii) to estimate parameters and compare models with different complexity. But it is worth the effort: After all, producing academic publications is a social endeavour, and our results shed more light on social feedback mechanisms and successful career paths of authors.

[1] V. Nanumyan, C. Gote, F. Schweitzer: Multilayer network approach to modeling authorship influence on citation dynamics in physics journals, *Physical Review E* 102, 032303 (2020)

[2] C. Zingg, V. Nanumyan, F. Schweitzer: Citations Driven by Social Connections? A Multi-Layer Representation of Coauthorship Networks, *Quantitative Science Studies* 1, 1493-1509 (2020)

SOE 14.3 Wed 16:00 H11

Idea engines: Innovation & obsolescence in markets, genetic evolution, science — •EDWARD LEE¹, CHRISTOPHER KEMPES², and GEOFFREY WEST² — ¹Complexity Science Hub Vienna, Vienna, Austria — ²Santa Fe Institute, Santa Fe, USA

Innovation and obsolescence describe dynamics of ever-churning and adapting systems from the development of economic markets and scientific progress to biological evolution. The shared aspect is that agents destroy and extend the "idea lattice" in which they live, finding new possibilities and rendering old solutions irrelevant. We focus on this aspect with a simple model to study the central relationship between the rates at which replicating agents discover new ideas and at which old ideas are rendered obsolete. When the rates match, the space of the possible (e.g. ideas, markets, technologies, mutations) is static. A positive or negative difference distinguishes flourishing, ever-expanding idea lattices from Schumpeterian dystopias in which the system collapses. We map the phase space in terms of rates at which agents enter, replicate, and die. With higher dimensions, cooperative agents, or obsolescence-driven innovation, we find that the essential features of the model are preserved. In all cases, we predict a density profile of agents that drops close to new and old frontiers. With data, we reveal that the density signals a follow-the-leader dynamic in firm cost efficiency and biological evolution, whereas scientific progress reflects consensus that waits on old ideas to go obsolete. We show how the fundamental forces of innovation and obsolescence provide a unifying perspective on complex systems.

SOE 14.4 Wed 16:15 H11

Loss of sustainability in scientific work — •NIKLAS REISZ¹, VITO DOMENICO PIETRO SERVEDIO¹, VITTORIO LORETO^{1,2,3}, WILLIAM SCHUELLER², MÁRCIA FERREIRA¹, and STEFAN THURNER^{1,4,5} — ¹Complexity Science Hub Vienna, Vienna, Austria — ²Sony Computer Science Lab, Paris, France — ³Sapienza University, Rome, Italy — ⁴Medical University of Vienna, Vienna, Austria — ⁵Santa Fe Institute, Santa Fe, USA

For decades the number of scientific publications has been rapidly increasing, effectively out-dating knowledge at a tremendous rate. Only few scientific milestones remain relevant and continuously attract citations. Here we quantify how long scientific work remains being utilized, how long it takes before today's work is forgotten, and how milestone papers differ from those forgotten. To answer these questions, we study the complete temporal citation network of all APS journals. We quantify the probability of attracting citations for individual publications. We capture both aspects, the forgetting and the tendency to cite already popular works, in a microscopic generative model. We find that the probability of citing a specific paper declines with age as a power law with an exponent of $\alpha = 1.4$. Whenever a paper in its early years can be characterized by a scaling exponent above a critical value, α_c , the paper is likely to become "ever-lasting". We validate the model with out-of-sample predictions. The model also allows us to predict that 95% of papers cited in 2050 have yet to be published. Our findings suggest a worrying tendency toward information overload and raises concerns about scientific publishing's long-term sustainability.

SOE 14.5 Wed 16:30 H11

On the empirical distribution functions of examination performance in beginning semesters in mathematics and physics — •MAGDA SCHIEGL — University of Applied Sciences Landshut, Am Lurzenhof 1, D-84036 Landshut
With increasing heterogeneity of student groups, the measurement and interpretation of individual study performance becomes more and more important,

both in terms of classification in group performance and under developmental aspects. We investigate the empirical distribution of study performance in the 1st and 2nd semesters of industrial engineering over several years. The basis of the study is the exam performance of large groups (approx. 100 students and more per year). We compare the subjects mathematics and physics. Characteristics of the empirical CDFs of the respective cohorts (year groups) are examined. The results are compared, summarised and interpreted.

SOE 15: Traffic Dynamics, Urban and Regional Systems

Time: Wednesday 17:00–18:15

Location: H11

SOE 15.1 Wed 17:00 H11

Gravity Model in Estimating Park Visitation Pre and during COVID-19 Pandemic — ZAHRA GHADIRI¹, AFRA MASHHADI², and •FAKHTEH GHANBARNEJAD^{1,3} — ¹Department of Physics, Sharif University of Technology, Tehran, Iran — ²Computing and Software Systems, University of Washington, Bothell, WA, USA — ³Chair for Network Dynamics, Institute for Theoretical Physics and Center for Advancing Electronics Dresden (cfaed), Technical University of Dresden, 01062 Dresden, Germany

The COVID-19 pandemic and the resulting economic recession have negatively affected many people's social, and psychological health. Parks may have ameliorated the negative effects of the pandemic by creating opportunities for outdoor recreation. At the same time, other public activities were restricted due to the risk of disease transmissions. In our study, we seek to improve our understanding of how the COVID-19 pandemic impacts park visitations by performing a longitudinal study based on the aggregated telecommunication data. To do so, we introduce a novel approach based on the Gravity Model to understand, quantify and model the relationship between distance and the visitation patterns. Particularly, we aim to find out how the park visitation behavior changes post-pandemic and how this change of visitation varies for different socio-economic groups of visitors. Our results show that the park visitation pattern in Washington state (U.S.A) obeys the gravity law. Moreover, we show that, although parameters of the model may vary, the gravity model can still accurately estimate the visitation after applying socio-economic and spatial filters.

SOE 15.2 Wed 17:30 H11

Bimodal transport: Making door-to-door transport sustainable and convenient — •PUNEET SHARMA^{1,2}, HELGE HEUER¹, STEFFEN MUEHLE¹, STEPHAN HERMINGHAUS^{1,2}, and KNUT HEIDEMANN¹ — ¹Max Planck Institute for Dynamics and Self Organization, Goettingen — ²Georg-August-Universität Göttingen

Decarbonization of passenger transport is essential for fighting climate emergency. While modern cities offer various modes of transportation, considered

separately, none of them is both, sustainable and convenient. A taxi service is convenient, in a sense, due to door-to-door service, but is inefficient since it usually serves one customer only. Demand-responsive ridepooling (DRRP) with minibuses is more efficient, but leads to undue competition with line services (LS), which provide even better pooling but are less convenient due to fixed routes and stops. A combination of both modes, DRRP and LS, may provide an ideal solution but is challenging to organize. Here we introduce a model for such bimodal on-demand transportation based on a square-grid geometry. Our model quantifies under what circumstances bimodal public transportation is feasible, both in terms of convenience and ecological footprint. Moreover, the model yields estimates for how to operate (LS frequency, modal split) a bimodal transportation system optimally. Perhaps surprisingly, we find that operating LS at maximum capacity is not necessarily optimal. We also consider the intricate interplay between LS operations and DRRP performance, i.e., detours, waiting times, and occupancy, via simulations.

SOE 15.3 Wed 17:45 H11

Urban road networks: Geometric characteristics and generative models — •REIK DONNER — Hochschule Magdeburg-Stendal, Magdeburg, Germany — Potsdam Institute for Climate Impact Research, Potsdam, Germany

Urban road networks provide the spatial backbone of the development of cities. As planar networks, they possess characteristic size, shape and orientation distributions of their basic constituting elements (road segments and cellular structures). Comparisons with simple benchmark planar graph models show that the latter commonly fail to mimic those characteristic features of the real-world networks, including heavy-tailed object size distributions, specific shapes of node and cell degree distributions, and the predominant orthogonality of street patterns. In order to account for these discrepancies, I introduce a hierarchy of planar network models combining the successive evolution of the network with a perpendicular splitting of road segments controlled by a spatial potential function. The resulting model networks can be used as benchmarks for generating *surrogate cities* for further testing dynamical models of urban traffic.

SOE 16: Members' Assembly

Annual General Assembly of SOE (all participants of SOE sessions are welcome). Agenda: 1. Report on Activities, 2. Announcements, 3. Elections, 4. Miscellaneous.

Time: Wednesday 18:15–19:30

Location: H11

All members of the Physics of Socio-economic Systems Division are invited to participate.

SOE 17: Poster

Time: Thursday 15:00–18:00

Location: P2

SOE 17.1 Thu 15:00 P2

CaosDB – a scientific research data management toolkit — •FLORIAN SPRECKELSEN¹, DANIEL HORNING¹, and JOHANNES FREITAG² — ¹IndiScale GmbH, Göttingen — ²Alfred Wegener Institute, Helmholtz Centre for Polar and Marine Research, Bremerhaven

Processing interconnected, multi-modal data poses a challenge in many fields, especially when the data model, i.e. the way how data is organized, changes over time or when its structure is poorly documented. The open-source software **CaosDB** is a toolkit for research data management which was originally developed at the Max Planck Institute for Dynamics and Self-Organization (Göttingen) because existing software could not fulfill the needs of the scientists.

We present examples where CaosDB helped make data FAIR (Findable, Accessible, Interoperable, Retrievable) and how it can simplify the workflows for researchers: Automated data collection and integration, export to data repositories, API libraries for third-party programs, integrated revisioning and workflow

state machines. If the data model needs to change, existing data can remain as-is and future search queries will return matching results containing “old” and “new” data. We demonstrate how raw and processed data, analysis settings and results, and even labnotebooks and publications can be linked against each other, to improve long-term usability of data and reproducibility of results.

We show how CaosDB can make semantic data AI ready in science.

SOE 17.2 Thu 15:00 P2

contagion dynamics of self-propelled particles in porous media — EHSAN IRANI¹, ABBAS SHOJAKANI², MOHADDESE SADAT ASGARI², and •FAKHTEH GHANBARNEJAD^{2,3} — ¹Max Delbrück Center for Molecular Medicine in the Helmholtz Association (MDC), The Berlin Institute for Medical Systems Biology (BIMSB), 10115 Berlin, Germany — ²Department of Physics, Sharif University of Technology, Tehran, Iran — ³Chair for Network Dynamics, Institute for Theoretical Physics and Center for Advancing Electronics Dresden (cfaed), Technical University of Dresden, 01062 Dresden, Germany

We investigate the effect of heterogeneous environment on the spread of disease in systems of active agents. Here we couple susceptible-infected-recovered (S-I-R) contagion dynamics to a system of self-propelled active particles with polar alignment, in the presence of randomly distributed obstacles. The heterogeneity of the environment is controlled by the density of obstacles. The temporal-spatial dynamics of the system is determined by the alignment strength and Peclet number as well as the density of the obstacles. We analyze how the heterogeneity of the environment results in rich set of spatial structures which significantly affect the epidemic dynamics of the disease. We further show that increasing the heterogeneity of the environment could change the outbreaks statistics in a non-monotonic way.

SOE 17.3 Thu 15:00 P2

Modelling discussion dynamics across Reddit communities — •RICCARDO CARLUCCI and JOÃO PINHEIRO NETO — Max Planck Institute for Dynamics and Self-Organization, Am Faßberg 17, 37077 Göttingen, Germany

Understanding the dynamics of online discussions is an important research challenge, not only in its own right but also in relation to e.g. the study of political polarization. With more than 20 million contributing monthly users, Reddit is one of the largest and most influential social media platforms in the world. Here we analyse the distribution of the number of comments-per-discussion within the largest 500 Reddit communities from an almost fully-sampled dataset, focusing on content created between 2019 and 2021. We find that about 60% of these communities exhibit a distribution which is well-approximated by a power-law with an upper exponential cut-off. However, the width and the exponent of the power-law regime are specific to each particular community. In order to explain this variability we develop a preferential attachment model where the ability of a discussion to attract comments is affected by its age and also by an intrinsic fitness value. After estimating aging and fitness from data, we find that the model is able to reproduce both non-power-law and power-law behaviour. In particular, the width and the exponent of the power-law regime are correlated with the average number of comments and discussion created per day in a community.

SOE 17.4 Thu 15:00 P2

Population dynamics and Nash equilibria in optimizing complexity measures — •ARCHAN MUKHOPADHYAY and JENS CHRISTIAN CLAUSSEN — University of Birmingham, UK

Do natural networks evolve towards complexity? In a related project (Mukhopadhyay and Clausen, to be submitted) we utilize graph complexity measures as fitness function for an evolutionary algorithm. This effectively leads to an evolutionary dynamics between complexity measures as "species" or "strategies". Here we rephrase each complexity measure value from the numerical simulations (when optimizing towards another complexity measure as co-evolutionary fitness value of one species within a population where another species is highly abundant). We analyze the resulting payoff matrix with respect

to their Nash equilibria and evolutionarily stable strategies, if interpreted within the context of evolutionary game theory.

SOE 17.5 Thu 15:00 P2

Die Nützlichkeit der mathematischen Begriffstheorie von E.K. Vojschvillo zur Kulturwissenschaft und Gender-Studies — •MARINA ZAKHARCHUK — Moskau, Russland

In der mathematischen Logik gibt es eine Begriffstheorie von E.K. Vojschvillo, die heute von D.V. Zaitsev und A.A. Iljin entwickelt wird, die die Begriffen als Mengen analysiert. Dieses Begriffsverständnis kann mit einem Venn-Diagramm dargestellt werden. Diese Theorie kann man auch in der Kunstforschung benutzen. Wir zeigen, wie das beschriebene Schema konkret zur Klassifizierung von Drag-Künstlern angewendet werden kann. Als Parameter nehmen wir das biologische Geschlecht einer Person und das Geschlecht ihrer Spielfigur. Wir unterteilen jeden der Parameter dichtomisch: biologisch ein Mann, biologisch kein Mann; Spielfigur ist ein Mann, Spielfigur ist kein Mann. Dieses Schema umfasst Bioqueen, Bioking, Drag Queen, Drag King sowie Künstler, die sich keiner dieser Klassen zuordnen. Darüber hinaus kann das Schema erweitert werden, indem eine Unterteilung nach der Modifikation der Grundlage eingeführt wird, wobei die Geschlechtsidentität des Künstlers als Grundlage genommen wird. Zum Beispiel: biologisch männlich -> Spielfigur ist nicht männlich -> Transgender. Diese Klassifikation ist innovativ und fortschrittlich im Bereich der Kulturwissenschaft und Gender-Studies; es ist übersichtlich und macht es einfacher zu definieren, wer welcher Drag-Künstler ist.

SOE 17.6 Thu 15:00 P2

Organisation der soziotechnischen Systeme mit dem industriellen Internet der Dinge (IIOT) — •DMITRII ABUSHEK — Moscow, Russia

Das Verwenden der Konzepte von Internet der Dinge kann helfen Kosten für Produktion und Entsorgung senken. Zum Beispiel, die Lösungen des Russischen Unternehmens "Strizh" als ein von mehreren. Auf Basis dieser Technologie können wir intelligente Gas-, Wasser- und Stromzähler erstellen. Die Erfassung und Analyse von Ressourcenverbrauchsdaten hilft uns, sie besser zu verwalten und Unfälle und Lecks zu erkennen. Die Grundlage der Plattform "Strizh" modifiziert die LPWAN Technologie. Dank der Energieeinsparung kann die Heizung der Wohnhäuser billiger werden, besonders in Systemen, in denen grüne Energie verwendet wird. Die Strizh-Plattform besteht aus Sensoren, Daten, und Auswertungsprogrammen unter XNB Protocol mit DBPSK Modulation. Sie kommunizieren miteinander und helfen Lösungen der unvermeidlichen zu machen. Die Einführung von IIOT bei Volvo ist zudem interessant. Das System von Volvo ermöglicht die Kommunikation zwischen Wagen, Volvo-Ingenieure, und Reparaturwerkstatt. Das ist möglich dank IIOT. Es verbessert die Qualität von Kundenservice. Aufgrund des kommerziellen Erfolges von IIOT kann man sagen dass diese Technologie eine große Zukunft hat.

SOE 18: Invited Talk Kathy Lüdge (joint session DY/SOE)

Time: Friday 9:30–10:00

Location: H19

See DY 48 for details of this session.

SOE 19: Machine Learning in Dynamics and Statistical Physics (joint session DY/SOE)

Time: Friday 10:00–11:15

Location: H19

See DY 51 for details of this session.

SOE 20: Nonlinear Dynamics 2: Stochastic and Complex Systems, Networks (joint session DY/SOE)

Time: Friday 11:30–12:45

Location: H19

SOE 20.1 Fri 11:30 H19

Thermodynamic uncertainty relations for many-body systems with fast jump rates and large occupancies — •OHAD SHPIELBERG¹ and ARNAB PAL² — ¹University of Haifa, Haifa, Israel. — ²Department of Physics, Indian Institute of Technology, Kanpur, India

The thermodynamic uncertainty relations constitute an important inequality, bounding the entropy production through current fluctuations. The results have been successfully applied, in particular for single body dynamics. Here we present uncertainty relations and other useful inequalities for the many body systems, in the limit of highly occupied systems. The resulting coarse grained theory also accounts for tighter inequalities than the single body case.

SOE 20.2 Fri 11:45 H19

Effects of measures on phase transitions in two cooperative susceptible-infectious-recovered dynamics — ADIB KHAZAEI¹ and •FAKHTEH GHANBARNEJAD^{1,2} — ¹Sharif University of Technology, Tehran, Iran — ²Chair for Network Dynamics, Institute for Theoretical Physics and Center for Advancing Electronics Dresden (cfaed), Technical University of Dresden, 01062 Dresden, Germany

In recent studies, it has been shown that a cooperative interaction in a co-infection spread can lead to a discontinuous transition at a decreased threshold. Here, we investigate effects of immunization with a rate proportional to the extent of the infection on phase transitions of a cooperative co-infection. We use the mean-field approximation to illustrate how measures that remove a portion of the susceptible compartment, like vaccination, with high enough rates

can change discontinuous transitions in two coupled susceptible-infectious-recovered dynamics into continuous ones while increasing the threshold of transitions. First, we introduce vaccination with a fixed rate into a symmetric spread of two diseases and investigate the numerical results. Second, we set the rate of measures proportional to the size of the infectious compartment and scrutinize the dynamics. We solve the equations numerically and analytically and probe the transitions for a wide range of parameters. We also determine transition points from the analytical solutions. Third, we adopt a heterogeneous mean-field approach to include heterogeneity and asymmetry in the dynamics and see if the results corresponding to homogeneous symmetric case stand. (Physical Review E 105 (3), 034311)

SOE 20.3 Fri 12:00 H19

ANDOR and beyond: Dynamically switchable logic gates as modules for flexible information processing in biochemical regulatory networks — •MOHAMMADREZA BAHADORIAN^{1,2} and CARL D. MODES^{1,2,3} — ¹Max Planck Institut for Molecular Cell Biology and Genetics (MPI-CBG), 01307 Dresden, Germany — ²Center for Systems Biology Dresden (CSBD), 01307 Dresden, Germany — ³Cluster of Excellence Physics of Life, TU Dresden, 01069 Dresden, Germany

Understanding how complex (bio-)chemical regulatory networks may be capable of processing information in flexible, yet robust ways is a key question with implications in biology and dynamical systems theory. Considerable effort has been focused on identification and characterization of structural and dynamical motifs of biological information processing, but a framework for studying flexibility and robustness of the motifs is lacking. We here propose a small set of effective modules capable of performing different logical operations based on the basin of attraction in which the system resides. These dynamically switchable logic gates require fewer components than their traditional analogs where static, separate gates are used for each desired function. We demonstrate the applicability and limits of these circuits by determining a robust range of parameters over which they correctly operate and then characterize their resilience against

intrinsic noise of the constituent reactions using the theory of large deviations. Trade-offs between multi-functionality and robustness against various types of noise are shown.

SOE 20.4 Fri 12:15 H19

Memory formation in adaptive networks — •KOMAL BHATTACHARYYA¹, DAVID ZWICKER¹, and KAREN ALIM^{1,2} — ¹Max Planck Institute for Dynamics and Self-Organization, 37077 Göttingen, Germany — ²Physik-Department, Technische Universität München, Garching, Germany

Continuous adaptation of networks like our vasculature ensures optimal network performance when challenged with changing loads. Here, we show that adaptation dynamics allow a network to memorize the position of an applied load within its network morphology. We identify that the irreversible dynamics of vanishing network links encode memory. Our analytical theory successfully predicts the role of all system parameters during memory formation, including parameter values which prevent memory formation. We thus provide an analytically tractable theory of memory formation in disordered systems.

SOE 20.5 Fri 12:30 H19

Inference of fractional nonlinear models from temperature time series and application to predictions — •JOHANNES A. KASSEL and HOLGER KANTZ — MPI for the Physics of Complex Systems, Dresden, Germany

We introduce a method to reconstruct macroscopic models of one-dimensional nonlinear stochastic processes with long-range correlations from sparsely sampled time series by combining fractional calculus and discrete-time Langevin equations. We reconstruct a model for daily mean temperature data recorded at Potsdam (Germany) and use it to predict the first frost date. Including the Arctic Oscillation Index as an external driver into our model, we predict extreme temperatures for several European weather stations, illustrating the potential of long-memory models for predictions in the subseasonal-to-seasonal range.

[1] Johannes A. Kassel and Holger Kantz, Phys. Rev. Research 4, 013206

Low Temperature Physics Division Fachverband Tiefe Temperaturen (TT)

Elke Scheer
Universität Konstanz
Fachbereich Physik
78457 Konstanz
elke.scheer@uni-konstanz.de

Overview of Invited Talks and Sessions

(Lecture halls H3, H10, H22, and H23; Poster P1)

Plenary Talk

PLV I Mon 8:30– 9:15 H1 **Intrinsic Josephson junctions in $\text{Bi}_2\text{Sr}_2\text{CaCu}_2\text{O}_8$: Generation of Terahertz radiation and beyond** — •REINHOLD KLEINER

Invited Talks

TT 1.1	Mon	9:30–10:00	H10	Stability of Floquet Majorana box qubits — •ANNE MATTHIES
TT 5.1	Mon	15:00–15:30	H10	Dynamics of visons and thermal Hall effect in perturbed Kitaev models — •APREM JOY
TT 10.1	Tue	9:30–10:00	H3	Two-fold symmetric superconductivity in few-layer NbSe_2 — •VLAD PRIBIAG
TT 10.2	Tue	10:00–10:30	H3	Spin-orbit coupling and triplet pairing in mesoscopic superconductors — •MARCO APRILI
TT 10.3	Tue	10:30–11:00	H3	Supercurrent diode effect in few-layer NbSe_2 — •NICOLA PARADISO
TT 10.4	Tue	11:15–11:45	H3	Superconducting devices in magic-angle twisted bilayer graphene — •FOLKERT DE VRIES
TT 10.5	Tue	11:45–12:15	H3	Minigap and Andreev bound states in ballistic graphene — •LUCA BANSZERUS
TT 16.1	Wed	9:30–10:00	H10	Multimethod, multimessenger approaches to models of strong correlations — •THOMAS SCHÄFER
TT 22.1	Wed	15:00–15:30	H10	Evidence for orbital loop current magnetism in Sr_2RuO_4 — •A. DI BERNARDO
TT 22.8	Wed	17:15–17:45	H10	Role of the film geometry in the electronic reconstruction of infinite-layer nickelates on $\text{SrTiO}_3(001)$ — •BENJAMIN GEISLER
TT 25.1	Thu	9:30–10:00	H3	Topology: Open and with diverse backgrounds — •TOBIAS MENG
TT 28.5	Thu	10:30–11:00	H23	Towards an <i>ab-initio</i> theory of Anderson localization for correlated electrons — •LIVIU CHIONCEL
TT 32.1	Thu	15:00–15:30	H10	Supercurrents in HgTe-based topological nanowires — •DIETER WEISS
TT 32.2	Thu	15:30–16:00	H10	Majorana bound states and non-reciprocal transport in topological insulator nanowire devices — •HENRY LEGG
TT 32.3	Thu	16:00–16:30	H10	Integration of topological insulator Josephson junctions in superconducting qubit circuits — •TOBIAS W. SCHMITT
TT 32.4	Thu	16:45–17:15	H10	Universal fluctuations of the induced superconducting gap in an elemental nanowire — •MATTHIEU DELBECQ
TT 32.5	Thu	17:15–17:45	H10	Exploring the full potential of edge channel transport in HgTe based two-dimensional topological insulators — •SAQUIB SHAMIM
TT 36.1	Fri	9:30–10:00	H10	Coherent control of lattice and electronic states — •STEVEN JOHNSON
TT 36.2	Fri	10:00–10:30	H10	New opportunities for light-matter control of quantum materials — •MICHAEL SENTEF
TT 36.3	Fri	10:30–11:00	H10	Coherent electronic control of an insulator-to-metal transition — •CLAUDIO GIANNETTI
TT 36.4	Fri	11:15–11:45	H10	Nanoscale transient magnetization dynamics: A comprehensive EUV TG study — •LAURA FOGLIA
TT 36.5	Fri	11:45–12:15	H10	Ultrafast magnetism of antiferromagnets — •ALEXEY KIMEL

Invited Talks of the joint Symposium **Frontiers of Orbital Physics: Statics, Dynamics, and Transport of Orbital Angular Momentum (SYOP)**

See SYOP for the full program of the symposium.

SYOP 1.1 Mon 9:30–10:00 H1 **Orbital degeneracy in transition metal compounds: Jahn-Teller effect, spin-orbit coupling and quantum effects** — •DANIEL KHOMSKII

SYOP 1.2	Mon	10:00–10:30	H1	Orbital magnetism out of equilibrium: driving orbital motion with fluctuations, fields and currents — •YURIY MOKROUSOV
SYOP 1.3	Mon	10:30–11:00	H1	Orbitronics: new torques and magnetoresistance effects — •MATHIAS KLÄUI
SYOP 1.4	Mon	11:15–11:45	H1	Orbital and total angular momenta dichroism of the THz vortex beams at the antiferromagnetic resonances — •ANDREI SIRENKO
SYOP 1.5	Mon	11:45–12:15	H1	Observation of the orbital Hall effect in a light metal Ti — •GYUNG-MIN CHOI

Invited Talks of the joint Symposium SKM Dissertation Prize 2022 (SYSD)

See SYSD for the full program of the symposium.

SYSD 1.1	Mon	10:15–10:45	H2	Charge localisation in halide perovskites from bulk to nano for efficient optoelectronic applications — •SASCHA FELDMANN
SYSD 1.2	Mon	10:45–11:15	H2	Nonequilibrium Transport and Dynamics in Conventional and Topological Superconducting Junctions — •RAFFAEL L. KLEES
SYSD 1.3	Mon	11:15–11:45	H2	Probing magnetostatic and magnetotransport properties of the antiferromagnetic iron oxide hematite — •ANDREW ROSS
SYSD 1.4	Mon	11:45–12:15	H2	Quantum dot optomechanics with surface acoustic waves — •MATTHIAS WEISS

Invited Talks of the joint Symposium United Kingdom as Guest of Honor (SYUK)

See SYUK for the full program of the symposium.

SYUK 1.1	Wed	9:30–10:00	H2	Structure and Dynamics of Interfacial Water — •ANGELOS MICHAELIDES
SYUK 1.2	Wed	10:00–10:30	H2	A molecular view of the water interface — •MISCHA BONN
SYUK 1.3	Wed	10:30–11:00	H2	Motile cilia waves: creating and responding to flow — •PIETRO CICUTA
SYUK 1.4	Wed	11:00–11:30	H2	Cilia and flagella: Building blocks of life and a physicist's playground — •OLIVER BÄUMCHEN
SYUK 1.5	Wed	11:45–12:15	H2	Computational modelling of the physics of rare earth - transition metal permanent magnets from SmCo_5 to $\text{Nd}_2\text{Fe}_{14}\text{B}$ — •JULIE STAUNTON
SYUK 2.1	Wed	15:00–15:30	H2	Hysteresis Design of Magnetic Materials for Efficient Energy Conversion — •OLIVER GUTFLEISCH
SYUK 2.2	Wed	15:30–16:00	H2	Non-equilibrium dynamics of many-body quantum systems versus quantum technologies — •IRENE D'AMICO
SYUK 2.3	Wed	16:00–16:30	H2	Quantum computing with trapped ions — •FERDINAND SCHMIDT-KALER
SYUK 2.4	Wed	16:45–17:15	H2	Breaking the millikelvin barrier in cooling nanoelectronic devices — •RICHARD HALEY
SYUK 2.5	Wed	17:15–17:45	H2	Superconducting Quantum Interference Devices for applications at mK temperatures — •SEBASTIAN KEMPF

Invited Talks of the joint Symposium Complexity and Topology in Quantum Matter (SYQM)

See SYQM for the full program of the symposium.

SYQM 1.1	Fri	9:30–10:00	H1	The role of crystalline symmetries in topological materials: the topological materials database — •MAIA VERGNIORY
SYQM 1.2	Fri	10:00–10:30	H1	Microwave Bulk and Edge Transport in HgTe-Based 2D Topological Insulators — •ERWANN BOCQUILLON
SYQM 1.3	Fri	10:30–11:00	H1	Spectral Sensitivity of Non-Hermitian Topological Systems — •JAN CARL BUDICH
SYQM 1.4	Fri	11:15–11:45	H1	Topological photonics and topological lasers with coupled vertical resonators — •SEBASTIAN KLEMBT
SYQM 1.5	Fri	11:45–12:15	H1	Spectroscopic Studies of the Topological Magnon Band Structure in a Skyrmion Lattice — •MARKUS GARST

Sessions

TT 1.1–1.13	Mon	9:30–13:15	H10	Topology: Majorana Physics
TT 2.1–2.14	Mon	9:30–13:15	H22	Nanotubes, Nanoribbons and Graphene
TT 3.1–3.13	Mon	9:30–13:00	H23	Superconductivity: Properties and Electronic Structure
TT 4.1–4.10	Mon	10:00–12:45	H20	Many-Body Quantum Dynamics 1 (joint session DY/TT)
TT 5.1–5.7	Mon	15:00–17:00	H10	Frustrated Magnets – Spin Liquids
TT 6.1–6.12	Mon	15:00–18:15	H22	Kondo Physics, f-Electron Systems and Heavy Fermions
TT 7.1–7.11	Mon	15:00–18:00	H23	Fluctuations, Noise, Magnetotransport, and Related Topics

TT 8.1–8.7	Mon	17:15–19:00	H10	Frustrated Magnets – Strong Spin-Orbit Coupling
TT 9.1–9.5	Mon	18:00–19:15	H23	Cold Atomic Gases and Superfluids
TT 10.1–10.9	Tue	9:30–13:15	H3	Focus Session: Superconductivity in 2d-Materials and their Heterostructures
TT 11.1–11.11	Tue	9:30–12:30	H10	Topology: Quantum Hall Systems
TT 12.1–12.13	Tue	9:30–13:00	H22	Correlated Electrons: Materials
TT 13.1–13.6	Tue	9:30–11:00	H23	Quantum Dots, Quantum Wires, Point Contacts
TT 14.1–14.6	Tue	11:30–13:00	H20	Many-Body Quantum Dynamics 2 (joint session DY/TT)
TT 15.1–15.6	Tue	11:15–12:45	H23	Nano- and Optomechanics
TT 16.1–16.13	Wed	9:30–13:15	H10	Correlated Electrons: Method Development
TT 17.1–17.9	Wed	9:30–12:00	H22	Cryogenic Detectors and Cryotechnique
TT 18.1–18.9	Wed	9:30–11:45	H23	Topological Insulators
TT 19.1–19.5	Wed	11:45–13:00	H23	Topological Superconductors
TT 20.1–20.11	Wed	15:00–18:00	P1	Topology: Poster Session
TT 21.1–21.38	Wed	15:00–18:00	P1	Correlated Electrons: Poster Session
TT 22.1–22.14	Wed	15:00–19:15	H10	Unconventional Superconductors
TT 23.1–23.13	Wed	15:00–18:30	H22	Frustrated Magnets - General
TT 24.1–24.15	Wed	15:00–19:00	H23	Quantum-Critical Phenomena
TT 25.1–25.13	Thu	9:30–13:15	H3	Topological Semimetals
TT 26.1–26.13	Thu	9:30–13:00	H10	Superconductivity: Tunnelling and Josephson Junctions
TT 27.1–27.11	Thu	9:30–12:30	H22	Quantum Coherence and Quantum Information Systems (joint session TT/DY)
TT 28.1–28.12	Thu	9:30–13:00	H23	Correlated Electrons: Theory 1
TT 29.1–29.18	Thu	15:00–18:00	P1	Transport: Poster Session
TT 30.1–30.24	Thu	15:00–18:00	P1	Superconductivity: Poster Session
TT 31.1–31.26	Thu	15:00–18:00	P1	Superconducting Electronics and Cryogenics: Poster Session
TT 32.1–32.8	Thu	15:00–18:30	H10	Focus Session: Topological Devices (joint session TT/KFM)
TT 33.1–33.12	Thu	15:00–18:15	H22	Nonequilibrium Quantum Many-Body Systems (joint session TT/DY)
TT 34.1–34.14	Thu	15:00–18:45	H23	Correlated Electrons: Theory 2
TT 35	Thu	19:00–20:00	H22	Members' Assembly
TT 36.1–36.5	Fri	9:30–12:15	H10	Focus Session: Ultrafast Spin, Lattice and Charge Dynamics of Solids
TT 37.1–37.14	Fri	9:30–13:15	H22	Superconducting Electronics: SQUIDS, Qubits, Circuit QED
TT 38.1–38.6	Fri	9:30–11:00	H23	Superconductivity: Theory
TT 39.1–39.8	Fri	11:15–13:15	H23	Correlated Electrons: Charge Order

Members' Assembly of the Low Temperature Physics Division

Thursday 19:00–20:00 H22

- Bericht
- Verschiedenes

I gratefully acknowledge the invaluable support of R. Hott in composing the program. Many thanks to the former divisional spokespersons C. Enss and U. Eckern for their careful cross reading and advice.

Sessions

– Invited Talks, Contributed Talks, and Posters –

TT 1: Topology: Majorana Physics

Time: Monday 9:30–13:15

Location: H10

Invited Talk

TT 1.1 Mon 9:30 H10

Stability of Floquet Majorana box qubits — •ANNE MATTHIES — Institute for Theoretical Physics, University of Cologne, Germany

A topological superconductor in one dimension can host Majorana zero modes at its edge. By driving the system periodically, so-called π modes (also named Floquet-Majoranas) can arise. These are topologically protected modes with the quasi-energy π/T , where T is the period of the drive. We consider the role of π modes in the presence of long-range Coulomb interactions and therefore study a Cooper pair box made of two Josephson coupled superconducting topological quantum wires. Time-dependent gate voltages periodically drive the system and can induce π modes. The presence of four Majoranas and four π Majoranas in our setup allows us to define three topological qubits in a fixed fermion parity sector within one single box. We investigate how to obtain and control the π modes and study their stability in the presence of interactions. The stability of the Floquet-Majorana box qubit depends crucially on the initialization of the Floquet state. If the system is prepared by adiabatically increasing the amplitude of the oscillating gate voltage, the topological Floquet phase is always inherently unstable. The instability arises due to resonant quasi-particle creation mediated by interactions. However, a stable Floquet phase can be reached by using a two-step protocol. First, the amplitude of the oscillating gate voltage is adiabatically increased, while the frequency of the oscillation is small. Then, the oscillation frequency is increased slowly. With this frequency-sweep protocol, we can achieve a stable Floquet device despite interactions.

[1] PRL 128, 127702

TT 1.2 Mon 10:00 H10

Quantized phase-coherent heat transport of counterpropagating Majorana modes — ALEXANDER G. BAUER¹, BENEDIKT SCHARF², LAURENS W. MOLENKAMP³, EWELINA M. HANKIEWICZ², and •BJÖRN SOTHMANN¹ — ¹Theoretische Physik, Universität Duisburg-Essen and CENIDE, D-47048 Duisburg, Germany — ²Institute of Theoretical Physics and Astrophysics and Würzburg-Dresden Cluster of Excellence ct.qmat, University of Würzburg, Am Hubland, 97074 Würzburg, Germany — ³Experimentelle Physik III, Physikalisches Institut, Universität Würzburg, Am Hubland, D-97074 Würzburg, Germany

We demonstrate that phase-coherent heat transport constitutes a powerful tool to probe Majorana physics in topological Josephson junctions. We predict that the thermal conductance transverse to the direction of the superconducting phase bias is universally quantized by half the thermal conductance quantum at phase difference $\phi = \pi$. This is a direct consequence of the parity-protected counterpropagating Majorana modes which are hosted at the superconducting interfaces. Away from $\phi = \pi$, we find a strong suppression of the thermal conductance due to the opening of a gap in the Andreev spectrum. This behavior is very robust with respect to the presence of magnetic fields. It is in direct contrast to the thermal conductance of a trivial Josephson junction which is suppressed at any phase difference ϕ .

[1] A. G. Bauer, B. Scharf, L. W. Molenkamp, E. M. Hankiewicz, B. Sothmann, Phys. Rev. B **104**, L201410 (2021)

TT 1.3 Mon 10:15 H10

Cookbook for perfect topological Majorana fermions — •PRATHYUSH P. PODUVAL^{1,2}, THOMAS L. SCHMIDT¹, and ANDREAS HALLER¹ — ¹University of Luxembourg, Luxembourg, Luxembourg — ²Indian Institute of Science, Bangalore, India

It has been demonstrated that Majorana corner modes of higher order topological insulators (HOTI) can be rotated by magnetic and superconducting pairing fields which pump the corner modes through the edges, and effectively realise a two-fold particle exchange [1]. These results are based on exact diagonalization of quadratic Hamiltonians that predict extended corner Majorana modes. Here, we show analytically that the topological phase of the 2D Majorana HOTI model can be adiabatically deformed to a scenario we dub "sweet spot limit", with perfectly localized Majorana corner modes. The existence of sweet spot limits are important for obtaining analytical solutions and also for possible experimental realizations with constraints on the total number of lattice nodes. Our findings are based on a systematic corner mode construction, which we apply to known lattice models in one and two spatial dimensions. The key idea is to obtain the typical lattice dimerization picture of the Hamiltonian matrix elements in a simultaneous eigenbasis of Majorana fermions and the symmetry operator which protects the corner modes. Based on our findings, we propose a novel 3D model featuring perfectly localized Majorana corner modes which avoids the dimen-

sional obstruction encountered in 2D and may pave the way towards braiding. [1] Phys. Rev. Res. **2**, 032068

TT 1.4 Mon 10:30 H10

Edge \mathbb{Z}_3 parafermions in fermionic lattices. — •RAPHAEL L R C TEIXEIRA^{1,2} and LUIS G G V DIAS DA SILVA¹ — ¹Instituto de Física - Universidade de Sao Paulo, Sao Paulo Brazil — ²Department of Physics and Materials Science Université du Luxembourg, Luxembourg, Luxembourg

Parafermions modes are non-Abelian anyons which were introduced as \mathbb{Z}_N generalizations of \mathbb{Z}_2 Majorana states. In particular, \mathbb{Z}_3 parafermions can be used to produce Fibonacci anyons, laying a path towards universal topological quantum computation. Due to their fractional nature, much of theoretical work on \mathbb{Z}_3 parafermions has relied on bosonization methods or parafermionic operators. In this work, we introduce a representation of \mathbb{Z}_3 parafermions in terms of purely fermionic models operators in the single-occupancy basis ($t - J$ regime). We establish the equivalency of a family of 1D-lattice fermionic models written in the $t - J$ model basis supporting free \mathbb{Z}_3 parafermionic modes at its ends. By using density matrix renormalization group calculations, we are able to characterize the topological phase transition and study the effect of local operators (doping and magnetic fields) on the spatial localization of the parafermionic modes and their stability. Moreover, we discuss the necessary ingredients towards realizing \mathbb{Z}_3 parafermions in strongly interacting electronic systems.

TT 1.5 Mon 10:45 H10

2π domain walls for tunable Majorana devices — •DANIEL HAUCK¹, STEFAN REX^{2,3}, and MARKUS GARST¹ — ¹Karlsruhe Institute of Technology, Institute for Theoretical Solid State Physics, Wolfgang-Gaede-Str. 1, 76131 Karlsruhe — ²Institute for Quantum Materials and Technologies, Karlsruhe Institute of Technology, 76021 Karlsruhe, Germany — ³Institute for Theoretical Condensed Matter Physics, Karlsruhe Institute of Technology, 76131 Karlsruhe

Superconductor-magnet hybrid structures provide a platform for investigating topological phases with localized Majorana states. Such states have previously been predicted for elongated Skyrmions in the magnetic layer. Here we consider 2π domain walls which are easier to realize and tweak experimentally. We show that localized Majorana states can be found in these systems and investigate possible ranges of parameters. This establishes 2π domain walls as tunable elements for the realization of Majorana devices.

TT 1.6 Mon 11:00 H10

Fraunhofer pattern in the presence of Majorana modes — •FERNANDO DOMINGUEZ¹, ELENA G. NOVIK², and PATRIK RECHER^{1,3} — ¹Institute for Mathematical Physics, TU Braunschweig, Germany — ²Institute of Theoretical Physics, Technische Universität Dresden, Germany — ³Laboratory for Emerging Nanometrology, Braunschweig, Germany

We investigate signatures of the presence of Majorana bound states that can arise in the Fraunhofer pattern of Josephson junctions made of Top.Sc/Qu.Spin Hall/Top.Sc. In this setup, the presence of Majorana bound states at the NS interfaces introduces electron-hole reflections with parallel spin, which due to spin-momentum locking, are forced to take place between opposite edges. In contrast to local electron-hole reflections (with opposite spin), the presence of such non-local processes do not accumulate a geometrical phase and therefore, they can change drastically or partially the periodicity of the Fraunhofer pattern. In order to observe such a change in the Fraunhofer pattern, the quantum spin-Hall edges have to be coupled either directly or through the bulk. Here, we propose two different scenarios where this can occur and provide numerical results from a scattering and tight-binding models.

15 min. break

TT 1.7 Mon 11:30 H10

Photonic noise as a probe of Majorana bound states — •LENA BITTERMANN¹, FERNANDO DOMINGUEZ¹, and PATRIK RECHER^{1,2} — ¹Institut für Mathematische Physik, Technische Universität Braunschweig, D-38106 Braunschweig, Germany — ²Laboratory for Emerging Nanometrology Braunschweig, D-38106 Braunschweig, Germany

We propose a route to detect Majorana bound states (MBSs) by coupling a topological superconductor to a quantum dot (QD) in a pn-junction. Here, two MBSs are coherently coupled to electrons on the QD, which recombine with holes in situ to photons. Importantly, the polarization of the emitted photons provides

direct information on the spin structure [1,2] and nonlocality [2,3] of the MBSs. Here, we focus on the shot noise of the emitted photons which allows to clearly distinguish the cases of well separated MBSs at zero energy from overlapping MBSs. In addition, we show that quasiparticle poisoning changes the shot noise from super-Poissonian to sub-Poissonian. Furthermore, this setup can be extended by coupling a second QD close to the second MBS which gives rise to more resonances in the shot noise leading to additional signatures of the MBSs. [1] D. Sticlet, C. Bena, P. Simon, PRL 108, 096802 (2012)
[2] E. Prada, R. Aguado, P. San-Jose, PRB 96, 085418 (2017)
[3] A. Schuray, L. Weithofer, P. Recher, PRB 96, 085417 (2017)

TT 1.8 Mon 11:45 H10

Zero energy modes of artificial spin chains from ab initio calculations — •BENDEGÚZ NYÁRI¹, ANDRÁS LÁSZLÓFFY², LÁSZLÓ SZUNYOGH¹, and BALÁZS ÚJFALUSSY² — ¹Department of Theoretical Physics, Budapest University of Technology and Economics, Hungary — ²Wigner Research Centre for Physics, Institute for Solid State Physics and Optics, Hungary

The conditions under which Majorana zero modes (MZM) appear and their physical properties in realistic materials have been of high interest over the past few years triggered by their possible applications as fault tolerant quantum bits. The MZMs are topological states corresponding to triplet pairing at zero energy emerging in an inner gap inside the superconducting gap. However, experimentally it is very challenging to identify MZMs based solely on the spectral properties. Ab initio calculations are able to reproduce the measured spectral quantities and provide additional information on the nature of the in-gap states reported in corresponding experiments.

In this work we present ab initio calculations in the superconducting state of the in-gap density of states and the singlet and triplet order parameters for Fe chains on Nb(110) surface covered by one monolayer of Au. The Fe chains are also assumed to be in various artificial spin-spiral states. In a wide range of the spin-spiral wavelength we find an inner gap with states at zero-energy and large triplet pairing order parameter. A similar behavior to previous studies based on tight-binding models further supports the conjecture that there are MZMs in this system.

TT 1.9 Mon 12:00 H10

Quantitative theory of Yu-Shiba-Rusinov states of magnetic adatoms on Nb(110) surface and various overlayers — •BALÁZS ÚJFALUSSY¹, ANDRÁS LÁSZLÓFFY¹, BENDEGÚZ NYÁRI², KYUNGWHA PARK³, and LASZLO SZUNYOGH² — ¹Wigner Research Centre for Physics, Budapest, Hungary — ²Budapest University of Technology, Budapest, Hungary — ³Department of Physics, Virginia Tech, Blacksburg, Virginia, USA

We present a fully relativistic first-principles-based theoretical approach for the calculation of the spectral properties of Fe, Co, Cr and Mn adatoms on the surface of Nb(110) substrate in the superconducting state, providing a material-specific framework for the investigation of the Yu-Shiba-Rusinov (YSR) states. We study the effect of spin-orbit coupling, the strength of the exchange field and induced moments. Furthermore, we attempt to explain certain features of the STM experiments, and to link some properties to the normal state density of states. In order to study the effect of the substrate, we provide results for the YSR states in the case of impurities on various Nb(110)/overlayer systems as well. We also study the formation of a zero-bias peak for single adatoms and dimers.

TT 1.10 Mon 12:15 H10

Matrix modelling of potential disorder effects on in-gap spectra of a vortex on a proximitized topological insulator surface — •ALEXANDER ZIESEN and FABIAN HASSLER — RWTH Aachen University, Aachen, Germany

We study a heterostructure of a three-dimensional topological insulator and an s-wave superconductor. If a single superconducting flux quantum is trapped on the proximitized surface of the topological insulator, it is theoretically predicted that a Majorana zero mode is hosted in this vortex core. To enable the usage of this non-Abelian anyon for quantum computation, it is essential to maximize the spectral gap between the Majorana zero mode and the first excited in-gap state. For clean systems tuned close to the charge neutrality point of the topological insulator and vortex radii close to the superconducting coherence length, this excitation gap is predicted to be comparable to the superconducting gap. On the other hand, for strongly disordered topological insulators, supersymmetric

σ -models of symmetry class BD predict a finite, but experimentally barely resolvable excitation gap. In this work, we build the bridge between both limits with a matrix description of an effective two-dimensional surface model for strong proximitization and potential disorder. With it, we quantify the amount of disorder tolerable in the system to allow for experimental resolution.

TT 1.11 Mon 12:30 H10

Steering Majorana braiding via skyrmion-vortex pairs: a scalable platform — JONAS NOTHHELPER¹, •SEBASTIÁN A. DÍAZ¹, STEPHAN KESSLER², TOBIAS MENG³, MATTEO RIZZI^{4,5}, KJETIL M. D. HALS⁶, and KARIN EVERSCHOR-SITTE¹ — ¹University of Duisburg-Essen, Duisburg, Germany — ²Johannes Gutenberg University of Mainz, Mainz, Germany — ³Technische Universität Dresden, Dresden, Germany — ⁴Forschungszentrum Jülich, Jülich, Germany — ⁵University of Cologne, Cologne, Germany — ⁶University of Agder, Grimstad, Norway

Majorana zero modes are quasiparticles that hold promise as building blocks for topological quantum computing. However, the litmus test for their detection, the observation of exotic non-abelian statistics revealed by braiding, has so far eluded experimental efforts. Here we take advantage of the fact that skyrmion-vortex pairs in superconductor-ferromagnet heterostructures harboring Majorana zero modes can be easily manipulated in two spatial dimensions. We adiabatically braid the hybrid topological structures and explicitly confirm the non-abelian statistics of the Majorana zero modes numerically using a self-consistent calculation of the superconducting order parameter. Our proposal of controlling skyrmion-vortex pairs provides the necessary leeway toward a scalable topological quantum computing platform.

[1] J. Nothhelfer, S. A. Díaz, S. Kessler, T. Meng, M. Rizzi, K. M. D. Hals, K. Everschor-Sitte, arXiv:2110.13983

TT 1.12 Mon 12:45 H10

Sachdev-Ye-Kitaev circuits for braiding and charging Majorana zero modes — •JAN BEHRENDTS¹ and BENJAMIN BÉRI^{1,2} — ¹TCM Group, Cavendish Laboratory, University of Cambridge, J.J. Thomson Avenue, Cambridge CB3 0HE, United Kingdom — ²DAMTP, University of Cambridge, Wilberforce Road, Cambridge CB3 0WA, United Kingdom

The Sachdev-Ye-Kitaev (SYK) model is an all-to-all interacting Majorana fermion model for many-body quantum chaos and the holographic correspondence. Here we construct fermionic all-to-all Floquet quantum circuits of random four-body gates designed to capture key features of SYK dynamics. Our circuits can be built using local ingredients in Majorana devices, namely, charging-mediated interactions and braiding Majorana zero modes. This offers an analog-digital route to SYK quantum simulations that reconciles all-to-all interactions with the topological protection of Majorana zero modes, a key feature missing in existing proposals for analog SYK simulation. We also describe how dynamical, including out-of-time-ordered, correlation functions can be measured in such analog-digital implementations by employing foreseen capabilities in Majorana devices.

TT 1.13 Mon 13:00 H10

Symplectic topological Kondo effect — •ELIO KOENIG¹, JUKKA VAYRYNEN², and GUANGJIE LI² — ¹Max-Planck-Institute for Solid State Research, Heisenbergstr. 1, 70569 Stuttgart, Germany — ²Purdue University, West Lafayette, IN 47907-2036, USA

The topological Kondo effect describes the stable, strongly coupled, non-Fermi liquid state obtained by screening a topological quantum dot, a so-called Majorana Cooper pair box, by means of external metallic leads. The symmetry group describing this exotic Kondo effect is the orthogonal group of rotations of real Majorana fermions. In this talk, I am going to present a symplectic topological Kondo effect, which, crucially, does not rely on the presence of Majorana modes. As I present in detail, this system can be implemented by coupling leads to a quantum dot consisting of a floating conventional s-wave superconductor coupled to spinful fermionic zero modes, as obtained e.g., in arrays of 1D topological insulators. Combining the solution of this problem at strong coupling with known results from Bethe Ansatz and conformal field theory demonstrates that this model harbors emergent anyonic excitations, including Fibonacci anyons, depending on the number of external leads. Importantly, the non-trivial physics is stable to anisotropies in the coupling to different leads.

TT 2: Nanotubes, Nanoribbons and Graphene

Time: Monday 9:30–13:15

Location: H22

TT 2.1 Mon 9:30 H22

Magnetic field control of the Franck-Condon coupling of few-electron quantum states — PETER L. STILLER, DANIEL R. SCHMID, ALOIS DIRNAICHER, and •ANDREAS K. HÜTTEL — Institute for Experimental and Applied Physics, Universität Regensburg, Regensburg, Germany

The longitudinal vibration of a suspended carbon nanotube has been observed many times in low temperature transport spectra via distinct harmonic Franck-Condon sidebands. Typically, strong Franck-Condon coupling has been attributed to disorder-induced or deliberately targeted charge localization. Here, we present the observation of a strong, tunable coupling in an ultra-clean car-

bon nanotube with $N = 1$ or $N = 2$ electrons in the conduction band. The clean transport spectrum allows a tentative identification of the electronic base quantum states according to their valley quantum number. Interestingly, the Franck-Condon coupling strength g , as extracted from our data, both depends on the magnetic field and on the precise electronic quantum states participating in transport. While spin-dependent Franck-Condon phenomena have already been observed, our results clearly point towards a valley-dependent origin. As possible cause of this phenomenon, re-shaping of the electronic wavefunction envelope by the magnetic field is discussed. A simple calculation demonstrates that variations of g as observed in the experiment can be reproduced by the theory, paving the way towards more realistic and detailed quantum-mechanical modelling.

TT 2.2 Mon 9:45 H22

Transparent low-temperature contacts to MoS₂ microtubes — •ROBIN T. K. SCHOCK¹, JONATHAN NEUWALD¹, MATTHIAS KRONSEDER¹, SIMON REINHARDT¹, LUKA PIRKER², MAJA REMŠKAR², and ANDREAS K. HÜTTEL¹ — ¹Institute for Experimental and Applied Physics, University of Regensburg, 93040 Regensburg, Germany — ²Solid State Physics Department, Institute Jožef Stefan, 1000 Ljubljana, Slovenia

Even though synthesis procedures of transition metal dichalcogenide (TMDC) based nanotubes have been established for many years, the quantum transport properties remain largely unexplored to date. First low-temperature transport spectroscopy results clearly show Coulomb blockage at 300 mK [1]. However, the contact material still remains a limiting factor due to the Fermi level pinning near the conduction band. Recently, for planar MoS₂ materials [2], the use of bismuth improved room-temperature contact resistances drastically. Here we present first transport measurements on MoS₂ microtubes with bismuth contacts at millikelvin temperatures. Our MoS₂ tubes are grown via a chemical transport reaction, yielding diameters down to 7 nm and lengths up to several millimeters. After transferring the tubes onto a Si/SiO₂ substrate, contacts are deposited using electron beam lithography. The resulting devices show Coulomb blockade, with in many cases, a transition from transparent conduction into a band gap. Disorder, compared with previous scandium-based devices, is significantly reduced.

[1] S. Reinhardt *et al.*, Phys. Stat. Sol. RRL **13**, 1900251 (2019)

[2] P. C. Shen *et al.*, Nature **593**, 211 (2021).

TT 2.3 Mon 10:00 H22

Topological transitions in dc+ac-driven superconductor nanotubes — •VLADIMIR M. FOMIN¹ and OLEKSANDR V. DOBROVOLSKIY² — ¹Institute for Integrative Nanosciences, Leibniz IFW Dresden, 01069 Dresden — ²Superconductivity and Spintronics Laboratory, Nanomagnetism and Magnonics, Faculty of Physics, University of Vienna, 1090 Vienna

A complex interplay of the patterns of superconducting screening currents with the 3D geometry unveils a plethora of emerging effects in the dynamics of topological defects in curved 3D superconductor nanoarchitectures [1]. We discuss topological transitions in the dynamics of vortices and slips of the phase of the order parameter in open superconductor nanotubes under a modulated dc+ac transport current [2]. Relying upon the time-dependent Ginzburg-Landau equation, we reveal two voltage dynamics regimes. The first regime with a pronounced first harmonic in the FFT spectrum of the induced voltage occurs when the dominant area of the open tube is in the superconducting or normal state. The second regime entails a rich FFT spectrum of the induced voltage because of the complex interplay between the dynamics of vortices/phase slips and the screening currents. Our findings represent novel dynamical states in superconductor open nanotubes, in particular, paraxial and azimuthal phase-slip regions, their branching and coexistence with vortices, and allow for their control by superimposed dc+ac current stimuli.

[1] V. M. Fomin, O. V. Dobrovolskiy, Appl. Phys. Lett. **120**, 090501 (2022)

[2] V. M. Fomin, R. O. Rezaev, O. V. Dobrovolskiy, Scientific Reports **12**, accepted (2022)

TT 2.4 Mon 10:15 H22

Graphene nanomembranes as valleytronic devices — •NIKODEM SZPAK¹, WALTER ORTIZ^{2,3}, and THOMAS STEGMANN³ — ¹Fakultät für Physik, Universität Duisburg-Essen, Duisburg, Germany — ²Instituto de Investigación en Ciencias Básicas y Aplicadas, Universidad Autónoma del Estado de Morelos, Cuernavaca, Mexico — ³Instituto de Ciencias Físicas, Universidad Nacional Autónoma de México, Cuernavaca, México

We investigate the electronic transport in graphene nanoelectromechanical resonators (GrNEMS), known also as graphene nanodrums or nanomembranes. We demonstrate that these devices, despite small values of strain, between 0.1 and 1%, can be used as efficient and robust valley polarizers and filters. Their working principle is based on the pseudomagnetic field generated by the strain of the graphene membrane. They work for ballistic electron beams as well as for strongly dispersed ones and can be also used as electron beam collimators due to the focusing effect of the pseudomagnetic field. We show additionally that the current flow can be estimated by semiclassical trajectories which represent a computationally efficient tool for predicting the functionality of the devices.

[1] W. Ortiz, N. Szpak, T. Stegmann, arXiv:2202.01739 (2022), submitted

TT 2.5 Mon 10:30 H22

Quantum interference in graphene by dynamic strain — •CHRISTIAN GLASENAPP, PAI ZHAO, MARTA PRADA, LARS TIEMANN, and ROBERT H. BLICK — Center for Hybrid Nanostructures, Universität Hamburg, Luruper Chaussee 149, 22761 Hamburg, Germany

We exploit surface acoustic waves (SAW) as a time-dependent strain wave that propagates through graphene [1] and study its influence on the weak localization (WL) phenomenon at 4 Kelvin. WL is a quantum interference effect that occurs due to the wave nature of charge carriers. In the case of graphene, it can be characterized by inelastic scattering and elastic inter- and intravalley scattering [2]. We fabricated interdigital transducers (IDTs) on a piezoelectric LiNbO₃ substrate, which can be actuated by a radiofrequency (RF) signal to generate a SAW. A large sheet of CVD-grown monolayer graphene was transferred onto the substrate and a Hall bar was patterned in the path of the SAW. In low-field magnetotransport measurements without SAW we observe a well-defined WL effect. When we launch a SAW that strains the graphene layer, WL becomes progressively suppressed with increasing SAW intensity. In this presentation we will show how SAW-induced dynamic strain affects the scattering mechanisms of WL.

[1] P. Zhao *et al.*, Appl. Phys. Lett. **116**, 103102 (2020)

[2] E. McCann *et al.*, Phys. Phys. Lett. **97**, 146805 (2006)

TT 2.6 Mon 10:45 H22

Tunable geometric phase in graphene quantum dots with spin-orbit coupling — •DARIO BERCIUOX^{1,2}, DIEGO FRUSTAGLIA³, and ALESSANDRO DE MARTINO⁴ — ¹Donostia International Physics Center (DIPC), Manuel de Lardizabal 4, E-20018 San Sebastián, Spain — ²IKERBASQUE, Basque Foundation for Science, Euskadi Plaza, 5, 48009 Bilbao, Spain — ³Departamento de Física Aplicada II, Universidad de Sevilla, E-41012 Sevilla, Spain — ⁴Department of Mathematics, City, University of London, London EC1V 0HB, United Kingdom

We show how chiral states in circular graphene pn junctions subject to normal magnetic fields and strong proximitized spin-orbit coupling can mimic those of propagating spin carriers in semiconducting quantum rings. We derive the effective one-dimensional Hamiltonian governing the spin dynamics of the zero-mode and calculate the associated geometric phase. We find that for a given polarity of the junction, it exists a special point in parameter space where the spin is fully polarized along the radial direction in the graphene plane. We further propose a quantum-Hall interferometer where these features can be readily identified.

TT 2.7 Mon 11:00 H22

Effective short distance interacting Hamiltonians for higher Landau levels in graphene — •NIKOLAOS STEFANIDIS¹ and INTI SODEMANN^{2,1} — ¹Max-Planck Institute for the Physics of Complex Systems, D-01187 Dresden, Germany — ²Institut für Theoretische Physik, Universität Leipzig, D-04103 Leipzig, Germany

We study the many body problem in graphene in the quantum Hall regime. Although dominated by Coulomb interactions, short range corrections can select among the degenerate ground states. For the $N = 0$ Landau level (LL) their importance has been demonstrated [1,2] and recent work [3] suggests that this remains true in the $N = 1$ LL. In this talk, we will present results on effective Hamiltonians with $N \neq 0$. We analyse the point group symmetries of graphene and find the Hamiltonians dictated by those.

[1] M. Kharitonov, Phys. Rev. B **85**, 155439 (2012)

[2] I. Sodemann, A. H. MacDonald, Phys. Rev. Lett. **112**, 126804 (2014)

[3] Fangyuan Yang *et al.*, Phys. Rev. Lett. **126**, 156802 (2021)

TT 2.8 Mon 11:15 H22

Massless Dirac fermions with time-dependent magnetic barriers — •NICO LEUMER¹ and WOLFGANG HÄUSLER² — ¹IPCMS, CNRS, University of Strasbourg, France — ²University of Augsburg, Germany

Potential barriers controlled by gate electrodes, as common for 2D-electron gases, are inefficient to guide graphene carriers, due to the Klein tunneling phenomenon. One well known way out consists in using inhomogeneous magnetic fields [1]. However, when considering temporal variations, fundamental differences arise between electric and magnetic fields. While to good approximation the former can be treated on its own, time dependent magnetic fields always will induce electric fields of comparable strengths, according to Maxwell's equations. Following Ref. [2] we report on the complete analytical solution for transmission through a weakly, ω -periodically modulated magnetic barrier, homogeneous along the y -direction, accounting for side bands that appear at energies $E \pm \omega$ in first order perturbation theory. Inherently, magnetic fields generalize the scattering problem to two dimensions. We find that sideband transport requires the static barrier to be permeable, while momentum conservation imposes new, independent conditions for complete reflection.

[1] A. De Martino, L. Dell'Anna, R. Egger, PRL **98**, 066802 (2007)

[2] M. Büttiker, R. Landauer, PRL **49**, 1739 (1982)

15 min. break

TT 2.9 Mon 11:45 H22

Measuring correlated phases in encapsulated bilayer graphene via graphite contacts — •ISABELL WEIMER, ANNA SEILER, and THOMAS WEITZ — 1st Physical Institute, Faculty of Physics, University of Göttingen, Friedrich-Hund-Platz 1, Göttingen 37077, Germany

Encapsulation of graphene in hexagonal Boron Nitride (hBN) as well as the addition of graphite top and bottom gates to the sample have been central to a lot of the research done on graphene in the recent years. This has allowed the observation of multiple new correlated phases including Stoner metals [1-3], correlated insulators [1] and superconductivity [2] at large electric fields in trigonal warped bilayer graphene.

The extent to which the phase space of Bernal bilayer graphene can be even further explored is amongst other parameters limited by the maximum electric field and thus by the maximum values of gate voltages that can be applied to the sample without breaking through the dielectric. With the aim of increasing these maximum voltages, we have explored the method of using graphite contacts to contact bilayer graphene flakes within van-der-Waals heterostructures [1]. Using graphite contacts instead of commonly used 1D edge contacts [4] removes the necessity to etch into the hBN flakes, which had previously been a limiting factor for the applied electric fields.

[1] A. M. Seiler et al., arXiv:2111.06413 (2021)

[2] H. Zhou et al., Science 375, 774 (2022)

[3] S. C. de la Barrera et al., arXiv:2110.13907 (2021)

[4] L. Wang et al., Science 342, 614 (2013)

TT 2.10 Mon 12:00 H22

Mapping electrostatically tunable bands in twisted double bilayer graphene in magnetic fields — •YULIA MAXIMENKO^{1,2}, MARLOU SLOT^{1,3}, SUNGMIN KIM^{1,2}, DANIEL WALKUP¹, EVGHENI STRELCOV¹, EN-MIN SHIH^{1,3}, DILEK YILDIZ^{1,2}, STEVEN BLANKENSHIP¹, KENJI WATANABE⁴, TAKASHI TANIGUCHI⁴, YAFIS BARLAS⁵, PAUL HANEY¹, NIKOLAI ZHITENEV¹, FERESHTE GHAHARI⁶, and JOSEPH STROSCIO¹ — ¹NIST MD USA — ²U of Maryland USA — ³Georgetown U DC USA — ⁴NIMS Tsukuba Japan — ⁵U of Nevada-Reno NV USA — ⁶George Mason U VA USA

After the first demonstration of superconductivity in magic-angle twisted bilayer graphene (MATBG), 2D moiré superlattices proved to be valuable systems for band engineering and studying correlated quantum phases. An imposed periodic potential can drive a crystal into a flat-band phase facilitating strong electron-electron interactions. In MATBG, flat bands appear only at a few precise values of the twist angle. In contrast, small-angle twisted double bilayer graphene (TDBG) can be tuned in and out of the correlated regime using electrostatic fields in a continuous range of twist angles. Local probe studies are key to avoid the common complication of angle disorder. Here we employ scanning tunneling microscopy and electrostatic gating to study TDBG with atomic spatial and high energy resolution in magnetic fields up to 15 T. We observe Landau quantization and map out the TDBG band structure in response to the applied electric field. We use theoretical modeling of the effects of displacement fields, Berry curvature, and magnetic fields to support our experimental findings.

TT 2.11 Mon 12:15 H22

Novel correlated phases near the van Hove singularity in Bernal bilayer graphene — •ANNA SEILER¹, FAN ZHANG², and THOMAS WEITZ¹ — ¹1st Physical Institute, Faculty of Physics, University of Göttingen, Friedrich-Hund-Platz 1, 37077 Göttingen, Germany — ²Department of Physics, University of Texas at Dallas, Richardson, TX, 75080, USA

Diverging density of states offers a unique opportunity to explore a wide variety of correlated phases in low dimensional systems. Graphene few-layers can host electric-field controlled Lifshitz transitions and concomitant van-Hove-singularities in the density of states. Here, we present the observation of experimental signatures consistent with various interaction-driven phases in trigonally warped Bernal bilayer graphene including the fractional metals of Stoner type (1-3). More prominently, we have found a Chern-insulating phase that emerges at finite densities in between two Lifshitz transitions and even survives at zero magnetic field (1). This phase is consistent with a topologically nontrivial Wigner-Hall crystalline phase, i.e., an electron crystal with a quantized Hall conductance as originally proposed at finite magnetic fields in 1989 (4). Evidently, our discovery shows that the reproducible, tunable, and simple Bernal bilayer graphene is

a fertile ground for exploring new, rich, and intrincating many-body physics.

[1] A. M. Seiler et al., arXiv:2111.06413 (2021)

[2] H. Zhou et al., Science 375, 774 (2022)

[3] S. C. de la Barrera et al., arXiv:2110.13907413 (2021)

[4] Z. Tešanović, F. Axel, B. I. Halperin, Phys. Rev. B 39, 8525 (1989)

TT 2.12 Mon 12:30 H22

Towards quantum transport measurements on encapsulated rhombohedrally stacked multilayer graphene — •MONICA KOLEK MARTINEZ DE AZAGRA and THOMAS WEITZ — 1. Physikalisches Institut, Georg August Universität Göttingen

In the recent past flat band multilayer graphene systems have become an experimental playground to explore a plethora of highly correlated many body phenomena such as superconductivity, topological insulators and ferromagnetic phases. However, so far the broad range of phenomena across the different systems, i.e., bilayer, twisted bilayer and rhombohedral trilayer graphene, still hold open questions to the origins and physical limitations of these phenomena. To further investigate these phenomena, we prepare high quality encapsulated multilayer graphene samples, using a variety of techniques such as Raman spectroscopy, scanning near field microscopy, atomic force microscopy and the dry transfer method with the goal to study these samples through magneto quantum transport measurements in the milli Kelvin regime.

TT 2.13 Mon 12:45 H22

Effective mass measurements near electric field controlled Lifshitz transitions in trigonally warped bilayer graphene — •MARTIN STATZ¹, ANNA SEILER¹, FRANCESCA FALORSI¹, JONAS PÖHLS¹, KENJI WATANABE², TAKASHI TANIGUCHI³, and R. THOMAS WEITZ¹ — ¹Univ. of Göttingen, Göttingen, Germany — ²Research Cent. for Funct. Mater., Tsukuba, Japan — ³Int. Cent. for Mater. Nanoarchitectonics, Tsukuba, Japan

Various spontaneous symmetry broken phases such as Stoner ferromagnetism, spin-polarized superconductivity, a quantum anomalous Hall octet and a topologically non-trivial Wigner-Hall crystal phase have recently been reported in bilayer graphene (BLG). Since these interaction-driven phenomena are dictated by the ratio of the Coulomb and kinetic energy of carriers, they can be promoted by the formation of flat bands and a divergent density of states (DoS) near Lifshitz transitions (LT). Trigonally warped BLG at low vertical displacement fields (D-field) and carrier densities ($\sim 10^{11} \text{ cm}^{-2}$) displays one centre and three off-centre Dirac cones in each valley and therefore offers a rich playground for correlated phases (CP) by inducing charge density and D-field driven LT. Insights into the renormalized bandstr. and eff. masses of carriers near such LT will foster a deeper understanding of the formation of these CP. Here, we report on our status on eff. mass measurements via T -dep. (1.9-25 K) Shubnikov-de Haas osc. in the vicinity of charge density and D-field driven LT in trigonally warped BLG. To minimize effects from pot. disorder, we encapsulate BLG in hex. boron-nitride and employ graphite contacts and graphite gates.

TT 2.14 Mon 13:00 H22

Ising superconductivity induced from valley symmetry breaking in twisted trilayer graphene — •TOBIAS STAUBER¹ and JOSE GONZALEZ² — ¹Instituto de Ciencia de Materiales de Madrid, CSIC — ²Instituto de Estructura de la Materia, CSIC

We show that the e-e interaction induces a strong breakdown of valley symmetry in twisted trilayer graphene, just before the superconducting instability develops in the hole-doped material. We analyze this effect by means of an atomistic self-consistent Hartree-Fock approximation, which is a sensible approach as the Fock part becomes crucial to capture the breakdown of symmetry. This effect allows us to reproduce the experimental observation of the Hall density, including the reset at 2-hole doping. Moreover, the breakdown of valley symmetry has important consequences for the superconductivity, as it implies a reduction of symmetry down to the C3 group. This leads to spin-splitting with respect to the two different valleys, suggesting Ising superconductivity and leading to a Pauli-violation with a factor 2-3 as seen in experiments [1]. We also find spin-layer locking which might explain the strong-coupling limit of superconductivity seen in general moiré-samples. We stress that the breakdown of symmetry down to C3 and subsequent spin-valley and spin-layer locking may be shared by other materials with valley symmetry breaking.

[1] J. González and T. Stauber, arXiv:2110.11294

TT 3: Superconductivity: Properties and Electronic Structure

Time: Monday 9:30–13:00

Location: H23

TT 3.1 Mon 9:30 H23

Is lead really a prototypical type I superconductor? New results on the phase diagram at ultra-low temperatures — THOMAS GOZLINSKI, QILI LI, ROLF HEID, JÖRG SCHMALIAN, and •WULF WULFHEKEL — Karlsruhe Institute of Technology

Superconductors are classified by their behavior in a magnetic field into type I, which transitions from a superconducting Meissner to a normal state at the critical field and type II, which have an additional Shubnikov phase consisting of magnetic vortices with one magnetic flux quantum, each. For type I superconductors of finite lateral dimensions, the transition to the normal state is, however,

known to occur locally in form of domains in the so-called intermediate Landau state. Basis for this classification are thermodynamic considerations near the critical temperature and a single band description of superconductivity. Although bulk lead (Pb) is classified as a prototypical type I superconductor, we surprisingly observe single and multi-flux quanta vortices in the intermediate state at temperatures far below the critical temperature using a 25 mK scanning tunneling microscope hand in hand with a complex superconducting behaviour of the two distinct Fermi surfaces of Pb. By probing the quasiparticle local density of states (LDOS) inside the vortices and comparison with quasi-classical simulations based on DFT band-structure calculations, we identify the Caroli-de-Gennes-Matricon states of the two superconducting bands of Pb and are consequently able to determine their winding number.

TT 3.2 Mon 9:45 H23

High-precision impedance measurements near the Berezinski-Kosterlitz-Thouless transition in strongly disordered superconductors — •LEA PFAFFINGER¹, ALEXANDER WEITZEL¹, THOMAS HUBER¹, KLAUS KRONFELDNER¹, LORENZ FUCHS¹, SVEN LINZEN², EVGENI IL'ICHEV², NICOLA PARADISO¹, and CHRISTOPH STRUNK¹ — ¹University of Regensburg, Germany — ²Leibniz Institute of Photonic Technology, Jena, Germany

We investigate the Berezinskii-Kosterlitz-Thouless (BKT) transition - a vortex induced topological phase transition - in 3 nm thin atomically layer deposited NbN films. The samples are placed inside a RLC-resonator, whose design enables us to perform AC measurements of the superfluid stiffness J_s and four-probe current-voltage (IV) characteristics in the same cooling cycle. In contrast to earlier experiments, we observe a sharp discontinuous jump of J_s at the BKT transition temperature T_{BKT} . Comparison of the J_s and the DC resistance measurements reveal quantitative agreement of both T_{BKT} and T_{c0} . Powerlaw exponents extracted of IV characteristics agree quantitatively with J_s and calculations based on renormalization group. Surprisingly, if a DC current is added to the rf-drive, $J_s(I)$ reaches a pronounced maximum before dropping sharply to zero at a current much smaller than the pair breaking critical current. This behaviour may be tentatively explained as a cut-off of the BKT renormalisation flow by the current.

TT 3.3 Mon 10:00 H23

Prediction of ambient-pressure superconductivity in ternary hydride PdCuH_x — •RICCARDO VOCATURO¹, CESARE TRESCA², GIACOMO GHIRINGHELLI³, and GIANNI PROFETA^{2,4} — ¹IFW-ITF, Dresden, Germany — ²Università degli studi dell'Aquila, L'Aquila, Italy — ³Politecnico di Milano, Milano, Italy — ⁴CNR-SPIN, L'Aquila, Italy

We present an ab initio study of the ternary hydride PdCuH_x, a parent compound of the superconducting PdH, at different hydrogen content ($x=1,2$). We investigate its structural, electronic, dynamical, and superconducting properties, demonstrating that, at low hydrogen content, the system is not a superconductor above 1K; however, the highly hydrogenated structure is a strongly coupled superconductor. We give a solid rationale for the unusual increase of the superconducting critical temperature in hydrogenated palladium when alloyed with noble metals (Cu, Ag, and Au), as observed in Stritzker's experiments in 1972 but never investigated with modern experimental and theoretical techniques. We highlight the important role played by H-derived phonon modes at intermediate frequencies, dynamically stabilized by anharmonic effects, as they strongly couple with states at the Fermi level. We hope that the present results will stimulate additional experimental investigations of structural, electronic, and superconducting properties of hydrogenated palladium-noble metal alloys. Indeed, if confirmed, these compounds could be considered a novel class of superconducting hydrides, showing different coupling mechanisms, which can be exploited to engineer new ambient-pressure superconductors.

TT 3.4 Mon 10:15 H23

Theory of spin-excitation anisotropy in the nematic phase of FeSe obtained from RIXS measurements — •ANDREAS KREISEL¹, PETER HIRSCHFELD², and BRIAN M. ANDERSEN³ — ¹Institut für Theoretische Physik, Universität Leipzig — ²Department of Physics, University of Florida, Gainesville — ³Niels Bohr Institute, University of Copenhagen

Recent resonant inelastic x-ray scattering (RIXS) experiments have detected a significant high-energy spin-excitation anisotropy in the nematic phase of the enigmatic iron-based superconductor FeSe [1], whose origin remains controversial. We apply an itinerant model previously used to describe the spin-excitation anisotropy as measured by neutron scattering measurements [2], with magnetic fluctuations included within the RPA approximation. The calculated RIXS cross section exhibits overall agreement with the RIXS data [3], including the high energy spin-excitation anisotropy such that the picture of a localized Heisenberg model does not need to be evoked in order to explain the experimental data.

[1] X. Lu et al., Nat. Phys. (2022)

[2] T. Chen et al. Nat. Mater. **18**, 709 (2019)[3] A. Kreisel, P. J. Hirschfeld, B. M. Andersen, Frontiers in Physics **10**, 859424 (2022)

TT 3.5 Mon 10:30 H23

Local measurements of (super-)conducting microstructure in Rb_xFe_{2-y}Se₂ — •DONALD M EVANS¹, STEPHAN KROHNS¹, DORINA CROITORI², VLADIMIR TSURKAN^{1,2}, and ISTVÁN KÉZSMÁRKI¹ — ¹Experimental Physics V, University of Augsburg, 86135 Germany — ²Institute of Applied Physics, MD 2028 Chisinau, Moldova.

There are many reports on the bulk coexistence of competing orders in iron-based superconductors. In some of these systems, such as RbFe₂Se₂, this is because even single crystals spontaneously phase separate into a superconducting phase made up of micron scale islands, within an antiferromagnetic host matrix. Such phase coexistence makes any bulk data challenging to interpret and, rather, requires local measurement techniques.

In this work, we use low-temperature conducting atomic force microscopy (cAFM) to map the local current response of the superconducting islands in RbFe₂Se₂. Below T_c (~ 32 K) these islands show large current values, as expected for a superconductor. Unexpectedly, there is no distinct change in these current values when heating through T_c : rather, the high currents persist within the islands until they becoming as insulating as the bulk matrix at ~ 150 K. This enhanced conductivity vanishes in response to external magnetic fields. This implies that the reported bulk T_c is the temperature at which the superconductivity is strong enough to connect the islands, i.e. the percolation limit, while the superconductivity within individual islands persists to higher temperatures. This work shows the strength of cAFM to understand the local properties of inhomogeneous superconductors.

TT 3.6 Mon 10:45 H23

Cascade of collapsed phases in SrNi₂P₂ and CaKFe₂As₂ under various strain conditions — •ADRIAN VALADKHANI¹, SHUYANG XIAO², IGOR MAZIN³, SEOK-WOO LEE², PAUL CANFIELD⁴, and ROSER VALENTI¹ — ¹Goethe University, Frankfurt am Main, Germany — ²University of Connecticut, Connecticut, United States — ³George Mason University, Fairfax, USA — ⁴Iowa State University, Ames, United States

Most of crystalline solids have a maximum recoverable strain of less than 1%. Further strain will cause plastic deformation or fractures. In the current work we present SrNi₂P₂, whose maximum recoverable compressive strain is $\sim 14\%$ and tensile is $\sim 6\%$. These widespread values of strain are realizable due to a double lattice collapse-expansion mechanism. The ab initio density functional theory calculations are in very good agreement with the experiment[1,2]. Instead of the usual uncollapsed to collapsed tetragonal transition for the generic tetragonal 122s, a second transition to an orthorhombic superstructure is observed. By a detailed investigation of the electronic and geometric structures for various strains, and substitutions of the Sr, Ni, (and /) or P from first principles, we are able to give a deeper insight in the theory description of this doubly lattice collapse-expansion mechanism. Within this framework we will also discuss structural phases in CaKFe₂As₂ under various strain conditions.

This work is support by the Deutsche Forschungsgemeinschaft (DFG, German Research Foundation) for funding through TRR 288.

[1] Nano Lett. 2021, 21, 19, 7913

[2] Phys. Rev. B 56, 13796 (1997)

TT 3.7 Mon 11:00 H23

3DSC - A new dataset of superconductors including crystal structures — •TIMO SOMMER, ROLAND WILLA, JÖRG SCHMALIAN, and PASCAL FRIEDERICH — Karlsruhe Institute of Technology (KIT), Karlsruhe, Germany

More than 100 years after the discovery of superconductivity in mercury, the search for new superconducting materials still remains challenging. In contrast to most other phenomena, making theoretical predictions about the superconductivity of a certain material is extremely difficult, due to the need to model the comparably tiny energy gain of the superconducting phase, compared to the other energy scales of the problem. Data-driven methods, in particular machine learning, are well-known for finding complex patterns in existing datasets. In the case of superconductors, the use of data science tools is to date slowed down by a lack of accessible data. Here we present a new and publicly available superconductivity dataset ("3DSC"), featuring the critical temperature T_c of superconducting materials additionally to tested non-superconductors. In contrast to existing databases such as the SuperCon database, the 3DSC contains not only the chemical composition, but also the approximate three-dimensional crystal structure of each material. We perform machine learning experiments which show that access to this structural information improves the prediction of the critical temperature T_c . Additionally, we provide ideas for further research to improve the 3DSC in multiple ways. We argue that expanding and developing the 3DSC is a promising direction towards the reliable prediction of new superconductors using machine learning.

15 min. break

TT 3.8 Mon 11:30 H23

Control of the critical temperature of a superconductor/chiral magnet heterostructure — •JULIUS GREFE¹, JANNIS WILLWATER¹, RODRIGO DE VASCONCELLOS LOURENÇO², MARKUS ETZKORN^{2,3}, STEFAN SÜLLOW¹, and DIRK MENZEL^{1,3} — ¹IPKM, TU Braunschweig, Germany — ²IAP, TU Braunschweig, Germany — ³LENA, TU Braunschweig, Germany

Recently, theory has predicted that spin valves consisting of a superconducting film and a magnetic substrate exhibiting a non-collinear spin structure can be controlled via the proximity effect by changing the spin orientation of the magnet. The critical temperature T_c of a thin superconducting Nb film on top of a magnetic MnSi substrate is supposed to be altered when the spin helix vector switches from the in-plane to the out-of-plane direction [1]. We have prepared substrates for molecular beam epitaxy from MnSi single crystals. After preparation the surface roughness has been investigated by AFM and TEM and is in the order of 1 nm. Afterwards, a 20 nm superconducting Nb thin film has been deposited on top of the MnSi substrate. In dependence of the orientation of the external magnetic field and, thus, the direction of the spin helix vector in the MnSi substrate, we observe a change of T_c in the Nb film. To distinguish between the influence of the helix on T_c and pure geometry effects, we compare the result with observations on a Nb film deposited on an isostructural but non-magnetic CoSi substrate.

[1] N. G. Pugach et al., Appl. Phys. Lett. **111**, 162601 (2017)

TT 3.9 Mon 11:45 H23

Gate controlled switching in A15 and non-centrosymmetric superconducting devices — •JENNIFER KOCH, LEON RUF, SIMON HAUS, ROMAN HARTMANN, ELKE SCHEER, and ANGELO DI BERNARDO — Universität Konstanz, Konstanz, Germany

Gate-controlled superconducting devices have become of great interest for the development of energy-efficient hybrid superconductor/semiconductor computing architectures. The idea behind this technology stems from the recent discovery that superconducting devices can be controlled electrically with the application of a gate voltage [1-3]. We investigate gate-controlled switching devices made of A15 and non-centrosymmetric superconductors like Nb₃Ge (A15) and Nb_{0.18}Re_{0.82} (non-centrosymmetric). These materials promise a low switching voltage due to their disordered structure and high spin-orbit coupling and should therefore be more suitable for the realization of devices working at voltages comparable to those used for the control of CMOS transistors.

[1] G. de Simoni et al., Nat. Nanotechnol. **13**, 802 (2018)

[2] F. Paolucci et al., Nano Lett. **18**, 4195 (2018)

[3] F. Paolucci et al., Phys. Rev. Applied **11**, 024061 (2019)

TT 3.10 Mon 12:00 H23

Fano interference of the Higgs response and CDW fluctuations in cuprate high- T_c superconductors — •LIWEN FENG^{1,2,3}, HAO CHU^{1,2,4}, SERGEY KOVALEV⁵, LUKAS SCHWARZ¹, TAO DONG⁶, MIN-JAE KIM^{1,2,3}, GIDEOK KIM¹, GENNADY LOGVENOV¹, BERNHARD KEIMER¹, DIRK MANSKE¹, NANLIN WANG⁶, JAN-CHRISTOPH DEINERT⁵, and STEFAN KAISER^{1,2,3} — ¹Max Planck Institute for Solid State Research, Stuttgart, Germany — ²4th Physics Institute, University of Stuttgart, Stuttgart, Germany — ³Institute of Solid State and Materials Physics, Technical University Dresden, Dresden, Germany — ⁴Quantum Matter Institute, University of British Columbia, Vancouver, Canada — ⁵Helmholtz-Zentrum Dresden-Rossendorf, Dresden, Germany — ⁶International Center for Quantum Materials, Peking University, Beijing, China

Cuprate high- T_c superconductors exhibit a rich phase diagram due to the presence of multiple orders. The interplay of these orders is difficult to access directly by experimental probes. Here, we introduce phase-resolved Higgs spectroscopy, i.e. THz driven amplitude oscillations of the superconducting order parameter. We find a Fano interference of the driven Higgs mode with charge density fluctuations in superconducting La_{2-x}Sr_xCuO₂ ($0.05 \leq x \leq 0.25$). The interference manifests itself as a distinct jump in the phase of the driven Higgs oscillation, which we characterize in an extensive doping- and magnetic field-dependent study. As such, Higgs spectroscopy provides a novel and direct view

on the intriguing interplay of charge density fluctuations and superconductivity in high- T_c cuprates.

TT 3.11 Mon 12:15 H23

Clarifying the origin of CDW and finding the routes to superconductivity in Ti-Se systems. — •ANDRII KUIBAROV, YULIA SHERMERLIUK, ALEXANDER FEDOROV, and SERGEY BORISENKO — IFW Dresden, Deutschland

Two-dimensional chalcogenides have gained renewed attention mainly because of the novel topological properties observed in single crystals and thin films. Although TiSe₂ has been intensively researched over the last 20 years, the true nature of its charge density waves (CDW) state remains controversial. Several different theories have been proposed during these years to explain CDW formation: Fermi surface nesting, Jahn-Teller effect and excitonic insulator.

We try to answer this question using high-resolution ARPES measurements and DFT calculations for different Ti-Se systems: TiSe₂, Cu_xTiSe₂, TiSeS. We show that the CDW state does disappear at various Cu-doping in Cu_xTiSe₂ as it was thought before.

TT 3.12 Mon 12:30 H23

Superconductivity in the type-I Weyl semimetal trigonal-PtBi₂ — •ARTHUR VEYRAT¹, VALENTIN LABRACHERIE¹, FEDERICO CAGLIERIS^{1,2}, JORGE I. FACIO¹, GRIGORY SHIPUNOV¹, JEROEN VAN DER BRINK^{1,3}, BERND BÜCHNER^{1,3}, SAICHARAN ASWARTHAM¹, and JOSEPH DUFOULEUR^{1,4} — ¹Leibniz Institute for Solid State and Materials Research (IFW Dresden), Dresden, Germany — ²CNR-SPIN, Genova, Italy — ³Department of Physics, TU Dresden, Dresden, Germany — ⁴Center for Transport and Devices, TU Dresden, Dresden, Germany

Symmetry breaking in topological matter became a key concept in condensed matter physics to unveil novel electronic states. In particular, the interplay between topology and superconductivity in topologically non-trivial materials is of great interest for the study of unconventional superconducting states. In this talk, I present DFT calculations showing a type-I Weyl semimetal band structure in trigonal PtBi₂. We also evidenced, via transport measurements, that single crystals of trigonal PtBi₂ are superconducting ($T_c \sim 600mK$), which represents the first unambiguous report of bulk superconductivity in a type-I Weyl semimetal. We further characterized the superconductivity in exfoliated thin flakes of trigonal PtBi₂ to be 2-dimensional, up to 126 nm, and we evidence a Berezinskii-Kosterlitz-Thouless transition in flakes up to 60nm thick, with $T_{BKT} \sim 310mK$. This discovery makes trigonal PtBi₂ a very interesting platform to study the interplay between low dimensional superconductivity and topology, into relatively thick and easily fabricated samples.

TT 3.13 Mon 12:45 H23

Vortex inductance as a directional probe of Lifshitz invariants in synthetic Rashba-superconductors — LORENZ FUCHS¹, DENIS KOCHAN¹, CHRISTIAN BAUMGARTNER¹, SIMON REINHARDT¹, SERGEI GRONIN², GEOFFREY C. GARDNER², TYLER LINDEMANN², MICHAEL J. MANFRA², CHRISTOPH STRUNK¹, and •NICOLA PARADISO¹ — ¹University of Regensburg — ²Purdue University

In type II superconductors, the magnetic field penetrates the sample in quantized units of flux, which correspond to vortices in the superfluid. To save condensation energy, vortices tend to be pinned to defects. If these are sharp, the pinning potential $U(\vec{r})$ is harmonic near the vortex core, where it mirrors the superfluid density $|\Psi(\vec{r})|^2$. In this work, we show that in 2D Rashba superconductors the combination of spin orbit interaction and in-plane magnetic field leads to an anisotropic squeezing of the vortex core. This, in turn, produces a strong enhancement of the pinning strength, which can be measured by vortex inductance measurements. To this end, we developed a technique to measure small inductances which is compatible with the application of both DC bias and strong magnetic fields. Vortex inductance is sensitive to the curvature of the pinning potential along the direction perpendicular to the supercurrent. Thus, our method enables a full tomography of the vortex core, obtained by measuring inductance as a function of the angle between current and field. Our results can be interpreted as the effect of the spin orbit-induced Lifshitz invariant term in the Ginzburg-Landau free energy.

TT 4: Many-Body Quantum Dynamics 1 (joint session DY/TT)

Time: Monday 10:00–12:45

Location: H20

See DY 5 for details of this session.

TT 5: Frustrated Magnets – Spin Liquids

Time: Monday 15:00–17:00

Location: H10

Invited Talk

TT 5.1 Mon 15:00 H10

Dynamics of visons and thermal Hall effect in perturbed Kitaev models — •APREM JOY and ACHIM ROSCH — Institute for Theoretical Physics, University of Cologne, Cologne, Germany

A vison is an excitation of the Kitaev spin liquid which carries a \mathbb{Z}_2 gauge flux. While immobile in the pure Kitaev model, it becomes a dynamical degree of freedom in the presence of perturbations. We study an isolated vison in the isotropic Kitaev model perturbed by a small external magnetic field h , an offdiagonal exchange interactions Γ and a Heisenberg coupling J . In the ferromagnetic Kitaev model, the dressed vison obtains a dispersion linear in Γ and h and a fully universal low- T mobility, $\mu = 6v_m^2/T^2$, where v_m is the velocity of Majorana fermions. In contrast, in the antiferromagnetic Kitaev model interference effects preclude coherent propagation and an incoherent Majorana-assisted hopping leads to a T -independent mobility. The motion of a single vison due to Heisenberg interactions is strongly suppressed for both signs of the Kitaev coupling. Vison bands induced by h in the AFM Kitaev model are topological and contribute to the thermal Hall effect.

TT 5.2 Mon 15:30 H10

Microscopic modeling of the Kitaev spin liquid candidates $\text{Li}_3\text{Co}_2\text{SbO}_6$ and $\text{Na}_3\text{Co}_2\text{SbO}_6$ under uniaxial strain — •WILLI ROSCHER, HUIMEI LIU, JEROEN VAN DEN BRINK, and OLEG JANSON — Leibniz Institute for Solid State and Materials Research IFW Dresden, 01069 Dresden, Germany

We have studied the magnetic properties of two Kitaev spin liquid candidates $\text{Li}_3\text{Co}_2\text{SbO}_6$ [1] and $\text{Na}_3\text{Co}_2\text{SbO}_6$ [2] under strain effect by using a microscopic density functional theory (DFT)-based analysis. Previous theoretical work [3] suggested that honeycomb cobaltates are promising candidates to realize the Kitaev spin liquid phase and can be driven there by lattice engineering. Following this conjecture, we simulate the effect of uniaxial strain along the c -axis. Low-energy tight-binding Hamiltonians were first obtained using DFT calculations and Wannier projections. Using the DFT-estimated parameters, we calculate the exchange parameters of the extended Kitaev-Heisenberg model. In this way, we get insights into the magnetic behavior of these materials under uniaxial strain. A small reduction of the trigonal splitting is found for tensile strain. Even though the strain is insufficient to drive the compounds into the spin liquid phase, the non-Kitaev terms are greatly suppressed in the investigated strain range. Our quantitative calculations shed light for the materialization of the Kitaev model.

[1] M. Stratan *et al.*, New J. Chem. **43**, 13545 (2019)

[2] L. Viciu *et al.*, J. Solid State Chem. **180**, 1060 (2007)

[3] H. Liu *et al.*, Phys. Rev. Lett. **125**, 047201 (2020)

TT 5.3 Mon 15:45 H10

Thermal conductivity of a new quantum Kagome antiferromagnet $\text{YCu}_3(\text{OH})_{6.5}\text{Br}_{2.5}$ — •XIAOCHEN HONG^{1,2}, MAHDI BEHNAMI², LONG YUAN³, BOQIANG LI³, WOLFRAM BRENIG⁴, BERND BÜCHNER², YUESHENG LI³, and CHRISTIAN HESS^{1,2} — ¹Bergische Universität Wuppertal — ²IFW-Dresden — ³Huazhong University of Sci. and Tech., Wuhan, China — ⁴TU Braunschweig

Herbertsmithite $\text{ZnCu}_3(\text{OH})_6\text{Cl}_2$ has long been studied as the archetypal quantum Kagome antiferromagnet whose ground state is anticipated to be a spin liquid. However, there is no consensus on the ground state properties of Herbertsmithite, in particular whether a spin gap exist or not, due to its Cu/Zn site mixing effect that distorts the Kagome plane.

Here we report low temperature thermal conductivity measurements of a newly synthesized quantum Kagome antiferromagnet $\text{YCu}_3(\text{OH})_{6.5}\text{Br}_{2.5}$. We observe a downwards deviation of its thermal conductivity κ from a standard phonon power-law temperature dependence beyond a characteristic temperature T^* and a systematic enhancement of this deviation upon application of a magnetic field. Furthermore, up to 16 T no residual κ/T occurs. Our findings imply that the thermal conductivity is dominated by phonons in the mK range, excluding itinerant gapless excitations contributing to it. We interpret the suppression of κ in magnetic field as a consequence of enhanced scattering of the phonons off magnetic fluctuations beyond T^* . Our analysis favors a small gap in the magnetic excitations, which is suppressed by the magnetic field.

TT 5.4 Mon 16:00 H10

Spinless fermions in a \mathbb{Z}_2 gauge theory on a triangular ladder — •WOLFRAM BRENIG — Institute for Theoretical Physics, Technical University Braunschweig, D-38106 Braunschweig, Germany

A study of spinless matter fermions coupled to a constrained \mathbb{Z}_2 lattice gauge theory on a triangular ladder is presented. The triangular unit cell and the ladder geometry lead to a physics different from that on the square lattice. In the static case, even and odd gauge theories are identical. The gauge field dynamics is strongly influenced by the absence of periodic boundary conditions, rendering the deconfinement-confinement process a crossover in general and a quantum phase transition only for decorated electric coupling. At finite doping and in the static case, distinct flux phases can be identified versus magnetic energy. As for the square lattice, a single transition into a confined fermionic phase is found versus electric coupling, however dimer resonances in the confined phase are second order processes only. Global scans of the quantum phases in the intermediate coupling regime are provided.

TT 5.5 Mon 16:15 H10

Nesting instability of gapless U(1) spin liquids with spinon Fermi pockets in two dimensions — •WILHELM KRÜGER and LUKAS JANSSEN — Institut für Theoretische Physik und Würzburg-Dresden Cluster of Excellence ct.qmat, Technische Universität Dresden, 01062 Dresden, Germany

Quantum spin liquids are exotic states of matter that may be realized in frustrated quantum magnets and feature fractionalized excitations and emergent gauge fields. Here, we consider a gapless U(1) spin liquid with spinon Fermi pockets in two spatial dimensions. Such a state appears to be the most promising candidate to describe the exotic field-induced behavior observed in numerical simulations of the antiferromagnetic Kitaev honeycomb model. We consider the regime close to a Lifshitz transition, at which the spinon Fermi pockets shrink to small circles around high-symmetry points in the Brillouin zone. By employing renormalization group and mean-field arguments, we demonstrate that interactions lead to a gap opening in the spinon spectrum at low temperatures, which can be understood as a nesting instability of the spinon Fermi surface. This leads to proliferation of monopole operators of the emergent U(1) gauge field and confinement of spinons. While signatures of fractionalization may be observable at finite temperatures, the gapless U(1) spin liquid state with nested spinon Fermi pockets is ultimately unstable at low temperatures towards a conventional long-range-ordered ground state, such as a valence bond solid.

TT 5.6 Mon 16:30 H10

Frustrated magnetism in pyrochlore rare earth materials: a pseudofermion-FRG study — •BERNHARD WORTMANN — Universität zu Köln — Köln — Deutschland

The family of rare earth pyrochlore materials is intensely scrutinized in the search for quantum spin-ice and quantum spin liquid phases. On the theoretical side, an initial focus has been to explore frustration phenomena in Heisenberg models in order to model the low temperature physics of these materials. It has, however, become increasingly clear that one has to also consider the sometime dominating effect of anisotropic exchange interactions, such as bond-directional Kitaev or Gamma couplings. In this talk, I will discuss the phase diagram of the Heisenberg-Kitaev-Gamma model on the pyrochlore lattice, calculated for $S=1/2$ quantum spins using the pseudofermion functional renormalization group. The rich phase diagram obtained when considering the competition of antiferromagnetic and ferromagnetic exchanges allows us to identify coupling regimes where we find agreement with recent neutron scattering experiments.

TT 5.7 Mon 16:45 H10

Competition between X-Cube and Toric Code in three dimensions — •MATTHIAS MÜHLHAUSER¹, KAI PHILLIP SCHMIDT¹, JULIEN VIDAL², and MATTHIAS REIMUND WALTHER¹ — ¹Institute for Theoretical Physics I, Friedrich-Alexander-Universität Erlangen-Nürnberg, Germany — ²Sorbonne Université, CNRS, Laboratoire de Physique Théorique de la Matière Condensée, LPTMC, F-75005 Paris, France

We investigate the competition of the X-Cube model with the 3D Toric Code using high-order series expansions. We determine the complete phase diagram, which interestingly consists of four regions, i.e. apart from the topologically ordered Toric-Code phase and the X-Cube fracton phase we find two regions which are adiabatically connected to classical spin-liquid phases.

[1] M. Mühlhauser, K. P. Schmidt, J. Vidal, M. R. Walther. SciPost Phys. **12**, 069 (2022)

TT 6: Kondo Physics, f-Electron Systems and Heavy Fermions

Time: Monday 15:00–18:15

Location: H22

TT 6.1 Mon 15:00 H22

Zooming in on heavy fermions in Kondo lattice models — BIMLA DANU¹, ZIHONG LIU¹, FAKHER ASSAAD¹, and MARCIN RACZKOWSKI² — ¹Institut für Theoretische Physik und Astrophysik and Würzburg-Dresden Cluster of Excellence ct.qmat, Universität Würzburg, 97074 Würzburg, Germany — ²Institut für Theoretische Physik und Astrophysik, Universität Würzburg, 97074 Würzburg, Germany

Resolving the heavy fermion band in the conduction electron momentum resolved spectral function of the Kondo lattice model (KLM) is challenging since, in the weak coupling limit, its spectral weight is exponentially small. To alleviate this limitation we consider a composite fermion operator, consisting of a conduction electron dressed by spin fluctuations that shares the same quantum numbers as the electron. Using auxiliary field quantum Monte Carlo simulations we show that for the SU(2) spin-symmetric model on the square lattice at half filling, the quasiparticle residue of the composite fermion tracks the Kondo coupling J_k . This result holds down to $J_k/W = 0.05$, with W the bandwidth, and confirms that magnetic ordering, present below $J_k/W = 0.18$, does not destroy the heavy quasiparticle. We also study the spectral function of the composite fermion in the ground state and at finite temperatures, for SU(N) generalizations of the KLM, as well as for ferromagnetic Kondo couplings, and compare our results to analytical calculations in the limit of high temperatures, large- N , large- S and large J_k .

TT 6.2 Mon 15:15 H22

Two-channel Kondo effect in locally non-centrosymmetric systems — DANIEL HAFNER — Max Planck Institute for Chemical Physics of Solids, Dresden, Germany

A scalable model is presented, which shows that two-channel Kondo (2CK) physics is possible in centrosymmetric crystals, in which the spin-orbit (SO) energy splitting α of conduction electron states is stronger than the hopping parameter t between an inversion symmetric pair of them. The potential difference introduced by the SO coupling effectively suppresses the hopping and disentangles the conduction states into two channels, allowing them to independently couple to impurity spins. If the impurity sites are located on inversion centers, the identical Kondo coupling strengths lead to a symmetrical 2CK effect below the Kondo temperature T_{2CK} . Since the coupling between sectors is still present, the impurity spin is eventually fully quenched by the entangled part of the conduction electrons in a single-channel Kondo effect below T_{1CK} . For $\alpha/t > \sqrt{2}$, a temperature region $T_{2CK} > T > T_{1CK}$ with dominant 2CK physics is found. If the impurities are not located on inversion centers, the resulting channel-asymmetric 2CK model introduces a third temperature scale. Below this, each of two inversion-symmetric impurity sites is screened by one of the two channels, creating a Fermi liquid made up of two types of Kondo singlets linked by inversion symmetry. The similarity of the presented 2CK model to the well established 2CK effect in quantum dots is discussed as well as possible candidate materials like the locally non-centrosymmetric heavy-fermion superconductor CeRh₂As₂.

TT 6.3 Mon 15:30 H22

Spin chain on a metallic surface: Dissipation-induced order vs. Kondo entanglement — BIMLA DANU¹, MATTHIAS VOJTA², TARUN GROVER³, and FAKHER F. ASSAAD¹ — ¹Institut für Theoretische Physik und Astrophysik and Würzburg-Dresden Cluster of Excellence ct.qmat, Universität Würzburg, 97074 Würzburg, Germany — ²Institut für Theoretische Physik and Würzburg-Dresden Cluster of Excellence ct.qmat, Technische Universität Dresden, 01062 Dresden, Germany — ³Department of Physics, University of California at San Diego, La Jolla, CA 92093, USA

We study the physics of an antiferromagnetic spin-1/2 chain Kondo coupled to a two dimensional metal as realized, for example, by depositing an array of magnetic adatoms on a metallic surface with scanning tunneling microscopy (STM) methods. Based on a field theoretical perturbative approach we show that at weak Kondo coupling this system maps onto a spin-1/2 chain coupled to a dissipative Ohmic bath. We argue that in this limit the dissipation induces long-range antiferromagnetic order along the spin chain. Using auxiliary field quantum Monte-Carlo simulations we show that the spin chain as a function of the Kondo coupling exhibits a quantum phase transition from an antiferromagnetic phase to a paramagnetic heavy fermi liquid phase. Since the heavy quasiparticle is not destroyed in the magnetic phase and at the critical point, this quantum phase transition falls in a Hertz-Millis-Moriya type quantum criticality. We discuss the relevance of our results in the context of STM experiments of magnetic adatom chains on metallic surfaces.

TT 6.4 Mon 15:45 H22

Quasiparticle critical slowing down in a heavy-fermion system — CHIA-JUNG YANG¹, KRISTIN KLIEMT², CORNELIUS KRELLNER², JOHANN KROHA³, MANFRED FIEBIG¹, and SHOVOV PAL^{1,4} — ¹Department of Materials, ETH Zurich, 8093 Zurich, Switzerland — ²Physikalisches Institut, Goethe-Universität Frankfurt, 60438 Frankfurt, Germany — ³Physikalisches Institut and Bethe Center for Theoretical Physics, Universität Bonn, 53115 Bonn, Germany — ⁴School of Physical Sciences, National Institute of Science Education and Research, HBNI, Jatni, 752 050 Odisha, India

Critical slowing down (CSD) is a universal phenomenon in phase transitions. A system, after suffering an initial perturbation, takes a very long time to return to its equilibrium state. While CSD is universally observed in the dynamics of bosonic excitations, it is not observed to occur for fermionic excitations. This is because of the half-integer nature of the fermionic spin. In this contribution, we show a fermionic CSD in the heavy-fermion (HF) compound YbRh₂Si₂ (YRS) by using phase-sensitive terahertz time-domain spectroscopy (THz-TDS). THz-TDS has recently been introduced as a novel tool to investigate the quasiparticle dynamics across quantum phase transition (QPT) in HF compounds [1–3]. We see that near the QPT in YRS, the build-up of spectral weight towards the Kondo temperature $T_K^* = 25$ K is followed by a logarithmic rise of the quasiparticle excitation rate on the heavy-Fermi-liquid side below 10 K. A critical two-band HF liquid theory shows that this is indicative of fermionic CSD, the softening of the HF quasiparticle dispersion.

TT 6.5 Mon 16:00 H22

Pressure tuning of the low-temperature states of CeRh₂As₂ — MEIKE PFEIFFER¹, KONSTANTIN SEMENIUK², and ELENA HASSINGER^{1,2} — ¹Technische Universität München, 85748 Garching, Germany — ²Max Planck Institut für chemische Physik fester Stoffe, 01187 Dresden, Germany

CeRh₂As₂ is a heavy-fermion superconductor with a centrosymmetric tetragonal crystal structure lacking local inversion symmetry at the Ce sites. It presents two-phase superconductivity with an exceptionally high ratio of critical field (> 15 T) to critical temperature ($T_c = 0.3$ K). An additional phase can be observed below 0.4 K, believed to be a quadrupole-density wave (QDW) order. We conducted an electrical resistivity study of CeRh₂As₂ down to 30 mK applying hydrostatic pressure up to 3 GPa. We find that under pressure the Kondo coherence peak shifts linearly to higher temperature at a rate of 10 K/GPa. The QDW order is highly sensitive to lattice compression and gets fully suppressed at about 0.7 GPa. The superconducting T_c decreases with a significantly lower rate suggesting no influence of QDW on superconductivity. The upper critical fields show an anisotropic behaviour: for $H \parallel c$ it decreases, whereas for $H \parallel a, b$ it increases for pressures up to ≈ 0.9 GPa and then also decreases. We relate our observations to the change of the relevant energy scales, such as Kondo temperature, Rashba spin-orbit coupling, and interlayer hopping.

TT 6.6 Mon 16:15 H22

The quadrupole density wave and its interplay with superconductivity in CeRh₂As₂: A thermodynamic study — PAVLO KHANENKO^{1,2}, DANIEL HAFNER¹, ROBERT KÜCHLER¹, JACINTHA BANDA¹, THOMAS LÜHMANN¹, JAVIER F. LANDAETA¹, FLORIAN BÄRTL³, TOMMY KOTTE³, JOACHIM WOSNITZA^{2,3}, CHRISTOPH GEIBEL¹, SEUNGHYUN KHIM¹, ELENA HASSINGER^{1,4}, and MANUEL BRANDO¹ — ¹Max Planck Institute for Chemical Physics of Solids, Germany — ²Institut für Festkörper- und Materialphysik, Technische Universität Dresden, Germany — ³Hochfeld-Magnetlabor Dresden (HLD-EMFL) and Würzburg-Dresden Cluster of Excellence, Germany — ⁴Technical University Munich, Germany

The heavy-fermion CeRh₂As₂ is a rare case of multi-phase superconductor ($T_c = 0.26$ K) located in the vicinity of a quantum critical point. Two different superconducting (SC) phases are observed for a magnetic field applied along the c -axis of the tetragonal locally-non-centrosymmetric crystalline structure. The upper critical field along c -axis ($B \parallel c$) is huge, $B_{c2} = 14$ T, but with field within the basal ab -plane ($B \perp c$) only a single SC phase is observed with $B_{c2} = 2$ T. Thermodynamic measurements have detected another non-magnetic phase transition at $T_0 = 0.4$ K which was interpreted as a quadrupole-density-wave (QDW) state. Here, we present new zero-field-cooled and field-cooled specific heat and thermal expansion measurements on a single crystal of CeRh₂As₂ with $B \parallel c$ and $B \perp c$. These allow to extend the phase diagram for $B \parallel c$ and to discuss the interplay between the SC and QDW states.

15 min. break

TT 6.7 Mon 16:45 H22

Heavy quasiparticles in Fermi surface and electronic instabilities in the heavy-fermion superconductor CeRh₂As₂ — •EVRARD-OUICEM ELJAOUHARI and GERTRUD ZWICKNAGL — Institut f. Mathemat. Physik, TU Braunschweig, Braunschweig, Germany

We present calculations of the heavy quasiparticles in the heavy-fermion compound CeRh₂As₂ which exhibits multi-phase superconductivity [1]. The narrow quasiparticle bands that are derived from the Ce-4f degrees of freedom are calculated by means of the Renormalized Band (RB) method. The RB scheme provides a framework for a realistic description of the coherent low-energy excitations in a Fermi liquid which combines material-specific ab-initio methods and phenomenological considerations in the spirit of the Landau theory of Fermi liquids. The central focus of the present study is the role played by the non-symorphic lattice structure and the consequences of the Crystalline Electric Field (CEF) which removes the orbital degeneracy of the Ce 4f states. We conjecture that the quasi-quartet CEF ground state in combination with pronounced nesting features of the Fermi surface may give rise to a quadrupole density wave [2].

This work is supported by the ANR-DFG program Fermi-NES.

[1] S. Khim et al., *Science* 373, 1012 (2021)

[2] D. Hafner et al., *Phys. Rev. X* 12, 011023 (2022)

TT 6.8 Mon 17:00 H22

Muon spin rotation/relaxation studies on the heavy-fermion superconductor CeRh₂As₂ — •SEUNGHYUN KHIM¹, MANUEL BRANDO¹, OLIVER STOCKERT¹, CHRISTOPH GEIBEL¹, ZURAB GUGUCHIA², ROBERT SCHEUERMANN², DEBARCHAN DAS², and TONI SHIROKA² — ¹Max-Planck-Institut für Chemische Physik fester Stoffe, Dresden, Germany — ²Laboratory for Muon Spin Spectroscopy, Paul Scherrer Institute, Villigen PSI, Switzerland

We study magnetic and superconducting (SC) properties of the unconventional superconductor CeRh₂As₂ ($T_c \sim 0.3$ K) by means of muon spin rotation/relaxation (μ SR) experiments. No clear evidence of oscillation is identified in zero-field μ SR spectra down to 0.27 K while the relaxation rate moderately increases below ~ 0.4 K. This could be associated with the suggested quadrupole-density-wave order at $T_0 \approx 0.4$ K and the antiferromagnetic order at $T_N \approx 0.27$ K. In weak transverse-field (TF) μ SR measurements, a pronounced increase in the relaxation rate was observed in the SC state. The relaxation rate (σ_c), regarded as a direct measure of the magnetic penetration depth λ ($\sigma_c \propto 1/\lambda^2$), almost flattens below $T/T_c \sim 0.2$, being strongly indicative of suppressed quasiparticle excitations. TF- μ SR measurements under 2 T reveal a power-law-like T -dependent relaxation rate in the normal state, indicating critical fluctuations. Furthermore, this relaxation rate increases with fields in both the normal and SC state, implying unusual magnetism. Our observations suggest CeRh₂As₂ to have a nearly fully-gapped SC behavior in the vicinity of a peculiar quantum critical point.

TT 6.9 Mon 17:15 H22

Anisotropy of resistivity and magnetotransport in CeRh₂As₂ — •KONSTANTIN SEMENIUK, SEUNGHYUN KHIM, and ELENA HASSINGER — Max Planck Institute for Chemical Physics of Solids, 01187 Dresden, Germany

The recently discovered heavy-fermion superconductor CeRh₂As₂ exhibits an intriguing low-temperature phase diagram containing two superconducting states [1], a quadrupole density wave order [2], and an antiferromagnetic state [3]. The underlying mechanisms of such a behaviour are currently being explored. However, symmetry-induced Rashba spin-orbit effect, Kondo interaction and interlayer coupling have already emerged as the primary ingredients.

To quantify the electronic properties of the compound further, we conducted a comprehensive study of charge transport in CeRh₂As₂. Precise control over sample dimensions and current flow direction were achieved via focused ion beam micromachining of single crystals in a strain-free manner. Based on resistivity anisotropy measurements the three-dimensional character of the electronic structure is established. We also examine magnetoresistance and Hall effect for different orientations of magnetic field with respect to the lattice.

[1] J. Landaeta et al., *Phys. Rev. X*, accepted (2022)

[2] D. Hafner et al., *Phys. Rev. X* 12, 011023 (2022)

[3] M. Kibune et al., *Phys. Rev. Lett.* 128, 057002 (2022)

TT 6.10 Mon 17:30 H22

Influence of substrate clamping in epitaxial EuPd₂Si₂ thin films — •SEBASTIAN KÖLSCH¹, CORNELIUS KRELLNER¹, HANS-JOACHIM ELMERS², and MICHAEL HUTH¹ — ¹Goethe Universität, Frankfurt (Main) — ²Johannes Gutenberg-Universität, Mainz

Europium-based ternary compounds, which crystallize in the tetragonal ThCr₂Si₂ structure, reveal a variety of interesting phenomena, which are attributed to strong electronic correlations and a competition between Kondo effect and the RKKY interaction. Recently EuPd₂Si₂ gained increased interest due to a temperature-driven valence transition from nearly Eu²⁺ above 200 K to Eu³⁺ below about 50 K. This rapid but continuous change of the Europium mean valence is accompanied by a relative change of the EuPd₂Si₂ a lattice constant by about -2% reflecting the strong coupling of lattice and electronic degrees of freedom. For epitaxial thin films of this material the underlying substrate has to be taken into account. In this case the change of the lattice constants due to clamping to the substrate impacts the possible thermal expansion of the corresponding in-plane components. So far research has focused on optimizing single crystal growth conditions under different doping scenarios to tune the system into a critical endpoint. Epitaxial thin films instead offer the possibility to strain-engineer this correlated system by applying biaxial strain to the thin film material upon cooling.

Here we present for the first time the successful growth of EuPd₂Si₂ as epitaxial thin film and report our recent results regarding its clearly distinct properties as compared to single crystals.

TT 6.11 Mon 17:45 H22

Theory of valence-band photoemission from Am metal — •JINDRICH KOLORENC — Institute of Physics (FZU), Czech Academy of Sciences, Praha, Czech Republic

The 5f states in americium metal are generally agreed to be localized, similar to 4f states in lanthanides, being in a well-defined 5f⁶ configuration (Am³⁺). In the same time, the valence-band photoemission spectrum [1,2] cannot be interpreted as a single set of multiplet transitions (5f⁶ → 5f⁵) like in lanthanides [3], and a second set of multiplets (5f⁷ → 5f⁶) has to be introduced [4]. Two mechanisms were suggested as a possible origin of these additional transitions: (i) Am²⁺ layer forming at the surface of the sample or (ii) a second screening channel for the 5f hole created during the photoemission process, with the second mechanism later determined as more likely [2]. Up to now, there does not seem to be a quantitative theory that would substantiate these empirical ideas. The best attempt to date [5] combined the DFT+DMFT method with a generalized Hubbard-I impurity solver, which reproduced the 5f⁷ → 5f⁶ part of the spectrum well, but it also generated a spurious 5f intensity at the Fermi level. Here I report a DFT+DMFT study employing a more accurate impurity solver (exact diagonalization) and demonstrate the mechanism leading to the 5f⁷ → 5f⁶ multiplets in the Am PES spectra.

[1] J. R. Naegele et al., *Phys. Rev. Lett.* 52, 1834 (1984)

[2] T. Gouder et al., *Phys. Rev. B* 72, 115122 (2005)

[3] J. K. Lang et al., *J. Phys. F: Met. Phys.* 11, 121 (1981)

[4] N. Mártensson et al., *Phys. Rev. B* 35, 1437 (1987)

[5] A. Svane, *Solid State Commun.* 140, 364 (2006)

TT 6.12 Mon 18:00 H22

Kondo systems with periodically driven dipole transitions — •MICHAEL TURAEV and JOHANN KROHA — Physikalisches Institut, Universität Bonn, Nufallee 12, 53115 Bonn, Germany

In this work, we study the effects of light irradiation on a magnetic impurity. The impurity is modelled by the single impurity Anderson model where the local impurity is coupled to the conduction electrons via dipole coupling. Therefore, the application of a strong laser field induces a time-periodic hybridization. This can be treated within Floquet Green's function method combined with the slave boson non-crossing approximation [1]. What we see is that the Kondo peak is robust against small driving strengths, and then it gets strongly suppressed when the driving strength increases. However, we find that the destruction of the Kondo effect occurs much faster in terms of driving strength compared to a situation where the energy level of the impurity is itself driven independently.

[1] B. H. Wu and J. C. Cao, *Physical Review B* 81, 085327 (2010)

TT 7: Fluctuations, Noise, Magnetotransport, and Related Topics

Time: Monday 15:00–18:00

Location: H23

TT 7.1 Mon 15:00 H23

Large Hall and Nernst effect from chiral spin fluctuations — KAMIL K. KOLINCIO¹, MAX HIRSCHBERGER^{2,3}, and JAN MASELL^{3,4} — ¹Gdansk Tech, Gdansk, Poland — ²University of Tokyo, Tokyo, Japan — ³RIKEN CEMS, Wako, Japan — ⁴Karlsruhe Institute of Technology (KIT), Karlsruhe, Germany

Magnetic materials with tilted electron spins exhibit conducting behaviour that is explained by the geometrical Berry phase, driven by a chiral (left- or right-handed) spin-habit. Dynamical and nearly random spin fluctuations, with a slight trend towards left- or right-handed chirality, represent a promising route to realizing Berry-phase phenomena at elevated temperatures. [1] Here, we re-

port thermoelectric and electric transport experiments on a triangular and on a slightly distorted kagomé lattice material, respectively. We show that the impact of chiral spin fluctuations is strongly enhanced for the kagomé lattice. Our modelling shows that the geometry of the kagomé lattice plays a crucial role as it helps to avoid cancellation of Berry-phase contributions already in the disordered (paramagnetic) state. Hence, the observations for the kagomé material contrast with theoretical models treating magnetization as a continuous field, and emphasize the role of lattice geometry on emergent electrodynamic phenomena.

[1] K. K. Kolincio, M. Hirschberger, J. Masell, S. Gao, A. Kikkawa, Y. Taguchi, T.-h. Arima, N. Nagaosa, Y. Tokura, PNAS 118, e2023588118 (2021)

[2] K. K. Kolincio et al., submitted

TT 7.2 Mon 15:15 H23

Revealing channel polarization of atomic contacts of ferromagnets and strong paramagnets by shot-noise measurements — MARTIN PRESTEL, •MARCEL STROHMEIER, WOLFGANG BELZIG, and ELKE SCHEER — University of Konstanz, 78457 Konstanz, Germany

We report measurements of the shot noise of atomic contacts using the mechanically controllable break junction (MCBJ) technique at low temperatures. In accordance with theoretical predictions [1, 2] single-atom contacts of the ferromagnets Co and Gd with conductance smaller than the conductance quantum show reduced noise compared to the expectation for the spin-degenerate single-channel transport. Additionally we focus on the strong paramagnets Pt [3], Pd [4], and Ir [5], where a nonmonotonic magnetoresistance has been reported for atomic contacts, interpreted as emerging magnetic ordering in small dimension, which is triggered by the vicinity of the respective bulk metals to a Stoner instability. Our recent measurements on Pd, Pt, and Ir reveal noise levels which are above, but close to the threshold to the spin-degenerate single-channel situation [6]. An anticorrelation between the minimum noise and the bulk Stoner parameter of these elements is observed. We discuss by how far this might indicate that spin polarization is reflected in the noise signal.

[1] Olivera et al., PRB 95, 075409 (2017)

[2] Häfner et al., PRB 77, 104409 (2008)

[3] Strigl et al., Nature Comm. 6, 6172 (2015)

[4] Strigl et al., PRB 94, 144431 (2016)

[5] Prestel et al., PRB 100, 214439 (2019)

[6] Prestel et al., PRB 104, 115434 (2021)

TT 7.3 Mon 15:30 H23

Synchronization in Josephson photonics devices with shot noise — •FLORIAN HÖHE¹, LUKAS DANNER^{1,2}, BRECHT DONVIL¹, CIPRIAN PADURARIU¹, BJÖRN KUBALA^{1,2}, and JOACHIM ANKERHOLD¹ — ¹ICQ and IQST, Ulm University, Ulm, Germany — ²Institute of Quantum Technologies, German Aerospace Center (DLR), Ulm, Germany

Phase stability is an important characteristic of radiation sources. For quantum sources exploitation and characterization of many quantum properties, such as entanglement and squeezing, may be hampered by phase instability. Josephson photonics devices, where microwave radiation is created by inelastic Cooper pair tunneling across a *dc-biased* Josephson junction connected in-series with a microwave resonator are particularly vulnerable lacking the reference phase provided by an ac-drive. To counter this issue, sophisticated measurement schemes have been used in [1] to prove entanglement, while in [2] a weak ac-signal was put in to lock phase and frequency of the emission.

The intrinsic shot noise of the Josephson-photonics device inevitably diffuses the oscillators phase and requires an extension of the classical theory [3] describing locking and synchronization to the quantum regime. Here, the shot noise, which is linked to the Full Counting Statistics, induces phase slips. Injection locking and synchronization lead to a strong narrowing of the photon emission statistics.

[1] A. Peugeot et al., Phys. Rev. X 11, 031008 (2021).

[2] M. C. Cassidy et al., Science 355, 939 (2017).

[3] L. Danner et al., Phys. Rev. B 104, 054517 (2021).

TT 7.4 Mon 15:45 H23

Theory of difference frequency quantum oscillations — •VALENTIN LEEB¹ and JOHANNES KNOLLE^{1,2,3} — ¹Department of Physics TQM, Technische Universität München, James-Frank-Straße 1, D-85748 Garching, Germany — ²Munich Center for Quantum Science and Technology (MCQST), 80799 Munich, Germany — ³Blackett Laboratory, Imperial College London, London SW7 2AZ, United Kingdom

Quantum oscillations (QO) describe the periodic variation of physical observables as a function of inverse magnetic field in metals. The Onsager relation connects the basic QO frequencies with the extremal areas of closed Fermi surface pockets, and the theory of magnetic breakdown explains the observation of sums of QO frequencies at high magnetic fields. Here we develop a quantitative theory of *difference frequency* QOs in metals with multiple Fermi pockets with parabolic or linearly dispersing excitations. We show that a non-linear interband coupling, e.g. in the form of interband impurity scattering, can give rise to otherwise forbidden QO frequencies which can persist to much higher temperatures

compared to the basis frequencies. We discuss the experimental implications of our findings, for example, for materials with multifold fermion excitations.

TT 7.5 Mon 16:00 H23

General bounds of electronic shot noise in the absence of currents — JAKOB ERIKSSON¹, •MATTEO ACCIARI^{1,2}, LUDOVICO TESSER¹, and JANINE SPLETTSTOESSER¹ — ¹Department of Microtechnology and Nanoscience (MC2), Chalmers University of Technology, S-412 96 Göteborg, Sweden — ²University of Gothenburg, S-412 96 Göteborg, Sweden

We investigate the charge and heat electronic noise in a generic two-terminal mesoscopic conductor in the absence of the corresponding charge and heat currents. Despite these currents being zero, shot noise is generated in the system. We show that, irrespective of the conductor's details and the specific nonequilibrium conditions, the charge shot noise never exceeds its thermal counterpart, thus establishing a general bound [1]. Such a bound does not exist in the case of heat noise, which reveals a fundamental difference between charge and heat transport under zero-current conditions.

[1] Eriksson et al., Phys. Rev. Lett. 127, 136801 (2021)

15 min. break

TT 7.6 Mon 16:30 H23

Direct observation of vortices in an electron fluid — •TOBIAS VÖLKL¹, AMIT AHARON-STEINBERG¹, ARKADY KAPLAN¹, ARNAB PARIARI¹, INDRANIL ROY¹, TOBIAS HOLDER¹, YOTAM WOLF¹, ALEXANDER MELTZER¹, YURI MYASOEDOV¹, MARTIN HÜBER², BINGHAI YAN¹, GREGORY FALKOVICH³, LEONID LEVITOV⁴, MARKUS HÜCKER¹, and ELI ZELDOV¹ — ¹Department of Condensed Matter Physics, Weizmann Institute of Science, Rehovot, Israel — ²Departments of Physics and Electrical Engineering, University of Colorado Denver, Denver, USA — ³Department of Physics of Complex Systems, Weizmann Institute of Science, Rehovot, Israel — ⁴Department of Physics, Massachusetts Institute of Technology, Cambridge, USA

Strongly-interacting electrons in ultrapure conductors have been shown to display signatures of hydrodynamic behavior including negative nonlocal resistance and Poiseuille flow in narrow channels. Here we provide the first visualization of current vortices in an electron fluid. By utilizing a nanoscale scanning superconducting quantum interference device on a tip we image the current distribution in a circular chamber connected through a small aperture to a current-carrying strip in the high-purity type-II Weyl semimetal WTe₂. We find that vortices are present only for small apertures, whereas the flow is laminar (non-vortical) for larger apertures. Our findings suggest a novel mechanism of hydrodynamic flow in thin pure crystals: the spatial diffusion of electrons' momenta is enabled by small-angle scattering at the surfaces, instead of the routinely invoked electron-electron scattering.

TT 7.7 Mon 16:45 H23

Optical dipole orientation of interlayer excitons in MoSe₂-WSe₂ heterostacks — •MIRCO TROUE¹, LUKAS SIGL¹, MANUEL KATZER², MALTE SELIG², FLORIAN SIGGER¹, JONAS KIEMLE¹, JOHANNES FIGUEIREDO¹, MAURO BROTONS-GISBERT³, BRIAN GERARDOT³, ANDREAS KNORR², URSULA WURSTBAUER⁴, and ALEXANDER HOLLEITNER¹ — ¹TU Munich — ²Technical University Berlin — ³Heriot-Watt University — ⁴University of Münster

Transition metal dichalcogenide monolayers exhibit strong light-matter interactions, which promotes them as ideal candidates for novel 2D optoelectronic applications. A vertical stacking into van der Waals heterostacks leads to the formation of long-lived interlayer excitons in adjacent layers. We present the far-field photoluminescence intensity distribution of interlayer excitons in MoSe₂-WSe₂ heterostacks as measured by back focal plane imaging in the temperature range between 1.7K and 20K. An analytical model describing the emission pattern from a dielectric heterostructure is used to obtain the relative contributions of the in- and out-of-plane transition dipole moments associated with the interlayer exciton photon emission. We determine the transition dipole moments for all observed interlayer exciton transitions to be (99 ± 1)% in-plane for R- and H-type stacking, independent of the excitation power and therefore the density of the exciton ensemble in the experimentally examined range. Moreover, we discuss the limitations of the presented measurement technique to observe correlation effects for many-body states in dense ensembles of interlayer excitons.

TT 7.8 Mon 17:00 H23

Magnetic and transport behaviour of quasi 2D NiS₂ flakes — •ROMAN HARTMANN¹, MARIO AMADO MONTERO², ELKE SCHEER¹, and ANGELO DI BERNARDO¹ — ¹Fachbereich Physik, Universität Konstanz, Germany — ²Department of Physics, University of Salamanca, Spain

Spintronics with 2D materials is emerging as a new field which enables development of devices with novel functionality compared to their three-dimensional counterparts.

We have recently managed to cleave single crystal NiS₂ down to the quasi 2D limit despite it not being a layered material. Bulk NiS₂ is a Mott insulator that has an interesting magnetic structure with an antiferromagnetic phase below 39 K and weak ferromagnetic ordering with a Curie temperature of 29 K. [1]

In transport measurements of thin flakes we see an increase in conductivity compared to the bulk, presumably due to the presence of metallic surface states. The ferromagnetic transition is clearly visible as kinks in the R-T curves and R-H curves. With magnetic field applied there is a complex hysteretic behaviour in the resistance with a strong asymmetry with respect to the direction of the applied field.

As a next step we are also looking into coupling the NiS₂ flakes to 2D superconductors to create two-dimensional superconducting spintronic devices.

[1] T. Thio et al., Phys. Rev. B 52, 5 (1995)

TT 7.9 Mon 17:15 H23

Spectral properties of the herringbone lattice — •MIGUEL ANGEL JIMÉNEZ HERRERA^{1,2} and DARIO BERCIUOX^{2,3} — ¹Centro de Física de Materiales (CFM-MPC) Centro Mixto CSIC-UPV/EHU, 20018 Donostia-San Sebastián, Basque Country, Spain — ²Donostia International Physics Center, 20018 San Sebastián, Spain — ³IKERBASQUE, Basque Foundation for Science, Euskadi Plaza, 5, 48009 Bilbao, Spain

We investigate the spectral properties of a two-dimensional electronic lattice that belongs to a non-symmorphic space group. More specifically, we look at the herringbone lattice that is characterised by two sets of glide symmetries applied in two orthogonal directions. We describe the system using a tight-binding model with nearest neighbors divided into horizontal and vertical hopping terms. We find two non-equivalent Dirac cones inside the first Brillouin zone along a high-symmetry paths, among other features, which react to different perturbations applied to the Hamiltonian. These perturbations break the symmetries of the lattice: we begin by placing different onsite potentials in the lattice sites. We observe annihilation of Dirac cones into semi-Dirac cones and nodal lines along high symmetry paths. Finally, we perturb the system by applying a dimerization on the hoppings. We report a flow of Dirac cones inside the first Brillouin zone describing quasi-hyperbolic curves

TT 7.10 Mon 17:30 H23

Hierarchical equations of motions approach to the study of thermodynamic uncertainty relations — SALVATORE GATTO and •MICHAEL THOSS — Institute of Physics, Albert-Ludwigs-Universität Freiburg

Thermodynamic uncertainty relations (TUR) are cost-precision trade-off relations in transport systems, relating the fluctuations in the heat and particle currents to the reversibility of the operation regime. While some violations have been reported for the TUR in classical systems, it has been found out that the geometry of quantum non-equilibrium steady-states alone directly implies the existence of a general quantum TUR. In this contribution, we investigate the relationship between quantum effects and current fluctuations in quantum systems. The hierarchical equation of motion approach is employed, which allows a numerically exact simulation of nonequilibrium transport in general open quantum systems involving multiple bosonic and fermionic environments.

TT 7.11 Mon 17:45 H23

Bosonization for Q = 0 particle-hole excitations of 2D gapless fermions — •SEBASTIAN MANTILLA¹ and INTI SODEMANN^{1,2} — ¹Max Planck Institute for the Physics of Complex Systems, 01187 Dresden, Germany — ²Institut für Theoretische Physik, Universität Leipzig, 04103 Leipzig, Germany

Understanding the non-perturbative effects of strong interactions on gapless phases of fermions in two-spatial dimensions is one of the major challenges in quantum condensed matter physics. Bosonization in one- and higher-dimensional systems has successfully captured such effects, where the picture of excitations in higher dimensions consists of small deformations of the Fermi surface. We discuss an extension for gapless phases in fermionic systems (e.g., nodal semimetals, Dirac fermions), not describable by the previous formalism since the Fermi surface shrinks to a point and the deformation picture breaks down. The new picture consists of a collection of excitons that considers non-perturbative effects in the weak- and strong-coupling regimes. We apply the formalism in two cases involving interacting electrons in graphene: the corrections to the optical response of 2D free fermions in monolayer graphene, and the weak coupling instability due to electron-hole attractive interactions in bilayer graphene. Our results contribute to understanding the effects of strong interactions in gapless fermions and extend bosonization beyond the picture of Fermi surface deformations.

TT 8: Frustrated Magnets – Strong Spin-Orbit Coupling

Time: Monday 17:15–19:00

Location: H10

TT 8.1 Mon 17:15 H10

α -RuCl₃ probed by ultrasound under hydrostatic pressure — •ANDREAS HAUSPURG^{1,2}, S. ZHERLITSYN¹, T. HELM¹, T. YANAGISAWA³, V. TSURKAN⁴, and J. WOSNITZA^{1,2} — ¹Hochfeld-Magnetlabor Dresden (HLD-EMFL), HZDR, Dresden, Germany — ²Institut für Festkörper- und Materialphysik, TU Dresden, Germany — ³Department of Physics, Hokkaido University, Sapporo, Japan — ⁴Institute of Physics, University of Augsburg, Germany

As a prime candidate for a quantum spin liquid (QSL) in the frame of the Kitaev model, is the honeycomb material α -RuCl₃ of particular interest. Although α -RuCl₃ exhibits antiferromagnetic order below 7K, it is considered as proximate to the QSL. The QSL features fractionalized quasiparticle excitations. A promising approach to investigate such excitations is to study the coupling between fractionalized quasiparticles and phonons. This affects the attenuation coefficient and the sound velocity of ultrasound. Our recent studies of the elastic properties of α -RuCl₃ show a promising path to unveil the unconventional physics of the debated QSL phase. Here, we present low-temperature results of the sound velocity and attenuation in external magnetic fields and under hydrostatic pressures. The observed anomalies in the acoustic properties and strong magnetoelastic couplings shed new light on the unconventional physics in this compound. At a pressure of 11.3 kbar the antiferromagnetic order is completely suppressed.

TT 8.2 Mon 17:30 H10

Fractional Excitation-induced Phonon Renormalization in α -RuCl₃ — •ADRIAN MERRITT¹, XIAO WANG¹, ALEXEI BOSAK², LUIGI PAOLASINI², ALEXANDRE IVANOV³, ROLF HEID⁴, and YIXI SU¹ — ¹Jülich Centre for Neutron Science JCNS-FRM II, Forschungszentrum Jülich GmbH, Garching, Germany — ²European Synchrotron Radiation Facility (ESRF), Grenoble, France — ³Institut Laue-Langevin, Grenoble, France — ⁴Institute for Quantum Materials and Technologies, Karlsruhe Institute of Technology, Karlsruhe, Germany

The quantum spin liquid (QSL) phase is of immense interest to condensed matter physicists, and have been studied for decades. With a Kitaev model that is exactly solvable and gives a QSL ground state, more recent work has focused on the $J_{eff}=1/2$ materials and in particular, α -RuCl₃. Above the critical magnetic field B_c 7T and below T 6K there is evidence for the half-integer quantized plateau possibly arising from the fractional excitations in the QSL phase. Recent theoretical work has shown that the fractional excitations can induce phonon

renormalization via the spin-lattice coupling, and would in particular affect the acoustic phonons near the zone boundary. Our measurements have focused on the phonon dispersion in α -RuCl₃ to observe this phonon renormalization effect in the putative QSL phase. We have been able to survey the acoustic phonons in the relevant scattering directions under magnetic fields using single crystals. We will discuss our results with a focus on examining the low-energy acoustic phonon branches we measured in comparison to published work as well as the observed phonon renormalization effect.

TT 8.3 Mon 17:45 H10

Quantum Monte Carlo simulations of generalized Kitaev models: applications to α -RuCl₃ — •TOSHIHIRO SATO¹ and FAKHER F. ASSAAD^{1,2} — ¹Institut für Theoretische Physik und Astrophysik, Universität Würzburg, Germany — ²Würzburg-Dresden Cluster of Excellence ct.qmat, Germany

We introduce a phase pinning approach in the realm of the auxiliary field quantum Monte Carlo (QMC) algorithm that mitigates the severity of the negative sign problem inherent to QMC methods of frustrated spin systems [1]. This allows us to access high-temperature thermodynamic and dynamical properties of the aforementioned systems and, for instance, carry out exact QMC simulations in a window of temperatures relevant to experiments for various frustrated magnets. We use our method to carry out extensive simulations of thermodynamic properties under magnetic fields in generalized Kitaev models describing α -RuCl₃, and discuss the characteristic feature in the field-direction dependence of the magnetic susceptibility, the specific heat as well as the magnetotropic coefficient. Our numerical results allow for direct comparison with recent measurements of the magnetotropic coefficient in α -RuCl₃ [2].

[1] T. Sato and F. F. Assaad, Phys. Rev. B. 104, L081106 (2021)

[2] K. A. Modic et al., Nat. Phys. (2020)

TT 8.4 Mon 18:00 H10

RuCl₃: Phonon (Hall) transport and sibling compounds RuBr₃, RuI₃ — •DAVID A S KAIB¹, SANANDA BISWAS¹, STEPHEN M WINTER², KIRA RIEDL¹, ALEKSANDAR RAZPOPOV¹, YING LI³, STEFFEN BACKES⁴, IGOR I MAZIN⁵, and ROSER VALENTI¹ — ¹Goethe-Universität, Frankfurt, Germany — ²Wake Forest University, Winston-Salem, NC 27109, USA — ³School of Physics, Xi'an Jiaotong University, Xi'an 710049, China — ⁴Institut Polytechnique de Paris, Route de Saclay, 91128 Palaiseau, France — ⁵George Mason University, Fairfax, VA 22030, USA

We present results of two studies related to the Kitaev candidate material RuCl_3 :

Recent experimental studies have pointed to the presence of significant magnetoelastic coupling in RuCl_3 and have highlighted unusual thermal transport signatures under magnetic field. We compute the pseudospin-phonon coupling in RuCl_3 from first principles and use it to model the intrinsic thermal transport from phonons scattered by spin fluctuations. This includes both the longitudinal as well as the transversal (Hall) conductivity.

In the second part of the talk, we analyze two new sibling compounds to RuCl_3 : RuBr_3 and RuI_3 . While current samples show a bad metal behavior in RuI_3 , our first principles calculations predict a Mott insulator close to the Mott-metal transition in the pristine parent compound, with a dominant Kitaev interaction and negligible Heisenberg exchange.

TT 8.5 Mon 18:15 H10

High-field ESR studies of the cubic Iridium hexahalide compounds $(\text{NH}_4)_2\text{IrCl}_6$ and K_2IrCl_6 — •LAKSHMI BHASKARAN¹, ALEXEY N. PONOMARYOV², JOCHEN WOSNITZA^{1,3}, NAZIR KHAN⁴, ALEXANDER A. TSIRLIN⁴, MIKE E. ZHITOMIRSKY⁵, and SERGEI A. ZVYAGIN¹ — ¹Dresden High Magnetic Field Laboratory (HLD-EMFL) and Würzburg-Dresden Cluster of Excellence ct.qmat, Helmholtz-Zentrum Dresden-Rossendorf, Dresden, Germany — ²Institute of Radiation Physics, Helmholtz-Zentrum Dresden-Rossendorf, Dresden, Germany — ³Institut für Festkörper- und Materialphysik, TU Dresden, Dresden, Germany — ⁴University of Augsburg, Augsburg, Germany — ⁵University Grenoble Alpes, Grenoble, France

We report on high-field electron spin resonance studies of two iridium hexahalide compounds, $(\text{NH}_4)_2\text{IrCl}_6$ and K_2IrCl_6 [1]. In the paramagnetic state, our measurements reveal isotropic g -factors $g = 1.79(1)$ for the Ir^{4+} ions, in agreement with their cubic symmetries. Most importantly, in the magnetically ordered state, we observe two magnon modes with zero-field gaps of 11.3 and 14.2 K for $(\text{NH}_4)_2\text{IrCl}_6$ and K_2IrCl_6 , respectively. Based on that and using linear spin-wave theory, we estimate the nearest-neighbor exchange couplings and anisotropic Kitaev interactions, $J_1/k_B = 10.3$ K, $K/k_B = 0.7$ K for $(\text{NH}_4)_2\text{IrCl}_6$, and $J_1/k_B = 13.8$ K, $K/k_B = 0.9$ K for K_2IrCl_6 , revealing the nearest-neighbor Heisenberg coupling as the leading interaction term, with only a weak Kitaev anisotropy.

[1] L. Bhaskaran et al., Phys. Rev. B **104**, 184404 (2021).

TT 8.6 Mon 18:30 H10

Spin-orbit excitons in the $j_{\text{eff}}=1/2$ compound K_2IrCl_6 — •PHILIPP WARZANOWSKI¹, MARCO MAGNATERRA¹, KAROLIN HOPFER¹, CHRISTOPH SAHLE², MARCO MORRETI SALA³, GIULIO MONACO⁴, PETRA BECKER⁵,

LADISLAV BOHATÝ⁵, and MARKUS GRÜNINGER¹ — ¹Inst. of Physics II, University of Cologne — ²European Synchrotron Radiation Facility, Grenoble Cedex, France — ³Dip. di Fisica, Politecnico di Milano, Italy — ⁴Dip. di Fisica e Astronomia, Università di Padova, Italy — ⁵Sect. Crystallography, Inst. of Geology and Mineralogy, University of Cologne

Spin-orbit entangled Mott insulators offer new playgrounds to explore novel ground states. Iridates with a t_{2g}^5 electron configuration are popular platforms to realize $j_{\text{eff}}=1/2$ systems due to the large cubic crystal field and strong spin-orbit coupling. Spectroscopies, RIXS in particular, show that thus far all iridates harbour non-cubic crystal field distortions, which turn the ground state away from an ideal $j_{\text{eff}}=1/2$ state. In this context, the (globally) cubic compound K_2IrCl_6 is a promising candidate to host ideal $j_{\text{eff}}=1/2$ moments. However, both RIXS and infrared spectroscopy show a splitting of the spin-orbit exciton. Within a single-site scenario, we extract a spin-orbit coupling $\lambda = 435$ meV and a non-cubic crystal field $\Delta = 60$ meV, yielding a ground state of 99.8% $j_{\text{eff}}=1/2$ character. To explore the origin of non-cubic distortions, we discuss the possible effects of i) librations [1], ii) the coupling to phonons, and iii) defects [2].

[1] N. Khan et al., Phys Rev B **103**, 125158 (2021)

[2] S.-S. Bao et al., Inorg. Chem. **57**, 13252 (2018)

TT 8.7 Mon 18:45 H10

Fragility of charge frustration in high-pressure CsW_2O_6 — •PASCAL REISS¹, MASAHIKO ISOBE¹, and HIDENORI TAKAGI^{1,2} — ¹Max Planck Institute for Solid State Research, Stuttgart, Germany — ²Department of Physics, The University of Tokyo, Bunkyo, Tokyo, Japan

The transition metal compound CsW_2O_6 represents an intriguing example of a pyrochlore structure at quarter filling. Starting from a nominal $\text{W}^{5.5+}$ oxidation state, the system suffers a metal-to-insulator transition around $T_c \approx 215$ K where a breathing distortion leads to the formation of regular molecular W_3 trimers with 2 localised electrons each, and a remaining W^{6+} site devoid of 5d electrons [1]. Recently, it was proposed that in this low-temperature phase, the interplay between a strong spin-orbital coupling and the transfer integral could realise a rare case of an intrinsically half-filled flat band dispersion with a stiff spin chirality [2].

In this talk, we will present our recent high pressures transport measurement on CsW_2O_6 . With increasing pressure, we find that the low-temperature insulating phase is stabilised as the metal-to-insulator transition shifts to higher temperatures. We will discuss our results in the light of recent theoretical proposals.

[1] Y. Okamoto et al., Nat. Commun. **11** (2020)

[2] N. Nakai and C. Hotta, Nat. Commun. **13** (2022)

TT 9: Cold Atomic Gases and Superfluids

Time: Monday 18:00–19:15

Location: H23

TT 9.1 Mon 18:00 H23

Symmetry-protected Bose-Einstein condensation of interacting hardcore bosons — •REJA WILKE¹, THOMAS KÖHLER², FELIX PALM¹, and SEBASTIAN PAECKEL¹ — ¹Department of Physics, Arnold Sommerfeld Center for Theoretical Physics, University of Munich, Germany — ²Department of Physics and Astronomy, Uppsala University, Sweden

We introduce a mechanism stabilizing a one-dimensional quantum many-body phase, characterized by a certain wave vector via the protection of an emergent \mathbb{Z}_2 symmetry. We illustrate this mechanism by constructing the solution of the full quantum many-body problem of hardcore bosons on a wheel geometry, which are known to form a Bose-Einstein condensate. The robustness of the condensate is shown numerically by adding nearest-neighbor interactions to the wheel Hamiltonian. We discuss further applications such as geometrically inducing finite-momentum condensates.

TT 9.2 Mon 18:15 H23

Quantum light-matter fluctuations in driven open cavity BEC systems — •LEON MIXA and MICHAEL THORWART — I. Institut für Theoretische Physik, Universität Hamburg

When an ultracold atom gas strongly interacts with a pumped cavity light field, effective retarded long-range interactions are induced. They give rise to non-classical states in the light sector, which do not necessarily require non-classical fluctuations in the matter sector. We study theoretically the quantum fluctuations in the light and the matter sectors in different driving regimes. In particular, the photon dissipation channel of the cavity allows for the direct nondestructive measurement of the fluctuations driving the phase transition known in this system. Light-induced density fluctuations drive a superradiant nonequilibrium Dicke quantum phase transition of the atom gas. The photon statistics in the presence of the strongly coupled, pumped atom gas is calculated within a Bogoliubov approach combined with analytic imaginary time path integrals

including photon leakage of the cavity. Parameter regimes for squeezed cavity light are identified.

TT 9.3 Mon 18:30 H23

The free energy of the two-dimensional dilute Bose gas — •ANDREAS DEUCHERT¹, SIMON MAYER², and ROBERT SEIRINGER² — ¹University of Zurich, Institute of Mathematics, Zurich, Switzerland — ²Institute of Science and Technology Austria, Klosterneuburg, Austria

We prove bounds for the specific free energy of the two-dimensional Bose gas in the thermodynamic limit. We show that the free energy at density ρ and inverse temperature β differs from the one of the non-interacting system by the correction term $4\pi\rho^2 |\ln(a^2\rho)|^{-1} (2 - [1 - \beta_c/\beta]_+^2)$. Here a is the scattering length of the interaction potential, $[x]_+ = \max\{0, x\}$ and β_c is the inverse Berezinskii-Kosterlitz-Thouless critical temperature for superfluidity. The result is valid in the dilute limit $a^2\rho \ll 1$ and if $\beta\rho \geq 1$.

TT 9.4 Mon 18:45 H23

Chaos in the three-site Bose-Hubbard model - classical vs quantum — •GORAN NAKERST¹ and MASUDUL HAQUE^{1,2} — ¹Institut für Theoretische Physik, Technische Universität Dresden, Dresden, Germany — ²Max-Planck-Institut für Physik komplexer Systeme, Dresden, Germany

We consider a quantum many-body system - the Bose-Hubbard system on three sites - which has a classical limit, and which is neither strongly chaotic nor integrable but rather shows a mixture of the two types of behavior. We compare quantum measures of chaos (eigenvalue statistics and eigenvector structure) in the quantum system, with classical measures of chaos (Lyapunov exponents) in the corresponding classical system. As a function of energy and interaction strength, we demonstrate a strong overall correspondence between the two cases. In contrast to both strongly chaotic and integrable systems, the largest Lyapunov exponent is shown to be a multi-valued function of energy.

TT 9.5 Mon 19:00 H23

Out-of-equilibrium dynamics of bosons on a 2D Hubbard lattice — •ULLI POHL, SAYAK RAY, and JOHANN KROHA — Physikalisches Institut, Rheinische Friedrich-Wilhelms-Universität Bonn, Nußallee 12, 53115 Bonn, Germany
We study the collective excitations of bosons in two-dimensional optical Hubbard lattices, described by the Bose-Hubbard model, using the cluster mean field theory at zero temperature. The method has been shown to be very powerful to determine the phase boundaries both at zero and finite temperatures [1]. From

the low-lying excitations, we identify the presence of the Higgs and the Goldstone modes of the superfluid, as well as the particle- and hole-like excitations in the Mott insulator phase and calculate their dispersion relations. The effective mass of the quasiparticles and -holes vanish at the tip of the Mott lobe where the Higgs energy gap also vanishes. Finally, we present the real time dynamics of the collective excitations, particularly, the Higgs mode. Our findings, particularly the dynamics of excitations support the previous mean-field-like calculations and can be relevant for cold-atom experiments.

[1] U. Pohl, S. Ray, J. Kroha arXiv:2106.14860

TT 10: Focus Session: Superconductivity in 2d-Materials and their Heterostructures

Two-dimensional crystals have become important throughout condensed matter physics. Only a few of them are intrinsic superconductors, most of these containing heavy elements. Hence, Cooper pairing is strongly affected by spin-orbit interactions that lead to exotic features like Ising pairing and mixed singlet-triplet correlations. The unconventional pairing offers novel degrees of freedom and integrates superconductivity with topological and even higher-order topological edge and hinge states. Moreover, proximity induced superconductivity displays characteristic features owing to the ballistic character and the Dirac dispersion relation of today's high-quality hexagonal boron nitride/graphene heterostructures. This makes graphene-based heterostructures an interesting platform for Andreev billiards and similar systems.

Organizers: Christoph Stampfer, RWTH Aachen University and Christoph Strunk, University of Regensburg

Time: Tuesday 9:30–13:15

Location: H3

Invited Talk

TT 10.1 Tue 9:30 H3

Two-fold symmetric superconductivity in few-layer NbSe₂ — •VLAD PRIBIAG — University of Minnesota, USA

Few-layer samples of transition metal dichalcogenides (TMDs) feature a wide array of properties such as layer-dependent inversion symmetry, valley-contrasted Berry curvatures, and strong spin-orbit coupling (SOC). Among the superconducting TMDs, NbSe₂ is profoundly affected by Ising SOC. Ising SOC not only helps stabilize the superconducting state against large in-plane magnetic fields, but in conjunction with other forms of SOC, it could also give rise to exotic superconducting states such as nodal topological superconductivity. This talk will discuss recent transport measurements of few-layer NbSe₂, and NbSe₂/CrBr₃ junctions, studied under in-plane external magnetic fields. Surprisingly, although the crystal lattice has a three-fold symmetry, the magneto-resistance and critical field show a two-fold anisotropy, which is absent in the normal state. We will discuss these results in the context of a competition between the conventional s-wave pairing instability characteristic of the bulk and a competing d- or p-wave instability that emerges in the few-layer limit. These results [1] suggest an unconventional character for superconducting pairing in NbSe₂ and open the possibility for further discoveries, such as non-trivial topologies, in few-layer TMDs.

[1] A. Hamill et al., Nat. Phys. 17, 949 (2021)

Invited Talk

TT 10.2 Tue 10:00 H3

Spin-orbit coupling and triplet pairing in mesoscopic superconductors — •MARCO APRILI¹, MARKO KUZMANOVIC¹, TOM DVIR², DAVID LEBOEUF³, STEFAN ILIC⁴, MENASHE HAIM², MAXIM KHODAS², JULIA MEYER⁴, HADAR STEINBERG², and CHARIS QUAY¹ — ¹Laboratoire de Physique des Solides, Bâtiment 510, Université Paris-Saclay 91405 Orsay, France — ²Racah Institute of Physics, Hebrew University of Jerusalem, Givat Ram, Jerusalem 91904 Israel — ³Laboratoire National des Champs Magnétiques Intenses, CNRS, Grenoble, France — ⁴Université Grenoble Alpes, CEA, Grenoble INP, 38000 Grenoble, France

The spin-orbit coupling which is present in 2D materials because of inversion breaking symmetry allows a triplet component of the superconducting order parameter to appear.

In presence of an external magnetic field acting on the spin degree of freedom of the electron pairs forming the condensate, this spin-orbit coupling originates a spontaneous supercurrent and hence a phase difference. In a monolayer of a superconducting transition-metal-dichalcogenides such as NbSe₂, the lack of in-plane crystal inversion symmetry, results instead in a large valley Zeeman splitting which pins the spins out-of-plane and protects in fact superconductivity. Adding an external magnetic field results in a mix singlet-triplet superconducting state where the two order parameters are linearly coupled by the field. The triplet is an equal spin pairing state. In this talk I'll present a series of quantum transport and tunneling spectroscopy experiments in mesoscopic superconductors that address these issues.

Invited Talk

TT 10.3 Tue 10:30 H3

Supercurrent diode effect in few-layer NbSe₂ — LORENZ BAURIEDL¹, CHRISTIAN BÄUML¹, LORENZ FUCHS¹, CHRISTIAN BAUMGARTNER¹, NICOLAS PAULIK¹, JONAS M. BAUER¹, KAI-QIANG LIN¹, JOHN M. LUPTON¹, TAKASHI TANIGUCHI², KENJI WATANABE², CHRISTOPH STRUNK¹, and •NICOLA PARADISO¹ — ¹Institut für Experimentelle und Angewandte Physik, University of Regensburg, Regensburg, Germany — ²International Center for Materials Nanoarchitectonics, National Institute for Materials Science, Tsukuba, Japan

Current rectifiers are devices which display a largely different resistance for the two opposite bias polarities. Recent seminal works on Rashba superconductors have demonstrated that a simultaneous breaking of time- and inversion-symmetry leads to supercurrent rectification, where for one direction the resistance is strictly zero. Owing to the symmetry of the Rashba spin-orbit interaction, the effect is controlled by the in-plane field. In this work, we report on a supercurrent diode effect in few layer-thick NbSe₂ constrictions. As predicted by theory for valley Zeeman spin-orbit interaction (SOI), the observed supercurrent rectification is controlled by the *out-of-plane* field B_z . Remarkably, the in-plane field does play a role: it determines a preferred direction for the out-of-plane field, making the rectification effect asymmetric in B_z . Such asymmetry is in contrast to theory expectations for pure valley Zeeman spin-orbit. Instead, it points toward the presence of an additional Rashba SOI component in NbSe₂.

15 min. break

Invited Talk

TT 10.4 Tue 11:15 H3

Superconducting devices in magic-angle twisted bilayer graphene — •FOLKERT DE VRIES¹, ELIAS PORTOLES¹, GIULIA ZHENG¹, SHUICHI IWAKIRI¹, KENJI WATANABE², TAKASHI TANIGUCHI², THOMAS IHN¹, and KLAUS ENSSLIN¹ — ¹Laboratory for Solid State Physics, ETH Zurich, Otto-Stern-Weg 1, Zurich, Switzerland — ²National Institute for Materials Science, 1-1 Namiki, Tsukuba 305-0044, Japan

In situ electrostatic control of two-dimensional superconductivity is commonly limited due to large charge carrier densities, and gate-defined superconducting devices are therefore rare. Magic-angle twisted bilayer graphene (MATBG) has recently emerged as a versatile platform that combines metallic, superconducting, magnetic and insulating phases in a single crystal. Here we use multilayer gate technology and physical etching to create devices based on distinct phases in adjustable regions of MATBG. We electrostatically define the superconducting and insulating regions of a Josephson junction and observe tunable d.c. and a.c. Josephson effects. Furthermore, we form a ring shaped geometry with two Josephson junctions known as a superconducting quantum interference device. We observe the expected coherent oscillations of the supercurrent and extract characteristics such as the current phase relation and inductance. These works are an initial steps towards devices where gate-defined correlated states are connected in single-crystal nanostructures. We envision applications in superconducting electronics and quantum information technology.

Invited Talk

TT 10.5 Tue 11:45 H3

Minigap and Andreev bound states in ballistic graphene — •LUCA BANSZERUS^{1,2}, FLORIAN LIBISCH³, ANDREA CERUTI¹, STEFAN BLIEN⁴, KENJI WATANABE⁵, TAKASHI TANIGUCHI⁵, ANDREAS HÜTTEL⁴, BERND BESCHOTEN¹, FABIAN HASSLER¹, and CHRISTOPH STAMPFER¹ — ¹RWTH Aachen University, Germany — ²Forschungszentrum Jülich, Germany — ³TU Vienna, Austria — ⁴University of Regensburg, Germany — ⁵National Institute for Materials Science, Japan

A finite-size normal conductor, proximity-coupled to a superconductor has been predicted to exhibit a so-called minigap, in which quasiparticle excitations are prohibited. In this talk, we demonstrate the direct observation of such a minigap through transport measurements on partially gated ballistic graphene, coupled to superconducting MoRe contacts [1]. The minigap is probed by finite bias spectroscopy through a weakly coupled junction in the graphene region and its value is given by the dimensions of the device. Besides the minigap, a distinct peak in the differential resistance is observed, which we attribute to weakly coupled Andreev bound states (ABS) located near the superconductor-graphene interface. For weak magnetic fields, the phase accumulated in the normal-conducting region shifts the ABS in quantitative agreement with predictions from tight-binding calculations based on the Bogoliubov-de Gennes equation as well as with an analytical semiclassical model.

[1] arXiv:2011.11471

TT 10.6 Tue 12:15 H3

Competition of Density Waves and Superconductivity in Twisted Tungsten Diselenide — •LENNART KLEBL¹, AMMON FISCHER¹, LAURA CLASSEN², MICHAEL M. SCHERER³, and DANTE M. KENNES^{1,4} — ¹Institut für Theorie der Statistischen Physik, RWTH Aachen University and JARA-Fundamentals of Future Information Technology, D-52056 Aachen, Germany — ²Max Planck Institute for Solid State Research, D-70569 Stuttgart, Germany — ³Institut für Theoretische Physik III, Ruhr-Universität Bochum, D-44801 Bochum, Germany — ⁴Max Planck Institute for the Structure and Dynamics of Matter, Center for Free Electron Laser Science, D-22761 Hamburg, Germany

Evidence for correlated insulating and superconducting phases around regions of high density of states was reported in the strongly spin-orbit coupled van-der Waals material twisted tungsten diselenide (*t*WSe₂). We investigate their origin and interplay by using a functional renormalization group approach that allows to describe superconducting and spin/charge instabilities in an unbiased way. We map out the phase diagram as function of filling and perpendicular electric field, and find that the moiré Hubbard model for *t*WSe₂ features mixed-parity superconducting order parameters with *s/f*-wave and topological *d/p*-wave symmetry next to (incommensurate) density wave states. Our work systematically characterizes competing interaction-driven phases in *t*WSe₂ beyond mean-field approximations and provides guidance for experimental measurements by outlining the fingerprint of correlated states in interacting susceptibilities.

TT 10.7 Tue 12:30 H3

Tuning lower dimensional superconductivity with hybridization at a superconducting-semiconducting interface — •M. SIMONATO¹, A. KAMLAPURE¹, E. SIERDA¹, M. STEINBRECHER¹, U. KAMBER¹, E. J. KNOL¹, P. KROGSTROP^{2,3}, M.I. KATSNELSON¹, A.A. KHAJETOORIAN¹, and M. RÖSNER¹ — ¹Radboud University, Institute for Molecules and Materials, Nijmegen, The Netherlands — ²Center for Quantum Devices, Niels Bohr Institute, University of Copenhagen, Copenhagen, Denmark — ³Microsoft Quantum Materials Lab Copenhagen, Lyngby, Denmark

TT 11: Topology: Quantum Hall Systems

Time: Tuesday 9:30–12:30

Location: H10

TT 11.1 Tue 9:30 H10

Quantum Hall effect induced by chiral Landau levels in topological semimetal films — •DUY-HOANG-MINH NGUYEN¹, KOJI KOBAYASHI², JAN-ERIK REINHARD WICHMANN³, and KENTARO NOMURA² — ¹Donostia International Physics Center, Donostia-San Sebastian, Spain — ²Department of Physics, Kyushu University, Fukuoka, Japan — ³Institute for Materials Research, Tohoku University, Sendai, Japan

Motivated by recent transport experiments, we theoretically study the quantum Hall effect in topological semimetal films. Owing to the confinement effect, the bulk subbands originating from the chiral Landau levels establish energy gaps that have quantized Hall conductance and can be observed in relatively thick films. We find that the quantum Hall state is strongly anisotropic for different confinement directions not only due to the presence of the surface states but also because of the bulk chiral Landau levels. As a result, we re-examine the quantum Hall effect from the surface Fermi arcs and chiral modes in Weyl semimetals and give a more general view into this problem. Also, we find that when a topological Dirac semimetal is confined in its rotational symmetry axis, it hosts both

We demonstrate that the hybrid electronic structure derived at the interface between semiconducting black phosphorus and atomically thin films of lead can drastically modify the superconducting properties of the thin metallic film. Using ultra-low temperature scanning tunneling microscopy and spectroscopy, we observe a strongly anisotropic renormalization of the superconducting gap. To study the effect of hybridization, we develop a hybrid two-band model as an extension to conventional BCS theory in the Nambu-Gorkov formalism. In this model, we obtain analytical expressions for the effective gap and link the hybridization-driven renormalization to a weighting of the superconducting order parameter that quantitatively reproduces the measured spectra. These results illustrate the effect of interfacial hybridization at superconductor-semiconductor heterostructures, and pathways for engineering quantum technologies based on gate-tunable superconducting electronics.

TT 10.8 Tue 12:45 H3

Ab initio study of the van der Waals Superconductor NbSe₂ — •MOHAMMAD HEMMATI, PHILIPP RÜSSMANN, and STEFAN BLÜGEL — Peter Grünberg Institut and Institute for Advanced Simulation, Forschungszentrum Jülich and JARA, Jülich, Germany

Transition metal dichalcogenides (TMDCs) are a very versatile material class in which a plethora of physical phenomena can be realized. This ranges from the topological electronic structure in Weyl and Dirac semimetals to magnetic and even superconducting systems that can furthermore be combined due to the intrinsic van der Waals stacking in these materials. The TMDC NbSe₂ is an example of a layered superconducting material which shows, for instance, the unconventional Ising superconductivity that is particularly robust against magnetic fields [1]. We study bulk and single-layer NbSe₂ on the basis of first-principles calculations within the Korringa-Kohn-Rostoker Green function method which allows combining the accurate description of the electronic structure on the basis of density functional theory with a description of the superconductivity via the Bogoliubov-de Gennes formalism [2,3].

This work was funded by the Deutsche Forschungsgemeinschaft (DFG, German Research Foundation) under Germany's Excellence Strategy - Cluster of Excellence Matter and Light for Quantum Computing (ML4Q) EXC 2004/1 - 390534769.

[1] D. Wickramaratne *et al.*, Phys. Rev. X **10**, 041003 (2020)[2] <https://jukkr.fz-juelich.de>

[3] P. Rüßmann, S. Blügel, arXiv:2110.01713 (2021)

TT 10.9 Tue 13:00 H3

Emergence of unconventional proximity effect in Cr_{1/3}NbS₂/NbS₂ heterostructures — •ALFREDO SPURI, ROMAN HARTMANN, ELKE SCHEER, and ANGELO DI BERNARDO — University of Konstanz

The helimagnetic metal Cr_{1/3}NbS₂ has been reported to host soliton excitations based on magnetotransport measurements which have been performed on flakes of this material down to the 2D limit. Investigating the proximity effect between 2D flakes of such a magnetic material and conventional 2D superconductors could lead to the discovery of unconventional spin-triplet superconducting states, with possible applications for superconducting spintronics and quantum computing. Based on these motivations, we have fabricated 2D Cr_{1/3}NbS₂/NbS₂ and Cr_{1/3}NbS₂/NbS₂ bilayers and investigated their low temperature magnetotransport and spectroscopic properties. In addition, we have also realized /NbS₂/Cr_{1/3}NbS₂/NbS₂ Josephson junctions and performed measurements on them. The results obtained give indication for the emergence of an unconventional proximity effect, possibly due to the emergence of spin-triplet pairing correlations.

TT 11: Topology: Quantum Hall Systems

Time: Tuesday 9:30–12:30

Location: H10

TT 11.1 Tue 9:30 H10

Quantum Hall effect induced by chiral Landau levels in topological semimetal films — •DUY-HOANG-MINH NGUYEN¹, KOJI KOBAYASHI², JAN-ERIK REINHARD WICHMANN³, and KENTARO NOMURA² — ¹Donostia International Physics Center, Donostia-San Sebastian, Spain — ²Department of Physics, Kyushu University, Fukuoka, Japan — ³Institute for Materials Research, Tohoku University, Sendai, Japan

Motivated by recent transport experiments, we theoretically study the quantum Hall effect in topological semimetal films. Owing to the confinement effect, the bulk subbands originating from the chiral Landau levels establish energy gaps that have quantized Hall conductance and can be observed in relatively thick films. We find that the quantum Hall state is strongly anisotropic for different confinement directions not only due to the presence of the surface states but also because of the bulk chiral Landau levels. As a result, we re-examine the quantum Hall effect from the surface Fermi arcs and chiral modes in Weyl semimetals and give a more general view into this problem. Also, we find that when a topological Dirac semimetal is confined in its rotational symmetry axis, it hosts both

quantum Hall and quantum spin Hall states, in which the helical edge states are protected by the conservation of the spin-z component.

TT 11.2 Tue 9:45 H10

Quantum Hall critical phase at topological insulator surfaces — •JOHANNES DIEPLINGER¹, MATEO MORENO-GONZALEZ², SOUMYA BERA³, MARTIN PUSCHMANN¹, MATTHEW FOSTER⁴, FERDINAND EVERS¹, and ALEXANDER ALTLAND² — ¹University of Regensburg, Regensburg, Germany — ²University of Cologne, Cologne, Germany — ³IIT Bombay, Mumbai, India — ⁴Rice University, Houston, Texas, USA

We show that an AIII three-dimensional topological insulator, when tuned away from the critical point at zero energy, realizes a finite class A critical phase on its surface, i.e. a continuum of quantum Hall critical states, instead of a naively expected quantum Hall insulator. Criticality is characterized numerically via an analysis of the multifractal exponents of the wave functions at the surface of the three dimensional bulk.

This numerical work supports a recently proposed first principle theory explaining the existence of the quantum Hall critical phase. Open questions re-

main concerning the nature of disordered surface states with higher topological index.

TT 11.3 Tue 10:00 H10

Universal properties of boundary and interface charges in multichannel models of one-dimensional insulators — •KIRYL PIASOTSKI¹, NIKLAS MULLER¹, DANTE KENNES^{1,2}, HERBERT SCHOELLER¹, and MIKHAIL PLETYUKHOV¹ — ¹Institut für Theorie der Statistischen Physik, RWTH Aachen, 52056 Aachen, Germany — ²Max Planck Institute for the Structure and Dynamics of Matter, Center for Free Electron Laser Science, 22761 Hamburg, Germany

Generalizing our previous results on a one-dimensional single-channel continuum [1] and multichannel tight-binding [2] models, we present novel topological invariants to characterize boundary and interface charges in systems described by one-dimensional Schrödinger operators with periodic non-Abelian vector and scalar potentials. In particular, we prove that the change in boundary charge upon the continuous shift of the system towards the boundary by the distance $x_p \in [0, L]$ (L -period) is given by the sum of the linear function of x_p and an integer-valued topological index $I(x_p)$ - the boundary invariant, and provide two equivalent representations of $I(x_p)$. In addition, we study translationally invariant systems interrupted by a localized impurity, we show that an excess charge on the impurity is a quantized integer quantity given by a winding number expression.

[1] Phys. Rev. B **104**, 155409 (2021)

[2] Phys. Rev. B **104**, 125447 (2021)

TT 11.4 Tue 10:15 H10

antiferromagnetic chern insulator in a centrosymmetric system — •MORAD EBRAHIMKHAS¹, MOHSEN HAFEZ-TORBATI², and WALTER HOFSTETTER¹ — ¹Institut für Theoretische Physik, Goethe-Universität, 60438 Frankfurt/Main, Germany — ²Lehrstuhl für Theoretische Physik I, Technische Universität Dortmund, Otto-Hahn-Straße 4, 44221 Dortmund, Germany

An antiferromagnetic Chern insulator (AFCI) can exist if the effect of the time-reversal transformation on the AF state cannot be compensated by a space group operation. Such a state has recently been reported in a noncentrosymmetric Kane-Mele-Hubbard model. We investigate the possible emergence of this phase in a centrosymmetric system. We consider a minimal extension of the time-reversal invariant Harper-Hofstadter-Hatsugai model. The next-nearest-neighbor hopping opens a gap at half-filling and allows for the realization of a quantum spin Hall insulator. We add to the system a staggered potential Δ and the Hubbard interaction U favoring a normal insulator and a Mott insulator, respectively. We map out the phase diagram of the model in the U - Δ plane and show that an APCI with the Chern number $C = 1$ appears for $(U \sim 2\Delta) \gg t$. We find that for a fixed Δ upon increasing U a spin-flop transition from the $C = 1$ z-APCI to a topologically trivial xy-AF phase takes place. Our findings can be used as a guideline in future investigations searching for an APCI in optical lattices.

TT 11.5 Tue 10:30 H10

Supercurrent-enabled Andreev reflection in a chiral quantum Hall edge state — ANDREAS BOCK MICHELSEN^{1,2}, PATRIK RECHER³, BERND BRAUNECKER¹, and •THOMAS L. SCHMIDT² — ¹University of St Andrews, UK — ²University of Luxembourg, Luxembourg — ³Technische Universität Braunschweig, Germany

A chiral quantum Hall (QH) edge state placed in proximity to an s-wave superconductor experiences induced superconducting correlations. Recent experiments have observed the effect of proximity-coupling in QH edge states through signatures of the mediating process of Andreev reflection. We present the microscopic theory behind this effect by modeling the system with a many-body Hamiltonian, consisting of an s-wave superconductor, subject to spin-orbit coupling and a magnetic field, which is coupled by electron tunneling to a QH edge state. By integrating out the superconductor we obtain an effective pairing Hamiltonian in the QH edge state. We clarify the qualitative appearance of nonlocal superconducting correlations in a chiral edge state and analytically predict the suppression of electron-hole conversion at low energies (Pauli blocking) and negative resistance as experimental signatures of Andreev reflection in this setup. In particular, we show how two surface phenomena of the superconductor, namely Rashba spin-orbit coupling and a supercurrent due to the Meissner effect, are essential for the Andreev reflection. Our work provides a promising pathway to the realization of Majorana zero-modes and their parafermionic generalizations.

15 min. break

TT 11.6 Tue 11:00 H10

Synthetic gravitational horizons in low-dimensional quantum matter — •CORENTIN MORICE¹, ALI G. MOGHADDAM^{2,3}, DMITRY CHERNYAVSKY², JASPER VAN WEZEL¹, and JEROEN VAN DEN BRINK^{2,4} — ¹Institute for Theoretical Physics and Delta Institute for Theoretical Physics, University of Amsterdam, 1090 GL Amsterdam, The Netherlands — ²Institute for Theoretical Solid State Physics, IFW Dresden, Helmholtzstrasse 20, 01069 Dresden, Germany — ³Department of Physics, Institute for Advanced Studies in Basic Sciences (IASBS), Zanjan

45137-66731, Iran — ⁴Institute for Theoretical Physics and Würzburg-Dresden Cluster of Excellence ct.qmat, Technische Universität Dresden, 01069 Dresden, Germany

We propose a class of lattice models realizable in a wide range of setups whose low-energy dynamics exactly reduces to Dirac fields subjected to (1+1)-dimensional gravitational backgrounds, including (anti-)de Sitter spacetime. Wave-packets propagating on the lattice exhibit an eternal slowdown for power-law position-dependent hopping integrals $t(x) \propto x^\gamma$ when $\gamma \geq 1$, signalling the formation of black hole event horizons. For $\gamma < 1$ instead the wave-packets behave radically different and bounce off the horizon. We show that the eternal slowdown relates to a zero-energy spectral singularity of the lattice model and that the semiclassical wave packets trajectories coincide with the geodesics on (1+1)D dilaton gravity, paving the way for new and experimentally feasible routes to mimic black hole horizons and realize (1+1)D spacetimes as they appear in certain gravity theories.

TT 11.7 Tue 11:15 H10

Adiabatic preparation of fractional quantum Hall phases from the thin torus limit — •BENJAMIN MICHEN¹, CÉCILE REPELLIN², and JAN CARL BUDICH¹ — ¹Institute of Theoretical Physics, Technische Universität Dresden — ²Univ. Grenoble-Alpes, CNRS, LPMCM, 38000 Grenoble, France

We explore as to what extent reversing the thin torus (TT) limit enables the adiabatic preparation of fractional quantum Hall (FQH) states in quantum simulators. As a novel approach, the TT limit is taken by increasing the hopping amplitude in one direction in order to make the system effectively one-dimensional.

The regime of strongly anisotropic coupling features the expected charge density wave (CDW) ground state. The CDW state can be adiabatically connected to the FQH state by tuning the coupling back to the isotropic regime without closing the many-body excitation gap along the way. This may provide an experimental path to the adiabatic preparation of FQH states from topologically trivial CDW states.

We find that the many-body excitation gap in the TT limit decreases with system size for fully discrete models, which limits the adiabatic preparation. However, there appears to be no such restriction in a semicontinuous setup of coupled wires. In that sense, the proposed protocol could be experimentally relevant for arbitrary system sizes.

TT 11.8 Tue 11:30 H10

Non-Hermitian topological signatures in a quantum Hall system — •RAGHAV CHATURVEDI¹, KYRYLO OCHKAN¹, VIKTOR KÖNYE¹, EWELINA HANKIEWICZ², JEROEN VAN DEN BRINK¹, JOSEPH DUFOULEUR¹, and COSMA FULGA¹ — ¹IFW Dresden, Deutschland — ²Julius Maximilian University of Würzburg

Reflection matrices describing waves reflected from the boundaries of insulators exhibit non-Hermitian topological signatures. Drawing from this, we propose to realize non-Hermitian topology in the quantum regime of a two dimensional condensed-matter system. Our work is based on the insight that, in the limit of maximal non-reciprocity, the Hamiltonian for the simplest topological non-Hermitian system - the Hatano-Nelson chain - effectively describes a one-dimensional, unidirectionally propagating mode. This is analogous to the unidirectional boundary mode of a fully Hermitian topological insulator: the quantum Hall system. We show that the multi-terminal conductance matrix of this system exhibits a topologically protected non-Hermitian skin effect. Moreover, we show that the topological invariant characterizing these features is more robust than the Chern number, as it remains well-quantized even across quantum Hall plateau transitions. Our work shows that the transport properties of Chern insulators may exhibit signatures of non-Hermitian topology, and this paves the way for the first experimental observation of non-Hermitian topology in a quantum condensed-matter system, which will be presented by another author.

TT 11.9 Tue 11:45 H10

Observation of non-Hermitian topology in a multi-terminal quantum Hall device — •KYRYLO OCHKAN¹, RAGHAV CHATURVEDI¹, VIKTOR KÖNYE¹, EWELINA HANKIEWICZ², JEROEN VAN DEN BRINK¹, JOSEPH DUFOULEUR¹, and COSMA FULGA¹ — ¹IFW Dresden, Deutschland — ²Julius-Maximilians-Universität Würzburg, Deutschland

One of the simplest examples of non-Hermitian topology is encountered in the Hatano-Nelson (HN) model, a one-dimensional chain where the hopping in one direction is larger than in the opposite direction. We present here the first experimental observation of non-Hermitian topology in a quantum condensed-matter system. The measurements are done in a multi-terminal quantum Hall device etched in a high mobility GaAs/AlGaAs two-dimensional electron gas ring. The conductance matrix that connects the currents flowing from the active contacts to the ground with the voltage of the active contacts is topologically equivalent to the HN Hamiltonian.

In our device, we directly measure and evidence the non-Hermitian skin effect. We also compute for our experimental device two topological invariants that are found to be more robust than the Chern number. We finally use the unique properties of our system and continuously tune the system configuration between open and periodic boundary conditions.

We focus here on the experimental results, whereas the theoretical aspects of the non-Hermitian skin effect and the topological invariants will be discussed in another presentation.

TT 11.10 Tue 12:00 H10

Emergent non-Hermitian topology and boundary sensitivity in interacting Su-Schrieffer-Heeger chains — •TOMMASO MICALLO, CARL LEHMANN, and JAN CARL BUDICH — Institute of Theoretical Physics, Technische Universität Dresden and Würzburg-Dresden Cluster of Excellence ct.qmat, 01062 Dresden, Germany

The exponential sensitivity of effective Non-Hermitian (NH) Hamiltonians with respect to boundary conditions has recently been predicted and observed in a broad range of settings. Here, we discuss as to what extent this remarkable phenomenon may occur in closed correlated fermionic systems that are governed by a Hermitian many-body Hamiltonian. There, an effectively NH quasiparticle description naturally arises in the Green's function formalism due to inter-particle scattering that represents a source of inherent dissipation. Using exact diagonalization, we analyze as a concrete platform extended Su-Schrieffer-Heeger (SSH) chains with interactions subject to varying boundary conditions.

TT 11.11 Tue 12:15 H10

Absent thermal equilibration on fractional quantum Hall edges over macroscopic scale — •RON MELCER¹, BIVAS DUTTA¹, CHRISTIAN SPANSLATT^{2,3,4}, JINHONG PARK⁵, ALEXANDER MIRLIN^{3,4}, and VLADIMIR UMANSKY¹ — ¹Braun Center for Submicron Research, Department of Condensed Matter Physics, Weizmann Institute of Science, Rehovot, 761001, Israel — ²Department of Microtechnology and Nanoscience, Chalmers University of Technology, S-412 96, Göteborg, Sweden — ³Institute for Quantum Materials and Technologies, Karlsruhe Institute of Technology, 76021, Karlsruhe, Germany — ⁴Institut für Theorie der Kondensierten Materie, Karlsruhe Institute of Technology, 76128, Karlsruhe, Germany — ⁵Institute for Theoretical Physics, University of Cologne, Zùlpicher Str. 77, 50937, Köln, Germany

Two-dimensional topological insulators, and in particular quantum Hall states, are characterized by an insulating bulk and a conducting edge. Fractional states may host both downstream (dictated by the magnetic field) and upstream propagating edge modes, which leads to complex transport behavior. Here, we combine two measurement techniques, local noise thermometry and thermal conductance, to study thermal properties of states with counter-propagating edge modes. We find that, while charge equilibration between counter-propagating edge modes is very fast, the equilibration of heat is extremely inefficient, leading to an almost ballistic heat transport over macroscopic distances. Moreover, we observe an emergent quantization of the heat conductance associated with a strong interaction fixed point of the edge modes.

TT 12: Correlated Electrons: Materials

Time: Tuesday 9:30–13:00

Location: H22

TT 12.1 Tue 9:30 H22

Low-dimensional magnetism in ordered perovskite and Ruddlesden-Popper variants — •RYAN MORROW, ANASTASIIA SMERCHUK, TAMARA HOLUB, SABINE WURMEHL, and BERND BÜCHNER — Leibniz Institute for Solid-State and Materials Research, IFW-Dresden, 01069 Dresden, Germany

Perovskites and their myriad of structural permutations have long been studied for their intriguing properties and interplay of degrees of freedom, both chemical and physical. While generally three dimensional in nature, perovskites can provide multiple means of access to low dimensional properties as well. In this talk, new results in three different directions pertaining to this concept will be presented. The first, most common approach, is the use of the Ruddlesden-Popper and similar phases, which separate perovskite-like layers with intercalated AO layers, rendering them primarily two dimensional. Several new cation-ordered iridate and rhodate Ruddlesden-Popper phases will be presented. The second approach is that of orbital order using Cu^{2+} in the double perovskite structure to yield in-plane only square lattice like magnetic interactions (e.g. Ba_2CuWO_6). New compounds produced by substitution series and high pressure methods will be shown. The third is that of vacancy ordering. By ordering of vacancies in combination with cation ordering, hexagonal perovskite phases can be reduced to well separated triangular two dimensional magnets with variable spin sizes and frustration. Again, new compounds will be shown. In all three directions, primarily crystallographic and magnetometry data on these new inorganic transition metal oxides will be presented.

TT 12.2 Tue 9:45 H22

Strain mediated phase transitions in SrCrO_3 — •ALBERTO CARTA and CLAUDE EDERER — Materials Theory, ETH Zurich, Switzerland

SrCrO_3 is a complex perovskite oxides that can exhibit a plethora of interesting and technologically promising characteristics. However, available experimental reports still disagree on whether the material is metallic or semiconducting, or whether it is paramagnetic or antiferromagnetic. In a recent pre-print, Bertino et al. also reported a transition from conducting to insulating behavior for thin films of SrCrO_3 grown at different levels of epitaxial strain [1]. In our work, we use density functional theory (DFT) and DFT+U to establish the basic properties of SrCrO_3 . Our calculations clearly suggest a metallic C-type antiferromagnetic ground state, consistent with previous DFT studies[2]. Furthermore, we show that the electronic and magnetic properties of SrCrO_3 are strongly influenced by epitaxial strain, and that the system can develop orbital order coupled to a Jahn-Teller structural distortion under tensile strain. We explore the regime where this distortion is possible and propose a mechanism for the transition to the insulating state that is consistent with the observations of [1].

[1] G. Bertino, H.C. Hsing, A. Gura, X. Chen, T. Sauyet, M. Liu, C.Y. Nam, M. Dawber, arXiv: 2104.02738 (2021)

[2] K.W. Lee, W. E. Pickett, Phys. Rev. B 80, 1 (2009)

TT 12.3 Tue 10:00 H22

Thermodynamic Signatures of the Soliton Lattice in Single-Crystal TbFeO_3 — •ALEXANDER ENGELHARDT¹, JOHANNA JOCHUM², ANDREAS BAUER¹, ANDREAS ERB³, ASTRID SCHNEIDEWIND⁴, and CHRISTIAN PFLEIDERER¹ — ¹TU München, Garching, Germany — ²Heinz Maier-Leibnitz Zentrum (MLZ), TU München, Garching, Germany — ³Walther-Meißner-Institut, Garching, Germany — ⁴Forschungszentrum Jülich GmbH, Jülich Center for Neutron Sciences at MLZ, Garching, Germany

The properties of the orthorhombic perovskite TbFeO_3 originate from the interplay of a Tb and Fe magnetic sublattices, resulting in a complex magnetic phase diagram. Perhaps most remarkable, at low temperatures, a complex and anharmonic magnetic structure, a so-called magnetic soliton lattice, was identified by means of neutron scattering under magnetic fields up to 4 T [1]. Here, we report the single-crystal growth of TbFeO_3 using a combination of a solid-state reactions and optical float-zoning. Measurements of the magnetic ac susceptibility and the specific heat are characteristic of strong easy-plane magnetic anisotropy with two prominent magnetic phase transitions in zero magnetic field at 8 K and 3 K, consistent with the literature. By combining transverse-field ac susceptibility measurements with neutron scattering, we have determined the magnetic phase diagram. When a magnetic field is applied along the hard magnetic c axis, the soliton lattice may be traced up to 12 T, the highest field studied.

[1] S. Artyukhin et al., Nat. Mater. 11, 694 (2012)

TT 12.4 Tue 10:15 H22

Lattice dynamic of LiReO_3 across the continuous ferroelectric-like structural transition — •KSENIA DENISOVA¹, PETER LEMMENS¹, KANTARO MURAYAMA², XIANGYU GU², HIROSHI TAKATSU², CEDRIC TASSEL², and HIROSHI KAGEYAMA² — ¹IPKM, TU BS, Braunschweig, Germany — ²Kyoto University, Kyoto, Japan

The observation of a ferroelectric instability in metallic LiOsO_3 [1] with strongly correlated electrons [2] has fueled an intense discussion on the origin of polar metallicity. A comparative Raman study [3] of the isostructural compound LiReO_3 reveals that the enlarged lattice parameters leads to softer Li vibrations and enhances fluctuations in the system. The phonon anomalies point to the phase transition at $T=175$ K with a crossover regime to temperatures as low as 140 K. The hysteresis in the temperature evolution of ReO_6 related modes as opposed to an abrupt softening of Li vibrations in the ferroelectric phase speaks in favour of a decoupling of polar degrees of freedom and itinerant electrons.

Work supported by the DFG EXC-2123-390837967 Quantum-Frontiers, DFG Le967/16-1, and DFG-RTG 1952/1.

[1] Y. Shi et al., Nat. Mater. 12, 1024 (2013)

[2] J.S. Zhou et al., PRB 104, 115130 (2021)

[3] F. Jin et al., PNAS 116, 20322 (2019)

TT 12.5 Tue 10:30 H22

Magnetic anisotropy, magnetoelastic coupling and the phase diagram of $\text{Ni}_{0.25}\text{Mn}_{0.75}\text{TiO}_3$ — •AHMED ELGHANDOUR, LUKAS GRIES, LENNART SINGER, KAUSTAV DEY, and RÜDIGER KLINGELER — Kirchhoff Institute for Physics, Heidelberg University, Heidelberg, Germany

Thermodynamic studies on high-quality single crystals of $\text{Ni}_{0.25}\text{Mn}_{0.75}\text{TiO}_3$ have been used to investigate magneto-structural coupling and to construct the magnetic phase diagram. Clear anomalies in the thermal expansion at the spin ordering and spin reorientation temperatures, T_N and T_R , evidence pronounced magneto-elastic effects. Notably, magnetic entropy is released mainly above T_N implying considerable short range magnetic order up to about $4T_N$. This is associated with a large regime of negative thermal expansion of the c axis. Both T_N and T_R exhibit the same sign of uniaxial pressure dependence which is positive (negative) for pressure applied along the b (c) axis. In addition, while our data indicate a glassy behaviour below $T^* \approx 3.7$ K, a significant amount of Ni^{2+} moments seems neither involved in long-range order nor in the glassy state.

TT 12.6 Tue 10:45 H22

NMR investigations of a quasi-two-dimensional Heisenberg antiferromagnet under pressure — •F. BÄRTL^{1,2}, D. OPPERDEN^{1,2}, C. P. LANDEE³, S. MOLATTA^{1,2}, J. WOSNITZA^{1,2}, M. BAENITZ⁴, and H. KÜHNE¹ — ¹Hochfeld-Magnetlabor Dresden (HLD-EMFL), HZDR, Dresden, Germany — ²Institut für Festkörper- und Materialphysik, TU Dresden, Germany — ³Department of Physics, Clark University, Worcester, Massachusetts, USA — ⁴MPI for Chemical Physics of Solids, Dresden, Germany

The molecular-based material $[\text{Cu}(\text{pz})_2(2\text{-HOPy})_2](\text{PF}_6)_2$ (CuPOF) is an excellent realization of a two-dimensional square-lattice quantum $S = 1/2$ Heisenberg antiferromagnet, with an intralayer exchange coupling $J/k_B = 6.8$ K and an interlayer coupling $J' \approx 10^{-4}J$. Previously reported nuclear magnetic resonance (NMR) data revealed a low-temperature transition to a commensurate antiferromagnetic (AF) quasistatic long-range order (LRO), with a preceding crossover from isotropic Heisenberg to anisotropic XY behavior. We present further NMR studies of the low-temperature correlations in magnetic fields up to 7 T and temperatures down to 0.3 K. The application of hydrostatic pressure up to 10 kbar leads to a change of the interlayer coupling and, therefore, the magnetic correlations in the critical regime. The transition regime is probed by ¹H and ³¹P spectroscopy and relaxometry, revealing a monotonic change of T_N with increasing pressure. The commensurate AF LRO below T_N persists at high pressures, as revealed by a splitting of the ¹H NMR lines, stemming from the broken symmetry of the local spin polarizations in the LRO regime.

TT 12.7 Tue 11:00 H22

Electronic structure of CeTAl₃ (T=Ag, Au, Cu, Pd, Pt) studied with density functional theory — •ANDRÉ DEYERLING¹, ANDREAS BAUER¹, CHRISTIAN FRANZ², MARC A. WILDE¹, and CHRISTIAN PFLIEDERER¹ — ¹Physics Department, Technical University Munich, Garching, Germany — ²Jülich Centre for Neutron Science (JCNS) at Heinz Maier-Leibnitz Zentrum (MLZ), Garching, Germany

The CeTAl₃ family (T=Ag, Au, Cu, Pd, Pt) is prototypical of strongly correlated electron systems with a large variety of different magnetic ordering phenomena [1,2,3,4], such as ferromagnetism in CeAgAl₃ and incommensurate antiferromagnetism in CeAuAl₃. Further, in CeAuAl₃ [5] and CeCuAl₃ [6] magneto-elastic hybrid excitations between crystal electric fields and phonons have been observed. The electronic structure, and in particular the role of the Ce-4f electron, is key for understanding the mechanism driving these phenomena. We report electronic structure calculations for selected members of the CeTAl₃ family, where the Ce-4f electrons are described either as being itinerant or localized using DFT or DFT+U, respectively. The results of our calculations treating the 4f electrons as localized are in good agreement with the experimental data available.

- [1] C. Franz et al., J. Alloy. Comp. 668, 978 (2016)
- [2] D.T. Adroja et al., Phys. Rev. B 91, 134425 (2015)
- [3] M. Klippera et al., Phys. Rev. B 91, 224419 (2015)
- [4] M. Stekiel et al., arXiv:2106.08194 (2021)
- [5] P. Čermák et al., Proc. Natl. Acad. Sci. 116, 6695 (2019)
- [6] D.T Adroja et al., Phys. Rev. Lett. 108, 216402 (2012)

15 min. break

TT 12.8 Tue 11:30 H22

Charge-carrier properties near the bandwidth-controlled Mott transition in layered organic conductors probed by magnetic quantum oscillations — •MARK V. KARTSOVNIK¹, SEBASTIAN OBERBAUER^{1,2}, SHAMIL ERKNOV^{1,2}, WERNER BIBERACHER¹, and NATALIA D. KUSHCH¹ — ¹Walther-Meißner-Institut, Garching, Germany — ²Technische Universität München, Garching, Germany

Despite the great amount of work devoted to the Mott metal-insulator transition (MIT), some key theoretical predictions in this field are still awaiting experimental verification. In particular, there is no clarity about the exact behavior of the quasiparticle mass renormalized by many-body interactions, or about the pseudogap formation in the metallic ground state close to the bandwidth-controlled first-order MIT. Here we address these issues by employing organic κ -type salts as exemplary quasi-2D Mott systems and gaining direct access to their charge carrier properties via magnetic quantum oscillations. We trace the evolution of

the effective cyclotron mass as the conduction bandwidth is tuned very close to the MIT by means of precisely controlled external pressure. We find that the sensitivity of the mass renormalization to subtle changes of the bandwidth strongly exceeds the theoretical predictions and is even further enhanced upon entering the transition region where the metallic and insulating phases coexist. On the other hand, even at this very edge of stability of the metallic ground state its Fermi surface remains fully coherent.

TT 12.9 Tue 11:45 H22

Anisotropic quasiparticle life times and magnetotransport in the doped Hubbard model — •NIKLAS WITT¹, ERIK VAN LOON², SERGEY BRENER¹, MIKHAIL KATSNELSON³, ALEXANDER LICHTENSTEIN¹, and TIM WEHLING¹ — ¹University of Hamburg, Hamburg, Germany — ²Lund University, Lund, Sweden — ³Radboud University, Nijmegen, The Netherlands

The strange metal phase of high-temperature superconducting copper oxide (cuprate) materials exhibits several unconventional transport properties like T-linear resistivity that do not conform to a conventional Fermi liquid description. The crossover to a normal metal for large dopings and the origin of the anomalous electronic properties remain unsolved problems.

Recent transport measurements [1,2] suggest that two different charge sectors exist, one with coherent quasiparticle charge carriers and the other with incoherent non-quasiparticle excitations. Only the former contributes to transport, leading to a drop of the Hall carrier density for small doping. To examine this hypothesis, we study the hole-doped Hubbard model using complementary many-body methods from the weak- and strong-coupling limit. We demonstrate that a dichotomy of the scattering rates between charge carriers from different momentum regions emerges which can lead to the reduction of the Hall carrier density already in the framework of semiclassical Boltzmann theory.

- [1] M. Culo et al., SciPost Physics 11 (2021)
- [2] J. Ayres et al., Nature 595, 661 (2021)

TT 12.10 Tue 12:00 H22

Electron spin resonance studies on layered van-der-Waals magnets — •JOYAL JOHN ABRAHAM^{1,2}, YURI SENYK¹, ALEXEY ALFONSOV¹, YULIA SHERMERLIUK¹, SEBASTIAN SELTER¹, SAICHARAN ASWARTHAM¹, BERND BÜCHNER^{1,3}, and VLADISLAV KATAEV¹ — ¹Leibniz IFW Dresden, D-01069 — ²Institute for Solid State and Materials Physics, TU Dresden, D-01069 — ³Institute for Solid State and Materials Physics and Würzburg-Dresden Cluster of Excellence ct.qmat, TU Dresden, D-01062

Magnetic van-der-Waals (vdW) materials are compounds in which the planes consisting of magnetic atoms are held by weak vdW bonds. With a striking advantage of mechanical exfoliation to produce atomically thin layers, they are considered as promising candidates for studying exotic quantum phenomena and device application. Here, we present the investigation of magnetic vdW single crystals $\text{Mn}_2\text{P}_2\text{S}_6$ and MnNiP_2S_6 , using high field/frequency electron spin resonance. Frequency dependence of resonance field reveals a change of the anisotropy from easy-axis-like in the pure Mn compound to an easy-plane-like in the mixed compound. Temperature dependence of resonance field and linewidth for in-plane and out-of-plane orientations of magnetic field reveals a shift in resonance from the paramagnetic position even above the transition temperature (T_N). This could be indicative of the presence of quasi-static spin-spin short-range correlations and hence provides insight about magnetic dimensionality of the studied material.

TT 12.11 Tue 12:15 H22

Magnon excitations, spin-lattice coupling and the emerging anisotropic nature of short-range order in van-der-Waals ferromagnets — M. JONAK¹, J. ARNETH¹, A. ELGHANDOUR¹, E. WALDENDY¹, S. SPACHMANN¹, C. KOO¹, M. ABDEL-HAFIEZ², S. SELTER³, S. ASWARTHAM³, and •RÜDIGER KLINGELER¹ — ¹Kirchhoff Institute for Physics, Heidelberg University, Germany — ²Dep. of Physics & Astronomy, Uppsala University, Sweden — ³IFW Dresden, Germany

CrI_3 and $\text{Cr}_2\text{Ge}_2\text{Te}_6$ are quasi-2D semiconducting van der Waals ferromagnets which evolve long-range order down to the single- or double-layer limit. Quantitative determination of magnetic anisotropy and spin-lattice coupling are crucial to further exploit these materials. We report ferromagnetic resonance studies in a broad frequency regime of 30 - 330 GHz and in magnetic fields up to 18 T and high-resolution capacitance dilatometry. Our data prove significant magneto-elastic coupling and provide quantitative values of the uniaxial pressure effects. Modelling the magnon branches in CrI_3 by means of a domain-based ferromagnetic resonance model provides the microscopic parameters such the anisotropy gap of 80 GHz at 2 K which remarkably remains finite at T_C and vanishes only above 80 K. In addition, we detect short-range magnetic correlations up to at least 160 K. Notably, the nature of the short-range correlations in CrI_3 changes, confirming the importance of spin-orbit coupling for the evolution of long-range ferromagnetism which develops from magnetically anisotropic short-range order.

TT 12.12 Tue 12:30 H22

Orbital order and nematic instability in the antiferromagnetic phase of BaCoS₂ — •BENJAMIN LENZ¹, MICHELE FABRIZIO², and MICHELE CASULA¹ — ¹Institut de minéralogie, de physique des matériaux et de cosmochimie (IMPMC), Sorbonne University - CNRS - MNHN, Paris, France — ²Scuola Internazionale Superiore di Studi Avanzati (SISSA), Trieste, Italy

We present evidence for a nematic instability in the antiferromagnetic insulating phase of BaCoS₂, which shows a Néel transition at a surprisingly high temperature of $T_N \sim 300$ K. Based on *ab initio* simulations, we discuss several competing orders in terms of magnetic order, orbital composition and structural distortions to identify a set of nematic and orbital ordered states as possible candidates for the ground state. From these considerations we derive an effective spin-model of $J_1 - J_2$ type and discuss the consequences of the most probable, orbital ordered ground state for its parametrization. We finally identify a driving mechanism which allows to explain the high Néel temperature by \mathcal{C}_4 -symmetry breaking through orbital order and draw parallels to other quasi-2D materials such as pnictides.

TT 12.13 Tue 12:45 H22

Tuning the multiorbital Mott transition of BaCoS₂ — •HANEEN ABUSHAMMALA^{1,2}, YANNICK KLEIN¹, and ANDREA GAUZZI¹ — ¹IMPMC, Sorbonne University, 4, place Jussieu, 75005 Paris, France — ²Institute for Experimental Physics IV, Ruhr-Universität Bochum, Germany

The quasi-2D BaCoS₂ system displays an unusual Mott state concomitant with a stipe-type antiferromagnetic (AFM) ordering at $T_N=305$ K in a square-lattice of Co²⁺. Electron doping by partial Co/Ni substitution, or hydrostatic pressure drives the system into a paramagnetic and Fermi Liquid (FL) metallic phase. Interestingly, this metal-insulator transition (MIT) is not accompanied by any significant structural distortion, which offers ideal conditions to investigate the FL to non-FL crossover in a model square-lattice system in the regime of moderate electronic correlations typical of sulphides. In order to investigate the interplay between AFM order and Mott state, we have studied the effect of chemical pressure and hole doping on the AFM order by partially substituting Sr and K for Ba respectively. Contrary to the case of hydrostatic pressure, we find that chemical pressure significantly reduces T_N down to 240 K for a substitution level of 8 at%, corresponding to an effective pressure of 0.3 GPa. The K-substitution is found to induce similar suppression of the AFM order as compared to the Sr-substitution. However, its sizable value of Sommerfeld coefficient (5.7 mJ/mol.K²) suggests a metallic state induced by hole doping. Studies on single crystals may unveil whether the metallic state induced by K-doping displays FL-properties.

TT 13: Quantum Dots, Quantum Wires, Point Contacts

Time: Tuesday 9:30–11:00

Location: H23

TT 13.1 Tue 9:30 H23

Precession of entangled spin and pseudospin in double quantum dots — •CHRISTOPH ROHRMEIER and ANDREA DONARINI — University Regensburg
Quantum dot spin valves are characterized by exchange fields [1] which induce spin precession and generate anomalous spin resonances [2]. Analogous effects have been studied in double quantum dots, in which the orbital degree of freedom replaces the role of the spin in the valve configuration [3]. We generalize, now, this setup to allow for arbitrary spin and orbital polarization of the leads, thus obtaining an even richer variety of current resonances, stemming from the entangled precession dynamics of the spin and pseudospin [4]. We observe for both vectors a delicate interplay of decoherence, pumping and precession which can only be understood by including the dynamics of the spin-pseudospin correlators. The results are obtained in the framework of a generalized master equation within the cotunneling approximation and are complemented by a coherent sequential tunneling model.

[1] Braun et al., Phys. Rev. B 70 (2004) 195345

[2] Hell et al., Phys. Rev. B 91 (2015) 195404

[3] Rohrmeier et al., Phys. Rev. B 103 (2021) 205420

[4] Rohrmeier et al., Phys. Rev. B 105 (2022) 205418

TT 13.2 Tue 9:45 H23

Pair-amplitude dynamics in superconductor-quantum dot hybrids — •MARKUS HECKSCHEN and BJÖRN SOTHMANN — Universität Duisburg-Essen, Duisburg, Deutschland

We consider a three-terminal system consisting of a quantum dot strongly coupled to two superconducting reservoirs in the infinite gap limit and weakly coupled to a normal metal. Using a real-time diagrammatic approach, we calculate the dynamics of the proximity-induced pair amplitude on the quantum dot. We find that after a quench the pair amplitude shows pronounced oscillations with a frequency determined by the coupling to the superconductors. In addition, it decays exponentially on a time scale set by the coupling to the normal metal. Strong oscillations of the pair amplitude occur also when the system is periodically driven both in the adiabatic and fast-driving limit. We relate the dynamics of the pair amplitude to the Josephson and Andreev current through the dot to demonstrate that it is an experimentally accessible quantity.

[1] M. Heckschen and B. Sothmann, Phys. Rev. B 105 (2022) 045420

TT 13.3 Tue 10:00 H23

Staggered spin-orbit interaction in a nanoscale device — LAURIANE CONTAMIN¹, TINO CUBAYNES¹, WILLIAM LEGRAND¹, •MAGDALENA MARGANSKA², MATTHIEU DESJARDINS¹, MATTHIEU DARTAILH¹, ZAKI LEGHTAS^{1,3,4}, ANDRE THIUVILLE⁵, STANISLAS ROHART⁵, AUDREY COTTET¹, MATTHIEU DELBECQ¹, and TAKIS KONTOS¹ — ¹Laboratoire de Physique de l'Ecole Normale Supérieure, ENS, Université PSL, CNRS, Sorbonne Université, Université Paris-Diderot, Sorbonne Paris Cité, Paris, France — ²Institute for Theoretical Physics, University of Regensburg, Germany — ³QUANTIC Team, INRIA de Paris, Paris, France — ⁴Centre Automatique et Systemes, Mines Paris-Tech, PSL Research University, Paris, France — ⁵Laboratoire de Physique des Solides, Université Paris-Saclay, CNRS, UMR 8502, Orsay, France

The coupling of the spin and the motion of charge carriers is an important ingredient for the manipulation of the spin degree of freedom and for the emergence of topological matter. Creating domain walls in the spin-orbit interaction at the nanoscale may turn out to be a crucial resource for engineering topological excitations suitable for universal topological quantum computing or for new schemes for spin quantum bits. Realizing this in natural platforms remains a challenge. Using high resolution circuit quantum electrodynamics magneto-spectroscopy, we show how this can be implemented in carbon nanotubes with a staggered synthetic spin-orbit interaction induced by two lithographically patterned magnetically textured gates.

TT 13.4 Tue 10:15 H23

Jahn-Teller effects in charge transport through single-molecule junctions: a hierarchical equation of motion approach — •CHRISTOPH KASPAR and MICHAEL THOSS — University of Freiburg

Molecules with degenerate electronic states may exhibit Jahn-Teller effects [1]. In this contribution, we investigate charge transport through such molecules bound to metal electrodes within a molecular junction [2]. The study employs the hierarchical equation of motion approach [3,4] to open quantum system dynamics. This method generalizes perturbative master equation methods by including higher-order contributions as well as non-Markovian memory, thus allowing for a systematic convergence of the results. Extending previous studies [5], we find that the molecule can become trapped in a nonconducting state resulting in a current-blockade, out of which only higher-order processes such as cotunneling provide an escape mechanism.

[1] M. O'Brien et al., Am. J. Phys. 61, 688 (1993)

[2] C. Kaspar et al., Phys. Rev. B 105, 195435 (2022)

[3] Y. Tanimura, J. Chem. Phys. 153, 020901 (2020)

[4] C. Schinabeck et al., Phys. Rev. B 94, 201407R (2016)

[5] M. Schultz et al., Phys. Rev. B 77, 075323 (2008)

TT 13.5 Tue 10:30 H23

Evolution of single-level-model parameters in the mechanically controllable break junctions — •M. LOKAMANI^{1,2}, F. KILIBARDA², F. GÜNTHER³, J. KELLING¹, A. STROBEL², P. ZAHN², G. JUCKELAND¹, K. GOTHELF⁴, E. SCHEER⁵, S. GEMMING⁶, and A. ERBE² — ¹FWCC, HZDR, Dresden, Germany — ²FWIO, HZDR, Dresden, Germany — ³IFSC, São Carlos, Brazil — ⁴INANO, Aarhus, Denmark — ⁵Department of Physics, Uni Konstanz, Germany — ⁶Institute of Physics, TU Chemnitz, Germany

The electrical properties of single molecules can be investigated using atomically sharp metallic electrodes in mechanically controllable break junctions (MCBJs). The current-voltage (IV) characteristics of single molecules in such junctions are influenced by the binding positions of the end groups on the tip-facets and tip-tip separation. In this talk, we present MCBJ experiments on N,N'-Bis(5-ethynylbenzenethiol-salicylidene)ethylenediamine (Salen). We discuss the evolution of the single level model (SLM) parameters namely, a) the energetic level ϵ of the dominant conducting channel and b) the coupling Γ of the dominant conducting channel to the metallic electrodes. The SLM-parameters were evaluated for IV-curves recorded during opening measurements and fitted to the

single level model. We propose a novel, high-throughput approach to model the evolution of the SLM-parameters and explain the recurring peak-like features in the experimentally measured evolution of Γ with increasing tip-tip separation, which we relate to the deformation of the molecule and the sliding of the anchor group above the electrode surface.

TT 13.6 Tue 10:45 H23

Relaxation dynamics in a Hubbard trimer and tetramer coupled to fermionic baths: antiferromagnetic order and persistent spin currents — •NIKODEM SZPAK¹, GERNOT SCHALLER², FRIEDEMANN QUEISSER², RALF SCHÜTZHOLD^{2,3}, and JÜRGEN KÖNIG¹ — ¹Theoretische Physik, Universität Duisburg-Essen, Lotharstr. 1, 47048 Duisburg — ²Helmholtz-Zentrum Dresden-Rossendorf, Bautzner Landstraße 400, 01328 Dresden — ³Institut für Theoretische Physik, Technische Universität Dresden, 01062 Dresden

We study relaxation dynamics in a strongly-interacting three and four-site Fermi-Hubbard system (quantum dots) coupled to environment represented by fermionic baths. Starting with an ab initio approach, we derive several variants of the Lindblad master equation for the quantum dots systems by applying different approaches: local and global, secular and coherent [1,2]. At low temperatures, depending on the particular parameter ratios and applied approximations, the system tends to or destroys antiferromagnetic order [2]. In three quantum dots, the system becomes spin-frustrated and relaxes to a stable persistent spin current.

[1] E. Kleinherbers, N. Szpak, J. König, and R. Schützhold, Phys. Rev. B 101, 125131

[2] G. Schaller, F. Queisser, N. Szpak, J. König, and R. Schützhold, Phys. Rev. B 105, 115139

TT 14: Many-Body Quantum Dynamics 2 (joint session DY/TT)

Time: Tuesday 11:30–13:00

Location: H20

See DY 19 for details of this session.

TT 15: Nano- and Optomechanics

Time: Tuesday 11:15–12:45

Location: H23

TT 15.1 Tue 11:15 H23

Mechanical frequency control in inductively coupled electromechanical systems — •THOMAS LUSCHMANN^{1,2,3}, PHILIP SCHMIDT^{1,2}, FRANK DEPPE^{1,2,3}, ACHIM MARX¹, ALVARO SANCHEZ⁴, RUDOLF GROSS^{1,2,3}, and HANS HUEBL^{1,2,3} — ¹Walther-Meißner-Institut, Bayerische Akademie der Wissenschaften, Garching, Germany — ²Physik-Department, Technische Universität München, Garching, Germany — ³Munich Center for Quantum Science and Technology, Munich, Germany — ⁴Department of Physics, Universitat Autònoma de Barcelona, Bellaterra, Spain

Nano-electromechanical systems couple mechanical motion to superconducting quantum circuits at microwave frequencies. While traditional, capacitive coupling strategies operate in the weak coupling regime, inductive coupling schemes based on partially suspended superconducting interference devices (SQUID) have demonstrated significantly improved coupling rates. Such systems are expected to allow for the exploration of phenomena beyond the linearized optomechanical interaction. Here, we present an investigation into the tuning of the mechanical resonance frequency in an inductively coupled system. The experimental data quantitatively corroborates theoretical predictions for SQUID-based electromechanical systems. In addition, we observe a magnetic field dependent tuning of the mechanical resonance frequency, which we attribute to an effective interaction of the atomic lattice and the superconducting vortex lattice.

TT 15.2 Tue 11:30 H23

Current-induced forces in nano-electromechanical systems: A hierarchical equations of motion approach — •SAMUEL RUDGE and MICHAEL THOSS — Physikalisches Institut, Albert-Ludwigs Universität Freiburg

Current-induced forces in nanostructures provide valuable insight into the mechanisms of nonequilibrium charge transport through nano-electromechanical systems [1]. In this contribution, we investigate specifically the electronic friction in molecular junctions using the hierarchical equations of motion approach [2-3]. Since this method is, in principle, numerically exact, it allows us to extend previous studies [4] beyond the Born-Markov approximation and incorporate strong intra-system interactions. To demonstrate the approach, we consider a resonant level model coupled to a low-frequency vibrational mode, which is treated semi-classically, and reproduce the exact electronic friction known from nonequilibrium Green's function theory [4]. We then also incorporate a high-frequency vibrational mode, which is strongly coupled to the electronic degrees of freedom and is treated fully quantum mechanically.

[1] J. T. Lü *et al.*, Phys. Rev. B 85, 245444 (2012)

[2] Y. Tanimura, J. Chem. Phys. 153, 020901 (2020)

[3] J. Bätge *et al.*, Phys. Rev. B 103, 235413 (2021)

[4] W. Dou *et al.*, J. Chem. Phys. 143 054103 (2015)

TT 15.3 Tue 11:45 H23

Generation of coherent acoustic phonons at the atomic scale with femtosecond Coulomb forces — •SHAOXIANG SHENG¹, ANNE-CATHERINE OETER¹, MOHAMAD ABDO¹, KURT LICHTENBERG¹, MARIO HENTSCHEL³, and SEBASTIAN LOTH^{1,2} — ¹University of Stuttgart, Institute for Functional Matter and Quantum Technologies, Stuttgart, Germany — ²Max Planck Institute for Solid State Research, Stuttgart, Germany — ³University of Stuttgart, 4th Physics Institute, Stuttgart, Germany

Coherent acoustic phonons enable ultrafast control of solids and have been exploited for applications in various acoustic devices. We find that localized coherent acoustic phonon wavepackets can be launched by THz-induced ultrafast Coulomb forces in a scanning tunneling microscope (STM) junction. The wavepackets induce an ultrafast displacement of the surface with several picometers amplitude and propagate into the sample with low losses. The surface displacement can be precisely controlled by varying the tip-sample distance. This non-thermal femtosecond force excitation enables localized measurements of phonon propagation with nanometer spatial resolution, can be used for diagnostics below surfaces and opens new perspectives in exploiting coherent phonons at the atomic scale.

TT 15.4 Tue 12:00 H23

Josephson optomechanics — •SURANGANA SEN GUPTA¹, BJOERN KUBALA^{1,2}, CIPRIAN PADURARIU¹, and JOACHIM ANKERHOLD¹ — ¹ICQ and IQST, Ulm University, Germany — ²Institute of Quantum Technologies, German Aerospace Center (DLR), Ulm, Germany

Optomechanical phenomena can be investigated in the microwave regime using a circuit-QED setup combining superconducting microwave cavities and a mechanical degree of freedom. In conventional optomechanics the cavity is usually driven to a coherent state by a laser. In contrast, in circuit optomechanics, the cavity can be driven by inelastic tunneling in a Josephson junction, which provides a large inherent non-linearity and leads to complex quantum states of light [1]. Here, we theoretically investigate a superconducting cavity with a single mode ω_0 coupled to a mechanical resonator. The cavity is driven by a dc-biased Josephson junction at $2eV_{dc} = p\hbar\omega_0$ where each Cooper pair excites $p = 1, 2, 3$ photons.

(i) We characterise signatures of the mechanics in the emission spectrum for squeezed light ($p = 2$) and for the $p = 3$ case, which is challenging for optical cavities, but easily realised in our microwave cavities. The inherent nonlinearity not only allows efficient driving at $p \geq 2$, but can also drastically change the spectrum at $p = 1$, where for stronger driving Mollow-like features arise. (ii) We calculate heating and cooling rates for the mechanical degree of freedom and find in the non-linear regime enhanced and non-monotonous rates.

[1] G. C. Ménard *et al.*, Phys. Rev. X 12, 021006 (2022).

TT 15.5 Tue 12:15 H23

Magnomechanics in suspended magnetic beams — KALLE S. U. KANSANEN¹, •CAMILLO TASSI², HARSHAD MISHRA³, MIKA A. SILLANPÄÄ³, and TERO T. HEIKKILÄ¹ — ¹Department of Physics and Nanoscience Center, University of Jyväskylä, P.O. Box 35 (YFL), FI-40014 Jyväskylä, Finland — ²Donostia International Physics Center, 20018 Donostia-San Sebastian, Spain — ³Department of Applied Physics, Aalto University, P.O. Box 15100, FI-00076 Aalto, Finland

Cavity optomechanical systems have become a popular playground for studies of controllable nonlinear interactions between light and motion. An alternative scheme with much smaller footprint is provided by magnomechanics, where phonons interact with magnons, instead of photons. Here, we consider the magnomechanical interaction occurring in a suspended magnetic beam, a scheme in which both magnetic and mechanical modes physically overlap and can be detected and also driven individually. We show that a sizable interaction - originated from both magnetoelastic and demagnetizing coupling - can be produced if the beam has some initial static deformation.

TT 15.6 Tue 12:30 H23

Improving device parameters in nanotube microwave optomechanics — NICOLE KELLNER, •FABIAN STADLER, NIKLAS HÜTTNER, and ANDREAS K. HÜTTEL — Institute for Experimental and Applied Physics, Universität Regensburg, Regensburg, Germany

In recent work [1,2], we have demonstrated optomechanical coupling between a carbon nanotube with an embedded quantum dot and a coplanar microwave resonator. The experiment displayed enhancement of the coupling by several or-

ders of magnitude via the nonlinearity of Coulomb blockade. The resulting novel optomechanical system can have figures of merit close to several interesting parameter regimes, as, e.g., strong optomechanical coupling (with hybridization of vibrons and photons) and the quantum coherent limit (where manipulation is faster than thermal decoherence). With this in mind, here we discuss our ongoing work to improve the components of this system, the optomechanical coupling, and its addressing and readout. — [1] S. Blien *et al.*, Nat. Comm. **11**, 1636 (2020); [2] N. Hüttner *et al.*, in preparation.

TT 16: Correlated Electrons: Method Development

Time: Wednesday 9:30–13:15

Location: H10

Invited Talk

TT 16.1 Wed 9:30 H10

Multimethod, multimessenger approaches to models of strong correlations — •THOMAS SCHÄFER — Max Planck Research Group “Theory of Strongly Correlated Quantum Matter” (SCQM), Max Planck Institute for Solid State Research, Stuttgart, Germany

The Hubbard model is the paradigmatic model for electronic correlations. In this talk I present a general framework for the reliable calculation of its properties, which we coined multi-method, multi-messenger approach. I will illustrate the power of this approach with three recent studies: (i) an extensive synopsis of arguably all available finite-temperature methods for the half-filled Hubbard model on a simple square lattice in its weak-coupling regime, fully clarifying the impact of spin fluctuations and tracking their footprints on the one- and two-particle level, (ii) a complementary subset of those applied to the Hubbard model on a triangular geometry, exhibiting the intriguing interplay of geometric frustration (magnetism) and strong correlations (Mottness) and (iii) a multi-method study of a model for magnetism in infinite-layer nickelates. These examples may work as a blueprint of similar future studies of strongly correlated systems.

TT 16.2 Wed 10:00 H10

Random phase approximation for gapped systems: Role of vertex corrections and applicability of the constrained random phase approximation — •ERIK VAN LOON¹, MALTE RÖSNER², MIKHAIL KATSNELSON², and TIM WEHLING³ — ¹Lund University, Lund, Sweden — ²Radboud University, Nijmegen, the Netherlands — ³University of Bremen, Bremen, Germany

The many-body theory of interacting electrons poses an intrinsically difficult problem that requires simplifying assumptions. For the determination of electronic screening properties of the Coulomb interaction, the random phase approximation (RPA) provides such a simplification. Here we explicitly show that this approximation is justified for band structures with sizable band gaps. This is when the electronic states responsible for the screening are energetically far away from the Fermi level, which is equivalent to a short electronic propagation length of these states. The RPA contains exactly those diagrams in which the classical Coulomb interaction covers all distances, whereas neglected vertex corrections involve quantum tunneling through the barrier formed by the band gap. Our analysis of electron-electron interactions provides a real-space analogy to Migdal’s theorem on the smallness of vertex corrections in electron-phonon problems. An important application is the increasing use of constrained RPA calculations of effective interactions. We find that their usage of Kohn-Sham energies accounts for the leading local (excitonic) vertex correction in insulators.

TT 16.3 Wed 10:15 H10

Consistency of potential energy in the diagrammatic vertex approximation — •JULIAN STOBBE and GEORG ROHRINGER — Institute of Theoretical Physics, University of Hamburg, 20355 Hamburg, Germany

In the last decades, dynamical mean field theory (DMFT) and its diagrammatic extensions have been successfully applied to describe local and nonlocal correlation effects in correlated electron systems. Unfortunately, both of them suffer from intrinsic inconsistencies which lead to a violation of the Pauli principle (and related sum rules) as well as the conservation laws of the system. This limits the predictive power of these approaches as fundamental observables such as the kinetic and/or potential energies are not unambiguously defined. Here, we will discuss an approach to overcome the ambiguity in the calculation of the potential energy within the ladder dynamical vertex approximation (DΓA) by introducing an effective mass renormalization parameter in both the charge and the spin susceptibility of the system. The applicability of the method is then demonstrated on the half filled single-band Hubbard model on a three-dimensional cubic lattice. Furthermore, the solution method will be discussed, since the new method requires careful consideration of finite approximation of infinite Matsubara sums.

TT 16.4 Wed 10:30 H10

Vertex divergences in the Anderson impurity model - From real to imaginary frequencies — •MICHAEL MEIXNER¹, JOHANNES HALBINGER², SEUNG-SUP LEE³, FABIAN KUGLER⁴, PATRICK CHALUPA-GANTNER⁵, ALESSANDRO TOSCHI⁵, JAN VON DELFT², and THOMAS SCHÄFER¹ — ¹Max Planck Institute for Solid State Research, Stuttgart, Germany — ²Arnold Sommerfeld Center for Theoretical Physics, Ludwig-Maximilians-Universität München, Munich, Germany — ³Department of Physics and Astronomy, National University, Seoul, South Korea — ⁴Department of Physics and Astronomy, Rutgers University, Piscataway, NJ, USA — ⁵Institute for Solid State Physics, TU Wien, Vienna, Austria

Generalized susceptibilities not only are at the heart of calculating momentum- and frequency-dependent response functions, but can also provide direct physical insights into local magnetic moment formation and Kondo screening. In particular, recent literature has investigated the implications of divergences of the irreducible vertex function on the Matsubara axis in the charge and particle-particle channels on the physics of the Anderson impurity model. In this study we examine the divergent properties of the two-particle irreducible vertex function in the Anderson impurity model employing the numerical renormalization group (NRG). In a first step data is benchmarked against state of the art results from continuous-time quantum Monte Carlo on the imaginary frequency axis. In a second step NRG allows us to access not only imaginary frequencies but also real frequencies via the Keldysh contour at very low temperatures and without analytic continuation.

TT 16.5 Wed 10:45 H10

Exact continuum representation of long-range interacting systems — •ANDREAS ALEXANDER BUCHHEIT¹, TORSTEN KESSLER¹, PETER SCHUHMACHER², and BENEDIKT FAUSEWEH² — ¹Saarland University, 66123 Saarbrücken, Germany — ²German Aerospace Center (DLR), 51147 Cologne, Germany

Continuum limits are a powerful tool in the study of many-body systems, yet their validity is often unclear when long-range interactions are present. In this work, we rigorously address this issue and put forth an exact representation of long-range interacting lattices that separates the model into a term describing its continuous analogue, the integral contribution, and a term that fully resolves the microstructure, the lattice contribution. For any system dimension, any lattice, any power-law interaction and for linear, nonlinear, and multi-atomic lattices, we show that the lattice contribution can be described by a differential operator based on the multidimensional generalization of the Riemann zeta function, namely the Epstein zeta function. Our representation provides a broad set of tools for studying the analytical properties of the system and it yields an efficient numerical method for the evaluation of the arising lattice sums. We benchmark its performance by computing classical forces and energies in three important physical examples, in which the standard continuum approximation fails: Skyrmions, defects in ion chains, and spin waves in a pyrochlore lattice with dipolar interactions. We demonstrate that our method exhibits the accuracy of exact summation at the numerical cost of an integral approximation.

TT 16.6 Wed 11:00 H10

Exotic phases in long-range interacting quantum lattices — ANDREAS A. BUCHHEIT¹, •TORSTEN KESSLER¹, PETER K. SCHUHMACHER², and BENEDIKT FAUSEWEH² — ¹Saarland University, Saarbrücken, Germany — ²German Aerospace Center (DLR), Cologne, Germany

We provide a rigorous analysis of the effects of power-law long-range interactions on the phase diagram of a multi-dimensional quantum spin lattice. Starting from the discrete Hamiltonian, we use the recently developed singular Euler-Maclaurin expansion and derive an exact and parameter-free field theory that fully captures the effects due to the inherent discreteness of the lattice. For any lattice and any system dimension, we derive analytic expressions for the phase boundaries to ferromagnetic and anti-ferromagnetic phases and outline their dependence on the exponent of the power-law interaction and of the system dimension.

TT 16.7 Wed 11:15 H10

SU(2)-symmetric tensor network study of the classical Heisenberg model — •PHILIPP SCHMOLL¹, AUGUSTINE KSHETRIMAYUM^{1,2}, JENS EISERT^{1,2}, ROMAN ORUS^{3,4,5}, and MATTEO RIZZI^{6,7} — ¹Dahlem Center for Complex Quantum Systems, Freie Universität Berlin, 14195 Berlin, Germany — ²Helmholtz Center Berlin, 14109 Berlin, Germany — ³Donostia International Physics Center, E-20018 San Sebastián, Spain — ⁴Ikerbasque Foundation for Science, E-48013 Bilbao, Spain — ⁵Multiverse Computing, E-20014 San Sebastián, Spain — ⁶Forschungszentrum Jülich, Institute of Quantum Control (PGI-8), 52425 Jülich, Germany — ⁷Institute for Theoretical Physics, University of Cologne, D-50937 Köln, Germany

The classical Heisenberg model in two spatial dimensions constitutes one of the most paradigmatic spin models, taking an important role in statistical and condensed matter physics to understand magnetism. Despite its paradigmatic character controversies remain whether the model exhibits a phase transition at finite temperature. In this work, we make use of state-of-the-art tensor network approaches, representing the classical partition function in the thermodynamic limit over a large range of temperatures. By implementing an SU(2) symmetry in our tensor network, we are able to handle very large bond dimensions, which is crucial in detecting phase transitions. With decreasing temperatures, we find a rapidly diverging correlation length, whose behaviour is apparently compatible with the two main contradictory hypotheses known in the literature, namely a finite-T transition and asymptotic freedom, though with a slight preference for the second.

15 min. break

TT 16.8 Wed 11:45 H10

Matrix-product-state-based band-Lanczos solver for quantum cluster approaches — SEBASTIAN PAECKEL^{1,2}, THOMAS KÖHLER³, SALVATORE R. MANMANA⁴, and •BENJAMIN LENZ⁵ — ¹Arnold Sommerfeld Center of Theoretical Physics, University of Munich, Germany — ²Munich Center for Quantum Science and Technology (MCQST), Munich, Germany — ³Department of Physics and Astronomy, Uppsala University, Sweden — ⁴Institute for Theoretical Physics, Georg August University of Göttingen, Germany — ⁵Institut de minéralogie, de physique des matériaux et de cosmochimie (IMPMC), Sorbonne University, Paris, France

We present a matrix-product-states-based band-Lanczos method as a solver for quantum cluster techniques. Based on a traditional band-Lanczos technique for the calculation of the cluster Green's function, we introduce and motivate different convergence criteria and discuss their impact on the stability of the results at the example of the variational cluster approximation. The capabilities of this method to calculate the self-energy functional are demonstrated for Hubbard-like models on different cluster geometries. Finally, we show a finite-size scaling of order parameters using cluster sizes, which are out of reach for traditional exact-diagonalization-based solvers.

TT 16.9 Wed 12:00 H10

Hierarchical equations of motion approach to open quantum system dynamics: Matrix product state formulation in twin space — •YALING KE¹, RAFAELE BORRELLI², and MICHAEL THOSS¹ — ¹Institute of Physics, Albert-Ludwig University Freiburg, Hermann-Herder-Strasse 3, 79104 Freiburg, Germany — ²DISAFA, Università di Torino, I-10095 Grugliasco, Italy

The hierarchical equations of motion (HEOM) approach is a numerically exact method to study the dynamics of open quantum systems with non-perturbative system-environment interaction and non-Markovian memory at finite temperatures. Although considerable progress has been made over the past few decades to extend the applicability of the HEOM approach, the numerical cost is still very expensive for reasonably large systems.

In this contribution, we present the twin-space formulation of the HEOM approach in combination with the matrix product state representation for open quantum systems coupled to a hybrid fermionic and bosonic environment. The key ideas of the approach are a reformulation of a set of differential equations for the auxiliary density matrices into a time-dependent Schrödinger-like equation for an augmented multi-dimensional wave function as well as its tensor decomposition into a product of low-rank matrices. The new approach facilitates accurate simulations of non-equilibrium quantum dynamics in larger and more complex open quantum systems with both factorized and correlated initial conditions.

TT 16.10 Wed 12:15 H10

Single-boson-exchange-fRG application to the two-dimensional Hubbard model at weak coupling — SARAH HEINZELMANN¹, KILIAN FRABOULET¹, PIETRO BONETTI², AÍMAN AL-ERYANI¹, DEMETRIO VILARDI², •ALESSANDRO TOSCHI³, and SABINE ANDERGASSEN¹ — ¹Eberhard Karls Universität Tübingen — ²Max Planck Institut Stuttgart — ³Technische Universität Wien

We illustrate the computational advantages of the recently introduced single-boson exchange (SBE) formulation for the one-loop functional renormalization group (fRG) applied to the two-dimensional Hubbard model. We present a detailed analysis of the physical susceptibilities and their evolution with temperature and interaction strength, both at half filling and finite doping. We find that the rest functions describing the corrections beyond the SBE contributions play a negligible role in the weak coupling regime. The SBE formulation of the fRG flow hence allows for a substantial reduction of the numerical effort in the treatment of the two-particle vertex function, paving a promising route for future multiboson and multiloop extensions.

TT 16.11 Wed 12:30 H10

Connecting real- and imaginary-frequency axis for two-particle many-body propagators — •SELINA DIRNBÖCK¹, SEBASTIAN HUBER¹, SEUNG-SUP LEE^{2,3}, FABIAN KUGLER⁴, JAN VON DELFT³, KARSTEN HELD¹, and MARKUS WALLERBERGER¹ — ¹TU Wien, Austria — ²Seoul National University, South Korea — ³Ludwig-Maximilians-Universität München, Germany — ⁴Rutgers University, New Jersey, USA

Two-particle response functions are a centerpiece of quantum many-body physics, relating both to experiment, where they can be observed as susceptibilities, and to theory, where they form the basis of advanced self-consistent field theories. Yet, due to their size and complex structure, they are challenging to handle numerically.

Recently, two advances have been made to tackle this problem: firstly, the intermediate representation together with an overcomplete basis (IR+OB), which provides a highly efficient compression of propagators in imaginary frequency, and secondly, partial spectral functions (PSFs), which allow for the efficient evaluation in real frequency, by, for example, using the numerical renormalization group (NRG).

In this talk, we connect these two approaches: we show that the IR+OB and PSFs are intimately connected. We also show that the two-particle propagator obtained from NRG/PSFs on the real-frequency axis can be compressed efficiently using IR+OB on imaginary-frequency axis, reducing the memory demand by more than three orders of magnitude. Finally, we use the guidance from PSFs to develop a physical regularization scheme for the IR+OB.

TT 16.12 Wed 12:45 H10

Trie-based ranking of quantum many-body states — •MARKUS WALLERBERGER and KARSTEN HELD — TU Wien, Vienna, Austria

Ranking bit patterns – finding the index of a given pattern in an ordered sequence – is a major bottleneck scaling up numerical quantum many-body calculations, as fermionic and hard-core bosonic states translate naturally to bit patterns. Traditionally, ranking is done by bisectioning search, which has poor cache performance on modern machines.

We instead propose to use tries (prefix trees), thereby achieving a two- to ten-fold speed-up in numerical experiments with only moderate memory overhead. For the important problem of ranking permutations, the corresponding tries can be compressed. These compressed “staggered” lookups allow for an additional speed-up while retaining the memory requirements of prior algorithms based on the combinatorial number system.

We use these improvements to go to larger system sizes for which three- and four-point propagators can be computed.

TT 16.13 Wed 13:00 H10

Tetranacci polynomials in solid state physics — •NICO LEUMER — IPCMS, CNRS, Strasbourg

In mesoscopic physics, state of the art theoretical research relies not solely but to large extent on numerical investigations. Naturally, support from analytical side is important whenever possible, in particular to appeal physical intuition. For the first time, I will introduce to a broader audience so called Tetranacci polynomials, which offer a generic technique to analytic diagonalize a variety of model Hamiltonians for finite system size and when open/free boundary conditions are imposed. As perspective, this approach is applicable on discrete physical (sub-) systems owing at least two degrees of freedom per atom, such as the Kitaev chain or the 1d Rashba-nanowire in magnetic field positioned on superconducting substrate. The use extends further to the famous Su-Schrieffer-Heeger model or to topological trivial tight-binding chains having nearest and next nearest neighbor hopping. In my presentation, I elaborate that Tetranacci polynomials extend Bloch's theorem and how they are related to eigenvectors and eigenvalues. Within the frame drawn by the illustrative example of the X-Y-chain in transverse magnetic field, I demonstrate how previous diagonalization approaches are recovered by the more general Tetranacci technique. The final part of my presentation is devoted to an overview of physically distinct systems hosting Tetranacci polynomials and their common spectral features overlooked in earlier studies.

[1] N. Leumer et al., J. Condens. Matter Phys. 32 445502 (2020)

[2] N. Leumer et al., Phys. Rev. B 103, 165432 (2021)

TT 17: Cryogenic Detectors and Cryotechnique

Time: Wednesday 9:30–12:00

Location: H22

TT 17.1 Wed 9:30 H22

TES sensors design for the CRESST experiment — •FRANCESCA PUCCI¹, ANTONIO BENTO^{1,2}, ANNA BERTOLINI¹, LUCIA CANONICA¹, NAHUEL FERREIRO IACHELLINI^{1,3}, ABHIJ GARAI¹, DIETER HAUFF¹, ATHOY NILIMA¹, MICHELE MANCUSO¹, FEDERICA PETRICCA¹, FRANZ PROEBST¹, and DOMINIK FUCHS¹ — ¹Max-Planck-Institut für Physik, D-80805 München, Germany — ²LIBPhys-UC, Departamento de Física, Universidade de Coimbra, P3004 516 Coimbra, Portugal — ³Excellence Cluster Origins, D-85748 Garching, Germany

The CRESST experiment aims at the direct detection of sub-GeV dark matter particles via elastic scattering off nuclei in different target crystals at cryogenic temperatures. Each detector consists of an absorber crystal and a Transition Edge Sensors (TES), which measures the temperature variations caused by an energy deposition in the crystal. The TES are made of tungsten thin films and they are operated in the middle of their superconducting transition, at around 15 mK. These very sensitive detectors allow for a leading energy threshold worldwide. The studies on the TES sensor design and its development at the Max Planck Institute for Physics are presented.

TT 17.2 Wed 9:45 H22

Beta spectrometry measurements with metallic magnetic calorimeters — •MICHAEL PAULSEN¹, JÖRN BEYER¹, CHRISTIAN ENNS^{2,6}, SEBASTIAN KEMPF^{3,6}, KARSTEN KOSSERT⁴, MARTIN LOIDL⁵, RIHAM MARIAM⁵, OLE NÄHLE⁴, PHILIPP RANITZSCH⁴, MATIAS RODRIGUES⁵, and MATHIAS WEGNER^{6,3} — ¹Physikalisch-Technische Bundesanstalt, Berlin, Germany — ²Kirchhoff-Institute for Physics, Heidelberg University, Germany — ³Institute of Micro- and Nanoelectronic Systems, Karlsruhe Institute of Technology, Germany — ⁴Physikalisch-Technische Bundesanstalt, Braunschweig, Germany — ⁵Université Paris-Saclay, CEA, List, Laboratoire National Henri Becquerel, Palaiseau, France — ⁶Institute for Data Processing and Electronics, Karlsruhe Institute of Technology, Germany

Precise beta spectra measurements are important for radionuclide metrology, the validation of theoretical calculations and nuclear medicine. Metallic Magnetic Calorimeters (MMCs) with the radionuclide sample embedded in a 4π absorber have proven to be among the best beta spectrometers in terms of energy resolution and threshold, linearity and detection efficiency, notably for low energy beta transitions. In this work, two measurements of the spectrum of the 2nd forbidden non-unique beta transition of ^{99}Tc ($Q^- = 297.5$ keV) are presented. They were acquired using two independent MMC based detectors in two different laboratories and show excellent agreement. The results suggest a spectral shape which deviates significantly from hitherto theoretical calculations and semi-empirical extrapolations at lower energies (< 50 keV) reported in the literature.

TT 17.3 Wed 10:00 H22

Low-noise, impedance matched current-sensing dc-SQUIDS for magnetic microcalorimeter readout — •FABIENNE BAUER^{1,2}, CHRISTIAN ENNS¹, and SEBASTIAN KEMPF^{1,2} — ¹Kirchhoff-Institute for Physics, Heidelberg University, Im Neuenheimer Feld 227, 69120 Heidelberg — ²Institute of Micro- and Nanoelectronic Systems, Karlsruhe Institute of Technology, Hertzstraße 16, 76187 Karlsruhe

Direct-current superconducting quantum interference devices (dc-SQUIDS) are the devices of choice for reading out low-impedance cryogenic particle detectors such as magnetic microcalorimeters (MMCs). MMCs use a paramagnetic or superconducting temperature sensor, placed in a weak magnetic field and inductively coupled to a superconducting pickup coil, to convert deposited energy into a change of magnetic flux threading the pickup coil. The latter is sensed using a low-noise SQUID. To maximize sensitivity and hence energy resolving power, impedance matching between SQUID and pickup coil as well as a SQUID white noise level close to the quantum limit are crucial. As current-sensing SQUIDS with input inductances between 1 nH and 10 nH and suited for mK-operation temperatures are rarely or not at all commercially available, custom SQUIDS for MMC readout must be developed. In this context, we discuss design and performance of three current-sensing dc-SQUIDS impedance matched to MMCs that are foreseen for neutrino mass investigation, X-ray spectroscopy and mass spectrometry, respectively. To achieve low-noise performance, the SQUIDS rely on the use of cross-type Josephson junctions to minimize junction capacitance and hence readout noise.

TT 17.4 Wed 10:15 H22

Flux ramp modulation based hybrid microwave SQUID multiplexer — •CONSTANTIN SCHUSTER^{1,2}, MATHIAS WEGNER^{1,2}, CHRISTIAN ENNS¹, and SEBASTIAN KEMPF^{1,2} — ¹Kirchhoff-Institute for Physics, Heidelberg University, Heidelberg — ²Institute of Micro- and Nanoelectronic Systems, Karlsruhe Institute of Technology, Karlsruhe

For the readout of cryogenic detector arrays, microwave SQUID multiplexers (μMUXes) are presently being developed. Using non-hysteretic rf-SQUIDS, each

multiplexer channel transforms the detector signal into a change of amplitude or phase of a microwave signal probing the resonance frequency of a superconducting resonator. In this way, numerous detectors can be simultaneously read out by coupling multiple resonators to a common transmission line. The resonator bandwidth is adjusted according to the detector speed and sets a lower limit for the frequency spacing of resonators. This limit, however, can in practice only be reached if the fabrication accuracy is very high. As a result, the channel density is very often limited by fabrication rather than the inherent channel capacity of the transmission line. We present a hybrid microwave SQUID multiplexer combining two frequency-division readout techniques to allow multiplexing a given number of detectors with only a fraction of readout resonators. We present insights of our approach based on information theory and discuss benefits and drawbacks using Monte-Carlo simulations. We further discuss the performance of a prototype device indicating that our technique is very well suited for reading out ultra-large bolometric detector arrays.

TT 17.5 Wed 10:30 H22

Transport properties of superconducting thin films and superconducting single-photon detectors — •FABIAN WIETSCHORKE¹, STEFAN STROHAUER², RASMUS FLASCHMANN¹, LUCIO ZUGLIANI¹, CHRISTIAN SCHMID¹, SVEN ERNST², STEFANIE GROTOWSKI², SIMONE SPEDICATO², BJÖRN JONAS¹, MIRCO METZ¹, KAI MÜLLER¹, and JONATHAN FINLEY² — ¹Walter Schottky Institute and Department for Electrical and Computer Engineering, Technical University of Munich, 85748 Garching, Germany — ²Walter Schottky Institute and Physics Department, Technical University of Munich, 85748 Garching, Germany

Superconducting single-photon detectors (SSPDs) play a crucial role in the rapidly growing field of quantum communication and computation. Hereby, NbTiN is an established candidate for superconducting thin films that is used as the active part of the SSPDs. To achieve high detection efficiencies, the superconducting properties of NbTiN films, deposited via magnetron sputtering, need to be optimized. In this contribution, we present transport measurements characterizing the influence of the deposition process onto the superconducting properties, which assists in a systematic optimization of the detectors. We are able to estimate detection efficiency and depairing current of the SSPDs, even before fabricating the nanostructures, utilizing the hotspot model and the Ginzburg-Landau model. Finally, we use the thin film transport measurements and detector measurements to assess the quality of our nanofabrication process.

15 min. break

TT 17.6 Wed 11:00 H22

Optimization of MoSi film deposition for superconducting single-photon detectors in the telecom c-band — •STEFANIE GROTOWSKI¹, LUCIO ZUGLIANI², RASMUS FLASCHMANN², STEFAN STROHAUER¹, CHRISTIAN SCHMID², FABIAN WIETSCHORKE², SVEN ERNST¹, SIMONE SPEDICATO¹, MIRCO METZ², BJÖRN JONAS², KAI MÜLLER², and JONATHAN FINLEY¹ — ¹Walter Schottky Institute and Physics Department, Technical University of Munich, Germany — ²Walter Schottky Institute and Department for Electrical and Computer Engineering, Technical University of Munich, Germany

Superconducting single-photon detectors (SSPDs) are a crucial building block for photonic quantum technologies. With regard to the telecommunication infrastructure, SSPDs sensitive in the telecom c-band are required. A promising material in this regard is MoSi, as it unites a small superconducting energy gap enabling high sensitivity while maintaining a high transition temperature. In this work we aim at optimizing the magnetron co-sputtering deposition to achieve high transition temperatures (T_c). We vary the stoichiometry and find maximized T_c values for Mo rich films until an upper limit of around 80% Mo is reached. Above this critical concentration grazing incidence diffraction reveals the transition to a polycrystalline phase in the material. Moreover, the working pressure during deposition influences both T_c and structure as well. We find that a low working pressure improves the T_c , but a minimum pressure is required to ensure an amorphous deposition. Finally, with the optimized parameter set we measured a T_c of 8.4 K for 20 nm and 6.2 K for 4.5 nm thin films.

TT 17.7 Wed 11:15 H22

Superconducting single-photon detectors on lithium-niobate-on-insulator — •CHRISTIAN SCHMID¹, RASMUS FLASCHMANN¹, LUCIO ZUGLIANI¹, STEFAN STROHAUER², BJÖRN JONAS¹, FABIAN WIETSCHORKE¹, SVEN ERNST², STEFANIE GROTOWSKI², SIMONE SPEDICATO², MIRCO METZ¹, KAI MÜLLER¹, and JONATHAN FINLEY² — ¹Walter Schottky Institute and Department for Electrical and Computer Engineering, Technical University of Munich, Germany — ²Walter Schottky Institute and Physics Department, Technical University of Munich, Germany

Superconducting single-photon detectors (SSPDs) are a key building block in photon-based quantum computation and communication. To realize a scal-

able photonic quantum computer, integration of single-photon sources, electronics and crucially SSPDs is necessary. One of the most promising material platforms for quantum photonic integration is lithium-niobate-on-insulator (LNOI), which offers a broad optical window and a large non-linearity. In this work, we present the thin film superconducting properties of NbTiN grown on crystalline LNOI and compare them to films deposited on amorphous Si/SiO₂ wafer. SSPDs fabricated from films on both substrates are further characterized with respect to their quantum efficiency, dark count rate, recovery time and timing jitter.

TT 17.8 Wed 11:30 H22

Cooling performance of a 4 K two-stage pulse tube cryocooler in tilted operation along main azimuthal orientations — •JACK-ANDRE SCHMIDT^{1,2}, BERND SCHMIDT^{1,2}, JENS FALTER^{1,2}, and ANDRE SCHIRMEISEN^{1,2} — ¹Justus-Liebig-University Giessen — ²TransMIT GmbH

Closed-cycle cryocoolers, here Gifford-McMahon (GM) type pulse tube cryocoolers (PTC), offer long measurement periods and low maintenance, but they exhibit undesired intrinsic effects due to the working principle [1]. Cooling performance of GM-type PTCs is strongly depending on the orientation and is set to be strictly vertical, which is not suitable for experiments where the cryostat needs to be tilted [2, 3]. We report an experimental study of the effect of tilting from vertical orientation on the cooling performance of a U-shaped 4 K pulse tube cryocooler (PTC) with 7 kW electrical input power. An investigation of cooling performance over tilt angles from 0 to 60 degree for selected azimuthal orientations of the PTC is performed. The non-coaxial arrangement of the tubes suggests an asymmetric cooling performance while tilting along the first or second stage heat exchanger due to natural convection in the pulse tubes [3]. The increase of no-load temperatures upon tilting by +/- 50 degree will be discussed. While the regime of tilt angles within 30 show moderate loss in cooling power

an almost sudden decrease of cooling power is revealed and analyzed for high tilt angles.

- [1] G. Thummes et al., Cryocoolers 9 (1997) 393
- [2] T. Tsan et al., Cryogenics 117 (2021) 103323
- [3] C. Risacher et al., IEEE 39 (2014)
- [4] L. Zhang, et al., Cryogenics 51 (2011) 85

TT 17.9 Wed 11:45 H22

Cross Correlated Current Noise Thermometer for Milli-Kelvin Temperatures — •CHRISTIAN STÄNDER, PASCAL WILLER, NATHALIE PROBST, ANDREAS REIFENBERGER, ANDREAS REISER, ANDREAS FLEISCHMANN, and CHRISTIAN ENSS — Kirchhoff Institute for Physics, Heidelberg University.

Within our search for easy-to-use and reliable thermometers for milli-Kelvin and micro-Kelvin temperatures we developed a noise thermometer, where the Johnson noise of a massive cylinder of high purity silver is monitored simultaneously by two current sensing dc-SQUIDS. Operating each SQUID in voltage bias mode in a 2-stage configuration allows to reduce the power dissipation of the SQUIDS to a minimum. To further reduce the parasitic effect of correlated amplifier noise, a mathematical method to suppress the noise coupled from the feedback to the input coil of the SQUIDS is introduced. By cross-correlating the two SQUID signals, the noise contribution of the read-out electronics is suppressed to a marginal level.

We recently assembled a first small series of such thermometers to best reliability, reproducibility and user friendliness. In the complete investigated temperature range from 4 K down to 5 mK, the measured noise power is linear in temperature. The 12 thermometers of the series agree within less than 0.1% in the complete temperature range and show a good agreement with the PTLs-2000 temperature scale. Also a new sensor material, with the goal of counteraction observed ageing effects, is introduced.

TT 18: Topological Insulators

Time: Wednesday 9:30–11:45

Location: H23

TT 18.1 Wed 9:30 H23

Exceptional topological insulators — •MICHAEL DENNER¹, ANASTASIA SKURATIVSKA¹, FRANK SCHINDLER^{1,2}, MARK FISCHER¹, RONNY THOMALE³, TOMÁS BZDUSEK^{1,4}, and TITUS NEUPERT¹ — ¹Department of Physics, University of Zurich, Switzerland — ²Princeton Center for Theoretical Science, Princeton University, USA — ³Institut für Theoretische Physik und Astrophysik, Universität Würzburg, Germany — ⁴Condensed Matter Theory Group, Paul Scherrer Institute, Switzerland

Since their theoretical conception and experimental discovery, 3-dimensional topological insulators have become the focal point for research on topological quantum matter. Their key feature is a single Dirac electron on the surface, representing an anomaly: in purely 2D such a state can neither be regularized on a lattice nor in the continuum. I will introduce an analog in dissipative systems, which are described by non-Hermitian operators, the exceptional topological insulator (ETI). Like normal topological insulators, the ETI hosts exotic surface states. It is characterized by a bulk energy point gap and exhibits robust surface states that cover the bulk gap as a single sheet of complex eigenvalues or with a single exceptional point. Even though it does not require any symmetry to be stabilized, I will explain how this non-Hermitian topological phase can also be inferred using symmetry-indicators of the bulk Hamiltonian. Furthermore, I will demonstrate how the ETI can be induced in gapless solid-state systems and metamaterials, thereby setting a paradigm for non-Hermitian topological matter.

TT 18.2 Wed 9:45 H23

Berry curvature effects in high-harmonic generation in topological insulator surface states — •VANESSA JUNK¹, COSIMO GORINI², and KLAUS RICHTER¹ — ¹Institut für Theoretische Physik, Universität Regensburg, Germany — ²Université Paris-Saclay, CEA, CNRS, SPEC, 91191, Gif-sur-Yvette, France

When strong-field light is interacting with a solid, it acts as an a.c. bias accelerating electrons through the bandstructure and driving non-perturbative transitions. These processes can lead to the emission of high-order harmonics containing fingerprints of the materials properties. Since in topological insulator surface states scattering is strongly suppressed, signatures of coherent transport can be found in the resulting spectra.

Recently, high-harmonics generation from the surface states of the three-dimensional topological insulator Bi₂Te₃ has been observed experimentally [1]. Here, we show fully quantum mechanical simulations of the electron dynamics and compare them with the experimental results. We find that the Berry curvature can not only lead to high-harmonics polarized perpendicularly to incoming radiation but also to an alternating polarization of odd and even order harmonics. This being one of the key observations in the experiment suggests the importance of Berry curvature effects in coherent high-harmonics emission.

[1] C. Schmid, L. Weigl, P. Grössing, V. Junk, C. Gorini, S. Schlauderer, S. Ito, M. Meierhofer, N. Hofmann, D. Afanasiev, J. Crewse, K. Kokh, O. Tereshchenko, J. Gütde, F. Evers, J. Wilhelm, K. Richter, U. Höfer, R. Huber, Nature **593**, 385 (2021)

TT 18.3 Wed 10:00 H23

Spin-polarized surface state transport in gate-tunable topological insulator — •LINH DANG¹, OLIVER BREUNIG¹, HENRY LEGG², and YOICHI ANDO¹ — ¹II. Physikalisches Institut, Universität zu Köln, Zùlpicher Str. 77, 50937 Köln, Germany — ²Department of Physics, University of Basel, Klingelbergstrasse 82, CH-4056 Basel, Switzerland

Topological insulators (TIs) possess helical spin-momentum locked surface states that can be harnessed to create a non-zero spin polarization by applying a current through the TI. Two opposite types of spin polarization have been reported on the same material, suggesting the interplay between topological surface state and Rashba spin splitting state of 2-dimensional surface electrons. These two contributing effects might be used to create a spin transistor device. In this report, we discuss the sign switching of the spin polarization by electrostatic gating based on data acquired from devices that were microfabricated on TI flakes.

TT 18.4 Wed 10:15 H23

Chern insulating phases and thermoelectric properties of EuO/MgO(001) superlattices — •OKAN KOEKAL and ROSSITZA PENTCHEVA — Department of Physics and Center of Nanointegration (CENIDE), University of Duisburg-Essen, 47057 Duisburg

The effect of confinement and strain on the topological and thermoelectric properties of (EuO)_n/(MgO)_m(001) superlattices (SLs) are investigated by means of DFT + *U* + spin-orbit coupling (SOC) calculations in conjunction with semiclassical Boltzmann transport theory. A particularly strong effect is observed in the ferromagnetic (EuO)₁/(MgO)₃(001) SL at the lateral lattice constant of MgO (*a* = 4.24 Å) where SOC opens a band gap of 0.51 eV due to an inversion between occupied localized Eu 4*f* and itinerant 5*d* conduction bands. This band inversion between bands of opposite parity is accompanied by a spin reorientation in the spin-texture along the contour of band surrounding the Γ point. The resulting Chern insulating phase with *C* = -1, confirmed by a single topological edge state, exhibits promising thermoelectric properties, i.e., a high Seebeck coefficient between 400 and 800 μVK^{-1} . Somewhat lower thermoelectric values are obtained for the ferromagnetic semimetallic (EuO)₂/(MgO)₂(001) SL, where SOC also induces a band inversion and AHC with values up to $-1.04 e^2/h$. This work emphasizes the correlation between non-trivial topology and thermoelectricity in (EuO)_n/(MgO)_m(001) SLs with broken time-reversal symmetry [1].

Support by the DFG within CRC/TRR80, project G3 is gratefully acknowledged.
[1] O. Kökcal and R. Pentcheva, Phys. Rev. B **103**, 045135 (2021)

TT 18.5 Wed 10:30 H23

Stacking faults in weak topological insulators with time reversal symmetry — •GABRIELE NASELLI, VIKTOR KÖNYE, and ION COSMA FULGA — Leibniz-Institut für Festkörper- und Werkstofforschung, Dresden, Germany

In experimental observation stacking faults can play a significant role in hiding the topological properties of topological insulators. The defects break lattice symmetries which can be required for the protection of the topological states in weak topological insulators. We studied stacking faults in 3D weak topological insulators like Bi₂TeI and Bi₁₄Rh₃I₉. Both these materials are formed by 2D topological insulating layers (with time reversal symmetry and quantum spin Hall effect) stacked on top of each other in the *z* direction with trivial insulating spacers between them. We have built a simple tight binding model for both of these materials and got the topological properties solving the eigenvalue problem numerically. We introduced a stacking fault in our model by shifting half of the system by a fraction of the unit cell in the *z* direction. We mapped the stacking surface in the WTI into a Su-Schrieffer-Heeger chain, considering the effective hoppings between the TI layers on the left and right side of the stacking fault. When all the TI layers on the left side are strongly interacting with the TI layers on the right side of the defect the corresponding SSH model is in the trivial phase and we did not find conducting states. Instead when the stacking fault has two weakly interacting TI layers at its boundaries the corresponding SSH chain is in the topological phase and we have found localized conducting states at the defect.

TT 18.6 Wed 10:45 H23

Dynamic impurities in two-dimensional topological insulator edge states — •SIMON WOZNY¹, MARTIN LEIJNSE¹, and SIGURDUR I. ERLINGSSON² — ¹Division of Solid State Physics and NanoLund, Lund University, Box 118, S-22100 Lund, Sweden — ²School of Science and Engineering, Reykjavik University, Menntavegi 1, IS-101 Reykjavik, Iceland

Two-dimensional topological insulators host one-dimensional helical states at the edges. These are characterized by spin-momentum locking and time-reversal symmetry protects the states from backscattering by potential impurities. Magnetic impurities break time-reversal symmetry and allow for backscattering.

We have investigated the effects of random, aligned but harmonically rotating magnetic impurities. Using the time dependent Green's function (GF) for the system we calculate the time-averaged density of states (DOS) and extract the transmission via a Floquet scattering formalism. For slow driving the DOS and transmission match an average over static impurity orientations, whereas fast driving results in a flat low-energy DOS and transmission with resonances at higher energies related to Floquet sub-band crossings. Resonant driving leads to a nontrivial DOS and transmission. We also investigate the dependence on the ratio between potential and magnetic strength of the impurities.

TT 18.7 Wed 11:00 H23

Quantum phase transitions and a disorder-based filter in a Floquet system — •BHARGAVA BALAGANCHI ANANTHA RAMU, SANJIB KUMAR DAS, and ION COSMA FULGA — IFW Dresden and Würzburg-Dresden Cluster of Excellence ct.qmat, Helmholtzstrasse 20, 01069 Dresden, Germany

Two-dimensional periodically-driven topological insulators have been shown to exhibit numerous topological phases, including ones which have no static analog, such as anomalous Floquet topological phases. We study a two dimensional

model of spinless fermions on a honeycomb lattice with periodic driving. We show that this model exhibits a rich mixture of weak and strong topological phases, which we identify by computing their scattering matrix invariants. Further, we do an in-depth analysis of these topological phases in the presence of spatial disorder and show the relative robustness of these phases against imperfections. Making use of this robustness against spatial disorder, we propose a filter which allows the passage of only edge states, and which can be realized using existing experimental techniques.

TT 18.8 Wed 11:15 H23

Topological phases of Su-Schrieffer-Heeger alternating ladders — •ANAS ABDELWAHAB — Leibniz Universität Hannover, Hannover, Germany

Alternating ladders are constructed from unit cells consisting of rungs with odd number of sites connected with rungs with even number of sites [1]. These systems can be constructed using several options of equivalent unit cells. Two one-site rungs connected with two two-site rungs as well as two three-site rungs connected with two two-site rungs are investigated. Rich phase diagrams of topological insulating phases separated by critical lines are identified using the Su-Schrieffer-Heeger (SSH) model that describe such ladder systems. The phase diagrams depend on the choices between the equivalent unit cells. One could identify cases with flat bands close to the Fermi level. In principle, these simple models can be realized in designer quantum materials such as artificial lattices constructed by manipulation of atoms using a tip of scanning tunnelling microscope (STM) [2,3].

[1] K. Essalah, A. Benali, A. Abdelwahab, E. Jeckelmann, and R. T. Scalettar, Phys. Rev. B 103, 165127 (2021)

[2] R. Drost, T. Ojanen, A. Harju and P. Liljeroth, Nat. Phys. 13, 668 (2017)

[3] M. N. Huda, S. Kezilebieke, T. Ojanen, R. Drost and P. Liljeroth, npj Quantum Materials 5, 17 (2020)

TT 18.9 Wed 11:30 H23

Coulomb-blockade spectroscopy in topological insulator-superconductor hybrid devices — •BENEDIKT FROHN, TOBIAS W. SCHMITT, WILHELM WITTL, DENNIS HEFFELS, MICHAEL SCHLEENVOIGT, ABDUR R. JALIL, DETLEV GRÜTZMACHER, and PETER SCHÜFFELGEN — Peter Grünberg Institut, Forschungszentrum Jülich & JARA Jülich-Aachen Research Alliance, D-52425 Jülich, Germany

In the search for fault tolerant quantum computing, Majorana zero modes resemble a promising platform [1]. We investigate an island of a topological insulator (TI) nanoribbon, (Bi,Sb)₂Te₃, proximitized with a superconductor (S) for signatures of these states using Coulomb-blockade spectroscopy. One possible signature would be a change in charge periodicity once the island is tuned into the topological regime. We successfully created tunneling barriers made from Al₂O₃ and obtained the characteristic Coulomb diamond structure. Nb provides excellent interface transparency towards TI and was capped *in situ*, yet we found no change in charge periodicity. Al, however, is known to show these signatures in comparable experiments. Since Al diffuses heavily into the TI when put directly into contact, we fabricated Josephson junctions (JJs) with different thin interlayers between (Bi,Sb)₂Te₃ and Al to characterize the influence of these diffusion barriers on the transport properties of the JJs. We find four possible interlayers that allow for engineering a transparent S-TI interface. These results will enable us to perform Coulomb-blockade experiments with Al as a S.

[1] A.Y. Kitaev, Ann. Phys. 303, 2 (2003)

TT 19: Topological Superconductors

Time: Wednesday 11:45–13:00

Location: H23

TT 19.1 Wed 11:45 H23

Periodic supercurrent oscillations in topological insulator nanowire Josephson junctions in an axial magnetic field — •MICHAEL BARTH¹, JACOB FUCHS¹, COSIMO GORINI^{1,2}, and KLAUS RICHTER¹ — ¹Institute of Theoretical Physics, University of Regensburg, D-93040 Regensburg, Germany — ²Université Paris-Saclay, CEA, CNRS, SPEC, 91191, Gif-sur-Yvette, France

Helical surface states of 3-dimensional topological insulator (TI) nanowires are expected to have very promising physical properties like forbidden backscattering [1]. Moreover it is predicted that a topological superconducting state which could possibly host Majorana fermions can be realized by bringing a normal s-wave superconductor in close proximity to a TI [2]. We theoretically study the influence of an axial magnetic field on the supercurrent flow in TI nanowire Josephson junctions. The wire is modeled by an effective 2 dimensional setup and we take into account the special surface geometry by incorporating the partial superconducting coverage of the wire circumference. By employing numerical tight-binding simulations [3] and a semiclassical analytical approach [4], we show that the critical current can exhibit periodic oscillations, where the period corresponds to half of the superconducting flux quantum.

[1] X.-L. Qi and S.-C. Zhang, Rev. Mod. Phys. 83, 1057 (2011)

[2] A. Cook and M. Franz, Phys. Rev. B 84, 201105(R) (2011)

[3] Kun Zuo et al., Phys. Rev. Lett. 119, 187704 (2017)

[4] V. P. Ostroukh et al., Phys. Rev. B 94, 094514 (2016)

TT 19.2 Wed 12:00 H23

Superconductivity in HgTe based quantum point contacts — •JOHANNES BAUMANN, MARTIN STEHNO, HARTMUT BUHMANN, and LAURENS MOLENKAMP — Institute for Topological Insulators and Physikalisches Institut, Experimentelle Physik 3, Universität Würzburg, 97074 Würzburg, Germany

Quantum point contacts have been suggested as tunable transmission elements in topological quantum circuits. We etched narrow constrictions into the weak links of topological Josephson junctions prepared from high-mobility, band-inverted HgTe quantum wells (2D topological insulator). In such devices, the conductance and supercurrent transmission decrease step-wise as we deplete the carriers in the constriction electrostatically with a gate. In the entire gating range, the supercurrent diffraction pattern in a perpendicular magnetic field exhibits a slow decay indicative of a small number of Andreev bound states funnelling through the constriction. Under microwave irradiation, odd Shapiro steps are suppressed in the current-voltage characteristic of the open constriction. This observation has been linked to the appearance of a 4π-periodic contribution to the supercurrent of topological Josephson devices. Surprisingly, we recover all

steps as we reduce the transmission to a small number of channels. We discuss possible origins of the effect and implications for topological quantum devices.

TT 19.3 Wed 12:15 H23

Tunable 4π -periodic supercurrent in HgTe-based topological nanowires — •RALF FISCHER¹, JORDI PICÓ-CORTÉS^{2,3}, WOLFGANG HIMMLER¹, GLORIA PLATERO², MILENA GRIFONI³, DIMITRY KOZLOV⁴, NIKOLAY MIKHAILOV⁴, SERGEY DVORETSKY⁴, CHRISTOPH STRUNK¹, and DIETER WEISS¹ — ¹Experimental and Applied Physics, University of Regensburg — ²Instituto de Ciencia de Materiales de Madrid — ³Institute of Theoretical Physics, University of Regensburg — ⁴Novosibirsk, Russia

Topological insulator nanowires in proximity to conventional superconductors have been proposed as a tunable platform to realize topological superconductivity. The tuning is done using an axial magnetic flux Φ which allows transforming the system from trivial at $\Phi = 0$ to topologically nontrivial when half a magnetic flux quantum $\Phi = \Phi_0/2$ threads the cross-sectional area of the wire.

In our work, we investigate Josephson junctions based on HgTe nanowires and probe the Shapiro step spectrum. From the suppression of odd Shapiro steps, we extract the 4π - and 2π -periodic portion of the supercurrent $I_{4\pi}$ and $I_{2\pi}$ using a resistively and capacitively shunted junction model. The ratio $I_{4\pi}/I_{2\pi}$ changes from a small value of few percent at $\Phi = 0$ up to a maximum at $\Phi = \Phi_0/2$. The presence of $I_{4\pi}$ at $\Phi = 0$ and small magnetic fields indicate that in this regime Landau-Zener transitions cause the 4π -periodic current. By disentangling the 4π -periodic supercurrent of trivial and topological origin, our data suggest that topological 4π -periodic supercurrents dominate at axial magnetic fields above $\Phi_0/4$.

TT 19.4 Wed 12:30 H23

Complex magnetic ground states and topological electronic phases of atomic spin chains on superconductors — •JANNIS NEUHAUS-STEINMETZ¹, ELENA VEDMEDENKO¹, THORE POSSKE², and ROLAND WIESENDANGER¹ — ¹Department of Physics, University of Hamburg, 20355 Hamburg, Germany — ²I. Institute for Theoretical Physics, University of Hamburg, D-20355 Hamburg, Germany

Understanding the magnetic properties of atomic chains and nanoscopic wires on superconductors is an essential cornerstone on the road towards controlling and constructing topological matter. Yet, even in the simplest models of sus-

pending chains, the classes of available magnetic ground states remain debated. Ferromagnetic (FM), antiferromagnetic (AFM), and spiral configurations have been suggested and experimentally detected, while additionally non-coplanar and complex collinear phases have been conjectured. Here, we resolve a recent controversy by determining the magnetic ground states of chains of magnetic atoms in proximity to a superconductor with Monte-Carlo methods, which employ the initial tight-binding model directly without further simplifications. We confirm the existence of FM, AFM and spiral ground states, and identify additional more complex ground states. We topologically classify the electronic structures, and investigate the stability of the magnetic states against increasing superconductivity. In addition, we introduce a computationally efficient alternative for approximating the magnetic ground state with an effective Heisenberg model, which we demonstrate by using our previous results as a benchmark for this new method.

TT 19.5 Wed 12:45 H23

Density functional Bogoliubov - de Gennes calculations for a topological superconductor — •PHILIPP RÜSSMANN^{1,2} and STEFAN BLÜGEL² — ¹Institute of Theoretical Physics and Astrophysics, University of Würzburg, Würzburg, Germany — ²Peter Grünberg Institut and Institute for Advanced Simulation, Forschungszentrum Jülich and JARA, Jülich, Germany

The possibility to combine topological electronic band structures and superconductivity (SC) opens new pathways towards engineering exotic quantum matter. Proximity induced superconductivity in the topological surface state of topological insulators (TIs) offers the possibility to realize a chiral p -wave superconductor. Such a superconductor is an exotic state of matter which supports non-Abelian anyons and is of great interest for Majorana-based quantum computing applications. Material-specific insights into the microscopic details of such SC/TI interfaces are of great interest and an indispensable ingredient in the challenging materials optimization problem.

Here we first introduce the recent Bogoliubov de-Gennes (BdG) extension to the all electron full potential relativistic Korringa-Kohn-Rostoker (KKR) Green function code JuKKR [1]. We apply the KKR-BdG method to the s -wave superconductor Nb [2] and investigate the proximity induced superconductivity in the topological surface state of a SC/TI heterostructure.

[1] <https://jukkr.fz-juelich.de>

[2] PRB **105**, 125143 (2022)

TT 20: Topology: Poster Session

In case the presenters cannot be present at their posters for the full duration of the poster session, they are kindly requested to leave a note at their poster indicating when they will be available for discussion.

Time: Wednesday 15:00–18:00

Location: P1

TT 20.1 Wed 15:00 P1

Effects of in-plane polarised light on graphene: Band gap, spin and topological quantum numbers — •FREDERIK BARTELMANN¹, MARTA PRADA², and DANIELA PFANNKUCHE^{1,3} — ¹University of Hamburg, I. Institute of Theoretical Physics — ²University of Hamburg, Institute of Nanostructure and Solid State Physics — ³The Hamburg Centre for Ultrafast Imaging

If it were not for the effects of spin-orbit interaction, the band gap in graphene would close at the K-points, resulting in perfect Dirac cones. In this work, a graphene tight-binding band structure involving atomic s -, p - and d -orbitals is modified by irradiation with light. The light is polarised in-plane to affect the d_{xz} - and d_{yz} -orbitals, which are coupled via spin-orbit interaction, and the p_z -orbitals, which are predominant in the valence and conduction band. Floquet formalism is used to obtain dressed states and an altered band structure. The changes to valence and conduction band and thus the band gap are studied for a range of frequencies in the PHz regime. Along these studies, the correlation between real- and sublattice spin is probed as well as topological properties and how they behave under a change of frequency. Since the focus lies on the effects due to changes in the orbital composition of the dressed states, inter-band couplings are prioritised over intra-band ones. The goal of the studies is to gauge the effect of different irradiated frequencies on graphene and to evaluate possible applications of dressed states for topological quantum computers.

TT 20.2 Wed 15:00 P1

Static and dynamic magnetism of $(\text{MnBi}_2\text{Te}_4)(\text{Bi}_2\text{Te}_3)_n$ ($n = 0, 1$) probed by electron spin resonance technique. — •ALEXEY ALFONSOV¹, KAVITA MEHLAWAT^{1,2}, JORGE I. FACIO¹, ALI G. MOGHADDAM^{1,3}, RAJYAVARDHAN RAY¹, ALEXANDER ZEUGNER^{4,5}, MANUEL RICHTER^{1,5}, ANNA ISAEVA^{1,6}, JEROEN VAN DEN BRINK^{1,2,5}, BERND BÜCHNER^{1,2,5}, and VLADISLAV KATAEV¹ — ¹Leibniz IFW Dresden, 01069 Dresden, Germany — ²Würzburg-Dresden Cluster of Excellence ct.qmat — ³IASBS, Zanjan 45137-66731, Iran — ⁴H.C. Starck Tungsten GmbH, 38642 Goslar, Germany — ⁵TU Dresden, 01062 Dresden, Germany — ⁶University of Amsterdam, 1098 XH Amsterdam, The Netherlands

$(\text{MnBi}_2\text{Te}_4)(\text{Bi}_2\text{Te}_3)_n$ ($n = 0, 1$) are van der Waals materials which exhibit a co-existence of topologically nontrivial surface states with intrinsic magnetism. In this work we address static and dynamic magnetic properties of the title materials in the ordered and disordered states using multifrequency and high field electron spin resonance technique. We show that the spin dynamics of the magnetic building blocks of these compounds, the Mn-based septuple layers (SLs), is inherently ferromagnetic (FM) featuring persisting short-range FM correlations far above the magnetic ordering temperature as soon as the SLs get decoupled either by introducing a nonmagnetic quintuple interlayer, as in MnBi_4Te_7 , or by applying a moderate magnetic field, as in MnBi_2Te_4 . Additionally, MnBi_2Te_4 exhibits a strongly anisotropic Mn spin relaxation in the paramagnetic state, which we explain by the sensitivity of the local electronic structure to the Mn spin orientation.

TT 20.3 Wed 15:00 P1

Low-dimensional spin correlations in $\text{Mn}_2\text{P}_2\text{S}_6$ and MnNiP_2S_6 as revealed by ESR spectroscopy — •YURIY SENYK¹, JOYAL JOHN ABRAHAM^{1,2}, ALEXEY ALFONSOV¹, YULIYA SHERMERLIUK¹, SEBASTIAN SELTER^{1,2}, SAICHARAN ASWARTHAM¹, BERND BÜCHNER^{1,3}, and VLADISLAV KATAEV¹ — ¹Leibniz IFW Dresden, D-01069 — ²Institute for Solid State and Materials Physics, TU Dresden, D-01069 — ³Institute for Solid State and Materials Physics and Würzburg-Dresden Cluster of Excellence ct.qmat, TU Dresden, D-01062

$\text{Mn}_2\text{P}_2\text{S}_6$ and MnNiP_2S_6 are members of the transition metal phosphorus trichalcogenide family which belongs to the layered van der Waals (vdW) materials class. Such compounds are considered to be attractive for designing novel spintronic devices due to their remarkable structural and magnetic properties. Here we report the electron spin resonance studies on single crystals of $\text{Mn}_2\text{P}_2\text{S}_6$ and MnNiP_2S_6 using an X-band (9.56 GHz) spectrometer. Measurements were done in a wide temperature range and at various angles between the applied magnetic field and crystal axes. The obtained spectra can be well fitted to the Lorentzian lineshape enabling an accurate determination of the linewidth and the resonance field. Remarkably, the angular temperature dependences of the

linewidth show signatures of the low-dimensional spin-spin correlations in the pure Mn compound whereas the mixed compound demonstrates a rather three-dimensional behaviour.

TT 20.4 Wed 15:00 P1

Quantum anomalous hall devices on magnetically doped topological insulator films — •ROOZBEH YAZDANPANAH RAVARI¹, GERTJAN LIPPERTZ^{1,2}, ANJANA UDAY¹, ANDREA BLIESENER¹, ALEXEY TASKIN¹, and YOICHI ANDO¹ — ¹University of Cologne, Cologne, Germany — ²KU Leuven, Leuven, Belgium
Magnetic doping opens an exchange gap in the surface states of topological insulators (TIs) at the Dirac point by breaking time reversal symmetry. Such systems manifest the quantum anomalous Hall (QAH) effect which is characterized by quantized Hall resistance and zero longitudinal resistance. To explore this phenomena, devices are fabricated on thin films of V-doped $(\text{Bi}_{1-x}\text{Sb}_x)_2\text{Te}_3$. This contribution highlights our effort to better understand this effect, including a study of the QAH breakdown where in high current densities or small dimensions, the quantized state is lost. Another ongoing effort focuses on interfacing the quantum anomalous hall insulator (QAH) system with a superconductor (SC) through devices with different geometries, where the obtained results suggest high transparency of the QAH/SC interface.

TT 20.5 Wed 15:00 P1

Entanglement spectrum of Su-Schrieffer-Heeger model — •MAHSA ALSADAT SEYED HEYDARI¹ and JAHANFAR ABOUEI² — ¹University of Konstanz, Germany — ²Institute for Advanced Studies in Basic Sciences (IASBS), Iran
We investigate the ground state properties of a one dimensional topological insulator, the Su-Schrieffer-Heeger (SSH) chain in the absence/presence of an alternative spin-orbit coupling (SOC), employing single-particle entanglement spectrum (ES). In the presence of SOC, owing to the spin-flip processes, different topologically trivial and non-trivial phases appear in the ground state phase diagram of the model. Using the matrix of single-particle correlation functions, we obtain the single-particle ES as well as the entanglement entropy, and show that they behave differently in these phases. We introduce an indicator, called entanglement gap, defined as the difference between the lowest positive entanglement level and the highest negative level, and demonstrate that this indicator distinguishes the topological phases from the trivial phase of the model.

TT 20.6 Wed 15:00 P1

Current increase by weakening site-site interaction in SSH lattices — •MIRKO ROSSINI, BRECHT DONVIL, and JOACHIM ANKERHOLD — Institute for Complex Quantum Systems and IQST, Ulm University, Germany
One of the simplest models supporting topologically protected states is the well-known Su-Schrieffer-Heeger (SSH) model. As a 1D chain with staggered NN hopping amplitudes, it can host two protected 0-energy modes when the distribution of hopping amplitudes is properly adjusted. These edge states are energetically relatively stable against ambient noise. thus providing natural protection from any excitation living on an edge of the chain.
In this poster, we show the realization of a current through such a chain, which in the topological regime could provide a naturally protected channel for the safe transport of excitations in space. The current is created by terminating the SSH chain at particle reservoirs. It has been shown that the edge-to-edge transport of particles in such a system is exponentially suppressed with respect to the length of the chain, preventing the practical use of this model for the stated purposes. Therefore we propose, after a brief introduction to the main properties of the SSH model, an extended model for the 1D lattice that, by weakening a small selection of hopping parameters along the chain, is able to increase the current through the edges while preserving some of the topological protection offered by the original SSH model.

TT 20.7 Wed 15:00 P1

Search for new europium-based intermetallic 122 materials with non-trivial topological properties — •SARAH KREBBER, KRISTIN KLIEMT, CORNELIUS KRELLNER, and ASMAA EL MARD — Max-von-Laue Straße 1, 60438 Frankfurt am Main, Physikalisches Institut
Today, more and more Eu-based compounds come into focus of magnetic topological nontrivial materials. The first examples were thin films of EuS on Bi_2Se_3 [1]. In recent studies, the material EuCd_2As_2 has attracted a lot of attention due to emergence of a variety of topological phases and magnetic phenomena [2,3]. Recently, a spin fluctuation induced Weyl semimetal state in the paramagnetic phase of EuCd_2As_2 [2] and its tunability by pressure [4] was discovered. Furthermore, the similar material EuCd_2P_2 has been explored due to its strong colossal magnetoresistance effect [5]. In this work we present the single crystal growth and characterization of the related system EuT_2X_2 , with T = Cd, Zn, Mn and X = P, crystallizing in the same trigonal structure (P-3m1) in order to search for similar effects in these materials. The physical properties of the compounds are explored via magnetization, electrical transport and heat capacity.
[1] Katmis et al., Nature 533, 513 (2016)
[2] Ma et al., Science Adv. 5, eaaw4718 (2019)
[3] Jo et al., Phys. Rev. B 101, 140402(R) (2020)

- [4] Gati et al., Phys. Rev. B 104, 155124 (2021)
[5] Wang et al., Adv.Mater. 33, 2005755 (2021)

TT 20.8 Wed 15:00 P1

Band structure and effective masses of the topological semimetal PdGa — •F. HUSTEDT^{1,2}, B.V. SCHWARZE^{1,2}, M. UHLARZ¹, S. CHATTOPADHYAY¹, K. MANNA^{3,4}, S. SHEKHAR³, C. FELSER³, and J. WOSNITZA^{1,2} — ¹Hochfeld-Magnetlabor Dresden (HLD-EMFL) and Würzburg-Dresden Cluster of Excellence ct.qmat, HZDR, Germany — ²Institut für Festkörper- und Materialphysik, TU Dresden, Germany — ³Max Planck Institute for Chemical Physics of Solids, Germany — ⁴Indian Institute of Technology Delhi, India
De Haas-van Alphen (dHvA) measurements at low temperatures and fields up to 18 T provided insight into the band structure of the topological semimetal PdGa which is presented in this poster. Previous investigation of PtGa revealed the topological character [1] of this sister compound of PdGa. Hence, angle-resolved measurements of the dHvA effect were performed on PdGa and showed a good agreement with the calculated band structure. This revealed a multitude of Fermi surfaces and eight spin-split bands crossing the Fermi energy. In particular, the calculations show a similar band structure as for PtGa, including two topologically protected multifold degenerate band-touching nodes. Furthermore, we analyzed the temperature dependence of the dHvA oscillations to determine the effective masses for field aligned along the crystallographic [100] axis. The low masses also show a good agreement to the calculations and, therefore, indicate insignificant correlations of the electrons.
[1] M. Yao, K. Manna et al., Nat. Commun. 11, 2033 (2020).

TT 20.9 Wed 15:00 P1

Current phase relation of HgTe nanowire Josephson junctions in an axial magnetic field — •N. HÜTTNER¹, W. HIMMLER¹, D. A. KOZLOV², N. N. MIKHAILOV², S. A. DVORETSKY², D. WEISS¹, and C. STRUNK¹ — ¹Experimental and Applied Physics, University of Regensburg, D-93040 Regensburg, Germany — ²Novosibirsk, Russia
Topological insulators (TIs) such as HgTe nanowires host topological surface states. Their band structure can be tuned to a Dirac shape via the application of an axial magnetic field (B_{\parallel}) [1]. For proximitized nanowires this is expected to tune between trivial and topological supercurrents as recent experiments suggest [2]. Here we directly probe the current phase relation (CPR) of a tunable TI Josephson junction. The TI junction consists of a HgTe nanowire proximitized by superconducting Nb contacts embedded into an asymmetric DC-SQUID together with an Al/AlOx/Al junction. Being in the short junction regime [2], the TI junction features a strongly anharmonic CPR [3,4] with a high average transparency of $D \approx 0.95$ for $n \approx 9 \pm 2$ channels [4]. Varying B_{\parallel} controls the magnetic flux enclosed by the nanowire surface. In the range $0 - 1.5\Phi_0$ we observe a strong modulation of the critical current and interference of phase shifted contributions of individual channels creating a great variety of CPR shapes.
[1] A. Cook et al., Phys. Rev. B 84, 201105 (2011).
[2] R. Fischer et al., Phys. Rev. Res. 4, 013087 (2022).
[3] A. A. Golubov et al., Rev. Mod. Phys. 76, 411 (2004).
[4] C. Baumgartner et al., Phys. Rev. Lett. 126, 037001 (2021).

TT 20.10 Wed 15:00 P1

Ground-state splitting of parafermions zero modes at a finite distance — •RAPHAEL L R C TEIXEIRA^{1,2}, AMAL MATHEW^{2,3}, ROSHNI SINGH^{2,3}, SOLOFO GROENEDIJK², ANDREAS HALLER², EDVIN G IDRISOV², LUIS G G V DIAS DA SILVA¹, and THOMAS L SCHMIDT² — ¹Instituto de Física - Universidade de Sao Paulo, Sao Paulo Brazil — ²Department of Physics and Materials Science Université du Luxembourg, Luxembourg, Luxembourg — ³Indian Institute of Technology, Bombay, India
Parafermion bound states can be regarded as fractional excitations that generalize Majorana bound states. Parafermions appear in strongly-correlated systems, and in particular, fractional Quantum Hall (FQH) edge states with induced superconductivity can be used to create localized \mathbb{Z}_{2n} parafermion modes. Previous works have used the single-instanton approximation to calculate the ground-state energy splitting in the limit of a large distance between the parafermions. In this work, we go beyond this approximation to determine the energy splitting in shorter systems, paving the way to better understanding experimentally relevant systems. We discuss the implications of a finite length in the coupling between parafermions and how it goes beyond the corresponding effect for Majorana bound states. The analytical results agreed with Monte Carlo simulations implying the corrections we found cannot be neglected.

TT 20.11 Wed 15:00 P1

Full counting statistics of electron transport through a Majorana single-charge transistor — •ERIC KLEINHERRBERS, ALEXANDER SCHÜNEMANN, and JÜRGEN KÖNIG — Faculty of Physics and CENIDE, University Duisburg-Essen, 47057 Duisburg, Germany
We study full counting statistics of electron transport through a Majorana single-charge transistor (MSCT) [1]. The MSCT can host both Majorana bound states and Cooper pairs. In addition, the system is coupled to a superconducting

and a metallic lead. A current through the system is realized by means of the Josephson-Majorana cycle [2], where sequential tunneling (normal and anomalous) of two electrons into the system is followed by the transfer of a Cooper pair into the superconductor. We find a highly correlated electron transfer which can be indicated by a sign violation of factorial cumulants. Moreover, when the

superconductor is only weakly coupled to the MSCT, we find for large bias voltages a strong suppression of the electron current. This effect is explained by the excitation of a dark state that effectively decouples from the leads.

- [1] A. Zazunov et al., Phys. Rev. B 84, 165440 (2011)
[2] N. Didier et al., Phys. Rev. B 88, 024512 (2013)

TT 21: Correlated Electrons: Poster Session

In case the presenters cannot be present at their posters for the full duration of the poster session, they are kindly requested to leave a note at their poster indicating when they will be available for discussion.

Time: Wednesday 15:00–18:00

Location: P1

TT 21.1 Wed 15:00 P1

Single crystal growth and characterization of CeCoIn₅ and GdCoIn₅ — •LEONARD ESSICH, ANJA PHILIPP, ALEXEJ KRAIKER, KRISTIN KLIEMT, and CORNELIUS KRELLNER — Physikalisches Institut, Goethe Universität Frankfurt, 60438 Frankfurt am Main

The family of 115 rare-earth compounds RTIn₅ (T = Co, Rh, Ir) with tetragonal crystal structure received growing attention over the past decades. Low-temperature phenomenologies associated with the strong correlations of the 4f-electrons of the rare-earth element and the quasi-two-dimensionality of the Fermi surface such as spin and valence fluctuations [1], heavy fermions [2], and anisotropic superconductivity [3] are observed for the Ce-based compounds. The GdTIn₅ series show magnetic ordering of local 4f-moments with a reduced interplane coupling for GdCoIn₅ [3].

In this contribution, we show our results of the self-flux growth of CeCoIn₅ and GdCoIn₅ single crystals. The crystallographic orientation was determined using microscopy and Laue X-ray diffraction along with the characterization by powder X-ray diffraction, magnetization, specific-heat and specific-resistivity measurements for both compounds.

- [1] D. Betancourth et al., JMMM 375, 744 (2015)
[2] Y. Onuki et al., J. Phys. Soc. Jpn. 71, 162 (2002)
[3] J.I. Facio et al., PRB 91, 014409 (2015)

TT 21.2 Wed 15:00 P1

Single crystal growth and characterization of Eu(Pd_{1-x}Au_x)₂Si₂ — •ROBERT MÖLLER, MARIUS PETERS, CORNELIUS KRELLNER, and KRISTIN KLIEMT — Physikalisches Institut, Goethe-Universität Frankfurt, Germany

In a general phase diagram for Eu compounds [1], the intermediate valent EuPd₂Si₂, T_V ~ 150 K, is located very close, but slightly at the high-pressure side of a second order critical endpoint [2]. The analysis of polycrystalline samples of Eu(Pd_{1-x}Au_x)₂Si₂ revealed that in this series a critical endpoint can be found which separates the region of continuous from first order transitions. It was shown that the valence state of the material can be tuned via Au substitution and that for x between 0.05 and 0.2 the transition becomes a first order phase transition [3]. In this contribution, we present the Czochralski growth and the characterization of Eu(Pd_{1-x}Au_x)₂Si₂ single crystals. Using magnetization and heat capacity measurements, we study the changes in the nature of the phase transition in detail.

- [1] Y. Onuki et al., Philosophical Magazine 97, 3399 (2017)
[2] B. Batlogg et al., in: Wachter, Boppart (eds.): Valence Instabilities, North-Holland publishing company (1982)
[3] C. U. Segre et al., Physical Review Letters 49, 1947 (1982)

TT 21.3 Wed 15:00 P1

Single crystal growth of EuPd₂Si₂ under enhanced gas pressure — •ALEXEJ KRAIKER, MARIUS PETERS, KRISTIN KLIEMT, and CORNELIUS KRELLNER — Physikalisches Institut, Goethe Universität Frankfurt, 60438 Frankfurt am Main, Germany

The study of collective phenomena raising from enhanced coupling between electrons and phonons is focussed on materials exhibiting phase transitions involving both, electronic and lattice-degrees of freedom. One system providing such a strongly coupled phase transition is EuPd₂Si₂ crystallizing in the ThCr₂Si₂ structure type. Because of the the high vapor pressure of Eu, high-quality single crystals of EuT₂X₂-compounds are very challenging to grow in larger size. One way to prevent Eu from evaporating out of the melt, is growing the crystals in argon overpressure. In this contribution, we present the crystal growth of EuPd₂Si₂ single crystals with a 20 bar Czochralski-furnace as well as the commissioning of a 150 bar high-pressure furnace which will provide the possibility of both the growth by the Czochralski and the Bridgman method.

TT 21.4 Wed 15:00 P1

YbIn_{1-x}Ag_xCu₄: single crystal growth and characterisation — •MICHELLE OCKER, BEREKET GHEBRETINSAE, KRISTIN KLIEMT und CORNELIUS KRELLNER — Physikalisches Institut, Goethe-Universität Frankfurt, 60438 Frankfurt/Main, Germany

The compound YbInCu₄ undergoes a 1st order valence transition at T_v = 42 K by changing the temperature. Thus, ytterbium in the compound is present in the Yb^{2.9+} state at high temperatures and as Yb^{2.7+} at low temperatures [1]. In analogy to Eu compounds, the first order valence transition is suspected to end in a second order critical endpoint [2]. In order to study this valence transition in more detail, single crystal samples can be prepared in In-Cu flux which are substituted with silver [3]. With increasing Ag content, negative chemical pressure within the crystal is increased and the characteristics of the valence transition changes significantly. Here, we report on the single crystal growth with different Ag substitution levels and the results of our structural, chemical and physical characterization.

- [1] H.Sato et al., Physica B 351, (2004) 298
[2] Y. Ōnuki et al., J. Phys. Soc. Jpn. 89, (2020) 102001
[3] J. L. Sarrao et al., Phys. Rev. B 54, (1996) 12207

TT 21.5 Wed 15:00 P1

Elastoresistance of Eu₂T₂P₂ (T=Fe, Ru, Co) systems close to a collapsed tetragonal phase transition — •TESLIN ROSE THOMAS¹, N. S. SANGEETHA¹, THANH DUC NGUYEN², JULIAN REUSCH², MARIUS PETERS², KRISTIN KLIEMT¹, CORNELIUS KRELLNER², and ANNA E. BÖHMER¹ — ¹Lehrstuhl für Experimentalphysik IV, Ruhr-Universität Bochum, Universitätsstraße 150, 44801 Bochum — ²Physikalisches Institut, Goethe-Universität Frankfurt, Max-von-Laue-Straße 1, 60438 Frankfurt am Main

Manipulation of the properties of materials by applying anisotropic strain is an increasingly common method used in the study of correlated electron materials. In particular, the nematic state of several unconventional superconductors has been studied intensively using elastoresistance as a probing tool. In the current project, we employ elastoresistance to study the state close to the uncollapsed to collapsed- tetragonal transitions in Eu₂T₂P₂ (T=Fe, Ru, Co) and CaCo₂As₂ 122 systems. In contrast to investigations of nematicity, where the response to uniaxial strain is studied, we apply bi-axial strain which is by symmetry well suited. The corresponding elastoresistance is compared for the different compounds and at different temperatures. The results are then compared with the temperature and pressure dependence of lattice constants, which show the tetragonal collapse.

We acknowledge support from the German Research Foundation (DFG) under CRC/TRR 288 (Project A02).

TT 21.6 Wed 15:00 P1

Valence fluctuations and structural collapse in Eu-based phosphides EuT₂P₂ — MARIUS PETERS¹, •KRISTIN KLIEMT¹, JULIAN DOMINIK REUSCH¹, THANH DUC NGUYEN¹, FRANZISKA WALTHER¹, MICHAEL MERZ², GASTON GARBARINO³, SOFIA MICHAELA SOULIOU², MATTHIEU LE TACON², AMIR-ABBAS HAGHIGHIRAD², and CORNELIUS KRELLNER¹ — ¹Kristall- und Materiallabor, Physikalisches Institut, Goethe University Frankfurt, Max-von-Laue-Str. 1, D-60438 Frankfurt — ²Karlsruhe Institute of Technology, Institute for Quantum Materials and Technology, D-76021 Karlsruhe — ³European Synchrotron Radiation Facility (ESRF), F-38043 Grenoble

Studies of enhanced coupling between electrons and phonons is focussed on materials exhibiting phase transitions involving both electronic and lattice degrees of freedom. Europium in intermetallic systems can exhibit different magnetic ground states: If the ground state is Eu²⁺, the system shows long range magnetic order; if the ground state is Eu³⁺, no magnetic order is observed. Instead, valence fluctuations occur in intermediate valent states [1].

In this work, we report on the structural collapse in divalent europium systems EuT₂P₂ (T = Fe, Co, Ru), which is connected to a change of europium's ground state by using single crystal diffractometry at pressures up to 15 GPa at 15 K and 300 K. Additionally, we show characterizations of the electronic and structural contributions to valence fluctuations in EuNi₂P₂.

- [1] Y. Onuki et al., Philos. Mag. 97, 3399 (2017).

TT 21.7 Wed 15:00 P1

Crystal growth and characterization of LnCo_2P_2 ($\text{Ln} = \text{Pr}, \text{Nd}$) — •FABIAN FIEDLER, MARIUS PETERS, KRISTIN KLIEMT, and CORNELIUS KRELLNER — Physikalisches Institut, Goethe-Universität Frankfurt, 60438 Frankfurt/Main, Germany

In condensed matter systems, the 4f-driven temperature scales at the surfaces of correlated materials have increasingly come into the focus of research efforts. Here, we present the crystal growth of LnCo_2P_2 ($\text{Ln} = \text{Pr}, \text{Nd}$) in tin flux and the corresponding structural/physical characterization.

Using temperatures of up to 1400°C and a vertical temperature-gradient, we optimized the growth, resulting in large high-quality single crystals, allowing for physical characterization, especially by means of thermodynamic measurements and angle-resolved photoemission spectroscopy.

The structural and chemical characterization is performed by X-ray powder diffractometry, energy-dispersive X-ray spectroscopy and the Laue-method.

Magnetic properties of these systems, arising from the combination of the 4f-moments of Ln^{3+} -ions and the 3d-moments of Co^{3+} , are investigated by measurements of magnetization, heat capacity and resistivity.

TT 21.8 Wed 15:00 P1

Growth and characterization of $\text{KFe}_{1-x}\text{Ag}_{1+y}\text{Ch}_2$ — •JUTTA PÜTTMANN, N. S. SANGEETHA, ANDREAS KREYSSIG, and ANNA E. BÖHMER — Experimentalphysik IV, Universitätstraße 150, 44801 Bochum

Iron-based 122-compounds with ThCr_2Si_2 structure have been intensely studied over the past decades. K-based chalcogenides, such as $\text{K}_x\text{Fe}_{2-\delta}\text{Se}_2$ have attracted attention due to their high-temperature superconductivity, their strong electronic correlations, and their complex microstructure dominated by vacancies and phase separation. Recently, $\text{KFe}_{0.8}\text{Ag}_{1.2}\text{Te}_2$ has been found to provide the possibility to study an iron chalcogenide 122-systems without vacancies on the alkali site and to investigate a superstructure in the Fe/Ag plane with an interesting magnetic and nematic ordering [1, 2].

The growth of K-based single crystals is challenging due to the high vapor pressure and reactivity of potassium. We developed a new, affordable and efficient growth technique using containers made from high-temperature resistant stainless steel that can be sealed without any air-exposure of the starting materials. The growth of $\text{KFe}_{1-x}\text{Ag}_{1+y}\text{Ch}_2$ -crystals by self-flux was optimized with respect to the starting material composition. The obtained crystals were characterized by EDX and XRD. The XRD patterns were analyzed for signs of superstructure in the Fe/Ag plane. Additionally, low-temperature measurements were carried out to confirm the magnetic transitions.

[1] Yu Song et al., Phys. Rev. Lett. 122, 087201 (2019)

[2] Yu Song et al. Phys. Rev. Lett. 123, 247205 (2019)

TT 21.9 Wed 15:00 P1

Classical Ising-like dipolar antiferromagnet DyScO_3 with slow spin dynamics — •NIKITA ANDRIUSHIN¹, STANISLAV NIKITIN^{2,3}, and ANDREY PODLESNYAK⁴ — ¹TU Dresden, Germany — ²MPI CPFS, Dresden, Germany — ³PSI, Villigen, Switzerland — ⁴ORNL, Tennessee, USA

The usual timescale of the spin flip process in common magnetic systems is femto- to picoseconds. In this work we show with the help of both AC and DC magnetization measurements and classical Monte-Carlo calculations that the spin dynamics in DyScO_3 can be slowed down to milliseconds and further. The orthorhombic DyScO_3 has a large uniaxial anisotropy caused by the strong crystalline electric field (CFT), which freezes magnetic moments below a certain temperature. Large anisotropy and long-range dipolar interaction result in an Ising-like antiferromagnetic ordering with critical temperature $T_C = 3.14$ K. Magnetization and susceptibility measurements revealed a magnetization relaxation on a timescale of minutes, which is unexpected for an antiferromagnet. As a classical approach for modeling Ising-like spin systems, the Monte-Carlo calculations with METROPOLIS algorithm were used. Our calculations, taking into account the dipole-dipole interaction energy, comprehensively reproduce the observed magnetic behavior, correctly predict the ground state, critical temperature and capture slow magnetization dynamics.

TT 21.10 Wed 15:00 P1

Hierarchical equations of motion approach to open quantum dynamics: Matrix product state formulation in twin space — •YALING KE¹, RAFFAELE BORRELLI², and MICHAEL THOSS¹ — ¹Institute of Physics, Albert-Ludwig University Freiburg, Hermann-Herder-Strasse 3, 79104 Freiburg, Germany — ²DISAFA, Università di Torino, I-10095 Grugliasco, Italy

The hierarchical equations of motion (HEOM) is a numerically exact approach to studying open quantum dynamics with strong non-perturbative and non-Markovian system-environment interactions at finite temperatures. Although considerable progress has been made over the past few decades to extend the applicability of the HEOM approach, the numerical cost is still very expensive for reasonably large systems.

In this contribution, we present the twin-space formulation of the HEOM approach in combination with the matrix product state representation for an open quantum system coupled to a hybrid fermionic and bosonic environment. The

key ideas are a reformulation of a set of differential equations for the auxiliary density matrices into a time-dependent Schroedinger-like equation for an augmented multi-dimensional wave function as well as its tensor decomposition into a product of low-rank matrices. The new approach facilitates accurate simulations of non-equilibrium quantum dynamics in larger and more complex open quantum systems with both factorized and correlated initial condition.

TT 21.11 Wed 15:00 P1

Quantum criticality of $2k_F$ density wave order in two-dimensional metals — •LUKAS DEBBELER and WALTER METZNER — Max Planck Institute for Solid State Research

We analyze the quantum critical point at the transition towards incommensurate charge or spin density wave order with a $2k_F$ wave vector that connects a single pair of hot spots on the Fermi surface. Perturbative renormalization group (RG) calculations confirm non-Fermi liquid behavior with anomalous frequency scaling and renormalization of the Fermi surface in proximity to the hot spots. Employing a functional RG approach we treat frequency and momentum dependence as well as fermionic and bosonic degrees of freedom on equal footing. This approach does not lead to a self consistent solution with a peak of the static polarization function at the $2k_F$ -vector. We explore the possibility of a self consistent quantum critical solution via a scaling ansatz.

TT 21.12 Wed 15:00 P1

Field dependence of the low-energy magnon modes and a spin-cholesteric phase in $\text{Sr}_3\text{Fe}_2\text{O}_7$ — •NIKOLAI PAVLOVSKII¹, YULIYA TYMOSHENKO¹, DARREN C. PEETS¹, ALEXANDRE IVANOV², JACQUES OLLIVIER², BERNHARD KEIMER³, and DMYTRO INOSOV¹ — ¹TU Dresden, Germany — ²ILL, Grenoble, France — ³MPI for Solid State Research, Stuttgart, Germany

We systematically studied low-energy magnon excitations in the helimagnetically ordered bilayer perovskite $\text{Sr}_3\text{Fe}_2\text{O}_7$. The magnetic ground state was previously believed to be characterized with a single-q magnetic order parameter that results from a frustration of exchange interactions, resulting in two types of equivalent helimagnetic domains. Our present results suggest that it could be instead a double-q state. Our elastic neutron-scattering measurements in a magnetic field applied along one of the (110) crystal directions further reveal an additional phase transition within the magnetic phase, associated with the destruction of long-range order along the direction orthogonal to the field, leading to an unusual spin-cholesteric magnetic phase that breaks both chiral symmetry and translational symmetry along only one of the crystal directions. In the orthogonal direction, we observe only short-range quasielastic spin dynamics. Across the transition from the magnetically ordered to the spin-cholesteric phase, these slow spin fluctuations fill in the spin gap in the spin-wave spectrum, as we can see in the high-resolution inelastic neutron-scattering spectra, and ultimately dominate the low-energy magnetic excitation spectrum after the long-range magnetic order is destroyed.

TT 21.13 Wed 15:00 P1

Crystal Growth and Characterization of ZrFe_4Si_2 — •KATHARINA M. ZOCH, ISABEL REISER, ALEXANDER BODACH, KRISTIN KLIEMT, and CORNELIUS KRELLNER — Physikalisches Institut, Goethe-Universität Frankfurt, 60438 Frankfurt am Main, Germany

The ZrFe_4Si_2 -structure consists of edge-linked Fe-tetrahedra along the crystallographic c-direction. This type of arrangement is prone to show frustration and low dimensional fluctuations. First results on polycrystalline samples indicate that ZrFe_4Si_2 displays some sort of weak magnetic order, for an Fe-based compound, unusual low temperatures as well as deviant behavior in specific heat and resistivity compared to normal metals [1,2]. To investigate these features further, we are in need of single crystals. The crystal growth is a challenging subject. The compound is strongly peritectic melting and its elements are reactive with common crucible materials. Crystal growth experiments utilizing the Czochralski methods were performed, and the structure as well as magnetic, thermodynamic and electrical transport properties of the material were analyzed.

[1] M. O. Ajeesh et al., Phys. Rev. B, **102**, 184403 (2020)

[2] K. Weber, PhD thesis Technische Universität Dresden (2017)

TT 21.14 Wed 15:00 P1

Magnetic properties of monoclinic euchoite $\text{Cu}_2(\text{AsO}_4)(\text{OH})_3(\text{H}_2\text{O})$ — •YANNIS HILGERS, LEONIE HEINZE, DIRK MENZEL, and STEFAN SÜLLOW — IPKM, TU Braunschweig, Braunschweig, Germany

Previous studies of magnetic susceptibility and magnetisation on a natural polycrystalline sample of euchoite ($\text{Cu}_2(\text{AsO}_4)(\text{OH})_3(\text{H}_2\text{O})$) suggested that euchoite may be understood as a representation of a delta spin chain and exhibits a spin gap of about 50 K. In order to test this notion, we have performed a corresponding study on a monoclinic sample, determining these properties along the three crystallographic axes. Magnetic susceptibility from 2 K to 300 K and magnetisation for magnetic fields up to 5 T were measured on a natural monoclinic sample, previously characterized for crystallinity by Laue diffraction, of euchoite. From our data, we establish Curie-Weiss temperatures $\Theta_{CW,a} = -150(20)$ K, $\Theta_{CW,b} = -140(10)$ K, $\Theta_{CW,c} = -$

140(10) K, significantly larger in value than $\Theta_{CW} = -50$ K by Kikuchi et al. Moreover, we find that at low temperatures, magnetic susceptibility exhibits a spin gap, and a residual magnetisation at low temperatures can be understood in terms of about 1 % free magnetic impurity ($S = 1/2$) moments. Fitting a Brillouin-function to the magnetisation data with $S = 1/2$ results in saturation magnetisations of $M_{s,a} = 89,2(2,1)$ emu mol⁻¹, $M_{s,b} = 94,0(1,7)$ emu mol⁻¹, $M_{s,c} = 108,2(5,8)$ emu mol⁻¹. From this, the minimal length l_{min} of the delta spin chain segments can be estimated to $l_{min} = 350(50)$ Å. Altogether, our data are consistent with euchroite as a delta spin chain material with a spin gap of about 50 K.

TT 21.15 Wed 15:00 P1

Bond-directional nearest-neighbor excitations in the proximate Kitaev spin liquid Na₂IrO₃ probed by RIXS — •MARCO MAGNATERRA¹, ALESSANDRO REVELLI¹, KAROLIN HOPFER¹, CHRISTOPH SAHLE², MARCO MORETTI SALA³, GIULIO MONACO⁴, JAN ATTIG⁵, CIARÁN HICKEY⁵, ANTON JESCHE⁶, PHILIPP GEGENWART⁶, SIMON TREBST⁵, PAUL H. M. VAN LOOSDRECHT¹, JEROEN VAN DEN BRINK⁷, and MARKUS GRÜNINGER¹ — ¹II. Physik. Inst., Universität zu Köln — ²ESRF, Grenoble, France — ³Dip. di Fisica, Politecnico di Milano, Italy — ⁴Dip. di Fisica, Università di Padova, Italy — ⁵Inst. für Theo. Physik, Universität zu Köln — ⁶Exp. Physics VI, University of Augsburg — ⁷Inst. for Theo. Solid State Physics, IFW Dresden

The Kitaev model hosts a spin-liquid ground state with Majorana fermion excitations. It is based on bond-directional exchange, i.e. Ising-like interactions that couple different spin components on different bonds. In Na₂IrO₃, resonant inelastic x-ray scattering (RIXS) revealed fingerprints of Kitaev physics in the magnetic excitations [1]. In fact, the RIXS intensity shows a sinusoidal \mathbf{q} dependence that proves the nearest-neighbor or single-bond character of the excitations. We report on refined RIXS measurements where we exploit the polarization dependence of the different spin channels and the \mathbf{q} dependence of the different bonds to demonstrate the direct connection between spin component and bond direction. Our results establish the bond-directional nearest-neighbor character of magnetic excitations in Na₂IrO₃.

[1] A. Revelli et al., Phys. Rev. Research 2, 043094 (2020).

TT 21.16 Wed 15:00 P1

Asymmetric melting of the 1/3-plateau for the Kagome lattice antiferromagnet — •HENRIK SCHLÜTER¹, JÜRGEN SCHNACK¹, and JOHANNES RICHTER² — ¹Bielefeld University, Germany — ²University of Magdeburg and MPIPKS Dresden, Germany

The kagome lattice Heisenberg antiferromagnet (KHAF) is a rich source of unconventional physics not only regarding its spin-liquid ground state but also with respect to its behavior at non-zero field and temperature.

Here we investigate the phenomenon of the asymmetric melting of the magnetization plateau at 1/3 of the saturation magnetization, see Refs. [1, 2]. We explain the effect by discussing the energy diagram and the density of states constructed from finite-temperature Lanczos data for KHAF with up to 48 sites [3].

[1] J. Schnack, J. Schulenburg, J. Richter, Phys. Rev. B **98**, 094423 (2018)

[2] T. Misawa, Y. Motoyama, Y. Yamaji, Phys. Rev. B **102**, 094419 (2020)

[3] H. Schlüter, F. Gayk, H.-J. Schmidt, A. Honecker, J. Schnack, Z. Naturforsch. A **76**, 823 (2021)

TT 21.17 Wed 15:00 P1

Berry Phases of Vison Transport in Z₂ Topological Ordered States from Exact Fermion-Flux Lattice Dualities — CHUAN CHEN^{1,2}, •PENG RAO², and SODEMANN INTI^{2,3} — ¹Institute for Advanced Study, Tsinghua University, 100084 Beijing, China — ²Max-Planck Institute for the Physics of Complex Systems, 01187 Dresden, Germany — ³Institut für Theoretische Physik, Universität Leipzig, 04103 Leipzig, Germany

We develop an exact map of all states and operators from 2D lattices of spins-1/2 into lattices of fermions and bosons with mutual semionic statistical interaction that goes beyond previous dualities of Z₂ lattice gauge theories because it does not rely on imposing local conservation laws and captures the motion of ‘charges’ and ‘fluxes’ on equal footing. This map allows to explicitly compute the Berry phases for the transport of fluxes in symmetry enriched topologically ordered states that can be either chiral, non-chiral, abelian or non-abelian, and whose numerical complexity reduces to diagonalizing free-fermion Hamiltonians. Among other results, we establish numerically the conditions under which the Majorana-carrying flux excitation in Ising-Topologically-Ordered states enriched by translations acquires 0 or π phase when moving around a single plaquette.

TT 21.18 Wed 15:00 P1

Linked cluster expansions for a perturbed topological phase — •VIKTOR KOTT, MATTHIAS MÜHLHAUSER, and KAI PHILLIP SCHMIDT — Friedrich-Alexander-Universität, Erlangen-Nürnberg, Germany

We investigate the robustness of Kitaev’s toric code in a uniform magnetic field on several two-dimensional lattices by perturbative linked cluster expansions using a full graph decomposition. In particular, the full graph decomposition al-

lows to correctly take into account the non-trivial mutual exchange statistics of the anyonic elementary excitations. This allows us to calculate the ground-state energy and excitation energies of the topological phase which are then used to study the quantum phase transitions out of the topologically ordered phase as a function of the field direction.

TT 21.19 Wed 15:00 P1

Linked-cluster expansions for Rydberg atom arrays on the Kagome lattice — •ANTONIA DUFT, MATTHIAS MÜHLHAUSER, PATRICK ADELHARDT, and KAI PHILLIP SCHMIDT — Friedrich-Alexander-Universität Erlangen-Nürnberg, Erlangen, Deutschland

We investigate a model of hardcore bosons on the links of a Kagome lattice subject to a long-range decaying van-der-Waals interaction. This model is known to be the relevant microscopic description of Rydberg atom arrays excited by a detuned laser field which has been realized in experiments recently. We apply high-order linked cluster expansions about different limits to investigate the quantum phase diagram. One particular interest is to find further evidence for the proposed topological phase in this quantum platform.

TT 21.20 Wed 15:00 P1

Fractal quantum criticality in the Newman-Moore model in a transverse field investigated by linked cluster expansions — •RAYMOND WIEDMANN, MATTHIAS MÜHLHAUSER, and KAI PHILLIP SCHMIDT — Friedrich-Alexander-Universität, Erlangen-Nürnberg, Germany

The zero-temperature phase transition in the two-dimensional self-dual quantum Newman-Moore model is investigated using perturbative linked cluster expansions. The model exhibits type-II fracton excitations that have a highly restricted mobility on the lattice. High-order series expansions of the energy gap for different quasi-particle sectors as well as the vacuum energy are calculated using perturbative continuous unitary transformations and matrix perturbation theory, respectively. Our results indicate a first-order phase transition between the fractal phase and the polarized phase at the self-dual point in the model.

TT 21.21 Wed 15:00 P1

Improved EPR spectroscopy on single molecular magnets — •MICHAEL SCHULZE¹, DANIEL SCHROLLER¹, GHEORGHE TARAN¹, EUFEMIO PINEDA³, MARIO RUBEN², CHRISTOPH SÜRGER¹, and WOLFGANG WERNSDORFER¹ — ¹Physikalisches Institut, KIT, Karlsruhe — ²Institut für Nanotechnologie, KIT, Karlsruhe — ³Departamento de Química, Universidad de Panamá, Panama City

The quantum nature and large magnetic anisotropies in lanthanide-based single molecular magnets (SMMs) provides potential for interesting applications in quantum computing and information storage. The development of the micro-SQUID technique provides a tool for high-resolution magnetization measurements of SMM single crystals from the mK-range up to several Kelvin. EPR spectroscopy, where different spin states are excited by resonant absorption of radiofrequency radiation, serves as a powerful extension of the micro-SQUID technique to gain further insight into the magnetic properties of SMMs. This project strives to improve various features of this combined setup, such as higher coupling strengths, better thermalization, and coherent spin manipulation of SMMs.

TT 21.22 Wed 15:00 P1

Electrical read out of the nuclear spin and implementation of quantum algorithms on Tb₂Pc₃ triple decker — •LUCA KOSCHE¹, FRANCK BALESTRO², MARIO RUBEN^{3,4,5}, and WOLFGANG WERNSDORFER^{1,2,3,4} — ¹Physikalisches Institut, Karlsruhe Institute of Technology (KIT), Karlsruhe — ²CNRS, Institut Néel, Univ. Grenoble Alpes, France — ³Institute of Nanotechnology (INT), KIT — ⁴Institute for Quantum Materials and Technology (IQMT), KIT — ⁵Centre Européen de Sciences Quantiques (CESQ), Strasbourg Cedex, France

Single-molecular magnets (SMMs) have emerged as an excellent link between the two disciplines of spintronics and molecular electronics. Their ultimate small size, excellent single spin characteristics, and long coherence times at low temperatures make them promising candidates for fundamental quantum operations. In this project we investigate spin-transistors comprising a SMM trapped in a nanometer sized gap coupled to a back gate thereby forming a quantum dot. The gap is achieved by electromigration of a gold constriction. Low-noise electrical transport measurements enable the read out of the four nuclear spin states of a single terbium ion in a TbPc₂ double decker. First quantum algorithms, most importantly the Grover’s algorithm, have been implemented on this system. Recent measurements of more complex multi-state systems such as the Tb₂Pc₃ triple decker showed that the interactions between the two terbium nuclear spins can be detected. Here we pursue to use the increased Hilbert space dimension of coupled molecular spins for more complex quantum algorithms.

TT 21.23 Wed 15:00 P1

Synthesis, structure and property investigations of low-dimensional magnetism in double perovskite variants — •ANASTASIIA SMERCHUK, SABINE WÜRMEHL, BERND BÜCHNER, and RYAN MORROW — Leibniz Institute for Solid-State and Materials Research, IFW-Dresden, 01069 Dresden, Germany

For many years perovskites in various modifications have been occupying a significant place in solid-state physics. The main feature of these materials is a large number of possible permutations of the structure. Although perovskites are mostly three-dimensional materials, low-dimensional magnetism can also be achieved in the special case. Current research is focused on two different approaches for that purpose. Experiments with the substitution of various compounds in double perovskites with Cu^{2+} were conducted at ambient and high pressure to acquire the magnetic interactions on a square lattice. Also, our research was concentrated on defect double perovskites, where vacancies have been ordered along with the ordering of cations. Then the hexagonal phases of perovskite can be transformed into triangular frustrated two-dimensional magnets. New inorganic transition metal oxides were synthesized. The crystallographic and magnetometry data will be discussed in detail in the poster.

TT 21.24 Wed 15:00 P1

Electronic properties of strongly correlated ruthenates — •NEDA RAHISAMANI and EVA PAVARINI — Institute for Advanced Simulation, Forschungszentrum Jülich, D-52425, Germany

We study the electronic properties of strongly correlated ruthenates by using the LDA+DMFT method. We construct materials-specific models for the t_{2g} bands via maximally localized Wannier functions. We solve the DMFT quantum impurity problem by adopting as solver the weak coupling continuous-time Quantum Monte Carlo approach, in the implementation of Refs. [1, 2, 3]. General trends will be discussed.

[1] E. Gorelov, M. Karolak, T. O. Wehling, F. Lechermann, A. I. Lichtenstein, E. Pavarini, Phys. Rev. Lett. **104**, 226401 (2010)

[2] G. Zhang, E. Gorelov, E. Sarvestani, E. Pavarini, Phys. Rev. Lett. **116**, 106402 (2016)

[3] E. Sarvestani, G. Zhang, E. Gorelov, E. Pavarini, Phys. Rev. B **97**, 085141 (2018)

TT 21.25 Wed 15:00 P1

Magnetic quantum oscillations in the molecular conductor κ -(BEDT-TTF)₂Cu[N(CN)₂]Cl near and away from the Mott transition — •SHAMIL ERKNOV^{1,2}, SEBASTIAN OBERBAUER^{1,2}, VLADIMIR ZVEREV³, WERNER BIBERACHER¹, NATALIA KUSHCH¹, and MARK KARTSOVNIK¹ — ¹Walther-Meißner-Institut, Garching, Germany — ²Technische Universität München, Garching, Germany — ³Chernogolovka, Russia

Magnetic quantum oscillations have been extensively used for exploring correlated-electron materials near various correlation-driven instabilities of the normal metallic state. Applying this technique to the quasi-two-dimensional bandwidth-controlled Mott insulator κ -(BEDT-TTF)₂Cu[N(CN)₂]Cl, we have recently disclosed several anomalies in the behavior of the effective mass and scattering rate, apparently inconsistent with theoretical predictions. For clarifying the role of the proximity to the Mott transition in these anomalies it is instructive to track their evolution in a broader range of the phase diagram, both very close to and far away from the metal-insulator phase boundary. To this end, we have measured quantum oscillations of magnetoresistance in the pressure interval 20 to 1000 MPa, which drives the system from the very edge of stability of the metallic phase to a “good metal” region of the phase diagram by means of the conducting bandwidth variation. We have also studied the possibility of changing the balance between the charge correlations and magnetic interactions governing the insulating instability by applying a strong magnetic field.

TT 21.26 Wed 15:00 P1

Building Blocks for Cluster Mott Insulators — •VAISHNAVI JAYAKUMAR and CIARÁN HICKEY — Institute for Theoretical Physics, University of Cologne, Germany

The Hubbard model provides a rich playground for investigating the physics of a wide range of strongly correlated systems. An important limit in the model is the Mott insulating regime, where, at half-filling, electrons get localized on single atomic sites. In this work, we investigate extensions of the idea to cluster Mott insulators—where electrons are now localized on clusters of sites. To that end, we study the Hubbard model on a plethora of different clusters, at different integer fillings, by constructing a general Hamiltonian for each cluster. This allows us to explore different regimes of the interplay of strong correlations and hopping within these clusters, and their respective emergent effective degrees of freedom. We then go beyond the single-orbital “cluster” Hubbard model and include multiple orbitals and interactions between them. Once these building blocks have been established, it is possible to introduce inter-cluster hopping terms into the picture; depending on the nature of the resulting effective interactions, they can give rise to novel Hamiltonians, which might possibly host highly correlated and/or frustrated phases.

TT 21.27 Wed 15:00 P1

Chern insulators in twisted bilayer graphene under hydrostatic pressure — •ISRAEL DÍAZ¹, JOSÉ GONZÁLEZ², and TOBIAS STAUBER¹ — ¹Materials Science Factory, Instituto de Ciencia de Materiales de Madrid, CSIC, E-28049, Madrid, Spain — ²Instituto de Estructura de la Materia, CSIC, E-28006, Madrid, Spain

It is well-known that high hydrostatic pressures can be used to induce flat bands in twisted bilayer graphene, at twist angles larger than those realizing the usual magic-angle condition. We show that these twisted graphene bilayers, tuned at such larger magic angles, are prone to fall into Chern insulator phases. We characterize such states by relying on a self-consistent real-space Hartree-Fock approach that accounts for the long-range Coulomb interaction between all the carbon atoms in the moiré unit cell, and which is exact at the Hartree-Fock level as we incorporate all the moiré minibands in the calculation. In our flat-band models with twist angles between 2 and 4 degrees, we show that a gap opens up at the charge neutrality point due to the dynamical breakdown of time-reversal invariance. At 2 hole-doping, the dominant order parameter corresponds instead to valley symmetry breaking, but there is a critical coupling of the interaction above which a gap opens up due to the condensation of the Haldane mass. These Chern insulator phases seem to be absent in twisted bilayer graphene at the usual small magic angle, probably because they are hindered by the effects of in-plane relaxation, but they become manifest at the larger twist angles we study, leading to interesting phenomena like dissipationless edge states and anomalous Hall effect.

TT 21.28 Wed 15:00 P1

Calculating moments for many-electrons systems — •ÉLAHEH ADIBI and ERIK KOCH — Institute for Advanced Simulation, Forschungszentrum Jülich, 52425 Jülich, Germany

We present a technique for computing the moments $\langle E^M \rangle = \text{Tr} H^M$ of the many-electron spectrum. Taking the trace over a basis of Slater determinants $|I\rangle$ and expressing the Hamiltonian in the same orbital basis, matrix elements $\langle I|H^M|I\rangle$ can only be non-zero when the orbital indices of the creation operators are a permutation of those of the annihilation operators. Writing the permutations in cycle notation and realizing that the trace over a cycle with different orbital indices only depends on the number of descends, we can write the trace as a sum over products of Eulerian numbers times binomial factors involving the number of orbitals and electrons. For non-interacting electrons this further simplifies to a sum over Bell polynomials.

TT 21.29 Wed 15:00 P1

Multiloop fRG analysis of the attractive Hubbard model — •AIMAN AL-ERYANI¹, SARAH HEINZELMANN¹, ANNA KAUCH², ALESSANDRO TOSCHI², and SABINE ANDERGASSEN¹ — ¹University of Tuebingen — ²TU Wien

We analyse the effect of multiloop corrections in the 2D Attractive Hubbard Model. In a TU-fRG scheme where the conventional multi-loop self-energy flow equations are replaced with a Schwinger-Dyson flow, we demonstrate the importance of self-energy iteration in the convergence to reference Parquet results. Furthermore, we study the feedback of the s-wave pairing fluctuations on the charge density wave order.

TT 21.30 Wed 15:00 P1

Single-boson exchange fRG application to the two-dimensional Hubbard model at weak coupling — KILIAN FRABOULET¹, •SARAH HEINZELMANN¹, PIETRO BONETTI², AIMAN AL-ERYANI¹, DEMETRIO VILARDI², ALESSANDRO TOSCHI³, and SABINE ANDERGASSEN¹ — ¹Institut für Theoretische Physik and Center for Quantum Science, Universität Tübingen, Auf der Morgenstelle 14, 72076 Tübingen, Germany — ²Max Planck Institute for Solid State Research, Heisenbergstrasse 1, D-70569 Stuttgart, Germany — ³Institute of Solid State Physics, Vienna University of Technology, 1040 Vienna, Austria

The functional renormalization group (fRG) is one of the most modern implementation of the renormalization group and has proven successful in the description of various many-body quantum systems, in condensed matter theory and beyond (quantum chromodynamics, nuclear physics, ...). We illustrate in this work the computational advantages of the recently introduced single-boson exchange (SBE) formulation for the one-loop fRG applied to the two-dimensional Hubbard model.

We present a detailed analysis of the physical susceptibilities and their evolution with temperature and interaction strength, both at half filling and finite doping. We find that the rest functions describing the corrections beyond the SBE contributions play a negligible role in the weak coupling regime. The SBE formulation of the fRG flow hence allows for a substantial reduction of the numerical effort in the treatment of the two-particle vertex function, paving a promising route for future multiboson and multiloop extensions.

TT 21.31 Wed 15:00 P1

Linked cluster expansions via hypergraph decompositions — •MATTHIAS MÜHLHAUSER and KAI PHILLIP SCHMIDT — Institute for Theoretical Physics I, Friedrich-Alexander-Universität Erlangen-Nürnberg, Germany

We present a hypergraph expansion which facilitates the direct treatment of quantum-spin-models with effective many-site interactions via perturbative linked cluster expansions. The main idea is to generate all relevant subclusters and sort them into equivalence classes essentially governed by hypergraph isomorphism. Concretely, a reduced König representation of the hypergraphs is used to make the equivalence relation accessible by graph isomorphism.

[1] M. Mühlhauser and K. P. Schmidt, arXiv:2202.03366 (2022)

TT 21.32 Wed 15:00 P1

Efficient and flexible approach to simulate low-dimensional quantum lattice models with large local Hilbert spaces at the example of the Holstein model — •THOMAS KÖHLER¹, JAN STOLPP², and SEBASTIAN PAECKEL³ — ¹Uppsala University, Sweden — ²Georg-August-Universität Göttingen, Germany — ³University of Munich, Germany

Quantum lattice models with large local Hilbert spaces emerge across various fields in quantum many-body physics. Problems such as the interplay between fermions and phonons, the BCS-BEC crossover of interacting bosons, or decoherence in quantum simulators have been extensively studied both theoretically and experimentally. In recent years, tensor network methods have become a successful tool to treat such lattice systems numerically. Nevertheless, systems with large local Hilbert spaces remain challenging. Here, we introduce a mapping that allows to construct artificial $U(1)$ symmetries for any type of lattice model. Exploiting the generated symmetries, numerical expenses that are related to the local degrees of freedom decrease significantly. Based on an intimate connection between the Schmidt values of the corresponding matrix-product-state representation and the single-site reduced density matrix, this allows for an efficient treatment of systems with large local dimensions. We demonstrate this new mapping, provide an implementation recipe, and perform example calculations for the Holstein model at half filling. We studied systems with a very large number of lattice sites up to $L = 501$ while accounting for $N_{\text{ph}} = 63$ phonons per site with high precision in the CDW phase.

TT 21.33 Wed 15:00 P1

Electronic correlations in inhomogeneous model systems: Numerical simulation of spectra and transmission — •ANDREAS WEH¹, WILHELM H. APPELT¹, ANDREAS ÖSTLIN², LIVIU CHIONCEL², and ULRICH ECKERN¹ — ¹Institute of Physics, University of Augsburg, 86135 Augsburg — ²EKM & ACIT, Institute of Physics, University of Augsburg, 86135 Augsburg

We investigate the effects of electronic correlations on the spectral and transport properties of inhomogeneous model systems. The models are based on the single-band Hubbard Hamiltonian, and electronic correlations are treated within dynamical mean-field theory (DMFT). In particular, continuous-time quantum Monte Carlo (CT-QMC) as well as the more recent tensor network methods (DMRG+TDVP) are employed as impurity solvers to study the spectral function of half-metallic ferromagnets; a Bethe lattice as well as layered square-lattice structures are considered [1]. The transport properties through a barrier made of such a single interacting half-metallic layer is studied [2] employing the Meir-Wingreen formalism. In particular, we demonstrate that even for a single half-metallic layer, highly polarized transmissions are achievable.

[1] A. Weh, J. Otsuki, H. Schnait, H. G. Evertz, U. Eckern, A. I. Lichtenstein, L. Chioncel, Phys. Rev. Res. 2, 043263 (2020)

[2] A. Weh, W. H. Appelt, A. Östlin, L. Chioncel, U. Eckern, Phys. Status Solidi B 259, 2100157 (2021)

TT 21.34 Wed 15:00 P1

Fifth harmonic generated currents in conventional s-wave superconductor — •PASCAL DERENDORF and ILYA EREMIN — Institut für Theoretische Physik III, Ruhr-Universität Bochum, Bochum, Germany

Recent advances in the field of THz spectroscopy allow for controlled experiments to measure the Higgs modes signature in the Fifth Harmonic Generation (FHG), which was first measured by Z. X. Wang et al [1]. Here, we analyze a periodic multicycle pulse setup, where the driving electromagnetic field solely points into the direction of a lattice vector. We investigate the role of the Higgs mode in the clean-limit FHG of a s-wave superconductor and compare it to other contributing mechanisms, such as charge density fluctuations (CDF) and the phase mode. Further, we show that the signal in the FHG is dominated by the CDF, similar to the third harmonic generated currents. We predict a double peak signature in the frequency resolved intensity amplitude of the FHG for all three mechanisms with one peak being located at $2\Omega = 2\Delta$ and the other one at $2\Omega = \Delta$. The resonant enhancement at $2\Omega = \Delta$ is indicative of the next higher order coupling to the Higgs mode implying that it carries 4Ω . The other resonance at $2\Omega = 2\Delta$ is reminiscent of the Third Harmonic Generation and could therefore describe e.g. the Higgs mode interacting with 3 single photons.

[1] Z. X. Wang et al., arXiv: 2107.07488

TT 21.35 Wed 15:00 P1

Transfer-matrix summation of path integrals for transport through nanostructures — •ALEXANDER HAHN, SIMON MUNDINAR, JÜRGEN KÖNIG, and ALFRED HUCHT — Theoretische Physik, Universität Duisburg-Essen and CENIDE, 47048 Duisburg, Germany

We develop a transfer-matrix style approach based on the numerical iterative summation of path integrals (ISPI) scheme [1,2] to solve non-equilibrium quantum transport. The usage of a transfer-matrix approach combined with further simplifications allows for the development of a method able to work in the stationary limit (TraSPI). Additionally, using the numerical properties of the transfer-matrix element calculation and Gray code, one can use the Woodbury formula to move inside the configuration space. Afterwards, the method is applied to a single-electron transistor with a single-level quantum dot as a central island.

[1] S. Mundinar *et al.*, Phys. Rev. B **99**, 195457 (2019)

[2] S. Mundinar *et al.*, Phys. Rev. B **102**, 045404 (2020)

TT 21.36 Wed 15:00 P1

Driven magnets: Domain wall motion in ferrimagnets in an oscillating magnetic field — •DENNIS HARDT and ACHIM ROSCH — Institute for Theoretical Physics, University of Cologne, Germany

Transition regions between two magnetic domains are described by domain walls (DWs).

In this work, we numerically study a 1D ferrimagnet with anisotropy term given by a symmetric double-well potential in magnetization in z-direction. This establishes a Goldstone mode as rotation in the x-y-plane which can be activated by driving the system with an oscillating magnetic field in z-direction.

At $T = 0$ (noise-free case) this leads to a spontaneous symmetry breaking visible in the collective movement of all DWs in one direction (left or right). We also found an analytical description for this limit.

At finite temperature, DW-pairs can also be created meaning that there is a competition between the annihilation (2 DWs meet due to diffusion and driving) and the creation (due to noise).

The noise-created domain walls are driven randomly in left or right direction. This leads to a suppression of the total number of DWs compared to the non-driven thermal case.

TT 21.37 Wed 15:00 P1

Rate functions and quantum adiabatic theorem in many-body systems — •VIBHU MISHRA — Institute for Theoretical Physics, Georg-August-Universität Göttingen, Friedrich-Hund-Platz 1, 37077 Göttingen, Germany

We investigate the quantum adiabatic theorem in many body systems for XXZ and ANNNI spin chains. In order to have a well-defined quantitative measure of adiabaticity in the thermodynamic limit we calculate a rate function defined via the overlap between the ground state of the final Hamiltonian and the time evolved initial state. The parameters in the Hamiltonian are varied with a linear ramp and we investigate how the rate function behaves with decreasing ramping speed (adiabatic limit). Our main tool is exact diagonalization, which is complemented by bosonization in the XY phase of the XXZ spin chain.

TT 21.38 Wed 15:00 P1

Pump-probe AC susceptibility of $\text{LiHo}_x\text{Y}_{1-x}\text{F}_4$ ($x = 4.5\%$) — •MICHAEL LAMPL, ANDREAS WENDL, MARKUS KLEINHANS, LAURA STAPF, MARC A. WILDE, and CHRISTIAN PFLEIDERER — Physik Department, Technical University of Munich, 85748 Garching, Germany

LiHoF_4 under a transverse magnetic field exhibits one of the best understood examples of a quantum critical point. Substitutional doping of Ho with non-magnetic Yttrium may be used to study the effects of disorder [1]. In the highly diluted system $\text{LiHo}_x\text{Y}_{1-x}\text{F}_4$ ($x = 4.5\%$), investigated in our study, the nature of the ground state is still subject to intense experimental and theoretical studies [2]. To explore the ground state properties of this system, multiple studies employed so-called pump-probe susceptibility measurements [3-5]. We revisit this question and report a study of the pump-probe susceptibility as a function temperature and field orientation, covering a wide parameter range.

[1] J. P. Gingras and P. Henelius, J. Phys.: Conf. Ser. **320**, 012001 (2011)

[2] J. A. Quilliam *et al.*, Phys. Rev. Lett. **101**, 187204 (2008)

[3] S. Ghosh *et al.*, Science **296**, 2195 (2002)

[4] M. A. Schmidt *et al.*, Proc. Natl. Acad. Sci. USA **111**, 3689 (2014)

[5] D. M. Silevitch *et al.*, Nat. Commun. **10**, 4001 (2019)

TT 22: Unconventional Superconductors

Time: Wednesday 15:00–19:15

Location: H10

Invited Talk

TT 22.1 Wed 15:00 H10

Evidence for orbital loop current magnetism in Sr_2RuO_4 — R. FITTIPALDI¹, R. HARTMANN², M.T. MERCALDO¹, S. KOMORI³, A. BJØRLIG⁴, W. KYUNG⁵, Y. YASUI⁶, T. MIYOSHI⁶, L.A.B. OLDE OLTHOF³, C.M. PALOMARES GARCIA³, V. GRANATA¹, I. KEREN⁷, W. HIGEMOTO⁸, A. SUTER⁷, T. PROKSCHA⁷, A. ROMANO¹, C. NOCE¹, C. KIM⁵, Y. MAENO⁶, E. SCHEER², B. KALISKY⁴, J.W.A. ROBINSON³, M. CUOCO¹, Z. SALMAN⁷, A. VECCHIONE¹, and •A. DI BERNARDO² — ¹CNR-SPIN, University of Salerno, Italy — ²University of Konstanz, Germany — ³University of Cambridge, UK — ⁴Bar-Ilan University, Israel — ⁵Seoul National University, South Korea — ⁶Kyoto University, Japan — ⁷Paul Scherrer Institute, Switzerland — ⁸Japan Atomic Energy Agency

A deeper understanding of the normal-state properties of Sr_2RuO_4 is crucial also to determine its superconducting state symmetry. Using low-energy muon spin rotation spectroscopy, we have found evidence for a new form of magnetism on the surface of Sr_2RuO_4 in its normal state. We detect weak static dipolar fields with a relatively high onset temperature above 50 K. The magnetism observed is not conventional, and we demonstrate that it arises due to orbital loop currents at the reconstructed Sr_2RuO_4 surface. Our results [1] set a reference for the observation of orbital loop current magnetism in other materials and shed light onto a new mechanism that can affect the superconducting state of Sr_2RuO_4 .
[1] R. Fittipaldi et al., Nat. Commun. 12, 5792 (2021)

TT 22.2 Wed 15:30 H10

Optimization of Sr_2RuO_4 thin films and devices based on single-crystals flakes — •PRIYANA PULIYAPPARA BABU¹, ROMAN HARTMANN¹, SOHAILA ZAGHLOUL NOBY¹, ELKE SCHEER¹, ANGELO DI BERNARDO¹, ROSALBA FITTIPALDI², and ANTONIO VECCHIONE² — ¹University of Konstanz, 78457 Konstanz, Germany — ²University of Salerno, 84084 Fisciano, Italy

Since its discovery in 1994, Sr_2RuO_4 has been the subject of intensive studies aiming at shedding light on the nature of its superconducting order parameter (OP). Despite earlier reports suggesting an unconventional nature of the Sr_2RuO_4 superconductivity, conflicting results have been recently reported and a definitive conclusion about the superconducting OP symmetry has not been yet achieved.

To address some of the open questions, it is crucial to fabricate superconducting devices based on high-quality superconducting thin films of Sr_2RuO_4 . Thin films of Sr_2RuO_4 with very low density of defects, high residual resistivity ratio (> 30) and fully metallic down to low temperatures have been grown from single crystal target of $\text{Sr}_3\text{Ru}_2\text{O}_7$. The growth parameters that can be further optimized to get fully superconducting thin films have also been identified. In parallel, we are also fabricating superconducting devices based on Sr_2RuO_4 flakes produced by mechanical exfoliation of single crystals. Different fabrication routes involving lithography patterning followed by Inductively Coupled Plasma (ICP) etching and patterning with a helium ion microscope have been successfully employed to fabricate superconducting devices from Sr_2RuO_4 single-crystal flakes.

TT 22.3 Wed 15:45 H10

Angular dependence of superfluid density in Sr_2RuO_4 — •JAVIER LANDAETA¹, KONSTANTIN SEMENIUK¹, JOOST ARETZ¹, ISMARDO BONALDE², and ELENA HASSINGER¹ — ¹Max Planck Institute for Chemical Physics of Solids, 01187 Dresden, Germany — ²Centro de Física, Instituto Venezolano de Investigaciones Científicas, Caracas 1020-A, Venezuela

Although being extensively studied for more than 25 years, the nature of the superconducting order parameter (SOP) of Sr_2RuO_4 is still debated. In recent years, experimental evidence revealed the possibility of two component SOPs. These results constrain the SOP to only a few allowed symmetries. To get insight on the nodal structure of the SOP, we carried out a comprehensive study of the temperature dependence of the superfluid density n_s at various angles. By measuring the superconducting lower critical field $H_{c1}(T)$ in a spherical sample with ac-susceptibility, we obtained the temperature dependence of $n_s = H_{c1}(T)/H_{c1}(0)$ down to $0.03 T_c$. Our results show that $n_s(T)$ is identical for all the studied angles showing a low temperature power law of T^2 , which rules out the possibility of horizontal line nodes in Sr_2RuO_4 . These results impose strong constraints over the remaining allowed symmetries for SOPs.

TT 22.4 Wed 16:00 H10

Spin-fluctuation pairing and Hund's pairing in Sr_2RuO_4 — MERÇÉ ROIG¹, ASTRID T. RØMER¹, THOMAS A. MAIER², •ANDREAS KREISEL³, PETER J. HIRSCHFELD⁴, and BRIAN M. ANDERSEN¹ — ¹Niels Bohr Institute, University of Copenhagen — ²Center for Nanophase Materials Sciences, Oak Ridge National Laboratory — ³Institut für Theoretische Physik, Universität Leipzig — ⁴Department of Physics, University of Florida

The unconventional superconductor Sr_2RuO_4 has been subject of enormous experimental investigations in the last two decades, but until now the form of its order parameter has not been explicitly determined. Given the exclusion of spin-

triplet superconductivity by recent experiments, the time-reversal symmetry breaking linear combinations of s -, d - and g -wave one-dimensional (1D) irreducible representations are strong candidates. However, also a two-dimensional representation E_g , stabilized within the so-called Hund's coupling mean-field pairing scenario, has been proposed. In this work, we examine Hund's pairing on equal footing with spin-fluctuation pairing using a three dimensional electronic structure for Sr_2RuO_4 and a model that does not exhibit clear nesting features. For the latter, the superconducting state generated by the Hund's mechanism agrees well with that from the full fluctuation exchange vertex for large J/U ratios. On the other hand, for systems characterized by a peaked finite-momentum susceptibility, spin-fluctuation pairing generally dominates over Hund's pairing. We conclude that Hund's pairing states (and therefore also the E_g pairing) are unlikely to be realized in systems like Sr_2RuO_4 .

TT 22.5 Wed 16:15 H10

Thermal conductivity of the two-phase superconductor CeRh_2As_2 — SEITA ONISHI¹, •ULRIKE STOCKERT¹, SEUNGHYUN KHIM¹, JACINTHA BANDA¹, MANUEL BRANDO¹, and ELENA HASSINGER^{1,2} — ¹MPI for Chemical Physics of Solids, Dresden, Germany — ²Physics Department, Technical University Munich, Germany

CeRh_2As_2 is an unconventional superconductor with $T_c = 0.26$ K. Two neighbouring superconducting phases are observed for a magnetic field H applied along the c -axis with an almost constant transition field H^* of about 4 T. In addition, antiferromagnetic order, quadrupole-density-wave order and the proximity of this material to a quantum-critical point have been reported: The coexistence of these phenomena with superconductivity is currently under discussion.

We present thermal conductivity, κ , and electrical resistivity, ρ , measured on single crystals of CeRh_2As_2 between 60 mK and 200 K and in magnetic fields ($H \parallel c$) up to 8 T. The extrapolation of our normal-state data to zero temperature is in line with the Wiedemann-Franz law. No clear anomaly is observed in the temperature dependence of κ at any of the reported phase transitions. Instead, $\kappa(T)$ shows a pronounced, field-dependent drop below T_c which is attributed to superconductivity. The field-dependence of the normalized thermal conductivity at 120 mK exhibits a change in slope around H^* , similar to the specific heat coefficient γ . Measurements at higher fields and lower T are required to confirm that this is really due to the transition between the two superconducting phases.

TT 22.6 Wed 16:30 H10

Consequences of density-wave order in a staggered Rashba superconductor — •ANASTASIIA SKURATIVSKA^{1,2}, MANFRED SIGRIST¹, and MARK H FISCHER³ — ¹University of Zurich, Zurich, Switzerland — ²Donostia International Physics Center, Donostia-San Sebastian, Spain — ³Institute for Theoretical Physics, ETH Zurich, Zurich, Switzerland

Superconductors with local inversion-symmetry breaking can exhibit properties usually associated with non-centrosymmetric systems, such as local mixing of even and odd superconducting order parameters or unusual magnetic response. An example of a system with such local non-centrosymmetry is a stack of layers with alternating Rashba spin-orbit coupling due to mirror symmetry breaking with respect to the individual layers. Motivated by recent experiments on the Ce-based superconductor CeRh_2As_2 , which were interpreted as showing possible quadrupole-density-wave order, we investigate the effect of density-wave order on the physics related to local inversion-symmetry breaking. In particular, we study how the partial gapping out of the Fermi surface changes the effect of local inversion-symmetry breaking.

TT 22.7 Wed 16:45 H10

Anisotropic vortex squeezing in Rashba superconductors: a manifestation of Lifshitz invariants — LORENZ FUCHS¹, •DENIS KOCHAN², CHRISTIAN BAUMGARTNER¹, SIMON REINHARDT¹, SERGEI GRONIN³, GEOFFREY GARDNER³, TYLER TYLER LINDEMANN⁴, MICHAEL MANFRA³, CHRISTOPH STRUNK¹, and NICOLA PARADISO¹ — ¹Institut für Experimentelle und Angewandte Physik, University of Regensburg, 930 40 Regensburg, Germany — ²Institut für Theoretische Physik, University of Regensburg, 930 40 Regensburg, Germany — ³Microsoft Quantum Purdue, Purdue University, West Lafayette, Indiana 47907 USA — ⁴Birck Nanotechnology Center, Purdue University, West Lafayette, Indiana 47907 USA

Most of 2D superconductors are of type II, i.e., they are penetrated by quantized vortices when exposed to out-of-plane magnetic fields. In a presence of a supercurrent, a Lorentz-like force acts on the vortices, leading to drift and dissipation. The current-induced vortex motion is impeded by pinning at defects. Usually, the pinning strength decreases upon any type of pair-breaking interaction perturbs a system.

In the talk we will discuss surprising experimental evidences showing an unexpected enhancement of pinning in synthetic Rashba 2D superconductors when applying an in-plane magnetic field. When rotating the in-plane component of

the field with respect to the driving current, the vortex inductance turns out to be highly anisotropic. We explain this phenomenon as a direct manifestation of Lifshitz invariant that is allowed in the Ginzburg-Landau free energy by symmetry when space-inversion and time-reversal symmetries are broken.

15 min. break

Invited Talk

TT 22.8 Wed 17:15 H10

Role of the film geometry in the electronic reconstruction of infinite-layer nickelates on SrTiO₃(001) — •BENJAMIN GEISLER — Fakultät für Physik, Universität Duisburg-Essen

The recent discovery of superconductivity in infinite-layer NdNiO₂ films on SrTiO₃(001) has sparked significant interest [1]. However, details of the physical mechanism behind this observation remained so far elusive, since in contrast to the thin films [2] bulk NdNiO₂ shows neither superconductivity nor the antiferromagnetic interactions characteristic of high- T_c cuprates.

First-principles simulations unravel the key role of the interface: Polarity mismatch drives a surprising electronic reconstruction that results in the emergence of a correlated two-dimensional electron gas (2DEG) in the SrTiO₃(001) substrate. The concomitant depletion of the self-doping Nd 5*d* states renders infinite-layer nickelates close to cuprate superconductors [3,4]. Recent work identifies an unexpected interface composition that completely quenches the 2DEG, but preserves the electronic reconstruction in the nickelate film [5]. This supports the notion of nickelate superconductivity as novel quantum phase, induced in film geometry by electronic reconstruction.

[1] D. Li *et al.*, Nature **572**, 624 (2019)

[2] H. Lu *et al.*, Science **373**, 213 (2021)

[3] B. Geisler and R. Pentcheva, PRB **102**, 020502(R) (2020)

[4] B. Geisler and R. Pentcheva, Phys. Rev. Res. **3**, 013261 (2021)

[5] B. H. Goodge, B. Geisler, K. Lee, M. Osada, B. Y. Wang, D. Li, H. Y. Hwang, R. Pentcheva, L. F. Kourkoutis, arXiv:2201.03613

TT 22.9 Wed 17:45 H10

Importance of electronic correlations in nickelates — •PAUL WORM¹, LIANG SI¹, MOTOHARU KITATANI², RYOTARO ARITA^{3,4}, and KARSTEN HELD¹ — ¹Institute of Solid State Physics, TU Wien, 1040 Vienna, Austria — ²Department of Material Science, University of Hyogo, Ako, Hyogo 678-1297, Japan — ³RIKEN Center for Emergent Matter Sciences (CEMS), Wako, Saitama, 351-0198, Japan — ⁴Research Center for Advanced Science and Technology, University of Tokyo, Komaba, Tokyo, 153-8904, Japan

Motivated by the recent discovery of superconductivity in the pentalayer nickelate Nd₆Ni₅O₁₂ [1], we calculate its electronic structure and superconducting critical temperature. First we analyse the compound by means of state of the art density functional theory and dynamical mean field theory (DFT+DMFT) and find that electronic correlations remove the Nd pockets from the Fermi surface, which crucially changes the filling of the Ni $d_{x^2-y^2}$ band. An *effective* single-orbital Hamiltonian can be constructed for the five layers and we show that its properties are stunningly similar to the infinite layer case. Subsequently we solve this *effective* model within the dynamical vertex approximation to determine the transition temperature. We further study the related bilayer nickelate and propose a suitable dopant to achieve a doping level where superconductivity is expected.

[1] Nature Materials **10**.1038

[2] P. Worm *et al.*, arXiv:2111.12697 (2021)

[3] K. Held *et al.*, Front. Phys. **9**:810394 (2021)

TT 22.10 Wed 18:00 H10

Collective Modes Contributions in Third-Harmonic Generation in Non-centrosymmetric Superconductors — •SIMON KLEIN, MATTEO PUVIANI, and DIRK MANSKE — Max Planck Institute for Solid State Research, Stuttgart, Germany

Recent interest for collective amplitude (Higgs) and phase (Leggett) excitations in single- and multi-band superconductors have led to various studies focused on third-harmonic generation (THG) experiments, both for singlet *s*- and *d*-wave gap structure. A resonance in the THG intensity appears, when matching the driving frequency to the energy of the corresponding investigated mode, leading to a phase jump at the resonance frequency. We extend these studies to superconductors without an inversion symmetry, which can be effectively described by a two-band model with an order parameter, consisting of spin singlet (even parity) and spin triplet (odd parity) components. We calculate the THG signal for the non-centrosymmetric compound CePt₃Si, showing that it contains contributions from three distinguishable sources, namely the Higgs mode, the Leggett mode and quasiparticles. In the clean limit, only diamagnetic Raman-like processes contribute to the THG signal, whereas the quasiparticle contributions dominate the collective modes for all singlet-triplet ratios of the gap structure. In the dirty limit, we find a significant enhancement of the Higgs mode contributions to the THG signal, due to the inclusion of non-vanishing paramagnetic diagrams. We notice a significant change in the phase jump, which helps to differentiate between diamagnetic and paramagnetic results and thus between clean and dirty superconductors.

TT 22.11 Wed 18:15 H10

High-field superconductivity in UTe₂ — •TONI HELM^{1,2}, MOTOI KIMATA³, KENTA SUDO³, JULIA STIRNAT^{1,5}, ATSUSHIKO MIYATA¹, MARKUS KÖNIG², TOBIAS FÖRSTER¹, JEAN-PASCAL HORNUNG^{1,5}, GERARD LAPERTOT⁴, JEAN-PASCAL BRISON⁴, ALEXANDRE POURRET⁴, GEORG KNEBEL⁴, DAI AOKI³, and JOCHEN WOSNITZA^{1,5} — ¹Dresden High Magnetic Field Laboratory, HZDR, Germany — ²MPI CPfS Dresden, Germany — ³Tohoku University, Oarai, Ibaraki, Japan — ⁴CEA, IRG-PHELIQS, Grenoble, France — ⁵Technical University Dresden, Germany

The potential spin-triplet superconductor UTe₂ with $T_c = 1.6$ K has attracted a lot of attention recently. The material is a highly anisotropic paramagnet that exhibits a metamagnetic transition at $H_M = 35$ T. In addition to its field-enhanced and pressure-induced superconducting ground state, high-field superconductivity (hfSC) was observed setting in for a particular field orientation just above H_M . We investigated magnetotransport and magnetic torque in pulsed magnetic fields up to 70 T for FIB-microfabricated samples of UTe₂. Our findings confirm the existence of the hfSC above 40 T for a narrow angular range around $\approx 30^\circ$ tilt off the *b* axis. The upper critical field, H_{c2} , reaches almost 75 T and exhibits a temperature dependence that strongly deviates from the low-field SC phase. Excitingly, the Hall effect experiences a drastic suppression for field orientations exactly where the hfSC emerges. The anomalous angle-dependence in high field poses a challenge to the theoretical understanding of the electronic ground state of UTe₂.

TT 22.12 Wed 18:30 H10

Two bands Ising superconductivity from Coulomb interactions in monolayer NbSe₂ — SEBASTIAN HÖRHHOLD, JULIANE GRAF, •MAGDALENA MARGANSKA, and MILENA GRIFONI — Institute for Theoretical Physics, University of Regensburg, Germany

The nature of superconductivity in monolayer transition metal dichalcogenides is still object of debate. It has already been argued that repulsive Coulomb interactions, combined with the disjoint Fermi surfaces around the K, K' valleys and at the Γ point, can lead to superconducting instabilities in monolayer NbSe₂. Here, we demonstrate the two bands nature of superconductivity in NbSe₂. In our approach it arises from repulsive Coulomb interactions, long range (resulting in intravalley scattering) and short range (intervalley scattering), together with Ising spin-orbit coupling. The two distinct superconducting gaps, one for the upper and one for the lower spin-orbit splitted band, both consist of a mixture of *s*-wave and *f*-wave components. Using a microscopic multiband BCS approach, we derive and self-consistently solve the gap equation, demonstrating the stability of nontrivial solutions in a realistic parameter range. The temperature dependence of the gaps and of the critical in-plane field are consistent with various sets of existing experimental data. Our results, although derived for NbSe₂, are however universal and apply to almost all systems with disjoint Fermi surfaces connected by two competing scattering processes.

TT 22.13 Wed 18:45 H10

Superconductivity in CrB₂ under pressure: Role of electron-phonon coupling and spin-fluctuations — •SANANDA BISWAS¹, ANDREAS KREISEL², RONNY THOMALE³, ROSER VALENTÍ¹, and IGOR MAZIN⁴ — ¹Goethe Universität, Frankfurt, Germany — ²Universität Leipzig, Leipzig, Germany — ³Julius-Maximilians-Universität Würzburg, Würzburg, Germany — ⁴George Mason University, Fairfax, VA, USA

Superconductivity has recently been discovered in CrB₂ under pressure with maximum reported T_c to be 7 K. Iso-structural to MgB₂, CrB₂ exhibits spin-density-wave (SDW) ground state at ambient pressure. In this talk, I will focus on the role of spin-fluctuations and electron-phonon coupling (EPC) in determining the T_c . We have performed ab-initio density functional perturbation theory to determine the EPC of this system and to study the spin-fluctuation, random-phase-approximation (RPA) has been employed.

TT 22.14 Wed 19:00 H10

p-wave superconductivity in Luttinger semimetals — •JULIA M. LINK¹ and IGOR F. HERBUT² — ¹TU Dresden, Dresden, Germany — ²Simon Fraser University, Burnaby, Canada

We consider the three-dimensional spin-orbit-coupled Luttinger semimetal of "spin" $3/2$ particles in presence of weak attractive interaction in the $l=1$ (p-wave) channel, and determine the low-temperature phase diagram for both particle- and hole-dopings [1]. The phase diagram depends crucially on the sign of the chemical potential, with two different states (with total angular momentum $j=0$ and $j=3$) competing on the hole-doped side, and three (one $j=1$ and two different $j=2$) states on the particle-doped side. The ground state condensates of Cooper pairs with the total angular momentum $j=1,2,3$ are selected by the quartic, and even sextic terms in the Ginzburg-Landau free energy. Interestingly, we find that all the p-wave ground states that appear in the phase diagram, while displaying different patterns of reduction of the rotational symmetry, preserve the time reversal symmetry. The resulting quasiparticle spectrum is either fully gapped or with point nodes, with nodal lines being absent.

[1] J. M. Link and I. F. Herbut, Phys. Rev. B **105**, 134522 (2022)

TT 23: Frustrated Magnets - General

Time: Wednesday 15:00–18:30

Location: H22

TT 23.1 Wed 15:00 H22

Numerical linked cluster expansion for magnetostriction of frustrated magnets — •ALEXANDER SCHWENKE and WOLFRAM BREINIG — Institute for Theoretical Physics, Technical University Braunschweig, D-38106 Braunschweig, Germany

Thermodynamic and magnetoelastic properties of the frustrated J - K - T quantum spin model for proximate Kitaev magnets on the honeycomb lattice in a finite magnetic field \vec{B} are studied using the numerical linked cluster expansion (NLCE) [1]. Calculations are performed on clusters of sizes up to $\sim \mathcal{O}(11)$. First, the specific heat and the magnetization are analyzed for in- as well as for out-of-plane configurations of \vec{B} . Second, we present results of the linear magnetostriction coefficient $\lambda(\vec{B}, T)$. This displays strongly anisotropic behavior and a clear indication for a field-induced transition. Third, employing exchange parameters as proposed for the proximate quantum spin-liquid (QSL) candidate α - RuCl_3 , we show that our results for λ are very similar to recently observed experimental data [2] on this material.

[1] M. Rigol et al., Phys. Rev. Lett. **97**, 187202 (2006)[2] V. Kocsis et al., Phys. Rev. B **105**, 094410 (2022)

TT 23.2 Wed 15:15 H22

Dynamic structure factor of the antiferromagnetic Kitaev model in large magnetic fields — •ANDREAS SCHELLENBERGER, MAX HÖRMANN, and KAI PHILLIP SCHMIDT — FAU Erlangen-Nürnberg, Erlangen, Deutschland

We investigate the dynamic structure factor of the antiferromagnetic Kitaev honeycomb model in a magnetic field by applying perturbative continuous unitary transformations about the high-field limit. One- and two-quasi-particle properties of the dressed elementary spin flip excitations of the high-field polarized phase are calculated which account for most of the spectral weight in the dynamic structure factor. We discuss the evolution of spectral features in these quasi-particle sectors in terms of one-quasi-particle dispersions, two-quasi-particle continua, the formation of anti-bound states, and quasi-particle decay. In particular, a comparably strong spectral feature above the upper edge of the upmost two-quasi-particle continuum represents three anti-bound states which form due to nearest-neighbor density-density interactions. [1]arXiv:2203.13546 [cond-mat.str-el]

TT 23.3 Wed 15:30 H22

Fractionalized quantum criticality in spin-orbital liquids from field theory beyond the leading order — SHOURYYA RAY¹, BERNHARD IHRIG², •DANIEL KRUTI³, JOHN A. GRACEY⁴, MICHAEL M. SCHERER², and LUKAS JANSSEN¹ — ¹TU Dresden — ²University of Cologne — ³University of Cologne and Jülich Research Centre — ⁴University of Liverpool

Two-dimensional spin-orbital magnets with strong exchange frustration have recently been predicted to realise a quantum critical point in the Gross-Neveu-SO(3) universality class. In contrast to previously known Gross-Neveu-type universality classes, this quantum critical point separates a Dirac semimetal and a long-range-ordered phase, in which the fermion spectrum is only partially gapped out. Here, we characterise the quantum critical behaviour of the Gross-Neveu-SO(3) universality class by employing three complementary field-theoretical techniques beyond their leading orders. We compute the correlation-length exponent ν , the order-parameter anomalous dimension η_ϕ , and the fermion anomalous dimension η_ψ using a three-loop $4-\epsilon$ expansion, a second-order large- N expansion (with the fermion anomalous dimension obtained even at the third order), as well as a functional renormalisation group approach. The results from the different methods agree well with each other and provide a prime benchmark for future complementary calculations. Averaging over them, we obtain the estimates $1/\nu = 1.03(15)$, $\eta_\phi = 0.42(7)$, and $\eta_\psi = 0.180(10)$ for the physically relevant case of $N = 3$ flavours of two-component Dirac fermions in 2+1 space-time dimensions.

TT 23.4 Wed 15:45 H22

Spin excitations in the frustrated helimagnet FeP — •ALEKSANDR SUKHANOV, YULIA TYMOSHENKO, ANTON KULBAKOV, and DMYTRO INOSOV — Institut für Festkörper- und Materialphysik, Technische Universität Dresden, D-01069 Dresden

The metallic compound FeP belongs to the class of materials that feature a complex noncollinear spin order driven by the magnetic frustration. While its double-helix magnetic structure with a period $\lambda_s \approx 5c$, where c is the lattice constant, was previously well determined, the relevant spin-spin interactions that lead to that ground state remain unknown. By performing extensive inelastic neutron scattering measurements, we obtained the spin-excitation spectra in a large part of the momentum-energy space. The spectra show that the magnons are gapped with a gap energy of ~ 5 meV. Despite the 3D crystal structure, the magnon modes display strongly anisotropic dispersions, revealing quasi-one-dimensional character of the magnetic interactions in FeP. The physics of the

material, however, is not determined by the dominating exchange, which is ferromagnetic. Instead, the weaker two-dimensional antiferromagnetic interactions between the rigid ferromagnetic spin chains drive the magnetic frustration. Using linear spin-wave theory, we were able to construct an effective Heisenberg Hamiltonian with an anisotropy term capable of reproducing the observed spectra. This enabled us to quantify the exchange interactions in FeP and determine the mechanism of its magnetic frustration.

TT 23.5 Wed 16:00 H22

NMR and magnetization studies of helical correlations within the stretched diamond lattice of LiYbO_2 — •S. LUTHER^{1,2}, S. WILSON³, M. M. BORDELON³, J. WOSNITZA^{1,2}, M. BAENITZ⁴, and H. KÜHNE¹ — ¹Hochfeld-Magnetlabor Dresden (HLD-EMFL), HZDR, Dresden, Germany — ²Institut für Festkörper- und Materialphysik, TU Dresden, Germany — ³University of California, Santa Barbara, USA — ⁴MPI for Chemical Physics of Solids, Dresden, Germany

The Yb-based delafossite LiYbO_2 hosts a stretched diamond lattice. The resulting three-dimensional geometric frustration is in strong contrast to the recently reported 2D-type Yb-based triangular-lattice delafossites. Further, the combination of a strong spin-orbit coupling together with crystalline-electric-field effects leads to a pseudospin-1/2 ground state of the Yb^{3+} ions. A recent study of LiYbO_2 by means of specific heat and neutron powder diffraction established the formation of helical order with non-trivial phasing between the two interpenetrating Yb sublattices below 1.1 K [1]. In order to further explore the H-T phase diagram and magnetic correlations, we performed low-temperature magnetometry and ^7Li NMR of polycrystalline LiYbO_2 . Our magnetometry and $1/T_1$ NMR data are fully consistent with the reported specific-heat results. The ^7Li NMR spectroscopy yields a monotonic and asymmetric spectral broadening towards low temperatures in the paramagnetic state. In the helical ordered state, a spontaneous and pronounced increase of the spectral width is observed, in agreement with the neutron-diffraction experiments.

[1] Bordelon et al., Phys. Rev. B **103**, 014420 (2021)

TT 23.6 Wed 16:15 H22

Nonlinear stress-strain relation of PdCrO_2 — •NINA STILKERICH^{1,2}, HILARY NOAD¹, SEUNGHYUN KHIM¹, ANDREW MACKENZIE^{1,3}, and CLIFFORD HICKS^{1,4} — ¹Max Planck Institute for Chemical Physics of Solids, Nöthnitzer Str. 40, 01187 Dresden, Germany — ²Institut für Festkörper- und Materialphysik, Technische Universität Dresden, 01062 Dresden, Germany — ³Scottish Universities Physics Alliance (SUPA), School of Physics and Astronomy, University of St. Andrews, St. Andrews KY16 9SS, United Kingdom — ⁴School of Physics and Astronomy, University of Birmingham, Birmingham B15 2TT, United Kingdom

PdCrO_2 is a delafossite with an antiferromagnetic triangular lattice and a Neel temperature of 38 K. It has a double-q magnetic structure, in which the direction of spin rotation alternates from layer to layer. Under uniaxial stress, PdCrO_2 undergoes a transition from this double- to a single-q structure. Here, we will show stress-strain data on PdCrO_2 , collected using a piezoelectric-driven strain cell that allows simultaneous measurement of uniaxial stress and strain. We will show that the change in lattice constant across this magnetic transition is quite large and that the transition evolves in a nontrivial way as temperature is raised.

15 min. break

TT 23.7 Wed 16:45 H22

Magneto-thermodynamics of the J_1 - J_2 Heisenberg antiferromagnet on the square lattice — •ANDREAS HONECKER¹, JOHANNES RICHTER^{2,3}, JÜRGEN SCHNACK⁴, ALEXANDER WIETEK³, and MIKE E. ZHITOMIRSKY⁵ — ¹LPTM, CY Cergy Paris Université, France — ²Institut für Physik, Universität Magdeburg, Germany — ³Max Planck Institute for the Physics of Complex Systems, Dresden, Germany — ⁴Fakultät für Physik, Universität Bielefeld, Germany — ⁵Université Grenoble Alpes, CEA, IRIG, PHELIQS, France

We investigate the finite-temperature properties of the J_1 - J_2 Heisenberg antiferromagnet on the square lattice in the presence of an external magnetic field. We focus on the highly frustrated regime around $J_2 \approx J_1/2$. The H - T phase diagram is investigated with particular emphasis on the finite-temperature transition into the “up-up-up-down” state that is stabilized by thermal and quantum fluctuations and manifests itself as a plateau at one half of the saturation magnetization in the quantum case. Furthermore, we discuss the enhanced magnetocaloric effect associated to the ground-state degeneracy that arises at the saturation field for $J_2 = J_1/2$. Computations for the spin-1/2 system are carried out using finite-temperature Lanczos and quantum typicality approaches.

TT 23.8 Wed 17:00 H22

One- and two-particle dynamics of the J_1 - J_2 -Heisenberg bilayer — •ERIK WAGNER and WOLFRAM BREINIG — TU Braunschweig, Braunschweig, Germany
The antiferromagnetic J_1 - J_2 Heisenberg-model on the square lattice is one of

the pillars of frustrated quantum magnetism, with Néel- and collinearly ordered ground states competing for large and small J_1/J_2 , and with a quantum disordered phase of still unsettled nature in between. Probing fingerprints of such phases by approaching them out of a well controlled dimer phase is one of the rationals for studying bilayer versions of frustrated spin models. Here, and starting from the limit of decoupled dimers, we use the perturbative Continuous Unitary Transformation (pCUT), based on the flow equation method, to perform series expansion in order to analyze the spectrum of the square lattice J_1 - J_2 -Heisenberg bilayer up to the two-triplon excitations. Evaluating the ground state energy and the one-particle dispersion up to 7th order in $J_{1,2}$ as well as the two-particle interactions and spectrum up to 5th order, we find emerging (anti-)bound two-particle states, which can be classified by total spin and real-space symmetry, consistent with results found for the J_1 -only bilayer on the square lattice [1]. We analyze the phase boundary of the dimer phase with respect to one- and two-particle excitations and find reasonable agreement with recent coupled-cluster calculations [2], while also uncovering prospects for an additional phase introduced by two-particle boundstate condensation.

- [1] A. Collins, C.J. Hamer, PRB 78, 054419 (2008)
 [2] R.F. Bishop et al., PRB 100, 024401 (2019)

TT 23.9 Wed 17:15 H22

Entanglement measures of a frustrated spin-1/2 Heisenberg octahedral chain within the localized-magnon approach — •OLEŚIA KRUPNITSKA — Institute for Theoretical Physics, Technical University Braunschweig, D-38106 Braunschweig, Germany — Institute for Condensed Matter Physics, NASU, Svientsitskii Str. 1, 79011 Lviv, Ukraine

The localized-magnon theory [1] is a powerful tool for the rigorous determination of the ground state and detailed study of the thermodynamic properties of a special class of frustrated quantum Heisenberg antiferromagnets at high magnetic fields and low temperatures. We study different measures of two-spin entanglement [2] between the nearest- and between next-nearest-neighbor spins on the square of the spin-1/2 octahedral Heisenberg chain. It was shown that the localized-magnon theory can be modified for simpler calculation of concurrence [3], which may serve as a measure of the bipartite entanglement of the octahedral chain. Furthermore, we calculate the entanglement of formation and the negativity [4] within the localized-magnon concept. We demonstrate that localized-magnon theory can be straightforwardly adapted in order to calculate the respective entanglement measures for a wide class of flat-band quantum Heisenberg antiferromagnets.

- [1] J. Schulenburg et al., Phys. Rev. Lett. **88**, 167207 (2002).
 [2] L. Amico et al., Rev. Mod. Phys. **80**, 517 (2008).
 [3] J. Strečka, O. Krupnitska and J. Richter, EPL, **132** 30004 (2020).
 [4] A. Peres, Phys. Rev. Lett. **77**, 1413 (1996).

TT 23.10 Wed 17:30 H22

Interacting magnons in the easy-axis square-lattice XXZ-model and extensions towards ring exchange — •DAG-BJÖRN HERING¹, MATTHIAS R. WALTHER², KAI P. SCHMIDT¹, and GÖTZ S. UHRIG¹ — ¹Technische Universität Dortmund, Department of Physics, Condensed Matter Theory, Otto-Hahn-Str. 4, 44227 Dortmund — ²Friedrich-Alexander-Universität Erlangen-Nürnberg, Institut für Theoretische Physik I, Staudtstraße 7, 91058 Erlangen

The method of non-perturbative continuous similarity transformations (CST) in momentum space captures the physics of the isotropic spin 1/2 antiferromagnetic Heisenberg model on the square lattice (IHM) quantitatively [1-2]. We extend these studies to single- and two-particle properties of models related to the IHM. We start with easy-axis square-lattice XXZ-model as simplest extension of the IHM. Here, we present and discuss the CST results for the gap [3], the roton mode [4] and the bound-states [3] between the Ising limit to isotropic point in comparison to other methods. In addition, we outline further applications of the CST to models with ring-exchange [5] relevant for cuprates and the J-Q Model as a variant of ring-exchange without frustration [6].

- [1] M. Powalski et al., Phys. Rev. Lett. **115**, 207202 (2015)
 [2] M. Powalski et al., SciPost Phys. **4**, 001 (2018)
 [3] S. Dusuel et al., Phys. Rev. B **81**, 064412 (2010)
 [4] R. Verresen et al., Phys. Rev. B **98**, 155102 (2018)
 [5] K. Majumdar et al., Phys. Rev. B **85**, 144420 (2012)
 [6] A. W. Sandvik Phys. Rev. Lett. **98**, 227202 (2007)

TT 24: Quantum-Critical Phenomena

Time: Wednesday 15:00–19:00

Location: H23

TT 24.1 Wed 15:00 H23

Quantum criticality on a compressible lattice — •SAHELI SARKAR, LARS FRANKE, NIKOLAS GRIVAS, and MARKUS GARST — Karlsruhe Institute of Technology, Karlsruhe, Germany

TT 23.11 Wed 17:45 H22

Towards analyzing phase-transitions with continuous similarity transformation: Easy-axis square-lattice XXZ and J_1 - J_2 models — •MATTHIAS R. WALTHER¹, DAG-BJÖRN HERING², GÖTZ S. UHRIG², and KAI P. SCHMIDT¹ — ¹Friedrich-Alexander-Universität Erlangen-Nürnberg, Institut für Theoretische Physik I, Staudtstraße 7, 91058 Erlangen — ²Technische Universität Dortmund, Department of Physics, Condensed Matter Theory, Otto-Hahn-Str. 4, 44227 Dortmund

The method of non-perturbative continuous similarity transformations (CST) in momentum space captures the physics of the isotropic spin 1/2 antiferromagnetic Heisenberg model on the square lattice (IHM) quantitatively [1,2]. We discuss the potential of the CST to study critical behavior. To this end, the easy-axis square-lattice XXZ-model serves as a straight-forward extension of the IHM with a gapped phase away from the isotropic point. Its critical behavior is described by an established mean-field theory [3]. The CST is able to capture this criticality quantitatively. For further insights on the general capability of the CST for spin models we extend the study towards the frustrated square-lattice spin 1/2 antiferromagnetic J_1 - J_2 model and analyze the breakdown of the magnetically ordered quantum phases and their gapless spin wave excitations [4,5].

- [1] M. Powalski et al., Rev. Lett. **115**, 207202 (2015)
 [2] M. Powalski et al., SciPost Phys. **4**, 001 (2018)
 [3] W. Zheng et al., Phys. Rev. B **71**, 184440 (2005)
 [4] Götz S. Uhrig et al., Phys. Rev. B **79**, 092416 (2009)
 [5] R. R. P. Singh et al., Phys. Rev. Lett. **91**, 017201 (2003)

TT 23.12 Wed 18:00 H22

“Stripe- yz ” magnetic order in KCeS_2 — •ANTON KULBAKOV^{1,2}, STANISLAV AVDOSHENKO³, INÉS PUENTE-ORENCH^{4,5}, JACQUES OLLIVIER⁵, MAHMOUD DEEB¹, MATHIAS DOERR¹, PHILIPP SCHLENDER⁶, THOMAS DOERT⁶, and DMYTRO INOSOV^{1,2} — ¹IFMP, TU Dresden, Germany — ²Würzburg-Dresden ct.qmat, TUD, Dresden, Germany — ³IFW, Dresden, Germany — ⁴INMA, Zaragoza, Spain — ⁵ILL, Grenoble, France — ⁶Fakultät für Chemie und Lebensmittelchemie, TU Dresden, Germany

We have solved the magnetic structure for the antiferromagnetic state below $T_N = 400$ mK, which was recently revealed in the effective spin-1/2 triangular-lattice antiferromagnet KCeS_2 . It represents the so-called “stripe- yz ” type of antiferromagnetic order with spins lying approximately in the triangular-lattice planes orthogonal to the nearest-neighbor Ce–Ce bonds, possibly with a small out-of-plane canting of the magnetic moments. The thermal expansion remains very small below 120 K, which we confirmed for the c lattice constant using capacitive dilatometry. Our experimental results also indicate that cerium oxy-sulphide, $\text{Ce}_2\text{O}_2\text{S}$, which was present in our sample as a minority phase, does not order magnetically down to 20 mK and may therefore represent a promising spin-liquid candidate deserving a separate study. For details, see [1]. Neutron time-of-flight spectroscopy of low-energy excitations in the ordered state of KCeS_2 reveals an unusual spin-wave band with an intensity maximum at $\mathbf{Q} = 0$, unlike in KCeO_2 and KYbSe_2 .

- [1] J. Phys.: Condens. Matter **33**, 425802 (2021)

TT 23.13 Wed 18:15 H22

Quantum Skyrmion lattices in Heisenberg ferromagnets — •ANDREAS HALLER, SOLOFO GROENENDIJK, ALIREZA HABIBI, ANDREAS MICHELS, and THOMAS L. SCHMIDT — Department of Physics and Materials Science, University of Luxembourg, L-1511 Luxembourg, Luxembourg

Skyrmions are topological magnetic textures that can arise in non-centrosymmetric ferromagnetic materials. In most systems experimentally investigated to date, skyrmions emerge as classical objects. However, the discovery of skyrmions with nanometer length scales has sparked interest in their quantum properties. In this talk, we present the results of our matrix product state simulations of the ground states of two-dimensional spin-1/2 Heisenberg lattices with Dzyaloshinskii-Moriya interactions. We discovered a broad region in the zero-temperature phase diagram which hosts quantum skyrmion lattices. The quantum skyrmion lattice phase can be detected experimentally in the magnetization profile via local magnetic polarization measurements as well as in the spin structure factor measurable via neutron scattering experiments. Finally, we show the real-space polarization profile of individual quantum skyrmions and show that it is a non-classical state featuring entanglement between quasiparticle and environment mainly localized near the boundary spins of the skyrmion.

We compute the one-loop renormalization group equations treating the Φ field as well as the phonons on the same footing. We find that the velocities of the Φ field as well as of the phonons are renormalized yielding an effective dynamical exponent $z > 1$. The renormalization group flow is found to depend on the number of components N . Whereas we find run-away flow for $N < 4$ a new fixed-point emerges for $N \geq 4$. We discuss the relation to known results for classical criticality. Our findings are directly relevant to insulating quantum critical antiferromagnets.

TT 24.2 Wed 15:15 H23

Metallic and deconfined quantum criticality in Dirac systems — •ZHONG LIU¹, MATTHIAS VOJTA², FAKHER ASSAAD¹, and LUKAS JANSSEN² — ¹Institut für Theoretische Physik und Astrophysik and Würzburg-Dresden Cluster of Excellence ct.qmat, Universität Würzburg, 97074 Würzburg, Germany — ²Institut für Theoretische Physik und Würzburg-Dresden Cluster of Excellence ct.qmat, Technische Universität Dresden, 01062 Dresden, Germany

Motivated by the physics of spin-orbital liquids, we study a model of interacting Dirac fermions on a bilayer honeycomb lattice at half filling, featuring an explicit global $SO(3) \times U(1)$ symmetry. Using large-scale auxiliary-field quantum Monte Carlo (QMC) simulations, we locate two zero-temperature phase transitions as function of increasing interaction strength. First, we observe a continuous transition from the weakly-interacting semimetal to a different semimetallic phase in which the $SO(3)$ symmetry is spontaneously broken and where two out of three Dirac cones acquire a mass gap. The associated quantum critical point can be understood in terms of a Gross-Neveu- $SO(3)$ theory. Second, we subsequently observe a transition towards an insulating phase in which the $SO(3)$ symmetry is restored and the $U(1)$ symmetry is spontaneously broken. While strongly first order at the mean-field level, the QMC data is consistent with a direct and continuous transition. It is thus a candidate for a new type of deconfined quantum critical point that features gapless fermionic degrees of freedom.

TT 24.3 Wed 15:30 H23

Deconfined multi-critical point — •ZHENJIU WANG¹ and ADAM NAHUM² — ¹Max-Planck Institute for the Physics of Complex Systems, D-01187, Dresden, Germany — ²Laboratoire de Physique, Ecole Normale Supérieure, CNRS, Université PSL, Sorbonne Université, Université de Paris, 75005 Paris, France

We numerically investigate a deconfined quantum critical point (DQCP) that happens between Neel and valence bond solid phase in a 3-dimensional loop model. Amazingly, this DQCP is an Lifshitz tricritical point due to an explicit lattice symmetry breaking term. This perturbation breaks lattice translational symmetry as well as a mirror-reflection symmetry whereas production of these two operations leave system invariant, hence only an additional vector potential term is coupled to the non-linear sigma model in IR theory. A helical valence bond solid state with spatially modulated valence bond order parameter separates VBS and Neel state due to this explicit vector potential, and a continuous phase transition between Neel and HVB state is simply described by the criticality of DQCP with an emergent Lorenz invariance in IR limit.

TT 24.4 Wed 15:45 H23

Specific heat and magnetocaloric effect at transverse-field quantum criticality in $LiHoF_4$ — •ANDREAS WENDL¹, HEIKE EISENLOHR², JAN SPALLEK¹, CHRISTOPHER DUVINAGE¹, MATTHIAS VOJTA², and CHRISTIAN PFLEIDERER^{1,3,4} — ¹Physik Department, TU München, Garching, Germany — ²Institut für Theoretische Physik und Würzburg-Dresden Cluster of Excellence ct.qmat, TU Dresden, Dresden, Germany — ³Centre for QuantumEngineering (ZQE), TU München, Garching, Germany — ⁴Munich Centre for Quantum Science and Technology (MCQST), TU München, Garching, Germany

The perhaps best understood example of a quantum critical point is the response of the dipolar Ising ferromagnet $LiHoF_4$ under a transverse field [1-3]. We report an experimental and theoretical study of the specific heat and magneto-caloric effect of $LiHoF_4$ as a function magnetic field down to mK temperatures using a bespoke experimental set-up permitting studies under arbitrary magnetic field orientations. We derive the low temperature entropy landscape and discuss our findings in terms of a theoretical model taking quantitatively into account the non-Kramers nature of the Ho ions, the effects of hyperfine coupling and the presence of magnetic domains.

[1] D. Bitko et al., Phys. Rev. Lett. 77, 940 (1996)

[2] H. M. Ronnow et al., Science 308, 389 (2005)

[3] P. B. Chakraborty et al., Phys. Rev. B 70, 144411 (2004).

TT 24.5 Wed 16:00 H23

Muon spin rotation and relaxation study on $Nb_{1-y}Fe_{2+y}$ — •JANNIS WILLWATER¹, DANIELA EPPERS^{1,2}, THOMAS KIMMEL¹, ELAHEH SADROLLAHI^{1,3}, JOCHEN LITTERST¹, MALTE GROSCHKE⁴, CHRISTOPHER BAINES⁵, and STEFAN SÜLLOW¹ — ¹IPKM, TU Braunschweig, Germany — ²PTB, Braunschweig, Germany — ³IFMP, TU Dresden, Germany — ⁴Cavendish Laboratory, University of Cambridge, United Kingdom — ⁵PSI, Villigen, Switzerland

The study of metallic materials with a ferromagnetic quantum critical transition revealed a plethora of novel and exotic behavior. In $Nb_{1-y}Fe_{2+y}$, a well-known example, the magnetic ground state reacts extremely sensitively to the chemical

composition. Previous experiments show that by varying y , two ferromagnetic ultralow-moment and a SDW phase can be reached in the phase diagram. In particular, the magnetism disappears in a narrow range which is associated with the occurrence of a quantum critical point.

Here, we present a comprehensive study of the magnetic behaviour of $Nb_{1-y}Fe_{2+y}$ by means of muon spin rotation and relaxation. After establishing the muon stopping site, we studied and validated the magnetic phase diagram on different single and polycrystals. The focus of our study was the first investigation of a quantum critical sample, which shows no signs of long-range order, using a microscopic measurement technique. We demonstrate that magnetism at the lowest temperatures is dominated by magnetic fluctuations and that $Nb_{1-y}Fe_{2+y}$ emerges to be uniquely suited to study quantum criticality close to weak itinerant ferromagnetic order.

TT 24.6 Wed 16:15 H23

Quantum criticality of the long-transverse-field Ising model extracted by Quantum Monte Carlo simulations — •JAN ALEXANDER KOZIOL, ANJA LANGHELD, SEBASTIAN C. KAPFER, and KAI PHILLIP SCHMIDT — Lehrstuhl für Theoretische Physik I, Staudtstraße 7, Friedrich-Alexander Universität Erlangen-Nürnberg, D-91058 Erlangen, Germany

The quantum criticality of the ferromagnetic transverse-field Ising model with algebraically decaying interactions is investigated by means of stochastic series expansion quantum Monte Carlo, on both the one-dimensional linear chain and the two-dimensional square lattice. Utilizing finite-size scaling (FSS), we extract the full set of critical exponents as a function of the decay exponents of the long-range interactions. We resolve the three different regimes predicted by field theory, ranging from the nearest-neighbor Ising to the long-range Gaussian universality classes with an intermediate regime giving rise to a continuum of critical exponents. Focusing on the non-trivial intermediate regime, we verify our study by the well-known limiting regimes. In the long-range Gaussian regime, we treat the effect of dangerous irrelevant variables on the homogeneity laws by means of a modern FSS formalism.

TT 24.7 Wed 16:30 H23

Quantum criticality of the long-range antiferromagnetic Heisenberg ladder — •PATRICK ADELHARDT and KAI PHILLIP SCHMIDT — Friedrich-Alexander-Universität Erlangen-Nürnberg

The Mermin-Wagner theorem excludes the breaking of a continuous symmetry in one-dimensional spin systems at zero temperature for sufficiently short-ranged interactions. Introducing algebraically decaying long-range couplings on the antiferromagnetic Heisenberg two-leg ladder, we show that a direct second-order quantum phase transition between the topologically ordered rung-singlet phase in the short-range limit and a conventionally Néel-ordered antiferromagnet can be realized in a one-dimensional system. We study the quantum-critical breakdown in the rung-singlet phase using the method of perturbative continuous unitary transformations (pCUT) on white graphs in combination with classical Monte Carlo simulations for the graph embedding in the thermodynamic limit supplemented with linear spin-wave calculations to extract the critical point. Exploiting (hyper-)scaling relations, the pCUT method is used to determine the entire set of canonical critical exponents as a function of the decay exponent. We find that the critical behavior can be divided into a long-range mean-field regime and a regime of continuously-varying exponents similar to the long-range transverse-field Ising model despite the presence of distinct orders on different sides of the critical point and the absence of criticality in the short-range limit.

TT 24.8 Wed 16:45 H23

Electronuclear quantum criticality — JACINTHA BANDA¹, DANIEL HAFNER¹, JAVIER F. LANDAETA¹, ELENA HASSINGER^{1,2}, KEISUKE MITSUMOTO³, MAURO GIOVANNINI⁴, JULIAN SERENI⁵, CHRISTOPH GEIBEL¹, and •MANUEL BRANDO¹ — ¹Max Planck Institute for Chemical Physics of Solids, D-01187 Dresden, Germany — ²Technical University Munich, Physics department, 85748 Garching, Germany — ³Liberal Arts and Sciences, Toyama Prefectural University, Imizu, Toyama 939-0398, Japan — ⁴Department of Chemistry and Industrial Chemistry (DCCI), University of Genova, 16100 Genova, Italy — ⁵Department of Physics, CAB-CNEA, CONICET, 8400 San Carlos de Bariloche, Argentina

We present here a rare example of electronuclear quantum criticality in a metal. The compound $YCu_4.6Au_{0.4}$ is located at an unconventional quantum critical point (QCP). The relevant Kondo and RKKY exchange interactions are very weak, of the order of 1 K with a strong competition between antiferromagnetic and ferromagnetic correlations, possibly due to geometrical frustration within the fcc Yb sublattice. This causes strong spin fluctuations which prevent the system to order magnetically. Because of the very low Kondo temperature the $Yb^{3+} 4f$ -electrons couple weakly with the conduction electrons allowing the coupling to the nuclear moments of the ¹⁷¹Yb and ¹⁷³Yb isotopes to become important. Thus, the quantum critical fluctuations observed at the QCP derive not from purely electronic states but from entangled 'electronuclear' states. This is evidenced in the anomalous temperature and field dependence of the specific heat at very low temperatures.

15 min. break

TT 24.9 Wed 17:15 H23

Bosonization duality in 2+1 dimensions and critical current correlation functions in Chern-Simons U(1)*U(1) Abelian Higgs model — •VIRA SHYTA¹, FLAVIO NOGUEIRA¹, and JEROEN VAN DEN BRINK^{1,2} — ¹Institute for Theoretical Solid State Physics, IFW Dresden, Helmholtzstr. 20, 01069 Dresden, Germany — ²Institute for Theoretical Physics and Würzburg-Dresden Cluster of Excellence ct.qmat, TU Dresden, 01069 Dresden, Germany

While the phase structure of the U(1)*U(1)-symmetric Higgs theory is still under debate, we have shown that a version of this theory with an additional Chern-Simons term undergoes a second-order phase transition. We established that such a theory is a bosonized dual of a topological field theory of massless fermions featuring two gauge fields. Here we elaborate on several aspects of this duality, focusing on the critical current correlators and on the nature of the critical point as reflected by the bosonization duality. The current correlators associated to the U(1)*U(1) symmetry and the topological current are shown to coincide up to a universal prefactor, which we find to be the same for both U(1) and U(1)*U(1) topological Higgs theories. The established duality offers in addition another way to substantiate the claim about the existence of a critical point in the bosonic Chern-Simons U(1)*U(1) Higgs model: a Schwinger-Dyson analysis of the fermionic dual model shows that no dynamical mass generation occurs. The same cannot be said for the theory without the Chern-Simons term in the action.

TT 24.10 Wed 17:30 H23

Fixed-point structure and critical behavior of generalized Gross-Neveu models in 2+1 dimensions — •KONSTANTINOS LADOVRECHIS, SHOURYYA RAY, TOBIAS MENG, and LUKAS JANSSEN — Institute for Theoretical Physics and Würzburg-Dresden Cluster of Excellence ct.qmat, Technische Universität Dresden, Germany

The universal behavior of matter near points of continuous phase transitions is an intriguing phenomenon in condensed matter and statistical physics. At quantum critical points, the presence of gapless fermion degrees of freedom leads to new quantum universality classes without any classical analogues. Here, we discuss zero-temperature phase transitions between two-dimensional Dirac semimetals and long-range-ordered phases, in which spin and/or charge symmetries are spontaneously broken. These transitions are described by generalized Gross-Neveu models in 2+1 dimensions. We identify and classify fixed points of the renormalization group in the theory space spanned by a basis of short-range interactions compatible with the given symmetries, and we compute the corresponding quantum critical behaviors. Implications for the physics of interacting Dirac systems will be discussed as well.

TT 24.11 Wed 17:45 H23

Torus spectroscopy of the chiral Heisenberg quantum phase transition — •THOMAS C. LANG¹, DAVIDE BREONI^{1,2}, SETH WHITSITT³, MICHAEL SCHULER¹, STEFAN WESSEL⁴, and ANDREAS M. LÄUCHLI^{1,5} — ¹Institute for Theoretical Physics, University of Innsbruck, Austria — ²Institute for Theoretical Physics II: Soft Matter, Heinrich Heine-Universität Düsseldorf, Germany — ³Joint Quantum Institute, NIST and the University of Maryland, College Park, Maryland, USA — ⁴Institut für Theoretische Festkörperphysik, JARA-FIT and JARA-HPC, RWTH Aachen University, 52056 Aachen, Germany — ⁵Institute of Physics, École Polytechnique Fédérale de Lausanne (EPFL), 1015 Lausanne, Switzerland

We establish the universal torus low-energy spectra at the strongly coupled chiral Heisenberg fixed point in $D = (2 + 1)$ dimensions by means of quantum Monte Carlo simulations and exact diagonalization. The fixed point and the associated Gross-Neveu-Yukawa field theory are directly relevant for the long-wavelength physics of certain interacting Dirac systems, such as repulsive spinful fermions on the honeycomb lattice, or π -flux square lattice and are compared against results from SLAC fermions. The torus energy spectrum has been shown previously to serve as a characteristic fingerprint of relativistic fixed points and is a powerful tool to discriminate quantum critical behavior in numerical simulations. We are able to address the subtle crossover physics of the low-energy spectrum flowing from the Dirac fixed point to the chiral Heisenberg fixed point, and compare against earlier attempts to extract the Fermi velocity renormalization.

TT 24.12 Wed 18:00 H23

Finite size spectrum of the staggered six-vertex model with $U_q(\mathfrak{sl}(2))$ -invariant boundary conditions — •SASCHA GEHRMANN¹ and HOLGER FRAHM² — ¹Institute of Theoretical Physics, Leibniz University Hannover, Germany — ²Institute of Theoretical Physics, Leibniz University Hannover, Germany

The finite-size spectrum of the critical \mathbb{Z}_2 -staggered spin-1/2 XXZ model with quantum group invariant boundary conditions is presented. The conformal weights, which are found to have a continuous component, can be described in terms of the non-compact $SU(2, R)/U(1)$ Euclidean black hole conformal field theory (CFT) for a range of the staggering parameter. Besides the continuous part of the spectrum of this CFT, we find also levels from the discrete part emerging as the anisotropy is lowered. The finite size amplitudes of both the continuous and the discrete levels can be parameterized by the corresponding eigenvalues of a quasi-momentum operator which commutes with the Hamiltonian and the transfer matrix of the model.

TT 24.13 Wed 18:15 H23

Fixed-point annihilation and duality in the SU(2)-symmetric spin-boson model — •MANUEL WEBER¹ and MATTHIAS VOJTA² — ¹Max-Planck-Institut für Physik komplexer Systeme, Dresden, Germany — ²Institut für Theoretische Physik und Würzburg-Dresden Cluster of Excellence ct.qmat, Technische Universität Dresden, Germany

The annihilation of two intermediate-coupling renormalization-group (RG) fixed points is of interest in diverse fields from statistical mechanics to high-energy physics and has so far been studied using perturbative techniques. Here we present high-accuracy quantum Monte Carlo results for the SU(2)-symmetric $S = 1/2$ spin-boson (or Bose-Kondo) model. We study the model with a power-law bath spectrum $\propto \omega^5$ where, in addition to a critical phase predicted by perturbative RG, a stable strong-coupling phase is present. Using a detailed scaling analysis, we provide direct numerical evidence for the collision and annihilation of two RG fixed points at $s^* = 0.6540(2)$, causing the critical phase to disappear for $s < s^*$. Moreover, we uncover a surprising duality between the two fixed points, corresponding to a reflection symmetry of the RG beta function, which we utilize to make analytical predictions at strong coupling which are in excellent agreement with numerics. We comment on the consequences for impurity moments in critical magnets.

TT 24.14 Wed 18:30 H23

Applying continuous unitary transformations to open quantum systems — •LEA LENKE, MATTHIAS MÜHLHAUSER, and KAI PHILLIP SCHMIDT — Lehrstuhl für Theoretische Physik I, Staudtstraße 7, Universität Erlangen-Nürnberg, D-91058 Erlangen, Germany

We generalize the method of continuous unitary transformations (CUTs) to certain types of open systems. In some cases – such as gain-loss Hamiltonians – there exists an effective description in terms of non-Hermitian Hamiltonians. For the latter we successfully apply a perturbative CUT (pCUT) to two non-Hermitian PT-symmetric quantum spin models in order to determine their low-energy physics [1]. In a next step, we aim at generalizing this method further to dissipative frustrated systems described by a Lindblad master equation.

[1] L. Lenke, M. Mühlhauser, K. P. Schmidt, Phys. Rev. B 104, 195137 (2021)

TT 24.15 Wed 18:45 H23

Finite-size scaling at quantum phase transitions above the upper critical dimension — •ANJA LANGHELD, JAN ALEXANDER KOZIOL, PATRICK ADELHARDT, SEBASTIAN C. KAPFER, and KAI PHILLIP SCHMIDT — Lehrstuhl für Theoretische Physik I, Staudtstraße 7, Friedrich-Alexander Universität Erlangen-Nürnberg, D-91058 Erlangen, Germany

The hyperscaling relation and standard finite-size scaling (FSS) are known to break down above the upper critical dimension due to dangerous irrelevant variables. The upper critical dimension becomes experimentally accessible, for instance, in systems with long-range interactions such as the long-range transverse-field Ising model, which can be realized in systems of trapped ions.

We present a coherent formalism for FSS at quantum phase transitions above the upper critical dimension following the recently introduced Q-FSS formalism for thermal phase transitions. Contrary to long-standing belief, the correlation sector is affected by dangerous irrelevant variables. The presented formalism recovers a generalized hyperscaling relation and FSS form.

Using this new FSS formalism, we determine the full set of critical exponents for the long-range transverse-field Ising chain in all criticality regimes ranging from the nearest-neighbor to the long-range mean field regime. For the same model, we also explicitly confirm the effect of dangerous irrelevant variables on the characteristic length scale.

TT 25: Topological Semimetals

Time: Thursday 9:30–13:15

Location: H3

Invited Talk

TT 25.1 Thu 9:30 H3

Topology: Open and with diverse backgrounds — •TOBIAS MENG — Institute of Theoretical Physics and Würzburg-Dresden Cluster of Excellence ct.qmat, Technische Universität Dresden, 01069 Dresden, Germany

The advent of topological physics has been a major disruption in the way we think about condensed matter physics. In its most basic form, topological physics relies on the definition of topological invariants defined from the wave functions in the Brillouin zone, including for example the Chern number governing the Hall effect. Implicitly, this view of topological physics requires closed systems with translation invariance.

In this talk, I will show that the fact that any experimental system is open (coupled to its environment) and never fully translationally invariant can be a resource rather than a nuisance. When suitable couplings to environments and inhomogeneities are induced, topological systems exhibit a plethora of novel phenomena, including black hole analogies and new Hall responses. This highlights that the study of topological systems out of their "comfort zone" (closed and translational invariant) is a worthwhile direction for future research.

TT 25.2 Thu 10:00 H3

Chirality flip of Weyl nodes and its manifestation in strained MoTe₂ — •VIKTOR KÖNYE¹, ADRIEN BOUHON², ION COSMA FULGA¹, ROBERT-JAN SLAGER³, JEROEN VAN DEN BRINK^{1,4}, and JORGE I. FACIO¹ — ¹IFW Dresden and Würzburg-Dresden Cluster of Excellence ct.qmat, Dresden, Germany — ²Nordic Institute for Theoretical Physics (NORDITA), Stockholm, Sweden — ³CM Group, Cavendish Laboratory, University of Cambridge, Cambridge, United Kingdom — ⁴Institute for Theoretical Physics, TU Dresden, Dresden, Germany

Due to their topological charge, or chirality, the Weyl cones present in topological semimetals are considered robust against arbitrary perturbations. One well-understood exception to this robustness is the pairwise creation or annihilation of Weyl cones, which involves the overlap in energy and momentum of two oppositely charged nodes. Here we show that the topological charge can in fact change sign, in a process that involves the merging of not two, but three Weyl nodes. This is facilitated by the presence of rotation and time-reversal symmetries, which constrain the relative positions of Weyl cones in momentum space. We analyze the chirality flip process, showing that transport properties distinguish it from the conventional, double Weyl merging. Moreover, we predict that the chirality flip occurs in MoTe₂, where experimentally accessible strain leads to the merging of three Weyl cones close to the Fermi level. Our work sets the stage to further investigate and observe such chirality flipping processes in different topological materials.

TT 25.3 Thu 10:15 H3

Thermoelectric properties in TaRhTe₄, TaIrTe₄ and Mo_xW_{1-x}Te₂ Weyl semimetals — •MAHDI BEHNAMI¹, HELENA REICHOVA^{1,3}, FEDERICO CAGLIERIS^{1,2}, MATTHIAS GILLIG¹, DMITRIY EFREMOV¹, GRIGORY SHIPUNOV¹, SAICHARAN ASWARTHAM¹, OCHKAN KYRYLO¹, JOSEPH DUFOULEUR¹, and BERND BÜCHNER^{1,3} — ¹IFW Dresden, P.O. Box 270116, 01171 Dresden, Germany — ²SPIN Consiglio Nazionale delle Ricerche — ³Technische Universität Dresden, 01062 Dresden, Germany

Magneto- and thermo transport are the key properties of metals that not only can be used to study the electronic bands [1] but also have potential applications for heat harvesting. Here we report our results on the thermoelectric properties of Weyl semimetals TaRhTe₄, TaIrTe₄ and Mo_xW_{1-x}Te₂ [2,3,4]. All of these materials show an anomaly in the Nernst and Seebeck effects, while no anomaly can be seen in the standard magnetotransport. We discuss the origin of this anomaly and compare the results obtained with those for two compounds from the same family of materials, WTe₂ and MoTe₂.

[1] J. Noky et al., Phys. Rev. B 98, 241106 (2018)

[2] E. Haubold et al. Phys. Rev. B 95, 241108 (2017)

[3] K. Koepernik et al. Phys. Rev. B 93, 201101 (2016)

[4] G. Shipunov et al., J. Phys. Chem. Lett. 12, 28, 67306735 (2021)

TT 25.4 Thu 10:30 H3

Ab initio study of nonlinear optical effects on the Weyl semimetal TaIrTe₄ — •ÁLVARO RUIZ PUENTE¹, IVO SOUZA^{1,2}, STEPAN S. TSIRKIN³, and JULEN IBAÑEZ-AZPIROZ^{1,2} — ¹Centro de Física de Materiales, Universidad del País Vasco, 20018 Donostia-San Sebastián, Spain — ²Ikerbasque Foundation, 48013 Bilbao, Spain — ³Department of Physics, University of Zurich, Winterthurerstrasse 190, 8057 Zurich, Switzerland

We investigate the bulk photovoltaic effect (BPE), which describes a d.c. nonlinear photocurrent taking place in crystals lacking inversion symmetry. TaIrTe₄ is a type II Weyl semimetal displaying such a large d.c. response [1]. In this work we use nonlinear response theory to address the optical properties of the solid and isolate the contribution of the Weyl points to it, calculating the 2nd

order shift [2] and 3rd order jerk [3] current contributions. Our analysis relies on a Wannier-interpolation scheme built over *ab initio* calculations. We put our theoretical calculations in context with the experimentally measured data, since these effects are expected to account for the measured photocurrent.

Funding provided by the European Union's Horizon 2020 research and innovation programme under the European Research Council (ERC) grant agreement No 946629.

[1] J. Ma et al., Nat. Mater. 18, 476 (2019)

[2] J. Ibañez-Azpiroz, S. S. Tsirkin, I. Souza, Phys. Rev. B 97, 245143 (2018)

[3] B. M. Fregoso, R. A. Muniz, J. E. Sipe, Phys. Rev. Lett. 121, 176604 (2018)

TT 25.5 Thu 10:45 H3

Control of topological nodal planes in MnSi — •MARC A. WILDE^{1,2}, MATTHIAS DODENHÖFT¹, ARTHUR NIEDERMAYR¹, ANDREAS BAUER^{1,2}, MORITZ M. HIRSCHMANN³, KIRILL ALPIN³, ANDREAS P. SCHNYDER³, and CHRISTIAN PFLEIDERER^{1,2,4} — ¹Physik Department, Technische Universität München, Garching, Germany — ²Center for QuantumEngineering (ZQE), Technische Universität München, Garching, Germany — ³Max Planck Institute for Solid State Research, Stuttgart, Germany — ⁴MCQST, Technische Universität München, Garching, Germany

Topologically protected band crossings occurring at points or along lines in reciprocal space have generated widespread interest. In contrast, the existence of entire surfaces on which bands are forced to cross and which can also carry a topological charge has been largely overlooked. This is especially intriguing, since (i) the conditions required for the crossing to occur exactly at the Fermi levels are dramatically relaxed by the two-dimensional nature of the planes and (ii) the reciprocal space separation between partner charges is maximal.

In the field-polarized phase of the chiral magnet MnSi the existence or absence of such topological nodal planes is enforced by the existence of absence of magnetic screw rotation symmetries. By using a combination of symmetry analysis, density functional theory and de Haas-van Alphen quantum oscillation experiments we demonstrate switching of the topological nodal planes by an applied magnetic field [1].

[1] M.A. Wilde et al., Nature 594, 374 (2021)

TT 25.6 Thu 11:00 H3

High-mobility surface conduction in FeSi at low temperatures — •CAROLINA BURGER, ANDREAS BAUER, VIVEK KUMAR, MICHAEL WAGNER, RALF KORNTNER, and CHRISTIAN PFLEIDERER — Physik-Department, Technische Universität München, D-85748 Garching, Germany

We report a study of the correlated small-band-gap semiconductor FeSi, exhibiting a saturation of resistivity below temperatures of a few Kelvin. The magnetic field dependence of the electrical transport properties provides strong evidence of a high-mobility surface conduction channel, that is insensitive to the additional presence of an impurity band in the bulk. The surface conduction channel shares great similarities with properties reported for topological insulators, but displays a striking lack of sensitivity to the presence of ferromagnetic impurities as studied by means of a series of single crystals with slightly different starting compositions. Here, we report measurements of the specific heat and the magnetic torque in order to shed further light on the nature of the high-mobility surface conduction.

[1] Y. Fang, S. Ran, W. Xie, S. Wang, Y. S. Meng, M. B. Maple, Proc. Natl. Acad. Sci. 115, 8558 (2018)

[2] B. Yang, M. Uphoff, Y. Zhang, J. Reichert, A. P. Seitsonen, A. Bauer, C. Pfleiderer, J. V. Barth, Proc. Natl. Acad. Sci. 118, e2021203118 (2021)

15 min. break

TT 25.7 Thu 11:30 H3

Network of topological nodal planes, multifold degeneracies, and Weyl points in CoSi — •NICO HUBER¹, KIRILL ALPIN², ANDREAS P. SCHNYDER², CHRISTIAN PFLEIDERER¹, and MARC A. WILDE¹ — ¹TU Munich — ²MPI for Solid State Research, Stuttgart

The discovery of multifold-fermions [1,2] and symmetry-enforced topological band crossings that are generically located at the Fermi level [3] has recently generated tremendous interest. However, the putative relationship between all topological charges remained unexplored up to now. We report the experimental identification of symmetry-enforced nodal planes (NPs) in CoSi which together with point degeneracies form a network of topological band crossings. In our study [4] we combined measurements of Shubnikov-de Haas (SdH) oscillations with first-principle electronic structure calculations, a symmetry analysis of SG 198, as well as a direct calculation of the topological charges. The observation of two nearly dispersionless SdH frequency branches is shown to provide clear evidence of four Fermi surface sheets around the R point and their pairwise degeneracy at the NPs on the Brillouin zone boundary. Our results further show

that the crystalline symmetry enforces a topological charge of the NPs. Taken together, the comprehensive identification of all topological band crossings in the electronic structure of CoSi we report represents a showcase of an entire network of interconnected topological charges.

[1] Rao et al., Nature 567, 496 (2019)

[2] Sanchez et al., Nature 567, 500 (2019)

[3] Wilde et al., Nature 594, 374 (2021)

[4] Huber et al., arXiv:2107.02820 (accepted in PRL) (2022)

TT 25.8 Thu 11:45 H3

Anomalous evolution of the Nernst effect in trigonal PtBi₂ — •FEDERICO CAGLIERIS^{1,2,3}, DMITRIY EFREMOV³, GRIGORY SHIPUNOV³, SAICHARAN ASWARTHAM³, ARTHUR VEYRAT³, JOSEPH DUFOULEUR³, CHRISTIAN HESS^{5,3}, BERND BUECHNER^{3,4}, and DANIELE MARRÉ^{1,2} — ¹University of Genova, Via Dodecaneso 33, 16146 Genova (IT) — ²CNR-SPIN, Corso Perrone 24, 16142 Genova (IT) — ³Leibniz-Institute for Solid State and Materials Research IFW-Dresden, 01069 Dresden (DE) — ⁴Institut fuer Festkoerperphysik, TU Dresden, 01069 Dresden (DE) — ⁵Fakultaet fuer Mathematik und Naturwissenschaften, Bergische Universitaet Wuppertal, 42097 Wuppertal (DE)

Trigonal PtBi₂ represents an exceptional playground for the exploration of topological materials. In fact, it is a Weyl semimetal with broken inversion symmetry and strong spin-orbit coupling, showing also superconductivity at low temperatures. The Nernst effect has been proven to be a powerful technique to investigate the fermiology of unconventional materials. Moreover, in systems characterized by non-trivial topology, the Nernst coefficient often assumes distinctive features, as observed in various Weyl semimetals. In this work, we deeply investigate the evolution of the Nernst coefficient in a single crystal of trigonal-PtBi₂ as a function of different parameters: temperature (T), magnetic field (B) and angle (θ) between the magnetic field direction and the c-axis of the sample. In particular, we found an anomalous phenomenology, which could be ascribed to peculiar properties of the Fermi surface.

TT 25.9 Thu 12:00 H3

Fermi surface of the chiral topological semimetal PtGa — •B.V. SCHWARZE^{1,2}, M. UHLARZ¹, J. HORNUNG^{1,2}, S. CHATTOPADHYAY¹, K. MANNA^{3,4}, S. SHEKHAR³, C. FELSER³, and J. WOSNITZA^{1,2} — ¹Hochfeld-Magnetlabor Dresden (HLD-EMFL) and Würzburg-Dresden Cluster of Excellence ct.qmat, HZDR, Germany — ²Institut für Festkörper- und Materialphysik, TU Dresden, Germany — ³Max Planck Institute for Chemical Physics of Solids, Germany — ⁴Indian Institute of Technology Delhi, India

PtGa is a chiral topological semimetal hosting two band-touching nodes with a maximal Chern number of four. Previously, we reported on angle-resolved photoemission spectroscopy measurements revealing giant spin-split Fermi arcs verifying the topology [1]. Here, we present our detailed investigation of the bulk Fermi surfaces of PtGa with angular-dependent de Haas-van Alphen (dHvA) measurements and band-structure calculations. Strong spin-orbit coupling leads to well separated spin-split bands. Eight bands cross the Fermi energy forming a multitude of Fermi surfaces resulting in intricate dHvA spectra. The assignment of the experimentally observed dHvA frequencies to the corresponding calculated extremal orbits is challenging, because of their considerable quantity and proximity. Yet, the experiment is in good agreement with the calculations further confirming the topological character of PtGa.

[1] M. Yao, K. Manna et al., Nat. Commun. 11, 2033 (2020).

TT 25.10 Thu 12:15 H3

Raman Spectroscopy with Twisted Light on Chiral Semimetal PdGa — •FLORIAN BÜSCHER¹, PETER LEMMENS¹, CHANDRA SHEKHAR², and CLAUDIA FELSER² — ¹LENA, TU-BS, Braunschweig, Germany — ²CPFS, MPI, Dresden, Germany

We use Raman spectroscopy to study phonon intensities as a function of light polarization and magnetic field. The investigated system is the chiral Weyl semimetal PdGa. PdGa has chirally ordered Pd and Ga atoms along the c-axis, forming a helix with a distinct handedness. We observed a unique phonon effect with twisted light on specific modes of PdGa depending on the direction of the magnetic field and the handedness of the incident light.

Work supported by DFG EXC-2123-390837967 Quantum-Frontiers, DFG Le967/16-1, DFG-RTG 1952/1, and the Quantum- and Nano-Metrology (QUANOMET) initiative of Lower Saxony within project NL-4.

TT 26: Superconductivity: Tunnelling and Josephson Junctions

Time: Thursday 9:30–13:00

Location: H10

TT 26.1 Thu 9:30 H10

Microwave spectroscopy of a long Josephson junction strongly coupled to a resonator — •MICHA WILDERMUTH¹, MIKHAIL FISTUL², JAN NICOLAS VOSS¹, ANDRE SCHNEIDER¹, HANNES ROTZINGER^{1,3}, and ALEXEY V. USTINOV^{1,3} —

TT 25.11 Thu 12:30 H3
Magnetic Kagome metal ErMn₆Sn₆ — YISHUI ZHOU¹, FABIO ORLANDI², DMITRY KHALYAVIN², PASCAL MANUEL², THOMAS BRÜCKEL³, and YIXI SU¹ — ¹Jülich Centre for Neutron Science JCNS at MLZ, Forschungszentrum Jülich, 85747 Garching, Germany — ²ISIS Facility, STFC, Rutherford Appleton Laboratory, Didcot OX11 0QX, UK — ³Jülich Centre for Neutron Science JCNS-2 and Peter Grünberg Institute PGI-4, Forschungszentrum Jülich, 52425 Jülich, Germany

Following the discovery of a quantum-limit magnetic Chern phase in TbMn₆Sn₆, the correlated topological metal series RMn₆Sn₆ (R=Gd-Yb, and Y, Lu etc.), that possess an ideal kagome lattice of Mn, have emerged as a new platform to explore the interplay between geometric frustration, non-trivial band topology and magnetism. In particular, for magnetic rare-earth ions contained RMn₆Sn₆, it has been recently found that the topological transport properties, such as the anomalous Hall effect (AHE) and the topological Hall effect (THE), can be engineered intrinsically by rare-earth ions, thus suggesting a close relationship between the localized rare-earth magnetism, itinerant Mn magnetism and non-trivial band-structure topology. We have carried out the single-crystal growth and physical properties characterization of this series of magnetic kagome metals. Our single-crystal neutron diffraction investigation of ErMn₆Sn₆ has uncovered a range of magnetic field induced complex magnetic orders that are likely associated to the observed THE in this compound.

TT 25.12 Thu 12:45 H3

Designing 3-dimensional flat bands in nodal-line semimetals — •ALEXANDER LAU¹, TIMO HYART², CARMINE AUTIERI¹, ANFFANY CHEN³, and DMITRY I. PIKULIN⁴ — ¹Institute of Physics Polish Academy of Sciences, Warsaw, Poland — ²Aalto University, Espoo, Finland — ³University of British Columbia, Vancouver, Canada — ⁴Microsoft Quantum, Redmond, USA

In materials with flat energy bands, the kinetic energy of the electrons is quenched leading to an enhancement of correlation effects. Research efforts, both theoretically and experimentally, have so far focused on materials and superlattices with two-dimensional energy bands. Two dimensions, however, put severe restrictions on the stability of the low-temperature phases due to enhanced fluctuations. Only three-dimensional flat bands can solve the conundrum of combining exotic flat-band phases with stable order existing at high temperatures. Here, we present a viable way to generate three-dimensional flat bands through strain engineering in topological nodal-line semimetals. We shed light on the underlying mechanism and discuss the competition of the arising superconducting and magnetic orders. The required strain profile can be realized, for instance, by bending the sample, which allows for in situ tuning of the emerging correlated phases and the transition temperatures. We show that these systems support a nontrivial 3D quantum geometry giving rise to large superfluid weight and supercurrents along all directions. Moreover, we identify rhombohedral graphite and CaAgP as promising material candidates to realize our proposal.

TT 25.13 Thu 13:00 H3

Weyl-point teleportation — •GYÖRGY FRANK^{1,2}, DÁNIEL VARJAS³, GERGŐ PINTÉR^{1,2}, and ANDRÁS PÁLYI^{1,2} — ¹Department of Theoretical Physics, Budapest University of Technology and Economics, Hungary — ²MTA-BME Exotic Quantum Phases Group, Budapest University of Technology and Economics, Hungary — ³Department of Physics, Stockholm University, AlbaNova University Center, 106 91 Stockholm, Sweden

In this work, we describe the phenomenon of Weyl-point teleportation. Weyl points usually move continuously in the configuration parameter space of a quantum system when the control parameters are varied continuously. However, there are special transition points in the control space where the continuous motion of the Weyl points is disrupted. In such transition points, an extended nodal structure (nodal line or nodal surface) emerges, serving as a wormhole for the Weyl points, allowing their teleportation in the configuration space. A characteristic side effect of the teleportation is that the motional susceptibility of the Weyl point diverges in the vicinity of the transition point, and this divergence is characterized by a universal scaling law. We exemplify these effects via a two-spin model and a Weyl Josephson circuit model. We expect that these effects generalize to many other settings including electronic band structures of topological semimetals.

¹Institute of Physics, Karlsruhe Institute of Technology, 76131 Karlsruhe, Germany — ²Theoretische Physik III, Ruhr-Universität Bochum, 44801 Bochum Germany — ³Institute for Quantum Materials and Technology, Karlsruhe Institute of Technology, 76131 Karlsruhe, Germany

Long Josephson junctions are interesting physical systems due to their strongly nonlinear spatial and temporal dynamics. In the past, most of experiments were performed by coupling long junctions galvanically to measurement lines and recording their DC current-voltage characteristics. Here we explore an alternative approach, where the long junction is attached to a passive microwave resonator and the whole coupled system is measured with an RF technique. This configuration opens up new opportunities of low-dissipative tests and applications, in particular, for Josephson vortex qubits. We present fabrication results, microwave spectroscopy data and numerical simulations of this high-impedance hybrid system.

TT 26.2 Thu 9:45 H10

Quantum interference in a 1d array of three-terminal Josephson junctions — •JOHANNA BERGER¹, CHRISTIAN BAUMGARTNER¹, LORENZ FUCHS¹, SERGEI GRONIN², GEOFF GARDNER², MICHAEL MANFRA², NICOLA PARADISO¹, and CHRISTOPH STRUNK¹ — ¹Experimental and Applied Physics, University of Regensburg (Germany) — ²Purdue University, West Lafayette, Indiana (USA)

We present DC transport measurements of an 1d array of three-terminal Josephson junctions based upon an epitaxial Al-InAs heterostructure. Two terminals are connected via a superconducting loop. Under the influence of perpendicular magnetic fields the critical current displays a complex diffraction pattern resembling the superposition of a Fraunhofer pattern-like envelope and SQUID oscillations. In the presence of an additional in-plane magnetic field this pattern develops two asymmetries: The main lobe shows clear supercurrent diode behavior [1], which results in different critical currents depending on the applied current direction. With increasing in-plane magnetic field the diffraction pattern acquires an overall skewness with respect to the perpendicular magnetic field, leading to differently pronounced side lobes. Unlike the diode effect this skewness is not suppressed at higher magnetic fields.

[1] C. Baumgartner *et al.*, Nat. Nanotechnol. 17, 39 (2022)

TT 26.3 Thu 10:00 H10

Highly-packed Nb-C Josephson junction arrays prepared by focused-ion-beam nanoprinting — •FABRIZIO PORRATI¹, FELIX JUNGWIRTH¹, SVEN BARTH¹, GIAN CARLO GAZZADI², STEFANO FRABONI², OLEKSANDR V. DOBROVOLSKIY³, and MICHAEL HUTH¹ — ¹Goethe-University, Institut of Physics, Frankfurt a. M. — ²Nanoscience Institute-CNR, Modena — ³University of Vienna, Faculty of Physics, Vienna

Focused ion beam-induced deposition (FIBID) is a direct-write technique for the fabrication of nanostructures of any shape and dimension with high lateral resolution. Here, FIBID is employed to prepare Josephson junction arrays (JJA) consisting of superconducting Nb-C dots coupled through the proximity effect via a thin granular metal layer. The fabrication of the device is straightforward and it takes place in a few seconds. The microstructure and the composition of the JJA are investigated by transmission electron microscopy (TEM) and energy dispersive x-ray spectroscopy (EDS). The superconductor-to-metal transition of the JJA is studied directly by tuning the Josephson junction resistance in 70 nm-spaced Nb-C dots. The observed magnetoresistance oscillations with a period determined by the flux quantum give evidence for the coherent charge transport by paired electrons.

TT 26.4 Thu 10:15 H10

A particle conserving approach to AC-DC driven interacting quantum dots with superconducting leads — •JULIAN SIEGL, JORDI PICÓ-CORTÉS, and MILENA GRIFONI — Universität Regensburg, Regensburg, Germany

The combined action of a DC bias and a microwave drive on the transport characteristic of a superconductor-quantum dot-superconductor junction is investigated. To cope with non-equilibrium effects and interactions in the quantum dot, we develop a general formalism for the dynamics of the density operator based on a particle conserving approach to superconductivity. An exact generalized master equation for the reduced dot operator is obtained that treats the interaction inside the dot exactly and showcases the characteristic bichromatic response due to the combination of the AC Josephson effect and an AC voltage. In the weak coupling limit, analytical expressions for the stationary current and the reduced dot operator are provided. In this regime, beside quasiparticle transport, we show that superconducting correlations manifest in anomalous pair tunneling processes involving the tunneling of a Cooper pair. Photon assisted processes allow for subgap transport and rich current-voltage characteristics. For example, we find total current inversion, in which the current flows against the applied DC bias for suitable parameter regimes.

TT 26.5 Thu 10:30 H10

Model-independent determination of the gap function of nearly localized superconductors — •DUŠAN KAVICKÝ¹, FRANTIŠEK HERMAN^{1,2}, and RICHARD HLUBINA¹ — ¹Department of Experimental Physics, Comenius University, Mlynská Dolina F2, 842 48 Bratislava, Slovakia — ²Institute for Theoretical Physics, ETH Zurich, CH-8093, Switzerland

The gap function $\Delta(\omega)$ carries essential information on both, the pairing glue as well as the pair-breaking processes in a superconductor. Unfortunately, in nearly

localized superconductors with a non-constant density of states in the normal state, the standard procedure for extraction of $\Delta(\omega)$ cannot be applied. Here, we introduce a model-independent method that makes it possible to extract $\Delta(\omega)$ also in this case. The feasibility of the procedure is demonstrated on the tunneling data for the disordered thin films of TiN. We find an unconventional feature of $\Delta(\omega)$ which suggests that the electrons in TiN are coupled to a very soft pair-breaking mode.

TT 26.6 Thu 10:45 H10

The DC Josephson effect for a single level weak link: a Green's function formulation within a particle conserving theory of superconductivity — •ANTON BLEIBAUM and MILENA GRIFONI — Institute for Theoretical Physics, University of Regensburg, 93053 Regensburg, Germany

In traditional transport set-ups a current only flows when a bias voltage is applied. In the presence of superconducting electrodes a super-current can flow through a tunneling barrier even in thermodynamic equilibrium. This phenomenon is called DC-Josephson effect. Most of its features can be captured within mean field BCS-theory, according to which the supercurrent is a function of the phase difference between the two superconductors.

How can this result be reconciled with charge conservation in a physical system? In this work we compute the DC Josephson current in transport set-ups consisting of two superconducting electrodes coupled to a single level non-interacting quantum dot. The computation is based on a particle conserving theory of superconductivity. We first provide a current formula in terms of particle conserving Green's functions. In a second step the infinite hierarchy of equations for the relevant Green's function is solved. The Andreev bound states spectrum naturally follows from the poles of the retarded Green's function, and the DC-current has the form known from BCS theory.

TT 26.7 Thu 11:00 H10

Engineering the speedup of quantum tunneling in Josephson systems via dissipation — •DOMINIK MAILE¹, JOACHIM ANKERHOLD¹, SABINE ANDERGASSEN², WOLFGANG BELZIG³, and GIANLUCA RASTELLI⁴ — ¹Institut für komplexe Quantensysteme, Universität Ulm, Germany — ²Institut für Theoretische Physik, Universität Tübingen, Germany — ³Fachbereich Physik, Universität Konstanz, Germany — ⁴NO-CNR BEC Center and Dipartimento di Fisica, Università di Trento, Povo, Italy

We theoretically investigate the escape rate occurring via quantum tunneling in a system affected by tailored dissipation [1]. Specifically, we study the environmental assisted quantum tunneling of the superconducting phase in a current-biased Josephson junction. We consider Ohmic resistors inducing dissipation both in the phase and in the charge of the quantum circuit. We find that the charge dissipation leads to an enhancement of the quantum escape rate. This effect appears already in the low Ohmic regime and also occurs in the presence of phase dissipation that favors localization. Inserting realistic circuit parameters, we address the question of its experimental observability and discuss suitable parameter spaces for the observation of the enhanced rate.

[1] D. Maile, J. Ankerhold, S. Andergassen, W. Belzig, G. Rastelli, arXiv:2203.08075 (2022)

15 min. break

TT 26.8 Thu 11:30 H10

Nonreciprocity in current-biased Josephson junctions in the presence of Yu-Shiba-Rusinov bound states — •MARTINA TRAHMS¹, BHARTI MAHENDRU¹, IDAN TAMIR¹, LARISSA MELISCHEK¹, JACOB F. STEINER¹, NILS BOGDANOFF¹, OLOF PETERS¹, GAËL REECHT¹, CLEMES B. WINKELMANN², FELIX VON OPPEN¹, and KATHARINA J. FRANKE¹ — ¹Fachbereich Physik, Freie Universität Berlin, 14195 Berlin, Germany — ²Univ. Grenoble Alpes, Institute Néel, 38042 Grenoble, France

Magnetic impurities on superconducting surfaces are known to locally disturb Cooper pairs and form Yu-Shiba-Rusinov (YSR) states. We employ current-biased Josephson spectroscopy in a scanning tunnelling microscope to study the phase dynamics of Josephson junctions in the presence of YSR states. For that purpose Mn and Cr adatoms are evaporated on a superconducting Pb(111) surface and investigated with a superconducting Pb tip. We observe switching currents that are significantly larger than the retrapping currents, identifying the junction as underdamped. In the presence of magnetic atoms, a local reduction of switching currents is observed. Additionally, we find a nonreciprocal behavior of the retrapping currents with respect to the current-sweep direction, i.e., the absolute value of the retrapping current depends on whether the current sweep starts at positive or negative bias values. In our experiment both species of magnetic atoms lead to a nonreciprocal retrapping-current behavior, albeit with a different directionality. We suggest a correlation between the damping of the Josephson junction and the electron-hole asymmetry of the YSR states.

TT 26.9 Thu 11:45 H10

Josephson effect through two superconducting magnetic impurity states — •FABIAN ZIESEL¹, CIPRIAN PADURARIU¹, BJÖRN KUBALA^{1,2}, and JOACHIM ANKERHOLD¹ — ¹ICQ and IQST, Ulm University, Germany — ²Institute of Quantum Technologies, German Aerospace Center (DLR), Ulm, Germany

A mK-STM functionalized with a magnetic impurity at the tip can probe a sample with a second impurity, thus realizing tunneling between Yu-Shiba-Rusinov (YSR) states [1]. We study the Josephson effect in such a system as a sensitive probe of the magnetic orientation of the impurities. Using Keldysh Green's functions, we show that the subgap bound states are spin-polarized and give rise to a spin polarized Josephson current. At low transmission, the YSR states of the impurities hybridize weakly, whereas at large transmission, the bound states are strongly phase-dependent, resembling spin split Andreev bound states [2]. The spin structure of the current becomes strongly phase-dependent. For aligned or anti-aligned magnetic impurities, we show that an unusual quantum phase transition emerges. While such a Josephson current can be used as a sensitive spin probe, we find that it is accompanied by significant feedback in the form of a Josephson spin torque acting to align/anti-align the impurities.

- [1] H. Huang *et al.*, Nat. Phys. **16**, 1227 (2020)
[2] B. Bujnowski *et al.*, EPL **115**, 67001 (2016)

TT 26.10 Thu 12:00 H10

Spin-orbit coupling assisted transport phenomena in superconducting magnetic tunnel junctions — •ANDREAS COSTA and JAROSLAV FABIAN — University of Regensburg, Germany

Superconducting magnetic junctions exhibit fascinating physical phenomena, making them essential building blocks for modern technologies like quantum computing. Particularly attractive are multicomponent junctions in which the broken space-inversion symmetry additionally rises strong spin-orbit coupling (SOC). Pairing the interplay of these two most important spin interactions—exchange and SOC—with superconducting coherence has already been demonstrated to lead to unique signatures in spectroscopy and transport, and is furthermore expected to induce topological superconductivity hosting Majorana states. In this theory talk, we will focus on the most intriguing transport ramifications of SOC in superconducting magnetic junctions, covering giant transport magnetoanisotropies in the junctions' conductance and Josephson-current flow [1], the possibility to generate sizable transverse anomalous (Josephson) Hall effects [2,3], as well as nonreciprocal transport and supercurrent-diode characteristics in proximitized 2DEG Josephson junctions [4] that were experimentally classified through robust Josephson-inductance measurements.

This work was supported by ENB IDK Top. Insulators, DFG SFB 1277 (B07), and DFG Grant 454646522.

- [1] PRB **95**, 024514 (2017)
[2] PRB **100**, 060507(R) (2019)
[3] PRB **101**, 104508 (2020)
[4] Nat. Nanotechnol. (2021)

TT 26.11 Thu 12:15 H10

Non-equilibrium transport in Josephson junctions through interacting nanostructures — •JORDI PICÓ CORTÉS^{1,2}, GLORIA PLATERO², and MILENA GRIFONI¹ — ¹Theoretische Physik, Universität Regensburg, 93040 Regensburg, Germany — ²Instituto de Ciencia de Materiales de Madrid (CSIC) E-28049, Spain

Studying transport through interacting nanostructures is challenging due to the interplay between strong interactions and the coupling to large thermalized leads. In the case of superconducting leads, this is further complicated by a number of features particular to Josephson junctions, chiefly the effect of Cooper pairs and the resulting anomalous transport. In this work, we develop a diagrammatic approach to transport through weakly coupled Josephson junctions [1,2,3] which treats the interaction inside the dot exactly and employ it to describe the conventional and Josephson currents. The dynamics of Cooper pairs out of equilibrium are described in a particle-conserving formalism, which avoids issues arising from the usual BCS treatment, allowing us to extend the description of electron pairing inside the dot and the $0 - \pi$ transition beyond the usual equilibrium treatment.

- [1] M. Governale, M.G. Pala, J. König, Phys. Rev. B **77**, 134513 (2008)
[2] B. Hiltcher, M. Governale, J. König, Physical Review B **86**, 235427 (2012)
[3] J. Siegl, J. Picó-Cortés, M. Grifoni, arXiv:2205.13936 (2022)

TT 26.12 Thu 12:30 H10

Interplay of Cooper pair and quasiparticle tunneling in the dynamics of an Anderson pseudospin — •CHRISTOPH ROHRMEIER, JORDI PICÓ-CORTÉS, ANDREA DONARINI, and MILENA GRIFONI — Institute of Theoretical Physics, University of Regensburg, Germany

In an interacting quantum dot coupled to superconducting reservoirs, the state of the system can be described in terms of a pseudospin [1] where "up" represents a fully occupied and "down" means an empty dot [2]. We investigate the dynamics of this Anderson pseudospin with the help of a generalized master equation based on a particle-conserving approach to superconductivity [3]. Superconducting correlations involved in Cooper pair and quasiparticle tunneling manifest in the pseudospin dynamics. The pseudospin precession is governed by an effective magnetic field [4] of which we give an analytical expression including finite gap, bias as well as interaction.

- [1] P. Anderson, Phys. Rev. **112**, 1900 (1958)
[2] M. Governale, M. Pala, Jürgen König, Phys. Rev. B **77**, 134513 (2008)
[3] J. Siegl, J. Picó-Cortés, M. Grifoni, arXiv:2205.13936 (2022)
[4] C. Rohrmeier and A. Donarini, Phys. Rev. B **105**, 205418 (2022)

TT 26.13 Thu 12:45 H10

Evolution of Andreev bands in half-filled superconducting periodic Anderson model — •VLADISLAV POKORNY¹ and PANCH RAM² — ¹Institute of Physics, Czech Academy of Sciences, Na Slovance 2, CZ-18221 Praha 8, Czech Republic — ²Faculty of Mathematics and Physics, Charles University, Ke Karlovu 5, CZ-12116 Praha 2, Czech Republic

Two-dimensional systems where the surface of a superconductor is coated with a molecular layer draw recently a lot of attention as they represent ideal setups for studying the competition between magnetism and superconductivity. The physics of such system can be studied using the superconducting periodic Anderson model which describes a conduction band with superconducting pairing hybridized with a non-dispersive band of correlated electrons. We use the dynamical mean-field theory to solve this problem by mapping the lattice model to the superconducting impurity Anderson model with a self-consistent bath. This method neglects spatial correlations between lattice sites while local quantum fluctuations are fully taken into account. We show the behavior of the in-gap Andreev bands and how the singlet-doublet (zero- π) quantum phase transition in the impurity model is reflected in the induced pairing in the correlated band.

TT 27: Quantum Coherence and Quantum Information Systems (joint session TT/DY)

Time: Thursday 9:30–12:30

Location: H22

TT 27.1 Thu 9:30 H22

Design of a granular aluminum Fluxonium qubit in a coplanar waveguide architecture — •PATRICK PALUCH, MARTIN SPIECKER, NICOLAS GOSLING, ALEXANDRU IONITA, SIMON GÜNZLER, DARIA GUSENKOVA, DENNIS RIEGER, IVAN TAKMAKOV, FRANCESCO VALENTI, PATRICK WINKEL, WOLFGANG WERNSDORFER, and IOAN-MIHAI POP — Karlsruhe Institute of Technology

Fluxonium qubits are often embedded in rectangular waveguides which dilute the electric field and favor high coherence [1,2]. However, this configuration complicates in-situ flux gates and multi-qubit experiments. Here, we present a fluxonium qubit placed in a coplanar waveguide architecture with an integrated fast-flux coil, surrounded by a normal metal ground plane. The superinductor is made out of granular aluminum (grAl) [3] and the use of a comparably large silver ground plane potentially decreases the number of quasiparticles in the system via phonon trapping [4].

- [1] Pop *et al.*, Nature **508**, 369 (2014)
[2] Somoroff *et al.*, arXiv:2103.08578 (2021)
[3] Grünhaupt *et al.*, Nat. Mater. **18**, 816 (2019)
[4] Henriques *et al.*, Appl. Phys. Lett. **115**, 212601 (2019)

TT 27.2 Thu 9:45 H22

Gralmonium: Granular aluminum nano-junction Fluxonium qubit — •DENNIS RIEGER, SIMON GÜNZLER, MARTIN SPIECKER, PATRICK PALUCH, PATRICK WINKEL, LOTHAR HAHN, JUDITH K. HOHMANN, ANDREAS BACHER, WOLFGANG WERNSDORFER, and IOAN M. POP — Karlsruhe Institute of Technology, Germany

Mesoscopic Josephson junctions (JJs), consisting of overlapping superconducting electrodes separated by a nanometer thin oxide layer, provide a precious source of nonlinearity for superconducting quantum circuits and are at the heart of state-of-the-art qubits, such as the transmon and fluxonium. Here, we show that in a fluxonium qubit the role of the JJ can also be played by a lithographically defined, self-structured granular aluminum (grAl) nano-junction: a superconductor-insulator-superconductor (SIS) JJ obtained in a single layer, zero-angle evaporation. The measured spectrum of the resulting qubit, which we nickname gralmonium, is indistinguishable from the one of a standard fluxonium qubit. Remarkably, the lack of a mesoscopic parallel plate capacitor gives rise to an intrinsically large grAl nano-junction charging energy in the range of $10 - 100$ GHz, comparable to its Josephson energy E_J . We measure average energy relaxation times of $T_1 = 10 \mu\text{s}$ and Hahn echo coherence times of

$T_2^{\text{echo}} = 9\mu\text{s}$. The exponential sensitivity of the gralmonium to the E_J of the grAl nano-junction provides a highly susceptible detector. Indeed, we observe spontaneous jumps of the value of E_J on timescales from milliseconds to days, which offer a powerful diagnostics tool for microscopic defects in superconducting materials.

TT 27.3 Thu 10:00 H22

Quantum dynamics of disordered arrays of interacting superconducting qubits: Signatures of quantum collective states — MIKHAIL FISTUL, OLIVER NEYENHUIS, ANTONIA BOCAZ, and ILYA EREMIN — Theoretische Physik III, Ruhr-Universität Bochum, Bochum 44801, Germany

We study theoretically the collective quantum dynamics occurring in various interacting superconducting qubits arrays (SQAs) in the presence of a spread of individual qubit frequencies. The interaction is provided by mutual inductive coupling between adjacent qubits (short-range Ising interaction) or inductive coupling to a low-dissipative resonator (long-range Ising exchange interaction). In the absence of interaction the Fourier transform of the temporal correlation function of the total polarization (z-projection of the total spin), i.e. the dynamic susceptibility $C(\omega)$, demonstrates a set of sharp small magnitude resonances corresponding to the transitions of individual superconducting qubits. We show that even a weak interaction between qubits can overcome the disorder with a simultaneous formation of the collective excited states. This collective behavior manifests itself by a single large resonance in $C(\omega)$. In the presence of a weak non-resonant microwave photon field in the low-dissipative resonator, the positions of dominant resonances depend on the number of photons, i.e. the collective ac Stark effect. Coupling of an SQA to the transmission line allows a straightforward experimental access of the collective states in microwave transmission experiments and, at the same time, to employ SQAs as sensitive single-photon detectors.

TT 27.4 Thu 10:15 H22

Heat transport and rectification in an ultrastrongly-coupled qubit-resonator system — LUCA MAGAZZU¹, MILENA GRIFONI¹, and ELISABETTA PALADINO² — ¹University of Regensburg — ²University of Catania

Inspired by the recent experimental developments in the field of heat transport in the quantum regime, we consider a flux qubit coupled to a superconducting resonator as a composite open quantum system. The two elements of this open quantum Rabi system interact with two heat baths held at different temperatures. At the steady state, a heat current is established which is the result of photon exchanges between the system and the baths. Due to the geometry of the setup, the coupling to the heat baths is asymmetric. In turn this entails the presence of a preferred direction for the heat current, to a degree quantified by the heat rectification.

We calculate the heat current and rectification in different coupling regimes and considering a periodic driving applied to the qubit. The rectification displays the signatures of multi-photon processes that occur when the qubit-resonator coupling enters the nonperturbative regime

[1] A. Ronzani et al., Nat. Phys. 14, 991 (2018)

[2] J. Senior, A. Gubaydullin, B. Karimi, J. T. Peltonen, J. Ankerhold, J. P. Pekola, Commun. Phys. 3, 40 (2020)

[3] B. Bhandari, P. Andrea Erdman, R. Fazio, E. Paladino, and F. Taddei. Phys. Rev. B 103, 155434 (2021)

[4] L. Tesser, B. Bhandari, P. A. Erdman, R. Fazio, E. Paladino, F. Taddei, New J. Phys. 24, 035001 (2022)

TT 27.5 Thu 10:30 H22

Probing the coherence of superconducting Fluxmon qubits — BENEDIKT BERLITZ, ALEXANDER NEUMANN, ALEXANDER BILMES, JÜRGEN LISENFELD, and ALEXEY V. USTINOV — Physikalisches Institut, Karlsruhe Institute of Technology (KIT), Karlsruhe, Germany

The Fluxmon qubit combines a transmission line resonator with a DC-SQUID and offers wide control over the circuit's potential energy via two independently applied bias flux channels. This allows one to operate the qubit as a phase or flux qubit, provides means for fast single-shot qubit readout, and offers a path to characterize decoherence due to surface spins and tunneling defects in a wide frequency range. We will review the Fluxmon qubit design and fabrication, and present measurements of its potential energy landscape which demonstrate single- and double well qubit physics. Our time-resolved measurements confirm that the Fluxmon qubit's performance is strongly limited by microscopic sources of decoherence, which might render it a suitable detector for defect spectroscopy applications.

TT 27.6 Thu 10:45 H22

Mapping the positions of individual material defects in superconducting transmon qubits — ALEXANDER K. HÄNDEL, BENEDIKT BERLITZ, ALEXANDER BILMES, JÜRGEN LISENFELD, and ALEXEY V. USTINOV — Physikalisches Institut, Karlsruhe Institute of Technology, 76131 Karlsruhe, Germany

In superconducting quantum bits, material defects at the surface of circuit electrodes and the substrate constitute a major source of decoherence. In our experiment, we detect individual defects with a transmon qubit while tuning their resonance frequencies with applied static electric fields. We fabricated samples

that feature on-chip gate electrodes that are placed close to the qubit island. By measuring the coupling strength of each detected defect to various electrodes, we are able to deduce the defect's position on the qubit chip. Our goal is to create two-dimensional maps of defect distribution over qubit electrodes. This will help to identify circuit components which contain majority of coherence-breaking defects and improve fabrication methods towards more coherent qubits.

15 min. break

TT 27.7 Thu 11:15 H22

Quantum memory based on spin donors in silicon — PATRICIA OEHL^{1,2}, JULIAN FRANZ^{1,2}, FLORIAN FESQUET^{1,2}, NADEZHDA KUKHARCHYK^{1,2}, KIRILL G. FEDOROV^{1,2}, RUDOLF GROSS^{1,2,3}, and HANS HUEBL^{1,2,3} — ¹Walther-Meißner-Institut, Bayerische Akademie der Wissenschaften, Garching, Germany — ²Physik-Department, Technische Universität München, Garching, Germany — ³Munich Center for Quantum Science and Technologies (MCQST), Germany

Quantum memories are considered as key elements for the successful realization of quantum communication [1]. In order to allow for the connection of several quantum nodes into a quantum network without frequency conversion, several requirements have to be met such as frequency compatibility and connectability to the quantum system of choice. As superconducting quantum processors operate in the microwave regime, solid-state spin ensembles with their exceptional coherence times are promising candidates [2]. Here, we present a hybrid system consisting of a superconducting lumped-element microwave resonator coupled to a phosphorus donor electron spin ensemble hosted in isotopically engineered silicon. We present experimental results on the storage of coherent microwave states and their retrieval using a Hahn-echo type pulse sequence. In detail, we discuss the impact of the resonator design, the classical storage times and outline strategies towards storing quantum signals.

We acknowledge financial support from the Federal Ministry of Education and Research of Germany (project number 16KISQ036).

[1] H. J. Kimble, Nature 453, 1023 (2008)

[2] C. Gezes et al., Phys. Rev. X 4, 021049 (2014)

TT 27.8 Thu 11:30 H22

Crystal electric field effects in yttrium orthosilicate doped with paramagnetic rare-earth ions — TIM HOFMANN, ANDREAS BAUER, FABIAN KESSLER, and CHRISTIAN PFLEIDERER — Chair for the Topology of Correlated Systems, Department of Physics, Technical University of Munich, Germany

Monoclinic yttrium orthosilicate Y_2SiO_5 doped with several ten ppm of rare-earth ions, such as Er^{3+} , Yb^{3+} , or Nd^{3+} , represents a candidate material for optical applications in quantum information technology. The amount of dopants directly influences key properties, such as the linewidth or the coherence time, and in turn precise control on the doping levels is essential. The quantitative determination of doping on ppm level is challenging when using conventional characterization techniques. Here, we report the magnetic characterization of rare-earth doped yttrium orthosilicate single crystals. We infer information from magnetization measurements at low temperatures down to 2 K for magnetic fields up to 14 T applied along the optical axes b , $D1$, and $D2$, exhibiting paramagnetic contributions characteristic of rare-earth ions. Distinct crystalline anisotropy and the substitution of yttrium on two magnetically inequivalent sites is observed, indicating the importance of crystal electric field effects for both the fundamental characterization and potential applications in quantum information technology.

TT 27.9 Thu 11:45 H22

Synchronized coherent charge oscillations in coupled double quantum dots — ERIC KLEINHERBERS¹, PHILIPP STEGMANN², and JÜRGEN KÖNIG¹ — ¹Faculty of Physics and CENIDE, University Duisburg-Essen, 47057 Duisburg, Germany — ²Department of Chemistry, Massachusetts Institute of Technology, Cambridge, Massachusetts 02139, USA

We study coherent charge oscillations in double quantum dots tunnel-coupled to metallic leads [1]. If two such systems are coupled by Coulomb interaction, there are in total six (instead of only two) oscillation modes of the entangled system with interaction-dependent oscillation frequencies. By tuning the bias voltage, one can engineer decoherence such that only one of the six modes, in which the charge oscillations in both double quantum dots become synchronized in antiphase, is singled out. We suggest to use waiting-time distributions and the $g^{(2)}$ -correlation function to detect the common frequency and the phase locking.

[1] E. Kleinherbers et al., Phys. Rev. B 104, 165304 (2021)

TT 27.10 Thu 12:00 H22

Electrically driven spin resonance with bichromatic driving — ZOLTÁN GYÖRGY¹, ANDRÁS PÁLYI², and GÁBOR SZÉCHENYI¹ — ¹Institute of Physics, Eötvös University, H-1117 Budapest, Hungary — ²Department of Theoretical Physics, Institute of Physics, Budapest University of Technology and Economics, H-1111 Budapest, Hungary

Electrically driven spin resonance (EDSR) is an established tool for controlling semiconductor spin qubits. Here, we theoretically study a frequency-mixing

variant of EDSR, where two driving tones with different drive frequencies are applied, and the resonance condition connects the spin Larmor frequency with the sum of the two drive frequencies. Focusing on flopping-mode operation, we calculate the parameter dependence of the Rabi frequency and the Bloch-Siegert shift. A shared-control spin qubit architecture could benefit from this bichromatic EDSR scheme, as it enables simultaneous single-qubit gates.

TT 27.11 Thu 12:15 H22

Cavity-mediated superconductor-ferromagnet interaction — ANDREAS T. G. JANSSØNN, •HENNING G. HUGDAL, ARNE BRATAAS, and SOL H. JACOBSEN — Center for Quantum Spintronics, Department of Physics, NTNU, Norwegian University of Science and Technology, Trondheim, Norway

TT 28: Correlated Electrons: Theory 1

Time: Thursday 9:30–13:00

Location: H23

TT 28.1 Thu 9:30 H23

General super-exchange Hamiltonians for magnetic and orbital physics in e_g and t_{2g} systems — •XUEJING ZHANG¹, ERIK KOCH^{1,2}, and EVA PAVARINI^{1,2} — ¹Institute for Advanced Simulation, Forschungszentrum Jülich, D-52425 Jülich, Germany — ²JARA High-Performance Computing, 52062, Aachen, Germany
In strongly-correlated transition-metal oxides, spin- and orbital-ordering or spin- and orbital-liquid phenomena are often studied with low-energy super-exchange Hamiltonians, derived from multi-band Hubbard models in highly symmetric cases and in the basis of pseudo-spin operators. This captures the essence of the Kugel-Khomskii[1] super-exchange mechanism. Recently, via an irreducible-tensor operator representation, we derived the orbital super-exchange Hamiltonian for t_{2g}^1 perovskites and successfully used it, in combination with many-body calculations based on dynamical mean-field theory, to explain the orbital physics in these systems. Then, we generalize our method to e_g^n and t_{2g}^n systems at arbitrary integer filling n , including both spin and orbital interactions[2,3]. Here, we identified the t_{2g}^2 perovskite LaVO_3 as a rare case in which orbital-ordering is indeed controlled by the KK super-exchange interaction[4].

[1] K. I. Kugel' and D. I. Khomskii, Zh. Eksp. Teor. Fiz. **64**, 1429 (1973) [Sov. Phys. JETP **37**, 725 (1973)]

[2] X. J. Zhang, E. Koch, E. Pavarini, Phys. Rev. B **102**, 035113 (2020)

[3] X. J. Zhang, E. Koch, E. Pavarini, Phys. Rev. B **105**, 115104 (2022)

[3] X. J. Zhang, E. Koch, and E. Pavarini, Submitted to Phys. Rev. Lett.

TT 28.2 Thu 9:45 H23

Fluctuations analysis of the spin susceptibility: Néel ordering revisited in dynamical mean field theory — •GEORG ROHRINGER¹ and LORENZO DEL RE² — ¹Institute of Theoretical Physic, University of Hamburg, 20355 Hamburg, Germany — ²Department of Physics, Georgetown University, 37th and O Sts., NW, Washington, DC 20057, USA

We revisit the antiferromagnetic (AF) phase diagram of the single-band three-dimensional Hubbard model on a simple cubic lattice studied within the dynamical mean field theory. Although this problem has been investigated extensively in the literature, a comprehensive understanding of the impact of the different one- and, in particular, two-particle local correlation functions of DMFT on the AF transition temperature is still missing. We have, hence, performed a fluctuation analysis of T_N with respect to different local bosonic fluctuations (charge, spin, particle-particle) contained in the two-particle vertex of DMFT. Our results indicate that, beyond weak coupling, the screening of the DMFT vertex by local fluctuations leads to an enhancement of T_N with respect to a random phase approximation (RPA) like calculation where this vertex is replaced by the bare interaction. The overall suppression of T_N in DMFT with respect to RPA is then solely due to the incoherence introduced by the DMFT self-energy in the one-particle Green's functions. This illustrates the Janus-faced role of the local moment formation in the DMFT solution of the Hubbard model, which leads to completely opposite effects in the one- and two-particle correlation functions.

TT 28.3 Thu 10:00 H23

Phase diagram of $SU(N)$ antiferromagnet on a square lattice — •JONAS SCHWAB, FRANCESCO PARISEN TOLDIN, and FAKHER F. ASSAAD — Institut für Theoretische Physik und Astrophysik and Würzburg-Dresden Cluster of Excellence ct.qmat, Universität Würzburg, 97074 Würzburg, Germany

We investigate the ground state phase diagram of an antiferromagnetic, $SU(N)$ -symmetric spin model on a square lattice, where the chosen irreducible representation of the $su(N)$ algebra is described by a square Young tableaux with $N/2$ rows and $2S$ columns. Using approximation-free fermionic quantum Monte Carlo simulations for $S \in \{1/2, 1, 3/2\}$ and even values of N in the range $N \in [2, 20]$, we present a phase diagram for this model. Our results are in line with the seminal work of Read and Sachdev. For any value S , we find Néel order

We present a microscopic theoretical analysis of interactions between a ferromagnet (FM) and superconductor (SC) mediated by photons in a cavity. This facilitates interactions over macroscopic distances, in contrast with extensively researched FM-SC proximity systems, and ensures there is no interfacial suppression of their respective order parameters. The spatial separation between the materials also means the FM and SC may be held at different temperatures, and has potential applications as a bridge in spintronic-superconducting circuitry. Specifically, we deduce the anisotropy field induced across the FM due to the presence of the SC when the system is subjected to a symmetry-breaking external field. Other quantities such as renormalized dispersion relations can also be deduced. The model is a modification and quantum mechanical extension of the principle presented in Jansson et al. PRB 102, 180506(R) (2020).

at small values of N , and disordered valence-bond solid (VBS) states at large N . The degeneracy of the VBS state, 4 for $S = 1/2$ and $3/2$ and 2 for $S = 1$, close to the Néel state follows the lower bound obtained by analyzing monopole singularities in the large- S limit. In contrast in the large- N limit, the VBS ground state shows a four fold degeneracy for all values of S . In order to best image the dimerization patterns, so as to confirm the above, we use a pinning field approach.

TT 28.4 Thu 10:15 H23

Field-tunable Berezinskii-Kosterlitz-Thouless correlations in a quasi-2d spin-1/2 Heisenberg lattice — D. OPPERDEN¹, M.S.J. TEPASKE^{2,3}, F. BÄRTL^{1,4}, M. WEBER³, M.M. TURNBULL⁵, T. LANCASTER⁶, S.J. BLUNDELL⁷, M. BAENITZ⁸, J. WOSNITZA^{1,4}, C.P. LANDEE⁹, R. MOESSNER³, D.J. LUITZ^{2,3}, and •H. KÜHNE¹ — ¹Hochfeld-Magnetlabor Dresden, HZDR — ²Physikalisches Institut, Univ. Bonn — ³MPI PKS, Dresden — ⁴IFMP, TU Dresden — ⁵Carlson School of Chemistry, Clark Univ. — ⁶Durham Univ., Centre for Materials Physics — ⁷Clarendon Laboratory, Univ. of Oxford — ⁸MPI CPFS, Dresden — ⁹Department of Physics, Clark Univ.

We discuss the manifestation of field-induced Berezinskii-Kosterlitz-Thouless (BKT) correlations in the weakly-coupled spin-1/2 Heisenberg layers of the material $[\text{Cu}(\text{pz})_2(2\text{-HOpy})_2](\text{PF}_6)_2$ (CuPOF). Due to the moderate intralayer exchange coupling of $J/k_B = 6.8$ K, laboratory magnetic fields induce a substantial XY anisotropy of the spin correlations. This provides a significant BKT regime, as the tiny interlayer exchange $J'/k_B \approx 1$ mK only induces 3d correlations upon close approach to the BKT transition. We employed NMR and μ^+ SR measurements to probe the spin correlations that determine the critical temperatures of the long-range order and the BKT transition. Further, we performed stochastic series expansion QMC simulations based on the experimentally determined model parameters. Finite-size scaling of the spin stiffness yields an excellent agreement of the critical temperatures between theory and experiment.

Invited Talk

TT 28.5 Thu 10:30 H23

Towards an *ab-initio* theory of Anderson localization for correlated electrons — •LIVIU CHIONCEL — University of Augsburg, Augsburg, Germany

Great progress has been made in recent years towards understanding the properties of disordered electronic systems. This is made possible by recent advances in quantum effective medium methods which include Dynamical Mean-Field Theory and the Coherent Potential Approximation, and their cluster extension, the Dynamical Cluster Approximation. The recently developed typical medium dynamical cluster approximation captures disorder-induced localization and provides an order parameter for the Anderson localized states. We present an overview of various recent applications of the typical medium single-site and dynamical cluster approximation to the Hubbard model, and its combination to realistic systems in the framework of Density Functional Theory.

15 min. break

TT 28.6 Thu 11:15 H23

The crucial influence of side groups on magnetic superexchange - a modification of the Goodenough-Kanamori-rules — DIJANA MILOSAVLJEVIĆ¹, OLEG JANSON², STEFAN-LUDWIG DRECHSLER², and •HELGE ROSNER¹ — ¹Max-Planck-Institut für Chemische Physik fester Stoffe, 01187 Dresden, Germany — ²IFW Dresden, Helmholtzstraße 20, 01069 Dresden, Germany

According to the famous Goodenough-Kanamori-Anderson rules, the key structural feature that determines the magnetic exchange coupling constant for superexchange in magnetic insulators is the magnetic ion-ligand-magnetic ion bond angle. Here, we demonstrate that this angle is not the only factor. An at least equally important influence on the exchange coupling has the presence of the side groups attached to the ligands. Applying density functional calculations and subsequently derived realistic parameters for a multiband model tight-binding model, we provide a quantitative analysis for the example case of edge-sharing

Cu-O chains with bond angles near 90 degrees. We find that a single parameter, the difference in onsite energies of the ligand orbitals parallel and perpendicular to the Cu-O chain, is at least as important as the bond angle for sign and size of the superexchange. This parameter strongly depends on the position of side groups outside the superexchange pathway. For a fixed bond angle, changes of a side group position, only, can cause changes in the superexchange of several hundred Kelvin and thus dramatic changes in the magnetic ground state.

TT 28.7 Thu 11:30 H23

The shared universality of charged black holes and the many many-body SYK model — •JAN LOUW — Institute for Theoretical Physics, Georg-August-Universität Goettingen, Friedrich-Hund-Platz 1, 37077 Goettingen, Germany

We investigate the charged $q/2$ -body interacting Sachdev-Ye-Kitaev (SYK) model in the grand-canonical ensemble. By treating q as a large parameter, we are able to analytically study its phase diagram. By varying the chemical potential or temperature, we find that the system undergoes a phase transition between low and high entropies, in the maximally chaotic regime. A similar transition in entropy is seen in charged AdS black holes transitioning between a large and small event horizon. Approaching zero temperature, we find a first-order chaotic-to-integrable quantum phase transition, where the finite extensive entropy drops to zero. This again has a gravitational analogue—the Hawking-Page (HP) transition between a large black hole and thermal radiation. An analytical study of the critical phenomena associated with the continuous phase transition provides us with two sets of critical exponents. These sets define two separate universality classes, both of which include several charged AdS black hole phase-transitions. Together, these findings indicate a connection between the charged large q SYK model and black holes.

TT 28.8 Thu 11:45 H23

Scrambling and Many-Body Localization in the XXZ-Chain — •NIKLAS BÖLTER and STEFAN KEHREIN — Institut für Theoretische Physik, Universität Göttingen

The tripartite information is an observable-independent measure for scrambling and delocalization of information. Therefore one can expect that the tripartite information is a good observable-independent indicator for distinguishing between many-body localized and delocalized regimes, which we confirm for the XXZ-chain in a random field. Specifically, we find that the tripartite information signal spreads inside a lightcone that only grows logarithmically in time in the many-body localized regime similar to the entanglement entropy. We also find that the tripartite information eventually reaches a plateau with an asymptotic value that is suppressed by strong disorder.

[1] N. Bölter and S. Kehrein, Phys. Rev. B 105, 104202

TT 28.9 Thu 12:00 H23

Nonlinear response theory and three-particle diagrams in strongly correlated systems — •PATRICK KAPPL, FRIEDRICH KRIEN, CLEMENS WATZENBÖCK, and KARSTEN HELD — Institute of Solid State Physics, TU Wien, Austria

We study three-particle correlation functions of the Anderson impurity model by means of quantum Monte Carlo simulations in the hybridization expansion. We analyze the parameter regime in which vertex corrections beyond the bare bubble term become relevant for the three-particle correlator. Such three-particle correlators are hitherto by-and-large terra incognita and become relevant for the next level of diagrammatic extensions of dynamical mean-field theory. We here restrict ourselves to correlators consisting of three densities n and spins $S_{x,y,z}$. These are related to nonlinear response theory and its zero-frequency component to the density-dependence of the electronic compressibility.

TT 28.10 Thu 12:15 H23

Superconductivity in 2D and 3D lattice models of correlated fermions - combining matrix-product states with mean-field theory — GUNNAR BOLLMARK¹, SVENJA MARTEN², •THOMAS KÖHLER¹, LORENZO PIZZINO³, YIQI YANG⁴, JOHANNES-STEPHAN HOFMANN⁵, HAO SHI⁶, SHIWEI ZHANG⁷, SAL-

VATORE R. MANMANA², THIERRY GIAMARCHI³, and ADRIAN KANTIAN^{1,8} — ¹Uppsala University, Sweden — ²Georg-August-Universität Göttingen, Germany — ³University of Geneva, Switzerland — ⁴College of William and Mary, Williamsburg, Virginia, USA — ⁵Weizmann Institute of Science, Rehovot, Israel — ⁶University of Delaware, Newark, USA — ⁷Flatiron Institute, New York, USA — ⁸Heriot-Watt University, Edinburgh, United Kingdom

Correlated electron states are at the root of many important phenomena including unconventional superconductivity (USC), where electron-pairing arises from repulsive interactions. Computing the properties of correlated electrons, such as the critical temperature T_c for the onset of USC, efficiently and unbiased remains a major challenge. Here, we combine matrix-product states (MPS) with static mean field (MF) to provide a solution to this challenge for 2D/3D materials comprised of weakly coupled correlated chains. This framework of Q1D fermions is developed and validated for attractive Hubbard systems and further enhanced via analytical field theory. Finally, we investigate the formation of transient non-equilibrium SC by a real-time evolution of a 3D extended Hubbard system out-of-equilibrium.

TT 28.11 Thu 12:30 H23

Non-local correlations and criticality in the triangular lattice Hubbard model — •MARIO MALCOLMS DE OLIVEIRA¹, JULIAN STOBBE², HENRY MENKE³, MARCEL KLETT¹, GEORG ROHRINGER², and THOMAS SCHÄFER¹ — ¹Max Planck Institute for Solid State Research — ²University of Hamburg — ³University of Erlangen-Nuremberg

We investigate the role of non-local electronic correlations at finite temperatures in the half-filled triangular lattice Hubbard model using the dynamical vertex approximation (DVA), a diagrammatic extension [1] of the dynamical mean-field theory (DMFT). We analyze the impact of (quantum) phase transitions on finite temperature properties at the one- and two-particle level. We discuss the absence of magnetic ordering at finite temperatures due to the fulfilment of the Mermin-Wagner theorem and the (Mott) metal-insulator crossover. In addition we compare the results of this method to the ones obtained by other cutting-edge techniques like DMFT, its real-space cluster extension cellular dynamical mean-field theory (CDMFT) and diagrammatic Monte Carlo (DiagMC) [2].

[1] G. Rohringer, H. Hafermann, A. Toschi, A.A. Katanin, A.E. Antipov, M.I. Katsnelson, A.I. Lichtenstein, A.N. Rubtsov, K. Held, Rev. Mod. Phys. 90, 025003 (2018)

[2] A. Wietek, R. Rossi, F. Šimkovic IV, M. Klett, P. Hansmann, M. Ferrero, E.M. Stoudenmire, T. Schäfer, A. Georges, Phys. Rev. X 11, 041013 (2021)

TT 28.12 Thu 12:45 H23

Non-local correlation and entanglement of ultracold bosons in the two-dimensional Bose-Hubbard lattice at finite temperature — ULLI POHL, •SAYAK RAY, and JOHANN KROHA — Physikalisches Institut, Rheinische Friedrich-Wilhelms-Universität Bonn, Nußallee 12, 53115, Bonn, Germany

The temperature-dependent behavior emerging in the vicinity of the superfluid (SF) to Mott-insulator (MI) transition of interacting bosons in a 2D optical lattice, described by the Bose-Hubbard model is investigated. The equilibrium phase diagram at finite temperature is computed using the cluster mean-field (CMF) theory including a finite-cluster-size-scaling. The SF, MI, and normal fluid (NF) phases are characterized as well as the transition or crossover temperatures between them are estimated by computing physical quantities such as the superfluid fraction, compressibility and sound velocity using the CMF method. It is found that the nonlocal correlations included in a finite cluster, when extrapolated to infinite size, leads to quantitative agreement of the phase boundaries with quantum Monte Carlo results as well as with experiments. Moreover, it is shown that the von Neumann entanglement entropy within a cluster corresponds to the system's entropy density and that it is enhanced near the SF-MI quantum critical point (QCP) and at the SF-NF boundary. The behavior of the transition lines near this QCP, at and away from the particle-hole symmetric point located at the Mott-tip, is also discussed.

[1] U. Pohl, S. Ray, J. Kroha, Ann. Phys. (Berlin) 2100581 (2022)

TT 29: Transport: Poster Session

In case the presenters cannot be present at their posters for the full duration of the poster session, they are kindly requested to leave a note at their poster indicating when they will be available for discussion.

Time: Thursday 15:00–18:00

Location: P1

TT 29.1 Thu 15:00 P1

Relaxation dynamics in two quantum dots coupled to the environment: The role of coupling asymmetry — •LUKAS LITZBA, ERIC KLEINHERBERS, NIKODEM SZPAK, and JÜRGEN KÖNIG — Fakultät für Physik, Universität Duisburg-Essen, Lotharstraße 1, 47057 Duisburg, Germany

We study a strongly interacting two-site Fermi-Hubbard model representing two coupled quantum dots and couple them each with different strengths to Marko-

vian baths. We start with the Born-Redfield equation (without second Markov approximation) and approximate it by the coherent Lindblad master equations [1]. Using this technique we observe that the long-time dynamics of a quantum state, in particular the contribution from the energy coherences, depends strongly on the asymmetry between the bath coupling strengths of the dots. In contrast to the Born-Redfield equation and the coherent Lindblad master equations the popular secular approximation fails to properly describe the interdot

and bath-dot currents in the asymmetric coupling case. To compare the quality of the approximations we use the exact solution in the case of no Coulomb interaction.

[1] E. Kleinherbers, N. Szpak, J. König, R. Schützhold, Phys. Rev. B 101, 125131 (2020)

TT 29.2 Thu 15:00 P1

Manipulating molecular spins with carbon nanotube SQUIDS — •TIM ALTHUON, ALJOSCHA AUER, TINO CUBAYNES, and WOLFGANG WERNSDORFER — Karlsruhe Institut für Technologie (KIT), 76131 Karlsruhe

Single-molecule magnets (SMMs) are promising candidates for spin-qubits due to their small size, cheap and reproducible chemical synthesis in a bottom-up approach and the opportunity to engineer their chemical properties such as the magnetic moment. However, an integration of SMMs with nanoscale diameters into electronic circuits is challenging. A solution to this problem could be to graft these molecules on carbon nanotubes (CNTs) which are comparable to SMMs in the diameter and possess unique sensing properties.

The CNT can be included as a weak-link Josephson junction into a superconducting quantum interference device (SQUID). Such a nano-SQUID is expected to have a large coupling between the magnetic moment of a molecule grafted on the CNT and the flux through the SQUID loop, giving rise to a very simple and precise detection of the spin of a single molecule.

Our CNTs are grown on separate chips with chemical vapor deposition and can then be integrated into prepatterned electronic circuits. For this purpose we use a novel, ultraclean, dry-transfer technique of CNTs where the CNTs are never exposed to air. This contribution will mainly focus on the integration of suspended CNTs into electronic circuits including preliminary results on the characterization of the devices at room and milli-Kelvin temperatures.

TT 29.3 Thu 15:00 P1

A carbon-nanotube nanoelectromechanical system coupled to a single-molecule magnet — •ALJOSCHA AUER, SVENJA MÜLLER, TIM ALTHUON, TINO CUBAYNES, and WOLFGANG WERNSDORFER — Karlsruhe Institut für Technologie, 76131 Karlsruhe

The one-dimensional structure of carbon nanotubes (CNTs) as well as their low weight and high Young's modulus make them an excellent candidate for nanoelectromechanical systems (NEMS). With their mechanical resonance frequency in the hundreds of MHz regime combined with a large quality factor they are suited for high sensitivity experiments. In addition, the conductivity of CNTs can be tuned nicely by applying an electric field tuning the energy levels of charge carriers. For our experiments we want to use a suspended, top-down fabricated carbon nanotube, grown by chemical vapour deposition connecting two electrodes or using a stamping technique where the CNT is grown on a separate chip. Five local gates below the suspended nanotube enable us to manipulate the system by application of a tunable electric field. Furthermore, we want to attach a single-molecule magnet (SMM) to the nanotube by thermal evaporation, therefore creating a system using spin-phonon-coupling to address a single individual spin. The possible measurements in this configuration are manifold, ranging from magnetoresistive effects, spin valves respectively, and double quantum dot transport measurements to electron-phonon coupling measurable in transport measurements in a mechanical resonator.

TT 29.4 Thu 15:00 P1

Investigation of Hall effects in freestanding SrRuO₃ nanomembranes — •STEFAN PETERSEN, ROMAN HARTMANN, ELKE SCHEER, and ANGELO DI BERNARDO — University of Konstanz, Konstanz, Germany

SrRuO₃ (SRO) is one of the most intensively studied ferromagnetic oxides with a Curie temperature of about 150 K. In addition to being ferromagnetic, SRO is also interesting because of its high conductivity at low temperatures, high chemical stability and good lattice matching with other oxides.

Recently, a new technique has been developed to manufacture freestanding nanomembranes of oxide thin films grown on a water-soluble Sr₃Al₂O₆ (SAO) sacrificial layer [1]. In our group, we have recently reproduced this process and been able to obtain freestanding nanomembranes of SRO.

We have investigated the anomalous Hall effect (AHE) and topological hall effect (THE) in SRO nanomembranes as a function of thickness and temperature, using SRO thin films grown on SrTiO₃ substrates as benchmark for comparison. We have also studied the evolution of these effects in SRO nanomembranes under a voltage-driven strain exerted by a piezoelectric substrate in contact with the nanomembrane. Our results are preliminary to the fabrication of devices with electric control of the AHE and THE.

[1] D. Lu et al., Nat. Mater. 15, 1255 (2016)

TT 29.5 Thu 15:00 P1

Curvature control of the superconducting proximity effect in diffusive ferromagnetic nanowires — •TANCREDI SALAMONE¹, HENNING HUGDAL¹, MORTEN AMUNDSEN², and SOL JACOBSEN¹ — ¹QuSpin Center for Quantum Spintronics, NTNU, Trondheim, Norway — ²Nordita, KTH Royal Institute of Technology, Stockholm, Sweden

There is currently great interest in the inclusion of superconducting components in spintronic devices, because they can provide dissipationless currents, greatly enhancing device performances for spin-based data processing. Coupling a conventional s-wave superconductor to a ferromagnet allows, via the proximity effect, to generate superconducting triplet correlations. The generation of triplet correlations can be employed to achieve a superconducting triplet spin-valve effect in superconductor-ferromagnet (SF) hybrid structures, for example by switching the magnetizations of the ferromagnets between parallel and antiparallel configurations in F₁SF₂ and SF₁F₂ trilayers, or in SF bilayers with both Rashba and Dresselhaus spin-orbit coupling. It was recently reported that geometric curvature can control the generation of long ranged triplets [1]. In our most recent work [2], we use this feature to show that the superconducting critical temperature of the hybrid structure can be tuned by varying the curvature of the ferromagnetic wire alone, with no need of another ferromagnet or SOC. Furthermore, we show that the variation of the critical temperature as a function of the curvature can be exploited to obtain a robust, curvature-controlled, superconducting triplet spin-valve effect.

[1] Phys. Rev. B 104, L060505

[2] Phys. Rev. B 105, 134511

TT 29.6 Thu 15:00 P1

Electronic transport through single-molecule junctions of photoswitchable diarylethenes — •VALENTIN BARTH¹, LUKAS HOLZ¹, THOMAS HUHN¹, FRANZ HERBST¹, GAUTAM MITRA¹, CHRISTOPHER WEAVER², SERGI NENEGRI¹, TIM ALBRECHT², and ELKE SCHEER¹ — ¹University of Konstanz, Konstanz, Germany — ²University of Birmingham, Birmingham, UK

Single-molecule junctions represent the conceptually simplest molecular devices. It is important to determine their electronic transport properties. Here we report on the transport characteristics of diarylethene-oligophenylene (DAE-OPE) molecule junctions at room and low temperature [1]. DAE molecules exist in two distinct stable states switched by irradiation of either visible or UV-light. Measurements are executed with the mechanically controllable break junction (MCBJ) method. Connection between the molecule and the gold electrodes is achieved by thiol end groups. The aim of the project is to distinguish the two states by their electrical transport properties. For this purpose, conductance histograms and current-voltage curves are measured separately for both states and compared afterwards. At room temperature, the conductance histograms of the states show small differences. These can be highlighted with the help of dimension reduction methods and neural networks [2]. Molecular vibration modes and thereby the current pathway through the molecule are determined for both states, by Inelastic electron tunneling spectroscopy (IETS).

[1] Sendler et al., Adv. Sci. 2 (2015) 1500017

[2] Albrecht et al., Nanotechnology 28 (2017) 423001

TT 29.7 Thu 15:00 P1

Low-temperature contact engineering for MoS₂ microtubes — •JONATHAN NEUWALD¹, ROBIN T. K. SCHOCK¹, MATTHIAS KRONSEDER¹, WOLFGANG MÖCKEL¹, SIMON REINHARDT¹, LUKA PIRKER², MAJA REMŠKAR², and ANDREAS K. HÜTTEL¹ — ¹Institute for Experimental and Applied Physics, University of Regensburg, 93040 Regensburg, Germany — ²Solid State Physics Department, Institute Jožef Stefan, 1000 Ljubljana, Slovenia

Planar molybdenum disulphide MoS₂, a 2d material similar to graphene, displays a multitude of interesting electronic properties. Nevertheless, only few electronic experiments on MoS₂ nanotubes and microtubes exist. A central reason for this is the difficulty of obtaining stable and transparent Ohmic contacts to transition metal dichalcogenides in general. At the metal-semiconductor interface, the Fermi level in MoS₂ is typically strongly pinned close to the conduction band edge. To avoid a high contact resistance from the formation of a Schottky-barrier, low-work function metals have to be chosen. However, these etch into the MoS₂ structure and therefore damage the tube. Following a recent publication,¹ we use the half-metal bismuth as a contact material, which disables the Fermi level pinning. We optimize the bismuth layer thickness to lower contact resistance and therefore improve the controllability and clarity of transport effects at millikelvin temperatures.

[1] P.C. Shen et al., Nature 593, 211 (2021)

TT 29.8 Thu 15:00 P1

Andreev reflection in gated bilayer graphene — •PANCH RAM¹, DETLEF BECKMANN², ROMAIN DANNEAU², and WOLFGANG BELZIG¹ — ¹Fachbereich Physik, Universität Konstanz, D-78457 Konstanz, Germany — ²Institute for Quantum Materials and Technologies, Karlsruhe Institute of Technology, D-76021 Karlsruhe, Germany

In this poster, we will present our recent theoretical study of the NS junction Andreev reflection and differential conductance on the bilayer graphene including different (equal and opposite) onsite potential for each monolayer graphene. We employ the Dirac-Bogoliubov de Gennes (DBdG) equation for the low-energy bilayer graphene Hamiltonian and calculate the Andreev reflection (retroreflection as well as specular) and differential conductance (within the Blonder-Tinkham-Klapwijk formalism [1-2]) for the junction in two different parame-

ters limits: (i) interlayer coupling is larger energy scale (ii) superconducting-side doping potential is larger energy scale [3-5]. We obtain the Andreev retro-reflection (specular reflection) below (above) the normal-side Fermi energy when the bias voltage is less than the superconducting gap. We also observe that both retro and specular Andreev reflections are strongly modified by the gate field.

- [1] A. F. Andreev, Sov. Phys. JETP 19, 1228 (1964)
 [2] G. E. Blonder et. al, Phys. Rev. B 25, 4515 (1984)
 [3] C. W. J. Beenakker, Phys. Rev. Lett. 97, 067007 (2006)
 [4] T. Ludwig, Phys. Rev. B 75, 195322 (2007)
 [5] D. K. Efetov and K. B. Efetov, Phys. Rev. B 94, 075403 (2016)

TT 29.9 Thu 15:00 P1

Coulomb blockade effects in minimally twisted bilayer graphene — •PATRICK WITTIG¹, FERNANDO DOMINGUEZ¹, CRISTOPHE DE BEULE², and PATRIK RECHER^{1,3} — ¹Institute for Mathematical Physics, TU Braunschweig, 38106 Braunschweig, Germany — ²Department of Physics and Materials Science, University of Luxembourg, L-1511 Luxembourg — ³Laboratory of Emerging Nanometrology, 38106 Braunschweig, Germany

In the presence of a finite interlayer electric field, minimally twisted bilayer graphene displays a triangular network of chiral valley Hall states that propagate along the AB/BA interfaces and scatter at the metallic AA regions. Previous studies model the chiral network using a phenomenological scattering matrix approach based entirely on the symmetries of the system. So far, the physics of the metallic AA scattering regions has been disregarded, and indeed, the finite size of the AA regions (order of nm) can give rise to similar physics as quantum dots: a discrete energy spectrum and also interacting effects such as Coulomb blockade physics. In our contribution, we include these effects and study the resulting network of chiral modes and quantum dots through the energy spectrum and magneto-conductance calculations.

TT 29.10 Thu 15:00 P1

Interaction effects in graphene/2D polymer heterostructures — •FRANCESCA FALORSI¹, KEJUN LIU², MIROSLAV POLOZIJ², CHRISTIAN ECKEL¹, THOMAS HEINE², XINLIANG FENG², RENHAO DONG², and THOMAS WEITZ¹ — ¹Physical Institute -Georg-August-University, Friedrich-Hund-Platz 1 37077 Göttingen Göttingen — ²Faculty of chemistry and food chemistry, Technische Universität Dresden, Mommsenstraße 4 01069 Dresden

This work explores the interlayer interaction effects of van-der-Walls heterostructures (HS) formed by graphene and a new class of two-dimensional polymers bonded by covalent bonds (C2DPs). These materials can be synthesized with multiple compositions and topology and therefore offer large tunability of their electronic properties. Via density functional theory calculations, it was possible to predict that coupling of different C2DPs with monolayer graphene should generate new interesting physical phenomena, including band flattening and trivial and non-trivial bandgap opening. The first system studied is the HSs formed by a mechanically exfoliated graphene on top of a C2DP that comprises metal-free porphyrin and perylene units linked by imide bonds. Different techniques are used for the first characterization of the structure: Raman, KPFM, SNOM, and ARPES. These different measurement techniques indicate the existence of interaction effects in the HSs. Electrical measurements on the HSs were also performed and showed that the polymer highly p-dopes the graphene.

TT 29.11 Thu 15:00 P1

Inductive coupling schemes in nano-electromechanics — •LUKAS NIEKAMP^{1,2}, THOMAS LUSCHMANN^{1,2,3}, PHILIP SCHMIDT^{1,2}, FRANK DEPPE^{1,2,3}, ACHIM MARX¹, RUDOLF GROSS^{1,2,3}, and HANS HUEBL^{1,2,3} — ¹Walther-Meißner-Institut, Bayerische Akademie der Wissenschaften, 85748 Garching, Germany — ²Physik-Department, Technische Universität München, 85748 Garching, Germany — ³Munich Center for Quantum Science and Technology, 80799 Munich

Nano-electromechanics studies the opto-mechanical interaction between microwave frequency resonators and mechanical components in the nanometer regime. Recently, the concept of inductive coupling has been demonstrated, allowing for the modulation of the resonator frequency by the mechanical displacement [1, 2]. This coupling scheme results in higher vacuum opto-mechanical coupling rates compared to previous capacitive coupling schemes. Therefore, devices based on inductive coupling are considered as potential pathway for realizing vacuum strong-coupling. This regime allows to harness the full nonlinearity of the optomechanical interaction offering opportunities like the generation of mechanical quantum states. The device presented here consists of a flux-tunable dc-SQUID with mechanically compliant strings integrated into a microwave resonator. The mechanical displacement of the strings modulates the external flux and hence the microwave resonator's frequency. Here, we present recent experiments on the path to strong photon-phonon interaction.

- [1] Rodrigues, Bothner, Steele, Nat. Commun. 10, 5359 (2019)
 [2] Schmidt et al., Commun. Phys. 3, 233 (2020)

TT 29.12 Thu 15:00 P1

Full counting statistics in periodically driven systems — •JOHANN ZÖLLNER, ERIC KLEINHERBERS, and JÜRGEN KÖNIG — Theoretische Physik, Universität Duisburg-Essen and CENIDE, Lotharstr. 1, 47048 Duisburg

By calculating the full counting statistics of tunnelling electrons one can obtain information about quantum dot systems. We focus on the factorial cumulants [1] of the full counting statistics in periodically driven systems, which can be calculated using Floquet theory [2]. Higher-order factorial cumulants show signatures that can not be observed in the tunnelling current. To obtain analytical expressions we use the adiabatic approximation for small frequencies or the Magnus expansion for large frequencies. For the adiabatic limit we observe frequency-doubling in all factorial cumulants.

- [1] P. Stegmann et al., Phys. Rev. B 92, 155413 (2015)
 [2] E. Potanina et al., Phys. Rev. B 99, 035437 (2019)

TT 29.13 Thu 15:00 P1

Light emission in ΔT -driven mesoscopic conductors — •MATTHIAS HÜBLER and WOLFGANG BELZIG — University Konstanz

The scattering approach paves the way for the description of electron transport and current fluctuations in mesoscopic conductors. If fluctuations are coupled to an electromagnetic field, then they are related to the rate at which the field transfers energy to or receives energy from the conductor. The non-symmetrized current-current correlator characterizes the emission and absorption spectrum. Recent interest is concerned with ΔT noise, which is the non-equilibrium noise caused by a temperature difference between the terminals. Here we generalize the notion of ΔT noise to the non-symmetrized current-current correlator at finite frequencies. The spectrum is investigated for energy-independent scattering and for a resonant level as an example of energy-dependent scattering. We find that a temperature difference ΔT leads to a partially negative ΔT noise spectrum. This is a consequence of temperature broadening in combination with a frequency shift of the involved Fermi distributions. In the case of energy-independent scattering, the lowest order is a quadratic $\propto (\Delta T)^2$ correction of the thermal-like noise spectrum. For the resonance, there arises an additional contribution to the ΔT noise spectrum that is $\propto \Delta T$ at the lowest order.

TT 29.14 Thu 15:00 P1

Symmetry-protected Bose-Einstein condensation of interacting hardcore bosons — •REJA WILKE¹, THOMAS KÖHLER², FELIX PALM¹, and SEBASTIAN PAECKEL¹ — ¹Department of Physics, Arnold Sommerfeld Center for Theoretical Physics, University of Munich, Germany — ²Department of Physics and Astronomy, Uppsala University, Sweden

We introduce a mechanism stabilizing a one-dimensional quantum many-body phase, characterized by a certain wave vector via the protection of an emergent Z2 symmetry. We illustrate this mechanism by constructing the solution of the full quantum many-body problem of hardcore bosons on a wheel geometry, which are known to form a Bose-Einstein condensate. The robustness of the condensate is shown numerically by adding nearest-neighbor interactions to the wheel Hamiltonian. We discuss further applications such as geometrically inducing finite-momentum condensates.

TT 29.15 Thu 15:00 P1

Low temperature photoluminescence investigation of light-induced degradation in boron doped CZ-silicon — •KATHARINA PEH¹, KEVIN LAUER^{1,2}, AARON FLÖTTO¹, DIRK SCHULZE¹, and STEFAN KRISCHOK¹ — ¹TU Ilmenau, Institut für Physik und Institut für Mikro- und Nanotechnologien, Ilmenau, Germany — ²CIS Forschungsinstitut für Mikrosensorik GmbH, Konrad-Zuse-Str. 14, 99099 Erfurt, Germany

Light-induced degradation (LID) in boron doped Czochralski grown (CZ) silicon is a severe problem for silicon devices such as solar cells or radiation detectors. In this contribution boron doped CZ silicon is investigated by low temperature photoluminescence (LTPL) spectroscopy. As already demonstrated on indium p-doped silicon samples, we suspect an AsI-Sii defect also in boron p-doped silicon samples [1]. To find the defect in connection with an additional LID PL peak which was also published by Vaqueiro-Contreras et al. [2], we carried out numerous measurements on boron-doped samples with the help of LTPL at 10 K.

- [1] K. Lauer, C. Möller, D. Schulze, C. Ahrens, AIP Advances 5, 017101 (2015)
 [2] M. Vaqueiro-Contreras, V.P. Markevich, J. Coutinho, P. Santos, I.F. Crowe, M.P. Halsall, I. Hawkins, S.B. Lastovskii, L.I. Murin, A.R. Peaker, J. Appl. Phys. 125, 185704 (2019)

TT 29.16 Thu 15:00 P1

Design and construction of low temperature probe for transport measurement — •REZA FIROUZMANDI, VILMOS KOCIS, PABLO PEDRAZZINI, TINO SCHREINER, DANNY BAUMANN, and BERND BÜCHNER — Leibniz Institute for Solid State and Materials Research (IFW), 01069 Dresden, Germany

Electrical and thermal transport experiments are fundamental tools of basic research not only because of their potential to reveal new phenomena in condensed matter physics but also to discover novel applications. Here we report on

our newly constructed, highly versatile, custom-built, low-temperature transport probes, which will allow us to perform high-precision measurements of electrical and thermal transport properties in a wide series of materials. The probes will allow measurements in the temperature range between 5K and 300K, under applied magnetic fields up to 16T, as well as high electric voltages up to 500V. The probes will be used in the investigation of novel quantum materials and multiferroics.

TT 29.17 Thu 15:00 P1

Lab::Measurement - measurement control with Perl 5 — MIA SCHAMBECK, ERIK FABRIZZI, FABIAN WEINELT, SIMON REINHARDT, and •ANDREAS K. HÜTTEL — Institute for Experimental and Applied Physics, Universität Regensburg, Regensburg, Germany

Lab::Measurement is a collection of object-oriented Perl 5 modules providing control of test and measurement devices. It allows for quickly setting up complex tasks with diverse hardware. Instruments can be connected via GPIB (IEEE 488.2), USB or VXI-11 / raw network sockets on Ethernet. Internally, third-party backends as, e.g., Linux-GPIB, the NI-VISA library, or Zurich Instruments' LabOne API are used, in addition to lightweight drivers for USB and TCP/IP-based protocols. The wide range of supported backends enables cross-platform portability of measurement scripts between Linux and Windows machines. Based on roles within Moose that provide communication standards such as SCPI, dedicated instrument driver classes take care of internal details. A high-level sweep layer allows for fast and flexible creation of nested measure-

ment loops, where, e.g., several input variables are varied and data is logged into a customizable folder structure. Features include live plotting or obtaining at-tested timestamps for measurement data.

Lab::Measurement is free software and available at <https://www.labmeasurement.com>.
— Reference: S. Reinhardt *et al.*, *Comp. Phys. Comm.* **234**, 216 (2019)

TT 29.18 Thu 15:00 P1

Theory of difference frequency quantum oscillations — •VALENTIN LEEB¹ and JOHANNES KNOLLE^{1,2,3} — ¹Department of Physics TQM, Technische Universität München, James-Frank-Straße 1, D-85748 Garching, Germany — ²Munich Center for Quantum Science and Technology (MCQST), 80799 Munich, Germany — ³Blackett Laboratory, Imperial College London, London SW7 2AZ, United Kingdom

Quantum oscillations (QO) describe the periodic variation of physical observables as a function of inverse magnetic field in metals. The Onsager relation connects the basic QO frequencies with the extremal areas of closed Fermi surface pockets, and the theory of magnetic breakdown explains the observation of sums of QO frequencies at high magnetic fields. Here we develop a quantitative theory of *difference frequency* QOs in metals with multiple Fermi pockets with parabolic or linearly dispersing excitations. We show that a non-linear interband coupling, e.g. in the form of interband impurity scattering, can give rise to otherwise forbidden QO frequencies which can persist to much higher temperatures compared to the basis frequencies. We discuss the experimental implications of our findings, for example, for materials with multifold fermion excitations.

TT 30: Superconductivity: Poster Session

By tradition the poster sessions in the Low Temperature Physics Division are long (3-4 hours). Since temporal overlap with interesting oral sessions cannot be completely avoided, we suggest the poster presenters to leave a note at their posters indicating when they would be available for discussion.

Time: Thursday 15:00–18:00

Location: P1

TT 30.1 Thu 15:00 P1

Optimization of single-crystal growth of Fe(Se,S) — •MAIK GOLOMBIEWSKI, TESLIN ROSE THOMAS, N. S. SANGEETHA, ANDREAS KREYSSIG, and ANNA E. BÖHMER — Lehrstuhl für Experimentalphysik IV, Fakultät für Physik und Astronomie, Ruhr-Universität Bochum, Universitätsstraße 150, 44801 Bochum
The iron-based superconductor FeSe and its substitution series Fe(Se,S) have been studied intensively for over a decade. Large (mm-sized) homogeneous single crystals are highly desirable for the accurate characterization of this material. An effective technique to grow Fe(Se,S) single crystals is chemical vapor transport with Cl-salts. However, the sulfur substitution makes the growth of large single crystals harder the higher the substitution percentage is.

We examine which parameters have an influence on the size and homogeneity of our Fe(Se,S) single crystals, namely furnace tilt, quartz ampoule dimensions and form, starting material preparation and temperature gradient. The composition of the single crystals is analyzed with a scanning electron microscope and properties are characterized by resistance measurements as well as x-ray diffraction experiments.

We find that we can consistently grow single crystals with masses ranging from 3 mg to more than 10 mg, depending on S-content. Other types of chemical substitution are explored.

TT 30.2 Thu 15:00 P1

Magnetic order in transition-metal doped CaKFe₄As₄ and the interplay with superconductivity — •ANDREAS KREYSSIG — Institute for Experimental Physics 4, Ruhr-Universität Bochum, 44801 Bochum, Germany — Ames Laboratory, U.S. DOE, and Department of Physics and Astronomy, Iowa State University, Ames, Iowa 50011, USA

CaKFe₄As₄ is an iron arsenide superconductor in which partial substitution of Fe by a transition metal shifts the ground state from superconducting to antiferromagnetically ordered. The magnetic structure is a hedgehog spin-vortex crystal arrangement within the Fe planes. This magnetic order is different from the stripe-type spin density wave observed in other iron arsenide superconductor, however, related to the same entangled propagation vectors based on Fermi-surface nesting. In this presentation the determination of the magnetic order will be reviewed and the interplay of the magnetism with superconductivity will be discussed in detail.

This work was supported by the U. S. DOE, BES, DMSE, under Contract DE-AC02-07CH11358. This research used resources at HFIR, a U. S. DOE Office of Science User Facility operated by the Oak Ridge National Laboratory.

TT 30.3 Thu 15:00 P1

Feedback of non-local d_{xy} nematicity on the magnetic anisotropy in FeSe — •STEFFEN BÖTZEL and ILYA EREMIN — Institut für theoretische Physik III, Ruhr-Universität Bochum, Bochum, Germany

Details of the nematic state in FeSe and its connection to superconductivity are still a matter of debate. We analyze theoretically the magnetic anisotropy in this state by computing the spin and the orbital susceptibilities from a microscopic multi-orbital model. In particular, we consider both the xz/yz and the recently proposed non-local xy nematic ordering. The latter is believed to have a significant impact on the bandstructure and to force a Lifshitz transition. Its inclusion could play a crucial role in reproducing the experimentally measured temperature dependence of the magnetic anisotropy. This provides a direct fingerprint of the different nematic scenarios on the magnetic properties of FeSe.

TT 30.4 Thu 15:00 P1

Microscopic theory of the multi-orbital FFLO phase in the iron-based superconductors — •LUKA JIBUTI and ILYA EREMIN — Institute für Theoretische Physik III, Ruhr-Universität Bochum, D-44801 Bochum, Deutschland

We study the superconducting Frude-Ferrel-Larnik-Ovchinnikov (FFLO) phase, a superconducting phase, where Cooper pairs having non-zero center-of-mass momentum \vec{q} , in iron-based superconductors. We develop a microscopic theory model considering two Γ -centered hole pockets created by xz and yz orbitals. We write the low energy effective Hamiltonian of the form $\hat{H} = \hat{H}_0 + \hat{H}_{int}$, where the first term includes the kinetic term, the \vec{k} -independent spin orbit coupling and the Zeeman field. We introduce the superconducting pairing between fermions in xz and yz orbitals and we restrict ourselves with the interactions which lead to the inter-band pairing of Cooper pairs. Writing the system Hamiltonian initially in orbital basis allows us to observe the changes of the orbital weights at the Fermi energy when making the transition from Normal to FFLO phase and pinpoint the direction and value of the center-of-mass momentum \vec{q} that connects particles within the same orbital. From the mean field calculations for magnetic field just above the Pauli limit and for temperatures close to absolute zero, we are able to observe that $\pm\vec{q}$ vectors connect particles within yz and xz orbitals respectively. We also observe that \vec{q} is highly dependent on the magnetic field and temperature, and the increase of the SOC constant destroys the FFLO phase.

TT 30.5 Thu 15:00 P1

In search of the superconducting symmetries of CeRh₂As₂ — •FABIAN JAKUBCZYK^{1,2}, JULIA M. LINK^{1,2}, and CARSTEN TIMM^{1,2} — ¹Institute of Theoretical Physics, Technische Universität Dresden, 01062 Dresden, Germany — ²Würzburg-Dresden Cluster of Excellence ct.qmat, Technische Universität Dresden, 01062 Dresden, Germany

Multiphase unconventional superconductivity is a rare phenomenon, which has recently been discovered in the heavy-fermion compound CeRh₂As₂. Here, the transition between two distinct superconducting phases occurs as a function of magnetic field applied along the c axis. At $\mu_0 H^* \approx 4$ T the superconductor changes from a low-field to a high-field state with a large critical field of

$\mu_0 H_{c2} = 14$ T. However, for in-plane fields only the low-field phase appears, with $\mu_0 H_{c2} = 2$ T. Furthermore, at $T_0 \approx 0.4$ K a transition to a suggested quadrupole-density-wave state was reported, whilst the low-field superconducting state is reached at $T_c = 0.26$ K. Intriguingly, this quadrupole-density-wave state seems to be suppressed by a c axis field of about H^* , such that the low-field phase lies within it, whereas the high-field state does not. It seems reasonable to assume that the change of superconducting properties might be triggered by the disappearing density-wave state. In order to analyze this and other possible scenarios, we first conduct a symmetry analysis of the locally noncentrosymmetric CeRh₂As₂. Moreover, we construct a Landau-type energy functional including the superconducting and density-wave order parameters, as well as the applied magnetic field. From this we can give a statement about the potential symmetries of the superconducting phases.

TT 30.6 Thu 15:00 P1

Ising superconductors: the signatures of triplet pairings in the density of states and vanishing of the "mirage" gap — •SOURABH PATIL¹, GAOMIN TANG², and WOLFGANG BELZIG¹ — ¹Universität Konstanz, Konstanz, Germany — ²University of Basel, Basel, Switzerland

The conventional 2D superconductors are governed by the critical in-plane magnetic field above which the superconductivity is destroyed. Monolayer transition-metal dichalcogenides lack inversion symmetry and along with a strong spin-orbit coupling, lead to valley-dependent Zeeman-like spin splitting. This is the Ising spin-orbit coupling (ISOC) which then lifts the degeneracy of the two valleys and enhances the in-plane critical magnetic field. The finite energy pairings are thus obtained in such systems. The main superconducting gap-like feature shifted to finite energy is observed and termed a mirage gap.

The triplet pairings are introduced by the applied field. The equal-spin triplet pairing is always coupled to the singlet pairing, reflected in the self-consistent equations. Importantly, as the applied field is increased, we observe that the mirage gap closes (vanishes) and reopens. We obtain a phase diagram for such vanishing of the mirage gap in the 3D parameter space of the applied field, temperature, and the critical triplet temperature, for a fixed ISOC. The role of topology in such a mirage gap closing and any observable physical effects on the superconductivity would be our topic of study.

- [1] G. Tang et. al., Phys. Rev. Lett. 126, 237001 (2021)
 [2] M. Kuzmanović et. al., arXiv:2104.00328 (2021)

TT 30.7 Thu 15:00 P1

Time-reversal symmetry breaking in the superconducting state of ScS — •ARUSHI ARUSHI^{1,2}, ROSHAN KUMAR KUSHWAHA¹, DEEPAK SINGH³, ADRIAN HILLIER³, MATHIAS S SCHEURER⁴, and RAVI PRAKASH SINGH¹ — ¹Indian Institute of Science Education and Research Bhopal, Bhopal, India — ²Max Planck Institute for Chemical Physics of Solids, Dresden, Germany — ³ISIS Facility, STFC Rutherford Appleton Laboratory, Didcot, United Kingdom — ⁴Institute for Theoretical Physics, University of Innsbruck, Innsbruck, Austria

The study of unconventional superconductors, which go beyond the BCS theory, is a crucial pillar of modern condensed-matter research and it is driven by the potential of these superconductors for applications and by fundamental scientific question, such as understanding their pairing mechanism. For the latter, time reversal-symmetry-breaking superconductivity might be particularly interesting since it is rare in nature and the underlying pairing mechanism must involve more than the conventional electron-phonon coupling. In this regard, we studied the superconducting state of ScS(rocksalt structure) using macroscopic and microscopic measurements such as muon spin rotation/relaxation(μ SR). All the performed measurements confirmed the bulk superconductivity at 5.1(1) K. Specific heat together with transverse-field μ SR measurements indicate a full gap, while our zero-field μ SR study reveals the presence of spontaneous static or quasi-static magnetic fields emerging when entering the superconducting state. We discuss various theoretical possibilities of pairing mechanisms, hint towards an unconventional superconducting state in ScS.

TT 30.8 Thu 15:00 P1

Topological phase transition away from the Fermi surface in multiband superconductors — •MASOUD BAHARI¹, SONG-BO ZHANG², CHANG-AN LI¹, CARSTEN TIMM³, and BJÖRN TRAUZETTEL¹ — ¹Institute for Theoretical Physics and Astrophysics, University of Würzburg, D-97074 Würzburg, Germany — ²Department of Physics, University of Zurich, Winterthurerstrasse 190, 8057, Zurich, Switzerland — ³Institute of Theoretical Physics, Technische Universität Dresden, 01062 Dresden, Germany

We demonstrate theoretically that odd-parity multiband superconductors with inversion symmetry host dispersive topological surface states induced solely by interband pairing away from the Fermi surface. The normal state requires to have at least a pair of energy bands with different effective masses. In this regard, spin-orbit coupling is a key ingredient. The topological phase transition occurs between electrons with different quantum numbers at finite excitation energies. Such phase transition happens at direction where the inter- and intra-band electron pairings are finite and vanishing at the same time. To capture the underlying physics, we develop a generic theory in the interband representation

of Bogoliubov-de Gennes Hamiltonian. We apply our theory to $j=3/2$ systems and we discuss the pairing channels hosting such surface states.

TT 30.9 Thu 15:00 P1

Majorana flat bands at structured surfaces of nodal noncentrosymmetric superconductors — •CLARA JOHANNA LAPP and CARSTEN TIMM — Institute of Theoretical Physics, Technische Universität Dresden, 01062 Dresden, Germany
 Surfaces of nodal noncentrosymmetric superconductors can host flat bands of Majorana modes, which provide a promising platform for quantum computation if one can find methods for manipulating localized Majorana wave packets. We study the fate of such flat bands when part of the surface is subjected to an exchange field induced by a ferromagnetic insulator. Exact diagonalization is used to find the eigenstates and eigenenergies of the Bogoliubov-de Gennes Hamiltonian of a model system, for which an exchange field is applied along a strip on the surface of a slab. Moreover, we discuss a setup with a small exchange field applied to the previously field-free strip with the goal of introducing a linear dispersion. By switching this dispersion on and off, a wave packet could be moved in a certain direction. We find that in our model system, a linear dispersion can indeed be achieved. The qualitative features of this dispersion can be predicted from the momentum-dependent spin polarization of the field-free surface.

TT 30.10 Thu 15:00 P1

Piezoelectric control of the electrical field-effect in superconductors — •LEON RUF, SARA KHORSHIDIAN, SOHAILA NOBY, JENNIFER KOCH, ELKE SCHEER, and ANGELO DI BERNARDO — Department of Physics, University of Konstanz, Konstanz, Germany

Superconducting (sc) transistors are promising building blocks for future superconductors by virtue of their low energy consumption. For real applications this requires devices with Complementary metal-oxide-semiconductor (CMOS) compatibility, high switching speed and high scalability. Some realizations of superconductor/semiconductor hybrid systems, such as Nanocryotrons (nTrons) [1] or thermal driven sc-nanowires (hTron) [2] have already been put forward. An alternative promising architecture are gate-controlled sc devices. Reversible switching via gate-controlled sc-transistors (EF-Trons) has been independently seen for various BCS superconductors, such as Ti [3] and V [4]. Still the physical effect of the EF-Trons is not fully understood and is under debate [5]. By coupling epitaxial piezo-/ferroelectrics to the EF-Trons, we investigate the role of strain and amplification of the electric field through these materials on the switching behavior. We present first results of the growth of epitaxial piezo-/ferroelectrics and characterization of EF-Trons coupled with piezo-/ferroelectrics.

- [1] A. N. McCaughan et al., Nano Lett. 14, 5748 (2014)
 [2] A. N. McCaughan et al., Nat. Electron. 2, 451 (2019)
 [3] G. De Simoni et al., Nat. Nanotechnol. 13, 802 (2018)
 [4] F. Paolucci et al., AVS Quantum Sci. 1, 016501 (2019)
 [5] I. Golokolenov et al., Nat. Commun. 12, 2747 (2021)

TT 30.11 Thu 15:00 P1

Gate effect on superconducting metal and metal oxide-based nanodevices — •SOHAILA MOHAMMED, SARA KHORSHIDIAN, ANGELO DI BERNARDO, and ELKE SCHEER — Physics Department, University of Konstanz

Quantum devices based on superconducting materials provide various technological applications, such as e.g. current limiters, electronic filters, routers, digital receivers, and photon detectors. The recent discovery of the reversible modulation of the superconducting critical current (I_c) in nanowires and Dayem bridges under the application of a gate voltage has raised a lot of interest for the possible application of this phenomenon towards the realization of superconducting logic devices. The threshold voltages necessary for the full suppression of I_c , however, remain high and correspond to an electrostatic field of ~ 4 MV/cm. Also, the physical origin of the effect remains controversial. To better understand the mechanism responsible for the suppression of I_c and to determine the physical parameters that can be useful to reduce the high electrostatic fields currently needed for the switching, we have performed a systematic investigation of gate-controlled superconducting devices made of different metal and metal-oxide superconductor materials. We report on our findings and discuss the physical parameters relevant to assess the performance of gate-controlled superconducting devices including their maximum operational temperature, kinetic inductance, leakage currents and switching voltages.

TT 30.12 Thu 15:00 P1

Gate-voltage mediated supercurrent suppression in a superconducting nano-bridge — •SUBRATA CHAKRABORTY, DANILO NIKOLIC, and WOLFGANG BELZIG — Fachbereich Physik, Universität Konstanz, D-78467 Konstanz, Germany

Voltage-gated supercurrent suppression in a superconducting nano-bridge is a hot topic for research in present days. Recent experiments on this effect demonstrate a sudden supercurrent suppression in the bridge with high gate-voltage [1-6]. The microscopic understanding of this is not settled till now. According to the experimental researches, there are three distinct tentative mechanisms, which could be responsible for this event. These mechanisms suggest that at high gate voltage there could be either a direct surface-pair breaking-induced phase

transition, superconductivity suppression with induced nonequilibrium phonon distribution due to Joule heating in the gate or supercurrent suppression due to nonequilibrium electronic quasiparticles via a direct small leakage current. In our work, we theoretically investigate the role of gate-voltage induced surface-pair breaking on the supercurrent suppression of superconducting nano-bridge. We speculate this work would present some generic theoretical predictions of this effect allowing to further test it experimentally.

- [1] M. Rocci *et al.*, *ACS Nano*, **14**, 12621 (2020)
 [2] I. Golokolenov *et al.*, *Nat. Commun.*, **12**, 2747 (2021)
 [3] L.D. Alegria *et al.*, *Nat. Nanotechnol.*, **16**, 404 (2021)

TT 30.13 Thu 15:00 P1

Tunable superconducting single electron transistors: from weak to strong-coupling regime — •OLIVER IRTENKAUF¹, LAURA SOBRAL-REY¹, DAVID OHNMACHT¹, WOLFGANG BELZIG¹, JENS SIEWERT², and ELKE SCHEER¹ — ¹Univ. Konstanz — ²Univ. del Pais Basque, Bilbao, Spain

An island coupled to two leads and a gate forms a single electron transistor (SET) that shows Coulomb blockade (CB). All-superconducting SETs have shown to enable a multitude of possible charge transport processes, not all of them are well understood [1], in particular in the strong-coupling regime [2]. The conceptually simpler SSN-SET reduces the number of possible processes. We study a device consisting of a S island coupled to a N lead via an oxide tunnel barrier, and to a S lead with a mechanically controlled break junction (MCBJ). Via the MCBJ, different coupling regimes can be studied from a tunnel contact to a point contact [2]. For weak coupling, our experimental findings in the N state can be understood in terms of the Orthodox Theory of CB [3,4]. For stronger coupling, we observe Andreev and Josephson transport as well as, in the N state, a renormalization of the charging energy [5,6]. We describe our experimental results in the S state with simulations based on a generalized master equation approach [7].

- [1] J.M. Hergenrother *et al.*, *PRL* **72**, 1742 (1994)
 [2] T. Lorenz *et al.*, *JLTP* **191**, 301 (2017)
 [3] D. V. Averin, K. K. Likharev, *JLTP* **62**, 345 (1986)
 [4] H. Grabert, M. H. Devoret, *NATO Sci. Ser. B*, **294** (1992)
 [5] P. Joyez *et al.*, *PRL* **79**, 1349 (1997)
 [6] S. Jezouin *et al.*, *Nature* **536**, 58 (2016)
 [7] J. Siewert, G. Schön, *PRB* **54**, 7421 (1996)

TT 30.14 Thu 15:00 P1

Interplay between charging effects and superconducting transport in a tunable SET — •DAVID CHRISTIAN OHNMACHT¹, LAURA SOBRAL REY¹, JENS SIEWERT², WOLFGANG BELZIG¹, and ELKE SCHEER¹ — ¹Universität Konstanz, Konstanz, Deutschland — ²University of the Basque Country, Bilbao, Spain

All-superconducting single electron transistors (SSS-SETs) have shown to enable a multitude of possible charge transport processes which are not well understood, in particular in the strong-coupling regime [1]. To disentangle these processes, the conceptually simpler (SSN)-SET, which has never been investigated experimentally before is considered [2]. Electron tunneling, Cooper pair tunneling and (multiple) Andreev reflection ((M)AR) are possible in the S-S mechanically controlled break junction (MCBJ) which can be adjusted to cover all coupling regimes: from a tunnel contact to a point contact with a small number of highly transmissive transport channels. The experimental data is compared to theoretical results obtained by using a master equation approach, including the rates of different transport mechanisms [3]. In order to account for MAR, we include the rates for the individual processes which are obtained from the theory of full counting statistics into the master equation framework [4]. The rates for MAR are computed using transmission probabilities according to the experimental data taking into account the presence of multiple transport channels. The limits of this master equation approach for a SSN-SET with a MCBJ are discussed in detail. Finally, it is shown that the charging energy decreases as the coupling of the MCBJ increases.

TT 30.15 Thu 15:00 P1

Preparation of Nb/MnSi heterostructures — •JULIUS GREFE¹, RODRIGO DE VASCONCELLOS LOURENÇO², MARKUS ETZKORN^{2,3}, STEFAN SÜLLOW¹, and DIRK MENZEL^{1,3} — ¹IPKM, TU Braunschweig, Germany — ²IAP, TU Braunschweig, Germany — ³LENA, TU Braunschweig, Germany

Motivated from theoretical predictions [1], the preparation of Nb/MnSi heterostructures, which are candidates for the usage as superconducting spin valves, is introduced. The substrates are obtained by cutting oriented Triarc-Czochralski grown MnSi single crystals into thin disc-shaped wafers. The surfaces of these substrates are prepared by various polishing steps, wet chemical etching, Ar sputtering and thermal annealing. After these processes the surfaces have been investigated by AFM and TEM and show surface roughnesses in the order of 1 nm. In order to investigate proximity effects between the chiral magnet MnSi and a superconductor we have deposited onto the substrates thin Nb films using molecular beam epitaxy. These heterostructures have been investigated in terms of magnetoresistivity measurements.

- [1] N. G. Pugach *et al.*, *Appl. Phys. Lett.* **111**, 162601 (2017)

TT 30.16 Thu 15:00 P1

Orientation-dependent magnetoresistance of Nb/MnSi heterostructures — •PHILIP SCHRÖDER¹, JULIUS GREFE¹, STEFAN SÜLLOW¹, and DIRK MENZEL^{1,2} — ¹Institut für Physik der Kondensierten Materie, TU Braunschweig, Germany — ²Laboratory for Emerging Nanometrology, TU Braunschweig, Germany

During high-resolution four probe (magneto-)resistivity measurements the reliability of the data strongly depends on the contacts' characteristics. If a vector magnet is not available the change of the sample orientation with respect to the field always requires demounting, reorientation and recontacting of the sample. We have measured the resistivity of a superconducting Nb thin film deposited on a helimagnetic MnSi substrate as function of the angle between the surface and the external magnetic field. In order to maintain the same four-probe configuration without recontacting an experimental setup has been developed allowing 720° sample rotation in a homogeneous field up to 1.1 T. The setup is used to accurately investigate the shift due to the proximity effect of the critical temperature T_c of the Nb film in contact to a magnetic system exhibiting a non-collinear spin structure. We show that the spin-helix orientation of the MnSi substrate is able to tune the T_c of Nb so that this heterostructure can be used as a two-component superconducting spin valve.

TT 30.17 Thu 15:00 P1

Decoupling of NbSe₂ monolayers in tailored SnSe-based multilayers — •O. CHIATTI¹, K. MIHOV¹, T. GRIFFIN¹, C. GROSSE¹, M. B. ALEMAYEHU², K. HITE², D. HAMANN², A. MOGLATENKO³, D. C. JOHNSON², and S. F. FISCHER¹ — ¹Novel Materials Group, Humboldt-Universität zu Berlin, 10099 Berlin, Germany — ²Solid State Chemistry, University of Oregon, Eugene OR 97403-1253, U.S.A. — ³Ferdinand-Braun-Institut, Leibniz-Institut für Höchstfrequenztechnik, 12489 Berlin, Germany

Van-der-Waals superlattices with two-dimensional (2D) superconducting layers of a transition-metal dichalcogenide (TMD) embedded between other materials have received a lot of attention [1]. Here, we examine the coupling between the NbSe₂ monolayers in [(SnSe)_{1+δ}]_m[NbSe₂] ferecrystals [2]. m is an adjustable parameter to control the spacing between NbSe₂ layers and tune the inter-layer coupling, with a crossover from 3D to 2D superconductivity. The electric transport shows three regions: I. for $m = 1 - 4$ the films resemble "good" metals and 3D anisotropic superconductors, with inter-layer coupling enhanced by proximity effect in the SnSe layers and charge transfer from NbSe₂ to SnSe; II. for $m = 5 - 9$ the films are "dirty" metals and 3D anisotropic superconductors, with inter-layer coupling reduced by disorder and smaller charge transfer; III. for $m > 9$ they are "bad" insulators and a stack of disordered quasi-2D superconductors, with Josephson coupling between NbSe₂ monolayers.

- [1] A. Devarakonda *et al.*, *Science* **370**, 231 (2020)
 [2] M. Trahms *et al.*, *Supercond. Sci. Technol.* **31**, 065006 (2018)

TT 30.18 Thu 15:00 P1

Spin-orbit effects in the vortex inductance of Al/InAs heterostructures — •JAYDEAN SCHMIDT, LORENZ FUCHS, DENIS KOCHAN, MAXIMILLIAN UFER, SIMON REINHARDT, MICHAEL PRAGER, MATTHIAS KRONSEDER, DOMINIQUE BOUGEARD, NICOLA PARADISO, and CHRISTOPH STRUNK — University of Regensburg (Germany)

In this work, we demonstrate the interplay of spin-orbit interaction and in-plane magnetic field in synthetic Rashba superconductors. We investigate the vortex inductance of epitaxially grown Al/InAs heterostructures containing an high-mobility surface-near InAs quantum well covered with an epitaxial layer of aluminum. An AC-current drives vortex oscillations around pinning centers which can be probed via inductance. The vortex inductance was found to be orders of magnitude larger than the kinetic inductance. When applying an in-plane field, the vortex inductance drops in particular for $B_{\parallel} \perp I_{AC}$ signaling an increase of the pinning force. With respect to the angle between magnetic field and current, a prominent two-fold anisotropy is observed. The unusual behavior of the vortex inductance signals a deformation of the vortex cores and can be theoretically explained by introducing an additional term in the Ginzburg-Landau free energy of a superconductor, resulting from the Rashba spin-orbit interaction [1].

- [1] L. Fuchs *et al.*, arXiv: 2201.02512

TT 30.19 Thu 15:00 P1

Generalising Beenakker equation to take into account evanescent modes — •DANIEL KRUTI and ROMAN-PASCAL RIWAR — Institute for Theoretical Nanoelectronics (PGI-2), Jülich Research Centre and Institute for Theoretical Physics, University of Cologne

Superconductor-normal-metal-superconductor Josephson junctions have been examined extensively in past years. In particular, the case where the normal region is modelled by an ideal normal conductor with an intermittent scattering region can be well described by the celebrated Beenakker equation. Strictly speaking however, this equation is applicable only in the asymptotic plain wave limit, neglecting evanescent modes. However, the situation is changing by recent experimental advances. First, conductor regions are now fabricated with significantly decreased impurity scattering, leading to situations where scattering is

dominated by the junction geometry. Second, miniaturisation is advancing such that evanescent modes should no longer be neglected. While this regime has already been captured by numerical methods, we here strive for an explicit analytical treatment, and generalise the Beenakker equation to short junctions with geometric scattering.

TT 30.20 Thu 15:00 P1

Controlling the Critical Current in Ferromagnetic Josephson-Junctions by Magnetization and Microwave Irradiation — •LUKAS KAMMERMEIER, ANDREAS BLOCH, OLIVER IRTENKAUF, and ELKE SCHEER — Universität Konstanz, Konstanz, Germany

A key building block in superconducting spintronics is a controllable superconducting device that accommodates long-ranged triplet currents [1]. It has been suggested to create long range triplets with the help of ferromagnetic resonance in superconductor-ferromagnet-superconductor (SFS) structures made of conventional s-wave superconductors [2]. Here we explore this possibility by studying the electronic transport in SFS junctions in different geometries and realizations of the F spacer, subject to microwave irradiation, with spin injection and as function of the magnetization state of the ferromagnet. We show that we can manipulate the critical current of overdamped S-S/F-S proximity junctions by several percent by flipping a single domain in the ferromagnet. First results on spin injection will be presented.

[1] J. Linder, W. A. Robinson, Nat. Phys. 11, 307 (2015)

[2] S. Takahashi, S. Hikino, M. Mori, J. Martinek, S. Meakawa, Phys. Rev. Lett. 99, 057003 (2007)

TT 30.21 Thu 15:00 P1

A Ballistic Graphene Cooper Pair Splitter — PREETI PANDEY¹, ROMAIN DANNEAU², and •DETLEF BECKMANN² — ¹Institute of Nanotechnology, Karlsruhe Institute of Technology, D-76021 Karlsruhe, Germany — ²Institute for Quantum Materials and Technologies, Karlsruhe Institute of Technology, D-76021 Karlsruhe, Germany

We report an experimental study of a Cooper pair splitter based on ballistic graphene multiterminal junctions. In a two transverse junction geometry, namely the superconductor-graphene-superconductor and the normal metal-graphene-normal metal, we observe clear signatures of Cooper pair splitting in the local as well as nonlocal electronic transport measurements. Our experimental data can be very well described by our beam splitter model. These results open up possibilities to design new entangled state detection experiments using ballistic Cooper pair splitters.

[1] Phys. Rev. Lett. 126, 147701 (2021)

TT 30.22 Thu 15:00 P1

Coupling of supercurrent and quasiparticle excitations in superconductor nanostructures — •PAUL MAIER and DETLEF BECKMANN — Institut für Quantenmaterialien und Technologien, Karlsruher Institut für Technologie

We report on the experimental observation of coupling between nonequilibrium modes of the quasiparticle excitations in thin superconducting films in the presence of supercurrent and high parallel magnetic fields. The coupling is due to a difference in the number of available quasiparticle states, depending on their relative propagation direction to the supercurrent. Recently the occurrence of a spin-energy (spin-antisymmetric charge imbalance) current in the presence of energy imbalance was predicted [1]. Here the resulting spin-energy imbalance

for a spatial gradient in the energy imbalance was probed in nonlocal conductance measurements with spectral resolution. The measurements show excellent agreement with numerical models and provide proof of the coupling of energy and spin-energy modes.

[1] F. Aikebaier et al., Phys. Rev. B 98, 024516 (2018)

TT 30.23 Thu 15:00 P1

Bloch oscillation effects in ultrasmall Josephson junctions embedded in high-inductance environment — •FABIAN KAAP and SERGEY LOTKHOV — Physikalisch-Technische Bundesanstalt, Bundesallee 100 38116, Deutschland Braunschweig

The adiabatic transport of Cooper pairs, also known as Bloch oscillations (BO), can be of high interest in future applications for metrology, due to the fundamental current-to-frequency relation, $I_B = 2e \times f_B$. In order for the BO in ultrasmall Josephson junctions to be observed, one has to suppress the quantum fluctuations of charge by means of embedding the junctions into a high impedance environment.

For this purpose, we elaborated a dedicated inductively-resistive planar biasing circuit, which includes high-kinetic-inductance meanders made from granulated aluminium and high-ohmic microstrips of partially oxidized titanium. Using this approach, we were able to measure the characteristic back-bending in an IV-curve of a dc-biased SQUID with Josephson junction of sub-100nm-sizes. By varying the ratio of the Josephson energy E_J and the charging energy E_C , using an external magnetic field, we were able to manipulate the shape of the IV-curves back-bending, which can be explained by a modification of the lowest Bloch energy band of Cooper pairs. With this biasing technique the way is paved to circumvent the microwave coupling issues hindering the realization of dual Shapiro step experiments.

TT 30.24 Thu 15:00 P1

Superconductor-insulator transition in ultra-thin granular aluminum films — •THOMAS HUBER¹, AVIV MOSHE², GUY DEUTSCHER², and CHRISTOPH STRUNK¹ — ¹Institute for Experimental and Applied Physics, University of Regensburg, Regensburg, Germany — ²Raymond and Beverly Sackler School of Physics and Astronomy, Tel Aviv University, Tel Aviv, Israel

The relation between homogeneously disordered and granular superconductors is so far not clearly understood. In particular, the existence of highly insulating states in grAl has yet not been demonstrated. Here we investigate ultra-thin grAl films in the truly 2D limit and find a superconducting transition for sample S with $R_{\square}(4K) \approx 3k\Omega$ and insulating behavior for sample I with $R_{\square}(4K) \approx 7.75k\Omega$ (d-SIT). By increasing the perpendicular magnetic field we drive both samples (deeper) into the insulating regime (B-SIT), where we find activated behavior in a temperature range $T^*(B) < T < \approx 800mK$. For $T < T^*$ and $B < \approx 1T$, the $R(T)$ curves saturate, indicating an intermediate anomalous metallic state [1] on both sides of the SIT [2]. The resistance R_{\square} , the activation energy E_A and the threshold voltage V_T depend on magnetic field and show strong similarities to the behavior of both regular Josephson junction arrays [3] and homogeneously disordered films [4].

[1] A. Kapitulnik et al., Rev. Mod. Phys. 91, 011002 (2019)

[2] X. Zhang et al., arXiv:2201.08801 [cond-mat.supr-con] (21.01.2021)

[3] P. Delsing et al., AIP Conference Proceedings 427, 313 (1998)

[4] T.I. Baturina et al., Phys. Rev. Lett. 99, 257003 (2007)

TT 31: Superconducting Electronics and Cryogenics: Poster Session

In case the presenters cannot be present at their posters for the full duration of the poster session, they are kindly requested to leave a note at their poster indicating when they will be available for discussion.

Time: Thursday 15:00–18:00

Location: P1

TT 31.1 Thu 15:00 P1

Modular architecture for circuit quantum electrodynamics — •SOEREN IHSEN¹, SIMON GEISERT¹, MARTIN SPIECKER², PATRICK PALUCH², ELIE DE SEZE^{1,3}, WOLFGANG WERNSDORFER^{1,2}, PATRICK WINKEL⁴, and IOAN POP^{1,2} — ¹Institute for Quantum Materials and Technologies, KIT, Germany — ²Physikalisches Institut, KIT, Germany — ³ENS Paris-Saclay, France — ⁴Yale University, USA

Superconducting quantum circuits play a pioneering role in finding a scalable architecture for the realization of a coherent quantum processor. In this context, keeping the integrity, individual addressability and controllability of each circuit component while increasing the complexity of the whole system is paramount to building a functional device. Fulfilling these key requirements becomes more difficult when increasing the connectivity in the circuit since parasitic cross-talk and the number of decay channels increase at the same time. Therefore, the coupling, readout and control mechanisms of every architecture need to be understood in great detail. Here, we investigate a flip-chip architecture in which

we implement the readout and flux control of generalized flux qubits. With our approach, circuits serving different tasks within the system can be prepared individually and exchanged in case they do not fulfil the requirements. In our first realization, a bandpass Purcell filter for readout and an on-chip flux bias line are fabricated and tested regarding their microwave properties. The developed circuit enables a suitable easy-access framework for future experiments on qubit-qubit coupling in a well-controlled microwave environment.

TT 31.2 Thu 15:00 P1

Flip chip implementation for generalized flux qubits — •SIMON GEISERT¹, SÖREN IHSEN¹, MARTIN SPIECKER^{1,2}, PATRICK PALUCH^{1,2}, DENNIS RIEGER², SIMON GÜNZLER², ELIE DE SEZE³, WOLFGANG WERNSDORFER^{1,2}, PATRICK WINKEL^{1,4}, and IOAN POP^{1,2} — ¹Institute for Quantum Materials and Technologies, Karlsruhe Institute of Technology (KIT), Germany — ²Physikalisches Institut, KIT, Germany — ³ENS Paris-Saclay, France — ⁴Yale University, USA

Superconducting flux qubits are a versatile and promising platform to implement coherent and tunable qubits with high anharmonicity. In this work, we

investigate a generalized flux qubit consisting of a single Josephson junction (JJ) shunted by a capacitance and a granular aluminum inductor. When biased at the flux degeneracy point, the potential landscape can be widely engineered by exploring the parameter space of the flux qubit, which includes the loop inductance, the Josephson energy of the JJ and the total capacitance across the latter. We demonstrate a high engineerability of the qubit frequency, yielding flux qubits in the range of 150 MHz to 7.6 GHz. Dispersive readout of the qubit state is performed via an embedded harmonic mode that is inductively coupled through an asymmetry of the qubit loop. The readout mode is capacitively coupled to a control chip, which is used to excite, read out and flux bias the qubit. This flip chip approach allows very well isolated qubits to be tested in a modular architecture and enables coupling to two distinct coupler chips, effectively creating a unit cell that can be scaled up to an array of coupled qubits.

TT 31.3 Thu 15:00 P1

Simultaneous quantum jumps on multiple Fluxonium qubits — •NICOLAS GOSLING, MARTIN SPIECKER, PATRICK PALUCH, SIMON GEISERT, and IOAN M POP — Karlsruhe Institut of Technology

Superconducting quantum circuits have become one of the front runners for the implementation of scalable quantum processors. Hereby, the ability to design and implement multiple artificial atoms and their couplings has become an important task for many researchers. Therefore it is imperative to understand how events on one qubit influence other qubits on the same chip. Here, we take simultaneous quantum jump traces of multiple Fluxonium qubits on the same chip using a frequency multiplexed readout scheme through dispersive measurement. The simultaneity is ensured by the frequency multiplexing, enabling both signals to use the same input and output lines. The resulting quantum jump traces are then analysed for simultaneous events in respect to the stochastically expected coherences for perfectly uncoupled quantum systems.

TT 31.4 Thu 15:00 P1

Characterization of Josephson photonic devices as microwave sources for a quantum radar — •LUKAS DANNER^{1,2}, CIPRIAN PADURARIU², JOACHIM ANKERHOLD², and BJÖRN KUBALA^{1,2} — ¹Institute for Quantum Technologies, German Aerospace Center (DLR), Ulm, Germany — ²ICQ and IQST, Ulm University, Ulm, Germany

In Josephson photonic devices, microwave radiation is created by inelastic Cooper pair tunneling across a dc-biased Josephson junction connected in-series with a microwave resonator [1]. Various resonances are accessed by tuning the dc-voltage, where, e.g., each tunneling Cooper pair creates one, two or three photonic excitations in the resonator. If excitations are created in two different resonators, the device could be used in a quantum radar which exploits the quantum correlations of the photons [2]. The source can be characterized by the steady-state Wigner density of the cavities, showing e.g. two-mode squeezing or other phase-space symmetries for multi-photon creation. Wigner-state tomography is expensive and in Josephson photonic devices especially challenging due to lacking phase stability. Therefore, we propose an alternative approximative characterization scheme which requires measuring only a few expectation values. A different way of dealing with the instability of the phase-space angle by a locking mechanism [3] is discussed in the contribution of F. Höhe.

[1] M. Hofheinz et al., Phys. Rev. Lett. 106, 217005 (2011)

[2] A. Peugeot et al., Phys. Rev. X 11, 031008 (2021)

[3] L. Danner et al., Phys. Rev. B 104, 054517 (2021)

TT 31.5 Thu 15:00 P1

Reflection-type superconducting microwave resonators for spin-based quantum memories — •JULIAN FRANZ^{1,2}, PATRICIA OEHRL^{1,2}, MANUEL MÜLLER^{1,2}, THOMAS LUSCHMANN^{1,2,3}, RUDOLF GROSS^{1,2,3}, and HANS HUEBL^{1,2,3} — ¹Walther-Meißner-Institut, Bayerische Akademie der Wissenschaften, Garching, Germany — ²Physik-Department, Technische Universität München, Garching, Germany — ³Munich Center for Quantum Science and Technologies (MCQST), Munich, Germany

Solid-state spin ensembles are considered as excellent candidates for quantum memory applications due to their long coherence times and frequency compatibility with superconducting quantum circuits. The realization of such quantum memory requires the conversion of quantum microwave signals to excitations in the spin ensemble, their storage, and retrieval. This requires the detailed understanding and design optimization of the employed microwave circuit. The excitation transfer is typically measured by using a hanger type resonator. However, in a reflection-type geometry, all of the signal power is available for measurement, which gives nominally a factor of 2 improvement of the signal-to-noise ratio relative to the hanger configuration [1]. Here, we discuss the design concepts for superconducting microwave circuits with emphasis on tuning the coupling rates to the microwave circuit environment and the spin ensemble. In addition, we present experimental data using thin film NbTiN and Nb reflection-type resonators and characterize their performance at mK temperatures.

[1] H. Wang et al., Quantum Sci. Technol., 6 (3), 035015 (2021)

TT 31.6 Thu 15:00 P1

MOCCA: A 4k-pixel molecule camera for the position and energy resolved detection of neutral molecule fragments — •DANIEL KREUZBERGER¹, CHRISTIAN ENSS¹, ANDREAS FLEISCHMANN¹, LISA GAMER², LOREDANA GASTALDO¹, CHRISTOPHER JAKOB², ANSGAR LOWACK¹, OLDŘICH NOVOTNY², ANDREAS REIFENBERGER¹, DENNIS SCHULZ¹, and ANDREAS WOLF² — ¹Heidelberg University — ²Max Planck Institute for Nuclear Physics, Heidelberg

The MOCCA detector is a 4k-pixel high-resolution molecule camera based on metallic magnetic calorimeters and read out with SQUIDs that is able to detect neutral molecule fragments with keV kinetic energies. It will be deployed at the Cryogenic Storage Ring CSR at the Max Planck Institute for Nuclear Physics in Heidelberg, a storage ring built to prepare and store molecular ions in their rotational and vibrational ground states, enabling studies on electron-ion interactions. To reconstruct the reaction kinematics, MOCCA measures the energy and position of incident particles on the detector, even with multiple particles hitting the detector simultaneously.

We present a new read-out scheme which uses only 32 SQUID channels for the 4096 pixels of the detector as well as some new fabrication details including a new thermalization system and first experimental results.

TT 31.7 Thu 15:00 P1

From ECHO-1k to ECHO-100k: Optimisation of the High-Resolution Metallic Magnetic Calorimeters with Embedded ¹⁶³Ho — •MARKUS GRIEDEL¹, ARNULF BARTH¹, SEBASTIAN BERNDT^{2,3}, LORENZO CALZA¹, HOLGER DORRER³, CHRISTOPH DÜLLMANN^{3,4,5}, CHRISTIAN ENSS¹, ANDREAS FLEISCHMANN¹, DANIEL HENGSTLER¹, TOM KIECK^{3,4,5}, NINA KNEIP², NEVEN KOVAC¹, FEDERICA MANTEGAZZINI¹, ANDREAS REIFENBERGER¹, ALEXANDER KAROL SLAWIK¹, KLAUS WENDT², and LOREDANA GASTALDO¹ — ¹Kirchhoff-Institute for Physics, Heidelberg University — ²Institute of Physics, Johannes Gutenberg University Mainz — ³Department of Chemistry - TRIGA Site, Johannes Gutenberg University Mainz — ⁴GSI Helmholtzzentrum für Schwerionenforschung GmbH — ⁵Helmholtz Institute Mainz

The ECHO collaboration aims to determine $m(\nu_e)$ by analysing the ¹⁶³Ho electron capture spectrum. Arrays of tens to hundreds of Metallic Magnetic Calorimeters (MMCs) implanted with ¹⁶³Ho have been chosen because of their excellent energy resolution in the range of a few eV, their fast response time below 1 μ s and their good linearity. The MMC array enclosing ¹⁶³Ho fabricated for the ECHO-1k phase has been fully characterised in terms of detector response, energy resolution and ¹⁶³Ho activity. Based on these results a new 64-pixel-array design has been conceived for ECHO-100k, featuring an optimised single pixel geometry and allowing for a ¹⁶³Ho activity of 10 Bq per pixel. First wafers, each with 40 ECHO-100k chips, have been fabricated and characterised. The obtained results show that the ECHO-100k array achieved the expected performance, especially an average energy resolution of 3.5 eV, fulfilling the requirements for the ECHO-100k phase.

TT 31.8 Thu 15:00 P1

Towards large-area 256-pixel MMC arrays with multiplexed read-out based on flux-ramp modulated dc-SQUIDS — •A. ABELN, S. ALGIEIER, L. EISENMANN, D. HENGSTLER, N. KAHNE, F. KRÄMER, D. MAZIBRADA, L. MÜNCH, A. STOLL, A. FLEISCHMANN, and C. ENSS — Kirchhoff-institute for Physics, Heidelberg University

Metallic Magnetic Calorimeters (MMCs) are energy-dispersive cryogenic particle detectors. Operated at about 20 mK, they provide very good energy resolution of down to 1.6 eV at 6 keV, high quantum efficiency as well as linearity over a large energy range. In many precision based experiments on high resolution X-ray spectroscopy the photon flux is small, thus a large active detection area is desirable. Therefore, arrays with a large number of MMC pixels are beneficial. For a cost-effective read-out of a growing number of detector channels we develop different multiplexing techniques.

In this contribution we present the design of a novel 16 \times 16 pixel MMC array. Each pixel provides an active detection area of 250 μ m \times 250 μ m yielding a total active detection area of about 4 mm \times 4 mm. With a thickness of 5 μ m the absorbers made of gold ensure a quantum efficiency of at least 50 % for energies up to 20 keV. The designed energy resolution according to numerical simulations is $\Delta E_{FWHM} = 1.4$ eV at an operation temperature of 20 mK. We also present the current status of flux-ramp multiplexing that allows to reduce the number of read-out channels by at least a factor of four compared to a conventional read-out.

TT 31.9 Thu 15:00 P1

PrimA-LTD: Magnetic microcalorimeters for primary activity standardization — •MICHAEL MÜLLER, RIA-HELEN ZÜHLKE, PETER KÄHLER, and SEBASTIAN KEMPF — Institute of Micro- and Nanoelectronic Systems, Karlsruhe Institute of Technology, Karlsruhe

Magnetic microcalorimeters (MMC) are cryogenic, energy-dispersive single-particle detectors that consist of a paramagnetic temperature sensor which is in strong thermal contact with a particle absorber. The sensor is magnetized by a magnetic field generated by a persistent current in an underlying super-

conducting pickup coil. The resulting change of sensor magnetization upon an energy input into the detector is read out by a SQUID. Due to their excellent energy resolution as well as the very low threshold, MMCs are a key technology in the frame of the EMPIR-project "PrimA-LTD" aiming to measure decay spectra of several isotopes with unprecedented precision to enable activity standardization for medicine and industry. Within this project we designed three MMC based layouts optimized for measuring the spectra of α -, β - and electron capture-decaying nuclides. We further developed a novel electroplating setup for the microfabrication of highly pure, 3D-structured particle absorbers made of Au to enable fast thermalization of the detector without position dependencies. Moreover, we started to develop a passive persistent current switch for injecting the persistent current allowing for easier detector handling and higher integration density in comparison to conventionally used heat switches. We summarize the present state of the project and outline ongoing next steps.

TT 31.10 Thu 15:00 P1

PrimA-LTD: Towards new primary activity standardization methods based on low-temperature detectors — ALEXANDER GÖGGMANN¹, JOERN BEYER², CHRISTIAN ENSS^{3,6}, SEBASTIAN KEMPF^{4,6}, KARSTEN KOSSERT¹, MARTIN LOIDL⁵, MICHAEL MÜLLER⁴, OLE NÄHLE¹, MICHAEL PAULSEN², PHILIPP CHUNG-ON RANITZSCH¹, MATIAS RODRIGUES⁵, and MATHIAS WEGNER^{4,6} — ¹Physikalisch-Technische Bundesanstalt (PTB), Braunschweig, Germany — ²Physikalisch-Technische Bundesanstalt (PTB), Berlin, Germany — ³Kirchhoff-Institute for Physics, Heidelberg University, Germany — ⁴Institute of Micro- and Nanoelectronic Systems, Karlsruhe Institute of Technology, Karlsruhe, Germany — ⁵CEA, LIST, Laboratoire National Henri Bequerel, Saclay, France — ⁶Institute for Data Processing and Electronics, Karlsruhe Institute of Technology, Karlsruhe, Germany

Radionuclide metrology, and in particular, activity standardization, is based on well-established measurement techniques that have been used and improved for decades. The methods and the achievable uncertainty are, however, very dependent on the type of radiation that is emitted and the quality of the available decay data. A major part of the EMPIR project "PrimA-LTD" consists in developing new primary techniques and in particular the high-resolution spectrometry of ²⁴¹Am, ¹²⁹I and ⁵⁵Fe using magnetic microcalorimeters (MMCs). The presentation will focus on the experimental details including the MMC detector setup, sample preparation and planned spectral measurements with more than 108 counts and energy thresholds below 50 eV.

TT 31.11 Thu 15:00 P1

Fabrication process for Nb/Al-AIO_x/Nb Josephson tunnel junction based SQUIDs for magnetic microcalorimeter readout — MARTIN NEIDIG, PAUL KAHRMANN, and SEBASTIAN KEMPF — Institute of Micro- and Nanoelectronic Systems, Karlsruhe Institute of Technology, Karlsruhe, Germany

Magnetic microcalorimeters (MMCs) are cryogenic particle detectors providing an excellent energy resolution, very fast signal rise time, an almost ideal linear detector response and a large dynamic range. These properties combined with a maturing fabrication process motivate the implementation of large MMC based detector arrays which poses the challenge of developing a suitable readout method. Small-scale arrays are typically readout using single-channel dc-SQUIDs with individual wiring, while large-scale arrays require a multiplexed readout scheme. One such multiplexing scheme is the microwave SQUID multiplexer which allows for the readout of hundreds of detectors via a common feedline. The realization of either readout method requires the use of SQUIDs and therefore a reliable fabrication process for high quality Josephson junctions.

For this purpose we established a fabrication process for Nb/Al-AIO_x/Nb based window-type Josephson tunnel junctions. Within this contribution, we outline the present status of our fabrication technology and, moreover, we discuss the performance of the fabricated junctions and results of our prototype dc-SQUIDs, which are presently used for several MMC based experiments.

TT 31.12 Thu 15:00 P1

Noise Thermometers for Milli-Kelvin Measurements in High Magnetic Fields and for Micro-Kelvin Temperatures — PASCAL WILLER, CHRISTIAN STÄNDER, NATHALIE PROBST, SARAH PHILIPS, ANDREAS REISER, ANDREAS FLEISCHMANN, and CHRISTIAN ENSS — Kirchhoff-Institute for Physics, Heidelberg University. To measure the temperature in the presence of high magnetic fields is one of the big challenges in solid state physics labs. We recently started to construct a prototype of a cross-correlated, current sensing noise thermometer for mK-temperatures for application in high magnetic fields. The basic concept relies on the thermal movement of charge carriers in a resistor. DC-SQUIDs detect the corresponding noise signal which is then recorded via two identical but independent amplifier chains. The method of cross correlation is used to eliminate uncorrelated noise contributions from the amplifier chains. As resistor material we use an alloy of platinum and tungsten, Pt₉₂W₈, since this material is characterized by an extremely small temperature dependence of the electrical resistivity as well as the smallest magneto-resistance known to date. We show that this approach towards a relative primary thermometer for high magnetic fields is able to operate over a wide range of temperatures within less than 1% uncertainty.

Additionally, we developed a second noise thermometer based on an alloy of copper and silver called "CuSil" to measure down to μ K-temperatures in the absence of magnetic fields.

We discuss the design and the necessary considerations of both thermometers and present first experimental results at mK temperatures.

TT 31.13 Thu 15:00 P1

Microprocessor controlled temperature measurement with Allen-Bradley-carbon- and Platinum-100-Sensors — JELKO SEIBOTH and ANDREAS WIECK — Lehrstuhl für Angewandte Festkörperphysik, Ruhr-Universität Bochum

This poster illustrates the setup of a device for the determination of temperatures between RT (294 K) and 4 K using Pt100 sensors and Allen-Bradley resistors with a RT value between 100 Ω and 1 k Ω . To measure the resistance, a Raspberry Pi with an analog-to-digital converter and upstream connected operational amplifiers is used. This combination provides a low price and easy further development.

The measurement is carried out with four-point technology, whereby, to reduce the temperature increase due to the electrical power consumed by the sensor, the supply of the Pt100 sensors is provided with constant current and that of the Allen-Bradley sensors with constant voltage. The device allows calibration for specific resistors and calculates the temperature from a polynomial fit function [1,2].

The determined value is shown on a display, recorded in a subsequently exportable file and output to a proportional connector with a voltage corresponding to the temperature. As the Raspberry Pi supports network connections via Ethernet and Wi-Fi, a remote retrieval or external database storage of the measurements may be implemented in the future. Calibration and temperature measurements were successfully taken to prove the functionality.

[1] B. Fellmuth, Guide to the Realization of the ITS-90. BIPM, 2018

[2] Star et al., J. Phys. [E] 2, 257 (1969)

TT 31.14 Thu 15:00 P1

Characterization and optimization of different regenerator matrices on a single-stage pulse tube cryocooler — DOMINIK SOARE^{1,2}, JACK-ANDRÉ SCHMIDT^{1,2}, BERND SCHMIDT^{1,2}, JENS FALTER², and ANDRÉ SCHIRMEISEN^{1,2} — ¹Justus-Liebig University Giessen — ²TransMIT GmbH

Closed-cycle cryocoolers have become an important cooling concept tool for scientific research at low temperatures [1]. We here focus on Gifford-McMahon (GM) type pulse tube cryocoolers (PTC), which offer long measurement periods and low maintenance. The regenerator of any regenerative cryocooler is essential for the cooling process [2]. The regenerator offers heat capacity as a storage for the gas temperature during the cooling cycle. It pre-cools or -heats the working gas and therefore the regenerator matrix is an important optimization factor.

The poster will display the influence of different regenerator matrices on the cooling performance of a single stage pulse tube cryocooler driven by a helium compressor with 2kW input power. Using the results, it is possible to get new insights of the optimization of the first stage of two-stage cryocoolers and therefore their overall cooling performance.

[1] R. Güsten et al., Nature 568 (2019) 357

[2] P. P. Steijaert, Thermodynamical aspects of pulse-tube refrigerators (1999) 10

TT 31.15 Thu 15:00 P1

Materials losses in superconducting circuits based on tantalum thin films — RITIKA DHUNDHWAL¹, THOMAS REISINGER¹, HAORAN DUAN², DIRK FUCHS¹, MATTHIEU LE TACON¹, JASMIN AGHASSI-HAGMANN², and IOAN M. POP¹ — ¹Institut für Quantenmaterialien und technologien (IQMT), Karlsruher Institut für Technologie (KIT) — ²Institut für Nanotechnologie (INT), Karlsruher Institut für Technologie (KIT)

Superconducting quantum circuits have very promising applications in the fields of quantum computing and detection. In general, their performance is limited by a variety of dissipation and noise sources. For mitigating these, the focus has been on improving microwave design and better fabrication processes. Another approach, recently in the spotlight, is to explore new materials entirely. One promising candidate superconducting material is Tantalum (Ta), which recently enabled record-breaking Transmon qubit lifetimes. However, there is a lack of conclusive evidence of the dominant loss mechanisms related to Ta. Here, we present a study of losses in epitaxial Ta films deposited using magnetron sputtering, with the aim of relating basic material properties and loss mechanisms. A variation in the deposition parameters (mainly substrate temperature) leads to structurally different films. We characterized these using high-resolution X-ray diffraction, scanning electron microscopy and measurements of the superconducting transition temperature. In addition, we fabricated lumped element resonators from the films using e-beam lithography and measured their quality factors as a function of photon number and temperature.

TT 31.16 Thu 15:00 P1

The Influence of Continuous Electric Bias Fields on the Dielectric Loss of Atomic Tunneling Systems — •JAN BLICKBERNDT, CHRISTIAN STÄNDER, LUKAS MÜNCH, MARCEL HAAS, ANDREAS REISER, ANDREAS FLEISCHMANN, and CHRISTIAN ENSS — Kirchhoff-Institute for Physics, Heidelberg, Germany

The low temperature properties of amorphous solids are mainly determined by atomic tunneling systems (TSs), which are known to act as a major source of noise and decoherence in superconducting quantum devices. We investigate the non-equilibrium dielectric loss of atomic tunneling systems under the influence of continuous electric bias fields at very low temperatures. By measuring the quality factor of a micro-fabricated superconducting resonator, the dielectric loss of the sample is obtained. Simultaneously, an electric bias field can be applied via a cover electrode, which allows us to sweep TSs through resonance by modulating their energy splitting. Experimentally, we found that for slow changing bias fields, TSs are saturated by the driving field leading to a constant loss. For faster bias rates, more and more TSs are swept through resonance and therefore contribute to an increasing loss. In the limit of fast continuous bias sweeps relaxation in between consecutive crossings diminishes and multiple coherent Landau-Zener transitions are possible, reducing the loss back to the saturation limit. We are able to verify these experimental results with a Monte Carlo based numerical simulation that shows good qualitative agreement.

TT 31.17 Thu 15:00 P1

Electrically and Acoustically Biased Resonators for Investigations of Dielectric Low Temperature Properties of Amorphous Solids — •CHRISTIAN STÄNDER, JAN BLICKBERNDT, JOYCE GLASS, BENEDIKT FREY, ANDREAS REIFENBERGER, ANDREAS FLEISCHMANN, ANDREAS REISER, and CHRISTIAN ENSS — Kirchhoff Institute for Physics, Heidelberg University, D-69120 Heidelberg

The low temperature properties of amorphous solids are governed by atomic tunnelling systems, which can be described as two-level systems (TLS) with a distribution of their energy splitting E , as assumed by the phenomenological standard tunnelling model. Recent interest in these systems due to their deteriorative effects on the performance of superconducting quantum devices lead to novel experimental investigations of atomic tunnelling systems driven by novel measurement techniques.

We use newly designed microfabricated superconducting LC-resonators to study the dielectric rf-response of the amorphous sample in the presence of an electric bias field. A novel method of applying this electrical bias field was introduced to the resonators. Compared to previous experiments, the bias field is applied via an electrode placed above the resonator chip. We present first results of this new way of introducing a bias, which modifies the energy splitting E of a TLS.

In addition we tried to achieve a similar effect as with the electrical bias field with a mechanical strain field. To induce such a strain field, the amorphous substrate of the resonator chip was flexed by a piezo-actuator.

TT 31.18 Thu 15:00 P1

Quantum electrodynamics of cold deposited granular aluminum — •AMEYA NAMBISAN¹, DENNIS RIEGER², SIMON GÜNZLER¹, WOLFGANG WERNSDORFER^{1,2,3}, and IOAN M POP^{1,2} — ¹Institute for Quantum Materials and Technology (IQMT), Karlsruhe Institute of Technology (KIT), Germany — ²Physikalisches Institut (PHI), Karlsruhe Institute of Technology (KIT), Germany — ³Institute Néel, CNRS Grenoble, France

In recent times, superconducting granular aluminium (grAl) has found increasing interest in the superconducting quantum circuits community because of its promising characteristics such as its tunable kinetic inductance, low microwave losses, high in-plane critical magnetic field, and a higher critical temperature compared with pure Al.

In general, the critical temperature of a grAl film depends on its resistivity until it reaches a superconducting-to-insulator transition. For samples evaporated at room temperature, a maximum of around 2.2K is reached for resistivity of about 1000 $\mu\Omega$. The critical temperature rises even above 3K when grAl is deposited on a substrate held at a lower temperature of 100K.

This project aims to answer the question of increased T_c , which is yet to be understood microscopically, and other consequences of cold deposition, such as how a generally smaller – while more homogeneous – grain size positively affects the electrodynamics of the film. The test-bed used to characterise the electrodynamics are stripline resonators fabricated entirely from cold-deposited grAl, and measured in a cylindrical copper waveguide sample holder at cryogenic temperatures.

TT 31.19 Thu 15:00 P1

Compact high-kinetic inductance using stacked Josephson junctions — •ALEX S. KREUZER¹, THILO KRUMREY¹, HANNES ROTZINGER^{1,2}, and ALEXEY V. USTINOV^{1,2} — ¹Physikalisches Institut (PHI), Karlsruher Institut für Technologie (KIT) — ²Institut für Quantenmaterialien und -technologien (IQMT), Karlsruher Institut für Technologie (KIT)

Highly inductive elements are often required in modern superconducting quantum circuits, e.g. to form, together with a suitable capacitance, a large non-dissipative impedance. One way of creating such a high inductance is to em-

ploy series arrays of Josephson junctions, as it is done in the fluxonium qubit. For conventionally made chains of Josephson junctions, a major limitation arises from the stray capacitance of the islands forming the junctions. This capacitance leads to undesirable parasitic resonances at GHz frequencies, which degrade the quantum coherence of the qubit.

We propose a new way of creating high-inductance elements by stacking Josephson junctions vertically thus avoiding the influence of the through-substrate capacitive coupling of the junction electrodes to the environment. Furthermore, we demonstrate that our approach allows for making extremely compact circuit components.

TT 31.20 Thu 15:00 P1

Towards machine learning models for NISQ processors — •ANDRAS DI GIOVANNI¹, HANNES ROTZINGER^{1,2}, ALEXEY V. USTINOV^{1,2}, ADRIAN AASEN³, MORITZ REH³, and MARTIN GÄRTNER³ — ¹Karlsruhe Institute for Technology, Karlsruhe, Germany — ²Institut für QuantenMaterialien und Technologien, Karlsruhe, Germany — ³Heidelberg University, Heidelberg, Germany

Quantum simulators promise insights into quantum many-body problems in regimes where classical simulation methods hit a complexity wall. One challenge towards this goal is to develop well characterized building blocks that allow to scale up system sizes while conserving reliability in terms of errors. A promising platform for building such NISQ (noisy, intermediate-scale quantum) devices are superconducting quantum circuits. Our goal is to characterize small scale quantum processors with minimal experimental and post-processing cost. For this we implement schemes for machine learning assisted adaptive Bayesian tomography and apply them to experimental data obtained from a prototype few-qubit superconducting chip.

TT 31.21 Thu 15:00 P1

Exploring the parameter regimes of superconducting Quarton qubits coupled via cross-Kerr nonlinearity — •HOSSAM TOHAMY¹, ALEX SIEGFRIED KREUZER¹, THILO KRUMREY¹, HANNES ROTZINGER^{1,2}, and ALEXEY V. USTINOV^{1,2} — ¹Physikalisches Institut, Karlsruhe Institute of Technology, 76131 Karlsruhe, Germany — ²Institute for Quantum Materials and Technologies, Karlsruhe Institute of Technology, 76021 Karlsruhe, Germany

Over the last two decades, tremendous efforts have been directed into studying superconducting qubits as a promising architecture for noisy intermediate-scale quantum processors to implement quantum simulations and algorithms. A recent superconducting qubit named the "Quarton" represents a generalized flux qubit featured by a quartic potential profile. It can offer positive, strong cross-Kerr nonlinearity compared to the ordinary linear dispersive coupling between qubits and resonators. This nonlinearity can be essential, e.g., to achieve the next milestones in quantum simulation, such as the simulation of model Hamiltonians where strong photon-photon interactions are possible via nonlinear elements.

To employ the quarton as a qubit and a coupler, a system of two primary quarton qubits coupled via a quarton qubit coupler is studied. We report on numerical results demonstrating the normal modes of the system. The calculations are based on a Hamiltonian derived from a circuit quantization model. The work is linked to ongoing experimental efforts for realizing multiqubit architecture based on quartons.

TT 31.22 Thu 15:00 P1

Multilayer surface acoustic wave resonators at cryogenic temperatures — •ALEXANDER JUNG^{1,2}, THOMAS LUSCHMANN^{1,2,3}, ACHIM MARX¹, RUDOLF GROSS^{1,2,3}, and HANS HUEBL^{1,2,3} — ¹Walther-Meißner-Institut, Bayerische Akademie der Wissenschaften, Garching, Germany — ²Physik-Department, Technische Universität München, Garching, Germany — ³Munich Center for Quantum Science and Technologies (MCQST), Munich, Germany

Circuit quantum acoustodynamics uses the piezoelectric coupling of surface acoustic waves (SAW) to superconducting qubits for the implementation of concepts known from circuit quantum electrodynamics [1,2]. In this approach, the role of electromagnetic field is replaced by an acoustic wave propagating at the speed of sound. Moreover, the wavelength of acoustic waves is of the order of the size of the artificial atom, and thus their interaction with the qubit can no longer be treated pointlike. SAW resonators are an essential building block for quantum acoustodynamics. Of particular interest is the integration of SAWs using a piezoelectric on a silicon substrate to combine highly coherent qubits with excellent SAW properties. However, this changes the properties of the SAWs in particular for thin piezoelectric films. Here, we present simulations and experimental studies of SAW resonators fabricated on bulk and thin film piezoelectric substrates at cryogenic temperatures to understand the SAW as multilayer system.

[1] A.F.Kockum, International Symposium on Mathematics, Quantum Theory, and Cryptography (2021)

[2] Mathematics for Industry, 33, 125 (2020)

TT 31.23 Thu 15:00 P1

Flux-pumped Josephson Traveling Wave Parametric Amplifier — •DANIIL E. BAZULIN^{1,2}, KEDAR E. HONASOGE^{1,2}, LEON KOCH^{1,2}, YUKI NOJIRI^{1,2}, THOMAS LUSCHMANN^{1,2}, ACHIM MARX¹, STEFAN FILIPP^{1,2,3}, and KIRILL G. FEDOROV^{1,2} — ¹Walther-Meißner-Institut, 85748 Garching, Germany — ²Physik-Department, Technische Universität München, 85748 Garching, Germany — ³Munich Center for Quantum Science and Technology (MCQST), 80799 Munich, Germany

Development of scalable superconducting quantum computers requires an efficient read-out of multiple quantum bits. This goal can be achieved by exploiting broadband Josephson Traveling Wave Parametric Amplifiers (JTWPAs). These are typically based on arrays of superconducting nonlinear elements, such as various types of Superconducting Quantum Interference Devices (SQUIDs). Here, we report on fabrication and characterization of a specific type of the JTWPA based on aluminium asymmetric SQUIDs exploiting the three-wave mixing down-conversion process. With this approach we circumvent inherent JTWPA problems with phase-matching and are able to spatially separate signal and pump paths.

TT 31.24 Thu 15:00 P1

Measurement of single NV centers inside a solid immersion lens at mK temperature — •AMER HASECIC, IOANNIS KARAPATZAKIS, MARCEL SCHRODIN, RAINER KRAFT, and WOLFGANG WERNSDORFER — Physikalisches Institut, Karlsruher Institut für Technologie, Karlsruhe, Deutschland

A solid immersion lens (SIL) prevents refraction on a diamond-air surface and therefore increases the collection efficiency of detected photons [1]. SILs are nanofabricated by removing bulk material via focused ion beam technique. Here, we rely on accelerated gallium ions. The photon collection from single Nitrogen-Vacancy (NV) centers inside a solid immersion lens in bulk diamond is examined at mK temperatures. We aim to improve readout times for electron spin and nuclear spin states with the later being a promising system in quantum computing [2].

[1] M. Jamali, Rev. Sci. Instrum. 85, 123703 (2014)

[2] M. Abobeih, Nature (2022)

TT 31.25 Thu 15:00 P1

Quantum manipulation of NV centers in diamond with on-chip coplanar waveguides at mK temperatures — •IOANNIS KARAPATZAKIS, AMER HASECIC, MARCEL SCHRODIN, RAINER KRAFT, and WOLFGANG WERNSDORFER — Physikalisches Institut, Karlsruher Institut für Technologie, Karlsruhe, Deutschland

Quantum information technology is advancing in several physical fields. Optically addressable spins such as Nitrogen-Vacancy (NV) centers in the solid-state structure of diamond stand out for their versatile applications in quantum mechanics which range from quantum processing of information [1] to magnetic field sensing [2]. NV centers can be reliably initialized optically and have long coherence and relaxation times.

Here, the quantum manipulation of NV centers is shown inside a dilution refrigerator (sionludi) at mK temperatures. Using lithographically fabricated on-chip coplanar waveguide circuits, Rabi oscillations can be driven with frequencies above 100 MHz at comparatively low microwave insertion power of 100 mW (20 dBm). This allows for fast manipulation of the NV center spin states at mK temperatures without excessive heating of the sample.

[1] A. Tsukanov, Russian Microelectronics 41, 91 (2012)

[2] L. Rondin, Reports on Progress in Physics 77, 056503 (2014)

TT 31.26 Thu 15:00 P1

Navigation system for a low temperature STM — •TIMO KANDRA, ROMAN HARTMANN, MARCEL STROHMEIER, SARA KHORSHIDIAN, and ELKE SCHEER — University of Konstanz, Germany

To obtain spatially resolved spectroscopic information in laterally confined superconducting heterostructures, such as nanowires and flakes on insulating substrates, tunneling spectroscopy on distinct locations on those structures shall be performed. For this purpose a coarse approach system is needed that allows to locate the STM tip at the point of interest without crashing the tip and while operating at very low temperature, here, 300 mK. We developed a braille-like pattern that allows to determine the absolute position of the tip within a $100 \times 100 \mu\text{m}^2$ scan range by scanning any area of size $1 \times 1 \mu\text{m}^2$. The search structure made of gold is patterned by electron beam lithography and is realized by a topographical pattern composed of squares. With this method it is possible to navigate to the point of interest by using an xy -table.

TT 32: Focus Session: Topological Devices (joint session TT/KFM)

The properties of topological phases of matter give rise to unique phenomena, such as edge or surface transport, spin-momentum locking, or topological protection against perturbations. Many years after their conception, several topological platforms have reached maturity, and research interests have shifted towards mesoscopic devices unveiling rich and new topological physics, driven in part by the perspectives of novel topological quantum computation. Within this Focus Session, recent examples of devices exploring or exploiting the topological properties of various phases of matter shall be discussed.

Organizers: Erwann Bocquillon, Oliver Breunig, Yoichi Ando (all Universität zu Köln)

Time: Thursday 15:00–18:30

Location: H10

Invited Talk

TT 32.1 Thu 15:00 H10

Supercurrents in HgTe-based topological nanowires — •DIETER WEISS — Institute for Experimental and Applied Physics, University of Regensburg, 93040 Regensburg/Germany

Topological insulator (TI) nanowires in proximity to conventional superconductors constitute a tunable platform to realize topological superconductivity and Majorana zero modes [1]. Tuning is done by an axial magnetic flux ϕ transforming the system from trivial at $\phi = 0$ to topologically nontrivial when a magnetic flux quantum $\phi_0 = h/2e$ threads the wire's cross-section. Here, we investigate the evolution of the supercurrent in ballistic HgTe Josephson junctions as a function of axial magnetic flux ϕ and examine the periodicity of the supercurrent utilizing microwave irradiation and probing Shapiro steps. Suppressed odd Shapiro steps herald the existence of 4π -periodic supercurrents, a signature of topological superconductivity. Our data suggest that at small ϕ this 4π -periodic supercurrent is of trivial origin but that at magnetic fields above $\phi_0/2$, topological 4π -periodic supercurrents take over [2].

Work done in cooperation with Ralf Fischer, Wolfgang Himmler, Johannes Ziegler, Jordi Picó-Cortés, Gloria Platero, Milena Grifoni, Dmitriy A. Kozlov, N. N. Mikhailov, Sergey A. Dvoretzky, Michael Barth, Jakob Fuchs, Cosimo Gorini, Klaus Richter, and Christoph Strunk.

[1] A. Cook and M. Franz, PRB 84, 201105(R) (2011)

[2] R. Fischer et al., PRR 4, 013087 (2022)

Invited Talk

TT 32.2 Thu 15:30 H10

Majorana bound states and non-reciprocal transport in topological insulator nanowire devices — •HENRY LEGG — Department of Physics, University of Basel

I consider devices consisting of a three-dimensional topological insulator (TI) nanowire placed in proximity to an s-wave superconductor.

First, I will show that a non-uniform chemical potential induced, for instance, by gating enables the device to be brought into a topological superconducting phase at relatively weak magnetic fields with Majorana bound states (MBSs) present for an exceptionally large region of parameter space in realistic systems. I also consider the experimental challenges posed by the metallization effect that occurs as a result of bringing a TI nanowire into proximity with a superconductor.

Second, I will discuss non-reciprocal transport evidence for the subband splitting that is central to the proposal to achieve MBSs in TI nanowires. I will show that a giant magnetochiral anisotropy observed in the normal state of the TI nanowire provides strong evidence for the artificial breaking of inversion symmetry due to gating effects. Furthermore, I will argue that the superconducting diode effect can be used as measure of inversion symmetry breaking in the presence of a superconductor and to determine when the TI nanowire is in the region of parameter space where topological superconductivity is expected.

Invited Talk TT 32.3 Thu 16:00 H10

Integration of topological insulator Josephson junctions in superconducting qubit circuits — •TOBIAS W. SCHMITT¹, MALCOLM R. CONNOLLY^{2,3}, MICHAEL SCHLEENVOIGT¹, CHENLU LIU², OSCAR KENNEDY³, JOSÉ M. CHÁVEZ-GARCÍA⁴, ANNE SCHMIDT¹, ALBERT HERTEL¹, TOBIAS LINDSTRÖM⁵, SEBASTIAN E. DE GRAAF⁵, KARL D. PETERSSON⁴, DETLEV GRÜTZMACHER¹, and PETER SCHÜFFELGEN¹ — ¹Peter Grünberg Institute & Jülich-Aachen Research Alliance, Forschungszentrum Jülich — ²Blackett Laboratory, Imperial College London — ³London Centre for Nanotechnology, University College London — ⁴Center for Quantum Devices, University of Copenhagen — ⁵National Physical Laboratory

Since the prediction of topological superconductivity in hybrid devices of topological insulators (TIs) and conventional s-wave superconductors (S), S-TI-S Josephson junctions have been studied intensively in electrical transport experiments. The integration of these Josephson junctions in superconducting qubit circuits allows to investigate them via circuit quantum electrodynamic techniques, which promises novel insights into their exotic characteristics. In this talk, I will present the implementation of transmon qubits with *in situ* fabricated S-TI-S Josephson junctions and outline fabrication challenges. I will further show results on coherent qubit control as well as temporal quantum coherence and discuss possible limitations on qubit coherence for the first generation of TI transmon devices [1]. An outlook on qubit improvements and developments towards the detection of topological superconductivity will be given.

[1] Nano Lett. 22, 7, 2595 (2022)

15 min. break

Invited Talk TT 32.4 Thu 16:45 H10

Universal fluctuations of the induced superconducting gap in an elemental nanowire — LAURIANE CONTAMIN, LUCAS JARJAT, WILLIAM LEGRAND, AUDREY COTTET, TAKIS KONTOS, and •MATTHIEU DELBECQ — Laboratoire de Physique de l'École Normale Supérieure, ENS, Université PSL, CNRS, Sorbonne Université, Université Paris-Diderot, Sorbonne Paris Cité, Paris, France.

Proximity induced superconductivity in a normal conductor is a rich field of experimental and theoretical investigations. Lately it has been at the heart of the quest for realizing topological modes in hybrid superconductor-nanowire nanodevices. Yet it turns out that there was a lack of investigations in elemental systems. In this work we therefore investigate an ultra-clean carbon nanotube coupled to a superconducting lead. We observe for the first time a long standing prediction of random matrix theory (RMT) that mesoscopic fluctuations of the mini-gap in a conductor follow a universal distribution with a clear transition when time reversal symmetry is broken, as predicted by RMT. Interestingly, mesoscopic fluctuations of the minigap were precisely predicted to lead to ubiquitous nontopological edge states clustering towards zero energy. We do indeed observe ubiquitous and robust zero bias conductance peaks under magnetic field in our device that cannot host topological modes by design. The RMT predictions that are compatible with our observations are very general and should be present in any system showing disorder. It therefore calls for alternatives to transport measurement to identify Majorana modes in 1D systems with microwave photons in a cavity as a promising platform.

Invited Talk TT 32.5 Thu 17:15 H10

Exploring the full potential of edge channel transport in HgTe based two-dimensional topological insulators — •SAQUIB SHAMIM^{1,2}, WOUTER BEUGELING^{1,2}, PRAGYA SHEKHAR^{1,2}, JAN BÖTTCHER³, ANDREAS BUDEWITZ^{1,2}, JULIAN-BENEDIKT MAYER³, LUKAS LUNCZER^{1,2}, JONAS STRUNZ^{1,2}, JOHANNES KLEINLEIN^{1,2}, EWELINA HANKIEWICZ³, BJÖRN TRAUZETTEL³, HARTMUT BUHMANN^{1,2}, and LAURENS MOLENKAMP^{1,2} — ¹Experimentelle Physik III, Physikalisches Institut, Universität Würzburg, Am Hubland, Würzburg, Germany — ²Institute for Topological Insulators, Universität Würzburg, Am Hubland, Würzburg, Germany — ³Institut für Theoretische Physik und Astrophysik, Universität Würzburg, Am Hubland, 97074 Würzburg, Germany.

In this talk, I will discuss some of our recent results on HgTe-based two-dimensional topological insulators. Over the past few years, we have developed a chemical wet-etch technique to fabricate high-quality microstructures in HgTe quantum wells. Firstly, I will discuss some important achievements due to the wet-etch fabrication process: We fabricated quantum point contacts in topological HgTe quantum wells and investigated the interactions among helical edge channels. We also fabricated microstructures from (Hg,Mn)Te quantum wells and observed quantized conductance in these devices. Secondly, I will introduce a gate training method that allows us to approach conductance quantization in macroscopic devices. Finally, I will present recent magnetotransport results on

(Hg,Mn)Te quantum wells and the emergence of quantum Hall plateaus at extremely low magnetic fields (~ 50 mT).

TT 32.6 Thu 17:45 H10

Quantum non-Hermitian topological sensors — •FLORIAN KOCH and JAN CARL BUDICH — Institute of Theoretical Physics, Technische Universität Dresden

Recent discoveries regarding the exceptional spectral and topological properties of non-Hermitian (NH) tight-binding models, e.g. their striking boundary-sensitivity, have triggered the quest for constructing novel sensors [1,2]. Here, using quantum master equations we promote the architecture of such sensing devices to a fully quantum-mechanical framework. Specifically, we study a setting of weakly-coupled bosonic modes arranged in an array with broken ring geometry that would realize a NH topological phase in the classical limit. Employing methods from quantum-information theory of Gaussian states, we show that a small coupling induced between the ends of the broken ring may be detected with a precision that increases exponentially in the number of coupled modes. Our findings pave the way towards designing quantum NH topological sensors (QUANTOS) that may observe with high precision any physical observable that couples to the boundary conditions of the device [3].

[1] J.C. Budich and E.J. Bergholtz, Phys. Rev. Lett. **125**, 180403 (2020).

[2] E.J. Bergholtz, J.C. Budich, and F.K. Kunst, Rev. Mod. Phys. **93**, 015005 (2021).

[3] F. Koch and J.C. Budich, Phys. Rev. Res. **4**, 013113 (2022).

TT 32.7 Thu 18:00 H10

First magnetic field measurements of a topological insulator based Transmon Qubit — •ANNE SCHMIDT¹, TOBIAS W. SCHMITT¹, CHENLU LIU², ALBERT HERTEL¹, CHRISTIAN DICKEL³, MICHAEL SCHLEENVOIGT¹, MALCOLM R. CONNOLLY^{2,4}, YOICHI ANDO³, DETLEV GRÜTZMACHER¹, and PETER SCHÜFFELGEN¹ — ¹Peter Grünberg Institute & Jülich-Aachen Research Alliance, Forschungszentrum Jülich — ²Blackett Laboratory, Imperial College London — ³Institute of Physics II, University of Cologne — ⁴London Centre for Nanotechnology, University College London

Hybrid topological insulator (TI) – superconductor (S) heterostructures are a promising platform for the realization of topologically protected quantum computation based on Majorana zero modes. This promises fewer physical qubits for creating a logical qubit compared to conventional superconducting qubits. Our full *in situ* device fabrication, which combines selective area growth of thin (Bi,Sb)₂Te₃ films and stencil deposition of superconductive Nb has already shown to create highly transparent S-TI interfaces. Recently, we have demonstrated that this fabrication process can readily be integrated into cQED structures as building block for a transmon qubit and performed coherence measurements at zero magnetic field. Here, we will expand these measurements to finite magnetic fields, as in-plane magnetic fields are a requirement for restoring the topological phase in confined (Bi,Sb)₂Te₃ nanostructures. We present initial results on the magnetic field dependence of the T₁ lifetime and the qubit's anharmonicity.

TT 32.8 Thu 18:15 H10

Kondo interactions of quantum spin Hall edge channels with charge puddles — •CHRISTOPHER FUCHS^{1,2}, PRAGYA SHEKHAR^{1,2}, SAQUIB SHAMIM^{1,2}, LENA FÜRST^{1,2}, JOHANNES KLEINLEIN^{1,2}, JUKKA I. VÄRYNEN³, HARTMUT BUHMANN^{1,2}, and LAURENS W. MOLENKAMP^{1,2} — ¹Physikalisches Institut, Universität Würzburg, Würzburg, Germany — ²Institute for Topological Insulators, Universität Würzburg, Würzburg, Germany — ³Department of Physics and Astronomy, Purdue University, West Lafayette, USA

Quantum spin Hall edge channels are protected against backscattering by time-reversal symmetry. However, since the first observation of the quantum spin Hall effect in HgTe in 2007 it is known that reproducible fluctuations shape the quantization plateau when the chemical potential is tuned through the bulk gap. Here, those fluctuations are examined in high-quality micron-sized quantum well structures of HgTe at millikelvin temperatures. By performing temperature and gate-dependent measurements, we conclude that the observed conductance fluctuations indicate interactions of the edge channel electrons with individual charge puddles – microscopic fluctuations in the potential landscape commonly observed in narrow gap semiconductors – that act like Kondo correlated quantum dots. The resulting spin-flip backscattering gives rise to a distinct Kondo-like temperature dependence of the conductance fluctuations, which is backed up by theoretical modelling. Our results provide insight into the leading mechanism of decoherence of quantum spin Hall edge channels.

TT 33: Nonequilibrium Quantum Many-Body Systems (joint session TT/DY)

Time: Thursday 15:00–18:15

Location: H22

TT 33.1 Thu 15:00 H22

Investigating the non-equilibrium dynamics of two-level systems at low temperature — •MARCEL HAAS, MAREIKE DINGER, LUKAS MÜNCH, JAN BLICKBERNDT, ANDREAS REISER, ANDREAS FLEISCHMANN, and CHRISTIAN ENSS — Kirchhoff-Institute for Physics, Heidelberg, Germany

The dielectric loss of amorphous materials along with noise and decoherence is the major limiting factor in many applications like superconducting circuits, Josephson junctions and quantum computing. It is mainly determined by atomic tunneling systems described by quantum mechanical two-level systems (TLS), which are broadly distributed low-energy excitations in the sample. The spontaneous phonon emission of an excited TLS gives rise to a relaxation time T_1 and the interaction between TLSs with their thermally excited surrounding induces a decoherence time T_2 . These effects mainly determine the measurable dielectric loss in the observed material, which we ascertain by measuring the quality factor of a bridge type superconducting LC-resonator. The dielectric medium in between the capacitor plates is a sputter deposited a-SiO₂ film. The setup shows a unique property when two off-resonant pump tones are applied symmetrically. In this limit, the resonator is emitting at the intermediate frequency of the driving fields. The underlying mechanism can therefore be explained by a nonlinear interaction of the rf-field with the TLSs and the resonator which is creating additional lines in the frequency spectrum. We present first measurements at a frequency of 1 GHz performed with a micro-fabricated superconducting resonator.

TT 33.2 Thu 15:15 H22

Photoinduced prethermal order parameter dynamics in the two-dimensional large-N Hubbard-Heisenberg model — •ALEXANDER OSTERKORN and STEFAN KEHREIN — University of Göttingen, Göttingen, Germany

A central topic in current research in non-equilibrium physics is the design of pathways to control and induce order in correlated electron materials with time-dependent electromagnetic fields. The theoretical description of such processes, in particular in two spatial dimensions, is very challenging and often relies on phenomenological modelling in terms of free energy landscapes. We discuss a semiclassical time evolution scheme that includes dephasing dynamics beyond mean-field and allows to simulate the light-induced manipulation of prethermal order in a two-dimensional model [1] with competing phases microscopically. We calculate the time evolution of the relevant order parameters subsequent to driving with a short laser pulse [2]. The induced prethermal order does not depend on the amount of absorbed energy alone but also explicitly on the driving frequency and amplitude. While this dependency is pronounced in the low-frequency regime, it is suppressed at high driving frequencies.

[1] Phys. Rev. B 39, 11538 (1989)

[2] arXiv:2205.06620

TT 33.3 Thu 15:30 H22

Nonequilibrium dynamics in pumped Mott insulators — •SATOSHI EJIMA¹, FLORIAN LANGE², and HOLGER FEHSKE^{1,2} — ¹Institut für Physik, Universität Greifswald, Greifswald, Germany — ²Erlangen National High Performance Computing Center, Friedrich-Alexander-Universität Erlangen-Nürnberg, Erlangen, Germany

The study of systems under optical excitation receives tremendous attention because of both the recent rapid developments of ultrafast pump lasers and the discovery of striking phenomena not observable in equilibrium. Various numerical techniques have been applied to optically excited systems to study nonequilibrium dynamics, e.g., the time-dependent version of exact-diagonalization technique or dynamical mean-field theory. Results for nonequilibrium dynamics based on tensor-network algorithms are still rare, however.

In this talk, we propose a direct numerical scheme in the matrix-product-states (MPS) representation for the computation of nonequilibrium dynamic response functions, which can be used for general (quasi-)one-dimensional systems. Using time-evolution techniques for (infinite) MPS, we calculate, directly in the thermodynamic limit, the time-dependent photoemission spectra and dynamic structure factors of the half-filled Hubbard chain after pulse irradiation. These quantities exhibit clear signatures of the photoinduced phase transition from insulator to metal that occurs because of the formation of so-called η pairs.

[1] S. Ejima et al., Phys. Rev. Res. 2, 032008(R) (2020)

[2] Phys. Rev. Res. 4, L012012 (2022)

[3] arXiv:2204.09085

TT 33.4 Thu 15:45 H22

Nonequilibrium non-Markovian steady states in open quantum many-body systems: Persistent oscillations in Heisenberg quantum spin chains — •REGINA FINSTERHOELZL¹, MANUEL KATZER², and ALEXANDER CARMELE² — ¹Department of Physics, University of Konstanz, Germany — ²Institute of Theoretical Physics, Technical University Berlin, Germany

We investigate the effect of a non-Markovian, structured reservoir on an open Heisenberg spin chain by applying coherent time-delayed feedback control to it. The structured reservoir couples frequency-dependent to the spin chain and therefore induces a memory, thus the spin chain interacts partially with its own past. We demonstrate that with this new paradigm of a non-Markovian temporal driving scheme, it is possible to generate persistent oscillations within the many-body system and thus induce highly non-trivial states which dynamically store excitation within the chain. These oscillations occur at special points in the stability landscape and persist for different chain lengths and different initial excitations within the chain. We propose a non-invasive partial characterization of the chain by exploiting the fact that the different trapping conditions which arise each relate to specific steady states within the chain.

TT 33.5 Thu 16:00 H22

Approaching the time-dependent quantum many-body problem with Artificial Neural Networks — •PIT NEITEMEIER and DANTE KENNES — RWTH Aachen Institut für Theorie der statistischen Physik

Numerical solutions to quantum many body problems pose a significant challenge due to the curse of dimensionality. In this work I propose a novel Artificial Neural Network (ANN) ansatz and an unsupervised learning scheme to efficiently and flexibly solve time dependent quantum many-body problems. Contrary to previous work I do not rely on ODE Solvers for the time evolution, but parametrize the full wave function using an ANN. This enables a constant cost evaluation and full differentiability of the wave function. Furthermore I show that it is possible to learn solution bundles that continuously represent the solution for a range of external parameters. The training of these ANNs is highly parallelizable and reduces sequential operations significantly in comparison to previous work. I benchmark the ansatz for quantum quenches, ramps and pulses of the magnetic field using 1D Ising and Heisenberg Chains.

TT 33.6 Thu 16:15 H22

Entanglement phase transitions in correlated 1D spin chains — •MONALISA SINGH ROY, JONATHAN RUHMAN, EMANUELE G. DALLA TORRE, and EFRAT SHIMSHONI — Department of Physics, Bar-Ilan University, Ramat Gan, Israel

Entanglement phase transitions have attracted immense attention in recent years especially in the context of monitored quantum circuits. In such systems the dynamics due to unitary evolution compete with the localization induced by measurements. The phase transition of quantum systems from a phase where its entanglement entropy exhibits volume law for weak monitoring, to a quantum Zeno like phase with where the entanglement entropy obeys area law is well known in many models with unitary dynamics. Some recently proposals have identified a critical phase with a logarithmic scaling of entanglement in non-Hermitian models. We explore such a critical transition in a monitored quantum spin chain model and identify the entanglement transitions in the system under both unitary and non-unitary evolutions.

TT 33.7 Thu 16:30 H22

Feynman-Vernon influence functional approach to quantum transport in interacting nanojunctions: An analytical hierarchical study — •LUCA MAGAZZU and MILENA GRIFONI — University of Regensburg

We present a nonperturbative and formally-exact approach to the charge transport in interacting nanojunctions using a real-time path-integral method based on the Feynman-Vernon influence functional. Expansion of the influence functional in terms of the number of tunneling transitions results in an exact generalized master equation for the populations in the occupation-number representation, and in a formally exact expression for the current. We apply our method to the exactly solvable resonant level model (RLM) and to the single-impurity Anderson model (SIAM). For both systems, we demonstrate a hierarchical diagrammatic structure. While the hierarchy closes at the second tier for the RLM, this is not the case for the interacting SIAM. Upon inspection of the current kernel, known results from various perturbative and nonperturbative approximation schemes to quantum transport in the SIAM are recovered. Using a simplified fourth-tier scheme, analytical results for the interacting SIAM are presented both in equilibrium and nonequilibrium and with an applied magnetic field.

[1] L. Magazzù and M. Grifoni, Phys. Rev. B 105, 125417 (2022)

15 min. break

TT 33.8 Thu 17:00 H22

In-Gap Band Formation in a Periodically Driven Charge Density Wave Insulator — •ALEXANDER OSTERKORN, CONSTANTIN MEYER, and SALVATORE MANMANA — University of Göttingen, Göttingen, Germany

Periodically driven quantum many-body systems host unconventional behavior not realized at equilibrium. Here we investigate such a setup for strongly interacting spinless fermions on a chain, which at zero temperature and strong

interactions form a charge density wave insulator. Using unbiased numerical matrix product state methods for time-dependent spectral functions, we find that driving of the correlated charge-density wave insulator leads not only to a renormalization of the excitation spectrum as predicted by an effective Floquet Hamiltonian [1], but also to a cosine-like in-gap feature [2]. This is not obtained for a charge density wave model without interactions. A mean-field treatment provides a partial explanation in terms of doublon excitations. However, the full picture needs to take into account strong correlation effects. [1] Phys. Rev. Lett. 120, 127601 (2018) [2] arXiv:2205.09557

TT 33.9 Thu 17:15 H22

Non-equilibrium phases of matter in 2D using Projected Entangled Pair States — •AUGUSTINE KSHETRIMAYUM^{1,2}, DANTE KENNES³, and JENS EISERT^{1,2} — ¹Freie University Berlin, Germany — ²Helmholtz-Zentrum Berlin, Germany — ³RWTH Aachen University, Germany

We explore the highly challenging realm of non-equilibrium physics in two spatial dimensions using infinite Projected Entangled Pair States (iPEPS), a two-dimensional tensor network ansatz directly in the thermodynamic limit. By adding disorder in a translationally invariant setting through the use of auxiliary states, we find evidence of Many-body localization (MBL) and Quantum time crystals in 2D.

In our discrete disorder setting, we show that many levels of disorder is required in order to achieve localization and ultimately time crystalline behavior. We discuss how our setting can be realized in programmable quantum simulators.

TT 33.10 Thu 17:30 H22

Charge transport in hybrid semiconductor-cavity systems: an exact diagonalization study — •SEBASTIAN STUMPER and JUNICHI OKAMOTO — Institute of Physics, University of Freiburg, Freiburg, Germany

Recent experiments demonstrate that the conductivity of organic semiconductors can be enhanced by hybridization with a plasmonic surface [Nat. Mat. 14, 1123 (2015)]. Motivated by these findings, we study a two-band tight-binding chain resonantly coupled to a photonic mode by an exact diagonalization technique. First, we argue that the exciton density and photon number are suppressed by the band gap, an effect which is neglected by the commonly used rotating wave approximation. Second, we determine the excitation of the semiconductor and its impact on the conductivity beyond the rotating wave approximation, i.e., including the off-resonant terms. Clean and disordered cases are compared. Finally, we discuss the real-time dynamics of electrons and holes under a uniform electric field.

TT 34: Correlated Electrons: Theory 2

Time: Thursday 15:00–18:45

Location: H23

TT 34.1 Thu 15:00 H23

The fate of the spin polaron in the 1D t-J model — •PIOTR WRZOSEK — Institute of Theoretical Physics, Faculty of Physics, University of Warsaw, Pasteura 5, PL-02093 Warsaw, Poland

We study the intrinsic origin of the well-established differences in the motion of a single hole in the 1D and 2D antiferromagnet. To this end, we consider a 1D t-J model, perform the slave fermion transformation to the holon-magnon basis, and solve the obtained model in a numerically exact manner. We explicitly show that the spin polaron quasiparticle, which is well-known from the studies of a single hole in the 2D antiferromagnet, is destroyed in the 1D t-J model by the magnon-magnon interactions. Nevertheless, we observe surprising similarities between the spectra obtained with and without magnon-magnon interactions, indicating that some of the key features of the spin polaron physics are still preserved in 1D.

TT 34.2 Thu 15:15 H23

Huge enhancement of the thermal conductivity in the Tomonaga-Luttinger-liquid region of YbAlO₃ — •PARISA MOKHTARI^{1,2}, ULRIKE STOCKERT¹, and ELENA HASSINGER^{1,2} — ¹Max-Planck-Institute for Chemical Physics of Solids, Dresden, Germany — ²Physics Department, Technical University of Munich, Garching, Germany

In 2019, Wu et al. found the typical excitation spectrum of the spinons in the Q-1D material YbAlO₃ via neutron scattering at 1 K. YbAlO₃ exhibit AFM ($J_c=2.3$ K) and FM ($J_a b=0.8$ K) exchange interaction along and perpendicular to the chain direction, respectively [1, 2]. In zero field, a 3D AFM order is established at 0.88 K. For fields along a, perpendicular to the chain, this order is suppressed and replaced by an IC-AFM state, until the FI-FM state occurs for $B > 1.5$ T.

It is an open question, if magnetic excitations in this material carry heat, and how they interact with phonons. Hence, we investigate the low-T κ of YbAlO₃ down to 30 mK in fields up to 4 T. The phase diagram is successfully reproduced with pronounced anomalies in both T and B sweeps. A clear additional anomaly

TT 33.11 Thu 17:45 H22

Interplay of disorder and interactions in a periodically driven ultracold atomic system — •ARIJIT DUTTA — Institut für Theoretische Physik, Goethe-Universität, 60438 Frankfurt am Main, Germany

Periodically driven clean noninteracting systems are known to host several interesting topological phases. Particularly, for high frequency driving, they have been found to host the analogues of equilibrium topological phases, like the Haldane phase. However, upon lowering the driving frequencies these systems have been found to host anomalous phases with robust edge modes despite all Chern numbers being zero. Moreover, theoretical works have shown that adding disorder to such anomalous phases leads to quantized charge pumping through the edge modes even when all bulk states become localised. We investigate the fate of these phases in presence of electron-electron interactions of the Falicov-Kimball type.

TT 33.12 Thu 18:00 H22

Non-equilibrium optical conductivity for striped states: A time-dependent Gutzwiller analysis for the single-band Hubbard model — •CHRISTIAN MARTENS and GÖTZ SEIBOLD — BTU Cottbus-Senftenberg, Institute of Physics, 03046 Cottbus, Germany

In recent years pump-probe experiments have turned out as a powerful tool to investigate the dynamics of correlated materials, e.g. transition metals or heavy fermion systems. In these experiments the system is prepared in a non-equilibrium state by a strong laser pulse, where the relaxation is afterwards examined by standard optical techniques. This method has also been applied to stripe ordered nickelates and cuprate superconductors where it allows to study the coupled order-parameter dynamics of charge- and spin-density waves and superconductivity.

Here we use the time-dependent Gutzwiller approximation for the single-band Hubbard model to analyse the non-equilibrium dynamics for stripe ground states of different symmetry. In particular we are interested in the interplay between spin and charge dynamics which is analysed by quenching the system in the charge or spin sector. This allows us to investigate the coupled relaxation dynamics as a function of the inserted energy. In contrast to the Hartree-Fock + random-phase-approximation the optical conductivity shows high-energy double occupancy fluctuations in addition to the low-energy collective mode. In the out-of equilibrium regime we find a softening of both modes depending on the inserted energy. Moreover the double occupancy excitation broadens into a continuum.

in the field dependence at low T confirms a crossover within the IC phase, which was suggested before based only on a tiny plateau appearing in the magnetisation. We find a large variation of the κ throughout the phase diagram indicating strong magneto-elastic coupling. In addition, a substantial enhancement of κ is observed in the proposed TLL region.

[1] L. S. Wu et al., Nat. Commun. 10, 698 (2019)

[2] L. S. Wu et al., Phys. Rev. B 99, 195117 (2019)

TT 34.3 Thu 15:30 H23

Counting statistics in interacting one-dimensional conductors — •OLEKSIY KASHUBA¹, ROMAN RIWAR¹, FABIAN HASSLER², and THOMAS SCHMIDT³ — ¹Forschungszentrum Jülich — ²RWTH Aachen — ³Luxemburg Uni

The calculation of the cumulant generating function of a given observable, such as the charge, is nontrivial even for the non-interacting systems. This problem is closely connected to the problem of Toeplitz eigenvalues and the Szegő-Kac theorem [1]. The application of the latter leads to a violation of the moment generating function's periodicity along the counting field. This periodicity can be restored using the Fisher-Hartwig conjecture, as was shown for non-interacting one-dimensional electrons [2]. Here, we aim to go beyond and include interactions. For weak interactions, a modification of the Matsubara diagrammatic approach was developed, allowing us explicit calculation of the interaction corrections to the cumulant generating function. All obtained terms preserve the periodic constraint of the moment generating function. The obtained result is in a good agreement at low filling with the noise suppression in Luttinger liquid for $K < 1$. We also found a surprising counterpart of the charge-density wave effect in the cumulant generating function.

[1] Basor, Morrison, Linear Algebra and its Appl. 202 (1994), 129

[2] Aristov, Phys. Rev. B 57 (1998), 12825

TT 34.4 Thu 15:45 H23

Enhancement of pair correlations in the asymmetric Hubbard ladder — •ANAS ABDELWAHAB and ERIC JECKELMANN — Leibniz Universität Hannover, Hannover, Germany

We investigated an extension of the asymmetric two-leg Hubbard ladder model [1,2] that consists of different on-site interaction U_y and intra-hopping t_y on each leg y using the density matrix renormalization group method. We calculated pair binding energy, charge, spin and single particle gaps as well as pairing correlation functions for several sets of model parameters. It is possible to adjust the asymmetry of model parameters to retain finite pair binding energy and enhanced pairing correlation functions similar to those appearing in symmetric two-leg Hubbard ladders. Such adjustment represents an interpolation between doped Mott insulator and doped charge transfer insulator.

[1] A. Abdelwahab, E. Jeckelmann, M. Hohenadler, Phys. Rev. B 91, 155119 (2015)

[2] A. Abdelwahab and E. Jeckelmann, Eur. Phys. J. B 91, 207 (2018).

TT 34.5 Thu 16:00 H23

Magnetic properties of a quantum spin ladder material in proximity to the isotropic limit — •SERGEI ZVYAGIN — Dresden High Magnetic Field Laboratory (HLD-EMFL), Helmholtz-Zentrum Dresden-Rossendorf, 01328 Dresden, Germany

We report on the synthesis, crystal structure, magnetic, thermodynamic, and electron-spin-resonance properties of the coordination complex $[\text{Cu}_2(\text{pz})_3(4\text{-HOpy})_4](\text{ClO}_4)_4$ [pz = pyrazine; 4-HOpy = 4-hydroxypyridine] [1]. This material is identified as a spin-1/2 Heisenberg ladder system with exchange-coupling parameters $J_{\text{rung}}/k_B = 12.1(1)$ K and $J_{\text{leg}}/k_B = 10.5(3)$ K [$J_{\text{rung}}/J_{\text{leg}} = 1.15(4)$]. For single crystals our measurements revealed two critical fields, $\mu_0 H_{c1} = 4.63(5)$ T and $\mu_0 H_{c2} = 22.78(5)$ T (for $H \parallel a^*$), separating the gapped spin-liquid, gapless Tomonaga-Luttinger-liquid, and fully spin-polarized phase. No signature of a field-induced transition into a magnetically ordered phase was found at temperatures down to 450 mK. The material bridges an important gap by providing an excellent physical realization of an almost isotropic spin-1/2 strong-rung Heisenberg ladder system with modest exchange-coupling energy and critical-field scales.

[1] S. A. Zvyagin, A. N. Ponomaryov, M. Ozerov, E. Schulze, Y. Skourski, R. Beyer, T. Reimann, L. I. Zviagina, E. L. Green, J. Wosnitzer, I. Sheikin, P. Bouillot, T. Giamarchi, J. L. Wikara, M. M. Turnbull, and C. P. Landee, Phys. Rev. B 103, 205131 (2021)

TT 34.6 Thu 16:15 H23

Finite-temperature optical conductivity with density-matrix renormalization group methods for the Holstein polaron and bipolaron with dispersive phonons — •DAVID JANSEN¹, JANEZ BONČA^{2,3}, and FABIAN HEIDRICH-MEISNER¹ — ¹Institute for Theoretical Physics, University of Göttingen — ²J. Stefan Institute, Ljubljana — ³Faculty of Mathematics and Physics, University of Ljubljana

We compute the optical conductivity for the Holstein polaron and bipolaron with dispersive phonons at finite temperature using a matrix-product state based method. We combine purification [1], to obtain the finite-temperature states, together with the parallel time-dependent variational principle (pTDVP) [2] algorithm to compute the real time current-current correlation functions. The pTDVP algorithm utilizes local basis optimization [3] to efficiently treat the phononic degrees of freedom. For the polaron, we find that the phonon dispersion alters the optical conductivity at several temperatures in the weak, intermediate, and strong coupling regime. In the two first cases, we see that the spectrum goes from being continuous to discrete when going from a downwards to an upwards phonon dispersion. In the strong coupling regime, the dispersion leads to a shift of the center of the spectrum. For the bipolaron, we study the effect of dispersion in both the weak and strong electron-phonon coupling regime, and thus see its influence on both a delocalized and a localized bipolaron.

This research was supported by the DFG via SFB 1073.

[1] Verstraete et al., Phys. Rev. Lett. 93, 207204 (2004)

[2] Secular et al., Phys. Rev. B 101, 235123 (2020)

[3] Zhang et al., Phys. Rev. Lett. 80, 2661 (1998)

TT 34.7 Thu 16:30 H23

Cavity-induced long-range interactions in strongly correlated systems — •PAUL FADLER¹, JIAJUN LI², KAI PHILLIP SCHMIDT¹, and MARTIN ECKSTEIN¹ — ¹Friedrich-Alexander-Universität Erlangen-Nürnberg — ²Paul Scherrer Institut

In recent years, the coupling of optical cavity modes to solid states systems has emerged as a possible way to control material properties. Here we investigate cavity-induced long-range interactions between spins in a Mott insulator, which are a new feature of the coupling to the quantized cavity field, and are absent in a control of magnetism by classical light. In detail, for the Fermi-Hubbard model at half filling we show that the cavity coupling leads to long-range four-spin terms in the effective low spin model at large onsite interaction U , in addition to the conventional antiferromagnetic Heisenberg exchange interaction.

To obtain these long-range interactions, we compare exact diagonalization, a perturbative approach based on the effective spin-photon Hamiltonian descrip-

tion of the system, and fourth-order perturbation theory in the Hubbard model. We show that the phenomenologically motivated spin-photon Hamiltonian fails to describe the interactions properly close to resonances of the cavity and charge excitations. It is therefore not possible to perturbatively treat cavity coupled correlated systems in an effective spin basis.

15 min. break

TT 34.8 Thu 17:00 H23

Magnetism and Mottness in the anisotropic triangular lattice Hubbard model: a cellular dynamical mean-field study — •MARCEL KLETT¹, HENRI MENKE², MICHEL FERRERO³, ANTOINE GEORGES³, and THOMAS SCHÄFER¹ — ¹Max Planck Institute for Solid State Research, Stuttgart, Germany — ²University of Erlangen-Nuremberg, Erlangen, Germany — ³College de France, Paris, France

We investigate the phase diagram of the anisotropic triangular lattice Hubbard model in a center-focused cellular dynamical mean-field theory (CDMFT) approach using an impurity with 7 sites. We investigate the Mott metal-to-insulator transition and crossover region as well as the superconducting phase. Using a spin symmetry-broken approach of the CDMFT, allowing for a rotations of spins on the Bloch sphere, we are able to investigate the magnetic ordering of the different cluster schemes.

TT 34.9 Thu 17:15 H23

Competing orders in a two-dimensional Su-Schrieffer-Heeger model — •ANIKA GÖTZ¹, MARTIN HOHENADLER^{1,2}, and FAKHER ASSAAD^{1,3} — ¹Institut für Theoretische Physik und Astrophysik, Universität Würzburg, 97074 Würzburg, Germany — ²Independent Researcher, Josef-Retzler-Str. 7, 81241 Munich, Germany — ³Würzburg-Dresden Cluster of Excellence ct.qmat, Am Hubland, 97074 Würzburg, Germany

We study a two-dimensional Su-Schrieffer-Heeger model of electrons coupled to Einstein phonons with auxiliary-field quantum Monte Carlo simulations. By adding a symmetry-allowed interaction, the phonons can be integrated out at the expense of imaginary-time correlations of the discrete Hubbard-Stratonovich fields. Using single spin-flip updates, we investigate the phase diagram at the $O(4)$ -symmetric point as a function of hopping t and phonon frequency ω_0 . For low phonon frequencies, the C_4 lattice symmetry is broken by valence bond order. Depending on t , the ordering wavevector is either (π, π) or $(\pi, 0)$, the latter value being accompanied by a dynamically generated π -flux in each plaquette. At larger ω_0 , the $O(4)$ symmetry is spontaneously broken by long-range antiferromagnetic (AFM) order. In the limit $t \rightarrow 0$, the model maps onto an unconstrained Z_2 gauge theory coupled to fermions which is in its confined phase for the parameters considered. Whereas the $(\pi, 0)$ -VBS to AFM transition is a candidate for a deconfined quantum critical point, the details of the $(\pi, 0)$ -VBS to (π, π) -VBS and (π, π) -VBS to AFM transitions are still under investigation.

TT 34.10 Thu 17:30 H23

Splitting of topological charge pumping in an interacting two-component fermionic Rice-Mele Hubbard model — •ERIC BERTOK¹, FABIAN HEIDRICH-MEISNER¹, and ARMANDO A. ALIGIA² — ¹Institute for Theoretical Physics, Georg-August-Universität Göttingen — ²Centro Atómico Bariloche and Instituto Balseiro, Bariloche, Argentina

A Thouless pump transports an integer amount of charge when pumping adiabatically around a singularity. We study the splitting of such a critical point into two separate critical points by adding a Hubbard interaction. Furthermore, we consider extensions to a spinful Rice-Mele model, namely a staggered magnetic field or an Ising-type spin coupling, further reducing the spin symmetry. The resulting models additionally allow for the transport of a single charge in a two-component system of spinful fermions, whereas in the absence of interactions, zero or two charges are pumped. In the $SU(2)$ -symmetric case, the ionic Hubbard model is visited once along pump cycles that enclose a single singularity. Adding a staggered magnetic field additionally transports an integer amount of spin while the Ising term realizes a pure charge pump. We employ real-time simulations in finite and infinite systems to calculate the adiabatic charge and spin transport, complemented by the analysis of gaps and the many-body polarization to confirm the adiabatic nature of the pump. The resulting charge pumps are expected to be measurable in finite-pumping speed experiments in ultra-cold atomic gases. We discuss the implications of our results for a related quantum-gas experiment by Walter et al. [arXiv:2204.06561].

TT 34.11 Thu 17:45 H23

Thermodynamics of the metal-insulator transition in the extended Hubbard model from determinantal quantum Monte Carlo — •ALEXANDER SUSHCHYEV and STEFAN WESSEL — RWTH Aachen University

We use finite-temperature determinantal quantum Monte Carlo simulations to study the thermodynamic properties of the extended Hubbard model on the square lattice at half-filling. In particular, we consider the effect of a nearest-neighbor and a long-range Coulomb repulsion on the thermal metal-insulator transition in the Slater regime at intermediate coupling. Within the parameter

regime accessible to sign-free quantum Monte Carlo simulations we explore in detail the temperature dependence of the double occupancy and entropy. Notably, we probe for signatures of a first-order metal-insulator transition driven by the suppression of correlation effects by the non-local interactions, as proposed in [1].

[1] M.Schueler et al., *Sci. Post. Phys.* 6, 067 (2019)

TT 34.12 Thu 18:00 H23

Surrogate models for quantum spin systems based on reduced order modeling — •STEFAN WESSEL¹, MICHAEL HERBST¹, BENJAMIN STAMM¹, and MATTEO RIZZI² — ¹RWTH Aachen University — ²University of Cologne and FZ Jülich

We present a methodology to investigate phase-diagrams of quantum spin models based on the principle of the reduced basis method. It is based on constructing a low-dimensional basis built from solutions of snapshots, i.e., ground states corresponding to particular and well-chosen parameter values. We propose to use a greedy-strategy to assemble the reduced basis and thus to select the parameter points where the full model is solved. Once the reduced basis is computed, observables required for the computation of phase-diagrams can be computed with a computational complexity independent of the underlying Hilbert space for any parameter value. We illustrate the accuracy of this approach for a geometrically frustrated antiferromagnetic two-dimensional lattice model and quantum spin model that describes a chain of excited Rydberg atoms.

TT 34.13 Thu 18:15 H23

Bound by three-body interactions — •GARY FERKINGHOFF¹, LEANNA MÜLLER¹, UMESH KUMAR², GÖTZ S. UHRIG¹, and BENEDIKT FAUSEWEH³ — ¹Condensed Matter Theory, Technische Universität Dortmund, Otto-Hahn-Straße 4, 44227 Dortmund, Germany — ²Theoretical Division, Los Alamos National Laboratory, Los Alamos, New Mexico 87545, USA — ³Institute for Software Technology, German Aerospace Center (DLR), Linder Höhe, 51147 Cologne, Germany

Stable bound quantum states are ubiquitous in nature. Mostly, they result from the interaction of only pairs of particles, so called two-body interactions, even when complex many-particle structures are formed. We show that three-quasi-particle bound states occur in a generic, experimentally accessible solid state system: antiferromagnetic spin ladders, related to high-temperature superconductors. Strikingly, this binding is induced by genuine three-quasi-particle interactions; without them there is no bound state. We compute the dynamic exchange structure factor required for the experimental detection of the predicted state by resonant inelastic x-ray scattering for realistic material parameters. Our work enables us to quantify these elusive interactions and unambiguously establishes their effect on the dynamics of the quantum many-particle state. In this talk we will present the main results of our study, briefly explain the theoretical tools that we used and present an experimental setting for verifying our theoretical results.

TT 34.14 Thu 18:30 H23

Non-linear response functions and disorder: The case of the photo galvanic effect — •KONSTANTINOS LADOVRECHIS and TOBIAS MENG — Institute for Theoretical Physics and Würzburg-Dresden Cluster of Excellence ct.qmat, Technische Universität Dresden, Germany

The circular photogalvanic effect (CPGE) is a non-linear photocurrent which is generated in materials with broken inversion symmetry when they are shed with circularly polarised light. In Weyl semi-metals, the CPGE is quantized in terms of fundamental constants and the Chern numbers associated with the Weyl nodes. In this work, we investigate the effect of pointlike disorder onto the quantization of CPGE. Implementing 1st-order and self-consistent Born approximations, we identify that the quantization of CPGE is broken and perturbative corrections in the scattering strength emerge, which we further classify in terms of self-energy and vertex corrections.

TT 35: Members' Assembly

Time: Thursday 19:00–20:00

Location: H22

All members of the Low Temperature Physics Division are invited to participate.

TT 36: Focus Session: Ultrafast Spin, Lattice and Charge Dynamics of Solids

This focus session deals with a current and interdisciplinary topic, which is of interest to many researchers in solid state physics. The focus is on the generation and manipulation of new effects such as switching the macroscopic magnetic order, the driving of metal-insulator transitions, and the observation of purely quantum mechanical phenomena in excited states (e.g., the squeezing of phonons) on the femtosecond time scale using laser pulses. The long-term goal is the coherent control of degrees of freedom in solids. The relevant issues are light-matter interaction on the ultrashort time scale, non-equilibrium dynamics of magnetic, phononic and electronic degrees of freedom, many-particle physics and strong correlations.

Organizers:

Davide Bossini, University of Konstanz and Götz S. Uhrig, TU Dortmund University

Time: Friday 9:30–12:15

Location: H10

Invited Talk

TT 36.1 Fri 9:30 H10

Coherent control of lattice and electronic states — •STEVEN JOHNSON — ETH Zurich, Zurich, Switzerland — Paul Scherrer Institut, Villigen, Switzerland

In this presentation I discuss a selection of recent efforts to use ultrafast light pulse excitation ranging from near-infrared to THz wavelengths to achieve control over both structural and electronic degrees of freedom in condensed phase materials. In one example, ultrafast excitation of a quasi-2D material results in a large-scale coherent modulation of structure (as seen by femtosecond x-ray diffraction) and associated carrier effective masses. These modulations are strongly connected to a nearby topological phase transition. In another example I discuss experiments using high field THz pulses to drive both coherent and incoherent carrier dynamics in a narrow-gap semiconductor, and describe how these dynamics can be inferred from multidimensional THz spectroscopy. The results demonstrate that carrier multiplication effects become dominant at moderately intense field strengths. In the final example I will discuss ongoing efforts to use combinations of high- and low-frequency light excitation to drive nonlinear structural dynamics in a soft mode ferroelectric.

Invited Talk

TT 36.2 Fri 10:00 H10

New opportunities for light-matter control of quantum materials — •MICHAEL SENTEF — Max Planck Institute for the Structure and Dynamics of Matter, Hamburg

In this talk I will discuss recent progress in controlling and inducing materials properties with light [1]. Specifically I will discuss recent experiments showing light-induced superconducting-like optical responses through phonon driving in an organic kappa salt [2], and their possible theoretical explanation via dynamical Hubbard U [3]. I will then highlight some recent theoretical and experimental progress in cavity quantum materials [4,5], where the classical laser as a driving field of light-induced properties is replaced by quantum fluctuations of light in confined geometries. Ideas and open questions for future work will be outlined.

[1] *Rev. Mod. Phys.* 93, 041002 (2021)

[2] *Phys. Rev. X* 10, 031028 (2020)

[3] *Phys. Rev. Lett.* 125, 137001 (2020)

[4] *Applied Physics Reviews* 9, 011312 (2022)

[5] *J. Phys. Mater.* 5, 024006 (2022)

Invited Talk TT 36.3 Fri 10:30 H10

Coherent electronic control of an insulator-to-metal transition — •CLAUDIO GIANNETTI, PAOLO FRANCESCHINI, and ALESSANDRA MILLOCH — Università Cattolica del Sacro Cuore, Brescia (Italy)

Managing light-matter interaction on timescales faster than the loss of electronic coherence is key for achieving the full quantum control of final products in solid-solid transformations. Here, we demonstrate coherent electronic control of the photoinduced insulator-to-metal transition in the prototypical Mott insulator V_2O_3 . Selective excitation of a specific interband transition with two phase-locked light pulses manipulates the orbital occupation of the correlated bands in a way that depends on the coherent evolution of the photoinduced superposition of states.

Comparison between experimental results and numerical solutions of the optical Bloch equations indicates an electronic coherence time on the order of 5 fs. Temperature dependent experiments suggest that the electronic coherence time is enhanced in the vicinity of the insulator-to-metal transition critical temperature, thus highlighting the role of fluctuations in determining the electronic coherence. These results open new routes to selectively switch functionalities of quantum materials and store quantum information in solid-solid transformations.

15 min. break

Invited Talk TT 36.4 Fri 11:15 H10

Nanoscale transient magnetization dynamics: A comprehensive EUV TG study — •LAURA FOGLIA — Elettra Sincrotrone Trieste, Trieste, Italy

The advent of X-ray free electron lasers (FELs) has allowed to overcome the wavelength limitations of optical radiation to manipulate and study magnetic phenomena on nanometer length- and femtosecond time-scale, which is paramount for light-controlled ultrafast magnetic data processing and storage applications. In this talk, we review the most recent advances on the EUV TG-based investigation of nanoscale transient magnetization dynamics, a technique pioneered at the FERMI FEL in Trieste, Italy. First, we show how EUV-TG is capable of inducing transient magnetization gratings which decay within tens of picoseconds

via thermal diffusion. Building upon this first demonstration, we investigate the transition from ultrafast demagnetization to all-optical switching (AOS) by looking at the ratio between the first and the second order of diffraction as a function of excitation fluence. Indeed, the non-linear fluence dependence of AOS induces a non-uniform spacing of the magnetization pattern that results in the appearance of even diffraction orders. Finally, we compare the magnetization dynamics induced by intensity gratings with those launched by polarization gratings, obtained when the two excitation beams have orthogonal polarization. Here, the intensity distribution on the sample is uniform and ultrafast the formation of transient magnetization gratings has to be associated to the coupling of majority and minority spins with the electric field polarization.

Invited Talk TT 36.5 Fri 11:45 H10

Ultrafast magnetism of antiferromagnets — •ALEXEY KIMEL — Radboud University, Nijmegen, The Netherlands

Antiferromagnets are ideal candidates to reach the THz landmark in data storage with no additional energy costs. However, the lack of a net magnetization in the antiferromagnetic ground state requires exceedingly high magnetic fields to manipulate the spins, hindering even fundamental studies on the control and switching of antiferromagnets. Here we propose an approach to empower THz control of antiferromagnetic order by pushing antiferromagnet out of equilibrium through a generation of coherent magnonic states. We will show that an antiferromagnet out of equilibrium is practically a different material. Generation of coherent magnonic states in antiferromagnets substantially modifies the susceptibility of antiferromagnetic spins to THz magnetic fields and facilitates energy transfer between otherwise noninteracting phononic and magnonic modes [1,2]. In this case, the generated impact on spins goes far beyond trivial superposition of excitations and can facilitate conceptually new ways for controlling antiferromagnetism. The proposed theoretical description suggests that spin dynamics in antiferromagnets is intrinsically non-linear and once coherent magnonic state is induced, additional channels of energy transfer between otherwise orthogonal modes open up.

[1] E. A. Mashkovich, K. Grishunin, R. Dubrovin, R. V. Pisarev, A. K. Zvezdin and A. V. Kimel, *Science* 374, 1608 (2021)

[2] Th. Blank et al. (in preparation)

TT 37: Superconducting Electronics: SQUIDs, Qubits, Circuit QED

Time: Friday 9:30–13:15

Location: H22

TT 37.1 Fri 9:30 H22

Nb constriction Josephson junctions and nanoSQUIDs patterned by He and Ne focused ion beams — •SIMON PFANDER¹, TIMUR GRIENER¹, JULIAN LINEK¹, THOMAS WEIMANN², UTE DRECHSLER³, REINHOLD KLEINER¹, ARMIN KNOLL³, OLIVER KIELER², and DIETER KOELLE¹ — ¹Physikalisches Institut, Center for Quantum Science (CQ) and LISA⁺, Universität Tübingen, 72076 Tübingen, Germany — ²Department Quantum Electronics, Physikalisches-Technische Bundesanstalt (PTB), 38116 Braunschweig, Germany — ³IBM Research Europe – Zürich, 8803 Rüschlikon, Switzerland

Nanopatterning of superconducting thin film structures with focused He or Ne ion beams (He/Ne-FIB) offers a flexible tool for creating constriction-type Josephson junctions (cJJs) and strongly miniaturized superconducting quantum interference devices (nanoSQUIDs) for magnetic sensing on the nanoscale. We present our attempts to use He/Ne-FIB for fabricating Nb cJJs and nanoSQUIDs which shall provide ultra-low noise and high spatial resolution for their application in scanning SQUID microscopy (SSM). The nanoSQUIDs are designed as sensors for magnetic flux and dissipation. They shall be integrated on custom-made Si cantilevers, which will provide the possibility of simultaneous conventional topographic imaging by atomic force microscopy (AFM). We will discuss the status of this project and challenges that have to be met on the way to combine SSM and AFM on the nanoscale.

We acknowledge the European Commission under H2020 FET Open grant FIB-superProbes (number 892427).

TT 37.2 Fri 9:45 H22

Development of a three-wave-mixing Josephson traveling-wave parametric amplifier — •VICTOR GAYDAMACHENKO¹, CHRISTOPH KISSLING^{1,2}, LUKAS GRÜNHaupt¹, RALF DOLATA¹, and ALEXANDER B. ZORIN¹ — ¹Physikalisch-Technische Bundesanstalt, Braunschweig, Germany — ²Technische Universität Ilmenau, Germany

Modern quantum experiments profit from wideband amplification of small microwave signals with noise approaching the quantum-limit. A promising approach to design an amplifier having a bandwidth of several GHz, power gain of 20 dB, and quantum-limited noise are traveling-wave parametric amplifiers (TWPAs). We develop a Josephson traveling-wave parametric amplifier (JTWPA), based on a series array of 1500 rf-SQUIDs, and utilising the three-wave mixing regime. One of the main challenges of TWPAs is power leakage to

unwanted processes like the generation of higher harmonics and mixing products, which significantly limit the gain. To solve this obstacle, we apply a dispersion engineering technique. Here, we present numerically optimised parameter sets for practical realisation of our concept. Simulations of the device operation show a signal gain of 20 dB in the frequency range from 3 GHz to 9 GHz.

TT 37.3 Fri 10:00 H22

Charge-mediated quantum phase slip interference — •JAN NICOLAS VOSS¹, MICHA WILDERMUTH¹, MAX KRISTEN^{1,2}, HANNES ROTZINGER^{1,2}, and ALEXEY V. USTINOV^{1,2} — ¹Physikalisches Institut, Karlsruher Institut für Technologie, Karlsruhe, Germany — ²Institut für Quantenmaterialien und Technologien (IQMT), Karlsruher Institut für Technologie, Karlsruhe, Germany

The duality between quantum phase slip junctions and Josephson junctions has triggered a variety of theoretical and experimental works and set the basis for a new type of quantum device based on coherent quantum phase slips. We present a realization of a quantum phase slip interferometer based on two strongly coupled superconducting nanowires. The interference is controlled by a gate voltage and visible as a periodic modulation of the critical Coulomb blockade voltage. The strength of the modulation strongly depends on the homogeneity of the wires, as the phase slip rates exponentially depend on the normal state resistances of the wires. We use the intrinsic electromigration technique ([1]) to adjust and homogenize the resistances of the wires in-situ and therefore are able to study a large range of wire impedances for single devices.

[1] J. N. Voss, Y. Schön, M. Wildermuth, D. Dorer, J. H. Cole, H. Rotzinger, A. V. Ustinov, *ACS Nano* 15, 4108 (2021)

TT 37.4 Fri 10:15 H22

RF superconducting arbitrary waveform generator for Qubit control — •HAO TIAN, OLIVER KIELER, ALEXANDER FERNANDEZ SCARIONI, SILKE WOLTER, ROLF-WERNER GERDAU, JOHANNES KOHLMANN, and MARK BIELER — Physikalisches Technische Bundesanstalt

The Josephson Arbitrary Waveform Synthesizer (JAWS) allows for the quantum-accurate-generation of spectrally-pure, arbitrary waveforms. It consists of a series array of Josephson junctions and is driven by GHz bit sequences (current pulses). So far, JAWS circuits are mainly used at National Metrology Institutes for metrological purposes with output frequencies in the kHz to MHz frequency range. Within the scope of the national QuMIC project, PTB and other partners

are currently further developing JAWS circuits with the aim to realize a compact and robust module, which is suitable for control and readout of superconducting qubits. In this talk, we will present the work, which is currently undertaken at PTB to reach this goal. Here, the main focus lies on the design and the fabrication of novel JAWS circuits and complex waveguide filters, capable of synthesizing arbitrary waveforms at GHz frequencies. This work was partly supported by German Federal Ministry of Education and Research (contract number: 13N15934).

TT 37.5 Fri 10:30 H22

Gate-tunable kinetic inductance in proximitized nanowires — •LUKAS JOHANNES SPLITTHOFF¹, ARNO BARGERBOS¹, LUKAS GRÜNHaupt¹, MARTA PITAVIDAL¹, JAAP JOACHIM WESDORP¹, YU LIU², ANGELA KOU³, CHRISTIAN KRAGLUND ANDERSEN¹, and BERNARD VAN HECK⁴ — ¹Delft University of Technology, Delft, The Netherlands — ²Center for Quantum Devices, Niels Bohr Institute, University of Copenhagen, Copenhagen, Denmark — ³Department of Physics and Frederick Seitz Materials Research Laboratory, University of Illinois Urbana-Champaign, Urbana, USA — ⁴Leiden Institute of Physics, Leiden University, Leiden, The Netherlands

Superconducting-semiconducting nanowires combine two frontiers of condensed matter in a hybrid state, which offers formidable possibilities for quantum computing and quantum sensing devices. In this talk, we study a quarter-wave coplanar waveguide resonator shunted by a hybrid InAs/Al nanowire. We show a gate voltage controllable resonance frequency and demonstrate a frequency shift of up to 8 MHz. We relate the frequency shift to the change in kinetic inductance of the hybrid nanowire which arises from the gate-tunable hybridization of the superconductor to semiconductor interface. From our measurement results we extract the normal state conductivity and the superconducting gap of the hybrid nanowire. The measurement technique demonstrated in this work complements existing characterization methods for hybrid nanowires and forms a promising path towards gate-controlled superconducting electronics.

TT 37.6 Fri 10:45 H22

Microwave photonics in high kinetic inductance microstrip networks — •NIKLAS GAISER¹, SAMUEL GOLDSTEIN², GUY PARDO², NAFTALI KIRSH², CIPRIAN PADURARIU¹, BJÖRN KUBALA^{1,3}, NADAV KATZ², and JOACHIM ANKERHOLD¹ — ¹ICQ and IQST, University of Ulm, Ulm, Germany — ²The Racah Institute of Physics, The Hebrew University of Jerusalem, Israel — ³Institute of Quantum Technologies, German Aerospace Center (DLR), Ulm, Germany

Microwave photonics based on superconducting circuits is a promising candidate for many quantum-technological applications. Progress towards compact integrated photonics devices in the microwave regime, however, is constrained by their long wavelengths.

Here, we discuss a solution to these difficulties via compact networks of high-kinetic inductance microstrip waveguides with strongly reduced phase velocities experimentally realized in [1]. We describe, how the Kirchhoff equations of a periodic network map to a tight-binding model, which allows a description in terms of Bloch waves and band structures, to explain experimental features. The ability to employ band-structure design techniques together with the unique properties of compactness, reduced speed of light, and strong non-linear features allows the design of highly versatile on-chip microwave networks. Furthermore utilizing this platform, we present first theoretical device proposals of linear and non-linear functional units, such as beamsplitters, filters, resonators and diodes exploiting non-reciprocity.

[1] S. Goldstein, G. Pardo, N. Kirsh, N. Gaiser, C. Padurariu, B. Kubala, J. Ankerhold, and N. Katz, *New J. Phys.* 24 023022 (2022)

TT 37.7 Fri 11:00 H22

Emission of photon multiplets by a dc-biased superconducting circuit — •BJÖRN KUBALA^{1,2}, GERBOLD MENARD³, AMBROISE PEUGEOT³, CIPRIAN PADURARIU², CHLOE ROLLAND³, YURI MUKHARSKY³, ZUBAIR IFTIKHAR³, CARLES ALTIMIRAS³, PATRICE ROCHE³, HELENE LE SUEUR³, PHILIPPE JOYEZ³, DENIS VION³, DANIEL ESTEVE³, JOACHIM ANKERHOLD², and FABIEN PORTIER³ — ¹Institute of Quantum Technologies, German Aerospace Center (DLR), Ulm, Germany — ²ICQ and IQST, Ulm University, Germany — ³SPEC, CEA Paris-Saclay, France

We show experimentally that a dc-biased Josephson junction in series with a high-impedance microwave resonator can emit up to $k = 6$ photons simultaneously for each Cooper pair tunneling through the junction [1]. Our resonator is made of a simple micro-fabricated spiral coil that resonates at 4.4 GHz and reaches a 1.97 k Ω characteristic impedance, corresponding to an effective fine-structure constant, $\alpha \sim 1$. Measuring the second order correlation function of the emission from the resonator allows computing the Fano factor F of the emitted photons, found to coincide with the naive prediction $F = k$ in the weak driving regime. At larger Josephson coupling E_J , a more complex behavior is observed in quantitative agreement with numerical simulations. This simple scheme highlights the ability of superconducting devices operating in the microwave domain to reach strong-coupling regimes of matter-light coupling inaccessible to conventional quantum optics experiments in the visible domain.

[1] G. C. Menard, et al., *Phys. Rev. X* 12, 021006 (2022).

TT 37.8 Fri 11:15 H22

Waveguide quantum electrodynamics in high impedance networks — •MIRIAM RESCH¹, CIPRIAN PADURARIU¹, BJÖRN KUBALA^{1,2}, and JOACHIM ANKERHOLD¹ — ¹ICQ and IQST, Ulm University, Ulm, Germany — ²Institute of Quantum Technologies, German Aerospace Center (DLR), Ulm, Germany

The emerging field of high impedance quantum circuits aims to exploit the extraordinary properties of high kinetic inductance materials, such as granular superconductors. The low propagation speed of electromagnetic excitations in such devices enables to strongly couple sub-units of quantum information devices, namely various types of qubits or resonators and waveguides. Theoretical description of such strongly coupled systems is challenging as the localized modes of the sub-unit typically couples to many waveguide modes simultaneously so that many common approximation schemes break down. While strong-coupling effects in closed systems have been widely investigated, showing, e.g. the breakdown of the Jaynes-Cummings model, our project aims at describing strongly coupled open quantum systems and photon emission. With experimental collaborators, we ultimately want to identify strong-coupling signatures in observables of the emitted radiation. Here, we present as preliminary steps towards the description of more complicated systems first investigations based on an ansatz, where the wave function of the complete system (unit + waveguide) is described by superposition of coherent states as proposed in [1], which allows to solve the system dynamics in a numerically efficient way.

[1] Nicolas Gheeraert et al., *New J. Phys.* 19 (2017) 023036

15 min. break

TT 37.9 Fri 11:45 H22

Fano interference in microwave resonator measurements — •SIMON GÜNZLER^{1,2}, DENNIS RIEGER², MARTIN SPIEKER^{1,2}, WOLFGANG WERNSDORFER^{1,2}, and IOAN POP^{1,2} — ¹IQMT, Karlsruhe Institute of Technology, Germany — ²PHI, Karlsruhe Institute of Technology, Germany

Resonator measurements are a simple but powerful tool to characterize a material's microwave response. The losses of a resonant mode are quantified by its internal quality factor Q_i , which can be extracted from the scattering coefficient in a microwave reflection or transmission measurement. Here we show that a systematic error on Q_i arises from Fano interference of the signal with a background path. Limited knowledge of the interfering paths and their relative amplitudes in a given setup translates into a range of uncertainty for Q_i , which increases with the coupling coefficient. We experimentally illustrate the relevance of Fano interference in typical microwave resonator measurements and the associated pitfalls encountered in extracting Q_i . On the other hand, we show how to characterize and utilize the Fano interference to eliminate the systematic error.

TT 37.10 Fri 12:00 H22

Direct observation of microscopic tow-level systems in granular aluminum films — •MAXIMILLIAN KRISTEN^{1,2}, JAN N. VOSS², MICHA WILDERMUTH², ANDRE SCHNEIDER², HANNES ROTZINGER^{1,2}, and ALEXEY V. USTINOV^{1,2} — ¹Institut für QuantenMaterialien und Technologien (IQMT), Karlsruher Institut für Technologie — ²Physikalisches Institut, Karlsruher Institut für Technologie

Thin films of disordered superconductors are extensively studied due to their applicability in quantum circuits and detectors, where they can provide kinetic inductances orders of magnitude higher than their geometric inductance. While these films generally show very high quality factors in microwave measurements, their disordered microscopic structure favors the presence of numerous material defects behaving as two-level systems (TLS). TLS have been shown to be a major source of dielectric loss in microwave circuits and are limiting the coherence properties of modern superconducting qubits.

We present microwave spectroscopy measurements of resonators made from highly resistive granular aluminum films. By applying mechanical strain and electric fields, we observe several TLS strongly interacting with the resonator modes. We compare the measured data to an analytical model for the single-photon interaction with TLS and estimate relevant physical properties.

TT 37.11 Fri 12:15 H22

Magnetic 1/f noise in superconducting microstructures and the fluctuation-dissipation theorem — •M. HERBST, A. FLEISCHMANN, L. GASTALDO, D. HENGSTLER, L. MÜNCH, A. REIFENBERGER, C. STÄNDER, and C. ENSS — Uni Heidelberg

The performance of superconducting devices like SQUIDs and qubits is often limited by 1/f-noise and finite coherence times. Various types of slow fluctuators in the Josephson-junctions and in the passive parts of these superconducting circuits can cause such noise, and devices most likely suffer from a combination of different noise sources, which are hard to disentangle and therefore hard to eliminate. Magnetic flux noise caused by fluctuating magnetic moments of magnetic impurities or dangling bonds in superconducting inductances, surface oxides, insulating oxide layers and adsorbates should be a very likely contribution in many cases. We present an experimental setup to measure at Millikelvin temperatures both, the complex impedance of superconducting micro-structures as well

as the magnetic flux noise that is picked-up by these structures. This allows for very important sanity checks by connecting both quantities via the fluctuation-dissipation-theorem. In order to allow for state-of-the-art sensitivity in both experiments, the structures under investigation are part of a Wheatstone-like bridge, read-out by two cross-correlated independent dc-SQUID readout chains. We present measurements of the insulating SiO₂ layers of our devices, the superconducting structures themselves, and magnetically doped noble-metal layers in the vicinity of the pickup coils at $T = 20\text{--}800\text{mK}$ and $f = 100\text{mHz--}100\text{kHz}$.

TT 37.12 Fri 12:30 H22

A quantum Szilard engine for two-level systems coupled to a qubit — •MARTIN SPIECKER¹, PATRICK PALUCH¹, NIV DRUCKER², SHLOMI MATITYAHU¹, DARIA GUSENKOVA¹, NICOLAS GOSLING¹, SIMON GÜNZLER¹, DENNIS RIEGER¹, IVAN TAKMAKOV¹, FRANCESCO VALENTI¹, PATRICK WINKEL¹, RICHARD GEBAUER¹, OLIVER SANDER¹, GIANLUIGI CATELANI³, ALEXANDER SHNIRMAN¹, ALEXEY V. USTINOV¹, WOLFGANG WERNSDORFER¹, YONATAN COHEN², and IOAN M. POP¹ — ¹Karlsruher Institut für Technologie, Karlsruhe, Germany — ²Quantum Machines, Tel Aviv-Yafo, Israel — ³Forschungszentrum Jülich, Jülich, Germany

The innate complexity of solid state physics exposes superconducting quantum circuits to interactions with uncontrolled degrees of freedom degrading their coherence. By using a simple stabilization sequence we show that a superconducting fluxonium qubit is coupled to a two-level system (TLS) environment of unknown origin, with a relatively long energy relaxation time exceeding 50ms. Implementing a quantum Szilard engine with an active feedback control loop allows us to decide whether the qubit heats or cools its TLS environment. The TLSs can be cooled down resulting in a four times lower qubit population, or they can be heated to manifest themselves as a negative temperature environment corresponding to a qubit population of 80%. We show that the TLSs and the qubit are each other's dominant loss mechanism and that the qubit relaxation is independent of the TLS populations. Mitigating TLS environments is therefore not only crucial to improve qubit lifetimes but also to avoid non-Markovian qubit dynamics.

TT 37.13 Fri 12:45 H22

Green's function approach to modelling finite size systems for applications in superconducting waveguide QED — •PRADEEPKUMAR NANDAKUMAR¹, ANDRES ROSARIO HAMANN^{1,2}, ROHIT NAVARATHNA¹, MAXIMILIAN ZANNER³, MIKHAIL PLETYUKHOV⁴, and ARKADY FEDOROV¹ — ¹ARC Centre of Excellence for Engineered Quantum Systems, School of Mathematics and Physics, The Uni-

versity of Queensland, Saint Lucia, Queensland 4072, Australia — ²Department of Physics, ETH Zurich, CH-8093 Zurich, Switzerland — ³Center for Quantum Physics, and Institute for Experimental Physics, University of Innsbruck, A-6020 Innsbruck, Austria — ⁴Institute for Theory of Statistical Physics, RWTH Aachen University, 52056 Aachen, Germany

In superconducting waveguide QED, artificial atoms are coupled to a 1D radiation channel that consists of continuum of electromagnetic modes. Waveguides are often modelled as infinite in size with open boundary conditions for the ease of understanding. However, while modelling waveguides employed in experiments, one should consider both the finite size of the waveguide as well as its coupling to measurement apparatus. To this end, we have developed a general method to realistically model any waveguide QED system using the Green's function methods that is often employed in studying electronic transport. We apply our formalism and experimentally study the formation of Atom-Photon Bound States (APBS) using two transmon qubits coupled to a 3D rectangular waveguide. Our results identify the prospects for using APBS for studying bosonic impurity models.

TT 37.14 Fri 13:00 H22

Dirac physics and charge localization due to quasiperiodic nonlinear capacitances — •TOBIAS HERRIG¹, JEDEDIAH PEXLEY², ELIO KÖNIG³, and ROMAN-PASCAL RIWAR¹ — ¹Forschungszentrum Jülich, Germany — ²Rutgers University, Piscataway, New Jersey, USA — ³Max-Planck Institute, Stuttgart, Germany

Superconducting circuits are an extremely versatile platform to realize quantum information hardware, and, as was recently realized, to emulate topological materials, such as Weyl semimetals or Chern insulators. We here show how a simple arrangement of capacitors and conventional SIS junctions can realize a nonlinear capacitive element with a surprising property: it can be quasiperiodic with respect to the quantized Cooper-pair charge. Integrating this element into a larger circuit opens the door towards the engineering of an even broader class of systems. First, we use it to simulate a protected Dirac material defined in the transport degrees of freedom. The presence of the Dirac point leads to a suppression of the classical part of the finite-frequency noise. Second, we are able to exploit the quasiperiodicity to implement the Aubry-André model, and thereby to emulate Anderson localization in charge space. Our setup implements a truly non-interacting version of the model, in which the macroscopic quantum mechanics of the circuit already incorporates microscopic interaction effects. This should be contrasted to conventional solid state and cold atomic realizations, where competition between interaction and localization are a common side effect. We predict that quantum charge fluctuations directly probe the localization effect.

TT 38: Superconductivity: Theory

Time: Friday 9:30–11:00

Location: H23

TT 38.1 Fri 9:30 H23

Unconventional superconductivity in the Hubbard model on the pyrochlore lattice — SHINGO KOBAYASHI¹, ANKITA BHATTACHARYA², •CARSTEN TIMM², and PHILIP M. R. BRYDON³ — ¹RIKEN Center for Emergent Matter Science, Saitama, Japan — ²TU Dresden, Germany — ³University of Otago, Dunedin, New Zealand

The Hubbard model on the pyrochlore lattice is studied close to half filling. In the normal state, the band structure realizes a $j = 3/2$ semimetal. Remarkably, the repulsive Hubbard interaction leads to an *attractive* superconducting pairing interaction in the E_g channel, which allows a two-component order parameter, whereas the interaction is repulsive in the trivial A_{1g} channel. The attractive interaction relies on the fact that the E_g pairing avoids the detrimental on-site repulsion. The solution of the BCS gap equation shows that a time-reversal-symmetry-breaking superconducting phase is favored, which displays Bogoliubov Fermi surfaces.

TT 38.2 Fri 9:45 H23

Pairing instabilities of the Yukawa-SYK models with controlled fermion incoherence — •WONJUNE CHOI^{1,2}, OMID TAVAKOL³, and YONG BAEK KIM³ — ¹Department of Physics, Technical University of Munich, 85748 Garching, Germany — ²Munich Center for Quantum Science and Technology (MCQST), Schellingstr. 4, 80799 München, Germany — ³Department of Physics, University of Toronto, Toronto, Ontario M5S 1A7, Canada

As a solvable platform of the strongly correlated superconductors, we study the pairing instabilities of the Yukawa-Sachdev-Ye-Kitaev (Yukawa-SYK) model, which describes spin-1/2 fermions coupled to bosons by the random, all-to-all Yukawa interactions. In contrast to the previously studied models, the random Yukawa couplings are sampled from a collection of Gaussian ensembles whose variances follow a continuous distribution rather than being fixed to a constant. By tuning the analytic behaviour of the distribution, we control the fermion incoherence to systematically examine various normal states ranging from the Fermi liquid to non-Fermi liquids that are different from the conformal solution of the

SYK model with a constant variance. Using the linearised Eliashberg theory, we show that the onset of the unconventional spin-triplet pairing is preferred with the spin-dependent interactions. Although the interactions shorten the lifetime of the fermions in the non-Fermi liquid, the same interactions also dress the bosons to strengthen the tendency to pair the incoherent fermions. As a consequence, the onset temperature of the pairing is enhanced in the non-Fermi liquid compared to the case of the Fermi liquid.

TT 38.3 Fri 10:00 H23

Superconducting pairing from repulsive interactions of fermions in a flat-band system — IMAN MAHYAEH¹, •THOMAS KÖHLER¹, ANNICA M. BLACK-SCHAFFER¹, and ADRIAN KANTIAN^{1,2} — ¹Department of Physics and Astronomy, Uppsala University, Sweden — ²SUPA, Institute of Photonics and Quantum Sciences, Heriot-Watt University, Edinburgh EH14 4AS, United Kingdom

Many-body quantum systems of fermions with flat bands at the Fermi level are intensely studied for their potential to boost superconductivity by enhancement of the density of states. We use quasiexact numerical methods to show that repulsive interactions between spinless fermions in a model one-dimensional flat band system, the Creutz ladder, lead to a finite pairing energy that increases with repulsion. Pure repulsion however leaves charge-order as the dominant quasi-order over the superconductivity. Adding an additional attractive component to the interaction shifts the balance fully in favor of superconductivity. In this regime we find that the interactions of two flat bands further yields a remarkable enhancement to superconductivity far above and outside the known paradigms for one-dimensional fermions.

TT 38.4 Fri 10:15 H23

Degenerate plaquette physics as key ingredient of high-temperature superconductivity in cuprates — MIKHAIL DANILOV¹, VAN LOON ERIK G. C. P.², •BRENER SERGEY^{1,3}, ISKAKOV SERGEY⁴, KATSNELSON MIKHAIL⁵, and LICHTENSTEIN ALEXANDER^{1,3} — ¹Institute of Theoretical Physics, University of Hamburg — ²Department of Physics, Lund University — ³The Hamburg Centre for Ultra-

fast imaging — ⁴Department of Physics, University of Michigan — ⁵Radboud University, Institute for Molecules and Materials

A major pathway towards understanding complex systems is given by exactly solvable reference systems that contain the essential physics of the system. For the $t - t' - U$ Hubbard model, the four-site plaquette is known to have a point in the $U - \mu$ space where states with electron occupations $N = 2, 3, 4$ per plaquette are degenerate. Such a degenerate point causes strong fluctuations when a lattice of plaquettes is constructed. The next-nearest-neighbour hopping is shown to play a crucial role in the formation of strongly bound electronic bipolarons whose coherence at lower temperature could be the explanation for superconductivity. A complementary approach to the lattice of plaquettes is given by dual fermion perturbation theory starting from a single degenerate plaquette as a reference system. This perturbation theory already contains the relevant short-ranged fluctuations from the beginning via the two-particle correlations of the plaquette. We find that d-wave superconductivity remains a leading instability channel under a reasonably broad range of parameters.

TT 38.5 Fri 10:30 H23

Charge 4e skyrmion superconductivity? — •GABRIEL REIN^{1,2}, MARCIN RACZKOWSKI¹, and FAKHER F. ASSAAD^{1,2} — ¹Institut für Theoretische Physik und Astrophysik Universität Würzburg, 97074 Würzburg, Germany — ²Würzburg-Dresden Cluster of Excellence ct.qmat, Universität Würzburg, 97074 Würzburg, Germany

We consider a dynamically generated quantum spin Hall (QSH) state which has as characteristic that skyrmion excitations of the SO(3) order parameter carry charge $2e$. In Refs. [1,2] a model was defined with a single parameter λ that drives a continuous transition akin to deconfined quantum criticality from a QSH insulator to an s-wave superconductor via the condensation of charge $2e$ skyrmions.

Our aim here is to modify this Hamiltonian by adding flavor degrees of freedom N_f , such that the charge of the skyrmion reads $N_f 2e$. In this talk we will map out the phase diagram of the model at $N_f = 2$. Although, to date charge 4e skyrmion superconductivity remains elusive, the phase diagram in the N_f versus λ plane is very rich with additional Kekule ordered phases.

[1] Y. Liu, Z. Wang, T. Sato, M. Hohenadler, C. Wang, W. Guo, and F. F. Assaad, Nat. Commun. 10 (2019) 2658

[2] Z. Wang, Y. Liu, T. Sato, M. Hohenadler, C. Wang, W. Guo, F. F. Assaad, Phys. Rev. Lett. 126 (2021) 205701

TT 38.6 Fri 10:45 H23

Groundstate phase diagrams of variants of the two-leg t - J ladder at low fillings — •STEFFEN BOLLMANN^{1,2}, ALEXANDER OSTERKORN², ELIO KÖNIG¹, and SALVATORE R. MANMANA² — ¹Max-Planck Institute for Solid State Research, 70569 Stuttgart, Germany — ²Institut für Theoretische Physik, Georg-August-Universität Göttingen, 37077 Göttingen, Germany

We study variants of the two-leg t - J ladder at low fillings using matrix product states (MPS) and perturbative approaches. While the groundstate phase diagram for the usual t - J ladder with spatially isotropic couplings at fillings $n > 0.5$ has been studied in detail, relatively little is known at low fillings. We address the phase diagram at these low fillings and investigate the influence of nearest-neighbor Coulomb interactions V and asymmetries in the spin-exchange $J_z \neq J_x = J_y$, on the size and nature of superconducting phases. For $V = 0$ the superconducting phase is enhanced, and we find a crossover within this phase from s -wave pairing to d -wave pairing when increasing the filling. For $J_z = 0$, the size of the superconducting region is reduced. In this talk, I will present the phase diagrams, discuss the physics, briefly introduce the methods used to classify the different phases, and give an outlook to possible realizations in experiments.

TT 39: Correlated Electrons: Charge Order

Time: Friday 11:15–13:15

Location: H23

TT 39.1 Fri 11:15 H23

Stripe discommensuration and spin dynamics of charge and spin stripe ordered $\text{Pr}_{3/2}\text{Sr}_{1/2}\text{NiO}_4$ — •AVISHEK MAITY¹, RAJESH DUTTA^{2,3}, and WERNER PAULUS⁴ — ¹Heinz Maier-Leibnitz Zentrum (MLZ), Technische Universität München, 85747 Garching, Germany — ²Institut für Kristallographie, RWTH Aachen Universität, 52066 Aachen, Germany — ³Jülich Centre for Neutron Science (JCNS) at Heinz Maier-Leibnitz Zentrum (MLZ), 85747 Garching, Germany — ⁴Institut Charles Gerhardt Montpellier, Université de Montpellier, 34095 Montpellier, France

Magnetic excitations in the charge and spin stripe ordered phases of La-based 214-nickelates have been vigorously explored using inelastic neutron scattering (INS) studies. In view of so far reported two-dimensional antiferromagnetic nature, out-of-plane interaction is not generally expected in 214-nickelates. Here we will present our results on the magnetic excitations of $\text{Pr}_{3/2}\text{Sr}_{1/2}\text{NiO}_4$, with stripe incommensurability $\epsilon = 0.4$, showing a very compelling evidence for the presence of a sizable out-of-plane interaction ($J_{\perp} \sim 2.2$ meV) manifesting a symmetrical outward shift of the spin wave dispersion from the antiferromagnetic zone center. Our linear spin wave calculation using an unconventional three-dimensional model of discommensurated spin stripe (DCSS) unit for $\epsilon = 0.4$ could explicitly show such outward shift results from the overlap of a mode originating exclusively from the out-of-plane interaction. Our study suggests that a careful consideration of the out-of-plane interaction is necessary in the stripe discommensurated 214-nickelates.

[1] A. Maity et al., PRL 124, 147202 (2020).

TT 39.2 Fri 11:30 H23

Quantum oscillations in the Kagome superconductor CsV_3Sb_5 — •ANMOL SHUKLA¹, LIRAN WANG¹, FRÉDÉRIC HARDY¹, AMIR-ABBAS HAGHIGHIRAD¹, MINGQUAN HE², WEI XIA³, YANFENG GUO³, and CHRISTOPH MEINGAST¹ — ¹Institute for Quantum Materials and Technologies, Karlsruhe Institute of Technology, 76021 Karlsruhe, Germany — ²Low Temperature Physics Lab, College of Physics & Center of Quantum Materials and Devices, Chongqing University, Chongqing 401331, China — ³School of Physical Science and Technology, ShanghaiTech University, Shanghai 201210, China

The recently discovered layered Kagome metals AV_3Sb_5 ($A = \text{K}, \text{Rb}, \text{Cs}$) exhibit a unique combination of nontrivial band topology, competing for the charge- and superconducting orders with clear signatures of electron correlations. Using magnetization, resistivity, thermal expansion, magnetostriction and heat capacity, we have investigated the normal- and superconducting-state properties of single crystals of the kagome superconductor CsV_3Sb_5 . The magnetization and magnetostriction data show clear signatures of quantum oscillations with at least two distinct frequencies. These are much less evident in the heat capacity. Combining the results from these thermodynamic probes and transport mea-

surement, we discuss the nature of the Fermi surface and the interplay between the charge order and superconductivity.

TT 39.3 Fri 11:45 H23

Statistical learning of engineered topological phases in the Kagome superlattice of AV_3Sb_5 — THOMAS MERTZ, •PAUL WUNDERLICH, SHINIBALI BHATTACHARYYA, FRANCESCO FERRARI, and ROSER VALENTÍ — Institut für Theoretische Physik, Goethe-Universität, 60438 Frankfurt am Main, Germany

Recently, the kagome metals AV_3Sb_5 ($A = \text{K}, \text{Rb}, \text{Cs}$) have gained intense research interest, as they display a wide spectrum of exotic topological properties, in addition to superconductivity, charge, orbital momentum and spin density waves. Motivated by a plethora of experimental evidence for unconventional charge orders in the enlarged (2×2) unit-cell of the vanadium based kagome metals, we investigate the type of topological phases that can manifest within the electronic parameter space of such kagome superlattices. Unlike conventional theoretical approaches, we employ a recently introduced statistical method capable of constructing topological models for any generic lattice, in an unbiased way without prior knowledge of its phase diagram. By extracting physically meaningful information from large datasets of randomized hopping parameters for the kagome superlattice, we find possible real-space manifestations of charge and bond modulations and associated flux patterns for different topological classes. Our results agree with contemporary theoretical propositions and experimental observations for the AV_3Sb_5 family. Simultaneously, we predict new higher-order topological phases that may be realized by appropriately manipulating the currently known systems.

TT 39.4 Fri 12:00 H23

High-pressure IR investigations unveil modifications in the electronic structure of the superconducting Kagome metal CsV_3Sb_5 — •MAXIM WENZEL¹, YUK T. CHAN¹, BRENDEN R. ORTIZ^{2,3}, STEPHEN D. WILSON³, MARTIN DRESSEL¹, ALEXANDER A. TSIRLIN⁴, and ECE UYKUR¹ — ¹Physikalisches Institut, Universität Stuttgart, 70569 Stuttgart, Germany — ²California Nanosystems Institute, University of California Santa Barbara, Santa Barbara, CA, 93106, United States — ³Materials Department, University of California Santa Barbara, Santa Barbara, CA, 93106, United States — ⁴Experimental Physics VI, Center for Electronic Correlations and Magnetism, University of Augsburg, 86159 Augsburg, Germany

The non-magnetic Kagome metal series AV_3Sb_5 with $A = \text{K}, \text{Cs}$, or Rb is known for the coexistence of charge-density-wave and superconducting orders at low temperatures. Previously, the tunability of both orders has been investigated extensively via high-pressure transport studies; however, the pressure-induced modifications of the electronic band structure, especially the position of the saddle points, remain the subject of current research. While theoretical studies

present conflicting suggestions regarding the pressure effects on the band structure, it has been shown that the interband optical transitions are highly sensitive to the position of the saddle points and hence, can probe them experimentally. Therefore, we performed high-pressure infrared studies on the model compound CsV_3Sb_5 at room temperature to trace the behavior of the interband optical transitions up to 17 GPa.

TT 39.5 Fri 12:15 H23

Charge-density waves in Kagome-lattice extended Hubbard models at the van Hove filling — •FRANCESCO FERRARI¹, FEDERICO BECCA², and ROSER VALENTÍ¹ — ¹Goethe University, Frankfurt am Main, Germany — ²University of Trieste, Trieste, Italy

The Hubbard model on the kagome lattice is presently often considered as a minimal model to describe the rich low-temperature behavior of AV_3Sb_5 compounds (with $A=\text{K, Rb, Cs}$), including charge-density waves (CDWs), superconductivity, and possibly broken time-reversal symmetry. We investigate, via variational Jastrow-Slater wave functions, the properties of its ground state when both on-site U and nearest-neighbor V Coulomb repulsions are considered at the van Hove filling. Our calculations reveal the presence of different interaction-driven CDWs and, contrary to previous renormalization-group studies, the absence of ferromagnetism and charge- or spin-bond order. No signatures of chiral phases are detected. Remarkably, the CDWs triggered by the nearest-neighbor repulsion possess charge isoproportionations that are not compatible with the ones observed in AV_3Sb_5 . As an alternative mechanism to stabilize charge-bond order, we consider the electron-phonon interaction, modeled by coupling the hopping amplitudes to quantum phonons, as in the Su-Schrieffer-Heeger model. Our results show the instability towards a tri-hexagonal distortion with 2×2 periodicity, in a closer agreement with experimental findings.

TT 39.6 Fri 12:30 H23

Chalcogenic orbital density waves in the weak- and strong-coupling limit — •ADAM KLOSINSKI¹, ANDRZEJ M. OLES^{2,3}, CLIO EFTHIMIA AGRAPIDIS¹, JASPER VAN WEZEL⁴, and KRZYSZTOF WOHLFELD¹ — ¹University of Warsaw, Warsaw, Poland — ²Jagiellonian University, Krakow, Poland — ³Max Planck Institute for Solid State Research, Stuttgart, Germany — ⁴University of Amsterdam, Amsterdam, The Netherlands

Stimulated by recent works highlighting the indispensable role of Coulomb interactions in the formation of helical chains and chiral electronic order in the elemental chalcogens, we explore the p-orbital Hubbard model on a one-dimensional helical chain. By solving it in the Hartree approximation we find a stable ground state with a period-3 orbital density wave. We establish that the precise form of the emerging order strongly depends on the Hubbard interaction strength. In the strong-coupling limit, the Coulomb interactions support an orbital density wave that is qualitatively different from that in the weak-coupling regime. We identify the phase transition separating these two orbital ordered phases and show that realistic values for the interorbital Coulomb repulsion in

elemental chalcogens place them in the weak-coupling phase, in agreement with observations of the order in the elemental chalcogens.

TT 39.7 Fri 12:45 H23

Understanding the transition from metal to Hund's insulator in CaFeO_3 — •MAXIMILIAN MERKEL and CLAUDE EDERER — Materials Theory Group, ETH Zürich, Switzerland

Materials where strong correlations are caused by the Hund's interaction have recently attracted a lot of attention. In some cases, a dominant Hund's interaction can even lead to the emergence of a charge-disproportionated insulating (CDI) or "Hund's insulating" state. One example is the perovskite transition-metal oxide CaFeO_3 (CFO), which exhibits a transition from metal to Hund's insulator around room temperature. This transition couples to a structural distortion that creates alternating large and small FeO_6 octahedra, leading to two inequivalent Fe sites with nominal Fe^{5+} and Fe^{3+} charge states. We study CFO using density functional theory (DFT) and dynamical mean-field theory (DMFT). To characterize the CDI state, we first apply DMFT to a five-orbital Hubbard model applicable to CFO and demonstrate the emergence of the CDI phase here [1]. We then investigate the energetics of the transition using fully self-consistent DFT+DMFT calculations. We discuss the ligand-hole character of the charge disproportionation due to the zero or even negative charge-transfer energy. Our calculations show that both structural and electronic properties of the CDI state are well described within DFT+DMFT but also that the subtle interplay of several effects represents a big challenge for any quantitative, predictive theory.

[1] M. E. Merkel and C. Ederer, Phys. Rev. B 104, 165135 (2021)

TT 39.8 Fri 13:00 H23

Reinvestigating the metallic region of the half-filled Hubbard Holstein model — SAM MARDAZAD¹, MARTIN GRUNDNER¹, ULRICH SCHOLLWÖCK¹, ADRIAN KANTIAN², THOMAS KÖHLER³, and •SEBASTIAN PAECKEL¹ — ¹Department of Physics, Arnold Sommerfeld Center of Theoretical Physics, University of Munich, Germany — ²Institute of Photonics and Quantum Sciences, Heriot-Watt University, Edinburgh, UK — ³Department of Physics and Astronomy, Uppsala University, Sweden

The one-dimensional Hubbard-Holstein model is the paradigmatic system to study the interplay between strongly correlated electrons and dispersionless lattice vibrations. Particularly, the intermediate regime of competing interactions has been heavily debated and only with the advent of powerful numerical techniques such as density-matrix renormalization group (DMRG) or advanced quantum Monte Carlo (QMC), the realization of an intermediate metallic phase has been established. However, these early studies are characterized by significant truncations of the phononic Hilbert spaces. Here, we exploit recent advances in the efficient representation of large local Hilbert spaces to re-examine the phase diagram by large-scale DMRG calculations, focussing on the regime of competing, strong interactions. This allows us to systematically study the complex competition between correlations, overcoming previous limitations.

Vacuum Science and Technology Division Fachverband Vakuumphysik und Vakuumtechnik (VA)

Stylios Varoutis
Karlsruhe Institute of Technology
Institute for Technical Physics (ITEP)
Hermann-von-Helmholtz-Platz 1
76344 Eggenstein-Leopoldshafen
stylios.varoutis@kit.edu

Overview of Sessions

(Lecture hall H12)

Sessions

VA 1.1–1.3	Mon	9:30–11:30	H12	Rarefied gas dynamics and novel numerical approaches
VA 2.1–2.4	Mon	12:30–15:10	H12	Vacuum technology: New developments and applications

Invited Talks of the joint Symposium SKM Dissertation Prize 2022 (SYSD)

See SYSD for the full program of the symposium.

SYSD 1.1	Mon	10:15–10:45	H2	Charge localisation in halide perovskites from bulk to nano for efficient optoelectronic applications — •SASCHA FELDMANN
SYSD 1.2	Mon	10:45–11:15	H2	Nonequilibrium Transport and Dynamics in Conventional and Topological Superconducting Junctions — •RAFFAEL L. KLEES
SYSD 1.3	Mon	11:15–11:45	H2	Probing magnetostatic and magnetotransport properties of the antiferromagnetic iron oxide hematite — •ANDREW ROSS
SYSD 1.4	Mon	11:45–12:15	H2	Quantum dot optomechanics with surface acoustic waves — •MATTHIAS WEISS

Invited Talks of the joint Symposium United Kingdom as Guest of Honor (SYUK)

See SYUK for the full program of the symposium.

SYUK 1.1	Wed	9:30–10:00	H2	Structure and Dynamics of Interfacial Water — •ANGELOS MICHAELIDES
SYUK 1.2	Wed	10:00–10:30	H2	A molecular view of the water interface — •MISCHA BONN
SYUK 1.3	Wed	10:30–11:00	H2	Motile cilia waves: creating and responding to flow — •PIETRO CICUTA
SYUK 1.4	Wed	11:00–11:30	H2	Cilia and flagella: Building blocks of life and a physicist's playground — •OLIVER BÄUMCHEN
SYUK 1.5	Wed	11:45–12:15	H2	Computational modelling of the physics of rare earth - transition metal permanent magnets from SmCo_5 to $\text{Nd}_2\text{Fe}_{14}\text{B}$ — •JULIE STAUNTON
SYUK 2.1	Wed	15:00–15:30	H2	Hysteresis Design of Magnetic Materials for Efficient Energy Conversion — •OLIVER GUTFLEISCH
SYUK 2.2	Wed	15:30–16:00	H2	Non-equilibrium dynamics of many-body quantum systems versus quantum technologies — •IRENE D'AMICO
SYUK 2.3	Wed	16:00–16:30	H2	Quantum computing with trapped ions — •FERDINAND SCHMIDT-KALER
SYUK 2.4	Wed	16:45–17:15	H2	Breaking the millikelvin barrier in cooling nanoelectronic devices — •RICHARD HALEY
SYUK 2.5	Wed	17:15–17:45	H2	Superconducting Quantum Interference Devices for applications at mK temperatures — •SEBASTIAN KEMPF

Sessions

– Talks –

VA 1: Rarefied gas dynamics and novel numerical approaches

Time: Monday 9:30–11:30

Location: H12

VA 1.1 Mon 9:30 H12

Direct Simulation Monte Carlo of diffusion pumps for the application in fusion reactors — •TIM TEICHMANN, THOMAS GIEGERICH, and CHRISTIAN DAY — Karlsruhe Institute of Technology, Eggenstein-Leopoldshafen, Germany

Active R&D is performed on developing of a continuously working pumping train for the future European demonstration fusion power plant (DEMO). Diffusion pumps operated with mercury have been identified as candidates for the high vacuum pumps. The numerical simulation of these pumps is challenging because they operate in a wide gas rarefaction range. A simulation framework based on the Direct Simulation Monte Carlo (DSMC) method has been established over the last years. The present talk aims to give an update on the present state of the simulations and their projected impact on the diffusion pump design for DEMO.

VA 1.2 Mon 10:10 H12

Transient modeling of the gas flows in the gas injection systems of fusion reactors — •CHRISTOS TANTOS, STYLIANOS VAROUTIS, and CHRISTIAN DAY — Karlsruhe Institute of Technology, Karlsruhe, Germany

This work presents an assessment of the flow evolution inside the gas pipes of the gas injection system (GIS) of fusion reactors during a control action. A successful gas injection system design requires on the one hand the ability to meet the technical requirements under steady state conditions that are in line with the operating requirements of the reactor and on the other hand the appropriate prediction of the dynamic change of the system response times. In this framework, in the present work a state-of-the-art methodology has been utilized analyzing the transient behavior of the argon and deuterium-tritium gas flows in the GIS of DEMO (DEMOstration Power Plant) fusion reactor. The applied methodology allows for an accurate description of the gas flow in the whole range of the gas rarefaction and compared to other widely applied particle-based approaches it requires low computational effort using an ordinary workstation. The main

output of the present work, namely the delay time, representing the time it takes the flow to reach the outlet as well as the time needed to recover steady state conditions, is estimated in a wide range of the operating conditions and ratios length-to-diameter of the GIS tubes. The obtained data show that the response times of the GIS are unfeasibly high and this may have a strong impact on the design of the piping of the DEMO gas injection system.

VA 1.3 Mon 10:50 H12

The Regularized 13-Moment Equations for Rarefied Gas Simulations — •MANUEL TORRILHON — RWTH Aachen University

The Regularized 13-Moment-Equations (R13) are using moment approximations for the Boltzmann equation in kinetic gas theory to describe gas flows when the Knudsen number - the ratio between mean free path and observation scale - becomes significant. Classical fluid theories like the constitutive laws of Navier-Stokes and Fourier are valid only close to equilibrium and fail for processes at Knudsen numbers as low as 0.05 because there are not sufficient particle collisions within the gas to maintain equilibrium.

The derivation of the R13-equations relies on the combination of moment approximations and asymptotic expansions in kinetic gas theory. The system has been shown to be stable and of high asymptotic accuracy yet using only a relatively small set of variables, namely density, velocity, temperature, stress deviator and heat flux - in total 13 fields. It has been demonstrated to succeed on the prediction of various non-equilibrium processes like shock waves or channel flows with Knudsen layers. The system of equations also exhibits desirable mathematical features like an entropy and is easy to use in numerical simulations. An overview of the equations and their features can be found in the review in *Ann. Rev. Fluid Mech.* 48, (2016), 429-458.

This talk will introduce the model and discuss recent developments like the efficient implementation in finite element frameworks, polyatomic collision models, and nonlinear extensions.

VA 2: Vacuum technology: New developments and applications

Time: Monday 12:30–15:10

Location: H12

VA 2.1 Mon 12:30 H12

Experimental characterisation of a NEG pump of novel size - a major step to its application in neutral beam injectors of future fusion devices — •STEFAN HANKE¹, CHRISTIAN DAY¹, THOMAS GIEGERICH¹, XUELI LUO¹, FABRIZIO SIVIERO², MICHELE MURA², ENRICO MACCALLINI², PAOLO MANINI², EMANUELE SARTORI³, MARCO SIRAGUSA³, and PIERGIORGIO SONATO³ — ¹KIT, Karlsruhe, Germany — ²SAES Getters, Lainate, Italy — ³Consorzio RFX, Padova, Italy

Future fusion plants require plasma heating including neutral beam injectors (NBI), demanding pumping speeds of several 1000 m³/s. A concept to replace the currently used customized cryopumps is based on the high capacity getter ZAO. In a 6 years systematic technology development, the concept of a NBI NEG pump was derived, starting with comprehensive material characterisation, expanded to pumping and regeneration characteristics of ZAO and to heating and thermal management of larger arrangements for scalability and control. The recent step was design, manufacturing and operation of a large NEG pump for demonstration and to confirm scalability. The resulting pump with 15 kg of ZAO was tested in the TIMO facility at KIT. The achieved experimental results, regarding sorption characteristics (depending on pressure, gas flux, getter temperature, loading of the getter with gas, isotope) and regeneration behaviour are described. Subsequently the entire setup was replicated in detail in the TPMC code ProVac3D to find the real sticking factor. With this, the performance of any advanced future arrangement of NEG cartridges can be predicted now.

VA 2.2 Mon 13:10 H12

Design process of the DTT divertor cryopump — •VOLKER HAUER and CHRISTIAN DAY — Karlsruhe Institute of Technology, Institute for Technical Physics, Karlsruhe, Germany

DTT is a planned, superconducting tokamak, which is to be built in Italy in the next few years. It will provide enough flexibility to test different divertor concepts and find the best concept for a subsequent demonstration power plant.

The plasma chamber in the center of the tokamak is actively pumped during operation. Nine cryopumps are used for this purpose due to the high pumping speed required.

The presentation shows the design process of the cryopumps starting from the boundary conditions, the calculation of pumping speeds by means of Test Particle Monte Carlo Simulation (TPMC), the selection of the optimal design and the necessary calculations for mechanical stability to the planned design of the cryopumps.

VA 2.3 Mon 13:50 H12

Outgassing rate studies and Monte Carlo simulations for the design of the cryogenic vacuum system of the Einstein Telescope — •KATHARINA BATTES, STEFAN HANKE, XUELI LUO, and CHRISTIAN DAY — Karlsruhe Institute of Technology, Eggenstein-Leopoldshafen, Germany

The Einstein Telescope (ET) is a third-generation underground gravitational wave observatory, currently under development in Europe. It is designed as an equilateral triangle with 10 km long arms and detectors in each corner. Two interferometers will be used to detect both low-frequency (LF) and high-frequency gravitational wave signals.

In order to reduce thermal noise, the main optics will partly be cooled to cryogenic temperatures below 20 K for ET-LF. The integral ET vacuum system requires high to ultra-high vacuum conditions and comprises three different parts: (i) the beamline vacuum characterised by outgassing from the pipe walls, (ii) the tower vacuum characterised by outgassing from the suspension arrangement, and (iii) the cryogenic vacuum systems around the LF mirror.

In this paper, the outgassing behavior of potential materials such as mild steel is studied at the Outgassing Measurement Apparatus OMA. Using this input, a Test Particle Monte Carlo model has been established with the KIT in-house code ProVac3D, to allow for a system analysis of the cryogenic vacuum area. It assesses the impinging rate of residual gas on the cryogenic mirror, depending on the particle sources. With that, the expected speed of frost formation is estimated, which is critical due to degradations of the optical performance.

VA 2.4 Mon 14:30 H12

Prevention of Carbon Contamination in Transmission Electron Microscopy by Sample-Specific Preparation — JULIA MENTEN¹, DANIELA RAMERMANN¹, ROBERT SCHLÖGL^{1,2}, and WALID HETABA¹ — ¹Max Planck Institute for Chemical Energy Conversion, Mülheim an der Ruhr, Germany — ²Fritz Haber Institute of the Max Planck Society, Berlin, Germany

Transmission electron microscopy (TEM) offers a powerful tool for the analysis of specimens down to an atomic scale. In order to achieve the best possible image resolution and quality of obtained data, sample preparation is a crucial step. Many samples contain a high carbon content, e.g. as organic ligands or solvents.

Electron beam exposure can lead to the deposition of carbon on the specimen surface and limit the quality of the measurements.

In our work we focus on the removal of undesirable carbon species before the sample is inserted in the microscope. Our sample cleaning setup allows for investigation of the influence of different preparation parameters, e.g. drying time or temperature, on how long solvents remain in the vacuum system and therefore can have an impact on the TEM analysis. Evaluation of the decrease in pressure while pumping our setup with a TEM sample gives insight in necessary drying times. The effect of our sample treatment can be verified in the TEM by contrast and thickness measurements after electron beam exposure of the sample.

Quantum Information Division Fachverband Quanteninformatik (QI)

Otfried Gühne
Universität Siegen
Walter-Flex-Str. 3
57068 Siegen
otfried.guehne@uni-siegen.de

Guido Burkard
Universität Konstanz
Universitätsstraße 10
78464 Konstanz
guido.burkard@uni-konstanz.de

Overview of Invited Talks and Sessions

(Lecture halls H8 and H9; Poster P2)

Invited Talks

QI 1.1	Mon	9:30–10:00	H8	Coherence of spin qubits in planar germanium — •NICO WILLEM HENDRICKX
QI 2.1	Mon	9:30–10:00	H9	Measuring the thermodynamic cost of timekeeping — •YELENA GURYANOVA
QI 2.6	Mon	11:15–11:45	H9	Finite-size effects in quantum thermodynamics — •KAMIL KORZEKWA
QI 3.1	Mon	15:00–15:30	H8	Generalized randomized benchmarking with short random quantum circuits — MARKUS HEINRICH, •MARTIN KLIESCH, INGOR ROTH
QI 5.1	Tue	9:30–10:00	H8	Towards universal quantum computation and simulation with NV centre in diamond — •VADIM VOROBYOV
QI 6.1	Tue	9:30–10:00	H9	Towards an Artificial Muse for new Ideas in Quantum Physics — •MARIO KRENN
QI 8.1	Wed	15:00–15:30	H9	Exploring Quantum Materials with Quantum Sensors — •URI VOOL
QI 10.1	Thu	9:30–10:00	H9	Entanglement Transition in the Projective Transverse Field Ising Model — •HANS PETER BÜCHLER
QI 13.1	Fri	9:30–10:00	H8	Scalable control of superconducting qubits — •STEFAN FILIPP
QI 14.1	Fri	9:30–10:00	H9	Testing quantum theory with generalized noncontextuality — •MARKUS P. MÜLLER, ANDREW J. P. GARNER

Invited Talks of the joint Symposium Entanglement Distribution in Quantum Networks (SYED)

See SYED for the full program of the symposium.

SYED 1.1	Wed	9:30–10:00	H1	A multi-node quantum network of remote solid-state qubits — •RONALD HANSON
SYED 1.2	Wed	10:00–10:30	H1	Quantum key distribution with highly entangled photons from GaAs quantum dots — •ARMANDO RASTELLI, SANTANU MANNA, SAIMON COVRE DA SILVA, GABRIEL UNDEUTSCH, CHRISTIAN SCHIMPF
SYED 1.3	Wed	10:30–11:00	H1	Entanglement distribution with minimal memory requirements using time-bin photonic qudits — •JOHANNES BORREGAARD
SYED 1.4	Wed	11:15–11:45	H1	Quantum photonics: interference beyond HOM and quantum networks — •STEFANIE BARZ
SYED 1.5	Wed	11:45–12:15	H1	Photonic cluster-state generation for memory-free quantum repeaters — •TOBIAS HUBER

Sessions

QI 1.1–1.11	Mon	9:30–12:45	H8	Implementations: Spin Qubits, Atoms, and Photons
QI 2.1–2.10	Mon	9:30–12:45	H9	Quantum Thermodynamics and Open Quantum Systems
QI 3.1–3.10	Mon	15:00–18:00	H8	Certification and Benchmarking of Quantum Systems
QI 4.1–4.41	Mon	18:00–20:00	P2	Poster: Quantum Information
QI 5.1–5.9	Tue	9:30–12:15	H8	Implementations: Solid state systems
QI 6.1–6.11	Tue	9:30–12:45	H9	Quantum Information: Concepts and Methods
QI 7.1–7.10	Wed	15:00–17:45	H8	Quantum Communication and Networks
QI 8.1–8.9	Wed	15:00–17:45	H9	Quantum Sensors and Metrology
QI 9.1–9.10	Thu	9:30–12:15	H8	Quantum Correlations
QI 10.1–10.9	Thu	9:30–12:15	H9	Quantum Simulation and Many-Body Systems
QI 11	Thu	14:00–15:00	H8	Members' Assembly

QI 12.1–12.12	Thu	15:00–18:15	H8	Quantum Computing and Algorithms
QI 13.1–13.11	Fri	9:30–12:45	H8	Implementations: Superconducting Qubits
QI 14.1–14.10	Fri	9:30–12:30	H9	Quantum Foundations

Members' Assembly of the Quantum Information Division

Donnerstag, 8. September 2022 14:00–15:00 H8

More information will be sent to the members of the division by e-mail.

Sessions

– Invited Talks, Contributed Talks, and Posters –

QI 1: Implementations: Spin Qubits, Atoms, and Photons

Time: Monday 9:30–12:45

Location: H8

Invited Talk

QI 1.1 Mon 9:30 H8

Coherence of spin qubits in planar germanium — •NICO WILLEM HENDRICKX — IBM Research Zurich, Switzerland

The prospect of building quantum circuits using advanced semiconductor manufacturing techniques position quantum dots as an attractive platform for quantum information processing. Initial demonstrations of one and two-qubit logic have been performed in gallium arsenide and later silicon. However, until recently, interconnecting larger spin qubit systems has remained a challenge.

Over the past years, hole states in strained germanium quantum wells have emerged as a host for spin qubits. These states have favourable properties for defining extended spin qubit arrays. The small effective mass relaxes constraints on lithography, the low degree of disorder enables reproducible quantum dots, the lack of a valley degeneracy ensures a well-defined qubit state and the strong spin-orbit coupling allows for local and electrical qubit control.

Over the past years, this platform has rapidly evolved from materials growth to supporting multi-qubit logic. I will first give an overview of the development of this system, starting from material growth to recent results on operating a highly-connected two-dimensional qubit array. Next, we will discuss the impact of noise on the qubit coherence, as well as strategies to mitigate this. We study the magnetic field dependence of various qubit properties in order to find sweet spots for operation. Finally, we will discuss strategies, challenges, and opportunities in scaling these systems up as a step towards the realisation of scalable qubit tiles for fault-tolerant quantum processors.

QI 1.2 Mon 10:00 H8

Spin relaxation times of single-electrons in bilayer graphene quantum dots —

•KATRIN HECKER^{1,2}, LUCA BANSZERUS^{1,2}, SAMUEL MÖLLER^{1,2}, EIKE ICKING^{1,2}, KENJI WATANABE³, TAKASHI TANIGUCHI³, CHRISTIAN VOLK^{1,2}, and CHRISTOPH STAMPFER^{1,2} — ¹2nd Institute of Physics, RWTH Aachen University, Germany — ²Peter Grünberg Institute (PGI-9), Forschungszentrum Jülich, Germany — ³National Institute for Materials Science, Japan

Thanks to its weak spin-orbit coupling and low nuclear spin density, bilayer graphene (BLG) promises long spin relaxation and coherence times, making this material a potentially interesting platform for spin based solid state quantum computation. Although the electrostatic confinement of single electrons in BLG quantum dot (QD) devices has been demonstrated, and their single particle spectrum has been studied in detail [1], their relaxation dynamics remain so far mostly unexplored [2]. Here, we report on measurements of the spin relaxation times (T1) of single-electron spin states in a BLG QD. Using pulsed gate spectroscopy, we extract T1 times exceeding 0.2ms at out-of-plane magnetic fields below 2T. The measured values for T1 show a strong dependence on the spin splitting and increase by about two orders of magnitude when decreasing the magnetic field from 2-3T, suggesting that T1 could be significantly larger at low magnetic fields [3].

[1] A. Kurzman et al., Phys. Rev. Lett. 123, 026803 (2019).

[2] L. Banszerus et al., Phys. Rev. B 103, L081404 (2021).

[3] L. Banszerus et al., arXiv 2110.13051 (2021).

QI 1.3 Mon 10:15 H8

Microwave spectroscopy of rare earth spin ensembles at zero magnetic field —

•ANA STRINIC^{1,2}, KIRILL G. FEDOROV^{1,2}, RUDOLF GROSS^{1,2,3}, and NADEZHDA KUKHARCHYK^{1,3} — ¹Walther-Meißner-Institut, Bayerische Akademie der Wissenschaften, Garching, Germany — ²Physik-Department, Technische Universität München, Garching, Germany — ³Munich Center for Quantum Science and Technologies, Munich, Germany

Operating at microwave frequencies and in the absence of external magnetic fields, superconducting circuits show exceptional potential for the development of quantum processors. Realizing a quantum memory, which operates in the microwave regime and in the vicinity of zero magnetic field, would allow for a direct interface to such quantum processors. In this regard, rare earth doped crystals are highly attractive, as they exhibit long optical and spin coherence times and possess transitions in the microwave frequency range [1,2]. In order to identify transitions, which form a suitable quantum memory scheme, we have performed microwave spectroscopy on a ¹⁶⁷Er:⁷LiYF₄ crystal in a magnetically shielded environment. The experimental findings of the spectroscopy study are then compared to simulations of the spin Hamiltonian. [1] N. Kukharchyk et al. New J. Phys. 20, 023044 (2018) [2] J.V. Rakonjac et al. Phys. Rev. B 101, 184430 (2020)

QI 1.4 Mon 10:30 H8

Nuclear Spin Quantum Memory in Silicon Carbide — •BENEDIKT TISSOT¹, MICHAEL TRUPKE^{2,3}, PHILIPP KOLLER², THOMAS ASTNER², and GUIDO BURKARD¹ — ¹Department of Physics, University of Konstanz, D-78457 Konstanz, Germany — ²Faculty of Physics, University of Vienna, Boltzmanngasse 5, 1090 Vienna, Austria — ³Institute for Quantum Optics and Quantum Information (IQOQI) Vienna, Austrian Academy of Sciences, Boltzmanngasse 3, 1090 Vienna, Austria

Transition metal (TM) defects in silicon carbide (SiC) are a promising platform for applications in quantum technology. Some TM defects, e.g. vanadium, emit in one of the telecom bands, but the large ground state hyperfine manifold poses a problem for applications which require pure quantum states. We develop a driven, dissipative protocol to polarize the nuclear spin, based on a rigorous theoretical model of the defect. We further show that nuclear-spin polarization enables the use of well-known methods for initialization and long-time coherent storage of quantum states. The proposed nuclear-spin preparation protocol thus marks the first step towards an all-optically controlled integrated platform for quantum technology with TM defects in SiC.

QI 1.5 Mon 10:45 H8

Cavity-mediated quantum gates between driven remote spin qubits — •FLORIAN KAYATZ, JONAS MIELKE, and GUIDO BURKARD — University of Konstanz, Konstanz D-78457, Germany

The implementation of two-qubit gates between distant qubits is of fundamental importance for quantum computing architectures involving many qubits. Considering cold ions confined in a linear trap, the Cirac-Zoller gate (CZ-gate) [1,2] constitutes such a two-qubit gate by exploiting the coupling of the ions through the collective quantized ion motion.

Here, we theoretically demonstrate a CZ-like gate between two spin qubits realized in gate defined semiconductor double quantum dots. In the envisioned system both spin qubits are coupled to a microwave resonator mode that has a similar function as the collective ion motion in the original CZ-gate. Recently, strong spin-photon coupling has been demonstrated [3] and, thus, allows for coherent population exchange between the spin qubit and the resonator mode. Thereby, two of the three main steps in the CZ-gate protocol can be realized. We describe in detail how the remaining step that requires the generation of a phase depending on the state of the second qubit and the resonator photon number can be implemented by driving the second DQD-system.

[1] Cirac, J. I. and Zoller, P., PRL 74, 4091 (1995)

[2] Schmidt-Kaler et al., Nature 422, 408-411 (2003)

[3] Mi et al., Nature 555, 7698 (2018)

15 min. break

QI 1.6 Mon 11:15 H8

Coherence improvements at a higher-order sweet spot in double quantum dots — •MORTEN I. K. MUNK^{1,2}, MARTIN LEIJNSE¹, and PETER SAMUELSSON² —

¹NanoLund and Division of Solid State Physics, Lund University, Lund, Sweden — ²NanoLund and Division of Mathematical Physics, Lund University, Lund, Sweden

One of the main limiting factors for designing a useful qubit is its dephasing time. In order to improve this, qubits are often operated at optimal points, or so-called "sweet spots", but in recent years, several systems have been proposed which can be tuned to higher-order sweet spots. These qubits often fail in practice, due for example to coupling to leakage states or a lack of protection against other relevant noise sources. In this work we propose a straightforward way of achieving a third-order sweet spot in a double quantum dot with two electrons in the singlet sector. This experimentally feasible qubit has the combined advantages of being operated at strong tunneling strengths, where leakage states are well separated from the qubit states, as well as being possible to construct in a way in which there are no relevant unprotected noise channels. We investigate the decoherence rate due to pure dephasing for a broad range of system parameters and for different noise spectral densities. It is found, in general, that higher-order sweet spots allow for substantially increased dephasing times, suggesting a guiding principle in optimizing the coherence properties of charge qubits in double quantum dots and related systems.

QI 1.7 Mon 11:30 H8

Quantum-optical Characterization of Single-photon Sources based on Chlorine-doped ZnSe/ZnMgSe Nanopillars — •CHRISTINE FALTER, YURI KUTOVYI, NILS VON DEN DRIESCH, THORSTEN BRAZDA, DETLEV GRÜTZMACHER, and ALEXANDER PAWLIS — Peter Grünberg Institute PGI-9, Forschungszentrum Jülich GmbH

The realization of optical quantum computers and secure quantum communication networks requires the development of efficient and scalable sources of single, indistinguishable photons that can be integrated onto photonic chips. Here we report on a novel type of single-photon source (SPS) device based on individual Cl donors in ZnSe/ZnMgSe quantum well nanopillars. On top of each nanopillar a solid immersion lens is fabricated, employing the photoresist previously used to define the nanopillars. For optimized conditions the external quantum efficiency is increased by up to one order of magnitude. Excitation-power-dependent photoluminescence measurements confirm that the emission stems from a true two-level system and the single photon purity of the source is verified by measuring the second order correlation function. Finally, we investigate the grade of sequential indistinguishability of subsequent single-photons from our devices by Hong-Ou-Mandel type experiments. This work paves the way for efficient generation of polarization entanglement between two sufficiently indistinguishable photons. Consequently, future applications of these SPSs are envisioned in all-optical based quantum cryptography or to interconnect distant nodes in quantum networks.

QI 1.8 Mon 11:45 H8

A Reversible Classical Half-Adder Implemented with Trapped Ion Qubits — •PATRICK HUBER¹, SAGAR PRATAPSI^{2,3}, PATRICK BARTHEL¹, SOUGATO BOSE^{4,5}, YASSER OMAR^{2,3,6}, and CHRISTOF WUNDERLICH¹ — ¹Department of Physics, School of Science and Technology, University of Siegen, 57068 Siegen, Germany — ²Physics of Information and Quantum Technologies Group, Instituto de Telecomunicações, Portugal — ³Instituto Superior Técnico, U. Lisbon, Portugal — ⁴Department of Physics and Astronomy, University College London, London WC1E 6BT, UK — ⁵Department of Electronic & Electrical Engineering, University College London, WC1E 7JE London, UK — ⁶Portuguese Quantum Institute, Portugal

We experimentally realise a Toffoli gate and a Half-Adder circuit suitable for classical computation, using qubits encoded into trapped $^{171}\text{Yb}^+$ ions. The microwave-controlled qubits are coupled by an all-to-all $\sigma_z\sigma_z$ interaction. A comprehensive analysis is given of the energy required to operate the gates, both from first principles and by experimental measurements. This allows for identifying decisive improvements that could lead to energetically efficient classical computation. Our analysis indicates that a novel planar ion trap-setup will already be 10^5 times more efficient.

QI 1.9 Mon 12:00 H8

Improving quantum state detection with adaptive sequential observations — SHAWN GELLER^{1,2}, DANIEL COLE¹, SCOTT GLANCY^{1,2}, and •EMANUEL KNILL^{1,2} — ¹National Institute of Standards and Technology, Boulder, CO, USA — ²University of Colorado at Boulder, Boulder, CO USA

For many quantum systems intended for information processing, one detects the logical state of a qubit by integrating a continuously observed quantity over time. For example, ion and atom qubits are typically measured by driving a cycling transition and counting the number of photons observed from the resulting fluorescence. Instead of recording only the total observed count in a fixed time

interval, one can observe the photon arrival times and get a state detection advantage by using the temporal structure in a model such as a Hidden Markov Model. We study what further advantage may be achieved by applying pulses to adaptively transform the state during the observation. We give a three-state example where adaptively chosen transformations yield a clear advantage, and we compare performances on an ion example, where we see improvements in some regimes.

QI 1.10 Mon 12:15 H8

Quantum Information Transfer in a Chain of Trapped Ions — •THEERAPHOT SRIARUNOTHAI, PATRICK BARTHEL, PATRICK HUBER, GOURI S. GIRI, and CHRISTOF WUNDERLICH — Department of Physics, School of Science and Technology, University of Siegen, 57068 Siegen, Germany

We explore a quantum teleportation scheme with four trapped $^{171}\text{Yb}^+$ ions in a non-segmented linear Paul trap, each radiofrequency-controlled ion representing one qubit. The $\sigma_z\sigma_z$ interaction between qubits is mediated by Magnetic Gradient Induced Coupling (MAGIC) [1]. The 4×4 interaction matrix of the qubit-system is measured and, taking advantage of all-to-all connectivity, is used to create Bell states between pairs of nearest neighbours and second-nearest neighbours, respectively. Furthermore, it is demonstrated how, while creating an entangled pair, another qubit serves as a decoupled quantum memory. This memory qubit is protected from decoherence with the same dynamical decoupling sequence as the one applied to perform the Bell-state operations. We developed and implemented a blueprint to demonstrate quantum state transfer using a quantum teleportation scheme. First experimental results on teleportation indicate the transfer of a superposition state from one end to another end of a quantum register. The method and techniques developed here can be applied to a larger system, for example, a full quantum byte or across quantum registers.

[1] Ch. Piltz et al., *Science Advances* **2**, e1600093 (2016).

QI 1.11 Mon 12:30 H8

Dressed $^{171}\text{Yb}^+$ Hyperfine Qubits in a Multi-layer Planar Ion Trap — •ELHAM ESTEKI¹, BOGDAN OKHRIMENKO¹, FRIEDERIKE GIEBEL^{2,3,4}, EIKE ISEKE^{2,3,4}, KONSTANTIN THRONBERENS^{3,4}, NILA KRISHNAKUMAR^{2,4}, JACOB STUPP^{2,3}, AMADO BAUTISTA SALVADOR^{2,3,4}, CHRISTIAN OSPELKAUS^{2,3,4}, IVAN BOLDIN¹, and CHRISTOF WUNDERLICH¹ — ¹Dept. Physik, Nat.-Techn. Fak., Universität Siegen, 57068 Siegen — ²Leibniz Universität Hannover, Welfengarten 1, 30167 Hannover — ³Laboratory for Nano - and Quantum Engineering, Schneiderberg 39, 30167 Hannover — ⁴Physikalisch-Technische Bundesanstalt, Bundesallee 100, 38116 Braunschweig

Dressed qubit states – the eigenstates of the Hamiltonian of a qubit subject to a near-resonant driving field – can be used to store and process quantum information instead of bare state qubits. We present a microfabricated ion trap chip, designed for the realization of quantum information processing based on radiofrequency-dressed qubits using hyperfine states of $^{171}\text{Yb}^+$ ions [1]. The ion trap chip consists of multiple layers [2], one of which includes an integrated microwave resonator. It creates a gradient of the microwave magnetic field amplitude which is needed for the realization of qubit addressing and qubit-qubit coupling. We experimentally characterize this novel ion trap chip and demonstrate preparation and detection of RF-dressed qubits, as well as single-qubit and two-qubit operations.

[1] S. Wölk, Ch. Wunderlich, *New J. Phys.* **19**, 083021 (2017).[2] A. Bautista-Salvador et al., *New J. Phys.* **21**, 043011 (2019).

QI 2: Quantum Thermodynamics and Open Quantum Systems

Time: Monday 9:30–12:45

Location: H9

Invited Talk

QI 2.1 Mon 9:30 H9

Measuring the thermodynamic cost of timekeeping — •YELENA GURYANOVA — Institute for Quantum Optics and Quantum Information (IQOQI), Austrian Academy of Sciences, Boltzmanngasse 3, 1090 Vienna, Austria

All clocks, in some form or another, use the evolution towards higher entropy states to quantify the passage of time. Because of the statistical nature of the second law and corresponding entropy flows, fluctuations fundamentally limit the performance of any clock. This suggests a deep relation between the increase in entropy and the quality of clock ticks. Indeed, minimal models for autonomous clocks in the quantum realm revealed that a linear relation can be derived, where for a limited regime entropy linearly increases with the accuracy. Does a linear relation persist as we move toward a more classical system? We answer this in the affirmative by presenting the first experimental investigation of this thermodynamic relation in a nanoscale clock. We stochastically drive a nanometer-thick membrane and read out its displacement with a radio-frequency cavity, allowing us to identify the ticks. We show theoretically that the maximum possible accuracy for this classical clock is proportional to the entropy created per tick, similar to the known limit for a weakly coupled quantum clock but with a dif-

ferent proportionality constant. We measure both the accuracy and the entropy. Once non-thermal noise is accounted for, we find that there is also a linear relation between accuracy and entropy.

QI 2.2 Mon 10:00 H9

Thermodynamics of Permutation-Invariant Quantum Many-Body Systems: A Group-Theoretical Framework — •BENJAMIN YADIN¹, BENJAMIN MORRIS^{2,3}, and KAY BRANDNER^{2,3} — ¹Naturwissenschaftlich-Technische Fakultät, Universität Siegen, Walter-Flex-Straße 3, 57068 Siegen, Germany — ²School of Physics and Astronomy, University of Nottingham, Nottingham NG7 2RD, United Kingdom — ³Centre for the Mathematics and Theoretical Physics of Quantum Non-equilibrium Systems, University of Nottingham, Nottingham NG7 2RD, United Kingdom

Classical thermodynamics originally described ensembles of many particles controlled collectively without addressing individual particles. However, quantum phenomena such as entanglement may lead to very different collective behaviour. We study non-identical particles that interact identically with their environment and control systems. Such collective dynamics are generally generated by a Hamiltonian invariant under particle permutations.

We develop a general framework for such systems, finding a quantum state space containing additional non-classical degrees of freedom. While the permutation symmetry prevents full thermalisation, we prove that a sufficiently complex bath interaction enables maximum possible thermalisation. For systems initialised out of equilibrium with the bath, we calculate steady-state properties and determine the performance of a heat engine model. Compared with previous models using $SU(2)$ spin interactions, we show that $SU(d)$ -based couplings for d -dimensional particles can lead to thermodynamical advantages.

QI 2.3 Mon 10:15 H9

Geometric structure of thermal cones — •ALEXSSANDRE DE OLIVEIRA JUNIOR, JAKUB CZARKOWSKI, KAROL ZYCZKOWSKI, and KAMIL KORZEKWA — Faculty of Physics, Astronomy and Applied Computer Science, Jagiellonian University, 30-348 Kraków, Poland.

The second law of thermodynamics imposes a fundamental asymmetry in the flow of events. The so-called thermodynamic arrow of time introduces an ordering on the space of states that can be distinguished according to the system's evolution as past, incomparable, and future thermal cones. In this work, we analyse the structure of the thermodynamic arrow of time within a resource-theoretic framework, where one investigates the accessibility of quantum state transformations under thermodynamic constraints. Specifically, for a d -dimensional classical state interacting with a heat bath at a fixed temperature T , we found the necessary and sufficient conditions to construct its incomparable and past thermal cones. By introducing a new thermodynamic monotone, the volume of the future thermal cone, we provide a detailed analysis of the behaviour of the thermal cones. In a general context, while the future thermal cone can be seen as a generalisation of the Hardy-Littlewood-Polya theorem, the past and incomparable region can be interpreted as its extensions. Moreover, our results also apply to other majorisation-based resource theories, such as entanglement, since in the limit of infinite temperature, the partial order that emerges is the same (precisely: the opposite) as defined on the set of bipartite pure entangled states by local operations and classical communication

QI 2.4 Mon 10:30 H9

Continuous measurement feedback for adaptive qubit thermometry — •JULIA BOEYENS and STEFAN NIMMRICHTER — Naturwissenschaftlich-Technische Fakultät, Universität Siegen, Siegen 57068, Germany

Bayesian estimation was recently applied to quantum thermometry since it allows for better estimation accuracy when data is limited and admits adaptive estimation schemes. Here, we apply the Bayesian framework to the setting of continuous temperature measurement. We model a qubit probe, subject to continuous monitoring interacting with a bosonic bath of unknown temperature. The Kushner-Stratonovich equation from classical filtering theory is simulated to find the posterior distribution. Bayesian estimation is then used to infer the temperature from this probability distribution using. This is compared to the discrete analogue, collisional thermometry. An adaptive strategy for improved accuracy is described where Hamiltonian parameters of the qubit can be changed continuously by measurement feedback.

QI 2.5 Mon 10:45 H9

Quantum trajectories beyond weak coupling — •BRECHT DONVIL¹ and PAOLO MURATORE GINANNESCHI² — ¹Institute for Complex Quantum Systems, Albert-Einstein-Allee 11, D-89069, Ulm — ²University of Helsinki, Department of Mathematics and Statistics P.O. Box 68 FIN-00014, Helsinki, Finland

Master equations are one of the main avenues to study open quantum systems. In situations where the interaction between a dedicated system and its environment is weak, the master equation is of the Lindblad form. In this case, the solution of the master equation can be “unraveled in quantum trajectories” i.e. represented as an average over the realizations of a Markov process in the Hilbert space of the system. Quantum trajectories of this type are both an element of quantum measurement theory as well as a numerical tool for systems in large Hilbert spaces.

In this talk, I show that I show how this procedure can be generalized to arbitrary trace-preserving master equations with time-local dissipation rates. In contrast to the conventional setting, these rates can take also negative values, thus mimicking back-flow of information. Such master equations typically arrive from exactly solvable models or time convolutionless perturbation theory. The crucial ingredient for our unraveling is to weigh averages by a probability pseudo-measure which we call the “influence martingale”. The influence martingale satisfies a $1d$ stochastic differential equation enslaved to the ones governing the quantum trajectories. The influence martingale thus extends the existing theory without increasing the computational complexity.

15 min. break

Invited Talk

QI 2.6 Mon 11:15 H9

Finite-size effects in quantum thermodynamics — •KAMIL KORZEKWA — Jagiellonian University, Kraków, Poland

The necessity to go beyond classical thermodynamics is usually motivated by the fact that at the nanoscale quantum effects, like coherence and entanglement,

start playing an important role. However, in the quantum regime one also deals with systems composed of a finite number n of particles, whereas the theory of thermodynamics is traditionally constrained to the study of macroscopic systems with $n \rightarrow \infty$, whose energy fluctuations are negligible compared to their average energy. In this talk I will address this problem and describe recent developments allowing one to go beyond the thermodynamic limit and rigorously investigate thermodynamic transformations of finite-size systems. I will explain why such transformations are generally irreversible and consume free energy, and how this affects the performance of thermodynamic protocols. A new version of the famous fluctuation-dissipation theorem will also be presented, linking the minimal amount of free energy dissipated in the process to the amount of free energy fluctuations present in the initial state of the system. Moreover, I will discuss a novel resource resonance phenomenon, which allows one to significantly reduce dissipation for transformations between states whose fluctuations are properly tuned. Finally, I will also explain how quantum coherence may bring states closer to resonance effectively decreasing the dissipation of free energy.

QI 2.7 Mon 11:45 H9

Work fluctuations and entanglement in quantum batteries — •SATOYA IMAI, OTFRIED GÜHNE, and STEFAN NIMMRICHTER — Universität Siegen Department Physik Emmy-Noether-Campus Walter-Flex-Straße 3 57068 Siegen Germany

We consider quantum batteries given by composite interacting quantum systems in terms of the thermodynamic work cost of local random unitary processes. We characterize quantum correlations by monitoring the average energy change and its fluctuations in the high-dimensional bipartite systems. We derive a hierarchy of bounds on high-dimensional entanglement (the so-called Schmidt number) from the work fluctuations and thereby show that larger work fluctuations can verify the presence of stronger entanglement in the system. Finally, we develop two-point measurement protocols with noisy detectors that can estimate work fluctuations, showing that the dimensionality of entanglement can be probed in this manner.

QI 2.8 Mon 12:00 H9

Large fluctuations of qubit decoherence under $1/f$ noise of a sparse bath of two-level fluctuators — •MOHAMMAD MEHMANDOOST and VIATCHESLAV DOBROVITSKI — QuTech and Kavli Institute of Nanoscience, Delft University of Technology, Lorentzweg 1, 2628 CJ Delft, The Netherlands

We theoretically study the qubit decoherence caused by $1/f$ noise of a sparse bath of Two-Level Fluctuators (TLFs) in the Ramsey and Hahn echo experiments. We focus on the role of bath density d , defined as the ratio of the number of TLFs n to the logarithmic frequency range $\ln(\gamma_M/\gamma_m)$, on the qubit decoherence. The first spectral density of $1/f$ noise produced by sparse bath samples, small d , are roughly similar. The qubit decoherence in this regime is, however, not fully characterized by the noise first spectral density. We therefore use the exact expressions describing the qubit decoherence coupled to a sample TLF bath. Using Monte Carlo simulations, we show that the qubit decoherence is subject to large sample-to-sample fluctuations in sparse baths of fixed density d . This highlights the necessity to adopt a statistical approach to characterize the qubit decoherence in this regime. We also found that the qubit decoherence under $1/f$ noise of sparse TLF baths is governed by only a few TLFs. We show that if these TLFs are removed, the coherence times are substantially improved. We hope the latter finding opens up a way to improve the coherence times of the state-of-the-art qubits affected by $1/f$ noise.

QI 2.9 Mon 12:15 H9

Entanglement Preservation in Open Quantum System — •MEI YU, STEFAN NIMMRICHTER, and OTFRIED GÜHNE — Universität Siegen, Siegen, Germany

It's widely known that the entanglement will decay when system is exposed to the environment. In this paper, we study how to keep the entanglement against destructive effect from environment at different temperatures. Within the spin gases model, we firstly investigate the entangling ability of two-qubit gate in Markovian and non-Markovian dephasing environment. Then, we implement the specific reset operation on two-qubit system at stochastic times in order to keep entanglement in steady state. The steady-state entanglement behavior is analysed in both cases of Markovian and non-Markovian dephasing noise with different temperatures. Excepting for considerable entanglement value, the difference between Markovian and non-Markovian effect can be observed directly.

QI 2.10 Mon 12:30 H9

Quantum thermodynamics of rare earth spin ensembles embedded into Y_2SiO_5 — ANDREAS MEYER^{1,2}, RUDOLF GROSS^{1,2,3}, and •NADEZHDA P. KUKHARCHYK^{1,3} — ¹Walther-Meißner-Institut, Bavarian Academy of Sciences, Garching, Germany — ²Physics Department, Technical University of Munich, Garching, Germany — ³Munich Center for Quantum Science and Technologies, Munich, Germany

Interest in the field of quantum thermodynamic has emerged recently supported by advances in quantum information field. While quantum systems themselves require an optimized approach for characterisation of entropy and work, also the temperature range at which such systems operate is highly sensitive to even small

excitation. The rare earth spin ensembles belong to those systems, which are in the focus of quantum thermodynamics. When these ensembles are cooled down to millikelvin temperatures, even short controlling pulses result in a strong perturbation of thermal equilibrium in the host crystal, which reveals itself in the observed dynamics of the excited spin ensemble [1]. In this talk, we will discuss the dynamics of the non-equilibrium state within the Y_2SiO_5 crystal, as well as

its impact on the relaxation and decoherence processes within the rare earth spin ensembles. The analytical modelling of the heat dynamics will be compared to the experimental finding of the coherence study of $^{167}Er:Y_2SiO_5$ at millikelvin temperatures.

1. N. Kukharchyk et al, "Enhancement of optical coherence in $^{167}Er:Y_2SiO_5$ crystal at millikelvin temperatures", arXiv: 1910.03096

QI 3: Certification and Benchmarking of Quantum Systems

Time: Monday 15:00–18:00

Location: H8

Invited Talk

QI 3.1 Mon 15:00 H8

Generalized randomized benchmarking with short random quantum circuits — MARKUS HEINRICH¹, MARTIN KLIESCH¹, and INGOR ROTH² — ¹Heinrich Heine University Düsseldorf, Germany — ²Technology Innovation Institute, Abu Dhabi, United Arab Emirates

The characterization of the quality of quantum gate implementations is among the most important certification tasks in the quantum sciences. State preparation and measurement errors render this task a challenge, in particular for large qubit numbers. Randomized benchmarking (RB) is among the most popular approaches to address this challenge. Rigorous theoretical guarantees for RB methods rely on sequences of unitary operations each of which is drawn uniformly from a group, often the Clifford group. Due to compiling, such RB strategies effectively require the implementation of quantum circuits with an unfavourable scaling of the circuit depth with the number of qubits. In practice, this scaling results in a restriction to a few qubits.

This talk starts with an introduction to RB, a generalized version thereof and a review of the idea of drawing the unitaries from a generating gate set of the group rather than from its uniform distribution in order to reduce the required circuit depths. Then we show analytically how this changes the exponential decay behaviour observed in RB. In particular, shorter circuits can result in decays that are a combination of the usual RB decay plus a decay corresponding to mixing properties (spectral gap of the moment operator) of the gate set. In this way, we shine new light on the important question of how quantum gates can be certified using short circuits.

QI 3.2 Mon 15:30 H8

Compressive gate set tomography — RAPHAEL BRIEGER¹, INGO ROTH², and MARTIN KLIESCH¹ — ¹Quantum technology, Heinrich Heine University Düsseldorf, Germany — ²Quantum Research Centre, Technology Innovation Institute, Abu Dhabi, UAE

Flexible characterization techniques that identify and quantify experimental imperfections under realistic assumptions are crucial for the development of quantum computers. Gate set tomography is a characterization approach that simultaneously and self-consistently extracts a tomographic description of the implementation of an entire set of quantum gates, as well as the initial state and measurement, from experimental data. Obtaining such a detailed picture of the experimental implementation is associated with high requirements on the number of sequences and their design, making gate set tomography a challenging task even for only two qubits. In this work, we show that low-rank approximations of gate sets can be obtained from significantly fewer gate sequences and that it is sufficient to draw them randomly. To this end, we formulate the data processing problem of gate set tomography as a rank-constrained tensor completion problem. We provide an algorithm to solve this problem while respecting the usual positivity and normalization constraints of quantum mechanics by using second-order geometrical optimization methods on the complex Stiefel manifold. Besides the reduction in sequences, we demonstrate numerically that the algorithm does not rely on structured gate sets or an elaborate circuit design to robustly perform gate set tomography and is therefore more broadly applicable than traditional approaches.

QI 3.3 Mon 15:45 H8

Spin squeezing inequalities meet randomized measurements — JAN LENNART BÖNSEL, SATOYA IMAI, YE-CHAO LIU, and OTFRIED GÜHNE — University of Siegen, Siegen, Germany

Due to the recent advances in quantum control, large quantum systems containing thousands of atoms can nowadays be prepared in the lab. Here, the characterization of quantum correlations is of special interest. For systems where the individual atoms are difficult to address, the measurement of collective angular momentum observables and the evaluation of the corresponding spin squeezing inequalities are a possibility to characterize entanglement and its usefulness for metrology.

In this contribution, we first study the number of quantum state samples that are necessary to verify entanglement with a certain confidence. For this purpose, we compare different estimators of spin squeezing parameters. We characterize the probability that the estimator deviates from its mean using simulations as well as analytical bounds derived from concentration inequalities, like Cantelli's

and Hoeffding's inequality. Second, we analyse if it is possible to obtain a good estimate from fewer measurements made only on a randomly chosen subset of the atoms.

QI 3.4 Mon 16:00 H8

Machine learning approaches to Optimal Gate Sequences for Quantum State Tomography under Noise — VIOLETA N. IVANOVA-ROHLING^{1,2,3}, NIKLAS ROHLING¹, and GUIDO BURKARD¹ — ¹Department of Physics, University of Konstanz, D-78457 Konstanz — ²Zukunftskolleg, University of Konstanz, D-78457 Konstanz — ³Department of Mathematical Foundations of Computer Sciences, IMI, Bulgarian Academy of Sciences

For limited scenarios, depending on projector rank and system size, optimal measurement schemes for efficient quantum state tomography (QST) are known. In the case of errorless non-degenerate measurements, using mutually unbiased bases yields the optimal QST scheme [1]. However, in the general case, the optimal measurement scheme for efficient QST is not known and, may need to be numerically approximated. Here, we investigate the effect of noise on the optimal QST measurement sets using two noise models: the depolarizing channel, and over- and under-rotation in two-qubit gates [2]. Furthermore, we apply reinforcement learning for optimizing the effective times each quantum gate is switched on in a set of gate sequences which – combined with an elementary projective measurement – realizes a QST quorum. We extend the model by including errors from single-qubit gates and allow for longer gate sequences than necessary for realizing arbitrary measurements aiming at higher noise resilience overall.

[1] Wootters, Fields, Ann. Phys. 191, 363 (1989)

[2] Ivanova-Rohling, Rohling, Burkard, arXiv:2203.05677

QI 3.5 Mon 16:15 H8

Verifying arbitrary entangled state with homogeneous local measurements — YE-CHAO LIU^{1,2}, YINFEI LI², JIANGWEI SHANG², and XIANGDONG ZHANG² — ¹Universität Siegen, Siegen, Germany — ²Beijing Institute of Technology, Beijing, China

Quantum state verification is the task that uses only local measurements to judge whether one unknown state is the pure state that we desire. Recently, with the rapid growth in the size of manipulated quantum systems, such a fundamental task attracts more and more attention due to the weakness of the standard tomography method in the efficiency, and many entangled states can be verified efficiently or even optimally. However, how to design a verification protocol for an arbitrary entangled state is still an open problem. In this paper, we present a systematic framework to solve the problem by considering the locality of what we call choice-independent measurement protocols, whose operators can be achieved directly when it is homogeneous. Taking several kinds of entangled states as examples, we demonstrate the concrete processes and results of the design method under the most common Pauli projections. Moreover, our framework can tackle the local protocol design of other tasks, like entanglement witness, which is also an important problem. Finally, all these tasks can be converted into corresponding parameter estimation tasks, whose local protocols can be always easily achieved by our methods.

15 min. break

QI 3.6 Mon 16:45 H8

Dynamic Uncertainty Propagation with Noisy Quantum Parameters — FELIX MOTZOI¹, MOGENS DALGAARD², and CARRIE WEIDNER³ — ¹Forschungszentrum Juelich — ²Aarhus University — ³Bristol University

Many quantum technologies rely on high-precision dynamics, which raises the question of how these are influenced by the experimental uncertainties that are always present in real-life settings. A standard approach in the literature to assess this is Monte Carlo sampling, which suffers from two major drawbacks. First, it is computationally expensive. Second, it does not reveal the effect that each individual uncertainty parameter has on the state of the system. In this talk, we evade both these drawbacks by incorporating propagation of uncertainty directly into simulations of quantum dynamics, thereby obtaining a method that is orders of magnitude faster than Monte Carlo simulations and directly provides information on how each uncertainty parameter influences the system dynamics. Ad-

ditionally, we compare our method to experimental results obtained using the IBM quantum computers.

Dalgaard et al., Phys. Rev. Lett. 128, 150503 (2022)

QI 3.7 Mon 17:00 H8

Error mitigation - handling noisy quantum hardware — •KATHRIN KÖNIG and THOMAS WELLENS — Fraunhofer IAF, Freiburg, Germany

Currently available quantum computing hardware suffers from errors due to environmental influences, nearest-neighbour interactions and imperfect gate operations. To achieve robust quantum computing, there are techniques like error mitigation by zero-noise extrapolation [1]. To reduce the impact of gate errors on observable expectation values, arbitrary noise can also be converted into stochastic Pauli errors by so called noise tailoring [2]. We elaborate on the implementation of error mitigation on a superconducting quantum computer and its impact on the computation of expectation values.

[1] He, A. et al., *Zero-noise extrapolation for quantum-gate error mitigation with identity insertions*, Phys. Rev. A 102, 012426 (2020)

[2] Wallman, J. J.; Emerson, J., *Noise tailoring for scalable quantum computation via randomized compiling*, Phys.Rev. A 94, 052325 (2016)

QI 3.8 Mon 17:15 H8

Break-even point of the quantum repetition code — ÁRON ROZGONYI and •GÁBOR SZÉCHENYI — Eötvös University, Budapest

Repetition code is not a real quantum error correction code in the sense, that it cannot protect the logical information against any Pauli error. However, for simplicity repetition code is widely investigated theoretically and used for benchmarking state-of-the-art quantum devices. In our work, we analyze the efficiency of the phase-flip code as a quantum memory in presence of relaxation and dephasing. We take into account noisy two-qubit gates suffering from depolarizing and coherent error. We determine the parameter regime, where the repetition code performs better than an idle qubit.

QI 3.9 Mon 17:30 H8

Benchmarking quantum error correcting codes on near-term devices — •REGINA FINSTERHOELZL and GUIDO BURKARD — Department of Physics, University of Konstanz

We evaluate the performance of small error-correcting codes which we implement on hardware platforms of very different connectivity and coherence: On a superconducting processor and on a spintronic quantum register consisting of a color center in diamond. Taking the hardware-specific errors and connectivity into account, we investigate the dependence of the resulting logical error rate on the platform features such as the native gates, the native connectivity, gate times, and coherence times. Using a standard error model parametrized for the given hardware, we simulate the performance and benchmark these predictions with experimental results when running the code on a real quantum device. The results indicate that for small codes, the hexagonal layout of the superconducting processor proves advantageous, yet for larger codes with multi-qubit controlled operations, the star-like connectivity of the color centers enables lower error rates.

QI 3.10 Mon 17:45 H8

Quantum Lifelong Learning — •LUKAS SIGL^{1,2}, TATJANA WILK², ANNA DONHAUSER^{3,2}, STEFAN KÜCHEMANN^{3,2}, BERNHARD KRAUS¹, JAN VON DELFT^{3,2}, JOCHEN KUHN^{3,2}, and ALEXANDER HOLLEITNER^{1,2} — ¹TU Munich, Germany — ²MCQST, Germany — ³LMU Munich, Germany

Quantum technologies comprise rapidly growing scientific fields with great potential for applications in industry. The current challenge for Germany and Europe is to educate a sufficiently large number of students in quantum technologies and to transfer knowledge as well as technological expertise from the research laboratories to the industrial sector.¹ A key role is played by the specialists and executives of the high-tech industry, who have to recognize and implement the specific potential of quantum technologies for the respective company. We present our Munich project Quantum LifeLong Learning (QL3), a targeted education and training program of the Munich universities in the field of quantum technologies according to a university certificate and ECTS system with the target group of specialists and executives in industry. We acknowledge financial support by the Bundesministerium für Bildung und Forschung (BMBF) of Germany.

References: 1. C.D. Aiello, et al. *Achieving a quantum smart workforce*. Quantum Science and Technology 6, 030501 (2021)

QI 4: Poster: Quantum Information

Time: Monday 18:00–20:00

Location: P2

QI 4.1 Mon 18:00 P2

Toward Digital-Analog Simulations using Superconducting Qubits and Resonators — •RICCARDO ROMA¹, FRANK WILHELM-MAUCH^{1,2}, and DMITRY BAGRETS^{2,3} — ¹Theoretical Physics, Universität des Saarlandes, 66123 Saarbrücken, Germany — ²Forschungszentrum Jülich GmbH, Germany — ³Institut für Theoretische Physik, Universität zu Köln, Zùlpicher Straße 77, 50937 Köln, Germany

We propose a novel architecture for processors based on superconducting qubits coupled to resonators for digital-analog simulations of bosonic-fermionic systems. More in detail we present some preliminary results of the numerical analysis of a system composed of a pair of superconducting qubits, each coupled to an ancillary qubit via a resonator, interacting with a cross-resonance gate.

QI 4.2 Mon 18:00 P2

Electronic Structure Simulations for Batteries and Fuel Cells Using a Quantum Computer — •KONSTANTIN LAMP^{1,2}, ALEJANDRO D. SOMOZA¹, FELIX RUPPRECHT¹, MARINA WALT³, NICOLAS VOGT³, GIORGIO SILVI³, and BIRGER HORSTMANN^{1,2} — ¹German Aerospace Center, Wilhelm-Runge Straße 10, 89081 Ulm — ²Helmholtz Institute Ulm, Helmholtzstraße 11, 89081 Ulm — ³HQS Quantum Simulations GmbH, Haid-und-Neu-Strasse 7, 76131 Karlsruhe

In the context of modern energy devices like batteries and fuel cells a description of challenging molecular structures is vital for the advancement of these technologies. However, classical algorithms for the simulation of such systems suffer from an exponential growth in required resources, which may be avoided by exploiting the correspondence between chemical orbitals and qubits of a quantum computer.

In this work, we show a variety of hybrid quantum algorithms for electronic structure calculations performed on the IBM System One quantum computer with state-of-the-art techniques of error mitigation and noise characterization. In particular, we focus on a class of hybrid algorithms that leverage additional measurements on the quantum processor without an increase in the complexity of the quantum circuits, like VQSE [Phys.Rev.X 10, 011004] and an extension of the QEOM method [Phys.Rev.Res. 2, 043140]. Furthermore, we investigate techniques like Entanglement Forging [arXiv:2104.10220] that exploit partitions of the initial problem into strongly correlated sectors in order to achieve efficient quantum simulations of larger systems.

QI 4.3 Mon 18:00 P2

Quantum simulation of the transverse field Ising models — •SUMEET SUMEET and KAI PHILLIP SCHMIDT — Friedrich-Alexander-Universität Erlangen-Nürnberg, Department of Physics, Staudtstraße 7, 91058 Erlangen, Germany

With the advancements in quantum technologies, it has become inevitable to investigate the potential existence of quantum advantages for quantum many-body systems. One of the most paradigmatic model is the transverse field Ising model (TFIM) that can be simulated on a quantum computer to compute properties such as the ground-state energy. This problem, when tackled on a classical computer, leads to an exponential surge in the cost of computation with increasing system size. Classical-quantum hybrid algorithms such as the Variational Quantum Eigensolver (VQE) algorithm, is considered reasonably good for obtaining the ground-state energy of quantum many-body systems in the current NISQ era. Here we explore various ansatzes, focusing mainly on the Hamiltonian variational ansatz, for calculating the ground-state energy of one-dimensional TFIMs. We devise strategies to compute the ground-state energy for relatively large spin systems leveraging the power of quantum computers. In addition to that, we explore the quantum advantage and access the resource requirement for a quantum computer to evaluate the properties of systems in difficult regions around the quantum phase transition, which is a computationally difficult problem for a classical computer. Further, we extend our considerations to explore geometrically frustrated TFIMs using quantum simulation.

QI 4.4 Mon 18:00 P2

Estimating the entangling power of a two-qubit gate from measurement data: artificial neural networks and randomized measurements versus standard tomography methods — •SALWA SHAGLEL — Universität Siegen, Siegen, Germany

Quantum logic gates are the building blocks of quantum circuits and algorithms, where the generation of entanglement is essential to perform quantum computations. The amount of entanglement that a unitary quantum gate can produce from product states can be quantified by the so-called entangling power, which is a function of the gate's unitary or Choi matrix representation.

I introduce two efficient approaches to the practical problem of estimating the entangling power of an unknown two-qubit gate from measurement data. The first approach is using a deep neural network trained with noisy data simulating the outcomes of prepare-and-measure experiments on random gates. The train-

ing data is restricted to 48 measurement settings, which is significantly less than the 256 dimensions of the ambient space of 16×16 Choi matrices and very close to the minimum number of settings that guarantees the recovery of a two-qubit unitary gate using the compressed sensing technique at an acceptable error rate. The second approach to determine the entangling power is based on the second moments of correlation functions obtained from locally randomized measurements. The two approaches do not make any prior assumptions about the quantum gate, and they also avoid the need for standard reconstruction tools based on full quantum process tomography, which is prone to systematic errors.

QI 4.5 Mon 18:00 P2

Frequency-degenerate Josephson mixer for quantum illumination — •FABIAN KRONOWETTER^{1,2,3}, FLORIAN FESQUET^{1,2}, MARIA-TERESA HANDSCHUH^{1,2}, KEDAR HONASOGE^{1,2}, YUKI NOJIRI^{1,2}, MICHAEL RENGER^{1,2}, ACHIM MARX¹, FRANK DEPPE^{1,2,4}, RUDOLF GROSS^{1,2,4}, and KIRILL G. FEDOROV^{1,2} — ¹Walther-Meißner-Institut, BADW, 85748 Garching, Germany — ²Physik-Department, TUM, 85748 Garching, Germany — ³Rohde & Schwarz GmbH, 81671 Munich, Germany — ⁴Munich Center for Quantum Science and Technology (MCQST), 80799 Munich, Germany

In quantum illumination, the joint measurement of the signal and idler beams enables a quantum advantage in target detection, as compared to the ideal classical radar. This advantage is predicted to exist for the case of weak quantum signals propagating in a bright thermal background, where the latter potentially contains a weakly reflecting target. The joint measurement exploits non-classical correlations between the signal and idler modes. A promising detector concept allowing for a theoretical 3 dB quantum advantage implements this joint measurement by exploiting a frequency-degenerate Josephson mixer (JM). The circuit of this JM consists of two 180° hybrid ring beam splitters and two flux-driven Josephson parametric amplifiers. We present the first successful operation of the frequency-degenerate JM with Gaussian states and, thus, demonstrate an important milestone for the realization of the microwave quantum radar.

QI 4.6 Mon 18:00 P2

Fabrication of low-loss Josephson parametric circuits — •KEDAR E. HONASOGE^{1,2}, YUKI NOJIRI^{1,2}, DANIL E. BAZULIN^{1,2}, LEON KOCH^{1,2}, THOMAS LUSCHMANN^{1,2}, NIKLAS BRUCKMOSER^{1,2}, MARIA-TERESA HANDSCHUH¹, FLORIAN FESQUET^{1,2}, MICHAEL RENGER^{1,2}, FABIAN KRONOWETTER^{1,2,4}, ACHIM MARX¹, STEFAN FILIPP^{1,2,3}, RUDOLF GROSS^{1,2,3}, and KIRILL G. FEDOROV^{1,2} — ¹Walther-Meißner-Institut, 85748 Garching, Germany — ²Physik-Department, Technische Universität München, 85748 Garching, Germany — ³Munich Center for Quantum Science and Technology (MCQST), 80799 Munich, Germany — ⁴Rohde & Schwarz GmbH, Munich, Germany

Interest in quantum-limited amplification based on Josephson superconducting circuits has increased drastically in the past decade due to the rapidly advancing field of quantum information processing. In this context, a key challenge lies in realizing low-loss superconducting devices by minimizing energy dissipation. We achieve this goal by employing various cleaning steps during fabrication of superconducting circuits. Respectively, we fabricate Josephson parametric amplifiers with internal quality factors in excess of 10^4 . We characterize bandwidth, gain, noise, dynamic range, and other properties of the realized devices. Based on these investigations, we derive useful criteria for development of more intricate Josephson parametric circuits, such as Josephson parametric converters.

QI 4.7 Mon 18:00 P2

Perspectives of microwave quantum key distribution — •FLORIAN FESQUET^{1,2}, FABIAN KRONOWETTER^{1,2,4}, MICHAEL RENGER^{1,2}, KEDAR HONASOGE^{1,2}, YUKI NOJIRI^{1,2}, MARIA-TERESA HANDSCHUH^{1,2}, ACHIM MARX^{1,2}, RUDOLF GROSS^{1,2,3}, and KIRILL G. FEDOROV^{1,2} — ¹Walther-Meißner-Institut, 85748 Garching, Germany — ²Physik-Department, TUM, 85748 Garching, Germany — ³Munich Center for Quantum Science and Technology (MCQST), 80799 Munich, Germany — ⁴Rohde & Schwarz GmbH, 81671 Munich, Germany

One of the cornerstones of quantum communication is an unconditionally secure distribution of classical keys between remote parties. This can be achieved by exploiting quantum features of electromagnetic waves, such as entanglement or the no-cloning theorem. However, these quantum resources are known to be susceptible to noise and losses, which are omnipresent in open-air communication scenarios. Here, we theoretically investigate the perspectives of continuous-variable open-air quantum key distribution (QKD) at microwave frequencies. We demonstrate that continuous-variable QKD with propagating microwaves can be unconditionally secure at room temperatures at distances up to 200 meters. Furthermore, we show that microwave QKD provides the potential to outperform conventional QKD protocols at telecom wavelengths for certain weather conditions

QI 4.8 Mon 18:00 P2

Simulating quantum repeaters with experimentally relevant parameters — •JULIUS WALLNÖFER¹, FABIAN WIESNER¹, FREDERIK HAHN¹, NATHAN WALK¹, and JENS EISERT^{1,2} — ¹Dahlem Center for Complex Quantum Systems, Freie Universität Berlin, 14195 Berlin, Germany — ²Helmholtz-Zentrum Berlin für Materialien und Energie, 14109 Berlin, Germany

The quantum repeater protocol is a well established standard for distributing entanglement over long distances. However, there are a number of open questions when considering setups that go beyond the standard scenarios and error models. We have developed a numerical simulation platform for quantum repeaters to explore in multiple directions:

(i) With experiments of small scale quantum repeaters becoming a reality, it is of high interest to explore detailed error models that are close to the real situations found in the experiment. Our simulation allows us to not only compare setups with different parameters, but also to assess the effect of improving certain aspects has on e.g. the achievable key rate.

(ii) We explore conceptual questions in larger scale quantum repeaters outside of standard situations - especially in asymmetric setups where e.g. the length or quality of quantum channels is not identical. Furthermore, we investigate strategies for quantum repeaters when considering entanglement purification and multi-mode memories.

QI 4.9 Mon 18:00 P2

Rare earth ion materials in micro-cavities as optically addressable qubits for quantum information — •JANNIS HESSENAUER¹, CHRISTINA IOANNOU¹, KUMAR SENTHIL KUPPUSAMY¹, MARIO RUBEN¹, DIANA SERRANO², PHILIPPE GOLDNER², and DAVID HUNGER¹ — ¹Karlsruher Institut für Technologie, Karlsruhe, Germany — ²Université PSL, Chimie ParisTech, CNRS, Paris, France

Rare earth ions retain long optical and spin coherence times in solid state hosts and are therefore a promising realization of optically addressable spin qubits. Due to the dipole forbidden nature of the optical transitions, an efficient spin-photon interface for quantum information technology requires the coupling of single ions to an optical cavity to enhance the transitions via the Purcell effect. Recently, rare earth ions in molecular crystals have demonstrated outstanding coherence properties, while also promising a large parameter space for optimization by chemically engineering of the host molecule. We characterize the optical properties of molecular materials at low temperature using techniques such as photoluminescence spectroscopy, absorption spectroscopy and spectral hole burning. Furthermore, we present our progress towards integrating Yb³⁺-doped materials into stable high finesse fiber-based Fabry-Pérot cavities.

QI 4.10 Mon 18:00 P2

Circular Bragg gratings for Integrated Enhancement of Quantum Emitters — •DARIO MEKLE, JONAS GRAMMEL, and DAVID HUNGER — Physikalisches Institut, Karlsruher Institut für Technologie

Surface-emitting center-disk cavities, composed of circular Bragg gratings have been successfully employed for distributed feedback lasers and quantum emitter applications based on nitrogen vacancy centers and semiconductor quantum dots.

We aim to transfer this approach to achieve greater collection efficiencies of rare earth ion based emitters in the form of nanocrystals and molecules. The collection efficiency is improved through the use of cavity induced Purcell enhancement and by utilizing directional field emission patterns. A finite element analysis is used to perform geometric parameter optimizations of circular Bragg cavities consisting of PMMA (or similar polymers) and air layers.

The simulation predicts a Purcell factor of more than 140, significantly higher than previously published results. We report on progress in fabricating the simulated structures using electron beam lithography on gold substrates.

QI 4.11 Mon 18:00 P2

Enhancing the optical emission of erbium dopants in silicon with photonic crystals — •FLORIAN BURGER^{1,2}, LORENZ WEISS^{1,2}, ANDREAS GRITSCH^{1,2}, STEPHAN RINNER^{1,2}, JOHANNES FRÜH^{1,2}, and ANDREAS REISERER^{1,2} — ¹Max Planck Institute of Quantum Optics, Garching bei München, Germany — ²Munich Center for Quantum Science and Technology (MCQST), LMU Munich, Germany

Silicon photonics has developed into a mature technology platform that allows for rapid development cycles using standardized tools. Integrating coherent optical emitters into silicon chips would pave the way towards large-scale quantum networks. In this context, we explore the use of erbium dopants which feature both long spin coherence times and coherent optical transitions in the telecom C band, where the loss in optical fibers is minimal. Using low-loss nanowire waveguides, we performed resonant spectroscopy and were able to confirm the integration of erbium dopants at well-defined lattice sites, with narrow inhomogeneous linewidths of approximately 1 GHz and homogeneous linewidths of less than 20 kHz at temperatures below 8 K. As the practical use of the investigated transitions is hampered by their long excited-state lifetime, we plan to enhance the emission with tailored photonic nanostructures. To this end, we have designed and fabricated nanophotonic cavities, offering strong narrow-band Purcell en-

hancement, as well as photonic-crystal waveguides with moderate broadband Purcell enhancement. We will present details about the design and fabrication of these structures, and give an outlook on the control of single erbium dopants in silicon.

QI 4.12 Mon 18:00 P2

Cavity-enhanced spectroscopy of molecular quantum emitters — •EVGENIJ VASILENKO, WEIZHE LI, NICHOLAS JOBBITT, SETHIL KUPPUSAMY, MARIO RUBEN, and DAVID HUNGER — Karlsruhe Institute of Technology (KIT)

Rare earth ions in solid-state hosts are a promising candidate for optically addressable spin qubits, owing to their excellent optical and spin coherence times. Recently, also rare earth ion-based molecular complexes have shown excellent optical coherence properties [1]. Due to the long optical lifetime of the optical transition ${}^3D_0-{}^7F_0$, an efficient spin-photon interface for quantum information processing requires the coupling of single ions to a microcavity. Open-access Fabry-Pérot fiber cavities have been demonstrated to achieve high quality factors and low mode volumes, while simultaneously offering large tunability and efficient collection of the cavity mode [2]. Since the used molecular quantum emitters require a cryogenic environment, the demands on mechanical stability of the cavity setup have a high priority. To tackle these challenges, we report on the development of a monolithic type of cavity assembly, sacrificing some lateral scanning ability for the purpose of significantly increasing the passive stability. We integrate molecules into the cavity in the form of a crystalline thin film on a macroscopic mirror and identify a sub-nanometer local surface roughness, sufficient to avoid excessive scattering loss. We report on first studies of cavity-enhanced emission spectroscopy.

[1] Serrano et al., to appear in Nature, arXiv:2105.07081

[2] Hunger et al., New J. Phys 12, 065038 (2010)

QI 4.13 Mon 18:00 P2

Finite-range multiplexing in tripartite quantum networks — •JULIA ALINA KUNZELMANN, HERMANN KAMPERMANN, and DAGMAR BRUSS — Institut für Theoretische Physik III, Heinrich-Heine-Universität Düsseldorf

Due to the interaction between qubits and their environment, long-distance communication still poses a challenge. To overcome this problem, quantum repeaters are used, in which the repeater rate can be maximized by utilizing multiplexing. In previous work (Abruzzo et al. (2014)), a finite-range multiplexing protocol for two parties was investigated. We extend this protocol to three parties and it turns out that also in the tripartite network, full-range multiplexing does not provide substantial advantages over finite-range multiplexing. We also analyze decoherence of quantum memories and various strategies to lower the experimental requirements. To achieve this, different three-dimensional matching strategies are analyzed.

QI 4.14 Mon 18:00 P2

Integrated Photonic Information Processing for Quantum Networks — •JELDRIK HUSTER¹, SIMON ABDANI¹, JONAS ZATSCH¹, CHRISTIAN SCHWEIKERT², ROUVEN KLENK², and STEFANIE BARZ¹ — ¹Institute for Functional Matter and Quantum Technologies & IQST, University of Stuttgart, 70569 Stuttgart, Germany — ²Institute of Electrical and Optical Communications Engineering, University of Stuttgart, 70569 Stuttgart, Germany

The steady progression of photonic quantum systems allows the realisation of quantum computation, communication and networked applications. Key in pursuit of scalable photonic quantum technology are integrated devices operating in the telecom regime, due to their small footprint, high phase stability and low loss connectivity. Particularly, the generation of multipartite entangled states is of special interest. These states are the basis for measurement-based quantum computing and multiparty key exchange. Here, we present our recent progress on silicon-photonic quantum circuits operating at the single-photon level. The circuits consist of tuneable beam splitters, phase shifters and highly efficient grating couplers. They are powered by spontaneous parametric down conversion sources and used in combination with superconducting single-photon detectors. We show the characterisation of integrated devices and a pathway to generate complex entangled states in an integrated manner.

QI 4.15 Mon 18:00 P2

Entanglement distribution over a cryogenic microwave link — •SIMON GANDORFER^{1,2}, MICHAEL RENGER^{1,2}, WUN KWAN YAM^{1,2}, FLORIAN FESQUET^{1,2}, KEDAR HONASOGE^{1,2}, FABIAN KRONOWETTER^{1,2,3}, YUKI NOJIRI^{1,2}, MARIA-TERESA HANDSCHUH^{1,2}, ACHIM MARX¹, RUDOLF GROSS^{1,2,4}, and KIRILL G. FEDOROV^{1,2} — ¹Walther-Meißner-Institut, 85748 Garching, Germany — ²Physik-Department, TUM, 85748 Garching, Germany — ³Rohde & Schwarz GmbH & Co. KG, 81671 Munich, Germany — ⁴Munich Center for Quantum Science and Technology, 80799 Munich, Germany

In the context of rapid progress in quantum technologies, the realization of hardware platforms for quantum communication networks is of utmost importance. Quantum local area networks connecting remote superconducting quantum nodes are crucial for the implementation of distributed quantum computing architectures. In this regard, we demonstrate a 6.5 m cryogenic link connect-

ing two dilution cryostats via a cold network node. The respective microwave quantum communication channel is realized with superconducting microwave coaxial cables cooled to temperatures below 100 mK. By using this system, we demonstrate a successful distribution of squeezed states and two-mode entanglement between the remote dilution fridges and validate robustness of the quantum state transfer up to channel temperatures of 1 K.

QI 4.16 Mon 18:00 P2

Efficient spin-photon interface for NV centers in diamond — •JEREMIAS RESCH¹, KERIM KÖSTER¹, MAXIMILIAN PALLMANN¹, JULIA HEUPEL², CYRIL POPOV², and DAVID HUNGER¹ — ¹Karlsruher Institut für Technologie (KIT) — ²Universität Kassel

In order to achieve spin-photon-based quantum computers, we require excellent control of the qubit spin states, in addition to long coherence times of the nuclear spin states. By combining several computing nodes, and linking them to a global register via optical networks, scalability is achieved. A crucial component of this optical network is an efficient, coherent single-photon source. Coupling colour centers in diamond, such as the nitrogen-vacancy or tin-vacancy centers, to a microcavity is a promising approach in order to achieve efficient single-photon sources. In our experiment, we integrate a diamond membrane into an open access fiber-based Fabry-Perot microcavity to attain emission enhancement into a single well-defined mode. We present our fully tunable, cryogenic cavity platform operating in a closed-cycle cryostat, and we achieve a sub-picometer mechanical stability during quiet periods. We observe cavity-enhanced fluorescence spectra of an ensemble of shallow-implanted nitrogen-vacancy centers in diamond, showing Purcell-enhancement of the zero-phonon line.

QI 4.17 Mon 18:00 P2

Designing a microwave antenna for spectroscopy of nitrogen vacancy centers in a fiber-based cavity — •MATTHIAS KLAUSMANN, MAXIMILIAN PALLMANN, JEREMIAS RESCH, and DAVID HUNGER — Karlsruher Institut für Technologie

Overcoming losses in long distance fiber-based quantum networks is one of the big challenges in the field of quantum communication, which requires the development of a quantum repeater. Color centers in diamond are a promising platform for realizing the needed spin-photon interfaces due to the possibility of optical readout and initialization. The optical readout of coherent photons can be enhanced by integrating the diamond in a cavity by exploiting the Purcell-effect. In addition, the coherent control of the electron spin of the color center and nearby nuclear spins is necessary for such a device.

In our experiment, we look for different designs of microwave antennas to manipulate the electron spin of nitrogen vacancy centers in a fiber-based Fabry-Pérot micro-cavity with regard that this can also be used under cryogenic conditions. Testing the antenna designs is performed in a room-temperature confocal microscope setup. We observe large ensembles of shallow implanted nitrogen-vacancy centers but also single centers at a depth of a few micrometers below the diamond surface. With our antennas we are able to perform pulsed optically detected magnetic resonance, Rabi and Echo measurements. Using this measurement protocols, the hyperfine interaction between the electron spin and the nuclear spin of the hosting nitrogen atom as well as the interaction with a nearby ¹³C nuclear spin can be resolved.

QI 4.18 Mon 18:00 P2

Microwave quantum teleportation over thermal channels — •WUN KWAN YAM^{1,2}, MICHAEL RENGER^{1,2}, SIMON GANDORFER^{1,2}, FLORIAN FESQUET^{1,2}, KEDAR HONASOGE^{1,2}, FABIAN KRONOWETTER^{1,2,3}, YUKI NOJIRI^{1,2}, MARIA-TERESA HANDSCHUH^{1,2}, ACHIM MARX¹, RUDOLF GROSS^{1,2,4}, and KIRILL G. FEDOROV^{1,2} — ¹Walther-Meißner-Institut, BAdW, 85748 Garching, Germany — ²Physik-Department, TUM, 85748 Garching, Germany — ³Rohde & Schwarz GmbH & Co. KG, 81671 Munich, Germany — ⁴Munich Center for Quantum Science and Technology, 80799 Munich, Germany

Microwave quantum communication enables quantum local area networks between superconducting quantum processors and, thereby, paves the way towards distributed quantum computing. Quantum teleportation belongs to the most relevant quantum communication protocols. It permits efficient and unconditionally secure transfer of quantum states. Recent experimental demonstration of quantum teleportation with propagating microwaves [1] motivates the investigation of its resilience against experimental imperfections. To this end, we analyze the effect of thermal noise in the analog feedforward channel. We show that quantum teleportation implements an error correction scheme for loss and noise in the feedforward signal. Furthermore, we consider realistic operating parameters and find that the teleportation fidelity can exceed the no-cloning threshold for finite energy codebooks.

[1] K. G. Fedorov et al., "Experimental quantum teleportation of propagating microwaves", Sci. Adv. 7, eabk0891 (2021)

QI 4.19 Mon 18:00 P2

Quantum Polyspectra - Grand Unified Theory of Continuous Quantum Measurements — •MARKUS SIFFT and DANIEL HÄGELE — Ruhr University Bochum, Faculty of Physics and Astronomy, Experimental Physics VI (AG), Germany

The evaluation of continuous quantum measurements is a challenge in research areas like circuit quantum electrodynamics, spin noise spectroscopy, and quantum sensing. Measurement records can exhibit as diverse results as quantum jumps, mainly Gaussian noise, or even stochastic peaks from detectors with single photon resolution. Until now, specialized theories were used to model and eventually evaluate such measurement records. The poster reports on our recent progress in unifying all continuous measurement schemes into one theory. The theory is based on the measurement record, its power spectrum, and its third and fourth order generalizations, so-called polyspectra. Expressions for quantum polyspectra can be derived without approximation from the stochastic master equation [1]. System parameters follow from fitting quantum polyspectra to measured spectra [2]. This approach allows for a systematic evaluation of quantum measurements including coherent quantum dynamics, environmental damping, and measurement backaction at arbitrary measurement strength (Zeno-physics). We present and interpret quantum polyspectra of conventional spin noise spectroscopy, quantum transport through quantum dots, and spin noise spectroscopy in the single-photon regime.

[1] Hägele et al., PRB 98, 205143 (2018), [2] Sift et al., PRR 3, 033123 (2021)

QI 4.20 Mon 18:00 P2

Multipartite High-dimensional Quantum Steering — •SOPHIE EGELHAAF and ROOPE UOLA — Department of Applied Physics, University of Geneva, 1211 Geneva, Switzerland

Bipartite low dimensional entanglement has been studied extensively. However, many findings cannot be extrapolated to multiple parties and moreover, increasing the dimensions of the systems adds complexity to the entanglement structure.

We are interested in characterising the degree of high-dimensional entanglement, specifically focusing on various multipartite quantum steering scenarios. One such example is a triangle network with only one trusted party, or more generally a line network with some trusted parties. We investigate what can be deduced about the strength of entanglement between the different nodes of the network in such scenarios. We are especially interested in entanglement dimensionality, i.e. the question of how many degrees of freedom can be certified to be entangled, for which we provide analytical bounds.

QI 4.21 Mon 18:00 P2

Gate-error characterization via long-sequence quantum process tomography — •ANDREAS KETTERER and THOMAS WELLENS — Fraunhofer Institut für Angewandte Festkörperphysik (IAF), Tullastr. 72, 79108 Freiburg, Germany

Currently available quantum computing hardware realizes networks of tens of superconducting qubits with the possibility of controlled nearest-neighbor interactions. However, the inherent noise and decoherence effects of such quantum chips considerably alter basic gate operations and lead to imperfect outputs of the targeted quantum computation. We show how to characterize such quantum gate errors in detail using a combination of quantum process and gate set tomography in order to estimate a complete set of single- and two-qubit gate operations. Key ingredients of our approach are the efficient characterization of a universal single qubit gate set via gate-set tomography and the subsequent reconstruction of one additional two-qubit entangling gate using a long-sequence version of quantum process tomography. The latter involves repeated applications of the respective target gate in combination with appropriately chosen single-qubit operations in order to assure a precise estimation of all involved error parameters. Lastly, we demonstrate the devised protocol by implementing it on IBMQ hardware and briefly discuss the impact of crosstalk effects on near-term quantum algorithms.

QI 4.22 Mon 18:00 P2

Solvable projected entangled pair states for ternary unitary quantum gates — •RICHARD MAXIMILIAN MILBRADT¹, CHRISTOPHER ASSMUS¹, and CHRISTIAN BERNHARD MENDL^{1,2} — ¹Technical University of Munich, Department of Informatics, Boltzmannstraße 3, 85748 Garching, Germany — ²Technical University of Munich, Institute for Advanced Study, Lichtenbergstraße 2a, 85748 Garching, Germany

Recently we introduced the so-called ternary unitary quantum gates. These are four-particle gates acting in $2 + 1$ -dimensions and are unitary in time and both spatial dimensions. Now we generalise the concept of solvable MPS [Phys. Rev. B 101, 094304 (2020)] to two spatial dimensions with cylindrical boundary conditions. We show that such *solvable PEPS* can be identified with matrix product unitaries. In the resulting tensor network for evaluating equal-time correlation functions, the bulk ternary unitary gates cancel out, and we delineate and implement a numerical algorithm for computing such correlations.

QI 4.23 Mon 18:00 P2

Towards digital-analog quantum computing with superconducting qubits — JULIA LAMPRICH¹, NICOLA WÜRZ¹, •STEFAN POGORZALEK¹, MANISH THAPA¹, VICENTE PINA-CANELLES¹, ANTTI VEPSÄLÄINEN², MIHA PAPIĆ¹, JAYSHANKAR NATH¹, FLORIAN VIGNEAU¹, DARIA GUSENKOVA¹, PING YANG¹, HERMANN HEIMONEN², HSIANG-SHENG KU¹, ADRIAN AUER¹, JOHANNES HEINSOO², FRANK DEPPE¹, and INÉS DE VEGA¹ — ¹IQM Quantum Computers, Nymphenburgerstr. 86, 80636 Munich, Germany — ²IQM Quantum Computers, Keilarenta 19, FI-02150 Espoo, Finland

Digital-Analog Quantum Computing (DAQC) is a novel approach to quantum computing. Here, one variant is banded DAQC where single qubit gates are applied on top of an analog (entangling) evolution. We have investigated the experimental and fundamental challenges in realizing banded DAQC for the example of preparing a Bell state. The main challenge in banded DAQC is the correct execution of single qubit gates under simultaneous qubit-qubit interaction. The latter is induced by a flux-tunable coupler element, which allows for the accumulation of conditional phase during the analog block. In addition, banded DAQC is compared to an alternative approach called stepwise DAQC, where the single qubit gates are executed only when the qubits do not interact. For both approaches, the relevant error sources are identified and fidelities are compared to the purely digital case.

We acknowledge support from the German Federal Ministry of Education and Research via the projects DAQC (13N15686) and Q-Exa (13N16062).

QI 4.24 Mon 18:00 P2

Thermo-optical properties of superconducting thin films for waveguide-integrated single-photon detectors. — •ANTHONY CHUKWUNSO OGBUEHI^{1,2}, PIERRE PIEL^{1,2}, MARTIN WOLFF^{1,2}, MATTHIAS HÄUSSLER^{1,2}, CARSTEN SCHUCK^{1,2}, and URSULA WURSTBAUER^{1,2} — ¹Institute of Physics, Münster University, Germany — ²Center for Soft Nanoscience SoN, Münster University, Germany

Integrated quantum photonics relies on the generation, manipulation, and measurement of single quantum states of light. The latter can be achieved with superconducting nanowire single-photon detectors (SNSPD) embedded into photonic integrated circuits [1]. While SNSPDs show attractive detection efficiency and high timing accuracy [2], it remains largely unknown how detector performance characteristics are connected to superconducting material properties. Here we study the temperature-dependent dielectric function of niobium-titanium nitride (NbTiN) thin films above and below the critical temperature by means of spectroscopic ellipsometry by varying a number of parameters. Material optimization guided by spectroscopic ellipsometry provides a novel approach for both getting new insight into key parameters of the detection process and improving single-photon detector benchmarks, benefitting a wide range of integrated quantum technology applications.

[1] S. Ferrari et al., Nanophotonics 7, 1725 (2018) [2] M. A. Wolff et al., Appl. Phys. Lett. 118, 154004 (2021).

QI 4.25 Mon 18:00 P2

Quantum Possibilistic Paradoxes and Logical Contextuality — •LEONARDO SANTOS — Universität Siegen, Siegen, Germany

Contextuality and nonlocality are nonclassical properties exhibited by quantum statistics whose implications profoundly impact both the foundations and applications of quantum theory. In this contribution we provide some insights into logical contextuality and inequality-free proofs. The former concept can be understood as the possibility version of contextuality, while the latter refers to proofs of quantum contextuality or nonlocality that are not based on violations of some noncontextuality (or Bell) inequality. By *possibilistic* we mean a description in terms of possibilities for the outcomes, which are Boolean variables assuming value 1 when the corresponding probability is strictly larger than zero and 0 otherwise. In this work we built a bridge between these two concepts from what we call possibilistic paradoxes, which are sets of possibilistic conditions whose occurrence implies contextuality and nonlocality. As the main result, we demonstrate the existence of possibilistic paradoxes whose occurrence is a necessary and sufficient condition for logical contextuality in a very important class of scenarios. Finally, we discuss some interesting consequences arising from the completeness of these possibilistic paradoxes.

QI 4.26 Mon 18:00 P2

Generating Entangled States on IBM Quantum — SEBASTIAN BRANDHOFER¹, JELENA MACKEPFRANG², •DANIEL BHATTI², ILIA POLIAN¹, and STEFANIE BARZ² — ¹Institute of Computer Architecture and Computer Engineering & IQST, University of Stuttgart, Germany — ²Institute for Functional Matter and Quantum Technologies & IQST, University of Stuttgart, Germany

Commercially available quantum computers have reached the NISQ era and already can be employed to run basic quantum algorithms. One of the most important resources for quantum computations are entangled multi-qubit quantum states. Therefore, it is necessary to produce these states deterministically and with a high fidelity. Based on the specific physical architectures of different IBM quantum computers we produce graph states and GHZ states with the help of CPHASE and CNOT gates, respectively, and assess the quality of the state preparation. To optimize the resulting state fidelities, we develop and implement a classical optimization algorithm that considers various error characteristics of the qubits and the two-qubit gates.

QI 4.27 Mon 18:00 P2

Quantum circuits for the preparation of spin eigenfunctions on quantum computers — •ALESSANDRO CARBONE^{1,2}, DAVIDE EMILIO GALLI², MARIO MOTTA³, and BARBARA JONES³ — ¹Theory and Simulations of Materials (THEOS), and National Centre for Computational Design and Discovery of Novel Materials (MARVEL), École Polytechnique Fédérale de Lausanne, 1015 Lausanne, Switzerland — ²Dipartimento di Fisica, Università degli Studi di Milano, via Celoria 16, 20133 Milano, Italy — ³IBM Quantum, IBM Research Almaden, 650 Harry Road, San Jose, CA 95120, USA

The preparation of accurate and efficient approximations for Hamiltonian eigenstates on quantum computers is a crucial step for building the quantum advantage when studying many-body quantum systems. If we can describe molecules or materials with a coarse-grained spin Hamiltonian, spin eigenfunctions can be a useful starting point for simulations which aim to understand their electronic structure. In particular the purpose of this work is to delve into the description of the quantum circuits which prepare total spin eigenfunctions in the case of spin-1/2 systems. We investigate the balance between generality, accuracy, and computational cost in the encoding of spin eigenfunctions by quantum circuits without ancillary qubits, by pursuing two approaches: an exact recursive construction of spin eigenstates, and a heuristic variational construction of approximate spin eigenstates. We have tested the described quantum circuits on the available IBM (classical) simulators and quantum devices in the cases of 3-spin and 5-spin systems.

QI 4.28 Mon 18:00 P2

Performances and limitations of variational quantum algorithms under realistic noise models — •MARCO SCHUMANN, FRANK WILHELM-MAUCH, and ALESSANDRO CIANI — Institute for Quantum Computing Analytics (PGI-12), Forschungszentrum Jülich, 52425 Jülich, Germany

As the field of quantum computing progresses, an intriguing question is if the currently available NISQ devices can deliver a quantum advantage for practical applications, like Variational Quantum Algorithms (VQAs). Due to the lack of error correction, noise limits the performance of these algorithms. Recently it was shown that a quantum state undergoing a variational quantum circuit with general Pauli noise approaches the completely mixed state with increasing circuit depth. In this ongoing project, we study the question of how variational quantum circuits behave under more realistic noise models, like dephasing or amplitude damping noise. We use the Quantum Approximate Optimization Algorithm (QAOA), which is a specific VQA, to solve combinatorial optimization problems. Considering the problem of MaxCut on different d -regular graphs with different qubit numbers, we run the circuit for many instances of randomly chosen circuit parameters. We find that for weak amplitude damping or dephasing noise the average purity of the output state of the circuit approaches the purity of the completely mixed state while the variance of the purity approaches zero with increasing circuit depth. The decrease of the average purity is well described by an exponential decay, where the decay rate is approximately linear in the noise strength.

QI 4.29 Mon 18:00 P2

A multi-qubit Bloch vector representation of density matrices in Julia — •QUNSHENG HUANG and CHRISTIAN MENDEL — Technische Universität München. Fakultät für Informatik. Boltzmannstraße 3. 85748 Garching

In the Bloch sphere picture, one finds the coefficients for expanding a single-qubit density operator in terms of the identity and Pauli matrices. A generalization to n qubits via tensor products represents a density operator by a real vector of length 4^n , conceptually similar to a statevector.

The tensor structure leads to computationally efficient algorithms for applying circuit gates and performing few-qubit quantum operations. In view of variational circuit optimization, we study backpropagation through a quantum circuit and gradient computation based on this representation, and generalize our analysis to the Lindblad equation for modeling the (non-unitary) time evolution of a density operator.

QI 4.30 Mon 18:00 P2

Efficient energy estimation for variational quantum algorithms using ShadowGrouping — •ALEXANDER GRESCH and MARTIN KLIESCH — Quantum Technology Research Group, Heinrich Heine University, Düsseldorf

Hybrid variational quantum algorithms (VQAs) are one of the main candidates for relevant applications of quantum computation in the near future. However, due to the hybrid quantum-classical nature of VQAs, a large number of repeated energy measurements for various trial states is needed. Each of these states requires an estimate \hat{E} of the target energy E .

In our work, we aim to find the optimal strategy with single-qubit measurements that yields the highest provable accuracy given a total measurement budget. To this end, we derive a new upper bound to the failure probability $\mathbb{P}[|\hat{E} - E| > \epsilon]$ for a given tolerable accuracy ϵ , which improves upon previous bounds obtained in the context of derandomized classical shadows. Moreover, we combine strategies that measure groups of commuting Hamiltonian terms with that framework. This combination results in a measurement allocation

scheme which we call *ShadowGrouping*. Numerically, we demonstrate that ShadowGrouping outperforms state-of-the-art methods in estimating the electronic ground-state energies of various small molecules. Hence, this work provides a promising way to approach the measurement bottleneck of VQAs.

QI 4.31 Mon 18:00 P2

Single Photon Sources at Telecom Wavelengths — •JONAS GRAMMEL¹, DARIO MEKLE¹, ANDRÁS LAUKÓ¹, THOMAS HERZOG², SIMONE LUCA PORTALUPI², PETER MICHLER², and DAVID HUNGER¹ — ¹Physikalisches Institut, Karlsruher Institut für Technologie — ²Institut für Halbleitertechnik und Funktionelle Grenzflächen, Universität Stuttgart

Semiconductor single photon sources are fundamental building blocks for quantum information applications. The current limitations of such quantum dot sources are the emitting wavelength and insufficient collection efficiency in fiber-based implementations. In the project *Telecom Single Photon Sources* we aim to realize high brightness, fiber coupled sources of single and indistinguishable photons at the telecom wavelength for the upcoming realization of fiber-based quantum networks. We employ open cavities realized with fiber-based mirrors, in combination with InGaAs quantum dots emitting in the telecom O-band and C-band. To achieve Fourier-limited photons we utilize the lifetime reduction of the emitters via the Purcell effect. We optimize the mode matching between the cavity mode and the guided fiber mode by introducing a fiber-integrated mode-matching optics that can basically reach near-unity collection efficiency. Fundamentally new is also the combination of Fabry-Perot micro-cavity modes with lateral micro and nano structures to reduce the cavity mode volume and thereby boost the emission enhancement and efficiency of the single photon emitters.

QI 4.32 Mon 18:00 P2

Towards downscaling of inter-electrode spacing in PDMR for quantum sensing applications — •JAN HEIDEN, MARCEL SCHRODIN, and WOLFGANG WERNSDORFER — KIT, Karlsruhe, Germany

Photoelectric Detection of Magnetic Resonances (PDMR) states a novel technique for the detection of electronic spin-states in nitrogen vacancy centers (NV centers). Contrary to the currently established optical detection (ODMR), which measures the spin-dependent fluorescence of the negatively charged NV⁻ center, the new method relies on the selectivity of the photocurrent induced by the ionizing conversion between NV0 and NV⁻. Therefore, gold electrodes are deposited directly onto the diamond surface with current inter-electrode distances of down to 2 μm .

Besides improved selectivity, PDMR promises enhanced spatial resolution, purely dependent on the process of micro-fabrication. Further advantages arise from the separation of excitation and signal processing paths towards integration of optical systems into on-chip electronic environments.

The work presented focuses on proceeding the down-scaling of the inter-electrode spacing towards the nanometer regime for diamond-spin based quantum information applications at millikelvin temperatures.

QI 4.33 Mon 18:00 P2

Addressing of superconducting qubit in rectangular waveguide. — •ROMAIN ALBERT¹, MAXIMILIAN ZANNER¹, ERIC ROSENTHAL², SILVIA CASULLERAS¹, MATHIEU L. JUAN³, KONRAD LEHNERT², ORIOL ROMERO-ISART¹, and GERHARD KIRCHMAIR¹ — ¹University of Innsbruck, Innsbruck, Austria — ²JILA - University of Colorado, Boulder, United States — ³Université de Sherbrooke, Sherbrooke, Canada

Superconducting qubits embedded into microwave waveguides have shown great potential for analog quantum simulation. Such systems present a unique combination of short-range direct qubit interactions and long-range waveguide mediated interactions which make it possible to model a wide variety of Hamiltonians. However, it is challenging to address individual qubits in such systems, as they are often separated by less than the wavelength of their control field. One possible solution is to use the non-linear dispersion of the waveguide to focus frequency chirped pulses to a specific location and it was shown theoretically that such a pulse can be used to selectively control a qubit[1]. We experimentally demonstrate this control using transmon qubits embedded in a rectangular waveguide.

[1] Casulleras, Silvia, et al. "Remote individual addressing of quantum emitters with chirped pulses." *Phys Rev Let* (2021)

QI 4.34 Mon 18:00 P2

Reduction of frequency spread in superconducting quantum coherent circuits — •TAMMO SIEVERS^{1,2,3}, LEON KOCH^{1,2,3}, NIKLAS BRUCKMOSER^{1,2,3}, YUKI NOJIRI^{1,2,3}, THOMAS LUSCHMANN^{1,2,3}, KIRILL FEDOROV^{1,2,3}, and STEFAN FILIPP^{1,2,3} — ¹Physik- Department, Technische Universität München, 85748 Garching, Germany — ²Walther-Meißner-Institut, Bayerische Akademie der Wissenschaften, 85748 Garching, Germany — ³Munich Center for Quantum Science and Technology (MCQST)

Superconducting quantum circuits form the basis of emerging applications in quantum computing and other quantum technologies. A prominent example is the transmon qubit, a superconducting Josephson junction shunted with a large

capacitance. To become practically useful, reliable fabrication methods are required to produce highperformance transmon qubits with lifetimes exceeding several hundred μs and well-controlled parameters, such as the junction frequency. Here, we present our results of different fabrication methods to reduce frequency variations of Manhattan-style Al-AlOx-Al Josephson junctions. To compare the influence of the investigated fabrication techniques, we measure the room temperature resistivity of Josephson junctions and use the Ambegaokar-Baratoff relation in order to quantify the critical current spread of the junctions.

QI 4.35 Mon 18:00 P2

Minimization of Loss Channels in Superconducting Resonators — •NIKLAS BRUCKMOSER^{1,2}, LEON KOCH^{1,2}, LEONHARD HÖLSCHER^{1,2}, DAVID BUNCH^{1,2}, TAMMO SIEVERS^{1,2}, KEDAR E. HONASOGE^{1,2}, YUKI NOJIRI^{1,2}, THOMAS LUSCHMANN^{1,2}, KIRILL G. FEDOROV^{1,2}, and STEFAN FILIPP^{1,2,3} — ¹Walther-Meißner-Institut, Bayerische Akademie der Wissenschaften, Garching, Germany — ²Physik-Department, Technische Universität München, Garching, Germany — ³Munich Center for Quantum Science and Technology (MCQST), München, Germany

Realizing a fault-tolerant quantum computer is the goal of an ever-growing number of publicly funded and commercial research and development activities. Amongst many potential platforms, quantum computers based on superconducting quantum circuits with Josephson junctions are a promising candidate. However, the fidelity of superconducting qubits is limited by decoherence due to noise arising from various sources, in particular the local environment of the qubit. Driven by the development of partially noise-protected qubit designs, related lifetimes increased significantly from several nanoseconds to a few hundred microseconds. Nonetheless, it is crucial to gain an even better understanding of the origin of loss channels to further improve the qubit coherence by tailored design and fabrication processes. Here, we demonstrate a process for fabricating coplanar waveguide resonators and qubits based on niobium thin films sputtered on silicon substrates. We achieve qubit lifetimes up to 150 μs by systematically analyzing fabrication steps, such as surface treatment and thin film deposition.

QI 4.36 Mon 18:00 P2

Reduction of frequency spread in superconducting quantum circuits — •TAMMO SIEVERS^{1,2,3}, LEON KOCH^{1,2,3}, NIKLAS BRUCKMOSER^{1,2,3}, YUKI NOJIRI^{1,2,3}, THOMAS LUSCHMANN^{1,2,3}, KEDAR E. HONASOGE^{1,2,3}, KIRILL G. FEDOROV^{1,2,3}, and STEFAN FILIPP^{1,2,3} — ¹Physik- Department, Technische Universität München, 85748 Garching, Germany — ²Walther-Meißner-Institut, Bayerische Akademie der Wissenschaften, 85748 Garching, Germany — ³Munich Center for Quantum Science and Technology (MCQST)

Superconducting quantum circuits form the basis of emerging applications in quantum computing and other quantum technologies. A prominent example is the transmon qubit, a superconducting Josephson junction shunted with a large capacitance. As quantum processors scale to larger sizes, avoiding frequency collisions becomes a formidable task. Here, we present our results on different fabrication methods to reduce frequency variations of Manhattan-style Al-AlOx-Al Josephson junctions. To compare the influence of the investigated fabrication techniques, we measure the room temperature resistivity of Josephson junctions and use the Ambegaokar-Baratoff relation in order to quantify the critical current spread of the fabricated junctions.

QI 4.37 Mon 18:00 P2

Optimizing Fabrication Parameters for Superconducting Coplanar Waveguide Resonators — •DAVID BUNCH^{1,2,3}, LEON KOCH^{1,2,3}, NIKLAS BRUCKMOSER^{1,2,3}, KEDAR E. HONASOGE^{1,2}, YUKI NOJIRI^{1,2,3}, THOMAS LUSCHMANN^{1,2,3}, TAMMO SIEVERS^{1,2,3}, KIRILL G. FEDOROV^{1,2}, and STEFAN FILIPP^{1,2,3} — ¹Physik-Department, Technische Universität München, 85748 Garching, Germany — ²Walther-Meißner-Institut, Bayerische Akademie der Wissenschaften, 85748 Garching, Germany — ³Munich Center for Quantum Science and Technology (MCQST)

Superconducting circuits are a promising platform for the implementation of a universal quantum computer. However, the coherence times of superconducting qubits that make up such systems are limited by material losses, leading to errors in quantum gates. In particular, the coherence time is predominantly limited by coupling to unwanted two level systems (TLS) located at material interfaces. Identifying fabrication techniques, materials, and thin-film dielectrics that reduce losses is essential to achieve scalable architectures for superconducting quantum computing. To evaluate the efficacy of different fabrication techniques we measure the quality factor of superconducting microwave resonators. We present results on optimal sputtering parameters for enhancing the internal quality factor of superconducting coplanar waveguide resonators and investigate the effects of different etching processes, cleaning methods, and surface treatments on these resonators. We validate our results by fabricating qubits with high coherence times.

QI 4.38 Mon 18:00 P2

Nb/AlOx/Nb-trilayer based Dimer Josephson Junction Array Amplifiers — FABIAN KAAP¹, SERGEY LOTHKOV¹, CHRISTOPH KISSLING¹, VICTOR GAYDAMACHENKO¹, MARAT KHABIPOV¹, MARK BIELER¹, and •LUKAS GRÜNHaupt^{1,2} — ¹Physikalisch-Technische Bundesanstalt, Department Quantum Electronics, 38116 Braunschweig, Germany — ²Physikalisch-Technische Bundesanstalt, Quantum Technology Competence Center, 38116 Braunschweig, Germany

Josephson parametric amplifiers are crucial components for superconducting quantum circuits as they enable high fidelity readout of qubits by improving the signal-to-noise ratio. Among them, Dimer Josephson Junction Array Amplifiers (DJJAA) [1] have shown promise as user-friendly devices with gain on the order of 20 dB, low added noise, saturation powers larger than approximately -110 dBm, and non-degenerate amplification over a bandwidth of up to ~10 MHz. Due to the use of dc-SQUIDS and multiple dimer modes the operating frequency can be tuned in the range of 2-10 GHz. Using results obtained on DJJAAs with Al/AlOx/Al Josephson junctions as a baseline, we present our progress towards realizing DJJAAs with Nb/AlOx/Nb-trilayer Josephson junctions. We will discuss the circuit design, our fabrication processes, and show preliminary cryogenic measurements of the device.

[1] P. Winkel et al., Phys. Rev. Applied 13, 024015 (2020)

QI 4.39 Mon 18:00 P2

High-fidelity gates and readout for scalable multi-qubit superconducting quantum processors — •FLORIAN WALLNER^{1,2}, MALAY SINGH^{1,2}, GLEB KRYLOV^{1,2}, IVAN TSITSILIN^{1,2}, GERHARD HUBER^{1,2}, NIKLAS BRUCKMOSER^{1,2}, LEON KOCH^{1,2}, NIKLAS GLASER^{1,2}, CHRISTIAN SCHWEIZER^{1,2}, and STEFAN FILIPP^{1,2,3} — ¹Physik- Department, Technische Universität München, 85748 Garching, Germany — ²Walther-Meißner-Institut, Bayerische Akademie der Wissenschaften, 85748 Garching, German — ³Munich Center for Quantum Science and Technology (MCQST)

To reach the goal of implementing an error-corrected quantum computer, qubits with long coherence times need to be manipulated in real time with high fidelity, followed by a fast and accurate readout. Currently, the main challenge for all hardware platforms is to scale up the number of qubits while at the same time maintain high quality gate operations.

Here, we report on our recent advances to build superconducting multi-qubit devices. Through a dedicated fabrication process we reach coherence times of up to 150 μs . We show single-qubit characterization measurements of gates and high fidelity dispersive readout. By applying this method to multi-qubit systems, we achieve simultaneous multiplexed readout of several qubits coupled to the same feed line. Furthermore, we demonstrate first randomized benchmarking results for single- and two-qubit gates. In addition we give an outlook on our efforts to build multi-qubit devices and qubits on alternative architectures that promise substantial longer coherence times.

QI 4.40 Mon 18:00 P2

Improving the Sørensen-Mølmer gate using analytical optimal control — •SUSANNA KIRCHHOFF^{1,2}, FRANK K. WILHELM^{1,2}, and FELIX MOTZOI³ — ¹Forschungszentrum Jülich, Quantum Computing Analytics (PGI 12), D-52425 Jülich, Germany — ²Theoretical Physics, Saarland University, 66123 Saarbrücken, Germany — ³Forschungszentrum Jülich, Institute of Quantum Control (PGI-8), D-52425 Jülich, Germany

The Sørensen-Mølmer gate is an entangling gate for ion qubits [1]. The entangled state is obtained by the application of a bichromatic light beam which collectively drives the ions. This leads to an entangling gate if certain conditions on gate time, drive frequency and amplitude are fulfilled. These conditions can be derived from the propagator. However, the gate is not perfect. In [1] the authors apply the Lamb-Dicke approximation and neglect some fast rotating terms as well as the single qubit rotation before calculating the propagator. This leads to gate errors. We investigate how the approximations affect the gate fidelity and explore methods to avoid those errors and make the gate more robust against heating.

[1] Sørensen and Mølmer: Entanglement and quantum computation with ions in thermal motion. In: Physical Review A 62.2 (2000)

QI 4.41 Mon 18:00 P2

Spin defects in hBN as promising temperature, pressure and magnetic field quantum sensor — •PAUL KONRAD¹, ANDREAS GOTTSCHOLL¹, ANDREAS SPERLICH¹, IGOR AHARONOVICH², and VLADIMIR DYAKONOV¹ — ¹Experimental Physics 6, Julius Maximilian University of Würzburg, 97074 Würzburg — ²School of Mathematics and Physical Sciences, University of Technology Sydney, Ultimo, NSW 2007, Australia

Colour centres in solid-state materials show great potential in quantum information technology and sensing applications. The lately discovered negatively charged boron vacancy (V_B^-) in hexagonal boron nitride (hBN)^[1] has shown the defect to be host to a spin-triplet ground state with spin-dependent photoluminescence. The system can be exploited in terms of its application as temperature, magnetic field, and pressure sensor^[2,3] which extends the already known appli-

cations of e.g. NV-centers in diamond not only due to its 2D character but also by highly improved temperature sensing especially at low temperatures.

Yet, the irradiation protocol is still unoptimized and achieving high contrast optically detected magnetic resonance (ODMR) on increasingly thinner flakes remains a challenge. We are on our way to tackle aforementioned challenges by performing measurements on V_B^- created by various types of irradiation and

achieve tremendous improvement of ODMR contrast on flakes of down to 80nm thickness.

- [1] Gottscholl et al., *Nat. Mat.*, **19**, 5, 540 (2020).
- [2] Gottscholl et al., *Sci. Adv.*, **7** (14), eabf3630 (2021).
- [3] Gottscholl et al., *Nat. Commun.*, **12**, 4480 (2021).

QI 5: Implementations: Solid state systems

Time: Tuesday 9:30–12:15

Location: H8

Invited Talk

QI 5.1 Tue 9:30 H8

Towards universal quantum computation and simulation with NV centre in diamond — •VADIM VOROBYOV — 3rd Physical Institute, University of Stuttgart
NV centre in diamond is a mature platform for quantum technologies having applications ranging from quantum sensing to quantum communication and quantum information processing. Numerous implementation of NV centres in coupe with relative simplicity of the experiment enabled implementation of the NV magnetometry within complementary analysis methods such as X ray spectrometers and high pressure diamond anvil cells scanning probe experiments enabled discovery of 2D antiferromagnetic domain walls and single layer magnetism in layered magnetic materials proving its firm niche among nanoscale quantum sensors.

For quantum information processing a well addressable, readable interacting qubits are essential. NV centre - as optically readable single electron spin forms an interface to nearby nuclear spin baths, allowing to realize a star shape central spin model. In this work we discuss the computational potential of such system and compare it to planar architecture adapted by superconducting qubit systems.

We perform a randomised benchmarking of a room temperature operational system and benchmark important building blocks for quantum information processing: QFT and Toffoli gates on a qubits and discuss their possible applications in quantum sensing.

QI 5.2 Tue 10:00 H8

Probing the quantum noise of metals and spin liquids with NV center spin qubits — JUN YONG KHO^{1,5}, FALKO PIENKA^{2,5}, PATRICK A. LEE³, and •INTI SODEMANN VILLADIEGO^{4,5} — ¹Institute of High Performance Computing, Agency for Science, Technology, and Research, Singapore — ²Institut für Theoretische Physik, Goethe-Universität Frankfurt a.M. — ³Department of Physics, Massachusetts Institute of Technology, Cambridge Massachusetts, USA — ⁴Institut für Theoretische Physik, Universität Leipzig — ⁵Max-Planck-Institut für Physik komplexer Systeme

Finding tailored probes that allow to identify the presence of exotic fractionalized states in quantum materials is a major open challenge. Recently, spin qubits based on NV centers are emerging as a new tool to investigate the magnetic noise emanating from complex correlated materials.

Here we study the magnetic noise emerging from a U(1) spin liquid state with a spinon Fermi surface. We show that at low frequencies the noise from this state has the same distance and frequency dependence as a metal but is reduced by a dimensionless pre-factor controlled by the diamagnetic susceptibilities of emergent fractionalized particles in this state. We estimate that the regime to detect this behavior can be comfortably accessed by the typical NV center splittings of a few GHz and estimate that the expected T1 times for an NV center placed above candidate materials, such as the organic dmit and ET salts, monolayer 1T-TaS2/Se2, would range from several tens to a few hundred milliseconds.

QI 5.3 Tue 10:15 H8

Fidelities of quantum algorithms for a spin register in diamond in presence of magnetic impurities. — •DOMINIK MAILE, JÜRGEN STOCKBURGER, and JOACHIM ANKERHOLD — Institut für komplexe Quantensysteme, Universität Ulm, Germany

The Nitrogen Vacancy Center in diamond coupled to addressable surrounding nuclear spins forms a versatile building block for future quantum technologies. We theoretically study quantum information protocols of a small spin register built out of this constituents in presence of a common bath of impurity spins. Using a cluster correlation expansion, we predict the coherence and relaxation properties as well as the fidelities for different quantum algorithms. Further, we study the influence of the volume density and the geometry of the spin bath consisting of substitutional nitrogen atoms. Our investigations yield insight how to efficiently use such a platform for quantum information purposes in presence of unavoidable magnetic impurities.

QI 5.4 Tue 10:30 H8

Nitrogen vacancy centers in diamond membranes coupled to an optical microcavity — •MAXIMILIAN PALLMANN¹, KERIM KÖSTER¹, JONATHAN KÖRBER³, JULIA HEUPEL², RAINER STÖHR³, TIMON EICHHORN¹, LARISSA KOHLER¹, CYRIL POPOV², and DAVID HUNGER¹ — ¹Karlsruher Institut für Technologie — ²Universität Kassel — ³Universität Stuttgart

Color centers in diamond centers are very promising candidates for applications in quantum communication and metrology. The nitrogen vacancy center (NV) stands out due to its exceptional spin coherence properties. On the other hand, it suffers from rather bad optical properties due to significant phonon coupling, and only 3% of the emitted light belongs to the Zero phonon line (ZPL). This can be overcome by coupling the emitters to optical cavities, making use of the Purcell effect.

In our experiment, we integrate a diamond membrane to an open access fiber-based Fabry-Perot microcavity [1] to attain emission enhancement into a single well-collectable mode as well as spectral filtering. We investigate the influence of the diamond membrane on the optical properties of the cavity.

We present Purcell-enhanced ensemble-fluorescence of shallow-implanted NV centers and observe cavity-induced collective effects that lead to a bunching behavior in the emission.

- [1] Heupel, Pallmann, Körber. *Micromachines* 2020, 11, 1080;

QI 5.5 Tue 10:45 H8

Cavity-free microwave spectral hole burning in ¹⁶⁶Er:Y₂SiO₅ below 1K — ANTON MLADENOV¹, NATALIA PANKRATOVA², DMITRIY SHOLOKHOV¹, VLADIMIR MANUCHARYAN², PAVEL BUSHEV^{1,3}, and •NADEZHDA KUKHARCHYK^{1,4,5} — ¹Experimental physics, University of Saarland, Saarbruecken, Germany — ²Department of Physics, Joint Quantum Institute and Center for Nanophysics and Advanced Materials, University of Maryland, College Park, USA — ³JARA-Institute for Quantum Information (PGI-11), Forschungszentrum Jülich, Jülich, Germany — ⁴Walther-Meißner-Institut, Bavarian academy of sciences, Garching, Germany — ⁵Munich Center for Quantum Science and Technologies, Munich, Germany

Deterministic narrow spectral hole burning on a microwave transition would allow for realization of microwave atomic frequency combs (mwAFC). On the way towards realisation an mwAFC, we present our recent results in spectral hole burning in Er:Y₂SiO₅ crystal in cavity-free regime at the variation of magnetic field and at temperatures below 1 K.

15 min. break

QI 5.6 Tue 11:15 H8

Modelling and engineering cQED devices via effective Hamiltonians — •BOXI LI^{1,2}, TOMMASO CALARCO^{1,2}, and FELIX MOTZOI¹ — ¹Forschungszentrum Jülich, D-52425 Jülich, Germany — ²Institute for Theoretical Physics, University of Cologne, D-50937 Cologne, Germany

Deriving effective Hamiltonian models plays an essential role in quantum theory, with particular emphasis in recent years on control and engineering problems. To develop fast, high-fidelity operations on cQED devices, there are also increasing demands on modelling tools that go beyond the strong perturbative regime and accurately capture the dynamics.

To this goal, we present two symbolic methods for computing effective Hamiltonian models. The first method makes use of the Jacobi iteration and works without the assumptions of perturbation theory while retaining convergence. In the perturbation regime, it reduces to a variant of the Schrieffer-Wolff method, which takes advantage of a recursive structure and exponentially decreases the number of terms in the high-order expansion. Both methods consist of algebraic expressions and can be easily automated for symbolic computation.

Based on these methods, we perform (semi-)analytical calculations that compute the effective Hamiltonian. We investigate both the ZZ and the cross-resonance interaction in the quasi-dispersive regimes. By choosing a proper frame transformation, we show that one can develop control pulses to suppress noises such as leakage and dynamical ZZ crosstalk, improving upon the conventional perturbative calculation.

QI 5.7 Tue 11:30 H8

Demonstration of an integrated optomechanical microcavity with a suspended frequency-dependent photonic crystal reflector — •SUSHANTH KINI M¹, ANASTASIA CIERS¹, JULIETTE MONSEL¹, CINDY PERALLE², SHU MIN WANG¹, PHILIPPE TASSIN², and WITLIF WIECZOREK¹ — ¹Dept of Microtechnology and Nanoscience, Chalmers University, Göteborg, Sweden — ²Dept of Physics, Chalmers University, Göteborg, Sweden

Optical microcavities confine the light field on sub-wavelength length scales leading to stronger light-matter interactions. Using microcavities in cavity optomechanics, which explores the interaction between an optical cavity and mechanical motion, one drastically increases the optomechanical interaction. In our work, we use this concept in on-chip optomechanical microcavities fabricated from AlGaAs heterostructures. In our realization, the mechanically-compliant element is a suspended photonic crystal (PhC) reflector slab, whose distance to a distributed Bragg reflector (DBR) mirror is less than the optical wavelength. We demonstrate a precise control over the microcavity resonance wavelength by varying the PhC hole radius, notably keeping cavity length constant. Importantly, we demonstrate that the frequency dependence of the optical reflectivity of the PhC slab modifies the optomechanical effects compared to a conventional optomechanical system. In the future, this integrated optomechanical microcavity platform offers novel capabilities in manipulating mechanical motion, such as offering more efficient cooling schemes or the capability to generate mechanical squeezing in the ultra-strong coupling regime.

QI 5.8 Tue 11:45 H8

Quantum reservoir computing with coupled cavity arrays — •FREDERIK LOHOF, NICLAS GÖTTING, and CHRISTOPHER GIES — Institute for Theoretical Physics, University of Bremen, Bremen

Arrays of coupled cavities with embedded semiconducting quantum dots are a

potential platform for the realization of a photonic quantum reservoir computer. The quantum reservoir paradigm is intriguing as it can be realized with preexisting technology and does not rely on fine-tuning of the system parameters as it is the case with gate-based quantum computing. Crucially, the performance of a quantum reservoir relies on a sampling of the exponentially increasing phase-space dimension. We provide theoretical benchmarks on how the topology of a quantum reservoir influences the reservoir's performance and discuss prospects for implementing quantum reservoir computing on a platform of arrays of semiconducting microcavities.

QI 5.9 Tue 12:00 H8

Ultra-stable open micro-cavity platform for closed cycle cryostats — •MICHAEL FÖRG^{1,2}, JONATHAN NOÉ^{1,2}, MANUEL NUTZ^{1,2}, THEODOR W. HÄNSCH^{1,3}, and THOMAS HÜMMER^{1,2,3} — ¹Fakultät für Physik, Ludwig-Maximilians-Universität Munich, Germany — ²Qlibri GmbH, Munich, Germany — ³Max-Planck-Institut für Quantenoptik, Garching, Germany

High-finesse, open-access, mechanical tunable, optical micro-cavities offer a compelling system to enhance light matter interaction in numerous systems, e.g. for quantum repeaters, single-photon sources, quantum computation and spectroscopy of nanoscale solid-state systems. Combining a scannable microscopic fiber-based mirror and a macroscopic planar mirror creates a versatile experimental platform. A large variety of solid-state quantum systems can be brought onto the planar mirror, analyzed, addressed individually, and (strongly) coupled to the cavity. We present a fully 3D-scannable, yet highly stable micro-cavity setup, which features a stability on the sub-pm scale under ambient conditions and unprecedented stability inside closed-cycle cryostats. An optimized mechanical geometry, custom built stiff micro-positioning, vibration isolation and fast active locking enables quantum optics experiments even in the strongly vibrating environment of closed-cycle cryostats.

QI 6: Quantum Information: Concepts and Methods

Time: Tuesday 9:30–12:45

Location: H9

Invited Talk

QI 6.1 Tue 9:30 H9

Towards an Artificial Muse for new Ideas in Quantum Physics — •MARIO KRENN — Max Planck Institute for the Science of Light (MPL), Erlangen, Germany

Artificial intelligence (AI) is a potentially disruptive tool for physics and science in general. One crucial question is how this technology can contribute at a conceptual level to help acquire new scientific understanding or inspire new surprising ideas. I will talk about how AI can be used as an artificial muse in quantum physics, which suggests surprising and unconventional ideas and techniques that the human scientist can interpret, understand and generalize.

[1] Krenn, Kottmann, Tischler, Aspuru-Guzik, Conceptual understanding through efficient automated design of quantum optical experiments. *Physical Review X* 11(3), 031044 (2021).

[2] Krenn, Pollice, Guo, Aldeghi, Cervera-Lierta, Friederich, Gomes, Häse, Jinich, Nigam, Yao, Aspuru-Guzik, On scientific understanding with artificial intelligence. *arXiv:2204.01467* (2022).

[3] Krenn, Zeilinger, Predicting research trends with semantic and neural networks with an application in quantum physics. *PNAS* 117(4), 1910-1916 (2020).

QI 6.2 Tue 10:00 H9

Learning variable quantum processes — MARCO FANIZZA¹, YIHUI QUEK², and •MATTEO ROSATI³ — ¹IFT: IFQ, Universitat Autònoma de Barcelona, 08193 Bellaterra (Barcelona) Spain — ²Dahlem Center for Complex Quantum Systems, Freie Universität Berlin, 14195 Berlin, Germany — ³Electrical Engineering and Computer Science, Technische Universität Berlin, 10587 Berlin, Germany

Much of the current research on characterizing quantum processes via statistical learning theory assumes a highly controlled learning setting. Typically, the learner is allowed to use the unknown process as a black-box that may be applied to well-crafted inputs. In this work, we relax this assumption. How hard is it to learn a quantum process observed 'in-the-wild', without control over the inputs? This is the case, for instance, in learning astronomical processes induced by random celestial events, Hamiltonians at variable temperature and biological processes triggered by mechanisms which we can observe but not control. We reformulate this problem as one where a learner has access to a source that outputs classical-quantum states $\sum_x p(x)|x\rangle\langle x| \otimes \psi(x)$ where ψ is the unknown process mapping an input classical random variable x to an output quantum state. The goal is to learn ψ . When ψ is drawn from a class of functions \mathcal{C} , we show that the complexity of this task scales polynomially in a combinatorial dimension of \mathcal{C} (a measure of its effective size) that we define, and further give algorithms that achieve this complexity. We show, for the first time to our knowledge, that quantum states and processes can be learned efficiently even when identical repetitions of the same experiment are not possible.

QI 6.3 Tue 10:15 H9

Shortening Quantum Convolutional Neural Networks to Constant Depth — •NATHAN MCMAHON, PETR ZAPLETAL, and MICHAEL HARTMANN — Friedrich-Alexander-Universität Erlangen-Nürnberg, Erlangen, Germany

The quantum convolutional neural network (QCNN) is a quantum circuit that detects symmetry protected topological (SPT) phases, with its construction drawing from ideas of renormalisation theory. In this talk I will discuss a special class of these circuits that are equivalent to constant depth quantum circuits, local measurements, and classical post-processing, including an earlier example from Cong et al for a Z2 x Z2 SPT phase detection circuit. We modify this circuit and demonstrate how to shorten it to constant depth, while improving both the time complexity and signal fidelity.

Surprisingly, while the quantum component circuit is constant depth on N -qubits, we still observe a provably exponential (in N) sample complexity speed up compared to only local Pauli measurements and post-processing of the input state. To understand how this happens we demonstrate that a reduced complexity of the input state leads to a guaranteed reduction in the sample complexity speedup.

We finally consider how to explain the effectiveness of the QCNN as a phase recognition algorithm through quantum fidelity approaches to phase transitions. We do this by deriving a sufficient condition for the layers of the QCNN for its output to perform phase recognition. In the process, also making a tantalising connection between the renormalisation group and optimisation.

QI 6.4 Tue 10:30 H9

Quantum Convolutional Neural Network as a Phase Detection Circuit on the Toric Code — •LEON SANDER, NATHAN MCMAHON, and MICHAEL HARTMANN — Chair of Theoretical Physics, Friedrich-Alexander-Universität Erlangen-Nürnberg, Germany

Understanding macroscopic behaviour of quantum materials is an interesting challenge in the field of quantum technologies. This macroscopic behaviour can be evaluated by the examination of quantum phases. Consequently, recognising the phase of a given input state is an important problem, which is often solved by measuring the corresponding order parameter. However, previous work by Cong et al. and Hermann et al. suggests quantum convolutional neural networks (QCNN) are an alternative method of phase detection that can also improve sampling efficiency near the phase boundary compared to direct measurements.

We construct a QCNN designed to act as a phase recognition circuit that determines whether certain magnetic/Ising type perturbations are sufficient to induce a phase transition in the toric code. The choice to study this quantum error correcting code can be motivated as it promises to reveal connections between quantum information and quantum phase transitions.

QI 6.5 Tue 10:45 H9

Evaluating the power and performance of sigmoid quantum perceptrons. — •SAMUEL WILKINSON and MICHAEL HARMAN — Department of Physics, Friedrich-Alexander-Universität Erlangen-Nürnberg (FAU), Staudtstr. 7, 91058 Erlangen, Germa

Quantum neural networks (QNN) have been proposed as a promising architecture for quantum machine learning. There exist a number of different quantum circuit designs being branded as QNNs, however no clear candidate has presented itself as more suitable than the others. Rather, the search for a “quantum perceptron” – the fundamental building block of a QNN – is still underway.

One candidate is quantum perceptrons designed to emulate the nonlinear activation functions of classical perceptrons. Such sigmoid quantum perceptrons (SQPs) inherit the universal approximation property that guarantees that classical neural networks can approximate any continuous function. However, this does not guarantee that QNNs built from SQPs will have any quantum advantage over their classical counterparts. Here we critically investigate both the capabilities and performance of SQP networks by computing general measures of the dimension and capacity of the network, as well as its performance on real learning problems. The results are compared to those obtained for other candidate networks which lack activation functions. It is found that simpler, easier-to-implement parametric quantum circuits actually perform better than SQPs. This indicates that the universal approximation theorem, which a cornerstone of the theory of classical neural networks, is not a relevant criterion for QNNs.

15 min. break

QI 6.6 Tue 11:15 H9

An algorithm to factorize quantum walks into shift and coin operations — •CHRISTOPHER CEDZICH¹, TOBIAS GEIB², and REINHARD F. WERNER² — ¹Quantum Technology Group, Heinrich Heine Universität Düsseldorf, Universitätsstr. 1, 40225 Düsseldorf — ²Institut für Theoretische Physik, Leibniz Universität Hannover, Appelstr. 2, 30167 Hannover

Quantum walks provide a basic architecture for implementing quantum information processing and computing. It is therefore important to resolve a given task into available operations, i.e., to “compile” a targeted program. We provide such a method, showing that an arbitrary one-dimensional quantum operation can be resolved into a protocol of two basic operations: A fixed conditional shift that transports particles between cells and suitable coin operators that act locally in each cell. This allows to tailor quantum walk protocols to any experimental setup by rephrasing it on the cell structure determined by the experimental limitations.

QI 6.7 Tue 11:30 H9

Improved Bell state measurement — •SIMONE D’AURELIO, MATTHIAS BAYERBACH, and STEFANIE BARZ — Institute for Functional Matter and Quantum Technologies & IQST, University of Stuttgart, 70569 Stuttgart, Germany
Bell-state measurements play an important role in many quantum technologies, e.g. in quantum repeaters, certain quantum communication protocols and photonic quantum computing. However, using linear-optics only, such a Bell-state measurement has a success probability of 50%. Here, we show the implementation of a novel scheme that allows overcoming this limit.

We give details on the experimental setup. We show how we generate Bell-states in a linear Mach-Zehnder-like scheme as well as how we create ancillary N00N states from single photons. Both states interfere in a linear-optical setup and photon-number measurements at the output allow determining the respective Bell state.

QI 6.8 Tue 11:45 H9

Preparation of maximally entangled states with digital-analog quantum computing — •NICOLA WÜRZ¹, JULIA LAMPRICH¹, MANISH THAPA¹, VICENTE PINA CANELLES¹, STEFAN POGORZALEK¹, ANTTI VEPSÄLÄINEN², MIHA PAPIĆ¹, JAYSHANKAR NATH¹, FLORIAN VIGNEAU¹, DARIA GUSENKOVA¹, PING YANG¹, HERMANN HEIMONEN², HSIANG-SHENG KU¹, ADRIAN AUER¹, JOHANNES HEINSOO², FRANK DEPPE¹, and INÉS DE VEGA¹ — ¹IQM Quantum Computers, Munich, Germany — ²IQM Quantum Computers, Espoo, Finland

Digital-Analog Quantum Computing (DAQC) is a novel approach, which combines digital single qubit gates with analog multi-qubit blocks. The DAQC concept distinguishes between stepwise and banded DAQC, where the single qubit gates are placed in between analog blocks or applied simultaneously with the analog (entangling) evolution, respectively. We have identified relevant sources of error for both DAQC protocols. When preparing a maximally entangled two-qubit state using either stepwise or banded DAQC, we reach similar fidelities as in the purely digital case. The multi-qubit version of the implemented circuit allows us to create GHZ states by parallelizing several two-qubit interactions. For the case of three qubits, we have investigated infidelities arising due to the multi-qubit nature of the interaction, including parasitic and higher order couplings.

We acknowledge support from the German Federal Ministry of Education and Research via the projects DAQC (13N15686) and Q-Exa (13N16062).

QI 6.9 Tue 12:00 H9

Momentum-Space Entanglement and the Wilsonian Effective Action — •MATHEUS HENRIQUE MARTINS COSTA^{1,2}, GASTAO INACIO KREIN², FLAVIO DE SOUZA NOGUEIRA¹, and JEROEN VAN DEN BRINK¹ — ¹Institute for Theoretical Solid State Physics - IFW Dresden, Dresden, Germany — ²Instituto de Física Teórica - Universidade Estadual Paulista, Sao Paulo, Brazil

The entanglement between momentum modes of a quantum field theory at different scales is not as well studied as its counterpart in real space, despite the natural connection with the Wilsonian idea of integrating out the high-momentum degrees of freedom. Here, we push such connection further by developing a novel method to calculate the Rényi and entanglement entropies between slow and fast modes which is based on the Wilsonian effective action at a given scale and apply it to the perturbative regime of some scalar theories, comparing the lowest-order results with those from the literature and giving them an interpretation in terms of Feynman diagrams. Our results open the way for further work in exploring the relation between renormalization and entanglement and the role of the latter in phase transitions.

QI 6.10 Tue 12:15 H9

Holographic code in the laboratory — •GERARD ANGLÈS MUNNÉ¹, VALENTIN KASPER², and FELIX HUBER¹ — ¹Faculty of Physics, Astronomy and Applied Computer Science, Jagiellonian University, 30-348 Kraków, Poland. — ²Institut de Ciències Fotòniques (ICFO), Mediterranean Technology Park, 08860 Castelldefels, Barcelona, Spain

We propose a method to prepare the holographic pentagon code in the laboratory. The code states can be described by graph states whose interactions patterns are optimized for experimental purposes. Taking a small instance of the holographic code on 12 qubits, we show how to do encoding and decoding. Furthermore, we demonstrate how to test the holographic property - any bulk part is determined by its nearby boundary - through a partial recovery procedure.

QI 6.11 Tue 12:30 H9

Universal ground state entanglement entropy in strongly biased bipartite systems — •OHAD SHPIELBERG — University of Haifa, Haifa, Israel

Consider the AB bipartite system with a single conserved quantity, say a particle number. The particle bias R is defined as the expectation of the particle number in subsystem A over the expectation in subsystem B. At the limit of large R , the ground state entanglement entropy is shown to universally scale like $\log R/R$, independent of the Hamiltonian details. A $1/\sqrt{R}$ universal power law is obtained for multiple conserved quantities. Moreover, the analysis shows a similar universal structure of the Rényi entropy.

This universal behavior could be exploited to optimize entanglement-assisted control over large many body systems, using systems with a small degree of freedom. Alternatively, one can use the different scaling of the entanglement entropy to detect hidden conserved quantities.

Part of the announced results are available at Phys. Rev. A 105, 042420 (2022).

QI 7: Quantum Communication and Networks

Time: Wednesday 15:00–17:45

Location: H8

QI 7.1 Wed 15:00 H8

Quantum networks and symmetries — •KIARA HANSENNE¹, ZHEN-PENG XU¹, TRISTAN KRAFT², and OTFRIED GÜHNE¹ — ¹Naturwissenschaftlich-Technische Fakultät, Universität Siegen, Siegen, Germany — ²Institute for Theoretical Physics, University of Innsbruck, Innsbruck, Austria

Quantum networks are promising tools for the implementation of long-range quantum communication. The characterization of quantum correlations in net-

works and their usefulness for information processing is therefore central for the progress of the field, but so far only results for small basic network structures or pure quantum states are known. Here we show that symmetries provide a versatile tool for the analysis of correlations in quantum networks. We provide an analytical approach to characterize correlations in large network structures with arbitrary topologies. As examples, we show that entangled quantum states with a bosonic or fermionic symmetry can not be generated in networks; moreover,

cluster and graph states are not accessible. Our methods can be used to design certification methods for the functionality of specific links in a network and have implications for the design of future network structures.

QI 7.2 Wed 15:15 H8

Secure Anonymous Conferencing in Quantum Networks — •FEDERICO GRASSELLI¹, GLÁUCIA MURTA¹, JARN DE JONG², FREDERIK HAHN³, DAGMAR BRUSS¹, HERMANN KAMPERMANN¹, and ANNA PAPPA^{2,4} — ¹Heinrich-Heine-Universität Düsseldorf — ²Technische Universität Berlin — ³Freie Universität Berlin — ⁴Fraunhofer Institut for Open Communication Systems

Users of quantum networks can securely exchange classical messages via quantum conference key agreement (CKA), which requires the users' identities to be publicly known. In numerous scenarios, however, communicating users demand anonymity with respect to the other network users, the network manager and even between themselves.

We introduce a security framework for anonymous conference key agreement with different levels of anonymity, generalizing the security of quantum key distribution (QKD). We present efficient and noise-tolerant protocols exploiting multipartite Greenberger-Horne-Zeilinger (GHZ) states and prove their security against general quantum attacks in the finite-key regime. We analyze their performance in noisy and lossy quantum networks and compare with protocols that only use bipartite entanglement to achieve the same functionalities. Our simulations show that GHZ-based protocols can outperform protocols based on bipartite entanglement and that the advantage increases for protocols with stronger anonymity requirements.

Our work advocates the use of multipartite entanglement for cryptographic tasks involving several users and enables the implementation of quantum communication protocols beyond QKD and CKA.

QI 7.3 Wed 15:30 H8

Prepare-and-measure conference key agreement protocol based on single-photon interference — •GIACOMO CARRARA, FEDERICO GRASSELLI, GLÁUCIA MURTA, HERMANN KAMPERMANN, and DAGMAR BRUSS — Institut für Theoretische Physik III, Heinrich-Heine-Universität Düsseldorf, Germany

Quantum Key Distribution (QKD) and its multipartite counterpart, Conference Key Agreement, (CKA) are fundamental cryptographic tasks, where two or more parties try to establish a common, secret key. The so-called Twin-Field Quantum Key Distribution (TF-QKD) setup recently received great attention as it only requires lasers and linear optical devices. TF-QKD has been generalized to many parties, where a CKA protocol based on single-photon interference has been proposed [F. Grasselli *et al.*, 2019, New J. Phys., **21** 123002]. This multipartite protocol, however, has a big drawback: it does not have a prepare-and-measure formulation and thus lacks a simple, practical implementation. In this work we propose a CKA protocol that allows for a prepare-and-measure implementation, where the parties are required only to produce weak coherent pulses. We provide for this protocol a security analysis based on the decoy state method and analyze how the protocol performs compared to the well-known repeaterless bound, considering different network architectures.

QI 7.4 Wed 15:45 H8

Experimental anonymous conference key agreement using linear cluster states — •LUKAS RÜCKLE, JAKOB BUDDE, and STEFANIE BARZ — Institute for Functional Matter and Quantum Technologies and IQST, University of Stuttgart, 70569 Stuttgart

Quantum networks allow for secure communication between more than just two parties. One example is the conference key agreement, where multiple parties exchange a secure key. Interestingly, quantum networks can provide another security feature: protecting the identity of the participants. Here, we realize such anonymous quantum conference key agreement in a linear network architecture using photonic cluster states. We show how different parties of the network can exchange a key anonymously by extracting a smaller GHZ state from the cluster state. We further study how noise affects the finite and asymptotic key rate and show that we achieve a positive asymptotic key rate.

QI 7.5 Wed 16:00 H8

Average waiting times for entanglement links in multiplexed quantum networks — •LISA WEINBRENNER, LINA VANDRÉ, and OTFRIED GÜHNE — Universität Siegen, Deutschland

In quantum communication protocols using noisy channels, the error probability typically scales exponentially with the length of the channel. To reach long-distance entanglement distribution, one can use quantum repeaters. These schemes involve first a generation of elementary bipartite entanglement links between two nodes and then measurements to combine the elementary links to a long-distance link.

Since the generation of an elementary link is probabilistic and quantum memories have a limited storage time, the generation of a long-distance link is probabilistic, too [1]. One possibility to speed up the generation of a long-distance link is a multiplexed system, in which there is more than one elementary link between two nodes [2]. In this contribution, we will present estimates and bounds

on waiting times in such a system. Our results rely on an analytical treatment of the underlying stochastic process, as well as numerical investigations using the matrix product state formalism.

[1] S. Khatri *et al.*, Phys. Rev. Research **1**, 023032 (2019)

[2] O. A. Collins *et al.*, Phys. Rev. Lett **98**, 060502 (2007)

QI 7.6 Wed 16:15 H8

Fiber communication with collective quantum measurements: a machine learning perspective with applications — •MATTEO ROSATI¹ and JANIS NÖTZEL² — ¹Electrical Engineering and Computer Science, Technische Universität Berlin, 10587 Berlin, Germany — ²Emmy-Noether Gruppe Theoretisches Quantensystemdesign Lehrstuhl für Theoretische Informationstechnik Technische Universität München.

The transmission rate of classical bits on optical fiber is ultimately governed by the Holevo capacity. Achieving such rate requires writing information into coherent states of light and then performing a collective quantum measurement on multiple received signals at once, known as quantum joint-detection receiver (QJDR).

We find that the realization of a QJDR would enable two key advantages in current communication networks: (i) an estimated 55% decrease in energy consumption of optical amplifiers; (ii) an unbounded logarithmic growth of the channel capacity with the signal pulse rate, as opposed to the bounded rate attained by conventional detectors.

We then develop a machine learning framework to discover approximate implementations of the QJDR with a state-of-the-art photonic circuit. We compute the theoretical learning complexity of such photonic circuits, showing that it is polynomial in the number of optical modes, and introduce a simple algorithm to optimize them. Finally, we show that our algorithm is able to discover decoder setups that are both realizable at the state of the art and can attain a decoding success rate as high as 93% of the optimal QJDR.

15 min. break

QI 7.7 Wed 16:45 H8

A Graphical Formalism for Entanglement Purification — •LINA VANDRÉ and OTFRIED GÜHNE — Universität Siegen, Germany

Hypergraph states form an interesting family of multi-qubit quantum states which are useful for quantum error correction, non-locality and measurement-based quantum computing. They are a generalisation of graph and cluster states. The states can be represented by hypergraphs, where the vertices and hyperedges represent qubits and entangling gates, respectively.

For quantum information processing, one needs high-fidelity entangled states, but in practice most states are noisy. Purification protocols address this problem and provide a method to transform a certain number of copies of a noisy state into single high-fidelity state. There exists a purification protocol for hypergraph states [1]. In my talk, I will first reformulate the purification protocol in a graphical manner, which makes it intuitively understandable. Based on this, I will propose systematic extensions, which naturally arise from the graphical formalism.

[1] T. Carle *et al.*, Phys. Rev. A **87**, 012328 (2013))

QI 7.8 Wed 17:00 H8

Quantum memories for space: from ideas to experimental roadmap — •MUSTAFA GÜNDOĞAN, MARTIN JUTISZ, ELISA DA ROS, and MARKUS KRUTZIK — Humboldt-Universität zu Berlin, Berlin, Germany

Quantum communication is usually limited to around a few hundred kilometers due to the exponential losses in optical fibers. Quantum repeaters (QR) based on the heralded storage of entangled states have been proposed to overcome this direct transmission limit. However, they are still limited to around a few thousand kms. On the other hand, space-based quantum links where channel loss scales mainly polynomially offer another solution to this problem. In this case, however, the communication distance is limited to the line-of-sight distance of the satellite which is around 2000 km for low earth orbit. In order to reach truly global distances, we have recently proposed an architecture that combines the above two approaches [1]: a quantum repeater operating in space. We show that this scheme provides a three orders of magnitude faster entanglement distribution rate across global distances than ground-based and hybrid space-ground architectures.

In this talk, after summarizing our findings and presenting a comparison of our scheme with already existing architectures I will finish with presenting our experimental work towards building space-compatible quantum memories with warm and cold atomic gases.

[1] M. Gündoğan *et al.*, npj Quantum Information **7**, 128 (2021)

(This work has been supported by DLR through the funds provided by BMWi: 50WM1958, 50WM2055 and 50RP2090.)

QI 7.9 Wed 17:15 H8

Employing Atomically-thin Single-Photon Sources in Quantum Communication — •TIMM GAO¹, MARTIN V. HELVERSEN¹, CARLOS ANTON-SOLANAS², CHRISTIAN SCHNEIDER², and TOBIAS HEINDEL¹ — ¹Institut für Festkörperphysik, Technische Universität Berlin, 10623 Berlin, Germany — ²Institut für Physik, Carl von Ossietzky Universität Oldenburg, 26111 Oldenburg, Germany

Confined excitons in monolayers of transition metal dichalcogenides (TMDCs) emerged as a novel type of quantum emitter showing appealing prospects for large-scale and low-cost device integration for quantum information technologies. Here, we pioneer the practical suitability of TMDC devices in quantum communication by evaluating the performance of a single-photon source (SPS) based on a strain engineered WSe₂ monolayer for applications in quantum key distribution (QKD) [1]. Employed in a QKD-testbed emulating the BB84 protocol we achieve raw key rates of up to 66.95 kHz and antibunching values down to 0.034 - competitive with QKD experiments using semiconductor quantum dots or color centers in diamond [2]. Furthermore, we exploit routines for the performance optimization developed in our group. Our work thus sets the direction for wider applications of emerging materials in quantum information processing.

[1] T. Gao, M. v. Helversen, C. Anton-Solanas, C. Schneider, and T. Heindel, Atomically-thin Single-photon Sources for Quantum Communication, arXiv:2204.06427 (2022)

[2] D. Vajner et al., Adv. Quantum Technol. 2100116 (2022).

QI 7.10 Wed 17:30 H8

Restoring quantum communication efficiency over high loss optical fibres — •FRANCESCO ANNA MELE — Scuola Normale Superiore, Pisa, Italy

In the absence of quantum repeaters, quantum communication proved to be nearly impossible across optical fibres longer than approximately 20 km due to the drop of transmissivity below the critical threshold of 1/2. However, if the signals fed into the fibre are separated by a sufficiently short time interval, memory effects must be taken into account. In this talk we show that by properly accounting for these effects it is possible to devise schemes that enable unassisted quantum communication across arbitrarily long optical fibres at a fixed positive qubit transmission rate. We also demonstrate how to achieve entanglement-assisted communication over arbitrarily long distances at a rate of the same order of the maximum achievable in the unassisted noiseless case.

This talk is based on <https://arxiv.org/abs/2204.13128> and <https://arxiv.org/abs/2204.13129>.

QI 8: Quantum Sensors and Metrology

Time: Wednesday 15:00–17:45

Location: H9

Invited Talk

QI 8.1 Wed 15:00 H9

Exploring Quantum Materials with Quantum Sensors — •URI VOOL — Max Planck Institute for Chemical Physics of Solids, Dresden, Germany

In recent years, improvements in crystal growth and sample fabrication have given us access to an expanding variety of quantum materials which exhibit exotic macroscopic phenomena directly tied to the strong quantum effects in their microscopic structure. These are exciting for basic research and potential technology applications, but there are still fundamental open questions about the structure of such systems, and the ability to control their quantum effects.

Meanwhile, there has been rapid growth in the ability to control coherent quantum effects in various solid state systems, from atomic defects to macroscopic electromagnetic circuits. These quantum systems can be efficiently manipulated and tuned while maintaining high coherence, making them leading quantum computing platforms. These advantages also make them excellent quantum sensors, and their operation at cryogenic temperatures and material compatibility make them especially suited for exploring quantum materials.

This talk will present several recent and ongoing experiments using coherent quantum systems for material exploration. We will focus on two experimental techniques: 1. Nitrogen-vacancy centers as cryogenic scanning probes for imaging hydrodynamic electron flow. 2. Hybrid superconducting circuits as probes of the superconducting structure in novel materials. Finally, we will discuss the prospective of this approach for material exploration and quantum technology.

QI 8.2 Wed 15:30 H9

Fractional Josephson effect induced by weak measurement — •MOHAMMAD ATIF JAVED, JAKOB SCHWIBBERT, and ROMAN-PASCAL RIWAR — Forschungszentrum Jülich, Peter Grünberg Institute (PGI-2), 52425, Jülich, Deutschland

The fractional Josephson effect is commonly directly linked to the presence of Majorana- and parafermions, which are important candidates to implement (universally) protected quantum gates in superconducting quantum hardware. However, these exotic particles still seem notoriously challenging to realize in experiment, and difficult to unambiguously identify via transport measurements. Moreover, a proper understanding of the topological transport properties requires a generalization to an open quantum system context.

Here, we study a standard quantum dot in proximity to two conventional superconducting contacts, including a weak transport measurement and a nonequilibrium quasiparticle source. The non-hermitian system dynamics are analysed by means of exceptional points, leading to a braiding of the complex eigenspectrum. Based on this analysis, we show that this system exhibits an open system version of a fractional Josephson effect, in spite of using only conventional materials.

QI 8.3 Wed 15:45 H9

Defects in semi-conductors for Quantum Applications — •SAJID ALI, FABIAN BERTOLDO, SIMONE MANTI, and KRISTIAN THYGESEN — CAMD, Computational Atomic-Scale Materials Design, Department of Physics, Technical University of Denmark, 2800 Kgs. Lyngby Denmark

Discovery of single photon emission (SPE) from 2D materials has opened a new arena of research because of the unique electric, magnetic and optical properties possessed by these SPE's systems. Based on these superior properties, such systems provide very attractive platform that can help to realize, control, ma-

nipulate and measure individual quantum states. The defect systems with similar properties must be explored in other 2D materials, as this will broaden the range of materials available for such applications, consequently revolutionising this field. In the present work we have shortlisted/ the defect systems with optimal properties for various quantum applications e.g. qubits, quantum key distribution, brain magnetometers etc., based on our screening study of intrinsic point defects in dynamically and thermodynamically stable and non-magnetic host systems from C2DB database. We study various aspects and properties of these defect systems e.g. photoluminescence (PL) line shape, Transition dipole moment, Radiative recombination rates, Inter-system crossing rates, Hyperfine coupling parameters, Zero field splitting, Spin-Coherence times etc. We identify a set of defect systems, with ideal properties, which can be exploited for various quantum technologies.

QI 8.4 Wed 16:00 H9

Iterative adaptive spectroscopy with a two-level nanomechanical platform — •AVISHEK CHOWDHURY¹, ANH TUAN LE¹, HUGO RIBEIRO³, and EVA M. WEIG^{1,2}

— ¹Department of Electrical and Computer Engineering, Technical University of Munich, 85748 Garching, Germany — ²Munich Center for Quantum Science and Technology (MCQST), Schellingstr. 4, 80799, Munich, Germany — ³Department of Physics and Applied Physics, University of Massachusetts Lowell, Lowell, MA 01854, USA

We develop an iterative, adaptive frequency sensing protocol based on Ramsey interferometry of a two-level system. Our scheme allows one to estimate unknown frequencies with a high precision from short, finite signals. It avoids several issues related to processing of decaying signals and reduces the experimental overhead related to sampling. High precision is achieved by enhancing the Ramsey sequence to prepare with high fidelity both the sensing and read-out state and by using an iterative procedure built to mitigate systematic errors when estimating frequencies from Fourier transform. Furthermore, we implement the protocol to demonstrate a proof-of-principle study on a classical two-level nanomechanical platform. We demonstrate that the protocol can detect the coupling between two normal modes with an accuracy higher than their individual dissipation rate. Moreover, the protocol can detect small DC fluctuation of the surrounding electrical field around our nanomechanical oscillator.

QI 8.5 Wed 16:15 H9

Quantum enhancement of multiphoton absorption signals in nonlinear interferometers — •SHAHRAM PANAHYAN^{1,2} and FRANK SCHLAWIN^{1,2} — ¹Max Planck Institute for the Structure and Dynamics of Matter, Center for Free Electron Laser Science, Luruper Chaussee 149, 22761 Hamburg, Germany — ²The Hamburg Centre for Ultrafast Imaging, Luruper Chaussee 149, 22761 Hamburg, Germany

SU(1,1)-interferometers are novel nonlinear interferometers [1] in which optical parametric amplifiers create quantum states of light by squeezing and anti-squeezing the light fields [2]. By taking advantage of these quantum states of light, SU(1,1)-interferometers have been employed for spectroscopy [3], imaging [4], quantum state engineering, and quantum information purposes.

Motivated by these applications, we study the precision of multiphoton absorption measurements in a nonlinear SU(1,1)-interferometer. We analyze multiphoton absorption signals, characterize the absorption as a function of nonlinear order, and derive sensitivity bounds from the Fisher Information. We show

that the precision of multiphoton absorption measurements can be enhanced compared to classical measurement strategies. Finally, we highlight that this enhancement is robust against experimental imperfections in detection devices.

[1] M. V. Chekhova and Z. Y. Ou, *Adv. Opt. Photon.* 8, 104 (2016).

[2] S. Panahiyan, C. S. Muñoz, M. V. Chekhova, F. Schlawin, [arXiv:2205.10675].

[3] K. E. Dorfman, *Light: Science & Applications* 9, 123 (2020).

[4] M. Manceau et al., *Phys. Rev. Lett.* 119, 223604 (2017).

15 min. break

QI 8.6 Wed 16:45 H9

Multicopy metrology with many-particle quantum states — •RÓBERT TRÉNYI^{1,2,3}, ÁRPÁD LUKÁCS^{1,4,3}, PAWEŁ HORODECKI^{5,6}, RYSZARD HORODECKI⁵, TAMÁS VÉRTESI⁷, and GÉZA TÓTH^{1,2,8,3} — ¹Dept. of Theoretical Physics, U. of the Basque Country UPV/EHU, Bilbao, Spain — ²DIPC, San Sebastián, Spain — ³Wigner Research Centre for Physics, Budapest, Hungary — ⁴Dept. of Mathematical Sciences, Durham University, United Kingdom — ⁵International Centre for Theory of Quantum Technologies, University of Gdansk, Gdansk, Poland — ⁶Faculty of Applied Physics and Mathematics, National Quantum Information Centre, Gdansk University of Technology, Gdansk, Poland — ⁷Institute for Nuclear Research, Debrecen, Hungary — ⁸IKERBASQUE, Bilbao, Spain

We consider quantum metrology with several copies of bipartite and multipartite quantum states. We characterize the metrological usefulness by determining how much the state outperforms separable states. We identify a large class of entangled states that become maximally useful for metrology in the limit of infinite number of copies. The maximally achievable metrological usefulness is attained exponentially fast in the number of copies. We show that, on the other hand, pure entangled states with even a small amount of white noise do not become maximally useful even in the limit of infinite number of copies. We also make general statements about the usefulness of a single copy of pure entangled states. We show that the multiqubit states presented in Hyllus et al. [*Phys. Rev. A* 82, 012337 (2010)], which are not useful, become useful if we embed the qubits locally in qutrits.

QI 8.7 Wed 17:00 H9

Quantum metrology in the non-asymptotic regime — •JOHANNES JAKOB MEYER¹, SUMEET KHATRI¹, PHILIPPE FAIST¹, DANIEL STILCK-FRANÇA², GIACOMO GUARNIERI¹, and JENS EISERT^{1,3,4} — ¹Dahlem Center for Complex Quantum Systems, Freie Universität Berlin, 14195 Berlin, Germany — ²Univ Lyon, ENS Lyon, UCBL, CNRS, Inria, LIP, F-69342, Lyon Cedex 07, France — ³Fraunhofer Heinrich Hertz Institute, 10587 Berlin, Germany — ⁴Helmholtz-Zentrum Berlin für Materialien und Energie, 14109 Berlin, Germany

The main concern of quantum metrology is to determine how we can achieve the best possible precision in estimating parameters of physical processes. One of the main tools used in the field is the Quantum Cramér-Rao bound. However, it is a relation that is only tight and meaningful asymptotically and, conversely, too optimistic for finite numbers of experimental repetitions. We analyze how a change of perspective to an operationally motivated measure of estimation success can be used to achieve more meaningful bounds. We show that the measure can be

evaluated using a semidefinite program and detail how it can be used to establish minimax guarantees against any prior distribution of the underlying parameter. We focus on the analysis of group-covariant estimation on pure states, which is relevant because of its relation to phase estimation. We prove that the optimal measurement in this setting is given by the pretty good measurement and exhibit a construction of a probe state that numerically saturates the optimal asymptotic minimax rate.

QI 8.8 Wed 17:15 H9

Gradient Magnetometry with Atomic Ensembles — •IAGOBA APELLANIZ¹, IÑIGO URIZAR-LANZ¹, ZOLTÁN ZIMBORÁS^{1,2,3}, PHILIPP HYLLUS¹, and GÉZA TÓTH^{1,2,4} — ¹Department of Physics, University of the Basque Country UPV/EHU, P.O. Box 644, E-48080 Bilbao, Spain — ²Dahlem Center for Complex Quantum Systems, Freie Universität Berlin, 14195 Berlin, Germany — ³Wigner Research Centre for Physics, Hungarian Academy of Sciences, P.O. Box 49, H-1525 Budapest, Hungary — ⁴IKERBASQUE, Basque Foundation for Science, E-48013 Bilbao, Spain

We study gradient magnetometry with ensembles of atoms with arbitrary spin. We calculate precision bounds for estimating the gradient of the magnetic field based on the quantum Fisher information. For states that are sensitive to homogeneous fields, a simultaneous measurement is needed, as the homogeneous field must also be estimated.

We present a method to calculate precision bounds for gradient estimation with two spatially separated atomic ensembles. We also consider a single atomic ensemble with an arbitrary density profile, where the atoms cannot be addressed individually, and which is a very relevant case for experiments.

[1] I. Apellaniz et al., *Phys. Rev. A*, 97 053603 (2018)

[2] G. Vitagliano et al., arXiv:2104.05663 (2021)

QI 8.9 Wed 17:30 H9

Ultra-low perturbation quantum measurements via random-time sampling — •MARKUS SIFFT and DANIEL HÄGELE — Ruhr University Bochum, Faculty of Physics and Astronomy, Experimental Physics VI (AG), Germany

Random-time sampling of a quantum system is introduced as a new approach to continuous quantum measurements with prospects for ultra-low-perturbation measurements [1]. Random sampling is, e.g., naturally realized in an optical spin noise experiment when weak probe-laser light exhibits random single-photon events in the detector [2]. Our theory shows that a direct evaluation of these detector click events yields power spectra that are equivalent but not identical to those of the usual Gaussian continuous measurement regime [3]. Surprisingly, this holds true even for average sampling rates much lower than the typical frequency range of the measured quantum dynamics. The third-order quantum polyspectrum (bispectrum) also contains the same information as its continuous counterpart. System characterization can, therefore, be performed using the analytic form of the quantum polyspectra [4]. Many applications of random-time sampling are envisioned for high-resolution spectroscopy, circuit quantum electrodynamics, quantum sensing, and quantum measurements in general.

[1] <https://arxiv.org/abs/2109.05862>, [2] G. M. Müller et al., *Physica E* 43, 569 (2010), [3] M. Siffert et al., *Phys. Rev. Res.* 3, 033123 (2021) [4] D. Hägele et al., *Phys. Rev. B* 98, 205143 (2018)

QI 9: Quantum Correlations

Time: Thursday 9:30–12:15

Location: H8

QI 9.1 Thu 9:30 H8

Dimension-free entanglement detection in multipartite Werner states — •FELIX HUBER¹, IGOR KLEP², VICTOR MAGRON³, and JURIJ VOLČIČ⁴ — ¹Institute of Theoretical Physics, Jagiellonian University, 30-348 Kraków, Poland — ²Faculty of Mathematics and Physics, University of Ljubljana, Slovenia — ³LAAS-CNRS & Institute of Mathematics from Toulouse, France — ⁴Department of Mathematical Sciences, University of Copenhagen, Denmark

Werner states are multipartite quantum states that are invariant under the diagonal conjugate action of the unitary group. We give a complete characterization of their entanglement that is independent of the underlying local Hilbert space: for every entangled Werner state there exists a dimension-free entanglement witness. The construction of such a witness is formulated as an optimization problem. To solve it, two semidefinite programming hierarchies are introduced. The first one is derived using real algebraic geometry applied to positive polynomials in the entries of a Gram matrix, and is complete in the sense that for every entangled Werner state it converges to an entanglement witness. The second one is based on a sum-of-squares certificate for the positivity of trace polynomials in noncommuting variables, and is a relaxation that involves smaller semidefinite constraints.

QI 9.2 Thu 9:45 H8

Constructing entanglement witnesses based on the Schmidt decomposition of operators — •SOPHIA DENKER¹, CHENGJIE ZHANG², ALI ASADIAN³, and OTFRIED GÜHNE¹ — ¹Naturwissenschaftlich-Technische Fakultät, Universität Siegen, Walter-Flex-Straße 3, 57068 Siegen, Germany — ²School of Physical Science and Technology, Ningbo University, Ningbo, 315211, China — ³Department of Physics, Institute for Advanced Studies in Basic Sciences (IASBS), Gava Zang, Zanjan 45137-66731, Iran

Characterizing entanglement is an important issue in quantum information, as entanglement is considered to be a resource for quantum key distribution or quantum metrology. One useful tool to detect and quantify entanglement are witness operators. A standard way to design entanglement witnesses for two or more particles is based on the fidelity of a pure quantum state; in mathematical terms this construction relies on the Schmidt decomposition of vectors. In this contribution, we present a method to build entanglement witnesses based on the Schmidt decomposition of operators. Our scheme works for the bipartite and the multipartite case and is found to be strictly stronger than the concept of fidelity-based witnesses. We discuss various examples and demonstrate that our approach can also be used to quantify quantum correlations as well as characterize the dimensionality of entanglement.

QI 9.3 Thu 10:00 H8

Nonlinear Entanglement Detection from Immanent Inequalities — •ALBERT RICO and FELIX HUBER — Faculty of Physics, Astronomy and Applied Computer Science, Jagiellonian University, 30-348 Kraków, Poland

We develop a method for nonlinear entanglement detection which is based on inequalities for immanants. This allows to use multipartite witnesses to detect bipartite states in a non-conventional way. We give examples and compare their effectiveness to the standard usage of witnesses. We show that this type of nonlinear entanglement detection can outperform its linear version, and how the detection can be performed in the laboratory through randomized measurements.

QI 9.4 Thu 10:15 H8

The shape of higher-dimensional state space: Bloch ball analog for a qutrit — CHRISTOPHER ELTSCHKA¹, MARCUS HUBER^{2,3}, SIMON MORELLI^{2,3}, and •JENS SIEWERT^{4,5} — ¹Institut für Theoretische Physik, Universität Regensburg, Regensburg, Germany — ²IQOQI Vienna, Vienna, Austria — ³Atominstytut TU Wien, Vienna, Austria — ⁴University of the Basque Country UPV/EHU and EHU Quantum Center, Bilbao, Spain — ⁵Ikerbasque, Basque Foundation for Science, Bilbao, Spain

The Bloch ball as a geometric representation of the state space for qubits is an ubiquitous tool to gain deeper insight and intuitive understanding of quantum-mechanical phenomena. Unfortunately, even for the next more complex system, the qutrit, such a geometric representation (rather than cross sections or projections) is not known. In order to serve as a model for higher-dimensional state space, it should display a number of desirable properties, such as different surface parts corresponding to pure or mixed states, convexity, inner and outer sphere with the corresponding radii, pure states should form a connected set, etc. [1]. We show that, based on the Bloch representation of qutrit states, such a model can be constructed that captures many of the geometric features discussed in Ref. [1].

[1] I. Bengtsson, S. Weis, K. Zyczkowski, Geometry of the Set of Mixed Quantum States: An Apophatic Approach. In: P. Kielanowski et al (eds) Geometric Methods in Physics. Trends in Mathematics (Birkhäuser, Basel, 2013).

QI 9.5 Thu 10:30 H8

Nearly optimal separability certification of quantum states — •TIES-ALBRECHT OHST¹, CHAU NGUYEN¹, OTFRIED GÜHNE¹, and XIAO-DONG YU² — ¹Naturwissenschaftlich-Technische Fakultät, Universität Siegen — ²Department of Physics, Shandong University, Jinan

Entanglement describes the possibility of local parties sharing a joint global system state that cannot be expressed as a probabilistic mixture of locally prepared states. The question on whether some given state is entangled or separable, on the contrary, is generically difficult to answer. We present an algorithm for the quantum separability problem for intermediate dimensions with evidences of being nearly optimal. The basic idea of our considerations can in general be described by a systematic search for separable decompositions of a given state by polytope approximations to a local system. As a benchmark we can compute the separability thresholds for known bound entangled states of two coupled qutrits with an accuracy that has not been achieved before. Also, for bi-partite systems of higher dimension we can certify the separability of states reliably which follows from the comparison with data by known entanglement criteria. For three coupled qubit systems, our ideas allow for an efficient distinction between different separability classes that lie at the heart of the theory of multi-partite entanglement. We developed an algorithm for the search among all fully bi-separable states to find the one whose entanglement robustness is as large as possible. Quite interestingly, the obtained states show a deep connection to the post measurement states in the teleportation protocol.

QI 9.6 Thu 10:45 H8

Hilbert-Schmidt geometry of two-qubit correlations — •SANTIAGO LLORENS¹ and JENS SIEWERT^{2,3} — ¹Grup d'Informació Quàntica, Universitat Autònoma de Barcelona, Barcelona, Spain — ²University of the Basque Country and EHU Quantum Center, Bilbao, Spain — ³Ikerbasque, Basque Foundation for Science, Bilbao, Spain

The Bloch representation of quantum states endows the state space with a natural Euclidean geometry via the Hilbert-Schmidt scalar product. Based on this, a Bloch ball-type global view of the state space for a qutrit was found recently. This imposes the question whether an analogous method exists for the simplest quantum correlations – those in a system of two qubits. From such a visualization one may expect a better understanding of the links between the algebraic

correlation constraints and their geometric background. We show that indeed the 2-sector (aka as the correlation tensor) of two-qubit states allows for a geometric representation of the algebraic constraints to the entries of the Bloch vector. In this context we provide novel insight into the relation between entanglement quantifiers and characteristic parameters of the Bloch representation of bipartite systems.

15 min. break

QI 9.7 Thu 11:15 H8

Schmidt number witnesses for high-dimensional quantum states in photonic temporal mode setups — •NIKOLAI WYDERKA¹, GIOVANNI CHESI², HERMANN KAMPERMANN¹, and DAGMAR BRUSS¹ — ¹Institut für Theoretische Physik III, Heinrich-Heine-Universität Düsseldorf, D-40225 Düsseldorf, Germany — ²Istituto Nazionale di Fisica Nucleare Sezione di Pavia, Via Agostino Bassi 6, I-27100 Pavia, Italy

Photonic temporal modes offer a robust and efficient toolbox for high-dimensional quantum information applications. In order to characterize the experimentally generated quantum states, we aim to use witnesses to certify their Schmidt numbers as a robust entanglement measure. To that end, we develop an iterative algorithm that yields Schmidt number witness candidates that require only a few of those measurements inherent to the temporal mode framework using quantum pulse gates. Finally, we use the numerical candidates to derive a proper Schmidt number witness for states close to the maximally entangled state.

QI 9.8 Thu 11:30 H8

Complete hierarchy for high-dimensional steering certification — •CARLOS DE GOIS, MARTIN PLÁVALA, and OTFRIED GÜHNE — Naturwissenschaftlich Technische Fakultät, Universität Siegen

Steerability can be employed as a semi-device independent test of the Schmidt number. As such, it is a promising component in quantum informational protocols that make use of entanglement dimension certification. Recently proposed and experimentally demonstrated for the special case in which the assemblage is prepared from two choices of measurements, high-dimensional steering is so far lacking a general certification procedure. Herein, we provide necessary and, at a limit, sufficient conditions to certify the entanglement dimension of a steering assemblage. These conditions are stated in terms of a hierarchy of semidefinite programs, which can also be used to compute the steering dimension robustness.

QI 9.9 Thu 11:45 H8

Distance-based resource quantification for sets of quantum measurements — •LUCAS TENDICK, MARTIN KLIESCH, HERMANN KAMPERMANN, and DAGMAR BRUSS — Institute for Theoretical Physics, Heinrich Heine University Düsseldorf, D-40225 Düsseldorf, Germany

The advantage that quantum systems provide for certain quantum information processing tasks over their classical counterparts can be quantified within the general framework of resource theories. Certain distance functions between quantum states have successfully been used to quantify resources like entanglement and coherence. Perhaps surprisingly, such a distance-based approach has not been adopted to study resources of quantum measurements, where other geometric quantifiers are used instead. Here, we define distance functions between sets of quantum measurements and show that they naturally induce resource monotones for convex resource theories of measurements. By focusing on a distance based on the diamond norm, we establish a hierarchy of measurement resources and derive analytical bounds on the incompatibility of any set of measurements. We show that these bounds are tight for certain projective measurements based on mutually unbiased bases and identify scenarios where different measurement resources attain the same value when quantified by our resource monotone. Our results provide a general framework to compare distance-based resources for sets of measurements and allow us to obtain limitations on Bell-type experiments.

QI 9.10 Thu 12:00 H8

On entanglement swapping and teleportation with local hidden variables — •EUGEN MUCHOWSKI — Primelstrasse 10, 85591 Vaterstetten

A model with local hidden variables is presented, which describes phenomena such as entanglement swapping and teleportation and also reproduces the quantum mechanical expectation values for the measurement of entangled photons. It refutes Bell's theorem and at the same time expands our physical understanding of entangled states since it can also explain the phenomena mentioned above.

QI 10: Quantum Simulation and Many-Body Systems

Time: Thursday 9:30–12:15

Location: H9

Invited Talk

QI 10.1 Thu 9:30 H9

Entanglement Transition in the Projective Transverse Field Ising Model — •HANS PETER BÜCHLER — Institut für theoretische Physik III, Universität Stuttgart

Discrete quantum trajectories of systems under random unitary gates and projective measurements have been shown to feature transitions in the entanglement scaling that are not encoded in the density matrix. Here we present the projective transverse field Ising model, a stochastic model with two noncommuting projective measurements and no unitary dynamics, and demonstrate the appearance of an entanglement transition. This transition is connected to quantum error correction, and we demonstrate the most efficient decoding of stored quantum information. Especially, we show that the ability to retrieve stored quantum information can serve as an experimental tool to detect such entanglement phase transitions.

QI 10.2 Thu 10:00 H9

Efficient Quantum Computation of Floquet Hamiltonians — •BENEDIKT FAUSEWEH¹ and JIAN-XIN ZHU^{2,3} — ¹Institute for Software Technology, German Aerospace Center (DLR), Germany — ²Theoretical Division, Los Alamos National Laboratory, USA — ³Center for Integrated Nanotechnologies, Los Alamos National Laboratory, USA

The Floquet formalism describes the control over quantum systems using external periodic fields. With recent advances in ultrafast spectroscopy of solid-state systems, Floquet engineering, that is, a targeted design of quantum systems driven by laser pulse, has led to an increasing interest in computational methods that can simulate light-matter interactions. Although the perturbative regime, in which the fundamental driving frequency is much larger than the energy bandwidth of the quantum system, shows interesting phenomena, it is the non-perturbative regime that presents the most exciting opportunity to study the interplay with strong correlations and which remains largely unexplored. Here we describe hybrid quantum algorithms that make use of quantum computers to tackle this problem. The required quantum resources are within reach for current day NISQ devices and allow the efficient computation of Floquet Hamiltonians. We demonstrate applications of these algorithms and discuss their performance for small scale driven quantum systems.

This work was carried out under the auspices of the U.S. DOE NNSA (Contract No. 89233218CNA000001) and was supported by the LANL LDRD Program.

QI 10.3 Thu 10:15 H9

Noise-utilizing quantum simulation of a system coupled to a structured bath — •JUHA LEPPÄKANGAS, NICOLAS VOGT, KIRSTEN BARK, KEITH FRATUS, JAN-MICHAEL REINER, SEBASTIAN ZANKER, and MICHAEL MARTHALER — HQS Quantum Simulations GmbH, Haid-und-Neu-Strasse 7, 76131 Karlsruhe, Germany

We consider noisy gate-based quantum computers for the purpose of simulating the spin-boson model. We establish a bosonic bath by an ensemble of qubits with finite coherence times. The energy-level broadening of qubits is mapped to broadening of the simulated bath spectral function. We study how desired forms of the spectral density can be constructed by optimizing simulated spin-bath couplings and bath energies. We study the effect of different gate decompositions and system connectivity on the quality of the mapping to the desired form. In the ideal situation, the spin-bath couplings can be decomposed using only variable angle two-qubit gates, such as a variable Mølmer-Sørensen gate. In other cases, qubit noise can get mapped to two-body noise in the simulated spin-bath system, which does not have exact correspondence in the spin-boson model. We show a numeric comparison of the quality of the mapping for various decompositions. Furthermore we compare the full inclusion of the two-body noise terms with an approximate mapping of the effects on the spectral density of the simulated spin-boson problem.

QI 10.4 Thu 10:30 H9

Distributed Multipartite Entanglement Generation in Coupled Cavities — •MARC BOSTELMANN, FREDERIK LOHOF, and CHRISTOPHER GIES — Institute for Theoretical Physics, University of Bremen, Germany

The generation of spatially distributed entanglement is important for the realization of quantum information protocols and quantum computing, leading to new fields of research like quantum machine learning. Coupled cavities offer a platform to create this kind of entanglement between spatially separated qubits [1]. By carefully tailoring excitations with external light pulses we theoretically examine the generation of entangled states, such as GHZ or Dicke states. Starting with a system of two qubits for generating bipartite entanglement, we extend the discussion to the multipartite case, exploiting symmetries of the system. Bridging the gap to experimental realizations, we study robustness of the generated entangled states to dissipation and asymmetry in the system. [1] Aron et al., PRA, 90, 062305 (2014).

QI 10.5 Thu 10:45 H9

Probing confinement in a \mathbb{Z}_2 lattice gauge theory on a quantum computer — •JULIUS MILDENBERGER¹, WOJCIECH MRUCZKIEWICZ², JAD HALIMEH^{3,4}, ZHANG JIANG², and PHILIPP HAUKE¹ — ¹INO-CNR BEC Center and Department of Physics, University of Trento, Italy — ²Google Quantum AI, Venice, CA, USA — ³Department of Physics and ASC, Ludwig-Maximilians-Universität München, Germany — ⁴MCQST, Munich, Germany

Digital quantum simulators provide a table-top platform for addressing salient questions in particle and condensed-matter physics. A particularly rewarding target is given by lattice gauge theories. Their constituents, e.g., charged matter and the electric gauge field, are governed by local gauge constraints, which are highly challenging to engineer and lead to intriguing yet not fully understood features such as confinement of particles. We simulate confinement dynamics in a \mathbb{Z}_2 LGT on a superconducting quantum chip. The charge-gauge-field interaction is synthesized using only 6 native two-qubit gates, enabling us to reach simulation times of up to 25 Trotter steps. We observe how tuning a term that couples only to the electric field confines the charges, a manifestation of the tight bond that the local gauge constraint generates between both. Moreover, we study a different mechanism, where a modification of the gauge constraint from \mathbb{Z}_2 to $U(1)$ symmetry freezes the system dynamics. Our work showcases the strong restriction that the underlying gauge constraint imposes on the dynamics of an LGT, illustrates how gauge constraints can be modified and protected, and paves the way for studying other models with many-body interactions.

15 min. break

QI 10.6 Thu 11:15 H9

Quantum Information Scrambling in Thermalizing Spin Chains with Non-local Interactions — •DARVIN WANISCH^{1,2,3} and STEPHAN FRITZSCHE^{1,2,3} — ¹Theoretisch-Physikalisches Institut, Friedrich-Schiller-Universität Jena, Max-Wien-Platz 1, 07743 Jena, Germany — ²Helmholtz-Institut Jena, Fröbelstieg 3, 07743 Jena, Germany — ³GSI Helmholtzzentrum für Schwerionenforschung GmbH, Planckstraße 1, 64291 Darmstadt, Germany

Motivated by recent works on information scrambling in spin systems with non-local interactions, and their potential of sharing features of quantum gravity, we study scrambling in different variants of the Ising model. Our results demonstrate that out-of-time-order correlators (OTOCs) might not be sufficient to properly characterize information scrambling in the presence of nonlocal interactions. In particular, two models that exhibit a highly nonlinear lightcone can vary widely in their thermalization timescale. More elaborate measures of operator growth can distinguish these two scenarios and reveal very different operator dynamics. Moreover, we find a distinct analogy between the growth of a local operator under time-evolution and the entanglement entropy following a quantum quench. Our work gives new insights into scrambling properties of systems that are within reach of state-of-the-art experimental platforms and complements results on the possibility of observing features of quantum gravity in the laboratory.

QI 10.7 Thu 11:30 H9

Quantum simulation of \mathbb{Z}_2 lattice gauge theories with dynamical matter from two-body interactions in $(2+1)D$ — •LUKAS HOMEIER^{1,2,3}, ANNABELLE BOHRDT^{3,4}, SIMON LINSEL^{1,2}, EUGENE DEMLER⁵, JAD C. HALIMEH^{1,2}, and FABIAN GRUSDIT^{1,2} — ¹LMU Munich, Germany — ²MCQST, Munich, Germany — ³Harvard University, Cambridge (MA), USA — ⁴ITAMP, Cambridge (MA), USA — ⁵ETH Zurich, Switzerland

Gauge fields coupled to dynamical matter are a universal framework in many disciplines of physics, ranging from particle to condensed matter physics, but remain poorly understood at strong couplings. Through the steadily increasing control over numerically inaccessible Hilbert spaces, analog quantum simulation platforms have become a powerful tool to study interacting quantum many-body systems. Here we propose a scheme in which a \mathbb{Z}_2 gauge structure emerges from local two-body interactions and one-body terms in two spatial dimensions. The scheme is suitable for Rydberg atom arrays and enables the experimental study of both $(2+1)D$ \mathbb{Z}_2 lattice gauge theories coupled to dynamical matter (\mathbb{Z}_2 mLGTS) and quantum dimer models on the honeycomb lattice, for which we derive effective Hamiltonians. We discuss ground-state phase diagrams of the experimentally relevant effective \mathbb{Z}_2 mLGT for $U(1)$ and quantum- \mathbb{Z}_2 matter featuring deconfined phases. Our proposed scheme allows to experimentally study not only longstanding goals of theoretical physics, such as Fradkin and Shenker's [PRD 19, 1979] conjectured phase diagram, but also go beyond regimes accessible with current numerical techniques.

QI 10.8 Thu 11:45 H9

Digital quantum simulation of the BCS model with a central-spin-like quantum processor — •JANNIS RUH, REGINA FINSTERHOEHLZ, and GUIDO BURKARD — University of Konstanz, Konstanz, Germany

The simulation of quantum systems is one of the most promising applications of quantum computers. We present a quantum algorithm to perform digital quantum simulations of the Bardeen-Cooper-Schrieffer (BCS) superconductivity model on a quantum register with a star shaped connectivity map, as it is, e.g., featured by color centers in diamond. We show how to effectively translate the problem onto the quantum computer and implement the algorithm using only the native interactions between the qubits. Furthermore, we use the algorithm to simulate the dynamics of the BCS model by subjecting its mean-field ground state to a time-dependent perturbation. The quantum simulation algorithm is studied using a classically simulated quantum computer.

QI 10.9 Thu 12:00 H9

Characterizing quantum correlations among magnons in antiferromagnets — •VAHID AZIMI MOUSOLOU^{1,2}, YUEFEI LIU³, ANDERS BERGMAN¹, ANNA DELIN³, OLLE ERIKSSON^{1,4}, MANUEL PEREIRO¹, DANNY THONIG⁴, and ERIK SJÖQVIST¹ — ¹Uppsala University, Uppsala, Sweden — ²University of Isfahan, Isfahan, Iran — ³KTH Royal Institute of Technology, Stockholm, Sweden — ⁴Örebro University, Örebro, Sweden

Quantum magnonics provides promising hybrid platforms for accessing unique quantum phenomena and using them to realize stable and energy-efficient nanoscale quantum technologies. Clearly, quantum correlations are the major non-classical resources in such quantum systems. Here we discuss how an antiferromagnetic coupling generates experimentally detectable bipartite continuous variable magnon-entanglement [1, 2]. We present feasible experimental setups based on hybrid magnon+X systems to quantify the demonstrated magnon-entanglement through an uncertainty relation.

[1] V. Azimi-Mousolou, et al., Hierarchy of magnon mode entanglement in antiferromagnets, Phys. Rev. B 102, 224418 (2020).

[2] V. Azimi-Mousolou, et al., Magnon-magnon entanglement and its quantification via a microwave cavity, Phys. Rev. B 104, 224302 (2021).

QI 11: Members' Assembly

Time: Thursday 14:00–15:00

Location: H8

All members of the Quantum Information Division are invited to participate.

QI 12: Quantum Computing and Algorithms

Time: Thursday 15:00–18:15

Location: H8

QI 12.1 Thu 15:00 H8

Partitioning methods for solving optimization problems on NISQ-devices — •FEDERICO DOMINGUEZ¹, KAONAN CAMPOS MICADEI¹, CHRISTIAN ERTLER¹, and WOLFGANG LECHNER^{1,2} — ¹Parity QC Germany GmbH, Munich, Germany — ²Institute for Theoretical Physics, LFUI, and Parity QC GmbH, Innsbruck, Austria

Partitioning methods are hybrid quantum-classical algorithms aimed at overcoming the memory limitations of current quantum devices. These methods decompose large problems into smaller pieces suitable for running on small quantum devices. The partial solutions to the problem are recombined using classical algorithms that can deal with both the error from the partition approximation and the intrinsic errors of the NISQ devices.

In this work, we solve optimization problems by developing partitioning methods based on the Parity encoding [1,2] and we benchmark the results using simulated quantum annealing. The Parity transformation is capable of encoding all-to-all graphs, hypergraphs, and side conditions of optimization problems using only local qubit interactions and allowing for a high gate parallelizability and hence scalability [3,4]. The resulting locality property is especially suited for the partitioning approach. The performance of our method shows that large optimization problems can be efficiently run on small quantum devices. [1] Lechner, W. et al. (2015). Science advances, 1(9), e1500838. [2] Ender, K. et al. (2021). arXiv preprint arXiv:2105.06233. [3] Lechner, W. (2020). IEEE Transactions on Quantum Engineering, 1, 1-6. [4] Drieb-Schön, M. et al. (2021). arXiv preprint arXiv:2105.06235.

QI 12.2 Thu 15:15 H8

Calculation of Correlated Electronic States on Noisy Intermediate Scale Quantum Computers — •JANNIS EHRlich¹, DANIEL URBAN¹, and CHRISTIAN ELSÄSSER^{1,2} — ¹Fraunhofer-Institut für Werkstoffmechanik IWM, Freiburg, Germany — ²Freiburger Materialforschungszentrum, Universität Freiburg, Germany

The numerical description of correlated electrons on conventional computers is limited to small system sizes. For the exact diagonalization approach, for example, all configurations in the many-particle space have to be considered, and their number grows exponentially with the number of one-particle states. This limitation can be overcome by simulating the correlated electrons with one of the artificial quantum systems that recently became available through the advance in quantum computing technologies. On such systems, each one-particle state can be represented by one qubit, which can be entangled with each other to generate superpositions. Thus, a linear scaling in the number of qubits is sufficient to cover the full many-particle space. Here, we describe strongly correlated systems within the dynamical mean-field theory (DMFT) and investigate its possible realization on a quantum computer. As a proof of concept, we study the simplified version of two-site DMFT both, by using simulators and an IBMQ quantum computer. We show that a solution of this model can be obtained using the quantum-classical variational quantum eigensolver (VQE). As the quality of the

results is limited by the noise level of current quantum computers (NISQ type), we further investigate how different error mitigation strategies can improve the results.

QI 12.3 Thu 15:30 H8

Optimal gradient estimation for variational quantum algorithms — •LENNART BITTEL, JENS WATTY, and MARTIN KLIESCH — Heinrich Heine Universität, Düsseldorf

Variational quantum algorithms (VQAs) are a leading approach for achieving a practically relevant near-term quantum advantage. A bottleneck of this approach is the estimation of derivatives of a given energy functional w.r.t. the parameters of the underlying variational quantum circuit. The parameter shift rule and its extensions allow for such and estimation without systematic errors. However, due to the measurement shot noise, they can have a large statistical error. As a consequence, many measurement rounds are required, which result in non-optimal VQA run-times.

In this work, we reduce this measurement overhead by using a Bayesian estimation framework. For this, we use prior knowledge about the circuit to then determine optimal measurement settings that minimize the expected statistical and systematic errors simultaneously. With accurate priors, this approach can significantly outperform traditional methods. We test our estimation algorithm numerically for a common quantum approximate optimization algorithm (QAOA). For a desired estimation accuracy we can reduce the number of measurements by an order of magnitude compared to traditional estimation methods. This also leads to significantly improved convergence times for the gradient descent algorithm.

QI 12.4 Thu 15:45 H8

Synthesis of and compilation with time-optimal multi-qubit gates — •PASCAL BASSLER¹, MATTHIAS ZIPPER¹, CHRISTOPHER CEDZICH¹, PATRICK HUBER², MICHAEL JOHANNING², MARKUS HEINRICH¹, and MARTIN KLIESCH¹ — ¹Heinrich Heine University Düsseldorf, Germany — ²University of Siegen, Germany

We develop a method to synthesize a class of entangling multi-qubit gates for a quantum computing platform with fixed Ising-type interaction with all-to-all connectivity. The only requirement on the flexibility of the interaction is that it can be switched on and off for individual qubits. Our method yields a time-optimal implementation of the multi-qubit gates. We numerically demonstrate that the total multi-qubit gate time scales approximately linear in the number of qubits. Using this gate synthesis as a subroutine, we provide compilation strategies for important use cases: (i) we show that any Clifford circuit on n qubits can be implemented using at most n multi-qubit gates without requiring ancilla qubits, (ii) we decompose the quantum Fourier transform in a similar fashion, (iii) we compile a simulation of molecular dynamics into native gates, and (iv) we propose a method for the compilation of diagonal unitaries with time-optimal multi-qubit gates, as a step towards general unitaries. As motivation, we provide

a detailed discussion on a microwave controlled ion trap architecture with magnetic gradient induced coupling (MAGIC) for the generation of the Ising-type interactions.

QI 12.5 Thu 16:00 H8

Estimating molecular forces and other energy gradients efficiently on a quantum computer — •MICHAEL STREIF², THOMAS O'BRIEN¹, NICHOLAS C. RUBIN¹, RAFFAELE SANTAGATI², YUAN SU¹, WILLIAM J. HUGGINS¹, JOSHUA J. GOINGS¹, NIKOLAJ MOLL², ELICA KYOSEVA², MATTHIAS DEGROOTE², CHRISTOFER S. TAUTERMANN³, JOONHO LEE^{1,4}, DOMINIC W. BERRY⁵, NATHAN WIEBE^{6,7}, and RYAN BABBUSH¹ — ¹Google Research, USA — ²Quantum Lab, Boehringer Ingelheim, Germany — ³Boehringer Ingelheim Pharma GmbH & Co KG, Germany — ⁴Department of Chemistry, Columbia University, USA — ⁵Department of Physics and Astronomy, Macquarie University, Australia — ⁶Department of Computer Science, University of Toronto, Canada — ⁷Pacific Northwest National Laboratory, USA

The calculation of energy derivatives underpins many fundamental properties for molecular systems, such as dipole moments or molecular forces. Nevertheless, most methods for quantum chemistry on quantum computers have focused on electronic structure calculations, even though energy derivatives are fundamental for many practical applications. Here, I will introduce quantum algorithms for the calculation of energy derivatives on noisy intermediate scale (NISQ) and fault tolerant (FTQC) quantum computers, with substantially reduced cost compared to previous methods. Our results suggest that the calculation of molecular forces has a similar cost to estimating energies. However, since molecular dynamics (MD) simulations typically require millions of force calculations, current known methods for MD on quantum computers are impractical and new approaches need to be found.

QI 12.6 Thu 16:15 H8

Towards the Simulation of Large Scale Protein-Ligand Interactions on NISQ-era Quantum Computers — •NIKOLAJ MOLL¹, FIONN D. MALONE², ROBERT M. PARRISH², ALICIA R. WELDEN², THOMAS FOX³, MATTHIAS DEGROOTE¹, ELICA KYOSEVA¹, RAFFAELE SANTAGATI¹, and MICHAEL STREIF¹ — ¹Quantum Lab, Boehringer Ingelheim, 55218 Ingelheim, Germany — ²QC Ware Corporation, Palo Alto, CA, 94301, USA — ³Medicinal Chemistry, Boehringer Ingelheim Pharma GmbH & Co. KG, 88397 Biberach, Germany

Most quantum computing research for quantum chemistry applications has focused on the calculation of ground state energies, while in the pharmaceutical industry, one is often more interested in gaining insight into the interaction of drugs and proteins. The interaction energy together with entropic contributions allows the determination of the efficacy of a potential drug. Here we explore the use of symmetry-adapted perturbation theory (SAPT) as a simple means to compute interaction energies between two molecular systems with a hybrid method combining NISQ-era quantum and classical computers. From the one- and two-particle reduced density matrices of the monomer wavefunctions obtained by the variational quantum eigensolver (VQE), we compute SAPT contributions to the interaction energy. At first order, this energy yields the electrostatic and exchange contributions for non-covalently bound systems. Ideal statevector simulations show that the SAPT(VQE) interaction energy components display orders of magnitude lower absolute errors than the corresponding VQE total energies which sub kcal/mol accuracy in the SAPT interaction energies.

15 min. break

QI 12.7 Thu 16:45 H8

Resilience of quantum approximate optimization against correlated errors — JORIS KATTEMÖLLE and •GUIDO BURKARD — Universität Konstanz, Konstanz, Deutschland

The Quantum Approximate Optimization Algorithm (QAOA) has the potential of providing a quantum advantage in large-scale optimization problems, as well as in finding the ground state of spin glasses. This algorithm is especially suited for Noisy Intermediate Scale Quantum (NISQ) devices because of its noise resilience. So far, this noise resilience has only been studied under the assumption of uncorrelated noise. However, in recent years, it has become increasingly clear that the noise impacting NISQ devices is significantly correlated. In this work, we introduce a model for both spatially and temporally (non-Markovian) correlated errors that allows for the independent variation of the marginalized local error probability and the correlation strength. Using this model, we study the effects of noise correlations on QAOA by full density matrix simulation. We find evidence that the performance of QAOA improves as the strength of noise correlations is increased at fixed marginalized local error probability. This shows that, as opposed to algorithms for fully error-corrected quantum computers, noise correlations need not be detrimental for NISQ algorithms such as QAOA, and may actually improve the performance thereof.

QI 12.8 Thu 17:00 H8

Exploiting symmetry in variational quantum machine learning — JOHANNES JAKOB MEYER¹, MARIAN MULARSKI^{1,2}, ELIES GIL-FUSTER^{1,3}, •ANTONIO ANNA MELE¹, FRANCESCO ARZANI¹, ALISSA WILMS^{1,2}, and JENS EISERT^{1,3,4} — ¹Dahlem Center for Complex Quantum Systems, Freie Universität Berlin, 14195 Berlin, Germany — ²Porsche Digital GmbH, 71636 Ludwigsburg, Germany — ³Fraunhofer Heinrich Hertz Institute, 10587 Berlin, Germany — ⁴Helmholtz-Zentrum Berlin für Materialien und Energie, 14109 Berlin, Germany

Variational quantum machine learning is an extensively studied NISQ application. The success of variational quantum learning models crucially depends on finding a suitable parametrization of the model that encodes an inductive bias relevant to the learning task. However, little is known about guiding principles for constructing suitable parametrizations. We explore when and how symmetries of the learning problem can be exploited to construct quantum learning models with outcomes invariant under the symmetry of the learning task. Using tools from representation theory, we show how a standard gateset can be transformed into an equivariant one that respects the symmetries of the problem through a process of symmetrization. We benchmark the proposed methods on two toy problems that feature a non-trivial symmetry and observe a substantial increase in generalization performance. As our tools can also be applied in a straightforward way to other variational problems with symmetric structure, we show how equivariant gatesets can be used in variational quantum eigensolvers.

QI 12.9 Thu 17:15 H8

Preparation of Hardware-Efficient Graph States on IBM QX — •SEBASTIAN BRANDHOFFER¹, JELENA MACKEPFRANG², DANIEL BHATTI², ILIA POLIAN¹, and STEFANIE BARZ² — ¹Institute of Computer Architecture and Computer Engineering & IQST, University of Stuttgart, Germany — ²Institute for Functional Matter and Quantum Technologies & IQST, University of Stuttgart, Germany

Near-term quantum computers are characterized by heterogeneous errors that occur at a high rate, a short decoherence time, and a limited number of qubits. Preparing a quantum state on these near-term quantum computers must be performed with these limitations in mind. Especially, when preparing highly entangled multi-qubit quantum states one would like to reach quantum state fidelities as high as possible. For this, the quantum state preparation algorithm needs to be adapted to the specific quantum hardware and the respective limitations. In this work, a method is proposed for determining the optimal preparation algorithm of a specific class of graph states. The proposed method is based on one of the winning submissions to the 2020 IBM Quantum's Open Science Prize - Graph State Challenge.

QI 12.10 Thu 17:30 H8

A single T-gate makes distribution learning hard — MARCEL HINSCHKE¹, MARIOS IOANNOU¹, •ALEXANDER NIETNER¹, JONAS HAFERKAMP¹, YIHUI QUEK¹, DOMINIK HANGLEITER², JEAN-PIERRE SEIFERT³, JENS EISERT^{1,4,5}, and RYAN SWEKE¹ — ¹FU Berlin, 14195 Berlin, Germany — ²University of Maryland, MD 20742, USA — ³TU Berlin, 10587 Berlin, Germany — ⁴Helmholtz-Zentrum Berlin, 14109 Berlin, Germany — ⁵Fraunhofer Heinrich Hertz Institute, 10587 Berlin, Germany

The task of probabilistic modelling is at the core of many practical applications. As such, the efficient learnability of natural classes of probability distributions is a question of both fundamental and practical interest. The output distributions of local quantum circuits is a particularly interesting class of distributions, of key importance both to quantum advantage proposals and a variety of quantum machine learning algorithms. In this work, we provide an extensive characterization of the learnability of the output distributions of local quantum circuits. We prove that the density modelling problem can be solved efficiently in case of Clifford circuits, while adding a single T gate renders the task computationally hard. Evidently, the simulability of this class does not imply its learnability. Next we show that the generative modelling task is hard for depth $n^{\Omega(1)}$ universal local quantum circuits for both, classical and quantum algorithms. Finally we obtain a similar hardness result already for depth $\omega(\log(n))$ local Clifford circuits when restricting to practically relevant learning algorithms, such hybrid-quantum classical algorithms.

QI 12.11 Thu 17:45 H8

Avoiding barren plateaus via transferability of smooth solutions in Hamiltonian Variational Ansatz — ANTONIO ANNA MELE^{1,2}, GLEN BIGAN MBENG³, GIUSEPPE ERNESTO SANTORO², MARIO COLLURA², and •PIETRO TORTA² — ¹Dahlem Center for Complex Quantum Systems, Freie Universität Berlin, 14195 Berlin, Germany — ²SISSA, Via Bonomea 265, I-34136 Trieste, Italy — ³Universität Innsbruck, Technikerstraße 21 a, A-6020 Innsbruck, Austria

A large ongoing research effort focuses on Variational Quantum Algorithms (VQAs), representing leading candidates to achieve computational speed-ups on current quantum devices. The scalability of VQAs to a large number of qubits, beyond the simulation capabilities of classical computers, is still debated. Two major hurdles are the proliferation of low-quality variational local minima, and the exponential vanishing of gradients in the cost function landscape, a phenomenon referred to as barren plateaus. Here we show that, by employing it-

erative search schemes one can effectively prepare the ground state of paradigmatic quantum many-body models, circumventing also the barren plateau phenomenon. This is accomplished by leveraging the transferability to larger system sizes of iterative solutions, displaying an intrinsic smoothness of the variational parameters, a result that does not extend to other solutions found via random-start local optimization. Our scheme could be directly tested on near-term quantum devices, running a refinement optimization in a favorable local landscape with non-vanishing gradients.

QI 12.12 Thu 18:00 H8

Hay from the haystack: explicit examples of exponential quantum circuit complexity — •YIFAN JIA and MICHAEL M. WOLF — Department of Mathematics, Technische Universität München, Germany

QI 13: Implementations: Superconducting Qubits

Time: Friday 9:30–12:45

Location: H8

Invited Talk

QI 13.1 Fri 9:30 H8

Scalable control of superconducting qubits — •STEFAN FILIPP — Walther-Meißner-Institut, 85748 Garching — TU Munich, Physics-Department, 85748 Garching

The rapid development of quantum technologies in the recent past has led to the realization of first quantum computer prototypes that promise to outperform conventional computers in specific types of problems. However, before practical real-life problems can be solved efficiently on quantum computers we have to still tackle numerous challenges not only to enhance the coherence, but also the control of qubits. To improve the fidelity of single qubit operations we utilize closed-loop optimization methods based on high duty-cycle measurements. With piecewise-constant pulse parameterizations we are able to demonstrate short, 4ns single-qubit pulses with high fidelity and low leakage. We further explore architectures that contain 'hidden' qubits, which are not directly addressable, and experimentally demonstrate full control and measurement capabilities of such a hidden qubit. I will then discuss the impact of such restricted control capabilities on the performance of specific qubit coupling networks. I will further preview promising future directions such as the use of adiabatic gates for quantum feed-forward neural networks and multi-qubit gate operations for the efficient implementation of quantum algorithms as part of the newly formed Munich Quantum Valley, a cross-disciplinary initiative to realize a full-stack quantum computer.

QI 13.2 Fri 10:00 H8

Test and diagnostics speed up for characterizing few-qubit superconducting quantum processors — •THORSTEN LAST, GARRELT ALBERTS, ADAM LAWRENCE, KELVIN LOH, VIACHESLAV OSTROUKH, and ADRIAAN ROL — Orange Quantum Systems B.V., Lorentzweg 1, 2628 CJ Delft, NL

The combined challenge of increasing the qubit count on a quantum processor and a requirement to further reduce the qubit's error rates require novel approaches in test and qubit diagnostics. An important aspect to improve the situation is an acceleration of the development cycle for quantum processors [1]. Here we present benchmarking and diagnostic tools based on the recently established open-source platform Quantify [2] to perform end-to-end data analytics. Structured (human-assisted) characterization and a gradual enhancement of automation already led to a reduction of time for basic qubit diagnostics from months to days. The diagnostic tools for characterizing small scale superconducting quantum processors are available as software packages or fully integrated into room temperature electronic control racks. They are organized in complexity classes ranging from hardware verification, and basic single-qubit analytics up to the level of algorithmic benchmarking. Besides quantum processor diagnostics these tools are also used for full-stack system verification through experiment. [1] G.J.N. Alberts, et al., EPJ Quantum Technol. 8: 18 (2021). [2] https://quantify-quantify-core.readthedocs-hosted.com/en/0.5.3_a/

QI 13.3 Fri 10:15 H8

How to correctly account for time-varying fluxes in superconducting circuits — •AHMED KENAWY¹, FABIAN HASSLER², DAVID DIVINCENZO¹, and ROMAN RIWAR¹ — ¹Peter Grünberg Institute, Theoretical Nanoelectronics, Forschungszentrum Jülich — ²JARA-Institute for Quantum Information, RWTH Aachen University

Time-varying fluxes are a ubiquitous tool to control superconducting hardware. Surprisingly, however, the existing literature has never fully accounted for the electro-motive force induced by the magnetic field. Here, we propose a general recipe to construct a low-energy Hamiltonian, taking as input only the circuit geometry and the solution of the external magnetic fields. We apply this recipe to the example of a dc SQUID and show that the assignment of individual capacitances to each Josephson junction is possible only if we permit those capacitances to be negative, time-dependent, or even momentarily singular. Such anomalous

The vast majority of quantum states and unitaries have circuit complexity exponential in the number of qubits. In a similar vein, most of them also have exponential minimum description length, which makes it difficult to pinpoint examples of exponential complexity. In this work, we construct examples of constant description length but exponential circuit complexity. We provide infinite families such that each element requires an exponential number of two-qubit gates to be generated exactly from a product and where the same is true for the approximate generation of the vast majority of elements in the family. The results are based on sets of large transcendence degree and discussed for tensor networks, diagonal unitaries and maximally coherent states.

QI 13.4 Fri 10:30 H8

Majorana fermions revealing the true nature of quantum phase slip junctions — •CHRISTINA KOLIOFOTI and ROMAN-PASCAL RIWAR — Forschungszentrum Jülich, Peter Grünberg Institut (PGI-2), 52425 Jülich, Deutschland

Quantum circuit theory is a powerful and ever-evolving tool to predict the dynamics of superconducting circuits. In its language, quantum phase slips are famously considered to be the exact dual to the Josephson effect. However, if taken at face value, this duality stipulates that charge must be continuous. We propose a charge-quantization conserving description of quantum phase slips and show that this seemingly minute change gives rise to some very different predictions. When shunting a quantum phase slip junction with a topological Josephson junction, the new description leads to a complete disappearance of the Hofstadter butterfly spectrum. For topologically trivial circuits we argue that adhering to charge quantization renders realizations of the Gottesman-Kitaev-Preskill code impossible.

QI 13.5 Fri 10:45 H8

Tunable-coupler mediated controlled-controlled-phase gate with superconducting qubits — •NIKLAS J GLASER^{1,2}, FEDERICO ROY^{1,3}, and STEFAN FILIPP^{1,2,4} — ¹Walther-Meißner-Institut, Bayerische Akademie der Wissenschaften, 85748 Garching, Germany — ²Physik-Department, Technische Universität München, 85748 Garching, Germany — ³Theoretical Physics, Saarland University, 66123 Saarbrücken, Germany — ⁴Munich Center for Quantum Science and Technology (MCQST), 80799 München, Germany

Applications for noisy intermediate scale quantum computing devices rely on the efficient entanglement of many qubits to reach a potential quantum advantage. Although entanglement is typically generated using two-qubit gates, direct control of strong multi-qubit interactions can improve the efficiency of the process. We investigate a system of three superconducting transmon-type qubits coupled via a single flux-tunable coupler. Tuning the frequency of the coupler by adiabatic flux pulses enables us to control the conditional energy shifts between the qubits and directly realize multi-qubit interactions. To accurately adjust the resulting controlled relative phases, we describe a gate protocol involving refocusing pulses and adjustable interaction times. This enables the implementation of the full family of pairwise controlled-phase (CPHASE) and controlled-controlled-phase (CCPHASE) gates. Numerical simulations result in fidelities around 99% and gate times below 300 ns using currently achievable system parameters and decoherence rates.

15 min. break

QI 13.6 Fri 11:15 H8

Coupler-mediated unconditional reset of fixed-frequency superconducting qubits — •GERHARD HUBER^{1,2}, FEDERICO ROY^{1,2}, and STEFAN FILIPP^{1,2,3} — ¹Walther-Meißner-Institut, Bayerische Akademie der Wissenschaften, 85748 Garching, Germany — ²Physik-Department, Technische Universität München, 85748 Garching, Germany — ³Munich Center for Quantum Science and Technology (MCQST), 80799 München, Germany

Advances in superconducting qubit fabrication procedures have led to energy relaxation times regularly exceeding 100 μ s. Therefore, passive reset via relaxation has become unpractical, and an active reset protocol is required to achieve high repetition rate of quantum algorithms. Previous unconditional qubit reset schemes have relied on flux tunable qubits or multiple transitions over higher qubit states. We extend a previous reset scheme using flux tunable qubits to

fixed frequency transmon qubits with tunable couplers. The reset pulse consists of a single parametric flux pulse on the coupler to transfer qubit excitations to a quickly decaying resonator. Our protocol does not rely on additional control lines and can be implemented on current multi-qubit architectures. Further, it can be extended to architectures where a single coupler allows for reset of multiple qubits. We present preliminary numerical and experimental results for this reset protocol demonstrating its potential usefulness.

QI 13.7 Fri 11:30 H8

Analysis of calibration techniques for single-qubit gates on a superconducting quantum computer — •KATHRIN KÖNIG¹, NAOKI KANAZAWA², and SHOTA NAKASUJI³ — ¹Fraunhofer IAF, Freiburg, Germany — ²IBM Research, Tokyo, Japan — ³University of Tokyo, Tokyo, Japan

Inexact calibrated gates and environmental influences lead to imperfect outcomes of a quantum computation. We investigate two calibration techniques on an IBM quantum computer. The state-of-the-art calibration uses an empirical formula to update the optimal control parameter. The compared new technique can directly estimate the parameter at arbitrary precision. We confirmed that the new technique shows higher precision with comparable accuracy.

QI 13.8 Fri 11:45 H8

Pulse class meta-optimization of continuous quantum gates in transmon systems — •FRANCESCO PRETI — Forschungszentrum Jülich, Jülich, Germany

Reducing the circuit depth of quantum circuits is a crucial bottleneck to enabling quantum technology. This depth is inversely proportional to the number of available quantum gates that have been synthesized. Moreover, quantum gate synthesis and control problems exhibit a vast range of external parameter dependencies, both physical and application-specific. We address the possibility of learning families of optimal control pulses in transmon systems, which depend adaptively on various parameters, in order to obtain a global optimal mapping from the space of potential parameter values to the control space, and hence continuous classes of gates. Our proposed method is tested on different experimentally relevant quantum gates and proves capable of producing high-fidelity pulses even in presence of multiple variables or uncertain parameters with wide ranges.

QI 13.9 Fri 12:00 H8

Magnetic field dependence of the quasiparticle parity lifetime in 3D transmons with thin-film Al – AlO_x – Al Josephson junctions — •JONAS KRAUSE¹, LUCAS JANNSSEN¹, CHRISTIAN DICKEL¹, ELMORE VAAL¹, MICHEL VIELMETTER¹, JUREK FREY², FELIX MOTZOI³, SHAI MACHNESS², KELVIN LOH⁴, MICHIEL ADRIAAN ROL⁴, GIANLUIGI CATELANI⁵, and YOICHI ANDO¹ — ¹Physics Institute II, University of Cologne — ²Quantum Computing Analytics (PGI 12), Forschungszentrum Jülich — ³Institute of Quantum Control (PGI-8), Forschungszentrum Jülich — ⁴Orange Quantum Systems — ⁵JARA Institute for Quantum Information (PGI-11), Forschungszentrum Jülich

Magnetic-field resilient superconducting circuits enable quantum sensing applications, hybrid quantum computing architectures, as well as studying flux noise and quasiparticle loss. Placing a thin-film aluminum transmon in a 3D copper cavity, we can measure its quasiparticle parity lifetime over a large range of magnetic fields, with in-plane fields approaching 1T. The magnetic field reduces

the Josephson Energy E_J , while the charging energy E_C is virtually unaffected. The transmon exhibits a parity-dependent frequency splitting. We are working on optimal control techniques for fast parity-selective gates which together with single-shot readout allow measuring the parity lifetime. The magnetic-field dependence of the parity lifetime is of interest for future topological qubits, which rely on combining superconductors with magnetic fields; additionally, it could improve the understanding quasiparticle loss in conventional superconducting qubits.

QI 13.10 Fri 12:15 H8

Towards cQED experiments with in-situ fabrication of topological insulator Josephson junctions — •LUCAS JANNSSEN, JONAS KRAUSE, CHRISTIAN DICKEL, ALEXEY TASKIN, ROOZBEH YAZDAMPANAH RAVARI, ANJANA UDAY, GERTJAN LIPPERTZ, and YOICHI ANDO — AG Ando, PH2, Universität zu Köln, Germany
Circuit quantum electrodynamics experiments with topological insulator (TI) Josephson junctions (JJs) are a promising path towards finding and studying Majorana zero modes. However, the fabrication of TI JJs is challenging. For our topological insulator, we use MBE grown ternary TI (BiSb)₂Te₃. The interface between the proximitising superconductor and the TI film is critically important for the quality of the JJ, which in turn is vital for microwave performance. Hence, we have been fabricating TI JJs with in-situ deposited niobium. However, etching the niobium to define a JJ has proven challenging. We are exploring a combination of titanium and aluminium as an alternative superconductor. An alternative to this etching step is stencil mask technology. We will present our progress in JJ fabrication and possibly first cQED measurements.

QI 13.11 Fri 12:30 H8

Mitigation of quasiparticle loss in superconducting qubits by phonon scattering — ARNO BARGERBOS¹, LUKAS J. SPLITTHOFF¹, MARTA PITA-VIDAL¹, JAAP J. WESDORP¹, YU LIU², PETER KROGSTROP³, LEO P. KOUWENHOVEN¹, CHRISTIAN K. ANDERSEN¹, and •LUKAS GRÜNHaupt^{1,4} — ¹QuTech and Kavli Institute of Nanoscience, Delft University of Technology, Delft, The Netherlands — ²Center for Quantum Devices, Niels Bohr Institute, University of Copenhagen, Copenhagen, Denmark — ³Niels Bohr Institute, University of Copenhagen, Copenhagen, Denmark — ⁴Physikalisch-Technische Bundesanstalt, Braunschweig, Germany

Most error correction schemes for future quantum processors rely on the assumption that errors are uncorrelated. However, in superconducting devices this assumption is drastically violated in the presence of ionizing radiation, which creates bursts of high energy phonons in the substrate. A mitigation technique is to place large volumes of metal on the device, capable of reducing the phonon energy to below the superconducting gap of the qubits. To investigate the effectiveness of this method we fabricate a device with four nominally identical nanowire-based transmon qubits and replace one half of the niobium titanium nitride ground plane with aluminum (Al), which has a much lower superconducting gap. We inject phonons into the substrate by voltage biasing a galvanically isolated Josephson junction and we find protection due to the Al by a factor of 2-4 in terms of qubit lifetime and excited state population. Furthermore, we turn the Al normal with a magnetic field, finding no marked change in the phonon-protection.

QI 14: Quantum Foundations

Time: Friday 9:30–12:30

Location: H9

Invited Talk

QI 14.1 Fri 9:30 H9

Testing quantum theory with generalized noncontextuality — •MARKUS P. MÜLLER^{1,2,3} and ANDREW J. P. GARNER¹ — ¹Institute for Quantum Optics and Quantum Information, Austrian Academy of Sciences, Boltzmanngasse 3, A-1090 Vienna, Austria — ²Vienna Center for Quantum Science and Technology (VCQ), Faculty of Physics, University of Vienna, Boltzmanngasse 5, A-1090 Vienna, Austria — ³Perimeter Institute for Theoretical Physics, 31 Caroline Street North, Waterloo, ON N2L 2Y5, Canada

It is a fundamental prediction of quantum theory that states of physical systems are described by complex vectors or density operators on a Hilbert space. However, many experiments admit effective descriptions in terms of other state spaces, such as classical probability distributions or quantum systems with superselection rules. Here, we ask which probabilistic theories could reasonably be found as effective descriptions of physical systems if nature is fundamentally quantum. To this end, we employ a generalized version of noncontextuality: processes that are statistically indistinguishable in an effective theory should not require explanation by multiple distinguishable processes in a more fundamental theory. We formulate this principle in terms of embeddings and simulations of one probabilistic theory by another, show how this concept subsumes standard notions of contextuality, and prove a multitude of fundamental results on approximate embeddings. We show how results on Bell inequalities can be used

for the robust certification of generalized contextuality, and use this to propose a novel type of experimental test of quantum theory.

QI 14.2 Fri 10:00 H9

Proposal for demonstrating hidden nonlocality without assumptions — •JONATHAN STEINBERG, H. CHAU NGUYEN, and MATTHIAS KLEINMANN — University of Siegen, Siegen, Germany

A quantum state with hidden nonlocality does not violate any Bell inequality unless its hidden nonlocality is activated using local filters. This phenomenon has been demonstrated in experiments, however only when special Bell inequalities are considered [Kwiat et al., Nature 409, 1014 (2001)], or under the assumption that the quantum state is constrained to a special form which has a known local hidden variable [Opt. Express 28, 13638 (2020)]. Developing a general method for constructing local models for bipartite systems of a qubit and a qudit, we propose a protocol which allows one to conclusively demonstrate hidden nonlocality which is free from assumptions on both, the form of Bell inequalities and the special form of the state. By an optimization over the states and measurement directions we obtain that the required precision is within reach of near future experiments.

QI 14.3 Fri 10:15 H9

Non-locality with overlapping marginals — •MOISÉS BERMEJO MORÁN — Jagiellonian University, Krakow, Poland

We investigate how non-locality can be shared in multi-partite physical systems. Going beyond the standard scenario with disjoint subsystems, we focus on the case where the subsystems participating in the Bell inequality can have overlap. The analytical methods are limited in generality and the standard numerical tools do not effectively provide good bounds when measurements with overlapping support are involved. We overcome these limitations by considering the Navascués-Pironio-Acín hierarchy for finite-dimensional systems, for a fixed dimension. Finding the optimal value via convex combinations of random states and PVMs. These allow us to find non-trivial monogamy bounds in simple scenarios.

QI 14.4 Fri 10:30 H9

Optimal convergence rate in the quantum Zeno effect for open quantum systems in infinite dimensions — •TIM MÖBUS and CAMBYSE ROUZÉ — Technical University Munich, Germany

In open quantum systems, the quantum Zeno effect consists in frequent applications of a given quantum operation, e.g. a measurement, used to restrict the time evolution (due e.g. to decoherence) to states that are invariant under the quantum operation. In an abstract setting, the Zeno sequence is an alternating concatenation of a contraction operator (quantum operation) and a strongly continuous contraction semigroup (time evolution) on a Banach space. In this paper, we prove the optimal convergence rate of order $1/n$ of the Zeno sequence by proving explicit error bounds. For that, we derive a new Chernoff-type lemma, which we believe to be of independent interest. Moreover, we generalize the Zeno effect in two directions: We weaken the assumptions on the generator, which induce a Zeno dynamics generated by an unbounded generator and we improve the convergence to the uniform topology. Finally, we provide a large class of examples arising from our assumptions.

QI 14.5 Fri 10:45 H9

Gravitational redshift induces quantum interference — •DAVID EDWARD BRUSCHI¹ and ANDREAS WOLFGANG SCHELL^{2,3} — ¹Institute for Quantum Computing Analytics (PGI-12), Forschungszentrum Jülich, Jülich, Germany — ²Institut für Festkörperphysik, Leibniz Universität Hannover, Hannover, Germany — ³Physikalisch-Technische Bundesanstalt, Braunschweig, Germany

We use quantum field theory in curved spacetime to show that gravitational redshift induces a unitary transformation on the quantum state of propagating photons. This occurs for realistic photons characterized by a finite bandwidth, while ideal photons with sharp frequencies do not transform unitarily. We find that the transformation is a mode-mixing operation, and we devise a protocol that exploits gravity to induce a Hong-Ou-Mandel-like interference effect on the state of two photons. Testing the results of this work can provide a demonstration of quantum field theory in curved spacetime.

15 min. break

QI 14.6 Fri 11:15 H9

Dynamical Theories in Phase-Space: The Almost Hydrogen Atom — •MARTIN PLÁVALA and MATTHIAS KLEINMANN — Universität Siegen, Siegen, Deutschland

We construct a large class of operational theories of hydrogen atom that includes both classical and quantum theory as special cases. We show that one can formulate a well-defined theory of stationary bound states even without uniquely defined time-evolution and we prove that the ground state energy is finite only if the theory exhibits preparation uncertainty relation between position and momentum observables. We perturb the Hamiltonian by including external magnetic field, which leads to breaking of the degeneracy of the energy spectrum; in this setting we show that the magnetic quantum number is bounded by the principal quantum number, similarly as in quantum theory. We also perturb the Hamiltonian by nonstationary electric field and we show that this leads to excitations of the atom. Finally we investigate scattering theory where we show that Rutherford formula for scattering holds in all investigated operational theories.

QI 14.7 Fri 11:30 H9

Uncertainty relations with the variance and the quantum Fisher information — •GÉZA TÓTH^{1,2,3,4} and FLORIAN FRÖWIS⁵ — ¹Theoretical Physics and EHU Quantum Center, University of the Basque Country UPV/EHU, E-48080 Bilbao, Spain — ²Donostia International Physics Center (DIPC), E-20080 San Sebastián, Spain — ³IKERBASQUE, Basque Foundation for Science, E-48011 Bilbao, Spain — ⁴Wigner Research Centre for Physics, H-1525 Budapest, Hungary — ⁵Group of Applied Physics, University of Geneva, CH-1211 Geneva, Switzerland

We present several inequalities related to the Robertson-Schrödinger uncertainty relation. In all these inequalities, we consider a decomposition of the density matrix into a mixture of states, and use the fact that the Robertson-Schrödinger uncertainty relation is valid for all these components. By considering a convex roof of the bound, we obtain an alternative derivation of the relation in Fröwis et al. [Phys. Rev. A 92, 012102 (2015)], and we can also list a number of conditions that are needed to saturate the relation. We present a formulation of the Cramér-Rao bound involving the convex roof of the variance. By considering a concave roof of the bound in the Robertson-Schrödinger uncertainty relation over decompositions to mixed states, we obtain an improvement of the Robertson-Schrödinger uncertainty relation. We consider similar techniques for uncertainty relations with three variances. Finally, we present further uncertainty relations that provide lower bounds on the metrological usefulness of bipartite quantum states in two-mode and two-spin systems.

QI 14.8 Fri 11:45 H9

Geometry of expectation values of non-commuting observables — •KONRAD SZYMANSKI — Universität Siegen, Siegen, Deutschland

Non-commutativity lies at the heart of quantum theory and provides a rich set of mathematical and physical questions. Here, I address this topic through the concept of the Joint Numerical Range (JNR) – the set of simultaneously attainable expectation values for multiple quantum observables, which in general need not commute. I discuss mathematical and physical implications of the geometry of JNR: classification of the possible shapes of the set, as well as development of novel uncertainty relations, entanglement and Schmidt rank witnesses, and detection of vanishing energy gap.

QI 14.9 Fri 12:00 H9

Measurement-based models of friction and dissipative collapse — •MICHAEL GAIDA and STEFAN NIMMRICHTER — Universität Siegen

Collapse models are objective modifications of quantum theory that aim to solve the measurement problem. One of the most studied models is the Continuous Spontaneous Localisation (CSL) model and its dissipative extension. We present a protocol based on randomly occurring Gaussian position measurements and unitary feedback operations that reproduces the single particle dynamics of dissipative CSL. Inspired by this protocol, we introduce a class of measurement-based models, implementing classical friction forces. We find that the specific model for linear Stokes friction reproduces the single-particle dissipative CSL master equation, as well.

QI 14.10 Fri 12:15 H9

Transcendental properties of entropy-constrained sets — •VJOSA BLAKAJ^{1,2} and MICHAEL WOLF^{1,2} — ¹Technical University of Munich — ²Munich Center for Quantum Science and Technology (MCQST), Munich, Germany

For information-theoretic quantities with an asymptotic operational characterization, the question arises whether an alternative single-shot characterization exists, possibly including an optimization over an ancilla system. If the expressions are algebraic and the ancilla is finite, this leads to semialgebraic level sets. In this work, we provide a criterion for disproving that a set is semialgebraic based on an analytic continuation of the Gauss map. Applied to the von Neumann entropy, this shows that its level sets are nowhere semialgebraic in dimension $d > 2$, ruling out algebraic single-shot characterizations with finite ancilla (e.g., via catalytic transformations). We show similar results for related quantities, including the relative entropy, and discuss under which conditions entropy values are transcendental, algebraic, or rational.

Working Group on Equal Opportunities Arbeitskreis Chancengleichheit (AKC)

Agnes Sandner
Sprecherin des AKC
sandner@akc.dpg-physik.de

Overview of Invited Talks and Sessions (Lecture hall H2)

Invited Talk

AKC 1.1 Fri 9:30–10:00 H2 Closing the gender gap: avoid dropout in the postdoc and junior professor phase — •PETRA RUDOLF

Session

AKC 1.1–1.2 Fri 9:30–12:00 H2 Career in Academia

Sessions

– Invited Talks and Discussions –

AKC 1: Career in Academia

Time: Friday 9:30–12:00

Location: H2

Invited Talk

AKC 1.1 Fri 9:30 H2

Closing the gender gap: avoid dropout in the postdoc and junior professor phase — •PETRA RUDOLF — Zernike Institute for Advanced Materials, University of Groningen, The Netherlands

The first big drop out from the scientific career for both women and men happens after the postdoc phase. In this talk I shall analyze the reasons why the postdoc phase is the most vulnerable phase in every young researcher's career and discuss what institutions and young researchers can do to better move on to a fulfilling position inside and outside academia. Of course every young scientist has to be good to make it but as a community we have a clear responsibility to foster talent development in physics.

Then I shall concentrate on academic careers and suggest some support actions for junior professor/ tenure track assistant professors to help these young talents to develop their full potential. Proper onboarding and mentoring in addition to practical help to easier reconcile professional and family duties can avoid losing the young academics at this stage of their career.

Discussion

AKC 1.2 Fri 10:00 H2

University career – yes, but how to? — •PETRA RUDOLF¹, DORIS REITER², ULRICH ECKERN³, and MONIKA MÜHLBAUER⁴ — ¹Zernike Institute for Advanced Materials, University of Groningen, The Netherlands — ²Condensed Matter Theory, TU Dortmund, Germany — ³Professor emeritus, Theoretische Physik II, Universität Augsburg, Germany — ⁴University of Applied Sciences, München, Germany

With the successful defense of the PhD dissertation, many graduates wish to continue their **career in academia**, aiming to work in a somehow independent position. This initially results in making life in temporary postdoc positions. On the long run, this desire leads to an academic career, with the prospect of later employment as a **group leader** in research centers of the scientific societies (MPG, HGF, FHG, ...) or as a university **professor**.

In combination with research-oriented teaching, a professorship is particularly attractive, bridging among generations with its orientation towards future, in largely open-ended and respected positions.

What obstacles are to be met, how to get on track? Comprehensive general information on the framework of preconditions and careful planning are essential for the targeted implementation of the necessary career steps. In particular, the sharing experiences with forerunners allows participation, including gender-specific aspects. All of this enhances the success probabilities of the **candidates**.

We are offering this **open format panel discussion** in our intention to encourage **young women and men** to pursue a scientific career in physics.

The **AKC** is continuously evaluating data from the Federal Statistical Office for physics. We are committed to booster the proportion of female professors (currently 13%), optimally up to their relative population fraction (51%). There is still a long path to go for this goal.

The major concern of this event is hence the link to role models – professionally successful physicists in science-oriented careers. Prof. Petra Rudolf (U Groningen, former first female president of the EPS) will give the introductory lecture and chair the session. Jun. Prof. Doris Reiter, Prof. Ulrike Diebold, Prof. Ulrich Eckern and Prof. Monika Mühlbauer will contribute and share their experiences. Prof. Mühlbauer will also present the “**Get to be a professor**” campaign that promotes this career choice by specific guidance and support.

The activity shall take place as a lively and informative **platform for everyone** such as to encourage physicists, in particular females among them, to pursue an academic career. The event will provide information, and it shall support the formation of professional networks by getting acquainted to each other. We aim at active contributions from all participants: questions, comments and reports on own experiences are explicitly invited.

Author Index

- A. Bich, Justin DS 26.1
A. Borysenko, Yelyzaveta .. MA 10.3
A. Egger, David HL 5.6
A. Khajetoorians, Alexander .. O 74.5
A. Kolmangadi, Mohamed .. MM 18.11
A. Reus, Manuel CPP 12.47, CPP 12.67
A. Rutten, Bram O 74.5
A. Ryndyk, Dmitry O 29.5
A. Sato, Shunsuke DY 35.1
A. Scheel, Manuel CPP 28.4
A. Shelykh, Ivan HL 15.7
Aarts, Dirk G. A. L. DY 23.8, DY 50.6
Aasen, Adrian TT 31.20
Abadizaman, Farzin MA 6.3
Abajyan, Pavel HL 4.3
Abanin, Dmitry DY 5.4
Abassi, Fatemeh BP 12.12
Abate, Antonio HL 5.4
Abbasi, Fatemeh ..BP 12.6, BP 12.15, BP 12.37
Abbasli, Madad O 42.1
Abbaspour, Leila BP 10.8
Abdala, Paula M. MM 7.4
Abdalbaqi, Shaimaa HL 28.4
Abdani, Simon QI 4.14
Abdelbarey, Doaa DS 25.4
Abdel-Hafiez, M. TT 12.11
Abdel-Hafiez, Mahmoud .. KFM 8.3, MA 9.1
Abdelkawy, Ahmed MM 33.7
Abdelwahab, Anas ..TT 18.8, TT 34.4
Abdelwahab, Ibrahim O 81.1
Abdo, Mohamad O 78.8, TT 15.3
Abdou Ahmed, Marwan .. HL 4.11
Abeln, A. TT 31.8
Abert, Claas MA 19.31
Ablets, Yevhen MA 35.61
Aboue, Jahanfar TT 20.5
Abouelela, Aya MA 35.75
Abou-Ras, Daniel .. HL 25.32, HL 34.3
Abou-Zied, Osama K. CPP 12.58
Abraham, Joyal John .. TT 20.3
Abrosimov, Nicolay V. HL 25.93
Abrosimov, Nikolay V. HL 19.8
Abt, Martin BP 10.4
Abtahi, F. HL 42.2
Abtahi, Fatemeh HL 42.2
Abtahi, Fatemeh alsadat .. DS 20.15
AbuAwwad, Nihad MA 3.1
Abusaa, Muayyad .. MA 30.1, MA 37.1
AbuSara, Hazem MA 3.1
Abushammala, Haneen .. TT 12.13
Abushek, Dmitrii SOE 17.6
Acciai, Matteo TT 7.5
Acet, Mehmet MA 32.1, MA 32.2
Aceves, Uriel MA 30.7
Acharya, Swagata MA 38.4
Achenbach, Tim ..CPP 27.5, CPP 27.6
Achinuq, B. MA 27.1
Acremann, Y. O 68.10
Actas, Ali Can MA 35.34
Adabifiroozjaei, Esmail .. MA 23.1
Adam, Ruth MM 13.4
Adam, Viktor HL 25.60, HL 30.5
Adamantopoulos, Theodoros .. MA 21.8
Adame-Arana, Omar BP 8.9
Adamkiewicz, Alexa O 68.7
Adamsen, Kraen Christoffer .. O 32.5
Adel Aly, Mohammed .. HL 25.16
Adeleke-Larodo, Tunrayo .. BP 26.5
Adelhardt, Patrick TT 21.19, TT 24.7, TT 24.15
Adhikari, Rajdeep MA 21.11
Adhikari, Ronjooy .. DY 28.2, DY 40.3
Adibi, Elaheh TT 21.28
Adler, Peter MM 7.4
Adnan, Mohammad .. HL 30.30
Ado, Ivan MA 18.4
Aeschlimann, Martin MA 8.8, MA 19.50, MA 25.5, MA 25.8, MA 35.19, MA 35.27, MA 35.28, O 2.2, O 5.4, O 9.12, O 16.2, O 17.6, O 33.1, O 59.4, O 68.6
Afanasyev, Dmytro HL 13.8, O 9.13
Agar, Joshua KFM 14.6
Agarwal, Naman MA 25.2
Aggoune, Wahib DS 14.2
Aghassi-Hagman, Jasmin .. TT 31.15
Agradidis, Clio Efthimia .. TT 39.6
Agudo-Canalejo, Jaime .. BP 8.7, BP 26.5, DY 3.8, DY 31.9
Aguirre, Andrea O 51.3
Agustsson, S.Y. O 68.10
Agustsson, Steinn Ymir .. O 63.5
Aharonovich, Igor QI 4.41
Aharon-Steinberg, Amit .. TT 7.6
Ahkmerov, Anton O 51.2
Ahles, Sebastian O 6.2, O 14.2
Ahmadi, A. HL 2.3
Ahmadian, Nahid DS 20.18
Ahn, Taehong O 51.7
Ahrens, Heiko BP 17.4, CPP 33.4, CPP 45.6
Ahrens-lwers, Ludwig O 31.2
Ahrling, Robin HL 25.33, HL 25.34
Aiboudi, Oumaima O 32.8
Aiello, Gaetano ..KFM 18.3, KFM 25.10
Aizpurua, Javier O 35.6
Ajay, Akhil HL 3.9, HL 3.10, HL 12.4
Ajdari, Mohsen O 40.2
Akashdeep, Akashdeep .. MA 22.1, MA 35.1
Akay, Melda CPP 1.11
akbarian, ziba O 13.4
Akhmetov, Vladimir .. O 40.1, O 79.2
Akhmetshina, Tatiana .. MM 3.9
Akhmina, Polina CPP 12.53
Akhundzada, Sapida .. MA 19.2, MA 27.5, MA 35.47, MA 35.64
Akimov, Ilya A. HL 5.2, O 35.5, O 37.8
Akerman, Quinten HL 30.32
Akerman, Quinten A. HL 5.7
akkoush, alaa O 48.1, O 58.1
Akmaz, Necmettin E. HL 12.9
Ako Khajetoorians, Alexander .. O 19.3
Alam, Shahidul ..CPP 1.3, CPP 12.60, CPP 12.62, CPP 12.63
Aland, Sebastian ..SYSM 1.2, BP 4.4, BP 10.7, CPP 7.5
Alarab, Fatima DS 20.36
Albar, Esra Ilke O 37.3
Albe, Karsten MM 20.5, MM 23.5, MM 30.3, MM 33.2
Albers, Christian .. DS 20.14, KFM 6.2, KFM 25.11, KFM 25.13
Albers, Tony DY 45.3
Albert, Romain QI 4.33
Alberti, Tommaso .. DY 8.10, DY 18.6, SOE 6.10, SOE 10.6
Albertini, Franca MA 42.4
Alberts, Garrelt QI 13.2
Albes, Tim HL 4.3
Albons Caldentey, Llorenç .. O 53.1
Albons, Llorenç O 44.8
Albrecht, Florian O 62.8
Albrecht, Manfred MA 21.10, MA 28.7, MA 35.9, MA 35.23, MA 35.25, MA 39.3
Albrecht, Martin DS 14.2, HL 14.3
Albrecht, Steve HL 5.4
Albrecht, Tim TT 29.6
Albus, Marie-Irene .. DS 20.19, O 12.4
Aldarawsheh, Amal MA 37.1
Aldosari, Haya CPP 1.3
Alemani, Tilman Diego SOE 5.1
Alemayehu, M. B. TT 30.17
Alemayehu, Rekiukua DS 20.52
Al-Eryani, Aiman .. TT 16.10, TT 21.29, TT 21.30
Alessandretti, Laura Maria ..SYSO 1.2
Aletsee, Clara O 42.5
Alexakis, Alexakis E. CPP 18.3
Alexander, Aji O 3.2, O 44.8, O 53.1
Alexander, Demianenko .. HL 28.3
Alexander, Lichtenstein .. TT 38.4
Alfaro, Gabriel BP 12.51
Alff, Lambert MA 22.4
Alfken, Jette BP 9.4, BP 12.54, BP 17.6
Alfonsov, Alexey .. MA 14.8, TT 12.10, TT 20.2, TT 20.3
Al-Ghattami, Eklas CPP 12.58
Al-Hamdo, Hassan MA 19.59, MA 35.50
Ali, Ahmed BP 7.19
Ali, Khadiza O 26.4
ALI, SAJID QI 8.3
Ali, Syed Yunus .. DY 24.6, DY 44.7
Aligia, Armando A. TT 34.10
Alijani, Farbod DY 12.3
Alim, Karen BP 7.15, BP 10.1, BP 10.5, BP 12.5, BP 12.34, BP 12.36, BP 12.46, BP 12.47, DY 52.4, SOE 20.4
Alimi, Kayode. L. DS 20.25
Alirezaeizanjani, Zahara .. BP 12.55
Aljaseem, Farouk HL 30.12
Aljic, Ervin HL 30.34
Alkaales, Mohanad HL 25.57
Allan, Milan P O 58.14
Allegretti, Francesco O 62.9
Allen, Rosalind J. BP 12.18
Allerbeck, Jonas .. HL 21.6, O 18.19
Allgaier, Jürgen CPP 33.1
Allgeier, S. TT 31.8
Allison, Morgan C. MM 7.4
Alloidi, Giuseppe MA 42.4
Allwang, Johannes CPP 44.3
Al-Maskari, Saleem ..CPP 12.58
Almeida, Trevor .. MA 2.2, MA 19.27
AlMutairi, AbdulAziz .. O 9.10, O 16.9, O 48.9
Alonso Orts, Manuel HL 10.11
Alonso-Orts, Manuel DS 20.6, DS 26.1, DS 26.2
Alouani, M'ebarek MA 19.35
Alova, Anna BP 14.10
Alpin, Kirill TT 25.5, TT 25.7
Alqurashi, Maryam CPP 1.3
Al-Shamery, Noah O 12.8
Alten, Fabian MA 27.3
Althammer, Matthias .. MA 19.41, MA 22.2, MA 34.4, MA 35.6, MA 35.7, MA 35.35, MA 35.37
Althobaiti, Wejdan CPP 1.3
Althouon, Tim TT 29.2, TT 29.3
Altimiras, Carles TT 37.7
Altland, Alexander TT 11.2
Althaler, Markus KFM 14.1
Alu, Andrea O 37.5, O 37.7
Álvarez Herrera, Pablo A. ..CPP 44.3
Álvarez-Garrido, Fabián DY 34.5
Amado Montero, Mario .. TT 7.8
Amador, Raymond O 29.6
Amann, Julia HL 6.7, HL 29.5
Amann-Winkel, Katrin .. CPP 18.1, HL 5.5
Amari, Houari DS 14.2
Amati, Matteo O 52.7, O 52.8
Ambacher, Oliver DS 2.2, DS 9.2
Ambrosio, Francesco .. HL 18.11
Ameri, Tayebbeh CPP 1.1
Americo, Stefano O 42.4
Amersdorffer, Ines HL 25.23
Ames, Benedikt DY 44.12
Amiri, Aboutaleb BP 27.3
Amiri, Behnam BP 22.9
Amit, Tomer DS 17.5
Ammon, Maximilian .. O 5.6, O 54.9
Amsalem, Patrick O 32.7
Amsharov, Konstantin .. O 40.1
Amsharov, Konstantin Y. .. O 79.2
Amundsen, Morten TT 29.5
An, Zhao HL 12.10, HL 15.2
Anand, Aman CPP 1.7, CPP 12.60, CPP 12.62
Anchutkin, Gordei ..DY 46.18, DY 46.18
Andergassen, Sabine TT 16.10, TT 21.29, TT 21.30, TT 26.7
Anders, André O 13.9
Anders, Daniel DS 21.1, HL 40.3
Anders, Frithjof B. MA 28.10, MA 38.3
Andersen, Brian M. .. TT 3.4, TT 22.4
Andersen, Christian K. QI 13.11
Andersen, Christian Kraglund TT 37.5
Andersen, Mie O 8.1, O 62.4
Anderson, Harry O 64.3
Anderson, Lennart DY 35.4
Andleeb, Shaista O 18.14
Ando, Yoichi MA 31.4, MA 31.7, MA 35.74, TT 18.3, TT 20.4, TT 32.7, QI 13.9, QI 13.10
Andre, Doreen MM 4.5
Andreas Wilde, Marc MA 27.11
Andreasson, J. HL 21.2
Andreasson, Jakob .. HL 13.3, HL 13.9, O 16.1
Andreotti, Bruno SYSM 1.1
Andres, Georges ..SOE 5.2, SOE 12.4
Andrienko, Denis CPP 28.7
Andrieu, Stéphane MA 9.2
Andriushin, Nikita TT 21.9
Anggara, Kelvin O 13.2, O 69.6
Anghel, Sergiu HL 2.2
Anglès Munné, Gerard .. QI 6.10
Ångqvist, Mattias MM 10.28
Angrick, Christoph O 82.3
Anhäuser, Sebastian .. CPP 12.55, CPP 39.1
Anjum, Taseer HL 25.66
Ankerhold, Elias HL 25.29
Ankerhold, Joachim .. MA 35.5, O 7.8, O 80.6, TT 7.3, TT 15.4, TT 20.6, TT 26.7, TT 26.9, TT 31.4, TT 37.6, TT 37.7, TT 37.8, QI 5.3
Annegarn, Marco CPP 17.18, CPP 34.2
Annett, James F MM 23.3
Anniés, Simon MM 8.9
Ansari, Mohammed Suhail .. O 17.11
Anselmetti, Dario .. BP 7.37, BP 12.49, BP 12.66, MM 18.16, MM 18.17
Anson, Christopher E. MA 19.22, MA 26.2
Anstett, Martin MA 35.19
Anton, A.M. CPP 12.71
Antoniadis, Nadia Olympia ..HL 2.5
Antón-Solanas, Carlos .. DS 17.4, HL 11.8, HL 15.4, HL 15.7, HL 20.6, QI 7.9
Antrack, Tobias DS 20.3
Antunes, Goncalo DY 16.7
Anwander, Emanuel CPP 12.68
Anwar, Md Shadab MA 4.3
Anwar, Shadab MA 4.2, MA 4.4
Anyfantis, Dimitrios MA 35.51
Ao, Lingyi KFM 8.3
Aoki, Dai TT 22.11
Aouane, Othmane DY 4.1, DY 4.2, DY 23.6
Apellaniz, Iagoba QI 8.8
Apetrei, Teodor O 8.5
Apfelbeck, Fabian CPP 12.15
Apfelbeck, Fabian A.C. ..CPP 12.13, CPP 20.4, CPP 37.6
Apfelbeck, Fabian Alexander Christian HL 6.4
Appel, Heiko ... O 37.3, O 58.1, O 78.2
Appel, Stephan HL 25.65
Appelt, Wilhelm H. TT 21.33
apriili, marco TT 10.2
Aprojanz, J. O 25.3
Apsite, Indra CPP 7.5
Arab, Arian O 73.9
Aradi, Bálint .. O 58.6, O 58.7, O 58.8
Aramberri Del Vigo, Hugo Imanol MM 23.2
Aranson, Igor S. DY 50.4
Arapan, Sergiu MA 32.8
Ardavan, Arzhang O 63.4
Ardenghi, Andrea HL 18.5
Arefi, Hadi O 5.5
Arefi, Hadi H. O 74.11
Aretz, Joost TT 22.3
Arima, Taka-hisa KFM 2.4
Arita, Ryotaro TT 22.9
Arjariya, Richa O 15.7
Armbrüster, Marc O 45.1
Armer, Melina CPP 19.3, CPP 19.5
Arndt, Hans-Dieter CPP 17.2
Arndt, Mira MA 35.70, O 55.9
Arndt-Staufenbiel, Norbert .. O 13.8
Arneth, J. TT 12.11
Andergassen, Sabine MA 9.1
Arnhold, Lukas O 71.6
Arnold, Florian HL 7.6
Arnoldi, Benito .. O 9.12, O 16.2, O 17.6
Aron, Marcel DY 39.5
Arora, A. MA 35.24
Arora, Himani HL 11.10
Arrighi, Everton TUT 2.2, HL 1.2
Artacho Cortés, Emilio .. O 51.10
Artacho, Emilio O 80.1
Artuk, Kerem HL 5.11
Artuykhin, Sergey .. HL 33.10, MA 11.8, MA 15.6
Arunakiri, Kumarahgiri DS 20.25
Arushi, Arushi TT 30.7
Arzani, Francesco QI 12.8
As, Donat J. HL 21.4
Asadian, Ali QI 9.2
Asaithambi, Aswin HL 31.3
Aschauer, Ulrich O 44.6, O 79.1, O 79.3
Asgari, Mohaddese Sadat .. SOE 17.2
Asgari, Nasrin BP 5.6
Asghari, Ehsan BP 7.37
Ashok, Sanjay MA 8.5, MA 8.9, MA 25.8, MA 35.31, MA 35.32
Ashurbekov, Nazim HL 35.3
Aßmann, Marc HL 30.2, HL 33.5
Aßmus, Christopher QI 4.22
Assaad, Fakher TT 6.1, TT 24.2, TT 34.9
Assaad, Fakher F. TT 6.3, TT 28.3, TT 38.5
Ast, Christian O 57.1
Ast, Christian R. .. O 7.8, O 47.8, O 71.2, O 80.6
Astakhov, Georgy V. HL 19.8, HL 25.41, MA 28.11

Author Index

Astner, Thomas QI 1.4
 Åstrand, Mattias KFM 3.4
 Astvatsurov, Dmitriy A. O 32.3
 Aswartham, S. TT 12.11
 Aswartham, Saicharan MA 14.7,
 MA 14.8, MM 18.37, MM 18.38,
 TT 3.12, TT 12.10, TT 20.3, TT 25.3,
 TT 25.8
 Asyuda, Andika CPP 17.9
 Athanopoulos, Stavros HL 41.2
 Atila, Achraf MM 6.1
 Atkinson, Paola HL 30.10
 Attallah, Ahmed Gamal KFM 3.3
 Atteia, Jonathan MA 13.12
 Attig, Jan TT 21.15
 Attou, Aymen BP 7.17, BP 7.20
 Atxitia, Unai MA 8.4
 Au Yeung, Kwan Ho O 32.8
 Auer, Adrian QI 4.23, QI 6.8
 Auer, Aljoscha TT 29.2, TT 29.3
 Auer, Andrea O 8.1, O 8.2, O 20.6
 Auerbach, Paul CPP 7.5
 Auernhammer, Günter CPP 17.15,
 CPP 20.2
 Auernhammer, Günter K DY 11.9
 Auge, Manuel HL 25.20, KFM 6.1
 August, Sophie-Charlotte BP 7.34
 Aull, Thorsten MA 42.1
 Auth, Thorsten BP 2.2, BP 17.7
 Autier, Carmine TT 25.12
 Auwärter, Willi O 55.1
 Au-Yeung, Kwan Ho O 29.2, O 29.5
 Avdeev, Maxim MA 35.42
 Avdoshenko, Stanislav TT 23.12
 Avdoshenko, Stanislav M. O 80.2
 Avila, J. MM 7.5
 Avila, Jose O 54.1
 Avilov, Ivan BP 12.17
 Awan, Wajid HL 25.17
 Axt, Marleen O 9.11
 Axt, Vollrath Martin HL 26.7, HL 30.46
 Aytuna, Ziyaad MM 13.5
 Aytuna, Ziyaad Talha MM 13.3
 Ayzer, Kartik O 61.2
 Azevedo Antunes, Luis KFM 10.1
 Azhar, Maria MA 10.4
 Azimi Mouoslou, Vahid QI 10.9
 Azizi, Maryam HL 25.44
 Azipour, Sahel BP 2.9
 Azuma, Hikaru KFM 2.7, MM 10.19
 B. Amabilino, David O 29.3
 B. Guedes, E. O 66.2
 Baaske, Martin D. BP 5.6
 Baba, Yuriko DS 20.23
 Babaki, Mehrnaz BP 19.4
 Babbush, Ryan QI 12.5
 Babin, Hans-Georg HL 12.2,
 HL 25.73, HL 25.81, HL 25.86,
 HL 25.6
 Bach, Nora HL 30.49
 Bacher, Andreas TT 27.2
 Bachmann, Jan Timo BP 7.22
 Bachmann, Julien O 45.2
 Bachmann, Michael HL 22.3
 Bachmann, Philipp O 56.1
 Bačić, Vladimir O 58.6
 Back, Christian PLV XI, DS 20.41,
 MA 24.7, MA 28.4, MA 35.14
 Back, Christian H. MA 28.3, MA 35.17
 Bäcker, Arnd DY 35.3, DY 35.7,
 DY 43.3, DY 43.4
 Backes, Steffen TT 8.4
 Backus, Ellen CPP 37.2
 Badami Behjat, Arash O 6.10
 Badarneh, Mohamad MA 15.5
 Badarneh, Mohammad H. A. MA 15.4
 Badenhorst, Chris MA 35.65
 Bader, Rainer BP 7.28
 Badr, Rodrigue CPP 7.8, CPP 17.37
 Badrtdinov, D. O 6.9
 Badrtdinov, Danis I. O 51.4
 Bae, Yujeong MA 26.3, O 47.1,
 O 47.4, O 51.7, O 54.3, O 80.5
 Baek, Euncheon MA 15.2
 Baenitz, M. TT 12.6, TT 23.5, TT 28.4
 Baenitz, Michael MM 23.1
 Baer, Andreas CPP 17.25
 Bag, Soumen DS 25.1
 Bagchi, Mahasweta MA 35.74
 Bagrets, Dmitry QI 4.1
 Bagrov, Andrey MA 30.5, O 53.3
 Bahadorian, Mohammadreza
 DY 52.3, SOE 20.3
 Bahari, Masoud TT 30.8
 Bahmanyar, Sina HL 25.4, HL 25.15
 Bahr, Christian CPP 7.1

Bähr, Mathias DY 45.13
 Bahramy, Saeed MA 17.3
 Baier, Felix O 63.7
 Baier, Thomas CPP 12.43
 Baines, Christopher TT 24.5
 Bajpai, Gaurav BP 8.9
 Bakhchova, Liubov DY 50.9
 Bakkers, Erik HL 25.50, HL 25.77
 Balaganchi Anantha Ramu, Bhargava
 TT 18.7
 Balajka, Jan O 58.11
 Balakrishnan, Geetha MA 17.3
 balashov, timofey O 80.3
 Balasubramanian, T. O 25.3
 Balasubramanian, Vijay BP 6.6
 Baldassarre, Leonetta HL 11.10
 Baldini, Edoardo MA 30.8
 Baldrati, Lorenzo MA 19.62, MA 25.5,
 MA 34.3, MA 35.28
 Balestro, Franck TT 21.22
 Bali, Rantej MA 4.2, MA 4.3, MA 4.4,
 MA 35.36, MA 35.68
 Ballani, Camillo MA 19.45, MA 35.51
 Ballif, Christophe HL 5.11
 Balmes, Aylin BP 12.11
 Balocchi, Andrea HL 20.8
 Baltazar, Samuel MM 20.7,
 MM 33.10
 Baltrusch, Simone BP 7.42
 Balzer, Bizan BP 15.2
 Balzer, Bizan N. BP 15.7
 Balzer, Nico O 61.5, O 61.7, O 74.6
 Bampoulis, Pantelis O 54.14, O 65.1
 Ban, Ivana BP 23.2
 Banda, Jacintha TT 6.6, TT 22.5,
 TT 24.8
 Bandarenka, Aliaksandr O 7.1
 Bandarenka, Aliaksandr S. CPP 48.3
 Bande, Annika CPP 12.26
 Bandyopadhyay, Souvik DY 33.1
 Banerjee, Atreyee CPP 9.3
 Banerjee, Ayan DY 44.13
 Banerjee, Hrishit MM 2.1, MM 14.2
 Banerjee, Somak O 49.6
 Banerjee, Sourish HL 17.3
 Banerjee, Varsha DY 26.6
 Bang, Joohee KFM 8.6
 Bange, Jan Philipp O 2.9, O 9.10,
 O 16.6, O 16.9, O 48.9
 Bange, Jan Phillip O 2.2, O 33.3
 Bange, Sebastian DS 17.6
 Banisch, Sven SYSO 1.3, SOE 14.1
 Bansal, Namrata O 26.1
 Bansmann, Joachim HL 18.2
 Banzserus, Luca HL 29.2, TT 10.5,
 QI 1.2
 Bapari, Sambit MM 17.1
 Bapat, Nikhil MM 10.1, MM 34.5
 Baptist, Anna BP 26.7
 Bär, Christian CPP 33.6
 Bar, M. HL 21.1, HL 33.4
 Bär, Marcus O 45.4
 Bär, Markus DY 39.7, DY 46.7
 Bar, Michael HL 13.9, HL 18.7
 Baranowski, Daniel MA 19.55
 Baranowski, Piotr HL 39.3
 Baratech, Juan HL 19.8
 Barbara, Paola HL 6.9
 Barbour, Andi MA 2.3
 Barcikowski, Stephan MA 35.52,
 MA 39.4
 Barcza, Alexander MA 29.9
 Bäreis, Johannes MM 1.1
 Barends, Rami PLV V
 Bärenfänger, Jan DS 22.6
 Barfüßer, Anja HL 5.7, HL 30.32
 Bargerbos, Arno TT 37.5, QI 13.11
 Bargheer, Matias DS 20.41, DS 20.52,
 HL 30.47, O 78.5
 Bark, Kirsten QI 10.3
 Barke, Ingo BP 7.28, BP 7.42,
 BP 12.43, BP 12.44, DS 5.6, O 17.9,
 O 34.7, O 59.6
 Barkemeyer, Kisa HL 8.6
 Barkhausen, Franziska HL 21.7
 Barlas, Yafis TT 2.10
 Barnasas, Alexandros MA 35.51
 Barnett, Julian O 37.2
 Baron, Elias HL 21.4
 Barreteau, Cyrille MA 38.6
 Barrett, Rhyon O 83.2
 Barros, Eduardo B. HL 33.6
 Barros, Kipton CPP 9.1
 Bärschneider, Toni CPP 1.10
 Bart, N. HL 25.1
 Bart, Nikolai HL 12.1, HL 12.2,

HL 25.67, HL 25.72, HL 30.7
 Bartell, Jason M. MA 2.3
 Bartelmann, Frederik TT 20.1
 Barth, Arnulf TT 31.7
 Barth, Johannes O 62.9
 Barth, Johannes V O 23.8
 Barth, Michael TT 19.1
 Barth, Sven MA 35.11, TT 26.3
 Barth, Valentin TT 29.6
 Barthele, Juri MA 33.2
 Barthele, Patrick QI 1.8, QI 1.10
 Barthelmi, Katja DS 17.5
 Bartkowiak, Maciej MA 6.4
 Bärtil, F. TT 12.6, TT 28.4
 Bärtil, Florian TT 6.6
 Barts, Evgenii MA 33.4
 Bartsch, Christian H. DY 8.2, SOE 6.2
 Bartsch, Heike DS 23.8
 Bartsch, Manfred O 26.2
 Barua, Avijit HL 25.74
 Barua, Sajib BP 7.36
 Barz, Stefanie SYED 1.4, QI 4.14,
 QI 4.26, QI 6.7, QI 7.4, QI 12.9
 Basaric, Farah HL 25.98
 Baschnagel, Joerg CPP 41.3
 Baše, Tomáš O 65.5
 Basermann, Achim BP 2.3
 Bashlakov, Dmytro MM 18.37,
 MM 18.38
 Baßler, Pascal QI 12.4
 Basletić, Mario O 81.2
 Bassallo, Mauricio HL 30.25
 Bassi, Nicolò O 23.9
 Bässler, Heinz HL 41.4
 Basso Basset, Francesco HL 19.2
 Bastiaans, Koen M O 58.14
 Bastianello, Alvisè DY 43.2
 Bastianello, Michele DS 21.1
 Bastonero, Lorenzo MM 33.3,
 MM 33.3
 Basu, Abhik DY 26.4, DY 44.18
 Basu, Nandita CPP 12.16
 Basulto, Guillermo Farias CPP 28.5
 Basute, Joshua L. HL 14.8
 Bätge, Jakob DY 3.9
 Battistelli, Riccardo MA 12.2
 Battes, Katharina VA 2.3
 Battistelli, Riccardo MA 2.1, MA 2.3,
 MA 23.3
 Bauch, David HL 26.4
 Bauch, Fabian CPP 40.3
 Bauduz, Arn HL 25.58, HL 25.83
 Bauer, Alexander G. TT 1.2
 Bauer, Andreas MA 10.6, MA 12.6,
 MA 19.7, MA 27.11, TT 12.3, TT 12.7,
 TT 25.5, TT 25.6, TT 27.8
 Bauer, Anja O 74.1
 Bauer, D. Janka BP 7.27, BP 18.5
 Bauer, Ernst MM 10.9
 Bauer, Fabienne TT 17.3
 Bauer, Gerrit E. W. MA 7.2
 Bauer, Hans G. MA 28.1, MA 28.2
 Bauer, Jonas M. DS 17.6, TT 10.3
 Bauer, Magnus BP 15.1
 Bauer, Michael O 9.4, O 16.7, O 16.8,
 O 33.1
 Bauer, Stephanie HL 17.1, HL 25.62,
 HL 25.70, HL 25.88
 Bauer, Udo O 56.1
 Baul, Upayan CPP 9.6
 Baule, Adrian DY 11.3
 Baum, Peter MA 8.7
 Baumann, Aljoscha MM 8.5
 Baumann, Danny TT 29.16
 Baumann, Johannes TT 19.2
 Baumann, Susanne O 71.6, O 71.7,
 O 71.8
 Baumann, Tim R. BP 12.49,
 BP 12.66
 Baumchen, Oliver SYUK 1.4, BP 3.2,
 BP 10.2, BP 10.3, BP 10.8, BP 12.60
 Baumert, Thomas BP 7.40, HL 30.39,
 HL 30.49, HL 30.50, HL 30.51
 Baumgarten, Lutz DS 20.36
 Baumgartner, Christian TT 3.13,
 TT 10.3, TT 22.7, TT 26.2
 Baumgärtner, Kiana O 55.15, O 68.3
 Bäumli, Christian TT 10.3
 Baunthiyal, Aman DS 13.5
 Bauri, Prashanta DY 44.7
 Bauriedl, Lorenz TT 10.3
 Bausch, Andreas BP 4.3
 Bauters, Stephen MM 18.35
 Bautista Salvador, Amado QI 1.11
 Bayani, Amirhossein HL 23.1, O 18.2
 Bayer, Andreas O 15.2, O 15.4

Bayer, Florian HL 25.41
 Bayer, Johannes HL 25.69
 Bayer, Johannes C. HL 3.8
 Bayer, Manfred HL 2.1, HL 2.4, HL 5.2,
 HL 23.11, HL 25.92, HL 26.9, HL 32.2,
 HL 39.5, MA 14.9, O 35.5, O 37.8
 Bayerbach, Matthias QI 6.7
 Bayliff, Samuel HL 32.1
 Bayo, Djénabou DY 51.3
 Bayrak, Türkan HL 25.68
 Bazarnik, Maciej O 26.6
 Bažiková, Martina HL 22.2
 Bazulin, Daniil E. TT 31.23, QI 4.6
 Beach, Geoffrey MA 34.5
 Beach, Geoffrey S.D. MA 2.3
 Bean, Richard BP 12.54
 Beaulés, Léa DY 23.7
 Beaulieu, S. O 9.5
 Beaume, Cédric DY 34.6
 Beauvois, Ketty MA 42.5
 Becca, Federico TT 39.5
 Becher, Manuel CPP 13.5
 Becherer, Markus MA 35.3
 Bechinger, Clemens BP 6.1, BP 14.1,
 BP 14.2, BP 14.3, DY 3.7, DY 28.6,
 DY 38.2, DY 49.5
 Bechstein, Ralf O 15.3, O 69.2
 Becht, Conny HL 10.3, HL 30.13
 Bechtle, Philip DY 8.9, SOE 6.9
 Becic, Berin BP 7.21
 Beck, Philip MA 9.4, MA 30.2
 Beck, Reinhard MM 7.3, MM 18.13
 Becker, Andreas DS 4.3
 Becker, Conrad O 12.3
 Becker, Julia MM 4.1
 Becker, Jürgen HL 30.9
 Becker, Lara BP 12.64
 Becker, Martin DS 20.44
 Becker, Moritz BP 2.6
 Becker, Nils B. BP 24.3
 Becker, Petra TT 8.6
 Becker, S. MA 19.63
 Becker, Stefan MA 19.16
 Becker, Sven MA 22.1, MA 35.1
 Becker-Bohatý, Petra MA 16.9
 Beckert, Sebastian MA 29.4,
 MA 29.6
 Beckmann, Benedict MA 29.9
 Beckmann, Benedikt MA 19.12,
 MA 19.14, MA 29.7
 Beckmann, Christian O 22.2
 Beckmann, Detlef TT 29.8, TT 30.21,
 TT 30.22
 Beckstein, Michael O 63.7
 Bednarz, Beatrice MA 19.60
 Beenken, Wichard CPP 12.69,
 HL 24.3, HL 24.6
 Beer, Andreas DS 20.27
 Beer, Sebastian DS 20.15
 Beg, Marjan MA 19.10
 Behle, Eric BP 7.18, BP 7.26
 Behler, Jörg SYES 1.3, MM 10.3,
 MM 29.5, O 46.4, O 49.2, O 58.5,
 O 67.4
 Behnami, Mahdi TT 5.3, TT 25.3
 Behner, Gerrit HL 7.3, HL 19.7
 Behovits, Yannic MA 19.47, MA 21.5
 Behrends, Jan TT 1.12
 Behrens, Peter HL 12.9
 Behrens, Silke MA 35.60
 Beigang, René MA 19.53
 Beigelbeck, Roman KFM 10.4
 Bein, Thomas CPP 19.3, HL 5.9
 Beinke, Daniel MM 22.3
 Beinlich, Simeon D. O 8.3
 Bejarano, Mauricio MA 28.11,
 MA 35.8
 Bekemeier, Simon MA 19.37
 Bekir, Marek DY 46.12
 Bektas, Onurcan BP 12.46, BP 12.47
 Bellamy-Carter, Abigail O 29.3
 Bellenbaum, Nils O 17.6
 Bellini, Dom BP 7.16
 Bellmann, Jonas CPP 12.56
 Bellón, Bárbara DS 4.2
 Belmeguenai, Mohamed MA 18.5
 Belova, Irina CPP 17.34
 Belova, Valentina CPP 26.5, O 41.3
 Belyth, Kendra O 70.9
 Belykh, Vasilli V. HL 25.92
 Belzig, Wolfgang MA 13.7, TT 7.2,
 TT 26.7, TT 29.8, TT 29.13, TT 30.6,
 TT 30.12, TT 30.13, TT 30.14
 Ben Mahmoud, Chiheb O 83.7
 Ben Moussa, Firas HL 25.29
 Benckiser, Eva DS 14.1, DS 14.4

Author Index

- Bendias, Kalle SYQM 1.2
Bendixen, Alexandra BP 18.3
Benduhn, Johannes CPP 1.12,
CPP 26.1, CPP 26.2, HL 22.4, HL 28.8
Benedikt, Jiri KFM 11.1
Benediktová, Anna *KFM 11.1
Beneke, Grisca MA 19.30
Benelli, Rebecca *BP 7.30
Benetatos, Panayotis *CPP 9.5
Benfatto, Lara O 44.10
Bengel, Christopher DS 18.1
Benival, Sumit O 40.1
Benka, Georg MA 10.6
Benndorf, G. HL 21.1
Bennecke, Wiebke O 2.2, O 9.10,
O 16.9, *O 33.3, O 48.9
Bennenhei, Christoph *HL 28.7
Benschop, Tjerk O 58.14
Ben-Shalom, Shir MM 30.10
Bensmann, Jannis HL 25.27,
*MA 21.10
Benthin, Frederik HL 8.3, *HL 8.5,
HL 12.10, HL 25.82
Bentkamp, Lukas *DY 34.4
Bentmann, H. O 21.5
Bentmann, Hendrik O 4.1, O 4.2, O 9.1,
O 73.4
Bento, Antonio TT 17.1
Benyoucef, Mohamed CPP 17.32,
CPP 17.33, HL 25.57, HL 36.10
Benz, Sebastian Leonard DS 20.44
Benzinger, Walther CPP 37.5
Bera, Soumya DY 44.19, TT 11.2
Berakdar, Jamal MA 28.1
Berciaud, Stéphane O 18.25
Bercioux, Dario *TT 2.6, TT 7.9
Bereciartua Perez, Pablo J. MM 7.4
Bereck, Franz P. DY 8.2, SOE 6.2
Bereczuk, Andreas *O 82.4
Berencén, Yonder HL 19.8, MA 28.11
Berends, Dennis DS 20.49
Berezovska, Lisa *BP 2.1
Berg, Lukas *HL 3.7
Berg, Sebastian DY 45.13
Bergeal, Nicolas O 44.10
Bergelt, Jason *O 18.12
Bergemann, Nils MM 17.5
Berger, Andreas *MA 14.1, MA 22.3,
MA 22.5
Berger, Christian HL 25.41
Berger, Christoph DS 6.3, *HL 30.16
Berger, Helmut MA 19.6
Berger, Johanna *TT 26.2
Berger, Leopold MM 3.9
Berger, Richard *O 29.7
Berger, Richard K. O 17.2
Berger, Rüdiger CPP 7.3, *CPP 7.4,
CPP 20.6, *CPP 37.2
Berger, Stefan A. *MM 32.2
Bergeret, F. Sebastian O 80.7
Bergeret, Sebastian O 51.5
Berges, Jan *KFM 11.3, *O 11.3
Berges, Ulf O 65.2
Bergman, Anders MA 11.2, MA 25.6,
MA 32.6, MA 38.6, O 53.3, QI 10.9
Bergmann, Anders MA 30.3
Bergmann, Nicolas *O 8.7
Bergmeier, Tim *O 33.2
Béri, Benjamin TT 1.12
Berkels, Benjamin MM 22.6
Berlin, Johannes *MM 3.3, MM 18.9
Berlitz, Benedikt *TT 27.5, TT 27.6
Berman, Samuel *O 23.4
Berman, Yonatan SOE 3.3
Bermejo Morán, Moisés *QI 14.3
Bernardi, Johannes MM 20.4
Berndt, Sebastian TT 31.7
Berner, Rico SOE 12.1
Bernhardt, Annika O 17.12
Bernholc, Jerzy O 21.1
Bernstorff, Sigrid DS 20.50
Bernstorff, Sigrid CPP 12.49,
CPP 20.4, CPP 48.2
Berrod, Quentin MA 26.2
Berroir, Jean-Marc SYQM 1.2
Berry, Dominic W. QI 12.5
Bertel, Erminald O 65.7
Berthier, Estelle BP 19.3
Berthod, C. O 66.2
Bertin, Eric *DY 29.1
Bertok, Eric *TT 34.10
Bertoldo, Fabian QI 8.3
Bertolini, Anna TT 17.1
Bertram, Frank DS 2.3, DS 6.3,
HL 22.9, HL 30.16
Bertram, Jo *DS 28.8
Bertrang, Kevin O 56.3, *O 56.5
Beschoten, Bernd DS 22.8, HL 29.2,
TT 10.5
Besocke, Kai *O 56.6
Bessarab, Pavel MA 15.5
Bessarab, Pavel F. MA 12.12, MA 15.4,
MA 37.9
Best, Andreas CPP 28.3
Best, James P. MM 28.1
Bester, Abderrezak O 18.23
Bester, Gabriel HL 12.8, HL 36.9,
O 18.23, O 18.24
Bestha, Kranthi Kumar *MA 14.7
Beta, Carsten *BP 24.1, DY 46.12,
DY 50.5
Betker, Marie CPP 12.3, CPP 12.59,
CPP 18.3
Bett, Andreas HL 23.10, HL 24.2
Betune, Julia MA 35.65
Betz, Markus HL 2.2
Betz, Nicolaj O 71.6, O 71.7, *O 71.8
Betz, Timo BP 7.2, BP 7.41, BP 12.6,
BP 12.10, BP 12.12, BP 12.13,
BP 12.15, BP 12.17, BP 12.37,
BP 12.39, BP 12.40, BP 19.8,
*BP 22.5, BP 22.8, DY 49.8
Betzold, Simon HL 22.7, HL 41.3
Beugeling, Wouter TT 32.5
Beyazit, Yasin O 2.4, O 16.11
Beye, M. MA 25.4
Beye, Martin MA 31.6, O 68.3
Beyer, André CPP 17.1, CPP 17.3,
CPP 17.4, O 23.5
Beyer, David *CPP 12.10, *CPP 34.1
Beyer, Hauke O 16.7, *O 33.1
Beyer, Joern TT 31.10
Beyer, Jörn MA 33.7, TT 17.2
Beyer, Paul CPP 26.5
Bez, Elena *O 13.9
Bezvershenko, Alla *MA 12.5
Bhadraj, Aman MM 13.3
Bharadwaj, Swaminath *CPP 9.8
Bhardwaj, Aman MM 13.4
Bhardwaj, Atmika *CPP 17.8
Bhaskaran, Lakshmi *TT 8.5
Bhatnagar-Schöffmann, Tanvi *MA 18.5, MA 33.2
Bhatt, Bidisha *CPP 7.7, CPP 12.37
Bhatt, Shalini *O 46.7
Bhattacharya, Ahana HL 11.2,
*HL 42.1
Bhattacharya, Ankita TT 38.1
Bhattacharyya, Komal *DY 52.4,
*SOE 20.4
Bhattacharyya, Shinibali TT 39.3
Bhatti, Daniel *QI 4.26, QI 12.9
Bhayani, Ghata Satish HL 3.5,
HL 12.6, HL 25.78
Bhowmick, Deb Kumar O 33.9
Bhowmik, Arghya *O 43.10
Bhukta, Mona *MA 10.2
Bialek, William BP 24.4
Bian, Baixue *MM 21.8
Bianchi, M. MM 7.5, O 68.10
Bianchi, Marco *O 54.5, O 72.1
Biba, Josef DS 16.3
Biberacher, Werner TT 12.8, TT 21.25
Biberger, Simon CPP 12.42, HL 5.3,
*HL 23.2, HL 30.36
Bibes, Manuel O 44.10
Bich, Justin Andreas *DS 20.6
Bidinakis, Konstantinos *HL 30.33
Biedenweg, Doreen BP 12.16,
BP 12.20, BP 12.23
Bieder, Steffen *DS 20.14
Biedinger, Jan CPP 17.10, *DS 5.2,
KFM 15.3, MA 19.17
Biele, Robert DS 22.1
Bielecki, Johan BP 12.54
Bieler, Mark TT 37.4, QI 4.38
Bieneck, Oliver HL 24.10
Bierhance, Genaro *MA 19.51
Biermann, Klaus HL 36.7
Biersack, Matthias DY 11.1
Bierwagen, Oliver *HL 14.3, HL 18.5
Biesuz, Mattia *MM 24.7
Bigi, Chiara MM 23.1
Bihlmayer, Gustav MA 3.2, MA 11.3,
MA 19.56, *O 13.3, O 48.7
Bilchenko, F. *HL 10.5
Bilchenko, Fedir HL 10.10
Bilgrim Otto Seibertz, Bertwin CPP 12.67
Billinge, Simon J.L. KFM 25.5
Bilmes, Alexander TT 27.5, TT 27.6
Bilous, Oksana DY 11.1
Bimberg, Dieter *PSV III
Bin Anooz, Saud DS 6.4, DS 20.1
Binder, Fabian CPP 12.72, *CPP 12.73,
CPP 12.77
Binder, Michael HL 10.3
Binder, Patrick *BP 24.3
Biniskos, Nikolaos MA 28.12
Birch, Max MA 27.3
Birge, Norman MA 34.5
Birk, Tobias *O 74.1, O 80.2
Birkhold, Moritz *HL 4.6
Birla, Hariom O 74.12
Birnkammer, Stefan *DY 43.2
Birschtzky, Viktor O 27.5
Bischof, Daniel CPP 12.55, *CPP 39.1
Bischoff, Lothar MA 28.8
Bischoff, P. HL 33.4
Bishara, Hanna MM 14.4
Bissolo, Michele HL 42.4
Bista, Pravash CPP 17.31, *CPP 20.1,
CPP 20.6
Biswas, Abin BP 12.24
Biswas, Deep MA 17.3
Biswas, Deepnarayan O 9.2, O 54.1
Biswas, Deepnarayan O 72.4
Biswas, Kalyan *O 79.6
Biswas, Naireeta CPP 1.4
Biswas, Sananda TT 8.4, *TT 22.13
Biswas, Subhajit HL 17.9
Bittel, Lennart *QI 12.3
Bittermann, Lena *TT 1.7
Bittihn, Philip BP 6.3
Bittner, Carina CPP 8.2
Bittrich, Eva CPP 26.2
Bitzke, Erik MM 6.1, MM 10.18,
MM 10.21, MM 10.24, MM 16.3,
MM 34.1
Björk, Jonas O 62.9
Björkman, Torbjörn MA 29.8
Björlig, A. TT 22.1
Black, Maximilian Johannes *O 78.7
Black, Sahara *MM 10.9
Black-Schaffer, Annica M. TT 38.3
Blagojevic, Niklas CPP 17.38,
*CPP 50.2
Blair, Paulina BP 7.3, *BP 7.4
Blakaj, Vjosa *QI 14.10
Blanchoin, Laurent BP 13.10
Blanco, Pablo M. *CPP 12.24,
*CPP 45.4
Blanco-Rey, Maria *O 26.4
Blank, Kerstin G. *BP 18.1
Blankenship, Steven TT 2.10
Blascke, Daniel HL 18.1
Blasco, Eva CPP 39.3
Bläsing, Jürgen HL 18.6, HL 22.9,
HL 30.16
Blasius, Jan *O 45.6
Blatnik, Matthias *O 12.7, O 49.10
Blaurock, S. HL 21.1
Blaurock, Steffen HL 18.7, HL 25.45
Bleibaum, Anton *TT 26.6
Blevins, Brianna DS 23.6
Bley, Michael CPP 9.6
Bleyer, Gudrun *CPP 8.2
Blick, Robert MA 35.65
Blick, Robert h. TT 2.5
Blickberndt, Jan *TT 31.16, TT 31.17,
TT 33.1
Bliem, Roland DS 1.2
Blien, Stefan TT 10.5
Bliesener, Andrea MA 31.4, MA 31.7,
TT 20.4
Blob, Anna *BP 13.7
Bloch, Andreas TT 30.20
Blöchl, Peter MM 7.3, MM 29.5
Blom, Paul W.M. HL 30.33
Blomberg, Sara O 69.5
Blonski, Markus *HL 10.4
Blowey, Phil J. O 40.5
Blowey, Philip O 14.3
Blügel, Stefan HL 33.1, MA 3.2,
MA 8.6, MA 11.3, MA 14.3, MA 14.4,
MA 15.8, MA 19.1, MA 19.56,
MA 20.6, MA 21.8, MA 24.1, MA 24.8,
MA 24.11, MA 27.4, MA 27.6,
MA 28.12, MA 35.13, MA 37.1,
MA 37.2, MA 37.4, MA 37.8,
*MA 38.5, MM 18.3, O 13.3, O 48.7,
TT 10.8, TT 19.5
Bluhm, Hendrik HL 19.10, HL 25.60,
HL 36.2, *O 36.1
Blum, Monika O 70.4
Blum, Volker O 50.2, O 50.4, O 50.9
Blumberg, Johannes BP 12.9
Blumberg, Johannes W. *BP 12.21
Blumenfeld, Raphael DY 46.6
Blundell, S.J. TT 28.4
Boa, Andrea G. MM 18.13
Boatner, Lynn A. O 57.5
Boban, Honey *MA 19.55, O 73.7
Bocaz, Antonia TT 27.3
Bochkarev, Anton *MM 25.2,
MM 31.2, MM 34.2
Bochud, Nicolas MM 35.7
Bock, Douglas J. HL 11.12
Bock, Martin MA 8.2
Bockhauer, Sandor MM 22.1
Bockhorn, Lina HL 25.10, *HL 29.6
Böckle, Raphael *HL 22.2
Bocquet, François C. O 18.5, O 18.6,
O 68.7
Bocquet, Lydéric *PRV II, CPP 18.5,
O 46.2
Bocquet, Marie-Laure O 19.1, *O 31.7
Bocquillon, Erwann *SYQM 1.2
Bodach, Alexander TT 21.3
Böddeker, Thomas J. *BP 8.6
Bode, Matthias O 22.5, O 26.5, O 26.9,
O 40.7, O 71.10, O 73.11, O 82.1
Bodesheim, David *DS 22.1
Bodnar, Stanislav *HL 28.6, MA 21.5
Boeglin, C. MA 25.4
Boehm, Benny MA 4.3
Boehm, M. MA 14.6
Boehme, Hans-Joachim BP 10.7
Boero, Giovanni O 63.4
Boeyens, Julia *QI 2.4
Bogdan, Tabea MA 39.6
Bogdanoff, Nils O 71.5, TT 26.8
Bøggild, Peter O 72.4
Bohatý, Ladislav MA 16.9, TT 8.6
Böhm, Benny MA 35.49
Böhm, Gregor CPP 14.1
Bohm, Sebastian *DY 46.10, *HL 13.4,
*HL 30.42
Böhme, Frank CPP 2.3
Böhme, Hans-Joachim BP 10.6
Böhmer, Anna E. DS 9.1, TT 21.5,
TT 21.8, TT 30.1
Böhmer, Michael CPP 28.6
Böhning, Martin CPP 49.1
Böhnke, Jan *O 9.9
Bohorquez, Laura Teresa Corredor MA 14.7
Bohrdt, Annabelle QI 10.7
Boix de la Cruz, Virginia O 54.14
Boix-Constant, Carla MA 21.1
Bojer, Mareike DY 45.5
Bokdam, Menno HL 21.8
Bökemeier, Sven *DS 20.39
Bolat, Rustem O 5.5, O 13.5
Boldin, Ivan QI 1.11
Boldt, Regine CPP 37.6
Boley, Mario *SYNM 1.2, MM 29.3
Bolkenbaas, Olaf O 41.6
Boll, Torben MM 4.1, MM 4.8,
MM 18.29
Bollmann, Steffen *TT 38.6
Bollmark, Gunnar TT 28.10
Bolotin, Kirill HL 25.29, HL 25.31,
HL 31.4, MA 35.30, O 54.10, O 54.13
Bolotin, Kirill I. HL 11.12, HL 31.1
Bölter, Niklas *TT 28.8
Boltynjuk, Evgeniy MM 30.8
Bölükbaşı, Ismail *HL 25.58, HL 25.83
Bömerich, Thomas *MM 10.12
Bomers, Mario PSV V
Bonafé, Franco O 37.3, O 58.1, *O 78.2
Bonafé, Franco P. O 81.4
Bonalde, Ismarco TT 22.3
Bonanni, Alberta MA 21.1
Bonča, Janez TT 34.6
Bondzio, Laila DS 4.3, MA 19.58,
*MA 35.63
Bonetti, Pietro TT 16.10, TT 21.30
Bonetti, Stefano MA 21.7
Bonfà, Pietro MA 42.4
Bongers, Marian David MM 17.4
Bonifazi, Davide O 55.1
Bonino, Valentina HL 21.11, HL 25.46
Bonn, Mischa *SYUK 1.2, CPP 37.7
Bönsel, Jan Lennart *QI 3.3
Boos, K. HL 2.3
Bopp, F. HL 2.3
Bopp, Frederik HL 30.7
Borchert, James W. *DS 16.3,
HL 25.54
Borchert, Martin *MA 8.3, MA 35.30
Bordács, Sándor MA 40.1
Bordelon, M. M. TT 23.5
Borgmann, Ralf *HL 22.9

Author Index

- Borisenko, Sergey TT 3.11
 Borisov, Andrei G. O 35.6
 Borisov, Vladislav•MA 12.11
 Bork, Sophie•MA 35.22
 Borkenhagen, Benjamin O 30.6
 Born, Philip•DY 11.2, •DY 11.8
 Borne, Vincent•BP 22.6
 Bornscheuer, Uwe T. MA 35.65
 Borregaard, Johannes•SYED 1.3
 Borrelli, Raffaele CPP 1.5, TT 16.9, TT 21.10
 Borsch, Markus HL 13.8
 Börsch, Michael BP 12.31
 Bortis, A. MA 33.6
 Bortis, Amadé KFM 19.1, •MA 11.1
 Börzsönyi, Tamás DY 11.4
 Bosak, Alexei TT 8.2
 Bose, Sougato QI 1.8
 bosse, harald O 13.4
 Bossini, Davide HL 40.6, MA 21.11, MA 28.10, MA 35.21, MA 35.26, MA 38.3
 Bostelmann, Marc•QI 10.4
 Bostwick, Aaron O 72.4
 Both, Jon Henrick O 55.10
 Böttcher, Artur DS 5.1, •O 52.7, •O 52.8
 Böttcher, Jan TT 32.5
 Böttcher, Lukas BP 7.28, •O 34.7
 Böttcher, Philipp C.•SOE 13.2
 Botti, S. HL 25.49, HL 33.4
 Botti, Silvana HL 13.9, HL 20.2
 Bötzel, Steffen•TT 30.3
 Bou Sanayah, Marwan HL 25.90
 Bouaziz, Juba•MA 20.6, •MA 37.4, O 71.3
 Boucher, Richard MA 4.2, MA 35.68
 Bougeard, Dominique HL 40.1, HL 40.5, MA 24.7, TT 30.18
 Bouhon, Adrien DS 19.2, HL 14.4, TT 25.2
 Bounouar, Samir HL 8.6
 Bourgnod, Alexander O 70.1
 Bourianoff, George MA 27.13
 Bourret, Edith KFM 7.3, KFM 7.5, KFM 7.6, KFM 14.6
 Bouvier, Mathilde DS 20.4
 Bovensiepen, U. MA 25.4
 Bovensiepen, Uwe MA 25.7, •O 2.4, O 16.11
 Box, Connor L.•O 46.6, O 50.8, O 61.8
 Boy, Johannes HL 25.89
 Božan, Domagoj BP 3.6, •BP 13.5
 Bozhko, Sergey I. O 23.4
 Braakman, Floris MA 41.4
 Bracht, Thomas HL 8.7
 Bracht, Thomas K. HL 26.7
 Brackmann, Stefan CPP 14.7
 Braden, Markus MA 35.72
 Bradforth, Stephen O 64.1
 Brägelmann, Katharina•HL 33.5
 Brand, Andreas HL 24.2
 Brand, Christian O 16.3, O 18.4, •O 30.2, O 65.1
 Brand, Julia-Sarita MA 35.55
 Brand, Richard MA 19.14
 Brandhofer, Sebastian QI 4.26, •QI 12.9
 Brandl, Hanja•SYSO 1.5
 Brandner, Kay QI 2.2
 Brando, Manuel TT 6.6, TT 6.8, TT 22.5, •TT 24.8
 Brandt, Martin Stefan HL 36.3
 Brandt, Matthias BP 12.6, BP 12.15
 Brandt, Oliver HL 25.66
 Brandt, Robert KFM 6.3
 Brataas, Arne TT 27.11
 Bratek, Dominik•HL 24.5
 Bratschitsch, Rudolf HL 19.9, HL 20.1, HL 25.25, HL 25.26, HL 25.27, HL 30.30, HL 30.48, MA 21.10
 Brauch, Uwe HL 4.11
 Braun, Hendrike BP 7.40
 Braun, Ina•BP 12.12
 Braun, Jürgen O 82.3
 Braun, Tobias MA 32.4
 Braun, Wolfgang DS 9.5
 Braunecker, Bernd TT 11.5
 Brazda, Thorsten HL 25.20, HL 37.2, QI 1.7
 Brechtken, Benedikt HL 12.7, HL 12.10, HL 36.8
 Brede, Mariana MA 8.1, MA 35.20
 Brede, Thomas•MM 9.2
 Bredow, Thomas O 12.8
 Bréhin, Julien•HL 14.2, O 44.10
 Brehm, Lucas BP 7.35
 Brehm, Mario•BP 12.28
 Brehm, Simon•CPP 12.4
 Brehm, Verena•MA 13.5
 Breitbach, David MA 13.8
 Breiterfeld, Juliane O 35.1
 Brem, Matthias HL 25.12
 Brem, Samuel HL 11.8, HL 20.1, HL 20.2, O 9.10, O 16.9, O 33.7, O 48.9, O 68.4
 Bremer, Lucas HL 25.74, HL 30.7, HL 36.10
 Bremerich, Alice O 81.2
 Bremers, Heiko HL 10.12, HL 10.13, HL 30.12, HL 30.17, HL 30.18
 Bremholm, Martin MM 28.2
 Brems, Maarten A.•MA 12.9, MA 19.30, MA 37.7
 Brendel, Lothar DY 3.6
 Brener, Sergey KFM 11.3, TT 12.9
 Brenig, Wolfram TT 5.3, •TT 5.4, TT 23.1, TT 23.8
 Brenner, G. O 68.10
 Brenner, Kilian O 63.2
 Brenner, Maxwell J. MM 12.5
 Breoni, Davide TT 24.11
 Bretel, Rémi O 5.8
 Brett, Calvin CPP 18.3
 Brett, Calvin J. CPP 1.8, MA 41.5
 Breuer, Tobias CPP 39.1, DS 5.4, O 12.1
 Breuer, Uwe HL 22.5
 Breunig, Oliver MA 35.74, TT 18.3
 Brida, Daniele HL 21.6, HL 22.10, HL 32.6
 Briega, Valentin O 20.4
 Brieger, Raphael•QI 3.2
 Briesenick, Simon DS 20.47
 Briggs, Emil O 21.1
 Briggs, Nathalie DS 22.2
 Brill, Lorenz•O 34.6
 Bringa, Eduardo MM 33.10
 Brink, Jeroen van den TT 5.2
 Brink, T. MM 21.7
 Brink, Tobias MM 3.5, •MM 3.6
 Brinker, Manuel MM 18.34, MM 35.7
 Brinker, Sascha MA 37.1
 Brinkop, Achim Theo•BP 9.6
 Briones, Johan MA 8.9, MA 35.32
 Brison, Jean-Pascal TT 22.11
 Brixner, Tobias O 61.3, O 82.5
 Broch, Katharina CPP 39.2, CPP 39.4
 Brockhagen, Bennet CPP 17.10, KFM 15.3
 Brockmann, Dirk•SOE 11.1
 Broedersz, Chase BP 19.3
 Broedersz, Chase P. BP 12.3
 Broekhoven, Rik O 47.6, O 47.7, •O 51.2
 Bronsch, Wibke O 9.2
 Brooks, Charles KFM 7.2
 Broqvist, Peter O 58.6
 Bröring, Martin DS 20.19
 Brorsson, Joakim MM 10.28, MM 18.2
 Brosda, Nico HL 25.37, •HL 25.77
 Brotons-Gisbert, Mauro TT 7.7
 Brousseau-Couture, V. HL 21.12
 Brown, Timothy•O 14.3
 Brown, Tom SOE 13.2
 Brozyniak, Aleksander MA 30.4
 Bruchmann-Bamberg, Vitaly DS 20.33, DS 20.37, •DS 20.40, MA 35.41
 Brückel, Thomas MA 28.12, MA 33.2, MA 40.3, TT 25.11
 Bruckhoff, Mike J.•O 2.8
 Brückl, Hubert KFM 10.4
 Bruckmeier, Lukas•O 9.6
 Bruckmoser, Niklas QI 4.6, QI 4.34, •QI 4.35, QI 4.36, QI 4.37, QI 4.39
 Brückner, David•PRV III
 Brüderl, Georg HL 10.2
 Brumm, Jannik MA 35.41
 Brumm, Pauline O 58.13
 Brumme, Thomas•DS 17.1, HL 25.13, MM 35.1
 Brummel, Olaf O 20.1, O 70.2
 Brune, Oliver•HL 24.7
 Bruß, Dagmar QI 4.13, QI 7.3, QI 9.7, QI 9.9
 Bruschi, David Edward•QI 14.5
 Bruss, Dagmar QI 7.2
 Brust, Felix CPP 19.5
 Brütting, Wolfgang CPP 12.75, CPP 12.78, CPP 26.5, CPP 28.7, HL 28.4
 Bryce, Martin O 12.2
 Brydon, Philip M. R. TT 38.1
 Bryja, Leszek HL 11.4
 Buba, Jonas•DY 45.9
 Buca, Dan HL 37.2
 Bucher, Dominik MA 19.28
 Bucher, T. HL 42.2, O 81.6
 Buchgeister, J. HL 4.7, •HL 4.9
 Buchheit, Andreas A. TT 16.6
 Buchheit, Andreas Alexander•TT 16.5
 Buchholz, Sven S. HL 7.7
 Buchinger, Quirin•HL 19.5
 Buchleitner, Andreas DY 5.6
 Büchler, Hans Peter•QI 10.1
 Büchner, B. MA 20.4
 Büchner, Bernd BP 7.29, DS 20.34, MA 5.3, MA 14.8, MA 31.5, MA 35.59, MA 35.73, MM 18.37, MM 18.38, MM 35.1, TT 3.12, TT 5.3, TT 12.1, TT 12.10, TT 20.2, TT 20.3, TT 21.23, TT 25.3, TT 29.16
 Büchner, Carsten CPP 19.3
 Buck, Jens MA 31.6, O 18.21, O 48.10
 Bučko, Tomáš O 83.9
 Buczek, Pawel MA 15.7
 Budde, Jakob QI 7.4
 Budewitz, Andreas TT 32.5
 Budich, Jan Carl•SYQM 1.3, DY 19.3, TT 11.7, TT 11.10, TT 32.6
 Budinská, B. MA 35.12
 Buechner, Bernd MA 14.7, TT 25.8
 Bühlman, K. O 68.10
 Bühlmeyer, Hanna•O 32.5
 Buhmann, Hartmut SYQM 1.2, HL 7.5, HL 25.41, HL 30.47, TT 19.2, TT 32.5, TT 32.8
 Bui, Minh HL 25.20, HL 25.84
 Bukas, Vanessa J. O 31.4, O 31.5
 Bükler, Björn MA 2.2, MA 19.25, MA 19.27, MA 35.63
 Bullerjahn, Jakob T. BP 15.7
 Bullerjahn, Jakob Tómas•BP 15.2, •BP 15.3
 Bültmann, Moritz•DY 46.15, •DY 49.4
 Bulut, Nebahat•MM 18.43
 Bulut, Yusuf•CPP 17.26
 Bulychew, Alexander BP 14.10
 Bunch, David QI 4.35, •QI 4.37
 Bunk, Carolin CPP 2.3
 Bünthe, Judith•MA 19.25
 Bunte, Paula MA 19.16
 Burakovskaya, Alesya O 83.3
 Burger, Carolin•TT 25.6
 Bürger, Felicitas MM 22.3
 Burger, Florian•QI 4.11
 Bürger, Jasmin-Clara•KFM 25.2, •MM 35.10
 Bürger, Julius•DS 1.4, DS 17.7, HL 25.1
 Burghammer, Manfred BP 7.34, BP 9.5
 Burghard, Marko DS 19.1, MA 27.3
 Bürgler, Daniel E. O 5.9
 Burkard, Guido HL 30.43, QI 1.4, QI 1.5, QI 3.4, QI 3.9, QI 10.8, •QI 12.7
 Burkart, Tom•BP 19.1
 Burke, Declan HL 7.4
 Burke, Kieron•SYES 1.4
 Burkel, Eberhard MM 24.4
 Burn, David MA 17.3
 Burwitz, Vassily Vadimovitch MM 4.4
 Buß, Lars O 65.3, O 69.10
 busch, ingo O 13.4
 Busch, Luisa•DS 20.49
 Busch, Mark•CPP 12.39
 Busch, Oliver•MA 8.11, •MA 19.39
 Busch, Ralf MM 30.2
 Busch, Sebastian MM 31.3
 Büscher, Florian•TT 25.10
 Bushati, Rezind MA 30.8
 Bushuev, Pavel QI 5.5
 Buss, Florenz O 79.8
 Busse, Carsten O 42.1, •O 81.2
 Busse, David•HL 25.50
 Busse, Sandra MA 35.49
 Bussmann, Lena•KFM 6.2
 Bütefisch, Sebastian KFM 25.8
 Butt, Hans-Jürgen CPP 7.3, CPP 7.4, CPP 17.13, CPP 17.31, CPP 20.1, CPP 20.6, CPP 28.3, CPP 37.2
 Butté, Raphaël HL 22.5, O 82.7
 Buttenschön, Sönke•O 20.9
 Butterling, Maik•KFM 3.3
 Buttersack, Tillmann•O 64.1
 Büttner, Felix•PRV I, MA 2.1, MA 2.3, MA 12.2, MA 23.3, MA 34.5
 Bykov, E.•MA 29.3
 Bykov, Eduard MA 19.13, MA 29.1
 Bzdusek, Tomáš TT 18.1
 C. Dacanal, Gustavo MM 18.23
 Cacho, Cephise O 33.5
 Cacci, Nils•MA 14.2
 Caddeo, Francesco•DS 13.4, HL 25.79
 Cagliaris, Federico TT 3.12, TT 25.3, •TT 25.8
 Caha, Ondřej O 18.20
 Cahill, David G. MA 15.1, MM 21.1
 Cahlik, Aleš MA 35.58, O 51.1, •O 71.9
 Cahoon, James F. HL 22.2
 Cai, Hao DS 18.1
 Cai, Jiaqi O 42.1, O 81.2
 Cai, Jiming O 79.4
 Cai, Wanhao BP 15.2, BP 15.7
 Cai, Wanzhu CPP 12.74
 Cai, Zhuoyun CPP 7.2
 Caicedo Davila, Sebastian HL 23.7
 Caicedo-Dávila, Sebastián CPP 28.1, HL 5.6, •HL 23.3
 Cakir, Asli•MA 32.1, MA 32.2
 Calarco, Tommaso HL 36.2, QI 5.6
 Calati, Stefano O 16.10
 Calcinelli, Fabio•O 28.8
 Caldas, Lucas de Souza O 52.11
 Caldwell, Joshua D. O 37.5, O 37.6, O 37.7
 Callsen, Gordon HL 25.95, HL 33.8, HL 37.3
 Callsen, Gordon J. HL 37.1
 Caltzidis, Ioannis DS 17.7, DS 20.46, HL 17.8, •HL 25.1
 Calvet, Laurie E. HL 28.2
 Calza, Lorenzo TT 31.7
 Camacho Ibarra, Oscar•DS 20.46, HL 17.8
 Camargo, Chico Q. BP 23.1
 Campanini, Marco KFM 19.3
 Campen, Richard Kramer O 48.8
 Campi, Davide O 6.8
 Campos Micadei, Kaonan QI 12.1
 Canali, Carlo Maria MA 41.3
 Canfield, Paul TT 3.6
 Cangi, Attilia MM 12.9
 Cannavacciuolo, M. MM 7.5
 Canola, Sofia O 55.14, O 74.10
 Canonica, Lucia TT 17.1
 cansever, Hamza MA 4.3
 Cao, Hujun MM 17.5
 Cao, Jiawen O 12.6, O 55.10
 Cao, Nan O 23.8, O 62.9
 Cao, Shixun KFM 10.4
 Cao, Wei CPP 26.3, CPP 48.3
 Cao, Xin•DY 28.6, HL 12.7, HL 12.10, HL 30.9, HL 36.8
 Cao, Yunjun•O 74.8
 Caprini, Lorenzo DY 31.7
 Caputo, M. O 66.2
 Car, Diana HL 25.77
 Carbogno, Christian MM 21.2, MM 29.2, O 11.1, O 50.2, O 67.1, O 83.10
 Carbone, Alessandro•QI 4.27
 Carbone, Dina•MA 20.3
 Carbone, Johanna P. MA 24.2
 Carbone, Maurizio•DY 34.3
 Cardias, Ramon MA 38.6
 Cardillo, Alessio SOE 9.1
 Cardinali, Giulia HL 10.4, HL 10.7, HL 10.9
 Carillo-Aravena, Eduardo O 21.2
 Carinan, Cammille MA 25.7
 Carini, Giulia O 37.5, •O 37.7
 Carleo, Giuseppe DY 43.7
 Carley, R. MA 25.4
 Carley, Robert MA 25.2, MA 25.7
 Carlin, Jean-François HL 22.5, HL 25.95, O 82.7
 Carlucci, Riccardo•SOE 17.3
 Carmele, Alexander HL 8.6, TT 33.4
 Carmesin, Christian HL 25.30
 Carnio, Edoardo DY 5.6
 Carrara, Giacomo•QI 7.3
 Carron, Romain•HL 34.1
 Carstens, Niko CPP 37.3
 Carta, Alberto•TT 12.2
 Cartus, Johannes MM 10.2, O 28.7
 Cartus, Johannes J. O 28.9
 Caruso, Fabio HL 11.3, O 50.5
 Carva, Karel O 18.18, O 18.20
 Casari, Carlo O 40.9

Author Index

- Casiraghi, Giona SOE 12.4
 Caspari, Verena •O 19.9
 Caspers, Juliana DY 3.7, •DY 38.2,
 •DY 49.5
 Cassella, Gino MA 16.4
 Cassini, Chiara BP 7.34
 Castelli, Ivano E. O 44.6
 Castillo-Bodero, Rodrigo O 26.4
 Castro, Alberto •MM 9.4
 Castro, Jose Martinez MA 19.5
 Castro, Silvia O 80.1
 Casula, Michele TT 12.12
 Casulleras, Silvia QI 4.33
 Catalan, Rodrigo •BP 10.2
 Catelani, Gianluigi TT 37.12, QI 13.9
 Cates, Michael E. DY 50.11
 Causer, Grace MA 19.7
 Cavagna, Andrea BP 14.8
 Cavar, Lukas Drago O 19.4
 Cazadilla, Miguel Angel O 51.5
 Cazalilla, Miguel.A O 80.7
 Čechal, Jan O 12.7, O 40.4, O 58.4
 Cedzich, Christopher •QI 6.6, QI 12.4
 Ceirotti, Michele O 43.5
 Cerchez, Mihai HL 7.9
 Cerhan Haink, Asena •CPP 41.2
 Ceriotti, Michele CPP 9.2, DY 51.4,
 O 43.4, O 58.9, O 67.2, O 67.5, O 67.6,
 O 83.1, O 83.7
 Čermak, Patrik O 18.20
 Černá, Lenka O 40.4, O 58.4
 Černoch, Peter CPP 45.4
 Černočová, Zulfiya CPP 45.4
 Černý, Miroslav MA 11.4, MM 6.4
 Cerrata, Andrea CPP 12.9
 Cersonsky, Rose DY 51.4
 Ceruti, Andrea TT 10.5
 Cervellera, Luca •DY 44.17
 Chaabani, Montassar CPP 12.69
 Chacon, Alfonso MA 12.6, MA 19.7
 Chae, Jungseok O 18.9
 Chahshouri, Fatemeh •O 59.8
 Chai, Liraz BP 12.35
 Chai, Ziwei •O 11.4
 Chakrabarti, Prerana KFM 6.3
 Chakraborti, Subhadip •DY 31.5
 Chakraborty, Nilotpal •DY 19.1
 Chakraborty, Poulami •MM 15.2
 Chakraborty, Subrata •TT 30.12
 Chalupa-Gantner, Patrick TT 16.4
 Chamard, Virginie BP 9.5, MA 20.3
 Chan, Clement CPP 8.3
 Chan, Yuk T. TT 39.4
 Chan, Yu-Te •O 82.2
 Chandran, Sivasunder CPP 7.7,
 CPP 37.1
 Chang, Cui-Zu O 21.1
 Chang, Hung-Tzu O 9.3
 Changiarath Sivasadan, Arya •BP 7.14
 Chao, Youchuang •CPP 7.1
 Charlier, Jean-Christophe TUT 2.2,
 HL 1.2
 Charrier, Marie J. •MM 30.3
 Charron, Gaëlle •SYM 15.5
 Charvin, Titouan •MA 35.73
 Chatain, Dominique DS 4.2
 Chaté, Hugues DY 16.3
 Chatterjee, Banhi •MM 23.8
 Chatterjee, Madhumita BP 3.8
 Chatterjee, Rakesh •BP 8.3, BP 26.3
 Chatterjee, Sangam DS 20.44,
 DS 21.1, DS 23.3, HL 6.2, HL 13.6,
 HL 13.10, HL 15.6, HL 32.1, HL 40.1,
 HL 40.3
 Chatterjee, Swarnajit •DY 46.21,
 DY 46.22
 Chattopadhyay, Jayeeta •DY 50.7
 Chattopadhyay, S. TT 20.8, TT 25.9
 Chaturvedi, Raghav •TT 11.8, TT 11.9
 Chatzichrysaifis, Dimos •MA 24.1
 Chatzitzi, Michalis •BP 26.5
 Chaulagain, Narendra CPP 12.54
 Chauraud, Dimitri MM 6.1
 Chava, Phanish HL 25.17, HL 25.19
 Chavez Rojas, Daniel •BP 8.8
 Chávez-García, José M. TT 32.3
 Che, Ping MA 19.6
 Checkelsky, Joseph MA 13.10
 Chehaimi, Omar O 39.2
 Chekhov, Alex MA 19.47
 Chekhov, Alexander MA 21.5
 Chen, Anffany TT 25.12
 Chen, Chuan MA 16.6, TT 21.7
 Chen, Chun-Jen •BP 14.2
 Chen, Hao O 49.10
 chen, hongyan •O 80.3
 Chen, Hongyen O 79.3
 Chen, Hui MM 22.5
 Chen, Ji O 43.6
 Chen, Jie •MM 24.5
 Chen, Ke •CPP 40.2
 Chen, Lijue DS 17.6
 Chen, Lin •MA 24.7
 Chen, Pin-Chuan •DY 45.4
 Chen, Qing •CPP 12.3, CPP 18.3
 chen, shuang •O 30.7
 Chen, Si CPP 1.3
 Chen, Siyu •BP 10.5
 Chen, Wei CPP 12.52, CPP 12.67,
 CPP 26.3, CPP 28.4, CPP 37.3,
 CPP 37.6
 Chen, Wei-Jhong MA 35.38
 Chen, Xi •BP 8.5, O 18.15
 Chen, Xianzhang •DY 19.5, •DY 46.20
 Chen, Xiao HL 20.5
 Chen, Xing-Yu O 12.6, O 55.10
 Chen, Y.-J. O 68.10
 Chen, Yi O 47.4
 Chen, Ying-Jiun MA 30.3
 Chen, Yong O 9.2, O 73.8
 Chen, Ziang •DS 18.1
 chen, zimei •CPP 12.59
 Cheng, Jin-Guang KFM 8.3
 Cheng, Xing CPP 1.11
 Cheng, Yajun CPP 17.27, CPP 27.3,
 CPP 37.3
 Cheng, Yanjun CPP 17.5
 Cheong, Sang-Wook KFM 7.1
 Cherasse, Marie HL 23.6
 Cherepanov, Vasily O 4.3
 Cherevko, Serhiy O 20.4
 Chernyavsky, Dmitry DY 3.4,
 •MM 22.8, TT 11.6
 Chernyshov, Dmitry MA 35.42
 Chesi, Giovanni QI 9.7
 Chhajed, Kartik •BP 27.5
 Chi, Lifeng O 32.7, O 62.9
 Chiang, Cheng-Tien O 73.10
 Chiang, Hsin-Yin CPP 12.7, CPP 45.3
 Chiang, Kuo-Yang CPP 37.7
 Chiappisi, Leonardo CPP 33.5,
 CPP 44.3
 Chiari, Luca KFM 3.3
 Chiarotti, Tommaso •O 11.6
 Chiatti, O. •TT 30.17
 Chiatti, Olivio HL 7.7, HL 25.33,
 HL 25.34, •HL 25.89
 Chicco, Simone MA 42.4
 Chico, Jonathan MA 11.2
 Chikina, A. MM 7.5
 Chimenti, Ada HL 37.2
 Chin, Xin Yu HL 5.11
 Chioncel, Liviu MA 40.1, O 42.3,
 TT 21.33, •TT 28.5
 Chitra, R. DY 12.4
 Cho, Deok-Yong •DS 18.3
 Cho, Franklin H. O 63.4
 Chochos, C.L. CPP 12.71
 Choe, Jungho MM 21.6
 Choeffel, Marisa DS 22.7
 Choi, Deung-Jang •O 80.5
 Choi, E. S. MA 14.6
 Choi, Gyung-Min •SYOP 1.5
 Choi, Heechea •MM 9.1
 Choi, Kwang-Yong MA 9.1
 Choi, Nuri •MM 21.6
 Choi, Taeyoung O 5.3
 Choi, Wonjune •TT 38.2
 Choi, Won-Young MA 19.44
 Choi, Woojae O 9.1
 Chojowski, Robert •BP 3.3
 Chou, Ta-Shun DS 6.4
 Choudhary, A. CPP 12.12
 Choudhary, Akash •BP 14.9
 Choudhary, Ankita HL 12.6, •HL 25.78
 Choupanian, Shiva •DS 1.1, DS 20.31
 Chow, W. W. HL 4.7, HL 4.9
 Chowdhury, Avishek •QI 8.4
 Chowdhury, Mithun CPP 12.16
 Christ, Andreas O 22.5, •O 82.1
 Christen, Jürgen DS 2.3, DS 6.3,
 HL 22.9, HL 30.16
 Christianen, Peter C. M. HL 39.5
 Christiani, Georg DS 14.4
 Christiansen, Dominik DS 20.12,
 HL 31.4
 Christis, Maximilian •O 30.3
 Chrystos, Leon •MM 4.4
 Chu, Hao TT 3.10
 Chu, Weibin HL 23.9
 Chumak, A. V. MA 35.12
 Chumak, Andrii MA 13.2, MA 19.31,
 MA 28.6, MA 35.11
 Chumak, Andrii V. MA 13.8
 Chumakov, Andrei CPP 18.3,
 CPP 19.4, •MA 41.5
 Chuman, Victor •BP 7.45
 Chumokov, Andrei CPP 12.3
 Chung, Ming-Chiang •O 67.8
 Chung, Simon O 54.14
 Churikova, Alexandra MA 34.5
 Chusnutdinov, Sergij O 35.5, O 37.8
 Chyrkin, Anton MM 15.3
 Ciani, Alessandro QI 4.28
 Ciccone, Giuseppe •HL 28.1
 Cichos, Frank BP 7.43, CPP 12.5,
 CPP 49.3, DY 40.2, DY 45.4, DY 46.11
 Cicuta, Pietro •SYUK 1.3
 Cierpinsky, Daniel HL 18.5
 Ciers, Anastasiia QI 5.7
 Ciers, Joachim HL 25.95
 Ciesielski, Richard O 13.1
 Cignarella, Chiara •O 8.8
 Cihan, Ebru •O 39.7
 Cilent, Federico O 9.2
 Cinchetti, Mirko MA 21.11, MA 28.10,
 MA 35.21, MA 35.22, MA 35.26,
 MA 35.70, O 12.5, O 34.8, O 34.9,
 O 42.3, O 55.5, O 55.9, O 68.9
 Cinquemani, Eugenio BP 24.6
 Ciobotea, Elena Ramela •BP 7.40
 Ciola, Riccardo •MA 19.6
 Ciomaga Hatnean, Monica MA 17.3
 Ciorga, Mariusz DS 22.6
 Cisternas, Eduardo KFM 15.6
 Cisternas, Marcelo A. BP 12.50,
 BP 12.51
 Ciuti, Cristiano HL 40.5
 Civita, Donato •O 74.3
 Çivitoğlu, Burak •O 67.9
 Cizek, Rebecca •O 55.8
 Claassen, Martin DY 43.7
 Claessen, Ralph DS 20.28, DS 20.34,
 DS 20.35
 Claramunt, Sara CPP 37.5
 Clarke, Michael •O 29.3
 Classen, Laura TT 10.6
 Claude, Jean-Benoît BP 7.5
 Claussen, Jens Christian •DY 45.6,
 •SOE 12.6, SOE 17.4
 Clementi, Cecilia •SYES 1.5
 Clough, Jessica •CPP 8.5
 Coasne, Benoit CPP 9.9, CPP 18.5
 Cobet, Christoph O 15.6, O 15.8
 Cocchi, Caterina CPP 12.44, •MM 2.6,
 MM 10.27, MM 23.6, O 5.2, O 55.12
 Codutti, Agnese •BP 10.1
 Coen, Sebastian •CPP 12.65
 Coenen, Jan Willem MM 4.10
 Coffey, David O 47.6, O 47.7
 Cohen, Galit DS 17.5
 Cohen, Lesley F. MA 29.6
 Cohen, Yonatan TT 37.12
 Cojocariu, Iulia MA 19.55, O 12.5,
 O 42.3
 Cojocaru-Mirédin, Oana HL 27.3,
 KFM 25.4
 Colazzo, Luciano MA 26.3, O 51.6,
 O 54.3, O 63.4
 Cole, Daniel QI 1.9
 Coletti, Camilla O 2.5, O 2.6, O 2.7,
 O 9.6, O 9.8, O 33.5
 Cölfen, Helmut MM 35.3
 Colin, Remy BP 12.61, DY 16.1
 Collard, Ylona DY 46.16
 Collomb, David O 34.4
 Collura, Mario QI 12.11
 Colombi Ciacchi, Lucio MM 12.1
 Concepción, Omar HL 37.2
 Connolly, Lara •BP 18.4
 Connolly, Malcolm R. HL 7.4, TT 32.3,
 TT 32.7
 Conrads, Lukas O 35.2, O 35.3,
 O 59.3, •O 78.1
 Conroy, Shelly •TUT 3.3, •KFM 1.3,
 •KFM 2.5
 Consiglio, Armando O 21.2
 Constable, Evan MM 10.9
 Constante, Gissela •CPP 7.5
 Constantini, Giovanni O 40.5
 Constantinou, Anna P. CPP 12.32
 Contamin, Lauriane TT 13.3, TT 32.4
 Contreras, Noemi O 6.3
 Contreras, Sebastian DY 8.9, SOE 6.9
 Cop, Pascal O 20.5
 Coppersmith, Susan O 71.7
 Coppey, Mathieu BP 6.7
 Coquelin, Daniel BP 2.3
 Coquinot, Baptiste •O 46.2
 Cordova, Dmitri L. M. DS 22.7
 Corken, Daniel O 74.11
 Cornelius, Steffen DS 20.14
 Cornil, Jerome DS 5.4
 Coronado, Eugenio MA 21.11
 Coronado Miralles, Eugenio DS 20.2
 Corrales, Tomás P. BP 12.50, BP 12.51
 Corredor, Laura MA 31.3
 Corredor, Laura T. •MA 14.8
 Corrias, Marco O 27.5
 Corso, Martina O 80.1
 Cortes, Louis B. G. DY 23.8
 Cosma Fulga, Ion TT 18.7
 Costa, Andreas •TT 26.10
 Côté, M. HL 21.12
 Cottet, Audrey TT 13.3, TT 32.4
 Cotton, Matthew W. BP 8.7
 Coudert, Francois-Xavier O 31.7
 Covre da Silva, Saimon SYED 1.2,
 O 35.8
 Covre da Silva, Saimon Filipe HL 8.1,
 HL 8.10, HL 19.2, HL 22.8
 Cozlin, D. MM 21.7
 Crampton, Andrew O 56.2
 Cremer, Jonas BP 10.1
 Cremer, Julian BP 7.37, •MM 18.16,
 •MM 18.17
 Creutzburg, Marcus O 56.4
 Creutzburg, Nelson HL 3.4
 Cristiani, Georg HL 13.7
 Croitor, Dorina TT 3.5
 Crompton, Anita MM 2.9
 Crosta, Martina O 55.1
 Croy, Alexander DS 22.1
 Cruz-Hidalgo, Raúl DY 11.4
 Csaba, György MA 35.3
 Csanyi, Gabor MM 14.1, MM 34.3,
 O 62.1
 Csire, Gabor MM 23.3
 Čtveráková, Lucie CPP 45.4
 Cubaynes, Tino TT 13.3, TT 29.2,
 TT 29.3
 Cubitt, Robert CPP 44.4
 Cuevas, Juan Carlos O 7.8, O 71.2
 Cugini, Francesco MA 42.4
 Cui, Mengnan •MM 33.4
 Cullip, C. HL 2.3
 Cuniberti, Gianarelio DS 22.1, O 29.2
 Cuni, Nicolas DY 29.1
 Cuoco, M. TT 22.1
 Cuperus, Jan •O 54.8
 Curcio, D. •MM 7.5, O 68.10
 Curcio, Davide O 54.5, O 72.1
 Curtarolo, Stefano MM 12.5, MM 34.9
 Čutuk, Ana HL 4.11
 Cuxart, Marc G. O 55.1
 Cyganik, Piotr CPP 11.2
 Cygorek, Moritz •SYOP 1.1, HL 8.8,
 •HL 30.46
 Czarkowski, Jakub QI 2.3
 Czerner, Michael MA 19.34, MM 6.6,
 MM 10.13
 D. Sheka, Denis MA 10.3
 Da, Binbin •O 5.6
 da Cruz, Miguel O 18.24
 Da Ros, Elisa QI 7.8
 da Silva Pinto, Manoel W. •MM 3.2,
 •MM 30.4
 da Silva, Saimon Covre HL 8.7
 Daddi-Moussa-Ider, Abdallah •BP 4.7
 Dadgar, Armin DS 9.2, HL 22.9,
 HL 30.16
 Daerr, Adrian •SYM 1.5
 Dagar, Janardan CPP 28.5
 Dahmann, Christian BP 3.1
 Dähne, Mario O 69.9
 Dai, Mian •MM 29.4
 Dake, Jules MM 18.29
 Dale, Philip HL 22.10, HL 32.6
 Dalgaard, Kirstine J. MM 28.2
 Dalgaard, Mogens QI 3.6
 Dalgicdir, Cahit CPP 9.8
 Dalla Torre, Emanuele G. TT 33.6
 Dalpke, Raphael CPP 17.3, DS 5.2
 Damanet, François DY 43.5
 D'Amico, Irene •SYUK 2.2
 Damm, Joshua HL 34.5
 Dammann, Lars MM 10.15,
 •MM 18.27
 Danegger, Tobias MA 28.9
 Dang, Linh •TT 18.3
 Dang, Thanh T. •MM 18.13
 Dang, Thien Thanh MM 7.3
 Dangel, Christian HL 12.1, HL 25.72,
 HL 26.6, HL 30.7

- Dani, Keshav•O 68.1
 Dani, Olfa•HL 3.8, •HL 25.69
 Daniel, Rostislav O 43.2
 Danieli, Carlo•DY 26.3
 Danilov, Mikhail TT 38.4
 Daninger, Kevin O 3.3
 Danneau, Romain TT 29.8, TT 30.21
 Dannegger, Tobias MA 8.10, •MA 15.2
 Dannenberg, Simon•BP 12.58
 Danner, Lukas TT 7.3, •TT 31.4
 Danon, Jeroen MA 13.6
 Danu, Bima TT 6.1, •TT 3.8
 Danz, Thomas O 78.5
 Daou, Ramzy MM 21.4
 Daqiqshirazi, Mohammadreza
 DS 17.1, MM 35.1
 Dargasz, Michelle •BP 7.10, BP 12.52
 Dartiaihl, Matthieu TT 13.3
 Dartiaihl, Matthieu C.•SYQM 1.2
 Darvish, Fahimeh CPP 7.3
 Das, Biswajit DY 44.13
 Das, Chittaranjan HL 5.4
 Das, Debarchan TT 6.8
 Das, Hena KFM 7.2
 Das Mohapatra, Bikash•MA 21.2
 Das, Shubhankar MA 15.2
 Dasgupta, Chandan DY 50.7
 Däster, S. O 68.10
 D'Astolfo, Philipp O 79.3
 Datta, Biswajit MA 30.8
 Dau, Huy Tung BP 12.23
 Daum, Lydia•MM 32.1
 Daum, Winfried O 30.6
 D'Aurelio, Simone•QI 6.7
 Davassuren, Bambar KFM 15.7
 David, Alessandro•HL 36.2
 David, C. MA 25.4
 Davide Marenduzzo, Davide•BP 4.1
 Davidkova, K. MA 35.12
 Davies, A. Giles HL 4.3
 Dávila López, Alexandra C.•O 38.3
 Davis, Timothy O 78.3
 Dawley, Natalie DS 20.32
 Day, Christian VA 1.1, VA 1.2, VA 2.1,
 VA 2.2, VA 2.3
 de Abreu, J.C. HL 21.12
 de, Anulekha•MA 19.50
 de Beer, Sissi•SYSM 1.3
 De Beule, Christophe TT 29.9
 De Boissieu, Marc O 66.4
 de Campos Ferreira, Rodrigo Cezar
 •O 55.14
 de Giovannini, Umberto MM 9.4
 de Gois, Carlos•QI 9.8
 de Graaf, Sebastian E. TT 32.3
 De Gregorio, Marco•HL 26.11
 De Groot, F. MA 25.4
 de Heuvel, Jorge BP 2.6
 de Jong, Hidde BP 24.6
 de Jong, Jarn QI 7.2
 de Juan, Fernando O 25.2
 de Kinkelder, Eloy BP 4.4
 de la Rie, Joris•O 5.7
 de la Torre, Bruno O 14.5
 de la Trobe, Yu Alice BP 4.3
 De Liberato, Simone O 37.6
 De Martino, Alessandro TT 2.6
 de Melo, Claudia MA 9.2
 de Oliveira Junior, Alexssandre
 •QI 2.3
 de Oliveira, Mario Malcolms•TT 28.11
 De Pas, Marco O 44.5
 De Renzi, Roberto MA 42.4
 De, Sandip MM 25.4
 de Seze, Elie TT 31.1, TT 31.2
 de Silva, Ranielle Oliveira CPP 12.26
 de Souza Nogueira, Flavio QI 6.9
 De Vasconcellos Lourenco, Rodrigo
 HL 10.13, •HL 30.18, TT 3.8, TT 30.15
 de Vega, Inés QI 4.23, QI 6.8
 de Visser, Anne DS 1.2
 de Vries, Folkert•TT 10.4
 de Vries, Insa•MM 18.1
 de Vries, N. O 25.3
 de Wijn, Raphael BP 12.54
 de Wolff, Timo O 17.5, O 28.6
 Deák, András MA 15.2
 Deak, Peter HL 18.8
 Deald, Cory O 54.1, O 72.4
 Deban, Arne DS 2.3
 Debbeler, Lukas•TT 21.11
 Debnath, Tushar HL 5.7, HL 30.32
 Debot, Alice HL 22.10, HL 32.6
 Debus, Charlotte BP 2.3
 Debus, Jörg HL 11.4, HL 36.5, O 22.1,
 O 22.2
 Deckert, Thomas HL 21.6
 Deconinck, Marielle HL 30.7
 Decurtins, Silvio O 79.1, O 79.3
 Deeb, Mahmoud TT 23.12
 Deffner, Michael HL 39.2
 Degroote, Matthias QI 12.5, QI 12.6
 Degünther, Julius•DY 24.4
 Dehm, G. MM 21.7
 Dehm, Gerhard DS 4.2, MM 3.5,
 MM 3.6, MM 15.4, MM 28.1, O 70.5
 Dehnert, Martin BP 18.3, •CPP 12.6
 Dehnhardt, Natalie HL 32.1
 Dehning, Jonas•DY 8.9, •SOE 6.9
 Deilmann, Thorsten•O 60.1, O 72.3,
 O 72.6
 Deinert, Jan-Christoph TT 3.10
 Deinhart, Victor MA 12.2, O 35.4
 Deisenhofer, Joachim MA 33.3,
 MA 33.4
 Deka, Antaran BP 7.39, BP 10.8
 del Pino, Javier DY 12.4
 Del Re, Lorenzo TT 28.2
 del Valle, Elena HL 8.10
 del Valle, Javier DS 25.1
 Delatowski, Felix-Florian HL 13.9,
 •O 16.1
 Delbecq, Matthieu TT 13.3, •TT 32.4
 Delcea, Mihaela MA 35.65
 Delhomme, Alex DS 17.5
 Delić, Selma•HL 30.10
 Delin, Anna MA 11.2, MA 12.11,
 MA 25.6, MA 38.6, QI 10.9
 Delis, Wassilios•MM 4.2
 Dellago, Christoph MM 10.3
 Deltenre, Kira•MA 28.10
 Dembecki, Marco HL 42.4
 Dementyev, Petr O 8.4, O 23.3, O 23.5
 Demidov, V. E. MA 35.12
 Demir, Johannes•MA 19.16
 Demir, Merve HL 27.4
 Demler, Eugene QI 10.7
 Demming, Maximilian•MM 10.8
 Demming, Maximilian MM 10.7
 Demokritov, S. O. MA 35.12
 Dempewolf, Anja HL 22.9
 Demsar, J. O 68.10
 den Hertog, Martien I. HL 22.2
 Dendzik, M. O 68.10
 Denecke, Reinhard MA 19.7
 Deng, Xin O 20.51
 Dengre, S. MA 4.1
 Denis, Hakan MA 24.4
 Denisenko, Andrej MA 2.4
 Denisova, Ksenia•TT 12.4
 Denker, Christian MA 19.46,
 MA 19.49, MA 35.65
 Denker, Sophia•QI 9.2
 Denner, Michael•TT 18.1
 Denneulin, Thibaud MA 23.4
 Denning, Emil HL 25.91
 Deppe, Frank TT 15.1, TT 29.11, QI 4.5,
 QI 4.23, QI 6.8
 Deppe, Michael HL 21.4
 Derelli, Davide CPP 41.7
 Derenbach, Gabriel O 61.5, O 80.3
 Derendorf, Pascal•TT 21.34
 Dergainlis, Vasilis HL 25.2
 Deringer, Volker MM 33.2
 Deringer, Volker L.•SYES 1.1, O 43.1,
 O 43.7, O 83.6
 Dernbach, Daniel•DY 11.6
 Deschler, Felix CPP 28.1, HL 28.6
 Deshpande, Veeresh HL 17.3
 Desjardins, Matthieu TT 13.3
 Dethloff, Christiane•DS 20.45
 Detlefs, Blanka MM 18.35
 Dette, Holger MM 6.5
 Dette, Ulrike MM 32.2
 Detzler, Skrollan•HL 25.36
 Deuchert, Andreas•TT 9.3
 Deumer, Jérôme•KFM 3.1
 Deussen, Andreas BP 12.45
 Deutscher, Guy TT 30.24
 Devarajulu, Mirunalini O 5.6, O 40.1
 Devereaux, Thomas MA 6.1
 Devi, Parul•MA 27.8
 Devishvili, Anton MA 42.5
 Dewangan, Jayant Kumar•CPP 12.16
 Dey, Amrita HL 5.7, HL 30.32
 Dey, Kaustav TT 12.5
 Dey, Raunak DY 44.13
 Deyrling, André•TT 12.7
 Dhara, Sushovan HL 14.1
 Dheenan, Ashok HL 14.1
 Dhillon, Sukhep S. HL 4.3
 Dhundhwal, Ritika•TT 31.15
 di Battista, Giorgio HL 33.3, HL 40.7
 Di Bernardo, A.•TT 22.1
 Di Bernardo, Angelo TT 3.9, TT 7.8,
 TT 10.9, TT 22.2, TT 29.4, TT 30.10,
 TT 30.11
 Di Carlo, Luca BP 14.8
 Di Dio, Giacomo•BP 12.61
 Di Giovanni, Andras•TT 31.20
 Di Luca, Mario TUT 2.2, HL 1.2
 Di Lucente, Enrico•MM 18.26
 Di Sante, Domenico O 4.1, O 4.2,
 O 21.2, O 73.4
 Di Santo, Giovanni O 82.6
 Dianat, Arezoo DS 22.1
 Diaz Carral, Angel•MM 34.7
 Diaz, Israel•TT 21.27
 Díaz, Sebastián A.•TT 1.11
 Diaz-Granados, Katja O 37.5
 Dichtl, Valentin•HL 30.41
 Dick, Leonard O 45.6
 Dick, Michael•DY 3.5
 Dickbreder, Tobias•O 69.2
 Dickel, Christian TT 32.7, QI 13.9,
 QI 13.10
 Diddens, Christian CPP 7.6
 Diebel, Laura HL 40.5
 Diebold, Ulrike•PLV IV, O 3.3, O 3.7,
 O 3.8, O 10.3, O 10.5, O 10.6, O 16.12,
 O 27.5, O 32.9, O 38.2, O 44.3, O 44.4,
 O 44.7, O 49.4, O 49.10, O 57.5,
 O 58.11, O 58.12, O 63.6
 Dieckmann, Niklas DY 11.5
 Diekmann, Jan•CPP 20.7
 Diekmann, Jonas HL 23.5
 Dielmann, Fabian O 79.8
 Diener, Alexander O 14.4
 Dieplinger, Johannes•TT 11.2
 Dierker, Tim•O 55.6
 Diesen, Elias•O 27.1, O 31.4, •O 31.5
 Diesing, Detlef O 2.4, O 16.11
 Diestelhorst, Elise CPP 17.10,
 KFM 15.3
 Dieterich, Peter BP 12.45
 Dietrich, Fabian•KFM 15.6
 Dietrich, Johannes•MM 32.4
 Dietrich, Siegfried DY 16.7
 Dietrich, Stefan MM 17.4
 Dietzel, Dirk O 39.3, •O 39.6, O 39.7
 Diez, Georg•BP 7.7, BP 15.6
 Diez, Karl Josef CPP 17.3
 Diez-Cabanes, Valentin DS 5.4
 Dil, J. H. O 66.2
 Dimitrova, Anna O 57.2
 Dimou, Aris•KFM 14.4
 Ding, Fei HL 8.3, HL 8.4, HL 8.5,
 HL 12.7, HL 12.10, HL 15.2, HL 25.82,
 HL 25.85, HL 30.9, HL 36.8, HL 39.4
 Ding, Pan CPP 12.15
 Ding, Yong CPP 28.2
 Dinger, Mareike TT 33.1
 Dioguardi, Adam P. BP 7.29
 Dippel, Ann-Christin KFM 25.5,
 MM 18.35
 Dirba, Imants MA 35.61
 Dirin, Dmitry HL 23.11
 Dirksen, Maxim CPP 34.2
 Dirnacher, Alois TT 2.2
 Dirnberger, Florian•MA 30.8
 Dirnböck, Selina•TT 16.11
 Dittmar, M. O 21.5
 Dittmeyer, Roland CPP 37.5
 Dittrich, Guido•CPP 12.38
 Dittrich, Lars DY 46.10
 Dittus, Anna O 34.7
 Ditz, Nikolas DY 38.2
 DiVincenzo, David QI 13.3
 Divinski, S. V. MM 21.7
 Divinski, Sergiy MM 10.7, MM 15.3,
 MM 21.6, MM 21.8, MM 21.10,
 MM 30.8
 Divinski, Sergiy V. MM 10.25,
 MM 20.1, MM 20.2
 Djoumessi, Aurelien Sokeng
 CPP 12.60
 Dobener, Florian HL 32.1
 Dobsch, Daniel MM 32.5
 Döblinger, Marcus HL 3.9
 Döblinger, Markus HL 12.4
 Dobner, Christoph•O 23.7, O 63.7
 Dobrovitski, Viatcheslav DY 5.8,
 QI 2.8
 Dobrovolskiy, O. V. MA 35.12
 Dobrovolskiy, Aleksandr MA 35.11
 Dobrovolskiy, Aleksandr V. TT 2.3,
 TT 26.3
 Dockalová, Lucie O 58.12
 Dodenhöft, Matthias TT 25.5
 Doener, Ali•DY 44.20
 Doerr, Florian O 63.6
 Doerr, Mark MA 35.65
 Doerr, Mathias MA 16.8, TT 23.12
 Doert, Thomas TT 23.12
 Dogan, Susanne DS 20.14
 Dohi, Takaaki MA 10.2, MA 12.9,
 MA 19.30, MA 35.46, MA 37.7
 Dohnalek, Zdenek•O 10.4
 Dolata, Ralf TT 37.2
 Doležal, Jiří O 55.14, •O 74.10
 Doll, Andrin MA 26.3
 Dolling, Daniel Silvan•O 56.4
 Doltsinis, Nikos MM 18.1
 Dolynchuk, Oleksandr CPP 12.70,
 •CPP 41.1
 Dombrowski, Pierre-Martin•O 12.1
 Domenici, Sara•DS 20.48
 Domínguez, Claribel DS 25.1
 Domínguez, Federico•QI 12.1
 Domínguez, Fernando•TT 1.6, TT 1.7,
 TT 29.9
 Domínguez-Adame, Francisco
 DS 20.23
 Domínguez-Celorrío, Amelia O 18.13
 Donarini, Andrea O 28.2, TT 13.1,
 TT 26.12
 Donat Natterer, Fabian MA 35.58
 Donath, Markus O 48.5, O 73.1,
 O 73.2, O 73.3, O 73.5, O 82.3
 Donati, Fabio MA 26.3, O 54.3, O 63.4
 Dong, Chuan-Ding CPP 40.3, HL 32.1
 Dong, Renhao HL 42.8, TT 29.10
 Dong, S. O 9.5, O 68.10
 Dong, Tao TT 3.10
 Dong, Yulian•KFM 15.2, •MM 18.24
 Donges, Andreas MA 8.7, MA 8.10,
 MA 28.9
 Donges, Jan•HL 30.3, HL 36.10
 Donges, Jan-Niklas HL 17.10
 Dönges, Philipp DY 8.9, SOE 6.9
 Donhauser, Anna•QI 3.10
 Donner, Reik•SOE 15.3
 Donner, Reik V.•DY 8.10, •DY 18.6,
 •SOE 6.10, •SOE 10.6
 Donner, Wolfgang MA 19.12
 Donnert, Gerald•BP 9.11
 Donvil, Brecht TT 7.3, TT 20.6, •QI 2.5
 Doppagne, Benjamin O 35.6
 Dorbath, Emanuel•BP 7.9
 Dörrflinger, Patrick CPP 19.3,
 •CPP 28.2
 Dorfner, Maximilian F. X.•CPP 1.5
 Döring, F. MA 25.4
 Dorn, Franziska•BP 12.43
 d'Ornellas, Peru•MA 16.4
 Dornheim, Martin MM 17.5
 Dornheim, Tobias MM 12.9
 Dornseifer, Jan L. MM 21.9
 Dörr, Andreas O 40.1, •O 79.2
 Dörr, Kathrin•CPP 48.1, MA 35.48
 Dorrer, Holger TT 31.7
 Dortaj, Sina•DY 8.5, •SOE 6.5
 dos Santos Dias, Manuel MA 3.1,
 •MA 28.12, MA 30.1, O 72.7
 dos Santos, Flaviano José MA 28.12
 Dos Santos, Gonzalo KFM 15.6
 Dosanjh, Pinder MM 7.4
 Dösinger, Christoph MM 25.8,
 •MM 34.6
 Dossow, Lisa DY 11.2
 Dötting, M.•O 66.2
 Dou, Baoying HL 24.11, •HL 34.4
 Dou, Wenjie DY 3.9
 Douglas-Gallardo, Oscar A. DY 35.5,
 O 32.4, •O 61.8
 Dowinton, Oliver MA 17.3
 Drachev, Vladimir P. MM 12.10
 Drašar, Čestmir O 18.20
 Dratz, Ralf MM 6.10
 Drautz, Ralf MM 15.1, MM 15.3,
 MM 18.14, MM 20.8, MM 23.4,
 MM 25.2, MM 25.3, MM 31.2,
 MM 34.2, MM 34.4, O 83.3
 Drawer, Jens-Christian•HL 15.4
 Draxl, Claudia•SYNM 1.1, DS 14.2,
 HL 11.3, O 50.1, O 50.5, O 50.11,
 O 67.1, O 67.7
 Drechsel, Carl O 79.3
 Drechsler, M. L. HL 4.9
 Drechsler, Monty Leon•HL 4.5,
 •HL 4.7
 Drechsler, Stefan-Ludwig TT 28.6
 Drechsler, Ute TT 37.1
 Dreher, Maximilian•O 12.9

Author Index

- Dreher, Pascal •O 2.10, O 33.8, O 65.1, O 78.3
Dreher, Paul O 25.2, O 48.6
Dreißigacker, Christoph CPP 28.6
Drescher, Jörg CPP 28.6
Drescher, Knut BP 10.4
Drescher, Markus •MA 16.3
Dressel, Martin TT 39.4
Dreuw, Andreas O 40.2
Drevelow, Tim •MA 19.4
Drewes, Jonas CPP 17.26, CPP 37.3
Dreyer, Anna CPP 17.3
Dreyer, Rouven •MA 28.1, MA 28.2, MA 28.5, MA 35.4
Driessens, Kurt O 14.4
Drnec, Jakub O 20.0
Droghetti, Andrea O 42.3
Drossel, Barbara BP 12.64
Drozowski, Oliver M. •BP 22.3
Drucker, Niv TT 37.12
Dsouza, Raynol •MM 31.4
D'Souza, Sunil Wilfred O 73.9
Du, Haifeng MA 27.6
Du, Nan DS 18.1
Duan, Haoran TT 31.15
Duarte Correa, Maria Jazmin DS 4.2, •MM 15.4
Duarte Ruiz, Daniel MM 2.6
Duarte-Correa, Liseth MM 33.5
Dubey, Astita MM 18.13
Dubinina, Tatiana V. O 32.3
Duboisset, Julien BP 9.5
Dubourdieu, Cathrine HL 17.3
Dubourg, Raphaël O 73.8
Dubroka, Adam MA 6.6
Dubs, Carsten MA 13.8, MA 28.3
Duclut, Charlie •BP 22.2, BP 22.4, BP 27.3
Duden, Thomas O 16.3
Dudin, P. MM 7.5
Dudin, Pavel O 54.1
Dudy, Lenart O 9.1
Dudzinski, Alexandra M. •O 31.4, O 31.5
Duesberg, Georg HL 22.3
Duesberg, Georg S. DS 16.3
Dufouleur, Joseph MA 31.5, MA 35.73, TT 3.12, TT 11.8, TT 11.9, TT 25.3, TT 25.8
Dufresne, Eric BP 25.2, CPP 17.41
Dufresne, Eric R. BP 8.6
Duft, Antonia •TT 21.19
Duhamel, C. MM 21.7
Duine, Rembert A. MA 7.4
Düll, Fabian •O 56.1
Düllmann, Christoph TT 31.7
Duncan, David A. O 40.5, O 41.1
Dunin-Borkowski, R.E. MA 20.4
Dunin-Borkowski, Rafal MA 19.1, MA 41.2
Dunin-Borkowski, Rafal E. HL 22.5, MA 23.4, MA 27.6, MM 18.39, O 22.7
Dunin-Borkowski, Rafal Edward O 82.7
Düputell, Christian •HL 36.5
Düputell, Christian HL 25.47
Durdiev, Dilshod •KFM 2.7, MM 10.19
Düreth, Johannes •HL 41.3
Düring, Pia M. •DS 20.36
Dürr, Michael O 30.8
Durst, Simon •O 61.4
Dusabirane, Félix •MA 8.5, MA 35.31
Dusanowski, Lukasz HL 17.7
Düsberg, Felix HL 22.3
Dusel, Marco HL 20.6, HL 41.3
Dutta, Amit DY 33.1
Dutta, Arijit •TT 33.11
Dutta, Bivas TT 11.11
Dutta, Rajesh TT 39.1
Duva, Giuliano CPP 26.5
Düvel, Marten O 2.9
Duvintage, Christopher TT 24.4
Düzel, Birkan •HL 7.2
dvir, tom TT 10.7
Dvoretzky, S. A. TT 20.9
Dvoretzky, Sergey TT 19.3
Dwedari, Magdulim •DY 3.6
Dyakonov, Vladimir CPP 12.72, CPP 12.73, CPP 12.77, •CPP 12.79, CPP 19.3, CPP 19.5, CPP 28.2, HL 5.2, QI 4.41
Dzhagan, Volodymyr DS 23.1, HL 39.1
Dziarzhyski, S. O 68.10
Dzinnik, Marvin J. •HL 12.9
Dzubiella, Joachim CPP 9.6, CPP 9.10, CPP 12.26
E. Faria Junior, Paulo HL 20.4
E, Juncheng BP 12.54
E. Toimil-Molares, Maria CPP 12.3
Ebeling, Daniel •O 6.2, O 14.2, O 40.6, O 41.2, O 79.5
Eberheim, Florian O 20.5
Ebert, Adrian O 23.7
Ebert, H. MA 38.2
Ebert, Hubert HL 5.9, HL 7.10, MA 18.2, MA 24.3, MA 28.13, MA 38.2, MA 38.7
Ebert, Philipp HL 22.5, MA 23.4, MM 18.39, O 22.7, O 69.9, O 82.7
Ebmeier, Florian BP 10.3
Ebrahimi Viand, Roya •CPP 49.6
ebrahimkhas, morad •TT 11.4
E-Castillo, Marianela MM 18.13
Ećija, David O 79.6
Eck, Philipp O 4.1, O 4.2, O 73.4
Eckel, Christian •HL 29.3, TT 29.10
Eckern, Ulrich TT 21.33, AKC 1.2
Eckert, Jürgen MM 30.1, MM 30.5, MM 30.7
Eckert, Marius O 20.5
Eckhard, Jan O 3.4
Eckhardt, Christian J. •MM 9.3
Eckhoff, Marco MM 29.5
Ecksel, Jannis •DY 43.6
Eckstein, Martin TT 34.7
Eda, Goki MA 18.3
Edalatmanesh, Shayan •O 81.1
Edens, Leonard •O 18.13
Eder, Bernhard O 20.6
Eder, Moritz O 3.7, O 3.8, •O 49.4, O 70.4, O 70.6
Eder, Peter DS 16.3
Ederer, Claude •MA 32.3, TT 12.2, TT 39.7
Edler, Simon HL 22.3
Edmondson, Matthew •O 29.4, O 41.1
Edte, Moritz BP 9.2
Edwards, Brendan MA 17.3
Edzards, Joshua •MM 10.27
Efe, Ipek •KFM 14.2
Efetov, Dmitri HL 33.3, HL 40.7
Efremov, Dmitri MM 18.37, MM 18.38
Efremov, Dmitriy TT 25.3, TT 25.8
Efremova, Maria V. MA 39.2
Egelhaaf, Sophie •QI 4.20
Egging, Christian BP 12.31
Egger, David CPP 28.1, HL 24.9, MM 23.7
Egger, David A. HL 23.3, HL 23.7, O 83.9
Eggert, Benedikt MA 4.3, MA 4.4, MA 19.14, •MA 19.15, MA 39.5
Eggert, Thorben O 38.3, •O 38.5
Eggle-Sievers, Benedikt •MM 10.18
Egner, Alexander BP 5.2
Egorov, Aleksei •MM 23.4
Egorov, Oleg HL 20.6
Egunov, Aleksandr I. BP 7.29
Ehgartner, Caroline CPP 17.23
Ehlert, Sascha CPP 33.2
Ehm, Alexander •O 55.7
Ehrens, Julian DS 20.1
Ehrentraut, Lutz MA 8.2
Ehresmann, Arno DS 20.2, MA 19.2, MA 27.5, MA 35.47, MA 35.64
Ehring, Ina CPP 17.18
Ehrler, Jonathan MA 35.36
Ehrler, Rico •MA 22.6
Ehrlich, Jannis •QI 12.2
Ehrmann, Andreas •BP 26.8
Eich, Manfred O 61.6
Eich, Sebastian •MM 6.3
Eich, Sebastian Manuel MM 10.14
Eichel, Rüdiger-A. DY 8.2, MM 8.8, MM 14.3, SOE 6.2
Eichhorn, Johanna CPP 12.65, DS 18.4, HL 24.4, HL 24.9
Eichhorn, Timon QI 5.4
Eichler, Alexander DY 12.4
Eichler-Volf, Anna HL 19.8
Eickhoff, Martin DS 20.6, DS 26.1, DS 26.2, HL 10.11, HL 30.11, HL 42.3
Eigner, Christof HL 33.9
Eilenberger, F HL 42.2, O 81.6
Eilenberger, Falk DS 20.15, HL 15.7, HL 20.6, HL 28.7, HL 42.7
Einfeldt, Sven HL 30.13
Eisebitt, Stefan MA 2.1, MA 2.3, MA 8.2, MA 8.3, MA 12.2, MA 35.30
Eisele, Holger HL 22.5, O 49.3, O 69.9, O 82.7
Eisenlohr, Heike TT 24.4
Eisenmann, L. TT 31.8
Eisenmenger-Sittner, Christoph MM 20.4
Eisenstein, Gadi HL 8.2
Eisert, Jens TT 16.7, TT 33.9, QI 4.8, QI 8.7, QI 12.8, QI 12.10
Eisfeld, Alexander CPP 40.7, DY 45.7
Ejima, Satoshi •TT 33.3
Ekborg-Tanner, Pernilla MM 10.28
El Mard, Asmaa TT 20.7
Elbers, Mirko KFM 6.2
Elbertse, Robbie J. G. O 51.7
El-Gainayni, Nora HL 25.32
Elghandour, A. TT 12.11
Elghandour, Ahmed MA 35.43, •TT 12.5
Elhajhasan, Mahmoud HL 25.95, HL 37.1, •HL 37.3
Elhanoty, M. F. MA 25.4
Eljaouhari, Evrard-Ouicem •TT 6.7
Eller, Fabian CPP 12.21, CPP 12.66
Ellinger, Florian •O 44.4
Elliott, Peter HL 11.12
Elm, Matthias T. •DS 18.2, DS 21.1, HL 25.97
El-Machachi, Zakariya •O 43.7
Elmers, H.-J. O 68.10
Elmers, Hans-Joachim TT 6.10
Elsässer, Christian HL 5.1, HL 19.6, HL 23.1, HL 30.1, HL 36.1, MM 8.1, MM 8.3, MM 8.5, MM 14.3, MM 24.1, MM 24.2, MM 24.3, MM 33.6, QI 12.2
Elsässer, Philipp •DY 38.5
Elsner, Jakob •O 58.2
Elster, Clemens O 7.9
Eltschka, Christopher QI 9.4
Elyas, Khairi F. •O 54.10, •O 54.13
Emamverdi, Farnaz •CPP 49.1
Embrechts, Paul •TUT 4.3, •SOE 1.3
Emerse, Megha •DY 39.2
Emge, Steffen O 43.3
Emmerling, Monika HL 22.7, HL 41.3
Emminger, C HL 21.2
Emminger, Carola •HL 13.9, HL 21.3
Emuna, Moran MM 30.10
Enache, Mihaela O 5.7, O 15.5, O 23.6
Encheva, Mirela CPP 37.2
Enderlein, Niklas •O 6.6
Enders, Axel O 23.7, O 63.7
Enders, Michael MA 35.48
Enekel, Vivien •O 41.8
Eng, Lukas KFM 14.5
Eng, Lukas M. O 37.5
Engel, Dieter MA 8.2, MA 8.3, MA 12.2
Engel, Lena HL 26.3
Engel, R. Y. MA 25.4
Engelhardt, Alexander •TT 12.3
Engel-Herbert, Roman DS 25.2
Engels, Stephan HL 29.2
Engin, Ibrahim HL 25.58
Engin, Ibrahim Azad •HL 25.83
Engler, Thea •KFM 3.2
Engster, Katharina •O 17.9, O 59.6
Engwer, Christoph BP 19.8
Enke, Dirk O 63.3
Ennen, Inga DS 4.3, MA 2.2, MA 19.25, •MA 19.27, MA 19.58
Enniful, Henry R.N.B. •O 63.3
Eninger, Wolfgang MA 29.9
Enss, C. TT 31.8, TT 37.11
Enss, Christian TT 17.2, TT 17.3, TT 17.4, TT 17.9, TT 31.6, TT 31.7, TT 31.10, TT 31.12, TT 31.16, TT 31.17, TT 33.1
Ensslin, Klaus TT 10.4
Eobaldt, Edwin •HL 4.4
Eom, Ki-Tae MM 10.30
Eppers, Daniela TT 24.5
Erb, Andreas TT 12.3
Erbe, A. TT 13.5
Erbe, Artur HL 11.10, HL 17.9, HL 19.8, HL 25.17, HL 25.19, HL 25.68
Erben, Daniel •HL 15.3, •HL 25.30
Erben, Elena BP 3.5, •DY 4.7
Erbes, Elisabeth •CPP 1.4, CPP 18.3
Erbil, Gökyay •CPP 12.7, CPP 45.3
Ercole, Loris MM 2.7
Erdene-Ochir, Otgonbayar •DS 20.10
Eremin, Alexey BP 14.10, DY 4.6, DY 31.2, DY 50.9
Eremin, Ilya TT 21.34, TT 27.3, TT 30.3, TT 30.4
Eremin, Mikhail MA 33.3
Eremin, Mikhail V. MA 14.9
Eremina, R. M. MA 4.1
Ergönenc Yavas, Zeynep HL 21.8
Erhard, Linus •MM 33.2
Erhardt, Andreas CPP 12.70
Erhardt, Jonas DS 20.28
Erhart, Andreas DS 13.1
Erhart, Paul MM 7.2, MM 10.28, MM 18.2, MM 21.1
Erik G. C. P., van Loon TT 38.4
Eriksson, Fredrik MM 7.2, MM 18.2, •MM 21.1
Eriksson, Jakob TT 7.5
Eriksson, O. MA 25.4
Eriksson, Olle KFM 8.5, MA 11.2, MA 12.11, MA 19.35, MA 23.6, MA 29.8, MA 30.5, MA 32.6, MA 32.7, MA 37.5, MA 38.6, O 53.3, QI 10.9
Erk, Hermann O 9.4, •O 16.8
Erkenov, Shamil TT 12.8, •TT 21.25
Erlingsson, Sigurdur I. TT 18.6
Ermonait, Lasse •HL 19.11
Ernst, Arthur MA 15.7, MA 34.6
Ernst, Karl-Heinz O 55.16
Ernst, Marcel •BP 7.11
Ernst, Sven HL 36.4, TT 17.5, TT 17.6, TT 17.7
Ernstorfer, R. O 9.5, O 68.10
Eroms, Jonathan DS 22.6, •HL 6.7, HL 25.21, HL 29.5
Er-raji, Oussama HL 23.10
Errea, Ion O 25.2
Ersfeld, Klaus BP 7.35
Ersfeld, Manfred DS 22.8
Ertel, Benjamin DY 24.5, •DY 44.2
Ertler, Christian QI 12.1
Erzberger, Anna BP 6.2
Esat, Taner O 5.5, •O 64.2
Esch, Friedrich O 69.3, O 70.1, O 70.3, O 70.10
Eschenlohr, A. MA 25.4
Eschenlohr, Andrea MA 25.7
Eschmann, Lukas •O 28.3
Escudero, Carlos HL 5.4
Esin, V. E. MM 21.7
Eskandari, Mohammad Amin •BP 7.2, BP 7.41
Eskandari, Mohammad Armin BP 12.12
Esmann, Martin HL 11.8, HL 15.4, HL 15.7, •HL 19.4, HL 28.7
Espada Burriel, Silvia •DY 16.1
Espinoza, S HL 21.2
Espinoza, Shirley •DS 23.4, HL 13.3, HL 13.9, HL 21.4, O 16.1
Esposito, Massimiliano •DY 3.2
Essich, Leonard •TT 21.1
Essig, Sarah MA 35.60
Essing, Nicolas MA 14.4
Estabrook, Ian D. BP 12.32, •BP 13.3
Estebanez, Pablo KFM 25.10
Esteki, Elham •QI 1.11
Esters, Marco MM 12.5
Esteve, Daniel TT 37.7
Estrecho, Eliezer •HL 9.3
Etemadi, Ahmad-Reza •HL 11.2
Etzkon, Markus HL 30.17, •O 35.1, O 55.11, TT 3.8, TT 30.15
Euchler, Eric CPP 37.6
Eul, Tobias O 17.6, •O 68.6
Eusterholz, Michael •MM 4.8
Evans, Donald KFM 14.1
Evans, Donald M. KFM 7.3, KFM 7.4, •TT 3.5
Evans, Paul MA 20.3
Everett, Christopher R CPP 12.45
Evers, Eiko HL 2.1, HL 2.4, HL 25.92, •HL 26.9
Evers, Ferdinand DY 44.19, HL 30.40, O 74.4, O 74.6, TT 11.2
Evers, Martin MA 8.7, MA 8.10, MA 28.9
Everschor-Sitte, Karin DY 44.8, DY 45.8, MA 12.3, MA 12.9, MA 27.13, MA 35.16, TT 1.11
Evertz, Simon •MM 28.1
Everts, Lee MM 2.9
Ewald, Björn •CPP 12.56, CPP 12.57
Ewert, Moritz •O 65.3
Ewertowski, Simon HL 30.34
Exner, Daniela O 52.7
Eychmüller, Alexander MM 35.9
Eyre, Lissa HL 28.6
F. Assaad, Fakher TT 8.3
Faber, Christian BP 2.3, •BP 27.6
Faber, Samuel DS 2.4
Fabian, Jaroslav DS 20.26, HL 6.7, HL 15.2, HL 20.4, HL 29.1, MA 24.7, MM 18.6, TT 26.10

- Fabiani, GiammarcoDY 43.7
 Fabrizio, MicheleTT 12.12
 Fabrizio, ErikTT 29.17
 Facio, JorgeMA 31.3
 Facio, Jorge I.MA 18.7, TT 3.12,
 TT 20.2, TT 25.2
 Fackso, StefanO 72.8
 Fadaly, ElhamHL 25.50
 Fadler, Paul•TT 34.7
 Fairuschin, ViktorMM 22.7, O 58.2
 Faist, PhilippeQI 8.7
 Fajman, Christian E.CPP 50.1
 Fakhri, NiktaBP 19.1
 Falch, Ken VidarKFM 6.3
 Falcke, MartinBP 22.9
 Falkenberg, GeraldKFM 6.3
 Falkenstein, AndreasHL 18.5
 Fal'ko, VladimirDS 19.3
 Falkovich, GregoryTT 7.6
 Fall, William•CPP 41.3
 Fallarino, LorenzoMA 22.5, MA 22.7,
 MA 22.8
 Falletta, StefanoHL 24.11, HL 34.4
 Falorsi, FrancescaHL 29.3, TT 2.13,
 •TT 29.10
 Falta, JensDS 13.5, O 52.11, O 65.3,
 O 69.10
 Falter, Christine•QI 1.7
 Falter, DennisHL 20.4
 Falter, JensTT 17.8, TT 31.14
 Faluweki, Mixon•BP 10.9
 Fan, Bo•DY 11.4
 Fan, GuozhengO 58.7, •O 58.8
 Fan, QitangO 5.5, O 12.4, O 12.6,
 O 32.3, O 52.6, O 55.13
 Fan, ZheyongMM 18.2
 Fanciulli, MauroO 73.6
 Fandrich, Pascal•CPP 17.8
 Fandrich, TomHL 8.3, HL 8.5,
 HL 12.10, •HL 25.82, HL 36.8
 Fangohr, HansMA 12.4, MA 19.10
 Fanizza, MarcoQI 6.2
 Fanselow, Benjamin•BP 7.43
 Farajian, Mahboubeh•BP 12.37
 Faranda, DavideDY 8.10, DY 18.6,
 SOE 6.10, SOE 10.6
 Farheen, HennaHL 21.10, •HL 33.9
 faria junior, paulo e.HL 15.2
 Faria Junior, Paulo E.•HL 6.1
 Farinacci, LaëtitiaO 34.3, •O 47.3,
 O 47.6, O 47.7
 Farle, MichaelCPP 45.2, DS 21.3,
 MA 19.23, MA 19.64, MA 32.1,
 MA 32.2, MA 35.34, MA 35.36,
 MA 39.2, MM 13.6
 Farzam, Farnaz•DS 4.2
 Faßbender, JürgenMA 4.2, MA 4.3
 Fasel, RomanO 17.12, O 18.19, O 23.9
 Fassbender, JürgenMA 10.3,
 MA 13.3, MA 21.7, MA 35.8,
 MA 35.68
 Fässler, Thomas F.CPP 50.1
 Fatayer, ShadiO 62.8
 Fathabad, Sobhan M.•KFM 25.1,
 MM 18.13
 Fattuoui, MouadMA 23.5
 Faugeras, ClémentDS 17.5
 Faupel, FranzCPP 37.3, MA 9.3,
 MA 35.62
 Fauseweh, BenediktTT 16.5, TT 16.6,
 TT 34.13, •QI 10.2
 Faust Akl, Dario•O 3.5
 Faustmann, AntonHL 25.98
 Fay, MichaelHL 14.5
 Fecher, GerhardMA 35.40
 Fechner, MichaelMA 33.7
 Federl, Maria-ElisabethO 2.5, •O 2.6
 Federolf, Mathias•HL 20.9
 Fedorov, AlexanderTT 3.11
 Fedorov, ArkadyTT 37.13
 Fedorov, KirillQI 4.34
 Fedorov, Kirill G.TT 27.7, TT 31.23,
 QI 1.3, QI 4.5, QI 4.6, QI 4.7, QI 4.15,
 QI 4.18, QI 4.35, QI 4.36, QI 4.37
 Fedosov, Dmitry•BP 17.7, BP 19.4
 Feeser, Katharina D.O 33.3
 Fehlinger, Sebastian•DY 31.1
 Fehn, NatalieCPP 28.1, •O 13.6,
 O 13.7
 Fehrs, Jan Ole•O 20.4
 Fehske, HolgerTT 33.3
 Feichtner, ThorstenO 35.4
 Feige, Michael•MM 18.40
 Feil, Niclas M.DS 9.2
 Feist, Armin•O 37.1, O 78.5
 Fekri, Zahra•HL 25.17, HL 25.19
 Feld, ArturHL 39.2
 Feld, YannickDY 45.1
 Felde, NHL 42.2
 Feldt, SimonHL 20.4
 Feldmann, JochenHL 4.10, HL 5.7,
 HL 30.32
 Feldmann, LutzKFM 25.7
 Feldmann, Sascha•SYSD 1.1
 Feldt, MilicaO 79.8
 Felekary, Arash•BP 13.11
 Felsen, Frederic•O 69.4
 Felser, C.MA 27.1, TT 20.8, TT 25.9
 Felser, Claudia•PLV II, MA 42.5,
 O 9.4, O 73.9, TT 25.10
 Fendler, CorneliusMA 35.65
 Feneberg, MartinHL 14.5, HL 14.7,
 HL 21.4, HL 22.6, HL 25.40
 Feng, JiaguiMA 17.3
 Feng, KaiDY 16.5
 Feng, Liwen•TT 3.10
 Feng, ShuanglongHL 25.38
 Feng, XinliangO 29.2, O 29.5,
 TT 29.10
 Feng, YaoyuanMA 23.3
 Fenske, MarkusCPP 28.5
 Fenzel, FlorianCPP 12.75
 Feofilova, Maria•BP 25.2
 Ferarri, FrancescoMA 16.7
 Ferchane, Selmane•CPP 40.7
 Ferkinghoff, Gary•TT 34.13
 Fernandes, Imara LimaMA 37.1
 Fernández Herrero, AnalíaO 13.1
 Fernandez Lahore, Rodrigo Gaston
 HL 28.1
 Fernandez, LauraO 26.4
 Fernandez, Lea•DY 44.5
 Fernandez, SaletaO 51.3
 Fernandez Scarioni, Alexander
 TT 37.4
 Fernández-Busnadiego, Rubén BP 9.4
 Fernández-Rico, CarlaCPP 17.1
 Fernengel, Bernd Michael•DY 35.2
 Ferrari, FrancescoTT 39.3, •TT 39.5
 Ferrario, MauroO 39.2
 Ferreira, MárciaSOE 14.4
 Ferreira, RodrigoO 74.10
 Ferreiro lachellini, NahuelTT 17.1
 Ferrero, Julian•HL 25.60
 Ferrero, MichelTT 34.8
 Ferretti, AndreaO 11.6
 Fersch, DanielO 61.3, •O 82.5
 Fery, AndreasCPP 17.15, CPP 20.2
 Fesquet, FlorianTT 27.7, QI 4.5,
 QI 4.6, •QI 4.7, QI 4.15, QI 4.18
 Fetai, Omer•MA 35.16
 Feuerbach, TobiasO 5.4
 Fève, GwendalSYQM 1.2
 Fevola, GiovanniKFM 6.3
 Fey, MelanieHL 13.6
 Feya, OlegMM 18.38
 Feyer, VitaliyMA 19.55, MA 30.3,
 O 12.5, O 42.3, O 55.9
 Feyherm, RalfMA 33.7
 Fidanyan, Karen•O 50.3
 Fiebig, M.KFM 2.3, MA 33.6
 Fiebig, Manfred•TUT 1.1, DS 13.3,
 KFM 2.4, KFM 7.1, KFM 14.2,
 KFM 14.3, KFM 19.1, KFM 19.3,
 •MA 1.1, MA 11.1, MA 25.1, MA 33.5,
 TT 6.4
 Fiedler, Fabian•TT 21.7
 Fiedler, Lenz•MM 12.9
 Figge, StephanDS 26.2, HL 10.11,
 HL 30.11
 Figgemeier, Tim•O 4.1, O 4.2, O 73.4
 Figueiredo, Johannes HL 6.5, HL 6.8,
 •HL 11.5, HL 25.14, TT 7.7
 Fikar, Ondřej•MM 10.23
 Filimonov, Aleksandr•MM 18.36
 Filimonova, Evgenia•CPP 12.23
 Filipiak, Zuzanna hMM 21.3
 Filipová, MarcelaCPP 45.4
 Filipp, StefanTT 31.23, QI 4.6,
 QI 4.34, QI 4.35, QI 4.36, QI 4.37,
 QI 4.39, •QI 13.1, QI 13.5, QI 13.6
 Filser, Jakob•O 46.1
 Findeisen, RolfO 14.4
 Fingscheidt, TimO 17.5, O 28.6
 Finizo, SimoneMA 41.2
 Fink, RainerDS 20.22
 Fink, Rainer H.BP 25.3, CPP 1.11
 finke, birkO 18.4, O 54.4
 Finkler, JonasMM 10.3, O 58.5
 Finley, J. J.HL 2.3
 Finley, Jon J.HL 42.9
 Finley, Jonathan•PLV X, DS 17.5,
 HL 3.10, HL 8.1, HL 11.9, HL 12.1,
 HL 20.3, HL 25.50, HL 25.65,
 HL 25.72, HL 26.6, HL 36.4, TT 17.5,
 TT 17.6, TT 17.7
 Finley, Jonathan J.HL 3.9, HL 8.10,
 HL 15.2, HL 15.5, HL 25.13, HL 30.7,
 HL 42.4, MA 19.28
 Finocchio, GiovanniMA 34.3
 Finsterhoelzl, Regina•TT 33.4,
 •QI 3.9, QI 10.8
 Firlus, Alexander•MM 30.6
 Firouzmandi, Reza•TT 29.16
 Fischer, AlfonsO 22.2
 Fischer, AmmonTT 10.6
 Fischer, AndreasO 13.1
 Fischer, FelixMM 6.3
 Fischer, Franz•O 18.23
 Fischer, I.HL 22.1
 Fischer, Jan•KFM 19.2
 Fischer, JeisonO 18.12, O 18.16,
 O 71.4
 Fischer, LukasBP 18.7, •CPP 18.4
 Fischer, Marisa•CPP 17.15, CPP 20.2
 Fischer, MarkTT 18.1
 Fischer, Mark HTT 22.6
 Fischer, PeterCPP 12.60, •HL 40.6
 Fischer, Ralf•TT 19.3
 Fischer, S. F.TT 30.17
 Fischer, Sabine C.BP 12.57
 Fischer, Saskia F.DS 25.2, HL 7.7,
 HL 25.33, HL 25.34, HL 25.89
 Fischer, ThomasMM 18.42
 Fischer, UtzHL 41.3
 Fischer-Friedrich, Elisabeth•BP 3.1
 Fischer-Posovszky, PamelaBP 12.4
 Fistul, MikhailTT 26.1, TT 27.3
 Fittipaldi, R.TT 22.1
 Fittipaldi, RosalbaTT 22.2
 Fitzky, GabrielHL 40.6
 Fix, MarioMA 21.10, MA 35.25
 Flacke, LuisMA 28.7, MA 35.35
 Flannigan, StuartDY 43.5
 Flaschmann, RasmusHL 36.4,
 TT 17.5, TT 17.6, TT 17.7
 Flathmann, ChristophHL 25.36
 Fleck, Michael•MM 31.5
 Flege, Jan IngoHL 5.4, •O 52.11,
 O 65.3, O 69.10
 Fleig, Philipp•BP 6.6
 Fleischhaker, JohannO 49.6
 Fleischmann, A.TT 31.8, TT 37.11
 Fleischmann, AndreasTT 17.9,
 TT 31.6, TT 31.7, TT 31.12, TT 31.16,
 TT 31.17, TT 33.1
 Flipse, C.F.J.O 25.3
 Flommersfeld, JohannesBP 12.3
 Florian, MatthiasHL 15.5, HL 25.30,
 HL 30.7
 Flötotto, Aaron•HL 24.3, HL 24.5,
 TT 29.15
 Fodor, EtienneDY 16.2, DY 24.1
 Foerster, MichaelMA 35.17
 Foglia, Laura•TT 36.4
 Fokin, NadineMA 35.63
 Folkers, LauraMA 31.3
 Folland, Thomas G.O 37.5, O 37.7
 Fomin, Mykola•BP 7.8
 Fomin, Vladimir M.•TT 2.3
 Fonin, MikhailO 41.8, O 74.1, O 80.2
 Foppa, LucasSYNM 1.2, •MM 25.4,
 MM 29.3, O 62.2, O 70.9
 Förg, Michael•QI 5.9
 Forker, RomanO 17.1, O 18.26, O 34.6,
 O 41.5, O 65.6
 Fornari, C. I.O 21.5
 Fornari, RobertoHL 18.5
 Förner, AndreasMM 18.14
 Forró, LászlóO 54.11
 Forslund, Ola K.CPP 1.8
 Forster, Lea•KFM 2.4
 Förster, StefanO 66.4, O 66.5, O 66.6,
 O 66.7, O 66.9
 Förster, StephanCPP 33.2
 Förster, TobiasTT 22.11
 Forsting, JohannaBP 13.6
 Förstner, JensHL 3.6, HL 21.10,
 HL 26.4, HL 33.9, MM 18.4, O 78.6
 Forti, Mariano•O 83.3
 Forti, StivenO 2.5, O 2.6, O 2.7, O 9.6,
 O 9.8, O 33.5
 Fortmann, JillDS 9.1
 Fortmann, Jonas•O 16.3, O 30.2
 Fortunato, Nuno M.MA 19.12
 Foschino, Eleonora•DY 46.13
 Föslleitner, Elias•MM 10.2
 Foster, Adam S.O 15.3, O 66.8
 Foster, MatthewTT 11.2
 Foster, Simon J.BP 12.18
 Foteinou, VarvaraHL 36.5
 Fowley, CiaránHL 19.8
 Fox, ThomasQI 12.6
 Frabboni, StefanoTT 26.3
 Fraboulet, KilianTT 16.10, TT 21.30
 Fragopoulos, AlexandrosBP 3.2,
 BP 10.2, •BP 10.3, •BP 12.60
 Frahm, HolgerTT 24.12
 Franceschi, GiadaO 3.7, O 3.8,
 O 16.12
 Franceschini, MarcoO 55.1
 Franceschini, PaoloTT 36.3
 Franchini, CesareHL 21.8, O 3.3,
 O 3.8, O 10.5, O 10.6, O 27.5, O 44.4,
 O 44.7, O 49.4, O 57.5, •O 66.1
 Francoual, SoniaMA 19.14, MM 7.4
 Frang Christiansen, EmilKFM 14.6
 Frank, BettinaO 78.3
 Frank, FreimuthMA 19.44
 Frank, György•TT 25.13
 Frank, Jonathan•DS 20.13
 Frank, KilianCPP 39.6, •CPP 41.7,
 MM 18.35
 Frank, Markus•BP 7.42
 Frank, Maximilian•CPP 13.6,
 DS 20.21
 Frank, StienkemeierHL 28.3
 Frank, TobiasMM 18.6
 Frank, Veronika•BP 7.5
 Franke, Florian•BP 10.7
 Franke, Katharina J.O 5.2, O 19.9,
 O 51.8, O 53.4, O 55.12, O 71.5,
 O 80.4, TT 26.8
 Franke, Lars•MA 37.13, TT 24.1
 Franke, SebastianHL 30.4
 Franke, Moritz•O 28.2
 Fransson, Erik•MM 7.2, •MM 10.28,
 •MM 18.2, MM 21.1
 Franz, ChristianMA 19.7, MA 35.54,
 TT 12.7
 Franz, JulianTT 27.7, •TT 31.5
 Franz, MartinO 49.3
 Franz, Maximilian•O 16.4
 Franzka, SteffenMA 32.2
 Fratus, KeithQI 10.3
 Frauendorf, André Philipp•HL 20.7
 Frauenheim, Thomas HL 18.8, O 58.6,
 O 58.7, O 58.8, O 81.4
 frauhammer, timoO 80.3
 Fraupeul, FranzCPP 17.26
 Fraux, Guillaume•DY 44.15, •DY 51.4,
 O 58.9, O 83.1
 Frederiksen, ThomasO 28.2, O 51.3,
 O 80.1
 Freeman, JoshuaHL 4.3
 Fregin, Bob•BP 12.1, BP 12.16,
 BP 12.20, BP 12.23
 Freiburger, Eva Marie•O 18.27, O 52.4
 Freier, ErikHL 30.13
 Freimuth, FrankMA 21.8
 Freire, RafaelMM 20.7
 Freitag, JohannesSOE 7.2, SOE 17.1
 Freitas, RodrigoMM 3.6
 Frej, AntoniMA 25.2
 Frenzel, Jan•BP 18.8
 Frenzel, Maximilian•HL 23.6
 Frenzke, SusannCPP 1.4
 Frese, NatalieCPP 17.10, CPP 17.39,
 DS 5.2, KFM 15.3, O 23.5
 Freter, Lars HL 22.5, MA 23.4, •O 82.7
 Freudenstein, Josef•HL 13.8, O 9.13
 Freund, Martina•MM 4.5
 Frey, BenediktTT 31.17
 Frey, ErwinBP 19.1, BP 19.7, DY 26.4,
 DY 39.8, DY 44.18, DY 50.4
 Frey, Felix•BP 5.7
 Frey, JohannesBP 12.60
 Frey, JurekQI 13.9
 Frey, Martha•O 65.5
 Freychet, GuillaumeCPP 12.21
 Freysoldt, Christoph•HL 24.11,
 HL 34.4, MM 22.2, O 27.2
 Friák, MartinMM 10.26
 Fribiczek, NoraCPP 2.3
 Fricker, DavidHL 25.84
 Friedel, Anna M.•MA 9.2
 Friedrich, PascalMM 22.4, TT 3.7
 Friedrich, Benjamin M.BP 12.32,
 BP 13.3, DY 40.4
 Friedrich, Christoph HL 33.1, MA 38.5
 Friedrich, DanielO 61.3
 Friedrich, Florentine•O 17.1
 Friedrich, JanDY 8.4, SOE 6.4
 Friedrich, Markus S.•MM 21.9

- Friedrich, Niklas O 51.3, O 51.10, O 80.1
 Friedrich, RicoMM 12.5, •MM 34.9
 Fries, Maximilian MA 29.9
 Frisch, Benjamin O 68.6
 Frisch, Johannes O 45.4
 Frisk, Thomas KFM 3.4
 Frison, Ruggero KFM 2.6
 Fritsch, Anatol BP 8.12
 Fritsch, Kilian HL 40.1
 Fritz, Torsten O 17.1, O 18.26, O 34.6, O 41.5, O 65.4, O 65.6
 Fritzsche, Stephan QI 10.6
 Frka-Petecic, Bruno CPP 8.4
 Frohn, Benedikt HL 19.7, HL 36.6, •TT 18.9
 Frohoff-Hülsmann, Tobias DY 46.3
 Froitzheim, Jan MM 15.3
 Frolov, Timofey MM 3.6
 Frömberg, Daniela DY 40.6
 Fromm, Lukas O 6.4, O 79.2
 Frommeyer, Lena •MM 3.5, MM 3.6
 Frömter, Robert MA 10.2, MA 19.44
 Frost, J.M. HL 21.12
 Frosz, Michael HL 15.8
 Fröwis, Florian QI 14.7
 Früh, Johannes QI 4.11
 Frühauf, Dietmar DS 9.3
 Frustagial, Diego TT 2.6
 Frysztacki, Martha Maria SOE 13.2
 Fu, Mengqi DY 12.2, •DY 12.5
 Fuchs, Christian HL 13.6
 Fuchs, Christopher •TT 32.8
 Fuchs, Dirk TT 31.15
 Fuchs, Dominik TT 17.1
 Fuchs, Jacob TT 19.1
 Fuchs, Lorenz TT 3.2, TT 3.13, TT 10.3, TT 22.7, TT 26.2, TT 30.18
 Fuchs, Matthias DY 38.2
 Fuchs, Maximilian •CPP 14.1
 Fuchs, Robert •HL 30.4
 Fuchs, Timo O 20.4
 Fuhrmann, Felix •MA 22.1
 Fuhrmann, Jürgen O 8.8
 Fuhrmann, Sindy KFM 6.2
 Fujinami, Masanori KFM 3.3
 Fulga, Cosma MA 18.7, TT 11.8, TT 11.9
 Fulga, Ion Cosma MM 23.9, TT 18.5, TT 25.2
 Fuller, Chloe MA 35.42
 Fünfingerlings, Achim •O 49.9
 Furchner, Andreas DS 23.6, MA 8.2
 Fürsich, Katrin DS 14.4
 Fürst, Lena HL 7.5, HL 25.41, TT 32.8
 Furuta, Kanji •HL 25.77
 Fusek, Lukáš O 3.2, O 20.1, O 70.2
 Fyta, Maria MM 34.7
 G G V Dias da Silva, Luis TT 1.4, TT 20.10
 G. Gopakumar, Thiruvancheril •O 74.12
 G Idrisov, Edvin TT 20.10
 G. Schlom, Darrell DS 26.1
 Gabaj, Šimon •O 67.7
 Gabriel, Vít O 16.12
 Gadelmeier, Christian MM 20.1
 Gader, Hardik BP 7.36, CPP 12.74
 Gaerner, Maik •MA 5.1
 Gaertner, D. •MM 21.7
 Gagel, Philipp HL 22.7
 Gagliardi, Alessio HL 32.4
 Gahl, Cornelius HL 11.12, HL 25.29, O 9.9
 Gaida, John MA 23.3
 Gaida, Michael •QI 14.9
 Gail, Michael HL 10.9
 Gaiser, Niklas •TT 37.6
 Galante, Mario DY 44.12
 Galazka, Zbigniew O 49.3
 Galazka, Zbigniew DS 6.4, DS 14.2, HL 18.5, HL 25.33, HL 25.34
 Galbierz, Vanessa KFM 6.3
 Galeotti, Gianluca •O 6.5
 Gali, Ádám MA 2.4
 Galifi, Emanuelle O 37.5
 Galindez Ruales, E. F. MA 15.2
 Galindez-Ruales, E.F. •MA 19.63
 Galla, Tobias •TUT 4.2, •SOE 1.2, •SOE 5.4
 Gallardo, Aurelio •O 14.5
 Gallardo, Laura •MM 10.16
 Gallardo, Rodolfo MA 19.36, MA 22.7
 Gallardo, Rodolfo MA 4.3
 Gallei, Markus •CPP 8.1
 Galler, Bastian HL 10.3
 Galli, Davide Emilio QI 4.27
 Gambardella, Pietro O 47.2, O 47.5
 Gamer, Lisa TT 31.6
 Gammelgaard, Lene O 72.4
 Gammer, Christoph MM 8.4, MM 20.1
 Gan, Z HL 42.2, O 81.6
 Gan, Ziyang HL 6.4, HL 25.21, HL 42.7, O 65.4
 Gandhi, Poshika •DY 23.3
 Gandorfer, Simon •QI 4.15, QI 4.18
 Ganesh, Panchapakesan O 21.1, O 81.3
 Ganichev, Sergey HL 33.3, HL 40.7
 Ganichev, Sergey D. HL 40.4
 Ganschow, Steffen DS 20.32
 Ganswindt, Patrick HL 32.3
 Ganzella, Marcelo BP 9.4, BP 17.6
 Gao, Hao •O 41.3
 Gao, Lei O 79.4
 Gao, Timm HL 17.10, •QI 7.9
 Gao, Xiang O 39.4
 Gao, Yongxiang DY 50.6
 Gappa, Dominik •CPP 13.5
 Garai, Abhiji TT 17.1
 Garbarino, Gaston TT 21.6
 Garcia, Alejandra MM 33.10
 Garcia-Goiricelaya, Peio •O 50.10
 Gardner, Geoff TT 26.2
 Gardner, Geoffrey TT 22.7
 Gardner, Geoffrey C. TT 3.13
 Gardner, James •DY 35.5, O 32.4, O 74.11
 Garg, Manish O 7.4, O 7.5
 Gargiani, Pierluigi MA 23.3
 Gariglio, Stefano DS 25.1
 Garmroudi, Fabian MM 10.9
 Garner, Andrew J. P. QI 14.1
 Garvoet, Jan KFM 6.3
 Garro, Ane O 51.5, O 80.7
 Garst, Markus •SYQM 1.5, MA 10.4, MA 19.6, MA 27.11, MA 37.3, MA 37.13, TT 1.5, TT 24.1
 Gärtner, Martin TT 31.20
 Gashnikova, Daria O 70.8
 Gaspar Quarenta, Mario A. MA 7.4
 Gastaldo, L. TT 37.1
 Gastaldo, Loredana TT 31.7
 Gatti, Teresa DS 16.1
 Gattinoni, Chiara •HL 14.8
 Gatto, Salvatore TT 7.10
 Gaub, Hermann BP 15.1
 Gauger, Erik M. SYQP 1.1, HL 8.8, HL 30.46
 Gault, Baptiste MA 23.1, MM 14.4, MM 15.2, MM 22.2
 Gaultois, Michael W. MM 10.6
 Gauzzi, Andrea TT 12.13
 Gavra Edo, Miguel DS 20.2
 Gawel, Przemyslaw O 64.3
 Gaydamachenko, Victor •TT 37.2, QI 4.38
 Gayen, Diptesh •CPP 9.10
 Gazibegovic, Sasa HL 25.77
 Gazizullin, Ilias •O 17.7
 Gazzadi, Gian Carlo TT 26.3
 Ge, Jianfeng O 58.14
 Ge, Yuqing MA 37.7
 Gebauer, Julian MM 4.8
 Gebauer, Richard TT 37.12
 Gebert, Aaron O 5.4
 Gebhardt, Julian •HL 5.1, HL 23.1, MM 8.3, O 6.4
 Gebhardt, Marius CPP 26.5
 Geburt, Sebastian HL 18.1
 Geck, Jochen MA 16.10, MM 7.4
 Geelhaar, Lutz HL 25.66
 Geers, Patrick •O 48.5
 Geese, Andre O 78.5
 Geesmann, Fridolin O 19.5
 Gegenwart, Philipp TT 21.15
 Gehle, Sven MA 19.37
 Gehr, Simone BP 7.23, BP 12.22
 Gehrig, Jonas CPP 12.56
 Gehring, Helge HL 25.27
 Gehrke, Kai DS 20.49
 Gehrman, Christian HL 5.6, HL 23.3, HL 23.7
 Gehrman, Sascha •TT 24.12
 Geib, Tobias QI 6.6
 Geibel, Christoph TT 6.6, TT 6.8, TT 24.8
 Geier, Philipp MA 19.45
 Geiger, Christina CPP 44.4, CPP 50.1
 Geiger, Daniel DY 4.4
 Geiger, Sophie •BP 12.41
 Geilen, Moritz MA 35.9
 Geilenkeuser, Julian BP 12.59
 Geirhos, Korbinian MA 33.1
 Geis, Clemens CPP 26.4
 Geisel, Theo •SOE 8.1
 Geisert, Simon TT 31.1, •TT 31.2, TT 31.3
 Geishendorf, Kevin MA 34.7
 Geisler, Benjamin DS 14.4, •O 83.5, •TT 22.8
 Geisler, Claudia BP 5.2
 Gekle, Stephan BP 3.7, BP 12.2, BP 12.14, CPP 17.36, DY 34.1
 Geldiyev, Begmuhammet O 4.2, •O 73.4
 Gelen, Ismet O 54.7
 Gelin, Maxim F. CPP 1.5
 Geller, Martin HL 3.1, HL 3.4, HL 8.9, HL 25.2, HL 25.59, HL 25.63, HL 26.10
 Geller, Martin P. HL 26.8
 Geller, Shawn QI 1.9
 Gellert, Florian •BP 17.4
 Gellert, Manuela BP 12.23
 Gemmer, Jochen DY 19.4
 Gemming, S. TT 13.5
 Gemming, Sibylle HL 25.19
 Geng, Zhansong O 18.21, O 48.10
 Genreith-Schriever, Annalena •MM 14.2
 Gensch, Marc CPP 18.3, CPP 37.3
 Genuzio, Francesca O 65.3, O 69.10
 Genzow, Meike BP 12.43
 George, A. HL 42.2, O 81.6
 George, Antony DS 20.27, HL 6.4, HL 25.17, HL 25.21, HL 42.7, O 65.4
 Georges, Antoine TT 34.8
 Georgeta, Salvan HL 28.5
 Georgiev, Y. HL 22.1
 Georgiev, Yordan M. HL 17.9, HL 25.87
 Georgiou, Theoni K. CPP 12.32
 Geprags, Stephan MA 19.40, MA 20.3, MA 34.4, MA 35.7, MA 35.35, MA 35.37
 Gerami, Adeleh M. MM 18.13
 Gerardot, Brian TT 7.7
 Gerasimenko, Y. A. O 9.5
 Gerasimenko, Yaroslav O 33.7, O 68.4
 Gerasimova, N. MA 25.4
 Gerasimova, Natalia MA 25.2, MA 25.7
 Gerber, Iann C. HL 20.8
 Gerber, Simon •O 7.7
 Gerdau, Rolf-Werner TT 37.4
 Gerhard, Lukas DS 5.1, O 61.5, •O 61.7, O 74.6
 Gerhard, Marina CPP 12.55, CPP 14.7, CPP 39.1, CPP 39.2, HL 25.16
 Gerhard, Nils HL 4.1
 Gerhard, Holger BP 12.26
 Gericke, Dirk O. O 33.4
 Gerland, Ulrich DY 39.6, DY 45.5
 Gerlinger, Kathinka MA 2.1, MA 12.2
 Germann, Timothy CPP 9.1
 Gernhäuser, Roman CPP 28.6
 Gerritsen, Jan W. O 51.4
 Gersdorf, Sophie DS 9.6
 Gerstel, Miriam •CPP 17.32
 Gerstmann, Uwe DS 20.8
 Geske, Michael O 62.6
 Gessert, Denis •DY 26.5
 Getzlaff, Mathias O 56.6, O 70.5
 Gewinner, Sandy O 44.5
 Geyer, Dominik •DY 23.6
 Geyer, Philipp •MA 7.1, MA 28.5
 Gezmis, Afra O 15.2, •O 15.4, O 45.9
 Ghabboun, Jamal MA 24.2
 Ghaderzadeh, Sadegh O 72.8
 Ghadiri, Zahra SOE 15.1
 Ghaebi, Omid •HL 29.4
 Ghahari, Fereshte TT 2.10
 Ghan, Simiam •O 46.3
 Ghanbarnejad, Fakhteh •DY 52.2, SOE 9.1, •SOE 15.1, •SOE 17.2, •SOE 20.2
 Ghara, Somnath KFM 7.4, KFM 14.1, MA 33.1, •MA 33.4
 Gharabeiki, Sevan •HL 34.7
 Ghardi, El Mehdi •MM 2.9
 Ghassemzadeh, Reyhaneh •HL 30.1, •HL 36.1
 Ghebretinsae, Bereket TT 21.4
 Ghidelli, Matteo DS 4.2
 Ghim, Minsu •MM 12.3
 Ghiringhelli, Giacomo TT 3.3
 Ghiringhelli, Luca O 67.1
 Ghiringhelli, Luca M. MM 25.4, MM 29.2, MM 34.10, O 62.7
 Gholivand, Amirreza •BP 25.4
 Ghorbani-Asl, Mahdi MM 34.9
 Ghosal, C. O 41.7
 Ghosal, Chitran DS 20.8, O 18.7, •O 18.8, O 18.14, •O 25.6, O 25.7
 Ghosh, Debadrita •BP 5.2
 Ghosh, Pratyay •MA 16.1
 Ghosh, Sayantan •HL 17.9
 Ghosh, Sheuly •MM 25.6
 Ghosh, Subhrokoli •O 39.5
 Ghosh, Sumit •MA 8.6
 Ghosh, Supriya O 26.8
 Ghrayeb, Mnar BP 12.35
 Giamarchi, Thierry TT 28.10
 Giannakou, Marios •CPP 17.35
 Giannetti, Claudio •TT 36.3
 Giantomassi, M. HL 21.12
 Giantomassi, Matteo HL 25.44
 Giardina, Irene BP 14.8
 Gibertini, Marco MA 11.7
 Giebel, Friederike QI 11.1
 Giebel, Michael A. CPP 50.5
 Giegerich, Thomas VA 1.1, VA 2.1
 Gierss, Peter •HL 4.11
 Gierz, Isabella O 2.5, O 2.6, O 2.7, O 9.6, O 9.8, O 30.5, O 33.5
 Gieß, Aaron •HL 30.15
 Gies, C. HL 4.7, HL 4.9
 Gies, Christopher DS 17.2, HL 4.5, HL 19.3, HL 30.7, QI 5.8, QI 10.4
 Gieschen, S. O 68.10
 Giessbil, Franz Josef O 82.4
 Giessen, Harald O 78.3
 Giessibl, Franz O 20.6
 Giessibl, Franz J. O 4.4, O 21.3, O 57.3, O 57.4
 Giessibl, Franz Josef O 22.8, O 74.9
 Gietl, Hanns MM 4.10
 Giger, Michael MA 11.1
 Gigli, Lorenzo •O 43.4, O 43.5
 Gil-Fuster, Elies QI 12.8
 Gilkes, Joe •O 83.2
 Gillen, Roland DS 20.9, HL 18.5, HL 25.14, O 6.6
 Gilles, Ralph CPP 12.14, CPP 17.28
 Gillig, Matthias TT 25.3
 Gimperlein, Matthias •DY 46.17
 Ginot, Félix •DY 3.7, DY 38.2, DY 49.5
 Giovannini, Mauro TT 24.8
 Giraldo, M. •KFM 2.3, •MA 33.6
 Giraldo, Marcela KFM 7.1
 Girard, Martin BP 8.8, •BP 17.5, CPP 41.6
 Giraud, Romain MA 31.5, MA 35.73
 Gires, Pierre-Yves BP 26.6
 Giri, Gouri S. QI 1.10
 Girnghuber, Anna HL 13.8
 Giron, Stefan MA 23.1
 Girones Paya, Paula •BP 7.12
 Giroto, Antoine •BP 3.2, BP 10.2, BP 10.8
 Giroto, Nina O 11.3
 Gittinger, Moritz HL 28.7
 Gizer, Gokhan MM 17.5
 Gkouzia, Georgia MA 22.4
 Glaab, Johannes HL 10.1, HL 10.6
 Gladrow, Jannes DY 40.3
 Glancy, Scott QI 1.9
 Glasenapp, Christian •TT 2.5
 Glaser, Niklas QI 4.39
 Glaser, Niklas J •QI 13.5
 Glaser, Timo •O 30.8
 Glass, Joyce TT 31.17
 Glatzel, Fabian DY 49.7
 Glatzel, Thilo O 17.10, O 22.6
 Glatzel, Uwe MM 20.1
 Glazov, Mikhail M. HL 40.4
 Gliga, Sebastian •MA 10.1, MA 41.2
 Glittenberg, Marvin •O 19.6
 Gloskovskii, Andrei •MA 35.40
 Glück, Lorenz KFM 7.4
 Glukhov, Konstantin MM 18.13
 Gmelch, Max CPP 27.5
 Gmitra, Martin DS 20.26
 Gnavarro, Gema O 22.6
 Gnecco, Enrico CPP 12.62
 Gnedel, Maximilian MM 3.1
 Go, Dongwook MA 21.8, MA 24.1, MA 24.2, MA 24.8, •MA 24.11, O 26.1
 Gobeil, Jeremie O 47.6, O 47.7
 Göbel, Borge •MA 12.10, MA 19.39, MA 37.12, O 44.10
 Göbel, Sophie •O 20.3, O 20.5
 Godara, Prakhar •SOE 5.1

- Godinho, João MA 29.6
 Goedecke, Julia J. MA 35.71
 Goedecker, Stefan O 58.5
 Goehring, Lucas BP 10.9, •DY 34.6, DY 39.2
 Goennenwein, Sebastian T. B. MA 7.2, MA 8.10, MA 28.9, MA 29.4, MA 29.6
 Goennenwein, Sebastian Tobias
 Benedikt MA 34.7
 Goerbig, Mark-Oliver MA 13.12
 Goering, Eberhard DS 14.4
 Goerlitzer, Eric CPP 8.2
 Goerzen, Moritz A. •MA 37.9
 Göggelmann, Alexander •TT 31.10
 Goh, Segun •BP 14.5, •CPP 2.2
 Göhler, Fabian DS 20.29, •DS 22.7
 Gohlke, Holger •BP 2.4
 Göhls, Beatrix MM 4.10
 Goian, Veronica •DS 20.32
 Goings, Joshua J. QI 12.5
 Goirand, Florian •BP 12.65
 Gökce, Bilal MA 39.5
 Golder, Katharina •O 62.3
 Goldhahn, Rüdiger HL 14.5, HL 14.7, HL 21.4, HL 22.6, HL 25.40
 Goldner, Philippe QI 4.9
 Goldsche, Matthias HL 29.2
 Goldstein, Samuel TT 37.6
 Golestanian, Ramin BP 4.7, BP 6.3, BP 8.7, BP 26.5, DY 3.8, DY 31.9
 Golež, Denis MM 23.8
 Golias, Evangelos MA 19.19, MA 35.25, O 54.7
 Golibrzuch, Matthias MA 35.3
 Gollwitzer, Christian KFM 3.1
 Golombiewski, Maik •TT 30.1
 Golubeva, Elizaveta MA 9.3, •MA 35.62
 Golze, Dorothea MM 31.1, O 50.4
 Götzhäuser, Armin DS 5.2, O 8.4, O 23.3, O 23.5
 Gomell, Leonie •MM 14.4
 Gomez-Vierling, Nancy •BP 12.50, BP 12.51
 Gomonay, O. MA 19.63
 Gomonay, Olena •MA 13.4, MA 19.45, MA 19.59, MA 19.62, MA 24.11, MA 25.5, MA 34.5, MA 35.15, MA 35.28, MA 35.45, MA 35.50
 Gompper, Gerhard BP 2.2, BP 4.6, BP 14.5, BP 14.7, BP 17.7, DY 46.8, DY 50.6
 Goncalves, Francisco J. T. MA 28.11
 Gonçalves, João N. MM 18.13
 gong, qingmei •MM 21.10
 Gong, Yilun •MM 20.3
 Gong, ZiZhou KFM 25.5
 Gönninger, Nils •MM 10.22
 Gonzalez Betancourt, Ruben Dario •MA 34.7
 Gonzalez Hernandez, Rafael Julian MA 34.7
 González, José MA 19.24, TT 2.14, TT 21.27
 Gonzalez, Marco A. DS 20.25
 Gonzalez Oliva, Ignacio •O 50.5
 González-Hernández, Rafael MA 34.1
 Gonzalez-Julian, Jesus DS 26.4, MM 4.9
 Gonze, X. HL 21.12
 Gonze, Xavier HL 25.44
 Goodner, Stephen DS 20.22
 Goodrich, Carl BP 26.8
 Gopakumar, Thiruvancheril G O 15.7
 Göpprich, Kerstin BP 26.3, BP 26.4
 Gördes, Jendrik MA 19.19, MA 35.25
 Gordyeva, Korneliya CPP 12.3, MA 41.5
 Gorfer, Alexander O 27.5
 Gori, Matteo DY 44.12
 Gorini, Cosimo TT 18.2, TT 19.1
 Göring, Andreas O 6.4, O 40.1, O 45.3, O 79.2
 Gorlova, Irina KFM 8.3
 Gort, R. MA 25.4, O 68.10
 Goscinski, Alexander •O 58.9
 Gosling, Nicolas TT 27.1, •TT 31.3, TT 37.12
 Gossler, Mattis •O 52.10
 Göth, Nils •CPP 9.6
 Gotthelf, K. TT 13.5
 Götsch, Thomas O 49.8
 Gottfried, J. Michael DS 20.19, O 5.5, O 12.1, O 12.4, O 12.6, O 32.3, O 41.2, O 52.6, O 55.10, O 55.13
 Gottfried, Michael O 79.4
 Götting, Niclas •DS 17.2, QI 5.8
 Gottschalk, Kay-E BP 12.4
 Gottschall, T. MA 19.11, MA 29.2, MA 29.3
 Gottschall, Tino •MA 19.13, MA 29.1, MA 29.7
 Gottscholl, Andreas QI 4.41
 Götz, Anika •TT 34.9
 Götz, Klaus CPP 33.6
 Götz, Markus BP 2.3
 Götz, Uhrig HL 2.4
 Gourmelon, Alexandre SYQM 1.2
 Gouzé, Jean-Luc BP 24.6
 Gozłinski, Thomas TT 3.1
 Graalmann, Jan-Hauke •O 48.3
 Grabowski, Blazej MM 6.8, MM 10.14, MM 31.4
 Gracey, John A. TT 23.3
 Gradauskaite, E. KFM 2.3
 Gradauskaite, Elzbieta KFM 14.2, •KFM 19.3
 Gradl, Johannes O 2.5, O 2.6, O 2.7, O 9.6, O 9.8, •O 33.5
 Graessel, Katharina •BP 3.7
 Graeve, Olivia A. •MM 13.1
 Graf, Ansgar •MA 40.5
 Graf, Felix •BP 12.20
 Graf, Juliane TT 22.12
 Graf, Thomas HL 4.11
 Grafe, Hans-Joachim BP 7.29
 Gräff, Kevin CPP 17.20
 Grafke, Tobias DY 28.1
 Graml, Maximilian •HL 30.40
 Gramlich, Moritz HL 30.38
 Grammel, Jonas HL 17.5, QI 4.10, •QI 4.31
 Grammer, Matthias MA 19.41
 Grånäs, O. MA 25.4
 Granata, V. MM 7.5, TT 22.1
 Grandjean, Nicolas HL 22.5, HL 25.95, HL 37.3, O 82.7
 Granovsky, Sergey MA 16.8
 Granwehr, Josef DY 8.2, MM 8.8, O 28.5, SOE 6.2
 Gräper, Leon MA 19.54, MA 21.3
 Gräper, Leon A. DS 20.25
 Grassano, Davide •MA 40.4
 Grasselli, Federico O 83.7, •QI 7.2, QI 7.3
 Grassl, Florian HL 28.4
 Gratzfeld, Kristin •O 20.8
 Grauer, Rainer DY 8.4, DY 28.1, SOE 6.4
 Graulich, Dominik MA 2.2, MA 19.27
 Graupeter, Sarina •HL 10.9, HL 10.10
 Gong, Sven •KFM 25.3
 Gravelle, Simon CPP 12.36
 Grawitter, Josua •CPP 20.5
 Gray, Alexander O 73.9
 Gray, Natascha KFM 19.3
 Greben, Kyrilo HL 31.4
 Green, Ben PLV III
 Greenberg, Yaron MM 30.10
 Grefe, Julius •TT 3.8, •TT 30.15, TT 30.16
 Gregg, John MA 35.2
 Gregor, Thomas BP 24.4
 Gregoratti, Luca O 52.7, O 52.8
 Greil, Johannes •MA 35.3
 Greilich, Alex •HL 2.1, HL 2.4, HL 26.9
 Greiner, Christian •MM 27.1
 Greiner, Johannes CPP 11.1
 Greiner, Michèle G. •HL 30.38
 Grenz, Pascal J. O 73.3
 Grenz, Pascal Jona •O 73.5
 Gresch, Alexander •QI 4.30
 Gresista, Lasse •MA 19.33
 Gretaarsson, Hlynur KFM 6.2, KFM 25.13
 Gretén, Lara •HL 6.10
 Gretz, Oliver O 14.1, O 22.8, O 74.9
 Greve, Christopher R. •CPP 12.21
 Greve, Matthias O 34.1
 Grewo, Nedal DS 20.25
 Grey, Clare O 43.3
 Grey, Clare P. MM 2.1, MM 14.2
 Grieb, Tim HL 10.11, HL 42.3
 Griedel, Markus •TT 31.7
 Griener, Timur TT 37.1
 Gries, Lukas MA 35.43, TT 12.5
 Gries, Stella MM 18.27, •MM 18.34
 Griebner, Christoph O 38.7
 Griesser, Christoph •O 15.9, O 15.10
 Griffin, Sinead KFM 2.5
 Griffin, T. TT 30.17
 Grifoni, Milena TT 19.3, TT 22.12, TT 26.4, TT 26.6, TT 26.11, TT 26.12, TT 27.4, TT 33.7
 Grigera, Tomas BP 14.8
 Grigoletto, Massimo HL 10.9, •HL 10.10
 Grill, Leonhard BP 12.25, O 6.1, O 17.7, O 20.11, O 23.2, O 29.1, O 58.15, O 74.2, O 74.3, O 74.7
 Grill, Stephan •PLV VIII
 Grimm, Philip O 17.1, •O 18.26
 Grimm, Uwe DY 49.3
 Grisafi, Andrea O 67.5
 Grisar, Stefan •HL 5.2
 Gritsch, Andreas QI 4.11
 Grivas, Nikolas TT 24.1
 Gröbmeyer, Johannes HL 7.8, •HL 13.1
 Groene, Tjark HL 25.79
 Groenedijk, Solofo TT 20.10
 Groenenboom, G. C. O 6.9
 Groenenboom, Gerrit C. O 51.4
 Groenedijk, Solofo TT 23.13
 Groening, Oliver O 29.6
 Gröger, Harald BP 12.49
 Groh, Sebastian CPP 9.10
 Groll, Daniel HL 25.48, •HL 30.48
 Groll, Maja DS 1.4, •DS 17.7, HL 25.1
 Gronin, Sergei TT 3.13, TT 22.7, TT 26.2
 Gröning, Oliver O 18.19
 Gros, Claudius •SOE 3.1
 Grosche, Malte TT 24.5
 Große, Jan HL 4.1
 Große, Nicolai O 19.2
 Grosjean, Benoit O 31.7
 Großmann, Max HL 13.4, HL 30.42
 Großmann, Robert DY 46.12, •DY 50.5
 Gross, Axel O 69.7
 Gross, Leo O 62.8, O 64.3
 Gross, Rudolf MA 19.40, MA 19.41, MA 20.3, MA 22.2, MA 34.4, MA 35.6, MA 35.7, MA 35.35, MA 35.37, TT 15.1, TT 27.7, TT 29.11, TT 31.5, TT 31.22, QI 1.3, QI 2.10, QI 4.5, QI 4.6, QI 4.7, QI 4.15, QI 4.18
 Gross, Stefan BP 12.23
 Grosse, C. TT 30.17
 Grossmann, Lukas O 12.10
 Grosu, Cristina MM 8.8, O 82.2
 Grote, Lukas KFM 3.4, MM 18.35
 Grothe, Alexander O 13.1
 Grothe, Isa Hedda •HL 26.5
 Grotowski, Stefanie HL 36.4, TT 17.5, •TT 17.6, TT 17.7
 Grott, Sebastian CPP 28.6
 Grötzner, Gabriel DS 18.4, HL 24.4
 Groven, Thorben O 16.3
 Grover, Tarun TT 6.3
 Grübel, Gerhard MA 31.6
 Gruber, Florian DS 20.14
 Gruber, Manuel MA 25.7
 Gruber, Maximilian •HL 32.3
 Gruber, Raphael MA 12.9, MA 37.7
 Gruber, Sophia BP 15.1
 Gruenewald, Marco HL 25.7, O 17.1, O 65.4, O 65.6
 Grüger, Benedikt Johannes •DY 28.5
 Grumbach, Justus •MA 16.8
 Grumbel, Manu •HL 14.7
 Grumet, Manuel •O 83.9
 Grumm, Jonas •O 59.1
 Grünberger, Alexander BP 12.49
 Grundler, Dirk MA 19.6
 Grundmann, M. HL 18.3, HL 21.1, HL 25.49, HL 30.20, HL 33.4
 Grundmann, Marius DS 20.45, DS 20.47, HL 9.5, HL 13.9, HL 18.7, HL 25.45, HL 30.21, HL 30.22, HL 30.23, HL 30.24, HL 30.25
 Grundner, Martin CPP 40.9, DY 43.5, TT 39.8
 Grüne, Jeannine CPP 12.77, CPP 12.79
 Grünebohm, Anna KFM 8.4, KFM 10.5, KFM 14.4, KFM 25.9
 Grün-eis, Andreas MM 12.7
 Gruner, Markus MA 19.12, O 2.4
 Gruner, Markus E. MA 19.14, MA 19.15, MA 42.4, O 2.8
 Gruner, Markus Ernst O 2.3
 Grünewald, Marco O 34.6
 Grünewald, Tilman •BP 9.5
 Grünhaupt, Lukas TT 37.2, TT 37.5, •QI 4.38, •QI 13.11
 Grüning, Martina BP 12.43
 Grüninger, Helen HL 23.2
 Grüninger, Markus TT 8.6, TT 21.15
 Grünleitner, Theresa HL 42.6, HL 42.9
 Grunwald, Jan-Dirk O 70.8
 Gruschwitz, M. •O 25.3, •O 41.7
 Gruschwitz, Markus O 25.6
 Grusdt, Fabian QI 10.7
 Grutter, Alexander J. MA 33.2
 Grützmacher, Detlev DS 21.2, HL 7.3, HL 7.4, HL 19.7, HL 25.20, HL 25.84, HL 25.98, HL 30.10, HL 33.7, HL 36.6, HL 37.2, O 4.3, TT 18.9, TT 32.3, TT 32.7, QI 1.7
 Gu, Bin MM 18.8
 Gu, Hongri •BP 14.3
 Gu, Xiangyu TT 12.4
 Guan, Pin-Wen MM 33.8
 Guan, Tianfu CPP 12.13, CPP 12.15, •CPP 12.52, CPP 17.23, CPP 17.26
 Guardi, Giorgia MM 18.18
 Guardia-Arce, Verónica HL 19.8
 Guarnieri, Giacomo QI 8.7
 Guatieri, Francesco •O 63.2
 Gubanov, Kirill •CPP 1.11
 Gubbin, Christopher R. O 37.6
 Gubkin, A.F. MA 29.2
 Guck, Jochen BP 12.24
 Guckel, Jannik O 35.1
 Gückelhorn, Janine MA 19.41, •MA 34.4, MA 35.6, MA 35.35
 Güdde, Jens •O 9.13, O 33.2, O 33.7, O 68.4
 Gueckstock, Oliver MA 19.51, •MA 21.9
 Guénolé, Julien MM 6.1
 Guénon, Stefan DS 25.1, •DS 25.3
 Guerra Santillan, Karla Yanin BP 3.1
 Guerrero Felipe, Juan Pablo O 5.2, •O 55.12
 Guevara, Jose M. •O 13.5, O 17.3
 Guglietta, Fabio •DY 4.1, DY 4.2
 Guguchia, Zurab TT 6.8
 Günhe, Otfried QI 2.7, QI 2.9, QI 3.3, QI 7.1, QI 7.5, QI 7.7, QI 9.2, QI 9.5, QI 9.8
 Guidat, Margot O 15.11, O 20.10
 Guido, Isabella BP 12.48, BP 26.2
 Guillén-Gosálbez, Gonzalo O 3.5
 Guimaraes, Filipe MA 30.7
 Guimaraes, Filipe S. M. O 71.3
 Guimarães Leal Lealdini, Leonardo •DS 26.4
 Gulans, Andris O 50.1
 Gulati, Lovish DS 19.1
 Gullick, Imogen PLV III
 Gulzar, Adnan BP 7.19
 Gumbel, Lukas DS 21.1, •HL 15.6, O 20.5
 Gumeniuk, Roman MM 18.43
 Günay, Benu •O 20.11
 Günder, Darius •DS 5.4, O 12.9
 Gündoğan, Mustafa •QI 7.8
 Gunkel, Felix O 37.2
 Günther, Christian MA 12.2
 Günther, Christian M. MA 2.1, MA 2.3
 Günther, F. TT 13.5
 Günther, Sebastian O 70.4
 Güzüing, Damian MA 4.4, •MA 22.4, MA 25.7
 Günzler, Simon TT 27.1, TT 27.2, TT 31.2, TT 31.18, •TT 37.9, TT 37.12
 Guo, Don-Sheng CPP 12.8
 Guo, Na O 81.1
 Guo, Renjun CPP 12.64, CPP 17.23, CPP 19.4, •CPP 28.4, CPP 28.6
 Guo, Yanfeng TT 39.2
 Guo, Yaqian •MA 18.7
 Gupalo, Marina •CPP 44.2
 Gupta, Priti HL 10.1
 Gupta, Shivam CPP 7.7, •CPP 12.37
 Gurevich, Svetlana V. DY 15.3, DY 15.4, DY 39.3
 Gurrath, Martin O 5.6
 Gurrieri, Maria Vittoria •HL 25.91
 Guruciaga, Pamela •BP 6.2
 Guryanova, Yelena •QI 2.1
 Gusenkova, Daria TT 27.1, TT 37.12, QI 4.23, QI 6.8
 Guskova, Olga •CPP 12.29, CPP 12.30, •CPP 40.4
 Guster, B. •HL 21.12
 Gütay, Levent DS 20.25
 Gutekunst, Jeremias •BP 12.27
 Guterding, Daniel •SOE 4.1
 Gutfleisch, Oliver •SYUK 2.1, MA 19.12, MA 19.14, MA 19.15, MA 23.1, MA 29.1, MA 29.7, MA 29.9

MA 32.4, MA 35.52, MA 35.61,
MM 13.7, MM 18.25
Gutfreund, Philipp CPP 33.4
Gutnikov, Michael •O 55.9
Gutowski, Jürgen HL 33.8
Gutsch, Sebastian KFM 25.2,
MM 35.10
Guttman, M. HL 10.5
Guttmann, Martin HL 10.1, HL 10.4,
HL 10.6, HL 10.8
Gutzeit, Mara MA 19.4
Gyger, Samuel DS 20.46
György, Zoltán TT 27.10
Györök, Michael O 12.3
H. Heenen, Hendrik MM 34.5
H. Mir, Showkat O 74.12
H. Strik, Julian O 74.5
Haaf, Magdalena •BP 12.30
Haag, Felix O 62.9
Haag, Florian O 5.4
Haager, Lena O 3.7
Haas, Benedikt MM 22.1
Haas, Marcel TT 31.16, •TT 33.1
Haas, Max •KFM 2.2
haas, stephan wolfgang O 18.15
Haataja, Johannes CPP 8.4
Habershon, Scott DY 35.5
Habibi, Alireza TT 23.13
Habicht, Klaus MA 6.4
Hache, Toni •MA 2.4, MA 28.11
Haddadi, Fatemeh •MA 11.7
Hader, Jörg HL 13.10
Hadjab, Moufdi CPP 40.4
Hadjadj, Sebastien MA 19.19,
MA 35.25
Hadjadi, Sebastien Elie O 18.22,
•O 54.7
Haerberle, Jan DY 11.8
Haeger, Tobias MM 14.4
Haerer, Manuel •HL 25.90
Haertl, Patrick •O 26.5
Haeussler, Ellen MA 16.8
Hafeez, Asad BP 7.33, BP 12.31
Häfele, Sophie CPP 19.3
Haferkamp, Jonas QI 12.10
Hafermann, Martin HL 18.1
Hafez-Torbati, Mohsen •MA 38.3,
TT 11.4
Hafner, Daniel •TT 6.2, TT 6.6,
TT 24.8
Hagag, Samar •HL 10.12
Hagedorn, Sylvia HL 10.9
Hägele, Daniel KFM 19.2, QI 4.19,
QI 8.9
Hagemann, Johannes CPP 12.39,
KFM 3.2
Hagemann, Philipp BP 7.3, BP 7.4
Hagemann, Ulrich O 65.1
Hagen, Jakob •KFM 8.1
Hager, Mareike CPP 12.17
Haghighirad, Amir-Abbas O 26.1,
TT 21.6, TT 39.2
Hagiwara, Kenta MA 30.3
Haglund, Åsa HL 25.95
Hagmann, Kevin •CPP 2.3
Hagymás, Imre MA 15.3
Hahn, Alexander •TT 21.35
Hahn, Frederik QI 4.8, QI 7.2
Hahn, Horst MM 30.8
Hahn, Lothar TT 27.2
Hahn, Thilo •HL 25.8, HL 30.48
Hahn, Walter •DY 5.8
Hähnel, David •O 78.6
Haider, Ferdinand MM 3.1, MM 3.3,
MM 3.4, MM 4.7, MM 18.9
haim, menashe TT 10.2
Halbauer, Max •O 55.3
Halhuber, Maïke HL 40.5
Halbinger, Johannes TT 16.4
Halbritter, Thomas O 74.12
Haldar, Astik DY 26.4, DY 44.18
Haldar, Ritesh CPP 17.4, CPP 48.4
Haldar, Soumyajyoti •MA 30.6,
MA 37.10
Haley, Richard •SYUK 2.4
Halimeh, Jad QI 10.5
Halimeh, Jad C. QI 10.7
Hall, Amelia MA 17.3
Hall, Samuel J. •O 28.4, O 41.2
Hallidin Stenlid, Joakim O 10.2
Haller, Andreas TT 1.3, TT 20.10,
•TT 23.13
Haller, Martin •O 66.5
Hallerberg, Sarah DY 8.1, SOE 6.1
Hallfarth, Freya MM 18.1
Hallstedt, Bengt MM 4.2

Hals, Kjetil M. D. TT 1.11
Hals, Kjetil Magne Dørheim MA 21.4
Hamada, Ikutaro O 7.6
Hamann, D. TT 30.17
Hamann, Danielle M. DS 20.29
Hamed, Mai H. MA 33.2
Hamer, Sebastian CPP 17.4
Hamm, Magnus MM 17.4
Hammer, Lutz O 54.9, O 63.6, O 73.4
Hammer, Natalie O 6.4
Hammer, Sebastian CPP 39.6
Hammerschmidt, Thomas MM 18.14,
MM 23.4, O 83.3
Hammud, Adnan O 7.6
Hampel, Hana K. MA 35.33
Hampel, Silke MA 35.73
Hamrle, Jaroslav MA 5.1
Hamzayev, Tarlan •HL 6.3, HL 20.5
Han, Bo •HL 11.8, HL 15.7, HL 20.6
Han, Dan •HL 5.9, HL 7.10
Han, Jeong Woo HL 6.9
Han, JeongWoo HL 42.1
Han, Peize HL 6.9
Han, Seung Heon •HL 42.7
Han, Xu •MM 29.1
Han, Yi CPP 12.80
Händel, Alexander K. •TT 27.6
Handschuh, Maria-Teresa QI 4.5,
QI 4.6, QI 4.7, QI 4.15, QI 4.18
Haneder, Fabian DY 5.10
Haneke, Markus •DY 40.7, •DY 44.11
Haney, Paul TT 2.10
Hangleiter, Andreas HL 10.12,
HL 10.13, HL 30.12, HL 30.17,
HL 30.18
Hangleiter, Dominik QI 12.10
Hangleiter, Tobias HL 19.10
Hänisch, Christian HL 41.5
Hanke, Michael DS 22.5, HL 35.3
Hanke, Stefan •VA 2.1, VA 2.3
Hankiewicz, Ewelina TT 11.8, TT 11.9,
TT 32.5
Hankiewicz, Ewelina M. TT 1.2
Hannappel, Thomas HL 13.4,
HL 25.55, HL 30.42, O 30.6
Hannebauer, Adrian HL 12.9
Hannezo, Edouard BP 27.2
Hans, Marcus MM 28.5
Hänsch, Theodor W. QI 5.9
Hanschke, Lukas HL 8.1, •HL 8.10,
HL 17.8, HL 25.56
Hanseman, Moritz N.L. O 69.9
Hansen, Felix MA 35.73
Hansen, Thomas W. O 27.3
Hansen, Wolfgang HL 25.89
Hansenne, Kiara •QI 7.1
Hanson, Ronald •SYED 1.1
Hänze, Max O 71.7, O 71.8
Hapala, Prokop O 55.14, O 74.10
Haque, Masudul TT 9.4
Haque, Mohammad Ahsanul O 63.5
Harati, Mariam HL 33.5
Harbich, Wolfgang O 69.3
Harbig, Jana MA 35.52
Harder, Constantin CPP 1.4,
CPP 12.59, •CPP 18.3, CPP 27.2,
CPP 37.6
Harder, Tristan H. HL 22.7
Hardian, Rifan MM 17.5
Hardt, Dennis •TT 21.36
Hardt, Steffen CPP 20.6
Hardy, Frédéric TT 39.2
Harisko, Dimitrios HL 34.5
Hariskos, Dimitrios HL 25.32
Harkort, Carolin •O 35.5
Harling, Benno •O 18.11
Harman, Michael QI 6.5
Harmon, Tyler •BP 8.4, BP 8.5,
BP 8.12
Harneit, Wolfgang CPP 12.8
Harouna-Mayer, Sani HL 25.79,
MM 18.35
Harouna-Mayer, Sani Y. •KFM 25.5
Harouri, Abdelmounaim HL 19.4
Harper, Angela •O 43.3
Harrington, David O 20.4
Harsh, Moshir •DY 28.7
Harsh, Rishav O 25.2, O 48.6
Härtel, Andreas •DY 38.1, DY 46.15,
DY 49.4, DY 49.7
Hartelt, Michael O 59.4, O 68.6
Hartge, Hannah M. •CPP 17.11
HARTH, Kirsten DY 4.5, •DY 11.7,
•DY 23.5
HARTH, Milan HL 32.4
Harting, Jens CPP 19.2, DY 4.1,

DY 4.2, DY 4.8, DY 16.7, DY 23.6,
DY 46.16
Hartinger, Simon SYQM 1.2
Härtl, Patrick O 71.10, O 82.1
Hartl, Tobias •O 54.14
Hartmann, Alexander K. DY 24.2,
•DY 26.2, DY 44.14, DY 44.16,
DY 45.1, DY 49.1
Hartmann, Markus KFM 6.3
Hartmann, Michael QI 6.3, QI 6.4
Hartmann, Nils O 65.1
Hartmann, R. TT 22.1
Hartmann, Roman TT 3.9, •TT 7.8,
TT 10.9, TT 22.2, TT 29.4, TT 31.26
Hartmann, Simon •CPP 7.6
Hartmann, Vincent •DS 17.3
Hartnoll, Sean A MM 21.3, MM 21.4
Härtter, Daniel •BP 3.10
Hartung, Lisa DY 28.3
Hartung, Stefan DY 18.2, SOE 10.2
Harvey, Tyler R. O 78.5
Haschke, Heiko BP 9.10, BP 13.9
Hasecic, Amer •TT 31.24, TT 31.25
Häser, Maria DS 20.7
Hashemi, Zohreh •CPP 39.5
Hashtroud, Aida •BP 6.4
Haslberger, Andreas MA 19.40,
MA 35.35
Hassani Abdollahi, Younes •O 8.8
Hassanien, Ahmed HL 30.39,
HL 30.49, HL 30.51
Hassanpour, Ehsan KFM 7.1, MA 33.5
Hassinger, Elena TT 6.5, TT 6.6,
TT 6.9, TT 22.3, TT 22.5, TT 24.8,
TT 34.2
Hassler, Fabian TT 1.10, TT 10.5,
TT 34.3, QI 13.3
Hasssanien, Ahmed •HL 30.50
Hatzoglou, Constantinos KFM 7.2
Hauck, Daniel •TT 1.5
Hauaise, Vincent MA 35.7
Hauer, J. O 68.10
Hauer, Lukas •CPP 7.2, CPP 7.8
Hauer Vidal, Daniel HL 10.4
Hauer, Volker •VA 2.2
Hauff, Dieter TT 17.1
Haug, Rolf J. HL 3.8, HL 12.7, HL 12.9,
HL 12.10, HL 25.10, HL 25.69,
HL 29.6, HL 36.8
Haugerud, Ivar Svalheim •BP 8.10
Hauke, Lara BP 3.10
Hauke, Philipp QI 10.5
Hauns, Jakob •DS 5.1, O 52.7, O 52.8
Hauptmann, Nadine O 19.3
Haus, Simon TT 3.9
Hausch, Julian CPP 39.2
Hauser, Christoph MA 19.45
Häuser, Simon MA 25.8, MA 35.19
Häusel, Fabian BP 12.14, DY 34.1
Häusler, Wolfgang MA 12.7, TT 2.8
Häuspurg, Andreas •TT 8.1
Häussler, Matthias QI 4.24
Haverkort, Jos HL 25.50
Havryliuk, Yevhenii •DS 23.1
Hayenga, William E. HL 4.8
Hayes, Jack O 54.7
Hayes, Johannes HL 40.1
Hazra, Binoy K. MA 34.6
He, Jiali •KFM 7.3, KFM 14.6
he, lianyi O 18.15
He, Lu •DS 26.3
He, Mingquan TT 39.2
He, Wen DS 22.2
He, Yunbin DS 13.2
Heber, M. O 68.10
Heber, Michael O 9.1, O 34.10, O 68.3
Hebert, Cecile •MM 22.5
Hecht, Bert O 61.3
Hecht, Lukas •DY 16.8
Hecht, Sandra •MM 20.2
Hecht, Stefan O 5.2, O 32.7, O 55.12
Heckel, Alexander O 74.12
Hecker, Daniel •HL 3.4
Hecker, Katrin •QI 1.2
Heckl, Wolfgang O 6.10, O 12.10,
O 40.8
Heckmann, Olivier O 73.6
Heckötter, Julian HL 33.5
Heckschen, Markus O 2.4, •TT 13.2
Heczko, Martin •MM 10.20
Heczko, Oleg MA 11.4
Hedrich, Carina DS 13.4
Hedwig, Sebastian •O 9.12, O 16.2
Heedt, Sebastian HL 25.77
Heermeier, Niels •HL 4.1
Heenen, Hendrik MM 14.1

Heenen, Hendrik H. MM 10.1,
MM 29.1, O 31.4, O 31.5, O 41.3,
•O 45.5
Heep, Julian O 30.8
Heermant, Saskia O 22.2
Hefele, Andreas MA 28.7
Heffels, Dennis HL 7.3, •HL 7.4,
TT 18.9
Hefner, Simon •DY 44.6
Hegde, Omkar •MM 4.6
Hege, Judith •CPP 17.24
Hegemann, Peter BP 10.2, HL 28.1
Heger, Julian E. CPP 12.13,
CPP 12.45, CPP 12.49, CPP 12.64,
•CPP 37.6, CPP 48.2
Heggemann, Jonas O 66.8
Hegselmann, Rainer •SOE 2.1
Heid, Rolf TT 3.1, TT 8.2
Heide, Gerhard KFM 6.2
Heidelmann, Markus MA 39.2
Heidemann, Knut SOE 15.2
Heiden, Jan •QI 4.32
Heidenreich, Alexander O 6.4
Heidenreich, Sebastian DY 46.7
Heider, Michael KFM 7.4
Heider, Tristan O 48.7
Heiderhoff, Ralf MM 14.4
Heidrich-Meisner, Fabian TT 34.6,
TT 34.10
Heifetz, Eyal DY 46.3
Heigl, Michael MA 28.7
Heikkilä, Tero T. TT 15.5
Heiliger, Christian DS 18.2, DS 21.1,
MA 19.34, MM 6.6, MM 10.13
Heilmair, Martin MM 4.1, MM 4.8
Heilmann, Anke MA 8.2
Heimbrott, Wolfram CPP 39.2
Heimig, Connor HL 32.3
Heimonen, Hermanni QI 4.23, QI 6.8
Heimrich, Karl MA 7.1
Hein, Petra O 9.4, O 16.8, O 33.1
Heindel, Tobias HL 17.10, QI 7.9
Heindl, Markus CPP 28.1
Heindl, Moritz O 59.2
Heindl, Moritz B. •O 78.4
Heine, Johanna HL 25.16, HL 32.1
Heine, Thomas HL 7.6, O 29.2,
TT 29.10
Heinig, Karl-Heinz MM 2.3
Heinig, Peter •MA 22.8
Heinrich, Andreas MA 26.3, O 47.4,
•O 47.10, O 51.6, O 54.3, O 63.4,
O 80.5
Heinrich, Andreas J. O 5.3, O 18.9,
O 51.7
Heinrich, Markus QI 3.1, QI 12.4
Heinrich, Tobias •O 9.3
Heins, Christopher MA 28.11,
•MA 35.8
Heinsoo, Johannes QI 4.23, QI 6.8
Heintzmann, Rainer BP 7.33,
BP 12.29, BP 12.31
Heinz, Björn MA 13.8, MA 28.6
Heinze, Dirk HL 26.1, HL 26.4
Heinze, Jonathan DS 22.1
Heinze, Karl •HL 32.5
Heinze, Leonie TT 21.14
Heinze, Stefan •MA 12.1, MA 12.12,
MA 19.4, MA 30.6, MA 37.9,
MA 37.10
Heinzel, Thomas HL 3.7, HL 7.9
Heinzelmann, Sarah TT 16.10,
TT 21.29, •TT 21.30
Heißenbüttel, Marie-Christin •O 72.3
Heiserer, Stefan DS 16.3
heißler, stefan O 30.7, O 70.8
Heissler, Stefan O 79.7
Heitkamp, Denis O 19.10
Heitmann, Tjark •DY 19.4
Heitzig, Jobst SOE 3.4, SOE 3.5
Heiz, Ueli O 3.4, O 13.6, O 13.7, O 42.5,
O 56.2, O 56.3, O 56.5, O 69.3, O 70.1,
O 70.3, O 70.4, O 70.6
Hেকে, Joscha O 50.9
Held, Andreas DY 34.1, HL 7.10
Held, Karsten TT 16.11, TT 16.12,
TT 22.9, TT 28.9
Held, Tobias •O 33.10
Helfrecht, Benjamin DY 51.4
Helias, Moritz DY 3.5
Helli, Michael HL 3.11
Helleman, Jan •HL 35.2, HL 35.3
Hellenes, Anna B. •MA 34.1
Heller, Jörg O 17.9
Heller, Maximilian HL 30.9
Heller, R. HL 22.1

Author Index

Hellmich, Celina•KFM 25.8
 Hellweg, Thomas CPP 17.18,
 CPP 34.2
 Hellwig, Lina BP 27.1
 Hellwig, Olav MA 4.3, MA 21.7,
 MA 22.6, MA 22.7, MA 22.8,
 MA 35.49
 Helm, Christiane A. BP 12.43, BP 17.4,
 CPP 13.3, CPP 33.4, CPP 45.6
 Helm, Christina DS 23.2
 Helm, M. HL 22.1
 Helm, Manfred HL 11.10, HL 19.8,
 HL 25.17, HL 25.41, HL 40.2
 Helm, T. TT 8.1
 Helm, Toni TT 22.11
 Helvoort, Antonius T. J. KFM 7.2
 Helvoort, Antonius T. J. van KFM 7.3
 Helwig, O. O 26.2
 Hemauer, Felix O 18.27, •O 52.3,
 O 52.4
 Hemm, Ralf O 2.2, O 5.4
 Hemmati, Mohammad TT 10.8
 Hemmida, Mamoun MA 27.2
 Hemmleb, Matthias KFM 25.8
 Hempel, Alexander MA 13.3,
 •MA 19.36
 Hendrickx, Nico Willem •QI 1.1
 Hengstler, D. TT 31.8, TT 37.11
 Hengstler, Daniel TT 31.7
 Henk, Jürgen MA 8.11, MA 31.8
 Henke, Nina HL 30.38, HL 32.3,
 HL 32.4
 Henke, Paul BP 7.28
 Henkel, Carsten DS 20.41
 Henkelmann, Gideon •MM 18.31
 Henksmeier, Tobias HL 22.6,
 •HL 25.40
 Henn, Sebastian •DS 20.47, •HL 9.5
 Hennecke, Martin •MA 8.2
 Hennes, Marc SYSM 1.5
 Hennig, Andreas CPP 12.8
 Hennig, Richard O 18.19
 Hennig, Richard G. O 67.3
 Henning, Alex DS 18.4, HL 42.6,
 HL 42.9
 Henning, Peter DS 20.43
 Henning, Pia •DS 20.33, •DS 20.37,
 DS 20.40
 Henry, Jack O 14.3
 Henry, Yves MA 19.36
 Hens, Zeger KFM 11.5
 Henschel, Cristiane CPP 44.3,
 DS 20.50
 Hensen, Matthias •O 61.3, O 82.5
 Hentschel, Mario TT 15.3
 Hentschel, Martina DS 19.4, DY 35.8,
 DY 43.8
 Henz, Jakob DS 20.39, •DS 22.4
 Heo, Y. KFM 2.3
 Hepting, Matthias MA 6.4
 Herb, Michael •O 30.5
 Herbold, Marius MM 10.4
 Herbst, Andreas MA 28.9
 Herbst, Franz TT 29.6
 Herbst, M. •TT 37.11
 Herbst, Michael TT 34.12
 Herbst, Timothy J. BP 12.21
 Herbut, Igor F. TT 22.14
 Herdl, Florian HL 22.3
 Herfort, Jens DS 22.5
 Hergert, Hannes •HL 25.97
 Herges, Rainer CPP 17.4
 Hergett, Waldemar MA 35.43
 Herich, Ondrej O 40.4, O 58.4
 Hering, Dag-Björn •TT 23.10, TT 23.11
 Hering, David •O 58.3
 Herink, Georg HL 25.96, O 59.2,
 O 78.4
 Herkenrath, Fabian BP 22.8
 Herman, Alexander MA 4.4
 Herman, František TT 26.5
 Hermannsdörfer, Thomas MA 27.8
 Hermes, Ilka HL 5.5
 Hermes, Ilka M. CPP 12.9, •CPP 28.3
 Herminghaus, Stephan SOE 5.1,
 SOE 15.2
 Hernández-Delfin, Dariel DY 11.4
 Hernangómez-Pérez, Daniel DS 17.5,
 DY 44.19
 Herold, Julian BP 7.18, •BP 7.26
 Herper, Heike MA 32.7
 Herper, Heike C. MA 29.8, •MA 32.6,
 MA 42.2
 Herr, Ulrich HL 18.2, •MA 39.1
 Herrera Diez, Liza MA 18.5
 Herrero, A. MA 29.2

Herrfurth, O. HL 21.1, HL 21.2
 Herrgen, Paul MA 25.5, •MA 35.28
 Herrig, Tobias •TT 37.14
 Herring, Max MA 16.7
 Herritsch, Jan DS 20.19, •O 12.4,
 O 12.6, O 55.10, •O 55.13
 Herrmann, Carmen MA 35.57
 Herrmann, Hannes •O 66.3, O 66.9
 Herrmann, Paul •HL 25.5
 Herrmann, Tabea •DY 35.3
 Herschel, Manuel MA 39.1
 Hertel, Albert TT 32.3, TT 32.7
 Hertel, Dirk CPP 12.80, DS 20.10,
 HL 30.34
 Herzig, Eva M. CPP 12.21, CPP 12.66,
 CPP 12.76, CPP 41.2
 Herzog, Marc •DS 20.41, HL 30.47
 Herzog, Max CPP 26.2
 Herzog, Sebastian BP 12.39, DY 45.12
 Herzog, Thomas HL 17.5, QI 4.31
 Heßdörfer, Johannes •O 21.2
 Hesjedal, T. MA 27.2
 Hesjedal, Thorsten MA 17.3
 Heßler, Andreas O 35.3, O 78.1
 Heßler, Martin •DY 8.3, •SOE 6.3
 Hess, Christian TT 5.3, TT 25.8
 Hess, Franziska O 52.1
 Hesselmann, Jonas HL 29.2
 Hessenauer, Jannis •QI 4.9
 Hessing, Piet MA 8.2
 Hessler, Andreas O 35.2
 Hetaba, Walid •MM 33.5, VA 2.4
 Heuer, Helge SOE 15.2
 Heuer, Sabrina MM 14.3
 Heuer-Jungemann, Amelie •BP 26.7
 Heugel, Toni L. DY 12.4
 Heuken, Michael DS 2.3
 Heupel, Julia QI 4.16, QI 5.4
 Heuplick, Lukas O 52.6
 Heuplick, Lukas J. O 12.4, •O 32.3,
 O 55.13
 Heuser, Tobias HL 4.1
 Heuthe, Veit-Lorenz •BP 6.1
 Hexemer, Alexander CPP 12.21
 Heyder, Stefan HL 13.4, HL 30.42
 Heyen, Hauke MA 35.65
 Heyen, Hauke Lars •MA 19.3
 Heyl, Markus DY 19.1
 Heyn, Christian HL 25.89
 Heyn, Johannes Clemens Julius
 •BP 22.9
 Hickel, Tilmann MA 14.4, MM 4.6,
 •MM 6.9, MM 10.25, MM 15.2,
 MM 15.5, MM 16.4, MM 20.6,
 MM 25.1
 Hickey, Ciarán TT 21.15, TT 21.26
 Hickin, David MA 25.7
 Hicks, Clifford TT 23.6
 Hicks, David MM 12.5
 Hiekel, Karl MM 35.9
 Hieulle, Jeremy O 42.1, O 80.1
 Higemoto, W. TT 22.1
 Hiiragi, Takashi BP 6.2
 Hilbert, Lennart BP 8.2, •BP 26.3
 Hilbrunner, Constantin •HL 25.22
 Hild, Marcel HL 33.3, HL 40.4,
 HL 40.7
 Hildebrandt, R. HL 21.1, •HL 25.49
 Hildner, Richard CPP 41.2
 Hilgers, Stefanie •O 18.28, O 65.2
 Hilgers, Yannis •TT 21.14
 Hilgert, Katharina •O 33.11
 Hille, Lukas DY 45.3
 Hillebrands, Burkard MA 13.8,
 MA 13.9, MA 19.52, MA 19.53,
 MA 35.10, MA 35.19
 Hillier, Adrian TT 30.7
 Hillmann, Leon •CPP 17.38
 Hilt, Gerhard O 12.6
 Hilt, Oliver DS 6.4
 Himcinschi, Cameliu CPP 12.4,
 MM 18.43
 Himmerlich, Marcel O 13.9
 Himmeler, W. TT 20.9
 Himmeler, Wolfgang TT 19.3
 Hinaut, Antoine O 17.10, O 22.6,
 O 39.4
 Hinderhofer, Alexander CPP 26.5
 Hinduja, Chirag CPP 7.3, CPP 7.4
 Hinger, Kurt O 15.6, O 15.8
 Hinke, Tobias •O 56.2, O 56.3, O 56.5
 Hinkov, Vladimir MA 31.3
 Hinrichs, Karsten •DS 23.6
 Hintsche, Marcel QI 12.10
 Hintermayr, Julian MA 35.23
 Hinz, Alexander HL 30.11

Hinz, Sandra •KFM 11.5
 Hinzke, Denise MA 8.12
 Hirel, Pierre KFM 14.4
 Hirn, Ulrich CPP 14.5
 Hirsch, Lisa •O 38.4
 Hirschberger, Max TT 7.1
 Hirscher, Michael •MM 17.2
 Hirschfeld, Peter TT 3.4
 Hirschfeld, Peter J. TT 22.4
 Hirschmann, Eric KFM 3.3
 Hirschmann, Moritz M. TT 25.5
 Hite, K. TT 30.17
 Hlawacek, Gregor DS 1.5, HL 25.17,
 MA 4.2, MA 28.8
 Hlubina, Richard TT 26.5
 Hobbs, Jamie K. BP 12.18
 Hochgesang, Adrian CPP 12.78
 Hochhaus, Julian A. O 18.28
 Hochhaus, Julian Andreas •O 65.2
 Hocke, Manuela •O 40.8
 Höcker, Julian CPP 19.3, •CPP 19.5,
 HL 5.2
 Hod, Oded O 39.4
 Hodson, Tom MA 16.4
 Hoefler, Jonas MA 35.19
 Hoegen, Michael horn-von O 65.1
 Hoehl, Arne O 7.9
 Hoepfl, Raphael •MA 35.37
 Hofeditz, Nico •CPP 39.2
 Hofemeier, Arne BP 12.13
 Hofer, André •O 45.2
 Hofer, Bianca HL 25.31
 Hofer, Thomas BP 24.3
 Höfer, Ulrich O 9.11, O 9.13, O 33.2,
 O 33.7, O 68.4, O 68.7
 Hoff, Felix DS 20.13, •DS 23.5
 Hoffelner, Lisa CPP 14.5
 Hoffer, Marvin O 58.13
 Hoffmann, Georg HL 14.3
 Hoffmann, GERMAR O 55.2
 Hoffmann, Ingo CPP 33.1
 Hoffmann, Karl Heinz CPP 9.7
 Hoffmann, Markus O 26.1
 Hoffmann, Marvin O 40.2
 Hoffmann, Veit HL 30.13
 Hoffmann-Vogel, Regina O 30.4
 Hoffmann-Vogel, Regina O 22.3
 Höfler, Mathias •BP 7.15
 Höflich, Katja DS 20.30, MA 12.2,
 O 35.4, O 54.10, O 54.13
 Höfling, Felix CPP 49.6, •DY 40.6,
 •DY 50.8
 Höfling, Sven HL 15.4, HL 15.7,
 HL 17.7, HL 19.5, HL 20.6, HL 20.9,
 HL 22.7, HL 25.80, HL 26.11, HL 30.2,
 HL 41.3
 Hofmann, Alexander HL 28.4
 Hofmann, Anna-Lena •CPP 26.2
 Hofmann, Damian •DY 43.7
 Hofmann, Detlev M. HL 32.1
 Hofmann, Johannes-Stephan
 TT 28.10
 Hofmann, Jonathan O 4.3
 Hofmann, Jonathan K. •O 49.3
 Hofmann, Kay DY 44.3
 Hofmann, Martin HL 4.1
 Hofmann, Niklas O 2.5, O 2.6, O 2.7,
 O 9.6, •O 9.8, O 33.5
 Hofmann, Oliver O 28.7, O 28.8,
 O 29.7
 Hofmann, Oliver T. MM 10.2, O 6.1,
 O 13.5, O 17.2, O 28.1, O 28.9
 Hofmann, P. MM 7.5
 Hofmann, Ph. O 68.10
 Hofmann, Philip O 54.5, O 63.5, O 72.1
 Hofmann, Philipp E. CPP 39.1
 Hofmann, Stephan O 9.10, O 16.9,
 O 48.9
 Hofmann, Tim •TT 27.8
 Hofmeier, Arne •BP 22.8
 Hofsäss, Hans HL 25.20, KFM 6.1,
 O 82.6
 Hofsäss, Hans Christian MM 7.3
 Hofstetter, Walter MA 31.10, TT 11.4
 Högele, Alexander HL 25.23, HL 30.6
 Hogg, Mark Richard HL 2.5
 Hohage, Michael MA 30.4
 Höhe, Florian •TT 7.3
 Hohenader, Martin TT 34.9
 Hoheneder, Alexander O 44.3
 Hohlstamm, Anselm •BP 12.45
 Hohmann, Judith K. TT 27.2
 Höhn, Fabian •O 13.8
 Hohn, Marcel •HL 8.6
 Höing, Dominik O 37.4, •O 61.2
 Holbach, Simon DY 28.3

Holder, Jacob •CPP 17.7
 Holder, Tobias TT 7.6
 Holderer, Olaf •CPP 33.3
 Hölderle, Tobias •KFM 25.18
 Holec, David KFM 8.2, •MM 28.5,
 O 43.2
 Holeňák, Radek DS 1.5
 Holl, Max Philipp •DY 50.10
 Holleitner, Alexander DS 17.5, DS 19.1,
 HL 6.5, HL 6.8, HL 7.2, HL 7.8,
 HL 11.1, HL 11.5, HL 11.9, HL 13.1,
 HL 25.14, TT 7.7, QI 3.10
 Hollenbach, Michael HL 19.8,
 MA 28.11
 Höllmer, Philipp •DY 49.2
 Hollricher, Michelle MA 27.11,
 •MA 35.56
 Höllring, Kevin •BP 7.23, BP 22.7,
 •CPP 17.25
 Hollweger, Simon •O 17.2
 Holm, Christian CPP 12.10,
 CPP 12.36, CPP 13.2, CPP 34.1,
 DY 8.7, DY 16.9, DY 46.14, SOE 6.7
 Holmes, Justin HL 17.9
 Hölscher, Leonhard QI 4.35
 Hölscher, Torsten HL 27.4
 Holstad, Theodor KFM 7.6
 Holstad, Theodor S. KFM 7.3
 Holt, Ann Julie U. O 72.1
 Holtmann, Marcel O 48.5, •O 73.3
 Holtz, Megan KFM 7.2
 Holub, Tamara TT 12.1
 Holubec, Viktor •DY 45.4, DY 46.18
 Holý, Václav O 18.20
 Holz, Lukas TT 29.6
 Holzer, Christof O 61.7
 Holzer, Marco HL 17.3
 Holzhaacker, Daniel •O 32.1
 Holzmann, Thomas O 14.1, •O 22.8
 Homeier, Lukas •QI 10.7
 Hommel, Caroline O 51.6
 Honasoge, Kedar QI 4.5, QI 4.7,
 QI 4.15, QI 4.18
 Honasoge, Kedar E. TT 31.23, •QI 4.6,
 QI 4.35, QI 4.36, QI 4.37
 Honecker, Andreas •DY 51.3, O 67.9,
 •TT 23.7
 Hong, Ping •KFM 25.15, •MM 8.6
 Hong, Seung-Ju •O 7.3
 Hong, Sung Ju HL 29.6
 Hong, Xiaochen •TT 5.3
 Honig, Hauke DS 9.3
 Honig, Hauke-Lars DS 23.2
 Honné, Natalie •O 35.3
 Honolka, Jan O 18.18, O 18.20
 Hoore, Masoud BP 17.7
 Hopfer, Karolin TT 8.6, TT 21.15
 Hopfmann, Caspar HL 3.5, HL 8.3,
 •HL 8.4, HL 8.5, HL 12.6, HL 25.78,
 HL 25.82
 Höpfner, Jakob •HL 10.1, HL 10.8
 Hoppe, H. CPP 12.71
 Hoppe, Harald CPP 1.7, CPP 12.50,
 CPP 12.60, CPP 12.62, CPP 12.63
 Hoppe, Wolfgang •MA 18.1, MA 24.4
 Hoppstock, Paul DS 20.21
 Hordiuchuk, Oleh HL 23.11
 Hörhold, Sebastian TT 22.12
 Hörlich, Florian HL 22.9
 Hörmann, Lukas MM 10.2, •O 28.1,
 O 28.8, O 28.9, O 29.7
 Hörmann, Max TT 23.2
 Hörmann, Nicolas O 8.1, O 38.7
 Hörmann, Nicolas G. O 8.3, O 8.7,
 •O 31.1, O 31.3, O 31.6, O 38.3, O 38.5
 Hormozi, Mohammadali •O 58.13
 Horn, Alexander CPP 12.62, MA 35.49
 Horn, Jonas CPP 12.51
 Horn-Cosfeld, Beate HL 7.9
 Hornemann, Andrea O 7.9
 Hörner, Andreas MA 28.7
 Hornung, Daniel SOE 7.2, SOE 17.1
 Hornung, Florian HL 25.62
 Hornung, J. TT 25.9
 Hornung, Jean-Pascal TT 22.11
 Horn-von Hoegen, Michael HL 13.2,
 HL 30.44, O 2.10, O 16.3, O 18.4,
 O 18.10, O 30.2, O 33.8, O 54.4, O 78.3
 Horodecki, Paweł QI 8.6
 Horodecki, Ryszard QI 8.6
 Horsfield, Andrew O 83.8
 Horstmann, Birger QI 4.2
 Horstmann, Jan Gerrit O 16.4
 Horstmann, Julia HL 27.4
 Horstmann, Robin •DY 40.7, •DY 44.6
 Horvath, Raphael DS 23.6

Author Index

- Höschen, Till MM 4.10
Hoshiyaripour, Sheila •BP 12.18
Hossain, MD Faruq BP 12.23
Hosseini Fard, Mohsen •HL 30.34
Hosseinfar, Rahil MA 19.19,
•MA 35.25
Hosseini-Toudeshki, Hamed MM 13.1
Hossenfelder, Sabine DY 3.3
Hötger, Alexander •DS 17.5, HL 11.1,
HL 11.9, HL 25.23
Hötzel, Rudolfo •HL 10.11
Hou, Shujin CPP 48.3
Hou, Xiao •O 21.4, O 73.7
Houska, Karina MA 19.28
Hövel, Philipp •SOE 9.1
Hovořáková, Kristýna MA 8.12,
MA 19.26
Howard, Ian CPP 17.4
Hoye, Robert •CPP 19.1
Hricovini, Karol O 73.6
Hruby, Martin CPP 45.4
Hsieh, Tzung-En O 45.4
Hsieh, Yu-Ling HL 31.1
Hsu, Chiao-Peng •BP 4.3
Hsu, Hsiao-ping CPP 9.3, •CPP 49.5
Hsu, Hua Shu MA 35.38
Hsu, Lan-Tien •KFM 25.9
Hsu, Li-Yun CPP 39.3
Hsu, Pin-Jui O 13.3
Hu, Guangwei O 37.7
Hu, Kun •MA 42.3
Hu, Wen MA 2.3
Hu, Zhixin O 69.6
Huang, Di-Jing MA 6.1
Huang, Haonan O 7.8, O 57.1, O 80.6
Huang, Hsiao-Yu MA 6.1
Huang, Jiasheng HL 17.1
Huang, Jun Hui HL 25.10
Huang, Junwei KFM 8.3
Huang, Liang DY 19.5
Huang, Mantao MA 2.3
Huang, Qunsheng •QI 4.29
Huang, Shuyu O 17.10, •O 22.6, O 39.4
huang, wantong •O 18.15, O 34.4
Huang, X. O 6.9
Huang, Xiaochun O 25.5
Huang, Xiaohui MM 17.3
Huang, Yen-Lin DS 13.3
Hubatsch, Lars •BP 8.12
Hübener, Hannes MM 9.4
Huber, Bernhard O 61.3
Huber, Dominik •BP 5.5
Huber, Felix •O 34.5, QI 6.10, •QI 9.1,
QI 9.3
Huber, Gerhard HL 7.8, QI 4.39,
•QI 13.6
Huber, Liam MM 31.4, MM 34.1
Huber, Linus F. •CPP 17.6
Huber, Lucas HL 23.6
Huber, Marcus QI 9.4
Huber, Markus A. HL 20.2
Huber, Martin TT 7.6
Huber, Nico •TT 25.7
Huber, Patrick CPP 12.38, CPP 12.39,
MM 10.15, MM 10.16, MM 18.11,
MM 18.27, MM 18.34, MM 35.7,
•QI 1.8, QI 1.10, QI 12.4
Huber, Phillip MM 4.10
Huber, Renato BP 7.29
Huber, Rupert HL 4.3, HL 13.8,
HL 20.2, HL 40.1, HL 40.5, O 9.13,
O 33.7, O 68.4
Huber, Sebastian TT 16.11
Huber, Thomas TT 3.2, •TT 30.24
Huber, Tobias •SYED 1.5, HL 17.7,
HL 19.5, HL 25.80, HL 26.11
Huberich, Lysander •O 18.19
Hubert, Maxime BP 7.23, BP 12.22,
BP 14.4, •BP 22.7, •DY 44.9,
•DY 46.16
Hübler, Matthias •TT 29.13
Hubmann, Stefan •HL 33.3, •HL 40.7
Hübner, Jens HL 20.7, •HL 25.93,
HL 25.94
Hübner, R. HL 22.1
Hübner, René MA 4.3, MA 28.8
Hübner, Ruven •HL 15.5
Hübner, U. O 81.6
Hübner, Uwe BP 7.36, CPP 11.2,
HL 6.4, HL 42.7
Hucht, Alfred DY 44.17, O 30.2,
TT 21.35
Hucht, Fred •DY 49.10
Huck, Christian O 40.2
Hücker, Markus TT 7.6
Huckfeldt, Pia MM 4.2
Huebl, Hans MA 7.2, MA 19.41,
MA 22.2, MA 34.4, MA 35.6, MA 35.7,
MA 35.35, MA 35.37, TT 15.1,
TT 27.7, TT 29.11, TT 31.5, TT 31.22
Huempfer, Tobias O 41.5
Hug, Hans Josef MA 23.3
Hugdall, Henning TT 29.5
Hugdall, Henning G. •TT 27.11
Hugel, Thorsten BP 7.5, BP 15.2,
BP 15.7
Hugenschmidt, Christoph MM 4.4,
•O 63.1, O 63.2
Hüger, Daniel CPP 11.2
Huggins, William J. QI 12.5
Huguenin-Dumittan, Kevin K. CPP 9.2
Hühn, Kai •HL 25.94
Huhn, Simon KFM 25.12
Huhn, Thomas TT 29.6
Hula, Tobias MA 28.11, MA 35.8
Hüllen, Isabell HL 19.3, HL 25.95,
HL 30.7, •HL 37.1, HL 37.3
Hültsberg, Marcel •DY 40.1
Humberg, Niklas •O 5.8
Hummel, Felix MM 12.7
Hummer, Gerhard BP 15.3
Hümmer, Thomas HL 25.23, HL 30.6,
QI 5.9
Humphol, Simon HL 19.10
Hung, Tzu-Chao •O 74.5
Hunger, David BP 7.32, HL 17.5,
HL 25.23, HL 30.6, QI 4.9, QI 4.10,
QI 4.12, QI 4.16, QI 4.17, QI 4.31, QI 5.4
Hunnestad, Kasper •KFM 7.2
Hunnestad, Kasper A. KFM 7.3
Hunt, Benjamin M. O 81.3
Huse, Nils MA 31.6
Husel, Lukas •HL 30.6
Hüsgen, Bruno CPP 17.39
Hüsing, Nicola CPP 17.23
Huss, Tabea •MM 2.4
Hussak, Sarah-Alexandra KFM 3.4
Hussein, Robert HL 3.8
Hussin, Anas •BP 12.33
Hustedt, F. •TT 20.8
Huster, Constantin BP 12.4, CPP 9.7
Huster, Jeldrik •QI 4.14
Huth, Michael MA 35.11, TT 6.10,
TT 26.3
Hutsch, Sebastian CPP 1.5, CPP 1.12,
CPP 26.6, •CPP 40.6
Hüttel, Andreas TT 10.5
Hüttel, Andreas K. •TT 2.1, TT 2.2,
TT 15.6, TT 29.7, •TT 29.17
Hütten, Andreas BP 7.37, DS 4.3,
DS 5.2, MA 2.2, MA 19.25, MA 19.27,
MA 19.32, MA 35.63, MM 18.16,
MM 18.17
Hutter, Mark DS 20.19, O 18.5, •O 18.6,
O 55.13
Huttner, Andrea DS 5.4
Hüttner, N. •TT 20.9
Hüttner, Niklas TT 15.6
Hwang, Jiyoung O 51.7, O 80.5
Hyart, Timo TT 25.12
Hyllus, Philipp QI 8.8
Hyman, Anthony BP 8.12
I. K. Munk, Morten •QI 1.6
I. Mazin, Igor O 48.6
I. Urgel, José O 79.6
I. Vasyuchka, Vitaliy MA 19.59
Ibañez-Azpiroz, Julen O 48.2, O 50.10,
TT 25.4
Ibarra, Rebeca •MA 42.5
Ibbeken, Gregor •CPP 45.5
Ibrahim, Eslam •MM 25.3
Ibrahim, Mohamed •O 12.2
Ichikawa, Masatoshi BP 14.6
Ichikawa, Takafumi BP 6.2
Ickert, Karina DS 6.4
Icking, Eike QI 1.2
Icking, Eike Thomas •HL 29.2
Idriss, Hicham •O 70.7
Iftikhar, Emil DY 8.9, SOE 6.9
Iftikhar, Zubair TT 37.7
Iglesias, Alvaro Gomez HL 10.3
Igliev, Hristo CPP 12.64, O 13.7
Ihle, Alexander O 6.2, O 14.2, •O 40.6,
O 41.2
Ihle, Thomas •DY 50.3
Ihn, Thomas TT 10.4
Ihrig, Bernhard TT 23.3
Ihssen, Soeren •TT 31.1
Ihssen, Sören TT 31.2
ilic, stefan TT 10.2
Il'ichev, Evgeni TT 3.2
Illas, Francesc O 62.7
Illien, Pierre BP 26.5
Illig, Maja BP 26.4
Illner, Hannah •O 69.7
Ilse, Sven DS 14.4
Ilyakov, Igor MA 21.7
Ilyin, Maxim O 22.4
Imai, Satoya •QI 2.7, QI 3.3
Imbalzano, Giulio O 58.9
Imlau, Robert MM 33.5
Imre, Alexander M. •O 63.6
Inamdar, Mandar M. BP 22.2
Indris, Sylvio KFM 15.7
Iniguez, Jorge •TUT 3.2, •KFM 1.2,
•KFM 10.2, MM 23.2
Inosov, D. S. •MA 4.1, MA 14.6,
MA 35.53
Inosov, Dmytro MA 35.42, MA 42.5,
TT 21.12, TT 23.4, TT 23.12
Inti, Sodemann TT 21.17
Ioannou, Christina QI 4.9
Ioannou, Marios QI 12.10
Ionita, Alexandru TT 27.1
Ionov, Andrey O 23.4
Ionov, Leonid CPP 7.5
Iorsh, Helmut HL 15.7
Irani, Ehsan SOE 17.2
Irländer, Kilian •MA 19.20
Irmer, D. MM 21.7
Irmiler, Andreas MM 12.7
Irrazábal-Moreda, Olvido DS 20.4
Irtlenkauf, Oliver •TT 30.13, TT 30.20
Irvin, Patrick MM 10.30
Isaeva, Anna MA 31.3, MA 31.5,
TT 20.2
Iseke, Eike QI 1.11
Isele, Marc •DY 44.3
Ishida, Hiroshi MA 20.6
Ishii, Ayumu O 52.5
Islam, M.M. •CPP 12.71
Islam, Md Fhokrul MA 41.3
Islam, Md Moidul CPP 1.7, CPP 12.60
Islam, Sourav •CPP 14.6
Ismail, Maneesha •O 47.8, O 71.2
Isobe, Masahiko MA 6.4, TT 8.7
Issac, Abey CPP 12.58
Ito, Suguru O 9.13, O 33.2
Ito, Yuichi •DY 40.5
Iurchuk, Vadym MA 35.8
Iuşan, Diana MA 30.5, O 53.3
Ivandekic, Goran CPP 28.6
Ivanisenko, Julia MM 18.18
Ivanov, Alexander TT 8.2, TT 21.12
Ivanov, Tzvetan DS 16.4
Ivanov, Viktor CPP 12.23, •CPP 12.28
Ivanova, Daniela •MM 18.3
Ivanova-Rohling, Violeta N. •QI 3.4
Ivashko, Oleh MM 18.35
Ivec, Arian •BP 13.4, BP 13.8
Ivlev, Sergei I. CPP 39.1
Iwakiri, Shuichi TT 10.4
Iyer, Priyanka BP 17.7
Izadi, Sepideh HL 42.1
Izardar, Ankit MA 32.3
J. Giessible, Franz O 14.1
J. Lopes, Joao Marcelo •DS 22.5
J. Rost, Marcel O 8.6
Jabeen, Fauzia HL 22.7
Jäckering, Lina •O 59.5
Jacob, David •O 50.6
Jacobs, Daniel HL 5.11
Jacobsen, Sol TT 29.5
Jacobsen, Sol H. TT 27.11
Jacobson, Peter O 74.2
Jadczak, Joanna HL 11.4
Jaeger, Arndt HL 25.90
Jaekel, Simon •O 15.2, O 15.4, •O 74.7
Jaeschke-Ubierno, Rodrigo •MA 19.42
Jäger, Daniel CPP 17.21
Jäger, Henrik Konstantin •CPP 12.25
Jäger, Lukas HL 21.11, HL 25.46
Jäger, Miriam •BP 15.7
Jagodkin, Denis MA 35.30
Jagtap, Nagesh S. •HL 19.8
Jahn, Reinhard BP 9.4, BP 17.6
Jahn, Reinhart BP 12.54
Jahnke, F. HL 4.7, HL 4.9
Jahnke, Frank HL 8.2, HL 15.3,
HL 25.30, HL 30.7
Jahnke, Kevin •BP 26.4
Jain, Archana HL 25.68
Jain, Mitisha •DS 20.30
Jaiswal, Pranay BP 8.10
Jaitner, Noah •DY 45.11
Jakes, Peter MM 8.8
Jakob, Christopher TT 31.6
Jakob, Franziska •CPP 12.1,
CPP 17.20
Jakob, G. MA 19.63
Jakob, Gerhard MA 18.8, MA 19.43,
MA 19.60, MA 22.1, MA 35.1,
MA 35.46
Jakob, Peter O 17.4, O 17.8, O 17.11
Jakschik, Jens •HL 17.2
Jakub, Zdenek O 10.5, •O 40.4,
O 44.7, O 57.5, O 58.4
Jakubczyk, Fabian •TT 30.5
Jalaal, Mazi BP 4.2
Jalaal, Maziyar CPP 7.6
Jalabert, Rodolfo DY 46.20
Jalil, Abdur R. TT 18.9
Jalil, Abdur Rehman DS 21.2, HL 7.3,
HL 19.7
Jamebozorgi, Vahid •O 53.2
Jana, Sanchayeeta •O 35.7
JANA, SUBHADIP •MA 40.2, MA 40.3
Janas, David MA 35.70, •O 42.3,
O 55.5, O 55.9
Jandová, Dagmar KFM 11.1
Janik, Alexander •BP 12.19
Janisch, Rebecca MM 6.5
Janke, Svenja M. DY 35.5
Janke, Wolfhard DY 26.5
Jankowski, Maciej O 41.3
Janssen, Lucas QI 13.9
Janoschek, Marc MA 31.9
Janoschka, David O 2.10, O 33.8,
O 65.1, O 78.3
Jansen, David •TT 34.6
Jansen, G. S. Matthijs MA 8.1,
MA 35.20, •O 2.2, O 2.9, O 9.10,
O 16.6, O 16.9, O 33.3, O 48.9
Janßen, Marten L. DS 20.25
Jansen, Marvin M. HL 25.98
Jansen, Marvin Marco HL 33.7
Janshoff, Andreas •BP 13.1
Janson, O. •MA 4.1
Janson, Oleg MA 18.7, O 43.8, TT 5.2,
TT 28.6
Janssen, Henning •MA 11.3
Janssen, Jan •MM 25.1
Janssen, Lucas •QI 13.10
Janssen, Lukas TT 5.5, TT 23.3,
TT 24.2, TT 24.10
Janszonn, Andreas T. G. TT 27.11
Janz, Stefan HL 30.26
Janzen, Benjamin M. •HL 18.5
Janzen, Christian MA 27.5, MA 35.47,
•MA 35.64
Jaouen, N. MA 27.1
Jaques, Ygor Morais O 15.3
Jarjat, Lucas TT 32.4
Jarman, John HL 25.65
Jarosik, Alexander •DY 31.2
Jauernik, Stephan O 9.4, O 16.8
Jauho, Antti-Pekka O 72.4
Jauk, Thomas •MA 35.33
Jaurigke, Lina •DY 45.10, DY 45.11,
DY 48.1
Javadi, Alisa HL 2.5, HL 19.1, HL 35.4
Javaloyes, Julien DY 15.3, DY 15.4
Javed, Mohammad Atif •QI 8.2
Jayabalan, Jesumony O 16.11
Jayabalan, Roshini •CPP 28.7
Jayakumar, Vaishnavi •TT 21.26
Jazavandi-Ghamsari, Shima HL 25.68
Jeangros, Quentin HL 5.11
Jeckelmann, Eric TT 34.4
Jede, Ralf O 35.5, O 37.8
Jeggler, Julian •DY 49.6
Jeindl, Andreas O 6.1, O 28.1, O 28.7,
O 28.8, O 28.9, O 29.7
Jekat, Felix HL 25.77
Jelínek, Pavel O 14.5, O 51.1, O 79.1,
O 79.6, O 81.1
Jelli, Eric •BP 10.4
Jena, Jagannath MA 12.10
Jenewein, Christian MM 35.3
Jenni, Kevin MA 35.72
Jentgens, Henrik MA 23.2
Jentzsch, Jana BP 7.35
Jeon, Dae-Woo HL 14.7
Jeon, Hansol •CPP 20.3, •MM 18.33
Jeon, Serim •O 51.6
Jeong, Hyowon •HL 3.9, HL 12.4
Jeong, Yejin O 63.4
Jesche, Anton TT 21.15
Jesche, Harald MA 16.7
Jessen, Bjarke O 54.1, O 72.4
Jetter, Michael HL 4.6, HL 4.11,
HL 12.3, HL 17.1, HL 17.4, HL 17.5,

- HL 17.7, HL 25.62, HL 25.70,
HL 25.88, HL 26.2, HL 26.3
JHA, MANI CHANDRAMM 18.12
Jha, NehaMA 35.65
Ji, Keyan•O 22.7
Ji, QingCPP 27.3
Ji, RanDS 20.3
ji, shuai-huaO 18.15
Jia, Baoxin•O 15.5
Jia, Yifan•QI 12.12
Jiang, BinO 46.6
Jiang, Chang-MingHL 24.9
jiang, haihong•MM 16.2
Jiang, KailiMM 12.9
Jiang, Xinyu•CPP 1.6, CPP 12.49,
CPP 12.65, CPP 12.67, CPP 48.3
Jiang, Xiongzhuo•HL 30.29
Jiang, YuxuanDY 12.2, DY 12.5
Jiang, ZhangQI 10.5
Jiang, Zhihao•O 54.1, O 73.8
Jibuti, Luka•TT 30.4
Jimenez Divins, NuriaO 52.12
Jiménez Herrera, Miguel Angel
•TT 7.9
Jimenez-Cavero, PilarMA 21.9
Jiménez-Siebert, EvaBP 10.4
Jin, DongliangCPP 18.5
Jin, Hui-KeMA 35.44
Jin, KedaMA 19.55, •O 54.6
Jin, LeiMA 23.4
Jin, Limei•DY 8.2, •SOE 6.2
Jin, Ou•MM 17.3
Jin, Xuelin•HL 25.84
Jiruschek, ChristianHL 4.3
Jinawali, GirirajO 30.2
Joachim Graf von Westarp, Mark
KFM 25.21
Jobbitt, NicholasQI 4.12
Jochum, JohannaMA 35.54, TT 12.3
Johánek, ViktorO 3.2, O 20.1, O 70.2
Johanning, MichaelQI 12.4
Johansson, AnnikaMA 24.6,
MA 35.76, O 44.10
John, Karin•BP 13.10
John, RobinMA 8.12
John, ThomasBP 3.7
John Weymouth, AlfredO 14.1
Johnson, D. C.TT 30.17
Johnson, David C.DS 20.29, DS 22.7
Johnson, FreyaMA 29.6
Johnson, ManuelCPP 1.11
Johnson, Steven•TT 36.1
Jolie, WouterO 18.16, •O 71.4
Jonak, M.TT 12.11
Jonak, MartinMA 9.1
Jonas, BjörnHL 3.6, HL 25.56,
•HL 26.1, HL 36.4, TT 17.5, TT 17.6,
TT 17.7
Jonda, Lukas•MA 35.32
Jones, Alfred•O 72.4
Jones, BarbaraQI 4.27
Jong, PatrickHL 3.10
Jöns, KlausDS 17.7
Jöns, Klaus D.DS 20.46, HL 8.1,
HL 8.10, HL 17.8, HL 19.2, HL 25.1,
HL 25.56, HL 26.1, HL 26.4
Jönsson, HannesMA 12.12
Jönsson, J.MA 25.4
Joos, Raphael•HL 17.1
Jooss, ChristianHL 30.27, O 20.7
Jorba, PauMA 35.72
Jorde, LaraBP 7.8
Jorgensen, PeterO 43.10
Jörns, Arne•HL 30.21
Joseph, Dijo Moonnukandathil
•CPP 12.74
JOSHI, HIMANSHU•BP 15.1
Jost, Daniel•MA 6.5
Josten, Nicolas•MA 32.2
Josten, SabineCPP 37.8
Jourdan, MartinMA 19.59, MA 21.5,
MA 35.50
Jovic, VedranDS 20.35
Joy, Aprem•TT 5.1
Joyez, PhilippeTT 37.7
Jozwiak, ChrisO 72.4
Juan, Mathieu L.QI 4.33
Juckeland, G.TT 13.5
Jülicher, FrankBP 8.5, BP 8.11,
BP 8.12, BP 22.2, BP 22.4, BP 27.3,
BP 27.5
Julien, Jean-DanielBP 10.5
Jung, Alexander•TT 31.22
Jung, Florian A.CPP 12.35
Jung, Hyein•O 9.7
Jung, Hyunwook•O 62.5
Jung, JannisO 79.5
Jung, NatalieHL 4.1
Jung, Soon JungO 65.8
Jungwirth, FelixTT 26.3
Jungwirth, PavelO 64.1
Jungwirth, TomasMA 13.11,
•MA 17.2, MA 34.1, MA 34.7
Junk, Vanessa•TT 18.2
Juo, Jz-Yuan•O 65.8
Jurado, Alejandro BP 12.39, BP 12.40,
•BP 19.8
Jurado Jimenez, Alejandro BP 12.37
Jürgens, Kevin•HL 25.48
Juríček, MichalO 17.12
Justus, Christian•O 59.3, O 59.5
Jutisz, MartinQI 7.8
Jüttner, VinzenzMA 35.55
Jux, NorbertO 5.6
Jyoti, DivyaO 80.5
K. Maiti, PrabalDY 50.7
K. Reb, Lennart CPP 12.47, CPP 28.4
K. Singh, JayantO 74.12
Kaa, JohannesKFM 6.2, KFM 25.13
Kaap, Fabian•TT 30.23, QI 4.38
Kachel, Stefan R.O 12.6, O 41.2,
O 55.13
Kachel, Stefan Renato DS 20.19,
O 12.1
Kachel, TorstenMA 25.7
Kadashchuk, AndreyHL 41.4
Kadasshchuk, Andrey CPP 12.79
Kadlec, Christelle DS 20.32
Kadow, Wilhelm•MA 16.5
Kadzielawa, Andrzej MA 32.8
Kafar, AnnaHL 30.14
Kaganskiy, ArsentyHL 8.6
Kagerer, P.O 21.5
Kagerer, PhilippO 48.10
Kageyama, HiroshiTT 12.4
Kahl, Robert•CPP 12.70, CPP 41.1
Kähler, PeterTT 31.9
Kahne, N.TT 31.8
Kahrmann, PaulTT 31.11
Kaib, David A S•TT 8.4
Kainikkara, GaanaO 17.8
Kaiser, Angelika•HL 18.2
Kaiser, D.O 81.6
Kaiser, FranzSOE 13.2
Kaiser, Katharina•O 64.3
Kaiser, SebastianO 69.3, O 70.1,
•O 70.3
Kaiser, StefanHL 13.7, TT 3.10
Kaiser, U.O 81.6
Kákay, AttilaMA 13.3, MA 19.36,
MA 21.7, MA 22.8, MA 35.8
Kakugo, Akira•BP 26.1
Kalarickal, Nidhin KurianHL 14.1
Kalashnikova, Alexandra M. MA 21.1
Kalbacova, JanaHL 31.2
Kalcheim, YoavDS 25.3
Kaleva, Galina M.KFM 25.1
Kaliman, SaraBP 7.23, BP 12.22
Kalisch, HolgerDS 2.3
Kalisky, B.TT 22.1
Kalitukha, InaHL 32.2
Kalitukha, Ina V.HL 25.92
Kalkan, Sirri Batuhan•HL 6.4,
HL 25.52
Kalläne, Matthias MA 31.6, O 9.1,
O 18.21, O 48.10
Kallert, Patricia•HL 25.56, HL 26.1
Kaltschmidt, BarbaraBP 7.37
Kaltschmidt, Bernhard•BP 7.37,
DS 5.2, MM 18.16, MM 18.17
Kaltschmidt, ChristianBP 7.37
Kalwa, Paul•BP 18.6
Kamata, HiroshiSYQM 1.2
Kamba, StanislavDS 20.32
Kamber, U.TT 10.7
Kamber, UmutMA 30.5, O 53.3,
O 72.5
Kamencek, Tomas CPP 40.5, HL 41.1
Kamenskyi, DmytroMA 33.4
Kamlapure, A.TT 10.7
Kamlapure, AnandO 25.5, •O 72.5
Kammerbauer, FabianMA 19.30,
MA 19.43, •MA 19.44, MA 37.7
Kämmerer, Gérald MA 25.7, •MA 26.1
Kammermeier, Lukas•TT 30.20
Kamp, MartinDS 20.34
Kampermann, HermannQI 4.13,
QI 7.2, QI 7.3, QI 9.7, QI 9.9
Kampfrath, TobiasMA 19.47,
MA 19.51, MA 21.2, MA 21.5,
MA 21.6, MA 21.9, MA 24.4
Kamps, OliverDY 8.3, SOE 6.3
Kampshoff, ChristophBP 9.9
Kamra, Akashdeep•MA 13.6,
MA 34.4
Kamrta, Robin•O 73.10
Kan, Q.HL 4.9
Kan, QiangHL 4.8
Kanai, YosukeO 50.4, O 50.9
Kanani, Mansour•HL 5.10, •HL 23.4,
•HL 23.8
Kanazawa, NaokiQI 13.7
Kandra, Timo•TT 31.26
Kang, HyunminO 18.9
Kang, Ji-HyeHL 30.13
Kang, Kisung•MA 15.1
Kang, KyungnamHL 6.2
Kangsabanik, Jiban•DS 16.2
Kanistras, NikolaosMA 35.51
Kansanen, Kalle S. U.TT 15.5
Kantelberg, Richard•CPP 27.6
Kantian, AdrianTT 28.10, TT 38.3,
TT 39.8
Kantner, MarkusHL 19.11
Kantorovich, SofiaCPP 34.3,
CPP 44.2, DY 11.1
Kantz, HolgerDY 52.5, SOE 20.5
Kapfer, MaëlleO 54.1
Kapfer, Sebastian C.TT 24.6,
TT 24.15
Kapil, Venkat•O 43.6
Kaplan, ArkadyTT 7.6
Kappe, FlorianHL 8.7, HL 26.7
Kappen, Hilbert J.O 23.1
Kappes, ManfredDS 5.1, O 52.7,
O 52.8
Kappl, Patrick•TT 28.9
Kappler, Julian•DY 28.2, •DY 40.3
Karakachian, H.O 25.3
Karakachian, HragO 41.8
Karami, Azam•HL 27.3
Karan, SujoyO 7.8, O 57.1
Karapatzakis, IoannisTT 31.24,
•TT 31.25
Karczewski, GrzegorzO 35.5, O 37.8
Kardynał, BeataHL 25.20, HL 25.84,
HL 30.10
Karetta, Bennet•MA 35.15
Karg, Alexander•DS 26.2
Karg, MatthiasCPP 17.16, CPP 41.8
Karimi, Amin•O 17.3
Karli, Yusuf•HL 8.7, HL 26.7
Karmakar, MintuDY 46.21
Karmo, MarselHL 25.39
Karnaushenko, DaniilBP 7.29
Karnaushenko, Dmitry D.BP 7.29
Karpitschka, Stefan BP 7.39, BP 10.8,
BP 12.48, BP 26.2, CPP 7.1, CPP 20.3
Karpov, PetrDY 19.1
Karras, PanagiotisO 63.5
Karthein, JanHL 19.7
Kartouzian, ArasCPP 28.1, O 13.6,
O 13.7
Kartsovnik, MarkTT 21.25
Kartsovnik, Mark V.•TT 12.8
Karube, KosukeMA 27.2, MA 27.7,
MA 27.10
Karzel, MarekHL 23.11, •HL 32.2
Käsebieber, THL 42.2
Kaßen, Alexander HL 13.2, •HL 30.44
Kashuba, Oleksiy•TT 34.3
Kaspar, Christoph•TT 13.4
Kasper, ChristianCPP 26.5
Kasper, ValentinQI 6.10
Kasprzak, JacekHL 25.8
Kassel, Johannes A.•DY 52.5,
•SOE 20.5
Kasten, PeerO 17.5, •O 28.6
Kastenmeier, MaximilianO 3.6,
•O 20.1, O 70.2
Kastl, ChristophDS 17.5, DS 19.1,
HL 7.2, HL 11.1, HL 25.23
Kästner, Bernd•O 7.9
Kästner, ChristianCPP 12.60
Kastner, Johann LucaDY 18.4,
SOE 10.4
Kästner, JohannesMM 32.3
Kastner, LukasHL 40.1
Kataev, ElmarO 12.12
Kataev, Vladislav MA 14.8, TT 12.10,
TT 20.2, TT 20.3
Katnagallu, Shyam•O 27.2
Kats, MikhailHL 18.1
Katsnelson, M. I.O 6.9, TT 10.7
Katsnelson, Mikhail MA 15.7, TT 12.9,
TT 16.2
Katsnelson, Mikhail I.MA 30.5,
MA 38.4, O 51.4, O 53.3, O 72.5
Katsumoto, Hiroshi•MA 14.3
Kattemölle, JorisQI 12.7
Katter, MatthiasMA 29.9
Katz, NadavTT 37.6
Katzer, ManuelHL 11.7, HL 11.10,
•HL 11.11, HL 25.14, TT 7.7, TT 33.4
Kauch, AnnaTT 21.29
Kauffmann, AlexanderMM 4.8
Kaur, GagandeepO 15.7
Kaur, RanbirCPP 17.33, •HL 25.57,
HL 36.10
Kaushik, Ravi•HL 33.10
Kavický, Dušan•TT 26.5
Kavokine, NikitaO 46.2
Kaya, NaziaMA 25.1
Kaya, SarpO 10.2
Kayatz, Florian•QI 1.5
Kaymazlar, KorayHL 17.10
Kaznacheeva, MargaritaDS 13.1
Ke, Yaling•TT 16.9, •TT 21.10
Keeling, JonathanHL 30.46
Keeney, LynetteKFM 2.5, •O 44.2,
•O 44.9
Kegelmann, LukasHL 5.4
Kehagias, ThomasMA 19.53
Kehlberger, AndreasMA 23.5
Kehr, SusanneO 37.5
Kehrein, StefanTT 28.8, TT 33.2
Keil, RobertHL 8.3, HL 8.5, HL 12.10,
HL 25.82
Keil, Waldemar CPP 17.10, CPP 17.39,
KFM 15.3
Keimer, BernhardHL 13.7, MA 6.4,
MM 7.4, TT 3.10, TT 21.12
Keller, Elisabeth•MM 33.1
Keller, FlorianO 15.11, •O 73.11
Keller, ThomasMM 7.4
Keller, Thomas F.CPP 17.12
Kelling, J.TT 13.5
Kellnberger, Richard•BP 12.14
Kellner, NicoleTT 15.6
Kelly, DanielO 27.3
Kelterborn, SimonBP 10.2
Kempa, HeikoHL 25.32, HL 27.3,
HL 27.4, HL 34.5
Kempes, ChristopherSOE 14.3
Kempf, Sebastian •SYUK 2.5, TT 17.2,
TT 17.3, TT 17.4, TT 31.9, TT 31.10,
TT 31.11
Kenawy, Ahmed•QI 13.3
Kendzo, GutenbergMA 19.59,
•MA 35.50
Kennedy, OscarTT 32.3
Kennes, DanteTT 11.3, TT 33.5,
TT 33.9
Kennes, Dante M.MM 9.3, TT 10.6
Kentsch, UlrichHL 17.9, HL 19.8,
MA 4.3, MA 35.68
Kentzinger, EmmanuelMA 33.2
Keppeler, DanielBP 9.9
Kerber, NicoMA 12.9, MA 37.7
Keren, I.TT 22.1
Kern, ChristianO 2.2
Kern, FelixMM 35.1
Kern, JohannesHL 19.9, HL 20.1,
HL 25.27
Kern, KlausBP 9.2, MA 2.4, MA 27.3,
O 7.4, O 7.5, O 13.2, O 57.1, O 65.8
Kern, Lisa-MarieMA 2.1, •MA 12.2
Kerres, Peter•DS 4.1, DS 20.42,
DS 23.5
Kerschbaumer, SamuelO 22.4
Kerski, Jens HL 3.4, •HL 8.9, HL 26.8,
HL 26.10
Kerth, GeraldBP 23.3
Keskeklar, Ata•DY 12.3
Keßler, Torsten•TT 16.6
Kesper, LukasO 65.2
Kesselheim, StefanBP 2.3
Kessler, FabianTT 27.8
Kessler, Jill•DS 20.44
Kessler, PhilippDS 20.35
Kessler, StephanTT 1.11
Kessler, TorstenTT 16.5
Kestler, Matthias•HL 4.10
kettemann, stefanO 18.15
Ketterer, Andreas•QI 4.21
Ketzmerick, RolandDY 35.7, DY 43.4
Keyser, Ulrich F.DY 40.3
Kezsmarki, Istvan KFM 14.1, MA 27.2,
MA 32.5, MA 33.1, MA 33.3, MA 33.4,
TT 3.5
Khabipov, MaratQI 4.38
Khademorezaian, Saba•MM 10.7
Khadivianazar, Saba•MM 10.21
Khajavikhan, MercedehHL 4.8,

- HL 9.2
- Khajetoorians, A. A. . . . O 6.9, TT 10.7
- Khajetoorians, Alexander A. MA 30.5, O 23.1, O 25.5, O 51.4, O 51.8, O 53.3, O 72.5
- Khakurel, Krishna O 16.1
- Khalaji, Samira BP 12.4
- Khalil Hezarjaribi, Mahdi . . . •HL 30.17
- Khaliq, Muhammad Waqas MA 35.17
- Khalliulin, Giniyat MA 6.4
- Khalyavin, Dmitry TT 25.11
- Khan, Jafar I. CPP 1.3, CPP 12.60
- Khan, M. HL 22.1
- Khan, Muhammad Bilal HL 17.9
- Khan, Muhammad Moazzam •HL 25.87
- Khan, Nazir TT 8.5
- Khan, Safe MA 18.3
- Khan, Saleem Ayaz •O 73.6
- Khanenko, Pavlo •TT 6.6
- Khanonkin, Igor HL 8.2
- Khare, Krishnacharya CPP 7.7, CPP 12.37
- Khatri, Sumeet QI 8.7
- Khavlyuk, Pavel MM 35.9
- Khaymovich, Ivan •DY 19.6
- Khayya, En-Neita •O 8.4
- Khazae, Adib DY 52.2, SOE 20.2
- Khim, Seunghyun TT 6.6, •TT 6.8, TT 6.9, TT 22.5, TT 23.6
- khodas, maxim TT 10.2
- Kholina, Yevheniia •KFM 11.2
- Khomskii, Daniel •SYOP 1.1
- Khoo, Jun Yong QI 5.2
- Khoroshkaia, Diana •BP 19.6
- Khorshidian, Sara TT 30.10, TT 30.11, TT 31.26
- Khurram, Muhammad •CPP 37.5
- Khusniyarov, Marat DS 20.22
- Ki, Stuart MM 12.5
- Kiaba, Michal MA 6.3
- Kick, Matthias O 82.2
- Kick, Michael •HL 7.5
- Kiechle, Martina MA 35.3
- Kieck, Tom TT 31.7
- Kiefer, Klaus MA 33.7
- Kiel, Annika BP 7.37
- Kiel, Lorenz CPP 12.18
- Kieler, Maximilian F. I. DY 35.3
- Kieler, Maximilian Friedrich Irenäus •DY 43.3
- Kieler, Oliver TT 37.1, TT 37.4
- Kiemle, Jonas •DS 19.1, HL 11.5, HL 25.14, TT 7.7
- Kienberger, Reinhard CPP 12.64, O 13.7
- Kiese, Dominik MA 19.33
- Kieslich, Gregor CPP 28.1
- Kiessler, Filippo BP 2.5, •BP 9.7
- Kiessling, Tobias HL 25.41
- Kikkawa, Akiko MA 27.10
- Kikkawa, Takashi MA 25.5, MA 35.28
- Kikuchi, Lukas DY 28.2
- Kikugawa, Naoki MM 21.3, MM 21.4
- Kilchoer, Cédric CPP 8.5
- Kilibarda, F. TT 13.5
- Kim, C. TT 22.1
- Kim, Eun-Ah •SYES 1.2
- Kim, Gideok TT 3.10
- Kim, Hakseong HL 19.8
- Kim, Hongwon •CPP 12.75, CPP 26.5
- Kim, Jinkyung •O 47.4, O 80.5
- Kim, Jongmin O 15.11, •O 20.10
- Kim, Jung-Hwa MM 7.4
- Kim, Kyoohyun BP 12.24
- Kim, Min-Jae HL 13.7, TT 3.10
- Kim, Sangwon HL 30.43
- Kim, Seo-Jin •MM 23.1
- Kim, Shi En MM 21.1
- Kim, Sungmin TT 2.10
- Kim, Tae Yun •MA 22.9
- Kim, Yong Baek TT 38.2
- Kimák, Jozef MA 29.6
- Kimata, Motoi TT 22.11
- Kimel, Alexey •TT 36.5
- Kimmel, Thomas TT 24.5
- Kimouche, Amina •O 6.3
- Kinast, Angelina DS 13.1
- Kindel, Sebastian HL 30.10
- King, Phil •MA 17.3
- King, Phil D. C. MM 23.1
- Kini M, Sushanth •QI 5.7
- Kippen, Lalminthang MA 19.19
- Kipp, Jonathan •MA 10.5, MA 37.8
- Kira, Mackillo HL 13.8, HL 15.5, HL 40.1
- Kiraly, B. O 6.9
- Kiraly, Brian O 23.1, O 74.5
- Kirby, Brian J. MA 33.2
- Kirch, Anton CPP 27.6
- Kirchheim, Reiner •MM 5.1, MM 9.2
- Kirchhof, Jan HL 25.31
- Kirchhof, Jan N. HL 31.1
- Kirchhoff, Alexander •O 72.6
- Kirchhoff, Susanna •QI 4.40
- Kirchmair, Gerhard QI 4.33
- Kirchmann, P. S. O 9.5
- Kirchner, Barbara O 45.6
- Kiremit, Sinan MM 18.16
- Kirilyuk, Andrei O 44.5
- Kirkpatrick, William O 43.1
- Kirkwood, Nicholas O 78.4
- Kirsan, Azad O 52.10
- Kirsch, Christopher CPP 12.78, CPP 28.7
- Kirschner, Johannes MM 20.4
- Kirsh, Naftali TT 37.6
- Kirshon, Yuri •MM 30.10
- Kirstein, Erik •HL 25.92
- Kirstein, Mark •SOE 3.3
- Kiselev, Nikolai MA 19.1, MA 37.2
- Kiselev, Nikolai S. •MA 27.4, •MA 27.6
- Kißlinger, Tilman O 63.6, O 73.4
- Kissling, Christoph TT 37.2, QI 4.38
- Kisslinger, Tilman O 54.9
- Kitatani, Motoharu TT 22.9
- Kittel, Achim O 12.2, O 19.5, O 19.6
- Kivala, Milan O 5.7, O 6.4, O 15.5, O 40.2, O 40.3
- Klapp, Sabine •DY 14.1
- Klapp, Sabine H. L. DY 15.1, DY 16.4, DY 23.4, DY 31.3, DY 40.1, DY 44.5, DY 46.7
- Klar, Peter HL 42.5, MA 41.1
- Klar, Peter J. DS 13.2, DS 18.2, DS 23.3, HL 25.97, HL 32.1, MM 21.9
- Klar, Thomas CPP 14.6
- Klare, Johann P. CPP 12.8
- Klassen, Alexander •CPP 12.9
- Klaßen, Philipp MA 4.4
- Klassen, Thomas MM 17.5
- Kläui, M. MA 19.63
- Kläui, Mathias •SYOP 1.3, MA 10.2, MA 12.4, MA 12.9, MA 15.2, MA 18.8, MA 19.10, MA 19.30, MA 19.43, MA 19.44, MA 19.59, MA 19.60, MA 19.62, MA 21.5, MA 22.1, MA 23.5, MA 24.2, MA 24.8, MA 25.5, MA 34.3, MA 35.28, MA 35.46, MA 35.50, MA 37.7
- Klausmann, Matthias •QI 4.17
- Klauss, H.-H. MA 4.1
- Klauss, Hans-Henning MA 19.21
- Klebl, Lennart •TT 10.6
- Kleeman, Hans HL 28.1
- Kleemann, Anja BP 12.4
- Kleemann, Felix BP 12.50, BP 12.51
- Kleemann, Hans CPP 1.9, HL 28.2
- Klees, Raffael L. •SYSD 1.2
- Kleimeier, Nils Fabian O 33.9
- Klein, Benedikt P. O 12.6, O 28.4, O 41.1, •O 41.2
- Klein, Julian DS 17.5, DS 22.3, HL 25.13
- Klein, Simon •TT 22.10
- Klein, Yannick TT 12.13
- Kleine, Hannah •O 50.1
- Kleiner, Reinhold •PLV I, DS 25.1, DS 25.3, TT 37.1
- Kleinhans, Markus TT 21.38
- Kleinherbers, Eric DY 35.9, •HL 3.1, HL 8.9, •TT 20.11, •TT 27.9, TT 29.1, TT 29.12
- KleinJan, Fenneke BP 12.4
- Kleinke, Tobias MA 19.46, •MA 19.48
- Kleinlein, Johannes HL 7.5, TT 32.5, TT 32.8
- Kleinmann, Matthias QI 14.2, QI 14.6
- Kleinschmidt, Peter HL 13.4, HL 25.55, HL 30.42, O 30.6
- Klembt, Sebastian •SYQM 1.4, HL 15.7, HL 22.7, HL 41.3
- Klement, Philip •DS 21.1, HL 6.2, HL 15.6, •HL 32.1
- Klemeyer, Lars •HL 25.79
- Klemke, Bastian MA 33.7
- Klenk, Rouven QI 4.14
- Klenovsky, Petr •HL 22.8, •HL 39.3
- Klep, Igor QI 9.1
- Klepzig, Lars HL 39.4
- Klett, Marcel TT 28.11, •TT 34.8
- Kliemt, K. MA 35.24
- Kliemt, Kristin KFM 25.21, MA 25.1, TT 6.4, TT 20.7, TT 21.1, TT 21.2, TT 21.3, TT 21.4, TT 21.5, •TT 21.6, TT 21.7, TT 21.13
- Kliesch, Martin •QI 3.1, QI 3.2, QI 4.30, QI 9.9, QI 12.3, QI 12.4
- Klimmer, Sebastian •HL 15.1, HL 25.5, HL 25.7, HL 29.4
- Klingberg, Tim •BP 8.2
- Klingeler, Rüdiger MA 9.1, •MA 26.4, MA 35.43, TT 12.5, •TT 12.11
- Klingner, Nico DS 1.5, MA 28.8
- Klippenstein, Viktor •CPP 9.4, CPP 12.27, •DY 38.6
- Klöffel, Tobias O 58.10
- Klomp, Arne J. MM 20.5, MM 30.3
- Klompmaker, Lars O 35.5, •O 37.8
- Klopp, Christoph •DY 4.6, •DY 38.4
- Klos, Kyra •DY 45.8
- Klose, Christopher •MA 2.3
- Klosinski, Adam •TT 39.6
- Kloth, Sebastian •DY 28.4
- Klumpp, Stefan BP 10.8, BP 12.33, BP 12.58, BP 13.6, DY 44.10
- Klunnikova, Yulia •MM 20.5
- Klupsch, Michael DS 6.4
- Klushin, Leonid CPP 17.37
- Kluth, Elias •HL 14.5, HL 22.6, HL 25.40
- klyatskaya, svetlana O 80.3
- Klykov, Sergei DY 4.7
- Knap, Michael DY 43.2, MA 16.5
- Napman, Ross •MA 12.3
- Knauer, Arne HL 10.1
- Knauer, S. MA 35.12
- Knauer, Sebastian MA 13.2
- Knebel, Alexander O 79.7
- Knebel, Georg TT 22.11
- Knechtges, Philipp BP 2.3
- Kneip, Nina TT 31.7
- Kneiß, M. HL 18.3
- Kneiß, Max HL 30.24
- Kneiss, Max HL 30.25
- Kneissl, M. HL 10.5
- Kneissl, Michael HL 10.1, HL 10.4, HL 10.6, HL 10.7, HL 10.8, HL 10.9, HL 10.10
- Knill, Emanuel •QI 1.9
- Knodt, Matthias CPP 39.5
- Knol, E. J. O 6.9, TT 10.7
- Knol, Elze J. O 23.1, O 72.5
- Knol, Marvin O 13.5, O 74.11
- Knölker, Hans-Joachim MA 19.21
- Knoll, Alexander MM 10.4, •O 46.4
- Knoll, Armin TT 37.1
- Knolle, Johannes DY 5.2, DY 43.1, MA 16.4, MA 35.44, TT 7.4, TT 29.18
- Knoller, Fabian O 70.1
- Knoop, Florian •MM 21.2, O 83.10
- Knoop, Franz Niklas •O 30.6
- Knopf, H HL 42.2
- Knopf, Heiko HL 20.6, HL 28.7
- Knop-Gericke, Axel O 49.8
- Knorr, Andreas DS 20.12, HL 6.10, HL 11.7, HL 11.10, HL 11.11, HL 25.14, HL 30.4, HL 31.4, O 37.4, O 59.1, O 61.2, TT 7.7
- Knorr, Matthias HL 13.8
- Knorr, Roland L. •SYSM 1.4
- Knothe, Angelika •DS 19.3, •DS 19.4
- Knotz, Gabriel BP 22.5, •DY 49.8
- Knudsen, Jan O 54.14
- Kny, Anna O 20.8
- Kny, Anna Juliana •O 12.8
- Ko, Tsz Wai MM 10.3, O 46.4
- Ko, Wonhee O 21.1
- Koall, Maximilian •O 19.10
- Kobayashi, Koji TT 11.1
- Kobayashi, Shingo TT 38.1
- Kobin, Björn O 5.2, O 32.7, O 55.12
- Kobitski, Andrei Yu BP 8.2
- Köbl, Julia O 12.11, O 12.12
- Kobl Müller, Gregor HL 3.9, HL 3.10, HL 12.4, HL 25.50, HL 42.4
- Köbrich, Manuel MM 18.14
- Kocán, Pavel O 16.12, O 44.8
- Kocer, Emir •MM 10.3
- Koch, Alexander •HL 18.1
- Koch, Christoph T. •MM 22.1
- Koch, Colin-Marius •DY 16.6
- Koch, David •MA 19.12, MA 29.7, MM 18.25
- Koch, Elias R. •DY 15.4
- Koch, Erik TT 21.28, TT 28.1
- Koch, Florian •TT 32.6
- Koch, J. O 41.7
- Koch, Jennifer •TT 3.9, TT 30.10
- Koch, Julian •DS 25.4, O 18.7, O 18.14
- Koch, Juliane •HL 25.55
- Koch, Leon TT 31.23, QI 4.6, QI 4.34, QI 4.35, QI 4.36, QI 4.37, QI 4.39
- Koch, Martin CPP 14.7, CPP 48.1, HL 25.16
- Koch, Martin Michael MA 35.48
- Koch, Norbert CPP 28.7, HL 28.4, O 32.7
- Koch, Roland O 72.4
- Koch, Stephan W. HL 13.10, HL 25.18
- Koch, Thomas HL 25.60
- Kochan, Denis HL 6.7, TT 3.13, •TT 22.7, TT 30.18
- Köcher, Simone •MA 11.5
- Kochetov, Vladislav MM 8.2
- Kocic, Nemanja O 79.2
- Kociurzynski, Raisa BP 2.1
- Kocsis, Vilmos MA 14.7, TT 29.16
- Koebler, Hans HL 5.4
- Koeksal, Okan •TT 18.4
- Koelle, Dieter DS 25.1, DS 25.3, TT 37.1
- Koenig, Elio MA 3.3, •TT 1.13
- Koermann, Fritz MM 20.3, MM 25.6
- Koert, Ulrich CPP 39.1, O 17.3, O 30.8
- Koethe, Ulrrich BP 12.21
- Kohanoff, Jorge •MM 18.8
- Kohantorabi, Mona •O 52.9
- Kohl, Peter •PSV II
- Köhler, Anna CPP 12.79, HL 23.2, HL 41.2, HL 41.4
- Kohler, Hannah •O 18.10
- Kohler, Larissa BP 7.32, QI 5.4
- Kohler, Sigmund HL 3.8
- Köhler, Thomas DY 43.5, TT 9.1, TT 16.8, •TT 21.32, •TT 28.10, TT 29.14, •TT 38.3, TT 39.8
- Köhler, Ulrich •KFM 25.3
- Köhler, Werner CPP 12.17, CPP 12.18
- Kohli, Nipin O 49.3
- Kohlmann, Johannes TT 37.4
- Kohlmann, Marcel •MA 8.12, MA 19.26, MA 35.65
- Kohlrantz, Niklas HL 29.3
- Kohminaev, Danial HL 25.73, HL 25.81, •HL 25.86
- Köhne, Ingo CPP 17.32, CPP 17.33
- Kohns, Richard O 63.3
- Kohrs, Daniel O 40.6, O 79.5
- Kokalj, David •KFM 25.6
- Kokott, Sebastian •O 50.2
- Koladi, Vivek HL 25.17
- Kolar, Ken •O 58.15
- Kolatschek, Sascha HL 17.1
- Kolbe, Tim HL 10.1
- Kolbeck, Pauline BP 15.1
- Kolek Martinez de Azagra, Monica •TT 2.12
- Kolhep, Maximilian •HL 18.6
- Kolincio, Kamil K. TT 7.1
- Koliofoti, Christina •QI 13.4
- Kolk, Jasper van der DY 44.18
- Kolker, Jannis CPP 18.4
- Kolle, Mathias BP 19.5
- Koller, Philipp QI 1.4
- Kolley, Francine •BP 12.32, BP 13.3
- Kolmer, Marek O 21.1
- Kolobkova, Elena V. HL 39.5
- Kolomiets, Alexandr MA 35.39
- Kolorenc, Jindric O 51.1
- Kolorenč, Jindrich O 26.3, •TT 6.11
- kölpin, nadja CPP 12.59
- Kölsch, Sebastian •TT 6.10
- Koltchanov, Alexej HL 12.5
- Kölzer, Jonas HL 7.3
- Komaragiri, Yesaswini BP 12.20, •BP 12.23
- Komatsu, Kazma MA 35.33
- Komori, S. TT 22.1
- Konde, Srumika •CPP 14.7
- Konetschny, Alexander DS 18.2
- König, Elio TT 37.14, TT 38.6
- König, Jürgen DY 35.9, HL 3.1, HL 8.9, TT 13.6, TT 20.11, TT 21.35, TT 27.9, TT 29.1, TT 29.12
- König, Kathrin •QI 3.7, •QI 13.7
- König, Markus TT 22.11
- König, Patricia •MM 34.8
- Kononenko, Denys Y. •O 43.8
- Konoplyuk, Sergiy •MA 35.39
- Konrad, Jennifer •O 39.3
- Konrad, Paul •QI 4.41
- Kontermann, Stefan HL 30.31

- Kontos, Takis TT 13.3, TT 32.4
Könye, Viktor TT 11.8, TT 11.9,
TT 18.5, +TT 25.2
Koo, C. TT 12.11
Koo, Changhaiun MA 26.4
Kooij, Floris O 54.8
Koopmans, Bert MA 35.23
Kopatz, Severin +MM 21.5
Kopp, Juri +MA 35.60
Kopp, Robin A. +DY 15.1
Köpp, S. +HL 30.20
Koppe, Nicklas BP 3.4
Koprucki, Thomas HL 19.11
Kopteva, Natalia +HL 23.11
Kopteva, Natalia E. HL 32.2, MA 14.9
Kopteva, Nataliia E. HL 26.9
Kopyshv, Alexey CPP 12.29
Koralan, Sabri MA 35.11
Körbel, Sabine +HL 14.6
Körber, Jonathan QI 5.4
Körber, Lukas +MA 13.3, MA 19.36,
MA 21.7, MA 35.8
Kordisch, Thomas MM 18.16
Kordus, David +O 52.12
Körmann, Fritz +MM 19.1
Körner, Dennis O 32.3
Kormoš, Lukáš O 40.4, O 58.4
Korn, Tobias DS 5.6
Körner, Carolin +MM 1.1
Körner, Chris +MA 28.2
Körner, Wolfgang HL 19.6, HL 36.1
Korneychuk, Svetlana +KFM 15.4
Körnig, André BP 9.10, BP 13.9
Korniienko, Anastasiia +MA 35.17
Korntner, Ralf TT 25.6
Kornyschenko, Anna +MM 18.30
Korolkov, Vladimir CPP 12.9
Korshunov, A. MA 4.1
Körstgens, Volker CPP 12.3, CPP 12.7,
+CPP 45.3
Korte-Kerzel, Sandra MM 4.2, MM 6.1
Kort-Kerzel, Sandra MM 4.5
Kortus, Jens CPP 12.4, MM 18.43,
O 57.7
Korytár, Richard O 11.2, +O 74.4
Korzekwa, Kamil QI 2.3, +QI 2.6
Korzetz, Riko +CPP 17.1, CPP 17.3
Kosarev, Aleksandr N. HL 5.2
Košata, Jan DY 12.4
Kosbahn, David P. +CPP 12.48
Kosche, Luca +TT 21.22
Kosiol, Lasse HL 17.3
Kosmala, Tomasz O 20.8
Košovan, Peter CPP 12.10, CPP 12.24,
+CPP 13.2, CPP 34.1, CPP 45.4
Kossert, Karsten TT 17.2, TT 31.10
Köster, Felix DY 48.1, DY 51.5
Köster, Kerim QI 4.16, QI 5.4
Köster, Sarah BP 7.34, BP 12.7,
BP 12.8, BP 12.9, BP 12.30, BP 13.6,
BP 13.7
Köster, Ulli MM 7.3
Kosto, Yulia O 3.6
Kot, Małgorzata +HL 5.4
Kot, Piot O 71.2
Kot, Piotr O 7.8, O 47.8
Kotewitz, Luca DS 22.2
Kotiuga, Michele O 43.4, O 43.5
Kotomin, E. KFM 18.1
Kott, Viktor +TT 21.18
Kotte, Tommy TT 6.6
Kottke, Josua MM 21.6
Kottke, Tilman CPP 17.18
Kottlarz, Inga DY 8.6, +DY 8.8,
+DY 45.12, +DY 45.13, SOE 6.6,
+SOE 6.8
Kotur, Mladen HL 23.11
Kou, Angela TT 37.5
Koufakis, Eleftherios CPP 20.4
Koulas-Simos, A. HL 4.7, HL 4.9
Koulas-Simos, Aris +HL 4.8, HL 17.3
Kouroudis, Ioannis HL 32.4
Koutná, Nikola KFM 8.2
Kouwenhoven, Leo P. QI 13.11
Kouyate, Maryke +CPP 26.6
Kovacs, Neven TT 31.7
Kovács, A. MA 20.4
Kovács, Alexander KFM 10.4
Kovács, András MA 23.4, MA 27.6,
MA 41.2
Koval, Natalia O 51.10
Koval, Natalia E. O 80.1
Kovalchuk, Sviatoslav HL 11.12,
+HL 31.4
Kovalenko, Maksym HL 23.11
Kovalenko, Maksym V. HL 32.2
Kovalenko, Maxim V. HL 25.92
Kovalev, Sergey HL 25.41, MA 21.7,
TT 3.10
Kovalyuk, Zakhar D. HL 11.10
Kovarik, Stepan O 47.2, +O 47.5
Kowalec, Igor O 62.2
Kowalska, Joanna PSV V
Kowalski, Hagen-Henrik +O 11.1
Kowarik, Stefan +CPP 17.9, DS 1.3
Koynov, Kaloian CPP 28.3, CPP 37.2
Koyuk, Timur DY 24.4
Koziej, Dorota CPP 41.7, DS 13.4,
HL 25.79, KFM 3.4, KFM 25.5,
MM 18.35
Kozioł, Jan Alexander +TT 24.6,
TT 24.15
Kozlov, D. A. TT 20.9
Kozlov, Dimitry TT 19.3
Kozubek, Roland HL 31.3
Krabbe, Phil +DY 24.2
Kraehnert, Ralph O 62.6
Kraft, Bastian MM 4.8
Kraft, Rainer TT 31.24, TT 31.25
Kraft, Tristan QI 7.1
Krahn, Oliver O 66.4, O 66.7
Kraiker, Alexej TT 21.1, +TT 21.3
Krajňak, Thomáš O 12.7
Krajl, Marko O 81.2
Kramar, Mirna +BP 6.7
Krämer, F. TT 31.8
Krane, Nils +O 17.12
Krashennikov, Arkady DS 20.30
Krashennikov, Arkady V. MM 34.9,
O 72.8
Kratky, Tim O 70.4
kratzer, peter HL 25.11, MA 25.7,
MA 26.1, O 30.2, +O 50.9
Kraus, Andreas BP 9.10
Kraus, Bernhard QI 3.10
Kraus, Jakob CPP 12.4, +O 57.7
Kraus, Stefan O 18.12
Krauß, Tamara MM 6.3
Krause, Jonas +QI 13.9, QI 13.10
Krause, Maximilian O 56.2
Krause, Oliver +HL 37.2
Kraushofer, Florian O 3.7, O 3.8,
O 16.12, O 63.6, O 70.10
Krauss, Gert CPP 12.70
Krauss, Sebastian BP 7.35
Krauss, Sebastian W. BP 7.12,
+BP 26.6
Kraut, Manfred CPP 37.5
Krauth, Werner DY 49.2
Krautscheid, H. HL 21.1, HL 33.4
Krautscheid, Harald HL 18.7,
HL 25.45
Kravchuk, Volodymyr MA 10.4,
+MA 37.3
Kraxner, Julia +BP 12.26
Kraych, Antoine MM 6.2
Krabber, Sarah +TT 20.7
Krebs, Olivier HL 19.4
Krecinic, Faruk O 33.6
Kredl, Jana MA 19.54, MA 21.3,
MA 35.33, +MA 35.65
Kreft, Maximilian M. BP 12.3
Kreger, Klaus CPP 41.2
Krehs, Sebastian HL 3.6, HL 26.1
Kreienkamp, Kim L. +DY 16.4
Kreil, Alexander J.E. MA 13.9
Krein, Gastao Ignacio QI 6.9
Kreis, Alex +BP 7.28
Kreis, Christian BP 3.2
Kreisel, Andreas +TT 3.4, +TT 22.4,
TT 22.13
Krejčí, Ondřej O 66.8
Krellner, C. MA 35.24
Krellner, Cornelius HL 30.19,
KFM 25.21, MA 25.1, TT 6.4, TT 6.10,
TT 20.7, TT 21.1, TT 21.2, TT 21.3,
TT 21.4, TT 21.5, TT 21.6, TT 21.7,
TT 21.13
Kremer, Kurt CPP 9.3, CPP 49.5
Kremer, Markus MM 6.6, +MM 10.13
kremeyer, laurenz O 18.4
Kremser, Malte HL 15.5
Kremser, Stephan +DY 39.6, +DY 45.5
Krenn, Mario +QI 6.1
Krenner, Hubert HL 25.3, HL 35.1
Kresse, Georg HL 21.8
Kretschmer, Andreas MM 28.5
Kretschmer, Silvan DS 20.30, +O 72.8
Kreuzberger, Daniel +TT 31.6
Kreuzer, Alex S. +TT 31.19
Kreuzer, Alex Siegfried TT 31.21
Kreuzer, Lucas P. CPP 1.8, CPP 50.1
Kreyßig, Andreas DS 9.1, TT 21.8,
TT 30.1
Kreysing, Moritz BP 3.5, DY 4.7
Kreyszig, Andreas +TT 30.2
Krieg, David +CPP 2.4
Kriegel, Marko +O 54.4, O 65.1
Krieger, D. MA 20.4
Kriegner, Dominik MA 29.6, MA 34.7
Krien, Friedrich TT 28.9
Krifa, Ahmed +CPP 12.47
Krill, Carl E. MM 18.29
Krill III, Carl E. DY 46.1
Krininger, Matthias +O 70.10
Krischer, Katharina DY 18.1, SOE 10.1
Krischok, Stefan DS 9.3, DS 20.17,
DS 23.2, HL 13.3, HL 13.5, HL 24.5,
HL 24.6, HL 30.15, HL 30.45, O 13.8,
O 57.2, TT 29.15
Krishna, Jyoti +O 48.2, O 50.10
Krishna Kumar, Karthika DY 38.2,
DY 49.5
Krishna, Vipin +HL 20.5
Krishnakumar, Nila QI 1.11
Krispeneit, Jon-Olaf DS 13.5
Kristen, Max TT 37.3
Kristen, Maximilian +TT 37.10
Kristen, Melina HL 27.4
Kristensen, Philip HL 25.91
Kristo, Maximilian +HL 25.37
Krivoruchko, Vladimir MA 35.13
Kröger, Jörg O 18.1, O 19.1, O 55.4,
O 55.8
Kröger, Philipp DS 25.4
Krogstrop, P. TT 10.7
Krogstrup, Peter O 25.5, O 72.5,
QI 13.11
Kroha, Johann MA 25.1, TT 6.4,
TT 6.12, TT 9.5, TT 28.12
Kroha, Johannes MA 35.75
Krohn, Sonja HL 39.2, KFM 11.5
Krohns, Stephan KFM 7.4, KFM 14.1,
MA 33.1, TT 3.5
Kroker, Stefanie KFM 25.8
Kröll, Eva +KFM 10.6
Kroll, Martin CPP 26.2, DS 20.3,
MM 6.5
Kromin, Raphael MA 35.16
Kronast, Florian MA 34.5, MA 35.25
Kronawitter, Silva CPP 28.1
Kronfeldner, Klaus TT 3.2
Kronowetter, Fabian +QI 4.5, QI 4.6,
QI 4.7, QI 4.15, QI 4.18
Kronseder, Matthias DS 20.41,
MA 24.7, MA 35.17, TT 2.2, TT 29.7,
TT 30.18
Krörner, Wolfgang HL 30.1
Kroy, Klaus BP 15.2, DY 40.2, DY 45.4
Kruck, Timo HL 25.71, +HL 25.73,
HL 25.81, HL 25.86
Krueger, Marco DS 13.4
Krug von Nidda, Hans-Albrecht
MA 27.2
Krüger, E. +HL 21.1, +HL 33.4
Krüger, Evgeny HL 9.5, HL 13.9,
HL 18.7, HL 25.45
Krüger, Manja MM 4.1
Krüger, Matthias BP 22.5, DY 3.7,
DY 23.2, DY 38.2, DY 49.5, DY 49.8
Krüger, Peter O 72.3, O 72.6, O 73.1,
O 73.2, O 73.3, O 73.5
Krüger, Timo BP 19.7
Krüger, Wilhelm +TT 5.5
Kruk, Monika CPP 11.2
Krumm, Bianca O 38.4
Krumrey, Michael KFM 3.1
Krumrey, Thilo TT 31.19, TT 31.21
Krupnitska, Olesia +TT 23.9
Kruse, Johannes SOE 7.1, SOE 13.1,
SOE 13.2
Kruse, Mads KFM 14.7, O 81.5
Krüsmann, Marcel +CPP 41.8
Kruteva, Margarita +CPP 33.1,
CPP 33.2
Kruti, Daniel +TT 23.3, +TT 30.19
Krutzik, Markus QI 7.8
Krutzke, Konstantin +BP 9.3
Krylov, Denis MA 26.3
Krylov, Gleb QI 4.39
Kshetrimayum, Augustine TT 16.7,
+TT 33.9
Ku, Hsiang-Sheng QI 4.23, QI 6.8
Kuan, Hui-Shun BP 8.3
Kubacka, Dorota MM 6.10
Kubala, Bjørn TT 15.4
Kubala, Björn O 7.8, O 80.6, TT 7.3,
TT 26.9, TT 31.4, TT 37.6, +TT 37.7,
TT 37.8
Kuban, Martin O 67.7
Kübel, Christian MM 17.3
Kubetzka, André MA 27.9, MA 30.6,
O 42.2
Kublitski, Jonas CPP 1.12, HL 28.8
Kuc, Agnieszka HL 7.6, HL 25.13
Kuch, Wolfgang MA 19.19, MA 35.25,
O 18.22, O 54.7
Küchemann, Stefan QI 3.10
Kuchkin, Vladyslav MA 37.2
Kuchkin, Vladyslav M. MA 27.4
Küchler, Robert TT 6.6
Kuckla, Daniel BP 7.3, BP 7.4,
+MA 35.55
Kudlaciak, Dennis HL 23.11, HL 25.92,
HL 32.2, +MA 14.9
Kudrawiec, R. HL 22.1
Kudrinskyi, Zakhar R. HL 11.10
Kuechle, Theresa +HL 25.7
Kuehne, Tim O 29.5
Kugler, Fabian TT 16.4, TT 16.11
Kühbach, Markus MM 22.1
Kuhfuss, Michel MM 9.2
Kuhl, Matthias +DS 18.4, HL 24.9
Kuhlbrodt, Kilian O 16.4
Kuhn, Christian HL 10.6
Kühn, Franziska +MA 35.10
Kuhn, Jochem QI 3.10
Kuhn, Meike CPP 12.21, +CPP 12.76
Kühn, Michael MA 39.3
Kuhn, Tilmann HL 25.8, HL 25.48,
HL 30.48
Kühne, Florian O 2.4, +O 16.11
Kühne, H. TT 12.6, TT 23.5, +TT 28.4
Kühne, Julius +HL 24.10
Kühne, Thomas MM 18.4
Kühne, Tim O 29.2, +O 32.8
Kuhnen, Raphael DS 9.3
Kuhnhold, Anja DY 23.3, DY 23.7,
+DY 23.9, DY 38.5, DY 46.13
Kühnle, Angelika +O 15.1, O 15.3,
O 69.2
Kuibarov, Andrii +TT 3.11
Kujawa, Stephan MM 33.5
Kuk, Keumkyung CPP 17.16
Kukharczyk, Nadezhda TT 27.7,
QI 1.3, +QI 5.5
Kukharczyk, Nadezhda P. +QI 2.10
Kukharensko, Oleksandra CPP 7.3,
CPP 9.3
Kulbakov, A. MA 4.1
Kulbakov, Anton TT 23.4, +TT 23.12
Kulitckii, Vladislav MM 15.3, MM 21.6
Külkens, Mike +HL 33.7
Kullgren, Jolla O 58.6
Küllmer, Florian CPP 17.2
Küllmer, Maria CPP 17.2
Kumagai, Takashi +DS 10.1, O 7.6,
O 33.6, O 55.3, O 78.2
Kumar, Abhijeet +HL 11.12, HL 25.29,
HL 31.4, MA 35.30
Kumar, Ajesh MA 30.8
Kumar Das, Sanjib TT 18.7
Kumar, Manoj DY 26.6
Kumar, Nitesh O 73.9
Kumar, Shiv O 73.3
Kumar, Umesh TT 34.13
Kumar, Vivek +MA 27.11, TT 25.6
Kumberg, Ivar MA 19.19, MA 35.25,
O 54.7
Kumpf, Christian O 18.5, O 18.6,
O 68.7
Kundu, Avijit +DY 44.13
Kungl, Hans MM 14.3
Kunkel, Christian CPP 14.2, CPP 40.2,
O 46.8
Kunkemöller, Stefan MA 35.72
Kuntscher, Christine MA 40.1
Kunz, Matthias HL 8.6
Kunz, Yannik +MA 35.9
Kunze, Fynn HL 42.5
Kunze-Liebhäuser, Julia O 8.1, O 8.2,
O 15.9, O 15.10, O 38.7
Kunzelmann, Julia Alina +QI 4.13
Kunzelmann, Viktoria Franziska
HL 18.9
Kunzmann, Dominic HL 10.2
Kunzmann, Dominic J. +HL 30.14
Kunz-Schughart, Leoni A. BP 7.31
Kupenko, Ilya HL 25.26
Kupferer, Astrid BP 18.8
Kupnik, Mario CPP 17.19
Kuppadaekhat, A +HL 42.2
Küpper, Jochem O 61.2
Küppers, Philipp MA 31.2

Author Index

- Kuppusamy, Kumar Senthil QI 4.9
 Kuppusamy, Senthil QI 4.12
 Kuppusamy, Senthil Kumar MA 25.7
 Kurban, Esma •DY 11.3
 Kurebayashi, Daichi MA 24.12
 Kurebayashi, Hidekazu MA 18.3
 Kurihara, Takayuki MA 8.10, MA 28.9
 Kurjahn, Maximilian BP 7.39, •BP 10.8
 Kurowská, Anna O 40.4, O 58.4
 Kurschat, Timo A. •HL 25.43
 Kürsten, Rüdiger DY 50.3
 Kurth, Stefan O 50.6
 Kurzmann, Annika HL 3.1, HL 8.9,
 HL 26.8
 Kūš, Matthias MA 35.9
 Kuschel, Olga MA 19.16
 Kuschel, Timo MA 2.2, MA 5.1,
 MA 19.16, MA 19.17, MA 19.27,
 •MA 20.2
 Kushch, Natalia TT 21.25
 Kushch, Natalia D. TT 12.8
 Kushwaha, Niraj •SOE 5.3
 Kushwaha, Roshan Kumar TT 30.7
 Küss, Matthias •MA 28.7
 Küster, Kathrin O 41.6
 Kuświk, Piotr MA 27.5, MA 35.64
 Kutnyakhov, D. •O 68.10
 Kutnyakhov, Dmytro O 9.1, O 34.10,
 O 68.3
 Kutovy, Yurii QI 1.7
 Kutrowska-Girzycka, Joanna HL 11.4
 Kuwabata, Susumu O 45.8
 kuzmanovic, marko TT 10.2
 Kuz'min, M. D. MA 29.3
 Kuznetsov, Alexander •HL 36.7
 Kuznetsova, Tatiana DS 25.2
 Kuzovkov, V KFM 18.1
 Kvashnin, Y. MA 25.4
 Kvashnina, Kristina MM 18.35
 Kvitnitskaya, Oksana •MM 18.37,
 •MM 18.38
 Kvon, Ze-Don HL 40.4
 Kwaaitaal, Maarten O 44.5
 Kwiatkowski, Grzegorz J. •MA 15.4
 Kwiatkowski, Grzegorz MA 12.12,
 MA 15.5
 Kwiatkowski, Grzegorz J. MA 37.9
 Kwon, Yong Seung O 9.1
 Kyoseva, Elica QI 12.5, QI 12.6
 Kyrylo, Ochkan TT 25.3
 Kyung, W. TT 22.1
 L. Chinelaatto, Adilson MM 18.23
 L R C Teixeira, Raphael •TT 1.4,
 •TT 20.10
 L Schmidt, Thomas TT 20.10
 L. Weindl, Christian CPP 12.52,
 CPP 17.29
 Labousse, Matthieu DY 44.9
 Labracherie, Valentin TT 3.12
 Lackinger, Markus O 6.5, O 6.10,
 O 12.10, O 15.7, O 40.8
 Lackner, David HL 30.35
 Lackner, Florian MA 35.33
 Lackner, Lukas •HL 20.6, HL 28.7
 Lacovig, Paolo O 54.5, O 54.14, O 72.1
 Ladovrechis, Konstantinos •TT 24.10,
 •TT 34.14
 Lagarde, Delphine HL 20.8
 Lägel, Bert MA 13.8
 Lahmidi, Khalid •HL 24.2
 Lai, King Chun •MM 2.8, MM 10.22
 Laiho, K. HL 4.7, HL 4.9
 Lake, Stephanie •MA 28.5
 Lakshminpathy, Tarakeshwar •MM 16.3
 Lal Sharma, Nand HL 3.6
 lalenejad, meelad •BP 7.44
 Ialkens, birka O 13.4, O 35.1
 Lallemand, Max BP 15.2
 Lamb-Camarena, Sebastian •MA 35.11
 Lambers, Hendrik •HL 6.5, HL 6.8,
 HL 11.6, HL 25.3, HL 25.4, •HL 25.6,
 HL 25.15
 Lambert, C. MA 25.4
 Lambert, Sascha BP 12.33
 Lammert, Janus •HL 7.9
 Lammich, Lutz O 32.5
 Lamon, Denny •MA 19.22
 Lamothe, Maximilian MM 33.5
 Lamp, Konstantin •QI 4.2
 Lampe, Carola HL 30.38, HL 32.2
 Lampe, Rasmus O 59.7
 Lampi, Michael •TT 21.38
 Lamprich, Julia QI 4.23, QI 6.8
 Lan, Qianqian HL 22.5, •MA 23.4,
 MM 18.39, O 22.7
 Lan, Zhenyun O 44.6
 Lanatà, Nicola O 72.1
 Lancaster, T. TT 28.4
 Lancaster, Tom MA 31.9
 Lanco, Loic HL 19.4
 Landaeta, Javier •TT 22.3
 Landaeta, Javier F. TT 6.6, TT 24.8
 Landee, C. P. TT 12.6, TT 28.4
 Landers, Joachim MA 35.60,
 MA 39.4, •MA 39.5, MA 39.6
 Landini, Elisabetta •O 43.9
 Landman, Uzi O 56.2
 Lang, Bruno DY 44.19
 Lang, Julia A. •HL 25.96, O 78.4
 Lang, Karl-Heinz MM 17.4
 Lang, Martin MA 19.10
 Lang, Michael •CPP 2.1
 Lang, Thomas MM 28.3
 Lang, Thomas C. •TT 24.11
 Lange, Christoph HL 4.3, HL 40.5
 Lange, Florian TT 33.3
 Lange, Gunnar •DS 19.2
 Lange, H. MA 38.1
 Lange, Hannah •MA 8.7, •MA 38.2
 Lange, Holger HL 33.6, HL 39.2,
 KFM 11.5, O 37.4, O 61.2
 Lange, Matthias DS 25.3
 Lange, Regina BP 7.28, BP 7.42,
 BP 12.43, BP 12.44
 Lange, Steffen BP 7.31, BP 10.6,
 BP 10.7
 Langendorf, Mattis O 33.3
 Langenkämper, Alexander DS 13.1
 Länger, Christian O 30.8
 Langer, Jürgen MA 18.5, MA 35.46
 Langer, Marcel F. O 83.10
 Langer, Moritz •HL 12.6, HL 25.78
 Langer, Timo HL 3.6, HL 26.1
 Langguth, Inga Christina •O 32.2
 Langheld, Anja TT 24.6, •TT 24.15
 Langrock, Veit HL 36.2
 Lanzer, Michael BP 5.3
 Lanzillotti-Kimura, Daniel HL 19.4
 Lapertot, Gerard TT 22.11
 Lapp, Clara Johanna •TT 30.9
 Lapteva, Margarita HL 4.4
 Laquai, Frédéric CPP 1.3, CPP 12.60
 Largo, Francisca HL 25.66
 Laroche, Alexandre CPP 7.4
 Larsson, Karin O 18.2
 Laschat, Sabine MM 18.11
 Laschewsky, Andre CPP 12.31,
 CPP 12.65, CPP 44.3, CPP 44.4,
 DS 20.50
 Lassauinière, Margaux •DS 22.2,
 DS 22.3
 Lasser, Jana •SOE 9.2
 Lassunière, Margaux DS 20.39,
 DS 22.4
 Last, Thorsten •QI 13.2
 Lászlóffy, András MA 19.38, TT 1.8,
 TT 1.9
 Lau, Alexander •MM 4.10, •TT 25.12
 Lau, Michael •MA 12.7
 Laube, Mandy BP 3.4
 Läuchli, Andreas MM 28.3
 Läuchli, Andreas M. TT 24.11
 Lauer, Kevin HL 24.5, •HL 24.6,
 TT 29.15
 Laukó, András QI 4.31
 Lauritsen, Jeppe V. O 72.1
 Lauritsen, Jeppe Vang O 32.5
 Lausch, Knut Nikolas •MM 29.5
 Laussy, Fabrice P. HL 8.10
 Lauster, Tobias O 78.4
 Lauth, Jannika HL 20.7, HL 39.4
 Lauwaet, Koen O 79.6
 Lavrentyev, Sergey •HL 7.8
 Lawrence, Adam QI 13.2
 Lawundy, Stefanie •HL 30.26
 Lazzaroni, Paolo •O 50.12
 Le, Anh Tuan QI 8.4
 Le Borgne, Tanguy BP 12.65
 Le Dü, Morgan •DS 20.50
 Le Guyader, L. MA 25.4
 le Guyader, Loic MA 25.7
 Le, Khan MM 13.3, MM 13.5,
 •MM 18.42
 Le Menn, Flora-Maud BP 12.60
 le Sueur, Helene TT 37.7
 Le Tacou, Matthieu KFM 25.21,
 O 26.1, TT 21.6, TT 31.15
 Le, Thi Thu MM 17.3, MM 17.5
 leboeuf, david TT 10.2
 Lebrun, R. MA 19.63
 Lechermann, Frank DS 20.36
 Lechner, Barbara O 70.4
 Lechner, Barbara A.J. O 69.3, •O 70.1,
 O 70.3, O 70.10
 Lechner, Wolfgang QI 12.1
 Leckron, Kai MA 8.5, MA 25.3
 Lecompte, William BP 13.10
 Ledentsov Jr., Nikolay HL 25.90
 Ledentsov, Nikolay N. HL 25.90
 Ledue, Denis MA 11.4
 Lee, Alpha •SYNM 1.5
 Lee, Changmin MA 13.10
 Lee, Edward SOE 5.3, •SOE 14.3
 Lee, Hyenkwon MM 13.3
 Lee, Jaehyun •MA 26.3, O 54.3
 Lee, Jai Sung MM 21.6
 Lee, Joonho QI 12.5
 Lee, Kyujoon MA 19.44
 Lee, Martin DY 12.3
 Lee, Miru DY 16.9
 Lee, Patrick A. QI 5.2
 Lee, S.E. MA 35.24
 Lee, Seok-Woo TT 3.6
 Lee, Seungjae •DY 18.1, •SOE 10.1
 Lee, Seung-Sup TT 16.4, TT 16.11
 Lee, Taehun O 49.1
 Lee, Tien-Lin O 18.6, O 40.5, O 41.1,
 O 73.9
 Lee, Wei-Sheng MA 6.1
 Lee, William MM 2.9
 Lee, Woo HL 19.8
 Lee, Y. KFM 11.4
 Lee, Yang-Jun •KFM 8.5
 Lee, Yejin MA 19.5
 Lee, Yonghun MA 6.1
 Lee, Yonghyuk MM 34.8, •O 69.8
 Lee, Yoonhee •MM 10.14, •MM 32.5
 Lee, Yunjae O 49.1
 Leeb, Valentin •TT 7.4, •TT 29.18
 Legenstein, Lukas CPP 40.5, •HL 41.1
 Legg, Henry TT 18.3, •TT 32.2
 Leghtas, Zaki TT 13.3
 Legrand, Jacqueline BP 9.5
 Legrand, William TT 13.3, TT 32.4
 Leguay, Lucie •HL 17.6
 Legut, Dominik •MA 32.8
 Lehmann, Carl •DY 19.3, TT 11.10
 Lehmann, Moritz BP 12.14, •DY 34.1
 Lehmann, Philippe •SOE 3.5
 Lehnert, Konrad QI 4.33
 Lehnert, T. O 81.6
 Lehniger, Kevin •KFM 25.7
 Lei, Shiming MM 28.2
 Lei, Yong DS 17.3, HL 24.1, KFM 15.1,
 KFM 15.2, KFM 15.5, KFM 25.15,
 KFM 25.16, KFM 25.17, MM 8.6,
 MM 14.5, MM 18.19, MM 18.21,
 MM 18.22, MM 18.24, O 13.10
 Leibauer, Benjamin •CPP 17.13
 Leijnse, Martin DY 35.6, HL 3.2,
 HL 3.3, HL 3.11, TT 18.6, QI 1.6
 Leimeroth, Niklas MM 10.4
 Leinen, Philipp O 13.5
 Leiner, Jonathan •MA 35.54
 Leiner, Thomas •KFM 8.2
 Leis, Arthur O 4.3
 Leisegang, Markus O 22.5, O 26.5,
 •O 71.10, O 82.1
 Leisgang, Nadine HL 20.8
 Leist, Justus O 15.11
 Leitenberger, Wolfram HL 30.47
 Leitenstorfer, Alfred HL 40.6, MA 28.9
 Leitherer, Andreas •MM 34.10
 Leitner, Erich CPP 14.5
 Leitner, Matthias O 15.10
 Leiva, Sergio •MA 24.6
 Lejček, Pavel MM 6.4
 Leliert, Jonathan MA 27.13
 Lemaître, Aristide HL 19.4
 Lemaury, Vincent DS 5.4
 Lemesh, Ivan MA 2.3
 Lemmens, Peter TT 12.4, TT 25.10
 Lenart, Peter BP 12.17
 Lendackel, Uwe BP 12.23
 Leng, Kai O 81.1
 Lengers, Frank HL 25.48
 Lenke, Lea •TT 24.14
 Lensing, Philipp O 19.10
 Lentfart, Akira MA 19.50
 Lentz, Adrian •BP 7.3, BP 7.4
 Lenz, Benjamin •TT 12.12, •TT 16.8
 Lenz, Kilian MA 4.3, MA 21.7,
 MA 22.7, •MA 28.8, MA 35.36
 Leo, Karl CPP 1.9, CPP 1.12, CPP 26.1,
 CPP 26.2, DS 20.3, HL 22.4, HL 28.1,
 HL 28.2, HL 28.8
 Leo, Ulrich HL 30.38, HL 32.3
 Leoni, Thomas O 12.3
 Leppäkangas, Juha •QI 10.3
 Leppenen, Nikita V. HL 2.1
 Leppert, Linn CPP 39.5
 Lepucki, Piotr BP 7.29
 Lerose, Alessio •DY 5.4
 Lesch, Harald •PSV IV
 Lesne, Edouard MA 42.5
 Letterier, Christophe •BP 5.1
 Leth Larsen, Matthew Helmi O 27.3
 Letrun, Romain BP 12.54
 Lettermann, Leon •BP 12.39, BP 12.40
 Lettinga, Minne Paul BP 19.4, BP 25.4
 Lettner, Thomas HL 8.1, HL 8.10
 Leu, Charlott BP 12.46, BP 12.47
 Leuenberger, D. O 9.5
 Leumer, Nico •TT 2.8, •TT 16.13
 Leung, Lydia O 69.6
 Leupold, Nico HL 5.3, HL 23.2
 Leuteritz, Till HL 33.9
 Leutner, Kilian •MA 12.4
 Levashov, Sergej •HL 42.9
 Levchenko, Alex MA 3.3
 Levchenko, Sergey V. HL 24.12,
 MM 12.10, O 62.7
 Leven, Richard MA 35.22
 Levin, Nikita O 56.5
 Levina, Anna BP 2.9
 Levis, Demian SOE 9.3
 Levitov, Leonid TT 7.6
 Levy, Amikam DY 3.9
 Levy, Jeremy MM 10.30
 Levy Yeyati, Alfredo O 7.8
 Lewin, Daniil •MA 35.67, MM 18.13
 Lewis, Alan O 50.12, •O 67.5
 Lexow, Matthias O 15.2
 Lexow, Matthias O 45.8
 Leyens, Christoph MA 35.68
 Leyzner, Maxim HL 4.11
 Lezuou, Luca •O 58.12
 Lhost, Olivier CPP 41.3
 Li, An-Ping O 21.1
 Li, Baijin O 79.4
 Li Bassi, Andrea O 40.9
 Li, Boqiang TT 5.3
 Li, Botao DY 49.2
 Li, Boxi •QI 5.6
 Li, Chang-An TT 30.8
 Li, Dapeng •DY 5.1
 Li, Dongzhe •MA 37.10
 Li, Guangjie TT 1.13
 Li, Haobo O 38.7
 li, hongshuai •MM 16.1
 Li, Jiajun TT 34.7
 Li, Jiehua MM 10.10
 Li, Jing O 81.1
 Li, Jingchen O 51.5, O 80.7
 Li, Jingcheng O 18.13, O 51.9
 Li, Jingwen •MA 25.1
 Li, Lang •O 31.3
 Li, Lianhe H. HL 4.3
 Li, Maxwell MA 19.2
 Li, Meng MA 39.1
 Li, Nian CPP 17.23, CPP 28.8,
 CPP 48.2, CPP 48.3
 Li, Peng MA 20.3
 Li, Pengji HL 8.3, HL 12.10, HL 25.85,
 •HL 39.4
 Li, Qili TT 3.1
 Li, Qing O 62.9
 Li, Quiyang O 16.10
 Li, Shulun HL 25.75, HL 25.76
 Li, Shutong HL 25.9
 Li, Siying MM 33.8
 Li, Weizhe QI 4.12
 Li, Xiaomei CPP 7.3, CPP 20.6,
 CPP 37.2
 Li, Yanan CPP 27.3, •CPP 28.8
 Li, Yinfei QI 3.5
 Li, Ying TT 8.4
 Li, Yuesheng TT 5.3
 Li, Yujiao HL 36.5
 Li, Zerui •CPP 12.61, CPP 12.65,
 DS 20.50
 Li, Zhongyang •MM 18.10
 Li, Zhuoqing •CPP 12.39, •MM 18.11
 Li, Zhuoqing MM 10.15
 Liang, Kevin •O 13.7
 Liang, Suzhe •CPP 12.52, CPP 17.23,
 CPP 17.26, CPP 27.4, •CPP 37.3
 Liang, Yanyan •MM 20.8
 Liang, Yongfeng MM 18.15
 Liang, Yuxin •CPP 12.15
 Libisch, Florian TT 10.5
 Liborius, Lisa HL 25.55

Author Index

- Libuda, Jörg ... O 3.6, O 20.1, O 32.5, O 70.2
- Lichtenberg, Kurt ... •O 78.8, TT 15.3
- Lichtenegger, Michael ... HL 32.3
- Lichtenstein, Alexander ... TT 12.9
- Lichtenstein, Alexander I ... MA 38.4
- Lichtl, Henrik ... O 71.6
- Lidal, Jonas ... MA 13.6
- Liebchen, Benno ... CPP 17.31, DY 16.5, DY 16.8, DY 31.1, DY 46.4, DY 51.1, DY 51.2
- Lieberwirth, Eric ... •BP 7.42
- Liebetrau, Martin ... •O 49.2
- Liebhauer, Eva ... O 80.4
- Liebich, Marlene ... HL 13.8
- Liebig, Alexander ... O 4.4, O 21.3
- Liebing, Niklas ... MA 28.1, MA 28.2, MA 28.5
- Liebisch, Tim ... BP 12.57
- Liebmann, Marcus ... HL 25.77, •MA 31.2
- Liebsch, Yossarian ... •DS 20.51
- Liebscher, Christian ... MM 3.5
- Liebscher, Christian H. ... MM 3.6
- Liedke, Maciej Oskar ... KFM 3.3
- lienau, Christoph ... HL 11.8, HL 28.7
- Lien-Medrano, Carlos R. ... •O 81.4
- Liensberger, Lukas ... MA 22.2
- Liese, Susanne ... •BP 8.11
- Lieske, Leonard-Alexander ... KFM 6.6
- Liestmann, Tjark ... DS 20.6, DS 26.1
- Lietzow, Finn-Frederik ... MA 19.48
- Ligthart, Rian ... •O 18.17
- Lihm, Jae-Mo ... •MM 12.8, O 7.3
- Lilienblum, M. ... KFM 2.3
- Lilienkamp, Gerhard ... O 30.6
- Lilienkamp, Thomas ... DY 39.5
- Liljeroth, Peter ... •O 25.1
- Lill, Johanna ... •MA 19.14, MA 19.15
- Lilleodden, Erica ... MM 18.33
- Lillig, Christopher ... BP 12.23
- Lim, Ji Soo ... DS 20.34
- Limame, Imad ... •HL 12.5, HL 17.3, HL 25.76, HL 30.3
- Lin, Baojun ... CPP 1.2
- lin, haicheng ... O 18.15
- Lin, Jun-Xiao ... MA 35.38
- Lin, Kai-Qiang ... DS 17.6, TT 10.3
- Lin, Nan ... •KFM 25.4
- Lin, Yen-Hui ... O 13.3
- Lin, You-Ron ... O 18.6
- Lin, Yu-Chuan ... O 18.19
- Linares Mardegan, Jose R. ... MA 19.14
- Lindemann, Markus ... HL 4.1
- Lindemann, Tyler ... TT 3.13
- Linden, Stefan ... HL 33.9
- Lindenmeir, Christoph G. ... •CPP 12.46
- Lindenthal, Jakob ... •HL 22.4
- Lindfors, Klas ... MM 18.42
- Lindfors, Lennart ... BP 12.56
- Lindfors-Vrejoiu, Ionela ... MA 6.2
- Lindgren, Eric ... •MM 18.5
- Lindner, Benjamin ... DY 50.3
- Lindner, Jonas ... O 20.7
- Lindner, Jörg ... DS 17.7
- Lindner, Jörg K. N. ... DS 1.4, HL 25.1
- Lindner, Julian ... MA 33.7
- Lindner, Jürgen ... MA 4.2, MA 4.3, MA 21.7, MA 22.7, MA 28.8, MA 35.8, MA 35.36, MA 35.68
- Lindner, Michael ... MA 35.14
- Lindner, Patrick ... HL 25.58, HL 25.83, HL 36.5
- Lindström, Tobias ... TT 32.3
- Linek, Julian ... TT 37.1
- Linfield, Edmund H. ... HL 4.3
- Link, Julia M. ... •TT 22.14, TT 30.5
- Link, Rabea ... •BP 19.2
- Linkenheil, Anna ... DS 16.4
- Linscott, Edward ... MA 11.7
- Linsel, Simon ... QI 10.7
- Linsmeier, Christian ... MM 4.9, MM 4.10, MM 24.5
- Linzen, Sven ... TT 3.2
- Lipfert, Jan ... •BP 15.1
- Lippertz, Gertjan ... MA 31.4, •MA 31.7, TT 20.4, QI 13.10
- Lippitz, Markus ... HL 30.41, O 35.7, O 35.8, •O 61.1, O 61.4
- Lippmann, Milena ... CPP 12.39, MM 18.27
- Lischner, Johannes ... O 83.8
- Lisenfeld, Jürgen ... TT 27.5, TT 27.6
- Liserer, Marco ... •DS 2.5
- Lisinetskaya, Polina ... DS 5.1
- Lisinetskii, Victor ... O 61.3, O 82.5
- Lissel, Franziska ... O 32.8
- Lisson, Julian ... •DS 20.31
- Litman, Yair ... •CPP 37.7, •O 50.8, •O 58.1
- Litnovsky, Andrey ... DS 26.4, MM 4.9, MM 24.5
- litterst, jochen ... MA 14.5, TT 24.5
- Litvin, Leonid V. ... O 35.5, O 37.8
- Litzba, Lukas ... DY 35.9, •TT 29.1
- Litzius, Kai ... MA 2.1, MA 2.3, MA 23.3, •MA 27.3, MA 34.5
- Liu, Bo ... MA 35.29
- Liu, Chenlu ... TT 32.3, TT 32.7
- Liu, Danyang ... •MA 35.58, O 7.2, O 71.9
- Liu, Dongdong ... O 74.2
- Liu, Feng ... DS 18.1
- Liu, Fupin ... O 80.2
- Liu, Hui ... MA 18.7, •MM 23.9
- Liu, Huimei ... TT 5.2
- Liu, Jianing ... •MA 35.52
- Liu, Jie ... •DY 26.3
- Liu, Jinghui ... BP 19.1
- Liu, Jung-Ching ... •O 79.3
- Liu, Junjie ... O 63.4
- Liu, Kejun ... TT 29.10
- Liu, Limin ... O 11.4
- Liu, Lingzhi ... MM 32.2
- Liu, Maowen ... •MM 3.8, MM 18.31
- Liu, Na ... BP 26.4
- Liu, Pei ... O 27.3
- Liu, Peitao ... HL 21.8
- Liu, Pengcai ... O 12.6, O 55.10
- Liu, Pin-Chi ... MA 19.19
- Liu, Shangpu ... •CPP 28.1, HL 28.6
- Liu, Shi-Xia ... •O 79.1, O 79.3
- Liu, Shuyi ... O 7.6, O 78.2
- Liu, Tsai-Jung ... HL 7.6
- Liu, Wei ... •MA 29.1
- Liu, Ye-Chao ... QI 3.3, •QI 3.5
- Liu, Yi ... O 5.6, O 6.4
- Liu, Yijing ... HL 6.9
- Liu, Yizhou ... MA 24.12
- Liu, Yu ... TT 37.5, QI 13.11
- Liu, Yuefei ... QI 10.9
- Liu, Yuzhou ... HL 9.2
- Liu, Zhe ... O 35.1
- Liu, Zihong ... TT 6.1, •TT 24.2
- Liu, Zitong ... O 33.9
- Livraghi, Mattia ... CPP 17.22, MM 18.7
- Lizzit, Daniel ... O 54.5
- Lizzit, Silvano ... O 54.5, O 54.14, O 72.1
- Llorens, Santiago ... •QI 9.6
- Lobe, Sandra ... MM 8.4
- Löbl, Mattias C. ... HL 19.1
- Locatelli, Andrea ... O 65.3, O 69.10
- Lochbrunner, Stefan ... DS 5.6
- Loche, Philip ... •CPP 9.2
- Löchner, F. ... HL 42.2
- Lochner, Pia ... HL 8.9, HL 26.8, HL 26.10
- Lodahl, Peter ... HL 35.4
- Loewe, Konrad ... MA 29.9
- Löffler, Jörg ... MM 3.7
- Löffler, Jörg F. ... MM 3.9, •MM 11.1, MM 30.6
- Löffler, Robert C. ... •BP 14.1
- Logal, Jutta ... MM 6.10
- Logsdail, Andrew ... O 62.2
- Logvenov, Gennady ... DS 14.4, HL 13.7, TT 3.10
- Loh, Kelvin ... QI 13.2, QI 13.9
- Loh, Kian Ping ... O 81.1
- Lohmann, Svenja ... •DS 1.5
- Lohmüller, Theobald ... HL 4.10
- Lohof, F. ... HL 4.7, HL 4.9
- Lohof, Frederik ... DS 17.2, HL 4.5, HL 19.3, •QI 5.8, QI 10.4
- Lohr, Leonhard ... •O 13.1
- Lohrmann, Christoph ... DY 8.7, •DY 16.9, SOE 6.7
- Lohse, Leon Merten ... KFM 25.12
- Lohstroh, Wiebke ... CPP 49.4
- loidl, alois ... TT 14.10
- loidl, Martin ... TT 17.2, TT 31.5
- Lojewski, T. ... •MA 25.4
- Lojewski, Tobias ... MA 25.7
- Lokamani, M. ... •TT 13.5
- Lomholdt, William B. ... O 27.3
- Long, Teng ... MM 25.7
- Longo, Danilo ... O 22.4, O 51.9
- Lopanitsyna, Nataliya ... •O 83.1
- Lopes Dias, Filipe ... O 22.1
- Lopes Dias, Nelson Filipe ... KFM 25.6
- Lopes, Joao Marcelo J. ... DS 20.30
- López Carreño, Juan Camilo ... HL 8.10
- López Díaz, Luis ... MA 23.5
- López-Posadas, Claudia ... •O 12.3
- Loran, Edwin ... •DY 51.2
- Lorber, Dana ... BP 8.9
- Lord, Sally ... •MA 35.2
- Lorente, Nicolas ... O 47.5, •O 71.1, O 74.5, O 80.5
- Lorenz, Charlotta ... •BP 13.6, •CPP 17.41
- Lorenz, Jaccomo ... O 19.10
- Lorenz, Janine ... HL 13.10
- Lorenz, Maïke ... BP 10.8
- Lorenz, Pierre ... O 13.9
- Lorenz, Thomas ... MA 16.9, MA 35.74
- Loreto, Vittorio ... SOE 14.4
- Lorke, Axel ... PSV II, HL 3.1, HL 3.4, HL 8.9, HL 25.2, HL 25.59, HL 25.63, HL 26.8, HL 26.10, HL 31.3
- Lorke, Michael ... •HL 8.2, HL 15.3, •HL 18.8, HL 25.30
- Löser, Patricia ... MM 25.4
- Löser, Thomas ... SOE 12.1
- Losi, Gabriele ... O 39.2
- Lötfering, Jakob Johannes ... •MM 2.10
- Lotfy, Ahmed Samir ... •KFM 14.5
- Loth, Sebastian ... O 34.5, O 71.6, O 71.7, O 71.8, O 78.8, TT 15.3
- Löther, Mona ... CPP 12.72, CPP 12.73, •CPP 12.77
- Lothkov, Sergey ... QI 4.38
- Lothkov, Sergey ... TT 30.23
- Lottenburger, Ben ... O 30.4
- Lottemoser, Th. ... KFM 2.3, MA 33.6
- Lottemoser, Thomas ... KFM 7.1, KFM 19.1, MA 11.1, MA 33.5
- Lotze, Christian ... O 5.2, O 19.9, O 54.7, O 55.12, •O 71.5
- Louis, Ard A. ... BP 23.1
- Lounis, Samir ... MA 3.1, MA 20.6, MA 20.7, MA 28.12, MA 30.1, MA 30.7, MA 37.1, •O 71.3, O 72.7
- Lourenço-Martins, Hugo ... O 78.5
- Lourens, Daniel ... O 44.5
- Louw, Jan ... •TT 28.7
- Love, Jaden ... HL 21.3
- Love, Jake ... MA 27.13
- Lovett, Brendon W. ... HL 30.46
- Löw, Mario ... O 15.11, O 20.10
- Lowack, Ansgar ... TT 31.6
- Löwen, Hartmut ... CPP 2.2, CPP 18.4, DY 16.8, DY 23.8, DY 31.7, DY 46.2, DY 50.1, DY 50.2
- Lu, Guanyu ... O 37.6
- Lu, Hao ... •DS 13.2
- Lu, Jianchen ... O 79.4
- Lu, Jiong ... O 81.1
- Lu, Wenbo ... O 5.7, •O 23.6
- Lu, Wenchang ... O 21.1
- Lu, Yan ... CPP 12.26, HL 22.5, •MM 18.39, O 22.7
- Luan, Yigong ... O 37.2
- Lubbers, Nicholas ... CPP 9.1
- Lubeck, Sven ... O 50.1, O 67.1
- Luber, Mattias ... BP 7.2, •BP 7.41
- Lubk, A. ... MA 20.4
- Lubk, Axel ... DS 20.34, MA 19.5, MM 35.1, MM 35.9
- Lübke, Jeremiah ... •DY 8.4, •SOE 6.4
- Luca Portalupi, Simone ... HL 12.3
- Lucas, Irene ... MA 21.9
- Lucas Kern, Felix ... MA 19.5
- Lucht, Jens ... •KFM 25.12
- Ludacka, Ursula ... KFM 7.3, •KFM 14.6
- Lüdemann, Kevin ... •DY 34.2
- Lüders, Anton ... •DS 9.4
- Lüders, Carolin ... •HL 30.2
- Lüdge, Kathy ... DY 15.2, DY 45.10, DY 45.11, •DY 48.1, DY 51.5
- Ludwig, A. ... HL 2.3
- Ludwig, Alfred ... DS 9.1
- Ludwig, Arne ... •SYPQ 1.2, HL 2.5, HL 3.4, HL 3.7, HL 8.9, HL 12.1, HL 12.2, HL 19.1, HL 25.37, HL 25.43, HL 25.47, HL 25.58, HL 25.59, HL 25.63, HL 25.64, HL 25.67, HL 25.71, HL 25.72, HL 25.73, HL 25.81, HL 25.83, HL 25.86, HL 26.2, HL 26.3, HL 26.6, HL 26.8, HL 26.10, HL 30.7, HL 35.4, HL 36.5
- Ludwig, Stefan ... HL 35.2, HL 35.3
- Ludwig, Tim ... •MA 7.4
- Ludwig-Petsch, Kim ... •PSV VII
- Luetkens, H. ... MA 4.1
- Lühmann, Thomas ... TT 6.6
- Lühmann, Tobias ... KFM 25.3
- Lührs, Lukas ... MM 18.10, MM 18.31
- Lui, Ming Hong ... •BP 12.40
- Luibrand, Theodor ... •DS 25.1, DS 25.3
- Luitz, D.J. ... TT 28.4
- Luitz, David ... MA 15.3
- Lukács, Árpád ... QI 8.6
- Lukianova, Olga ... •MM 15.3
- Lulei, Sebastian ... CPP 12.79
- Luley, Peter ... BP 12.7, BP 12.8
- Luncker, Lukas ... SYQM 1.2, HL 30.47, TT 32.5
- Lund, H. E. ... MM 7.5
- Lund, Mike Alexander ... •MA 21.4
- Lundgren, Edvin ... O 69.5
- Lungerich, Dominik ... O 5.6
- Lunkenbein, T. ... KFM 11.4
- Lunkenbein, Thomas ... MM 33.5, O 49.8
- Lunkenheimer, Peter ... CPP 17.4
- Luntz, Alan C. ... O 27.1
- Luo, Chen ... MA 19.19, MA 23.3
- Luo, Jian ... •MM 24.6
- Luo, Xueli ... VA 2.1, VA 2.3
- Luo, Yang ... O 7.4, •O 7.5
- Luong, Felix ... SYNMM 1.2, MM 29.3
- Lupascu, Doru ... KFM 10.5, KFM 10.6
- Lupascu, Doru C. ... •MA 35.67, MM 18.13
- Lupascu, Doru C. ... KFM 25.1
- Lupke, Felix ... MA 19.55, O 4.3, •O 21.1, O 54.12, •O 81.3
- Lupton, John M. ... DS 17.6, TT 10.3
- Luschmann, Thomas ... •TT 15.1, TT 29.11, TT 31.5, TT 31.22, TT 31.23, QI 4.6, QI 4.34, QI 4.35, QI 4.36, QI 4.37
- Lushchik, A ... KFM 18.1
- Lüth, Hans ... HL 7.3, HL 19.7, HL 25.98
- Luther, Klaus-Dieter ... HL 30.19
- Luther, S. ... •TT 23.5
- Luther, Stefan ... DY 8.6, DY 39.5, DY 45.12, DY 45.13, SOE 6.6
- Lutter, Klaus ... •MM 22.7
- Lüttich, Christopher ... DS 9.2
- Lutz, Tyler ... •BP 18.7
- Lützen, Arne ... HL 28.7
- Lux, Fabian ... MA 10.5, MA 14.3, MA 37.8
- Lux, Fabian R. ... MA 24.11, MA 27.12
- Luzzietti, Nicholas Luzzietti ... BP 7.1
- Lv, Hua ... DS 22.5
- Lykhach, Yaroslava ... O 3.6, O 20.1, •O 70.2
- Lykov, Vladimir ... •O 79.8
- Lymperakis, Liverios ... •DS 6.2, O 64.5
- Lysovorskiy, Yury ... MM 20.8, MM 25.2, MM 25.3, MM 31.2, •MM 34.2
- Lytken, Ole ... O 12.11, O 12.12
- Lytvynenko, Yaryna ... MA 19.59, MA 35.50
- Lyu, Lu ... O 17.6
- M. Gallego, José ... O 79.6
- M. J. A. Pallone, Eliria ... MM 18.23
- M. Jesus, Lilian ... MM 18.23
- M. May, Matthias ... O 20.10
- M. Papadakis, Christine ... CPP 12.33
- M. Pop, Ioan ... TT 31.15, TT 31.18
- Ma, Changqi ... CPP 12.61
- Ma, Chenxi ... HL 12.7, HL 12.10, HL 25.85, •HL 30.9
- Ma, Haibo ... CPP 40.9
- Ma, Wei ... CPP 1.2
- Ma, Wenhui ... KFM 25.17, MM 14.5
- Ma, Xuekai ... HL 21.7, HL 21.9
- Ma, Yingqiao ... MA 35.71
- Maass, Corinna C. ... DY 31.4
- Maass, Friedrich ... O 40.2
- Maccallini, Enrico ... VA 2.1
- Maccari, Fernando ... •MM 13.7, MM 18.25
- MacDonald, Allan H. ... MA 30.8
- Machado Chary, Eduardo ... CPP 14.1
- Macher, Lucca ... •DS 20.21
- Machness, Shai ... QI 13.9
- Machnikowski, Paweł ... HL 30.48
- Macieszczak, Katarzyna ... DY 35.6
- Macke, Eric ... •MM 12.1
- Mackenzie, Andrew ... TT 23.6
- Mackenzie, Andrew P. ... MM 21.3, MM 21.4
- Mackeprang, Jelena ... QI 4.26, QI 12.9
- Mackewicz, Sonia ... O 70.4, •O 70.6
- Maczko, H. ... HL 22.1
- Madalaimuthu, Jose Prince ... CPP 12.62, CPP 12.63
- Madeira, Teresa I. ... DS 20.18, DS 26.3
- Madeira, Teresa Isabel Picoto Pena ... HL 28.5

- Madej, Ewa MA 19.55
Mader, Dorothee •O 44.5
Madhukar, S. CPP 12.12
Mädler, Lutz MM 18.36
Maehrlin, Sebastian F. HL 23.6,
O 44.5
Maeno, Y. TT 22.1
Maffione, Gaia TUT 2.2, HL 1.2
Magazu, Luca •TT 27.4, •TT 33.7
Magerle, Robert BP 18.3, CPP 12.6
Maggs, A. C. DY 49.2
Maghelli, Nicola BP 3.5, DY 4.7
Magnaterra, Marco TT 8.6, •TT 21.15
Magnussen, Olaf DS 20.4, O 20.4,
O 34.1
Magrez, Arnaud MA 19.6
Magron, Victor QI 9.1
Magusin, Pieter O 43.3
Mahatha, Sanjoy MA 31.6
Mahault, Benoît •DY 16.3
Mahdian, Seyed Majid DS 13.5
Mahendru, Bharti •O 53.4, TT 26.8
Mahmoud, Mohamed •HL 23.10
Mahyaeh, Iman TT 38.3
Mai, Alexander •HL 22.3
Maiberg, Matthias •HL 34.5
Maier, Florian O 15.2, O 15.4, O 20.2,
O 45.7, O 45.8, O 45.9
Maier, Niclas DS 20.27
Maier, Paul •TT 30.22
Maier, Sabine O 5.6, O 6.4, O 6.6,
•O 40.1, O 79.2
Maier, Thomas A. TT 22.4
Maile, Dominik MA 35.5, •TT 26.7,
•QI 5.3
Mailly, Dominique TUT 2.2, HL 1.2,
HL 7.9
Mairegger, Thomas •O 38.7
Maisel, Sven O 40.1, O 45.3
Maiti, Kalobaran O 82.6
Maitra, Tulika MA 35.66
Maity, Avishek •TT 39.1
Maiworm, Michael O 14.4
Majchrzak, Paulina •O 9.2, O 54.1,
O 73.8
Majer, Lena Nadine •DS 9.5
Majewski, Martin •CPP 19.2
Majka, Maciej •BP 24.5
Makadir, Nabil •MA 35.31
Makarov, Denys MA 10.3
Makarov, Oleg Yu. HL 25.90
Maklar, J. O 9.5
makov, guy MM 12.6, MM 30.10
Makoveev, Anton O 12.7
Makowski, Marcin BP 3.2
Maksimov, Dmitrii O 5.2, O 55.12,
•O 83.4
Makvandi, Ardavan •MM 8.4
Malagrecia, Ferdinando O 29.3
Malavolti, Luigi BP 9.2, O 78.8
Maleki, Farahnaz O 69.3
Malgaretti, Paolo DY 4.8, DY 16.7,
DY 23.6
Malic, Ermin HL 11.8, HL 20.1,
HL 20.2, O 9.10, O 16.9, O 33.7,
O 48.9, O 68.4
Malik, Ali Muhammad •MM 23.5
Malik, Bilal HL 25.20
Malindretos, Joerg HL 25.22
Maljuk, Andrey MM 7.4
Mallada, Benjamin O 14.5
Mallik, Srijani •O 44.10
Malmström, Eva CPP 18.3
Malone, Ethan O 23.6
Malone, Fionn D. QI 12.6
Malý, Pavel O 82.5
Mameka, Nadiia MM 35.5, MM 35.6
Mamiyev, Z. O 41.7
Mamiyev, Zamin •O 25.7
Mamontova, Irina BP 8.2
Manara, Jochen DS 5.5
Mañas-Valero, Samuel MA 21.11
Mancuso, Adrian BP 12.54
Mancuso, Michele TT 17.1
Mandal, Mukundha CPP 28.7
Mandal, Rituparno •DY 31.6
Mandal, Sagarmoy O 58.10
Mandal, Suvendu DY 16.8
Mandal, Swadhin MA 35.65
Mandru, Andrada-Oana MA 23.3
Mandrus, David G. O 81.3
Mandziak, Anna MA 19.55
Manesco, Antonio O 51.2
Manfra, Michael TT 22.7, TT 26.2
Manfra, Michael J. TT 3.13
Mang, Christian •MA 35.7
Mangeat, Matthieu DY 46.21,
•DY 46.22
Mangold, Lena •SOE 12.3
Mangold, Markus DS 23.6
Manini, Nicola DY 28.6
Manini, Paolo VA 2.1
Mankovsky, S. •MA 38.7
Mankovsky, Sergey MA 24.3
Mankovsky, Sergiy MA 28.13,
MA 38.2, MA 38.7
Manmana, Salvatore TT 33.8
Manmana, Salvatore R. TT 16.8,
TT 28.10, TT 38.6
Manna, K. TT 20.8, TT 25.9
Manna, Santanu SYED 1.2
Mannathanath Chakkingal, Aswathi
•MA 35.42
Mannel, Hendrik HL 8.9, HL 25.59,
HL 25.63, HL 26.8, •HL 26.10
Mannhart, Jochen DS 9.5
Mannix, Dan MA 20.3
Mannsfield, Stefan CPP 1.12
Mano, Takaaki HL 2.2
Manouras, Theodore CPP 20.4
Mansano, Ronaldo MM 7.3
Manske, Dirk TT 3.10, TT 22.10
Mansour, Ahmed HL 28.4
Mansson, Martin CPP 1.8
Mantegazzini, Federica TT 31.7
Mantel, E. •O 21.5
Manthel, Tobias HL 6.6
Manti, Simone QI 8.3
Mantilla, Sebastian •TT 7.11
Manucharyan, Vladimir QI 5.5
Manuel, Pascal TT 25.11
Mao, Wenwen •DY 35.1
Mao, Yiran MM 4.10
Marathe, Madhura •KFM 10.5,
•MA 42.2
Marconi, Umberto M. B. DY 31.7
Marcos, José Carlos Ureña DY 16.5
Mardazad, Sam •CPP 40.9, DY 43.5,
TT 39.8
Mardegan, Jose R. L. MM 7.4
Marecek, David •DS 1.3
Marek, Štěpán •O 11.2
Marganska, Magdalena •TT 13.3,
•TT 22.12
Margenfeld, Christoph DS 2.4
Margraf, Johannes MM 2.4, MM 14.1
Margraf, Johannes T. CPP 14.2,
CPP 40.2, MM 10.1, MM 10.22,
MM 33.1, MM 33.4, MM 34.3, O 58.3,
O 62.1, O 62.5
Marguet, Sylvie KFM 3.1
Mari, Romain DY 29.1
Maria, Häser DS 23.5
Mariam, Riham TT 17.2
Marie, Xavier HL 20.8
Markl, Matthias MM 1.1
Markmann, Jürgen MM 18.32,
MM 18.33, MM 32.2, MM 35.8
Markou, Anastasios MA 42.5
Markovic, Igor MM 21.3
Marks, Timo •DY 45.1
Markus, Philipp O 74.6
Marlow, Frank CPP 37.8
Marmodoro, Alberto •MA 13.11,
•MA 18.2, •MA 28.13, MA 38.7
Marnitz, Luca MA 19.17
Marotzke, Simon •MA 31.6
Maroun, Fouad DS 20.4
Marré, Daniele TT 25.8
Marsalek, Ondrej O 46.5
Marschall, Holger CPP 20.6
Marschall, Manuel O 7.9
Marschick, Georg MM 18.13
Marszalek, Tomasz HL 30.33
Martel, Anne CPP 33.6
Martemyanova, Julia CPP 12.28
Marten, Svenja TT 28.10
Martens, Christian •TT 33.12
Martens, Ulrike MA 19.46, MA 19.48
Marthaler, Michael QI 10.3
Martí, Othmar BP 12.19, BP 12.62,
DY 4.4, DY 46.1, •DY 46.6
Martí, Roger O 3.5
Martin Axt, Vollrath HL 8.7
Martin, B.A.A. HL 21.12
Martin, Christoph DY 8.1, SOE 6.1
Martin, Fernando O 7.4
Martin, Manfred HL 18.5
Martin, Nora S. •BP 23.1
Martín Sabanés, Natalia O 33.6
Martin, Stefan •HL 32.4
Martín Valderrama, Carmen
•MA 22.3, MA 22.5
Martinazzo, Rocco O 50.8
Martínez-Castro, Jose •O 5.5, O 54.6
Martínez-Criado, Gema HL 21.11,
HL 25.46
Martín-Jiménez, Alberto •O 7.4, O 7.5
Martín-Jiménez, Daniel •O 14.2
Martino, Edoardo O 54.11
Martins Costa, Matheus Henrique
•QI 6.9
Marx, Achim TT 15.1, TT 29.11,
TT 31.22, TT 31.23, QI 4.5, QI 4.6,
QI 4.7, QI 4.15, QI 4.18
Maryshev, Ivan •BP 19.7, DY 50.4
Marzari, N. O 66.2
Marzari, Nicola MA 11.7, MA 28.12,
MA 40.4, MM 2.7, MM 12.1,
MM 18.26, O 6.8, O 11.3, O 11.6,
O 43.4, O 43.5
Marzena, Petter HL 20.4
Maschio, Lorenzo HL 25.13
Masciocchi, Giovanni •MA 23.5
Masell, Jan MA 12.3, •MA 24.12,
•MA 27.2, •MA 27.7, •MA 27.10,
•TT 7.1
Masenda, Hilary HL 25.16
Mashhadi, Afra SOE 15.1
Masliuk, L. KFM 11.4
Mason, Philip O 64.1
Massabuau, Fabien HL 14.5
Massicot, Stephen O 20.2, •O 45.8,
O 45.9
Matczak, Michał MA 35.64
Matěj, Adam O 79.6
Matera, Sebastian DY 8.5, MM 2.8,
MM 8.8, O 8.8, •O 69.5, SOE 6.5
Matern, Stephanie •DY 35.6
Materne, Anne •BP 22.4
Mathes, Lucian MM 4.4
Mathew, Amal TT 20.10
Mathias, Stefan DS 20.16, MA 8.1,
MA 35.18, MA 35.20, MA 35.41,
O 2.2, O 2.9, O 9.10, O 16.6, O 16.9,
O 33.3, O 48.9, •O 68.2
Mathijssen, Arnold J.T.M. DY 31.4
Mathur, Sanjay MM 13.3, MM 13.4,
MM 13.5, MM 18.42
Matioli, Elison •DS 6.1
Matityahu, Shlomi TT 37.12
Matolínová, Iva O 3.6
Matschy, Sebastian HL 11.2
Matson, Joseph R. O 37.5, O 37.7
Matsubara, Masakazu MA 25.1
Matsyshyn, Oles HL 33.2
Matta, Bharti •O 41.6
Mattern, Maximilian HL 30.47
Mattevi, Cecilia HL 31.3
Matthäus, Franziska BP 12.57
Matthes, Frank O 5.9
Matthies, Anne •TT 1.1
Matts, Olga •MM 35.6
Matzner, Margherita MA 21.11
Maucher, Fabian DY 39.3
Maultzsch, Janina DS 20.9, HL 18.5,
KFM 11.5, O 6.6
Maurer, Felix M. BP 3.7
Maurer, Florian O 70.8
Maurer, Reinhard J. DY 35.5, O 13.5,
O 28.4, O 32.4, O 40.5, O 41.1, O 41.2,
O 46.6, O 50.8, O 61.8, O 74.11, O 83.2
Mauri, Marco BP 12.18, •BP 24.6
Mauritz, Tanja HL 18.2
Maurya, Arvind •MA 16.11
Mavridou, Kalliopi •HL 40.2
Mavrodiev, Pavlin BP 23.3
Mawass, Mohamad MA 34.5
Maximenko, Yulia •TT 2.10
May, Benjamin MM 13.3
May, Matthias M. •O 15.11
Mayer, Benjamin HL 25.3
Mayer, Christian •HL 22.7
Mayer, Julian-Benedikt TT 32.5
Mayer Martins, Jonas •DY 16.10
Mayer, Simon TT 9.3
Mayländer, Amelie DY 46.6
Mayor, Marcel O 61.5, O 61.7, O 74.6
Mayr, Stefan MM 32.4
Mayr, Stefan G. BP 18.8
Mayrhofer, Paul H. KFM 8.2, MM 28.5
Mayr-Schmölzer, Wernfried
•MM 20.4, MM 20.9, O 49.6
Mazarov, Paul MA 28.8
Mazhar, Hussain •O 32.6
Mazheko, Aliaksei •O 62.6, •O 62.7
Mazhijka, Donya •MA 3.2, •MA 19.56
Mazibrada, D. TT 31.8
Mazin, Igor MA 16.7, TT 3.6, TT 22.13
Mazin, Igor I TT 8.4
Mazitova, Dina I. •HL 24.12
Maznev, Alexei DS 20.41
Mazurenko, Vladimir V. O 51.4
Mazza, F. •MA 14.6
Mazza, Marco G. BP 10.3, BP 12.60
Mazzilli, Raffaele •MA 3.3
Mazzocchi, Francesco •KFM 18.4
Mazzoli, Claudio MA 2.3
Mazzolini, Piero HL 18.5
Mbeng, Glen Bigan QI 12.11
McCandless, Jonathan DS 20.6,
DS 26.1
McCord, Jeffrey MA 9.3, MA 19.3,
MA 35.62
McDougal, Anthony BP 19.5
McGlinchey, Amy •DS 20.5
McGuinness, Philippa H MM 21.3
McMahon, Nathan •QI 6.3, QI 6.4
McMullen, Ryan O 64.1
McMurtree, Gregory O 71.7, O 71.8
McNeill, Chris CPP 12.76
McSloy, Adam O 58.7, O 58.8
McVitie, Stephen MA 2.2, MA 19.27
Mecke, Joscha •DY 50.6
Meckenstock, Ralf MA 35.36
Medarde, Marisa KFM 2.6
Medicus, Sophie DS 13.4
Medina, Alberto DY 50.6
Medjanik, K. O 68.10
Medlin, Rostislav KFM 11.1
Medvedeva, Daria •O 26.3
Meer, Hendrik MA 19.60, •MA 19.62,
MA 25.5, MA 35.28
Meerholz, Klaus CPP 12.80, DS 20.10,
HL 30.34
mehdipour, hamid •HL 25.11, O 30.2
Mehl, Michael J. MM 12.5
Mehl, Sascha O 3.6, O 12.11, •O 49.5,
O 70.2
Mehlawat, Kavita TT 20.2
Mehler, Alexander O 18.1
Mehlhorn, Borge •MA 35.59
Mehlig, Bernhard •TUT 4.1, •DY 17.1,
•SOE 1.1
Mehmandoust, Mohammad •QI 2.8
Mehnke, Frank HL 10.6, HL 10.7
Mehrtrens, Thorsten DS 13.5
Mei, Hongyan HL 18.1
Meibohm, Jan •DY 3.2
Meier, Andreas KFM 18.3, KFM 25.10
Meier, Dennis •TUT 3.1, •KFM 1.1,
KFM 2.2, KFM 7.2, KFM 7.3, KFM 7.5,
KFM 7.6, KFM 14.6, MA 33.7
Meier, Matthias O 3.3, O 3.8, •O 10.5,
O 10.6, O 49.4, O 57.5
Meier, Q. N. MA 33.6
Meier, Quintin KFM 7.1
Meier, Quentin N. KFM 19.3
Meier, Torsten •HL 13.10
Meierhofer, Manuel HL 13.8, O 9.13
Meigel, Felix J. •BP 27.1
Meijer, Jan KFM 25.3
Meinecke, Jannick O 30.8
Meinecke, Moritz •HL 25.80
Meinecke, Stefan DY 15.2
Meineke, Christian •HL 40.1
Meinert, Helmut HL 25.90
Meingast, Christoph TT 39.2
Meinhardt, Alexander •CPP 17.12
Meisel, Tino CPP 26.5
Meißner, Kevin DY 50.5
Meißner, Robert MM 20.9, O 31.2,
O 49.6
Meister, Eduard CPP 26.5
Meitzner, R. CPP 12.71
Meitzner, Rico CPP 1.7, CPP 12.60,
CPP 12.62, CPP 12.63
Meixner, Michael •TT 16.4
Mejuto-Zaera, Carlos •MM 12.4
Mekle, Dario •QI 4.10, QI 4.31
Melampianaki, Eirini CPP 12.32
Melcer, Ron •TT 11.11
Mele, Antonio Anna •QI 12.8, QI 12.11
Mele, Francesco Anna •QI 7.10
Meléndez, Adrián MA 22.5
Melinte, Georgian KFM 15.4
Melischek, Larissa TT 26.8
Melles, Stephan HL 30.27
Melnikov, Alexey HL 11.12
Melo, P.M.M.C. HL 21.12
Meloni, Ilenia HL 28.1
Meltzer, Alexander TT 7.6
Ménard, Gerbold O 44.10, TT 37.7
Mendieta-Moreno, Jesus O 81.1

Author Index

- Mendirek, Gizem •MA 30.4
Mendive Tapia, Eduardo ... •MA 14.4
Mendive-Tapia, Eduardo ... MA 37.4
Mendl, Christian ... •DY 49.9, QI 4.29
Mendl, Christian Bernhard ... QI 4.22
Meneghini, Giuseppe ... O 16.9, O 48.9
Meneghini, Guiseppa ... O 9.10
Meng, Kuan ... •MM 35.4
Meng, Tobias ... TT 1.11, TT 24.10,
•TT 25.1, TT 34.14
Meninno, Antonella ... O 25.2
Menke, Henri ... TT 34.8
Menke, Henry ... TT 28.11
Menon, Vinod M. ... MA 30.8
Menou, Lucas ... •DY 45.2
Mensink, Liz ... •SYM 1.3
Menten, Julia ... •VA 2.4
Menteş, Tevfik Onur ... O 65.3, O 69.10
Mentink, Johan ... DY 43.7, •MA 17.1
Mentink, Johan H. ... MA 19.30
Menzel, Andreas ... BP 18.7
Menzel, Andreas M. ... CPP 2.8,
CPP 18.4, •DY 16.11
Menzel, Dirk ... MA 41.5, TT 3.2,
TT 21.14, TT 30.15, TT 30.16
Menzel, Stephan ... DS 18.1, HL 18.4
Merboldt, Marco ... •O 2.9, O 16.6
Mercadier, L. ... MA 25.4
Mercadier, Laurent ... MA 25.2, MA 25.7
Mercaldo, M.T. ... TT 22.1
Mercurio, G. ... MA 25.4
Mercurio, Giuseppe ... MA 25.2,
MA 25.7
Mergenthaler, Philipp ... BP 27.1
Merino, Pablo ... O 55.14, O 74.10
Merino-Diez, Nestor ... O 29.6
Merkel, Konrad ... •CPP 11.1
Merkel, Maximilian ... •TT 39.7
Merker, S. ... HL 33.4
Merker, Stefan ... HL 18.7
Merkl, Philipp ... HL 20.2
Merkl, Valentino ... HL 25.70
Merritt, Adrian ... •TT 8.2
Merschroth, Holger ... MA 35.52
Merte, Maximilian ... MA 21.8
Mertens, Fabian ... •MA 21.11,
•MA 35.21, MA 35.22
Mertens, Florian ... •DS 9.6
Mertens, Julian ... DS 20.13
Mertens, Lotte ... •DY 3.4
Mertig, Ingrid ... MA 8.11, MA 12.10,
MA 19.39, MA 24.4, MA 24.6,
MA 31.8, MA 35.76, MA 37.12,
MA 42.1, O 44.10
Mertin, Paul ... CPP 17.32
Mertz, Thomas ... TT 39.3
Merz, Florian ... O 50.2
Merz, Michael ... TT 21.6
Merz, Steffen ... MM 8.8
Messow, Adrian ... DS 26.2
Mette, Gerson ... O 9.11
Metternich, Daniel ... MA 2.1, MA 12.2,
•MA 23.3
Mettus, Denis ... •MA 12.6, •MA 19.7
Metwalli, Ezzeldin ... •CPP 33.6
Metz, Mirco ... HL 36.4, TT 17.5, TT 17.6,
TT 17.7
Metzger, Christian ... O 55.15, O 68.3
Metzner, Selma ... O 7.9
Metzner, Walter ... TT 21.11
Meusel, Manuel ... O 15.2, O 15.4
Mewes, Claudia ... MA 13.1
Mewes, Tim ... MA 13.1, MA 19.2
Mey, Oliver ... HL 30.8
Meyer, Andreas ... CPP 28.6, QI 2.10
Meyer, Bernd ... HL 30.37, MM 10.17,
O 5.6, O 32.9, •O 38.2, O 49.10,
O 52.10, O 58.10
Meyer, Carola ... BP 7.8
Meyer, Constantin ... TT 33.8
Meyer, Ernst ... O 17.10, O 22.6, O 39.4,
O 79.1, O 79.3
Meyer, Fabian ... MA 28.8
Meyer, H. ... O 68.10
Meyer, Hendrik ... CPP 41.3
Meyer, Johannes Jakob ... •QI 8.7,
QI 12.8
meyer, julia ... TT 10.2
Meyer, Lorenz ... •O 51.10, O 80.1
Meyer, Miriam ... O 58.15
Meyer, Nina ... MA 35.65
Meyer, Paul ... •KFM 25.14
Meyer, Ruth ... •BP 12.7, BP 12.8
Meyer, Sebastian ... MA 30.6
Meyer, Tamara ... O 38.4
Meyer, Tobias ... O 20.7
Meyer zu Heringdorf, Frank ... O 2.10,
O 18.4, O 18.10, O 54.4
Meyer zu Heringdorf, Frank-J. ... O 33.8,
O 78.3
Meyerheim, Holger L. ... MA 34.6,
O 66.4
Meyer-Ortmanns, Hildegard ... •DY 18.3,
SOE 10.3
Micallo, Tommaso ... •TT 11.10
Micevic, Ana ... HL 11.1
Michael, Marios ... MM 9.3
Michael Sauther, Schorsch ... MA 27.11
Michael, Stephan ... HL 8.2
Michaelides, Angelos ... •SYUK 1.1,
O 43.6, O 46.5
Michaelis de Vasconcellos, Steffen
•TUT 2.3, •HL 1.3, HL 19.9, HL 20.1,
HL 25.25, HL 25.26, HL 25.27,
HL 30.48, MA 21.10
Michalik, Stefan ... MM 30.6
Michalsky, Ina ... O 40.2, O 40.3
Michel, Fabian ... DS 21.1
Michels, Andreas ... TT 23.13
Michelsen, Andreas Bock ... TT 11.5
Michely, Thomas ... O 18.12, O 18.16,
O 54.14, O 65.1, O 71.4
Michen, Benjamin ... •TT 11.7
Michl, Johannes ... •HL 17.7
Michler, Peter ... •SYPQ 1.4, HL 4.6,
HL 4.11, HL 12.3, HL 17.1, HL 17.4,
HL 17.5, HL 17.7, HL 25.62, HL 25.70,
HL 25.88, HL 26.2, HL 26.3, QI 4.31
Michlikova, Sona ... BP 7.31
Middleburgh, Simon ... MM 2.9
Midolo, Leonardo ... HL 35.4
Midya, Jiarul ... •BP 2.2
Miedema, P. ... MA 25.4
Mielke, Jonas ... QI 1.5
Mier, Cristina ... O 80.5
Miglio, A. ... HL 21.12
Miguel, Maxi San ... SOE 5.4
Miguez-Lago, Sandra ... O 15.5
Mihalovic, D. ... O 9.5
Mihalic, Saskia ... •DS 9.2
Mihlan, Levin ... •DS 20.11
Mihov, K. ... TT 30.7
Mikhail, Katsnelson ... TT 38.4
Mikhailov, N. N. ... TT 20.9
Mikhailov, Nikolay ... TT 19.3
Milbradt, Richard Maximilian ... •QI 4.22
Mildenberger, Julius ... •QI 10.5
Milekhin, Ilya ... HL 25.9
Milkin, Pavel ... CPP 7.5
Miller, Daniel ... O 27.4
Miller, Fabian ... •MM 18.9
Miller, Michael ... MA 27.3
Milloch, Alessandro ... TT 36.3
Milosavljevic, Djana ... TT 28.6
Milovanovic, Dragomir ... BP 9.4
Milow, Barbara ... MM 10.29
Min, Chul hee ... •O 9.1
Minár, Ján ... KFM 11.1, MA 28.13,
O 48.7, O 73.6, O 73.9
Minko, Sergij ... DS 23.6
Minola, Matteo ... MA 6.4
Minopoli, Antonio ... DY 4.7
Mintert, Florian ... DY 5.2, DY 43.1
Mir, Mashood ... HL 30.49
Mir, Mashood Tariq ... •HL 30.39,
HL 30.50, HL 30.51
Miranda, Ivan ... MA 25.6
Miranda, Rodolfo ... O 79.6
Mirau, Luca ... •CPP 17.19
Mirhajvarzaneh, Alaleh ... •BP 7.29
Mirlin, Alexander ... TT 11.11
Mirolo, Marta ... O 20.4
Miroshkina, Olga ... MA 19.12
Miroshkina, Olga N. ... MA 19.14,
MA 19.15, •MA 42.4
Mirzapour-Shafiyi, Fatemeh
•BP 12.36
Mischke, Valentin ... •O 55.5
Mishra, Harshad ... TT 15.5
Mishra, Neeraj ... O 2.5, O 2.6, O 2.7,
O 9.6, O 9.8, O 33.5
Mishra, Simli ... MM 21.3, •MM 21.3
Mishra, Vibhu ... •TT 21.47
Mishra, Vipin ... O 15.7
Misof, Philipp ... MM 10.3
Mitchell, John ... MA 6.1
Mitchell, Roger ... MA 5.2
Mitchell, Sharon ... O 3.5, •O 10.1
Mitschank, Rüdiger ... HL 25.33, HL 25.34
Mithun, Devapriyo ... •HL 15.8
Mitkov, Martin ... •O 5.4
Mitra, Gautam ... TT 29.6
Mitric, Roland ... DS 5.5
Mitsumoto, Keisuke ... TT 24.8
Mittendorfer, Florian ... O 65.7
Mittendorff, Martin ... •HL 6.9, HL 11.2,
HL 42.1
Mittenzwey, Henry ... •HL 11.7
Miwa, J.A. ... O 68.10
Miwa, Jill ... O 54.5
Mix, Torsten ... MA 29.4
Mixa, Leon ... •TT 9.2
Miyamoto, Koji ... O 73.3
Miyata, Atsuhiko ... HL 20.3, TT 22.11
Miyazaki, Ray ... •O 70.9
Miyoshi, T. ... TT 22.1
Mladenov, Anton ... QI 5.5
Moaddeli, Mohammad ... HL 5.10,
HL 23.4, HL 23.8
Möbus, Tim ... •QI 14.7
Möckel, Wolfgang ... TT 29.7
Mockute, Aurelija ... DS 9.1
Modes, Carl D. ... BP 22.2, DY 52.3,
SOE 20.3
Modregger, Peter ... •KFM 6.3
Moerman, Evgeny ... •MM 12.7
Moessner, R. ... TT 28.4
Moessner, Roderich ... DY 5.2, DY 19.1,
DY 43.1, MA 15.3, MA 16.3
Moghaddam, Ali G. ... DY 3.4, TT 11.6,
TT 20.2
Mogilatenko, A. ... TT 30.17
Mohamed, Elalyaa ... •CPP 37.8
Mohammadejad, Sarah ... BP 12.58
Mohammadzadeh, Hossein ... •MA 35.5
Mohammed, Sohaila ... •TT 30.11
Mohanad, Alkaales ... HL 36.10
Mohandes, Aminreza ... HL 5.10
Mohapatra, Subhadra ... •O 16.10
Mohite, Atul Tanajuni ... •DY 24.1
Mohlentkamp, Laurens W. ... HL 7.5
Mohr, Sebastian B. ... DY 8.9, SOE 6.9
Mokhtari, Parisa ... •TT 34.2
Mokhtari, Zahra ... DY 50.8
Mokrousov, Yuriy ... •SYPQ 1.2, MA 8.6,
MA 10.5, MA 14.3, MA 15.8,
MA 19.44, MA 21.8, MA 24.2,
MA 24.8, MA 24.11, MA 25.5,
MA 27.12, MA 35.28, MA 37.8, O 26.1
Molatta, S. ... TT 12.6
Moldabekov, Zhandos A. ... MM 12.9
Molenkamp, Laurens ... SYQM 1.2,
HL 30.47, TT 19.2, TT 32.5
Molenkamp, Laurens W. ... HL 25.41,
TT 1.2, TT 32.8
Molina-Ferández, Rafael A. ... DS 20.23
Molinari, Elisa ... O 74.2
Moll, Nikolaj ... QI 12.5, •QI 12.6
Mollavali, Saied ... HL 23.4
Mollenhauer, Doreen ... O 79.5
Möller, Björn ... O 17.5, O 28.6
Möller, Christina ... MA 8.1, MA 35.20
Möller, Marcel ... MA 23.3
Möller, Nadir ... CPP 17.31, DY 23.1
Möller, Robert ... KFM 25.21, •TT 21.2
Möller, Samuel ... QI 1.2
Möller, Wolfhard ... DS 1.1
Möllers, Paul Valerian ... •O 26.8,
O 55.16
Moloney, Jerry ... HL 13.10
Momeni, Davood ... O 2.9
Momeni Pakdehi, Davood ... O 41.4
Monaco, Giulio ... TT 8.6, TT 21.15
Mondal, Badal ... •HL 21.5
Mondal, Debasish ... •DY 24.6, DY 44.4,
DY 44.7
Monderkamp, Paul A. ... DY 23.8,
DY 46.2
Mönig, Harry ... O 18.20
Mönkebüscher, David ... MA 21.11,
MA 35.21, •MA 35.26
Monkenbusch, Michael ... CPP 33.1
Monsel, Juliette ... QI 5.7
Monserrat, Bartomeu ... DS 19.2,
HL 14.4
Montag, Verena ... •HL 10.6
Monter, Samuel ... BP 6.1
Montibeller, Samuel ... MM 3.9
Monzel, Cornelia ... BP 7.3, BP 7.4,
CPP 45.2, MA 35.55
Mook, Alexander ... MA 31.8
Moonnukandathil Joseph, Dijo
BP 7.33, •BP 12.31
Moor, Anne-Lena ... •BP 24.2
Moore, Kalani ... KFM 2.5
Moore, R. G. ... O 9.5
Moors, Kristof ... HL 7.4
Moors, Kristoff ... HL 7.3
Moos, Eduard ... •O 16.7
Moos, Ralf ... HL 5.3, HL 23.2
Mooshammer, Fabian ... HL 20.2
Mora, Thierry ... BP 6.7
Moraga, Nicolás ... BP 12.50, •BP 12.51
Morales, Carlos ... O 52.11
Morawski, Marcin ... HL 27.3, HL 34.5
Mørch Nielsen, Carl Emil ... •O 18.24
Morelli, Simon ... QI 9.4
Morellon, Luis ... MA 21.9
Moreno, Juan Nicolas ... •DY 45.7
Moreno-Gonzalez, Mateo ... TT 11.2
moreno-pineda, eufemio ... O 80.3
Moresco, Francesca ... O 29.2, O 29.5,
O 32.8
Moretti Sala, Marco ... TT 21.15
Morgenstern, Annika ... •HL 25.51,
HL 28.5
Morgenstern, Karina ... O 27.4, O 32.2,
O 32.6, O 52.2, O 74.8, O 79.8
Morgenstern, Markus ... HL 25.77,
MA 31.2
Morice, Corentin ... DY 3.4, •TT 11.6
Moritz, Brian ... MA 6.1
Moritz, Michael ... •O 45.3
Moritz, Micheal ... O 45.4
Moritz, Michelbach ... •HL 28.3
Mork, Jesper ... HL 25.91
Mornhinweg, Joshua ... •HL 40.5
Moroder, Mattia ... •DY 43.5
Morreti Sala, Marco ... TT 8.6
Morris, Andrew ... O 43.3
Morris, Andrew J. ... MM 2.1, MM 14.2
Morris, Benjamin ... QI 2.2
Morrison, Abigail ... MA 37.8
Morrow, Joe D. ... •O 83.6
Morrow, Ryan ... •TT 12.1, TT 21.23
Morscher, Christoph Burghard
BP 7.40
Moser, Philipp ... •HL 20.3
Moser, Simon ... DS 20.28, DS 20.35
Moser, Tobias ... BP 9.9
Moser, Toni ... •O 8.2, O 15.9, O 15.10
Moshe, Aviv ... TT 30.24
Moshkina, E. M. ... MA 4.1
Moshnyaga, Vasily ... DS 20.16,
DS 20.33, DS 20.37, DS 20.40,
MA 35.18, MA 35.20, MA 35.41
Moskalenko, Andrey S. ... •HL 30.43
Mößle, Michael ... •PSV V
Mostofi, Arash A. ... MM 12.2
Mostovoy, Maxim ... MA 33.4
Motta, Mario ... QI 4.27
Mottin, Davide ... O 63.5
Motzoi, Felix ... HL 36.2, •QI 3.6, QI 4.40,
QI 5.6, QI 13.9
Mouhat, Felix ... O 31.7
Mravlje, Jernej ... MM 23.8
Mrovec, Matous ... MM 6.2, MM 15.1,
MM 20.8, MM 25.2, MM 25.3,
MM 31.2, MM 34.4
Mruczkiewicz, Wojciech ... QI 10.5
Msall, Madeleine ... HL 35.2, HL 35.3
Msiska, Robin ... •MA 27.13, MA 35.16
Mu, Xiaoke ... MM 17.3
Muchowski, Eugen ... •QI 9.10
Mudi, Priyabrata ... HL 30.10
Mudryk, Y. ... MA 29.3
Muehle, Steffen ... SOE 15.2
Mueller, David N. ... •MM 13.2
Mueller, Kai ... HL 25.65
Mueller, Matthias ... O 62.6
Mueller, Maximilian ... DS 23.5
Mueller, Niclas S. ... •HL 33.6
Mueller, Ulrich ... CPP 12.56
Muenker, Till ... BP 22.8
Muenker, Till M ... •BP 12.10
Muenzenberg, Markus ... MA 19.61
Mugarza, Aitor ... O 6.3
Muhin, A. ... HL 10.5
Muhin, Anton ... HL 10.7, HL 10.8,
HL 10.10
Mühl, Thomas ... MA 5.3
Mühlbacher, Peter ... MA 14.2
Mühlbauer, Martin ... MM 8.2
Mühlbauer, Monika ... AKC 1.2
Mühlbauer, Sebastian ... MA 19.7
Mühlhauser, Matthias ... •TT 5.7,
TT 21.18, TT 21.19, TT 21.20,
•TT 21.31, TT 24.14
Mujid, Fauzia ... MM 21.1
Mukharsky, Yuri ... TT 37.7
Mukhopadhyay, Archan ... DY 45.6,
SOE 12.6, •SOE 17.4
Mukhopadhyay, Aritra K. ... •DY 16.5
Mukhopadhyay, Soham ... •BP 7.38

Author Index

- Mukhundhan, Nitin . . . HL 3.9, HL 12.4
 Mułarski, Marian . . . QI 12.8
 Mülbauer, Sebastian . . . MA 12.6
 Mulkers, Jeroen . . . MA 27.13
 Müllen, Klaus . . . O 17.10, O 23.9
 Müller, A. . . . HL 21.1
 Müller, Aaron Merlin . . . •KFM 19.1
 Müller, Andreas . . . •HL 25.45
 Müller, Claudius . . . MM 28.2
 Müller, David . . . MM 13.3
 Müller, David A. . . . MM 21.1
 Müller, Eckhard . . . MM 21.5
 Müller, Erich A. . . . O 46.5
 Müller, Felix . . . HL 30.27
 Müller, Philipp . . . HL 35.2
 Müller, Isabel . . . DS 20.44
 Müller, Jens . . . DS 23.2
 Müller, Judith . . . •BP 12.55
 Müller, K. . . . HL 2.3
 Müller, Kai . . . HL 8.1, HL 8.10, HL 12.1,
 HL 15.5, HL 25.13, HL 25.72, HL 26.6,
 HL 36.4, TT 17.5, TT 17.6, TT 17.7
 Müller, Leanna . . . TT 34.13
 Müller, Leonard . . . MA 31.6
 Müller, Mahni . . . •DS 25.2
 Müller, Manuel . . . MA 19.40, MA 19.41,
 •MA 22.2, MA 35.6, MA 35.7,
 MA 35.35, MA 35.37, TT 31.5
 Müller, Marcus . . . BP 17.3, BP 18.2,
 CPP 17.38, CPP 45.5, CPP 50.2
 Müller, Markus P. . . . •QI 14.1
 Müller, Martin . . . MM 31.3
 Müller, Martina . . . DS 20.36, MA 23.2,
 MA 33.2, MA 35.26
 Müller, Marvin . . . •DS 13.3
 Müller, Melanie . . . MA 21.1, •O 7.6,
 O 33.6
 Müller, Michael . . . •TT 31.9, TT 31.10
 Müller, Niels . . . DY 44.11
 Müller, Niklas . . . •O 59.7, TT 11.3
 Müller, Robert . . . MA 35.60
 Müller, Sebastian . . . BP 12.2
 Müller, Simon . . . O 9.1
 Müller, Svenja . . . TT 29.3
 Müller, Tobias . . . MA 16.1, •MM 10.17
 Müller, Toni . . . CPP 2.1
 Müller, Torsten . . . BP 13.9
 Müller, Verena . . . •CPP 17.2
 Müller-Bender, David . . . •DY 18.4,
 DY 45.3, •SOE 10.4
 Müller-Buschbaum, Peter . . . •CPP 1.2,
 CPP 1.6, CPP 1.8, CPP 12.3, CPP 12.7,
 CPP 12.13, CPP 12.14, CPP 12.15,
 CPP 12.31, CPP 12.40, CPP 12.43,
 CPP 12.46, CPP 12.47, CPP 12.48,
 CPP 12.49, CPP 12.52, CPP 12.54,
 CPP 12.61, CPP 12.64, CPP 12.65,
 CPP 12.67, CPP 12.68, CPP 17.5,
 CPP 17.6, CPP 17.17, CPP 17.23,
 CPP 17.26, CPP 17.27, CPP 17.28,
 CPP 17.29, CPP 18.3, CPP 19.4,
 CPP 20.4, CPP 26.3, CPP 27.2,
 CPP 27.3, CPP 28.4, CPP 28.4,
 CPP 28.6, CPP 28.8, CPP 37.3,
 CPP 37.6, CPP 44.4, CPP 45.3,
 CPP 48.2, CPP 48.3, CPP 49.4,
 CPP 50.1, DS 20.50, HL 30.29,
 KFM 25.18, KFM 25.20
 Müller-Buschbaum, Peter
 Müller-Buschbaum . . . CPP 12.45
 Müller-Deku, Adrian . . . BP 17.2
 Mulvaney, Paul . . . O 78.4
 Munch, Falk . . . MA 29.9
 Münch, L. . . . TT 31.8, TT 37.11
 Münch, Lukas . . . TT 31.16, TT 33.1
 Müncker, Till . . . BP 12.17
 Mundinar, Simon . . . TT 21.35
 Mundy, Julia . . . KFM 7.2
 Munk, Axel . . . BP 13.7
 Munker, Till . . . BP 22.5
 Münker, Till moritz . . . DY 49.8
 Muñoz, Omar . . . •BP 12.24
 Muñoz, Sergio Alonso . . . DY 39.7
 Muñoz-Santiburcio, Daniel . . . •MM 18.8
 Münster, Florian . . . DS 20.19, O 12.6,
 •O 55.10, O 55.13
 Münster, Lambert . . . •DY 26.1
 Münster, Lasse . . . O 33.7, •O 68.4
 Münzberg, Julian . . . HL 8.7
 Münzenberg, Markus . . . MA 8.12,
 MA 19.3, MA 19.26, MA 19.46,
 MA 19.48, MA 19.49, MA 19.54,
 MA 21.3, MA 35.33, MA 35.65
 Mura, Michele . . . VA 2.1
 Muralikrishna, G. M. . . . MM 21.7
 Muratore Ginanneschi, Paolo . . . QI 2.5
 Muraveva, Valeriia . . . •DY 46.12
 Murawski, Caroline . . . HL 28.1
 Murayama, Kantaro . . . TT 12.4
 Murillo Navarro, Diana Elisa
 •MM 23.2
 Murphey, Corban G.E. . . . HL 22.2
 Murphy, Bridget . . . KFM 25.7
 Murphy, Thomas E. . . . HL 6.9
 Murray, Seán . . . BP 13.2, BP 18.4
 Murta, Gláucia . . . QI 7.2, QI 7.3
 Musekamp, Jens . . . MA 32.4
 Musil, Félix . . . O 58.9
 Mussler, Gregor . . . DS 21.2, HL 7.3,
 HL 19.7, O 4.3
 Mustafa, Luqman . . . •DS 9.1
 Muth, Dominik . . . •CPP 12.55
 Muth, Maximilian . . . O 12.11, •O 12.12
 Mutombo, Pingo . . . O 79.6
 Mutschler, Julius . . . MA 19.22, •MA 26.2
 Mutter, Daniel . . . MM 8.1, MM 8.5,
 •MM 14.3, MM 24.3, •MM 33.6
 Mützel, Carina . . . O 40.7
 Myasoedov, Yuri . . . TT 7.6
 Myint, Hsu Thazin . . . •CPP 12.54
 Myroshnychenko, Viktor . . . HL 21.10,
 HL 33.9, O 78.6
 Mysliveček, Josef . . . O 3.2, O 20.1,
 O 70.2
 Nabok, Dmitrii . . . HL 33.1, MA 38.5
 Nacci, Christophe . . . O 17.7, O 20.11,
 •O 23.2, O 58.15
 Nachtigall, Matyás . . . O 81.1
 Nadarajah, Ruksan . . . MA 39.5
 Nadvornik, Lukas . . . MA 21.9
 Nagaosa, Naoto . . . MA 24.12
 Nagata, Yuki . . . CPP 37.7
 Nagel, Daniel . . . BP 7.7, •BP 15.6
 Nagel, Sören . . . •SOE 3.4
 Nagyfalusi, Balázs . . . MA 7.3, •MA 37.6
 Nähle, Ole . . . TT 17.2, TT 31.10
 Nahum, Adam . . . TT 24.3
 Naidyuk, Yurii . . . MM 18.37
 Naimer, Thomas . . . •DS 20.26
 Najafidehaghani, E . . . HL 42.2, •O 81.6
 Najafidehaghani, Emad . . . HL 6.4,
 HL 42.7
 Nakajima, Makoto . . . MA 28.9
 Nakasuiji, Shota . . . QI 13.7
 Nakerst, Goran . . . •TT 9.4
 Nam, K. . . . •KFM 11.4
 Nam, Shinjae . . . •O 14.1, O 22.8
 Nambiar, Sankalp . . . BP 14.9
 Nambisan, Ameya . . . •TT 31.18
 Nandakumar, Pradeepkumar
 •TT 37.13
 Nandi, Shibabrata . . . MA 40.3
 Nandy, Manali . . . O 30.6
 Narita, Akimitsu . . . O 17.10, O 23.9
 Narkevicius, Aurimas . . . CPP 8.4
 Narkowicz, Ryszard . . . MA 28.8
 Nase, Michael . . . CPP 2.4
 Naselli, Gabriele . . . •TT 18.5
 Nasiri, Mahdi . . . •DY 51.1, DY 51.2
 Nasirimarekani, Vahid . . . •BP 12.48,
 •BP 26.2
 Nataf, Guillaume . . . •KFM 2.1
 Nath, Jayshankar . . . QI 4.23, QI 6.8
 Natori, Willian . . . MA 16.4
 Natterer, Fabian . . . O 71.9
 Natterer, Fabian D. . . . O 51.4
 Natterer, Fabian Donat . . . •O 7.2
 Naujoks, Jonas . . . •DY 51.5
 Naujoks, Tassilo . . . •CPP 12.78,
 CPP 28.7
 Naumann, Jonas . . . •BP 3.4
 Naumann, Tim . . . •O 52.6
 Navarathna, Rohit . . . TT 37.13
 Navarro, Gema . . . •O 17.10
 Navarro-Quezada, Andrea . . . MA 30.4
 Navas, Salman Fariz . . . •DY 23.4
 Nawrath, Cornelius . . . HL 17.1, HL 17.4,
 HL 17.7
 Nayak, Ganesh K. . . . MM 28.5
 Nayak, Ganesh Kumar . . . •O 43.2
 Nayar, Divya . . . CPP 9.8
 Nazarenko, Olga . . . HL 23.11, HL 25.92
 Nazeeruddin, Mohammad Khaja
 CPP 28.2
 N'Diaye, Alpha T. . . . MA 22.4
 Ndiaye, Waly . . . •O 73.6
 Ndione, Pascal D. . . . O 33.4
 Nebe, Barbara . . . BP 12.43, BP 12.44
 Neckernuß, Tobias . . . BP 12.19
 Neckernuss, Tobias . . . •DY 4.4
 Nedelea, Vitalie . . . HL 2.1
 Neduck, Felix . . . HL 34.5
 Néel, Nicolas . . . O 18.1, •O 19.1, O 55.4,
 O 55.8
 Nees, Nico . . . CPP 8.2
 Neethirajan, Jeffrey N. . . . MA 2.4
 nefedov, alexei . . . O 30.7, O 70.8, O 79.7
 Negi, Rajendra Singh . . . •BP 4.6
 Neidig, Martin . . . •TT 31.11
 Neitemeier, Pit . . . •TT 33.5
 Nellesen, Jan . . . •O 48.4
 Nelson, Andrew . . . DS 1.3
 Némec, Petr . . . MA 29.6
 Nerf, Hannah C. . . . O 54.10, O 54.13
 Nerreter, Svenja . . . •HL 20.2
 Nest, Leona . . . HL 23.6
 Nessler, Peter . . . CPP 13.3, CPP 45.6
 Nethewala, Aditi . . . MM 10.30
 Netter, Niklas . . . BP 10.4
 Neu, Jennifer . . . O 4.1
 Neubauer, Manuel . . . HL 30.34
 Neuber, Nico . . . MM 30.2
 Neuber, Sven . . . BP 12.43, •CPP 45.6
 Neuendorf, Jan . . . O 28.3
 Neugebauer, Joerg . . . MM 10.4,
 MM 20.3, MM 25.6, MM 34.1
 Neugebauer, Jörg . . . DS 6.2, HL 24.11,
 HL 34.4, MA 14.4, MM 4.6, MM 6.9,
 MM 15.2, MM 15.5, MM 16.4,
 MM 20.6, MM 20.10, MM 22.2,
 MM 25.1, MM 31.4, MM 33.7, O 38.6,
 O 64.5
 Neugebauer, Nils . . . MA 19.34, •MA 41.1
 Neuhaus, Alexander . . . O 2.10, •O 33.8,
 O 78.3
 Neuhaus, Charlotte . . . BP 9.4, BP 12.54,
 •BP 17.6
 Neuhaus, Josefina . . . •HL 25.18
 Neuhaus, Konstantin . . . BP 10.4
 Neuhaus, Leonard . . . •DS 20.19, O 12.1,
 O 12.4, O 12.6, O 55.10
 Neuhaus-Steinmetz, Jannis . . . •TT 19.4
 Neuman, Tomáš . . . O 35.6
 Neumann, Alexander . . . TT 27.5
 Neumann, C. . . . O 81.6
 Neumann, Christof . . . CPP 11.2, HL 4.4,
 HL 42.7, O 65.4, O 65.5
 Neumann, Robin R. . . . •MA 31.8
 Neumann, Tanja . . . BP 13.9
 Neumark, Daniel . . . O 64.1
 Neumeier, Steffen . . . MM 18.14
 Neupert, Titus . . . TT 18.1
 Neusch, Andreas . . . •CPP 45.2
 Neuwald, Jonathan . . . TT 2.2, •TT 29.7
 Newsom, Chloe . . . PLV III
 Newton, Mark . . . •PLV III
 Neyenhuys, Oliver . . . •TT 27.3
 Ngo, G. . . . HL 42.2
 Ngo, G. Q. . . . O 81.6
 Nguyen, Chau . . . QI 9.5
 Nguyen, Duy-Hoang-Minh . . . •TT 11.1
 Nguyen, Gia Huy Philipp . . . •DY 50.2
 Nguyen, Giang Nam . . . •HL 19.1, HL 35.4
 Nguyen, H. Chau . . . QI 14.2
 nguyen, long . . . •MM 12.6
 Nguyen, T.T.N. . . . O 25.3
 Nguyen, Thanh Duc . . . TT 21.5, TT 21.6
 Nguyen, Thi Hai Quyen . . . O 20.3,
 •O 20.5
 Nguyen Thi, Thuy Linh . . . •HL 25.42
 Nguyen, Viet-Hung . . . TUT 2.2, HL 1.2
 Ni, Bing . . . MM 35.3
 Ni, Xiang . . . O 37.5, O 37.7
 Nickel, Bert . . . •BP 17.2, BP 26.7,
 CPP 39.6, CPP 41.7, HL 6.4,
 HL 25.52, MM 18.35
 Nickl, Andreas . . . HL 26.6
 Nicolai, Laurent . . . O 73.6, O 73.9
 Nicolini, Nina . . . MM 28.1
 Nie, Weijie . . . HL 8.3, HL 8.4, HL 8.5,
 HL 25.82
 Niebur, André . . . HL 20.7
 Niebuur, Bart-Jan . . . CPP 33.5
 Niedermayr, Arthur . . . TT 25.5
 Niehaus, Jan Steffen . . . HL 39.2,
 KFM 11.5
 Niehoff, T. . . . •MA 29.2
 Niehoff, Timo . . . MA 19.13
 Niehues, Iris . . . HL 20.1
 Niekamp, Lukas . . . •TT 29.11
 Nieken, Ulrich . . . •MM 32.5
 Nielaba, Peter . . . CPP 17.7, DS 9.4,
 DY 44.3
 Niemann, Leonhard . . . •MM 10.11
 Niemann, Richarda . . . •O 37.6, O 44.5
 Nienhaus, Gerd Ulrich . . . BP 8.2
 Nierhauve, Alena . . . O 18.21, •O 48.10
 Nieswicz, Kathrin . . . •O 52.1
 Nietner, Alexander . . . •QI 12.10
 Nieves, Pablo . . . MA 32.8
 Nigam, Jigyasa . . . •O 67.6
 Niggli, Lorena . . . •MA 30.5, O 53.3
 Nikitin, Stanislav . . . TT 21.9
 Nikolai, Rafal E. . . . MA 27.4
 Nkolic, Danilo . . . TT 30.12
 Nikolo, M. . . . MA 14.6
 Nikoubashman, Arash . . . BP 7.27,
 BP 18.5
 Nilima, Athoy . . . TT 17.1
 Nilsson, Anders . . . O 27.1
 Nimmrichter, Stefan . . . QI 2.4, QI 2.7,
 QI 2.9, QI 14.9
 Ning, C.-Z. . . . HL 4.7, HL 4.9
 Ning, Cun-Zheng . . . HL 4.8
 Ning, Jiaoyi . . . CPP 12.26
 Niño, Miguel Ángel . . . MA 35.17
 Nishigami, Yukinori . . . BP 14.6
 Nisi, Katharina . . . DS 22.2
 Nitsch, Maximilian . . . •HL 3.3, HL 30.40
 Nitschke, Jonah . . . O 55.9
 Nitschke, Jonah E. . . . O 55.5
 Nitschke, Jonah Elias . . . •O 12.5
 Niu, Gang . . . DS 20.1
 Niu, Jiasen . . . O 58.14
 Niu, Kaifeng . . . O 62.9
 Niu, Ran . . . DY 16.5
 Niu, Shuo . . . DS 26.3
 Niu, Zhichuan . . . DS 25.75
 Noack, Philipp . . . •HL 25.61
 Noad, Hilary . . . TT 23.6
 Noby, Sohaila . . . TT 30.10
 Noce, C. . . . TT 22.1
 Nocerino, Elisabetta . . . CPP 1.8
 Noda, Takeshi . . . HL 2.2
 Nöding, Lukas . . . HL 30.39, HL 30.49,
 HL 30.50, •HL 30.51
 Noé, Jonathan . . . QI 5.9
 Noei, Heshmat . . . O 52.9, O 56.4
 Noei, Neda . . . O 55.11
 Nogueira, Flavio . . . TT 24.9
 Noh, Kyungju . . . MA 26.3, O 47.4, O 54.3
 Noirault, Nicolas . . . DY 49.2
 Nojiri, Yuki . . . TT 31.23, QI 4.5, QI 4.6,
 QI 4.7, QI 4.15, QI 4.18, QI 4.34,
 QI 4.35, QI 4.36, QI 4.37
 Noll, Cornelia . . . MM 7.3, MM 18.13
 Nolte, Stefan . . . DS 20.15
 Nolte, Ulla . . . BP 12.4
 Nomura, Kentaro . . . TT 11.1
 Nong, Hanond . . . HL 4.3
 Norbert, Norbert . . . MA 28.6
 Nordström, Lars . . . MA 30.5, O 53.3
 Nothel, Tabata . . . CPP 11.2
 Nothelfer, Jonas . . . TT 1.11
 Nötzel, Janis . . . QI 7.6
 Nouri, Hamid . . . •DS 20.24
 Novak, Ekaterina . . . CPP 34.3, CPP 44.2,
 DY 46.5
 Novak, Maja . . . BP 13.4, •BP 13.8,
 DY 40.4
 Novik, Elena G. . . . TT 1.6
 Novikau, Ivan . . . •CPP 34.3, DY 46.5
 Novko, Dino . . . O 2.9, O 81.2
 Novoselova, Iuliia . . . CPP 45.2
 Novotny, Oldřich . . . TT 31.6
 Nowak, D. . . . MA 33.6
 Nowak, U. . . . MA 38.1
 Nowak, Ulrich . . . MA 8.4, MA 8.7,
 MA 8.10, MA 8.12, MA 12.8, MA 15.2,
 MA 28.9, MA 38.2
 Nowicki, Marek . . . O 20.8
 Nowotnick, Adrian . . . •HL 25.46
 Nuzaki, Kyoko . . . O 55.3
 Nobar, Matthias . . . CPP 12.64
 Nuegebauer, Jörg . . . O 27.2
 Nuić, Lovro . . . BP 7.23, BP 22.7
 Nuñez Valencia, Cuauhtemoc . . . •O 27.3
 Nurmukhametov, Alexey . . . MA 33.3
 Nurmukhametov, Alexey R. . . . MA 14.9
 Nutz, Manuel . . . HL 25.23, HL 30.6,
 QI 5.9
 Nyári, Bendegúz . . . MA 19.38, •TT 1.8,
 TT 1.9
 Nysten, Emeline . . . •HL 35.1
 O. von Rohr, Fabian . . . MA 35.58
 Ober, Martina . . . BP 17.2, BP 26.7
 Oberbauer, Sebastian . . . TT 12.8,
 TT 21.25
 Oberhofer, Harald . . . •CPP 40.1, O 11.4,
 O 43.9, O 46.1, O 46.3, O 46.8, O 82.2
 Oberreiter, Julian . . . DS 1.3
 O'Brien, Thomas . . . QI 12.5
 Obst, Maximilian . . . O 37.5
 Ochkan, Kyrilo . . . TT 11.8, •TT 11.9

Author Index

- Ochner, Hannah•BP 9.2
 Ocker, Michelle•TT 21.4
 O'Connell, Eoghan KFM 2.5
 Odobesko, Artem O 73.11
 O'Driscoll, Luke O 12.2
 Oechsle, Anna Lena CPP 12.40,
 •CPP 48.2
 Oechsle, Anna-Lena CPP 27.2,
 CPP 48.3
 Oehlschlägel, Lisa Marie DY 34.1
 Oehme, M. HL 22.1
 Oehrl, Patricia•TT 27.7, TT 31.5
 Oelschläger, Anne•O 66.9
 Oelsner, A. O 68.10
 Oestreich, Michael HL 20.7, HL 25.93,
 HL 25.94
 Oeter, Anne-Catherine TT 15.3
 Oettel, Martin•DY 2.1
 Off, Jürgen HL 10.3
 Ogata, Shuji KFM 2.7, MM 10.19
 Ogawa, Naoki KFM 2.4
 Ogbuehi, Anthony Chukwunonso
 •QI 4.24
 Ogunmoye, Kehinde CPP 12.50
 Ogura, Masako•HL 7.10
 Oh, Jeongmin O 51.7
 Ohlerth, Thorsten MM 14.3
 Ohlin, Hanna KFM 3.4
 Ohlmann, Jens HL 30.35
 Ohmann, Robin O 42.1, O 81.2
 Ohmer, Jürgen HL 41.3
 Ohmura, Takuya BP 10.4, •BP 14.6
 Ohnmacht, David TT 30.13
 Ohnmacht, David Christian•TT 30.14
 Ohresser, Philippe MA 33.2
 Ohst, Ties-Albrecht•QI 9.5
 Ohta, Hitoshi MA 14.8
 Okamoto, Junichi TT 33.10
 Okhrimenko, Bogdan QI 1.11
 Okuda, Taichi O 73.3
 Okulov, Ilya MM 18.36
 Olbrich, Eckehard•SOE 14.1
 Olde Olthoff, L.A.B. TT 22.1
 Oldenburg, Kevin O 59.6
 Oleaga, A. MA 29.2
 Olejnik, Kamil MA 29.6, MA 34.7
 Oles, Andrzej M. TT 39.6
 Oliveira, Thales HL 25.41
 Oliver, Rachel HL 25.65
 Ollefs, K. MA 25.4
 Ollefs, Katharina MA 19.14, MA 19.15,
 MA 22.4, MA 25.7
 Ollivier, Héléne HL 19.4
 Ollivier, Jacques MA 26.2, TT 21.12,
 TT 23.12
 Olsen, Thomas KFM 14.7, •O 72.2,
 O 81.5
 Olthof, Selina DS 20.3, HL 30.34,
 O 12.8
 omambac, karim O 18.4, O 54.4,
 •O 65.1
 Omar, Alan O 34.9, O 68.9
 Omar, Hassan•CPP 37.4
 Omar, Yasser QI 1.8
 Ong, Chin Shen•KFM 8.3
 Onishi, Hiroshi O 15.3
 Onishi, Seita TT 22.5
 Ono, Ryota•MA 15.6
 Ono, Shimpei MA 18.5
 Opdam, Joeri DY 23.3
 Opel, Matthias MA 34.4, MA 35.37
 Opherden, D. TT 12.6, TT 28.4
 Opitz, Andreas CPP 12.75, CPP 17.9,
 •CPP 26.5, CPP 28.7, HL 28.4
 Oppeneer, Peter MA 8.12
 Oppliger, Jens MA 35.58, O 7.2
 Ordejón, Pablo MM 28.4
 O'Regan, David D. O 23.4
 Orenstein, Joseph MA 13.10
 Orenstein, Joseph W MM 21.3
 Orio, Hibiki•O 55.15
 Orlandi, Fabio MA 42.4, TT 25.11
 Orloff, Nathan D. DS 20.32
 Orrit, Michel BP 5.6
 Ortega, Enrique O 26.4
 Ortego Larrazabal, Maialen•O 58.14
 Ortiz, Brenden R. TT 39.4
 Ortiz, Ricardo O 51.3
 Ortiz, Walter TT 2.4
 Ortmann, Frank CPP 1.5, CPP 1.12,
 CPP 11.1, CPP 26.6, CPP 40.6,
 CPP 40.8, HL 7.1
 Ortmann, Tobias•DS 13.1
 Ortuzar, Jon O 22.4, •O 51.5, O 51.9,
 •O 80.7
 Orus, Roman TT 16.7
 Oschinski, Hedda•O 31.6
 Oses, Corey MM 12.5
 Osipov, Vasilii•CPP 12.80
 Ospelkaus, Christian QI 1.11
 Ossig, Christina KFM 6.3
 Ossinger, Sascha MA 19.19
 Ostendorf, Stefan MM 32.1
 Österbacka, Nicklas•HL 18.11
 Osterhage, Hermann O 51.8
 Osterhoff, Markus BP 12.54
 Osterkorn, Alexander•TT 33.2,
 •TT 33.8, TT 38.6
 Ostermaier, Florian MA 39.1
 Ostthues, Helena MM 18.1
 Östlin, Andreas TT 21.33
 ostovar, hossein•HL 11.6, HL 25.15
 Ostroukh, Viacheslav QI 13.2
 Ott, Florian MA 19.2
 Ott, Jonas MM 18.28
 Ott, Vincent MM 4.8
 Otte, Magdalena BP 7.42
 Otte, Sander O 34.3, O 47.3, •O 47.6,
 O 47.7, O 51.2, O 51.7
 Otteneder, Maximilian•HL 40.4
 Otto, Andreas BP 18.3, MA 13.3,
 MA 19.36
 Otto, Felix O 17.1, O 18.26, •O 41.5,
 O 65.4, O 65.6
 Otto, Nicolas•CPP 28.5
 Otto, Oliver BP 12.1, BP 12.16,
 BP 12.20, BP 12.23
 Ouazan-Reboul, Vincent•DY 31.9
 Ouerfelli, Hamza HL 36.3
 Ouladdiaf, Bachir MA 42.5
 Ourdani, Djoudi MA 18.5
 Öz, Seren Dilara DS 20.3
 Özden, Ayberk MM 18.43
 Öztürk, Osman MA 5.4
 Paap, Ulrike•O 45.7
 Paarmann, Alexander MA 35.65,
 O 37.5, O 37.6, O 37.7, O 44.5
 Pablo-Navarro, Javier MA 28.8
 Pabst, Falk MA 35.42
 Pacchioni, Gianfranco•O 3.1, O 69.3
 Pace, M. MA 25.4
 Pachat, Rohit MA 18.6
 Padurariu, Ciprian O 7.8, •O 80.6,
 TT 7.3, TT 15.4, TT 26.9, TT 31.4,
 TT 37.6, TT 37.7, TT 37.8
 Paekkel, Sebastian CPP 40.9,
 DY 43.5, TT 9.1, TT 16.8, TT 21.32,
 TT 29.14, •TT 39.8
 Paetel, Stefan HL 25.32
 Paetzold, Lukas•MA 35.47
 Pahi, Sampannai•MM 18.7
 Pahlke, Andreas HL 22.3
 Pajmans, Joris BP 22.2
 Paischer, Sebastian•MA 15.7
 Pakdel, Sahar O 72.1, •O 81.5
 Pal, Amrita CPP 12.29
 Pal, Arijet DY 5.3
 Pal, Arnab DY 52.1, SOE 20.1
 Pal, Shovon MA 25.1, TT 6.4
 Paladino, Elisabetta TT 27.4
 Palankar, Raghvendra MA 35.65
 Palato, Samuel O 19.2
 Palberg, Thomas CPP 17.31, •DY 23.1
 Palekar, Chirag DS 17.4, •HL 6.6,
 HL 25.24, •HL 42.5
 Paleschke, Maximilian•O 26.7
 Palin, Victor MA 9.2
 Palkhivala, Shalom•BP 7.32
 Pallmann, Maximilian QI 4.17, •QI 5.4
 Pallmann, Maximilian QI 4.16
 Palm, Felix TT 9.1, TT 29.14
 Palma, Carlos-Andres O 81.4
 Palomares Garcia, C.M. TT 22.1
 Palomba, S HL 42.2
 Palotás, Krisztián•MA 7.3, •O 49.1,
 O 55.4
 Paltiel, Y. O 26.2
 Paluch, Patrick•TT 27.1, TT 27.2,
 TT 31.1, TT 31.2, TT 31.3, TT 37.12
 Pályi, András TT 25.13, TT 27.10
 Pampel, Benjamin•DY 28.3
 Pan, Guangjiu•CPP 17.23
 Pan, Wun-Chang•O 40.7
 Pan, Xing-chen O 9.2, O 73.8
 Pan, Yang•HL 25.9
 Pan, Yiming HL 11.3
 Pan, Yong-He•O 55.2
 Panahiyani, Shahram•QI 8.5
 Panayis, James BP 7.6, BP 7.16
 Panchami Raj, Shilpa•O 20.11
 Pancholi, Agnieszka BP 8.2
 Panda, Binod HL 33.5
 Pandey, Preeti TT 30.21
 Pandit, Pallavi MM 18.35
 Paneff, Florian CPP 17.4
 Pánek, Jiří CPP 45.4
 Panhans, Michel CPP 1.12, •HL 7.1
 Panizon, Emanuele BP 6.1, BP 14.1,
 DY 28.6
 Pankratova, Maryna•MA 25.6
 Pankratova, Natalia QI 5.5
 Pannir-Sivajothi, Sindhana•DY 50.7
 Panosetti, Chiara•MM 8.8, MM 8.9,
 MM 34.8
 Pantawane, Sanwardhini•CPP 17.36
 Panzer, Fabian CPP 12.42, HL 5.3,
 HL 23.2, HL 30.36
 Paolasini, Luigi TT 8.2
 Paoluzzi, Matteo SOE 9.3
 Paone, Domenico MA 2.4
 Pap, Leonie O 40.2
 Papa, Lorenzo O 27.5
 Papadakis, Christine M. CPP 12.31,
 CPP 12.32, CPP 12.34, CPP 12.35,
 CPP 27.3, •CPP 33.5, CPP 44.3,
 CPP 44.4
 Papaianina, Olena O 40.1
 Papaioannou, Evangelos MA 19.53,
 MA 21.2, MA 28.5
 Papaioannou, Evangelos Th.
 •MA 19.45, •MA 35.51
 Papenfuß, Franziska•BP 7.39
 Papez, Pavel•MM 10.26
 Papić, Miha QI 4.23, QI 6.8
 Papp, Adám MA 35.3
 Papp, Christian O 18.27, O 45.3,
 O 45.4, O 52.3, O 52.4, O 56.1
 Pappa, Anna QI 7.2
 Pappenberger, Ronja O 40.2
 Paradisano, Ioannis HL 20.8
 Paradiso, Nicola TT 3.2, •TT 3.13,
 •TT 10.3, TT 22.7, TT 26.2, TT 30.18
 Paramekanti, Arun MA 37.11
 Parcheon, Sergii•MA 25.2
 Pardo, Guy TT 37.6
 Pareek, Devendra•DS 20.25
 Pariari, Arnab TT 7.6
 Parisen Toldin, Francesco TT 28.3
 Parisi, Jürgen DS 20.25
 Park, Cheol-Hwan KFM 8.5, MA 22.9,
 MM 12.3, MM 12.8, O 7.3
 Park, Chibeom MM 21.1
 Park, Daesung O 35.1
 Park, J.-G. KFM 2.3
 Park, Jeyong•O 50.7
 Park, Jinhong MM 10.12, O 50.7,
 TT 11.11
 Park, Jiwoong MM 21.1
 Park, Joo Hyun MM 21.6
 Park, Juyoung•O 63.4
 Park, Kyungwha TT 1.9
 Park, Seongae DS 16.4
 Park, Soyoung O 32.8
 Parker, Richard•CPP 8.3, CPP 8.4
 Parkin, Stuart MA 12.10, MA 24.4
 Parkin, Stuart S. P. MA 18.1, MA 34.6
 Parkinson, Gareth•O 3.8, O 44.7,
 O 49.4, O 58.12
 Parkinson, Gareth S. O 3.3, O 3.7,
 O 10.3, O 10.5, O 10.6, O 16.12, O 57.5
 Parlak, Umüt MA 21.11, MA 35.22,
 MA 35.26
 Parlitz, Ulrich DY 8.6, DY 8.8, •DY 18.5,
 DY 39.5, DY 45.12, DY 45.13, SOE 6.6,
 SOE 6.8, •SOE 10.5
 Parmentier, Christopher HL 14.5
 Parmentier, François MA 13.12
 Parmer, Rahul O 52.7, O 52.8
 Parra Lopez, Luis•O 18.25
 Parra Lopez, Luis Enrique MA 21.1,
 O 33.6
 Parrish, Robert M. QI 12.6
 Partington, James BP 7.6
 Parton, Thomas•CPP 8.4
 Partovi-Azar, Pouya•MM 2.2
 Parvini, Tahereh Sadat•MA 19.61
 Parzefall, Philipp•HL 25.12
 Parzer, Michael MM 10.9
 Paschen, S. MA 14.6
 Paschke, Fabian O 41.8, O 74.1,
 •O 80.2
 Pascual, José Ignacio O 22.4, O 51.5,
 O 51.9, O 51.10, O 80.1, O 80.7
 Pascual, Nacho O 18.13
 Pashkin, Alexej HL 11.10, HL 25.41,
 HL 40.2
 Pashov, Dimitar MA 38.4
 Pasinetti, Marcelo KFM 15.6
 Paßlack, Felix•O 34.8
 Paspalides, Christos•HL 25.14
 Passerone, Daniele O 29.6
 Passetti, Giacomo MM 9.3
 Passler, Nikolai C. O 37.7
 Paszúk, Agnieszka O 30.6
 Patane, Amalia HL 11.10
 Patel, Gauravkumar•MA 22.7
 Patel, Hemangi•MM 10.29
 Patel, Himanshu P•DY 11.9
 Patel, Kuntal•DY 4.3
 Patera, Laerte O 28.2
 Patera, Laerte L. O 79.1
 Patil, Sourabh•TT 30.6
 Patoka, Piotr O 7.9
 Patra, Pintu•BP 5.3
 Pattavina, Luca DS 13.1
 Patte, Renaud MA 11.4
 Patterson, Robert I. A. DY 50.8
 Pattison, Philip MM 7.4
 Pätzold, Marius•DY 46.1
 Paul, Ganesh C.•MM 7.1
 Paul, Neelima•CPP 13.1
 Paul, P HL 42.2
 Paul, Pallabi DS 20.15, •DS 21.4
 Paul, Patrick BP 12.4
 Paul, Raja DY 46.21
 Paul, Wolfgang CPP 12.28, CPP 41.4
 Paulik, Nicolas TT 10.3
 Paulsen, Michael•MA 33.7, •TT 17.2,
 TT 31.10
 Paulus, Michael BP 7.10, BP 12.52,
 DS 20.14, KFM 25.6, KFM 25.7,
 KFM 25.11
 Paulus, Simon HL 30.31
 Paulus, Werner TT 39.1
 Pausch, Lukas DY 5.6
 Pauw, Brian Richard KFM 3.1
 Pavanello, Michele MM 12.9
 Pavarini, Eva TT 21.24, TT 28.1
 Pavelec, Jiri O 3.7, O 3.8, O 10.3,
 O 10.5, O 10.6, O 49.4, O 58.11,
 O 58.12
 Pavin, Nenad BP 3.6, BP 13.4,
 BP 13.8, BP 23.2
 Pavlova, Ewa CPP 45.4
 Pavlovskii, Nikolai•TT 21.12
 Pavone, Pasquale O 50.5
 Pawlak, Rémy O 79.1, O 79.3
 Pawlis, Alexander HL 25.84,
 HL 25.98, HL 33.7, HL 33.8, QI 1.7
 Pazniak, Hanna DS 21.3
 Pearce, Fiona MM 2.9
 Pecharsky, V. MA 29.3
 Pedersen, Thomas O 72.4
 Pedrazzini, Pablo TT 29.16
 Peeters, Wouter HL 25.50
 Peets, Darren MA 35.42
 Peets, Darren C.•MM 7.4, TT 21.12
 Peh, Katharina HL 24.5, HL 24.6,
 •TT 29.15
 Pehlke, Eckhard O 20.9
 Peil, Oleg MM 25.8, MM 34.6
 Peixoto, Tiago•SOE 12.5
 Pelagejev, Philipp DY 46.15, •DY 49.7
 Pelini, Thomas DS 17.5
 Pellegrin, Theodore DS 20.35
 Peltason, Vivien F. S. HL 18.5
 Pelusi, Francesca DY 4.1, •DY 4.2
 Peña, Diego O 18.13, O 51.3, O 62.8,
 O 80.1
 Peña Gil, Diego O 51.10
 Peña-Camargo, Francisco•HL 5.8
 Peng, Bo•HL 14.4
 Peng, Licong MA 27.2, MA 27.7
 Peng, Yan MA 26.2
 Pengerla, Monica HL 25.74, HL 30.3,
 •HL 36.10
 Pentcheva, Rossitza•DS 14.3,
 DS 14.4, O 2.3, O 2.4, O 2.8, O 49.7,
 O 49.9, TT 18.4
 Pentz, Sebastian•MM 4.7
 Peralle, Cindy QI 5.7
 Perea-Causín, Raúl HL 20.1, HL 20.2,
 O 33.7, O 68.4
 Pereira, Lino M.C. MA 31.7
 Pereiro, Manuel MA 11.2, MA 25.6,
 MA 38.6, QI 10.9
 Perekrestov, Vyacheslav MM 18.30
 Perez, Danny•SYNM 1.4
 Pérez-Ramírez, Javier O 3.5, O 10.1
 Perlin, Piotr HL 30.14
 Pernice, Wolfram H. P. HL 25.27
 Perrard, Stéphanie DY 44.9
 Perrodin, Didier KFM 7.6
 Perry, Robin S MM 21.4

Perßon, Jörg	MA 40.3	Pietzonka, Patrick	•DY 50.11	Pop, Ioan-Mihai	TT 27.1	Protik, Nakib	•O 50.11
Persson, Jörg	MA 28.12	Pignedoli, Alessandro	•DY 44.8	Popescu, H.	MA 27.1	Prucnal, S.	HL 22.1
Persson, Mats	O 29.1	Pikulin, Dmitry I.	TT 25.12	Popov, Alexey A.	O 80.2	Prucnal, Slawomir	HL 17.9, HL 25.87
Pertsch, T	HL 42.2	Piliiai, Lesia	O 3.6	Popov, Anatoli I.	•KFM 18.1	Pruy, Pascal	HL 17.1, •HL 17.4
Pertsch, Thomas	HL 4.2	Pillich, Cynthia	•MA 39.6	Popov, Cyril	QI 4.16, QI 5.4	Pucci, Fabrizio	BP 2.3
Peruani, Fernando	DY 50.5	Pilz, Wolfgang	MA 28.8	Popova, Gorelova, Daria	O 68.3	Pucci, Francesca	•TT 17.1
Perugachi Israëls, Cintia	BP 4.2	Pimenov, Andrei	MM 10.9	Popović, Marko	•BP 27.3, BP 27.4, BP 27.5	Pudell, Jan	•HL 30.47
Peschka, Dirk	CPP 17.14	Pina Canelles, Vicente	QI 6.8	Popp, Andreas	DS 6.4, HL 25.33	Pudell, Jan-Etienne	DS 20.41
Pessel, Simon	HL 31.4	Pina-Canelles, Vicente	QI 4.23	Porcar, Lionel	CPP 1.8, CPP 33.6	Puente-Orench, Inés	TT 23.12
Pestka, Benjamin	HL 25.77	Pinar Sole, Andres	•O 51.1	Porrali, Fabrizio	MA 35.11, •TT 26.3	Pukrop, Matthias	HL 21.7, HL 21.9, HL 30.2
Petaccia, Luca	O 82.6	Pincelli, T.	O 9.5	Portalupei, Simone	HL 17.1, HL 17.7, HL 25.62, HL 26.2, HL 26.3	Pula, Taner	BP 12.4
Peter, Nicolas J.	MM 4.5	Pineda, Eufemio	TT 21.21	Portalupei, Simone L.	HL 17.1, HL 17.7, HL 25.62, HL 26.2, HL 26.3	Puliappara Babu, Priyana	•TT 22.2
Peterlechner, Martin	MM 3.2, MM 8.4, MM 10.5, MM 10.8, MM 16.1, MM 16.2, MM 20.1, MM 30.2	Pinheiro Neto, João	SOE 17.3	Porta, Nikita	MA 19.29	Pulkin, Artem	O 51.2
Peters, Lukas	DS 2.4	Pinna, Daniele	MA 37.8	Porter, Fabien	TT 37.7	Pulis, Florian	MA 19.21
Peters, Marius	•KFM 25.21, TT 21.2, TT 21.3, TT 21.5, TT 21.6, TT 21.7	Pintér, Gergő	TT 25.13	Portnichenko, P. Y.	MA 4.1, MA 14.6, MA 35.53	Pundt, Astrid	•KFM 15.4, MM 17.3, •MM 17.4, MM 18.18, MM 18.29
Peters, Olof	TT 26.8	Pinto, Dinesh	MA 2.4	Portoles, Elias	TT 10.4	Punj, Deep	BP 5.6
Peters, Tobias	MA 5.1, MA 19.17, •MA 19.58	Pirard, Geoffrey	•HL 12.8, •HL 36.9	Porwal, Nikita	MA 19.29	Puntel, Denny	O 9.2
Petersen, C.	•HL 18.3, HL 30.20	Pires, Ricardo Hugo	BP 12.23	Pos, Eszter S.	O 50.8	Puntigam, Lukas	•KFM 7.4, •KFM 14.1
Petersen, Clemens	HL 30.23	Pirker, Luka	TT 2.2, TT 29.7	Posske, Thore	MA 30.2, TT 19.4	Puntscher, Lena	•O 3.3, O 3.8, O 10.6
Petersen, Nanning	•CPP 41.6	Pirro, Philipp	MA 9.2, MA 13.8, MA 19.50, MA 19.52, MA 19.59, MA 28.6, MA 35.9, MA 35.19, MA 35.50	Potapov, Pavel	DS 20.34, MM 35.9	Purcell, Thomas	•MM 29.2
Petersen, Nina	MM 18.10	Pisarev, Roman V.	MA 14.9	Potemski, Marek	DS 17.5	Purcell, Thomas A.R.	MM 21.2
Petersen, Stefan	•TT 29.4	Pisarra, Michele	O 7.4	Potzger, Kay	MA 4.2, MA 4.3, MA 35.36	Puri, Sanjay	DY 26.6
Petersson, Karl D.	TT 32.3	Pisegna, Giulia	•BP 14.8	Poul, Marvin	•MM 10.4, •MM 34.1	Püring, Thorben	•MA 37.8
Petit-Watelot, Sébastien	MA 9.2	Pister, Daniel	MA 19.18	Pouloupoulos, Panagiotis	MA 35.51	Puschmann, Martin	•DY 44.19, TT 11.2
Petralanda, Urko	•KFM 14.7	Pistidda, Claudio	MM 17.3, •MM 17.5	Pourret, Alexandre	TT 22.11	Puschnig, Peter	O 2.2, O 12.5
Petrić, Marko M.	HL 15.5	Pistor, Julian	MM 13.1	Povstugar, Ivan	MM 4.9	Pushkin, Dmitri O.	DY 31.4
Petricca, Federica	TT 17.1	Pistor, Paul	HL 32.5	Powalla, Lukas	DS 19.1, MA 27.3	Putatunda, Aditya	•MM 11.8
Petrich, Rebecca	•DS 9.3, DS 23.2	Pisula, Wojciech	HL 30.33	Powell, Annie K.	MA 19.22, MA 26.2	Pütter, Sabine	MA 33.2
Petrov, Alexander	O 61.6	Pitala, Krzysztof	MM 18.35	Pozarowska, Emilia	O 52.11	Püttmann, Jutta	•TT 21.8
Petrovic, Arsen	BP 9.4	Pita-Vidal, Marta	TT 37.5, QI 13.11	Pozdnyakov, Sergey	•O 67.2	Pütz, Sebastian	•SOE 7.1
Petrovic, Marin	O 54.4, O 65.1, O 81.2	Pithan, Linus	CPP 17.9, CPP 26.5	Pozdnyakow, Sergey	O 58.9	Putzky, Daniel	DS 14.4
Pettinger, Nina	•HL 11.1	Pivarníková, Ivana	•CPP 17.28	Pozo, Iago	O 62.8	Puviani, Matteo	TT 22.10
Petton, Bruno	BP 9.5	Pixelley, Jedediah	TT 37.14	Prada, Claire	MM 35.7	Puzrev, Dmitriy	DY 4.5, DY 11.5, DY 11.7, DY 50.9
Petz, Dominik	•KFM 25.20, MM 8.2	Pizzi, Giovanni	O 43.4, O 43.5	Prada, Marta	TT 2.5, TT 20.1	Pyanzina, Elena	CPP 34.3, CPP 44.2
Petzold, Silke	DS 6.3	Pizzino, Lorenzo	TT 28.10	Pradhan, Tapaswani	MM 15.1	Qahosh, Mohammed	O 21.4, •O 73.7
Petzoldt, Philip	•O 70.4, O 70.6	Placer, Bernard	•SYQM 1.2	Prager, Michael	HL 40.1, TT 30.18	Qaiumzadeh, Alireza	MA 13.5
Peugeot, Ambroise	TT 37.7	Planer, Jakub	O 12.7, O 58.4	PRAKASH, MEHER	BP 15.5	Qamar, Minaam	•MM 31.2
Pfaff, Sebastian	O 69.5	Plankl, Markus	HL 20.2	Pramanik, Arindam	O 82.6	Qi, Jing	O 26.9, O 40.7
Pfaffinger, Lea	•TT 3.2	Plansky, Johanna	•O 69.3, O 70.1, O 70.3	Pramann, Axel	•KFM 6.4	Qi, Yangpen	O 9.4
Pfalzgraf, Daniel	•MM 8.1, •MM 24.2	Plass, Christian	•HL 21.11, HL 25.46	Prasad, Aniruddha Sathzadharna	MA 5.3	Qi, Yubo	•O 23.3, O 23.5
Pfander, Simon	•TT 37.1	Platero, Gloria	TT 19.3, TT 26.11	Prass, Pascal	•MA 27.12	Qian, Chenjiang	•HL 11.9, HL 42.9
Pfannkuche, Daniela	TT 20.1	Plattner, Moritz	HL 12.5	Pratapasi, Sagar	QI 1.8	Qiang, Gang	•HL 39.5
Pfau, Bastian	MA 2.1, MA 2.3, MA 8.2, MA 8.3, MA 12.2	Plávála, Martin	QI 9.8, •QI 14.6	Predeeschly, Benjamin	CPP 28.6	Qiao, Le	•CPP 13.4
Pfeifer, Torben	MA 35.9	Plazanet, Marie	CPP 9.9	Predejevic, Ana	•SYPQ 1.5	Qiao, Siqi	HL 33.8, HL 33.9
Pfeiffer, Maurice	•O 61.6	Pleines, Linus	O 52.11, •O 69.10	Prehl, Janett	•CPP 9.7	Qiao, Yu	•HL 24.1, •MM 18.21
Pfeiffer, Meike	•TT 6.5	Plessl, Christian	MM 18.4	Prentice, Joseph C. A.	•MM 12.2	Qin, Lin	•MM 6.10
Pfeiffer, Walter	O 61.3	Pletyukhov, Mikhail	TT 11.3, TT 37.13	Pres, Sebastian	O 61.3	Qin, Shuyu	KFM 14.6
Pfeil, Jonas	•BP 12.62, DY 4.4	Plucinski, Lukasz	MA 19.55, O 21.4, •O 48.7, O 73.7	Press, Adrian T.	BP 12.29	Qiu, Canrong	DS 20.4
Pfeuffer, Lukas	MA 29.7	Plumb, N. C.	O 66.2	Pressacco, F.	O 68.10	Qiu, Jiajia	•KFM 25.17, •MM 14.5
Pfister, Ulrich	•HL 25.62	Poddar, Preeti	MM 21.1	Pressacco, Federico	O 9.1, O 34.10	Quasebarth, Gwendolyn	MA 13.3
Pflaum, Jens	CPP 12.56, CPP 12.57, CPP 13.6, CPP 26.5, CPP 27.1, CPP 39.6, DS 5.5, DS 20.20, DS 20.21	Poddubny, Alexander N.	O 35.5, O 37.8	Prestel, Martin	TT 7.2	quay, charis	TT 10.2
Pfleiderer, Christian	MA 10.6, MA 12.6, MA 19.7, MA 27.11, MA 35.54, MA 35.56, MA 35.72, MA 35.64, MA 35.56, MA 35.72, TT 12.3, TT 12.7, TT 21.38, TT 24.4, TT 25.5, TT 25.6, TT 25.7, TT 27.8	Podlesnyak, Andrey	TT 21.9	Preti, Francesco	•QI 13.8	Queisser, Friedemann	TT 13.6
Pflug, Theo	CPP 12.62	Poduval, Prathyush P.	•TT 1.3	Pretsch, Thorsten	CPP 7.5	Quek, Su Ying	DS 22.2
Pfnür, Herbert	DS 25.4	Poggio, Martino	MA 41.4	Preuß, Johann	HL 25.25	Quek, Yihui	QI 6.2, QI 12.10
Pfützenreuter, Daniel	DS 14.2	Pogodaeva, Maria K.	•MM 12.10	Preuß, Johann A.	HL 30.48	Quenter, Ruwen	•O 55.16
Pham, Anh	O 21.1, O 81.3	Pogorzalek, Stefan	•QI 4.23, QI 6.8	Preuß, Johann Adrian	•HL 19.9, HL 20.1	Quincke, Moritz	MA 39.1
Pham, Jonathan T.	CPP 7.2	Pohl, D.	MA 20.4	Preuß, Johann Adrian	•HL 19.9, HL 20.1	Quintana, Mikel	MA 22.3, •MA 22.5
Pham, Thien An	•CPP 12.14	Pohl, Darius	MA 27.7	Preuß, Johann Adrian	•HL 19.9, HL 20.1	Quintanilla, Jorge	•MM 23.3
Phi, Hai Binh	DY 46.10	Pohl, Ulli	•TT 9.5, TT 28.12	Prezzi, Deborah	O 74.2	Quiring, Viktor	HL 33.9
Philipp, Anja	TT 21.1	Pöhls, Jonas	•HL 42.8, TT 2.13	Prezzi, Michael	O 27.5	R. Everett, Christopher	CPP 12.67
Philipp, Julian	•BP 12.56	Poier, Dario	O 3.5	Pribiag, Vlad	•TT 10.1	R. Lara, Francisco	•O 80.1
Philipp-Kobs, André	MA 31.6	Pokorny, Vladislav	•TT 26.13	Pries, Julian	MM 10.6	R. Monteiro, Fábulo	•MM 18.23
Philipps, Christian A.	•BP 14.7	Pokrovskii, Vadim	KFM 8.3	Priesemann, Viola	BP 2.6, BP 2.9, DY 8.9, SOE 6.9	R. T. Zahn, Dietrich	HL 25.9
Philips, Sarah	TT 31.12	Polanyi, John C.	O 69.6	Priessnitz, Tim	•HL 13.7	Raab, Aileen	MM 18.11
Piasotski, Kiryl	•TT 11.3	Polesya, S.	MA 38.1	Prieto, Mauricio J.	O 52.11	Raab, Jürgen	HL 4.3
Piccinni, Viviana	•O 28.5	Polesya, Svitlana	MA 38.2, •MA 38.7	Primetzhofner, Daniel	DS 15.5, MM 28.1	Raab, Klaus	•MA 19.30
Pickard, Chris	O 43.6	Poletto, Daniele	O 55.1	Prinz, Eva	•MA 8.8, O 59.4, O 68.6	Raabe, Dierk	MM 4.2
Picker, Julian	HL 42.7, •O 65.4, O 65.5, O 65.6	Polian, Ilia	QI 4.26, QI 12.9	Prinz, Günther	HL 25.2, •HL 31.3	Raabgrund, Andreas	•O 54.9
Picó Cortés, Jordi	•TT 26.11	Polin, Nikita	•MA 23.1, MM 22.2	Privalov, Alexei	DY 46.9	Rabia, Andi	O 40.9
Picó-Cortés, Jordi	TT 19.3, TT 26.4, TT 26.12	Politova, Ekaterina D.	KFM 25.1	Priya, Priya	HL 19.4	Raczkowski, Marcin	•TT 6.1, TT 38.5
Piéchon, Frédéric	MA 40.5	Polkovnikov, Anatoli	•DY 33.1	Priya, Ravi	•O 17.4, O 17.8, O 17.11	Rader, Oliver	MA 31.2, O 9.9
Piebler, Jacob	BP 7.8	Pollack, Yoav G.	•BP 6.3	Prizak, Roshan	BP 8.2	Radhakrishnan, A.V.	CPP 12.12
Piel, Pierre	MA 35.63, QI 4.24	Polley, C.	MM 7.5, O 25.3	Probst, Henrike	•MA 8.1, MA 35.18, MA 35.20	Radhakrishnan, Padma	•DS 14.4
Piel, Pierre-Maurice	DS 20.39, •DS 22.3, DS 22.4	Pollymann, Erik	HL 31.3, O 48.8	Probst, Nathalie	TT 17.9, TT 31.12	Radiev, Yurii	•DS 5.3
Pielić, Borna	O 81.2	Pollmann, Frank	MA 16.3	Procházka, Pavel	O 12.7, O 40.4, O 58.4	Rädler, Joachim	BP 12.46, BP 12.47, BP 12.55, BP 12.56, BP 12.59
Pientka, Falko	QI 5.2	Polozij, Miroslav	TT 29.10	Prodan, Lilian	KFM 14.1, MA 14.5, •MA 32.5, MA 33.1, MA 33.3, MA 33.4, MA 40.1	Rädler, Joachim Oskar	BP 22.9
Pierz, Klaus	HL 7.9, O 2.9, O 41.4	Polyudov, Katharina	DS 19.1	Proebst, Franz	TT 17.1	Radonjić, Milos	O 42.3
Pietka, Isabel	•MM 18.14	Pomjakushina, E.	MA 19.63	Profeta, Gianni	TT 3.3	Radons, Günter	DY 18.4, DY 45.3, SOE 10.4
Pietras, Bastian	BP 2.7	Pompe, Ruben	O 61.3	Prokscha, Jan	O 18.20	Radović, M.	O 66.2
Pietsch, Ullrich	HL 25.66	Poncé, S.	O 66.2	Prokscha, T.	TT 22.1	Radu, Florin	MA 19.19, MA 23.3, MA 25.7
Pietschnig, Rudolf	CPP 17.32, CPP 17.33	Poncé, Samuel	O 11.3	Prokleska, Jan	O 18.20	Radulov, Iliya	MA 19.14, MM 18.25

Ragunathan, V.A. •CPP 12.12
 Raghuraman, Swetha BP 12.37
 Raghuvansy, Sushma DS 20.6,
 •DS 26.1
 Raghuvanshi, Mohit DS 20.13
 Rahaman, Mahfuju HL 25.9
 Rahe, Philipp O 19.10, O 55.6, •O 66.8
 Rahimi-Iman, Arash HL 6.2, HL 30.8,
 HL 42.5
 Rahimzadeh, Amin CPP 17.19
 Rahlff, Ivo •HL 30.35
 Rahm, J. Magnus MM 10.28
 Rahm, Marco MA 19.53
 Rahn, M. MA 27.1
 Rahn, Marein MA 16.10, •MA 31.9
 Rahn, Marein Christopher MA 35.42
 Rai, Akash MM 21.1
 rai, gautam O 18.15
 Rai, Pranav •MM 18.41
 Rai, Venus •MA 40.3
 Rai, Vibhuti •O 61.5, O 61.7
 Raiber, Simon •HL 20.4
 Rajabpour, Siavash DS 20.39,
 DS 22.2, DS 22.4
 Rajak, Sanam K. DS 22.7
 Rajan, Adithya MA 19.60
 Rajan, Akhil MA 17.3
 Rajan, Siddharth •HL 14.1
 Ram, Panch TT 26.13, •TT 29.8
 Ramachandran, Ranjani •MM 10.30
 Raman, Narayanan O 45.3
 Ramani, Madhura •BP 12.22
 Ramasubramanian, Shrinidhi DS 22.7
 Ramaswamy, Sriram DY 50.7
 Ramermann, Daniela •MA 2.2,
 MA 19.25, MA 19.27, VA 2.4
 Ramesh, Prashanth •DY 31.4
 Ramesh, Ramamoorthy DS 13.3
 Ramirez, Lucia SOE 5.4
 Ramirez Sierra, Michael Alexander
 •BP 12.57
 Ramirez-soto, Olinka BP 12.48,
 BP 26.2, CPP 7.1
 Ramming, Philipp HL 5.3, HL 23.2
 Ramos, Rafael MA 19.62, MA 25.5,
 MA 34.3, MA 35.28
 Rampp, Markus O 50.2
 Ramsauer, Bernhard R. •O 6.1
 Ramsteiner, Manfred DS 22.5
 Rana, Debkumar CPP 39.4, CPP 48.4
 Rana, Rakesh HL 40.2
 Ranawat, Yashasvi O 66.8
 Ranftl, Demian •HL 30.19
 Rani, Renu •HL 25.20, HL 25.84
 Ranitzsch, Philipp TT 17.2
 Ranitzsch, Philipp Chung-On TT 31.10
 Rao, Jing MM 15.4
 Rao, Peng •TT 21.17
 Rao, Zhonghao HL 24.1, MM 18.21
 Rappich, Jörg CPP 12.26, O 16.1
 Raptakis, Antonios DS 22.1
 Rasabathina, L. O 26.2
 Rasabathina, Lokesh •MA 35.49
 Raßhofer, Florian •DY 26.4, DY 44.18
 Rasmussen, Asbjørn O 81.5
 Rastelli, Armando •SYED 1.2, HL 8.1,
 HL 8.7, HL 8.10, HL 19.2, HL 22.8,
 HL 26.7, HL 35.1, O 35.8
 Rastelli, Gianluca TT 26.7
 Rata, Aurora Diana MA 35.48
 Rata, Diana CPP 48.1
 Rath, David •O 10.3
 Rathje, Christopher MA 19.54,
 •MA 21.3, O 53.5, O 59.7
 Raths, Miriam O 18.5, O 68.7
 Rauch, Darius BP 10.2
 Rauch, Philipp BP 7.1
 Rauls, Simon MA 4.3, •MA 4.4
 Raumann, Leonard MM 4.10
 Rauschenbach, Stephan BP 9.2
 Rauschendorfer, Tassilo O 18.3
 Rautiyal, Prince MM 2.9
 Ravankhah, Mahboobeh O 56.6,
 •O 70.5
 Ravelosona, Dafiné MA 18.5
 Ray, Ariana MM 21.1
 Ray, Purusattam DY 39.1
 Ray, Rajyavardhan TT 20.2
 Ray, Sayak TT 9.5, •TT 28.2
 Ray, Shouryya TT 23.3, TT 24.10
 Razpopov, Aleksandar •MA 16.7,
 TT 8.4
 Razumskii, V. MM 21.7
 Razumovskiy, Vsevolod MM 25.8,
 MM 34.6
 Reale, Francesco HL 31.3

Reale, Stefano MA 26.3
 Reascos Portilla, Ana Karen O 13.9
 Reb, Lennart •CPP 28.6
 Reb, Lennart K. CPP 12.43,
 CPP 12.46, CPP 12.54, CPP 19.4,
 CPP 48.3
 Rebarz, M HL 21.2
 Rebarz, Mateusz HL 13.3, HL 13.9,
 O 16.1
 Rebber, Matthias MM 18.35
 Rebehn, Lydia •BP 12.4
 Reber, Simone BP 12.24
 Recher, Patrik MM 7.1, TT 1.6, TT 1.7,
 TT 11.5, TT 29.9
 Reck, Kristian CPP 17.26
 Recktenwald, Steffen M. BP 3.7
 Reddy, Laxman Nagi O 73.6
 Redies, Matthias MA 24.2
 Redinger, Alex HL 34.7, O 42.1
 Redondo, Jesús O 3.2, •O 16.12,
 O 44.3, O 44.8
 Reecht, Gaël O 53.4, O 80.4, TT 26.8
 Reeh, Jana CPP 17.24
 Reehuis, Manfred MM 7.4
 Refaely-Abramson, Sivan DS 17.5,
 O 9.8
 Rege, Ameya MM 10.29
 Reglinski, Katharina BP 12.31
 Reh, Moritz TT 31.20
 Reh, Roman •CPP 12.17, •CPP 12.18
 Rehberg, Ingo •DY 18.2, •SOE 10.2
 Rehfeldt, Florian BP 12.22
 Reich, Stephanie HL 33.6
 Reich, Veronika •MM 31.3
 Reichel, Peter O 19.4
 Reichenberger, Sven MA 39.4
 Reichlova, Helena MA 29.4, MA 29.6,
 MA 34.7, TT 25.3
 Reichmann, Alexander •MM 25.8,
 MM 34.6
 Reichert, Lukas •CPP 40.5, HL 41.1
 Reifemberger, A. TT 37.11
 Reifemberger, Andreas TT 17.9,
 TT 31.6, TT 31.7, TT 31.17
 Reiker, Tobias •O 33.9
 Reimer, Max CPP 12.80, O 12.8
 Rein, Gabriel •TT 38.5
 Reina Galvez, Jose •MA 35.69
 Reina, José O 71.1
 Reinalter, Luis DY 49.5
 Reinalter, Luis Frieder DY 38.2
 Reinauer, Alexander •DY 46.14
 Reindl, Marcus HL 8.1, HL 8.10
 Reineke, Sebastian CPP 1.10,
 CPP 12.41, CPP 27.5, CPP 27.6,
 HL 41.5
 Reiner, Jan-Michael QI 10.3
 Reinert, F. O 21.5
 Reinert, Friedrich O 4.1, O 4.2, O 9.1,
 O 21.2, O 48.7, O 55.15, O 68.3, O 73.4
 Reinhardt, Simon TT 2.2, TT 3.13,
 TT 22.7, TT 29.7, TT 29.17, TT 30.18
 Reinken, Henning •DY 31.3, •DY 46.7
 Reis, Edgar M. S. D. •MM 18.13
 Reisbeck, Patrick MM 18.35
 Reiser, Andreas TT 17.9, TT 31.12,
 TT 31.16, TT 31.17, TT 33.1
 Reiser, Anita BP 12.55
 Reiser, Christopher DS 20.35
 Reiser, Isabel MA 25.1, TT 21.13
 Reiser, Patrick MM 22.4
 Reiserer, Andreas QI 4.11
 Reisinger, Thomas TT 31.15
 Reissner, Veronika •HL 25.52
 Reiss, Günter CPP 17.10, DS 5.2,
 KFM 15.3, MA 19.58
 Reiss, Pascal •TT 8.7
 Reisz, Niklas •SOE 14.4
 Reitenbach, Julija CPP 1.6, •CPP 44.4
 Reiter, Doris HL 8.7, AKC 1.2
 Reiter, Doris E. HL 25.48, •HL 26.7
 Reiter, Günter •CPP 37.1
 Reiter, Lukas DY 46.6
 Reithmaier, Johann Peter CPP 17.32,
 CPP 17.33, HL 8.2, HL 25.57
 Reitzenstein, S. HL 2.3, HL 4.7, HL 4.9
 Reitzenstein, Stephan DS 17.4, HL 4.1,
 HL 4.8, HL 6.6, HL 8.6, HL 12.5,
 HL 17.3, HL 25.24, HL 25.74,
 HL 25.75, HL 25.76, HL 30.3, HL 30.7,
 HL 36.10, HL 42.5, O 35.8
 Reitzenstein, Stephan HL 17.10
 Rejali, Rasa O 47.6, O 47.7
 Rellinghaus, B. •MA 20.4, MA 27.1
 Rellinghaus, Bernd MA 27.7
 Remes, Zdenek MA 35.38

Remesh, Vikas HL 8.7, HL 26.7
 Remini, Khalil •CPP 17.14
 Remlein, Benedikt •DY 24.3
 Remškar, Maja TT 2.2, TT 29.7
 Ren, Wei DS 20.1, KFM 10.4
 Ren, Zengyao MA 22.1, MA 35.1
 Renaud, Gilles O 41.3
 Renger, Michael QI 4.5, QI 4.6, QI 4.7,
 QI 4.15, QI 4.18
 Renger, Roman •BP 7.1
 Renn, Lukas •HL 25.53
 Rennert, Mirko CPP 2.4
 Rensberg, Jura HL 18.1
 Renzi, Enrico Maria O 37.5
 Repellin, Cécile TT 11.7
 Repp, Daniel HL 4.2
 Repp, Jascha O 28.2, O 47.9, O 62.8,
 O 79.1
 Resch, Christoph •MA 10.6
 Resch, Jeremias •QI 4.16, QI 4.17
 Resch, Miriam •TT 37.8
 Resel, Roland CPP 14.1
 Retamal, María José BP 12.50,
 BP 12.51
 Rethfeld, Baerbel MA 25.3, MA 25.5,
 MA 25.8, MA 35.27, MA 35.28,
 MA 35.31, MA 35.32, •O 1.1, O 16.5,
 O 33.4, O 33.10
 Rethfeld, Bärbel MA 8.5, MA 8.9
 Reticcioli, Michele •O 27.5, O 44.4,
 O 44.7, •O 57.5
 Retsch, Markus O 78.4
 Rettig, L. MA 35.24, O 9.5, O 68.10
 Rettig, Laurenz •O 68.8
 Rettinger, David O 52.7, O 52.8
 Reuban, Anicha •MM 4.9
 Reuner, Marvin O 68.3
 Reus, Manuel A. CPP 1.2, CPP 1.6,
 CPP 12.43, CPP 12.46, CPP 12.48,
 CPP 12.49, CPP 12.54, CPP 17.6,
 •CPP 19.4, CPP 48.3
 Reus, Manuel Andree DS 20.50
 Reusch, Julian TT 21.5
 Reusch, Julian Dominik TT 21.6
 Reuter, D. HL 2.3
 Reuter, Daniel CPP 17.4
 Reuter, Dirk HL 3.6, HL 7.7, HL 22.6,
 HL 25.40, HL 26.1, HL 30.7
 Reuter, K. KFM 11.4
 Reuter, Karsten CPP 14.2, CPP 40.2,
 DY 8.2, MM 2.4, MM 2.5, MM 2.8,
 MM 10.1, MM 10.22, MM 14.1,
 MM 29.1, MM 33.1, MM 33.4,
 MM 34.3, MM 34.5, MM 34.8, O 8.1,
 O 8.3, O 8.7, O 11.4, O 28.5, O 31.3,
 O 31.4, O 31.5, O 31.6, O 38.3, O 38.5,
 O 38.7, O 41.3, O 43.9, O 46.1, O 46.3,
 O 46.8, O 49.8, O 58.3, O 62.1, O 62.4,
 O 62.5, O 69.4, O 69.8, SOE 6.2
 Reuther, Johannes MA 16.7
 Reutter, Andreas •O 55.11
 Reutter, Eric HL 25.62
 Reutzel, Marcel MA 8.1, MA 35.20,
 O 2.2, O 2.9, O 9.10, O 16.6, •O 16.9,
 O 33.3, O 48.9
 Revelli, Alessandro TT 21.15
 Revenga, N. HL 2.3
 Rex, Stefan TT 1.5
 Rey, Dulce O 80.1
 Rey, Sergio DS 17.5
 Rezvani, J. MA 25.4
 Rheinfrank, Erik O 16.12
 Rheinlaender, Johannes BP 3.8,
 •BP 3.9, BP 9.3
 Riahisamani, Neda •TT 21.24
 Riaz, Abdullah •MM 24.4
 Riazanova, Anastasia V. MA 41.5
 Ribeiro de Assis, Ismael •MA 37.12
 Ribeiro, Hugo QI 8.4
 Ribeiro-Palau, Rebeca •TUT 2.2,
 •HL 1.2
 Richarz, Leonie •KFM 7.5
 Richter, Dieter CPP 33.1, CPP 33.2
 Richter, Johanna HL 25.29, O 54.10,
 O 54.13
 Richter, Johannes TT 21.16, TT 23.7
 Richter, Jonas •DY 5.3, DY 19.4
 Richter, Klaus DS 19.4, DY 5.5,
 DY 5.10, O 82.4, TT 18.2, TT 19.1
 Richter, Manuel TT 20.2
 Richter, Maria Christine O 73.6
 Richter, Marten HL 30.4
 Richter, Martin •CPP 39.4, CPP 48.4
 Richter, Peter O 18.11
 Richter, Reinhard •DY 11.1
 Richter, S HL 21.2

Richter, Sonja BP 18.7
 Richter, Tilman •DY 4.8
 Rickert, Lucas HL 17.10, HL 25.74,
 HL 30.3
 Rickhaus, Peter MA 41.4
 Rico, Albert •QI 9.3
 Rieche, Antonia •MA 35.48
 Rieck, Katharina •BP 12.15
 Riedel, Christian •MA 28.3, MA 35.14
 Riedel, Lukas •MM 18.32
 Riedinger, Andreas CPP 41.6
 Riedl, H. HL 2.3
 Riedl, Kira TT 8.4
 Riedl, Thomas DS 1.4, MM 14.4
 Riedmüller, Benjamin MA 39.1
 Riegel, Elisabeth O 74.9
 Rieger, Dennis TT 27.1, •TT 27.2,
 TT 31.2, TT 31.18, TT 37.9, TT 37.12
 Rieger, Heiko •DY 46.21, DY 46.22
 Rieger, Manuel HL 25.65, •HL 26.6
 Rieger, Robert MA 9.3
 Rieger, Sebastian HL 5.7
 Riegg, Stefan MA 32.4
 Rienitz, Olaf •KFM 6.4
 Riepl, Josef •HL 4.3, HL 40.5
 Ries, Jonas •BP 5.4
 Riesch, Johann DS 13.1, MM 4.10
 Rieth, Tim •HL 24.8, HL 24.10,
 HL 25.35
 Rietveld, Jörn C. O 51.7
 Rigamonti, Santiago O 67.7
 Righi, Lara MA 42.4
 Righi, M. Clelia O 39.2
 Rigoni, Christian Aaron •MM 30.8
 Riha, Christian HL 25.89
 Rimek, Fabio •HL 25.59, HL 25.63,
 HL 26.10
 Rimmler, Berthold H. •MA 34.6
 Rinaldi, Matteo •MM 34.4
 Ringel, Eva •O 12.10
 Ringkamp, Christoph •DS 21.2
 Ringleb, Andreas DS 20.48, O 32.1
 Ringling, Julian •CPP 17.16
 Rinke, Patrick O 50.4
 Rinner, Stephan QI 4.11
 Ripoll, Marisol DY 46.8, DY 50.6
 Rischau, Willem DS 25.1
 Ristau, Mariam •BP 12.13
 Ristow, Florian O 13.7
 Ritman-Meer, Tom •MA 5.2
 Ritschel, Tobias MM 7.4
 Ritsema van Eck, Guido SYSM 1.3
 Ritter, Oliver MA 19.17
 Ritterhoff, Christian •O 58.10
 Ritzer, Maurizio HL 21.11, HL 25.46
 Ritzinger, Philipp •MA 18.6
 Ritzmann, Julian HL 19.1
 Riva, Michele O 3.7, O 3.8, O 16.12,
 O 63.6
 Rivera-Arrieta, Herzain I. •O 62.2
 Rivero Arias, Melissa HL 21.3
 Rivetti, Marco BP 3.2
 Riwar, Roman TT 34.3, QI 13.3
 Riwar, Roman-Pascal TT 30.19,
 TT 37.14, QI 8.2, QI 13.4
 Rizzi, Angela HL 25.22
 Rizzo, Matteo TT 1.11, TT 16.7,
 TT 34.12
 Robert, Cedric HL 20.8
 Roberts, Joseph HL 14.5
 Robertson, Elizabeth DY 45.11
 Robinson, J.W.A. TT 22.1
 Robinson, Joshua •TUT 2.1, DS 20.39,
 DS 22.2, DS 22.4, •HL 1.1, O 18.19
 Robles, Roberto O 6.3, O 47.5, O 74.5
 Rocabert, Ulysse •MA 29.9
 Roccia, Emanuele HL 19.2
 Rodolfo, Rodolfo DS 25.1
 Roche, Léo •HL 25.76
 Roche, Patrice TT 37.7
 Rochford, Luke A. O 41.1
 Rockinger, Tobias HL 6.7, •HL 25.21
 Rockstuhl, Carsten O 61.7
 Rodatis, Vladimir MM 17.4
 Roddaro, Stefano HL 37.2
 Rode, Daniel Karl-Heinz BP 10.4
 Rode, Johannes C. HL 29.6
 Rode, Julian •DY 40.4
 Rodehutsors, Sophie •O 19.5
 Rödel, Maximilian •DS 5.5, DS 20.21
 Rodemund, Tom •DY 35.8
 Roden, Stephanie •MA 35.27,
 MA 35.31
 Roder, Sebastian HL 24.2
 Rodier, Clement BP 12.32, BP 13.3
 Rödl, Alexandra •O 78.3

Author Index

Rodrigues, Davi MA 35.16
 Rodrigues, Davi R MA 12.3, MA 12.9
 Rodrigues, Matias TT 17.2, TT 31.10
 Rodríguez, Alberto •DY 5.6
 Rodríguez, Jorge P •SOE 9.3
 Rodríguez Martín, Miguel •DY 44.10
 rodriguez sota, arturo MA 34.2,
 •O 42.2
 Rodríguez-Barea, Borja •HL 25.68
 Rodríguez-Fernández, Jonathan
 O 72.1
 Rodt, Sven HL 8.6, HL 12.5, HL 17.10,
 HL 25.75, HL 30.3, HL 30.7, HL 36.10
 Rodyakina, Ekaterina E. HL 40.4
 Roede, Erik D. KFM 7.3
 Roemling, Lukas CPP 8.2
 Roesch, Roland CPP 12.62
 Roessner, Michael O 57.3
 Rogero, Celia O 22.4
 Rogić, Luca BP 7.23
 Rog-Zielinska, Eva BP 13.11
 Rohart, Stanislas TT 13.3
 Rohde, Lisa •DY 46.11
 Rohleder, Darius KFM 15.4
 Rohlfing, Michael O 6.7, O 28.3,
 O 48.3, O 48.4, O 72.3, O 72.6
 Rohling, Niklas MA 13.7, •MA 24.9,
 QI 3.4
 Rohrbach, Alexander BP 5.5, BP 7.44,
 BP 7.45, BP 7.46, BP 9.8, BP 12.27,
 BP 12.28, BP 13.11, O 39.5
 Rohrbach, Pascal HL 30.28, •O 19.4
 Rohrer, Jochen MM 23.5, MM 33.2
 Rohringer, Georg TT 16.3, •TT 28.2,
 TT 28.11
 Rohrmeier, Christoph •TT 13.1,
 •TT 26.12
 Roig, Mercè TT 22.4
 Rojas, Javier MM 20.7
 Rojas-Aedo, Ricardo HL 22.10,
 HL 32.6
 Rojas-Nunez, Javier •MM 33.10
 Rol, Adriaan QI 13.2
 Rol, Michiel Adriaan QI 13.9
 Roldan Cuenya, Beatriz O 52.12
 Rolland, Chloe TT 37.7
 Roma, Riccardo •QI 4.1
 Romanczuk, Pawel •SYSO 1.4
 Romaner, Lorenz MM 25.8, MM 34.6
 Romano, A. TT 22.1
 Romdhane, Samir CPP 12.69
 Romeo, Michelangelo O 35.6
 Rømer, Astrid T. TT 22.4
 Römer, F. HL 10.5
 Römer, Friedhard DS 2.4
 Römer, Rudolf A. •BP 7.6, •BP 7.16,
 DY 26.3, •DY 49.3, DY 51.3, O 67.9
 Romero, Francisco O 18.13, O 51.3
 Romero Lara, Francisco O 51.10
 Romero-Isart, Oriol QI 4.33
 Römer-Stumm, Malte MA 19.3
 Ronceray, Pierre •BP 19.3
 Rong, Alena MA 35.65
 Ronning, Carsten DS 1.1, DS 20.31,
 HL 4.2, HL 4.4, HL 18.1, HL 21.11,
 HL 25.46
 Ronning, Filip MA 31.9
 Rønnow, Henrik MA 19.6
 Ronsin, Olivier CPP 19.2
 Roos, Aycke •DY 15.2
 Röper, Sina •KFM 3.4
 Ropers, Claus KFM 8.1, MA 23.3,
 O 9.3, O 16.4, O 78.5
 Rosa, Bárbara DS 17.4, HL 6.6,
 •HL 25.24
 Rosander, Petter MM 7.2
 Rosario Hamann, Andres TT 37.13
 Rosati, Matteo •QI 6.2, •QI 7.6
 Rosati, Roberto •HL 20.1
 Rosch, Achim MA 12.5, MM 10.12,
 O 50.7, O 71.4, TT 5.1, TT 21.36
 Rösch, Niels •DS 20.29, DS 22.7
 Roscher, Moritz MM 14.4
 Roscher, Willi •TT 5.2
 Roseker, Wojciech MA 31.6
 Rosenauer, Andreas DS 13.5, DS 20.6,
 HL 42.3
 Rosenberger, David •CPP 9.1
 Rosenberger, Paul DS 20.36,
 MA 23.2, MA 35.26
 Rosenkranz, Marco BP 7.29
 Rosenthal, Eric QI 4.33
 Rosenzweig, Dorothee O 49.3
 Rosenzweig, Dorothee S. O 69.9
 Rosenzweig, Philipp O 41.6, O 41.8
 Rosillo-Orozco, Luis •O 15.6

Rosinus Serrano, Bruno •MA 19.47
 Roslowska, Anna O 18.25, •O 35.6
 Rößler, Ulrich K. O 43.8
 Rösner, B. MA 25.4
 Rösner, Harald MM 20.1, MM 30.2,
 MM 30.4
 Rosner, Helge MM 23.1, •TT 28.6
 Rösner, M. O 6.9, TT 10.7
 Rösner, Malte O 72.5, TT 16.2
 Rosowski, Frank O 62.6
 Rosowski, Kathryn A. BP 8.6
 Ross, A. MA 19.63
 Ross, Andrew •SYSD 1.3
 Ross, Ulrich •O 20.7
 Rossbach, Philipp •BP 10.6
 Rossell, M. KFM 2.3
 Rossell, Marta D. KFM 14.3, KFM 19.3
 Rossi, Mariana KFM 11.3, O 5.2,
 O 11.1, O 48.1, O 50.3, O 50.8, O 50.12,
 O 55.12, O 58.1, O 67.5, O 83.4
 Rossi, Matteo MA 6.1
 Rossini, Mirko •TT 20.6
 Rössle, Matthias DS 20.52, HL 25.66,
 •HL 30.47
 Rössler, U.K. MA 20.4
 Rossnagel, K. O 68.10
 Rossnagel, Kai MA 31.6, O 9.1,
 O 18.21, O 33.1, O 34.10, O 48.10,
 O 55.15, O 68.3, O 80.4
 Rossow, Uwe HL 10.12, HL 10.13,
 HL 30.17, HL 30.18
 Rossow, Uwe Rossow HL 30.12
 Rostami, Habib HL 29.4
 Rota, Michele B. HL 19.2
 Rotenberg, Eli O 72.4
 Roth, Camille SOE 12.3
 Roth, Ingo QI 3.2
 Roth, Ingor QI 3.1
 Roth, Robert CPP 48.1
 Roth, Stenphan V. CPP 37.3
 Roth, Stephan CPP 12.3
 Roth, Stephan V. CPP 1.4, CPP 1.6,
 •CPP 1.8, CPP 12.13, CPP 12.59,
 CPP 12.64, CPP 17.6, CPP 17.26,
 CPP 18.3, CPP 19.4, CPP 27.2,
 CPP 27.3, CPP 27.4, CPP 37.6,
 CPP 48.3, CPP 50.1, MA 41.5
 Rothe, Johannes DS 13.1
 Rothe, Karl •O 18.1, O 19.1
 Rothenbach, N. MA 25.4
 Rothhardt, Daniel •O 22.3, O 30.4
 Rothlör, Jan MA 19.30, •MA 37.7
 Rott, Karsten MA 19.17
 Rötzer, Marian O 56.2
 Rotzinger, Hannes TT 26.1, TT 31.19,
 TT 31.20, TT 31.21, TT 37.3, TT 37.10
 Roulleau, Preden MA 13.12
 Rousseau, Ian HL 37.3
 Roussigné, Yves MA 18.5
 Rouzé, Cambyse QI 14.4
 Rouzegar, Reza MA 21.2, MA 24.4
 Rowe, Patrick O 46.5
 Rowen, Julien O 32.6
 Roy, Federico QI 13.5, QI 13.6
 Roy, Indranil TT 7.6
 Roy, Reshmi •DY 39.1
 Rozas, Elena HL 30.2
 Rozenberg, Marcelo DS 25.1
 Rozgonyi, Áron QI 3.8
 Rózsa, Levente •MA 8.4, MA 12.8,
 MA 30.2
 Ruan, Zilin •O 79.4
 Ruban, Andrei MM 6.8
 Rubeck, Jan CPP 18.3
 Ruben, Mario MA 25.7, O 80.3,
 TT 21.21, TT 21.22, QI 4.9, QI 4.12
 Rubin, Nicholas C. QI 12.5
 Rubio, Angel DY 35.1, MM 9.4, O 78.2
 Rubrecht, Bastian MA 14.8, MA 31.3
 Rüchardt, Baltasar DY 8.6, DY 45.12,
 SOE 6.6
 Ruck, Michael O 21.2
 Rückle, Lukas •QI 7.4
 Rudenko, Alexander N. O 51.4
 Rudge, Samuel •TT 15.2
 Rudi, Eduard HL 19.9
 Rudloff, Maximilian DS 5.5
 Rudolf, Petra •AKC 1.1, •AKC 1.2
 Rudolph, Jörg KFM 19.2
 Rudolf, Sophia BP 12.55
 Rudzinski, Joseph BP 8.8
 Rueßmann, Philipp O 26.1
 Ruess, Raffael O 32.1
 Ruf, Leon TT 3.9, •TT 30.10
 Ruf, Thomas •MA 19.57
 Ruffieux, Pascal O 17.12, O 18.19,
 O 23.9

Rugeramigabo, Eddy P. HL 12.7,
 HL 12.10, HL 30.9, •HL 36.8
 Rugeramigabo, Eddy Patric HL 8.3
 Ruh, Jannis •QI 10.8
 Rühle, Jessica O 82.5
 Rühl, Eckart O 7.9
 Rühman, Jonathan TT 33.6
 Rührmair, Ulrich DS 16.3
 Ruhstorfer, Daniel HL 3.10
 Ruhwedel, Moritz MA 19.53,
 MA 19.59
 Ruiz Alvarado, Isaac Azahel HL 25.39
 Ruiz, Daniel O 6.3
 Ruiz Puente, Álvaro •TT 25.4
 Ruiz, Victor G. CPP 12.26
 Ruiz-Gomes, Sandra MA 35.17
 Rulands, Steffen BP 6.4, BP 27.1
 Rullkötter, Leon O 71.6
 Runge, Erich DY 46.10, HL 13.3,
 HL 13.4, HL 13.5, HL 24.3, HL 24.6,
 •HL 25.39, HL 30.42, HL 30.45
 Rungger, Ivan O 42.3
 Rupp, Matthias •O 67.3, •O 83.10
 Ruppenstein, Cordula O 40.1
 Ruppenthal, Lukas DS 20.19, O 12.4,
 •O 12.6, O 41.2, O 52.6, O 55.10
 Ruppert, Michael G. O 14.2
 Ruppert, Thomas MA 19.22, MA 26.2
 Rupprecht, Felix QI 4.2
 Rupprecht, Verena •BP 22.1
 Ruschel, Jan HL 10.1
 Rüschoff, Josef BP 7.40
 Rushton, Michael MM 2.9
 Rüsing, Michael KFM 14.5
 Rübmann, Philipp TT 10.8, •TT 19.5
 Rutsch, Matthias CPP 17.19
 Rütten, Lisa M. •O 80.4
 Ryabov, Artem DY 46.18
 Ryan, Paul T. P. O 40.5
 Rybakov, Filipp MA 19.1, MA 37.2,
 •MA 37.5
 Rybakov, Filipp N. MA 27.4, MA 27.6
 Rybakowski, Lawrence •MA 35.57
 Ryndyk, Dmitry A. O 29.2
 Ryu, Shinsei MM 23.9
 S. Cabaco, Joao •MA 35.68
 Saal, Alexander CPP 7.3
 Saalfeld, Jürgen HL 18.1
 Saalwächter, Kay CPP 41.5
 Saavedra, Daniel BP 12.51
 Saavedra, Rodrigo •DY 46.8
 Sabota, J. A. O 9.5
 Sadat, Sayed HL 25.73
 Sadat, Sayed Shkeebullah •HL 25.81,
 HL 25.86
 Sadre-Momtaz, Zahra HL 22.2
 sadrollahi, elaheh •MA 14.5, TT 24.5
 Safari, Mohammad Reza •O 5.9
 Safer, Affan O 18.12
 Safiri, M. •MA 35.53
 Safran, Samuel •BP 8.1
 Safran, Samuel A. BP 8.9
 Sagkovits, Dimitrios MA 18.3
 Sagnes, Isabelle HL 19.4
 Saha, Suropriya •DY 3.8
 Sahinovic, Armin O 83.5
 Sahle, Christoph TT 8.6, TT 21.15
 Saigal, Nihit HL 6.5, •HL 6.8, HL 11.6,
 HL 25.4, HL 25.6, HL 25.15
 Saikia, Ujjal •MM 10.25
 Saitoh, Eiji MA 19.62, MA 25.5,
 MA 34.3, MA 35.28
 Saiz, Guilhem O 44.10
 Sajan, Sandra O 25.2
 Sakar, Baha •MA 5.4
 Sakong, Sung O 69.7
 Sakrowski, Robin KFM 25.11,
 KFM 25.13
 Sakurai, Takahiro MA 14.8
 Sala, Alessandro O 12.5
 Salamon, Soma MA 25.7, MA 35.60,
 •MA 39.4, MA 39.5, O 26.8
 Salamone, Tancredi •TT 29.5
 Salánki, Miklós MA 19.38
 Salas, Clara Ortegón BP 12.23
 Salazar Mejia, C. MA 19.11, MA 29.2,
 MA 29.3
 Salazar, Raphaël O 44.10
 Salazar-Mejia, Catalina MA 19.13
 Salbaum, Katja BP 2.5, BP 9.7
 Salbreux, Guillaume BP 19.6
 Salditt, Tim BP 9.4, BP 9.9, BP 12.54,
 BP 17.6, KFM 25.12, KFM 25.14
 Salehi, Waheed HL 25.66
 Salgado-Cabaço, João MA 4.2

Salikhov, Ruslan •MA 21.7, MA 22.7,
 MA 22.8
 Salimath, Akshaykumar MA 21.4
 Sallermann, Moritz MA 24.11, MA 37.1
 Salloum, Sarah HL 42.1
 Salman, Jad HL 18.1
 Salman, Z. TT 22.1
 Saltzman, Tobias •PSV 1
 Salusti, Francesco •HL 19.2
 Salvan, G. O 26.2
 Salvan, Georgeta HL 25.51, MA 35.49
 Salzwedel, Robert HL 6.10, •O 37.4,
 O 59.1, O 61.2
 Samad, Fabian MA 22.8, MA 35.49
 Samano, Enrique HL 25.68
 Samanta, Tapas DS 4.3
 Sambale, Anna K. CPP 37.6
 Samigullina, Dinara •HL 41.5
 Samir, A. KFM 2.3
 Samuelsson, Peter QI 1.6
 Sanchez, Alvaro TT 15.1
 Sanchez, Cecilia P BP 5.3
 Sánchez, Cristián G. O 81.4
 Sanchez, Juan •MM 10.15, MM 10.16
 Sánchez, Miguel •MA 19.24
 Sanchez, Pedro DY 11.1
 Sánchez-Barriga, Jaime O 9.9
 Sánchez-Grande, Ana O 79.6
 Sanchez-Tejerina, Luis MA 34.3
 Sanchez-Valle, Carmen HL 25.26
 Sander, Leon •QI 6.4
 Sander, Oliver TT 37.12
 Sander, Wolfram O 32.6
 Sanders, C. E. MM 7.5
 Sanders, Ch. O 68.10
 Sanders, Charlotte O 54.5
 Sanders, Charlotte E. •O 72.1
 Sandfeld, Stefan •MM 25.5
 Sandlöbes-Haut, Stefanie MM 4.2
 Sandner, Fabian HL 13.8, HL 20.2
 Sangeetha, N. S. TT 21.5, TT 21.8,
 TT 30.1
 Sangermano, Marco CPP 14.6
 Sangiovanni, Giorgio O 4.1, O 4.2,
 O 73.4
 Santagati, Raffaele QI 12.5, QI 12.6
 Santer, Svetlana CPP 12.29, DY 46.12
 Santoro, Giuseppe Ernesto QI 12.11
 Santos, Leonardo •QI 4.25
 Santos, Luis MM 7.1
 Santos, Paulo HL 35.3, HL 36.7
 Santos, Paulo V. HL 35.2
 Santra, Saswati O 8.5
 Sanvito, Stefano MA 11.5
 Sanz, Sofia O 18.13, O 80.1
 Saphiannikova, Marina CPP 49.2
 Saraceno, Clara O 34.9, O 68.9
 Sarhan, Radwan M. O 78.5
 Sarkar, Anirban MA 33.2
 Sarkar, J. MA 35.24, •O 9.5
 Sarkar, R. MA 4.1
 Sarkar, Saheli •TT 24.1
 Sarkar, Suchetana •O 29.5, O 32.8
 Sarker, Debalaya HL 24.12
 Sarker, Mamun O 23.7, O 63.7
 Sarott, Martin KFM 8.6
 Sarott, Martin F. •KFM 14.3
 Sarpe, Cristian BP 7.40
 Sartison, Marc DS 17.7, DS 20.46,
 •HL 17.8
 Sartore, Sofia •BP 7.25
 Sartori, Emanuele VA 2.1
 Sasaki, Tomoya O 45.8
 Sasioglu, Ersoy MA 24.4, MA 42.1
 Saßnick, Holger-Dietrich MM 10.27,
 MM 23.6
 Satison, Marc HL 25.1
 Sato, Shunsuke MM 9.4
 Sato, Takuma MA 7.2
 Sato, Toshihiro •TT 8.3
 Sattar, Shahid •MA 41.3
 Sattler, Klaus CPP 17.10, KFM 15.3
 Sattler, Lars E. O 12.6
 Sauer, Mikkel O 72.4
 Sauderson, Tom G MA 24.2,
 •MA 24.8
 Sauter, Eduard HL 25.93
 sauter, eric O 30.7, •O 70.8
 Savchenko, Andrii •MA 19.1,
 •MA 35.13, •MA 37.2
 Savchenko, Vladyslav •CPP 12.30
 Savelkoul, Jaqueline BP 7.10,
 •BP 12.52
 Savey-Bennett, Marc MA 5.2
 Sawicki, Jakub SOE 12.1
 Saxena, Alaukik MA 23.1, •MM 22.2

- Saxena, Rishabh ... •HL 41.2, HL 41.4
saxena, vishesh ... •MA 34.2, O 42.2
Saymung, Rungarune ... •CPP 12.33
Saywell, Alex ... O 29.4
Saywell, Alexander ... O 29.3, O 41.1
Sbierski, Björn ... •MA 16.2
Sbresny, F. ... HL 2.3
Sbresny, Friedrich ... HL 8.1
Scagnoli, Valerio ... •MA 20.1
Scandolo, Mattia ... BP 14.8
Scaparra, Bianca ... HL 25.65
Schaaf, Peter ... DS 23.2
Schaal, Maximilian ... O 17.1, O 18.26,
O 65.4, •O 65.6
Schädlich, Philip ... O 18.11, •O 41.4,
O 54.2
Schady, Pascal ... •CPP 12.72,
CPP 12.77
Schaedel, Laura ... BP 13.7
Schaeper, Anja ... BP 7.42
Schaeper, Jannis Justus ... •BP 9.9
Schäfer, Ansgar ... MM 25.4
Schäfer, Benjamin SOE 7.1, •SOE 13.1
Schäfer, Felix ... HL 13.10
Schäfer, Gerhard ... HL 30.41
Schäfer, Julian ... •MA 19.52
Schäfer, Kilian ... •MA 32.4
Schäfer, Luca ... •BP 12.64
Schäfer, Lukas MA 35.52, •MM 18.25
Schäfer, Mareen ... CPP 41.5
Schäfer, Moritz R. ... •O 58.5
Schäfer, Robin ... •MA 15.3
Schäfer, Sascha DS 20.25, HL 30.49,
MA 19.29, MA 19.54, MA 21.3,
O 53.5, O 59.7
Schäfer, Sören ... HL 30.31
Schäfer, Thomas ... •TT 16.1, TT 16.4,
TT 28.11, TT 34.8
Schäffer, Alexander F. ... MA 28.1
Schäffer, Tilman ... BP 18.6
Schäffer, Tilman E. ... BP 3.8, BP 3.9,
BP 9.3, BP 12.11
Schäffler, Nathalie ... •BP 12.59
Schaible, Sophie ... •HL 30.27
Schalk, Martin ... HL 20.3, MA 19.28
Schall, J. ... HL 2.3
Schall, Johannes HL 17.10, HL 25.75,
HL 30.3, •HL 30.7, HL 36.10
Schaller, Gernot ... TT 13.6
Schambeck, Mia ... TT 29.17
Schanzenbach, Dirk ... CPP 44.4
Schaper, Simon J. ... CPP 37.3
Schaper, Steffen ... BP 23.1
Schäpers, Thomas ... DS 21.2, HL 7.3,
HL 19.7, HL 25.77, HL 25.98
Scharf, Benedikt ... TT 1.2
Scharf, Carl Hendric ... •DS 20.4
Scharffetter-Kockanek, Karin BP 12.4
Scharmer, Selim ... DS 20.46
Schart, Maximilian ... CPP 12.35
Schatz, Enno ... O 61.3
Schäublin, Robin E. MM 3.9, MM 30.6
Schaumburg, Felix ... •HL 25.2
Schawe, Hendrik ... DY 24.2
Schawe, Jürgen ... MM 3.7
Schebek, Maximilian ... •HL 11.3
Scheblykin, Ivan G. ... CPP 12.74
Scheele, Marcus ... CPP 12.78,
CPP 28.7, HL 28.4
Scheer, E. ... TT 13.5, TT 22.1
Scheer, Elke ... •TUT 2.4, DY 12.2,
DY 12.5, •HL 1.4, TT 3.9, TT 7.2,
TT 7.8, TT 10.9, TT 22.2, TT 29.4,
TT 29.6, TT 30.10, TT 30.11, TT 30.13,
TT 30.14, TT 30.20, TT 31.26
Scheer, Roland ... •HL 27.3, •HL 27.4,
HL 32.5, HL 34.5
Scheffel, Jakob ... O 13.7
Scheffler, Daniel ... •MA 29.4
Scheffler, Matthias ... SYNM 1.2,
MM 12.7, MM 21.2, MM 25.4,
MM 29.2, MM 29.3, O 11.1, O 50.2,
O 62.2, O 62.7, O 67.1, O 70.9, O 83.10
Scheibel, Franziska ... MA 29.1,
MA 29.7, MA 32.2
Scheiber, Daniel ... MM 25.8, MM 34.6
Scheidt, Joshua ... •O 14.4
Schell, Andreas ... HL 25.85
Schell, Andreas Wolfgang ... QI 14.5
Schell, Juliana ... MM 7.3, MM 18.13
Schellenberger, Andreas ... •TT 23.2
Schellhammer, Karl Sebastian
HL 41.5
Schellhammer, Sebastian ... •CPP 40.8
Schels, Andreas ... HL 22.3
Schemmelmann, Sven ... O 73.1, •O 73.2
- Schenk, Sebastian ... •O 66.4, O 66.5,
O 66.7
Schepers, Anna ... BP 12.30
Schepers, Anna V. ... •BP 12.7, •BP 12.8
Scherb, Sebastian ... O 17.10, O 22.6,
O 39.4
Scherer, Michael M. ... TT 10.6, TT 23.3
Scherer, Theo ... •KFM 18.2, KFM 18.3,
KFM 18.4, •KFM 18.5, KFM 25.10
Scherer, Theo A ... KFM 18.1
Schering, Philipp ... HL 2.4
Scherm, Clara ... HL 24.8
Schermer, Nicole ... DS 13.1
Scherz, A. ... MA 25.4
Scherz, Andreas ... MA 25.2, MA 25.7
Scherzad, Sohraab ... •DS 20.20
Scheu, Christina ... MM 14.4
Scheuer, Laura ... MA 19.50, MA 19.52,
•MA 19.53, MA 35.19
Scheuerer, Philipp ... O 47.9
Scheuermann, Robert ... TT 6.8
Scheufole, Monika ... MA 35.7,
•MA 35.35
Scheurer, C. ... KFM 11.4
Scheurer, Christoph ... DY 8.2, MM 2.4,
MM 2.5, MM 2.8, MM 8.8, MM 8.9,
MM 14.1, MM 34.8, O 28.5, O 49.8,
O 69.4, O 69.8, O 82.2, SOE 6.2
Scheurer, Fabrice ... O 18.25, O 35.6
Scheurer, Mathias ... MM 28.3
Scheurer, Mathias S ... TT 30.7
Schewe, Christian ... O 64.1
Schick, Daniel ... MA 8.2, MA 8.3,
•MA 12.8
Schick, Lisa ... •BP 12.34
Schickel, Jonas ... MM 10.21
Schied, Monika ... •O 74.2
Schied, Monika T. ... O 54.5
Schiegl, Felix ... HL 20.2
Schiegl, Magda ... •SOE 4.2, •SOE 14.5
Schier, Richard ... •MM 23.6
Schierholz, Roland ... MM 14.3
Schierning, Gabi ... HL 42.1
Schilberth, Felix ... •MA 40.1
Schilcher, Maximilian ... MM 23.7
Schilfgaarde, Mark van ... MA 38.4
Schiller, Frederik ... O 26.4
Schiller, Karl ... HL 2.2, O 34.9, •O 68.9
Schilling, James S. ... MA 35.72
Schilling, Marcel ... •HL 10.7, HL 10.8
Schilling, Tanja ... DY 23.3, DY 23.7
Schimpf, Christian ... SYED 1.2
Schindler, Frank ... TT 18.1
Schißt, Jakob ... O 27.3
Schirmeisen, Andre ... O 6.2, O 14.2,
O 39.3, O 39.6, O 39.7, O 40.6, O 41.2,
O 79.5, TT 17.8, TT 31.14
Schlabach, Sabine ... •MM 18.18
Schlagel, D. L. ... MA 29.3
Schlauch, Alexander ... •CPP 9.9,
CPP 12.25, •CPP 12.36, •CPP 18.5
Schlappa, J. ... MA 25.4
Schlappa, Justine ... MA 25.2
Schlatmann, Rutger ... CPP 28.5
Schlaugat, Paul ... DS 17.4
Schlawin, Frank ... MM 9.3, QI 8.5
Schleberger, Marika ... HL 31.3, O 48.8
Schleenvoigt, Michael ... HL 19.7,
HL 36.6, O 4.3, TT 18.9, TT 32.3,
TT 32.7
Schlegel, Julius ... •MA 8.10, MA 28.9
Schleife, André ... MA 15.1
Schleifer, Felix ... MM 31.5
Schlein, Carolin ... •BP 13.7
Schlemmer, Alexander ... •DY 8.6,
DY 45.13, •SOE 6.6
Schlender, Philipp ... TT 23.2
Schlenhoff, Anika ... •O 26.6
Schlenz, Patrick ... DS 20.14
Schlereth, Raimund ... SYQM 1.2
Schlettwein, Derck ... CPP 12.51,
CPP 26.4, DS 20.48, O 20.3, O 20.5,
O 32.1
Schlichting, Antonia-Louisa
CPP 17.24
Schlickriede, Christian ... HL 33.9
Schlickum, uta ... O 13.4, O 17.5, O 28.6,
O 55.11
Schlischka, Marvin ... HL 30.3
Schlitz, Richard ... •MA 7.2, O 47.5
Schliwa, Andrei ... HL 17.6
Schlögl, Robert ... O 49.8, VA 2.4
Schlom, Darrell ... KFM 7.2
Schlom, Darrell G. ... DS 20.32
Schlombs, Simon ... •HL 25.67
Schlothauer, Thomas ... KFM 6.2
- Schluck, Jakob ... HL 7.9
Schlueter, Christoph ... MA 35.40
Schlüter, Henrik ... •TT 21.16
Schmalian, Jörg ... TT 3.1, TT 3.7
Schmalofski, Timo ... •MM 6.5
Schmalz, Veronika ... O 17.3
Schmalz, Karin ... MA 28.12
Schmauder, Siegfried ... MM 6.8,
MM 34.7
Schmeller, Leonie ... CPP 17.14
Schmid, Christian ... HL 36.4, TT 17.5,
TT 17.6, •TT 17.7
Schmid, Christoph Peter ... HL 13.8
Schmid, Daniel R. ... TT 2.1
Schmid, Friederike BP 7.27, BP 12.53,
CPP 7.8, CPP 12.11, CPP 17.35,
CPP 17.40, DY 45.8
Schmid, Harald ... O 80.4
Schmid, Michael ... O 3.3, O 3.7, O 3.8,
O 10.3, O 10.5, O 10.6, O 16.12, O 27.5,
O 38.2, O 44.3, O 44.7, O 49.4,
O 49.10, O 57.5, O 58.11, O 63.6
Schmid, Ralf ... CPP 17.7
Schmid, Stephanie ... BP 13.11
Schmid, Valentin ... CPP 28.2
Schmidbauer, Martin ... DS 20.1, MA 8.2
Schmidt, Anne ... TT 32.3, O 28.5
Schmidt, Bernd ... TT 17.8, TT 31.14
Schmidt, Christoph F. ... BP 3.10
Schmidt, Claudia ... CPP 17.10,
CPP 17.39, KFM 15.3
Schmidt, Constantin ... HL 12.10,
HL 30.9
Schmidt, Franz-Philipp ... O 49.8
Schmidt, Georg ... MA 7.1, MA 19.45,
MA 19.57, MA 21.2, MA 28.5,
MA 35.51
Schmidt, Gordon ... •DS 2.3, DS 6.3,
HL 22.9, HL 30.16
Schmidt, Hannes ... BP 12.11
Schmidt, Hans-Werner ... CPP 41.2
Schmidt, Heidemarie ... DS 18.1, HL 18.1
Schmidt, Heinz-Jürgen ... DY 5.7,
MA 19.20
Schmidt, Jack-Andre ... •TT 17.8,
TT 31.14
Schmidt, Jan Robert ... •DY 35.7
Schmidt, Jaydean ... •TT 30.18
Schmidt, Kai P. ... TT 23.10, TT 23.11
Schmidt, Kai Phillip ... TT 5.7, TT 21.18,
TT 21.19, TT 21.20, TT 21.31, TT 23.2,
TT 24.6, TT 24.7, TT 24.14, TT 24.15,
TT 34.7, QI 4.3
Schmidt, M. ... MA 20.4
Schmidt, Marcel ... HL 12.1, HL 12.2,
HL 26.2, HL 26.3
Schmidt, Marcus ... MM 23.1
Schmidt, Nico ... O 5.7
Schmidt, Oliver G. ... BP 7.29, HL 3.5,
HL 8.3, HL 8.4, HL 8.5, HL 12.6,
HL 25.82
Schmidt, Paul Philip ... •O 30.4
Schmidt, Philip ... TT 15.1, TT 29.11
Schmidt, Philipp ... HL 29.2
Schmidt, Robert ... HL 19.9, HL 20.1,
HL 25.25, HL 25.26, •HL 25.27,
HL 30.48
Schmidt, Ronny ... HL 30.7
Schmidt, Thomas ... •DS 20.42, O 52.11,
TT 34.3
Schmidt, Thomas L. ... TT 1.3, •TT 11.5,
TT 23.13
Schmidt, Wolf Gero ... HL 25.39, •O 30.1
Schmidt, Wolfgang ... MA 40.3
Schmidt-Grund, R ... HL 21.2
Schmidt-Grund, Rüdiger ... DS 20.17,
DS 23.2, •HL 13.3, HL 13.5, HL 30.45
Schmidt-Kaler, Ferdinand ... •SYUK 2.3
Schmidt-Mende, Lukas ... HL 5.5,
HL 30.28, MM 35.3
Schmiedeborg, Michael ... •DY 31.8,
DY 39.4, DY 44.20, DY 45.9, DY 46.17,
DY 46.19
Schmitt, Cedric ... •DS 20.28
Schmitt, Christin ... MA 19.60, MA 19.62,
MA 25.5, •MA 34.3, MA 35.28
Schmitt, David ... O 2.2, O 9.10, O 16.9,
O 33.3, •O 48.9
Schmitt, Robert ... O 35.3
Schmitt, Tanja ... •CPP 39.3
Schmitt, Tobias ... HL 19.7
Schmitt, Tobias W. ... TT 18.9, •TT 32.3,
TT 32.7
Schmittel, Michael ... O 6.10, O 40.8
Schmitz, Fabian ... •DS 16.1
Schmitz, Guido ... MM 8.10, MM 10.10,
- MM 10.14, MM 18.20, MM 18.28,
MM 22.3, MM 32.3, MM 32.5,
MM 35.2, MM 35.4
Schmitz-Antoniak, Carolin ... MA 25.7
Schmoll, D. ... MA 35.12
Schmoll, David ... •MA 13.2
Schmoll, Philipp ... •TT 16.7
Schmoranzzerová, Eva ... MA 8.12,
MA 19.26, MA 29.6
Schmude, Tobias ... HL 30.43
Schmülling, Bastian ... •HL 25.71
Schmunk, Waldemar ... •HL 7.2
Schmutz, Valentin ... BP 2.7
Schmutzler, Stephan ... O 9.9
Schnack, Jürgen ... DS 20.11, •DY 5.7,
DY 43.6, MA 19.18, MA 19.20,
TT 21.16, TT 23.7
Schnauß, Jörg ... CPP 12.5
Schnedler, Michael ... •HL 22.5,
MA 23.4, MM 18.39, O 22.7, O 69.9,
O 82.7
Schneider, Andre ... TT 26.1, TT 37.10
Schneider, Benedikt ... •MA 11.6
Schneider, Carina ... •CPP 17.20
Schneider, Christian ... DS 17.4, HL 11.8,
HL 15.4, HL 15.7, HL 20.6, HL 28.7,
HL 30.2, HL 41.3, QI 7.9
Schneider, Claus M. ... MA 30.3, O 5.9,
O 48.7, •O 84.1
Schneider, Claus Michael ... MA 19.55,
O 21.4
Schneider, Claus-Michael ... O 73.7
Schneider, Daniel ... O 63.3
Schneider, Eric ... •KFM 25.6
Schneider, H. Christian ... MA 35.31
Schneider, Hans Christian ... MA 8.5,
MA 25.3, MA 25.5, MA 25.8,
MA 35.27, MA 35.28
Schneider, Harald ... HL 11.10
Schneider, Jale ... HL 24.2
Schneider, Jochen M. ... MM 28.5
Schneider, Konrad ... CPP 37.6
Schneider, Lucas ... •MA 9.4, •MA 30.2,
MA 35.71
Schneider, M. Alexander ... O 54.9,
O 73.4
Schneider, Michael ... MA 2.1, MA 2.3,
MA 12.2, •MA 13.8, MA 28.6, MA 35.9
Schneider, Robert ... HL 20.1, HL 25.27,
MA 21.10
Schneider, S. ... MA 20.4, MA 27.1
Schneider, Sebastian ... MA 27.7
Schneider, Thomas ... HL 27.4
Schneider, Tim P. ... •CPP 12.51, O 20.5
Schneidewind, A. ... MA 4.1
Schneidewind, Astrid ... TT 12.3
Schnellbacher, Nikolas D. ... BP 24.3
Schnelle, Walter ... MA 42.5
Schnitzlerin, Miriam ... •BP 12.38
Schnitzspan, Leo ... •MA 18.8
Schnorr, Laurin ... •HL 3.7
Schnorrer, Frank ... BP 12.32, BP 13.3
Schnuerer, Matthias ... MA 8.2
Schnupfagn, Christoph ... O 61.4
Schnyder, Andreas P. ... TT 25.5, TT 25.7
Schober, Jan-Christian ... O 56.4
Schobert, Arne ... •KFM 11.3
Schock, Robin T. K. ... •TT 2.2, TT 29.7
Schoeller, Herbert ... TT 11.3
Schoen, Carl-Friedrich ... DS 23.5
Schoenmaker, Steven ... •MA 19.9
Schöffmann, Patrick ... •MA 33.2
Schöll, Eckehard ... SOE 3.4, SOE 3.5,
•SOE 12.1
Schöll, Eva ... •HL 8.1, HL 8.10, HL 17.8,
HL 25.56, HL 26.1
Schöllkopf, Wieland ... O 44.5
Schollwöck, Ulrich ... CPP 40.9, DY 43.5,
TT 39.8
Scholz, Markus ... O 55.15, •O 68.3
Scholz, Monika ... •BP 2.8
Scholze, Frank ... O 13.1
Schön, Carl-Friedrich ... DS 20.7, •O 57.6
Schöndelmaier, Daniel ... HL 25.51,
HL 28.5
Schönenberger, Thomas ... MA 19.6
Schöner, Tobias ... •CPP 12.40
Schönert, Stefan ... DS 13.1
Schönfeld, Dennis ... CPP 7.5
Schönhals, Andreas ... CPP 37.4,
CPP 49.1, MM 18.11
Schönhense, G. ... O 68.10
Schönig, Marco ... O 38.1
Schöniger, Maik ... DS 20.19
Schöning, Sonja ... MA 19.32, MM 18.40
Schoop, Leslie M ... •MM 28.2

Author Index

- Schöpf, Jörg •MA 6.2
Schopmans, Henrik •MM 22.4
Schöppach, Fabian •HL 30.22
Schorlepp, Timo •DY 28.1
Schörmann, Jörg DS 21.1, HL 10.11
Schorre, Florian BP 9.6
Schott, Christina O 33.11
Schött, Johann MA 19.35
Schott, Rüdiger HL 2.5
Schöttke, Fabian •O 73.1, O 73.2
Schöttner, Johannes •DY 46.19
Schötz, Konstantin CPP 12.42, HL 5.3, HL 23.2
Schötz, Simon O 15.2
Schowalter, Marco DS 13.5, DS 20.6
Schoz, Markus O 9.1
Schraa, Lucas CPP 37.6
Schradner, Malte HL 10.12, •HL 10.13, HL 30.18
Schrage, Jenny O 42.1
Schramm, Tim •DS 20.3
Schramma, Nico •BP 4.2
Schran, Christoph O 43.6, •O 46.5
Schraut-May, Lisa •CPP 39.6
Schrautzer, Hendrik •MA 12.12
Schreck, Sabine KFM 18.3, •KFM 25.10
Schrefl, Thomas •KFM 10.4
Schreiber, D. MM 21.7
Schreiber, F. MM 19.63
Schreiber, Felix MA 19.62
Schreiber, Frank CPP 26.5, •CPP 44.1
Schreiber, Lars HL 25.60
Schreiber, Lars R. HL 19.10, HL 36.2
Schreiber, Waldemar HL 30.26
Schreiner, Tino TT 29.16
Schreitmüller, Tobias •HL 3.10, HL 12.4
Schrüder, Alexander •O 53.5
Schrüder, Benjamin O 19.8
Schrüder, Christian DY 5.7, MA 19.37
Schrüder, Philip •TT 30.16
Schrüder, S HL 42.2
Schrüder, Tim HL 26.6
Schrodin, Marcel TT 31.24, TT 31.25, QI 4.32
Schroeder, Jonas DS 16.3
Schroer, Christian CPP 12.39, KFM 3.2, KFM 3.4
Schrüer, Julian •HL 11.4
Schrüfel, Fabian •O 34.1
Schrollner, Daniel HL 25.60, TT 21.21
Schropp, Andreas CPP 12.39, KFM 3.4
Schubert, Alina DS 5.6
Schubert, Jürgen DS 22.5
Schubert, Mathias O 37.7
Schubert, U.S. CPP 12.71
Schubert, Ulrich S. CPP 1.7, CPP 12.50, CPP 12.60, CPP 12.62, CPP 12.63
Schubotz, Simon CPP 17.15, •CPP 20.2
Schuck, Carsten QI 4.24
Schueler, Leonard MA 35.41
Schueller, William SOE 14.0
Schuetze, Yannik CPP 9.14
Schüffelgen, Peter DS 21.2, HL 7.4, HL 19.7, HL 36.6, O 4.3, O 21.4, TT 18.9, TT 32.3, TT 32.7
Schug, Alexander •BP 2.3, BP 7.18, BP 7.26, BP 27.6
Schug, Felix •MA 19.34
Schuh, Dieter HL 40.1, MA 24.7
Schuhmacher, Peter TT 16.6
Schuhmacher, Peter K. TT 16.6
Schuler, Bruno O 18.19
Schüler, Leonard •DS 20.16
Schüler, Michael DY 19.3, O 2.1, TT 24.11
Schull, Guillaume O 18.25, O 35.6, •O 77.1
Schüller, Christian DS 20.27, HL 20.4, HL 25.12
Schuller, Ivan K DS 25.3
Schulli, Tobias HL 35.3
Schulte, Alfons CPP 33.5, CPP 44.3
Schulte, Lennart CPP 17.1, •CPP 17.3
Schulte, Malte G. H. O 18.28
Schulte, Stefan O 55.4
Schultheiß, Jan KFM 2.2, KFM 7.5
Schultheiß, Helmut MA 28.11, MA 35.8, MA 41.1
Schultheiß, Katrin MA 35.8
Schultz, Christof CPP 28.5
Schultz, Johannes •MM 35.9
Schultze, Martin MA 35.33
Schulz, Christian MA 6.4
Schulz, Dennis TT 31.6
Schulz, Fabian MA 21.1, O 33.6, O 64.3
Schulz, Florian HL 33.6
Schulz, Friedemann HL 25.40
Schulz, Johann Friedemann •HL 22.6
Schulz, Martha CPP 41.5
Schulz, Oliver DY 8.9, SOE 6.9
Schulz, Stephan HL 42.1
Schulz, Tobias HL 32.5
Schulze, Celina S. O 49.3
Schulze, Dirk HL 24.5, TT 29.15
Schulze, J. HL 22.1
Schulze, Manuel O 22.3, O 30.4
Schulze, Michael •TT 21.21
Schulze, Patricia HL 23.10
Schumacher, Claus HL 30.47
Schumacher, Hans Werner HL 7.9, MA 5.4, O 2.9
Schumacher, Maren MA 8.1, •MA 35.20
Schumacher, Stefan CPP 40.3, •HL 9.4, HL 21.7, HL 21.9, HL 26.1, HL 26.4, HL 30.2, HL 32.1
Schumacher, Thorsten O 35.8
Schumann, Florian O 66.3
Schumann, Frank Oliver O 73.10
Schumann, Marco •QI 4.28
Schünemann, Alexander TT 20.11
Schunk, Stephan MM 25.4, O 62.6
Schupp, Stefan Manuel •MM 35.3
Schürmann, Hannes HL 30.16
Schusser, Jakob O 4.1, O 48.7, O 73.4
Schusser, Laura HL 25.4
Schusser, Laura Nicolette •HL 25.15
Schüssler-Langeheine, Ch. MA 35.24
Schuster, Constantin •TT 17.4
Schuster, Patrick DS 16.3
Schuster, Rolf •O 38.1, O 38.4
Schütt, Freerk •CPP 12.44
Schütte, Ole M. BP 17.1
Schütz, Emilia HL 30.28
Schütz, Gisela MA 27.3, MA 34.5
Schütze, Adrian DS 22.7, •O 54.2
Schütze, Yannik •CPP 12.26
Schützhold, Ralf TT 13.6
Schwaab, Valentin O 18.27, O 52.3, •O 52.4
Schwab, Jonas •TT 28.3
Schwade, Martin •MM 23.7
Schwaiger, Dominik M. •CPP 49.4
Schwabe, Gerlinde BP 12.55
Schwalenberg, Daniel MM 4.10
Schwalger, Tilo •BP 2.7
Schwan, Lennart MA 19.16, •MA 19.32
Schwartzkopf, Matthias CPP 1.4, CPP 1.6, CPP 12.3, CPP 12.13, CPP 12.64, CPP 12.67, CPP 17.26, CPP 18.3, CPP 19.4, CPP 27.3, CPP 27.4, CPP 28.4, CPP 37.3, CPP 37.6, CPP 48.3, CPP 50.1
Schwarz, D. HL 22.1
Schwarz, Fabian •MM 6.7
Schwarz, Holger •DS 20.43
Schwarz, Lukas TT 3.10
Schwarz, Tim Maximilian •MM 18.28, •MM 32.3
Schwarz, Ulrich BP 12.21
Schwarz, Ulrich S. BP 3.3, BP 5.3, BP 5.7, BP 12.9, BP 22.3, BP 24.3
Schwarz, Ulrich Sebastian BP 19.2
Schwarz, Ulrich T. HL 10.2, HL 10.3, HL 30.13, HL 30.14
Schwarzburg, Klaus HL 13.4, HL 30.42
Schwarze, B.V. TT 20.8, •TT 25.9
Schwarzendahl, Fabian Jan •DY 50.1
Schwarzkopf, Jutta DS 14.2, DS 20.1
schwarzkopf, matthias CPP 12.59
Schweer, Paul •O 52.2
Schweickert, Lucas HL 8.1, HL 8.10, HL 19.2
Schweikert, Christian QI 4.14
Schweinberger, Florian O 56.2
Schweitzer, Frank •SYSO 1.1, •BP 23.3, SOE 5.2, SOE 12.4, •SOE 14.2
Schweitzer, Pascal •CPP 26.4
Schweizer, Christian QI 4.39
Schweizer, Matthias R. •MA 13.9, MA 35.10
Schweizer, Pirmin •HL 22.10, •HL 32.6
Schwendke, Philipp •O 19.2
Schwenke, Alexander •TT 23.1
Schwenke, Philipp •MA 19.40
Schweyen, Peter DS 20.19
Schwibbert, Jakob QI 8.2
Schwier, Frank O 18.21, O 48.10
Schwilling, Patricia BP 12.62, DY 4.4
Schylliga, Patrick HL 30.35
Sciaini, Germán HL 13.2
Sciani, Germán HL 30.44
Sciortino, Alfredo BP 4.3
Scriven, Lorel O 64.3
Sebastian, Hartweg HL 28.3
Seegers, Kai SOE 9.1
Seeja Sivakumar, Nikhil •O 19.3
Seelbinder, Benjamin BP 3.5, DY 4.7
Seema, Seema •MA 23.2
Seemann, Lukas DS 19.4, •DY 43.8
Seemann, Ralf CPP 17.14
Seemann, Susanne BP 12.44
Seemann, Wilken •HL 25.95, •HL 33.8, HL 37.1, HL 37.3
Seewald, Felix •MA 19.21
Seewald, Tobias HL 5.5
Sega, Marcello DY 4.1, DY 4.2
Segev, Mordechai •PLV VII
Segreto, Nico MM 32.3
Segura-Ruiz, Jaime HL 21.11, HL 25.46
Seibel, Christopher MA 8.9, MA 25.5, MA 25.8, MA 35.27, MA 35.28, MA 35.32
Seibel, Johannes DS 5.1
Seibert, Sebastian O 15.3
Seibold, Götz TT 33.12
Seiboth, Jelko •TT 31.13
Seibt, Michael HL 25.36, HL 30.27, HL 30.31, O 20.7
Seick, Cinja MA 35.20
Seide, Ralf HL 25.68
Seidel, Michael HL 25.96, HL 30.41, •O 35.8
Seidel, Robert O 64.1
Seidel, Thomas G. •DY 15.3, DY 15.4
Seidemann, Tim HL 8.7, HL 26.7
Seidl, Angelika HL 40.2
Seidl, Stefan •HL 23.7
Seidler, Inga HL 19.10, HL 25.60
Seifert, Jan BP 9.3
Seifert, Jean-Pierre QI 12.10
Seifert, Johannes Tim •O 17.5, O 28.6
Seifert, M. HL 25.49, HL 33.4
Seifert, Michael MA 35.72
Seifert, Ralf HL 13.9
Seifert, Tom S. •MA 21.6, MA 21.9, •O 47.2
Seifert, Tom Sebastian MA 21.1, O 47.5
Seifert, Udo DY 24.3, DY 24.4, DY 24.5, DY 44.2
Seiffert, Sebastian CPP 2.3
Seiler, Anna HL 29.3, TT 2.9, •TT 2.11, TT 2.13
Seipel, Philipp •KFM 15.7
Seiringer, Robert TT 9.3
Seith, Adrian HL 30.40
Seitz, Hermann MM 24.4
Seitz, Manuel •O 22.5
Seki, Takakazu CPP 37.7
Selbach, Sverre M. KFM 7.3
Selhuber-Uinkel, Christine BP 12.41
Selig, Malte DS 20.12, HL 6.10, HL 11.7, HL 11.10, HL 11.11, HL 25.14, HL 31.4, O 37.4, O 59.1, O 61.2, TT 7.7
Sellies, Lisanne •O 47.9
Sellschopp, Kai MM 20.9, O 49.6
Selter, S. TT 12.11
Selter, Sebastian MA 14.7, MA 14.8, TT 12.10, TT 20.3
Selyshchev, Oleksandr DS 23.1, HL 25.42, •HL 39.1, O 55.7
Selzer, Severin MA 8.4
Semeniuk, Konstantin •O 54.11, TT 6.5, •TT 6.9, TT 22.3
Semisalova, Anna MA 35.34, •MA 35.36
Sen Gupta, Surangana •TT 15.4
Sen, Kaushik O 26.1
Sen, Parongama DY 39.1
Sen, Swati •BP 12.63
Senellart, Pascale HL 19.4
Senf, Felix DY 46.1
Senftleben, Arne BP 7.40, HL 30.39, HL 30.49, HL 30.50, HL 30.51
Seng, Boris MA 12.9
Sentef, Michael DY 43.7, KFM 11.3, •TT 36.2
Sentef, Michael A. MM 9.3
Senyk, Yurii TT 12.10, •TT 20.3
Senyshyn, Anatoliy KFM 25.18, KFM 25.20, •MM 8.2
Seo, Jeong Ah •O 18.9
Seoane, Luis F •SOE 3.2
Seoane Souto, Rubén HL 3.2, HL 3.3
Sepulveda, Pamela MM 20.7
Serebrennikova, Alexandra •CPP 14.5
Sereni, Julian TT 24.8
Serga, Alexander A. MA 13.8, MA 13.9, MA 35.10
Sergey, Brener •TT 38.4
Sergey, Iskakov TT 38.4
Sergii, Urs MA 25.2
Serha, R. O. •MA 35.12
Serha, Rostyslav MA 13.2
Serralta, Eduardo DS 1.5
Serrano, Diana QI 4.9
Serrano Escalante, Valentina •HL 34.6
Serrate, David O 18.13
Servedio, Vito Domenico Pietro SOE 14.4
Serwane, Friedhelm BP 2.5, BP 9.6, BP 9.7
Šesták, Petr •MM 6.4, MM 10.20
Setescak, Christoph •O 4.4, O 21.3
Setvin, Martin O 3.2, O 16.12, O 27.5, O 38.2, O 44.3, O 44.4, •O 44.7, O 44.8, O 53.1, O 57.5
Sevlikar, S. V. MM 21.7
Sewidan, Muhamed •O 59.6
Seyd, Johannes •MA 35.23
Seyed Heydari, Mahsa Alsadat •TT 20.5
Seyller, T. O 41.7
Seyller, Thomas DS 20.29, DS 20.43, DS 22.7, O 18.3, O 18.6, O 18.11, O 41.4, O 54.2
Seyrich, Martin KFM 3.4
Seyring, Martin DS 1.1
Sglavo, Vincenzo Maria MM 24.7
Sha, Mo •KFM 25.16, •O 13.10
Shabbir, Huzaifa •CPP 12.22
Shahib, Sherjeel MM 22.1
Shagle, Salwa •QI 4.4
Shah, Manan •HL 6.2, •HL 30.8, HL 42.5
Shah, Sahil •HL 23.5
Shaharukh, Muhammad CPP 17.32, CPP 17.33
Shahsavar, Azin O 40.4, •O 58.4
Shakirov, Timur CPP 12.23, CPP 12.28, •CPP 41.4
Shall, Johannes HL 12.5
Shamim, Saquib HL 7.5, •TT 32.5, TT 32.8
Shamseldeen Ali Alhassan, Amel •MM 22.6
Shamsulbaharin, Sofia MA 35.67
Shan, Hangyong HL 11.8, HL 15.4, •HL 15.7
Shang, Jiangwei QI 3.5
Shang, Xiaoyue BP 7.4
Shang, Yuanyan MM 17.3, MM 17.5
Shankar, Karthik •CPP 12.54, O 13.6
Shanmugam, Sankaran MM 10.25
Shao, Xuecheng MM 12.9
Shao-Horn, Yang •O 24.1
Shapeev, Alexander MM 20.3, MM 25.6
Shapoval, Oleg DS 20.33, DS 20.37
Shapovalov, Konstantin KFM 7.3
Sharafi, Nahal •DY 8.1, •SOE 6.1
Sharma, A. O 26.2
Sharma, Aakash •CPP 33.2
Sharma, Apoorva HL 25.51, MA 35.49
Sharma, Maneesha •MA 5.3
Sharma, Meenaxi CPP 12.37
Sharma, Mukesh •MA 35.66
Sharma, Nand Lal •HL 3.5, HL 8.3, HL 8.4, HL 8.5, HL 12.6, HL 25.78, HL 25.82
Sharma, Puneet •SOE 15.2
Sharma, Rohit MA 16.9, •MA 35.74
Sharma, Sangeeta HL 11.12, MA 8.1, MA 35.33
Sharp, Ian DS 18.4, HL 18.9, HL 24.8, HL 25.35, HL 42.6
Sharp, Ian D. HL 24.4, HL 24.7, HL 24.9, HL 24.10, HL 42.9, O 8.5
Shcherbakov, Andrii HL 28.6
SHEHAD, SUFYAN •MA 30.1
Shekar, C. •MA 27.1
Shekhar, Chandra TT 25.10

- Shekhar, Pragma TT 32.5, TT 32.8
 Shekhar, S. TT 20.8, TT 25.9
 Shelton, Elijah •BP 2.5, BP 9.7
 Shemerliuk, Yulia TT 3.11
 Shemerliuk, Yuliia MM 18.37, TT 12.10, TT 20.3
 Shen, Chen •MM 33.9
 Shen, Dan CPP 1.11
 Shen, Jun HL 25.38
 Shen, Z.-X. O 9.5
 Shen, Zhi-Xun MA 6.1
 Sheng, Shaoxiang O 78.8, •TT 15.3
 Sheverdyaeva, Polina O 26.4
 Shi, Hao TT 28.10
 Shi, Haofei HL 25.38
 Shi, Hexia •O 6.4
 Shi, Juanzi CPP 12.74
 Shi, L. F. KFM 8.3
 Shi, Li-kun HL 33.2
 Shi, Shan MM 18.32, MM 18.33, MM 35.8
 Shibli, Sakhir •HL 25.34
 Shick, Alexander MA 11.3
 Shih, Ching-Wen HL 12.5, •HL 17.3, HL 25.76, HL 30.3
 Shih, En-Min TT 2.10
 Shimshoni, Efrat TT 33.6
 Shin, Bong Gyu O 65.8
 Shin, ChaeHo HL 19.8
 Shin, Sunghwan O 45.8
 Shinwari, Tauqir MA 19.19
 Shiotari, Akitoshi •O 52.5, O 55.3
 Shipunov, Grigory MM 18.38, TT 3.12, TT 25.3, TT 25.8
 Shiroka, Toni TT 6.8
 Shkodich, Natalia •MM 13.6
 Shnirman, Alexander TT 37.12
 Shohani, Oriël DY 12.2
 Shojakani, Abbas SOE 17.3
 Sholokhov, Dmitriy QI 5.5
 Shomali, Elaheh •O 2.3, O 2.4
 Shornikova, Elena V. HL 39.5
 Shpielberg, Ohad •DY 52.1, •SOE 20.1, •QI 6.11
 Shradha, S HL 42.2
 Shree, Shivangi HL 20.8
 Shubbak, Yahya •DS 20.2
 Shukla, Anmol •TT 39.2
 Shumaly, Sajjad •CPP 7.3, CPP 7.4
 Shvartsman, Vladimir KFM 10.5, KFM 10.6
 Shvartsman, Vladimir V. KFM 25.1, MA 35.67
 Shvets, Igor V. O 23.4
 Shyta, Vira •TT 24.9
 Si, Liang TT 22.9
 Siboni, Henrik •BP 12.25, O 58.15
 Siday, Thomas HL 20.2
 Sidiropoulos, Themistoklis MA 8.2
 Sidler, Elizaveta CPP 12.28
 Siebenkotten, Dario O 59.3
 Siebentritt, Susanne •HL 27.1, HL 34.7
 Sieberer, Lukas DY 3.1
 Siebert, Dustin •HL 3.6
 Siebrecht, Janis •O 7.8
 Stiefke, Thomas HL 4.2
 Siegel, M. MA 35.53
 Siegele, Flora •O 56.3
 Siegert, Marie •CPP 27.1, DS 20.20
 Siegert, Tobias •CPP 12.42
 Siegl, Julian •TT 26.4
 Siegl, Luise MA 7.2
 Siegrist, Theo O 4.1
 Siemann, Gesa MM 23.1
 Sierda, E. •O 6.9, TT 10.7
 Sierda, Emil O 72.5
 Sievers, Sibylle MA 5.4
 Sievers, Tammo •QI 4.34, QI 4.35, •QI 4.36, QI 4.37
 Siewert, Jens TT 30.13, TT 30.14, •QI 9.4, QI 9.6
 Siffit, Markus •QI 4.19, •QI 8.9
 Sigel, Reinhard •CPP 12.19
 Sigger, Florian HL 6.5, HL 6.8, HL 11.5, HL 25.14, HL 25.23, TT 7.7
 Sigl, Lukas HL 6.5, HL 6.8, HL 11.5, HL 25.14, TT 7.7, •QI 3.10
 Sigmund, Ivan •BP 3.6
 Sigrist, Manfred TT 22.6
 Silber, Robin MA 5.1, MA 35.65
 Silies, Martin DS 20.25, HL 11.8, HL 28.7
 Sill, Annekatrin •CPP 13.3, •CPP 33.4, CPP 45.6
 Sillanpää, Mika A. TT 15.5
 Silly, Mathieu O 30.8
 Silva, Andrea DY 28.6
 Silvi, Giorgio QI 4.2
 Silvioli, Riccardo •MA 19.28
 Sim, H. KFM 2.3
 Simanenko, Alexander •O 3.6
 Simmet, Bianca •O 74.9
 Simon, Eszter MA 38.7
 Simon, J. Rika •O 5.2, O 55.12
 Simonato, M. •TT 10.7
 Simonato, Manuel O 72.5
 Simoncelli, Michele MM 18.26
 Simonov, A. KFM 2.3
 Simonov, Arkadiy •KFM 2.6, KFM 11.2
 Simons, Hugh KFM 14.7
 Simpson, Grant O 58.15, O 74.3
 Simpson, Grant J. O 6.1, •O 29.1
 Simson, Clemens MM 20.4
 Sinatkas, G. HL 4.7, HL 4.9
 Sinatkas, Georgios HL 4.8
 Sinelnik, Artem HL 15.1
 Sing, Michael DS 20.34
 Singer, Lennart TT 12.5
 Singh, Ajay HL 34.7
 Singh, Amol MA 6.1
 Singh, Bahadur O 82.6
 Singh, Deepak TT 30.7
 Singh, Karmveer BP 12.4
 Singh, Maanwinder DS 19.1, HL 7.2
 Singh, Malay QI 4.39
 Singh, Ravi Prakash TT 30.7
 Singh, Roshni TT 20.10
 Singh Roy, Monalisa •TT 33.6
 Singh, Sanjay MA 27.8
 Singha, Aparajita MA 2.4
 Singldinger, Andreas HL 30.38
 Singraber, Andreas MM 10.3
 Sinitskii, Alexander O 23.7, O 63.7
 Sinova, Jairo MA 19.9, MA 19.42, MA 19.62, MA 24.10, MA 25.5, MA 34.1, MA 34.5, MA 35.15, MA 35.28
 Sinterhauf, Anna O 18.11
 Šipr, Ondřej MA 13.11, MA 18.2, •MA 24.3, MA 28.13
 Siragusa, Marco VA 2.1
 Sirenko, Andrei •SYOP 1.4
 Siri, Olivier O 12.3
 Sirotti, Elise HL 24.9
 Sirtl, Maximilian T. CPP 19.3
 Sistani, Masjar HL 22.2
 Sittig, Robert HL 12.3, HL 17.1, HL 17.4, HL 17.5, HL 25.70
 Siuda, Emil •MA 29.5
 Sivanesan, Vipilan •CPP 48.4
 Sivankutty, Devika •HL 25.25
 Siviero, Fabrizio VA 2.1
 Sivas, Murat KFM 8.1, O 9.3, •O 78.5
 Sjöqvist, Erik MA 11.2, MA 25.6, MA 38.6, QI 10.9
 Skála, Tomáš O 3.6, O 18.18, O 20.1, O 70.2
 Skogvoll, Ida MA 13.6
 Skokov, Konstantin MA 19.14, MA 19.15, MA 29.1, MA 35.52, MM 18.25
 Skokov, Konstantin P. MA 29.7
 Skolaut, Julian •O 74.6
 Skourski, Y. MA 29.3
 Skroblin, Dieter KFM 3.1
 Skurativska, Anastasiia TT 18.1, •TT 22.6
 Slager, Robert-Jan DS 19.2, HL 14.4, TT 25.2
 Slater, Gary W. CPP 13.4
 Slavin, Andrei N. MA 13.8
 Slawik, Alexander Karol TT 31.7
 Sleziona, Stephan O 48.8
 Sleziona, Vivien MA 21.1, •O 33.6
 Slimi, Younes DS 9.3, DS 20.17, •DS 23.2
 Slot, Marlou TT 2.10
 Slotosch, Thorben •HL 30.23
 Šlouf, Miroslav CPP 45.4
 Slowik, Josef CPP 12.60, CPP 12.62
 Slowik, Josef Bernd CPP 12.63
 Småbråten, Didrik R. O 44.6
 Smallenburg, Frank DY 23.8
 Smarsly, Bernd M. O 20.5
 Šmejkal, Libor MA 19.42, MA 34.1, MA 34.7
 Smerechuk, Anastasiia TT 12.1, •TT 21.23
 Smink, Sander DS 9.5
 Smirnov, Dmitry HL 2.4
 Smirnov, Dmitry S. HL 2.1
 Smirnova, Daria •MM 10.24, •MM 15.1
 Smith, Ana-Sunčana BP 7.23, BP 12.22, BP 12.42, BP 14.4, BP 22.7, CPP 17.22, CPP 17.25, DY 46.16, MM 18.7
 Smith, David M. CPP 17.25
 Smith, David Matthew •CPP 17.22
 Smoliarova, Tatiana •MA 19.23
 Smorka, Rudolf •MA 24.5
 Snegir, Sergii TT 29.6
 Snoeijer, Jacco SYSM 1.3
 Soare, Dominik •TT 31.14
 Soavi, Giancarlo HL 4.4, HL 6.3, HL 15.1, HL 15.8, HL 20.5, HL 25.5, HL 25.7, HL 29.4
 Šobán, Zbyněk MA 29.6, MA 34.7
 Sobral Rey, Laura TT 30.14
 Sobral-Rey, Laura TT 30.13
 Sobucki, Marcel BP 8.2
 Sochor, Benedikt CPP 1.4, CPP 12.3, CPP 12.59, CPP 18.3, •CPP 27.2
 Sodemann, Inti TT 2.7, TT 7.11
 Sodemann Villadiego, Inti •HL 33.2, •MA 16.6, •QI 5.2
 Söderberg, Daniel CPP 12.3, CPP 12.59, CPP 18.3, •CPP 45.1
 Söderberg, L. Daniel •CPP 1.8
 Soederberg, Daniel MA 41.5
 Sofer, Zdenek MA 19.28
 Sofin, R.G. Sumesh CPP 12.58
 Soh, Jian-Rui MA 40.3
 Sohail, Billal •O 40.5
 Sohn, Seoyun •MM 35.8
 Sokalski, Vincent MA 19.2
 Sokeng Djoumessi, Aurelien •CPP 12.62
 Sokolov, Dmitry A MM 21.3
 Sokolova, Anna MA 19.7
 Sokolović, Igor O 16.12, O 27.5, •O 44.3, O 44.4, O 44.8, O 53.1, O 57.5
 Sokolowski, Moritz O 5.8, O 12.8, O 20.8
 Sokolowski, Thomas R. BP 12.57, •BP 24.4
 Sokolowski-Tinten, Klaus MA 25.7
 Sokoluk, Dominik MA 19.53
 Soldemo, Markus O 10.2
 Sole, Ricard •PLV IX
 Soler, Diego O 79.6
 Solignac, Aurélie MA 18.5
 Sollich, Peter DY 23.2, DY 28.5, DY 28.7, DY 31.6
 Solodenko, Helena MM 18.28, •MM 35.2
 Sologub, Sergii •O 18.7
 Soltaninezhad, Mohammad BP 7.33, BP 12.31
 Soltaninezhad, Mohammad •BP 12.29, CPP 12.74
 Softwedel, Olaf CPP 33.4
 Soltwisch, Victor O 13.1
 Solzi, Massimo MA 42.4
 Sombut, Panukorn O 3.3, O 3.8, •O 10.6, O 49.4
 Sommer, Denny MA 8.3
 Sommer, Felix O 59.2
 Sommer, Jens Uwe CPP 12.22
 Sommer, Jens-Uwe BP 8.5, CPP 17.8, CPP 17.15, CPP 20.2
 Sommer, Marco •CPP 12.8
 Sommer, Nils •HL 18.4
 Sommer, Timo •TT 3.7
 Somoza, Alejandro D. QI 4.2
 Sonato, Piergiorgio VA 2.1
 Sonek, Paul Louis •BP 12.53
 Song, Chang-Yun HL 25.32, HL 34.5
 Song, Dongsheng MA 27.6
 Song, Jimin •O 79.7
 Song, Jin-Dong HL 25.74
 Song, Justin C. W. HL 33.2
 Song, Yiming O 17.10, O 22.6, •O 39.4
 Song, Young Jae O 18.9
 Söngen, Hagen O 15.3
 Sonkusare, Reshma •MM 4.1, MM 4.8
 Sonner, Michael DY 5.4
 Sonntag, Selina BP 2.5, BP 9.7
 Soon, Aloysius O 49.1
 Sophie Härtel, Marlene CPP 12.67
 Şöpu, Daniel •MM 30.1, MM 30.5, MM 30.7
 Soraru, Gian Domenico MM 24.7
 Sorgenfrei, Felix •MA 19.35
 Sorn, Sopheap •MA 37.11
 Sorokin, Serhii •MA 4.2
 Sostina, Daria •O 34.4
 Sothmann, Björn HL 25.58, HL 25.83, O 2.4, O 30.2, •TT 1.2, TT 13.2
 Soto-Arriaza, Marco A. BP 12.50, BP 12.51
 Sotskov, Vadim MM 25.6
 Soubatch, Serguei O 18.6
 Soubelet, Pedro HL 11.9, HL 15.2, •HL 25.13
 Soul, Philipp HL 33.3, HL 40.7
 Souliou, Sofia Michaela TT 21.6
 Souliou, Sofia-Michaela KFM 25.21
 Sourjik, Victor BP 12.61, DY 16.1
 Sourpis, Anastasios •CPP 12.11
 Souza, Ivo TT 25.4
 Spachmann, S. TT 12.11
 Spachtholz, Raffael O 47.9
 Spaldin, N. A. MA 33.6
 Spaldin, Nicola •O 44.1
 Spaldin, Nicola N. KFM 7.1
 Spallek, Jan TT 24.4
 Spangenberg, Katharina MM 30.4
 Spanheimer, Kai Luca •CPP 17.21
 Spanier, Lukas CPP 12.65, CPP 28.6
 Spanier, Lukas V CPP 12.45, CPP 12.49, •CPP 12.64, CPP 12.68
 Spanslatt, Christian TT 11.11
 Spantzel, Lukas BP 12.31
 Spasova, Marina MA 19.23, MA 39.2, MM 13.6
 Spasova, Maryna •MA 19.64
 Späth, Andreas BP 25.3
 Späth, Florian •O 56.1
 Späth, Thomas O 22.3
 Speck, Florian O 18.3, O 41.4
 Speckhard, Daniel •O 67.1
 Spedicato, Simone HL 36.4, TT 17.5, TT 17.6
 Speller, Sylvia BP 7.28, BP 7.42, BP 12.43, BP 12.44, DS 5.6, O 17.9, O 34.7, O 59.6
 Spencer, Russell •BP 18.2
 Sperl, Matthias DY 11.8
 Sperlch, Andreas CPP 12.72, CPP 12.73, CPP 12.77, CPP 12.79, QI 4.41
 Sperling, Jan HL 30.2
 Spethmann, Jonas •MA 27.9, O 42.2
 Speticato, Simone TT 17.7
 Spetzler, Benjamin •DS 16.4, •MA 9.3, MA 35.62
 Spiecker, Erdmann O 45.4
 Spiecker, Martin TT 27.1, TT 27.2, TT 31.1, TT 31.2, TT 31.3, TT 37.9, •TT 37.12
 Spiegler, Stefanie BP 12.1, BP 12.16, BP 12.20, BP 12.23
 Spieker, L. MA 25.4
 Spieker, Lea •MA 25.7
 Spieker, Stephan O 34.5
 Spies, Maximilian •HL 30.36
 Spijker, Peter O 15.3
 Spillecke, Lena MA 26.4
 Spinner, Clemens HL 19.1, •HL 35.4
 Spitzer, Nikolai HL 12.1, HL 12.2, •HL 25.64, HL 25.67
 Spitzner, Laurens HL 21.6
 Splettsdoesser, Janine TT 7.5
 Splith, Daniel DS 20.45
 Splitthoff, Lukas J. QI 13.11
 Splitthoff, Lukas Johannes •TT 37.5
 Spohn, Herbert DY 49.9
 Spolenak, Ralph MM 6.7
 Spoltore, Donato CPP 26.1
 Sponfeldner, Lukas •HL 20.8
 Spreafico, Samuele •HL 30.37
 Spreckelsen, Florian •SOE 7.2, •SOE 17.1
 Spree, Lukas O 51.6
 Sprenger, Alexander R. DY 31.7
 Spreyer, Florian HL 33.9
 Spring, Merit •DS 20.34
 Springer, Armin BP 7.42
 Springholz, Gunther MA 31.2, MA 34.7, O 18.18
 Spuri, Alfredo •TT 10.9
 Sreekala, Lekshmi MM 6.9
 Sriarunothai, Theeraphot •QI 1.10
 Srinivasan, Prashanth O 43.2
 srivastava, prashant •O 27.4
 Srot, Vesna O 13.2
 Šrūt Rakić, Iva O 81.2
 Staab, Franziska MA 32.2
 Staacke, Carsten MM 2.4, •MM 14.1
 Staacke, Carsten G. •MM 29.1
 Stachelin, Yannic •HL 39.2
 Stachnik, Karolina KFM 3.4
 Stadler, Fabian •TT 15.6
 Stadtmueller, Benjamin O 16.2,

- O 68.5
 Stadtmüller, Benjamin MA 8.8,
 MA 19.50, MA 25.3, MA 25.5,
 MA 25.8, MA 35.19, MA 35.27,
 MA 35.28, O 2.2, O 5.4, O 9.12, O 17.6,
 O 33.11, O 59.4, O 68.6
 Stahl, Lucas •HL 25.63
 Stähler, Julia O 16.10, O 19.2
 Stamm, Benjamin TT 34.12
 Stamm, C. •MA 25.4
 Stammer, Moritz •BP 9.4, •BP 12.54,
 BP 17.6
 Stamov, Dimitar •BP 9.10, •BP 13.9
 Stampfer, Christoph DS 22.8,
 HL 29.2, TT 10.5, QI 1.2
 Stanczyk, Szymon HL 30.14
 Ständer, C. TT 37.11
 Ständer, Christian •TT 17.9, TT 31.12,
 TT 31.16, •TT 31.17
 Stangier, Dominic KFM 25.6, O 22.1
 Stankeyvych, Andrei CPP 12.79,
 •HL 41.4
 Stanko, Štefan •MM 3.7
 Stannarius, Ralf DY 4.5, DY 4.6,
 •DY 9.1, DY 11.4, DY 11.5, DY 11.7,
 DY 23.5, DY 38.4
 Staño, Roman CPP 13.2, CPP 45.4
 Stapf, Laura TT 21.38
 Stará, Veronika O 12.7
 Starchl, Elias •DY 3.1
 Starikov, Sergei •MM 6.2, MM 15.1,
 MM 15.3
 Stark, Alexander MA 41.4
 Stark, Holger BP 14.9, CPP 20.5,
 DY 4.3, DY 38.3
 Stark, Mate O 34.4
 Stärk, Philipp •CPP 12.2, CPP 12.25,
 •CPP 17.30
 Stark, Thomas DS 5.5
 Stark, Wojciech G. DY 35.5, •O 32.4
 Starke, Jens O 34.7
 Starke, U. O 25.3
 Starke, Ulrich O 41.6, O 41.8
 Starnini, Michele SOE 9.3
 Statz, Martin •TT 2.13
 Stauber, Tobias MA 19.24, •TT 2.14,
 TT 21.27
 Staude, I HL 42.2, O 81.6
 Staude, Isabelle HL 15.1
 Stauffer, Oskar •BP 25.1
 Staunton, Julie •SYUK 1.5, MA 37.4
 Stecher, Maximilian •O 2.5
 Steeger, Paul HL 25.25, •HL 25.26,
 HL 25.27
 Steenbeck, Torben MA 35.57
 Steenekon, Peter DY 12.3
 Stefan Blügel, Stefan MA 24.2
 Stefanidis, Nikolaos •TT 2.7
 Stefanucci, Gianluca O 50.6
 Steffen, Werner CPP 7.3, CPP 17.13
 Steffens, P. MA 14.6
 Stegemann, Bert CPP 28.5
 Stegmann, Philipp HL 3.1, TT 27.9
 Stegmann, Thomas TT 2.4
 Stegmüller, Tobias MM 3.3, •MM 3.4,
 MM 18.9
 Stehl, Willy Frederik HL 2.5
 Stehno, Martin TT 19.2
 Steidel, Jakob •O 40.3
 Steil, Daniel DS 20.16, MA 8.1,
 MA 35.18, MA 35.20, MA 35.41,
 O 2.2, O 2.9, O 9.10, O 16.6, O 16.9,
 O 33.3, O 48.9
 Steil, Sabine MA 35.20, O 2.2, O 2.9,
 O 9.10, O 16.6, O 16.9, O 33.3, O 48.9
 Stein, David •MM 3.1
 Stein, Markus •HL 13.6, •HL 13.10,
 HL 40.1, HL 40.3
 Steinacker, Lorenz DS 9.3
 Steinau, Martin O 82.4
 Steinbach, Daniel DS 9.6
 Steinbach, Felix MA 35.30
 Steinberg, Alina B. •DY 39.3
 Steinberg, hadar TT 10.2
 Steinberg, Jonathan •QI 14.2
 Steinbrecher, M. TT 10.7
 Steinbrecher, Manuel O 25.5, •O 51.4,
 O 51.8, O 72.5
 Steinbrecher, René CPP 12.31
 Steinem, Claudia •BP 17.1
 Steiner, Christian O 6.4
 Steiner, Corinne HL 29.2
 Steiner, Dominik O 65.7
 Steiner, Jacob F. TT 26.8
 Steiner, Johannes HL 13.10
 Steinert, Michael CPP 11.2
 Steingelb, Genrietta •HL 30.11
 Steinhauer, Johann O 52.3, O 56.1
 Steinhoff, Alexander HL 15.3, HL 15.5,
 O 9.8
 Steinhuber, Mathias •DY 5.5
 Steinigeweg, Robin DY 19.4
 Steinmann, Iris DY 45.13
 Steinmann, Ulrike DY 50.9
 Steinrück, Hans-Peter O 12.11,
 O 12.12, O 15.2, O 15.4, O 18.27,
 O 20.2, O 45.3, O 45.4, O 45.7, O 45.8,
 O 45.9, O 52.3, O 52.4
 Steinrück, Elisa CPP 13.5
 Stellbrink, Michael O 2.9
 Stellhorn, Annika MA 33.2
 steizl, Lukas BP 7.14, BP 18.5
 Stender, Patrick MM 10.10, MM 10.14,
 MM 18.28, •MM 22.3, MM 32.3,
 MM 32.5, MM 35.2
 Stenger, Roland DY 45.12
 Stenz, Christian •MM 10.6
 Štěpánek, Miroslav CPP 45.4
 Stepanow, Sebastian O 47.2, O 47.5
 Stephan, Sven HL 11.8
 Šterin, Pavel HL 25.94
 Sternemann, Christian DS 20.14,
 KFM 6.2, KFM 25.7, KFM 25.11,
 KFM 25.13
 Sternemann, Lasse •O 34.9, O 68.9
 Stetsovych, Oleksandr O 51.1
 Stetten, Amy Z. CPP 20.1
 Stettner, Jochim DS 20.4
 Stettner, Monja O 68.7
 Stetzuh, Nele HL 11.12, •MA 35.30
 Steuer, O. •HL 22.1
 Steuer, Oliver HL 25.87
 Stiehl, Martin MA 25.8, MA 35.27
 Stiehm, Noah HL 13.3, •HL 13.5,
 •HL 30.45
 Stiehm, Torsten HL 6.5, HL 6.8
 Stienen, Sven MA 22.7
 Stier, Andreas DS 17.5, HL 11.9,
 HL 20.3
 stier, andreas v. HL 15.2, HL 15.5,
 HL 25.13, MA 19.28
 Stier, Fabian •MA 16.10
 Stierl, Dario •DS 4.3
 Stierle, Andreas O 52.9, O 54.14,
 O 56.4
 Stiewe, Finn-F. MA 35.65
 Stiewe, Finn-Frederik •MA 19.46,
 MA 19.49
 Stilck-França, Daniel QI 8.7
 Stilkerich, Nina •TT 23.6
 Stiller, Peter L. TT 2.1
 Stilp, Fabian O 57.3, •O 57.4, O 82.4
 Stiphout, Koen V. MM 18.13
 Stirnat, Julia TT 22.11
 Stobbe, Julian •TT 16.3, TT 28.11
 Stöber, Jonas •DY 43.4
 Stöberl, Stefan BP 9.6, •BP 12.3
 Stock, Gerhard BP 7.7, BP 7.9,
 BP 7.19, BP 15.6
 Stock, Sebastian CPP 17.19,
 CPP 17.20, CPP 17.21
 Stockburger, Jürgen QI 5.3
 Stocker, Sina •O 62.1, O 62.5
 Stockert, Oliver TT 6.8
 Stockert, Ulrike MM 21.4, •TT 22.5,
 TT 34.2
 Stoev, Iliya •BP 3.5
 Stoev, Iliya D. •DY 4.7
 Stöhler, Jörn •HL 33.1
 Stöhr, Meike •O 5.1, O 5.7, O 15.5,
 O 23.6
 Stöhr, Rainer MA 2.4, QI 5.4
 Stoica, Mihai MM 30.6
 Stoll, A. TT 31.8
 Stölmacker, Christoph HL 30.13
 Stolpp, Jan TT 21.32
 Stolte, Evert •O 34.2
 Stollerfoht, Martin HL 5.8
 Stolz, Samuel O 29.6
 Stolz, Wolfgang HL 13.6
 Stone, Howard MM 10.15
 Stoodley, Matthew A. •O 41.1
 Strack, Alexander G. •MM 21.9
 Straka, Ladislav MA 11.4
 Stralka, Tillmann DS 20.45, •HL 18.10
 Straßburger, Julian •MA 19.17
 Straßheim, M. •MA 19.11
 Strassburg, Martin HL 10.3
 Strassen, Robert •DY 44.16
 Strassheim, Marc MA 19.13
 Strauch, Andreas •HL 21.10, •MM 18.4
 Strauch, Hannah O 2.9, •O 16.6
 Straumal, Boris MM 21.8
 Strauß, Raimund DS 13.1
 Strauss, Dirk KFM 18.3, KFM 18.4,
 KFM 25.10
 Streib, Simon •MA 38.6
 Streibel, Verena HL 24.7, HL 24.9,
 O 8.5
 Streif, Michael •QI 12.5, QI 12.6
 Streit, Achim BP 2.3
 Strelcov, Evgheni TT 2.10
 Streller, Fabian •DS 20.22
 Streller, Matthias •BP 7.31
 Stempel, Klaas DS 2.4
 Stringe, Mark MM 10.8, MM 30.4
 Strinic, Ana •QI 1.3
 Strinic, Anna MA 33.3
 Strittmatter, André DS 6.3, DS 9.2,
 HL 22.9, HL 30.16
 Stritzke, Mandy O 17.5, O 28.6
 Strkalj, Nives KFM 8.6
 Strobel, A. TT 13.5
 Strobel, Tim •HL 26.2, HL 26.3
 Strobl, Clemens •HL 25.3, HL 25.4
 Strocov, Vladimír N. DS 20.36
 Stroganov, Vladislav •CPP 11.2
 Stroh, Karen DS 20.33, DS 20.37,
 DS 20.40, MA 8.1, MA 35.20
 Stroh, Karen P. •MA 35.18
 Strohauer, Stefan HL 36.4, TT 17.5,
 TT 17.6, TT 17.7
 Strohmair, Simone HL 30.32
 Strohmeier, Marcel •TT 7.2, TT 31.26
 Stroschio, Joseph TT 2.10
 Strothmann, Robert •CPP 14.2
 Stroucken, Tineke HL 25.18
 Struck, Tom HL 19.10
 Strunk, C. TT 20.9
 Strunk, Christoph TT 3.2, TT 3.13,
 TT 10.3, TT 19.3, TT 22.7, TT 26.2,
 TT 30.18, TT 30.24
 Strunkus, Thomas CPP 17.26
 Strunskus, Thomas CPP 37.3
 Strunz, Jonas TT 32.5
 Strusch, Tanja MA 35.36
 Stüber, Michael MM 4.8
 Stuckelberger, Michael KFM 6.3
 Stuckert, Rouven DS 9.4
 Studt, Felix •O 69.1
 Stummvoll, Mike O 55.11
 Stumper, Sebastian •TT 33.10
 Stunault, Anne MA 40.3
 Stupakiewicz, Andrzej MA 25.2
 Stupar, Matija O 34.9, O 68.9
 Stupp, Jacob QI 1.11
 Sturm, C. HL 21.1, HL 25.49, HL 33.4
 Sturm, Chris DS 20.47, •HL 9.1,
 HL 9.5, HL 13.9, HL 25.45
 Sturm, Joris •DS 20.12
 Sturmeit, Henning O 12.5
 Style, Robert W. BP 8.6
 Su, Xiaoya •DY 40.2
 Su, Yixi •MA 31.1, TT 8.2, •TT 25.11
 Su, Yuan QI 12.5
 Subakti, Subakti •MM 35.1
 Subramanian, Shruti DS 22.2
 Subramanian, Srikanth •BP 13.2
 Subramanyam, Aparna MM 23.4
 Sudo, Kenta TT 22.11
 Suess, Dieter MA 19.31, MA 35.11
 Sugimoto, Yoshiaki O 52.5
 Suh, Joonki MM 21.1
 Sukhanov, A. S. MA 4.1
 Sukhanov, Aleksandr •TT 23.4
 Sukhanov, Alexandr MA 42.5
 Sukhov, Alexander DY 46.16
 Süllow, Stefan TT 3.8, TT 21.14,
 TT 24.5, TT 30.15, TT 30.16
 Sulmoni, Luca HL 10.6, HL 10.8
 Sumathi, Vasudevan CPP 7.7
 Sumeet, Sumeet •QI 4.3
 Sun, Dianming HL 41.2
 Sun, Fei •MM 21.3, MM 21.4
 Sun, Kun CPP 12.15, •CPP 12.49,
 CPP 17.6, DS 20.50
 Sun, Mengru •HL 30.31
 Sun, Pei-Ling MM 4.2, MM 4.5
 Sun, Shih Jye MA 35.38
 Sun, Shih-jye •MA 18.9
 Sun, Shijie O 79.4
 Sun, Wenbo •O 58.7
 Sun, Yan O 9.4
 Sun, Yue •MA 13.10
 Sun, Yuhao •MA 19.41
 Sun, Zhaozong O 72.1
 Sündermann, Eric •BP 12.16
 Sundermann, Martin KFM 6.2,
 KFM 25.13
 Sundermeier, Jörg O 52.6
 Sundermeyer, Jörg O 5.5
 Sunko, Veronika MA 13.10, MM 21.3,
 MM 21.4
 Supplie, Oliver O 30.6
 Sürgers, Christoph O 34.4, TT 21.21
 Surmeier, Göran BP 12.52
 Surta, T. Wesley MM 10.6
 Sushchyev, Alexander •TT 34.11
 Susilo, Norman HL 10.4, HL 10.7,
 HL 10.10
 Suter, A. TT 22.1
 Sutorius, Anja •MM 13.5
 Sutton, Christopher MM 25.4
 Švec, Martin O 55.14, O 74.10
 Svendsen, Mark Kamper DS 16.2
 Swart, Ingmar O 18.17, O 54.8, O 58.14
 Sweetman, Adam O 14.3
 Sweke, Ryan QI 12.10
 Swiderski, Richard DY 26.4, •DY 44.18
 Swinburne, Thomas SYNMM 1.4
 Sydow, Stephan •CPP 12.5
 Sylvie, Lorthois BP 12.65
 Syskaki, M-A. MA 10.2
 Syskaki, Maria-Andromachi MA 18.5,
 •MA 35.46
 Szabó, Dorothée Vinga MM 17.3,
 MM 18.29
 Széchenyi, Gábor TT 27.10, •QI 3.8
 Szeghalimi, Adriana DS 20.15
 Szeghalmi, A HL 42.2
 Szeghalmi, Adriana DS 21.4
 Szilagyi, Sven BP 9.2
 Szpak, Nikodem •DY 35.9, •TT 2.4,
 •TT 13.6, TT 29.1
 Sztucki, Michael BP 9.5
 Szunyogh, László MA 7.3, MA 15.2,
 •MA 19.38, MA 37.6, TT 1.8, TT 1.9
 Szymanski, Konrad •QI 14.8
 Szymoniak, Paulina CPP 37.4
 T.M. Koper, Marc O 8.6
 T. Margraf, Johannes MM 34.5
 T. N. Ha, Nguyen •O 26.2
 T. P. Ryan, Paul •O 58.11
 Taborelli, Mauro O 13.9
 Taccardi, Nicola O 45.2, O 45.3
 Taché, Olivier KFM 3.1
 Tadano, Terumasa MM 7.2, MM 33.9
 Taftershofner, Nicola •HL 25.35
 Taghizadeh, Alireza DS 16.2, O 81.5
 Tagliabue, Andrea CPP 13.2
 Taguchi, Yasujiro MA 27.2, MA 27.7,
 MA 27.10, MA 33.5
 Tahaei, Ali •BP 27.4
 Taheriniya, Shabnam •MM 20.1
 Tahir, Shabbir MA 39.5
 Tahouni, Farnaz DS 25.3
 Tahouni-Bonab, Farnaz DS 25.1
 Tailleur, Julien SYSM 1.5
 Tajik, Mohammad O 16.3, •O 18.4,
 O 30.2
 Takagi, Hidenori TT 8.7
 Takatsu, Hiroshi TT 12.4
 Takei, Hiroyuki O 23.5
 Takmakov, Ivan TT 27.1, TT 37.12
 Taleb, Masoud O 59.8
 Talebi, Nahid O 59.8, O 78.7
 Talnack, Felix CPP 11.2
 Talwar, Timo •O 20.2
 Tamir, Idan O 19.9, TT 26.8
 Tan, Anne Marie O 18.19
 Tan, Xiaoyue MM 24.5
 Tan, Xin Liang •MA 30.3
 Tânase, Liviu C. O 52.11
 Tang, Gaomin TT 30.6
 Tang, Hua •CPP 1.3
 Taniguchi, Takashi TUT 2.2, DS 17.5,
 DS 22.6, DS 22.8, HL 1.2, HL 6.7,
 HL 11.8, HL 11.9, HL 20.4, HL 20.8,
 HL 25.17, HL 25.19, HL 25.21,
 HL 29.2, HL 29.5, HL 33.3, HL 40.7,
 O 7.4, TT 2.10, TT 2.13, TT 10.3,
 TT 10.4, TT 10.5, QI 1.2
 Taniguchi, Takuya MA 28.3, MA 28.4,
 •MA 35.14
 Tanimura, Katsumi O 33.7, O 68.4
 Tannoury, Lama CPP 17.37
 Tantos, Christos •VA 1.2
 Tänzler, Victor •BP 7.24
 Tao, Cong •MM 24.3
 Tapias, Diego DY 28.5
 Taran, Gheorghe TT 21.21
 Tarasov, Ivan •DS 21.3
 Tarhouni, Karsten O 34.1
 Tariq, Muhammad CPP 41.1

Author Index

- Tas, B. MM 21.7
Tas, Bengü MM 21.6
Taskin, Alexey MA 31.4, MA 31.7, TT 20.4, QI 13.10
Tassel, Cedric TT 12.4
Tassi, Camillo TT 15.5
Tassin, Philippe QI 5.7
Tasto, Janosch MA 39.6
Taubel, Andreas MA 29.7
Täuber, Daniela BP 7.33, BP 7.36, •BP 9.1, BP 12.29, BP 12.31, CPP 12.74
Taubert, Oskar BP 2.3
Taubner, Thomas O 35.2, O 35.3, O 37.2, O 59.3, O 59.5, O 78.1
Tauchert, Sonja MA 8.7
Tauer, Maximilian HL 10.3
Tautermann, Christof S. QI 12.5
Tautz, F. Stefan O 4.3, O 5.5, O 13.5, O 14.4, O 17.3, O 18.6, O 54.12, O 68.7, O 74.11
Tautz, Stefan F. O 54.6
Tavakol, Omid TT 38.2
Tavernelli, Ivano O 62.8
Taylor, Robert HL 25.65
Tayo, Joel O 57.2
Tcakaev, Abdul-Vakhab •MA 31.3
Te Vrugt, Michael •DY 3.3, •DY 44.1, •DY 46.2, •DY 46.3
Team, SPB BP 17.6
Techert, Simone CPP 1.4
Tedeschi, Davide HL 19.2
Tegeder, Petra CPP 39.3, CPP 39.4, CPP 48.4, O 40.2, O 40.3
Tegenkamp, C. O 25.3, O 26.2, O 41.7
Tegenkamp, Christoph DS 20.8, DS 25.4, O 18.7, O 18.8, O 18.14, O 25.6, O 25.7
Tehranchi, Ali •MM 15.5, •MM 20.6
Teichert, Fabian •DS 20.8
Teichgreber, Robin •CPP 12.66
Teichmann, M. MA 25.4
Teichmann, Marlo •O 19.7
Teichmann, Marlo H. O 19.8
Teichmann, Martin MA 25.7
Teichmann, Tim •VA 1.1
Teichrib, Christian DS 20.7, •DS 20.38
Teiwes, Nikolas K. BP 17.1
Teklu, Zekarias CPP 12.60
Telychko, Mykola O 81.1
Temirov, Ruslan O 5.5, O 13.5
Tendick, Lucas •QI 9.9
Teng, Sheng-Han •KFM 8.4
Tenne, Ron HL 40.6
Tepaß, Jannina J. •HL 10.2, HL 30.14
Tepaske, M.S.J. TT 28.4
Terfort, Andreas CPP 39.1
Ternes, Markus O 5.5, O 47.6, O 47.7, O 54.6
Terra, Alexis MM 4.10
Terschanski, Marc MA 35.21, MA 35.22
Teshuva, Simon SYNMM 1.2, •MM 29.3
Teske, Julian D. HL 36.2
Tessarek, Christian HL 33.8, •HL 42.3
Tesser, Ludovico TT 7.5
Tetos, Nikolaos CPP 45.2
Tetzner, Kornelius •DS 6.4
Teubler, Raimund CPP 14.5
Teurtrie, Adrien MM 22.5
Tezak, Nikolai O 73.4
Thakur, Bhumika •DY 18.3, •SOE 10.3
Thakur, Sangeeta MA 19.19, MA 35.25, O 18.22, O 54.7, •O 82.6
Thakur, Tushar •MM 2.7
Thalacker, C. •HL 2.3
Thaler, Marco •O 65.7
Thalheim, Tobias BP 7.43, CPP 12.5, •CPP 49.3
Thalmann, Fabrice BP 2.1
Thalmann, Karin S. O 83.9
Thampi, Arsha •MA 19.5
Thampi, Mithun BP 26.6
Thaomponpun, Jutathip •MA 35.38
Thapa, Manish QI 4.23, QI 6.8
Theis-Bröhl, Katharina MM 4.10
Thelakkat, Mukundan CPP 12.70, CPP 12.78, CPP 41.1
Thelen, Marc •MM 35.7
Théry, Manuel BP 13.10
Theurer, Christoph CPP 39.4
Theurer, Christoph P. CPP 39.2
Thewes, Filipe •DY 23.2
Thiagarajan, B. MM 7.5
Thiaville, Andre TT 13.3
Thiede, Andreas HL 3.6
Thiele, Uwe CPP 7.6, CPP 20.7, DY 39.3, DY 46.3, DY 50.10
Thiemann, Fabian •HL 13.2, HL 30.44
Thiemann, Fabian L. O 46.5
Thiering, Nicola DS 20.14, KFM 6.2, •KFM 25.11, •KFM 25.13
Thiesbrummel, Jarla HL 23.5
Thiyagarajan, Raman KFM 8.3
Thoenness, Julian DY 5.4
Thomale, Ronny MA 16.1, TT 18.1, TT 22.13
Thomann, Carl Arne •O 22.1
Thomann, Kim •BP 25.3, CPP 1.11
Thomas, A. MA 20.4
Thomas, Andy MA 19.5, MA 29.4, MA 29.6, MA 34.7
Thomas, Antony O 12.3
Thomas, Heidi •CPP 12.41, CPP 27.5
Thomas, Priscila F. S. MA 31.9
Thomas, Sinju •HL 25.32
Thomas, Teslin Rose •TT 21.5, TT 30.1
Thome, Ulrich Herbert BP 3.4
Thompson, Joshua J.P. HL 11.8
Thomson, Steven •DY 5.9
Thonig, Danny MA 11.2, MA 25.6, MA 38.6, QI 10.9
Thonke, Klaus HL 18.2
Thorn-Seshold, Oliver BP 17.2
Thorwart, Michael MA 12.7, TT 9.2
Thoss, Michael DY 3.9, DY 19.2, MA 24.5, •TT 7.10, TT 13.4, TT 15.2, TT 16.9, TT 21.10
Thran, Peter CPP 13.3
Thränhardt, Angela DS 20.8
Threadgold, Matthew DY 34.6
Thronberens, Konstantin QI 1.11
Thunström, P. MA 25.4
Thunström, Patrik MA 12.11, MA 19.35
Thurau, Philipp O 19.5
Thürmer, Stephan O 64.1
Thurn, Andreas HL 3.10
Thurn-Albrecht, Thomas CPP 12.70, CPP 41.1, •CPP 41.5
Turner, Stefan SOE 14.4
Thyen, Laurenz •HL 30.24, HL 30.25
Thygesen, Kristian QI 8.3
Thygesen, Kristian S. DS 16.2, O 42.4
Thygesen, Kristian Sommer O 81.5
Tian, Hao •TT 37.4
Tian, Ting CPP 27.3, •CPP 27.4, CPP 48.3, CPP 50.1
tiede, david HL 11.6
Tiemann, Lars TT 2.5
Tietz, Frank KFM 15.7
Tilger, Thomas •CPP 18.2
Tilgner, Andreas DY 34.2
Tilgner, Niclas O 18.3
Till, Sebastian BP 10.3
Tillmann, Wolfgang KFM 25.6, O 22.1
Timm, Carsten TT 30.5, TT 30.8, TT 30.9, •TT 38.1
Timm, Matthew J. •O 69.6
Timmermann, Jakob O 69.8
Timoshenko, Janis O 52.12
Timrov, Iurii MA 11.7, MM 12.1
Tissot, Benedikt •QI 1.4
Tissot, Héloïs O 10.2
Titkov, Ilya E. HL 25.90
Titov, Mikhail MA 18.4
Titvinidze, Irakli MA 31.10
Titze, Tim DS 20.16, MA 35.18, MA 35.20, •MA 35.41
Tiwari, Aarti O 52.11
Tkačik, Gašper BP 24.4
Tkatchenko, Alexandre DY 44.12
Tobias, Steve DY 34.6
Todenhagen, Lina Maria •HL 36.3
Todorova, Mira MM 20.10, MM 33.7, O 38.6, O 64.5
Todt, Juraj O 43.2
Tohamy, Hossam •TT 31.21
Toher, Cormac MM 12.5
Tokita, Alea Miako •O 67.4
Tokunaga, Yusuke KFM 7.1, MA 33.5
Tokura, Yoshinori KFM 2.4, KFM 7.1, MA 27.2, MA 27.7, MA 27.10, MA 33.5
Tolan, Metin KFM 25.7, KFM 25.11, KFM 25.13
Tolić, Iva BP 13.4, BP 23.2
Tolić, Iva M. BP 13.8
Tolmachev, Danil O. HL 39.5
Tomar, Ritu O 12.8
Tomašić, Lucija •BP 23.2
Tömekce, Birce Sena •O 55.1
Tomm, Natasha HL 2.5
Tomut, Marilena MM 10.7, MM 20.1
Ton That, Khai •MA 35.71
Tong, Anh •MA 35.72
Tong, Yujin O 48.8
Toninelli, Costanza •SYPP 1.3
Tonisch, Katja DS 9.3
Tonner-Zech, Ralf HL 21.5, O 41.2
Torche, Abderrezak O 18.24
Tornatzky, Hans HL 18.5
Török, János DY 11.4
Török, Máttyás MA 19.8
Torošyan, Garik MA 19.53
Torres, Jorge •MA 19.19, MA 35.25, O 18.22, O 54.7
Torres, Tomás O 79.6
Torres-Herrador, Francisco DY 8.7, SOE 6.7
Torrihlon, Manuel •VA 1.3
Torsi, Riccardo O 18.19
Torta, Pietro •QI 12.11
Tosatti, Erio DY 28.6
Toscano-Tejeda, Diana DY 45.13
Toschi, Alessandro TT 16.4, •TT 16.10, TT 21.29, TT 21.30
Tosi, Ezequiel O 54.5
Tosoni, Sergio •O 40.9, O 69.3
Tosun, Ahmet HL 5.7, •HL 30.32
Tóth, Géza QI 8.6, QI 8.8, •QI 14.7
Totz, Jan •BP 19.5
Tour, James M. O 74.2
Tovey, Samuel DY 8.7, SOE 6.7
Toyoda, Shingo KFM 2.4, MA 13.10
Trabs, Matthias KFM 3.2
Traeger, Georg O 19.7
Traeger, Georg A. •O 19.8
Trahms, Martina O 53.4, •TT 26.8
Traiphol, Nisanart CPP 12.33, CPP 12.34
Traiphol, Rakchart CPP 12.33, CPP 12.34
Trakala, Marianna BP 23.2
Tran, Loi V. •O 66.6
Tran, Mai BP 26.3
Trapp, Julian HL 30.6
Trassin, M. KFM 2.3
Trassin, Morgan DS 13.3, KFM 8.6, KFM 14.2, KFM 14.3, KFM 19.3
Trauzettel, Björn TT 30.8, TT 32.5
Trebst, Simon MA 19.33, TT 21.15
Trefflich, L. HL 21.1
Trefflich, Lukas HL 25.45
Treit, Michael MM 4.10
Trempler, Philip MA 7.1, MA 19.45, MA 19.57, MA 28.5
Trényi, Róbert •QI 8.6
Tresca, Cesare TT 3.3
Triclin, Sarah BP 13.10
Trifonov, Artur V. HL 5.2
Trinker, Florian O 64.1
Tripathy, Madhusmita •CPP 12.27
Tripp, Matthias W. CPP 39.1
Triscone, Jean-Marc DS 25.1
Trishin, Sergey O 71.5
Trittel, Torsten •DY 11.5, DY 11.7, DY 38.4
Trivedi, Rahul HL 8.1, HL 25.65
Trivini, Stefano O 22.4, O 51.5, O 51.9, O 80.7
Trocha, Piotr MA 29.5
Tröger, Lucas •BP 12.5
Troglia, Alessandro •DS 1.2
Trommer, Clara O 18.22
Trommer, Clara W.A. MA 19.19
Troncoso, Roberto E. MA 24.9
Trosman, Oleg DY 46.16
Trotta, Rinaldo HL 8.1, HL 8.10, HL 19.2
Troue, Mirco HL 6.5, HL 6.8, HL 11.5, HL 25.14, •TT 7.7
Trunschke, A. KFM 11.4
Truong, Dong-Juunn Jeffery BP 12.59
Trupinic, Monika BP 13.4
Trupke, Michael QI 1.4
Tsarapkin, Aleksei •O 35.4
Tschurikov, Xenia BP 26.3
Tschurl, Martin •O 3.4, O 42.5, O 56.5, O 70.4, O 70.6
Tseng, Hsin •CPP 1.9, HL 28.2
Tshintzis, Athanasios •HL 3.2, HL 3.11
Tsirkin, Stepan S. TT 25.4
Tsilin, Alexander A. TT 8.5, TT 39.4
Tsitilianis, Constantinos CPP 12.35
Tsitiliani, Ivan QI 4.39
Tsotsalas, Manuel O 79.7
Tsud, Nataliya O 3.6, O 12.11, O 20.1, O 70.2
Tsurkan, V. TT 8.1
Tsurkan, Vladimir KFM 14.1, MA 14.5, MA 32.5, MA 33.1, MA 33.3, MA 33.4, TT 3.5
Tszuki, Takahiro KFM 2.7, •MM 10.19
Tu, Suo CPP 1.6, CPP 27.4, •CPP 48.3
Tubandt, Tobias MA 35.65
Tuchecker, Paul K. MM 21.9
Tucholski, David •MM 2.3
Tuczek, Felix MA 19.19, O 18.22
Tuinier, Remco DY 23.3
Tumino, Francesco O 40.9
Tuniz, A HL 42.2
Turaev, Michael •TT 6.12
Turchanin, A HL 42.2, O 81.6
Turchanin, Andrey CPP 11.2, CPP 17.2, DS 20.27, HL 4.4, HL 6.4, HL 25.17, HL 25.21, HL 42.7, O 65.4, O 65.5
Turco, Elia O 17.12
Türk, Hanna MM 34.8, •O 49.8
Türkyay, Deniz HL 5.11
Turnbull, M.M. TT 28.4
Tusche, C. O 68.10
Tusche, Christian MA 30.3
Tuttles, Ute MM 32.5
Tüysüz, Harun O 70.9
Tverdokhle, Nina •CPP 49.2
Tvingstedt, Kristofer CPP 19.3
Tybell, Thomas KFM 7.6
Tyberkevich, Vasily S. MA 13.8
Tyler, Bonnie MM 30.8
Tyler Lindemann, Tyler TT 22.7
Tymoshenko, Yuliia TT 21.12, TT 23.4
Uaman Svetikova, Tatiana Aureliia •HL 25.41
Ucar, Mehmet Can •BP 27.2
Uday, Anjana •MA 31.4, MA 31.7, TT 20.4, QI 13.10
Uderhardt, Stefan BP 12.38
Udod, Tetiana •BP 9.8
Udvardi, László •MA 19.8, MA 37.6
Udvarhelyi, Péter MA 2.4
Uecker, Reinhard DS 20.32
Ueda, Hiroki MA 25.2
Uehlein, Markus •O 16.5
Ueltschi, Daniel MA 14.2
Ufer, Maximilian TT 30.18
Ugeda, Miguel •O 25.2, O 48.6
Ugokwe, Chikezie Williams •CPP 12.50
Uhlarz, M. TT 20.8, TT 25.9
Uhlenbruck, Sven MM 8.4
Uhlig, Lukas HL 10.2, •HL 30.13, HL 30.14
Uhlig, Thomas DS 20.43
Uhlig, Tino MA 22.6
Uhlmann, Petra CPP 20.2
Uhrig, Goetz S. MA 38.3
Uhrig, Götz S. MA 28.10, TT 23.10, TT 23.11, TT 34.13
Újfalussy, Balazs MM 23.3, TT 1.8, •TT 1.9
Ullmann, Fabian HL 30.15, O 13.8, •O 57.2
Ulrich, Aladin HL 28.4, •MA 39.3
Ulmsperger, T. HL 42.2
Ull, Andreas O 35.3
Ulreich, Manuel O 10.6
Ulrich, Nils CPP 12.3
Ulrich, Sven MM 4.8
Ulstrup, S. O 68.10
Ulstrup, Søren O 9.2, O 54.1, O 72.4, O 73.8
Umansky, Vladimir TT 11.11
Undeutsch, Gabriel SYED 1.2
Ungeheuer, Arne HL 30.39, •HL 30.49, HL 30.50, HL 30.51
Unger, Eva CPP 28.5
Unger, Ralph-Stephan DS 6.4
Unglert, Nico MA 40.1
Ünlü, Feray MM 18.42
Unruh, Tobias CPP 33.6
Ünzelmann, Maximilian O 4.1, •O 4.2, O 73.4
Uola, Roope QI 4.20
Uphues, Thorsten MM 22.7, O 58.2
Uranagase, Masayuki KFM 2.7, MM 10.19
Urbakh, Michael O 39.4
Urban, Alexander HL 32.3, HL 32.4
Urban, Alexander S. HL 30.38
Urban, Daniel •HL 19.6, HL 30.1, HL 36.1, MM 8.1, MM 8.3, MM 8.5,

Author Index

- MM 14.3, •MM 24.1, MM 24.2,
MM 24.3, MM 33.6, Q1 12.2
- Urban, Joanna HL 23.6
- Urbánek, M. MA 35.12
- Urbánek, Michal MA 28.6, MA 35.11
- Urbani, Maxence O 79.6
- Urbaszek, Bernhard HL 20.8
- Urbina, Juan-Diego DY 5.5, DY 5.10
- Urcan, Özlem •CPP 17.33
- Urdaniz, Corina O 51.6, •O 54.3
- Ureña Marcos, José Carlos DY 46.4
- Uriarte Amiano, Unai O 51.10
- Uriarte-Amiano, Unai O 80.1
- Urizar-Lanz, Iñigo Q1 8.8
- Urteaga, Raul CPP 12.38
- Ushakov, Ivan •KFM 7.6
- Usman, Arslan HL 25.16
- Ustinov, Alexey V. TT 26.1, TT 27.5,
TT 27.6, TT 31.19, TT 31.21, TT 37.3,
TT 37.10, TT 37.12
- Utt, Daniel T. MM 30.3
- Uykur, Ece TT 39.4
- V. Campos, João MM 18.23
- v.d. Avoird, Ad O 51.4
- v. Helversen, Martin Q1 7.9
- v. Korff Schmising, Clemens MA 8.3
- v. Malotki, Stephan MA 37.9
- v. Mullekom, Niels P.E. O 51.4
- v. Pylypovskiy, Oleksandr MA 10.3
- V. Roth, Stephan CPP 12.67, CPP 28.4
- V. Spanier, Lukas CPP 12.67
- V. Ustinov, Alexey TT 31.20
- v. Weerdenburg, Werner M.J. O 51.4
- v. Zimmermann, Martin KFM 25.5
- Vaal, Elmore Q1 13.9
- Vaccario, Giacomo SOE 12.4
- Vachier, Jeremy •BP 4.5, BP 12.60
- Vaerst, Olivia •MM 10.5
- Vafae-Khanjani, Mehran MA 12.9
- Vagias, Apostolos CPP 12.65,
•CPP 20.4, CPP 28.8
- Vahidzadeh, Ehsan O 13.6
- Vaidya, M. MM 21.7
- Vaitsi, Alkisti •MA 21.1, O 33.6
- Vajdi Hokmabad, Babak DY 31.4
- Vajner, Daniel •HL 17.10
- Valadkhani, Adrian •TT 3.6
- Valášek, Michal O 61.5, O 61.7, O 74.6
- Valencia, Ana M. CPP 12.44, O 5.2,
O 55.12
- Valencia, Ana Maria MM 10.27
- Valenti, Francesco TT 27.1, TT 37.12
- Valenti, Roser MA 16.7, TT 3.6,
TT 8.4, TT 22.13, TT 39.3, TT 39.5
- Valentin, Sascha René HL 2.5
- Valerius, Philipp O 65.1
- Valero, Rosendo O 62.7
- Valiullin, Rustem O 63.3
- Valls Mascaro, Francesc O 8.6
- Valsson, Omar CPP 41.6, DY 28.3
- Valvidares, M. MA 27.1
- Valvidares, Manuel MA 23.3
- Vamvakaki, Maria CPP 20.4
- van Aken, Peter DS 14.4
- van Aken, Peter A. DS 9.5, O 13.2
- Van Avermaet, Hannes KFM 11.5
- van Buel, Reinier •DY 38.3
- van de Groep, Jorik DS 1.2
- van de Kerkhof, Gea CPP 8.4
- van de Walle, Chris O 64.5
- van den Brink, Jeroen DY 3.4,
MA 10.3, MA 18.7, O 43.8, TT 11.6,
TT 11.8, TT 11.9, TT 20.2, TT 21.15,
TT 24.9, TT 25.2, Q1 6.9
- van der Brink, Jeroen TT 3.12
- van der Heide, Tammo •O 58.6,
O 58.7
- van der Kolk, Jasper DY 26.4
- Van der Laan, G. MA 27.1
- van der Laan, Gerrit MA 17.3,
•MA 20.5
- van der Meer, Jann •DY 24.5, DY 44.2
- van der Schoot, Paul DY 23.9
- van der Vegt, Nico CPP 9.8
- Van Der Vegt, Nico F. A. CPP 9.4,
DY 38.6
- van der Vegt, Nico FA CPP 12.27
- van der Zant, Herre DY 12.3, •DY 12.6
- van Efferen, Camiel •O 18.16, O 71.4
- van Heck, Bernard TT 37.5
- van Helvoort, Antonius KFM 14.6
- van Helvoort, Antonius T.J. KFM 7.5
- Van Kuiken, B. MA 25.4
- van Kuiken, Benjamin MA 25.7
- van Lange, Victor HL 25.50
- van Loon, Erik KFM 11.3, TT 12.9,
•TT 16.2
- van Loosdrecht, Paul H.M. MA 6.2,
TT 21.15
- van Meege, Alex DY 3.5
- van Mullekom, Niels P.E. O 25.5,
•O 51.8
- van Stiphout, Koen •KFM 6.1
- van Straten, Duco MA 27.12
- van Waas, T. P. O 66.2
- van Weerdenburg, Werner M.J.
•O 23.1, •O 25.5, O 51.8
- van Wezel, Jasper DY 3.4, TT 11.6,
TT 39.6
- Vana, Philipp KFM 15.4
- Vandamme, Matthieu CPP 9.9
- Vanderlinden, Willem BP 15.1
- Vanderstraeten, Laurens MA 16.3,
MA 16.5
- Vandewalle, Nicolas DY 44.9,
DY 46.16
- Vandré, Lina Q1 7.5, •Q1 7.7
- Vanossi, Andrea DY 28.6
- Varanasi, SR CPP 12.58
- Varbaro, Lucia DS 25.9
- Vardhan, Vaishali HL 17.1
- Varjas, Dániel TT 25.13
- Varma, Kaarthik DY 50.7
- Varotto, Sara O 44.10
- Varoutis, Stylianos VA 1.2
- Varrasi, Lorenzo •HL 21.8
- Vasconcelos, Samuel •O 6.7
- Vaßen-Carl, Max •HL 36.6, O 21.4
- Vasilenko, Evgenij •Q1 4.12
- Vasilyev, D. O 68.10
- Vasin, Kirill •MA 33.3, MA 33.4
- Vasylieva, Olga HL 25.79
- Vasyuchka, Vitaliy MA 19.43,
MA 35.50
- Vaxevani, Katerina O 22.4, O 51.5,
•O 51.9, O 80.7
- Vaynzof, Yana DS 20.3
- Vayrynen, Jukka TT 1.13
- Väyrynen, Jukka I. TT 32.8
- Vazquez, Hector •O 11.5
- Vazquez-Miranda, Saul •O 15.8
- Vecchione, A. MM 7.5, TT 22.1
- Vecchione, Antonio TT 22.2
- Vedmedenko, Elena TT 19.4
- Vedmedenko, Elena Y. MA 27.9
- Vegge, Tejs O 44.6
- Vegliante, Alessio •O 51.3, O 51.10,
O 80.1
- Veit, Max O 43.4, •O 43.5
- Veit, Peter DS 2.3, DS 6.3, HL 30.16
- Veith, Lothar HL 5.5
- Vekariya, Yagnika •HL 25.19
- Veldman, Lukas O 47.6, •O 47.7
- Veldman, Lukas M. O 47.3
- Veldscholte, Lars SYSM 1.3
- Vélez, Saül DS 13.3
- Venanzi, Tommaso •HL 11.10,
HL 25.17
- Vennema, Hester •O 34.3
- Venturini, Rok O 48.10
- Ventzke, Roman David BP 13.7
- Vepsäläinen, Antti Q1 4.23, Q1 6.8
- Vera, Alexander DS 20.39, DS 22.2,
DS 22.4
- Verba, Roman MA 28.2
- Vercelli, Gabriel DY 39.6
- Vereijken, Arne •MA 19.2, MA 35.64
- Vergniory, Maia •SYQM 1.1
- Verlhac, Benjamin MA 30.5, O 51.8,
•O 53.3
- Verma, Sandeep O 15.7
- Veroutis, Emmanouil O 28.5
- Verstraete, M.J. HL 21.12
- Verstraete, Matthieu J. MM 28.4
- Vértesi, Tamás Q1 8.6
- Verzhbitskiy, Ivan MA 18.3
- Vescan, Andrei DS 3.3
- Vetrik, Miroslav CPP 45.4
- Vettori, Marco HL 25.50
- Veyrat, Arthur •TT 3.12, TT 25.8
- Veyrat, Louis DS 20.34
- Vezzoni, Vincenzo MA 42.4
- Vicente-Arche, Luis M. O 44.10
- Vidal, Julien TT 5.7
- Vidal-Dupiol, Jeremie BP 9.5
- Vieffhues, Martina BP 12.49, BP 12.66
- Vieira, Rafael •MA 29.8
- Vielmetter, Michel Q1 13.9
- Vierck, Paula •HL 10.8
- Viertel, Klaus CPP 17.39
- Vieyra, Hugo MA 29.9
- Vigneau, Florian Q1 4.23, Q1 6.8
- Vignolini, Silvia CPP 8.3, CPP 8.4
- Vijaya Prakash, Gaddam HL 30.30
- Vijayan, Ponraj •HL 12.3, HL 17.1,
HL 17.5
- Vilardi, Demetrio TT 16.10, TT 21.30
- Vilas Varela, Manuel O 51.10
- Vilas-Varela, Manuel O 18.13, O 80.1
- Vilfan, Andrej BP 4.7
- Vilgis, Thomas A. CPP 17.11,
CPP 17.24
- Villafañe, Viviana HL 11.9, HL 15.5,
•HL 25.65, HL 26.6
- Villiou, Maria BP 12.41
- Vilsmeyer, Franz •MA 28.4
- Vinai, Giovanni MA 17.3
- Viñas Boström, Florinda •HL 3.11
- Vincent, Olivier MM 10.16
- Vines, Francesc O 62.7
- Vinogradova, Olga •MM 33.8
- Vion, Denis TT 37.7
- Vir, P. MA 27.1
- Virnaou, Peter MA 12.9, MA 37.7
- Vishina, Alena MA 32.6, •MA 32.7
- Vishnu, Jude Ann •CPP 17.40
- Višňák, Jakub O 65.5
- Viswanathan, Venkatasubramanian
MM 33.8
- Vitale, Francesco •HL 4.2, HL 4.4
- Vitalie, Nedelea •HL 2.4
- Vitaloni, Andrea CPP 12.46
- Vitroler, Daniel •HL 25.54
- Vlček, Vojtěch MM 12.4
- Vo, Trung-Phuc •O 73.9
- Vocaturu, Riccardo •TT 3.3
- Vögel, Domenik CPP 12.75
- Vogel, Michael CPP 13.5, DY 28.4,
DY 40.7, DY 44.6, DY 44.11, DY 46.9,
KFM 15.7, •MA 13.1, MA 19.2,
MA 27.5, MA 35.47, MA 35.64
- Vogel, Nicolas CPP 8.2
- Vogel, Peter •CPP 17.31
- Vogel, Tobias HL 42.7
- Vögl, F. HL 2.3
- Vogl, T. O 81.6
- Vogt, Nicolas Q1 4.2, Q1 10.3
- Vogt, Patrick DS 20.6, DS 26.1,
DS 26.2
- Vogt, S. HL 18.3
- Vogt, Sofie DS 20.45
- Vogt, Ulrich KFM 3.4
- Voigt, Axel DY 46.2
- Voigt, Hendrik •MM 30.2, MM 30.8
- Voigtländer, Bert •O 4.3
- Vojta, Matthias TT 6.3, TT 24.2,
TT 24.4, TT 24.13
- Volčič, Jurij Q1 9.1
- Volckaert, K. O 68.10
- Volckaert, Klara O 9.2, •O 73.8
- Volk, Christian HL 29.2, Q1 1.2
- Volk, Talia BP 8.9
- Volkert, Cynthia MM 9.2
- Völk, Tobias HL 6.7, •TT 7.6
- Volkmann, Ulrich G. BP 12.50,
BP 12.51
- Volkmer, Dirk CPP 17.4
- Völkner, Christian BP 7.42, BP 12.43,
BP 12.44
- Volkov, Mikhail MA 8.7
- Vollgraff, Tobias O 52.6
- Vollmer, Doris CPP 7.2, CPP 7.4,
CPP 7.8
- Vollmer, Jürgen DY 11.6
- Vollmer, Sergej HL 4.6
- Vollroth, Lucas MA 8.12, •MA 19.26
- Volmer, Frank DS 22.8, HL 29.2
- Volobueva, Evgeniia •MM 10.10
- Volz, Kerstin HL 13.6
- Volz, Matthias •MA 35.4
- Völzer, Tim •DS 5.6
- von Allwörden, Henning O 19.3
- von Bergmann, Kirsten •MA 17.4,
MA 27.9, MA 34.2, O 42.2
- von Delft, Jan TT 16.4, TT 16.11,
Q1 3.10
- Von den driesch, Nils HL 25.84,
HL 38.8, Q1 1.7
- von der Lehr, Fabrice BP 2.3
- von der Oelsnitz, Erik DS 5.6
- von Eysmond, Hendrik •BP 3.8
- von Freymann, Georg MA 13.9,
MA 19.50, MA 35.10
- von Helversen, Martin •DS 17.4,
HL 30.7
- von Klitzing, Regine CPP 2.3,
CPP 12.1, CPP 17.19, CPP 17.20,
CPP 17.21, CPP 18.2, O 58.13
- von Korff Schmising, Clemens
MA 8.2, MA 35.30
- von Oppen, Felix O 71.5, O 80.4,
TT 26.8
- von Reppert, Alexander DS 20.41
- von Roeder, Maximilian •DS 23.3
- von Rüling, Florian •BP 14.10, DY 31.2,
•DY 50.9
- von Seggern, Rieke •MA 19.54,
MA 21.3
- von Toperczer, Florian MM 18.42
- von Wenckstern, H. HL 18.3, HL 21.1,
HL 30.20
- von Wenckstern, Holger DS 20.45,
HL 18.7, HL 30.21, HL 30.22,
HL 30.23, HL 30.24, HL 30.25
- Vona, Cecilia HL 11.3
- Vonbun-Feldbauer, Gregor MM 20.4,
•MM 20.9, O 31.2, •O 49.6
- Vondráček, Martin •O 18.18, O 18.20
- Vondrák, Martin MM 10.1, •MM 34.5
- Vonk, Vedran O 54.14
- Vonrüti, Nathalie O 44.6
- Vool, Uri HL 25.78, •Q1 8.1
- Vorndamme, Patrick DY 5.7
- Vorobiev, Alexei CPP 27.2
- Vorobyov, Vadim •Q1 5.1
- Vorokhta, Mikhailo HL 5.4
- Vorokhta, Mykhailo O 3.6
- Voronenko, Maria MM 8.9
- Voronov, Andrey •MA 19.31
- Vos, Bart BP 7.2, •BP 12.17
- Voss, Jan N. TT 37.10
- Voss, Jan Nicolas TT 26.1, •TT 37.3
- Voss, Johannes O 27.1
- Voss-Boehme, Anja BP 7.31, BP 10.7
- Voss-Böhme, Anja BP 10.6
- Vosse, Gerrit O 59.7
- Vozmediano, Maria A.H. KFM 8.5
- Všianská, Monika MA 11.4, MM 6.4
- Vu Thanh Trung, Nam MA 18.3
- Vučković, Jelena HL 8.1
- Vuilleumier, Rodolphe O 31.7
- Vujičić, Nataša O 81.2
- Vyalikh, D.V. MA 35.24
- Vyborny, Karel MA 18.6
- Waack, Jan M. •MM 6.6
- Waag, Andreas •DS 2.4
- Wächtler, Christopher w. DY 45.7
- Wacker, Andreas HL 4.3
- Waentig, Albrecht O 29.5
- Wagener, Martin MA 28.2
- Wagner, Andreas KFM 3.3
- Wagner, Barbara CPP 17.14
- Wagner, Bettina HL 25.16
- Wagner, Christian BP 3.7, O 5.5,
O 13.5, O 14.4, O 17.3, •O 74.11
- Wagner, Erik •TT 23.8
- Wagner, Guntram DS 20.43
- Wagner, Laura DS 18.4
- Wagner, Laura I. HL 24.4, HL 24.7,
•HL 24.9
- Wagner, Lukas HL 26.2, •HL 26.3
- Wagner, Margareta O 15.2, O 32.9,
O 38.2, •O 49.10
- Wagner, Markus R. HL 18.5, HL 37.1
- Wagner, Michael TT 25.6
- Wagner, Stefan KFM 15.4, MM 17.3,
MM 18.18, MM 18.29
- Wagner, Thorsten O 17.9
- Wagner, Timo HL 25.69
- Wagner, Tobias •MA 35.45
- Wagner, Victoria DS 13.1
- Wagstaffe, Michael O 52.9
- Wahada, Mohamed Amine MA 18.1,
•MA 24.4
- Wahl, Jan CPP 28.7
- Wahl, Sophia •DS 20.7, O 59.3
- Waibel, Martin CPP 28.7
- Wakerlin, Christian O 51.1
- Walczak, Aleksandra BP 6.7
- Waldeck, David O 26.8
- Waldendy, E. TT 12.11
- Waldmann, Oliver MA 19.22, MA 26.2
- Waldow, Diana MM 18.31
- Waldsauer, Tim •DS 20.35
- Waleska, Natalie O 52.4
- Waleska, Natalie J. O 18.27, •O 56.1
- Walk, Nathan Q1 4.8
- Walker, Marc O 41.1
- Walkup, Daniel TT 2.10
- Wallauer, Robert O 33.7, O 68.4,
O 68.7
- Wallerberger, Markus TT 16.11,
•TT 16.12
- Wallmeyer, Bernhard BP 19.8

Author Index

- Wallner, Florian•Q1 4.39
 Wallnöfer, Julius•Q1 4.8
 Walls, Brian O 23.4
 Walowski, Jakob MA 8.12, MA 19.3,
 MA 19.26, MA 19.46, MA 19.48,
 MA 19.49, MA 19.54, MA 19.61,
 MA 21.3, MA 35.33, MA 35.65
 Walraven, Etienne F. O 51.4
 Walshe, Killian O 23.4
 Walt, Marina Q1 4.2
 Walter, Marcel MA 19.19, •O 18.22,
 O 54.7
 Walter, Michael CPP 12.20, CPP 14.4,
 CPP 40.7
 Walters, Andrew C. MM 7.4
 Walther, Eva O 17.6, O 33.11
 Walther, Franziska TT 21.6
 Walther, Jonas•BP 12.42
 Walther, Matthias R. TT 23.10,
 •TT 23.11
 Walther, Matthias Reimund TT 5.7
 Waluk, Jacek O 74.7
 Wambold, Raymond HL 18.1
 Wan, Chenghao HL 18.1
 Wan, Wen O 25.2, •O 48.6
 Wand, Tobias•SOE 12.2
 Wandelt, Klaus O 20.8
 Wang, Chunlei O 3.8, •O 10.2, O 10.6,
 O 49.4
 Wang, Dongfei MA 35.71, •O 22.4,
 O 51.9
 Wang, Dongze•HL 25.88
 Wang, Feifan HL 23.6, •HL 23.9
 Wang, Hao•MA 15.8
 Wang, Heng HL 10.3
 Wang, Hongguang DS 9.5
 Wang, Hsin-Yi O 27.1
 Wang, Jing•DY 4.5
 Wang, Ke•MM 8.10, •MM 18.20
 Wang, Lichen MA 6.4
 Wang, Lingyan DS 20.1
 Wang, Liran TT 39.2
 Wang, Nanlin TT 3.10
 Wang, Peixi•CPP 17.17, CPP 20.4,
 CPP 44.4
 Wang, Q. MA 35.12
 Wang, Qi MA 13.2, MA 19.31,
 •MA 28.6, MA 35.11
 Wang, Qiang•O 32.7
 Wang, Qiankun O 5.7
 Wang, Shizhe HL 5.9
 Wang, Shu Min Q1 5.7
 Wang, Shuanglong HL 30.33
 Wang, Shun KFM 15.5, MM 18.22
 Wang, Taowen HL 34.7
 Wang, Wen O 39.6
 Wang, Xiangzun DY 45.4
 Wang, Xiao•MA 16.9, TT 8.2
 Wang, Xiao-Ye O 12.6, O 55.10
 Wang, Xing O 79.3
 Wang, Yanggang O 62.7
 Wang, Yankun•DS 20.1
 Wang, Yazhong CPP 26.1
 Wang, Yi DS 14.4
 Wang, Yinan HL 12.7, •HL 25.85
 Wang, Ying HL 35.4
 Wang, Yiran MA 35.42
 Wang, Yu O 5.3
 Wang, Yude KFM 15.1, KFM 25.15,
 MM 8.6, MM 18.19
 wang, yuemin O 30.7, O 70.8, O 79.7
 Wang, Yuhan HL 22.5, O 82.7
 Wang, YuHuang HL 30.6
 Wang, Yujiao CPP 7.4
 Wang, Yutong•BP 7.33, BP 12.31
 Wang, Zhen CPP 8.3
 Wang, Zhenjiu•TT 24.3
 Wang, Zhenyu•O 38.6
 Wang, Zhichang O 44.7, O 57.5
 Wang, Zhiyong HL 42.8
 Wang, Zidong•KFM 15.1, •MM 18.19
 Wang, Zunhao O 35.1
 Wanierke, Friedrich O 18.26
 Wanisch, Darvin•Q1 10.6
 Wanjura, Clara C. DY 46.6
 Warburton, Richard J. HL 19.1,
 HL 20.8, HL 35.4
 Warburton, Richard John HL 2.5
 Wartelle, Alexis MA 28.4, MA 35.17
 Warzanowski, Philipp•TT 8.6
 Waseda, Sam•MM 16.4
 Waser, Rainer HL 18.4
 Waßerroth, Sören O 37.6
 Wasielewski, Radosław O 20.8
 Wassermann, Lea BP 26.7
 Wassermann, Tobias O 12.4
 Wasserroth, Sören•O 37.5, O 44.5
 Wasserscheid, Peter O 45.2, O 45.3
 Watanabe, Kenji TUT 2.2, DS 17.5,
 DS 22.6, DS 22.8, HL 1.2, HL 6.7,
 HL 11.8, HL 11.9, HL 20.4, HL 20.8,
 HL 25.17, HL 25.19, HL 25.21,
 HL 29.2, HL 29.5, HL 33.3, HL 40.7,
 O 72.4, TT 2.10, TT 2.13, TT 10.3,
 TT 10.4, TT 10.5, Q1 1.2
 Watermeyer, Philipp O 70.5
 Waters, Dacen O 81.3
 Watson, Matt MA 17.3
 Watts, Anthony•BP 15.4
 Watty, Jens Q1 12.3
 Watzenböck, Clemens TT 28.9
 Wawrzyńczak, Rafał MA 42.5
 Weaver, Christopher TT 29.6
 Weber, Cedric MA 38.4, MM 23.10
 Weber, Christoph BP 8.10, BP 8.11,
 BP 8.12
 Weber, Dominik HL 25.51, •HL 28.5,
 •O 59.2
 Weber, Johannes MA 35.7
 Weber, Jonas H. HL 26.2, HL 26.3
 Weber, Jonathan Tilman MA 19.29
 Weber, M. TT 28.4
 Weber, M. C. MA 33.6
 Weber, Mads C.•KFM 7.1, MA 33.5
 Weber, Malte Luca•HL 18.9
 Weber, Manuel•TT 24.13
 Weber, Marius•MA 25.3, MA 25.8,
 MA 35.27
 Weber, Paula O 40.7
 Weber, Paula M.•O 26.9
 Weber, Sebastian M. O 12.6
 Weber, Sebastian T. MA 8.9,
 •MA 25.8, MA 35.27, MA 35.31,
 MA 35.32, O 16.5, O 33.4, O 33.10
 Weber, Stefan CPP 17.31
 Weber, Stefan A.L. CPP 20.1,
 •CPP 20.6, CPP 28.3, HL 5.5,
 HL 30.28, HL 30.33, O 19.4
 Weber, Thomas KFM 8.6
 Weber, Torsten•DY 5.10
 Weber, Walter M. HL 22.2
 Wecker, Julia•HL 17.5
 Wedemann, Gero BP 7.17, BP 7.20
 Weder, Chris CPP 8.5
 Wegener, Martin O 61.7
 Wegner, Anja BP 12.38
 Wegner, D. O 6.9
 Wegner, Daniel MA 30.5, O 19.3,
 O 53.3, O 74.5
 Wegner, Hermann A. O 6.2, O 14.2,
 O 40.6, O 79.5
 Wegner, Mathias TT 17.2, TT 17.4,
 TT 31.10
 Weh, Andreas•TT 21.33
 Wehling, Tim HL 25.28, KFM 11.3,
 O 2.6, O 9.8, O 11.3, •O 25.4, TT 12.9,
 TT 16.2
 Wei, Jimeng O 26.8
 Wei, Shuai•MM 30.9
 Wei, Wei•MM 8.3
 Wei, Xian-Kui MA 23.4, O 21.4
 Wei, Xingzhan HL 25.38
 Wei, Yao•MM 23.10
 Weick, Guillaume DY 46.20
 Weidenhiller, Franz•MA 35.6
 Weidenkaff, Anke MM 33.9
 Weidner, Anja MM 4.8
 Weidner, Carrie Q1 3.6
 Weiel, Marie BP 2.3
 Weig, Eva•DY 12.1
 Weig, Eva M. Q1 8.4
 Weigand, Markus MA 27.3, MA 34.5
 Weigel, Martin DY 26.1, DY 26.5,
 •DY 26.6
 Weigel, Robert F. B.•DY 39.4
 Weigelt, Carmen HL 8.4
 Weigl, Leonard O 2.5, O 2.6, •O 2.7,
 O 9.6, O 9.8, O 33.5
 Weigold, Matthias MA 35.52
 Weihs, Gregor HL 8.7, HL 26.7
 Weiler, Mathias MA 19.43, MA 19.59,
 MA 22.1, MA 22.2, MA 28.7, MA 35.9,
 MA 35.35, MA 35.50
 Weimann, Nils HL 25.55
 Weimann, Thomas KFM 25.8, TT 37.1
 Weimann, Agnes HL 39.2
 Weimer, Isabell•TT 2.9
 Wein, Konstantin•DS 6.3
 Weinbrenner, Lisa•Q1 7.5
 Weindl, Adrian O 4.4, •O 21.3
 Weindl, Anna DS 20.27
 Weindl, Christian CPP 28.6
 Weindl, Christian L. CPP 1.6,
 CPP 19.4, CPP 27.3, CPP 27.4,
 •CPP 50.1
 Weinelt, Fabian TT 29.17
 Weinelt, Martin MA 35.29, O 9.9
 weinert, michelle O 13.4
 Weinhold, Marcel DS 18.2
 Weinmann, Dietmar DY 46.20
 Weintrub, Benjamin Isaac•HL 31.1
 Weinzierl, Alexander CPP 37.6
 Weinzierl, Alexander F. CPP 19.4
 Weiß, Christopher•O 59.4
 Weiß, Cornelius O 52.3
 Weis, Jürgen HL 25.62
 Weiß, Lorenz Q1 4.11
 Weisenburger, Pascal O 52.8
 Weißenhofer, Markus MA 12.8,
 MA 38.2
 Weißmüller, Jörg MM 17.1, MM 18.31,
 MM 18.32
 Weiss, D. TT 20.9
 Weiss, Dieter DS 22.6, HL 6.7,
 HL 25.21, HL 29.5, MA 24.7, TT 19.3,
 •TT 32.1
 Weiss, Marco•O 57.3, O 57.4
 Weiss, Marvin MA 8.10, •MA 28.9
 Weiss, Matthias•SYSD 1.4, BP 7.12,
 BP 7.30, BP 7.35, BP 22.6, BP 26.6
 Weiss, Stephan•DY 32.1
 Weiss, Thomas Paul HL 34.6
 Weissbach, Anton CPP 1.9, •HL 28.2
 Weissenhofer, M. MA 38.1
 Weissenrieder, Jonas O 10.2
 Weissmüller, Jörg MM 3.8, MM 18.10,
 MM 32.2, MM 35.8
 Weitkamp, Philipp CPP 12.80
 Weitz, R. Thomas DS 16.3, HL 25.54,
 O 9.10, O 16.9, O 48.9, TT 2.13
 Weitz, Thomas HL 25.53, HL 29.3,
 HL 42.8, TT 2.9, TT 2.11, TT 2.12,
 TT 29.10
 Weitzel, Alexander TT 3.2
 Welden, Alicia R. Q1 12.6
 Wellens, Thomas Q1 3.7, Q1 4.21
 Wellert, Stefan CPP 33.3
 Wen, Qiannan HL 40.1
 Wende, H. MA 25.4
 Wende, Heiko MA 4.3, MA 4.4,
 MA 19.14, MA 19.15, MA 22.4,
 MA 25.7, MA 35.60, MA 39.4,
 MA 39.5, MA 39.6, O 26.8
 Wendelin, Andreas•MA 19.29
 Wenderoth, Martin O 18.11, O 19.7,
 O 19.8, O 82.6
 Wenderoth, Sebastian•DY 19.2
 Wendl, Andreas TT 21.38, •TT 24.4
 Wendler, Frank KFM 2.7, KFM 25.9,
 MM 10.19
 Wendt, Klaus TT 31.7
 Wendt, Stefan O 32.5
 Wenger, Jérôme BP 7.5
 Wengert, Simon•MM 34.3
 Wenk, Marius•O 33.4
 Wenthaus, L. O 68.10
 Wenthaus, Lukas O 9.1
 Wenzel, Alina•MA 35.76
 Wenzel, Felix CPP 41.2
 Wenzel, Maxim•TT 39.4
 Wervkovits, Anna O 17.2, •O 28.7,
 •O 28.9
 Werner, Marco CPP 12.22, •CPP 14.3,
 CPP 17.8
 Werner, Peter•DY 49.1
 Werner, Reinhard F. Q1 6.6
 Werner, Simon O 5.5, O 52.6
 Wernicke, T. HL 10.5
 Wernicke, Tim HL 10.1, HL 10.4,
 HL 10.6, HL 10.7, HL 10.8, HL 10.9,
 HL 10.10
 Wernsdorfer, Wolfgang HL 25.60,
 HL 30.5, O 34.4, TT 21.21, TT 21.22,
 TT 27.1, TT 27.2, TT 29.2, TT 29.3,
 TT 31.1, TT 31.2, TT 31.18, TT 31.24,
 TT 31.25, TT 37.9, TT 37.12, Q1 4.32
 Wesdorp, Jaap J. Q1 13.11
 Wesdorp, Jaap Joachim TT 37.5
 Weßels, Teresa•MA 41.2
 Wesenberg, Lucia•BP 17.3
 Wessel, Stefan MA 14.2, TT 24.11,
 TT 34.11, •TT 34.12
 Wessels, Teresa MA 22.4
 West, Geoffrey SOE 14.3
 Westerbeck, Dennis•MA 19.18
 Westermayr, Julia DY 35.5, O 32.4,
 O 83.2
 Westmeyer, Gil BP 12.59
 Westphal, Carsten O 18.28, O 65.2
 Westphal, Michael CPP 17.10,
 KFM 15.3, •O 23.5
 Westphal, Tobias HL 30.27, HL 30.31
 Wettlaufer, John S. BP 4.5
 Wex, Alexander DS 13.1
 Weyer, Henrik•DY 39.8
 Weyers, Markus HL 10.1, HL 10.6,
 HL 10.9
 Weymouth, Alfred John O 22.8,
 O 74.9
 Whitsitt, Seth TT 24.11
 Wichmann, Christoph O 45.3, •O 45.4
 Wichmann, Jan-Erik Reinhard TT 11.1
 Wichmann, Tobias MA 19.55,
 •O 54.12
 Wick, Christian CPP 17.22, MM 18.7
 Wickramaratne, Darshana O 48.6
 Widdra, Wolf O 26.7, O 66.3, O 66.4,
 O 66.5, O 66.6, O 66.7, O 66.9,
 O 73.10
 Widhalm, Alex HL 3.6, HL 26.1
 Widmer, Roland O 29.6
 Wiebe, Jens MA 9.4, MA 30.2,
 MA 35.71
 Wiebe, Nathan Q1 12.5
 Wiechers, Paul O 5.2, O 55.12
 Wieck, A. HL 2.3
 Wieck, Andreas DY 35.4, HL 25.47,
 HL 25.63, HL 25.64, HL 25.67,
 HL 25.81, HL 25.83, HL 26.6,
 HL 26.10, TT 31.13
 Wieck, Andreas D. HL 3.4, HL 7.7,
 HL 8.9, HL 12.1, HL 12.2, HL 19.1,
 HL 25.37, HL 25.43, HL 25.58,
 HL 25.59, HL 25.71, HL 25.72,
 HL 25.73, HL 25.86, HL 26.2, HL 26.3,
 HL 26.8, HL 30.7, HL 35.4, HL 36.5
 Wieck, Andreas Dirk HL 2.5, HL 3.7
 Wiczorek, Witlef Q1 5.7
 Wiedland, Ulf CPP 45.2
 Wiedmann, Raymond•TT 21.20
 Wiedmann, Steffen MM 28.2
 Wiedwald, Ulf DS 21.3, MA 19.23,
 •MA 39.2
 Wiegand, Patrick MA 9.3
 Wiegart, Lutz CPP 12.21
 Wiehemeier, Lars CPP 17.18
 Wiemeler, Jonas•MA 35.34
 Wienhold, Kerstin S. CPP 1.2,
 CPP 27.3, CPP 27.4, CPP 50.1
 Wiercinski, Julian•HL 8.8
 Wiersig, Jan HL 26.5
 Wierzbowski, Jakob HL 25.13
 Wiesendanger, Roland MA 9.4,
 MA 27.9, MA 30.2, MA 34.2,
 MA 35.71, O 42.2, TT 19.4
 Wiesener, Philipp O 12.2, O 19.6
 Wieser, Sandro CPP 40.5, HL 41.1
 Wiesner, Fabian Q1 4.8
 Wietek, Alexander TT 23.7
 Wietschorke, Fabian HL 36.4,
 •TT 17.5, TT 17.6, TT 17.7
 Wigger, Daniel HL 25.8, HL 25.48,
 HL 30.48
 Wiktor, Julia HL 18.11
 Wilczek, Michael BP 12.60, DY 16.6,
 DY 31.3, DY 34.3, DY 34.4, DY 34.5
 Wild, Johannes•MM 18.29
 Wilde, G. MM 21.7
 Wilde, Gerhard MM 3.2, MM 8.4,
 MM 10.5, MM 10.7, MM 10.8,
 MM 10.25, MM 15.3, MM 16.1,
 MM 16.2, MM 18.30, MM 20.1,
 MM 20.2, MM 21.6, MM 21.8,
 MM 21.10, MM 30.2, MM 30.4,
 MM 30.8, MM 32.1
 Wilde, Marc A. MA 35.56, TT 12.7,
 TT 21.38, •TT 25.5, TT 25.7
 Wildeis, Anna KFM 6.3
 Wilden, Kilian•O 35.2
 Wildermuth, Micha•TT 26.1, TT 37.3,
 TT 37.10
 Wilhelm, Frank K. Q1 4.40
 Wilhelm, Jan HL 30.40, •MM 31.1,
 O 74.6
 Wilhelm, Michael MM 13.3, •MM 13.4,
 MM 13.5
 Wilhelm, Patrick•MM 28.3
 Wilhelm, Philipp DS 17.6
 Wilhelm, Richard•DS 10.2
 Wilhelm-Mauch, Frank Q1 4.1, Q1 4.28
 Wilk, Tatjana Q1 3.10
 Wilke, Max KFM 25.13
 Wilke, Melanie DY 45.13
 Wilke, Reja•TT 9.1, •TT 29.14

Author Index

- Wilkins, Stuart B. MA 2.3
 Wilkinson, Samuel •QI 6.5
 Wilksen, Steffen •HL 19.3
 Will, Moritz O 54.14
 Willa, Roland TT 3.7
 Willatt, Michael O 67.6
 Willems, Felix MA 8.2
 Willer, Pascal TT 17.9, •TT 31.12
 Willke, Philip •DS 10.3, O 5.3, O 34.4,
 O 47.3, O 82.6
 willner, arik CPP 12.59
 Willner, Lutz CPP 33.1
 Willock, David O 62.2
 Willsher, Josef •MA 35.44
 Willwater, Jannis TT 3.8, •TT 24.5
 Wilms, Alissa QI 12.8
 Wilson, Mark O 43.7
 Wilson, Murray N. MA 31.9
 Wilson, Nathan HL 11.9
 Wilson, Nathan P. HL 15.5
 Wilson, S. TT 23.5
 Wilson, Stephen D. TT 39.4
 Wilting, Jens BP 2.6
 Wilts, Bodo CPP 8.5
 Wimmer, Markus A. O 22.2
 Wimmer, Michael O 51.2
 Wimmer, Stefan MA 31.2
 Wimmer, Tobias MA 34.4
 Wind, Lukas HL 22.2
 Wind, Niklas MA 31.6, •O 34.10
 Windbacher, Niklas MA 8.4
 Windischbacher, Andreas O 2.2,
 O 12.5
 Windsor, Y.W. MA 35.24
 Wingenbach, Jan •HL 21.9
 Winkel, Patrick TT 27.1, TT 27.2,
 TT 31.1, TT 31.2, TT 37.12
 Winkel, Tristan MA 19.46, •MA 19.49,
 MA 35.65
 Winkelmann, Clemes B. TT 26.8
 Winker, Roland G. BP 4.6, BP 14.5
 Winkler, Benjamin •DY 39.7
 Winkler, Daniel O 15.9, •O 15.10
 Winkler, Julius HL 32.1
 Winkler, Louis Conrad CPP 26.1,
 •HL 28.8
 Winkler, Lucy CPP 26.2
 Winkler, Maximilian •MA 33.1
 Winkler, Roland G. BP 14.7
 Winkler, Thomas Brian MA 12.4,
 •MA 19.10
 Winkhofer, Michael MA 19.29
 Winnerl, Stephan HL 11.10, HL 25.41,
 HL 40.2
 Winter, Bernd O 64.1
 Winter, Carsten O 33.9
 Winter, Dominik •CPP 12.57
 Winter, Edda KFM 15.7
 Winter, Leonhard •O 45.9
 Winter, M. MA 27.1
 Winter, Michael •HL 25.28
 Winter, Rainer O 74.1
 Winter, Stephen M TT 8.4
 Winterott, Moritz •MA 20.7
 Wintterlin, Joost O 62.3, O 69.7
 Wintz, Sebastian MA 23.3, MA 27.3,
 MA 34.5
 Wirth, Konstantin O 59.5, O 78.1
 Wirth, Konstantin G. O 59.3
 Wischnewski, Andreas CPP 33.1
 Wismath, Sonja CPP 17.19
 Wissmann, Michael •MA 31.5
 Witt, Christina •HL 5.3
 Witt, Hugo O 44.10
 Witt, Niklas O 2.6, •TT 12.9
 Witte, Gregor CPP 12.55, CPP 39.1,
 DS 5.3, DS 5.4, O 12.1, O 12.9
 Witte, Wanda •BP 12.44
 Witte, Wolfram HL 25.32, •HL 27.2,
 HL 34.5
 Wittemann, Alexander DS 9.4
 Wittemeier, Nils •MM 28.4
 Witteveen, Catherine MA 35.58
 Witthaut, Dirk SOE 7.1, SOE 13.1,
 SOE 13.2
 Wittig, Alexandra O 22.1
 Wittig, Patrick •TT 29.9
 Wittkämper, Haiko O 45.3, O 45.4
 Wittkowski, Raphael DY 3.3, DY 16.10,
 DY 46.2, DY 46.3, DY 49.6
 Wittl, Wilhelm TT 18.9
 Wittmann, Angela •MA 34.5
 Wittmann, René •DY 23.8, •DY 31.7,
 DY 46.2, DY 50.2
 Wittrock, Adrian O 22.1, •O 22.2
 Wittwer, Lucas BP 4.4
 Witzigmann, B. HL 10.5
 Witzigmann, Bernd CPP 17.32,
 DS 2.4, HL 10.4
 Witzky, Yannick •BP 7.27
 Wixforth, Achim MA 28.7
 Woche, Susanne HL 12.10
 Wochner, Peter DS 14.4
 Wohlfeld, Krzysztof TT 39.6
 Wohlrab, Sebastian •BP 12.2
 Wöhrl, Nicolas •PSV II
 Wojewoda, Ondřej MA 28.6
 Wojnar, Piotr HL 39.3
 Wojtowicz, Tomasz O 35.5, O 37.8
 Wolansky, Jakob •CPP 1.12, CPP 26.2
 Wolf, Adriana HL 22.7
 Wolf, Andreas TT 31.6
 Wolf, Bettina BP 9.9
 Wolf, Christoph MA 26.3, •O 5.3,
 O 47.4, O 51.6, O 54.3, O 71.1
 Wolf, D. MA 20.4, MA 27.1
 Wolf, Daniel MA 19.5, MM 35.1
 Wolf, Dietrich DY 3.6
 Wolf, M. O 9.5
 Wolf, Marcell CPP 20.4
 Wolf, Martin •PSV VI, HL 23.6,
 MA 21.1, O 7.6, O 33.6, O 37.5, O 37.6,
 O 37.7, O 44.5, O 55.3, O 78.2
 Wolf, Michael QI 14.10
 Wolf, Michael M. QI 12.7
 Wolf, Steffen BP 7.9, BP 7.19, BP 15.17
 Wolf, Yotam TT 7.6
 Wolff, Christian M. •HL 5.11
 Wolff, Martin QI 4.24
 Wolff, Max •CPP 44.5
 Wolff, Michael MM 8.4
 Wolff, S. O 41.7
 Wolff, Stefan •DS 20.9
 Wolff, Susanne DS 22.7, •O 18.3,
 O 18.6
 Wolfram, Alexander •O 12.11, O 12.12
 wöll, christof O 30.7, O 70.8, O 79.7
 Wöll, Christoph CPP 48.4
 Wollmann, Philipp DS 20.14
 Wolloch, Michael O 39.1, •O 39.2
 Wollschläger, Joachim MA 19.16
 Wolter, Anja MA 31.3, MA 35.59
 Wolter, Anja U. B. MA 14.7, MA 14.8
 Wolter, Celine •DY 46.9
 Wolter, Silke TT 37.4
 Wolters, Janik DY 45.11
 Woltersdorf, Georg MA 18.1, MA 24.4,
 MA 28.1, MA 28.2, MA 28.5, MA 35.4
 Wolverton, Chris •SYNM 1.3
 Wolz, Lukas M. •HL 24.4
 Wong, Deniz MA 6.4
 Wong, Eric DS 20.43
 Wong, William S.Y CPP 20.1
 Woodcock, Thomas G. MA 29.4
 Woodruff, D. Phil O 40.5
 Wörgötter, Florentin BP 12.39
 Wörle, Simon •HL 42.6
 Worm, Paul •TT 22.9
 Wörtche, Frederike HL 29.9
 Wortmann, Bernhard •TT 5.6
 Wortmann, Daniel MM 18.3
 Wortmann, Martin •CPP 17.10,
 •CPP 17.39, DS 5.2, •KFM 15.3
 Woschée, Daniel BP 12.55
 Wosnitza, J. MA 19.11, MA 29.2,
 MA 29.3, TT 8.1, TT 12.6, TT 20.8,
 TT 23.5, TT 25.9, TT 28.4
 Wosnitza, Joachim HL 20.3, MA 27.8,
 TT 6.6
 Wosnitza, Jochen MA 19.13, TT 8.5,
 TT 22.11
 Wozny, Simon DY 35.6, •TT 18.6
 Wrachtrup, Jörg MA 2.4
 Wrana, Dominik O 3.2, O 16.12,
 O 44.3, •O 44.8, O 53.1, O 57.5
 Wrzosek, Piotr •TT 34.1
 Wu, Bingyu MM 18.18
 Wu, Kai •O 10.7
 Wu, Kexin •CPP 17.29
 Wu, Mingjian O 45.4
 Wu, Weishan O 17.4
 Wu, Xiaojian HL 30.6
 Wu, Xinyan O 61.6
 Wu, Xu O 13.2
 Wübbeler, Gerd O 7.9
 Wührer, Dennis •MA 13.7
 Wüthrl, Friederike •O 66.7
 Wulf, Wulfhchel MA 24.2
 Wulff, Harm BP 17.4
 Wulfhchel, Wulf DS 5.1, O 7.7, O 26.1,
 O 61.5, O 61.7, O 74.6, O 79.3, O 80.3,
 •TT 3.1
 Wunderlich, Christof QI 1.8, QI 1.10,
 QI 1.11
 Wunderlich, Hannes •BP 7.35
 Wunderlich, Joerg MA 29.6
 Wunderlich, Paul •TT 39.3
 Würdemann, Rolf •CPP 12.20,
 •CPP 14.4
 Würfl, Joachim DS 6.4
 Wurm, Gerhard MA 39.6
 Wurmehl, Sabine TT 12.1, TT 21.23
 Wurstbauer, Ursula DS 20.39,
 DS 22.2, DS 22.3, DS 22.4, HL 6.5,
 HL 6.8, HL 11.5, HL 11.6, HL 25.3,
 HL 25.4, HL 25.6, HL 25.14, HL 25.15,
 TT 7.7, QI 4.24
 Würthner, Frank O 40.7, O 82.5
 Würthner, Laeschkir DY 39.8
 Wurz, Nicola QI 4.23, •QI 6.8
 Wust, Stephan •MA 25.5, MA 35.28
 Wuttig, Matthias DS 20.7, DS 20.13,
 DS 20.38, DS 20.42, DS 23.5,
 KFM 25.4, MM 2.10, MM 10.6,
 MM 18.3, O 35.2, O 35.3, O 57.6,
 O 59.3, O 78.1
 Wyderka, Nikolai •QI 9.7
 Wysmolek, Paulina BP 2.5, BP 9.7
 Xang, Xuexiao CPP 40.9
 Xia, Wei TT 39.2
 Xia, Yonggao CPP 17.5
 Xian, R.P. O 68.10
 Xiang, Bo HL 23.6
 Xiang, Feifei O 18.19, O 23.9, O 40.1
 Xiao, Huijuan •MA 35.29
 Xiao, Shuyang TT 3.6
 Xiao, Tianxiao CPP 19.4, •CPP 26.3,
 CPP 37.6
 Xiao, Xingxing MM 33.9
 Xie, Ruiwen MA 22.4
 Xie, Stephen R. O 67.3
 Xie, Wenjie MM 33.9
 Xie, Zhuocheng •MM 6.1
 Xing, Xinlai O 53.5
 Xu, Bai-Xiang •KFM 10.3
 Xu, Changfan •KFM 25.19, •MM 8.7
 Xu, J. HL 4.7, HL 4.9
 Xu, Jia-Lu HL 4.8
 Xu, Qi •MM 30.7
 Xu, Qichen •MA 11.2
 Xu, Tao O 32.5
 Xu, Wenbin •O 62.4
 Xu, Wenqi CPP 12.32
 Xu, Xiang •MM 6.8, MM 34.7
 Xu, Xuefei MM 29.1
 Xu, Yihe CPP 40.9
 Xu, Youjiang •MA 31.10
 Xu, Zhen-Peng QI 7.1
 Xu, Zhuijun CPP 12.15, •CPP 17.5
 Xu, Zhuo •CPP 12.63
 xue, qi-kun O 18.15
 Xue, Ran •HL 19.10, HL 25.60
 Yadav, Bharti CPP 49.2
 Yadav, Devinder MM 18.41
 Yadav, Khushboo O 74.12
 Yadavalli, Nataraja Sekhar DS 23.6
 Yadin, Benjamin •QI 2.2
 Yagodkin, Denis HL 11.12, •HL 25.29
 Yahel, Eyal MM 30.10
 Yakovlev, Dimitri R. MA 14.9
 Yakovlev, Dmitri HL 2.4, HL 23.11
 Yakovlev, Dmitri R. HL 26.9, HL 32.2,
 HL 39.5, O 35.5, O 37.8
 Yakovlev, Dmitrii R. HL 5.2
 Yakovlev, Dmtri R. HL 25.92
 Yalcin, Eyüp O 37.8
 Yalcin, Firat •O 39.1, O 39.2
 Yalcinkaya, Yenal •HL 5.5, •HL 30.28
 Yam, Chi Yung O 81.4
 Yam, Chi-Yung O 58.8
 Yam, Wun Kwan QI 4.15, •QI 4.18
 Yamada, Norifumi L. CPP 1.8
 Yan, Binghai TT 7.6
 Yan, Chengzhan •KFM 15.5,
 •MM 18.22
 Yan, Jiaqiang O 81.3
 Yan, Lok-Yee HL 33.9
 Yan, Zewu KFM 7.3, KFM 7.5
 Yan3, Zewu KFM 14.6
 Yanagisawa, T. TT 8.1
 Yang, Biao O 23.8, •O 62.9
 Yang, Chan •HL 25.38
 Yang, Chia-Jung •TT 6.4
 Yang, Dan CPP 1.2
 Yang, Dengyu MM 10.30
 Yang, Eui-Hyeok HL 6.2
 Yang, Fan •DY 12.2, DY 12.5
 Yang, Hung-Hsiang O 26.1
 Yang, Jing •MM 20.10
 Yang, Jingzhong •HL 8.3, HL 8.5,
 HL 12.10, HL 25.82, HL 30.9, HL 36.8,
 HL 39.4
 Yang, Lexian O 9.4
 Yang, Liang O 61.7
 Yang, Luyan MA 19.1, MA 27.4
 Yang, Luyi MA 37.11
 Yang, Ping QI 4.23, QI 6.8
 Yang, S.-L. O 9.5
 Yang, Sangsun MM 21.6
 Yang, Tao •O 48.8
 Yang, Yangyiwei MA 23.1
 Yang, Ying MA 35.52
 Yang, Yiqi TT 28.10
 Yang, Yuhui •HL 25.75, HL 25.76,
 O 35.8
 Yao, Yi O 50.2, •O 50.4, O 50.9
 Yao, Yong-Xin O 72.1
 Yao, Yuxuan •O 46.8
 Yap, Ian C. J. MM 18.13
 Yap, Ian Chang Jie •MM 7.3
 Yaqoob, Misbah •MA 19.43, MA 19.59
 Yaroslavtsev, A. MA 25.4
 Yaroslavtsev, Alexander MA 25.2
 Yasin, Fehmi S. MA 27.7, MA 27.10
 Yasui, Y. TT 22.1
 Yatish, Yatish •BP 7.46
 Yazdampannah Ravari, Roozbeh
 QI 13.10
 Yazdan Yar, Azade MM 34.7
 Yazdampannah Ravari, Roozbeh
 •TT 20.4
 Yazdanshenas, Bahar •CPP 12.35
 Ye, Jingjing HL 25.68
 Ye, Linda MA 13.10
 Ye, Mai •KFM 25.21
 Ye, Xingchen MA 41.1
 Ye, Yusong •BP 12.35
 Yen, Yun •O 2.1
 Yesilpinar, Damla •O 18.20
 Yildirim, Haydar Altug O 9.9
 Yildiz, Dilek TT 2.10
 Yimkao, Watsapon •CPP 12.34
 Yin, Hao •O 18.5
 Yin, Rongrong O 46.6
 Yin, Shanshan CPP 12.45, CPP 12.67,
 CPP 17.23, •CPP 27.3, CPP 27.4,
 CPP 37.3, CPP 48.2, CPP 48.3,
 CPP 50.1
 yin, yuguo O 18.15
 Yochellis, S. O 26.2
 Yogi, Arvind MA 6.4
 Yogi, Priyanka DS 25.4
 Yokaichiya, F. MA 4.1
 Yoo, Su-Hyun DS 6.2, •O 64.5
 Yoon, Bokwoon O 56.2
 Yordanov, Petar HL 13.7
 You, Changjiang BP 7.8
 You, Jih-Shih MM 23.9
 Yu, Sifan O 32.7
 Yu, Boram •BP 7.34
 Yu, Haiting •HL 12.4
 Yu, Ji Hun MM 21.6
 Yu, Jisoo O 63.4
 Yu, Ka Man O 5.4
 Yu, KaMan O 33.11
 Yu, Mei •QI 2.9
 Yu, Muqing MM 10.30
 Yu, Weichao MA 7.2
 Yu, Xiao-Dong QI 9.5
 yu, xiaojuan O 30.7, O 79.7
 Yu, Xiuzhen MA 27.2, MA 27.7,
 MA 27.10
 Yu, Yinye HL 25.38
 Yu, Yuan DS 20.7, KFM 25.4
 Yu, Yuefeng •HL 25.31
 Yuan, Chentian O 20.4
 Yuan, Hongtao KFM 8.3
 Yuan, Huaiyang MA 7.4
 Yuan, Long TT 5.3
 Yuan, Ning •MA 35.43
 Yuan, Xudong MM 30.1, •MM 30.5
 Yuan, Xueyong HL 22.8
 Yucel, Oguzhan HL 25.31
 Yugova, Irina A. HL 26.9
 Yunus Ali, Syed DY 44.4
 Yusa, Go HL 2.2
 Zabolocki, Jennifer HL 28.7
 Zabolotnyy, Volodymyr MA 31.3
 Zaburdaev, Vasily •BP 6.5, BP 8.2,
 BP 8.3, BP 12.24, BP 12.35, BP 12.38,
 BP 26.3
 Zacharias, Helmut O 26.8, O 33.9,
 O 55.16
 Zacharias, Margit HL 18.6, KFM 25.2,

- MM 35.10
Zaghoul Noby, Sohaila TT 22.2
Zahn, Dietrich R.T. DS 20.18, DS 23.1,
DS 26.3, HL 25.42, HL 25.51, HL 28.5,
HL 39.1, O 55.7
Zahn, Manuel •KFM 7.4, KFM 14.5
Zahn, P. TT 13.5
Zaharov, M HL 21.2
Zahradník, Martin .. HL 13.3, HL 13.9,
HL 21.4, O 16.1
Zajac, Peter HL 12.1, •HL 25.72
Zajusch, Sarah •O 33.7, O 68.4
Zakeri, K. O 66.2
Zakharchuk, Marina •SOE 17.5
Zakharov, A.A. O 25.3
Zallo, Eugenio •HL 42.4
Zamarripa, Cesy HL 21.3
Zamborlini, Giovanni .. MA 35.70,
O 12.5, O 34.8, O 42.3, O 55.5, O 55.9
Zamponi, Michaela CPP 33.1,
CPP 33.2
Zander, Ellen DS 9.4
Zanker, Sebastian QI 10.3
Zanner, Maximilian .. TT 37.13, QI 4.33
Zanolli, Zeila MM 28.4
Zanotti, Jean-Marc MA 26.2
Zaper, Liza •MA 41.4
Zapf, Daniel CPP 12.18
Zapf, Maximilian HL 4.4
Zaplétal, Petr QI 6.3
Zaraket, Jean O 73.6
Zardbani, Fatemeh O 63.5
Zarzuela, Ricardo MA 19.9, •MA 24.10
Zatsch, Jonas QI 4.14
Zatterin, Edoardo HL 35.3
Zauchner, Mario •O 83.8
Zayko, Sergey MA 2.1, O 9.3
Zázvorka, Jakub MA 12.9
Zech, Paul •BP 18.3, CPP 12.6
Zech, Tobias CPP 33.6
Zechner, Christoph BP 24.2
Zeer, Mahmoud •MA 24.2
Zeinger, Johannes •O 64.4
Zeitner, U HL 42.2
Zeitner, Uwe HL 4.2
Zeldov, Eli TT 7.6
Zelena, Anna •BP 12.9
Zelenina, Anastasia •HL 34.2
Zelený, Martin .. •MA 11.4, MM 10.20,
MM 10.23, MM 10.26
Železný, Jakub MA 34.7
Zeller, Rudolf MA 14.4
Zeller, Viola HL 40.5
Zemen, Jan MA 29.6
Zemp, Yannik KFM 7.1, •MA 33.5
Zen, Andrea O 43.6
Zeng, Xianzhe •O 57.1
Zengin, Berk O 71.9
Zenner, Jannik MA 31.2
Zentgraf, Thomas HL 33.9
Zeplichal, Marc CPP 39.1
Zeppenfeld, Peter .. MA 30.4, O 12.3
Zerebecki, Swen MA 39.4
Zerhoch, Jonathan HL 28.6
Zerihun, Mehari BP 2.3
Zerson, Mario CPP 12.6
Zetterberg, Johan O 69.5
Zeugner, Alexander TT 20.2
Zeuner, Katharina D. .. HL 8.1, HL 8.10
Zhai, Liang HL 19.1, HL 35.4
Zhan, Pengfei BP 26.4
Zhang, Chao O 18.21, O 48.10
Zhang, Chengjie QI 9.2
Zhang, Chun O 81.1
Zhang, Deqing O 33.9
Zhang, Fan TT 2.11
Zhang, Haijing MM 23.1
Zhang, Haiming O 62.9
Zhang, Heng •MM 18.15
Zhang, Hongbin .. DS 20.24, HL 13.5,
HL 30.45, MA 19.12, MA 22.4,
•MM 25.7, MM 29.4, MM 33.9
Zhang, Jiahuan CPP 12.67
Zhang, Jingshu DS 20.32
Zhang, Juli HL 25.22
Zhang, Junjie O 62.9
Zhang, Ke O 69.3, O 70.1
Zhang, Lichuan O 26.1
Zhang, Peiran •CPP 12.31
Zhang, R. K. HL 4.9
Zhang, Ruifeng MA 32.8
Zhang, Ruikang K. HL 4.8
Zhang, Shihao MA 32.8
Zhang, Shiwei TT 28.10
Zhang, Songbo •MM 4.3, TT 30.8
Zhang, T. HL 4.7, HL 4.9
Zhang, Taiping HL 4.8
Zhang, Tianyi •CPP 26.1
Zhang, Weichun BP 8.2
Zhang, Xi MM 6.8, MM 10.14
Zhang, Xiangdong QI 3.5
Zhang, Xianghui •CPP 17.4
Zhang, Xiao Yue .. HL 25.10
Zhang, Xin •MM 35.5
Zhang, Xue O 5.3
Zhang, Xuejiao •O 13.2
Zhang, Xuejing •TT 28.1
Zhang, Yaolong O 46.6
Zhang, Yiteng •HL 12.7, HL 12.10,
HL 30.9, HL 36.8
Zhang, Yiwei •DY 16.2
Zhang, Yixuan .. HL 13.5, HL 30.45,
MM 29.4
Zhang, Yong O 79.4
Zhang, Yu O 33.5, O 72.1
Zhang, Zongbao DS 20.3
Zhao, Gloria PLV III
Zhao, Heng CPP 1.2
Zhao, Hongzheng .. •DY 5.2, •DY 43.1
Zhao, Huan MM 15.2
Zhao, Huaping .. HL 24.1, KFM 15.1,
KFM 15.2, KFM 25.15, KFM 25.16,
KFM 25.17, MM 8.6, MM 14.5,
MM 18.19, MM 18.21, MM 18.24,
O 13.10
Zhao, Jin HL 23.9
Zhao, Pai TT 2.5
Zhao, Qiang DY 16.5
Zhao, Tianheng CPP 8.3
Zhao, Weisheng O 72.7
Zhao, Wenchao •O 23.8
Zhao, Xianyue DS 18.1
Zhao, Xueping BP 8.11
Zhao, Yi-Fan O 21.1
Zheng, Andreas CPP 45.3
Zheng, Bei •HL 25.10, HL 29.6
Zheng, Feifei .. •CPP 12.32, CPP 44.3
Zheng, Fengshan .. HL 22.5, MA 19.1,
MA 27.4, MA 27.6, MM 18.39
Zheng, Giulia TT 10.4
Zheng, Tianle •CPP 17.27
Zherlitsyn, S. TT 8.1
Zhitenev, Nikolai TT 2.10
Zhitomirsky, Mike E. TT 23.7
Zhitomirsky, Mike E. TT 8.5
Zhong, Huaying .. •CPP 12.67, CPP 37.6
Zhong, Jianxin DY 26.3
Zhong, Qigang O 6.2, •O 79.5
Zhong, Xiaoyan MA 23.4
Zhong, Yu MM 21.1
Zhou, Hangyu •O 72.7
Zhou, Jianfeng O 69.5
Zhou, Ling-Jie O 21.1
Zhou, Ping O 2.4, O 16.11, O 79.3
Zhou, S. HL 22.1
Zhou, Shengqiang MA 4.3
Zhou, Xilin MA 24.4
Zhou, Xinyu •DS 20.17
Zhou, Yiming DS 23.5
Zhou, Yishui TT 25.11
Zhou, Yuxing •O 43.1
Zhu, Jian-Xin QI 10.2
Zhu, Tongtong HL 25.65
Zhu, X.-Y. HL 23.6, HL 23.9
Zhu, Xiangzhou .. •HL 5.6, HL 23.3,
HL 23.7
Zhu, Xiaoyang O 16.10
Zhukouskaya, Hanna CPP 45.4
Zhukov, Evgeny HL 2.4
Zhukov, Evgeny A. HL 25.92
zhumagullo, yaroslav .. HL 15.2
Zhumagulov, Yaroslav •MM 18.6
Zhussupbekov, Kuanysh O 23.4
Zhussupbekova, Ainur O 23.4
Ziebert, Falko BP 3.3, BP 22.3
Ziefuß, Anna MA 35.52
Ziegler, Andreas •O 32.9
Ziegler, Martin DS 16.4, O 18.21,
O 48.10
Ziegler, Sebastian •BP 14.4
Ziegler, Sina •MM 2.5
Zielinski, Bastian BP 7.40
Ziepke, Alexander .. BP 19.1, •DY 50.4
Zierenberg, Johannes •BP 2.6,
•BP 2.9
Zierold, Robert DS 13.4
Ziesel, Fabian •TT 26.9
Ziesen, Alexander •TT 1.10
Ziethen, Noah •BP 7.13
Ziffer, Eviathar HL 10.10
Zilberberg, Oded •DY 12.4
Ziletti, Angelo MM 34.10
Zills, Fabian •DY 8.7, •SOE 6.7
Zilz, Alexander HL 30.5
Zimborás, Zoltán QI 8.8
Zimmer, Andreas BP 12.25
Zimmer, Klaus O 13.9
Zimmer, Michael HL 4.6
Zimmermann, Erik ... DS 21.2, HL 7.3,
•HL 19.7, HL 25.98
Zimmermann, Jonas E. O 9.11
Zimmermann, Philipp HL 13.1
Zimmermann, Tammo •O 18.21,
O 48.10
Zimmermann, Valentin •MA 6.4
Zimmermann, Wolfram-Hubertus
BP 3.10
Zink, Mareike BP 3.4, BP 18.8
Zinke, Gregor O 9.12, •O 16.2
Zinkevich, Tatiana KFM 15.7
Ziolkowski, Franziska MA 8.11
Ziolkowski, Pawel MM 21.5
Zippelius, Annette •PLV VI
Zipper, Matthias QI 12.4
Zito, Cecilia •MM 18.35
Zitterich, Julian •DY 44.14
Zitz, Stefan DY 4.8
Zivanovic, Lidija O 15.3
Zizlsperger, Martin HL 20.2
Zoch, Katharina M. •TT 21.13
Zohair, Fazeel HL 14.3
Zojer, Egbert CPP 40.5, HL 41.1
Zojer, Karin CPP 14.1, CPP 14.5
Zollitsch, Christoph W. •MA 18.3
Zöllner, Johann DS 29.12
Zollner, Klaus DS 20.26, •HL 29.1
Zöllner, Marcel HL 25.2, HL 25.59,
HL 25.63, •HL 26.8, HL 26.10, HL 31.3
Zollner, S •HL 21.2
Zollner, Stefan •HL 21.3
Zonda, Martin MA 24.5
Zopf, Michael HL 8.3, HL 8.5, HL 12.7,
•HL 12.10, HL 15.2, HL 25.82,
HL 25.85, HL 30.9, HL 36.8, HL 39.4
Zorin, Alexander B. TT 37.2
Zöttl, Andreas BP 7.22
Zou, Yuqin •CPP 12.45, CPP 12.64,
CPP 17.23
Zrenner, Artur HL 3.6, HL 26.1
Zu, Fengshuo CPP 28.7
zu Heringdorf, Frank-J. Meyer .. O 65.1
Zubáč, Jan MA 34.7
Zubizarreta Casalegua, Eduardo
HL 8.10
Zugliani, Lucio •HL 36.4, TT 17.5,
TT 17.6, TT 17.7
Zühlke, Ria-Helen TT 31.9
Zülske, Tilo BP 7.17, •BP 7.20
Zuniga Puelles, Esteban .. MM 18.43
Zupancic, Martina .. •DS 14.2, HL 14.3
Zverev, Vladimir ... •DY 46.5, TT 21.25
Zvyagin, Sergei •TT 34.5
Zvyagin, Sergei A. TT 8.5
Zweipfennig, Thorsten DS 2.3
Zwicker, David BP 7.11, BP 7.13,
BP 12.60, BP 12.63, •DY 37.1,
DY 45.2, DY 52.4, SOE 20.4
Zwicknagl, Gertrud .. HL 25.69, TT 6.7
Zwiller, Val .. HL 8.1, HL 8.10, HL 19.2
Zyabkin, Dmitry MM 18.13
Zybtsev, Sergey KFM 8.3
Zyczkowski, Karol QI 2.3
Zysman-Colman, Eli HL 41.2

Index of Exhibitors Regensburg 2022

Exhibition Venue:

Campus University of Regensburg, Universitätsstraße 31, 93053 Regensburg

- Foyer Main Lecture Hall (A)
- Main Lecture Hall area H6 (H6)
- Law & Economy Building (E)
- Tent close to Physics Building (Tent Physics)

Opening hours exhibition:

- Tuesday, Sept 6 09:00 – 18:00 (optional until 14:30 due to the award ceremony)
- Wednesday, Sept 7 09:00 – 18:00
- Thursday, Sept 8 09:00 – 18:00

The entrance is free!

Company	Location	Booth No.
ADDITIVE Soft- und Hardware für Technik und Wissenschaft GmbH Max-Planck-Straße 22 b, 61381 Friedrichsdorf <i>ADDITIVE Soft- und Hardware für Technik und Wissenschaft GmbH</i>	Audimax Foyer	A47
ADL Analoge & Digitale Leistungselektronik GmbH Bunsenstraße 30, 64293 Darmstadt <i>Plasmastromversorgungen/Stromversorgungen für Ionenquellen</i>	Audimax Foyer	A39
Agilent Technologies Sales & Services GmbH & Co. KG Hewlett-Packard-Straße 8, 76337 Waldbronn <i>Agilent is a leader in life sciences, diagnostics and applied chemical markets. The company provides laboratories worldwide with instruments, services, consumables, applications and expertise.</i>	Audimax Foyer	A20
AHF analysentechnik AG Kohlplattenweg 18, 72074 Tübingen <i>AHF provides optical filters, LED/laser light sources, image splitters and quality monitoring tools for professional and challenging (fluorescence) microscopy. Customers benefit from long-term and interdisciplinary expertise.</i>	Audimax Foyer	A43
Allectra GmbH Traubeneichenstraße 62-66, 16567 Schönfließ <i>Vakuumkomponenten, elektrische Durchführungen, Kabel</i>	Tent Physics	P05
Almax easyLab bvba Wagenmakerijstraat 5, 8600 Diksmuide, BELGIUM <i>High Pressure (0.50 - 400 GPA), Science Solutions, Quantum Diamond, Polishing Services, Diamond Anvil Cell, Piston Cylinder Cell, Optical Diamond Component, High Pressure Tools and Accessories</i>	Audimax Foyer	A36
Amplitude Laser Group 11 avenue de Canteranne, 33600 Pessac, FRANCE <i>Diodengepumpte Femtosekunden-Festkörperlaser (Yb, TiSa), diodengepumpte Ultrakurzpuls-Faserlaser und Femtosekunden-Faserlaser (Yb), hochenergetische Nanosekunden-Laser</i>	H6	A52
AMT Andreas Mattil – Technischer Vertrieb Talstraße 33, 67737 Frankelbach <i>UHV Manipulators, Magnetrons & Power Supply's, Vacuum Components, Right Angle & Leak Valves, Linear & Rotation. Transfer, Load Locks & Chamber, Custom Solution, Instruments & Electronics, Thickness Measurement, Gauges and Controller</i>	Tent Physics	P01

<p>attocube systems AG Eglfinger Weg 2, 85540 Haar <i>Piezo-based nanopositioners, low temperature microscopes, dry and liquid cryostats</i></p>	Audimax Foyer	A14+A15
<p>Bernhard Halle Nachfl. GmbH Optische Werkstätten Hubertusstraße 10, 12163 Berlin <i>Polarisationsoptik, Linsensysteme, Optische Komponenten</i></p>	Economy Bldg.	E11
<p>Bluefors Oy Vojko Kunej Arinatie 10, 003700 Helsinki, FINLAND <i>We offer a variety of models of dilution refrigerator measurement systems which can be further equipped with a wide range of options, e.g., experimental wiring, optical access, and magnet integration</i></p>	Audimax Foyer	A29
<p>Bruker Nano GmbH Am Studio 2D, 12489 Berlin <i>Bruker provides industry-leading surface analysis instruments for nanoscale materials characterization and process monitoring, addressing R&D and QA/QC questions with speed, accuracy, and ease. More information: www.Bruker.com</i></p>	Economy Bldg.	E02
<p>CAEN ELS S.R.L. AREA Science Park - SS14 km 163,5, 34149 Basovizza, Trieste, ITALY <i>High Performance Power Supplies, ZERO FLUCS Precision Current Measurements, Beamline Electronic Instrumentation, MicroTCA and FMC</i></p>	Economy Bldg.	E05
<p>CLASS 5 PHOTONICS GmbH Notkestraße 85, 22607 Hamburg <i>Ultrafast High Intensity Laser Systems, HHG-Sources, XUV-, VIS-, N/MIR-Sources, OPCPA, MPC</i></p>	Audimax Foyer	A02
<p>CreaPhys GmbH Niedersedlitzer Straße 75 (Eingang A), 01257 Dresden <i>Technology leader in purification & vacuum deposition of molecular organic & inorganic compounds for research & manufacturing of opto-electronic devices, perovskite solar cells & lithium-ion batteries</i></p>	Audimax Foyer	A40
<p>CreaTec Fischer & Co. GmbH Industriestraße 9, 74391 Erligheim <i>Manufacturer of customized LT-STM/AFM, MBE, RTA and molecular spray systems including associated electronics with software solutions as well as a wide range of equipment for use in (ultra-high) vacuum.</i></p>	Economy Bldg.	E21
<p>Cryoandmore Budzylek GbR Hermann-Cossmann-Straße 19, 41472 Neuss <i>4K Cryostats, Pulse Tube Cryocooler up to 2.7W@4.2K, GM Cryocooler up to 2W@4.2K Ultra Low Vibration Cryostats, Custom Cryostats</i></p>	Audimax Foyer	A12
<p>Cryogenic Unit 6, Acton Park Estate, The Vale, London, W3 7QE, UNITED KINGDOM <i>Cryogen-free, superconducting, 20 tesla, magnets, measurement, beamline, neutron, scattering, 3He, magnetism, VSM, conductivity, electrical, transport, low-temperature, UHV, SQUID, resonance, NMR, EPR, dilution refrigerator</i></p>	Audimax Foyer	A09
<p>CryoVac GmbH & Co. KG Langbaughstraße 13, 53842 Troisdorf <i>CRYOVAC designs and manufactures custom and standard cryogenic and vacuum systems. We offer a wide range of cryogenic products and equipment ranging from benchtop laboratory research to large-scale astronomical applications.</i></p>	Economy Bldg.	E10

Delft Circuits BV Lorentzweg 1, 2628CJ, Delft, NETHERLANDS <i>Delft Circuits is the manufacturer of cryogenic microwave flex cables. Cri/oFlex provides excellent microwave performance, low thermal load, flexibility, ease of installation, and reliability</i>	Audimax Foyer	A34
Deutsche Forschungsgemeinschaft (DFG) – Physik, Mathematik, Geowissenschaften 53170 Bonn <i>Information und Beratung zu den Förderprogrammen der DFG</i>	Audimax Foyer	A31
Digital Surf 16 rue Lavoisier, 25000 Besancon, FRANCE <i>Digital Surf provides software solutions for analyzing data from a range of instruments including Scanning Probe Microscopes (SPM), Scanning Electron Microscopes (SEM), profilometers and spectroscopy.</i>	Audimax Foyer	A23
Dr. Eberl MBE-Komponenten GmbH Josef-Beyerle-Straße 18/1, 71263 Weil der Stadt <i>Effusionszellen, Elektronenstrahlverdampfer, Dotierquellen, kundenspezifische Verdampfer</i>	Economy Bldg.	E06
Edwards High Vacuum International Ltd. Burgess Hill, West Sussex, RH15 9TW, UNITED KINGDOM <i>Complete Vacuum Solutions: Edwards stellt seine Vakuumpumpen aus der nXDS Serie sowie Zubehör/Messgeräte (wie APG200) vor - z.B. für die Halbleiterbranche zur Überwachung von Foreline-/allgemeinen Drücken.</i>	H6	A53
Focus GmbH Neukirchner Straße 2, 65510 Hünstetten-Kesselbach <i>Instruments for surface science</i>	Economy Bldg.	E01
GVL Cryoengineering Dr. George V. Lecomte GmbH Aachener Straße 89, 52223 Stolberg <i>Mischkryostate, Magnete und Zubehör für Kryotechnik</i>	Economy Bldg.	E13
GWU-Lasertechnik Vertriebsgesellschaft mbH Bonner Ring 9, 50374 Erftstadt <i>Abstimmbare Lasersysteme & OPOs; Kristalle (Laser, nicht-lineare); Spektrometer; Fiberlaser</i>	Economy Bldg.	E04
Hamamatsu Photonics Deutschland GmbH Arzbergerstraße 10, 82211 Herrsching a. Ammersee <i>Hamamatsu Photonics supplies award winning, high-quality detectors, which not only have contributed to achieve major scientific milestones but enable science every day. So, let us talk about your project.</i>	Tent Physics	P06
Heidelberg Instruments Mikrotechnik GmbH Mittelgewannweg 27, 69123 Heidelberg <i>Fotolithographie-Systeme und Nanofabrikationswerkzeuge zur Erstellung von Mikro- und Nanostrukturen.</i>	Audimax Foyer	A06
Hidden Analytical Europe GmbH Kaiserswerther Straße 215, 40474 Düsseldorf <i>Mass Spectrometers</i>	Audimax Foyer	A38
HORIBA Jobin Yvon GmbH Neuhofstraße 9, 64625 Bensheim <i>Your trusted partner for innovative spectroscopy</i>	Tent Physics	P02

Hositrad Deutschland Lindnergasse 2, 93047 Regensburg <i>CF, KF, ISO, UHV-Vakuumbauteile, Elektrische Durchführungen, Membranbalgen, Special Products</i>	Audimax Foyer	A17
Hübner Photonics Heinrich-Hertz-Straße 2, 34123 Kassel <i>Manufacturer of high performance lasers and thz systems</i>	Tent Physics	P11
HZDR Innovation GmbH Bautzner Landstraße 400, 01328 Dresden <i>Tensormeter, Rotax</i>	Tent Physics	P08
ICEoxford Avenue 4, Station Lane, Witney, Oxon, OX28 4BN, UNITED KINGDOM <i>Dry and Wet Cryogenic Systems, Dilution Refrigerators, Cryogenic Spares</i>	H6	A49
Incidenta Technologie GmbH Pommernstraße 22, 63110 Rodgau-Weiskirchen <i>Closed cycle & flow cryostats, custom cryogenic systems & probe Stations, ferro- & piezoelectric testers, analytical tools, thin film deposition: systems & components, custom UHV components.</i>	Audimax Foyer	A28
Institute of Physics Publishing Temple Circus, Temple Way, Bristol, BS1 6BE, UNITED KINGDOM <i>Publishers of journals, magazines, community websites</i>	Audimax Foyer	A05
Interdisciplinary Center for Analytics on the Nanoscale – ICAN Carl-Benz-Straße 199, 47057 Duisburg <i>Interdisciplinary Center for Analytics on the Nanoscale, XPS, AFM, SEM, TOF-SIMS, TEM, Raman, Präparation, Auftragsanalysen, Beratung</i>	Tent Physics	P09
JCM Dr. Jürgen Christian Müller Zeilweg 19, 60439 Frankfurt / Main <i>Vakuumtechnik, Dünnschichttechnik, Tieftemperaturtechnik, supraleitende Magnete</i>	Audimax Foyer	A09
Kashiyama Europe GmbH Leopoldstraße 244, 80807 München <i>Vacuum solutions</i>	Audimax Foyer	A18
kiutra GmbH Flößergasse 2, 81369 München <i>Cryogen-free Crostat</i>	Audimax Foyer	A24
Kleindiek Nanotechnik GmbH Aspenhaustraße 25, 72770 Reutlingen <i>Micromanipulators, nanopositioners, nanoprobing, in situ AFM, cryo TEM sample liftout, nanoassembly, manipulators for UHV, force measurement, etc. Give your microscope a hand! www.kleindiek.com</i>	Audimax Foyer	A46
LASER 2000 GmbH Argelsrieder Feld 14, 82234 Weßling <i>Laser & Strahlquellen, Optik & Optomechanik, Optische Messtechnik, Laserschutz, LWL-/Netzwerktechnik</i>	H6	A55
Leiden Probe Microscopy B.V. J.H. Oortweg 19, 2333 CH Leiden, THE NETHERLANDS <i>High Pressure STM, Fast SPM, SXRD, CVD, Graphene, Variable Temperature STM</i>	Economy Bldg.	E18

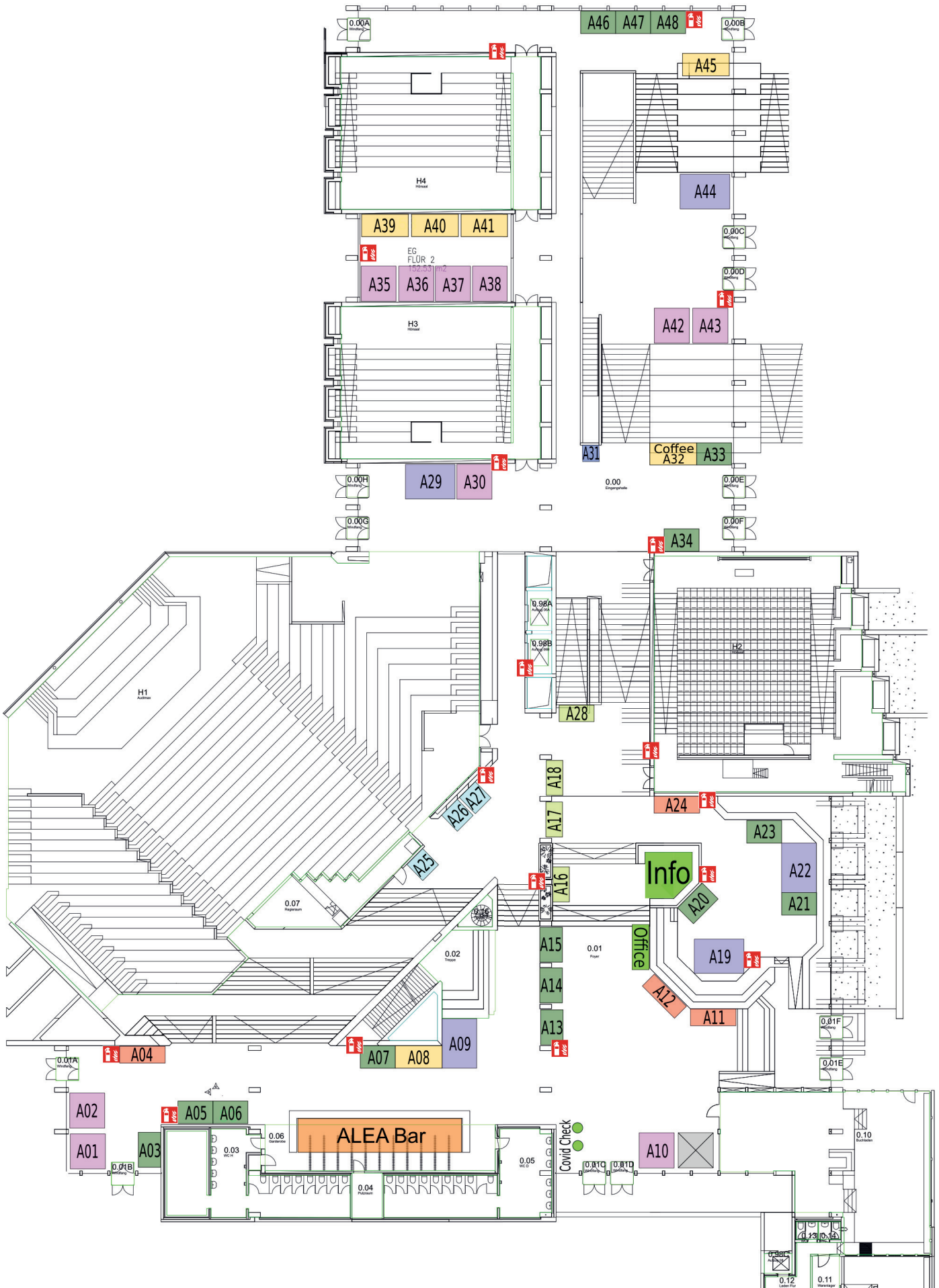
Leybold GmbH Bonner Straße 498, 50968 Köln <i>Vakuumpumpen</i>	H6	A50
LIOP-TEC GmbH Industriestraße 4, 42477 Radevormwald <i>Optomechanik</i>	Tent Physics	P13
Ludwig-Maximilians-Universität München (Prof. Alexander Högele) Geschwister-Scholl-Platz 1, 80539 München <i>Qlibri Projekt LMU München</i>	Audimax Foyer	A03
MaTeck – Material-Technologie & Kristalle GmbH Im Langenbroich 20, 52428 Jülich <i>Einkristalle, Sputtertargets, Substrate, hochreine Materialien, Isotope, Halbleiterkristalle</i>	H6	A57
Menlo Systems GmbH Bunsenstraße 5, 82152 Martinsried <i>Femtosecond Fiber Lasers, THz Time Domain Systems, Ultrastable Lasers, Optical Frequency Combs</i>	Audimax Foyer	A11
ML4Q Office Cologne Matter and Light for Quantum Computing Pohligstraße 3, 50969 Köln <i>Cluster of Excellence „Matter and Light for Quantum Computing“ representing the Quantum Alliance, the consortium of German clusters and research centers working in quantum science and technology</i>	Tent Physics	P10
Moorfield Nanotechnology LTD Unit 1 Parkgate Industrial Estate, Knutsford, Cheshire, WA16 8XJ, UNITED KINGDOM <i>Deposition systems for magnetron sputtering, thermal and e-beam evaporation, as well as etching tools. Benchtop, free-standing and glovebox models. Field-proven MiniLab, nanoPVD and nanoETCH ranges.</i>	Economy Bldg.	E17
Nanosurf GmbH Rheinstraße 5, 63225 Langen <i>Rasterkraftmikroskope, Atomic Force Microscope, AFM, SPM</i>	Audimax Foyer	A07+A08
Nikalyste Ltd 77 Heyford Park, OX25 5HD Upper Heyford, Bicester, UNITED KINGDOM <i>Nikalyste is a supplier of nanoparticle deposition equipment</i>	Economy Bldg.	E19
Onnes Technologies B.V. Kenauweg 21, 2331 BA Leiden; THE NETHERLANDS <i>ONNES TECHNOLOGIES introduces ARKTIKA, a new cryogenic nanopositioner. Our WALKING TECHNOLOGY distinguishes itself from stick-slip in superior characteristics. Visit us at Regensburg22, stand E14.</i>	Economy Bldg.	E14
Orange Quantum Systems Lorentzweg 1, 2628 CJ Delft, THE NETHERLANDS <i>Orange QS provides solutions that enable our partners to create the best quantumchips</i>	Audimax Foyer	A41
Owis GmbH Feinmechanische und optische Systemtechnik Im Gaisgraben 7, 79219 Staufen i. Br. <i>Strahlführungs- und Positioniersysteme</i>	Tent Physics	P16

Oxford Instruments GmbH Borsigstraße 15 a, 65205 Wiesbaden <i>Oxford Instruments produces leading-edge analytical solutions including: Raman imaging systems from WITec, atomic force microscopes from Asylum Research, and cryogenic systems for low temperature environments from NanoScience.</i>	Audimax Foyer	A30
Oxford University Press Academic Division Great Clarendon Street, Oxford OX2 6DP, UNITED KINGDOM <i>Books, Catalogues</i>	Economy Bldg.	E09
Park Systems Europe GmbH Schildkrötstraße 15, 68199 Mannheim <i>Atomic Force Microscopy</i>	Audimax Foyer	A13
Pfeiffer Vacuum GmbH Berliner Straße 43, 35614 Asslar <i>Vakuumumpfen, Messgeräte, Turbopumpen, Lecksucher</i>	Audimax Foyer	A33
Picovac Ziegelhüttenweg 30a, 65232 Taunusstein <i>Thin Film Deposition Systems, Instruments for In-situ/Operando Research, Nanoparticle Deposition. Representing Korvus Technology, Leiden Probe Microscopy, Moorfield Nanotechnology, Nikalyte</i>	Economy Bldg.	E20
PINK GmbH Vakuumtechnik Gyula-Horn-Straße 20, 97877 Wertheim <i>Vakuum- u. UHV-Kammern, Beschleunigerkomponenten, Vakuumtechnische Anlagen u. Systeme, Manipulatoren</i>	Economy Bldg.	E16
PREVAC sp. z o.o. Raciborska Str. 61, 44362 Rogów, POLEN <i>uhv, xps, ups, arpes, deposition, sputtering, mbe, pld, research, science, customized solutions.</i>	Audimax Foyer	A26+A27
Qioptiq Photonics GmbH & Co. KG Hans-Riedl-Straße 9, 85622 Feldkirchen (München) <i>Präzisionsoptik und Mechanik, Faseroptik, Aufbausysteme, Laser</i>	Audimax Foyer	A35
Qnami AG Hofackerstrasse 40B, 4132 Muttenz, SWITZERLAND <i>Quantum Sensor</i>	Economy Bldg.	E15
Quantum Design GmbH Im Tiefen See 58, 64293 Darmstadt <i>Kryostate, Optische Kryostate, Kryogene Probe-Stations, Magnetsysteme für die Materialcharakterisierung, Magnetometer, Heliumverflüssiger, Temperatur Sensoren & Controller, Elektrische Messtechnik, CCD-, ICCD-, EMCCD-Detektoren, Spektrographen</i>	Audimax Foyer	A44
Quantum Machines Fruebjergvej 3, 2100 Copenhagen, DENMARK <i>QDevil presents its product lineup for quantum computing applications. Cryogenic sample holders for Spin and Superconductivity qubit chips. Cryogenic filters, Control electronics and hardware.</i>	Audimax Foyer	A21
Raith GmbH Konrad-Adenauer-Allee 8, 44263 Dortmund <i>Raith is a leading precision technology manufacturer for nanofabrication, electron beam lithography, FIB SEM nanofabrication, nanoengineering, process control and reverse engineering applications.</i>	Audimax Foyer	A10

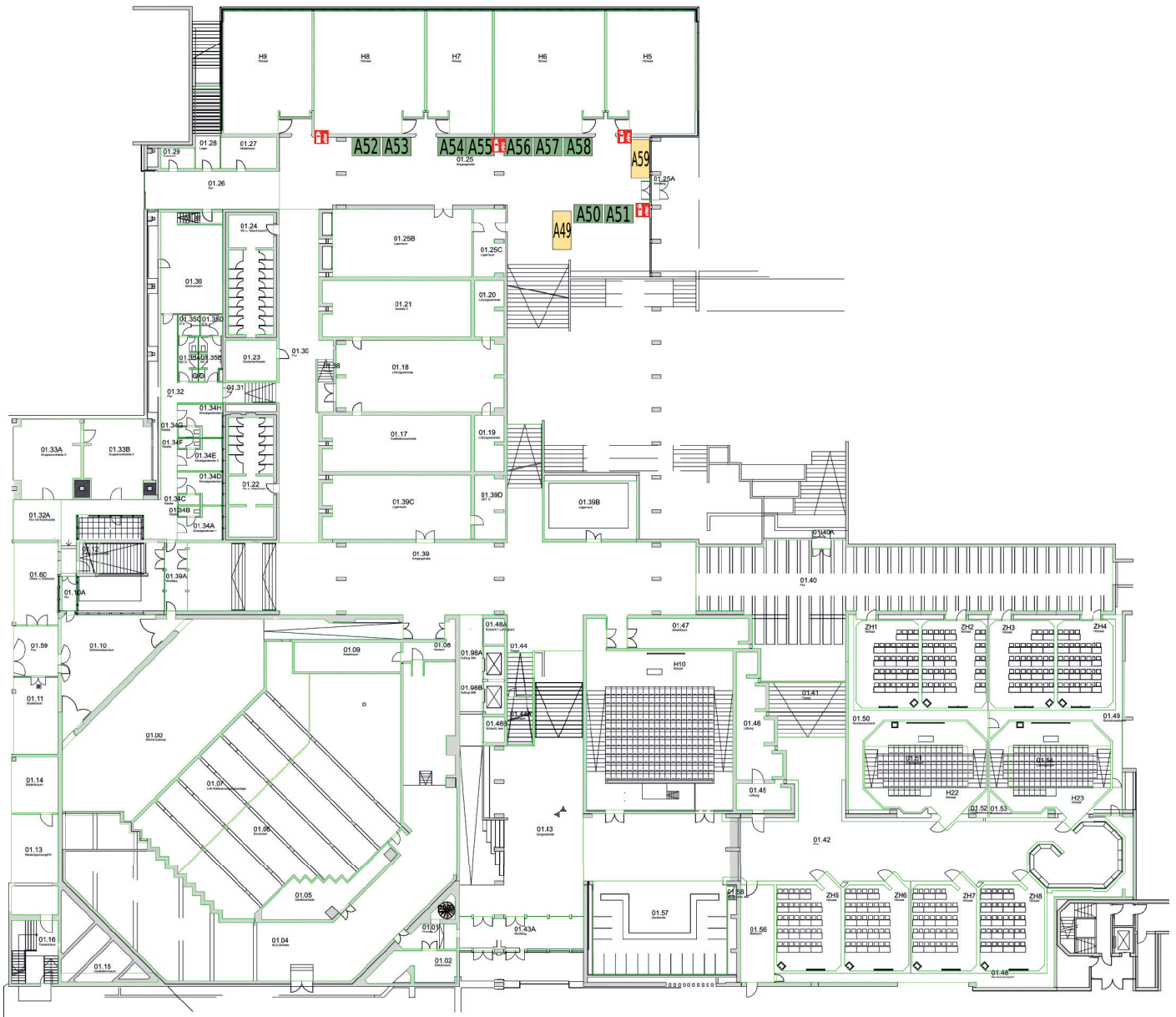
SAES Getters S.p.A. Viale Italia, 77, 20020 Lainate (Milan), ITALY <i>UHV NEG-Pumpen, Alkalimetall-Dispenser, Hochvakuumpumpen, Getter</i>	Tent Physics	P07
Schaefer Technologie GmbH Robert-Bosch-Straße 31, 63225 Langen <i>Rastersondenmikroskopie, optische 3D-Mikroskopie, Dünnschicht-Technologie, Nano-Analytik</i>	H6	A58+A59
Scienta Omicron GmbH Limburger Straße 75, 65232 Taunusstein <i>Systems and Instruments for Surface Science and Thin Film Technology</i>	Economy Bldg.	E12
SEKELS GmbH Dieselstraße 6, 61239 Ober-Mörlen <i>Magnetische Abschirmungen, Magnetsysteme, weichmagnetische Halbzeuge, induktive Bauelemente</i>	H6	A56
Sensific GmbH Paukengasse 14, 89077 Ulm <i>Camera-based high-speed analysis and control systems with integrated real-time image processing for applications in droplet microfluidics, particle and cell analysis</i>	Audimax Foyer	A48
SENTECH Instruments GmbH Schwarzschildstraße 2, 12489 Berlin <i>Plasma Prozess technologie und Ellipsometer</i>	Audimax Foyer	A01
SI Scientific Instruments GmbH Römerstraße 67, 82205 Gilching <i>Spektrometer, Lock-In Verstärker</i>	Tent Physics	P14
SmarAct GmbH Schütte-Lanz-Straße 9, 26135 Oldenburg <i>SmarAct Kleingeräte</i>	Tent Physics	P17
SPECS Surface Nano Analysis GmbH Voltastraße 5, 13355 Berlin <i>Photoelektronenspektroskopie, Rastersondenmikroskopie, winkelaufgelöste Photoemission, Elektronenmikroskopie</i>	Audimax Foyer	A19
Springer-Verlag GmbH Tiergartenstraße 17, 69121 Heidelberg <i>Wissenschaftliche Bücher und Zeitschriften</i>	Audimax Foyer	A45
Staub Instrumente GmbH Hagenastraße 22, 85416 Langenbach <i>In situ growth monitoring for MBE, RHEED, TorrRHEEDTM, AUGERProbeTM, AES, XPS, UPS, REELS, electron and ion sources, complete surface analysis systems, STAIB MultitecTM</i>	Tent Physics	P15
Surface Concept GmbH Am Sägewerk 23 a, 55124 Mainz <i>Scientific cameras, ToF momentum microscopes, imaging & time-resolved MCP based detection, analoge pulse processing</i>	H6	A51

<p>Swabian Instruments GmbH Stammheimer Straße 41, 70435 Stuttgart <i>TCSPC, Time Taggers, Pulse Streamer</i></p>	Audimax Foyer	A42
<p>Technische Informationsbibliothek Hannover (TIB) Welfengarten 1B, 30167 Hannover <i>Wissenschaftliche Fachliteratur</i></p>	Tent Physics	P03
<p>Tecuum AG Applied Vacuum Technology Gertrudstrasse 1, 8400 Winterthur, SWITZERLAND <i>VCM600 is the standard Vacuum Thermal Evaporator. "Plug and Play", compact, desktop/bench top, Rack type and Glove Box systems. No running cables mesh. No special operating system. No PLC bugs. Robust, fast, versatile systems.</i></p>	Tent Physics	P04
<p>THORLABS GmbH Münchner Weg 1, 85232 Bergkirchen <i>Optische und optomechanische Komponenten, Test & Measurement Systeme, optische Tische und Vibrationskontrolle, Nanopositionierungen, Lichtquellen sowie Imaging, Mikroskopie und Life Science Komponenten</i></p>	Audimax Foyer	A16+A25
<p>TOPAG Lasertechnik GmbH Nieder-Ramstädter Straße 247, 64285 Darmstadt <i>Laser und Optische Messtechnik</i></p>	H6	A54
<p>TOPTICA Photonics AG Lochhamer Schlag 19, 82166 Gräfelfing / München <i>Laser Rack Systems, Tunable Diode Lasers, Laser Frequency Stabilization, Femto Fiber Lasers, Wavelength Meters</i></p>	Audimax Foyer	A37
<p>TransMIT GmbH Kerkrader Straße 3, 35394 Gießen <i>TransMIT GmbH - Center for Adaptive Cryotechnology and Sensors</i></p>	Economy Bldg.	E08
<p>Ulrich Neumann Tschiedererstraße 3, 86609 Donauwörth <i>Ausstellung des Buches „Das wunderbare Universum verstehen – Physik 2.0“</i></p>	Tent Physics	P12
<p>Vaqtec-scientific Mario Melzer Thulestraße 18B, 13189 Berlin <i>Komponenten der UHV- und HV-Technik: u.a. Stromdurchführungen, Schaugläser, Schichtdicken-Messgeräte</i></p>	Economy Bldg.	E07
<p>Wiley-VCH GmbH Boschstraße 12, 69469 Weinheim <i>Fachverlag, Fachbücher, Fachzeitschriften, Online Produkte</i></p>	Audimax Foyer	A04
<p>Zurich Instruments AG Marketing and Sales Technoparkstrasse 1, 8005 Zurich, Schweiz <i>Lock-in Amplifiers, Test & Measurement</i></p>	Audimax Foyer	A22

Audimax DPG 2022



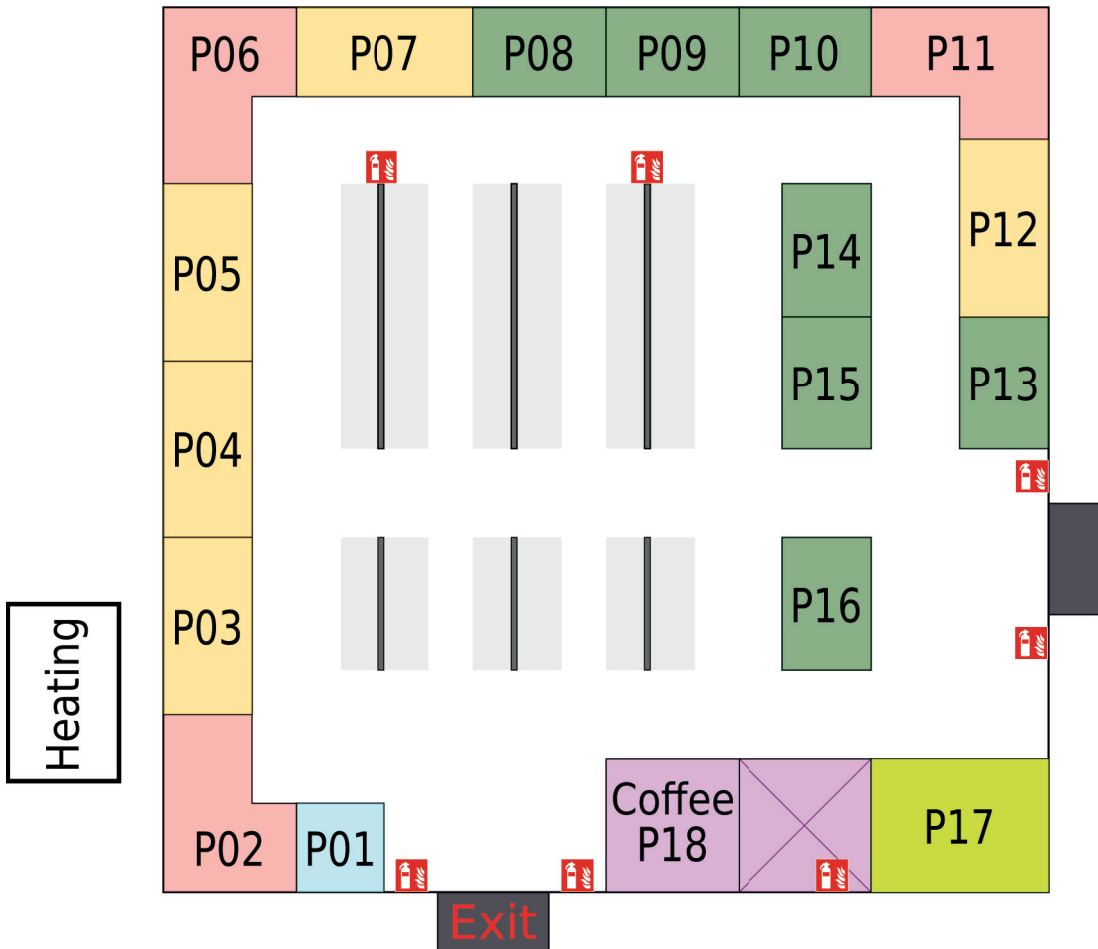
Audimax - H6 DPG 2022



Wirtschaft & Recht DPG 2022



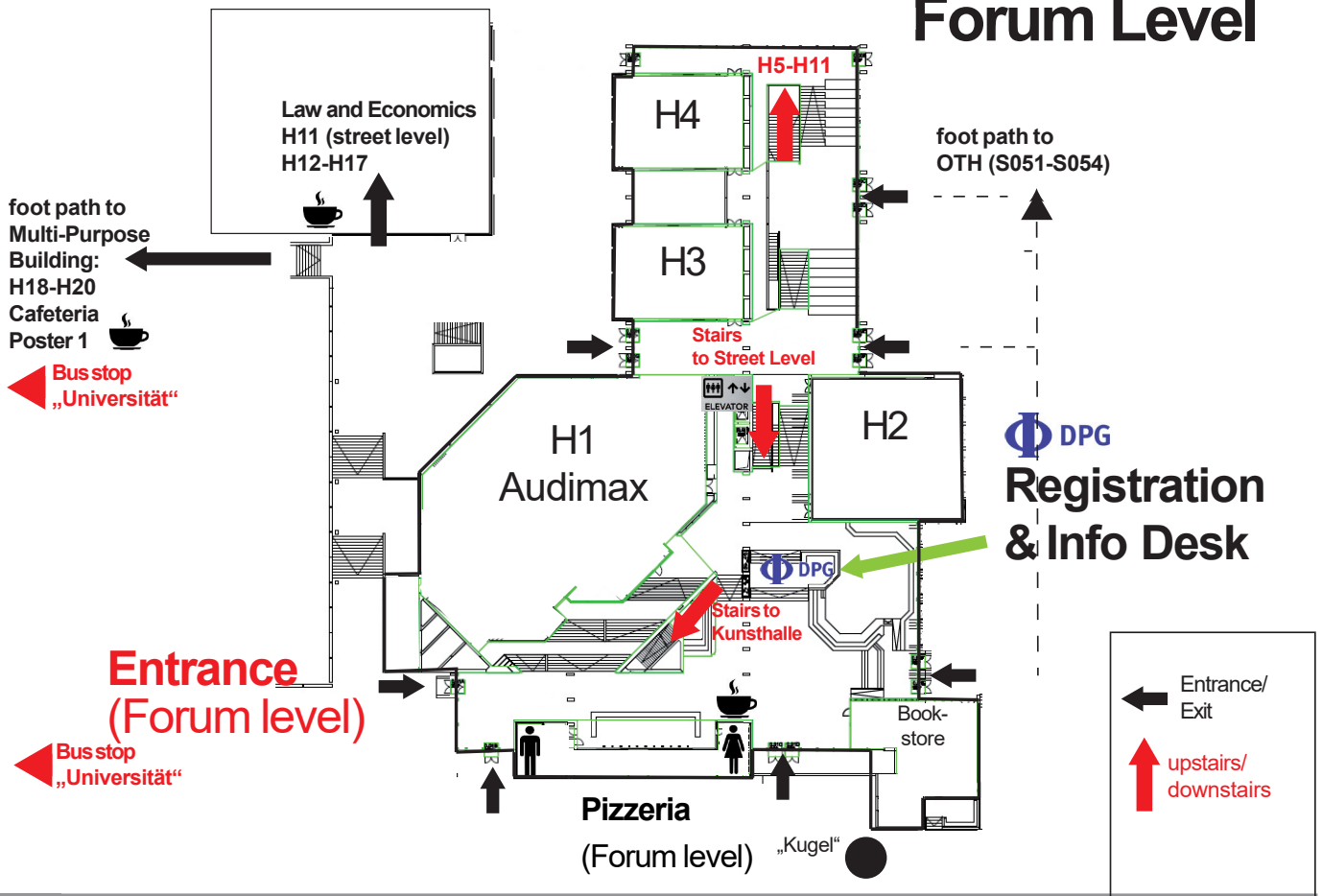
Tent at Physics department



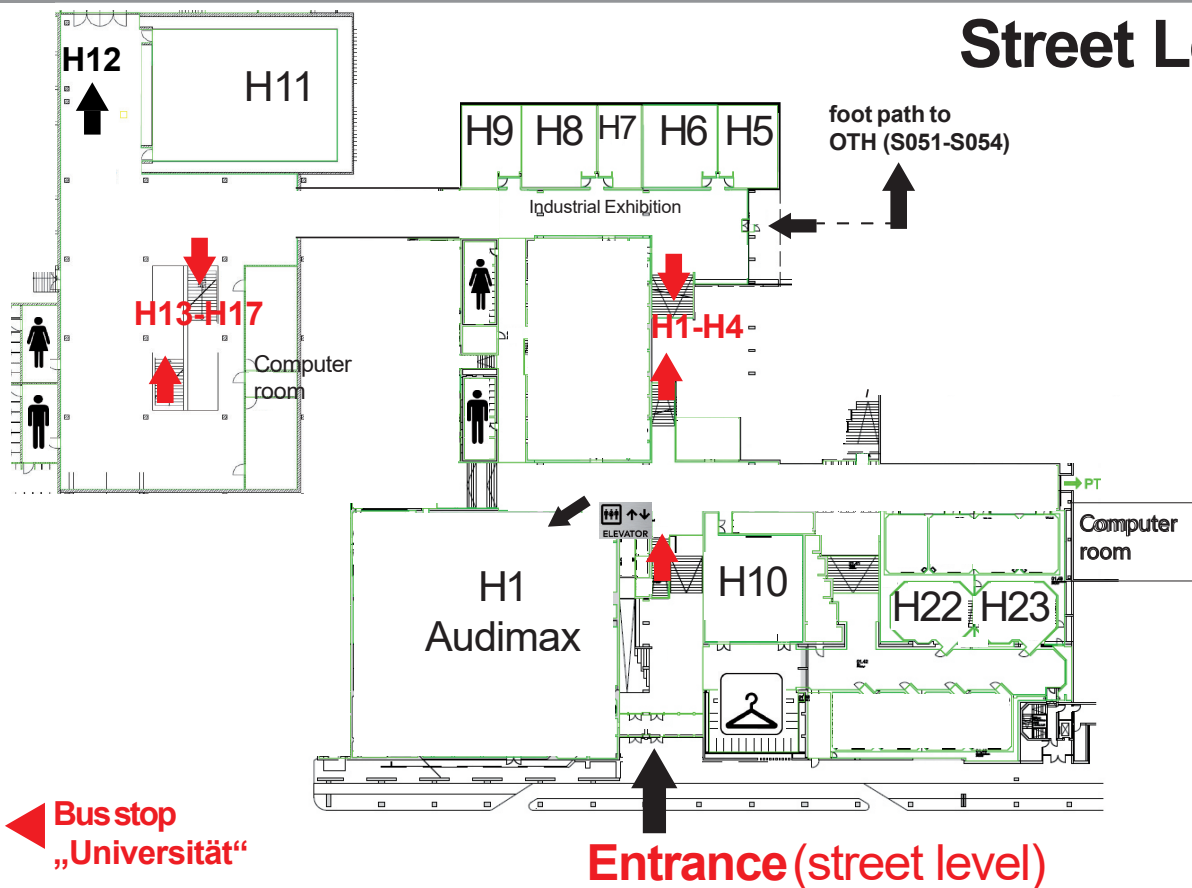
Quelle: Universität Regensburg
Einzeichnung Stände: Stefan Hartl

Map of the Main Lecture Hall

Forum Level



Street Level



Universität Regensburg - Campus Map DPG Spring meeting 2022

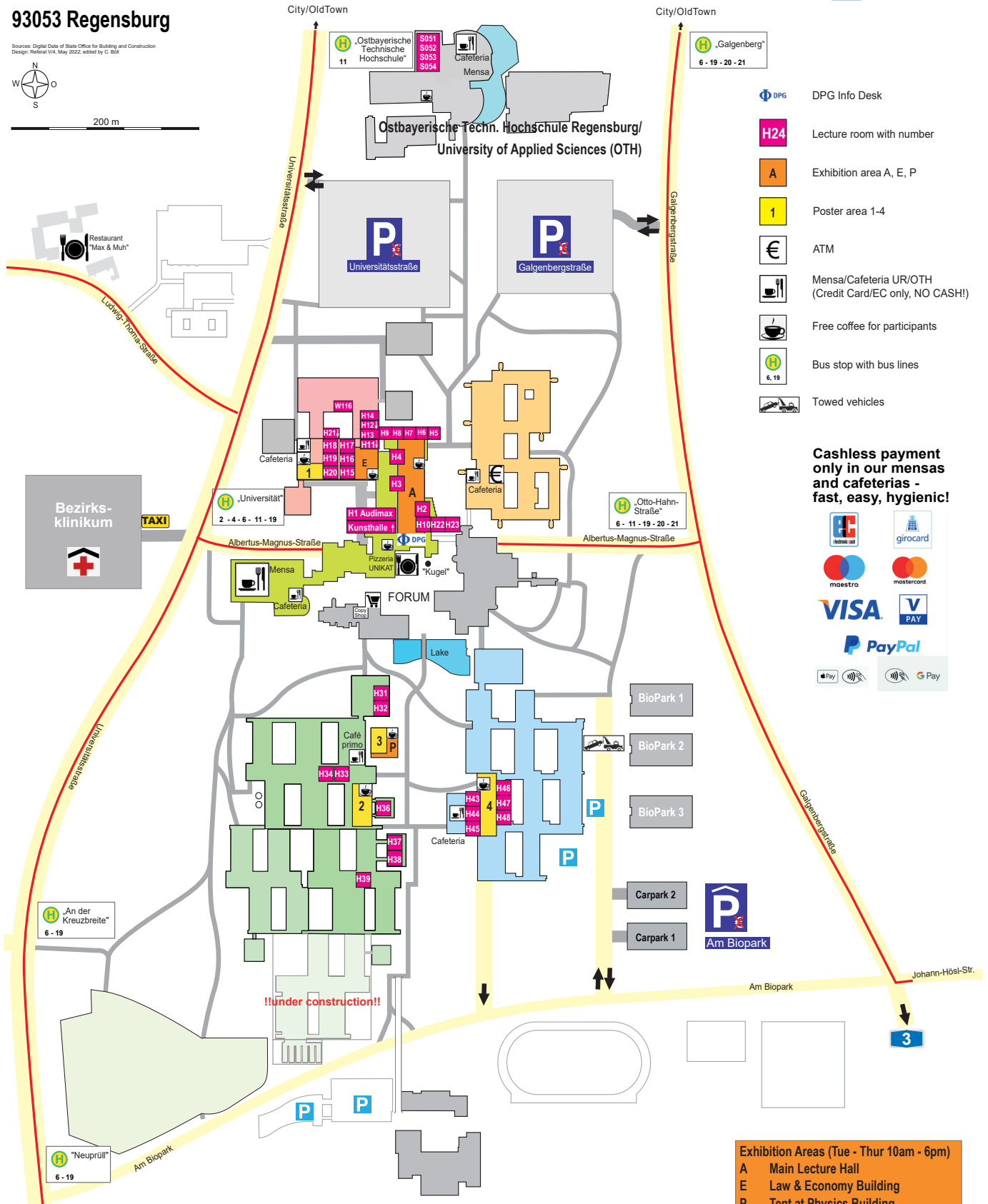


Universitätsstraße 31
93053 Regensburg

Sources: Digital Data of State Office for Building and Construction
Design: Robert Vils, May 2022, edited by C. Böt

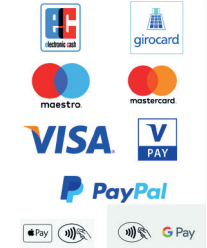


200 m



- DPG Info Desk
- Lecture room with number
- Exhibition area A, E, P
- Poster area 1-4
- ATM
- Mensa/Cafeteria UR/OTH (Credit Card/EC only, NO CASH!)
- Free coffee for participants
- Bus stop with bus lines
- Towed vehicles

Cashless payment only in our mensas and cafeterias - fast, easy, hygienic!



Sammelgebäude / Multi-purpose Building
 H18 H19 H20 H21
Recht & Wirtschaft / Law/Business/Economics
 H11 H12 H13 H14
 H15 H16 H17

Zentrales Hörsaalgebäude / Main Lecture Hall
 H1 Audimax H2 H3 H4
 H5 H6 H7 H8 H9
 H10 H22 H23
 Kunstthalle

Chemie & Pharmazie / Chemistry & Pharmacy
 H43 H44 H45
 H46 H47 H48

Exhibition Areas (Tue - Thur 10am - 6pm)
 A Main Lecture Hall
 E Law & Economy Building
 P Tent at Physics Building

Mathematik / Mathematics H31 H32
Physik / Physics H33 H34 H36
Vorklinik/ Pre-Clinical Medicine H37 H38 H39

Timetable

Start	Sunday, September 4	Monday, September 5	Tuesday, September 6	Wednesday, September 7	Thursday, September 8	Friday, September 9
08:15		08:25 Opening remarks (Audimax)				
08:30		Plenary Talk (Audimax)	Plenary Talk (Audimax)	Plenary Talk (Audimax)	Plenary Talk (Audimax)	Plenary Talk (Audimax)
08:45						
09:00						
09:15						
09:30						
09:45						
10:00						
10:15						
10:30						
10:45		STOP (Audimax)	SYPQ (Audimax)	SYED (Audimax)	SYSO (Audimax)	SYQM (Audimax)
11:00						
11:15		SKM Diss. Prize Symp. (H2)	Sessions of divisions	SYUK I (H2)	Sessions of divisions	Panel Discussion AKC (H2)
11:30						
11:45						
12:00						
12:15						
12:30						
12:45						
13:00						
13:15		Prize Talk (Audimax)	Prize Talk (Audimax)	Prize Talk (Audimax)	Lunch Talk (Audimax)	Closing Talk (OTH - S054)
13:30			Lunch Talk (H2)	Lunch Talk (H2)	Lunch Talk (H2)	
13:45						
14:00		Plenary Talks (Audimax + H2)		Plenary Talks (Audimax + H2)	Plenary Talks (Audimax + H2)	
14:15						
14:30						
14:45						
15:00						
15:15						
15:30						
15:45						
16:00						
16:15	15:00-19:00 Registration		14:30-17:15 Ceremonial Session with Award Ceremony and Ceremonial Talk (Audimax)			
16:30		SYNM (Audimax)	Sessions of divisions	SYSM (Audimax)	SYES (Audimax)	Annual General Meetings of the DPG divisions
16:45						
17:00	16:00-18:15 Tutorials (Audimax, H2, H3, H4)			SYUK II (H2)		
17:15						
17:30						
17:45						
18:00						
18:15						
18:30						
18:45						
19:00						
19:15						
19:30	18:30-21:30 Welcome Evening (Mensa)		19:00-20:00 Public Evening Talk (in German) (Audimax + H2)			
19:45						
20:00						
20:15						
20:30						
20:45						
21:00						
21:15						
21:30						
21:45						
21:55						
22:00						
22:15						
22:30						
22:45						
23:00						
23:15						
23:30						
23:45						